TRANSACTIONS

OF THE

AMERICAN SOCIETY

OF

MECHANICAL ENGINEERS

1942

VOLUME 64

PUBLISHED BY
THE AMERICAN SOCIETY OF MECHANICAL ENGINEERS
29 WEST THIRTY-NINTH STREET, NEW YORK, N. Y.

Copyright, 1943, by
THE AMERICAN SOCIETY OF MECHANICAL ENGINEERS

Printed in the United States of America by
The Mack Printing Co., Easton, Pa.

Engin Lib
4-20-43

Foreword

VOLUME 64 of the Transactions of The American Society of Mechanical Engineers contains the individual papers published during 1942 under the sponsorship of the Society's professional divisions and technical committees, including the contributions of the Applied Mechanics Division, issued originally in a quarterly known as *Journal of Applied Mechanics*, and the 1942 Society Records and Index. The technical papers and reports that make up this volume represent the Society's annual contribution to the permanent record of mechanical-engineering achievement. Most of these papers and reports were presented at meetings of the Society and its professional divisions and local sections and were published in monthly issues, eight being distributed as the Transactions of The American Society of Mechanical Engineers and four as the *Journal of Applied Mechanics*. Indexes to other A.S.M.E. papers and publications will be found on page RI-81 at the end of this volume.

In view of the fact that material of which this volume is composed was originally issued periodically as Transactions, *Journal of Applied Mechanics*, and Society Records, three sets of page numbers will be found. Numbers without letter symbols are those of the eight issues of the Transactions, those with letter symbol A preceding the number refer to the pages of the *Journal of Applied Mechanics*, which follow, and those with letter symbol RI to the Society Records section, which concludes the volume.

All sections of the Transactions are bound together at the end of the year for the convenience of libraries and of engineers who wish all of the papers in permanent form. Copies of the bound Transactions will be found in depositories located in selected engineering, university, and public libraries throughout the world. A complete list of these depositories will be found on pages RI-77 to RI-80 of the Society Records and Index. Copies of the Transactions have also been set aside for sale.

The Society Records of the A.S.M.E. for 1942, which form a part of these Transactions, are the permanent records of the Society's activities for the year, including lists of committees and memorial biographies. The Index provides a means of locating special A.S.M.E. publications and articles in *Mechanical Engineering* as well as those in the Transactions.

THE COMMITTEE ON PUBLICATIONS

Modern Steam Passenger Locomotives—Research and Design

By P. W. KIEFER,[1] NEW YORK, N. Y.

This paper traces the progress of development of passenger locomotives on the New York Central System from the heavy Pacific type of 1925, to the latest combination passenger and freight design of 1940, showing the continued demand for increased power and the methods used to satisfy the requirements. A brief résumé of actual results obtained is presented and in conclusion, an expression of views is offered on possibilities for further improvement in the near future without departure from the conventional reciprocating design.

IN RECENT years, much valuable information and data on the modern steam locomotive, its elements and adjuncts, have been published or otherwise made available by many eminent engineers interested in railroad motive power. As a result of these painstaking efforts, the subject as a whole and the factors into which it subdivides have been particularly well covered. Nevertheless, when dealing with the subject of motive power from the standpoint of meeting the constantly changing needs of the modern railroad, even over a relatively short period of time, it soon becomes evident that the problems to be faced and solved are both complex and numerous and usually urgent.

With these circumstances indicated, it will be the author's main purpose to review the practical aspects of the problems which have been involved in supplying high-capacity steam motive power for fast and heavy service on the New York Central System during the last 15 years; to recite the several design and performance objectives, as determined in advance for this motive power; to submit information indicating the extent to which these objectives have been attained, as checked through performance tests under regular passenger-train operating conditions; and, finally, to express some thoughts on trends for the near future in design improvement.

While many of the problems confronted are similar to those encountered on other large railroads and the solutions in a number of respects are alike, it is desired to discuss specific matters which can be directly handled and to avoid the use of generalities so far as practicable. For these reasons, the content of this paper has been confined to the motive power of the System with which the author is connected.

It is not the intention to detail the features of the motive-power units here included but instead to limit the descriptive matter to major characteristics of design, supplemented in some instances by reference to special equipment items and to avoid, as far as practicable, repetition of what is already well known or is readily procurable from various sources.

Historical Background

In 1904, when the "Consolidation," "Ten-Wheeler," "Atlantic," and "Prairie" types were still the conventional freight and passenger locomotives in common use for heavy duty on the System, the first of a series of "Pacifics," class K-80, was introduced on the Michigan Central Railroad. During the following year, passenger locomotives of the same type were placed in service on the Boston & Albany and on the C.C.C.& St.L. Railroads. In 1907, the New York Central and the Lake Shore and Michigan Southern, now New York Central Lines West, received modifications of this type in the form of somewhat larger locomotives, designated as class K-2.

These engines successfully handled the work assigned to them and succeeding lots of the same type were installed until 1911, when a somewhat heavier and more powerful Pacific type was produced. This design is known as the class K-3, a considerable number of which are still in active service.

Continuing Demand for Increased Power

Shortly after the introduction of the last of the K-3 class, it became evident that a further substantial increase in power was required and an attempt was made to meet this demand by a yet larger Pacific, having 25-in. × 28-in. cylinders instead of 23½-in. × 26-in., and with firebox and boiler capacity increased proportionately. With 79-in-diam driving wheels and a working boiler pressure of 200 psi, these locomotives developed a rated main-engine tractive effort of 37,650 lb which, by the use of a booster, was increased to 47,350 lb. This design was designated as class K-5, and, in view of its increased size, hand firing was no longer practicable for capacity operation, so mechanical stokers were installed.

The progressive development of the Pacific type from the original class K-80 on the Michigan Central, built in 1904, to the latest class K-5, built in 1926, is shown in Figs. 1 to 5, inclusive, the principal characteristics of each typical design being indicated. Fig. 6 shows the drawbar pull and drawbar horsepower versus speed for each of these distinct designs, the curves being typical of actual performance on the road under regular operation with locomotives in good condition.

The K-5 class, built in 1925 and 1926, was supplied with a tender carrying 15,000 gal of water on two 6-wheel trucks, which marked the introduction of the large-capacity tender for System passenger operation, the progressive elimination of service stops, and the extension of locomotive runs.

A survey undertaken in 1926 of the facts and conditions as related to the necessity for a further increase in the power of main-line passenger locomotives, together with consideration of probable future needs, led quickly to the definite conclusion that a unit of an entirely new design and type must be developed.

A New Type Locomotive

The basic problem presented was to create a design of locomotive having the following characteristics, as compared with the Pacific types heretofore used:

1 Somewhat greater starting tractive effort with increased horsepower capacity and maximum output at much higher speed.

2 Boiler of ample sustained capacity to satisfy the cylinder requirements for maximum power development, under severe weather and other conditions.

3 Weight distribution, wheel loads, and counterbalance to be such that impact forces and rail stresses could be confined to

---

[1] Chief Engineer, Motive Power and Rolling Stock, New York Central System. Mem. A.S.M.E.

Contributed by the Railroad Division and presented at the Semi-Annual Meeting, June 16–19, 1941, Kansas City, Mo., of The American Society of Mechanical Engineers.

Note: Statements and opinions advanced in papers are to be understood as individual expressions of their authors, and not those of the Society.

CYLS. 22 DIA. × 26 STROKE
BOILER PRESSURE 200 LBS
MAX. TRACTIVE FORCE 28500 LBS

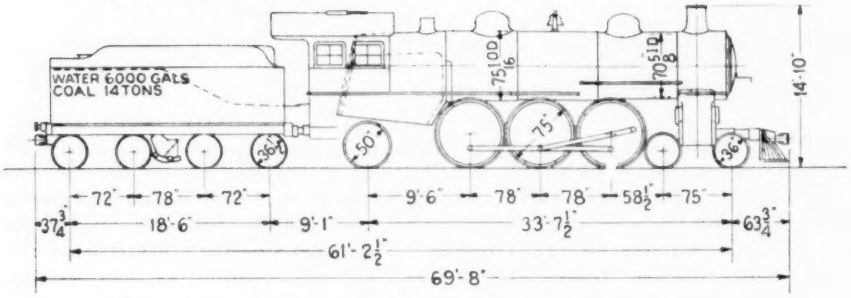


FIG. 1 MICHIGAN CENTRAL CLASS K-80 PACIFIC TYPE LOCOMOTIVE, BUILT 1904

CLASS K80 BUILT 1904

WEIGHTS		HEATING SURFACE	
DRIVERS	142,500 LBS.	EVAPORATIVE	3283 SQ. FT.
TOTAL ENGINE	224,000 LBS.	SUPERHEATED	672 SQ. FT.
HORSEPOWER			
MAX. INDICATED	1700 AT 39 M.P.H.	GRATE AREA	50.2 SQ. FT.
MAX. DRAWBAR	1430 AT 35 M.P.H.		

CYLS. 22 DIA × 28 STROKE
BOILER PRESSURE 200 LBS
MAX TRACTIVE FORCE 29160 LBS.

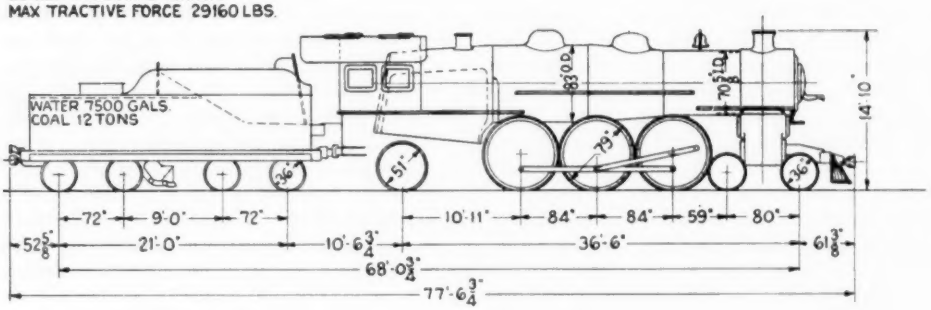


FIG. 2 CLASS K-2A LOCOMOTIVE, BUILT 1907

CLASS K2A BUILT 1907

WEIGHTS		HEATING SURFACE	
DRIVERS	173,000 LBS.	EVAPORATIVE	3789 SQ. FT.
TOTAL ENGINE	268,000 LBS	SUPERHEATED	724 SQ. FT.
HORSEPOWER			
MAX. INDICATED	2000 AT 45 M.P.H.	GRATE AREA	56.5 SQ. FT.
MAX. DRAWBAR	1655 AT 40 M.P.H.		

CYLS. 23½ DIA. × 26 STROKE
BOILER PRESSURE 200 LBS.
MAX. TRACTIVE FORCE MAIN ENGINE 30900 LBS.
" " " BOOSTER 9700 LBS.

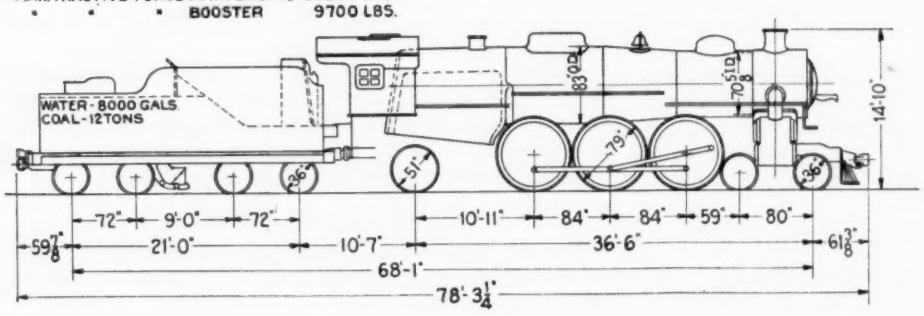
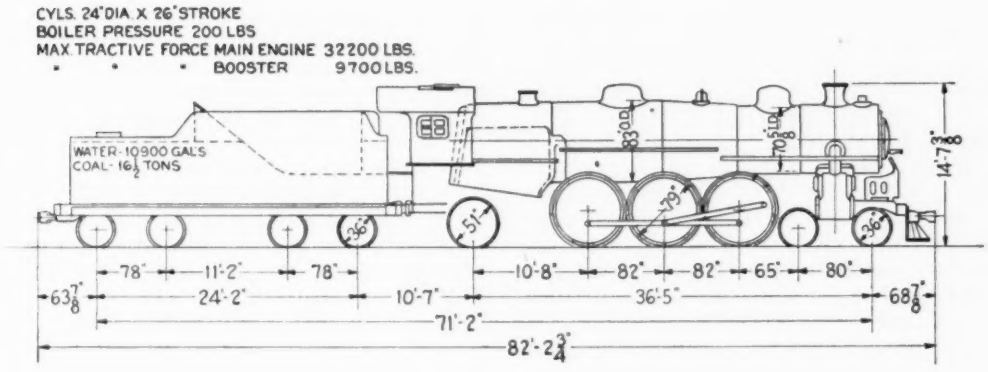


FIG. 3 CLASS K-3Q LOCOMOTIVE, BUILT 1923

CLASS K3Q BUILT 1923

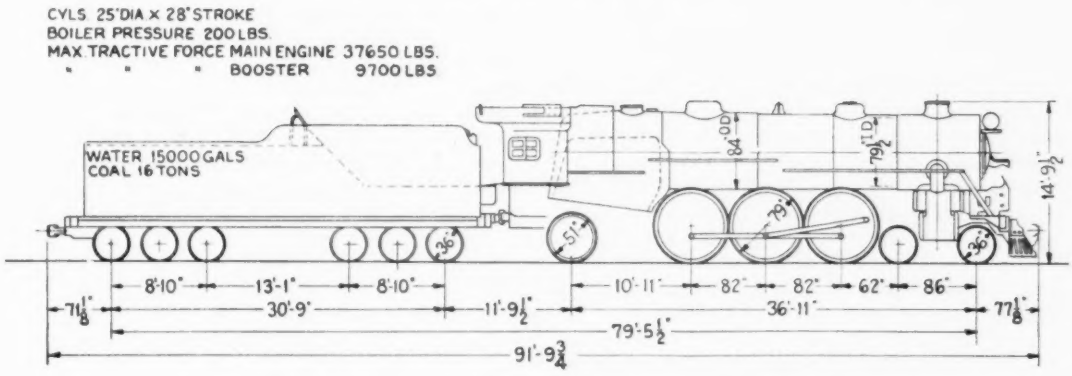
WEIGHTS		HEATING SURFACE	
DRIVERS	194,500 LBS.	EVAPORATIVE	3424 SQ. FT.
TOTAL ENGINE	295,500 LBS.	SUPERHEATED	832 SQ. FT.
HORSEPOWER			
MAX. INDICATED	2100 AT 45 M.P.H.	GRATE AREA	56.5 SQ. FT.
MAX. DRAWBAR	1720 AT 40 M.P.H.		



CLASS K3R BUILT 1925

WEIGHTS		HEATING SURFACE	
DRIVERS	169,000 LBS.	EVAPORATIVE	3421 SQ.FT.
TOTAL ENGINE	278,000 LBS.	SUPERHEATED	839 SQ.FT.
HORSEPOWER			
MAX. INDICATED	2140 AT 45 M.P.H.	GRATE AREA	56.7 SQ.FT.
MAX. DRAWBAR	1750 AT 40 M.P.H.		

FIG. 4 CLASS K-3R LOCOMOTIVE, BUILT 1925



CLASS K5B BUILT 1926

WEIGHTS		HEATING SURFACE	
DRIVERS	185,000 LBS.	EVAPORATIVE	3952 SQ.FT.
TOTAL ENGINE	302,000 LBS.	SUPERHEATED	1150 SQ.FT.
HORSEPOWER			
MAX. INDICATED	3200 AT 54 M.P.H.	GRATE AREA	67.8 SQ.FT.
MAX. DRAWBAR	2530 AT 45 M.P.H.		

FIG. 5 CLASS K-5B LOCOMOTIVE, BUILT 1926

lower limits than heretofore observed, thus contributing to higher standards of track maintenance and obtaining better train riding characteristics.

4 Increased thermal efficiency.

5 Clearances to permit operation without restriction on the various parts of the System.

6 Symmetrical appearance with smooth lines, free from the effects of miscellaneous appliances, piping, and other details.

7 A high degree of reliability for uninterrupted service under conditions of dense traffic, especially on the eastern section of the System, requiring relatively simple but adequate machinery, combined with the use of well proved auxiliary equipment, such as feedwater heaters and mechanical stokers.

After the preparation of several preliminary designs, in which the American Locomotive Company, the Superheater Company, and others cooperated to the fullest extent, the conclusion was reached that the objectives could be most efficiently attained by using a 4-6-4 wheel arrangement which would satisfy the requirements for capacity and weight and avoid the addition of a fourth

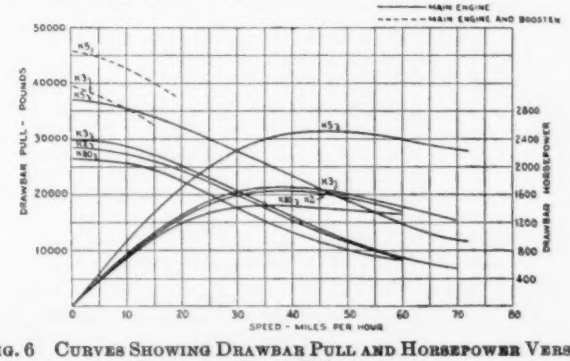


FIG. 6 CURVES SHOWING DRAWBAR PULL AND HORSEPOWER VERSUS SPEED FOR CLASS K LOCOMOTIVES

pair of driving wheels, with a resultant increase in size, weight, and first cost, as well as higher maintenance costs.

This arrangement represented the first 6-driver locomotive, built with 4-wheel leading and trailing trucks for service in America.

To meet the demand for exceptional steaming capacity at sustained high speed with heavy load, the size and proportions of the boiler were given first consideration, ample heating surfaces being essential, with extra-large superheater and a grate area sufficient to insure an economical rate of firing under maximum conditions of steam generation. To carry the added weight thus imposed on the rear of the locomotive, without excessive loads on trailing or coupled axles, the 4-wheel trailing truck was used, thus securing the advantage of providing for large firebox capacity with comparatively light individual axle loads and consequent low rail stresses. The boiler as finally designed had the following general dimensions and proportions:

Firebox 130 in. long × 90 1/4 in. wide
Volume of firebox, 428 cu ft
Diameter of boiler at smokebox, 82 7/16 in.
Diameter of boiler at back tube sheet, 87 5/8 in.
Tubes, 201–3 1/2 in. and 37–2 1/4 in., 20 ft 6 in. long
Heating surface; tubes, 4203 sq ft
Heating surface; firebox, 281 sq ft
Heating surface; total, 4484 sq ft
Superheater, type E; heating surface 1951 sq ft
Gas area through flues and tubes, 9.67 sq ft
Grate area, 81.5 sq ft

In developing the boiler design, the provision of a combustion chamber was carefully considered but, because of serious difficulties then being experienced with riveted-seam construction, it was finally omitted.

To reduce the pressure drop and other losses and to provide for more efficient use of the steam in the cylinders, the steam and exhaust passages were enlarged, as compared with the K-5 Pacific type, and a front-end throttle was installed. A large-volume steam chest with valves 14 in. diam, similar to those of the K-5 type, was retained.

Other special features included air compressors mounted on the front deck for improved weight distribution and, for the first time, a specially designed cast-steel pilot and drop coupler, providing a surface free from the projection of coupler and pocket for clearing effectively possible obstructions on the right of way. The centrifugal-type boiler feed pump was first introduced on this design with the heater located in a recessed portion of the smokebox top and a large portion of the piping placed under the jacket. Careful attention was given to the arrangement of controls and gages in the cab for convenient access and clear vision.

Fig. 7 illustrates the last of the J-1 class as received in 1931 and also shows the principal engine dimensions and proportions of the design as finally determined for the first sample J-1A, No. 5200,[2] built in 1927, except that the weight on drivers was 182,000 lb and total engine weight was 343,000 lb. A tender with 4-wheel trucks was used with this first engine having a capacity of 10,000 gal of water and 18 tons of coal.

From 1927 to 1931, a total of 205 of these locomotives, designated as the "Hudson" type, were received and placed in service.

Subsequently, all of the J-1 class were dynamically counterbalanced to provide smoother operation and to permit the use of shorter running cutoff, as well as to improve the track effects. Roller bearings were installed on all engine and tender trucks and to the drivers of eight locomotives. All engines received speed recorders, later augmented by cutoff-selection equipment.

Cast-steel beds with integral cylinders were applied, the engines already being equipped with one-piece cast-steel tender frames, engine-truck, trailer-truck, and tender-truck frames. The substitution of integral construction for the multiple-bolted parts of earlier locomotives eliminated a large number of bolts and contributed to increased availability and continuity of operation with substantial reduction in maintenance costs.

At the end of 1940, a total of 437 locomotives of this 4-6-4 type had been placed in service in the United States and Canada, including the 275 on the New York Central System. The total weight in working order for each of these locomotives ranged from 310,000 to 415,000 lb, with corresponding variations in maximum tractive force.

Performance and Capacity Tests, J-1 Hudson Versus K-5 Pacific Type

Class J-1A No. 5200 was subjected to complete performance

[2] "First Hudson Type Locomotive," *Railway Age*, vol. 82, 1927, pp. 523–526.

"Hudson Type Locomotive on N.Y.C.," *Railway Mechanical Engineer*, vol. 101, 1927, pp. 139–141.

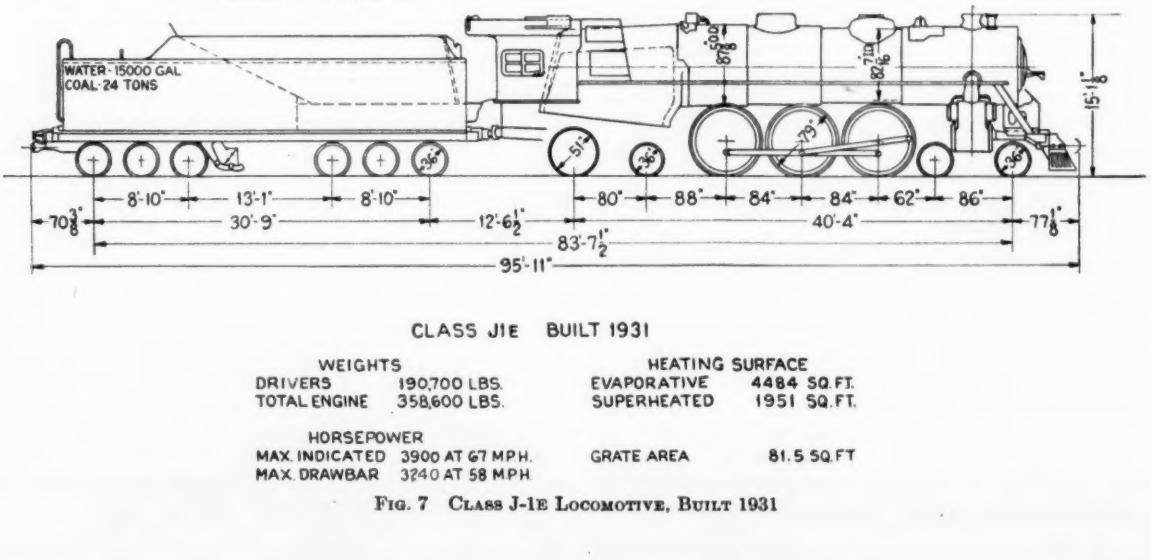


Fig. 7 Class J-1E Locomotive, Built 1931

and capacity tests shortly after delivery in 1927. Because of the total engine weight being held to 343,000 lb and the smaller and lighter tender used, this locomotive delivered a maximum drawbar horsepower of 3300 at 58 mph. However, subsequent improvements already referred to increased the weight of the Hudson-type locomotives and, consequently, the principal test results here given are for the last-built and heavier class J-1E tested in 1937.

The complete performance and capacity tests of classes J-1E (No. 5339) and K-5B (No. 8363) were conducted under spring and summer weather conditions over the Mohawk Division of the New York Central between Albany and Syracuse, a distance of 140 miles. This division is generally representative in profile and operating characteristics of the main line between New York and Chicago with the exception of the severe though comparatively short grade westbound between Albany and West Albany, a distance of about 3 miles, where the maximum grade is 1.63 per cent on a curvature of 3½ deg. With a total rise westbound of 384 ft in the 140-mile division over a rolling profile, the average grade is 0.05 per cent with a maximum of about 0.5 per cent for approximately 1.5 miles westbound and about 0.75 per cent for slightly over 2 miles eastbound.

All tests were made under regular-road-service conditions of operation, the trains consisting of empty standard steel passenger coaches varying in number from ten to twenty which, with a dynamometer car, provided train weights of 780 to 1465 tons. These trains were selected as representative of normal daily operation expected of the locomotive. Average test results demonstrated that the class J-1 Hudson type surpassed all previous New York Central locomotives in maximum horsepower, coal and water consumption per horsepower, weight per horsepower, and over-all efficiency.

A comparison of the principal results obtained for a single division run with representative trains is given in Table 1. It should be especially noted that, except for the maximum-power characteristics which may be duplicated at will with full boiler pressure and locomotive in good condition, the results shown are on the basis of over-all averages for the complete division runs, and indicate regular daily service performance rather than maximum values for short periods or under controlled conditions for the separate items.

TABLE 1 COMPARISON OF TEST RUN FOR K-5 AND J-1 LOCOMOTIVES

	Maximum power K-5	Maximum power J-1	Improvement, J-1, per cent
Tractive effort with booster, lb	48750	55100	13.0
Main-engine tractive effort, lb	40000	45400	13.5
Main-engine drawbar pull, lb	37000	41300	11.6
Cylinder horsepower	3200 at 54 mph	3900 at 67 mph	22.0 24.1
Drawbar horsepower	2530 at 45 mph	3240 at 58 mph	28.1 28.9
Average-performance data			
Number of cars and weight in tons	15–1053	18–1244	..
Average working speed, mph	51.2	55	..
Average firing rate, lb dry coal per hr	5867	6940	..
Water delivered to boiler, lb per hr	40636	57200	..
Evaporation per lb of dry coal, lb	6.94	8.24	18.7
Combined efficiency—boiler, feedwater heater and superheater, per cent	67.8	74.6	10.0
Steam per indicated horsepower-hour, lb			
Cylinders only	15.42	15.44	..
Including auxiliaries	17.00	17.28	..
Dry coal per indicated horsepower-hour, lb			
Cylinders only	2.22	1.94	12.6
Including auxiliaries	2.46	2.10	14.6
Coal as fired per car mile, lb	7.22	7.03	2.6
Weight per indicated horsepower, lb	94	90	4.3
Based on working-order weight, lb	302000	352000	..

Comparative curves representing the drawbar pull and drawbar horsepower versus speed are shown in Fig. 8, which also includes curves for locomotives of more recent design as discussed later. With a starting effort approximately 12 per cent greater than the K-5, increasing to 37 per cent more at a speed of 70 mph, and with an increase of 28 per cent in maximum drawbar horsepower at a speed 29 per cent higher, the weight per horsepower of the J-1 Hudson type has been decreased.

The Improved Hudson Type, Class J-3

As early as 1931, when the last of the J-1 class was built, consideration was already being given to the future development of this type in anticipation of greater power demand necessitated by the constantly increasing weight of trains and shortening of schedules. In order to reduce weight and also to gain some experience in the use of alloy steel of high tensile strength, with a view toward increasing the steam pressure, three of these loco-

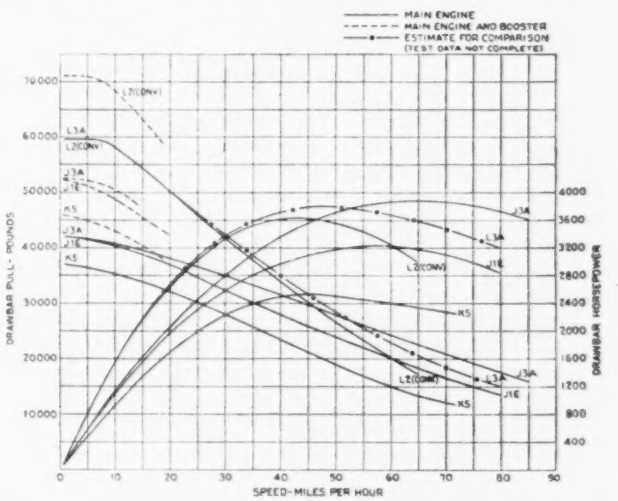


FIG. 8 CURVES SHOWING DRAWBAR PULL AND HORSEPOWER VERSUS SPEED FOR VARIOUS TYPES OF LOCOMOTIVES

motives were equipped with nickel-steel boilers. Two of the three also had roller bearings on all wheels except on the trailing truck, and the entire lot had roller bearings on the engine truck and tender wheels.

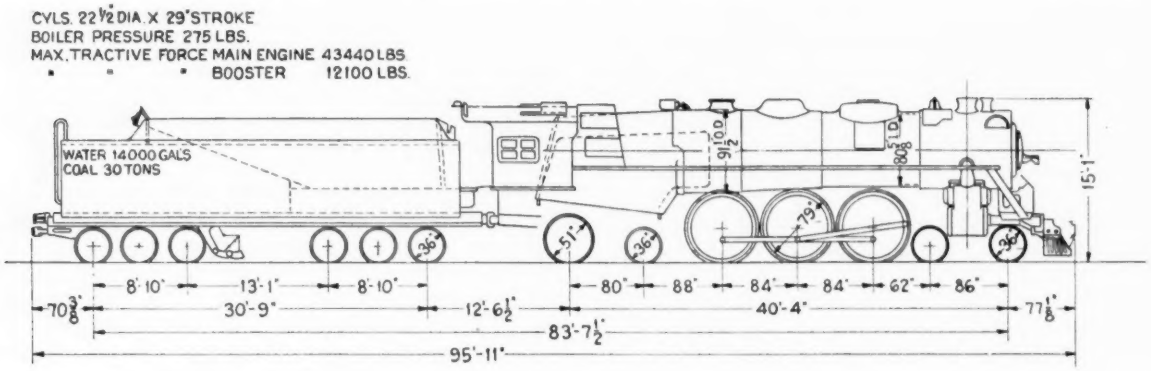
Subsequently, one of the three, No. 5344, received lightweight roller-bearing rotating and reciprocating parts and the counterbalance was reduced proportionately, providing lower rail stresses and improved riding qualities. At this time, the boiler pressure was raised from 225 to 250 psi and the cylinders were bushed to preserve the same starting tractive effort and adhesion factor as on others of the same class.

As previously explained, successive lots of the J-1 class had received various improvements when built and subsequently with gradual increase in the weight of engine and tender. The weights of the original class J-1A and the latest class J-1E compare as follows:

	Original J-1A	Latest J-1E
Engine truck, lb	63500	65700
Drivers, lb	182000	190700
Four-wheel trailing truck, lb	97500	102200
Total engine, working order, lb	343000	358600
Tender, fully loaded, lb	212200	305600

On the basis of the J-1 test results, the experience accumulated with the altered locomotives of this class, and other considerations, the general objectives for the new design were set as follows:

1 Maximum cylinder horsepower approximately 20 per cent greater at a much higher speed.



CLASS J3A BUILT 1937

WEIGHTS		*HEATING SURFACE	
DRIVERS	201,500 LBS.	EVAPORATIVE	4187 SQ. FT.
TOTAL ENGINE	360,000 LBS.	SUPERHEATED	1745 SQ. FT.
HORSEPOWER			
MAX. INDICATED	4725 AT 75 M.P.H.	GRATE AREA	82.0 SQ. FT.
MAX. DRAWBAR	3880 AT 65 M.P.H.		

FIG. 9 CLASS J-3A LOCOMOTIVE, BUILT 1937

2 Boiler pressure 275 psi versus 225 psi.

3 Equal main-engine starting tractive effort, with some additional help from booster because of increased pressure.

4 Boiler and superheater proportioned for higher capacity demand and to insure ample supply of steam under all conditions.

5 Approximately same over-all length and clearance limitations.

6 Highest capacity tender possible within the then total length limitation.

7 Least possible increase in weight, and weight distribution no less favorable from track standpoint.

Careful study of the situation indicated that, with the utmost attention to all details of design, these objectives could be attained and still adhere to the 4-6-4 wheel arrangement rather than using another pair of driving wheels, thus effecting substantial savings in size, weight, first cost, and operating expense.

In the development of the new design, the cooperation given by The American Locomotive Company, the Superheater Company, the Timken Roller Bearing Company, and others was of the utmost value.

Fifty of these locomotives were built in the fall of 1937 and the spring of 1938, ten of which were streamlined and five of these had roller bearings on main and side rods. The principal dimensions and proportions[3] are shown in Fig. 9.

As indicative of the design characteristics of the boiler, without elaboration of the details, the following information is given:

Material, nickel steel
Working pressure, 275 psi
Firebox, 130 13/16 in. long × 90 1/4 in. wide
Volume of firebox, 519 cu ft
Diameter of boiler at smokebox, 80 5/8 in.
Diameter of boiler at back tube sheet, 91 1/2 in.
Combustion chamber, 43 in. long
Tubes, 183–3 1/2 in. and 59–2 1/4 in., 19 ft long
Heating surface; tubes, 3827 sq ft
Heating surface; firebox, 360 sq ft
Heating surface; total, 4187 sq ft
Superheater, type E; heating surface 1745 sq ft
Gas area through flues and tubes, 8.91 sq ft
Grate area, 82 sq ft

[3] "New N. Y. C. Locomotives Show High Power Concentration," *Railway Age*, vol. 104, 1938, pp. 597–605.
"The New York Central Receives Fifty Powerful 4-6-4 Locomotives," *Railway Mechanical Engineer*, vol. 112, 1938, pp. 165–173.

With a boiler pressure of 275 psi, cylinder sizes of 22 1/2 in. diam and 29 in. stroke were fixed to produce a main-engine starting tractive effort of 43,440 lb, slightly more than the 42,360 lb of the J-1 class. The booster provided an additional 12,100 lb starting effort. A large-volume steam chest with 14-in-diam valves, similar to the J-1 class, was retained but the steam passages from dome to exhaust were enlarged in proportion to the cylinder area to provide free passage of the steam and reduce losses in transmission.

Special design and equipment features were as follows:

Roller bearings applied to all wheels.
Reciprocating parts of special lightweight design.
Revolving parts reduced in weight.
Dynamic counterbalancing.
Reverse-gear cylinder located on center line of engine to assist in reducing irregularities or inequalities in valve travel due to deflection or other causes.
Speed recorder and cutoff-selection equipment.
Rubber twin-cushion double-acting draft gear at rear of tender to eliminate free slack in both directions of gear movement substituting controlled resiliency to obtain smooth and efficient operation of trains. The ten streamlined engines received tight-lock couplers.

The requirements for increased cylinder power and consequent greater boiler capacity and higher working steam pressure, together with the roller-bearing equipment, improved brakes, additional sand-box capacity, and certain minor items, indicated a weight increase of about 14,750 lb over that of the latest class J-1E, but, as previously stated, one of the major objectives was to hold the weight as closely as possible to that of the J-1 class and to accomplish this the following features were incorporated in the design:

Nickel-steel boiler-shell sheets.
Cast-steel unit-bar grates.
High-tensile-steel drop coupler.
Cor-Ten steel main air reservoirs.
Aluminum cab, running boards, casings, and gage board.
Magnesia-block lagging of light weight.
Tubes and flues to close tolerance.
Booster exhaust piped to tender instead of to stack.

Integral cast-steel frames and cylinders, cradle, engine-truck and trailing-truck frames of lightened design.

Lightweight new-design valve gear.

Lightweight reciprocating parts and alloy-steel rods also contributed to the saving in weight.

The resulting weight reduction amounted to 13,350 lb, making the net addition only 1400 lb with a total weight of engine in working order of 360,000 lb, of which 201,500 lb were placed on the drivers.

With this total weight and the distribution obtained, together with the use of reduced-weight rotating and reciprocating parts and dynamic counterbalancing, the calculated stresses on the track structure were satisfactory and well within permissible limits.

Performance and Capacity Tests, J-3 Versus J-1

The tests of the J-3 were conducted with engine No. 5408 during the last 3 months of 1937, over the Mohawk Division under regular service conditions of operation, the trains consisting of 22, 17, and 10 cars, which with the dynamometer car, furnished

TABLE 2 PERFORMANCE OF J-3 CLASS LOCOMOTIVE COMPARED WITH J-1 CLASS

	Maximum power J-1	Maximum power J-3	Improvement, J-3, per cent
Tractive effort with booster, lb	55100	55000	..
Main-engine tractive effort, lb	45400	45000	..
Main-engine drawbar pull, lb	41300	41500	..
Cylinder horsepower	3900 at 67 mph	4725 at 75 mph	21.1 11.9
Cylinder horsepower per pair of driving wheels	1300	1575	21.1
Drawbar horsepower	3240 at 58 mph	3880 at 65 mph	19.75 12.1
	Average performance, division run of 140 miles		
Number of cars and weight in tons	18–1244	18–1253	
Working speed, mph	55	59	
Firing rate, dry coal per hour, lb	6940	6419	
Water delivered to boiler per hour, lb	57200	54900	
Evaporation per pound of dry coal, lb	8.24	8.32	1.0
Combined efficiency; boiler, feedwater heater, and superheater, per cent	74.6	76.3	2.3
Steam per indicated horsepower-hour, lb			
Cylinders only	15.44	14.76	4.4
Including auxiliaries	17.28	16.89	2.3
Dry coal per indicated horsepower-hour, lb			
Cylinders only	1.94	1.84	5.15
Including auxiliaries	2.10	2.03	3.3
Coal fired per car mile, lb	7.03	6.21	11.7
Weight per indicated horsepower, lb	90	76	15.5
Based on weight of engine in working order, as tested, lb	352000	360000	

weights back of the tender of 1609, 1244, and 766 tons, or heavy, medium, and lightweight trains.

The principal results of representative performance are given in Table 2, the figures for the class J-1 being repeated for ready comparison.

The drawbar pull and drawbar horsepower throughout the speed range are included in Fig. 8, with other types for comparison. Fig. 10 also shows the cylinder tractive effort and horsepower for the J-3a class only.

While the same main-engine starting tractive effort has been obtained in the new design, as desired, the drawbar pull at 70 mph has increased nearly 25 per cent, and the maximum drawbar horsepower is 20 per cent greater at a speed 12 per cent higher than the J-1. Coal and steam consumption per horsepower-hour have been decreased with a reduction of 15 per cent in weight per horsepower. An average thermal efficiency of 6.06 per cent at the drawbar was obtained for a complete division run, corresponding to 9.6 per cent at the cylinder.

Thermal Efficiency at Tender Drawbar Referred to Fuel

Reference to this value for the conventional-design steam locomotive usually affords an opportunity for considerable argument, although it is a fact that, during recent years, gradual improvement in this respect has been achieved.

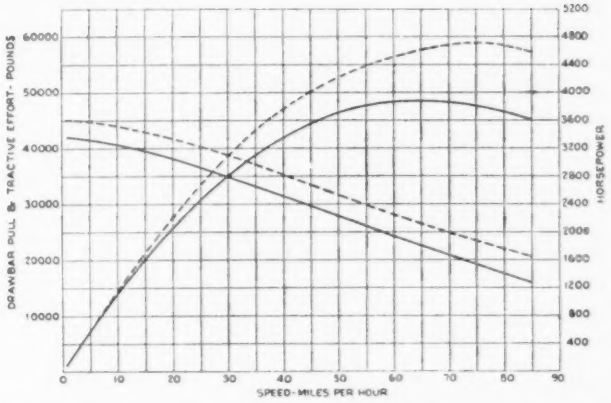


Fig. 10 Tractive Effort and Horsepower Versus Speed; and Drawbar Pull and Horsepower Versus Speed for J-3a Locomotives

Without questioning the fact that it is highly desirable to improve this performance characteristic, it is prudent to review some of the reasons for the relatively low thermal-efficiency value, and to consider the practical advantages inherent in this form of motive-power plant.

The conventional locomotive is a noncondensing self-contained and self-propelled unit, confined within close and definite limits of weight, height, width, and in most cases length, because of operating clearance and load limitations. The necessarily high horsepower requirement naturally is accompanied by a high combustion rate and Btu heat release per cubic foot of firebox volume per hour. Furthermore, this complete power plant, including all auxiliary equipment and its own fuel and water supply, is handled successively by different crews of only two men each at high speeds in dense traffic under widely and rapidly fluctuating load requirements.

Steam-locomotive efficiency at the tender drawbar is affected by the non-power-producing wheels and by the weight carried thereby. The modern tender when fully loaded may represent the equivalent of $1^1/_2$ loaded 70-ton coal cars or more. However, the hauling of this nonadhesive weight is amply justified through sustained power output and the attendant advantages obtained.

Simplification of design, particularly with respect to cylinders and valve gear, penalizes the thermal efficiency, but repayment is secured and augmented in terms of high serviceability and reasonable freedom from excessive maintenance troubles. Moderate first cost for an active motive-power unit is essential unless the net return on additional investment can be clearly established. The measure of the value of a locomotive is its use, idle motive power representing a total loss of investment and a constant expense. It is currently demonstrated that economically, maximum over-all-performance efficiency is secured through the use of a unit capable of providing uninterrupted service and consistently high mileage throughout its life, with the best available design of boiler, cylinder, and related parts to fulfill these conditions.

Slipping Tests

As previously noted, the J-3 class was equipped with roller bearings throughout, including the driving wheels. The possibility was recognized that forced vibrations of the unsprung mass of the closely fitted roller-bearing driving-wheel assemblies caused by the overbalance and the elastic foundation of the track structure might be sufficient during high-speed slipping to cause

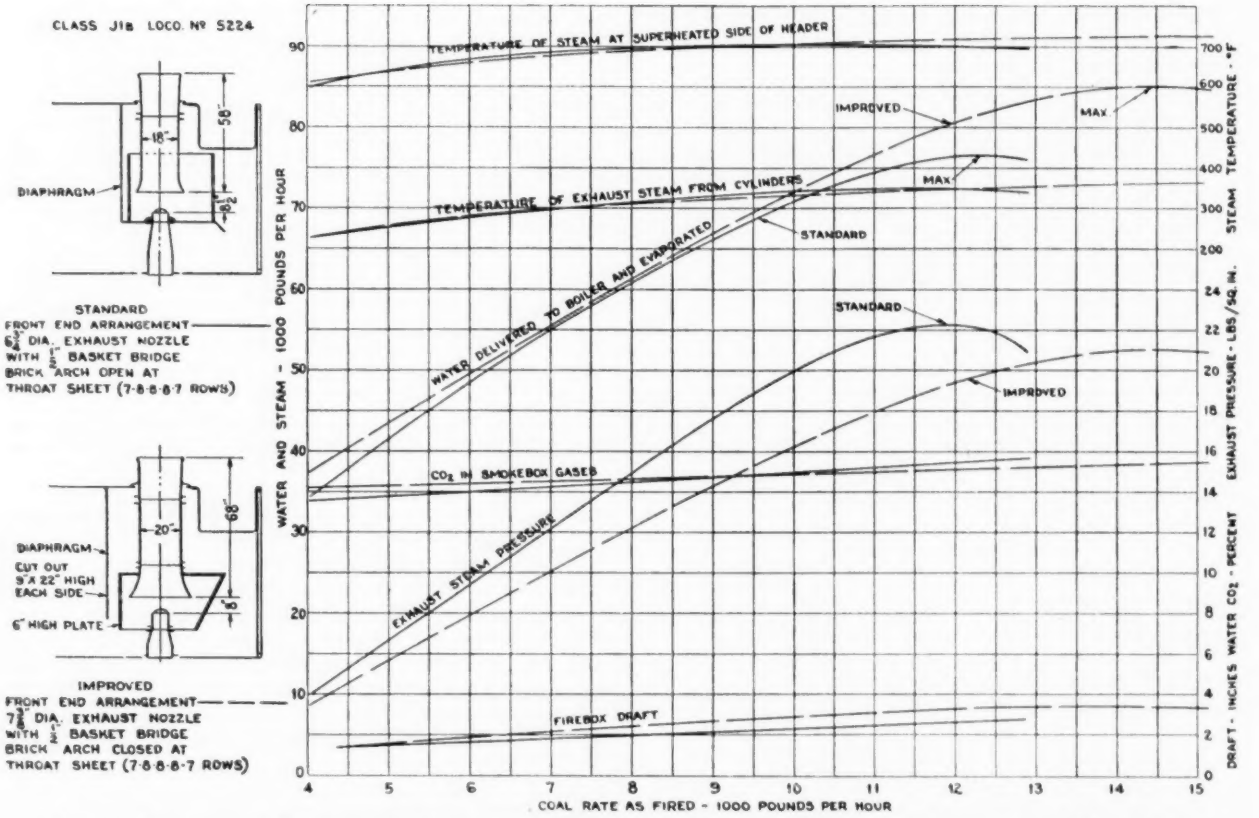


FIG. 11 PERFORMANCE CURVES FOR STANDARD AND IMPROVED FRONT-END ARRANGEMENTS, AS APPLIED ON J-1 LOCOMOTIVES

the wheels to lift from the rail. Freedom from lost motion and smooth-running machinery are highly desirable characteristics of this type of driving-wheel-and-axle assembly, and in order definitely to determine (1) the rotational speed at which the driving wheels actually lift from the rail, and (2) whether this speed would approach or possibly fall below the maximum recorded slipping speed of 120 mph on this class of engine, a program of slipping tests was formulated and conducted in April, 1938, on a short stretch of main-line track with a train of eight cars for trailing load. The rail was 127-lb section on rock ballast as later described under "Track Tests, L-2D Converted."

To promote slipping, the heads of both rails were greased before each run for a distance of 230 ft. Scratch gages to measure rail deflection and movement of driving boxes with respect to frame were located at marked positions on the rail and on the locomotive. The train speed and the maximum revolving speed of the driving wheels during slips were obtained by a positively driven electrical speed indicator of the Weston generator type, and high-speed motion-picture cameras were used to record any lifting of wheels from the rail.

Four test runs were made at train speeds varying from 61 to 82 mph and with maximum slipping speeds of 123, 130, 135, and 164 mph while working steam. In the three tests at the lower speeds, there were no indications that the wheels had lifted. In the final test at 164 mph, the main drivers definitely left the rail and later examination disclosed a number of very slight markings on the rails which were without significance and had no disturbing effect on the track structure requiring attention of maintenance forces.

No damage to the locomotive occurred in any of these tests and the two questions postulated were definitely answered because the rotational speed of 164 mph necessary to lift the wheels from the rail exceeded by 44 mph the highest known slipping speed of these engines.

SUBSEQUENT IMPROVEMENTS IN BOILER CAPACITY AND ENGINE EFFICIENCY

In the year 1937, a series of standing tests was undertaken to determine the extent to which improvement in capacity and efficiency of the class J-1 and J-3 boilers and cylinders could be secured by redesign of the smokebox arrangement. The primary objectives were to increase the capacity of the boiler, accompanied by a reduction in back pressure, which would be reflected in increased cylinder horsepower and efficiency. Prior to this time, standing tests had been conducted and had furnished valuable information but were not conclusive because no means had been developed for reducing the temperature of the exhaust steam corresponding to the temperature drop, when mechanical work was being performed under service conditions.

In the tests under consideration, this reduction in temperature was effected and controlled through the medium of a spray of water mist introduced into the cylinders, the water being subsequently removed, so that the condition of the exhaust steam during the standing tests was made identical with the thermal conditions experienced in road service.[4]

---

[4] A complete description of the apparatus used and results obtained was presented by W. F. Collins, Engineer of Tests, New York Central System, at the 1940 Annual Meeting of the Railway Fuel and Traveling Engineer's Association. Reports were published as follows:

"Standing Locomotive Tests of the New York Central," *Railway Age*, Jan. 18, 1941, pp. 177–181, 186.

"New York Central's Standing Locomotive Tests," *Railway Mechanical Engineer*, part 1, Feb., 1941, pp. 56–59; part 2, March, 1941, pp. 96–100.

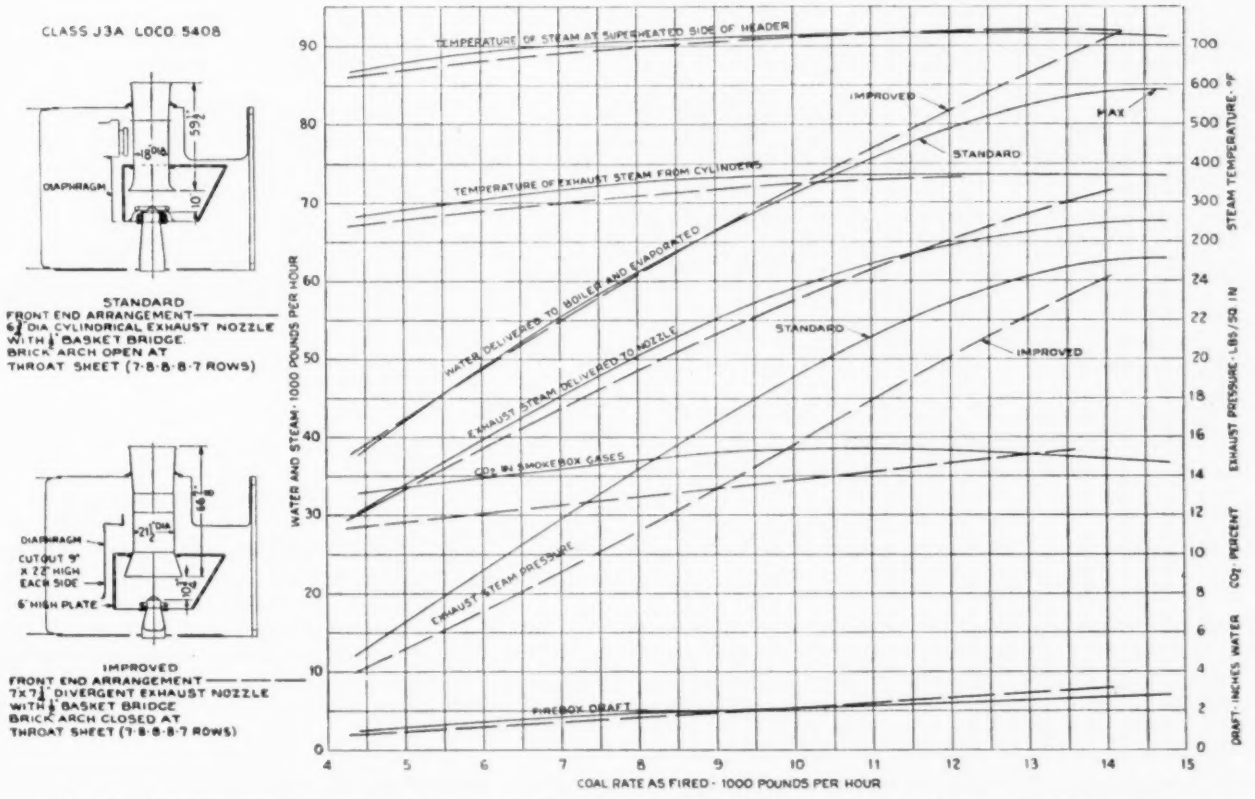


FIG. 12 PERFORMANCE CURVES FOR STANDARD AND IMPROVED FRONT-END ARRANGEMENTS, AS APPLIED ON J-3 LOCOMOTIVES

Several different smokebox arrangements were tested during these experiments, which were first conducted on J-1 No. 5224 at the Selkirk Engine Terminal. The design finally approved as producing the best performance is shown in Fig. 11, the previous standard arrangement also being shown, together with curves

TABLE 3 SMOKEBOX TESTS FOR J-1 AND J-3 LOCOMOTIVES AT MAXIMUM EVAPORATION RATE

Item no.		J-1 Class		J-3 Class	
		Original	Improved	Original	Improved
1	Coal fired per hour, lb....	12300	14500	14700	14200
2	Coal fired per square foot of grate area per hour, lb...	151	178	179	173
3	Water evaporated per hour, lb.....	76800	85500	84500	92000
4	Increase, Item 3, per cent.	..	11.3	..	8.9
5	Evaporation per pound of coal fired, lb.....	6.24	5.89	5.76	6.48
6	Exhaust passageway pressure, psi.....	22.3	21.4	25.3	24.5
7	Decrease, Item 6, per cent.	..	6.4	..	3.2
8	Firebox draft, in. of water	2.7	3.4	2.8	3.2
9	Combined efficiency, boiler and superheater (dry coal basis), per cent....	56.8	52.6	53.0	56.0
10	Diameter of basket-bridge exhaust nozzle, in.....	6¾	7⅛	6¾	7

TABLE 4 SMOKEBOX TESTS FOR J-1 AND J-3 LOCOMOTIVES, AVERAGE VALUES

Item no.		J-1 Class		J-3 Class	
		Original	Improved	Original	Improved
1	Coal fired per hour, lb.....	7131	7131	7175	7175
2	Coal fired per square foot of grate area per hour, lb...	87.5	87.5	87.5	87.5
3	Evaporation per pound of coal fired, lb.....	7.87	7.90	7.89	7.82
4	Exhaust pressure, psi.....	12.5	10.3	12.0	9.3
5	Decrease, Item 4, per cent.	..	17.6	..	22.5
6	Firebox draft, in. of water	1.8	2.2	1.6	1.4
7	Combined efficiency, boiler and superheater (dry coal basis), per cent.....	68.5	70.0	69.4	67.8
8	Combustion efficiency (dry coal basis), per cent.....	86.0	87.8	86.0	88.1
9	Diameter of basket-bridge exhaust nozzle, in.....	6¾	7⅛	6¾	7

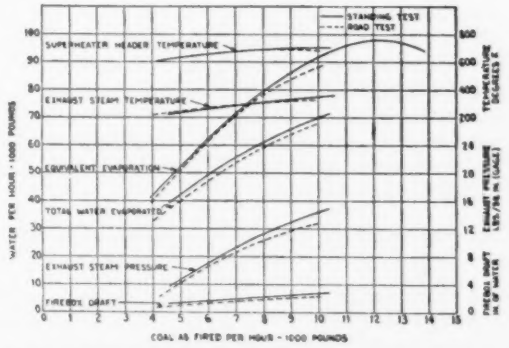


FIG. 13 COMPARATIVE RESULTS OF STANDING TESTS VERSUS ROAD DYNAMOMETER TESTS FOR CLASS J-1, ENGINE NO. 5224
(Original front end, 7⅛-in. nozzle.)

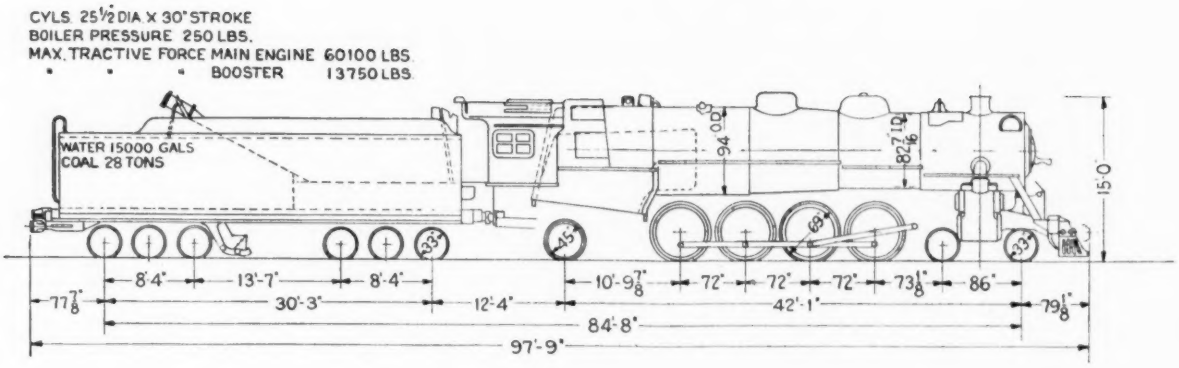
illustrating the comparative performance. Fig. 12 shows similar information for the J-3 class.

Tables 3 and 4 outline briefly the principal results for both the J-1 and the J-3 classes, the data being given at maximum evaporation rates and also for an average firing rate of about 7100 lb per hr, corresponding to 87.5 lb of coal per hr per sq ft of grate area.

While the combined efficiency of the boiler and superheater is shown as lower for the J-1 with the improved front end, this is due to the much higher coal rate made possible with this front end. The maximum evaporation has been increased about 11 per cent, with a decrease in back pressure of 6 per cent.

For the class J-3 the combined efficiency of the boiler and superheater is increased slightly at approximately the same coal rate, and at the same time the maximum evaporation is increased almost 9 per cent with some reduction in back pressure.

The fundamental means of accomplishing these results was by



CLASS L2D (CONV) BUILT 1930-CONVERTED 1939

WEIGHTS		HEATING SURFACE	
DRIVERS	257,000 LBS.	EVAPORATIVE	4556 SQ.FT.
TOTAL ENGINE	385,100 LBS.	SUPERHEATED	1931 SQ.FT.
HORSEPOWER			
INDICATED	4200 AT 50 M.P.H.	GRATE AREA	75.3 SQ.FT.
DRAWBAR	3640 AT 43 M.P.H.		

FIG. 14 CHARACTERISTICS AND PRINCIPAL DIMENSIONS OF L-2D CLASS LOCOMOTIVES, BUILT IN 1930, AND CONVERTED IN 1939

providing a smokebox arrangement which, with the proper relation of exhaust nozzle and stack, resulted in moving a greater quantity of gas with the same quantity of steam.

Under average conditions of firing, representing normal operation of the locomotive, the evaporation and efficiency of the boiler have been maintained with a reduction in exhaust pressure, which is reflected in increased cylinder horsepower and over-all thermal efficiency.

Fig. 13 has been prepared to show graphically the results from a road dynamometer test and a standing test for the same class J-1 locomotive with identical arrangement of smokebox, firebox, and exhaust nozzle, illustrating the close degree to which the standing tests duplicate the thermal conditions which occur when steam is used during road operations.

As a result of the experiments, installations of the improved design of front-end arrangement have been proceeding and approximately 520 engines are now equipped.

CONVERSION OF TWO 4-8-2 LOCOMOTIVES FOR PASSENGER SERVICE

With the full complement of 275 Hudson type on the System, it was found that the passenger traffic could be handled satisfactorily under normal conditions but that, during peak periods in the holiday seasons, it was necessary to use some of the older K-3 Pacific type for the excess traffic. As these units were gradually retired and assigned to secondary or branch-line service, there remained an insufficient number available for this supplemental operation and, as the trains handled often demanded greater power than these engines possessed, they were not satisfactory for this purpose.

For these reasons the 4-8-2 Mohawk-type freight engines, class L-2, were occasionally used in emergency passenger service during heavy-traffic periods but were limited to 60 mph due to riding qualities and the difficulty of maintaining satisfactory running conditions with the friction-bearing driving boxes.

These engines were built during the years 1926 to 1930. When the acquisition of new freight power was lately under consideration, necessitating complete review of the design, with a number of important changes, the question arose as to whether the new design could be so arranged as to preserve the general character of freight locomotives and at the same time serve satisfactorily in passenger service during periods of peak traffic. Such additions to the freight motive power would also accomplish an increase in the available passenger power without actually involving additional units, designed especially for passenger service.

Consideration was given to the design and construction of a sample locomotive to be given a thorough test and trial but, because of the time involved and the complications usually present in an undertaking of this kind, it was decided that one or two of the L-2 class should be converted for high-speed passenger service, thus making possible early development of experience background for the design of the new engines, an order for which could then be placed without undue delay.

Two of the L-2 class, Nos. 2995 and 2998, were selected for this purpose and the following principal changes were made to provide satisfactory operation in passenger service at speeds of 80 mph and at the same time maintain suitability for freight operation equal to the L-2 class:

1 Boiler pressure increased from 225 to 250 psi.
2 Cylinder diameter reduced from 27 in. to 25½ in. for starting tractive effort equal to the L-2.
3 Lightweight reciprocating parts.
4 Dynamic counterbalancing of all drivers.
5 Roller bearings on engine truck, tender truck, and drivers on No. 2998.
6 Roller bearings on engine truck and tender truck on No. 2995.
7 Coal pushers in tender.
8 Lateral-motion device on front drivers.
9 Improved radial buffers between engine and tender.
10 Cast-steel pilots and drop couplers.

The weights before and after conversion were as follows:

Weight in working order, lb	L-2 Freight	L-2 Converted
Engine truck	59150	65400
Drivers	250000	257000
Trailing truck	61000	62700
Total engine	370150	385100

The two locomotives were released for service in August, 1939, and have been successfully handling main-line passenger trains since that time, except that one of them was removed from service for exhibition at the World's Fair throughout the 1940 season. As of December 31, 1940, a total of 200,000 miles had been accumulated on the two engines and no special difficulties of

operation or maintenance have been experienced during this period of service. Fig. 14 shows the dimensions and principal characteristics of the converted engines.

Track Tests, L-2d Converted

The weight of the two converted class L-2 locomotives had been increased about 15,000 lb over the standard L-2 and it was essential to determine whether these engines, with 69-in. driving wheels and the modifications referred to, could be operated at the passenger-train speed of 80 mph without imposing excessive stresses on the track structure. For this purpose, track tests were conducted in September, 1939, which included one of the J-1 class as well as the two converted engines, in order to obtain comparative information, as the J-1 class, during approximately 200,000,000 miles of operation, had never been known to produce any harmful effects on the track.

Two 170-ft test sections were used, located about $^1/_2$ mile apart on the inside westbound high-speed main track No. 1 of a 4-track system. Both sections are on an ascending grade of 0.315 per cent, one comprising tangent track and the other a curve of 1 deg 8 min, selected so that each test was run continuously over both sections without reduction in speed for the curve.

The rail was 127-lb New York Central standard section laid on sound creosote-treated ties spaced about 1 ft 8 in. center to center with canted tie plates having an outside shoulder only. The ballast was 2-in. crushed rock.

Strain gages placed in groups at 10-ft intervals were used to measure the stresses in the rails on the outside of the rail head, underneath the rail at the center line, and on top of the outer and inner flanges. Slow-motion pictures were taken at each test section to determine the position of the crankpin for each stress recorded.

The results showed that up to 87 mph, the maximum speed operated, the converted L-2 imposed no greater stress on the track than the J-1 and that the maximum stresses in both cases were well within permissible limits, proving that such a 69-in-diam-driver locomotive could be operated at the same maximum speeds as the one with 79-in-diam drivers and substantiating the correctness of the method of balancing used for the converted L-2, which had taken into account the complete theoretical analysis. In this work much valuable assistance was rendered by the Timken Roller Bearing Company.

TABLE 5 SUMMARY OF MAXIMUM STRESSES; TANGENT SECTION

Locomotive	Speed range, mph	Strain-gage location on rails	Rail	No. of stresses above 15,000 psi	Five highest maximum stresses, psi — Average	Five highest maximum stresses, psi — Range
2995	54.4 to	Underneath the rail	Left (S)	64	21400	22100 to 20900
L-2d	87.2		Right(N)	17	18800	23300 to 17100
(conv)	(9 runs)					
5330	66.2 to		Left (S)	34	21200	22600 to 19500
J-1e	85.9		Right(N)	16	18800	20500 to 17800
	(5 runs)					
5435	72 to		Left (S)	21	24200	29100 to 20200
J-3a	83.2		Right(N)	11	19200	20800 to 18300
	(4 runs)					
2995	54.5 to	Outside of head of rail	Left (S)	43	20500	23000 to 18500
L-2d	87.2		Right(N)	26	20200	23400 to 18600
(conv)	(9 runs)					
5330	66.2 to		Left (S)	33	19400	20500 to 18500
J-1e	85.9		Right(N)	20	22000	27700 to 19100
	(5 runs)					
5435	72 to		Left (S)	19	17700	18400 to 17400
J-3a	83.2		Right(N)	10	19500	22000 to 18400
	(4 runs)					

The ranges of comparative stresses for the two locomotives and for one of the J-3 class tested at the same time are given in Table 5.

New L-3 Combination Passenger-and-Freight Locomotive

On the basis of the experience gained with the two converted L-2 engines and the study that had been given to the design, with the close cooperation of The American Locomotive Company, the Superheater Company, the Timken Roller Bearing Company, and others, fifty of the L-3 class were ordered and have lately been delivered, twenty five of which are arranged for operation in either passenger or freight service, while the remaining twenty five are strictly freight locomotives but having the same characteristics with respect to speed versus track structure. The combination engines are equipped with a cast-steel pilot and drop coupler, steam heat, air signal, engine-truck brake, and roller bearings on all wheels including drivers. Boosters were omitted although arrangements were made for convenient application if subsequently found desirable.

The 4-8-2 wheel arrangement was retained as it was found that for this design the required weight distribution could be secured without the use of a 4-wheel trailing truck and also because it was desired to supply the largest possible tender, particularly with reference to coal capacity, without extending the over-all length of engine and tender beyond the limits of the 100-ft turntables now in use at principal main-line terminals.

The extra large coal capacity of 43 tons was provided to increase materially the length of runs and through intensive use to obtain high monthly mileage which would be equivalent to additional locomotives.

A waterscoop of improved quick-acting design, which had recently been developed and tested, and which supplies approximately 20 per cent more water with a substantial reduction in the amount spilled, was applied.

The standard 69-in. driving wheels were retained as experience had proved this size best for high-speed main-line freight service in which the engines would be used the greater portion of the time. Provision was made, however, by increasing the driving wheel base and the over-all length, for the future application of 72-in. driving wheels, as a margin of protection for high-speed running.

For reasons beyond the scope of this paper, it was decided to use carbon steel instead of nickel steel for the boilers and, in order to conform to the desired limits of total weight and wheel loads, this necessitated using a working boiler pressure of 250 psi instead of the 275 psi originally planned. With this pressure and cylinders of $25^1/_2$ in. diam and 30 in. stroke, a rated starting tractive effort of 60,100 lb was obtained, about equal to the 60,620 lb of the L-2 class as desired.

The increase in driving wheel base permitted the use of a combustion chamber 12 in. longer than on the L-2 for increased firebox volume and greater combustion efficiency; greater gas area through an enlarged superheater was provided to increase the superheat temperature.

An improved front end, as developed by the Selkirk tests heretofore mentioned, was installed.

Particular attention was given to the proportioning of steam passages from dome to exhaust to provide free steam passage and reduce transmission losses, and the large-volume steam chest with the standard 14-in. valves was retained.

Reciprocating parts are of special lightweight design similar to those used on the two converted L-2 class, and all wheels were dynamically balanced in accordance with the theoretically correct principles established for those engines.

The following modifications were made with a resulting decrease in weight:

Cor-Ten steel main air reservoirs.

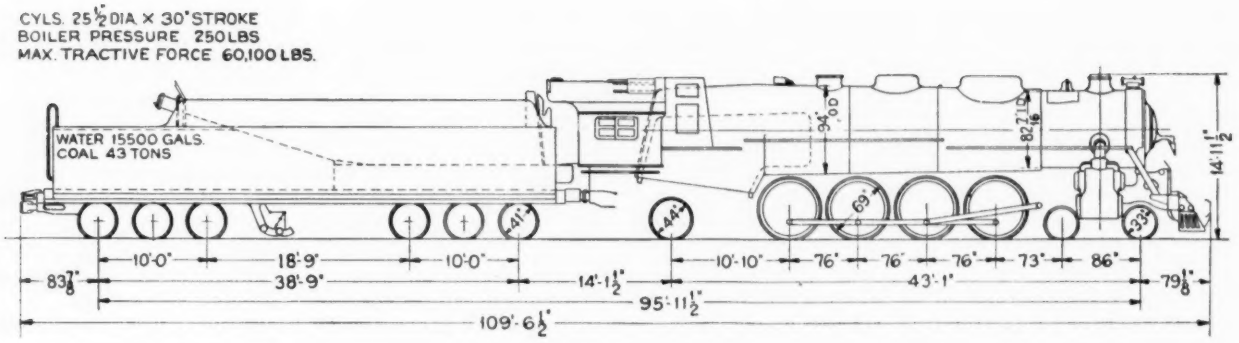
Aluminum cab, running boards, cylinder and valve casings dome and turret casings, and gage board.

High-tensile-steel drop coupler.

Lightweight magnesia block lagging.

Tubes and flues to one gage tolerance.

New design lightweight valve gear.



CLASS L3A BUILT 1940

WEIGHTS		HEATING SURFACE	
DRIVERS	262,000 LBS	EVAPORATIVE	4676 SQ FT.
TOTAL ENGINE	388,500 LBS.	SUPERHEATED	2082 SQ. FT.
HORSEPOWER			
ESTIMATED INDICATED	4400 AT 55 M.P.H.	GRATE AREA	75.3 SQ FT.
ESTIMATED DRAWBAR	3800 AT 48 M.P.H.		

FIG. 15 CHARACTERISTICS AND PRINCIPAL DIMENSIONS OF LATEST COMBINATION PASSENGER-AND-FREIGHT LOCOMOTIVE, CLASS L-3A

Other special features incorporated were complete speed-recorder and cutoff-selection equipment, coal pusher, Alemite grease equipment for rods and other parts, roller bearings on all axles, and lateral-motion device on front and main drivers.

TABLE 6 CHARACTERISTICS OF L-3 TYPE LOCOMOTIVE COMPARED WITH L-2D FREIGHT AND L-2D CONVERTED

	L-2D Freight	L-2D Converted	L-3A Combination
Wheel base:			
Driving		18 ft 0 in.	19 ft 0 in.
Engine		42 ft 1 in.	43 ft 1 in.
Engine and tender		84 ft 8 in.	95 ft 11½ in.
Weight in working order, lb			
Engine truck	59150	65400	70400
Drivers	250000	257000	262000
Trailing truck	61000	62700	56100
Total engine	370150	385100	388500
Tender loaded	313500	313500	373900
Boiler pressure, psi	225	250	250
Cylinders, diameter and stroke, in.	27 × 30	25½ × 30	25½ × 30
Rated tractive effort			
With booster, lb	73020	73850	...
Main engine, lb	60620	60100	60100
Factor of adhesion	4.12	4.28	4.36
Permissible operating speed, mph	60	80	80
Boiler:			
Inside diameter, first course, in.	..	82⅞	82⅞
Outside diameter, third course, in.	..	94	94
Tubes, number and diameter, in.	..	40–2¼	50–2¼
Flues, number and diameter, in.	..	199–3½	198–3½
Length of tubes and flues, ft-in.	..	20-6	20-6
Firebox, length and width, in.	..	120¼ × 90¼	120¼ × 90¼
Grate area, sq ft	..	75.3	75.3
Combustion chamber length, in.	..	51	63
Firebox volume, cu ft	..	510	538
Gas area through flues and tubes, sq ft	..	9.45	9.33
Heating surface, sq ft			
Firebox	..	354	373
Tubes and flues	..	4202	4303
Total	..	4556	4676
Superheater	..	1931	2082
Tender:			
Coal capacity, tons	..	28	43
Water capacity, gal	..	15000	15500
Size of axle journals, in.	..	6 × 11	6½ × 12
Cylinder horsepower	3800 at 48 mph	4200 at 50 mph (est)	4400 at 55 mph (est)
Engine weight per horsepower, lb	97	92	88 (est)

The estimated drawbar pull and horsepower versus speed for the L-3 are shown by the curves included in Fig. 8. Capacity and performance tests for the L-3 are now in progress and the characteristics shown are believed to be conservative.[5] The principal dimensions and the proportions are shown in Fig. 15.

TABLE 7 SUMMARY OF PRINCIPAL WEIGHT AND POWER CHARACTERISTICS FOR LOCOMOTIVE DESIGNS DISCUSSED

Class	Type	Last built	Locomotive weight, lb	Maximum horsepower and speed at which attained, mph — Cylinder	Maximum horsepower and speed at which attained, mph — Drawbar	Weight per horsepower, lb — Cylinder	Weight per horsepower, lb — Drawbar
K-80	4-6-2	1912	252500	1700–39	1430–35	149	177
K-2	4-6-2	1910	273000	2000–45	1655–40	137	165
K-3Q	4-6-2	1923	295500	2100–45	1720–40	141	172
K-3R	4-6-2	1925	278000	2140–45	1750–40	130	159
K-5	4-6-2	1926	302000	3200–54	2530–45	94	119
J-1a No. 5200	4-6-4	1927	343000	3900–67	3300–58	88	104
J-1E	4-6-4	1931	358600	3900–67	3240–58	92	111
J-3	4-6-4	1937	360000	4725–75	3880–65	76	93
Converted L-2	4-8-2	1930	385100	4200–50	3640–43	92	106
L-3	4-8-2	1940	388500	4400–55	3800–48	88	102

For convenient reference, some of the characteristics, as compared with the L-2D converted class and the L-2 freight engine, are given in Table 6, the data for the L-2 freight only being shown where different from the converted L-2.

PRESENT THOUGHTS ON TRENDS OF STEAM-LOCOMOTIVE-DESIGN IMPROVEMENT FOR THE NEAR FUTURE

While this paper is confined to the subject of the conventional steam passenger locomotive, the author is fully cognizant of the rapid strides being made by other forms of motive power, their possibilities, advantages, and growing importance to the railroads for certain classes of service.

This may be illustrated by stating that on the New York Central, 127 Diesel-electric locomotives are used in intensive daily service. As early as 1924, a 60-ton 300-hp Diesel-electric locomotive was operated in switcher and puller service in New York City territory with favorable results, followed in 1928 by a road freight and in 1929 by a road passenger locomotive. The first straight electric was introduced in 1904, and there are now 168 of various types and capacities in use on the System. Within the last 6 years, limited operating experience has been obtained with a 5000-hp experimental turboelectric locomotive and a 3600-hp Diesel-electric, both designed for high-speed main-line service, and a 5400-hp Diesel-electric freight locomotive.

Future development of the steam locomotive in some radically new form, such as the steam-turbine condensing or combustion type, as recently proposed, should show a substantial increase in thermal efficiency but, until the stage has been reached where such units of proved dependability in daily operation can be pro-

[5] "New York Central Buys All-Round Road Locomotives," *Railway Age*, vol. 109, 1940, pp. 856–861, 864.

"New York Central Buys 50 4-8-2 Type Locomotives," *Railway Mechanical Engineer*, January, 1941, pp. 1–8, 21.

duced of moderate size, weight, and cost, it is the author's belief that basic lines of development should be continued by taking advantage of the possibilities for further betterment of the conventional reciprocating design without radical changes in the type of boiler or resorting to the mechanical complication of multiple expansion of steam. It should be possible now to produce a highly serviceable two-cylinder single-expansion locomotive of the 4-8-4 type at a weight per indicated horsepower closely approaching that represented by the 4-6-4 class J-3A described in this paper, capable of delivering 6000 cylinder hp when required.

Such a design should include the largest practicable superheater, with ample firebox volume and grate area, carefully proportioned steam passages from boiler to exhaust, and a working steam pressure probably up to 300 psi.

Roller bearings on all locomotive and tender axle journals and to a lesser degree in rods and motion work have resulted in increased serviceability because of freedom from heating failures. Their extended utilization should receive careful consideration.

For the future extension of steam-locomotive productive capacity, design study leading to a better proportioned and more efficient boiler is proposed. The development of a suitable drier arrangement to provide high-quality steam, taken directly from the boiler barrel, would permit elimination of the steam dome with corresponding possibilities within given weight or clearance limitations for increased diameter of barrel with improved tube and flue layouts and larger gas areas and superheater, additional firebox depth and volume, and more nearly level grates without restricting the highly important features of adequate ash-pan capacity and arrangement necessary for long locomotive runs.

Design studies and performance experiments are now in progress to improve the poppet-valve arrangement of steam distribution and these efforts may result in making available for practical use the better cylinder performance in relation to power output and efficiency inherent therein, without prohibitive increase in the size and weight of the boiler.

Other interesting experiments now in operation include locomotives having four simple cylinders and two separate sets of running gear or combined within a single rigid wheel base, with which improved wheel loadings and rail effects should be obtained, together with lower dynamic forces in machinery and running-gear parts, as well as other advantages.

Ability to extend the length of locomotive runs in either freight or passenger service without stops for fuel depends to a great extent upon the size of the tender. This, in turn, may be limited by possible restrictions on over-all length. One leading western railroad now has in service back of a considerable number of modern design steam locomotives a new arrangement of tender running gear and underframe which possesses possibilities of materially increased tender capacity within given dimensional restrictions.

Discussion

T. V. Buckwalter.[6] This paper reviews the detailed development of the six-coupled locomotive, starting with the New York Central class K-80 in 1904, to its ultimate development, culminating in the Hudson type class J-3A in 1937. The improvement in locomotives from year to year is gradual and does not afford an outstanding contrast when comparing the 1904 locomotive with the 1937 locomotive. The improvement of from 1430 to 3880 drawbar horsepower has been made in the short span of 33 years, the power development of 1937 being 2.71-fold that of 1904, or an annual increase of 8.2 per cent.

This development was made in two stages in so far as the New York Central System is concerned, the first being the Hudson type class J-1E developed in 1927, developing 3300 hp, an increase of 30 per cent over that of its predecessor, the K-5 locomotive, built in 1926, and the second step, the Hudson J-3A in 1937.

The Hudson locomotive served the New York Central System so well that a total of 225 were built, replacing the older "K" type Pacific locomotives on main-line service.

The Hudson type was further improved in 1937, increasing capacity in drawbar horsepower to 3880, or 17 per cent; this in itself being an outstanding improvement, considering that the weight on the drivers of the J-3A is only 11,000 lb more than that of the J-1E, while the actual engine is only 1400 lb additional weight. The use of lightweight reciprocating parts, effecting a reduction of more than 50 per cent in weight, afforded an opportunity to redistribute the counterbalance, the typical practice being to distribute 66⅔ to 75 per cent of this reciprocating-weight reduction to lightening the counterbalance and, therefore, the dynamic augment on the rail, and utilizing the balance to reduce nosing. Together these have an important influence on improved riding qualities of the locomotive and also tend to reduce rail reaction. As the author mentions, the Hudson engines have operated 200,000,000 miles without a single case of rail damage attributable to this class of locomotive.

A further outstanding development, since the origin of the Pacific engine, is the increase of speed from 35 mph to 65 mph, at which maximum horsepower is developed; this being an increase of 85 per cent. At the same time the weight reduction per draw-

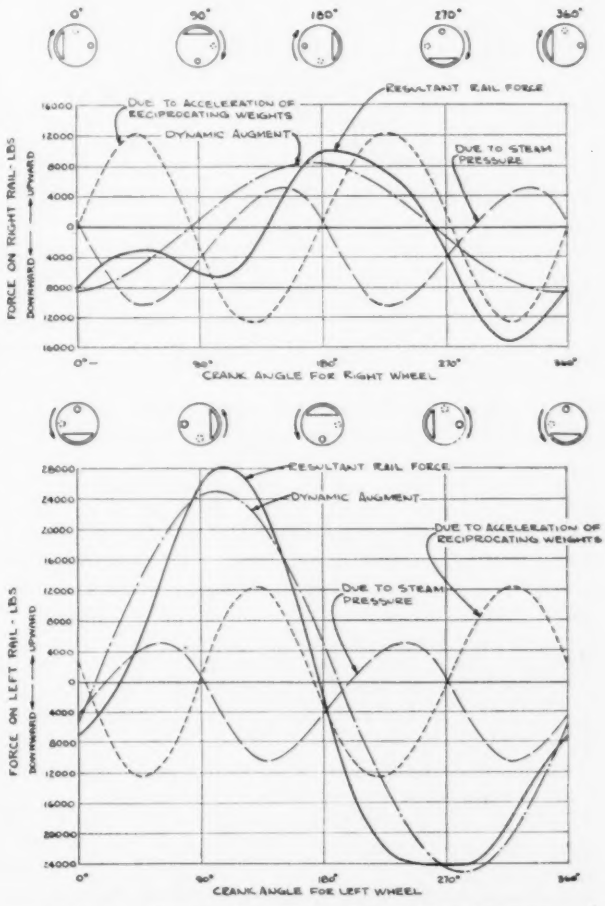


Fig. 16 Dynamic Rail Force Under Main Drivers
(N.Y.C. type L-2D locomotive, plain-bearing drivers and heavy reciprocating parts.)

[6] Vice-President, Timken Roller Bearing Company, Canton, Ohio. Mem. A.S.M.E.

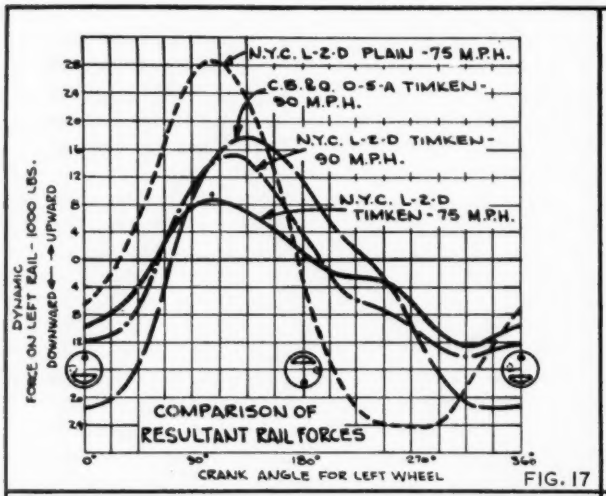


FIG. 17

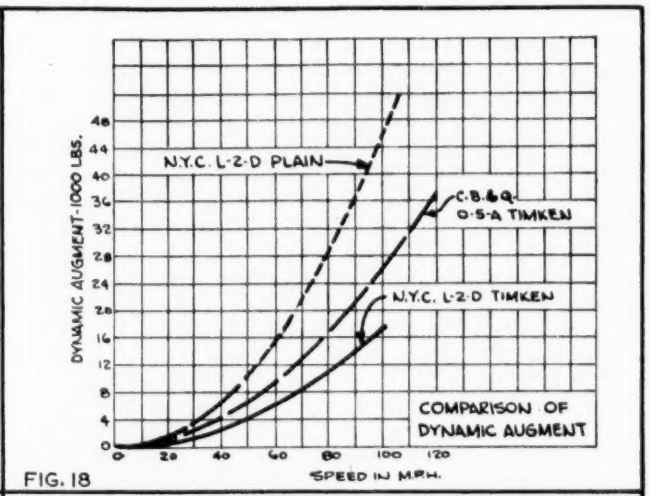


FIG. 18

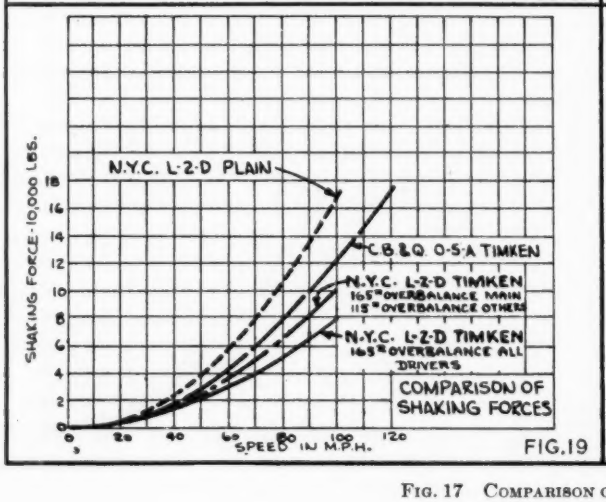


FIG. 19

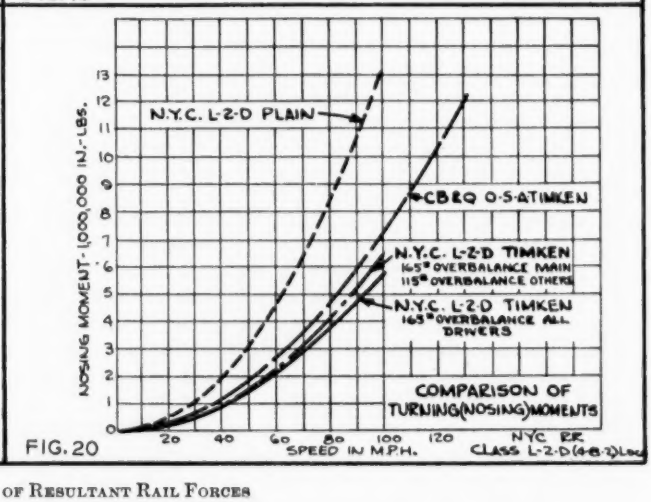


FIG. 20

FIG. 17 COMPARISON OF RESULTANT RAIL FORCES

FIG. 18 COMPARISON OF DYNAMIC AUGMENTS

FIG. 19 COMPARISON OF SHAKING FORCES

FIG. 20 COMPARISON OF TURNING, OR NOSING, MOMENTS

bar horsepower from 177 lb to 93 lb, or 48 per cent, is noteworthy.

Probably the major improvement in steam passenger locomotives is the increase in capacity for work, as measured in ton-miles per month. The average of the fifty J-3 locomotives for the month of December, 1940, was 11,689 miles each, giving effect to engines in shop and engines partially employed during the month. Ten of these locomotives actually made over 16,000 miles in that month. It is doubtful whether the typical passenger locomotive prior to 1925 averaged more than one third of that figure and handled trains, giving effect to the air-conditioning drag about one half as heavy. This would indicate that the modern Hudson locomotive has 6 times the capacity for work, as compared with the locomotive of only 15 years ago. This is a noteworthy development and affords a further indication that the replacement of the steam passenger locomotive by other forms of motive power is still a long distance in the future.

The New York Central received delivery of fifty class L-3 Mohawk locomotives during 1940. This followed the experimental conversion in 1939 of two class L-2D Mohawk, type 4-8-2 freight locomotives. Much thought was given to the conversion locomotive No. 2998. The reciprocating weight was reduced from 2143 to 1239 lb, a reduction of 904 lb. The overbalance in the plane of the rail on the left main driver was reduced from 441 lb to 171 lb and a corresponding dynamic augment at diameter speed from 21,200 lb to 8220 lb, a reduction of 12,980 lb, or 158 per cent of the remaining dynamic augment.

The rail reaction on the main driver at 75 mph was reduced from 28,100 lb to 8200 lb, upward against the spring rigging, and from 24,000 lb to 12,200 lb, downward against the rail. The nosing moment was reduced from 8,400,000 in-lb to 4,000,000 in-lb at 80 mph, and the fore-and-aft shaking force from 108,000 lb to 64,000 lb. These figures are reflected in the relatively low rail stresses at speeds up to 87 mph, as indicated in Table 5 of the paper.

Curves of dynamic rail force under the main drivers for the L-2D Mohawk are shown in Fig. 16. Comparisons of resultant rail forces, dynamic augments, shaking forces, and turning moments of this type locomotive with others at various speeds are given in Figs. 17 to 20, inclusive.

The Mohawk engine, having 69-in. drivers, balanced as described, ranks with the best of the results obtained from the J-1E and J-3A Hudson type locomotives at high speeds measured in lower stress in rails and good riding qualities.

The experience with 25 of the L-3's, equipped for passenger-

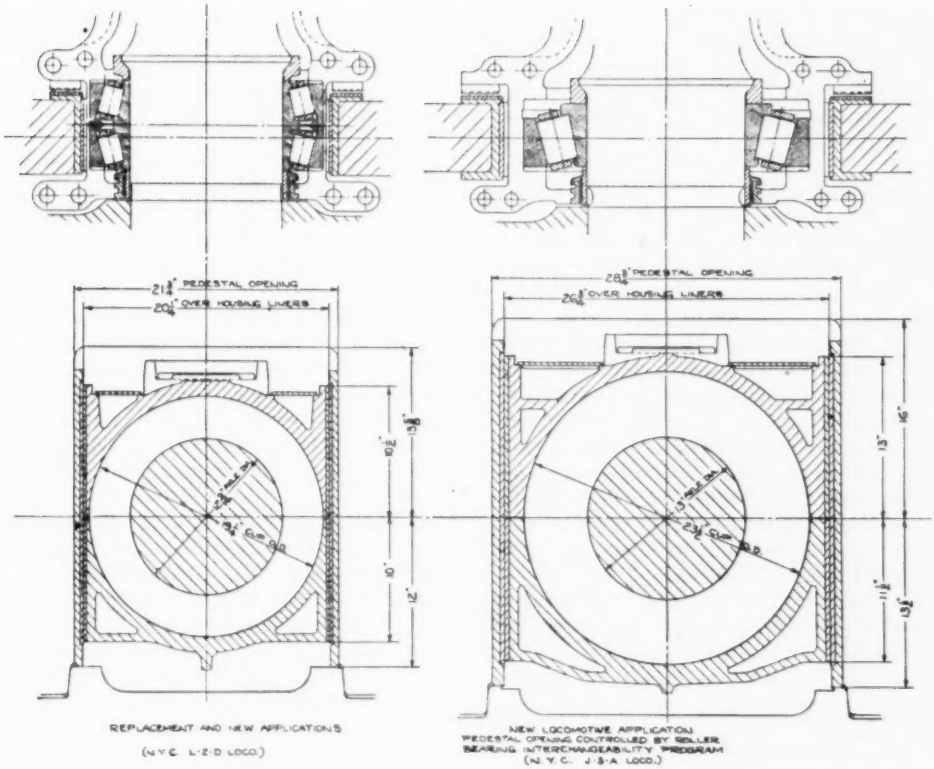


FIG. 21

train operation, proves that the new Mohawks can be used interchangeably in passenger and freight service. This equipment defers the increase in Hudson locomotive inventory for the handling of peak loads in midwinter and midsummer, and the Labor Day holidays. At the same time, these locomotives are available for freight-traffic peaks developing in the early fall. Notwithstanding the general improvement in passenger service, this locomotive has also been improved in its capacity to handle freight traffic.

Table 7 of the paper, showing the capabilities of this locomotive for high-speed operation as ranking with the best passenger locomotives, together with its greatly increased drawbar capacity at low and medium speeds, indicates that this locomotive is capable of handling heavy passenger and express trains in congested traffic at a higher average rate of speed than any other locomotive available. It is believed to be the outstanding locomotive achievement in recent years.

The New York Central J-3A (Hudson) and L-3A (Mohawk) locomotives afford an additional interesting comparison, shown in Fig. 21, entitled "main-pedestal-opening comparison." The J-3A driver-bearing application, shown at the right in Fig. 21, is based on interchangeability with other types of roller bearings. The pedestal opening of 28¾ in. and pedestal clearance of 16 in. above the center line of the axle are derived from the space requirements of other roller bearings.

The L-2D and L-3A pedestal opening is based on the space requirements of the taper roller bearing of the double-row type. The pedestal opening is 21¼ in. and the pedestal clearance is 13⅝ in. which interchange exactly with the plain-bearing requirements. In addition, there are outstanding reductions in unsprung weight and provision of more space for spring rigging with the advantages of an equal degree of reliability and greater economy in the plain-bearing interchangeable layout. Most current locomotive construction is based on this interchangeable layout.

R. M. OSTERMANN.[7] This paper discloses a very creditable engineering achievement. It is remarkable how greatly the sustained capacity of the New York Central J class locomotives was increased by attention to details and by refinement in design. In the section "Thermal Efficiency at Tender Drawbar Referred to Fuel," the author explains the circumstances which led him to compromise between that thermal efficiency and practical operating advantages, and he thus exhibits the very logical view of a railroad operating man.

However, the engineer sitting on the sidelines wonders whether steam-locomotive designers will not eventually be forced to far-reaching modifications of the design of steam locomotives because of the pressure of the competition which the conventional steam locomotive is experiencing from the Diesel-engine-powered locomotive. This type of motive power has great advantages of thermal efficiency. Steam-locomotive designers may be forced, in self-defense, in their future designs, to embody some of the principles, the application of which has produced such eminent progress in the economy of stationary power plants within the last 15 years. For instance, it is seen that the J-3 engine, at its best, works with a heat drop per pound of steam of about 160 Btu. It is not at all unreasonable to expect that steam locomotives may someday be worked with nearly double that heat drop, in an entirely practical manner.

As the author points out it is perfectly true that, in railroad locomotives, we are confronted with acute limitations of weight, height, width, and length of structure, but it seems to the writer that, just because of them, every physical means should be tried

[7] Vice-President, Western Territory, The Superheater Company, Chicago, Ill. Mem. A.S.M.E.

in order to get a maximum of capacity into a given cubic space. The writer feels that men such as the author who have been able to refine the design of conventional steam locomotives to such a remarkable degree, by painstaking engineering analysis, will also be able to make entirely new forms of steam locomotives practicable.

JAMES PARTINGTON.[8] In this paper we have a very complete picture of the development of main-line steam locomotives for passenger service. These modern locomotives show wonderful sustained horsepower output and are making a yearly mileage of well over 200,000.

To keep within the railroad company's weight limits on the L-3 locomotives, the cabs, runboards, and dome casing are made of aluminum. On the J-3, all of the important casings, dome casing, cylinder-head casing, etc., were aluminum, and the cabs were aluminum on forty engines; ten engines were Cor-Ten steel. Here we have a situation where the saving of weight was urgently necessary and the use of expensive material was resorted to for a weight saving of about 2000 lb per locomotive. Twice this saving could be obtained if the boilers of these locomotives were of welded construction. Therefore, the writer would like to discuss briefly the welded boiler for locomotives.

Soon after the rules for fusion welding were adopted by the A.S.M.E. Boiler Code Committee, they were placed in the Code for Power Boilers. The use of these rules proved them to be safe and satisfactory, and after several years' experience the Code Committee suggested that they be incorporated into the Code for Boilers for Locomotives.

After several conferences with the I.C.C. Bureau of Locomotive Inspection, and largely through the efforts of the late L. F. Loree, then president of the Delaware & Hudson Railroad, permission was granted to that company to build and operate a locomotive with a welded boiler. This boiler was built by the American Locomotive Company to meet the requirements of the A.S.M.E. Power Boiler Code, and the locomotive was placed in freight service on the D.&H. in the fall of 1937. This welded boiler will soon have a service record of 4 years. During this time thorough inspections made frequently have shown that it has a performance record of 100 per cent.

When the Interstate Commerce Commission gave its permission for the operation of this locomotive with a welded boiler, it was in response to a request sponsored by many of the leading railroads that an experimental installation be allowed. In granting this request it was stipulated that no additional welded boilers would be permitted pending a test period of 5 years. For the operation of additional locomotives with welded boilers, the railroads will have to secure authorization from the I.C.C. through a procedure similar to that used by the D.&H. Company for this first welded boiler.

The advantages of the welded locomotive-type boiler are that there are no rivets; no overlaps; no obstructions inside or outside; no joint repairs or failures; lower upkeep expense; higher efficiency; lighter weight; easier handling; quicker washing; neater appearance. Finally, this form of construction eliminates caustic embrittlement, which has caused rivet failures and cracked sheets in the region of both circumferential and longitudinal seams of riveted boilers. In a number of cases this has made expensive repairs necessary.

Welding has supplanted riveting for high-pressure stationary boilers and for nearly all pressure-vessel construction.

There are several hundred locomotive-type welded boilers in use for power purposes in the United States, and these boilers are operating at pressures up to 350 psi.

Will more welded boilers for locomotives be built?

This will depend upon the attitude of the railroads and the decision of the Interstate Commerce Commission.

The locomotive builders are ready to give full assistance and cooperation in this development

F. E. RUSSELL.[9] Our experience with the development of high-speed steam locomotives agrees closely with that of the author, in that we have been able to increase the efficiency and output of the steam locomotive by intensive development and improvement in design. By providing ample firebox volume and gas area through tubes and flues, it is possible to increase the evaporation considerably without excessive losses in combustion and absorption efficiency, as is shown by the performance curves in the author's paper. In this regard, on the Southern Pacific, we are more fortunate, in that the combustion efficiency of the locomotive boiler with oil fuel is high, and there is little falling off in over-all boiler efficiency as the firing rate is increased; and high outputs can be obtained with a moderate draft and back pressure.

Steam-flow conditions are extremely important if the maximum potential output of a steam locomotive is to be obtained in practice. The dry pipe, superheater header, and superheater units should be of ample area, and the flow should be as direct and "streamlined" as the design will permit. The writer considers the design of the steam and exhaust passages in the cylinder especially important. Much of the increase in horsepower per unit volume in our more recent locomotives is due to careful cylinder design, with our insistence on definite steam, exhaust, and valve bushing area in relation to piston size. In this respect the increase in boiler pressure, with subsequent decrease in cylinder size for a given power, has been a great advantage, as it is possible to provide greater area in the passages per unit volume of steam handled.

Prior to 1927, apparently little attention was paid to increasing the area of exhaust passages in the cylinders in proportion to the cylinder diameter, resulting in high back pressure and low power output at high speeds. During that year we made an analysis of the proportion of exhaust passages, as related to piston area, and since then all our locomotives have been built with improved exhaust passages, resulting in increased horsepower output and reduced back pressure and decreased fuel consumption.

In 1920, we made some dynamometer tests on 2-10-2 type superheater locomotives and determined that for superheated locomotives we should get away from saturated-steam practice. It was also decided that, in order to obtain maximum fuel economy, the cylinder diameter should be reduced and the stroke increased over the proportions normally used at that time. In 1921, when we purchased our first heavy Pacifics for service between Sparks, Nevada, and Ogden, Utah, handling heavy transcontinental trains, we went to a 30-in. stroke with a 25-in. cylinder, using 73-in. drivers. These locomotives were so satisfactory in passenger service, not only in high-speed hauling capacity but also in their ability to start heavy trains without taking slack, that we have continued the practice of using a relatively long stroke. Our latest 4-8-4 type locomotives have 25½-in. × 32-in. cylinders with 80-in. drivers. We find these proportions very satisfactory for starting heavy trains and for high-speed full-power operation.

Given a boiler designed for high output and high superheat, and steam and exhaust passages capable of handling the steam required for high power output, the remaining problem is that of utilizing this steam with the greatest efficiency in the cylinders. In this regard, the present form of piston valve with interconnected timing of events is certainly not ideal. The writer con-

[8] Manager, Engineering Department, American Locomotive Company, New York, N. Y. Mem. A.S.M.E.

[9] Mechanical Engineer, Southern Pacific Company, San Francisco, Calif. Mem. A.S.M.E.

fidently looks forward to the perfection of some form of valve with independent timing, to obtain more adequate valve openings at high speeds and short cutoffs, together with a reduction in the present distortion of exhaust events. In this connection, the poppet-valve gear mentioned in the paper is of great interest, and is believed to be very promising.

As an example of what a modern high-power steam locomotive can do, the writer has analyzed some of the performance records of our latest 4-8-4 type passenger locomotives purchased in 1940. These locomotives have cylinders 25½ in. × 32 in., with 80-in. drivers, and carry 300-psi boiler pressure. They are equipped with type E superheaters, Worthington SA feedwater heaters, and have oil lubrication on all axle bearings. These locomotives are used to handle the streamline "Daylight" trains between San Francisco and Los Angeles, which are frequently as heavy as 16 cars, weighing 924 tons loaded. On these trains, the portion of the run that requires the highest power output is eastbound from Camarillo to Santa Susanna, Calif., a distance of 20.9 miles, with an average opposing grade over the entire district of 0.75 per cent. Between these points the schedule speed is 62.7 mph. Examining the speed-record tapes, the writer finds that, on one 7-mile continuous stretch of compensated 1 per cent grade in this territory, the maximum speed maintained steadily is 55 mph with the 16-car 924-ton train, which performance requires a calculated drawbar horsepower on the level of 4750; the equivalent cylinder horsepower is estimated at 5400. On other occasions, these locomotives have handled the "Daylight" with 13 cars, weighing 729 tons, on the 2.2 per cent Cuesta grade, making speeds of 28 mph without a helper.

On our Salt Lake Division, a slightly older type of 4-8-4 locomotive is handling trains of 20 cars, weighing approximately 1400 tons, on fast schedules.

The writer is in complete agreement with the author that research and design have greatly improved the high-speed steam passenger locomotive, and that continued development and testing will result in future locomotives of higher output and efficiency than yet obtained.

C. J. Surdy.[10] We are fully aware that present-day traffic demands result in a radical change in operating methods. In many instances this traffic is seasonal and, during such periods, there is a heavy demand for high-speed power in both passenger and freight service. Few, if any, roads can afford to hold in reserve power to meet such seasonal demands, therefore, it is quite evident that the solution of this problem is the dual-service locomotive, described so well in this paper.

Of more than usual interest is that portion of the paper in which the author presents his thoughts on trends of steam-locomotive design and improvement for the future. With the experience on the New York Central, including the experimental use of a 5400-hp Diesel-electric locomotive and a 5000-hp turboelectric locomotive, the author's endorsement of the conventional reciprocating-design locomotive should be regarded by motive-power designers as a challenge. Apparently, his choice of motive power is made on the basis that nothing better has yet been offered, when due consideration is given to all factors.

There is much more to consider in the selection of motive power than the known advantages which are derived from more expensive power, such as Diesel-electrics or turboelectrics of the experimental type proposed in recent years. Practical railroad men must also give full consideration to the economic forces which, in a considerable measure, determine whether or not coal must be used as a source of power. They must also take into account the effect which their use of certain kinds of coal may have on the consumer market which their railroad serves. Obviously, to take off the market a coal that is desired by the consumer only results in loss of the haul to the railroad. In 1939 bituminous coal accounted for one sixth of the total railroad freight revenue in the United States. From this, it appears the railroads need the coal freight haul, while the coal-mine operators apparently need the railroad fuel business to stabilize their output.

On the premise that many railroads will continue to regard coal as a primary fuel for their motive power, it appears that sufficient incentive exists for locomotive designers to give more thought to producing a coal-burning motive-power unit with the characteristics of the Diesel-electric. Some work of a preliminary nature has been done in this respect, but apparently the development is not complete.

It is not within the scope of this discussion to promote a new system of motive power, but this paper, which takes us step by step through the development of steam locomotives on the New York Central, indicates that, as greater demands are made for sustained power output of steam locomotives, more study will have to be given to some arrangement for increasing the diameter of the boiler barrel which will result in improved tube and flue layouts with larger gas areas and superheater. Since the diameter of the boiler cannot in any event, with steam-locomotive-design trends leading toward larger drivers, be increased greatly over present dimension, the thought of other systems of motive power naturally arises.

With the wide experience gained through the use of the locomotive boiler, of simple construction and high steam-generating capacity, a logical starting point for development of a turboelectric locomotive is present. The boiler of a New York Central Hudson-type locomotive can generate a maximum of about 100,000 lb of steam per hr. By the use of a water-tube firebox, it should be possible to generate steam at a pressure in the neighborhood of 700 psi. This capacity would exceed the steam requirements of two or even three 2500-hp turbines, so that a 7500-hp turboelectric locomotive, using coal as a primary source of fuel in a boiler and firebox somewhat along present conventional lines, is within the realm of possibility.

Author's Closure

The author is grateful for the privilege of submitting brief comments on the valuable and helpful discussions contributed to the subject matter of his paper.

Mr. Buckwalter's discussion has been reviewed with much interest and appreciation. The material presented is consistent with our experience and records. The information given in terms of "increase in capacity for work," as pertaining to the modern steam passenger locomotive, provides a practical illustration of progress in this field.

Mr. Buckwalter refers to the increase of 17 per cent in drawbar horsepower obtained in the Hudson type locomotives with an increase of only 11,000 lb on drivers and 1400 lb in total weight. It should be pointed out that the increase of 11,000 lb on drivers was arranged deliberately to produce a higher factor of adhesion for this extremely high-powered locomotive, and was practicable because of the reduced rail reactions secured by the methods indicated. If considered desirable, the small increase in total weight could have been distributed to leading and trailing trucks by proper equalization, with weight on drivers held to that of the previous Hudsons.

Later in his discussion Mr. Buckwalter refers to the latest class L-3, equipped for passenger-train operation, the estimated power characteristics of which were shown in Table 7 of the author's paper.

Preliminary results of the tests of this class conducted under

[10] Assistant to General Manager, The Standard Stoker Company, Inc., New York, N. Y.

regular road service conditions of operation may now be reported as follows

Maximum cylinder horsepower	5120 at 67 mph
Maximum drawbar horsepower	4320 at 62 mph
Engine weight per cylinder horsepower	76 lb
Engine weight per drawbar horsepower	90 lb
Drawbar pull at 85 mph	17000 lb

The final report has not as yet been completed, and minor corrections may be required after all dynamometer records have been thoroughly checked.

Although Mr. Ostermann has commented favorably on the increase in sustained capacity on the New York Central class J locomotives through attention to detail and by refinement in design, he may have gained the impression from the section on "Thermal Efficiency at Tender Drawbar Referred to Fuel," that the treatment of this subject was intended to explain the circumstances which led to a compromise between thermal efficiency and practical operating advantages in the design of the Hudson type class J-3. The section on thermal efficiency was included for reasons given in the opening paragraphs, inasmuch as the paper was addressed to the subject of modern steam passenger locomotives for handling heavy high-speed passenger traffic at the present time. It is not the author's belief that it will be necessary to force steam-locomotive designers to modifications in design, because what is constantly sought by progressive railroads, locomotive builders, and manufacturers engaged in related activities, is the most efficient and economical form of motive power which may be produced to meet the changing needs of the railroad industry.

Under the concluding heading, "Present Thoughts on Trends of Steam-Locomotive-Design Improvement for the Near Future," attention has been directed to these circumstances with a view to stimulating interest and efforts of all concerned in the direction of increasing the thermal efficiency of motive-power units. However, to insure progress in rail transportation, it is necessary before introducing radically different designs in quantities sufficient to permit handling some reasonable proportion of the total traffic that such units be of proved dependability and of practicable size, weight, and cost. It is the author's belief that any contribution along these lines, from those skilled and experienced in the art, which appears to have reasonable prospect of success, would immediately receive due attention and consideration by all concerned.

Mr. Partington's discussion of the welded boiler for locomotives is pertinent and timely. He has supplied a concise outline of the numerous advantages to be gained through this form of locomotive-boiler construction, which has become widely used in the fabrication of boilers for stationary plants, marine and other services, and for various types of pressure vessels.

It may be said that this subject is now under active consideration through official channels of the Association of American Railroads in cooperation with the locomotive builders. It is hoped that, through negotiations with the Interstate Commerce Commission, additional boilers for locomotive use may be constructed by the fusion-welding process and placed in service within a reasonable time.

The author is gratified to note that Mr. Russell's experience agrees with his own on the matter of increased efficiency and capacity of the steam locomotive, obtained by extensive development and improvement in design, with particular reference to steam-flow conditions, and shares his belief that continued development and testing will result in future steam locomotives of still higher output and efficiency than any yet obtained. Further work of this character is being actively prosecuted by the New York Central, and the hope is expressed that a similar procedure will be carried on throughout the rail-transportation industry.

The interest expressed by Mr. Surdy and the specific ideas he has offered in reference to the thoughts presented on trends of steam-locomotive design and improvement for the future have been noted with appreciation. As indicated under this section of the paper, extensive experience has been obtained on the New York Central with certain types of Diesel-electric locomotives, and the results have been fully up to expectations. At the same time, limited experience has been gained with other experimental locomotives, designed for road service, and continued progress is anticipated in the design of steam, Diesel, and other forms of motive power. As this progress continues, supplemented by service and economic experience, a wider choice of motive-power types should be made available, subject to an analysis of the different conditions to be met.

Francis-Turbine Installations of the Norris and Hiwassee Projects

By GEORGE R. RICH[1] AND J. F. ROBERTS,[2] KNOXVILLE, TENN.

The Hiwassee turbine, having a rated output of 80,000 hp at 190-ft head, is believed to be the highest-powered Francis wheel in the eastern United States. The Norris turbines are identical in physical size with the Hiwassee unit and have a rated output of 66,000 hp at 165-ft head. In this paper, considerations affecting the selection of these machines are discussed, and principal features of the design and acceptance testing are described.

THE Tennessee Valley Authority is a Federal corporation invested with statutory power to develop the Tennessee River in the combined interests of navigation, flood control, and electric-power generation. The ultimate plan of development will provide a channel for 9-ft navigation for a distance of 650 miles from the confluence of the Tennessee with the Ohio at Paducah, Ky., to the headwaters at Knoxville. The flood-control storage afforded by the main river and tributary storage reservoirs, about 10,000,000 acre-ft, will be sufficient to reduce flood crests on the Mississippi River about 2 ft and possibly 3 ft at Cairo, Ill. The ultimate installed hydroelectric capacity will be about 2,000,000 kw. As part of the National Defense Program, there is now under construction a modern steam plant of 120,000-kw capacity for the purpose of priming high-grade secondary hydro energy during periods of water deficiency. This station, together with other properties obtained by acquisition, will afford a total steam capacity of about 300,000 kw, giving a high degree of flexibility to the system, which is favorably located in close proximity to an extensive supply of high-grade steam coal. Fig. 1 and Table 1 show the geographic location and physical features of the various water-control projects.

The Norris and Hiwassee projects are essentially storage developments for operation at low capacity factor on the nonnavigable tributary streams, and have the primary function of impounding headwater floods and augmenting the flow of the main river in the interests of navigation and power during the dry season. Long-term records establish the low-flow period from September 15 to December 1, in an average year and from July 15 to January 15, in an extremely dry year. Both long-term records and modern analyses of storm movements indicate that floods of major magnitude will occur only in the interval from December 15 to April 15. The cycle of operation of the storage reservoirs is predicated upon this hydrologic pattern. Under such rational advance planning, the requirements of navigation, flood control, and power generation are not at all incompatible, and very satisfactory operating results have been obtained.

From Table 2 it will be noted that the Norris project has a drainage area of 2950 sq miles and an average annual runoff of 4600 cfs. There are two 66,000-hp turbines which operate at heads varying from 194 ft to 129 ft. The storage available between elevations 955 and 1020, amounting to 1,500,000 acre-ft, is sufficient to provide an average daily discharge of 6000 cfs, exclusive of normal inflow, for a period of about 4 months. The Hiwassee project has a drainage area of 966 sq miles and an average annual runoff of 2150 cfs. While provision has been made for an ultimate installation of two units, only a single unit has been installed initially. This turbine operates at heads varying from 254 ft to 143 ft and is rated 80,000 hp at 190 ft head. The available storage is 365,000 acre-ft, which is sufficient to supply an average discharge of 3200 cfs, exclusive of normal inflow, for a period of about 2 months.

Reservoir Operation

The present schedule of reservoir operation is as follows: At the end of the flood period, April 15, the restriction that part of the reservoir be reserved for flood storage is lifted, and the remainder may be filled to the normal level as rapidly as stream flow permits. In a normal year, no release from storage would be required until September 15, although in a dry year, such as 1925, low flow in the lower river might require release of stored water by July 15, or on rare occasions, even during June. During the period of storing water, one unit at Norris and the unit at Hiwassee are operated as synchronous condensers with the guide vanes fully closed, but with the scroll case full of water, and with the runner and the draft tube vented to atmospheric pressure, and drawing about 2.75 per cent of normal generator rating from the transmission system. Under these conditions, the governor is so adjusted that, in case the frequency drops approximately 1/4 cycle, the guide vanes open up and the turbine picks up load. During storms or other interruptions, the Norris plant has picked up as much as 50,000 kw in 8 sec. When normal conditions have been restored, the tributary plants are again motored.

Since such occurrences are infrequent and of short duration, the amount of water used is negligible, but the emergency value of such units to the generating system as a whole is considerable. While motoring, one of the Norris units consumes about 10 cfs of water, this consisting of leakage through the guide vanes and the amount required to lubricate the runner seals and stuffing box and for cooling of the thrust bearing and the generator.

If the reservoirs reach normal full level before additional water is required for either navigation or power in the lower river, then the units are operated part of the time as generators so as just to utilize the inflow and hold the reservoirs full. Since the load on the Authority's system has been such as to require steam operation for a considerable part of each year, part-time operation of the storage plants results in a material saving of coal.

As the dry season approaches, the release from storage is gradually increased so as to maintain a steady flow in the lower river between Pickwick Dam and Kentucky Dam, where navigation is still definitely dependent upon stream flow to maintain an interim depth of 6 ft for navigation. When the Kentucky Dam is completed, probably in 1945, this stream flow will not be required for navigation on the lower Tennessee River and the storage may be released in the manner most beneficial for power generation in the Tennessee River plants and for improving

[1] Assistant Chief Design Engineer, Tennessee Valley Authority. Mem. A.S.M.E.

[2] Principal Mechanical Engineer, Tennessee Valley Authority. Mem. A.S.M.E.

Contributed by the Hydraulic Division and presented at the Spring Meeting, Atlanta, Ga., March 31–April 3, 1941, of THE AMERICAN SOCIETY OF MECHANICAL ENGINEERS.

NOTE: Statements and opinions advanced in papers are to be understood as individual expressions of their authors and not those of the Society.

TABLE 1 PROJECT FEATURES

	Navigation		Reservoir						Power					
Project	Size of Lock Chamber (feet)	Maximum Lift of Lock (feet)	Area at Top of Gates (acres)	Volume at Top of Gates (acre-feet)	Controlled Flood Storage (acre-feet)	Length of Spillway (feet)	Spillway Capacity (second-feet)	Backwater Length (miles)	Rated Head (feet)	Head for Best Efficiency (feet)	Present[4] Plant Capacity (kw)	Ultimate[4] Plant Capacity (kw)	Effective Capacity During High Flow - 1926-1927 Flood (kw)	Type of Turbines
Kentucky[1]	110x600	73	256,000	6,100,000	4,570,000	960	1,100,000	184.4	48	51	--	160,000	74,000	Kaplan
Pickwick Landing	110x600	63	46,800	1,091,000	418,000	880	670,000	52.7	43	56	72,000	216,000	36,000	Kaplan
Wilson	60x300[2]	90	16,200	600,000	--	2,212	629,000	15.5	95 & 92	95 & 92	184,000	444,000	419,000	Francis
Wheeler	60x360	53	68,300	1,150,000	429,000	2,400	687,000	74.1	48	48	64,800	259,200	245,000	Propeller
Guntersville	60x360	45	70,700	1,019,000	282,000	720	625,000	82.1	36	36	72,900	97,200	69,000	Kaplan
Hales Bar	60x267	37	5,800	126,000	--	1,200	--	39.8	35	36	50,500	50,500	20,000	Francis
Chickamauga	60x360	56	37,200	655,000	377,000	720	600,000	59.0	36	48	81,000	108,000	67,000	Kaplan
Watts Bar[1]	60x360	70	41,500	1,132,000	370,000	800	550,000	72.4	52	82	90,000	150,000	150,000	Kaplan
Fort Loudoun[1]	60x360	80	14,900	365,500	106,000	800	550,000	55.0	68	70	--	96,000	64,000	Kaplan
Norris	--	--	40,160	2,567,000	2,020,000	300	54,000	72.0	185	180	100,800	100,800	100,000	Francis
Hiwassee	--	--	6,280	438,000	365,000	224	130,000	22.0	190	200	57,600	115,200	115,000	Francis
Cherokee[1]	--	--	32,200	1,640,000	1,473,000	360	300,000	58.5	100	110	90,000	120,000	120,000	Francis
Blue Ridge[3]	--	--	3,290	197,500	183,000	110	55,000	10.0	147	--	20,000	20,000	20,000	Francis
Ocoee No. 1[3]	--	--	1,380	78,700	25,900	582	--	7.8	110	--	18,000	18,000	18,000	Francis
Ocoee No. 2[3]	--	--	--	--	--	--	--	--	250	--	28,800	28,800	18,000	Francis
Great Falls[3]	--	--	2,290	55,100	49,900	450	180,000	--	142	--	29,400	29,400	29,000	Francis

1 Under construction.
2 Two lock chambers.
3 Acquired by purchase of completed projects; dependable flood storage not fully determined.
4 Generating capacities are based upon actual performance which exceeds guaranteed performance.

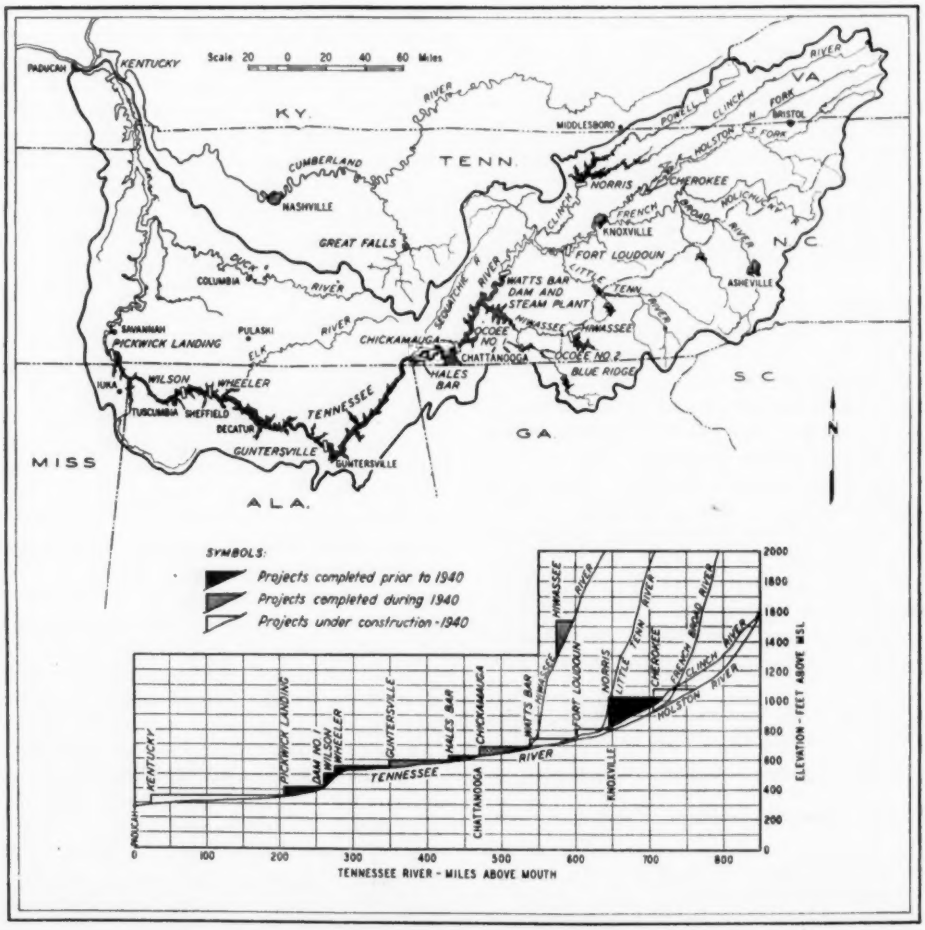


FIG. 1 MAP OF THE TENNESSEE VALLEY

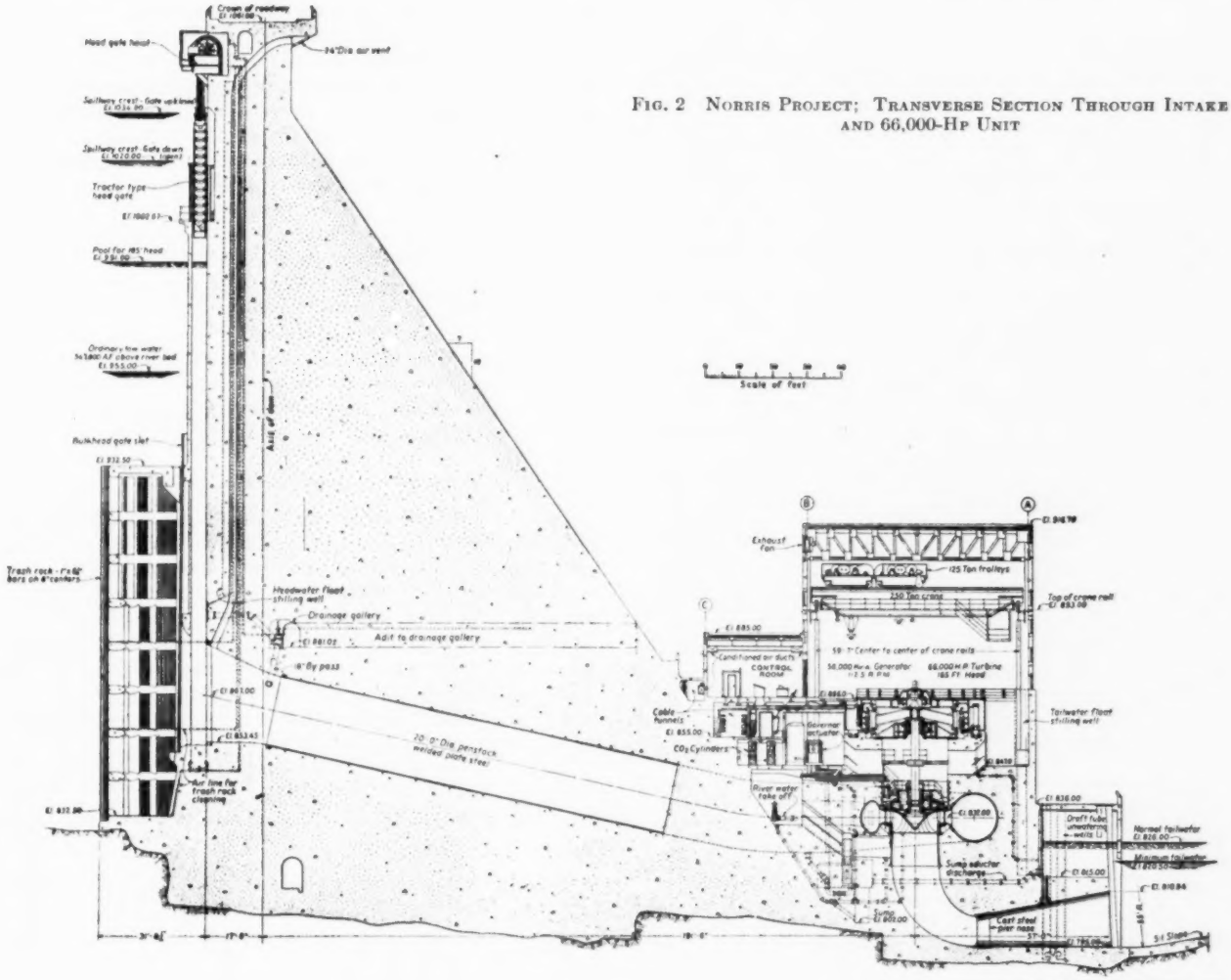


Fig. 2 Norris Project; Transverse Section Through Intake and 66,000-Hp Unit

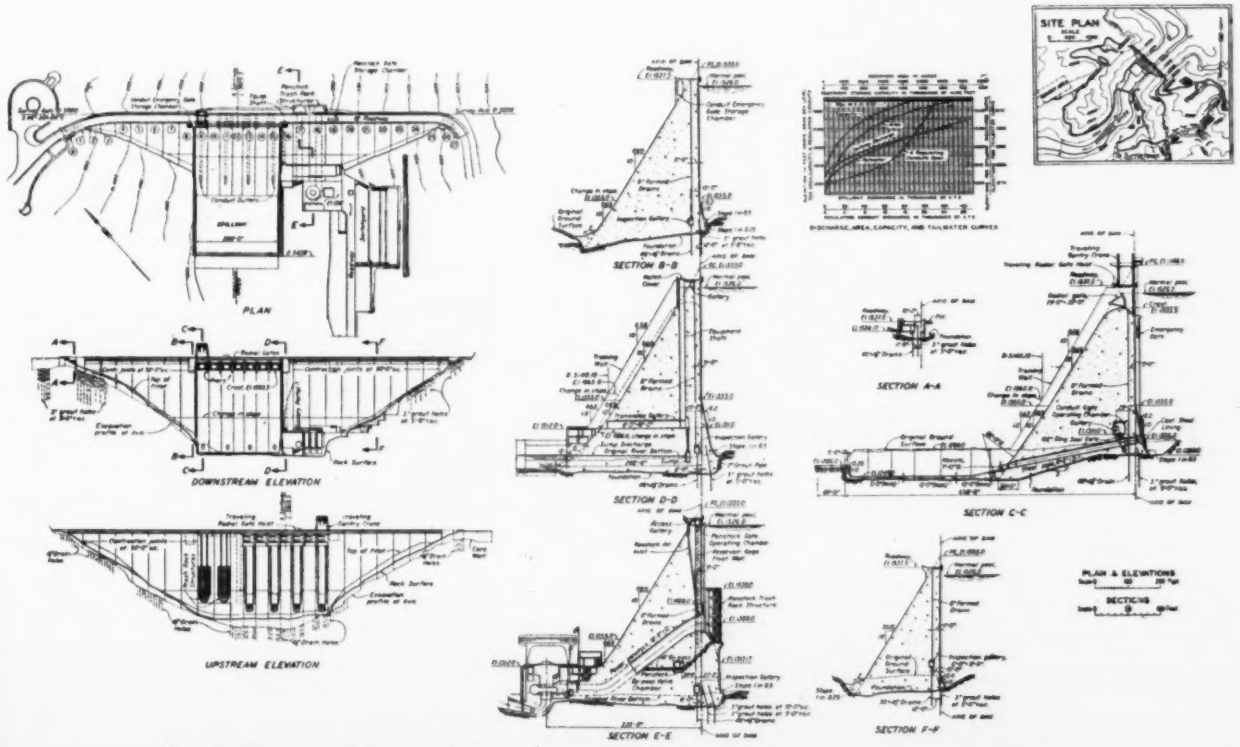


Fig. 3 Hiwassee Project; General Arrangement, Plan, Elevation, and Sections of Dam

TABLE 2 PHYSICAL FEATURES

	Norris	Hiwassee
Project started	Oct. 1933	July 1936
Machinery ordered	Oct. 1934	Sept. 1938
Machinery operating	July 1936	May 1940
Drainage area - sq mi	2912	966
Average run-off - cfs	4600	2100
Maximum recorded flood - cfs	115,000	42,000
Minimum recorded flow - cfs	200	134
Flood capacity - cfs - sluices	36,000	20,000
- overflow	54,000	130,000
- total	90,000	150,000
Number of sluices	8	4
Spillway gates	3-100'x14'	7-23'x32'
Elevation of gate sills	1020	1503.5
Pond levels - elevation and storage volumes - ac.-ft		
Ordinary minimum	955.....554,000	1415.....73,000
Normal storage	1020...2,047,000	1526.5..438,000
Controlled flood storage	1034....2,567,000	1532....474,000
Tailwater - normal elevation - ft	826	1272
- minimum elevation - ft	820.5	1266
Head - gross - maximum ft	194 (Elev.1020-826)	255 (Elev.1525-1272)
- minimum ft	129 (Elev. 955-826)	143 (Elev.1415-1272)
Head - net for turbine rating - ft	165	190
Turbine horsepower and number of units	132,000 in 2 units	80,000 in 1 unit
Turbine discharge - rated capacity - cfs	8500	4500
Provision for additional capacity	None	A 2d 80,000-hp unit
Increase in dry river flow downstream - approximate cfs	6000	3200
Generator rating - kva	2 @ 56,000	1 @ 64,000
- kw	2 @ 50,400	1 @ 57,600

navigation conditions during periods of low flow in the lower Mississippi River.

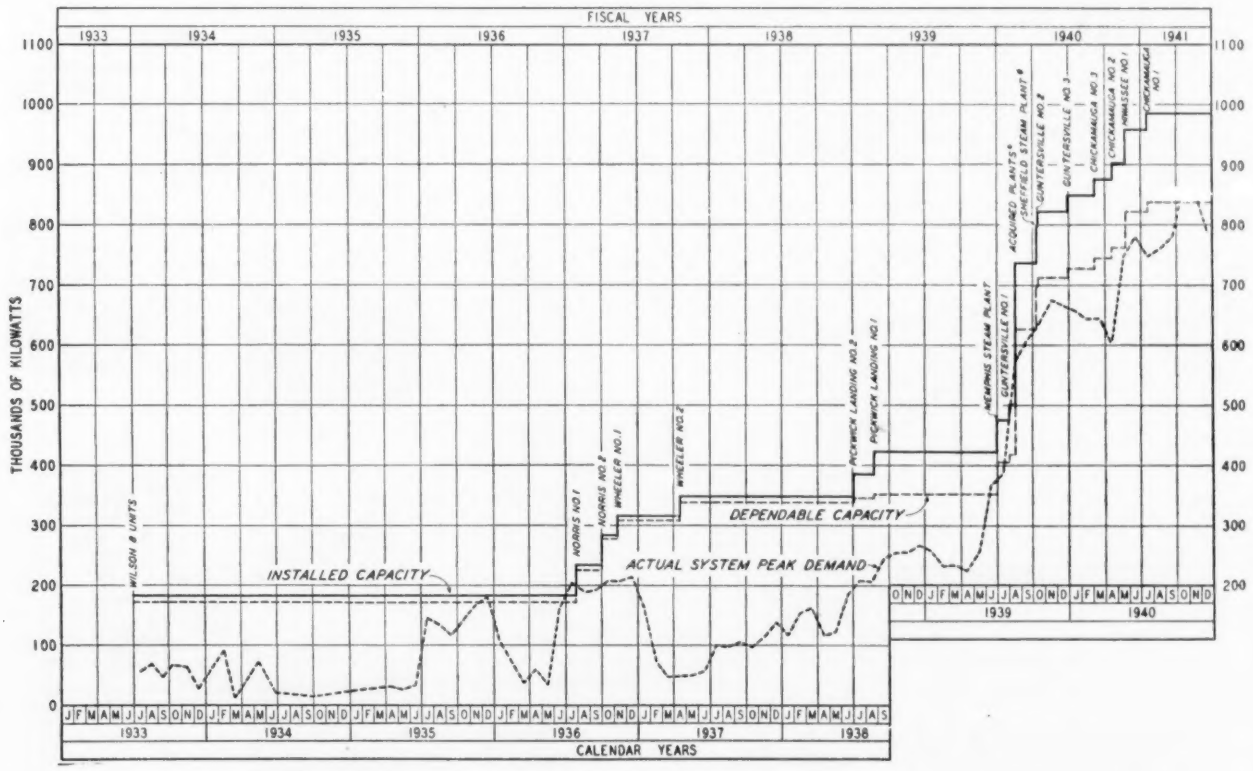
The approximate flow required for interim 6-ft navigation between Pickwick and Paducah under present conditions is about 17,000 cfs. During this period of drawdown there is very little conflict between the requirements for navigation and power. The present electrical load of the Authority is largely industrial, relatively steady with a high load factor, and not subject to appreciable seasonal variations. Consequently, any water drawn out of storage to maintain a flow of 17,000 cfs in the lower Tennessee for navigation is utilized nearly 100 per cent for power generation. At the present stage of completion of the development as a whole storage water released from both Norris and Hiwassee is used over a total head of 323 ft in the six main river plants already completed, not including the variable head at the storage dams.

On December 15, the operating schedule requires that the reservoirs be practically empty to accommodate flood storage between that date and April 15. This sometimes requires water to be drawn out of storage which would be held if operation were controlled solely by power requirements.

During the period from December 15 to April 15, the elevation of the reservoirs is limited to certain maximum levels, excess water being either wasted or used through the generating units at Norris and Hiwassee if the rate of discharge permits.

Determination of Turbine Capacity

When, in 1933 and 1934, studies were being made for the installation of generating machinery at Norris Dam, the size, type, and characteristics of the Authority's electrical system were somewhat nebulous. Wilson Dam and generating plant, with 182,000 kw installed, was the only operating station. Wheeler Dam was under construction, and one unit was contemplated as the initial installation. As will be seen from Fig. 4 the total load on the TVA system in 1934 was less than 50,000 kw, part of which was on short-time contracts to neighboring utilities and which could be taken or not at their option.



* HYDRO:
Blue Ridge
Ocoee No.2
Ocoee No.1
Hales Bar
Great Falls

STEAM:
Hales Bar
Nashville
Parksville

Sheffield Steam Plant available since July 1, 1933, but not in operation until October 10, 1939.

Fig. 4 Available System Capacity and Actual Peak Loads, 1933-1940

Based on the storage available, the maximum discharge necessary to improve the extreme low flows of the Tennessee, and future probable six-plant TVA system, with a total installation of approximately 525,000 kw, the capacity of the Norris plant was planned to be 100,800 kw, in two units rated 50,400 kw, 66,000 hp, 165-ft head.

In 1936, when funds were first appropriated for the start of construction on Fowler Bend Dam, later called Hiwassee, no power installation was planned initially, although provision was to be made for a future installation of two 40,000-kw units. The

TABLE 3 HYDRAULIC-TURBINE DATA

	Norris	Hiwassee
Rpm	112-1/2	120
Name plate rating - hp	66,000	80,000
Rated head - ft	165	190
Specific speed	48.8	48.1
Head for best efficiency - ft	180	200
Maximum usable hp	75,000	93,000
Maximum gross head - ft	194	254
Minimum gross head - ft	129	143
Elevation - center line of turbine - ft	832	1277
Elevation - normal tailwater - ft	826	1272
Runner inlet - inches	161	161
Discharge diameter - inches	165-1/2	165-1/2
Height - inches	41-7/8	41-7/8
Penstock diameter - ft	20	18
Penstock length - ft	154	220
Turbine scroll case inlet diameter	17'-8"	17'-8"
Scroll case design pressure - lb/sq in	125	140
Maximum scroll case plate thickness - inches	1-11/16	1-11/16
Governor cylinders - diameter - inches	28	28
- stroke - inches	13-3/4	13-3/4
Runaway speed at maximum head - rpm	215	235
Main shaft diameter - inches	35	36
Length of main shaft	14'-0"	12'-4"
Turbine bearing diameter - inches	36	37
Length of turbine bearing - inches	36	36
Weight of turbine runner and shaft - lb	153,500	142,500
Hydraulic thrust - lb	385,000	410,000
Weight generator rotor - lb	483,000	489,000
Total weight revolving parts - lb	1,104,000	1,106,000
Thrust bearing diameter - inches	74	76
Thrust bearing manufacturer	Kingsbury	Kingsbury
Powerhouse crane capacity - tons	250	275
Generator rating - kva	56,000	64,000
- kw	50,400	57,600
Generator WR^2 - lb ft sq	70,000,000	60,000,000
Reverse power required for motoring - kw	1350	1580

1936 report to Congress, made at about that time, indicates that four plants with an installed capacity of 348,000 kw and a continuous capacity of 225,000 kw were to be the nucleus of the TVA generating system and that at some possible future date machinery having a total continuous capacity of 660,000 kw might be installed in eleven plants. Fig. 4 shows how soon this expectation was surpassed.

Two 36,000-kw generators were authorized for Pickwick in the summer of 1936, and, in the summer of 1937, two 25,000-kw units for Guntersville and two 27,000-kw units for Chickamauga. In 1938, when the first Pickwick unit was nearing completion, overtime work was authorized to hasten the completion date so as to accommodate the increase in load. With continued steady growth of the TVA load, a third unit was authorized for both the Guntersville and Chickamauga plants. At that time, final studies were being made to determine the exact capacity of the generating units for Hiwassee Dam. The final decision was for an ultimate installation of two 57,600-kw units driven by 80,000-hp, 190-ft head, 120-rpm hydraulic turbines, although the use of three 40,000-kw units with an initial installation of two units was seriously considered.

The 115,200-kw ultimate installation increases that contemplated in preliminary studies by 44 per cent. This was due to the changed perspective resulting from the unpredictably rapid growth of the TVA system and the desirability of having larger units and greater installed capacity for peak loads and for spinning reserve in case of emergencies.

Features of Design

A fortunate set of circumstances made it possible to have the Hiwassee turbine almost an exact duplicate of the Norris turbines, both turbines being furnished by the Newport News Shipbuilding and Drydock Company. Only slight modifications were made, such as a larger shaft diameter and higher tensile strength in the plates of the spiral casing, together with slightly thicker metal in some other parts, in order to take care of the larger power output and higher head conditions. Table 3 shows the principal physical features of both the Norris and Hiwassee installations.

Much thought and discussion were given to the design of the

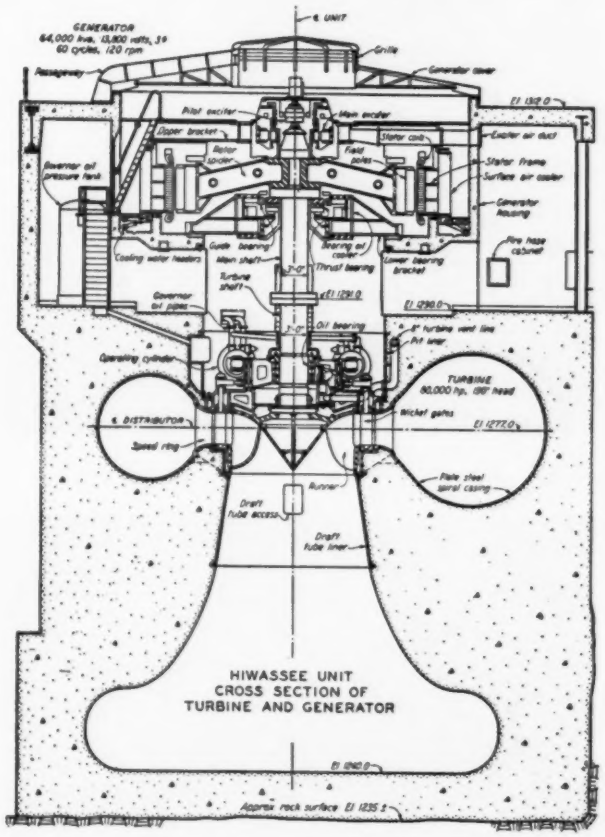


FIG. 5 HIWASSEE UNIT; CROSS SECTION OF TURBINE AND GENERATOR

plate-steel scroll case, particularly at the terminal point of the volute, where the smaller areas usually require elliptical sections. The speed ring must be designed for the largest or inlet section of the scroll case. With a guide-vane height of 41$^7/_8$ in. and a scroll-case inlet diameter of 17 ft 8 in. the speed-ring flanges have an angle of 50 deg with the horizontal and an outside width of 7 ft 1$^3/_4$ in. Since the scroll-case area is decreased around the turbine as the water is fed into the runner, a point is reached about $^1/_8$ of the way around the circumference, where a circle of 7 ft diam would have the required area of $^1/_8$ of the inlet area. Obviously, the vertical height of the casing must be greater than the height of the speed ring in order that the 50-deg flanges of the speed ring (100 deg total included angle) shall come tangent to the circle. One method of reducing the area and still maintaining the vertical height of the casing is to make the scroll-case sections elliptical at the small end.

Elliptical sections, however, when subjected to internal pres-

sure, tend to become round and, in a complicated structure of this type, exact determination of the resulting stresses is difficult. In order to reduce these stresses the Newport News Shipbuilding and Drydock Company proposed using a special steel casting which forms the terminal section of the scroll case and also the junction between the terminal and inlet sections. While this has a complicated shape, it could be heavily ribbed and stiffened so as to form a rigid connection. This special casting was used on both the Norris and Hiwassee turbines. In addition, in view

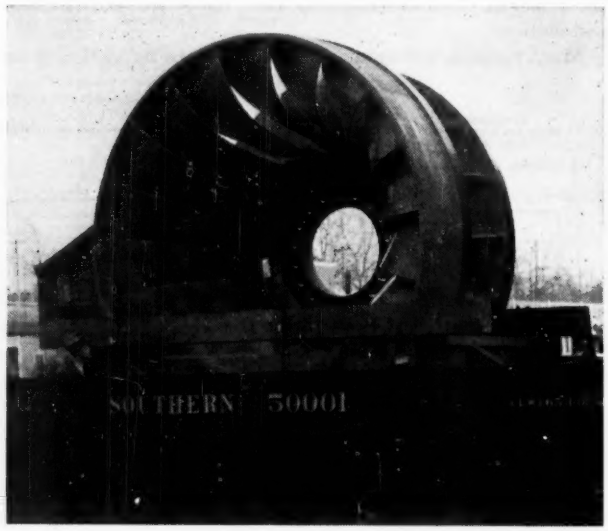


FIG. 6 161-IN. RUNNER FOR NORRIS DAM

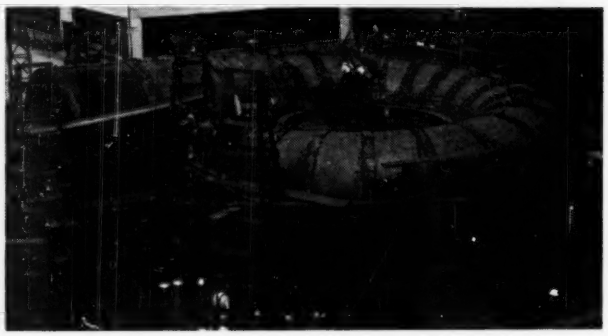


FIG. 7 SPIRAL CASING FOR 80,000-HP TURBINE FOR HIWASSEE DAM

of the impracticability of trying to hold the full stress in the casing metal in the small one quarter of the casing, that section was embedded solidly in concrete and sufficient reinforcing added to assist the plate-steel structure.

Over the balance of the scroll case, from the inlet around approximately three quarters of the circumference, a layer of cork and felt $^3/_4$ in. thick is laid over the plates so that the expansion of the casing under pressure will not be transmitted to the concrete.

The Norris scroll case, with an inlet diameter of 17 ft 8 in. and designed for a pressure of 125 psi, used a maximum plate thickness of $1^{11}/_{16}$ in. with $1^1/_4$-in. rivets. Even rivets of this size are difficult to drive by hand, so when the Hiwassee scroll case, of practically the same size and for a pressure of 140 psi, was under discussion, it was decided to use a higher-strength steel so as not to require thicker plates or rivets larger than $1^1/_4$ in. diam.

While the harder plate and harder rivets increased the difficulties of assembly and riveting somewhat, a tight job was obtained. An interesting method of testing joints was developed and consisted of smearing soapy water on the outside of a joint and directing a stream of compressed air at 100 lb pressure at the inside. Any bubbles indicated leaks which required additional calking.

On the Hiwassee turbine, in order to guard against corrosion and rusting of the guide-vane stems, where they pass through the grease- and water-lubricated bearings adjacent to the waterway, a special hard bronze bushing or sleeve $^1/_4$ in. thick was shrunk on the guide-vane stem in addition to the usual bronze bushing in the head cover and curb plate.

Similarly, the top and bottom of the guide vanes were protected by a piece of 12 to 14 per cent chromium-steel plate $^1/_2$ in. thick cut to the exact profile of the guide vane and welded to both the top and bottom of the guide vanes. The facing plates adjacent to the guide vanes on both the head cover and the curb ring were also of 12 to 14 per cent chromium-steel plate, $^3/_4$ in. thick. The clearance between the ends of the guide vanes and the stationary plates was about 0.015 in. top and bottom. It was very gratifying, after 7 months' operation of the Hiwassee turbine, to note the bright clean surfaces of these chromium-steel facing plates as contrasted to the usual rust-pitted surface where the ordinary plate steel is used.

TABLE 4 COMPARISON OF SCROLL-CASE FEATURES

	Norris	Hiwassee
Casing design pressure - lb/sq in	125	140
Steel used - ASTM	A89-33, Grade B Flange, low tensile carbon steel	A149-36, Grade A Firebox quality silicon steel
Ultimate strength - lb/sq in	50,000	65-77,000
ASTM designation - Rivets	Boiler rivet steel, A31-24	Structural rivet steel, A141-39
Ultimate strength - lb/sq in	45-55,000	52-62,000
Allowable stress in spiral casing - lb	12,000	14,000

Both the stationary and rotating clearances adjacent to the runner are protected with steel wearing rings, the stationary rings being of hard silicon steel, those on the runner being of mild steel.

When the Norris turbines were purchased, it was felt that a more accurate alignment of the runner clearances could be obtained by grinding the stationary wearing rings in the head cover and curb ring after the spiral casing and speed ring were embedded in the concrete. For this purpose a special grinding ring was supplied with the turbines, and, after the concrete had set and most of the heat had been dissipated, these clearances were very accurately ground out.

The design clearance between the runner crown and the head cover is 0.040 in. radially and 0.060 in. at the runner band. At Norris this grinding was completed about February 1, 1936, before any water had been impounded in Norris Lake. Filling of the reservoir started early in March. Early in June it was found that these runner clearances had shifted materially, the tight side being upstream. With no contraction joint between the power station and dam, the water load against the dam caused a slight tilting of the powerhouse and a deformation of the substructure, which forced the stationary parts of the turbine slightly out of round. While it would have been possible to remove the internal parts of the turbine and regrind the clearances, this was not considered necessary. A slight realignment of the bearings was made and the unit put into operation, with satisfactory results. The minimum runner clearances after readjusting the bearings was about 0.025 inch.

In view of the building settlement and resulting distortion of

the stationary rings at Norris, the grinding device was not used at Hiwassee, but the parts were all machined to final dimensions in the shop. However, the proper contraction joint between the dam and powerhouse was provided at Hiwassee, and no appreciable distortion occurred in the Hiwassee turbine parts due to deflection from the water load on the dam.

The Norris penstocks are 20 ft in diam and have field-welded circumferential joints. The Hiwassee penstocks are only 18 ft in diam and have riveted joints throughout. The smaller size of the Hiwassee penstocks is justified because of the lower capacity factor at which the Hiwassee plant will operate after the second unit has been installed. Furthermore, as additional storage is provided, the period over which that storage must be utilized becomes longer, resulting in yet lower capacity factor even during the period of drawdown. The total entrance loss, penstock friction loss, and rack loss at Norris for a flow of 4472

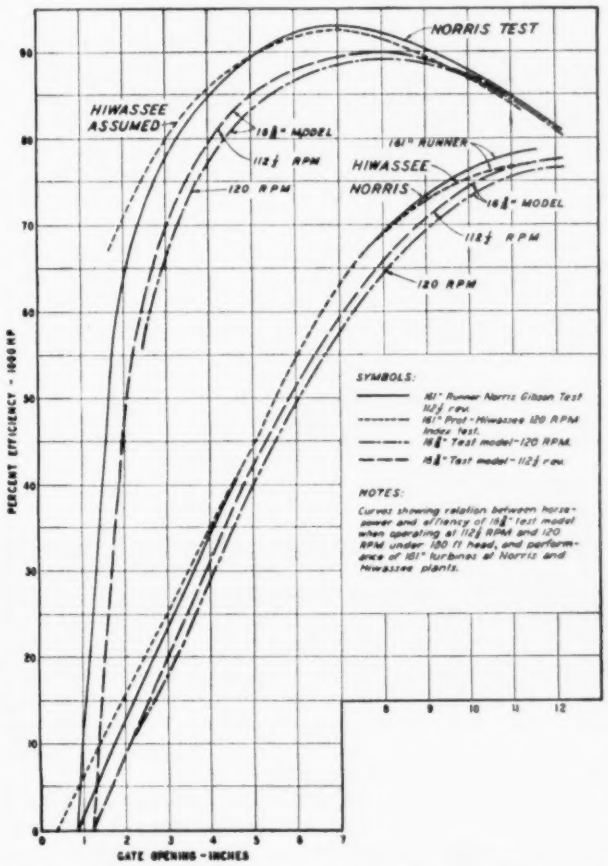


FIG. 8 CURVES SHOWING HORSEPOWER AND EFFICIENCY OF NORRIS AND HIWASSEE TURBINE PLOTTED AGAINST GATE OPENING

cfs was 0.6-ft head. At Hiwassee, the corresponding loss amounted to 1.95-ft head for a flow of 4470 cfs. This difference of 1.35 ft amounts to 0.71 of 1 per cent at full load but reduces to 0.56 ft or 0.3 of 1 per cent head at best efficiency load.

The stress-relieving system used for the field-welded circumferential joints in the Norris penstocks consisted of electric heaters, the heat being applied to the area about 10 in. on either side of the weld. While this procedure removed all stresses from the neighborhood of the weld, it apparently set up rather severe strains at the edge of the heated section. As a result, field stress relieving was discontinued, but a thorough peening of the weld metal was employed, after laying in each bead, and a satisfactory job was obtained.

EFFICIENCY TESTS ON NORRIS TURBINES

Efficiency tests on the Norris turbines were conducted after installation was completed, using the Gibson method of water measurement, which is based upon the equation of impulse and momentum. The differential system was used wherein the instantaneous difference between changes in pressure between two fixed cross sections in the conduit was recorded. The cross sections with four piezometer taps at each section were 91 ft 10 in. apart in the straight part of the 20-ft-diam penstocks.

TABLE 5 TURBINE-EFFICIENCY TESTS: NORRIS PROJECT

	Guaranteed Performance	Test Results Unit 1	Unit 2
Performance at 60,000 hp efficiency - percent	91.0	93.1	93.3
Maximum efficiency - percent	91.0	93.2	93.3
Hp at maximum efficiency	60,000	62,000	60,000
Maximum output - hp	75,200	78,300	78,300
Efficiency at 75,200 hp - percent	86.0	88.9	89.9
Efficiency at maximum output - percent		84.1	84.0
Discharge - cfs, maximum	4275	4560	4562
Generator efficiency - percent			
100 percent p.f. - 56,000 kva	97.75	98.25	98.25
90 percent p.f. - 56,000 kva	97.3	97.97	97.97

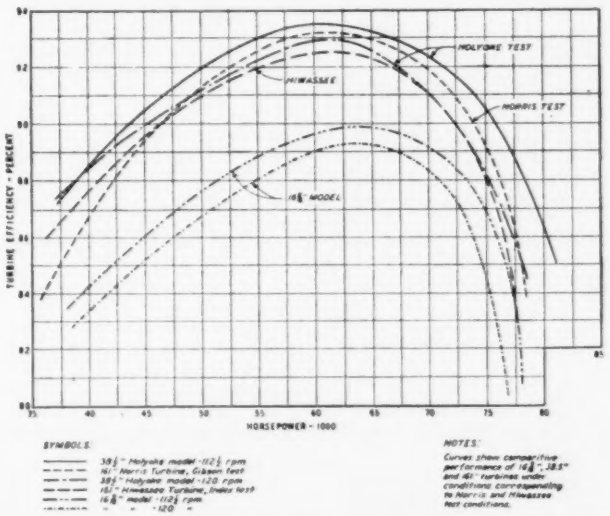


FIG. 9 EFFICIENCY CURVES OF NORRIS AND HIWASSEE TURBINES PLOTTED AGAINST HORSEPOWER

The head measurement was obtained from float-operated headwater and tailwater gages located in stilling wells near the intake gates and the tailrace. The corrections for rack loss and penstock friction were obtained by differential manometers connected to piezometers located just downstream of the trashracks and at the entrance to the turbine scroll case.

The power output of the generator was measured by two sets of calibrated wattmeters connected to the generator terminals. Since the generators had been tested for efficiency, the turbine output could be obtained by dividing the generator output by the known generator efficiency. These tests were conducted in accordance with the A.S.M.E. 1926 Power Test Code.

The results of the efficiency tests on the Norris turbines are shown in Table 5 and in Figs. 8 and 9, the performance of the two units being so nearly alike that the difference is not perceptible. These data are for 180 ft net head.

Fig. 8 shows a comparison between the performance of a 16$^{3}/_{16}$-in-diam model runner tested at the laboratory of the Newport News Shipbuilding and Drydock Company and the 161-in-diam Norris turbine. Horsepower at 180 ft head and efficiency are plotted against inches of opening of the wicket gates. While the horsepower output at any given gate opening shows an increase

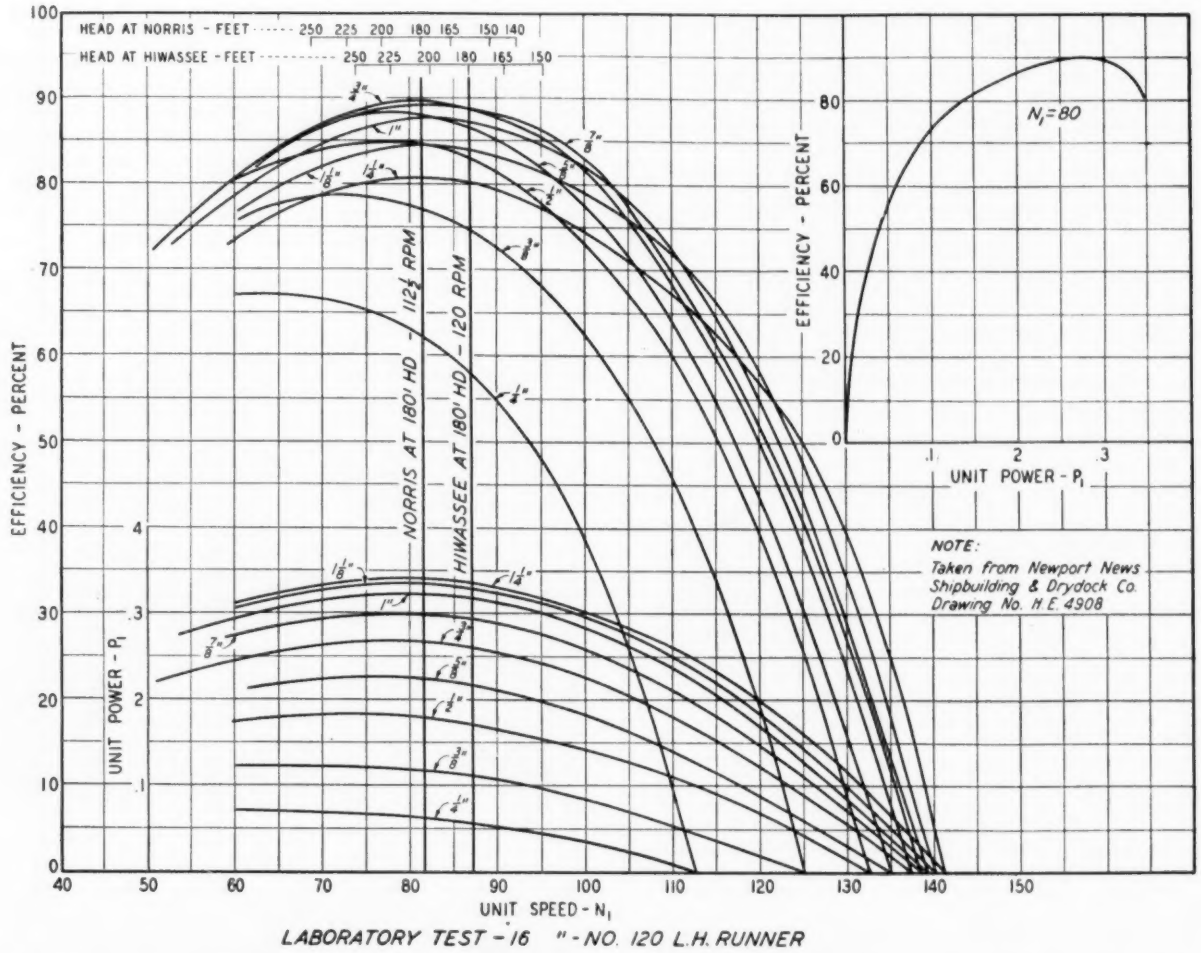


FIG. 10 TEST OF 16⁹/₁₆-IN-DIAM RUNNER AT THE LABORATORY OF THE NEWPORT NEWS SHIPBUILDING AND DRY DOCK COMPANY

of approximately 5 per cent when comparing the 161-in. prototype at Norris with the 16⁹/₁₆-in. test model, the maximum output only increased about 1½ per cent, although the 161-in. prototype required less opening of the wicket gates to produce the same output. The laboratory test on the 16⁹/₁₆-in. model runner is shown in Fig. 10.

The 161-in. Norris runner also shows the greatest gain in efficiency at the smaller power outputs. This may be due in part to the effect of the spiral casing, as the 16⁹/₁₆-in. test model was not tested with a spiral casing.

Fig. 9 shows the comparison between the performance of the 16⁹/₁₆-in. model and the 161-in. Norris runner plotted with efficiency against horsepower. On this basis, the increase in efficiency at part load, while appreciable, is less noticeable than when plotted on the other basis. Plotting efficiency against horsepower is the most generally accepted method of comparison. Large turbines in scroll-case settings usually develop their power at a smaller wicket-gate opening, owing probably to the effect of the scroll-case velocity at the entrance to the wicket gates.

Fig. 9 also shows the performance of a 38.5-in. test model at the Holyoke testing flume. This test was made in 1926, on a homologous runner, but with a straight-tapered draft tube and with a different number and type of wicket gates, so that the performances are not exactly comparable. The Holyoke test shows a maximum of 93.6 per cent efficiency, as compared with 93.3 per cent at Norris.

To date no actual efficiency tests have been made on the Hiwassee turbine, although index tests show very closely the performance of that unit. As at Norris, the tests were made with a gross head of between 175 and 185 ft, but since the Hiwassee unit operates at 120 rpm as against a speed of 112½ rpm for the Norris turbines, the results cannot be compared directly, but a reasonable comparison may be obtained by taking the performance of the 16⁹/₁₆-in. model at the different unit speeds, which are approximately 6 per cent apart.

Fig. 8 shows the difference in the horsepower and efficiency of the 16⁹/₁₆-in. model turbine plotted against inches of gate opening at the two different speeds. In all cases, the Hiwassee conditions require greater gate opening for the same horsepower and give about 1.5 per cent less output at full gate. The efficiency curve for the Hiwassee conditions is also about 1 per cent lower for all gate openings. It should be pointed out that, while the Hiwassee turbine is operating at a lower efficiency than the Norris turbine under the particular test condition of 180 ft head, this is not true throughout the full range of operating heads. The Norris turbines were designed for best efficiency under about 185-ft head, and the tests were run at about 97.5 per cent of this head. The Hiwassee turbine operates at best speed under about 212-ft head, and the tests were run at only 85 per cent of this head, hence, the difference in efficiency for the test conditions.

The 161-in. Hiwassee turbine shows the same output for gate openings between 4½ and 7 inches. At full gate it shows about 2 per cent less power, and at small gate openings it shows up to 5 per cent greater output than the Norris turbine, as shown in Fig.

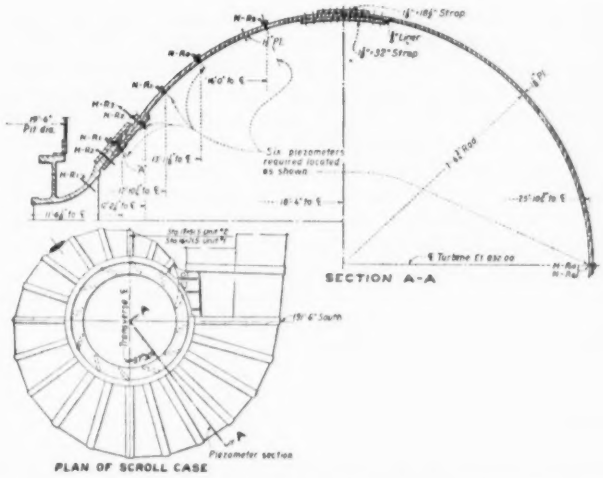


FIG. 11 NORRIS POWER PLANT; PIEZOMETER LOCATION

8. The increased output at the small gate openings is probably accounted for by the fact that during the Hiwassee tests the air valve, admitting air to the space between the runner and head cover and then through the runner into the draft tube, was blocked wide open at all gates. Originally this was operated by a cam which started to open the valve at approximately 40 per cent gate and held it wide open at 30 per cent gate and below. Some preliminary tests indicated that quieter operation and greater output could be obtained with the turbine vented even at considerably larger gate openings.

A study of the horsepower-gate curves of the $16^{9}/_{16}$-in. model and of the Norris and Hiwassee tests indicates that, under the test conditions of 180 ft head, the efficiency of the Hiwassee turbine should be slightly less than the efficiency of the Norris turbines.

All the turbines installed by the Authority are provided with the Winter-Kennedy type of differential pressure piezometers in the scroll case. Fig. 11 shows the arrangement of these piezometers for both the Norris and Hiwassee turbines. During the Gibson tests on the Norris turbines readings were taken on water columns connected to each of these piezometers; and after the discharge had been accurately determined, it was possible to obtain an equation for any set of piezometers reading as follows:

$$\text{cfs} = KD^N \text{ where}$$

cfs = discharge of turbine in cubic feet per second

K = constant obtained experimentally

D = head difference in feet of water between piezometer on outside of scroll case, called R_0 in Fig. 11, and one of the piezometers on inside of scroll case, R_1, R_2, R_3, or R_4, Fig. 11.

N = coefficient, usually very close to 0.5, as in venturimeter formula

The equations for two sets of the piezometers at Norris, based on the water measurements by the Gibson method, were as follows:

For unit 1.....	cfs = 1334	$D^{0.509}$ for R_0-R_1
	cfs = 1652	$D^{0.503}$ for R_0-R_3
For unit 2.....	cfs = 1293	$D^{0.509}$ for R_0-R_1
	cfs = 1620	$D^{0.510}$ for R_0-R_3

It will be noted that the coefficient N is very close to the 0.5

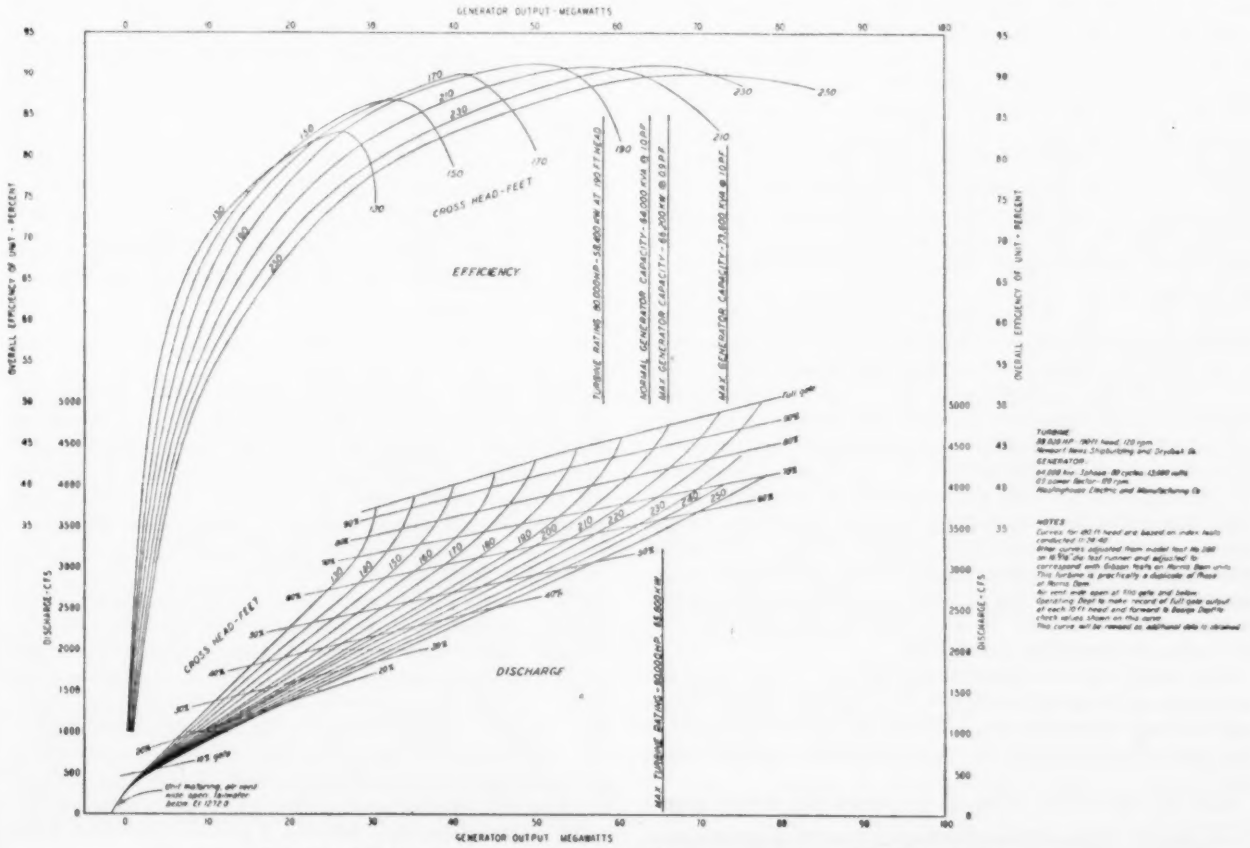


FIG. 12 HIWASSEE PROJECT; OPERATING CHARACTERISTICS OF 64,000-KVA UNIT

power; and, in accordance with the conclusion of J. M. Mousson,[3] the square root may be used without appreciable error.

Where no accurate water measurements are made, it is necessary to arrive at the coefficient K in a different manner, the exponent N being assumed to be 0.5. The generally accepted method is to plot a curve of $hp/D^{1/2}$, this curve having the general shape of the over-all-efficiency curve of the unit. After determination from an inspection of the horsepower-gate curves in Fig. 8, that the maximum turbine efficiency of the Hiwassee turbine under 180 ft head should be about 1 per cent less than at Norris, or about 92.3 per cent, the discharge for the maximum efficiency can be computed and from this the coefficient can be derived for the discharge formula. In the case of the Hiwassee turbine, this was computed to be $Q = 1535D^{1/2}$. Calculating the discharge and efficiency for the Hiwassee turbine, we obtain the curve shown in Figs. 8 and 9, which lies slightly above the Norris efficiency curve for part loads but lies below the Norris curve at maximum efficiency and at full load.

The Department of Operations of the Authority uses a curve, such as that shown in Fig. 12, giving over-all efficiency and discharge against kilowatt output for various heads between 130 ft minimum and 250 ft maximum. The curve for 180 ft head is taken directly from the index test, but the other curves are based on the $16^{9}/_{16}$-in. model test adjusted in accordance with the field performance; in this particular case, upon the performance of the Norris turbines at various heads.

[3] "Water Gaging for Low-Head Units of High Capacity," by J. M. Mousson, Trans. A.S.M.E., vol. 57, 1935, pp. 303–316.

Discussion

R. V. Terry.[4] It is seldom that a manufacturer has the opportunity of furnishing large turbines of identical design for two or more power plants. In this case, the three Norris and Hiwassee turbines are practically identical, as mentioned by the authors. A fourth turbine of the same design was furnished for the Flathead plant of the Rocky Mountain Power Company in Montana, rated 77,000 hp, 189 ft head, 112.5 rpm.

Fabrication of the heavy steel-plate casings was a major job, especially the casing for Hiwassee which was made from the higher-tensile-strength material. The casings were built by men originally trained in the construction of Scotch boilers for marine use. A brief outline of the procedure for building a casing of this type is as follows: Each plate, which is of irregular shape, is developed one quarter size in the drawing room. Full-size molds for laying off the plates are then made from offsets, following a procedure generally used in shipbuilding. After laying out, the plates are cut to size and partially drilled ($^{1}/_{16}$ in. undersize) for the fitting-up bolts. The plates are rolled to the correct curvature and the butt straps are knuckled where necessary on a hydraulic press. Adjoining plates are fitted together and the joints ironed out locally as necessary on a hydraulic press. After each plate has been temporarily fitted to its adjacent plate, the complete shop assembly with the speed ring is started, beginning with the large end of the casing. Considerable use is made of heavy jacks, shoring, chain falls, bolting machines, etc.

After all sections of the casing are in place around the speed ring, the joints are laid up by local heating as necessary, and by a liberal use of fitting-up bolts. The rivet holes are then drilled to size. The general alignment of the casing is checked several times during the assembly processes, but the final center lines are not established until the shop assembly has been completed. After the assembly is dismantled, the speed ring is finally machined and drilled for its several other connecting members, using the center lines established from the assembly. In this way, a correct field assembly is assured. Each of the drilled rivet holes serves as a dowel hole so that no difficulty is experienced in relocating the plates in the field assembly exactly as they were in the shop. No rivets are driven until all parts of the casing are assembled and aligned.

The special cast-steel piece at the junction of the small and large ends of the casing resulted in some simplification in design and economy in construction. This part was actually made in two pieces, one at the top and one at the bottom, joined by steel plates.

Some of the $1^{1}/_{4}$-in. rivets at the speed-ring flanges passed through four thicknesses of material and had a grip length of 5 in. The rivets were driven with 90-lb hand guns, using dies with a special shaped shank to prevent breakage. Standard rivet sets with straight shanks were found to be unsuitable for this service. It was also found from experience in driving the rivets that the longer rivets had to be made longer, by amounts up to $^{1}/_{8}$ in., than the lengths determined by conventional methods.

The main-shaft stuffing boxes, which were about 40 in. diam, were packed with six rings of $1^{1}/_{4}$-in-square braided asbestos packing, lubricated with graphite. A lantern ring for the admission of cooling water was placed at the middle of the box. No grease is used in the boxes as previous experience with similar large units demonstrated that better service was secured by omitting all lubricants other than the graphite and water. When grease was used, the packing rotated and tended to jam and cause excessive heating.

The main-bearing oil sump is located in the crown plate where it is cooled by the adjacent water. No cooling coils were found necessary. The maximum temperatures were found to be about 130 F.

Some of the more important weights of each turbine were approximately as follows:

Runner	45 Tons
Turbine shaft	25 Tons
Speed ring	65 Tons
Crown plate	30 Tons
Spiral casing	225 Tons

The total weight of one complete turbine, exclusive of governor equipment, was about 450 tons.

The Holyoke model tests were made in 1926. The 93.6 per cent efficiency obtained on these tests is on a par with the best efficiencies ever obtained in that testing flume. However, while comparative, the Holyoke results must be discounted somewhat and cannot be stepped up in the customary way as is done with the more accurate results secured in modern hydraulic laboratories. It is often considered fortunate if the Holyoke efficiencies are equaled by the field results.

The laboratory model really should have included a model of the spiral casing. A riveted casing of the Norris and Hiwassee types probably results in relatively higher frictional losses near full load, which prevents full realization of the maximum power output that might otherwise be obtained. This is borne out by the comparative results shown in the authors' Fig. 8, where it is seen that very little gain in power or efficiency at the higher gate openings was obtained in the field, as compared with the model results. If the model had included a duplication of the casing construction, it is believed a greater differential would have been noted near full load.

[4] Hydraulic Engineer, Newport News Shipbuilding and Drydock Company, Newport News, Va. Mem. A.S.M.E.

The medium specific speed employed with these turbines results in a very satisfactory power-efficiency curve that is quite flat, and approaches the shape of curve that can be realized with the newer adjustable-blade type turbines suitable for the lower heads up to about 80 ft.

R. E. B. SHARP.[5] The Norris and Hiwassee casings were, presumably, completely riveted in the field, with the sections nested into each other for compactness during shipment. The external girth butt straps, it is noted, were located at the section joints and were, therefore, crimped to suit the angles between the sections.

As a contrast to this design are shown Figs. 13 and 14 of this discussion, a shop view of a welded-plate steel casing for one of the I. P. Morris turbines for the Lower Colorado River Authority, for installation in the Marshall Ford Plant near Austin, Texas. The turbines are rated at 27,000 hp under a head of 120 ft, with a maximum head of 216 ft. The casings were fabricated in the Baldwin Locomotive Works at Eddystone, Pa. The diameter at intake to the casing is 172 in., with a maximum plate thickness of $1^{9}/_{16}$ in. This thickness exists in the vicinity of the intake near the speed ring, while that at the intake around the periphery is only 1 in. The difference is due to considering the casing as a torus with the greatest radial loads near the center.

[5] Chief Engineer, I. P. Morris Department, Baldwin Locomotive Works, Philadelphia, Pa. Mem. A.S.M.E.



FIG. 13 WELDED-PLATE: TURBINE CASING

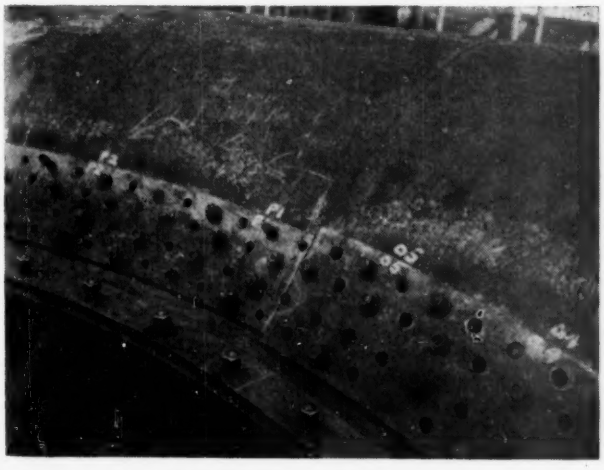


FIG. 14 DETAIL OF FIG. 13

As will be noted from Fig. 13, there are six joints for field riveting. These are located between sections and, therefore, no crimping was required of the butt straps.

All welds were radiographed, and were chipped out and rewelded where the films showed more defects than permitted by A.S.M.E. Class 1 weld. The sections were then stress-relieved, and finally fitted to the speed ring and to each other.

With a given allowable stress, this construction permits the use of thinner plate than does riveting, due to the superior efficiency of the butt-weld joint. The plate thickness at the speed ring, however, is determined by the riveted joints at that location. Also smoother flow surface is obtained than with girth-lap joints, which would have been employed otherwise; rivet heads are also avoided.

A different treatment of the terminal section of the casing from that described by the authors is illustrated in Fig. 13, which shows the section to be constructed entirely of plate. The outside wall of the casing is continued past the baffle vane to a welded junction with the intake portion, while a vertical baffle plate inside of the scroll curves inward to meet the cast baffle vane of the stay ring. The hollow space between the baffle plate and the outside wall is filled with grout, which effectively supports the baffle plate and retains its shape.

It is the writer's experience that had the Norris model been tested with a casing, the efficiency and power developed therefrom would have been slightly reduced. This would have had the effect of increasing above 1.5 per cent the relative increase of the prototype power above the model. It is also the writer's experience that the coefficient of flow through the wicket gates of the prototype is greater than for the model, even where a casing is employed in both instances. In making close comparisons of models and prototypes involving gate opening, it should also be borne in mind that the true value of ϕ tends to be lower on the prototype than on the model, due to the higher efficiency of the former.

A further explanation for the slight discrepancies between the model and prototype performances might lie in slight differences in design which result in the model and the large unit not being exactly homologous. It is noted that the power at best efficiency of the prototype is about 2 per cent less than that of the model. If the power-efficiency curve of the large unit is shifted to the right by this amount, the curve becomes very closely parallel with that of the model. Similar consideration would, to some extent at least, account for the convergence of the power-gate curves of the prototype and model.

It is believed that the authors' curve of the Norris test, Fig. 9, is incorrectly low at the smallest values of power, as in this respect it does not appear to check Fig. 8. The Holyoke test curves, while probably too high all along the line, do show the gain in efficiency at maximum and minimum values of power, due to the straight tube.

It is believed that the Hiwassee turbine is suffering a loss in power at the higher gate openings (authors' Fig. 8), due to air admission. The model curves, Fig. 11 of the paper, do not justify this relative decrease in power as compared to Norris. Air admission at full load generally results in some loss of power, but in smoother operation.

AUTHORS' CLOSURE

Mr. Terry calls attention to practical obstacles attending the use of $1^{1}/_{4}$-in. rivets with very long grip. The field erection forces experienced much difficulty in maintaining sufficient heat to insure workability in driving without actually burning the rivet steel.

Mr. Sharp gives an interesting description of the welded-plate-steel casing for the Lower Colorado River Authority. Such pro-

TABLE 6 POWER READINGS WITH AIR VENT CLOSED AND OPEN

Turbine gate opening	Gross head, ft	Air vent	Kw by watthour meter	Kw at 180 ft gross head	Loss power, air valve open	Power loss, per cent
100	181.66	Closed	55861	55200	...	...
90	181.58	Closed	54800	54100	...	...
80	181.63	Closed	52650	52000	...	...
70	181.74	Closed	49200	48500	...	...
60	181.92	Closed	43650	43000	...	...
50	182.47	Closed	35950	35250	...	...
40	182.76	Closed	27330	26750	...	...
60	182.08	Open	43650	42950	50	0.116
50	182.26	Open	35600	34950	300	0.86
40	182.90	Open	27250	26600	150	0.56
40	184.37	Open	27300	26350	400	1.52
50	183.61	Open	35780	34720	530	1.52
60	182.87	Open	43950	42950	50	0.116
70	182.45	Open	49400	48400	100	0.21
80	181.68	Open	52950	52250	—250	—0.48
90	181.56	Open	54600	53900	200	0.37
100	181.39	Open	55650	55000	200	0.36

cedure was unheard of in 1934, when the Norris turbines were ordered; and, even in 1938, when the Hiwassee turbine was awarded, there was no actual experience on welding the scroll case of a turbine of this size. A paper describing in detail the construction of a welded-plate scroll case and of the X-ray and pressure tests would undoubtedly be of great interest and value.

Mr. Sharp is correct regarding the lower part of the Norris test curve in Fig. 9 of the paper. This curve is in error from 50,000 hp down to 35,000 hp and should cross the 86 per cent line at 35,000 hp, which would bring it just above the Hiwassee curve.

Referring to the last paragraph of Mr. Sharp's comment, the authors submit Table 6 of this closure, giving power readings taken at Hiwassee with the air vent closed and open. Omitting the reading at 80 per cent gate, which is probably in error, the tests indicate that, with the air valve open at gates from 60 per cent to 100 per cent, there is a decrease in output of from 50 to 200 kw, or from 0.1 per cent to 0.37 per cent, which is too small to show on the curves of Figs. 8 or 9.

The Separation of Liquid From Vapor, Using Cyclones

By ARTHUR POLLAK[1] AND L. T. WORK,[2] NEW YORK, N. Y.

In this paper, the various types of cyclones are reviewed and the data on their performance are summarized. Experiments with cyclones for separating liquids from vapors are described. The performance data obtained conform to the equation log $[L_e (V/L)^a] = b + cV$; where L_e is the entrainment or liquid remaining in the effluent vapor, V is the vapor velocity, L is the liquid velocity, all in units of pounds per minute per square foot of inlet-duct cross section. Terms a, b, and c are constants associated with the equipment and its mode of operation. The principal source of the entrainment is shown to be the wall creep of liquid in the cyclone, impelled by the radial component of the vapor velocity.

Introduction

THE separation of liquids from vapors is frequently a serious problem in industry. The performance and capacity of boilers, evaporators, gas scrubbers, and distillation units are often limited for a lack of adequate means for removing entrained liquid from vapor streams. Separators operated with such vapor-liquid streams frequently function at comparatively high vapor velocities, and often, large quantities of liquid must be separated. Cyclones are widely used for this work.

The performance of cyclones is governed predominantly by variables of two categories; (*a*) operating variables, relating to the properties and to the states and rates of the solids, liquids, and gases handled, and (*b*) design variables, involving the types, arrangements of parts, and dimensions of cyclones.

The number of operating variables is reduced considerably if interest be limited to the field of greatest practical importance; i.e., the separation of steam from aqueous solutions.

Design variables are affected in some measure by these operating variables. Thus, the velocity and relative amounts of liquid and of vapor influence the design of a cyclone. Very few systematic series of experiments have been published on cyclone design variables, and those only on dust separation. The cyclones most commonly used today are of simple construction, containing few parts. Simple cyclones are, therefore, of considerable practical interest and are the most likely to yield performance data capable of correlations which would be comparatively independent of physical dimensions.

If some relation among the separating efficiency of a specific cyclone, the velocity of the vapor, and the amount of liquid could be established and, perhaps, extended to other cyclones and vapor-liquid streams, an insight into the nature of the entrainment might be gained and some useful generalizations might be achieved.

While some experimental data have been published on the separating efficiency of cyclones on dusts, no data have been discovered on the effectiveness of cyclones for separating liquids from vapors.

Types of Cyclones

In reviewing the many variations in cyclone design, a system of classification appeared to be desirable. Accordingly, cyclones were classified in terms of the relative complexity of the path of an element of the gas or vapor stream. Such a grouping closely parallels the structural variations. With this functional definition in mind, the following classes were identified; examples of the various groups are also being considered:

1 "Simple Cyclones:" In this type the path of the vapor within the cyclone is unimpeded, an element of vapor traveling smoothly from a tangential inlet to a central exit.

(*a*) "Standard cyclones" in which the path of the vapor is vortical, the vapor ascending through a central exit. Under this classification are cyclones in which the vortical path is of large diameter in relation to its length, and those in which the vortical-path diameter is small in relation to its length; this ratio being stated by some to be about 0.2 or less.

(*b*) "Webre cyclones" in which the path of the vapor is vortical, the vapor descending through a central exit.

(*c*) "Spiral cyclones" in which the path of the vapor is spiral, the vapor having no vertical velocity in the cyclone.

2 "Complex Cyclones:" In this type the path of the vapor within the cyclone is guided or modified by means of special features or parts of the following categories:

(*a*) Inlets, (*b*) internal parts, (*c*) vapor outlets, (*d*) liquid and dust outlets.

3 "Compound Cyclones:" In this type the vortical path of the vapor within the cyclone is divided into separate vortical paths.

These various types will be outlined briefly. While such performance data as have been published always refer to the separation of dusts from gases and, therefore, may not be analogous to performance data for vapor-liquid streams, the comparison is of interest.

Simple Standard Cyclones of Large Diameter

A simple standard cyclone of large diameter is illustrated in Fig. 1. Reams (49)[3] has tabulated the dimensions of units varying from 4 to 18 ft diam. The American Blower Corporation (5) lists optimum dimensional relations. Dedrick (21) states that the volume of a cyclone should be from $^1/_{20}$ to $^1/_{30}$ that of air handled per minute.

These cyclones are applied most frequently to the separation of coarse dusts and are also used extensively in air-classifying systems, as steam separators. They also appear to be the preferred device for disengaging steam in discharging wood-pulp digesters. Others (8, 14, 61) consider its application for cleaning dust from gases, whereby the gases are sprayed with liquid and

---

[1] Graduate Student at Columbia University, and Director of Research and Development on By-Products, West Virginia Pulp and Paper Company.

[2] Formerly Associate Professor of Chemical Engineering at Columbia University, now Director of Research and Development, Metal and Thermit Corporation.

Contributed by the Process Industries Division and presented at the Spring Meeting, Atlanta, Ga., March 31–April 3, 1941, of The American Society of Mechanical Engineers.

Note: Statements and opinions advanced in papers are to be understood as individual expressions of their authors and not those of the Society.

[3] Numbers in parentheses refer to the Bibliography at the end of the paper.

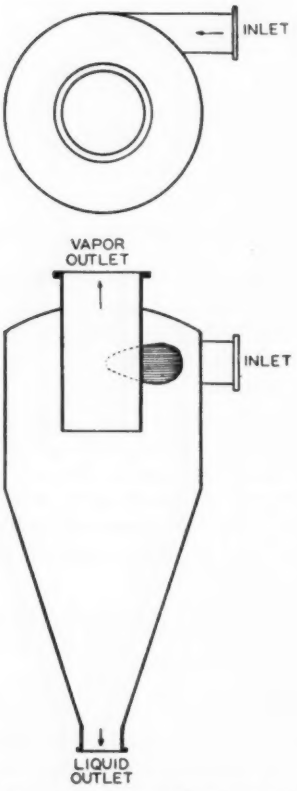


FIG. 1 STANDARD CYCLONE OF LARGE DIAMETER

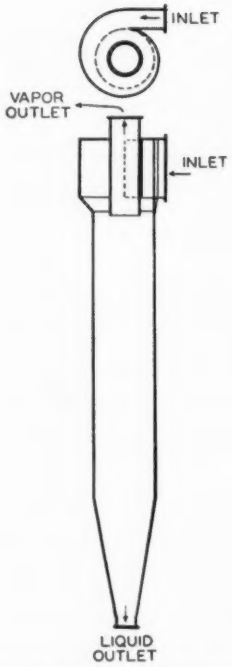


FIG. 2 STANDARD CYCLONE OF SMALL DIAMETER

the entrained, dust-bearing droplets are thus separated. Mauthe (42) proposes wetted-wall cyclones for cleaning gases.

For separating liquids from vapors, Webre (71) states that this type is comparatively unsuited because of the re-entrainment of liquid at the rim of the outlet tube. Alden (2) limits its effectiveness to dusts above 50 μ. According to the American Blower Corporation (6), the lighter the dust, the lower the air velocity should be; the inlet velocity should not exceed 40 fps. Barth (10) found, on an 8-in. model, that efficiency increases with velocity to a maximum and then decreases. Dedrick's data (21) also indicate that an optimum velocity exists. Drijver (22), on the other hand, reports only an increase with velocity. This was confirmed by Whiton (76) who also showed, testing cyclones 1, 2, and 3 ft in diam, that the smallest diameter gave the greatest dust recovery.

The only generalization which can be deduced from the foregoing references is that simple, large-diameter cyclones are not considered so effective as some of the modified types to be discussed.

SIMPLE STANDARD CYCLONES OF SMALL DIAMETER

The realization that high velocities improved the efficiency of dust separation led to the development of long narrow cyclones, typified in Fig. 2. They are dimensioned to attain a specific efficiency, increases in capacity being achieved by increasing the number of units. However, this gives rise to complicated distribution problems which, if not adequately solved, minimize the advantages of these cyclones. This type is applied mainly to dusts below 50 μ. Abrasive dusts cause excessive wear. According to Horne and Lissman (33), their vertical height should be at least 6 times their diameter. Lissman (40) discusses units with tubes as small as 4 in. diam. Horne and Lissman have also considered the application of these cyclones for separating entrained droplets from sprays. Various arrangements of distributing systems have been proposed (18, 33, 34, 35, 45, 46, 66, 67). Recently Freeman (28) has applied this type to the separation of dirt particles from thin slurries of wood pulp.

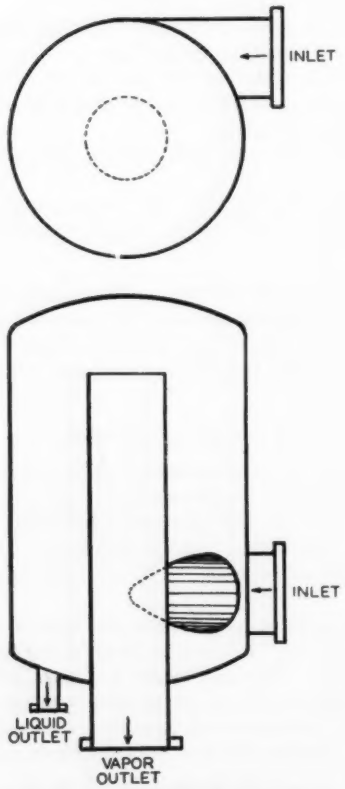


FIG. 3 WEBRE CYCLONE

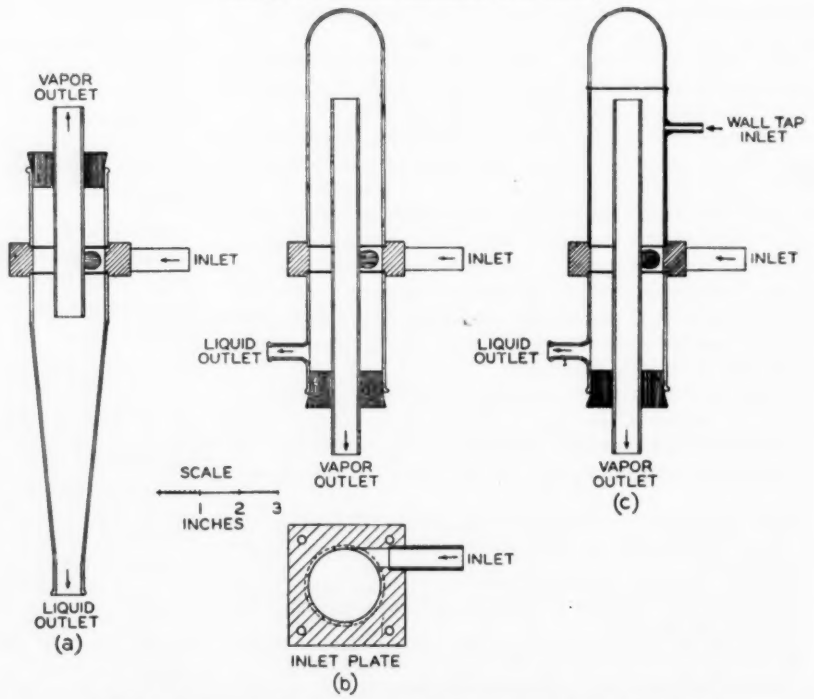


FIG. 4 STANDARD CYCLONE AND TWO TYPES OF WEBRE CYCLONE
(*a* Standard cyclone, glass model, 1.85 in. diam; *b* Webre cyclone, glass model, 1.85 in. diam; *c* Webre cyclone, 1.85 in. diam, fitted for wall injection.)

No data correlating efficiency and velocity have been published. According to Lissman (40), a collection efficiency exceeding 99 per cent is possible, using 4-in. cyclones, with particles averaging 5 μ. Alden (2) writes that such a cyclone handles 70 cfm.

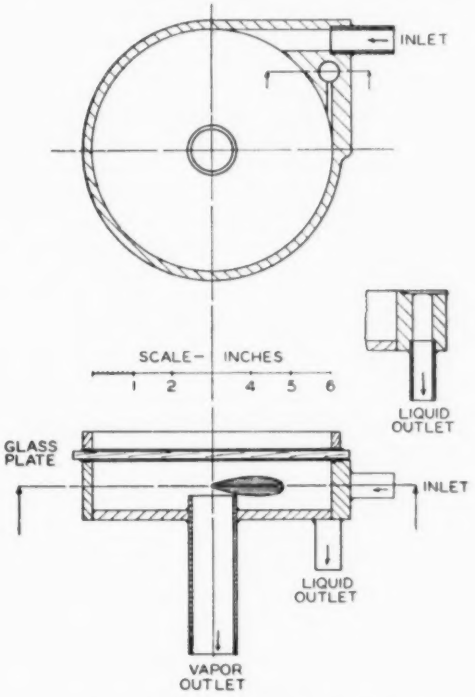


FIG. 5 SPIRAL CYCLONE, 6 IN. DIAM

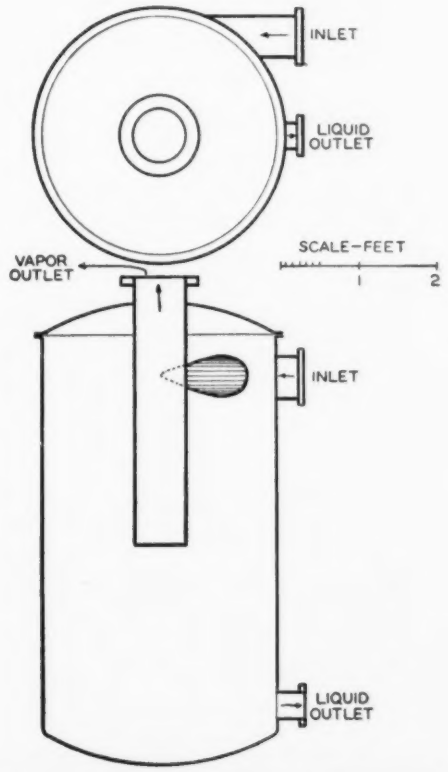


FIG. 6 STANDARD CYCLONE 36 IN. DIAM, USED FOR SEPARATING BLACK LIQUOR FROM STEAM

SIMPLE WEBRE CYCLONES

Webre cyclones are illustrated in Figs. 3 and 4 (*b*). No data have appeared in the literature on the sizes or dimensions, but units are known to be in operation which vary from 9 in. to over 6 ft in. diam. Webre cyclones have been frequently used as entrainment separators on vacuum evaporators and have also proved effective in diameters below 12 in. for separating liquid from vapor in the flash distillation of oils (27). This type of cyclone appears to be merely an inverted standard cyclone, but Webre and Robinson (71) pointed out that, unlike standard cyclones, liquid does not run along the central outlet pipe to be entrained at the rim.

SIMPLE SPIRAL CYCLONES

Spiral cyclones as, for example, that of Fig. 5, are usually considered to have the advantage of inducing an increasing centrifugal force on particles as they move toward the center outlet, thereby impelling them to move outward against the gas stream. Air grinding classifiers, or micronizers, utilize a somewhat similar design. Frequently, to insure a long spiral path, a spiral baffle is installed, whereby the gas is constrained to move in a spiral path of the desired pitch. Such separators will be considered as complex cyclones.

COMPLEX CYCLONES

Many modifications in cyclone design have been proposed to reduce velocity-head losses and to improve efficiencies. While reduced friction losses are comparatively simple to demonstrate, increased efficiency is not so readily ascertained, since variations in particle sizes must be taken into account. Numerous patents and other literature deal with modifications in the four principal structural elements of cyclones as follows:

(*a*) *Inlets.* Various vanes, baffles, or special ports are proposed for obtaining better entrance conditions.

(*b*) *Internal Parts.* Special shapes, baffles, or parts are offered for improving the efficiency of separation.

(*c*) *Vapor Outlets.* Modifications, involving louvers and ports, are devised for aiding the exit of cleaned vapor or gas.

(*d*) *Liquid and Dust Outlets.* Special designs for facilitating the exit of the separated liquid or dust.

Inlets. Alden (2) tabulates dimensional data for cyclones with helical tops used to reduce entrance losses. Capacities from 500 to 40,000 cfm, having diameters from 3 to 14 ft, are given. Deflector plates at the inlet also serve to reduce entrance losses. This has been confirmed by Shepherd and Lapple (54). The use of vanes to initiate the whirling motion is the subject of a number of patents (3, 4, 12, 25, 26, 32, 36, 37, 38, 48, 51, 62, 74). Others (11, 29, 30, 31) prefer louvers for this purpose. Scroll-shaped inlets have also been described (34, 65) Alexander (3, 4) describes a central baffle below the entering zone which forces the fluid material to flow near the wall of the cyclone. Various other inlets have been described (1, 15, 20, 70).

No systematic comparison data have appeared, comparing the efficiencies of any of the wide variety of inlets. Barth (10) demonstrated that a small-diameter inlet gives higher dust recoveries than a large inlet for the same volume of gas handled.

Internal Parts. Barth (10) tested identical cyclones with and without a spiral vane and found the empty cyclone more efficient. Webre (72) considers the spiral-baffled Hughes separator very effective as an entrainment separator in evaporators, but gives no data. The use of spiral vanes is also the subject of patents (11, 24, 44, 67). Drijver (22) tested vanes placed against the shell of a cyclone operated as a dust separator. With the

vanes pitched into the gas stream, he obtained a 35 per cent dust recovery. Pitched so as not to oppose the gas stream, the recovery was 55 per cent. Removed altogether, the recovery rose to 75 per cent. He attributed their detrimental action to re-entrainment. Alden states (2) that reversing vanes below the outlet pipe increased the resistance to a total of 1 to 2 velocity heads but that they also increased the separating efficiency for small particles. A disk or cone, centered below the outlet pipe, is also frequently seen. Other patents on this type of improvement have been granted (12, 15, 18, 20, 25, 41, 44, 51, 55, 56, 64, 66, 67, 68).

Vapor Outlets. Schaak (52) found that straightening vanes below the exit tube reduced the velocity-head losses approximately 50 per cent. Shepherd and Lapple (54) confirm this. No suggestion of its effect on separating efficiency is offered. Patents on the use of straightening vanes have been secured (36, 37, 48). Prockat (47), experimenting with dust, compared a cyclone containing a widely flared exit tube with one having no internal exit tube and found the latter much more efficient.

Many designs show louvers inserted into the exit tube. In the Van Tongeren cyclone (65), the exit tube is replaced by a ring of reversing louvers, whereby the gas reverses its flow. The length of the outlet tube does not appear to be important, according to Barth (10). As might be expected, supports and other obstructions were found to decrease the efficiency of separation.

Liquid and Dust Outlets. A number of improvements over the common hopper-bottom dust outlet have been devised. In some the dust is withdrawn as an annular ring near the wall by using baffles (3, 4, 63, 77). The use of vertical slots for skimming off liquid or dust has also been considered in patents (4, 13, 65, 68, 70), as have series of perforations (64, 66, 67).

Compound Cyclones

Increased efficiency is claimed for the compound cyclone. Re-entrainment, especially of the fine particles near the wall, is minimized by skimming off a layer of gas near the wall and transferring this dust-rich layer to a second cyclone. The Van Tongeren cyclone of this design is claimed to give 80 per cent efficiency with 10 μ particles (16, 65). Stebbins (59) and O'Mara (48) show similar arrangements. According to Alden (2), identical cyclones in series are not worth while.

Factors Influencing the Investigation of Cyclone Performance

When cyclones are used for separating liquids from vapors, the system consists of the following:

1 A vapor-liquid mixture entering the cyclone.

2 A cleaned-vapor effluent, containing a residual portion of unseparated or re-entrained liquid, the entrainment.

3 A liquid effluent, consisting of the separated liquid.

The entrainment is the main criterion of the performance of a cyclone. For a specific cyclone, handling a specific vapor-liquid stream, there should be some relation among the vapor velocity, the amount of liquid, and the particle-size distribution of any liquid in droplet form.

In discussing the action of cyclones, writers (78, 79, 80, 81) have generally reasoned that increasing the velocity increased the effectiveness of separation. However, it is also commonly recognized that a cyclone can be overloaded. Any adverse effect of velocity on the effectiveness of separation has always been tacitly ascribed to secondary effects arising from supposed structural defects in the particular cyclone. In spite of the many varied designs of special inlets, baffles, and outlets, which have been proposed, there appears to be an increasing agreement among experienced designers that baffles and other complicating features are of doubtful effectiveness.

In cyclones applied to the separation of dusts, the particle-size distribution is an important factor in the effectiveness of separation, especially when any considerable portion comprises particles below 50 μ. In separating vapor-liquid mixtures from stills, evaporators, or pressure vessels, the size of droplets is not always so important. In practice, cyclones are known to remove most of the entrained liquid. Consequently, it would seem likely that most of the liquid in such vapor-liquid streams occurs either in bulk or as droplets coarse enough to be separable by centrifugal force. The presence of any considerable amount of liquid in the form of droplets of a few μ diameter is also unlikely, in view of the large amount of energy required for disintegration. This would suggest that the presence of small droplets is not necessarily a dominant factor in the performance of cyclones separating considerable liquid.

Experimental Procedure

To facilitate the correlation of data, all quantities of liquid and vapor are expressed in terms of weight velocities referred to the cross section of the inlet tube as follows:

L_e = pounds of liquid leaving per minute in effluent vapor per square foot of inlet cross section, lb per min per sq ft

V = pounds of vapor entering per minute per square foot of inlet cross section, lb per min per sq ft

L = pounds of liquid entering per minute per square foot of inlet cross section, lb per min per sq ft

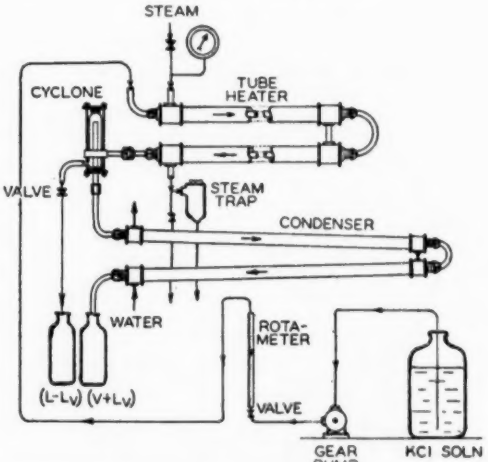


Fig. 7 General Arrangement of Apparatus for Entrainment Tests, Using Heater Tubes

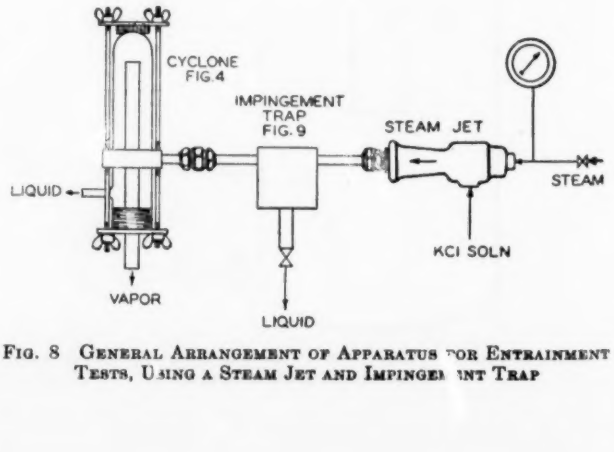


Fig. 8 General Arrangement of Apparatus for Entrainment Tests, Using a Steam Jet and Impingement Trap

Accordingly, the vapor-liquid mixture entering the cyclone is $(V + L)$; the cleaned vapor effluent containing residual liquid is $(V + L_v)$; the liquid effluent is $(L - L_v)$.

The entrainment in cyclones could be defined in a number of ways. Thus, viewed as an impurity in the vapor, the entrainment may be considered to be the ratio of (L_v/V) or, viewed as a loss of liquid, it may be (L_v/L). For the purpose of this research, the entrainment is defined as L_v, the pounds of liquid leaving per minute with the effluent vapor per square foot of inlet cross section.

The operating and design variables of various cyclones were investigated in 15 series of experiments. The cyclones used are illustrated in Figs. 4, 5, and 6. A jacketed-tube heater, Fig. 7, whereby water or dilute potassium-chloride solution could be partially vaporized, was used for generating continuous streams of steam-water mixtures. Fig. 8 illustrates the application of steam jets to supply such mixtures.

The condensed vapor effluent $(V + L_v)$ and the separated

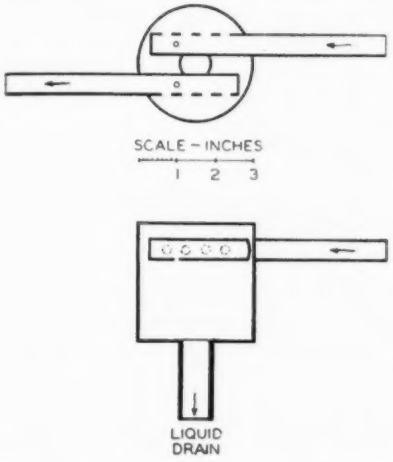


FIG. 9 IMPINGEMENT TRAP INSERTED IN VAPOR-LIQUID LINE BEFORE THE CYCLONE

liquid effluent $(L - L_v)$ were collected for one or more minutes and measured in suitable graduated cylinders. Both effluents were analyzed for chloride ion by titrating an aliquot with approximately 0.1 molar silver-nitrate solution, using sodium chromate as an indicator. Where the vapor effluent was too dilute to secure distinct end points, or the titer was too small, the potassium-chloride concentration was estimated by means of a Leeds and Northrup portable electrolytic resistance indicator and dip-type conductivity cells. Calibration curves for the two cells used were made from measurements using various dilutions of 0.1 molar potassium-chloride solution. Temperature corrections were made by cooling or warming samples to 25 ± 5 C and then noting the temperature to 0.5 deg, when reading the resistance meter. All resistances were converted to a 25 C basis by correcting readings 2 per cent per deg deviation. Wherever the concentrations permitted, the conductivity method was checked by the titration method. The results invariably checked within several per cent.

At the operating rates encountered in these experiments, errors due to vapor condensation in the cyclone or liquid flashing at the cyclone inlet could safely be ignored, so that the separated liquid, $(L - L_v)$, and the entrained liquid, L_v, were considered identical in potassium-chloride concentration. Since the potassium-chloride concentration in $(L - L_v)$ and in $(V + L_v)$ was determined, L_v could be computed.

The experiments are ordered chronologically, the upper-case letters referring to a specific arrangement of equipment and the numbers to individual experiments in which V or L was varied.

Some data were collected on the pressure drops in the cyclones but omitted from this paper since it did not appear to be pertinent. Efforts were also made to gage the velocity head at various points within the 1.85-inch Webre cyclone by inserting shaped copper capillary tubes but this cyclone was so small that excessive refinements in such a technique appeared necessary for consistent readings.

ENTRAINMENT CORRELATIONS IN 1.85-IN. WEBRE CYCLONE

Using the 1.85-in. Webre cyclone of Fig. 4 (*b*) and the jacketed-tube vapor generator, shown in Fig. 7, a very definite relation among the entrainment L_v, the vapor velocity V, and the liquid velocity L was found. The simplest correlation appears to be

$$L_v\left(\frac{V}{L}\right)^2 = c_1 V + b_1 \quad [1] \quad \text{or} \quad \text{Log}\left[L_v\left(\frac{V}{L}\right)^2\right] = b_2 + c_2 V \quad [2]$$

where a, b, and c are constants.

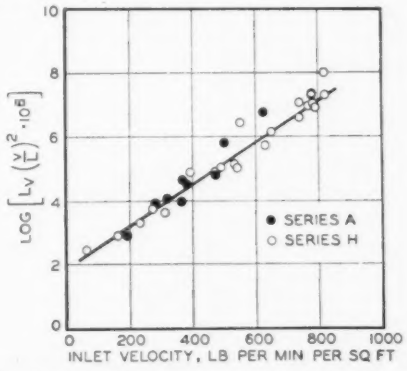


FIG. 10 ENTRAINMENT RELATION IN A 1.85-IN. WEBRE CYCLONE (Series A using 24-in. heater tubes; series H using 48-in. heater tubes, arranged as in Fig. 7. Data from Table 1.)

The results of 31 experiments in two series, covering wide variations in L and V, are summarized in Table 1 and the functional relation of L_v, V, and L is illustrated in Fig. 10. For the experiments of series A, two 24-in. heater tubes, 0.58 in. inside diam were used. In series H these were replaced with two 48-in.

TABLE 1 ENTRAINMENT CORRELATIONS IN A 1.85-IN. WEBRE CYCLONE

Experiment no.	Vapor velocity, lb per min per sq ft V	Liquid velocity, lb per min per sq ft L	Entrainment, lb per min per sq ft L_v	Entrainment function, $\log\left[L_v\left(\frac{V}{L}\right)^2 \times 10^8\right]$	Remarks
A- 1	620	960	13.0	6.73	KCl solution metered into two 24-in. heater tubes
A- 2	360	1310	0.13	3.98	
A- 3	500	1100	2.9	5.80	
A- 4	370	1280	0.53	4.66	
A- 5	380	1260	0.37	4.53	
A- 6	280	1360	0.18	3.90	
A- 7	320	1330	0.19	4.04	
A- 8	190	1560	0.052	2.86	
A- 9	470	1110	0.36	4.80	
H- 1	390	780	0.331	4.91	KCl solution metered into two 48-in. heater tubes filled with jack chain
H- 2	530	610	0.19	5.16	
H- 3	790	140	0.28	6.96	
H- 4	740	570	8.4	7.16	
H- 5	780	270	3.01	7.41	
H- 6	820	230	9.2	8.07	
H- 7	780	440	7.3	7.36	
H- 8	550	900	8.8	6.51	
H- 9	820	110	0.42	7.35	
H-10	630	1370	2.78	5.76	
H-11	650	1310	6.2	6.19	
H-12	540	2410	2.26	5.06	
H-13	770	130	0.31	7.03	
H-14	470	2840	2.9	4.89	
H-15	780	90	0.158	7.08	
H-16	310	430	0.008	3.64	
H-17	270	750	0.044	3.74	
H-18	490	530	0.139	5.08	
H-19	230	830	0.028	3.32	
H-20	160	870	0.00024	2.89	
H-21	740	150	0.173	6.63	
H-22	60	540	0.0254	2.47	

tubes of the same diameter but filled with brass jack chain to insure intimate mixture.

Entrainment Correlations in a 36-In. Standard Cyclone

A standard cyclone 36 in. diam, Fig. 6, was tested at the Tyrone, Pa., mill of the West Virginia Pulp and Paper Company, where it served to separate black liquor from steam. This cyclone was so installed that, while the effluent vapor ($V + L_v$) could be sampled and measured by means of a pitot tube in the piping from the cyclone to a condenser, the effluent-separated-liquid piping was accessible only for sampling the liquid ($L - L_v$).

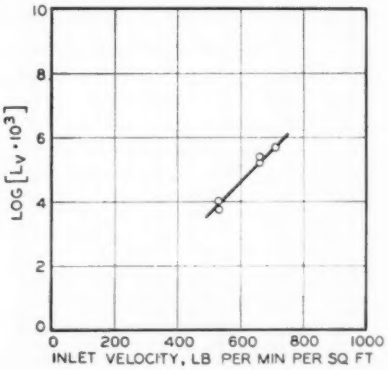


Fig. 11 Entrainment Relation in a 36-In. Standard Cyclone, Separating Black Liquor From Steam
(Data from Table 2.)

However, it was known that the ratio V/L was nearly constant, so that a simplified form of Equation [2] should apply, namely

$$\text{Log } L_v = b_3 + c_3 V \quad \ldots\ldots\ldots\ldots\ldots\ldots [3]$$

The data of Table 2 and the corresponding Fig. 11, would indicate such a relation. While this does not demonstrate that, if the ratio V/L had varied, Equation [2] would have applied, nevertheless, it serves to show that the entrainment increases with the inlet-weight velocity V in this cyclone also.

TABLE 2 ENTRAINMENT OF BLACK LIQUOR IN A 36-IN. STANDARD CYCLONE

Experiment no.	Vapor velocity, lb per min per sq ft V	Entrainment, lb per min per sq ft L_v	Entrainment function log $[L_v \times 10^3]$
P-1	530	6	3.78
P-2	530	11	4.04
P-3	660	260	5.41
P-4	660	170	5.23
P-5	710	530	5.72

The Influence of Droplet Size on Entrainment

To increase the proportion of liquid entering the cyclone in droplet form as compared to liquid of greater bulk, an impingement trap Fig. 9 was inserted in the vapor-liquid line before the cyclone. Most of the liquid present as large drops or in bulk was thus drained from the bottom of the trap. In some of the experiments, the tube heaters were replaced by two sizes of steam-jet injectors, Fig. 8.

The results of the four series of experiments so made are summarized in Table 3 and illustrated in Fig. 12. It will be seen that in all cases the entrainment function, Equation [2], furnished a definite correlation which may be compared with the results of series A and H in Fig. 10. The constants b and c, corresponding to the intercept and slope of the lines of Fig. 12, are thus seen to be influenced by the nature of the liquid, presumably by the particle-size distribution of the liquid in the liquid-vapor stream.

TABLE 3 INFLUENCE OF DROPLET SIZE ON ENTRAINMENT

Experiment no.	Vapor velocity, lb per min per sq ft V	Liquid velocity, lb per min per sq ft L	Entrainment, lb per min per sq ft L_v	Entrainment function log $\left[L_v \left(\frac{V}{L}\right)^2 \times 10^3\right]$	Steam-jet size, in.	Steam-jet pressure psi gage
D2a	530	21	1.09	8.82	3/8	43
b	230	34	0.65	7.49	3/8	43
D3a	550	29	1.02	8.57	3/8	42
b	240	32	0.63	7.56	3/8	42
E1a	700	89	0.15	6.97	3/4	11
b	470	121	0.094	6.16	3/4	11
E2a	790	118	0.26	7.06	3/4	13
b	380	126	0.18	6.21	3/4	13
E3a	870	134	0.40	7.24	3/4	17
b	550	173	0.21	6.34	3/4	17
F1a	520	31	0.92	8.41	3/8	43
b	240	25	0.58	7.75	3/8	43
F2a	130	7.8	3.0	8.92	3/8	20
b	210	9.2	4.6	9.37	3/8	20
c	290	14	8.6	9.59	3/8	20
F3a	510	22	0.91	8.70	3/8	40
b	420	25	0.76	8.34	3/8	40
c	220	21	0.66	7.89	3/8	40
F4a	290	8.0	4.1	9.73	3/8	20
b	120	8.1	3.8	8.97	3/8	20
G2a	640	155	0.28	6.69	two 48-in. tube heaters	
b	310	109	0.150	6.18		
G3a	720	200	0.45	6.76		
b	360	135	0.16	6.07		
G4a	710	260	0.44	6.53		
b	380	160	0.155	5.93		
G5a	830	140	0.32	7.08		
b	360	100	0.135	6.22		

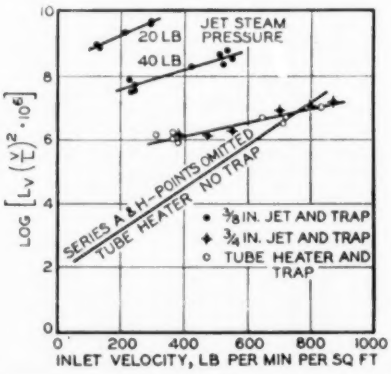


Fig. 12 Influence of Droplet Size on Entrainment, Using Webre Cyclone
(Data from Table 3.)

Thus, the small steam jet displaces the function to the greatest degree.

Design Variables in 1.85-In. Cyclones

Comparison of Webre and Standard Cyclones. A series of comparison tests was made, changing from Webre to standard cyclone by changing the glass parts of Fig. 4 (*b*) to those of Fig. 4 (*a*). The metal inlet plate was remachined to furnish a 0.25-in. tangential inlet in place of the 0.50-in. inlet used in previous experiments. Otherwise, the arrangement of apparatus was that of Fig. 7, no trap being used. The results are recorded in Table 4 and shown in Fig. 13.

The difference in operation between the cyclones was quite noticeable. Where, in the Webre cyclone, the outer wall of the exit tube remained dry and liquid spread over the shell only, in the standard cyclone, considerable liquid ran down the outer wall of the exit tube to be entrained in the vapor. Varying the height of the shell above the inlet plate from 0 to 2 in. did not appear to decrease the movement of liquid onto the exit-tube wall. These results confirm Webre's contention that a central exit tube in the top end of a cyclone aids entrainment.

Inlet Sizes of Webre Cyclone. The effect of varying the inlet size from 0.50 to 0.25 in. diam may be noted by comparing, in Fig. 13, the data of series L for a 0.25-in. inlet, with the earlier series H, where a 0.50-in. inlet was used. Increasing the inlet velocity displaced the entrainment function, Equation [2].

TABLE 4 DESIGN VARIABLES IN 1.85-IN. CYCLONES

Experiment no.	Vapor velocity, lb per min per sq ft V	Liquid velocity, lb per min per sq ft L	Entrainment, lb per min per sq ft L_v	Entrainment function $\log\left[L_v\left(\frac{L}{V}\right)^3\times 10^6\right]$	Cyclone
L-1	1320	8500	102	6.39	Webre, 0.25-in. inlet
L-2	1510	2040	102	7.75	
L-3	740	3160	0.17	4.00	
N-1	2030	1950	295	8.50	Standard, 0.25-in. inlet
N-2	380	1340	460	7.57	
N-3	940	1490	325	8.11	
M-1	1120	1840	0.74	5.43	Webre, 0.25-in. inlet

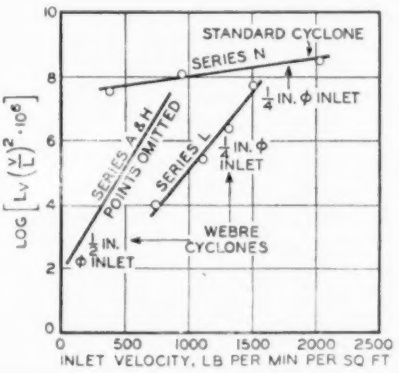


FIG. 13 EFFECT OF DESIGN VARIABLES ON ENTRAINMENT RELATION, USING 1.85-IN. CYCLONES
(Data from Table 4.)

THE CYCLONE AS THE SOURCE OF ENTRAINMENT

The entrainment relation expressed by Equation [2] has survived experiments involving wide variations in V and L and also some design variations. If then this function holds so generally, it would seem likely that it would be due to actions within the cyclone rather than to the states and rates of the vapor-liquid stream.

To investigate this consideration, a tap was machined, Fig. 4 (*c*), into the side wall of the 1.85-in. Webre cyclone, whereby a small stream of potassium-chloride solution could be pumped into the cyclone. By feeding tap water into the two 48-in. vaporizing tubes, all liquid entering the cyclone from the vaporizer was, within the limits of the authors' precision, free of chloride ion. Consequently, entrainment due to droplets of liquid formed outside the cyclone and contained in the inlet stream would not be detected by analyses of samples of the effluent vapor. On the other hand, liquid on the wall of the cyclone, being mixed with the potassium-chloride solution pumped in at the wall tap, would, if entrained, be measured by a corresponding amount of chloride ion in the effluent vapor ($V + Lv$).

The results of these experiments, series I, are listed in Table 5. In Fig. 14 the entrainment relation is compared with that for series A and H. It will be seen that curve I is somewhat displaced. This and the points off the curve were judged to be due to the incomplete mixing of the water on the wall with the potassium-chloride solution fed.

A confirmatory series of experiments was therefore made, using the same apparatus except that the 0.50-in. inlet was replaced by a 0.25-in. inlet. This smaller inlet resulted in higher inlet velocities and, therefore, better mixing of the wall liquids. The results of series L, already listed in Table 4, were found, as noted, to be similar to those of series A and H, potassium chloride being fed through the heater tubes. In another experiment M-1, the procedure of feeding potassium-chloride solution through the cyclone-wall tap was followed. Fig. 15 shows how this result conforms to those of series L. It would appear that the entrainment is due to actions within the cyclone in addition to the properties of V and L.

TABLE 5 ENTRAINMENT FROM LIQUID ON CYCLONE WALL

Experiment no.	Vapor velocity, lb per min per sq ft V	Liquid velocity, lb per min per sq ft L	Entrainment, lb per min per sq ft L_v	Entrainment function $\log\left[L_v\left(\frac{V}{L}\right)^3\times 10^6\right]$
I-1	720	250	5.7	7.69
I-2	740	250	2.7	7.38
I-3	720	250	2.1	7.24
I-4	710	250	2.4	7.20
I-5	550	1460	14.5	6.32
I-6	570	1410	17.8	6.47
I-7	560	1390	31.5	6.71
I-8	360	2970	56.5	5.91
I-9	270	3900	0.29	3.13

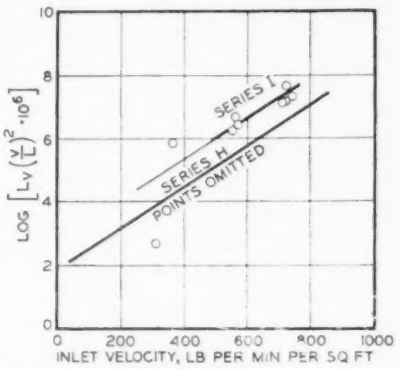


FIG. 14 ENTRAINMENT FROM LIQUID ON CYCLONE WALL; ENTRAINMENT RELATION USING 0.50-IN. INLET
(Data from Table 5.)

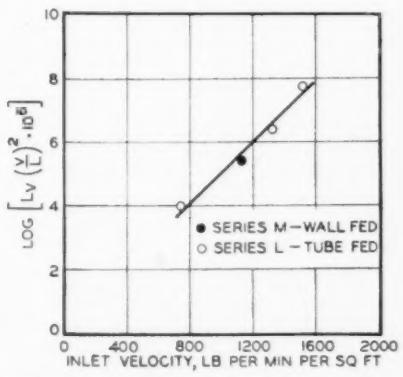


FIG. 15 ENTRAINMENT FROM LIQUID ON CYCLONE WALL; ENTRAINMENT RELATION USING 0.25-IN. INLET
(Data from Table 4.)

THE WALL CREEP OF LIQUID AS A SOURCE OF ENTRAINMENT

In all the cyclones which were tested by the authors, the entrainment is an increasing function of the vapor velocity. This function persists even when the entrainment due to droplets of L is discounted, as in series I and M, or when the proportion of L in droplet form is increased as in series D to G.

If the entrainment is to be attributed to some action occurring within the cyclone, then some explanation or description of the mechanism for this action is needed. Most of the liquid entering flows onto the wall of the cyclone, forming a turbulent, continuous layer which can be seen to move in the direction of the vapor with which it is in contact. It is obvious that the vapor entering a cyclone pursues a spiral or vortical path to a central outlet. Using standard cyclones Shepherd and Lapple (54) and others have shown that the flow consists of an outer downward vortex and an inner upward vortex. Secondary actions have also been

reported, notably by Van Tongeren (65) and Wellman (73). The former states, without giving data, the existence of a so-called double eddy current of gas which serves to transport dust inward at the extremities of a cyclone. Shepherd and Lapple were unable to detect the presence of such a current, nor did observations made during the authors' experiments suggest the action of such a current.

Perhaps a simpler explanation for entrainment actions within a cyclone is conceivable, at least in the separation of liquid from vapor. If, as most writers indicate, and as has been observed invariably in these experiments, the vapor entering a cyclone pursues some form of spiral or vortex, then the vapor velocity must at all places have a component radially inward. Liquid on the walls must then be induced to creep along surfaces toward the center exit.

TABLE 6 ENTRAINMENT CORRELATIONS IN A 6-IN. SPIRAL CYCLONE

Experiment no. (series O)	Vapor velocity, lb per min per sq ft V	Liquid velocity, lb per min per sq ft L	Entrainment, lb per min per sq ft L_v	Entrainment relation log $[L_v \times 10^3]$
1	640	310	68	4.83
2	290	530	105	5.02
3	121	690	0.76	2.88
4	97	650	0.26	2.41
5	153	1320	0.65	2.81
6	360	980	97	4.99
7	640	600	66	4.82
8	650	450	63	4.80
9	610	1280	71	4.85
10	600	1510	71	4.85
11	580	1550	73	4.86
12	510	1300	81	4.91
13	490	1270	81	4.91
14	490	1300	83	4.92
15	370	1390	105	5.02
16	360	1340	107	5.03
17	360	1380	111	5.05
18	121	1640	8.6	3.93
19	108	1700	10.3	4.02
20	162	1410	0.61	2.79
21	270	1130	123	5.09
22	230	1160	134	5.13
23	210	1360	129	5.11
24	210	1330	131	5.12
25	137	1280	0.5	2.68
26	162	1230	0.075	1.87
27	157	1250	0.81	2.91
28	111	1280	6.3	3.80
29	118	1250	7.3	3.86
30	400	3080	123	5.09
31	360	3400	131	5.12
32	190	2970	23.8	4.38
33	200	2970	27.5	4.44

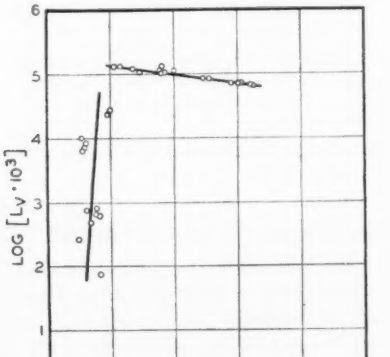


FIG. 16 ENTRAINMENT RELATION IN 6-IN. SPIRAL CYCLONE
(Data from Table 6.)

To enable better visual observations, in addition to the collection of data, a spiral cyclone 6 in. diam was made, fitted with a Pyrex plate-glass top, assembled as illustrated in Fig. 5. This cyclone was operated with the same vaporizing tubes and other equipment shown in Fig. 7, as was used in series H. In addition to the usual measurements for determining L_v, V, and L, the plate-glass top afforded visual evidence of the entrainment action.

The results of 33 experiments are summarized in Table 6. The correlation previously noted, Equation [2], did not hold for this cyclone. The data collected in this series of experiments would make it appear that there is a critical velocity below which L_v increases rapidly with V, and above which L_v decreases slowly with V. Variations in L do not appear to influence the entrainment. The functions appear to be of the form

$$\text{Log } L_v = b_4 + c_4 V \quad \ldots\ldots\ldots\ldots\ldots\ldots [4]$$

These relations are illustrated in Fig. 16. Surprisingly definite patterns of liquid flow were visible on the glass plate when the cyclone was in operation. At vapor velocities below the critical of 200 lb per min per sq ft of inlet section the pattern was unstable. Liquid would tend to remain near the wall of the cyclone. Some of the liquid on the glass plate would tend to move along the glass plate to the center, but reactions would develop periodically whereby centrifugal forces would sling the liquid back in waves. As the vapor velocity was increased toward the critical, liquid began to move toward the center with greater velocity and the beginnings of the much more stable high-velocity pattern could be discerned.

At vapor velocities above the critical, a definite geometric pattern was invariably established. The principal features of this pattern are easy to discern. Most prominent is the smooth, spiral streaming of liquid from the wall of the cyclone to the center. By focusing a camera on the interior surface of the glass cyclone cover plate, it was possible to high-light some of the streaming liquid and to photograph the spiral flow. Such a photograph, reproduced in Fig. 17, was taken with the cyclone operating at an inlet-vapor velocity of 780 lb per min per sq ft. Term L was nearly zero in order to reduce the liquid flow to a few well-defined streams. Two of the curves from opposite sides of the center of the cyclone were calipered from the photograph and the data, corrected for the photographic reduction, caliper $\times 1.29$ = actual size, is given in Table 7. It is of interest to note that these curves are logarithmic spirals

$$r = 2.79^{\theta} \quad \ldots\ldots\ldots\ldots\ldots\ldots [5]$$

where

r = radius vector, in. $\times$ 100
θ = vector angle, in radians

Fig. 18 shows the small deviation between the measured points and the logarithmic spiral of Equation [5].

A second feature of the liquid flow pattern is the presence of an inner spinning ring of liquid. The diameter and thickness of this ring vary inversely with the vapor velocity. This ring becomes unstable when, at low values of V, the diameter of the ring exceeds the inside diameter of the vapor outlet pipe, 1.06 in. As V increases, the ring becomes thinner and decreases in diameter until, at the highest values reached, about V = 800 lb per min per sq ft, the ring reduces to about 0.1 in. diam. At intermediate velocities, when the ring is about 0.5 in. diam, an inner spiral of liquid flowing outward from the center point of the plate and to the inner ring is clearly visible. This inner spiral of liquid rotates in a direction opposite to the large spiral and appears to sling back onto the inner ring any liquid which gets any nearer to the center point of the cyclone than the inner ring.

It appears, therefore, that the spinning ring marks the equilibrium of forces along the glass plate between the drag of the radial component of the vapor velocity and the centrifugal force of the liquid spinning at the center. Liquid can be seen to drop into the vapor outlet pipe from the spinning ring and also from the center of the inner spiral of liquid. These observations are illustrated

TABLE 7 SPIRAL-FLOW DATA CORRECTED FOR PHOTOGRAPHIC REDUCTION OF FIG. 17

Curve A		Curve B	
Degrees from reference axis	Radius, in. × 100	Degrees from reference axis	Radius, in. × 100
0	270	240	135
30	185	270	75
60	120	300	40
90	64	330	29
120	33	360	22
150	22	...	...
180	14	...	...



FIG. 17 WALL CREEP IN SPIRAL CYCLONE

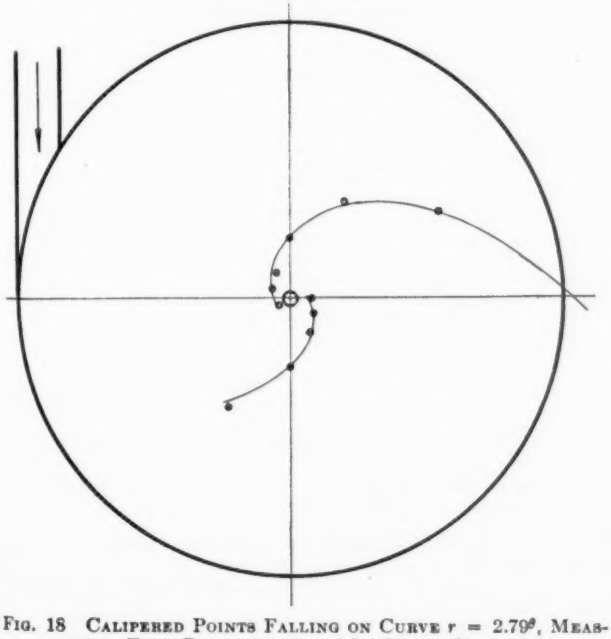


FIG. 18 CALIPERED POINTS FALLING ON CURVE $r = 2.79^{\theta}$, MEASURED FROM PHOTOGRAPH OF 6-IN. SPIRAL CYCLONE

in Fig. 19, showing plan and diametral section views of the cyclone. It is not difficult to observe an analogous wall creep in the case of the 1.85-in. Webre cyclone used in previous experiments. While the shape of this cyclone does not lend itself to photography or measurement, a sketch, Fig. 20, shows in section the typical liquid distribution. It will be seen that, in so far as the curved shell permits, the pattern of liquid distribution conforms to that for the spiral cyclone.

DISCUSSION OF EXPERIMENTAL RESULTS

The logarithmic spiral of Equation [5] describes the path of the liquid which is being entrained. Term θ, the angular velocity, must be a function of the inlet-vapor velocity. Radius vector r, must be a function of the radial velocity of the vapor as well as of the liquid being entrained.

The similarity of the two generalized functions of Equations [4] and [5]

$$L_e = c^{(V+b)} \quad [6]$$

and

$$r = n^{(\theta+m)} \quad [7]$$

suggests an analogy between the results of the experiments of series I, L, and M and the present observations. The parallelism suggests that the radial component of the vapor velocity is the force which induces this wall creep.

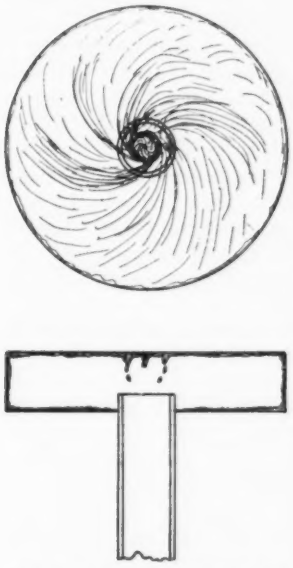


FIG. 19 WALL CREEP IN 6-IN. SPIRAL CYCLONE

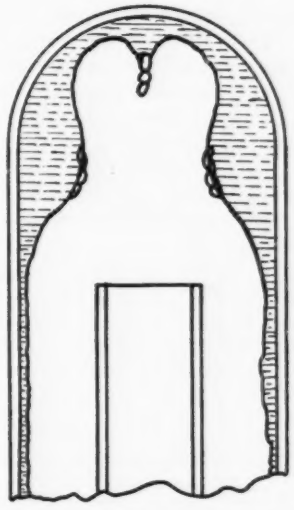


FIG. 20 WALL CREEP IN 1.85-IN. WEBRE CYCLONE

The significance of the factor $(V/L)^2$ in the more complicated entrainment function of Equations [1] and [2] is not clear. However, it may be noted that Equation [1] rewritten as

$$L_e = (L/V)^2 \times c^{(V+b)} \quad [8]$$

suggests that the factor $(L/V)^2$ may be associated with the energy required to lift liquid from the inlet level to the level where it may creep inward. Such a factor would not occur in the 6-in. spiral cyclone where no lift is required. In confirmation of this, it may be noted that the entrainment L_e is much greater for the spiral cyclone than for the Webre cyclone.

If such a lift is the explanation for the presence of this factor in Equation [1], then it would follow that the V in this factor is not the inlet velocity but rather the vertical component of the internal velocity. This could be investigated further by testing similar cyclones of varying dimensions. The results so far suggest the generalized form

$$\text{Log}\left[L_e\left(\frac{V}{L}\right)^a\right] = b + cV \quad [9]$$

where $a = 0$ in the case of the spiral cyclone and $a = 2$ in the cases of the other cyclones tested.

CONCLUSIONS

1 The entrainment, or liquid remaining in the cleaned vapor of cyclones, separating liquid from vapor, is a function of the liquid- and vapor-inlet weight velocities.

2 On the basis of this investigation, it appears that the entrainment is related to the liquid and vapor weight velocities by the function

$$\text{Log}\left[L_v\left(\frac{V}{L}\right)^a\right] = b + cV$$

where L_v is the entrainment, V is the vapor velocity, and L is the liquid velocity, all in the units of pounds per minute per square foot of inlet-duct cross section. Terms a, b, and c are constants associated with the type of cyclone and the condition of the liquid in the vapor-liquid stream.

3 Under all the operating conditions encountered in the cyclones tested, the constant a is zero in the case of a spiral cyclone and equals 2 in the case of a Webre cyclone.

4 The constants b and c are affected by variations in droplet size and also by the type of cyclone used.

5 In these experiments, at velocities below 1500 lb per min per sq ft, the entrainment with a Webre cyclone was lower than that with a similar standard cyclone.

6 From these experiments, a spiral cyclone appears to be less effective than a Webre cyclone.

7 The creep of liquid along the surfaces of a cyclone, leading to the central vapor-exit tube, was found to be a significant factor in the entrainment encountered in the cyclones used in this investigation.

8 In the case of a spiral cyclone, the path of liquid moving toward the central vapor-exit tube appears to be a logarithmic spiral.

9 The creep of liquid is induced by the inward radial component of the vapor velocity.

BIBLIOGRAPHY

1 U. S. Patent No. 1,825,990; R. C. Aland.

2 "Cyclones and Filters," by J. L. Alden, *Heating and Ventilating*, vol. 35, July, 1938, pp. 48–53.

3 U. S. Patent No. 1,960,887; W. Alexander.

4 U. S. Patent No. 1,898,608; W. Alexander.

5 "Air Conditioning and Engineering," American Blower Corporation, Detroit, Mich., 1935, p. 147.

6 "Air Conditioning and Engineering," American Blower Corporation, Detroit, Mich., 1935, p. 315.

7 U. S. Patent No. 2,032,827; N. H. Andrews.

8 U. S. Patent No. 2,155,853; A. W. Anthony, Jr.

9 "Heat Transfer and Evaporation," by W. L. Badger, Chemical Catalog Company, New York, N. Y., 1926, pp. 212–214.

10 "Die Anwendung des Modellversuches in der Staubtechnik," by W. Barth, *Rauch und Staub*, vol. 22, 1932, pp. 93–98.

11 U. S. Patent No. 1,950,285; R. Battle, and F. I. Ross.

12 U. S. Patent No. 1,734,030; A. C. Bennett.

13 U. S. Patent No. 1,953,948; T. C. Bieth.

14 U. S. Patent No. 1,979,189; D. W. Bowers.

15 U. S. Patent No. 1,774,588; C. P. Brockway.

16 "Fly-Ash Prevention," by S. Brown, TAPPI, Technical Association Papers, series 21, 1938, pp. 207–209.

17 U. S. Patent No. 1,780,641; S. N. Chew.

18 U. S. Patent No. 1,970,077; T. B. Collins.

19 U. S. Patent No. 1,756,909; L. V. Cram.

20 U. S. Patent No. 1,708,122; H. R. Davies.

21 "Cyclone Dust Collector Experiments," by B. W. Dedrick, *National and American Miller*, vol. 60, 1932, pp. 11, 12, 80, 82.

22 "Untersuchungen zur Verbesserung des Auffangwertes eines Zyklons für Hochofenstaub," by A. Drijver, *Wärme*, vol. 60, 1937, pp. 333–339.

23 U. S. Patent No. 1,784,664; F. Eickholt.

24 U. S. Patent No. 1,764,250; E. Falkenthal.

25 U. S. Patent No. 1,899,498; J. H. Fedeler.

26 U. S. Patent No. 1,824,713; J. P. Fisher and G. F. Downs.

27 U. S. Patent No. 2,143,344; E. M. Frankel and A. Pollak.

28 "The Vortrap," by H. Freeman, TAPPI, Technical Association Papers, series 21, 1938, pp. 225–228; "Separation of Solid Particles From Fluids," December, 1937, U. S. Patent No. 2,102,525.

29 U. S. Patent No. 1,684,022; C. G. Hawley.

30 U. S. Patent No. 1,883,908; C. G. Hawley.

31 U. S. Patent No. 2,004,467; C. G. Hawley.

32 U. S. Patent No. 2,004,468; C. G. Hawley.

33 U. S. Patent No. 1,886,548; G. H. Horne and M. A. Lissman.

34 U. S. Patent No. 1,930,806; G. H. Horne and M. A. Lissman.

35 U. S. Patent No. 1,973,764; G. H. Horne and M. A. Lissman.

36 U. S. Patent No. 1,746,218; H. G. Kamrath.

37 U. S. Patent No. 1,757,432; H. G. Kamrath.

38 U. S. Patent No. 1,761,923; H. G. Kamrath.

39 U. S. Patent No. 2,006,244; J. F. Kopsa.

40 "An Analysis of Mechanical Methods of Dust Collection," by M. A. Lissman, *Chemical and Metallurgical Engineering*, vol. 37, 1930, pp. 630–634.

41 U. S. Patent No. 1,939,710; M. A. Lissman.

42 U. S. Patent No. 1,888,603; J. L. Mauthe.

43 U. S. Patent No. 1,915,436; T. V. Moore and H. D. Wilde.

44 U. S. Patent No. 1,773,840; A. Nattcher and F. Seipp.

45 U. S. Patent No. 1,826,086; R. G. Neumann.

46 U. S. Patent No. 1,928,702; R. F. O'Mara.

47 "Trennung von Staubgasgemischen durch Fliehkraft," by F. Prockat, *Glasers Annalen*, vol. 107, 1930, pp. 47–54.

48 U. S. Patent No. 1,795,888; H. Rabezzana.

49 "Modern Blast Cleaning and Ventilation," by C. A. Reams, Penton Publishing Company, Cleveland, O., 1939, p. 106.

50 U. S. Patent No. 2,015,464; E. C. Saint-Jacques.

51 U. S. Patent No. 1,994,049; E. C. Saint-Jacques.

52 "Verbesserung des Wirkungsgrades von Staubabscheidern (Zyklonen) in Entstaubungsanlagen," by A. Schaak, *Rauch und Staub*, vol. 22, 1932, pp. 127–128.

53 U. S. Patent No. 1,846,365; F. Seipp.

54 "Flow Pattern and Pressure Drop in Cyclone Dust Collectors," by C. B. Shepherd and C. E. Lapple, *Industrial and Engineering Chemistry*, vol. 31, 1939, pp. 972–984.

"Flow Pattern and Pressure Drop in Cyclone Dust Collectors; Cyclone Without Inlet Vane," by C. B. Shepherd and C. E. Lapple; *Industrial and Engineering Chemistry*, vol. 32, 1940, pp. 1246–1248.

55 U. S. Patent No. 1,920,437; D. A. Sillers.

56 U. S. Patent No. 1,509,910; A. H. Stebbins.

57 U. S. Patent No. 1,509,911; A. H. Stebbins.

58 U. S. Patent No. 1,845,566; A. H. Stebbins.

59 U. S. Patent No. 1,845,567; A. H. Stebbins.

60 U. S. Patent No. 1,950,069; C. M. Stein.

61 U. S. Patent No. 1,548,066; A. Steinbert.

62 U. S. Patent No. 1,906,432; C. E. Summers.

63 U. S. Patent No. 1,835,445; T. Thomson and N. Nisbet.

64 U. S. Patent No. 1,595,268; O. W. Van Petten and R. Deming.

65 "A Modern Dust Collector," by H. Van Tongeren, *Mechanical Engineering*, vol. 57, 1935, pp. 753–759.

66 U. S. Patent No. 1,940,196; F. H. Wagner.

67 U. S. Patent No. 2,005,305; F. H. Wagner.

68 U. S. Patent No. 1,591,147; S. S. Wales.

69 U. S. Patent No. 1,797,812; H. Waring.

70 U. S. Patent No. 1,825,377; G. W. Watts.

71 "Evaporation," by A. L. Webre and C. S. Robinson, Chemical Catalog Company, New York, N. Y., 1926, p. 108.

72 "Evaporation," by A. L. Webre and C. S. Robinson, Chemical Catalog Company, New York, N. Y., 1926, p. 467.

73 "Bemerkenswerte Rauchgasentstaubungen der Bauart Van Tongeren," by F. Wellman, *Feuerungstechnik*, vol. 25, 1937, pp. 108–116.

"Die Strömungsvorgänge in Zyklonen," by F. Wellman, *Feuerungstechnik*, vol. 26, 1938, pp. 137–145.

74 U. S. Patent No. 1,734,507; L. L. Westling and M. R. Hickman.

75 U. S. Patent No. 1,760,617; J. Whitmore.

76 "Performance Characteristics of Cyclone Dust Collectors," by L. C. Whiton, Jr., *Chemical and Metallurgical Engineering*, vol. 39, 1932, pp. 150–152.

"Results of Research on Cyclone Dust Collectors," by L. C. Whiton, Jr., *Power*, vol. 75, 1932, pp. 344–346.

77 U. S. Patent No. 1,798,510; C. A. Winslow and E. J. Hall.

78 "Some Factors and Principles Involved in the Separation and Collection of Dust, Mist, and Fume From Gases," by E. Anderson, Trans. American Institute of Chemical Engineers, vol. 16, part 1, 1924, pp. 69–85.

79 "Trennung von Staubgasgemischen durch Fliehkraft," by F. Prockat, *Glasers Annalen*, vol. 107, 1930, pp. 43–45.

80 "Grundlagen und Grenzen der Zyklonentstaubung," by P. Rosin, E. Rammler, and W. Intelmann, *Zeit. V.D.I.*, vol. 76, 1932, pp. 433–437.

81 "Note sur les dépoussiéreurs centrifuges," by M. Seillan, *Chaleur et industrie*, vol. 10, 1929, pp. 233–238.

Discussion

H. C. Moore, Jr.[4] In discussing the flow pattern in a cyclone, the authors state that they were unable to find the evidence of a secondary component of flow. They cite Shepherd and Lapple (54) as also being unable to detect the presence of the double-eddy current. It would be interesting to know what means were used to investigate whether or not this phenomenon was evident. Obviously, a visual observation alone is not always sufficient. The secondary component of velocity is usually of such magnitude that it affects only the finer particles of dust and/or liquid. These particles are of a size individually invisible to the naked eye and, when dispersed throughout a gas, just give a homogeneous appearance of darker color. With the velocities encountered in cyclones, it is quite impossible to determine flow direction, unless the individual particles are visible. The solution would be to use an extremely light dust wherein particles of corresponding terminal velocities have a larger dimensional size.

The existence of the double-eddy current in a fluid caused to flow in a curved path was observed by such early investigators as Boussinesq[5] and Reynolds[6] in the study of the flow of water. Lorenz[7] shows by mathematical analysis that, for a circular fluid flow, there is a difference in pressure between fluid streamlines at different radii. This pressure difference, together with the static-pressure gradient built up in the fluid due to the slower moving strata in the region of the enveloping walls, causes a displacement of streamlines into a pattern of two similar spiral flows known as the double-eddy current. It has been demonstrated that this double-eddy current is present in the flow of gases as well as liquids.[8]

In the design of cyclones, therefore, either of two alternatives is possible, i.e., the cyclone may be designed to prevent the formation of the double-eddy flow, or the inherent formation of the double eddy may be utilized to enhance the efficiency of collection. In the former case, the prevention of the natural formation is translated into increased turbulence, with a resultant impairment of efficiency and increase in pressure loss. The latter method is the more logical. In allowing the double eddy to take its natural form, the turbulence is thus reduced to a minimum, resulting in a minimum re-entrainment. However, if the double eddy is allowed to form, it is necessary to make some provision in the design to remove the dust which will concentrate at the top of the cyclone, and which, in coming down, passes in close proximity to the gas-outlet pipe. This is accomplished in the van Tongeren design by means of a shave-off slot at the top, which draws off this upwardly moving dust and passes it through an exterior duct for reintroduction into the cyclone proper at a point where the influence of the lower eddy is definitely downward.

In considering cyclones for separation of liquids, the effect of turbulence is probably not as great as in the separation of dust. Once the droplets reach the enveloping surface and become part of the film thereon, there is slight possibility of re-entrainment with proper design. However, in dust separation, a particle which has reached the wall of the cyclone is always subject to the possibility of re-entrainment due to turbulent flow.

A. L. Webre.[9] The results of this research are particularly interesting to the writer, inasmuch as he has used the so-called Webre cyclone for about 30 years in connection with the prevention of entrainment losses in pans and evaporators in the sugar industry, as well as in others—always with success.

In all of our standardizations, we have always used the vapor velocities in feet per second, instead of pounds per minute per square foot, used in the paper. Presumably, the experiments were conducted at atmospheric pressure. It is, therefore, pertinent to consider what would happen to the cyclone if the same weight of vapor were passed through at the higher lineal velocities encountered at high vacua. In line with this thought, whereas we have never recorded any research work done on the cyclones, yet we have had to standardize on certain proportions, and these standards have always been based on the actual linear velocities at the vapor inlet.

Thus we have found that we must not exceed certain limits. At 4 in. abs, we use 250 fps; if we exceed 275 fps, we begin to have entrainment losses. At lower vacua, and at atmospheric pressure, we reduce the velocity gradually, standardizing on 100 fps at atmospheric pressure.

If the velocity is too slow, then the apparatus begins to lose efficiency. In the case of black-liquor evaporators, where there is a great deal of foam, the whirling action of the cyclone is used to break up the foam. To accomplish this, the velocity must be in the neighborhood of 100 fps. It has very often been necessary for us to insert reducers at the cyclone inlet to accomplish this, without which, the foam would not be broken up.

In all cyclones, there is a loss of head between the inlet and the outlet due to the centrifugal force of the vapor itself, and this can be observed by placing manometers at the proper points. Under extreme velocity conditions, we have observed as much as 3 in. of mercury difference between the outer periphery of the cyclone and the center of the cover. It was mostly on this account that we have now abandoned the use of cyclones in favor of a different design which has no loss of pressure and performs with equal efficiency.

Particularly in the sugar industry, we have a very satisfactory means of determining the losses by entrainment, for all vapors are condensed. By using the alpha-naphthol test, we can determine as small an amount as 1 part of sucrose in 5,000,000 parts of water. With a well-operated sugar factory, the entrainment loss is less than the figure cited.

It might be stated further that the amount of liquid usually present in the vapor leaving an evaporator, and entering the cyclone, is relatively small. In the ordinary sugar evaporator, it would certainly be less than 2 per cent. In certain types of black-liquor evaporators, it is assuredly many times more than this figure, and a guess would be from 10 to 12 per cent by weight. The percentage by volume is naturally very small.

We should like to thank the authors for their illuminating work, and hope that they may be able to supplement this along the lines suggested, namely, under high vacuum and with smaller ratios between liquor and vapor.

---

[4] Moore-Broach Engineering Company, Atlanta, Ga.

[5] "Essai sur la theorie des eaux courantes," by J. Boussinesq, Mémoires Présenté par Divers Savants, vol. 23, Académie des Science, Paris, 1877, p. 596.

[6] "On Certain Laws Relating to Rivers," by O. Reynolds, British Association for the Advancement of Science, Report, 1887, pp. 555–562.

[7] "Der Widerstand von Rohrkruemmern," by H. Lorenz, *Physikalische Zeitschrift*, vol. 30, 1929, pp. 228–230.

[8] "Vortrage aus dem Gebiete der Aerodynamik und Verwandte Gebiete," by A. Gilles, L. Hopf, and T. von Kármán, Julius Springer, Berlin, 1930, p. 10.

[9] Mechanical Engineer, Merion, Pa. Mem. A.S.M.E.

Analyzing Governor-System Performance

By A. F. SCHWENDNER,[1] PHILADELPHIA, PA.

All the characteristics of a turbine governor considered as an entity have their effect on the operating performance, expressed in terms of speed-regulation sensitivity, rate of response, and stability. The governor can only be judged adequately by observing its operation in conjunction with the system with which it is associated, which can only be done by employing instruments more sensitive and rapid in response than the governor itself. This paper describes the essential features of an instrument, developed specifically for this purpose, the methods of testing employed, and actual tests made with it.

THE turbine-generator-governing problem has attracted considerable attention in the last few years. Papers have been presented describing the effects of governor characteristics on the unit, station, tie line, and system. The desirable characteristics of governors have been pointed out, and the qualities of stability, sensitivity, and rate of response have been discussed.

Turbine users are mainly interested in the effect of governor performance on their systems. In other words, they are concerned with the operating-performance characteristics of their governors, for example, the unit-load changes corresponding to certain system-frequency changes as dependent upon unit loading. All the characteristics associated with a governor considered as an entity have their effect on the operating performance, i.e., speed-regulation (over-all and incremental) sensitivity, rate of response, and stability. In addition, the characteristics of associated units and the system-load conditions also affect operating performance. A governor cannot be adequately judged by observing only its behavior as an isolated mechanism or even by comparing the steam charts of different units. It must be carefully studied in conjunction with the system with which it is associated. Such study must be implemented with instruments more sensitive and rapid in response than the governor itself. An ideal set of such instruments would comprise a governor-performance analyzer capable of testing all the required governor characteristics in a short series of tests.

Governing-System Performance Characteristics

To discuss this subject intelligently there must be a well-defined nomenclature. The A.S.M.E. Power Test Code on speed-responsive governors does not cover all the terms and definitions used in recent years. The reorganized committee has not yet issued a new nomenclature. In the meantime something has to be used, but the terminology which has been adopted in this paper is not intended to establish new terms and definitions.

The operator judges the governor on the basis of its behavior when the unit is on the generating system. This behavior reveals what, for want of a better name, may be called the operating-performance characteristics of the governor. These are nothing more than the changes in load of the unit, corresponding to various classes of system-frequency change. The small frequency changes occurring in all systems, amounting to from 0.1 to 0.2 cycle, actuate the governing valves and change load to an extent depending upon the incremental speed regulation and sensitivity of the governor, for frequency changes slow in comparison to the rate of response of the governor. The operating performance approaches the incremental speed regulation as the sensitivity is increased.

A less sensitive governor or one with a rate of response slow, compared to the system frequency fluctuations or both will show a lower governor operating performance (effectively higher regulation) than the incremental speed regulation. Thus the operating performance of a governor can be measured by its deviation from the incremental speed regulation if the roughness or rate and magnitude of the frequency changes are also considered. The final decision on definition of and numerical expression of this deviation must be left to the joint A.S.M.E.-A.I.E.E. committee. The governor operating performance is so much dependent upon the individual governor-performance characteristics that all of them must be checked to enable us to analyze the former. Thus the following must be considered: Speed-regulation (over-all and incremental) sensitivity, rate of response, and stability.

Governor-Speed Regulation (Over-All). This is the sustained percentage of speed change of a prime mover for rated load change. Owing to the peculiarities of governors, this is not necessarily a unique value for a particular governor. The regulation for a no-load setting of the load-changing device may vary appreciably from the regulation for the full-load setting. Curves defining these variations are necessary to express fully the over-all speed regulation.

Governor-Speed Regulation (Incremental). This is the slope of the speed-load curve passing through 100 per cent speed at the load point in question, stated in percentage of rated load percentage of rated speed. If the governing valves had a linear steam-flow valve-lift characteristic and the turbine water rate were constant, the incremental and over-all regulations would be identical. The requirements for low valve pressure drops to obtain high efficiencies result in greater nonlinear flow-lift relationships.

Sensitivity. This is the speed change necessary to start movement of the governor and governing valves. It can be expressed in percentage of rated speed. It is important to be able to check the individual sensitivities of each of the elements of the governing system from the governor to the operating servomotor so that the source of insensitivity may be located.

Rate of Response. Perfect governing performance would be the exact following of speed by the governing valves. The governing valves actually lag behind their true speed position by an amount depending upon the shaft acceleration and the rate of governor response. The latter might, then, be measured in terms of the time required to initiate a corrective motion of the valves when the prime mover is accelerated at some constant and standard rate. Such an acceleration might be obtained by dumping an appropriate load. The effectiveness of a governor as applied to a particular unit is dependent not only upon its rate of response but also upon the inertia, rating, and speed regulation of the unit. This over-all effectiveness might be measured in terms of the time required to initiate corrective valve motion following the dumping of a definite fraction of the rated load.

---

[1] Control Engineer, Westinghouse Electric & Manufacturing Company, South Philadelphia Works.

Contributed by the Power Division and presented at the Semi-Annual Meeting, Kansas City, Mo., June 16–19, 1941, of The American Society of Mechanical Engineers.

Note: Statements and opinions advanced in papers are to be understood as individual expressions of their authors and not those of the Society.

It may be noted that broad transient regulation, introduced in some governors to obtain stability, will have a decided effect on the rate of response.

Stability. A stable governor is one which tends to damp rather than excite load or frequency oscillations. Small oscillations which may be revealed by a fast and sensitive recorder are not necessarily indications of fundamental instability.

Foregoing are the governor characteristics which should be measured to obtain a better conception of governor performance.

Specifications for a Governor-Testing Instrument

One of the first characteristics which should be demanded of a testing instrument is great flexibility. The many types of governor require an instrument readily adapted to the measurements of their various characteristics. This adaptability should be obtained without major alterations of the parts of the instrument. By using unit sections for the measurement of the different governor functions, the different elements can be interchanged quickly. It is also important to have a record of all the elements on a single chart. It is essential to be able to measure the following quantities: (*a*) Angular velocity of the turbine rotor; (*b*) travel of the governor and servomotors; (*c*) hydraulic pressures corresponding to motions in flyball governors; and (*d*) electrical output of the generator. A governor-testing equipment should be suitable not only for an initial determination of the governor-performance characteristics, but also for periodic checks to determine when the slow depreciation in performance justifies taking the governor out of service for repairs.

Equipment which may be used frequently should be designed with light compact units arranged so that the complete setup would require only a few hours. In a large power plant it should be possible either to move the instrument as a unit from turbine to turbine or to locate it centrally and provide for cable connections to the measuring elements which may be located on the various machines. The elaborate precautions necessary in transmitting and magnifying motions mechanically with levers and wires, and the difficulties in moving such an arrangement from unit to unit, suggest the advantage of transforming the motions into proportionate electrical quantities directly at the source.

Similarly, pressures are conveniently converted to electrical units and transmitted by electrical cables which are easily handled and laid. The pressure and travel elements should be so designed that after the type of elements has been selected as dictated by the governor to be tested, all the tests can be completed without changing the elements. Each element should have sufficient range so that the changes in characteristics, required for the different tests, can be obtained with easy and rapid adjustment. If the adjustments are obtained in definite steps, recalibration after a change may be omitted. The individual measuring elements should indicate the smallest significant change of the measured quantity without overtravel or time lag, regardless of the instrument magnification ratio. Analysis of records is considerably facilitated if the orders of magnitude of the deviations of the measured quantities as recorded are roughly equal, whatever their actual values.

The recording instrument can be a standard oscillograph. Direct recording with pen or stylus on a paper chart would be preferable if a multielement recorder with sufficiently high frequency response were available. Development of such an instrument has been interrupted by more pressing work. For a typical governor test, one frequency element, three travel, a load, and a timing element for a mechanical governor, or one frequency, two pressure, one travel, a load, and a timing element for an oil governor are required as a minimum. To analyze practically any governing system, one frequency element, three pressure, three travel, several load elements, and a time element would cover all requirements. A long-film seven-element oscillograph would be adequate for most purposes. A range of film speeds from $1/8$ to $1/2$ in. per sec to 3 in. per sec and an easily adjustable light intensity are desirable.

Speed-Measuring Element

The individual measuring elements should have the following characteristics:

The speed-measuring element should be arranged for attachment to the shaft end wherever possible. In many cases, the shaft ends are not available for this purpose. For this reason a synchronous motor, connected to the unit through the instrument transformers, can drive the speed-measuring element at an angular velocity reasonably close to that of the turbine. Error due to variations in phase angle of the terminal voltages and to electrical flexibility between generator and motor will limit this method to those cases in which such error is permissible.

Two full-scale speed ranges are required: A wide range from approximately 50 to 70 cycles per sec and a sensitive scale with full-scale deflection for about 0.25 cycle from a base frequency which may be set anywhere from 59 to 61 cycles. The full-scale deflection should be sufficient to show definitely a speed change of 0.01 per cent or less on the sensitive scale.

Motion-Measuring Element

To follow and record the motion of any part of the governing system the measuring element should have a substantially flat frequency response to about 60 cycles per sec. In order to obtain the required response, it is desirable to have a short, stiff connecting wire between the moving part and measuring element. Converting the motion into proportional electrical current permits mounting the element very close to the moving part. The element should be capable of a wide range of ratio adjustment to be able to record the different motions in a governing system. Besides the wide-range ratio required to give full-scale deflection for the total stroke of a movement, a sensitive range is also needed to give full-scale deflection to a motion corresponding to a change in frequency of 0.25 cycle. The changeover from one ratio to the other should not require more than a few minutes and the element should be so constructed that it can be attached to any part of a governing system without trouble. Some protection should be provided to allow sudden overtravels of the moving part, while the element is set to the sensitive range without damaging the element.

Pressure-Measuring Element

The oil pressures to be recorded for the purpose of analyzing governor performance vary about as much as the motion of the governing system. The pressure changes and ranges require a wide ratio of adjustment. Most of the pressures also require two complete ranges, a wide range which will record the deflection corresponding to the maximum pressure change, and a sensitive scale which will give full-scale deflection to an oil-pressure change corresponding to a change in frequency of 0.25 cycle. It is possible to develop an adjustable-ratio pressure-measuring element, or two elements may be used, having the proper ratios to permit analysis of the governing-system performance, using the same gage line with suitable cutover valves. In any case, the arrangement should be such as to permit changeover from one ratio recording to the other without appreciable loss of time. Wide variation in base pressures is also required.

Load-Measuring Element

The polyphase average-watt oscillograph galvanometer which is available for use in standard oscillographs measures true watts

in three-phase circuits. Such a galvanometer may advantageously be employed as the load-measuring element. The accuracy and response of this element must be matched reasonably closely to those of the other measuring elements. It is quite a task to draw up specifications for a universal governor-performance testing equipment. The specifications outlined cover the elements required to evaluate the governor-operating performance characteristics and to make all the other tests required to establish those characteristics. The elements described can be used to investigate and analyze governing and generating system performance, or tie-line characteristics, by using the proper combination of these elements. It is advisable to have all the elements so made as to be able to record both direct and alternating components with frequency-response characteristics substantially flat from zero to 50 or 60 cycles per sec (if feasible).

Testing a Governing System

Given an instrument which can readily be adapted to any unit for a quick determination of governor characteristics, we must also have a test program which will enable us to obtain all the necessary information with the least possible outage or system disturbance. The test method to be outlined is simple to follow and adequate to provide all necessary information to make possible an analysis of governing-system performance:

1 With the unit on the line and carrying maximum load, measure the speed-changer and governing-valve positions. Then reduce the load in small increments, preferably with a load-limiting device. Hold every load position long enough to run a short record on the oscillograph or to read the deflections directly. The steam conditions must, of course, be nearly identical for all of these readings. When rated load is reached, record also the speed-changer and governing-valve positions necessary to sustain this load at rated speed. Remove the remainder of the load in the same manner.

2 Take the generator off the line and, with the recorder running, move the speed changer from the no-load to rated- and maximum-load positions. Then return it to the no-load, full-speed position. Partly close the throttle valve and so drop speed until the governing valves open to the rated-load position, and then to the maximum-load position. Reopen the throttle valve and bring the turbine speed back to normal. While the speed changer is being moved, the steam pressure and vacuum should be kept constant within reasonable limits.

3 Synchronize and put the generator back on the line with the recorder running.

4 While the load on the unit is being brought up to its previous value, run the recorder for a short time at all settled load points, preferably identical with load points of the first test.

The first test requires only the load and governing-valve-travel measuring elements of the analyzing instrument. Both are set to the wide range and the recorder is run at a slow speed. The second test requires the speed and governing-valve-travel measuring elements. The governor-travel or governor-oil-pressure measuring element can be added to the others. All the elements are to be set to the wide recording range with the recorder set to run at a slow speed.

The third test requires the speed, governor-travel or pressure, and governing-valve-travel measuring elements. The load element can be added for a better over-all picture. All the elements are to be set to the sensitive recording range. The recorder should be set to run at high speed.

The fourth test requires all the governor-travel- or pressure-measuring elements with the speed-and-load element included.

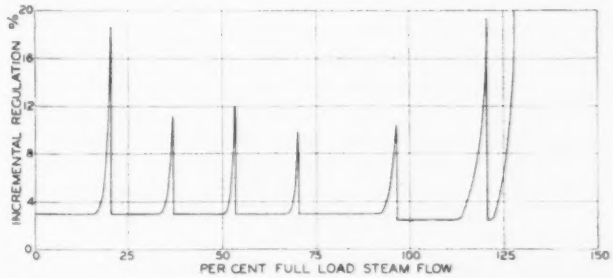


Fig. 1 Steady-State Incremental Regulation Vs. Steam Flow

All the elements are to be set to the sensitive recording range. The recorder should be set to run at slow speed.

Having the specification for the instrument and also having determined the program for a governor test, we now need the instrument itself and some test results to prove that the type of instrument and the method of test will provide all the required information about governor performance.

Some time ago J. E. Allen (1)[2] built an instrument which very

[2] Numbers in parentheses refer to the Bibliography.

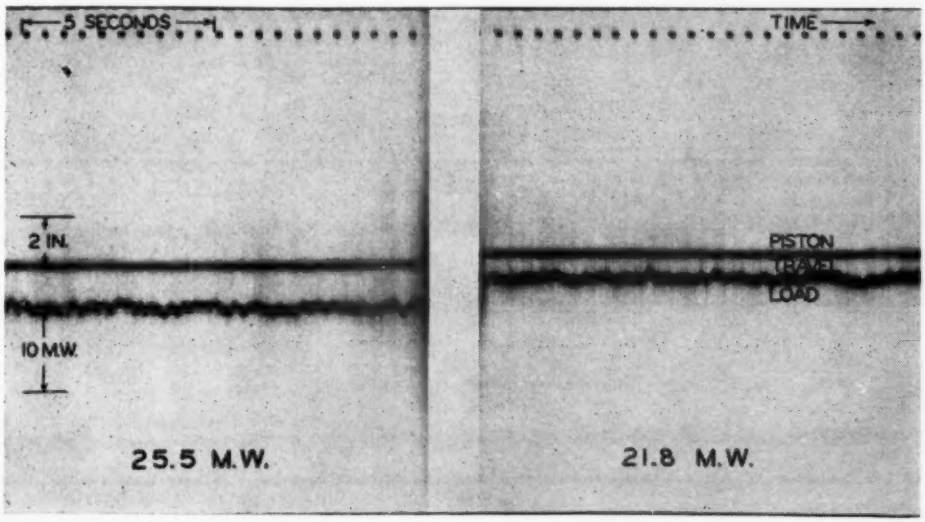


Fig. 2 Typical Records of Load and Valve Travel

nearly fulfills our requirements. The East Pittsburgh research laboratories have since built a governor-analyzing instrument which satisfies the specifications laid down. It will not be necessary to enter into a detailed description of this instrument, as it will be covered in a paper by W. O. Osbon (2).

Analyzing Test Results

We set out to check what the governing system of a specific unit will do when connected to a power-generating system. The results obtained should be prepared in such form that the operators will know the incremental regulation at each load point, for each unit in their system. For good system regulation it is important to know at any time at what regulation each component of the total system capacity is being generated. For that purpose a curve showing the load points of the unit plotted against the regulation at each load point will be the most useful. Fig. 1 shows a typical steam-flow incremental regulation curve. When the test results obtained with the analyzing instrument are worked up, we shall obtain a similar curve except that it will show load incremental regulation. It will, of course, also differ by the amount of the deviations due to change in water rate. The information obtained by the test can be used to plot the incremental regulation curve. Two methods are available and they can be used to cross check the results obtained.

The records of a test run taken under the conditions described in test paragraph 1 are shown in Fig. 2. The load and valve or governor travel obtained in this manner can then be plotted in curve form, as shown in Fig. 3. The curve shows steam flow, while the test will give load and the corresponding valve or governor position.

The curve shown in Fig. 3 can be transformed into the shape shown in Fig. 1 if the over-all speed regulation at the particular load point is known. The over-all speed regulation was checked during the second test.

The test results are best plotted in a curve of the shape shown in Fig. 4. The speed-changer travel is plotted against the percentage of normal speed. The speed increase, recorded while the

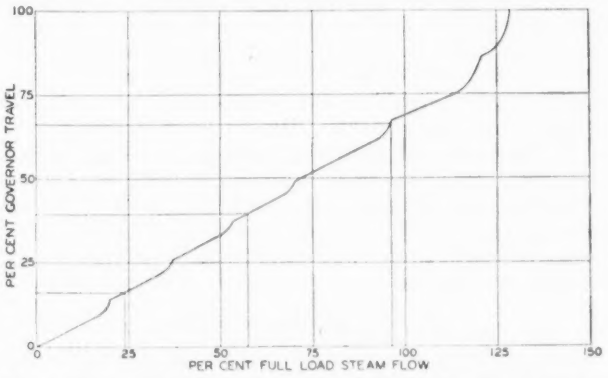


Fig. 3 Governor-Travel Versus Steam-Flow Characteristic of Multivalve Steam Flow

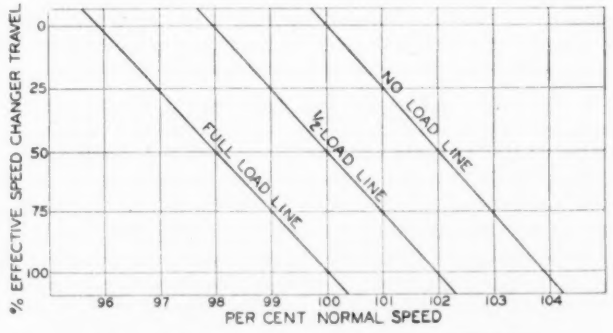


Fig. 4 Governor-Regulation Characteristic

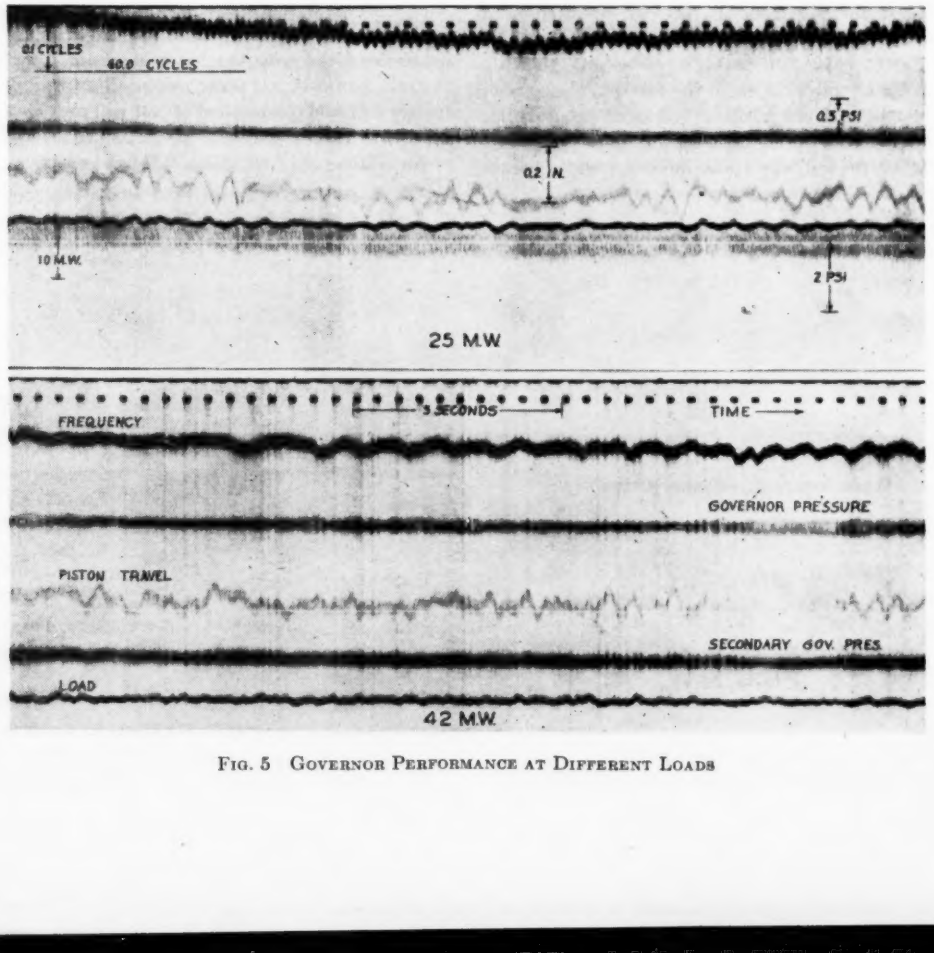


Fig. 5 Governor Performance at Different Loads

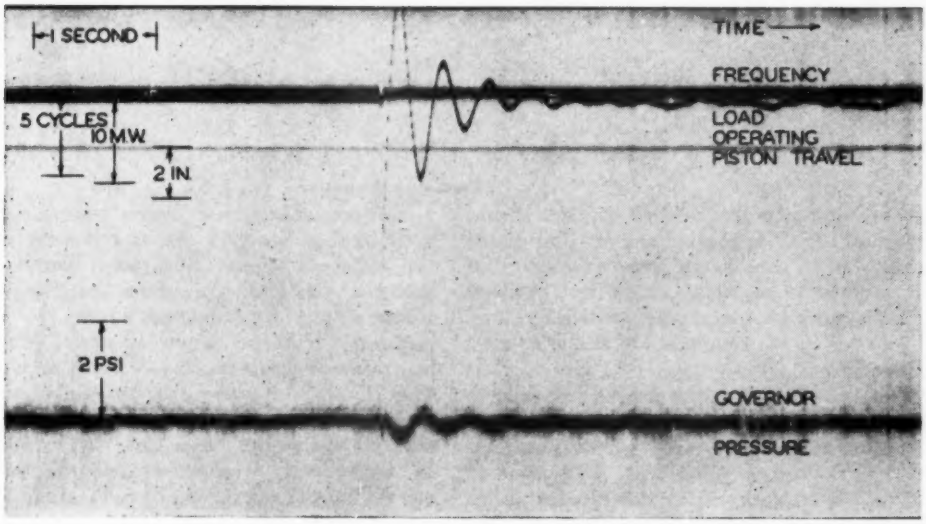


FIG. 6 SYNCHRONIZING TRANSIENTS

speed changer was moved from the no-load to the maximum-load position, should be marked on the chart and thus will become the no-load line.

The drop in speed which occurred when throttling until the maximum-load governing-valve positions were reached should be plotted on the horizontal zero line of the "effective speed-changer-travel" axis. Connecting this point with the 100 per cent speed-travel point gives us the full-load line and completes the chart. Fig. 4 shows almost parallel no-load full-load lines. Most of the travel governors have considerable variation between the two points. The actual over-all regulation for any load point should be taken from the horizontal line between the no-load full-load lines at the point where the particular load line crosses the 100 per cent normal speed line.

The second method of obtaining governor-operating characteristics is by analysis of the records obtained by the test outlined in test paragraph 4. Two records obtained at two load points are shown in Fig. 5. Even a casual observation of the two records shows that, while the frequency changes have been followed by the governing system, the load change has not followed them. The maximum frequency change of 0.07 cycle is followed by a valve travel of 0.11 in. and a load change of 1500 kw in the top record. The lower record shows a maximum frequency change of 0.05 cycle with a valve travel of 0.08 in. and practically no change in load.

If the changes in frequency are plotted against changes in load and a line drawn through to average all the points, the slope of the line will give us the incremental regulation for that particular load point. A considerable number of additional cases will have to be analyzed before it will be possible to evaluate the width of the band obtained.

J. E. Allen has developed a governor-analyzing instrument which records the frequency on one axis and the valve movement on the other axis simultaneously. This type of record would eliminate the rather cumbersome plotting of points, but it neglects the effect of valve-flow characteristics.

The stability of a governing system can be shown by means of the records obtained in the test indicated in test paragraph 3, as shown in Fig. 6. Frequency and governor pressure show no tendency toward oscillation up to the point of synchronization.

When checking sensitivity down to very small values, it is difficult to obtain definite results. Any ripple in a recorded quantity, regardless of its cause, reduces the accuracy and definiteness of the result. The frequency and motion records, shown in Fig. 5, indicate a motion with a frequency change of from 0.01 to 0.02 cycle.

To establish the rate of response of a governing system, it is necessary to arrange for a load-dump test. The instrument described is also suitable to obtain the type of records necessary to establish the rate of response in a load-dump test.

CONCLUSION

The test results so far obtained demonstrate that the instrument, built in accordance with the specifications given in this paper, is capable of analyzing the governor performance of almost any type of governor. The instrument can be set up to test a governor in about 3 hours, and the test itself requires less than 4 hours. Most of the tests thus far made were taken only recently, and not all of the records have been evaluated. Where test values were not available, calculated values have been substituted.

The sensitivity and rate of response of the few governors tested, in comparison with the rate and magnitude of the frequency changes, did not give us a measurable deviation from the incremental speed regulation at the few check points made. Further tests are required on units which will show a measurable deviation between the incremental speed regulation and the operating performance of the governor. Only after the completion of such a test can the method of testing and evaluating test results be established and completed information presented.

ACKNOWLEDGMENT

The author wishes to express appreciation for the assistance given by W. A. Wilson of the Steam Division of the Westinghouse Electric & Manufacturing Company in preparing this paper.

BIBLIOGRAPHY

1 "Oscillograph Analyzes Governor Performance," by J. E. Allen, *Power*, vol. 78, 1934, pp. 610–612.

2 "A Turbine Governor Performance Analyzer," by W. O. Osbon, Transactions A.I.E.E., vol. 60, 1941, November Section, pp. 963–967.

3 "Regulation of System Load and Frequency," by H. Estrada and H. A. Dryar, Trans. A.S.M.E., vol. 62, 1940, pp. 221–232.

4 "The Field of System Governing," by A. Davis, Trans. A.S.M.E., vol. 62, 1940, pp. 207–217.

5 "Prime-Mover Speed Governors for Interconnected Systems," by R. J. Caughey and J. B. McClure, *Electrical Engineering*, April, 1941, Transactions section, pp. 147–150.

Silica Removal by an Improved Magnesia Process

By H. L. TIGER,[1] NEW YORK, N. Y.

Modern high-pressure boilers with high feedwater make-up requirements frequently demand reduction of dissolved silica. A new magnesia process for silica removal has been developed, combining flexibility, simplicity, and economy. It can be applied to any type of water at any temperature; it can be carried out in conjunction with the usual precipitation water-softening process; and the increase in operating cost is very small.

These results are accomplished by a new method of combining a number of principles embodied in this process. Extensive investigations were conducted to determine the influence of each of various factors on the final result, and data are presented on the effects of the following: Form of magnesium used (whether precipitated ionic Mg or undissolved Mg compound), temperature, sludge-magnesium concentration, and agitation for sludge-water contact. The principles of increasing the Mg^{++} content, when required, by means of a novel sludge recycling process with a magnesium dissolver are described. A method of using cheap dolomitic lime as a low-cost source of magnesium is also presented.

The process lends itself advantageously to a modified Spaulding precipitator type of construction at either low or high temperature, to be followed by suitable treatment with carbonaceous-ion exchangers, when required, for complete removal of residual hardness and reduction of alkalinity to any predetermined figure.

THE trend toward higher pressures and higher percentages of make-up in steam boilers and toward lower alkalinites in boiler feedwater has resulted in siliceous deposits in boilers and turbines in several cases. Boiler-tube failures, due to such deposits, are described in many papers (1, 2, 3, 4, 5, 6).[2] Troubles from these deposits in superheaters and turbines, as a result of carry-over of silica-containing salines with the steam, are described in other papers (7, 8, 9, 10, 11, 12, 13). This has caused a demand for an effective and economical method of reducing silica in boiler feedwater or otherwise preventing silica deposits.

Dissolved silica is always present to some extent in all natural waters. Suspended silica is also present in surface waters containing turbidity. Such suspended silica or siliceous substances can be readily removed by the usual coagulation and filtration methods. It is the silica remaining in solution which offers the special problem with which we are concerned in this paper.

The factors which influence the formation of silica deposits in boilers and the nature of the deposit which forms have not been thoroughly explored. It is known, however, that the presence of calcium and magnesium in the feedwater tends to form calcium and magnesium silicates. The presence of aluminum tends to form alumino-silicates, of which analcite is a special form. Under certain conditions, pure silica alone may constitute the bulk of the deposit.

The "silica tolerance," i.e., the maximum allowable amount of silica that may be tolerated in the concentrated boiler saline, cannot be specified with accuracy at present, due to the lack of sufficient statistical information on that subject over a sufficiently broad range of boiler pressures, ratings, etc. This is a subject which deserves further investigation by our engineering societies. If the feedwater contains little or no dissolved calcium, if the ratio of alkalinity to silica is sufficiently high, for example, more than 1:1, and if the boiler circulation is satisfactory, the silica content of the boiler salines may be as high as 350 ppm. Several cases are on record where such conditions prevail in high-pressure boilers without resultant difficulties. In some cases when silica-scale troubles started, they have been overcome by increasing slightly the ratio of alkalinity to silica in the boiler saline. In other instances, such difficulties have been overcome by improving boiler circulation to avoid "hot spots" or "dry tubes," i.e., local areas in which the steam is formed more rapidly than it is carried away by the circulating water in the boiler.

The trend in modern boiler-feedwater-conditioning practice is to reduce the hardness and total solids to the lowest possible limits and also to reduce the alkalinity to a minimum in order to avoid carry-over and CO_2 in the steam. Such modern methods of feedwater conditioning have been described in previous papers (14, 15, 16). These methods are applicable even where raw water contains sodium bicarbonate which hitherto could be removed only by distillation (17).

This trend toward lower alkalinity has created a demand for a corresponding reduction in the silica content, because if the "silica tolerance" limits the amount of silica in the saline, then the amount of boiler blowoff is controlled in many cases by the silica in the feedwater rather than by the other solids present. The silica in the feedwater is concentrated along with other substances which are present in solution. The extent of such concentration can, of course, be controlled by regulating the amount of boiler blowoff which is replaced by a corresponding amount of fresh feedwater. However, if the silica in the feedwater is very high and the "silica tolerance" in the saline is very low, such control of the silica in the saline by blowoff becomes difficult and expensive. These considerations have led to a demand for an efficient method of reducing silica. However, it must be realized that the cost of reducing silica increases disproportionately with each additional ppm reduction as the silica desired in the effluent approaches zero. Therefore, a balance should be determined between the boiler blowoff and silica reduction by treatment of the feedwater to arrive at the most economical and satisfactory method of keeping below the silica tolerance.

If, for example, the boiler saline must be limited to total solids 1500 ppm and silica 30 ppm, and the total solids in the make-up

---

[1] Vice-President in charge of Research and Development, The Permutit Company. Mem. A.S.M.E.

[2] Numbers in parentheses refer to the Bibliography at the end of the paper.

Contributed by the Joint Research Committee on Feedwater Studies and presented at the Annual Meeting, New York, N. Y., December 2–6, 1940, of THE AMERICAN SOCIETY OF MECHANICAL ENGINEERS.

NOTE: Statements and opinions advanced in papers are to be understood as individual expressions of their authors and not those of the Society.

after treatment is 200 ppm, then the desired SiO_2 in the make-up water is calculated as follows

$$\frac{1500}{200} = 7.5 \text{ concentrations}$$

$$\frac{30}{7.5} = 4 \text{ ppm silica}$$

It is then only necessary to reduce the silica to 4 ppm in the make-up, since the amount of boiler blowoff required to maintain total solids below 1500 ppm will at the same time maintain silica in the boiler saline below 30 ppm.

Analytical Methods and Literature References to Silica Removal

The method used throughout the investigation described in this paper was that adopted by the A.P.H.A. (18) with some modifications. Swank and Mellon (19) buffered-chromate standards were used, because our tests confirmed the higher accuracy obtainable with these standards. This agrees with the findings of Knudson, Juday, and Meloche (20).

We also found it necessary to make all our silica determinations at 20 to 25 C, since variations in temperature affected the color of the silicomolybdate complex. This was especially noticeable in cold-water investigations, where determinations at the low temperature gave false low readings.

Experience showed also that glass vessels might seriously contaminate the solutions, particularly when they were highly alkaline and at high temperatures. To determine the extent of such contamination, tests were made with various types of containers, periods of contact, temperatures, and solution alkalinities. These tests led to the following conclusions:

(*a*) Hot-alkaline samples require suitable metal or rubber or other nonsiliceous containers.

(*b*) Pyrex glass is fairly satisfactory.

(*c*) Soft-glass containers may add considerable contamination and should only be used on cold waters of fairly high silica content and fairly low pH value (below pH = 8.3, the change point for phenolphthalein indicator).

M. C. Schwartz made an excellent study of the analytical methods for silica determination, and his paper (21) contains a comprehensive summary of the literature and a bibliography on this phase of the subject. Recently Kahler (22) presented data on improvements in the use of the Isaacs method which depends upon the blue color of the reduced silicomolybdate complex.

Very little was published on the removal of silica from water prior to 1930. Exploratory experiments were made before that time, but no practical processes were evolved (23, 24, 25).

Since 1930, a considerable amount of material has been published describing various processes. Most of these processes depend upon the removal of silica by absorption[3] or adsorption[3] by hydrous metallic oxides or hydrated oxides, such as, alumina, ferric oxide, magnesium oxide, zinc oxide, and other miscellaneous metal oxides.

In some of the processes described, the water is filtered through beds of metallic-oxide granules, which may or may not be capable of regeneration; in others, the metal oxides or hydroxides are precipitated in the water; while in others, the solid absorption materials are fed to the water. Processes have also been suggested in which calcium and magnesium aluminates are employed to precipitate the silica from the water.

[3] The more general term "absorption" is used throughout this paper, as it is possible that these processes involve other phenomena besides straight adsorption.

Silica removal by passage of water through beds of metallic-oxide granules has been described by Liebknecht (26), Kurz (27), but this method has not been adopted in practice because of high operating cost and operating difficulties.

Silica removal by precipitation of aluminum hydroxide at high pH and by various aluminates is described in detail by Christman, Holmes, and Thompson (28), Stumper (2, 29), Black, Bardwell, and Graham (30), Kaissling (9), Lindsay and Ryznar (31), Lindsay and Braithwaite (32), and Betz, Noll, and Maguire (33). However, high treatment cost, as well as the possibility of analcite-scale troubles in the boilers, due to residual alumina in the treated-water effluent, has discouraged the adoption of the aluminum-hydroxide and aluminate methods of silica removal.

Silica removal by precipitation of hydrous ferric oxide from ferric sulphate has been described by Smith (24), Stumper (2), Schwartz (34), Powell, Carpenter, Setter, and Coates (36), Behrman and Gustafson (37). The article by Schwartz (34) describes the characteristics of this hydrous-ferric-oxide process in detail. Several large boiler-feedwater-treatment plants, employing this process, have been in operation for a number of years with satisfactory results, Applebaum (15). However, the cost of treatment is high, especially when the initial silica in the water is high. Furthermore, the precipitation of ferric hydroxide from the ferric sulphate fed results in an increase of soluble sulphates, i.e., an increase in the total-dissolved-solids content of the boiler feedwater, which is frequently undesirable.

Reimers (38) suggested the precipitation of hydrous zinc oxide, cadmium oxide, manganese oxide, etc., but this process was never adopted in practice because of high operating cost.

Silica removal by magnesium oxide has been referred to frequently in the literature. Bohlig (39) referred to the use of calcined magnesite for reducing the calcium-bicarbonate content of water and noted that silica is also removed from the water in the same treatment. Stumper (29, 2) describes beaker tests on silica removal by calcined magnesite at high and low temperatures and concludes that MgO is of no value at room temperature but may be of some use at boiling-water temperatures. Christman, Holmes, and Thompson (28) present some laboratory test data indicating silica removal by precipitation of ionic magnesium at room temperature and at boiling-water temperatures. Hundeshagen (3) and Kurz (27) also recommended the removal of silica by precipitating $Mg(OH)_2$, or by the addition of calcined magnesite (MgO). Kuhnert (40) recommended the use of MgO and $MgCO_3$ for removing silica from natural brines. Straub (41) studied the removal of silica from boiler salines at 182 to 282 C by the addition of solid MgO inside the boiler. Geisler (7) fed dried precipitated MgO to the water to remove the silica in a hot-process softener and claimed excellent results. Wesly (42, 13) stated that phosphate ion interfered with the absorption of silica by solid MgO at high temperatures. Peters and Turner (43) recommend that partial lime softening of boiler feedwater be employed in order to avoid precipitating the Mg^{++} in the water softener. Then this Mg^{++} is precipitated in the boiler, and they state that this precipitation reduces the SiO_2 content of the boiler salines to very low values. Betz, Noll, and Maguire (44, 45) recommend the use of special forms of magnesium oxide for removal of silica in the hot-process treatment. Low-temperature treatment by magnesium oxide is not recommended by these investigators, even though it is claimed that longer retention periods will improve silica removal at low temperatures. Behrman and Gustafson (37) recommend the precipitation of $Mg(OH)_2$ for removing silica in cold treatment and suggest feeding magnesium carbonate or magnesium bicarbonate to increase the ionic Mg content of the water being treated without leading to an increase in total dissolved solids of the treated

water. They state that no improvement in silica removal is obtained by the use of dolomitic lime [$Ca(OH)_2 \cdot MgO$] instead of ordinary lime.

It is interesting to note that, despite the activity in this field during the last decade, no data have been presented hitherto on a widely applicable silica-removal process. On the other hand, the new magnesia-silica-removal process to be discussed presently has already been embodied in a large-scale installation, which has been operating for more than a year, and it may be added that further installations embodying this process are under construction at the present time.

Development of Magnesia Process for Silica Removal

The investigations discussed in this paper were carried out with a view to developing a silica-removal process that would

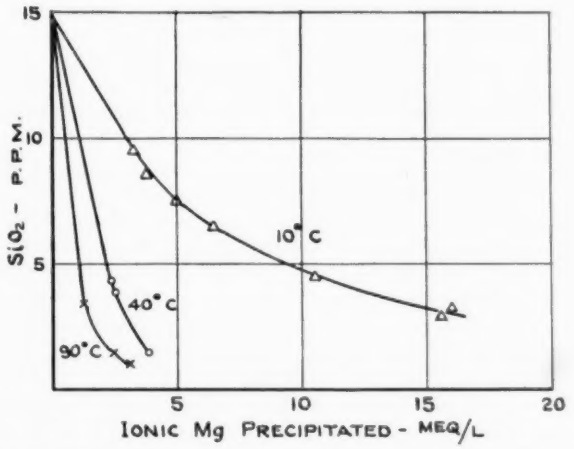


Fig. 1 Silica Removal by Ionic Mg Precipitated at Various Temperatures

Note: (a) Raw well water containing 15 ppm SiO_2; various amounts of Mg^{++} added in form of $Mg(HCO_3)_2$ or $MgCO_3$.
(b) Agitated with alkali for 30 min to precipitate the ionic Mg; decanted and filtered through paper, and SiO_2 determined on filtrate.
(c) Precipitated Mg^{++} only; no sludge added.

be simple and foolproof, in addition to being economical and sufficiently flexible to satisfy the wide variety of conditions which result from the various combinations of the following factors: Composition of the raw water, silica desired in the effluent, temperature of water to be treated, volume of water involved, other treating processes which must be applied to the water in addition to silica removal.

In order to determine the possibilities of developing such a process, several series of exploratory experiments were made during the early stages of this research. These investigations indicated that it would be possible to develop a simple and economical process and one that would be sufficiently flexible to meet the varying conditions enumerated. It was realized, however, that before such a process could be evolved, it would be necessary to carry out a systematic study of the influence of each of a number of factors affecting the process and to correlate these properly in designing equipment to suit each particular set of operating conditions.

The various aspects of the problem investigated include:

1 Silica removal by precipitating ionic Mg:
   (a) Effect of temperature and agitation
   (b) Methods of increasing the ionic Mg content of the raw water when that is necessary
   (c) Most suitable and economical sources of Mg in such cases.
2 Silica removal by solid, undissolved Mg compounds:
   (a) Effect of temperature and agitation
   (b) Influence of sludge; type of sludge, concentration, and degree of contamination
   (c) Most suitable and economical sources of Mg.
3 Silica removal by combining the effects of precipitation of ionic Mg and undissolved Mg compounds.

Precipitated Ionic Magnesium

Experiments were made to determine the controlling factors governing the silica reduction by precipitating ionic Mg, and in this series of tests, the sludge was eliminated in order to observe the effect of ionic Mg precipitation alone.

The Mg was added in the form of soluble $Mg(HCO_3)_2$ or $MgCO_3$ to a clear well water containing about 15 ppm SiO_2. The Mg was then precipitated by adding alkali and agitating for about 1 hr. These tests were also extended to various temperature ranges. The initial and final Mg and SiO_2 were measured, the results being summarized in Fig. 1.

These data show that:

(a) Silica reduction increases with increasing amounts of ionic Mg precipitated at any given temperature.

(b) The efficiency of silica absorption by precipitating ionic Mg increases greatly with rise in temperature.

It is apparent from these data that, from the technical point of view, it is feasible to reduce the silica to any desired extent by precipitating ionic Mg, but a number of questions immediately present themselves. What if there is not sufficient Mg in the raw water to permit precipitating the required amount of Mg for the desired silica reduction? In that event, how should it be added and in what form, and from what source should the Mg be obtained? Should the water be heated in order to take advantage of the great increase in silica-removal efficiency with rise in temperature?

The answers to these questions obviously involve considerations of design, availability and costs of Mg compounds, and local costs of heat. In order to study these matters adequately, it is first necessary to examine the reactions involved in the precipitation of ionic Mg and the dissolving of Mg compounds.

Principles of Dissolving and Precipitating Mg Compounds

The simplest method of adding Mg^{++} is to use a readily soluble salt, such as $MgSO_4$ which is usually available on the market in the form of Epsom salt, $MgSO_4 \cdot 7H_2O$. When Mg ion is precipitated from an $MgSO_4$ solution by a hydroxide like lime, the following reaction takes place

$$MgSO_4 + Ca(OH)_2 \rightarrow Mg(OH)_2 + CaSO_4 \quad \ldots\ldots [1]$$

The insoluble $Mg(OH)_2$ is precipitated, and the $CaSO_4$ is left in solution and is subsequently converted to a corresponding amount of Na_2SO_4 by the other steps in the treatment which are applied for removing the residual hardness. Thus each milliequivalent (meq) of $MgSO_4$ added leaves 1 meq of Na_2SO_4 in solution. The molecular weight of Na_2SO_4 = 142, and its equivalent weight = $\frac{142}{2}$ = 71. Therefore the addition of 1 meq of Mg per l in the form of $MgSO_4$ (weighing 60 mg) increases the total solids of the final effluent by 71 mg per l or 71 ppm.

If, on the other hand, the Mg^{++} is added in the form of $MgCO_3$ or $Mg(HCO_3)_2$ and is then precipitated by hydrate of lime, the reactions are as follows

$$MgCO_3 + Ca(OH)_2 \rightarrow Mg(OH)_2 + CaCO_3 \quad \ldots\ldots [2]$$

$$Mg(HCO_3)_2 + 2Ca(OH)_2 \rightarrow Mg(OH)_2 + 2CaCO_3 + 2H_2O \quad [3]$$

Both the reaction products, $Mg(OH)_2$ and $CaCO_3$, are relatively insoluble, and thus the dissolving of the Mg in this form and its subsequent precipitation do not leave any salts in solution, i.e., do not increase the total dissolved solids. It should be borne in mind, however, that commercial magnesite (which is the only fairly cheap form of $MgCO_3$) cannot be dissolved readily in water. But calcined magnesite (MgO) can be dissolved readily if brought into a fairly low pH environment, such as that prevailing in the usual raw water where HCO_3^- and CO_2 are present. When MgO is brought into contact with such a water, the following reactions take place

$$MgO + CO_2 \rightarrow MgCO_3 \quad [4]$$

or

$$MgO + 2\,HCO_3^- \rightarrow MgCO_3 + CO_3^- + H_2O \quad [5]$$

The reactions are essentially the same for dissolving $Mg(OH)_2$ which, as shown in Equations [2] and [3], is the form in which Mg is precipitated from solution.

Equations [4] and [5] show that the amount of Mg which can be dissolved from MgO depends upon the $HCO_3^- + CO_2$ content of the raw water. Where the raw water does not contain enough of these constituents to dissolve the required amount of Mg, CO_2 may be added readily and economically to the raw water by means of flue gas, in order to increase the MgO dissolved per Equation [4]. It is necessary to add a constant amount of CO_2 per unit volume of water for dissolving a constant amount of magnesium per unit volume of water. With this in mind, two arrangements may conveniently be used:

(*a*) *Presaturation of the Raw Water With CO_2.* This is accomplished by using a trickler-carbonator or bubbler arrangement, in which an excess of flue gas is contacted with the water to saturate all or a definite portion of the water with a constant amount of CO_2 under any given set of conditions. The water containing this constant amount of CO_2 is then admitted to the magnesium dissolver, where it is agitated with an excess of undissolved MgO.

(*b*) *Simultaneous Carbonation and Mg Dissolving.* This is carried out by using a flue-gas bubbler with measuring pump (compressor) to discharge a measured volume of flue gas directly into the agitated suspension of MgO in the magnesium dissolver. This dissolver is so designed that all the CO_2 added is absorbed by the water in the magnesium dissolver. Method (*b*) is useful when it is not possible to introduce sufficient CO_2 in the presaturation carbonator of (*a*) to dissolve the required amount of ionic Mg in the magnesium dissolver.

Sources of Ionic Magnesium

There are available several Mg compounds which are soluble directly in water containing HCO_3^- and CO_2. As mentioned, some of these, like $MgSO_4$, dissolve readily without reacting with the HCO_3^- and CO_2, while others, like MgO, require HCO_3^- and CO_2 to carry them into solution. In addition to the disadvantage of increasing total solids, as previously discussed, $MgSO_4$ has a high cost per unit Mg, as shown in Table 1.

In addition to MgO, there is another source of Mg which is even much less costly, namely, dolomitic lime. This product is made by calcining dolomite, and its composition is shown in Table 1. Although hitherto it has been customary to specify lime-free from Mg for water treatment (46), it is now found that these high Mg limes are a convenient and economical source of MgO for silica removal. The figures in Table 1 show it to be the cheapest source of Mg, after duly crediting the cost of the dolomitic lime with the value of the lime contained therein. This applies where the lime present in the dolomitic lime can be usefully consumed in the softening or other reactions. When the amount of MgO required carries with it too much lime, the dolomitic lime may be enriched by adding MgO so as to keep the lime dosage down to that which can be consumed usefully in the reactions. This is sometimes the case in waters that are low in Mg^{++}, HCO_3^-, and CO_2, so that little lime is required for treatment.

However, there is a special problem involved in transforming the undissolved MgO into the ionic Mg. Equations [4] and [5] showed that CO_2 or HCO_3^- must be present to dissolve MgO. It follows also that, so long as appreciable hydroxide is present (high pH), MgO does not dissolve. Such a condition prevails in the usual precipitation process, where sufficient excess hydroxide (usually in the form of lime) is added to complete the precipitation of ionic Mg after neutralizing the HCO_3^- and CO_2.

Thus, in order to dissolve any MgO, it is necessary to transfer it from the high pH lime-precipitation zone (i.e., the lime-softening reaction and settling tank) to an environment of low pH value (i.e., to a tank or compartment that is separate from the high pH zone).

The raw water, which usually contains some HCO_3^- and CO_2, constitutes such a low pH environment. Thus, if MgO is the source of ionic Mg, it is a simple matter to feed this MgO to the raw water (with or without additional CO_2 as outlined previously) in a separate tank or compartment, i.e., the magnesium dissolver.

But if calcined dolomitic lime [$Ca(OH)_2 \cdot MgO$] is used as the source of Mg, it becomes necessary to separate the MgO from the $Ca(OH)_2$ before the MgO can be dissolved to yield Mg^{++} in solution. This can be done in a lime-saturator type of apparatus, however, that is cumbersome and expensive. A much simpler method is to use the water-treating reaction and settling tank for this separation. The method of doing this is diagrammatically illustrated in Fig. 2.

This simple arrangement makes it possible to use the dolomitic lime as a source of low-cost ionic Mg by withdrawing the

TABLE 1 SOURCES AND COSTS OF MAGNESIUM IN SOLUBLE OR DISSOLVABLE COMPOUNDS

Commercial name	Chemical name	Chemical formula of usual commercial form	Average analysis CaO, per cent	Average analysis MgO, per cent	Cost of material, cents per lb	Value of lime (CaO) content, cent per lb	Balance of cost of material, cents per lb	Number of gram equivalents of MgO in 1 lb of commercial material	Cost per gram equivalent of MgO,[b] cent
Epsom salt	Magnesium sulphate	$MgSO_4 \cdot 7H_2O$	0	16	1.9	0[c]	1.9	3.6	0.53
Calcined magnesite	Magnesium oxide	MgO	1–2	92	3.0	0	3.0	21.0	0.14
Calcined dolomite (hydrated)	Calcium hydrate-magnesium oxide	$Ca(OH)_2 \cdot MgO$	47[a]	33[a]	0.6	0.3	0.3	7.5	0.04
Calcined dolomite (unhydrated)	Calcium magnesium oxide	$CaO \cdot MgO$	57[a]	42[a]	0.6	0.3	0.3	9.5	0.03

[a] These figures correspond to CaO MgO mole ratios = 1:1, which is to be expected from the fact that these materials are produced by calcining natural dolomite ($CaCO_3 \cdot MgCO_3$).

[b] 1 milliequivalent per liter of water (meq per l) corresponds to $\frac{1{,}000{,}000 \text{ lb}}{2.2 \text{ lb per l}} = 454{,}000$ meq or 454 g eq per million lb of water or 3.8 g eq per 1000 gal of water.

[c] In fact, $MgSO_4$ requires (in addition to the lime for precipitating the Mg^{++}) Na_2CO_3 for precipitating the $CaSO_4$ left in solution; this is usually a substantial item in operating cost.

MgO-containing thickened sludge from the settling tank after the lime is consumed in the reactions, the MgO of the dolomitic lime having dropped to the bottom of the settling tank with the precipitated $Mg(OH)_2$ and $CaCO_3$. This MgO-containing sludge is then agitated in the low pH environment in the magnesium dissolver, where it meets the HCO_3^-- and CO_2-containing raw water.

It should be noted that, although magnesium in the form of natural magnesite ($MgCO_3$) or dolomite ($CaCO_3 \cdot MgCO_3$) is even cheaper than in the corresponding calcined forms shown in Table 1, it is not practical to use these natural uncalcined materials as sources of Mg, because they cannot be dissolved in the presence of HCO_3^- and CO_2. However, under certain conditions, a partially calcined dolomite ($CaCO_3 \cdot MgO$) may be satisfactory and economical.

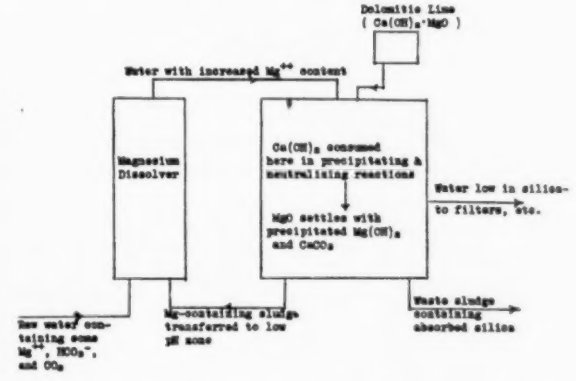


FIG. 2 DOLOMITIC LIME AND RECYCLED SLUDGE AS A SOURCE OF IONIC MG

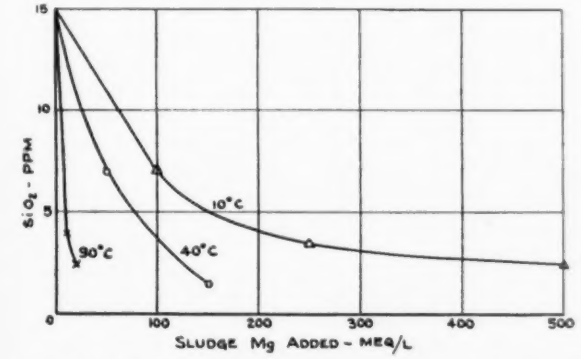


FIG. 3 SILICA REMOVAL BY UNDISSOLVED SPAULDING PRECIPITATOR SLUDGE AT VARIOUS TEMPERATURES

NOTE: (a) Raw well water containing 15 ppm SiO_2.
(b) Spaulding precipitator sludge containing 30 per cent by weight of MgO and $Mg(OH)_2$ and 70 per cent $CaCO_3$.
(c) Agitated with sludge 30 min; then centrifuged 5 min, decanted and filtered through paper, and SiO_2 determined on filtrate.
(d) No ionic Mg precipitated.

SILICA REMOVAL BY UNDISSOLVED MAGNESIUM COMPOUNDS (WITHOUT PRECIPITATING IONIC MG)

Exploratory tests made previously showed the advantages of accumulated Mg-containing sludges. It was clear from these observations that undissolved Mg compounds also have silica-absorption properties. This fact, as well as the desirability of avoiding the dissolving and reprecipitation of ionic Mg in some cases, made it necessary to study the role of undissolved Mg compounds.

These investigations included tests on various sludges and various commercial magnesium compounds. Precipitation of ionic Mg was eliminated so as to observe the effect of the undissolved compounds only; for this purpose, a low Mg^{++} water was used, and the HCO_3^- and CO_2 were neutralized before adding the Mg compound, so as to prevent any magnesium from passing into solution. The tests were also extended to various temperature ranges, and the initial and final SiO_2 were measured. The results are set forth in Fig. 3. The tests were conducted on the same well water used for the ionic Mg tests and containing about 15 ppm SiO_2. The sludge was taken from a precipitator which had been operating for some time on this well-water supply; thus the sludge was substantially contaminated with absorbed silica.

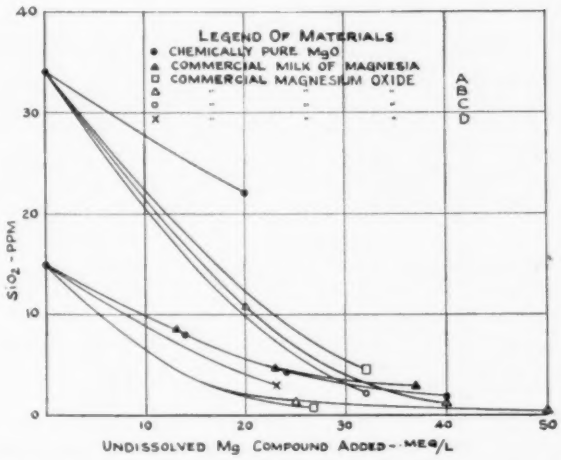


FIG. 4 INITIAL SILICA ABSORPTION BY VARIOUS UNDISSOLVED MG COMPOUNDS

NOTE: (a) Raw well water containing 15 to 16 ppm SiO_2 (lower set of curves) and 32 to 34 ppm SiO_2 (upper set of curves).
(b) Temperature 90 C.
(c) Water agitated 20 min with each material after neutralizing HCO_3^- and CO_2 to prevent MgO from passing into solution. Sample then decanted, filtered through paper, and SiO_2 determined on filtrate.
(d) No ionic Mg precipitated.

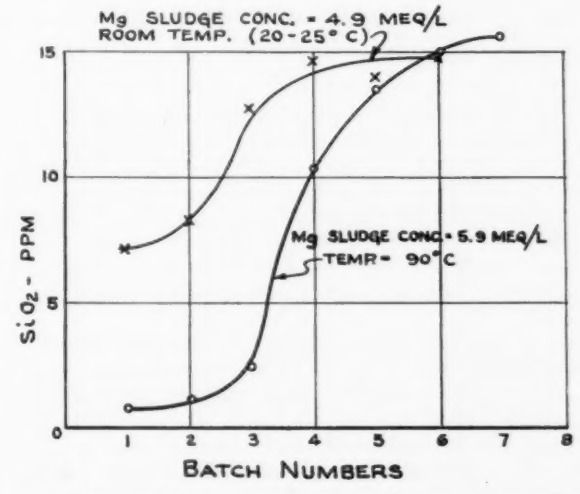


FIG. 5 ULTIMATE SILICA ABSORPTION BY VARIOUS UNDISSOLVED MG COMPOUNDS

NOTE: (a) Raw well water containing 15 to 16 ppm SiO_2.
(b) Successive batches of water treated with one batch of externally prepared $Mg(OH)_2$ sludge [by precipitation from $Mg(HCO_3)_2$ solution] in concentrations indicated on curves.
(c) Water agitated with sludge 1 hr on each test after neutralizing HCO_3^- and CO_2 to prevent $Mg(OH)_2$ from passing into solution. Sample then decanted, filtered through paper, and SiO_2 determined on filtrate.
(d) No ionic Mg precipitated.

These studies show that:

(*a*) The larger the amount of sludge magnesium added, the greater is the silica reduction.

(*b*) The amount of undissolved sludge Mg required to produce a given silica reduction is much greater than the amount of precipitated ionic Mg required.

(*c*) The efficiency of silica reduction increases with rise in temperature in the same general way as with precipitated ionic Mg.

These findings on silica absorption by Mg sludges were then supplemented by determining the silica-absorption characteristics of various other undissolved Mg compounds. The results are summarized in Fig. 4. The term "initial absorption" means the silica reduction obtained by contacting a water once with a given material. Such tests are made in the absence of ionic Mg precipitation or accumulated undissolved Mg compounds.

Since we already had indications of the value of accumulated sludge, further investigation was undertaken to determine more clearly the nature of this reaction. For this purpose, so-called "ultimate-absorption" tests were made as illustrated in Fig. 5. These tests show that, as successive batches of water are brought into contact with these undissolved Mg compounds, they continue to absorb more silica. It follows from this that there is economy to be realized by retaining these partially exhausted materials in the system for further contact with silica-containing water. It would be expected that such further silica absorption by the partially exhausted Mg compound would reduce the silica-absorption burden on new Mg compound added to the system (make-up Mg compound), and would therefore reduce the required quantity of such make-up Mg compound.

In order to check these theoretical conclusions, tests were conducted with various undissolved Mg compounds, and the material added was accumulated from one batch treatment to the next until certain desired concentrations of these accumulated compounds had been reached. These accumulations are referred to as "sludge accumulations," and their concentrations on the graphs are represented in terms of "sludge Mg concentrations—meq/L."

An alternative and more rapid method of accumulating such silica-contaminated sludge is to treat a large volume of water with the Mg compound in question, thereby contaminating the MgO with silica. The large amount of contaminated MgO thus obtained is separated from the water and used as the contaminated sludge for subsequent treatments of small volumes of water.

To these successive batches of water, specified amounts of make-up MgO are added until equilibrium is reached under each set of conditions for at least several batches, and just prior to adding the make-up MgO, a portion of the sludge is discharged to waste in an amount equal to the make-up MgO to be added to the system. Thus the total sludge Mg concentration is maintained at a constant figure for each series of measurements with a specific make-up MgO dosage. This provides a method for collecting equilibrium data which stimulate the results that are obtained in large-scale operation.

Figs. 6 and 7 summarize the results obtained for certain Mg compounds at 95 C and 20 to 25 C, respectively. The absorption of silica by adding make-up undissolved Mg compounds in the presence of Mg sludge accumulations is referred to as "operating absorption." These graphs show clearly that the accumulation of Mg sludges substantially reduces the amount of make-up MgO required for obtaining a given silica-removal result or, conversely, that the same amount of make-up MgO produces a better silica-removal result in the presence of Mg sludge accumulations.

Sources and Desirable Characteristics of Undissolved Mg Compounds

In general, the same materials as those mentioned under sources of ionic Mg are suitable for silica absorption in the undissolved form, calcined dolomite [$Ca(OH)_2 \cdot MgO$] being one of the cheapest sources (see Table 1). Usually it is necessary to add

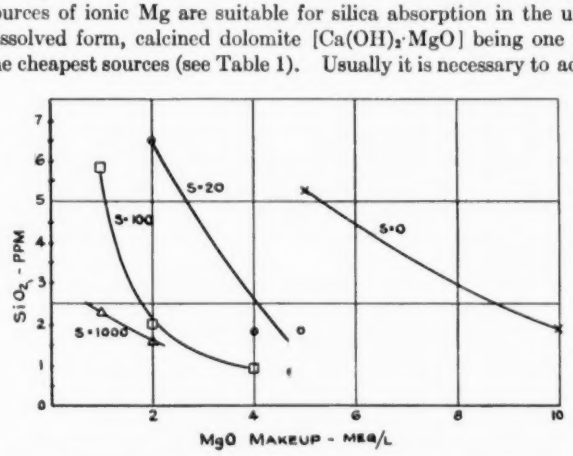


Fig. 6 Effect of Accumulating Mg Sludges on Silica Removal by Undissolved Mg Compounds; High Temperature

Note: (*a*) *S* represents sludge-magnesium concentration in meq/L.
(*b*) Material used as make-up and accumulated as sludge was a commercial calcined magnesite about 300 mesh.
(*c*) Raw well water containing 15 ppm SiO_2.
(*d*) Temperature 95 C.
(*e*) Agitated with sludge 20 min.
(*f*) pH of filtered effluent 10 to 10.3.
(*g*) HCO_3^- and CO_2 first neutralized with lime to prevent any of the Mg from passing through ionic stage.
(*h*) No ionic Mg precipitated.

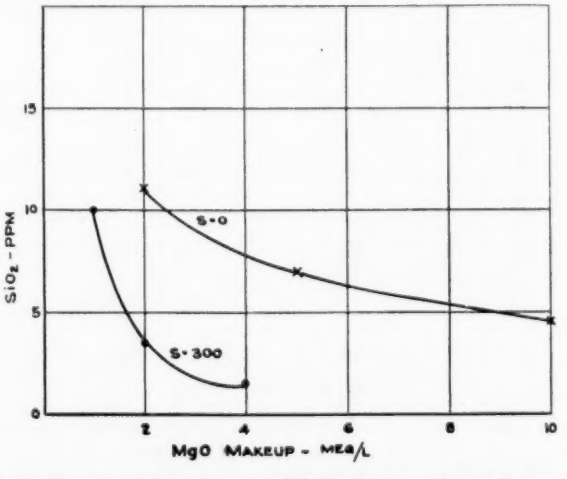


Fig. 7 Effect of Accumulating Mg Sludges on Silica Removal by Undissolved Mg Compounds; Low Temperature

Note: (*a*) *S* represents sludge-magnesium concentration in meq/L.
(*b*) Material used as make-up and accumulated as sludge was a commercial calcined magnesite about 300 mesh.
(*c*) Raw well water containing 15 ppm SiO_2.
(*d*) Temperature 20 to 25 C.
(*e*) Agitated with sludge 1 hr.
(*f*) pH of filtered effluent 10 to 10.3.
(*g*) HCO_3^- and CO_2 first neutralized with lime to prevent any of the Mg from passing through ionic stage.
(*h*) No ionic Mg precipitated.

some lime in the treatment even if Mg^{++} is not being precipitated; as a matter of fact, the HCO_3^- and CO_2 in the water must be neutralized to prevent the MgO from passing into solution. Thus, if dolomitic lime is used, there is added with each equivalent of $Ca(OH)_2$ one equivalent of low-cost MgO. If this is not sufficient, the dolomitic lime may be supplemented by magnesium oxide (MgO).

Tests show that, when dolomitic lime is used in this man-

ner, it is preferable to avoid feeding it in the form of a slurry, because the absorption of OH ion by the MgO from this concentrated-lime solution reduces the silica-absorption capacity of the MgO. (Some of our recent data contradict this statement, but there has not yet been an opportunity to determine the final answer to this question.) Our investigations have shown also that other things being equal, finer particle size enhances the silica absorption by undissolved Mg compounds. Also there is a relation between the calcining temperature of various materials and their ability to absorb silica.

Combined Use of Ionic Magnesium and Undissolved Magnesium Compounds

Although in the preceding discussion and in much of the investigation, these two types of Mg have been separated for purposes of study, in actual practice both forms of Mg are usually used in combination. This is due to the fact that most raw waters contain some Mg^{++}, and, if not, they usually contain some HCO_3^- and CO_2, so that some ionic Mg can be conveniently added by the simple expedient of agitating the raw water with an Mg-containing sludge in the magnesium dissolver (Equations [4] and [5]).

In this connection, it should be noted that, if ionic Mg is added to the water by dissolving MgO or $Mg(OH)_2$ and if no CO_2 is added to the system, the amount of lime required for the precipitation of this Mg^{++} is the same as that which would have been required for reacting with the $CO_2 + HCO_3^-$ in the usual lime treatment. This is apparent from a consideration of the following reactions, which take place in the usual lime treatment.

$$CO_2 + Ca(OH)_2 \rightarrow CaCO_3 + H_2O \quad \ldots\ldots\ldots\ldots [6]$$

$$2HCO_3^- + Ca(OH)_2 \rightarrow CaCO_3 + CO_3^- + 2H_2O \quad \ldots\ldots [7]$$

In each of these reactions, 1 equivalent of lime is consumed, while according to Equations [4] and [5], the reactions between MgO and the same amounts of CO_2 and HCO_3^- yield one equivalent of $MgCO_3$ in each case. As shown by Equation [2], each of these equivalents of $MgCO_3$ in turn requires only 1 equivalent of $Ca(OH)_2$, i.e., the same amount as required for the reactions directly with lime as set forth in Equations [6] and [7]. The OH ion liberated by the hydrolysis of the MgO or directly by the $Mg(OH)_2$ exactly balances the OH ion required in the form of lime (or other alkali) for the precipitation of the dissolved $MgCO_3$. It follows that the mere addition of ionic Mg, dissolved from MgO by the $CO_2 + HCO_3^-$ present in the raw water, does not cause any increase in the lime consumption. Also it is clear that the amount of Mg^{++} picked up in the magnesium dissolver does not alter the lime dosage in any way, i.e., the hardness and alkalinity of the effluent remain constant.

Where conditions require the precipitation of more ionic Mg than can be directly taken up by the raw water, the CO_2 content of the water is increased by means of flue gas as discussed previously. In that event, each added equivalent of CO_2 requires the addition of one equivalent of lime. Usually this does not increase the operating cost out of proportion to the added benefits obtained from the high Mg^{++}.

Silica Contamination of Sludge Accumulations

In practicing the combined ionic Mg and undissolved Mg process, the Mg^{++} which is precipitated as $Mg(OH)_2$ concentrates in the sludge zone of the settling tank with the MgO of the dolomite. During this cycle, the $Mg(OH)_2$ and MgO are contaminated with the silica which they absorb, and such contamination would increase indefinitely were it not for the fact that there is discharged to waste from the system a certain amount of silica-contaminated sludge, while there is being added to the system fresh Mg. If the Mg added to the system and wasted is increased, this ratio of $Mg:SiO_2$ in the sludge rises correspondingly, and the residual SiO_2 in the effluent decreases, Fig. 6. Therefore, in calculating the amount of make-up MgO to be added in the form of $Ca(OH)_2 \cdot MgO$ or MgO, this contamination factor must be considered, i.e., the amount of make-up MgO must bear a certain ratio to the SiO_2.

Spaulding Precipitator-Type Equipment Favorable for Process

In addition to the laboratory-scale tests on both the ionic Mg, the undissolved Mg compounds, and the combined process, extended tests were carried out on a miniature-plant scale using various combinations of ionic and undissolved Mg, at various temperatures, and with various sludge concentrations. These extensive tests indicate that the most favorable type of equipment is that illustrated in Fig. 8. The principles of the precipitator itself have been described (47), and it is clear that this equipment has certain characteristics which make it particularly suitable for carrying out this process.

For example, as shown in Fig. 8, the magnesium dissolver can be conveniently built into the upper section of the downcomer without any sacrifice of useful space. Also, this type of equipment lends itself readily to the insertion of so-called sludge-concentrator pockets in which the sludge is further thickened. This thickened sludge is especially suitable for recirculation into the

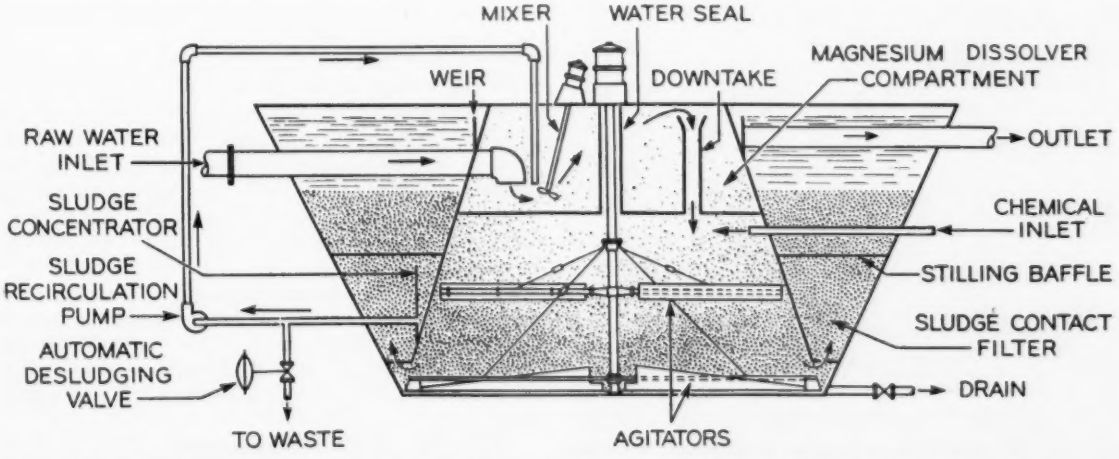


Fig. 8 Modified Spaulding Precipitator With Magnesium Dissolver, Etc., for Magnesia-Silica-Removal Process

magnesium dissolver, because the higher the sludge concentration in this recirculated stream, the smaller is the volume required to maintain the proper MgO concentration in the magnesium dissolver. Also, it is desirable to add as little as possible of the high pH liquid to the magnesium dissolver, because any OH^- or $CO_3^=$ in the recirculated liquid neutralizes some of the HCO_3^- and CO_2 in the raw water, and thereby reduces the amount of Mg^{++} that can be dissolved in the magnesium dissolver.

As shown previously, thorough and extended agitation of the concentrated sludge with the water enhances the silica-removal process. It is clear that the Spaulding precipitator affords this extended intimate contact between the water and the sludge, which is maintained in suspension in the lower part of the equipment. Briefly, the operation, illustrated in Fig. 8, is as follows: The raw water and recirculated sludge are mixed in the magnesium-dissolver compartment, where the water takes up the required amount of Mg^{++}. This water then passes into the downcomer, where it meets the stream of chemical reagents and undergoes thorough agitation for an extended period of time, during which the Mg^{++} is precipitated as $Mg(OH)_2$ and the Ca^{++} is precipitated as $CaCO_3$. The water containing these precipitates and the undissolved MgO from the dolomitic lime or other source then passes through the ports adjacent to the lower edge of the central downcomer and passes upward through the concentrated suspension of previously formed sludge in the outer compartment. As this compartment increases in cross-sectional area, the vertical velocity of the water continuously decreases as it rises toward the outlet. Finally, the upward velocity of the water decreases to such a point that it can no longer maintain the sludge particles in suspension. At this level, the sludge is left behind, and the clear water rises to the top of the equipment and overflows the collecting weir and passes through the outlet and into the filters.

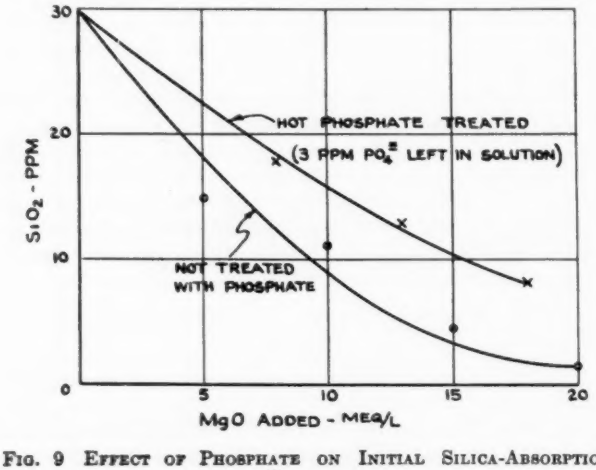


FIG. 9 EFFECT OF PHOSPHATE ON INITIAL SILICA-ABSORPTION CAPACITY

NOTE: (a) Raw water containing 30 to 33 ppm SiO_2.
(b) Commercial calcined magnesite (finer than 200 mesh) added without any sludge accumulations.
(c) Temperature 95 C.
(d) Agitated with MgO 20 min; then decanted and filtered, and SiO_2 determined on filtrate.
(e) HCO_3^- and CO_2 neutralized on untreated sample to prevent MgO passing into solution.
(f) No ionic Mg precipitated.

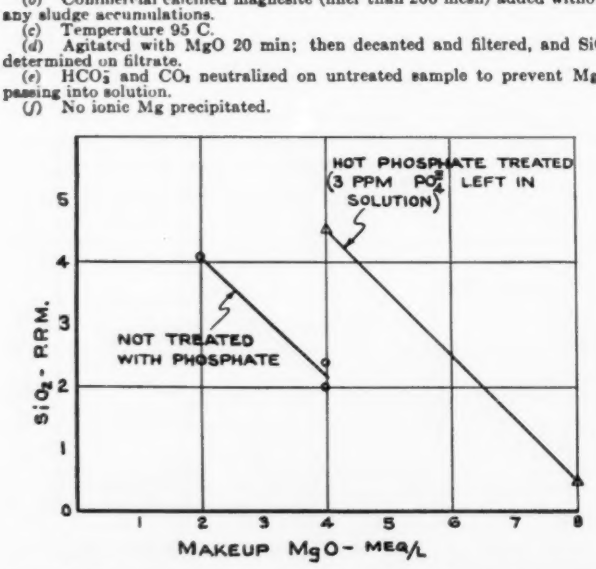


FIG. 10 EFFECT OF PHOSPHATE ON OPERATING SILICA-ABSORPTION CAPACITY IN PRESENCE OF CONCENTRATED SLUDGE ACCUMULATIONS

NOTE: (a) Raw water containing 30 to 33 ppm SiO_2.
(b) Commercial calcined magnesite (finer than 200 mesh) added in presence of 100 meq sludge Mg per l.
(c) Temperature 95 C.
(d) Agitated with MgO 20 min; then decanted and filtered, and SiO_2 determined on filtrate.
(e) HCO_3^- and CO_2 neutralized on untreated sample to prevent MgO passing into solution.
(f) No ionic Mg precipitated.

In addition to accomplishing the silica removal by the precipitation of Mg^{++} and by maintaining intimate contact between the sludge and the water, this equipment permits the usual lime-soda softening reactions to take place at the same time. Also the addition of coagulant provides for simultaneous turbidity removal. It is evident, therefore, that this silica-removal process can be incorporated in the lime-soda-coagulant-softening and turbidity-removal plant at little added initial cost or operating cost.

The process can also be incorporated into the usual hot-process lime-soda softener. For the most efficient results, it is desirable to incorporate the Spaulding sludge-agitation and sludge-contact features (and occasionally the magnesium-dissolver feature) in such equipment. With this in view, the construction principles, illustrated in Fig. 8, are being incorporated in a modified hot-process lime-soda softener which is under construction at the present time.

EFFECT OF PHOSPHATE ON SILICA REMOVAL

A question arises as to the effect of phosphates on this silica-removal process. In some cases where the raw-water hardness is very low, it is found desirable to soften the feedwater make-up by external hot-phosphate treatment, which is carried out in equipment similar to the conventional hot-process lime-soda softener. Since many such low-hardness waters have a high silica content, the effect of phosphate ion on the absorption of silica by undissolved MgO was investigated. Wesly (13, 42) reported that phosphate ion interfered with silica absorption by undissolved MgO, and our tests were made to determine the extent of this interference under conditions prevailing in the present process.

Two series of tests were carried out; one on the so-called initial silica absorption, where the MgO is contacted once with the water without sludge accumulations, and a second on the so-called operating silica absorption, which is carried out in the presence of concentrated accumulations of Mg compounds or sludge and only a certain amount of make-up Mg compound is added to the system. In each case, the results were compared on the hot-phosphate-treated water with those on a water which was not treated with phosphate.

Figs. 9 and 10 summarize the data. They show clearly that the presence of phosphate ion interferes substantially with the silica-absorption properties of MgO. It may be concluded, therefore, that in such cases it is usually preferable to apply the silica-removal process before applying the hot-phosphate treatment.

CONCLUSIONS

This research study has revealed the following:

(*a*) For any given set of conditions ionic Mg precipitated in situ as $Mg(OH)_2$ is most efficient, but undissolved Mg compounds of proper quality (fine-particle size, etc.) also give satisfactory results when favorable conditions of sludge concentration, agitation, etc., are maintained.

(*b*) The efficiency of removing silica by precipitating ionic Mg or by undissolved Mg compounds increases with temperature, but the application of other factors disclosed makes it possible to obtain satisfactory results at low temperature. Slight prewarming of the water to about 30 to 40 C (86 to 104 F) reduces the Mg required to obtain the desired result; waste heat is usually available for this purpose.

(*c*) Efficiency increases with the concentration of the Mg-containing sludge in contact with the water.

(*d*) Increasing the time of contact with the sludge absorbent in agitated suspension improves the results.

(*e*) Reducing the silica contamination of the retained concentrated sludge reduces the silica in the effluent; thus if the Mg added to the system is increased, the ratio of $Mg:SiO_2$ in the sludge rises correspondingly, and the residual SiO_2 in the effluent decreases.

(*f*) The presence of phosphate ion interferes with silica absorption by MgO.

(*g*) In those cases where additional Mg is required for the desired silica reduction, it can usually be obtained most economically from dolomitic lime ($Ca(OH)_2 \cdot MgO$); where no lime is required in the treatment, calcined magnesite (MgO) is used.

(*h*) Ionic Mg may be added to the raw water economically and without increasing the lime requirement or the total-solids content of the effluent by recirculating sludge into a magnesium-dissolver compartment or low pH zone, where the HCO_3^- and CO_2 in the raw water dissolves Mg^{++} from this sludge. If necessary, additional CO_2 may be added by flue-gas carbonation to increase further the amount of Mg^{++} introduced.

In applying this silica-removal process, the economic balancing of these findings to produce the desired result requires careful consideration of all the facts in any given case. The data show that the silica may be removed efficiently both at low and high temperatures. In general, the following may be stated with respect to the equipment:

(*a*) If hot-process lime-soda treatment is applied to reduce the hardness, superior silica-removal results are obtained by using equipment embodying positive agitation and intimate sludge contact like that provided by a Spaulding precipitator type of hot-process softener.

(*b*) If hot-phosphate softening is used, the silica-removal treatment should be carried out first, and the phosphate treatment should follow.

(*c*) If the treatment is applied at low or medium temperatures (cold-process treatment), the silica removal is applied first, and advantage may be taken of posttreatment by carbonaceous zeolites, which completely eliminate any residual hardness. Carbonaceous hydrogen-zeolite treatment (14) may also be included to reduce the final alkalinity to any predetermined figure. These carbonaceous zeolites, being nonsiliceous, can treat the effluent of the silica-removal plant without danger of silica pickup from the zeolite by the water.

Acknowledgment

The author wishes to acknowledge the cooperation of Mr. S. B. Applebaum, vice-president of The Permutit Company and of the following members of The Permutit Company's Research and Development staff in the development of this process and the preparation of this paper: Dr. P. C. Goetz, Dr. John G. Dean, Dr. Ray Riley, Mr. R. W. Jackson, Dr. Calvin Calmon, Mr. M. E. Gilwood, and several others.

BIBLIOGRAPHY

1 "Stellungnahme zu dem Bericht von Oberingenieur Pfadt," by K. Morawe, Vereinigung der Grosskesselbesitzer, Speisewasserpflege, Berlin, 1928, pp. 44–47.

2 "Untersuchungen über die Entkieselung des Wassers," by R. Stumper, *Die Wärme*, vol. 55, 1932, pp. 272–278.

3 "Zur Kenntnis der zementierenden, insbesondere der silicatischen Bestandteile des Kesselsteines," by F. Hundeshagen, *Chemiker Zeitung*, vol. 56, 1932, pp. 521–524, 542–544.

4 "Silicon in Boiler Waters," by R. E. Summers and C. S. Keevil, unpublished paper, presented at Annual Meeting, A.S.M.E., 1933; *Power Plant Engineering*, vol. 38, 1934, pp. 219–220.

5 "Treatment of Silica for High Pressure Boilers," by S. E. Tray, *Power Plant Engineering*, vol. 40, 1936, pp. 515 517.

6 "Complex Silicate Scales in High-Pressure Boilers," by S. T. Powell, L. V. Carpenter, and J. J. Coates, *Combustion*, vol. 11, no. 2, August, 1939, pp. 18–24.

7 "Die Entkieselung des Speisewassers der Höchstdruckanlage in Höchst," by W. Geisler, *Mitteilungen der Vereinigung der Grosskesselbesitzer*, vol. 64, 1937, pp. 267–269.

8 Discussion at Mechanical Engineers Meeting in Lone Star State, *Power*, vol. 80, 1936, p. 381.

9 "Zur Verkieselung der Dampfturbinen," by F. Kaissling, *Archiv für Wärmewirtschaft und Dampfkesselwesen*, vol. 20, 1939, pp. 89–91.

10 Abstract of paper by W. Wesly, *Die Wärme*, vol. 61, 1938, p. 576; refer to (13).

11 "Descaling Steam Turbines," by J. B. Entriken, *Industrial and Engineering Chemistry*, vol. 30, 1938, pp. 1279–1280.

12 "Die Kieselsäure und ihre Bedeutung im Hochdruck-Kesselbetrieb," by A. Splittgerber, *Mitteilungen der Vereinigung der Grosskesselbesitzer*, vol. 73, 1939, pp. 206–231.

13 "Neue Erfahrungen über die Speisung von Höchstdruckkesseln mit chemische aufbereitetem Wasser," by W. Wesly, *Chemische Fabrik*, vol. 12, 1939, pp. 137–142.

14 "Carbonaceous Zeolites—an Advance in Boiler-Feedwater Conditioning," by H. L. Tiger, Trans. A.S.M.E., vol. 60, 1938, pp. 315–325.

15 "Applications of Carbonaceous Zeolites to Water Softening," by S. B. Applebaum, *Journal*, American Water Works Assn., vol. 30, 1938, pp. 947–978.

16 "Treatment of Boiler Feedwater by Zeo-Karb Process," by J. D. Yoder, *Combustion*, vol. 10, no. 11, 1939, pp. 35–40.

17 "Zeo-Karb H: A New Method of Conditioning Water to Remove Sodium Bicarbonate," by S. B. Applebaum and R. Riley, *Industrial and Engineering Chemistry*, vol. 30, 1938, pp. 80–82.

18 "Standard Methods for the Examination of Water and Sewage," American Public Health Association, Eighth edition, New York, N. Y., 1936, pp. 103–105.

19 "Colorimetric Standards for Silica," by H. W. Swank and M. G. Mellon, *Industrial and Engineering Chemistry*, Analytical edition, vol. 6, 1934, pp. 348–350.

20 "Silicomolybdate Method for Silica," by H. W. Knudson, C. Juday, and V. W. Meloche, *Industrial and Engineering Chemistry*, Analytical edition, vol. 12, 1940, pp. 270–273.

21 "Silica in Water," by M. C. Schwartz, Louisiana State University Bulletin, vol. 30, N.S. no. 14, Oct., 1938.

22 "Determination of Soluble Silica in Water. A Photoelectric Method," by H. L. Kahler, presented at the 100th Meeting of the American Chemical Society, September 11, 1940.

23 "Precipitation of Silica in Drinking Water by Means of Soda and Alum," by A. Massink, Verslag Centr. Lab. t.b.u.h., Staatstaez. o.d. Volksgesend. h. over, 1918, pp. 76–83.

24 "Silicic Acid, Its Influence and Removal in Water Purification," by O. M. Smith, Illinois State Water Survey, Bulletin 16, 1918-1919, pp. 140–181.

25 "Über die Entkieselung von Kieselsäurehaltigen Wässern," by E. Berl and H. Staudinger, *Zeitschrift für Angewandte Chemie*, vol. 40, 1927, pp. 1313–1317.

26 "Removing Silica From Water," by Otto Liebknecht, U. S. Pat. 1,860,781, May 31, 1932, assigned to The Permutit Company.

27 "Verfahren zur Entfernung von in Wasser gelöster Kieselsäure," by A. G. Kurz, Austrian Pat. 133,757, June 15, 1933.

28 "Prevention of Silica Scale With Sodium Aluminate," by C. H. Christman, J. A. Holmes, and H. Thompson, *Industrial and Engineering Chemistry*, vol. 23, 1931, pp. 637–646.

29 "Kolloidchemische Fragen der Speisewasserbehandlung, . . ." by R. Stumper, *Die Wärme*, vol. 53, 1930, pp. 859–862.

30 "Coagulation as Applied to Industrial Waters," by A. P. Black, R. A. Bardwell, and B. W. Graham, *Journal*, American Water Works Assn., vol. 29, 1937, pp. 1533–1547.

31 "Removal of Silica From Water by Sodium Aluminate," by F. K. Lindsay and J. W. Ryznar, *Industrial and Engineering Chemistry*, vol. 31, 1939, pp. 859–861.

32 "Water Treatment," by F. K. Lindsay and D. G. Braithwaite, U. S. Pat. 2,194,524, March 26, 1940, assigned to National Aluminate Corporation.

33 "Removal of Silica From Water by Cold Process," by L. D. Betz, C. A. Noll, and J. J. Maguire, *Industrial and Engineering Chemistry*, vol. 32, 1940, pp. 1320–1323.

34 "The Removal of Silica From Water for Boiler Feed Purposes," by M. C. Schwartz, *Journal*, American Water Works Assn., vol. 30, 1938, pp. 659–678.

35 "Rohwasser-Entkieselung," by K. Hoell, *Archiv für Wärmewirtschaft*, vol. 19, 1938, pp. 323–324.

36 "Recent Trends in Water Treatment," by S. T. Powell, L. V. Carpenter, L. R. Setter, and J. J. Coates, *Chemical and Metallurgical Engineering*, vol. 46, 1939, pp. 481–484.

37 "Removal of Silica From Water," by A. S. Behrman and H. Gustafson, *Industrial and Engineering Chemistry*, vol. 32, 1940, pp. 468–472.

38 "Process for Purifying Water," by H. A. Reimers, U. S. Pat. 1,966,733, July 17, 1934, assigned to Dow Chemical Company.

39 "Verfahren zum Reinigen von Wasser unter Anwendung von Magnesiumoxyd oder basisch Kohlensaurer Magnesia," by E. Bohlig, German Pat. 3187, Jan. 16, 1879.

40 "Method of Removing Dissolved Silica From Natural Alkaline Brines," by W. A. Kuhnert, U. S. Pat. 1,992,532, Feb. 26, 1935.

41 "Removal of Silica From Solution at Boiler Temperatures," by F. G. Straub, *Industrial and Engineering Chemistry*, vol. 28, 1936, pp. 36–37.

42 Discussion of paper by W. Geisler (7), by W. Wesly, *Mitteilungen der Vereinigung der Grosskesselbesitzer*, vol. 64, 1937.

43 "Silica in Boiler Feed Water," by W. F. Peters, Jr., and W. D. Turner, *Power Plant Engineering*, vol. 44, no. 3, 1940, pp. 54–57; no. 4, 1940, pp. 47–49.

44 "Removal of Silica From Water by Hot Process," by L. D. Betz, C. A. Noll, and J. J. Maguire, *Industrial and Engineering Chemistry*, vol. 32, 1940, pp. 1323–1329.

45 "Adsorption of Soluble Silica From Water," by L. D. Betz, C. A. Noll, and J. J. Maguire, *Industrial and Engineering Chemistry*, June, 1941, pp. 814–820.

46 "Quality of Lime Desired for Water Treatment," by C. P. Hoover, A.S.T.M. Symposium on Lime, March 8, 1939, pp. 43–46.

47 "Cold Lime-Soda Water Softening," by S. B. Applebaum, *Industrial and Engineering Chemistry*, vol. 32, 1940, pp. 678–684.

Discussion

L. D. Betz,[4] C. A. Noll,[5] and J. J. Maguire.[6] This paper presents data which serves to confirm some of the conclusions previously reached by the writers.[7] We have previously pointed out the increase in efficiency of silica removal, which results from increase in temperature, increase in retention and recirculation of sludge, and are naturally pleased that independent investigators have confirmed the validity of our former conclusions.

Unlike the author, however, we have not found ionic magnesium precipitated in situ as $Mg(OH)_2$ to be more efficient in the removal of silica from solution than the use of properly prepared magnesium oxide, except within the limits of possible error in laboratory technique. Under full-scale-plant conditions, a study of the results obtained have indicated very little, if any, difference in the quantity of silica removed, per unit of magnesium added, whether in the dissolved form as a salt such as magnesium sulphate or from an undissolved compound such as a specially prepared form of magnesium oxide. It is evident that the author's conclusions on the greater efficiency of ionic magnesium were obtained by the comparison of a soluble salt, such as magnesium sulphate with an "undissolved compound," such as calcined magnesite. In the large amount of work we have done on silica removal, we have tested and reported on a great number of various types of calcined magnesite and have found the efficiency of numerous samples submitted to vary considerably. A special form of magnesium oxide, prepared from sea-water bitterns, has been found to possess qualities markedly superior to calcined magnesite for the removal of silica from water.

Under the heading, "Sources of Undissolved Magnesium Compounds," the author calls attention to the fact that "finer particle size enhances the silica absorption by undissolved magnesium compounds. Also there is a relation between the calcining temperature of various materials and their ability to absorb silica." This confirms work done in our laboratories quite some time ago and was the direct cause of cooperative research with the California Chemical Company, which led to the development, almost two years ago, of a highly efficient magnesium oxide prepared under controlled conditions. It is this specially prepared form of magnesium oxide which they have termed Remosil and which we have found to possess considerably superior silica-removal properties to any other form of magnesium oxide we have tested. It is for this reason they have specifically branded this to differentiate it from calcined magnesite. Such data, we have presented in our previous papers on this subject.

Examination of the data, shown in Fig. 4 of the paper, for the initial silica absorption by various undissolved magnesium compounds, indicates a rather low silica-removal efficiency (parts of silica removed per part reagent employed). For example, the work done on the raw water containing 32 to 34 ppm silica, the results illustrated for commercial calcined magnesite *A*, indicate a reduction of the silica content to approximately 5 ppm, employing approximately 32 meq per l of commercial calcined magnesite *A*. This is equivalent to the removal of 28 ppm of silica by 640 ppm calcined magnesite *A* or a silica removal of 0.044 per part of calcined magnesite. For commercial calcined magnesite *C*, silica reduction was effected down to approximately 3 ppm with the use of approximately 32 meq per l of calcined magnesite *C*, or 30 ppm of silica removed by 640 ppm of calcined magnesite. This is equivalent to 0.047 part of silica removed per part of calcined magnesite *C*.

Reference to Table 2, in a current paper[8] by the writers, will show that silica was reduced from 37.1 ppm to 3.6 ppm with the use of 200 ppm magnesium oxide. This shows the removal of 0.17 part of silica per part of magnesium oxide used. In another case, in Table 3 of the same paper, silica was reduced from 31 ppm to 3 ppm with the use of 150 ppm magnesium oxide. This shows a removal of 0.19 part of silica per part of magnesium oxide used. This information is summarized in Table 2 of this discussion. This represents a silica-removal efficiency four times as great for the specially prepared form of magnesium oxide we used in our work as was secured by the author, with the calcined magnesite which he employed. This checks quite closely with the results the writers obtained in their work, as shown in Fig. 9 of our current paper.[8]

Relatively low silica removal per part of calcined magnesite is also shown by the $S = 0$ curve of Figs. 6 and 7. Fig. 9 of the

[4] General Manager, W. H. & L. D. Betz, Philadelphia, Pa. Mem. A.S.M.E.

[5] Chief Chemist, W. H. & L. D. Betz.

[6] Director, Technical Division, W. H. & L. D. Betz.

[7] "Removal of Silica From Water by Hot Process," by L. D. Betz, C. A. Noll, and J. J. Maguire, *Industrial and Engineering Chemistry*, vol. 32, 1940, pp. 1323–1329.

"Removal of Silica From Water by Cold Process," by L. D. Betz, C. A. Noll, and J. J. Maguire, *Industrial and Engineering Chemistry*, vol. 32, 1940, pp. 1320–1323.

"Adsorption of Soluble Silica From Water," by L. D. Betz, C. A. Noll, and J. J. Maguire, *Industrial and Engineering Chemistry*, June, 1941, pp. 814–820.

"Removal of Soluble Silica From Water by Adsorption," by L. D. Betz, presented at Water Conference, Engineers' Society of Western Pennsylvania, November 13, 1940.

[8] "Adsorption Process for Removal of Soluble Silica From Water," by L. D. Betz, C. A. Noll, and J. J. Maguire, Trans. A.S.M.E., vol. 63, 1941, pp. 713–720.

TABLE 2 DATA ON REMOVAL OF SILICA BY USE OF MAGNESIUM OXIDE

	Silica in original water, ppm	Residual silica in treated water, ppm	Silica removed, ppm	Reagent employed, meq per l	Reagent employed, ppm	Silica removed per part of reagent employed
Calcined magnesite *A* (Fig. 4)	32–34[a]	5	28	32	640	0.044
Calcined magnesite *C* (Fig. 4)	32–34[a]	3	30	32	640	0.047
Remosil, MgO (Table 2)	37.1 [b]	3.6	33.5	10	200	0.170
Remosil, MgO (Table 3)	31.0 [b]	3	28	7.5	150	0.190
Remosil, MgO (Table 4)	48.0 [b]	2.5	35.5	13	260	0.175

[a] Reported in author's paper.
[b] Reported by writers.[8]

same paper[8] also shows low silica removal per unit of calcined magnesite. In general, the silica-removal efficiencies obtained check our previous observations that the various forms of calcined magnesite are considerably less efficient for the removal of silica, than the specially prepared highly adsorptive grade of magnesium oxide prepared from sea-water bitterns. Undoubtedly, the low removal efficiencies of the calcined magnesites employed in this work have led the author to the conclusions that ionic magnesium is considerably more effective in the removal of silica than magnesium added in the form of an undissolved magnesium compound. Where the magnesium oxide is added as calcined magnesite, this is true. However, the more adsorptive forms of magnesium oxide, with which most of our work was carried out, possess silica-removal properties per unit of magnesium, comparable with those possessed by soluble magnesium salts.

We have found that it is rather important to control the pH value of the silica-removal process at approximately 10.1. The author, in this paper, makes no mention of any control on the basis of pH.

We have not found it necessary in our experience to employ such a unit as the "magnesium dissolver." It is possible that such a device has been employed in this work because of the relatively low efficiency of the calcined magnesite used. Where a magnesium oxide of a higher degree of efficiency is employed, since there is no appreciable difference in the silica-removal properties of that magnesium oxide, when compared with soluble magnesium salts, the need for a dissolver is eliminated.

We have employed, with very successful results, the simple method of adding the specially prepared magnesium oxide directly to the chemical mixing tank of a softener, at the same time as the lime and soda ash employed for softening.

In this paper, the author, without reservation, concludes (*f*): "The presence of phosphate ion interferes with silica absorption by MgO." This conclusion is based on data shown in Figs. 9 and 10 of the paper. Our work with magnesium oxide is not in agreement with this conclusion. On the basis of laboratory work, with water containing about 30 ppm silica, 3 ppm phosphate ion in a treated water does not interfere with subsequent silica removal by magnesium oxide, within the degree of analytical accuracy.

T. E. Crossan.[9] This paper on silica comes at an opportune time when many high-pressure stations are giving serious consideration to the maintenance of low dissolved silica in boiler water without entailing excessive cost and blowdown. For over a year and a half, silica removal by dolomitic oxide, fed along with quicklime, has been accomplished in the double-cone precipitators at Louisiana Station of the Gulf States Utilities Company. Softening and removal of turbidity from the Mississippi River water are accomplished along with the removal of silica, but no recirculation of sludge is practiced.

Our experience to date, with a few exceptions, has agreed with the conclusions reached by the author. Increased ionic magnesium in the river water, higher temperature, higher sludge concentration in the agitation chamber, and longer agitation time, all aid toward the removal of dissolved silica.

There are, however, certain unfavorable aspects which we have encountered. The introduction of a coagulant (in this case ferric sulphate) definitely retards the silica reduction. During periods of river-water turbidities of over 800 ppm, the removal of silica becomes less effective. In some cases, when the incoming dissolved silica is under 4.5 ppm, and the river-water turbidity is high, no silica reduction resulted. With high dissolved silica and high turbidity in the river water good removal has been obtained.

For a constant percentage of total sludge in the agitation chamber of the precipitator, the percentage of magnesium sludge decreases to small proportions as the river-water turbidity increases. Thus, the silica removal is impaired as the proportion of magnesium in the sludge decreases. Furthermore, if this sludge is recirculated, considerable recirculation must be done before any appreciable magnesium can be dissolved in the incoming water. Recirculation of this sludge to this extent in an already highly turbid water would soon overload the sludge concentrators, and the tank effluent would soon be found to carry sludge. Recirculation of sludge, during periods of high turbidity of the inlet water, therefore, may be impractical. On the other hand, the decrease in silica removal may not entirely be one of decrease in magnesium concentration. It may be due to interference with the surface activity or adsorption properties of the magnesium by the finely divided clay.

Because of the constantly varying conditions of our inlet water, and the rather low river-water-dissolved silica, it is difficult to determine the effect of feeding a dolomitic-oxide slurry. In general, however, the dolomitic oxide (on the basis of equivalent magnesium) appears to be at least one half as effective as ionic magnesium. With entering dissolved-silica contents of over 4.5 ppm, even better results are obtained.

In a system such as ours, the water entering the zeolites must be reduced to 7 pH. For good silica removal with magnesium, higher pH values must be carried to precipitate the magnesium than would be required if only a maximum of calcium-hardness removal were required. This means a higher lime dose for silica removal and, eventually, before the zeolites, a higher sulphuric-acid dose to neutralize it than during periods when silica reduction is not required. Silica removal by magnesium therefore can be accompanied by a higher dissolved solids to the boilers than is experienced during normal operation without silica removal.

Because of the longer detention periods, and the greater sludge concentrations required for removal of silica in the cold with magnesium than is required for softening and clarification alone, a somewhat greater plant investment is required. This is especially so with waters having over 200 ppm turbidity.

When feeding dolomitic oxide along with the quicklime, practically no magnesium goes into solution. Even though this results in less effective silica removal, it does not subject the system to sudden fluctuations in hardness to the zeolites and thus endanger their being overrun, sending excessive hardness to the boilers. If conditions are not correct for silica removal, practically no hardness fluctuation results.

On the other hand, if the sludge-recirculation system of the author's company is used, the amount of magnesium in the sludge, the strength of the sludge, and the quantity of CO_2 must

[9] Superintendent of Production, Gulf States Utilities Company, Baton Rouge, La. Mem. A.S.M.E.

be controlled accurately at all times. Deficiency of CO_2 will result in high alkalinities and high calcium hardness. On the other hand too much CO_2 may result in high magnesium hardness, perhaps high calcium hardness, ineffective coagulation, and the sludge in the unit being carried over with the delivered water. With an unchanging water supply and with an unchanging rate t › be treated, the system has the additional need for accurate CO_2 control. However, with a variable water supply and a changing rate, the system will, as we now see it, require extremely careful control and observation.

One of the most important economical factors in the system, described by the author, is the pH of the water entering the downtake, Fig. 8 of the paper. It would be interesting to know the proportions and the amounts of magnesium and calcium dissolved by CO_2 at different pH values. If adequate dissolving of magnesium can be accomplished at 9.1 pH, without too much simultaneous dissolving of calcium, then considerable lime and CO_2 can be saved. At 7.5 pH both magnesium and calcium enter solution very readily, but more CO_2 is required to convert magnesium and calcium to the bicarbonate form, and considerable calcium is dissolved with the magnesium. The lime dose required to reprecipitate the redissolved calcium and magnesium becomes quite large. Therefore, the pH at which redissolving of magnesium takes place would seem to be highly important from an economical standpoint.

The maintenance of low dissolved silica in boiler waters, without high blowdown or excessive chemical cost, would seem to be within reasonable reach of many high-pressure stations, as a result of the comprehensive treatment of the subject in this paper.

C. E. Joos.[10] This paper treats comprehensively the various factors affecting the silica-removal process by magnesium salts. While the author discusses both the cold and hot treatments,

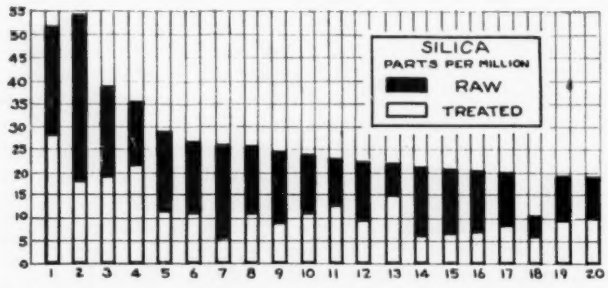


FIG. 11 REDUCTION IN SILICA BY USE OF HOT-PROCESS SOFTENER

the writer wishes to confine his comments to the hot-process treatment for silica reduction when combined with softening.

It has been recognized for many years that the hot-process softener, utilizing lime and soda ash in the treatment of fairly hard water supplies, resulted in considerable silica reduction. Fig. 11, of this discussion, illustrates a series of tests, made on raw and treated waters from hot-process-softener installations, showing the reduction in silica which took place during the softening process without regard to silica reduction as the principal objective. It was also noted that, the higher the magnesium hardness, the more effective was the silica removal, and that calcium precipitants were of slight value. These observations led to the process of fortifying the water with magnesium sulphate wherever the silica reduction was to be greater than that which could be obtained through the precipitation of the natural magnesium hardness of the raw water.

[10] Cochrane Corporation, Philadelphia, Pa.

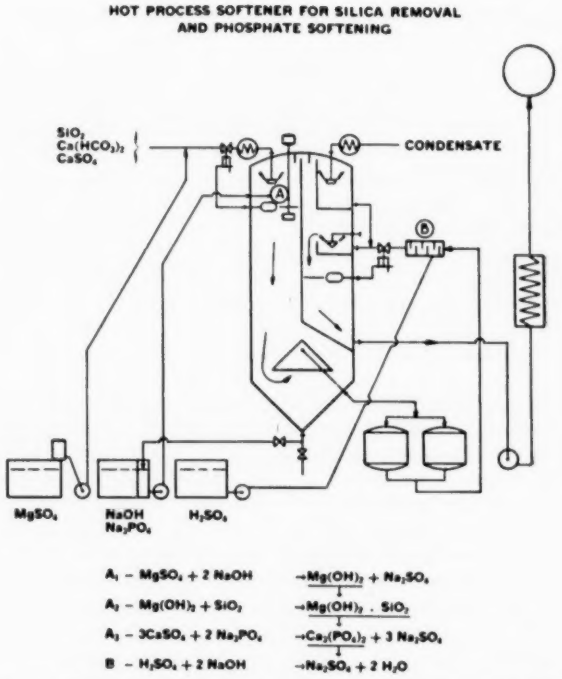


FIG. 12 HOT-PROCESS SOFTENER FOR SILICA REMOVAL AND PHOSPHATE SOFTENING

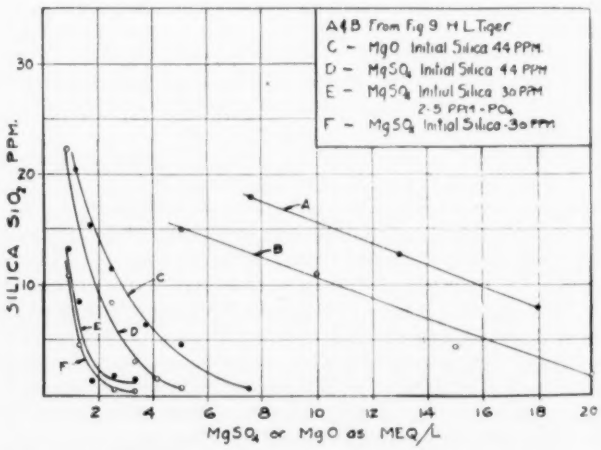


FIG. 13 COMPARISON OF RESULTS IN REDUCTION OF SILICA BY USE OF MAGNESIUM SALTS

Recommendations of this procedure were made as early as 1936, and a hot-process softener has been in operation for well over a year, specifically installed to reduce silica by the use of magnesium sulphate. Fig. 12, of this discussion, is a diagrammatic outline of this installation. Phosphate is used in this case as the softening agent, because of the low hardness of the raw water. Sludge is recirculated to reduce the consumption of magnesium sulphate and caustic soda.

During our research in the reduction of silica by the use of magnesium salts, it was recognized that magnesium sulphate, although very effective, was open to the objection that it produces a by-product of sodium sulphate which in some cases was objectionable. This objection was overcome by the use of magnesium oxide which is only slightly less effective than the sulphate and produces no by-product. Our work indicates that, while the ionic magnesium, in the form of the bicarbonate of

sulphate, is somewhat more effective than the magnesium oxide, the difference is not as great as that indicated by the author.

In Fig. 13 the curves *C* and *D* represent the difference on the basis of tests conducted on a natural water having a silica content of 44 ppm. Curve *D* represents results obtained by the use of magnesium sulphate, and *C* by the use of a commercial magnesium oxide. Curve *F* represents results with the use of magnesium sulphate on a water having an initial silica content of 30 ppm. Curves *A* and *B* are plotted from points taken from the author's paper, Fig. 9.

While the author's results showing the effectiveness of ionic magnesium (Fig. 1, curve for 90 C) agree closely with our own findings with magnesium sulphate, shown by curves *F* and *D*, Fig. 13, his data on the use of magnesium oxide indicate the necessity of using a quantity far in excess of that required by our research. This difference is indicated by a comparison of curves *F* and *B*, representing tests on a water having an initial silica content of 30 ppm. The difference in results can only be explained by the difference in the physical or chemical characteristics of the calcined magnesite which the author used and the magnesium oxide we employed. In view of the fact that the magnesium oxide we used is commercially available, it is obvious that the process can be much improved by proper selection of the reagents employed.

From the author's work with the absorption of silica in the presence of the phosphate ion, as illustrated in Fig. 9 of the paper, he comes to the conclusion, "the presence of phosphate ion interferes with silica absorption by magnesium oxide." His conclusions are not borne out by our own researches in the laboratory or observations made with hot-process water-softener installations. As an illustration, Fig. 13 of this discussion reproduces the author's findings in which curve *B* illustrates the reduction of silica obtained by the use of calcined magnesite, while curve *A*

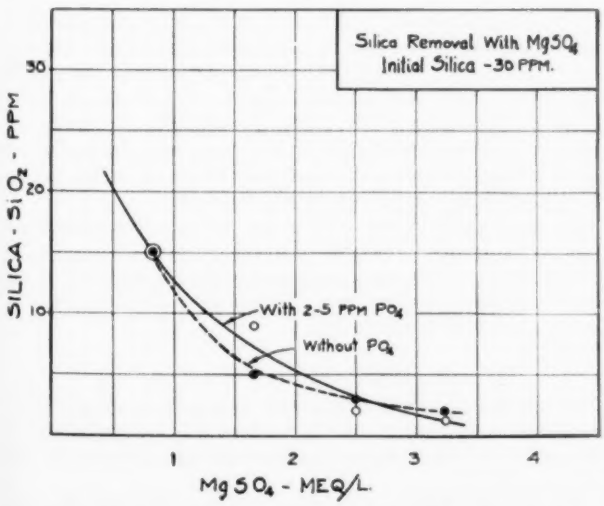


FIG. 14 SILICA REMOVAL WITH $MgSO_4$ WITH AND WITHOUT PO_4 ION
(Initial silica, 30 ppm.)

illustrates the same procedure, excepting that precipitation is conducted in the presence of approximately 3 ppm of phosphate ion. On a water containing 30 ppm of silica, which is the concentration the author uses for his explanation, we obtain by the use of magnesium sulphate with the presence of 2 to 5 ppm PO_4 a curve illustrated by *E*, and *F* illustrates the same procedure without the phosphate ion being present. It is quite evident from these curves that, while there may be a slight difference in the absorbing properties of magnesium-hydrate precipitate, it is quite evident that the author's differences cannot be reconciled with our own work.

Curves *E* and *F* resulted from gravimetric-silica tests, whereas, these same observations were made using colorimetric-silica procedures, and are illustrated in Fig. 14 of this discussion. It will be observed that their points are so close it would be impossible to draw the conclusion that the phosphate ion interferes with the absorbing properties of magnesium hydrate.

The reason for this may be in the type of reagents employed for it is quite clear from Fig. 13, with the comparison of curves *B* and *F*, that the author's efficiency of removal is very much less than our own findings. This cannot be ascribed to the differences existing between the use of magnesium oxide and ionic magnesium sulphate, as these differences are illustrated clearly by curves *C* and *D*.

Observation in the field verifies our research that, within the limits of concentrations of magnesium oxide and PO_4 ion used in practice, the presence of the PO_4 ion does not interfere perceptibly with the silica-removal process.

The author points out the effectiveness of sludge recirculation which is a substantiation of our own researches and practical experience in the field, in which the magnesium consumption can be reduced to approximately 50 per cent in normal cases by employing such means.

While he does not present in his paper the effect of magnesium oxide on the absorption of the phosphate ion, this subject has been brought up previously and used as a reason for conducting a silica-removal and phosphate-softening process in two stages. Analysis of the quantity of phosphate absorbed by the magnesium precipitate does not substantiate a sound basis for this recommendation. Our observations have indicated that when 5 ppm of phosphate ion are introduced as an excess, there is no absorption with the use of 50 ppm magnesium sulphate, absorption of only 1 ppm with the use of 100 ppm of magnesium sulphate, and 3 ppm with the use of 150 ppm. In view of the fact that recirculation of sludge is customarily employed in all processes, the quantity of magnesium salts necessary for the normal silica reduction will not generally exceed 100 ppm of magnesium sulphate, or its equivalent in magnesium oxide. Therefore, it does not appear to be economically justified to complicate hot-process softening apparatus merely for the saving of 1 ppm of phosphate.

Our work in the laboratory and in the field does not indicate that the silica-removal process need be separated from that of phosphate softening wherever the phosphate-softening process is applicable. The separation of these processes, as recommended by the author, would add unnecessarily to the equipment cost and attendance.

S. E. TRAY.[11] Current interest in methods of reducing the silica content of water used for boiler feed is not only a tribute to the advancement of the science of water treatment, but is indicative of the important role which research plays in the development of steam and power generation. The author is to be commended on the manner in which he has presented data which will prove an important contribution in the field of silica reduction. It is interesting to note that, while the effect of magnesium on the reduction of soluble silica has been quite well known for a number of years, there has been little effort to investigate all of the possibilities of the process until comparatively recently. It is also interesting to observe the number of investigators simultaneously engaged in the study of this process, which only serves to emphasize the importance of the subject.

The author makes an interesting observation on the subject of "silica tolerance," which is the maximum allowable amount of

[11] Allis-Chalmers Manufacturing Company, Milwaukee, Wis.

silica that may be tolerated in the concentrated boiler saline. From the standpoint of silica-scale deposits in boilers, it would appear that a minimum silica content of boiler water is as desirable as minimum alkalinity and total solids. The usual boiler-water sample taken from a boiler drum is assumed to represent average boiler-water conditions. Unfortunately, there have been no means developed thus far to obtain water samples from tubes in which the maximum heat transfer occurs. As a result, we are somewhat in the dark as to the actual boiler-water conditions at these points of greatest evaporation. It is entirely possible for the silica to remain in solution throughout most of the boiler, and yet to precipitate in the solid phase at these localized points. Until we have a better understanding of the conditions under which silica precipitates, it would seem wise to reduce the silica concentration to the lowest possible value.

From the standpoint of turbine operation, a study of a large number of plants indicates that if insoluble silica deposits on turbine blades are to be avoided, the soluble silica in the boiler water must not exceed 2 per cent of the total dissolved solids. From this standpoint as well, it is very desirable to reduce the soluble silica as low as possible.

The results reported by the author are apparently based on laboratory tests, rather than full-scale plant operation. A note of caution should be sounded against attempting to apply laboratory results directly to plant practice. The author has indicated that the reduction of silica is largely a physical process and, thus, the concentrations and character of the sludge are of prime importance. It is extremely difficult to reproduce in the laboratory the conditions which normally exist in large-scale operations. It would be interesting also to have more detailed information on the chemical characteristics of the effluent following treatment for silica reduction. The hardness and alkalinity of the effluent, as well as the control required to obtain maximum silica removal, are important considerations from the standpoint of practical operation.

This paper points out the effect of ionic magnesium on silica removal, and indicates this source of magnesium to be more efficient and to require less than magnesium derived from sludge. This is not entirely true, since the ionic magnesium must precipitate from solution, usually as the hydroxide, in order to remove silica. In the process of precipitation, the magnesium passes from the soluble to the insoluble state through a colloidal phase, and the particle size of the precipitate during this process ranges from zero to a definite, measurable size. The paper indicates that there is a particle size of sludge which is more effective in silica removal than any other, and obviously, in the case of ionic magnesium, this state must be reached some time during the process. However, undissolved magnesium compounds may also exist in this favorable state, provided a suitable form of magnesium is selected and the proper conditions are maintained. With these requirements satisfied, the undissolved magnesium compounds may be equally as effective in removing silica, without the necessity of recycling the sludge.

There is one inherent disadvantage in the magnesium dissolver which tends to reduce its effectiveness as a source of ionic magnesium. As the sludge is recycled and brought in contact with low pH water, $Mg(OH)_2$ will dissolve first. However this sludge also contains absorbed silica, the same as the waste sludge. This silica will also dissolve in low pH water and, hence, the SiO_2 content of the incoming water will be increased. As a consequence, the magnesium requirements will continue to increase in proportion to the silica added from the recycled sludge.

The author indicates that the removal of silica by magnesium is generally an adsorption process, but also states that it is possible this process involves other phenomena besides straight adsorption. Our experience confirms this thought, which is also borne out by the fact that the efficiency of the process definitely increases with temperature. In a true adsorption process, increased temperature reduces the rate of adsorption. The author finds that, as the ratio of $Mg:SiO_2$ rises in the sludge, the residual silica in the effluent decreases. This would be true in the case of straight adsorption, but experience in the field shows that the $Mg:SiO_2$ ratio in the sludge does not necessarily determine the degree of silica removal. The state of the sludge material seems to be quite important, and this likewise is contrary to what we would expect of straight adsorption. It is also inferred that if magnesium sludge were left indefinitely in the sludge zone, silica would be adsorbed indefinitely. After the sludge has reached equilibrium there will be no further removal of silica from solution.

Adsorption may be differentiated from precipitation by the fact that in an adsorption process no definite compound can be identified. It has been possible, however, by means of X-ray-diffraction analysis to identify certain combinations of magnesium and silica in the precipitated sludge. It is more likely, therefore, that removal of silica by magnesium is a combination of both adsorption and precipitation. The factors favorable to both phenomena must be maintained in order to obtain the maximum effectiveness of the treatment.

The effect of phosphate on silica removal with magnesium is well known, and it is interesting to learn that the tests reported by the author confirm this point. The fact that the phosphate ion interferes with the action of magnesium on silica is due in part to the respective solubilities of magnesium phosphate and magnesium silicate. It is also due to the blanketing effect of the phosphate ion, which is adsorbed by the magnesium along with the silica. This reduces the amount of silica which can be adsorbed by a given amount of magnesium. There is no doubt that the removal of silica, even from low-hardness waters, must be accomplished prior to the addition of the phosphate ion for softening.

The author makes an excellent point of the necessity for intimate contact between water and sludge for silica removal in the cold. It is very fortunate that the development of equipment designed for accelerated softening and clarification in cold water has been contemporary with the progress in silica removal. By providing this intimate sludge contact, these accelerated softeners reduce the time required for adsorption and provide the proper conditions for the removal of silica in the cold.

The application of this process, like other water-purification methods, requires a knowledge of the chemical characteristics of the raw water. It is not a panacea for all silica troubles; but, when intelligently applied, offers definite assistance in combating soluble silica in boiler feedwater.

Author's Closure

It is particularly gratifying to have such copious and pertinent discussion on this important subject, because it directs attention to those phases which require further investigation for the benefit of all concerned.

Messrs. Betz, Noll, and Maguire, and Mr. Joos call attention to the fact that the undissolved magnesium oxides on which data were presented in the paper do not appear to be as absorptive as other MgO products on the market. In this connection, it should be borne in mind that the primary focus of this entire paper is on various methods of silica removal which can be combined advantageously under various conditions to produce maximum silica removal *at minimum cost*. We were not attempting to present data on high-cost activated MgO products as we believe such data have been presented elsewhere by these discussers and some time previously by other investigators such as Wesly (see reference 42 in the Bibliography). This low-cost point of view is verified by the fact that Table 1 of the paper

states a price of 3 cents per pound for MgO, whereas the activated MgO products to which the discussers refer are marketed at more than double this price.

Another point on which there seems to be considerable confusion is the "magnesium dissolver" and its role in combining various methods of silica removal in an efficient low-cost process. Messrs. Betz, Noll, and Maguire, and Mr. Crossan seem to feel that this dissolver is not usually needed and that it adds undue complication to the operation of the plant. There is one important point to bear in mind in this connection, and that is that, so long as no CO_2 is added to the influent from any external source such as flue gas, the use of the magnesium dissolver does not involve either any increased operating cost or any additional operating control. This is fully discussed in the paper under the heading "Combined Use of Ionic Magnesium and Undissolved Magnesium Compounds," on page 55.

Mr. Tray has raised a question about the increase in silica content upon passing recirculated sludge through the magnesium dissolver. Actual tests show that the silica content of the treated water leaving the dissolver is not higher than that of the influent, while the use of the dissolver, as proved by experience, does reduce the final silica content without additional operating cost.

There seems to be considerable difference of opinion on the effect of PO_4 ion. These opinions are apparently based on different test results rather than on different interpretations of similar data. Messrs. Betz, Noll, and Maguire, and Mr. Joos, feel that the PO_4 ion does not have any significant effect, while Mr. Tray agrees with us that it does. It is pertinent to mention here that previous investigators (Wesly, references 13 and 42 of the paper) also find that PO_4 ion interferes with silica absorption by MgO. These conflicting data indicate that either there are some incorrect measurements involved or that different waters act differently in this respect. It is to be hoped that further parallel tests on various waters will clear up this question in due time.

Mr. Tray questions the "silica tolerance" and suggests the advisability of maintaining the SiO_2 concentration as low as possible in the boiler salines. There is much to be said for his point of view. . Furthermore, it makes it all the more desirable to combine all the advantages of ionic Mg precipitation, high Mg sludge concentration, recycling sludge through the magnesium dissolver, and utilizing the cheapest possible source of magnesium to obtain the best results at lowest operating cost. This is particularly true in those cases where the quantity of water to be treated is large, so that the operating cost per unit of water treated is important.

Some questions are also raised about the fact that this paper is based on laboratory tests. Although this point is well taken, it should be noted that special laboratory techniques were developed (as described in the paper) to simulate long-term, large-scale tests, and these techniques were verified by operating larger pilot plant equipment over a long period. As a matter of fact, Mr. Crossan points out that one modification of our dolomitic lime process has been in successful operation at his plant for over one and a half years. It may be added that considerable further experience has become available since this paper was presented about a year ago, and these large-scale experiences further verify the conclusions drawn from the tests presented in the paper. It is intended to present these operating data in another paper in the near future.

Combustion of Four Fuels in One Boiler

By W. J. LUTZ,[1] NEWARK, N. J.

Present-day fuel economics has decreed the desirability of a multifuel-burning boiler even in small and medium-sized installations. This paper describes the 100,000-lb per hr four-fuel boiler in the Harrison Gas Works of the Public Service Electric and Gas Company at Harrison, N. J. The difficulties encountered in burning oil, tar, pulverized coal, and pulverized fuel-pitch in the same burner and their successful solution are reported in detail.

GENERALLY speaking, the controlling factor in the design of a steam-generating unit is the selected fuel. In some instances, considerations of economics, of sources of supply, or of owner policies narrow the choice of fuels down to one particular type. In such cases, the boiler is designed to burn that one fuel as efficiently as possible. In other instances, the plant management has a choice of a number of available fuels not too far out of line economically. The fuel which may be selected today, however, may not be the first choice a year or even a few months from now when the economic picture has changed. Yet, it is necessary to make a decision. This problem of fuel selection is independent of the size of the plant, whether it be small, medium-sized, or a superpower station.

With price changes in the fuel market, it has often been advantageous to revamp boilers so as to burn the currently cheaper fuel. Another price swing might still later cause a return to the original fuel. Such cases are not uncommon, especially in the eastern-seaboard area where shifts in the relative prices of oil and coal have been pronounced.

In locations where competitive fuels are available, the experience of the last decade has definitely dictated the need of a universal boiler which can handle a number of fuels equally well without requiring extensive and costly alterations with each change of fuel. In fact, the change should be made from one fuel to another without even shutting down. Such a unit would permit the operator to select the most economical fuel and would extend the sources of his fuel supply.

The need for a universal burner and boiler became apparent in 1937 at the Harrison Gas Works of the Public Service Electric and Gas Company, Harrison, N. J., when plans were being made to extend the boiler plant, for there were available four fuels, i.e., oil, coal, tar, and fuel-pitch.

There were on the market at that time boilers of the integral-furnace type, successfully handling oil, pulverized coal, and gas, which seemed to meet the requirements of a universal boiler for small and medium-sized installations. There were also available successful combination oil-and-pulverized-coal burners. A two-fuel boiler was an established fact and was offered as a standard product by several leading boiler manufacturers. To add two more fuels, tar and pulverized fuel-pitch, thereby approaching more nearly to a hypothetical universal burner, was the particular problem put to the boiler manufacturers. It was further stipulated that all fuels must be as successfully burned as if the boiler and burner were designed for that particular fuel alone. It was to be a four-fuel combination burner and not a compromise burner.

Prior to this plant extension, the boiler equipment in this 40,000-Mcf per day carbureted water-gas plant at Harrison, N. J., consisted of four 50,000-lb per hr units with chain-grate stokers, firing river barley and coke breeze, and eight waste-heat boilers. Increased load and a desire for greater fuel flexibility were the motivating factors for the installation of a 100,000-lb per hr unit capable of handling four fuels, oil, tar, pulverized coal, and fuel-pitch.

New Unit at Harrison

The new unit is a standard Babcock & Wilcox integral-furnace boiler of the general arrangement shown in Figs. 1 and 2. It is designed to deliver 100,000 lb of steam per hr at 230 psi gage and 500 F total temperature.

When contracting to furnish a four-fuel boiler, the manufacturer was aware of the characteristics of pulverized fuel-pitch and had already concluded that the conventional circular pulverized-coal burner, which depended upon impellers and splash plates to obtain good distribution and turbulence of the primary air and pulverized fuel, would be unsatisfactory, for the pitch would adhere to the impeller or splash plate and eventually result in a stoppage.

Fuel-Pitch

Fuel-pitch is a by-product of water-gas or coal-gas tar. It is the solid residue of the distillation of these tars at about 800 F, which can either be flaked or broken into lumps that can be crushed to any size in an ordinary crusher. When flaked it consists of small, irregular, fragile, shiny black flat chips about $^1/_{16}$ in. thick and $^1/_2$ in. across. When handled in lumps, it is not unlike soft coal, porous and dirty.

To minimize the dust, when handling flaked pitch, bunker C oil in quantities of about 0.3 gal per net ton is sprayed on it. Water is unsatisfactory as the shiny flaked particles are water-repellent. When handling it in crushed lump form, water is added during the dry season in amounts to bring the surface moisture up to about 2 or 3 per cent by weight.

In either form, fuel-pitch has a softening temperature of 300 to 330 F, as determined by the $^1/_2$-in. cube-in-air test. It becomes tacky at about 190 to 200 F. The temperature rise resulting from the frictional impact of pulverized pitch against an impeller or splash plate would be sufficient to cause a building up of pitch. It is apparent that the mixing of pulverized pitch with the primary air must be done without impellers or splash plates or other devices which would cause too sudden a change in the velocity of the pitch particles, thereby transferring kinetic energy into heat energy.

New Babcock & Wilcox Burner

The Babcock & Wilcox Company were experimenting at that time with a new pulverized-coal burner in which the primary air and pulverized fuel are led through a volute-shaped burner casing and discharged axially into the primary-fuel pipe. The secondary air is similarly led through a volute-shaped burner casing and discharged axially into the secondary-air pipe concentric with and surrounding the primary-fuel pipe. The directional whirl of the secondary air is governed by the direction of the volute-shaped burner entrance and is opposite to that of the pulverized fuel. Thus when the primary air carrying the fuel and the

---

[1] Power Plant Engineer, Gas Department, Public Service Electric and Gas Company.

Contributed by the Fuels Division and presented at the Spring Meeting, Atlanta, Ga., March 31–April 3, 1941, of The American Society of Mechanical Engineers.

Note: Statements and opinions advanced in papers are to be understood as individual expressions of their authors, and not those of the Society.

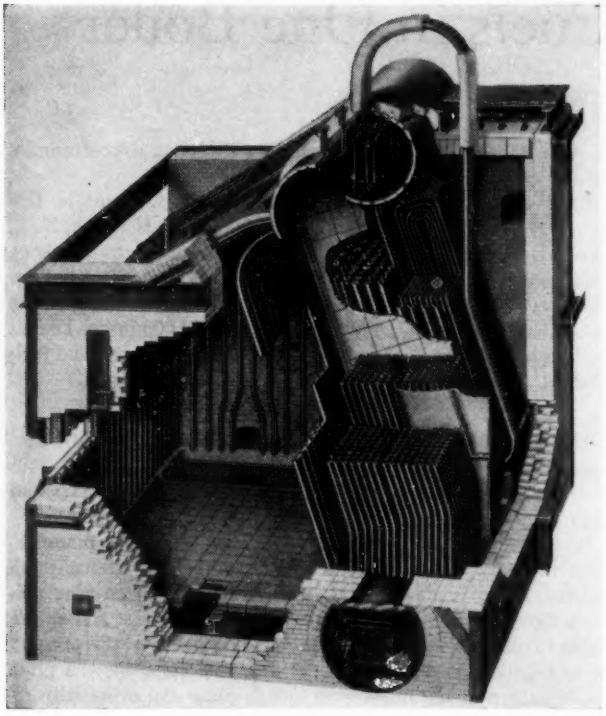


FIG. 1 BABCOCK & WILCOX INTEGRAL-FURNACE BOILER

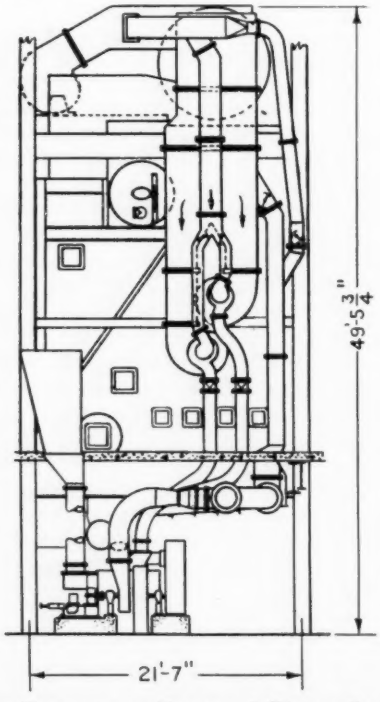


FIG. 2 FRONT ELEVATION OF BABCOCK & WILCOX INTEGRAL-FURNACE MULTIFUEL BOILER AT HARRISON GAS WORKS

secondary air meet at the burner exit the two are moving at high velocity and at right angles to each other. To assist in ignition and in the burning of high-volatile coals, atmospheric air can be drawn into the center of the primary-air fuel pipe through a short tertiary-air nozzle. Fig. 3 shows the essential features of this pulverized-coal burner, which somewhat resembles two superimposed fan casings on a common axis. The direction of flow, however, is from the periphery to the center, the reverse of that in a fan.

Results when firing pulverized coal at another plant justified the claims that good distribution and turbulence could be obtained by use of a volute casing and, hence, offered possibilities for firing pulverized fuel-pitch. It was, of course, realized by the manufacturer that this design had only been tried as a single-fuel burner. Its possibilities as a combination burner, even with such standard fuels as pulverized coal and oil, were still undetermined. The purchaser, too, realized that the introduction of fuel-pitch, especially in a combination four-fuel burner, added problems the solution of which could only be worked out cooperatively in the field.

Fig. 4 shows the combination burner as originally furnished. The assembly consists of three concentrically arranged volute-shaped casings and a liquid-fuel-burner pipe at the center. When firing pulverized coal, the coal is mixed with tempered air at the pulverizer in the basement and delivered through the intermediate pipe. Secondary air delivered by a forced-draft fan is forced through a Ljungström air preheater located on top of the

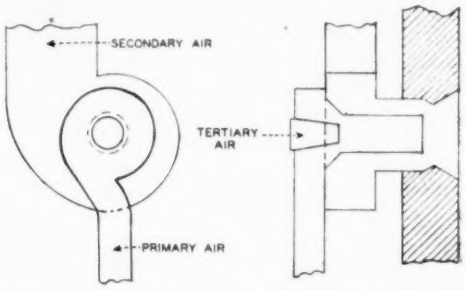


FIG. 3 NEW BABCOCK & WILCOX PULVERIZED-COAL BURNER

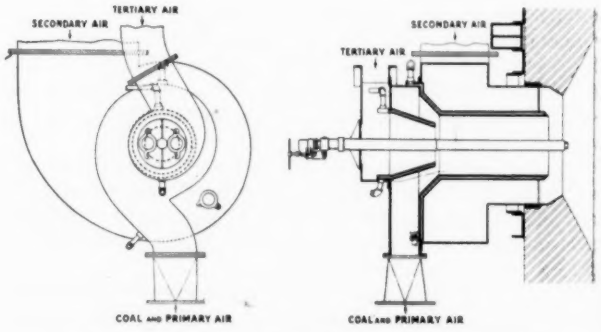


FIG. 4 ORIGINAL COMBINATION FOUR-FUEL BURNER

boiler and then down to the burner through the inner and largest duct. The direction of the secondary-air-casing volute is opposite to that of the primary air. Control of the secondary air is obtained indirectly by first changing the speed of the turbine-driven induced-draft fan which changes the furnace draft. In turn the forced-draft fan changes speed accordingly to maintain a predetermined constant furnace draft.

When firing liquid fuels, as oil or tar, the entire combustion air, except a very small amount of tertiary air for ignition purposes, is supplied through the secondary-air duct.

When firing pulverized fuel-pitch only cold primary air is used. It was believed necessary to use cold tertiary air under pressure to aid in the combustion of high-volatile fuel-pitch. This air is led into the center of the primary-air stream with a directional whirl opposite it. The primary-fuel-burner pipe is also water-

cooled to prevent pitch from approaching the tacky temperature of about 190 to 200 F before it reaches the burner tip.

Oil Firing

The boiler was first fired with oil and it was observed in this preliminary run that the whirl obtained in the secondary-air scroll was too great. The air left the burner throat at the periphery at too high a velocity, thereby resulting in but slight mixing with the oil spray. The flame was flat, pancake-shaped, hollow, and smoky in the center.

To slow down the secondary-air whirl to a point where the oil and air could mix properly, stationary air-guide vanes were installed in the annular secondary-air throat. Their value became apparent in subsequent trial runs, though it was necessary to change their setting and to alter the plastic burner throat from a 60-deg throat to a 30-deg throat, as well as to make several changes in the design of the sprayer plates, before the desired whirling, full-bodied, short, white-tipped flame was procured.

The oil burner is the standard Babcock & Wilcox mechanical-steam-atomizing unit, Figs. 5 and 6, external-mix type which

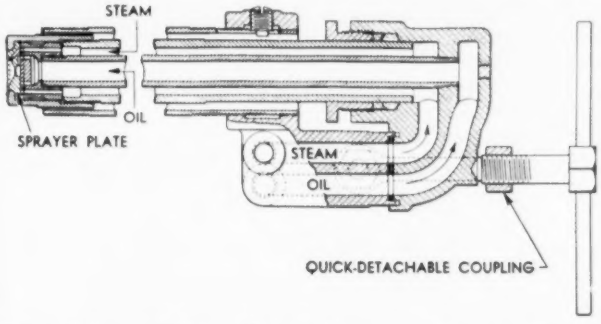


Fig. 5 Babcock & Wilcox Steam Mechanical Atomizing Burner for Oil Firing

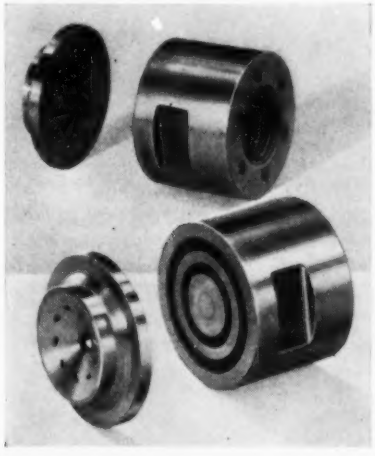


Fig. 6 Babcock & Wilcox Steam Mechanical Atomizing Sprayer Plate

operates as a steam-atomizing unit when the oil pressure is below 100 psi, and can be operated as a mechanical sprayer at pressures above that. The manufacturer definitely recommended the mechanical-steam type rather than a straight mechanical type for use in the "cold" or completely water-cooled furnace.

Pulverized-Coal Firing

Trial runs with pulverized coal disclosed that the secondary-air velocity was too high to burn even high-volatile coal. To reduce it, the diameter of the secondary-air throat was increased by cutting down the venturi lip on the outside of the throat. This lip was also streamlined in order to reduce the vena contracta and to secure full effective area of the throat. Observations of the secondary-air flow from the furnace side with pitot tubes when the boiler was cold indicated a uniform velocity and a good directional whirl. Subsequent runs with pulverized-coal firing showed a marked improvement, though it was necessary to change the angle of the stationary vanes about 10 deg from that found satisfactory for oil firing before the desired compact full-bodied pulverized-coal flame was obtained.

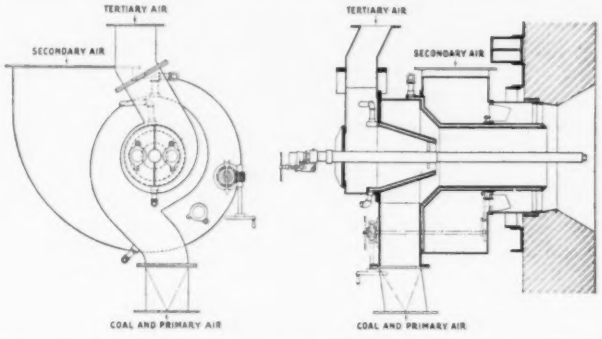


Fig. 7 Intermediate Development Stage of Combination Four-Fuel Burner

Upon operating the unit again on oil, it was found that the oil flame was unsatisfactory. Apparently, the changes in the combination burner necessitated to burn pulverized coal had seriously affected the successful oil firing. The vane angle was changed back to the original, and once more satisfactory oil-firing results were secured. Several rechecks on coal- and oil-burner operation showed that there appeared to be no one fixed secondary-air-vane setting for even this type of burner which would be satisfactory for pulverized-coal and oil firing and, since this burner had to burn pulverized fuel-pitch as well, there remained only one answer—install adjustable secondary-air vanes.

Upon completion of the installation of the adjustable secondary-air vanes, the burner appeared as shown in Fig. 7. To summarize, a comparison with the original shows the following changes:

1 A 30-deg plastic throat instead of the 60-deg throat.

2 A streamlined metal lip in place of the original sharp venturi.

3 The installation of adjustable guide vanes in the secondary-air throat.

Trial runs when firing either oil or pulverized coal proved the value of adjustable vanes, and a series of performance tests with these two fuels was conducted, before starting trial runs with tar and pulverized fuel-pitch. The results of these tests indicated the general attainment of the guaranteed test efficiencies of 87 per cent and over-all performance when firing these fuels.

Tar Firing

Little trouble was expected from tar firing in this combination burner, for the major problem of tar firing is one of conditioning the tar for proper handling and atomization. The Saybolt Furol viscosity of water-gas tar at 122 F (50 C) ranges from 400 to 2000 sec or, in terms of specific viscosity Engler 50 cc, 176 F (80 C), from 20 to 43. It contains breeze in small amounts and, as delivered to the boilerhouse at the Harrison plant, it has a water content of about 0.5 per cent. Tar-firing operations can

be grouped into (1) storage and pumping, (2) heating, and (3) atomization and combustion.

Due to its high viscosity, tar is stored in insulated, heated supply tanks at about 180 to 200 F. At this temperature, it flows readily to the reciprocating pumps and only slight strainer trouble is encountered. A change of strainers once per shift is

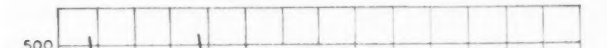


FIG. 8 TAR TEMPERATURE-VISCOSITY CURVE

normal. At lower temperatures such as 150 F or less, there is a marked increase in suction-strainer blockage, which is probably due to the presence of the breeze in the tar. The small breeze particles appear to form the nuclei about which the tar coagulates as it cools. At higher temperatures the suspended breeze particles flow freely through $^1/_{16}$-in. round-hole strainers.

The presence of this abrasive breeze in water-gas tar, even in small amounts, precludes the use of any close-clearance pump, such as a gear or screw type, for handling purposes. Reciprocating pumps equipped with alloy-steel liners, of iron, nickel, and copper composition, and stainless-steel valves have to date proved most satisfactory and should have a life equal to that of a pump handling ordinary fuel oil. Centrifugal pumps can also be used, provided a uniform tar-inlet temperature is maintained. The tar-temperature-viscosity curve for temperatures of 150 to 190 F is rather steep in this range, thus, even a 10 or 20 F variation results in a considerable viscosity and, hence, pump delivery change, Fig. 8.

To condition the tar to the desired 18 sec Saybolt Furol or 4 deg Engler at the burner tip requires heaters to bring the temperature up to about 220 to 250 F. No trouble with carbon deposits in the heater has been experienced. A yearly checkup and brushing of the tubes is the present extent of the maintenance.

No combustion troubles have been encountered with tar firing. The flame has the exact appearance of the oil flame. Steam-atomizing burners of the internal-mix type, equipped with sludge sprayer tips, Figs. 9 and 10, are used. Considerable wear in the sprayer plates and nozzles took place. Different materials, such as chrome-nickel alloys and casehardened steel, were tried but did not last 2 weeks. The latest development is a chrome-silicon-alloy tip which to date has shown signs of service measured in terms of months. To increase their life yet further the manufacturer is experimenting with tips which have been case-hardened by a new process of nitriding alloy steels. A set will be tried out shortly.

Mechanical atomization of tar can also be used. In fact it may be stated that any bunker C fuel-oil burner, steam-atomizing or mechanical, can successfully handle tar, provided the tar is conditioned to a viscosity equal to that of the oil for which the burner was designed. The presence of breeze in water-gas tar will require the use of abrasive-resisting material for the nozzle.

Steam-atomizing burners are preferred, especially for burners which operate intermittently and in completely water-cooled furnaces. The steam heats up the tar-burner pipe directly to the nozzle tip, thereby securing conditioned tar right at the start. Drooling, poor atomization, and smoke are the usual characteristics of a mechanical burner when starting up with tar.

Unfortunately, the suspended breeze particles in the tar do not burn up in the furnace, although they have a heat content of about 11,000 Btu per lb. They will drop out in the combustion

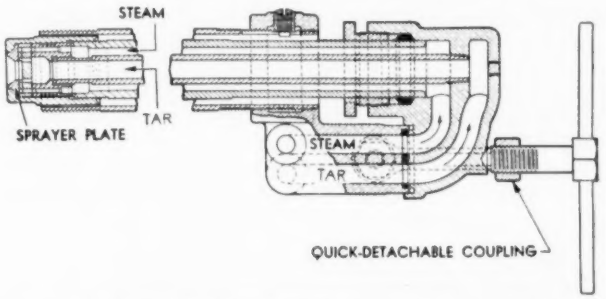


FIG. 9 BABCOCK & WILCOX STEAM-ATOMIZING BURNER FOR TAR FIRING

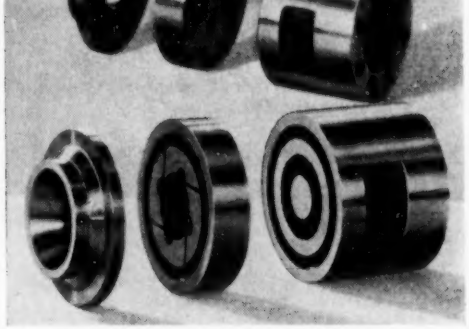


FIG. 10 BABCOCK & WILCOX STEAM-ATOMIZING SPRAYER PLATE

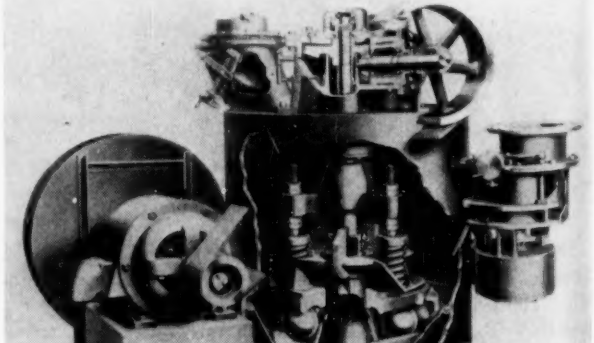


FIG. 11 BABCOCK & WILCOX TYPE-B COAL PULVERIZER

chamber or pass out into the stack. Their presence, though, has one beneficial effect in that, in passing through the air heater, they keep the heating surfaces absolutely clean. When operating with oil, it is necessary to take the heater out of service every 6 months to wash off the smudge coating which is not effectively removed with everyday soot blowing.

Pulverizing Fuel-Pitch

The next problem in the development of this four-fuel burner was to burn pulverized fuel-pitch, the main function of this burner and the reason for the deviation from the standard burner.

The pulverizing equipment, as originally furnished, consisted of a Babcock & Wilcox type-B ball-race mill with a water-cooled lower race and side-wall jacket to keep the temperature within the mill well below the tacky temperature of 190 F for fuel-pitch. When pulverizing coal no water cooling is used.

The first attempts to pulverize pitch in this ball-race mill, Fig. 11, met with failure. The balls crushed and packed the pitch in the ball race, thereby stopping the balls from rolling, while the upper race simply slid over them. This took place regardless of the spring pressure on the balls. The next move was to increase the primary-air velocity over the lower ball race by reducing the throat opening and the installation of directional baffles within the pulverizer. It was theorized that the higher primary-air velocity would sweep away the finely crushed pitch before packing could take place. This, too, met with failure.

A restudy of these failures led to the suggestion of using smaller balls in the same race. Pitch is very fragile and has a grindability of about 150 Hardgrove scale. Therefore, but little weight and pressure are required. Furthermore, the use of small balls in a race designed for larger balls means the balls have only point contact with the pitch.

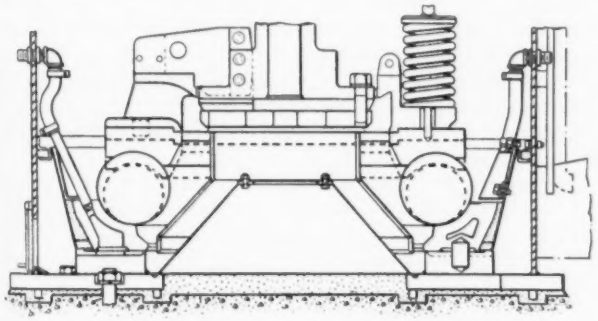


Fig. 12 Pulverizer Ball-Race Detail

There is also ample clearance between the ball and race for the crushed pitch to lie without being packed. The suggestion was put into effect and worked out successfully from the start. Fig. 12 shows this combination in the type-B pulverizer. Samples taken at the pulverizer outlet had a fineness of 92 per cent through 200 mesh.

Pulverized-Fuel-Pitch Firing

Combustion difficulties encountered in burning pulverized pitch were manifold and can be grouped into (*a*) dripping of the plastic pitch at the burner tip, (*b*) flashbacks in the burner, (*c*) poor fuel distribution, and (*d*) burner and pipe blockage. All these accounted in part for the low efficiency. The pulverized-pitch flame is much brighter than the pulverized-coal flame, and has semidistinct end boundaries. Rear-door observations clearly showed the presence of incandescent pitch particles in the bright combustion gases. These particles would shoot through like meteors. They were also descriptively referred to as burning "matchsticks" or as "butterflies." When cooled, these particles dropped out in the combustion chamber or swept beyond into the breeching and stack. Many of the particles had the appearance of small, round, broken Christmas-tree balls, ranging in size from a pin point to a BB shot. Apparently the bottled-up volatile gases within the incandescent plastic-pitch particle expanded and burst the surrounding shell after leaving the flame. It is these burning volatile gases which are identified as "matchsticks." The carbon shell quickly cools on leaving the combustion zone and drops out.

Observations of the flame at the burner tip clearly indicated that many pitch particles became plastic before reaching the tip and, on reaching the burner tip, would unite with others to form irregular plastic sheets. These remained suspended at the nozzle until knocked off by the operator or were swept away by the flame. Other plastic-pitch particles dropped onto the burner throat or the floor. Continual vigilance and considerable poking by the operator were necessary to keep the pulverized-pitch flame uniform and regular.

The worst trouble encountered was with flashbacks in the burner pipe. While operating at a constant rating and without warning, the pulverized pitch would suddenly ignite some 12 in. or so back in the burner pipe itself. If noticed immediately, the operator could rectify this by vigorously poking the burning plastic pitch forward into the furnace. But more often than not the plastic pitch built up so quickly that the burner was completely blocked. This was serious and necessitated a forced emergency shutdown.

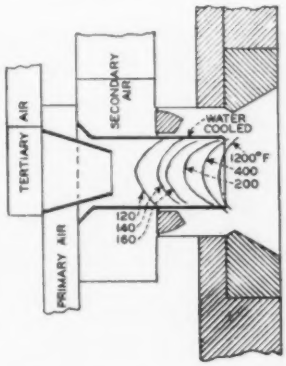


Fig. 13 Pitch Temperatures in Burner Pipe

These trial runs most forcibly pointed out the important fact that the temperature of the pulverized pitch must be kept below 190 F, the temperature at which pitch starts to become tacky, while it is still in the burner pipe. A series of temperature readings within the burner pipe were taken with a pyrometer while operating under the conditions described and with varying primary-air-fuel mixtures. They are plotted in Fig. 13. These tests served as the basis for a redesign of the burner and an altered mode of operation.

It was observed that the higher temperatures are in the center and that the temperatures varied with the primary-air-fuel ratio. The richer the fuel, the lower the temperature and, hence, decreased danger of flashbacks. This led to the conclusion that the incoming pulverized fuel must be shielded from the radiant furnace heat while still in the burner pipe. This could be partially effected by increasing the fuel density. The ignition zone would be advanced slightly away from the burner nozzle, and all other temperature zones would similarly be moved forward. The limiting factor, however, was the shape of this hot front zone or lines of equal fuel temperatures. To move the center forward sufficiently, so that its ignition took place at the burner tip and not within the burner pipe, meant that the ignition of the

outer ring of this paraboloidal-shaped fuel mixture took place too far away from the burner. Under these conditions, the ignition was unstable and the flame puffed.

These observations suggested the elimination of the center zone of the primary-air-fuel supply by extending the nozzle of the tertiary air to the burner tip, thereby confining the flow of the pulverized fuel to the annular space between the two water-cooled cylindrical nozzles. Temporary field changes were made on one

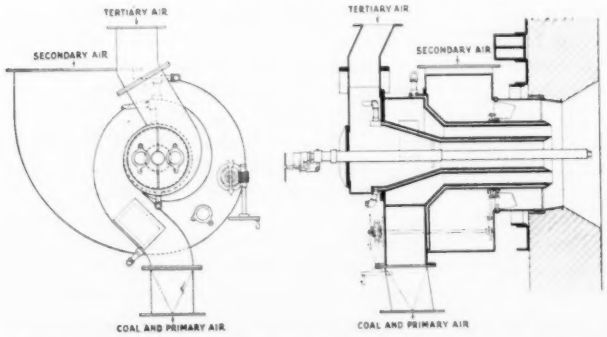


FIG. 14 FINAL DEVELOPMENT OF COMBINATION FOUR-FUEL BURNER

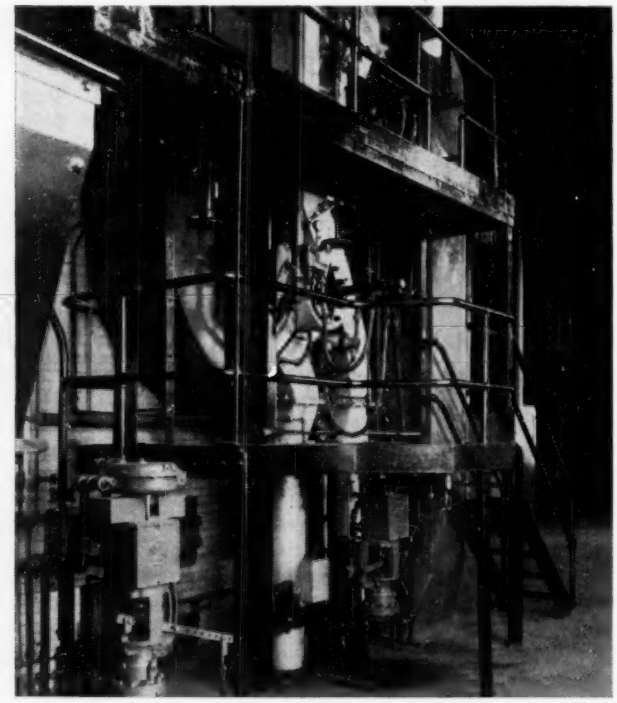


FIG. 15 COMBINATION FOUR-FUEL BURNER

burner. The improvement was marked. Dripping decreased, flashbacks were eliminated, but there still remained poor fuel distribution. Pitot-tube tests in the primary-air casing disclosed the presence of eddy currents at the junction of the inlet-supply pipe and casing. A good portion of the fuel would flow directly into the burner pipe without first passing around the volute casing. This by-passing was eliminated by the installation of a baffle at this point. Subsequent tests with pulverized pitch proved satisfactory.

To test these burner changes thoroughly, the unit was operated on pitch for a period of 40 days. During this period, temperature readings within the pulverizer were taken with and without water cooling. The difference was negligible and water cooling was discontinued even on the hottest days when the pulverizer air inlet was 100 F and outlet 105 F. Incidentally, it is important that there be no leakage of hot air into the pulverizer. The usual operating dampers are not tight and it was found necessary to blank off the hot air when operating on pitch.

At the end of this trial run, the burner, pipes, and pulverizer were thoroughly examined. The pulverizer was clean and showed no measurable wear in the race or balls. Pulverized fuel-pitch did coat the burner lead pipes, especially at the long sweep bends and the burner casing. It was deemed expedient to install clean-out doors at these points.

To note the effect of these burner changes on pulverized coal, the boiler was refired with this fuel. An improvement in burning this fuel was also noted, and it was therefore decided to rebuild both burners. In addition to the changes mentioned, the furnace ends of both the primary and tertiary nozzle were brought to a sharp edge in order to reduce the surface to which the plastic pitch might adhere. In the redesigned burner, more internal baffles were installed in the cooling jackets to insure the flow of cold water to the tip. All welds were ground down to obtain a uniform and smooth surface. Fig. 14 clearly shows these changed features. Fig. 15 illustrates the final combination four-fuel burner as it is today.

AUTOMATIC COMBUSTION CONTROL

During the development of this burner, the usual kinks encountered in adjusting a multifuel-firing boiler for 100 per cent automatic control were ironed out. A Smoot combustion-control system regulates the air-and-fuel input and automatically maintains their proper relation throughout the range, thereby resulting in a constant CO_2. A maximum-and-minimum-rating control is incorporated in the master controller to confine the rating of this unit between these two designated limits, regardless of the plant demand.

The Smoot control system, as applied to this unit, consists of an air-operated master controller and oil-operated regulators which measure and control the primary-air-fuel input when firing pulverized coal or pitch, the liquid-fuel input when firing oil or tar, air flow, and draft.

The master controller directly translates changes in header steam pressure into changes in air pressure (master loading) which pressure changes are pneumatically dispatched to the fuel-flow and air-flow regulators. Since the changes in steam-header pressure, the index of steam flow, vary as the square of the flow, it follows that changes in the master loading also vary as the square of the steam flow. This master-loading force, the impulse for air and fuel changes, is transmitted to the individual regulators. It is balanced against some measure or index of fuel-and-air flow which also varies as the square of the fuel flow or air flow. Thus, to control and measure liquid-fuel flow, the master loading is balanced against the pressure drop across an orifice in the fuel line. Since this pressure drop varies as the square of the fuel flow and the master loading varies as the square of the steam flow, the indexes of these flows can be directly balanced against each other. The regulator can be adjusted so that for a definite steam load there is a definite fuel input.

Air flow to this boiler is controlled indirectly by controlling the output of the combustion gases through the speed of the induced-draft fan. A change in the speed of this fan changes the furnace draft. A forced-draft fan, controlled by a weight-loaded regulator, automatically changes speed to maintain a predetermined furnace draft of 0.1 in. of water. In this manner the control of the output gases automatically controls the air input. As in the fuel regulator, the master loading is balanced against some measure of the gas flow which varies as the square

of the flow. Since gas flow is directly proportional to fan speed, and the pull of a speed governor, driven by the fan, varies as the square of the speed, the master loading can be balanced directly against the governor pull. This balance can be adjusted so that for a definite steam load there is a definite gas flow and, hence, air input. This relationship necessarily varies with different fuels but the regulator can easily and quickly be adjusted to follow the predetermined master-loading-speed curves for pulverized fuels and liquid fuels.

Since the master loading is an index of the quantity of fuel input and air input, it is only necessary to adjust the air master loading relative to the fuel master loading directly at the master

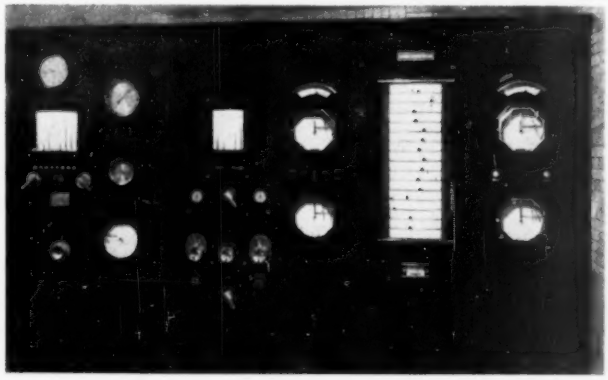


Fig. 16 Control and Gage Board

controller to alter the air-fuel ratio and, hence, CO_2. This the operator does from time to time as governed by the CO_2 reading, furnace observations, etc.

Numerous indicating pressure gages and thermometers of the multipointer type, as well as flowmeters, CO_2 recorders, haze combustion meter and smoke indicator, water-level recorder, and temperature recorders assist the operator in maintaining optimum conditions. A view of the control panel of this multi-fuel unit is shown in Fig. 16.

Among the interesting safety features installed on this boiler are the safety regulators which operate automatically to reduce the fuel input in case of partial failure of the air supply or induced-draft-fan failure. In case of complete failure, the electric interlocking of all auxiliaries automatically shuts down those ahead of the unit which failed. This electric interlocking of the auxiliaries also prevents their starting up in an improper and dangerous sequence. Each burner is equipped with an electric-eye flame detector which can be seen in Fig. 15. These and such important functions as feedwater pressure, primary-air pressure, oil pressure, furnace draft, and boiler differential are all equipped with electric alarm devices which operate to sound a signal gong and to light up their respective light signals on an annunciator board in case of partial failure. This trouble-analyzer-and-alarm signal system has proved its value on numerous occasions and is particularly helpful to the operator whose duties include the control of four stoker-fired boilers in an adjacent wing.

Flexibility of Four-Fuel Boiler

With the completion of the basic development of this four-fuel boiler, there remained yet to demonstrate its flexibility in changing from one fuel to another and to evaluate these fuels under normal plant-operating conditions. The switch from liquid-fuel firing, such as oil or tar, to pulverized coal or fuel-pitch is made without any change in rating and is fully controlled from the master controller. If desired, both liquid fuel and pulverized fuel can be fired at the same time in the same burner. To change from oil to tar or back to oil is a simple operation which entails no difficulties if the valve changes are made quickly and if both liquids have been conditioned to the proper viscosity. Tar is partially soluble in fuel oil and, in a mixture of about 50–50, there will be precipitated insoluble resins which form a liverlike substance which will be caught in the strainers. It is, therefore, good practice to minimize the time and area contact of tar and oil in this fuel change. Needless to say, oil should never be stored in a tar tank or vice versa, without first emptying the tank completely. A most troublesome sludge, impossible to handle with ordinary reciprocating pumps, will be the penalty.

The change from one pulverized fuel to another cannot be done directly, for different-sized balls are required as has been pointed out previously. The general practice has been to fire oil during the time required to change balls in the pulverizer, a period of about 4 hr, if continuity of service is desired.

Operating Results

During the last 2 years, the unit has been fired with oil, tar, and pulverized fuel-pitch. Changes in the prices of these fuels during this period warranted these switches. Compared to the prevailing prices of these fuels, pulverized-coal firing was uneconomical. Enough coal, though, was fired to obtain complete operating data and results under normal automatic operation to serve as the basis of comparison with these other fuels. Complete operating data and typical average daily results obtained with each fuel are listed in Tables 1 and 2.

The results given in the tables are those obtained under everyday operating conditions with a variable load and are, therefore, the results of interest to the management. Under test conditions with a constant load, the efficiency was found to be about 2 per cent higher. The blowdown and jacket-cooling-water losses, amounting to about 0.75 per cent and chargeable to the unit, are actually 90 per cent recovered in heat exchangers.

To determine the limits of minimum excess air, when firing liquid fuels, a series of tests was conducted with varying amounts of combustion air. Careful fuel-gas analyses of CO_2, O_2, CO, and unburned hydrocarbons were made with an Elliott gas analyzer. The tedious and lengthy task of analyzing for unburned hydrocarbons led to the suggestion of utilizing a standard commercial combustible-gas indicator, an instrument in common use with all gas and oil companies for routine check-up on gas- and vapor-explosion hazards. Parallel tests were conducted and in all cases the answer obtained with a combustible-gas indicator in less than 1 min agreed with that obtained on an Elliott apparatus. Thereafter, for a quick determination to detect the presence of any unburned combustible gases, carbon monoxide, hydrogen, or hydrocarbons in the boiler passes and exit the combustible-gas indicator was used. These tests indicated that with a fixed rating the minimum excess air can be reduced to 10 per cent without the occurrence of incombustible-gas losses when firing oil or tar. However, when operating with a variable load this must be increased to 15 per cent excess air.

It is noted that the efficiency when firing tar is about 1 per cent higher than with oil. The lower hydrogen content should actually result in a 2 per cent increase in efficiency. The carbon loss in the breeze, however, offsets this so the net gain is only about 1 per cent. The efficiency of pitch firing was expected to be somewhat lower, due to the use of cold primary air, but not to the extent experienced. This lower efficiency can be traced to the unburned carbon losses and, to date, this appears to be about the best that can be expected with this equipment and fuel. Whether it is the inherent characteristic of pitch remains only a speculation. Pitch is easily pulverized to a high state of fineness. In powdered form even at room temperature, it has a tendency

TABLE 1 LIQUID-FUEL FIRING

	Type of fuel: Oil		Tar	
Steam flow, M lb per hr	50	100	50	100
Number of burners	1	2	1	2
Boiler operation				
Pressure at drum outlet, psi	230	238	230	238
Pressure at superheater outlet, psi	227	227	227	227
Superheater pressure drop, psi	3	11	3	11
Feedwater temperature, F	220	220	220	220
Superheated-steam temperature, F	490	500	490	500
Factor of evaporation	1.103	1.108	1.103	1.108
Fuel				
Quantity, gph	417	847	377	766
Grade	Bunker C		Water gas	
API	12.9		....	
Specific gravity	0.98		1.18	
Lb per gal	8.18		9.86	
Viscosity, S F at 122 F, sec	68		900	
Flash point, deg F	183		156	
Pour point, deg F	23		75	
Ultimate analysis:	Per cent by weight			
Carbon	86.0		89.9	
Hydrogen	11.0		6.0	
Sulphur	1.2		1.2	
Oxygen	0.8		1.8	
Nitrogen	0.8		0.4	
Moisture	0.2		0.7	
Ash	0.0		0.0	
Total	100.0		100.0	
Btu per lb, dry	18400		16750	
Btu per gal, dry	150500		165200	
Fuel-pump-inlet temperature, F	110		190	
Fuel-pump-inlet pressure, psi	2		2	
Fuel-heater-outlet temperature, F	200		250	
Fuel pressure at burner, psi	170		70	
Viscosity at burner, S F, sec	18		18	
Type of atomizing	Steam-mech.		Steam	
Steam pressure at burner, psi	100		150	
B & W sprayer plate no.	H-08-30-48		3 WA-XCR	
Flue gases				
Analysis at boiler outlet:	Per cent by volume			
CO_2	13.9		15.7	
O_2	2.9		2.8	
CO	0.0		0.0	
N_2	83.2		81.5	
Total	100.0		100.0	
Analysis at air-heater outlet:	Per cent by volume			
CO_2	12.1		13.7	
O_2	5.2		5.2	
CO	0.0		0.0	
N_2	82.7		81.1	
Total	100.0		100.0	
Excess air, per cent	15		15	
Air-heater air leakage, per cent by volume	15		15	
Temperature leaving boiler, F	530	640	530	640
Temperature leaving air heater, F	275	340	270	335
Furnace draft, in. of water	0.1	0.1	0.1	0.1
Boiler-exit draft, in. of water	0.40	1.35	0.40	1.35
Air				
Air-heater-inlet temperature, F	90	90	90	90
Air-heater-outlet temperature, F	420	455	425	460
Miscellaneous				
Continuous blowdown, per cent	5	5	5	5
Calculated results				
Apparent evaporation, lb per gal	120	118	133	130
Heat balance:	Per cent			
Loss due to unburned combustible gases	0	0	0	0
Loss due to theoretical dry gases	3.3	4.5	3.3	4.5
Loss due to excess dry air	0.5	0.7	0.5	0.7
Loss due to H in fuel	6.1	6.2	3.6	3.7
Loss due to moisture in fuel	0	0	0	0
Loss due to moisture in air	0.1	0.1	0.1	0.1
Loss due to air-heater air leakage	0.5	0.7	0.5	0.7
Loss due to continuous blowdown	0.8	0.8	0.8	0.8
Radiation and unaccounted for (by diff)	3.2	2.5	4.7	4.0
Total losses	14.5	15.5	13.5	14.5
Efficiency	85.5	84.5	86.5	85.5

TABLE 2 PULVERIZED-FUEL FIRING

	Type of fuel: Coal		Pitch	
Steam flow, M lb per hr	50	100	50	100
Number of burners	1	2	1	2
Boiler operation				
Pressure at drum outlet, psi	230	238	230	238
Pressure at superheater outlet, psi	227	227	227	227
Superheater pressure drop, psi	3	11	3	11
Feedwater temperature, F	220	220	220	220
Superheated-steam temperature, F	495	505	500	510
Factor of evaporation	1.106	1.111	1.108	1.113
Fuel				
Quantity, lb per hr	4520	9200	4210	8570
Grade	med. vol. bit.		fuel-pitch	
Grindability, Hardgrove scale	80		150+	
Proximate analysis	Per cent by weight			
Moisture	3.0		2.2	
Volatile matter	21.2		48.2	
Fixed carbon	69.8		48.9	
Ash	6.0		0.7	
Total	100.0		100.0	
Softening temperature, F	2570		315	
Ultimate analysis:	Per cent by weight			
Carbon	78.0		90.1	
Hydrogen	4.1		4.9	
Sulphur	1.3		0.9	
Oxygen	6.5		0.6	
Nitrogen	1.1		0.6	
Moisture	3.0		2.2	
Ash	6.0		0.7	
Total	100.0		100.0	
Btu per lb, dry	14300		16200	
Pulverizer				
Air temperature to pulverizer, F	230	210	Atm	Atm
Pulverizer-outlet temperature, F	150	150	Atm+5	Atm+5
Through 50 U. S. sieve, per cent	99+	99	99+	99+
Through 200 U. S. sieve, per cent	90	83	92	90
Flue gases				
Analysis at boiler outlet:	Per cent by volume			
CO_2	15.8		14.2	
O_2	3.5		4.9	
CO	0.0		0.0	
N_2	80.7		80.9	
Total	100.0		100.0	
Analysis at air-heater outlet:	Per cent by volume			
CO_2	13.7		12.3	
O_2	5.8		7.0	
CO	0.0		0.0	
N_2	80.5		80.7	
Total	100.0		100.0	
Excess air, per cent	20		30	
Air-heater air leakage, per cent by volume	15		15	
Temperature leaving boiler, F	565	685	540	670
Temperature leaving air heater, F	290	355	325	400
Furnace draft, in. of water	0.1	0.1	0.1	0.1
Boiler-exit draft, in. of water	0.45	1.50	0.45	1.50
Air				
Air-heater-inlet temperature, F	90	90	90	90
Air-heater-outlet temperature, F	450	500	445	500
Primary-air burner pressure, in. of water	6.0	6.0	7.5	7.5
Secondary-air burner pressure, in. of water	3.5	3.6	3.2	3.3
Miscellaneous				
Continuous blowdown, per cent	5	5	5	5
Calculated results				
Apparent evaporation, lb per lb	11.1	10.9	11.9	11.7
Heat balance:	Per cent			
Loss due to unburned combustible gases	0	0	0	0
Loss due to theoretical dry gases	3.7	4.9	4.5	5.9
Loss due to excess dry air	0.7	0.9	1.3	1.7
Loss due to H in fuel	2.9	3.2	3.3	3.4
Loss due to moisture in fuel	0.3	0.3	0.2	0.2
Loss due to moisture in air	0	0.1	0.1	0.1
Loss due to air-heater air leakage	0.6	0.8	0.8	1.1
Loss due to continuous blowdown	0.8	0.8	0.7	0.7
Radiation and unaccounted for (by diff)	5.5	4.5	8.6	7.4
Total losses	14.5	15.5	19.5	20.5
Efficiency	85.5	84.5	80.5	79.5

to cake more easily than powdered coal. This characteristic is no doubt more pronounced at higher temperatures. In its flow through the burner at velocities of 4000 fpm, collisions between particles occur which tend to raise the temperature of the particles. Furthermore, as the particles approach the burner nozzle they are subjected to the radiant furnace heat. Both factors work toward the formation of larger particles. All pitch particles, large or small, pass through the plastic stage before ignition occurs. This is the critical stage in pitch firing for, while in this form, all particles will stick together on contact. Small particles will chemically unite with the air and are consumed while yet in the combustion zone. The larger plastic particles burn, but the plastic condition of the surface does not allow the air to come in contact with the inner material before they are out of the combustion zone. It is a question of which takes place first, the union of the plastic pitch particle with air, or its union with an adjacent plastic particle. To minimize carbon losses immediate contact with the combustion air must take place.

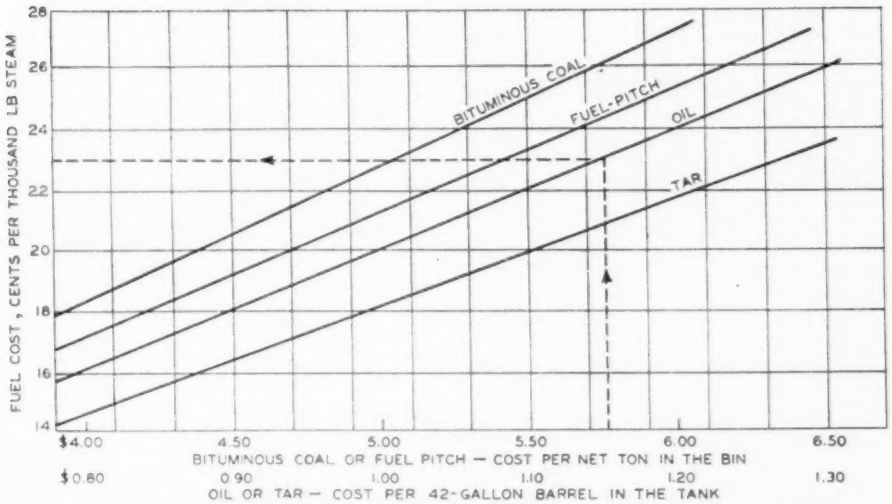


FIG. 17 FUEL COST PER 1000 LB OF STEAM FOR VARIOUS FUEL PRICES AND FUELS

Basis	Pulverized coal	Pulverized fuel-pitch	Oil	Tar
Steam pressure, lb per sq in...	227	227	227	227
Steam temperature, deg F.....	500	505	495	495
Feedwater temperature, deg F.	220	220	220	220
Apparent evaporation.....	11.0 lb per lb	11.8 lb per lb	119 lb per gal	132 lb per gal
Fuel per thousand lb steam....	91 lb	85 lb	8.4 gal	7.6 gal
Efficiency, per cent.....	85	80	85	86
Btu of fuel, dry.....	14,300 per lb	16,200 per lb	150,000 per gal	165,200 per gal
Moisture, per cent.....	3.0	2.2	0.2	0.7
Equivalent evaporation.....	12.6 lb per lb	13.4 lb per lb	132 lb per gal	147 lb per gal

FUEL ECONOMICS

Based on these day-in-and-day-out results, the economic value of each fuel which will produce the lowest over-all steam cost can be ascertained. Since supervision, labor, water, water treatment, and miscellaneous costs are common to all types of firing, with this unit the controlling factor remains fuel cost per 1000 lb of steam. Differential repair and power costs for the auxiliaries are contributing factors and must necessarily vary with different installations and methods of driving the auxiliaries. The curves in Fig. 17 are useful in determining the fuel cost in units of 1000 lb of steam for each type of firing and with varying fuel prices, or they can be used to arrive at the economic value of the other three fuels, compared to the price of one.

Thus, if fuel oil in the boilerhouse costs $1.15 per bbl the fuel cost per 1000 lb of steam is 23 cents. In similar manner, the fuel costs per 1000 lb of steam for the other three fuels, based on their respective delivered costs in the boilerhouse, can be read off this curve. Repairs and difference in boiler-auxiliary-power requirements modify these figures and, in the case at the Harrison Gas Works, these cost items are graphically presented in Fig. 18. If the average load were 75,000 lb per hr, these must be added to the fuel cost per 1000 lb of steam, as obtained in Fig. 17: 0.1 cent per M to the tar-firing cost, 0.5 cent per M to the pulverized coal-firing cost, and 0.7 cent per M to the pulverized fuel-pitch firing cost to obtain the true relative cost.

Similarly, the "break-even" price in the boilerhouse of the other fuels compared to fuel oil can be ascertained from these two curves. Thus, if fuel oil costs $1.15 per bbl in the boilerhouse, tar is worth 3 cents per gal, also in the boilerhouse; bituminous coal $4.95 per net ton, delivered in the boilerhouse, and fuel-pitch $5.25 per net ton, also delivered in the boilerhouse. To arrive at the contract price, all handling and conveying costs from the receiving point to the boilerhouse must, of course, be deducted from these figures.

Actually, due to local circumstances, the evaluation of fuels in the Harrison Gas Works is somewhat more complicated by the fact that the operating costs of the chain-grate barley-firing boilers must be considered. At least three are always under fire and there arises the problem of economic load division between these and the new four-fuel boiler.

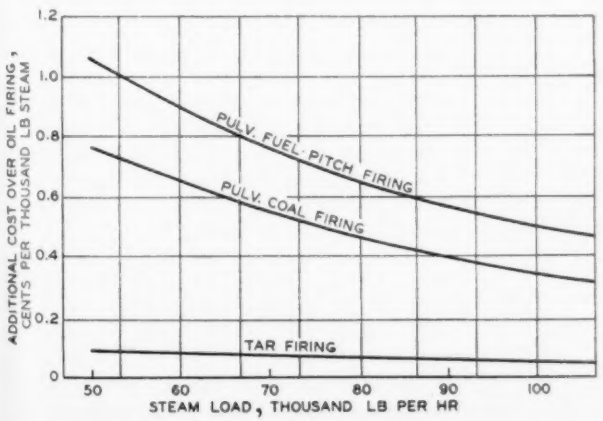


FIG. 18 AUXILIARY-POWER AND REPAIR COST CURVES

CONCLUSION

It is felt that this unit has met the general requirements of a multifuel boiler in its flexibility to change from one fuel to another even without shutting down, and its ability to handle all fuels equally well. It is a forward step toward the goal of a universal boiler and burner, a need of those who have a choice of fuels and demand continuity of service.

ACKNOWLEDGMENT

The writer gratefully acknowledges the assistance given by The Babcock & Wilcox Company, especially in the preparation of the illustrations.

Discussion

G. W. Concklin.[2] The writer would like to convey some of the facts which he has encountered in the burning of by-product fuels. No doubt the burning of fuel-pitch and water-gas tar holds the most interest. Up to date we have used as boiler fuel 5,000,000 gal of tar and 7000 tons of fuel-pitch.

The burning of fuel-pitch presented quite a burner problem at first. With a standard coal burner, it was impossible to fire more than 3 hr without removing the burner for cleaning. To overcome these frequent shutdowns, we used water-cooled burners with copper tips and impeller vanes. This change enabled us to run continuously for 5½ days. Although quite encouraging, it did not prevent the dripping and part-clogging of the burners. The melting of the pitch and the clogging at the tip resulted in frequent blowbacks lasting from 15 min to 8 hr. We achieved the best results by keeping the primary air at 25 per cent and the temperature at 120 F. The velocities at the burner giving the best results were 3500 to 5000 fpm. We found it impossible to operate at velocities below 2800 fpm.

The pulverizing was done with a tube mill. In addition to a ball charge, it was necessary to add scrap gears as grinding media to prevent the fuel from packing the liners. A fineness of 75 to 90 per cent through 200 mesh did not have a marked effect on the burning.

At no time were we able to get over 80.5 per cent efficiency with an air heater in use. The high carbon and unaccounted-for losses were so high that we had to discontinue the fuel-pitch for economic reasons. The availability of the steaming output when burning pitch was about 85 per cent, the balance being produced with liquid fuels, Table 3 of this discussion.

[2] Plant Engineer, Haverstraw Industrial Terminal, Haverstraw, N. Y.

TABLE 3 TYPICAL FUEL-PITCH FIRING BY MONTHS; GARNERVILLE BOILER NO. 1

	Jan., 1940	Feb., 1940	March, 1940
Total steam generated by boiler, lb	41,000,000	40,000,000	40,000,000
Steam generated from fuel-pitch, lb	37,500,000	34,000,000	31,500,000
Evaporation per pound of pitch	12.5	12.5	12.51
Availability, pitch firing, per cent	91.5	85	78.8
Balance of firing, per cent	8.5 (tar)	15 (tar)	21.2 (oil)
Efficiency, with pitch only, per cent	80.5	80.5	80.5

Notes:
Boiler designed for firing four fuels.
Capacity, 70,000 lb per hr.
Boiler has complete waterwalls.
Furnace width, 12 ft 6 in.
Two burners (angular placement).
Firing depth, 19 ft.
Average heat release per cubic foot = 24,000 Btu.
Boiler run at base load.
Content of steam = 1015 Btu.
Content of fuel-pitch = 16,000 Btu.
Temperature leaving boiler, 585 F.
Temperature leaving air heater, 370 F.
Secondary-air temperature, 305 F.
Primary air (25 per cent) and fuel, 120 F (room + 40 F).
Continuous blowdown, 0.6 per cent.
Average CO_2 = 14.8 per cent.
Excess air = 25 per cent.
Firing this boiler with oil, an efficiency of 85.5 per cent was obtained.
Firing with water-gas tar, an efficiency of 87 per cent was obtained.

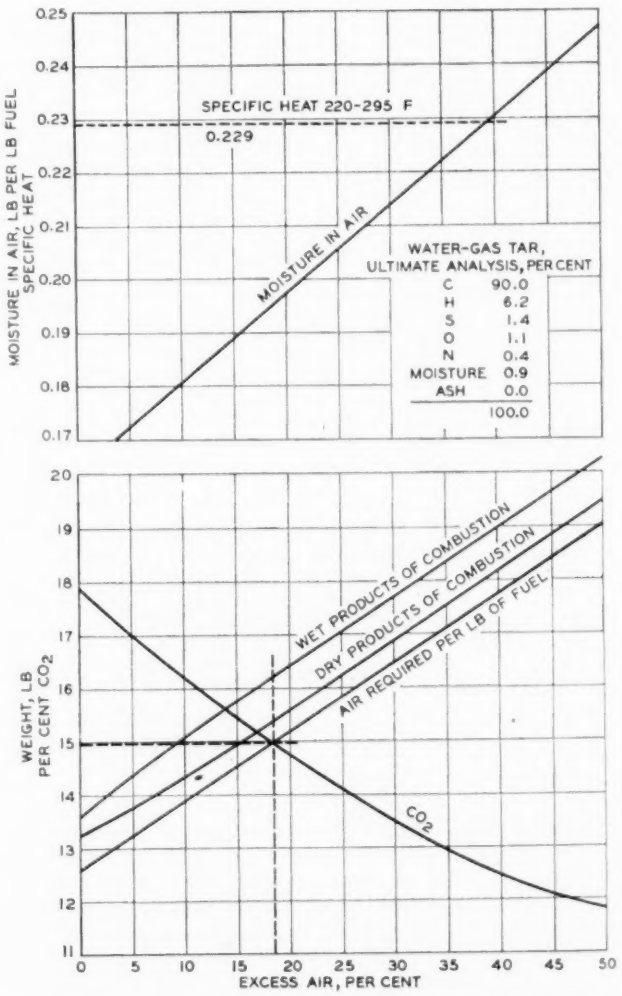


Fig. 19 Performance Data for Garnerville Boiler No. 3 Burning Liquid Tar; 16,480 Btu per Lb

TABLE 4 TYPICAL PERFORMANCE WITH WATER-GAS-TAR FIRING; GARNERVILLE BOILER NO. 3[a]

	Steaming rate, lb per hr			
	65000	55000	40000	30000
Furnace draft, in. water	—0.05	—0.05	—0.05	—0.04
Entrance to third pass, in. water	—0.20	—0.14	—0.075	—0.042
Air-heater-exit draft, in. water	—1.58	—1.10	—0.50	—0.28
CO_2, per cent	15	14.9	14.7	13
Excess air, per cent	18.5	19	21	35
Boiler-exit temperature, F	480	450	405	380
Air-heater-exit temperature, F	295	278	240	220
Air temperature, F:				
Entering	77	83.25	89	88
Leaving	275	268	265	257
Products of combustion per pound of fuel, lb:				
Wet	16.19	16.28	16.44	18.20
Dry	15.38	15.46	15.63	17.41
Air for combustion, lb	14.97	15.00	15.28	17.03
Heat release, Btu per cu ft per hr	19900	17000	12200	9200

Heat Balance

Evaporation, lb per hr	65000		55000		40000		30000	
	Btu	Per cent	Btu	Per cent	Btu	Per cent	Btu	Per cent
Dry-gas loss	792	4.81	736	4.47	610	3.70	598	3.64
H_2 and moisture in fuel	661	4.01	656	3.98	648	3.93	639	3.88
Moisture in air	21	0.13	20	0.12	16	0.10	16	0.10
Unburned carbon	165	1.00	165	1.00	165	1.00	165	1.00
Radiation	124	0.75	165	1.00	231	1.40	305	1.85
Unaccounted for	247	1.50	247	1.50	247	1.50	247	1.50
Total losses	2011	12.20	1989	12.07	1917	11.63	1970	11.97
Efficiency by difference		87.80		87.93		88.37		88.03
		100.00		100.00		100.00		100.00

[a] Boiler designed for firing liquid fuels; capacity 55,000 lb per hr; two burners, placed parallel 5 ft 3 in. center to center; furnace width, 14 ft; firing depth, 18 ft; water-cooled front, bottom, and roof; no waterwalls at sides (walls 22 in.).
This boiler is giving 87.5 per cent efficiency for a 6-day continuous run; continuous blowdown, 0.5 per cent.

We have burned more than 4,000,000 gal of water-gas tar during the last year and find it to be an excellent boiler fuel. The availability of all three boilers was 100 per cent when firing this fuel. There are some minor precautions to be taken, such as correct heating, storing, and atomizing. In general, we consider it equal to oil. The additional 1 to 1½ per cent efficiency gained compensates for the carbon loss. This carbon collects in the furnace and soot hoppers which are cleaned once or twice a week. We have found that this by-product fuel meets all theoretical expectations.

No. 3 boiler, which was designed especially for tar firing, has given a fine performance using this fuel. Performance data and the heat balance for this boiler, together with some observations therewith, are given in Table 4 and Fig. 19 of this discussion.

L. Coykendall.[3] This paper should prove to be of great service to the industry because it demonstrates the feasibility and economic advantage of burning various types and kinds of fuel in one unit. Particularly is this true at this time when warring nations are using great stores of oil, coal, and other fuels, with the resulting fluctuations in price. Many of the units sold for several years past, including large central-station boilers, have been designed for firing by several fuels.

A large percentage of the successful modifications and changes in the installation were suggested by the author, and to him should go a great deal of the credit for the present successful performance and operation of the equipment. However, he has not dwelt on the troubles experienced mainly because of the difficulty of burning fuel-pitch in a unit also adapted for three other fuels. If time permitted, he might have described the discouraging results of various changes before the final arrangement was obtained. These included the installation of various types of vanes and screw flights in the primary scroll to reduce pressure drop and correct poor distribution around the burner nozzle, and several changes to the secondary-air casing and burner throat.

The greatest difficulty was encountered with combustion of fuel-pitch, and the efficiency obtained will permit of considerable room for improvement. While the analysis of this fuel indicates that it is an ideal fuel from an efficiency standpoint, its potential value depends upon ability to overcome its peculiar properties. Among these are (1) the low softening temperature, and (2) the fact that, although the volatile content is high, the volatile constituents are all in the brackets which distill off at the higher temperatures. It will be noted that the efficiency of this fuel on this unit in everyday operations is around 80 per cent, whereas 85 to 86 per cent might be expected. This difference of about 5 per cent is attributed to unburned-carbon losses, as a result of the foregoing properties. An explanation covering the mechanics of this carbon loss is given in the paper in the first part of the section on "Fuel-Pitch." It is suggested for the benefit of those who may decide to use this fuel that probably a refractory furnace instead of one completely water-cooled would be beneficial in reducing this carbon loss. With the other fuels involved, however, this would be out of the question.

It should be pointed out that firing of gas could be adapted to this burner without effect on combustion of the other fuels and without any changes other than the installation of a standard gas ring at the burner throat.

Mention is made in the paper that breeze particles in gashouse tar are beneficial in cleaning soot or ash deposits from the air heater and other surfaces. In the last few years, slag and ash deposits on generating surfaces, resulting from bunker C oil firing, have become more troublesome as a result of new processes in the oil refineries. We know of several plants equipped for combination coal-and-oil firing where the operators fire coal periodically (say once a week for several hours) for the express purpose of cleaning the air heater and other surfaces. On this unit, it was found necessary to increase the steam pressure to the soot blowers to about 150 psi in order to clean the boiler surfaces effectively when firing bunker C oil. Provision was made to supply 90-lb-pressure steam when firing the other fuels.

The author is to be commended for his description of the instruments, automatic control, electric-eye flame detectors, electric interlocks, and other safety features. These are particularly necessary and useful in the efficient and safe operation of a multifuel unit.

D. S. Frank.[4] The paper is interesting from the standpoint of showing what can be done with equipment when time and effort is spent in making adjustments necessary for individual application.

Since the greatest difficulty was encountered with the fuel-pitch, the writer would question the necessity of burning this material in semisolid form. If the distillation had been carried out to a hard-coke residue, the handling characteristics would have been quite similar to coal. This should have eliminated the necessity for changing the ball race.

The writer is not familiar with the formation of fuel-pitch but, if the material is in a liquid form, as residue in the still, it should be possible to burn the pitch as a liquid. This would require suitable equipment for handling and atomizing. If this material could be removed from the still and burned as a liquid at such temperature as is required to obtain the desired viscosity of 18 sec Furol, no difficulty should be experienced.

Referring to Fig. 18 of the paper, it will be noted that the cost of burning fuel-pitch is 0.7 cent per 1000 lb of steam, higher than fuel oil. Based on a steam production of 75,000 pounds per hr, the daily cost of pulverized-fuel-pitch firing is $12.60. It is entirely possible that handling the material as a liquid might show a lower daily cost than $12.60.

The author states that a combination steam-mechanical burner is recommended over a straight mechanical burner in a "cold" furnace for oil firing. Does this hold true for both the 50,000- and 100,000-lb per hr production rate, or at what furnace-release rate in Btu per cubic foot are the burners equal? No mention is made of the cost of steam required for atomization, which may also have a bearing upon the choice of burners.

Author's Closure

When coal-gas or water-gas tar is distilled, there may be left, as a solid residue at atmospheric temperatures, a number of kinds of pitches depending upon the temperature of distillation and quantity of oils distilled. The higher the temperature and the more oils recovered, the higher will be the melting point of the pitch. Thus if about 14 per cent of the original charge is recovered as oils, there will remain a roofing pitch which has a melting point of 140 to 150 F. If this is increased to a point where about 22 per cent of the tar is recovered as oils, there will be left a briquette-pitch which has a melting point of 180 to 190 F. To continue to a point where tar is distilled at about 800 F, when about 49 per cent of the tar is recovered as oils, there will be left fuel pitch which has a melting point of 300 to 330 F. Therefore, it is understandable that the term pitch cannot be loosely used. It is important to describe the form specifically as roofing-pitch, briquette-pitch, or fuel-pitch.

Liquid roofing pitch has been successfully burned in boilers,

[3] Service Department, The Babcock & Wilcox Company, New York, N. Y.

[4] Pure Oil Company, Chicago, Ill.

for it need only be heated to about 350 F to obtain the desired viscosity of 18 sec Furol. However, to burn liquid fuel-pitch requires that it be heated to at least 700 F to obtain the proper viscosity for atomization. This, of course, requires special heating equipment, such as an externally fired boilerf or heating the fuel-pitch and special heated storage tanks. The pumping equipment, piping, and valves should all be steam-jacketed and designed for this temperature. The cost of this equipment, coupled with unduly high maintenance, is prohibitive compared to the advantages, if any, of liquid-fuel-pitch firing over pulverized-fuel-pitch firing.

The distillation of tars is often done to recover oils, in which case fuel-pitch is a by-product and not the end in itself. It must be handled as is, and up to now fuel-pitch is best handled and burned in boilers as a pulverized fuel. The author knows of no plant in this country where fuel-pitch is burned in liquid form. There are several installations where pitches of lower melting point, such as roofing pitch, are burned in liquid form.



FIG. 1 EAST PORTAL OF MOFFAT TUNNEL



FIG. 2 EAST PORTAL OF MOFFAT TUNNEL WITH CURTAIN RAISED

Piston Effect of Trains in Tunnels

BY R. L. DAUGHERTY,[1] PASADENA, CALIF.

The author was recently engaged by the Denver and Rio Grande Western Railroad to make a study of the ventilation of the Moffat Tunnel, which is 6.21 miles in length. In the course of this work measurements were made of the friction of air through the empty tunnel and also of the air pressures developed by different trains of various lengths passing through the tunnel at speeds ranging from 15 to 38 mph. The results of this investigation are presented in the form of curves for a wide variety of conditions. The mathematical analyses are given, which may be applied to the problem of tunnel ventilation in general. For the reason that but little information concerning the subject of "piston action" of trains in tunnels is available in the engineering literature, the author deems it desirable to make the present data a matter of record.

THE Moffat Tunnel, completed in 1928 at a cost of $18,000,000, pierces the Rocky Mountains some 50 miles northwest of Denver, Colorado, and is used jointly by the Denver and Rio Grande Western Railroad and the Denver and Salt Lake Railroad. Originally 16,593 ft of its length were timber-lined, but the timbering has been completely replaced with concrete by now. The remainder of the length is through granite rock which has been covered with gunite. This portion is naturally rough and irregular and varies in cross-sectional area. The standard concrete section is shown in Fig. 3. The essential dimensions of the tunnel sections are shown in Table 1.

TABLE 1 MOFFAT TUNNEL DIMENSIONS

Type	Length, ft	Area, sq ft	Perimeter, ft	Hydraulic mean radius, ft
Concrete-lined	17446	340	71	4.8
Concrete-lined	985	310	68	4.6
Rock, gunited	14374	340 to 450	77 Avg	5.2Avg

The east portal of the Moffat Tunnel is at an elevation of 9195 ft above sea level and the west portal is 112 ft lower. In order to secure drainage, the tunnel slopes both ways from a high point in its central portion, which is 42 ft higher than the east portal and 154 ft higher than the west portal. For equilibrium, the barometer at the west portal should be 0.087 in. of mercury higher than at the east portal. However, because of the high mountain range separating the two ends of the tunnel, the barometer differences are often much greater than this value. Occasionally the pressure at the west portal is as much as 2 in. of water more than at the east end, and at times it has been found to be 1.6 in. of water less. Any measurements of tunnel friction must be corrected for the barometric pressure differences, due allowance being made for the static difference because of the 112-ft difference in elevation. That is, for an air flow from east to west the tunnel pressure at the east portal will be increased not only by the tunnel friction but also by an amount

$$\Delta B = 13.6\ (B_w - B_e - 0.087) \quad \ldots [1]$$

[1] Professor of Mechanical Engineering, California Institute of Technology. Past Vice-President and Fellow A.S.M.E.

Contributed by the Hydraulic Division, and presented at the Semi-Annual Meeting, Kansas City, Mo., June 16–19, 1941, of THE AMERICAN SOCIETY OF MECHANICAL ENGINEERS.

NOTE: Statements and opinions advanced in papers are to be understood as individual expressions of their authors, and not those of the Society.

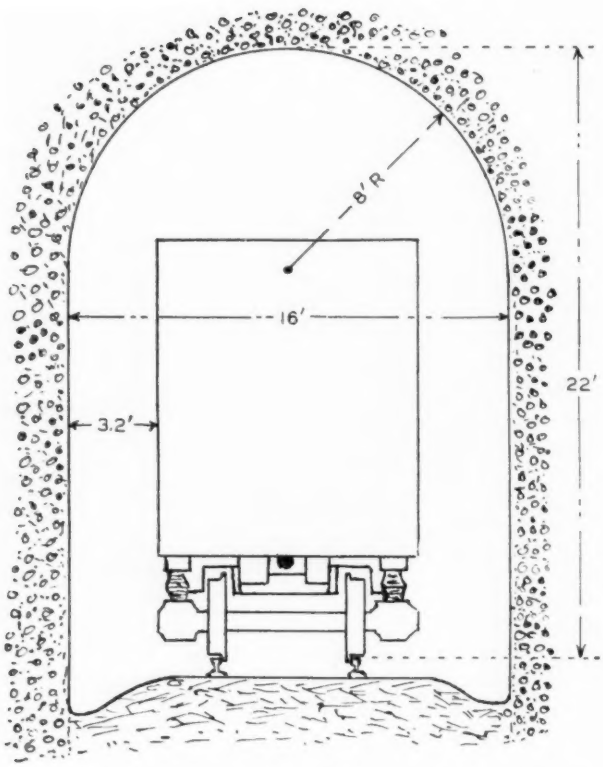


FIG. 3 STANDARD CONCRETE-LINED SECTION; MOFFAT TUNNEL

where ΔB = adverse barometer in inches of water
B_w = barometer at west portal in inches of mercury
B_e = barometer at east portal in inches of mercury

When the air is exhausted from the east portal so that the flow is from west to east, the vacuum at the east portal will be decreased by the same quantity.

At the elevation of the Moffat Tunnel, the barometer is normally about 21.2 in. of mercury or 10.4 psi. The outside-air temperature ranges from 80 F to —40 F, but the temperature in the tunnel is constant at 58 F. The specific weight of air at the time of the tests was 0.055 lb per cu ft.

SYSTEM OF VENTILATION

The tunnel is ventilated by fans which are housed at the east portal. By means of dampers, the fans may be so operated as to blow air into the tunnel and cause it to discharge at the west portal; or they may exhaust from the tunnel, thus producing a flow from west to east. Such operation is made possible by closing the east portal by means of a tightly fitting door or curtain made of numerous plys of heavy canvas. This curtain is raised only long enough for a train to pass the portal. It is made of canvas in case it should fail to open at the right time and the locomotive should then plow through it.

TUNNEL FRICTION

The friction of air in the tunnel, when no trains are passing through, can be determined by measuring the tunnel pressure just inside the closed door at the east portal by means of a water manometer, one leg of which is open to the outdoor air. The reading will be positive, if air is being blown into the tunnel and negative, if it is being exhausted. The true tunnel friction will be this reading corrected for the adverse barometer, if any, as defined by ΔB.

The quantity of air flowing through the tunnel was determined in these tests by the use of an anemometer at a section near the west portal. Air velocities were measured at 21 different points over the cross section. From determinations made at several different rates of flow, the equation for friction in the Moffat tunnel was found to be

$$F = 1.08 \times 10^{-11} Q^2 \quad \ldots\ldots\ldots\ldots\ldots\ldots [2]$$

where F = inches of water
Q = flow of air, cfm

In order to make this result useful in other cases, it is necessary to evaluate the friction coefficients involved. If the tunnel were uniform throughout its length, that would be a very simple matter. But the variation in the cross-section areas and in the character of the tunnel lining renders a direct procedure impossible. Consequently, the friction was computed on a purely theoretical basis to see if the total result would check. If it did, it would either prove that the individual assumptions were correct, or else that their errors were such as to compensate.

For air at 60 F, the absolute viscosity is 0.018 centipoises or 0.00000038 lb sec per sq ft, and this multiplied by g is 0.0000122 lb per ft sec. Dividing this latter by 0.055 lb per cu ft gives the kinematic viscosity of the air in question as 0.000222 sq ft per sec.

In the standard concrete-lined section, an air flow of 300,000 cfm would give a velocity of 14.7 fps. A section with a hydraulic-mean radius of 4.8 ft would correspond to a circular conduit with a diameter of 4 ft × 4.8 ft. Therefore, the Reynolds number would be

$$R = \frac{4 \times 4.8 \times 14.7}{0.000222} = 1{,}270{,}000$$

Using Pigott's diagram[2] for friction factor, rough-formed concrete would be in class E of his table.[3] For an equivalent diameter of 4 × 4.8 = 19.2 ft, the table would specify curve 2 of the diagram. For this curve and a Reynolds number of 1,270,000 the diagram would give $f = 0.013$.

For the standard concrete-lined section, the friction would then be

$$f \times \frac{L}{4m} \times \frac{V^2}{2g} = 0.013 \times \frac{17{,}446}{19.2} \times \frac{14.7^2}{64.4} = 39.7 \text{ ft of air}$$

which equals 0.418 in. of water in this case.

There can be little question as to the accuracy of the value of f for the concrete lining; and a similar computation for the 985-ft length gives a friction head of 2.8 ft of air.

The difficulty lies in the proper estimate of the value of f for the rough and irregular rock-wall sections. The Pigott diagram is hardly applicable to surfaces as irregular as this, and hence it seems desirable to turn to data on large open channels, many of which are equally rough and irregular. Because the gunite smooths up the minor roughnesses, a value of Kutter's n of 0.021 was finally decided upon. Using Manning's formula this gave a value of C of 92.5 in the well-known formula $V = C\sqrt{ms}$ and, since $f = 8g/C^2$, the value of f is 0.03. Therefore, for the gunited-rock portion, the friction would be

$$f \times \frac{L}{4m} \times \frac{V^2}{2g} = 0.03 \times \frac{14{,}374}{20.8} \times \frac{12.5^2}{64.4} = 50.5 \text{ ft of air}$$

Adding the friction losses in the three sections shown in Table 1, the result is 93 ft of air or 0.98 in. of water.

[2] "Hydraulics," by R. L. Daugherty, Fourth edition, McGraw-Hill Book Company, Inc., New York, N. Y., 1937, p. 211.

[3] "The Flow of Fluids in Closed Conduits," by R. J. S. Pigott, *Mechanical Engineering*, vol. 55, 1933, p. 497.

For a flow of air of 300,000 cfm, the experimental result, as given by Equation [2], is 0.972 in. of water. The close agreement obtained would indicate that the values of f employed are very nearly correct.

Time and Power Required to Clear Tunnel

Coal-burning steam locomotives are used through the Moffat Tunnel, and hence it is of great interest to know the time interval required to clear the tunnel of smoke after a train has passed through and the power required for the operation of the fans for different time intervals. In Fig. 4 is shown the relation between the volume of air supplied per minute and the time required for this air to traverse the tunnel. Because of mixing of the incoming air with the smoke, it is probable that the time required to clear the tunnel completely may be something like 50 per cent more than that shown in Fig. 4. The curve showing the relation between volume of air per minute and time required is a rectangular hyperbola and, as seen in Fig. 4, the quantity of air required increases rapidly as the time is decreased.

By the aid of Equation [2], which gives the friction head for the tunnel, it is now possible to compute the air horsepower required for any given rate of air flow, and hence for any given time of clearing. By assuming a constant fan efficiency, the actual horsepower required to operate the fan for these various rates of flow can be determined, as shown also in Fig. 4. Be-

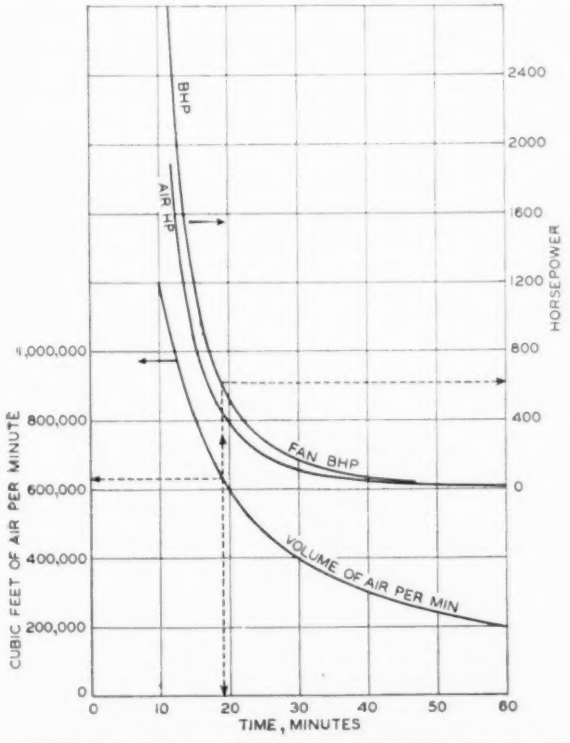


Fig. 4 Ventilation of Moffat Tunnel With No Train in Tunnel, Showing Time for Air to Traverse Tunnel; Time to Clear Tunnel Is Approximately 50 Per Cent More

cause the power required varies as the cube of the rate of air flow, it is seen that the power increases enormously as the time of clearing the tunnel is decreased. It is thus apparent that there is a minimum time for clearing the smoke from the tunnel below which it is not economical to go, because of the high power costs.

Thus for fresh air to traverse the length of the tunnel in 20 min, and probably clear it completely in 30 min, an air flow of 600,000 cfm is required, and the necessary power input to the fan will be 530 hp. But to traverse the tunnel in 15 min will require 1200 hp.

Piston Effect of Trains in Tunnel With One End Closed

A formula will now be developed for the train resistance when it is proceeding toward the closed end of the tunnel and air is being blown into the same end so that the air flow is in the opposite direction to the motion of the train.

It will be assumed that the train resistance, which is the same quantity as "piston effect," is proportional to the square of the relative velocity of the air past it. Let

A = tunnel cross-section area, sq ft
a = train cross-section area, sq ft
Q = volume of air from fan per unit time = AV, cfm
V = velocity of air in unobstructed tunnel = Q/A, fpm
S = train speed, fpm

Assume first that the fan is not operating so that $Q = 0$, $V = 0$. The train will then displace air in front of it at the rate aS. This volume of air per unit time will have to flow back past the train through the area $(A - a)$. If the fan is also operating, the total flow past the train will be $aS + Q = aS + AV$. The absolute velocity (i.e., relative to the tunnel wall) of the air past the train will then be $(aS + AV)/(A - a)$. But the velocity of this air relative to the moving train is

$$\frac{aS + AV}{A - a} + S = \frac{AS + AV}{A - a} = \frac{AS + Q}{A - a} \quad \ldots\ldots [3]$$

In accordance with the assumption previously made, the train resistance or its piston action is then given by

$$P = K(AS + Q)^2 \quad \ldots\ldots [4]$$

where K is a constant for each train in a given tunnel.

For the Moffat Tunnel, A is known and K was determined for a series of trains by observing the tunnel pressure in each case as well as by determining the fan discharge, and observing the train speed. However the preceding can be generalized.

From Equation [3] it can be seen that K must involve $(A - a)^2$. Also it would seem reasonable that it would be proportional to the length of the train as well as including an "end effect," and that it would be proportional to the density of the air. Therefore

$$K = \frac{M + NL}{(A - a)^2} w \quad \ldots\ldots [5]$$

where M and N are constants and L is the length of the train. For a single locomotive without any cars, it is probable that the end effect, represented by M, might be apparent, but for the trains involved in these tests, which ranged from a locomotive and tender with two cars making a total train length of 277 ft up to a 50-car freight train with a total length of 2410 ft, the end effect seemed to be negligible. Assuming then that $M = 0$, for all practical purposes, the formula for train resistance of any train at any speed in any tunnel with one end closed would be

$$P = \frac{wNL}{(A - a)^2} (AS + Q)^2 \quad \ldots\ldots [6]$$

From the data obtained with the trains in the Moffat Tunnel the value of N would seem to be 328×10^{-11}. Therefore, for this type of tunnel, the formula may be tentatively given as

$$P = \frac{328 \times 10^{-11} wL}{(A - a)^2} (AS + Q)^2 \quad \ldots\ldots [7]$$

With this value of the constant, the units on the right-hand side of the equation are in feet, pounds, and minutes, while P is the pressure produced by the train in inches of water.

The general formula given by Equation [6] is offered with some confidence, but the exact value of the constant appearing in Equation [7] is not so certain. The tunnel pressure readings varied considerably while trains were passing through the tunnel. The reasons for this are that the train speed is not constant, being less than the average upgrade and more than the

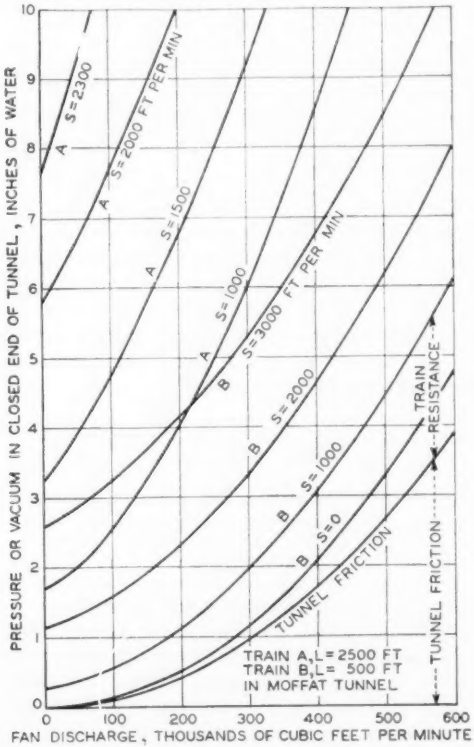


FIG. 5 AIR FLOW OPPOSITE TO DIRECTION OF TRAIN

average on the downgrade after passing over the summit in the center of the tunnel; the tunnel cross-section area varies as shown in Table 1; the roughness of the tunnel wall varies from place to place; the fan speeds were not kept constant because of certain operating necessities in the fan room; and thus the air flow was not the same throughout the train trip. Hence, it is obvious that these data lack the precision of laboratory values. But, in spite of these difficulties, it is believed that the results obtained are close approximations to the truth and may be used with all due allowances for these various uncertainties.

TOTAL TUNNEL PRESSURE AT CLOSED END

The total pressure in the closed end of the tunnel when air is blown against an approaching train is the sum of the foregoing, that is

$$T = F + P + \Delta B \quad [8]$$

If the train were proceeding in the opposite direction and air were being exhausted from the closed end of the tunnel, then a vacuum would be obtained, which would be

$$\text{Vacuum} = F + P - \Delta B \quad [9]$$

If it were not for the barometer effect, the increase in tunnel pressure above the atmospheric pressure for the one case would be the same as the vacuum obtained when the direction of both the air flow and the train was reversed. In both cases, the flow of air would be against the motion of the train. Equation [8] or [9] gives the value of the "head" which must be developed by a fan in order to provide the specified air flow. The performance of trains in a tunnel with a closed end and the air flow against the motion of the train is shown in Fig. 5, assuming $\Delta B = 0$. The effect of a barometer difference is merely to shift all of the curves up or down by the amount ΔB.

In Fig. 5 may be seen the effect of changing the speed of the same train and also the difference between a short train and a long train, when both are operated at the same speed. Pressures as high as 8.7 in. of water and vacuums as high as 8.2 in. of water have been observed when the fan was in operation. With the fan shut down and all dampers closed, a vacuum of 7 in. of water has been noted. Thus the diagram in Fig. 5 does not extend much beyond some of the operating points.

AIR FLOW IN SAME DIRECTION AS TRAIN MOTION

In the two cases previously cited, the air flow was against the motion of the train. If the air flow from the fan were in the same direction as the train travel, Equation [4] would be changed to

$$P = K(AS - Q)^2 \quad [10]$$

and the same change of sign would apply to Equations [6] and [7]. The effect of this change of sign is to decrease very greatly the value of the train resistance.

If AS is greater than Q, the train speed will be greater than

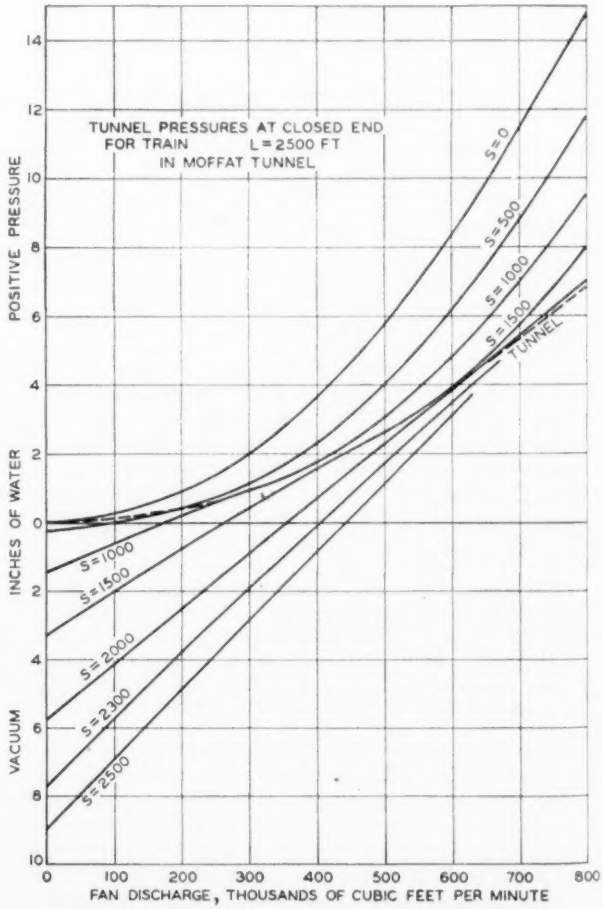


FIG. 6 AIR FLOW IN SAME DIRECTION AS TRAIN MOTION

the velocity of the air in the tunnel behind it, and some air will still flow past the train from the front to the rear. Equation [8] is then changed to

$$T = F - P + \Delta B \quad \ldots\ldots\ldots\ldots\ldots\ldots [11]$$

which shows the saving in power which may result from blowing air behind a train instead of against it. This is shown more clearly in Fig. 6.

When the train speed S is greater than the air velocity V the pressure in the tunnel at the closed end is less than that due to tunnel friction alone. If the piston action P is greater than the tunnel friction F, the tunnel pressure then becomes a vacuum. The maximum vacuum obtained is when the fan is not operated and all dampers are closed.

When the air velocity and the train speed are equal, the piston effect of the train becomes zero and the curves, shown in Fig. 6, then cross the tunnel-friction curve.

When the train speed is less than the air velocity, some air will flow past the train from the rear to the front. For this condition it is necessary to revert to Equation [8] which adds

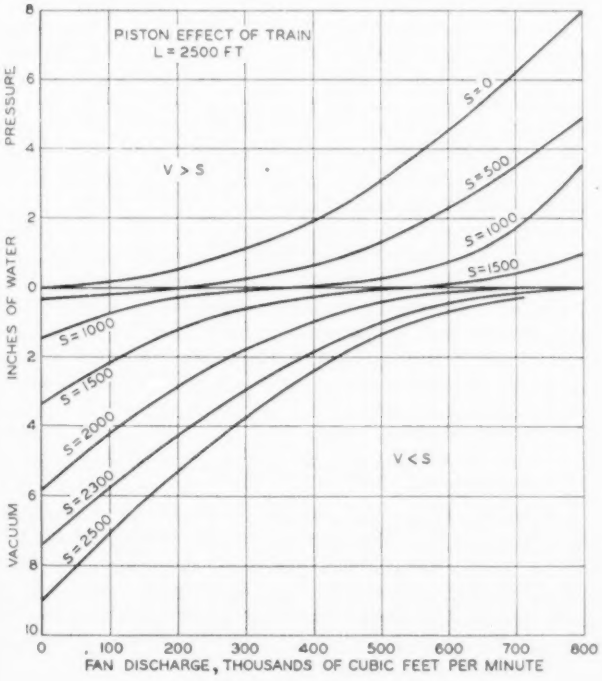


FIG. 7 AIR BLOWN BEHIND TRAIN

the train effect to the tunnel friction. However the tunnel pressure is still much less than with the same fan discharge blowing against the train, because P is still to be computed by Equation [10]. Comparing Figs. 5 and 6 for the large air flows, will show the great reduction in tunnel pressure and hence in fan power required.

The piston action of the train alone, for this condition of operation, separated from any effect of tunnel friction, is shown in Fig. 7. Each curve crosses the zero axis when the air velocity is equal to the train speed.

TRAIN TUNNEL WITH BOTH ENDS OPEN

The use of a door or curtain to close one end of the Moffat Tunnel was necessary in order that the fan could force air to flow through the tunnel from one end to the other. The cost of a separate duct to deliver air at intermediate points along the length of the tunnel would have been prohibitive, since it would have been comparable in size with the tunnel itself, or else would have required very high velocities and a large expenditure of power, if it were smaller. However tunnels with both ends open are much more common, the ventilation in such cases being provided in other ways.

The analysis made for the Moffat Tunnel can be modified so as to apply to a tunnel with both ends open. Since a fan can no longer be employed to produce a flow of air through the entire length of the tunnel, it will here be assumed that no fan is in service. Such a condition of operation might very reasonably be employed for the Moffat Tunnel, for example, if electric locomotives were used. In fact the ventilation obtained without the use of a fan might even be sufficient if Diesel locomotives were to replace the present coal-burning steam locomotives.

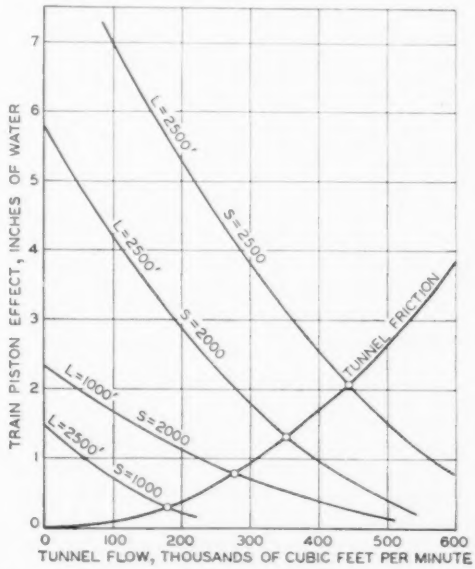


FIG. 8 PISTON EFFECT WITH BOTH ENDS OF TUNNEL OPEN

The physical facts in this case are then as follows: The train will displace air at the volume rate aS. Some of this air will be forced out of the open end of the tunnel ahead of the train and will be replaced by an equal volume of air drawn in at the rear portal of the tunnel. Also some of the air will flow back past the train from front to rear. If q is the volume of air which flows through the tunnel, as a result of the piston action of the train, and q' is the volume which flows back past the train, then

$$aS = q + q' \quad \ldots\ldots\ldots\ldots\ldots\ldots [12]$$

The quantity of air q is now the amount of the tunnel ventilation. The tunnel friction corresponding to it is then given by Equation [2], which may be written as

$$F = 1.08 \times 10^{-11} \times q^2 \quad \ldots\ldots\ldots\ldots\ldots\ldots [13]$$

This friction head, shown in Equation [13], can be supplied only by the action of the train. It is the same in value as the so-called "piston action," or is the same as the difference in pressures in front of and behind the train. This pressure difference is produced by the resistance to the flow of air past the train and relative to it. Therefore $F = P$.

The absolute velocity of the air past the train is $q'/(A - a) = (aS - q)/(A - a)$, while the relative velocity is

$$\frac{AS - q}{A - a} + S = \frac{AS - q}{A - a}$$

It will be assumed that the train resistance is proportional to the square of the relative velocity of flow past it, so that

$$P = K\,(AS - q)^2 \quad \ldots\ldots\ldots\ldots\ldots\ldots [14]$$

where K has the same numerical value as in Equation [4] or [10]. Since $F = P$, the value of q can be determined by equating the tunnel friction to the train resistance. When q is known, the train resistance can be computed.

Thus for the Moffat Tunnel, as an illustration

$$1.08 \times 10^{-11} \times q^2 = K\,(AS - q)^2$$

Assuming a train 1000 ft in length running at 2000 fpm, this expression becomes

$$1.08 \times 10^{-11} \times q^2 = 0.5 \times 10^{-11}(680{,}000 - q)^2$$

The solution of this equation gives the tunnel ventilation as q = 275,000 cfm of air with a tunnel friction of 0.82 in. of water. With a train displacement of aS = 190 × 2000 = 380,000 cfm, the flow of air past the train from front to rear is 380,000 — 275,000 = 105,000 cfm. The piston action of the train is, of course, also 0.82 in. of water.

The simultaneous solution of Equations [13] and [14] is shown graphically in Fig. 8. The solution in each case is the point of intersection of a train curve with the tunnel-friction curve. The co-ordinates of this point of intersection give the values of the tunnel ventilation and the piston effect. This diagram shows the value of tunnel speed in securing tunnel ventilation, and it also shows the effect of train length for the same speed.

Determination of K

The analysis, which has been presented in this paper, of the performance of trains in the Moffat Tunnel under all possible conditions of operation, rests upon two assumptions: (1) That the piston effect is properly expressed by Equation [4] or a modification thereof, and (2) that the value of K is constant for a given train, depending only upon the length. However, the value of K is affected by the area of the tunnel, as shown by Equation [5], and it is also affected by the wall roughness. Since the tunnel is not uniform throughout, obviously the value of K for a given train must vary according to the position of the train in the tunnel. Hence, the value of K used for each train is in reality an average value.

However, observations have been made of tunnel pressures with the air flow opposed to the motion of the train, with the air flow in the same direction as the train, and with zero flow with the fan not operating. The values so obtained are all consistent with the curves shown in Figs. 5 and 6.

While it is desirable that values of K be obtained by direct measurement with trains in the tunnel in question, the practical necessities of railroad operation are such that it is not always possible to maintain uniform conditions during a given run so that reliable values may be obtained. Where it is not feasible to measure the piston effect of a train at all, an approximate value of K might be computed in the following manner:

Assume the train to be stationary in some interior portion of the tunnel, which is an operating condition not to be tolerated in reality. Then Equation [4] reduces to $P = KQ^2$. The friction of air through the annular-like space between the train and the tunnel walls is

$$P = \frac{w}{5.2} \times f \times \frac{L}{4m} \times \frac{v^2}{2g} \quad \ldots\ldots\ldots\ldots [15]$$

where w is specific weight of air in lb per cu ft, 5.2 is a constant to give P in inches of water, L is the length of the train, m is the hydraulic radius for the space and equals $(A - a)$ divided by the entire perimeter, and $v = Q/60(A - a)$. If one can estimate the proper value of f for such a passage, then the value of K is established. Thus, for the value of K determined by experiment in the Moffat Tunnel, the corresponding value of f will be found to be 0.0301.

Results of Moffat-Tunnel Studies

In addition to providing information regarding the piston action of trains in tunnels in general, the tests made with trains in the Moffat Tunnel pointed the way to better operation with more rapid clearing of smoke from the tunnel and reduced cost of fan operation. The two fans originally installed were for too high a pressure and too low a capacity. By replacing one of these with a lower-pressure but higher-capacity fan, the smoke can be cleared from the empty tunnel more rapidly and with less expenditure of power. Also it was seen that much power could be saved by blowing air behind a train instead of against it. As long as the train speed is in excess of the air velocity in the tunnel, there will still be a flow of air from the front of the train to the rear. The train crews report more satisfactory conditions with this change of operation.

For the present, one of the old fans is still used to blow air against eastbound trains, because the latter climb more of a grade and hence move more slowly. Thus air is sent in only one direction through the tunnel at all times. Formerly when the air movement was against the train motion and when trains alternated in direction through the tunnel at frequent intervals, the smoke in the middle was shifted back and forth without having an opportunity to reach an exit.

Acknowledgments

The author wishes to express his appreciation to Mr. E. A. West, general manager of the Denver and Rio Grande Western Railroad, for permitting publication of the information obtained; to Mr. Durbin Van Law, Mem. A.S.M.E., for assistance in making the tests, as well as to the engineering staff of the D.andR. G.W. for their co-operation.

Discussion

J. C. Miles.[4] Has an investigation been made of the ventilating effect that could be obtained from a vertical "chimney" drilled from near the middle of the tunnel to the surface? This question is asked without knowledge of the prevailing temperatures, winds, and barometer, as well as depth of tunnel below the surface. Any of these factors, it is realized, may make the question pointless.

Durbin Van Law.[5] The investigation described in this paper was occasioned directly by unsatisfactory conditions prevailing in the ventilation of the Moffat Tunnel. Discomfort to passengers and to operating crews was not infrequent. That condition has been changed due to remedies which have been applied as the result of the author's studies. In the development of theory, it is interesting to find the conclusions sustained by facts in the nature of actual performance, and this discussion will be confined to a few statements of this specific character.

When the Moffat Tunnel was completed in 1928, it served one railroad, namely, The Denver & Salt Lake Railway, operating only approximately 200 miles of main-line track and having an expectancy of peak traffic amounting to not more than sixteen

[4] Instructor in Mechanical Engineering, University of Illinois, Urbana, Ill. Jun. A.S.M.E.

[5] Consulting Engineer for the Denver and Rio Grande Western Railroad, and the Denver & Salt Lake Railway, Denver, Colo. Mem. A.S.M.E.

train movements per day. Electrification of the tunnel was considered and discarded because of the expensive operation which would have been entailed for this very light degree of traffic. Careful searches had preceded tunnel construction to determine if possible the operating experiences of other comparable tunnels. Surprisingly meager data were available in general and nothing reliable was discovered which was applicable to the piston effect of trains. A ventilating plant was designed upon the basis of suppositions which did not materialize into fact, with the result that ventilating fans were installed to operate against a discharge pressure many times that actually developed after the tunnel was put into operation. To accentuate the difficulty, overloading-type fans were selected, with the result that the air quantity had to be throttled by artificial restrictions to hold the power within the limits of the motors used for fan drive. With tunnel friction so much less than was anticipated, operation of the fans with the tunnel empty became a most inefficient operation. When ventilating with a train actually in the tunnel, operating conditions were, from a mechanical standpoint, somewhat improved. This was, of course, due to the resistance or increased friction imparted by the train itself, which the author has classified as "piston effect" and which he has most capably reduced to specific formulas.

Now, since it appeared that the principal resistance in any blowing operation is imparted by the train rather than the tunnel walls, it became desirable to eliminate as much of this piston effect as was possible. The simplest way to accomplish this result was to blow behind trains instead of against them. It was not feasible to blow at such a rate that the products of combustion would be carried ahead of the engine. That would require too much power, in consideration of the fact that some of the passenger trains traverse the tunnel in as little as $8^1/_2$ min, and practically all the freight trains clear in 17 min or less. Therefore, it was decided that new fan equipment should be designed to blow behind westbound trains at a rate less than train speed. In reality, this procedure is based upon the theory that the ventilation provided by the train itself is sufficiently great so that it may actually be diminished to some slight degree by lessening the vacuum which would otherwise appear behind the train, and this through the medium of blowing at less than train speed. In this regard, it is startling, but nevertheless true, to state that were a train to enter the tunnel when it was filled with suffocating gases, no fan made within any reasonable limits of power input could possibly afford relief to the train crew until the train had actually traversed nearly two thirds of the tunnel length.

There is a definite reason why a following movement of air was not decreed in the case of eastbound trains—in fact, two reasons. The author states that the train movement eastbound is somewhat slower on account of the relatively steeper grade. In addition to this circumstance, it was desired that only clean air be taken through the fans on account of otherwise resulting corrosion to fan blades and dampers. The installation of new fan equipment has actually been used somewhat differently from that contemplated at the time of the author's studies. For eastbound train movements of passenger trains and certain freight trains, no fan whatever is used, and the train is allowed to proceed through the empty tunnel with the curtain or door on the east end closed during its passage, up to the point where it has to be opened to permit the train to emerge. This, again, is a manifestation of piston effect, this time in its simplest form and not complicated by air movement due to the effect of a fan.

The entire theory of tunnel operation in so far as ventilation is concerned is that trains are seldom bothered with the smoke from their own engines. If the tunnel is clear with the entrance of the train, ventilation is usually satisfactory. It was, therefore, the desire to create revised facilities which would clear the tunnel in the shortest space of time, thus permitting daily train movements of several times the number originally contemplated. Since the Denver & Rio Grande Western Railroad has established rail connection through the tunnel and on to its main line at Dotsero, the system has become one of the principal carriers to and from the Pacific Coast, and traffic intensity has grown by rapid bounds.

The Moffat Tunnel is the longest railroad tunnel in the world now utilizing steam power, and the only one of comparable length utilizing coal fuel. The ventilating plant has been revised through the installation of a new fan unit built to conform to pressure-volume characteristics as determined by the author's studies. Its performance almost exactly follows performance predictions for tunnel ventilation as laid down in his advance work. Cleaning time with the tunnel empty has been reduced by nearly 50 per cent, while power costs have been reduced by 35 per cent. Of primary importance is the fact that operation is now clean and, in consideration of the type of motive power, provides the very minimum of discomfort to train crews and none at all to passengers. In the latter respect it is very easy to forget that gases, like all fluids, tend to equalize as to pressure differences. Therefore, if a relatively high pressure exists within the tunnel and a normal pressure within the passenger coaches, there is certain to be an infiltration from the tunnel into the coaches. The lower this differential can be maintained, the less the infiltration effect. The present scheme of operation, with due cognizance of the pressure imparted by piston effect, holds down the tunnel pressure to the lowest point compatible with sufficient displacement to provide adequate ventilation.

Actual performance has attested the accuracy of the author's theoretical determination. The ventilating plant is operating according to schedule. To those who may be confronted with the problem of ventilating railroad tunnels, the author has made available an engineering contribution that has not existed heretofore.

EUGENE MURPHY.[6] Recently the Chicago newspapers have mentioned experiments made on the New York subways to improve the air flow in the Chicago subway, which is now under construction. Would the author care to comment on the application of his paper to subways in which ventilation depends largely upon piston effect and perhaps slightly on chimney effect, without the aid of fans? In subways, the air velocities past station platforms and upward through sidewalk gratings must be limited to avoid annoyance to patrons, regardless of consideration of friction.

AUTHOR'S CLOSURE

In reply to Mr. Miles, an investigation was made as to the possibility of ventilating the Moffat Tunnel by the construction of a vertical chimney from near the center of the tunnel to the surface. At the most favorable location the vertical distance to the surface is about 2200 ft. A shaft of this length and 8 ft in diam was estimated to cost about $175,000. However, it is believed that a shaft about 12 ft in diam would really be necessary for satisfactory results, with a corresponding increase in cost.

The temperature in the tunnel is constant at 58 F the entire year while the temperature at the top of the shaft would range from 80 F to below zero. It is believed that under these conditions the chimney could not be relied upon to produce a natural draft upward. In fact it seemed certain that at times there would be a downdraft and at others, no draft at all. Consequently it would be necessary to install a fan at the base of the chimney to insure operation at all times. Thus the scheme seemed to be impractical as a solution of the problem.

It is gratifying to the author that Mr. Van Law has been able

[6] Illinois Institute of Technology, Chicago, Ill.

to add his comments, based upon his observations of the ventilation of the tunnel after the changes in equipment and mode of operation, recommended by the author, had been carried out. The author's paper naturally ended with the analysis of the problem and the prediction of the results that might be obtained with a fan of very different characteristics from the old one, and with a change to blowing air behind a train instead of against it. Mr. Van Law's observations have shown that the predictions were correct, and that a great improvement in tunnel conditions has resulted.

In reply to Mr. Murphy, the ventilation of a subway by the piston effect of the trains without the aid of a fan is a direct application of the case which has been presented in this paper under the heading, "Train Tunnel With Both Ends Open," and illustrated in Fig. 8. Equations [12], [13], and [14] are directly applicable, except that the constant in Equation [13] will have to be changed to conform to the length of a subway section between openings to the outer air, and also modified if the roughness of the walls is materially different from that of the tunnel in question. For a subway, the length involved will be much less than that of the Moffat Tunnel and hence the curve for tunnel friction will have much lower values than those shown in Fig. 8.

Also subway trains will doubtless be shorter than railroad trains and an inspection of Fig. 8 will show that these two effects are such as to provide much less ventilation than in the case of the Moffat Tunnel. As seen by Equation [5], this reduction will be even more pronounced if the subway is a double-track one so that the train does not fill it to the same extent as shown in Fig. 3. Hence piston effect will merely aid subway ventilation but will probably not be adequate.

Developments in Regulating Outlet Valves

By G. J. HORNSBY,[1] DENVER, COLO.

This paper covers briefly the step-by-step progress in the development of high-pressure regulating outlet valves, as experienced by the Bureau of Reclamation. The author describes the various designs of outlet valves now in use, points out some of the good and bad features of present design practice, and proposes some ways and means of preventing cavitation. The conclusions reached are confirmed by model tests. A new and radically different type of regulating outlet valve, which model tests indicate will be free from cavitation and will have unusually favorable stilling-pool characteristics, is described.

OUTLET valves are usually employed wherever water is stored for future use, as for domestic consumption or irrigation purposes. Regulating outlet valves, or gates, are employed wherever regulation, or flow at variable rates, is desired. Regulation of flow by increments is sometimes accomplished by the use of a number of nonregulating valves, or gates, installed in parallel. This method was used at Grand Coulee Dam, which has 60 outlets of the same size installed in horizontal rows of 20 each at three different elevations. By selection of gates and elevations, very close regulation may be obtained.

Storage of water in reservoirs for municipal and irrigation purposes creates the necessity for the outlet valve. In the case of irrigation where water must be released according to current demands to avoid waste, close regulation is highly important. This condition is responsible for the development of the regulating outlet valve. The regulating outlet valve is not only called upon to control the flow of water but to meter it also. With the discharge coefficient of the valve established, the operator is provided with a chart showing the discharge of the valve for various heads and valve openings. From this chart he knows at all times the rate of discharge of the valve.

Need for High-Pressure Regulating Valves

Until about the beginning of the twentieth century, few high-head storage reservoirs were in use. The slide gate is adequate and economical for low-head regulation and hence there was no need for high-head regulating valves. However, when the Bureau of Reclamation came into existence it began to build high-head reservoirs. It was soon found that the slide gate was not practical for high heads due to both extreme hydraulic conditions and mechanical requirements. Friction on the sliding elements and the hoist requirements in many cases were found to be excessive. Also the poor hydraulic characteristics inherent in the slide gates were conducive to cavitation and its destructive effects on the confining walls of the water passages. It was then apparent that a balanced type of valve would be desirable.

Development of Balanced Valve

A crude type of balanced gate known as the cylinder gate had already been developed and used with satisfactory results, but this gate required the use of a hoist for operating. This type of gate is shown in Fig. 1. By means of two clever refinements the cylinder gate was made into the first needle valve to open and close by controlled manipulation of the water pressure from the reservoir. This development was credited to O. H. Ensign in 1906, and may well be regarded as a forward step in the development of balanced needle outlet valves. A flange, or "bull ring," somewhat larger in diameter was added to the head of the cylinder and a conical piece, conforming somewhat to the lines of flow, served to seal the downstream end of the cylinder. This entire assembly became a piston in a fixed cylinder whose machined inside diameter fitted the flange or "bull ring." The reservoir pressure exerted an opening force on the flange at all times, while the controlled pressure inside the fixed cylinder exerted a closing force on the valve which might be greater or less

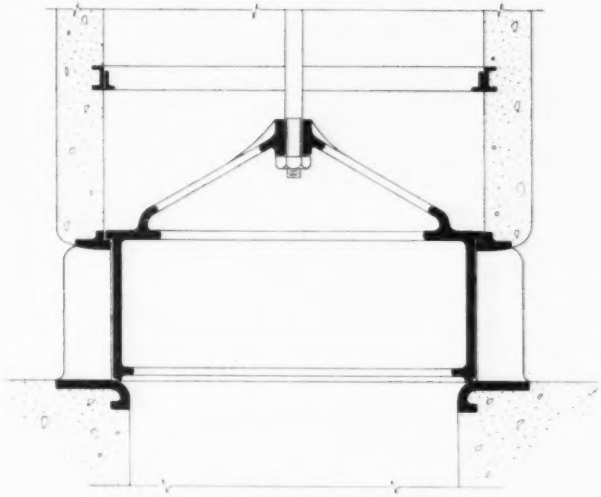


Fig. 1 Typical Cylinder Gate

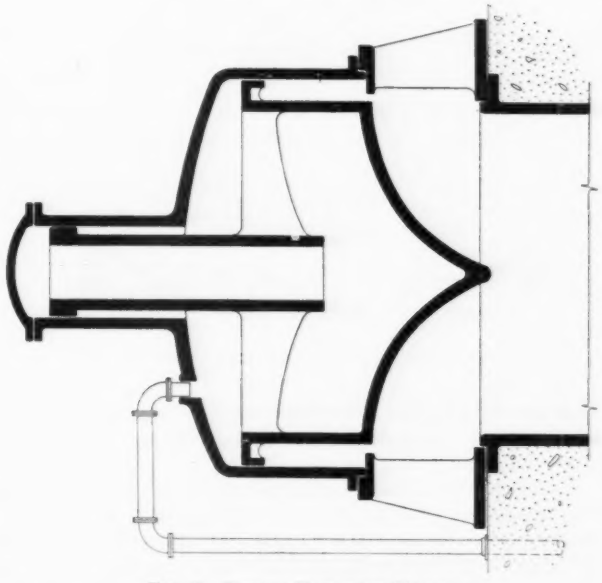


Fig. 2 Ensign Balanced Valve

[1] Engineer, Bureau of Reclamation, U. S. Department of the Interior.

Contributed by the Hydraulic Division and presented at the Semi-Annual Meeting, Kansas City, Mo., June 16–19, 1941, of The American Society of Mechanical Engineers.

Note: Statements and opinions advanced in papers are to be understood as individual expressions of their authors and not those of the Society.

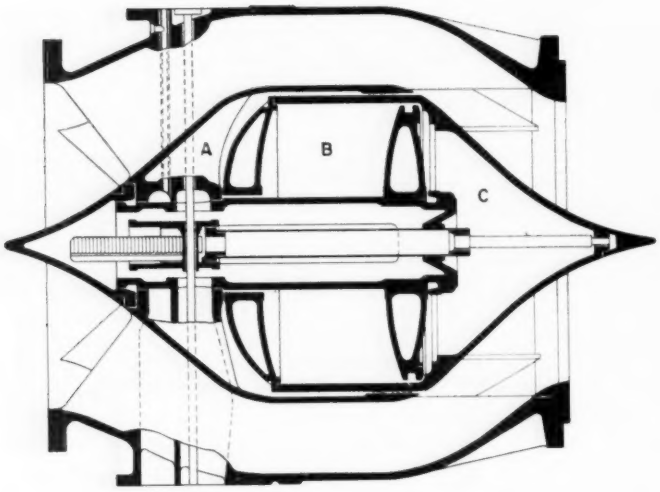


FIG. 3 INTERNAL-DIFFERENTIAL NEEDLE VALVE

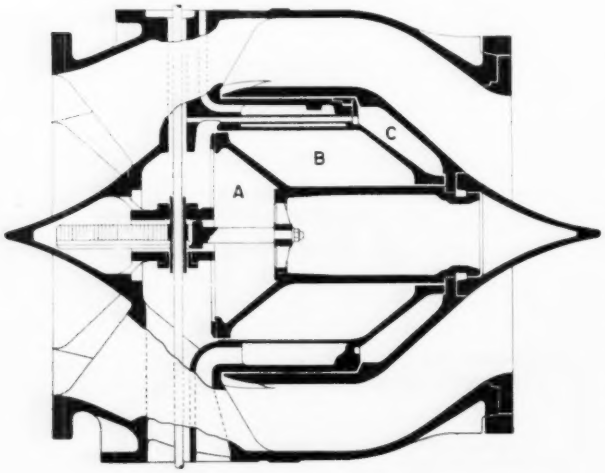


FIG. 4 INTERIOR-DIFFERENTIAL NEEDLE VALVE

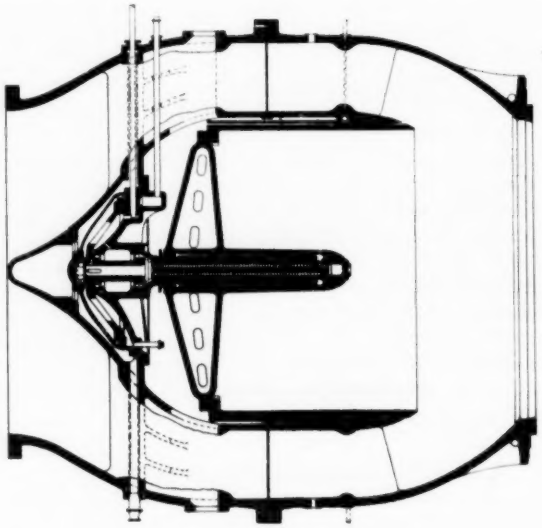


FIG. 5 TUBE VALVE

than the opening force. The valve may be held in any position by controlling the pressure in the fixed cylinder. This valve is shown in Fig. 2.

The next development was that of the internal-differential balanced valve. This valve is enclosed in an outer shell, or body, and is designed to be attached to the discharge end of a conduit. The water passages are streamlined throughout and the jet from this valve is intended to be smooth and round, similar to that of the needle valve developed by the Pelton Water Wheel Works for use in connection with the impulse turbine. For this reason the valve is frequently referred to as the needle valve. This valve is operated hydraulically by reservoir pressure acting on pistons within the valve body. The flange or "bull ring" has been turned inward, and a second piston has been added. In this valve the closing force is more than double the opening force. Referring to Fig. 3, it may be seen that chamber *A* communicates with chamber *C* so that the force reacting on the upstream cone exerts a force on the piston diaphragm between chambers *A* and *B*, and simultaneously the force reacting on the fixed diaphragm between chambers *B* and *C* exerts a force on the needle cone for closing the valve. For opening the valve, the force reacting on the fixed diaphragm between chambers *B* and *C* exerts a force on the piston diaphragm between chambers *A* and *B*. The valve may be held in any position by controlling the pressures in the respective chambers.

Further improvements are embodied in a later design known as the interior-differential balanced valve. The operating mechanisms of this valve are the same as those of the internal-differential valve. The principal difference is in the water passages. It will be seen in Fig. 4 that the supporting ribs between the outer shell and the valve core have been cut back and the valve cylinder slides on the outside of the valve supporting structure. This permits a longer radius for the shoulder between the needle cone and the cylinder to which it is attached. In this design, the outer shell may be made shorter and somewhat smaller in diameter, thus reducing the cost of the valve. The proportions of the water passages are maintained and the flow is not hampered by ribs in the region of high velocity. This results in less pitting on the needle cone and in the valve nozzle.

In an effort to reduce further the cost of balanced outlet valves the tube valve was developed. In this valve, the needle cone and both the fixed diaphragm and the piston diaphragm are eliminated. This, in effect, is the same as the cylinder gate. This type of valve was first operated mechanically by means of a large screw geared within the upstream needle cone and extending downstream through a tube nut in the spider attached to the partially balanced cylinder, as shown in Fig. 5. Later, operation of this type of valve was accomplished by means of a high-pressure oil cylinder attached to the interior of the upstream needle cone and carrying a piston connected to the spider through a piston rod. This design is being developed at the present time for the outlet valves for Shasta Dam.

The various types of balanced valves previously developed were subject more or less to cavitation and pitting, a matter which will be discussed later. Late in 1940, development work on a new and radically different type of free-discharge valve was started in the laboratory. It has been called the "hollow-jet valve," because of its peculiarity of discharging the water in the form of a smooth, hollow cylinder. The interior of this hollow jet requires a surprisingly small amount of aeration to prevent collapse of the jet, for which ample provision is made in the design of the valve. The valve is designed for complete regulation of flow throughout its entire range. Model tests have shown that the jet is smooth and steady, and that the pressure gradient is positive at all points where the water is in contact with the valve for all valve openings. The valve is, therefore, free from

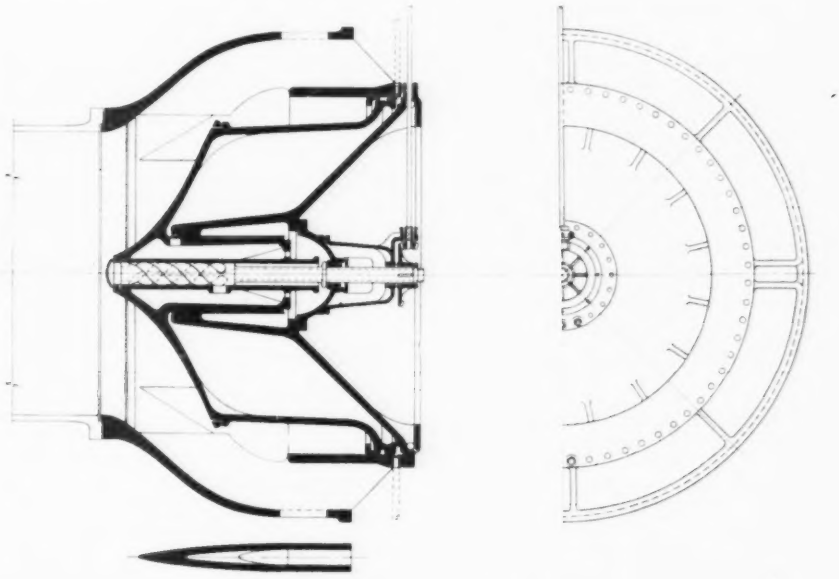


FIG. 6 HOLLOW-JET VALVE

cavitation and its destructive effects. Regardless of this fact, this valve will discharge a surprisingly large quantity of water for a given size and head. Hence, the cost per cubic foot per second of discharge is small, making it economical to build and install.

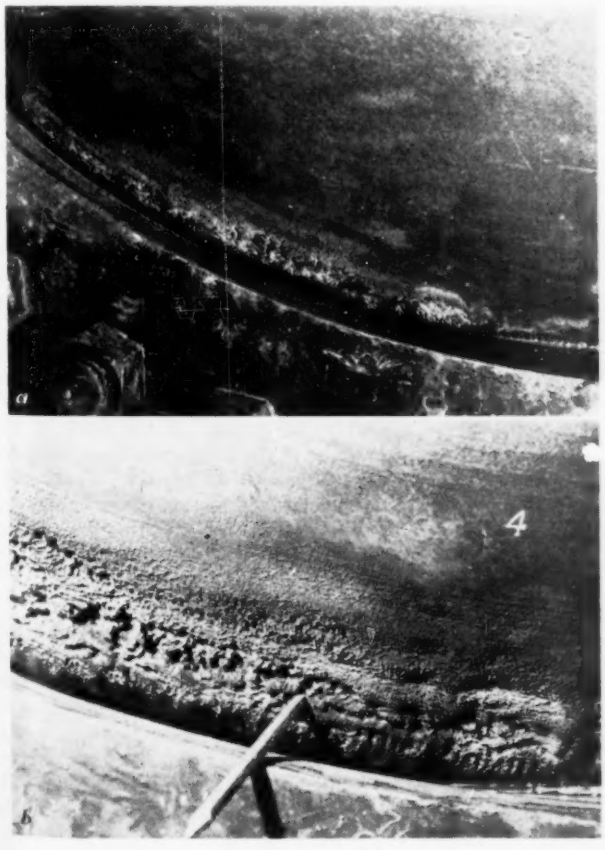


FIG. 7 PITTING IN INTERIOR-DIFFERENTIAL NEEDLE VALVES
(*a* Pitting on nozzle and needle. *b* Enlarged view showing extent of pitting.)

Fig. 6 shows the construction of the hollow-jet valve. By removing the smaller circle of flange bolts the spiral control and operating mechanism may be withdrawn for inspection, or by removing the outer circle of flange bolts the entire valve may be dismounted, leaving the valve body undisturbed. Under operating conditions the outer shell is never subjected to greater pressure than that imposed by the reaction of the jet which, by comparison, is small.

Another important feature of the hollow-jet valve is its action on the stilling pool. By making the outer shell of the valve in the form of a slightly diverging cone, the jet will take the form of a hollow cone instead of a hollow cylinder. This will cause the water to be a dispersed instead of a concentrated jet. Obviously this will result in far less erosion in the stilling pool than that produced by the solid jet discharging from earlier types of balanced valves.

CAVITATION IN OUTLET VALVES AND CONDUITS

Although cavitation is of great importance in high-head outlet valves and conduits, it appears that little was done about it, especially in the earlier designs. The Ensign valve was designed for use either on the inlet end or the outlet end of the conduit, but was best suited for installation on the inlet end. For that reason most installations were made placing the valve on the upstream face of the dam where the valve acted as a sort of plug for the conduit inlet. For full-discharge conditions the operation was good, but for partial openings the operation was extremely unsatisfactory due to cavitation which resulted in serious pitting on the inner walls of the conduit adjacent to the valve. Attempts were made to admit air to the region of most severe pitting but it was found to be extremely difficult to install an air duct of sufficient capacity in this location after the valves were in place. In fact, it was necessary to lower the reservoir level to a point below the valve before inspection or repairs could be attempted. Regardless of these difficulties a large number of installations of this character were made before it was finally concluded that the outlet end of the conduit was the proper place for the controlled regulating outlet valve.

The internal-differential valve was definitely designed for use on the outlet end of the conduit. Due to the large size and the carefully streamlined water passages of the earlier designs, this valve was comparatively free from pitting. However, in later

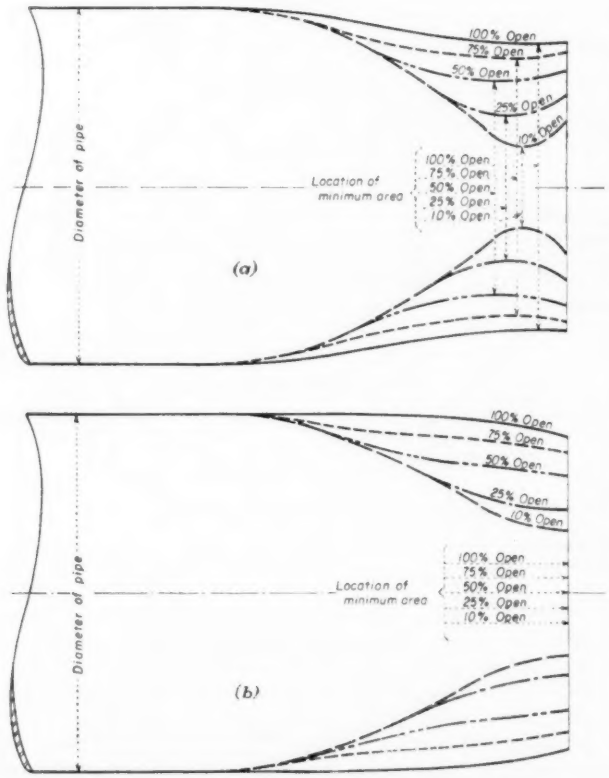


FIG. 8 EQUIVALENT AREAS FOR VARIOUS VALVE OPENINGS
(*a* Circular nozzle with areas equivalent to original interior-type needle valve. *b* Circular nozzle with areas equivalent to improved interior-type needle valve.)

designs, when an attempt was made to reduce the size and the cost per cubic foot per second discharge, the shorter bends in the water passages resulted in serious pitting. This was also found to be true of the interior-differential type of valve as shown in Fig. 7. However, it is possible to prevent pitting completely, even in the smaller and less costly valves, by the proper application of hydraulic principles as will presently be shown. The hollow-jet valve, designed for large discharges at small cost, embodies these principles and is not expected to have any of the defects found in the earlier types.

In case of the internal-differential-type outlet valves at Boulder Dam and the interior-differential-type outlet valves at Alcova Dam pitting became serious, Fig. 7, and the Bureau of Reclamation initiated a series of investigations to develop corrective measures. Prior to making model tests, a careful study of the hydraulic features of valves was undertaken to determine the cause of the pitting.

CAUSES OF CAVITATION

It is not considered necessary to go into a minute discussion of the intricacies of the phenomenon of cavitation and the manner in which it acts upon the confining walls of water passages, as this has been well and fully described and explained by Thomas and Schuleen.[2]

First, a careful study was made of the areas of the cross sections of the water passages at numerous points from the inlet flange to the nozzle of the valve. These areas were plotted against distance along the water passage for valve openings of 10 per cent, 25 per cent, 50 per cent, 75 per cent, and 100 per cent. From the curves, Fig. 8, it was found that at no position of the valve was the minimum, or control section, at the nozzle of the valve. Not only was this true but it was found to change location with each change in position of the valve. An examination of Fig. 8 will show that the control section was farthest upstream when the valve was about 40 per cent open and, as was later shown by model tests, the discharge coefficient was highest at this point. From the point of minimum section to the valve nozzle, the areas increased in the direction of flow in some cases so rapidly that the water could not follow. This produced reduced-pressure areas and cavitation, and pitting resulted in the nozzle and on the needle cone. This was confirmed by tests on models of the valves.

It was apparent from these studies, that the nozzle and needle cone must be so designed that the minimum or control section of the valve shall be stable, that this control section be located at the lip of the nozzle, and that there be a slight convergence of the water passages as the flow approaches this point. This condition must obtain for all valve openings if cavitation is to be eliminated. It was also apparent that in order to hold the control at one point in the nozzle and meet the stated conditions the nozzle should be sharp-edged.

Another point revealed by the studies was that the seat line on the valve was not on the cone portion of the needle but on the rounded shoulder between the cylindrical needle body and the point of tangency at the needle cone. This caused the water to have a tendency to leave the needle cone at small openings, resulting in severe pitting immediately downstream from the seating line in both nozzle and needle cone as shown in Fig. 7. This indicated that the seating line should be on the needle cone proper and not on the curved shoulder between the needle cone and the needle body.

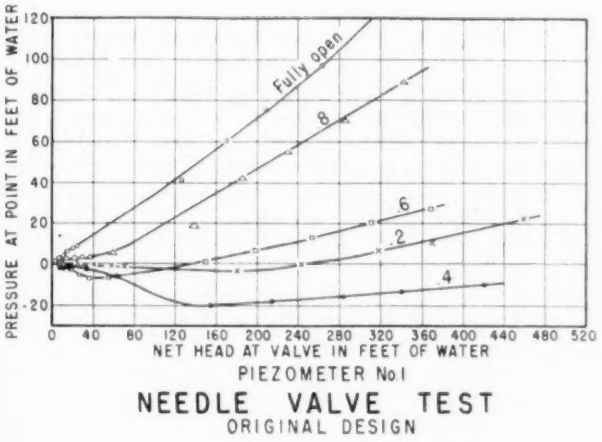
From the studies it was found that, by making the angle of the needle cone the same as, or slightly less than, that of the nozzle cone, there was sufficient convergence in the water passages in the direction of flow to maintain positive pressures throughout the valve for all valve openings. Further, by making the tangent circle between the needle cone and the rounded shoulder slightly larger in diameter than the sharp-edged nozzle, a narrow zone of contact instead of a line formed the valve seat. As the valve is so designed that tremendous pressure is exerted by the valve against the valve seat, the zone or band contact is far superior to the line contact used in former designs. Obviously the relation between the angle of the needle cone and that of the nozzle is of great importance since it determines whether or not the valve will be subject to cavitation. If the angle of the needle cone is greater than that of the nozzle cone there is danger of cavitation but the discharge will be greater. Conversely, if the angle of the needle cone is less than that of the nozzle, the safety factor is increased but the discharge will be less, due to greater convergence of areas in the direction of flow.

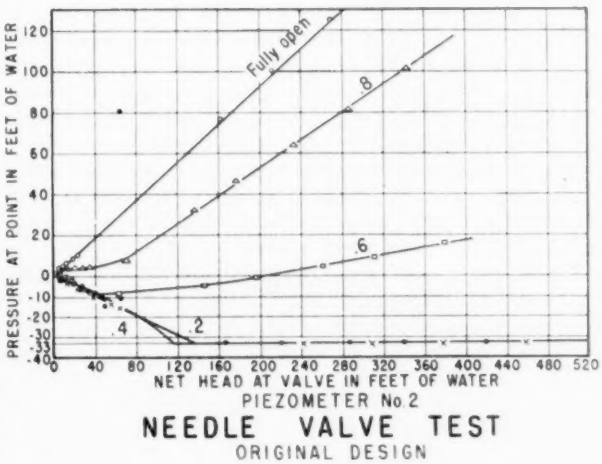
MODEL STUDIES

In order to test these conclusions, a model embodying these principles of design was constructed of a size to fit on a 6-in. outlet pipe. Having on hand a model of the older design of the same size, the models were tested in exactly the same manner so as to compare results. Pressure piezometers were located on the needle cones of both models as indicated on the curves of Figs. 9 and 10. It should be pointed out that the angle of the needle cone on the original design was 42 deg and that of the nozzle was 36 deg 22 min, Fig. 3, while on the new design the angle of the needle cone was 37 deg and that of the nozzle was 40 deg, Fig. 11.

Pressure piezometers were also placed in the nozzle and along

[2] "Cavitation in Outlet Conduits of High Dams," by Harold A. Thomas and Emil P. Schuleen, Proceedings of the American Society of Civil Engineers, vol. 66, 1940, p. 1623.





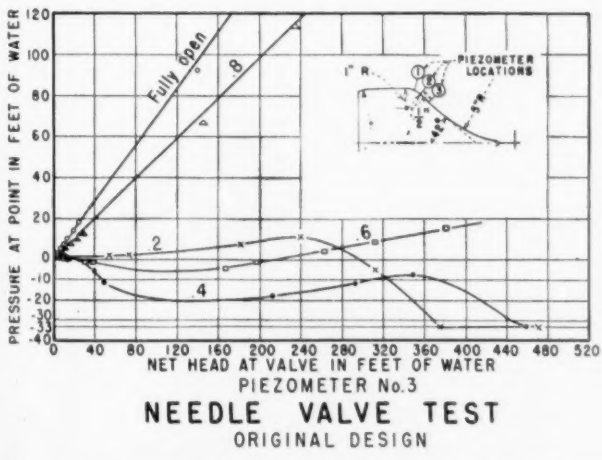
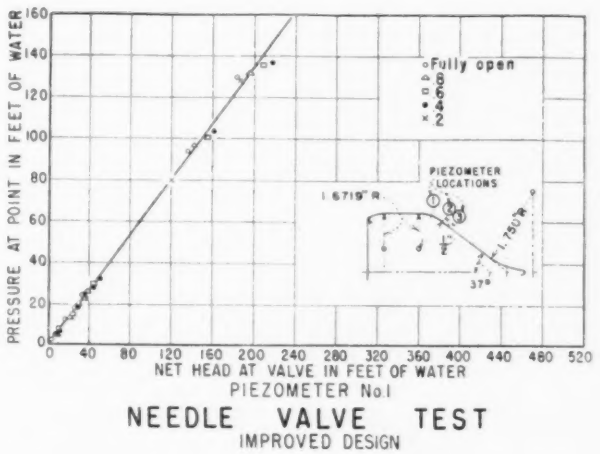
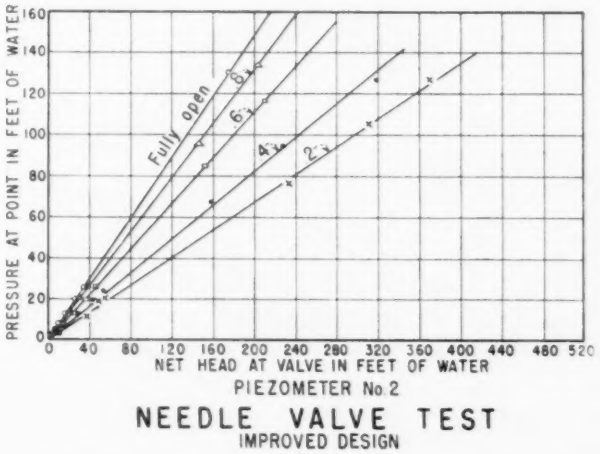


FIG. 9 PRESSURES ON NEEDLE CONE, ORIGINAL INTERIOR-DIFFERENTIAL NEEDLE VALVE





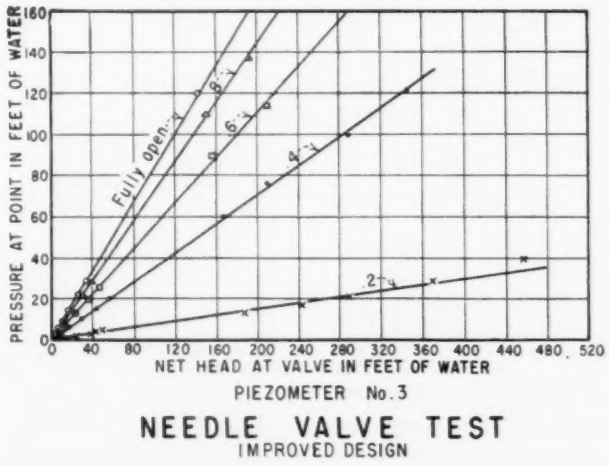


FIG. 10 PRESSURES ON NEEDLE CONE, IMPROVED-DESIGN INTERIOR-DIFFERENTIAL NEEDLE VALVE

the outer body of the valve up to the point where the outer body becomes cylindrical.

In the original design, subatmospheric pressures were indicated by the piezometers in the nozzle and for some distance back in the valve but the remaining piezometers showed positive pressures. This was true for all valve openings. The location of the piezometers and pressures recorded on the needle cone are shown in Fig. 9. The curve for piezometer No. 2, with the valve at 0.4 open, shows that the pressure at this point reaches zero when the head on the valve reaches 115 ft, while at full open all three piezometers showed positive pressures for all heads.

In the new design, all piezometers in the valve nozzle and outer body and all piezometers in the needle cone showed positive pressures for all valve openings and for all heads. The pressures

on the needle cone for the improved design are shown in Fig. 10.

After the laboratory tests were completed where heads of only about 70 ft were used, the question was raised as to what would happen under higher heads. The valve models were then taken to Boulder Dam where heads up to about 450 ft were available. The models were tested under these heads and the curves, Figs. 9 and 10, were extended accordingly. The lower points on the curves are those obtained in the laboratory and the higher points were obtained from the Boulder Dam tests.

Upon completion of the pressure tests, the model of the original design of the interior-differential valve and that of the improved design were left in operation under a head of about 500 ft. The valves were set at partial openings and were watched for the appearance of pitting. After 14 days, the original design was pitted, as shown in Fig. 12 (*a*), while the improved design showed no pitting after operating for 84 days, as shown in Fig. 12 (*b*).

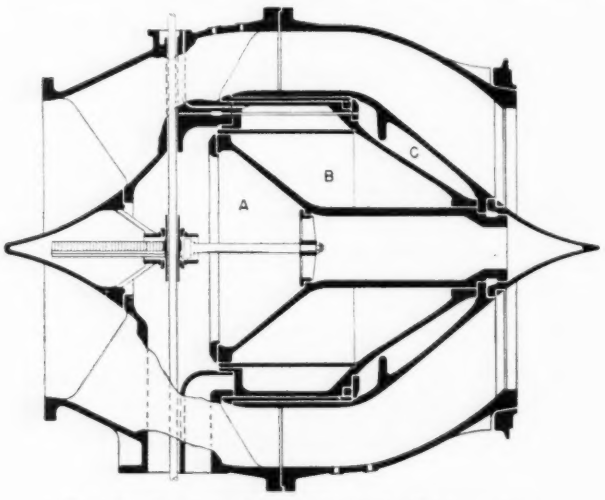


FIG. 11 IMPROVED-DESIGN INTERIOR-DIFFERENTIAL NEEDLE VALVE

In an attempt to improve the original design, the rounded nozzle was replaced with a sharp-edged nozzle, after which all the pressure piezometers in the nozzle and outer body of the valve showed substantially positive pressures and the pressures on the needle cone were greatly improved. However, it was still apparent that low pressures would occur in the region of piezometers Nos. 2 and 3 at 0.2 valve opening. It is interesting to note the discharge was reduced about 10 per cent by the sharp-edged nozzle.

In designing the hollow-jet valve, every effort was made to insure positive pressures at every point where the water at high velocities contacted metal surfaces. In other words, the design principles already developed were rigidly observed. A model of the hollow-jet valve was made to fit the same 6-in-diam pipe used for the tests previously described. Pressure piezometers were placed in the line of flow along the surface of the valve cone and along the outer body from the inlet flange to the discharge lip. All showed positive pressures. It is, therefore, concluded that this valve will be free from cavitation.

SUMMARY

The most desirable location for the outlet valve, either regulating or nonregulating, is at the discharge end of the conduit. Regulating valves may be used in a conduit only when adequate air relief is provided for the partially open positions.

Outlet valves of the balanced needle type, the tube type, or the hollow-jet type can be designed to eliminate cavitation by proportioning the water passages so that there will be positive pressures in all regions for all positions of valve opening.

The foregoing conditions can be complied with (1) by designing the nozzle with a sharp edge, (2) by making the base of the needle cone larger in diameter than the edge of the sharp-edged nozzle, (3) by making the angle of the nozzle cone equal to or greater than that of the needle cone. This is true except for the hollow-jet valve, in which case the angle of the nozzle cone must be considerably less than that of the needle cone to produce proper convergence and consequent pressures in the direction of flow.

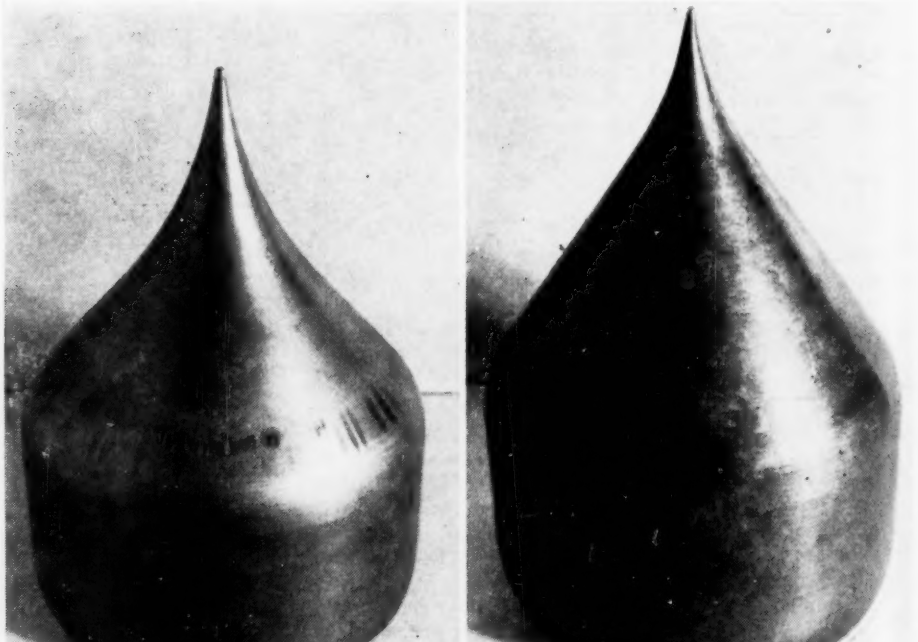


FIG. 12 MODEL NEEDLE CONES FOR INTERIOR-DIFFERENTIAL NEEDLE VALVES

(*a* Original design after operating 14 days under 500 ft head; *b* improved design after operating 84 days under 500 ft head.)

The Performance of Flat-Plate Solar-Heat Collectors[1]

By H. C. HOTTEL[2] and B. B. WOERTZ,[3] CAMBRIDGE, MASS.

The great magnitude of solar-energy flux on the earth has stimulated a number of attempts at its more effective utilization during the last 60 years. Mouchot (1, 2)[4] and Pifre (3, 2) in France, Shuman (4) in Egypt, Ericsson (5), Willsie (6), Shuman (7), and more recently Abbot (8) in America are but a few of the names associated with attempts to prove the economic feasibility of converting solar energy to heat and transferring that heat to the working fluid (steam, air, and sulphur dioxide have been used) of a heat engine. Recently Dr. Godfrey L. Cabot has made possible a continuing research on the problem by establishing an endowment at the Massachusetts Institute of Technology for studying means of more effective utilization of solar energy. Four projects are under way: three in the fields of photochemistry, photoelectricity, and thermoelectricity. The fourth follows the conventional attack on the problem, namely, the collection of solar energy in the form of heat in a fluid and the utilization of that heat. The present paper is a first quantitative report on progress in the last field.

SOLAR-HEAT collectors may be classified according to the type of insulation, degree of concentration of sunshine, and nature of orientation (whether, and how completely, they follow the sun). Insulation may consist of one or more spaced glass panes parallel to the absorbing surface of a flat collector, or one or more concentric glass tubes surrounding a heat-absorbing tube, with or without vacuum between the tubes. In the case of the flat-plate collector, the back side is also insulated. Concentration may vary from unity in flat-plate collectors to successively higher values as reflectors are employed in the shape of cylindrical parabolas, truncated cones, or paraboloids. Orientation varies greatly with the type of concentration; it includes stationary horizontal, stationary but tilted toward the equator, mounting on an East-West axis to follow the sun's seasonal motion, mounting on North-South horizontal or equatorial axes to follow the sun's diurnal motion, mounting on two axes, equatorial and transverse, to maintain the collector normal to the solar beam at all times, azimuth mounting, and others.

The engineering literature indicates that most of the possible combinations of insulation, concentration, and orientation of solar-heat collectors have been tried at one time or another. A final decision as to which is best involves quantitative knowledge of performance characteristics, combined with an economic balance of cost versus performance.

[1] Solar-Energy-Conversion Research Project, publication No. 3, the Massachusetts Institute of Technology, Cambridge, Mass., 1940.

[2] Associate Professor of Fuel Engineering, the Massachusetts Institute of Technology. Mem. A.S.M.E.

[3] Research Associate, the Massachusetts Institute of Technology.

[4] Numbers in parentheses refer to the Bibliography at the end of the paper.

Contributed by the Heat Transfer Division and presented at the Spring Meeting, Atlanta, Ga., March 31–April 3, 1941, of The American Society of Mechanical Engineers.

Note: Statements and opinions advanced in papers are to be understood as individual expressions of their authors and not those of the Society.

Because flat-plate collectors are the simplest and basic type, because a preliminary analysis indicated that they may have economic importance in connection with solar house heating, air conditioning, or power production, and because they are even now of some importance in connection with the supply of domestic hot water, the present project started with a study of their characteristics.

A flat-plate collector consists in general of an insulated flat absorbing surface painted black to increase absorption. This surface may be a sheet of metal or a number of tubes, with or without fins on their sides. In the case of a sheet-metal absorber, some form of piping is fastened on one side of it so that water or some liquid may be circulated through the piping to collect the heat. Below the absorbing surface some form of insulation is used, such as glass wool, mineral wool, aluminum foil, wood, or dead-air spaces. Desert sand has been tried (6) but found inadequate. Above the absorbing surface is one or more layers of a material substantially transparent to solar radiation, spaced approximately 1 in. apart. Glass has been used exclusively in the past, but certain plastics may be found to work satisfactorily.

A number of flat-plate collectors have been built and described. Tellier (9), in 1885, described a tilted flat-plate-collector system for heating ammonia, in connection with solar water pumping. Willsie (1902–1909) built horizontal flat-plate collectors in Needles, Calif., involving combinations, such as desert sand as an insulator, oil-covered water, water on an asphalt surface with one and with two layers of glass. He used the collected heat for operation of an engine with sulphur dioxide as the working fluid. Shuman, in Philadelphia (1906), built a flat-plate collector, consisting of water-immersed coils containing ether. Insulation consisted of one layer of glass. The ether was vaporized, used to drive a small engine, condensed in an air-cooled condenser, and pumped back into the collector. Flat-plate collectors have been in use for domestic water heating in Florida and California for a number of years. At present there are several companies manufacturing them. Brooks (10) has studied several types of natural-convection solar water heaters in use in California, and gives some quantitative data on performance but no correlation with measurements of solar intensity. Thus, it is seen that previous work on this problem has not yielded quantitative relations for predicting the effects of the many factors which contribute to the over-all performance of a flat-plate collector.

Description of Experimental Setup

An Eppley pyrheliometer (11) of the type installed at some eighteen Weather Bureau stations is in use for determining the rate of reception of total solar radiation on a horizontal surface; it is connected to a recording potentiometer. Although a calibration constant was provided by the Weather Bureau, the pyrheliometer was subjected to a detailed study of response to radiation from a constant source at various angles of incidence. The instrument was mounted equatorially and irradiated by a 1000-w projection bulb at various angles; the absolute calibration was established by comparison with a Smithsonian substandard silver-disk pyrheliometer. The instrument "constant" was substantially constant at 0.925 from normal incidence up to 50 deg, increased slowly to 0.995 at 70 deg, then rapidly to 1.17 at 80 deg

(these values are ratios to the average calibration constant recommended by the Weather Bureau).[5]

The special building constructed for this study consists of a laboratory and small office of approximate ground area 16 ft by 31 ft, Fig. 1, well insulated to compensate for its high surface-volume ratio. The walls are lapped board and plywood inside, paper-sealed, with 3⅝-in. rock-wool bats in the space between joists; windows are double-glazed and weatherstripped throughout; ceiling insulation consists of 4 in. of mineral wool. This construction gives 820 sq ft of wall with a calculated over-all

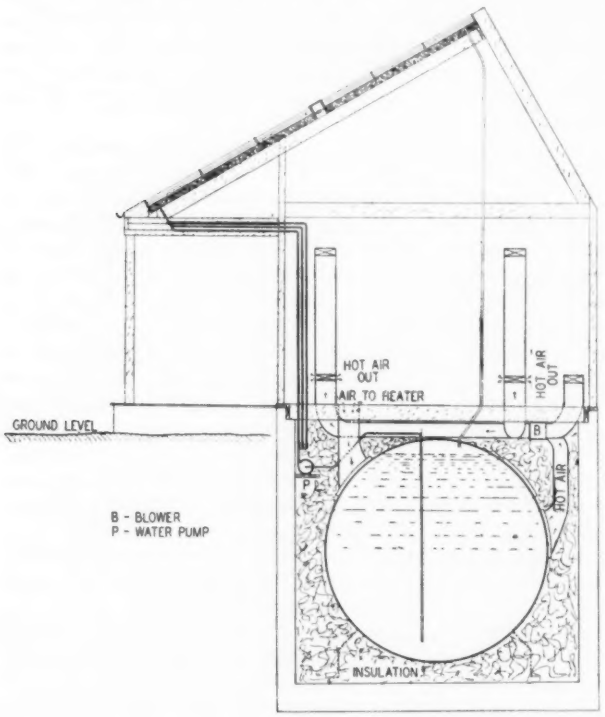


FIG. 1 SECTIONAL VIEW OF SOLAR-ENERGY BUILDING AT THE MASSACHUSETTS INSTITUTE OF TECHNOLOGY

coefficient of heat loss, per sq ft, of 0.075 Btu per deg F per hr, 483 sq ft of ceiling with an over-all coefficient of 0.055 Btu per deg F per hr, 75 sq ft of windows with a coefficient of 0.58 Btu per deg F per hr. One air change requires 73.3 Btu per deg F. There is no heat loss but rather a small heat gain through the floor, since the basement is filled with an insulated hot-water tank. In heat required per cubic foot, the building corresponds to a moderately insulated six-room house. Other features of the building were dictated by the intention to use it for studying the performance of various types of solar-heat collectors and the utilization of the heat so collected for house heating, air conditioning, and power generation.

The roof is of a special construction; the greater part of it slopes about 30 deg southward, and is recessed 9 in. deep except for a narrow strip at all edges. The area of the recess is approximately 533 sq ft; at present it is partially filled with 360 sq ft of exposed absorbing surface in collectors occupying 408 sq ft.

The basement is filled with a hot-water tank and insulation. The tank is 11 ft inside diam and 24.5 ft long, having a capacity of 17,400 gal (2320 cu ft). The average thickness of insulation is 2.18 ft; due to its nonuniform distribution around the tank, its effective thickness is 1.96 ft. These data yield a calculated heat loss of 390 Btu per deg-day using a k of 0.022 Btu per deg F per sq ft per hr per ft for the insulation.

The tank is equipped with a calibrated 10-junction copper-constantan differential thermocouple in a glass tube running from the top of the tank to within less than 6 in. of the bottom. The hot junctions can be run up and down the glass tube for a temperature traverse.

Before the space between the tank and the basement walls was filled with insulation, nine thermocouples were placed against the concrete walls, for use in calculating heat losses from the tank.

The size of the tank and the roof-collector area in use in this experimental building are not quantitatively significant for calculation of the cost of solar house heating. The unit is known to be highly uneconomical; its characteristics were dictated by considerations of need for flexibility in application to various problems. Economic studies will come later.

The building is heated by hot air, warmed by passage through a duct system, one side of which is the water-tank wall itself. The ducts, 2 in. by 30 in. in cross section, make three passes lengthwise of the tank and cover a tank area of 155 sq ft. The air fan, controlled by a thermostat, withdraws air from a register in the floor and delivers it through any of eight registers in the partition between the office and laboratory. Four of these are approximately 1 ft above the floor; the others 1½ ft from the

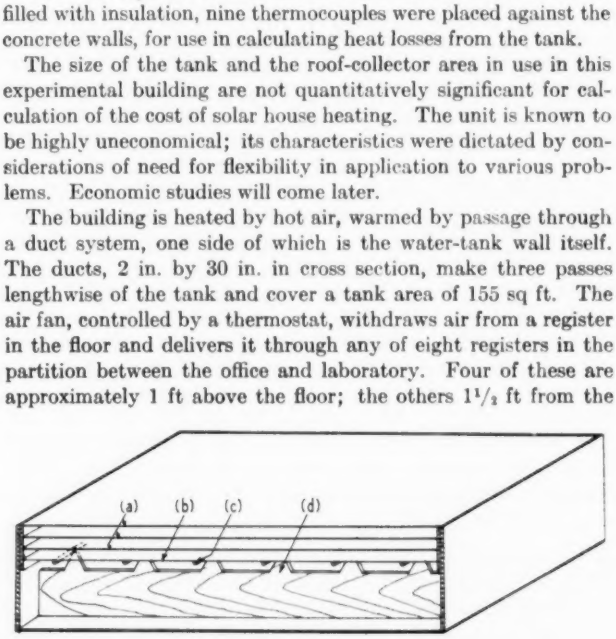


FIG. 2 CUTAWAY SECTION OF ONE OF THE SOLAR-HEAT COLLECTORS TESTED

(*a* Air-spaced glass panes; *b* blackened-metal absorbing surface; *c* copper tubes for circulation of water; *d* wooden cross supports for absorbing surface.)

ceiling. The latter were intended primarily for use with an air-conditioning unit in the summer.

There are fourteen collectors set in the roof recess. A cutaway section of one is shown in Fig. 2. The absorbing surface *b* is a 3-ft by 9-ft blackened-copper sheet 0.02 in. thick to which are soldered six parallel copper tubes, 0.375 in. outside diam, 0.016 in. wall, spaced 6 in. apart, running lengthwise of the collector, and silver-soldered at their ends into ¾-in-outside-diam copper header tubes. The absorbing surface is set into a ⅜-in. plywood box, and is supported by side strips and wooden cross supports *d*. The space between the metal and the box bottom, 5.5 in., is filled with insulation. Above the absorber are three air-spaced layers of double-strength glass of high quality (referred to later as glass C_2), in 3-ft by 3-ft panes. The supports for the glass divide each collector into three square cells. A nonhardening calking compound is used on the top panes.

The collectors are placed seven side by side running up the roof, with seven more above them. Water flows in series through two collectors. The three water-supply lines supply four, four, and six collectors. The water-circulating system, for transfer of heat from the roof to the basement tank, consists of a centrifugal pump withdrawing water from within 1 ft of the tank bottom and discharging it through three lines in parallel for supplying the three sets of collectors on test. Each line is provided with a calibrated thin-plate orifice, connected to a ligroin-water-filled inverted manometer. Except when the water is near its boiling point, the flow rate may be determined to within ½ per cent.

From the orifices, the water lines go to the collector inlets along

[5] A more detailed account of the calibration of the instrument appeared recently (21).

the lower edge of the roof. The collector outlets unite in the attic, and the returning water is delivered to the air space in the tank top. All tubing is sloped so that it drains into the tank when the pump is stopped. The pump is controlled by a galvanometer-photocell-relay combination, operated by a differential thermocouple (12), the two junctions of which are in the hot-water tank at the pump-inlet level and on a collector on the roof, respectively.

For measurement of water temperatures, there are five calibrated mercury-in-glass thermometers in use, graduated to 0.1 C and capable of being read to 0.01 C. The thermometers are located in wells at the tank outlet, the farthest collector inlet, and all three collector outlets. In addition, there is an independent system for recording temperature rise in any one of the three collector systems, consisting of resistance thermometers in an unbalanced Wheatstone-bridge circuit, connected to a recording millivoltmeter. The circuit contains actually two of the four resistance thermometers, one in the pump-inlet line and any one of the other three in the outlets from the three collector systems.

Most domestic solar hot-water heaters depend upon natural circulation, with the tank above the collector level. However, if flat-plate collectors ever achieve large-scale importance they will almost certainly be of the forced-circulation type, to which this discussion is restricted.

Experimental Data

The data taken for determining flat-plate-collector performance included the following:

(*a*) A continuous record of total solar radiation on a horizontal surface, determined by the Eppley pyrheliometer; and integration of the record to give hour-by-hour reception.

(*b*) Fraction of total radiation arriving as diffuse or sky radiation. This is based on results of occasionally shading the pyrheliometer from the sun and observing the lowest radiation indicated.

(*c*) Differential pressures across orifices in the water-supply lines of the three sets of collectors, from which flow rates are calculated.

(*d*) A continuous-chart record of temperature rise of the water flowing through one set of collectors, and integration over hourly periods.

(*e*) Readings of calibrated thermometers simultaneously with readings from the chart record (*d*), to determine the correction factor on the chart record; this comparison is made only during periods of steady sunlight.

(*f*) Outside air temperature.

(*g*) Attic and laboratory temperature, necessary for making thermometer-stem corrections.

(*h*) A qualitative estimation of dirtiness of uncleaned collector units. The top panes of glass of the east unit were maintained clean at all times. The west and center units were never cleaned except by rain or snow. Visual observations of dirtiness were recorded day by day in the form of a grading 1 to 5, grade 1 being clean and grade 5 being very dirty; all grading was done by the same individual.

In order accurately to establish the temperature of the collector plate, known to be a major factor in determining efficiency, the water rate was kept high enough to prevent a temperature rise in excess of 15 F. The collector temperature was taken as the arithmetic-mean water temperature.

A discussion of the results of many runs summarized in Table 5 must wait for an analytical treatment of the problem. Other data on transmittances and reflectivities of various materials for sunlight will be discussed in this paper under their proper heads.

Analysis of Collector Performance

The problem is to express the rate of useful-heat collection in the water stream in terms of the intensity of sunlight, air temperature, tilt of the collector plate, and properties of the collector parts. Pyrheliometric records most commonly available give the solar-energy flux density on a horizontal surface; call this H_S in cal per sq cm per hr. A portion of the energy comes from the entire sky rather than directly from the sun; call this diffuse-radiation flux density H_D. Then in unit time a unit surface, tilted somewhat toward the equator and covered with severa glass plates, will absorb as direct radiation the amount

$$(H_S - H_D)(\cos\theta_T/\cos\theta_Z)\tau\alpha \equiv (H_S - H_D)R\tau\alpha \quad [1]$$

where

θ_T and θ_Z = angles of incidence of direct sunlight on a tilted surface and on a horizontal surface, respectively (the latter is generally called the zenith angle of the sun)

τ = over-all transmittance of glass plates for direct solar radiation

α = absorptivity of the blackened collector surface for incident solar radiation

R = $(\cos\theta_T/\cos\theta_Z)$, the ratio of direct radiation intercepted by a tilted surface to that intercepted by a horizontal surface (the pyrheliometer)

A corresponding term $H_D R'\tau'\alpha'$ represents the contribution of diffuse solar radiation to the energy absorption by the collector plate; the primes differentiate the terms from similar ones for direct solar energy. The term R', representing sky radiation on a tilted surface relative to that on a horizontal one, is difficult to evaluate exactly. The incomplete "view" which the tilted receiver has of the sky is partially compensated by its being better oriented with respect to that brighter part of the sky which is near the sun. Because of inadequate knowledge of the distribution of sky radiation, the compensation will be assumed perfect, i.e., $R' = 1$. Diffuse radiation being less important than direct radiation this assumption is usually a minor source of error. The total absorbed energy q_A is now given by the relation

$$q_A/A = 3.69\,[(H_S - H_D)R\tau\alpha + H_D\tau'\alpha'] \quad [2]$$

The factor 3.69 is introduced to convert H from the units in which it is generally reported in Weather Bureau tables (cal per sq cm per hr) to English engineering units, Btu per sq ft per hr.

The energy q_A/A absorbed by the collector is available for transfer as useful heat q_U/A in a fluid stream in contact with the plate, for supplying the heat loss q_L/A from the plate through the air and glass layers to the air above, and for supplying the heat loss q_B/A from the plate through the insulation below it and out through the bottom of the box (temporarily, a system with no side losses is being considered). The useful heat-collection rate is then

$$q_U = q_A - q_L - q_B \quad [3]$$

and the problem is the evaluation of q_L/A, q_B/A, and the terms in Equation [2] giving q_A/A.

Solar Radiation on Tilted Surfaces

The total solar-energy intensity H_S on a horizontal surface is recorded at some eighteen stations in the United States. These recorded values are adequate for collectors located near the pyrheliometer; for other sections of the United States, few data are available. The use of data for another locality is at best an approximation. Cloudiness measurements are the most common of all those related to solar radiation and are perhaps the best criterion for selecting the station whose solar-radiation values are most nearly like those, of unknown magnitude, of the locality in

TABLE 1 CLOUDINESS AT OR NEAR STATIONS MEASURING SOLAR RADIATION

	Station	Latitude	Cloudiness at	Cloudiness (tenths) Feb.–Apr.	May–July	Aug.–Oct.	Nov.–Jan.	Mean
1	San Juan, Puerto Rico	18°28′	Same	5.0	5.8	5.9	5.2	5.5
2	Miami, Fla.	25°41′	Same	4.9	5.5	6.3	5.0	5.4
3	Gainesville, Fla.[a]	29°39′	Tampa	3.9	4.6	5.4	4.1	4.5
4	New Orleans, La.	29°56′	Same	5.8	5.3	5.3	4.5	5.2
5	Yuma, Ariz.[b]	32.7°	Same	2.4	0.6	1.7	2.5	1.8
6	La Jolla, Calif.	32°50′	San Diego	5.6	4.0	4.2	5.1	4.7
7	Riverside, Calif.	33°58′	Los Angeles	4.9	3.1	2.9	4.0	3.7
8	Albuquerque, N. Mex.	35.1°	Same	5.3	3.8	2.7	4.1	4.0
9	Santa Fe, N. Mex.[a]	35.7°	Same	5.1	4.4	4.1	4.0	4.4
10	Fresno, Calif.	36°43′	Same	6.3	2.1	2.4	6.1	4.2
11	Washington, D. C.	38°56′	Same	6.5	6.1	5.2	5.2	5.8
12	Pittsburgh, Pa.[a]	40°22′	Same	7.4	6.8	5.2	7.2	6.7
13	New York, N. Y.	40°46′	Same	6.5	6.3	5.5	5.3	5.9
14	Lincoln, Neb.	40°50′	Same	6.9	4.9	3.6	4.6	5.0
15	Newport, R. I.	41°30′	Providence	5.4	5.5	5.3	4.8	5.3
16	Chicago, Ill.	41°47′	Same	7.4	5.7	4.1	6.1	5.8
17	Blue Hill, Mass.	42°13′	Boston	6.1	6.4	5.5	5.5	5.9
18	Cambridge, Mass.	42°22′	Boston	6.1	6.4	5.5	5.5	5.9
19	Ithaca, N. Y.	42°27′	Same	7.6	6.2	5.8	7.7	6.8
20	Twin Falls, Idaho	42°29′	Boise	7.0	4.1	3.8	6.5	5.4
21	Madison, Wis.	43°05′	Same	7.0	6.5	5.6	5.9	6.3
22	Portland, Me.[b]	43.7°	Same	5.0	5.2	4.5	3.7	4.6
23	Mt. Washington, N. H.[a]	44°16′	Northfield, Vt.	7.1	6.1	6.3	6.5	6.5
24	Williston, N. Dak.[b]	48.2°	Same	6.5	3.8	3.9	4.0	4.6
25	Friday Harbor, Wash.	48°32′	Seattle	7.6	5.6	5.3	8.3	6.7
26	Fairbanks, Alaska	64°52′	None available	...	...	...	...	...
	Mean			6.0	5.0	4.6	5.3	5.2

[a] Discontinued station.
[b] Never any station.

TABLE 2 NUMBER OF CLEAR DAYS DURING PERIOD AUGUST 1–31, 1938;[a] SEPTEMBER, 1939–JULY, 1940

Location	Number
Boston, Mass.	105
Williston, N. D.	165
Portland, Me.	170
Yuma, Ariz.	287

[a] August, 1939, data were incomplete; August, 1940, not available at time table was prepared.

question. Summaries of average daily radiation at each of eighteen stations and cloudiness at approximately 200 United States cities and towns appear in the *U. S. Monthly Weather Review*. The complete hour-by-hour records of the eighteen solar stations are obtainable from the stations or from Solar Radiation Investigations, Blue Hill Observatory, Milton, Mass., on payment of the charge for photostating. Although the use of pyrheliometer data from a station having about the same latitude and cloudiness characteristics as the locality of interest may introduce considerable error, there is no better procedure except the installation locally of some type of pyrheliometric equipment.

Cloudiness as a function of season is shown in Table 1 for the region of each solar-radiation-measuring station. Three other localities are also included. It is seen that the period February to April is, in general, the cloudiest, while August to October is the clearest.

For purposes of comparison, the number of reported clear days in a year at Boston and three other localities is compiled in Table 2. It is seen that the percentage of clear days varies from 29 in Boston to 78 in Yuma. The percentage of possible sunshine is considerably higher.

The magnitude of solar radiation on a horizontal surface is shown by the fact that, during the year ending June 30, 1940, a total of 123,300 cal per sq cm (454,000 Btu per sq ft) was received at Cambridge, Mass. About 192,000 cal per sq cm would have been received with no clouds and high atmospheric transmissivity throughout the year. Hourly radiation as high as 93.4 cal per sq cm has been observed.

Data on diffuse, or sky, radiation H_D are rather meager, generally having been measured on relatively cloudless days by investigators not interested in the present use of the data. Values of 4 to 18 cal per sq cm per hr are reported for clear days (13), and indications are that sky radiation is relatively constant throughout most of the day. Measurements made at Cambridge between March 18 and June 30, 1940, in connection with the present project, indicate an average value of H_D of 16.3 cal per sq cm per hr for all hours in which heat could be collected at the prevailing tank temperature. For 0.5, 1.5, 2.5, 3.5, and 4.5 hr from solar noon, the corresponding average values of H_D were 18.2, 16.9, 16.7, 14.3, and 9.7 cal per sq cm per hr. During December, 1940, the values of H_D at 0.5, 1.5, and 2.5 hr from noon were 7.8, 7.7, and 6.

Diffuse radiation is highest on partly cloudy days and lowest on very cloudy days, extreme values of 52.7 and 1.5 cal per sq cm per hr having been recorded at the Cambridge station. The average noon value for days on which heat could be collected is around 20 cal per sq cm per hr at the summer solstice and 8 at the winter solstice. It is believed that summer-solstice values are proper to use until the latter part of August, since there are as many partly cloudy days in July and August as in June. On a cloudless day H_D probably averages not more than 9 cal per sq cm per hr, even in the summer.

The geometrical factor R involves the latitude ϕ, the tilt β of the collector from the horizontal toward the equator, the declination δ of the sun, and the time of day expressed as hour angle ω of the sun from the noon meridian (substantially 15 deg per hr). The zenith angle of the sun (14) is given by

$$\cos \theta_Z = \sin \phi \sin \delta + \cos \phi \cos \delta \cos \omega \quad [4]$$

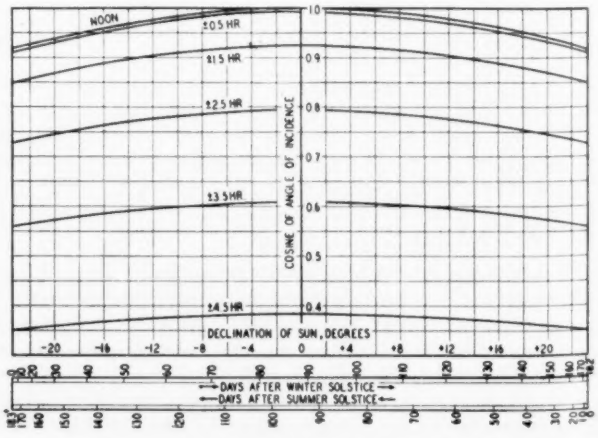


FIG. 3 COSINE OF ANGLE OF INCIDENCE OF DIRECT SUNLIGHT ON COLLECTORS TILTED β DEG TOWARD EQUATOR AT LATITUDE ϕ DEG, WHEN $\phi - \beta = 0$ DEG

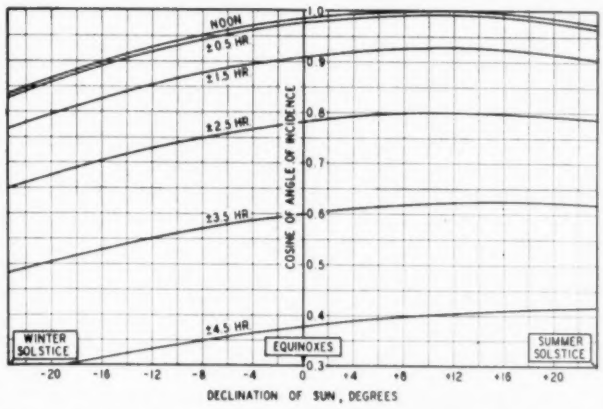


FIG. 4 COSINE OF ANGLE OF INCIDENCE OF DIRECT SUNLIGHT ON COLLECTORS TILTED β DEG TOWARD EQUATOR AT LATITUDE ϕ DEG, WHEN $\phi - \beta = 10$ DEG

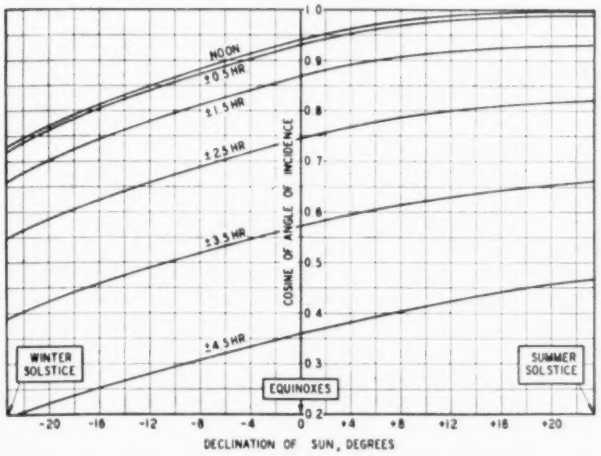


FIG. 5 COSINE OF ANGLE OF INCIDENCE OF DIRECT SUNLIGHT ON COLLECTORS TILTED β DEG TOWARD EQUATOR AT LATITUDE ϕ DEG, WHEN $\phi - \beta = 20$ DEG

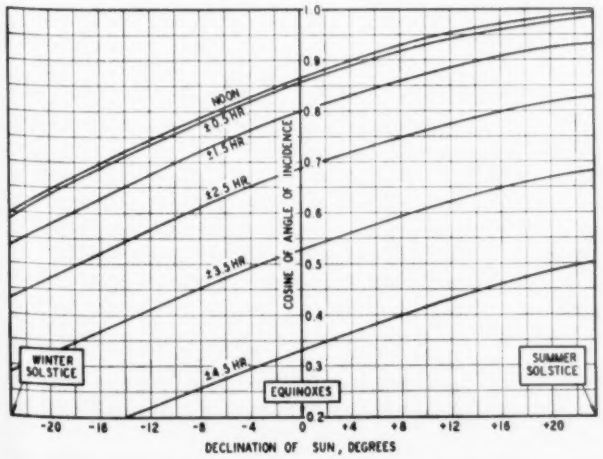


FIG. 6 COSINE OF ANGLE OF INCIDENCE OF DIRECT SUNLIGHT ON COLLECTORS TILTED β DEG TOWARD EQUATOR AT LATITUDE ϕ DEG, WHEN $\phi - \beta = 30$ DEG

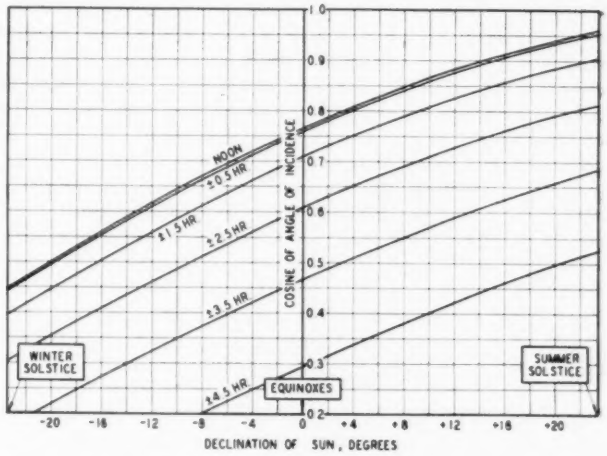


FIG. 7 COSINE OF ANGLE OF INCIDENCE OF DIRECT SUNLIGHT ON COLLECTORS TILTED β DEG TOWARD EQUATOR AT LATITUDE ϕ DEG, WHEN $\phi - \beta = 40$ DEG

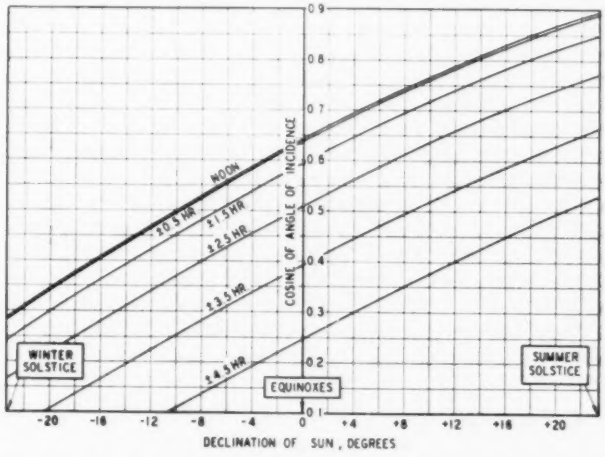


FIG. 8 COSINE OF ANGLE OF INCIDENCE OF DIRECT SUNLIGHT ON COLLECTORS TILTED β DEG TOWARD EQUATOR AT LATITUDE ϕ DEG, WHEN $\phi - \beta = 50$ DEG

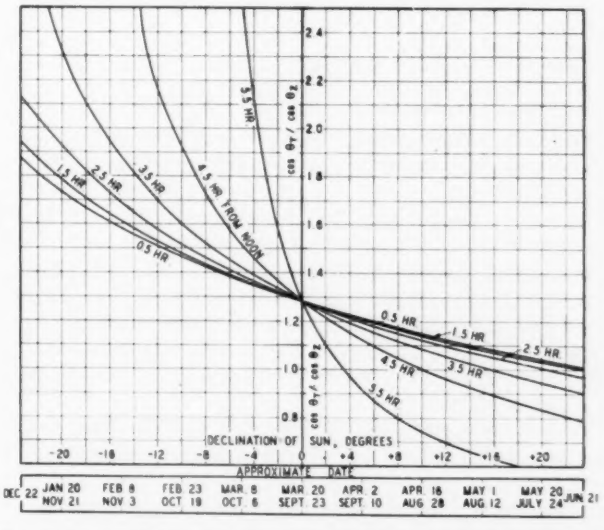


FIG. 9 COS θ_T/COS θ_Z, RATIO OF DIRECT SUNLIGHT FALLING ON A COLLECTOR TILTED 30 DEG TOWARD EQUATOR TO THAT FALLING ON A HORIZONTAL COLLECTOR, BOTH BEING AT 40 DEG LATITUDE

A little consideration will show that the angle of the sun θ_T on a surface tilted β deg from the horizontal toward the equator is the same as on a horizontal surface at an artificial latitude $(\phi - \beta)$. Values of $\cos \theta_T$ are given in Figs. 3 to 8 for values of $(\phi - \beta)$ in 10-deg intervals from 0 to 50 deg, for times of day corresponding to centers of successive hours from solar noon.

Reading from two of the plots, values may be obtained for $\cos \theta_T$ and $\cos \theta_Z$ and their ratio R for various combinations of latitude and tilt. One such combination, latitude 40 deg and tilt 30 deg, appears as Fig. 9. Such a plot serves to emphasize the gain from tilting, during the winter months, and the loss during the summer months because of so large a tilt. It is obvious that the choice of tilt is profoundly affected by whether a collector is to be used to supply heat for an absorption-refrigeration cycle for summer cooling or to heat a house in winter.

Transmission of Radiation Through a System of Glass Plates

The next factor appearing in Equation [2] is the over-all transmittance τ of the glass plates for a beam of solar energy. This depends upon surface reflection and internal absorption in the glass, and both of these depend upon angle of incidence of the beam. Consider first the surface-reflection losses in a system of nonabsorbing glass plates. The reflectivity of an optically smooth nonconductor is given in terms of angle of incidence θ and refractive index n by the Fresnel equations (15). The incident beam is split into its components of polarization, parallel and perpendicular to the plane of incidence, and each component is treated separately. Consider a unit beam, one component of polarization, having a reflectivity of r as calculated previously, and let it be incident on the first surface of the system of parallel plates. The fraction $(1 - r)$ is incident on the second surface. Of that beam, the fraction $r(1 - r)$ is lost back through the first surface, $(1 - r)$ is transmitted through the second surface, and the remainder repeats its division between the two sinks in the same ratio. Then the total amount getting through is

$$(1 - r)\frac{(1 - r)}{(1 - r) + r(1 - r)} \equiv (1 - r)/(1 + r) \equiv \tau_1$$

where τ_1 is the over-all transmittance of a pane of glass, allowing for reflection losses only. To consider two glass panes, let the over-all reflectivity of the first pane $= \rho_1 \equiv 1 - \tau_1$. By analogy to the previous derivation, the over-all transmittance of the two panes is

$$\tau_2 = \frac{1 - \rho_1}{1 + \rho_1} = \frac{1 - r}{1 + 3r} \quad \ldots\ldots\ldots\ldots\ldots [5]$$

Extension of this treatment yields the over-all transmittance τ_n of an n-plate system, containing $2n$ reflecting surfaces. It is

$$\tau_n = \frac{1 - r}{1 + (2n - 1)r} \quad \ldots\ldots\ldots\ldots\ldots [6]$$

This relation, with values of r from the Fresnel equations, is valid for either component of polarization. For a homogeneous beam (i.e., one with equal values of the two components of polarization), such as direct sunlight, the over-all transmittance is obviously the arithmetic mean of the two values of τ_n calculated from Equation [6].

Over-all transmittance (allowing for reflection losses only) has been calculated by this method and is plotted in Fig. 10, versus angle of incidence for one to four panes of glass of refractive index $n = 1.526$, the value at the D line for the glass used in the collectors tested. The transmittance is seen to vary but slightly for angles of incidence up to 30 deg. It is interesting to note that, for a large number of plates, the over-all transmittance actually increases with angle of incidence out to a value near the critical polarizing angle.

To determine the effect of the combined losses, due to reflection and internal absorption, on the over-all transmittances of various available glasses and partially transparent organic films, a one-junction thermopile was used in a series of measurements of an orienting character. The thermopile, suitably enclosed in concentric chambers for stability of reading, was pointed at the sun and its shutter alternately opened and closed every 20 sec. Open-shutter periods were alternately with and without the glass-plate or organic-film system between the thermopile and the sun. Even with a fairly unsteady solar irradiation, it was possible to obtain quite reliable and reproducible determinations of transmittance, provided several readings were averaged. The accuracy of the method was checked by replacing the thermopile by a Smithsonian silver-disk pyrheliometer, which indicated on one specimen an over-all transmittance of 0.76, compared to 0.755 by the thermopile. The results of such studies of various materials, four air-spaced parallel plates unless otherwise indicated, appear in Table 3. Notable is the variation among available window glasses, due probably to differences in iron content. Glass high in iron is greenish in tinge and in addition is a poor solar-radiation transmitter because of absorption in the near infrared. The glass finally chosen for construction of collectors was that designated by C_2, a rather expensive glass chosen on the ground that, if the demand were great enough, similar glass could be manufactured which would lie in the window-glass price range. Plate glass was used, not because the grinding operation added value to it for the present use, but because a supply of seconds was available.

Since transmittance for a normal beam of solar energy is inadequate for collector design, a more comprehensive study was made of glasses A_2 and C_2, to determine internal absorption versus thickness. Layers of glass were cemented together with a balsam-benzene mixture, the absorptivity of which for solar radiation was found to be low enough to justify a simple correction for it. (Extinction coefficient was 10 times that of glass C_2, 2.5 times that of glass A_2; equivalent thickness, expressed as glass, never exceeded 5 per cent of glass C_2.) When the data are plotted as transmittance on a log scale versus sample thickness on an arithmetic scale, a sufficiently straight line is obtained to justify the use of the conventional exponential relation, strictly applicable only to monochromatic radiation. Smooth curves indicated transmittances for 0.5 in. of glasses C_2 and A_2 of 0.948 and 0.806, respectively, when reflection loss was eliminated. Extinction coefficients K equivalent to these values are 0.107 in.$^{-1}$ (0.042 cm^{-1}) and 0.432 in.$^{-1}$ (0.170 cm^{-1}), respectively, for use in the relation

$$\tau_a = e^{-KL} \quad \ldots\ldots\ldots\ldots\ldots [7]$$

where τ_a is the transmittance of thickness L, allowing only for internal absorption losses in the glass.

With knowledge of extinction coefficients applicable for total solar radiation, it is possible to calculate the over-all transmittance τ of a system of plates. Stokes (16) treats this problem of the combined effects of multiple reflection and internal absorption. To a high degree of accuracy, however, τ is given by the simple relation

$$\tau = \tau_r \cdot \tau_a \quad \ldots\ldots\ldots\ldots\ldots [8]$$

where τ_r and τ_a are, respectively, the transmittance of the plate system, allowing for reflection losses only (Fig. 10), and the transmittance, allowing for internal absorption only. The simplified relation will break down when τ_r and τ_a are far from unity, but introduces an error of less than 1 per cent in the range of interest in collector design.

TABLE 3 NORMAL TRANSMITTANCE OF GLASSES, PLASTICS, ETC.

(Four parallel plates unless otherwise indicated. Thickness given is for a single plate)

		Per cent
Cellulose-acetate plastics from various sources:		
Source B_1	(0.103 in. thick)	41.1
D	(0.060 in. thick)	53.1
B_2	(0.010 in. thick)	61.4
E	(0.010 in. thick)	67.4
B_3	(0.006 in. thick)	64.1
Regenerated cellulose:		
Sample F (yellowish from age)		42.4
Samples G-J (all about 0.001 in. thick)		53.6–57.8
Cellulose nitrate (0.0275 in. thick)		45
Acrylic type resins:		
Source L	(0.122 in. thick)	53.2
M	(0.265 in. thick)	57.5
Glasses:		
Source N	greenish window glass (0.085 in. thick)	41.9
O	Belgian plate (0.239 in. thick)	52.4
P	S.S. window (0.096 in. thick)	55.2
A_3	grade A window (0.126 in. thick)	63.9
A_1	grade A window (0.089 in. thick)	65.8
A_2	grade A window (0.089 in. thick)	61.3
Q	water-white plate (0.242 in. thick)	67.8
C_3	water-white plate (0.247 in. thick)	68.0
C_2	water-white plate (0.117 in. thick)	68.8
C_1	water-white plate (0.117 in. thick)	69.9
C_3	water-white plate (0.117 in. thick, three layers)	75.5
R	Pyrex (three layers only)	77.5
Film-glass:		
Treated with MgF_2		80.0
Treated with Cryolite		82.8

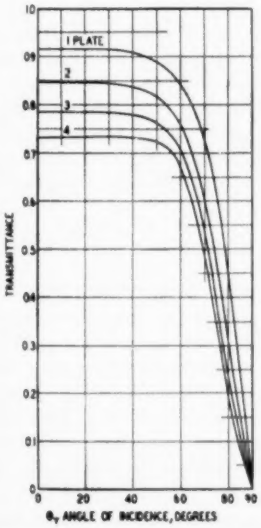


FIG. 10 CALCULATED TRANSMITTANCE τ_R OF A SYSTEM OF GLASS PLATES, ALLOWING FOR REFLECTION LOSSES ONLY

(Refractive index = 1.526.)

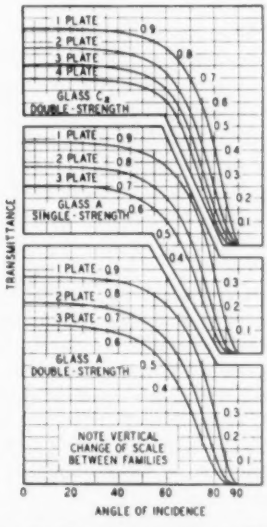


FIG. 12 TRANSMITTANCE τ OF SYSTEMS OF GLASS PLATES, ALLOWING FOR REFLECTION AND ABSORPTION LOSSES

(Top, middle, and bottom families are for glasses with KL per plate = 0.0125, 0.0370, and 0.0524, respectively.)

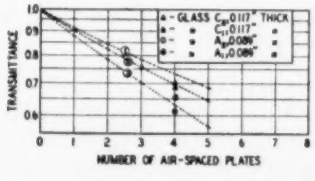


FIG. 11 TRANSMITTANCE FOR SUNLIGHT AT NORMAL INCIDENCE, OF PLATES OF VARIOUS GLASSES

(Data points experimental, smooth curves calculated. Curve 1 allows for reflection losses only; $n = 1.526$. Curves 2 and 3, for glasses C_2 and A_{avg}, allow for the effects of absorption and reflection. $K = 0.107$ in.$^{-1}$ and 0.419 in.$^{-1}$, respectively.)

Fig. 11, shows experimental points for the glasses A and C taken from Table 3, subscripts referring to samples from different batches. The glass used in the roof collectors was C_2. Attention is called to the considerable difference between the two samples of glass A. In the same figure appear some calculated curves for comparison. Curve 1 gives the transmittance τ_r of a nonabsorbing glass of refractive index $n = 1.526$ (applies to glass C and approximately to glass A); curve 2 is curve 1 multiplied by τ_a for the proper total thickness of glass C_2, using the previously determined extinction coefficient of 0.107 in.$^{-1}$; curve 3 is curve 1 multiplied by τ_a for the proper total thickness of glass A, using an extinction coefficient of 0.419 in.$^{-1}$ to make the curve go midway between the results for the two samples of glass A.

Using the extinction coefficients 0.107 in.$^{-1}$ and 0.419 in.$^{-1}$ for glasses C and A, respectively, and a refractive index of 1.526, over-all transmittances were calculated for systems consisting of one to four plates of double-strength glass C and one to three plates of single- or double-strength glass A. The results are given in graphical form in Fig. 12. Four panes of double-strength glass C transmit more than three panes of single-strength glass A or about as much as the average of two and three panes of double-strength glass A.

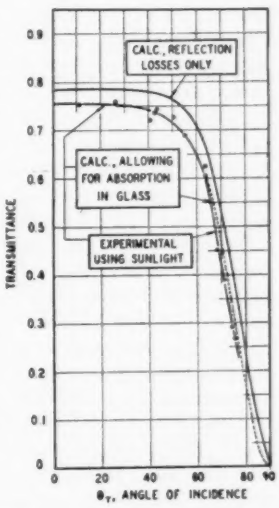


FIG. 13 TRANSMITTANCE OF THREE PLATES OF GLASS C_2, AS USED IN COLLECTORS TESTED

(Appropriate calculated curve from Fig. 12 and one from Fig. 10, allowing for reflection losses only, also shown.)

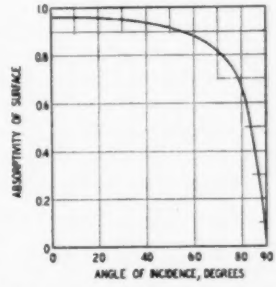


FIG. 14 ABSORPTIVITY OF A BLACKENED SURFACE FOR ARTIFICIAL SUNLIGHT TRANSMITTED THROUGH GLASS

(From reference 17 of Bibliography.)

As a final check on the calculated over-all transmittance of glass C_2, several determinations of τ for various angles of incidence were made using three panes of glass. In these measurements, the glass was maintained either horizontal or parallel to the roof, and variations in angle of incidence depended upon variation of position of the sun in the sky. The data are shown in Fig. 13, together with the calculated curve from Fig. 12 and a curve allowing for reflection losses only from Fig. 10. The agreement between the calculated curve and experimental data is excellent out to an angle of 65 deg. The small discrepancy at greater angles may well be due to the change in the quality of solar energy when the sun is low; an increase in the fraction of the energy in the infrared, which is most easily absorbed by glass. There is no indication from this study, however, of any need for complicating the problem of collector performance by attempting to allow for the effect of change in quality of solar energy.

ABSORPTIVITY OF BLACKENED SURFACES

The next factor in Equation [2] to be considered is the absorptivity α of the blackened collector plate for solar energy. The variation of α with angle of incidence of the beam has been

determined by the British Building Research Board (17) using a filtered-light source in imitation of sunlight. The results are given in Fig. 14. To obtain as perfect an absorber as possible, the monochromatic absorptivities of a number of surfaces covered with various mixtures of carbon black and vehicle were determined, using the Hardy spectrophotometer. An absorptivity in the visible spectrum of 98+ per cent at normal incidence is easily obtainable with blacks in which a minimum of vehicle is used, but adherence to the metal plate is poor.

The collectors under study were blackened with one coat of a primer consisting of 1 part by weight of special carbon-black pigment to 2 parts of alcohol-resisting varnish. The top-coat composition was 2.5 parts of the same pigment per part of 4 lb cut shellac. Enough thinner was added to reduce the paints to a thin brushing consistency. Test pieces finished with these had an absorptivity of 98.8+ per cent; but upon application to the collector surface, the paint had a definite tendency to crack and curl. This condition was not regarded as serious, and has become no worse since. However, due to the imperfection of the coat on the collectors, a value of 0.98 at normal incidence was judged to be sufficiently high for the finished collectors. Values at other angles of incidence were taken as 0.98/0.96 times the values read from Fig. 14.

Although not actually measured for absorptivity, test pieces later finished with drop black showed definitely superior adhesion characteristics of the paint and at the same time appeared to have substantially as high absorptivity.

The question arises as to what values to use for τ' and α', the transmittance and absorptivity for diffuse radiation. If one assumes a uniform sky, a graphical integration is possible which indicates that sky radiation is transmitted by three glass plates (C_3) and absorbed by the blackened surface as though it were all concentrated in a beam making an angle of 58 deg with the normal to the collector. For the present collector system, the corresponding value of $\tau'\alpha'$ is 0.61.

Heat Losses From Absorbing Surface to Atmosphere

The next factor to be considered is the upward heat loss q_L. Inasmuch as the absorption of solar energy within the glass plates covering the blackened metal surface of the collector is small, the loss of heat upward from the collector metal maintained at a definite temperature by circulating water may be calculated independently of the influx of solar radiation. Variables determining the upward heat flux are (*a*) temperature of the absorbing surface; (*b*) temperature of the outer air and sky; (*c*) number of glass plates and spacing; (*d*) tilt of the glass plates from the horizontal; and (*e*) wind velocity over the top plate.

The first four items are important in all cases. Wind velocity is important for collectors having one glass plate, less so for others. To prevent excessive complications, the relation for prediction of heat loss will be derived for a collector in steady-state operation and having no side losses. The effect of unsteady operation will be considered later; the effect of side losses can be allowed for independently of the present derivation.

The loss from the collector to the bottom glass plate is by radiation and convection. No radiant heat is transmitted through the glass since the latter is opaque to the long wave lengths characterizing radiation from sources at only a few hundred degrees Fahrenheit. The same quantity of heat is transferred through the glass, thence from its top face to the next plate, by radiation and convection. A preliminary calculation shows that thermal resistance within a glass plate is negligible compared with plate-to-plate resistance; consequently, a mean temperature may be assigned to each glass plate. Since air is diathermic to radiation, the loss of heat by convection from a plate to an air space equals the loss by convection from the air space to the next higher plate. The heat flux q_c/A by convection per sq ft of the collector surface to the bottom plate is given by

$$q_c/A = h(T - T_1) \quad [9]$$

where T and T_1 are the temperatures of the collector and the first glass plate, respectively. Convection coefficients h for transfer between parallel tilted plates are given by the relation

$$h = c(T - T_1)^{1/4} \quad [10]$$

where c is a constant dependent upon the tilt (referred to later). The total rate of heat loss q_L/A per sq ft from metal to first glass is then

$$q_L/A = c(T - T_1)^{5/4} + \frac{\sigma\,(T^4 - T_1^4)}{\frac{1}{\epsilon_C} + \frac{1}{\epsilon_G} - 1} \quad [11a]$$

where σ is the Stefan-Boltzmann constant, 0.1723×10^{-8} Btu per sq ft per hr per deg R^4, and the denominator of the second term allows for the effect, on radiant interchange between parallel plates, of the emissivity (and low-temperature absorptivity) ϵ_C of the collector surface and ϵ_G of the glass plate.

The same heat flux q_L/A occurs from the first to the second glass plate

$$q_L/A = c(T_1 - T_2)^{5/4} + \frac{\sigma(T_1^4 - T_2^4)}{\frac{2}{\epsilon_G} - 1} \quad [11b]$$

Similar relations hold up to the top or nth glass plate, but the formulation of the loss q_L/A from the top plate to the atmosphere is different, because convection loss is related to wind velocity and outer-air temperature T_a, and radiation loss is related to the effective radiation temperature of the sky. If, in the absence of adequate data on the latter, one uses air temperature instead, the error in q_L/A is small, particularly if the convection coefficient h_w due to wind is fairly high. Then

$$q_L/A = h_w(T_n - T_a) + \sigma\epsilon_G(T_n^4 - T_a^4) \quad [11\ n + 1]$$

Given the collector temperature and air temperature, there are $(n + 1)$ Equations [11] in $(n + 1)$ unknowns (n unknown glass temperatures $T_1 \ldots T_n$, and q_L/A), and solution for q_L/A is possible. The solution, however, is a very tedious stepwise trial and error, best accomplished by assigning values to q_L/A and T, calculating T_1 from Equation [11*a*], then T_2 from Equation [11*b*], etc., until T_a is found. If the emissivity factor F_ϵ were the same in all Equations [11], and the convection coefficient were always $c(T_n - T_{n+1})^{1/4}$ (even at the outside of the top plate), then the $(n + 1)$ Equations [11] could be added and divided by $(n + 1)$ to give

$$q_L/A = \frac{c}{n+1}(T - T_a)^{5/4} + \frac{F_\epsilon}{n+1}\sigma(T^4 - T_a^4) \quad [12]$$

This relation was used as a guide in seeking another, necessarily considerably more complicated and necessarily approximate, which is free from the restrictions on Equation [12]. Such a relation is

$$q_L/A = \frac{T - T_a}{\frac{n}{c\sqrt[4]{\frac{T - T_a}{n+f}}} + \frac{1}{h_w}} + \frac{\sigma(T^4 - T_a^4)}{\frac{1}{\epsilon_C} + \frac{2n + f - 1}{\epsilon_G} - n} \quad [13]$$

Although this relation may appear to be rather complicated, it is the only one the authors found which fits the exact relations of Equations [11] over the full range of variables one may expect

to encounter in solar collector design, and it is enormously simpler than the solution of simultaneous Equations [11]. The term f in Equation [13] represents the ratio of thermal resistance of the outer plate to that of an average inner plate. Consequently, its value varies with wind velocity as that affects h_w. For values of h_w of 1, 4.07, and 7, corresponding to winds of 0, 10, and 20 mph (18), values of f of 0.76, 0.36, and 0.24, respectively, are recommended. Since the effect on q_L/A of varying h_w and f is rather small for collectors having more than one glass plate, one is justified in using constant values corresponding to a 10-mph wind, which is close to the average for most of the United States.

The adequacy of Equation [13] as a substitute for Equations [11a] to [11 n + 1] was tested over the normal range of variables involved; the maximum difference was 1.8 per cent, the average 1 per cent. When ϵ_C is changed from 0.95 (the emissivity of a normally well-blackened surface) to 0.48 (of interest only if such a surface could be found which were at the same time a substantially perfect absorber of sunlight), the error due to use of Equation [13] may increase to 5 per cent.

Equation [13] involves a constant c from Equation [10] giving the convection coefficient for transfer between parallel tilted plates; and the question arises as to its numerical value. The results of various investigations (19) studying heat transfer from hot plates at temperature T_1 to air at T_a conform to the relation

$$q/A = c'(T_1 - T_a)^{5/4} \quad \ldots\ldots\ldots\ldots\ldots\ldots [14]$$

and are in substantial agreement as to the value of c' for vertical plates, 0.3 when temperature is F. For horizontal plates losing heat upward, the agreement is not good, values of c' varying from 10 to 55 per cent higher than for vertical plates. If one may assume this to hold for the collector system of present interest and to be applicable to transfer both from a plate to air and from the air to the next plate at T_2

$$q/A = c'(T_1 - T_a)^{5/4} = c'(T_a - T_2)^{5/4} \quad \ldots\ldots [15]$$

from which

$$T_1 - T_a = T_a - T_2 = \frac{T_1 - T_2}{2}$$

Then

$$q/A = \frac{c'}{2^{1.25}}(T_1 - T_2)^{1.25} \equiv c(T_1 - T_2)^{1.25} \quad \ldots\ldots [16]$$

Corresponding to the values given for c', c is 0.126 for vertical and 0.139 to 0.195 for horizontal parallel plates. Such a treatment of the problem is hardly justifiable, however, because of the effect of the closed system in changing the air-flow pattern. Fishenden and Saunders (19) have compared the data of various investigators on heat flow across an air gap between vertical plates (enclosed at all edges) and recommend Equation [16] with c = 0.126 (equivalent to c' = 0.3). For horizontal plates they recommend c = 0.16 (equivalent to c' = 0.38) when the spacing exceeds 2 in. Mull and Reiher's data on horizontal parallel plates (19) indicate an increase in heat transfer by convection of 10 per cent when plate spacing is decreased from 2 in. to 1 in. (the value used in the collectors under consideration).

Wilkes (20) on the basis of a more comprehensive experimental study of flow across an enclosed air gap recommends values for c of 0.18, 0.207, and 0.256 for plates which are vertical, tilted 45 deg with heat flow upward, and horizontal with heat flow upward, respectively. Fig. 15 gives values for c recommended by Wilkes, and by Fishenden and Saunders on the basis of experiments of Mull and Reiher.

Since the spread in recommendations for c is considerable and since neither set of experiments corresponded very closely to the present collector design, runs were made with the present collectors to determine heat losses independently of their action as solar-energy absorbers, by operating after sundown. Measuring the heat input to the collector from the water rate and its temperature drop (never more than a few degrees and measured to 0.01 C) and subtracting the bottom loss, the upward heat losses of Table 4 were obtained for collectors tilted 30 deg and covered with three glass panes with 1-in. air spaces. The recorded values of q_L/A were corrected to allow for the fact that, if the entire metal plate had been maintained at water temperature instead of only the lines of contact of the water tubes with the plate, the heat loss would have been about 3 per cent greater. This correction applies in the opposite direction where the collectors are in daytime use, since the metal between parallel water tubes is then warmer than the tubes.

TABLE 4 UPWARD HEAT LOSSES FROM COLLECTORS[a]

t Mean water temperature, F	t_a Air temperature, F	q_L/A Upward heat loss, Btu per sq ft per hr	U (corrected) Over-all coefficient of heat transfer	c Coefficient of Equations [10–13]
163.0	37.2	57.9	0.472	0.164
145.2	41.4	46.2	0.457	0.169

[a] Night runs.

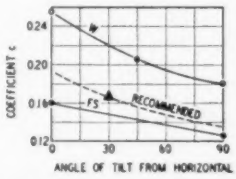


FIG. 15 COEFFICIENT OF CONVECTION c AS DETERMINED BY VARIOUS INVESTIGATORS
(Solid-triangle point calculated from tests of collectors under study.)

To evaluate c from the measured heat flux and Equation [11] or [13], values for ϵ_C, ϵ_G, and h_w must be known. The hemispherical reflectivity of glass for long-wave-length radiation (from a surface of say 140 to 300 F) is close to 4 per cent for all glasses; since glass is opaque to such radiation, the term ϵ_G is complementary to reflectivity, or 0.96. The hemispherical emissivity ϵ_C of the blackened-receiver surface is taken as 0.95, which should be in error by no more than 2 per cent for a well-blackened surface. The outside wind coefficient h_w is assumed to be 4.07 corresponding to a 10-mph wind. A considerable error in this assumption has little effect on a collector with three glass plates. Based on these values and the measured heat flux, the coefficient c in Table 4 was calculated by use of Equations [11]. Equation [13] would have given substantially the same result. The two values obtained are seen to be in excellent agreement. Their mean, 0.166, is plotted as a triangle in Fig. 15, for comparison with previous recommendations. Although the value obtained for c is to some extent dependent upon values taken for ϵ_C, ϵ_G, and h_w, the uncertainty in those values is not enough to explain the difference between the triangle c and the values given by Wilkes. The discrepancy is probably due to difference in plate-to-plate spacing or difference in lateral extent of the individual air chambers.

For collectors of the general design of those described here, it is recommended that values of c be read from the dotted curve of Fig. 15, which follows the trend with tilt of Wilkes's values but differs in absolute magnitude. Although Equation [13], with c from Fig. 15, may now be used for predicting heat losses, it is somewhat cumbersome. It has been used to calculate q_L/A over the normal range of t and t_a to be expected, for collectors tilted 30 deg and provided with one, two, or three glass plates. The results appear in Fig. 16, in the form of an over-all coefficient of heat transfer U for use in the relation

$$q_L/A = U(t - t_a) \quad \ldots\ldots\ldots\ldots\ldots [17]$$

TABLE 5 COMPARISON OF ACTUAL AND CALCULATED PERFORMANCE OF COLLECTORS

Q_U/A = useful heat into water stream, Btu per sq ft (experimental)
Q_B/A = loss through bottom of collector (calculated)
Q_L/A = loss through top of collector (calculated)
Q_A/A = heat absorbed by collector plate (calculated) (should = $[Q_U + Q_B + Q_L]/A$)

Period April 6 to July 1, 1940[a]

Cleanliness of center unit	Q_U/A experimental: Center unit	East unit	Calculated values: Q_B/A	Q_L/A	Q_A/A	Experimental $[Q_U$, East, $+ Q_B + Q_L]/A$	Comparison of: $(Q_A - Q_L)/A$ calculated	$(Q_U$, East, $+ Q_B)/A$
1	5397	5364	433	4279	11143	10076	6864	5797
2	8836	8869	446	4408	14939	13723	10531	9315
3	11009	11023	595	6055	19043	17673	12988	11618
4	7287	7435	369	3718	12360	11522	8642	7804
5	4042	4080	207	2094	6912	6381	4818	4287
Total[a]	36571	36771	2050	20554	64397	59375	43843	38821

Period May 9 to July 1, 1940[a]

Cleanliness of center and west units	Q_U/A experimental: West unit	Center unit	East unit	Calculated values: Q_B/A	Q_L/A	Q_A/A	Experimental $(Q_U$, East, $+ Q_B + Q_L)/A$	Comparison of: $(Q_A - Q_L)/A$	$(Q_U$, East, $+ Q_B)/A$
1	3904	3923	3910	303	3042	7981	7255	4939	4213
2	3575	3592	3587	203	2074	6386	5864	4312	3790
3	9277	9364	9367	519	5301	16439	15187	11138	9886
4	3587	3599	3716	214	2224	6529	6154	4305	3930
5	1099	1136	1173	76	796	2290	2045	1494	1249
Total[a]	21442	21614	21753	1315	13437	39625	36505	26188	23068

[a] Data were not taken on every sunny day during the period. Consequently the "total" is not a measure of total possible heat collection. The top table is based on 69 days data, the lower one on 44.

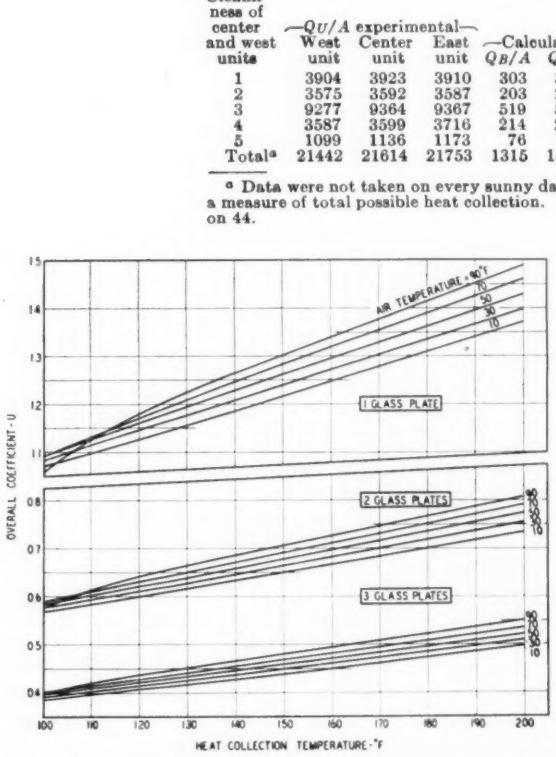


FIG. 16 OVER-ALL HEAT-TRANSFER COEFFICIENT FOR USE IN CALCULATION OF HEAT LOSSES FROM FLAT-PLATE COLLECTORS
(Tilt from horizontal = 30 deg; collector-surface emissivity = 0.95; wind coefficient = 4.07; 10 mph.)

Although this equation and Equation [13] are applicable strictly to a collector plate at a uniform temperature T, they apply with negligible error to the more important case of plate temperature varying continuously from water inlet to outlet, if T is replaced by the arithmetic-mean water temperature. This approximation would be exact if U were independent of T.

The heat loss through the bottom of the collector boxes may be calculated by conventional methods; by use of sufficient insulation it may be made as small as is consistent with the value of the heat saved. In the present installation, bottom losses were minimized to increase the accuracy of determinations of useful-heat collection. Insulation under the blackened plate consisted of an air gap, about 4 in. of glass wool and 1½ in. of mineral wool. For such construction, the heat loss through the bottom is 0.051 Btu per deg F per sq ft per hr. This makes no allowance for insulating value of the roof boards on which the collectors rest or the small air space between the collectors and the roof. However, the value of this air space is offset by the fact that a certain amount of air may circulate through it; and a 20 per cent error in the assumed over-all coefficient introduces an almost negligible error into the calculation of useful-heat collection.

CORRELATION AND INTERPRETATION OF ACTUAL AND CALCULATED RESULTS

With all the terms on the right side of Equation [3] evaluated, the calculated and actual performance of the collectors may be compared. It is to be remembered, however, that the formulation of terms in Equation [3] neglected the effects of dirt on the outer glass panes, shading of the blackened surface by the collector walls, heat capacity of the collectors, and resistance to lateral heat flow in the absorbing surface, which has been treated as a plate at uniform temperature rather than one cooled by attached parallel tubes 6 in. apart. Consequently, the calculated values of heat collection will be high until the quantitative relations given are modified to allow for the foregoing effects.

Table 5 (bottom) shows the results for the period May 9 to July 1, 1940, during which period all three sets of collectors were in operation. Table 5 (top) includes collection back to April 6,

TABLE 6 REDUCTION IN Q_U/A AND $(Q_U + Q_B + Q_L)/A$ DUE TO DIRT ON OUTER-COLLECTOR-GLASS SURFACE

Center and West, glass cleanliness	Reduction in Q_U/A, per cent	Reduction in $(Q_U + Q_B + Q_L)/A$, per cent
1	—0.090	—0.048
2	+0.098	+0.060
3	0.497	0.306
4	3.31	2.00
5	4.73	2.71
Weighted mean	1.03	0.62

1940. During April, only the East and center sets of collectors were in operation. The outside glass on the East collectors was kept clean; that on the others was cleaned only by rain, wind, and snow. Each day was classified as to cleanliness of the glass on the uncleaned collectors. The figures given in Table 5 include hours for which calculation indicated the possibility of useful-heat collection (i.e., $q_A > q_L + q_B$), even though the experimental measurements indicated no net collection (occasional early morning and late afternoon hours).

Table 5 (bottom) indicates that the heat collection by the center unit is slightly higher than by the West unit, neither of which was ever cleaned. The difference, 0.8 per cent, is a measure of the similarity of the units in construction and dirtiness. For grade-

TABLE 7 HEAT QUANTITIES FOR THREE PERIODS USED TO OBTAIN EFFECT OF HEAT CAPACITY

Period	Measured Q_U/A Morning	Measured Q_U/A Afternoon	$(Q_U + Q_L + Q_B)/Q_A$ Morning	$(Q_U + Q_L + Q_B)/Q_A$ Afternoon	Difference, column 5—column 4
1	3645	4225	0.885	0.945	0.060
2	4778	5221	0.903	0.948	0.045
3	3490	4173	0.871	0.957	0.086
Average					0.064

1 cleanliness, all three units may be compared. It is seen that the standard or east unit (always clean) is about midway between the other two, which differ by less than 0.5 per cent.

The effect of dirt on useful-heat collection may be obtained by comparing the mean of the West and center units with the clean East unit. Table 6, second column, shows the effect of dirt on useful-heat collection q_U/A; the third shows the effect on absorption q_A/A, calculated by adding $(q_B + q_L)/A$ to q_U/A. The third column is more readily interpreted since it is a direct measure of the effect of dirt on the transmittance of the glass plates. (Its value is later referred to as D.) The effect of dirtiness on net collector performance, 4.7 per cent maximum and 1 per cent average, is surprisingly small, especially considering the location of the test unit in an industrial district near a power plant and 100 yd from a four-track railroad. Horizontal collectors would probably not self-clean as effectively.

The data in Table 5 may be used to study the effect of heat capacity of the collectors, an effect manifested in an abnormally low useful-heat collection during the morning hours when a portion of the absorbed heat is utilized in bringing the glass plates and the insulation below the collector plate up to equilibrium temperature. A comparison was made of those days on which complete early morning and afternoon records were available (42 days), the days being divided chronologically into three groups of 14 days each. In order to make certain that thermal equilibrium was reached during each morning period, no such period was used of less than 3-hr duration. Morning and afternoon periods were chosen to balance in total number of hours and in total calculated heat absorption Q_A/A to within 1 per cent. Table 7, columns 2 and 3, gives the measured useful-heat collection during the periods. To make the morning and afternoon values for one period comparable, the measured Q_U/A values were increased by the calculated values of heat loss, Q_L/A and Q_B/A, and then divided by

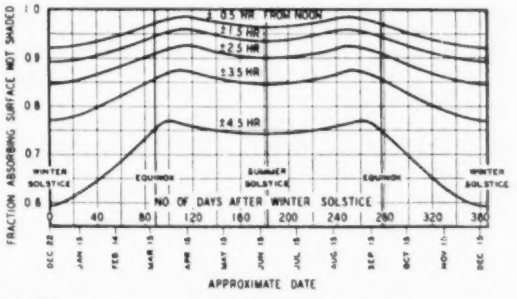


FIG. 17 SHADING EFFECT DUE TO SIDES OF SQUARE COLLECTOR HAVING DEPTH EQUAL TO 9.6 PER CENT OF SIDE DIMENSION, AS IN COLLECTORS TESTED, AND TILTED 30 DEG SOUTH AT 40 DEG NORTH LATITUDE

the respective calculated values of total absorption, Q_A/A. The results appear in columns 4 and 5, their difference in column 6. To obtain the heat lost by storage in the collectors in each period, column 6 is multiplied by the average value of Q_A/A for morning and afternoon. This loss amounts to 420, 378, and 632 Btu per sq ft for the successive 14-day periods, or to 30, 27, and 45 Btu per sq ft per day. By combining the average value 34, with the average difference 94 F between the temperature of heat collection and that of the early morning outside air, one obtains for the heat loss caused by heat capacity, a value of 0.36 Btu per sq ft per day per deg F temperature difference between collector and air. For comparison with this experimental value, the amount of heat stored in 1 sq ft of collector when at equilibrium temperature (calculated from the materials of construction and assuming linear temperature drop both ways from the plate) was divided by the temperature difference between collector and outside air. The resulting value, 0.57 Btu per deg F temperature difference per sq ft is higher than the experimental one. This was expected since the collector plate and glass and insulation surrounding it are preheated by solar radiation during the early morning period preceding the period of heat collection. For the prediction of heat-capacity losses in collectors of other design than those under discussion, it is suggested that the value corresponding to the 0.57 of the present collectors be estimated and then reduced by about one third to allow for early morning preheating. Calling this value C, the heat-capacity loss Q_H/A per sq ft per day is given by

$$Q_H/A = C(t - t_a) \quad [18]$$

The calculation of heat capacity of the present collectors indicates that the glass plates and bottom insulation contribute 52 per cent and 28 per cent, respectively, of the total, and that the copper absorbing surface and tubes attached to it account for but 20 per cent. Although the morning loss due to heat capacity is relatively small in the present collectors, such is not the case in a number of solar hot-water heaters on the market, due to too generous use of metal, large undrained pipes, and insulation of high density.

The calculation of useful-heat collection by Equation [3], with heat loss predicted from Equation [13] (or its equivalent Fig. 16, and Equation [17]), involves the assumption that the collector plate is at a uniform temperature T, whereas, in the collectors here studied, as well as in some of the commercial units, the temperature is at an average value of T only along the lines of contact of the plate with the pipes through which fluid flows, and higher in between. It may be shown that the ratio F of useful-heat collection from the latter system to one having a uniform plate temperature is given by

$$F = \frac{2}{a}\left(\frac{e^a - 1}{e^a + 1}\right) \quad [19]$$

where

$$a = W\sqrt{U'/kM}$$

$U' = U + U_D$

U = over-all loss coefficient, plate to upper air (Fig. 16)

U_D = over-all loss coefficient, plate to box bottom, through insulation

k = thermal conductivity of collector plate, Btu per deg F per ft per hr

W = minimum distance between parallel pipes, measured along collector plate, ft

M = thickness of collector plate, ft

The term F may be thought of as the efficiency of the plate-pipe combination. In the present collectors it has the high value 0.97; in some commercial units, it is considerably lower.

It is now possible to modify Equation [3] to allow for the various complicating factors discussed. The total useful heat Q_U/A collected per sq ft over a period including N days of actual operation is given by

$$Q_U/A = F\Sigma\{(q_A/A)(1 - D)(1 - S) - q_L/A - q_B/A\} - N\,Q_H/A \quad [20]$$

where q_A/A and q_L/A are evaluated as before from Equations [2]

and [13] or [17]; D is the fractional reduction in transmittance of the glass plates due to the presence of dirt; S is a factor to allow for shading of the collector plate by the walls supporting the glass; and Q_H/A is the heat-capacity loss evaluated from Equation [18]. All these terms have been discussed except the shading factor S. The data of Table 5 (bottom) may be used to evaluate it. If data from the East (clean) unit are used, $D = 0$. The total number of test periods $N = 44$. Q_H/A for the period in question averaged 36 (versus 34 given previously). $F = 0.97$. Substituting these values in Equation [20] together with values from Table 5

$$21{,}753 = 0.97\ [39{,}625\ (1 - S) - 13{,}437 - 1315] - 44 \times 36$$
$$S = 0.021$$

This factor, while called a shading factor, is obviously forced to carry the burden of all approximations in the derivations. It will be remembered that the loss of about 3 per cent by internal absorption in the glass panes was assumed a total loss, whereas it is partially effective in supplying the heat losses from the collector plate to the outer air. The true loss by shading is consequently probably more than the value 2.1 per cent (possibly 2.1 + 3/2 = 3.6 per cent), but the treatment of the problem would be enormously complicated by an attempt to make the equations rigorous in this respect.

The expected shading effect may be estimated. Geometrical relations permit construction of the curves of Fig. 17, showing the fraction of an incident beam of direct sunlight which reaches the collector surface directly, the remainder being intercepted by the walls. For the test period in question (Table 5 [bottom] data), the properly weighted average of values read from Fig. 17 is 0.9, indicating an average interception by the white-painted walls of 10 per cent. Of this, perhaps one half finally reaches the collector by diffuse reflection, and part of the remainder is useful in supplying heat losses q_L/A from the system. The residue, perhaps 3 to 5 per cent, is in good agreement with the experimental value of 2.1 per cent, modified upward to almost 4 per cent by consideration of internal absorption in the glass.

That there is no evidence of any unaccounted-for item being necessary to produce a balance is an indication of the quality of the data taken and the adequacy of the relations given for estimating the various losses. The recommendation may therefore be made that Equation [20] be used for the calculation of performance of flat-plate collectors of any desired number of glass plates at any tilt, absorbing heat at any desired water temperature. Evaluation of the terms of Equation [20] involves use of pyrheliometric data, Equations [2], [17], [18], [19], and values for dirtiness D and shading factor S. An average value of 0.006 has been found for D. For the shading factor S a value equal to about 30 per cent of the complement of the average of values read from Fig. 17 is recommended. Equation [20] and the equations giving its components will simplify considerably when restricted in applicability to a particular collector design. In its general form given here, it is useful for disclosing unsuspected causes of poor performance in commercial solar heaters.

Space prevents a discussion of the relative importance of the various terms of Equation [20], beyond pointing out that, as the heat loss q_L/A approaches in magnitude the heat absorbed q_A/A, the useful heat collected is very sensitive to small changes in the operating variables. Application of Equation [20] to the determination of expected performance of solar-heat collectors in various localities and economic studies of the feasibility of solar house heating and absorption refrigeration will constitute the subject matter of later papers of this series.

Nomenclature

A = area, sq ft

C = loss due to heat capacity, Btu per sq ft collector per deg F, temperature difference of collector plate and air, per cycle of operation

c = constant in Equation [10]

c' = constant in Equation [14]

D = fractional reduction in transmittance of glass plate system due to surface dirt

e = natural base of logarithms

F = ratio of useful heat collection by a finned surface to that by a surface of same area maintained at uniform temperature

F_e = factor to allow for emissivity of surfaces in heat-transfer relation, Equation [12]

f = effective thermal resistance of outer glass plate relative to others, Equation [13]. Numerical value = 0.36 for ten-mile wind

H_S = total solar irradiation of a horizontal surface, cal per sq cm × hr

H_D = diffuse irradiation of a horizontal surface, cal per sq cm × hr

h = convection coefficient, plate to plate, Btu per sq ft × hr × deg F, temperature difference

h_w = forced convection coefficient due to wind on top plate, Btu per sq ft × hr × deg F, temperature difference of top glass and air

K = extinction coefficient for total solar radiation through glass, in.$^{-1}$

k = thermal conductivity of collector plate, Btu per sq ft × hr × (deg F/ft)

L = thickness of glass, in.

M = thickness of collector plate, ft

N = number of days or heat collection periods in a long test period

n = number of glass plates (also used as refractive index, but not in equations)

Q = heat quantity, Btu

Q_H = loss, per collection period, due to heat capacity of collector, Btu

Q_U = useful heat collected over a period involving several cycles of heating and cooling, with allowance for dirt on glass, wall shading, heat capacity, and fin effects, Btu

q = rate of heat flow Btu per hr

q_A = rate of heat absorption by collector plate, Btu per hr

q_c = rate of heat transfer between two parallel plates by convection only, Btu per hr

q_B = rate of heat loss through bottom of collector, Btu per hr

q_L = rate of total heat loss through top of collector, Btu per hr

q_U = rate of net useful heat collection by a collector, assuming no losses due to dirt, wall shading, heat capacity, or fin effects, Btu per hr

R = ratio, direct solar radiation falling on tilted surface: same on horizontal surface

R' = ratio, diffuse solar radiation on tilted surface: same on horizontal surface

r = surface reflectivity of glass

S = factor allowing for shading of collector plate by walls

$T, (T_1, T_n, T_a)$ = absolute temperature of collector plate (first glass plate, nth plate, and outer air), deg F + 460 deg.

$t, (t_a)$ = temperature of collector plate (outer air), F

U = over-all coefficient of heat transfer for calculating upward losses from collector, Btu per sq ft × hr × deg F temperature difference of collector plate and outer air

U_D = over-all coefficient for loss through bottom of collector,

Btu per sq ft × hr × deg F temperature difference of collector plate and air below

U' = $U + U_D$

W = distance between water-cooling tubes on collector plates, ft (measured along collector plate, between nearest points)

$\alpha(\alpha')$ = absorptivity of surface of collector for direct (diffuse) solar radiation

β = tilt of collectors from horizontal toward equator, deg

δ = declination of sun, deg; + in summer

$\epsilon_C(\epsilon_G)$ = emissivity and absorptivity of collector plate (glass plate) for low-temperature radiation

θ_T = angle between solar beam and normal to tilted surface

θ_Z = angle between solar beam and normal to horizontal surface = zenith angle of sun

$\rho_1(\rho_n)$ = over-all reflectivity of one (n) plate(s) of nonabsorbing glass

σ = Stefan-Boltzmann constant, Btu per sq ft × hr × (deg R^4)

Σ = summation

$\tau_1(\tau_n)$ = over-all transmittance of one (n) plate(s) of nonabsorbing glass

$\tau_a(\tau_r)$ = over-all transmittance of a system of glass plates, allowing for absorption but not reflection losses (reflection but not absorption losses)

$\tau(\tau')$ = over-all transmittance, for direct (diffuse) sunlight, of a system of glass plates, allowing for absorption and reflection losses

ϕ = latitude

ω = hour angle of sun from solar noon, calc as 15 deg per hr

BIBLIOGRAPHY

1 M. L. Simonin, Revue des deux Mondes, May 1, 1876; "Solar Heat, Its Industrial Applications," by A. Mouchot, Gauthier-Villars, Paris, 1879.

2 "The Sun and the Welfare of Man," by C. G. Abbot, Smithsonian Scientific Series, vol. 2, Smithsonian Institution Series, New York, N. Y., 1934, pp. 196, 203.

3 "New Results on the Utilization of Solar Heat at Paris," by M. H. Mangon, Comptes Rendus, vol. 91, 1880, p. 388.

4 "The Utilization of Solar Energy," by A. S. E. Ackermann, *Journal of the Royal Society of Arts*, vol. 63, 1914–1915, p. 538.

5 "The Sun Motor and the Sun's Temperature," by J. Ericsson, *Scientific American Supplement*, vol. 17, 1884, p. 6727.

6 "Experiments in the Development of Power From the Sun's Heat," by H. E. Willsie, *Engineering News*, vol. 61, 1909, p. 511.

7 "Power From the Sun's Heat," *Engineering News*, vol. 61, 1909, p. 509.

8 "Utilizing Heat From the Sun," by C. G. Abbot, Smithsonian Miscellaneous Collections, vol. 98, no. 5, 1939.

9 "The Utilization of Solar Heat for the Elevation of Water," reprinted from *La Nature; Scientific American*, vol. 53, 1885, p. 214.

10 "Solar Energy and Its Use for Heating Water in California," by F. A. Brooks, University of California Agricultural Experiment Station, Bulletin No. 602, November, 1936.

11 "Review of U. S. Weather Bureau Solar Radiation Investigations," by I. F. Hand, *U. S. Monthly Weather Review*, vol. 65, 1937, p. 415.

12 F. J. Port, Jr., Doctor's Thesis in Chemical Engineering, Library, the Massachusetts Institute of Technology, Cambridge, Mass., 1939.

13 H. H. Kimball, U. S. Department of Agriculture, Weather Bureau Circular Q, no. 1051, 1931; N. N. Kalitin, *U. S. Monthly Weather Review*, vol. 57, 1929, p. 52; N. Shaw, Manual of Meteorology, vol. 3, chap. 4, Cambridge University Press, 1930, p. 139.

14 "A Time Analysis of Sunshine," by F. Benford and J. E. Bock, Trans. Illuminating Engineering Society, vol. 34, 1939, p. 200.

15 "The Principles of Optics," by A. C. Hardy and F. H. Perrin, McGraw-Hill Book Company, Inc., New York, N. Y., 1932, p. 26.

16 "On the Intensity of the Light Reflected From or Transmitted Through a Pile of Plates," by G. G. Stokes, Proceedings of the Royal Society of London, vol. 11, 1860–1862, p. 545.

17 British Building Research Board, Report for 1932, His Majesty's Stationery Office, London, 1933, p. 87.

18 "Heat Transmission," by W. H. McAdams, McGraw-Hill Book Company, Inc., New York, N. Y., 1933, p. 237.

19 "The Calculation of Heat Transmission," by M. Fishenden and O. A. Saunders, His Majesty's Stationery Office, London, 1932, pp. 104–120.

20 "Radiation and Convection Across Air Spaces in Frame Construction," by G. B. Wilkes and C. M. F. Peterson, *Heating, Piping, and Air Conditioning*, vol. 9, 1937, p. 505.

21 "The Characteristics of the Eppley Pyrheliometer," by B. B. Woertz and I. F. Hand, *U. S. Monthly Weather Review*, vol. 69, 1941, p. 146.

Discussion

F. A. Brooks.[6] This work on the utilization of solar energy is most welcome in that it advances the technique of utilizing directly the earth's primary energy and is another step toward saving our natural resources.

The flat-plate absorber is inherently the most efficient thermally but is difficult to make trouble-free over a long life. Possibly the copper tubing (for forced circulation) need not be rigidly soldered to the blackened receiving surface, although this proved necessary in the Carnes design.[7] For thermosiphon circulation, avoiding the troubles of pumps and thermostats, the flat absorber virtually means a flat tank which presents serious staybolt problems if used under city water pressure. Probably the best compromise for the thermosiphon absorber will be a commercial flattened-pipe heat exchanger laid on a grooved metal pan with some nonhardening adhesive for thermal bond.

The most disappointing feature of the fixed solar absorber is its sacrifice of solar energy with inclination of the sun's rays. It would be of interest to investigate the use of twin absorbers, one faced for maximum intake of the morning sunshine and the other for the afternoon. If the two absorbers operated separately the one not effectively exposed probably would not discharge any of the heat absorbed by the other because the diffuse sky radiation would be enough to counteract reverse circulation. Such a dual system would not be the same as a larger single absorber (except at noon time) because higher temperatures would be available in the directly exposed absorber.

For house heating, it would seem advantageous to arrange for the direct entry of the morning sunshine into the living quarters, if adequate reflector shades are provided to prevent overheating. In this case a southeast wall and roof of glass is needed and the construction might well follow the new greenhouse design of the Boyce-Thompson Institute[8] in which no heating other than by illuminating lamps has been found necessary. If direct sunshine is to be used with water-heating absorber pipes under the same roof glass, these pipes should not have wide fins, but the reflector shade might be designed so to surround the pipes that, when closed, all the glass area of sunshine would be utilized by reflection onto the pipes.

The writer's personal acquaintance with the project described is limited to the construction period and initial operation. Therefore, the only direct comments he might offer are that the need for absorber units of low heat capacity to respond quickly in partly cloudy weather is very different in Boston, an unfavorable location for solar heaters, than in the Southwest where one expects to find their most extensive use; and that the installed cost of the storage tank and its insulation is excessive.

---

[6] Agricultural Engineer, California Agricultural Experiment Station, Davis, Calif.

[7] "Heating Water by Solar Energy," by A. Carnes, *Agricultural Engineering*, vol. 13, 1932, pp. 156–159.

[8] "A New Type of Insulated Greenhouse Heated and Lighted by Mazda Lamps," by J. M. Arthur and L. C. Porter, Contributions from Boyce-Thompson Institute, vol. 7, no. 2, 1935, pp. 131–146.

Authors' Closure

Professor Brooks suggests that low heat capacity is a less necessary characteristic of solar absorbers in the Southwest than in Boston where the weather is more variable. Our discussion of "heat-capacity loss" by solar absorbers was perhaps misleading in failing to point out that, even in the variable sunshine of Boston, the operation of a solar-heat collector is generally continuous throughout the day, i.e., if the sun is bright enough to bring the collector up to operating temperature and start the circulating pump, diffuse radiation during subsequent cloudy periods is usually sufficient to prevent the collector temperature from dropping, although the useful transfer rate to the water may of course drop to almost nothing during the passage of a cloud.

The data of Table 5 of the paper indicate a heat collection of about 500 Btu per sq ft per day of operation, or about 400 Btu per sq ft per day, including all days in the period, without regard to operation. (Actual heat collection is slightly greater than indicated by Table 5; for various reasons certain heat collection on Sundays and early morning hours was not included in Table 5.) Storage-tank temperature averaged 153 F for the 3-month period of Table 5, 160 F for the shorter one.

Comparing the heat-capacity loss, 34 Btu per sq ft per day, with the average daily heat collection of about 500 Btu per sq ft per day, we see that heat-capacity loss is less than 7 per cent of the average daily heat collection, when collection occurs at a somewhat higher temperature than that characterizing domestic solar water heaters. Some commercial heaters would probably have 2 to 3 times as high a loss due to heat capacity. The magnitude of the loss per square foot of collector should be the same in California as in Boston; expressed as a fraction of the total heat collected it should, of course, be less in California. The authors believe it probable that many of the California solar heaters have a heat-capacity loss equal to at least 15 per cent of the useful collection.

With respect to Professor Brooks's comments that the installed cost of the storage tank and its insulation is excessive at Cambridge, we believe the paper clearly states that the storage system was not chosen with regard to cost but with the objective of permitting other experimental work than that related to solar house heating. If he refers to storage tanks in general, rather than the one at Cambridge, we can neither agree nor disagree; economic studies are now in process.

A Method for Determining Unsteady-State Heat Transfer by Means of an Electrical Analogy

By VICTOR PASCHKIS[1] AND H. D. BAKER,[2] NEW YORK, N. Y.

The known methods for solving unsteady-state or transient-heat-flow problems in solids are reviewed. The method of solution by means of an electric model is explained. A proof experiment is described. Finally, a permanent model, constructed at Columbia University, is described.

I—Introduction

THIS paper is a continuation of work carried out by the first author, in Europe, on a method first devised by C. L. Beuken (1, 2).[3]

When a solid mass is changing temperature as a result of heat exchange between it and the surroundings, there are variable temperature gradients in the mass, a series of isothermal surfaces, a nonuniform changing temperature field within it, related to the time rate of heat gained or lost by the mass, and a time to attain a steady state. This is known as the unsteady state of heat transfer and may be associated with transfer through the mass into one face and out from another.

Mathematical calculations of the effect of any imposed conditions on a given mass defined by shape, size, and physical properties of its materials have depended on the solution of Fourier's differential equations for this set of conditions. Those cases that can thus be solved with acceptable simplicity are relatively few in number and exclude most of those of industrial importance (3, 4, 5).

The difficulties imposed by the mathematical approach are partially overcome by the graphical method (6). This is based on the replacing of the differential equation by an equation of finite differences, a process sometimes called step integration. The method is, however, tedious and of likewise limited application.

Experimental solution of industrial problems of unsteady-state heat transfer, depending on inserted thermocouples or other thermometric devices and on some means of measuring rate of heat transfer, is difficult, expensive, and often impossible under service conditions.

The method presented here is based on an electrical analogy. Electrical models for the solution of heat problems have long been known (7, 8, 9). Such models have been based on a geometrical similarity between the body subjected to heat flow and the model body. A fundamentally different method is applied here; the model has no geometrical similarity to the body being investigated. Instead it is based on identity in form of the fundamental equations. In this type of model a single electrical installation is susceptible of immediate adaptation to a wide range of heat-transfer problems. The solutions are then rapidly obtained by direct manipulation of instruments.

The permanent model described in section V of this paper is designed primarily for solving problems of unsteady-state heat conduction in solids with definite radiation and convection boundary resistances. Regarding the latter, it is necessary here to assume a definite average value for the ambient temperature. A model adapted to deal fully with problems of radiation exchange between bodies of intricate shape and nonuniform temperatures requires a different design. Such a model has been built by one of the authors (10). Similarly, to deal only with complex steady-state conduction problems, a different design would be better suited.

In what follows, the method will be explained in theory and in practical application to unsteady-state problems. The results of an experiment performed to verify its soundness will be presented, the scope of the heat-transfer situations to which it is adaptable will be discussed, and the permanent electrical installation will be described.

II—Theory of the Method

The method rests on the fundamental similarity between the flow of heat within a rigid body and that of charge in a noninductive electric circuit. Conservation of the scalar quantity, charge, corresponds to conservation of heat. The scalar point function, electric potential, corresponds to the scalar point function, temperature. Ohm's law corresponds to Fourier's law. The concept "electric capacity of a conductor," corresponds to the concept "thermal capacity of a portion of mass."

The method is based directly on the identity in form between the defining equations for thermal and electric resistance, and those for thermal and electric capacity. Thus

$$R_e = \frac{\Delta V}{I} \qquad [1]$$

and

$$R_t = \frac{\Delta t}{q} \qquad [2]$$

where

R_e = electric resistance
R_t = thermal resistance
I = electric current through R_e
q = hourly heat flow through R_t
ΔV = difference in electric potential across R_e
Δt = difference in temperature across R_t

Similarly

$$C_e = \frac{Q_e}{\Delta V} \qquad [3]$$

and

$$C_t = \frac{Q_t}{\Delta t} \qquad [4]$$

---

[1] Research Associate in Mechanical-Engineering Department, Columbia University.

[2] Instructor in Mechanical-Engineering Dept., Columbia University.

[3] Numbers in parentheses refer to Bibliography at end of paper.

Contributed by the Heat Transfer Division and presented at the National Meeting of the Applied Mechanics Division, Philadelphia, Pa., June 20–21, 1941, of The American Society of Mechanical Engineers.

Note: Statements and opinions advanced in papers are to be understood as individual expression of their authors and not those of the Society.

where

C_e = electric capacity
C_t = thermal capacity
Q_e = charge stored in C_e
Q_t = heat stored in C_t
ΔV = rise in electric potential of C_e due to Q_e
Δt = rise in temperature of C_t due to Q_t.

Fundamentally, no other quantities than R_t, C_t, t, Q_t, q, and τ_t are involved in the derivation of the general Fourier heat-conduction equation

$$\frac{\partial t}{\partial \tau_t} = a\left(\frac{\partial^2 t}{\partial x_t^2} + \frac{\partial^2 t}{\partial y_t^2} + \frac{\partial^2 t}{\partial z_t^2}\right) \quad [5]$$

where

τ_t = time in the thermal circuit
$a = \frac{k}{c\rho}$ = thermal diffusivity
c = heat capacity per unit mass
k = thermal conductivity
ρ = density
t = temperature at point (x_t, y_t, z_t) at time τ_t.

The distribution of resistance and capacity in space, assumed in the Fourier equation to be uniform and continuous, is represented by the space coordinates x_t, y_t, z_t.

It follows from this identity in form of the fundamental defining equations that all mathematical developments based upon them, respectively, will likewise be identical in form. Thus, take the case of one-dimensional flow. In heat transfer this amounts to conduction across an infinite slab or along a rod insulated at the sides. There Fourier's equation reduces to

$$\frac{\partial t}{\partial \tau_t} = a\frac{\partial^2 t}{\partial x_t^2} \quad [6]$$

where

x_t = distance along the heat flow path
t = temperature at distance x_t at time τ_t.

In electricity the corresponding case is that of flow along an ideal "R_eC_e-cable." This is a linear conductor insulated at the sides and with resistance and capacity uniformly distributed along its length, but of negligible inductance. It is to be noted that there is no thermal analogue to inductance; hence, an electric circuit to be analogous must be noninductive. Here the well-known equation applying to transient phenomena is

$$\frac{\partial V}{\partial \tau_e} = \frac{1}{R_eC_e}\frac{\partial^2 V}{\partial x_e^2} \quad [7]$$

where

τ_e = time in the electric circuit
R_e = distributed resistance per unit length of cable
C_e = distributed capacity per unit length of cable
x_e = distance measured along the cable
V = electric potential at distance x_e and time τ_e.

Clearly [6] and [7] are identical in form; V replaces t, and $\frac{1}{R_eC_e}$ replaces a.

Then to represent a one-dimensional heat-conduction problem by an electric circuit, the following procedure applies. Express the various quantities R_t, C_t, q, t, and x_t and τ_t for the thermal circuit in any desired consistent system of units. Choose a consistent system of units (not necessarily the same) for R_e, C_e, I, V, x_e, and τ_e in the analogous electrical circuit. Then make $x_e = x_t$ and divide the thermal circuit into elements of Δx_t length, and the corresponding R_eC_e cable into an equal number of elements of length Δx_e. Give every element Δx_e the same number of units of electric resistance R_e and electric capacitance C_e, as the corresponding element Δx_t has units of thermal resistance R_t and thermal capacitance C_t. It is not necessary that the thermal path be of uniform cross section or that the elements Δx_t be equal. Then by Equations [1], [2], [3], and [4], or [6] and [7] all readings for V and I taken in the cable at points defined by x_e and τ_e will be numerically equal to the values of t and q in the thermal circuit at points defined by x_t and τ_t, for $x = x_t$ and $\tau_e = \tau_t$.

III—Practical Application of the Method

Since R_e and C_e occur in Equation [7] only as the product R_eC_e, the result will not be affected by changing R_e and C_e individually, provided their product is not changed. Thus C_e may be reduced to $\frac{C_e}{m}$ if R_e is correspondingly increased to mR_e. Moreover, m may have any convenient value. Also, since Equation [7] is homogeneous in V, V may be replaced by $l\,V$ without affecting anything else. It is evident from the dimensions in Equation [7] that, if R_eC_e is replaced by nR_eC_e, or $n(mR_e)\frac{C_e}{m}$ and τ_e is replaced by $n\tau_e$, the form of the solution will not be altered.

Equation [1] implies that if ΔV is thus replaced by $l\Delta V$ and R_e is replaced by nmR_e, I will be replaced by $\frac{lI}{nm}$. Similarly, Equation [3] implies that if ΔV is thus replaced by $l\Delta V$ and C_e is replaced by $\frac{C_e}{m}$, Q_e will be replaced by $\frac{l}{m}Q_e$.

By suitable choice of the scale factors, m, n, and l, the electric model may be operated at convenient voltages and transient time intervals and built with feasible magnitudes of resistance and capacitance. The possibility of changing the time scale is of paramount importance for the practicability of the method. A heat process actually taking hours or days may be condensed to a few minutes in the experiments. On the other hand, a short process requiring only fractions of a second may be stretched in the model so as to last several minutes; thus times are achieved which allow easy reading of instruments.

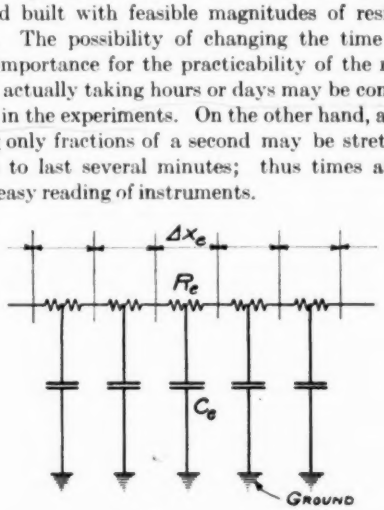


FIG. 1

In practice the R_eC_e-cable is replaced by a "lumped" cable. This amounts to replacing the resistances and capacitances of elements Δx_e by resistors in series and corresponding condensers in parallel, as indicated in Fig. 1. The smaller the "lumps," Δx_e, the more perfect will be the representation of the actual cable by the lumped cable. A feasible compromise is usually possible in practice.

This "lumping" procedure is a standard technique in electrical engineering, used when it is desired to represent an actual cable by a laboratory model (11). The number of sections required depends on the desired accuracy and the dimensions and properties of the body to be investigated. In this respect the model

method does not differ from the graphical method (6). Both are based essentially on the idea of replacing a differential equation by an equation of finite differences.

In a somewhat similar manner any three-dimensional heat-conduction problem may be represented by an electrical model. In this, the general case, the thermal capacity C_t of each volume element $\Delta x_t\ \Delta y_t\ \Delta z_t$ is replaced by a condenser and the three orthogonal components of thermal resistance are replaced by three electric resistors, as indicated in Fig. 2.

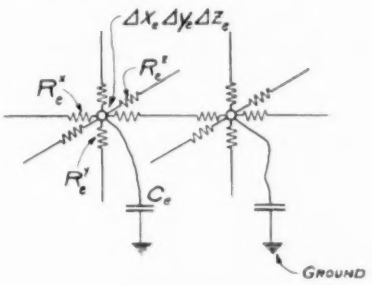


FIG. 2

Radiation and convection surface boundary resistances may be represented by electric resistors R_e without any corresponding condensers.

When the surface temperature differs by a large amount from the ambient temperature, the surface boundary resistance may be a fairly rapid function of temperature. This requires that the corresponding electrical resistor repeatedly be adjusted in magnitude during the period of an experiment. A similar degree of adjustment is required more generally, owing to variations in k and c with changing temperature.

A practical difficulty in applying this method to three-dimensional problems lies in the vastly increased number of resistors required. This implies, in addition to the added expense for equipment, an important increase in manipulation difficulties. The latter is particularly serious in the case of changing thermal resistance when this large number of resistors must repeatedly be adjusted in magnitude during the course of an experiment.

IV—Preliminary Experiment

In order to verify the theory and to determine the practicability of the method, a trial experiment was performed in the laboratory at Columbia University. A problem was selected for which actual thermal test data were available. The apparatus was built from such equipment as happened to be obtainable in the Columbia laboratories at the time. The problem may be stated thus:

A steam pipe line, $1^1/_4$ in. nominal diameter, is covered with cork insulation of 1.4 in. thickness. The inside of the pipe is suddenly raised in temperature from 88 F to 211 F by admitting steam. What will be the temperature distribution in the insulation as a function of time for a given time cycle of turning on and off the steam? What will be the heat loss compared to that for a continuously hot pipe?

Actual measurements of the temperature-time functions were made for this case by Perry and Berggren at the University of California. Thermocouples were inserted at various depths in the insulation. Steam was suddenly admitted and the several temperature rises were noted. The results are shown plotted in Fig. 5. It was found, however, that owing to the thermal capacity of the steel pipe, the temperature rise at the inner surface of the cork was subject to some lag. This lag is shown in Fig. 3. The heat loss was not measured.

The physical properties of the cork insulation must be known to solve this problem by means of the electric model. These are given by Perry and Berggren as follows:

Thermal conductivity k = 0.025 Btu per ft per F per hr

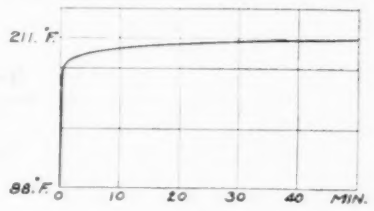
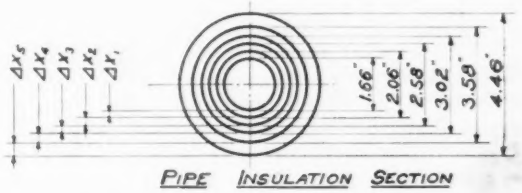


FIG. 3



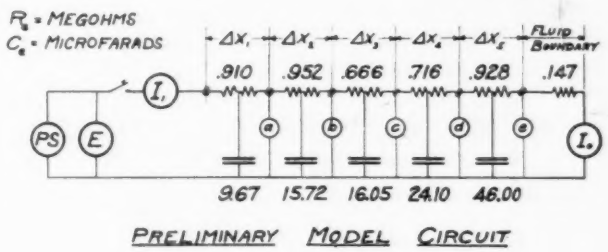


FIG. 4

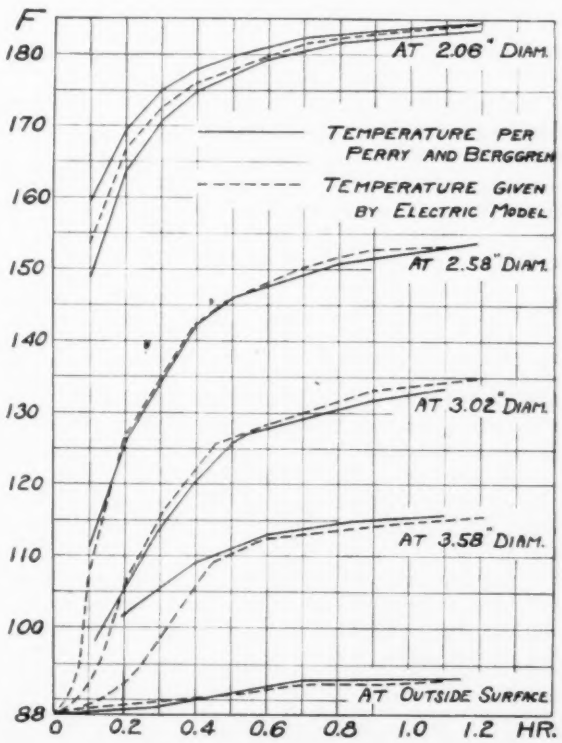


FIG. 5

Specific heat $c = 0.485$ Btu per lb per F
Density $\rho = 8.15$ lb per cu ft
Thermal diffusivity $a = 0.00633$ ft² per hr

The fluid boundary conductance on the outer surface may be deduced from the steady-state conditions as observed by Perry and Berggren. Here, the hourly heat flow through the insulation must equal the heat flow from the outside surface to the surroundings. The former may be computed from the radii, physical properties, and the temperature drop in the insulation. Perry and Berggren give the latter as 118.8 F for steady state. Assuming the ambient temperature to be 88 F implies 4.2 F drop from the outer surface to the surroundings. From these data the surface boundary conductance U is computed to be $3.85 \frac{\text{Btu}}{\text{ft}^2\ \text{F}\ \text{hr}}$. However, U will vary as the outer surface temperature varies.

In setting up the electric model the standard electric units were chosen. Thus R_e is in ohms, C_e is in farads, Q_e is in coulombs, V is in volts, I is in amperes, and τ_e is in seconds.

The usual thermal units are retained. Thus R_t is in F hr per Btu; C_t is in Btu per F; Q_t is in Btu; t is in F; q is in Btu per hr; and τ_t is in hours.

Preliminary trials suggested the following values for the scale factors:

$l = 2$ means: 2 volts in the electric circuit correspond to 1 F in the thermal circuit

$n = 200$ means: 200 sec in the electrical circuit correspond to one hour in the thermal circuit

$m = 0.329 \times 10^4$.

Then the numerical value of the thermal resistance in hr F/Btu for any element Δx_i in the thermal circuit must be multiplied by $nm = 0.658 \times 10^6$ to obtain the number of ohms to use for the corresponding resistor in the electric model. Similarly, the numerical value of the thermal capacity in Btu per F for any element Δx_i in the thermal circuit must be multiplied by $\frac{1}{m} = \frac{1}{0.329} \times 10^{-4}$ to obtain the number of farads to use for the corresponding condenser in the electric model.

Then by Equation [1] multiplying ΔV by factor $l = 2$ and multiplying R_e by factor $nm = 0.658 \times 10^6$ results in multiplying I by factor $\frac{l}{nm} = 3.04 \times 10^{-6}$. Thus 3.04 microamperes in the electric model will represent an hourly heat of 1 Btu per hr in the thermal circuit.

Similarly, by Equation [3], multiplying ΔV by factor $l = 2$ and multiplying C_e by factor $\frac{1}{m} = \frac{1}{0.329} \times 10^{-4}$ results in multiplying Q_e by factor $\frac{l}{m} = 6.08 \times 10^{-4}$. Thus 6.08×10^{-4} coulombs in the electric model will represent 1 Btu in the thermal circuit.

In order to effect the actual set-up of the electric model, the insulation on the steam pipe was divided into five layers or tubes, so chosen as to conform to the positions of the thermocouples in Perry and Berggren's work. The thermal capacity of each of these tubes was computed in Btu per F from the dimensions and the physical constants. Similarly, the thermal resistance of each tube for radial heat flow was computed in F hr/Btu. Then the number of farads and ohms to use in corresponding condensers and resistors in the electric model were obtained by multiplying these by $\frac{1}{0.329} \times 10^{-4}$ and 0.658×10^6, respectively.

The fluid boundary resistance was represented by a single resistor. Variations with temperature are neglected as being small in comparison with other resistances in series.

TABLE 1

Time "on" / Time "on" + time "off"	Cycles per 24 hr: "On" time = 1/2 hr	Cycles per 24 hr: "On" time = 1 hr	Loss in Btu per lineal ft of pipe per cycle: "On" time = 1/2 hr	Loss in Btu per lineal ft of pipe per cycle: "On" time = 1 hr	Loss in Btu per lineal ft of pipe per 24-hour period: "On" time = 1/2 hr	Loss in Btu per lineal ft of pipe per 24-hour period: "On" time = 1 hr
0.2	9.6	4.8	18.4	29.8	176.7	143.0
0.4	19.2	9.6	16.1	28.2	309.1	270.7
0.6	28.8	14.4	13.6	25.2	391.7	362.9
0.8	38.4	19.2	11.4	22.4	437.8	430.1

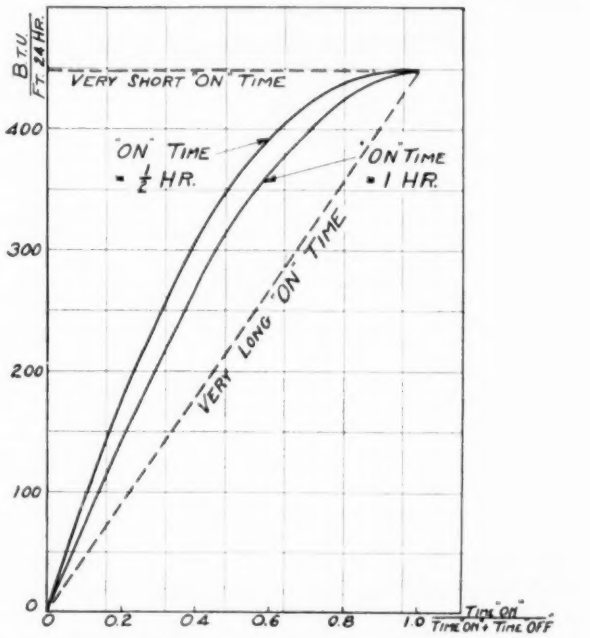


FIG. 6 HEAT LOSS FROM STEAM PIPE UNDER INTERMITTENT LOADING

The subdivision of the insulation and the corresponding circuit used in the electric model are shown in Fig. 4.

In taking data on the model it was found to be feasible to regulate E manually to simulate the actual temperature rise on the inner surface shown in Fig. 3. The readings in volts on the voltmeter E and on the electrostatic voltmeters a to d, Fig. 4, must be divided by two to give degrees Fahrenheit. Similarly, the readings in seconds on the stop-watch must be divided by 200 to give hours. After being thus converted back to thermal units, the results are plotted in Fig. 5. The curves representing the actual measurements made by Perry and Berggren are plotted superposed, upon those obtained with the electric model.

It is evident from Fig. 5 that the two sets of curves nearly coincide. Discrepancies may be attributed in part at least to two causes not inherent in the method. First, the difficult character of the measurements made by Perry and Berggren indicates that their data may be subject to appreciable error. Second, it was noted in the foregoing that the preliminary model was made of apparatus of varying quality such as happened to be available about the laboratory. Also, variations of resistances with temperature have been neglected.

The close check obtained in this trial experiment may be regarded as substantial evidence for the soundness of the principles on which this method is based. The experiment proves that the manipulation of the electric apparatus is practicable for problems of at least this degree of difficulty.

The electric model was also used to measure the heat loss from the steam pipe, not only in steady state, but also for periodic applications of steam. This is a practical problem. Perry and Berggren did not attempt to do this.

The procedure was as follows: Voltage was applied to *PS*, Fig. 4, for the "steam on" periods. The voltage was "switched off" at *PS* for the "steam off" periods. The current was read at I_b, Fig. 4, at intervals of 10 sec. This was continued until the current-time curves for successive cycles were identical. The values of the current in microamperes were then divided by 3.04 to give the heat flow from the outer surface to the surroundings in Btu per hr. Readings on the stop-watch in seconds were divided by 200 to give the time in hours. From the periodic plots of heat flow against time the total heat loss in Btu over a 24-hour period was computed. The results for various types of cycle are given in Table 1 and Fig. 6.

V—Permanent Apparatus

A permanent electric model, as indicated in Fig. 7, has been erected at Columbia University. This model differs from the original model of Beuken (1) by many modifications and improvements. The most important of these are arrangements for changing the capacity during the experiments and for automatically recording the voltages. The whole electrical and mechanical design has been changed. Nothing is retained but the basic idea.

This model contains 525 condensers, divided into 15 equal groups. One group is intended for each section of the model, representing C_i for Δx_i or $\Delta x_i\ \Delta y_i\ \Delta z_i$ in the one- and three-dimensional flow, respectively. The condensers range in size from 0.1 μf to 20 μf, in such a manner as to make the capacity of any section available in steps of 0.1 μf. The total capacity is 2280 μf or 152 μf per section. A number of reserve condensers bring the total available capacity to more than 2400 μf. All condensers are accurate to within plus or minus one per cent. Owing to the high resistance of the circuits ordinarily used in the model, high insulation resistance in the condenser is of paramount importance. All condensers have at least 15,000 megohms per microfarad insulation resistance.

The condensers in each section are assembled on six trays. Each tray has a plug board to which one terminal of each condenser is connected. The other terminal is grounded. Each tray is a self-contained unit, which can be withdrawn from the frame for cleaning and inspection. Each section has its own switchboard, resistor board, and bus plugboard.

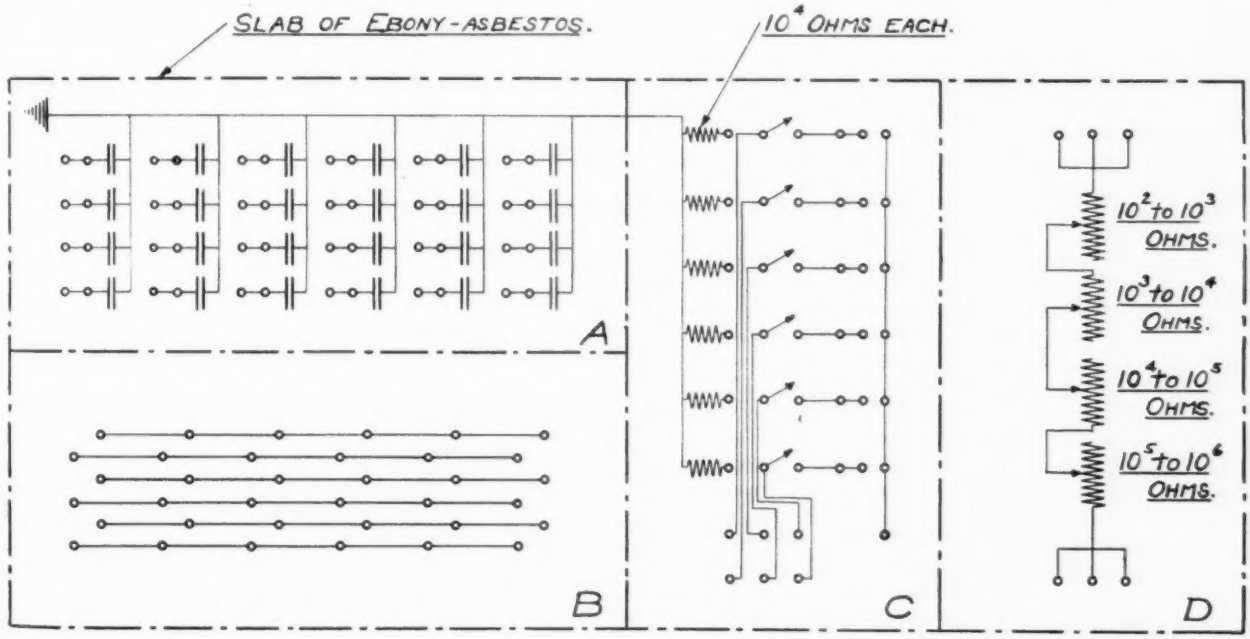
The condensers may be combined into six groups by means of flexible plug leads connecting the plugboards on the trays to the bus board. If necessary, condensers of one section can be connected to the bus board of another section. Each bus board contains six buses with a number of jacks (outlets). The six busses lead to six single-pole double-throw knife switches. In one position these knife switches connect to jacks on the resistor board. In the other position they ground the busses, and therewith the condensers connected to these busses.

The resistor boards contain four decade resistors each, which together yield any resistance value from 100 ohms to 1,111,000 ohms in steps of 100 ohms. The resistor boards can be connected by plugs and flexible leads to the busses coming from the condensers.

Ten busses run along the top of the installation of resistor and condenser sections. Their purpose is to make possible plugging in any of the instruments on any one of the sections. Furthermore, condensers and resistors can be interchanged in the different parts of the model.

A central instrument panel contains the power controls and all of the instruments.

Power supply is provided through a "regulated power" unit. When plugged in on an ordinary 110-volt alternating-current



A = 152 M.F. IN 6 CONDENSER TRAYS.
B BUS PLUGBOARD.
C = SWITCHBOARD.
D = RESISTOR BOARDS.

NOTE - SECTIONS ARE SERVED BY 10 BUSES NOT SHOWN.

Fig. 7 Wiring Diagram of One Section of Electric Model (15 Sections Available)

outlet, this unit furnishes a practically constant direct-current output, the voltage of which can be set at any value between 130 volts and 286 volts. A voltage divider (bleeder resistor) is provided to extend the range of voltage from 130 volts down to zero. It is possible to vary the voltage to correspond to changing temperatures in the thermal circuit.

A current regulator (constant-current device) is also provided. By means of electron tubes any current value between 0.1 ma and 30 ma can be set and maintained constant throughout an experiment, regardless of apparent changes in resistance resulting from the loading of the condensers.

Since the total current dealt with is small, the voltmeters must not draw more than an exceedingly small current. On the other hand, recording instruments are desirable in order to cut down

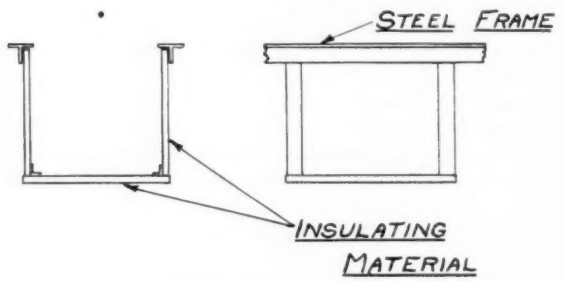


FIG. 8 INSULATING SUPPORTS

necessary assistance. Electrostatic voltmeters, which would satisfy the first condition, are ruled out by the second.

To satisfy both conditions, four two-stage amplifiers have been devised, which operate on two double-point recording millivoltmeters. Each millivoltmeter measures the voltage drop across a 100-ohm resistor and is calibrated in milliamperes. The current drawn from the model circuit by the amplifier is less than 10^{-9} amperes. This current may be neglected as compared with the leakage currents through the insulation in other parts of the model. Input voltage and current are measured by standard instruments.

In nearly every experiment need arises to determine total heat input. In the model this is represented by total charge in coulombs. To measure the total charge an ampere-hour meter is required. Because of the very small current values involved (0.03 amp and smaller) and the very short time intervals (only a few minutes) no standard instrument could be used directly. Hence an amplifier is provided. Because voltage amplification is easier than current amplification the current to be measured is passed through a resistance and the voltage drop is amplified. The amplifier used is that described by Treviño and Offner [12]. A volt-minute meter then accumulates a reading which is readily converted into total charge in coulombs.

The accuracy of the electric model method depends largely on the insulation resistance of the condensers and boards against the common ground. The resistors in the model are, generally speaking, connected in series. Hence the total resistance of the model is high, possibly more than 15 megohms. On the other hand the leakage paths are in parallel. Hence the total leakage resistance becomes only a fraction of the resistance of one leak.

Condenser leakage is kept at a minimum by use of condensers with insulation resistance of at least 15,000 megohms per microfarad. The leakage of the boards was reduced by permitting no board to be fastened directly to the steel frame. All boards are fastened by means of insulating slabs as shown in Fig. 8.

ACKNOWLEDGMENTS

The authors wish to express their gratitude to Dr. T. H. Chilton of E. I. du Pont de Nemours & Co., Wilmington, Del., and Prof. T. B. Drew of Columbia University, for making available the tests of Perry and Berggren; to Dean J. W. Barker, Prof. C. E. Lucke, and Prof. Geo. B. Karelitz of Columbia University, for their support of this project; to Dean J. W. Barker for the idea of the electronic voltmeter; to Dr. E. J. Williams, Leeds & Northrup Co.; and H. L. Anderson physicist, Columbia University, for the design of the amplifier for the voltmeter; to Prof. C. J. Russell for the design of the constant-current device and for frequent advice; to Prof. J. H. Dunning for assistance with the ampere-minute meter; and to Prof. W. A. Curry and Dr. M. Avrami for advice and analysis.

BIBLIOGRAPHY

1 In *Economish Technish Tijdschrift*, C. L. Beuken, Mastricht, Netherlands, 1937, no. 1.

2 "Die Berechnung der Durchwärmungszeiten von Gutstuecken auf Grund der relativen Mindertemperatur," by V. Paschkis and C. L. Beuken, *Elektrotechnik und Maschinenbau*, vol. 56, no. 8, 1938, pp. 98–100.

3 "Mathematical Theory of Conduction of Heat in Solids," by H. S. Carslaw, The Macmillan Co., New York, N. Y., 1921.

4 "Industrial Heat Transfer," by Alfred Schack, translated by Hans Goldschmidt & E. P. Partridge, The J. Wiley and Sons, Inc., New York, N. Y., 1933.

5 "Durchwärmezeit von Werkstücken in Industrieöfen," by V. Paschkis, *Archiv für Wärmewirtschaft und Dampfkesselwesen*, vol. 12, 1931, p. 356.

6 In "August Foeppl Denkschrift," by E. Schmidt, 1924, p. 179. The method is discussed in "The Calculation of Heat Transmission," by M. W. Fishenden and O. A. Saunders, H. M. Stationery Office, London, 1932.

7 "Flow of Heat Through Furnace Walls," by I. Langmuir, E. Q. Adams, and F. S. Meikle, Trans. American Electrochemical Society, vol. 24, 1913, pp. 53–84.

8 "Elektrische Modellversuche zur Loesung Waermetechnischer Aufgaben," by F. Bruckmayer, *Archiv. für Wärmewirtschaft und Dampfkesselwesen*, vol. 20, no. 1, 1939, pp. 23–25.

9 "Un Modello elettrico per lo studio dei campi termici dei sistemi di riscaldamento a turbi immersi nelle murature," by B. Finzi-Contini, *Il Politecnico*, vol. 85, 1937, p. 291.

10 "Elektrisches Modell zur Verfolgung von Waermestrahlungsvorgaengen, insbesondere in elektrischen Oefen," by V. Paschkis, *Elektrotechnik und Maschinenbau*, vol. 54, 1936, pp. 617–621.

11 "Heaviside's Electric Circuit Theory," by Louis Cohen, 1928, McGraw-Hill Book Co., Inc., New York, N. Y.

12 "An A.C. Operated D.C. Amplifier With Large Current Output," by S. N. Treviño and F. Offner, *Review of Scientific Instruments*, 1940, p. 412.

Discussion

J. A. DOYLE.[4] The interesting technique described by this paper holds promise of practical usefulness by meeting a need in industrial-heating practice involved in production of metal, ceramic, and chemical products.

In this field, the viewpoint of the engineer, relative to the rate at which heat *can* be transferred should be subordinate to that of the metallurgist, ceramist, or chemist in determining the rate at which heat *should* be transferred in heating and cooling a given product made from a given material.

Time and rate of heat transfer are equally as important as temperature in such practice because of the influence of both on the structure and uniformity of the ultimate product.

Each of these essential product requirements is of interest to the engineer. Too frequently he is embarassed by failure actually due to disregard of the important time and rate factors but attributed to some other cause.

Typical examples include the striking and repeated failure of large reduction gears on merchant ships during the previous world war; unfavorable effect of variations due to mass methods

[4] Vice-President, W. S. Rockwell Company, 50 Church Street, New York, N. Y.

of heating and cooling in annealing steel and malleable-iron castings; brass, copper, and steel products; forgings, etc. Age-old variations in structural-clay products are matters of common knowledge.

The importance of mass phenomena, in heating and cooling, is not generally sensed in commercial practice. This is indicated by the fact that a piece of carbon steel 1/2 in. diam, after quenching, may have a surface hardness of 600 Brinell; but a piece of the same steel 6 in. diam, subjected to the same treatment, may have a surface hardness of but 250 Brinell. The hardness tends to decrease as the mass increases, unless the rate factor varies accordingly.

Mechanical-property values in the handbooks may be misleading, if they are based on tests of smaller sections, but give no indication of allowance for variation incident to the mass effect in heat-treatment.

The cooling phase of the problem is frequently more critical than the heating phase, particularly with irregularly shaped products, because of the inverse relation of time and rate factors in comparison to the heating phase.

This relation may be in the ratio of hours and minutes, or even seconds. It is illustrated by the difference in time and rate of cooling metal products of equivalent mass, shape, and weight in annealing, normalizing, strain-relieving, tempering, and hardening by quenching. Similar relations exist in drying, burning, and cooling ceramic and chemical products.

The problem of heat transfer that confronts the metallurgist, concerned with various products of different physical characteristics, is much more complex than the problem as it usually confronts the engineer.

It is comparatively simple with relatively static conditions affecting heat transfer through insulation, refractories, metals, and other materials; or with equipment such as boilers, furnaces, prime movers, and transmission or other operating mechanisms.

Yet, the metallurgist has relatively few basic heat-transfer data as a foundation for his effort to determine the time and rate at which his products should be heated and cooled, even though he may understand the effect of heating and cooling on the material from which the product is made. That he should have such data is apparent to the engineer concerned with selection and use of metal products.

A fundamental defect in industrial-heating practice is the time-worn error of basing heat-treating shop specifications on a given material, without reference to physical structure and uniformity of products made from that material in the process of heating and cooling.

Essential factors, such as the method of heat transfer to and from the surface of the product, the method of loading the furnace, and the time, rate, and uniformity of such transfer, in heating and cooling, are usually left to the judgment of the furnace operator.

Naturally, the products frequently vary with the operatives in the same plant or in different plants producing similar products, even though the pyrometer records may be uniform. The several industries are loath to admit this because of shortsighted commercial policy, and the inertia that resists change until economic pressure forces improvement.

It has always been so and will so continue, unless and until the principles of heat transfer are better understood and effectively applied in shop practice.

Shop specifications should indicate a preferred method of controlling the operation of heating and cooling to guide the furnace operatives in producing products as uniform as the pyrometer chart indicates them to be.

Many improvements in heating practice have been effected in recent years that will decrease the great waste of metal products in the last war, but there is still much need for improvement. It will be effected in proportion as the engineer insists on higher standards of quality and uniformity in the product itself.

As reference to these vital factors is conspicuous by its absence in the literature of the several arts, and rarely referred to in production specifications, the method described by the paper may be of value in determining basic physical factors of heat transfer which, in turn, may serve as a basis for better specifications of the product itself.

The problem of uniformity is of acute interest at the moment because of the defense program. It is a fact that our armed forces have never been provided with ordnance matériel of desired uniformity. It is a physical impossibility to produce uniform products with the mass methods of heating and cooling which have been in vogue for generations. They represent more in the form of industrial folklore than rational technical development. Much of it is still in practice and condoned today by technical experts on the false assumption that a uniform pyrometer chart is proof of a uniform product.

For this reason, the procedure described by the paper is likely to be appreciated by those concerned with the use of heat-treated metallurgical, ceramic, and chemical products if, as, and when its merit is understood and publicized.

The authors, Columbia University, and this Society have rendered a constructive service in this presentation outlining accomplishment to date.

M. H. Mawhinney.[5] Without attempting to discuss the details of the method of heat-transfer determination described, it would appear to simplify greatly at least part of the unsatisfactory approach by mathematical calculation to the solution of problems in heat transfer. Tedious calculation is eliminated, but the necessity for the assumption of varying physical constants remains, which is the other weakness of the mathematical method. Assumptions of such constants by cut-and-try methods are possible, however, where a high-speed method is available for using them, and the way is paved for developments which are now retarded if not prevented by the necessity for so much effort.

The writer is primarily interested in the practical application of the method to the problems of industrial-heating-furnace design, and offers the mild criticism that the discussion of "the scope of the heat-transfer situations to which it (the method) is adaptable," which is promised in Part I fails to materialize in the remainder of the paper. Perhaps this can be remedied in the authors' closure.

The possible applications to which the method would seem to be adaptable are heat transfer through furnace linings, retorts and muffles of alloy and refractory, radiant-heating tubes, and gas-burner steels and cooling wells. The most important of these is the heat absorption of furnace linings, because the knowledge of this value and its variation with time from lighting the furnace is essential to calculations of fuel consumptions. "Steady-state" conditions are seldom reached, and, therefore, "unsteady-state" conditions are most commonly encountered. Such information is also of importance in evaluating the modern light refractory linings now used in industrial furnaces to reduce heat absorption.

A complication of this problem is the fact that furnace walls are almost always a combination of refractory and insulation. The writer would, therefore, appreciate a statement concerning the complications which this introduces into the electrical method described.

An article by the writer discussed this subject in some detail, and described the results of experimental determination in the

---

[5] Consulting Engineer, Salem, Ohio. Mem. A.S.M.E.

case of a furnace wall made up of 13½ in. of firebrick and 2½ in. of silocel insulation.[6] The inside of the furnace was held at 1700 F, and temperatures at various depths in the wall were determined by thermocouples for a period of 10 hr. Since at least 30 hr are required to approach a steady state, the variations in the first 10 hr are in the unsteady state for which the electrical method was devised.

Such a test is of strictly practical value, since it includes not only a combination of refractories in the wall, but also the effects of joints between bricks and other variables. A check of such tests, reported for industrial furnace walls by this electrical method, would be of great interest to furnace engineers.

In conclusion, the writer urges the application of this method by the authors of this interesting paper to further determination of heat flow in furnace walls of different thicknesses of firebrick and light brick, each with various thicknesses of insulation.

Authors' Closure

Mr. Doyle's statements are more timely today than when first given. The present war situation makes every waste detrimental to national interest; and waste must result, if heat-treatment and forging are carried out without due consideration of the problem of temperature uniformity in the individual piece. Referring to a previous paper[7] by Mr. Doyle on the relation of uniform pyrometer records to uniform products, the relation illustrated in his paper, which is given qualitatively, may in many instances be determined quantitatively by the authors' method.

Mr. Mawhinney's remarks may be summed up in four points, which will be answered separately:

1 The necessity of assuming the physical constants for evaluating a problem is not eliminated.

This is true. However (as Mr. Mawhinney himself indicates) the method offers the possibility of running a test on a certain problem with various physical constants. Thus the relative influence of the different constants on the result can be ascertained. This procedure is considered to be of considerable importance, because of the ease with which it shows the influence.

2 The scope of the heat-transfer situations to which the method is applicable is not outlined in the paper.

A complete list of applications would be too long, and probably incomplete, as well. The following applications, however, suggest themselves. In each of these applications, the model method can yield answers to the following questions:

a What is the temperature change and lapse of time on the hot or cold surface or at any point within the body (temperature differentials; temperature distribution in the body)?

b What is the quantity of heat stored or lost in any interval of time after the beginning of the thermal-time cycle?

c In order to select the material best suited for any job, the tests with the model may be repeated, changing systematically the physical properties. This type of investigation can serve (*a*) to select one of a number of available materials; (*b*) to find the desired properties of a material to be developed for a certain purpose.

The applications are as follows:

(1) *Metal Heating.*
- (*a*) Heat-treatment (heating, quenching, annealing).
- (*b*) Cooling conditions in casting.
- (*c*) Heating for the change of form (rolling, forging).

(2) *Metal Melting.* Conditions in molten baths and containers (open hearth, aluminum).

(3) *Glass and Ceramics, Including Refractories.* Glass-melting tank, glass cooling and annealing, temperature distribution in ceramic bodies in kilns.

(4) *Chemical Industry.* Heating of material.

(5) *Industrial Furnaces.* Walls of intermittently operated furnaces; regenerator design and operation.

(6) *Building Walls.* Heating and cooling load of houses, ships, vehicles.

(7) *Refrigeration.*

(8) *Food Industries.* Canning industry; necessary heating and cooling time; baking and roasting.

(9) *Industrial Ovens.* Drying of cores, lumber, japanning.

(10) *Internal-Combustion Engines.* Pistons, cylinders, heads, accessories, valves, spark plugs, sprayers.

(11) *Vehicle Equipment.* Brake linings, shoes, and drums or wheels; relation between load-time cycle and reaching of dangerous temperatures; clutches (friction).

(12) *Plastic Materials.* Temperature-time conditions in the state of manufacture of rubber, synthetic resin.

(13) *Localized Heating.* Heat concentrated in a local zone and transmitted from there to the rest of the material by conduction (flame-hardening, induction-hardening, chemical reaction).

Incidentally, the same electrical model can be applied to certain types of problems other than heat: (*a*) Flow of fluids or mass transfer; (*b*) chemical diffusion.

3 Do investigations of walls composed of several layers offer additional difficulties?

A wall composed of several materials "in series" does not offer any difficulty. Thermal conductivity and electrical resistance (also thermal capacity and electrical capacity) for each experiment are in a given relation. For example, consider a wall composed of two layers. The inside layer is 4½ in. thick, conductivity = 1, thermal capacity = 120; the outside layer is 9 in. thick, conductivity = 0.2, thermal capacity = 30. This wall might be represented by two groups of sections, the first group representing the inner layer, having a total resistance of 0.5 megohm, and a total capacity of 240 μf. The outer layer would be represented by the second group having a total resistance of

$$0.5 \times \frac{9}{4.5} \times \frac{10}{2} = 5 \text{ megohms}$$

and a total capacity of

$$240 \times \frac{9}{4.5} \times \frac{30}{120} = 120\ \mu f$$

4 Desirability of checking the method against actual temperature measurements.

The Johns-Manville Corporation carried out some experiments on an insulated furnace wall in its laboratories in Manville, N. J. These experiments were duplicated in the heat-transfer laboratory at Columbia University. A paper on this comparison will be published by C. E. Ernst and C. B. Bradley.

[6] "Heating Refractories From 'Cold' in Fuel-Fired Furnaces," by M. H. Mawhinney, *Iron Age*, vol. 128, pp. 1556–1559 and 1584; also "Heat Absorption by Refractories During Operation of Fuel-Fired Furnaces," by M. H. Mawhinney, *Iron Age*, vol. 128, pp. 1678–1682 and 1708.

[7] "Relation of Uniform Pyrometer Records to Uniform Products," by J. A. Doyle, appearing in "Temperature; Its Measurement and Control in Science and Industry" (a symposium held Nov., 1939, by the American Institute of Physics), Reinhold Publishing Corp., New York, N. Y., 1941, pp. 984–987.

Steels and Alloys Developed for Use at Elevated Temperatures in Petroleum Refineries as Still Tubes and Other Parts

By B. B. MORTON,[1] NEW YORK, N. Y.

This paper outlines the steps which have been taken in the development of steels and alloys for use at elevated temperatures. Various tests, such as creep, rupture, and relaxation, which have been used in this development, are briefly discussed. A review is also given of the effects of the different alloying elements upon the steels and alloys.

THE development of steels for use at elevated temperatures, in connection with the refining of petroleum, has been guided by two main considerations, namely, that the metal shall have adequate mechanical strength to resist the forces acting upon it, and that it shall possess such a degree of resistance to corrosion and oxidation as to insure an economical life for the parts. It will be appreciated that the two considerations are interrelated to a certain extent for, if corrosion proceeds at a lively rate, there is likelihood of so thinning parts that mechanical failures can occur.

Strength of Materials

The fact that the steels in use were not wholly elastic at elevated temperatures was thrust upon the attention of refiners at an early date. The steels showed a lack of elasticity by enlargement of tubes and other cylindrical forms, as well as by a tendency of parts to elongate. This elongation was often marked in the case of heating-coil tubes which were found draped between supports, after some hours of service, in a manner resembling spaghetti.

As pressures were increased in the refining operations, the behavior of metals at elevated temperatures became of prime importance from the standpoint of safety to life and property. Developments in the chemical industries and in steam generation brought the need for knowledge bearing on this problem before larger groups than were encompassed in the petroleum industry. The result was that intensive studies of the characteristics of metals at elevated temperatures were undertaken throughout the world.

The results that poured in from the earlier investigations reminded one of the first meeting of the seven blind men of India with the elephant. Like the reports of the blind men, each set of results bore some grain of truth but in the composite the accounts appeared garbled and confusing. However, certain facts were established at an early date:

1 Above a certain temperature level, which appeared to vary for different steels, the metal ceases to act as an elastic material and acts more in the manner of a plastic, in that "creep," i.e., continuous elongation in the direction of maximum stress, takes place.

2 Breaks which are transcrystalline when the metals are ruptured in short periods of time at temperatures below about 700 to 750 F take place around grain boundaries when the temperatures are higher. The location of the break in respect to the crystals varies with the speed of rupture and the temperature.

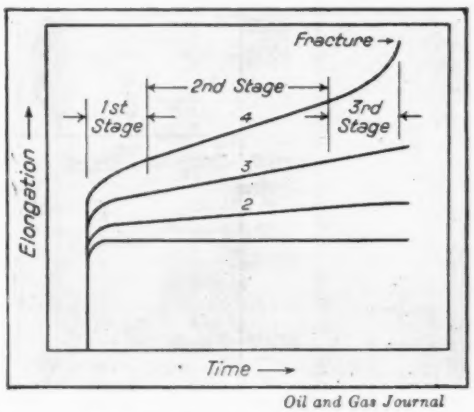
3 The transfer of major strength from the grain-boundary material (referred to as amorphous material) to the crystal apparently takes place in a gradual manner as the temperature is increased. A region of balanced strength of the two materials naturally exists at some temperature level. This point has been designated as the "equicohesive" temperature by Zay Jeffries(1),[2] and is of some significance in connection with the theory of the "creep of metals."

4 There appears to be no satisfactory correlation between any short-time tests and the results obtained from creep tests.

5 Within a certain temperature range, roughly, room to 700 F, the mechanical properties of steels used for design at room temperature can be applied, since the effects of carbon content and alloying elements, as well as of heat-treatment, can be felt and usefully employed within this range.

Creep Tests

With the thought fairly established that creep-test results were the only reliable means for determining the stresses to be imposed upon operating parts at elevated temperatures (above about 700 to 750 F), a great deal of creep testing was undertaken.



Oil and Gas Journal

FIG. 1 TYPICAL CREEP CURVES

It was soon developed that three distinct phenomena of creep could be observed during testing of ductile material; otherwise, only two phases appear, Fig. 1. There is an immediate elongation of the metal which results in a permanent set, amounting in some cases to 3 to 5 per cent of the total elongation of the specimen during the test. Following the initial elongation, the specimen continues to elongate at a speed set by the load and tem-

[1] Development and Research Division, The International Nickel Company, Inc. Mem. A.S.M.E.

Contributed by the Petroleum Division and presented at the Semi-Annual Meeting, Kansas City, Mo., June 16–19, 1941, of THE AMERICAN SOCIETY OF MECHANICAL ENGINEERS.

NOTE: Statements and opinions advanced in papers are to be understood as individual expressions of their authors and not those of the Society.

[2] Numbers in parentheses refer to the Bibliography at the end of the paper.

perature. This portion of the curve is used to arrive at the rate of creep; the creep rate being the slope of this portion of the strain-time curve. When uniform creep has proceeded for some time, there often develops a third phase in ductile material in which the rate of flow increases rapidly and rupture occurs.

The appearance of the third phase of rapid creep in a specimen which has been creeping at some low rate indicates the necessity for long periods of testing of the specimens, and, in fact, has greatly influenced the art of creep testing. This third phase distinctly indicates the danger of determining and reporting creep rates based on tests of short duration, say 1000 hr.

Since the creep rate is taken as the slope of the line representing the second phase of flow of the specimen, the necessity for intensely close controls of conditions surrounding the specimens can be imagined. Decided changes in temperature must be avoided, as well as shock and vibrations. A sensitive method of measuring strain is naturally essential, since each point on the curve in the second phase is a point denoting some increment of strain.

Considering the variables present and the care to be exercised in making creep tests, the amount of good creep data available today is remarkable. In this connection, reference is especially made to work on creep data (2) compiled by a joint committee of this Society and the American Society for Metals.

The presentation of creep data is in a number of forms. Each form has some particular use which recommends it. The method used by Kanter and Spring (3) of plotting creep data on

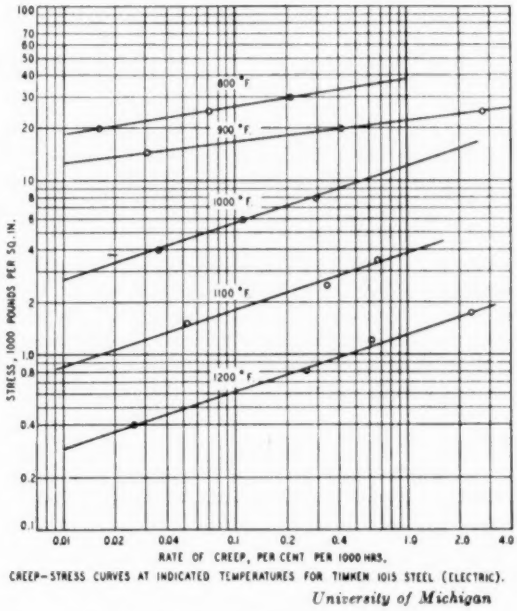


FIG. 3 LOGARITHMIC PLOTTING OF CREEP DATA

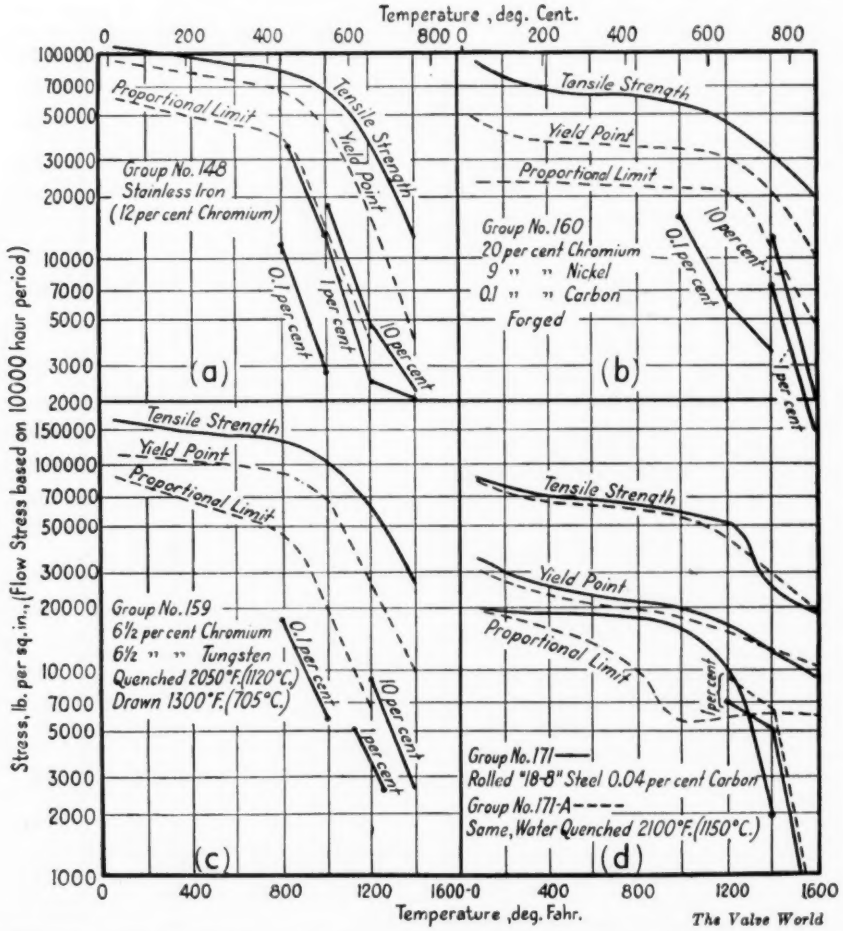


FIG. 2 STRESS-TEMPERATURE CURVES FOR "LONG-TIME" AND "SHORT-TIME" TENSILE TESTS, PLOTTED WITH LOGARITHMIC STRESS ORDINATE

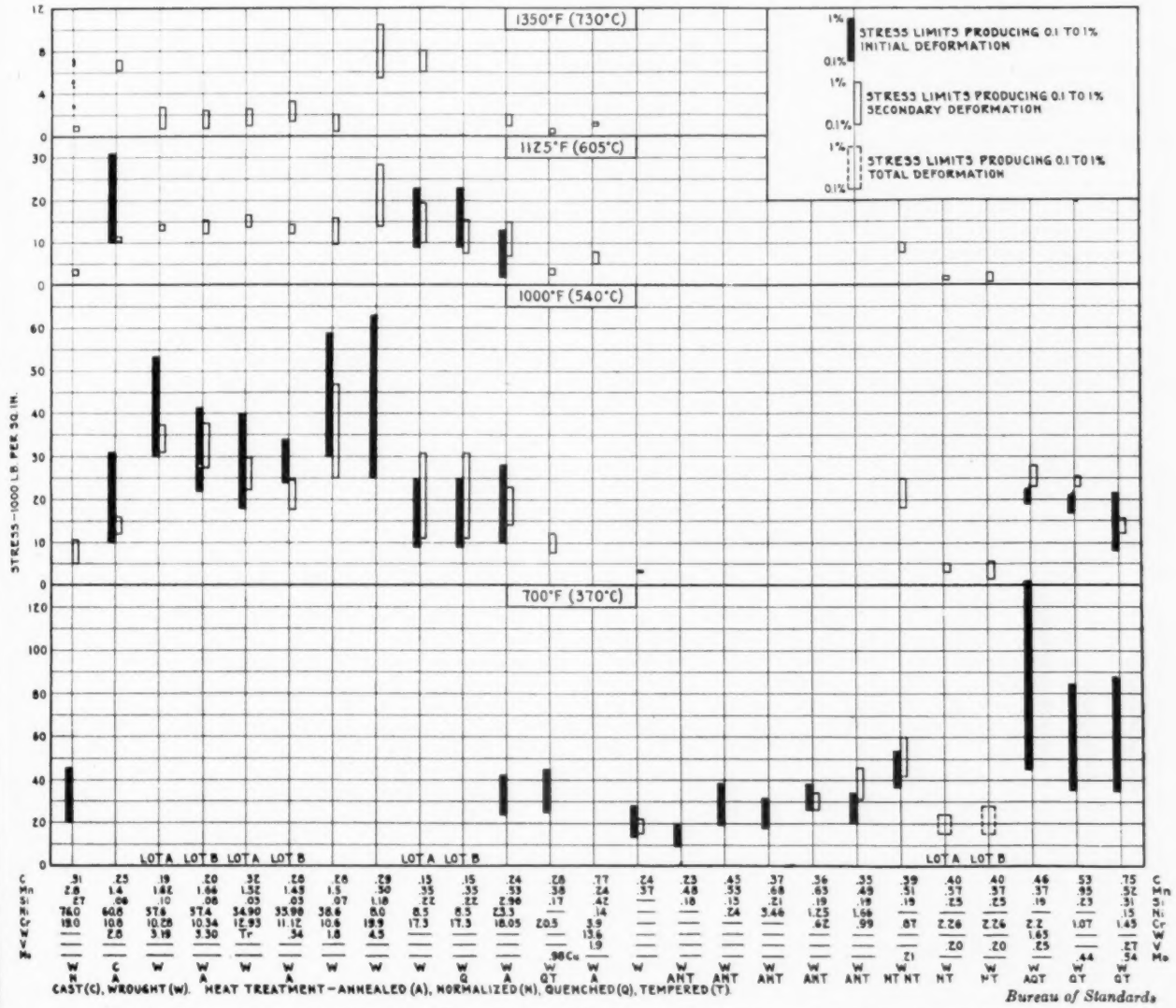


FIG. 4 COMPARISON OF ALLOYS ON THE BASIS OF STRESS PRODUCING DEFORMATION, BOTH INITIAL AND SECONDARY

the charts containing "short-time" test results, Fig. 2, was most useful at the time when the transition in thinking from the use of short-time results to creep results was taking place. The use of logarithmic stress ordinates enhanced the work of these distinguished authors.

The logarithmic plot of stress versus creep rates is widely used, and is particularly useful in indicating the effects of temperature on the rate of creep when several curves, representing results obtained at different temperature levels, are presented in a graph, as in Fig. 3.

The initial deformation which occurs in the creep specimen is often ignored in presenting creep data. In some cases, this deformation may be the controlling factor. Some work done at the Bureau of Standards, Fig. 4, indicates between 0 and 1 per cent the initial deformation to be expected from a given stress load. The secondary deformation (creep rate) is also given.

RUPTURE TESTS

Creep testing is a precision method, and, when properly conducted, should give precision results. Such results are necessary where close tolerances will exist in the parts used at elevated temperatures. There is an enormous field in petroleum refineries and elsewhere where close tolerances are not required and where slight distortion of parts is of no consequence. Where such conditions prevail, the rupture tests are receiving much attention, and appear to fulfill a distinct need. In the case of heating-coil tubes, the rupture test is considered by many as being more useful than creep testing, since it outlines the regions of stress and temperature within which actual failures may be

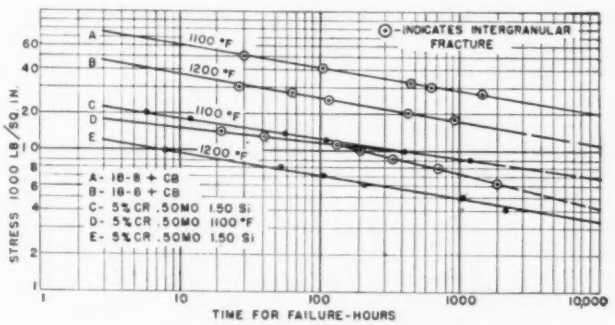


FIG. 5 RESULTS FROM RUPTURE TESTS

expected; and, further, it indicates whether or not a ductile type of failure will occur.

As the name implies, "rupture tests" are made by applying varying loads to a number of specimens held at a constant temperature until rupture occurs. The time and stress required to produce failure in each bar is plotted. When plotted on log-log paper a straight-line relation often results, Fig. 5. Elongation accompanying the rupture is often recorded and throws light on the ductility existing at the time of rupture.

A considerable literature bearing on rupture tests is being accumulated, and an accurate evaluation of the merits of such tests can probably be made in the near future. To one interested in the design of refinery equipment and conscious of the dangers attending failure of such equipment, there will probably be a tendency to use creep data in conjunction with data from rupture tests. The writer recalls the satisfaction gained from studying the early work of Messrs. Clark and White (4), dealing with the rupture tests made using tubing samples. Anything these early tests may have lacked in scientific nicety they made up in the assurance they gave that a certain stress acting at a given temperature over a period of time would or would not probably result in rupture. The data from the tube-rupture tests were of particular use in heating-coil investigations in connection with some creep data available at the time.

Relaxation Tests

The characteristic of the creep of many steels of taking a large permanent set when first loaded at elevated temperatures can be most annoying in the case of bolts, since this initial "strain" can release a definite amount of stress. Leakage of the joint may result from this so-called "relaxation" of the bolt. A special technique and apparatus is employed in studying the relaxing properties of different materials. It would appear from studies reported to date that structure and dispersion of reaction products in the steel are controlling factors in the tendency toward relaxation of a steel.

* * * *

From the preceding discussion, it is developed that the creep tests, rupture tests, and relaxation tests are employed in evaluating steels for use at temperatures above about 700 F. Below this temperature (actually 650 F), it is generally recognized that steels can be treated as elastic bodies, and design can be based on using a factor of safety in connection with the ultimate strength as determined in short-time tests. Reference may be made to the A.P.I.-A.S.M.E. code (5) for details in this connection.

Chemical Composition

As previously pointed out, steel to be used in refinery equipment at elevated temperatures often must possess resistance to corrosion and oxidation. Corrosion resistance is usually conferred on steels by alloying elements into their composition. Steel is also often protected from corrosion by cladding with suitable alloys and elements. There follows a brief discussion of certain elements used in connection with the steels employed in parts of refinery equipment.

Chromium. Chromium is probably the most useful element used to protect refinery equipment, operating at elevated temperatures, against corrosion. As an alloying agent, chromium forms carbides and also dissolves in ferrite. It possesses the useful property of taking upon itself a dense, closely adhering scale of oxide or sulphide which acts as a barrier to further attack. It confers this immunity to attack upon iron and nickel with which it is alloyed.

Chromium per se does not appear to affect appreciably the creep resistance of a steel within the usual commercial limits for

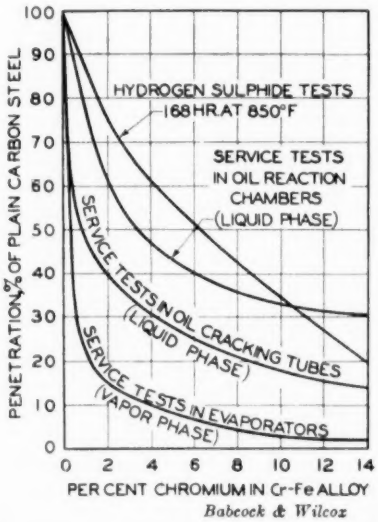


Fig. 6 Effects of Chromium in Retarding Sulphur Attack

this element. The benefits to be derived by the presence of chromium in resisting sulphur are shown in Fig. 6.

Molybdenum. Molybdenum, due to its potent effect upon the creep resistance of steel, is probably the most widely used alloying element entering refinery equipment which operates at temperatures of 700 to 1300 F. It is added to the chromium alloys containing 2 to 10 per cent chromium to inhibit temper brittleness and to improve creep resistance, and is effective in concentrations of 0.25 and 0.5 per cent. It is added in amounts up to 4 per cent to the 18 per cent chromium-8 per cent nickel alloys to improve the corrosion resistance to certain organic acids encountered in refining.

Tungsten. The element tungsten is also one of the carbide formers. It shares with molybdenum the property of rendering chrome steels less susceptible to temper brittleness. The presence of tungsten in steels enhances the resistance to creep.

Nickel. Nickel dissolves in ferrite and does not form carbides. This element does not add materially to the creep strength or corrosion resistance of the low-chromium (1 to 3 per cent chrome) alloys when it is used in low concentrations. When present in percentages greater than about 7 per cent in the presence of sufficient chromium, the useful, austenitic chromium-nickel alloys are formed, among which may be listed the 18 per cent chromium-8 per cent nickel, and the 25 per cent chromium-20 per cent nickel alloys.

Nickel in concentrations of 12 to 80 per cent is an important element in the heat-resisting alloys.

The chromium alloys rendered austenitic by the addition of nickel have the lowest creep rates at temperatures above about 1200 F. The structure of the austenite appears to account for the low creep rates.

Silicon. Silicon additions (up to 3 per cent) to the chromium and to the austenitic chromium-nickel steels appear to improve somewhat the resistance to attack by sulphur compounds and to improve greatly the resistance to oxidation. This element does not appear to improve creep resistance.

Carbon. Carbon, while having a profound effect upon the mechanical properties of steels at temperatures below about 900 F, does not appear to increase the creep resistance above that temperature. In general, low-carbon values (0.15 to 0.2 per cent) appear desirable in parts to be welded and worked. The carbon content of castings will usually exceed that of wrought materials of the same composition.

Application

The objects of the studies outlined in the preceding discussion have been to evolve steels and alloys for use at temperatures in excess of about 700 F. It has been indicated that chromium confers upon a steel base a resistance to sulphur attack and to oxidation. Also, that molybdenum, tungsten, nickel, and other elements can be used to improve the resistance to creep of steels and alloys. Mention will be made of the various alloys now in common usage. Tables 1, 2, and 3 list the alloys and indicate specifications covering the materials.

Carbon-Molybdenum Steels (1/2 *Per Cent Mo*). These steels find wide applications as tubes in heating coils where the metal temperatures will not exceed about 1050 F, and where better creep properties are required than are obtainable from carbon steels. No particular improvement in corrosion resistance can be expected. These steels are also employed as parts of vessels and piping.

Chromium-Molybdenum Steels. A useful series of steels containing from 0.8 to 10 per cent chromium with 0.15 to 1.3 per cent molybdenum have been evolved for use in refineries. These alloy steels make use of the chromium to resist sulphur attack and molybdenum to avoid temper brittleness, as well as to confer good creep properties.

On the lower end of this series, is found the alloy steel SAE 4140 (0.8 to 1.1 per cent chromium, 0.15 to 0.25 per cent molybdenum) which is widely used as a bolting material at elevated temperatures.

Steels containing 1 to 3 per cent chromium with 1/2 to 1 per cent molybdenum find use as the service becomes more severe from a standpoint of corrosion or oxidation.

The 4 to 6 per cent chromium-0.5 per cent molybdenum steel is widely used in heating coils and other locations where a good order of resistance to sulphur attack and to oxidation is required. In refineries, tubes of this material are used to approximately 1300 F. This alloy must be viewed as a very important contribution to the art of refining.

Additional amounts of chromium, up to about 10 per cent, are used in this series of alloys to give greater resistance to sulphur attack.

Silicon appears in the composition of many of the steels of the chromium-molybdenum series. The silicon improves the resistance to oxidation.

Alloys of 11 to 14 Per Cent Chromium. The resistance to sulphur obtained from chromium is taken advantage of in the use of the 11 to 14 per cent chromium alloys to protect reaction vessels. These alloys are applied as liners of vessels serving at elevated temperatures. The liners are welded, using an 18 per cent chromium-8 per cent nickel or a 25 per cent chromium-20 per cent nickel rod. The application of these liners, which serve as the "corrosion constant" required in design to meet the A.P.I.-A.S.M.E. Code (5), is in itself an art and has been thoroughly discussed in the literature (6, 7, 8).

Alloys of 18 Per Cent Chromium-8 Per Cent Nickel. These alloys, with additions of stabilizers as titanium and columbium and often with an addition of 2 to 4 per cent molybdenum, play an important part in refinery metallurgy due to their high order of resistance to sulphur and to good creep resistance.

The addition of molybdenum renders these alloys resistant to organic acids, such as naphthenic (against which the 18-8 is not especially resistant) and phosphoric, as well as other acids which are corrosive at high temperatures.

The 18-8 alloy has shown its worth against phenols in various forms. It is so highly resistant to sulphur at temperatures up to 1300 F that only slight corrosion is noted after several years' service. In this connection, Jamison reports (9), Case 1145, negligible corrosion of KA_2S (18 per cent chromium-8 per cent nickel alloy) in 50,000 hr. The crude used to furnish the feed stock was reported as West Texas Panhandle with 1.5 per cent sulphur. The sulphur content of the cracking-unit fresh feed is not given, but, judging from the attack upon the carbon-steel tubes, the feed was corrosive.

TABLE 1 LIST[a] OF A.S.T.M. SPECIFICATIONS FOR TUBES AND PIPES

Specification number	Materials covered
ASTM A-53-36.....	Seamless steel pipe
ASTM A-83-38T.....	Boiler tubes, seamless steel, and open-hearth iron
ASTM A-106-39.....	Seamless-steel pipe for high-temperature service
ASTM A-120-36.....	Seamless black and galvanized pipe for ordinary uses
ASTM A-158-38T....	Seamless alloy-steel pipe for high-temperature service
ASTM A-161-37.....	Seamless-steel cracking-still tubes for refinery service. (Including carbon-0.5 per cent molybdenum)
ASTM A-179-37.....	C.D. steel heat exchanger and condenser tubes for refinery service
ASTM A-187-38.....	C.D. heat exchanger and condenser tubes 5 per cent chrome; 5 per cent chromium with molybdenum; 5 per cent chromium with tungsten
ASTM A-188-38.....	Seamless cracking-still tubes 5 per cent chromium; 5 per cent with molybdenum; 5 per cent with tungsten
ASTM A-192-38T....	Seamless boiler tubes for high-pressure service
ASTM A-199-39.....	Seamless C.D. intermediate-alloy heat exchanger and condenser tubes
ASTM A-200-39.....	Seamless intermediate alloy-steel cracking-still tubes
ASTM A-206-39T....	Seamless carbon-molybdenum alloy-steel pipe for high-temperature service
ASTM A-209-38T....	Seamless carbon-molybdenum alloy-steel boiler tubes (Grades T-1 and T-1a)
ASTM A-210-38T....	Seamless medium-carbon-steel boiler tubes (grade C)
ASTM A-213-39T....	Seamless alloy-steel boiler and superheater tubes; low, medium, and high alloys
ASTM A-158-38T.... (P8a, b, c)	Seamless nickel-chromium austenitic alloy-stee cracking-still tubing, 18-8

[a] Based on "Technical Data Card No. 7," The Babcock & Wilcox Company, New York, N. Y.

TABLE 2 A.S.T.M. SPECIFICATIONS COVERING STEEL PLATE FOR ELEVATED-TEMPERATURE SERVICE

Specification number	Materials covered
ASTM A-7.....	Specifications for structural steel for bridges (plates only)
ASTM A-10.....	Specifications for mild-steel plates
ASTM A-30.....	Specifications for boiler and firebox steel for locomotives
ASTM A-70.....	Specifications for carbon-steel plates for boilers and other pressure vessels for stationary service
ASTM A-78.....	Specifications for steel plates for structural quality for forge welding (grades A and B)
ASTM A-113.....	Specifications for structural steel for locomotives and cars (plates for cold pressing only)
ASTM A-129.....	Specifications for open-hearth iron plates of flange quality
ASTM A-149.....	Specifications for high-tensile-strength carbon-steel plates for pressure vessels (2 in. and under in thickness)
ASTM A-150.....	Specifications for high-tensile-strength carbon-steel plates for fusion-welded pressure vessels (over 2 to 4 in., inclusive, in thickness)
ASTM A-201.....	Specifications for carbon-silicon-steel plates for ordinary tensile ranges for fusion-welded boilers and other pressure vessels, firebox and flange grades
ASTM A-202-39..	Specifications for chromium-manganese-silicon (CMS) alloy-steel plates for boilers and other pressure vessels
ASTM A-203-39..	Specifications for low-carbon nickel-steel plates for boilers and other pressure vessels
ASTM A-204-39..	Specifications for molybdenum-steel plates for boilers and other pressure vessels
ASTM A-167-39..	Specifications for corrosion-resisting chromium-nickel-steel sheet, strip, and plate

TABLE 3 A.S.T.M. SPECIFICATIONS COVERING CAST STEELS FOR USE AT ELEVATED TEMPERATURES

Specification number	Materials covered
ASTM A-95-40.....	Specifications for carbon-steel castings for valves, flanges, and fittings for high-temperature service
ASTM A-157-40.....	Specifications for alloy-steel castings for valves, flanges, and fittings for service at temperatures from 750–1100 F; carbon-molybdenum; chrome-molybdenum; 13 per cent chromium; nickel-chromium-molybdenum; 18-8; 25 chrome-20 nickel covered
	Welding Grades
ASTM A-216-40T....	Specifications for carbon-steel castings suitable for fusion welding for service at temperatures up to 850 F (tentative)
ASTM A-217-40T....	Specifications for alloy steel suitable for fusion welding for service at temperatures from 750–1100 F (tentative); carbon-molybdenum; nickel-chromium-molybdenum covered

Apparently, 18-8 is an excellent material for use as heating-coil tubes if a clean and refractory feed stock can be supplied. The alloy apparently should not exceed 1300 F in metal temperature during operation. The excellent corrosion resistance of this alloy has indicated its use as the protecting liner for vessels and pipes. Its coefficient of thermal expansion, which is approximately 50 per cent greater than that of steel, has somewhat limited its use in this service.

The failure of tubes of 18-8 are often spectacular, in that there occurs a violent rupture. The ruptured tube frequently shows little or no ductility in the region of the break. An explanation for the tendency for sudden rupture is that failure in many cases

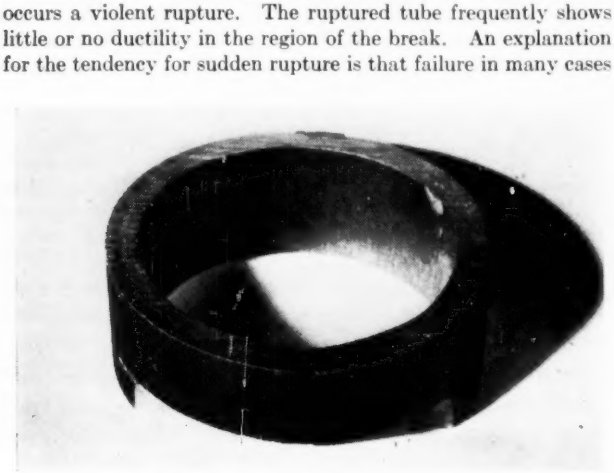


FIG. 7 CRACK IN WALL OF AN 18-8 TUBE
(The crack started on the outside and has not fully penetrated the wall.)

appears to result from a crack which originates at the outer wall and works inward. The origin of the crack at the outer skin is something of a mystery. It may be due to a fluctuating heat load that sets up a fatigue type of stress. Fig. 7 shows a section of wall of an 18-8 tube. The crack developed from the outer wall and was caught before the tube could rupture, that is, before it reached the inner wall.

HEAT-RESISTING ALLOYS

There is a wide variety of compositions used in heat-resisting alloys. One of the most common varieties used in oil refineries contains about 28 per cent chromium with 12 per cent nickel. This composition appears to give good economical life in such parts as tube supports, damper parts, and other parts which operate at temperatures of 1600 to 1800 F.

Much of the 25 per cent chromium-20 per cent nickel alloy, in both wrought and cast form, is used for temperatures of 1800 to 2000 F. The material has good resistance to oxidation and to sulphur in the form of the oxide.

It should be noted that, while many of the heat-resisting alloys can resist the effects of sulphur dioxide at high temperatures, they often can be destroyed by hydrogen sulphide at the same temperature. A firing system which permits unburned fuel to enter the firebox can set up conditions to form hydrogen sulphide from sulphur dioxide and can result in damage to the heat-resisting alloys. Sodium salts in a fuel can be damaging to heat-resisting alloys.

While there is a variety of compositions of heat-resisting alloys, they will be found to contain chromium to provide oxidation resistance and nickel to give load-carrying ability at high temperatures.

Calorizing, a method of placing an aluminum-aluminum oxide coating on a metal surface, is often invoked to protect parts operating at elevated temperatures. This form of coating is highly protective to the metal part and prevents or greatly retards oxidation and sulphur attack. Calorizing appears especially applicable to protection of bolts serving under conditions conducive to oxidation of the bolt material.

The decided effect of temperature upon the strength of heat-resisting alloys at elevated temperatures (1000 to 2000 F) can be seen from Fig. 8.

HEAT-RESISTING CAST IRONS

A considerable quantity of cast irons are used to resist moderate temperature conditions (700 to 1200 F) as tube supports, chiefly in the convection section of heating coils.

Desirable properties in cast irons when used as supports in fireboxes, burner parts, etc., are low rates of growth, resistance to oxidation, and a good order of strength.

Ni-Resist[3] cast iron, containing approximately 15 per cent nickel, 6 per cent copper, and 2 to 4 per cent chromium (10), has given good service as tube supports and as dampers. This alloyed iron shows low rates of growth at temperatures up to 1200 to 1300 F.

Special processed nickel-chromium irons have entered refinery

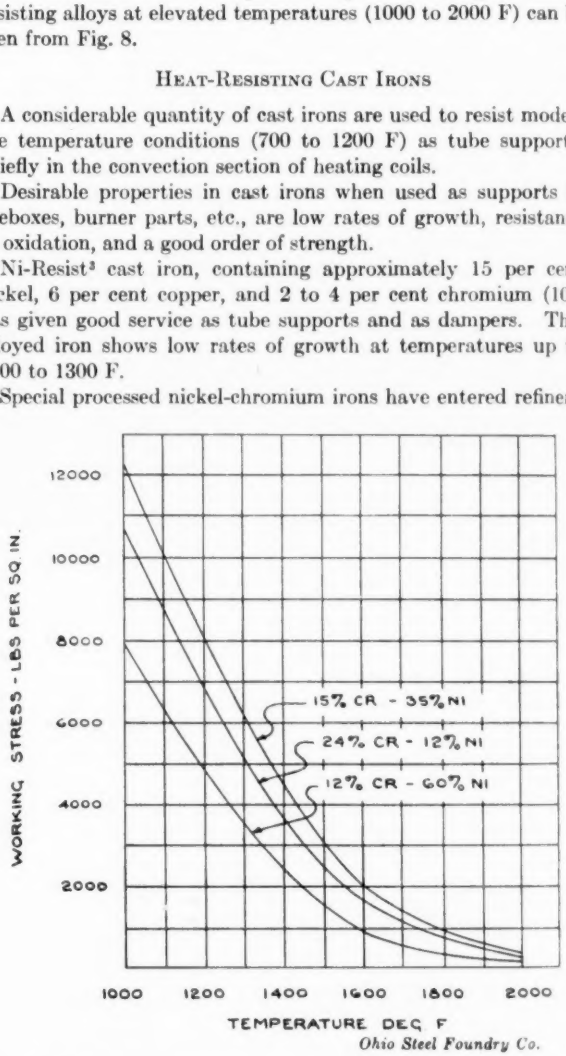


FIG. 8 WORKING STRESSES FOR SOME HEAT-RESISTING ALLOYS

service in large tonnage as tube supports. These irons contain 0.8 to 1.5 per cent nickel, 0.3 to 0.9 per cent chromium with 3.2 to 3.5 (maximum) carbon values, depending upon grade (11). In tests simulating conditions of furnace heating and cooling, these irons showed a remarkable resistance to growth and scaling, especially when considering the low alloy contents. The nickel appeared to induce a densely adhering scale which acted to protect the underlying metal.

There is often a temptation to use cast irons as furnace parts where the true nickel-chromium heat-resisting alloys are indicated. Yielding to such a temptation has rarely resulted in any benefit or saving.

CONCLUSIONS

In this paper, which is historical in nature, the purpose has been to show that, at an early date in refinery circles, it was noted that metals behaved in the manner of a plastic at certain

[3] Registered trade-mark.

temperature levels. Based on this observation, an extensive study of the behavior of metals at elevated temperatures was undertaken, often in collaboration with other industries. Creep tests, rupture tests, relaxation tests, and variations of these tests were developed, and results useful to industry have accumulated.

The use of chromium to confer upon steel resistance to oxidation and sulphur attack has been widely exploited, and a series of alloys are available today containing 1 to 28 per cent chromium, generally with other alloy elements present.

Molybdenum is added to a wide range of steels containing carbon and chromium to improve the resistance to creep. In the case of the chromium steels, the presence of molybdenum suppresses the tendency toward temper brittleness. It is added to 18-8 alloy to give greater resistance to certain agents, chiefly organic acids occurring in refinery operations.

Nickel, in amounts of 8 per cent and above, is added to the chromium-containing alloys to form the well-known austenitic alloys. These alloys possess a high order of resistance to sulphur at elevated temperatures. They also possess the best load-carrying ability at elevated temperatures (1100 F and above) of available commercial alloys.

A wide variety of chromium-nickel alloys are used as heat-resisting parts of furnaces. The 28 per cent chromium-12 per cent nickel alloy appears popular for this service.

BIBLIOGRAPHY

1 "Effect of Temperature, Deformation, and Grain Size on the Mechanical Properties of Metals," by Zay Jeffries, Trans. A.I.M.E. vol. 60, 1919, pp. 474–562; Fig. 74, p. 530.

2 "Compilation of Available High-Temperature Creep Characteristics of Metals and Alloys," Joint Research Committee on Effect of Temperature on the Properties of Metals, Creep Data Section, A.S.T.M.-A.S.M E., published 1938.

3 "Some Long-Time Tension Tests of Steel at Elevated Temperature," by J. J. Kanter and L. W. Spring, *The Valve World*, vol. 27, Crane Company, Chicago, Ill., 1930, pp. 443–460.

4 "The Stability of Metals at Elevated Temperatures," by C. L. Clark and A. E. White, Trans. American Society for Steel Treating, vol. 15, January-June, 1929, pp. 670–711.

5 "Unfired Pressure Vessels for Petroleum Liquids and Gases," A.P.I.-A.S.M.E. Code, Third edition, published jointly, 1938.

6 "Field Installation of Chromium Sheet Lining in Pressure Vessels," by J. T. Shaler. Proceedings, Ninth Mid-Year Meeting, A.P.I., Section III, "Refining," 1939, pp. 29–40.

7 "Field Lining of Refinery Vessels With Stainless Steel Sheets or Strips," by K. E. Luger, Mimeographed paper distributed by Stainless Steel Division, Carnegie-Illinois Steel Corporation, 1939.

8 "Layout and Application of Stainless Strip Lining to Refinery Vessels," by W. W. McClow, *Refiner and Natural Gasoline Manufacturer*, 1940, vol. 19, pp. 451–455.

9 "Corrosion Protection of Refinery Equipment," by J. A. Jamison, Proceedings, Nineteenth Annual Meeting, A.P.I., Section III, "Refining," 1938, pp. 46–89.

10 Specification K-6, The International Nickel Company, Inc., New York, N. Y. This covers four grades of Ni-Resist used in petroleum refineries.

11 Specification NT-FB 93-1-40, The International Nickel Company, Inc., New York, N. Y.

Experimental Study, Feedwater Treatment for 1400-Lb Boiler Operating Pressure

By D. C. CARMICHAEL,[1] WILMINGTON, DEL.

Study has shown that the future steam and electrical loads of the Dye Works of the author's company would be most economically supplied by a 1400-psi boiler-and-turbine installation, exhausting directly into the plant process mains, without the use of evaporators as are now used at the Deepwater plant of the Deepwater Operating Company. The development of a satisfactory water-purification system to permit 100 per cent treated soft water to be used in a 1400-lb boiler would eliminate the necessity of using intermediate evaporators with their consequent maintenance and loss of thermal potential. It has been calculated in connection with the study of increased steam and electrical capacity for the Dye Works that the elimination of the evaporators would permit the generation of up to 8000 kw of electricity from the same steam. Additional savings in maintenance would be realized. This paper reviews the various steps undertaken in developing, installing, and operating the experimental water-treatment system, followed later by the installation of a 1400-lb experimental boiler, operating with a heat absorption of 100,000 Btu per sq ft per hr. A 400,000-lb per hr boiler to operate at 1400 psi with 100 per cent treated soft water has been purchased and will start operation in January, 1942.

THE present steam and electrical load of the Dye Works of the author's company is largely supplied from the Deepwater plant of the Deepwater Operating Company. The boiler units at this plant generate steam at 1250 psi, which is delivered to a 12,000-kw turbine. The turbine exhausts at approximately 310 psi into high-pressure tubular evaporators, which in turn generate steam at 180 psi from the Dye Works' treated water. The turbine exhaust is condensed in the evaporators, after which it is returned to the 1250-lb boiler-feedwater system.

The development of a satisfactory water-purification system to permit treated water to be used in a 1400-lb-pressure boiler would eliminate the necessity of using intermediate evaporators with their consequent maintenance and loss of thermal potential.

Course Pursued in Study

An investigation was made of the successful operation of two 900-psi plants, using 100 per cent make-up, and it was believed that our problem was not materially different. However, reliable design information on the treatment equipment and proc- which would be necessary for the Dye Works could not be obtained without fairly large-scale experiments.

aboratory work was carried on with the available raw-water supply, using various treatments of caustic soda, ferric sulphate, and magnesium sulphate for color and silica removal. Typical analyses of the raw water are shown in Table 1.

The results indicated that color and silica could not be effectively removed by a single treatment but required two stages, the first at a pH of approximately 5 for color removal, and the second at a pH of approximately 10 for silica removal.

The experimental or semiworks equipment first proposed for color and silica removal consisted of batch settling tanks, equipped with decant pipes and floats so that, after adding the treating chemicals, agitating, and allowing the water to settle, the clear water would be decanted to a gravity filter.

Prior to the final design of the equipment for batch treatment, the use of continuous settling equipment, utilizing upward flow through a sludge blanket, was suggested, and further laboratory work was carried out. The results again indicated that a two-stage treatment was necessary for color and silica removal, but the important finding was that a continuous, rather than batch, system was feasible.

Based on the laboratory work, the semiworks plant for color and silica removal was designed as a continuous system of treating and settling, followed by filtration. The schematic layout of treatment equipment is shown in Fig. 1, and design details in Fig. 2.

The continuous settling equipment was so designed that the water and coagulating chemicals were thoroughly mixed by mechanical agitation in the lower part of the tank, then passed upward through a cone partition in the upper part of the tank. This design permits the settled water to pass upward through a layer of sludge before reaching the take-off pipe. At 3 gpm flow the volume of the mixing chamber allowed for 200 min mixing time, and the settling chamber, or cone, was of sufficient volume to allow for 50 min detention period. Later, the flow rate was increased to 7 gpm with satisfactory results.

Siphons were installed approximately 15 in. below the sludge level in each case, and continuous blowoff of sludge was regulated so as to keep the sludge level below the overflow openings.

The semiworks equipment was started June 16, 1938, and continued in operation until November 25.

Operating data and tests were taken every 2 hr and recorded on the log-sheet forms. At intervals of 2 to 5 days, samples of water were collected and sent to the laboratory for gravimetric silica analyses. Each sample was given a run number. The average, maximum, and minimum silica contents of 28 run sam-

TABLE 1 TYPICAL ANALYSES OF RAW WATER

Sample No.	1	2	3	4
Date	4/1/37	5/5/37	7/13/37	7/21/37
Calcium carbonate	..	14.0	26.0	30.0
Calcium sulphate	46.0	19.9	15.6	24.0
Magnesium carbonate	10.9	1.0	15.6	15.1
Magnesium sulphate	4.9	..	..	..
Magnesium chloride	..	9.9	..	6.0
Silica	7.0	24.0	8.0	7.0
Iron and alumina	7.0	3.9	3.3	7.0
Sodium sulphate	7.0	..	8.1	..
Sodium chloride	27.8	4.9	30.0	42.0
Volatile and organic matter	9.1	81.0	73.9	54.0
Total dissolved solids	119.7	158.0	180.0	184.2
Suspended matter	38.8	25.0	35.0	35.0
Phenolphthalein alkalinity as calcium carbonate	0	0	0	0
Methyl-orange alkalinity as calcium carbonate	8.6	10.0	30.8	32.5
pH value	6.9	7.1	6.1	6.1
Color	25.0	30.0	115.0	90.0
Soap hardness as calcium carbonate	51.0	39.5	51.5	71.5

NOTE: All quantities as parts per million.

[1] Industrial Engineer, E. I. du Pont de Nemours & Company.

Contributed by the Power Division and presented at the Spring Meeting, Atlanta, Ga., March 31–April 3, 1941, of THE AMERICAN SOCIETY OF MECHANICAL ENGINEERS.

NOTE: Statements and opinions advanced in papers are to be understood as individual expressions of their authors and not those of the Society.

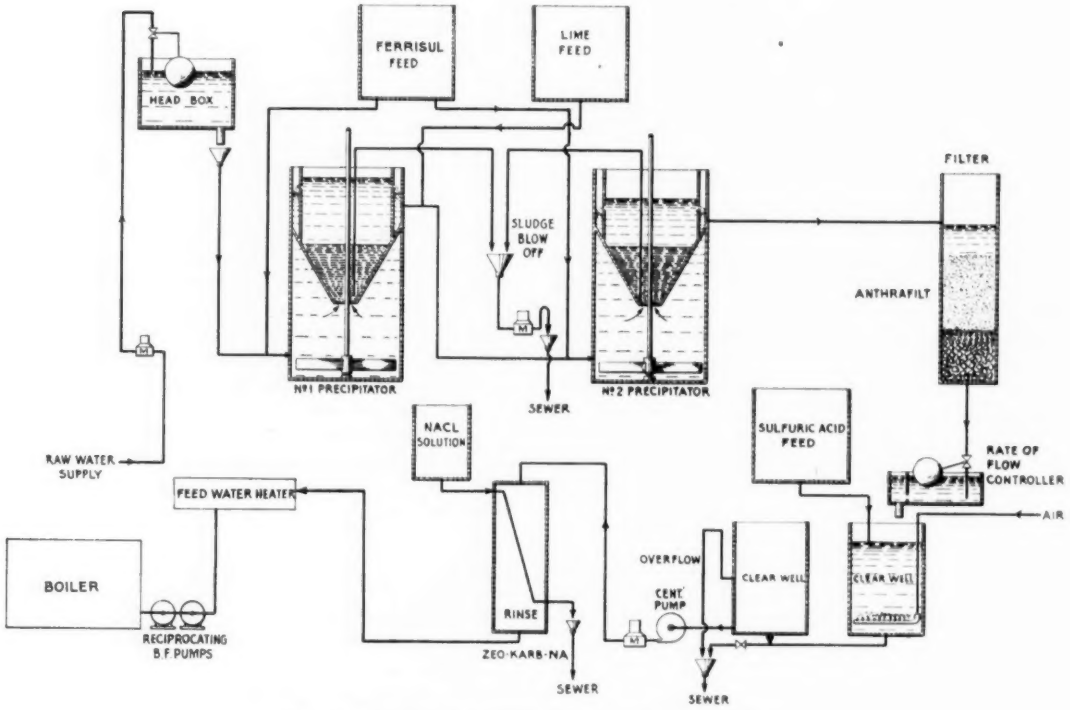


FIG. 1 SCHEMATIC LAYOUT OF WATER-TREATING UNIT

ples leaving No. 1 settling tank after color removal were 8.7, 13.5, and 2.5 ppm, respectively, and similar averages in the filtered water were 2, 5.2, and 0.4 ppm, respectively.

The silica content of the treated water was somewhat affected by the operating difficulties experienced in the control of the chemical feeders, this varying from shift to shift. During the week, Monday to Friday, inclusive, full-time operators were on duty from 8:00 a.m. to 12:00 midnight, but from 12:00 midnight to 8:00 a.m., the system was operated with very little or no attention. Over the week ends from 4:00 p.m. Friday to 4:00 p.m. Sunday, the operation of the system was discontinued, the only part in operation being the agitators in the mixing chambers. This type of operation, while keeping the labor requirements at a minimum, tended toward occasional erratic results on silica removal.

Prior to September 19, Ferrisul, which is anhydrous ferric sulphate, was used as the coagulant. During the remaining part of the test period, chlorinated ferrous sulphate in chemically equivalent amounts was used in place of Ferrisul. The results as to color and silica removal were the same with either coagulant.

After filtration, the pH value of the water was approximately 10 and, to prevent deposition of $CaCO_3$ on the softener beds, the pH value was lowered to 7.5 by the addition of sulphuric acid.

From the filtered-water storage tanks, the water was pumped to zeolite softeners where the hardness and total dissolved solids were reduced. The softeners consisted of two pressure shells, each 12 in. in diam and approximately 5 ft high.

The first softener was charged with Zeo-Karb, a carbonaceous zeolite and the second with De-acidite, a granular organic compound.

During the softening process, the cations (Ca, Mg, and Na) are replaced by H ions by exchange process in the Zeo-Karb unit. The effluent from this unit contains H_2CO_3, HCl, and H_2SO_4 due to replacement of the cations with hydrogen. This acid water then flows directly to the second or De-acidite unit where the HCl and H_2SO_4 are absorbed; thus, removal of the hardness and lowering of the total dissolved solids are accomplished.

TABLE 2 ANALYSIS OF WATER SAMPLES FROM EACH STEP IN WATER-TREATING SYSTEM

Results as ppm	Raw water	From No. 1 precipitator	From No. 2 precipitator	From effluent gravity filter	From effluent de-mineralite unit
Silica	10.0	9.0	1.8	1.5	1.5
Iron as Fe	0.8	6.0	0.4	0.1	0.1
Calcium bicarbonate as $CaCO_3$	..	..	..	..	3.7
Calcium carbonate as $CaCO_3$	..	..	14.0	12.0	..
Calcium chloride	..	..	43.4	43.4	..
Calcium sulphate	21.8	44.6	106.1	106.1	..
Calcium hydrate	..	..	1.0	..	..
Magnesium sulphate	..	..	9.7	9.7	..
Magnesium carbonate	13.4	..	..	..	1.7
Magnesium chloride	..	15.0	15.0	15.0	..
Sodium chloride	19.8	19.8	19.8	19.8	3.9
Sodium sulphate	21.7	21.7	21.7	21.7	.5
Total dissolved solids	87.5	116.1	232.9	230.2	19.7
Turbidity	35	20.0	15.0	0	..
Color	Turbid	15	10	10	..

The Zeo-Karb bed was regenerated with H_2SO_4 and the De-acidite with soda ash.

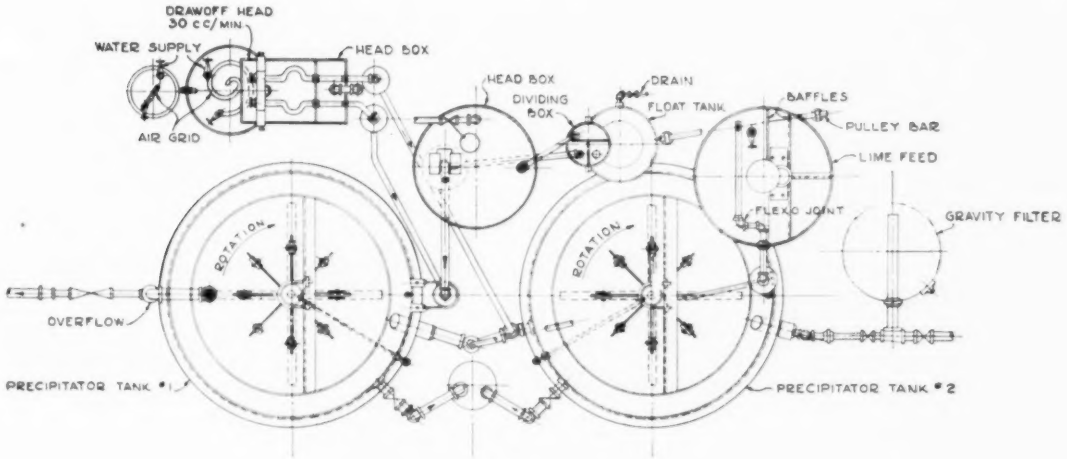
The complete analysis of a set of water samples collected through the water-treatment system is shown in Table 2.

TREATMENT COSTS

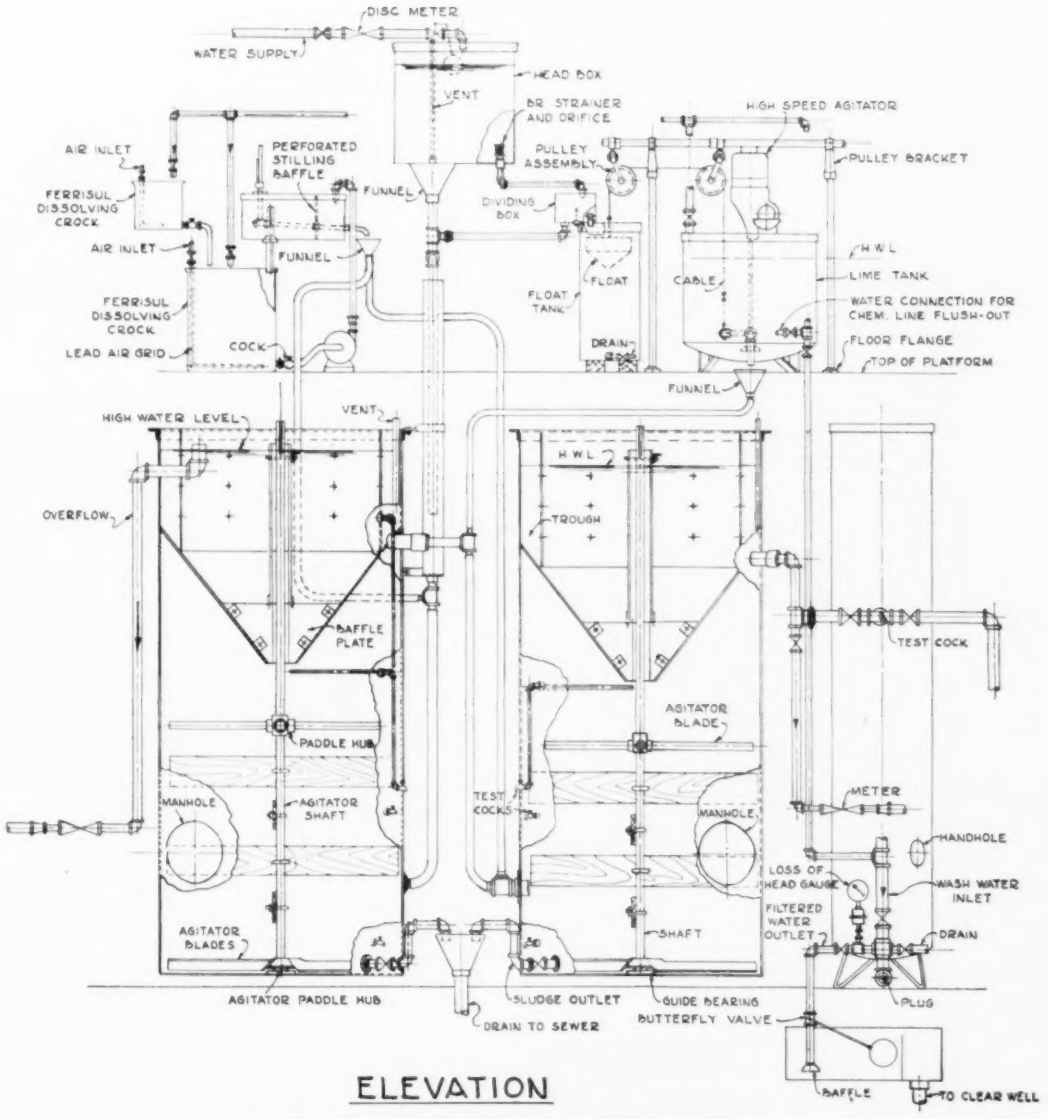
The treatment costs per million gallons were as follows:

Color removal	$ 1.90
Silica removal	16.10
Acid treatment	1.06
Zeo-Karb softening	26.20
De-acidite softening	56.60
Total	$101.86

These costs are based on using chlorinated ferrous sulphate and sulphuric acid in the color-removal treatment, chlorinated copperas and lime in the silica-removal treatment, sulphuric acid for lowering the pH value after filtration, sulphuric acid for re-



PLAN



ELEVATION

FIG. 2 DESIGN DETAILS OF WATER-TREATING UNIT

TABLE 3 ANALYSIS OF WATER; EVAPORATION TEST BY NATIONAL ALUMINATE CORPORATION

	Feedwater, ppm	Boiler water, ppm
Total dissolved solids	18.8	750
Suspended solids	..	145
Total hardness as $CaCO_3$	6.8	0
Noncarbonate hardness as $CaCO_3$	..	..
Calcium hardness as $CaCO_3$	1.7	..
Magnesium hardness as $CaCO_3$	5.1	..
Phenolphthalein alkalinity as $CaCO_3$	nil	345
Methyl-orange alkalinity as $CaCO_3$	8.5	448
Free CO_2 as $CaCO_3$	3.4	..
Chlorides as NaCl	8.5	103
Sulphates as NA_2SO_4	nil	47.9
Silica as SiO_2	0.85	19.5
Alumina as Al_2O_3	nil	1.4
Iron as Fe	..	..
Phosphate as PO_4	..	54

	Scale on tube, per cent
Loss at dull red heat	7
Silica (SiO_2)	nil
Ferric oxide (Fe_2O_3)	nil
Calcium oxide (CaO)	46
Magnesium oxide (MgO)	2
Sulphur trioxide (SO_3)	nil
Phosphorus pentoxide (P_2O_5)	40

generation of the Zeo-Karb unit and soda ash for regeneration of the De-acidite unit.

Evaporation Tests

In order to study the effect of the water treatment on scale formation, arrangements were made with the National Aluminate Corporation of Chicago to ship 250 gal of the final treated water in stainless-steel drums to its plant for evaporation in its laboratory boiler. Heating of the water was by means of electrical resistance elements inserted in the heating or boiler tube. This tube was 12 in. long and $1^1/_2$ in. outside diam.

The duration of the test was for a period of 294 hr, during which time, 200 gal of water were evaporated. An operating pressure of 1000 psi was maintained throughout the test, and the heat input was 35,000 Btu per sq ft per hr. The water was preheated to 210 F before being delivered to the boiler.

Trisodium phosphate was fed with the water in order to precipitate any residual hardness not removed by the zeolite softeners.

After completion of the test, the heating tube was removed and the adhering deposit examined physically and chemically. The physical examination showed a coral-like formation approximately 0.1 in. thick. The deposit was very soft when wet and could be readily crushed between the fingers. Chemical analysis showed it to consist entirely of calcium and magnesium phosphates.

Table 3 shows the analysis of "treated water," "boiler water," and "deposit on tube," as made in the National Aluminate Corporation's laboratory. Views of the boiler tube before and after the evaporation test are shown in Figs. 3 and 4.

The conclusions of part 1 of this experiment were as follows:

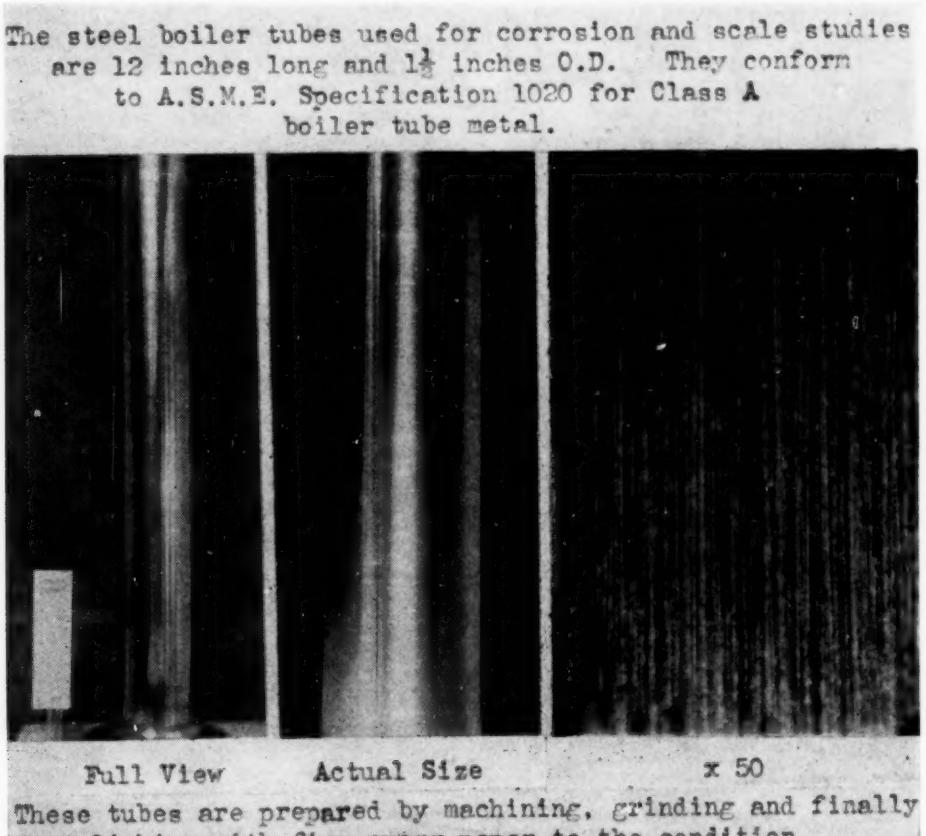


Fig. 3 Boiler Tube Before Evaporation Test

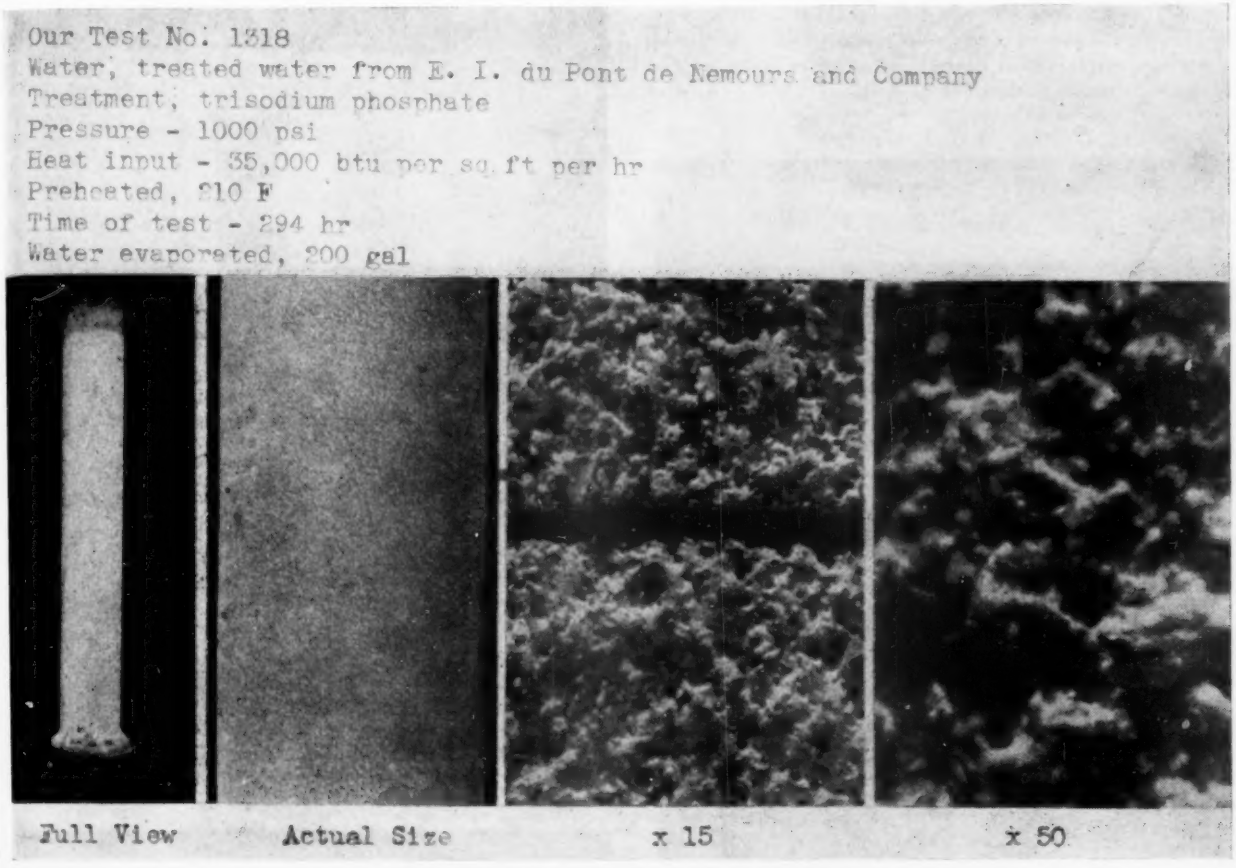


FIG. 4 BOILER TUBE AFTER EVAPORATION TEST

1 The silica content was lowered to 2 ppm or less.

2 Evaporation tests at 1000 psi working pressure and a heat input of 35,000 Btu per sq ft per hr showed no detrimental scale formation.

3 Before any definite conclusion was reached to construct a 1400-lb boiler, operating with 100 per cent make-up water, further evaporation tests should be made in an experimental boiler to be operated at 1400 psi and heat inputs up to 100,000 Btu per sq ft per hr.

Following the completion of part 1 of the experimental program, contact was made with several boiler companies regarding the design of an experimental boiler unit. This boiler consisted of an oil-fired unit for operation at a maximum pressure of 1400 psi, with a heating surface of 4.45 sq ft, and was enclosed in a suitable refractory-lined, steel-encased setting for oil burning. The oil burner was of the air-atomizing type, using oil from existing oil lines located in the boiler room and air from a low-pressure motor-driven blower.

Feedwater was supplied to the boiler room from the treating equipment previously described. The only major change made in the feedwater treatment was the use of Zeo-Karb zeolite on the sodium cycle rather than employing the two types of zeolite already discussed.

The design of the boiler allowed for operation at 1400-psi pressure with a heat input up to and including 100,000 Btu per sq ft per hr.

Figs. 5, 6, 7, and 8 show construction of the boiler pressure parts and furnace. Fig. 9 shows the boiler feed pump which is a motor-driven duplex unit.

BOILER OPERATION

The boiler was placed in operation on June 1, 1940, maintaining the gas temperatures entering and leaving the tubes as given in the expected performance, Table 4. It was not possible to obtain the desired heat absorption of 100,000 Btu per sq ft per hr and adjustments were made in the fuel and air. To obtain the mentioned heat absorption it was necessary to maintain a gas temperature of approximately 2900 F entering, and 2400 F leaving the tubes. This temperature greatly exceeded the gas temperature as originally calculated, and it was recommended that the furnace be rebuilt using brick to withstand temperatures of 3100 F.

The boiler unit was taken out of operation on June 7, and the furnace rebuilt by The Babcock & Wilcox Company. During the rebuilding, the furnace arch was changed from a suspended to a sprung arch. Operation of the boiler unit was resumed on June 17, at the expected heat absorption. Table 5 shows optical-pyrometer observations together with other related data as periodically collected by The Babcock & Wilcox Company. The

TABLE 4 EXPECTED PERFORMANCE OF EXPERIMENTAL BOILER UNIT

Temperature of water entering boiler, F	230
Steam generated, lb per hr	479
Heat absorption, Btu per sq ft per hr	100000
Total air, per cent	180
Oil fuel, lb per hr (18,500 Btu per lb)	258
Flue gas, lb per hr	6650
Input from fuel, Btu per hr	4775000
Boiler-tube surface, sq ft	4.26
Total absorption, Btu per hr	426000
Btu available per lb gas, Qg	630
Moisture in flue gas, per cent	5
Adiabatic gas temperature, F	2340
Gas temperature entering tubes, F	2240
Gas temperature leaving tubes, F	2060

maximum brick temperature was 3188 F, which would have resulted in forced shutdown of the boiler if rebuilding of the furnace had not been carried out at the first indications of distress. Fig. 10 shows the location of the thermocouple and optical-pyrometer observations as given in Table 5.

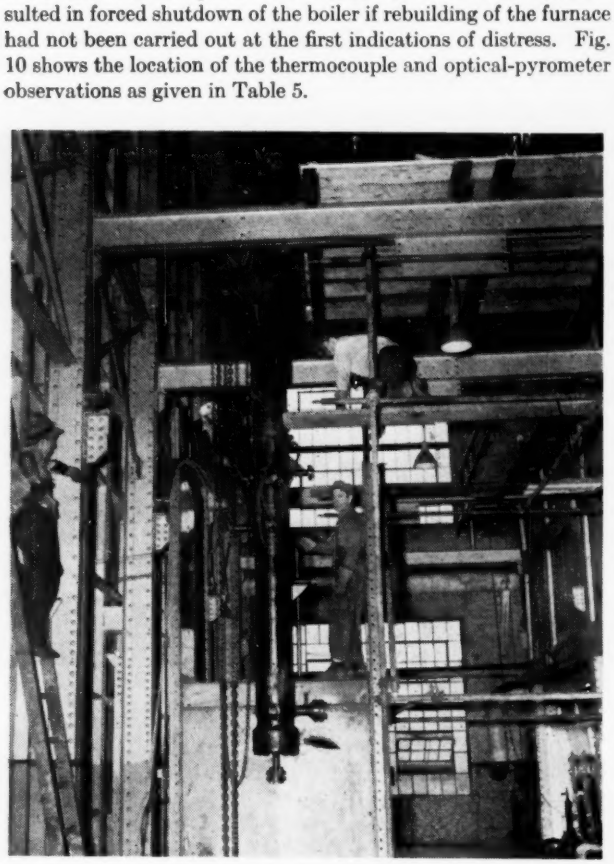


FIG. 5 BOILER DURING CONSTRUCTION

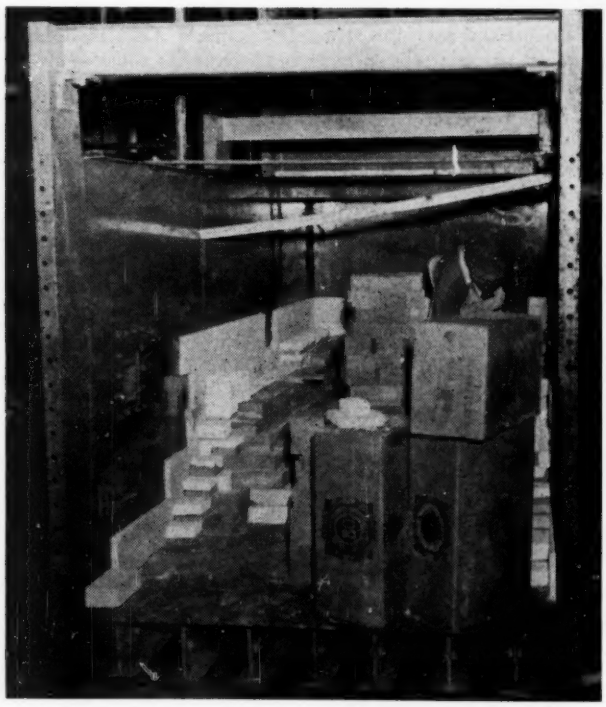


FIG. 6 BOILER FURNACE DURING CONSTRUCTION

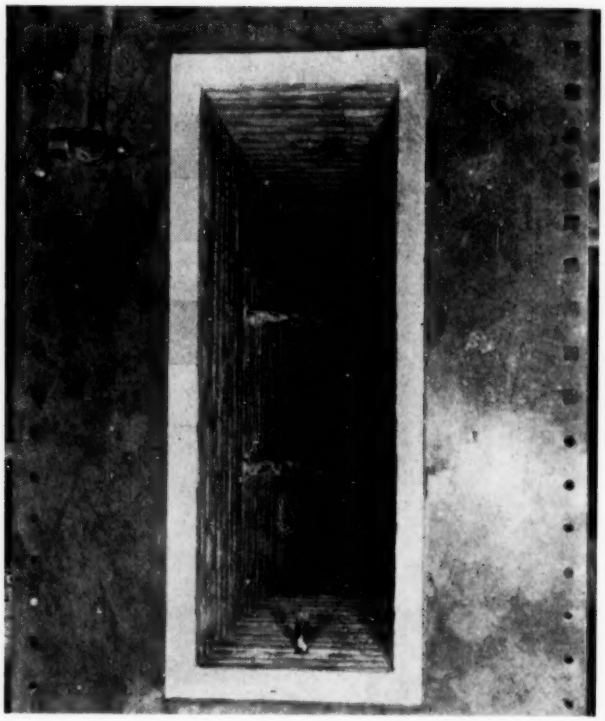


FIG. 7 VERTICAL FLUE OF FURNACE DURING CONSTRUCTION SHOWING BOILER TUBES AND THERMOCOUPLE NO. 2
(Photograph taken from top of vertical flue looking downward.)

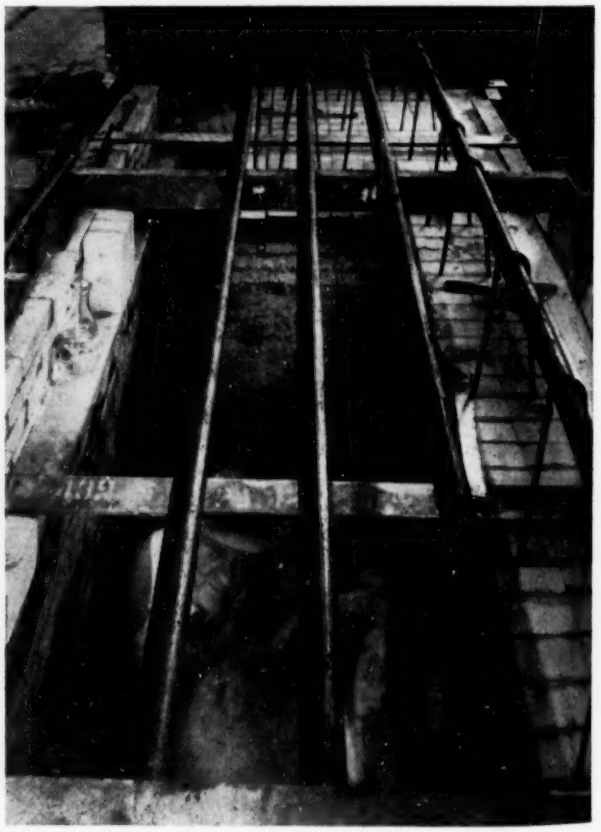


FIG. 8 CONSTRUCTION OF SUSPENDED BOILER FURNACE ARCH

TABLE 5 DATA ON FURNACE BRICK TEMPERATURES AS COLLECTED BY THE BABCOCK & WILCOX COMPANY

Date	June 25, 1940	July 9, 1940	July 18, 1940	August 6, 1940
Time				

TABLE 5 DATA ON FURNACE BRICK TEMPERATURES AS COLLECTED BY THE BABCOCK & WILCOX COMPANY

Date	June 25, 1940					July 9, 1940						July 18, 1940						August 6, 1940		
Time	11:00 a.m.	12:10 p.m.	1:35 p.m.	2:10 p.m.	2:30 p.m.	3:15 p.m.	4:30 p.m.	2:15 p.m.	3:00 p.m.	3:30 p.m.	4:30 p.m.	6:00 p.m.	2:45 p.m.	4:20 p.m.	5:40 p.m.	6:35 p.m.	1:45 p.m.	2:50 p.m.	5:20 p.m.
No. 1 T. C. deg F (thermocouple)	2930	2940	2950	2920		2930	2910	2910	2910	2904	2920	2910	2900	2900	2885	2890	2840	2820	2830
No. 2 T. C. deg F (thermocouple)	2410	2410	2420	2930		2405	2390	2430	2410	2410	2430	2410	2400	2420	2395	2440	2340	2330	2340
No. 1-A deg F (optical pyrometer)				3177		3188				3135									
No. 1-B deg F (optical pyrometer)				3004		2992				2996									
No. 2-A deg F (optical pyrometer)				3064		3004				2996									
No. 2-B deg F (optical pyrometer)				3028		3004				2960									
No. 3 deg F (optical pyrometer)				2743		2702				2615									
No. 4 deg F (optical pyrometer)				...		2435				2325									
Feedwater temperature, F	205	203	203				203	210	210		210	212	212	212	212	213	212	210	214
Temperature water entering tubes, F	595	600	595				600	...	...	...	...	590	590	589	589	588	588	589	591
Steam pressure, psi	1380	1405	1405				1400	1400	1400		1400	1400	1390	1400	1410	1400	1380	1400	1405
Absorption rate (total M Btu per hr)	437.3	437.6	439.4				416.6	457.3	457.5		460.0	457.4	450.4	460.6	443.8	459.9	462.9	453.1	455.3
(M Btu per sq ft per hr)	98.3	98.3	98.6				93.6	102.9	102.9		103.4	102.9	101.3	103.7	99.7	103.3	104.0	101.9	102.4
Steam output, lb per hr	405.5	405.5	412.0				388.0	411.0	411.0		414.0	412.0	416.0	435.0	412.0	435.0	424.0	411.0	417.0
Blowdown, lb per hr	74.5	75.0	61.9				64.5	115.1	115.0		113.7	115.0	88.7	70.2	82.8	68.6	101.9	104.6	101.0
Ratio water to steam at outlet of tubes (by weight)	5.94	6.03	5.94				6.40	5.15	5.14		5.11	5.15	5.25	5.15	5.44	5.16	6.0	6.16	6.12
CO_2, per cent					11.0					12.8									
Excess air, per cent					38.0					20.0									

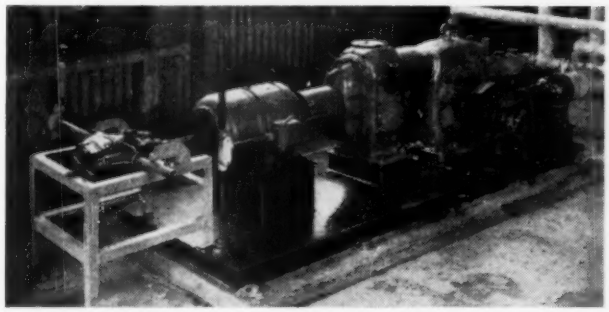
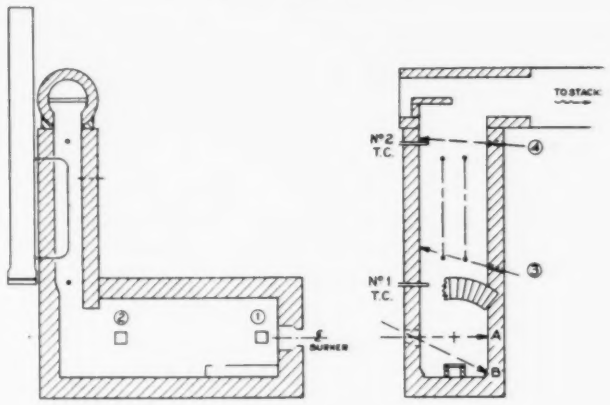


FIG. 9 BOILER FEED PUMP



N°1 T.C. = N°1 Thermocouple
N°2 T.C. = N°2 Thermocouple
1-A = (Flame) Front of primary furnace - horizontal
1-B = Front of primary furnace - downward
2-A = Rear of primary furnace - horizontal
2-B = Rear of primary furnace - downward
3 = Vertical flue - lower sidewall
4 = Vertical flue - upper sidewall

FIG. 10 LOCATION OF THERMOCOUPLE AND OPTICAL-PYROMETER OBSERVATIONS AS GIVEN IN TABLE 5

Fig. 11 is a diagrammatic arrangement, showing the manometer elevations and method of measuring steam output and blowdown water from the boiler. The manometers were installed by The Babcock & Wilcox Company and were used in measuring the circulation through the boiler tubes and also the water-to-steam ratios by weight at the outlet of the tubes.

A number of operating difficulties were experienced in maintaining continuous boiler operation at the rated heat input. Metering facilities of the condensed steam were found inadequate, due to the low steam flow, and arrangements were made to weigh separately the condensed steam and blowdown water. This change was found very satisfactory and, likewise, gave accurate means for calculating the heat absorption.

Operating difficulties were also experienced with the boiler feed pumps and, at frequent intervals, it was necessary to repack the pumps and finally install stainless-steel plungers. A number of changes were also made in the lubrication and method of its application.

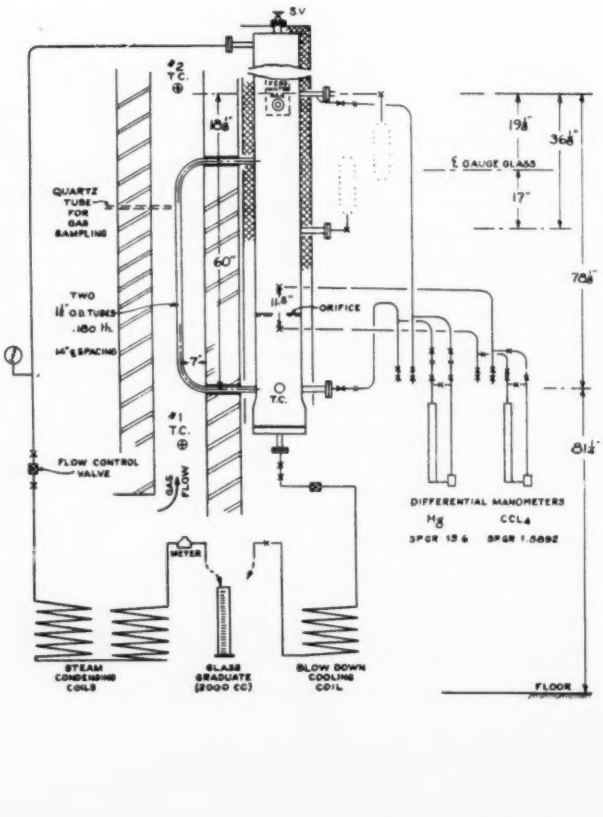
Data on the boiler operation were taken every 2 hr by the shift operators. A weekly summary of the daily average data on the furnace and evaporating conditions is given in Table 6.

TABLE 6 WEEKLY SUMMARY OF FURNACE CONDITIONS AND EVAPORATING CONDITIONS

	Furnace inlet temp, F	Furnace outlet temp, F	Feed-water temp, F	Circulation rate, lb per hr	Evaporation rate, lb per hr	Blowdown, lb per hr	Water-to-steam ratio	Heat absorption Btu per sq ft per hr, M
60-Day run:								
Week ending								
6/22/39	2884	2400	200	5219	399	84	5.8	97
6/29/39	2919	2404	205	5316	400	89	5.9	98
7/6/39	2923	2423	209	5340	405	97	5.8	98
7/13/39	2910	2419	207	4900	405	107	5.2	101
7/20/39	2885	2406	206	4680	413	85	4.9	100
7/27/39	2809	2367	209	4980	407	97	5.2	100
8/3/39	2803	2354	208	5680	410	101	6.1	101
8/10/39	2830	2334	210	5520	411	103	5.9	102
8/17/39	2841	2300	210	5400	395	96	..	97
First 30-day run:								
Week ending								
10/19/39	2283	1796	180	..	180	41	..	43
10/26/39	2460	1991	191	..	202	49	..	50
11/2/39	2502	2010	200	..	207	57	..	52
11/9/39	2495	2004	200	..	205	54	..	52
11/16/39	2501	2004	197	..	206	52	..	52
Second 30-day run:								
Week ending								
11/30/39	2726	2175	193	..	297	83	..	76
12/7/39	2756	2178	195	6250	298	72	9.7	75
12/15/39	2760	2161	197	6180	296	74	9.5	75
12/22/39	2772	2160	197	..	296	75	..	75

TABLE 7 WEEKLY SUMMARY ON DAILY OPERATION OF EXPERIMENTAL BOILER AND FEED-WATER TREATING SYSTEM

	Effluent No. 1 precipitator, silica, ppm	Filtered water, silica, ppm	Acid-treated water, total hardness, ppm	Soft water, total solids, ppm	Boiler water				
					Pht., ppm	M-O, ppm	NaCl, ppm	SiO_2, ppm	Total solids, ppm
60-Day run:									
Week ending									
6/22/39	6.0	1.8	149	246	105	194	397	18.5	1689
6/29/39	7.0	1.3	160	274	67	140	438	16.7	1723
7/6/39	8.0	1.6	186	287	57	128	455	14.5	1620
7/13/39	5.4	1.3	173	275	65	136	423	11.2	1854
7/20/39	6.9	1.8	137	247	69	156	421	18.2	1619
7/27/39	5.7	1.3	150	256	57	137	356	14.8	1553
8/3/39	4.6	1.6	149	288	55	135	308	11.7	1551
8/10/39	5.4	1.4	144	285	57	134	387	11.9	1638
8/17/39	4.4	1.3	153	270	..	..	..	..	766
First 30-day run:									
Week ending									
10/19/39	10.1	2.2	161	..	81	172	320	17.5	..
10/26/39	9.0	2.0	147	283	280	344	181	16.2	1821
11/2/39	10.4	2.1	152	285	133	184	147	10.4	1621
11/9/39	10.6	1.9	164	304	165	234	129	10.6	1726
11/16/39	9.0	1.8	168	300	151	210	111	10.9	1668
Second 30-day run:									
Week ending									
11/30/39	11.3	2.0	165	..	108	159	108	10.5	..
12/7/39	10.2	1.6	162	282	146	189	104	8.6	1627
12/15/39	11.9	1.8	178	287	164	210	108	12.1	1615
12/22/39	11.1	1.8	177	307	182	242	82	10.4	1720



Water Treatment

Throughout the operation of the boiler, 100 per cent treated make-up water was fed from the treating equipment as previously described. All stainless or monel-metal containers were used in collecting water samples for silica analyses, thus avoiding any such possible contamination as existed with Pyrex glassware.

A Diller photoelectric-cell color comparator was employed in all silica testing, thus enabling the operator to make frequent checks and changes in the chemical treatment when necessary. This method of testing for dissolved silica was a decided improvement over the visual color comparisons or gravimetric analyses.

Hourly tests were made on water samples for chemical control in the water-treatment plant. A weekly summary of these tests is given in Table 7.

A supplementary chemical treatment, consisting of definite amounts of sodium sulphite, trisodium phosphate, caustic soda and, occasionally, soda ash, was pumped as a single solution direct to the boiler. This treatment was used chemically to fix any traces of oxygen in the feedwater not removed in the deaerating heater and also to precipitate any hardness remaining in the feedwater as a tricalcium phosphate.

Analyses of the boiler blowdown water were made at least once every 4 hours to control the supplementary chemical treatment. Composite weekly samples of blowdown water were likewise sent to the laboratory for complete analyses.

FIG. 11 (LEFT) DIAGRAMMATIC ARRANGEMENT SHOWING MANOMETER ELEVATIONS AND METHOD OF MEASURING OUTPUT FROM BOILER

TABLE 8 CHEMICAL ANALYSES OF INTERNAL TUBE DEPOSITS

Sample No.	1	2	3	4	5	6	7	8	9
	Per cent	Per cent	Per cent	Per cent	Per cent	Per cent	Per cent	Per cent	Per cent
Ignition loss at 900 F	+0.30	−0.87	+1.31	+2.71	..	−0.77	−0.52	−0.39	−0.44
Ignition loss at 1200 F	+0.44	− .90	+1.64	+3.09	..	−1.33	−0.83	−0.63	−0.59
Ignition loss at 1500 F	+0.04	−1.08	+1.35	+2.28	..	−2.13	−1.22	−1.63	−1.31
Ignition loss at 1800 F	−0.41	−1.41	+0.11	+1.23	−0.54	−2.38	−1.41	−2.08	−1.49
Ether extractable	0.61	0.39	0.28	0.26	0.08	0.79	0.76	0.95	0.75
Silica as SiO_2	1.22	0.83	0.80	1.47	0.68	0.38	0.15	0.20	0.17
Iron as Fe	36.57	53.58	48.70	59.40	53.21	16.45	13.70	46.51	28.22
Aluminum as Al_2O_3	5.78	5.68	5.53	0.78	4.30	4.35	5.52	2.10	5.00
Phosphate as PO_4	24.33	16.69	14.31	9.00	11.29	43.46	39.79	13.00	29.93
Zinc as ZnO	..	..	..	..	..	12.10	12.26	1.94	6.08
Copper as Cu	..	..	..	..	..	..	..	Less than 0.001	0.05
Calcium as CaO	1.37	1.62	1.50	0.61	1.45	10.72	8.33	10.32	7.72
Magnesium as MgO	0.66	1.20	0.74	0.32	0.66	4.38	4.46	0.42	1.69
Sulphate as SO_4	0.26	0.73	0.49	0.26	0.27	0.28	0.24	0.24	0.54
Sodium as NA_2O	9.54	7.07	5.66	3.77	2.74	0.62	1.01	0 76	6.43
Acid insoluble loss on ignition	1.89	2.17	1.57	1.38	..	None in 0.3 g	None in 0.3 g	0.26	0.50
Water-soluble sulphate as SO_4	0.10	0.63	0.40	0.27	0.27	0.02	0.03	0.26	0.15
Water-soluble phosphate as PO_4	1.10	0.68	0.43	0.19	0.34	0.57	0.50	0.08	0.09
Water-soluble chloride as CL	0.07	0.04	0.08	0.03	nil	0.08	0.07	0.01	0.02

Sample no.

1 Loose patches from straight section
2 Scale from upper bend
3 Scale from lower bend
4 Scale from straight section—hard and fast } 60-day run
5 Sludge from header
6 Deposit from south tube after first 30-day run—Upper half straight section
7 Deposit from south tube after first 30-day run—Lower half straight section
8 Deposit from south tube after second 30-day run
9 Deposit from north tube formed during exposure of first and second 30-day run

NOTE:
+ = Gain in weight.
− = Loss in weight.

TUBE EXAMINATION

On August 14, after 60 days of operation of the experimental boiler, one of the tubes blistered and failed. Examination of the tubes, after they had been removed, showed that they were blistered at several points along the wall of the tube and on the side facing the fire. These tubes were cut up and the deposits were analyzed. Microscopic examination was also made of the tube metal.

Figs. 12 to 17, inclusive, are views of the tubes in the furnace and after being removed and sectioned.

Chemical and X-ray analyses were made of the deposits, the chemical analyses being given in Table 8 of samples Nos. 1 to 5, inclusive.

Although many opinions were expressed as to the possible cause of the failure, definite conclusions on this point were not reached. There were, however, several factors which may have contributed to the failure, these being:

1 Formation of analcite scale or other scales of this group, which have not been adequately identified.

2 Concentrated heat input at certain sections of the tube, due to cracking off of external scale which accumulated on the outside of the tube.

3 The presence of oil or grease brought into the feedwater from the lubrication of the feedwater pumps.

In order to study factor (1) further, additional X-ray analyses were made of the deposits.

In factor (2), it was recommended that the evaporation tests be repeated and the furnace temperature so regulated that the average heat input would be in the vicinity of 50,000 Btu per sq ft per hr. The evaporation tests, leading to the failure of the tube, had been made at an average heat input of 100,000 Btu. It was calculated that, with this average heat input, the lower half of the tube where failure occurred was subject to a heat absorption of 150,000 Btu and the upper half of the tube to 65,000 Btu.

This compares with a maximum and average heat input of the plant boiler of 50,000 and 25,000 Btu per sq ft per hr, respectively. During the week of August 5, the Deepwater contract was authorized and the boiler to be installed at Deepwater was purchased. This boiler was designed for a maximum and average heat input, respectively, as previously mentioned.

The recommendations for repeating the test run follow:

The proposed test run would be for 30 days, after which one tube would be removed and sectioned for examination. The second tube in the furnace would not be disturbed but the boiler would be put back on the line and continued in service to determine if scale would accumulate under the operating conditions proposed, after the second 30-day period of service.

The decision to increase or decrease the rate of heat input on the tubes, during the second 30-day run, would be determined after the first tube was cut and examined.

In order to eliminate as far as possible the presence of oil or grease in the feedwater from lubrication of the boiler feed pump, a metallic packing with a graphite base, which would not require the use of oil or grease, would be used.

BOILER OPERATION

The boiler was placed in operation October 18, and the furnace temperature so regulated that the average heat input was in the vicinity of 50,000 Btu per sq ft per hr.

The schedule of testing the water during the various steps in treatment was the same as previously discussed. The weekly summary of the tests on the water-treating system is part of Table 7. Data on the furnace and evaporating conditions on this run are given in Table 6.

No abnormal operating difficulties were experienced for the 30-day period, October 18 to November 17, the boiler being shut down on this last-mentioned date.

The south tube was removed and sectioned for examination. No blisters were noted along the wall of the tube and the internal deposit was of quite different appearance from that noted after the 60-day run. The deposit on the tube formed during the 30-day run was easily removed and had the appearance of sludge rather than showing any crystalline formation.

Illustrations of the straight section of the tube and a close-up view of the top portion before removing the internal deposits are shown in Figs. 18 and 19.

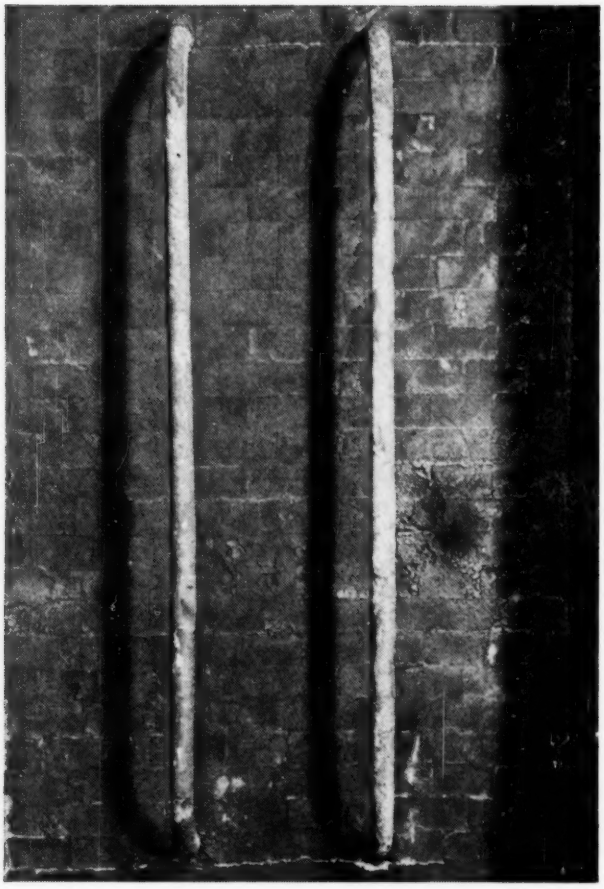


FIG. 12 SHOWING BOILER TUBES AFTER 60-DAY RUN
(Dark spot on right-hand side of photograph caused by steam impinging on brickwork from failure north tube.)

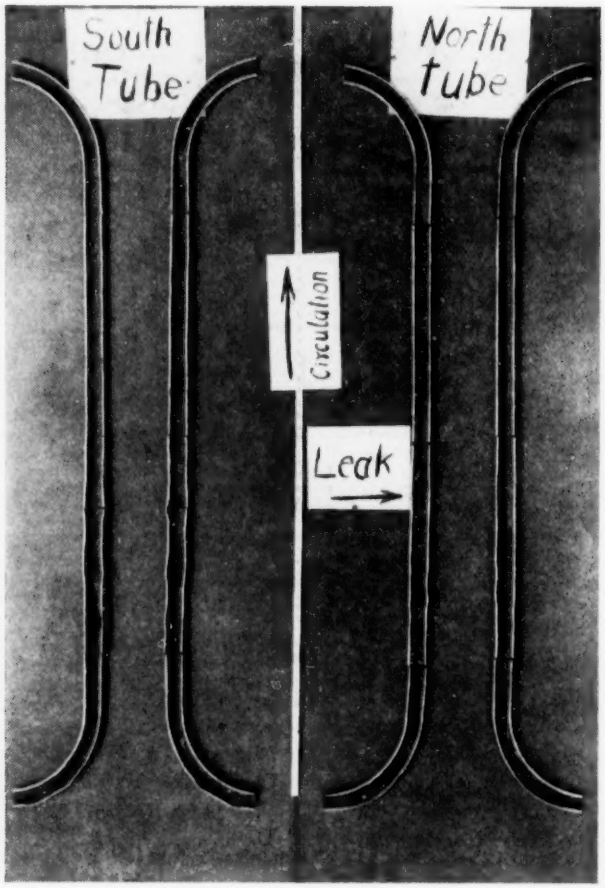


FIG. 13 SECTIONED NORTH AND SOUTH BOILER TUBES AFTER 60-DAY RUN

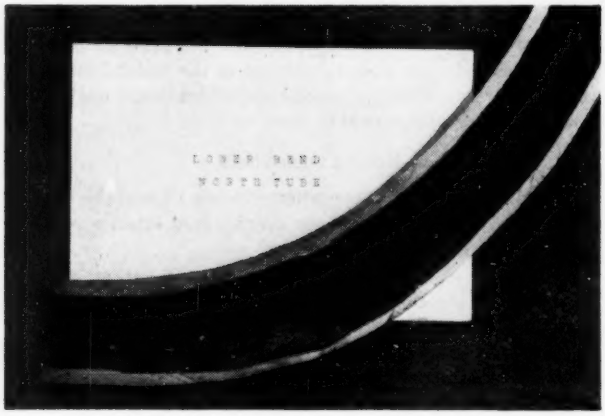


FIG. 14 SECTIONED LOWER BEND—NORTH TUBE AFTER 60-DAY RUN

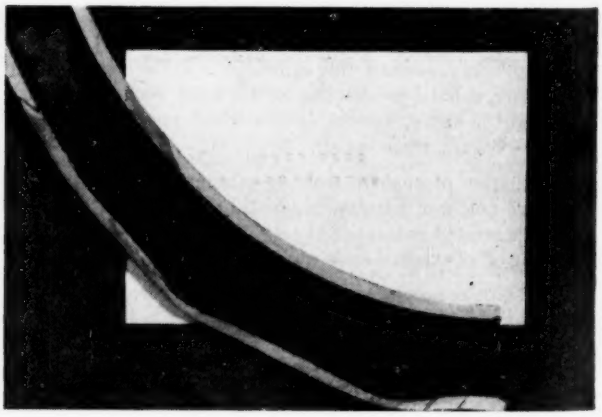


FIG. 15 SECTIONED LOWER BEND—SOUTH TUBE AFTER 60-DAY RUN

The internal-surface deposit was divided into two portions, namely, from the upper half and lower half. The chemical analysis of each portion is given in Table 8, samples Nos. 6 and 7. Microscopic examination of the tube metal was also made.

The zinc oxide, showing in the chemical analysis, resulted from contamination of the feedwater with zinc from a galvanized line between the softener and deaerating heater. This source of contamination was eliminated on the succeeding run.

THIRD BOILER RUN—SECOND 30-DAY RUN

The south tube was replaced with a new tube and boiler operation was again resumed on November 22. Due to the satisfactory internal condition of the south tube after the first 30-day run it was decided to increase the rate of heat absorption to 75,000 Btu per sq ft per hr during the second 30-day run. With this average heat input it was estimated that the maximum and minimum heat input would be 110,000 and 50,000 Btu per sq ft per hr, respectively.



FIG. 16 SECTION OF NORTH TUBE SHOWING INTERNAL LOCATION OF FAILURE AFTER 60-DAY RUN

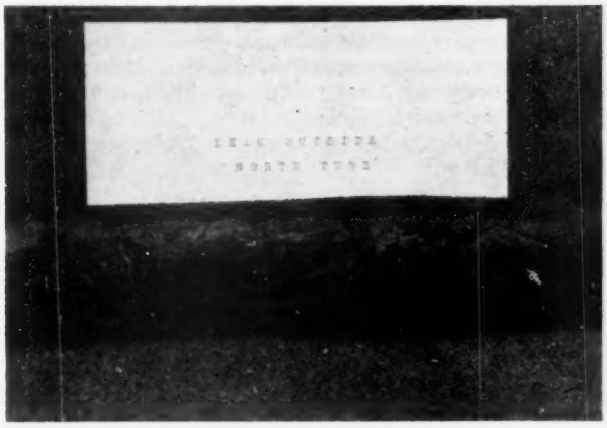


FIG. 17 SECTION OF NORTH TUBE SHOWING EXTERNAL LOCATION OF FAILURE AFTER 60-DAY RUN

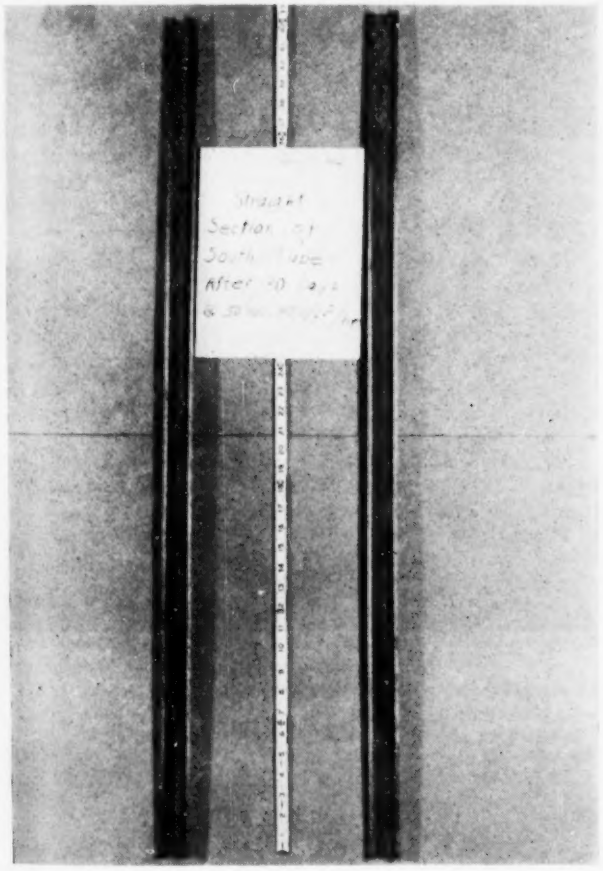


FIG. 18 STRAIGHT SECTION OF SOUTH TUBE AFTER FIRST 30-DAY RUN

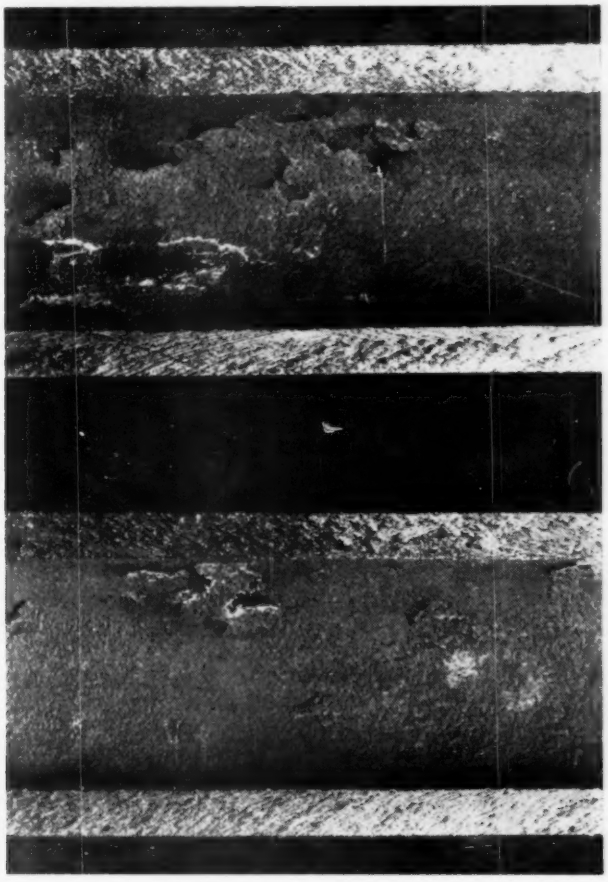


FIG. 19 CLOSE-UP VIEW OF TOP PORTION OF TUBE IN FIG. 18

During the operation of the first 30-day run it was noted that the boiler water from the continuous blowdown was quite clear, that is, free from suspended solids. This condition was further checked by the large accumulation of soft sludge in the bottom of the boiler header when opened after the run mentioned.

The continuous-blowdown line was connected to the bottom of the header and, from the appearance of the internal deposit in the south tube after the 30-day run, it was the opinion that adequate removal of sludge was not being obtained. The sludge probably accumulated ahead of the continuous-blowdown control valve and acted as a filter in preventing further sludge removal.

To overcome this condition in the second 30-day run arrangements were made to open the continuous-blowdown valve wide every 8 hr and rapidly blow down from 4 to 5 lb of water from the boiler. This volume of water was weighed, together with the normal continuous blowdown, in arriving at the total blowdown from the boiler.

The effectiveness of this intermittent blow may be noted from

the data in Table 9. Samples of boiler water were collected before, during, and after the intermittent blow.

The time interval between collecting the sample marked "during intermittent blow" and "after intermittent blow" was approximately 2 hours. It required that length of time to reset properly the continuous-blowdown control valve.

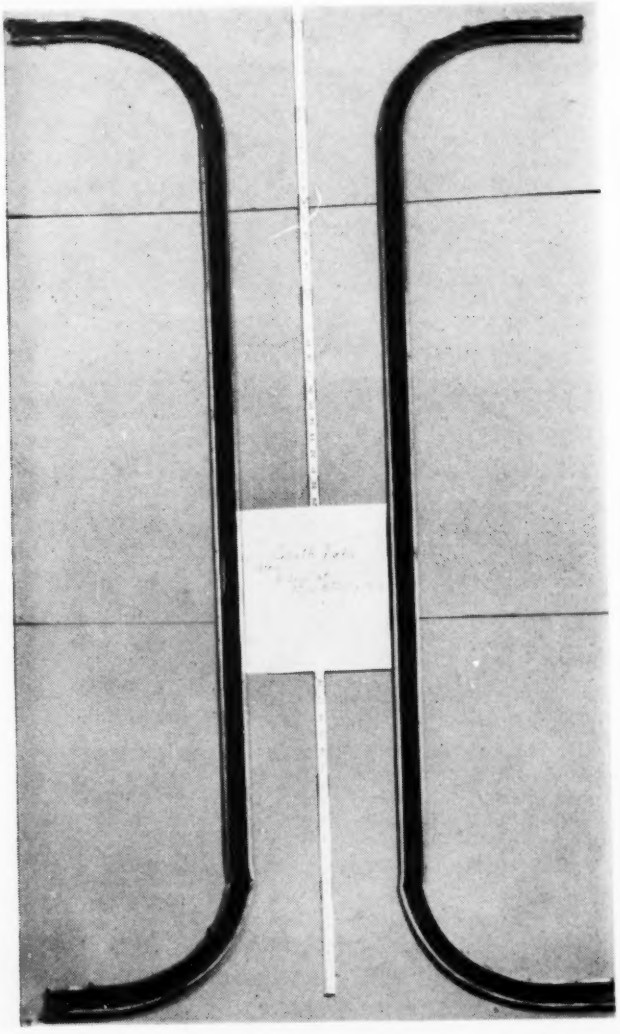


FIG. 20 SECTIONED SOUTH TUBE AFTER SECOND 30-DAY RUN



FIG. 21 CLOSE-UP VIEW OF SOUTH TUBE AS SHOWN IN FIG. 20

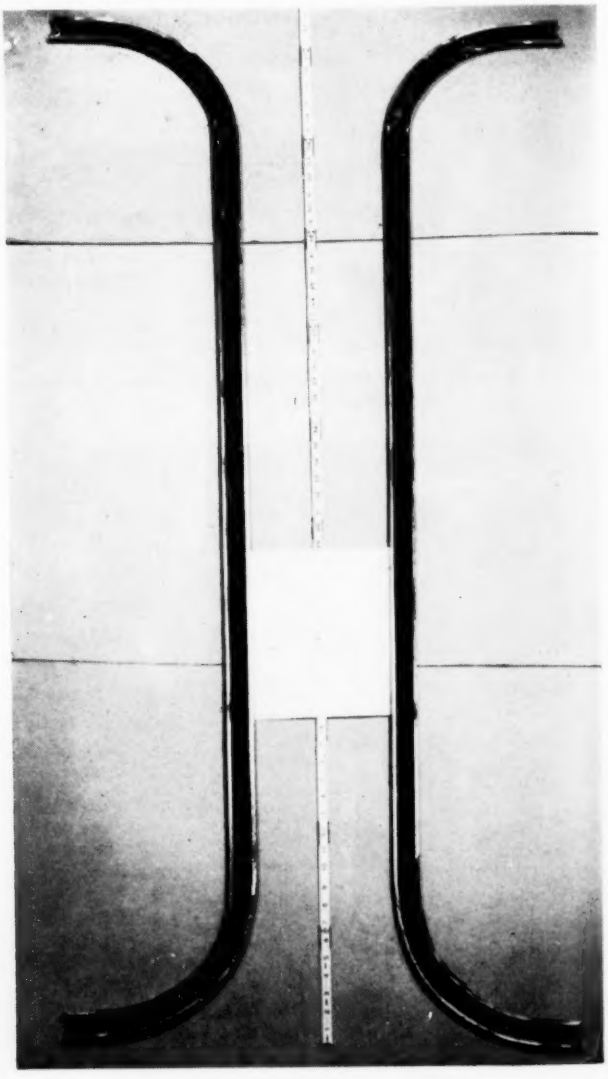


FIG. 22 SECTIONED NORTH TUBE
(Tube was exposed during first and second 30-day run.)

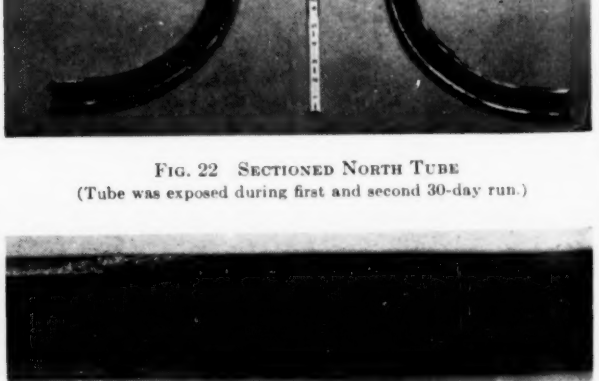


FIG. 23 TYPICAL STRAIGHT SECTION OF TUBE IN FIG. 22

Table 9 shows the effectiveness of removing the suspended solids by intermittent blow. As a check on the suspended solids, the suspended iron in each water sample was determined and reported in Table 9. Very little change was noted in the sodium-chloride content which indicated that not sufficient water was removed during the intermittent blow to affect the total dissolved-solids concentration.

TABLE 9 EFFECT OF INTERMITTENT BLOWDOWN IN REDUCING SUSPENDED SOLIDS

Blowdown	Date	Suspended solids, ppm	Suspended iron as Fe	Sodium chloride ppm
Before intermittent blow....	12/6/40	13.4	..	93.8
During intermittent blow....	12/6/40	251.4	..	99.7
After intermittent blow.....	12/6/40	0	..	93.8
Before intermittent blow....	12/10/40	4.4	..	82.1
During intermittent blow....	12/10/40	12.0	..	82.1
After intermittent blow.....	12/10/40	2.4	..	82.1
Before intermittent blow....	12/13/40	14.0	0.3	82.1
During intermittent blow....	12/13/40	173.6	57.2	82.1
After intermittent blow.....	12/13/40	22.4	0.3	82.1
Before intermittent blow....	12/18/40	21.4	0.2	82.0
During intermittent blow....	12/18/40	53.0	40.7	82.0
After intermittent blow.....	12/18/40	52.6	0.4	82.0
Before intermittent blow....	12/20/40	11.0	0.9	93.8
During intermittent blow....	12/20/40	186.0	90.1	93.8
After intermittent blow.....	12/20/40	4.6	0.9	87.9

The same procedure of testing, supplementary treatment, and furnace observations was followed as discussed under the first 30-day run. The data on the feedwater treatment and boiler-water test are part of Table 7, and on the furnace and evaporating conditions are part of Table 6.

The second 30-day run terminated on December 22 when the boiler was shut down.

Both tubes were removed and sectioned for examination. Figs. 20 and 21 show the south tube, and Figs. 22 and 23, the north tube, before any internal deposits were removed. A comparison of Figs. 20 and 21 with Figs. 18 and 19 will indicate the difference in quantity of sludge. Very little if any sludge accumulation showed in the south tube after 30 days of operation at 75,000-Btu heat input, as compared with 30 days of operation at 50,000-Btu heat input. The only major difference other than the heat input was the intermittent blow to remove suspended solids.

The north tube, which had been exposed for both 30-day runs, showed less sludge accumulation than was present in the south tube exposed for the first 30-day run. This likewise indicated that the intermittent blow not only prevented sludge from accumulating but also assisted in removing old sludge previously deposited.

The chemical analyses from the south and north tubes are given in Table 8 for samples Nos. 8 and 9.

The zinc content of the sludge from the south tube, after the second 30-day run, was 1.94 per cent as ZnO, compared to 12.1 per cent after the first 30-day run. The decrease of zinc in the sludge was due to a change in the feedwater piping, that is, from galvanized pipe to stainless steel. Complete elimination of zinc is quite problematical as the raw water contains varying amounts which are not entirely removed by the feedwater treatment.

Conclusions

1 The investigation showed that the Dye Works water supply can be treated so as to obtain a supply of suitable purity for high-pressure boiler-feed requirements. It was possible to remove the color and reduce the silica content to 2 ppm or lower, by suitable iron-salt coagulants.

2 During the operation of the zeolite softener for removal of hardness in the filtered water, it was found necessary to change the standards as to softener operation to obtain desirable low hardness at all times for boiler feed. This observation was of sufficient importance that special tests were made by the softener manufacturer, and the specifications and guarantees on softener capacities were completely revised. This represented a distinct change in the feed treatment which was directly applicable to the plant-size softening equipment, as a result of the experimental work.

3 The heat input on the experimental boiler was at a maximum of 150,000 Btu with an average of 100,000 Btu when the tubes failed. When lowering the average to 75,000 Btu, which represented a maximum of 110,000 Btu, no trouble with scale formation was experienced. This heat input considerably exceeded the maximum of 50,000 Btu, the expected operating condition on the plant unit. With more favorable water-treating conditions, as would be expected on a plant scale, there is every reason to believe that the plant unit can be operated for at least 6 months between inspections without forced outage.

4 The practice of intermittent blowdown for sludge removal on the experimental boiler has been directly applicable to a similar location of intermittent blow on the plant boiler. Without this information, it may be quite definitely stated that, the boiler manufacturer would not have agreed to intermittent blow from the lower drum on the plant unit. Engineers of the manufacturer have always been of the opinion, even at boiler pressures below 1400 lb, that intermittent blowdown from the lower drum was not necessary and advised against such procedure.

5 The experience on silica removal and operation of the experimental boiler, at heat-absorption values well above the maximum expected in the plant unit, show that considerable knowledge and confidence have been gained which will assist in avoiding forced outages and maintenance on the plant unit.

Discussion

S. B. Applebaum.[2] The work described in this paper represents a pioneer effort and a major advance in the field of feedwater treatment for high-pressure boilers.

Previous practice in this country for boilers having a pressure as high as 1400 psi has been more or less confined to a low percentage of make-up as in central power plants. All of these plants used evaporators to distill even that small percentage of make-up. There is only one other plant now in operation that approaches this boiler pressure which uses Zeo-Karb feedwater treatment instead of evaporators, and that is the Consolidated Edison Company, Waterside Station, New York, N. Y., but in that case the raw water comes from the New York City supply and is therefore of much superior quality as compared to the natural pond water involved in the Deepwater case. Furthermore, only 25 per cent make-up is involved at Waterside, whereas, the make-up at Deepwater will be 100 per cent.

It was due to the fact that no actual operating experience in this country was available on chemical feedwater treatment for 100 per cent make-up to boilers of such high pressure that this extensive experimental work was undertaken.

The successful development of high-pressure boilers has been more or less dependent upon equally successful development of improved feedwater-conditioning methods to permit such high-pressure boilers to function successfully with chemically treated feedwater. The du Pont Company is rendering a service to the engineering public in publishing the interesting data obtained in these tests, which should be of considerable help to the designers of future high-pressure plants.

The investigation brings out a point of increasing importance, i.e., that boiler design and the type of feedwater treatment to be selected must be considered simultaneously. In other words, the boiler designer, in order to insure successful operating re-

[2] Vice-President, The Permutit Company, New York, N. Y. Mem. A.S.M.E.

sults, must become more and more cognizant of the chemical composition of the feedwater and the effect of the various possible constituents of this feedwater on boiler operation. Likewise, the specialist in feedwater treatment must take into consideration boiler design before recommending any specific type of feedwater treatment for successful operating results with any particular boiler.

The raw water in this case will come from a pond or reservoir behind Munson Dam. It is a typical surface supply, such as is frequently encountered on the eastern seaboard and will be subjected to the usual contamination of color, organic matter, algae, turbidity, etc. It also has a rather high silica content, ranging from 8 ppm up to 25 ppm, or an average of about 14 ppm. Table 10, of this discussion, gives the average composition and maximum composition to be expected.

The chemical constituents which cause the major operating difficulties in high-pressure boilers are (1) hardness, (2) silica, (3) color and organic matter, (4) alkalinity, (5) oxygen.

The first two impurities, hardness and silica, are mainly responsible for the objectionable scale deposits in the boiler, as well as deposits in superheaters and turbines, which may result from carry-over. The third and fourth impurities, color and alkalinity, are mainly responsible for carry-over difficulties. The fifth impurity, oxygen, is mainly responsible for corrosion.

Therefore, the feedwater-treatment plant that was outlined in a preliminary manner to condition this surface water to make it suitable for feeding these high-pressure boilers involved:

1 Color removal to take care of the physical impurities mentioned.
2 Silica removal.
3 Hardness and alkalinity removal.
4 Deaeration to remove oxygen.

Our preliminary laboratory experiments also indicated that it would be difficult to accomplish the removal of the color and the silica simultaneously, because the peculiar nature of the color in this case made it necessary to coagulate at a pH of 4.5 to 5 to insure very good color removal. The silica removal, on the other hand, required an optimum pH of about 9 to 9.5. Some silica is removed in the color-removal step, as indicated in the author's Table 2, but the major silica removal is accomplished in step No. 2 at the higher pH values. Permutit Spaulding precipitators were used for both color removal and silica removal in the two stages mentioned because, in this design of reaction tank, the sludge, formed by the chemical reagents added, is kept suspended by the agitators in the bottom of these tanks and the sludge is accumulated to occupy most of the lower portion of the tank. This large amount of suspended sludge in the precipitators is especially advantageous for adsorption phenomena, such as color removal and silica removal. Furthermore, the large excess of sludge present tends to drive both the color and the silica down to lower values than could be obtained in the absence of sludge. Therefore, an economy of chemical reagent and consequent lower operating cost is realized, as well as a superior quality of effluent.

The filters following the precipitators use nonsiliceous filtering medium, such as Anthrafilt, to avoid pickup of silica during filtration. Similarly, in the case of zeolite water softeners, a nonsiliceous zeolite, "Zeo-Karb Na," is employed to avoid pickup of silica from the zeolite. In the paper, Table 2 gives the analysis of the water at each step of treatment and below Table 2 is given the treatment costs per million gallons. This was based on the first part of the experimental work where Zeo-Karb H for cation removal and De-acidite for anion removal were used in the experimental units. Later, when the experimental boiler was installed, the Zeo-Karb H and De-acidite were no longer employed, and instead, Zeo-Karb Na for hardness removal alone was utilized and no anions were removed. Table 11, of this discussion, shows the average results at each stage of treatment, which are anticipated for the large plant now being designed and constructed. At the bottom of Table 11, are given the chemical costs anticipated.

TABLE 10 RAW-WATER COMPOSITION AT MUNSON DAM OF DEEPWATER LIGHT & POWER COMPANY
(Analyses expressed in ppm)

Chemical Expression	Symbol	Expressed as	Average	Maximum
Total Hardness	TH	$CaCO_3$	45	60
Calcium "	CaH	"	28	33
Magnesium "	MgH	"	17	27
Bicarbonates	HCO_3	"	30	50
Carbonates	CO_3	"	0	0
Hydrates	OH	"	0	0
Non-Carb Hardness	NCH	"	15	30
Sodium Alkalinity	Alk Na	"	0	0
*Alkalinity M.O.	Alk A	"	30	50
" Phenol	Alk B	"	0	0
Free Carbon Dioxide	CO_2	CO_2	8	10
*Chlorides	Cl	NaCl	40	70
*Sulfates	SO_4	Na_2SO_4	40	70
Iron	Fe	Fe		
pH	—	—		
*Silica		SiO_2	14	25
Color			40	115
Total Dissolved Solids (items x)			124	215

TABLE 11 AVERAGE RESULTS AT EACH STAGE OF TREATMENT AT MUNSON DAM, AND CHEMICAL COSTS ANTICIPATED
(Analyses expressed in ppm)

1. Raw water
2. After color removal
3. After Aeration
4. After Silica Removal
5. After acid & sodium zeolite

Chemical Expression	Symbol	Expressed as	1.	2.	3.	4.	5.
Total Hardness	TH	$CaCO_3$	45	45	45	154	2
Calcium "	CaH	"	28	28	28	137	1
Magnesium "	MgH	"	17	17	17	17	1
Bicarbonates	HCO_3	"	30	0	0	4	11
Carbonates	CO_3	"	0	0	0	16	0
Hydrates	OH	"	0	0	0	0	0
Non-Carb Hardness	NCH	"	15	45	45	104	0
Sodium Alkalinity	Alk Na	"	0	0	0	0	9
*Alkalinity M.O.	Alk A	"	30	-1	-1	20	11
" Phenol	Alk B	"	0	0	0	8	0
Free Carbon Dioxide	CO_2	CO_2	8	34	10	0	1
*Chlorides	Cl	NaCl	40	40	40	40	40
*Sulfates	SO_4	Na_2SO_4	40	90	90	228	240
Iron	Fe	Fe					
pH	—	—	7.0	4.5	4.6	9.5	7.5
*Silica		SiO_2	14.0	10.0	10	3.0	3.0
Color			40	10	10	10	10
Total Dissolved Solids, (sum of items x)			124	140	140	291	294

APPROXIMATE CHEMICAL COSTS

Type Chemical and % Purity	lbs. Chemical per million gallons water	Cost Chemical c per lb	$ chemical cost per thousand gallons	
Color Removal (Ferrisul	283	1.25	3.54	
(Acid	75	0.84	0.63	
				4.17
SiO_2 Removal (Ferrisul	1040	1.25	13.00	
(Lime hydrate	725	0.55	4.00	
				17.00
Acid	84	0.84		0.71
Salt for Sodium Zeo-Karb	4760	0.275		13.55
				$31.43

(Note: The chemical costs are based upon present market prices, and may be subject to some fluctuations by the time the plant starts operation in 1942.)

As the author points out, the results anticipated in the large-scale plant will be superior to the results obtained in the pilot plant because of the greater ease of control and the greater depth of sludge, etc., in the large tanks.

The actual plant will also involve some changes from the experimental treatment, such as:

1 Acid will be added in addition to ferric sulphate for color removal. The acid feed will be pH-controlled and will save some ferric sulphate, thus reducing the chemical costs for this step.

2 Aeration will be employed after the color removal and before the silica removal, so as to reduce the free carbon dioxide in solution below 10 ppm. This will save an equivalent amount of

lime in the silica-removal step and will reduce the total hardness in the effluent of that step, which the sodium zeolite will have to remove, thus keeping the operating costs at a minimum.

It is to be noted in Table 11 that the anticipated hardness of the zeolite effluent will be under 2 ppm, and most of the time the hardness will be under 1 ppm. This will reduce the amount of phosphate employed for secondary treatment, added directly to the boilers, and will therefore reduce the amount of phosphate sludge that will be formed in the boiler. This very low hardness in the zeolite effluent is obtained by special attention to the design of the softeners and to their regeneration. Also, special soap tests are employed to test the zeolite effluent in order to make sure that the hardness does not exceed the low figures mentioned.

Our large-scale water-treatment plant is being designed in co-operation with the American Gas & Electric Company and the du Pont Company, and is expected to go into operation early in 1942. We all look forward to publication of the actual operating results obtained next year.

F. G. Ely.[3] The author is to be congratulated for the thoroughgoing manner in which he has undertaken and prosecuted this unique and interesting experiment in feedwater treatment. Means for obtaining the final proof of results, under pilot-plant conditions of evaporation which simulate, but in many respects exceed, those of plant operation, were necessarily elaborate and expensive, and the Society is indebted to the author and his company for this comprehensive record of their experience and data.

During the course of the steaming tests, certain observations were made of heat-transfer and circulation characteristics of the boiler system, as given in Table 6 of the paper. It will be of interest to note that, at the present time, the writer's company is conducting a short supplementary series of tests to extend these data beyond the range of temperature and rating which could be accommodated in the principal series of feedwater experiments. Condensate is being used in the system, and additional data are being taken with high-velocity thermocouple and thermal probe to explore the distribution of temperature and heat absorption in the vertical gas passage where the boiler tubes are located.

Incomplete and preliminary results indicate that the estimated values of maximum and minimum absorption rate, as stated by the author, are reasonably confirmed; also that, where no difficulty with internal cleanliness of the tubes is involved, the evaporating surfaces of this model boiler have withstood materially higher rates of heat transfer without distress.

It is perhaps significant to note that the maximum absorption rate sustained in the author's final 30-day run exceeds the minimum and average rates of the first 60-day run when overheating of the tube metal throughout its length was detected. This would seem to indicate that causes 1 and 3, in conjunction with the sludge condition, are primarily accountable for failure of the tubes in the initial run. Beyond doubt, however, any question of internal cleanliness is aggravated by high rates of heat absorption.

Fig. 11, of the paper, illustrates an arrangement of high-pressure manometers which were used in obtaining data on circulation flow. In this simple circulating system, the total downward flow of water in the header was passed through a concentric orifice, and differential pressure was indicated by a column of carbon tetrachloride, submerged by water in the connecting lines. In calculating the rate of flow entering the boiler tubes, as given in Table 6, of the paper, manometer readings were first corrected for fluid-density differences of the carbon tetrachloride, the cool water in the connecting piping, and the hot water, at saturation temperature, in the header. The separately measured blowdown rate was then subtracted from the total flow to obtain the net flow rate entering the tubes. From these data, and the accompanying values of latent heat and absorption rate, it was possible to calculate terminal ratios of water to steam in the mixture leaving the tubes, as given in Table 6, and also the corresponding flow velocities.

These measurements were undertaken for general confirmation of conditions existing during the feedwater experiments, and are not regarded as precision tests of circulation fundamentals. It is of interest, however, to add that the observed results are in good agreement with previously calculated characteristics of the system.

The second manometer, shown at the left in Fig. 11, of the paper, served primarily as an auxiliary indicator of boiler-water level.

The author has indicated that, in the design of the plant boiler, much lower average and maximum heat-absorption rates are to be expected. This is an important consideration for an operating unit that is to be supplied with high percentage make-up of treated water, and lends an added factor of safety against unexpected or inadvertent changes in the treating plant. It is reassuring to have obtained such tangible evidence of successful water treatment under accelerated conditions in the experimental unit.

E. B. Powell.[4] The author records for us another step in the utilization of chemically conditioned natural waters for the generation of steam at high pressures and under high rates of heat absorption. As in most fruitful experimental studies, the perfect attainment is not reached on the first attempt, and the difficulties encountered are accepted as mere warnings of avoidable hazards. In his summation of opinions, secured on the tube failure after the 60-day run, the author states that no definite conclusion was reached as to the cause. The inclusion of quantity values for the deposits removed from the different tubes following the 60-day run and the two succeeding 30-day runs would doubtless now make the cause of the failure somewhat clearer. However, the evidence which is presented would seem to leave little room for doubt that the essential cause of the tube over-heating had been excessive quantity and insufficient fluidity on the part of the sludge content of the boiler water. In fact, the conduct of the subsequent test runs would indicate that the author himself suspected sludge to be the cause of the difficulty.

Although primarily devoted to a discussion of those aspects of the experimental study on which the commercial treatment of feedwater for the Dye Works' boiler-plant extension was to be based, the paper includes numerous other data of much interest and value at this time. Such items which are especially noteworthy are the results of the water treatment during part 1 of the experimental program, as given in Table 2, of the paper, and the furnace-performance and boiler-circulation data of Tables 5 and 6, with Figs. 10 and 11. Full demineralizing of natural waters has yet to attain the truly commercial stage but, meanwhile, demonstrations of performance on different waters are genuine contributions to knowledge. There is also a serious deficiency of data on gas and brickwork temperatures under different furnace and combustion conditions and on rates of circulation under different conditions of heat absorption and shape and dimensions of path. The author's observations help fill in the gaps.

[3] Analytical Engineer, The Babcock & Wilcox Company, New York, N. Y.

[4] Consulting Engineer, Stone & Webster Engineering Corporation, Boston, Mass. Mem. A.S.M.E.

S. E. Tray.[5] The author is to be congratulated for the comprehensive information which he has developed from the test data obtained in this experimental project. This is perhaps the first time that such a complete series of tests has been made on other than a laboratory scale, prior to actual plant installation. The fact that all possible factors were taken into consideration, in order to simulate actual plant operation, makes the results of paramount importance to those contemplating the installation of high-pressure boilers with a high percentage of make-up.

Of particular interest are the results recorded at heat-transfer rates as high as 100,000 Btu per sq ft per hr. This is somewhat in excess of current design practice, but experience has indicated that such conditions may be reached on individual tubes at localized points in the boiler. Even at these high rates of heat transfer, there was no apparent distress noted on the heating surfaces of the boiler. This is an indication that, with the water in the proper condition to prevent deposits, no fear need be felt in operating at high rates of heat transfer as long as the heating surfaces are constantly supplied with water. While this experimental project has demonstrated the effectiveness of proper water treatment in a high-pressure test boiler, there may be some question as to whether a full-size boiler will have equally sufficient circulation. The results recorded by the author should encourage further investigation by boiler manufacturers to insure proper and adequate circulation at all ratings on full-size boilers.

The use of the X-ray diffraction method in studying the boiler deposits has proved of considerable value. This method not only provides a positive method of identification for the various constituents in the boiler deposits, but also indicates the manner in which formation occurs on the heating surfaces. All of the deposits contained an appreciable percentage of iron, which would render optical methods useless as a means of identifying the various combinations present. The use of the X ray in the study of boiler scales, while rather recent, has already pointed the way toward acquiring a more complete understanding of the methods of scale formation. This will be extremely valuable in suggesting definite means of preventing such deposits. As an illustration of the effectiveness of X-ray analysis, some five different types of silica scales have been identified. All of these were formed under widely varied conditions, and could not be differentiated by the usual chemical analysis.

The effect of external removal of silica from the feedwater is evidenced by the lack of any silica-scale formation in the deposits in the boiler. While silica is not completely absent in the feedwater, it has been reduced to a practical minimum. The question as to how low the silica should be carried in high-pressure boilers is as yet unanswered, but it is obvious that it should be as low as may be obtained, consistent with operating costs and capital investment. It is also obvious that water treatment should provide for a minimum of alkalinity and dissolved solids, if we are to operate boilers at 1400 psi or higher with large percentages of make-up water.

From the standpoint of boiler operation, this experimental project has been very informative, and has indicated that similar operation on a commercial scale is entirely feasible. Such plants will, of necessity, operate back-pressure turbines or topping units, in which the maximum kilowatt output must be obtained in order to justify the investment. In view of the influence of boiler water on steam conditions to high-pressure turbines, it will be interesting to observe the results obtained in actual plant operation. It is hardly feasible to construct a small turbine to operate in conjunction with a test boiler such as the author has described. Consequently, until actual operating data are available, the turbine characteristics for such a plant will not be known. It is reasonable to suppose, however, that, after all the factors have been considered which relate to proper steam conditions for high-pressure turbines, there should be a minimum of difficulty from this angle. Nevertheless, it should be recognized that reliable and continued operation of turbines, installed with boilers of the type under discussion, is absolutely essential. In this connection, the operating experience of 1400-lb turbines, operating in low-make-up plants, will be extremely valuable.

[5] Allis-Chalmers Mfg. Co., Milwaukee, Wis.

Author's Closure

Further data on the chemical cost of treating water indicate that the cost will be approximately $61 per million gallons. This cost is based on later market prices of chemicals than those given in Table 11.

A Study of Damper Characteristics

By P. S. DICKEY[1] and H. L. COPLEN,[2] CLEVELAND, OHIO

But meager information is at present available covering the design of dampers in spite of their universal use in furnace control. Tests made by the authors have shown that the size of the damper for a given application is the most important factor in determining the flow characteristic. A simplified procedure for predicting the flow characteristic of commonly used types of dampers is offered to stimulate interest in this subject among designing engineers. Mechanical features of design are discussed and suggestions for improvement offered. The relative merits of different types of dampers are considered.

Regulating Characteristics of Dampers

IN SPITE of the universal use of dampers as a means of controlling air and gas flow for furnaces of all types, there are but few published data covering the design of these devices. In boiler practice, prior to the introduction of mechanical-draft fans, the primary consideration in damper design was to avoid any pressure loss and thus reduction in capacity when the damper was wide open. To achieve this end, the dampers were usually made quite large, and the tendency has been to follow this practice without any thought as to their regulating characteristic.

A point which undoubtedly needs clarification is that of the meaning of a desirable flow characteristic in dampers. When the damper is used in combustion furnaces for regulating the air-fuel relation or for regulating the furnace pressure, it is desirable that the change in rate of gas flow per increment change in opening of the damper be reasonably uniform from the tightly closed position to the wide-open position. It is hardly possible to achieve this desirable result in dampers of conventional design but, with proper consideration of the size and general form of the damper, a reasonable approximation may be obtained.

It is not uncommon to find dampers installed which cause a change in the rate of gas flow 10 times as great per deg travel at 10 deg opening as is caused at 60 or 70 deg opening. This is bad for manual control since the operator cannot coordinate the effect and the cause and, hence, finds it difficult to obtain proper regulation. It is bad for automatic regulation as the regulator cannot be properly stabilized for the sensitive portion of the damper and yet achieve the maximum effective speed at the insensitive portion of the damper.

Since dampers are usually of considerable size, it is not ordinarily practicable to build them as precise mechanisms but, as will be pointed out later, this is entirely unnecessary. Dampers of simple and inexpensive construction and with quite reasonable clearances can be built to give good regulating characteristics for manual or automatic control if a few fundamental considerations are followed.

Mechanical Design

In selecting the most suitable damper design for a specific application, the designer must consider the following factors:

1 Is the damper to be used for regulating purposes or for complete shutoff only?

2 Is the duct in which the damper is located handling hot or cold gases?

3 Is the duct handling gases under pressure or under vacuum?

4 What size damper should be used?

5 Should the damper frame be round or rectangular?

6 Should single- or multiple-blade dampers be used?

7 What provisions shall be made for mechanical and dynamic balance?

8 What type of external linkage should be used for operating the damper?

If a damper is to be used for shutoff service only, the two prime considerations are the leakage possibilities and the power required to operate it. If the damper is to be used for regulating service, the leakage may or may not be important, depending upon how much range must be covered. The power required for operation is equally as important with the regulating damper as with the one used for shutoff only. The flow characteristic of the regulating damper must be considered if proper results are to be obtained.

Dampers of conventional design are suitable for use in ducts where gas temperatures do not exceed 800 F. They may also be used at higher temperatures if suitable allowance is made for the decreasing strength of materials at the elevated temperatures. For temperatures in excess of 1200 F, the usual practice is to use gates built of refractory materials which operate in water-cooled slides.

In general, the clearance between the damper blades and the damper frame must be increased as the gas temperature increases, due to possible warpage of the ductwork and damper frame at the elevated temperatures. The tests, made and described later, on typical types of dampers were carried out with models having close clearance and large clearance so that the effect on the flow characteristic may be determined. For ordinary work, the damper, having side and end clearances of 0.25 per cent of the cross-sectional dimensions of the frame, has been chosen as the design which will give good results without excessive manufacturing cost. For higher-temperature service, a design, having a side and end clearance of 2 per cent of the cross-sectional dimensions of the frame, has been chosen. It is believed that this added clearance will take care of any changes in the shape of the damper frame due to temperature variations.

Proper design of the damper shafts, shaft bearings, and seals is of utmost importance, particularly where the dampers are located in ducts in which the gases are under pressure and at high temperature and where there is any dust present in the flue gas. Both the sleeve type and ball-bearing type have been used with good success, though it is important that either type of bearing be located outside the damper frame and spaced some distance away from it with a suitable seal at the point where the damper shaft extends through the frame. Most bearing troubles are due either to misalignment or to hot gas or dust-laden gas being blown into the bearing through the opening between the damper shaft and damper frame.

In the smaller-size dampers, with rectangular or round frames, it is usually possible to provide frames of good rigidity, therefore, clearances may be small and leakage kept to very low values. A single-leaf damper, closing at right angles to the side wall, is the design which gives the best flow characteristic. There is no great

[1] Director of Research, Bailey Meter Company. Mem. A.S.M.E.
[2] Research Department, Bailey Meter Company.

Contributed by the Power Division and presented at the Spring Meeting, Atlanta, Ga., March 31–April 3, 1941, of The American Society of Mechanical Engineers.

Note: Statements and opinions advanced in papers are to be understood as individual expressions of their authors and not those of the Society.

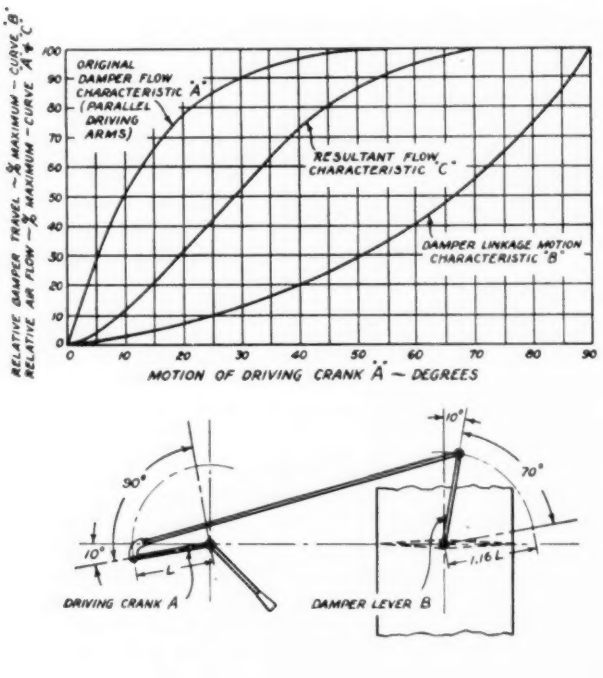


FIG. 1 STUDY OF LINKAGE FOR IMPROVING FLOW CHARACTERISTIC

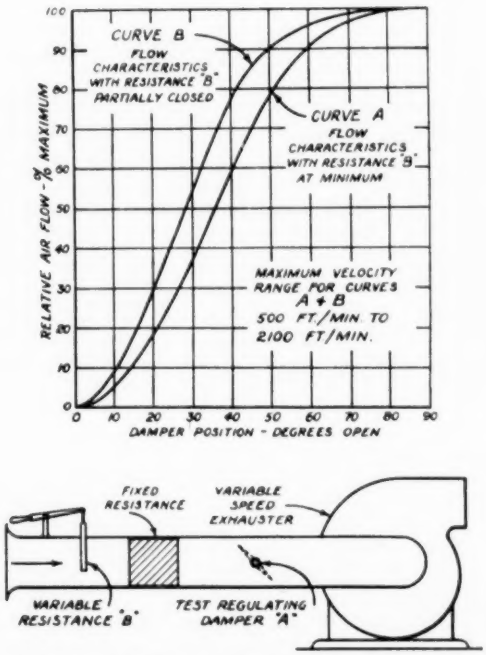


FIG. 3 TYPICAL DAMPER FLOW CHARACTERISTICS

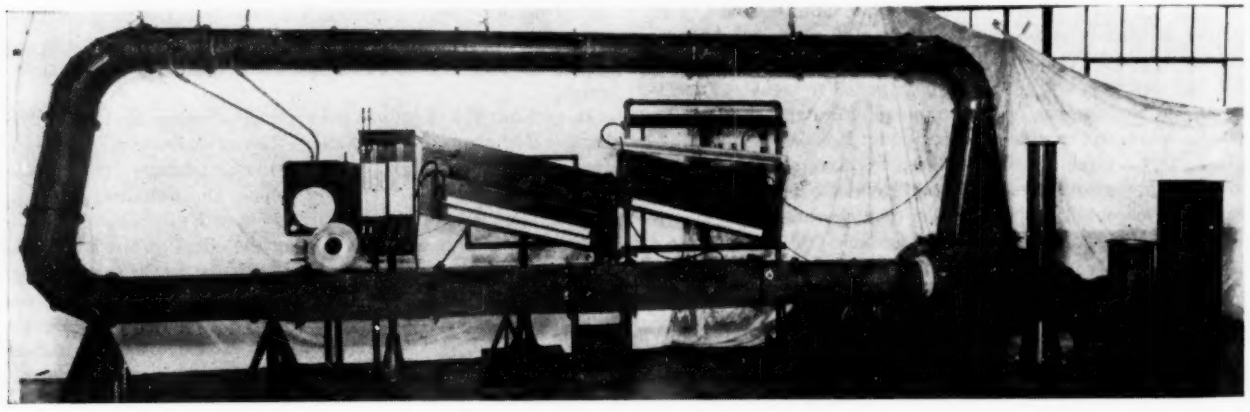


FIG. 2 VIEW OF TEST PLANT

difference between the area or flow characteristic of single-leaf dampers in rectangular or round ducts. Therefore, there is no reason for changing the shape of the duct at the point where the damper is installed until the duct size becomes large enough so that multiple-blade dampers are required.

In the larger sizes, where it is not practical to retain the single-leaf construction, in view of the large values of torque obtained due to small unbalance of the blade area, it becomes necessary to divide the damper into a number of blades or louvers. To accomplish the desirable flow characteristic of the single-leaf damper, a partition can be installed between blades. The use of this dividing partition not only gives the most desirable area and flow characteristic, but also provides a means of changing the over-all effective area of the damper after it is installed. In other words, if the damper is oversized it is possible after installation to block one or more of the louvers in the closed position and use only the remaining louvers for regulation.

Dividing partitions should be approximately the same length as the blade width to give proper results. The damper blade should be arranged to close at right angles to the dividing partitions as in the case of the single-leaf damper described. To overcome the increased leakage in the damper with the dividing partitions, which results because the blades cannot be closed against one another, side stops may be installed on the duct and on the dividing partition without seriously affecting the flow characteristic.

Another way in which to accomplish the flow characteristic of the single-leaf damper with multiple-louver dampers is to arrange the external linkage so that adjacent blades rotate in opposite directions. The principal difficulty with this arrangement, however, is that it is difficult to close the openings tightly between the louvers, unless sealing strips are installed between blades.

There is no reliable rule for determining the proper number of louvers for a given-size damper. It becomes necessary, therefore, for the designer, in a given-size frame, to select the number of blades which will keep the width of each blade, and thus the pos-

sible unbalanced force, within the limits of the driving mechanism. At the same time, he must keep the number of blades and thus the possible leakage area as low as possible.

Efforts have been made from time to time to obtain perfectly balanced dampers by adjusting the effective area of the blade on either side of the supporting or operating shaft. Such efforts are entirely justified as a means of reducing the torque necessary for operation, but this is strictly a field job as it is impractical for the designer to attempt to make a provision of this nature. In most cases, force unbalance is caused by area unbalance or by some unpredictable stratification of the gas flow in the duct. In dampers having louvers of considerable size, particularly width, an unbalanced area, caused by variations in manufacture well within the tolerance for this type of equipment, may result in considerable force being exerted on the operating shaft.

No doubt there is some unbalance exerted by the variable pressures existing over the area of the blade on the downstream side, but this likewise is difficult to predict, in view of the lack of standardization of damper types and sizes. Therefore, the best procedure for the designer is to strive for equal distribution at the areas of the damper blades and, if necessary, provide a balancing pendulum of suitable size on the outside of the duct, which may be used to offset any undesirable unbalance or to produce an unbalance in the opening or closing direction for those applications where this feature is desired.

When the desired flow characteristic cannot be obtained by using a proper size of damper as described later in the paper, approximate results may be obtained by the use of angularity in the driving linkage. For example, if an operating linkage is provided, as shown in Fig. 1, and the driving crank A starts close to the dead-center position when the damper is closed, a motion characteristic is obtained which provides only $^1/_8$ of the travel of the damper per deg motion of the driving crank at 10 deg that it does at 80 deg open. This motion characteristic is shown in Fig. 1, and it will be noted that the motion characteristic compensates for the poor flow characteristic of the oversize damper, which is usually similar to that also shown in the illustration. However, when using a linkage of this type to overcome a poor flow characteristic, it is essential that all bearings and all pins in the linkage be free of backlash or of lost motion, as otherwise all benefit of the retarded damper action near the closed position will be lost.

Investigation of Flow Characteristics

The misapprehension which too often exists among designers and users of dampers is that, because a specific damper has given good results in one application, it will likewise give good results in all applications. Efforts have frequently been made to standardize damper design and size for definite capacities, but the results are not always satisfactory for reasons which become obvious when further study is made of the problem.

For the purpose of the studies described later in the paper, the plant, illustrated in Fig. 2, was constructed. It was felt that models 12 in. square or of equivalent area would give reliable results and a blower was provided which would give velocities up to 5000 fpm, which is as high as ordinarily encountered in furnace work.

Twelve different damper types were tested and, of these twelve, nine have been selected as representative types. The characteristic curves and design details are included in Fig. 4 and Figs. 8 to 15. Of these Figs. 8 to 15 are grouped later in the paper for ready reference. During the tests, measurement of air flow was by means of an orifice-type Bailey Gas Meter, type CG35, and measurement of pressure losses was made by means of specially built inclined manometers.

The beginning of real progress in this investigation came with the realization of two factors of extreme importance in damper design:

1 The gas velocity through a given damper has no material effect on the flow characteristic if the total resistance of the system exclusive of the damper is unchanged.

2 The flow characteristic of a given damper is variable and is determined primarily by the ratio of its resistance at any given opening to the resistance of the system in which it is installed.

For example, in the system shown in Fig. 3, which consists of a fan drawing gas from a point of fixed pressure through a resistance, such as heat-transfer surface, when a damper of a definite size is installed in the system as at A, its flow characteristic is fixed. Changing the volume of gas or, in other words, the velocity through the system does not affect the flow characteristic in any way. At each damper setting the percentage of the maximum flow at a given fan speed is essentially constant. This is illustrated by curve A in Fig. 3, showing a series of tests on the fan-and-duct system used in these tests.

However, if the fixed resistance of the system is changed, or if an additional resistance is added to the system, as may be done with the gate at B in Fig. 3, the flow characteristic of the damper is changed even though the fan speed is adjusted to restore the maximum velocity through the duct to the original value. This new flow characteristic curve is illustrated by curve B in Fig. 3.

Now, if the new value of resistance, obtained by adding that of gate B to the original fixed system resistance, is not changed, the flow characteristic shown by curve B is fixed and will retain the same shape even though the velocity is adjusted, by changing the fan speed over the entire range.

The foregoing statements need to be qualified as they are dependent upon the use of a fan which has a flat pressure characteristic or, in other words, one which maintains a constant pressure at a given speed regardless of the capacity. Such a fan characteristic is seldom obtained but, since there is no occasion for precise determination of flow characteristic, the effects of the fan characteristic can be disregarded. The intent of this work is to provide means of predicting approximate flow characteristics of different types of dampers in typical applications. Since, ordinarily, the fan characteristic will not seriously change the damper characteristic and since the important thing is to get the right type and size of damper for a specific application, the complication of incorporating fan characteristic to obtain precise results is avoided.

From the curves in Fig. 3, it becomes obvious that a given size and type of damper in a specific system will have a fixed flow characteristic regardless of the maximum gas flow. Therefore, if means can be provided for calculating the resistance of different types of dampers and if the total resistance of the system in which the damper is installed is known in advance, the flow characteristic of a given damper in that application can be predicted.

Damper-Design Characteristic Curves

Information covering the various damper types was obtained and the following data plotted on the typical damper characteristic sheet, shown in Fig. 4, which covers the single-leaf damper:

1 Design features
2 Area characteristic
3 Combined approach factor and coefficient of discharge
4 Resistance ratio
5 Flow characteristic.

The principal features of design are shown in the sketch in the lower right-hand corner of Fig. 4. All factors which have an important bearing on the flow characteristic of the specific damper design are tabulated below the sketch.

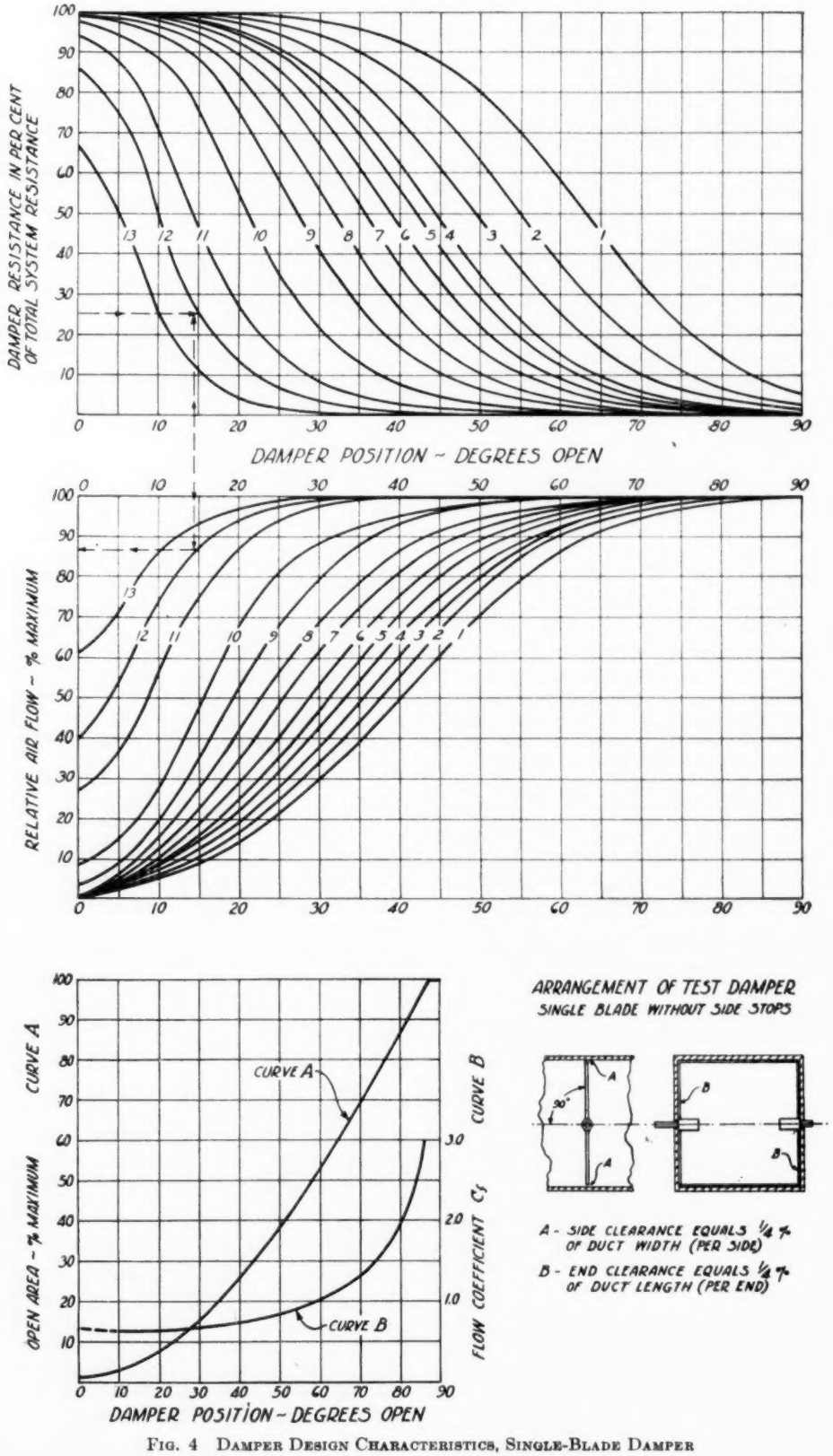


FIG. 4 DAMPER DESIGN CHARACTERISTICS, SINGLE-BLADE DAMPER

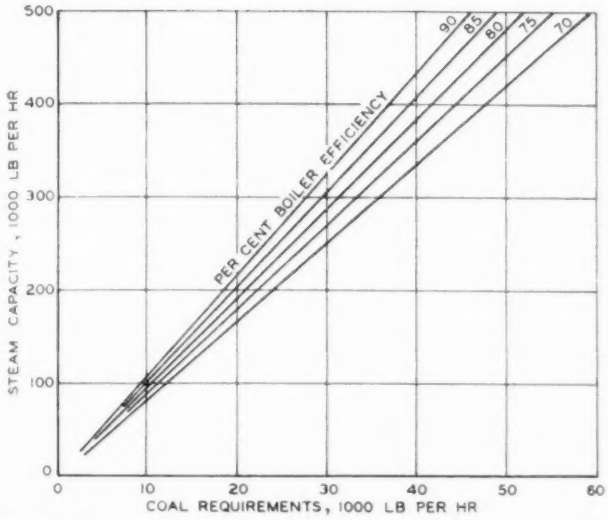


FIG. 5 FUEL-REQUIREMENT-PREDICTION CHART; COAL-FIRED BOILERS

Corrections for variation in operation

Chart based on { Heat input to feedwater 1150 Btu per lb; Higher heating value coal 13,800 Btu per lb }

Multiply table value by factors, K, corresponding to proper operating values

Heat input to feedwater	K	Heating value of coal	K
1100	.955	11,500	1.20
1200	1.04	12,000	1.15
1250	1.09	12,500	1.10
1300	1.13	13,000	1.06
1350	1.17	13,500	1.02
1400	1.22	14,000	.985
		14,500	.951

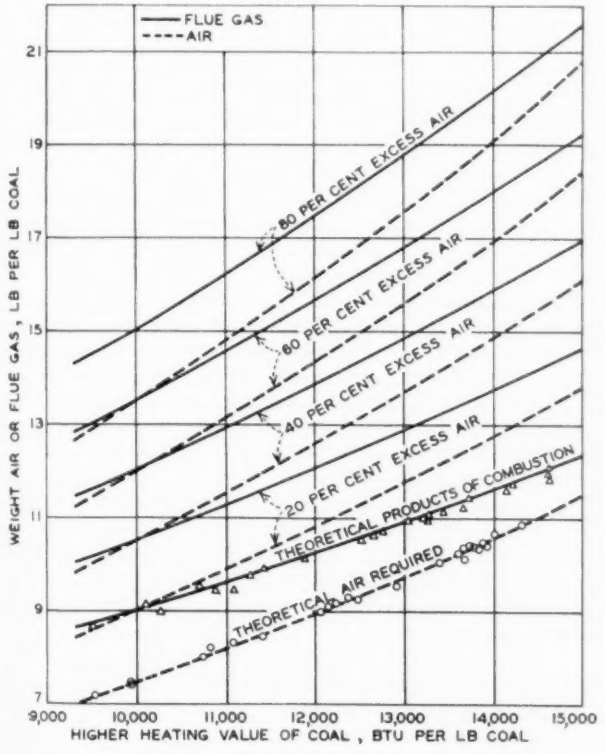


FIG. 6 AIR AND GAS QUANTITIES; COAL-FIRED FURNACES

TABLE 1 AIR AND GAS QUANTITIES FOR OIL- AND GAS-FIRED FURNACES

For average fuel oil

C = 84 per cent H_2 = 12.7 per cent O_2 = 1.2 per cent S = 0.4 per cent N = 1.7 per cent

Excess air, per cent	Weights, pound per pound of oil[a]: Air required	Flue gas produced
0	14.03	15.03
20	16.84	17.84
40	19.64	20.64
60	22.45	23.45
80	25.26	26.26

For various gases

Fuel gas	Theoretical volumes of air and gas: Volume of air required[a] per cu ft of gas, V_a	Volume of fuel gas produced[a] per cu ft of gas, V_g
Blast-furnace gas	0.70	9.974
Blue water gas	2.28	2.797
Carbureted water gas	4.85	5.512
Coal gas	5.50	6.215
Natural gas, W. Va.	21.55	23.329
Natural gas, Pa.	14.25	15.709
Natural gas, Ohio	10.04	11.112
Oil gas	4.25	4.977
Producer gas	1.08	1.916

For varying quantities of excess air

Q = cubic feet of fuel gas per hour

$$\times \left[V_g + (\text{Per cent excess air} \times V_a) \frac{460 + T_{FG}}{460 + T_G} \right]$$

Q_1 = cubic feet of fuel gas per hour

$$\times \left[1 + (\text{Per cent excess air} \times V_a) \frac{460 + T_{FG}}{460 + T_G} \right]$$

where

Q = flue-gas quantity, cfh
Q_1 = air quantity, cfh
V_a = theoretical air quantity cu ft per cu ft (refer to preceding table)
V_g = theoretical flue-gas quantity, cu ft per cu ft (refer to preceding table)
T_{FG} = air or flue-gas temperature at damper, F
T_G = temperature of flue gas, F

[a] "Principles of Combustion in the Steam-Boiler Furnace," by A. D. Pratt, The Babcock & Wilcox Company, New York, N. Y., 1920.

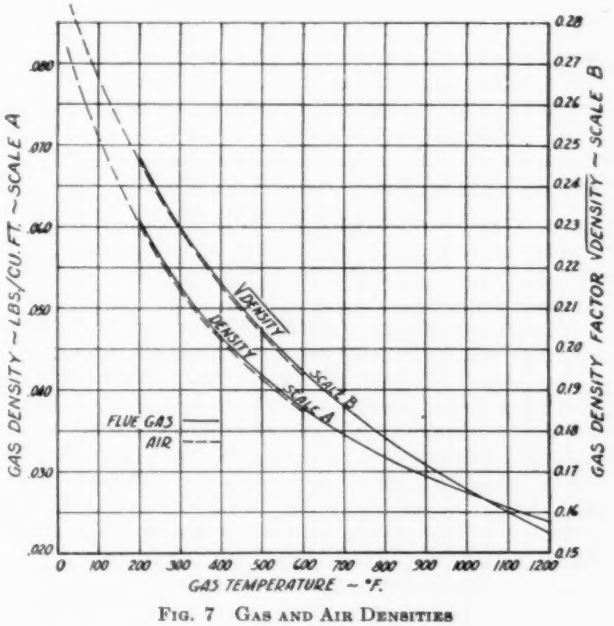


FIG. 7 GAS AND AIR DENSITIES

The area characteristic of the specific damper type is shown in curve A in the lower left-hand corner of Fig. 4. This information was obtained as accurately as possible on the model tested but, obviously, will be affected somewhat by variations in the manufacture of a given type of damper.

The combined approach factor and coefficient of discharge was determined by calculation from the test data in accordance with the equation

$$C_f = \frac{W}{124.3\, A_2 \sqrt{h_w}} \quad \ldots\ldots\ldots\ldots\ldots\ldots [1]$$

where

C_f = combined approach factor and coefficient of discharge
W = pounds of air per hour at 80 F
A_2 = open area of damper, sq in.
h_w = damper differential, in. of water

This information is plotted as curve B in the lower left-hand corner of Fig. 4.

The resistance-ratio curves at the top of Fig. 4, and the flow characteristic curves in the center were obtained by actual tests of all the different damper types with readings taken at each 10-deg increment from the closed to the wide-open position. In addition, tests were made with thirteen different values of system resistance and these values were distributed as equally as possible between the lowest and the highest practical quantities.

Prediction of the Flow Characteristic

The prediction of the flow characteristic of the damper in a specific application is a relatively simple procedure with these data available. Knowing the maximum gas or air flow in cubic feet per hour, and the type and size of the damper to be used, the pressure loss across the damper may be obtained from the equation

$$h_w = \left(\frac{Q \times \sqrt{d}}{457.7 \times C_f \times A_2} \right)^2 \quad \ldots\ldots\ldots\ldots [2]$$

where

h_w = damper pressure loss, in. of water
Q = gas flow, cfh
d = gas density at existing temperature, lb per cu ft (refer to Fig. 7)
A_2 = open area of damper at desired damper position, sq in.
C_f = combined approach factor and coefficient of discharge at desired damper position

Note: Obtain A_2 and C_f from damper characteristic curve for correct type. A_2 = per cent open area times open area of damper frame.

It will be noted that, in making this calculation, two different values are required from the damper characteristic curves covering the particular type being studied. Most accurate results are usually obtained by determining the pressure loss at damper openings from 20 to 40 deg. Therefore, a damper position should be selected between these values and, from the damper characteristic curves, the C_f value and the percentage of open area of the damper are obtained. Knowing the size of the damper, the maximum free opening can be determined and actual open area at the selected opening can then be calculated.

In furnace work, usually the system pressure loss at maximum gas flow is known and, in any case, it must be determined in order to predict the flow characteristic of the damper. It should be remembered that the system pressure loss means the total pressure loss from a point of constant pressure to the inlet of the fan or other draft-producing means. For example, a boiler furnace with forced- and induced-draft fans and a furnace-draft control consists of two complete systems. The forced-draft system consists of all ducts and heat-transfer surface from the forced-draft fan discharge to the furnace, which is the point of constant pressure. A calculation of the forced-draft damper characteristic must be made, using the air required for combustion and the resistance between the forced-draft fan discharge and the furnace. The induced-draft system includes all duct work and heat-transfer surface from the furnace to the uptake or induced-draft fan inlet. The flow characteristic of the induced-draft damper must be made on the basis of total gas volume and the pressure loss from the furnace to the uptake, or induced-draft fan inlet.

It may be found that, when a calculation is made on the basis of maximum gas flow and a damper opening of from 20 to 40 deg, the combined resistance of the damper plus the system is greater than the head available in the fan. This makes no difference, however, from the standpoint of determining the damper characteristic for, as pointed out previously, the damper flow characteristic is dependent entirely upon the ratio of its resistance at a given opening to that of the system. We can assume that a fan having a suitable static head is provided for the purpose of this determination. System pressure losses and damper pressure losses are determined with greater accuracy at the maximum gas flow and, since the form of the flow characteristic is not affected by the fan delivery, best results are obtained using these hypothetical values.

Knowing the system pressure loss and the damper pressure loss at a given opening, the relation between this damper loss and the combined damper-plus-system pressure loss is determined in per cent.

A point corresponding to this ratio or percentage at the specified damper opening is located on the resistance-ratio curves at the top of the damper-characteristic sheet. The particular one of the resistance-ratio curves, numbered from 1 to 13, which comes closest to intersecting this point, is selected and the flow-characteristic curve bearing the same number in the family of curves in the center of the damper-characteristic sheet is the correct one for that size and type of damper in the specific application. If the point located on the resistance-ratio curve comes between two curves, a reasonable approximation of the damper characteristic may be obtained by drawing a parallel curve correspondingly spaced between the two flow-characteristic curves in the center group which carry similar numbers.

The flow-characteristic curve, thus determined, gives the percentage of maximum gas flow at different damper openings and this may be converted to actual gas flow from the known maximum capacity. Likewise, if the capacity of the fan or other draft-producing medium is changed, these same percentage values will hold on the basis of the new maximum capacity; it is not necessary to make another flow-characteristic determination as outlined.

To assist in the determination of gas flow, curves and charts, showing approximate values of the air requirement and gas produced with combustion of various fuels, are included as Figs. 5, 6, and 7, and Table 1. In determining the gas volumes at the induced-draft damper, allowance should be made for increased gas flow due to infiltration.

Sample Solution of Damper Characteristics

Assume a steam boiler having a maximum capacity of 150,000 lb per hr at 400 lb pressure and 750 F, and a feed temperature of 200 F. Coal burned has a heating value of 13,500 Btu per lb. Boiler efficiency at maximum is 80 per cent with 140 per cent total air for combustion and 500 F gas-outlet temperature. Draft loss from furnace to induced-draft fan at maximum is 8.5 in. of water. Determine the flow characteristic of a four-leaf-louver induced-draft damper, 6 ft by 4.5 ft with no dividing plate, as shown in Fig. 13.

(*a*) From Fig. 5
Coal required = 16,000 (1.06 × 1.02) = 17,300 lb

(*b*) From Fig. 6
Pounds of gas per pound of coal = 15.4

(*c*) From Fig. 7
Gas density at 500 F = 0.042
Square root of density = 0.205

(*d*) From Fig. 13, at 30-deg damper opening
Flow coefficient, C_f = 0.60
Area = 45 per cent
Actual area = 0.45 × 144 × 27 = 1750 sq in.

(*e*) From (*a*), (*b*), and (*c*)

$$\text{Gas flow} = 17{,}300 \times 15.4 \times \frac{1}{0.042} = 6{,}340{,}000 \text{ cfh}$$

(*f*) From Equation [2]

$$\text{Damper resistance} = h_w = \left(\frac{6{,}340{,}000 \times 0.205}{457.7 \times 0.6 \times 1750}\right)^2 = 7.33 \text{ in.}$$

(*g*) Total system resistance = 7.33 + 8.5 = 15.83 in. of water

(*h*) Damper resistance in per cent of total resistance = $\frac{7.36}{15.86}$ = 46.3

(*i*) From upper series of curves Fig. 13, locate 46.3 per cent on vertical resistance-ratio scale and project to intersection with vertical at 30-deg damper opening (see dotted lines). Locate nearest resistance-ratio curve. Flow-characteristic curve in center group which has the same number is the flow characteristic of the damper under the system conditions specified.

Discussion of Types Tested

Figs. 8 to 15 (pp. 144 to 151) show the design characteristics of the various types tested, in addition to Fig 4, appearing earlier. It is believed that most of the types in general use are covered. The conclusions reached regarding the relative merit of the various types are as follows:

1 The single-leaf damper in a round or rectangular duct is a thoroughly practical design and, if built with clearances not exceeding 0.25 per cent of the duct width as well as properly sized to the job so that its resistance at 30-deg opening is not less than 55 per cent of the total system resistance, a good flow characteristic is obtained. A damper of this size will have a low loss at the wide-open position. The characteristics of these dampers are shown in Figs. 4 and 8.

2 The addition of side stops to dampers of single-leaf construction, as shown in Fig. 10, decreases the leakage without materially affecting the flow characteristic, assuming that the damper is properly sized as outlined. If side stops are used and the damper is properly sized to the job, the side clearance may be increased from 0.25 per cent of the duct width to approximately 2 per cent, as shown in Fig. 11, without materially affecting the flow characteristic. However, if the damper is oversize for the job, the increased side clearance will have an adverse effect on the flow characteristic, as indicated by flow-characteristic curves 11, 12, and 13 in Fig. 11.

3 A streamlined damper blade, as shown in Fig. 9, reduces the pressure loss at the wide-open position slightly, but not enough to be of any great importance. The flow characteristic of this design is not materially different from the flat-blade louver, and either will give good results if properly sized. The particular model tested had somewhat greater clearance than other types investigated, since it was felt that this damper could not be held to the same manufacturing tolerances. The leakage at low rates is therefore correspondingly higher. Side stops on this type of damper would reduce this leakage without materially affecting the flow characteristic.

4 Multiple-leaf-louver dampers, of the types shown in Figs. 12 and 13, give good regulating characteristics although it is much easier to obtain a good regulating characteristic with the damper having dividing partitions between the louvers than with the type which does not have the dividing partition. To obtain an equivalent flow characteristic, the damper without the dividing partition must be appreciably smaller, which may in some cases result in increased draft loss in the wide-open position. The characteristics of the model with the dividing partition could be improved by the use of side stops, which would reduce the leakage in the closed position. If these side stops were added, the flow characteristics would be similar to those in Fig. 10.

Butterfly dampers having cast frames and cast butterflies, as shown in Fig. 14, have a very satisfactory flow characteristic if properly sized to the job. These units can usually be made to close quite tightly in view of the rigidity of the frame and of the butterfly.

Radial-vane-type dampers, of the type shown in Fig. 15, will give good flow characteristics if properly sized, though most dampers of this type are oversize, which result in a very poor flow characteristic. If the damper is made small enough to obtain a reasonably straight flow characteristic, there is likely to be some pressure loss at the wide-open position. This type of damper has its maximum effective opening at about 65-deg travel, so that there is no occasion to use greater travel than this in an effort to obtain increased capacity. The vanes can be made relatively tight closing if properly built and if arranged to overlap slightly in the closed position. From the standpoint of flow characteristic alone, this type of damper is not as desirable as the other types described but, since it is used primarily for the purpose of directing the gas flow into the inlet of the fan, the advantages gained thereby probably offset the disadvantages as a regulating device. It would appear that, with proper attention to the sizing of the fan inlet and thus the vanes, a reasonably good flow characteristic could be obtained without sacrificing pressure loss. One difficulty, of course, is the necessity for using different-size fan inlets for each installation.

A general conclusion is reached that most of the difficulties with dampers are due entirely to a lack of proper selection of size for each application, principally because no information was available to the designer. It is hoped that this work will stimulate some interest in this matter and lead others to make similar investigations and suggestions for improvement of this device which is so universally used.

Discussion

C. B. Arnold.[3] In the past, many control systems have doubtless proved to be only mediocre, not because the control regulators were inadequate but because the pieces of equipment controlled, such as dampers and the like, have had characteristics which did not lend themselves to satisfactory control, thus placing an undue requirement on the regulators. This fact, of course, has long been recognized by engineers and efforts have been made to correct the situation. However, it is felt that, in most cases, interest in the problem waned as soon as a reasonable improvement of a particular situation had been realized.

For ideal results, equal incremental movements of damper actuators should render equal incremental changes in flow through the dampers. Practically, however, this degree of refinement is not frequently necessary. It is necessary, however, that the size of a damper be suited to the particular conditions for which it is

Discussion continued on page 152.

[3] Assistant Division Engineer, Mechanical Engineering Department, Consolidated Edison Company of New York, Inc., New York, N. Y. Mem. A.S.M.E.

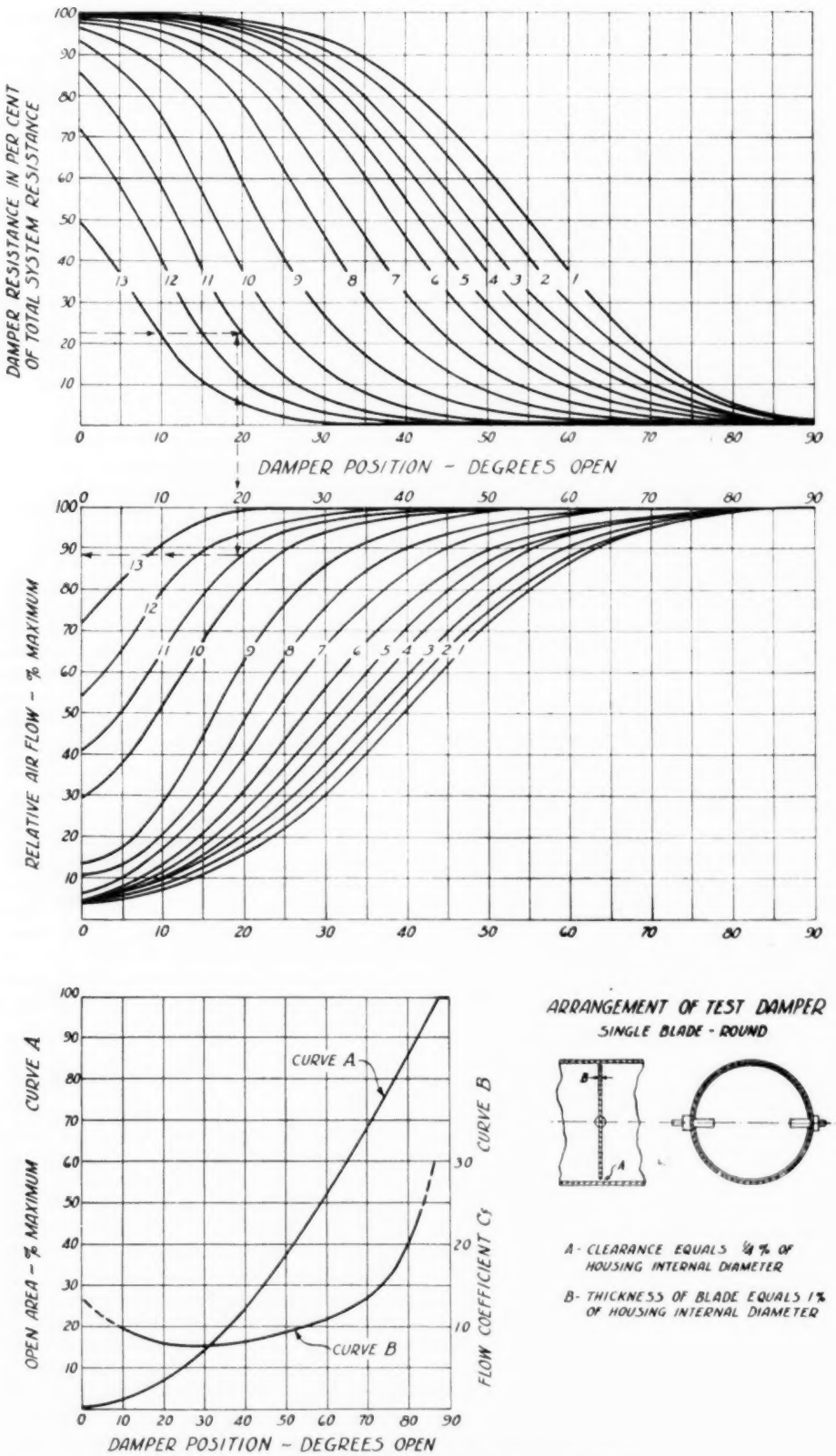


FIG. 8 SINGLE-BLADE DAMPER, ROUND DUCT

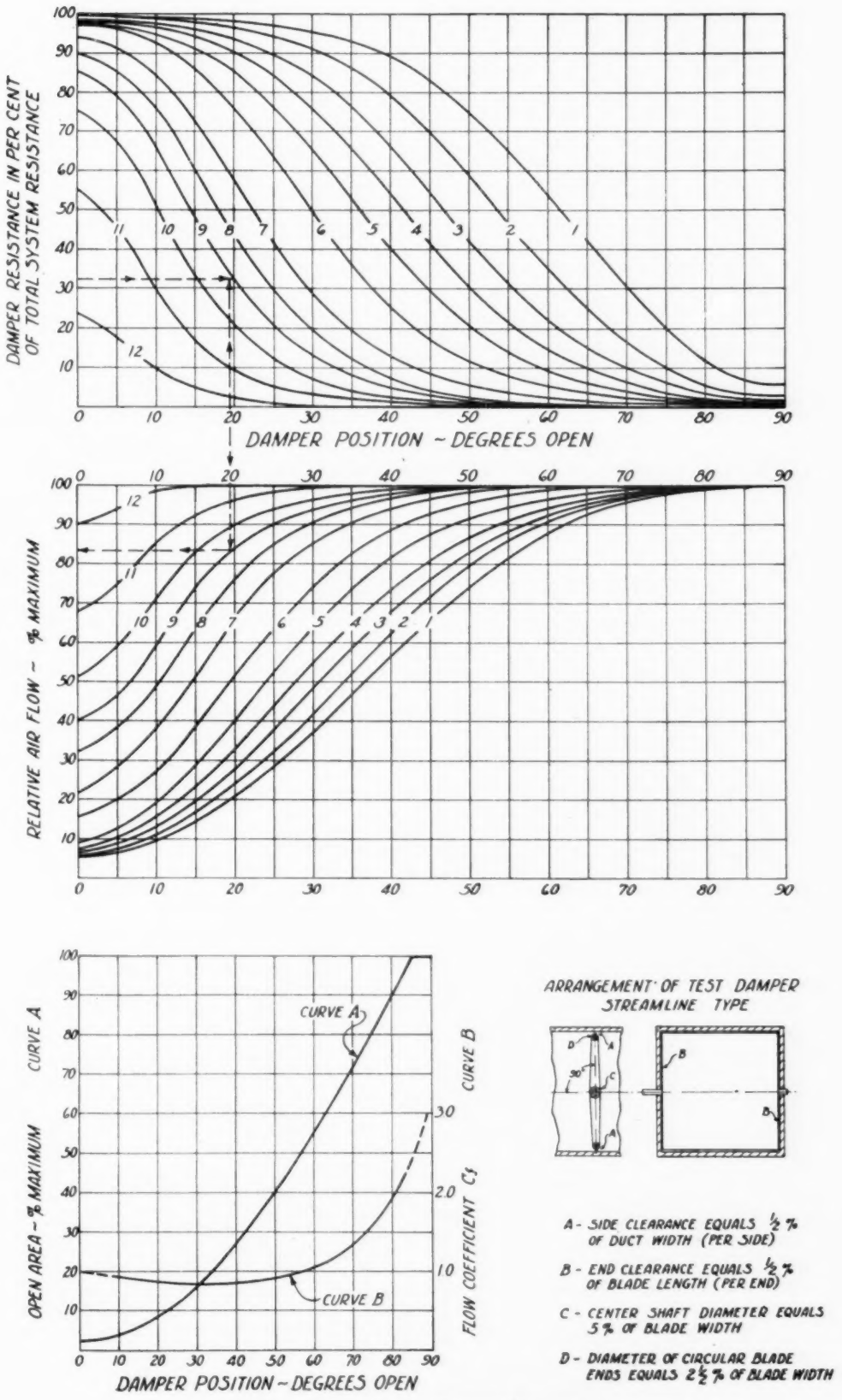


FIG. 9 SINGLE-BLADE DAMPER, STREAMLINED

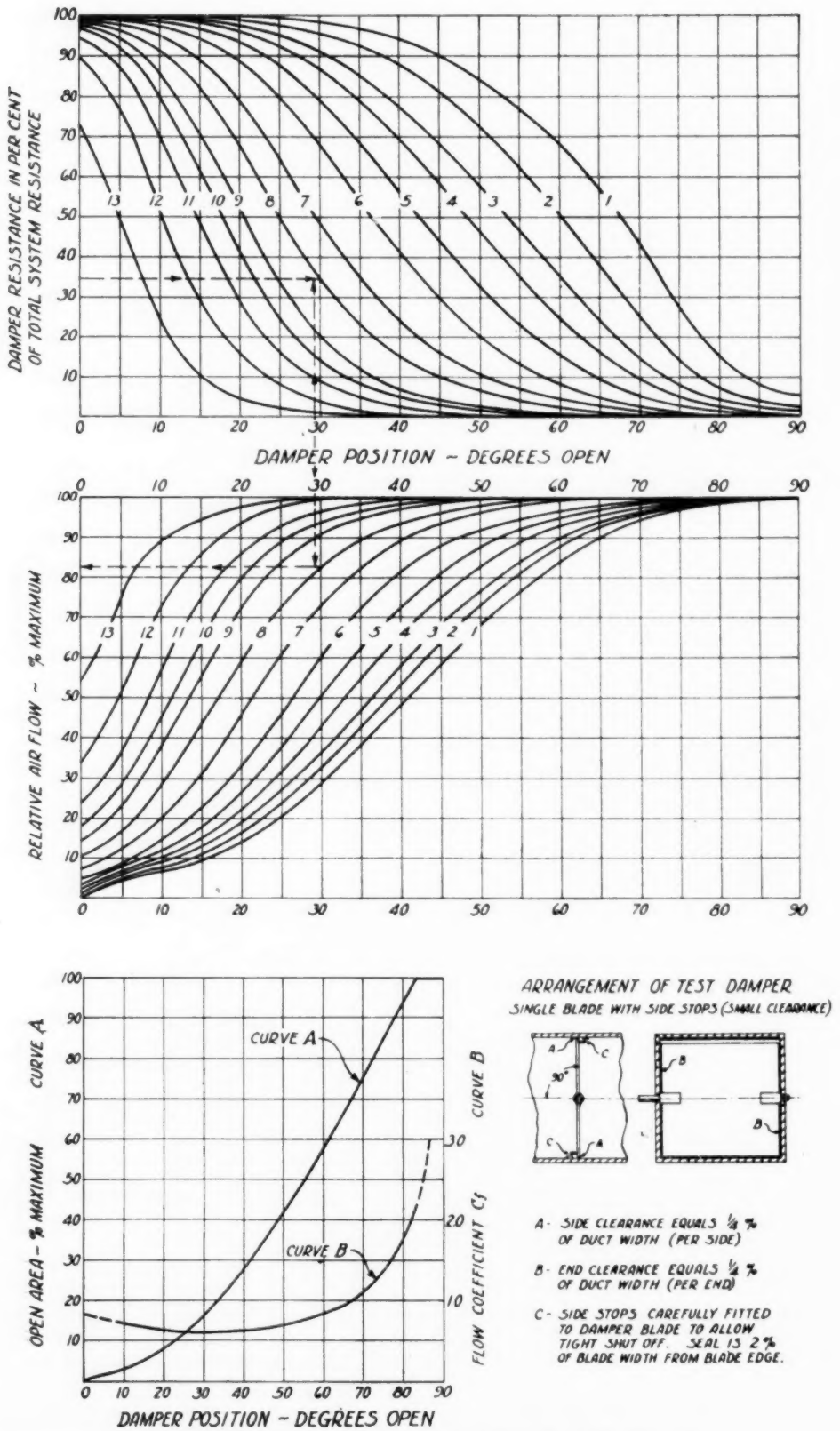


FIG. 10 SINGLE-BLADE DAMPER; SIDE STOPS; SMALL CLEARANCE

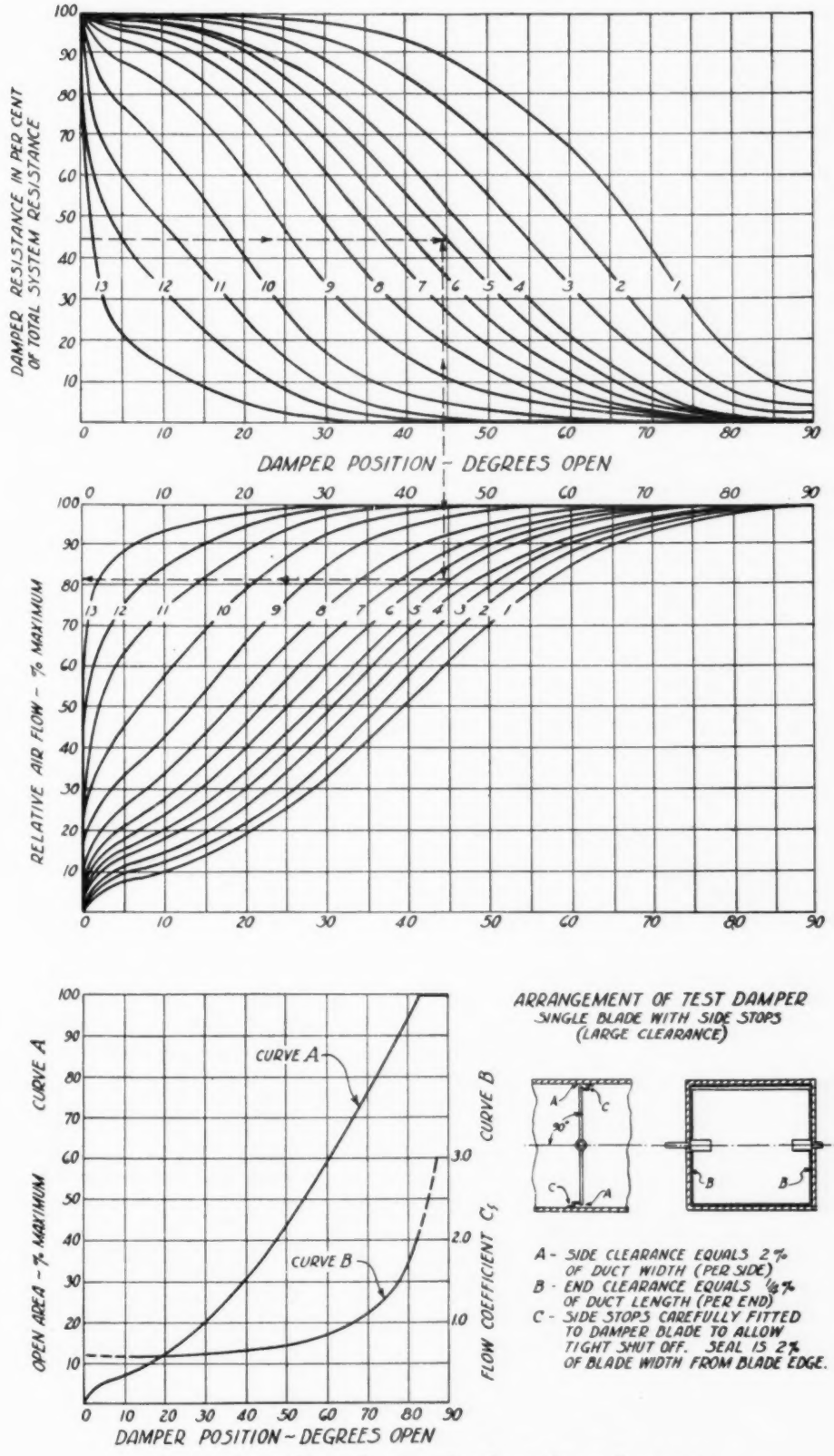


FIG. 11 SINGLE-BLADE DAMPER; SIDE STOPS; LARGE CLEARANCE

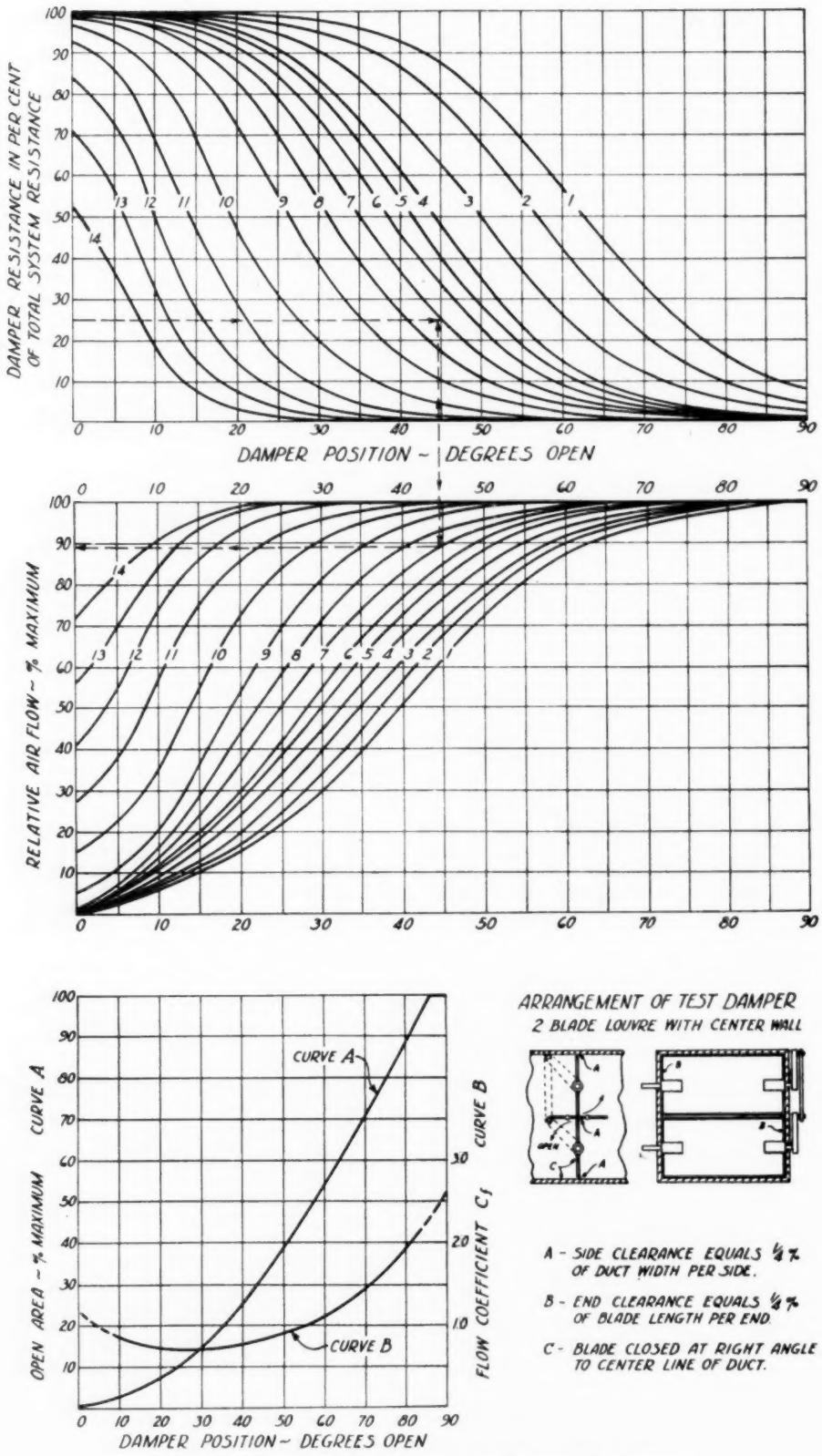


FIG. 12 MULTIPLE-LEAF LOUVER WITH DIVIDING PARTITIONS

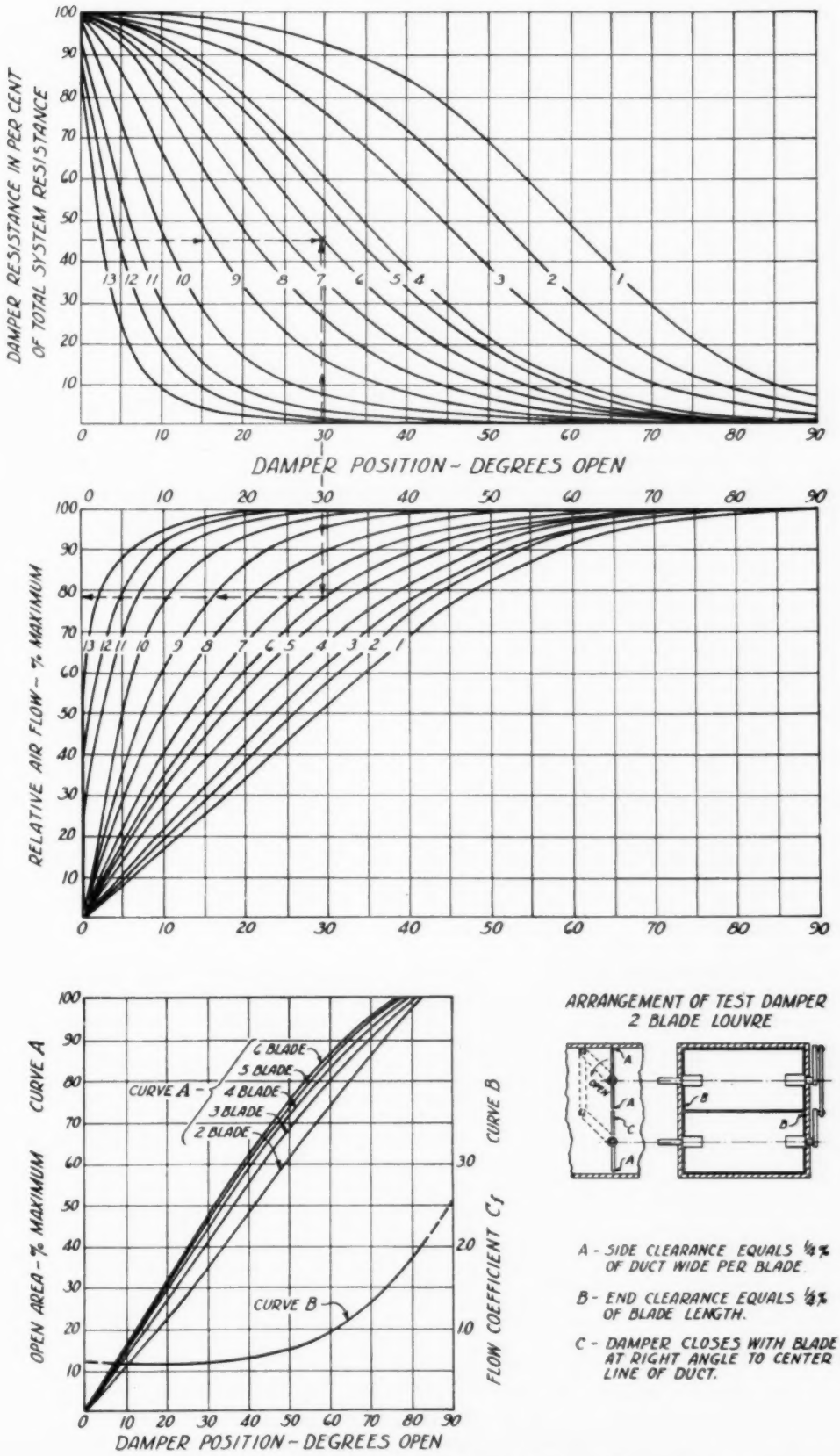


FIG. 13 MULTIPLE-LEAF LOUVER WITHOUT DIVIDING PARTITIONS

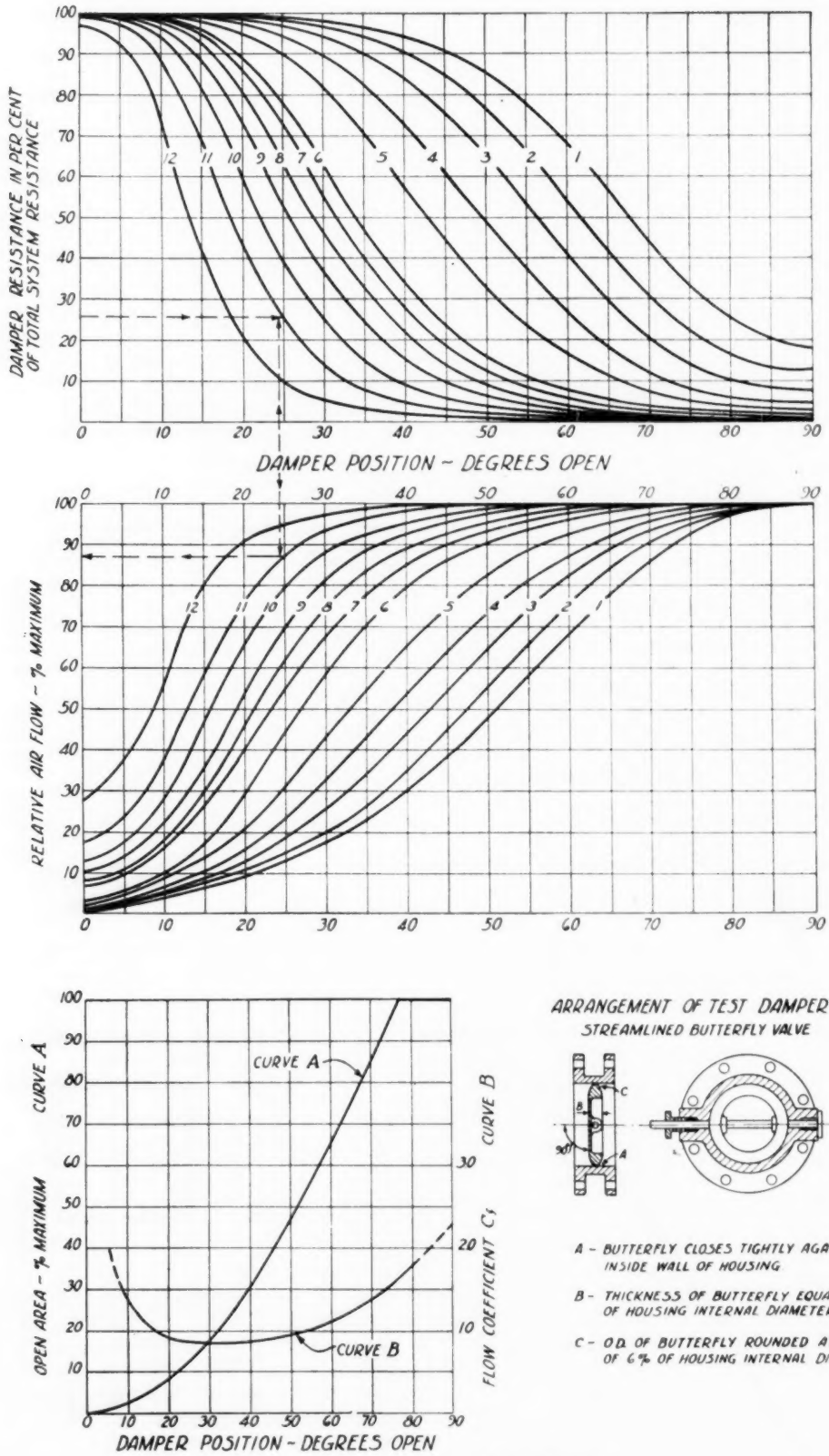
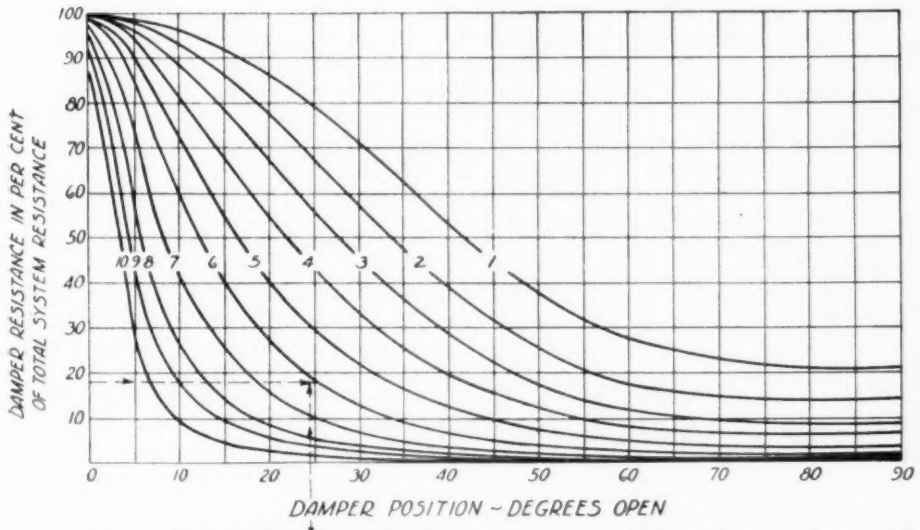
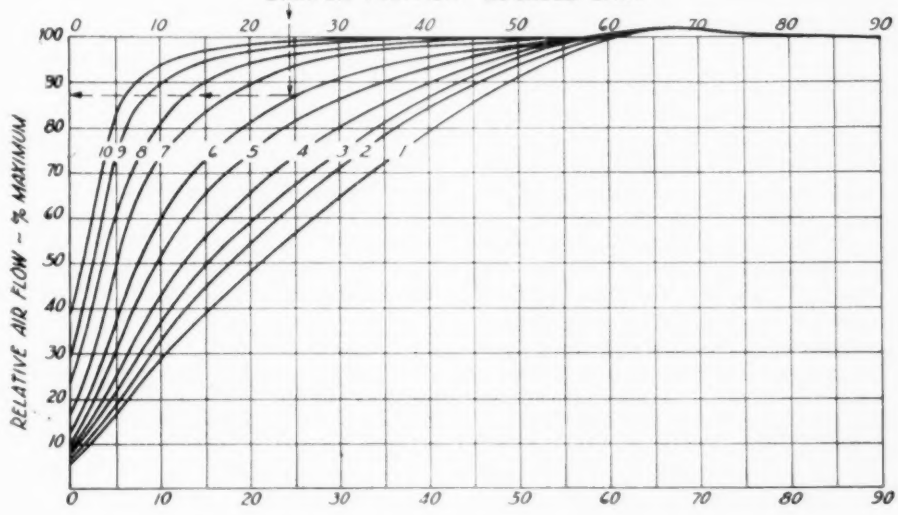
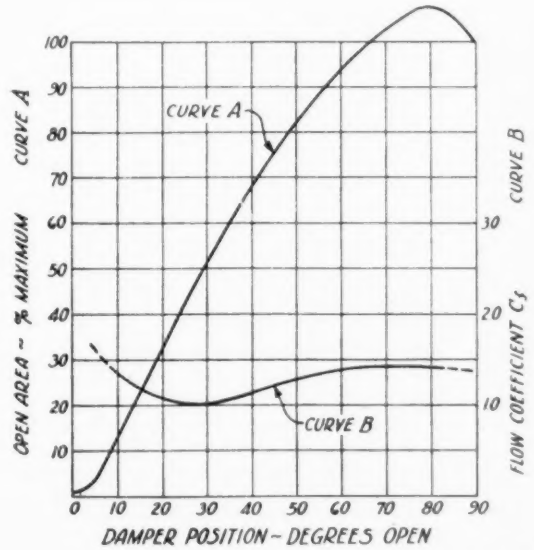


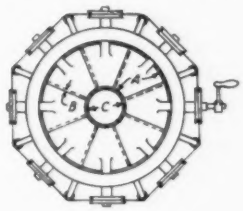
FIG. 14 BUTTERFLY-TYPE DAMPER







ARRANGEMENT OF TEST DAMPER
RADIAL MULTIVANE OVERLAPPING BLADE



A - CLEARANCE AROUND BLADE EQUALS 1/4% OF HOUSING INTERNAL DIAMETER.

B - VANES OVERLAP.

C - DIAMETER OF CENTER SECTION EQUALS 25% OF INTERNAL HOUSING DIAMETER.

FIG. 15 RADIAL-VANE-TYPE DAMPER

intended, otherwise not even a close approximation of this ideal will be had. It is felt, therefore, that the authors have offered a very useful contribution by outlining a method of determining damper size so that it can be designed correctly, prior to its installation.

After the proper size of a damper has been ascertained, the further refinements relative to the connecting means between the damper and its power actuator should be given consideration. The arrangement mentioned by the authors, whereby equal increments of actuator movement produce small incremental movements of the damper near the closed position and, larger incremental movements near the open position, can be used to advantage in many cases. The merits of such an arrangement are as follows:

1 Actuator movement bears a closer relationship to flow through the damper.

2 Greater mechanical advantage is available when the damper is near the closed position, and frequently more force is required to operate the damper in this position.

3 Because of the additional mechanical advantage where it is most needed, as mentioned, smaller power actuators may be employed.

Granted that the size of a damper has been properly selected and that means of connecting the damper to the actuator have been satisfactorily arranged, there is still one other factor which may cause unsatisfactory results. This factor is damper unbalance. True, as the authors have stated, the torque-requirement characteristics of dampers are quite unpredictable, because of the unpredictable flow pattern ahead of and leaving the dampers. It is felt, however, that this unsatisfactory condition which frequently prevails should not be treated too lightly. One of the greatest causes of damper unbalance is the reduction of pressure, brought about by the increased velocity of air or gas between the damper leaves and between the dampers and their respective sealing strips, when the dampers are in the nearly closed position. If there is considerable overlap of one damper over another or of the sealing strips over the dampers, extreme forces are required to open them, and they tend to snap shut when approaching the closed position. If this unbalanced force were to change but gradually and always be in the same direction, no serious consequence would result. However, in many cases, the unbalanced forces sometimes suddenly decrease or actually reverse in direction, as the dampers move through some critical point. These changes of force required to operate the damper cause overtravel in damper movement on either side of the critical point, due to lost motion or yield in the linkage, and are bound to produce a hunting condition which no regulator can stabilize.

The writer has had some experience with dampers which had these unsatisfactory unbalance characteristics and was able to produce a satisfactory improvement of the characteristics on two-leaf dampers by providing unequal damper areas on either side of the damper shafts. This caused a counter-unbalanced force sufficient to cancel out a major part of the unbalanced force which originally prevailed. It is felt, therefore, that further study of this condition would be beneficial and might reveal some general rules and useful techniques which would insure at least an improvement of the condition and indicate some of the pitfalls to be avoided.

F. C. Smith.[4] The writer has been greatly interested in the authors' comments with regard to unbalance caused by overlap of the damper on sealing strips. Further comment by the authors concerning sealing strips would be greatly appreciated. For instance, what has been done along the lines of making use of spring-type strips somewhat comparable to the principles employed in ordinary building weather stripping? It appears to me that use of such sealing might greatly decrease the unbalanced condition which has been discussed.

C. L. Myers.[5] The authors have selected a subject that well deserves attention. The annual loss resulting from faulty dampers would be startling if there were any reliable figures available to establish it. Some index may be taken from the fact that our records indicate an average efficiency increase of 5.7 per cent for one group of installations after the dampers had been replaced; this figure does not take into account the item of equipment maintenance which is frequently effected.

The authors have defined the ideal flow characteristic, as shown in Fig. 16 of this discussion, and suggest that dampers be reduced in size to a point where the ratio of damper resistance to total system resistance is not less than 55 per cent at 30-deg opening. In order to visualize this recommendation, Fig. 16 includes the several flow curves corresponding to 55 per cent resistance and also, for comparison, curve 1 from Fig. 4 and curve 12 from Fig. 9 of the paper, to indicate the limits to which the curves can be moved by extremes of damper-size adjustment. The former corresponds to 98 per cent resistance at 30-deg opening and the latter, to 0 per cent resistance at 30-deg opening.

It is suggested that designers may find some difficulty in reducing damper sizes to those recommended without encountering problems of flow distribution in the system. Another problem may be found in that the indicated damper area, when divided by the necessary width, may result in a small height. Such dampers are more difficult to build to close clearances due to sag.

[4] Editor, *Southern Power and Industry*, Atlanta, Ga. Jun. A.S.M.E.

[5] Heacon, Inc., Philadelphia, Pa.

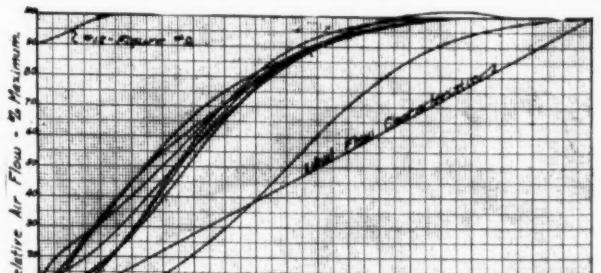


Fig. 16 Flow Curves Corresponding to 55 Per Cent Resistance

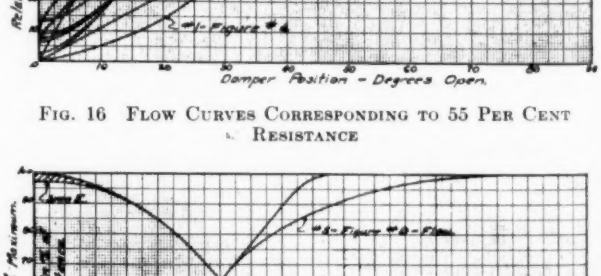
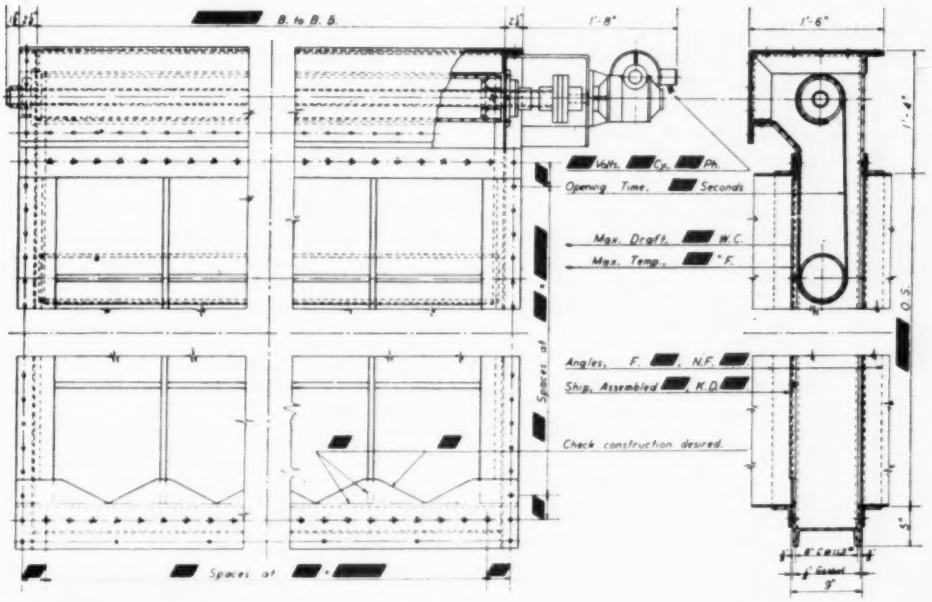


Fig. 17 Hypothetical "Modified-Flow" Curve and Curves 5 From Fig. 9 of the Paper



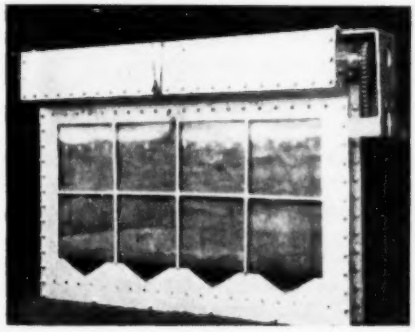


FIG. 18 MODERN DAMPER DESIGN

The increased leakage, resulting from the larger clearance necessary, has an adverse effect on the damper characteristic. These problems suggest a search for additional approaches.

The authors have made the alternative suggestion that the linkage, as shown in Fig. 1, be employed, but point out that such linkage must be maintained in perfect condition in order to obtain its benefits. They have also suggested that, in the case of multiple-leaf dampers with partitions, one or more sections can be blocked off. This procedure would seem to introduce distribution problems. Neither course will affect materially the leakage problem at the lower end of the curve.

Fig. 17 of this discussion shows curves 5 from Fig. 9 of the paper. Superimposed is an hypothetical "modified flow," which more nearly conforms to the desirable straight line and the "modified damper resistance" which would be required to produce such a flow curve. Area *D* indicates the need for less resistance which would be accomplished by more damper area. Area *E* indicates the need for more resistance or less damper area. This leads to the conclusion that the answer may be found in modification of the shape of the damper opening rather than rectilinear reduction of its size alone.

Such an approach to the problem is illustrated by Fig. 18 of this discussion. Obviously, the V-porting shown can be extended to provide any desired shape in the resistance curve, and thus any desired flow characteristic. Since there is no clearance between the moving part of the damper and its sealing strips, the leakage problem indicated by area *E* is eliminated, regardless of the size of the damper. Another thought involves the elimination of inclined planes in the path of flow, thus reducing turbulance and resistance. This is desirable in area *D* and modifies the amount of shaping necessary to obtain the desired result.

The authors have pointed out several other problems as follows:

1 Need for increased clearance for higher temperatures.
2 Power requirements.
3 Dynamic balance.
4 Shafts, bearings, and seals.
5 Leakage.

Examination of the design, illustrated by Fig. 18, establishes that large operating clearance is provided for the moving parts without introducing leakage. It also shows that ample strength to prevent sag in wide dampers is provided without introducing a large mass in the path of flow, that the weight to be supported is less and, further, that any sag which may develop does not require clearance effecting leakage. Since large operating clearance is provided, binding is eliminated. The problem of dynamic balance disappears automatically. Shafts can be made large in proportion to the weight supported. Bearings are in a favorable location more or less away from the flow and in a position which does not tend to distort to cause misalignment. Good seals should be provided in any case. These facts all add up to modest power requirements.

Leakage is a problem of a magnitude but little appreciated. Most dampers in service have been warped to an extent that the leakage has been materially increased from what it was when they were originally installed and the original leakage is usually considerable. The adverse effect of leakage on the flow characteristic is well illustrated by the several curves in the paper. Leakage of cold air into the breeching from cold boilers reduces available draft and thus capacity. Leakage of isolation dampers results in poor and even dangerous working conditions for maintenance crews. Elimination of leakage increases the range of efficient output. Leakage in an uptake damper results in a considerable loss of heat during banking periods. Leakage of air past a damper, controlling flow to a fuel bed, results in increased banking losses. Leakage in a by-pass damper permits heat to short-circuit the economizer or air heater. Leakage past an uptake damper to a breeching leading to an economizer reduces the temperature and increases the volume of gas passing through the

economizer, thus reducing its heat-absorbing efficiency and, passing on to the induced-draft fan, increases the power consumption, sometimes overloading the fan to the extent that full capacity is not attainable. Some dampers are so located that leakage results in recirculation, which leads to increased fan power and loss of capacity. Leakage, in some cases associated with air heaters or economizers, results in corrosion problems.

The authors have made a splendid contribution to a subject that can lead to very real improvement in the art of steam generation, conservation of fuel, and substantial economies.

Authors' Closure

The discussion by Mr. Arnold is appreciated as it emphasizes the need for greater care in the selection of dampers and the mechanisms for operating them. An important point brought out by Mr. Arnold is the fact that proper design of the linkage between the damper and the operating mechanism not only improves the flow characteristic, but reduces the torque requirements of the operating mechanism. We agree that the matter of damper unbalance requires further study, but this is beyond the scope of this paper. It is hoped that studies can be made later which will throw some additional light on this matter.

To answer Mr. Smith's question; the authors have had some experience with the use of sealing strips for decreasing the leakage in the closed position. We have used both weather-stripping construction and strips of flexible materials, such as asbestos tape, and find that satisfactory results can be obtained. The principal difficulty is the added cost, inasmuch as these strips must be fitted in the field, if satisfactory results are to be obtained. This adds considerably to the cost of the damper. The leakage on dampers of simple design, if properly sized, is not generally serious, and sufficient tightness can usually be obtained by the addition of metal stops on the damper frame.

The design of damper offered by Mr. Myers is interesting and unique. It offers the possibility of providing any desired area and flow characteristic. However, if suitable results are to be obtained, the area characteristic of this damper must be determined and a corresponding port-shape in the damper must be provided. It is for the purchaser to decide whether the desirable flow characteristic can be accomplished more easily and at less cost in this type of damper than in one of conventional design.

Mr. Myers is quite justified in pointing out that the damper which is properly sized does not give a straight-line relation between motion and flow increase. However, it will be noted that the average of the various curves, shown in Fig. 17 of his discussion, which incidentally do not represent the best that can be obtained for each damper type, still shows less than a $2^1/_2$ to 1 change in slope over the effective range of travel. By arranging the linkage between the operating mechanism and the damper to use only the effective portion of damper travel, which in this case is approximately 70 deg, and incorporating some angularity in the linkage, a very nearly uniform slope could be obtained. In most cases no difficulty would be encountered with dampers having a flow characteristic similar to the average of these curves with or without angularity in the linkage, as the change in slope is not sufficient to present any regulation problems.

Operating Experiences With High-Pressure High-Temperature Unit at Des Moines

By J. F. McLAUGHLIN,[1] DES MOINES, IOWA

Operating experiences, with performance records for 1939 and 1940, with a 35,000-kw turbine generator operating at 1290 psi and 925 F, and a steam generator which has a capacity of 420,000 lb per hr are presented, and changes made to overcome failures and outages are described.

THE latest addition to Des Moines power station No. 2 at Des Moines, Iowa, consists of one 35,000-kw turbine generator operating at 1290 psi 925 F, without reheat, running at 3600 rpm, and exhausting to a condenser. Steam is supplied by a steam-generator unit which has a capacity of 420,000 lb per hr and burns Iowa pulverized coal.

The station piping is so arranged that steam to the high-pressure turbine can be supplied from a group of 365-psi boilers and steam to the 365-psi turbines can be furnished from the high-pressure boiler through a desuperheater. One boiler feed pump is driven by a 1250-hp motor, the other by a 1250-hp turbine receiving steam normally from the 365-psi boilers. Steam for this turbine can also be obtained from the high-pressure boiler through an auxiliary desuperheater. All other auxiliaries are driven by electric motors.

The condenser has a divided water box with two circulating water pumps so arranged that either pump can furnish water to both sides of the condenser. The circulating water is automatically treated with chlorine.

The steam-generator unit has two induced-draft fans, two forced-draft fans, two air heaters, and three pulverizers of which any two are sufficient for full load.

The turbine was first started Nov. 23, 1938, with steam from the 365-psi boilers. The unit was operated at high pressure from Dec. 14 to Dec. 20, 1938, when it was shut down for completion of construction work.

The operating record of the unit for 1939 and 1940 is shown graphically in Figs. 1 and 2, and indicates the time, duration, and cause of each outage, major repair, and change made and the maximum daily load carried on the unit.

Turbine Generator Operation

The availability factor of the turbine was 79.8 for 1939 and 95.5 for 1940. There were ten outages of the unit in 1939, three of which were forced outages due to the turbine. There were seven outages of the unit in 1940, two of which were also forced outages due to the turbine.

The unit was placed in service Jan. 5, 1939, and the load was held at 15,000 kw until the next day when the load was increased to 32,000 kw. Wear, caused by misalignment of some of the parts, was noticed in the thrust bearing. Adjustments were made and the unit resumed operation. On Feb. 10 several groups of high-pressure reaction blading were replaced with a modified design to relieve the axial thrust. A different type of thrust bearing was also installed. Some broken blades were found in the two impulse rows, and both rows were replaced with blades of the original design. New dummies and nozzle blocks were also installed.

After starting the turbine on March 24 the load was increased to 18,000 kw at which time steam was found to be leaking through a thermometer well which had been installed in the casing at the reaction inlet. After the unit had been shut down it was found that the thermometer well had broken off inside the turbine casing. When the high-pressure cover was removed some broken blades were found in the second row of impulse blading. It was apparent that the turbine blades had broken first and the impact of the broken pieces caused the thermometer well to break. All of the impulse blades in the second row were removed and the unit was placed in service March 31. No restrictions of any kind were imposed on the amount of load to be carried, and on April 11 the unit carried a load of 43,750 kw at 100 per cent power factor which is full-load rating of the generator. The position of the turbine inlet valves indicated that the turbine could have carried considerably more load. The turbine was inspected April 21 to 29, and everything was found to be in good condition.

The unit was next taken out of service June 15, at which time new impulse blades were installed in both first and second rows. See Fig. 3. These blades had been redesigned, and in this redesign the results of latest design developments[2] in connection with partial-admission blading were taken into consideration.

The turbine was placed in service July 3 and operated without further inspection or changes until Feb. 6, 1940. There were five outages during this period but none of these was due to the turbine. The turbine was given a complete inspection during the outage between Feb. 6 and March 5. The first row of impulse blading was in good condition but one blade in the second row was broken immediately under the shroud and two other blades were cracked in the same region. Subsequent examination revealed that these three blades had extremely sharp corners with insufficient radii in the vicinity of the failures. New second-row blading was installed with the blades made heavier under the shrouding, welded in groups of two at the top and bottom of the blades, and stress-relieved before installation. See Fig. 4. The entire impulse element has since continued to operate satisfactorily without trouble of any kind.

Two forced outages of the unit due to the turbine took place in 1940, one caused by a leak in a weld on the oil piping and the other caused by a broken tension screw in the governor; the latter allowed the turbine inlet valves to close instantaneously.

The turbine was inspected in October, 1940, and all blading was found to be in good condition. Some difficulties had been experienced with sticking of the control valves. A new-type cage was installed on these valves during this outage and this has entirely corrected this trouble. A study has been made of the relation between governor movement and frequency and this showed especially good speed regulation.

---

[1] Mechanical Engineer, Iowa Power & Light Co. Mem. A.S.M.E.

Contributed by the Power Division and presented at the Semi-Annual Meeting, Kansas City, Mo., June 16–19, 1941, of The American Society of Mechanical Engineers.

Note: Statements and opinions advanced in papers are to be understood as individual expressions of their authors and not those of the Society.

[2] "Steam-Turbine Blading," by R. C. Allen, Trans. A.S.M.E., vol. 62, 1940, pp. 689–710.

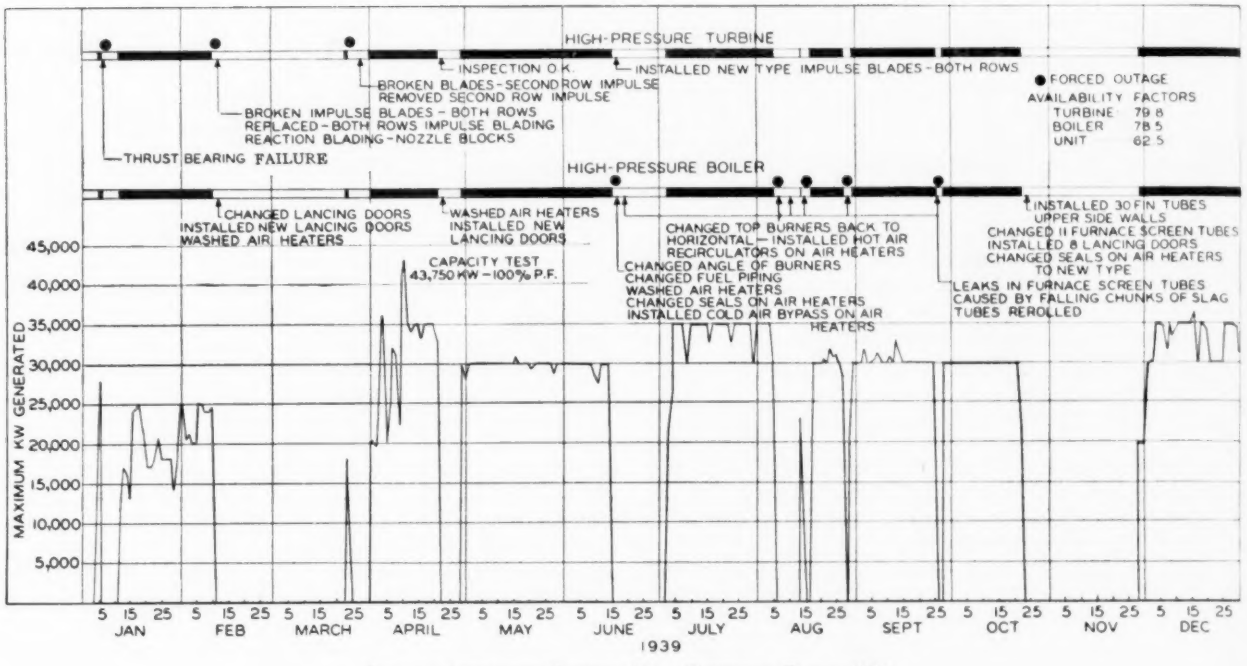


FIG. 1 OPERATING RECORD, HIGH-PRESSURE UNIT—1939

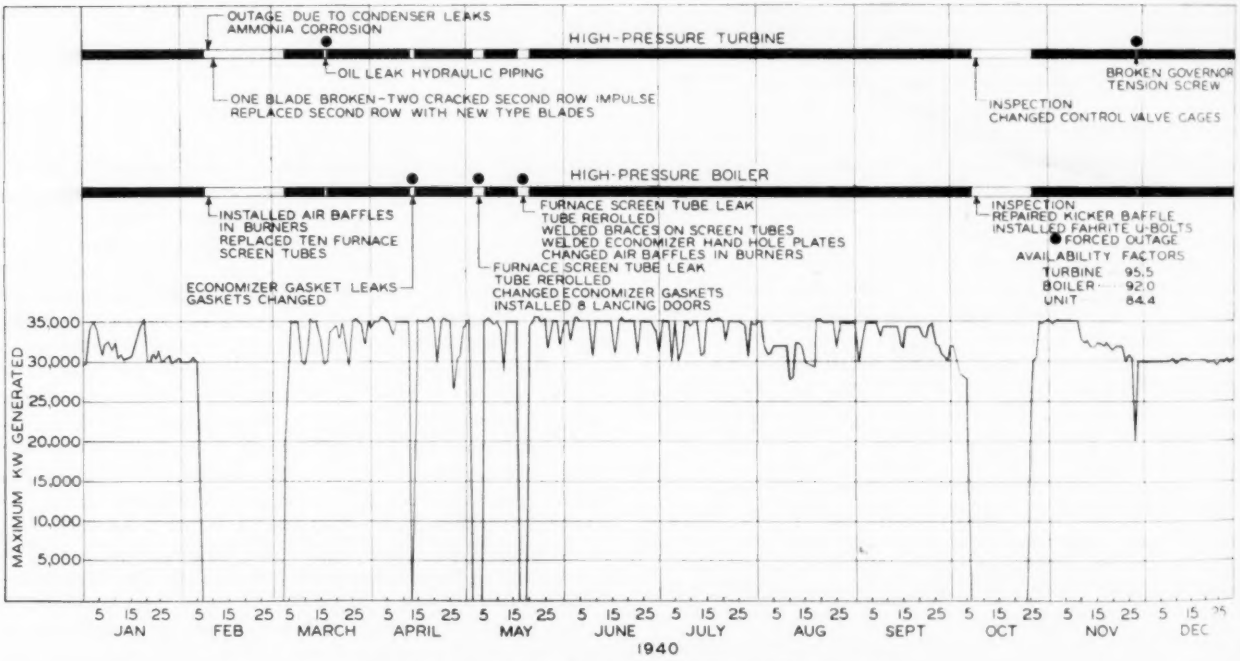


FIG. 2 OPERATING RECORD, HIGH-PRESSURE UNIT—1940

CONDENSER

No operating difficulties have been encountered with the condenser or its auxiliaries. Condenser air leakage at full load averages 0.43 cfm. In December, 1939, and January, 1940, the flow of the Des Moines River reached the lowest stage ever recorded with the result that the circulating water entering the condenser amounted to nothing more than sewage. This was before the Des Moines sewage-disposal plant was operating. Recirculation of the circulating water raised the temperature of the water to 75 F. Make-up for the evaporators was obtained by softening river water in a treating plant. Since there was no convenient means for reducing the ammonia content of the treated water, the steam and condensate became polluted with ammonia by way of the evaporator circuit. Measurements of the condensate at the hot well indicated presence of 5 to 6 ppm ammonia nitrogen.

On Jan. 17 a considerable condenser leak occurred, so that it seemed that a tube must have broken. One half of the condenser was drained at a time and it was found that 18 tubes were leaking. Further investigation proved that corrosion had taken



FIG. 3 NEW-TYPE IMPULSE BLADES INSTALLED IN JUNE, 1939

place from the steam side of the condenser. A few of the tubes was found to be split, but most of the leaks were in the tops of the tubes just inside of the tube sheet at the water inlet end of the first pass. The majority of the holes were found to be plugged with sewage, which no doubt accounts for the fact that there were no condenser leaks previous to Jan. 17. The air take-off of this condenser is at the top and at both ends, and although the concentration of ammonia at the air take-off was not measured, there is no doubt that it was exceptionally high. A total of 124 leaks was found before the unit was shut down Feb. 6. During the shutdown 1315 tubes were replaced owing to the corrosion, all of which was in the top half.

Make-up for the treated-water plant has since been obtained from a previously abandoned well which has only a trace of ammonia. Subsequent inspection of the condenser indicates that further corrosion has been eliminated.

STEAM GENERATOR

The availability factor of the steam generator was 78.5 in 1939 and 92.0 in 1940. Of the ten outages of the unit in 1939, six were due to the boiler, five of which were forced outages. Of the seven outages of the unit in 1940, three were due to the boilers, all of which were forced outages.

The boiler was placed in service Jan. 5, 1939. The first month's operation presented no difficulties, owing, apparently, to the reduced rating caused by turbine troubles. It did indicate, however, the necessity of moving lancing doors and the installation of others to facilitate the removal of slag. As noted in Figs. 1 and 2, lancing doors have been moved or installed at various times as further experience indicated where they could be used to advantage. Observations made during this first run also indicated the need for some changes on the air heaters to prevent plugging at the cold end. Air recirculators and a cold-air by-pass were later installed on the air heaters and these are used at light loads to prevent condensation of the moisture in the flue gas upon the air-heater plates. The average temperature of the air into and of the gas out of the air heaters is kept at or above 230 F. This, together with the use of superheated steam for sootblowers, has kept the air heaters clean.

The five forced outages between June 15 and Sept. 25 were due to leaks in the rolled joints of the furnace screen tubes caused by chunks of slag falling onto these tubes from the furnace side walls. The front and rear walls and the lower side walls of this furnace consisted of closely spaced finned tubes, but the upper side walls were built of plain tubes spaced $10^1/_4$ and $15^3/_8$ in. on centers with the firebrick between the tubes exposed to the furnace. The molten slag adhered to the firebrick and after solidifying by cooling gradually built up to considerable size. The weight of this slag eventually became too great to remain attached to the side walls and chunks would fall, striking the floor screen tubes 20 to 25 ft below. This slag weighed about 200 lb per cu ft, so that a piece two feet square and four inches thick might weigh 250 to 275 lb. See Fig. 5.

During the outage in November, 1939, these plain tubes in the upper side walls were removed and closely spaced finned tubes were installed. See Fig. 6. This change, together with changes in the angle of the burners and installation of air baffles to deflect the secondary air into the coal stream, materially reduced the amount of slag adhering to the walls.

A section through the steam generator is shown in Fig. 7.

Two more outages occurred in May, 1940, from leaks in the screen tubes caused by falling slag, although there had been no evidence of any heavy chunks in the ashpit as had previously been the case. It was found that a thin layer of slag averaging

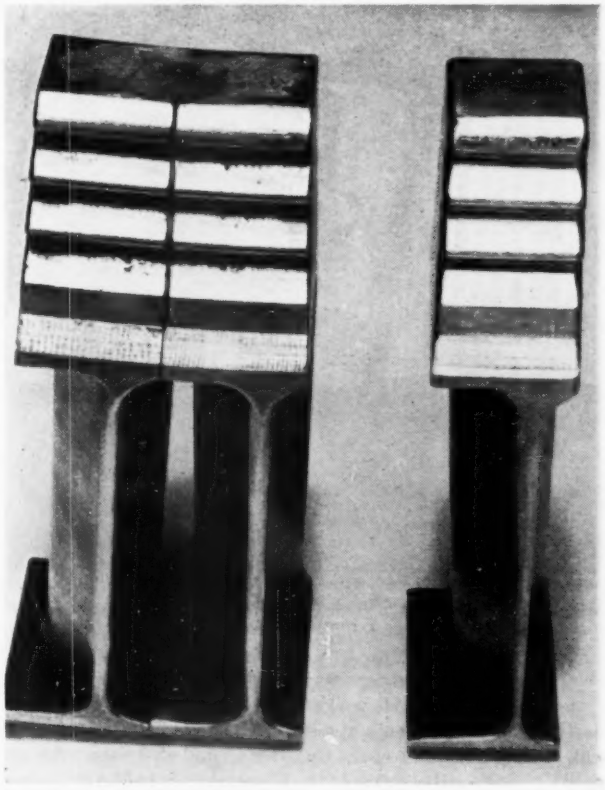


FIG. 4 NEW-TYPE IMPULSE BLADES INSTALLED IN SECOND ROW, FEBRUARY, 1940, AT LEFT, COMPARED WITH PREVIOUS BLADE

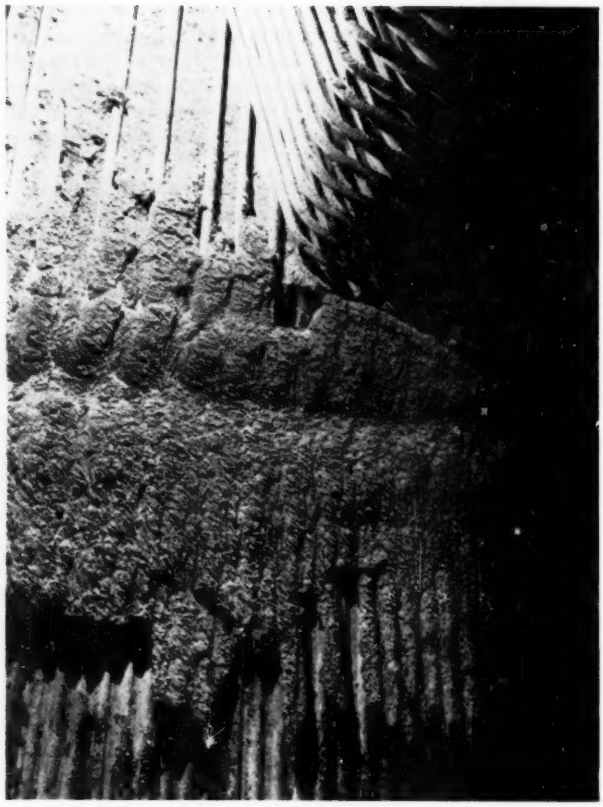


FIG. 5 SLAG ADHERING TO REFRACTORY BETWEEN UPPER SIDE-WALL TUBES, AUGUST, 1939

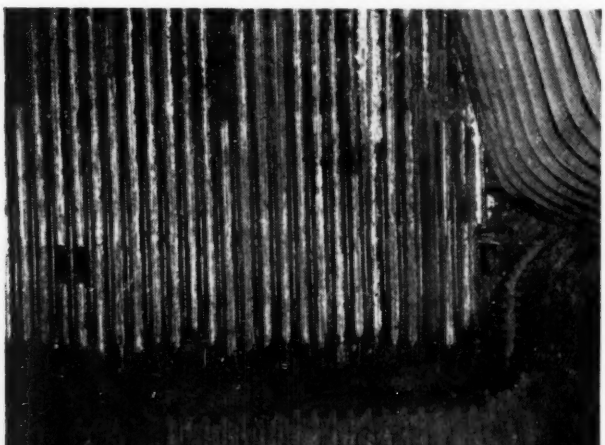


FIG. 6 NEW FINNED TUBES IN UPPER SIDE WALLS, INSTALLED NOVEMBER, 1939

about one inch in thickness and about four feet square had been accumulating on the side wall about 15 ft above the screen tubes. As this slab would weigh about 275 lb, it could readily cause a leak in the rolled joint of the tube if it should strike the tube just right. Additional changes in the secondary-air baffles with more frequency hand lancing at this location has eliminated this difficulty. Three screen tubes on each side of the furnace were tied together by welding steel braces to the tubes at two points to stiffen up the tubes.

One outage in 1940 was due to leaks in economizer hand-hole gaskets. As the piping and economizer tubes were welded to the header, the hand-hole plates were also welded, so no more leaking has taken place.

In the original installation, two stationary sootblowers designated *A* and *B* were located back of the second row of boiler tubes facing the furnace; a third blower of the rotary type designated *C* was installed in front of the convection superheater. Elements *A* and *B* were later changed to the rotary type. Although these three elements were made of the best possible material for the service, the life of the element was very short. In addition to the short life, one type of nozzle had a tendency to grow and close up; another type tended to disintegrate and cut out. Elements *A* and *B* were discontinued since they were ineffective in removing slag that formed on the front of the tubes. Element *C* was replaced with a telescopic blower installed in front of the superheater. Retractable wall blowers have also been installed in the side walls and front wall above the mud-drum elevation. Hand lancing has become unnecessary in those sections of the furnace provided with the telescopic and retractable blowers. No method other than hand lancing has been found which will effectively remove the slag where the temperature is high enough to make it sticky.

Some trouble was experienced with the burning of baffle castings and U-bolts in the high-temperature zone of the boiler. These troubles have been eliminated by the use of alloy steel of 25 per cent chromium, 12 per cent nickel.

There has been considerable erosion of the blades of the induced-draft fans at the center of the rotor. The worn parts of the blades were repaired by welding with "Abrasoweld" which was applied with the electric arc. This appears to be a satisfactory method of repair.

The induced- and forced-draft fans are driven by constant-speed motors through hydraulic couplings. Considerable sludging of oil was experienced when using oil having a viscosity of 195; however, since changing to an oil having a Saybolt Universal viscosity of 155 sec, this trouble has been eliminated.

The original rolls and rings in the pulverizers had a life of about 20,000 tons. Changes have been made in the shape and material which indicate a life of about 40,000 tons with a reduction in cost per ton. Different materials have also been used in the pulverizer liners, exhauster liners, and blades, all of which have reduced the cost per ton. The exhauster blades have a life of from 8500 to 10,500 tons. The blades have been made of structural plate, abrasive-resisting plate, four-way plate, and chrome-manganese plate. Structural-steel plates with beads of Abrasoweld are now being tried on one of these exhausters.

The pulverizers have a capacity of 12 tons per hr each and require 15 kwhr per ton at full load with a fineness of coal as follows: 98.0 per cent through 50-mesh screen; 92.0 per cent through 100-mesh screen; and 77.0 per cent through 200-mesh screen.

The coal used is Iowa screenings with the following analysis:

Moisture as received, per cent	16.50
Ash, per cent	17.50
Volatile, per cent	30.00
Carbon, per cent	36.00
Heating value, Btu per lb	9200
Sulphur, per cent	4.5
Ash: Initial deformation, F	1685
Softening point, F	1950
Fluid temperature, F	2110

The high amount of moisture, ash, and sulphur and the low softening point of the ash all tend to aggravate the difficulties

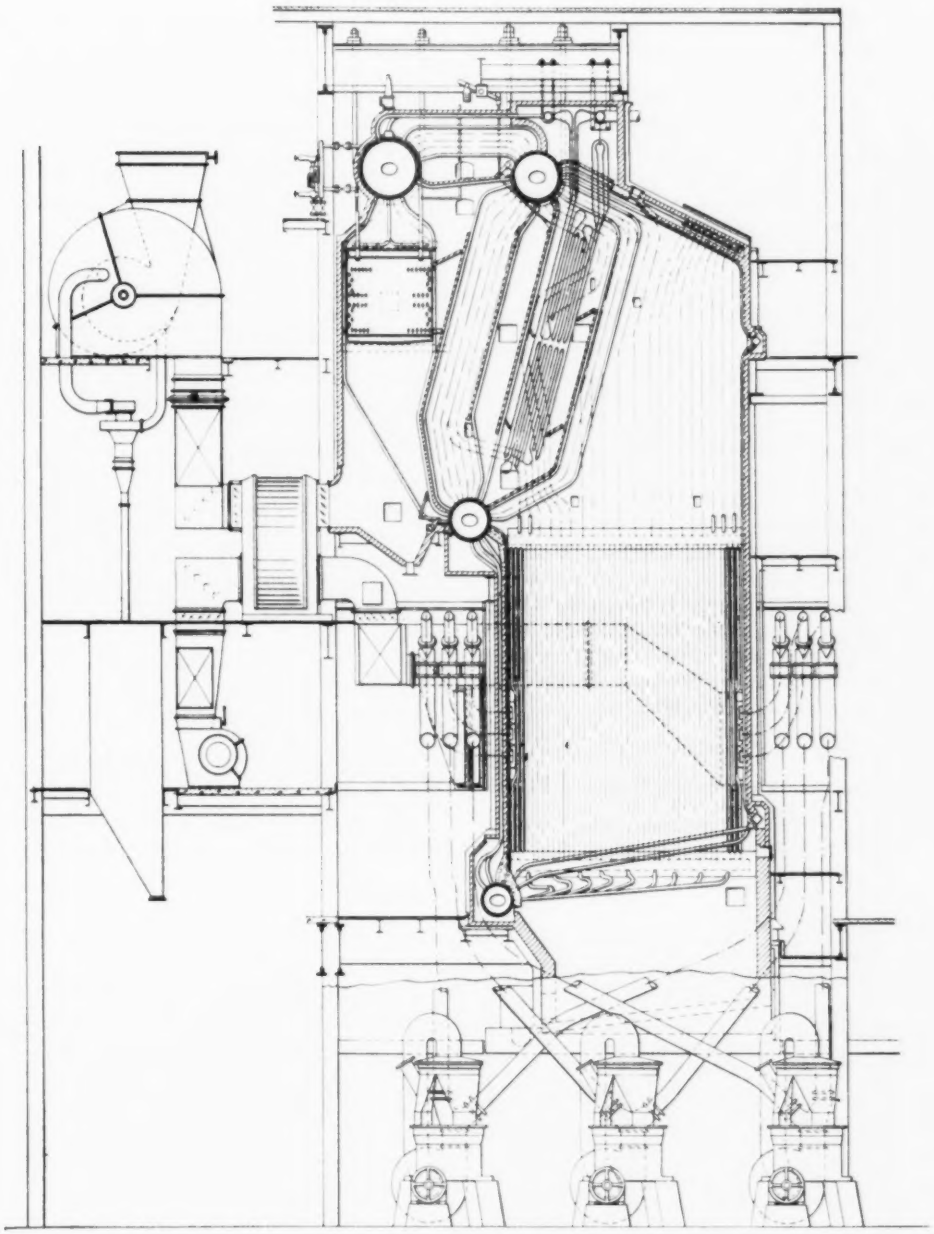


FIG. 7 SECTION THROUGH STEAM GENERATOR

inherent in pulverized fuel, yet owing to the fact that this station is located in the center of the Iowa coal field, it is the most economical fuel to use.

The combustion control has proved to be very reliable. It is completely automatic and regulates steam pressure and temperature, water, coal and air flow, and coal-air temperature from the pulverizers. Automatic regulation of steam pressure and temperature is also provided through the desuperheater, reducing the steam pressure to 365 psi and the temperature to 700 F for the 365-psi turbines in case of loss of the high-pressure turbine.

Some difficulty has been experienced with the motor-driven boiler feed pump owing to porous material in the pump diffusers, leaks having occurred mainly in the machined joints where two diffusers fit together, reducing the capacity of the pump. This happened in the original rotor twice and in a spare rotor once. These leaks did not develop until April, 1940, so that the difficulty has not yet been eliminated. However, the manufacturer is now rebuilding one of these rotors making use of different material.

The unit is equipped with five feedwater heaters, two of which are located between the hot-well pump and the boiler feed pump, and the other three between the boiler feed pump and the economizer. Heaters Nos. 3, 4, and 5 are designed for a working pressure of 1800 psi and are of the horizontal condenser type with floating heads. Nos. 3 and 4 had $^3/_4$-in. OD, 9 Bwg arsenical-copper tubes and No. 5 had $^3/_4$-in. OD, 12 Bwg copper-nickel tubes. Heaters Nos. 3 and 4 are subcooled. The drip cascades from No. 5, which is the high-pressure heater, through each of the other heaters to the drip pumps. Several leaks developed in No. 4 heater in both tube sheets, and although the tubes were rerolled sufficiently to stop the leaks under a hydrostatic test, the leaks persisted under operating conditions. It then became

impossible to stop the leaks by rerolling, so a new tube bundle was made for this heater using $^3/_4$-in. OD 12 Bwg, copper-nickel tubes with return bends instead of the floating heads.

No difficulties have been encountered with boiler-water circulation or carryover. Total solids in the boiler drum are maintained at 100 to 200 ppm by means of a continuous blowdown, amounting to about 0.5 per cent of the total evaporation. A continuous record of conductivity is made at the hot well, boiler-feed suction header, saturated or superheated steam, and distilled water from the evaporators.

Discussion

M. K. Drewry.[3] Coal, having an ash-fusion temperature of 1950 F, with 17.5 per cent ash, presents a difficult boiler-unit design and operating problem. That the Des Moines unit has been able to afford $4^1/_2$ months continuous service at high loads with this unfavorable fuel is creditable to the designers and operators.

About 90,000 Btu per sq ft per hr of furnace heat-absorbing surface is understood to be present in this furnace. This relatively low heat-release rate, or in other words, proportionately high "black" cooling surface, seems of major significance in explaining why the Des Moines unit operates well with bad fuel.

This case of controlling slagging under conditions of exaggerated difficulty points the way to its control in all other boiler units. It is a definite answer to the practicability of burning all coals when maintaining their ash in the dry state.

John Van Brunt.[4] This paper, dealing with operating experiences at Des Moines power station No. 2, is very interesting and instructive. The author should be given credit for his persistence in meeting and solving many problems that are inherent in burning coal of the character described and used in this plant. Some twenty or twenty-five mines are drawn upon for fuel, and the author will agree that some of the coal used is not as good as that referred to in his paper. Much of the coal contains as high as 6 per cent sulphur as well as a very considerable amount of iron.

This installation is one of the type requiring high steam temperature when burning low-fusion-ash coal. In order to avoid fusion of ash in the superheater, the furnace must be so designed as to give the lowest possible entering-gas temperature consistent with the superheater requirements. Despite the low softening temperature and the extremely low deformation temperature, there has been no troublesome fusion of ash in the superheater. Such ash as is deposited on the superheater elements can be easily removed by hand-lancing, and at the present time by telescopic soot blowers, as described by the author.

An availability factor of 92 per cent for 1940 shows that the operation is well organized and in competent hands.

The combustion in this furnace is excellent, as evidenced by repeated analyses of the fly ash, showing less than 1 per cent carbon in the fly ash, corresponding to a carbon loss of about 0.5 per cent.

A slagging-bottom furnace would be better suited for burning this type of coal. Less ash would pass through the boiler and superheater, and the handling of the ash from the slag-bottom furnace is simpler and easier than from a dry-bottom furnace. The gas temperature leaving the furnace would be the same or slightly lower, and less heavy slag would deposit on the walls. In all probability, such a furnace would be less affected by variations in the coal than is a dry-bottom furnace.

[3] Assistant Chief Engineer of Power Plants, Wisconsin Electric Power Company, Milwaukee, Wis. Mem. A.S.M.E.

[4] Vice-President in Charge of Engineering, Combustion Engineering Company, Inc., New York, N. Y. Mem. A.S.M.E.

An Improved Hand-Fired Furnace for High-Volatile Coals

By J. R. FELLOWS[1] and J. C. MILES,[2] URBANA, ILL.

This paper describes a furnace designed to burn high-volatile coal in two distinct phases: (1) Green coal is reduced to coke in the forward part of the furnace called a coking chamber; (2) when refiring is necessary, the resulting coke is pushed forward and down an inclined grate, where it burns as a smokeless fuel. The volatile gases from the coal pass under a baffle wall through which secondary air is admitted. Burning of the volatile gases occurs above the bed of hot coke. Air for coking the green coal and for burning the coke, as well as secondary air, is admitted through separate inlet openings. The furnace was found to produce no smoke and operated well on a variety of fuels. The temperature of the baffle wall was found to be proportional to the amount of air admitted to the coking chamber. The results indicate this method of burning bituminous coal is applicable to all types of hand-fired equipment, such as stoves, furnaces, and water heaters.

THE enormous amount of bituminous coal in the United States together with its wide geographical distribution makes it the most economical fuel for a large percentage of the population. That much of this coal will continue to be burned in low-cost hand-fired equipment is evidenced by the fact that approximately 7,000,000[3] coal- and wood-burning heating stoves were sold in the United States during the period from 1925 to 1937, and over 1,400,000 during the year 1937 alone, according to the latest report of the Census of Manufacturers.

The primary objections to the use of high-volatile coal in most hand-fired equipment comes from the amount of attention required and from the quantity of smoke produced. For both of these ills the stoker provides a satisfactory solution. However, until the use of stokers is economically feasible for a larger percentage of our population, the smoke palls are apt to hang over the poorer districts of most cities in the bituminous-coal area. If hand firing of high-volatile coal is prohibited by law, those least able to pay are forced to buy a premium fuel. This is made more significant by the fact that approximately 42 per cent[4] of the 29,000,000 family units in the United States, during the year 1937, had an income of less than $1000. The need for improving hand-fired bituminous-coal stoves and furnaces, with the object of eliminating smoke, increasing efficiency, and reducing the attention required, is quite evident.

There are two possible solutions for the problem of smoking fires: (1) that of processing the fuel, and (2) that of improving the furnace or stove. Fuel-processing operations such as coking and briquetting to produce a smokeless product must of necessity add to the cost of the fuel by virtue of those operations and the added transportation and handling costs. Therefore, the more logical solution of the smoke problem for families having low incomes would seem to be the development of suitable bituminous-coal-burning equipment, rather than reduction of the fuel to a "smokeless" form.

In this connection, it is interesting to note that, in the early stages of its development, the simple kerosene lamp was similarly handicapped, in that it produced much smoke. The present kerosene lamp which we are prone to regard as a crude primitive device is the result of very elaborate and painstaking research done more than half a century ago. Those interested are referred to a book[5] by Stepanoff, for which he was awarded the Nobel prize. Attempting to improve the oil rather than the lamp in this case would doubtlessly have proved futile.

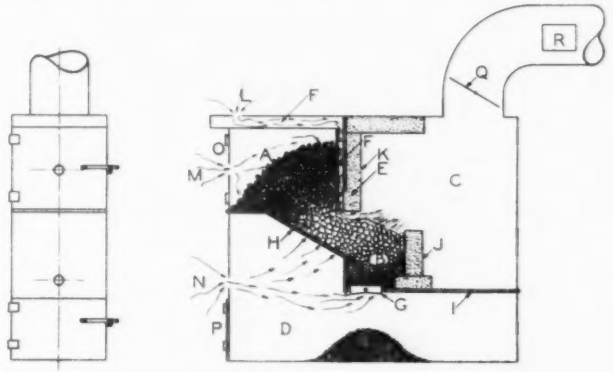


FIG. 1 SCHEMATIC SECTION OF TEST FURNACE

A	Coking chamber, intermittently charged with green coal by hand firing	I	Dead plate
B	Coke-burning chamber into which coke is pushed before refilling coking chamber with green coal	J	Back stop
C	Combustion chamber	K	Refractory block
D	Ashpit	L	Secondary-air inlet
E	Baffle wall	M	Coking-air inlet
F	Secondary-air passage	N	Undergrate-air inlet
G	Shaking grate	O	Firing door
H	Inclined grate	P	Ash door
		Q	Cross damper
		R	Check damper

The requirements for obtaining smokeless combustion of high-volatile coal have long been known, and have been briefly summarized by various authors as follows:

(*a*) Sufficient temperature for ignition.
(*b*) Sufficient air for oxidation.
(*c*) Thorough mixing of volatile gas and air.
(*d*) Sufficient time to complete oxidation.

It seems incredible that these few requirements could not be satisfied in some simple unit.

A good stove or furnace should incorporate those features essential to comfort, convenience, cleanliness, and economy. The major requirements are as follows:

[1] Assistant Professor of Mechanical Engineering, University of Illinois.

[2] Instructor in Mechanical Engineering, University of Illinois. Jun. A.S.M.E.

[3] "The Stove Market," editorial, *Coal Heat*, vol. 38, no. 6, December, 1940, p. 36.

[4] "Statistical Abstract of the United States—1939," U. S. Bureau of the Census, Washington, D. C., table of "Consumer Incomes," p. 313.

Contributed by the Fuels Division and presented at the Semi-Annual Meeting, Kansas City, Mo., June 16–19, 1941, of THE AMERICAN SOCIETY OF MECHANICAL ENGINEERS.

NOTE: Statements and opinions advanced in papers are to be understood as individual expressions of their authors and not those of the Society.

[5] "Oil Burning," by H. A. Romp, Martinus Nijhoff, The Hague, Holland, 1937; reference is made on page 87 to "Grundlagen der Lampentheorie," by Stepanoff (1894).

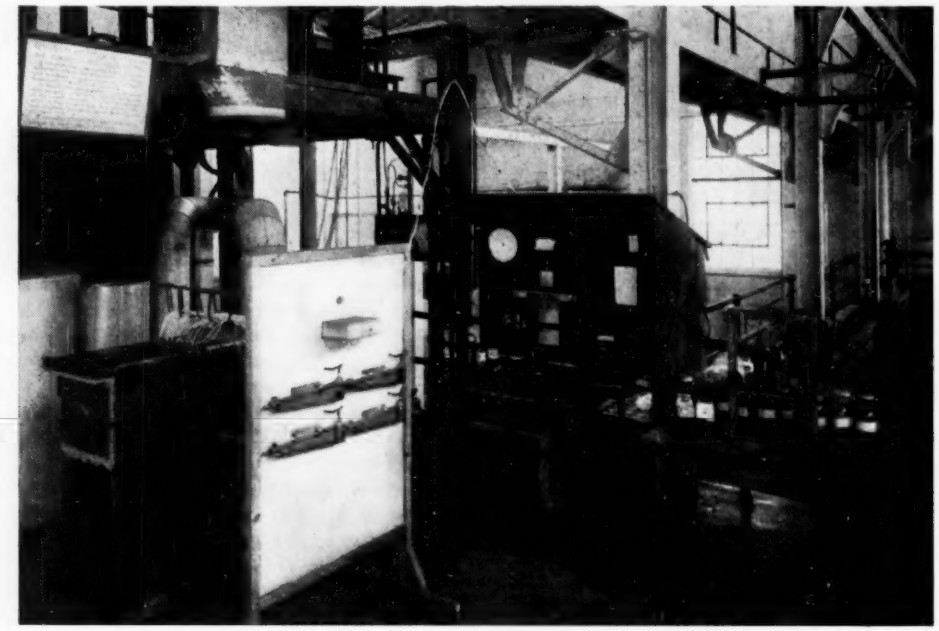


FIG. 2 ARRANGEMENT OF TEST APPARATUS

1 A large fuel capacity to eliminate frequent firing.
2 Adaptability to simple automatic temperature control.
3 Ashpan of sufficient size so that cleaning is not too frequently required.
4 Complete combustion with a minimum of excess air.
5 Smokeless operation.
6 Ability to burn fuel of various grades and sizes.

The furnace discussed in this paper was developed as the result of an attempt to incorporate these features in a simple unit for burning high-volatile coal. The furnace was designed by the authors and was tested in the Mechanical Engineering Experiment Station of the University of Illinois.[6]

The object of the tests was to determine how many of the different types of solid domestic fuels could be burned successfully in a unit of this type.

[6] The Engineering Experiment Station is under the direction of Dean M. L. Enger. Professor A. P. Kratz is in charge of research in mechanical engineering.

DESCRIPTION OF FURNACE

The principal features of the furnace design are shown in Fig. 1. The furnace was made of 1/4-in. firebox-steel plate in the shape of a simple rectangular box and was arranged in such a way that the proportional volumes of the coking chamber and the coke-burning chamber, and the slope and position of the inclined grate could be easily changed. The furnace was made airtight by welding the plates at the edges. Over-all dimensions were width, 16 inches; height, 41 inches; and length, 48 inches.

The baffle wall consisted of five narrow channel-shaped heat-resisting castings, attached to a supporting plate of 5/8-in. firebox steel by means of single-pin brackets. The castings provided air passages for secondary air which entered through the double roof and was discharged at the bottom of the baffle wall. A refractory block was placed at the rear of the baffle wall to shield it from radiant heat from the combustion chamber.

The inclined grate was arranged to facilitate the transfer of coke from coking chamber to coke-burning chamber. This in-

TABLE 1 GENERAL DATA

Test no.	Fuel	Fuel size, in.	Proximate analysis, per cent by weight as fired: Moisture	Volatile matter	Fixed carbon	Ash	Stack draft, in. water	Orifice diam, in.: Secondary air	Coking air	Undergrate air	Barometric pressure, in. Hg, avg	Outside temp, F, avg	Room temp at furnace, F, avg
1	West Va. "Pocahontas"	3/4 × 1	0.67	20.30	74.07	4.96	0.04	1.504	0.952	1.337	28.811	34	91
2	West Va. "Pocahontas"	3/4 × 1	0.67	20.30	74.07	4.96	0.12	1.504	0.952	1.337	29.031	27	90
3	Saline Co., Ill., "Sahara"	1/4 × 3/4	4.26	37.40	50.30	8.04	0.04	1.996	1.123	1.012	29.221	16	78
4	Saline Co., Ill., "Sahara"	1/4 × 3/4	4.26	37.40	50.30	8.04	0.12	1.996	1.123	1.012	29.049	16	82
5	Vermilion Co., Ill., "Danville"	1/4 × 3/4	7.25	37.30	46.30	9.15	0.04	2.061	0.952	1.012	28.907	15	80
6	Vermilion Co., Ill., "Danville"	1/4 × 3/4	7.25	37.30	46.30	9.15	0.12	2.061	0.952	1.012	28.907	15	80
7	Vermilion Co., Ill., "Danville"	1/4 × 3/4	7.25	37.30	46.30	9.15	[a]	2.061	0.952	1.012	29.264	7	72
8	East Kentucky	1/4 × 1	1.53	40.37	55.20	2.90	0.04	2.197	1.012	1.012	29.238	5	80
9	East Kentucky	1/4 × 1	1.53	40.37	55.20	2.90	0.12	2.197	1.012	1.012	29.234	9	91
10	Franklin Co., Ill.	1 × 2 nut	2.45	33.09	49.86	14.60	0.04	1.504	0.952	0.887	28.965	24	89
11	Franklin Co., Ill.	1 × 2 nut	2.45	33.09	49.86	14.60	0.12	1.504	0.952	0.887	28.965	24	90
12	Indiana "Brazil Block"	1 × 2 nut	8.26	33.42	49.45	8.87	0.04	2.197	1.012	1.012	29.213	30	90
13	Indiana "Brazil Block"	1 × 2 nut	8.26	33.42	49.45	8.87	0.12	2.197	1.012	1.012	29.400	27	95
14	Penn. Anthracite	1 × 2 nut	2.75	2.55	86.63	8.07	0.04	0.746	1.337	1.379	29.570	24	88
15	Penn. Anthracite	1 × 2 nut	2.75	2.55	86.63	8.07	0.12	0.746	1.337	1.379	29.569	25	92
16	Franklin Co., Ill.	Screenings	11.48	31.50	48.50	8.55	[a]	1.012	1.337	1.012	29.428	28	93
17	Coke	1 1/4 lump	0.42	0.00	91.94	7.64	0.04	0.495	1.012	1.504	29.138	24	85
18	Coke	1 1/4 lump	0.42	0.00	91.94	7.64	0.12	0.495	1.012	1.504	29.231	21	85
19	Sawdust and shavings	Fine, dry	Not analyzed			...	[a]	1.878	0.952	0.887	29.160	33	86
20	Wood scrap (hard and soft)	Small, dry	Not analyzed			...	[a]	1.878	1.123	0.746	29.797	52	92

[a] Variable stack draft.

TABLE 2 GENERAL RESULTS OF TEST

Test no.	Fuel	Flue-gas analysis, per cent by volume, avg			Carbon in refuse, per cent	Air flow, avg			Duration of test, hr	Total fuel burned, lb	Fuel burned, lb per hr	Smoke	No. of observations	Maximum temp of wall, F	Excess air, per cent
		CO_2	O_2	CO		Total air, lb per hr	Secondary air, per cent	Coking air, per cent	Under-grate air, per cent						
1	West Va. "Pocahontas"	9.77	10.07	0	44.0	54.3	44.8	20.2	35.0	8.38	35	4.17	none	23	1470	90
2	West Va. "Pocahontas"	10.61	8.71	0	44.0	96.6	43.3	19.7	37.0	9.00	80	8.89	none	28	1770	68
3	Saline Co., Ill., "Sahara"	9.77	9.50	0	30.6	63.5	59.9	21.2	18.9	7.53	38	5.02	none	19	1470	80
4	Saline Co., Ill., "Sahara"	8.85	10.18	0	30.6	110.2	59.9	20.8	19.3	8.50	70	8.24	none	26	1560	91
5	Vermilion Co., Ill., "Danville"	10.59	8.64	0	31.0	59.3	62.4	16.5	21.1	6.25	30	4.80	none	21	1420	68
6	Vermilion Co., Ill., "Danville"	10.38	8.88	0	31.0	104.7	64.4	16.0	19.6	4.00	30	7.50	none	13	1400	71
7	Vermilion Co., Ill., "Danville"	3.57	15.77	0	31.0	54.0	64.8	18.5	16.7	12.00	18	1.50	none	16	1550	285[b]
8	East Kentucky	9.08	9.65	0	30.3	58.0	60.3	20.7	19.0	8.33	25	3.00	none	25	1640	82
9	East Kentucky	9.74	9.00	0	30.3	109.5	64.8	16.9	18.3	8.33	65	7.80	none	25	1620	72
10	Franklin Co., Ill.	10.15	8.77	0	30.0	41.0	54.9	21.9	23.2	8.00	35	4.37	none	25	1490	69
11	Franklin Co., Ill.	11.75	7.18	0	30.0	68.5	56.2	23.4	20.4	4.25	22	5.18	none	13	1470	50
12	Indiana "Brazil Block"	9.96	9.60	0	43.5	64.5	63.6	18.6	17.8	8.00	30	3.75	none	25	1470	83
13	Indiana "Brazil Block"	9.74	9.90	0	43.5	108.6	64.0	17.1	18.9	4.00	30	7.50	none	13	1460	88
14	Penn. Anthracite	13.48	6.80	0	27.5	44.8	14.3	40.2	45.5	8.00	35	4.37	none	24	1800	48
15	Penn. Anthracite	14.13	6.25	0	27.5	75.4	15.3	41.2	43.8	4.00	30	7.50	none	13	2070	42
16	Franklin Co., Ill.	11.12	8.03	0	47.0	51.8[a]	32.4	38.6	29.0	9.50	65	6.85	none	26	1950	60
17	Coke	11.72	8.22	0	49.9	38.0	6.6	30.3	63.1	8.25	25	3.03	none	25	1730	63
18	Coke	12.75	7.46	0	49.4	69.4	7.2	29.4	63.4	5.75	25	4.35	none	18	1950	55
19	Sawdust and shavings	11.18	8.57	0	...	61.0[a]	64.0	19.6	16.4	5.25	55	10.48	[c]	15	1350	69
20	Wood scrap (hard and soft)	10.90	9.64	0	...	70.7[a]	60.2	27.4	12.4	3.00	36	12.00	[c]	13	1380	83

[a] Frequent firing allowed much air to enter unmetered.
[b] Banking test.
[c] Very light smoke, visible on one observation only.

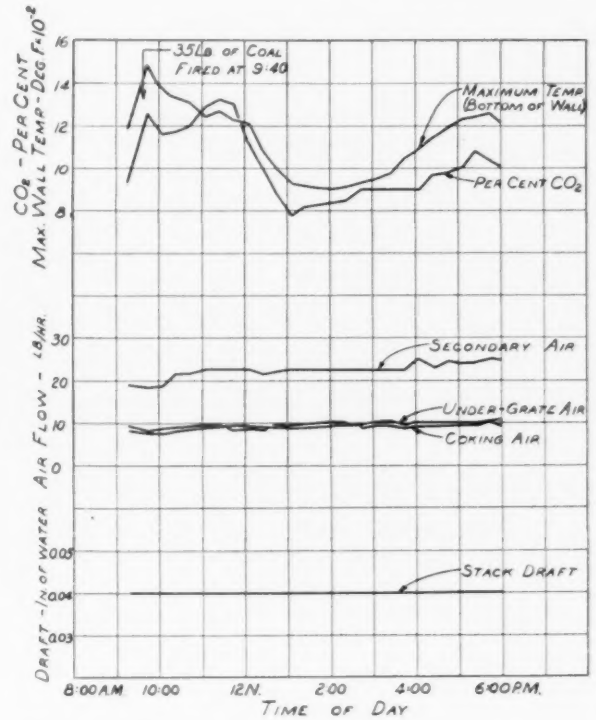


FIG. 3 GRAPHICAL LOG OF TEST NO. 10; FRANKLIN COUNTY, ILLINOIS, COAL

clined grate was provided with 1/4-in. holes on 1-in. centers for a distance of 6 in. nearest the baffle wall. The purpose of the holes was to promote sufficient combustion in the coke at this region to maintain below the baffle wall an ignition temperature high enough to assure ignition of all gases passing from the coking chamber.

Furnace Operation. The furnace was designed to burn high-volatile coal in two distinct phases and the operation is as follows: (1) A charge of green coal (about 35 lb) is converted to coke in the coking chamber; (2) when refiring is necessary, the coke is pushed down the inclined grate into the coke-burning chamber before a new charge of green coal is placed. While the green coal is being converted to coke, the volatile gases evolved pass beneath the baffle wall, where they become mixed with the secondary air entering through the baffle wall. The mixing occurs just above the bed of burning coke, in a region where the temperature is high enough to ignite the mixture.

The rate of distillation of gases from the green coal is determined by the amount of primary air entering the coking chamber. The rate at which the coke burns on the grate is determined by the amount of air admitted below the grate. Sufficient air to burn the volatile gases is admitted through the baffle wall.

By proportioning properly the three air-inlet openings, the green coal is completely coked before the coke from the previous charge is all consumed on the grate. With this cycle of operation a region of high temperature is always maintained, through which the volatile gases must pass. By supplying sufficient secondary air through the baffle wall, conditions are ideal for complete combustion of the volatile or smoke-forming content of the coal. The air flow through all three inlet openings and, consequently, the rate of combustion are controlled by use of a check or cross damper as in any conventional furnace.

Instruments and Calibration. Temperatures existing in the baffle wall were measured by means of thermocouples, made by peening the ends of No. 22 B.&S. gage Chromel and Alumel wires

into holes drilled 1/4 in. apart in the alloy castings. The thermocouples were spaced at varying distances from the bottom of the baffle wall. The wires were protected by porcelain insulators and brought out the top of the furnace to a cold-junction box mounted on a panel a short distance from the furnace. Copper-wire extensions were run from the cold-junction box to a selector switch and a potentiometer. The calibrations were checked by measuring the melting points of several chemically pure metals with a thermocouple made exactly as those in the test furnace. A mercury-in-glass thermometer was used to determine the temperature at the thermocouple cold junction.

Flue-gas analyses were made with a standard Orsat apparatus, and thin-plate orifices were used to measure the flow of air through the three separate inlets.

The orifices used were made by turning smooth holes in flat 23-gage-steel plates. The pressure drop through each orifice was measured with an inclined draft gage graduated in hundredths of an inch of water. A similar gage was also used for measuring the chimney draft at the outlet from the combustion chamber. The chimney draft was regulated by means of a check-draft damper and a cross damper in the smoke pipe. The general arrangement of the equipment is shown in Fig. 2.

Test Procedure

Tests were made on eleven types of fuels, representing the general range of types common in domestic firing. A test was made on each of these at a low combustion rate, and a second test was made at a high combustion rate, except in the cases of sawdust and wood scrap which were burned at the low rate only. The combustion rate was controlled by regulating the stack draft. During the low-rate tests, the stack draft was maintained at 0.04 in. of water and a draft of 0.12 in. of water was maintained during the high-rate tests. This range of draft was chosen as representing approximately the normal range encountered in domestic practice. The fuel was not disturbed during any test.

For each fuel tested, the proper orifices were selected so that the combination would give the highest average CO_2 consistent with completely smokeless operation. With any given fuel, the low-combustion-rate test was run first, as it was found to be more difficult to obtain smokeless combustion at this rate. The orifice combination which proved satisfactory for the low rate of combustion was also used for the high rate, thus only one orifice combination was used for each fuel.

Before starting a test, the furnace was fired with the kind of fuel to be tested in order that the residual coke would be from the fuel under test. The coke was broken up with an ordinary poker and the greater part pushed down the inclined grate into the coke-burning chamber. Sufficient coke was left on the lower part of the inclined grate to prevent any of the fresh charge from passing the lower edge of the baffle wall.

Immediately after placing a charge of fuel, the stack draft was adjusted to the desired value, and the doors and all places where possible leakage might occur were sealed with furnace cement. Temperatures, draft-gage readings, flue-gas analyses, and smoke observations were made at 20-min intervals. Smoke observations were made by placing an ordinary light bulb inside the stack or by observing the top of the stack against the sky. Samples were taken and proximate analyses were made of all fuels with the exception of sawdust and wood scrap. The refuse from each fuel was analyzed for unburned carbon.

Results of Tests

General data pertaining to the fuels and conditions are given in Table 1. General results are given in Table 2. Fig. 3 shows a typical graphical log.

The primary objectives were to determine whether all major types of fuel could be burned smokelessly and to measure the furnace-baffle-wall temperatures. More extensive tests are to be made to compare the performance of different fuels under a wider range of operating conditions. Furnace efficiency as calculated from heat losses was not determined, since the flue-gas and residue analyses give ample indication of the combustion efficiency. For the purpose of obtaining smokeless operation, there was no point in using coke or anthracite in this type of furnace. These fuels were tested, however, to see if they could be successfully burned.

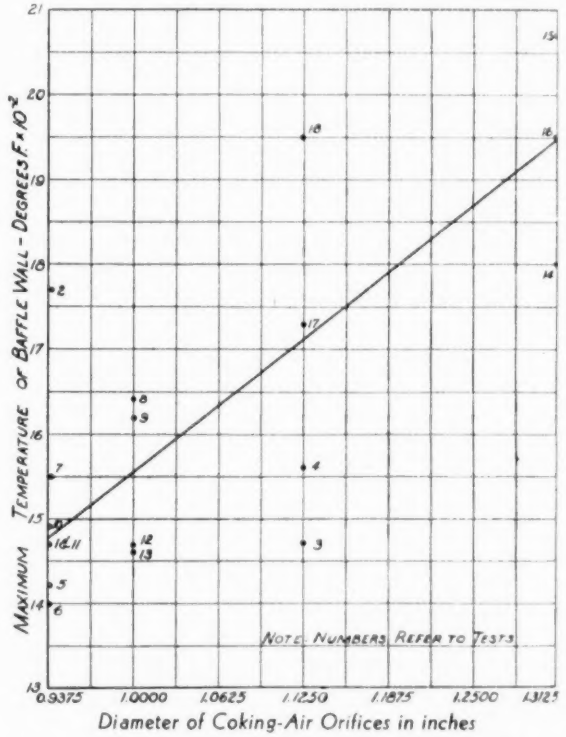


Fig. 4 Relation of Coking-Air-Orifice Size to Maximum Baffle-Wall Temperature

Temperatures in the Baffle Wall. The temperatures existing in the baffle wall were found to be proportional to the amount of air admitted to the coking chamber. This finding is logical since combustion in the coking chamber can proceed no faster than the supply of air will permit. Fig. 4 shows the relationship between coking-air-orifice size and maximum temperature of the baffle wall. No definite curve could be drawn to represent the test points, but there is a definite tendency for the higher baffle-wall temperatures to be associated with the larger flows of air to the coking chamber. The results, shown in Fig. 4, are incidental, since no tests were run specifically to determine this relationship. The latter could be more effectively established by a series of tests involving only one fuel.

During the operating cycle, a period of high baffle-wall temperature occurred at the time the coke was being pushed down, preliminary to firing a fresh charge of green coal. While the door was open, rapid oxidation occurred at the surface of the coke bed. This initial peak in wall temperature, coincident with the time of firing, is very evident in all the graphical logs.

The temperatures measured in the lower part of the baffle wall indicate the necessity for using special heat-resisting alloys or refractories for this part of the structure. The tem-

perature gradient in the baffle wall,[7] shown in Fig. 5, indicates the necessity for using a special sectional construction to resist warping.

Smoke. Observations made at 20-min intervals showed that no smoke whatever was produced during test runs with any of the fuels used, with the exception of sawdust and wood scrap, for which very light smoke was seen on one occasion only during each of the tests of these fuels. A total of 406 observations were made during which 784 lb of fuel were burned, thus proving that high-volatile coal can be burned in this type of furnace without the formation of smoke.

For each type or kind of fuel, it was necessary to determine by experiment the best combination of orifice sizes to be used. The coking-air orifice was made sufficiently small to prevent the wall temperatures from exceeding a safe value. An undergrate orifice was then selected which would supply sufficient air below the grate to consume the greater part of the coke in the coke-burning chamber by the time the coking operation was complete. With these orifice sizes determined, a secondary-air orifice was selected such that the secondary-air supply was ample to prevent the

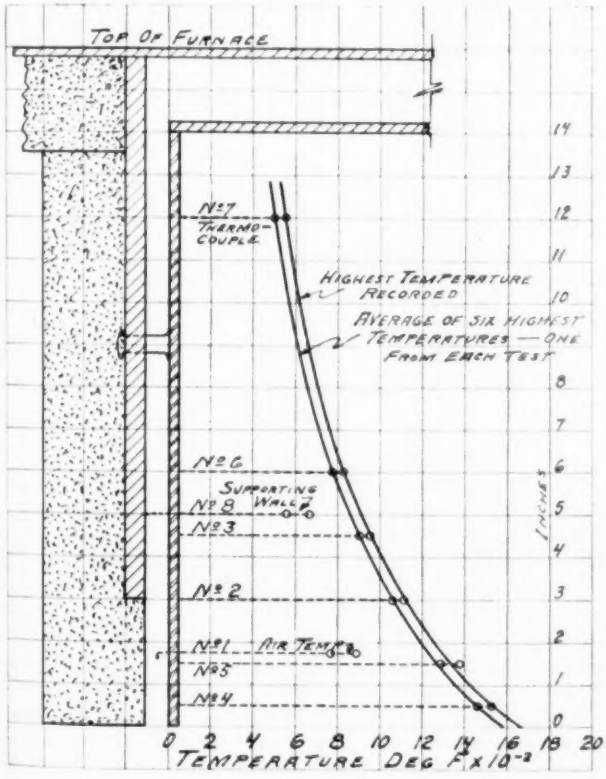


FIG. 5 TEMPERATURE GRADIENT IN BAFFLE WALL

formation of smoke throughout the operating cycle. During the preliminary work required to determine the proper orifice combination for a given fuel, smoke frequently occurred as a result of too small a secondary-air orifice.

With high-volatile coal, the peak demand for secondary air occurred approximately 1 hr after recharging the furnace. Since the rate of volatilization was highest at that time, it was generally coincident with the highest CO_2 content in the flue gas.

Fuel-Burning Rate. Using bituminous coal, the average fuel-burning rate was 7.5 lb per hr with 0.12 in. draft, and 4.2 lb per hr with 0.04 in. draft. These rates are comparable with those of updraft furnaces of similar physical dimensions. The minimum burning rate of 1.5 lb per hr was established during test No. 7 in which 18 lb of coal were sufficient to maintain slow combustion for 12 hr.

Fuel Sizes. The range in size of coal fired was not great enough to establish the effect of fuel size on furnace performance. It is significant, however, that screenings were successfully burned as well as 1 × 2-in. nut coal. During other tests 2 × 3-in. nut coal has been successfully burned. It therefore appears that

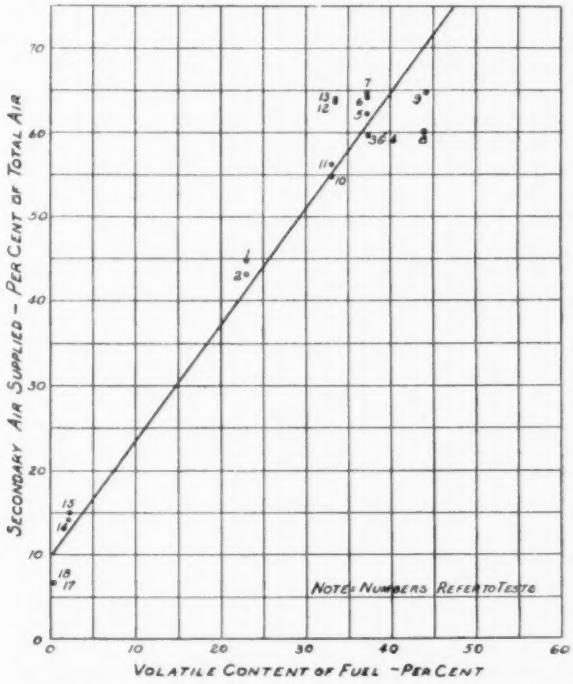


FIG. 6 RELATION OF VOLATILE CONTENT TO SECONDARY AIR

accurate sizing of coal is not essential for smokeless operation of this furnace.

Air Distribution. In order to obtain smokeless combustion, it was found necessary to supply from 55 to 65 per cent of the total air as secondary air for most Midwest bituminous coals. The relationship of volatile content to secondary air required is shown in Fig. 6.

A comparison of the orifices, selected by trial and error for each fuel, showed that practically the same combination was satisfactory for all bituminous coals having a volatile content of 30 to 40 per cent. The combination of orifices which would be suitable for practically all high-volatile bituminous coals was 2 in., 1 in., and 1 in. diam, respectively, for the secondary, coking, and undergrate air. This corresponds to an area relationship of 4 to 1 to 1, or on a percentage basis of 66.6, 16.6, and 16.6 per cent, respectively.

For a given temperature, and very small pressure drop across the orifice, the flow of atmospheric air may be expressed by the equation

$$W = KA(i)^{1/2}$$

in which W = air flow, lb per sec
A = area of orifice, sq ft
K = constant
i = pressure drop across orifice, in. of water

[7] Data from which this graph was made were obtained during tests made in August, 1939, while burning Franklin County, Illinois, coal in this same furnace.

into holes drilled 1/4 in. apart in the alloy castings. The thermocouples were spaced at varying distances from the bottom of the baffle wall. The wires were protected by porcelain insulators and brought out the top of the furnace to a cold-junction box mounted on a panel a short distance from the furnace. Copper-wire extensions were run from the cold-junction box to a selector switch and a potentiometer. The calibrations were checked by measuring the melting points of several chemically pure metals with a thermocouple made exactly as those in the test furnace. A mercury-in-glass thermometer was used to determine the temperature at the thermocouple cold junction.

Flue-gas analyses were made with a standard Orsat apparatus, and thin-plate orifices were used to measure the flow of air through the three separate inlets.

The orifices used were made by turning smooth holes in flat 23-gage-steel plates. The pressure drop through each orifice was measured with an inclined draft gage graduated in hundredths of an inch of water. A similar gage was also used for measuring the chimney draft at the outlet from the combustion chamber. The chimney draft was regulated by means of a check-draft damper and a cross damper in the smoke pipe. The general arrangement of the equipment is shown in Fig. 2.

Test Procedure

Tests were made on eleven types of fuels, representing the general range of types common in domestic firing. A test was made on each of these at a low combustion rate, and a second test was made at a high combustion rate, except in the cases of sawdust and wood scrap which were burned at the low rate only. The combustion rate was controlled by regulating the stack draft. During the low-rate tests, the stack draft was maintained at 0.04 in. of water and a draft of 0.12 in. of water was maintained during the high-rate tests. This range of draft was chosen as representing approximately the normal range encountered in domestic practice. The fuel was not disturbed during any test.

For each fuel tested, the proper orifices were selected so that the combination would give the highest average CO_2 consistent with completely smokeless operation. With any given fuel, the low-combustion-rate test was run first, as it was found to be more difficult to obtain smokeless combustion at this rate. The orifice combination which proved satisfactory for the low rate of combustion was also used for the high rate, thus only one orifice combination was used for each fuel.

Before starting a test, the furnace was fired with the kind of fuel to be tested in order that the residual coke would be from the fuel under test. The coke was broken up with an ordinary poker and the greater part pushed down the inclined grate into the coke-burning chamber. Sufficient coke was left on the lower part of the inclined grate to prevent any of the fresh charge from passing the lower edge of the baffle wall.

Immediately after placing a charge of fuel, the stack draft was adjusted to the desired value, and the doors and all places where possible leakage might occur were sealed with furnace cement. Temperatures, draft-gage readings, flue-gas analyses, and smoke observations were made at 20-min intervals. Smoke observations were made by placing an ordinary light bulb inside the stack or by observing the top of the stack against the sky. Samples were taken and proximate analyses were made of all fuels with the exception of sawdust and wood scrap. The refuse from each fuel was analyzed for unburned carbon.

Results of Tests

General data pertaining to the fuels and conditions are given in Table 1. General results are given in Table 2. Fig. 3 shows a typical graphical log.

The primary objectives were to determine whether all major types of fuel could be burned smokelessly and to measure the furnace-baffle-wall temperatures. More extensive tests are to be made to compare the performance of different fuels under a wider range of operating conditions. Furnace efficiency as calculated from heat losses was not determined, since the flue-gas and residue analyses give ample indication of the combustion efficiency. For the purpose of obtaining smokeless operation, there was no point in using coke or anthracite in this type of furnace. These fuels were tested, however, to see if they could be successfully burned.

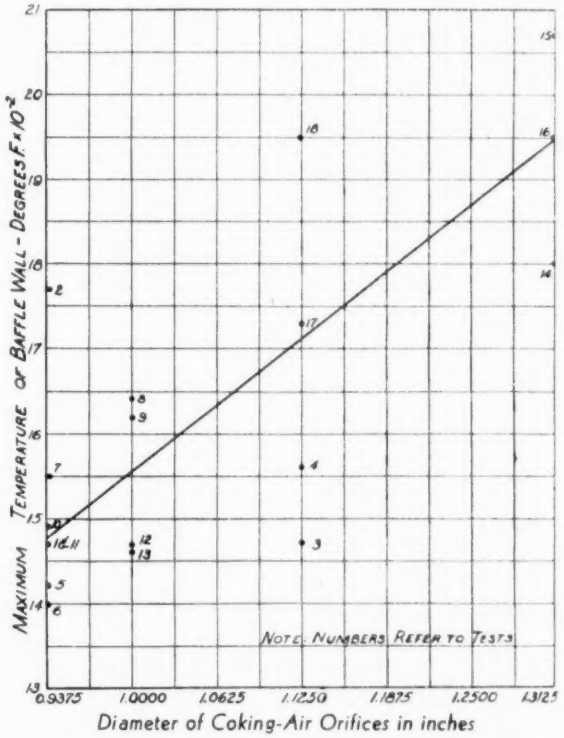


Fig. 4 Relation of Coking-Air-Orifice Size to Maximum Baffle-Wall Temperature

Temperatures in the Baffle Wall. The temperatures existing in the baffle wall were found to be proportional to the amount of air admitted to the coking chamber. This finding is logical since combustion in the coking chamber can proceed no faster than the supply of air will permit. Fig. 4 shows the relationship between coking-air-orifice size and maximum temperature of the baffle wall. No definite curve could be drawn to represent the test points, but there is a definite tendency for the higher baffle-wall temperatures to be associated with the larger flows of air to the coking chamber. The results, shown in Fig. 4, are incidental, since no tests were run specifically to determine this relationship. The latter could be more effectively established by a series of tests involving only one fuel.

During the operating cycle, a period of high baffle-wall temperature occurred at the time the coke was being pushed down, preliminary to firing a fresh charge of green coal. While the door was open, rapid oxidation occurred at the surface of the coke bed. This initial peak in wall temperature, coincident with the time of firing, is very evident in all the graphical logs.

The temperatures measured in the lower part of the baffle wall indicate the necessity for using special heat-resisting alloys or refractories for this part of the structure. The tem-

perature gradient in the baffle wall,[1] shown in Fig. 5, indicates the necessity for using a special sectional construction to resist warping.

Smoke. Observations made at 20-min intervals showed that no smoke whatever was produced during test runs with any of the fuels used, with the exception of sawdust and wood scrap, for which very light smoke was seen on one occasion only during each of the tests of these fuels. A total of 406 observations were made during which 784 lb of fuel were burned, thus proving that high-volatile coal can be burned in this type of furnace without the formation of smoke.

For each type or kind of fuel, it was necessary to determine by experiment the best combination of orifice sizes to be used. The coking-air orifice was made sufficiently small to prevent the wall temperatures from exceeding a safe value. An undergrate orifice was then selected which would supply sufficient air below the grate to consume the greater part of the coke in the coke-burning chamber by the time the coking operation was complete. With these orifice sizes determined, a secondary-air orifice was selected such that the secondary-air supply was ample to prevent the

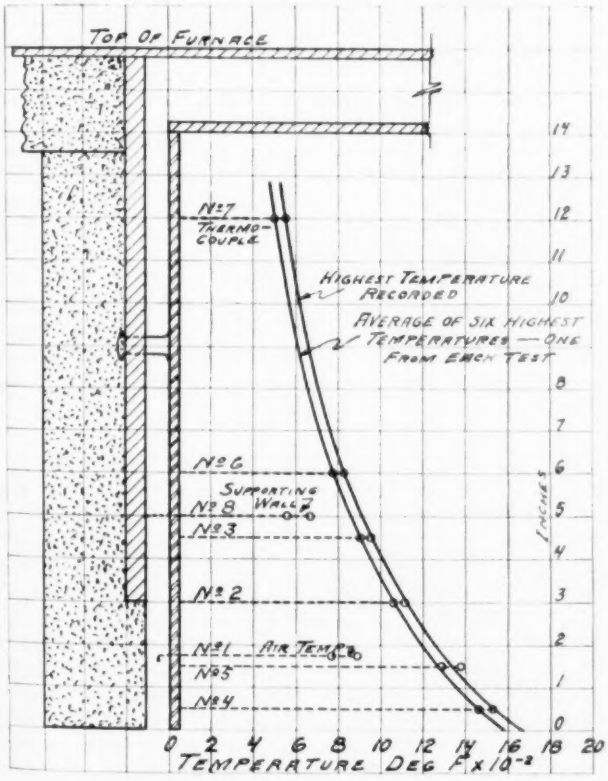


FIG. 5 TEMPERATURE GRADIENT IN BAFFLE WALL

formation of smoke throughout the operating cycle. During the preliminary work required to determine the proper orifice combination for a given fuel, smoke frequently occurred as a result of too small a secondary-air orifice.

With high-volatile coal, the peak demand for secondary air occurred approximately 1 hr after recharging the furnace. Since the rate of volatilization was highest at that time, it was generally coincident with the highest CO_2 content in the flue gas.

Fuel-Burning Rate. Using bituminous coal, the average fuel-burning rate was 7.5 lb per hr with 0.12 in. draft, and 4.2 lb per hr with 0.04 in. draft. These rates are comparable with those of updraft furnaces of similar physical dimensions. The minimum burning rate of 1.5 lb per hr was established during test No. 7 in which 18 lb of coal were sufficient to maintain slow combustion for 12 hr.

Fuel Sizes. The range in size of coal fired was not great enough to establish the effect of fuel size on furnace performance. It is significant, however, that screenings were successfully burned as well as 1 × 2-in. nut coal. During other tests 2 × 3-in. nut coal has been successfully burned. It therefore appears that

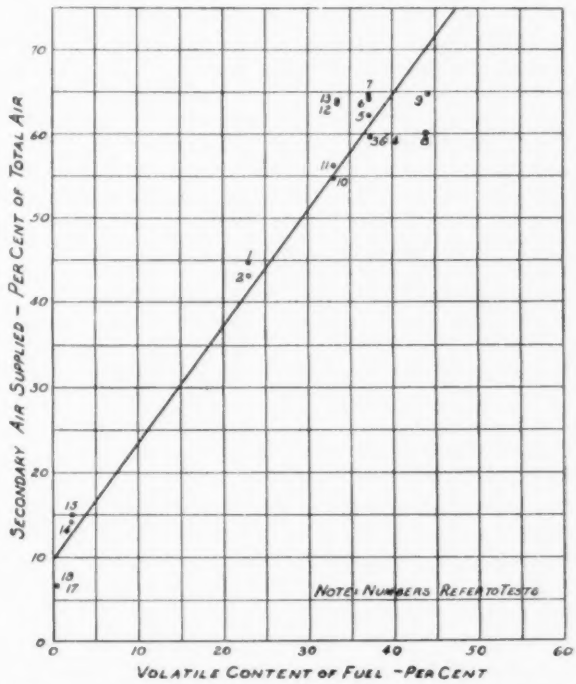


FIG. 6 RELATION OF VOLATILE CONTENT TO SECONDARY AIR

accurate sizing of coal is not essential for smokeless operation of this furnace.

Air Distribution. In order to obtain smokeless combustion, it was found necessary to supply from 55 to 65 per cent of the total air as secondary air for most Midwest bituminous coals. The relationship of volatile content to secondary air required is shown in Fig. 6.

A comparison of the orifices, selected by trial and error for each fuel, showed that practically the same combination was satisfactory for all bituminous coals having a volatile content of 30 to 40 per cent. The combination of orifices which would be suitable for practically all high-volatile bituminous coals was 2 in., 1 in., and 1 in. diam, respectively, for the secondary, coking, and undergrate air. This corresponds to an area relationship of 4 to 1 to 1, or on a percentage basis of 66.6, 16.6, and 16.6 per cent, respectively.

For a given temperature, and very small pressure drop across the orifice, the flow of atmospheric air may be expressed by the equation

$$W = KA(i)^{1/2}$$

in which W = air flow, lb per sec
A = area of orifice, sq ft
K = constant
i = pressure drop across orifice, in. of water

[1] Data from which this graph was made were obtained during tests made in August, 1939, while burning Franklin County, Illinois, coal in this same furnace.

From this equation, it is evident that orifice area is the major factor in determining the rate of air flow through the orifice. Since i is ordinarily less than 0.1 in. of water, the change in $(i)^{1/2}$ for a small change in draft is almost negligible. Thus, orifice size is the controlling factor in determining air flow to the several chambers, regardless of minor changes in the resistance of either fuel bed. Otherwise, burning would not be stable, but would accelerate or decelerate in either fuel chamber as the resistance of the respective fuel beds decreased or increased. This effect is shown in the graphical logs by the reasonably steady air flow to each compartment during the whole of each firing cycle.

Combustion Efficiency. The CO_2 content of the stack gases averaged 10.46 per cent for all tests with a complete absence of CO. This represents approximately 70 per cent excess air. During the period of maximum volatilization, the excess air averaged 30.6 per cent. The loss of combustible in the refuse was high because of a loose-fitting shaking grate and thorough cleaning of the fire between tests. No difficulty was encountered on any test as the result of clinker formation.

Frequency of Firing. The average firing period for coal (not including wood or coke) during the high-rate tests was 4 hr, and during the low-rate tests was 8.32 hr. For the "banking" test, the interval was 12 hr. This indicates relatively less attention than that necessary for conventional updraft units. The fact that this furnace will operate smokelessly at low combustion rates indicates the possibility of increasing the fuel capacity and, consequently, of decreasing the frequency of firing.

Summary of Results Attained

The following general statements can be made concerning the furnace and the results of the tests:

1 High-volatile bituminous coal was burned without the formation of smoke.

2 Temperatures in the baffle wall were directly proportional to, and could be controlled by limiting, the amount of air admitted to the coking chamber.

3 Reasonable combustion efficiency was obtained during all tests as indicated by an average CO_2 content, ranging from 8.85 to 14.13 per cent, with complete absence of CO.

4 The amount of secondary air necessary for smokeless operation varied directly with the volatile content of the coal.

5 Secondary-air requirements of from 55 to 65 per cent of the total air supplied were necessary when burning high-volatile coal smokelessly.

6 The furnace successfully burned bituminous coal, coke, wood, sawdust, and anthracite.

7 The furnace responded quickly and smokelessly when fired after high-rate, low-rate, or banking operations.

8 No difficulties were encountered from the formation of clinkers or in pushing coke from the coking chamber to the coke-burning chamber. The comparatively hard coke from certain coals was partially broken up with a short bar before using the ordinary poker for pushing it into the coke-burning chamber.

9 The draft requirements are not above those normally obtained from a typical domestic chimney.

10 No difficulties were encountered in maintaining draft with any fuel tested.

11 Coal ranging in size from screenings to 2 × 3-in. nut was successfully burned.

12 The fuel-burning rate, using bituminous coal, was comparable to that for an updraft furnace of the same physical dimensions. The maximum burning rate was 8.89 lb per hr during these tests.

13 One combination of orifices was found to be satisfactory for all rates of combustion of any given fuel.

14 One combination of orifices would be satisfactory for all Midwestern bituminous coals.

15 The results indicate that this method of burning bituminous coal may be applied to all types of hand-fired equipment such as stoves, furnaces, boilers, and water heaters.

Discussion

W. G. Christy.[8] The authors are to be congratulated for their experimental work in a field where more engineering work should be done. There is need for equipment which will burn, smokelessly, potentially smoky fuels such as high-volatile bituminous coal.

The writer would like to call attention to two requirements upon which the success of the equipment depends:

The cost should be very little higher than competitive equipment. Users will not pay very much additional for smokeless equipment. It would appear that the furnace described in this paper will qualify in this respect. Quantity production should make the price reasonable.

Such equipment should be as near foolproof as possible. It has been demonstrated that many people do the wrong things and pay little attention to firing instructions. While this furnace is not complicated, it is a radical departure from the usual type of hand-fired furnace. In order that the furnace may function properly, coked coal must be pushed back. With such furnaces installed in homes, some people might fire additional fresh coal without pushing back the coked coal, or they may push the coal back before it is fully coked. In the latter case considerable smoke will likely result.

This furnace is an ingenious device. If operated according to instructions, it should be successful, economical, and smokeless. It is very desirable that some manufacturer build 50 or 100 of these furnaces and get them installed in districts where high-volatile bituminous coal is the prevailing domestic fuel. It will be interesting to observe how they perform in the hands of the public.

A. S. Langsdorf.[9] In a previous paper,[10] V. J. Azbe described a furnace equipped with a baffle designed to utilize the same downdraft principle that has been used by the authors. There is no doubt that the principle is sound and that furnaces constructed along these lines will be effective in preventing smoke, provided the material of which the baffle is made will stand up under the punishment it must take. In experiments made in St. Louis, an attempt was made to install baffles, some of them made of a chrome-steel alloy, in standard types of furnaces made by different manufacturers. Difficulty was experienced in providing satisfactory means for attaching the baffles to the furnaces which had not been designed to accommodate them. Better results may be expected if the furnace is originally designed to be fitted with a baffle, and studies of the kind reported in the paper under discussion are to be encouraged, particularly if they lead to the commercial introduction of small domestic furnaces which embody sound engineering principles.

There is one feature of the design shown in the illustrations which should receive more attention than is usually accorded to it. It is to be noted that the air inlets to the furnace are simple openings in the stove casing, a characteristic shared by all other

[8] Smoke Abatement Engineer, in charge of Hudson County Department of Smoke Regulation, Jersey City, N. J. Mem. A.S.M.E.

[9] Dean, Schools of Engineering and Architecture, Washington University, St. Louis, Mo. Mem. A.S.M.E.

[10] "Smokeless and Efficient Firing of Domestic Furnaces," by V. J. Azbe, Trans. A.S.M.E., vol. 49-50, 1927-1928, paper FSP-50-23, pp. 175–182.

types which have come to the writer's attention. It appears to be taken for granted that the air required to support combustion will somehow find its way into the air-inlet openings; but in cold weather, when the stove is really needed, it is the common practice of householders to shut all doors and windows of the room in which the stove is installed, so that the air supply is restricted to the inadequate amount that leaks through the window sashes and door frames. Every stove manufacturer should be compelled to provide a positive source of air in the same way that he is obliged to provide a vent for the products of combustion. Conduits or ducts for air supply should be as much an integral part of the installation as is the smoke pipe.

EUGENE MURPHY.[11] Several questions on the application of this interesting new furnace occur to the writer. The authors state that relatively less attention will be required than that necessary for conventional updraft units. During typical weather in the region for which the furnace is designed, may a householder tend the furnace only in the morning and evening?

Will the average adult be able to operate the furnace properly without special skill or training?

Clearly the furnace shown was constructed as an experimental model. Have the authors attempted to remodel a commercially available furnace or to estimate costs of commercially constructed furnaces built to operate on the same fundamental principle?

AUTHORS' CLOSURE

The authors desire to thank Mr. Christy, Dean Langsdorf, and Mr. Murphy for their interesting comments.

In answer to Mr. Christy's question, concerning the proper operation of the furnace, the authors do not believe that it will be difficult to educate the public to use this type of furnace properly. The fire does not respond after the coke has burned out of the coke-burning chamber, and adding fresh fuel will not result in the production of an appreciable amount of heat unless the coke from the previous charge is first broken up and pushed into the coke-burning chamber. In other words, the authors feel that proper operation of the furnace is necessary to obtain satisfactory heating, and that smokeless combustion will result even though the operator is not particularly interested in smoke elimination.

In reply to Mr. Christy's suggestion, the authors are happy to report that a reliable furnace manufacturer is now working on a commercial design of this furnace to be placed on the market in the near future.

The authors recognize the need for positive air supply to any furnace, as pointed out by Dean Langsdorf. However, the need would not be as critical with this type of stove or furnace as with the conventional types, because periods of high rates of volatilization are eliminated and, consequently, the maximum air requirements are much lower for the same average combustion rate.

In answer to Mr. Murphy's first question, the authors wish to state that they believe furnaces of this type, if properly proportioned to the heat load, will perform satisfactorily during typical Illinois weather, if given attention only morning and evening.

The authors do not believe there is any question about the ability of the average person to operate the furnace. The only step in the firing procedure that is different from that used in firing any furnace is that of pushing the coke down before refiring. The shape of the coking chamber makes this operation much simpler than that of pushing coke to the back or side of the firepot of the conventional furnace.

The "downdraft conversion burner" for converting the conventional updraft furnace to this same downdraft principle of operation has been tried out in approximately 20 different homes, and has been operated by all types of people, with no difficulty in their learning to operate it satisfactorily.

[11] Instructor in Mechanical Engineering, Illinois Institute of Technology, Chicago, Ill. Jun. A.S.M.E.

Some Problems in Pulverizing and Burning Midwest Coals

By A. C. FOSTER,[1] NEW YORK, N. Y.

The author cites the characteristics of Midwest coals which require special consideration in the design of pulverizers and boiler furnaces to meet the conditions of combustion. The principal items to be provided are (1) large furnace volume with moderate heat-release rates, (2) ample furnace cooling surface, (3) preheated air at sufficient temperature to enable pulverizer to pulverize coal with maximum moisture content which may be encountered, (4) ample mill capacity. The paper includes a discussion of these various elements in the solution of the problem of burning Midwest coals efficiently.

THE successful pulverizing and burning of low-grade Midwest coals in boiler furnaces requires that adequate provisions be made in the original design for the following coal characteristics:

1 Low ash-softening and fusion temperatures.
2 Negligible coking tendency.
3 Generally high moisture content.
4 Low to moderate grindability.

The first two characteristics determine the design of the furnace and the selection of burners; the third and fourth influence the choice of coal-preparation and pulverizing equipment.

Noncoking Midwest coals are free-burning and, even when quite coarsely pulverized, they burn easily and with a relatively low unburned-carbon loss. However, the ash slags easily and, for this reason alone, these coals are more troublesome than most of our native coals. This inherent slagging tendency is one factor requiring the designer's closest attention.

Today operators everywhere demand equipment that is capable of staying on the line for long periods of time. It is not uncommon to find operators scheduling boilers "on the line" for periods of 6 months, and being able to maintain these schedules. Obviously, such performance requires, in addition to freedom from mechanical breakdown, also freedom from fouling of the furnace, boiler, and superheater with slag and ash. The heat-absorbing surfaces and the gas passages between them must be kept clean. How then can we best obtain such cleanliness as will enable the operator to keep the unit "on the line" for long periods, when low-grade, low-ash-fusion coals must be burned?

It is possible to make provisions in the original design of a steam-generating unit for the removal of ash and slag from heat-absorbing surfaces by mechanical soot blowers and deslaggers and by designing with free access to all parts for hand lancing. However, experience indicates that even the most elaborate provisions of this kind will not offset violations of sound furnace design and firing principles. So, rather than depend alone upon such methods to prevent slagging, close attention should be given to those design factors, which, if followed, will give the operator complete control of the slag problem and a minimum of hand cleaning when burning these coals.

The principal design factors influencing the fouling of steam-generator heating surfaces by low-fusion-temperature ash or slag are as follows:

1 Furnace proportions.
2 Arrangement of furnace cooling surface.
3 Type of cooling surface.
4 Location of burners.
5 Disposition of heating surface before the superheater.
6 Arrangement of superheater.
7 Fineness of pulverization.

Furnace Proportions

The furnace should be designed for a moderate heat release. For Midwest coals, while this will be predicated on other conditions, such as ratio of cooling surface in furnace to furnace volume, whether dry-bottom or slagging-bottom type, and arrangement of burners with respect to boiler entrance or furnace exit, heat releases of the order of 21,000 to 25,000 Btu per hr per cu ft have been found desirable.

The cross section of the furnace should be such that the gas velocity, in the clear space between the flame and the entrance to the boiler-tube bank, will be low enough to permit the larger particles of fuel and ash to "hover" or move about more slowly than the gas, and so give the radiant-heat-absorbing surfaces a greater opportunity to cool and solidify even the largest particles before they can reach the furnace outlet. It is also desirable to have the area of the furnace outlet arranged to provide a low gas velocity entering the boiler bank in order to minimize the fouling which results when those globules of ash, which are frozen only on the surface but are still molten within, impinge on the boiler tubes.

It would be interesting to have available, from Midwest operators, additional data on the capitalized value of deslagging, and hand-lancing costs, plus necessary outages for cleaning, versus excess of furnace-exit-gas temperature over the ash-sticking temperature. If furnace-exit temperatures are not available the average heat liberation per square foot of effectively exposed radiant surface could serve as a basis for comparison of these costs. It is believed that such a survey will tend to justify extremely conservative furnaces.

Arrangement of Furnace Cooling Surface

Many arrangements of furnace cooling surface are possible. With any of them the gases should be cooled sufficiently and the particles of ash in suspension chilled and solidified before they reach the furnace outlet or boiler entrance.

It is desirable that combustion be completed in minimum time and space and this may be accomplished by the use of turbulent burners which promote rapid and intimate mixing of the coal and air. With a short turbulent flame we obtain the maximum of clear atmosphere in the furnace, both from above the flame body to the gas outlet and from below the flame body to the floor or ash hopper, to effect the ready cooling of ash particles by radiation to the surrounding surfaces.

[1] Manager, Service Department, Foster Wheeler Corporation. Mem. A.S.M.E.

Contributed by the Fuels Division and presented at the Semi-Annual Meeting, Kansas City, Mo., June 16–19, 1941, of The American Society of Mechanical Engineers.

Note: Statements and opinions advanced in papers are to be understood as individual expressions of their authors and not those of the Society.

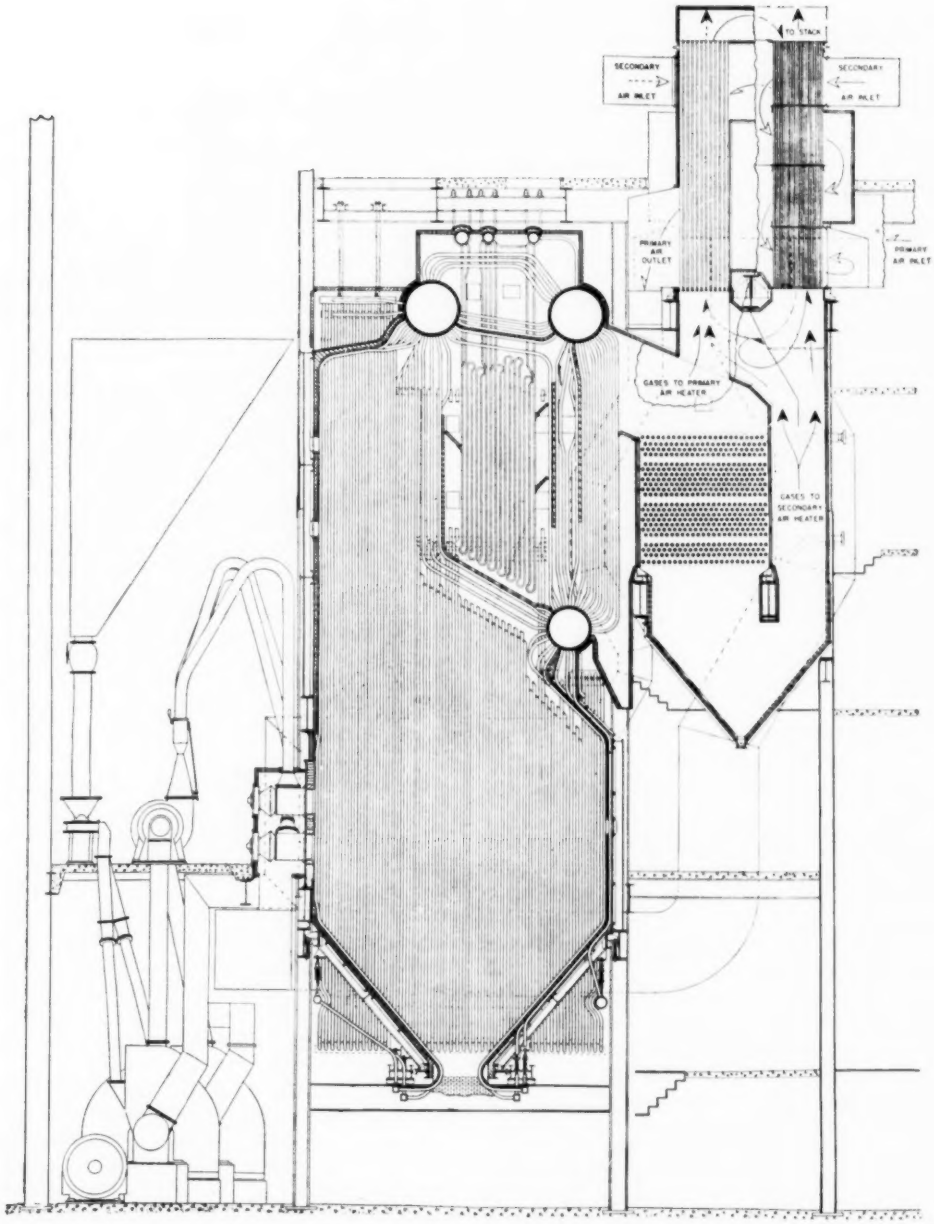


FIG. 1 CONVENTIONALLY DESIGNED UNIT FOR AN OUTPUT OF 550,000 LB PER HR AT 870 PSI AND 900 F WITH 300 F FEEDWATER

The highest gas temperatures prevail in that part of the furnace adjacent to the burners. It has been our experience that the most effective cooling surface should be available in this region to take full advantage of the high rates of heat absorption and corresponding rapid rates of ash cooling which are attainable in this zone. Any covering of cooling surface adjacent to the burners tends to restrict its effectiveness and defeat one of the purposes for which it was primarily installed. Bare tubes provide the most rapid heat-absorbing surface and are used even in this region. There need be no concern regarding blistering and tube failures if there is adequate circulation, freedom from violent flame impingement on the outer surface of the tubes, and the absence of scale or oil on the inner surface.

Of the various types of furnace cooling surface in use today, bare tangent tubes, that is, bare tubes so closely spaced as to leave very little space between them, provide the most effective cooling and the least furnace-wall slagging. This is due to the absence of anchorages, or high-temperature zones, between the tubes to which ash and slag may bond to form a continuous covering over the tubes.

LOCATION OF BURNERS

The most desirable location of burners will depend upon whether the furnace is of the dry-bottom or the slagging type. Too often the burner location is subordinated to some predetermined or existing arrangement of auxiliary equipment such as a stack, ash-handling equipment, coal bunker, etc.

In furnaces of the dry-bottom type, burners should be located high enough above the floor, or ash hopper, to assure cooling of the ash below the "sticky" temperature before it comes in contact with the cooler surfaces below the burners.

In furnaces of the slagging type, burners firing horizontally

near the slag floor and arranged to distribute the fuel evenly across the full width of the furnace have given excellent results. In this way a blanket of flame is interposed between the slag and the furnace cooling surface above the flame. The slag floor is thus maintained at a high temperature, because it cannot "see" the cooling areas through the flame. Where multiple burners are used it is extremely important that the coal be evenly distributed across the width of the furnace to avoid stratified zones of high temperature and accompanying spotty slag accumulations throughout the unit.

Assuming conventional types of steam generators, having the boiler located above a furnace of either dry-bottom or slagging type, the preferred direction of firing has been found to be away from the entrance to the boiler-tube bank, which usually means that the burners are set in the wall directly below the bottom drum. Such an arrangement insures minimum slagging of the boiler entrance.

Slag screens and boiler heating surface before the superheater, if arranged vertically, tend to be self-cleaning and give least trouble from slagging. The tubes should be spaced wide enough apart to prevent bridging across of such ash or slag as might stick to them.

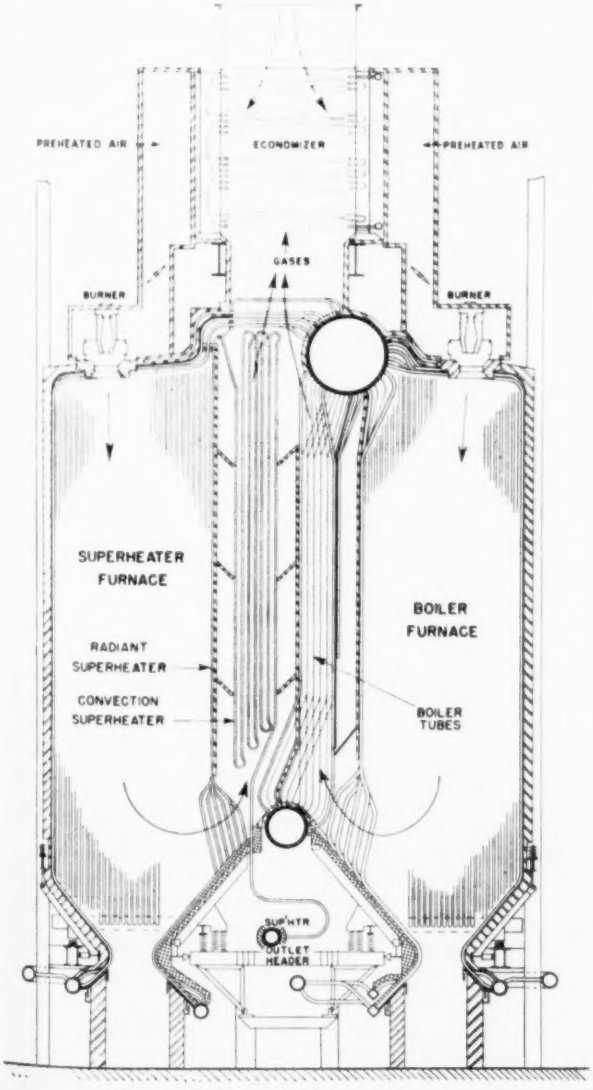


FIG. 2 TWIN-FURNACE DESIGN OF UNIT FOR OUTPUT OF 500,000 LB PER HR AT 865 PSI 910 F TEMPERATURE WITH 400 F FEEDWATER

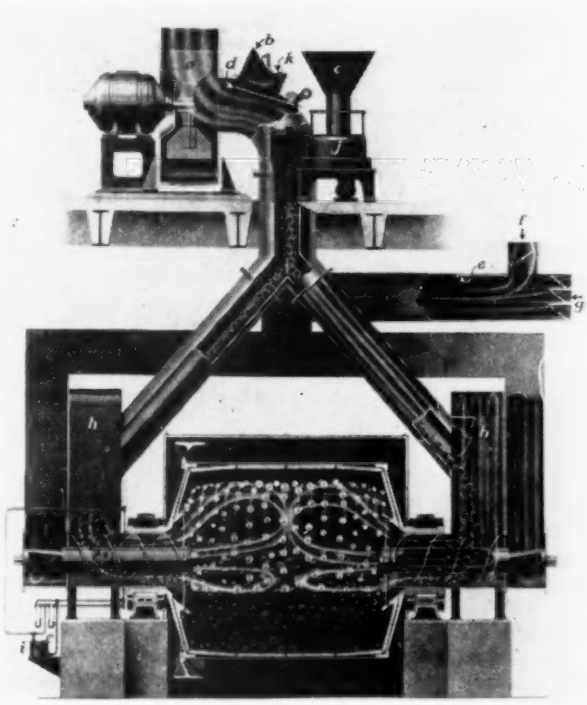


FIG. 3 DOUBLE-CLASSIFIER BALL MILL ARRANGED FOR UNIT SYSTEM OF PULVERIZED-FUEL FIRING

(*a* Shaft-mounted pulverizer-exhauster rotor; *b* damper trips open when exhauster shuts down allowing room air to sweep conduits and burners clean; *c* incoming coal to feeder; *d* mill-output-control damper; *e* hot-air shut-off damper; dampers *d* and *e* automatically isolate mill when exhauster shuts down; *f* tempering air from forced-draft fan; *g* hot air from air preheater; *h* classifiers, rejected oversize dries raw coal entering mill; *i* level controller to maintain constant level in mill regardless of mill output; *j* rotating-table feeder; *k* air added when necessary to maintain velocity at low loads.)

ARRANGEMENT OF SUPERHEATER

Superheater tubes give least trouble if arranged vertically as in the pendent, self-supporting superheater, in which the elements hang from external headers. This type of superheater promotes external cleanliness and inhibits fouling by slag and fly ash, due to the absence of large supports and hangers within the gas path. Attempts to economize in superheater surface, by designing for high gas-mass flow, with closely packed tubes, invite troublesome slagging. Such installations run the risk of subsequent unsatisfactory operation.

Fig. 1 shows a conventionally designed unit in which the designer has endeavored to follow these principles.

Fig. 2 shows a twin-furnace unit designed for about the same output. This design permits maximum cooling of the furnace gases because of the greater ratio of furnace cooling surface to furnace volume than is found in the conventional design. The arrangement of superheater surface in radiant and convection sections, with the radiant section in what is in reality a separately fired furnace, enables the maintenance of the maximum final steam temperature over an extremely wide range, with low gas temperature entering the convection superheater. This is accomplished with approximately two thirds of the superheater surface that would be required in a conventionally designed unit with an all-convection superheater.

FINENESS OF PULVERIZATION

Throughout the history of pulverized-coal firing in steam-

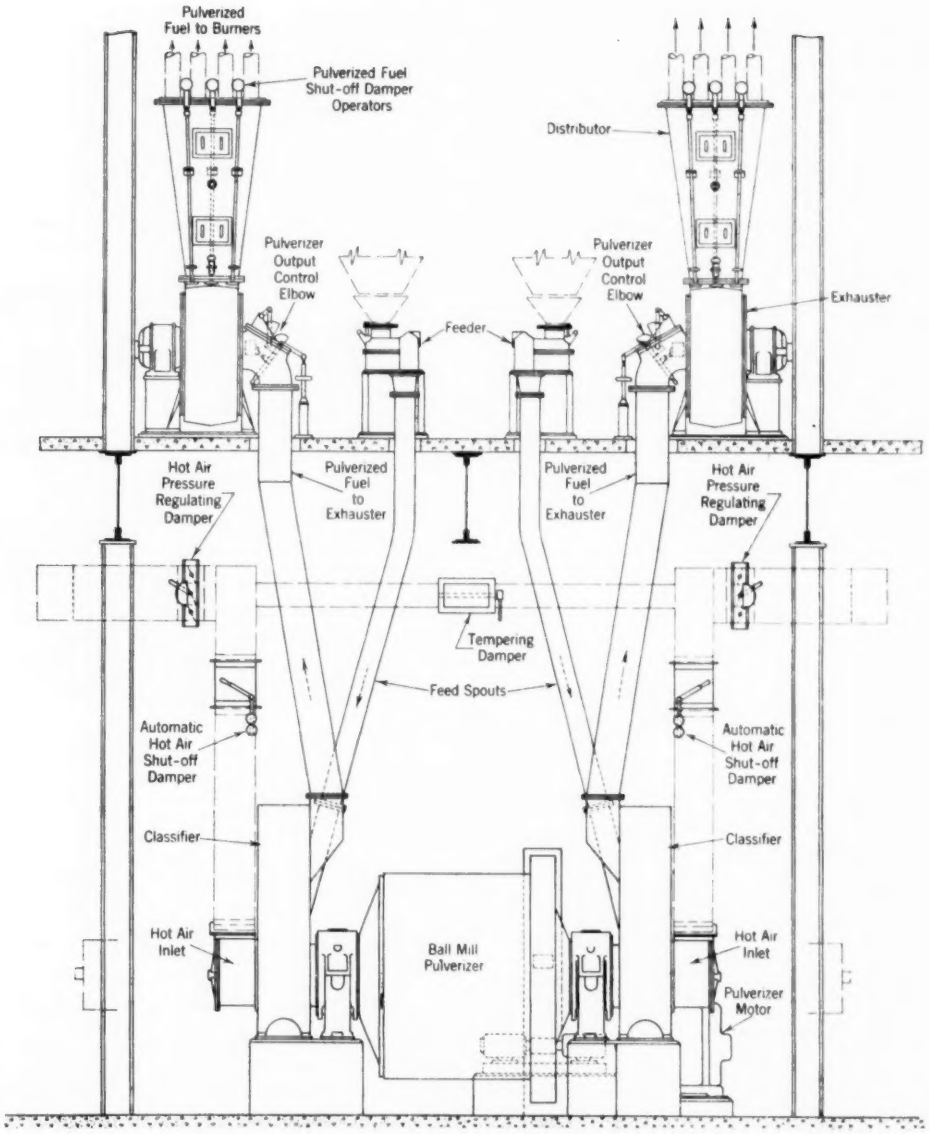


FIG. 4 DOUBLE-CLASSIFIER MILL WITH TWIN EXHAUSTERS AND TWIN FEEDERS

generating units coarse pulverization and boiler-entrance slagging have gone hand in hand. The effect of fine grinding on both combustible loss and slagging of the boiler entrance and superheater is more noticeable with the low-grade, low-ash-fusion-temperature coals than with the better coals. The smaller the particle the more certain it is to be cooled throughout by the time it passes into the boiler and superheater. Likewise, since the loss due to unburned combustible is reduced by finer grinding, it means that we have fewer particles reaching the boiler and superheater while still burning.

There are, of course, economical limits beyond which finer grinding may not pay dividends. These limits are not always easily defined. Finer grinding increases power consumption. In addition to the savings resulting from decreased carbon loss there are the more or less intangible savings resulting from the reduction in cleaning labor, steam, etc., the improvement in net over-all efficiency due to reduction in soot-blower operation, and time for hand lancing. The value of the reduced outage time for cleaning and the resulting increase in availability may be worth more than all of these savings put together. This is something that can only be determined by each individual plant.

The free-burning Midwest coals may easily be burned with a carbon loss of less than 1 per cent, with a fineness of about 70 per cent through 200 mesh. Nevertheless, experience has indicated that the fineness may advantageously be as high as 80 to 85 per cent through 200 mesh, in order to minimize boiler and superheater fouling.

The third and fourth characteristics affecting the successful pulverizing and burning of low-grade Midwest coals, namely, high moisture content and low to moderate grindability, as previously pointed out, influence the choice of coal preparation and pulverizing equipment.

Specifications for pulverizers to handle Midwest coals usually require that the pulverizer be capable of handling coal of 13 to 15 per cent moisture. In all probability the moisture specified is the average moisture over some period of time. It may happen that when the installation is placed in operation the total moisture content is greater than specified. We have had occasions where

it has been necessary to pulverize Midwest coals containing 19 to 20 per cent moisture. The conical ball mill will satisfactorily handle coals of this moisture content and even higher, providing preheated air at a high enough temperature is available.

Fig. 3 shows a double-classifier ball mill equipped with a single exhauster and a single feeder arranged to feed and remove the coal from both ends of the mill.

Preheated air, preferably at temperatures of 500 to 600 F, is admitted through pipes centrally located in the hollow trunnions at each end and the pulverized fuel is carried out through the annular openings between the hollow trunnions and the central pipes into the classifiers at each end of the mill. The finished product leaves the classifiers through two conduits which are, in this case, brought together at a Y connection and connected to the exhauster through the output-control elbow.

This arrangement of classifiers provides a large recirculating load. At times the rejected material being returned to the mill, from the classifiers, may amount to three or four times the quantity of coal being delivered to the exhausters. The raw incoming coal is fed in approximately equal amounts to each classifier. Here it is mixed with the partially dry and semipulverized rejects and fed into the mill by the double-flight ribbon conveyers which

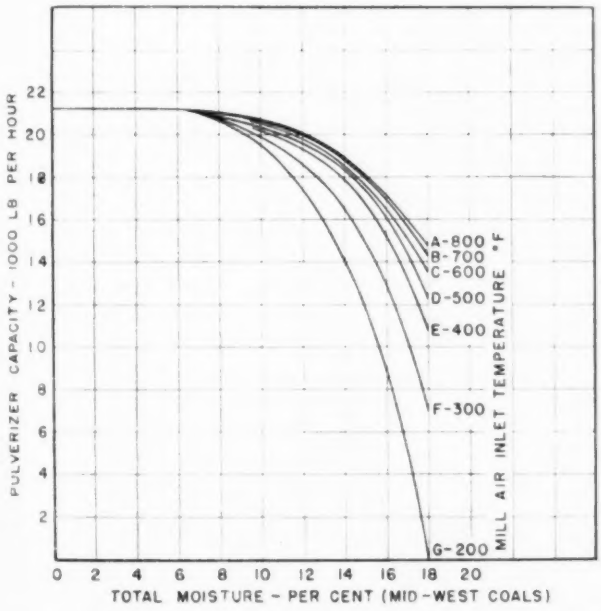


Fig. 5 Effect of Initial Moisture Content on Pulverizer Capacity With Varying Mill Air-Inlet Temperature

are attached to the rotating air-inlet tube. This air-inlet tube is driven by the mill through a spider shown at the mill end of the tube.

Mixing the raw incoming feed with the warm dried classifier rejects reduces the effect of surface moisture on mill capacity for the following reasons:

1 Part of the surface moisture is transferred to the warm rejects. Preliminary warming of the incoming wet coal takes place in the classifier; some drying takes place during the time required to convey the coal from the classifier to the mill. Thus, if the raw coal fed to the classifier contains a total of 15 to 20 per cent moisture, corresponding to a surface-moisture content of 8 to 13 per cent, the mixture of raw coal and rejects entering the mill from the classifier will have an average surface-moisture content of 2 to 4 per cent. This corresponds to an average total moisture content of 9 to 11 per cent, which is appreciably less than 15 to 20 per cent.

2 In transferring part of the surface moisture of the incoming coal to the warm semipulverized rejects, the moisture is transferred to a much larger and warmer surface area, from which it is more easily evaporated.

Fig. 4 shows a double-classifier mill, arranged with two exhausters and two feeders, with each feeder and each exhauster serving one classifier.

The question frequently arises as to how more grinding capacity can be obtained from mills which may be handling poorer grades of coal than was anticipated at the time they were purchased. Let us first consider the possibility that mill output is limited because the moisture of the incoming coal is higher than was anticipated. An increase in the temperature of the preheated air to the mill will improve the mill performance.

If the air temperature is below 300 F the installation of a steam air heater to increase the temperature to somewhere in the neighborhood of 400 F is possible, provided steam at a pressure of 350 to 400 psi is available. Such an air heater can usually be installed in the air ducts supplying preheated air to the mill.

Another method is to install a special primary-air-heater section on the gas side of the steam-generating unit. This should be arranged so that the partially preheated primary air from the outlet of the secondary-air preheater enters the primary-air heater to be further heated by gases taken from a higher-temperature region than those normally entering the secondary-air heater. This makes it possible to increase the primary-air temperature to 500 or 600 F, depending upon the gas temperature available. The unit, shown in Fig. 1, is equipped with such a primary-air heater. The lines having only one half an arrow head indicate the flow of gas and air through the primary-air-heater section, which is centrally located with twin secondary-air heaters on each side of it.

It may prove advantageous to increase the temperature of the air going to the mill by mixing with the air a small amount of flue gas taken from a section of the boiler where the gas temperature is in the neighborhood of 1000 to 1200 F. Only a limited amount of flue gas can be mixed with the primary air. This quantity will depend upon the volatile and ash content of the fuel being burned, and for Midwest coals will be about 20 per cent by weight. An excessive amount of flue gas added to the primary air may decrease the burner stability because of the inert gas present.

There is a limit to the improvement which may be expected from an increase in temperature of the air entering the mill. The law of diminishing returns sets a temperature of 600 to 650 F as the practical upper limit. This is shown in Fig. 5, where a series of curves indicates the effect of raw-coal moisture content on mill capacity with varying air temperatures entering the mill.

If we consider a pulverizer, selected for a capacity of 18,600 lb per hr with a total moisture content of 12 per cent and an air temperature to the mill of 300 F, it will be seen that an increase in raw-coal moisture content to 16 per cent will reduce the mill output to about 13,000 lb per hr. However, if an entering-air temperature of 600 F is available, the output will only be reduced to 16,500 lb per hr. Increasing the inlet-air temperature from 600 to 800 F will only increase the output, with 16 per cent moisture coal, from 16,500 to 17,100 lb per hr, a negligible amount. This same pulverizer will have the same capacity with 14 per cent moisture raw coal and 600 F entering air as it has with 12 per cent moisture and 300 F entering air. The effect of increased air temperatures diminishes with decreasing raw-coal moisture content.

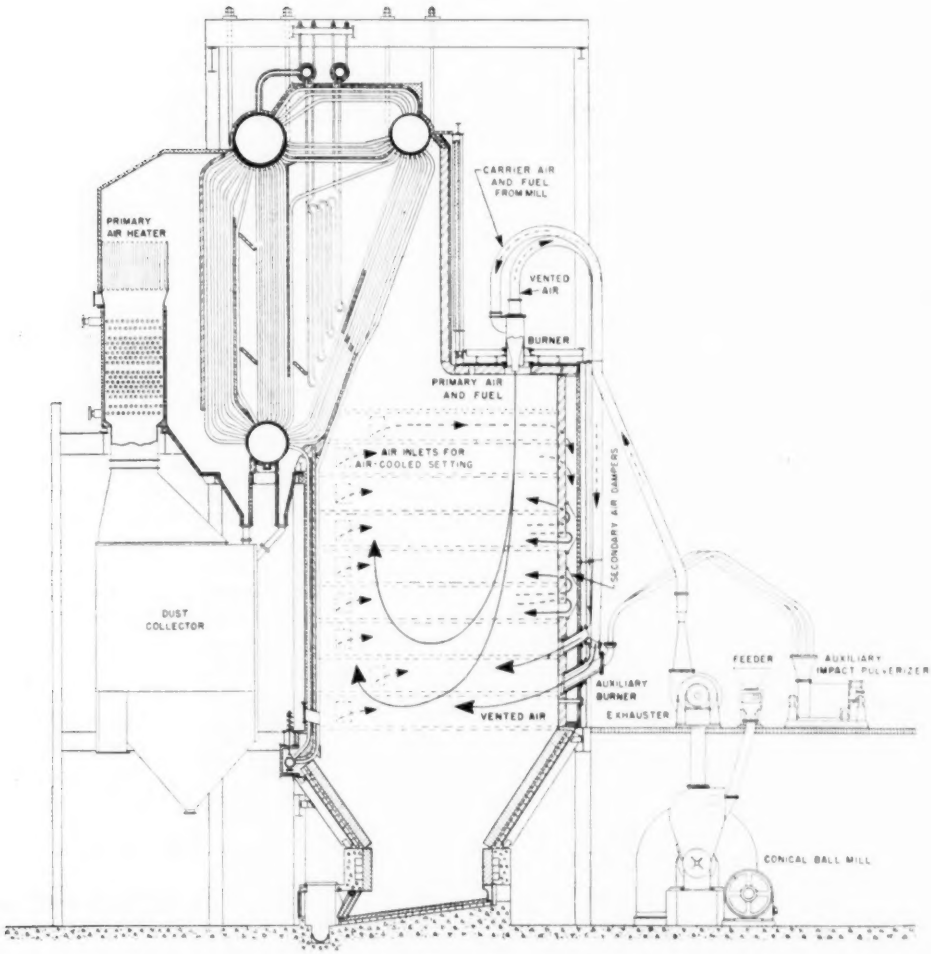


FIG. 6 UNIT HAVING SEPARATE HIGH-TEMPERATURE PLATE-TYPE PRIMARY-AIR HEATER FOR COAL CONTAINING UP TO 20 PER CENT MOISTURE

Fig. 6 shows a unit equipped with a separate plate-type heater which may be used with or without a secondary-air heater. Similar installations of horizontal-tubular type have also been made. Whether used singly or in conjunction with a secondary-air heater, this type of installation can be installed to give a primary-air temperature of 500 to 600 F, providing flue gas in the neighborhood of 900 F is available.

Most operators have seen occasions when it has been necessary to operate with water running from the raw-coal bunkers through the scales, feeders, and raw-coal conduits into the mill. These have been, of course, extraordinary conditions. Fig. 7 shows a simple arrangement that can be installed in any coal bunker to eliminate this condition. It consists of a short addition to the coal pipe, extending up into the bunker in such a manner that a trough is formed between this extension and the sides of the bunker. Suitable drain connections are provided to drain off the excess surface moisture, which will collect in the trough. In plants where coal takes fire easily in the bunker, if not kept moving, the dead space between the extension and the side of the bunker may be filled with crushed rock as shown. This will also reduce the necessity for cleaning out the drain lines. This device has been used in numerous plants, particularly in Canada, where large quantities of snow and ice find their way into the coal bunker during the winter. If, in connection with this moisture trap in the bunker, sufficient bunker capacity is available so that provisions can be made to allow the incoming coal

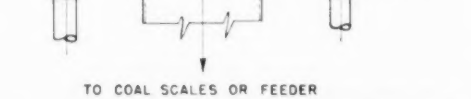


FIG. 7 ARRANGEMENT TO PREVENT RUN-OFF WATER ENTERING PULVERIZER

to remain in a section of the bunker for a period of 24 hours before it is fed to the mill, an appreciable reduction in the surface moisture content of the raw coal can be expected.

If it becomes necessary to grind harder coal a reduction in mill capacity must be expected, unless additional power for pulverizing is provided, or a reduction in fineness accepted. An increase in grinding capacity may be obtained, in the case of a

ball mill, by increasing the weight of the ball charge and by increasing the percentage of larger-diameter balls in the charge. In other types of mills this may involve an increase in the loading pressure on the grinding elements or an increase in speed.

All of these steps usually result in an increase in the power required for the mill motor. In cases where changes of this nature may be limited, because of such conditions as the mill motors' being fully loaded, or the motor circuits' being fully loaded, some improvement in mill capacity can be expected from crushing the incoming coal to smaller sizes.

The pulverizing and burning of low-grade Midwest coals offer problems not usually associated with the higher-grade Eastern coals. It is the designer's responsibility to recognize the important characteristics affecting the successful burning and pulverizing of these coals and provide:

1 Large furnace volume with moderate heat-release rates.

2 Ample cooling surface in the furnace.

3 Preheated air at sufficient temperature to enable the pulverizer to pulverize coal with the maximum moisture content that may be experienced.

4 Ample mill capacity to provide fine grinding with the worst coals likely to be encountered.

If these conditions are satisfied there should be no serious problems for the operators to overcome.

Discussion

RAY WINTERS.[1] It would seem that the information requested by the author on the cost of slagging with furnace-exit temperature above the ash-sticking temperature is a matter of checking past records. When pulverized coal was first used under steam boilers, most furnaces were too small and employed only refractory lining, which gave high gas temperatures. Generally lower ratings and additional excess air were resorted to rather than have continuous slagging conditions which required constant cleaning. When operating under such conditions, there is always the possibility of slag reducing the rating or shutting the boiler down.

[1] Results Engineer, Kansas City Power & Light Co., Kansas City, Mo.

If furnaces are designed to maintain gas temperatures below the sticking point, two men working 1 hour per shift or 6 man-hr per day will keep a 200,000 to 300,000-lb boiler clean. With the temperature above the sticking point, 48 or more man-hr would be required. At 80 cents per hour and 85 per cent service, the slagging would cost $10,250. The labor cost alone would justify an additional furnace cost of over $85,000. Therefore, it seems that furnaces should be designed to give furnace-exit temperatures with a generous margin under the ash-sticking temperature.

Increasing fineness of the coal not only reduces slagging but reduces the unburned-carbon loss. At Northeast Station the loss decreased from 0.69 per cent to 0.36 per cent by increasing the fineness through 200 mesh from 54 per cent to 71 per cent.

The author's discussion of the effect of moisture on mill capacity and power requirements should prevent the future installation of undersized units, as has occurred many times in the past.

AUTHOR'S CLOSURE

It is indeed gratifying to receive the data on boiler cleaning costs contained in Mr. Winters' discussion. The cost of boiler cleaning, particularly when such cleaning requires hand lancing in addition to regular mechanical soot-blower operation, is a phase of boiler operation and operation costs that sometimes is not even considered and too frequently is not given sufficient consideration in evaluating one type or size of steam-generating unit against another. As pointed out by Mr. Winters, removal of slag from boiler and superheater surface requires a considerable expenditure for labor and, therefore, a considerably higher capital investment may be justified for a unit designed to provide furnace-exit gas temperatures below the ash-sticking temperature.

The figures given for the decrease in carbon loss resulting from increased fineness confirm the author's findings in other installations. They are particularly interesting inasmuch as they show that, even with free-burning Midwestern coals that have relatively low combustible loss even when quite coarsely pulverized, a worthwhile improvement in efficiency can be obtained by pulverizing finer. With less-free-burning coals the effect of increased fineness on reduction in combustible loss will be even greater.

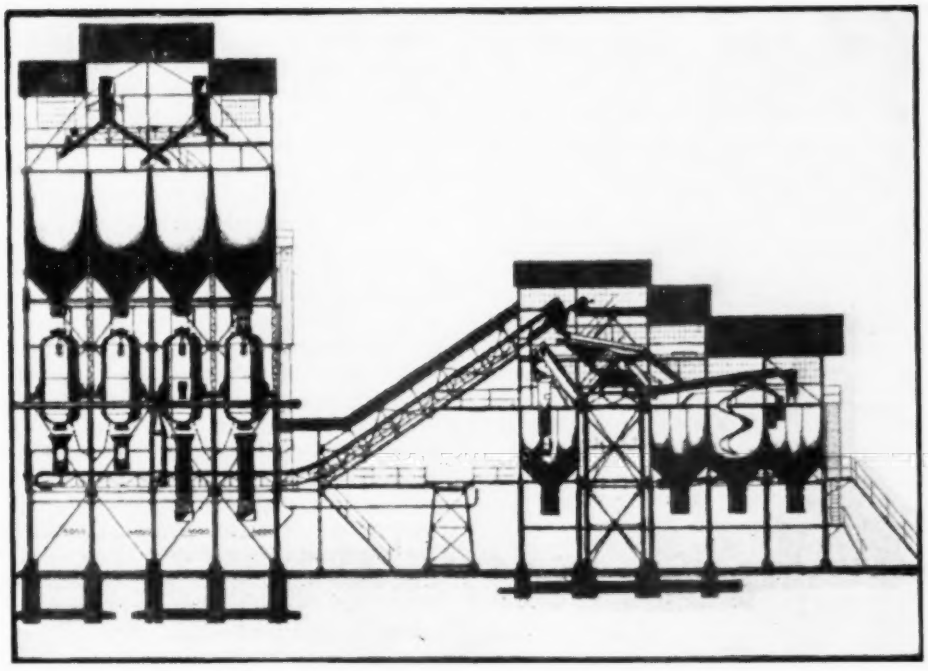


FIG. 1 LONGITUDINAL SECTION, KOEFLACH PLANT

The Preparation of Stable Nonslacking Fuel by Steam-Drying Subbituminous Coal and Lignite[1]

BY V. F. PARRY,[2] L. C. HARRINGTON,[3] AND ARTHUR KOTH[4]

Subbituminous coal and lignite, as mined, contain 20 to 40 per cent moisture, which limits their markets, due to slacking and to the costs of transporting this water. By drying these fuels with saturated steam at 400 psi pressure, by the Fleissner process, described in this paper, the free-moisture content may be lowered to 4 to 8 per cent, reducing slacking and increasing the available market. The properties of the dried fuel and processing data are presented and the construction and operating costs of plants are estimated.

ENLARGEMENT of the markets for the lower-rank coals is in accord with a thoughtful national policy on conservation of energy, which recommends that the lower-rank fuels should be used for generating power and heat where economically possible to conserve the highest-rank coking coals and oil or gas, which have a more limited reserve (1).[5] The subbituminous coals and lignites of the eastern slope of the Rocky Mountains and the Northern Great Plains area represent two fifths of all coal reserves of the United States but, owing to the distance and to the cost of transporting the moisture in the coal, these fuels have limited markets. In a normal year the production in this area averages about 3 per cent of the national output of coal. North Dakota alone has an estimated reserve of 600,000,000,000 tons of lignite, but its yearly production of 2,000,000 tons is consumed largely within the state. The economical boundary for shipments of lignite, owing to the weight of its high moisture content, is about 50 miles east of the state line and 100 to 200 miles into South Dakota. Beyond these points, lignite must compete with coals shipped through the Great Lakes from West Virginia and Kentucky; therefore, if the markets for lignite are to be enlarged, methods must be found to decrease the moisture at the mine. This paper summarizes some of the studies which have been made by the University of North Dakota, in co-operation with the Bureau of Mines, United States Department of the Interior, on improving subbituminous coal and lignite by drying with steam.

[1] Published by permission of the Director, Bureau of Mines, U. S. Department of the Interior, Washington, D. C.

[2] Senior Fuel Technologist, Bureau of Mines Field Office, Golden, Colorado.

[3] Dean, College of Engineering, and Director of the Division of Mines and Mining Experiments, University of North Dakota, Grand Forks, N. Dakota.

[4] Assistant Professor of Chemical Engineering, School of Mines, University of North Dakota, Grand Forks, N. Dakota.

[5] Numbers in parentheses refer to the Bibliography at the end of the paper.

Contributed by the Fuels Division and presented at the Semi-Annual Meeting, Kansas City, Mo., June 16–19, 1941, of THE AMERICAN SOCIETY OF MECHANICAL ENGINEERS.

NOTE: Statements and opinions advanced in papers are to be understood as individual expressions of their authors, and not those of the Society.

The object of the investigation was to determine the economic possibilities of applying the Fleissner steam-drying process to American coals.

Fleissner Steam-Drying Process

Lignite has been dried successfully in Europe for 13 years, and three plants having a total capacity of about 2000 tons daily are now in operation in the countries recently known as Austria, Czechoslovakia, and Hungary (2). A typical commercial plant is shown in Fig. 1. The steam-drying process involves heating

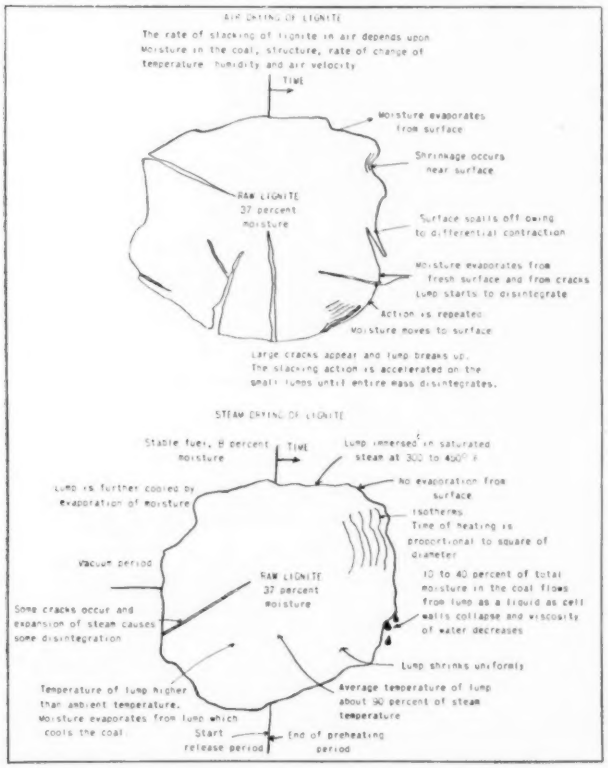


Fig. 2 Air Drying of Lignite and Steam Drying of Lignite

raw lignite with saturated steam until the lumps are heated to the center; the pressure is then released, and a vacuum is applied which cools the coal through evaporation of moisture.[6] When the lumps are heated with saturated steam no water can evaporate at the surface, consequently slacking does not take place as it does in atmospheric drying. It has been demonstrated experimentally that part of the natural bed moisture is forced from the coal as a liquid under the conditions imposed by heating with saturated steam. Owing to this effect, the thermal requirements for steam drying are less than for flue-gas drying because no latent heat of evaporation is necessary to remove the liquid water. Heating with saturated steam also affects the structure of the coal, either by collapsing the cells or by closing the capillaries. As a result, the dried lignites do not absorb water as readily, the slacking properties are reduced, and the fuels are more stable when exposed to the atmosphere. Fig. 2 is a schematic description of the sequence of events when a lump of lignite is dried in air and in saturated steam.

The action of high-pressure saturated steam on a lump of lignite produces the following effects: The lump is heated uniformly by its envelope of condensing steam. As the pressure increases and the temperature rises, part of the colloidal water is expelled from the lump as a liquid. The lump shrinks as water leaves and when the pressure is lowered more water evaporates owing to the sensible heat stored in the lump. When the pressure is lowered further by vacuum, additional moisture is evaporated, which cools the lignite to about 140 F. The apparent density of lignite is decreased about 20 per cent by drying.

Experimental Work at North Dakota University

Description of Pilot Plant and Tests

Experimental investigations of the application of the Fleissner steam-drying process to American coals and lignites had been made by the University of North Dakota, before the present investigation in co-operation with the Federal Bureau of Mines (3). The results of that work indicated that the process should be technically successful on American lignites.

The experimental work described in this paper was conducted in a small pilot plant having a capacity of 1 ton of coal per day. The plant is shown in Fig. 3. About 50 tons of raw lignite were dried under a variety of conditions to furnish data for a technical and economic appraisal of the process. Two series of tests were made to obtain comparable information on several coals. The first series was made on large samples of lignite from four mines in North Dakota and the second series on small samples of sub-

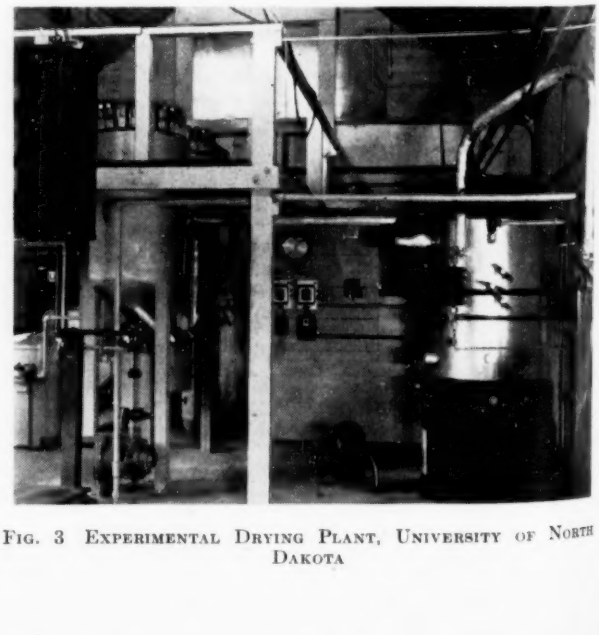


Fig. 3 Experimental Drying Plant, University of North Dakota

[6] Two autoclaves are required for proper operation of the process. Steam from the high-pressure autoclave is expanded into the low-pressure autoclave to preheat the raw coal. The cycle on two autoclaves is timed as follows:

Let A = time required for equalizing pressure between the two autoclaves
B = steaming time, using fresh steam from boiler
C = time required to evacuate autoclave containing dried coal after pressure is equalized
D = time required to charge and discharge one autoclave

Then B must equal $C + D$; $A + B$ = heating period; and $A + C$ = cooling period.

A 42-min cycle would be timed as follows:

Elapsed time, min	No. 1 autoclave, min		No. 2 autoclave, min	
0				
8	8 Equalize pressure	(A)	8 Preheating	(A)
16	8 Evacuate	(C)		
21	5 Empty and charge vessel	(D)	13 Steaming with fresh steam	(B)
29	8 Preheating	(A)	8 Equalize pressure	(A)
37			8 Evacuate	(C)
42	13 Steaming	(B)	5 Empty and charge	(D)
50	8 Equalize pressure		8 Preheating	

bituminous coal and lignite from nine mines in North Dakota, Wyoming, and Colorado. The large samples were shipped to the plant in railroad boxcars and stored in burlap sacks in concrete storage bins where they remained until sent to the drying plant. After drying, the processed lignite was stored in sacks in an open frame building where it remained for several months awaiting additional tests. The small samples were delivered to the drying plant in sealed drums and kept in the drums until dried. This precaution eliminated the questionable effects of open storage in concrete bins, and results showed that fresh lignite dries better than older lignite.

The effects of steam pressure, length of heating time, steam consumption, and size of lumps were studied. Most of the experimental work on the large samples was conducted in cycles aggregating about 140 min. The processing time was divided into a preheating period, a heating period, and a release period, followed by vacuum and aeration to cool the coal. European practice had defined these periods as definite parts of the process, but as more experience was obtained on processing the several lignites in the pilot plant, it was observed that steam drying can be considered best by dividing the processing time into only two periods, a heating period and a cooling period.[7] During the heating period, the temperature of the ambient steam is higher than that of the lumps, and the steam pressure is rising. The source of steam may be either from expansion from the previously heated autoclave or from a steam boiler. The length of the heating period depends upon the size of the lumps. When they have attained a temperature nearly equal to that corresponding to the maximum steam pressure, the heating period is complete and cooling can begin. Slight advantage is gained by extending the heating period beyond the time required to heat the lumps. Some liquid water is forced from the coal during heating. During the cooling period, the temperature of the coal is higher than the temperature of the ambient steam, and moisture evaporates constantly as the differential temperature is maintained, either by dropping the steam pressure or by application of vacuum. The time required for this period has not been fully investigated. If the pressure were suddenly released to atmospheric, the potential energy within the lumps might be sufficient to explode the coal, similar to the effect produced in

TABLE 1 PROPERTIES OF A TYPICAL LIGNITE AND A TYPICAL SUBBITUMINOUS COAL BEFORE AND AFTER DRYING AT 400 PSI STEAM PRESSURE

	North Dakota[a] lignite		Wyoming[b] subbituminous coal	
	Before	After	Before	After
Proximate analysis:				
Moisture, per cent	36.4	8.1	23.2	2.5
Volatile matter, per cent	29.2	42.0	31.2	42.5
Fixed carbon, per cent	30.4	44.1	41.7	50.8
Ash, per cent	4.0	5.8	3.9	4.2
Heating value, Btu per lb	6836	10101	9540	12079
Heating value, ratio	..	1.48	..	1.27
Available-heat ratio	..	1.57	..	1.31
Weight ratio	..	1.48	..	1.26
Screen analysis, square mesh				
Plus 2 in., per cent	100	75.4	..	..
1.05 × 2 in., per cent	..	14.3	100	55.6
0.525 × 1.05 in., per cent	..	4.9	..	32.2
0.263 × 0.525 in., per cent	..	2.2	..	8.3
0 × 0.263 in., per cent	..	3.2	..	3.9
Slacking index	56	32.3	50	[c]30.0
Friability, per cent	12.0	25.9	18.0	50.0
Specific gravity	1.22	0.96	1.25	1.07
Apparent shrinkage, per cent	..	22.8	..	12.4
Weight per cubic foot, lb	44	34	45	38.5
Available heat per cubic foot,[d] thousands of Btu	232	282	307	380

[a] Ward County.
[b] Sheridan County.
[c] Average of five tests.
[d] Available heat contained in 1 cu ft of loose coal or bin space.

[7] The heating period has been divided into two periods, the time required to raise the pressure to the maximum processing pressure and the time the lumps are allowed to "soak" at constant pressure while coming to temperature. The size of the lumps determines the relative length of these two parts of the heating period.

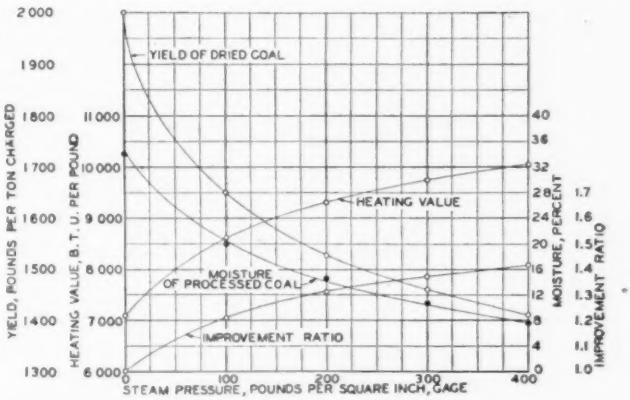


FIG. 4 EFFECTS OF PRESSURE ON STEAM DRYING OF AVERAGE NORTH DAKOTA LIGNITE

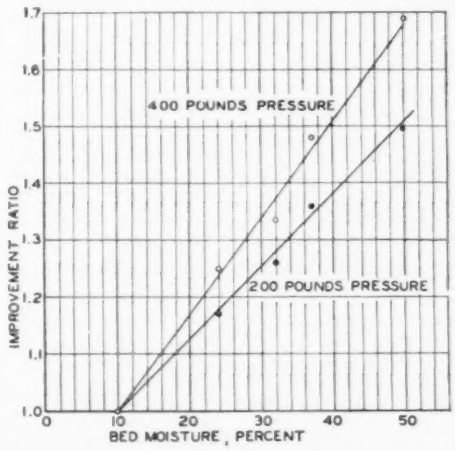


FIG. 5 RELATION BETWEEN BED MOISTURE AND IMPROVEMENT RATIO

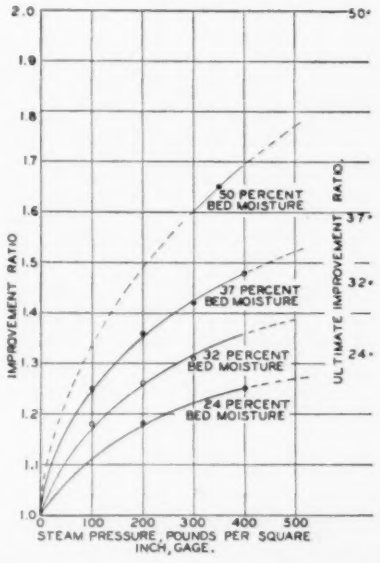


FIG. 6 RELATION BETWEEN STEAM PRESSURE, IMPROVEMENT RATIO, AND BED MOISTURE

making puffed rice. If the pressure is released gradually, this energy is restrained and fracturing probably is decreased. Experiments have shown that the cooling period can be less than 10 min on 1½-in. coal.

Summary of Results

Table 1 shows the average properties of raw and dried lignite and raw and dried subbituminous coal before and after processing at 400 psi pressure. It should be noted that the ratio of corresponding weights of raw coal to dry coal virtually equals the ratios of their gross heating value, volatile matter, and fixed carbon. This ratio is arbitrarily called the "improvement ratio" to define the degree of improvement due to drying. The available-heat ratio is higher than the weight ratio owing to the greater losses of latent and sensible heat when raw coal is burned.

Fig. 4 shows the relationship of improvement ratio, heating value, weight, and moisture content of the dried coal as the steam pressure increases. These curves represent the average results on North Dakota lignite. Lignites respond differently to saturated steam because the structure, bed moisture, and proportions of earthy and peaty material influence the drying properties. The most noticeable variation is that of improvement ratio with respect to bed moisture and steam pressure. Fig. 5 illustrates this relationship at two pressures and Fig. 6, at four moisture contents. Fig. 5 can be used to estimate the probable improvement ratio that can be attained on any high-moisture coal.

Consumption of Steam

The amount of steam required to remove a unit quantity of water from coal decreases as the total amount of water removed increases. Table 2 shows the measurements made on four lignites dried in the pilot plant at various pressures.

TABLE 2 NET STEAM IN POUNDS USED PER POUND OF WATER REMOVED FROM LIGNITE

	Steam pressure, psi gage						
	75	100	150	200	250	300	400
Lignite *A*	...	...	0.979	0.982	0.777	0.879	0.782
Lignite *B*	1.122	...	0.822	0.711	0.627	0.577	0.542
Lignite *C*	...	1.266	...	1.049	...	0.865	0.916
Lignite *D*	1.226	...	...	0.931	...	...	0.850
Average	1.176	1.266	0.900	0.923	0.702	0.774	0.773

These observations agree with the results of Klinger (4), who measured the steam consumed in an autoclave holding about 4 tons of lignite. The practice in commercial plants has been to dry large lumps of coal. To do so requires a long heating period; up to 100 min. This period has been divided into a preheating time and a steaming time, which have been described.[7] Klinger showed that about 75 per cent of the total steam required is consumed during preheating. The experiments on the pilot plant were substantially in agreement with Klinger's measurements but also showed that, when some lignites are dried, more than 75 per cent of the steam is used during the preheating period if higher final pressures are employed.

In general, it can be stated that the rate of consumption of steam is proportional to the rate of heating the lumps. When the lumps are large, the time of heating will be longer and the rate of heating lower, therefore the rate of consumption of steam will be less than when the lumps are small. Table 2 shows that an average of 0.77 lb of steam is required to remove 1 lb of water from coal. In drying North Dakota lignite at a pressure of 400 psi, 600 lb of moisture are removed from 1 ton, Fig. 4. The removal of 600 lb of water will require 600 × 0.77 = 462 lb of steam, and if it is assumed that 75 per cent of the steam is used during a 20-min heating period, then the rate of consumption of steam is 1000 lb per hr per ton of lignite being dried at 400 psi pressure. An autoclave having a capacity of 10 tons would require steam at a maximum-demand rate of 10,000 lb per hr for a 20-min heating period. Part of the steam would be supplied from the other autoclave, but the net steam from the boiler would still be required at this maximum rate. The fuel required to dry lignite by this process is estimated to be 4.5 per cent of the plant output, and for subbituminous coal, it is estimated to be 2.3 per cent, assuming in both cases the efficiency of steam generation is 75 per cent.

Effects of Size of Coal on Processing Time

From theoretical considerations of the time required to heat coal of different sizes to a given average temperature, it is evident that the size of the coal will determine the length of the drying period. Through theoretical deductions, Dr. Formanek (5) showed the importance of size in relation to the time required for drying. It was proved by Burke, Schumann, and Parry (6) that the law of squares can be applied to this problem even though the thermal constants may vary with the temperature and temperature with the time. The law of squares states that the time required to heat a body to a stated condition or distribution of heat is proportional to the square of some linear dimension of the body. For irregular lumps of coal, the time required is proportional to the square of the average diameter of the lump.[8] A formula for estimating the time of heating in minutes is as follows:

Estimated theoretical time of heating in minutes = 7 × diameter (inches) squared

Diameter of lump, in.	Heating time, min
0.25	0.44
0.50	1.75
0.75	3.9
1.00	7.0
1.25	10.9
1.50	15.7
1.75	21.4
2.00	27.9
2.50	43.5
3.00	63.0
3.50	85.0
4.00	112.0
5.00	175.0
6.00	252.0
7.00	340.0

[8] If it is assumed that average lignite has a specific heat of 0.58, a density of 78 lb per cu ft, and a thermal conductivity of 0.25 Btu per deg F per sq ft per hr per ft, the time required to heat the lump to any average temperature can be estimated from known laws of heat conduction using the graphic solution referred to in reference (6). If it is assumed that the temperature rise of the center of the lump is 95 per cent of the surface temperature rise, the time of heating in minutes equals 7 times the average diameter in inches squared.

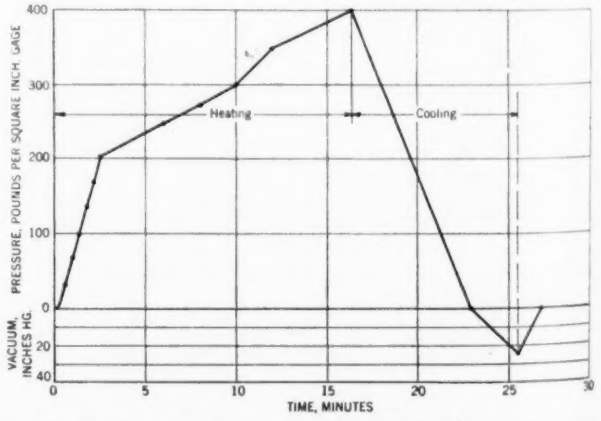


Fig. 7 Heating and Cooling Periods When Drying Subbituminous Coal at 400 Psi Pressure
(Size of coal ¼ in. × 1½ in.)

These estimates of the time of heating are in fair agreement with experimental measurements. European practice in large commercial plants has shown that cycles lasting 140 to 180 min are necessary to dry large lumps averaging 4 to 6 in. diam. One experiment conducted at the University of North Dakota on lumps of coal sized up to $1^1/_2$ in. diam is illustrated in Fig. 7. In this experiment, the time of heating was about 15 min and the time of cooling about 10 min.

From these considerations, it can be concluded that small stoker coal of a size less than 1 in. may be dried with steam in periods as short as 10 to 15 min.

Changes in Physical and Chemical Properties

Although alterations occur in the ultimate constituents during steam drying, the changes are so slight that they have but little significance. Dr. H. Klein (7) and Lavine (3) showed that approximately 30 cu ft of CO_2 is released when 1 ton of lignite is dried at 175 psi pressure. Some nitrogen is released, and the liberation of these inert gases improves the calorific value of the coal substance, but the effect is slight. A small amount of ash is leached out by the drying process.

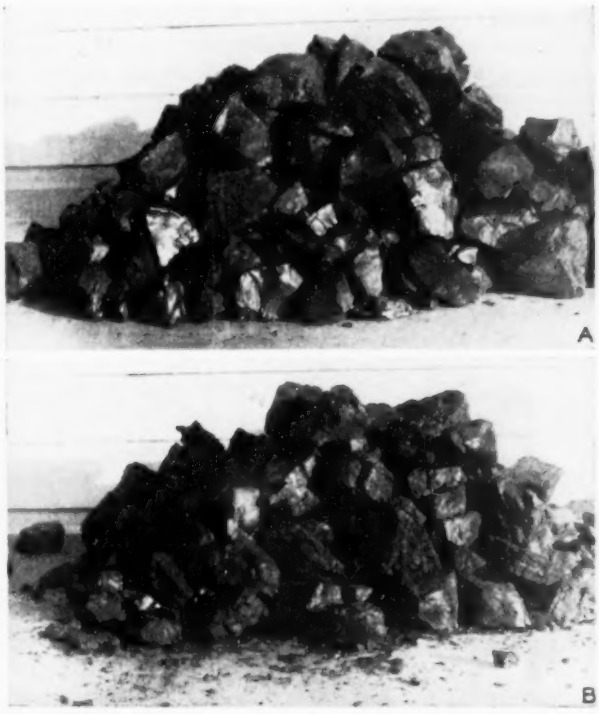


Fig. 8 (*A*) Subbituminous Coal Before Drying. (*B*) Subbituminous Coal After Drying With Steam at 200 Psi Pressure

All of the coals tested disintegrated to some extent. The data on screen sizes, in Table 1, indicate the average disintegration. Experiments on fresh 2 × 4-in. lignite show that about 15 per cent of the processed residue will pass a 1-in. screen after drying. Other experiments on lumps up to $2^1/_2$ inches in size indicate that the disintegration is less on the small sizes and amounts to about a 10 per cent reduction in average size. Fig. 8, showing large lumps of subbituminous coal before and after drying, indicates the amount of disintegration and the way in which the lumps fracture. This sample was handled carefully to avoid mechanical breakage.

TABLE 3 ESTIMATED COST OF CONSTRUCTION OF FLEISSNER STEAM-DRYING PLANTS

Location of plant	North Dakota		Wyoming	
Raw coal dried per day, tons	200	400	200	400
Dry coal per day, tons	138	276	158	316
Steam pressure, psi	400	400	400	400
Steam required per hour, lb, avg	5500	11000	4000	8000
Boiler unit:				
Boiler and stoker materials	$13900	$20000	$12200	$17400
Erection labor	2550	3500	2450	2950
Boilerhouse and foundations	7000	7000	7000	7000
Coal elevator	1000	1200	1000	1200
Coal bunker	500	800	500	800
Feedwater storage and treatment	3000	5000	3000	5000
Miscellaneous piping and valves	2000	2000	2000	2000
Total	29950	39500	28150	36350
Drying unit:				
Steel work, 75 tons	11000	11000	11500	11500
Sheeting, 3000 sq ft	200	200	225	225
Foundations	1000	1000	1000	1000
Coal bunker	1500	2500	1500	2500
Cooling hoppers	1500	2500	1500	2500
Autoclaves	12500	25000	12800	25600
Miscellaneous	3000	3500	3000	3500
Vacuum pump	840	840	875	875
Incidentals; ducts, insulation, painting, wiring, etc	5000	5000	5000	5000
Total	36540	51540	37400	52700
Coal-handling equipment:				
Track hopper	1400	1400	1500	1500
Feeder	1200	1200	1200	1200
Elevator for drying unit	2700	2700	2700	2700
Belt conveyer, 75 ft	2000	2000	2000	2000
Vibrating screen	1700	1700	1800	1800
Grading and railroad tracks, misc	5000	5000	5000	5000
Total	14000	14000	14200	14200
Total cost of plant:	80490	105040	79750	103250
Cost per ton of dry coal per day	582	381	505	327
Cost per ton of raw coal per day	402	263	400	258
Annual cost at 15 per cent	12050	15800	11900	15490
Cost per ton of raw coal, 300 operating days	0.205	0.132	0.198	0.129
Cost per ton of raw coal, 200 operating days	0.307	0.198	0.297	0.194

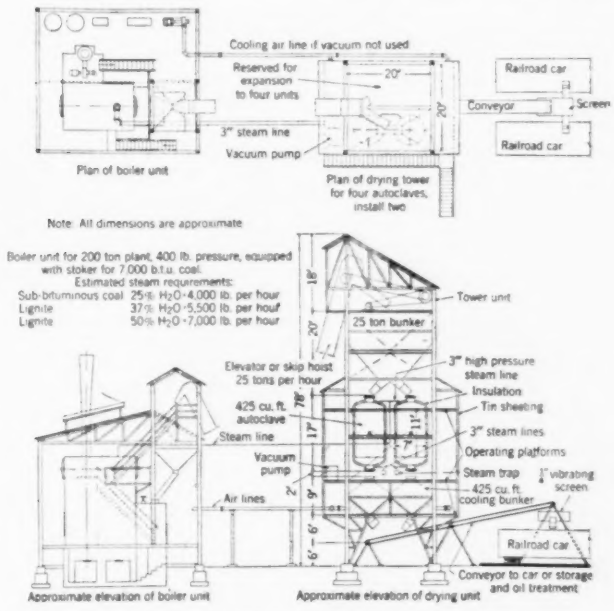


Fig. 9 Schematic Layout for Fleissner Drying Plant (Capacity, 200 to 400 tons wet lignite per day.)

Commercial Application of Fleissner Process to American Coals

A schematic design was made of a 400-ton plant to estimate costs, Fig. 9. Several equipment manufacturers in the United States contributed estimates of the cost of different parts. These costs are summarized in Table 3, which shows that a plant having two 425-cu-ft autoclaves will cost approximately $80,000 and a plant with four autoclaves will cost about $105,000 either in North Dakota or in Wyoming. The capacity of these plants

TABLE 4 ESTIMATED TOTAL COSTS FOR DRYING SUBBITUMINOUS COAL AND LIGNITE

	140-Min cycle				70-Min cycle			
	200-Ton plants		400-Ton plants		400-Ton plants		800-Ton plants	
	North Dakota	Wyoming	North Dakota	Wyoming	North Dakota	Wyoming	North Dakota	Wyoming
Cost of plants	$80,490	$79,750	$105,040	$103,250	$90,040	$87,950	$120,340	$114,900
Costs for plants operating 300 days a year:								
Annual charge at 15 per cent	12050	11900	15800	15490	13550	13200	18100	17200
Salaries and wages	22200	22200	29000	29000	29000	29000	34200	34200
Operating expenses	12400	11620	19460	18020	19460	18020	35200	32700
Total annual cost	46650	45720	64260	62510	62010	60220	87500	84100
Raw coal dried, tons	60000	60000	120000	120000	120000	120000	240000	240000
Cost per ton of raw coal[a]	0.778	0.762	0.535	0.521	0.517	0.501	0.364	0.350
Costs for plants operating 200 days a year:								
Annual charge at 15 per cent	12050	11900	15800	15490	13550	13200	18100	17200
Salaries and wages	18050	18050	23550	23550	23550	23550	28650	28650
Operating expenses	9400	8880	14480	13580	14480	13580	27800	26200
Total annual cost	39500	38830	53830	52620	51580	50330	74550	72050
Raw coal dried, tons	40000	40000	80000	80000	80000	80000	160000	160000
Cost per ton of raw coal[a]	0.988	0.971	0.673	0.658	0.644	0.629	0.466	0.451

[a] Cost in dollars.

will depend upon the length of the drying cycle. If 140 min are required for drying, the capacity will be 200 and 400 tons a day, respectively, and if the drying time can be reduced to 35 min, the capacity will be approximately 800 to 1600 tons daily. At 1600 tons daily, the steaming rate would be approximately 22,000 lb per hr for each pair of autoclaves, assuming a 13-min steaming period, and the maximum steam rate for a plant having four autoclaves would be 44,000 lb per hr.

Total investment and operating costs are estimated in Table 4, for plants operating 200 and 300 days a year on cycles of 70 and 140 min. As shown, the total cost of drying per ton of raw coal ranges from 98.8 to 35 cents, and the cost of drying is reduced one third when the drying time is halved, indicating that the cost of drying may be reduced to about 25 cents a ton if a drying time of 35 min can be attained.

TABLE 5 COMPARATIVE COSTS OF SLACK OR STOKER COAL IN NORTH DAKOTA, MINNESOTA, AND NORTHWESTERN WYOMING[a]

Freight rate, dollars	Cost in cents per million Btu of available heat[b]								
	A	*B*	*C*	*D*	*E*	*F*	*G*	*H*	*I*
0	22.8	9.4	14.9	13.0	12.1	9.2	12.1	10.9	10.2
0.50	25.0	14.1	17.9	16.1	15.2	12.5	14.7	13.4	12.8
0.75	26.1	16.5	19.5	17.6	16.7	14.2	15.9	14.7	13.9
1.00	27.2	18.9	21.0	19.1	18.2	15.8	17.2	15.9	15.3
1.25	28.3	21.2	22.5	20.6	19.7	17.4	18.4	17.2	16.6
1.50	29.4	23.6	24.0	22.1	21.2	19.1	19.7	18.5	17.8
1.75	30.2	26.0	25.5	23.7	22.7	20.7	20.9	19.7	19.0
2.00	31.6	28.3	27.0	25.2	24.3	22.4	22.2	21.0	20.3
2.25	32.7	30.7	28.5	26.7	25.8	24.0	23.4	22.2	21.6
2.50	33.8	33.0	30.0	28.2	27.3	25.7	24.7	23.5	22.8
3.00	35.8	37.7	33.1	31.2	30.3	29.0	27.2	26.0	25.3

[a] Excludes dealer's margin.

[b] Available heat is net heat minus the sensible heat of products of combustion above 32 F, when stack gases leave the furnace at 500 F with 30 per cent excess air.

(*A*) Millers Creek bituminous slack coal; $5.20 a net ton at Duluth, Minn., available heat = 22,900,000 Btu per ton.

(*B*) Raw lignite; $1 per ton at mine; available heat = 10,600,000 Btu per ton.

(*C*) Dried lignite, 140-min cycle, 400 psi steam pressure, 400-ton plant operating 200 days a year; available heat = 16,500,000 Btu per ton; cost at mine = $2.46 per ton.

(*D*) Dried lignite, 70-min cycle, 400 psi steam pressure, 800-ton plant operating 200 days a year; available heat = 16,500,000 Btu per ton; cost at plant = $2.15 per ton.

(*E*) Dried lignite, 70-min cycle, 400 psi steam pressure, 800-ton plant operating 300 days a year; available heat = 16,500,000 Btu per ton; cost at plant = $2 per ton.

(*F*) Raw subbituminous coal; available heat = 15,172,000 Btu per ton; cost at plant = $1.40 per ton.

(*G*) Dried subbituminous coal, 140-min cycle, 400 psi steam pressure, 400-ton plant operating 200 days a year; available heat = 19,846,000 Btu per ton; cost = $2.41 per ton.

(*H*) Dried subbituminous coal, 70-min cycle, 400 psi pressure, 800-ton plant, operating 200 days a year; available heat = 19,846,000 Btu per ton; cost = $2.17 per ton.

(*I*) Dried subbituminous coal, 70-min cycle, 400 psi pressure, 800-ton plant operating 300 days a year; available heat = 19,846,000 Btu per ton; cost = $2.04 per ton.

Table 5 and Fig. 10, show the estimated costs of available heat from bituminous coal and raw and dried lignite; Table 5, also includes costs for raw and dried subbituminous coal at various destinations. Available heat, instead of gross heat, is used in this comparison as it allows for the combustion characteristics of the different fuels. "Available heat" is defined as the amount of heat in excess of stack losses when fuel is burned at either 14 per cent CO_2, or with 30 per cent excess air, and the products of combustion leave the furnace at 500 F. The high moisture content of raw subbituminous coal and lignite and the relatively large amount of inert gases produced when these low-rank fuels

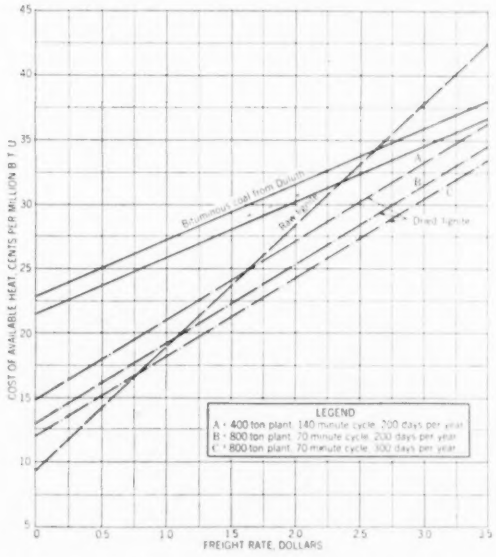


FIG. 10 DELIVERED COSTS OF BITUMINOUS COAL AND RAW AND DRIED LIGNITE

are burned cause disproportionate stack losses, compared with stack losses when the higher-rank fuels are burned. These losses do not permit good comparisons on the basis of gross heating value.

Table 5 presents the cost of available heat exclusive of the dealer's margin of profit or expense. The costs in column *A* are for available heat from bituminous coal delivered from the docks at Duluth. The costs shown in the other columns are for available heat from raw and dried subbituminous coal and lignite delivered from the mines. From this table the probable extension of markets for dried lignite can be determined. For example, the freight rate on bituminous coal from Duluth to Minneapolis is $1.32, making the cost of available heat 28.6 cents per million Btu. The freight rate on lignite to Minneapolis is $2.51, and the cost of available heat is 33.1 cents per million Btu. Raw lignite, therefore, cannot compete with bituminous coal in Minneapolis. On the other hand, the estimated cost of heat from dried lignite in Minneapolis is 27.4 cents per million Btu. Similarly, the freight rate on bituminous coal from Duluth

to Brainerd, Minn.,[9] is $1.27, which makes the cost of available heat 28.1 cents per million Btu. The freight rate on lignite is $2.47, and, if lignite can be dried under the conditions described in column *E*, the delivered cost in Brainerd, Minn., will be 27 cents per million Btu which is less than the cost of heat from bituminous coal. These comparisons indicate that the eastern markets for lignite could be extended approximately 150 miles by steam drying.

BIBLIOGRAPHY

1 Report of Energy Resources Committee, National Resources Committee, Jan., 1939, p. 12.

2 "A Technical and Economic Investigation of Northern Ontario Lignite," reprinted from Report of the Ontario Department of Mines, vol. 42, part 3, 1933.

3 "Studies in the Development of Dakota Lignite—III. Drying of Lignite Without Disintegration," by Irvin Lavine, A. W. Gauger and C. A. Mann, *Industrial and Engineering Chemistry*, vol. 22, 1930, p. 1347.

4 "Die Trocknung Der Brennstoffe als Veredlungsvorgang und das Trocknungsverfahren nach Patent Prof. Fleissner," by Herbert Klinger, *Montanistischen Rundschau*, Vienna, vol. 23, 1929. Also, translation: "The Drying of Lump Lignite," by G. A. Revell, Ontario Research Foundation, Lignite Report 22, 1933.

5 "Contributions to the Thermodynamics of the Drying of Brown Coal by the Fleissner Process," by J. Formanek, *Braunkohle*, vol. 40, 1931. Translation from original German title, by G. A. Revell and C. Tasker, Ontario Research Foundation, Lignite Report 27, 1933.

6 "The Physics of Coal Carbonization," by S. P. Burke, T. E. W. Schumann, and V. F. Parry, *Fuel in Science and Practice*, 1931, pp. 148–171.

7 "Die Vorgänge beim Fleissner-Kohlentrocknungsverfahren für Lignite und ihre chemischen und physikalischen Grundlagen," by Hermann Klein, *Braunkohle*, Hefte 1 and 2, 1930. Translation: "The Fleissner Process for Drying Lignite. Its Physical and Chemical Principles," by G. A. Revell, Ontario Research Foundation, Lignite Report 24, 1933.

[9] Brainerd, Minn., is 118 miles west of Duluth and 335 miles east of Bismarck, N. Dak., by rail.

A Method of Determining the Pressure Drop for Oil-Vapor Mixtures Flowing Through Furnace Coils

By F. W. DITTUS[1] and A. HILDEBRAND[1]

This paper outlines a procedure for calculating pressure drops which has been used by the authors in the design of furnaces over a period of several years. The resultant total pressure drops have in each case checked closely with the calculated values. The equations given in the paper are set up to determine the pressure gradient for the part of the furnace where a liquid-vapor composition exists, particularly in the case of a vaporizing petroleum oil. The method as outlined consists of a combination of mathematical equations and graphical solutions.

IN THE derivation of the equations in this paper, the following nomenclature is used:

Nomenclature

a = constant in equation for curve of heat content at initial boiling point, Fig. 3, Btu per lb
c_s = slope of heat-content curve for liquid-vapor mixture, Fig. 3 (pseudo specific heat of vaporizing mixtures), Btu per deg F per lb
c_p = slope of curve for heat content of oil at initial boiling point, Fig. 3, average specific heat of liquid, Btu per deg F per lb
D = inside diameter of tubes, in.
f = friction factor for two-phase mixture flowing through tube
F_v = weight fraction of liquid which has been vaporized at any point within heating coil
g = acceleration of gravity = 32.2 fps per sec
h = height of vertical section of heating coil, ft
H = heat content of fluid at any point within heating coil, Btu per lb
H_c = heat content of cold fluid at inlet to heating coil, Btu per lb
H_i = heat content of fluid at its initial boiling point at any given pressure P_1, P_2, P_3, etc., Btu per lb
H_M = heat content of fluid at inlet to or bottom of that section of heating coil lying in a vertical plane, Btu per lb
H_T = heat content of fluid at outlet or top of that section of heating coil lying in a vertical plane, Btu per lb
k_f = slope of flash-distillation curve, Fig. 2, F
k = slope of molecular-weight curve, Fig. 5
L = length of fluid travel, ft
l_t = length of single tube, ft
M = average molecular weight of oil vapor
M_i = hypothetical molecular weight of oil vapor at initial boiling point
n_p = number of tubes operating in parallel
n_r = number of velocity heads lost in each return header
P = pressure at any point within heating coil, psi abs
R = perfect-gas constant = 10.71, volume in cu ft and P psi
T = absolute temperature of fluid at any point in heating coil, deg Rankine
T_i = initial boiling point of liquid at any given pressure P, deg Rankine
u = mean velocity, fps
U = heat-absorption rate of inside tube area, Btu per sq ft per hr
v = mean specific volume of two-phase mixture, cu ft per lb
v_L = mean specific volume of liquid, cu ft per lb
v_v = volume of vapor per pound of two-phase mixture, Fig. 6, cu ft per lb
W = total mass flow rate, lb per hr
$X = \frac{ZR}{MP}(2k_fF_v + T_i)$, Fig. 6
y = elevation above any given reference plane, ft
Z = gas-law correction factor (molal volume of vaporized oil divided by volume of equivalent perfect gas)

The units indicated apply to the final equations which will be derived. The derivation of these equations is in absolute units however, for the purpose of eliminating a number of constants.

General Statement of Problem

The engineer is sometimes confronted with the problem of calculating the pressure drop for the flow of a boiling liquid through furnace tubes. As long as the pressures and temperatures within the tubes are such that vaporization is suppressed, the pressure-drop calculation is simple. As soon as the temperature has become high enough to cause vaporization, the pressure-drop calculations become involved, for the reason that the liquid-vapor composition changes all along the tube, resulting in a continual change of the pressure gradient. The equations given in this paper are set up to determine the pressure gradient for the part of the furnace where the latter condition exists; particularly for the case of a vaporizing petroleum oil. The procedure should, within limits, apply also to other fluids, but in such cases a check should be made on the various assumptions to insure that the physical properties of the fluid under consideration do not make the assumptions used in this paper invalid.

As far as the authors know, the general practice in solving a problem of this type is to divide the heating element into a number of convenient sections and calculate by trial-and-error method the pressure drop of each section, starting with the terminal section and moving backward along the heating element, section by section. Since the pressure, temperature, and heat content of the fluid vary all along the tube, this is a rather difficult and time-consuming job. To establish mathematical equations for an exact solution of this type of flow problem for such cases as oil-distillation furnaces is, while perhaps not impossible, certainly impractical because of the number of variables involved in such a problem. A method is herewith presented for solving such problems by using a combination of mathematical equations and

[1] Standard Oil Company of California, San Francisco, Calif.

Contributed by the Heat Transfer Division and presented at the Semi-Annual Meeting, Kansas City, Mo., June 16–19, 1941, of The American Society of Mechanical Engineers.

Note: Statements and opinions advanced in papers are to be understood as individual expressions of their authors, and not those of the Society.

graphical solutions. After once becoming acquainted with this method, a relatively rapid and accurate solution of such problems may be obtained.

Principle Used in Calculations

In principle the solution of the problem consists of first calculating the rate of pressure drop per unit length of tube, i.e., $(dP)/(dL)$, at several points in the furnace for each of a number of arbitrarily assumed constant pressures (P_1, P_2, P_3, etc.), then plotting these values as ordinates against the tube length, as shown in Fig. 1. The pressure gradient at constant pressure indicates the rate of pressure drop which would occur at any given point along the tube if the pressure at that point were equal to the assumed constant pressure.

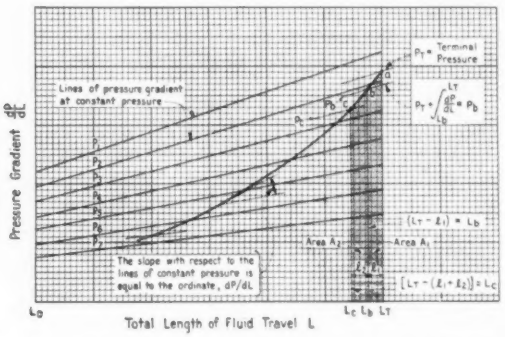


Fig. 1 Method of Graphical Integration to Determine Pressure Gradient Through Oil Furnace

To obtain the total pressure drop involves graphical integration, as shown in Fig. 1. This is accomplished by plotting a curve, beginning at the terminal pressure P_T, of such shape that the area A_1 under this curve between the limits of L_T and $(L_T - l_1)$ (which area represents the pressure drop for the length l_1) when added to the terminal pressure P_T is equal to the pressure P_b established by the intersection b of this curve with the pressure curve P_b at the point $(L_T - l_1)$. This pressure P_b is the pressure within the tube at point L_b. In order to secure the area A_1 under the curve ab the shape for the curve ab must be known. Actually, of course, the point b is unknown, and it is therefore necessary to make an assumption as to location of this point, i.e., the pressure P_b at point $(L_T - l_1)$, and then check if the area under the thus assumed curve ab when added to pressure P_T is equal to pressure P_b. This procedure is then repeated using pressure P_b as a starting point, and using the point P_c then found as a starting point for the next increment of tube length, and so on.

While this procedure is fundamentally a trial-and-error method, it will be found from experience that the solution is simple. The most time-consuming part of the work is to plot the curves of pressure gradient at constant pressures (P_1, P_2, P_3, etc.) against tube length, as shown in Fig. 1. The following discussion is concerned primarily with the simplified method developed for calculating the points necessary to plot these pressure-gradient curves. Experience has demonstrated that the simplifications employed affect the accuracy of the answer but little. Also it has been found that it simplifies matters some to use the heat absorbed instead of the tube length as the abscissa in Fig. 1, as will be explained.

Determining Pressure-Gradient Curve

Before proceeding to set up the various equations, it might be well to review briefly what factors must be considered in determining the pressure-gradient curve for any constant pressure P at any one point within the heating coil.

As a unit mass of liquid passes from the entrance of the heating coil L_0 to the exit or terminal of the heating coil L_T, the liquid absorbs heat equal to the heat absorption of the surface over which the liquid passes. The first simplification that is made is the assumption that the heat-absorption rate per unit area of tube surface is constant, and that therefore the heat absorbed by the liquid is directly proportional to the tube length traversed by the liquid. Thus, the heat content of the fluid can be established at any point along the tube. With this known, and considering the fluid under a constant pressure P, it is possible to calculate the fraction of fluid in vapor form. This permits evaluation of the mean density which in turn allows calculation of the friction loss per unit length of tube, the change in velocity head, and the change in static head, at the point corresponding to this density. In the event the heat-absorption rate is not uniform, the solution can still be secured by breaking up the heat-absorbing surface into a convenient number of sections, for each of which the heat-absorption rate is nearly constant, and then preparing a separate set of calculations for each one of the sections.

Since the rate of heat input per unit area and the tube diameter are assumed to be constant, the heat transferred is directly proportional to length. It is therefore possible to calculate the pressure gradient as a function of the heat absorbed instead of the tube length and thus plot a set of curves showing the pressure gradient as a function of the heat content of the fluid, instead of as a function of lengths, as was shown in Fig. 1. The pressure drop is then obtained by graphical integration in the same manner as is shown in Fig. 1. With this procedure in mind, the necessary equations required for plotting the pressure gradients at constant pressures will now be derived.

Fanning's and Bernoulli's equations state that the total change in pressure when a fluid is flowing through a conduit can be expressed as

$$dP = \frac{fu^2}{2vgD}\,dL + \frac{u\,du}{vg} + \frac{dy}{v} \qquad [1]$$

The first term in the right-hand side of Equation [1] represents the friction loss which is the major portion of the total pressure drop in a furnace. The second term represents the change in velocity head. The velocity head is usually a large factor only in a furnace whose outlet pressure is well below atmospheric. The third term represents the change in gravitational potential or liquid head. In the case of liquids partially vaporized this term is generally very small.

The first step in changing Equation [1] into the desired form for integration is to express the linear velocity u in terms of mass rate and specific volume

$$u = \frac{4Wv}{\pi D^2 n_p} \qquad [2]$$

$$du = \frac{4W}{\pi D^2 n_p}\,dv \qquad [3]$$

Substituting these in Equation [1], it becomes

$$dP = \frac{8fW^2v}{\pi^2 g n_p^2 D^5}\,dL + \frac{16W^2}{\pi^2 g n_p^2 D^4}\,dv + \frac{dy}{v} \qquad [4]$$

If coefficient of friction f is assumed constant, the specific volume v and the differentials dL, dv, and dy are the remaining variables on the right-hand side of the equation within a portion of the furnace having a constant tube size and the same number of parallel passes.

The average specific volume v is equal to the fraction vaporized F_v times the specific volume of the vapor, plus the fraction unvaporized $(1 - F_v)$ times the specific volume v_L of the liquid, or

$$v = F_v Z \frac{RT}{MP} + (1 - F_v)v_L \quad [5]$$

It is next necessary to establish the value of F_v at any point within the heating coil in terms of H, the heat content, and P, the pressure.

The first step in solving for F_v is to plot a flash- or equilibrium-distillation curve from laboratory data. Such a curve, as shown in Fig. 2, can be expressed as a straight line for any given pressure or, if a single straight line deviates too much from the curve, successive sections of straight lines can be used. The equation for such a straight line at any given pressure P is

$$F_v k_f = T - T_i \quad [6]$$

In most cases only a portion of the liquid is vaporized so that the straight line need only express that section of the curve over which vaporization takes place. By inspecting Fig. 2, which represents a typical equilibrium-distillation curve, it can be seen that the straight line *ab* expresses the flash-distillation curve very well if the total liquid vaporized is less than 50 per cent for this particular case. If 80 per cent were to be vaporized, it would be necessary to establish another line covering the 50 to 80 per cent vaporized section and make a second set of calculations for that part of the furnace.

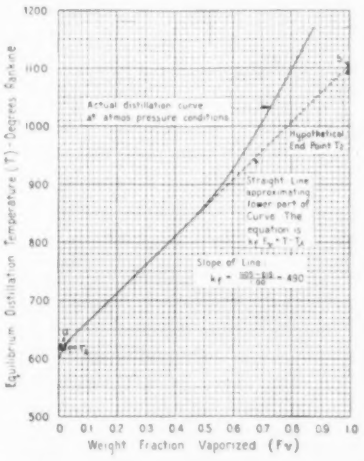


FIG. 2 FLASH- OR EQUILIBRIUM-DISTILLATION CURVE

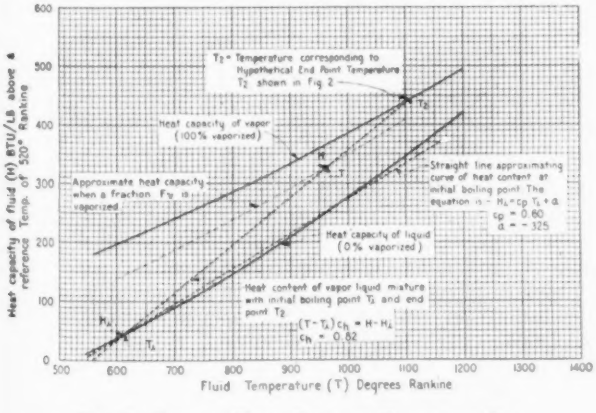


FIG. 3 TYPICAL HEAT-CONTENT CURVE FOR OIL

The next step is to express the value $(T - T_i)$ in terms of the heat content of the mixture of liquid and vapor at any temperature T and any pressure P. This can be done in an approximate manner with the aid of the heat-content curve shown in Fig. 3. In general, no great error is involved if the relation of heat content of the liquid-vapor mixture to temperature at a given pressure is expressed in a linear equation as long as we are concerned only with that section of the flash curve which can be expressed approximately by a linear equation. From Fig. 3, it can be seen that the equation for the heat-content curve of the liquid-vapor mixture at a given pressure P can be expressed by the equation

$$c_h(T - T_i) = (H - H_i) \quad [7]$$

The slopes of the curves represented by Equations [6] and [7], i.e., slopes k_f and c_h, are not independent of pressure, but the changes in slopes with pressures are not great and the error in assuming them constant over the entire range of pressures ordinarily occurring within a furnace will be quite small if the slopes used correspond approximately to the furnace-outlet pressure. The reason for selecting the values of k_f and c_h at pressures near the furnace outlet, or near the terminal pressure of a given section if the furnace is divided into sections for reasons previously mentioned, is that near the outlet the fraction vaporized is a maximum, and therefore the pressure gradient is a maximum. Ahead of that point the pressure is higher and the heat content lower, so that a much smaller fraction is vaporized and any errors in pressure gradients are of much less magnitude.

By combining Equations [6] and [7] and eliminating the term $(T - T_i)$, it is possible to express F_v in terms of H

$$F_v = \frac{(H - H_i)}{k_f c_h} \quad [8]$$

The quantity H_i is the heat content of the liquid at the point at which vaporization begins at any pressure P. Therefore, H_i will depend upon the pressure. To express it in terms of pressure, it is convenient first to express it in terms of T_i, which will be done as follows:

In Fig. 3, the lower line is the heat-content curve of the liquid. In general, this curve can be expressed as a simple linear function $H = a + kT$ and the point at which vaporization first begins can be expressed

$$H_i = a + c_p T_i \quad [9]$$

Substituting Equation [9] in Equation [8], the following equation is obtained

$$F_v = \frac{1}{k_f c_h}(H - c_p T_i - a) \quad [10]$$

The term T_i can be expressed as a function of pressure by the equation proposed by E. R. Cox.[1]

$$T_i = \frac{AB}{A - \log P} \quad [11]$$

where A is a constant and B is the boiling temperature at unit pressure.

The substitution of Equation [11] in Equation [10] results in an equation which is cumbersome to use. For this reason, it is better to assume several pressures and select T_i for each of these pressures from a Cox chart, as illustrated in Fig. 4. The value of T_i thus obtained can then be substituted in Equation [10] to determine the fraction vaporized F_v. In view of this, no further substitution will be made and the expression to be used for F_v in Equation [5] is the one shown as Equation [10]. For simplicity, Equation [10] will not be substituted in Equation [5], but will be carried through these calculations as F_v to be evaluated separately and then substituted in the final solution of the problem.

[1] "Hydrocarbon Vapor Pressures," by E. R. Cox, *Industrial and Engineering Chemistry*, vol. 28, 1936, pp. 613–616.

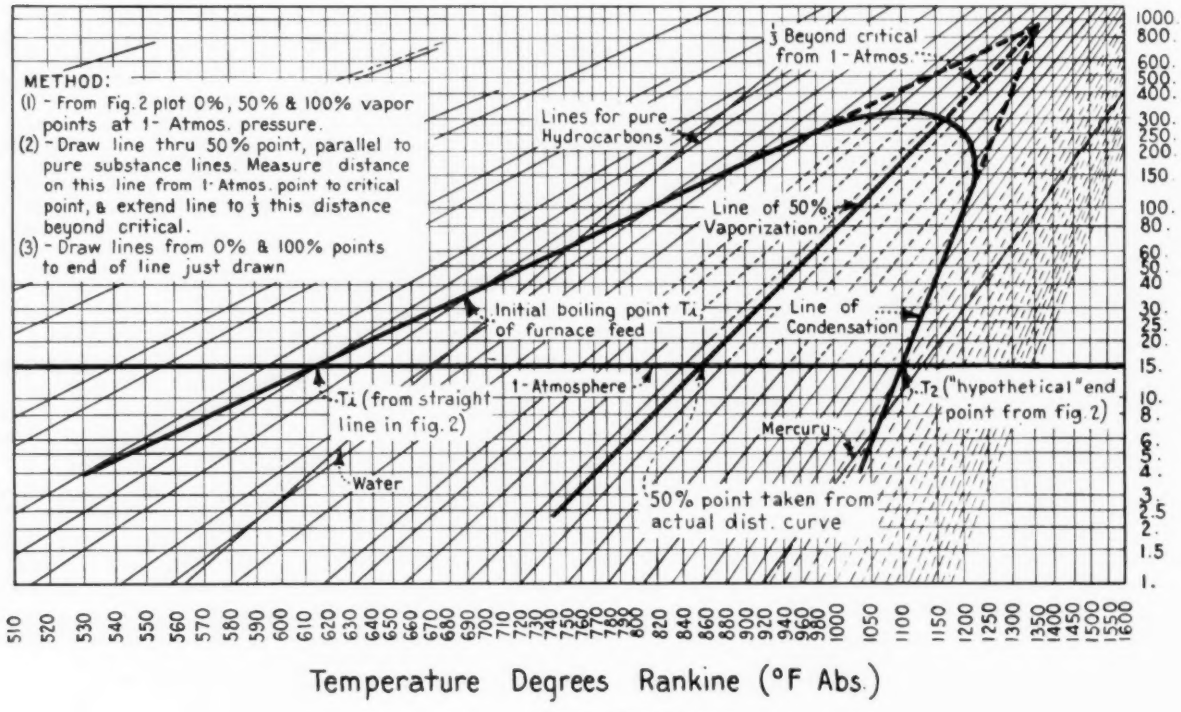


FIG. 4 COX CHART

The two other variables in Equation [5] for conditions of constant pressure are the values T and M.

The value of M can be fairly well expressed as a linear function of F_v without causing much error. It is relatively simple, however, to evaluate M separately from a curve, such as shown in Fig. 5 (which is based on laboratory data) and then substitute its value directly in the final solution.

The value of T in Equation [5] can be expressed in terms of Equation [6]

$$T = k_f F_v + T_i \quad \ldots\ldots [12]$$

Substituting Equation [12] in Equation [5], the latter then becomes

$$v = \frac{ZR}{MP} F_v(k_f F_v + T_i) + (1 - F_v)v_L \quad \ldots\ldots [13]$$

Differentiating Equation [13], with P (and hence T_i) constant, gives

$$dv = \left[\frac{ZR}{MP}(2k_f F_v + T_i) - v_L\right] dF_v - \left[\frac{ZR}{M^2P} F_v(k_f F_v + T_i)\, dM\right] \quad \ldots\ldots [14]$$

Similarly, differentiating Equation [10] gives

$$dF_v = \frac{dH}{k_f c_h} \quad \ldots\ldots [15]$$

Although the molecular weight M can be taken conveniently from an experimental curve, such as that shown in Fig. 5, it is necessary to use a line approximating this curve in order to obtain a simple expression for dM. If the equation of this line is taken as

$$M = k_m F_v + M_i \quad \ldots\ldots [16]$$

then

$$dM = k_m dF_v \quad \ldots\ldots [17]$$

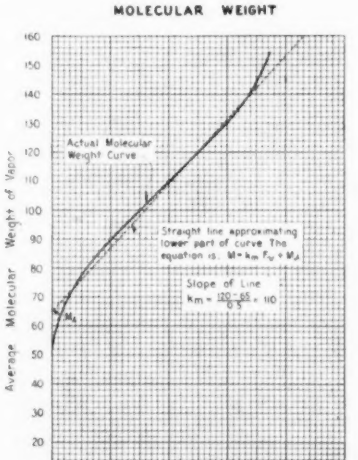


FIG. 5 MOLECULAR WEIGHT

By substituting Equations [15] and [17] in Equation [14], an expression for dv in terms of dH is obtained

$$dv = \left[\frac{ZR}{k_f c_h MP}(2k_f F_v + T_i) - \frac{v_L}{k_f c_h} - \frac{k_m ZR}{k_f c_h M^2 P} F_v(k_f F_v + T_i)\right] dH \quad \ldots\ldots [18]$$

Referring to Equation [4], it is seen that v and dv in that equation can now be expressed as functions of H and P by the use of Equations [10], [13], and [18], but expressions must still be obtained for dL and dy. The expression for dL will be obtained next.

If the absorption rate is constant throughout the furnace, or in

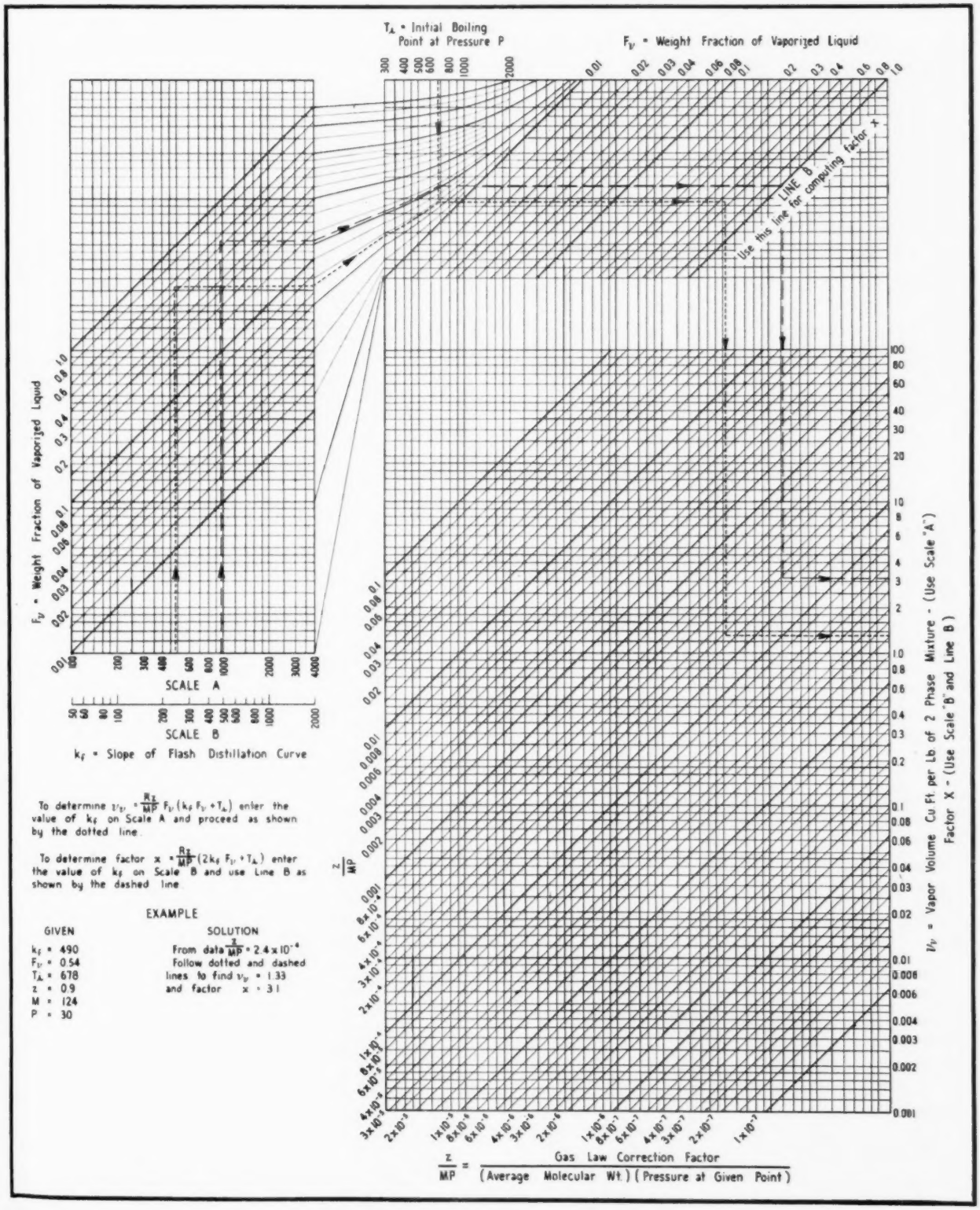


FIG. 6 CHART FOR COMPUTING FACTORS v_v AND x

any given section of the furnace, and if the number of passes and tube size are constant, then the total heat absorbed by the oil up to any point is equal to the heat transferred through the tubes up to that point, or

$$W(H - H_c) = \pi L n_p D U \quad \ldots\ldots\ldots\ldots [19]$$

Differentiating Equation [19] gives

$$dL = \frac{W}{\pi n_p D U}\, dH \quad \ldots\ldots\ldots\ldots [20]$$

The length represented by L is the actual distance traveled by a particle of fluid, but a multiplying factor must be applied to make an allowance for the friction loss in the return header at the end of each tube. If the pressure loss in each header is n_v velocity heads, the equivalent length of tube that will give the same loss of n_v velocity heads is $n_v D/f$. The friction length per tube will therefore be increased from l_t to $l_t + (n_v D/f)$. The simplest way to take care of this extra friction is to multiply the length dL by the ratio

$$\frac{l_t + \dfrac{n_v D}{f}}{l_t} \text{ or } 1 + \frac{n_v D}{l_t f}$$

When multiplied by this factor, Equation [20] becomes

$$dL' = \left(1 + \frac{n_v D}{l_t f}\right) dL = \left(1 + \frac{n_v D}{l_t f}\right) \frac{W}{\pi n_p D U}\, dH \ldots [21]$$

The method of expressing dy as a function of H may have to be varied somewhat to suit individual cases. Wherever the change in elevation is approximately proportional to the length of fluid travel or the heat absorbed, we can say that the elevation above (or below) the inlet of the coil is

$$y = h\,\frac{H - H_B}{H_T - H_B} \quad \ldots\ldots\ldots\ldots [22]$$

Differentiating Equation [22], we obtain

$$dy = \frac{h}{H_T - H_B}\, dH \quad \ldots\ldots\ldots\ldots [23]$$

Equation [4] can now be rewritten to give dP in terms of H and P by use of Equations [13], [18], [21], and [23]

$$dP = \left[\frac{8 f W^2}{\pi^2 g n_p^2 D^5}\left\{\frac{ZR}{MP} F_v(k_f F_v + T_i) + (1 - F_v) v_L\right\}\left(1 + \frac{n_v D}{l_t f}\right)\left(\frac{W}{\pi n_p D U}\right)\right] dH + \left[\frac{16 W^2}{\pi^2 g n_p^2 D^4}\left\{\frac{ZR}{k_f c_h MP}(2 k_f F_v + T_i) - \frac{v_L}{k_f c_h} - \frac{k_m ZR}{k_f c_h M^2 P} F_v(k_f F_v + T_i)\right\}\right] dH + \left[\frac{\dfrac{h}{H_T - H_B}}{\dfrac{ZR}{MP} F_v(k_f F_v + T_i) + (1 - F_v) v_L}\right] dH \ldots [24]$$

Rewriting and consolidating

$$\frac{dP}{dH} = \left[\left(f + \frac{n_v D}{l_t}\right)\left(\frac{8}{\pi^2 g U}\right)\left(\frac{W}{n_p D^2}\right)^2 \left\{\frac{ZR}{MP} F_v(k_f F_v + T_i) + (1 - F_v) v_L\right\}\right] + \left[\left(\frac{16}{\pi^2 g k_f c_h}\right)\left(\frac{W}{n_p D^2}\right)^2 \left\{\frac{ZR}{MP}(2 k_f F_v + T_i) - v_L - \frac{k_m ZR}{M^2 P} F_v(k_f F_v + T_i)\right\}\right] + \frac{h}{(H_T - H_B)\left[\dfrac{ZR}{MP} F_v(k_f F_v + T_i) + (1 - F_v) v_L\right]} \ldots [25]$$

Rewriting Equation [25] to employ the units shown in the nomenclature, and using the term v_v for $\frac{ZR}{MP} F_v(k_f F_v + T_i)$ and X for the term $\frac{ZR}{MP}(2 k_f F_v + T_i)$, Equation [25] becomes

$$\frac{dP}{dH} = \left[\left(\frac{12{,}820}{U}\right)\left(f + \frac{n_v D}{12 l_t}\right)\left(\frac{W}{1000 n_p D^2}\right)^2 \left\{v_v + (1 - F_v) v_L\right\}\right] + \left[\left(\frac{0.56}{k_f c_h}\right)\left(\frac{W}{1000 n_p D^2}\right)^2 \left(X - \frac{k_m}{M} v_v - v_L\right)\right] + \left[\frac{h}{144(H_T - H_B)\{v_v + (1 - F_v) v_L\}}\right] \ldots [26]$$

The values of v_v and X can be readily evaluated by the use of Fig. 6.

In general, it will be found that the friction loss, the first general term of Equation [26], makes up the predominant portion of the total pressure drop. As soon as any fair amount of vaporization takes place, the third term, i.e., the one accounting for the change in static head, can be neglected entirely since the mean density then becomes relatively low. This term is also omitted, of course, when the coil lies in a horizontal plane, since in that case $h = 0$. When the fraction vaporized is very small, such as is sometimes the case in reboilers, the static head may be appreciable, but in that case the change in velocity head is small and the second general term can be omitted altogether.

For all cases of furnace-pressure-drop calculations made by the authors, it was found that no serious error was introduced if both

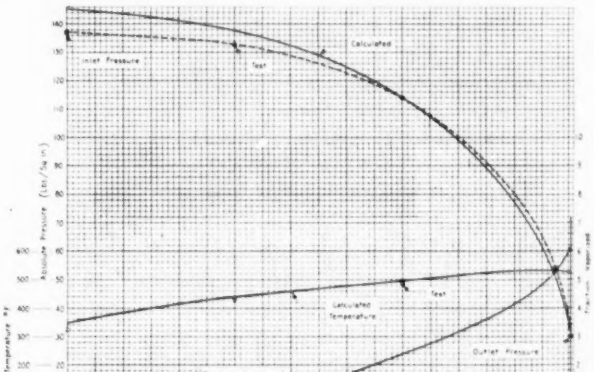


FIG. 7 COMPARISON OF CALCULATED AND ACTUAL PRESSURES IN FURNACE USED FOR SAMPLE CALCULATION

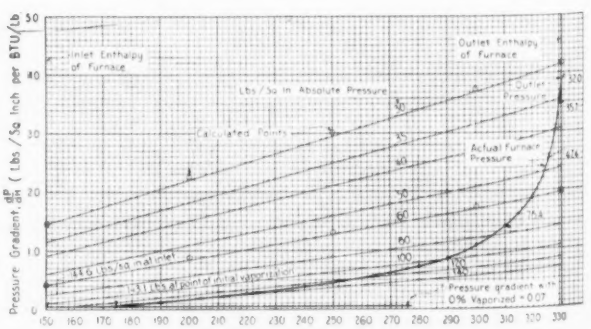


FIG. 8 GRAPHICAL INTEGRATION FOR SAMPLE CALCULATION

TABLE 1 PRESSURE GRADIENT CALCULATIONS

TABLE 1 PRESSURE GRADIENT CALCULATIONS

POSITION NO.	1	2	3	4	5	6	7	8	9	10	11	12	13	14	15	16	17	18
LOCATION OR ITEM	P	H	T_1	$C_p T_1$	$H-C_pT_1=A$	F_v	B	$\frac{A}{B}$	v_v	$v_L(1-F_v)$	v	$\frac{dP}{dH}$ friction	X	$\frac{dP}{dH}$	$\frac{1}{778}v_v-v_L$	$\frac{dP}{dH}$ (velocity)	$\frac{dP}{dH}$ (total)	$\frac{dP}{dH}$ (total)
SOURCE	Assumed	Arbitrarily Selected*	From Fig. 4	0.48 T_1	$H_{32.0^\circ F}=322$	Col.5 / 322	From Fig. 4 Figure 5		From Fig. 8	col.8 $(1-F_v)$	Column 9 plus 10	2.79 x Column 11	From Fig. 8	110 x Col. 9 / v	Col.13 minus 0.025	0.0146 x Col.14	Sum of Cols. 12, 16, and 17	
	30	331	678	407	249	0.620	322	0.00078	1.46	0.010	1.49	5.16	3.12	1.75	1.48	0.031	0.0007	4.19
	*	320	*	*	238	0.618	314	0.00074	1.35	0.012	1.34	4.64	3.12	1.62	1.32	0.028	0.0006	3.97
	*	290	*	*	208	0.548	284	0.00073	1.06	0.013	1.07	3.68	3.12	1.29	1.04	0.024	0.0010	3.01
	*	250	*	*	178	0.480	248	0.00072	0.75	0.018	0.80	2.75	3.12	0.97	0.75	0.017	0.0013	2.27
	*	190	*	*	118	0.319	86	0.00037	0.48	0.031	0.500	1.40	3.12	0.61	0.41	0.0097	0.0022	1.44
	35	331	690	414	242	0.602	330	0.00080	1.25	0.010	1.26	3.52	2.71	1.26	1.02	0.027	0.0008	3.55
	*	190	*	*	61	0.172	86	0.00030	0.38	0.031	0.397	1.11	2.71	0.48	0.31	0.0074	0.0028	1.19
	40	331	703	422	234	0.582	326	0.00016	1.08	0.011	1.09	3.04	2.40	1.44	1.01	0.024	0.0010	3.06
	*	190	*	*	53	0.132	82	0.00027	0.35	0.032	0.370	0.89	2.44	0.44	0.28	0.0068	0.0035	0.92
	50	331	720	432	218	0.542	324	0.00014	0.94	0.012	0.95	2.37	1.96	1.18	0.78	0.019	0.0012	2.19
	*	190	*	*	37	0.092	76	0.00024	0.33	0.033	0.364	0.87	2.06	0.43	0.26	0.0060	0.0052	0.90
	60	331	740	444	206	0.513	322	0.00012	0.88	0.012	0.892	1.97	1.65	1.09	0.69	0.017	0.0016	1.94
	*	300	*	*	177	0.440	314	0.00035	0.80	0.014	0.814	1.71	1.66	1.01	0.64	0.015	0.0017	1.73
	*	290	*	*	177	0.441	301	0.00031	0.64	0.017	0.661	1.39	1.68	0.84	0.53	0.012	0.0023	1.43
	*	250	*	*	147	0.366	259	0.00027	0.51	0.020	0.530	1.17	1.81	0.68	0.43	0.010	0.0034	1.20
	*	190	*	*	26	0.065	72	0.00021	0.31	0.033	0.343	0.76	1.81	0.39	0.25	0.0057	0.0077	0.63
	80	331	788	473	185	0.461	316	0.00010	0.68	0.014	0.694	1.75	1.27	0.86	0.54	0.013	0.0011	1.40
	*	270*	*	*	74	0.184	88	0.00013	0.52	0.020	0.540	1.07	1.32	0.67	0.42	0.0097	0.0044	1.09
	100	331	818	491	163	0.411	311	0.00008	0.56	0.016	0.578	1.46	1.06	0.67	0.42	0.011	0.0028	1.07
	*	220*	*	*	54	0.134	82	0.00011	0.34	0.032	0.372	0.93	1.11	0.42	0.26	0.0059	0.0065	0.47
	120	331	840	504	152	0.384	308	0.00049	0.59	0.016	0.605	1.51	0.90	0.68	0.43	0.010	0.0034	0.96
	*	220*	*	*	41	0.104	78	0.00036	0.37	0.032	0.402	1.00	0.97	0.28	0.17	0.0041	0.0081	0.54
	140	331	870	522	124	0.313	303	0.00065	0.25	0.017	0.267	0.67	0.68	0.24	0.15	0.0035	0.0043	0.68
	*	220*	*	*	25	0.057	70	0.00093	0.06	0.074	0.134	0.34	0.93	0.08	0.05	0.0012	0.0142	0.24

* H must be chosen sufficiently large so that F_v will not be negative, since F_v cannot be less than zero.

When $F_v=0$, the pressure gradient, $\frac{dP}{dH}=2.79\ v_L=2.79\times 0.025=0.07\ \frac{\text{lbs/sq.in.}}{\text{ft/lb}}$.

the second and the third general term of Equation [26], representing the change in velocity head and static head were omitted in the integration. The total pressure drop in this case is obtained by using the thus simplified equation to calculate the friction pressure drop and then adding the pressure loss due to the increase in the velocity head from the furnace inlet to the outlet and the change in static head based on a mean specific volume. For this particular mode of solution, the equation for the pressure gradient will then become

TABLE 2 INTEGRATION OF PRESSURE-GRADIENT CURVE
(All pressures are psi abs)

Section Under Consideration	ΔH	Average Value of $\frac{dP}{dH}$ from Fig. 7	Pressure Drop for Section $\frac{dP}{dH}\times\Delta H$	Outlet Pressure of Section	Inlet Pressure to Section
H=331 to H=330	1.0	3.7	3.7	32.0 (Given)	35.7
" 330 " " 329	1.0	3.3	3.3	35.7	39.0
" 329 " " 328	1.0	3.0	3.0	39.0	42.0
" 328 " " 326	2.0	2.7	5.4	42.0	47.4
" 326 " " 324	2.0	2.4	4.8	47.4	52.2
" 324 " " 320	4.0	2.05	8.2	52.2	60.4
" 320 " " 315	5.0	1.70	8.5	60.4	68.9
" 315 " " 310	5.0	1.5	7.5	68.9	76.4
" 310 " " 300	10.0	1.25	12.5	76.4	88.9
" 300 " " 290	10.0	0.95	9.5	88.9	98.4
" 290 " " 280	10.0	0.80	8.0	98.4	106.4
" 280 " " 250	30.0	0.60	18.0	106.4	124.5
" 250 " " 220	30.0	0.37	11.1	124.5	135.6
" 220 " " 190	30.0	0.20	6.0	135.6	141.6
" 190 " " 172	18.0	0.085	1.5	141.6	143.1
" 172 " " 150	22.0	0.07	1.5	143.1	144.6

TABLE 3 CALCULATIONS FOR FRACTION OF OIL VAPORIZED AND OIL TEMPERATURE

H (Btu/lb)	P (lbs/sq.in.)	T_1 (°R.)	F_v	T (°F)
Arbitrarily Selected	Taken from Fig. 7	From Cox Chart Fig.4	Equation (10)	Equation (12)
331	32	680	0.617	523
320	61	750	0.485	528
310	77	780	0.416	524
290	99	812	0.318	508
250	125	850	0.161	469
200	140	865	0.017	413
150				348*

* From liquid heat capacity curve, Figure 3.

$$\left(\frac{dP}{dH}\right)_{friction}=\left(\frac{12{,}820}{U}\right)\left(f+\frac{n_v D}{12l_t}\right)\left(\frac{W}{1000n_p D^2}\right)^2\left(v_v+(1-F_v)v_L\right)\ldots[27]$$

Column 12 in Table 1, shows the values obtained by the use of Equation [27], while column 18 lists the results of the exact calculations using Equation [26]. It will be noted that the differences are indeed small, although it should be noted also that, once the terms for Equation [27] have been set up, the solution of Equation [26] requires but very little more work.

Simplification of Problem

The solution of the problem can further be simplified for the reason that the values of $(dP)/(dH)$ when plotted against H form a curve that in most cases deviates but very little from a straight line so that it is only necessary to calculate and plot two points for each of the assumed pressures through which straight-line curves can then be drawn. The error caused by this simplification for all the cases the authors have encountered is well within the accuracy that can be expected considering the various simplifying assumptions made in the derivation of the equations.

Since the ease with which the values for the pressure gradients are calculated depends to some extent upon the procedure followed, sample calculations for an actual case will be given. The resultant calculated pressure gradient is compared with the test results in Fig. 7.

Perhaps the one item that is deserving of some comment is the value of the friction factor f for two-phase flow used

in the foregoing equations. The value of this term f can be obtained from the published curves of friction factors plotted against Reynolds number. The Reynolds number is calculated using the average specific volume v of the two-phase mixture, and the viscosity of the liquid. This procedure of establishing the friction factor is substantiated by test results published by Boelter and Kepner.[3]

As in the case of single-phase flow, the friction factor for commercial steel tubes apparently becomes nearly constant with increasingly large Reynolds numbers. The Reynolds number in a furnace is usually quite large so that a constant friction factor is a reasonable assumption to make. In crude-oil furnaces with steel tubes, where the Reynolds numbers are of the order of 1,000,000 to 20,000,000, it has been found by test results that the friction factor is of the order of 0.02, which checks fairly well with published data on friction factors for single-phase flow in commercial pipes.

Typical Pressure-Drop Calculation

The sample calculation to be carried through is for a section of a furnace in which the furnace feed has been split into two parallel streams. There are 34 tubes in each stream (68 total), arranged in a vertical bank with each tube lying horizontally, 10 in. above the preceding tube. The characteristics of the oil are shown in Figs. 2 to 5, inclusive, and the size of tubes, quantity of oil, and other constants describing the furnace and the heat duty are as follows:

a = —325 Btu per lb (see Fig. 3)
c_h = 0.82 Btu per deg F per lb (see Fig. 3)
c_p = 0.60 Btu per deg F per lb (see Fig. 3)
D = 4.5 in.
f = 0.02 (see foregoing discussion)
h = 27.5 ft
H_c = 150 Btu per lb (given condition)
$H_B = H_c$ = 150 Btu per lb (given condition)
H_T = 331 Btu per lb (given condition)
k_j = 490 deg Rankine (see Fig. 2)
k_m = 110 (see Fig. 5)
l_t = 27 ft
n_p = 2 tubes in parallel
n_v = 3 velocity heads per return header
U = 11,700 Btu per hr absorbed per sq ft of inside tube area
v_w = 0.025 cu ft per lb (assumed to be constant)
W = 140,000 lb per hr
Z = 0.9 (assumed to be constant

Substituting these values in Equation [26] gives

$$\frac{dP}{dH} = \left[\left(\frac{12{,}820}{11{,}700}\right)\left(0.02 + \frac{3 \times 4.5}{12 \times 27}\right)\left(\frac{140{,}000}{1000 \times 2(4.5)^2}\right)^3 \left\{v_v + (1 - F_v)\,0.025\right\}\right] + \left[\left(\frac{0.56}{490 \times 0.82}\right)\left(\frac{140{,}000}{1000 \times 2(4.5)^2}\right)^2 \left\{X - \frac{k_m}{M} v_v - 0.025\right\}\right] + \left[\frac{27.5}{144(331 - 150)\left\{v_v + (1 - F_v)0.025\right\}}\right]$$

Consolidating constants, the equation then becomes

$$\frac{dP}{dH} = \left[2.79\left\{v_v + 0.025(1 - F_v)\right\}\right] + \left[0.0166\left\{X - \frac{110}{M} v_v - 0.025\right\}\right] + \left[\frac{0.00105}{v_v + 0.025(1 - F_v)}\right]$$

The first step is to assume various values of constant pressure P and, for each of these values of P, assume various values of H, as shown in columns 1 and 2 of Table 1. Actually, in practice it is only necessary to assume two values of H for each given pressure since, as stated, the curves are nearly straight lines, so that two points are sufficient. In Table 1 more than two values of H have been carried through in the calculations for two given pressures to show how much the intermediate calculated points deviate from the straight line. From the Cox chart, Fig. 4, the value of T_i for each of the assumed pressures is then selected, as shown in column 3 of Table 1.

The next step is to solve for F_v, which can be done with the aid of Equation [10] which, with the proper values substituted, will read

$$490 \times 0.82 F_v = (H - 0.60 T_i + 325)$$

or

$$F_v = \frac{(H - 0.60\,T_i + 325)}{402}$$

The solution for F_v is carried through in columns 4, 5, and 6 of Table 1. From there on, the procedure of calculating the pressure-drop gradients can be clearly followed through from column to column. The resultant total pressure gradients are shown in column 18 and are plotted in Fig. 8. As has been mentioned, and as can be seen from the results listed in Table 1, the velocity-head and static-head terms can be neglected, in which case the work is reduced somewhat, except, of course, it will then be necessary to make an over-all correction for these values.

The pressure gradients, shown in Fig. 8, are then integrated graphically in accordance with the procedure discussed in connection with Fig. 1. The procedure can perhaps be somewhat better understood by following through Table 2, and the actual furnace-pressure curve shown in Fig. 8. The starting point is the given outlet pressure of 32 psi abs. The furnace-inlet pressure arrived at is 144.6 psi abs.

After the pressure gradient has once been established, it is then a simple matter to establish the fraction vaporized and the temperature of the oil at the various points within the furnace by the aid of Equations [10] and [6], respectively. This is done in Table 3 and the results are plotted in Fig. 8.

The foregoing outlined procedure of calculating pressure drops has been used by the authors in the design of several furnaces during the last few years. The resultant actual total pressure drops have in each case checked within a very few per cent of the values calculated by the foregoing procedure. While the authors have not yet had any occasion to apply this procedure to evaporators and other similar equipment, there appears to be no reason why it should not work equally well for such cases.

Discussion

L. M. K. Boelter.[4] This paper represents another step toward the solution of nonisothermal two-phase flow pressure-drop problems. A tentative analytical solution indicates that the pressure drop depends, among others, on the dimensionless modulus

$$\mathbf{R}_g \cdot \frac{\nu_g}{\nu_l} \cdot \frac{W_g}{W_l}$$

where

ν_g = kinematic viscosity of gaseous phase
ν_l = kinematic viscosity of liquid phase
W_g = weight rate of gas
W_l = weight rate of liquid
$\mathbf{R}_g$ = Reynolds modulus of the gas

Thus the procedure outlined by the authors for determination of the friction factor receives partial analytical confirmation.

[3] "Pressure Drop Accompanying Two-Component Flow Through Pipes," by L. M. K. Boelter and R. H. Kepner, *Industrial and Engineering Chemistry*, vol. 31, 1939, pp. 426–434.

[4] Professor of Mechanical Engineering, University of California, Berkeley, Calif. Mem. A.S.M.E.

Vaporization Inside Horizontal Tubes—II Benzene-Oil Mixtures

By W. H. McADAMS,[1] W. K. WOODS,[2] and L. C. HEROMAN, JR.[3]

This paper reports an investigation carried out to determine heat-transfer coefficients and pressure drops for mixtures of benzene and lubricating oil flowing inside a heated horizontal tube, and also includes an analysis of the pressure drops for the runs previously reported (1)[4] for the flow of benzene and of water. The present data cover the following ranges: Velocity, 0.4 to 1.0 fps at the inlet and 16 to 200 fps at the outlet; feed composition, 13 to 94 weight per cent benzene; gage steam pressures, 2 to 120 psi; product compositions, 4 to 76 weight per cent benzene; total pressure drops, 1 to 12 psi. Average over-all coefficients of heat transfer, in Btu per hr per sq ft per deg F, range from 40 to 140 in the preheating section, and 45 to 470 in the boiling section. For a given feed composition the average coefficients per pass in the boiling section increase as vaporization progresses, but pass through a maximum and decrease due to depletion of volatile solvent in the liquid phase. When the same data are grouped by composition of the liquid phase, rather than that of the feed, curves are obtained which are very similar to those obtained for pure liquids.

Nomenclature

THE following nomenclature is used in this paper:

A = area of inside heating surface, sq ft
C_p = specific heat, Btu per lb per deg F
D = diameter, inside, ft
DG/μ = Reynolds number, dimensionless, $= 4w/\pi D\mu$
F = friction, ft-lb per lb
f' = apparent friction factor, Equation [1], dimensionless; f'_m is mean value for one pass; f_i friction factor for single-phase flow based on $4w/\pi D\mu$; at $y = 0$, μ is that of the liquid; at $y = 1$, μ is that of the vapor. For the benzene-oil runs, the length mean μ of the liquid in the preheating section was used to obtain an estimate of f_i
G = mass velocity, lb per hr per sq ft, or lb per sec per sq ft
g_c = conversion factor = 32.2 lb × ft per (sec²) (force-pounds)
h = individual coefficient from inside wall to fluid inside tube, Btu per hr per sq ft per deg F
k = thermal conductivity of liquid, Btu per (hr) (sq ft) (deg F per ft)
L = equivalent frictional length, taken as 14 ft per pass for second, third, and fourth passes, and 12 ft for first pass
L_p = perimeter, circumference, ft
P = gage pressure of steam in jackets, psi
p = absolute pressure inside tube, force-pounds per sq ft; p' in cm of mercury, absolute
q = rate of heat flow, Btu per hr
q/A = local flux, Btu per hr per sq ft of inside surface
$(q/A)_m$ = average flux in boiling section, up to any y
R = gas constant = pv/T
S = total cross section, sq ft
T = absolute bulk temperature of fluid in tube, deg F absolute; T_m is taken midway through a pass
t_m = temperature, deg C, midway through a pass
U = over-all coefficient of heat transfer, Btu per hr per sq ft (inside) per deg F length-mean difference steam to fluid; substantially equal to h in benzene-oil runs. U and U_m refer to local and mean values in boiling section, respectively, U_p to preheating section
u = average velocity of fluid in tubes, fps
v = specific volume of mixture, cu ft per lb
v_l = specific volume of liquid, cu ft per lb
v_g = specific volume of vapor, cu ft per lb, v_{g1} at entrance to a pass, v_{g2} at entrance to next pass; $v_{gs} = 2RT_m/(p_1 + p_2)$, cu ft per lb of vapor
w = mass rate of flow inside tube, lb per hr
x = weight fraction of benzene in oil; x_1 entering a pass, x_2 entering next pass, x_m midway through a pass, x_0 for feed to first pass
y = cumulative weight fraction of feed in vapor state, dimensionless; y_1 at entrance to a pass, y_2 at entrance to next pass, y_m midway through a pass
Δp = observed decrease in absolute pressure from entrance to one pass to entrance to next, force-pounds per sq ft; $\Delta p'$ in cm mercury
Δt = over-all temperature difference in deg F; Δt_m is length-mean value
μ = viscosity of liquid at bulk temperature, lb per hr per ft; μ', in centipoises; μ'_p, length-mean value in preheating section, centipoises
π = 3.1416
τ = drag, pounds force

Procedure for Testing Benzene-Oil Mixtures

Results of tests on boiling benzene and boiling water in a four-pass, horizontal-tube evaporator have been presented previously (1). It is the purpose of this paper to give the results of tests on boiling mixtures of benzene and lubricating oil. An analysis of the pressure drops for all runs is also included.

The oil used in the investigation was a finished propane-treated bright stock of viscosity S.A.E. 50, and gravity 25.7 deg A.P.I. No light ends could be detected by steam distillation. Liquid viscosities for benzene-oil mixtures were obtained experimentally in a Hepler (falling-ball) viscosimeter at temperatures of 55 C, and less, were extrapolated to 3.7 centistokes by A.S.T.M.-

[1] Professor, Chemical Engineering, Massachusetts Institute of Technology, Cambridge, Mass.
[2] Technical Division, Engineering Department, Experimental Station, E. I. du Pont de Nemours & Company, Wilmington, Del.
[3] Technical Division, Process Engineering Department, Standard Oil Company of Louisiana, Baton Rouge, La.
[4] Numbers in parentheses refer to the Bibliography at the end of the paper.

Contributed by the Heat Transfer Division and presented at the Semi-Annual Meeting, Kansas City, Mo., June 16–19, 1941, of The American Society of Mechanical Engineers.

Note: Statements and opinions advanced in papers are to be understood as individual expressions of their authors, and not those of the Society.

chart D341-32T, and were finally extrapolated to lower viscosities by interpolating between the known viscosity of benzene at high temperatures and the specification for the oil (164 Saybolt Universal sec at 210 F) Fig. 1.

Only minor modifications had to be made in the apparatus prior to runs on benzene-oil mixtures. It was necessary to pass the hot liquid oil from the vapor-liquid separator through a cooler before the oil could be mixed with the condensed benzene. The frictional resistance of the cooler created a partial vacuum on the intake side of the pump, and caused some air to flow into the oil through leaks in the pipe connections. Accordingly, a large

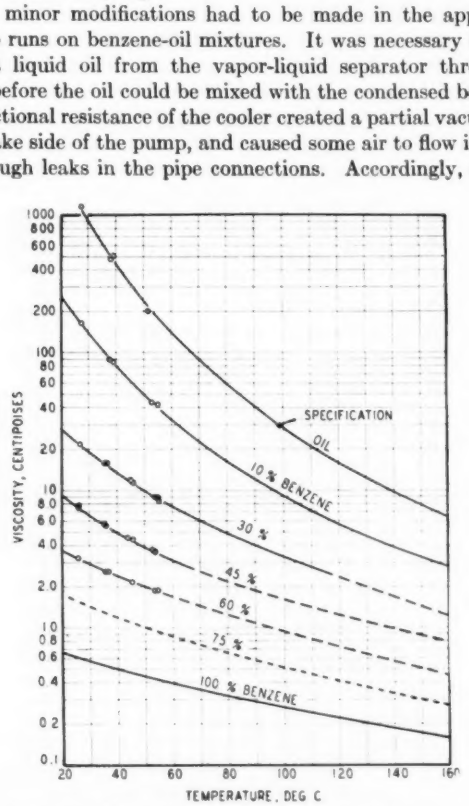


FIG. 1 VISCOSITY-TEMPERATURE CURVES FOR MIXTURES OF BENZENE AND FINISHED PROPANE—TREATED BRIGHT STOCK, S.A.E. 50; GRAVITY 25.7 DEG A.P.I. CURVE FOR BENZENE FROM BIBLIOGRAPHY REFERENCE 2

vertical drum was installed between the outlet of the pump and the feed orifice in order to allow this air to separate and be vented through a valve in the top of the drum, before the feed entered the heating section.

Samples of approximately 300 cu cm were withdrawn from the vapor-liquid separator and from the drum in the feed line during each run. One half of each sample was withdrawn at the start of the run, and the remainder at the end of the run; 100 cu cm of each sample was analyzed for volume per cent benzene by simple distillation at atmospheric pressure. The analysis was accurate to 0.5 cu cm of benzene. However, the product sample was taken from the separator at a slightly lower pressure than that at the end of the last steam-jacketed section, so a small amount of benzene may have flashed, causing the reported amount of benzene in the product to be slightly low. In mixing standard samples of benzene and oil, it was found that the volumes were substantially additive. The difference in density between the oil and the benzene is so small that analysis on a volume basis is substantially the same as analysis on a weight basis. The benzene distilled from the heavy oil was water-white.

An over-all heat balance was obtained from the rate of condensation of steam and from the rate of flow and temperature rise of the water in the condenser and in the cooler. The heat balances, corrected for estimated heat losses, checked within 7 per cent at all times, with an arithmetic average of very close to zero. The heat picked up by the cooler varied from 5 to 78 per cent of the total heat transfer. The feed rate reported in the tables was determined from heat and material balances on the test section; the feed rate indicated by the orifice usually checked closely with that from the heat and material balance.

Atmospheric boiling points were determined experimentally for various concentrations of benzene in oil. These data were smoothed by Raoult's law which indicated that the effective molecular weight was a function of the benzene concentration. For pressures above atmospheric the relation between boiling temperature and benzene concentration was calculated from Raoult's law, which involves the vapor pressure of pure benzene, assuming the effective molecular weight of the oil to be independent of temperature. The start of the boiling section for each heat-transfer run could then be estimated, since the initial boiling temperature of the feed was known for the pressure existing at the end of each pass and could be interpolated for the intermediate jackets. A fluid-temperature curve was then interpolated, pass-

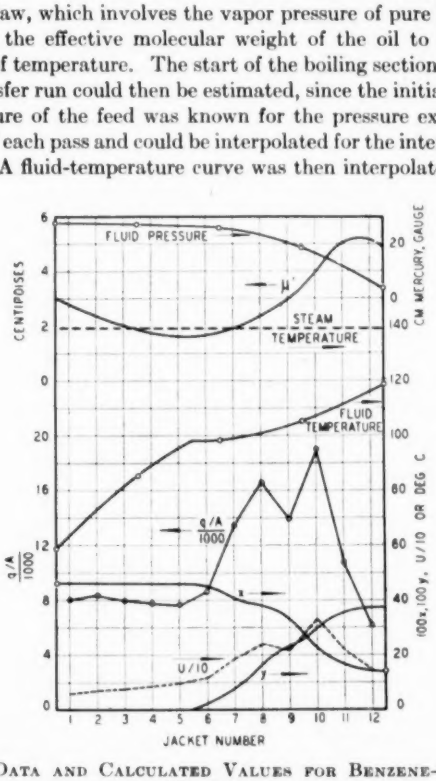


FIG. 2 DATA AND CALCULATED VALUES FOR BENZENE-OIL RUN NO. BO-22

(1015 lb per hr of feed containing 46 weight per cent benzene; steam gage pressure, 35.5 psi.)

ing through this initial boiling point and thence through the successive observed temperatures of the fluid at the end of each pass. Based on this temperature gradient, the rate of transfer of latent heat in any jacket was obtained by subtracting the rate of transfer of sensible heat from the total heat-transfer rate, based on condensate rates. From the initial feed composition, the feed rate, and the latent heat transferred, both the cumulative weight per cent $100y$ of the feed vaporized, and the weight per cent of benzene $100x$ remaining in the liquid phase at discharge from any specified steam-jacketed section, were calculated. The local over-all coefficients U in Btu per hr per sq ft per deg F were calculated by dividing the heat flux q/A in each jacket by the difference between the saturation temperature of the steam and the average fluid temperature.

RESULTS OF RUNS ON BOILING BENZENE-OIL MIXTURES

Local Coefficients. The results of a representative run on boiling a mixture of benzene and oil are shown in Fig. 2. In contrast with the runs on benzene or on water, it is noted that a progressive increase in fluid temperature occurs throughout the apparatus. While the decreasing static pressure through the apparatus tends to lower the boiling point of the liquid, the decrease in concentra-

TABLE 1 OVER-ALL RESULTS FOR BENZENE-OIL RUNS[a]

(Steam used in all twelve jackets in all runs)[b]

Run no.	Feed rate, lb per hr	Weight per cent benzene: Feed	Weight per cent benzene: Product	Feed temp, C	Steam pressure, psi gage	Heat[c] transfer, Btu per hr	Weight per cent of feed vaporized	U_p in preheating section	μ'_p centi-poises[d]	Start of boiling section, per cent of jacket	Total pressure drop,[e] cm of Hg
BO-1	702	90.5	60.5	53.0	1.8	105000	76.0	123	0.49	80 of J 3	17.9
BO-2	775	93.5	75.5	55.5	1.9	115000	73.5	131	0.45	60 of J 3	26.3
BO-6	498	88.5	10.5	46.0	26.0	102000	87.0	...	....	60 of J 1	33.6
BO-5	545	70.5	23.0	38.5	9.1	83000	62.0	87	1.00	20 of J 4	17.4
BO-24	884	76.0	7.0	56.0	74.0	169000	74.0	138	0.73	50 of J 2	....
BO-23	996	62.0	13.0	52.0	37.0	145000	56.0	97	1.3	20 of J 5	38.5
BO-21	990	56.5	4.0	66.0	120.0	170000	55.0	107	1.40	60 of J 2	60.4
BO-22	1015	46.0	14.0	58.5	35.5	111000	37.0	77	2.1	End of J 5	24.4
BO-17	1020	45.0	8.0	65.5	53.3	123000	40.0	79	2.2	60 of J 4	32.8
BO-16	1011	41.0	6.0	70.0	78.3	123000	37.0	79	2.4	10 of J 4	34.7
BO-20	1050	43.0	4.0	70.0	120.0	143000	40.5	101	2.3	30 of J 3	45.2
BO-7	984	33.5	18.5	59.0	22.0	69000	18.5	65	4.2	60 of J 7	10.2
BO-13	1080	25.7	15.4	68.0	36.0	62000	12.0	53	5.2	20 of J 9	11.0
BO-14	1093	31.3	10.7	68.0	52.0	86000	23.0	55	4.2	60 of J 6	16.5
BO-15	970	30.0	7.5	74.0	80.0	101000	24.0	58	4.1	90 of J 4	20.7
BO-19	1050	29.0	4.0	79.0	119.0	113000	26.0	76	4.0	80 of J 3	28.4
BO-8	1008	21.0	17.0	68.5	38.5	47000	5.0	43	7.0	60 of J 8	4.1
BO-11	1078	16.0	9.0	78.5	70.0	59000	8.0	59	7.3	60 of J 7	4.6
BO-18	1025	13.0	6.0	85.0	119.0	75000	7.5	74	6.6	End of J 5	9.7

[a] Refer to Bibliography (3).
[b] Inside heated area of copper pipe = 0.88 sq ft per jacket.
[c] Based on steam-condensate measurements, for all twelve jackets.
[d] Length-mean value for preheating section.
[e] Over-all pressure drop for all four passes (see also Table 2).

TABLE 2[a] RESULTS OF HEAT-TRANSFER COEFFICIENT CALCULATIONS

Run no.	Pass no.	U_m	Δt_m, deg F	$100x_m$	$100y_1$	$100(y_2 - y_1)$	$100y_m$	p'_a, cm of Hg	$\Delta p'$, cm of Hg	t_m, deg C	$1000/f'_m$
BO-1	2	160	32	90	1	9	5	97	1.0	88	6.1[b]
	3	360	32	88	10	27	19	95	4.8	88	9.9
	4	470	35	75	37	39	61	87	12.1	85	8.3
BO-2	2	171	31	93	2	8	6	105	0.6	88	1.2[b]
	3	410	31	92	10	27	21	101	9.5	88	18.7
	4	460	36	83	37	36	61	88	16.1	86	9.3
BO-6	1	396	79	81	0	73	41	109	5.6	95	13.8[c]
	2	147	38	33	73	12	83	103	7.6	111	10.1
	3	120	12	16	85	2	86	94	9.9	126	11.5
	4	110	3	10	87	0	87	83	10.5	131	10.6
BO-5	2	134	49	68	0	18	8	92	1.8	89	13.9[b]
	3	245	45	55	18	31	34	88	4.7	90	9.2
	4	170	34	29	49	13	58	82	9.3	96	11.9
BO-24	2	280	76	31	41	28	65	...	....	116	....
	3	195	37	15	69	3	72	126	27.7	139	15.6
	4	190	16	10	72	2	73	98	29.0	150	11.8
BO-23	3	325	66	38	17	30	38	110	11.9	103	7.2
	4	225	44	16	47	9	55	94	21.2	116	8.8
BO-21	2	265	90	21	24	26	45	133	13.1	124	8.8
	3	196	42	13	50	1	50	117	18.8	153	10.8
	4	210	22	5	51	4	54	96	24.0	163	9.7
BO-22	3	215	68	36	5	20	16	100	7.3	101	9.1
	4	240	50	17	25	12	35	88	15.2	111	8.9
BO-17	2	163	87	41	0	17	7	111	3.6	102	8.1
	3	235	66	21	17	18	30	103	11.6	113	8.6
	4	200	38	11	35	5	38	89	16.8	130	9.3
BO-16	2	171	99	32	0	24	14	111	5.3	104	6.3
	3	191	68	14	24	9	31	102	12.5	122	9.7
	4	196	36	6	33	4	37	88	15.9	141	8.9
BO-20	2	220	101	18	11	25	30	118	9.8	117	7.5
	3	181	55	9	36	2	37	107	14.5	146	9.3
	4	200	28	4	38	2	40	90	18.1	159	8.6
BO-7	3	93	59	32	0	7	2	85	2.1	96	15.5[b]
	4	177	49	23	7	12	14	80	6.5	101	8.2
BO-13	4	142	60	18	2	10	10	82	7.9	104	13.4
BO-14	3	121	79	26	2	10	7	89	4.3	105	8.5
	4	183	58	13	12	11	21	83	10.6	116	7.7
BO-15	2	89	102	28	0	9	2	96	2.3	106	13.5[b]
	3	150	79	16	9	11	16	92	7.1	117	9.9
	4	178	46	8	20	4	24	83	10.3	136	9.1
BO-19	2	148	104	20	1	16	12	103	5.2	116	7.5
	3	163	68	9	17	6	22	96	9.5	136	8.9
	4	192	37	4	23	3	26	84	12.0	155	8.2
BO-8	4	63	61	17	2	3	4	79	2.7	107	12.7[b]
BO-11	3	46	72	15	0	2	1	81	0.8	117	12.3[b]
	4	109	61	10	2	6	7	79	3.0	122	5.2
BO-18	3	84	71	9	3	1	4	82	3.2	135	16.4
	4	117	50	7	4	4	7	78	3.3	147	7.7

[a] Based on data of Bibliography (3).
[b] $\Delta p'$ is below 3 cm of mercury, and corresponding values of f'_m are not plotted.
[c] Value of f'_m is based on L of 12 ft, since the first pass did not include a U-bend.

tion of benzene in the liquid more than counterbalances the effect of the pressure drop.

For the run illustrated in Fig. 2, the over-all heat-transfer coefficient in the boiling section starts at 116 in jacket No. 6, passes through a maximum of 330 in jacket No. 10, and then decreases to 147 in jacket No. 12. Not only the heat-transfer coefficients but even the heat flux is larger in the later jackets than in the jacket where boiling begins, despite both the decreasing temperature difference and the increasing viscosity of the liquid. Hence, this initial increase in the heat-transfer coefficient must be ascribed to the turbulence resulting from an increase in the percentage of the feed vaporized.

The operating variables and the over-all results of runs on benzene-oil mixtures are summarized in Table 1. Out of a series of twenty-four runs, four were discarded because of unsatisfactory heat balances, and one because of inaccurate determination of rate of steam condensation in two of the twelve steam jackets. Subsequent to BO-6 all runs were taken at a feed rate close to 1000 lb per hr.

These results, obtained in a given steam-jacketed section are

a function of the distance of that jacket from the entrance to the pass. This function might conceivably be affected by feed rate, feed composition, and steam pressure, as well as being different for different passes. Correlation and presentation of the data are simplified by considering only the over-all results obtained for an entire pass (three jacketed sections).

Average Coefficient for Boiling in Each Pass. The average heat-transfer coefficient U_m for any pass is obtained by dividing the arithmetic average of the heat flux in the three jackets by the length-mean temperature difference in the pass. The results thus calculated are presented in Table 2. The values of $100x_m$ and $100y_m$ are the values existing at the mid-point of the pass, as indicated by graphs, such as Fig. 2. If boiling had not commenced before the end of the first jacket in any pass, the data are not included in Table 2. The heat-transfer coefficients for the preheating section are given in Table 1.

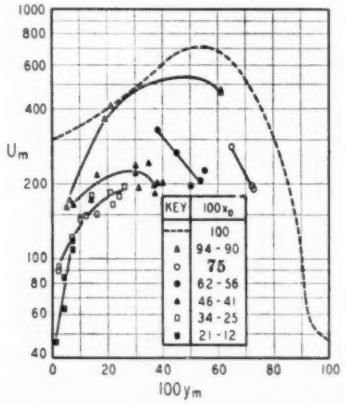


FIG. 3 AVERAGE BOILING COEFFICIENTS FOR EACH PASS, VERSUS $100y_m$, FOR VARIOUS FEED COMPOSITIONS, OMITTING RUNS AT LOW FEED RATES

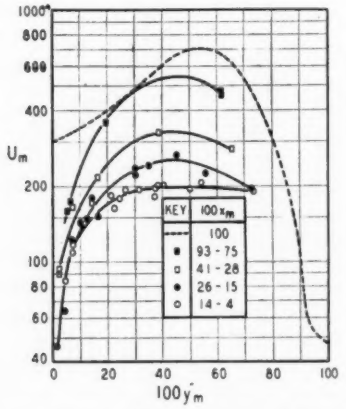


FIG. 4 AVERAGE BOILING COEFFICIENTS FOR EACH PASS, VERSUS $100y_m$, FOR VARIOUS AVERAGE COMPOSITIONS OF LIQUID PHASE MIDWAY THROUGH THE PASS; SAME DATA AS IN FIG. 3

The data of Table 2 are presented in Fig. 3 as a plot of the average heat-transfer coefficient for the pass versus the average cumulative per cent vapor, excluding the data from runs BO-5 and BO-6, which involved considerably lower feed rates. In Fig. 3 symbols are used to designate the various ranges in benzene concentration $100x_0$ of the feed. In general, the coefficient increases with an increase in benzene content of the feed. The plot indicates that the heat-transfer coefficient increases during the initial stages of boiling but subsequently decreases after some critical value of $100y_m$ has been obtained, the critical value of $100y_m$ being a function of the initial feed composition.

Fig. 4 involves the same data as Fig. 3 except that the points are designated, not according to feed composition, but according to average composition $100x_m$ of the liquid phase. The curves of Fig. 4 show a striking similarity to those obtained for pure liquids in this apparatus (1). For a given average composition of liquid, as $100y_m$ increases the coefficient goes through an initial increase. At high values of $100y_m$ (say, greater than 40 per cent) the coefficients may begin to decrease as $100y_m$ increases, due to vapor binding, resulting from insufficient liquid. No data are shown in Figs. 3 and 4 for values of $100y_m$ greater than 73 per cent and, therefore, no extreme cases of vapor binding are involved. There is a tendency for more serious vapor binding to occur when the liquid contains large amounts of benzene.

Fig. 4 is of value primarily because of the light it sheds upon the phenomena; Fig. 3 is the practical plot showing what happens as a given feed is progressively vaporized. For feeds containing 56 to 62 per cent benzene, the coefficient decreases from 320 to 200 as the cumulative vaporization increases from 38 to 54 per

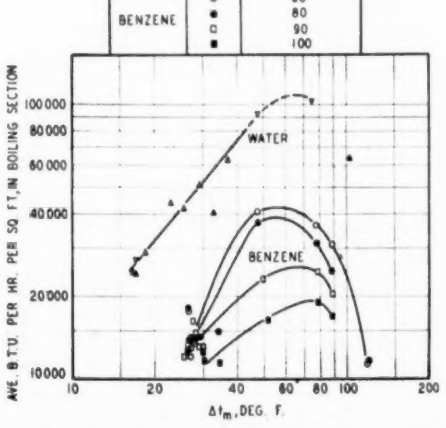


FIG. 5 AVERAGE FLUX IN BOILING SECTIONS VERSUS Δt_m FOR ALL WATER RUNS AND FOR BENZENE RUNS HAVING FEED RATES RANGING FROM 615 TO 618 LB PER HR, FOR VARIOUS CUMULATIVE WEIGHT PER CENT VAPORIZED

(For benzene, hot-wall vapor binding occurs at Δt_m exceeding 55–75 F, depending upon extent of vaporization. Data from Bibliography references 1 and 3.)

cent of the feed. Fig. 4 shows that this decrease in the coefficient is not due to vapor binding, but to the depletion of benzene in the liquid phase, the concentration in the liquid phase decreasing from (roughly) 35 to 10 per cent benzene.

The heat-transfer coefficients obtained in runs BO-5 and BO-6, if plotted in Figs. 3 and 4, would be lower than those shown. It is believed that this is due to the relatively low feed rates (545–498 lb per hr) used in these two runs, compared with feed rates averaging 984 for the other runs.

The minor effect of temperature difference probably results from the fact that the heat transferred not only goes into vaporizing some of the benzene but also into heating the residual liquid and vapor. Since coefficients for sensible-heat transfer are less dependent upon temperature difference, it is rational to believe that if large percentages of the heat transferred are used merely to warm the fluid the effect of temperature difference on the heat-transfer coefficient should be minimized. The heat transfer in this instance is rather different in mechanism from the heat trans-

fer by natural convection to liquids boiling at constant temperature outside of horizontal submerged tubes.

For benzene boiling in the same apparatus, with feed rates ranging from 615 to 818, two types of vapor binding were encountered, as shown in Fig. 5, where average flux, $(q/A)_m = U_m \Delta t_m$, is plotted versus the length mean Δt, for various final values of $100y$. Except at low Δt_m where the results were erratic, for a given final weight per cent vapor, the flux goes through a maximum at a critical value of Δt_m. This is due to the formation of a vapor film on the inside wall of the pipe, and is designated "hot-wall" vapor binding.

For a given Δt_m, say 50 F, the average flux decreases with increase in final per cent vapor by weight. This is due to the formation of spray which, at high values of y, is largely carried by the main stream. Such spray as hits the heated wall is evaporated, but since a considerable fraction of the wall is dry, the effective area is reduced, and the apparent coefficient decreases, being based on the entire area, whether wet or dry. This second phenomenon is designated "dry-wall" vapor binding. A few benzene runs were made at higher and lower feed rates and gave results similar to those in Fig. 5.

The data for all the water runs are shown in the upper part of Fig. 5. Although the data are insufficient to warrant curves for

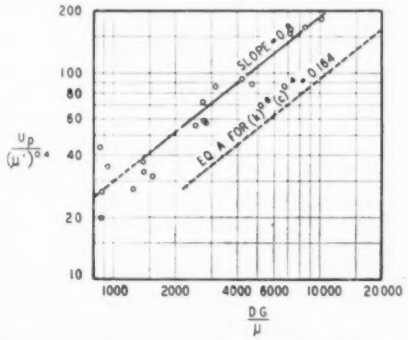


FIG. 6 PREHEATING COEFFICIENTS FOR ALL BENZENE-OIL RUNS, COMPARED WITH EQUATION [A]

various final values of y, it seems likely that dry-wall vapor binding occurred for y of 0.95 to 0.99.

Coefficients in Preheating Section. The warming of fluids inside of pipes, when the temperature of the pipe wall is considerably above the boiling point of the fluid, represents a problem which has not been intensively studied. The problem is especially complicated for the benzene-oil runs, since the Reynolds numbers (860 to 10,000) range from streamline flow, through the critical "dip" region, into turbulent flow. In Fig. 6 the data for the preheating sections are shown for all benzene-oil runs, with $U_p/(\mu')^{0.4}$ plotted versus the Reynolds number based on length-mean viscosity of the main body of the liquid. The dotted line represents (4) the equation

$$\frac{hD}{k} = 0.0225 \left(\frac{DG}{\mu}\right)^{0.8} \left(\frac{C_p \mu}{k}\right)^{0.4} \quad \ldots\ldots\ldots [A]$$

with D taken as 0.0884, k as 0.08, and C_p as 0.48, or any combination of values for k and C_p which make the product of $k^{0.8}$ and $C_p^{0.4}$ equal to 0.164. The solid line through the data gives coefficients twice those from Equation [A]; this may be due to the greater turbulence resulting from the surging flow, and/or to vaporization of benzene in the film next to the hot wall and condensation in the main body of the liquid.

A similar phenomenon was observed in the preheating section of the benzene runs (1).

PRESSURE DROP

In the present apparatus the pressures at a given point fluctuated somewhat with respect to time, as did the nature of the fluid flow. For example, at the end of the first pass where condensate measurements showed a time-average vapor generation equal to 8 per cent by weight of the feed in a certain run on water, photographs, Figs. 10 and 11 of the previous paper (1), taken a few seconds apart showed stratification into vapor and liquid layers in one case, and in the other an intimate mixture of vapor and liquid. At other times, alternate slugs of vapor and liquid flowed from the first pass. However, as the fluid flowed through two additional passes, and condensate measurements from the first three passes showed 47 per cent vapor by weight, drops of liquid were carried as spray in the vapor stream, which now had a velocity of almost 300 fps. Because of the time fluctuations in the pressures and in the mechanism of the fluid flow the following simplifying assumptions were made:

1 Vapor and liquid flow at the same velocity. The error introduced by this assumption is the greatest at low velocity of the mixture, where stratification into two layers occurs.[5]

2 The volume occupied by the liquid is negligible in relation to that of the vapor. This amounts to discarding the last term in the equation

$$v = yv_g + (1 - y)v_f$$

where v is the volume of 1 lb of vapor-liquid mixture, y is the weight fraction of vapor in the mixture, v_g is the specific volume of the vapor, and v_f is the specific volume of the liquid. The term $(1 - y)v_f$ is not negligible, compared with yv_g at small values of y, but in this range a substantial error is introduced by the assumption of no slip between vapor and liquid.

3 The wall drag τ may be correlated by an equation of the Fanning type, without allowance for any wall traction resulting from vaporization

$$d\tau = (f')(L_p dL)\frac{u^2}{2g_c v}, \text{ or } dF = \frac{v}{S}\,d\tau = \frac{f' dL u^2}{2g_c\left(\frac{S}{L_p}\right)}$$

which for a round pipe of diameter D reduces to

$$dF = \frac{4f' dL u^2}{2g_c D} \quad \ldots\ldots\ldots [1]$$

wherein f' is the apparent friction factor (dimensionless), L_p is the circumference or perimeter, S is the cross section, u is the average velocity of the mixture at the particular length L, and g_c is a conversion factor (gross dimensions ML/FT^2).

The familiar energy balance, with all terms having dimensions of FL/M, is

$$-vdp = \frac{udu}{\alpha g_c} + dF \quad \ldots\ldots\ldots [2]^*$$

wherein the dimensionless term α allows for nonuniformity in velocity distribution. (As usual for turbulent flow, this term was assumed equal to 1.0.)

By definition

$$u = Gv \quad \ldots\ldots\ldots [3]$$

where G is the mass velocity, equal to w/S, which remains constant. Assumption 2 gives

$$v = yv_g \quad \ldots\ldots\ldots [4]$$

[5] Isothermal runs, wherein no phase change was occurring, would simplify the problem so that estimates of the slip could be made, but in nonisothermal runs the ratio of velocities of vapor and liquid probably changes as vapor generation proceeds.

* In analyzing the pressure gradient for vaporization of a liquid flowing in a heated tube, R. Hoger (*Die Wärme*, vol. 63, 1940, pp. 209–212) employed essentially Equations [1] and [2] but ignored kinetic effects, which are not negligible for conditions encountered in this investigation.

Equations [1, 2, 3, and 4] may be combined, and rearranged, noting that du equals $Gy\,dv_g + Gv_g\,dy$, giving

$$-\frac{dp}{v_g} = \frac{G^2}{g_c}\,dy + y\,\frac{dv_g}{v_g} + \frac{2f'}{D}\,y\,dL \quad \ldots\ldots\ldots [5]$$

Equation [5] was multiplied by $D/2y$, and integrated between sections 1 and 2, calling y, T, and f' constant at y_m, T_m, and f'_m, respectively, giving

$$\frac{g_c D(p_1 - p_2)(p_1 + p_2)}{4G^2 R T_m y_m} = \frac{g_c D(\Delta p)}{2G^2 v_{g_a} y_m}$$

$$= \frac{D}{2}\ln\frac{y_2}{y_1} + \frac{D}{2}\ln\frac{v_{g1}}{v_{g2}} + f'_m L \quad \ldots [6]$$

Values of f'_m were then calculated from the original data and calculated values, using Equation [6], $D = 0.0884$ ft, $L = 14$ ft (which included the equivalent frictional length of the U-bend). The mean value of y for the pass was read from plot of y versus jacket number, at the mid-point of the three jackets; the values

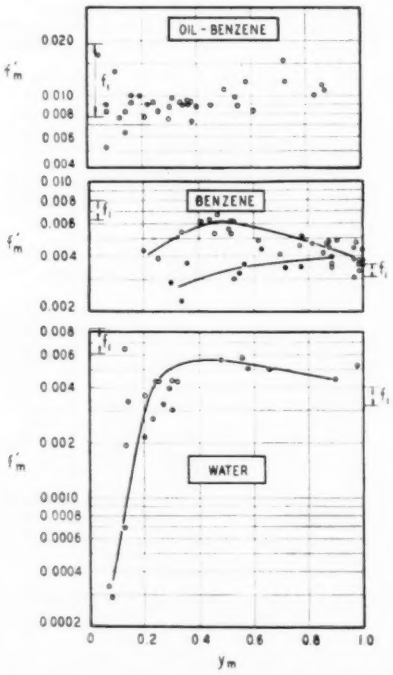


FIG. 7 APPARENT FRICTION FACTORS VERSUS $100y_m$
(Black circles designate benzene runs wherein hot-wall vapor binding occurs.)

of v_{g_a} were evaluated at the arithmetic-mean pressure as called for by Equation [6], and at T taken midway through the pass. The vapors at these moderate pressures were assumed to follow the gas laws. The values of the friction factor f'_m are shown in Tables 2 and 3. When y is small, there is a substantial percentage of error in estimating y_m which introduces a yet larger error in f'_m, which is obtained by subtracting two kinetic-energy corrections (one for increase in y and the other for increase in volume due to change in T and p) from a term containing the observed pressure drop divided by y_m; unfortunately, when y is small both Δp and y_m are small, hence values of f'_m at low values of y have poor precision. The fluctuation in pressure introduces a substantial percentage of error in Δp, when the latter is small; consequently, for the passes in which $\Delta p'$ did not exceed 3 cm of mercury, values of f'_m were not plotted, although they are given in the tables.

Fig. 7 shows the values of the apparent friction factors, plotted

TABLE 3[a] PRESSURE-DROP DATA AND APPARENT FRICTION FACTORS FOR RUNS WITH BENZENE AND WITH WATER

Run no.	Pass no.	p', cm of Hg	$\Delta p'$, cm of Hg	y_1	$(y_2 - y_1)$	y_m	t_m, deg C	1000 f'_m
			BENZENE RUNS					
B6	2	99.0	2.8	0.08	0.13	0.14	90	2.8[b]
	3	94.9	5.4	0.21	0.19	0.30	88	2.9
	4	86.8	10.8	0.40	0.26	0.55	85	3.2
B3	2	104.9	2.4	0.09	0.15	0.17	91	1.6[b]
	3	100.8	5.9	0.24	0.30	0.34	89	2.3
	4	91.2	13.3	0.54	0.28	0.72	85	3.4
B2	2	109.9	9.8	0.48	0.27	0.70	93	4.1
	3	99.6	10.9	0.75	0.19	0.89	90	3.4
	4	88.2	11.9	0.94	0.06	0.98	85	3.2
B4	2	101.7	1.5	0.004	0.11	0.05	90	0.8[b]
	3	97.8	6.3	0.11	0.22	0.20	89	4.3
	4	88.4	12.4	0.33	0.33	0.53	85	3.0
B7A	3	102.6	6.3	0.14	0.26	0.25	90	3.8
	4	90.9	17.0	0.40	0.33	0.62	87	4.8
B11	2	98.3	4.5	0.26	0.20	0.36	89	3.6
	3	92.8	6.5	0.46	0.18	0.57	87	3.6
	4	84.7	9.6	0.64	0.23	0.78	84	3.4
B10	2	97.9	7.4	0.57	0.28	0.77	91	4.6
	3	91.1	6.3	0.85	0.15	0.97	88	3.0
	4	83.9	8.0	1.00	0.0	1.00	99	3.8
B9	2	101.7	8.5	0.67	0.26	0.87	89	4.8
	3	93.1	8.7	0.93	0.07	1.00	86	4.4
	4	84.4	8.7	1.00	0.0	1.00	110	3.8
B8	2	103.5	8.9	0.59	0.28	0.82	90	4.6
	3	96.7	9.3	0.87	0.12	0.96	92	4.2
	4	85.1	9.3	0.99	0.01	1.00	114	3.6
B1	2	94.4	5.6	0.21	0.46	0.44	89	6.4
	3	88.1	7.0	0.67	0.26	0.88	86	4.4
	4	81.6	6.1	0.93	0.07	0.99	82	3.6
B5	2	95.2	1.3	0.08	0.20	0.18	89	1.4
	3	91.6	5.9	0.28	0.43	0.46	87	5.2
	4	84.1	9.1	0.71	0.25	0.91	84	4.8
B7	2	95.6	1.7	0.05	0.21	0.15	88	2.2[b]
	3	91.4	6.7	0.26	0.38	0.41	87	6.0
	4	83.5	9.1	0.64	0.27	0.86	84	4.2
B14	2	95.8	1.3	0.02	0.18	0.10	88	1.6[b]
	3	92.4	5.4	0.20	0.34	0.34	87	5.4
	4	84.5	10.4	0.54	0.31	0.78	84	5.1
B1A	2	97.6	1.8	0.07	0.23	0.16	89	2.0[b]
	3	92.7	8.1	0.30	0.41	0.47	87	6.7
	4	83.6	10.1	0.71	0.20	0.88	83	4.8
B4A	2	96.7	1.4	0.08	0.25	0.19	89	0.5[b]
	3	92.1	7.9	0.33	0.46	0.54	87	6.0
	4	83.4	9.4	0.79	0.21	0.97	82	4.4
B6A	2	97.1	1.1	0.07	0.25	0.18	89	—0.9[b]
	3	92.2	8.7	0.32	0.42	0.52	87	6.2
	4	83.7	8.3	0.74	0.18	0.89	85	3.6
B12	2	84.3	1.7	0.27	0.23	0.39	84	3.7[b]
	3	82.0	2.8	0.50	0.22	0.63	83	4.4
	4	78.8	3.7	0.72	0.26	0.89	82	3.9
B2A	2	86.1	3.4	0.25	0.58	0.51	85	5.6
	3	82.4	4.0	0.83	0.17	0.98	83	4.8
	4	78.8	3.2	1.00	0.0	1.00	92	3.9
B5A	2	86.8	3.6	0.25	0.57	0.52	85	5.3
	3	82.8	4.4	0.82	0.18	0.98	84	4.8
	4	79.0	3.2	1.00	0.0	1.00	96	3.5
B13	2	79.5	0.9	0.33	0.27	0.47	82	3.7[b]
	3	78.4	1.3	0.60	0.19	0.71	81	4.4
	4	77.0	1.5	0.79	0.21	0.94	80	3.8
B3A	2	79.5	1.8	0.64	0.36	0.95	83	4.5[b]
	3	78.0	1.2	1.00	0.00	1.00	93	3.5[b]
	4	76.8	1.2	1.00	0.00	1.00	99	3.4[b]
			WATER RUNS					
W5	2	135	2.8	0.03	0.08	0.07	117	—0.1[b]
	3	129	11.3	0.11	0.12	0.17	115	3.2
	4	110	29.7	0.23	0.18	0.32	110	4.3
W7	2	139	2.9	0.01	0.07	0.05	118	0.5[b]
	3	132	15.5	0.08	0.11	0.13	116	6.7
	4	108	30.2	0.19	0.20	0.29	110	4.0
W9	3	116	6.3[b]	0.03	0.11	0.08	112	0.3
	4	104	24.6	0.14	0.18	0.23	109	2.7
W10	4	95	16.3	0.10	0.21	0.20	106	2.0
	2	103	1.6	0.0	0.04	0.02	109	—1.3[b]
	3	100	3.6	0.04	0.06	0.07	108	0.3
	4	94	14.7	0.10	0.10	0.15	106	3.1
W13	4	112	33.8	0.38	0.38	0.66	111	5.0
W11	4	108	28.2	0.24	0.43	0.48	109	5.6
W6	2	98	1.0	0.02	0.06	0.05	108	—1.1[b]
	3	96	3.1	0.08	0.10	0.13	107	0.7
	4	90	13.1	0.18	0.15	0.25	105	4.3
W2	2	100	1.0	0.02	0.07	0.06	108	—1.4[b]
	3	97	4.1	0.09	0.09	0.13	107	1.9
	4	90	12.9	0.18	0.15	0.24	105	4.3
W8	3	93	2.1	0.03	0.09	0.08	106	—0.1[b]
	4	88	9.8	0.12	0.15	0.20	104	3.6
W12	4	86	12.9	0.82	0.18	0.98	103	5.2
W4	2	110	4.5	0.17	0.26	0.30	110	3.0
	3	103	11.0	0.43	0.32	0.58	108	5.0
	4	89	15.6	0.75	0.20	0.90	104	4.4
W1	2	96	1.2	0.06	0.14	0.13	107	0.8[b]
	3	93	4.7	0.20	0.23	0.31	106	4.2
	4	86	10.4	0.43	0.26	0.56	103	5.8

[a] Based on data of Bibliography (3). Additional data are given in Tables 1 and 2 of Bibliography (1).
[b] $\Delta p'$ is below 3 cm of mercury and corresponding f'_m is not plotted.

versus y_m on semilogarithmic paper. The abnormally low friction factors for water, at values of y of say 0.2 and less, are believed to be due to the error introduced by the assumption that the residual liquid travels at the same speed as the vapor, whereas, at the low values of y, apparently the liquid phase travels at only a fraction of the speed of the vapor. It should be recalled that f'_m was computed by deducting terms representing kinetic-energy changes for both liquid and vapor from the pressure-drop term. Hence, if the deduction for the kinetic energy of the liquid is excessive, the computed value of f'_m will be too low, especially in the range where the weight fraction of liquid is high. The range of ordinates, at y_m of 1, show the usual friction factors (5) f_i for isothermal flow of vapor, and the corresponding range at y_m of 0 shows the usual values of f_i for isothermal flow of liquid. In the range of y_m from 0.4 to 1, the values of f'_m for water are not much higher than would be obtained by a linear interpolation between the terminal values of f_i.

The results for benzene, shown by the open circles of Fig. 7, where the surface was not vapor bound, are similar to those for water. The benzene runs made with a vapor-bound surface (due to excessive wall temperature), shown by the black circles, give lower values of f'_m, probably due to the fact that viscosity of the vapor film is less than that of a liquid film of the same substance.

The values of f'_m for the benzene-oil runs, shown in the top section of Fig. 7, are quite erratic. This results from the fact that the range of Reynolds numbers for all liquid (at $y_m = 0$) is greater than for benzene. Because of the wide variation in benzene content of the feed, f_i ranges from 0.0076 to 0.019. Since the oil could not be vaporized under the conditions used, the f_i range is not shown for y_m of 1.0. The values of f'_m average 0.01, but would doubtless decrease at high Reynolds numbers characteristic of high velocity of flow in pipe stills. A correlation of the values of f'_m might be had in terms of a Reynolds number based on μ at the wall, which would be the viscosity at the wall temperature, of the equilibrium liquid at the existing temperature and pressure. However, it seemed unsafe to extrapolate the viscosities from 55 C to temperatures as high as 176 C.

Heat Transfer Versus Pressure Drop. Fig. 8 shows a plot of pressure drop per pass as abscissas and the mean U per pass as ordinates, and includes preheating data for all runs, and data for the boiling section for those passes where the final y did not exceed 0.74 for all the water runs, those benzene runs where serious hot-wall vapor binding did not occur (i.e., benzene runs where gage steam pressures were below 35 psi), and all the benzene-oil runs. For a given $\Delta p'$, the values of U_m are highest for water, next highest for benzene with moderate Δt_m, and lowest for benzene-oil mixtures, depending upon $100x_m$, the per cent benzene in the liquid midway through the pass. The benzene-oil runs could also be subdivided as to viscosity of the liquid. For a given liquid the curves are flat, and where binding is encountered at high values of $\Delta p'$, the points fall below the curve.

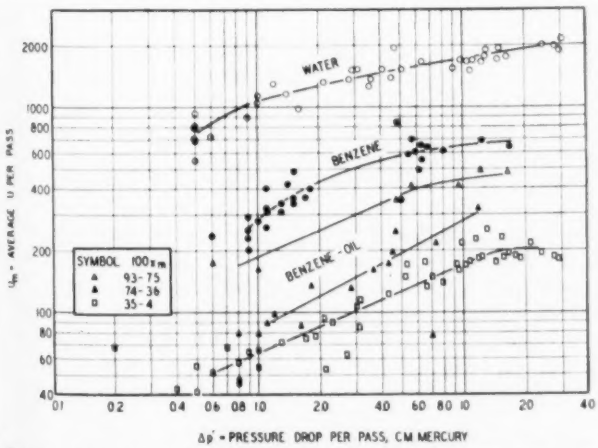


FIG. 8 AVERAGE COEFFICIENTS PER PASS IN PREHEATING AND BOILING SECTIONS, PLOTTED VERSUS PRESSURE DROP PER PASS (Curves for all water runs, all benzene runs for steam pressures below 35 psi, and all benzene-oil runs; omitting runs wherein the final y exceeds 0.74.)

CONCLUSIONS

1 The coefficients for preheating benzene-oil mixtures are considerably higher than would normally be expected (Fig. 6), and it is concluded that this is due to the surging nature of the flow, and/or to boiling in the film and condensation in the main stream. A similar effect was noted in the benzene runs.

2 Vapor binding, due to spray formation and insufficient wetted area, occurred in the benzene-oil runs (Fig. 4), but to a lesser extent than with benzene, since the oil was substantially nonvolatile and a liquid residue was always present.

3 A further analysis of the benzene runs (Fig. 5) shows both dry-wall and hot-wall vapor binding; the latter type was apparently not encountered in the benzene-oil runs.

4 The pressure-drop data for benzene-oil mixtures, benzene, and water are reported in terms of apparent friction factors (Fig. 7); further data are needed to clarify the situation.

5 In the region where serious vapor binding did not occur, the average heat-transfer coefficients per pass correlate fairly well with pressure drop per pass (Fig. 8), both for the preheating and boiling sections, for the runs on benzene-oil mixtures, benzene, and water.

ACKNOWLEDGMENT

The authors acknowledge the donation of the oil used in the tests from the Humble Oil and Refining Company, Baytown, Texas, as arranged by Dr. Henry D. Wilde.

BIBLIOGRAPHY

1 "Vaporization Inside Horizontal Tubes," by W. H. McAdams, W. K. Woods, and R. L. Bryan, Trans. A.S.M.E., August, 1941, pp. 545–552.

2 "International Critical Tables," McGraw-Hill Book Company, Inc., New York, N. Y., vol. 5, 1933, p. 2.

3 "Heat Transfer for Boiling Inside Tubes," by W. K. Woods, Doctor of Science Thesis in Chemical Engineering, Massachusetts Institute of Technology, 1940.

4 "Heat Transmission," by W. H. McAdams, McGraw-Hill Book Company, Inc., New York, N. Y., 1933, p. 169.

5 "Principles of Chemical Engineering," by W. H. Walker, W. K. Lewis, W. H. McAdams, and E. R. Gilliland, Third edition, McGraw-Hill Book Company, Inc., New York, N. Y., 1937, p. 78, based on curve by T. B. Drew and R. P. Generaux, Trans. American Institute of Chemical Engineers, vol. 32, 1936, pp. 17–19.

Discussion

M. A. MAYERS.[6] It seems possible that the concentration of oil droplets along the axis of the tubes, which appeared somewhat unaccountable, might be explained by the phenomenon that causes a clear space adjacent to a hot surface in a dust-filled space or stream. This phenomenon has been described and analyzed by Cawood[7] and Watson;[8] it has been applied to smoke-precipitating apparatus by Watson[8] and Blacktin,[9] and has been used

[6] Coal Research Laboratory, Carnegie Institute of Technology, Pittsburgh, Pa. Mem. A.S.M.E.

[7] "The Movement of Dust or Smoke Particles in a Temperature Gradient," by W. Cawood, Trans. Faraday Society, vol. 32, 1936, pp. 1068–1073.

[8] "The Dust-Free Space Surrounding Hot Bodies," by H. H. Watson, Trans. Faraday Society, vol. 32, 1936, pp. 1073–1084.

[9] "The Cleaning of Air and Gas by Thermal Repulsion—Part I," by S. C. Blacktin, *Journal of the Society of Chemical Industry*, Trans., vol. 58, 1939, pp. 334–381; Part II, vol. 59, 1940, pp. 153–154.

to prevent the collection of smoke and soot on the windows of smoke meters, using light-absorption methods.[10] There may be a question whether this effect would be observed in flows of as high Reynolds number as in the authors' experiments, but, if it were, the apparent repulsion of particles from a hot surface would account for the observations. It is to be noted that, if the fluid were being cooled, rather than heated, concentration of droplets along the axis from this cause would not be expected.

R. L. Scorah.[11] The authors have not made clear in the paper whether they are dealing with simple over-all heat-transfer coefficients which apply only to the particular type of apparatus employed, or the more fundamental film coefficient. Perhaps the question could be answered best if we could have a short statement regarding: (*a*) the method of determining the heat input of each pipe section, including any corrections found necessary; (*b*) the methods used in determining the temperature of the inside surface of the tube, and the temperature conditions within the flowing fluids; (*c*) the methods employed to study the velocity conditions throughout the length of the tube; and (*d*) a brief statement of the procedures found necessary to estimate the kind of heat-transfer coefficients here reported from a set of observed data.

[10] "The Measurement of Smoke Density—a New Kind of Kapnometer," by J. S. Hales, *Fuel*, vol. 19, 1940, pp. 231–234.

[11] Associate Professor of Mechanical Engineering, University of Missouri, Columbia, Mo. Mem. A.S.M.E.

Authors' Closure

In reply to Mr. Mayers, we share his doubt that the hot-surface effect has a bearing on the phenomena described in the present paper. The remainder of the closure deals with the questions asked by Professor Scorah.

As stated in the second column of page 194, all coefficients were over-all values based on over-all temperature differences. In the benzene-oil runs the resistance on the oil side is so large, relative to those of the tube wall and steam side, that little error would be introduced by assuming that the over-all and oil-side coefficients are substantially equal. The answers to questions (*a*) through (*d*) are as follows:

(*a*) As stated on page 194, the heat input to each section was determined from condensate rates from each section.

(*b*) Tube temperatures were not measured or calculated.

(*c*) Linear velocities were not measured. The mass velocity through the tube is necessarily constant and was calculated from the relation $G = w/S$. As stated on page 194, w was calculated from heat and material balances, and the over-all heat balances checked within 7 per cent; furthermore this value of w was supported by the orifice-meter measurements of feed rates. S was taken as $\pi D^2/4$. The terminal linear velocities were calculated by dividing G by ρ.

(*d*) The procedure used to calculate the over-all coefficients for the benzene-oil runs is given in the second column on page 194. The procedure for runs on water and benzene, together with a detailed description of the apparatus, is given in reference (1).

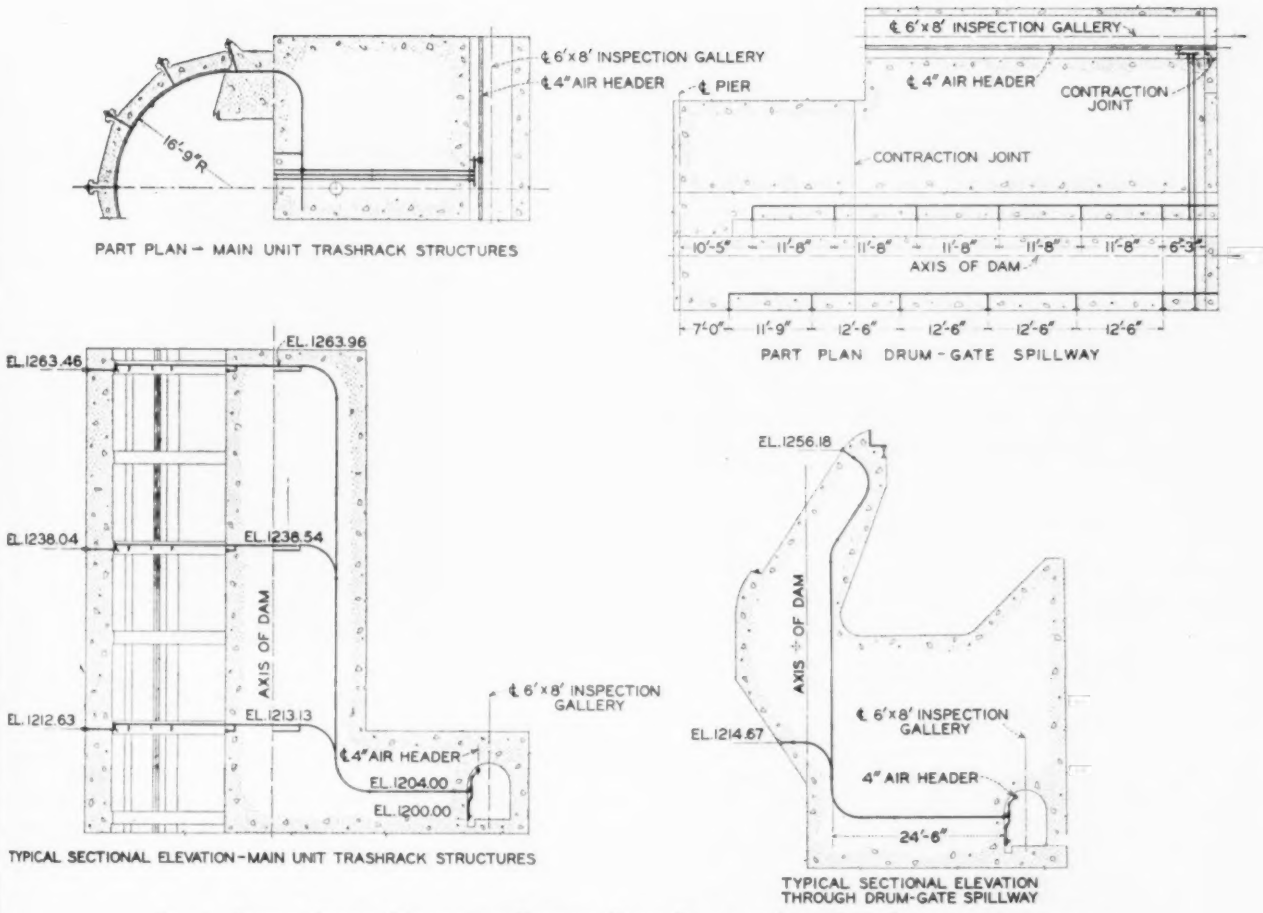


FIG. 1 TYPICAL ORIFICE LOCATIONS IN FRONT OF TRASH-RACK AND DRUM-GATE SPILLWAY STRUCTURES

Ice Prevention by the Air-Lift System at Grand Coulee

BY T. G. OWEN,[1] DENVER, COLO.

This paper deals with the results of a laboratory study of orifices for an air-lift deicing system at Grand Coulee Dam. The investigation included the testing of single- and multiple-hole arrangements of orifices of the short-tube type, the diverging-tube type, and various combinations of both. Flow patterns were studied with these various orifices discharging upward, horizontally, and downward. Special attention was devoted to the freezing phenomenon, and rules for designing a satisfactory nonfreezing orifice were proposed. An orifice was developed which gave a satisfactory balance between flow pattern, economy of operation, and nonfreezing characteristics.

ONE of the difficulties which has developed in connection with operations at Grand Coulee Dam, of the Columbia Basin Project, Washington, is the formation of ice in front of the trash racks and drum gates. Unless this condition could be adequately corrected during winter weather, it would prove to be both detrimental to good operation and dangerous to the structure. Temperatures of —28 F and of several days' duration have been recorded at the dam site. The problem confronting the designing engineers has been to develop a system whereby the reservoir surface immediately adjacent to the upstream face of the dam could be maintained free of ice. Many methods of accomplishing this result were studied but discarded in favor of the air-lift system because of its simplicity. In the air-lift system compressed air is forced into the reservoir adjacent to the structure at a depth at which the water temperature is at or near that corresponding to maximum density. The stirring and mixing action of the rising air induces the upward flow of

[1] Assistant Hydraulic Engineer, U. S. Department of the Interior, Bureau of Reclamation.

Contributed by the Hydraulic Division and presented at the Semi-Annual Meeting, Kansas City, Mo., June 16–19, 1941, of THE AMERICAN SOCIETY OF MECHANICAL ENGINEERS.

NOTE: Statements and opinions advanced in papers are to be understood as individual expressions of their authors and not those of the Society.

relatively warm currents of water which either melt the ice or prevent its formation.

A typical plan and section of the proposed location of the orifices in front of one trash rack and in front of one drum gate are shown in Fig. 1. Provision is made to introduce air at three different elevations in front of the trash racks and at two separate levels in front of the drum gates. This feature allows air to be introduced at a depth equal to or greater than 10 ft, which has been found to be the minimum depth for best results, regardless of the reservoir elevation.

Laboratory Tests of Orifices

The problems of determining the best size, shape, and direction of discharge of the orifice and the cooling effect due to expansion of the air at the orifice exit were studied in a 1 to 1 scale model in the hydraulic laboratory of the Bureau of Reclamation at Denver. The laboratory investigation was divided into two parts: (1) A preliminary examination of several orifice designs; (2) a detailed study concerning the cooling effect due to expansion.

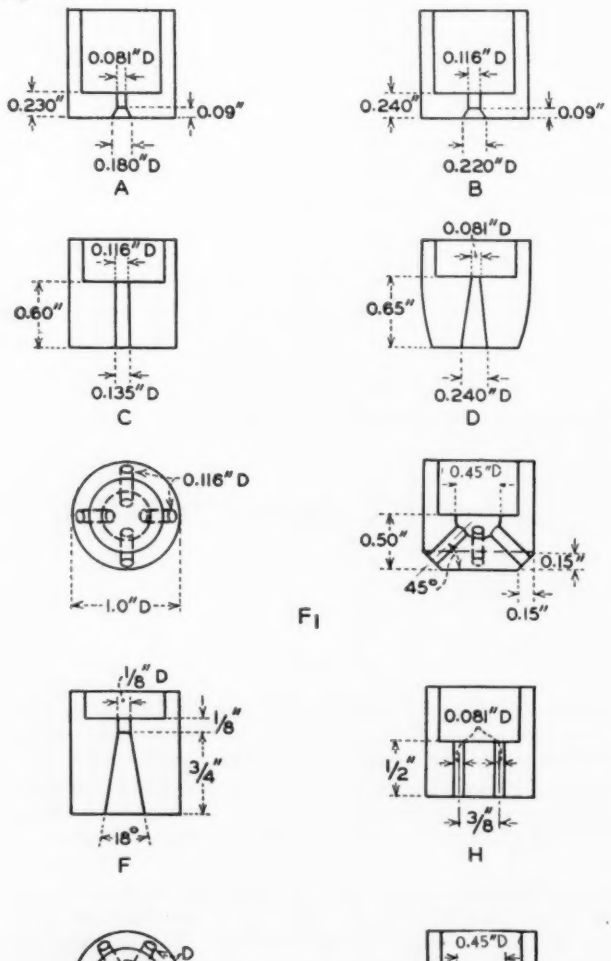


Fig. 2 Orifice Details

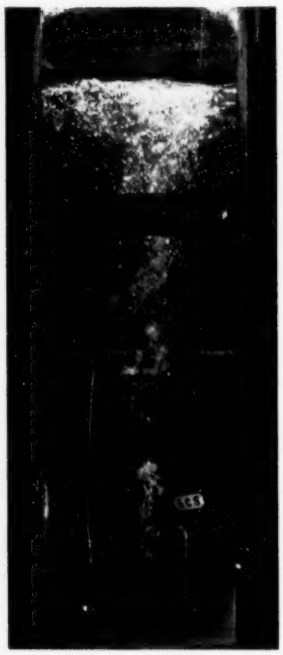


Fig. 3 Typical Vertical Discharge Flow Pattern at 3 Ps Differential Pressure; Orifice *C*

In the preliminary tests, the equipment consisted of a glass-sided tank, near the bottom of which was located the orifice to be tested. The orifice was connected with a high-pressure air line, and a throttling valve was placed in the line to control the pressure. Air-line pressure at the orifice and static water pressure at the orifice elevation were measured by mercury U-tubes, and the difference between these two observed pressures gave the differential pressure across the orifice.

In the experiments on orifices *A*, *B*, and *C*, the tests were purely visual. The general details of these orifices are shown in Fig. 2 and a typical flow pattern, in Fig. 3. From these tests, it was determined that discharge directed vertically downward gave the best flow pattern, the criterion being the largest cross-sectional area of the rising air current and the fineness of division of the air bubbles. It was observed further that an orifice of type *C* gave a better pattern than type *B*, which had the same cross-sectional area.

After these initial tests, a gas meter of the displacement type was installed to obtain the discharge characteristics of the various orifices. The flow pattern of orifice *D* was found to be good but its discharge was too low to establish a strong upward water current. Orifice *F* produced a good flow pattern and also a good upward circulation of water. The orifices thus far tested had only one hole. The multiple-hole nozzles were then examined. This group embraces orifices F_1, *H*, *I*, and *J*, Fig. 2. The flow pattern from nozzle *H* was no better than *F*, and the water current it established was inferior. Nozzles F_1, *I*, and *J* all gave excellent flow patterns and induced strong water currents but the discharge capacity of each was excessive. It was thought that if the diameters of the holes in these three nozzles were reduced to lower their discharge capacity, the holes would then be so small that they might easily become fouled or plugged by foreign matter.

Equipment Used for Testing Orifices

For the detailed investigation a special tank was constructed and equipped with instruments. The tank was made 12 ft deep

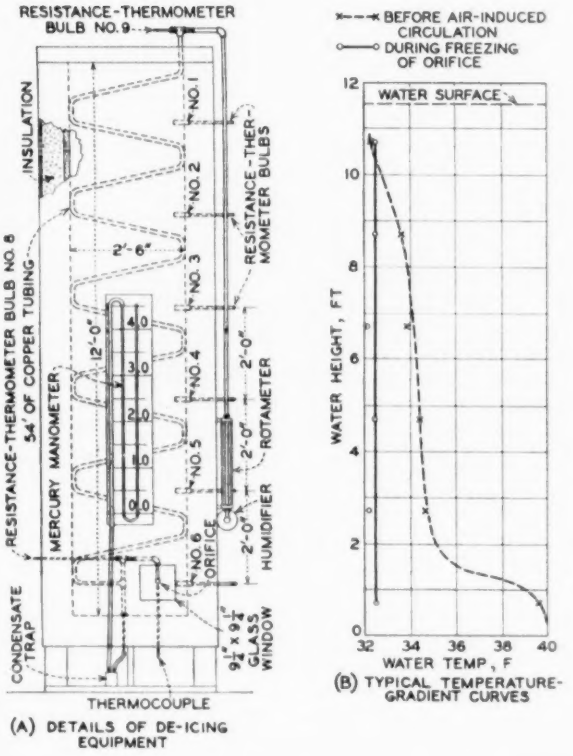


FIG. 4 DETAILS OF DEICING EQUIPMENT AND TYPICAL TEMPERATURE-GRADIENT CURVES

so that at least 10 ft of static waterhead could be imposed on the orifice. Inside the tank, about 54 ft of $^3/_4$-in. copper pipe was placed in coils at the end of which was located the orifice to be tested. In one side of the tank and at the elevation of the orifice, a piezometer opening and a resistance-thermometer bulb were located. Located in the same side of the tank at 2-ft intervals, vertically above the thermometer bulb at the orifice level, were five other thermometer bulbs to determine the temperature gradient during testing. These details are shown in Fig. 4 (*A*). The resistance thermometers were connected through a selector switch to a Wheatstone bridge and the resistance balance was indicated by a very sensitive light-beam galvanometer. The temperature of the air before entering the copper coils was measured by resistance thermometer No. 9, and the air temperature before expansion through the orifice, by thermometer bulb No. 8. Attempts were made to measure the temperature of the air stream issuing from the orifice by using a small resistance-thermometer bulb and also by a thermocouple. However, because of the oscillation of the air jet and the vibration of the thermocouple, it was thought that neither the resistance thermometer nor the thermocouple was continuously surrounded by air alone, and hence the indicated temperatures were unreliable.

Insulating material was placed between the inner and outer tank walls which were separated by 2 × 6-in. studding. The bottom of the tank was insulated and the top was equipped with a close-fitting removable cover, also insulated. The air pressure was controlled by a system of three valves, Fig. 5, so arranged that variations in the supply-line pressure would be minimized. The humidity of the air from the supply line was increased by passing the air through the humidifier, consisting of two atomizers which sprayed water on two porous baffles. Mechanically entrained water was removed by a system of three solid baffles, Fig. 5. From the humidifier, the air passed through the air rotameter, a device for measuring rate of flow. The air rotameter, Fig. 5, consists of an accurately machined glass tube tapered to increase in bore from bottom to top. A spinning metal rotor floats in the air stream and its position, read on a scale on the glass tube, indicates the amount of air flowing. Just above the rotameter, a Bourdon-type pressure gage was located. For more accurate air-pressure measurements, a mercury manometer was used. For visual observation and photographic recording, two $9^1/_4 \times 9^1/_4$-in. glass windows were located on opposite sides of the tank at the orifice level.

TESTING PROCEDURE

Before starting a test, the tank was charged with about 1200 lb of ice in pieces of about 25 lb each. The initial temperature gradient as indicated by thermometer bulbs Nos. 1 to 6, inclusive, Fig. 4 (*A*) was recorded. Fig. 4 (*B*) shows typical temperature-gradient curves. The static waterhead on the orifice was recorded and then the air flow was started. Water and air temperatures, air pressure, and the quantity of air discharged were observed. The differential pressure across the orifice was progressively increased by increments of about 1 psi until the orifice froze or the pressure limit of the apparatus was attained.

The preliminary tests indicated that orifice *F* had the most desirable properties. A check calibration was made on this orifice in the new model, as shown on the pressure-discharge curve plotted in Fig. 6. Tests on the cooling effect due to expansion of the air indicated that the orifice would freeze solidly, forming a cone of ice in the tapered exit when the air temperature before expansion was 32.38 F and the differential pressure was 5.4 psi.

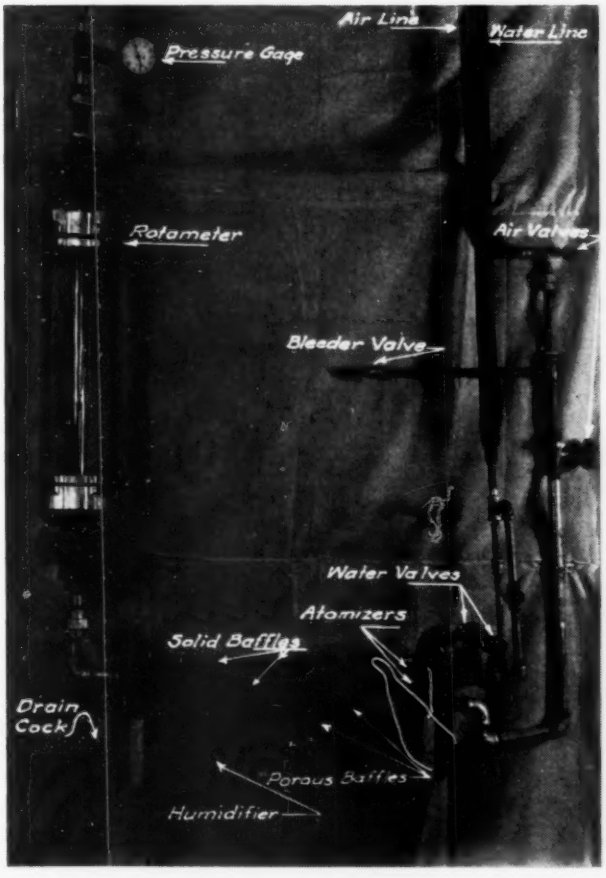


FIG. 5 HUMIDIFYING AND AIR-METERING APPARATUS

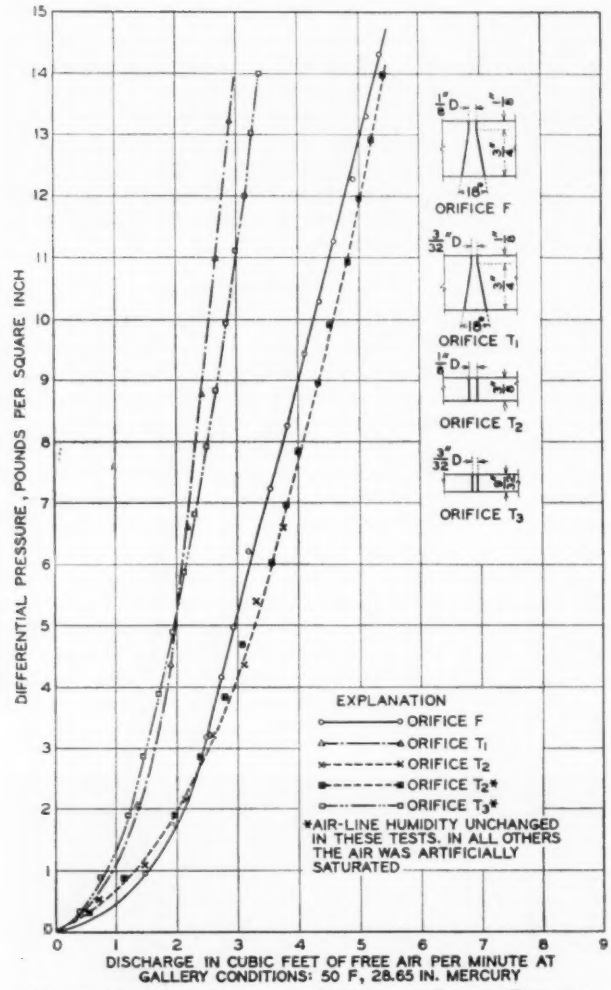


FIG. 6 PRESSURE-DISCHARGE CURVES AND ORIFICE DETAILS

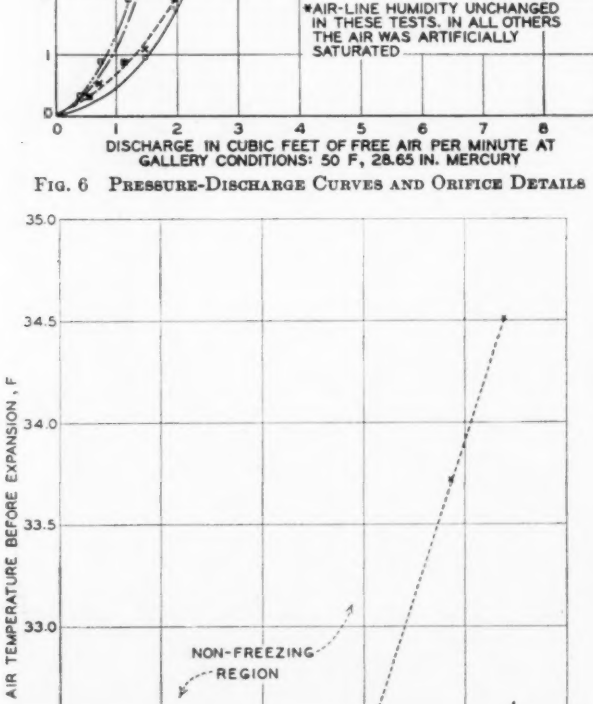
As an alternative design, orifice T_1 was built. It is the same in every detail as orifice F, except that its initial diameter is $^3/_{32}$ in. instead of $^1/_8$ in., which makes its area roughly one half that of orifice F. The calibration curve for this orifice is shown in Fig. 6. Temperature tests were made but the range of air temperature before expansion was too high to cause freezing. The highest differential pressure during the test was 17.54 psi, and the air temperature before expansion was 35.39 F. No further temperature tests were made on this orifice.

Orifice T_2 was tested because it was believed that it would have a lesser tendency to freeze than an orifice having a tapered exit, such as F or T_1. The general dimensions and calibration curve are shown in Fig. 6, and Fig. 8 shows orifice T_2 during a freezing cycle.

Orifice T_3 is a short tube similar to T_2, having its length equal to 3 diameters, Fig. 6. Its area, however, is approximately one half that of T_2. The calibration curve for this orifice is shown in Fig. 6. At this point in the test program, it was decided to adopt orifice T_2 so no further temperature investigations were conducted on T_3.

ICE FORMATION IN THE ORIFICE

From data on the freezing characteristics of orifice T_2 a "critical freezing curve" was constructed by plotting air temperature before expansion against differential pressure Fig. 7(*A*). This curve passes through the points which lie furthermost to the left and upward. Thus, it divides the temperature-pressure plane into two regions, i.e., one region lying upward and to the left of the curve, in which no combination of initial air temperature and differential pressure will cause freezing; the other lying downward and to the right of the curve, in which all combinations of initial temperature and pressure result in ice formation in the orifice. Ice formation in the orifice is a function of at least the differential pressure across the orifice, the air temperature before expansion, and temperature of the surrounding water; but since the air temperature before expansion is, in turn, a function of the temperature of the surrounding water, the initial air temperature was chosen as one of the co-ordinates for the freezing curve.



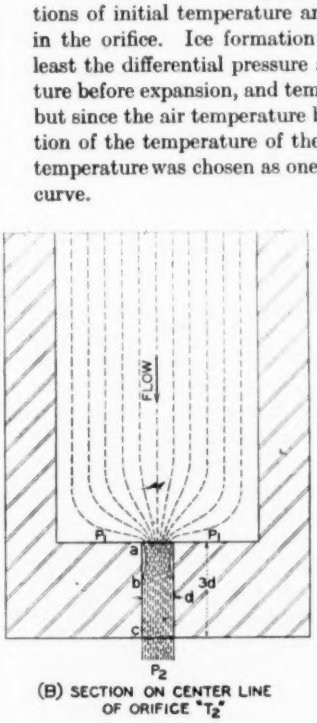


FIG. 7 CRITICAL FREEZING CURVE AND DIAGRAM FOR ORIFICE T_2



(*A*) Unobstructed flow prior to ice formation

(*B*) Deflected and restricted flow, due to ice formation

(*C*) Large dense ice cone, completely restricts flow

FIG. 8 ORIFICE T_2 DISCHARGING AT 19.25 PSI DIFFERENTIAL PRESSURE; AIR TEMPERATURE BEFORE EXPANSION, 32.37 F
(Thermocouple is seen immediately below orifice.)

In one test, the air temperature before entering the cooling coils was purposely raised about 90 deg F higher than in other tests, but the temperature before expansion was found to be about the same as in other tests. This indicates that the air temperature before expansion will be sensibly the same as that of the surrounding medium, regardless of its initial temperature.

The critical freezing curve, Fig. 7(*A*), does not give all the data in regard to the freezing of orifice T_2. While it gives the combinations of initial air temperature and differential pressure at which freezing starts, it does not indicate the degree or seriousness of freezing. In the range of initial air temperatures up to about 33 F, it was observed that it was possible to have the orifice freeze solidly at points lying on the critical freezing curve.

However, these instances were exceptions rather than the usual result; generally ice would start to form in the orifice, partially fill it, and then be removed by the passing air. In order to obtain quick freezing and ice cones, such as shown in Fig. 8, the differential pressure was increased to 19.25 psi.

In the range of initial air temperature lying above 33 F, freezing of the orifice was not such a serious factor within the differential-pressure range tested. The start of freezing in the range above 33 F became progressively more and more difficult to detect by visual observation of the jet as the differential pressure necessary to produce freezing increased, until in the vicinity of 10 or 11 psi it could only be detected by the instruments. When the mercury manometer, indicating the air-line gage pressure, showed an increase in pressure, and when the rotameter showed concurrently a decrease in discharge, it was definitely established that freezing had started.

In the region of temperature lying above 33 F, it was observed that the duration of the decreased discharge due to ice formation in the orifice became shorter as the values of temperature and differential pressure necessary to cause freezing became greater. Clearing of the orifice was manifested by a sudden increase in discharge and decrease in differential pressure.

THEORY ADVANCED FOR ICE FORMATION IN ORIFICE

In attempting to explain the phenomenon of ice formation in the orifices, the following interpretation is offered. A theoretical analysis was made for expansion of saturated air through orifice T_2, taking the actual values of initial and final pressure and initial air temperature found in one test. The expansion was considered adiabatic and account was taken of the variation of the specific heat of the saturated air with temperature, and of the heat of vaporization and heat of fusion given to the mixture by the moisture which condensed and froze. Thus, by approximation, the final temperature of the gas mixture was obtained, and found to be about 2.34 F. This analysis has taken no consideration of heat transfer from the orifice to the gas mixture, although there must have been some. It will be remembered that this set of values of pressure and initial temperature constituted one point on the critical freezing curve, which means that freezing of the orifice just started under these conditions. The theoretical final temperature of 2.34 F is far below the freezing point and it is difficult to conceive that the orifice whose temperature cannot be greater than that of the surrounding water (32.48 F) could raise the air temperature to such a point that freezing just starts under these conditions. Another question arising from a study of the freezing phenomenon is how frozen moisture particles can stick to the walls of the orifice when moving at such a high velocity, approximately 525 fps or 358 mph for orifice T_2 at a differential pressure of 6.01 psi.

A solution which would satisfactorily explain both of these points is proposed and reference will be made to Fig. 7(*B*). The mixture of air and water vapor at pressure P_1 expands through the orifice to pressure P_2 following the approximate streamlines as shown in Fig. 7(*B*). From point *a* to point *b* the jet contracts, passes through the vena contracta, and then expands again following the walls of the orifice between points *b* and *c*. The cold air cools the walls of the orifice between points *b* and *c* to some temperature which is higher than that of the air and lower than that of the water surrounding the orifice. As the saturated air expands, the temperature drops, resulting in moisture being removed from the air by condensation. The resulting fluid is then a mixture of moisture particles and saturated air, the air temperature being below freezing. It is conceivable that the particles of moisture do not freeze instantly because there must be a heat transfer before freezing can occur and, therefore, because of the high velocity through the orifice, it could be possible that unfrozen moisture particles could come in contact with the walls of the orifice between points *b* and *c*. It will be remembered from studies of refrigeration that a moist finger will stick instantly to a metal surface when that surface is at a temperature of 15 F or lower. This is known as the "stick test." If the walls of the orifice were at 15 F, then the moisture particles would stick instantly upon contact, and freezing of the orifice would start. This hypothesis would satisfy both the question of low air temperature and that of the high air velocity.

It is of interest to note that, for the one point on the critical freezing curve for which the theoretical final air temperature was computed and found to be 2.34 F, the average of this final air temperature and that of the surrounding water is exactly 15 F, which is the highest temperature at which the stick test will occur.

By extending this reasoning further it can be explained why freezing is more serious (that is, the orifice may freeze solidly) when it occurs with the temperature of the surrounding water in the region of 32 to 33 F. The orifices tested in the laboratory were made of wrought iron and lead. The thermal conductivity at 64 F is 20.1 for lead, and 34.9 for wrought iron.[2] For ice, the thermal conductivity[2] is given as 1.26. This means that a temperature gradient plotted from the surrounding water, through the metal forming the orifice and to the inside wall, can be of a relatively flat slope but, from the inside wall through the ice to the cold-air stream, the temperature gradient has relatively a very steep slope. Therefore, when freezing of the orifice starts with the temperature of the surrounding water in the region of 32 to 33 F, the temperature of the inside wall of the orifice can conceivably remain below the melting point, the bond between metal and ice remains unbroken, and the freezing process continues on to ultimate restriction of air flow. Whereas, with a higher temperature of the surrounding water, the freezing of the orifice may start but, as the ice deposit increases in thickness, the temperature of the inside wall of the orifice rises until the melting point is reached, the bond between the ice and metal is broken, the flow-restricting ice deposit is removed, and complete freezing of the orifice is prevented.

Conclusions

From this investigation it was concluded that:

(*a*) The direction of discharge vertically downward from the orifice gave a superior flow pattern.

(*b*) An orifice with an 18-deg tapered exit similar to type *F* gave the best flow pattern of all single-hole types tested. The multiple-hole types were at once abandoned because of the high discharge capacity or because of danger of becoming plugged if the diameter of the holes were decreased so that the discharge would be equivalent to the single-hole type.

(*c*) A discharge of 2 cu ft of free air per min at a differential pressure of 2 psi is sufficient to induce a strong upward water current. This value for discharge is also consistent with practical limits of compressor size required for the Grand Coulee air deicing system.

(*d*) An orifice of the short-tube type (T_2) was found to be somewhat superior to the type represented by orifice *F* as far as freezing is concerned; its flow pattern was not materially worse, and its discharge characteristics about the same. Therefore, this orifice was adopted for use in the Grand Coulee deicing system.

(*e*) When freezing in the orifice occurs with the initial air temperature and surrounding water temperature in the range of 32 to 33 F, the orifice may freeze completely, thus stopping the air flow. No complete freezing was observed in the tests when the temperatures of the air and surrounding water were above 33 F and the differential pressure was within the range available with the laboratory apparatus. However, complete freezing may be possible at higher differential pressures.

(*f*) Freezing of the orifice is a function of the initial air temperature, the differential pressure, the type of orifice, the temperature of the surrounding water, the thickness of the orifice walls, and the thermal conductivity of the material of which the orifice is made. It is presupposed that the air used has a sufficiently high initial humidity so that moisture will be condensed during expansion.

Where the danger of freezing is imminent, a sharp-edged orifice should be used. If, however, an orifice of the short-tube type is used because of its superior flow pattern, the freezing hazard may be decreased by making the operating differential pressure small, the walls of the tube as thin as possible and of a material of high thermal conductivity such as copper.

The hydraulic laboratory in which these studies were made is directed by J. E. Warnock, engineer, and is a section of the materials, testing, and control division, supervised by R. F. Blanks and Arthur Ruettgers, senior engineers, in the Denver office of the Bureau of Reclamation. Design studies and investigations are made under the direction of J. L. Savage, chief designing engineer. S. O. Harper is chief engineer for the Bureau and J. C. Page is Commissioner of Reclamation.

[2] "Mechanical Engineers' Handbook," by Lionel S. Marks, editor in chief, McGraw-Hill Book Company, Inc., New York, N. Y., Third edition, 1930, Tables 1 and 3, pp. 396–397.

Discussion

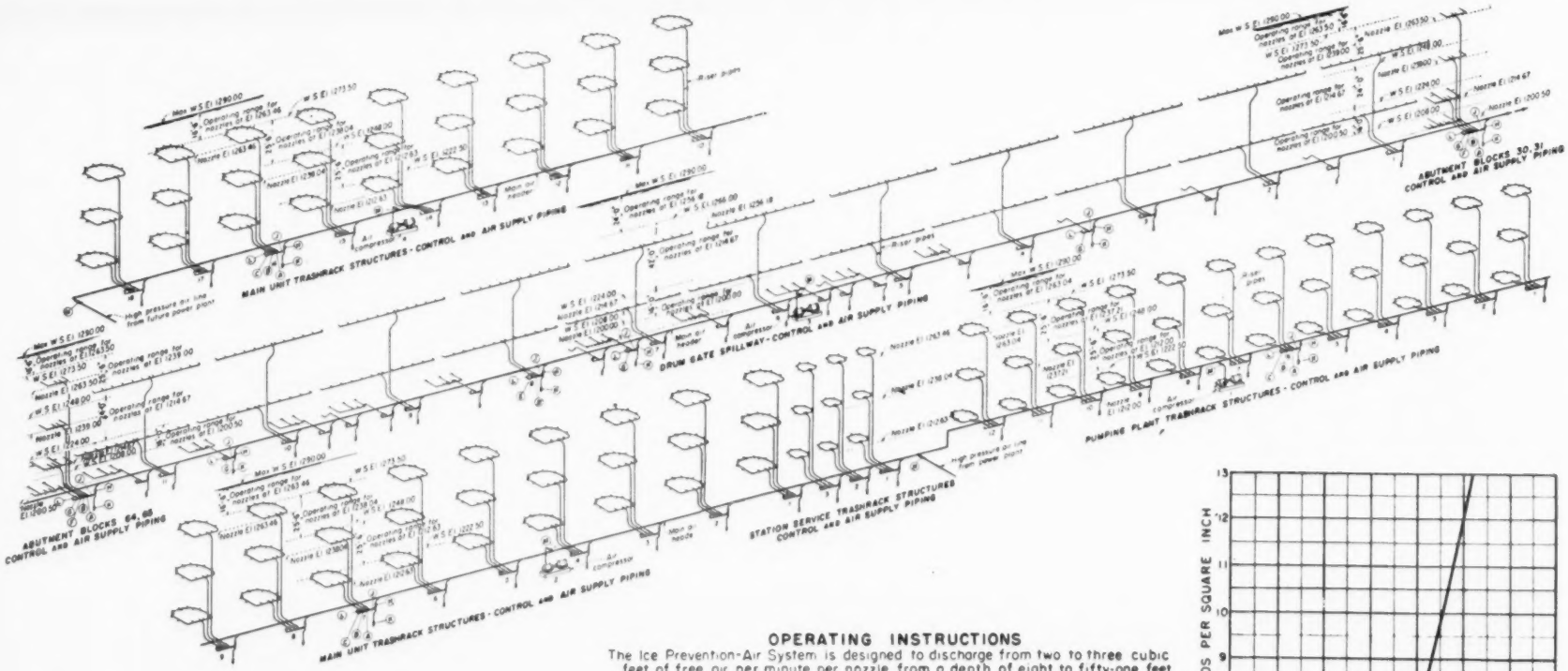
P. J. Bier.[3] This paper has presented primarily the laboratory experiments made on various air-discharge nozzles and orifices. It may be of added interest to the average engineer engaged in the design and operation of ice-prevention installations to learn something of the construction and operating features of the system developed for Grand Coulee Dam. As far as operating information is concerned, however, the preparation of the paper is somewhat premature, as data on operation will not be available until the ice-prevention system has been thoroughly tested in actual practice.

When the compressed-air system of ice prevention was first considered in connection with the design of the dam, a review was made of existing literature on the subject. While several installations of this nature were in use here and abroad, useful information was very meager. As far as known to the writer, all present installations were added to the dams after construction. Hence, the Grand Coulee ice-prevention system is presumably the first of its kind which has been designed and built into the structure as an integral part of the dam. The reported success of the ice-prevention systems used at Keokuk Dam and at other dams, and their operating economy was mainly responsible for the selection of this type of installation at Grand Coulee.

The lack of information relative to the best size, shape, and position of the orifice in the air nozzle, also the cooling effect and possible freezing which may be encountered when the expanding air leaves the nozzle, became apparent and the laboratory experiments described in the paper were undertaken at the request of the mechanical-design section. Another laboratory experiment was also made, which consisted of discharging compressed air into a vertical glass tube full of water representing the 1-in. distribution pipes which fill up with water between operating cycles. This demonstrated that, for sizes 1 in. diam and smaller, the water is blown out of the tube when the system is put in service, while for larger sizes the air simply blasts a passage through the water in the tube.

As the usual winter fluctuations of the Grand Coulee reservoir are expected to vary between a low level of 1230 and a high level of 1280, it was necessary to provide protection against ice formation for a 50-ft variation in water surface. This will be accomplished with three sets of air-distribution pipes placed at three different levels for the trash racks in front of the penstocks and pump intakes, and with two sets of distribution pipes at two different levels in front of the drum gates, as shown in Fig. 1 of the paper. A better illustration of the entire installation is given in

[3] Senior Engineer, United States Department of the Interior, Bureau of Reclamation, Denver, Colo. Mem. A.S.M.E.



EXPLANATION

A - Control valve - W S El 1273.50 to W S El. 1290.00
B - Control valve - W S El. 1248.00 to W S El. 1273.50
C - Control valve - W S El 1222.50 to W S El. 1248.00
D - Control valve - W S El 1266.00 to W S El. 1290.00
E - Control valve - W S El 1224.00 to W S El. 1266.00
F - Control valve - W S El 1224.00 to W S El. 1248.00
G - Control valve - W S El 1208.00 to W S El. 1224.00
H - Control header "shut-off" valve.
J - Control header throttling valve.
K - Control header drain valve.
L - Pressure gage.
M - Plug valve on compressor discharge lines.
N - Plug valve on high pressure air connections.

OPERATING INSTRUCTIONS

The Ice Prevention-Air System is designed to discharge from two to three cubic feet of free air per minute per nozzle from a depth of eight to fifty-one feet below the water surface. To discharge more than three cubic feet of free air per minute per nozzle, operate parts of the system intermittently.

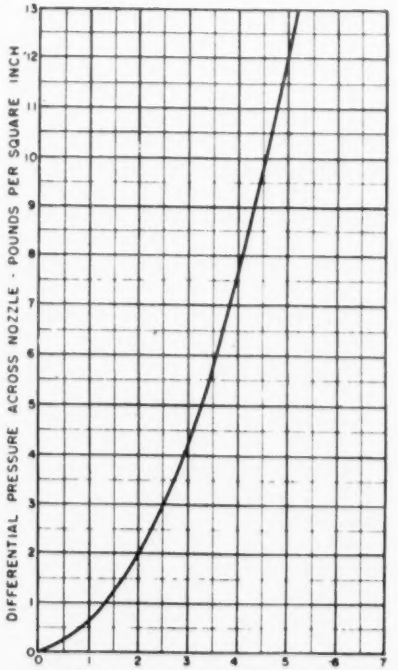
The table shows gage readings calculated to discharge two cubic feet of free air per minute per nozzle for water surface elevations of two foot intervals. The curve shows the cubic feet of free air per minute that will be discharged through the air nozzles for differential pressures across the nozzles from zero to thirteen pounds per square inch.

The air compressors are to be put in service and operated according to instructions furnished by the manufacturer.

Determine which nozzles to use from the water surface elevation. The operating ranges for air nozzles at different elevations and locations are shown on the diagram. When air is first supplied from the control header to the nozzles, valves "H", "J" and the control valve corresponding to the nozzle elevation should be opened wide, so that a maximum flow of air will blow the water out of the riser pipes. The flow of air may then be adjusted by the control valve until the gage reading shows the desired amount of air flowing. When the system is operating the accumulated moisture should be drained from the line through valve "K".

When the system is not in operation, valves "A", "B", "C", "D", "E", "F", "G", "H", and "N" should be closed and valves "J", "K", and "M" should be opened.

High pressure air from the power plant may be obtained for supplementary service and blowing-out lines by opening valve "N". To protect air compressors, valve "M" should be closed before opening valve "N".



PRESSURE - DISCHARGE CURVE

FIG. 9 OPERATING DIAGRAM AND INSTRUCTIONS FOR ICE-PREVENTION SYSTEM AT GRAND COULEE DAM

TABLE 1

CALCULATED GAGE READINGS					
WATER SURFACE ELEVATION	MAIN UNIT TRASHRACK STRUCTURES	STATION SERVICE TRASHRACK STRUCTURES	PUMPING PLANT TRASHRACK STRUCTURES	DRUM GATE SPILLWAY	ABUTMENT BLOCKS 30,31, AND 64,65
1290	13.9	13.3	13.8	16.8	13.1
1288	13.1	12.5	13.0	16.0	12.3
1286	12.4	11.7	12.2	15.2	11.5
1284	11.6	10.9	11.4	14.4	10.7
1282	10.8	10.1	10.6	13.6	9.9
1280	10.0	9.3	9.8	12.8	9.1
1278	9.2	8.5	9.0	12.0	8.3
1276	8.4	7.7	8.2	11.3	7.5
1274	7.7	6.9	7.5	10.5	6.6
1272	16.7	16.3	16.8	9.7	15.8
1270	15.9	15.5	16.0	8.9	15.0
1268	15.2	14.7	15.2	8.1	14.1
1266	14.4	13.9	14.4	7.3	13.3
1264	13.6	13.0	13.6	23.0	12.5
1262	12.8	12.2	12.8	22.2	11.7
1260	12.0	11.4	12.0	21.4	10.9
1258	11.2	10.6	11.2	20.6	10.1
1256	10.4	9.8	10.4	19.8	9.3
1254	9.6	9.0	9.6	19.0	8.5
1252	8.8	8.2	8.8	18.2	7.6
1250	8.0	7.4	8.0	17.4	6.8
1248	7.2	6.6	7.2	16.5	6.0
1246	16.3	16.0	16.4	15.7	15.3
1244	15.5	15.2	15.6	14.9	14.5
1242	14.7	14.4	14.8	14.1	13.6
1240	13.9	13.5	14.0	13.3	12.8
1238	13.1	12.7	13.2	12.5	12.0
1236	12.3	11.9	12.4	11.7	11.2
1234	11.5	11.1	11.6	10.9	10.4
1232	10.7	10.3	10.7	10.1	9.6
1230	9.9	9.5	9.9	9.3	8.8
1228	9.1	8.7	9.1	8.5	8.0
1226	8.3	7.9	8.3	7.7	7.2
1224	7.6	7.1	7.5	6.9	6.4
1222	6.8	6.2	6.7	11.5	11.2
1220				10.7	10.4
1218				9.9	9.6
1216				9.1	8.7
1214				8.3	7.9
1212				7.5	7.1
1210				6.6	6.3
1208				5.8	5.5

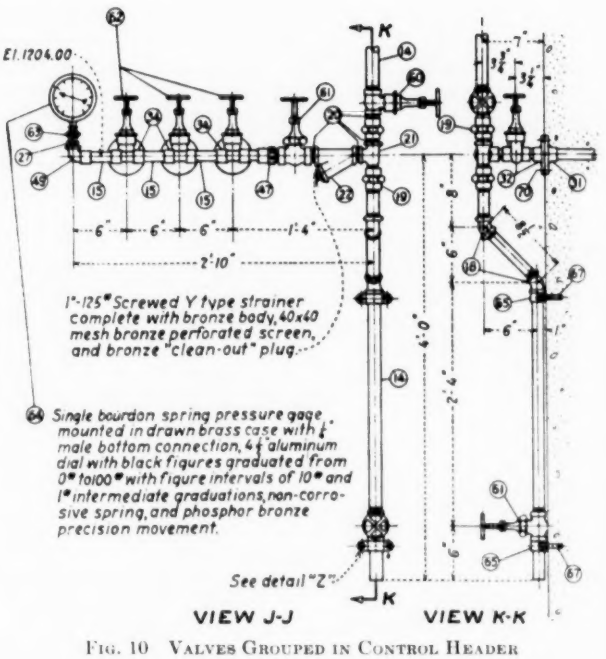


FIG. 10 VALVES GROUPED IN CONTROL HEADER

the isometric view, Fig. 9 of this discussion, which also contains the operating instructions for the system.

The compressed air required for the operation of the system is supplied by four single-stage, water-cooled, motor-driven, rotary-type air compressors, each with a capacity of 380 cfm of air at 40 psi gage pressure. Three of the compressors are located in separate chambers off the 1200-ft gallery in the main dam and one in a chamber off the 1210-ft gallery in the pumping-plant dam. The compressed air is collected in a 4-in. main header run through the gallery, from which the distribution pipes and discharge nozzles are supplied.

The air supply to the various distribution pipes, located at the different elevations to suit the reservoir level, is controlled with globe valves, having plug-type disks, and with gate valves, one for each level. These valves are grouped together in a control header for convenience in operating, as shown in Fig. 10 of this discussion, and each control header is equipped with shutoff and drain valves, strainer, and pressure gage. By means of a table giving a set of calculated pressure-gage readings for various reservoir levels and for a discharge of 2 cfm of free air for each nozzle on the distribution pipe to be placed in service, the operator will be in a position to throttle the globe valve to the required pressure to supply the quantity of air needed for the nozzles. For discharges in excess of 2 cfm, the globe valve will be set for the pressure given in the table corresponding to the reservoir elevation, plus the additional pressure given in the pressure-discharge curve in excess of the 2-lb differential pressure for a discharge of 2 cfm.

The entire system can be operated simultaneously, discharging 2 cfm of free air per nozzle for any one of the distribution pipes, with three of the available four air compressors operating.

For a discharge of 3 cfm of free air per nozzle for any one of the levels, it will be necessary to operate all four compressors. From the pressure-discharge curve in Fig. 9, it can be seen that discharges up to 5 cfm per nozzle can be provided with differential pressures up to 12 lb. If discharges in excess of 3 cfm per nozzle are desired at any section of the dam, it will be necessary to operate the system intermittently. The table of calculated gage readings given in Table 1 does not cover this remote possibility. The table is based on the assumption that the operating range shown for each distribution pipe or set of nozzles in Fig. 9 is adhered to. This range is 25 ft 6 in. for the two lower sets of trash-rack nozzles and 16 ft 6 in. for the upper set. For the drum-gate nozzles, the range is 42 ft and 24 ft, respectively, for the lower and upper set of nozzles.

The 4-in. main header is made of galvanized steel pipe, the control headers of 1-in. brass pipe, and the distribution lines of 1-in. seamless copper tubing with branches of $^1/_2$-in. copper tubing. The copper lines are connected with cast-bronze solder-joint fittings. The air nozzles are made from bronze with $^1/_8$-in. drilled orifices. Expansion joints are provided for pipe lines running through the contraction joints of the dam. The air-pipe system is cross-connected to a high-pressure air-line extension from the powerhouse, which may be used for supplementary service and for blowing out the operating lines.

While the compressed-air system has been designed for service in front of all trash racks and drum gates, the ends of the drum gates will be protected against freezing to their seats by electrical heating coils embedded behind the face plates of the concrete piers.

The air-lift system was designed by junior engineer J. C. Wright and associate engineer C. O. Selander under the direction of the writer. All mechanical designs are under the general supervision of W. C. Beatty, mechanical engineer, and L. N. McClellan, chief electrical and mechanical engineer, and all designs and investigations are under the general direction of J. L. Savage, chief designing engineer.

The Calculation of Critical Speeds of an Oil-Well Pumping System

By C. R. FREBERG[1] and E. N. KEMLER,[1] WEST LAFAYETTE, IND.

Because of the increasing economic necessity for using light oil-well pumping equipment, steps must be taken to keep loads and stresses at a minimum. Loads can be controlled to some extent by using proper speeds, stroke, and plunger size. Proper counterbalancing has a greater influence on peak loads and stresses than any other item of equipment design. Vibration and critical-speed problems are among the most difficult experienced in pumping systems. Such systems do not lend themselves to mathematical analyses so the authors have undertaken to solve the more complicated problems by replacing such involved systems by an equivalent system, which will have the same capacity for storage of kinetic and potential energy. A mathematical explanation of the procedure used in reducing a pumping system to equivalent mass, and equivalent elastic systems, followed by calculations of typical elements of the system and examples illustrating specific applications of the method, are given.

THE changes which have taken place in the oil-producing industry during the last few years have greatly altered the general equipment program. The low producing rates, imposed by proration requirements, and the increased difficulties of making a profit, together with the future uncertainties of the industry have made it necessary to watch the investment cost of a well. This has resulted in using as light equipment as possible. While such equipment, when used within its range, will operate as well as heavy equipment when operated at its capacity, there is a general tendency toward making the lighter equipment do as much as the heavier. The result of this general tendency is to cause the smaller equipment either to be overloaded or the factor of safety to be reduced to a very small value. Under these conditions, every possible provision should be made to operate the equipment in such a manner as to keep the loads and stresses at a minimum. The loads can be controlled to some extent by using proper speeds, stroke, and plunger size. Proper counterbalancing will influence peak loads and stresses more than any other single item. The use of proper counterbalance can reduce the peak torque by about one half, that is, the effective capacity of the equipment will be reduced about one half, if counterbalance is not used.

As factors of safety have been decreased and every effort expended toward reducing investment and getting the most out of equipment, it has become increasingly necessary to eliminate or investigate every possible source of trouble. Among the sources are vibration or critical-speed problems in connection with the pumping system. Among the problems of this type which have been studied are the investigation of vibrations in sucker-rod strings (1, 2),[2] torsional vibrations in the gear-reduction system of pumping units (3), and investigations of the peak loads, resulting from the engine impulses (4). These investigations have covered various phases of this general problem. The results have indicated that, under certain conditions, the loads and stresses, resulting from critical or resonance speeds, could be of the same order of magnitude as the normal stresses.

Figs. 1, 2, and 3 show cases where these effects have been

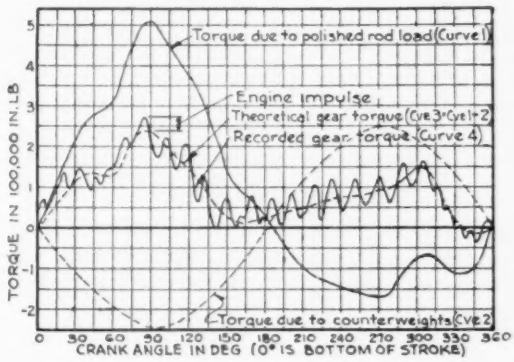


FIG. 1 INFLUENCE OF ENGINE IMPULSES ON ROD TORQUE (4)

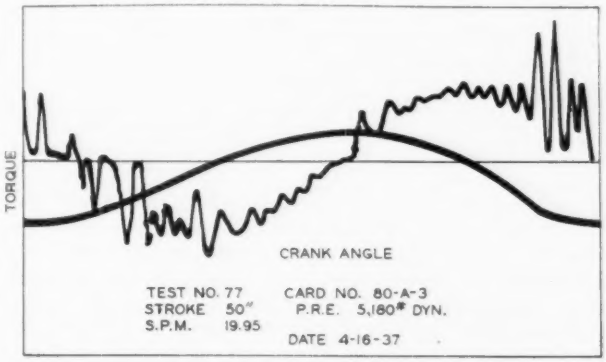


FIG. 2 TORQUE OBTAINED WITH ENGINE DRIVING COUNTERBALANCE (3)

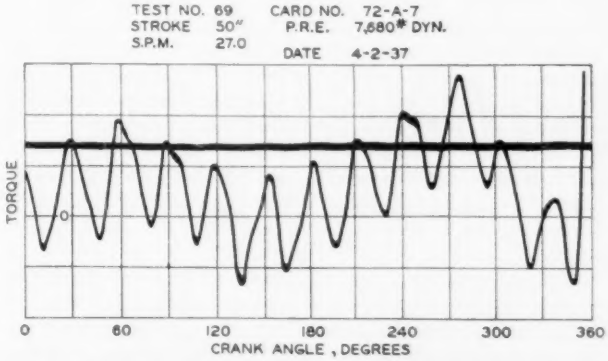


FIG. 3 LARGE VIBRATIONS SET UP IN RESONANCE WITH ENGINE EXPLOSIONS (3)

[1] School of Mechanical Engineering, Purdue University.

[2] Numbers in parentheses refer to the Bibliography at the end of the paper.

Contributed by the Petroleum Division and presented at the Semi-Annual Meeting, Kansas City, Mo., June 16–19, 1941, of THE AMERICAN SOCIETY OF MECHANICAL ENGINEERS.

NOTE: Statements and opinions advanced in papers are to be understood as individual expressions of their authors and not those of the Society.

measured. Fig. 1 shows the actual torque transmitted to a reduction gear by the engine, as measured by a torque dynamometer mounted in the driving pulley on the gear reducer. The engine explosions can be clearly seen on this diagram, and the impulses resulting from them are an appreciable percentage of the peak torque. The peak in this case would have been doubled had no counterbalance been used. Fig. 2 shows the torque obtained for a case where a higher-speed engine was used to drive only a counterbalance. A severe vibration occurred in this case as a result of the firing of the engine when the torque was a maximum. Fig. 3 shows a case where large vibrations in resonance with engine explosions were set up. In this case, the peaks of the vibrations are about twice the normal torque requirements. Another serious effect of such vibrations is also shown, i.e., the oscillation of the torque back and forth across the zero-torque line. When the torque is positive (above the line), the engine is driving the sucker rods. When the torque is negative (below the line), the rods are driving the engine. When the zero line is crossed backlash in the gears is taken up, resulting in impact stresses on the gears. This condition results in an increase in the number and magnitude of impacts, and as wear occurs this becomes more serious. It may account for wear or pitting on the back side of gear teeth when the normal load is always in one direction.

General Methods Used

The mathematical solution of certain types of vibration problems has received much attention and covers many types of engineering problems (5, 6, 7, 8). However, as is typical of many

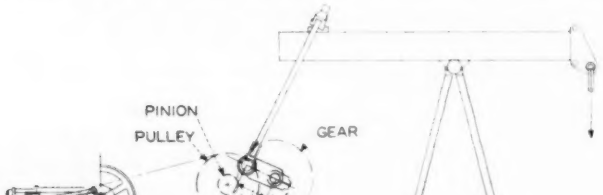


Fig. 4 Schematic Arrangement of Pumping-Unit System

engineering problems, certain types of elastic systems do not readily lend themselves to analytical solutions because of the involved nature of the problem, rather than the problem's not being adaptable to mathematical analysis. The system to be discussed in this paper comes under this latter heading so that some method of approach other than the purely mathematical one is necessary.

The natural vibrations of elastic systems involve the interchange of potential and kinetic energy. The potential energy in the system is present as elastic energy stored in the shafts or other elastic members. The kinetic energy is stored in the weight or mass of the system due to its velocity. Any system, therefore, must have elasticity and mass to be able to vibrate. As an example of such systems might be mentioned a weight on a spring where the weight is the mass of the system in which kinetic energy may be stored, and the spring is the elastic member where potential energy may be stored. The solutions of the more complicated types of vibration problems are based on the principle of replacing a complicated system by an equivalent system which will have the same capacity for storage of kinetic and potential energy.

In a pumping-unit system, as has been shown schematically in Fig. 4, the various parts operate at different speeds and have different elastic properties and masses. In an equivalent system, all parts are reduced to an equivalent rotating system, and the masses and elastic members are then varied to give an equivalent energy system. In this system, all elastic members are reduced to an equivalent shaft of unit diameter and of such a length as to give an equivalent energy-storage capacity at engine speed. The masses are likewise determined to give an equivalent energy-storage capacity at engine speed. In cases of members having a variable mass, the equivalent mass necessary to give the same effect over a cycle will be used.

Standard Solutions

In the calculations to be made, there are three general types of vibrations to be considered which have been treated in detail in the literature. To simplify the treatment, only the formulas for these cases will be considered in this paper. The first of these is the case of the vibration of a weight hung on a spring, as shown in Fig. 5. The natural frequency of such a system, i.e., the frequency with which the system will vibrate if displaced from its normal position, is



Fig. 5 Weight Suspended From Spring

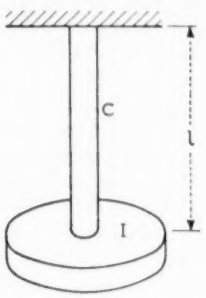


Fig. 6 Disk on End of Shaft

$$f = \frac{1}{2\pi}\sqrt{\frac{gk}{W}} \quad [1]$$

if the mass of the spring is neglected.

Where f = natural frequency in vibrations per second
g = in. sec^{-2} = 386
W = weight, lb
k = spring const, lb per in.

A second type of problem is that of a disk on the end of a shaft as is indicated in Fig. 6. The natural frequency of such a system is

$$f = \frac{1}{2\pi}\sqrt{\frac{C}{I}} \quad [2]$$

For a circular shaft of uniform cross section

$$C = \frac{E_s}{l} \times \frac{\pi d^4}{32} = \frac{E_s}{l} J \quad [3]$$

where E_s = torsional modulus of elasticity, psi
l = length of shaft, in.
J = polar moment of inertia of shaft, in.^{4}
d = shaft diameter, in.
I = moment of inertia of disk, lb in. sec^2
C = torque required to produce unit angle of twist

The moment of inertia for a circular disk of uniform thickness can be expressed as

$$I = \frac{WD^2}{8g} \quad [4]$$

where W = weight of disk, lb
D = diameter of disk, in.

In the case of a flywheel or pulley, the thickness is not uniform so that it is necessary to express the moment of inertia in terms of some calculated value. If it is assumed that the mass is concentrated in the rim, then

$$I = \frac{WD_r^2}{4g} \quad \text{[5]}$$

where D_r is the mean diameter of the rim in inches and g is 386 in. sec^{-2}.

If more exact calculations are made, taking into account the weight in the arms, hub, etc., the results are normally given as the sum of the individual WD^2 values for each part. In this case we have

$$I = \frac{\Sigma WD^2}{4g} = \frac{\Sigma Wr^2}{g} \quad \text{[6]}$$

where ΣWD^2 represents the sum of individual $W \times d^2$ values or ΣWr^2 represents the sum of the $W \times r^2$ values, where r is the radius of the weight W or of an element of weight W.

In all of the cases cited, the mass of the shaft has been neglected. Regardless of how the mass of the disk is expressed, the frequency can be calculated from Equation [2] by substituting the proper value for I.

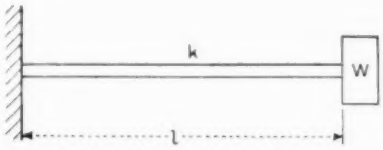


FIG. 7 WEIGHT ON END OF FIXED BEAM

The third case to be considered is that of a weight mounted on the end of a fixed beam as shown in Fig. 7. In this case, the spring constant k must be determined from the deflection characteristics of the beam. The beam deflection is given by

$$S = \frac{Wl^3}{3EI_b} \quad \text{[7]}$$

where S = beam deflection, in.
W = weight on end of beam, lb
E = modulus of elasticity, psi
I_b = moment of inertia of beam section, in.^{4}
k = spring constant of beam

$$k = \frac{W}{S} = \frac{3EI_b}{l^3} \quad \text{[8]}$$

EQUIVALENT-MASS SYSTEMS

It is necessary to reduce the complicated pumping system, shown in Fig. 4, to an equivalent system in order to determine the vibration characteristics of the system. The various rotating masses in the system operate at different speeds, and some of the masses, as in the case of the sucker rods, beam counterbalance, and engine piston, have motion of translation or have an oscillating motion instead of fixed rotation so that some method of converting these into equivalent rotating masses is necessary. The general principle, in reducing these various mass systems to an equivalent simple rotating system, is to make the conversion on the basis of equivalent kinetic-energy storage capacity.

The simplest of the cases involved is that existing in a speed reducer. This case is shown schematically in Fig. 8. Fig. 8(*a*) shows the actual gear train and Fig. 8(*b*) shows the reduced system. Let N_1 be the speed of masses i_1 and i_2, and N_2 be the speed of masses i_3 and i_4. In reducing the mass i_3 to an equivalent at the speed of shaft 1, it will be necessary to multiply i_3 by the square of the speed ratio, since the kinetic energy of the mass will vary as the square of angular velocity or speed. Since the elasticity of the gear teeth is negligible, compared with the shaft elasticity, mass i_2 and the reduced mass of i_3 will combine directly to give mass I_2. On the foregoing basis, we will have for the equivalent masses of this system

$$I_1 = i_1$$

$$I_2 = i_2 + \frac{N_2^2}{N_1^2} i_3$$

$$I_3 = i_4 \frac{N_2^2}{N_1^2}$$

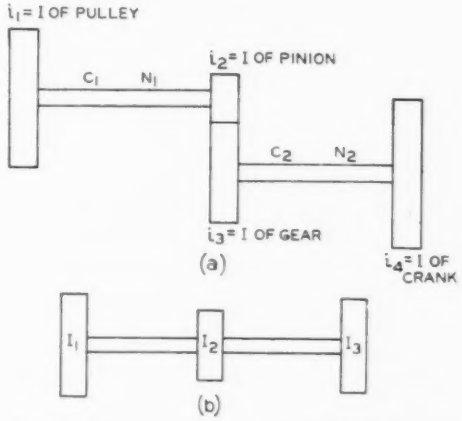


FIG. 8 SCHEMATIC DIAGRAM OF SPEED REDUCER



FIG. 9 SLIDER CRANK

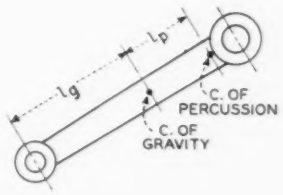


FIG. 10 CONNECTING-ROD SYSTEM

In general, the equivalent inertia of masses having rotary motion will be given by

$$I \text{ equivalent} = \frac{(\text{Speed of actual mass})^2}{(\text{Speed of equivalent mass})^2} \times I \text{ actual} \quad \text{[9]}$$

By using this formula, it is possible to reduce the mass directly to the required speed. In this paper, all masses will be reduced to the engine speed so that the term (speed of equivalent mass) will be the speed of the engine. This general formula applies regardless of the method of driving the mass, i.e., through gear, belt, or chain.

In the case of reciprocating masses, it is necessary to resort to approximations inasmuch as the actual systems become very difficult to solve mathematically. Under conditions considered, the approximations used will have little effect on the critical or resonant speeds. One case is the slider crank or engine mechanism shown in Fig. 9. This case has been treated by Timoshenko (5) who found that, for critical-speed calculations, the

weight or mass of this system can be replaced by an equivalent fixed mass at the crankshaft. As a first step in such a mass reduction, it is necessary to reduce the mass of the engine connecting rod with its complicated motion to a simple system. It can be shown that for the connecting-rod system, Fig. 10, the mass of the connecting rod can be replaced by a mass at the piston wristpin or crosshead as the case may be, and another mass at the center of percussion with respect to the wristpin axis. It is obvious that such a system does not simplify this particular problem. If this center of percussion is close to the crankpin center, the mass can be used at the crank center with sufficient accuracy. While this is obviously an approximation it will be used as the basis for reduction in this case. With this approximation we have

$$M_1 = \frac{l_p}{l_g + l_p} M$$

and

$$M_2 = \frac{l_g}{l_g + l_p} M$$

where M = mass of connecting rod
M_1 = mass of connecting rod concentrated at crankpin
M_2 = mass of connecting rod concentrated at wristpin
l_g = distance between wristpin and center of gravity, in.
l_p = distance between center of gravity and center of percussion, in.

After the connecting-rod mass has been concentrated at the wristpin and crankpin, it is necessary to convert the piston-mass

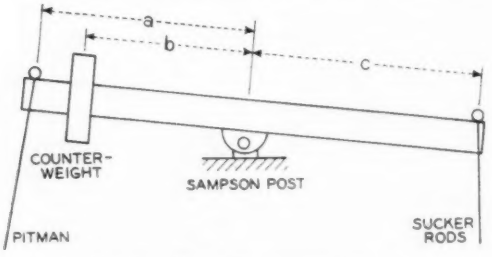


FIG. 11 BEAM COUNTERBALANCE

and connecting-rod-mass component at the wristpin to an equivalent mass or inertia at the crankpin. Timoshenko (5) shows that the mass or inertia of a disk which, concentrated at the crankshaft, will give the same kinetic-energy effect is

$$I_e = \left[M_1 + {}^1/_2(M_2 + M_p)\left(1 + \frac{r^2}{4l^2}\right)\right] r^2 \ldots\ldots [10]$$

where M_1 and M_2 are as given.

M_p = mass of piston and crosshead $= \frac{W_p}{g}$
r = crank throw, in.
l = length of connecting rod, in.
I_e = engine-parts inertia

Since for the cases considered $\frac{r}{l}$ is small, the term $\frac{r^2}{4l^2}$ will be negligible so that, for most cases, the equivalent moment of inertia will be given by

$$I_e = [M_1 + {}^1/_2(M_2 + M_p)]r^2 \text{ (approx)} \ldots\ldots [11]$$

For the case of beam counterbalance, as shown in Fig. 11, the mass can be reduced to an equivalent mass or rotating disk at the crank if the elasticity of the pitman is neglected. Beam counterbalance will, therefore, be similar to a rotary counterbalance. In working out the reduced beam mass, it is assumed that the pitman bearing on the beam has reciprocating motion. The making of this assumption is equivalent to reducing the system to that shown in Fig. 9, provided the mass of the counterbalance is first reduced to the upper pitman bearing. This can be done by making the kinetic energy of the reduced mass equal to that of the original mass. For the data shown in Fig. 11 we have

$$M_{CB} = \frac{b^2}{a^2} M_c \ldots\ldots [12]$$

where M_{CB} = reduced mass of beam counterbalance
b = distance from walking-beam center to counterbalance center of gravity, in.
a = distance from walking-beam center to wristpin center, in.
M_c = actual counterbalance mass

The equivalent inertia at the crank center will be given by

$$I_c = \frac{M_{CB}}{2}\left(\frac{L}{2}\right)^2\left(\frac{N_c}{N_1}\right)^2 \text{ (approx)} \ldots\ldots [13]$$

where $\frac{L}{2}$ = crank radius on pumping unit, in.
N_c = speed of crank or strokes per minute
I_C = equivalent counterbalance inertia, reduced to engine speed

The reduction of the sucker-rod-and-fluid system is somewhat more difficult. The sucker-rod system has sufficient length and elasticity so that it does not respond as a concentrated mass (2). The time required to transmit the motion is appreciable, and the fluid loading is intermittent so that any attempt to evaluate this system accurately is difficult. In order to arrive at a value which will serve as a basis to indicate the relative magnitude of the effect of the sucker rods on the system, it will be assumed that the integrated effect of the sucker-rod-and-fluid system will approximate that which would be obtained if the weight of the sucker rods were concentrated at the end of the walking beam. This amounts to saying that the loss of effectiveness of the sucker-rod mass, due to elasticity and time lag, is balanced by the intermittent effect of the fluid mass. On this basis, we would first reduce the sucker-rod weight at the walking beam to the pitman bearing on the basis of equivalent kinetic energy or inversely as the velocities squared. This mass would then be reduced, as is the beam counterbalance, giving

$$I_R = \frac{W_r}{2g}\left(\frac{c}{a}\right)^2\left(\frac{L}{2}\right)^2\left(\frac{N_c}{N_1}\right)^2 \text{ (approx)} \ldots\ldots [14]$$

where N_c, N_1, L are as before, c and a are as shown in Fig. 11, and W_r is the weight of sucker rods.

g = 386
I_r = effective inertia of rods at engine speed

A somewhat closer approximation of the sucker-rod-and-fluid system could be obtained by breaking the rod-and-fluid systems up into units of smaller mass and introducing elasticity between the small masses.

EQUIVALENT ELASTIC SYSTEMS

The members in a system, such as shown in Fig. 4, store elastic or potential energy. Since the various shafts rotate at different speeds and since some of the members, such as the belt and walking beam, are nonrotating members, it is necessary to reduce the system to an equivalent system of shafts rotating at engine speed. The equivalent shaft system involves both diameter and

length, since they are both involved in determining the energy which can be stored. In order to simplify the problem, the shafts will all be reduced to a unit diameter which is a diameter of 1 in. The length is then determined to give the proper energy storage. The longer the equivalent shaft, the greater its energy-storing capacity.

If a unit diameter is used as a basis for calculation, it is necessary to vary the length, in order to maintain a constant c value or energy-storage capacity. This can be arrived at by referring to Equation [3] from which

$$C = \frac{E_s}{l} \cdot \frac{\pi d^4}{32}$$

If d is made unit diameter, and l_e denotes the equivalent length we will have for a uniform shaft

$$\frac{E_s}{l} \times \frac{\pi d^4}{32} = \frac{E_s}{l_e} \times \frac{\pi \times 1^4}{32}$$

or

$$l_e = \frac{l}{d^4} \quad \ldots\ldots [15]$$

For a shaft which varies in diameter between supports, it is necessary to find the equivalent lengths of the various sections and add them together to obtain the total equivalent length of a shaft of unit diameter.

In the case of the gear-reduction system, shown in Fig. 8, it is necessary to find the equivalent torsional-rigidity constant C of shaft 2 at the engine speed. This can be determined from the equation

$$C \text{ equivalent} = \frac{(\text{Speed of actual shaft})^2}{(\text{Speed of engine shaft})^2} C \text{ actual}$$

or

$$C_e = \left(\frac{N}{N_1}\right)^2 C \quad \ldots\ldots [16]$$

where C_e = equivalent torsional rigidity of shaft
N = actual shaft speed
N_1 = engine-shaft speed
C = actual torsional rigidity of shaft

since

$$C_e = \frac{E_s}{l_e} \frac{\pi d_e^4}{32} = \frac{\pi E_s}{32 l_e} \text{ for } d_e = 1$$

and

$$C_e = \frac{\pi E_s}{32 l_e} = \left(\frac{N}{N_1}\right)^2 C = \left(\frac{N}{N_1}\right)^2 \frac{E_s}{l} \times \frac{\pi d^4}{32}$$

we have

$$l_e = \frac{l}{d^4} \times \left(\frac{N_1}{N}\right)^2 \quad \ldots\ldots [17]$$

which is the equivalent length for a shaft of unit diameter, at engine speed N_1.

The crankshaft can be presented schematically, as is shown in Fig. 12. As can be seen from this diagram it is quite difficult to arrive at an equivalent length of such a shaft. Several exact formulas based on certain assumed conditions have been worked out by Timoshenko (5). A simplified empirical formula, as given by Carter, appears to be satisfactory for normal conditions and will be used here. Using the dimensions, as given in Fig. 12, this formula can be expressed in the following form if unit diameter is assumed for the equivalent shaft, l_{ec}

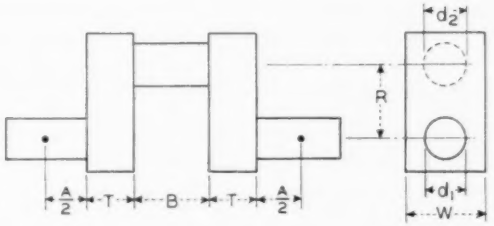


FIG. 12 SCHEMATIC DIAGRAM OF CRANKSHAFT

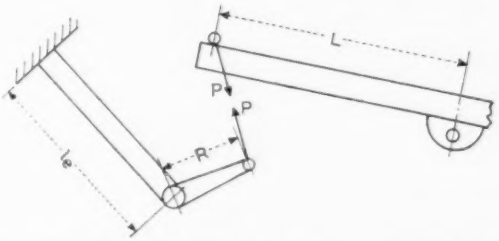


FIG. 13 SYSTEM FOR CALCULATING SHAFT EQUIVALENT TO WALKING BEAM

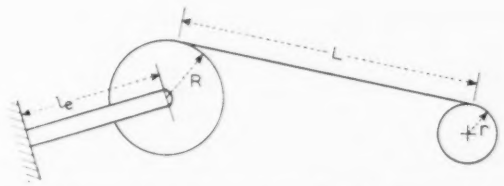


FIG. 14 EQUIVALENT DIAGRAM FOR BELT OR CHAIN DRIVE

$$l_{ec} = \left(\frac{A + 0.8T}{d^4}\right) + \left(\frac{0.75B}{d_2^4}\right) + \left(\frac{1.5R}{TW^3}\right) \quad \ldots\ldots [18]$$

The moment of inertia of the walking beam is negligible compared with the inertia of the other parts and will not be considered. This, however, does not mean that the elastic properties of the beam can be neglected. Fig. 13 shows schematically a system which will be used as a basis for calculating the equivalent shaft to have the same energy storage as the walking beam. If the beam and shaft be loaded as shown, the energy stored in the shaft is

$$U = \frac{1}{2} \frac{T^2 l_e}{E_s J} = \frac{1}{2} \frac{(PR)^2 l_e}{E_s J}$$

and that stored in the beam is

$$U = \frac{1}{6} \frac{(PL)^2 L}{EI}$$

If these are to be equal we then have

$$\frac{1}{2} \frac{(PR)^2 l_e}{E_s J} = \frac{1}{6} \frac{(PL)^2 L}{EI} \quad \ldots\ldots [19]$$

From which we find

$$l_e = \frac{1}{3} \frac{L^3}{R^2} \times \frac{E_s J}{EI} \quad \ldots\ldots [20]$$

Actually the elastic members from the crank on are effective only about one half the time. This same condition was true for the masses, and it was shown that the beam weights and the sucker rods were effective only one half the time, so that the value of the equivalent mass is only one half of the actual mass. An-

other manner of considering this problem is to note that the natural frequency of any system is a function only of the ratio of C to I. If then the mass in one part of the system is reduced, the C value will likewise have to be reduced. On this basis we have

$$l_e = \frac{1}{6}\frac{L^3}{R^2}\frac{E_e J}{EI}$$

Fig. 14 shows an equivalent diagram for a belt or chain drive. In this case the belt tension P represents only the effective pull. It is assumed that the slack-side tension does not influence the problem since it supposedly puts a constant stress or energy into the system. The energy stored in the belt will be given by

$$U = \frac{1}{2}\frac{P^2 L}{AE_B}$$

and in the shaft

$$U = \frac{T^2 l_e}{2E_e J} = \frac{(PR)^2 l_e}{2E_e J}$$

Equating these and solving for l_e we have

$$l_e = L \times \frac{E_s}{E_B}\frac{J}{AR^2}$$

For a shaft of unit diameter this reduces to

$$l_e = \frac{\pi L}{32A} \times \frac{E_s}{E_B}\frac{1}{R^2} \quad \text{[21]}$$

Fig. 15 shows a plot of data obtained from a belt test. These data show that, after the initial stretch is taken up, the modulus

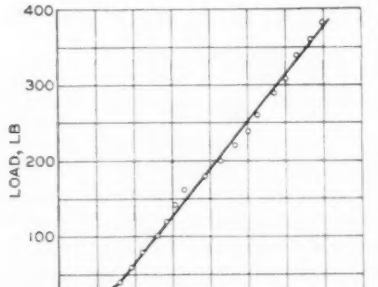


FIG. 15 DATA FROM BELT TEST

(4-ply rubber belt; 1 in. wide × 0.23 in. thick; breaking load 1200 lb; permanent stretch at B.P. = ½ in. in 18 in., Et = 22,640; stress at rupture 5454 psi.)

of elasticity for the rubber belt E_s = 22,600 psi. They will be used in determining the equivalent shaft length for a belt.

The reduction of the sucker-rod string to an elastic system, composed of several masses with elastic members in between, could be made using the same general formula. It would be necessary to reduce the sucker-rod system to the pitman and again take one half the value as was done in the case of the walking beam.

TORSIONAL VIBRATION OF WALKING BEAM

In addition to the conditions considered, it is possible for a walking beam carrying beam weights to have a torsional vibration. Under these conditions it would vibrate in a manner similar to the shaft and disk shown in Fig. 6, the inertia in this case being the inertia of the beam weights with respect to the longitudinal axis of the beam and the spring constant being the torque required to produce unit angle of twist in the beam. The calculation of the spring constant c of this system is complicated by the fact that the angle of twist and the stresses are not a function of the polar moment of inertia as used for circular shafting. Timoshenko (5) gives the following formula as an approximation to the angle of twist in an I-beam section subject to a torque T, where the dimensions are as shown in Fig. 16

$$\theta = \frac{3T}{(b_1 c_1^3 + 2b_2 c_2^3)E_s}$$

Since the spring constant $c = \frac{I}{\theta}$ we have

$$C = \frac{(b_1 c_1^3 + 2b_2 c_2^3)E_s}{3}$$

The shearing stress in a walking beam (not including stress concentration at re-entrant corners) is given by

$$S_s = \frac{3TC_2}{(b_1 c_1^2 + 2b_2 c_2^2)}$$

Since beam weights are generally rectangular in shape, their polar moment of inertia can be calculated approximately by the following formula (using dimensions as given in Fig. 17)

$$I_p = \frac{Wdt(d^2 + W^2)}{1065}$$

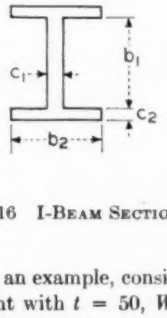


FIG. 16 I-BEAM SECTION

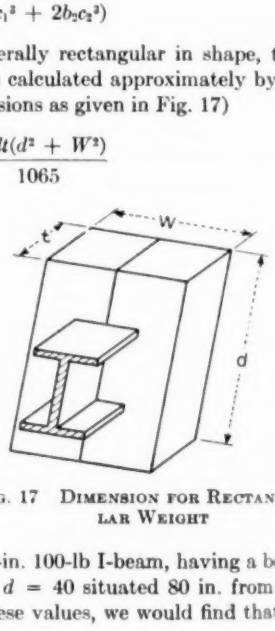


FIG. 17 DIMENSION FOR RECTANGULAR WEIGHT

As an example, consider a 24-in. 100-lb I-beam, having a beam weight with t = 50, W = 20, d = 40 situated 80 in. from the sampson-post bearing. For these values, we would find that, in round numbers

$$I_p = 75{,}000$$

$$C = 1 \times 10^6$$

and finally the frequency

$$f = \frac{1}{2\pi}\sqrt{\frac{1 \times 10^6}{75{,}000}} = 0.49 \text{ per sec} = 29 \text{ per min}$$

A 15-in. 55-lb beam with 6 weights 15 × 30 × 6 in. situated 90 in. out from the beam support would have a natural frequency of about 40 cycles per min.

In each of these cases, the natural frequency is close to the normal operating speeds. The magnitude of the natural frequency will vary with the location and magnitude of the weights. The point at which to consider the weights located will depend upon the method of anchoring the weights to the beam and may be difficult to determine.

Since the torque which may be safely carried by a beam is relatively small, it would not take a very large vibration to result in quite high stresses. A torsional vibration superimposed on a heavily loaded beam could result in an increase of stresses to the point where failure might ensue.

TABLE 1 DATA FOR PUMPING UNITS, WITH SUMMARY OF EQUIVALENT MOMENTS OF INERTIA AND ELASTICITIES

		Single cylinder		Four cylinder	
		Actual	Corrected	Actual	Corrected
	Engine speed, rpm	600		900	
	Engine pulley diameter, in.	10		8	
	Gear-reduction pulley diameter, in.	30		36	
	Gear reduction	10		10	
	Strokes per minute	20		20	
	Pulley centers, in.	60		60	
	Crank length, in.	20		20	
	Sucker rod weight, lb.	7200		7200	
	Beam balance, lb.	6000		6000	
	Beam, 7-ft centers, in-lb.	15-55		15-55	
	Belt, 6-ply rubber (approx 0.3 in. thick)	8 In. wide		8 In. wide	
	I—10-In. pulley and clutch, lb-in. per sec²	3.3	3.3		
	I—8-In. pulley, lb-in. per sec²			1.0	1.0
	I—Large pulley, lb-in. per sec²	70	7.8	140	6.9
	I—Rotary counterbalance, lb-in. per sec²	9350	10.4	9350	4.6
	I—Beam balance, lb-in. per sec²	3110	3.5	3110	1.5
	I—Sucker rod, lb-in. per sec²	3730	4.2	3730	1.8
	I—Large gear, lb-in. per sec²	240	0.27	240	0.12
	I—Pinion, lb-in. per sec²	0.1	0.01	0.1	0.005
	I—Piston, rod, crank lb-in., per sec²	9.8	9.8	0.5	0.5
	I—Flywheel, lb-in. per sec²	930	930	46.4	46.4
	l_e—Equivalent lengths of unit diameter, in:				
1	Flywheel to crank	0.074	0.074		
2	Crank to pulley	0.15	0.15		
3	First crank to second crank			0.14	0.14
	Second to third			0.22	0.22
	Third to fourth			0.14	0.14
	Fourth to flywheel			0.20	0.20
4	Flywheel to pulley			0.15	0.15
5	Belt	52	52	81.5	81.5
6	Pulley to pinion	0.179	1.61	0.179	3.62
7	Gear to crank	0.0236	21.2	0.0236	47.8
8	Pitman	Negligible		Negligible	
9	Beam	0.04	36	0.04	81

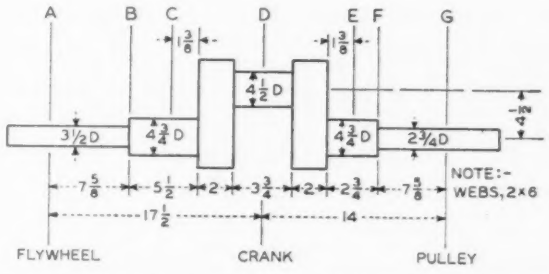


FIG. 18 DETERMINING EQUIVALENT LENGTH OF CRANKSHAFT

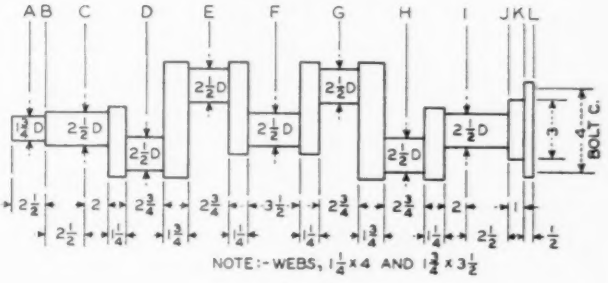


FIG. 19

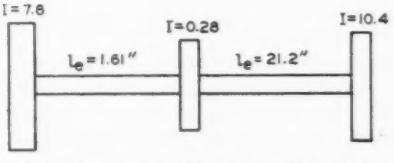


FIG. 20 EQUIVALENT LENGTH OF PINION SHAFT

CALCULATION OF TYPICAL ELEMENTS

The critical speeds in a pumping-unit system will be dependent upon the specific values of the sizes and weight of the many parts. Each case will have its own critical speeds and should, therefore, be analyzed separately.

A typical pumping unit can, however, be used to illustrate the method of solving for critical speeds and give some indication as to the relative importance of the various parts in the vibrating system. Two pumping units were selected, one with a single-cylinder and the other with a four-cylinder engine. The data for both cases, with a summary of the equivalent moments of inertia and elasticities, are given in Table 1.

The following examples should illustrate the methods used to calculate the equivalent elasticities. On the crankshaft in Fig. 18, the equivalent length from the flywheel to point B is, by Equation [15]

$$l_{ab} = \frac{7^1/_2}{(3^1/_2)^4} = 0.050 \text{ in.}$$

Since the equivalent shaft will be considered as rotating at engine speed, there is no correction for speed. The equivalent length between point B and the center of the main bearing C is found in like manner and added to l_{ab} to give the equivalent length of the unit diameter shaft. Section C-E is the crank. Using Carter's formula

$$l_{ac} = \frac{2 \times 1^3/_8 + 0.8 \times 2}{(4^3/_4)^4} + \frac{0.75 \times 3^3/_4}{(4^1/_2)^4} + \frac{1.5 \times 4^1/_2}{2 \times 6^3}$$

$$= 0.031 \text{ in.}$$

One half of this added to l_{ac} gives the equivalent length between the flywheel and the crank.

The equivalent length of the pinion shaft, Fig. 20, is

$$l_p = \frac{7}{(2^1/_2)^4} = 0.179 \text{ in.}$$

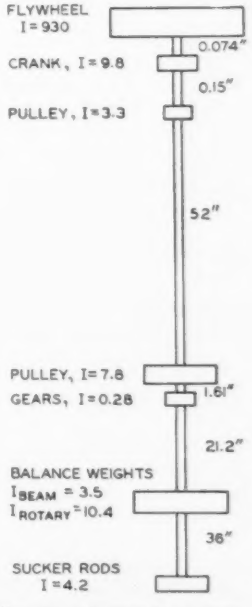


FIG. 21 SINGLE-CYLINDER EQUIVALENT SYSTEM

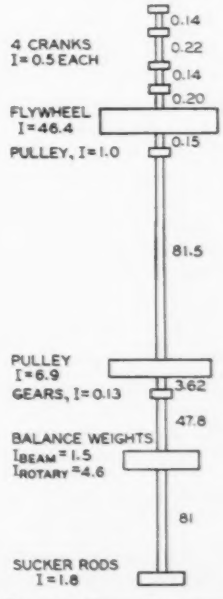


FIG. 22 FOUR-CYLINDER EQUIVALENT SYSTEM

This length is at the pinion-shaft speed so must be corrected to engine speed, giving

$$l_{p1} = 0.179 \times \left(\frac{600}{200}\right)^2 = 1.61 \text{ in.}$$

The equivalent length of the belt is based on Equation [21].

$$l_{belt} = \frac{\pi \times 60}{32 \times 0.3 \times 8} \times \frac{12{,}000{,}000}{22{,}600} \times \frac{1}{(5)^2} = 52 \text{ in.}$$

This length is based on the engine-pulley radius so no correction is necessary.

The equivalent length of the beam is based on Equation [20].

$$l_{beam} = \frac{1}{6} \times \frac{2(7 \times 12)^2}{20^2} \times \frac{12{,}000{,}000}{30{,}000{,}000} \times \frac{\frac{\pi(1)^4}{32}}{509} = 0.04 \text{ in.}$$

The moment of inertia of the beam cross section is 509 in.^{4} The value of l_{beam} must be corrected for speed.

$$l_{beam} = 0.04 \times \left(\frac{600}{20}\right)^2 = 36 \text{ in.}$$

After all the mass moments of inertia have been calculated, they must be corrected to engine speed. The rotary-counterbalance mass moment of inertia about the crank was found to be 9350 lb in. sec^2 at a crank speed of 20 rpm, therefore

$$I_{cb} = 9350 \times \left(\frac{20}{600}\right)^2 = 10.4 \text{ lb in. sec}^2$$

Summary

An analysis of the cases outlined in the previous section shows that the belt elasticity and the moment of inertia of the engine flywheel are the two outstanding parts of the system. The sucker rods and counterbalance are not nearly as effective as the lighter engine flywheel because of their slow speed.

The entire system may be closely approximated by a two-mass system since the equivalent length of the belt is long when compared to the lengths of the other equivalent lengths. The general formula for solving a two-mass system is

$$N = \frac{60}{2\pi} \sqrt{\frac{\pi E_s d^4 (I_1 + I_2)}{32 I_1 I_2 l}}$$

where N = vibrations per min
d = diameter of shaft, in.
I_1 = moment of inertia of one mass, lb in. sec^2
I_2 = moment of inertia of second mass, lb in. sec^2
l = length of shaft, in.

With this approximation, the critical speed of the single-cylinder unit with rotary counterbalance becomes

$$N = \frac{60}{2\pi} \sqrt{\frac{\pi \times 12{,}000{,}000 \times 1^4 (943 + 23)}{32(943)\,(23)\,52}} = 304 \text{ rpm}$$

Table 2 gives the remaining critical speeds calculated.

TABLE 2 CRITICAL SPEEDS

	Critical speeds, rpm	
	Rotary balance	Beam balance
Single cylinder	304	364
Four cylinder	354	393

These values indicate that pumping units do operate at values near the critical speed. Naturally, these speeds must be watched and kept a safe distance (20 to 30 per cent) from this critical speed.

To make a further analysis of the problem, the two ends of the complete unit may be analyzed individually without introducing any appreciable error. The belt is the elastic member separating the two ends.

In solving for the critical speeds of the pumping end of the system, it is to be noticed that there are four masses to be considered. However, the mass of the gears is very small and also relatively close to the mass of the pulley. Therefore, the mass of the pulley and the mass of the gears may be considered as one for most practical purposes. This assumption greatly simplifies the solution of the problem. The usual equation for solving three-mass systems is

$$\left(\frac{I_1 I_2 I_3}{k_1 k_2}\right)\omega^4 - \left(\frac{I_1 I_2 + I_1 I_3}{k_1} + \frac{I_2 I_3 + I_1 I_3}{k_2}\right)\omega^2 + (I_1 + I_2 + I_3) = 0$$

where I = moments of inertia, lb in. sec^2

$$k = \frac{E_s}{l_s} \times \frac{\pi d^4}{32}$$

ω = radians per sec

The critical points for the single-cylinder pumping unit with the rotary counterbalance are determined as follows

$$I_1 + I_2 + I_3 = 22.7$$

$$k_1 = \frac{12{,}000{,}000 \times \pi}{22.8 \times 32} = 51{,}600$$

$$k_2 = 32{,}700$$

$$\frac{I_1 I_2}{k_1} = \frac{8.1 \times 10.4}{51{,}600} = 0.00163$$

$$\frac{I_1 I_3}{k_2} = \frac{8.1 \times 4.2}{51{,}600} = 0.00066$$

$$\frac{I_1 I_3}{k_2} = \frac{8.1 \times 4.2}{32{,}700} = 0.00104$$

$$\frac{I_2 I_3}{k_2} = \frac{10.4 \times 4.2}{32{,}700} = 0.00134$$

$$\frac{I_1 I_2 I_3}{k_1 k_2}\omega^4 = \frac{8.1 \times 10.4 \times 4.2}{51{,}600 \times 32{,}700}\omega^4 = 0.00000021\omega^4$$

so $0.00000021\omega^4 - 0.00467\omega^2 + 22.7 = 0$

Solving by the quadratic equation

$$\omega^2 = 7220 \text{ or } 15000$$

$$\omega = 85 \text{ or } 122.5 \text{ radians per sec}$$

$$N_1 = \frac{122.5 \times 60}{2\pi} = 1170 \text{ rpm}$$

$$N_2 = \frac{85 \times 60}{2\pi} = 812 \text{ rpm}$$

The critical speeds for the other counterweights are given in Table 3.

TABLE 3 CRITICAL SPEEDS FOR COUNTERWEIGHTS

	Critical speeds, rpm	
Single cylinder		
Rotary balance	812	1170
Beam balance	808	1680
Zero balance	815	....
Four cylinder		
Rotary balance	680	1130
Beam balance	740	1680
Zero balance	755	....

A general study of these values indicates

1 That the second critical speed is of the same order of magnitude as the engine speed.

2 That the belt and engine flywheel are the largest items involved, and any change in their values may greatly affect the critical speed.

The fact that the various critical speeds are within the normal operating ranges for oil-well pumping conditions and the fact that the actual measured torque cards show the presence of such vibrations indicate that further study of this problem may be desirable. The presence of damped resonance vibrations may result in high gear-tooth and belt loads so any method of eliminating them will permit operation of equipment with a lower factor of safety or at a higher rating. Further work is contemplated on the study of the effect of engine explosions on the peak torque transmitted to gear teeth and the effect of this peak on rating formulas.

BIBLIOGRAPHY

1 "Vibration Problems in Oil Wells," by J. C. Slonneger, American Petroleum Institute, Drilling and Production Practice, 1937, pp. 179.
2 "An Investigation of Experimental Methods of Determining Sucker Rod Loads," by E. N. Kemler, Trans. American Institute of Mining and Metallurgical Engineers, vol. 118, 1936, pp. 89–99.
3 "Factors Influencing the Application of Pumping Units," by E. N. Kemler, American Petroleum Institute, Drilling and Production Practice, 1938, pp. 183–208.
4 "Progress Report on Engine Drive Factor," by J. R. Mahan, Proceedings, American Petroleum Institute, Ninth Mid-Year Meeting, May, 1939, Section 4, Division of Production, pp. 175–176.
5 "Vibration Problems in Engineering," by S. Timoshenko, D. Van Nostrand Co., Inc., New York, N. Y., 1937.
6 "Mechanical Vibrations," by J. P. Den Hartog, Second edition, 1940, McGraw-Hill Book Company, Inc., New York, N. Y.
7 "Practical Solution of Torsional Vibration Problems," by W. K. Wilson, second edition, 1940, John Wiley & Sons, Inc., New York, N. Y.
8 "Torsional Vibration," by W. A. Tuplin, John Wiley & Sons, Inc., New York, N. Y., 1934.

Discussion

EUGENE HOSFORD.[3] There have been various fundamental rules established for the selection of a pumping unit and engine, but in the past there seems to have been very little attention given to the speed at which the equipment should be operated. The general rule is to operate the unit at a speed which will pump the required amount of fluid. In this paper, the authors have shown that the critical speed of certain pumping systems can occur at normal operating speeds. Certainly, such operating speeds should be avoided if at all possible. The A.P.I. peak-torque rating of gears may be sufficiently high to allow for a reasonable increase in torque due to vibration without failure of the gears, but it is of real importance that this paper present a definite method of determining at which speeds the torque may be the highest. Before the formulas included in this paper can be accurately used for calculating torque on the gears, an evaluation of the effect of engine explosions must be made. It is fortunate that such an investigation is planned by the authors of this paper.

J. C. SLONNEGER.[4] The dominating masses in an oil-well pumping system are the engine flywheel (or flywheels), counterweight, and unit drive sheave, in the order named. The elastic system is primarily made up of the belt drive, the unit shaft, and, in the case of engines having a flywheel on the outer end, the crankshaft of the engine. All other masses and elastic members may be neglected in ordinary calculations for the purpose of predicting critical speeds. By comparing exact calculations with the foregoing assumption, it has been found that the difference in calculations is 3 per cent or less.

In making calculations it is usually more convenient to reduce the system to the high-speed shaft of the unit. In this way it is rather simple to compare various belt drives and engines on any given pumper. The authors have reduced the system to the engine shaft.

Single-noded vibrations are most bothersome to slow-speed engines. It should be remembered that the amplitude of any vibration is a function of the disturbing force, which in this case is a function of cyclical variation. The tuning of systems for this type of engine should be such that if criticals cannot be completely avoided, they should be chosen at the top of the engine speed range where the cyclical variation is smallest.

On the other hand, with multicylinder engines, single-noded vibrations usually have a frequency lower than that of the disturbing force, and therefore are harmless. However, the frequency of two-noded vibrations is very troublesome here in avoiding synchronism. The unit sheave because of its speed often has as much torsional inertia as the counterweight and dominates the two-noded vibrations. A study shows that two-noded vibrations are little influenced by the belt resilience because of the small amplitude of the flywheel, and also because the frequency is a function of the square root of the resilience. In V-belt drives, usually used with multicylinder engines, evidence of critical speeds is given by violent vibration of the belts.

Timoshenko's method of reducing a reciprocating mass to a rotary mass is applicable only in cases where the frequency of the disturbing force is equal to or less than the frequency of reciprocation. This applies to crankshafts of engines but not to a beam counterbalance. The disturbing force is usually more than 4 times as rapid as the reciprocating motion of the beam counterbalance; in some cases, it is as much as 150 times as rapid. The effect of the beam counterbalance is to change continuously the frequency of the system as its effectiveness changes with the crank angle. This is evidenced in the authors' Fig. 2. The variation in amplitude is due entirely to the system's falling in and out of synchronism from the causes just cited. Note that, in Fig. 1, the amplitude of vibration remains nearly constant since this is a rotary balance having constant tuning.

AUTHORS' CLOSURE

Mr. Slonneger has given a very concise discussion of the interpretation and application of vibration phenomena as applied to oil-well pumping systems. The authors have corrected an error in the preprint which Mr. Slonneger called to their attention. The approximations which he has suggested greatly simplify the solution of such problems. There is, however, danger from oversimplification; and each type of problem must be considered separately. As is indicated in Fig. 22 for example, the sucker rods may be as important as the rotary balance. The example shown in Fig. 2 is for a rotary counterbalance and not a beam balance as Mr. Slonneger infers.

The method of solution offered in the main paper is intended only as an approximation. To illustrate the accuracy to be expected, the critical speeds for a four-mass system are given in Table 4. These results are as accurate as any data that might be used. They show that the accuracy is much better when

TABLE 4 CRITICAL SPEEDS BASED ON A FOUR-MASS SYSTEM

	Critical speeds		
Single cylinder			
Rotary balance	325	774	1140
Beam balance	372	783	1660
Four cylinder			
Rotary balance	277	878	1230
Beam balance	344	878	1730

[3] Mechanical Engineer, Gulf Oil Corporation, Tulsa, Okla.
[4] Assistant Chief Engineer, The Continental Supply Company, Dallas, Texas.

the inertia of the engine and flywheel is great compared to the other elements. The results for the four-cylinder engine as determined by the approximate method are not in as good agreement as those of the single-cylinder.

The exact solution for the critical speeds of a four-mass system can be determined from the following equation. The use of this equation eliminates the necessity of making some of the approximations which Mr. Slonneger suggests or the approximations the authors made.

$$-w^6\frac{I_1I_2I_3I_4}{k_1k_2k_3}+w^4\left(\begin{array}{l}\dfrac{(I_1+I_2)I_3I_4}{k_2k_3}\\ +\dfrac{(I_2+I_3)I_1I_4}{k_1k_3}\\ +\dfrac{(I_3+I_4)I_1I_2}{k_1k_2}\end{array}\right)-w^2\left(\begin{array}{l}\dfrac{(I_1+I_2+I_3)I_4}{k_3}\\ +\dfrac{(I_1+I_2)(I_3+I_4)}{k_2}\\ +\dfrac{(I_2+I_3+I_4)I_1}{k_1}\end{array}\right)$$
$$+I_1+I_2+I_3+I_4=0$$

The authors appreciate the helpful suggestions and comments offered by Messrs. Hosford and Slonneger. It is hoped that further work along the lines suggested by Mr. Hosford will be possible in the near future.

Air-Heater Facts: 1926–1941

By E. L. HOPPING[1] and D. F. SCHICK, JR.,[2] PHILADELPHIA, PA.

In 1926, data were presented by N. E. Funk covering several types of air heaters used on boilers equipped with economizers and on some not so equipped. The equipment selected for discussion at the Chester and Richmond Stations of the Philadelphia Electric Company was relatively new at the time, but provided a valuable basis for future selection of air-heater units. The present paper gives facts pertaining to experience gained in operation of the air heaters previously mentioned; applications of new heaters to recently installed generating equipment; applications in associated industries; and trends evident in an analysis of new units. Further detail is given covering the selection of air heaters, corrosion problems, methods of eliminating corrosion, cleaning air-heater units, and troubles experienced with air-heater installations.

IN a paper[3] before this Society in 1926, N. E. Funk presented comparative data on several types of air heaters used on boilers equipped with economizers and on others not so equipped. Tubular, plate, and regenerative air heaters were used. Experience was confined to tests on relatively new equipment at the Chester, Delaware, and Richmond Stations of the Philadelphia Electric Company. The data presented for the various arrangements of air heaters provided a valuable reference source for the future selection of air-heater units.

The present paper gives facts pertaining to experience with the air heaters discussed in the original paper, applications of heaters with more recently installed generating equipment, a brief summary of air-heater applications in associated industries, and the trends evident in an analysis of new units.

References made to specific stations are those of the Philadelphia Electric Company.

Air heaters are generally classified in two groups, i.e., the recuperative, those which transfer heat through a partition, continuously heating the cool side by conductive transfer from the hot; and the regenerative, those which alternately heat and cool the same mass, regenerating it thermally by passing hot gas over its surface.

The recuperative type includes the plate air heater composed of alternately spaced plates for air and gas passage, and the tubular air heater composed of a nest of tubes with the gas usually passing through the tubes.

Regenerative heaters may be stationary multichambered heating elements provided with dampers to alternate the gas-air flow. Usually, however, they are of the rotating heating element type, such as Ljungström air-heater units.

Selection of Air Heater

Studies dealing with the air heater are primarily economic. For each British thermal unit received from the flue gases by the air for combustion, there is a like decrease of heat to be supplied by the fuel in heating the air to furnace temperature. Capitalization of the annual fuel saving, debited by additional cost of fans and fan-power requirements, represents a theoretical maximum that can be spent for an air heater.

Practically the most economic proportioning of heating surface leads to the selection of the largest-size air heater possible. The air heater offers a low-temperature heat-absorbing surface, making it possible to obtain high thermal efficiency. Air-heater surface is relatively low-cost surface in contrast to the pressure parts of a boiler unit. A limiting factor for maximum surface is temperature. The gas temperature cannot be carried too low because of sulphur corrosion when the temperature of the gas approaches the dew point for the sulphur in the fuel, while the maximum air temperature is limited by firing conditions. Within such limits lie the proper proportioning of air-heater and economizer surface.

Corrosion of air heaters is primarily brought about by lowering the flue-gas temperatures below the dew point of the acid constituents of the flue gas. The outgoing flue gas should not be lowered to such an extent that the metal temperature of the air heater approximates the dew point. In all probability, the rate of corrosion would be greatest at the temperature of the dew point because of the combined action of the acid film and of substances brought into solution. The dew point, as previous investigators have indicated, is higher than appears from the moisture content alone, especially because of the presence of sulphur compounds in the gas. On account of the high boiling point of sulphuric acid, a trace of this vapor in the flue gas is sufficient to cause a high dew point. The corroding agents in the soot and fly ash in the gas accelerate this action. In the following discussion of corrosion, a limiting factor for metal temperature is indicated to be the fuel composition.

The outgoing-air temperature is another limiting factor. Here, the type of firing limits the temperature to which the air can be heated. Stoker firing limits the air temperatures to 300 to 400 F, because of stoker maintenance, while pulverized fuels, oil, and gas allow considerably higher air temperatures of 500 to 600 F.

An additional margin of safety is desirable because of the inability to secure even distribution of gas over all air-heater surfaces, particularly at low loads, resulting in certain areas having temperatures below the average.

Additional factors of space requirements, draft losses in the air and gas passages, ease of cleaning and repair, are a few other items to be evaluated before making final selection of the air heater.

Corrosion

An investigation made by The Babcock & Wilcox Company, relative to external corrosion of economizers and one which would be equally applicable to air heaters, indicates the possibility of corrosion according to the relation between metal temperatures and the sulphur content of the fuels.

The information obtained was from operating data and observation of the equipment on various installations, with respect to the presence or absence of attack on the tubes. It was further indicated that an exact relationship could not be established since other conditions, such as moisture in the fuel, are a part of the problem. However, these other variable factors approximate an average for the normal range of fuels, leaving sulphur as an index of the corrosion probability.

[1] Mechanical Engineer, Philadelphia Electric Company. Mem. A.S.M.E.

[2] Engineer, Mechanical-Engineering Division, Philadelphia Electric Company. Mem. A.S.M.E.

[3] "Comparative Performance of Air Preheaters," by N. E. Funk, Trans. A.S.M.E., vol. 48, 1926, pp. 337–356.

Contributed by the Power Division and presented at the Semi-Annual Meeting, Kansas City, Mo., June 16–19, 1941, of The American Society of Mechanical Engineers.

Note: Statements and opinions advanced in papers are to be understood as individual expressions of their authors, and not those of the Society.

When burning pulverized coal, the limiting range between no active corrosion and active corrosion appeared to be a metal temperature of approximately 160 F with 2 per cent by weight of sulphur in the coal, extending to 250 F with 5 per cent by weight of sulphur in the coal.

Burning coal on a stoker indicated the desirability of maintaining somewhat higher gas-outlet temperatures to avoid corrosion through the same sulphur range. With pulverized fuel, the

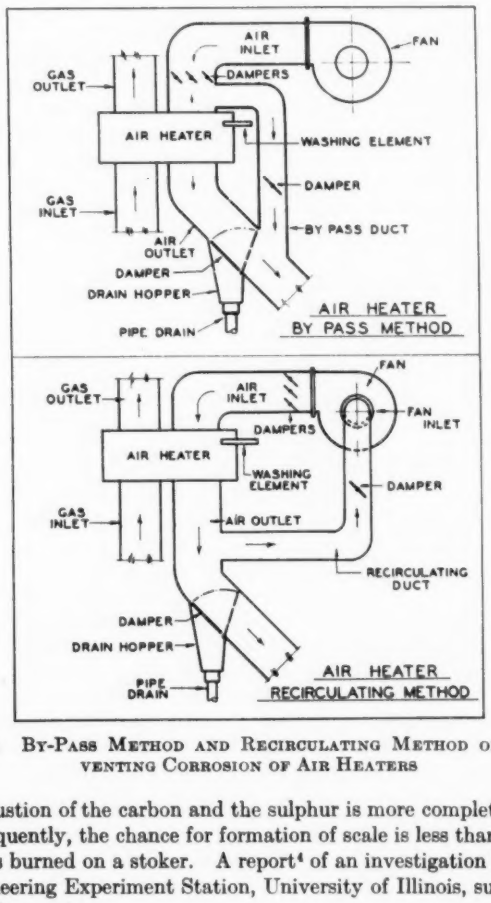


FIG. 1 BY-PASS METHOD AND RECIRCULATING METHOD OF PREVENTING CORROSION OF AIR HEATERS

combustion of the carbon and the sulphur is more complete and, consequently, the chance for formation of scale is less than when coal is burned on a stoker. A report[4] of an investigation by the Engineering Experiment Station, University of Illinois, supports this observation.

The results of the combustion of the sulphur in coal are not definitely known. Investigators assume, however, that for the most part the sulphur oxidizes to sulphur dioxide in the furnace. Then, as the colder portions of the system are reached, this gas is further partially oxidized to sulphur trioxide.

PREVENTION OF CORROSION BY BY-PASS AND OTHER MEANS

Since corrosion of air heaters, due to condensation of moisture carried by the flue gas, is most likely to occur at low ratings on the boiler, some simplified by-pass schemes are of value.

One of the most simplified schemes provides for a direct air by-pass duct for the air heater. This by-pass around the unit lowers the air-gas ratio and, therefore, increases the air temperature through the air heater and raises its metal temperature because of reduced heat transfer.

Another arrangement provides for recirculating the air. Air ducts are arranged so that some of the air discharged from the air heater returns to the inlet of the forced-draft fan. This arrangement increases the temperature of the entering air and raises the metal temperatures at the cold end. It is also possible to use a separate fan for recirculation.

Fig. 1 shows two arrangements as applied to the regenerative type of air heater. Similar arrangements are readily adaptable to the tubular-type air heater.

Where air heaters are operating under severe corrosion conditions special materials are used for the heating elements. Elements of varying depth on the cold end of Ljungström units are made replaceable and of special alloy. Corrosion tests show increased life with elements of Toncan iron and zinc-coated steel with only slightly increased initial cost. In other cases, heavier-gage tubes or heavier-gage elements are initially installed for tubular and regenerative units.

On pulverized-fuel-fired boilers at the Richmond and Schuylkill Stations of the Philadelphia Electric Company, provision has been made to by-pass Ljungström air heaters. The forced-draft fans are located above the air heaters. The by-pass duct takes a portion of cold air at the discharge of the fan and delivers the cold air to the warm-air-discharge side of the air heater. When outlet gas temperatures fall to 300 F, the by-pass duct is opened. This lowers the air-gas ratio, and outlet-flue-gas temperatures are raised to 300 F or higher. It is assumed that negligible corrosion will exist on the units above 300 F and, with this procedure, satisfactory corrosion experience has been the result. The Richmond air heaters have been in operation since 1935, and the Schuylkill units since 1938.

Limited experience when burning fuel oil in the Schuylkill boilers has not indicated any special problem, however, the sulphur content of this fuel oil was under 1 per cent.

The recirculating method has been installed with Ljungström units on pulverized-fuel-fired boilers at the Chester Station of the same company, but these units have only recently gone into operation. This method takes warm air, discharged from the air heater, and returns it to the inlet of the forced-draft fan. While the kilowatthour input to the forced-draft fan will increase during recirculation, this will occur only at low-load periods and does not increase the cost of fan or the normal power requirements. The increased air temperature to the boiler during this period may be a compensating item. The temperature of the air-heater elements should be increased, but whether the increase is substantial and formation of moisture and flue-dust corrosion will be eliminated remain to be determined after a period of longer operation and observation.

By means of the arrangements of duct work mentioned, an attempt is made to establish a relationship between condensation temperature and corrosion. In preventing the formation of a film of sulphuric acid on the metal, the temperature of the metal seems to be more important than that of the temperature of the gas or the air. The temperature of the gases may be well above the dew point, however, the metal may be below the dew point, due to the cooling effect of the cold forced-draft air.

Experience by the authors' company indicates that the tendency to clog tubes or air-heater sections, operating with stoker-fired boilers, is more likely than with pulverized-fuel-fired boilers. Since corrosion usually starts in clogged areas, the hazard then is greater with the stoker-fired boilers. As previously mentioned, this can be attributed to the fact that with pulverized fuel the combustion of the carbon and the sulphur in the coal is more complete.

Two Ljungström air heaters, installed at the Chester Station in 1925, and operating with a stoker-fired boiler, have required considerable maintenance of plates due to corrosion. This is in direct contrast to the very favorable, although shorter, experience with similar equipment on the pulverized-fuel-fired boilers previously mentioned.

[4] "The Corrosion of Power Plant Equipment by Flue Gases," by H. F. Johnstone, University of Illinois, Engineering Experiment Station, Bulletin No. 228, 1931.

Cleaning Air Heaters

Ljungström Units. Means should be provided for cleaning the surface of all air heaters as they are always subject to fouling from fly ash and dust in the flue gases.

With the Ljungström type of air heater, stationary steam soot blowers are usually located above and below the heating elements. Closely spaced nozzles sweep the heating elements as the rotor turns. To supplement this cleaning, a water-washing device using warm water is often provided for the air side. A hopper in the duct below the unit traps the waste water. This drain hopper is also shown in Fig. 1. During the washing period, it is necessary to reduce the rotor speed which is accomplished by means of a reducing gear. Air motors for slow-speed driving are being used with success, providing a minimum rotation of 1 revolution per 15 min.

Soot deposits materially increase the resistance to flow and the fan power consumption. However, the heat transfer is not necessarily materially affected, because of the regenerative principle, since the heat is not required to pass through the metal as is the case with plate and tubular units.

The Richmond Station air heaters are periodically water-washed. These 600,000-lb per hr boilers are not equipped with economizers, and outlet-gas temperatures from the air heaters are approximately 400 F at full load. At minimum boiler load, it is attempted to maintain 300 F or higher.

It has not been necessary to wash the air heaters on 600,000-lb per hr boilers at the Schuylkill Station. These latter units are equipped with economizers but outlet-gas temperatures from the heaters are higher than with the Richmond units. The higher gas temperature and the smaller quantity of fly ash through the heater because of ash trapped below the economizer probably accounts for the difference in operating practice.

Tubular Units. Cleaning the tubular air heater is usually more difficult. Water washing during periods of outage is most common. Some installations are successfully cleaned by means of high-pressure air lances alone.

Troubles Experienced

An analysis of troubles reported by one boiler manufacturer and experienced with various types of air heaters in utility and industrial service over a period of approximately 14 years indicates corrosion as the greatest offender. Such corrosion occurred with low unit gas temperatures and at the cold end. Recirculation methods either remedied this trouble or prolonged the life of the metals. In some cases, improved distribution of gases, installation of baffles, and tightening of the duct to prevent leakage improved performance of the equipment.

A discussion of troubles which have occurred should not overshadow the fact that in most cases they were rectified. Further, the troubles actually occurred in only a very small proportion of the total boiler installations.

Experience With Plate-Type Heaters at the Deepwater Station

During 1930, four plate-type sectional air heaters, five sections high by three sections wide, 90 plates per section, No. 14 gage sheet steel, containing 0.25 per cent Cu, 46,400 sq ft, were installed on pulverized-fuel-fired boilers. At maximum boiler load of 330,000 lb per hr evaporation, the gas temperature out of the unit is approximately 325 F.

Two plate-type sectional air heaters, five sections high by three sections wide, 102 plates per section, No. 14 gage sheet steel, containing 0.25 per cent Cu, 52,800 sq ft, were installed on reheat boilers. At maximum boiler load of 290,000 lb per hr evaporation, gas temperature out of the unit is approximately 325 F.

This station has operated at a very high load factor over the 11-year period, and no repairs nor replacements have been made on the air heaters. When the boilers are off at infrequent intervals, the air heaters are blown out with air and regular inspections are made for leakage.

However, during the first year the plant was operated, when burning a poor grade of coal, it was necessary to wash the air heaters frequently with high-pressure water, but this practice was not continued sufficiently long to cause any trouble. This experience applies to four standard and two reheat boilers installed in the plant.

TABLE 1 INVESTIGATION OF CORROSION ON TUBULAR AIR HEATERS; RICHMOND STATION BOILERS

Test no.	1	2	3	4	5	6	7	8	9	10
Gas temperature at air-heater outlet, F.....	244	246	280	278	352	...	255	257	269	275
Tube No. 7, temperature, F.....	174	170	182	179	193	210	237	242	247	250
Tube No. 8, temperature, F.....	158	155	163	160	151	191	218	224	227	230
Tube No. 9, temperature, F.....	152	150	158	155	179	150	191	198	207	210

Test Nos. 1 and 2.... Boiler rating, 155 per cent
Test Nos. 3 and 4.... Boiler rating, 220 per cent
Test No. 5..... Boiler rating, 280 per cent
Test No. 6..... Boiler banked but had a heavy fire; ashpit water on
Test Nos. 7 and 8.... Boiler on dead bank; ashpit water on
Test Nos. 9 and 10... Boiler on dead bank; ashpit water off

Test on No. 60 boiler. Tubes, 90 wide by 15 deep = 1350 tubes per unit
Tube No. 7... 35th tube; outside row; couple 6 in. below upper sheet
Tube No. 8... 21st tube; outside row; couple 6 in. below upper sheet
Tube No. 9... 4th tube; outside row; couple 6 in. below upper sheet

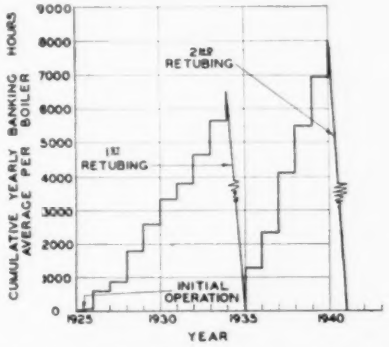


Fig. 2 Yearly Banking Hours, Showing Retubing of Air Heaters for Twelve Stoker-Fired Boilers at Richmond Station

Plate-Type Heaters at Chester Station

The paper[3] by N. E. Funk, previously referred to, included statistics for Nos. 5 and 6 plate-type heaters installed in the Chester Station. The life of these units was exceptionally short, 2 and 4 years, respectively. This short life is attributed to the inability to clean the plates properly, which resulted in excessive corrosion. Nonuniform gas flow, because of cleaning difficulties, probably accelerated the corrosion. These plate units were replaced with the tubular-design heater.

Tubular-Air-Heater Study

Richmond Station. Fig. 2 indicates the average life of tubes on twelve 200,000-lb per hr stoker-fired boilers at the Richmond Station. The original heater installation, 1925, consisted of hot-finished seamless-steel tubes, $2^1/_2$ in. outside diam, 25 ft $^1/_4$ in. long, No. 12 gage, having 22,072 sq ft of surface. During 1934 and 1935, after 10 years of operation, it was necessary to retube the air heaters because of excessive corrosion. Retubing was completed on the twelve units using electric-resistance and lap-welded No. 10 gage steel tubes. At the end of 1940, it was again necessary to retube the air heaters. The greatest number of defective tubes was at the back of the preheater, where the

tubes are first contacted by cold air. There was no apparent choice between the life of the electric-resistance and the lap-welded installations.

Boiler banking during the last 6 years was higher than during the previous 10-year period, as the chart, Fig. 2, indicates, so an investigation followed to determine if lower tube temperatures were maintained during the banking period, which might accelerate sulphur corrosion.

An analysis of recent conditions, Table 1, indicates that the coolest tubes in the air heater are warmer while the boiler is banked than during normal operation at higher rating. This is to be expected, since, during the banked period, the gases are entrapped and very small quantities of cold air are passed over the tubes. It is also possible that a distillation of the coal takes place, depositing moisture on the tubes, facilitating corrosion.

At low boiler ratings additional readings were taken. The gas temperatures are in the same range as during banking, but the tube temperatures have decreased, due to the introduction of cold air across the tubes. The short life of the tubes could not therefore be attributed directly to banking hours.

Chester Station. Table 2 gives a further case history of air heaters at the Chester Station over the life of the units. The corrosion conditions were in general similar to experience at the Richmond Station. Active corrosion occurred inside the gas tubes at the upper rear section where cold air sweeps the tubes. It will be noticed that boilers Nos. 2, 4, 6, and 8 have been relatively free from corrosion, as compared with Nos. 1, 3, 5, and 7 units. These latter units were affected to a greater extent because of their location in close proximity to a row of windows with an ambient temperature of 12 to 14 F below the opposite row. The higher gas-outlet temperature on No. 8 boiler, 400 F, compared to 300 F and below for the others, accounts for the satisfactory tube conditions with this unit.

These tubular units are designed so that the gases make one pass through the 25-ft-long tubes. The air makes four passes over the tubes from the fans to the boiler. Most severe corrosion extended to 6 in. below the second tube sheets with some corrosion showing below the third tube sheet. The remaining sections were relatively free from attack.

Conclusions on Corrosion

During periods of operation with low gas temperatures, particularly when gas temperatures are below approximately 300 F, severe corrosion may exist.

The tendency toward corrosion seems to be more severe with stoker-fired units than with pulverized-fuel-fired units.

On tubular air heaters, the corrosion exists inside the tube and is greatest in the vicinity where the incoming cold air passes over the hot tubes. The first bank of tubes struck by the cold air is most affected. Similarly, with the regenerative type of unit, most severe corrosion exists on the plates at the cold-air end.

The immediate cleaning of air heaters, when a boiler is taken off the line, may be an important factor in retarding corrosion.

TABLE 2 INVESTIGATION OF CORROSION ON SEVERAL TYPES OF AIR HEATERS; CHESTER STATION BOILERS

Unit no. and type	Installed	Retubed	Surface, sq ft	Repairs since retubing	Retubed
1 Tubular....	1925	1933	22072	446 New tubes	1940 291 Blanks
2 Tubular....	1925	1933	22072	....	....
3 Tubular....	1924	1933	22072	341 New tubes	1941 164 Blanks
4 Tubular....	1925	1933	22072	....	....
5 Plate, Connery P.E. design....	1925	Tubular 1927	22072	427 New tubes	1940 214 Blanks
6 Plate, B.&W. design....	1924	Tubular 1929	22072	....	....
7 Ljungström.	1925	New elements 1928–1929	2–32480	....	Severe corrosion
8 Tubular....	1925	....	50276	....	....

NOTE: Boilers Nos. 1, 3, 5, 7, heaters face windows.
Boilers Nos. 2, 4, 6, 8, heaters face bank of boilers.
Ambient temperature Nos. 1, 3, 5, 7, forced-draft fans 12 to 14 F below Nos. 2, 4, 6, 8.
No. 5 boiler generally used as regulating unit.

Maintenance Costs of Air Heaters

An investigation of Fig. 2, showing the life of tubular air heaters at Richmond, and Table 2, indicating experience with various types of air heaters at the Chester Station, has provided information for additional comparisons. When it becomes necessary to replace tubes due to corrosion, usually the entire tube nest is replaced. During the period, however, some new tubes may have been inserted and others blanked out of service. Replacement costs are negligible until the time for complete retubing, when an appreciable capital expenditure is required. During this period, leakage may be cumulative until retubing takes place, at which time with new tubes and tight tube sheets, it is again eliminated. An example of a method used by The Babcock & Wilcox Company to make a tight air-heater casing, particularly at the ends where the tube sheet has to move, is shown in Fig. 3. This construction employs a bellows-type expansion joint between the bottom plate and the casing channel.

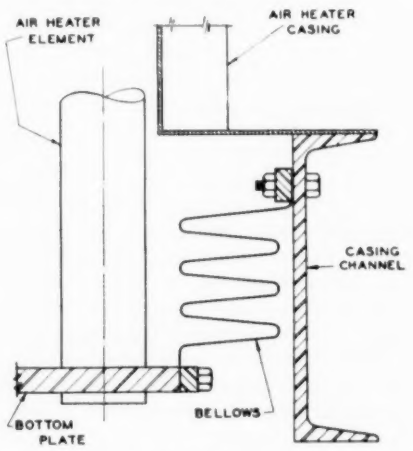


FIG. 3 BELLOWS-TYPE EXPANSION JOINT

With the Ljungström air heater, leakage is necessarily present, due to the rotating element and the method of sealing. Expressed in percentage of gas entering the unit, it ranges from 6 to 8 per cent at full load, increasing with decreasing boiler loads and wear. With proper maintenance of seals, this leakage should be held within normal limits. Variations in differential pressures will necessarily affect this leakage.

Figures compiled by The Air Preheater Corporation for the

TABLE 3 LJUNGSTRÖM AIR HEATERS

Year	1926	1927	1928	1929	1930	1931	1932	1933	1934	1935	1936	1937	1938	1939	1940
Number of heaters in operation	85	158	197	243	281	302	310	316	327	340	379	416	502	527	568
Average size of heater	16.33	17.20	17.23	16.93	17.07	17.08	17.08	17.06	17.04	16.97	16.84	16.75	16.81	16.79	16.81
Replacement value of heating surface expressed in percentage of heater cost	...	...	...	...	...	0.59	0.51	1.68	1.06	0.71	0.91	1.15	0.91	1.36	1.27
Replacement value of spare parts with exception of heating surface, expressed in percentage of heater cost	...	...	...	...	...	1.04	0.52	0.62	1.09	0.75	1.49	1.87	0.95	1.27	1.32

years 1926 to 1940, inclusive, are given in Table 3. The tabulation shows the number of Ljungström air heaters in operation by December 31, of the respective years indicated, average size of heater, replacement value of heating surface and of spare parts, expressed in percentage of heater cost f.o.b. Wellsville, N. Y. Cost of parts includes rebuilding of old units to rotor center support and center drive, but does not include replacement cost of fan parts where integral forced and induced fans are used.

Oil-Refinery Practice

A refiner reports that the main advantage to an oil refinery of using air heaters is that, in many cases on oil-cracking stills, the inlet oil temperature is in the neighborhood of 700 F, with the exit gas temperatures in the range of 950 F, when convection banks are used. When the inlet oil temperatures are around 700 F, it is necessary to install some heat-recovery equipment. A recent paper[5] by O. F. Campbell and T. B. Kimball presents further information relative to refinery practice. Among other items, they consider the economy of eliminating the convection bank of a cracking-still furnace and substituting an air heater.

Additional advantages when using an air heater lie in the fact that there are fewer oil tubes to clean, that there is less original cost of alloy tubes and headers, and that preheated-air temperature increases the rate of heat transfer by radiation, due to the higher furnace temperature.

An analysis of Ljungström air heaters of various sizes and varying quantities of flue gas and air handled reflects average high-temperature air-heater operation for oil-refinery practice as follows:

Flue-gas inlet temperatures to the air heaters range between 910 and 1275 F. Gas outlet temperatures range between 315 and 650 F. Air outlet temperatures from the air heater are similarly higher than experienced in public-utility practice and range from 700 to 1055 F.

One refiner, using the tubular-type air heater, reports this experience with refinery equipment during the last 10 years:

A tabulation of expected performance and test data on tubular-type air heaters indicates that the actual performance is closely in line with that specified and that these refinery air heaters also operate at rather high temperatures when compared to utility-boiler practice. These higher temperatures are accounted for through the use of heat exchangers providing feed temperatures above 500 F. With cracking stills and furnaces, a "soaking" section is usually included in the convection path of the furnace where the oil must be held at temperatures in the vicinity of 1000 F. The primary purpose of these refinery air heaters, therefore, is to reduce what would otherwise be excessive stack loss.

In marine installations, this same company finds it preferable to use sufficient stage heaters to give satisfactory boiler-feed temperatures without the use of economizers and to obtain a proper stack temperature and boiler efficiency by the use of an air heater. In this way, maintenance difficulties with economizers are eliminated and a higher air temperature is obtained which is of considerable advantage when using a very heavy low-grade fuel oil.

In refinery practice, generally higher temperatures account for the absence of corrosion difficulties.

Recent Applications of Air Heaters

An analysis of the last 2 years' sales of the regenerative air heater, applied to boilers for public-utility service, indicates a gradual increase in size of unit (square feet of heating surface) and in heat recovery. Twenty of the boilers considered are rated 500,000 lb per hr or above, Table 4.

TABLE 4 RECENT APPLICATIONS OF LJUNGSTRÖM AIR HEATER WITH BOILERS RATED 500,000 LB PER HR OR ABOVE

No. boilers	No. heaters	Capacity × 1000	Surface per boiler, sq ft	Efficiency of air heater, per cent	Resistance Air	Resistance Gas	Air temp., F In	Air temp., F Out	Gas temp., F In	Gas temp., F Out
1	2	1000	283000	63.2	4.4	3.2	80	580	660	294
2	4	750	47800	46.8	4.2	4.0	80	484	719	420
1	2	650	110000	62.6	4.35	3.7	80	529	635	288
1	2	650	..	53.0	3.10	3.6	80	595	730	386
2	4	615	148000	64.2	2.26	1.7	80	607	680	295
2	4	615	108200	58.3	1.74	1.74	80	505	619	305
2	4	600	59600	50.6	2.94	3.2	80	545	709	391
2	4	550	99400	58.4	2.12	2.34	80	602	720	346
2	4	550	99400	58.4	2.12	2.34	80	602	720	346
1	2	550	..	52.2	2.3	2.4	80	531	680	367
1	2	525	51600	55.2	2.88	2.74	80	530	682	350
1	2	535	51600	55.2	2.88	2.74	80	530	682	350
2	4	500	90000	60.8	2.44	2.25	80	510	610	288

TABLE 5 RECENT APPLICATIONS OF TUBULAR AIR HEATER WITH BOILERS RATED 300,000 LB PER HR OR ABOVE

No. boilers	Capacity × 1000	Surface per boiler, sq ft	Efficiency of air heater, per cent	Air temp, F In	Air temp, F Out	Gas temp, F In	Gas temp, F Out
1	900	147500	60.0	80	510	680	319
3	575	32630	42.5	80	415	690	430
1	550	133600	56.0	80	570	690	347
1	450	77300	53.5	80	502	618	330
3	424	30200	45.4	100	359	545	342
1	400	77400	54.5	100	515	650	350
2	375	26720	42.3	80	425	625	395
2	375	56077	53.6	100	486	642	350
2	350	55600	57.0	100	524	680	350
2	315	22075	43.5	80	395	646	400
2	300	34800	48.5	80	423	650	372

The efficiencies for the various installations 500,000 lb per hr and above are tabulated and range from 46.8 to 64.2 per cent. This efficiency is by definition $\frac{T \text{ gas in} - T \text{ gas out}}{T \text{ gas in} - T \text{ air in}}$ for the regenerative unit. The per cent efficiency of the air heater, compared with the square feet of air-heater surface per boiler, indicates the trend in increased size and recovery. The limiting factor for percentage of heat recovery appears to be the acceptable minimum gas temperature and maximum air temperature.

Table 4 gives further details regarding the resistance through the units, the air temperatures, and the gas temperatures for the twenty representative installations.

An analysis of recent sales of tubular-type air heaters indicates a somewhat similar trend. Again, twenty of the most recent sales are tabulated as installed on boilers rated 300,000 lb per hr and above, where the limiting factors are indicated as the minimum gas temperature and maximum air temperature, Table 5.

Trends in Air-Heater Selection—Explanation of Charts

Fig. 4 presents graphically data pertaining to air-heater installations for public-utility service, obtained from boiler statistics compiled for the A.E.I.C. in a report of the Committee on Power Generation, for a 5-year period to date. Table 6 shows the actual tabulation. Only boilers installed, having a capacity of 100,000 lb per hr or over, are included. These boiler data show a predominance of pulverized-coal, oil, or gas fuel installations during the last 5 years with practically an equal division between the tubular and the Ljungström air heater. Relatively insignificant in number were those installations having a plate or steam air heater or no air heater.

Figs. 5, 6, and 7 further subdivide the installations among three boiler-capacity ranges, i.e., 100,000 lb per hr to 295,000 lb per hr, 300,000 lb per hr to 495,000 lb per hr, and 500,000 lb per hr and higher. Table 7 itemizes this subdivision.

With the lower-capacity boilers, the tubular air heater predominates. With the intermediate-sized boilers, the Ljungström shows a marked increase in popularity; there is a corresponding decrease in the use of tubular units. An analysis of

[5] "Regenerative-Type Air Heaters for Refinery Use," by O. F. Campbell and T. B. Kimball, A.P.I. Meeting, Tulsa, Okla., May 19–22, 1941.

TABLE 6 AIR-HEATER TRENDS

Total boilers purchased	Type of firing and type of air heater: Pulverized-coal, oil, or gas units	Stoker units	Equipped with: Tubular type	Ljungström type	Plate, steam, no air heater
			1939–1940		
74	64	10	37	31	6
100%	87%	13%	50%	42%	8%
			1938–1939		
36	32	4	18	17	1
100%	89%	11%	50%	47%	3%
			1937–1938		
21	18	3	12	6	3
100%	86%	14%	57%	28%	15%
			1936–1937		
79	64	15	27	37	15
100%	81%	19%	34%	47%	19%
			1935–1936		
19	18	1	14	4	1
100%	95%	5%	74%	21%	5%
			Totals		
229	196	33	108	95	26
100%	86%	14%	47%	42%	11%

NOTE: Only boilers 100,000 lb per hr or above are included.

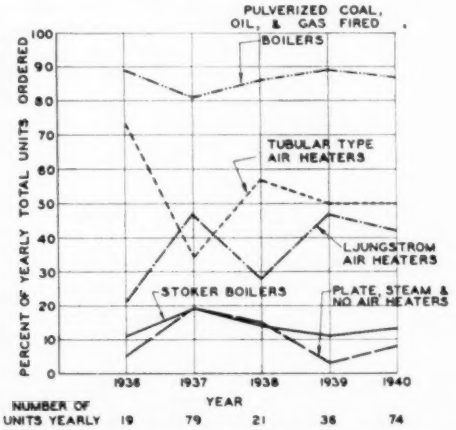


FIG. 4 TYPES OF AIR HEATERS INSTALLED IN BOILERS OF MORE THAN 100,000-LB PER HR CAPACITY, ORDERED DURING A 5-YEAR PERIOD FOR PUBLIC-UTILITY SERVICE

TABLE 7 AIR-HEATER TRENDS—CAPACITY OF BOILERS VERSUS TYPES OF FIRING AND TYPE OF AIR HEATER

Boiler rating: 100–295 M lb per hr	300–495 M lb per hr	500–1000 M lb per hr	Pulverized-coal, oil, or gas units	Stoker units	Tubular type	Ljungström type	Plate steam, no air heater
			1939–1940				
25			20	5	15	6	4
	33		28	5	18	14	1
		16	16	..	4	11	1
			1938–1939				
10			7	3	8	2	..
	15		14	1	9	5	1
		11	11	..	1	10	..
			1937–1938				
11			10	1	10	..	1
	8		6	2	2	4	2
		2	2	..	..	2	..
			1936–1937				
42			35	7	14	18	10
	26		18	8	12	9	5
		11	11	..	1	10	..
			1935–1936				
1			..	1	..	..	1
	12		12	..	11	1	..
		6	6	..	3	3	..

NOTE: Only boilers 100,000 lb per hr or above included.

large-size boilers indicates all to be of the pulverized-coal, oil, or gas type with the Ljungström heaters greatly predominating in this class of service.

Summarizing all the charts, we find a general trend toward the application of the Ljungström units with an increase in capacity of the steam generator. This is particularly noticeable during the period of increase in capacity in existing power-plant structures. During the latter part of the period, when entirely new plants and structures were being erected, this tendency was not so pronounced; perhaps due to greater space available in the new plant for the generally larger tubular-type air heater.

In conclusion, the authors wish to thank the various manufacturers and the users of air-heater equipment for their assistance in supplying information incorporated in this paper.

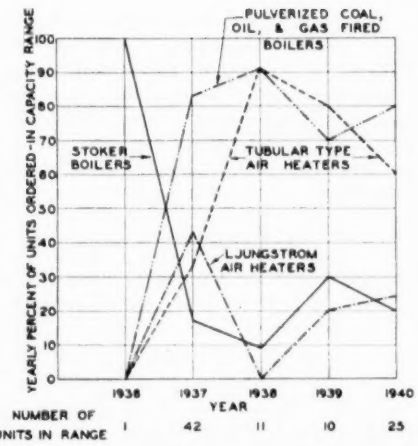


FIG. 5 TYPES OF AIR HEATERS INSTALLED IN BOILERS WITHIN THE CAPACITY RANGE OF 100,000 LB PER HR TO 295,000 LB PER HR

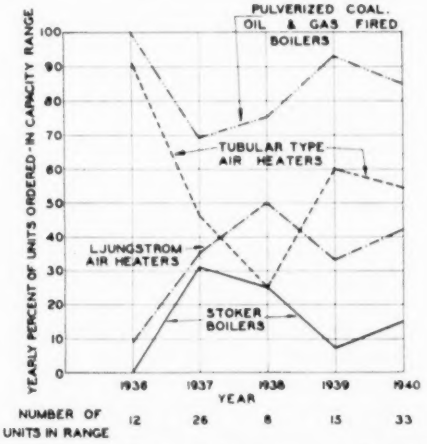


FIG. 6 TYPES OF AIR HEATERS INSTALLED IN BOILERS WITHIN THE CAPACITY RANGE OF 300,000 LB PER HR TO 495,000 LB PER HR

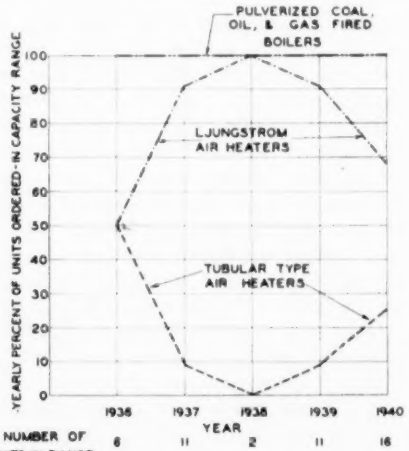


FIG. 7 TYPES OF AIR HEATERS INSTALLED IN BOILERS WITHIN THE CAPACITY RANGE OF 500,000 LB PER HR TO 1,000,000 LB PER HR

Discussion

O. F. Campbell.[6] The authors are to be complimented for their efforts in assembling pertinent air-heater data for 1926–1941. From the data included in the paper, it would appear that a purchaser of air heaters may make a more intelligent choice of a preheater for definite duty.

The corrosion of air heaters, which is apparently quite indefinite, occurs in many instances when the exit flue gases are well above the dew point. Several cases of air-heater corrosion have been attributed to condensation of acid after the flue gases have left the air heater, where the duct construction has been such as to allow the condensed acid to drip back on the air-heater elements or run down the sides of the exit flue-gas duct into the air heater. The cases referred to occurred where the installation of the air heater was placed outdoors, without insulation of the exit flue-gas duct or other protection. It is suggested that any air-heater installation made outdoors should be so designed as to guard against condensed acid falling or dripping back on the air-heater elements.

Each type of preheater has its own advantages and disadvantages. One of the advantages of the regenerative-type air heater is its apparent ability to stand abuse. An illustration of the severe duty imposed upon a Ljungström regenerative air heater is cited. The air heater was installed on a cracking still. The forced- and induced-draft fans were driven with an electric motor, and a power interruption occurred. Immediately after the power interruption, the soot and sulphur deposits on the air-heater elements ignited and two sections of the rotor were fused together or melted. Upon resumption of power, it was found that the rotor could not be turned with the ordinary driving mechanism. The rotor was then started manually by the application of a 48-in. pipe wrench to the pinion-gear shaft. After the rotor was loosened, the ordinary driving mechanism had sufficient power to turn it over. The still then continued to operate for approximately 50 days after the power interruption. Combustion conditions were not satisfactory because of the two sectors of the rotor which were destroyed but, nevertheless, the still continued in operation.

Where electrical energy is the sole source of power for the forced- and induced-draft fans, and power interruptions are likely to occur, smothering steam should be used at the entrance of the air heater in sufficient quantity to prevent burning of deposits on the air-heater elements and consequent destruction of the air-heater rotor. For refinery practice, smothering steam should be used on all air-heater installations to protect the air heater when power failure occurs.

J. H. Sengstaken.[7] The authors have given us a complete and extremely interesting report on air preheaters and their development since the paper[3] by N. E. Funk in 1926. This discussion will attempt to indicate how a number of operators, whose boilers have been designed for high over-all efficiency and low exit-gas temperatures at normal loads, have overcome the possibility of clogging and corrosion at low loads when the heating surface in the preheaters normally might be expected to reach the dew point of the gases.

With particular reference to the Ljungström air preheater, which operates on the regenerative cycle, the metal temperature is not affected by any deposit of soot on the heating surface at the cold end. Moreover, all of the surface passes through all of the gases and air so that all of the heating surface at any point along the path of gas travel is at the same average temperature.

These units are designed so that under normal conditions the rates of gas and air flows are very nearly equal. Thus, the average metal temperature at the cold end, during one revolution of the rotor, is an arithmetic average of the exit-gas and entering-air temperatures. During the course of one revolution of the rotor, the heating-surface temperature at the cold end will vary between 10 and 20 deg above and below the average temperature for that revolution. Thus, if the temperature of the air entering the preheater is added to that of the gases leaving, and a certain amount deducted for the variation in the cold-end metal temperature during a revolution, a totalized figure will be obtained which will indicate the actual minimum temperature of the heating surface. This can be maintained above the dew point by the use of air by-pass or air-recirculating ducts. The control can be either manual or made entirely automatic by the use of damper-operating equipment, actuated from the totalized temperature. In every case where this method of operation has been established, difficulties from clogging and corrosion have been entirely eliminated.

As to recirculation, the higher mass velocity of the air passing through the preheater tends to pull the metal temperature down toward that of the incoming air. The contrary is true with by-passing, since the mass velocity of the air is reduced and the heating surface then tends to rise toward the temperature of the gases. This is a safety factor in favor of air by-passing.

In a number of cases, the writer has discovered that, while apparently the temperature of the metal at the cold end, as indicated by the recording instruments measuring exit-gas temperature and room-air temperature should be safely above the dew point, clogging has occurred on perhaps one air preheater in a row. Investigation indicated that such a preheater was near an open window with the forced-draft fan taking air directly from outside. Thermocouples placed in the air inlet to the preheater have indicated this immediately. The control herein described can overcome difficulty from this source automatically.

Other examples of corrosion which have occurred, when apparently the temperatures were correct, have been solved by cleaning the preheater immediately after the boiler has been shut down and before the preheater has had an opportunity to cool off. It has been found that severe corrosion can sometimes take place during the shutdown period if the preheater has not been cleaned. Certain types of deposits on the surface absorb moisture from the cool air drifting through the preheater, resulting in severe corrosion. Cleaning the surfaces has taken off the deposits thereby entirely eliminating the corrosion.

Authors' Closure

The authors wish to express their thanks to those who offered discussion on this paper and, further, their appreciation of the interest shown by those who submitted material incorporated in the paper.

More recent experience obtained by the authors' company would indicate that the by-pass method for the reduction of corrosion is most satisfactory. The recirculation method, which was installed at Chester Station, whereby a portion of hot air was discharged from the air heater and returned to the forced-draft fan, did not prove practicable. With this arrangement there was a tendency for fly ash in small quantities to be carried through to the forced-draft ducts and to be discharged in the air near the forced-draft-fan inlet.

The heated air discharged in the vicinity of the forced-draft-fan floor was also an objectionable feature as the recirculating duct was opened directly before the forced-draft-fan inlets.

The system at Chester was adjusted to provide for a direct air by-pass.

[6] Combustion Engineer, Sinclair Refining Company, East Chicago, Ind. Mem. A.S.M.E.

[7] Sales Manager, The Air Preheater Corporation, New York, N. Y. Mem. A.S.M.E.

TABLE 6 AIR-HEATER TRENDS

Total boilers purchased	Type of firing and type of air heater: Pulverized-coal, oil, or gas units	Stoker units	Equipped with: Tubular type	Ljungström type	Plate, steam, no air heater
			1939–1940		
74	64	10	37	31	6
100%	87%	13%	50%	42%	8%
			1938–1939		
36	32	4	18	17	1
100%	89%	11%	50%	47%	3%
			1937–1938		
21	18	3	12	6	3
100%	86%	14%	57%	28%	15%
			1936–1937		
79	64	15	27	37	15
100%	81%	19%	34%	47%	19%
			1935–1936		
19	18	1	14	4	1
100%	95%	5%	74%	21%	5%
			Totals		
229	196	33	108	95	26
100%	86%	14%	47%	42%	11%

NOTE: Only boilers 100,000 lb per hr or above are included.

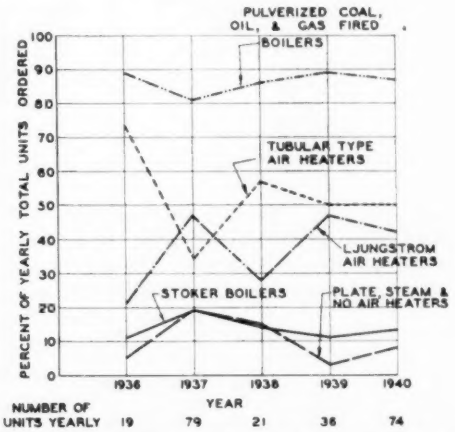


FIG. 4 TYPES OF AIR HEATERS INSTALLED IN BOILERS OF MORE THAN 100,000-LB PER HR CAPACITY, ORDERED DURING A 5-YEAR PERIOD FOR PUBLIC-UTILITY SERVICE

TABLE 7 AIR-HEATER TRENDS—CAPACITY OF BOILERS VERSUS TYPES OF FIRING AND TYPE OF AIR HEATER

Boiler rating: 100–295 M lb per hr	300–495 M lb per hr	500–1000 M lb per hr	Pulverized-coal, oil, or gas units	Stoker units	Tubular type	Ljungström type	Plate steam, no air heater
			1939–1940				
25			20	5	15	6	4
	33		28	5	18	14	1
		16	16	..	4	11	1
			1938–1939				
10			7	3	8	2	..
	15		14	1	9	5	1
		11	11	..	1	10	..
			1937–1938				
11			10	1	10	..	1
	8		6	2	2	4	2
		2	2	..	..	2	..
			1936–1937				
42			35	7	14	18	10
	26		18	8	12	9	5
		11	11	..	1	10	..
			1935–1936				
1			..	1	..	..	1
	12		12	..	11	1	..
		6	6	..	3	3	..

NOTE: Only boilers 100,000 lb per hr or above included.

large-size boilers indicates all to be of the pulverized-coal, oil, or gas type with the Ljungström heaters greatly predominating in this class of service.

Summarizing all the charts, we find a general trend toward the application of the Ljungström units with an increase in capacity of the steam generator. This is particularly noticeable during the period of increase in capacity in existing power-plant structures. During the latter part of the period, when entirely new plants and structures were being erected, this tendency was not so pronounced; perhaps due to greater space available in the new plant for the generally larger tubular-type air heater.

In conclusion, the authors wish to thank the various manufacturers and the users of air-heater equipment for their assistance in supplying information incorporated in this paper.

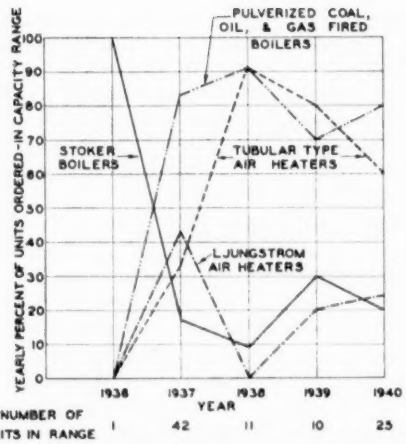


FIG. 5 TYPES OF AIR HEATERS INSTALLED IN BOILERS WITHIN THE CAPACITY RANGE OF 100,000 LB PER HR TO 295,000 LB PER HR

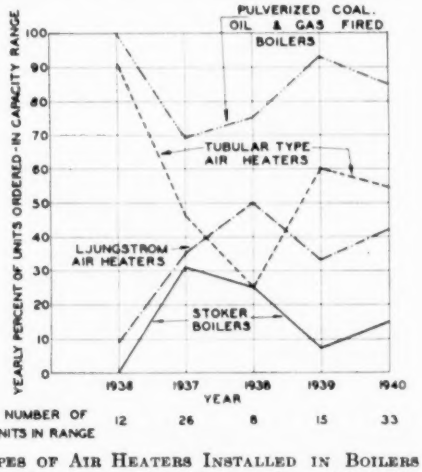


FIG. 6 TYPES OF AIR HEATERS INSTALLED IN BOILERS WITHIN THE CAPACITY RANGE OF 300,000 LB PER HR TO 495,000 LB PER HR

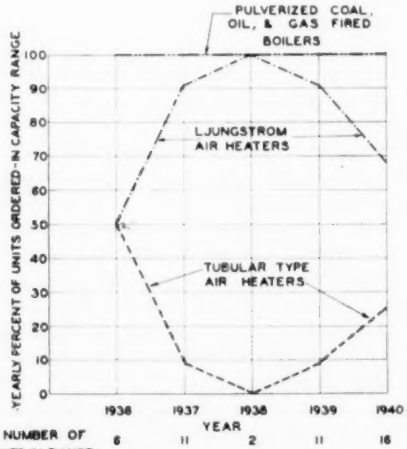


FIG. 7 TYPES OF AIR HEATERS INSTALLED IN BOILERS WITHIN THE CAPACITY RANGE OF 500,000 LB PER HR TO 1,000,000 LB PER HR

Discussion

O. F. CAMPBELL.[6] The authors are to be complimented for their efforts in assembling pertinent air-heater data for 1926–1941. From the data included in the paper, it would appear that a purchaser of air heaters may make a more intelligent choice of a preheater for definite duty.

The corrosion of air heaters, which is apparently quite indefinite, occurs in many instances when the exit flue gases are well above the dew point. Several cases of air-heater corrosion have been attributed to condensation of acid after the flue gases have left the air heater, where the duct construction has been such as to allow the condensed acid to drip back on the air-heater elements or run down the sides of the exit flue-gas duct into the air heater. The cases referred to occurred where the installation of the air heater was placed outdoors, without insulation of the exit flue-gas duct or other protection. It is suggested that any air-heater installation made outdoors should be so designed as to guard against condensed acid falling or dripping back on the air-heater elements.

Each type of preheater has its own advantages and disadvantages. One of the advantages of the regenerative-type air heater is its apparent ability to stand abuse. An illustration of the severe duty imposed upon a Ljungström regenerative air heater is cited. The air heater was installed on a cracking still. The forced- and induced-draft fans were driven with an electric motor, and a power interruption occurred. Immediately after the power interruption, the soot and sulphur deposits on the air-heater elements ignited and two sections of the rotor were fused together or melted. Upon resumption of power, it was found that the rotor could not be turned with the ordinary driving mechanism. The rotor was then started manually by the application of a 48-in. pipe wrench to the pinion-gear shaft. After the rotor was loosened, the ordinary driving mechanism had sufficient power to turn it over. The still then continued to operate for approximately 50 days after the power interruption. Combustion conditions were not satisfactory because of the two sectors of the rotor which were destroyed but, nevertheless, the still continued in operation.

Where electrical energy is the sole source of power for the forced- and induced-draft fans, and power interruptions are likely to occur, smothering steam should be used at the entrance of the air heater in sufficient quantity to prevent burning of deposits on the air-heater elements and consequent destruction of the air-heater rotor. For refinery practice, smothering steam should be used on all air-heater installations to protect the air heater when power failure occurs.

J. H. SENGSTAKEN.[7] The authors have given us a complete and extremely interesting report on air preheaters and their development since the paper[3] by N. E. Funk in 1926. This discussion will attempt to indicate how a number of operators, whose boilers have been designed for high over-all efficiency and low exit-gas temperatures at normal loads, have overcome the possibility of clogging and corrosion at low loads when the heating surface in the preheaters normally might be expected to reach the dew point of the gases.

With particular reference to the Ljungström air preheater, which operates on the regenerative cycle, the metal temperature is not affected by any deposit of soot on the heating surface at the cold end. Moreover, all of the surface passes through all of the gases and air so that all of the heating surface at any point along the path of gas travel is at the same average temperature.

These units are designed so that under normal conditions the rates of gas and air flows are very nearly equal. Thus, the average metal temperature at the cold end, during one revolution of the rotor, is an arithmetic average of the exit-gas and entering-air temperatures. During the course of one revolution of the rotor, the heating-surface temperature at the cold end will vary between 10 and 20 deg above and below the average temperature for that revolution. Thus, if the temperature of the air entering the preheater is added to that of the gases leaving, and a certain amount deducted for the variation in the cold-end metal temperature during a revolution, a totalized figure will be obtained which will indicate the actual minimum temperature of the heating surface. This can be maintained above the dew point by the use of air by-pass or air-recirculating ducts. The control can be either manual or made entirely automatic by the use of damper-operating equipment, actuated from the totalized temperature. In every case where this method of operation has been established, difficulties from clogging and corrosion have been entirely eliminated.

As to recirculation, the higher mass velocity of the air passing through the preheater tends to pull the metal temperature down toward that of the incoming air. The contrary is true with by-passing, since the mass velocity of the air is reduced and the heating surface then tends to rise toward the temperature of the gases. This is a safety factor in favor of air by-passing.

In a number of cases, the writer has discovered that, while apparently the temperature of the metal at the cold end, as indicated by the recording instruments measuring exit-gas temperature and room-air temperature should be safely above the dew point, clogging has occurred on perhaps one air preheater in a row. Investigation indicated that such a preheater was near an open window with the forced-draft fan taking air directly from outside. Thermocouples placed in the air inlet to the preheater have indicated this immediately. The control herein described can overcome difficulty from this source automatically.

Other examples of corrosion which have occurred, when apparently the temperatures were correct, have been solved by cleaning the preheater immediately after the boiler has been shut down and before the preheater has had an opportunity to cool off. It has been found that severe corrosion can sometimes take place during the shutdown period if the preheater has not been cleaned. Certain types of deposits on the surface absorb moisture from the cool air drifting through the preheater, resulting in severe corrosion. Cleaning the surfaces has taken off the deposits thereby entirely eliminating the corrosion.

AUTHORS' CLOSURE

The authors wish to express their thanks to those who offered discussion on this paper and, further, their appreciation of the interest shown by those who submitted material incorporated in the paper.

More recent experience obtained by the authors' company would indicate that the by-pass method for the reduction of corrosion is most satisfactory. The recirculation method, which was installed at Chester Station, whereby a portion of hot air was discharged from the air heater and returned to the forced-draft fan, did not prove practicable. With this arrangement there was a tendency for fly ash in small quantities to be carried through to the forced-draft ducts and to be discharged in the air near the forced-draft-fan inlet.

The heated air discharged in the vicinity of the forced-draft-fan floor was also an objectionable feature as the recirculating duct was opened directly before the forced-draft-fan inlets.

The system at Chester was adjusted to provide for a direct air by-pass.

[6] Combustion Engineer, Sinclair Refining Company, East Chicago, Ind. Mem. A.S.M.E.

[7] Sales Manager, The Air Preheater Corporation, New York, N. Y. Mem. A.S.M.E.

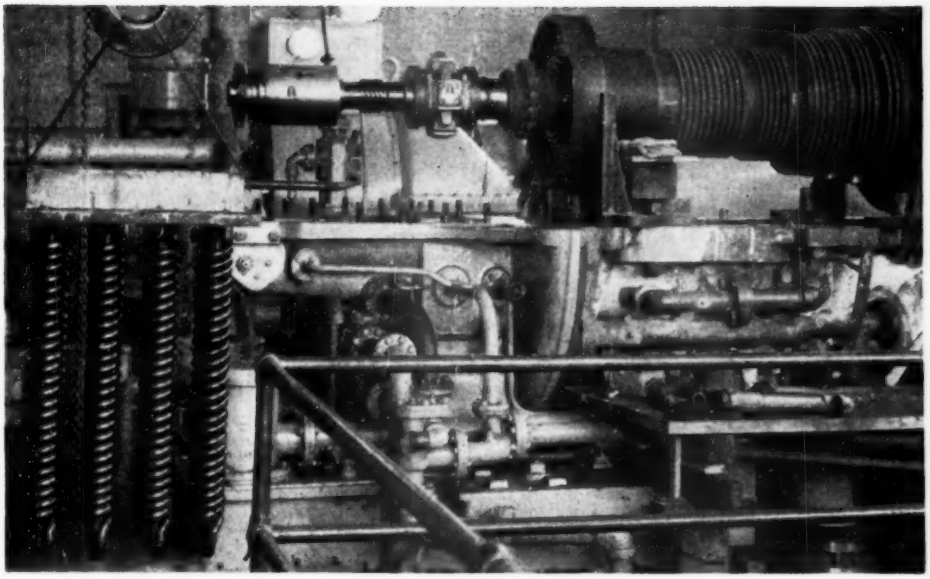


FIG. 1 OIL COOLER, SHOWN AT LEFT, REMOVED FROM A 5000-KW TURBINE FOR INSPECTION
(Inhibited turbine oil was installed in May, 1930; the cooler was removed for inspection in May, 1940, after 10 years of service without cleaning.)

Stability Characteristics of Turbine Oils

BY HOWARD R. PETERSON,[1] CHICAGO, ILL.

This paper reviews the phenomena of turbine oil oxidation, its effects on turbine lubrication, and the use of inhibitors. Service data on an inhibited turbine oil, free from asphaltene-forming constituents, manufactured by the author's company and used in 560 turbines, are presented. These data show a retention of essential properties after 14 years of service. The problem of turbine corrosion is briefly dealt with, responsibility for its prevention being placed upon designers and operators as well as upon oil refiners.

THE need for uninterrupted operation of turbines and turbogenerators, particularly during a period of emergency and rapidly increasing power demand, has led to an intensification of the study of lubricants and their influence on performance. The selection of an oil to meet the relatively broad specifications of most turbine designers, and provide satisfactory lubrication when new, is not a difficult task. The principal problem is one of selecting an oil which will retain its essential characteristics under service conditions. Turbine outage attributable to lubrication is largely caused by deposits resulting from chemical changes in the oil.

Petroleum oils are extremely complex mixtures of hydrocarbons of a variety of molecular sizes and types, varying from paraffinic to aromatic in structure. Various constituents differ in their resistance to oxygen absorption, some being very stable. Turbine oils, generally low in viscosity, are somewhat less resistant to oxidation than heavier oils.

The products of oxidation are of numerous types, depending upon the particular combination of oxygen with the hydrocarbons. Peroxides, alcohols, aldehydes, ketones, lactones, asphaltenes, and organic acids of various molecular weights, volatility, and corrosiveness are among the possible resultant products. Some of these, such as the asphaltenes, tend to precipitate as sludge, while both acids and asphaltenes serve as emulsifying agents in the presence of moisture. The acids may attack metal surfaces, forming metal soaps which not only are emulsifiers but, being relatively insoluble in oil at low temperatures, deposit in lines, coolers, and couplings. Other oxidation products may interfere with the operation of oil-actuated governors. Viscosity changes, sludging, emulsions, and acidity are fundamentally oxidation problems.

The complicated nature of the reactions to which oils are subject is shown by Dornte, Ferguson, and Haskins (1, 2, 3),[2] who describe three types of oils, viz.:

1 Those which oxidize autocatalytically, i.e., whose rate of oxidation is increased by the reaction products.

2 Those whose rate of oxidation is unaffected by nonvolatile reaction products.

3 Those whose rate of oxidation continuously decreases due to decreasing concentration of reacting compounds.

CONDITIONS FAVORABLE TO OXIDATION

The conditions to which turbine oils are exposed are favorable to oxidation. Rapid circulation in the presence of air, contact with various metals, of which some are active catalysts, and ex-

[1] Sales Technical Service Department, Standard Oil Company (Indiana).

Contributed by the Power Division and presented at the Semi-Annual Meeting, Kansas City, Mo., June 16–19, 1941, of THE AMERICAN SOCIETY OF MECHANICAL ENGINEERS.

NOTE: Statements and opinions advanced in papers are to be understood as individual expressions of their authors and not those of the Society.

[2] Numbers in parentheses refer to the Bibliography at the end of the paper.

posure to elevated temperatures are among the unfavorable influences. Other conditions being constant, the rate of oxygen sorption is an exponential function of temperature, doubling or each increase of 12 to 18 F. Careful control of temperature is therefore of prime importance.

Investigators who have studied the effects of various metals on the oxidation rate of turbine oils are in general agreement that copper is the most active, followed by brass, tin, and zinc. Iron, nickel, and aluminum have much less effect, although iron oxides may serve to promote oxidation. Staeger (4) also found that the area of immersed metal has an influence, but not a proportional one. These conclusions should be of value both in turbine design and in laboratory investigations of oxidation phenomena.

Accelerated Oxidation Tests

For purposes of investigation, accelerated oxidation tests are desirable. The literature describes a large number of tests, with temperatures varying from 212 to 392 F, and test periods from 5 to 500 hr. Some tests use oxygen and others air and water, or various metal catalysts may or may not be used. The Rogers stability test (5) has been largely employed by the author's company, since it was established that this test substantially duplicates oil behavior in a dry turbine. Later tests, such as the modified Farmer test, and the test now under consideration by the A.S.T.M. Turbine Oil Committee, impose more severe conditions. It is hoped that this investigation will lead to a generally accepted procedure. Accelerated oxidation tests are at best difficult to interpret. Conditions of service must be simulated or results will be misleading. Actual service data will continue to play the most important role in the evaluation of turbine oils.

Advance in refining technique has resulted in a marked improvement in the stability of turbine oils. Through acid treating and solvent extraction, unstable types of molecules may be removed while preserving the more stable ones. Insufficiently refined oils are subject to excessive deposit formation, whereas some highly refined oils are susceptible to rapid acidity development, presumably due to the removal of natural oxidation inhibitors. This hypothesis led to the use of added inhibitors which, in low concentrations, serve effectively to retard the absorption of oxygen by the petroleum hydrocarbons.

Addition of Inhibitors to Turbine Oils

Inhibitor response of turbine oils is affected by the degree of refining. Since highly treated oils are more uniform in chemical composition, the oxidation reactions to which they are subject are more limited and, hence, easier to control. The selection of a satisfactory inhibitor, however, is by no means a simple task and must be based upon a broad background of experience both with the oil and the inhibitor. Acidity development may be retarded by adding inhibitors to oils insufficiently refined to remove asphaltene-forming constituents completely. This may result in the formation of turbine deposits without a corresponding increase in acidity of the oil.

Patents issued on application filed by Rogers in 1926 (6) cover the addition of certain inhibitors to highly refined white viscous oils from which asphaltic constituents had been removed. Oxidation tests of turbine oils embodying this invention resulted in the conclusion that, under normal operating conditions, they might be expected to last indefinitely. This conclusion was confirmed by experience in a limited number of turbines prior to 1927, at which time an inhibited turbine oil was placed on the market. In 1931, Fitzgerald (7) reported an average acidity of 0.04 mg/KOH/gm on the inhibited oil in sixteen turbines after from 4 to 21 months of service.

Service Experience With Inhibited Turbine Oil

Fig. 2 shows the number of turbines in which this oil has been in service, as of December 31, for each year. Of the 560 turbines shown, 69 are of 10,000 kw capacity or over, and 32 are of 25,000 kw or more. Since it has been a practice to obtain samples from each turbine at regular 6-month intervals, there is now available

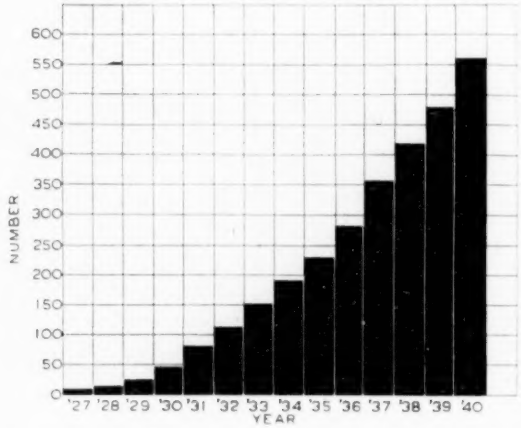


Fig. 2 Number of Turbines Operating on Inhibited Turbine Oil

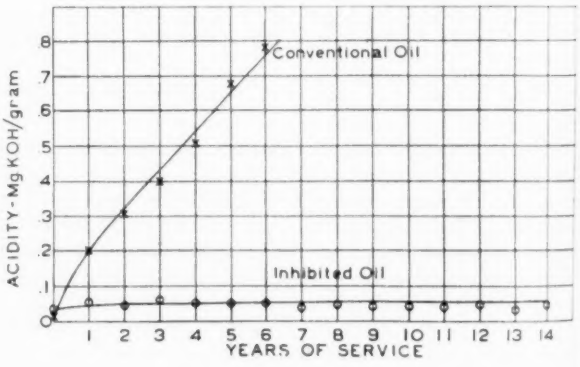


Fig. 3 Comparison of Acidity Development; Conventional Versus Inhibited Turbine Oil

a unique background of performance data which, in view of the increasing attention being given to inhibited oils, may prove of interest.

Two grades of this type of oil are in use, a medium grade of 155 to 160 sec viscosity for direct-connected turbogenerators, and a heavy grade of 310 to 320 sec for geared units. Under severe oxidizing conditions, the viscosity increase of conventional oils has frequently been troublesome. Inspections of samples from those units in which the inhibited oil has been in use for 9 years or more show a viscosity increase of 3 to 7 sec, the average viscosities being 159 and 319 sec for the medium and heavy grades, respectively.

Fig. 3 shows a comparison of acidity development between a conventional oil and the inhibited oil. Since asphaltic constituents have been entirely removed from the inhibited oil, acidity is an adequate criterion of its oxidation. Data on the conventional oil were secured from records of inspections of all samples of medium-grade oils from direct-connected turbogenerators examined during the last 3 years, for which length of service was known. Insufficient data were available to extend this over more than 6 years, since in a majority of cases the oil

is changed before expiration of that period. Data on the inhibited oil were secured from records of periodic sample inspections from 560 units.

In 1933, on the basis of experience with about 100 installations, it was found possible to guarantee that the neutralization number would not exceed 0.15 mg/KOH/gm during the life of the turbine, if the system is thoroughly cleaned prior to installation, and if the temperature of oil from the bearings does not exceed 170 F.

Steam Emulsion Values of Various Oils

Fig. 4 shows the A.S.T.M. steam emulsion values on conventional and inhibited oils of medium grade at the end of various periods of use. Data on conventional oil were secured by inspection of all samples of medium grade secured over a period of 6 months for which length of service was known. The results are not unexpected in that an initial rapid decrease in demulsibility is followed by a slower gradual decrease. Inasmuch as steam emulsion values are regularly determined on only about 25 per cent of all routine samples of the inhibited oil, it was necessary to supplement the available data by examination of not less than five samples, representing each of the various periods of service. All were of medium grade.

While the initial steam emulsion value of the inhibited oil is

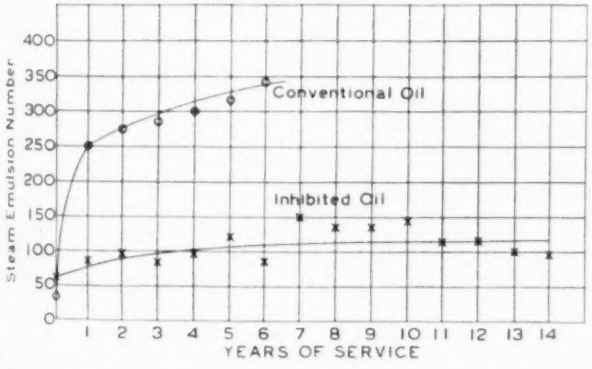


Fig. 4 Comparison of Demulsibility; Conventional Versus Inhibited Turbine Oil

somewhat higher than for a well-refined conventional oil, the decrease in demulsibility is comparatively slight, even after 10 to 14 years of service. This illustrates the inadvisability of establishing extremely restrictive demulsibility specifications on new oil.

It must be recognized that steam emulsion values are seriously affected by the presence of contaminants. Troublesome emulsions may occasionally result even with oils of excellent demulsibility and low acidity. Although such an emulsion may be termed "sludge" by operators, analysis reveals a significant distinction. A typical emulsion, involving a conventional oil, consists of the following:

	Per cent
Petroleum oil	41.7 (acidity 0.6)
Water	57.0
Naphtha insoluble	1.3
Chloroform soluble	0.9
Ash (iron oxide)	0.2

It is apparent from the high acidity and chloroform soluble that extensive oxidation of the oil has occurred. It is reasonable to assume that this emulsion was caused by oil oxidation.

In one case a very persistent emulsion, involving the inhibited oil, was found upon analysis to consist of the following:

	Per cent
Petroleum oil	34.0 (acidity 0.08)
Water	65.0
Naphtha insoluble	0.9
Chloroform soluble	0.01
Ash (iron oxide and silica)	0.9

In this case the low acidity and chloroform soluble show that oxidation is not extensive and that the emulsion was not caused by products of oxidation. The high ash indicates the presence of contaminants remaining in the oil as a result of not having equipment for their removal, and that the contaminants are responsible for the emulsion. In a similar case the emulsifier was found to be a product resulting from the oxidation of cereal dust which found ingress into the lubrication system.

Of the 560 turbines under discussion, about 60 per cent are provided with either filters or centrifuges, while the remaining 40 per cent are not. Even in the case of oils of high oxidation stability, adequate purification devices have a very important function in the removal of water, foreign contaminants, and iron oxide, and the prevention of their attendant ill effects on oil quality.

Turbine Corrosion Problem

During the last two or three years, considerable attention has been focused on the problem of turbine corrosion (8), especially in connection with marine turbines and gear sets. If severe, this may result in impairment of governor operation, particularly in governors of recent design having close tolerances. The problem is further aggravated by operation under constant load, resulting in a reduced flow of oil through the governor. Another unfavorable result of rusting is the fact that iron oxide in finely divided form may serve as an emulsifier and as an oxidation catalyst.

The admixture of small amounts of used oil having moderately high acidity with unused oil is undoubtedly effective in retarding corrosion and has been advocated by some for use in new turbines. It should be kept in mind, however, that this procedure will materially reduce the demulsibility of the new oil. The addition of even small amounts of highly oxidized oil may also greatly increase the oxidation rate of the new oil, as well as result in the precipitation of sludge. Unless specifically compounded to prevent corrosion, however, highly refined oils may be deficient in this property. Since 1927, the inhibited turbine oil described has been compounded to include an antirusting agent in order to provide the necessary degree of rust prevention.

Corrosion prevention is necessarily relative. Under certain conditions of temperature and humidity encountered in turbine operation, the most effective specially prepared rust preventives will give protection for only a short period. It will probably not be feasible to treat turbine oils to such an extent that protection will be provided under all conditions of service, although a reasonable degree is entirely proper. This should not be accomplished, however, at the expense of such desirable qualities as low acidity, good demulsibility, and high stability.

Accelerated tests for rusting tendency, such as the modified Kuebler test (8), will undoubtedly prove to be of assistance in the evaluation of oils. Minimum standards can be established, however, only after much correlation between laboratory results and service data.

Turbine design, metallurgy, improved protective coatings, and maintenance practices must share with turbine oil the responsibility for the correction of this problem, just as each has contributed toward the present high standard of performance.

BIBLIOGRAPHY

1 "Oxidation of White Oils," by R. W. Dornte, *Industrial and Engineering Chemistry*, vol. 28, 1936, pp. 26–30.

2 "Oil Oxidation," by R. W. Dornte and C. V. Ferguson, *Industrial and Engineering Chemistry*, vol. 28, 1936, pp. 863–866.

3 "Oil Oxidation," by R. W. Dornte, C. V. Ferguson, and C. P. Haskins, *Industrial and Engineering Chemistry*, vol. 28, 1936, pp. 1342–1345.

4 "Methods of Testing Transformer Oils," by Hans C. Staeger, *Industrial and Engineering Chemistry*, vol. 17, 1925, pp. 1272–1275.

5 "Evaluation of Turbine Oils," by T. H. Rogers and C. E. Miller, *Industrial and Engineering Chemistry*, vol. 19, 1927, pp. 308–312.

6 "Refined Viscous Hydrocarbon Oil," by T. H. Rogers, U. S. Patents No. 1,774,845, Sept. 2, 1930; No. 1,793,134, Feb. 17, 1931; No. 1,793,135, Feb. 17, 1931.

7 "Modern Turbine Lubrication Practice," by W. F. Fitzgerald, *Power Plant Engineering*, vol. 35, 1931, pp. 604–605.

8 "Lubrication of General Electric Steam Turbines," by C. Dantsizen, Trans. A.S.M.E., vol. 63, August, 1941, pp. 491–495.

The Steam-Turbine Regenerative Cycle—An Analytical Approach

By J. KENNETH SALISBURY,[1] SCHENECTADY, N. Y.

The author has found that with other conditions fixed the heat rate of a turbine depends only upon the fractional quantity of steam extracted, regardless of internal variations in the heater cycle. A method is presented in this paper for determining quickly and accurately the improvement in heat rate resulting from regenerative feedwater heating with any steam conditions. The results are shown in Fig. 1, which is useful in estimating heat rates and in settling the design of a feedwater-heating system before final design figures are completed.

Nomenclature

The following nomenclature is used in the paper:

- a = coefficient of x^2 in quadratic approximation
- b = coefficient of x in quadratic approximation
- c = subscript denoting state-line end point without exhaust loss (c denotes "condenser end")
- e = subscript referring to bleeding operation
- h = enthalpy of feedwater (saturated liquid)
- n = number of heaters
- p = $[(H - h) - t]$ at mid-rise
- r = heat rate, Btu per Btu (conversion constant 3412.75 omitted)
- s = subscript denoting throttle or saturation conditions; also
- s = $[(H_s - h_s) - t]$ (at throttle)
- t = $(H - h)$ at state-line end point, i.e. $(H_c - h_c)$
- w = pounds total extraction per pound condenser flow
- w_s = pounds extraction below any given extraction point per pound condenser flow
- x = fraction of rise in liquid enthalpy between hot well and throttle = $\dfrac{h - h_c}{h_s - h_c}$
- A = area used as a parameter ($= {}^1/_3\,a + {}^1/_2\,b$)
- C = condenser flow
- C_a = coefficient of ax^2 term $= f(n, R/t)$
- C_b = coefficient of bx term $= f(n, R/t)$
- E = extraction quantity
- A.E. = available energy
- E.L. = exhaust loss, Btu per pound of condenser flow. (Subscript N indicates nonextraction; e indicates extraction)
- F_1 = factor defined as ratio of extraction exhaust loss in Btu to nonextraction exhaust loss in Btu
- G = per cent reduction in nonextraction heat rate with infinite number of heaters
- H = enthalpy of steam from state line
- N = subscript referring to nonbleeding operation
- η = internal efficiency of turbine, from throttle to exhaust, including all losses except exhaust loss and mechanical losses
- P = per cent of G obtainable with a finite number of heaters
- P_p = per cent of G obtainable with a finite number of heaters at the optimum feedwater temperature
- R = rise in liquid enthalpy above hot well ($= xR_s$)
- U = turbine used energy without exhaust loss
- V = turbine used energy per pound throttle flow when extracting for feedwater heating

Introduction

The origin of the philosophy that reductions in the nonextraction heat rate depend upon a few relatively simple parameters is lost in antiquity. These parameters will be defined herein, together with a method for their use. We will also demonstrate in this paper the use of this philosophy in calculating many useful functions which occur frequently in heat-balance work.

In determining turbine performance, the nonextraction heat rate is always known or easily obtainable by the turbine designer and by the purchaser, from the nonextraction water rates. The nonextraction turbine heat rate is defined as the heat supplied in the boiler to the working fluid per kilowatthour generated at the generator terminals, when operating without regeneration. The "quadratic-approximation" method (Q.A. method) permits rapid calculation of the bleeding performance, with accuracy, from the nonbleeding heat rates.

Methods will be demonstrated whereby it is possible to calculate or find from curves:

1 The total quantity of extraction with an infinite number of heaters, heating to the saturation temperature corresponding to throttle pressure, for any turbine efficiency, or steam conditions.

2 The reduction in nonextraction heat rate, resulting from the use of such a hypothetical cycle.

3 The total extraction quantity with any finite number of heaters, heating to any feedwater temperature.

4 The reduction in nonextraction heat rate obtained with any finite number of heaters, heating to any feedwater temperature.

5 The variation in this reduction with variation in the number of heaters.

6 The variation in this reduction with variation in feedwater temperature.

7 The optimum feedwater temperature for any steam conditions.

8 A comparison of regenerative power-plant cycles, using only theoretical water-rate tables to supplement the curves given herein, or, alternatively, using the table of nonextraction heat rates (Table 2).

9 A method of dealing with all of these variables mathematically.

The desirability of such methods is unquestioned. It is highly desirable, for example, in the preliminary design of a power plant to be able to state definitely the number of feedwater heaters which is compatible with the economics of the particular installation. Invariably there is some question as to the steam conditions which should be chosen for a given power plant. It will be seen that the evaluation of various steam conditions depends to some extent upon the feedwater-heating cycle to be employed. There is always the early necessity of specifying a

[1] Turbine Engineering Dept., General Electric Co. Jun. A.S.M.E. Contributed by the Power Division and presented at the Semi-Annual Meeting, Kansas City, Mo., June 16–19, 1941, of The American Society of Mechanical Engineers.

Note: Statements and opinions advanced in papers are to be understood as individual expressions of their authors and not those of the Society.

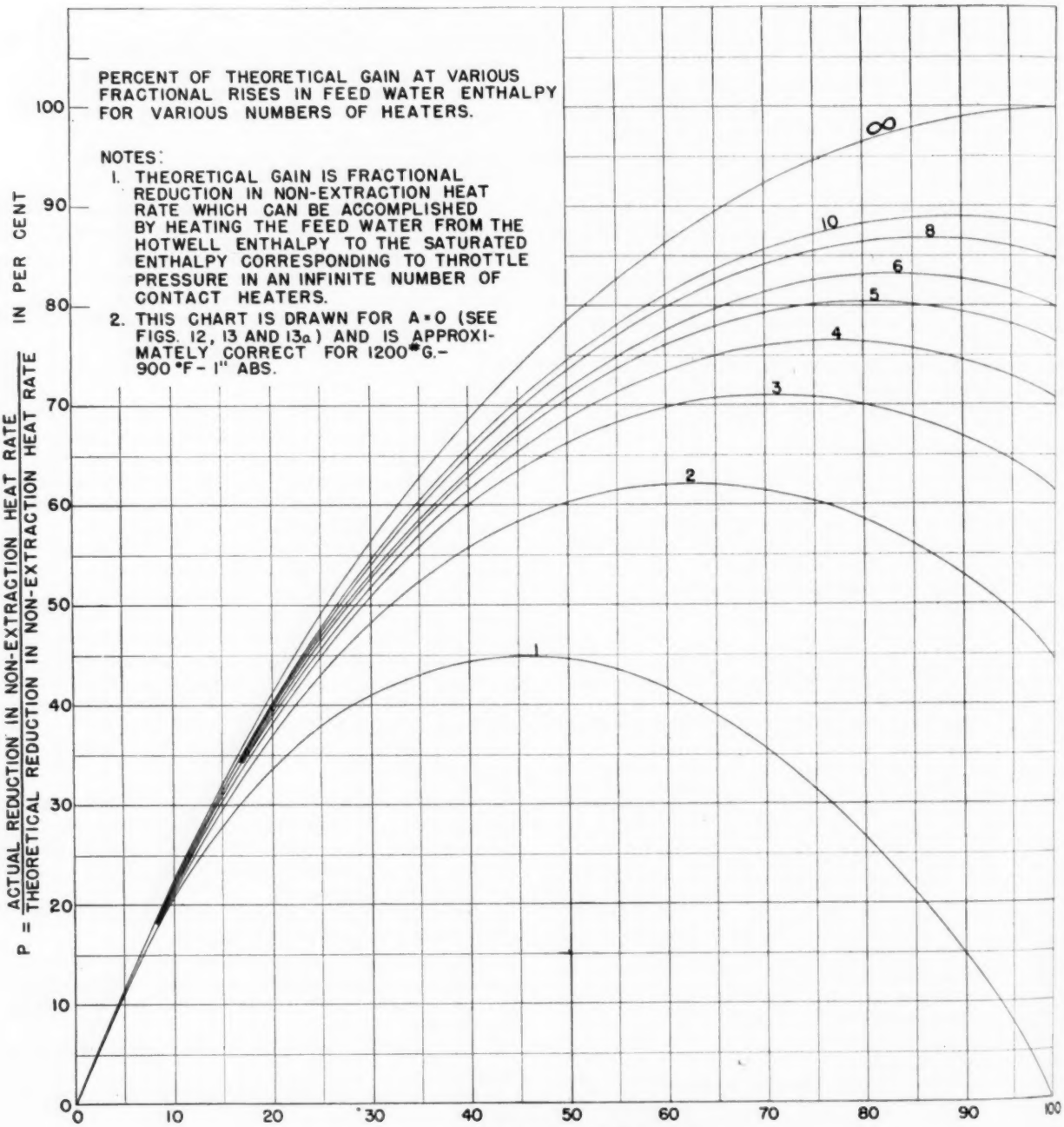


FIG. 1 CURVES CORRELATING FRACTION OF "THEORETICAL" GAIN AGAINST PERCENTAGE OF "POSSIBLE" RISE FOR VARIOUS NUMBERS OF HEATERS

condenser, in order that quotations may be obtained from manufacturers at an early date to aid in making preliminary arrangement drawings of the power plant. From the standpoint of the turbine designer, it is extremely vital that the duty of the exhaust end of the turbine be known in order that he may properly proportion it to handle the flows. The boiler manufacturer invariably is interested in the feedwater temperature in order that he may design his heating surface in both the economizer and the boiler. Use of the curves and of the methods presented herein will not only make possible rapid solutions of all these questions, but will also suggest many other uses of the basic Q.A. method.

Let the reader be assured that, although in some cases it has been necessary to resort to mathematical formulations far beyond the author's original intention, it is by no means necessary that the user concern himself with the derivations and theory in order to reap a full measure of benefit from the results. Only simple arithmetic is required.

Ideally, the most economical way to operate a power plant is to pass the condensate from the condenser hot well through an infinite number of infinitesimal heaters, each of which is supplied

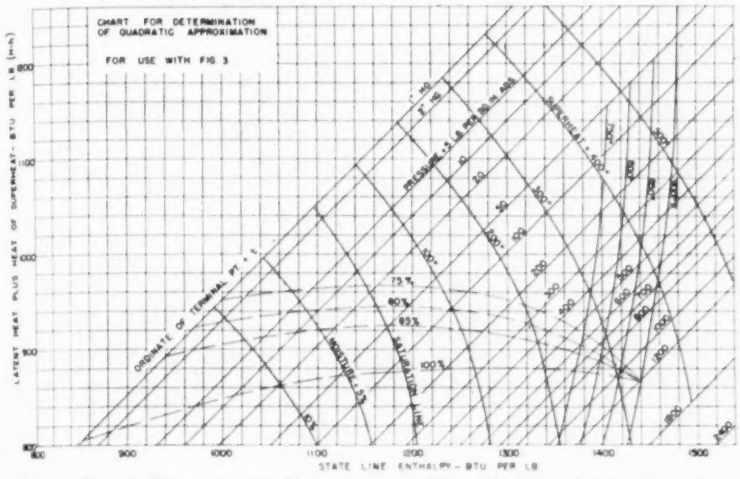


FIG. 2 CHART ILLUSTRATING VARIATION OF $(H - h)$ WITH STATE-LINE ENTHALPY FOR VARIOUS EFFICIENCIES

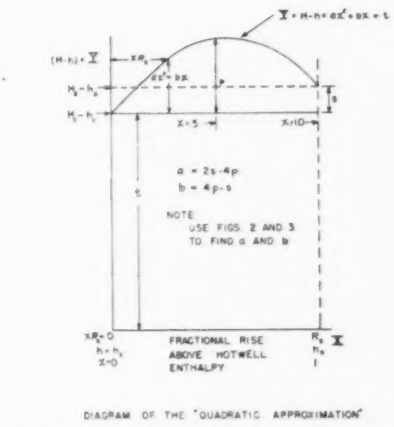


FIG. 4 DIAGRAM ILLUSTRATING METHOD OF OBTAINING QUADRATIC APPROXIMATION AND SHOWING NOMENCLATURE USED

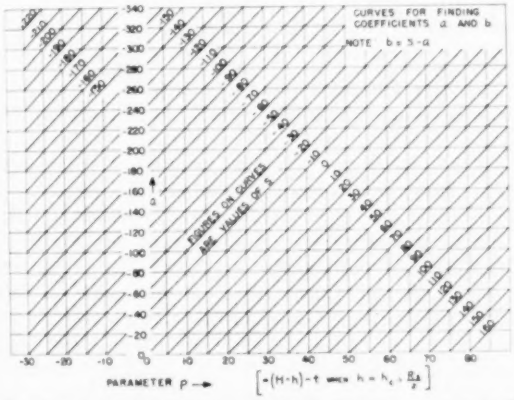


FIG. 3 CHART FOR DETERMINING COEFFICIENTS a AND b IN QUADRATIC APPROXIMATION $(H - h) = ax^2 + bx + t$

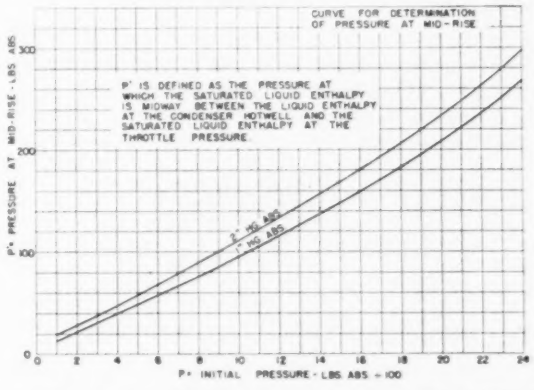


FIG. 5 CURVES FOR DETERMINING PRESSURE P' AT MID-RISE

by one of an infinite number of extractions in the turbine. In such a cycle, the heating of the feedwater most nearly approaches thermodynamically perfect reversibility, and the maximum "gain," or reduction in nonextraction heat rate, is obtained. Obviously, however, it is necessary to use a finite number of heaters; the smaller the number, the greater the degree of irreversibility and the greater the loss. With a finite number of heaters, the maximum gain is always obtained when the feedwater is heated to less than the saturation enthalpy corresponding to throttle pressure.

When the gains which result from heating in an ***infinite*** number of heaters to the saturated liquid enthalpy (corresponding to the throttle pressure) are known for various steam conditions, then it is possible to correlate the gains with ***finite*** numbers of heaters by plotting these gains as fractions of the "theoretical gain" against "fractional rise" for various numbers of heaters. The result of such correlation is shown in Fig. 1. The gains resulting from use of an infinite number of heaters could be obtained by numerical integration, using a large number of steps, but such a process is unsatisfactory, tedious, and subject to inaccuracies. Mathematical integration would be much more satisfying.

The regenerative feedwater-heating cycle has not heretofore been considered amenable to mathematical analysis. A method will be demonstrated by which turbine state lines[2] can be accurately described algebraically, using a "quadratic approximation." Further uses of the quadratic approximation suggest themselves as one becomes better acquainted with it.

[2] A turbine state line is the locus of the state points of the steam in the various stages of the turbine, with constant throttle flow.

PART 1

"QUADRATIC APPROXIMATION"

It has been observed that the heat available per pound of steam extracted for heating the feedwater is relatively constant throughout the whole state line. Using the method actually employed by turbine designers in drawing state lines, a curve of $(H - h)$ may be plotted against the fractional rise above the hot-well enthalpy which can be accurately approximated by the quadratic[3]

$$(H - h) = ax^2 + bx + t \quad \ldots\ldots\ldots\ldots\ldots\ldots [1]$$

From analytic geometry, the coefficients a and b may be determined by the value of $(H - h)$ at any two points on the state line. We have chosen for convenience and accuracy two easily defined points, i.e., mid-rise and throttle conditions, respectively. The constant t must be determined from a third point which we have chosen to be the state-line "end point." (The liquid enthalpy at mid-rise is defined as that enthalpy which is midway between the liquid enthalpy at the condenser hot well and the saturated liquid enthalpy, corresponding to the throttle pressure. The state-line end point is the lower terminus of the state line,

[3] Originally a quartic was used, and then a cubic, but the additional accuracy did not justify the complication introduced.

with no exhaust loss.) By using Figs. 2 and 3, the constants a and b may be readily determined. The accuracy of the quadratic approximation is found to be well within allowable limits.

Checks were made to determine the amount by which this approximation varies from the actual state line as it would normally be drawn. In most cases the maximum discrepancy is less than 0.5 Btu and in a few cases, such as at 2400 lb initial pressure, it reached a maximum value of about 2 Btu. By the derivation, there is an exact check at the turbine exhaust, at mid-rise, and at the throttle. Intermediate points are of slight significance because, normally, the turbine manufacturer does not know the efficiencies of the various parts of the turbine as well as he knows the over-all turbine efficiency, and no attempt is made to predict the exact enthalpies at the various stages.

Fig. 4 indicates the manner in which the Q.A. is determined. Fig. 5 is presented in order that the pressure corresponding to mid-rise may be easily determined.

PART 2

Gain With Perfectly Regenerative Feedwater Heating Using an Infinite Number of Heaters

Since we are now able mathematically to handle extraction data, an expression for the reduction in nonextraction heat rate due to feedwater heating may be easily deduced.

By definition, the heat rate of the turbine cycle is the heat supplied to the working fluid per unit of output, that is

$$r = \frac{\text{Heat supplied}^4}{\text{Output}} \quad [2]$$

$$= 1 + \frac{\text{Heat rejected}}{\text{Heat supplied} - \text{heat rejected}} \quad [3]$$

For a ***nonregenerative*** cycle the heat rejected is

$$\text{Heat rejected} = 1 \cdot (H_e - h_c) \text{ (per lb condenser flow)} \quad [4]$$

and the heat supplied minus the heat rejected is

$$\text{(Heat supplied} - \text{heat rejected)} = (H_s - H_e) =$$

$$\text{Used energy} = U \quad [5]$$

The heat rate, then, for a nonregenerative cycle is

$$r_n = 1 + \frac{H_e - h_c}{H_s - H_c} = 1 + \frac{t}{U} \quad [6]$$

For ***completely regenerative*** feedwater heating, that is, in a cycle in which the feedwater is heated to the saturated liquid enthalpy corresponding to the throttle pressure, the heat supplied is

$$\text{Heat supplied} = (H_s - h_s)(1 + w) \quad [7]$$

and the heat rejected per pound of condenser flow is

$$\text{Heat rejected} = 1 \cdot (H_c - h_c) \quad [8]$$

Then the heat rate r_s for a ***completely regenerative*** cycle is

$$r_s = 1 + \frac{(H_e - h_c)}{(1 + w)(H_s - h_s) - (H_e - h_e)} \quad [9]$$

For a cycle in which the feedwater is not heated to the saturated enthalpy corresponding to the throttle pressure, h_s is replaced by h, the enthalpy of the feedwater leaving the last heater.

[4] Exhaust loss will be considered later, since it is, in effect, an external loss. All of the following derivation is based upon "internal" heat rate, i.e., with no exhaust loss. The constant 3412.75 Btu per kwhr has been omitted throughout.

Subtracting Equation [9] from Equation [6], the reduction in heat rate is

$$r_n - r_s = \frac{t}{U}\left[1 - \frac{1}{1 - \left(\frac{R_s}{U}\right) + w\left(\frac{H_s - h_s}{U}\right)}\right] \quad [10]$$

The fractional reduction then is

$$\frac{r_n - r_s}{r_n} = \frac{t}{U + t}\left[\frac{1}{1 - \left(\frac{U}{R_s - w(H_s - h_s)}\right)}\right] \quad [11]$$

where all terms are known from the turbine efficiency and the assumed conditions, and w is as yet unknown.

Equation [11] may be rewritten as

$$\frac{r_n - r_s}{r_n} = \frac{t}{U + t}\left[\frac{w(H_s - h_s) - R_s}{w(H_s - h_s) - R_s + U}\right] \quad [11a]$$

when heating to h_s in any number of heaters or

$$\frac{r_n - r}{r_n} = \frac{t}{U + t}\left[\frac{w_x(H_s - h) - xR_s}{w_x(H_s - h) - xR_s + U}\right] \quad [11b]$$

when heating to h in any number of heaters.

These equations are strictly correct, providing the applicable value of w is used.

(Note that all of the heat rates mentioned are expressed in "Btu per Btu," the reciprocal of the thermal efficiency of the turbine cycle.)

It will be observed in the foregoing equations, which are general, that the gain over the nonextraction heat rate depends only upon the quantity of steam extracted per pound of condenser flow, the final feedwater enthalpy, the turbine efficiency, and the steam conditions. It may be generalized then, that with given steam conditions and turbine efficiency, the heat rate of a cycle depends only upon the fraction of the throttle steam extracted and the final feedwater enthalpy. This generalization may be carried even further: With given steam conditions, turbine efficiency, and final feedwater enthalpy, the heat rate of a cycle depends only upon the fraction of the throttle steam extracted. In other words, any change which reduces the amount of the extracted steam produces a poorer turbine heat rate. This change may, for example, be the use of more pressure drop between the turbine and the heater, or the use of a larger terminal difference in the heater. These two items both increase the difference between the enthalpy of the extracted steam and the feedwater leaving the heater, hence they reduce the quantity required to be extracted. Apparently, then, we need a method for calculating w, the total extraction.

Determination of w With an Infinite Number of Heaters

Assume that the condenser flow is 1 lb per hr. Then, for any infinitesimal contact heater, a heat balance may be set up

$$\text{Heat supplied} = \text{Heat required} \quad [12]$$

or

$$dw_x(H - h) = dh(1 + w_x) \quad [13]$$

Rearranging and integrating between the condenser hot well and the top heater to obtain w_x, the total amount extracted per pound of condenser flow

$$\log_e (1 + w_x) = \int_{h_c}^{h} \frac{dh}{H - h} \quad [14]$$

To evaluate $\int_{h_c}^{h} \frac{dh}{H - h}$ let us use the Q.A., Equation [1]

$$(H - h) = ax^2 + bx + t$$

where

$$x = \frac{h - h_c}{h_s - h_c} = \frac{h - h_c}{R_s} \quad \ldots\ldots\ldots\ldots [15]$$

whence

$$dh = R_s dx \quad \ldots\ldots\ldots\ldots\ldots\ldots [16]$$

Equation [14] then becomes

$$\log_e (1 + w_x) = R_s \int_0^x \frac{dx}{ax^2 + bx + t} \quad \ldots\ldots [17]$$

or, when the right-hand member is integrated, changed to its simplest form, and the antilog taken

$$(1 + w_x) = \left(\frac{bx + 2t + x\sqrt{b^2 - 4at}}{bx + 2t - x\sqrt{b^2 - 4at}} \right)^{R_s/\sqrt{b^2 - 4at}} \quad \ldots [18]$$

In the case where $x = 1$, Equation [18] becomes

$$(1 + w) = \left(\frac{b + 2t + \sqrt{b^2 - 4at}}{b + 2t - \sqrt{b^2 - 4at}} \right)^{R_s/\sqrt{b^2 - 4at}} \quad \ldots [18a]$$

and w is equal to the right-hand member, minus 1.

Using Equations [18a] and [11a] and actual turbine state lines, a large number of calculations were made with great accuracy to determine the value of G, the gain with an infinite number of heaters heating to the saturation point. It is felt that fewer minor inconsistencies are introduced by calculation of the value of G along an actual turbine state line than by calculation of this value along an isentropic or 100 per cent efficiency line. The latter, although perfectly defined, never occurs in practice and its use would require additional correction, not only because of the abnormally low values of $(H - h)$, but also because it is a straight line, whereas normally, a curved state line is used.

The values of G are shown in Figs. 6 and 7, plotted against pressure for various temperatures, and in Fig. 8, plotted against temperature for various pressures. It was found that the variation of G with temperature is exactly linear as might be expected. Fig. 8(a) illustrates the variation in G, caused by departure from the base turbine efficiency of 80 per cent. Fig. 8(b) shows values of G plotted against back pressures higher than the usual range of condensing machines.

PART 3

The cycle which has been assumed in these studies is shown in Fig. 9, together with the nomenclature. We have used throughout this investigation that cycle which is most easily defined, and which is frequently approximated in practice, i.e., one in which the heaters have zero terminal differences and in which the rise in enthalpy per heater is constant and equal to

$$\frac{\text{Total rise in enthalpy}}{\text{Number of heaters}}$$

In practice the rises are usually very nearly equal, and any normally encountered departure from this situation does not affect the validity of the present analysis. The methods herein demonstrated make corrections for terminal difference, pressure drop, boiler-feed-pump work, heater distribution, etc., easily obtainable. It is the author's intention to present in a subsequent paper a method of using this analysis to determine the variation in heat rate with such minor variables as these, but it is not considered within the scope of the present paper to discuss them.

Determination of w_x With a Finite Number of Heaters

It has been shown necessary to calculate the extraction quantity. A determination of the extraction quantity with a finite number of heaters is made readily possible from the hypothesis that the rise in enthalpy per heater is constant, and equal to

$$\frac{\text{Total rise in enthalpy}}{\text{Number of heaters}}$$

Assume for the moment that $(H - h)$ is constant for all extractions and equal to

$$(H_c - h_c) = t \quad \ldots\ldots\ldots\ldots\ldots [19]$$

In this case

$$w_x = \sum_1^n E = \left(1 + \frac{R}{nt}\right)^n - 1 \quad \ldots\ldots\ldots [20]$$

This is a first approximation to the true quantity, but it is shown in the Appendix that a correction for the assumption that t = constant may be made. It is there shown that an approximate expression[5] for the actual total extraction is

$$w_x = \frac{t}{t + \Delta_w} \left[\left(1 + \frac{R}{nt}\right)^n - 1 \right] \quad \ldots\ldots\ldots [21]$$

where

$$\Delta_w = C_a ax^2 + C_b bx \quad \ldots\ldots\ldots\ldots\ldots [22]$$

or, inserting coefficients C_a and C_b, which are plotted in Fig. 10

$$\Delta_w = \left[\frac{(2n + 1)(n + 1)}{6n^2} + \frac{(n + 1)(n^2 - 1)}{12n^3} \left(\frac{R}{t}\right) \right] ax^2 + \left[\left(\frac{n + 1}{2n}\right) + \frac{n(n^2 - 1)}{12n^3} \left(\frac{R}{t}\right) \right] bx \quad \ldots [23]$$

Typical curves showing the variation of Δ_w with number of heaters and x are shown in Fig. 11, which has been drawn for 1200 psi, 900 F, 1 in. Hg. It will be noted that for one heater the value of Δ_w is equal to the value of $(ax^2 + bx)$. This is because, when one heater is used, the actual value of $(H - h)$ is that obtained from the plot of $(H - h)$ against x, the fractional rise. We have determined the constants a and b, so that

$$(H - h) - t = ax^2 + bx \quad \ldots\ldots\ldots\ldots [1a]$$

and when $n = 1$, C_a and C_b also become unity.

For two heaters at $x = 0.5$, it will be noted that the value of Δ_w is approximately equal to the average of the values read at $x = 0.25$ and $x = 0.5$. It differs from the exact average only because the extraction for the top heater is greater than the extraction for the first heater by a small amount (since the second heater is required to heat not only the condenser flow but also the extraction for the first heater).

Since we can obtain the reduction in nonextraction heat rate for any *finite* number of heaters from Equations [11b] and [21],

[5] This method obviously gives a second approximation to the extraction quantity with a finite number of heaters. To obtain the accuracy desired in the final results (Fig. 1) it was necessary for large values of $\frac{R}{n}$ actually to calculate heat balances, obtaining the values of $(H - h)$ from the Q.A. for consistency. If an accurate value of w_x is desired, it is suggested that Equation [24] be used, utilizing the curves of P and G which are strictly accurate, in preference to this second approximation.

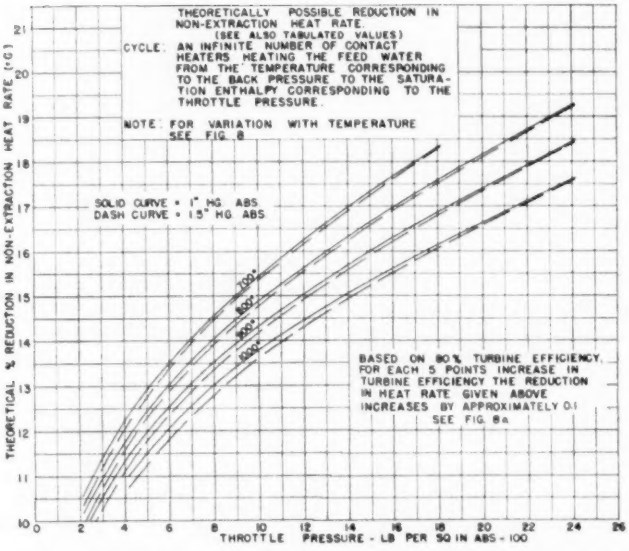


FIG. 6 THEORETICAL REDUCTION IN NONEXTRACTION HEAT RATE ACCOMPLISHED BY HEATING IN AN INFINITE NUMBER OF HEATERS FROM CONDENSER HOT WELL TO SATURATED LIQUID ENTHALPY, CORRESPONDING TO THROTTLE PRESSURE; DRAWN FOR BACK PRESSURES OF 1 IN. AND 1.5 IN. HG ABS

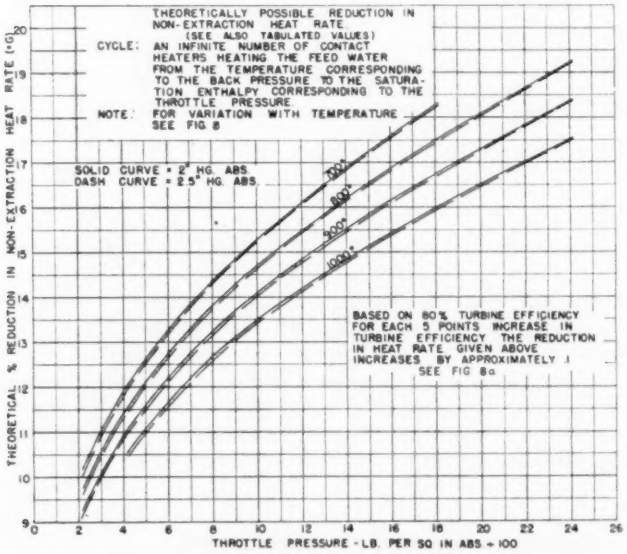


FIG. 7 THEORETICAL REDUCTION IN NONEXTRACTION HEAT RATE ACCOMPLISHED BY HEATING IN AN INFINITE NUMBER OF HEATERS FROM CONDENSER HOT WELL TO SATURATED LIQUID ENTHALPY, CORRESPONDING TO THROTTLE PRESSURE; DRAWN FOR BACK PRESSURES OF 2 IN. AND 2.5 IN. HG ABS

and from Equations [11*a*] and [18*a*] we can obtain the reduction in nonextraction heat rate with an *infinite* number of heaters heating to h_s, it is possible to find the ratio of these two gains for any combination of rise, number of heaters, and steam conditions. This ratio is designated by P and plotted in Fig. 1.

TABLES

In addition to the curves shown in Figs. 6, 7, and 8, Table 1 is presented showing the gains at various pressures and temperatures and for various vacuums, to two decimal places.

Table 2, of "Nonextraction Theoretical Heat Rates," will be found of great assistance when used with Figs. 14, 15, and 16.

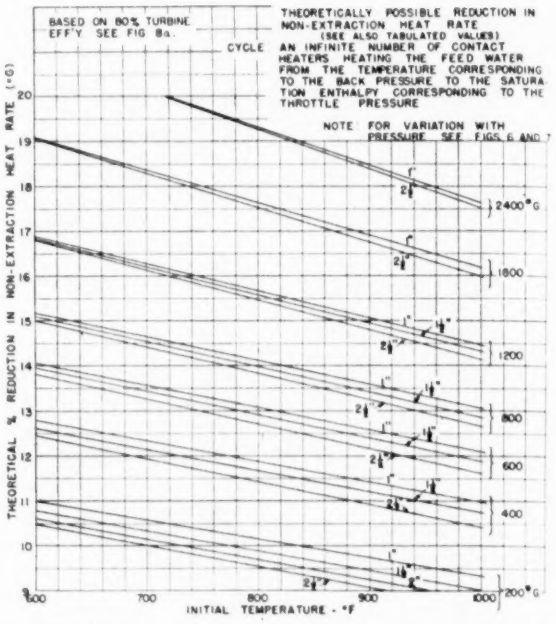


FIG. 8 THEORETICAL REDUCTION IN NONEXTRACTION HEAT RATE ACCOMPLISHED BY HEATING IN AN INFINITE NUMBER OF HEATERS FROM CONDENSER HOT WELL TO SATURATED LIQUID ENTHALPY, CORRESPONDING TO THROTTLE PRESSURE
(Plotted against temperature to show linear variation with temperature)

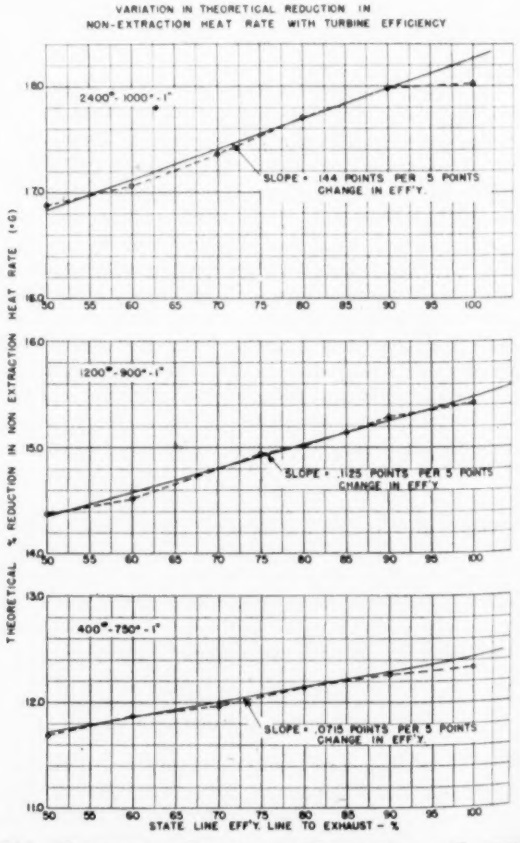


FIG. 8(*a*) THEORETICAL PERCENTAGE REDUCTION IN NONEXTRACTION HEAT RATE FOR TYPICAL STEAM CONDITIONS VERSUS TURBINE EFFICIENCY

TABLE 1 PERCENTAGE REDUCTIONS IN NONEXTRACTION HEAT RATES FOR VARIOUS INITIAL PRESSURES, TEMPERATURES, AND BACK PRESSURES[a]

Initial pressure, psi, gage	Initial temperature, F	Reduction in nonextraction heat rate, per cent— 1 in. Hg	1½ in. Hg	2 in. Hg	2½ in. Hg
200	700	10.57	10.33	10.15	10.01
	800	10.16	9.90	9.70	9.55
	900	9.75	9.46	9.25	9.08
400	700	12.34	12.17	12.04	11.94
	800	11.89	11.70	11.55	11.44
	900	11.44	11.22	11.06	10.93
	1000	10.99	10.75	10.57	10.43
600	700	13.57	13.44	13.34	13.26
	800	13.08	12.93	12.81	12.72
	900	12.59	12.41	12.28	12.18
	1000	12.10	11.90	11.75	11.63
800	700	14.64	14.54	14.47	14.41
	800	14.12	13.99	13.90	13.83
	900	13.60	13.45	13.33	13.24
	1000	13.08	12.90	12.77	12.67
1200	700	16.27	16.21	16.16	16.12
	800	15.67	15.58	15.52	15.47
	900	15.07	14.96	14.88	14.82
	1000	14.47	14.34	14.24	14.16
1800	700	18.35	18.32	18.30	18.28
	800	17.63	17.58	17.55	17.52
	900	16.91	16.85	16.80	16.76
	1000	16.19	16.11	16.05	16.00
2400	800	19.30	19.28	19.27	19.26
	900	18.47	18.44	18.41	18.39
	1000	17.64	17.59	17.55	17.52

[a] Values are plotted in Figs. 6, 7, and 8. Based on 80 per cent turbine efficiency. For each 5 points increase in turbine efficiency the reduction in heat rate given increases 0.1, on the average. See Fig. 8(*a*) for variation at typical steam conditions.

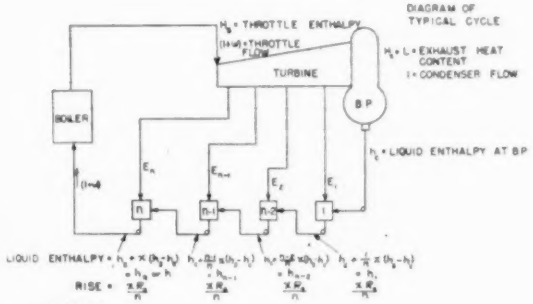


FIG. 9 DIAGRAM OF FEEDWATER-HEATING CYCLE ASSUMED AND NOMENCLATURE USED

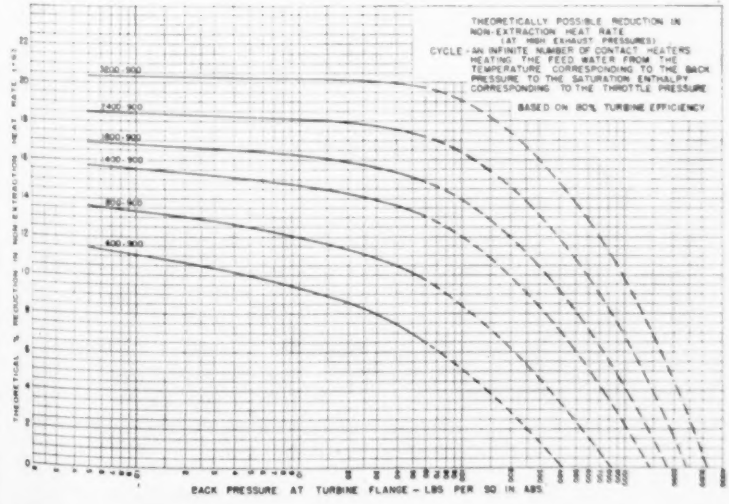


FIG. 8(*b*) THEORETICAL PERCENTAGE REDUCTION IN NONEXTRACTION HEAT RATE FOR TYPICAL STEAM CONDITIONS VERSUS EXHAUST PRESSURE

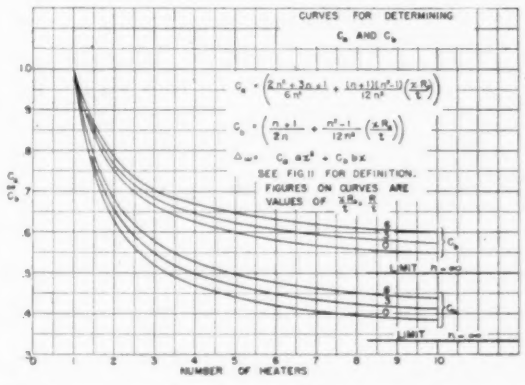


FIG. 10 CURVES FOR DETERMINING COEFFICIENTS C_a AND C_b FOR USE IN EQUATION [22]

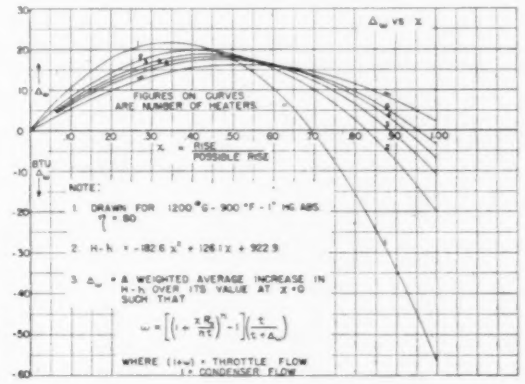


FIG. 11 CURVES ILLUSTRATING THE VARIATION OF Δ_w WITH x THE FRACTIONAL RISE AND n THE NUMBER OF HEATERS
(Specific curves for 1200 psi, 900 F, 1 in. Hg.)

The table gives the heat rate of nonregenerative cycles operating with hypothetical turbines of 100 per cent efficiency. To obtain a quick estimate of actual heat rates:

1 Divide the nonextraction theoretical heat rate by the overall nonextraction efficiency.

2 Obtain the gain due to feedwater heating by multiplying the ordinates of Fig. 14, and Fig. 15 or 16.

3 Apply this gain (as a reduction) to the nonextraction heat rate.

4 Reduce the resulting heat rate by from 1 to 2.5 per cent to allow for the reduction in exhaust loss, if a full-load heat rate is under consideration. (At lighter loads or with excessively large exhaust ends this nonthermodynamic gain will approach zero and may even become negative at very light loads due to loss in turbine efficiency with the reduction in exhaust flow resulting from extraction for feed heating.) More accurate calculation of the gain due to reduction in exhaust loss may be made using the method described in Part 7.

When the values of the percentage P of the theoretical gain G had been calculated, it was discovered that there was a small variation of corresponding points with respect to steam conditions. This variation can most logically and easily be related to a parameter A, as illustrated in Fig. 12, because the value of A is indicative of the history of the function $(H - h)$ between the condenser and the throttle, and uniquely determines the involved

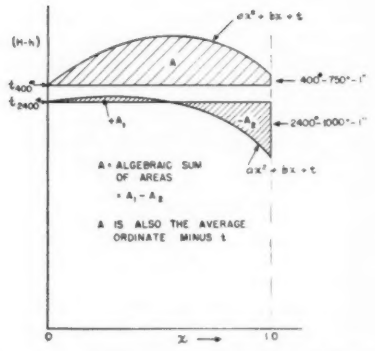


FIG. 12 DIAGRAM ILLUSTRATING SIGNIFICANCE OF PARAMETER *A*

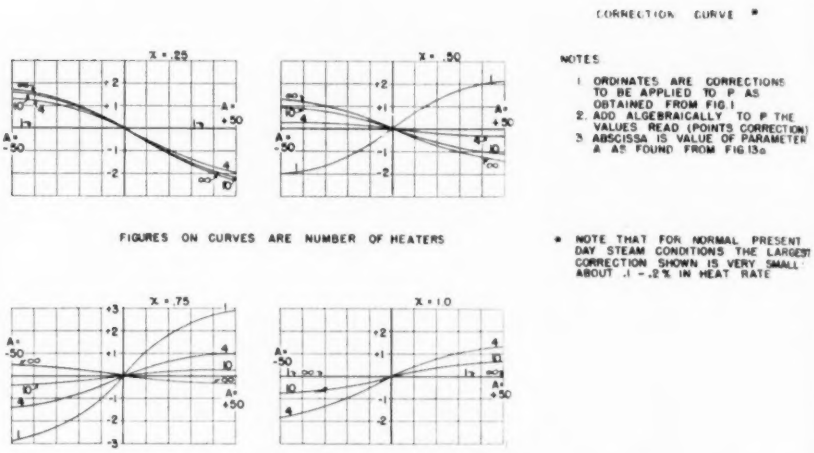


FIG. 13 CURVES SHOWING VARIATION WITH *A* OF FRACTION OF THEORETICAL GAIN

TABLE 2 THEORETICAL NONEXTRACTION HEAT RATES, BTU PER KWHR

Initial pressure, psi gage	Initial temperature, F	Back pressures 1 in. Hg	1.5 in. Hg	2 in. Hg	2.5 in. Hg
200	650	10140	10528	10840	11094
	700	10031	10405	10704	10953
	750	9919	10280	10568	10812
	800	9804	10153	10432	10670
	850	9686	10023	10296	10528
	900	9565	9891	10160	10386
300	650	9681	10009	10279	10502
	700	9581	9907	10167	10383
	750	9481	9801	10053	10261
	800	9380	9692	9937	10137
	850	9280	9580	9819	10011
	900	9179	9466	9699	9883
400	650	9371	9677	9923	10110
	700	9284	9583	9822	10006
	750	9195	9487	9719	9900
	800	9105	9389	9613	9792
	850	9013	9289	9505	9682
	900	8919	9186	9396	9570
	950	8823	9081	9284	9456
600	650	8995	9261	9465	9646
	700	8914	9175	9377	9549
	750	8832	9087	9287	9451
	800	8750	8998	9194	9352
	850	8667	8907	9098	9252
	900	8583	8816	9001	9151
	950	8498	8725	8902	9050
	1000	8411	8633	8801	8949
800	650	8757	8992	9184	9341
	700	8679	8913	9099	9251
	750	8601	8832	9013	9161
	800	8522	8749	8925	9070
	850	8443	8665	8837	8978
	900	8364	8580	8749	8886
	950	8284	8495	8658	8792
	1000	8204	8409	8566	8697
1000	700	8513	8730	8898	9043
	750	8436	8651	8817	8951
	800	8360	8571	8735	8871
	850	8284	8491	8651	8784
	900	8208	8411	8567	8697
	950	8132	8330	8483	8609
	1000	8056	8248	8398	8521
1200	750	8314	8516	8675	8808
	800	8240	8438	8593	8723
	850	8165	8360	8511	8638
	900	8090	8282	8429	8553
	950	8015	8203	8347	8468
	1000	7939	8124	8265	8383
1800	850	7929	8102	8238	8349
	900	7855	8025	8157	8266
	950	7781	7948	8076	8183
	1000	7707	7871	7995	8100
2400	850	7797	7952	8076	8180
	900	7720	7875	7996	8098
	950	7646	7799	7917	8017
	1000	7565	7724	7839	7937

NOTE: Table derived from "Theoretical Steam Rate Tables," by J. H. Keenan and F. G. Keyes, A.S.M.E., New York, N. Y., 1938.
The values obtained from the tables have been altered slightly in a few cases to give smooth curves.
Divide by the over-all turbine-generator efficiency to obtain the non-extraction heat rate.

variables, for a fixed state-line shape. Table 3 shows the values of *a*, *b*, and *A* as used in this investigation.

It will be noted in Fig. 13 that the variation of *P* with respect to *A* is small; hence for most purposes Fig. 1 may be used without this correction, especially for estimating. Fig. 13 is presented as a record and for the use of those who wish to take account of this secondary variation in the calculation of heat rates. Fig. 13(*a*) provides a convenient method of obtaining the value of *A* for any given conditions.

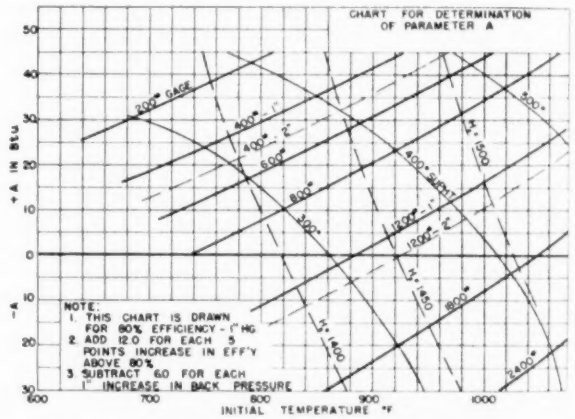


FIG. 13(*a*) CHART FOR DETERMINING PARAMETER *A*

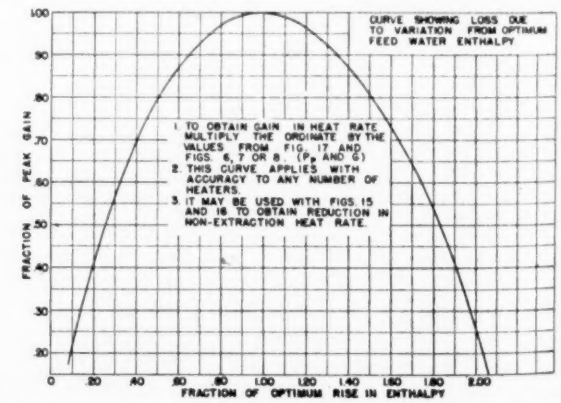


FIG. 14 CO-ORDINATION OF SHAPES OF CURVES SHOWN IN FIG. 1 (Fraction of peak gain plotted against fraction of optimum rise in feed-water enthalpy.)

PARTIAL-LOAD HEAT RATES

As the load on a turbine decreases, there is a rapid drop in the rise, hence, the duty, of the lowest pressure heater. Occasionally,

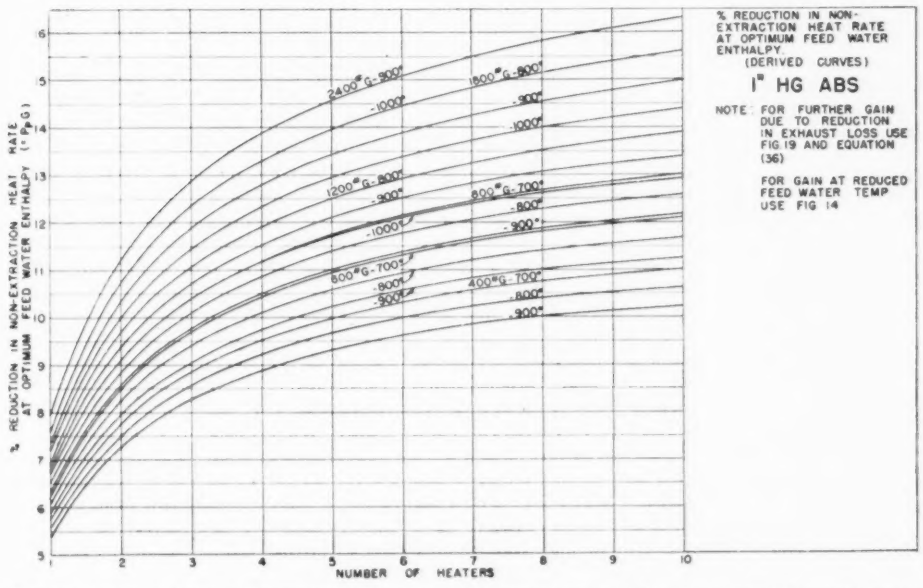


FIG. 15 SPECIFIC CURVES SHOWING ACTUAL FRACTIONAL GAIN OVER NONEXTRACTION HEAT RATE FOR VARIOUS STEAM CONDITIONS AND NUMBERS OF HEATERS AT 1 IN. HG ABS

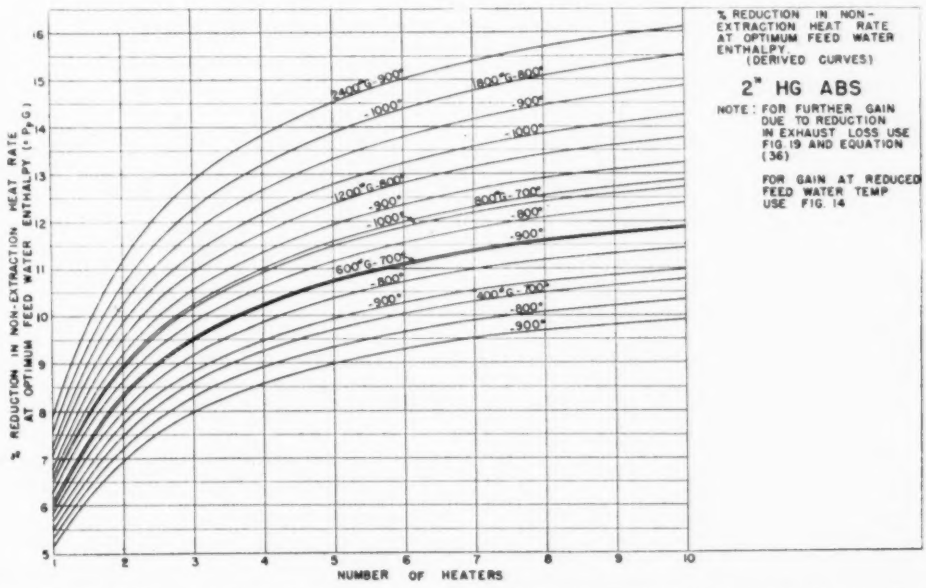


FIG. 16 SPECIFIC CURVES SHOWING ACTUAL FRACTIONAL GAIN OVER NONEXTRACTION HEAT RATE FOR VARIOUS STEAM CONDITIONS AND NUMBERS OF HEATERS AT 2 IN. HG ABS

where generator air coolers and steam jets are used in the condensate circuit, the extraction for this heater ceases to be required. At this point, the number of heaters obviously becomes $(n - 1)$. In the interval between normal load and this point, the effect of the progressive reduction in low-pressure-heater duty is equivalent to a reduction in the value of n, the number of heaters. In other words, in using Fig. 1, at partial loads, an interpolation should be made between n and $(n - 1)$. The reduction in duty of the low-pressure heater usually has little effect on the heat rate because of the convergence of the various lines in Fig. 1, at low fractional rises.

Due to the decrease in efficiency of the first stage at lighter loads, there is another small decrease in the gain, because of the concentration of output on the early stages with extraction operation. Several devices suggest themselves as a solution of this problem, if the user is unwilling to estimate the loss. One of the more easily understandable methods is to consider the initial pressure as that in the first stage, obtaining a heat rate by the method described herein. The first-stage output is then considered as being at 100 per cent thermal efficiency, and the heat rate reduced in proportion to the magnitude of this output. (Similar reasoning provides a method applicable to reheat cycles.)

PART 4

SPECIFIC CURVES

The curves shown in Fig. 1 have been converted and plotted in Fig. 14, against percentage of optimum rise with percentage of

TABLE 3 VALUES OF COEFFICIENTS a AND b AND PARAMETER A FOR VARIOUS STEAM CONDITIONS[a]

Pressure, gage	Temperature, F	a	b	A Btu
200	700	— 51.6	98.2	31.90
400	650	— 98.0	92.0	13.30
	750	— 90.4	107.6	23.70
	850	— 86.2	127.9	35.20
	950	— 88.2	155.5	48.40
600	700	—126.2	97.7	6.80
	800	—120.0	116.6	18.30
	900	—116.0	138.6	30.60
800	700	—151.0	91.9	— 4.35
	800	—142.6	110.1	7.55
	900	—138.6	132.9	20.25
1200	800	—186.4	101.0	—11.60
	900	—182.6	126.1	2.20
	1000	—182.2	154.7	16.60
1800	850	—239.6	96.6	—31.60
	900	—239.2	112.4	—23.50
	1000	—238.0	142.6	— 8.00
2400	900	—293.8	96.3	—49.75
	1000	—294.6	131.7	—32.35

[a] $(A = \frac{1}{2}a + \frac{1}{2}b)$.
Based on 80 per cent turbine efficiency and 1 in. Hg abs back pressure.
To estimate A for other efficiencies and back pressures:
For each 5 points increase in turbine efficiency, increase the value of A by 12 Btu.
For each increase of 1 in. Hg, decrease the value of A by 6 Btu.

peak gain as the ordinate. There is a remarkable correlation between the shapes of these curves. Because of this probably fortuitous relationship, it is relatively easy to determine the gain for any cycle by reading from the derived curves, Fig. 15 or 16, the gain (P_pG) with the specified number of heaters at the peak feedwater temperature and for the steam conditions involved. For any value of the abscissa (fraction of optimum rise), in Fig. 14, the required factor on this gain may be determined.

It will be found that the curves, Figs. 15 and 16, are very useful in comparing cycles with various steam conditions and regenerative feedwater heating, when used with a table of theoretical nonextraction heat rates, such as that shown in Table 2, using the method described in Part 3. Such calculations cannot take into account the variation in turbine efficiency, unless comparative nonextraction efficiencies are available. These efficiencies may be obtained by using the method described in a paper[6] by Warren and Knowlton.

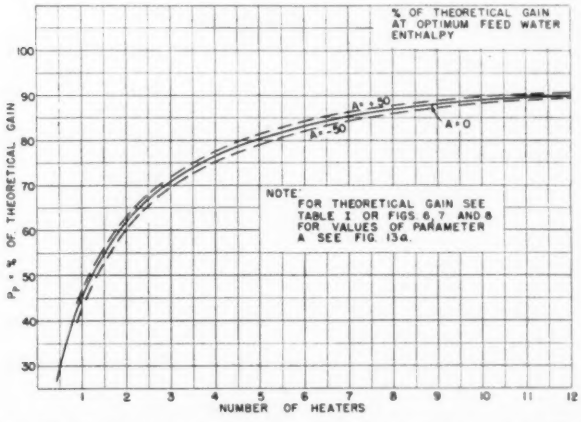


FIG. 17 FRACTION OF THEORETICAL GAIN OBTAINABLE WITH VARIOUS NUMBERS OF HEATERS WHEN HEATING TO OPTIMUM FEEDWATER TEMPERATURE

Fig. 17 illustrates the variation in the percentage of the possible gain G, with the number of feedwater heaters employed. The ordinate of this curve, when multiplied by the value of G, obtained from Figs. 6, 7, 8, or Table 1, yields the gain over the nonextraction heat rate which is obtained by heating to the optimum feedwater temperature in various numbers of heaters. The percentage correction for change in the number of heaters may be determined by subtracting any two ordinates in Fig. 17, and multiplying by the value of G, obtained from Figs. 6, 7, or 8. (Observe that the result usually is required in percentage of the extraction heat rate; hence it must be divided by $[1 - PG]$.) Fig. 17 may also be used to determine the fraction of the total rise necessary to obtain peak gains, which is identical numerically with the value P_p.

Fig. 18 is presented as a method of determining the theoretically optimum feedwater temperature at various steam conditions.[7] Horizontal lines are shown in Fig. 18, from which the extraction pressure required may be determined. This extraction pressure is that which would be required with no pressure drop between the turbine and the heater and with no terminal difference.

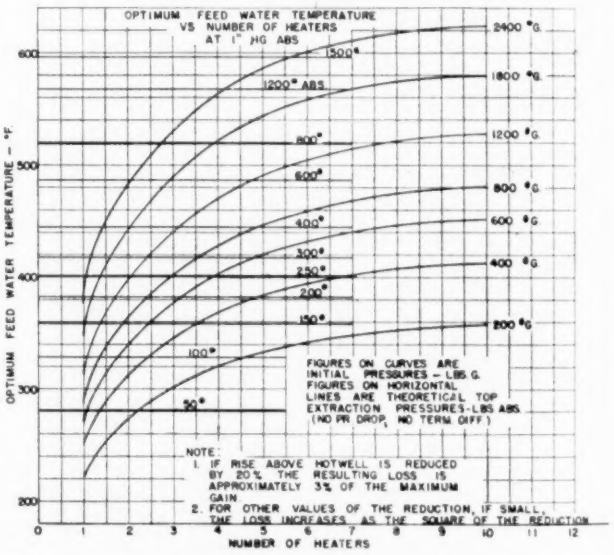


FIG. 18 THEORETICAL OPTIMUM FEEDWATER TEMPERATURE AT VARIOUS STEAM CONDITIONS VERSUS NUMBER OF HEATERS
(Horizontal lines indicate theoretical top extraction pressures with no terminal difference and no pressure drop. Add approximately 10 per cent to values shown to obtain true stage pressure.)

Under actual conditions, a slightly higher pressure must be used in order to compensate for these items (usually about 10 per cent higher pressure is required).

PART 5

DETERMINATION OF FRACTIONAL EXTRACTION

Occasionally it is desirable to determine directly the fraction of the total throttle flow extracted. The derivation of the expression is comparatively simple; hence only the result is presented herewith

[6] "Relative Engine Efficiencies Realizable From Large Modern Steam-Turbine Generator Units," by G. B. Warren and P. H. Knowlton, Trans. A.S.M.E., Feb., 1941, pp. 125–135.

[7] At first glance these feedwater temperatures may seem to be high. They are the exact peak of the curves in Fig. 1. In actual practice it is usually desirable to heat feedwater to somewhat less than these values for three reasons:

1 The loss in so doing is small as shown in Fig. 14.
2 The lower investment justifies this small loss.
3 Often, where a boiler economizer is used, the loss in boiler efficiency offsets the small gain which could be obtained with higher feedwater temperature.

Occasionally machines are sold with the anticipation of a low unit output factor. In these cases it may be desirable to approach or even exceed the theoretical feedwater temperature in order to affect favorably the light-load economy.

$\frac{w_x}{1+w_x}$ = Fraction of throttle flow extracted

$$= \frac{R + \left[\left(\frac{PG}{1-PG}\right)(H_s - h)\left(\frac{U}{t}\right)\right]}{U+t} \quad [24]$$

This expression is useful in determining the additional gain due to reduction in exhaust loss as discussed subsequently. Under actual conditions, appropriate allowance should be made in the value of PG for the effect of terminal differences and pressure drop between the stage and the heater. This expression is strictly accurate, providing only that the value of PG is known, together with the true correction to PG for such small items as those mentioned.

PART 6

Reduction in Load Due to Extraction With Constant Throttle Flow

In many cases, it is desirable to determine directly the reduction in load due to extraction of steam for feedwater heating. An expression for the ratio of the loads with extraction and without extraction is derived as follows:

$$r_n = \frac{t+U}{U} \quad [6a]$$

$$r_e = \frac{(t+U-R)}{V} \quad [25]$$

where V is the output per pound of throttle flow.

Then

$$\frac{V}{U} = \frac{\text{Extraction load}}{\text{Nonextraction load}} \quad [26]$$

with constant throttle flow.

Dividing Equation [25] by Equation [6a]

$$\frac{r_e}{r_n} = (1-PG)\left(\frac{t+U-R)}{t+U}\right)\frac{U}{V} \quad [27]$$

Solving for $\frac{V}{U}$

$$\frac{V}{U} = \frac{\left(1-\frac{R}{U+t}\right)}{(1-PG)} = \frac{\left(\frac{H_s-h}{H_s-h_c}\right)}{(1-PG)} \quad [28]$$

that is, the ratio of the internal output with extraction to the internal output without extraction is

$$\frac{\text{Internal extraction output}}{\text{Internal nonextraction output}} = \frac{1-\left(\frac{R}{U+t}\right)}{(1-PG)} \quad [29]$$

assuming constant exhaust loss. The change in exhaust loss may also be considered as demonstrated in Part 7. Equation [29], including this change, becomes

$$\frac{\text{Net extraction output}}{\text{Net nonextraction output}}$$

$$= \frac{\left(1-\frac{R}{U+t}\right)}{1-\frac{\text{E.L.}_N}{\text{A.E.}}\left\{1-F_1\left[1-PG\left(\frac{t+U}{t}\right)\right]\right\}} \quad [30]$$

(This expression has been simplified at a loss in accuracy of about 0.05 per cent, as is shown later.)

PART 7

Reduction in Heat Rate Due to Reduction in Exhaust Loss

The methods previously described provide the reduction in nonextraction heat rate accomplished thermodynamically by extracting for feedwater heating. In addition to the thermodynamic gain in thermal efficiency, resulting from regeneration, there is an additional gain which arises from the reduction in congestion of the flow in the exhaust passages. Although this gain is, in a sense, a reduction of an external loss, it is very real, and is intimately connected with the regenerative cycle.

The reduction in "exhaust loss" includes the reduction in kinetic energy of the steam leaving the last-stage buckets, as well as the reduction in pressure drop through the hood. (Exhaust loss is discussed at some length in Warren and Knowlton's paper.[8])

An expression, Equation [24], was given for the reduction in condenser flow resulting from extraction for feedwater heating

$$\frac{w_x}{1+w_x} = \frac{R + \left[\left(\frac{PG}{1-PG}\right)(H_s-h)\left(\frac{U}{t}\right)\right]}{U+t} \quad [24]$$

By using this expression we are able to determine from Fig. 19 the ratio of the Btu exhaust loss.[8] The ratio of exhaust losses in

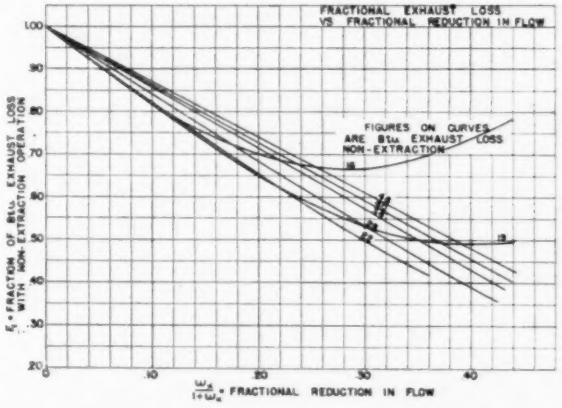


FIG. 19 FACTOR TO BE APPLIED TO NONEXTRACTION EXHAUST LOSS IN BTU TO OBTAIN EXTRACTION EXHAUST LOSS IN BTU
(See part 7 in text for use of this factor.)

Btu is not the true ratio of the effective exhaust losses until it has been corrected in the ratio of the respective exhaust flows and loads for extraction and nonextraction operation.

The effective exhaust loss is defined by the equations

$$\text{Per cent E.L.}_N = 100 \cdot \frac{\text{E.L.}_N \times \eta}{U}$$

$$= 100 \cdot \frac{\text{E.L.}_N \times \eta \times \text{throttle flow}}{\text{Nonextraction load} \times 3412.75} \quad [31]$$

$$\text{Per cent E.L.}_e = 100 \cdot \frac{\text{E.L.}_e \times \eta \times \text{condenser flow}}{\text{Extraction load} \times 3412.75} \quad [32]$$

Observe that these equations are ratios of exhaust loss in kilowatts to output in kilowatts.

[8] These curves apply to exhaust ends as built for General Electric turbines, but will probably be found to hold without intolerable error for other designs.

Now let

$$\frac{\text{E.L.}_e}{\text{E.L.}_N} = F_1 = \text{ratio of Btu exhaust losses} \quad [33]$$

F_1 has been plotted against $\frac{w_x}{1 + w_x}$, the fraction of the throttle flow extracted, in Fig. 19.

Since the exhaust loss may be thought of as an external loss, directly affecting the turbine output, hence also the heat rate, but caused by internal phenomena, the heat rate is reduced by reduction in exhaust loss in the ratio

$$\frac{100 - \text{per cent E.L.}_N}{100 - \text{per cent E.L.}_e} \quad [34]$$

Using Equations [24] and [29] this ratio may be written

$$\frac{1 - \left(\frac{\text{E.L.}_N}{\text{A.E.}}\right)}{1 - \frac{\text{E.L.}_N}{\text{A.E.}} F_1 \left[1 - PG\left(\frac{t + U}{t}\right)\right]} \quad [35]$$

where A.E. = available energy.

For most purposes expression [35] may be used with slight error by converting it to a fractional reduction in heat rate due to decreased exhaust loss

Fractional reduction in heat rate due to reduction in exhaust loss

$$= \frac{\text{E.L.}_N}{\text{A.E.}} \left\{1 - F_1 \left[1 - PG\left(\frac{t + U}{t}\right)\right]\right\} \quad [36]$$

This reduction may then be applied to the heat rate

r_e = (nonextraction W.R.)$(H_e - h_c)(1 - PG)$

$$\left[1 - \frac{\text{E.L.}_N}{\text{A.E.}} \left\{1 - F_1 \left[1 - PG\left(\frac{t + U}{t}\right)\right]\right\}\right] \quad [37]$$

(Mechanical and generator efficiency are assumed to be unchanged. If desired these may be handled separately.)

Appendix

Derivation of Expression for Quantity of Extraction With a Finite Number of Heaters

Let

$$(H - h) = ax^2 + bx + t \quad [1]$$

where $(H - h)$ is taken at any point along the state line.

If $a = b = 0$, then, with contact heaters, each succeeding heater must heat an increasing amount of feedwater, the increase being the amount of extraction which was added to the condensate flow at the preceding heater. In this case it will be seen that

$$w_x = \sum_1^n E = \left(1 + \frac{R}{nt}\right)^n - 1 \quad [20]$$

Since, in general

$$a \neq b \neq 0$$

it is necessary to apply a correction to Equation [20].

To obtain the correction let us expand Equation [20] by the binomial theorem

$$w_x = \sum_1^n E = \left[n\left(\frac{R}{nt}\right) + \frac{n(n-1)}{2!}\left(\frac{R}{nt}\right)^2 + \ldots\right] \quad [38]$$

This represents the total extraction from the turbine per pound of condenser flow. A similar expression may also be written for the total extraction up to and including the $(n - 1)$th heater

$$w_{\frac{n-1}{n}x} = \sum_1^{n-1} E = \left[(n-1)\left(\frac{R}{nt}\right) + \frac{(n-1)(n-2)}{2!}\left(\frac{R}{nt}\right)^2 + \ldots\right] \quad [39]$$

To obtain the extraction for the nth heater, subtract Equation [39] from Equation [38].

Extraction for nth heater

$$= \left[\left(\frac{R}{nt}\right) + (n-1)\left(\frac{R}{nt}\right)^2 + \ldots\right] \quad [40]$$

In similar fashion, the expression may be written for the extraction for any heater.

Because t has been assumed constant in Equation [20] and because the true value of $(H - h)$ exceeds the value of t by a small amount

$$\Delta_1 = ax_1^2 + bx_1 = ax^2\left(\frac{1}{n^2}\right) + bx\left(\frac{1}{n}\right) \quad [41]$$

the true value of the extraction for the first heater is

$$E_1 = \frac{t}{t + \Delta_1}\left[\frac{R}{nt} + 0\right] \quad [42]$$

$$= \left[1 - \frac{\Delta_1}{t + \Delta_1}\right]\left(\frac{R}{nt}\right) \quad [43]$$

In a similar fashion, the extraction for the second heater is given by

$$E_2 = \left[1 - \frac{\Delta_2}{t + \Delta_2}\right]\left[\left(\frac{R}{nt}\right) + 1 \cdot \left(\frac{R}{nt}\right)^2\right] \quad [44]$$

and for the third heater by

$$E_3 = \left[1 - \frac{\Delta_3}{t + \Delta_3}\right]\left[\left(\frac{R}{nt}\right) + 2 \cdot \left(\frac{R}{nt}\right)^2\right] \quad [45]$$

in which the second bracket is meant to indicate the complete series.

Equations [43], [44], and [45] may be rewritten in the following form (Equation [44] being taken as an example)

$$E_2 = \left[\left(\frac{R}{nt}\right) + 1 \cdot \left(\frac{R}{nt}\right)^2\right] - \left[\frac{\Delta_2}{t + \Delta_2}\right]\left[\left(\frac{R}{nt}\right) + 1 \cdot \left(\frac{R}{nt}\right)^2\right] \quad [46]$$

The total extraction w_x per pound of condenser flow will be the sum of all such expressions from E_1 to E_n, inclusive. Let us sum up from 1 to n expressions having the form

$$\Delta_2\left[\left(\frac{R}{nt}\right) + 1 \cdot \left(\frac{R}{nt}\right)^2 + \ldots\right] \quad [47]$$

which in Equation [46] is the second bracket of the second term multiplied by the numerator of its coefficient.

The summation is

$$= ax^2 \left\{ \left(\frac{1}{n}\right)^2 \left[\left(\frac{R}{nt}\right) + 0 \cdot \left(\frac{R}{nt}\right)^2 \right] + \left(\frac{2}{n}\right)^2 \left[\left(\frac{R}{nt}\right) + 1 \cdot \left(\frac{R}{nt}\right)^2 \right] \cdots + \left(\frac{n}{n}\right)^2 \left[\left(\frac{R}{nt}\right) + (n-1)\left(\frac{R}{nt}\right)^2 \right] \right\} + bx \left\{ \left(\frac{1}{n}\right) \left[\left(\frac{R}{nt}\right) + 0 \cdot \left(\frac{R}{nt}\right)^2 \right] + \left(\frac{2}{n}\right) \left[\left(\frac{R}{nt}\right) + 1 \cdot \left(\frac{R}{nt}\right)^2 \right] + \cdots \left(\frac{n}{n}\right) \left[\left(\frac{R}{nt}\right) + (n-1)\left(\frac{R}{nt}\right)^2 \right] \right\} \quad \ldots [48]^6$$

which is readily seen to be

$$= ax^2 \left\{ \left(\frac{R}{nt}\right) \frac{(2n+1)(n+1)n}{6n^2} + \left(\frac{R}{nt}\right)^2 \frac{n(3n+2)(n+1)(n-1)}{12n^2} \right\} + bx \left\{ \left(\frac{R}{nt}\right)\left(\frac{n+1}{2}\right) + \left(\frac{R}{nt}\right)^2 \frac{n(n-1)(n+1)}{3n} \right\} \quad \ldots [49]$$

$$= ax^2 \left\{ \left(\frac{R}{t}\right) + \frac{n(n-1)}{2!n^2}\left(\frac{R}{t}\right)^2 \right\} \left\{ \frac{(2n+1)(n+1)}{6n^2} + \frac{(n+1)(n^2-1)}{12n^3}\left(\frac{R}{t}\right) \right\} + bx \left\{ \left(\frac{R}{t}\right) + \frac{n(n-1)}{2!n^2}\left(\frac{R}{t}\right)^2 \right\} \left\{ \frac{n+1}{2n} + \frac{n(n^2-1)}{12n^3}\left(\frac{R}{t}\right) \right\} \quad \ldots [50]$$

$$= \left[\left(1 + \frac{R}{nt}\right)^n - 1 \right] [C_a ax^2 + C_b bx] \text{ (approximately)} \quad \ldots [51]$$

Since the first factor of Equation [51] is the total extraction w_z, the second factor is an average weighted value of Δ, by virtue of the operation which was performed, that is

$$\Delta_w = ax^2 \left[\frac{(2n+1)(n+1)}{6n^2} + \frac{(n+1)(n^2-1)}{12n^3}\left(\frac{R}{t}\right) \right] + bx \left[\left(\frac{n+1}{2n}\right) + \frac{n(n^2-1)}{12n^3}\left(\frac{R}{t}\right) \right] \quad \ldots [52]$$

The value of the coefficients of ax^2 and bx, respectively, for various values of R/t are plotted in Fig. 10, against n, the number of heaters. The total extraction w_x then is

$$w_x = \frac{t}{t + \Delta_w} \left\{ \left[1 + \left(\frac{R}{nt}\right)^n \right] - 1 \right\} \text{ (in second approximation)} \quad \ldots [21]$$

Knowing w_x, the fractional reduction in nonextraction heat rate, which can be obtained by feedwater heating, is seen to be that given in Equation [11b] in the text.

Parameter A

The parameter A (see Fig. 12) is defined as the area between the curve of $(H - h)$ and the horizontal line $(H_c - h_c) = t$ from $x = 0$ to $x = 1$. Since this curve is given by Equation [1]

$$ax^2 + bx + t$$

the area under this curve will be

$$A = \int_0^1 (ax^2 + bx)dx = \left[{}^1/_3 ax^3 + {}^1/_2 bx \right]_0^1 = {}^1/_3 a + {}^1/_2 b \quad \ldots [53]$$

It should be mentioned that the correlation between A and the variation in P is dependent upon the use of a specific state-line curvature. A similar correlation might be worked out for any other shape of state line, which would be equally good but would differ by a small amount from that given. In practice, it has been found that a very flat curvature most nearly fits actual turbine state lines. This type of curve has been used in the analysis, and is illustrated in Fig. 20. Although the state line quoted in Warren and Knowlton's paper[8] is truly representative, in this

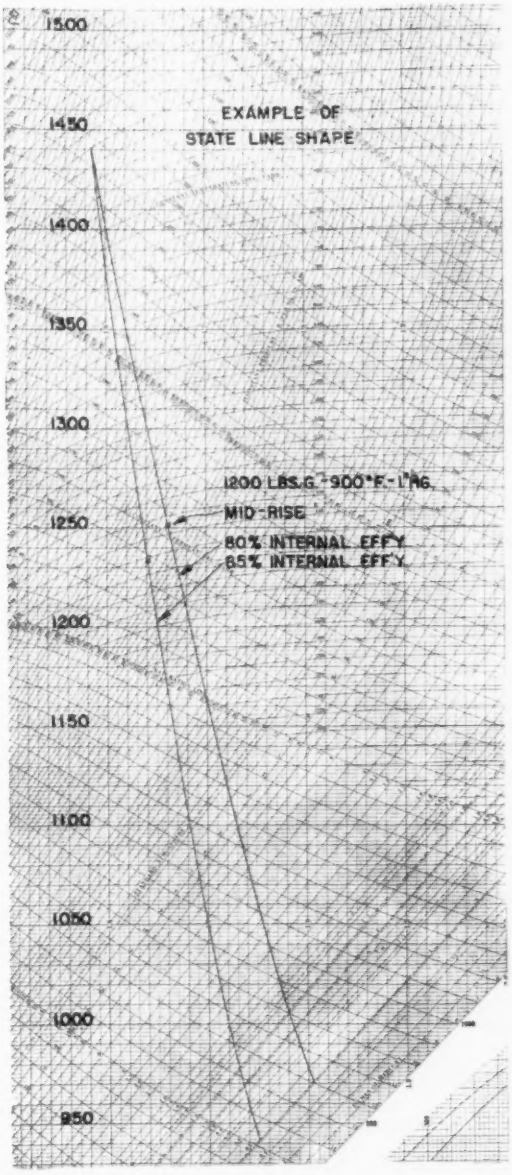


FIG. 20 TYPICAL STATE LINES AS USED IN THIS ANALYSIS

[6] Two terms only of the series give excellent accuracy for the small correction function Δ_w.

investigation, we have drawn it through the initial-state point, for purposes of consistency and accuracy of definition at all steam conditions. Obviously there is no appreciable difference in heat rate.

Correction for Actual Cycles

The P-x curves, of Fig. 1, are drawn for contact heaters and assume that the enthalpy leaving each heater is that of saturated liquid at the applicable temperature. For low feedwater pressures this is practically true. In recent years, with the advent of 1200-lb and higher pressure cycles, some engineers have considered the compressibility of the liquid in making heat balances, thus taking account of the recovery of part of the boiler-feed-pump input.

The major effect of the liquid compression is to reduce the extraction required from the next higher heater, thus offsetting part of the loss due to boiler-feed-pump power. In this paper no increase in liquid enthalpy due to liquid compression in any pump has been considered. A fairly accurate assumption, however, is that the boiler-feed-pump work is returned as heat to the cycle, and that for this reason the plant heat rate will suffer a fractional loss:

$$\text{Loss due to boiler feed pump} = \frac{\text{Boiler-feed-pump input}}{\text{Plant output}} \times (1 - \text{Cycle thermal efficiency}) \quad [54]$$

This modification is of the same character as that required by heater-terminal differences and pressure drop, and will be discussed by the author in a future paper.

As an interim approximation, the effect on heat rate of terminal difference and pressure drop aggregate in usual cases about 0.5 per cent in heat rate and may be so used. Evaporators, generator air or gas coolers, oil coolers, and steam-jet air-ejector condensers in the feedwater circuit can usually be taken care of separately if all the turbine data are known.

Example 1. What is an estimating heat rate for a plant operating at 800 psi gage, 900 F, 1 in. Hg, with six heaters? The nonextraction turbine efficiency is 81 per cent and the exhaust loss is 5 per cent.

Nonextraction heat rate from Table 2 $= \frac{8364}{0.81} =$ 10,326 Btu per kwhr

Gain from Fig. 15 = 11.38 per cent

Less cycle allowance $\frac{0.50}{10.88}$ 1123

9203 Btu per kwhr

Allow 2½ per cent for decrease in E.L.[10] 230

8973 Btu per kwhr

If it is desired to heat the feedwater to less than the optimum enthalpy, an additional allowance, usually in the order of 0.25 per cent, should be added to this heat rate.

Example 1a. What is the true gain due to reduction in exhaust loss if the feedwater is 400 F?

$$R_s = 512.3 - 47.1 = 465.2$$
$$R = 375.0 - 47.1 = 327.9$$
$$x = \frac{R}{R_s} = 0.705$$

From Fig. 17, the optimum rise is at $x = 0.83$ (= 453 F)

$$\text{Fraction of optimum rise} = \frac{0.705}{0.83} = 0.849$$

From Fig. 14, fraction of peak gain = 0.983

$$0.983 \times 11.38 = 11.19$$

Less cycle allowance $\frac{0.50}{10.69}$ per cent

Fractional extraction from Equation [24] =

$$\frac{327.9 + \left(\frac{10.69}{89.31} \times (1454.9 - 375)\frac{490}{917.8}\right)}{1407.8} = 0.282$$

Btu exhaust loss, nonextraction $= 0.05 \times \frac{3412.75}{5.941}$[11] $= 28.7$ Btu

From Fig. 19 and Equation [36], the fractional reduction in heat rate due to exhaust loss is

$$0.05\left\{1 - 0.565\left[1 - 0.1069\left(\frac{1407.8}{917.8}\right)\right]\right\} = 2.64 \text{ per cent}$$

Hence, the heat rate in example 1 would have been 0.14 per cent better than calculated because of the slight error in exhaust-loss-gain estimate and about 0.21 per cent poorer because the feedwater temperature is below the optimum.

Example 2. Find the loss which may be expected if only four heaters are used in example 1, keeping the feedwater temperature constant.

From Fig. 1 at $x = 0.705$

$$P_6 = 81.6$$
$$P_4 = 76.2$$

Gain with 4 heaters $= \frac{0.762}{0.816} \times 11.19 = 10.45$ per cent (no cycle allowance)

Percentage increase in heat rate $= 100 \times \frac{0.74}{88.81} = 0.833$ per cent

Example 2a. Note that the same result may be obtained from Fig. 1 and Fig. 6, but that this method neglects the slight variation in P with the parameter A; whereas this variation is included in Figs. 15 and 16.

$$0.054 \times 13.58 = 0.733$$

$$\frac{0.733}{1 - (0.816 \times 0.1358)} = 0.825 \text{ per cent}$$

Example 2b. A further alternative is the use of Figs. 17, 6, and 14; providing the final feedwater is at the *same fraction* of the optimum rise, such as 84.9 per cent in example 1*a*

$$(0.835 - 0.769)\ 0.1358 \times 0.983 = 0.881 \text{ per cent}$$

$$\frac{0.881}{0.8885} = 0.992 = \text{loss at comparable feedwater temperature.}$$

Example 3. What is the approximate difference in heat rate between the plant in example 1, designed with four heaters, and a comparable plant designed for 1200 psi gage, 950 F, 1 in. Hg, 6 heaters, assuming there is no difference in turbine efficiency or exhaust loss?

[10] Experience will soon develop the ability to estimate this value quite accurately. In this case the large number of heaters makes the allowance higher than usual.

[11] "Theoretical Steam Rate Tables," by J. H. Keenan and F. G. Keyes, The American Society of Mechanical Engineers, New York, N. Y., 1938.

Use Table 2 and Fig. 15

$$\text{Plant } A \quad \frac{8364(1-0.105)}{\eta} = \frac{7486}{\eta}$$

$$\text{Plant } B \quad \frac{8015(1-0.1227)}{\eta} = \frac{7032}{\eta}$$

With 80 per cent turbine efficiency and an assumed gain of 2 per cent in exhaust loss in both cases

$$\text{Plant } A = 9170$$
$$\text{Plant } B = 8614$$
$$\text{Difference} = \frac{556}{9170} = 6.06 \text{ per cent plant } B \text{ is better than plant } A$$

whereas, nonextraction cycles would indicate only

$$\frac{349}{8364} = 4.17 \text{ per cent plant } B \text{ is better than plant } A$$

Actually plant B is probably slightly more than 6.06 per cent better than plant A, because of the greater reduction in exhaust loss resulting from a better heater cycle, providing the exhaust losses are equal on a nonextraction basis.

The difference in turbine efficiency would have to be applied to the result to obtain a true comparison.

Acknowledgment

The author wishes to express his indebtedness to Miss E. T. Hannan and Miss Daisy Houghton for the large number of numerical calculations made in obtaining data for the curves presented in this paper.

Experimental Studies of Automatic Control

By J. C. PETERS,[1] PHILADELPHIA, PA.

It is important that new modes of automatic control and newly developed control mechanisms be proved in the laboratory, in so far as is possible. The first part of this paper describes an equipment for this purpose developed by the author's company during the last 10 years. Sufficient detail is given to be useful to others who may wish to build a similar equipment. The second part of the paper deals with typical results obtained, illustrated with actual test records.

IT IS important that field studies of automatic control be carried out with minimum disturbance to the controlled process. With modern high-capacity units, unnecessary shutdowns or loss of production, even for short periods, cannot be tolerated. In the refining industry, for example, neither operators nor management look with favor upon repeated changes in furnace or tower temperatures made just to learn how a controller will take care of them. It is, therefore, the responsibility of the manufacturer of control equipment to prove his product in the laboratory, in so far as is possible, before trying it out on an actual job. A suitable "dummy" process used for this purpose by the author's company will be described, together with examples of results obtained. Sufficient detail will be given to be useful to others, particularly teachers of instrumentation courses, who may wish to build a similar equipment.

Description of Laboratory Process

The principal elements of the laboratory process are shown in Fig. 1. While it is one involving temperature control only, it is proper to say at this point that the fundamentals of control are much the same regardless of the particular controlled variable involved. Peculiar to temperature control is the unfavorable effect of "transfer lag," which may be defined for present purposes as retardation, resulting from intervening thermal resistance, in the effect, at the point of measurement, of changes in the adjusted heat supply. Another unfavorable process lag, "distance-velocity lag," found particularly in pH control, can be introduced into the temperature process by a suitable artifice to be described later. In short, a temperature process is most convenient for general automatic-control studies.

Referring to Fig. 1, the automatic controller under test maintains temperature in a small tank[2] of water *B*. The controller adjusts rheostats to provide the proper rate of electric heating in a nichrome winding surrounding the tank. The heat output of this winding will be spoken of as the "supply." The "demand" will refer to the heat required by a flow of water which enters at *F* and overflows at *G*. A manually adjustable head device is provided so that the demand may be changed at will and the resulting control action observed.

The degree of difficulty of control is determined by the thermal relationship between the heater winding and the tank. A bare heater winding, immersed in the water, would result in such an easy process to control that special tests of it would not be worth while. By isolating the heater thermally from the tank to a certain extent, the control problem can be made just as difficult as is desired. In the particular arrangement shown, the tank is first covered by about 1/8 in. of asbestos sheet. The winding is then applied and on this is placed a layer of alundum cement, followed by glass wool. Typical test records to be given later will show the extent to which transfer lag affects control with this construction.

While an equipment of the type shown is simple in principle, unless considerable care is taken in the design, spontaneous changes in supply or demand will occur to obscure the results. On the supply end, line-voltage variations represented a considerable source of annoyance, until voltage regulators were applied, practically eliminating the trouble.

The scheme shown in Fig. 1 for handling the demand flow was evolved after various others were proved to be undependable. In this, every precaution was taken to eliminate the trapping of gas liberated from the water by heating.

Tank *A* is the source of water for the demand flow. Here the temperature is held at 50 C, using a contacting mercury thermometer with a special relay. Because the return flow is at a higher temperature, a fixed water flow through a closed coil is provided to make it possible to control by heating.

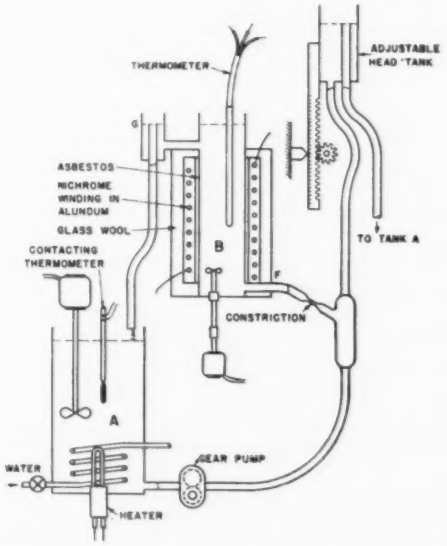


FIG. 1 SCHEMATIC REPRESENTATION OF LABORATORY PROCESS

A gear-type constant-displacement pump is induction-motor-driven to circulate approximately 40 cu in. of water per min. By setting the height of the adjustable head device, the water flow through *B* may be varied as desired. By tapping off for the useful flow as indicated, most of the liberated gas is carried directly through the system and passes out at the overflow in the variable head device. The expanded section near the tap-off point was introduced to eliminate the effect of eddies, which caused some change in the effective head, with normal variations in total flow, resulting from variable "slippage" in the pump.

---

[1] Chief of Automatic-Control Division, Research Department, Leeds and Northrup Company. Mem. A.S.M.E.

[2] Diameter 2.5 in., water depth 9 in., water capacity 44 cu in.

Contributed by the Committee on Industrial Instruments and Regulators of the Process Industries Division and presented at the Semi-Annual Meeting, Kansas City, Mo., June 16–19, 1941, of THE AMERICAN SOCIETY OF MECHANICAL ENGINEERS.

NOTE: Statements and opinions advanced in papers are to be understood as individual expressions of their authors and not those of the Society.

The constriction in the line to tank B is of a transparent plastic in which any stoppage is readily observed. Distilled water is used to cut down accumulation of solids in the closed system.

The power circuit for the heater of tank B is shown in Fig. 2, together with means for positioning the rheostats in response to air pressure, as is required when a pneumatic controller is under test.

For test purposes it is convenient to have a linear relationship between rheostat position and power input to the heater. This

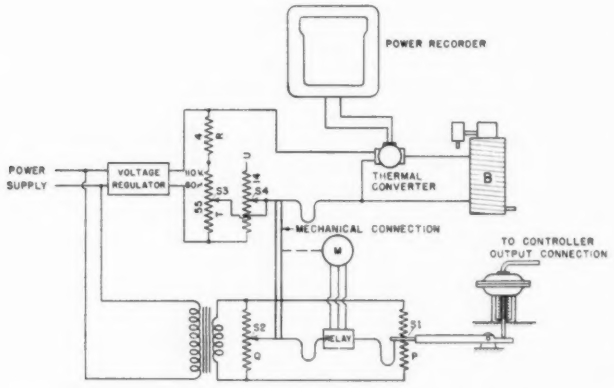


FIG. 2 HEATER CIRCUIT AND SCHEME FOR POSITIONING RHEOSTATS IN ACCORDANCE WITH AIR PRESSURE

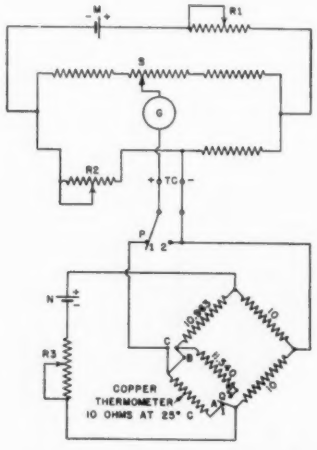


FIG. 3 SCHEME FOR USING A POTENTIOMETER RECORDER WITH A RESISTANCE THERMOMETER

relationship is closely obtained with the connection scheme shown. Resistance values, as indicated, are for use with a heater of 19 ohms resistance. The available power range is 40 to 660 w.

As indicated by the rigid connection, contacts $S2$, $S3$, and $S4$ always move together. The positions of these contacts are caused automatically to follow that of contact $S1$ on slide-wire P. Unless the Wheatstone bridge consisting of the parts of rheostats P and Q is balanced, a suitable contact is made in the differential relay to energize the motor which moves contact $S2$ to restore the balance.

In testing electrical control mechanisms, slide-wire P and the relay may be part of the controller under test. In testing pneumatic controllers contact $S1$ is moved by a diaphragm motor as indicated. An 11-in. diaphragm motor with valve positioner attached is provided.

Tank B is large enough to take mercury-filled- or vapor-pressure-type bulbs of suitable temperature range. With either resistance-thermometer- or thermocouple-type instruments, a resistance thermometer is used as the primary element. This is because the desired temperature range does not give enough sensitivity with thermocouples. The recorder range generally used is 50 to 80 C. A suitable auxiliary circuit, adaptable to a thermocouple potentiometer of almost any range, is shown in Fig. 3.

Referring to Fig. 3, the points marked TC, + and —, represent thermocouple terminals of a potentiometer recorder, the circuit of which is shown above these points. In this circuit, the nickel coil which provides for automatic reference junction compensation has been replaced by an adjustable resistance $R2$ of manganin, which should have a range of about 10 ohms in increments of 0.01 ohm.

Below the TC terminals is shown an unbalanced bridge arrangement providing an emf dependent upon the temperature of a copper resistance thermometer. The adjustment procedure is as follows:

First, the TC terminals are shorted by throwing switch P to position 2, and resistance $R2$ is adjusted until the recorder balances at the low end of the scale. The recorder circuit is then standardized against the standard cell (not shown) in the usual manner. Switch P is now thrown to position 1 and switch Q to position 2. Rheostat $R3$ is then adjusted until the recorder reads 65 C as it should, since 11.540 ohms is the resistance of the thermometer at this temperature. Because 10.963 ohms is the resistance of the thermometer at 50 C, and because $R2$ was adjusted for zero emf at the low end of the scale, this end of the scale will correspond to 50 C.

It should be noted that a highly accurate temperature scale is not necessary for the purpose of testing automatic controllers.

Figs. 4 and 5 are front and rear views, respectively, of the actual equipment. In Fig. 4 three rheostats are seen on the table to the left. Two of these in parallel constitute rheostat U of Fig. 2. Rheostat Q is not seen in Fig. 4, as it is behind the others. It is of a small rotary type, driven through a worm from one of the larger rheostats. The voltage regulators, two 500-w units in parallel, are seen under the rheostat table.

On the second table is seen tank B with the mark LN. What is seen is not the tank proper but a brass cylinder surrounding it. To the right of tank B is the adjustable head device. The large tank, mounted through a hole in the table, is tank A of Fig. 1. To the right of tank A and under the table is the No. 2 Oberdorfer gear pump, driven through a worm reduction at a speed of approximately 90 rpm.

The recorder on the left-hand side of the panel board is the power recorder of range 0–1000 w. Under this is a push-button station for use when it is desired to position the rheostats manually through operation of the motor. The differential relay is flush-mounted in a case below the push buttons.

The pneumatic control instrument on the right-hand side of the panel is used for general automatic-control studies and as a recorder only, when other controllers are being tested. It is provided with a Wheatstone-bridge circuit for the range of from 50 to 80 C.

Controllers under test are mounted either on the slat-type board seen at the extreme right or on a similar board, out of the view, on the left. The switching scheme is such that two controllers, one a pneumatic and the other an electric type, may be applied alternately without changing the wiring.

In the rear view, Fig. 5, the diaphragm motor for positioning rheostat P of Fig. 2 is seen at the left. To the right, on the corner of the table, is a small magnetic brake used to stop motion of the rheostats quickly.

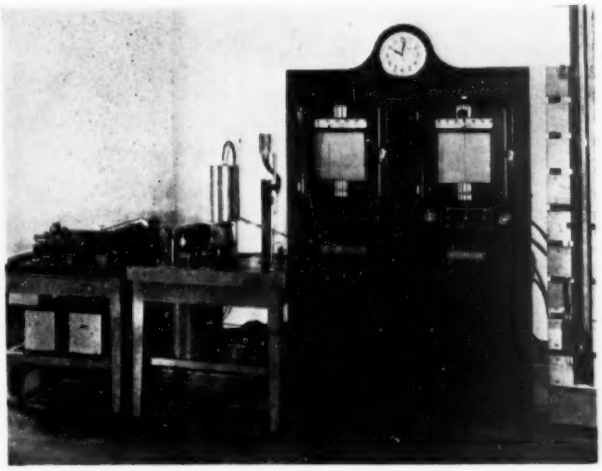


FIG. 4 FRONT VIEW OF AUTOMATIC-CONTROL TEST EQUIPMENT

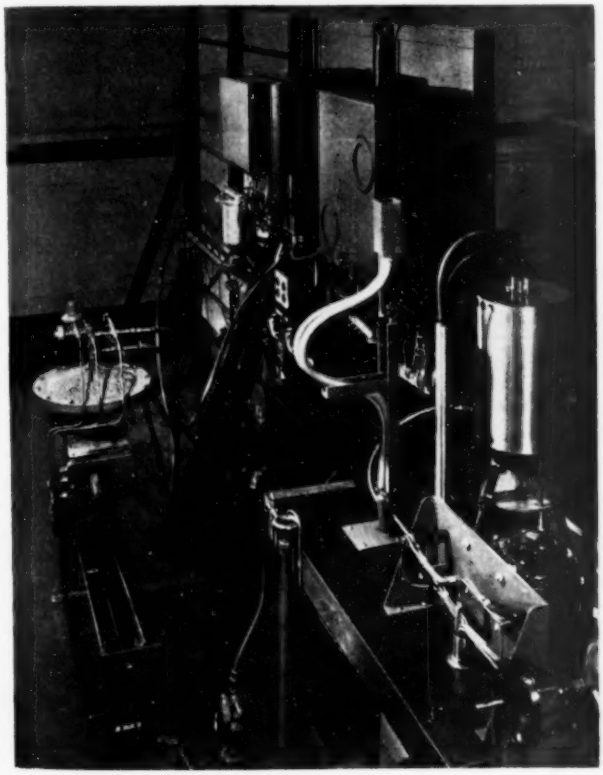


FIG. 5 REAR VIEW OF AUTOMATIC-CONTROL TEST EQUIPMENT

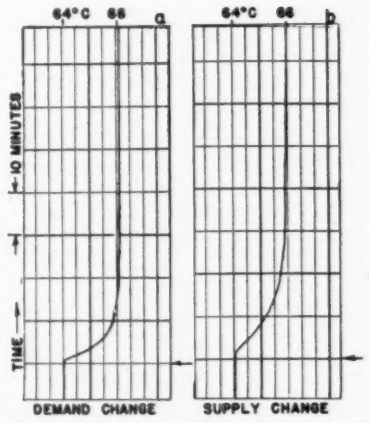


FIG. 6 RESPONSE OF PROCESS TO SUDDEN CHANGE, NO AUTOMATIC CONTROL

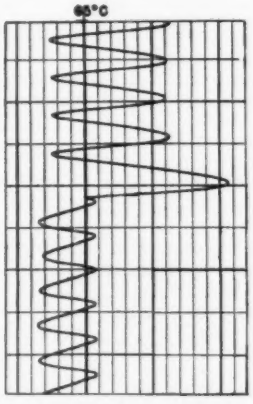


FIG. 7 TWO-POSITION CONTROL RECORD, SHOWING EFFECT OF SUDDEN DEMAND CHANGE

EXPERIMENTAL RESULTS

The illustrations which follow are all reproductions of photographs of actual test records. To simplify the marking of the records it will be mentioned here that, in all cases, the vertical scale is time, each scale division representing 10 min, and higher points are for later times; for temperature records, each scale division is 0.5 deg C, and for power records, each scale division represents 10 w.

(*a*) *Process Characteristics.* Figs. 6(*a*) and (*b*) show temperature-response curves, resulting from sudden changes in demand and supply, respectively. Changes were made at the times indicated by the arrows. The response to sudden demand change, e.g., a sudden decrease in rate of water flow, was evident on the record 40 sec after the change was made and the response was 60 per cent complete in 220 sec.

The response to a sudden supply change, e.g., change in rheostat position, was evident on the record in 90 sec, and the time required for the change to be 60 per cent complete was 645 sec.

Delay in the initial response to a demand change is mainly the result of detection lag in the resistance thermometer used, this particular element not being of a very rapid type.

(*b*) *Two-Position Control.* Fig. 7 shows the results obtained with two-position control under two different conditions of demand. The power changed between 40 and 660 w as the temperature crossed the 65-deg value. For the first portion of the curve, the power is at 660 w 79 per cent of the time, and at 40 w 21 per cent of the time, giving an average power of 530 w. After the decrease in load the average power is 235 w.

(*c*) *Proportional-Plus-Floating Control.*[3] The significance of the series of curves which follow will be evident after a discussion of the typical curves of Fig. 8. Curve 8(*a*) is the temperature response to a sudden change in demand, i.e., a sudden change in the rate of water flow through tank *B*, with proportional-plus-floating control. First the demand was increased, then 40 min later, it was decreased. Curve 8(*b*) is the corresponding record of

[3] This may be more completely specified as proportional-position plus proportional-speed-floating control. Refer to "Some Fundamental Considerations in the Application of Automatic Control to Continuous Processes," by E. S. Bristol and J. C. Peters, Trans. A.S.M.E., vol. 60, 1938, pp. 641–650.

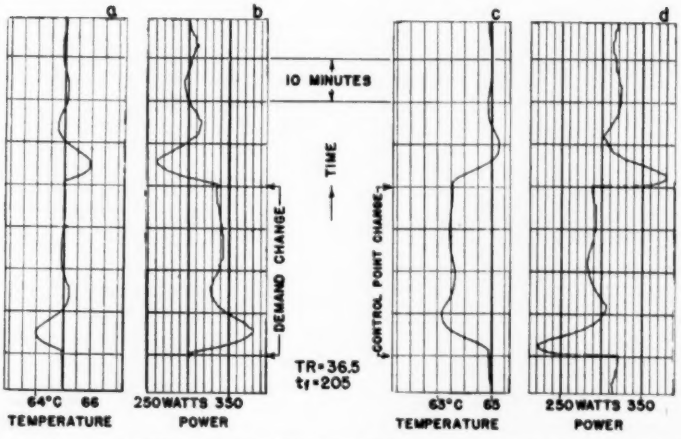


FIG. 8 TYPICAL RESPONSES TO SUDDEN DEMAND AND CONTROL-POINT CHANGES

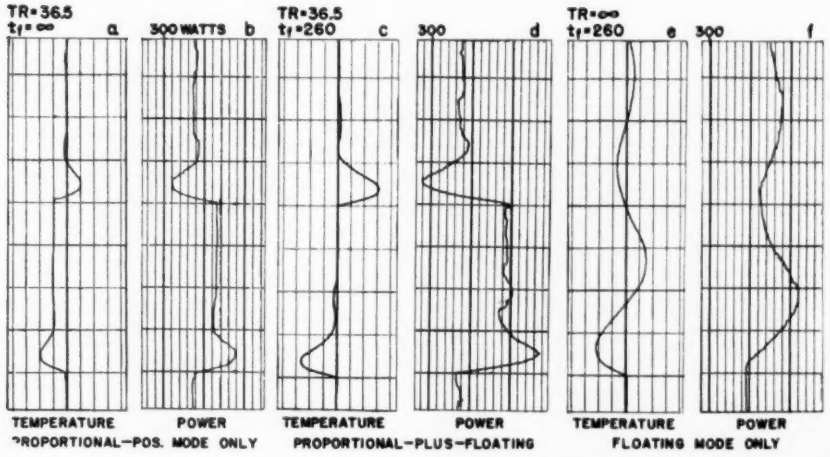


FIG. 9 EFFECT OF CUTTING OUT EITHER COMPONENT MODE IN PROPORTIONAL-PLUS-FLOATING CONTROL

power to the heater. From this it will be noted that the load change required an ultimate power change of 40 w.

Curve 8(*c*) is the temperature response to a sudden change in control point, the controller adjustments being exactly the same as for 8(*a*). For 8(*c*) the water flow was left unchanged but the control setter was moved for control at 63.5 C and then, 40 min later, turned to the original setting of 65 C. With the particular controller used, and this would be the case with most controllers operating in accordance with the same mode of control, the proportional-position action functions as soon as the setting is changed and shifts the power as though the temperature had deviated from the control point by the amount of the change in setting. The power record of curve 8(*d*) shows this effect followed by additional change due to the combined proportional-position and floating actions.

For these and records which follow, the *TR* (throttling-range) value is the apparent percentage of the scale range, 9.875 in., or 50 to 80 C, through which the pen would have to be moved to change the power over the entire adjustable range of 40 to 660 w. It is determined in the following manner:

With the power in the vicinity of the range covered in a particular test, the pen is moved by a small amount, say ΔS per cent of the scale range. The corresponding power change by proportional-position action only is noted. Calling this ΔP, the *TR* value is then calculated from the formula

$$TR = (660 - 40) \times \frac{\Delta S}{\Delta P}$$

The "floating time" t_f is the apparent time in minutes required to change the power through the entire adjustable range by floating action alone, when the deviation from the control point is 1 per cent of the scale range. This is determined by noting the power change ΔP_1 occurring in a given time t, when the deviation is ΔD per cent of the recorder scale range. Then

$$t_f = (660 - 40) \frac{\Delta D t}{\Delta P_1}$$

This figure applies to the throttling range used in the particular test. Generally and preferably, a change in throttling-range setting changes the floating time proportionately. If the floating-speed adjustment remains fixed, then

$$\frac{t_f}{TR} = \text{constant}$$

The value of this ratio is, therefore, an index of the setting for floating speed, and is inversely proportional to it.

The curves of Fig. 9 show what happens when one of the component modes of proportional-plus-floating control is cut out. Curve 9(*c*) is the response to a sudden demand change with proportional-plus-floating control adjusted so that the return to the control point is nearly "critically damped," i.e., it takes place about as rapidly as is possible without overshooting. Curve 9(*d*) is the corresponding power record.

Curve 9(*a*) was obtained with the floating action cut out. While the control is stable, the temperature is not returned to the

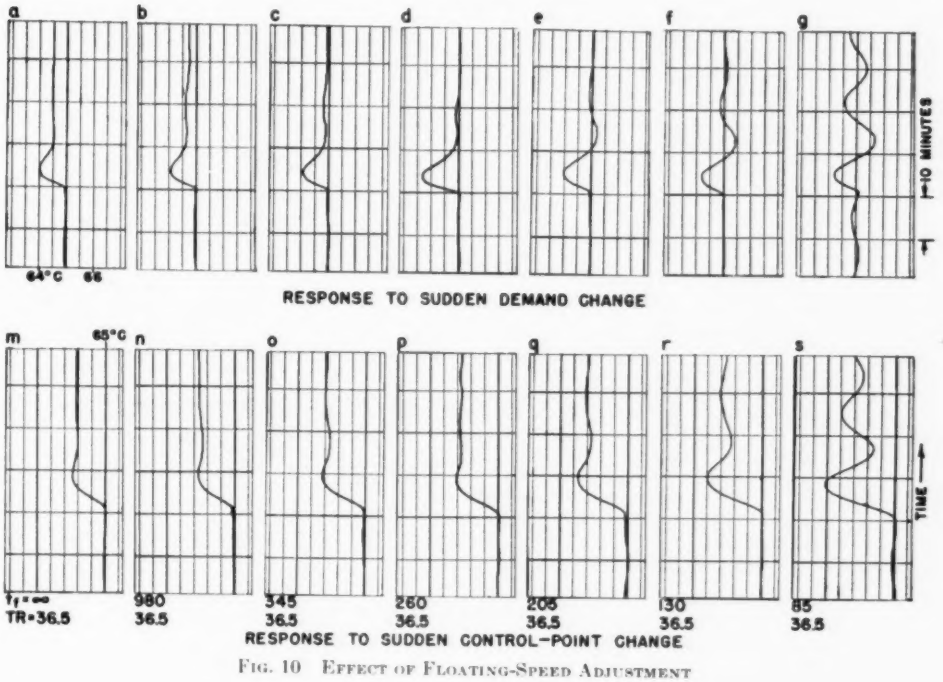


FIG. 10 EFFECT OF FLOATING-SPEED ADJUSTMENT

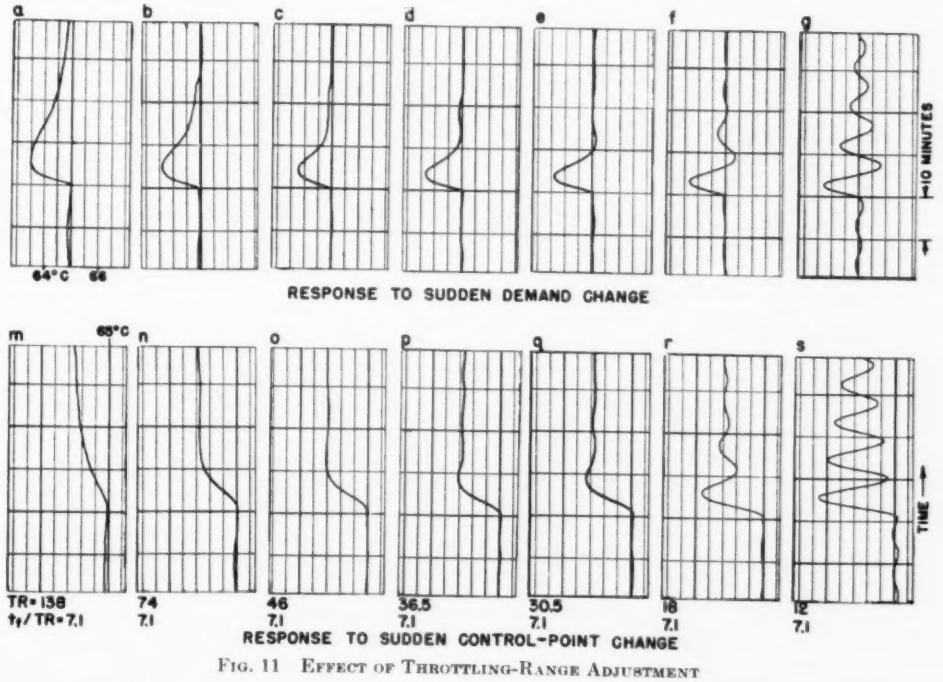


FIG. 11 EFFECT OF THROTTLING-RANGE ADJUSTMENT

initial value. In curve 9(*e*), with floating action only, return to the control point is seen to be taking place after a series of oscillations, the first overshoot being 70 per cent of the initial deviation. In comparing 9(*b*), (*d*), and (*f*), it should be noted that ultimate power shifts are not equal but have values of 30, 55, and 35 w, respectively, representing demand changes of different magnitudes.

The curves of Figs. 10 and 11 show how varying the adjustment of floating speed and throttling range affects the responses to sudden change of demand or of control point. Curve 10(*d*) is for adjustment giving a nearly critically damped response to demand change and 10(*p*) is the response to control point change obtained with the same controller adjustments. To the left of these are curves obtained with slower floating speeds or longer floating times, while the curves to the right are for more rapid floating action. For curve 10(*a*) there is no floating action and, as would be expected, the temperature does not return to the original value. In 10(*b*), the return is so slow that a record of several times the length given would be needed to show when it is nearly complete.

It is to be noted that the small oscillations about the return

curve, as seen in records 10(*b*), 10(*c*), and 10(*d*), are due to the proportional-position mode and could be removed by widening the throttling range slightly. The floating speed is adjusted correctly when this action is just sufficient to center the oscillations about the control point. In curve 10(*d*), the floating action is slightly less than sufficient.

By comparing the results of sudden control-point changes with those of sudden demand changes, it will be seen that characteristics as regards slow approach to final temperature or conditions of damped oscillation are similar. Frequently, the safest way to study the action of a controller, applied in the field, is to make small control-point changes and note the results.

In Fig. 11 curves (*d*) and (*p*) are identical with the correspondingly lettered curves of Fig. 10. The curves on either side of

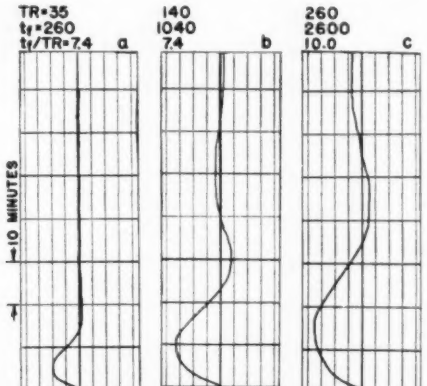


FIG. 12 EFFECT OF DISTANCE-VELOCITY LAG

11(*d*) and 11(*p*) show the effect of varying the throttling-range setting. As previously stated the floating time varies directly with the throttling-range setting.

As with the setting for floating speed, too weak an action means sluggish return and too strong an action introduces undesirable oscillations. Comparing 10(*d*) and 10(*f*) with 11(*d*) and 11(*f*), each representing an increase in strength of 50 per cent in the control action, it is seen that the decrement of the resulting oscillation is greater for a 50 per cent decrease in throttling range than it is for the same percentage reduction in floating time.

The temperature-response curves of Fig. 12 show results obtained with proportional-plus-floating control when distance-velocity[4] lag is introduced. This type of lag represents a definite delay between the time when a change takes place at the point at which the controlled variable should be held constant and the time when the controller is in a position to do something about it. In pH control, it is the time required for the solution to travel from the point at which a control agent is added to the point at which the electrodes for measurement are located.

In using a temperature-controlled process[5] for studies of the effect of distance-velocity lag, an artifice must be used to give a similar effect. The procedure which we have followed is to actuate the control mechanism from a pointer which is moved manually to follow the temperature curve, as produced at a specified previous time.

In Fig. 12 curve (*a*) is the response without distance-velocity lag. For curve (*b*) the lag is 5 min, and for curve (*c*) it is 10 min. Upon introducing the *D-V* lag of 5 min, the control was found to be unstable until the throttling range was widened. Upon changing the *TR* setting from 35 to 70 per cent (record not shown), the control was stable but the first overshoot was twice that of curve (*b*). A wider throttling range than the 140 per cent figure used for curve (*b*) would further reduce the oscillations.

Curve 12(*c*) shows that stable control is possible with a 10-min *D-V* lag, but it is required that the control actions be further weakened. In considering automatic control in the face of *D-V* lag, the point made by Callender and Stevenson[6] must be clearly kept in mind, namely, that any changes which occur during the delay period are inevitable. If means can be introduced to keep these within allowable limits, then satisfactory control may be obtained in spite of the lag.

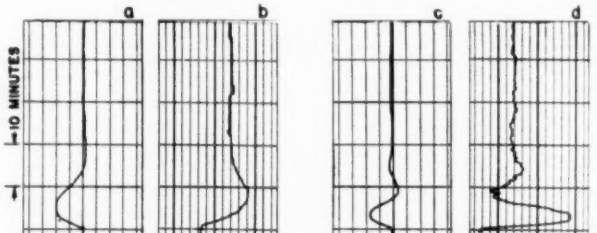


FIG. 13 CURVES SHOWING EFFECT OF ADDING SECOND-DERIVATIVE MODE

The effect of the addition of the second-derivative[7] mode of control to proportional-plus-floating control is illustrated by the curves of Fig. 13. Before discussing the curves, what is meant by second-derivative control will be explained. If we consider the action of the control valve (or rheostat) at any instant, the floating mode may be said to move the valve at a rate proportional to deviation from the control point, while the proportional-position mode simultaneously moves it at a rate proportional to the rate of change of the deviation with time. The second-derivative mode causes valve motion at a rate proportional to the rate of change of the rate of change of the temperature deviation, i.e., in accordance with the rate at which the slope of the temperature curve is changing. The resultant rate of valve movement is described by the equation

$$-\frac{dV}{dt} = A\theta + B\frac{d\theta}{dt} + C\frac{d^2\theta}{dt^2}$$

where V = valve position
θ = deviation of temperature from control point
A = a constant for floating action

[4] The term "distance-velocity lag" is preferred to the term "velocity-distance lag" originally suggested by C. E. Mason in his paper, "Science of Automatic Control in Petroleum Refining," *World Petroleum*, vol. 4, 1933, pp. 187–190. This is because the changed order of the words is more suggestive of the ratio of distance to velocity which has the dimensions of time, in numerical units of which this lag can usually be stated.

[5] Distance-velocity lag, referred to by another name, was introduced in a laboratory process for the study of pH control by J. J. Grebe, R. H. Boundy, and R. W. Cermak and is described in their paper, "The Control of Chemical Processes," Trans. American Institute of Chemical Engineers, vol. 29, 1933, pp. 211–256.

[6] "The Application of Automatic Control to a Typical Problem in Chemical Industry," by A. Callender, and A. B. Stevenson, Proc. of the Chemical Engineering Group, Society of Chemical Industry (London) vol. 18, 1936, pp. 108–116.

[7] This name arises from the fact that this mode is represented by a second-derivative term in the differential equation to be given shortly. Perhaps "rate-of-rate" control would be a more acceptable name for it.

B = a constant for proportional-position action
C = a constant for second-derivative action

Comparing temperature curves 13(*a*) and 13(*c*) it is seen that with second-derivative control the temperature is brought to within 0.2 C of the control point in 6.5 min, while without this mode the time required was 12 min. Power records 11(*b*) and 11(*c*) show clearly how the power is more quickly increased when second-derivative control is used and how it is cut back sharply to prevent serious overshooting.

While second-derivative control is the subject of several patents[8] and has been discussed in papers on automatic control, it has never been widely used. The chief factors in this have probably been the complication of most mechanisms proposed for the purpose, and the problem involved in making adjustments to fit the controller to a particular application. The combination of proportional-plus-floating plus second-derivative control requires the manipulation of three separate adjustments to fit it to the job.

ACKNOWLEDGMENT

In conclusion the writer wishes to express his appreciation to Mr. E. W. Yetter for his assistance, both in obtaining test records and in assembling material for the paper.

Discussion

N. B. NICHOLS[9] AND J. G. ZIEGLER.[10] The writers have developed a method of predicting optimum controller settings, and the data contained in this paper afford a trial of this method. This method will be described in a paper now in preparation. By optimum settings, we mean such adjustments of the controller response as will give a reasonable combination of small deviations from, and prompt return to, the control point. The data needed could be obtained from a study of the uncontrolled-process-response curve shown in Fig. 6(*b*) of the paper, but unfortunately the author does not give the magnitude of the supply change causing this response curve. However, they may also be obtained from the curves shown in Fig. 7. Using the writers' method on the larger load (bottom half) of Fig. 7, it may be predicted that the following controller settings would give good control

$$TR = 10 \text{ per cent}$$

$$t_f = 58 \frac{\text{Min}}{\text{Per cent}} \qquad \frac{t_f}{TR} = 5.8 \text{ min}$$

Using the small load (upper half) of Fig. 7

$$TR = 24 \text{ per cent}$$

$$t_f = 180 \frac{\text{Min}}{\text{Per cent}} \qquad \frac{t_f}{TR} = 7.5 \text{ min}$$

From these data, it would appear that the process is slightly easier to control at larger loads. Since it appears that most of the author's curves are run with loads of less than 540 w, we shall use the latter values. It will be observed that these values correspond to a controlled-response curve about halfway between the curves of Fig. 11(*e*) and 11(*f*), 11(*q*) and 11(*r*). It thus appears that for this example our method has predicted settings which give good control. Evidently, the author has not made the same load change in the various controlled-response curves given in Figs. 10 and 11. We believe a better comparison could be made if the relative magnitudes of the load changes were known.

[8] U. S. Patents 1,497,164, 1,988,458, 2,053,034, and 2,175,985.

[9] Engineering Research Department, Taylor Instrument Companies, Rochester, N. Y.

[10] Sales Engineering Department, Taylor Instrument Companies, Rochester, N. Y.

In the examples with distance-velocity lags our method would predict the following settings:

Distance-velocity lag of 5 min

$$TR = 80 \text{ per cent}$$

$$t_f = 1900 \frac{\text{Min}}{\text{Per cent}} \qquad \frac{t_f}{TR} = 25 \text{ min}$$

Distance-velocity lag of 10 min

$$TR = 133 \text{ per cent}$$

$$t_f = 5500 \frac{\text{Min}}{\text{Per cent}} \qquad \frac{t_f}{TR} = 42 \text{ min}$$

We believe the settings mentioned will give a somewhat smaller initial deviation and shorter period of oscillation than the values used by the author.

Concerning second-derivative response, we agree with the author's comment that it is a very useful type. It is being used very successfully on long-time-lag applications, such as rayon shredders, tube stills, juice heaters, fractionating columns, and in various air-conditioning processes. The author does not indicate the second-derivative setting used in obtaining Fig. 13(*c*), nor does he indicate what units he would use to measure it. We would suggest the term "pre-act time," PA, which we have found useful. If V is expressed in watts, θ in per cent of range, and t in minutes, the equation for $-\frac{dV}{dt}$ in the paper may be written

$$-\frac{dV}{dt} = \frac{660 - 40}{t_f}\theta + \frac{660 - 40}{TR}\frac{d\theta}{dt} + \frac{660 - 40}{TR}PA\frac{d^2\theta}{dt^2}$$

Our method indicates that PA should have a value near 1.1 min with the other settings as noted for the application of Fig. 13(*c*). This means the coefficient of the second derivative should be

$$C = 28 \frac{\text{Watts}}{\text{Per cent/Min}}$$

It would be interesting if the author would compare this with the value of C or PA used in Fig. 13(*c*). For the examples with distance-velocity lags, we would suggest the pre-act times of 3.6 min and 6.1 min. With TR and t_f values as suggested, the settings for good control are thus completely specified.

G. A. PHILBRICK.[11] This paper is a worthy contribution to the literature and a fitting continuation of the Bristol and Peters paper[3] given a few years ago. Models of controlled systems are exceedingly useful in the study and application of automatic control; and the disclosure in this paper of a carefully worked out experimental equipment should help to make such methods better known. Just as pilot plants aid in the construction and operation of full-scale processing equipment, so model systems offer a means for developing the specialized technique necessary for the successful adjustment of controllers.

While the author has described a model system principally thermal, it is true, as he states, that "the fundamentals of control are much the same regardless of the particular controlled variable involved." Thus, although transfer lag, for example, is defined by him in terms of thermal concepts, it is a property as well of other kinds of system (e.g., chemical), although in general it is perhaps not as prevalent nor as pernicious as in many thermal systems. With artificially constructed systems, of course, such lags may be introduced at will to simulate control-resisting properties; this may be done whether such (model) systems are thermal, hydraulic, pneumatic, or electrical. For instance, a two-capacitor ther-

[11] The Foxboro Company, Foxboro, Mass. Jun. Mem. A.S.M.E.

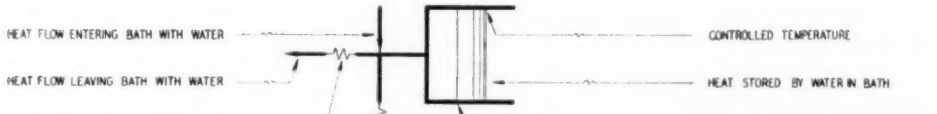


FIG. 14 LIQUID-LEVEL MODEL OF AUTHOR'S THERMAL SYSTEM

mal model was shown by Mason,[12] together with its hydraulic analog, in which transfer lag is the result of lumped, or concentrated, elements rather than of distributed elements as in the case of the thermal model described in this paper.

Since the subject matter of the present paper is coextensive in part with that of two earlier papers,[13, 14] by C. E. Mason and the present writer, it might not be out of place to point out some correspondences in nomenclature between the two presentations. "Throttling range" (Peters) and "proportional band" (Mason and Philbrick) are names for the same thing, the former expressed in percentage of the instrument scale, and the latter in actual units of the controlled variable. "Floating time" (Peters) is a derived expression and is the ratio of the "throttling range" (Peters) to the "reset constant" (Mason and Philbrick), the latter being referred to as "floating speed" by the author.

The collection of experimental curves included in the paper shows quite well the effect of controller adjustments following suddenly applied upsets of the two types chosen. For the proportional-plus-floating controller, a norm is chosen for both throttling range and floating speed adjustments, and the effect is indicated of changes in either adjustment from this norm, although not of changes in both adjustments together. This would require a complete square array, which would show in one corner, for example, the response obtainable with a large throttling range and a slow floating adjustment—the adjustments for averaging control.[14] Nevertheless, the author's results are unusually complete.

The experimental results, showing response in the presence of distance-velocity lag (or dead time) in the controlled system form a much-needed addition to the literature, especially since these results are compared with results for the same system, but from which such lag is absent. The method used by the author for simulating this kind of lag, and which was also used,[15, 16] in the analytical work of Callender, Hartree, Porter, and Stevenson, naturally may be followed in models other than thermal.

On the whole, the results presented corroborate the contention that model systems offer feasible representation of systems to which controllers must be applied in industry. The adequacy of the use of models, having lumped elements, is also upheld by the evidence now available. Theoretical results alone are poor comfort indeed without experimental support. In connection with the use of models and with the ability generally of one system to represent another, the writer would like to exhibit a simple liquid-level model, made of resistances and tanks, which has practically the same characteristics as the thermal system of the paper. Fig. 14 of this discussion is a diagram of such a system, with the analogies indicated in detail. Heat energy becomes quantity of liquid, and temperature becomes level. The relative sizes of the resistances and the capacitances (tank areas), corresponding to thermal resistances and capacitances, are indicated in Fig. 14. A wealth of confirming data[17] show that the reactions of hydraulic systems, such as this one, can be successfully computed from their known constants. This model is analytically simple, and it may readily be shown to react to flow changes in a manner indistinguishable from that shown in the paper for the thermal model. Automatic control, when applied to this system, yields response curves uncannily similar to those shown by the author.

E. S. SMITH.[18] The empirical approach of this paper is both sound and sensible. It challenges mathematicians to produce commensurate results, especially where two-position control or transportation lag, i.e., distance-velocity lag exists.

A better comparison would be obtained by taking the actual temperature instead of that recorded, since the latter has excessive lag. In the paper, much of the control lag was due to the response lag of the measuring which governed the controlling. It is desirable that the measurement used as a basis of the comparison should have considerably less response lag.

It is requested that the closure include basic diagrams of controllers used, which were stated to give proportional-and-floating and second-derivative control, respectively. Objection is made to the terminology of the paper, which probably will cause confusion by taking valve velocity instead of position, since "proportional" is generally accepted to mean that the valve position corresponds with departure. It is requested that the final equation be placed upon the integral basis. Its correctness is questioned, hence, the request for the basic diagrams.

It may be noted that the paper agrees with the unpublished discussion by P. D. Keppler of the Lowe-Smith paper,[19] emphasizing the usefulness of higher derivatives with hard-to-control systems, such as have transportation lag.

This discussion is not to be taken as in any way minimizing the value of the paper in helping the workers in the theory of the art of controlling to keep one foot on the ground.

[12] "Quantitative Analysis of Process Lags," by C. E. Mason, Trans. A.S.M.E., vol. 60, May, 1939, pp. 327–334.

[13] "Automatic Control in the Presence of Process Lags," by C. E. Mason and G. A. Philbrick, Trans. A.S.M.E., vol. 62, 1940, pp. 295–308.

[14] "Mathematics of Surge Vessels and Automatic Averaging Control," by C. E. Mason and G. A. Philbrick, Trans. A.S.M.E., vol. 63, 1941, pp. 589–601.

[15] "Time-Lag in a Control System," by A. Callender, D. R. Hartree, and A. Porter, *Philosophical Transactions*, series A, vol. 235, 1936, pp. 415–444.

[16] "Time-Lag in a Control System," by D. R. Hartree, A. Porter, A. Callender, and A. B. Stevenson, Proceedings of the Royal Society of London, series A, vol. 161, 1937, pp. 450–476.

[17] Pneumatic and hydraulic versions of such model systems have been used for a number of years by the writer's company for purposes of instruction.

[18] C. J. Tagliabue Manufacturing Company, Brooklyn, N. Y. Mem. A.S.M.E.

[19] "Reset Controller for Sump Pumps," by R. P. Lowe and E. S. Smith, *Power Plant Engineering*, May, 1941, pp. 79–80.

Author's Closure

The predictions of Messrs. Ziegler and Nichols check the experimental results closely enough to indicate that their methods have considerable promise. The author is glad to give additional power values, which they suggest as desirable for purposes of comparison. These will be found at the end of this closure.

While we have not made tests with the particular TR and t_f settings, suggested for use under the conditions applying to Fig. 12(*b*) and (*c*), it is evident from these curves, and from others obtained with different controller settings, that the suggested values would not give results as good as those shown. Decreased TR would increase the amplitude of oscillations following a disturbance, and an accompanying increase in floating time would increase the time required for these oscillations to center about that temperature corresponding to the control point. The maximum deviation cannot be reduced appreciably, because, in each case, the temperature has practically stabilized by self-regulation before control actions begin. Possibly this is the reason that the Ziegler and Nichols method of predicting settings does not seem to apply as well to these as to other conditions.

When the controller equation is considered in the form given in the Ziegler and Nichols discussion, the constants for the curves of Fig. 13(*a*) and (*c*) are approximately as follows:

	t_f	TR	PA
Fig. 13(*a*)	260	35	0
Fig. 13(*c*)	140	27	0.9

In this case, t_f and TR are in the same units as given in the paper. Term PA is in minutes. As applying to Fig. 13(*c*), t_f and TR are actual effective values and not merely those which applied before the second-derivative action was introduced. In explanation of this, the equation of the particular mechanism employed may be written in the form

$$-\frac{dv}{dt} = \frac{k_2}{1 - k_1 k_3}\left[k_1\,\theta + (1 + k_1 k_3)\frac{d\theta}{dt} + k_3\frac{d^2\theta}{dt^2}\right]$$

The adjustments for floating speed, proportional-control action, and second-derivative action, affect constants k_1, k_2, and k_3, respectively. It will be noted that when $k_3 = 0$ (no second-derivative action), the constants k_1 and k_2 represent the usual adjustments for proportional-and-floating control. An adjustment of k_1 then changes the floating speed only, while a change in k_2 changes both proportional and floating components by the same percentage.

The adjustment of k_3 for second-derivative action is seen to modify the coefficients for floating-and-proportional control as well. It may be worth noting here that in practice this relationship is found to be favorable as compared with one which affects the second-derivative action only.

Referring now to the settings listed for Fig. 13(*c*), the value of 0.9 for PA is reasonably close to that of 1.1 calculated by Ziegler and Nichols.

The author appreciates the remarks of Mr. Philbrick who, with Mr. C. E. Mason, has carried out a considerable amount of interesting analytical work, based on hydraulic analogies. When combinations can be found in which response characteristics are similar, the particular device used is often relatively unimportant. Since the author's company has a particular interest in temperature control, it has seemed preferable to set up a "dummy" process on this basis. When testing particular temperature-control mechanisms, it is desirable, not only that the response characteristics be similar, but that the actual rates of response be approximately those found in industry. It is considered somewhat easier to obtain corresponding time lags in a thermal laboratory system than would be the case if time constants of hydraulic or electric systems were involved.

If we were dealing with an actual industrial process, it would be important to know the actual temperature as suggested by Mr. Smith. However, when we are using a laboratory process for the sole purpose of studying automatic control, nothing is lost by considering the measured temperature as the actual temperature and the lag of the primary element as part of the process lag.

The equation, given in connection with comments on the Ziegler and Nichols discussion, shows clearly how three control adjustments affected the proportional, floating, and second-derivative modes. The equation is based on the particular type of pneumatic controller used. Whether it is preferable to write this and similar equations with respect to the actual magnitude of the power at any instant, or the rate at which the power is varied by the operation of the controller, is a matter of personal preference. The author finds it simpler, as given, in the last-mentioned form. Those who find the other form easier to understand can readily obtain it by integration.

The following table gives additional information for the use of those who may wish to compare their own results with those of the paper. Figure numbers apply to figures of the paper.

	—Ultimate change in watts—	
Fig. no.	from	to
6(*a*)	282	318
10(*a*)	337	366
10(*b*)	320	350
10(*c*)	320	354
10(*d*)	335	393
10(*e*)	300	340
10(*f*)	314	344
10(*g*)	320	354
11(*a*)	324	370
11(*b*)	315	360
11(*c*)	315	363
11(*d*)	337	395
11(*e*)	310	366
11(*f*)	290	353
11(*g*)	288	350
12(*a*)	234	270
12(*b*)	257	292
12(*c*)	225	262
13(*b*)	234	270
13(*d*)	228	270

Burning Pulverized Anthracite in Steam Power Plants

By C. H. FRICK,[1] ALLENTOWN, PA.

After citing early installations for burning pulverized anthracite in steam power plants, the author describes in some detail the present Pine Grove installation of the Pennsylvania Power & Light Company. This plant incorporates three boilers using pulverized anthracite exclusively, each boiler having a capacity of 180,000 lb of steam per hour. They have been operating successfully since 1927. A proposed two-boiler pulverized-fired installation at the Hauto plant of the company is also described. Each boiler, which is now on order, will be capable of producing 365,000 lb of steam per hour at 1325 psi and 930 F total temperature. Economic considerations entering into the decision to use this type of fuel are also considered in the paper.

THE Pennsylvania Power & Light Company is the largest single user of anthracite. In order for the system to supply the gas, electric, and steam-heat service required, 27,000 tons of large sizes, 594,000 tons of No. 3 buckwheat, 753,000 tons of No. 4 buckwheat, and 146,000 tons of yet smaller sizes are burned, making a total of 1,520,000 tons per year.

There are now 108 anthracite-fired boilers in the company's power plants, varying in size from approximately 4000 to 18,000 sq ft of heating surface. Two just recently put into service are capable of producing 185,000 lb of steam per hr. These, however, are stoker-fired, and thus far are the largest anthracite-burning boilers ever installed.

At present, three of the larger boilers are fired by pulverized anthracite, while two larger boilers now on order will also be similarly fired. These will operate at about 1325 psi pressure with 930 F total steam temperature. Each boiler will be capable of producing 365,000 lb of steam per hr.

On the basis of the existing installation experience was secured which governed the decision again to use pulverized fuel.

History of Burning Pulverized Anthracite

The first experimental boiler plant to burn pulverized anthracite was a small two-boiler installation, made in 1918 by a coal company. This plant was abandoned in 1928, after sufficient proof was established that low-volatile fuel could be burned in pulverized form in a properly designed furnace. In 1920 and 1921, the same coal company erected a larger plant containing twelve pulverized-fired boilers of 500 and 600 hp, which plant is still in operation. It was one of the first power plants[2] designed to utilize anthracite slush, which at that time constituted all sizes below No. 3 buckwheat, previously considered waste incidental to anthracite mining.

This plant produces steam and electricity for direct use in the coal mines. The coal used is comparatively soft and therefore easy to grind.

Early Research on Coals. Tests conducted at this coal company's plant in 1924 on coals from nine different sections of the anthracite field, on a screen-type ball-and-pusher mill, indicated that there is a rather wide variation in the grindability of the coal from the various fields. The results of these tests are shown in Fig. 1, with mill capacity and power per ton, expressed in percentage of that obtained with coal from the extreme western end of the anthracite region, plotted against distance. The chart is plotted in this manner, since quantitatively these data are of little value today, because of improvement in the design of equipment. Relatively, they would hold true with the original type of milling equipment. However, with the ball-and-tube type of mill there is practically no difference because of coal characteristics. This is substantiated by the dotted lines in Fig. 1, showing results of tests at Pine Grove on a ball-and-tube type of mill with coal from three sources plotted relatively against the coal nearest Pine Grove. These tests were of a month's duration, and indicate very little decrease in performance with variable coal hardness.

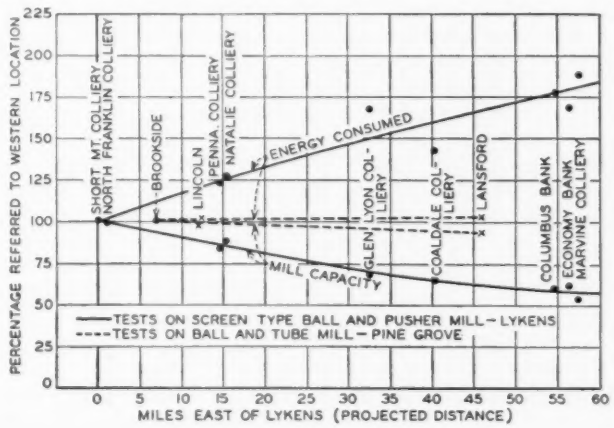


FIG. 1 RESULTS OF TESTS ON GRINDABILITY OF ANTHRACITE COAL FROM VARIOUS FIELDS

The first-mentioned coals were burned under an Edgemoor four-pass boiler having 5116 sq ft of heating surface and 680 sq ft of superheating surface. The furnace walls, of solid firebrick construction, contained a number of small ports for admission of secondary air. A suspended arch was used as a roof over the section of the furnace through which the coal was admitted. A stream of mine water, flowing continuously through a trough in the bottom of the boiler furnace, constituted the method of ash removal. Fig. 2 shows a sectional elevation.

Although these early installations and tests showed the practicability of using anthracite in pulverized form, no large installation was made until the Pennsylvania Power & Light Company, as a result of these investigations in the coal company's plant, decided to extend its Pine Grove plant by adding three large

---

[1] Plant Betterment Engineer, Pennsylvania Power & Light Company. Mem. A.S.M.E.

[2] "Pulverized Anthracite Slush Burned at Lykens," *Power*, vol. 60, 1924, pp. 2–7.

Presented at a Joint Meeting of the Fuels Division of THE AMERICAN SOCIETY OF MECHANICAL ENGINEERS and the Coal Division of the American Institute of Mining and Metallurgical Engineers, Easton, Pa., October 30–November 1, 1941.

NOTE: Statements and opinions advanced in papers are to be understood as individual expressions of their authors and not those of the Society.

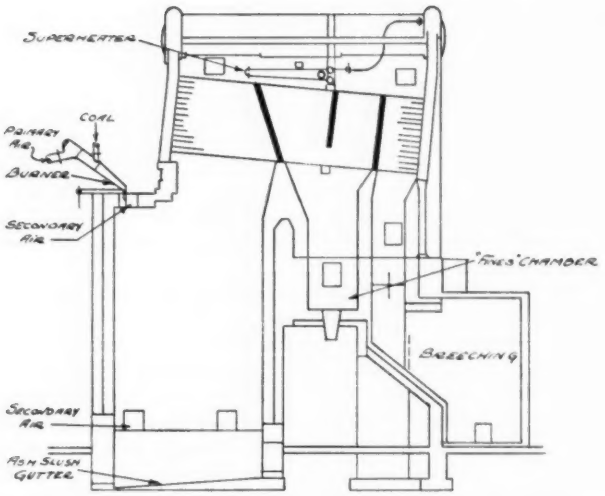


FIG. 2 SECTIONAL ELEVATION OF EDGEMOOR FOUR-PASS BOILER FIRST USED TO BURN PULVERIZED ANTHRACITE

pulverized-coal-fired boilers, which were put into service early in the year 1927.

PRESENT PINE GROVE INSTALLATION

PREPARATION PLANT

Handling and Drying. Incoming coal is taken by skip hoists and conveyers to an elevated raw-coal storage bunker of 1000 tons capacity. From this bunker by means of conveyers, the coal is taken to two single-shell indirect rotary driers of 23 tons per hr capacity each.

These driers are 7 ft 6 in. diam by 45 ft long, driven by motors through pinion and circumferential gears. Each drier rotates in a furnace equipped with stationary grates on which No. 3 buckwheat is hand-fired. The gas travel is counterflow to that of the coal. The raw coal is reduced from its original normal moisture content of 12 to 14 per cent (winter weather, up to 20 per cent) to 1 per cent.

Gas from each drier passes through a cyclone for removal of solids, thence through a washer for additional removal of solids, and is finally discharged to the boiler stack.

After drying, the coal is elevated and transported to the mill bins, each of 22 tons capacity.

Grinding Equipment. The original milling equipment consisted of four 70-in. screen-type mills, each driven by a 350-hp motor. These, except for gear drives, were larger units, identical in type to the 42-in. mills in the coal company's plant previously referred to.

Later, one of these mills was converted to an air-swept type, which depended on recirculation of the product for control of fineness. It partially overcame one of the inherent deficiencies of the screen-type mills, in which there was no continuous control of fineness.

Eventually, two of the original screen mills were removed and two horizontal air-swept ball-and-tube mills were installed. These are 8 ft in diam by 17 ft long, and normally supply the entire pulverized-fuel requirements.

Pulverized coal, transported by air through these mills, is collected in cyclones from which it is pumped through pipe lines, using air as the transport medium, to bins of 120 tons capacity at each boiler. From these it is fed by mechanical feeders to the boiler burners.

All the vents from the various bins, cyclones, etc. are connected to a common venthouse, used as a settling chamber for the coal dust, from which the vented air with a small amount of entrained coal is taken to the suction of the primary-air fans, so that no coal is lost to the atmosphere. No bag filters or other equipment of such nature are used in this plant.

Boiler Plant. Each of the three pulverized-fired boilers is of the single cross-drum type, having about 17,700 sq ft of heating surface proper. Protection to the rear-wall refractories is afforded by a waterwall, connected into the boiler-water circulation. Originally, no cooling surface was planned for the bottom of the furnace, except that the first boiler had a water screen, located several feet above the bottom. For reasons which will be explained, new water-cooled-furnace bottoms were installed, consisting of tubes at an angle of approximately 45 deg, which are covered with cast-iron blocks, also connected into the boiler-water circulation. Fig. 3 shows a sectional elevation of these boilers.

Each boiler is equipped with an air preheater, which raises the temperature of the secondary air from room temperature to approximately 550 F. This secondary air is about 80 per cent of the total requirement. The boiler side walls are hollow, and the front walls have staggered airports. The secondary air passes through the hollow side walls to keep down refractory temperatures and is discharged through the ports in the front walls to complete combustion of the coal.

The coal is fired vertically downward, so that the heat of combustion travels up to ignite additional coal coming into the furnace. This is the only way anthracite can be fired.

The ignition temperature for pulverized anthracite is about 300 F higher than for bituminous, therefore, it is not possible to be as liberal in the use of waterwall cooling with the former as with the latter.

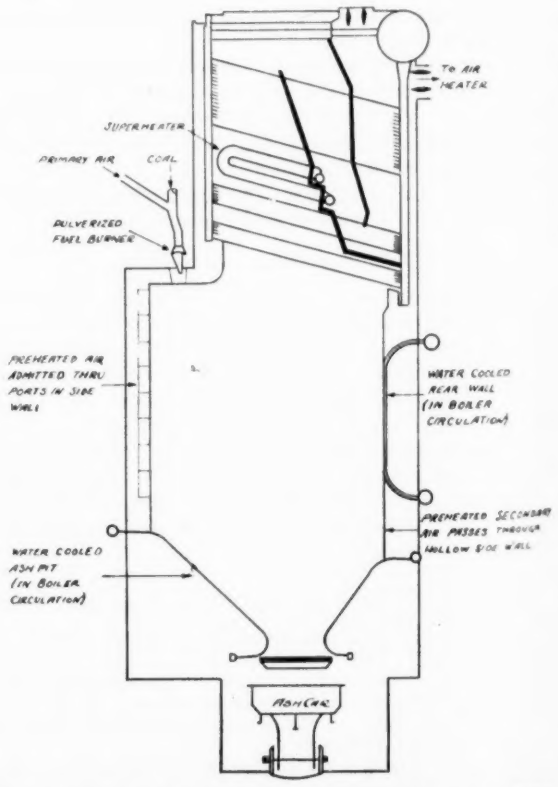


FIG. 3 SECTIONAL ELEVATION OF PULVERIZED-ANTHRACITE BOILER AT PINE GROVE PLANT

Operating Experiences

Preparation Plant. Shortly after being put into operation, it was evident that the maintenance of mills would be high and the capacity low. That the various mill changes made have produced improved results is evidenced by the statistics given in Table 1.

TABLE 1 PINE GROVE ANNUAL PREPARATION-PLANT DATA

	Preparation plant				
Year	Size, per cent through 200-mesh screen	Pulverized coal per mill-hour, net tons	Kwhr per net ton pulverized	Maintenance, cents per net ton pulverized: Mills	Total
1928	69.2	8.4	28.5	46.7	51.0
1929	73.3	9.3	29.8	28.8	36.1
1930[a]	74.0	10.3	33.1	43.2	52.1
1931	76.7	11.7	35.5	13.9	26.6
1932	75.4	11.6	36.0	20.4	22.2
1933	75.8	12.7	34.7	9.1	21.9
1934[b]	76.9	12.8	34.9	18.6	27.8
1935	76.6	12.2	34.1	4.8	11.4
1936	75.2	11.8	33.4	2.2[c]	7.9[c]
1937	76.2	12.3	31.3	8.5	13.5
1938	76.5	12.0	33.2	9.3	17.4
1939	77.2	12.5	34.5	6.2	13.7
1940	77.6	12.8	36.2	6.7	14.1

[a] First ball-and-tube mill in service.
[b] Second ball-and-tube mill in service.
[c] Low, due to credit for material returned to stock.

Generally, since 1934, all preparation-plant equipment has given satisfactory service at low cost. Certain limitations are imposed, such as keeping moisture of the pulverized fuel to 1 per cent or less, to prevent arching in bins.

Except for higher grinding costs and energy consumption, as is to be expected, there is no marked difference between preparation of anthracite as compared with bituminous. However, the former has one distinct advantage, i.e., there are no explosion hazards, principally because of the low volatile content.

Driers. The driers as originally designed did not retain the coal long enough, nor was there sufficient mixing of coal and air to produce thorough and economical drying. The installation of additional cascading angles and retarding baffles improved the condition materially.

To insure thorough drying under all initial moisture conditions, it was found necessary to maintain the exit coal temperature at about 300 F, with a drier exit gas temperature of about 225 F. These temperatures are considerably higher than allowable in drying bituminous coal, which under similar temperatures would lose part of its volatile matter.

These improvements resulted in drying to 1 per cent moisture or less, as compared to only about 50 per cent initial-moisture extraction originally.

Boilers. The boiler furnaces, having a volume of 16,900 cu ft, were originally designed for a maximum heat release of 16,000 Btu per cu ft per hr. This was conservative, in order that capacity could be maintained with high-ash coal, at little sacrifice in boiler efficiency. Various tests conducted from time to time have shown this to be true.

Trouble was experienced when the first boiler went into service from ash which stuck to the bottom of the furnace (fusion temperature about 2450 F). It required from two to five hours daily to loosen up and remove the ash from the floor, so that it could be dumped through the gates. It was necessary to operate with a higher percentage of excess air in order to prevent excessive temperatures, which would cause slagging of the entire screen and necessitate taking the boiler out of service for cleaning.

This condition could be alleviated by reducing the flame length well above the hearth screen. However, by so doing, the decreased flame travel produced excessive carbon losses in the stack gases, and transferred the slagging trouble to the boiler tubes themselves.

This experience immediately warranted a change in the design of the remaining two boilers to include Bailey furnace bottoms. Their successful performance later justified a similar installation in the first boiler.

After a period of test with varying air distribution through the front wall ports, operation became very well stabilized so that ash removal was simply a matter of opening the ash gates periodically. Boiler-tube slagging is effectively reduced by soot blowers in the first pass, so that continuous service periods of from two to three months are not exceptional for these boilers.

The operating data in Table 2 indicate the consistent, dependable, and economical performance obtained at this plant with pulverized anthracite.

TABLE 2 OPERATING DATA OF BOILERS AT PINE GROVE PLANT

Year	Boiler load factor,[a] per cent	Boiler availability, per cent	Per cent of ash in coal, dry basis	Over-all boiler efficiency, per cent	Dry flue-gas loss, per cent	Combustible in refuse loss,[b] per cent
1931	287	82.9	15.4	75.1	6.1	9.0
1932	276	88.0	14.0	77.2	7.2	5.4
1933	264	87.6	14.1	78.2	8.8	4.5
1934	279	85.9	14.3	80.5	8.6	4.8
1935	278	92.9	13.5	82.0	8.2	4.7
1936	284	92.5	13.2	83.2	8.0	4.2
1937	280	92.8	14.7	83.8	7.8	5.3
1938	273	89.6	14.8	81.5	7.9	5.8
1939	282	91.9	14.9	81.8	7.6	5.6
1940	282	91.0	15.0	80.8	7.8	5.2

[a] Boiler load factor as used here is intended to express the average monthly rating referred to 100 per cent rating as a base, and not the percentage of maximum capacity.
[b] Includes refuse up stack.

The present practice is to maintain a coal fineness of about 77 per cent through a 200-mesh screen, which has been found to be most economical for this particular installation. Successful operating results are secured by limiting the variation in fineness to a narrow range, and this is accomplished by having the operators take hourly samples of pulverized fuel, screen them immediately, and make mill-draft adjustments if necessary.

The total preparation-plant power requirement is about 3 per cent of the main unit capacity supplied. Because this plant incorporates a storage system, the preparation plant is shut down during peak-load hours.

Boilers are started from the cold state by means of several torches, which burn either kerosene or light oil, and which are inserted through the front walls of the furnace. They are left burning only long enough to ignite the coal which is turned on gradually from the overhead burners. Invariably, the torches are removed before the boiler is up to pressure. Once ignition is secured, maintaining it from about 90,000 lb of steam per hr to 180,000 lb per hr is possible without using torches.

New Developments at Hauto

As previously mentioned, the company has recently contracted for the two largest boilers ever designed to burn anthracite in any form. These will also be pulverized-coal-fired. After considerable study of the relative merits of the unit system versus the bin or storage system, it was decided to use a storage system similar to that at Pine Grove. The advantages in favor of extending the use of the bin system to this plant are as follows:

1 Capacity will be gained by shutting down the preparation plant over station-peak hours. This will amount to 1300 kw or about 4 per cent of the topping-unit capacity for which these boilers will supply steam.

2 One shift of preparation-plant labor will be saved.

3 Any failure of preparation-plant apparatus will not immediately affect the boiler output, because of the prepared fuel in storage bins which have a capacity of 240 tons, sufficient for 12 hr at maximum conditions.

4 Better control of product, since milling conditions can be set independently of boiler requirements for continuous maximum capacity consistent with fineness desired. This will reduce the energy requirements, as compared with the unit system, since there is only a variation of about 10 per cent in energy requirements between full load and no load, because the amount of coal in the mill is only a small percentage of the ball charge.

Reasonable evaluation of these advantages has justified the slightly higher cost of the bin over the unit system in this case. This is directly contrary to the usual practice when using bituminous coal, for the principal reason that almost double the milling capacity is required for anthracite than for soft coal, for equivalent initial moisture. However, with as much as 20 per cent moisture, which prevails in winter, this ratio probably would be 4 times as great, making the capacity value of the preparation plant an appreciable figure. There will be three mills with a total capacity of 57 tons per hr. The two boilers will be capable of burning a total of 40 tons per hr.

As at the Pine Grove plant referred to previously, the burners will project the coal vertically downward through a short horizontal arch. The point of entrance will be about one third of the distance between the top and bottom of the furnace.

The entire air supply for combustion will be preheated to a temperature of approximately 590 F at full boiler load. A portion of this preheated air, ranging from 5 to 10 per cent will be mixed with the coal streams through seven feeders, each one supplying two burners. Supplementary primary-air fans will act as boosters to maintain adequate air pressure at the burners.

Surrounding the coal burners will be tertiary-air nozzles, which will supply air amounting to anywhere from zero to approximately 40 per cent of the total air for combustion, as found necessary. The balance of the air will be injected through a series of ports in the front wall of the furnaces served by three horizontal ducts. This air, known as secondary air, will vary anywhere from 60 to 95 per cent of the total, as found necessary. Individual control dampers will be installed on the primary-air supply of each boiler, on each individual tertiary-air supply, and also on each duct of the secondary-air supply. The entire installation will be automatically controlled, using inlet-vane dampers on the forced-draft and the induced-draft fans, the actuating medium being primarily steam pressure.

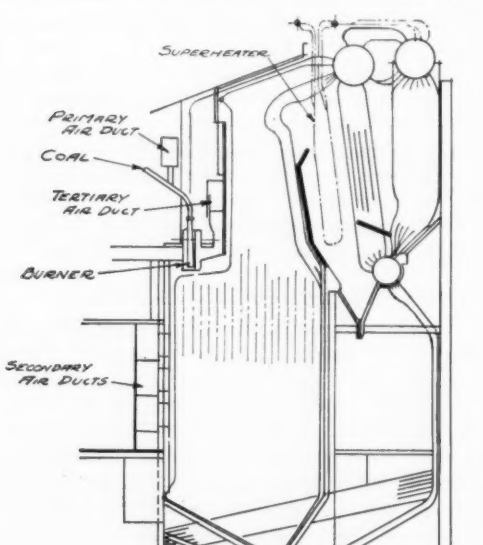


FIG. 4 CROSS SECTION THROUGH BOILERS TO BE INSTALLED AT THE HAUTO PLANT

Because of the size of the boilers, two forced-draft fans for each boiler have been specified to deliver the air through a common regeneration rotary-type air preheater. There will also be two induced-draft fans, so that, in case of trouble with either one, the remaining unit will enable about 60 per cent of the boiler output to be maintained.

The raw-fuel supply is expected to contain approximately 14 to 16 per cent ash (dry basis) and will be of such size that all particles will pass through a $^3/_{32}$-in. round mesh screen. The guaranteed boiler efficiency at full load is 81.5 per cent, with coal pulverized to 85 per cent through a 200-mesh screen. This sizing was specified to insure ample reserve milling capacity.

The furnace volume will be 25,000 cu ft, with an anticipated heat release of 20,000 Btu per cu ft of furnace volume per hr. The entire furnace bottom will have fin-type tubes. Fig. 4 shows a cross section of these boilers.

GENERAL CONSIDERATIONS FOR USE OF PULVERIZED ANTHRACITE

In general, the raw coal, used in a pulverized-anthracite installation, is smaller in size than it is practical to burn on stokers, and is usually the size remaining after all such usable stoker sizes have been removed from the raw material. There are millions of tons in banks in the anthracite territory, with additional tonnage being currently produced.

The moisture content of small anthracite is usually high, running from 8 to 15 per cent, or even more in some cases. This is particularly true of railroad-car deliveries during the cold-weather months, when coal is frozen. This condition is due to the large amount of water used in its preparation. The smaller the size of the coal, the more moisture it will inherently retain. Very small sizes of anthracite seem to act very much like a sponge, holding a considerable percentage of moisture. Samples of this kind of coal taken on the very hottest summer day will indicate as much as 8 to 10 per cent moisture at a distance of 2 to 3 ft below the surface of the pile. This even applies to coal which has been in storage for a very long time.

This high moisture content presents a handling problem in winter, necessitating a coal-thawing shed, since such coal frozen in railroad cars would entail an unloading cost of from 15 to 20 cents per ton, whereas, with proper thawing facilities it can be unloaded for about 25 per cent of this cost.

From an over-all standpoint, the economic use of such fuel is limited to the anthracite-producing centers or territory adjacent thereto, where large piles of these small sizes are within low-cost-transportation zones.

This can be readily understood by comparison of the figures in Table 3.

TABLE 3 RELATIVE DELIVERY COSTS OF VARIOUS COALS

Kind of fuel	Size	Method of burning	Ratio of cost per million Btu, to lowest-cost fuel: Delivered to plant	Delivered to boilers
1 For Low Freight Zones Within Anthracite Territory				
Anthracite	Slush or culm	Pulverized	1.00	1.00
Anthracite	No. 4 buckwheat	Stokers	1.30	1.04
Anthracite	No. 3 buckwheat	Stokers	1.80	1.36
Bituminous	Stoker	Stokers	3.20	2.50
2 For Freight Zones Immediately Outside of Anthracite Territory				
Anthracite	Culm	Pulverized	1.00	1.00
Anthracite	No. 4 buckwheat	Stokers	1.17	1.02
Anthracite	No. 3 buckwheat	Stokers	1.47	1.23
Bituminous	Stoker	Stokers	1.96	1.63
3 For Freight Zones Within Next Cheapest Bituminous Freight Zone				
Anthracite	Culm	Pulverized	1.00	1.00
Anthracite	No. 4 buckwheat	Stokers	1.12	1.02
Anthracite	No. 3 buckwheat	Stokers	1.35	1.18
Bituminous	Stoker	Stokers	1.41	1.24

All small sizes of anthracite take the same freight rate from a given source to a certain location within the anthracite territory. In section 1 of Table 3, the cost for the cheapest usable stoker fuel per million Btu at the boilers, on an as-received basis, is about 4 per cent higher than with fuel for pulverizing. To import bituminous coal would cost approximately 150 per cent more for the same steam costs, assuming equal boiler economies in all cases.

In the case of section 2, Table 3, by going immediately outside of the anthracite territory, say Allentown or Easton, we are confronted with an increased anthracite freight rate, with no change in bituminous rate, thereby decreasing the bituminous cost differential; and the next step, section 3, for further increased anthracite rate and lowered bituminous rate, cuts the original difference in half. This comparison is made on the basis of present mine prices and, as will be noted, the greatest favorable differential for pulverized-anthracite slush or culm occurs nearest the source.

Since the "cost per million Btu delivered to boilers" column includes the cost of pulverization for this fuel, the question can be raised whether the 4 per cent decrease in favor of utilizing this fuel warrants the increased investment required over a stoker plant for the cheapest stoker fuel listed. There are several reasons for giving preference to pulverized fuel, as follows:

1 The availability of No. 4 buckwheat is limited, dependent largely upon current mine production.

2 There is only about an 8 per cent investment differential in favor of stokers, for such an installation as is being considered, because with pulverized-firing only two boilers are contemplated, whereas, with stoker-firing, using the largest stokers obtainable for small anthracite, four boiler units would be necessary.

3 The final answer is that pulverization makes usable in the territory a natural resource which would otherwise be wasted, and heretofore not usable by any other means, at a total cost very close to that obtainable with marketable sizes of limited quantity.

Every case is a special problem, requiring consideration of all factors involved, before final selection of type of fuel and equipment can be made.

BIBLIOGRAPHY

1 "Use of Pulverized Anthracite for Steam Generation," by C. H. Frick, Proceedings of the Engineers Club of the Lehigh Valley, 1925, pp. 12–20.

2 "Operating Experience of Anthracite in Central Power Stations," by C. H. Frick, Transactions of Third Annual Anthracite Conference of Lehigh University, 1940, pp. 169–180.

Discussion

J. R. Baker.[1] The Holtwood steam-electric plant of the Pennsylvania Water & Power Company, consisting of three cross-drum boilers, each having 14,831 sq ft of heating surface, and equipped for burning coal in pulverized form, was placed in operation in 1925, with the expectation that anthracite coal, obtained from river-bottom deposits in the pool behind the Holtwood dam on the Susquehanna River, would become the principal fuel. Initially, dredging capacity was insufficient to supply the entire fuel requirements, and the available river-bottom anthracite was burned as a mixture with the necessary bituminous coal. Since 1931, almost all boiler coal has been river anthracite. At times during the early years, bituminous coal formed the entire fuel supply, so that opportunity has been had, with the equipment installed, to note the performance of the boiler plant with fuels of composition varying from 100 per cent bituminous to 100 per cent anthracite. The following will therefore supplement the author's data by a comparison of boiler-plant operation with the two different fuels.

The plan dimensions of the Holtwood furnaces below the horizontal firing arch are 17 ft wide by 23 ft from front to rear wall. Coal is fed vertically to the furnace through eight fantail burners, with axes parallel to side walls, placed in a horizontal arch near the top of the furnace. The arch extends about 9 ft from the front wall, thus reducing the front-to-back dimension of the upper portion of the furnace to 14 ft. The depth of the furnace under the firing arch to the water-screen tubes over the ashpit is 25 ft; the height of furnace above the elevation of the arch to the boiler tubes averages 10 ft. The furnace volume above the water screen is about 11,500 cu ft. The average length of travel of the coal from the burners to the first boiler pass is about 50 to 55 ft. The first boiler pass is adjacent to the front wall of the furnace above the firing arch. The path of the burning coal is thus downward along the front wall, backward toward the rear wall, up along the rear wall, gradually crossing toward the front wall above the firing arch, forming almost a closed loop in the upper part of the furnace.

The side and front walls are air-cooled refractory walls, and the rear wall is a solid refractory wall with 4-in-OD waterwall tubes on $10^1/_2$-in. centers in front of it opposite the front wall under the firing arch. Similar tubes on similar spacing screen the ash-hopper slopes and floor which form the bottom of the furnace. The projected area of the rear wall and ash-hopper screen tubes and of the boiler above the furnace is equivalent to about 17 per cent of the area of refractory walls and projected area of the refractory ash hopper. For comparison, in the Pine Grove furnaces, the ratio of projected area of water-cooled surface to refractory area appears to be 40 per cent; the Hauto furnaces appear to be almost entirely water-cooled. It is apparent that the Holtwood furnaces can be classed as refractory furnaces.

The bulk of the air for combustion in the Holtwood furnaces is induced by furnace draft through horizontal air lanes in the side and front walls, the air entering the lanes at the rear of the side walls and flowing into corresponding lanes in the front wall, from which the air passes at relatively low temperature into the furnace through some 60 ports in the front wall. Some air is induced through the burner casings and some, estimated at from 10 to 15 per cent of the total, enters through the burners at about atmospheric temperature with the coal, at several inches of forced draft.

The average steaming rate of the Holtwood boilers is about 110,000 lb of steam per hr, equivalent to about 250 per cent of normal rating. At this load, the Btu in coal per hour entering the furnace per cu ft of furnace volume is about 12,900, equal to about 56,300 Btu per sq ft of furnace-wall area.

The furnaces were not conveniently operated continuously at ratings of 250 per cent and higher on bituminous coal because of the slagging of the furnace walls, the entrance of the first boiler pass, and in the ash hopper. Ash is removed from the ash hopper by hand hoes through three doors at the level of the ash-hopper floor. When the ash slags materially it is difficult to dislodge it from the slopes of the ash hopper because of the distances involved. When burning bituminous coals, there was the constant liability of hot spots on the walls with consequent washing of the refractories. With coals having ash of low fusing temperatures, frequent hand-lancing of the first boiler pass was necessary to prevent plugging.

These difficulties diminished as the proportion of river anthracite was increased. The ash-fusion temperature of the river anthracite is over 2700 F. There is no slagging problem with anthracite, although the corners and upper parts of the ash

[1] Baltimore, Md. Mem. A.S.M.E.

hoppers must be cleaned by hand every few weeks by entering the ash hopper. Overheating of the furnace walls does not occur when burning anthracite, and the wear of the refractory walls results from gradual spalling with temperature changes rather than from active chemical deterioration by molten slag.

Probably the most noteworthy difference between the Holtwood furnaces and those described by the author is the use of preheated secondary combustion air under positive control in his furnaces. He mentions the higher ignition temperature of anthracite coal, but says nothing about the differences in volatile and fixed-carbon contents of the two coals. The high fixed-carbon content of anthracite causes it to be relatively slow-burning compared to bituminous, and this fact makes the mixing of the secondary air with the coal particles, as they move through the furnace, of the utmost importance. It was quickly found with the Holtwood furnaces that the distribution of admission of secondary air to the furnaces should be radically different with the two coals. When burning bituminous, better combustion results were obtained with most of the secondary air entering through the upper ports just below the burners, that is, the air was required near the point where the coal entered the furnace. This distribution is found to be almost impossible with anthracite, when most of the secondary air is admitted through the lower lanes; in fact, the upper air lanes are practically closed, except for some leakage. In the Holtwood furnaces, the problem of combustion is thus twofold, that is, to bring the coal to ignition temperature as quickly as possible and to promote mixing of the coal with the secondary air in a part of the furnace where the coal has lost its initial velocity energy. Such mixing must come from the slow-moving stream of induced secondary air.

The difference in ignition temperature between bituminous and anthracite of 300 F, mentioned by the author, would be neutralized to some extent by his secondary and tertiary combustion-air temperature of 550 to 590 F, but even if the anthracite coal would be brought quickly to the ignition temperature as it enters the furnace, the difference in burning characteristics still remains and presents the major problem of complete combustion of the fixed carbon before it leaves the furnace. The author states that the only way anthracite can be fired is vertically downward so that the heat of combustion travels up to ignite additional coal coming into the furnace. This, it is believed, can be amplified by pointing out that vertical firing with reverse flow of the furnace gases also gives the longest possible travel of the coal particles in the furnace, and that the scrubbing action of the oppositely moving streams of gases probably contributes to turbulence or mixing of the combustion air with the burning coal.

The cross sections of the Pine Grove and Hauto furnaces show that the coal travel in the later designed furnace is probably materially longer than in the first design of furnace. An exact comparison in this respect would be of interest. The Hauto furnace could be expected from the cross sections to give more turbulence than occurs in the Pine Grove furnace with resulting decrease in unburned combustible in the stack gases.

On the other hand, the Hauto furnace, Fig. 4 of the paper, indicates that all furnace walls as well as the ash hopper will be covered with fin tubes. If this is a correct interpretation of Fig. 4, it represents a distinct departure from the basis of design of the Holtwood and Pine Grove furnaces, both of which are largely refractory. It has been a moot question as to the relative amount of water-cooled surface which can be utilized when burning pulverized anthracite, and the Hauto design may provide an answer on this point.

Experience at Holtwood leads one to think that practically no slag would adhere to furnace waterwalls when burning river anthracite, certainly not to the extent reported in the case of some recently designed furnaces for burning bituminous coal. The walls should therefore remain cold in operation instead of approaching furnace temperature such as refractory walls do in service. However, since cold furnaces are lighted at Holtwood with the aid of only two small oil torches, continuously cold furnaces could tend to produce unburned combustible only in the relatively thin layer of gases along the wall surface. It seems reasonable to assume that the long gas travel in the Hauto furnace and its cross-sectional aspect will promote sufficient turbulence to keep the combustible loss to an acceptable amount. The performance of the Hauto furnace will be of interest in this regard.

Experience at Holtwood in drying and pulverizing river anthracite is quite similar to that reported by the author, and the data given by him for mill costs, boiler efficiencies, etc. are likewise applicable to Holtwood, after modification for the absence of air preheaters. His data indicate that the combustible loss in refuse is the next largest boiler loss after the dry-gas loss. It has been found at Holtwood that if the secondary-air admission is not properly adjusted, the combustible loss may equal the dry-gas loss. The fuel used in drying anthracite at Holtwood, preparatory to pulverizing, amounts to about 3 per cent of the boiler fuel. It is assumed that the author's data for over-all boiler efficiency includes this loss for drier fuel.

J. B. Cordiner, Jr.[4] What effect does a change in ash content have on the operation of pulverized anthracite in installations such as those described? In other words, if the ash content were suddenly changed from 11 per cent to 19 per cent, how would this affect ignition, output, and over-all efficiency?

It is admitted that the ash content should be as nearly constant as possible to insure best results. What keeps the ash content constant at the 14 to 15 per cent shown in the figures?

E. L. Willson.[5] The coal to which the author refers in his discussion of the economics of pulverized anthracite under various names of culm, silt, slush, etc. are by-product sizes which are produced necessarily as a result of the mining and preparation of anthracite in sizes intended for domestic use. There are several sizes smaller than those used generally for heating homes which have found a market in industrial use, so that the successful pulverization and combustion of coal which passes through $^3/_{32}$-in. round mesh screen appears to be the ultimate step in the utilization of the entire fuel value of anthracite.

Being a by-product of the preparation of coal for domestic use, the production of this fine size tends to become seasonal and is greater during the winter heating season when the problem of freezing in transit presents a serious unloading problem.

The necessity for the thawing shed, mentioned by the author as a means for reducing year-around unloading costs, is not necessary if ample ground storage is available close to the colliery. Reloading from a storage pile yields coal uniform in moisture and ash content, the latter approximating closely the calculated weighted average ash content of cars dumped into storage.

The selection of pulverized anthracite by the author's company for the important installation which he describes indicates that the technique of preparation and combustion of this fuel has been standardized. The prospect for increased utilization of anthracite fines minus $^3/_{32}$-in. mesh is therefore of interest to the anthracite-producing companies. However, if prospective users, in their desire to minimize investment cost, insist on the extreme minimum in ash content, they will find their sources of supply limited. Carrying the process of de-ashing beyond reasonable

[4] First Lieutenant, U.S.A., Office of the Chief of Engineers, Washington, D. C.

[5] Lehigh Navigation Coal Co., Philadelphia, Pa.

limits is accomplished at a great sacrifice in efficiency in the preparation process, a waste of good fuel values in the tailings, and costs increased beyond an economic return. An additional investment in mill capacity, sufficient to provide for the desired boiler output, using coal of ash content higher than the desired minimum, will be justified by a much larger source and greater reliability of supply.

Because of its high and uniform fixed-carbon ratio, anthracite lends itself to the premium-and-penalty basis of purchase contract, based on a uniform delivered cost per million Btu. The relation between Btu per pound and per cent of ash is a simple straight-line function from which can be developed a factor for adjusting a base price per ton of coal of an agreed base ash content to a price per ton above or below the base price for each 1 per cent of ash lower or greater than the base ash. Ash determination is a rapid and inexpensive test, which may be applied to individual cars by the shipper, and checked if desired by the purchaser.

Such contracts have been in force between some anthracite producers and their larger customers for nearly 10 years, and have proved satisfactory.

Author's Closure

For comparison with Mr. Baker's figures on Holtwood, the Btu in coal per hr entering the furnace per cu ft of furnace volume at Pine Grove is about 13,200, equal to about 56,000 Btu per sq ft of furnace-wall area at 282 per cent of normal rating.

In the case of the new Hauto boilers, the Btu input per cu ft of furnace volume will be about 20,000, equivalent to about 54,500 Btu per sq ft of wall area with a boiler output of 365,000 lb of steam per hr.

At Pine Grove most of the secondary air is also admitted though the lower lanes, and it is anticipated that similar practice will be followed at Hauto.

As a comparison to Mr. Baker's figure of 50 to 55 ft for the coal-travel distance in the Holtwood furnaces, at Pine Grove the comparable distance is about 50 ft and at Hauto it will be about 75 ft.

Not all of the furnace-wall area will be exposed. Initially about 20 per cent will be refractory-covered, subject to modification as experience indicates the necessity for changing after these boilers are in service.

The over-all boiler-efficiency figures given in Table 2 include drier fuel. This amounts to about 2.6 per cent of total fuel at Pine Grove; and for Hauto, it is estimated, it will run about 3 per cent.

Change in ash content, as indicated by Mr. Cordiner, would not have any appreciable effect on ignition; however, from tests conducted with coals of varying ash, boiler capacity varies inversely about 2.8 per cent for each per cent variation in ash for the same coal weight input. This, however, can usually be compensated for up to the limitations of the feeders, burners, etc., to handle the increased amount of coal required to maintain a fixed output.

Similarly with respect to boiler efficiency for anthracite within 12 to 20 per cent ash limits, there is an inverse variation of about 150 Btu per lb of dry coal for each per cent ash variation. Tests have indicated that the boiler heat absorption above feed varies inversely about 230 Btu for each per cent ash variation within these same limits. If, with a known coal of say 12,700 Btu per lb dry, corresponding to about 13.3 per cent ash, an absorption of 10,000 Btu per lb of dry coal is obtained in the boiler, the average over-all efficiency is 78.7 per cent. With an increase of 1 per cent ash in the coal, these relative quantities become 12,550 Btu per lb of dry coal and heat absorption of 9770 Btu per lb of dry coal, or an efficiency of 77.8 per cent, a decrease in efficiency of 0.9 point, or a 1.15 per cent decrease.

The ash content of the fuel delivered for the various years is nearly constant because coal companies are preparing coal to meet definite specifications. All coal is purchased on a bonus-and-penalty basis with a base price for coal having 14 to 16 per cent ash (dry basis). The uniformity in quality indicates the advantages of some such method.

Mr. Willson's statement relative to the necessity for a coal thawing shed is true if coal companies could deliver fuel uniformly to a power plant in winter months by loading from a storage pile. However, colliery production is higher as the weather gets colder, and consequently the quantity of smaller sizes of fuel also increases. This fuel when loaded wet in cars may be held in railroad yards for several days and arrives at the plant in a frozen condition, if shipped according to a definite delivery schedule; or if shipped as loaded, the plant unloading facilities are then taxed to a point where it must lay over in cars so that it freezes before it can be unloaded.

Automatic Burning Control in Rotary Kilns

By WILLIAM E. REASER,[1] EASTON, PA.

Significant developments in automatic regulation of the burning process in rotary cement kilns have occurred in the last decade, but general application of control devices has proceeded slowly. Indeed, neither the real import of the subject nor the extent of the progress is yet widely appreciated, though there are sufficient installations of various equipment to demonstrate the worth of a scientific approach to a problem which has been a typical rule-of-thumb operation. This paper discusses achievements in the field through reference to diagrams, charts, and illustrations in order to bring about a more universal understanding and to establish a background for additional thought which may encourage further experimentation. Moreover, although the discussion pertains especially to cement-clinker burning, the same basic principles of control are applicable to many other manufacturing processes employing rotary kilns.

THE bituminous-coal industry should be decidedly interested in the subject of automatic burning control in rotary kilns, because soft coal is the primary source of heat in cement mills. The latest complete figures available,[2] covering the fuel consumption of the cement industry for the year 1939, when 122,259,154 bbl of cement were finished, are as follows:

Bituminous coal, tons	5,227,756
Oil, bbl (42 gal)	2,378,762
Gas, cu ft	40,233,089,789

Analysis of these figures shows that approximately 70 per cent of all heat units purchased by cement manufacturers come from bituminous coal. Naturally, as production rises, the total tonnage will increase. In 1941, it is expected that approximately 150,000,000 bbl will be finished, requiring nearly 6,500,000 tons of coal of which about 95 per cent is burned in the kiln process. The remaining 5 per cent is consumed in the preparation of raw materials and pulverized fuel. Because of the evident importance of coal, reference to control apparatus will emphasize its use, although the fundamental ideas involved can be utilized for oil- and gas-fired kilns equally well.

Manufacturers of cement, too, have good reason to show marked concern in the problem, since the burning operation is one of the most important and most expensive processes in the sequence of production. Especially when waste-heat steam generators are used, the kiln department is truly the very "heart" of the entire mill, because a continuous balance must be maintained between clinker output and power generation to secure maximum over-all economy. Since, on the average, a barrel of clinker requires about 100 lb of coal, fuel may represent from 15 to 25 per cent of the total manufacturing cost, a far more important item than in the average industrial enterprise. Refractory maintenance is a very essential consideration as temperatures of 2600 to 2800 F must be attained for heating the material. But above all, there is the problem of striving constantly for improved quality and greater uniformity of clinker, aims which cannot be accomplished to the highest degree through manual operation, even with the use of instruments to act as "seeing eyes."

Automatic-control apparatus is helping to meet these difficulties. Plant records show savings ranging from 5 to 10 per cent of the fuel expense alone and, in addition, considerably lengthened life of refractories due to elimination of extreme temperature fluctuations in the burning zone. Positive control of firing conditions is responsible for uniform rates of waste-heat steam generation, while, at the same time, it is improving quality and uniformity of product to the extent that new and more precise specifications can be satisfied. To hold maximum clinker temperatures within limits of ± 25 F and to maintain kiln speeds at uniform rates without stoppages for "heating up" are some of the restrictions recently imposed on producers. Such requirements demand the intelligent application of modern instruments and control.

Methods of Kiln Operation

In order to comprehend the problem, it must be understood first that there are two general methods of operating a rotary kiln:

1 Maintain a constant combustion rate, that is, supply fixed safe maximum quantities of air and fuel, and vary the speed of the kiln to produce the necessary temperature of material in the burning zone.

2 Maintain a fixed speed of kiln and vary the combustion rate, that is, modify the supply of air and fuel to procure desired burning temperatures.

Such procedures might well be considered "ideals," which, because of certain practical limitations, cannot always be followed. Nevertheless, they provide basically sound patterns from which necessary deviations are expected and permitted.

Various attempts have been made to regulate automatically the flow of material through the hot zone, and to insure combustion at maximum efficiency, the two principal points of control. In no kiln, however, have both of these elements been completely governed by co-ordinated auxiliaries, although in several instances semiautomatic control has been installed with gratifying success. A typical example of the latter approach is an achievement worthy of attention because it deals adequately with a fundamental consideration, draft control. The arrangement of kiln and regulating apparatus is illustrated schematically in Fig. 1.

In operation, the scheme aims to set a constant combustion rate and, thereafter, to produce desired clinker temperatures by varying the rate of flow of material through changes in kiln speed.

Pulverized coal is supplied to the kiln through a blast pipe which receives hot primary air from a rotary cooler. Secondary air also comes from this source. The weight of air entering the hood depends upon the magnitude of the induced draft at this point, if it be assumed the openings and clearances are fixed in size and air density is constant. With proper precautions, these assumptions can be realized. Thus, to set the combustion rate, a simple draft control developed for furnaces of steam generators is applied. A controller, operating with compressed air as the power medium, adjusts a damper in the stack to maintain a predetermined hood draft. A typical chart, Fig. 2, illustrates the fact that the system functions to hold the draft throughout the day at 0.065 ± 0.005 in. of water regardless of variation in

[1] Assistant Professor of Mechanical Engineering, Lafayette College. Jun. A.S.M.E.

[2] "Minerals Year Book," U. S. Bureau of Mines, 1940, p. 1138.

Presented at a Joint Meeting of the Fuels Division of The American Society of Mechanical Engineers and the Coal Division of the American Institute of Mining and Metallurgical Engineers, Easton, Pa., October 30–November 1, 1941.

Note: Statements and opinions advanced in papers are to be understood as individual expressions of their authors, and not those of the Society.

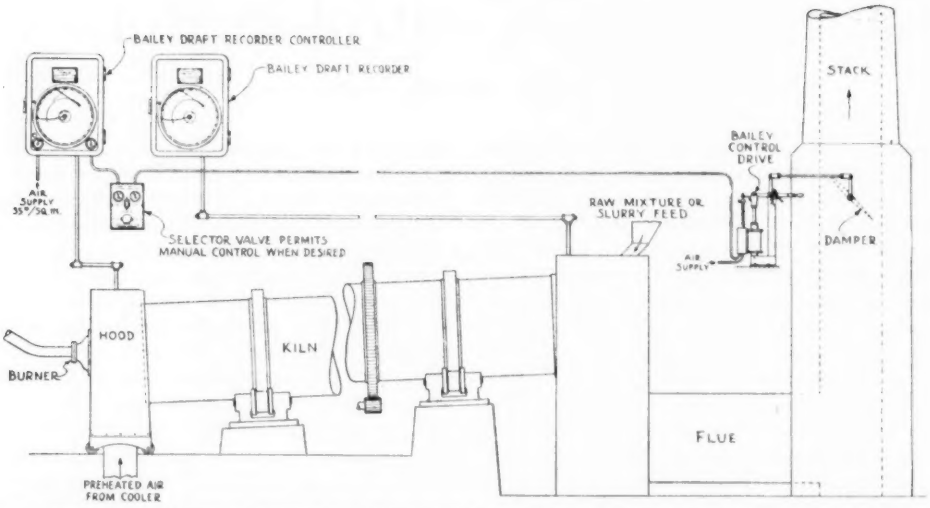


FIG. 1 DIAGRAM OF HOOD-DRAFT CONTROL SYSTEM FOR ROTARY KILN IN WHICH SECONDARY AIR IS SUPPLIED UNDER INDUCED DRAFT

draft loss through the kiln and gas passages. In addition to fixing the air supply, the effect of draft control is a definite aid in preventing undesirable movements of the position of the hot zone in the kiln.

Once the draft is set, primary air and fuel flow are selected to produce optimum combustion efficiency as determined by Orsat analyses of exit gases and consideration of the type of flame necessary to meet burning requirements. When the air-fuel ratio is fixed by the engineer in charge, the operator, commonly referred to as a "burner," is not permitted to adjust draft, primary air, or fuel, except in the event of an unusual circumstance, when temporary changes are in order. To complete the burning process, kiln speed is varied to maintain the necessary clinker conditions as shown by some temperature-measuring device, or simply by visual observation on the part of the burner.

Attention is directed to additional equipment considered essential. A feed-end-draft recorder is mounted in a convenient position alongside the instrument measuring hood draft, in order that the burner may observe at all times the draft loss across the kiln. An increase in draft loss generally indicates that a ring is forming (in rotary-kiln operation, a ring is a common term for the mass of material which occasionally builds up and restricts the opening in the kiln), and it is highly desirable to take immediate steps to eliminate the formation. One effort sometimes successful is to make an abrupt change in the draft, and this can be done readily by the means provided for manual adjustment of the damper. Such hand control is also useful when the fire is first lighted preliminary to starting production, and also when taking the kiln out of service.

Results from this mode of procedure are most satisfactory, yet certain limitations should be apparent. In attempting to establish a constant rate of heat release, a pulverized-coal feeder is set at some fixed speed which at the time delivers the correct quantity of fuel to produce desired combustion efficiency, as determined from an average of a number of gas samples. Unfortunately, even the best equipment does not continuously deliver an unvarying weight of fuel. However, experience has shown it to be possible to accomplish a setting of air-coal ratio which will be maintained within close practical limits from one day to the next. The general plant policy calls for a careful check on combustion conditions twice every 24 hr.

With regard to altering kiln speed to meet temperature specifications, certain authorities suggest that the action producing somewhat abrupt changes in velocity of material flowing down

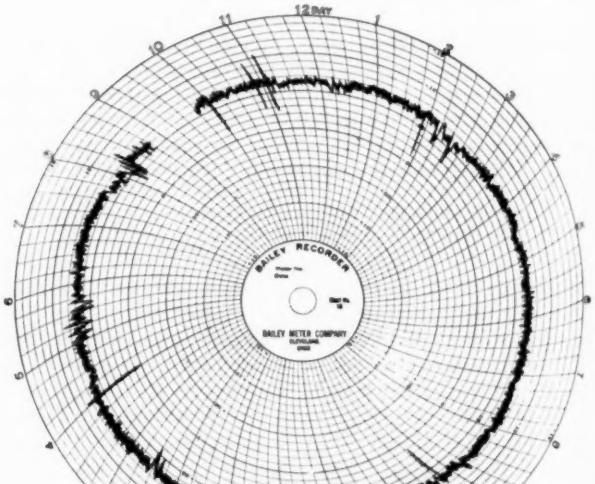


FIG. 2 TYPICAL CHART MADE BY RECORDER, ILLUSTRATING HOW CONSTANT-DRAFT CONDITIONS ARE AUTOMATICALLY MAINTAINED BY HOOD-DRAFT CONTROLLER OF FIG. 1

the kiln may be conducive to ring formation, and hence should be avoided. As a matter of fact, extreme variations in speed are not needed under ordinary circumstances if provision is made to control firing at the desired constant rate, and if adequate care is given to the preparation and delivery of material by the raw feeder. However, in cases where these requirements are not satisfied, especially when hood draft is not automatically regulated, attempts to operate in such a fashion, either by manual or automatic adjustment of the kiln speed controller, have resulted in speed fluctuations which could not be allowed.

Another development which provides for the same general operating philosophy of a constant combustion rate and variable kiln speed is illustrated in Fig. 3. One fundamental difference in the major plant equipment from that shown in Fig. 1 is in the method of cooling the clinker, that is, a so-called pressure cooler replaces the rotary type. In this case, one fan delivers air to the front section of the cooler grate and thence into the kiln hood

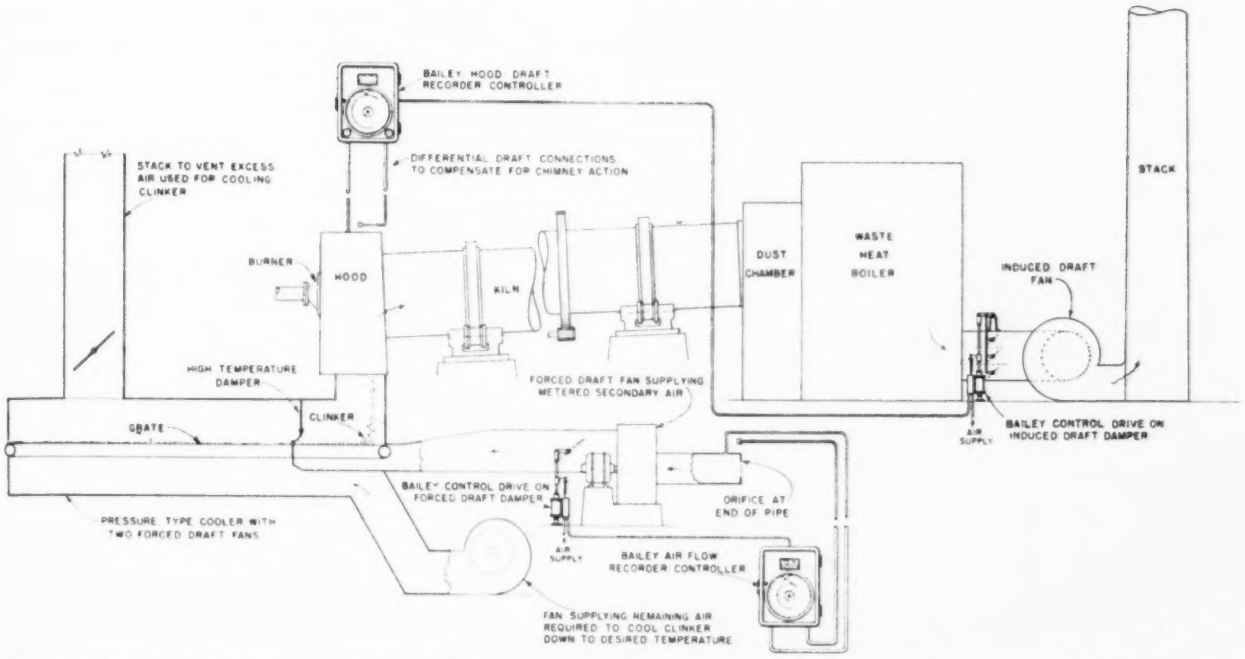


FIG. 3 SCHEMATIC DRAWING, DEMONSTRATING TYPE OF CONTROL REQUIRED FOR KILN WHEN SECONDARY AIR IS DELIVERED UNDER FORCED DRAFT

where it becomes secondary air for combustion, while another fan supplies additional cooling air to what may be termed the aftercooler. A primary-air fan draws hot air from the aftercooler and injects it into a blast pipe to act as the transporting medium for pulverized coal which is delivered by means of a helical screw.

It must be appreciated that the quantity of secondary air passing through the hot clinker to the hood will depend upon the thickness of bed and gradation of particles if the fan is operated at constant speed without compensating control. The variation in air flow would cause considerable difficulty in kiln burning. Consequently, a means is provided to establish the necessary air flow to meet combustion requirements and, thereafter, maintain the desired rate regardless of the variation in resistance to the passage of the air through the clinker to the hood. An orifice installed at the fan inlet produces a differential pressure which the instrument records in terms of air flow, after which the same mechanism functions as a controller by adjusting the damper in the duct leading to the cooler to hold the flow at the predetermined standard. Hood draft is also controlled by regulating the damper near the induced-draft fan for the purpose of maintaining a constant air leakage at the hood, to compensate for variation in resistance to gas flow through the kiln itself, and to aid in fixing the hot zone at the desired position in the kiln.

To complete the air-fuel setting, the speed of the coal feeder is adjusted to produce optimum combustion efficiency, an Orsat being used to analyze the gases. Again, it is found possible to operate in such a fashion long enough so that only periodic checks of the setting are required, say twice each day. The fuel-burning process is thus considerably simplified, and burners need only make occasional changes in kiln speed to obtain correct clinker temperature.

To demonstrate how satisfactorily the air-and-draft regulation is accomplished, Fig. 4 is presented. The upper two chart records indicate that secondary air and hood draft are maintained at practically constant standards even though the control is subjected to an unusually difficult task. It is to be observed that feed-end draft increases steadily from a value of about —0.15 to a magnitude of approximately —0.35 in. of water during the 24-hr period. The increased draft loss across the kiln is caused by the building up of rings. Hence, the draft controller must function in a manner to increase feed-end draft to overcome the additional resistance to gas flow. If this were not done, an increased pressure would develop at the hood which would change the air leakage through openings and cause the hot zone to move closer to the front of the kiln.

DRAFT CONTROL FOR ROTARY KILNS

At this point, it might be well to correct a common misconception concerning draft control as applied to rotary kilns. Prior to the two installations of equipment just described, cement-mill operators for many years talked about draft and its importance in maintaining satisfactory operating conditions, but they thought in terms of draft at the feed end of the kiln, not at the hood. Consequently, the very first attempt at draft control called for the draft connection to be made in the dust chamber at the raw-feed end, as shown in Fig. 5. This idea would be acceptable if the resistance across the kiln did not change, but the resistance is continually changing because of ring formations, both clinker and coal, and variations in level of material at various points throughout the kiln length. No one would consider a suggestion to control furnace draft in a steam generator by making the draft connection in the breeching leading to the stack, yet such an arrangement is analogous to the effort to regulate conditions in the front of the kiln by means of draft control at the feed end. The analysis, based on Table 1, should tend to clarify the situation by exposing the error in conception.

TABLE 1 HYPOTHETICAL CORRELATION BETWEEN GAS FLOW THROUGH KILN AND DRAFT IN DUST CHAMBER

Gas flow	Draft, inches of water
0	—0.5
2	—0.3
3	—0.2

Suppose the kiln is completely closed due to a solid ring; there

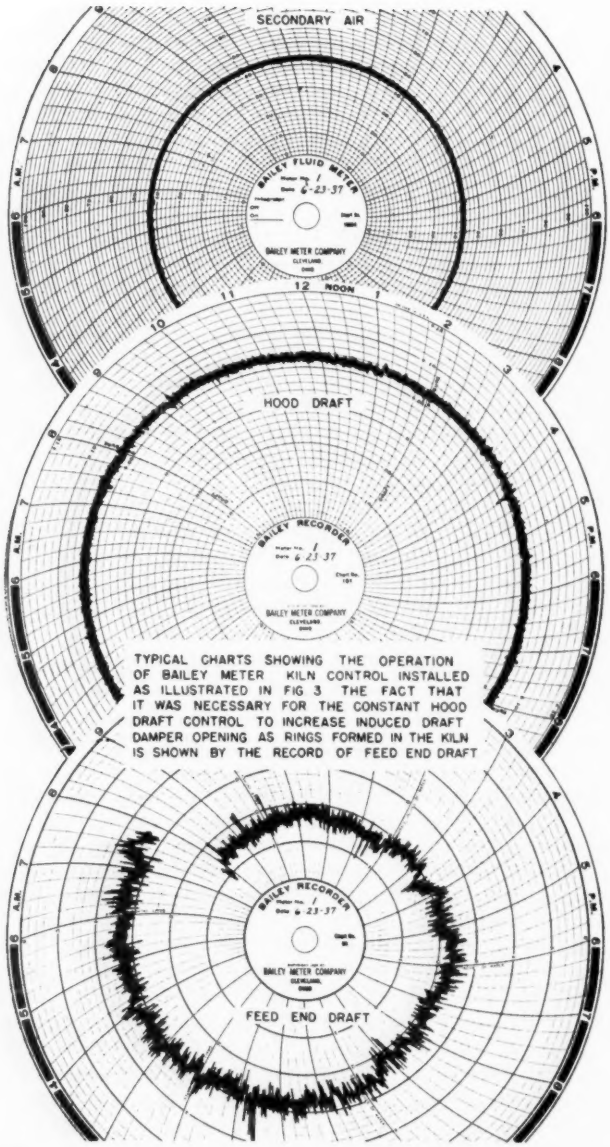


FIG. 4 REPRODUCTIONS OF CHARTS SHOWING OPERATION OF KILN-CONTROL SYSTEM, AS ILLUSTRATED IN FIG. 3

(The fact that it was necessary for the constant-hood-draft controller to increase induced-draft damper openings, as rings formed in the kiln, is shown by the record of raw-feed-end draft.)

is zero gas flow, and the draft in the dust chamber is a maximum, say —0.5 in. of water, as long as the gas in the stack remains at operating temperature. On the other hand, if the kiln is only partially obstructed, the flow of gas might be represented by a value of 2, while because of the gas flow the draft in the chamber will be somewhat lowered, say to —0.3. Under normal conditions with the kiln wide open, the flow may be represented by 3 and again the draft would be lower, say —0.2. Now, assume that a check on combustion conditions and the position of the burning zone is made when the situation within the kiln is normal, that is, gas flow equals 3 and draft is —0.2 and further, a draft controller is attached as illustrated in Fig. 5. Suppose a ring begins to build up in the kiln. Several undesirable results ensue. The first is a decreased gas flow because of the decreased opening. This causes increased feed-end draft. For example, if the flow is reduced to 2, the draft will increase to —0.3, as shown in Table 1. The second undesirable result now follows, for the control will function so as to restore the draft to the predetermined standard of —0.2, further reducing gas flow. This is not at all desirable, because raw feed and coal feed have remained unchanged. Obviously, feed-end draft control acts in a manner exactly contrary to that of a proper scheme, whereas control of hood draft maintains the correct conditions as long as there is sufficient draft created by the stack to overcome the additional draft losses caused by the restrictions.

The schematic layout of another type of control system is also shown in Fig. 5, in which an attempt is made to regulate the air-fuel ratio continuously even when the fuel rate is varied by the

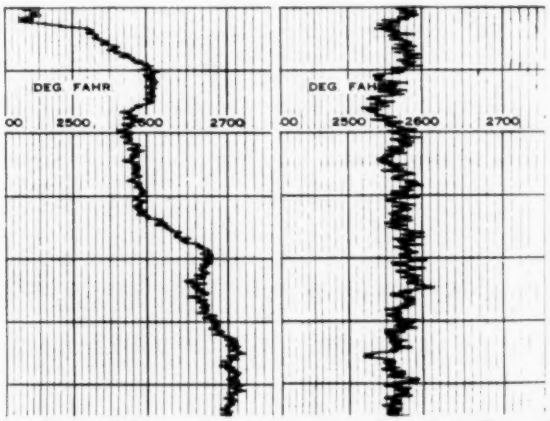


FIG. 6 CHARTS TAKEN FROM RECORDER OF RADIATION PYROMETER MEASURING BURNING-ZONE TEMPERATURES

(The chart at the left indicates results when the burner gave no attention to the instrument, while the chart at the right shows the record when the instrument was used as a guide.)

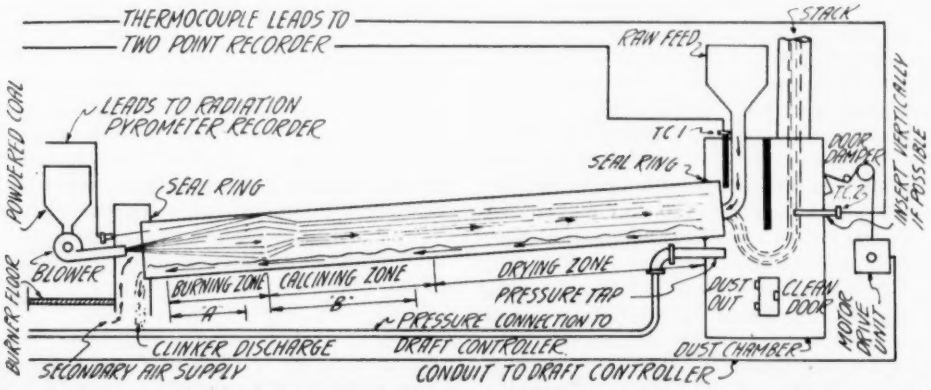


FIG. 5 DIAGRAMMATIC LAYOUT OF KILN EQUIPPED WITH TWO-POINT TEMPERATURE CONTROL AS A MEANS OF MAINTAINING AUTOMATICALLY OPTIMUM AIR-FUEL RATIO

(Note radiation pyrometer used to record burning-zone temperatures.)

burner. The major equipment is similar to that shown in Fig. 1, except that a comparatively long dust chamber connects the kiln to the stack. A thermocouple is installed so that it projects into the kiln and another is located far enough away in the dust chamber in the path of the gases so that an appreciable temperature drop occurs, due to air leakage around the tail seal and loss of heat from radiation. A potentiometer style of instrument, utilized to act as a recorder-controller, is designed to register continuously the temperature differential between the two couples. From Orsat analyses, the normal temperature drop under actual operating conditions can be determined when there is no unburned gas in the stream at the feed end, and the controller can be adjusted to maintain this differential. For instance, if the burner notices that the clinker temperature is too low, he may increase the coal feed which, if sufficient to cause a deficiency of air, will introduce some unburned gas in the stream at the feed end of the kiln. Experience shows that combustion is at least partially completed by the air which leaks past the seal and, consequently, the heat thus developed raises the temperature of the second thermocouple. This action decreases the differential as registered by the instrument, which then operates to adjust a check damper to increase the air flow to the kiln hood. The control continues to increase air flow until the original value of temperature differential is restored. On the other hand, if fuel flow is decreased, it is found that the temperature differential increases, and the controller operates to decrease the air flow to maintain the desired conditions. In such a fashion, the correct air-fuel ratio is continuously maintained within certain limits. Actually, the range of control of fuel feed is comparatively narrow; yet it is extremely helpful to burners when they are asked to keep the clinker temperature within close bounds.

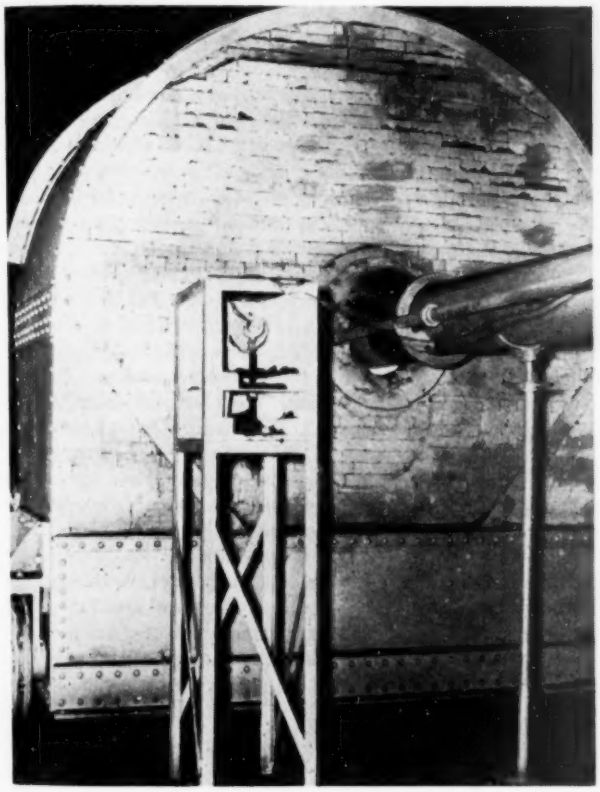


FIG. 7 RAYOTUBE MOUNTED IN FRONT OF KILN

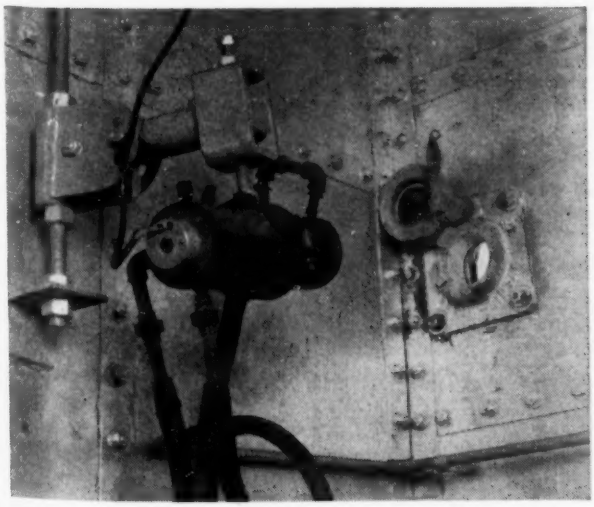


FIG. 8 RAYOTUBE SIGHTING THROUGH HOLE IN KILN HOOD
This instrument has a water jacket and is supplied with compressed air to prevent the entrance of dust, smoke, or flame.)

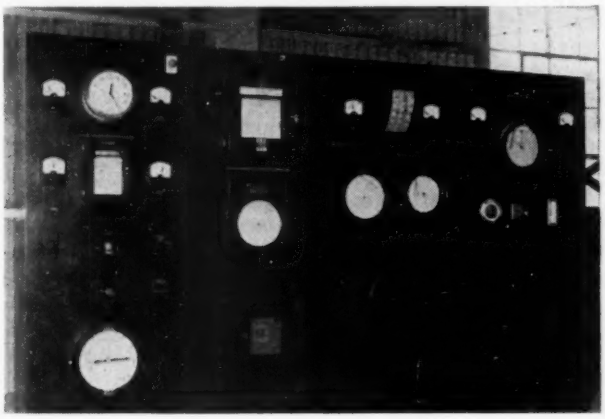


FIG. 9 INSTRUMENTS AND CONTROL EQUIPMENT MOUNTED ON SUITABLE PANEL BOARD IN MODERN KILN DEPARTMENT

In this type of installation, burning is controlled by varying both kiln speed and combustion rate, a radiation pyrometer being used for a temperature guide. As an example of the value of such an instrument to a burner, Fig. 6 is included. The chart at the left indicates the extreme variation in temperature in the burning zone when the burner gave no attention to the instrument, while the one at the right shows how closely the temperature was maintained when the burner used the instrument as a helpful guide.

Figs. 7 and 8 demonstrate two methods of positioning the rayotube element of such a temperature-recording instrument. It is to be noted in Fig. 8 that the device is equipped with a water-cooled jacket. Thus, provision is made for a stream of water to maintain the equipment within optimum operating temperatures, as well as for a jet of air to prevent the entrance of dust, smoke, or flame.

For the purpose of showing the close attention which is now given to obtain a satisfactory mounting of controls and instruments, a typical panel board is illustrated in Fig. 9. Included on the board are recorders and indicators used in conjunction with a radiation pyrometer, hood-draft controller, a fuel controller for a unit pulverizer, and various thermocouples for gas- and air-temperature measurement. This exhibit shows the extent to

which progressive mill operators are exerting their efforts to centralize control of the burning process and to eliminate the guesswork common in manual operation.

Co-ordinated Control System for Automatic Operation

Finally, the author wishes to propose a new scheme, one which provides a co-ordinated control system for the automatic operation of rotary kilns. Some may wonder why clinker burning is not controlled, like many other manufacturing processes, to maintain a predetermined production rate. The plan to be described aims to do just that, for the basic principle upon which the system functions is the second ideal of operation, namely, the preservation of a fixed speed of kiln and modification of the supply of air and fuel to secure the desired burning temperatures.

The major plant working equipment is illustrated schematically in Fig. 10. The raw mixture is supplied to the kiln by a suitable feeding device located at the high or raw-feed end. As the kiln rotates, the material passes down the kiln through the burning zone to be discharged as clinker to the perforated shaking grate of a pressure-type cooler. Air for cooling the hot particles is provided by a forced-draft fan. The air-quenched clinker passes from the cooler to the atmosphere through a swinging gate, or if further cooling is necessary, an aftercooler may be employed. In this event, an additional fan might be used to supply the air, or one fan of greater capacity could be arranged to discharge into a divided duct. Fuel is prepared in a unit air-swept pulverizer from which the coal is delivered to the kiln through the burner pipe. A portion of the air which cooled the clinker is drawn away from the cooler by the primary-air fan to dry the coal and transport it in suspension to the kiln. The remainder of the air passing through the clinker bed enters the hood to complete combustion of the fuel.

The procedure of operation, as previously stated, aims to establish a predetermined production rate. Thus, by trial, the optimum kiln speed is determined. Thereafter, it will remain constant, unless there is a pronounced change in the character of the raw mixture or in the type of product desired. At the same time, the optimum speed of the raw feeder is experimentally established and will remain fixed unless an emergency arises. Under these circumstances, what are the requirements of an ideal control scheme? Obviously, an adequate system should maintain the proper heat release to produce specified clinker temperatures. Further, it should maintain optimum combustion efficiency, that is, hold the air-fuel ratio continuously at the value which gives the best over-all economy.

In order to understand how the co-ordinated kiln-control system functions, it is important first to examine the method of regulating fuel flow to the kiln. As is well known by those familiar with the characteristics of an air-swept coal pulverizer, the quantity of fuel discharged is substantially proportional to the rate of flow of primary air through the unit, if a proportionate amount of coal is maintained therein. A controller is thus designed to vary the speed of the raw-coal-feeder motor to maintain a definite ratio of coal in the mill to the existing primary-air flow. The basis upon which this control operates is the relation between two differential pressures—one, the pressure drop across the mill proper; and the other, the pressure differential across the orifice in the air-supply line to the pulverizer. By such an arrangement it is possible to regulate the rate at which coal is delivered to the kiln by adjusting the damper which controls the flow of primary air. If an increased coal flow is demanded, the primary air is increased in proportion to the increase called for, and vice versa.

Now, consider that by trial the most desirable conditions of burning have been established. This means kiln and raw-feeder speeds are set. Heat release is sufficient to raise the temperature of the clinker to the desired standard. Combustion efficiency is at the optimum value, and the hood-draft controller has been adjusted to give the desired balance between forced and induced draft.

Then suppose a change occurs which decreases the temperature in the burning zone. The co-ordinated control apparatus, illustrated in Fig. 10, immediately functions. A photoelectric cell, sighted at the experimentally determined correct spot in the kiln, indicates that the temperature is too low, which means that the

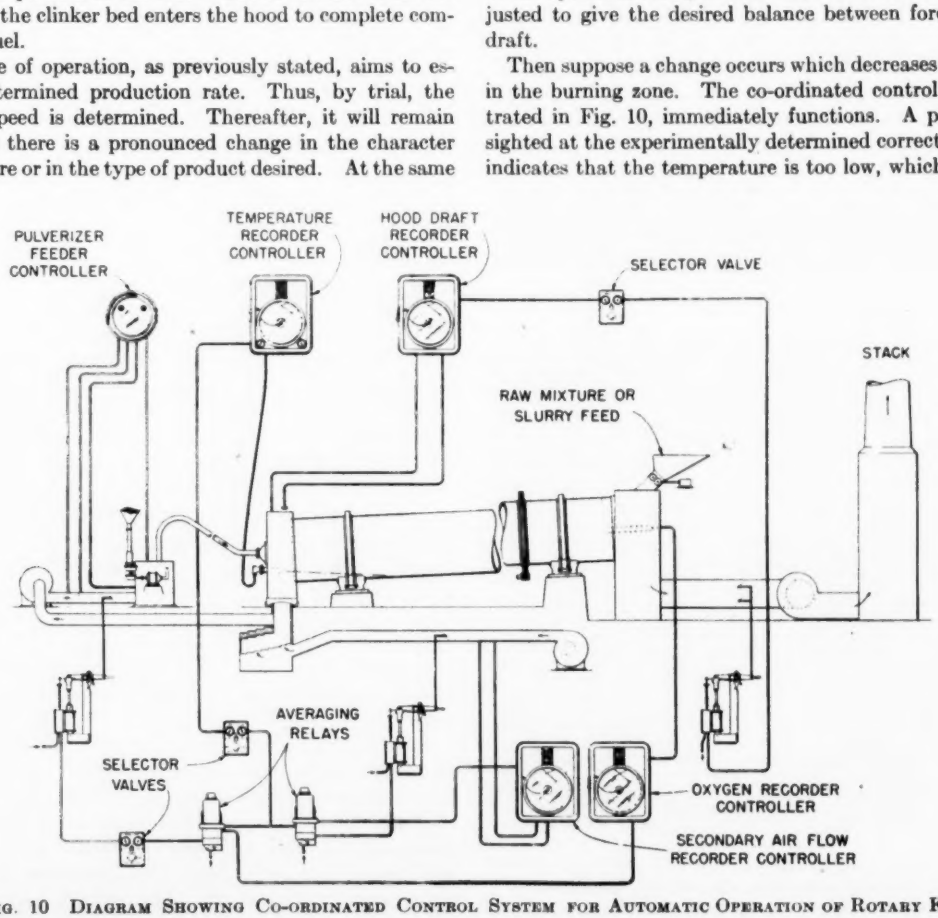


Fig. 10 Diagram Showing Co-ordinated Control System for Automatic Operation of Rotary Kiln

heat release is insufficient. The control operates to increase air and coal so that enough heat will be liberated to restore the temperature to the desired standard. A change in air flow is produced by a mechanism which positions the damper in the main air duct. This mechanism includes a metering device which operates through an averaging or two-element relay to establish a definite air flow rather than just a new damper position for each control impulse. Coincidental with the air increase, the same control impulse from the photoelectric cell increases fuel flow from the pulverizer. This latter action is effected by suitable means through a power drive which adjusts the damper controlling the flow of primary air to the unit mill.

Meanwhile, the exit gases are being continuously analyzed, preferably for oxygen content. A device capable of performing such a function acts as a recorder and as a controller to readjust the coal flow to maintain the optimum percentage of oxygen, since variation from such a value represents change in combustion efficiency. Impulses from this controller pass through the other averaging relay to readjust the primary-air damper. By this means, it is possible to compensate for the following:

1 Damper characteristics, that is, dampers of practical form do not necessarily work together to produce proportionate changes. For instance, to increase heat release, a new air flow is established in the main duct and, at the same time, the damper in the primary-air pipe is opened. It is not likely that both dampers have identical flow characteristics and hence the air-fuel ratio would vary.

2 Nonuniform performance of pulverizer, that is, relatively minor variations in the amount or character of coal within the pulverizer may cause momentary fluctuations in the Btu input of fuel to the kiln. In this connection, it might be pointed out that considerable progress has been made toward improving such characteristics of a unit pulverizer, yet further improvement is very much needed

3 Nonuniform coal, that is, the chemical analysis of the coal may vary to some degree.

The control makes one more significant adjustment when the increased heat release is demanded. Naturally, with a greater flow of air and fuel to the kiln, more combustion gases are generated and the damper at the induced-draft fan must be opened to exhaust the greater volume. Otherwise, the pressure in the hood would increase to cause greater air and gas leakage through openings and, in addition, the burning zone would move closer to the kiln front. Thus the purpose of the draft controller is to insure that combustion gases are carried away continuously from the burning zone through the kiln at the same rate at which they are generated.

In conclusion, a word is in order pertaining to the importance of continuous gas analysis as an essential guide in any fuel-burning process. Engineers have long realized the potential value of obtaining the oxygen content of combustion gases without the necessity of first analyzing for CO_2, for such a measurement is almost a direct determination of excess air. At the present time, there is at least one satisfactory device available to perform this function, and others are in the process of development. Consequently, there need be no delay in contemplating experimental work on the proposed system of control simply from the lack of such type of combustion-efficiency instrument. It is hoped that the suggestions which are outlined in this paper may create sufficient interest so that some effort in this direction will soon be forthcoming.

Acknowledgments

The author is grateful to the Leeds and Northrup Company and the Bailey Meter Company for the splendid co-operation extended by both organizations in the preparation of illustrative material for this paper.

Discussion

C. S. Burnett.[3] The author of this paper is to be congratulated on the presentation of a method of automatic kiln control which is apparently completely new as to ideas and completely automatic in its arrangement.

Control of burning-zone temperature automatically by regulation of the kiln fuel is not new, several installations now being at least partially automatic. However, as far as is known, none is capable of maintaining automatic operation a major portion of the time.

Kiln temperatures are relatively slow in responding to changes in fuel. If the temperature-controlling device is not properly compensated and adjusted to be in step with the speed of response of the temperature changes, a hunting cycle will result in which the fuel will chase the temperature up and down through a continuous cycle.

If some attempt is not made to change the air with and in approximately the proper ratio to the coal, smothering of the flame on increasing fuel, or excessive air and changed burning-zone position on decreasing fuel may result. Such instabilities limit the practical use of automatic temperature control.

It is, however, conceivable that, with air controlled in the proper proportion to the fuel, a greater stability of automatic operation would result.

The control arrangement proposed by the author is notable in that the air is the limiting factor. Coal cannot be fed by the control if there is insufficient air available to burn it. This feature is very desirable and has long been used in large steam-generating units, particularly where air, gas, or pulverized coal is used.

In considering the proposed arrangement, the plant operator will be concerned primarily with the sources of potential trouble. In studying the arrangement, it appears that there are several points to which particular attention should be paid.

The statement is made: "Meanwhile, the exit gases are being continuously analyzed, preferably for oxygen content." Since CO_2 is not a true indication of fuel-air ratio in a cement kiln, the analysis would necessarily have to be made by an oxygen-measuring instrument; and, since this instrument would be the heart of the system, we would all be interested in hearing more about it. Such a device should respond quickly to changes in fuel or air and, above all, should be able to operate for long periods without excessive maintenance being required.

The major sources of trouble in such an instrument would, no doubt, be in the sampling tube. This would, necessarily, be water-cooled and should be designed to prevent frequent stoppage by the kiln dust. Such a sampling tube is provided by at least one oxygen-measuring-instrument manufacturer.

Oxygen recorders have been used in power-generating stations for at least 2 years; hence, apparently, they have reached at least a semipractical stage of development. The usage they would receive around a cement kiln, however, would be much more severe than in power stations, particularly because of increased dust.

The present design of pressure cooler is not ideally arranged to permit fine control of secondary air. Designers have always considered the primary purpose of clinker coolers to be to cool clinker in order that it may grind more easily, or to quench the magnesia crystals in their amorphous state, in order to meet autoclave-expansion specifications. Now, we have a further use for these coolers.

[3] Alpha Portland Cement Co., Easton, Pa.

The arrangement, shown in Fig. 3 of the paper, is only partially satisfactory, as it is not possible to make the high-temperature-dividing damper very tight, and a considerable flow of air either away from or to the kiln would complicate matters.

Some thought in the design of clinker coolers to allow for better secondary-air control would be an effective step in advancing the cause of automatic kiln operation.

The system proposed by the author would, undoubtedly, be very desirable and, no doubt, practical in a kiln setup where there is an effective means of secondary-air control, furnace draft, and an accurate means of coal control.

There are, however, a great many kilns in service which, no doubt, will continue to be used, that are not arranged with the necessary equipment. It would be unfortunate if the developed instrument could not be applied to some of these existing kilns.

Considering a mill where there are several kilns discharging their gases into a common dust chamber and where kiln air is introduced only from the waste-heat fans, it is highly improbable that each of the kilns would get the same amount of air through it, as variations in coatings and other variables would affect its resistance to gas flow. With a draft controller maintaining the hood draft constant and approximately equal on all of the kilns, these variables would be efficiently removed.

The oxygen-measuring instrument could then be installed on each kiln, and from it the coal could be controlled to maintain the proper fuel-air ratio. Burning-zone temperature would be controlled by the kiln speed, and variations in the production of individual kilns could be regulated by varying slightly the value of the hot draft. Such a system does not have the flexibility of the author's scheme, but does allow the benefits of proper fuel-air ratio to be applied to this great number of existing kilns.

The discussion of the merits of controlled draft at the hood end of the kiln is well taken, and there is not much reason for discussion on this point.

The average modern steam-generating station is years ahead of the average cement plant in so far as utilizing combustion instruments to the fullest extent is concerned. It is true that central stations have their CO_2 recorders, steam and air flowmeters, and other fuel-air-ratio-efficiency instruments, which could not be adapted directly to our purpose.

The advent of the oxygen recorder, however, should fill a long-felt need in the cement industry, and it is hoped that this instrument can be developed to a point where it will be practical for use in the average plant.

It is suggested that the best way for the instrument manufacturer and the cement plant to get together for a mutually beneficial development would be to make a demonstration installation.

In the writer's district, there are numerous plants with equipment which would be adaptable to the proposed arrangement. Since this district produces much of the cement made in this country, it should be an ideal location for such an installation.

A. G. Christie.[4] Engineers who have studied cement production have marveled at the fact that so little has been done to apply control to the several steps of the process and particularly to rotary-kiln operation. Too often one is told that reliance can only be placed on the burner for proper operation. One who has watched burners handle a kiln must be impressed with the fact that much manipulation is unnecessary, because of the guesses made by the burner as to the cause of the trouble and the best method of correcting it. His decisions are based solely upon visual observation of the kiln interior without the aid of an accurate meter or device to inform him of the exact conditions. Some excellent indicating devices not widely used are available, such as the Smidth instruments, which assist the burner in diagnosing troubles and thus improve the efficiency of operation.

It is unfortunate that the author describes only briefly two of the systems now in use. By making operation fully automatic, less reliance is placed upon the skill of the burner and better average results are obtained. Before such systems are applied, many rotary-kiln installations should be largely rebuilt and modernized. For instance, relatively few kilns have proper preheating equipment for drying and preheating the contents of the slurry. Also, many old-fashioned clinker coolers could be profitably replaced by modern clinker air-quenching equipment which would lead to fuel savings, as well as to reduced power requirements for clinker grinding. Few kilns have fans for forced- and induced-draft control. When such kilns are modernized, automatic control can be considered.

While the control systems described in this paper have operated satisfactorily, much yet remains to be done to perfect kiln operation. In fact, further experience with such control systems must lead to improvements in the equipment itself and possibly to modifications of the kiln and its auxiliaries.

The author refers in a closing paragraph to the value of an oxygen analyzer for gases. The CO_2 content of the cement-kiln gases may come from the combustion of the fuel or from the calcining of the limestone, either of which may vary. Hence, this CO_2 as a measure of the efficiency of the combustion process is uncertain. On the other hand, the oxygen present must all come from the entering air, and its amount will serve as a measure of the excess air present. While this measurement is of value on cement kilns, an oxygen recorder on rotary kilns, burning lime or dolomite, would have equal value. A wide field for the application of a low-priced oxygen recorder would be its use on vertical lime kilns, of which there are hundreds in this country. In general, these vertical kilns have no instruments at present to indicate kiln conditions or to aid in control. However, many of them should be rebuilt or modernized before funds are expended on instruments or controls.

J. C. Witt.[5] The writer considers fuel control preferable to kiln-feed control, as outlined by the author. The industry is not yet ready for the completely automatic control of kilns (because of a number of factors), but this may come someday.

W. H. Sayler.[6] The writer's interest in the subject of this paper arises from the fact that his early professional life was spent in the cement industry, while the last several years have been devoted to the design, sale, and installation of automatic process-control systems.

In reviewing the paper, it will be helpful to consider the problem from a broader viewpoint than the author has been able to use, as his paper is confined basically to an excellent report of specific installations.

In a cement kiln we have the following variables:

1 The rate of feed of raw material.
2 Speed of kiln (in many cases fixed).
3 Rate of fuel feed.
4 Rate of air feed.
5 Air pressure in kiln.
6 Temperature in kiln.
7 Fuel-air ratio.
8 Heat input to raw-material input ratio.

[4] Professor of Mechanical Engineering, The Johns Hopkins University, Baltimore, Md. Mem. A.S.M.E.

[5] Technical Service, Manager, Marquette Cement Manufacturing Company, Chicago, Ill. Mem. A.S.M.E.

[6] Registered Professional Engineer, Specialty Sales Company, Salt Lake City, Utah.

Of these eight variables, 2 is the only one which can be maintained constant without automatic control. Variables 7 and 8 are really functions of 3 and 4 and 1, 3, and 4.

In the wet-process plant, control must start in the raw-grinding room. Unless the slurry is automatically controlled at constant density, a volumetric-type slurry feeder will introduce errors to begin with. Therefore, the slurry should be controlled to a constant density to obtain a uniform feed rate. In the dry plant, a constant-weight feeder should be used to insure the feed rate being the same as the management hopes it is. This eliminates variable 1 from the control problem. For this discussion we will assume variable 2 to be fixed.

The next important variable to be made constant is the air feed. When we remember that approximately 14 lb of air per lb of coal are required, or for a 1000-bbl-per-day kiln, 1,400,000 lb per day, it is seen that air is important in its effect on kiln economy. In the West, in many places, air temperature may vary tremendously over an 8-hr period. An examination of Weather Bureau reports shows that, at Salt Lake City, the density of air may vary, both because of temperature and barometric variation, as much as 13 per cent between 8 a.m. and 3 p.m. in clear summer weather. In case of sudden showers, the variation is more abrupt. During a 24-hr period, the variation is much greater.

Therefore, the writer proposes the following control scheme:

1 Meter raw material into the kiln at a truly constant weight rate (as described).

2 Meter air into the kiln, a constant weight ratio to raw-material feed.

3 Meter in the proper amount of fuel to react with the air at whatever ratio is decided upon as optimum.

4 Control draft at the firing hood.

5 Record kiln-firing-end temperature, if desired.

6 Record kiln-exit temperature.

7 Record, or occasionally check, oxygen content of flue gas.

Point 1: May be achieved by constant volume rate of slurry, if constant slurry density is maintained.

Point 2: May be maintained by a constant air-weight controller, such as has been applied to blast furnaces in the steel industry.

Point 3: May be handled by a standard air-to-fuel-ratio regulator.

Point 4: Adequately covered by the author.

Point 5: A record is sufficient in this case, since the precision of temperature measurement in the firing end of a cement kiln is not high enough to permit control by temperature.

Point 6: The record only is necessary, since this temperature is a measure of results.

Point 7: Most gas-percentage recorders are not precise enough to make reliable control mechanisms. This statement is open to dispute, but on a total oxygen percentage of, say, 1 per cent, in the flue gas, it is easy to compute the error in proportioning, caused by the oxygen-recorder reading 1.1 per cent when it should read 1 per cent.

Except for the oxygen recorder, with which the writer does not claim too great a familiarity, all of the devices described are more or less standard products with at least two nationally known manufacturers.

In conclusion, the writer wishes to express the hope that this paper will provoke a lively interest in the problem of applying automatic control to the cement industry.

Author's Closure

The author is grateful to those who have contributed discussions of this paper. Several thoughts expressed by the writers warrant further comment.

Mr. Burnett calls attention to the problem of applying control apparatus in a plant where a number of kilns discharge gases into a common flue. Obviously, satisfactory regulation of combustion requires hood-draft control on each kiln. The author has had considerable experience with just such a problem. A water-cooled sliding-gate damper was installed in the gas duct between the tail end of the kiln and the main dust chamber, while the draft measuring and controlling device was attached to the kiln hood. No difficulty in damper operation was encountered; only a small quantity of water was required to keep the damper reasonably cool; and hood draft was maintained continuously within limits of ± 0.005 in. of water. Such an arrangement can be thus utilized as part of a control layout in the type of plant to which Mr. Burnett refers. When clinker is discharged to rotary coolers or open pits, constant hood draft establishes the secondary-air supply; the O_2 controller maintains the desired fuel-air ratio; and burning-zone temperatures can be kept within required limits by changes in kiln speed, either by automatic adjustment from a sight temperature instrument or by manual control.

Professor Christie calls attention to the need for control development in the cement industry, especially as it concerns the rotary-kiln process. He points out that in many cases kiln installations need to be rebuilt and modernized before regulating apparatus can be applied with benefit. The great difficulty in the past has been to convince the many mill operators of the economic advantages of such rehabilitation. It should be of interest to know there are numerous instances where installation of controls, regulating just one element of the burning process, has directed attention to distinct shortcomings in major equipment. Modification of kiln and auxiliary design has brought about subsequent marked improvement, and further use of automatic control devices has been thus encouraged.

In general, the discussions emphasize the need for continued effort and experimentation, in order that rotary-kiln operation may approach the high degree of excellence already existent in many other manufacturing processes involving the combustion of fuels. It was not many years ago that complete automatic control of steam boilers was considered an ideal to be realized only in the distant future; today, this goal has been reached and a complete set of control appurtenances is an integral element of all modern steam-generator installations. Energetic research, sponsored by those responsible for the most efficient operation of rotary kilns, will accomplish a similar much-needed result.

A Method of Estimating the Circulation in Steam-Boiler-Furnace Circuits

By A. A. MARKSON,[1] T. RAVESE,[2] and C. G. R. HUMPHREYS[2]

The estimation of the quantity of circulation in modern high-pressure boiler-furnace circuits is not essentially new, especially to the literature abroad. Methods popularized by Münzinger and others are based on an air-lift analogy and, while straightforward, are tedious of application. The method developed by the authors is essentially an inversion of the problem as previously conceived. It consists of solving a simple equation by the use of parametric circulation curves for the heat absorption corresponding to the leaving quality of the mixture. These are given for two assumed conditions of heat transfer, that of principal heat absorption at the bottom of the tube, and that of uniform heat absorption at the length of the tube up to the critical pressure. Most commercial applications are intermediate between these two assumptions. Examples are worked out in detail to show the application. Some effects of changing circuit design are illustrated. A method of obtaining the point of maximum circulation with respect to heat absorption directly is outlined.

The following nomenclature is used in the paper:

A = internal circuit area
D = tube diameter
d = density, lb per cu ft
d_1 = density of solid water, lb per cu ft
d_2 = density of mixture leaving circuit, lb per cu ft
d_{2l} = logarithmic-mean density in heated circuit
F = frictional losses
f = friction coefficient
G = mass flow, lb per sq ft per sec
g = 32.2
H = total heat absorption of circuit, Btu per hr
h_{fg} = enthalpy of vaporization, Btu per lb
l = vertically projected length of circuit, ft
l_1, l_2 = developed length of circuit, ft
N = number of risers or downcomers
Q = heat absorption, Btu per sq ft per hr
P = pressure
p = pressure drop in tube, as defined
V = velocity
v = specific volume, cu ft per lb
v_f = specific volume saturated liquid, cu ft per lb
v_{fg} = volume of vaporization, cu ft per lb
W = rate of flow, lb per hr
w = rate of flow, lb per sec
X = steam quality of mixture

[1] Hagan Corporation, Pittsburgh, Pa. Formerly with Research Bureau, Consolidated Edison Co. of New York. Mem. A.S.M.E.

[2] Combustion Engineering Co., New York, N. Y. Formerly with Research Bureau, Consolidated Edison Co. of New York, New York, N. Y. Jun. A.S.M.E. and Mem. A.S.M.E., respectively.

Contributed by the Fuels Division and presented at the Fall Meeting, Louisville, Ky., October 12–15, 1941, of The American Society of Mechanical Engineers. This paper was also presented under the auspices of the Applied Mechanics and Power Divisions at a meeting of the A.S.M.E. Metropolitan Section held at Columbia University, New York, N. Y., November 18, 1941.

Note: Statements and opinions advanced in papers are to be understood as individual expressions of authors and not the Society.

The exact formulation of the quantity of circulation produced in the furnace circuits of an operating steam boiler is obviously of extraordinary complexity. The major evaporative zone of a modern high-pressure-boiler unit is the water-cooled furnace and first row of boiler tubes. From a hydraulic standpoint, these circuits lend themselves more to analysis than do those of the older units where the sectional boiler with its baffling constitutes the principal evaporative section.

Münzinger (1)[3] published a method of calculating boiler circulation which has since been used by many writers. Two recent papers in English by Van Brunt (2), and by Lewis and Robertson (3), illustrate the use of Münzinger's method. Briefly, it consists of analyzing the boiler circuit as though it were an air-lift pump.

Curves of hydraulic loss are plotted against velocity, usually for constant heat-absorption rate along the tube. The curves of available head, due to the density differences, are also plotted against velocity at constant heat absorption. The intersection of the loss and head curves marks the theoretical operating point of the unit for the assumed conditions.

The principal assumptions usually made in connection with these analyses are:

1 The rate of heat absorption is uniform along the heated tubes, and the heat absorbed per tube is the same.

2 The mixture of steam and water is essentially homogeneous. Bubble slip is neglected.

3 The coefficient of friction is usually taken as a constant throughout.

4 Individual hydraulic resistances are handled by some conventional method.

5 Evaporation starts immediately and there is no steam in the downcomers.

6 Drum velocities are negligible.

Each of these assumptions is open to criticism having varying degrees of validity. Nevertheless, the conclusion that approximations of value can be derived from them is not open to very serious objection (3), especially for the higher operating pressures where the steam and water phase differences become less marked.

While the artifices to be discussed constitute an important phase of the theory of boiler circulation, it is well to emphasize the fact that a complete picture of circuit design is not to be gained from a steady-state mechanism. It suffices to state as an example that a circuit having a low resistance also has a low damping characteristic. Tubes may never burn out in such a circuit but slight disturbances in operation conditions may produce annoying oscillations in water level.

The authors' method differs from Münzinger's. In the Münzinger method, simultaneous curves of available head and of losses against velocity must be drawn for each assumed condition, giving one set of curves to be constructed for each point. The construction of a complete circulation-heat absorption characteristic curve is therefore a drawn-out affair. The present

[3] Numbers in parentheses refer to the References at the end of the paper.

method inverts the problem. The resistance of the circuits having been formulated, an assumption is made as to the quality of the mixture coming from the circuit. A set of parametric curves is presented by which a basic equation is solved for the rate of heat transfer which must correspond to this quality. Having these, the velocity, mass flows, and other derived quantities are readily calculated.

The parametric curves of the circulation or Z function possess considerable interest by themselves. Constant heat absorption is represented by a horizontal line on the curves, so that, having located an operating point for an actual boiler on the diagram, the rough operating characteristic for this or an identical boiler at different pressures and heat absorptions may be quickly predicted. Such comparisons are less accurate if carried over too wide a range, because this procedure neglects secondary density effects.

Development

Throughout, all losses and heads will be expressed as head in feet of a column whose density is that of the mixture leaving the

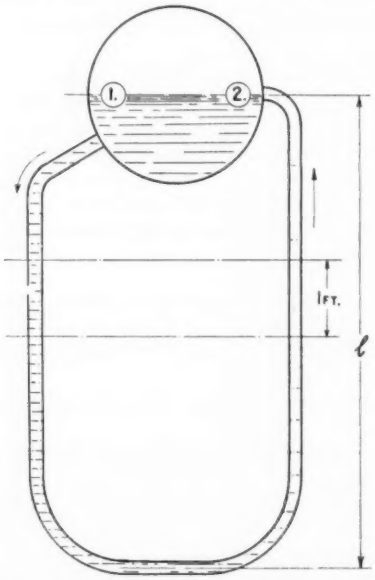


Fig. 1 U-Tube Circuit Connected to Drum

circuit. All velocities will be expressed in terms of the velocity leaving the circuit. This is convenient because there are usually but three densities involved, i.e., the density of solid water, the mean density of the heated column, and the actual density of the mixture leaving the circuit.

A comparison of the method with others indicates that the basic assumptions and the evaluation of the resistance coefficients are the same. The results obtained should be identical. The introduction, however, of the graphical parameters saves considerable purely mechanical labor and gives a better over-all picture of circulation, considered as a hydraulic process.

A considerable simplification can be achieved for some purposes in setting up the resistance coefficients by the device of adding so many pipe diameters to the friction length. Where this can be done discriminately the results should be good.

Fig. 1 is a U-tube circuit connected to a drum. The assumptions will be made that the tubes are heated on one leg, and that the feed, entering the heated section, is at the steaming point. It will also be assumed in a purely introductory way that (as in many modern boiler furnaces) the principal heat absorption is at the bottom so that, neglecting gravity head, the tube acts as though the mean density were roughly constant throughout the length. Thus, the mean density in the heated leg may be taken as approximately equal to the density leaving the tube. It will be shown that this assumption does not lead to radically different results than the assumption of uniform steam generation throughout the tube, which represents another extreme of practical operation.

By taking a 1-ft section across the tube, the gravitational head per foot of vertical length in terms of a column having a density d_2 is

$$\frac{d_1 - d_2}{d_2} \quad \ldots\ldots [1]$$

and for the total length, l is

$$l\left(\frac{d_1 - d_2}{d_2}\right) \quad \ldots\ldots [2]$$

where d_1 is the density in the downcomer and d_2 the average density in the riser. This head is the driving force of natural circulation. Balancing the available head are the appropriate circuit losses.

The section, under consideration in Fig. 1, is from point 1 in the drum to point 2 in the drum at the same elevation as point 1. The energy of circulation is wholly derived from the isothermal changes of state in evaporation. The circuit may be analyzed hydraulically by considering the forces which balance the head of circulation. The available head is considered as established by the density differences in the heated and unheated parts. This head is consumed or balanced by various losses occurring in the circuit. The losses, expressed in velocity heads, are equated to the head of circulation in a manner analogous to the application of the Bernoulli theorem. It may be easily shown that this procedure in its details lacks thermodynamic and even hydraulic rigor, but this lack is unimportant. It is equivalent to stating as a theorem that the net gravitational work done between points 1 and 2 is zero.

Consider 1 lb of water at saturation temperature at point 1. It enters the tubes with an entrance loss. There are further losses accountable as friction and change of section up to the evaporating tubes. There, the state commences to change and the similar losses from this point on must take this into account. At the discharge point 2, which is assumed to be at the same level as point 1, the mixture is delivered at some velocity into the drum. The drum velocity is assumed as zero. The use of the term "acceleration loss" has been introduced by practically every writer on the subject of boiler circulation to account for the reactive head which is developed when the particles, initially traveling with the velocity of solid water, are accelerated by the evaporative process in a section of constant cross section. Lewis and Robertson (3) go into considerable detail on this matter to explain that the reactive force rather than the whole exit kinetic energy should be balanced against the available head, because the excess energy has been generated directly by the fire as part of the latent-heat change. But the authors feel that it might be better, since the entire process of circulation stems from the change of state, to regard acceleration loss as an engineering coinage in accounting for part of the head. However, there is no doubt of its physical meaning. It is one of the principal forces involved in "pop-bottle" action in boilers. The foregoing is not meant to imply novelty other than of name for this, as every work on theoretical hydraulics and thermodynamics considers this force in the pipe-line flow of compressible fluids (4).[4]

[4] The concept of acceleration head stems directly from the general equation

$$-vdp = \frac{VdV}{g} + dF + dl$$

which is in effect integrated by the methods of the text.

Frictional losses will be defined quite conventionally as consisting principally of downcomer and riser friction amenable to treatment by the friction formula of the form

$$\frac{p}{d} = \frac{4flV^2}{2gD}$$

where

p = pressure drop, lb per sq ft
d = density of fluid, lb per cu ft
f = friction coefficient
V = velocity, fps
D = internal tube diameter, ft

These losses are reducible to a standard form in terms of d_2 and V_2.

Let A_1 be the combined area of all the downcomers and A_2 be the area of the risers. The riser friction in feet of d_2 is written as

$$\frac{4fl_2V_2^2}{2gD_2}$$

The downcomer friction likewise is

$$\frac{4fl_1V_1^2}{2gD_1} \text{ in feet of } d_1$$

To transform the downcomer friction into terms of V_2 and d_2 use the continuity expression

$$A_1V_1d_1 = A_2V_2d_2$$

giving for the downcomer friction in feet of d_1

$$\frac{4fl_1}{2gD_1}\left(V_2\frac{A_2d_2}{A_1d_1}\right)^2$$

Multiplying by $\frac{d_1}{d_2}$ transforms this into feet of d_2 reducing to

$$\frac{4fl_1}{2gD_1}\left(V_2^2C^2\right)\frac{d_2}{d_1}$$

where

$$C^2 = \left(\frac{A_2}{A_1}\right)^2$$

Kinetic Losses. This term will be taken to include all losses due to entrance, changes of section, and dissipated velocity up to the evaporating section.

These losses may be approximated as a function of V_2^2 and become on transformation similar to the foregoing

$$\frac{k_1V_2^2C^2}{2g}\cdot\frac{d_2}{d_1} \text{ in ft of } d_2$$

where k_1 is the summation of the usual loss coefficients. To these may be added similar evaporating-circuit losses, including moisture baffling, and drum losses as

$$k_2\frac{V_2^2}{2g} \text{ in ft of } d_2$$

k_1 and k_2 are evaluated as in ordinary hydraulic work.

Acceleration Loss. If w is the weight of fluid per second, its change of momentum due to evaporation is

$$\frac{w}{g}(V_2 - V_i)$$

where V_i is the inlet velocity to the heated section. The change of momentum per second is also numerically the reactive force. This, divided by area, gives pressure, and again by d_2 gives loss in feet of d_2, becoming

$$\frac{w}{d_2A_2g}(V_2 - V_i)$$

For V_i write $V_id_1 = V_2d_2$

$$V_i = V_2\frac{d_2}{d_1}$$

and finally after transformation the acceleration loss becomes in feet of d_2

$$\frac{V_2^2}{2g}\left(2 - 2\frac{d_2}{d_1}\right)$$

Collecting all the losses as a coefficient of $\frac{V_2^2}{2g}$ gives

$$\Sigma \text{ losses, ft } d_2 = \frac{V_2^2}{2g}\left[\frac{4fl_2}{D_2} \text{ risers}\right.$$
$$+ \frac{4fl_1}{D_1}C^2\frac{d_2}{d_1} \text{ downcomers}$$
$$+ k_1C^2\frac{d_2}{d_1} \text{ kinetic on water circuit}$$
$$+ k_2 \text{ kinetic on steam circuit}$$
$$\left. + 2 - 2\frac{d_2}{d_1}\right] \text{ acceleration}$$
$$= \frac{V_2^2}{2g}\left(\frac{4fl_2}{D_2} + \frac{d_2}{d_1}\left[\frac{4fl_1}{D_1}C^2 + k_1C^2 - 2\right] + k_2 + 2\right) \ldots [3]$$

This expression is equal to the available head which is $l\left(\frac{d_1 - d_2}{d_2}\right)$ giving

$$V_2 = \frac{(2g)^{1/2}l^{1/2}}{K^{1/2}}\left(\frac{d_1 - d_2}{d_2}\right)^{1/2}$$

where K is the coefficient of $\frac{V_2^2}{2g}$ in Equation [3]. For weight, we multiply by A_2d_2. Collecting constants

$$W = \frac{28{,}900\,A_2l^{1/2}d_2^{1/2}(d_1 - d_2)^{1/2}}{K^{1/2}}$$

where W is the rate of circulation in pounds per hour.

Multiplying by the quality and hfg, the heat absorption in Btu per hr

$$H = 28{,}900\cdot\frac{A_2l^{1/2}}{K^{1/2}}d_2^{1/2}(d_1 - d_2)^{1/2}\cdot X\cdot h_{fg}$$

$d_2^{1/2}(d_1 - d_2)^{1/2}\cdot X\cdot h_{fg}$ can be represented graphically by Fig. 2 as Z, so that the circulation equation reduces to the form

$$H = 28{,}900\cdot\frac{A_2l^{1/2}}{K^{1/2}}\cdot Z \ldots\ldots\ldots\ldots [4]$$

This result was based upon the hypothesis of principal heat absorption at the bottom of the circuit. It is pertinent to inquire how this compares with the assumption of uniform heat absorption along the tube, for between these two assumptions lies most of the cases encountered in practice.

We start with the unbalanced driving force due to uniform generation of steam, assuming no bubble slip.

The mean density of such a column in terms of d_1 and d_2 is

$$d_{22} = \frac{2.3}{Xv_{fg}}\log_{10}\left(\frac{d_1}{d_2}\right)$$

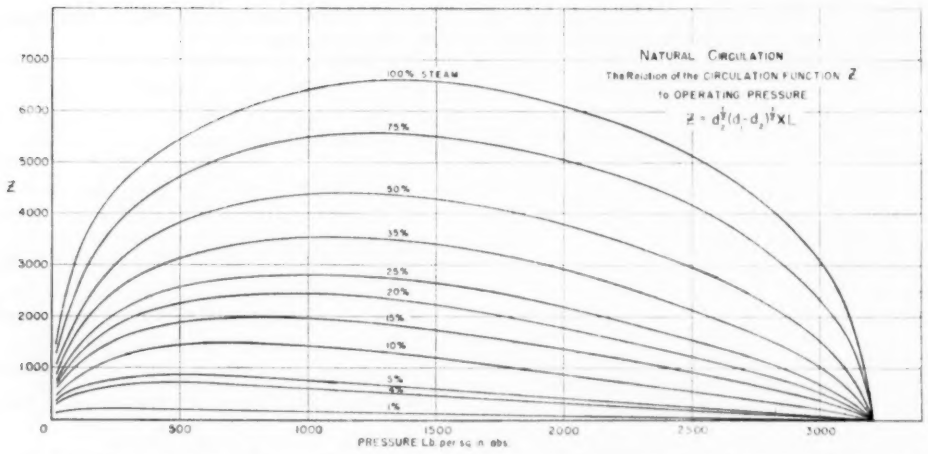


FIG. 2 NATURAL CIRCULATION: RELATION OF CIRCULATION FUNCTION Z TO OPERATING PRESSURE

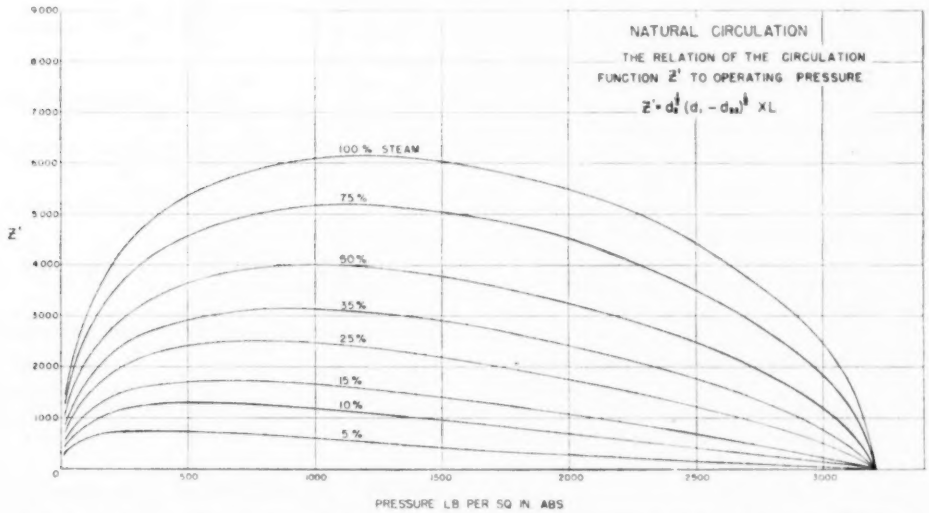


FIG. 3 NATURAL CIRCULATION: RELATION OF CIRCULATION FUNCTION Z' TO OPERATING PRESSURE

as derived in Appendix 1, where d_2 as usual is the density leaving the tube. In terms of d_2 the unbalanced head is $\frac{d_1 - d_{22}}{d_2}$, per foot.

We may write

$$l\left(\frac{d_1 - d_{22}}{d_2}\right) = K'\frac{V_2^2}{2g}$$

where K' is a loss coefficient.

In this loss coefficient, all the losses but the riser friction are defined much the same as by Equation [3]. The riser friction, however, does not depend upon V_2 but must follow the changing velocity and density along the tube. Term K' must correctly estimate the riser friction.

A better friction term for use in K' is

$$\frac{4fl_2}{D}\left(\frac{d_2 + d_1}{2d_1}\right)$$

as derived in Appendix 2. Thus, the riser friction term in K' for uniform heat absorption becomes

$$\frac{4fl_2}{D_2}\left(\frac{d_2 + d_1}{2d_1}\right) = \frac{4fl_2}{D_2}\left(\frac{1}{2}\cdot\frac{d_2}{d_1} + \frac{1}{2}\right)$$

By a process similar to that followed in deriving Equation [4], an expression relating the circulation to the heat absorption when the heat is uniformly absorbed is readily obtained as

$$H = \frac{28{,}900\, A_2 l^{1/2}}{(K')^{1/2}} Z' \qquad [5]$$

where $Z' = d_2^{1/2}(d_1 - d_{22})^{1/2} \cdot X \cdot h_{fg}$. Term Z' is represented graphically in Fig. 3. It is the authors' conclusion that all practical cases to which these methods may be applied will lie between the principal assumptions of heat absorption as given

APPLICATION

The application of the method to a furnace circuit of assumed characteristics will be shown. The circuit consists of 161 riser tubes of 3 in. OD, shown at top of work sheets, Figs. 4*a* and 4*b*. It is supplied by two 12-in-ID downcomers. The projected heating surface is 2700 sq ft. The vertical height is 50 ft. The developed length of the risers is taken as 90 ft and the downcomers as 60 ft. The assumed nominal rate of heat absorption is 49,000 Btu per sq ft of projected area per hr. Each tube absorbs the same quantity of heat. Densities of mixtures may be obtained from Fig. 5.

Example 1. The first problem will be to establish the circulation characteristics at 2200 lb abs as a function of heat ab-

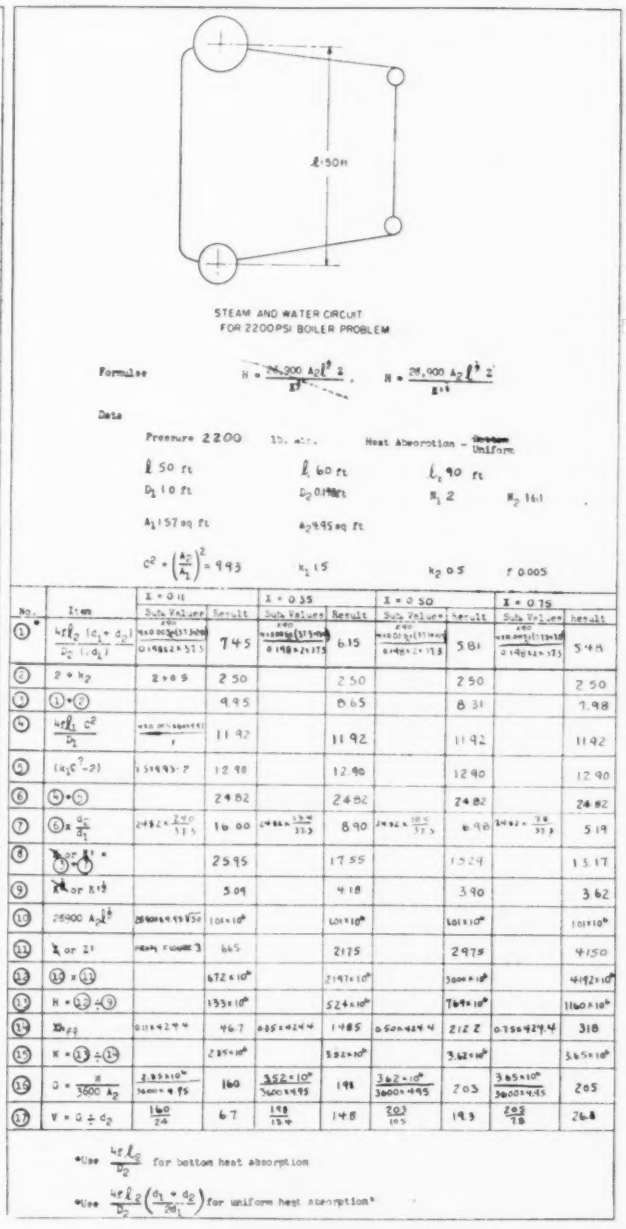


No.	Item	X = 0.095 Sub Values	Result	X = 0.35 Sub Values	Result	X = 0.50 Sub Values	Result	X = 0.75 Sub Values	Result
①	$\frac{4f\ell_2}{D_2}\frac{(t_1+d_2)}{(t_1 d_2)}$	400 / 0.198	908		908		908		908
②	2 × N_2	2×0.5	2.50		2.50		2.50		2.50
③	① + ②		11.58		11.58		11.58		11.58
④	$\frac{4f\ell_1}{D_1}\frac{c^2}{1}$		11.92		11.92		11.92		11.92
⑤	$(N_1 c^2 - 2)$	15×993 − 2	12.90		12.90		12.90		12.90
⑥	④ + ⑤		24.82		24.82		24.82		24.82
⑦	⑥ × $\frac{d_2}{d_1}$	24.82 × 20/373	16.00	24.82 × 13.9/37.3	8.90	24.82 × 10.5/37.3	6.98	24.82 × 7.0/37.3	5.19
⑧	③ or ⑦ + ①		28.38		20.48		18.56		16.77
⑨	$R^{\frac{1}{2}}$ or $R^{\frac{1}{3}}$		5.31		4.52		4.29		4.09
⑩	26900 $A_2 R^{\frac{1}{2}}$	26900×4.95×√5.31	101×10⁶		101×10⁶		101×10⁶		101×10⁶
⑪	Σ or Σ'	from Figure 2	7.00		34.25		34.75		47.75
⑫	⑩ × ⑪		707×10⁶		3460×10⁶		3500×10⁶		4820×10⁶
⑬	H = ⑫ ÷ ⑨		533×10⁶		349×10⁶		347×10⁶		464×10⁶
⑭	$\Sigma h f_3$	0.0954×4.95	4.73	0.35×4.95	1.485	0.50×4.95	2.12	0.75×4.95	3.18
⑮	K = ⑬ ÷ ⑭		113×10⁶		235×10⁶		164×10⁶		146×10⁶
⑯	Q = $\frac{H}{3600\ A_2}$	88×10⁶ / 36 × 4.95	165	395×10⁶ / 36 × 4.95	222	555×10⁶ / 36 × 4.95	216	371×10⁶ / 36 × 4.95	208
⑰	V = Q ÷ d_2	165 / 20.2	7.4	222 / 13.4	16.5	216 / 10.5	20.6	208 / 7.5	36.7

*Use $\frac{4f\ell_2}{D_2}$ for bottom heat absorption ✓

*Use $\frac{4f\ell_2}{D_2}\left(\frac{\sigma_1+\sigma_2}{2\sigma_1}\right)$ for uniform heat absorption

FIG. 4a STEAM-AND-WATER CIRCUIT AND WORK SHEET FOR 2200-PSI BOILER PROBLEM, EXAMPLE 1



No.	Item	X = 0.11 Sub Values	Result	X = 0.35 Sub Values	Result	X = 0.50 Sub Values	Result	X = 0.75 Sub Values	Result
①	$\frac{4f\ell_2}{D_2}\frac{(t_1+d_2)}{(t_1 d_2)}$	400 / 0.198×2.515	745	400 / 0.198×2.175	615	400 / 0.198×2.113	581	400 / 0.198×2.113	548
②	2 × N_2	2×0.5	2.50		2.50		2.50		2.50
③	① + ②		9.95		8.65		8.31		7.98
④	$\frac{4f\ell_1}{D_1}\frac{c^2}{1}$		11.92		11.92		11.92		11.92
⑤	$(N_1 c^2 - 2)$	15×993 − 2	12.90		12.90		12.90		12.90
⑥	④ + ⑤		24.82		24.82		24.82		24.82
⑦	⑥ × $\frac{d_2}{d_1}$	24.82 × 2.0/31.5	16.00	24.82 × 13.9/37.3	8.90	24.82 × 10.5/37.3	6.98	24.82 × 7.0/37.3	5.19
⑧	③ or ⑦ + ①		25.95		17.55		15.29		13.17
⑨	$R^{\frac{1}{2}}$ or $R^{\frac{1}{3}}$		5.09		4.18		3.90		3.62
⑩	26900 $A_2 R^{\frac{1}{2}}$	26900×4.95×√5.09	101×10⁶		101×10⁶		101×10⁶		101×10⁶
⑪	Σ or Σ'	from Figure 3	6.65		21.75		29.75		41.50
⑫	⑩ × ⑪		672×10⁶		2197×10⁶		3000×10⁶		4192×10⁶
⑬	H = ⑫ ÷ ⑨		133×10⁶		524×10⁶		769×10⁶		1160×10⁶
⑭	$\Sigma h f_3$	0.11×4.95	46.7	0.35×4.95	1.485	0.50×4.95	2.12	0.75×4.95	3.18
⑮	K = ⑬ ÷ ⑭		285×10⁶		3.52×10⁶		3.62×10⁶		3.65×10⁶
⑯	Q = $\frac{H}{3600\ A_2}$	2.85×10⁶ / 3600×4.95	160	3.52×10⁶ / 3600×4.95	198	3.62×10⁶ / 3600×4.95	203	3.65×10⁶ / 3600×4.95	205
⑰	V = Q ÷ d_2	160 / 24	6.7	198 / 15.9	14.8	203 / 10.5	19.3	205 / 7.8	26.8

*Use $\frac{4f\ell_2}{D_2}$ for bottom heat absorption

*Use $\frac{4f\ell_2}{D_2}\left(\frac{\sigma_1+\sigma_2}{2\sigma_1}\right)$ for uniform heat absorption

FIG. 4b STEAM-AND-WATER CIRCUIT AND WORK SHEET FOR 2200-PSI BOILER PROBLEM, EXAMPLE 2

sorption for both the cases of bottom and uniform heat absorption. Fig. 4*a* shows the computations made on the work sheet which was used and found to be convenient. Values of X are assumed; K is calculated for each value of X. The value of Z is obtained for 2200 lb from the Z curve for each value of X. The basic equation is then solved for H, the total heat absorption. Given X and H, the total weight per hour circulated is obtained. This divided by the appropriate area and time unit gives the mass flow G in pounds per second. Term G multiplied by the specific volume gives the velocity. The process is also undergone for the case of uniform heat absorption. The results are given in Table 1 and Fig. 6. Term f is taken as 0.005 throughout.

Example 2. The next application is the problem of defining the circulation characteristic of this circuit as pressure varies with constant heat absorption for both the case of uniform and bottom heat absorption. (See Fig. 4*b* for work sheet.) The riser-tube diameters have been recalculated for the pressures given by formula (6), which follows

$$P_o = \frac{27{,}600\ (t - 0.04)}{D} - 400 \quad \ldots\ldots\ldots\ldots [6]$$

where

t = wall thickness, in.
D = outside diameter of tube, in.
P_o = working pressure, psi

Table 2 and Fig. 7 give the results of this analysis. The method of working is slightly different. The rate of heat absorption being fixed, X is assumed as a first trial and K is tabulated. Term Z is solved for and generally will correspond to a

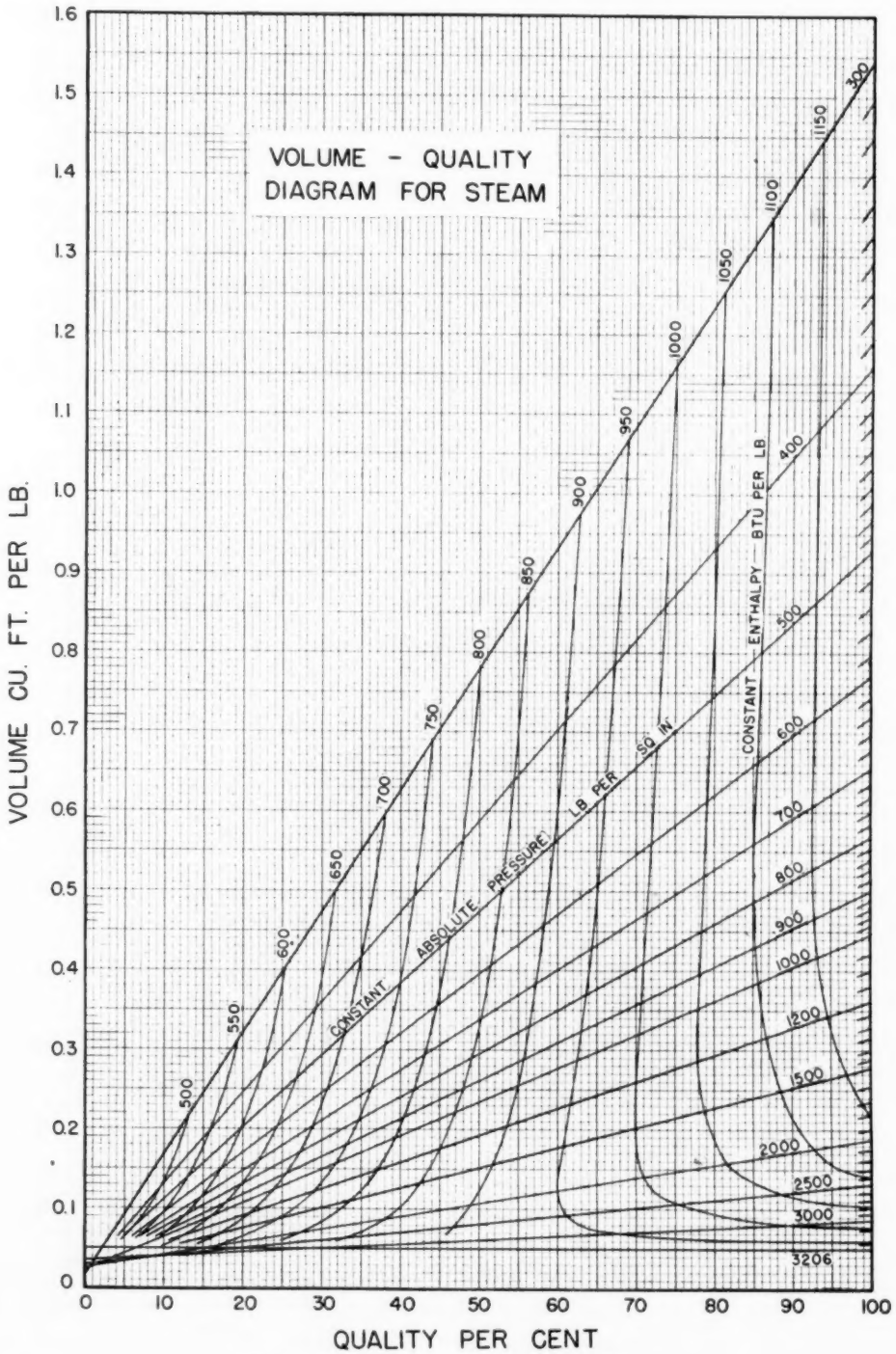


FIG. 5 VOLUME-QUALITY DIAGRAM FOR STEAM

different value of X. Term K is then reworked for a new assumed value of X and, as a rule, the second trial will be found exact enough.

Example 3. A problem of interest is the calculation of the circulation characteristic if one downcomer were removed. The results are given in Table 3 and Fig. 6 for the case of uniform heat absorption for 2200 lb.

ANALYSIS OF MORE COMPLICATED CIRCUITS

The analysis of more complicated circuits may be attempted as long as the circuits can be handled by the use of the continuity equation. The general method is to resolve all changes of section by means of area and density relationships into functions of outlet velocity and density. The proper densities to assume might be troublesome on the evaporating side were it not for the following: There are no section changes as a rule inside the furnace, which means that the density leaving the furnace is the same as that leaving the circuit. This being so, only one acceleration loss has to be computed.

Assuming, however, that the circuit consists of a number of

TABLE 1 CIRCULATION CHARACTERISTICS AT 2200 PSI ABS AS FUNCTION OF HEAT ABSORPTION

Bottom heat absorption				Uniform heat absorption			
Q	G	X	V_2	Q	G	X	V_2
49000	185	0.095	7.4	49000	160	0.11	6.7
217000	222	0.35	16.5	193000	198	0.35	14.8
301000	216	0.50	20.6	282000	203	0.50	19.3
435000	208	0.75	26.7	415000	205	0.75	26.3

TABLE 2 CIRCULATION CHARACTERISTICS AS PRESSURE VARIES WITH CONSTANT HEAT ABSORPTION

Pressure, psi	Internal tube diameter, in.	Bottom heat absorption			Uniform heat absorption		
		G	X	V_2	G'	X'	V'_2
1400	2 1/2	213	0.055	8.2	181	0.065	7.5
1800	2 7/16	202	0.07	7.7	177	0.08	7.1
2200	2 3/8	185	0.095	7.4	160	0.11	6.7
2600	2 1/4	176	0.14	7.4	145	0.17	6.5
2900	2 9/16	157	0.22	7.3	127	0.27	6.3
3100	2 1/8	138	0.40	7.2	122	0.50	6.8

TABLE 3 CIRCULATION CHARACTERISTICS WITH ONE DOWNCOMER REMOVED; UNIFORM HEAT ABSORPTION AT 2200 PSI

Q	G	X	V_2
28000	90	0.11	3.8
119000	122	0.35	9.1
179000	129	0.50	12.3
382000	138	1.00	22.4

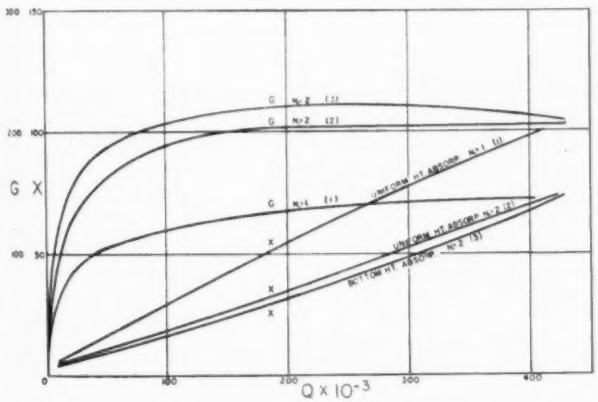


FIG. 6 CURVES SHOWING CIRCULATION CHARACTERISTICS AT 2200 PSI ABS AS FUNCTION OF HEAT ABSORPTION

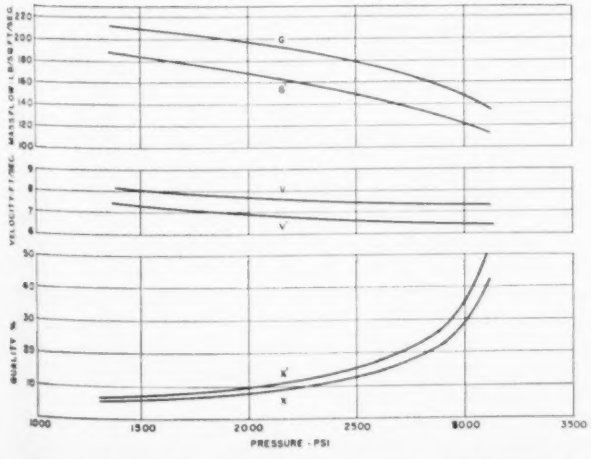


FIG. 7 CURVES SHOWING CIRCULATION CHARACTERISTICS AS PRESSURE VARIES WITH CONSTANT HEAT ABSORPSION

parallel tubes not heated with the same intensity, the analysis becomes intricate. A way to overcome this partially is to consider that, if the riser circuits were connected to a downcomer of low velocity, each circuit would produce an equilibrium quality exactly given by the simple analysis. From this point, by assuming velocities in the downcomers sufficient to produce considerable pressure drop, the qualitative behavior of the less strongly heated circuits can be predicted. In certain cases reversal of circulation or even no circulation is indicated (2, 5). The cause and the cure for such conditions reside in the downcomer part of the circuit. The analysis, however, is straightforward, although beyond the scope of the present paper.

The authors feel assured that if the method here presented will stand the test of discussion and experimental results, the intelligent analysis of natural-circulation problems by the use of models is a possibility.

ACKNOWLEDGMENT

The authors gratefully acknowledge the assistance and encouragement given them by their colleagues in the Research Bureau of their company, especially that of W. F. Davidson, director of research, A. R. Mumford, and T. Larsen. The authors' thanks are also extended to John Blizard.

Appendix 1

MEAN DENSITY IN A UNIFORMLY HEATED TUBE

The cumulative weight of steam generated per unit time up to any point l from the inlet is equal to kl, where k is the rate of heat absorption per foot of tube divided by h_{fg}. The quality of the mixture X is therefore equal to (kl/m) where m is the rate of total flow in the tube. At point l, the specific volume is therefore equal to

$$v_{fg}\,(kl/m) + v_f$$

The density at l is the reciprocal of this.

The weight dw of a unit area of height dl is equal to

$$\frac{dl}{v_{fg}\,(kl/m) + v_f}$$

The integral of this between l and 0 is

$$\frac{1}{(k/m)v_{fg}} \log_e \frac{v_f + (kl/m)v_{fg}}{v_f}$$

Dividing this by the length of the tube, and substituting the quality at the outlet for (kl/m), the mean density d_{22} in the tube in terms of the outlet quality X is

$$d_{22} = \frac{2.3}{Xv_{fg}} \log_{10}\left(\frac{d_1}{d_2}\right)$$

Appendix 2

FRICTION LOSS IN A UNIFORMLY HEATED TUBE

If dp is that part of the pressure drop across a length dl, which is due to friction

$$dp = \frac{4fV^2ddl}{2gD} = C'V^2ddl$$

where V is velocity and d density at point l. This can be integrated if V and d can be put in terms of l. This is readily done

$$V = \frac{V_0\,d_0}{d}$$

where V_0 and d_0 are the entering velocity and density, respectively.

$$dp = C' \frac{V_0^2 d_0^2}{d^2} d\,dl = C'' \frac{dl}{d} = C'' v dl$$

where v is the specific volume at point l. Again

$$v = v_{fg}\,(kl/m) + v_f$$

giving $$dp = \left[C'' v_{fg}\,(kl/m) + v_f\right] dl$$

which integrated between l and 0 gives

$$p = C'' v_{fg}\,(kl^2/2m) + C'' v_f l$$

$$= C'' l \left[\frac{(v_{fg}X) + 2v_f}{2}\right]$$

$$= \frac{4fl}{2gD} \cdot V_0^2 d_0^2 \left[\frac{(Xv_{fg}) + 2v_f}{2}\right]$$

$$= \frac{4fl}{2gD} \cdot V_2^2 d_2^2 \left[\frac{(Xv_{fg}) + 2v_f}{2}\right]$$

in which the bracketed expression is the arithmetic mean of the inlet and outlet specific volume and may be written

$$\left(\frac{1}{d_1} + \frac{1}{d_2}\right) \div 2 = \frac{d_2 + d_1}{2d_1 d_2}$$

$$p = \frac{4fl}{2gD} \cdot V_2^2 d_2 \left(\frac{d_2 + d_1}{2d_1}\right)$$

as a head in terms of d_2 is equal to

$$\frac{4fl}{2gD} V_2^2 \left(\frac{d_2 + d_1}{2d_1}\right)$$

Appendix 3

The ability to predict whether a given circuit, operating at a certain rate of heat absorption, will pass through the circulation maximum is of some interest.

The method of ascertaining this readily will be given for the case of principal absorption at the bottom of the circuit.

By use of the continuity equation we may rewrite Equation [3] in terms of downcomer velocity as

$$V_1 = \frac{C_1(R-1)^{1/2}}{(\beta R^2 + \alpha R)^{1/2}}$$

where

C_1 = constant, involving l, g, etc.

$R = \dfrac{d_1}{d_2}$

α = Σ resistance coefficients of $\dfrac{d_2}{d_1}$ in Equation [3]

β = Σ remainder of resistance term in Equation [3]

A maximum of V_1 results when

$$\frac{dV_1}{dR} = 0$$

After carrying out the necessary differentiation, it is found that V_1 has its maximum when

$$R = 1 + \sqrt{1 + \alpha/\beta} \qquad [7]$$

Two special cases are of interest.

When the downcomer resistance is negligible, the maximum velocity will occur when the density on the heated leg is one half the density of solid water. When the riser resistance is negligible the circuit will burn out before a maximum velocity is reached.

To locate the point of maximum circulation solve Equation [7] for R or $\dfrac{d_1}{d_2}$. This gives X, the exit quality. Having X, solve for the heat absorption by the method of the text.

REFERENCES

1 "Increase in the Output of Large Steam Boiler," by F. Münzinger, Julius Springer, Berlin, 1922.

2 "A Study of Circulation in High-Pressure Boilers and Water-Cooled Furnaces," by John Van Brunt, Trans. A.S.M.E., vol. 63, May, 1941, pp. 339–343; also discussion by E. F. Leib, pp. 344–347.

3 "The Circulation of Water and Steam in Water Tube Boilers," by W. Y. Lewis and S. A. Robertson, Proceedings of The Institution of Mechanical Engineers, Great Britain, vol. 143, 1940, pp. 147–175.

4 "Heat Transmission," by W. H. McAdams, McGraw-Hill Book Company, Inc., New York, N. Y., 1933.

5 "Tests of Marine Boilers," by H. Kreisinger, John Blizard, A. R. Mumford, B. J. Cross, W. R. Argyle, and R. A. Sherman, U. S. Bureau of Mines, Bulletin 214, 1924, pp. 163–168.

6 *Mechanical Engineering*, vol. 61, 1939, p. 322.

Discussion

N. Artsay.[6] My sincere commendation of this excellent paper may be best expressed by the suggestion of several changes which would make the proposed method of wider application. The method is an improvement over the current one in the easy way in which circulation data at various loads of the furnace may be obtained, by plotting quality and other data versus heat absorption and reading the curves back for various loads. However, for a boiler designer who has to do the work of checking circulation against certain criteria, the method must be extended.

(*a*) A coefficient C_1^2, added to the kinetic loss on the steaming side to take into account heavy losses in the fewer riser connections, i.e., side furnace waterwalls, for example.

(*b*) Most of the furnace walls are designed to be supplied from a common downcomer system and, since there is a marked difference in circulation rate per tube, amounting roughly to 25 to 30 per cent between the freely discharging front or rear walls and side walls discharging through a limited number of riser connections, Equation [3] of the paper and its derivatives become inapplicable. The resistance in a practicable downcomer distribution system is quite large and greater by far than the resistance in the wall tubes; hence the amount of water drawn by each waterwall of different size and construction depends substantially upon the total circulation in waterwalls. There are many furnaces in which one of the walls discharges into the lower drum of the unit, complicating the problem yet further. However, it is quite possible to use the method for the several waterwalls as follows:

Allow a set of reduced values l_1 of l to equal the effective height of the circuits and draw curves of V_1 versus heat absorption for every wall; then, according to actual heat absorption, check the valid points of V_1 versus l_1 and draw curves of total water to each wall versus l_1 and the total water of the walls. The intersection of the last curve with the flow in the downcomer system, corresponding to resistance equal to l_1, will give the correct solution for the total flow of circulating water and, knowing l_1, the correct values of circulation.

(*c*) The authors will find that referring all formulation to the inlet velocity into waterwall tubes and to the density of hot

[6] Foster Wheeler Corporation, New York, N. Y.

water will simplify the calculations, and avoid also the unfortunate picture in which the "effective head as the driving force," Equation [2], may be greater than the height of the circuit.

(*d*) The effect of entrainment of steam bubbles in the downcomer system which is quite usual has to be taken into account in a real nonacademic circulation check. With the method offered, it is possible to take this condition into account by reducing the effective circulation head 1 in proportion to water content in the mixture going into downcomers. As a variation a few sets of curves for functions Z and Z_1 with say 3, 5, 10 per cent steam by volume in the downcomers may be prepared.

Looking at the problem of circulation in general, the following is quite noticeable:

The cases, in which the amount of total circulation is insufficient, are extremely few, while the cases of poor distribution of the produced flow are quite frequent. Hence, every effort should be made to ascertain and evaluate the causes of uneven distribution of water between the parallel heated circuits and the effect of uneven distribution of heat absorption between them, which is quite a study in itself.

There is another question of equal importance. Just what is the safe criterion for average circulation in a waterwall and for each tube individually?

E. F. Leib.[6] The problem, as conceived by the authors, is to establish the circulation characteristics of a circuit for which all dimensions and the rate of heat absorption are given, while the problem of circulation usually appears in the following form: The layout of the furnace and the steam output are given; these determine the number, diameter, and length of all tubes in the furnace, the required heat supply, the kind of the individual resistances, and the heat-absorption rate per unit of heating surface. Thus, the only quantities which may still be disposed of are number and diameter of the unheated downcomer tubes. The problem, therefore, consists in determining the two latter quantities.

There are four points which must be considered in solving the problem:

1 The stability of flow in the steaming tube.
2 The steam generation due to self-steaming.
3 The location of the saturation point.
4 The steam flashing due to pressure reduction in the downcomer.

Points 2 and 3 are important for medium- and low-pressure boilers, while point 4 is of interest in forced-circulation boilers particularly. Formulated in this manner, the equilibrium equation for the circulation problem permits a straightforward solution as outlined in the following:

The assumptions are the same as those made by the authors, with their assumption 5 discarded later in this analysis. For the sake of simplicity, it may be assumed that only two different tube diameters occur as follows:

Radius of the m riser tubes and all other connections: R', ft; flow G', lb per sec.

Radius of the n unheated downcomer tubes: R'', ft; flow G'', lb per sec.

Then we have for the total flow in the circuit

$$G = m\,G' = n\,G''$$

which gives

$$G'' = \frac{m}{n}\,G' = \mu\,G' \quad \ldots\ldots\ldots\ldots\ldots\ldots [8]$$

The pressure difference between given points in the circuit consists of the difference in static head ΔP_s and the individual pressure losses, ΔP_L (entrance, acceleration, friction, exit). This pressure difference may be written separately for the two sections of the circuit with tube radius R' and R'', respectively, as follows

$$\Delta P' = \Delta P_s' + \Sigma\,\Delta P_L' \text{ (riser)} \ldots\ldots\ldots\ldots [9]$$

$$\Delta P'' = \Delta P_s'' - \Sigma\,\Delta P_L'' \text{ (downcomer)} \ldots\ldots\ldots [10]$$

The authors have shown how these quantities may be represented by the flow rate, tube radius, tube length (L), heat-absorption rate (Q), and the thermal properties of the steam and water. For these thermal properties we use the symbol θ, comprising any quantity obtainable from the steam tables, such as specific volume and enthalpy of water and steam, or the heat of evaporation. We then write for Equations [9] and [10] of this discussion

$$\Delta P' = f_1(G', R', L, Q, \theta) \ldots\ldots\ldots\ldots [11]$$

$$\Delta P'' = f_2(G'', R'', L, \theta) \ldots\ldots\ldots\ldots [12]$$

The exact determination of the functions f_1 and f_2 has to be done in accordance with the authors' formulas for the individual losses as they occur for the particular circuit under consideration.

Equilibrium requires that

$$\Delta P' = \Delta P''$$

or

$$f_1(G', R', L, Q, \theta) = f_2(G'', R'', L, \theta) \ldots\ldots\ldots [13]$$

It is possible to replace the flow rate by the top-dryness fraction x_0 by means of the relation for the total amount of heat supplied to each tube per unit time

$$Q = G' x_0 h_{fg} \text{ Btu per sec} \ldots\ldots\ldots\ldots [14]$$

We further introduce the diameter ratio

$$s = \frac{R''}{R'} \ldots\ldots\ldots\ldots\ldots\ldots [15]$$

Substituting from Equations [8, 14, 15], Equation [13] can be written

$$f_1(x_0, R', L, Q, \theta) = f_2(\mu, s, x_0, R', L, Q, \theta) \ldots\ldots [16]$$

Exact calculation shows that the function f_2 has the form

$$f_2 = \mu^2\,\frac{C_1 s + C_2(L/R')}{s^5} \times f_3(x_0, R', L, Q, \theta) \ldots\ldots [17]$$

Introducing Equation [17] into [16] and solving for μ^2 yields

$$\mu^2 = \frac{s^5}{C_1 s + C_2 L/R'} \times F_1(x_0, R', L, Q, \theta) \ldots\ldots [18]$$

where F_1 has been written for f_1/f_3, both functions having the same argument. In this equation, the constants C_1 and C_2 and the quantities R', L, Q, θ are given by the design data. As soon as the dryness fraction x_0 is given, Equation [18] gives pairs of values μ, s which all comply with the equilibrium condition of Equation [13]. Then, using Equations [8] and [15], we obtain from Equation [18] co-ordinated values for the radius and the number of downcomer tubes, which give the desired flow condition. The next objective is, therefore, the determination of x_0.

A maximum permissible value of x_0 is obtained from the postulate that the flow in the steaming (riser) tube must be stable. The calculation of stability conditions has been explained in detail by the writer.[7] The procedure is shown for a particular

[6] Combustion Engineering Company, New York, N. Y.

[7] "A Study of Circulation in High-Pressure Boilers and Water-Cooled Furnaces," by John Van Brunt, Trans. A.S.M.E., vol. 63, May, 1941, pp. 339–343; discussion by E. F. Leib, pp. 345–347.

example in Fig. 8 of this discussion. First set up the equation for the pressure through the steaming tube between both headers

$$\Delta P = \Delta P_s \pm \Sigma \Delta P_L$$

The plus sign holds for upward-directed flow (right branch of curve), and the minus sign holds for downward-directed flow (left branch of curve). Both equations can be represented in terms of the following variables

$$\text{Riser } (+ \text{ sign}) \quad \Delta P = f_4(x_0^+, R', L, Q, \theta) \ldots\ldots [19]$$

$$\text{Downcomer } (- \text{ sign}) \quad \Delta P = f_5(x_0^-, R', L, Q, \theta) \ldots\ldots [20]$$

Then find the maximum of the left branch by differentiating Equation [20] with respect to x_0^- and solving for x_0^- (point A). Substitute this value x_0^- into Equation [20] to obtain the pertaining pressure (point B). Substitute this pressure into Equation [19] and solve for x_0^+ to obtain the pertaining dryness fraction and flow rate (point C). Each flow condition to the right of C is stable. We will, therefore, select a value of x_0 slightly smaller than x_0^+ and introduce this value into Equation [18]. Then, all variables in the function F_1 are known.

As the liquid moves upward in the steaming tube, the pressure on the liquid is continuously reduced, partly due to a decrease in static pressure and partly due to pressure loss by friction. Fig. 9 of this discussion shows that, when the pressure decreases, the enthalpy of the saturated liquid decreases, too. Thus, a certain amount of heat is liberated for the generation of steam (change of state I → III in Fig. 9). At medium and lower pressures, this additional steam generation without heat supply, which is referred to as "self-steaming," is appreciable and has to be considered in order to obtain a correct circulation analysis. Consider the increase in steam content dx over the tube length dl. The mean steam content in this tube section is x. Then, the amount of liquid flowing in 1 sec through this section is $G'(1 - x)$. The pressure decreases in the tube section dl by the amount dp. The accompanying decrease in enthalpy is dh' which produces the steam quantity

$$dM_1 = -\frac{(1-x)G'}{h_{fg}}\, dh' \ldots\ldots [21]$$

The simultaneous evaporation due to the heat supply is

$$dM_2 = \frac{Q}{h_{fg}} \frac{dl}{L} \ldots\ldots [22]$$

with L as total tube length and Q the heat supplied over this total length. Thus, the evaporation in the tube section dl is

$$G'dx = dM_1 + dM_2 = \frac{1}{h_{fg}} \left[\frac{Q}{L}\, dl - (1-x)G' \frac{dh'}{dp}\, dp \right] \quad [23]$$

where dh'/dp is the change of enthalpy of saturated water for the pressure change dp and can be taken from the steam tables. Equation [23] can be written

$$dx = \left[\frac{Q}{G'L} - (1-x) \frac{dh'}{dp} \cdot \frac{dp}{dl} \right] \frac{dl}{h_{fg}} \ldots\ldots [24]$$

We have now to find dp/dl, which is the pressure reduction over the tube section dl. The reduction of the static head contributes

$$-dp_s = \frac{dl}{v} = \frac{dl}{v' + x(v'' - v')} = \frac{1}{1 + Bx} \cdot \frac{dl}{v'}$$

and the friction loss contributes

$$-dp_f = \frac{fG'^2}{g\pi^2 R'^5} [v' + x(v'' - v')] dl = \frac{fG'^2 v'}{g\pi^2 R'^5} (1 + Bx)\, dl$$

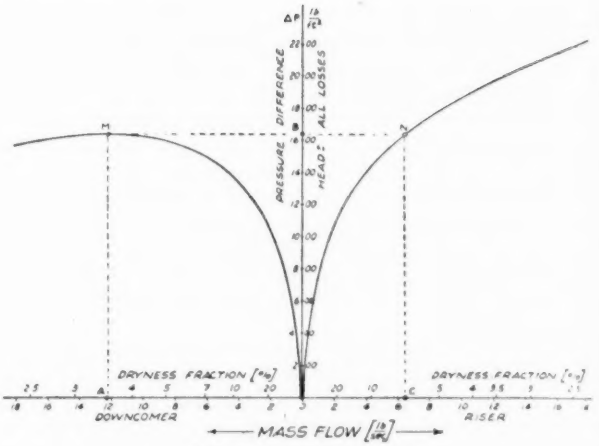


FIG. 8 STABILITY CURVE
(For 1350 psi pressure; 3-in. tube, 50 ft long; 72,000 Btu per sq ft per hr heat absorption.)

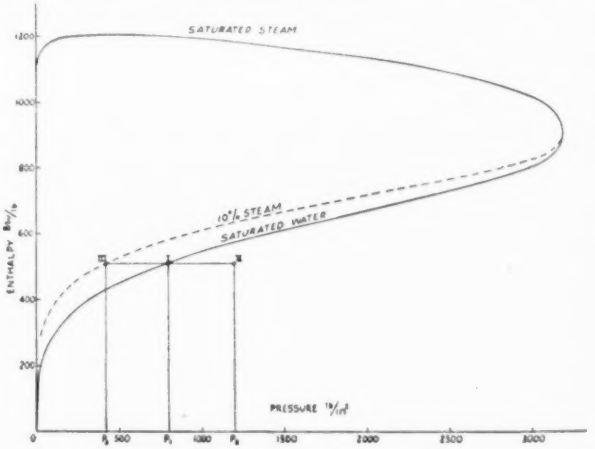


FIG. 9 PRESSURE-ENTHALPY DIAGRAM FOR SATURATED H_2O

where v' = specific volume of saturated water, v'' = specific volume of saturated steam, $B = \dfrac{v'' - v'}{v'}$

By adding dp_s and dp_f, we obtain

$$-\frac{dp}{dl} = \frac{1/v'}{1 + Bx} + \frac{fG'^2 v'}{g\pi^2 R'^5} (1 + Bx) \ldots\ldots [25]$$

By substituting Equation [25] into [24], and by separating the variables, we have the differential equation for the local dryness fraction in the tube

$$\frac{dx}{\dfrac{Q}{G'L} + \dfrac{1-x}{v'} \dfrac{dh'}{dp} \left[\dfrac{1}{1+Bx} + \dfrac{fG'^2 v'^2}{g\pi^2 R'^5} (1 + Bx) \right]} = \frac{1}{h_{fg}}\, dl \quad \ldots\ldots [26]$$

Fig. 10 of this discussion shows the result of the integration of Equation [26] for one particular example. In the two cases shown, the contribution of self-steaming to the total steam generation is 7 per cent and 15 per cent, respectively, an amount which cannot be neglected. Since, as a satisfactory approximation, the total steam generation can be represented by a straight line in Fig. [10] of this discussion, the local dryness fraction can be written as

$$x = \frac{zQ}{G'h_{fg}} \cdot \frac{l}{L} \ldots\ldots [27]$$

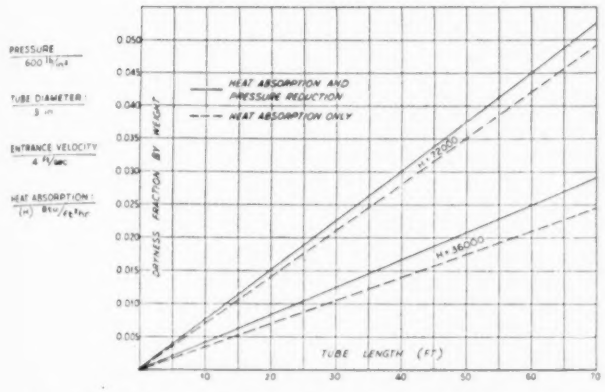


FIG. 10 EFFECT OF PRESSURE DROP ON STEAM GENERATION

where the value of $z > 1$ is found by integrating Equation [26]. Thus, the quantity of steam actually generated equals that which is obtained if the heat zQ instead of the heat Q were supplied to the tube.

The pressure drop through the tube is obtained by substituting z from Equation [27] into Equation [25] and integrating. The result is

$$\Delta P = \frac{G'h_{fg}L}{zQBv'} \ln\left(1 + \frac{zQB}{G'h_{fg}L}\, l\right) + \frac{fG'^2v'}{g\pi^2R'^5} l \times \left(1 + \frac{zQB}{G'h_{fg}L} \cdot \frac{l}{2}\right) \quad [28]$$

Thus, the pressure drop for a tube with self-steaming equals the pressure drop through a tube without self-steaming to which the heat zQ is supplied instead of Q.

In a circuit like that used for illustration by the authors, the steam-water mixture enters the drum from the end of the steaming tube. The feedwater entering the drum is then at saturation condition corresponding to this pressure. Since the evaporation in the steaming tube starts at a higher pressure, a corresponding amount of sensible heat must be supplied to the feedwater in order to bring it to the saturation condition pertaining to this pressure. Thus, a portion of the heating surface is needed to supply this heat, and the saturation point is not at the bottom of the tube. Of the total tube length L, the portion L'' is available for steam generation, while the portion $(L - L'')$ serves to supply the sensible heat to the water. The pressure drop through the steaming portion is obtained by substituting L'' for l into Equation [28]; then

$$\Delta P = \frac{G'h_{fg}L}{zQBv'} \ln\left(1 + \frac{zQB}{G'h_{fg}} \cdot \frac{L''}{L}\right) + \frac{fG'^2v'L''}{g\pi^2R'^5} \left(1 + \frac{zQB}{2G'h_{fg}} \cdot \frac{L''}{L}\right) \quad [29]$$

The sensible heat to be supplied to the feedwater to reach saturation condition at a pressure which surmounts the entrance pressure by ΔP is

$$Q' = G' \frac{dh'}{dp}\, \Delta P \quad [30]$$

For uniform heat absorption holds

$$Q' = Q\, \frac{L - L''}{L} \quad [31]$$

Equating Equations [30] and [31] and solving for ΔP gives

$$\Delta P = \frac{Q}{G'} \cdot \frac{dp}{dh'} \cdot \frac{L - L''}{L} \quad [32]$$

By equating Equations [29] and [32] an equation for the unknown quantity L'' is found. Solving for L'' gives the correct location of the saturation point. At medium and lower pressures, the portion of tube needed to supply the sensible heat is considerable. The pressure-drop calculation in Equation [11] must be carried out with the correct values for those portions of the steaming tube containing the solid water and the steam-water mixture, since the friction loss is very different for both portions. Therefore, the authors' assumption 5 is inaccurate for medium and lower pressures, and their diagrams can be used in this region only with caution.

Finally, the question arises whether a second relationship between the variables μ, s occurring in Equation [18] could be established, such that a single-valued solution for these two variables might be found. Such a relationship can be derived from the postulate that, in case of a sudden increase in load, a maximum of pressure reduction shall be permitted in the system without resulting in steam flashing in the unheated downcomer tubes. Since this condition is exclusively used in the determination of downcomer tubes for forced-circulation boilers, it may only be mentioned here.

W. H. ROWAND.[8] The authors' first assumption that all the steam is made at the bottom of the rising circuit, and the use of the density of the mixture leaving the circuit as the average density, and their second assumption that the average density is the log mean are simplifications for calculation work over the use of some other evaluated average density. While this results in circulating flows which are higher than will actually obtain, the error is not too great so long as the per cent steam by volume leaving the circuit is relatively low, and so long as the velocity of the mixture is high, compared with the relative velocity between the steam and the water. When limiting cases are being considered, however, it is important to evaluate the average density in such a way that it will agree closely with that obtained from actual test data in the field.

It is believed that the term, "per cent steam by volume" leaving a circuit, is a better yardstick for judging the safety of a tube from overheating than steam quality or per cent steam by weight, since it presents a physical picture of the degree to which the tube is being wetted regardless of the pressure.

The authors have reduced the differential head and all friction losses to feet of water corresponding to the density leaving the heated tube. While this procedure is satisfactory for a single simple circuit, it is impractical for multiple circuits where each circuit must not only be balanced within itself but also must be balanced with all the other circuits in the system; this being the usual case in most practical analysis work. It is suggested that a more practical reference base is 62.4-density water.

Table 4 of this discussion gives a comparison between a circulation test conducted recently by the writer's company on an open-pass-type boiler, operating at 1350 psi pressure, and the first method of calculation presented by the authors using the density leaving the circuit as the average density, modified to make it applicable to the many interconnected circuits, and also the method of calculation used by the writer's company for several years. In general, the authors' method results in more optimistic circulation than was actually obtained, and the company's method gives somewhat less circulation that the test results,

[8] Mechanical Engineer, The Babcock & Wilcox Company, New York, N. Y. Jun. A.S.M.E.

TABLE 4 COMPARISON OF CIRCULATION TEST BY B & W WITH AUTHORS' FIRST METHOD OF CALCULATION

Circuit	Steam flow	Test results			Authors' method using B. & W. method of balancing			B. & W. Co. method		
		Circulation	Mixture steam ratio	Steam by volume, per cent	Circulation	Mixture steam ratio	Steam by volume, per cent	Circulation	Mixture steam ratio	Steam by volume, per cent
A	109,800	1,738,000	15.8	48.5	1,610,000	14.7	49.3	1,118,000	10.2	59.0
B	102,800	1,610,000	15.7	48.5	1,988,000	19.4	42.5	1,376,000	13.4	51.7
C	50,000	1,220,000	24.4	36.5	1,657,000	33.1	29.1	1,105,000	22.1	38.2
D	27,300	568,000	20.8	40.5	860,000	31.5	30.5	563,000	20.6	41.0
E	18,600	354,400	19.1	42.5	434,000	23.3	38.0	283,000	15.2	49.0
F	33,500	308,400	9.2	62.0	440,000	13.1	52.3	248,000	7.4	67.2
G	64,800	956,000	14.8	49.3	1,104,000	17.0	45.4	928,000	14.3	50.0
H	17,600	355,000	20.2	41.0	361,000	20.5	40.3	258,000	14.6	49.4
I	78,400	1,210,000	15.4	48.0	1,320,000	16.8	45.6	816,000	10.4	58.3
J	77,700	621,000	8.0	65.5	699,000	9.0	62.5	400,000	5.2	77.0
K	68,200	544,000	8.0	65.5	636,000	9.3	62.0	358,000	5.8	74.5
Total and Average	648,700	9,484,800	14.6	50.0	11,109,000	17.1	46.0	7,453,000	11.5	55.0

which is on the conservative side. The total calculated circulation by the authors' method is 17 per cent above the actual test results, while, by the company's method, it is 20 per cent below.

Authors' Closure

The authors feel that there have not been many papers presented before this Society in which the discussion has done more to enhance the value of the original presentation than in the present instance. On the whole, criticism of the paper itself is minor.

Messrs. Rowand and Artsay believe that the choice of reference densities in terms of the mixture leaving the circuit was unhappy. We are inclined to agree with this reaction, since the choice of reference density is merely a matter of convenience. Having absorbed the principles, which somehow seem better illustrated by the use of exit conditions, there is no great difficulty in changing to a reference density of cold water or, what amounts to the same thing, in working directly with pressure drop. Artsay points out that where there is considerable loss in junction headers the kinetic losses are greater than in the illustrative example. This is easily taken care of by including these losses in the resistance tabulation. His suggestion for taking care of steam in the downcomers by constructing new Z curves is good as an educational exercise. Practically, we know now by experience that steam must be kept out of the downcomers if we are to have good boilers.

The remainder of Artsay's discussion is much to the point although we do not agree with his remark that the use of effective heads, which may be greater than the linear height of the circuit, is unfortunate. The concept of a head in terms of a homogeneous column of fluid is the first simple relationship which must be acquired before even the simplest hydraulic problems can be tackled away from a handbook.

The discussion by Lieb, which deals with the effect of flashing, due to sudden pressure drop on a boiler, is interesting. While clothed with a considerable (to the authors) mathematical treatment, the information presented will be valuable to students of the subject. His criticism of the authors' assumption of constant friction factor is good, and, fortunately, the authors can throw additional light on this subject before concluding.

It is to Rowand that we are most indebted. The paper as presented lacked experimental data to indicate to the engineer, who is interested in the application of novel methods of analysis, the amount of confidence that might be placed in them. Rowand shows in his comparison of actual measurements on a 1350-lb boiler with the calculated results that methods, such as the authors', or modifications thereof, are more than mere exercises. This, however, has been known for some time by a few of the boiler manufacturers. The authors wish to state that the publication of important and previously unpublished experimental results as a discussion of the work of others is a laudable act.

Until the Sherman Creek experiments on heat transfer and friction drop in tubes, in which water was boiling at high pressure, were concluded, we could do no more than assume constant friction factors for such analyses. The use of the data obtained in those experiments will bear out Rowand's contention that such methods fall progressively in error as the percentage of evaporation increases. These data will be published soon in the Transactions and will accommodate Rowand's criticism quantitatively. They will also show that "per cent steam by volume" presents no fundamentally clear technical concept of tube safety.

As to the proper density of the mixture to assume in an actual boiler for the purpose of useful calculations, it now appears from Rowand's comparison that the use of the logarithmic-mean density, with friction factors as indicated by the Sherman Creek data, may be expected to give results worthy of a better designation than mere estimates.

Turbines for Power Generation From Industrial-Process Gases

By JOHN GOLDSBURY[1] AND J. R. HENDERSON,[2] LYNN, MASS.

This paper presents a discussion of the fields of application for turbines operated by industrial-process gases and natural gases, examples of the mechanical details of actual turbines which have been built for such applications, a simple method for calculating the energy available in a pure or a compound gas for specific operating conditions, and the properties of various gases for use in such calculations. After a study of the available data on gas properties, the authors have selected for the working curves those which were considered to be most authentic.

Nomenclature

The following nomenclature is used in this paper:

- a = fractional part by volume (of a component in a mixture)
- b = fractional part by weight (of a component in a mixture)
- c_p = constant-pressure specific heat, Btu per deg F per lb
- c_v = constant-volume specific heat, Btu per deg F per lb
- E = available energy of isentropic expansion or compression, Btu per lb
- e = turbine efficiency, dimensionless
- k = exponent of isentropic expansion or compression
- M = molecular weight of a pure gas or equivalent molecular weight of a gas mixture
- m = molecular weight of a component in a gas mixture
- p = pressure, psi abs
- Q = gas flow, cfm at 60 F and 14.7 psi abs (i.e., free gas)
- R = gas constant = pv/T
- T = temperature, deg F abs, or deg Rankine
- v = specific volume, cu ft per lb
- $(\ )_0$ refers to condition of gas at zero pressure
- $(\ )_1$ refers to condition of gas before expansion or compression
- $(\ )_2$ refers to condition of gas after expansion or compression
- $(\ )_c$ refers to condition of gas at critical point
- $(\ )_m$ refers to mean value between $(\ )_1$ and $(\ )_2$

Field of Usefulness for Industrial-Process-Gas Turbines

Many modern industrial processes involve the production or use of gases or vapors under pressure. It is apparent that certain desirable reactions take place more effectively under pressures above atmosphere. In some cases, the gain in the quality or quantity of the product seems to be well worth the cost of air or gas compression. In the case of natural gas, the compression, as well as the gas itself, is contributed by nature. In any case, when a continuous flow of gas is available under pressure above atmosphere, it will be well to consider whether advantage cannot be derived from expanding the gas through an elastic-fluid turbine.

This term "elastic-fluid turbine" is used to denote the general class of turbines which are operated by the expansion of any gas or vapor. The general features are the same as those of the steam turbine, but the dimensions, materials, and design details will be determined by the particular elastic fluid used, as well as by the pressures and temperatures involved.

Not only may it be found that the use of a turbine will improve some established processes or increase the economy of operation, but the possible advantages of a turbine may turn the balance in favor of new processes being considered.

In some cases, certain difficulties may arise, such as corrosiveness of the gas, presence of liquid, gummy, or solid particles carried by the gas, or arising from physical or chemical changes, etc. If, however, the advantage of using the gas in a turbine is great, ways of overcoming these difficulties can frequently be found.

In general, the justification for a turbine would be the power which it could produce, but an increasing number of processes are being considered in which the advantage of the turbine is the reduction in gas temperature due to the energy absorbed by the turbine. At least one such application has been made and several others have been considered.

Application in Petroleum-Refining Processes

The most important development so far in the use of turbines, driven by industrial-process gases other than steam, is found in connection with certain catalytic petroleum-refining processes. In these processes carbon is deposited on the catalyst. The carbon must be burned off and the catalyst regenerated at frequent intervals. In several of these processes, it is apparently most effective and economical to burn off the carbon under pressure. In some cases, the pressure is as high as 300 psi, and much higher pressures have been proposed. Several catalyst retorts are frequently used so that one or more can be undergoing the regeneration processes continuously. The maximum regeneration temperature is controlled either by tubes through which a coolant is passed, or by recirculation of some of the products of combustion which have passed through a waste-heat boiler, or by other suitable means. There is, then, a steady flow of these products of combustion or flue gas which is of no further use to the process.

The heat could, of course, be partially recovered in a waste-heat boiler or other type of heat exchanger, but the pressure potential would be largely wasted. The pressure potential can be utilized and a large portion of the heat removed by passing the gas through a turbine.

Fig. 1 shows a 3500-hp flue-gas turbine on the test floor. A cross-sectional view through this turbine is shown in Fig. 2. The following description indicates some of the problems which must be considered in connection with such turbines.

With some grades of process charge, sulphur will be deposited on the catalyst. This will appear as SO_2 in the flue gas. In order to avoid corrosion from this, as well as from any other possible corrosive component in the gas, it was decided to make the

---

[1] Turbine Engineering Department, General Electric Company. Mem. A.S.M.E.

[2] Turbine Engineering Department, General Electric Company. Jun. A.S.M.E.

[3] In several cases the subscripts $(\ )_1$, $(\ )_2$, etc., are used to indicate individual values for the several components of a compound gas. In these cases this is stated in the text.

Contributed by the Power Division and presented at the Fall Meeting, Louisville, Ky., October 12–15, 1941, of The American Society of Mechanical Engineers.

Note: Statements and opinions advanced in papers are to be understood as individual expressions of their authors and not those of the Society.

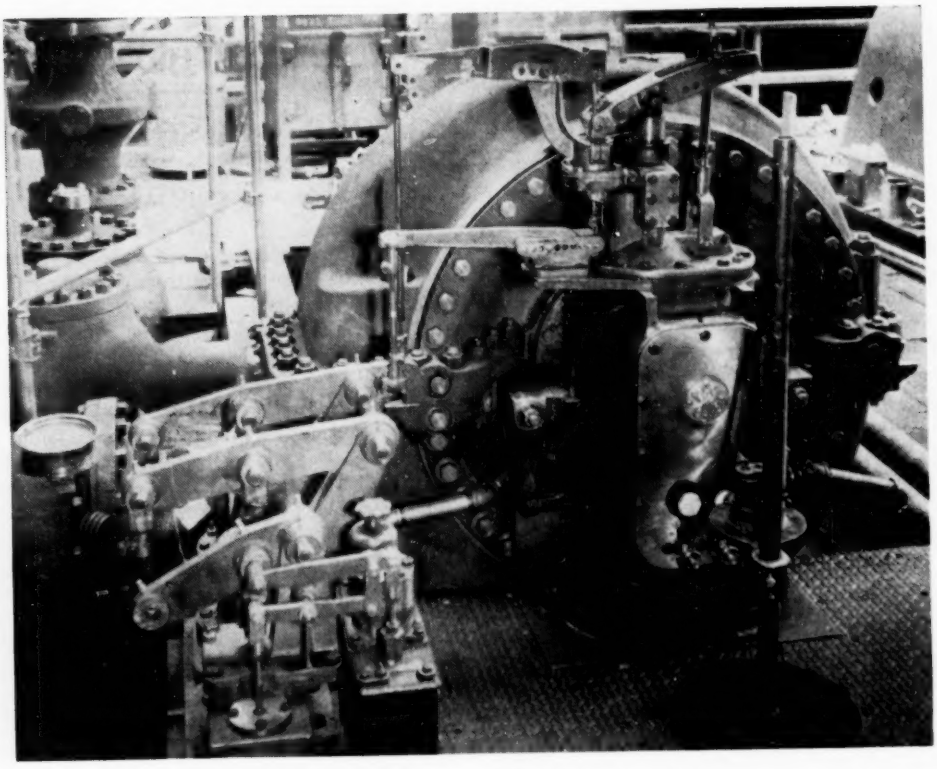


FIG. 1 FLUE-GAS TURBINE OF 3500 HP ON TEST FLOOR

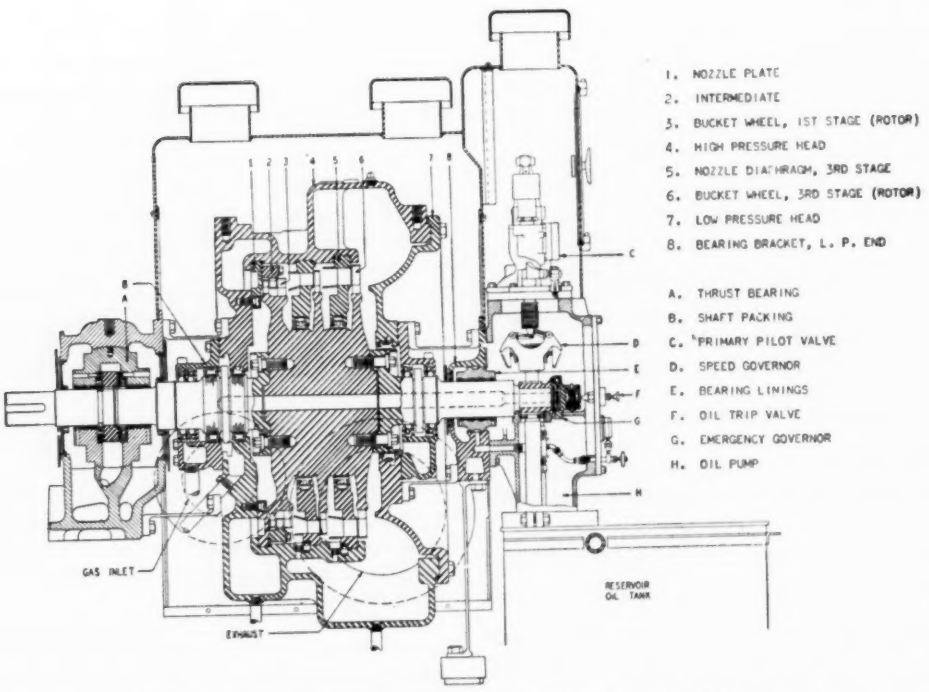


FIG. 2 CROSS-SECTIONAL VIEW THROUGH 3500-HP FLUE-GAS TURBINE

rotor, buckets, nozzles, and some other parts of this particular turbine of a high grade of stainless steel, while a low-alloy steel was used for the casing parts. Valve trim was of stellite, interior packings were of a special cast iron, and outer shaft packings of carbon. Recent tests have indicated that less expensive and more easily workable materials will probably be suitable for many of the parts when the corrosive components of the gas are only SO_2 and water.

As further protection against corrosion it is planned in so far as possible to operate the turbine only at exhaust temperatures well above the condensation points of any acids likely to be present in the gas. When the turbine is to be shut down for any extended period, hot dry air or neutral gas will be blown through the casing, packing glands, valves, etc., to purge out all traces of the gas, and precautions will be taken to prevent any gas from leaking into the turbine during such periods.

Although no solid materials in appreciable quantities are expected to be entrained with the gas, provision has been made for the admission of air to the shaft-packing glands, if that is necessary to prevent such material from settling in the packings. Space has been provided for assembly of special interstage packings which can also be sealed with air if experience indicates the need.

Because of the large coefficient of thermal expansion of the stainless-steel rotor, it was necessary to use particular care in designing packing and other clearances to prevent any possibility of rubbing, even under large and rapid changes in load or operating conditions. In general, the turbine was designed for simplicity and ruggedness rather than highest efficiency. The first of the three stages is velocity-compounded with two rotating bucket rows and with circular nozzle ports. Maximum turbine efficiency, together, doubtless, with other refinements contributing to plant economy, can come later, when the experience necessary for determining the best over-all arrangement is available.

Fig. 3 shows the control arrangement for this turbine. The mechanism is such that speed can be held constant at any set value within the setting range of the governor, in this particular case, from 2800 to 4000 rpm. The speed governor *a* controls a single admission valve *b* through an oil operating cylinder, not shown. In order to assist the speed governor in holding constant speed in spite of large variations in gas-main pressure, a constant-pressure governor *c* is used to control the pressure ahead of the speed-governing valve. The pressure governor controls a valve *d* which by-passes excess gas around the turbine. Fluid-restoring links, not shown in the diagram, permit very close net speed and pressure regulation, combined with instantaneous regulation which is broad enough to be stable.

This particular turbine was designed to be installed out of doors, and the sheet-metal lagging, oil-tank cover, etc., were consequently made weatherproof.

Details of 885-Hp Flue-Gas Turbine

In Fig. 4 is shown the control diagram for another flue-gas turbine of 885 hp capacity. In this case, a 1460-hp steam turbine is coupled to the same shaft for starting and for supplementing the gas-turbine power.

Referring to the diagram, it will be seen that both turbine admission valves, *b* and *d*, are controlled by one speed governor *a*, through oil relays. The linkage is arranged in such a manner that the gas-turbine valve *d* opens first, the steam-turbine valve *b* then opening to whatever extent is necessary to make up the difference between the load required and the power which can be obtained from the gas turbine under the particular conditions considered. The steam valve has an overtravel in the closed position, so that it does not lift above its seat until the gas valve is nearly wide open.

Although there is only one speed governor, a separate emergency overspeed governor is provided on each turbine, to prevent runaway of either turbine in case of loss of its load. The emergency governor *f* on the gas turbine will dump the oil pressure from the gas-admission-valve cylinder *e* only, while the emergency governor *g* on the steam turbine will dump the oil pressure from both the gas *e* and steam *c* admission-valve cylinders, to cover the case of complete loss of load on the compressor.

The governing mechanism also includes a device, not shown in Fig. 4, to admit a small steam flow to the steam turbine to carry away the heat resulting from windage of the buckets, rotating idly while the compressor is being driven by the gas turbine. Steam is also supplied to the shaft seals of the gas turbine, to prevent leakage of gas.

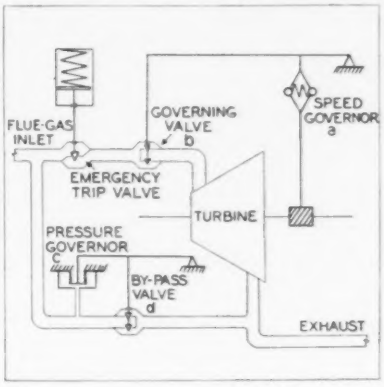


Fig. 3 Control Diagram for 3500-Hp Flue-Gas Turbine

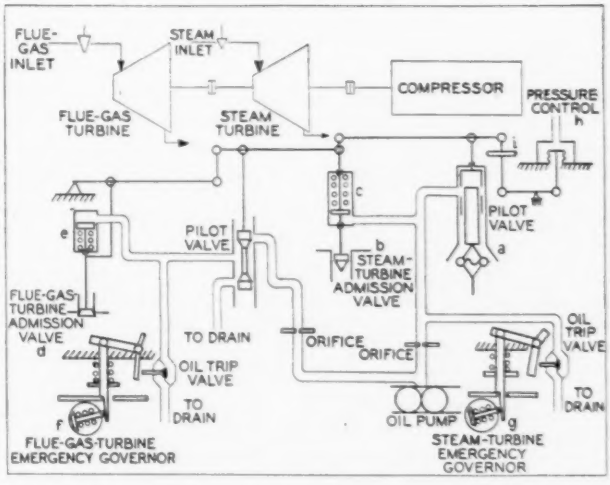


Fig. 4 Governing Mechanism for Dual-Drive Flue-Gas Turbine and Steam-Turbine Compressor Set

The speed setting of the governor *a* can be regulated either automatically by the pressure control *h* or manually by the handwheel *i*.

Natural-Gas Industry Offers Possibilities for Turbines

Another large potential field for power from expansion of gas through turbines is the natural-gas industry. It has been calculated that the total work which might theoretically be thus extracted from the annual production of natural gas in the United

States is of the order of 1,750,000,000 kwhr.[3] Numerous very small turbines of standard steam designs are being operated by natural gas and used to drive pumps and other apparatus. However, there are undoubtedly many cases where no power is derived from expansion of the gas, but where the pressure drop from the well to the point of use is much greater than is really needed to overcome friction losses in pipes of reasonable size.

In the repressuring process of liquid extraction from natural gas, well pressures run from 1500 to 3000 or more psi, while the pressure in the absorption tower is usually from 1000 to 1500 psi. Since the amount of liquid extracted increases with decrease in temperature, any power extracted by passing the gas through a turbine would contribute also to the yield. The turbine could be designed to separate out a large portion of the liquid from the gas by centrifugal force, and might thereby replace one or more of the extraction devices normally used. Taking a case where 50,000,000 cu ft of free gas per day are processed with a gas-main pressure of 2000 psi, dropping down to 1000 psi at the absorption towers, if we assume a temperature of 100 F at the main and a net pressure ratio of 1.8 for the turbine after allowing for pipe losses, the net power obtainable will be approximately 650 hp.

There are, of course, other processes than those mentioned in which gases are expanded through turbines, but it would seem probable that very much more can profitably be done along these lines.

Methods of Deriving Turbine Output

In order to determine in any particular case whether it will be profitable to expand a gas through a turbine, a calculation or estimate must be made of the power obtainable. The nomograph in Fig. 5 can be used for rough work to obtain quickly approximate outputs from given quantities of gases at various temperatures and pressure ratios. A formulation has been introduced whereby turbine efficiency is included on a basis which gives approximately the correct characteristic with respect to size, but of necessity many variables cannot be evaluated in such a chart. The reduced size of the chart, because of space restrictions, in itself precludes accurate results, but for very rough approximations it may be found useful.

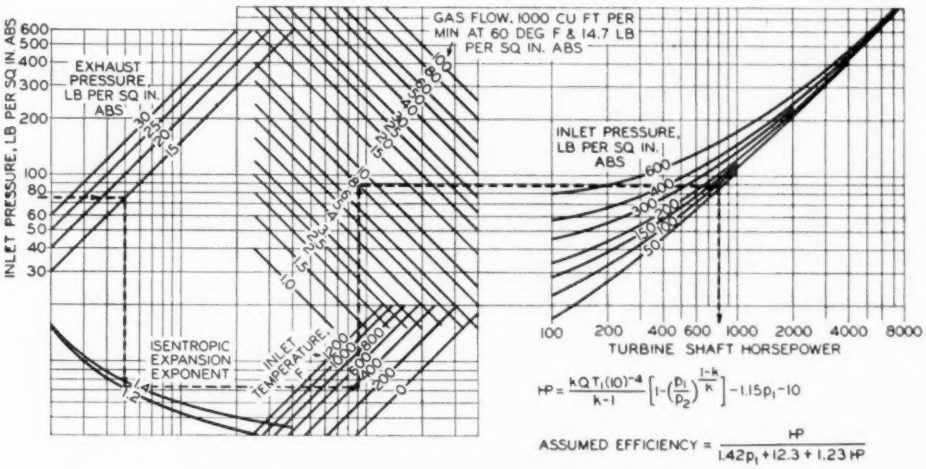


Fig. 5 Approximate Gas-Turbine Performance

An example of the derivation of turbine output by the use of the nomograph in Fig. 5 is given in the appendix. For comparison the same example is also worked out by the method to be described.

For more accurate determinations something must be known of the properties of the gas and suitable methods must be used to calculate the available expansion energy. Although much work has been done on measurement of the thermodynamic properties of the common gases, the reports of many of these measurements are scattered through the literature. A great amount of work is necessary to assemble these data and to convert the various quantities to common English units. For the convenience of engineers who wish to use these properties, the p-v-T relationships of several common gases are given herewith. In general, the complete range of temperatures for which data were found is given, and, in several cases, extrapolations have been made by means of the Beattie-Bridgman[4] equation of state or by other means.

The range of pressures for which data were given was usually more than adequate for normal use. These p-v-T relations are presented on charts which are necessarily of restricted size, but determinations from them will be accurate enough for most purposes.

Problems Entailed by Low Gas Temperatures and Fire Hazard

The temperature of natural hydrocarbon gas, as it issues from the wells, is very low compared with that of combustion gases. It is frequently less than 120 F. When such gas is expanded through a turbine, the temperature at the turbine outlet may be below freezing. This not only requires the use of materials which retain their ductility and strength at such low temperatures, but also introduces a possible difficulty from ice formation. If considered advisable, moisture, hydrates, and even carbon dioxide can be removed from the gas before it enters the turbine.

In one natural-gas application, where turbines were used to drive electric generators, special precautions were taken to avoid danger from ignition of gas which might leak from the packings. One of these precautions was the use of a fire wall between the turbine and the generator. Another was the use of beryllium copper for the trigger of the emergency overspeed governor in order to prevent sparks when the emergency governor bolt strikes the trigger. An explosion-proof speed-synchronizing control motor is also used.

[3] Based on 1939 production of 2,435,000,000,000 cu ft; *World Almanac*, 1941.

[4] Extrapolations of some of the p-v-T data which follow have been made by means of the Beattie-Bridgman formula as given in Bibliography reference (11).

Power Outputs for Superheated-Gas Expansions

A method for obtaining quite accurately turbine inputs or theoretical power outputs for superheated-gas expansions will be described. This method has been found very convenient for such calculations. For a pure gas, the accuracy of the results depends chiefly upon the accuracy of the available data on the properties of the gas, and upon the accuracy of the secondary data, derived from the basic data. In calculations with superheated steam through a very wide range of initial pressures, initial temperatures, and pressure ratios, the inaccuracies due to the approximations of the method itself are seldom as great as 0.5 per cent when compared on the basis of available energy per pound with those derived directly from the Keenan and Keyes tables (1).[5] Since both the basic and derived steam properties are also taken from these tables and from the accompanying curves, the comparison was between two methods of deriving available energies from these properties.

The method being described is based on the assumption that, if the initial specific volume can be found, and if a suitable mean value of isentropic exponent can be obtained, the available energy from the expansion of 1 lb of any gas from given initial pressure and temperature to a given final pressure can be determined from the formula

$$E = \frac{144}{778} p_1 v_1 \frac{k}{k-1}\left[1 - \left(\frac{p_1}{p_2}\right)^{\frac{1-k}{k}}\right] \quad \ldots\ldots\ldots [1]$$

where E = available energy, Btu per lb of gas
p_1 = initial pressure, psi abs
p_2 = final pressure, psi abs
v_1 = initial specific volume, cu ft per lb
k = mean isentropic-expansion exponent

If the gas flow is given in cubic feet per minute of free gas, (60 F, 14.7 psi abs) the turbine output in horsepower is

$$\frac{Q \times 60 \times M \times E \times e}{2545 \times 380} = 6.2(10)^{-5} QMEe \quad \ldots\ldots [2]$$

where Q = gas flow
M = molecular weight
e = turbine efficiency, which must be assumed or obtained from the manufacturers

For a perfect gas, k is constant throughout the expansion, and the formula is exact. Also, for a perfect gas, $p_1 v_1 = RT_1$. With temperature T_1, in degrees Rankine or Fahrenheit absolute, and p and v in the units given, $R = \frac{10.72}{M}$. With all actual gases pv/T is not constant. Curves of pv/T plotted against temperature at different pressures are shown in Figs. 6 to 14, inclusive, for several common gases. References are given in the Bibliography to the sources of the data for each chart.

Curves of $E/(p_1v_1)$ plotted against p_1/p_2 for various values of k are shown in Fig. 15. These curves may also be used for determining the energy of isentropic compression by using the curves above $k = 1$. In this case Equation [1] becomes

$$E = \frac{144}{778} p_1 v_1 \frac{k}{k-1}\left[\left(\frac{p_2}{p_1}\right)^{\frac{k-1}{k}} - 1\right] \quad \ldots\ldots\ldots [1a]$$

Enlarged curves for greater accuracy can readily be prepared from calculations using Equations [1] and [1a]. Plotting $E/(p_1v_1)$ against k for constant values of p_1/p_2 facilitates accurate interpolation, but many curves are required.

Curves of k versus T for constant values of p are shown in Figs. 16 to 18, inclusive, for three gases. The zero-pressure curves are calculated from the new values of c_{p0} derived from spectroscopic investigations. The formula used for k_0 was

$$k_0 = \frac{c_{p0}}{c_{p0} - \frac{1.985}{M}} = \frac{c_{p0}}{c_{v0}} \quad \ldots\ldots\ldots [3]$$

Values of k at pressures other than zero were derived from the formula

$$k = -\frac{v}{p}\left(\frac{\partial p}{\partial v}\right)_T \frac{c_p}{c_v} \quad \ldots\ldots\ldots [4]$$

where

$$c_p = c_{p0} - \int T\left(\frac{\partial^2 v}{\partial T^2}\right)_p dp \quad \ldots\ldots\ldots [5]$$

and

$$c_v = c_p + T\frac{(\partial v/\partial T)_p^2}{(\partial v/\partial p)_T} \quad \ldots\ldots\ldots [6]$$

Calculations of k using this formula are quite laborious. The derivatives were obtained by taking the ratios of differences at small intervals. The consistency of these differences was improved by taking second differences, and drawing smooth curves through them, then calculating new primary differences from the smoothed second differences. Fortunately, except at large pressure ratios, the energy per pound of gas is not sensitive to the magnitude of k, within the normal range. For this reason, it is often sufficiently accurate to use k_0 with no allowance for the pressure effect. This is particularly true for components of a gas mixture the partial pressures of which are low. Curves of k_0 plotted against T for several gases are shown in Fig. 19.

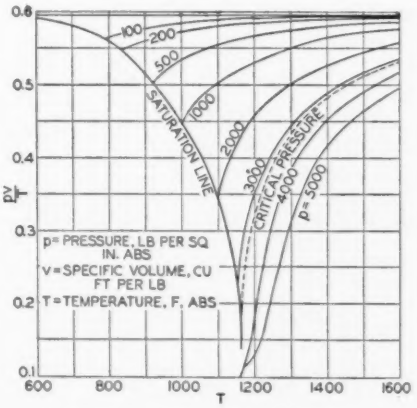


Fig. 6 pv/T for Steam (H_2O)
(Refer to Bibliography 1.)

Selecting Mean Isentropic-Expansion Exponent k

It is often possible to select, by inspection from the curves, a value of mean k which is sufficiently accurate for ordinary requirements. Where greater accuracy is required, the following method will help:

Consider first the case of a gas for which only curves of k_0 against temperature are available. The end temperature T_2

[5] Numbers in parentheses refer to the Bibliography at the end of the paper. References 1 to 12, inclusive, deal with p-v-T data; references 13 to 17, inclusive, deal with specific heats at zero pressure, as used in calculating isentropic-expansion exponents at zero pressure.

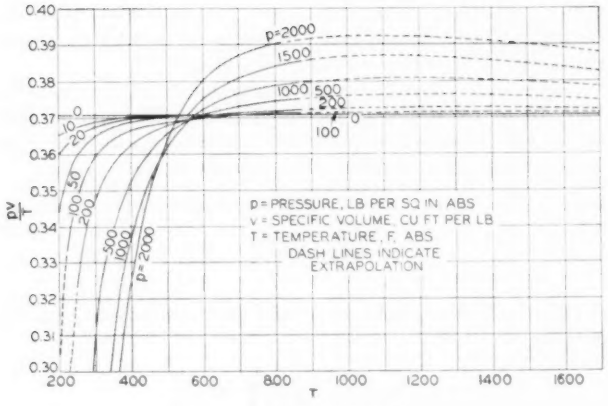


FIG. 7 pv/T FOR DRY AIR
(Refer to Bibliography 2.)

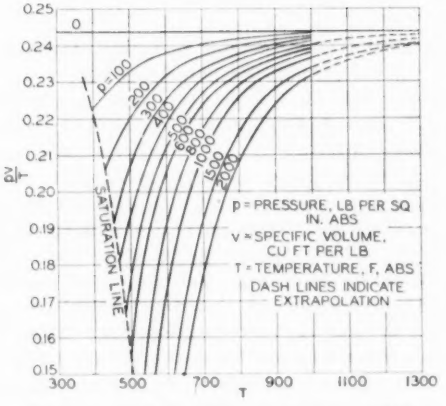


FIG. 10 pv/T FOR CARBON DIOXIDE (CO_2)
(Refer to Bibliography 5.)

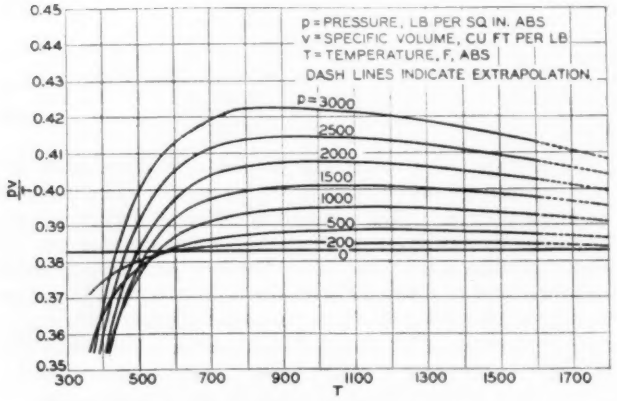


FIG. 8 pv/T FOR NITROGEN (N_2)
(Refer to Bibliography 3.)

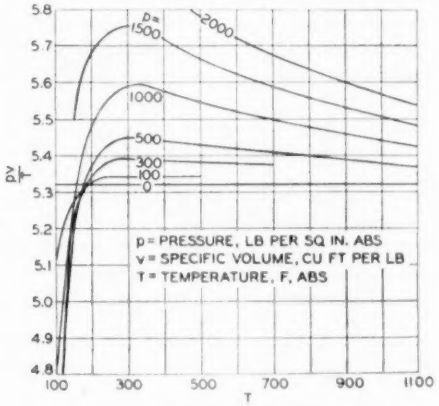


FIG. 11 pv/T FOR HYDROGEN (H_2)
(Refer to Bibliography 6.)

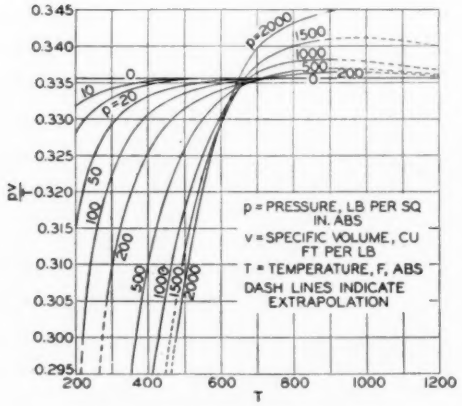


FIG. 9 pv/T FOR OXYGEN (O_2)
(Refer to Bibliography 4.)

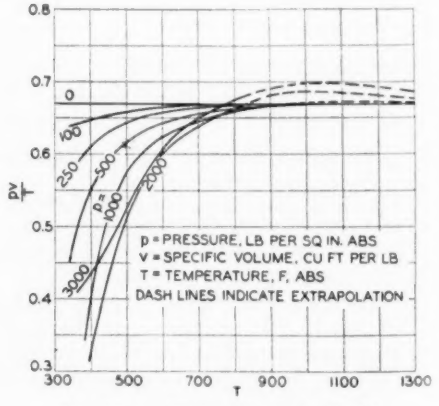


FIG. 12 pv/T FOR METHANE (CH_4)
(Refer to Bibliography 7.)

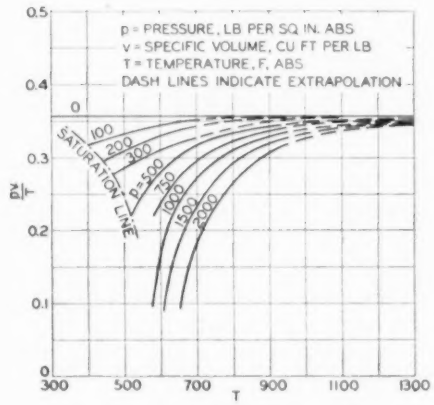


FIG. 13 pv/T FOR ETHANE (C_2H_6)
(Refer to Bibliography 8.)

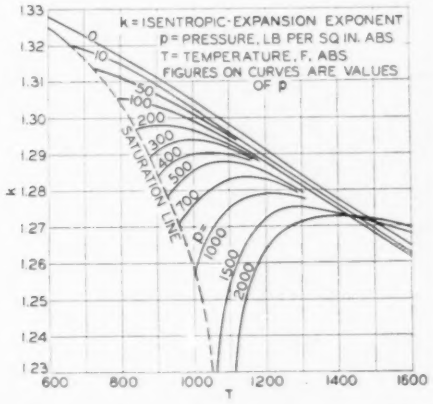


FIG. 16 ISENTROPIC-EXPANSION EXPONENT FOR STEAM (H_2O)

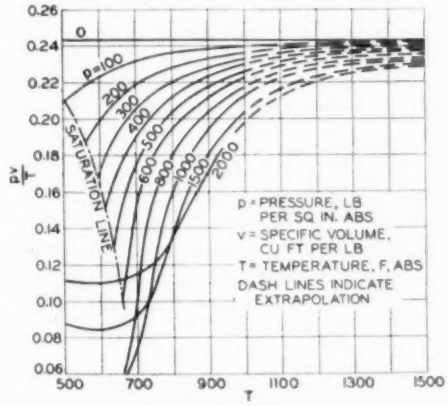


FIG. 14 pv/T FOR PROPANE (C_3H_8)
(Refer to Bibliography 9.)

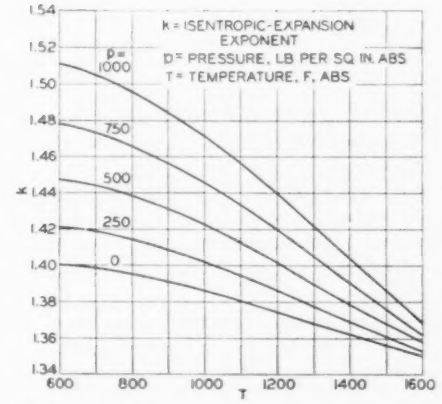


FIG. 17 ISENTROPIC-EXPANSION EXPONENT FOR NITROGEN (N_2)

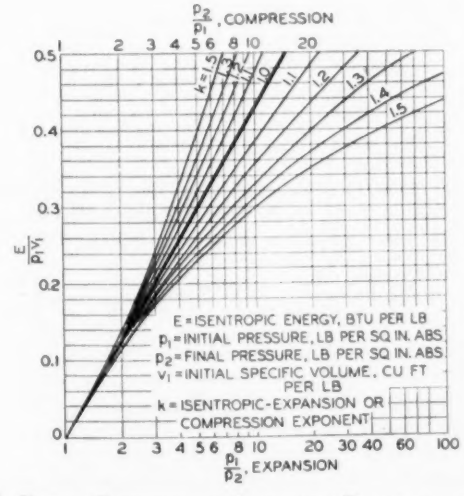


FIG. 15 ENERGY FUNCTION FOR ISENTROPIC EXPANSION AND COMPRESSION

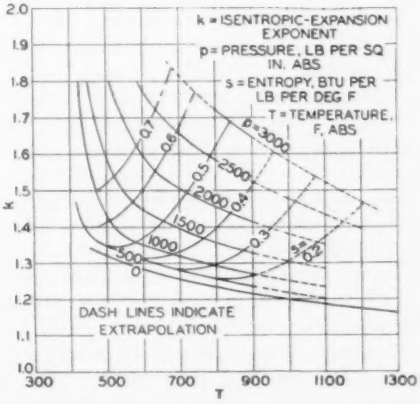


FIG. 18 ISENTROPIC-EXPANSION EXPONENT FOR METHANE (CH_4)

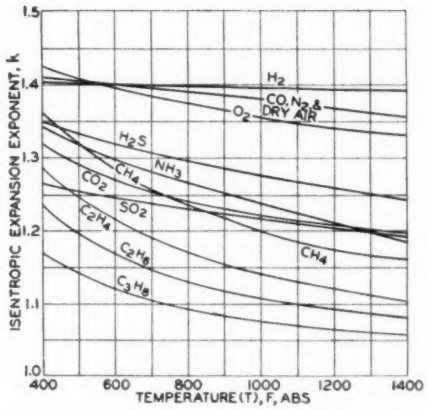


FIG. 19 ISENTROPIC-EXPANSION EXPONENT FOR VARIOUS GASES AT ZERO PRESSURE

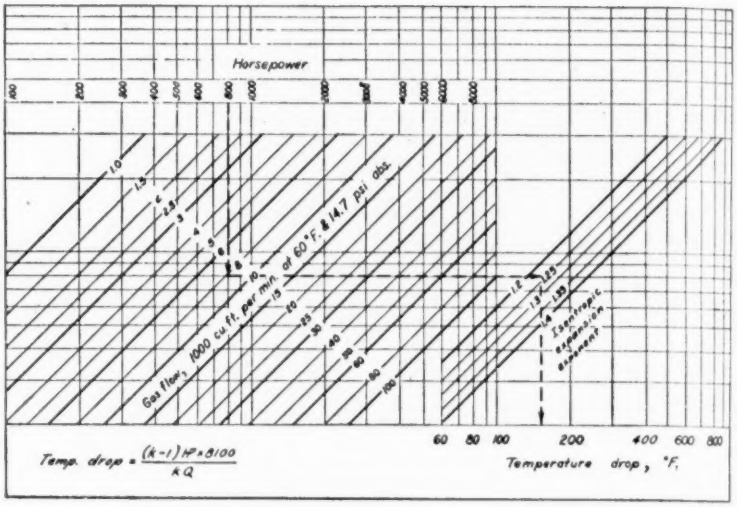


FIG. 20 GAS-TEMPERATURE DROP THROUGH TURBINE

for isentropic expansion can be calculated, using an assumed value of mean k from the formula

$$T_2 = T_1 \left(\frac{p_1}{p_2}\right)^{\frac{1-k}{k}} \quad \ldots\ldots\ldots\ldots\ldots\ldots [7]$$

A mean value of k between T_1 and T_2 can then be determined. Usually it is sufficiently accurate to use the value of k at the mean temperature $(T_1 + T_2)/2$.

If curves of k are available for a sufficient range of both temperature and pressure, calculate T_2 by Equation [7]. If the temperature drop is small, it will be sufficiently accurate to use $k_m = (k_1 + k_2)/2$, where k_1 is read from the curves at p_1 and T_1, and k_2 at p_2 and T_2.

Since the path of isentropic expansion on the $(k - T)$ plane may not be a straight line, it will be well, in the case of large pressure ratios, to divide the temperature drop into two or more approximately equal parts. The end pressure for each successive expansion can be determined from the formula

$$p_2 = p_1 \left(\frac{T_1}{T_2}\right)^{\frac{k}{1-k}} \quad \ldots\ldots\ldots\ldots\ldots\ldots [8]$$

the subscripts in this case referring to the beginning and end points of the partial expansions. A mean value of k can then be determined for each partial expansion and these averaged to obtain an over-all k_m.

If it is found that the assumed value of k_m used in Equation [7] is too far off from the final value, the process must be repeated.

In the case of gas mixtures the accuracy of this method will depend also upon the accuracy of the method used for obtaining the combined properties, as well as on the time which can be given to deriving curves of combined properties. Combined values of pv/T based on Amagat's law are usually more reliable at high pressure than those based on Dalton's law. Combined values of pv/T for many of the hydrocarbon gases and some others can be obtained with good accuracy from charts of generalized properties, based on reduced pressures and temperatures and on pseudo critical pressures and temperatures. This method was developed by W. B. Kay (10), and is described by Hougen and Watson (11). This book contains a great deal of useful information on gases and gas mixtures. What is probably a yet more accurate, but rather laborious method, also described by Hougen and Watson, was developed by Prof. E. R. Gilliland (12) of the Massachusetts Institute of Technology.

Assuming Amagat's law to hold, an assumption which is sufficiently accurate for most work at any but very high pressures, combined values of pv/T can be readily obtained from the formula

$$\text{Combined } \frac{pv}{T} = \frac{p_1 v_1}{T_1} b_1 + \frac{p_2 v_2}{T_2} b_2 + \ldots\ldots\ldots [9]$$

The subscripts 1, 2, etc., here refer to the individual values for the several component gases taken at the same pressure and temperature that are being considered for the mixture. Terms b_1, b_2, etc. are the fractional parts by weight of the component gases.

A method of obtaining values of combined k, which is justified by the perfect-gas laws, has been proposed by Allen Keller.[6] It is doubtful whether the effective error, due to the use of this method with actual gases is of appreciable magnitude except at extremely high pressures. No more suitable method is known to the authors. In this method

$$\text{Combined } k = \frac{\sum \frac{ak}{k-1}}{\sum \frac{a}{k-1}} \quad \ldots\ldots\ldots\ldots [10]$$

in which a is the fractional part by volume of a component.

Changes from fractional parts by weights to fractional parts by volume and vice versa can be made by means of the formulas

$$a = \frac{bM}{m}, \quad b = \frac{am}{M}, \quad M = \Sigma(am), \quad \frac{1}{M} = \Sigma\left(\frac{b}{m}\right)$$

If many energy calculations will be required for a given gas mixture, it will be well to compute values of combined pv/T and k over sufficiently wide ranges and plot curves. This will be found much simpler than working up a Mollier chart for the gas on a scale which will give corresponding accuracy.

The approximate temperature drop from turbine inlet to exhaust can be obtained from the nomograph in Fig. 20, when the horsepower, corresponding to a given volume flow and isentropic-expansion exponent, is known.

Although the calculation method just described is derived for theoretical power outputs of superheated gases, experience with steam and mercury indicates that the supersaturation effect will

[6] Mechanical Engineer, General Electric Company, Lynn, Mass.

TABLE 1 DATA FOR VARIOUS GASES FROM SMITHSONIAN TABLES, 1933

Gas	Formula	Molecular weight, M	Boiling temp at 14.7 psi abs, deg Rankine	Critical pressure, psi abs	Critical temp, (T_c), deg Rankine	Theoretical $\frac{p_2/T = R}{\frac{10.72}{M}}$
Air	...	28.97	....	547.0	238.5	0.3701
Ammonia	NH_3	17.03	431.3	1639.0	730.0	0.6295
Argon	A	39.93	157.5	706.0	272.2	0.2687
Carbon dioxide	CO_2	44.00	347.4	1073.0	548.0	0.2437
Carbon monoxide	CO	28.00	149.6	514.6	241.7	0.3829
Chlorine	Cl_2	70.91	429.3	1185.0	750.8	0.1512
Ethane	C_2H_6	30.05	332.9	717.5	550.0	0.3568
Ethylene	C_2H_4	28.03	305.0	748.2	509.0	0.3825
Helium	He	4.00	7.7	33.5	9.54	2.681
Hydrogen	H_2	2.016	36.7	188.2	59.96	5.319
Hydrogen chloride	HCl	36.47	342.1	1199.0	584.5	0.2939
Hydrogen sulphide	H_2S	34.08	379.6	1307.0	673.3	0.3147
Methane	CH_4	16.03	201.0	673.5	343.2	0.6690
Mercury	Hg	200.61	1134.0	....	....	0.0535
Neon	Ne	20.18	49.1	382.0	80.1	0.5320
Nitric oxide	NO	30.01	216.4	956.0	322.8	0.3572
Nitrogen	N_2	28.02	138.9	492.0	226.8	0.3826
Nitrous oxide	N_2O	44.02	330.1	1054.0	557.4	0.2435
Oxygen	O_2	32.00	162.4	730.8	277.8	0.3350
Propane	C_3H_8	44.06	411.7	632.2	663.7	0.2435
Sulphur dioxide	SO_2	64.06	474.1	1143.0	774.6	0.1674
Water	H_2O	18.02	671.6	3206.2	1164.5	0.5948

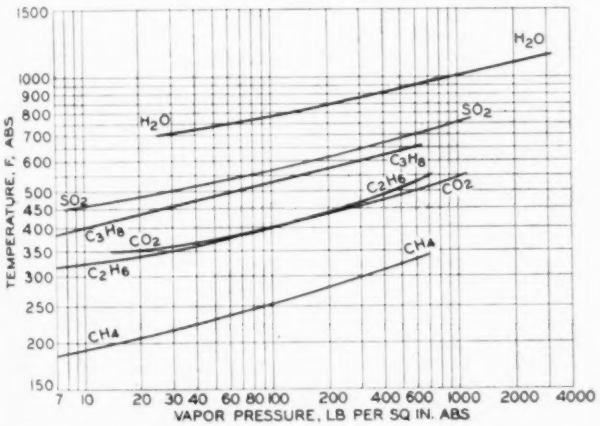


FIG. 21 VAPOR PRESSURE-TEMPERATURE CHARACTERISTICS FOR VARIOUS GASES

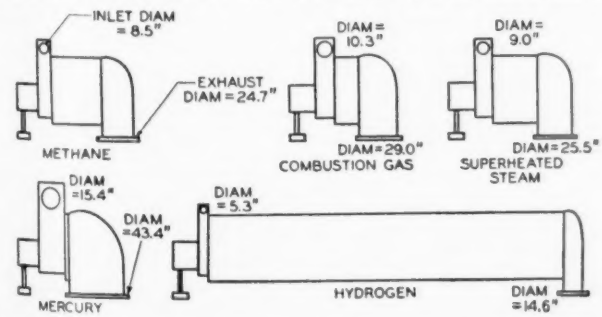


FIG. 22 COMPARISON OF TURBINES OPERATED BY VARIOUS GASES (3500 hp; inlet, 170 psi gage, 1000 F; back pressure, 5 psi gage.)

prevent any serious inaccuracy in using it for calculating turbine outputs for expansions down to approximately one half of the pressure at which the isentropic expansion crosses the saturation line or the dew line, in the case of a compound gas. The turbine efficiency used should be that based on complete superheated-gas expansion. Exhaust temperatures, determined from Fig. 20, may however be incorrect in such cases. Vapor-pressure curves for several gases are given in Fig. 21.

Fig. 22, showing the comparative physical sizes of turbines operated by several gases, may be of some interest. The turbine operated by mercury is assumed to have one expansion stage. The numbers of expansion stages for the other turbines are in proportion to the available energies of their gases, as compared to the available energy for the mercury. The relative number of stages is indicated by the turbine-barrel length, as compared with that of the mercury turbine. The comparative inlet and exhaust sizes, worked out on a consistent basis, are also shown in Fig. 22.

Certain useful data on various gases are given in Table 1.

SUMMARY

1 It is probable that many engineers, who are associated with or considering processes in which gases are available under pressure, will welcome a simple and accurate method of estimating the power output which can be obtained from a flow of gas expanding in a turbine between given pressures. Such a method is given in this paper.

2 Certain processes may be improved or operated more economically by the installation of turbines to derive power from the expansion of gases whose energy might otherwise be wasted or inefficiently used.

3 In some cases, the reduction in temperature resulting from expansion through a turbine may be more important than the power obtained.

4 By expanding gases through turbines rather than wastefully through valves and small pipe lines, power can often be derived which will replace power derived from the burning of fuel, and thus help to conserve our fuel resources.

Appendix

EXAMPLE OF DERIVATION OF TURBINE SHAFT HORSEPOWER

Gas composition by volume (molecular fraction)

Methane	0.8211
Ethane	0.0753
Propane	0.0426
Nitrogen	0.0140
Carbon dioxide	0.0470
	1.0000

Initial pressure, 75 psi abs
Final pressure, 15 psi abs
Initial temperature, 340 F
Gas flow, 8000 cfm at 60 F and 14.7 psi abs

(*a*) *Derivation of Output From Fig. 5.* From the k_0 curves in Fig. 19, select by inspection an approximate mean value of

isentropic exponent. The relative portions of the various component gases and the locations of the curves indicate that k_m for the combined gas will fall slightly below the curve for methane. As a mean temperature, we may take 100 less than the initial temperature. Since the k_0 curves are plotted against absolute temperature, the mean temperature will be 340 — 100 + 460 = 700 R. It would appear then that a value of 1.24 for mean k is approximately correct.

This example is shown plotted in Fig. 5, the dash lines and arrows indicating the path to be followed in working out a solution with this nomograph. The operating conditions chosen for the example, together with the efficiency assumed in the nomograph, give a turbine shaft horsepower of approximately 800.

(*b*) *Derivation of Output From Properties of Component Gases, the Perfect-Gas Energy Formula, and an Assumed Turbine Efficiency.*

Component	Volume fraction or molecular fraction a	Molecular weight m	am	Weight fraction $b = am/M$
Methane	0.8211	16.03	13.15	0.666
Ethane	0.0753	30.05	2.26	0.114
Propane	0.0426	44.06	1.88	0.095
Nitrogen	0.0140	28.02	0.39	0.020
Carbon dioxide	0.0470	44.00	2.07	0.105
		M =	19.75	1.000

Assume $k_m = 1.24$ as in example (*a*). From Equation [7]

$$T_2 = 800\left(\frac{75}{15}\right)^{-0.1935} = \frac{800}{1.365} = 586 \text{ F abs}$$

$$Tm = \frac{800 + 586}{2} = 693 \text{ F abs}$$

Values of k_m for the component gases are read from the curves in Fig. 19, at 693 R, and values of pv/T from Figs. 12, 13, 14, 8, and 10, at 75 psi abs and 800 F abs.

Component	k_m	$\frac{a}{k_m - 1}$	$\frac{a\,k_m}{k_m - 1}$	$\frac{p_1v_1}{T_1}$	$\frac{b \times p_1v_1}{T_1}$
Methane	1.26	3.156	3.977	0.669	0.445
Ethane	1.15	0.502	0.578	0.355	0.041
Propane	1.11	0.387	0.430	0.238	0.023
Nitrogen	1.395	0.035	0.049	0.384	0.008
Carbon dioxide	1.255	0.184	0.231	0.243	0.025
		4.264	5.265		0.542

$$\text{Combined } k_m = \frac{5.265}{4.264} = 1.235$$

$$\text{In Fig. 15, at } k = 1.235 \text{ and } \frac{p_1}{p_2} = 5, \frac{E}{p_1v_1} = 0.258$$

$$\text{Combined } \frac{p_1v_1}{T_1} = 0.542$$

$$E = 0.258 \times 0.542 \times 800 = 111.8 \text{ Btu per lb}$$

The gas flow is 8000 cfm at 60 F (520 F abs) and 14.7 psi abs

$$v = \frac{380}{M} = \frac{380}{19.75} = 19.23$$

$$\text{Weight flow} = \frac{8000 \times 60}{19.23} = 24{,}960 \text{ lb per hr}$$

$$\text{Theoretical horsepower} = \frac{24{,}960 \times 111.8}{2545} = 1096$$

Assuming a turbine efficiency of 0.725, the turbine shaft horsepower is 795.

BIBLIOGRAPHY

1 Steam: "Thermodynamic Properties of Steam," by J. H. Keenan and F. G. Keyes, John Wiley & Sons, Inc., New York, N. Y., 1936.

2 Air: "International Critical Tables," vol. 3, pp. 9–10, McGraw-Hill Book Company, Inc., New York, N. Y., 1928; references are given to articles by Amagat, Penning, Witkowski, Holborn and Otto.

3 Nitrogen: "Smithsonian Physical Tables," eighth edition, Smithsonian Institution, Washington, D. C., 1933, p. 146; references are given to articles by Bartlett and collaborators.

Nitrogen: "International Critical Tables," vol. 3, pp. 17–19; references are given to articles by Bartlett, Holborn and Otto, Kamerlingh, Onnes and Urk.

4 Oxygen: "International Critical Tables," vol. 3, pp. 8–9; references are given to articles by Holborn and Otto, Kuypers and Onnes, Nijhoff and Keeson.

5 Carbon Dioxide: "International Critical Tables," vol. 3, pp. 11–12; references are given to articles by Amagat.

6 Hydrogen: "International Critical Tables," vol. 3, pp. 4–6; references are given to articles by Holborn, Holborn and Otto, Verschoyle, Onnes and Penning, Crommelin and Swallow, Witkowski, Bartlett, Bartlett, Cupples and Tremearne.

7 Methane: "The Compressibility Isotherms of Methane at Pressures to 1000 Atmospheres and at Temperatures From —70 to 200," by H. M. Kvalnes and V. L. Gaddy, *Journal of the American Chemical Society*, vol. 53, 1931, pp. 394–399.

8 Ethane: "Compressibility of, and an Equation of State for, Gaseous Ethane," by J. A. Beattie, C. Hadlock, and N. Poffenberger, *Journal of Chemical Physics*, vol. 3, 1935, pp. 93–96.

9 Propane: "P-V-T Relations for Propane," by W. W. Deschner and G. G. Brown, *Industrial and Engineering Chemistry*, vol. 32, 1940, pp. 836–840.

10 "The Density of Hydrocarbon Gases and Vapors at High Temperature and Pressure," by W. B. Kay, *Industrial and Engineering Chemistry*, vol. 28, 1936, pp. 1014–1019.

11 "Industrial Chemical Calculations," by Hougen and Watson, second edition, John Wiley & Sons, Inc., New York, N. Y.

12 "P-V-T Relations of Gaseous Mixtures," by E. R. Gilliland, *Industrial and Engineering Chemistry*, vol. 28, 1936, pp. 212–215.

13 Steam, Nitrogen, Oxygen, Carbon Dioxide, Hydrogen, Carbon Monoxide: "The New Specific Heats," by R. C. H. Heck, *Mechanical Engineering*, vol. 62, 1940, pp. 9–12.

14 Air: "The New Specific Heats, Addenda to and Discussion of Paper by R. C. H. Heck," *Mechanical Engineering*, vol. 63, 1941, p. 126.

15 Methane, Ethane: "Empirical Specific Heat Equations Based Upon Spectroscopic Data," by R. L. Sweigert and M. W. Beardsley, Bulletin No. 2 of the Georgia School of Technology, 1938. Engineering Experiment Station.

16 Propane: Calculated from a generalized equation for hydrocarbon gases, "Empirical Specific Heat Equations Based Upon Spectroscopic Data," by Edminster, given in Bulletin No. 2 of the Georgia School of Technology.

17 Hydrogen Sulphide, Sulphur Dioxide: "Empirical Molecular Heat Equations From Spectroscopic Data," by W. M. D. Bryant, *Industrial and Engineering Chemistry*, vol. 25, 1933, pp. 820–822.

Discussion

D. J. BERGMAN.[7] From the viewpoint of the turbine manufacturer this presentation gives valuable information for establishing the power available from gas or vapor under pressure in industrial plants.

This subject is especially interesting, at the present time, to the oil refiner. For a number of years the refining industry has been improving the efficiency of its processes. In recent years, gas formerly burned in field torches has been processed in newly developed plants for the production not only of motor fuel but aviation fuel and chemicals as well. This has reduced the refiner's available fuel supply.

[7] Engineering and Development Department, Universal Oil Products Company, Chicago, Ill. Mem. A.S.M.E.

A further reduction has come about through elimination in large part of acid-treating and improvement of residual fuels to the point where there is practically no unsalable fuel product produced in a refinery. This has changed the refiner's fuel picture from one of disposal of a product for its nuisance value to that of the need for rigid economy in minimizing the use in the refinery of otherwise salable products. In line with the increasing trend toward fuel economy has been the installation of superheaters, steam generators, and the use of exhaust steam from other services in low-pressure turbines.

Under present conditions with the government's call for tripling the aviation-fuel capacity in this country, yet greater reduction in refinery-gas supply must result, and direct generation of power will be one answer to the problem.

Application of a turbine directly in a refining process, using gas or vapor, involves a number of considerations which do not occur in connection with generating power by steam. Aside from the very different thermodynamic properties of the material there are problems due to corrosion, dust, high temperatures, refrigeration of gas, formation of hydrates, and the hazards involved in using combustible materials.

Natural gas has been used as a motive power for driving pumps in many instances, particularly in connection with the natural-gasoline industry. However, leakage past stuffing boxes has been rather a serious matter and at least one bad refinery fire has occurred as a result. Where leakage of steam would be of no consequence whatever, careful thought must be given to the possible effects of leakage of combustible gas, and provisions for ventilation or sealing fluids must be made to cut down the hazards. In many cases, special alloys will be required because of the corrosive properties.

P. V. Keyser, Jr.[8] The authors have presented a method of estimating the energy available in gases under pressure for deriving power by the use of suitable expansion turbines. The work is of considerable engineering value for future developments in this field. In addition, the authors suggest specific applications for equipment of this type in process industries.

In this connection some comments regarding the use of gas turbines in catalytic cracking may be of interest. In our domestic refineries we now have nine gas-operated turbines, generating a total of more than 25,000 hp, and several more are under construction.

These turbines are used on Houdry catalytic cracking units. Their purpose is to drive the 2500-hp compressors which provide compressed air for burning deposits from the catalyst. The gas turbines are driven by the compressed air after it has served its purpose in the catalyst cases.

There is some pressure drop through the catalyst cases, but the temperature of the air increases during the burning operation so that enough power is usually derived from the regeneration gases to compress the air. It can be seen that a considerable saving in power is realized in this operation by the use of gas turbines.

The regeneration gases used to drive the turbines vary considerably in composition, being rich in CO_2 and poor in O_2 at the start of regeneration, and poor in CO_2 and rich in O_2 at the end of regeneration. The average composition is approximately as follows:

	Per cent
Water vapor	8
Carbon Dioxide	10
Oxygen	7
Nitrogen	75
	100

[8] Technical Service Division, Socony-Vacuum Oil Company, Brooklyn, N. Y.

Some of these turbines have been in operation for more than 2 years and have given remarkably little trouble, considering the high rotational speeds at which they operate.

As for other possible uses for gas turbines, the petroleum-refining industry offers many applications where power could be derived from high-pressure gases. The disadvantage in most cases is that the power produced must be used by the unit producing it, because the source of power will be eliminated when the unit is shut down for cleaning out or inspection.

If, for instance, the power is used to generate electricity for use at the refinery, there must be some other source of power during shutdowns of the unit producing the power. Demand charges of public-utility companies, or auxiliary-equipment costs, will often seriously reduce the savings made by use of the turbines.

One other problem in using gas turbines at oil refineries, even when the power is used at the unit producing the power, is that outside power must be used in many cases, when starting up the unit.

For the turbocompressors at the Houdry units, a burner is placed in the compressed-air line, so that the air can be heated even though no deposits are being burned. Also, a steam turbine or electric motor is connected to the system for use in starting. No doubt, similar solutions could be found for problems in connection with other applications of gas turbines in oil refineries.

The potential savings possible by using gas turbines in oil refineries are large. The principal reason why such installations have not been made in the past was doubt as to their reliability. The losses which would be suffered if a large cracking unit had to be shut down, because of a gas-turbine failure, would outweigh any savings which could be made by using the turbine. Now that gas turbines have been proved reliable, we believe that such installations will be made in increasing numbers in the future.

The paper under discussion should be of considerable value to engineers analyzing the operation of existing gas turbines and considering the economics of proposed installations.

Authors' Closure

The fact, mentioned by Dr. Bergman, that the oil refiner is now concerned with the generation of by-product power rather than the useful disposition of waste heat is a condition which is now more or less common to all thermodynamic processes, in which efficiency and economy are of first importance.

Dr. Bergman has also pointed out some of the special problems, such as corrosion, dirt, and inflammability, which will be encountered with certain gases. These problems must, of course, be anticipated in the design of the turbine. The hydrogen-cooled generator furnishes an example of what may be done to avoid explosion hazards.

The temperature of gases used in turbines will frequently be high. In recent years a wealth of operating experience has been accumulated with steam, mercury vapor, and combustion gases at temperatures between 900 and 1000 F. Some experience also has been obtained with combustion gases at still higher temperatures.

While the thermodynamic properties of a gas will have an important effect on the design of the turbine, designs can be made for efficient utilization of the expansion energy of almost any gas through wide ranges of flow, temperature, pressure, and pressure drop without exceeding the limits of stress and rotational speed encountered with steam turbines.

Mr. Keyser has brought out the very important point that in some turbine applications none of the normal operating gas will be available for starting. In some cases it may be practical to pass steam through the gas turbine to start it, then gradually change to operation with gas.

The authors have observed that nearly all engineering problems could be solved if economic considerations were neglected. Obviously economic considerations cannot be neglected, so the state of progress of gas turbines has been determined by the economics of gas processes into which the turbines fit. It is entirely possible that in the period immediately following the present emergency, the need for fuel economy will require the development of many new sources of power, and at that time further development of gas turbines and gas processes will be economically practical.

The Application of the Girbotol Process to Industry

By B. D. STORRS,[1] and R. M. REED[1]

Details of the Girbotol process for the removal and recovery of acid gases, such as hydrogen sulphide and carbon dioxide, with amine solutions are outlined in this paper, and its many applications to industry are described. These fields include: Purification of natural and refinery gases; removal of carbon dioxide from raw hydrogen and hydrogen-nitrogen mixtures; carbon-dioxide and hydrogen-sulphide recovery; and the production of inert atmospheres.

IN 1928, the necessity of finding an economical means of removing large percentages of carbon dioxide from helium-bearing natural gas led to the discovery of the Girbotol process. This is a simple cyclic process for scrubbing and recovering acid gases from gaseous mixtures. Gases are scrubbed with solutions of organic bases (amines) to remove acid gases such as hydrogen sulphide and carbon dioxide. The absorbed acid gases are then separated from the amine solutions by heating which reactivates the solutions for further use. This reactivation is made possible by the fact that amine salts of weak acids dissociate at moderately elevated temperatures so that the amines may be separated from acid gases which they have absorbed at lower temperatures. The process has become well established and has proved to be an efficient and economical method for separating hydrogen sulphide or carbon dioxide from natural, refinery, and other gases, as well as from the combustion products of various fuels. The purpose of this paper is to acquaint those not intimately associated with natural-gas or petroleum technology, or chemical manufacture, with the many and varied applications of this process, which is finding an increasing field of usefulness in industry.

The Girbotol Cycle

Fig. 1 shows a typical flow diagram of the process. The equipment consists of an absorber tower in which the gas is scrubbed by amine solution to remove hydrogen sulphide or carbon dioxide therefrom, a reactivator tower in which hydrogen sulphide or carbon dioxide is boiled out of the amine solution to reactivate it for further use, and the necessary heat exchangers and pumps for handling the solution. Raw gas, containing hydrogen sulphide or carbon dioxide, flows into the base of the absorber which is a bubble plate or packed tower. Lean amine solution enters the absorber near its top and flows in countercurrent relation to the rising gas, absorbing hydrogen sulphide or carbon dioxide in its downward passage. Purified gas leaves from the top of the absorber.

Rich amine solution, containing the removed acid gas, flows by absorber pressure or is pumped from the base of the absorber through the heat exchanger and thence into the upper section of the reactivator.

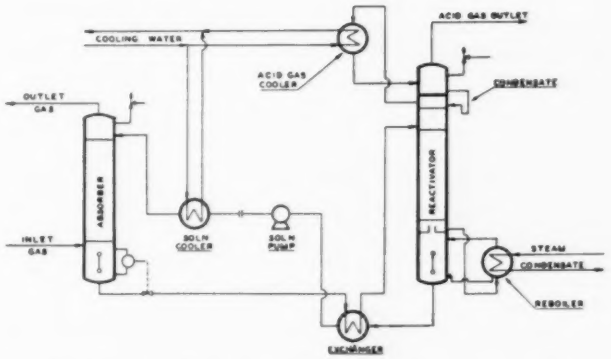


FIG. 1 FLOW DIAGRAM FOR TYPICAL GIRBOTOL PROCESS
(Patented.)

The reactivator is also a bubble plate or packed tower. In or near its base there is a reboiler which is an indirect-heating element supplied with low-pressure steam, or other suitable hot medium, for boiling the amine solution and expelling the acid gas. As the solution flows down the reactivator it is heated by ascending steam generated in the reboiler, and the hydrogen sulphide or carbon dioxide is expelled from the solution. In the reboiler, the solution reaches its boiling point which is usually slightly above the boiling point of water.

Reactivated amine solution flows through the heat exchanger and is then pumped through the solution cooler back to the top of the absorber.

Hydrogen sulphide or carbon dioxide and steam flow together from the top of the reactivator to the acid-gas cooler, where the temperature of the mixture is reduced to atmospheric and the steam is condensed. The condensate returns to the top of the reactivator as reflux, and the cooled acid gas in pure concentrated form flows to disposal or recovery.

Purification for Helium Extraction From Natural Gas

As mentioned, the first plant utilizing this process was built to treat a helium-bearing natural gas which contained a high concentration of carbon dioxide. Complete carbon-dioxide removal is necessary in helium extraction to prevent freezing difficulties in the liquefaction stage of the cycle. The early plants extracted helium from natural gases containing only small amounts of carbon dioxide which could be separated by caustic scrubbing. The helium content of these gases was in the order of 1 to 2 per cent so that it was necessary to process large volumes of gas per unit of helium recovered. A natural-gas pool containing 8 per cent helium was then discovered, but it was also found that the mixture contained about 15 per cent carbon dioxide. Caustic-soda scrubbing for this quantity of carbon dioxide would have been prohibitively expensive and, after investigating other available processes, it was decided that a new method for carbon-dioxide removal must be found—another case of necessity being the mother of invention. So it was for this original purpose that the Girbotol process was developed. It was soon recognized that the new process had general application for

[1] The Girdler Corporation, Louisville, Ky.

Contributed by the Process Industries Division and presented at the Fall Meeting, Louisville, Ky., October 12–15, 1941, of THE AMERICAN SOCIETY OF MECHANICAL ENGINEERS.

NOTE: Statements and opinions advanced in papers are to be understood as individual expressions of their authors and not those of the Society.

carbon-dioxide absorption, and that it was equally useful for separating hydrogen sulphide from gas mixtures.

Natural-Gas Purification

Following quickly upon the successful operation of the first carbon-dioxide-removal plant, the process was applied to the removal of hydrogen sulphide from sour natural gas. At present, this is its broadest field of usefulness, and one in which it accomplishes a high degree of purification. Regardless of the initial hydrogen-sulphide content, sour natural gas can be processed and made suitable for domestic and industrial purposes. Numerous Girbotol plants now purify natural gas for pipe-line distribution in this country and Canada.

Simultaneous Purification and Dehydration of Natural Gas

At this point, mention should be made of a more recent modification of this process to effect simultaneous purification and partial dehydration of natural gas. The amines themselves are extremely hygroscopic and when a concentrated amine solution, or one which is fortified with another hygroscopic agent such as diethylene glycol, is circulated in the Girbotol cycle, the mixture removes both hydrogen sulphide and moisture from the gas. In this manner the solution reduces the water dew point of the gas sufficiently to prevent the formation of hydrocarbon hydrates in the transmission lines, thus eliminating line-plugging and interference with compressor operation, two very troublesome factors in pipe-line distribution. Most of the natural-gas plants in which this process is applied have now incorporated dehydration. The combination process for separating acid gases and water vapor simultaneously has also found application in other fields, such as purification and dehydration of natural gas for liquefaction and storage.

Uses in Petroleum-Refining Operations

By 1930, petroleum refiners had developed hydrogenation processes for improving lubricating oils and other petroleum products. The large quantities of hydrogen needed were obtained by a new process in which refinery or natural gas is treated with steam at high temperatures in the presence of catalysts to produce hydrogen by a modified water-gas reaction. The raw hydrogen obtained by this process contains about 20 per cent carbon dioxide. The Girbotol process is widely employed for removing the carbon dioxide from this mixture to produce essentially pure hydrogen. These plants are highly successful and are now in use in refineries producing improved lubricating oils and aviation gasoline in the United States, England, and the Netherlands East and West Indies.

Perhaps the largest potential field for the process lies in petroleum refining for the removal of hydrogen sulphide and sometimes carbon dioxide from refinery gases and liquids. Polymerization processes, the synthesis of isooctane, neohexane, and various organic chemicals, such as the aliphatic alcohols and glycols, as well as the production of hydrogen and liquefied hydrocarbon gases, all are improved by the use of sulphur-free starting materials. In some instances, catalysts are injured by hydrogen sulphide. In others, expensive aftertreatment, or methods which impair the quality of the finished product must be resorted to if hydrogen sulphide is present in the charge stock. Frequently sulphur specifications are so rigid that pretreatment is essential. In all cases, the corrosive effect of hydrogen sulphide on the process equipment and pipe lines is eliminated by its removal.

Recovery of Hydrogen Sulphide for Sulphuric Acid

Another application for refinery-gas purification is the recovery of hydrogen sulphide for sulphuric-acid manufacture. Several refiners have plants in operation and others are contemplating installations. Hydrogen sulphide usually can be recovered more cheaply than sulphur can be purchased, and hydrogen sulphide can readily be burned to sulphur dioxide which is converted to sulphuric acid.

Liquid-Hydrocarbon Purification

Although the process is firmly established in the gas-purification field, it is not generally known that the same reagents and principles may be applied to the treatment of certain liquid hydrocarbons with equal or even better success. This fact is becoming increasingly important because many of the newer processes in the refining field, such as preparation of polymerization feed stocks, require the removal of hydrogen sulphide in the liquid phase.

Carbon-Dioxide Recovery

The process is useful in the separation and recovery of carbon dioxide from stack gas for the production of liquid carbon dioxide and dry ice. Many of the carbon-dioxide recovery plants operate as completely integrated units in which a fuel is burned in a boiler to produce stack gas and steam, the carbon dioxide is extracted from the stack gas, and the steam is used first for power for compression and then for heat for expelling the carbon dioxide from the absorbing solution. The fuel fired to the boiler furnishes the raw material, heat, and power. Ten years ago dry-ice manufacturers were using sodium- or potassium-carbonate solution as the absorbing medium for carbon dioxide, and had perfected a balanced system, firing just enough fuel to furnish the power and steam for the carbon dioxide which was recovered. Although balanced, this system was not efficient, since only about 50 to 70 per cent of the carbon dioxide produced could be absorbed from the stack gases by these absorbents. Excess carbon dioxide passed out the top of the absorbers unabsorbed. Since that time, improvements in steam-generating and power-producing equipment have greatly decreased the amount of fuel which must be burned to produce the power for compressing and liquefying carbon dioxide. With the old absorption processes, these improvements could not be put to profitable use, since the same amount of fuel had to be burned as before to recover a given quantity of carbon dioxide. Consequently, the newer power-production improvements threw the old carbon-dioxide-recovery cycle out of balance. In a modern Girbotol carbon-dioxide-recovery plant, as much as 95 per cent of the carbon-dioxide content of the stack gas is recovered. The liquefaction of this increased quantity of carbon dioxide utilizes all the power available from burning the fuel, while the exhaust steam from the compression cycle is sufficient to separate the absorbed carbon dioxide from the amine solution. The system is again balanced, but with a much higher over-all efficiency than was possible under the old system.

Operating on combustion gases from coal, coke, oil, and natural gas, the process is being employed to recover pure carbon dioxide for the many uses to which liquid carbon dioxide and dry ice are put. In addition, carbon dioxide being recovered by this process is used in the safety mining of coal, for the production of soda ash, and even in the manufacture of aspirin. Plants are located in the United States, England, Cuba, the Philippines, New Zealand, and the Malay States.

The process is particularly economical for carbon-dioxide recovery when natural gas is available as a fuel. Flue gas from natural-gas-fired boilers contains only about 10 per cent carbon dioxide, as against 14 to 20 per cent for solid and liquid fuels. The high absorptive capacity of the amines for carbon dioxide makes natural gas a practical fuel for carbon-dioxide production.

and natural gas has been substituted for coke in some existing plants after the alkali-carbonate solution has been replaced with the present process.

Production of Inert Atmospheres

Quite recently the importance of controlled atmospheres in the heat-treatment of steels and special metals has been recognized. In order to meet the steadily increasing standards of quality in metallurgical products, it has been necessary to produce an essentially inert atmosphere for use in treating certain grades of metals. The present crisis necessitates uninterrupted production, which is facilitated by the proper processing of working tools. The heat-treating processes employed are annealing, normalizing, quenching, and preheating for the hot-shaping of steels by rolling, forging, and pressing. All of these heat operations can be greatly improved if carried out in inert atmospheres. The most suitable atmosphere for heat-treating metals is one consisting essentially of pure nitrogen.

A nitrogen atmosphere is produced by burning fuel gas in the proper quantity of air to convert the oxygen to carbon dioxide and water. These are then removed from the products of combustion. Here again the process fits nicely into the picture. A combustion apparatus or "atmospheric-gas converter" is controlled to produce a gas essentially free from oxygen, but containing carbon dioxide and water vapor, which are removed by treatment with a dehydrating solution of amine and glycol. Final water removal is effected by aftercontact with silica or alumina gel. Since the inert atmosphere can be recirculated and make-up is required only for leakage, small generator plants are built. There are now many of these small plants operating in this country.

In the field of munitions manufacture, the process also plays an important role in supplying an inert atmosphere which is used to minimize explosion and fire hazards in powder-drying and bag-filling operations.

Removal of Carbon Dioxide Before Ammonia Synthesis

Yet another use of the process in the manufacture of munitions is the removal of carbon dioxide from a raw hydrogen-nitrogen mixture prior to ammonia synthesis. This is essentially the same problem that exists in the production of purified hydrogen for hydrogenation in petroleum refineries. The other commerical method of purification in this field is water scrubbing at high pressures. The Girbotol process is more effective in obtaining a carbon-dioxide-free product. However, the choice of process lies in the available fuel from which the hydrogen is produced, and the manner in which the investment may be written off. The Girbotol process shows higher economy when operated on synthesis gas from natural or refinery gas than from such starting materials as coal or coke. The temperature and availability of water is a factor which has a decided bearing on the water-scrubbing operation, but affects the subject process only slightly. This process permits the economical use of steam-driven compression equipment, employing the exhaust steam to reactivate the solution.

The manufacturers of hydrogenated edible oils also take advantage of the process in preparing their hydrogen. With improved methods of hydrogenation being developed for this industry, this process will play an important part in replacement of the older processes.

From this review of its applications it may be seen that the Girbotol process offers operating economies in many diversified fields. The simple invention of 1928, originally developed for the express purpose of removing carbon dioxide from helium-bearing natural gas, now occupies an important place industrially. There are now 102 plants in successful operation throughout the world, covering the many fields mentioned. There is every reason to believe that many new applications will be found and that the process will continue to make a worth-while contribution to industry, as it has done in the last 12 years.

BIBLIOGRAPHY

1 "Process for Separating Acidic Gases," U. S. Patent Reissue 18,958, Sept. 26, 1933, to R. R. Bottoms.

2 "Equilibrium Absorption of Carbon Dioxide by Solutions of the Ethanolamines," by J. W. Mason and B. F. Dodge, Trans. American Institute of Chemical Engineers, vol. 1, 1936, pp. 27–47.

3 "Carbon Dioxide Scrubbing by Amine Solutions," by L. B. Gregory and W. G. Scharmann, *Industrial and Engineering Chemistry*, vol. 29, 1937, pp. 514–519.

4 "The Girbotol Purification Process," by W. R. Wood and B. D. Storrs, Proceedings of the American Petroleum Institute, Eighth Midyear Meeting, Section III, vol. 19, 1938, pp. 34–36.

5 "Cost of Hydrogen-Sulphide Removal From Refinery and Sour Natural Gases," by B. D. Storrs, American Chemical Society, *News Edition*, vol. 17, 1939, pp. 627–628.

6 "Treatment of Sour Gas," by W. R. Wood, Proceedings of the American Gas Association, Technical Section, Houston, Tex., May 7–9, 1940.

7 "Annealing Atmospheres From the Combustion Products of Gaseous Fuels," by A. G. Hotchkiss, *Industrial and Engineering Chemistry*, vol. 33, 1941, pp. 32–38.

8 "Recent Design Developments in Amine Gas Purification Plants," by R. M. Reed and W. R. Wood, Trans. American Institute of Chemical Engineers, vol. 37, June 25, 1941, pp. 363–383.

Discussion

R. J. Bender.[2] One handicap of automotive Diesel engines on the highways is the strong acrid odor of the exhaust gases. Experiments seem to indicate that it is due to the presence in the exhaust of acrylic aldehydes in various proportions, according to the make of engine, process of combustion, etc.

Would the Girbotol process lend itself to the absorption of these objectionable aldehydes in the exhaust gases? If it is feasible, there might be a field for small portable installations to clean the exhaust gases on trucks and busses, powered by Diesel engines. Naturally the carbon dioxide present in the exhaust gases to the extent of 4 to 10 per cent would be absorbed at the same time, but inasmuch as the process is of the regenerative type and as some waste heat is available for that regeneration, CO_2 absorption would not be an objection

Authors' Closure

The Girbotol process has very recently found application in another industry, namely, the manufacture of magnesium. The chemical-engineering division of the Todd-California Shipbuilding Corporation is operating a new magnesium plant at Permanente, Calif., near San Jose. Published reports advise that this plant produces magnesium by the Hansgirg process, in which magnesium oxide (obtained by calcining magnesite) is reduced with coke in an electric reduction furnace at about 2000 C to produce metallic magnesium and carbon monoxide. The mixed vapors of magnesium and carbon monoxide emerge from the furnace and are quenched with a large volume of natural gas. This quenching with inert gas is necessary because, at lower temperatures, magnesium and carbon monoxide are recombined to give magnesium oxide.

The magnesium dust is separated by settling and by electrostatic precipitation from the stream of natural gas. A portion of the gas is then cooled and recycled through the quenching process. About one fourth of the gas is continuously withdrawn and is used for fuel in an adjoining cement plant, operated by the same company. This quantity is made up by fresh natural gas added continually to the system. The fresh gas is added in order to keep the carbon-monoxide content of the circulating quench gas at a low point.

[2] Fuel Oil Engineer, Sinclair Refining Co., Chicago, Ill. Mem. A.S.M.E.

When this plant was placed in operation, it was found that the natural-gas supply contained 1.5 per cent of carbon dioxide, which reacted with the magnesium and caused a considerable decrease in the yield of the reduction furnace.

A caustic-soda scrubber has been installed to handle the problem temporarily but the quantity of carbon dioxide to be removed is so large that the caustic-soda cost for complete removal amounts to several hundred dollars per day.

A Girbotol carbon-dioxide-removal plant is being installed at the present time to remove the carbon dioxide from this natural gas. In this case, the operating cost will be less than 10 per cent of that required to remove the carbon dioxide with caustic soda.

This new magnesium plant is another project carried out by Henry J. Kaiser who was one of the founders of Six Companies, Inc. which constructed the Boulder Dam. Construction of the plant was begun in March, 1941, and on September 10, the first unit with a capacity for producing 8,000,000 lb of magnesium per year was placed in operation. Two more similar units are under construction at the present time, and it is believed that more units will be installed after these have been placed in operation.

The crude magnesium obtained from the condenser on the outlet of the reduction furnace is purified by batch distillation, and a product is obtained with a final purity of about 99.97 per cent.

In answer to Mr. Shannon of the Henry Vogt Company, who asked if there are any impurities in the gases treated by the process which are detrimental to the solution, the following statement is made.

There are some constituents in the commercial-gas mixtures, which are treated by the process, which are undesirable. Sulphur dioxide is absorbed into the solution, forming amine sulphite, which regenerates incompletely. If there is also oxygen in the gas mixture being scrubbed, the sulphite is oxidized to sulphate in solution and the amine is thus neutralized by a strong, fixed acid. In such instances, it is possible to add caustic soda or soda ash to the solution in proportion to the amount of fixed amine. The addition of soda forms the sodium salt of the strong acid and frees the amine for further acid-gas absorption. After considerable quantities of the sodium salts have accumulated, it is necessary to discard the amine solution to prevent the crystallization of the sodium salts.

In reply to Mr. Bender; acrolein is an aldehyde, and it may be said generally that aldehydes react with the reagents of the subject process, forming undesirable decomposition products. The compounds which are formed cannot be readily regenerated in the reactivation cycle. Aldehydes are sometimes encountered in the treatment of industrial gases, and they may usually be effectively removed from such gases by an efficient water scrubber. Perhaps water scrubbing would be suitable for Mr. Bender's purification problem.

Corrosion of Unstressed Steel Specimens and Various Alloys by High-Temperature Steam

By H. L. SOLBERG,[1] G. A. HAWKINS,[2] AND A. A. POTTER[3]

Inasmuch as steam temperatures in modern central stations are approaching those used for the commercial production of hydrogen by reaction between steam and iron, an investigation was undertaken at Purdue University of the corrosion by steam of the various steels which are available for high-temperature service. Apparatus was constructed and techniques developed for measuring the amount of corrosion on unstressed specimens due to temperatures up to approximately 1400 F, and pressures up to at least 1600 psi gage. Data are presented showing the effect of various types of surface finish and methods of scale removal, time of exposure to steam at 1100 F for various intervals of time up to 2000 hr, exposure for 500 hr at steady steam temperatures from 1000 F to approximately 1400 F, and temperature fluctuations on the corrosion resistance and spalling of scale on round bars, as well as convex, concave, and flat surfaces. Data on the corrosion of cast steels and some special alloys are also given. The resistance of alloy steels to high-temperature steam is greatly influenced by the amount of chromium present. Alloy steels containing 7 per cent or more of chromium are very resistant to corrosion produced by steam at temperatures up to at least 1400 F. The 18-8 stainless steels showed practically no corrosion when subjected to steam up to 1400 F.

INASMUCH as steam temperatures in modern central stations are approaching those used for the commercial production of hydrogen by the reaction between steam and iron, an investigation was undertaken at Purdue University of the corrosion by steam of the various steels which are available for high-temperature-steam service. Apparatus was constructed and techniques developed for measuring the amount of oxidation due to temperatures up to 1200 F and pressures up to at least 1600 psi gage. Data were presented by the authors in a progress report,[4] which showed the effect of temperatures from 800 to 1200 F on the oxidation of low-carbon steel in contact with steam at 1200 psi gage. It was found that the rate of oxidation of low-carbon steel at 1100 F is independent of pressure between the minimum and maximum pressures used, which were 400 to 1200 psi.

The investigation has been continued upon unstressed specimens of a wide variety of steels and alloys and has had for its objective the determination of the effect of various types of surface finish and methods of scale removal; the effect of time of exposure to steam at 1100 F for various intervals of time up to 2000 hr; the effect of exposure for 500 hr at steady steam temperatures from 1000 F to 1300 F; the effect of temperature fluctuations on the corrosion resistance and spalling of scale on round bars as well as convex, concave, and flat surfaces; and the corrosion of cast steels and special alloys.

Methods Used for Measuring Corrosion Products

Steam reacts with steel according to the following equation

$$4H_2O + 3Fe = Fe_3O_4 + 4H_2$$

While this reaction indicates that the amount of corrosion could be measured from the quantity of hydrogen evolved, the occluded gases in the steel and the permeability of steel to hydrogen introduced variables which made the method unsuited for this investigation.

An attempt was made to measure the extent of corrosion by stripping the scale from corroded specimens by the use of hydrochloric acid, antimony trioxide, and stannous chloride. This solution failed to remove the scale from steels high in chromium, although it was satisfactory for low-carbon steel.

TABLE 1 EFFECT OF INHIBITORS ON ACTION OF ACIDS IN CONTACT WITH LOW-CARBON STEEL

	Loss of Weight in Milligrams per Square Inch in Six Hours at Room Temperature.									
Inhibitor Amount cc/liter	Concentrated Hydrochloric Acid						34 per cent Sulphuric Acid			
	Rodine No.101	Rodine No.102	Di-n-Amyl-amine	Tri-n-Amyl-amine	Tri-n-Butyl-amine	Wap No.22	Di-n-Amyl-amine	Tri-n-Amyl-amine	Tri-n-Butyl-amine	Wap No.22
0.0	613.5	-----	-----	-----	-----	-----	170.2	-----	-----	-----
0.25	68.4	32.4	-----	-----	-----	-----	-----	-----	-----	-----
0.4	-----	-----	302.3	290.0	336.5	-----	-----	50.8	123.0	-----
0.5	25.2	14.2	-----	-----	-----	79.5	-----	-----	-----	1.61
0.8	-----	-----	262.0	306.5	289.5	-----	50.6	65.4	78.2	-----
1.0	9.1	9.7	276.5	268.5	257.0	61.0	44.9	40.1	72.2	1.14
1.5	-----	-----	-----	-----	-----	58.0	-----	-----	-- -	-----
2.0	4.8	7.8	231.8	245.5	199.8	56.7	13.5	33.4	29.4	1.03
5.0	3.0	6.6	108.2	47.1	142.0	46.8	11.4	25.9	8.4	1.01
7.5	2.6	6.0	-----	-----	-----	38.2	-----	-----	-----	0.72
8.0	-----	-----	85.4	37.0	85.8	-----	6.4	20.7	10.4	-----
10.0	2.0	4.7	76.5	33.1	72.5	31.4	3.5	17.3	6.8	0.71

A series of experiments on other acid-and-inhibitor combinations was then undertaken. The main purpose of this phase of the work was to determine if possible an acid-and-inhibitor combination which would work equally well for removing the scales formed on low-carbon steel and alloys containing large amounts of chromium. Various mixtures and concentrations of nitric, sulphuric, and hydrochloric acids and inhibitors were used in an attempt to remove the scale formed on 18-8 stainless steel. A number of different inhibitors were used and it was found that a 34 per cent sulphuric-acid solution with 0.1 per cent quinoline ethiodide would remove the scale from low-alloy steels with no appreciable attack on the base metal. Table 1 gives the results for all of the inhibitors used, except quinoline ethiodide, with both 34 per cent sulphuric acid and concentrated hydrochloric acid.

---

[1] Head, School of Mechanical Engineering, Purdue University. Mem. A.S.M.E.

[2] Associate Professor of Mechanical Engineering, Purdue University. Mem. A.S.M.E.

[3] Dean, Schools of Engineering, and Director of the Engineering Experiment Station, Purdue University. Past-President A.S.M.E.

[4] "Investigations of the Oxidation of Metals by High-Temperature Steam," by A. A. Potter, H. L. Solberg, and G. A. Hawkins, Trans. A.S.M.E., vol. 59, 1937, p. 725.

Contributed by the Special Research Committee on Critical-Pressure Steam Boilers and presented at the Fall Meeting, Louisville, Ky., October 12–15, 1941, of The American Society of Mechanical Engineers.

Note: Statements and opinions advanced in papers are to be understood as individual expressions of their authors and not those of the Society.

TABLE 2 EFFECT ON LOW-CARBON STEEL OF CONCENTRATIONS OF QUINOLINE ETHIODIDE AS AN INHIBITOR IN DIFFERENT ACID SOLUTIONS

Grams of Quinoline Ethiodide per liter	Loss of weight in milligrams per square inch in six hours at room temperature	
	34 per cent Sulphuric acid	Concentrated Hydrochloric acid
0.1	3	---
0.2	2	405
0.5	---	390
0.75	1.5	371
1.0	1.2	344
1.5	---	258
2.0	0.9	229
2.5	---	103

TABLE 3 RESISTANCE OF CLEAN SPECIMENS OF LOW-CARBON STEEL TO ATTACK BY ELECTROLYTIC STRIPPING IN 10 PER CENT SULPHURIC ACID WITH 1 G PER L OF QUINOLINE ETHIODIDE

(Current density, 1 amp per sq in; time, 30 min)

Specimen	Weight of Specimen, grams		
	Before stripping	After stripping	Loss in Weight, grams
1	143.264	143.234	0.030
2	147.442	147.402	0.040
3	148.642	148.628	0.014
4	146.292	146.274	0.018
5	146.102	146.078	0.024
6	144.298	144.270	0.028
7	145.060	145.016	0.044

In all of the tests the low-carbon-steel samples were allowed to remain in the acid-inhibitor solution for six hours at room temperature. Quinoline ethiodide was found to be very effective in 34 per cent sulphuric acid and poor in concentrated hydrochloric acid, as shown in Table 2. The inhibiting action of quinoline ethiodide in 34 per cent sulphuric acid breaks down as the temperature of the acid increases. At 110 F very little inhibiting action remains.

While quinoline ethiodide in 34 per cent sulphuric acid worked very well for removing the scale on low-carbon steel, no combination of acids or concentrations of quinoline ethiodide could be found which would remove the scale from the steels containing 12 per cent chromium or more without pitting of the parent metal.

Consideration was given to measuring the extent of corrosion by weighing the corroded specimen, then reducing the scale by means of hydrogen at high temperature, and again weighing the specimen in order to determine the amount of oxygen present in the corrosion products. This method was discarded because of the stability of chromium oxide.

Scale removal by electrolysis was next considered. It was found that scale could be removed completely from low-alloy steels in 10 per cent sulphuric acid containing 1 g per l of quinoline ethiodide by using a current density of 1 amp per sq in. at room temperature. A density of 2 amp per sq in. removed the scale satisfactorily from 18-8 stainless steel. Tests were conducted to measure the attack on the bare metal. In 10 per cent sulphuric acid with no inhibitor and a current density of 2 amp per sq in., there was little loss in weight; however, the metal was dark in color, thus indicating some surface oxidation. With 1 g per l of quinoline ethiodide and 10 per cent sulphuric acid, no loss in weight of bare metal was detected. Additional tests were conducted to determine the effect of temperature. Up to 110 F, the metal was attacked no more than at room temperature. At higher temperatures, the attack on the metal became noticeable. Table 3 shows the results obtained in a series of tests on clean specimens of low-carbon steel when subjected to electrolytic action for 30 min at room temperature.

The method of determining the extent of corrosion by steam, which was finally adopted and used to obtain the results reported in this paper consisted of weighing the clean specimen before exposure to steam, removing the scale by electrolytic stripping after exposure to high-temperature steam, and reweighing the specimen. The solution consisted of 10 per cent sulphuric acid with 1 g per l of quinoline ethiodide. The specimen served as the cathode. The time required for effective stripping with a current density of 1 amp per sq in. was investigated and was found to vary with the chromium content of the specimen as follows:

Steel	Time required, hr
S.A.E. 1010	1/2
4-6 Cr-Moly	1
12 Cr	2
18-8	4

The earlier test specimens were made from tube stock 6 in. long, and $1\frac{1}{2}$ in. OD × 1 in. ID. Scale was stripped from these



FIG. 1 PHOTOGRAPH OF STRIPPING TANK AND BAR-STOCK SPECIMENS

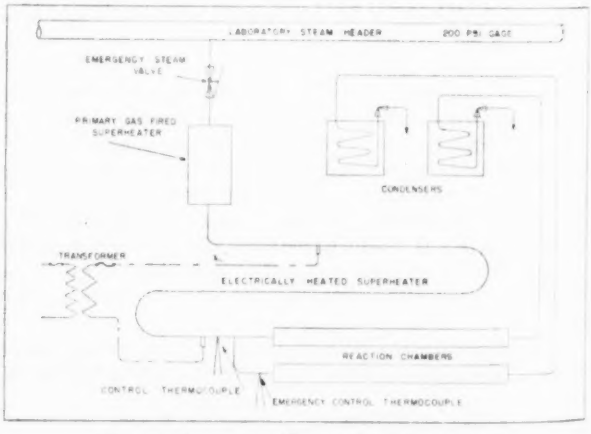


FIG. 2 SCHEMATIC DIAGRAM OF APPARATUS

specimens by use of a platinum rod as the anode. Difficulty in inspecting the inside surface of the specimens for complete scale removal resulted in the subsequent use of bar stock for all specimens. The specimens machined from bar stock were stripped by means of the apparatus shown in Fig. 1. The round bar stock samples were placed in a saddle as shown which in turn was placed on insulators located on the bottom of a lead container. The solution of sulphuric acid and quinoline ethiodide was placed in the lead jar which served as the anode. The current density was regulated by means of a large carbon-pile rheostat. Heat

losses from this lead case during the stripping action made cooling devices unnecessary.

Test Apparatus

Fig. 2 is a schematic diagram of the test apparatus. The steam, after leaving the laboratory main at about 200 psi gage, passed through a counterflow gas-fired superheater. A thermocouple was located in the discharge line from this superheater. After leaving the gas-fired superheater, the steam passed through 65 feet of 18-8 stabilized stainless-steel tubing, $^{5}/_{8}$ in. OD × $^{3}/_{8}$ in. ID. The ends of this pipe were connected to a current transformer, thus converting the tubing into a resistance heater in which the final heating of the steam was accomplished.

Leaving the electric superheater, the steam was divided and flowed into two 16-ft test sections, each made from 2-in. extra-heavy pipe. The discharge end of each test section was fitted with a standard pipe cap to facilitate insertion and removal of the test samples. The steam leaving each test section passed into a coiled-copper-tube condenser. The condensate was weighed at intervals in order to maintain the proper flow rates. Needle valves were used on the discharge side of the condenser for regulating steam flow and maintaining turbulent-flow conditions around the specimens. Bourdon-tube pressure gages were used to determine the pressure in each of the test sections.

Around each 16-ft test section or reaction chamber were wrapped three electric heaters, consisting of No. 13 chromel wire insulated with refractory beads. The heaters were divided into three sections consisting of two 4-ft end-guard heaters and one main heater having a length of 8 ft. The pipes and heaters were covered with 10-in. split sewer tiles over which was placed a very thick bed of loose diatomaceous-earth insulation. Chromel-alumel thermocouples were placed every 18 in. along each test section.

Electric Circuit

The temperature of the steam leaving the electric superheater was maintained constant by means of a thermocouple, controller,

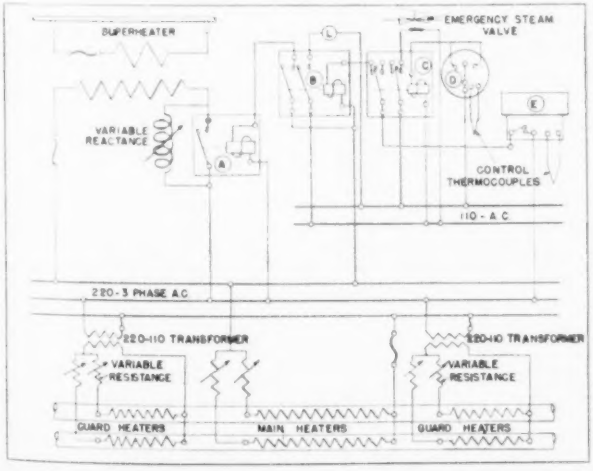


Fig. 3 Schematic Diagram of Electrical Apparatus

and magnetic switch. Fig. 3 shows a wiring diagram of the main electrical circuit. In the lower portion of the diagram are shown the main and guard heaters which surrounded the reaction chambers or test sections. The guard heaters operated on 110 v, while the main heaters were supplied from the 220-v line. Each heater was equipped with a variable resistance in order to maintain the temperature of the tubes at any desired value which was equal to the temperature of the steam supplied to them. The main power circuit for the electric superheater is shown in the upper left-hand corner of the diagram. The 2300-v winding was removed from an old transformer and replaced by a few turns of No. 0000 cable, which served as the secondary. The original 220-v winding was connected to the magnetic contactor (A) and variable reactance as shown. With the magnetic switch open only a fraction of the maximum current passed through the superheater circuit. By means of opening and closing the magnetic switch intermittently, it was possible to maintain the superheater temperature constant. The control for the magnetic switch is shown in the upper right-hand corner of Fig. 3. The thermocouple located in the discharge line from the electric superheater operated a controller (E) which actuated the magnetic switch (A) through relay (B), thereby opening and closing the circuit to the superheater transformer. Relay (C) together with the emergency controller (D) were used for opera-



Fig. 4 Tube Specimen

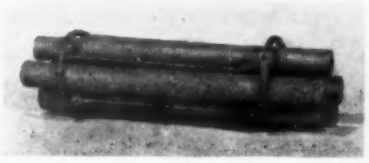


Fig. 5 Bar Specimen

tion of the emergency steam valve in the line supplying steam to the superheater. In case of a low or high superheater temperature, the emergency controller (D) operated relay (C) which opened the magnetic switch (A) and also actuated the coil connected to the quick-acting shutoff valve in the steam line. Thus the specimens were automatically protected from steam at any temperature other than the desired test temperature.

Lead wires from all of the thermocouples located in the reaction chambers were connected to a bakelite jack-board cold junction. All temperature readings were taken on a portable potentiometer.

Test Specimens

All test samples, other than those used in the surface-finish tests, were sandblasted and weighed, after which they were placed in the reaction chambers. Fig. 4 shows the type of tube specimens used. The tubes were supported on four small legs in order to align the test tube concentrically with the reaction chamber. The bar specimens were mounted in cages, as shown in Fig. 5. Upon completion of a test the bars were removed and the scale stripped, after which they were accurately weighed. Test specimens which had to be stored for any length of time were placed in a large can containing a layer of calcium chloride on the bottom and an opening on the side or top for the admission of nitrogen gas. All samples were handled as little as possible and only then with gloves in order to prevent any foreign material from contaminating the external sanded surface. All samples were carefully stamped with the classification number and the specimen number. The location of each specimen together with the cage was recorded both with regard to the position in the reaction chamber and thermocouples.

Heat-Treatment

In order to insure consistent heat-treatment of specimens, all of the steel received except the cast steels were heat-treated. Low-carbon steel was annealed at 1600 F, slow-cooled to 1200 F at a rate of 40 F per hr, and then air-cooled from 1200 F to room temperature. Steels having a chromium content between 1 and 12 per cent were annealed at 1580 F, slow-cooled to 1200 F at a rate of 40 F per hr, and air-cooled from 1200 F to room temperature. The high-chromium stainless steels were annealed at 1950 F and water-quenched. Several of the special alloy steels were annealed according to the methods suggested by the producers which deviated only slightly from the general procedure outlined.

The cast steels were received in the annealed condition which was reported to be as follows:

Cast steel	Heat-treatment
Carbon steel.....	Annealed 1650 F for 4 hr, furnace-cooled to 700 F, and air-cooled to room temperature
Carbon-Moly.....	Normalized at 1800 F for 4 hr, drawn at 1200 F for 4 hr, furnace-cooled to 700 F, and air-cooled to room temperature
Ni-Cr-Moly.....	Normalized at 1725 F for 4 hr, normalized at 1550 F for 5 hr, drawn at 1200 F for 4 hr, and air-cooled to room temperature
5 Cr-Moly.....	Normalized at 1800 F for 4 hr, normalized at 1600 F for 3 hr, drawn at 1280 F for 4 hr, and air-cooled to room temperature
9 Cr-1 1/2 Moly.....	Normalized at 1820 F for 4 hr, normalized at 1650 F for 4 hr, drawn at 1300 F for 4 hr

Preliminary Test on Low-Carbon-Steel Tube Specimens

As the first part of the general program it was decided to test a series of specimens from one heat of steel to determine the probable consistency of the results. Twelve identical tube specimens were cut from one tube, 1 1/2 in. OD × 1 in. ID, of open-hearth S.A.E. 1015 steel and machined to size. The specimens were sandblasted and placed in the reaction chamber at a mean temperature of 1095 F with steam at the same temperature flowing past the specimens for a period of 120 hr. Considering only specimens at a temperature of ± 5 F from the mean, the results shown in Table 4 were obtained. The results obtained seemed to indicate that the method of stripping the scale and general test technique were satisfactory.

TABLE 4 CORROSION OF LOW-CARBON-STEEL TUBES IN CONTACT WITH 1100 F STEAM FOR 120 HR

Specimen Number	Loss in Weight of individual sample, grams	Temperature Degrees, F	Variation from the average loss in weight, percent
17-1	5.650	1099	-16.07
20-2	6.544	1098	-2.79
21-2	7.222	1096	+7.36
31-4	6.308	1093	-6.33
25-3	6.555	1090	-2.63
18-1	6.582	1089	-2.23
19-1	6.677	1089	-0.82
32-5	6.837	1092	+1.56
26-3	6.918	1098	+2.76
29-3	7.013	1099	+4.17
30-3	7.079	1098	+5.15
27-3	7.405	1095	+10.00

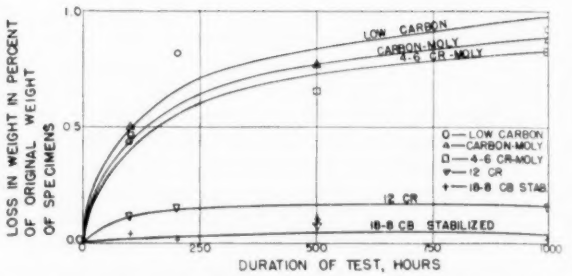


FIG. 6 CORROSION OF STEEL TUBES IN CONTACT WITH STEAM AT 1100 F FOR 100 HR, 200 HR, 500 HR, AND 1000 HR

Test on Tube Specimens to Determine Influence of Lengths of Test

A series of tests on five different alloy tubes was conducted at

TABLE 6 EFFECT OF ANNEALING, COLD-WORKING, AND SURFACE FINISH ON CORROSION OF 1/8-IN. ROUND S.A.E. 1020 SPECIMENS IN CONTACT WITH STEAM AT 1100 F FOR 500 HR

Method of preparing specimens	Average temperature of specimens, F	Loss in weight of individual sample, grams	Average loss in weight of individual sample, grams	Maximum per cent deviation from the average	Loss in weight in terms of annealed and sand blasted specimens
Annealed and surface sand blasted	1097	1.862 1.827 1.870 1.875 1.714 1.733 1.899	1.826	6.13	1.000
Annealed, surface ground, and lapped	1098	1.966 2.024 2.175 1.950 2.307 2.256 2.305	2.144	9.03	1.172
Annealed, surface sand blasted, specimen boiled in distilled water, & washed in alcohol and ether	1098	1.813 1.784 1.957 1.945 2.283 2.290 2.267	2.048	12.90	1.121
Unannealed, and surface sand blasted	1096	2.030 1.868 1.844 1.929 2.003 1.935 1.869	1.925	5.45	1.055
Unannealed, cold worked, and surface sand blasted	1097	2.013 2.035 2.008 2.012 1.917 1.890 1.908	1.969	4.02	1.078
Unannealed, surface sand blasted, and surface worked by peening hammer	1097	2.075 2.038 2.149 2.111	2.093	2.67	1.149
All sample average	----	1.995	1.995	----	1.091

TABLE 5 CORROSION OF STEEL TUBES IN CONTACT WITH STEAM AT 1100 F FOR 100, 200, 500, AND 1000 HR

Steel	Chemical Analysis (Ladle) Percent									Test: 100 Hour		200 Hour		500 Hour		1000 Hour	
	C	Mn	P	S	Si	Cr	Ni	Mo	Cb	Number of Samples	Average Loss in Weight, gms	Number of Samples	Average Loss in Weight, gms	Number of Samples	Average Loss in Weight, gms	Number of Samples	Average Loss in Weight gms
Low Carbon	0.1 -0.2	0.3 -0.6	0.045	0.055	--	--	--	--	--	2	4.43	3	8.17	--	--	3	9.38
Carbon-Moly	0.13	0.48	0.013	0.013	0.25	--	--	0.51	--	2	5.07	--	--	2	7.75	2	8.76
4-6 Cr-Moly	0.09	0.46	0.030	0.030	0.30	4.75	--	0.55	--	2	4.57	--	--	2	6.53	3	8.29
12 Cr	0.04	0.75	0.026	0.025	0.31	11.69	0.7	0.31	--	1	1.14	2	1.54	1	0.79	3	1.65
18-8-Cb stabilized	0.06	0.56	0.016	0.014	0.38	17.29	12.2	--	0.68	2	0.34	3	0.16	2	0.91	2	0.25

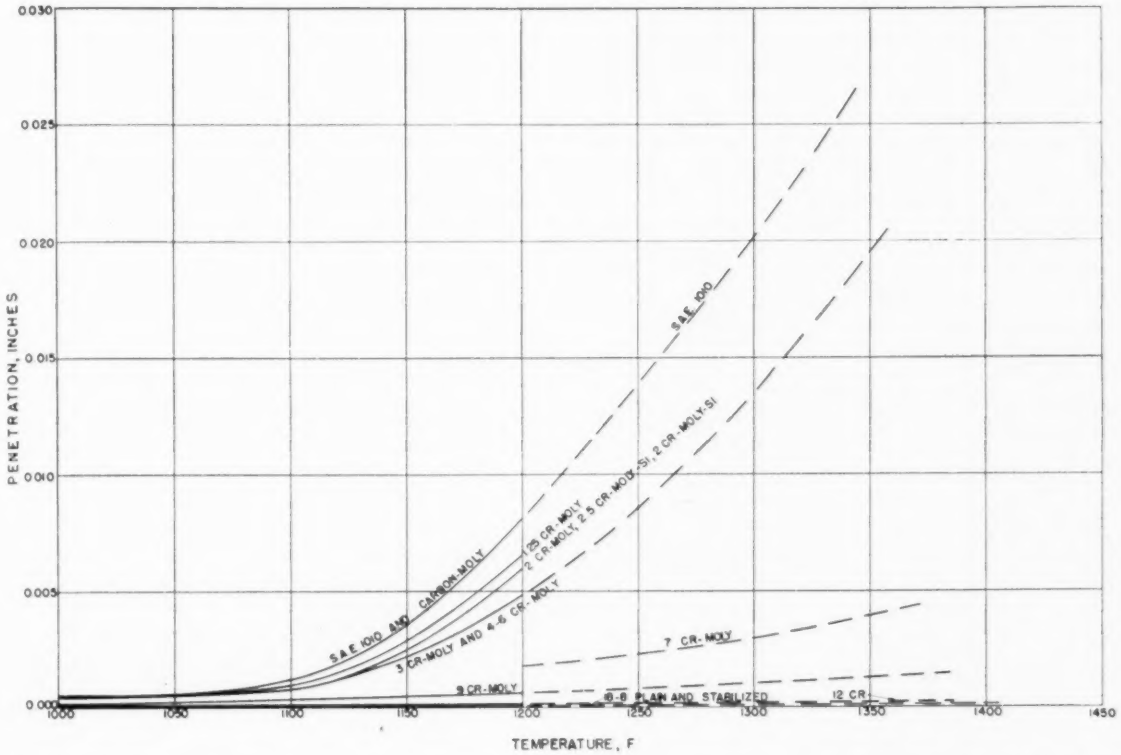


FIG. 8 CORROSION OF STEEL BARS IN CONTACT WITH STEAM FOR 500 HR AT VARIOUS TEMPERATURES

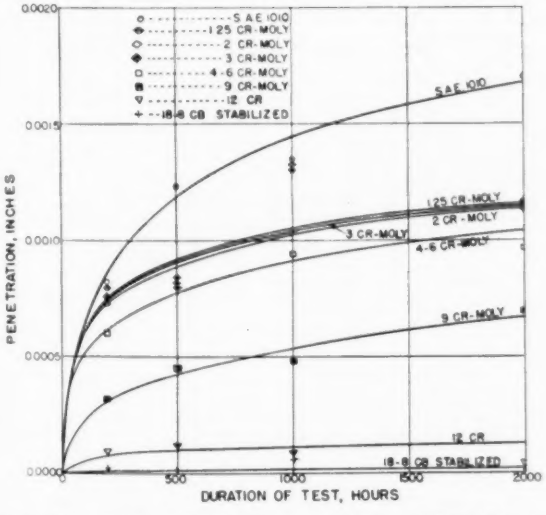


FIG. 7 CORROSION OF STEEL BARS IN CONTACT WITH STEAM AT 1100 F FOR 200 HR, 500 HR, 1000 HR, AND 2000 HR

1100 F ± 5 F for time intervals of 100 hr, 200 hr, 500 hr, and 1000 hr in order to determine the effect of time on the extent of corrosion. The analyses of the various steels are shown in Table 5. Specimens of each alloy were cut from $1^1/_2$-in-OD × 1-in-ID tube stock, machined to size, and sandblasted. The results are shown in Table 5 and are represented by smoothed curves in Fig. 6. The scattered results were attributed to irregular temperature distribution and the difficulty encountered in ascertaining whether or not the scale had been removed completely from the inside surface of the tube. Nevertheless, this test does show the great influence of the chromium content upon the extent of corrosion. Due to the difficulty of removing the scale from the inner surface of the tube it was decided to change from tube to bar specimens in subsequent tests.

EFFECT OF SURFACE FINISH

With the adoption of bar-stock specimens having accessible surfaces, a study was made of the effect of surface finish on the bar specimens in order to ascertain whether or not sandblasting

TABLE 7 CORROSION OF STEEL BARS IN CONTACT WITH STEAM AT 1100 F FOR 200, 500, 1000, AND 2000 HR

Steel	Chemical Analysis (Ladle) Percent									Test					
										200 Hour		500 Hour		1000 Hour		2000 Hour	
	C	Mn	P	S	Si	Cr	Ni	Mo	Cb	Number of Samples	Average Penetration, Inches	Number of Samples	Average Penetration, Inches	Number of Samples	Average Penetration, Inches	Number of Samples	Average Penetration, Inches
S.A.E. 1010	0.08	0.30	0.017	0.034	--	--	--	--	--	18	0.000826	8	0.001238	13	0.001348	16	0.001700
Carbon-Moly	0.15	0.44	0.014	0.025	0.17	--	--	0.54	--	--	---	--	---	--	---	--	---
1.25 Cr-Moly	0.11	0.43	0.012	0.012	0.80	1.22	--	0.53	--	8	0.000788	4	0.000796	6	---	8	0.001159
2 Cr-Moly	0.11	0.47	0.017	0.016	0.40	1.98	--	0.51	--	8	0.000738	8	0.000811	5	0.001349	8	0.001163
3 Cr-Moly	0.11	0.51	0.014	0.016	0.36	2.95	--	0.98	--	7	0.000748	5	0.000812	8	0.001348	8	0.001131
4-6 Cr-Moly	0.12	0.41	0.017	0.016	0.28	4.60	--	0.54	--	6	0.000604	--	---	5	0.000943	8	0.000956
9 Cr-Moly	0.11	0.36	0.010	0.016	0.27	9.00	--	1.22	--	3	0.000324	4	0.000459	7	0.000485	4	0.000694
12 Cr	0.05	1.19	0.021	0.025	0.38	11.92	--	--	--	8	0.000095	3	0.000122	8	0.000091	4	0.000045
18-8-Cb stabilized	0.07	0.36	0.015	0.012	0.39	18.62	9.9	--	1.11	8	0.000022	4	0.000019	8	0.000079	8	0.000012

TABLE 8 CORROSION OF STEELS IN CONTACT WITH STEAM BETWEEN 1343 AND 1405 F FOR 300 HR

Steel	Chemical Analysis (Ladle) Percent									Temp., F	Number of Samples	Average Penetration, Inches
	C	Mn	P	S	Si	Cr	Ni	Mo	Cb			
S.A.E. 1010	0.08	0.30	0.017	0.034	--	--	--	---	--	1343	4	0.02240
4-6 Cr-Moly	0.12	0.41	0.017	0.016	0.28	4.60	--	0.54	--	1357	4	0.01810
7 Cr-Moly	0.11	0.43	0.012	0.011	0.92	7.35	--	0.59	--	1371	4	0.00368
9 Cr-Moly	0.11	0.38	0.010	0.016	0.27	9.00	--	1.22	--	1382	4	0.00086
12 Cr	0.10	0.51	0.022	0.029	0.40	12.70	--	---	--	1382	4	0.00020
18-8-Cb stabilized	0.08	0.36	0.015	0.012	0.39	18.62	9.90	---	1.11	1386	4	0.00002
18-8	0.08	1.13	0.014	0.078	0.39	18.79	9.08	0.27	--	1405	2	0.00002

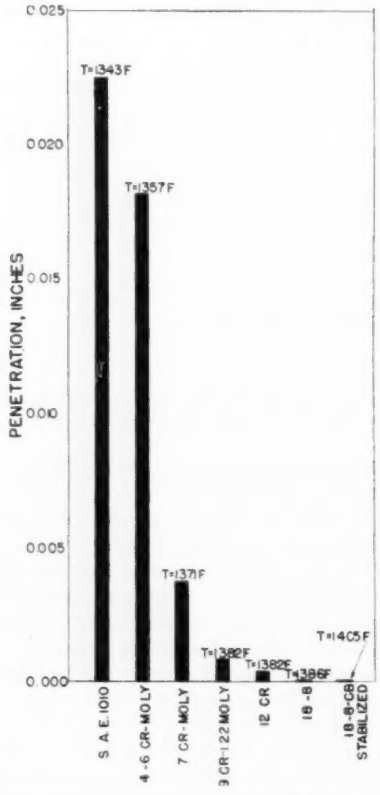


FIG. 9 CORROSION OF STEELS IN CONTACT WITH STEAM FROM 1343 F TO 1405 F FOR 300 HR

was suitable for standardizing the surfaces of the various alloys. For this study thirty-nine specimens were prepared from 1/2 in-diam S.A.E. 1020 steel. Twenty-one specimens were annealed for 30 min at 1600 F and air-cooled. Of these, fourteen were surface-sandblasted, and seven surface-ground and lapped. Of the sandblasted specimens, seven were boiled in distilled water for 24 hr and then washed in ether and 95 per cent ethyl alcohol immediately before being placed in the test section. Of the eighteen specimens which were unannealed, seven were cold-worked by severe bending and straightening and finally surface-

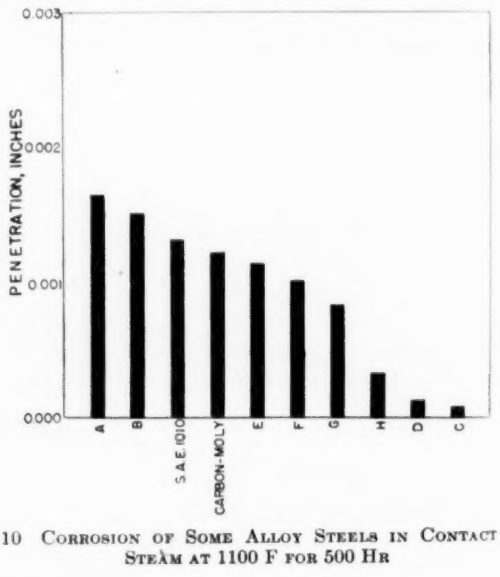


FIG. 10 CORROSION OF SOME ALLOY STEELS IN CONTACT WITH STEAM AT 1100 F FOR 500 HR

TABLE 9 CORROSION OF SOME ALLOY STEELS IN CONTACT WITH STEAM AT 1100 F FOR 500 HR

Steel	Chemical Analysis (Ladle) Percent											Number of Samples	Average Penetration, Inches
	C	Mn	P	S	Si	Cr	Ni	Mo	Al	Cu	Va		
S.A.E. 1010	0.08	0.30	0.017	0.034	--	--	---	--	--	--	--	16	0.001317
Carbon-Moly	0.15	0.44	0.014	0.025	0.17	--	---	0.54	--	--	--	16	0.001220
Alloy A	--	1.43	---	---	1.72	2.44	14.56	--	--	6.39	--	6	0.001650
Alloy B	0.18	0.52	---	---	0.24	1.23	---	0.23	1.18	--	--	6	0.001508
Alloy C	0.07	0.24	---	---	1.10	11.57	0.17	1.02	--	--	--	9	0.000076
Alloy D	0.06	0.28	---	---	0.34	12.02	0.12	1.16	--	--	--	8	0.000129
Alloy E	0.17	0.50	---	---	0.67	1.79	---	0.69	--	--	--	12	0.001141
Alloy F	0.20	0.46	---	---	0.16	0.96	---	--	--	--	0.15	12	0.001080
Alloy G	0.09	0.32	---	---	0.62	0.74	0.31	--	--	0.35	--	11	0.000832
Alloy H	0.11	0.38	---	---	0.27	9.00	---	1.22	--	--	--	11	0.000324

sandblasted, seven were sandblasted, and four were sandblasted and surface cold-worked by peening with a ball-peen hammer. The specimens were placed in cages and allowed to remain in contact with 1100 F steam for 500 hr.

The results are shown in Table 6. From a study of these data, it was decided that the method already adopted of annealing and sandblasting test bars was satisfactory when cost, time of preparation, and consistency of results were considered.

Test on Bar Specimens to Determine Influence of Length of Test

The effect of time on corrosion at 1100 F for a number of different-alloy bars was next studied. Four different tests were conducted on the various alloys; the lengths of these tests were 200 hr, 500 hr, 1000 hr, and 2000 hr. Specimens of each alloy steel and low-carbon steel as listed in Table 7 were used in each of the tests. The smoothed results are shown in Fig. 7. In general, the corrosion decreases as the chromium content of the steel increases. The high-chromium steels are practically corrosion-resistant. The various 4-6 Cr steels fall in one general class, and it is not possible from this test to segregate the steels within this group. The corrosion is very rapid during the first 100 hr after which the layer of corrosion products retards the oxidation rate under steady temperature conditions. During this series of tests, from 65 to more than 80 per cent of the corrosion occurring in 2000 hr took place during the first 500 hr.

Effect of Steam Temperature on Corrosion of Bar Specimens

A series of tests was completed to determine the effect of steam temperature for a constant time on the corrosion resistance of the same steels as listed in Table 7, together with samples of carbon-moly steel. The specimens were treated in the usual manner, and subjected to steam at various temperatures. The smoothed results are shown as solid lines in Fig. 8. Except for the high-chromium steels, corrosion increases very rapidly at temperatures in excess of about 1100 F. The high-chromium steels showed very little corrosion even at 1200 F.

A special test was conducted at very high steam temperatures in order to observe the corrosion of the high-chromium steels. Seven steels as listed in Table 8 were subjected to high-temperature steam for a period of 300 hr. Heater failures prevented continuation of the test beyond this time. The results are shown in Fig. 9 and Table 8. The temperatures at which each steel was tested are shown. Steels having 7 per cent chromium or more showed very little corrosion. The 18-8 stainless steels both stabilized and unstabilized were practically unattacked at these temperatures. The results of this 300-hr test were converted to a 500-hr basis by the use of Fig. 7. This extrapolated prediction has been plotted in Fig. 8 as dotted lines.

A test on the alloy steels, shown in Table 9, was conducted for 500 hr at 1100 F. The results are shown in Fig. 10 and Table 9. As has been shown in the other tests, the chromium content has a marked influence on the corrosion. The high-copper alloy (A), and the aluminum-and-low-silicon alloy (B) show a higher corrosion than either low-carbon steel or carbon-moly steel.

Corrosion Tests on Stellite, Hastelloy, Colmonoy, and Lamite

One bar of grade 3 and one of grade 6 Haynes Stellite each $\frac{1}{2}$ in. diam and 14 in. long were tested in contact with 1100 F steam for a total of 1300 hr. The cumulative test consisted of two 500-hr, one 200-hr, and one 100-hr tests. Examination of the surfaces after 1300 hr of testing showed that the amount of oxide

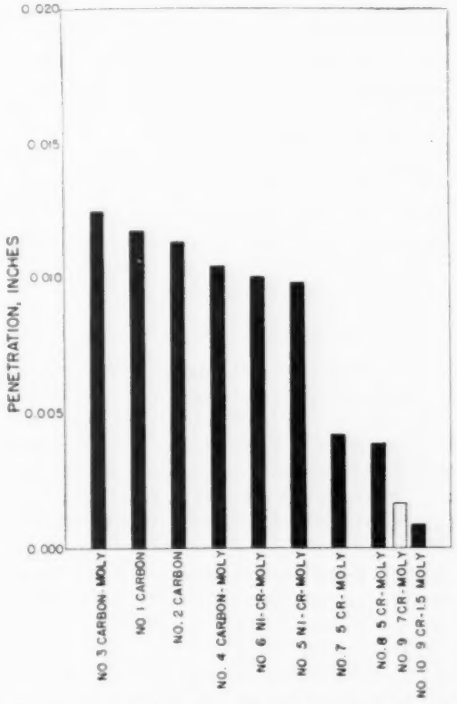


Fig. 11 Corrosion of Cast Steels in Contact With Steam at 1200 F for 570 Hr

TABLE 10 CORROSION OF CAST STEELS AT 1200 F FOR 570 HR

Specimen Number	Type of Cast Steel	Chemical Analysis (Ladle) Percent								Number of Samples	Average Penetration, Inches
		C	Mn	P	S	Si	Cr	Ni	Mo		
1	Carbon	0.24	0.95	0.020	0.010	0.44	----	----	----	2	0.01160
2	Carbon	0.25	0.75	0.022	0.018	0.44	----	----	----	2	0.01139
3	Carbon-Moly	0.21	0.64	0.020	0.012	0.43	----	----	0.49	2	0.01252
4	Carbon-Moly	0.20	0.71	0.020	0.015	0.37	----	----	0.49	2	0.01049
5	Ni-Cr-Moly	0.35	0.61	0.021	0.010	0.45	0.64	2.13	0.26	2	0.00992
6	Ni-Cr-Moly	0.28	0.62	0.018	0.010	0.44	0.73	2.25	0.26	2	0.01012
7	5 Cr-Moly	0.22	0.65	0.032	0.010	0.77	5.07	----	0.47	1	0.00429
8	5 Cr-Moly	0.27	0.63	0.026	0.010	0.87	5.49	----	0.43	2	0.00395
9	7 Cr-Moly *	0.11	0.43	0.012	0.011	0.92	7.33	----	0.59	2	0.00173
10	9 Cr-1.5 Moly	0.23	1.05	0.032	0.015	0.84	9.09	----	1.56	5	0.00088

* Not a cast steel

formed was too small to determine by the stripping method. Three specimens each of Hastelloy A, B, and C were placed in contact with 1100 F steam for a period of 500 hr. A very thin layer of corrosion products was observed, which was too thin to determine by the stripping operation. Three specimens each of Hastelloy A, B, and C together with pieces of grades 3 and 6 of Haynes Stellite were placed in contact with steam at 1200 F for 1300 hr. The scale formed was very thin and the amount could not be determined by the stripping process.

Rod samples of Colmonoy and Lamite No. 4, No. 5, and No. 6 were placed in contact with steam at 1200 F for 570 hr. A very thin layer of scale formed but was too thin to measure by the electrolytic stripping method. All of these special alloys are extremely resistant to steam corrosion.

Corrosion of Cast Steels

This test was performed to determine the oxidation of several types of cast steels, the analyses of which are given in Table 10. The test specimens were machined from cast test coupons. The final specimens were 6 in. long and $^1/_2$ in. diam. The specimens were exposed to steam at 1200 F for 570 hr. Along with the cast-steel specimens, samples of 7-Cr rolled steel were placed in the reaction chamber for purposes of comparison with earlier results. The results of the test are shown in Table 10 and Fig. 11. The results from the 7-Cr steel check earlier tests within the accuracy of the experimental measurements. The corrosion decreases as the chromium content increases, as was the case with other steels having similar compositions. In general, the corrosion of cast-steel specimens is not materially different in amount from the corrosion of rolled-steel specimens.

Effect of Temperature Changes on Corrosion Rate

This phase of the general test program was undertaken to determine the effect of extreme temperature fluctuations on the corrosion of various steels. Specimens of five different unstressed steels, as listed in Table 11, were placed in contact with superheated steam at a steady temperature of 1200 F for 500 hr. At the end of this period three specimens of each steel were removed and stripped electrolytically in order to measure the loss in weight due to corrosion. One half of the remaining specimens were held at 1200 F, with sudden cooling to room temperature in nitrogen and heating again to 1200 F every 100 hr until the total time in contact with 1200 F steam was 1200 hr. The remainder of the specimens were treated similarly except for a 50-hr cooling cycle. Specimens were removed after 700 hr and at the end of the test, in order to measure the extent of corrosion.

Fig. 12 shows typical specimens at the end of the test. The first visible evidence of extensive cracking of the scale occurred after a total exposure to steam of 700 hr. The result of visual observation during the test indicated that the layer of corrosion products is thinner and more brittle as the chromium content increases up to 5 per cent. An examination of the specimens, shown in Fig. 12, indicates that the scale on the low-carbon-steel specimens was very thick, porous, and, in spite of the severe temperature shocks, spalled only slightly as compared to the 4-6 Cr steel. The 2 per cent Cr steel spalled less than the 3 per cent Cr steel while the third layer of scale was cracking in the 4–6 per cent Cr steel at the end of 1200 hr. Little scale formed on the 9 per cent Cr steel and a microscopic examination of the surfaces at the end of the test failed to show evidence that the scale had cracked or checked.

Fig. 13 is a plot of the results. It is apparent that the difference in results from the 50- and 100-hr-cycle tests is not significant. The thickness of the scale or, in other words, the time of exposure is the factor which controls cracking and spalling under temperature fluctuations for any given steel. The corrosion decreases as the amount of chromium in the steel increases.

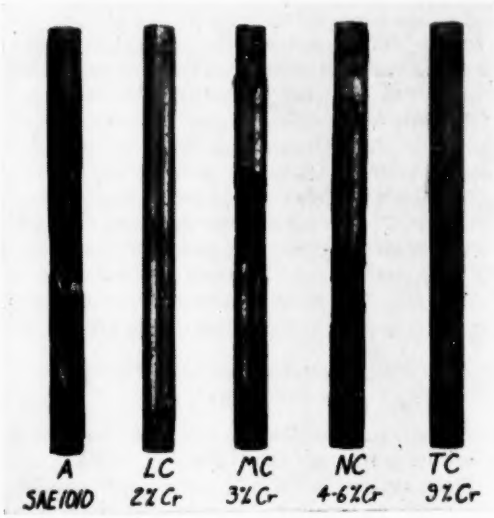


Fig. 12 Specimens Exposed to Steam at 1200 F for 1200 Hr (Specimens cooled to room temperature every 50 hr, after a continuous exposure to steam at 1200 F for 500 hr.)

Another test was conducted in order to continue the study on the effect of intermittent heating and cooling of the test samples, and to observe the effect of the specimen-surface shape.

The ladle analyses of the steels selected for the test are shown in Table 12. Pieces of 1.5-in-OD × 1-in-ID tubing, 4 in. long, were machined externally and internally to remove mill scale, after which hexagonal flats were machined on about 40 per cent of the external surface. The specimens were then split longitudinally. The three types of surface on each piece afforded a

TABLE 11 CORROSION OF FIVE STEELS BY STEAM AT 1200 F WHEN SUBJECTED TO EXTREME TEMPERATURE FLUCTUATIONS

Steel	Chemical Analysis (Ladle) Percent							Test							
								500 Hour Constant Temperature		700 Hour Intermittent				1200 Hour Intermittent	
										50 Hour Cycle		100 Hour Cycle		50 Hour Cycle		100 Hour Cycle	
	C	Mn	P	S	Si	Cr	Mo	Number of Samples	Average Penetration, Inches	Number of Samples	Average Penetration, Inches	Number of Samples	Average Penetration, Inches	Number of Samples	Average Penetration, Inches	Number of Samples	Average Penetration, Inches
S.A.E. 1010	0.08	0.30	0.017	0.034	--	--	--	3	0.0105	3	0.0123	3	0.0113	3	0.0156	4	0.0155
2 Cr-Moly	0.11	0.47	0.017	0.016	0.40	1.98	0.51	4	0.0094	4	0.0111	3	0.0105	3	0.0125	3	0.0118
3 Cr-Moly	0.11	0.51	0.014	0.016	0.36	2.95	0.98	2	0.0092	4	0.0096	3	0.0089	3	0.0108	3	0.0102
4-6 Cr-Moly	0.12	0.41	0.017	0.016	0.28	4.60	0.54	3	0.0075	3	0.0080	3	0.0084	4	0.0092	3	0.0100
9 Cr-1.22 Moly	0.11	0.38	0.010	0.016	0.27	9.00	1.22	3	0.0015	3	0.0011	3	0.0011	3	0.0013	4	0.0012

Note: Temperature was constant at 1200 F for 500 hours, followed by intermittent cooling to room temperature from 1200 F after 50 or 100 hour intervals at 1200 F.

TABLE 12 CORROSION OF STEELS IN CONTACT WITH STEAM DURING INTERMITTENT OPERATION AT 1200 F FOR 1300 HR

Steel	Chemical analysis (ladle), Per cent													Number of Samples	Average Penetration, Inches
	C	Mn	P	S	Si	Cr	Ni	Mo	Cb	Al	Cu	Ti	Va		
S.A.E. 1010	0.15	0.53	0.008	0.028	0.09	0.05	0.08	--	--	--	0.014	--	--	4	0.01560
Carbon-Moly	0.12	0.52	0.010	0.020	0.21	--	--	0.53	--	--	--	--	--	4	0.01520
S.A.E. 6120	0.21	0.43	--	--	--	1.00	--	--	--	--	--	--	0.18	4	0.00809
2 Cr-Moly-Al-Si	0.09	0.28	0.011	0.014	1.27	2.02	--	0.55	--	0.70	--	--	--	3	0.00501
3 Cr-Moly	0.15	0.48	0.011	0.016	0.45	3.12	--	0.80	--	--	--	--	--	3	0.00755
4-6 Cr-Moly	0.09	0.46	0.030	0.030	0.30	4.75	--	0.55	--	--	--	--	--	3	0.00597
4-6 Cr-Moly-Si	0.13	0.25	0.014	0.012	1.50	4.98	--	0.50	--	--	--	--	--	3	0.00002
4-6 Cr-Moly-Al-Si	0.13	0.34	0.012	0.012	0.82	5.20	--	0.54	--	0.55	--	--	--	3	0.00487
4-6 Cr-Moly-Cb stabilized	0.10	0.48	0.015	0.014	0.25	6.00	--	0.50	0.77	--	--	--	--	2	0.00467
4-6 Cr-Moly-Ti stabilized	0.08	0.31	0.015	0.013	0.47	5.18	0.25	0.54	--	--	--	0.63	--	4	0.00433
9 Cr-1 Moly	0.13	0.42	0.025	0.016	0.23	8.46	--	1.52	--	--	--	--	--	3	0.00266
12 Cr	0.04	0.75	0.026	0.025	0.31	11.69	0.66	0.31	--	--	--	--	--	2	0.00128
18-8	0.05	0.41	0.020	0.011	0.48	18.23	9.96	--	--	--	--	--	--	4	0.00004
18-8-Cb stabilized	0.06	0.58	0.016	0.014	0.38	17.29	12.20	--	0.68	--	--	--	--	4	0.00003

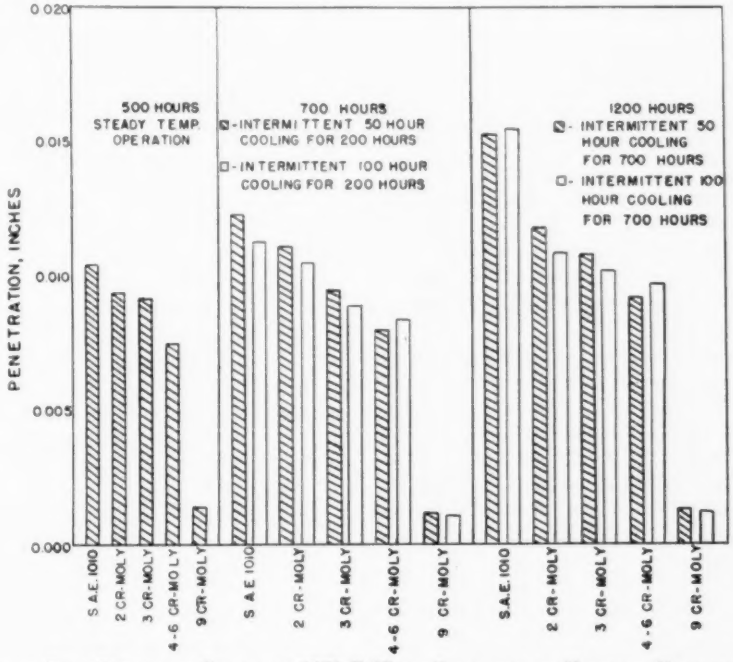


FIG. 13 CORROSION OF FIVE STEELS BY STEAM AT 1200 F WHEN SUBJECTED TO EXTREME TEMPERATURE FLUCTUATIONS

means for observing the effect of the shape of surface on the corrosion of the steel.

The specimens were placed in the steam reaction chamber at a temperature of 1200 F for 500 hr, after which they were removed and rapidly cooled in an atmosphere of nitrogen to room temperature. Two pieces of each steel were removed for use in establishing the oxidation rate for 500 hr. The remaining four pieces of each steel were placed in the reaction chamber at 1200 F. All specimens were removed, cooled to room temperature, examined, and replaced in the reaction chamber at 600, 700, 800, 900, 1000, and 1150 hr. At the end of 1300 hr of actual test time, the steel samples were removed and the penetration determined. The time intervals previously stated indicate the time the specimens were in contact with the steam and do not include the cooling or heating periods. The temperature-history chart for the test is shown in Fig. 14. This chart shows two heater failures. During these interruptions the reaction cham-

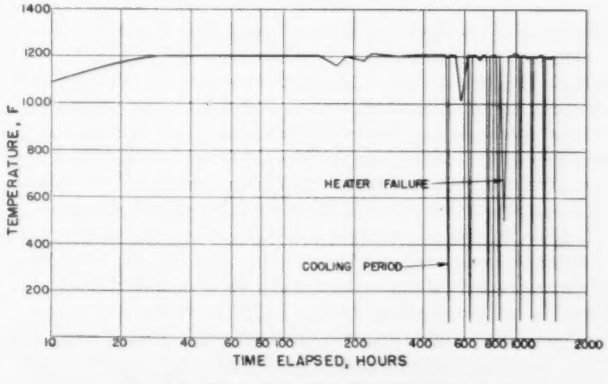


FIG. 14 TEMPERATURE-HISTORY CHART

bers were filled with nitrogen until the necessary repairs were made.

Before stripping the scale from the steel samples a 1.25-lb sphere, dropped from a height of 3 ft, struck the end of each piece four times in order to measure the adherent property of the scale.

The scale on all samples was removed at the conclusion of the impact test. After the scale was completely removed, the pieces of steel were weighed in order to determine the loss in weight from which the penetration was computed.

At the end of 500 hr, all the steel samples showed a smooth oxide coating without visible cracks in the scale. Several of the samples of 4-6 Cr-Moly-Ti stabilized showed signs of cracking of

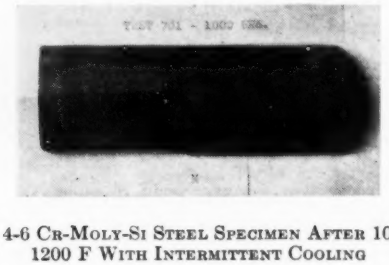


FIG. 15 4-6 CR-MOLY-SI STEEL SPECIMEN AFTER 1000 HR AT 1200 F WITH INTERMITTENT COOLING

the scale at the end of 600 hr. This was the first indication of the excessive scaling which was later observed. Samples of 18-8-Cb stabilized and 18-8 unstabilized showed very little scale formation. At the end of 700 hours flakes of scale had chipped off the samples of 4-6 Cr-Moly and 4-6 Cr-Moly-Si. The parent metal which had been exposed by the scale cracks on specimens of 4-6 Cr-Moly-Ti stabilized was again covered with a new layer of oxide. No new changes were observed when the specimens were examined at the end of 800 hours.

While the steel samples were being cooled at the 900-hr period, the noise of scale cracking from some of the specimens was audible. The scale on the specimen of S.A.E. 1010 was very thick but adhered rigidly to the metal. The scale on the pieces of 2 Cr-Moly-Al-Si and 4-6 Cr-Moly-Si flaked off in elliptical sections. This type of flaking occurred on the outer curved and flat surface, but did not exist on the inner curved surface. Scale on steels of S.A.E. 6120, 3 Cr-Moly, and Carbon-Moly, although thick, showed no signs of chipping. Complete layers of scale flaked off specimens of S.A.E. 1010 but in no case was the parent metal visible. In all the other steels the parent metal was visible after the scale flaked off. A very small scale layer formed on steels of 18-8-Cb stabilized, 18-8, 12 Cr, and 9 Cr-1$^1/_2$ Moly. The scale on 4-6 Cr-Moly-Cb stabilized was thicker than on 9 Cr-1$^1/_2$ Moly. Steels of 4-6 Cr-Moly-Ti stabilized, 4-6 Cr-Moly, 4-6 Cr-Moly-Si, and 4-6 Cr-Moly-Al-Si all showed sections where large pieces of scale had flaked off.

Fig. 15 is from a photograph, taken at the end of 1000 hr, of the 4-6 Cr-Moly-Si steel which clearly indicates the elliptical shape of the flakes of scale which had cracked from the external surface of the specimen. No appreciable changes were noticed at the end of 1150 hr. At the conclusion of the test, the scale formed on S.A.E. 1010, Carbon-Moly, 3 Cr-Moly, and S.A.E. 6120 steels was very thick but adhered tightly to the parent metal. Considerable flaking of the scale had occurred on specimens of 4-6 Cr-Moly-Ti stabilized, 4-6 Cr-Moly-Si, 4-6 Cr-Moly, 2 Cr-Moly-Al-Si, and 4-6 Cr-Moly-Al-Si. Very little scale had formed on 18-8-Cb stabilized, 18-8, 12 Cr, 9 Cr-1$^1/_2$ Moly.

The results of this test have been plotted in Figs. 16 and 17. The importance of chromium content on the resistance to corrosion is apparent from these figures. In Fig. 17, point (1) is

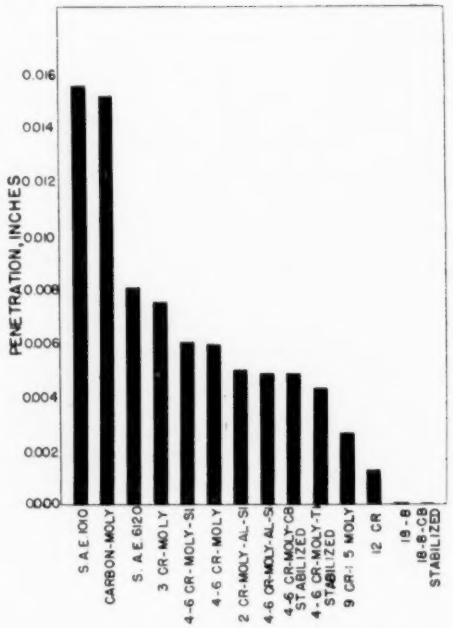


FIG. 16 CORROSION OF STEELS IN CONTACT WITH STEAM DURING INTERMITTENT OPERATION FOR 1300 HR AT 1200 F

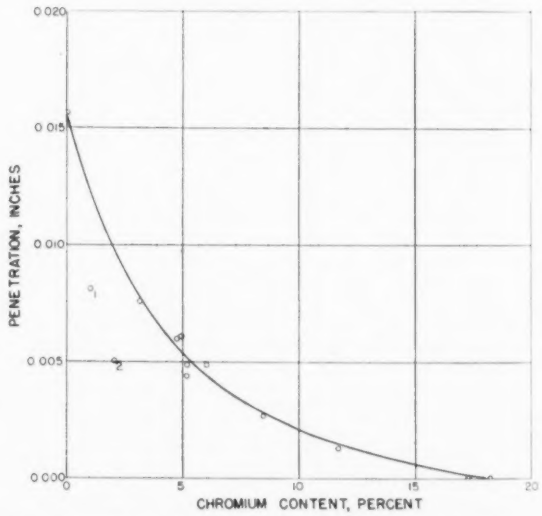


FIG. 17 INFLUENCE OF CHROMIUM CONTENT ON CORROSION OF STEELS DURING INTERMITTENT OPERATION AT 1200 F FOR 1300 HR

for S.A.E. 6120 which is high in vanadium and point (2) is for 2 Cr-Moly steel high in aluminum and silicon. With the exception of these two points which have been neglected in constructing the curve in Fig. 17, the test points for the other steels show a good correlation between chromium content and corrosion penetration.

The steels tested for 1300 hr may be grouped into three general classes according to the scale formed: The first group consists of specimens of Carbon-Moly, 3 Cr-Moly, S.A.E. 6120, and S.A.E. 1010 which were all covered with a thick porous tightly adhering scale.

The scale formed on the steels of the second group, 4-6 Cr-Moly-Cb stabilized, 4-6 Cr-Moly-Al-Si, 4-6 Cr-Moly-Si, 2 Cr-Moly-Al-Si, 4-6 Cr-Moly, and 4-6 Cr-Moly-Ti stabilized was very brittle and flaked off the specimens during the test. The scale formed on specimens of 4-6 Cr-Moly-Si and 2 Cr-Moly-Al-

Si which were exposed to the steam at 1200 F for 1300 hr flaked off in elliptical sections. This type of flaking may be due to the silicon in the steel, since the silicon contents of 4-6 Cr-Moly-Si and 2 Cr-Moly-Al-Si were 1.5 and 1.27 per cent, respectively. Specimens of 4-6 Cr-Moly-Al-Si, which has a silicon content of 0.82 per cent, showed a slight tendency toward this type of flaking. From the visual and microscopic examination of the specimens the scale found on the inside curved surface did not flake off as much as the scale formed on either the outer curved or flat surfaces. No difference in the amount of scale flaking off the outer curved and flat surfaces could be detected.

Alloys of the third group consisting of steels of 18-8-Cb stabilized, 18-8, 12 Cr, and 9 Cr-1½ Moly were covered with a very thin layer of scale which adhered tightly to the parent metal.

In Table 12 the penetration for steel of 3 Cr-Moly is higher than for steel of 2 Cr-Moly-Al-Si, in spite of the fact that steel of 3 Cr-Moly has a higher chromium content than the sample of 2 Cr-Moly-Al-Si. Since 2 Cr-Moly-Al-Si contained both silicon and aluminum it may be that the combination of these two elements reduces the rate of oxidation.

The impact test showed that the oxide layers formed on samples of Carbon-Moly, S.A.E. 6120, and S.A.E. 1010 adhere to the metal as was evident by a slight amount of flaking. Practically all the outer layers of scale on steel of 3 Cr-Moly were removed during the impact test. Considerable flaking of the scale formed on steels of 4-6 Cr-Moly-Cb stabilized, 4-6 Cr-Moly-Al-Si, 4-6 Cr-Moly-Si, 4-6 Cr-Moly, 4-6 Cr-Moly-Ti stabilized, and 2 Cr-Moly-Al-Si occurred during the impact test. No scale was removed from samples of 18-8 Cb stabilized, 18-8, 12 Cr, and 9 Cr-1½ Moly during the impact test.

General Conclusions

1 The resistance of alloy steels to high-temperature steam is greatly influenced by the amount of chromium present. Alloy steels containing 7 per cent or more of chromium are very resistant to corrosion produced by steam at temperatures up to at least 1400 F. The 18-8 stainless steels showed practically no corrosion when subjected to steam at temperatures up to 1400 F.

2 The corrosion rate is very rapid during the first 500 hr of testing and then gradually diminishes as the time of exposure to the steam continues.

3 Steam temperatures greatly influence the corrosion of steels. Except for steels containing 7 per cent or more of chromium, the corrosion rate increases very rapidly at temperatures in excess of 1100 F.

4 The steels tested may be grouped into three general classes according to the type of scale formed. The first group consists of low-carbon steel, carbon-moly, and the low-chromium steels which are covered with a thick, porous, tightly adhering scale. The scale which forms on the steels of the second group, that is, the 4-6 Cr steels and the 2 Cr-Moly-Al-Si steel, is very brittle and easily flakes off under fluctuating temperatures. The third group consists of steels having a chromium content of 7 per cent or more upon which a very thin, nonporous, tightly adhering scale is formed.

5 Scale formed on the inner surface of a tube does not flake off as readily as the scale which has formed on the outer surface of a tube.

Acknowledgments

This investigation has been sponsored by the A.S.M.E. Special Research Committee on Critical-Pressure Steam Boilers. The authors wish to express their appreciation of the valuable assistance rendered by the members of this Committee.

In this undertaking Purdue University had effective co-operation from the Engineering Foundation, The American Society of Mechanical Engineers, The Babcock and Wilcox Company, The Detroit Edison Company, the Timken Roller Bearing Company, the Superheater Company, the National Tube Company, the Crane Company, the International Nickel Company, The Haynes Stellite Company, and the Continental Steel Corporation.

The authors are particularly indebted to C. L. Clark, research metallurgical engineer of the Timken Roller Bearing Company, Steel and Tube Division, for constructive criticism and valuable assistance rendered. Special acknowledgment is due H. J. Kerr of The Babcock and Wilcox Company, C. H. Fellows and R. M. Van Duzer, of The Detroit Edison Company, E. L Robinson of the General Electric Company, W. H. Armacost of Combustion Engineering Company, E. C. Petrie and J. J. Kanter of the Crane Company.

To the recent graduates of Purdue University, J. G. Miller, H. Templeton, W. H. Winslow, J. T. Agnew, W. R. Shade, and M. H. Davis, the authors owe a debt of gratitude, for it was through their untiring efforts that this project was brought to a satisfactory conclusion.

Discussion

C. L. Clark.[8] The authors are to be complimented on their contribution to the general subject of the effect of alloy additions on the surface stability. The point of particular interest in this respect is Fig. 17, showing the influence of chromium content on the corrosion resistance in steam at 1200 F. On the basis of this figure, chromium appears to be the predominating factor in so far as the resistance to steam attack is concerned.

Certain alloy additions do not appear to exert the same degree of protection against steam attack as against air oxidation. This is well illustrated in Fig. 18 of this discussion, in which the steam-corrosion results have been replotted on the basis of their ratio to

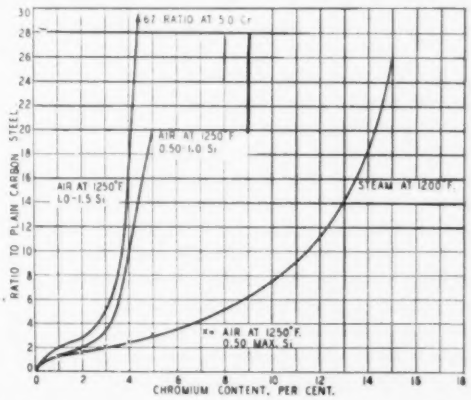


Fig. 18 Influence of Silicon Content on Oxidation Resistance in Steam and Air

carbon steel. Air oxidation tests at 1250 F, rather than at 1200 F, fall exactly on this same curve when the steels contain 0.50 per cent silicon maximum. If, however, the silicon content is either 0.50 to 1 or 1 to 1.5 per cent, then the resistance to attack in air is greatly superior to that in steam. In other words, increased silicon content is beneficial against air oxidation but not in steam.

The resistance of steels to the attack of hot petroleum products is another case in which chromium content is the main controlling factor, and a comparison of the relative influence of this element against steam and oil attack should be of interest. This condi-

[8] Research Metallurgical Engineer, The Timken Roller Bearing Company, Steel and Tube Division, Canton, Ohio.

tion is shown in Fig. 19 of this discusssion, with the results being expressed on the basis of their ratio to a 1 per cent chromium steel. The curve for the resistance to the attack of hot petroleum products expresses the results from four different refineries in which the corrosive conditions were entirely different, but in which, as shown, the relative influence of chromium content was exactly

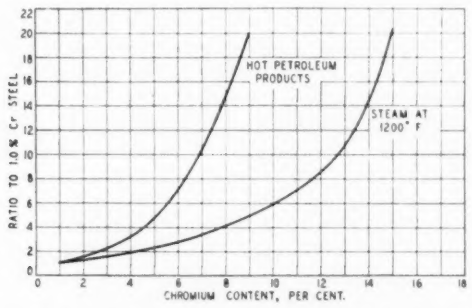


FIG. 19 COMPARATIVE CORROSION RESISTANCE IN STEAM AND HOT PETROLEUM PRODUCTS

the same. These results would indicate increasing chromium content to be more effective against hot petroleum products than against steam at 1200 F.

The mechanism of attack in steam, air, and hot petroleum products must be different; and it is hoped the authors in their future work will obtain data to explain these differences between steam and air attack. The hydrogen present, because of the dissociation of the steam, may have an important influence on the type of scale formed.

R. M. VAN DUZER, JR.[6] Those who have known of the steam-corrosion research program under way at Purdue University have awaited with interest the results published in this paper. It is hoped that this work will be continued and that the other phase of the research project, dealing with the corrosion of specimens subjected to high-temperature steam and stress, also will be made available.

The writer's company has been interested in the corrosion of alloy steel from the standpoint of its attack by 1100 F steam as part of an investigation conducted in the use of high-temperature steam for power production since 1929. The corrosion phase of this work, started first as an investigation of various materials suitable for superheater tubes, was later augmented by tests on materials usable for valves and turbines when subjected both to 925 and 1100 F steam.

The tests by The Detroit Edison Company have been made using $\frac{1}{2}$-in. round × 6-in. ground-and-polished specimens which were held in a cage slipped into a steam line. Cages were or are to be removed at 4000-, 8000-, 12,000-, and 16,000-hr intervals for investigation. One group of steels, at this time, has been examined after exposure to 1100 F steam for 15,000 hr.

Among these are two, similar in composition to the corresponding steels given in Table 7 of the paper, which were exposed to 1100 F for 2000 hr. The different conclusions, which may be drawn from the authors' data and that of the writer, collected over entirely different time intervals, may be of interest.

It should be mentioned that the Purdue tests were conducted under laboratory conditions, that is, close temperature control and continuous steam flow, while the Detroit Edison samples were subjected to heating and cooling cycles and temperature fluctuations which would be encountered in commercial practice. The authors' results are the average of a number of identical tests, while the writer's results are from one specimen in each case.

In Table 13 of this discussion are listed the analyses of the two steels, together with inches penetration, service hours, and number of heating and cooling periods. The specimens were annealed and the weight-loss determinations were made in a manner similar to that followed by the authors.

Plotting these results and drawing smooth curves by the method of least squares, the results shown in Fig. 20 of this discussion are obtained. If the smoothed values from Fig. 20 are plotted on log-log paper, together with the smoothed results from Fig. 7 of the paper, two different conceptions of steam corrosion are evident from Fig. 21 of this discussion.

The authors' results indicate that loss of weight with time follows a power relation, while the writer's results indicate the relationship is much more complex, and that there is not a pro-

TABLE 13 CORROSION OF SAMPLES SUBJECTED TO 1100 F STEAM

Specimen	Analysis, per cent by weight C	Si	Cr	Mo	Mu	P	S	Average penetration, in. 3840 hr	7585 hr	11427 hr	15143 hr
1.25 Cr, Mo	0.09	0.78	1.21	0.58	0.41	0.01	0.013	0.0033	0.0034	0.00362	0.0041
4–6 Cr, Mo	0.13	0.32	4.96	0.52	0.45	0.01	0.016	0.0022	0.0031	0.0038	0.0036
Heating and cooling cycles								6	12	19	31

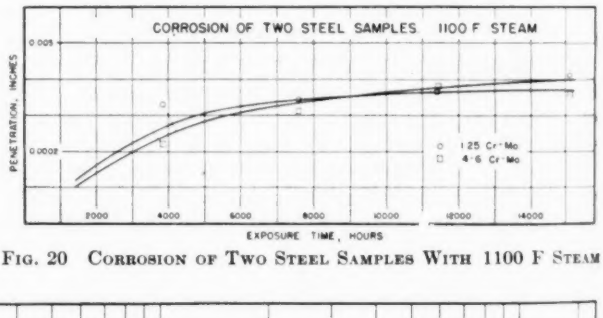


FIG. 20 CORROSION OF TWO STEEL SAMPLES WITH 1100 F STEAM

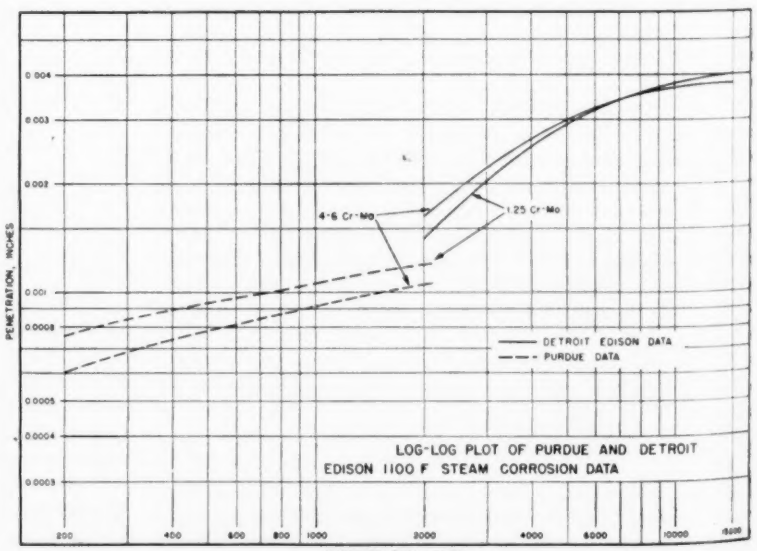


FIG. 21 LOG-LOG PLOT OF PURDUE AND DETROIT EDISON 1100 F STEAM-CORROSION DATA

[6] Engineer, Production Department, The Detroit Edison Company, Detroit, Mich. Mem. A.S.M.E.

gressive loss in weight with time, even when the specimens are subjected to heating and cooling cycles. This same tendency also was shown in examining the weight-loss data collected on samples of 0.15 C steel exposed for 15,000 hr. A further basis for the belief that there is stabilization of the surface of the corrosion specimen with exposure are results presented by White, Clark, and McCollam[7] on the analyses of the complex scale formed on the surface of unstressed furnace-heated corrosion samples.

Their analyses of the scale layers show that, in the case of the low-chromium alloys, there is an increase of as much as 40 to 50 per cent in the chromium content in the inner scale layer over that contained in the parent metal, while the alloy content of the outer scale layer is practically nil. This same condition was true where Mo and Si were present as alloying elements.

It is quite probable that a similar build-up of alloy-rich scale at the surface of steels subjected to high-temperature steam has a marked stabilizing influence on weight loss with exposure, as photomicrographs of the scale in steam-corrosion samples show that it is likewise of a complex nature.

The authors' statement, regarding the resistance of alloys containing more than 7 per cent chromium, perhaps should be more specific. A 12 Cr-2 Mo alloy steel, examined after 12,000-hr exposure to 1100 F, has shown a greater weight loss than C-Mo steel. The influence of alloy additions to low-chromium steels can be seen by comparing the penetration value obtained on 1.23 Cr, Alloy B, Table 9 of the paper, and that of the 1.25 Cr-Mo listed in Table 7 of the paper. Here, with the addition of aluminum, the weight loss in 500 hr was nearly doubled.

A. R. Mumford.[8] The authors of this paper and the Special Research Committee on Critical-Pressure Steam Boilers are to be congratulated on this contribution to the literature, concerning the occurrences of corrosion in water vapor at high temperatures.

The writer has long been interested in the corrosion of steel and iron exposed to steam and condensate at much lower temperatures, and the discussion which follows is largely influenced by the knowledge that, at low temperatures and pressures, the problem is exceedingly complex.

At first glance, if we assume that the reaction is almost solely that of the production of hydrogen, it may appear that the problem of corrosion under high temperatures is very simple, but a simple solution is exactly what we assumed at first in the study of corrosion of iron in contact with condensate. The writer feels that the paper should include some information on the analysis of the steam vapor supplied to the experimental corrosion chambers. It may well be that the contamination by oxygen and perhaps ammonia is so small that it will have no influence on the larger reaction, but a statement indicating the amounts of such gases originally present might well be included in the paper as a matter of record. We certainly are unaware of the solubilities of such contaminants in condensates at high total pressures and temperatures, and we are not aware of the effect on the reaction of such contaminants under these high-temperature conditions. Data on the composition of the condensate also might well be included for the record, even though the influence of any contaminants which might have been found cannot be evaluated at this time. Similarly, the gaseous phase over the surface of the condensate might indicate to future investigators more details of the action which took place within the chamber.

From a metallurgical standpoint, metallographic examinations of the specimens before and after exposure would have provided rather interesting information and might have made possible a full explanation of the differences in corrosion indicated by the weight losses. The writer feels that his experience in low-temperature corrosion makes it advisable to try fully to understand the mechanism of the reaction as soon as possible, in order to understand and explain the resistance of some materials under certain conditions of exposure.

It is assumed that the data presented in the paper, with particular reference to penetration of the specimen, are based on distributing the average weight loss over the exposed area of the specimen. If this assumption is correct, then the information differs only from other published information at low temperatures in presenting the total loss rather than a rate. Inches of penetration per year has been used as a rate figure for heating-system corrosion but, because of the duration of the tests reported in this paper, it might well be reported as a rate per 100 hr. The writer converted the average penetration, given in Table 11 of the paper, to average penetration per 100 hr and found that he could see more clearly the inferences drawn from the data than as presented with the total average penetration rather than a rate. The influence of the oxide coatings in slowing down the continuance of corrosion is clearly evident on the rate basis, as is also the indication of the minor significance of the cycle at which sudden cooling took place.

J. B. Romer.[9] Corrosion tests have always involved the problems incidental to the preparation of the surface of specimens, removal of the products of corrosion without marring or pitting the unattacked surface, as well as determination of the actual loss or damage sustained by the specimen.

The authors' data on surface preparation and on stripping of the oxidized surfaces clearly warrant the methods they have finally adopted.

Aside from their main problem, but nevertheless of great importance, are the data on inhibitors. This is a subject of growing importance both in research and in industry. The data, contained in Tables 1 and 2 of the paper, show that all inhibitors are not equally efficient; that the inhibitor should be selected in accordance with the acid to be used for stripping; that the efficiency of the inhibitor decreases with rise in temperature and may completely disappear if the temperature becomes too high. Of great economic importance is the fact that, beyond a critical point which varies with each inhibitor, increasing the amount of inhibitor used adds very little to its effectiveness.

The great resistance of certain alloys, such as Hastelloy, Stellite, Colmonoy, and Lamite, to oxidation by high-temperature steam may be of considerable value for certain applications. To date, these alloys either do not possess certain properties which make them suitable for steam generation, or else they are not commercially available in the required form.

Several important features have been proved by the authors, particularly:

1 The reduction in rate of oxidation with time because of the impenetrability of the oxide film, the thickness of which is increasing with time.

2 The sharp increase in rate of oxidation at certain temperature levels, notably at about 1100 F for low alloys, and at higher temperatures for the higher-alloy materials.

3 The effect of chromium in reducing the rate of oxidation. The effect of chromium is well shown by the authors in their Figs. 7, 8, and 17, the latter being at 1200 F. If we take the 1100 to 1350 F data from Fig. 8, and plot it in a manner similar to that of Fig. 17, the effect of chromium addition is outstanding. These data are presented herewith as Figs. 22 and 23.

[7] "Influence of Cr, Si, and Al on the Oxidation Resistance of Intermediate Alloy Steels," A. E. White, C. L. Clark, and C. H. McCollam, Trans. American Society for Metals, vol. 27, 1939, p. 139.

[8] Combustion Engineering Co., New York, N. Y. Formerly Associate Director of Research, Consolidated Edison Company of New York, Inc., New York, N. Y. Mem. A.S.M.E.

[9] The Babcock & Wilcox Company, Barberton, Ohio.

Chromium improves the physical properties of steel in many ways, and low-chromium alloys have very definite fields of usefulness. The authors' data on steam oxidation indicate that, when the operating temperature is below 1100 F, the gain from chromium additions is not large. However, a great deal is

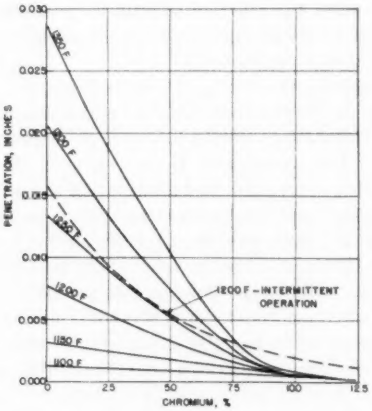


FIG. 22 INFLUENCE OF CHROMIUM CONTENT ON CORROSION OF STEELS DURING STEADY AND INTERMITTENT OPERATION

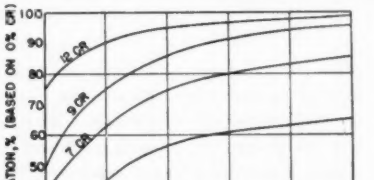


FIG. 23 DECREASE IN PENETRATION VS. TEMPERATURE FOR ALLOY STEELS

gained by adding at least 7 per cent of chromium, whenever the operating temperature is in excess of about 1150 F.

The quantitative nature of the data presented by the authors will be of great value to those engaged in high-temperature high-pressure steam design.

AUTHORS' CLOSURE

The authors are indebted to Messrs. Clark, Van Duzer, Mumford, and Romer for their excellent written discussions.

The charts presented by Dr. Clark, which show the influence of silicon content on the oxidation resistance in steam and air and compare the corrosion resistance in steam and hot petroleum products, are indeed interesting and instructive. It is hoped that it will be possible to conduct additional tests which will throw light on the mechanism of attack in steam and air as suggested by Dr. Clark.

The close relationship between the authors' results and those of Fleischmann[10] is shown in the accompanying Fig. 24. Apparently Fleischmann found that the same general relationship exists between the decrease in penetration and increased chromium content as is reported by the authors. Mr. Van Duzer stated that tests conducted by him showed that the corrosion of 12 Cr-2 Mo was greater than for C-Mo steel after 12,000 hr exposure to steam at 1100 F. He further shows that 4-6 Cr steel corrodes more than 1.25 Cr-Moly between 2000 and 7000 hr exposure, and then less after 7000 hr. The authors had hoped that a complete report would be published of the extensive tests conducted by Mr. Van Duzer and his colleagues at The Detroit Edison Company. Since these tests were made on single specimens, the extent to which conclusions may be drawn from them would depend upon the consistency of the results. In the absence of complete data, it is rather difficult to compare results.

Mr. Mumford suggested the inclusion of water analysis and results of metallographic studies. A number of water analyses were made by Dr. Chittum of the Purdue University chemistry department. These analyses revealed that no ammonia existed and the oxygen varied from a slight trace to a maximum of 0.08 cc per liter. In any case, the possibility that oxygen influenced the reaction of the specimens with steam is probably very slight. Before entering the main reaction chamber, the steam first was passed through a gas-fired iron-tube superheater which raised the temperature to between 800 and 900 F. The chances that oxygen passed through this long tube without reacting with the iron of the tube are slight. If small amounts were able to escape the gas-fired superheater tube, reaction would then probably take place in the high-temperature superheater. Examination that the superheater tubing revealed that a small amount of corrosion occurred in the gas-fired tube and only a trace in the high-temperature superheater tube.

A large number of photomicrographs were taken during the course of the investigation to show any structure changes; however, these were not intended for use in publication and would not make satisfactory prints. These plates are available in the laboratory files for examination by anyone interested in them and show no evidence of structural change.

The plots of the test data submitted by Mr. Romer are very interesting and show the marked influence of chromium content on the corrosion resistance for various temperatures.

In conclusion the authors wish to thank all of those who have presented oral and written discussions for their interest, comments and constructive criticisms.

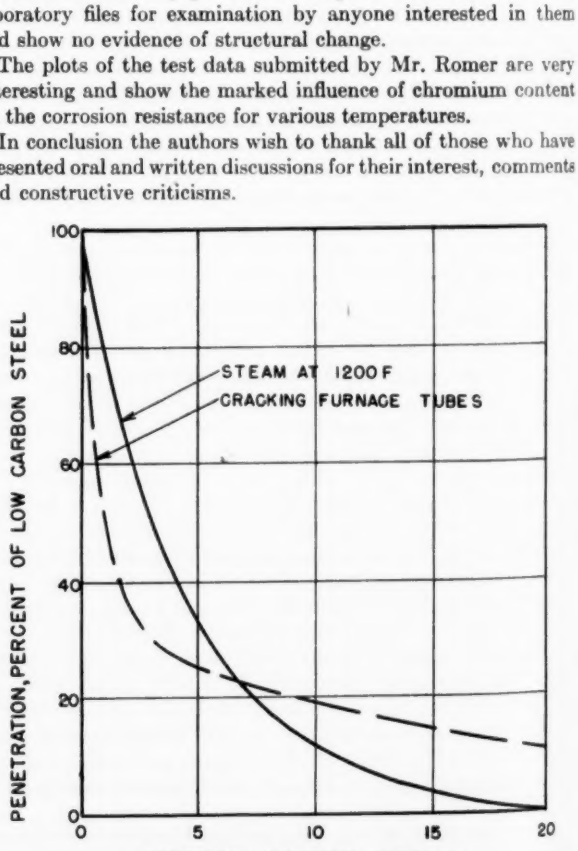


FIG. 24 COMPARISON OF CORROSION RATE AND CHROMIUM CONTENT FOR STEELS IN CONTACT WITH STEAM AND CRACKING FURNACE TUBES

[10] "Selection of Steels for High Temperature Service," M. Fleischmann, *Steel*, 1938, vol. 102, pp. 34–39.

Theoretical Consideration of Power Loss Caused by Combustion Knock

By C. W GOOD,[1] ANN ARBOR, MICHIGAN

In this paper the author presents a theoretical analysis to show that the power loss accompanying combustion knock may be attributed to a mass vibration of the gases within the combustion chamber rather than to radiation. Equations are developed, based on perfect gases, to show that, on the basis of assumptions made, pressure rise with normal combustion is proportional to the quantity of charge burned and to show the loss in effective pressure caused by the vibration resulting from knocking combustion. The latter have been developed for both the Otto and Diesel cycles and the relative theoretical losses for the two cycles is indicated. The author indicates the effect of differences between actual and assumed conditions.

POWER loss has been an accepted corollary of combustion knock for many years. This loss has been attributed to radiation. A theoretical analysis shows that it is actually due to a mass vibration or reciprocation of the gases within the combustion chamber. It is now generally accepted that a momentary high pressure is generated in that portion of the chamber where the detonation which is the source of the combustion knock occurs. The combustion in this zone is so rapid that there is insufficient time for the pressure to equalize. The gases in this region undergo a mass expansion, compressing the other portions. The inertia of the gases causes those being compressed to be compressed beyond the equalization pressure and those expanding to expand below the equalization pressure, thus starting the mass vibration in the chamber. The energy of the vibration is not effective in pushing the piston outward and thus represents a power loss. In so far as these vibrations are damped out by friction within the gas itself, the mechanical energy of the vibration reverts to heat and becomes effective. However, such motion improves the conditions for conduction of heat from the gas to the chamber walls and this increase is loss which is chargeable to the cause of the combustion knock.

While exact measurement of the various factors is difficult, an analysis based on the laws of perfect gases is relatively simple and serves to demonstrate that not only does such a loss exist but that it can be quite appreciable. In order to arrive at the loss due to combustion knock, it is first necessary to formulate the conditions for normal or nonknocking combustion and then show, by a similar type of formulation, the effect of detonation.

To facilitate calculation, the following assumptions are made:

1 The gases behave as perfect gases.

2 The number and size of molecules is unchanged by combustion.

3 The specific heats remain constant with changes in either temperature or pressure.

4 The mixture is homogeneous prior to ignition.

5 The temperature is uniform prior to ignition.

6 All the combustion occurs in the flame front.

7 The process is adiabatic, that is, there is no heat transfer between the gases and the chamber walls and there is no radiation or conduction of heat between molecules, except in the form of work.

8 The energy liberated by combustion is constant, irrespective of the temperature at which it is liberated.

9 The chamber volume remains constant.

10 Detonation is complete before any expansion of the detonating portions occurs.

Obviously, none of these assumptions hold more than approximately for actual engines, but their use permits a simplification of the problem so that an analysis can be made which will help to explain the actual phenomena.

Fig. 1 shows a diagram of pressure vs. specific volume for the compression and combustion of specific portions of a charge in which certain portions burn normally, that is, at constant pressure, while other portions burn under detonating conditions, that

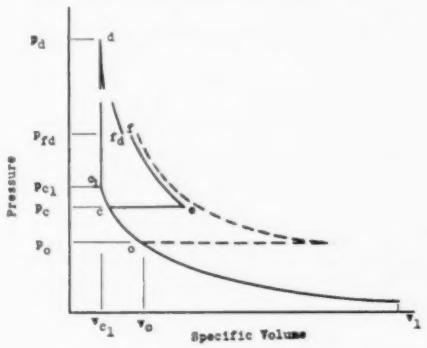


FIG. 1

is, at constant volume. The compression from 1 to *o* is accomplished by the piston. The piston is assumed to stay on top center until combustion is complete. The first portion is ignited at *o*, after which it expands during reaction along the horizontal dotted line. It is then compressed, as shown, by the other portions as they burn. As burning goes on, the portions remaining unburned are compressed adiabatically. *c* represents the point to which some specific infinitesimal portion is compressed when ignited. It then burns normally, expanding to *e*, after which burning of other portions compresses it along the adiabatic *ef*. When the pressure at which burning occurs reaches c_1, the remaining portions detonate. Their pressure and volume before expansion, based particularly on the assumption that detonation is complete before any expansion of the detonating portions occurs, is represented by *d*. They then expand along the curve df_d, compressing all the portions which had burned normally until the pressures of all the portions in the chamber have been equalized at a pressure, noted as p_{fd}, except for those variations in pressure caused by the mass vibration of gas.

On the basis of the assumptions made, the quantity of charge burned is proportional to the pressure rise with normal combus-

---

[1] Associate Professor of Mechanical Engineering, University of Michigan. Mem. A.S.M.E.

Presented at the National Meeting of the Oil and Gas Power Division, Kansas City, Mo., June 11–14, 1941, of THE AMERICAN SOCIETY OF MECHANICAL ENGINEERS.

NOTE: Statements and opinions advanced in papers are to be understood as individual expressions of their authors, and not those of the Society.

tion. This is shown by the following development. In Fig. 2, let the total volume of the cylinder be represented by v. Let the volume of a portion before burning, say the first tenth, be represented by v_b and the same portion after burning by v_a. During the burning of the first portion, the remaining portions would be compressed adiabatically from $v - v_b$ to $v - v_a$. The heat available as chemically stored energy in the volume of gas v_b may be represented by Av_b, where A may either be the British thermal units or foot-pounds of energy liberated by burning one cubic foot of the mixture at the original cylinder pressure. The heat liberation accomplishes two things: (*a*) Raises the internal energy of the portion of the gas in which the heat is liberated,

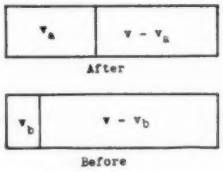


FIG. 2

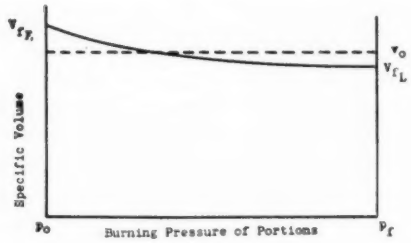


FIG. 3

which means raising its temperature; (*b*) does work on the remainder of the gases in the combustion space. Expressing this in the form of an equation

$$Av_b = dU_a + dW_r \quad \ldots\ldots [1]$$

where dU_a is the increase in internal energy of the burned portions and dW_r is the work done on the remaining portions.

$$dU_a = (p_a v_a - p_b v_b)/(k - 1) \quad \ldots\ldots [2]$$

$$dW_r = [p_a(v - v_a) - p_b(v - v_b)]/(k - 1) \quad \ldots\ldots [3]$$

By substituting Equations [2] and [3] in Equation [1]

$$Av_b = (p_a - p_b)v/(k - 1) \quad \ldots\ldots [4]$$

This is the typical equation for heat added at constant volume. The development shows, however, that with progressive combustion under the assumed conditions, the pressure rise is proportional to the quantity of gas burned. By letting $v_b = v$ in Equation [4], a relation is established between the mixture strength in terms of the heat available and the total pressure rise. This latter holds true only when the individual portions burn at constant pressure, that is, under what is here called normal burning.

Fig. 3 shows in a general way how the final specific volume of any infinitesimal portion varies with the pressure at which it starts to react.

Considering the diagram *ocef* in Fig. 1

$$v_f = (p_c/p_f)^{1/k} v_e \quad \ldots\ldots [5]$$

Using the general expression for heat added at constant pressure in terms of pressure, volume, and the ratio of specific heats k

$$Av_0 = p_c(v_e - v_c)k/(k - 1)$$

where A is in foot-pounds per cubic foot and represents the heat energy available as stored chemical energy in the mixture under the conditions of point *o*. From this

$$v_e = [A(k - 1)v_0/kp_c] + v_c \quad \ldots\ldots [6]$$

Also

$$v_c = (p_0/p_c)^{1/k} v_0 \quad \ldots\ldots [7]$$

By substitution of Equation [7] in [6] and then [6] in [5], v_f is found to be

$$v_f = p_c^{(1-k)/k} \frac{A(k - 1)v_0}{kp_f^{1/k}} + \left(\frac{p_0}{p_f}\right)^{1/k} v_0 \quad \ldots\ldots [8]$$

and Equation [4] shows that $(p_f - p_0)$ can be substituted for $A(k - 1)$ in Equation [8].

Since by assumption there has been no change in total volumes of the combustion chamber, the area under the curve v_f in Fig. 3 should be equal to the area under the dashed line v_0. This can be represented by

$$\sum_{p_0}^{p_f} v_f = (p_f - p_0)v_0 \quad \ldots\ldots [9]$$

The area under the v_f curve can be obtained from

$$\sum_{p_0}^{p_f} v_f = \int_{p_0}^{p_f} \left[p^{\frac{1-k}{k}} \frac{(p_f - p_0)v_0}{kp_f^{1/k}} + \left(\frac{p_0}{p_f}\right)^{1/k} v_0 \right] dp \quad \ldots\ldots [10]$$

and is found to prove the equality. Proceeding in the same manner, but assuming that the individual portions each burn at constant volume and expand, compressing the remainder of the charge, it can be shown that the equality expressed in Equation [9] does not exist, showing that the assumption of constant-pressure burning of the infinitesimal portions is correct.

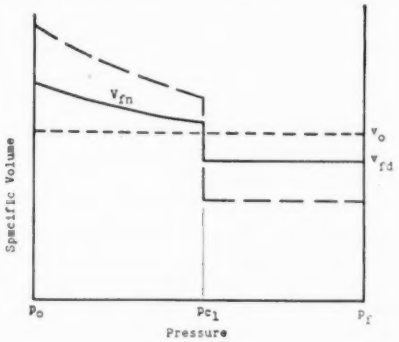


FIG. 4

In the case with detonation as assumed here, the final specific volumes of the respective portions burning normally will vary much as has been shown but the detonating portions will all have the same final specific volumes.

The variations are represented in Fig. 4. Here the full lines represent the final volumes at the equalized pressure while the dashed lines represent the respective specific volumes at the instant just prior to detonation. The dotted line is the specific volume of all the portions just prior to ignition. In Fig. 4, pressures were again used to indicate the portions burned. The final pressure with part of the charge detonating is not equal to the final pressure with normal burning, but is less depending on the proportion of the charge detonating, the compression pressure, the stored energy liberated by combustion, and the ratio of specific heats. The final pressure can be determined by integrating the areas under the v_{fn} and v_{fd} curves of Fig. 4 and equating the areas to $(p_f - p_0)v_0$.

$$\sum_{p_0}^{p_{c1}} v_{fn} + (p_f - p_{c1})v_{fd} = (p_f - p_0)v_0 \quad \ldots\ldots [11]$$

$$\sum_{p_0}^{p_{c1}} v_{fn} = \int_{p_0}^{p_{c1}} \left[p^{\frac{1-k}{k}} \frac{(p_f - p_0)v_0}{k{p_{fd}}^{1/k}} + \left(\frac{p_0}{p_{fd}}\right)^{1/k} v_0 \right] dp$$

$$= [(p_f - p_0)({p_{c1}}^{1/k} - {p_0}^{1/k})v_0 + {p_0}^{1/k}(p_{c1} - p_0)v_0]/{p_{fd}}^{1/k} \quad \ldots [12]$$

In order to combine the second term of Equation [11] with the first, v_{fd} must be evaluated in terms of v_0. Referring to Fig. 1

$$v_{fd} = (p_d/p_{fd})^{1/k} v_{c1} \quad \ldots\ldots [13]$$

$$v_{c1} = (p_0/p_{c1})^{1/k} v_0 \quad \ldots\ldots [14]$$

For the constant-volume burning

$$Av_0 = (p_d - p_{c1})v_{c1}/(k-1) = (p_f - p_0)v_0/(k-1)$$

So that

$$p_d = [(p_f - p_0)v_0/v_{c1}] + p_{c1} \quad \ldots\ldots [15]$$

And

$$v_{fd} = [(p_f - p_0)(p_0/p_{c1})^{(k-1)/k} + p_0]^{1/k} v_0/{p_{fd}}^{1/k} \quad \ldots [16]$$

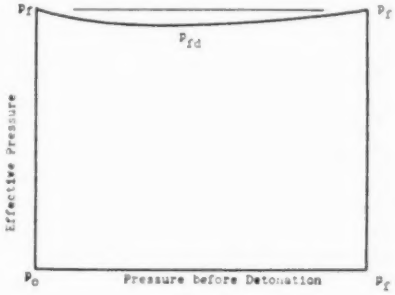


FIG. 5

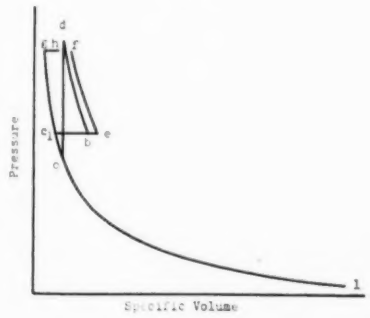


FIG. 6

Substituting Equations [12] and [16] in Equation [11] and rearranging terms

$$p_{fd} = \left(b^{1/k} - \left\{ 1 - \left[(a-1)\frac{1}{b^{(k-1)/k}} + 1 \right]^{1/k} \right\} \frac{a-b}{a-1} \right)^k p_0 \quad \ldots [17]$$

where

$$bp_0 = p_{c1} \text{ and } ap_0 = p_f$$

Fig. 5 shows the general nature of the variation of the final pressure with the pressure at which detonation occurs. It will be observed that, with one hundred per cent detonation, the final pressure is the same as with normal combustion. This is logical since all the portions are undergoing the same change at the same time.

In the case of the Diesel cycle the combustion knock occurs near the beginning of combustion rather than at the end as is the case with the Otto cycle just considered. In the actual combustion, some normal burning precedes the detonation responsible for the knock but, for purposes of this theoretical consideration, it will be considered as occurring at the beginning as indicated in Fig 6.

All the charge is compressed from point 1 to point *o* by the piston after which a portion detonates. Assume that the portion which burns under constant-volume conditions would, under

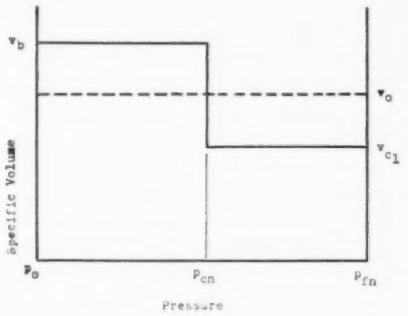


FIG. 7

normal burning conditions, have raised the pressure uniformly in the chamber to a pressure p_{cn}. It has already been shown in connection with Equation [4] that the pressure rise, with constant-volume combustion of the charge from point *o*, results from normal combustion of the charge, so the pressure p_d is equal to p_{fn}; the subscript n indicates normal burning. Now assume that the detonating portion expands so that the pressure of the unburned portion equals that of the burned portion, which is compressed.

Again using normal burning pressures to represent quantities burned, the specific volumes of the burned and unburned portions are shown in Fig. 7. The equalized pressure p_{c1} may be obtained by equating the areas under the v_b and v_{c1} lines to the area under the v_0 line.

$$(p_{cn} - p_0)v_b + (p_{fn} - p_{cn})v_{c1} = (p_{fn} - p_0)v_0 \quad \ldots [18]$$

However

$$v_b = (p_{fn}/p_{c1})^{1/k} v_0$$

and

$$v_{c1} = (p_0/p_{c1})^{1/k} v_0$$

so that

$$(p_{fn}/p_{c1})^{1/k}(p_{cn} - p_0) + (p_0/p_{c1})^{1/k}(p_{fn} - p_{cn}) = p_{fn} - p_0$$

or

$$p_{c1} = \{[{p_{fn}}^{1/k}(p_{cn} - p_0) + {p_0}^{1/k}(p_{fn} - p_{cn})]/(p_{fn} - p_0)\}^k \quad \ldots [19]$$

Letting $ap_0 = p_{fn}$ and $bp_0 = p_{cn}$

$$p_{c1} = \{[a^{1/k}(b-1) + a - b]/(a-1)\}^k p_0 \quad \ldots\ldots [20]$$

Since the pressure rise caused by the portions burning normally is proportional to the quantity burned, the loss in effective pressure is $p_{cn} - p_{c1}$ and the percentage power loss is

$$L_D = (p_{cn} - p_{c1})/(p_{fn} - p_0) \quad \ldots\ldots [21]$$

The power loss with detonation in the Otto cycle is

$$L_O = (p_{fn} - p_{fd})/(p_{fn} - p_0) \quad \ldots\ldots [22]$$

In Fig. 8, the per cent power losses are shown for the two cycles

when a is taken as 4 and k as 1.3. Here it must be remembered that, in the case of the Otto cycle, b is a measure of the portion of the charge which burns normally whereas with the Diesel cycle it is a measure of the quantity of charge detonating.

Since, with the Otto cycle, the specific energy of the charge is inherently greater than that of the Diesel, the dotted curve is included to show the effect on the Diesel loss when a is reduced to 3.

All of the foregoing is based on the theoretical conditions assumed at the beginning and therefore cannot be expected to hold absolutely in practice. In the following an attempt is made to predict, on a basis of present knowledge, the extent to which actual combustion varies from the assumed theoretical conditions.

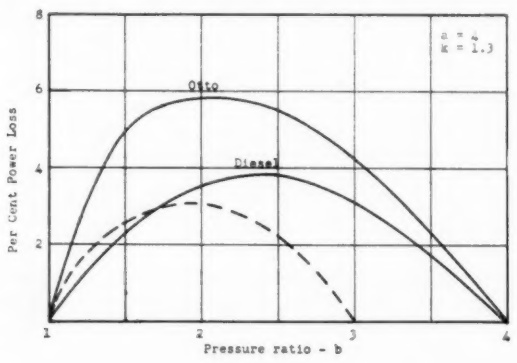


FIG. 8

The gases entering into the combustion do not behave as perfect gases. The principal difference of importance is the variation in specific heat with temperature and pressure. A study of the charts prepared by Hershey, Eberhardt, and Hottel[2] shows that in the ranges in which combustion occurs, k is in the neighborhood of 1.3. The equations show that the lower the value of k the less the loss for a given percentage of the charge detonating in either case.

Likewise the number and size of the molecules change. However, these changes do not affect the results appreciably. The mixtures are not homogeneous nor are the temperatures uniform prior to ignition. These, together with the fact that the reactions are known to be chain reactions, make it impossible to have all the combustion occur in the flame front. Recently published results by Withrow and Cornelius[3] indicate that as much as 30 per cent of the burning, under what are called normal burning conditions, does not occur in the flame front. Whether or not the same proportion holds for the detonating portions, in the time interval before the expansion of this portion becomes appreciable, has not yet been determined. This would cause an appreciable difference in either cycle.

The combustion process is not adiabatic, but in this case the lack of conformance tends to increase the power loss rather than decrease it, because the rapid vibration of the gases back and forth in the chamber is conducive to increased heat transfer to the chamber walls over that which would occur with normal combustion, where there is comparatively little gas motion, or that which would occur with one hundred per cent detonation. In all probability, the high radiation attributed to knocking combustion came from the chamber walls which were subjected to this high heat transfer from the rapidly moving gases.

[2] "Thermodynamic Properties of the Working Fluid in Internal-Combustion Engines," by R. L. Hershey, J. E. Eberhardt, and H. C. Hottel, *S.A.E. Journal*, vol. 39, 1936, pp. 409–424.

[3] "Effectiveness of the Burning Process in Non-Knocking Engine Explosions," by Lloyd Withrow and Walter Cornelius, *S.A.E. Journal*, vol. 47, 1940, pp. 526–545.

The chamber volume does not remain constant while combustion is in process; the change depends upon engine speed, and, in the case of the Otto cycle, affects the amount of detonation. One of the principal means of controlling detonation is to cause the latter portion of the burning to occur while the chamber volume is increasing.

Detonation is not complete before expansion of the detonating portion starts. In the case of the Diesel, where the detonating portions do not necessarily form one contiguous mass of gas it is quite probable that considerable such expansion does occur.

The fact that detonation probably does occur in disconnected masses of the charge in the Diesel probably promotes turbulence in the chamber. Professor Vincent[4] has advised the author that in his experimental work in the development of Diesel engines he has been able to improve efficiency with a small amount of detonation.

From these theoretical considerations it would appear that the cause of power loss with combustion knock or detonation is the vibratory motion set up in the chamber, and that the loss is represented by the kinetic energy of the vibration and the heat transferred to the chamber walls because of this motion. It also appears that the loss with the Diesel cycle is relatively less than with the Otto cycle.

Discussion

W. L. H. DOYLE.[5] Referring to Fig. 8 of the paper, the writer is interested in the use of a value of 1.3 for the coefficient k. This value seems to be widely divergent from values developed from various test-engine indicator cards, particularly in the case of high-compression oil engines. For spark-ignition gasoline engines the indicator cards evidence values somewhat above the 1.3 value. Studies of indicator cards for high-speed high-compression oil engines evidence appreciably higher mean values of k, ranging from 1.37 to 1.43 for the expansion stroke. How are the somewhat different values of k, found in actual engines, reconciled with the author's mathematical treatment?

C. B. ROSENBERG.[6] Do the author's assumptions on the Diesel-injection process, which to the writer is a sustained burning process, strictly substantiate his first assumption that there is a homogeneous mixture at the beginning of the combustion process. From observations made on work in the injection field, the writer feels that the primary charge of injection is perhaps the best example of homogeneous mixture which may be found, whereas the secondary and tertiary stages rather break down the first assumption that there is a homogeneous mixture.

AUTHOR'S CLOSURE

In consideration of Mr. Doyle's question relative to the use of a value of 1.3 for the coefficient k, it is necessary to differentiate between the expansion exponent n for the charge as a whole and the expansion exponent k for any infinitesimal portion of the charge. The former reflects a number of factors such as heat loss to the cylinder walls, blow-by, afterburning, etc., while the latter is understood to reflect only the ratio of the specific heats.

Considering these factors it is understandable that the value of n is appreciably higher than the value of k used in arriving at the data plotted in Fig. 8. The slope of the expansion line, on a log-log plot of the pressure-volume diagram for an engine, gives the value of n for any point on that expansion curve.

[4] E. T. Vincent, Professor of Mechanical Engineering, University of Michigan.

[5] Caterpillar Tractor Company, Peoria, Ill. Mem. A.S.M.E.

[6] Pure Oil Company, Chicago, Ill.

Such plots give values of n which normally vary from values less than 1 at the beginning of the expansion to values even above those given by Mr. Doyle, when afterburning has stopped and blow-by and heat loss to the cylinder walls are causing the temperature and pressure to drop more rapidly than would be the case with adiabatic expansion.

While k is supposed to reflect only the ratio of specific heats, it includes chemical-equilibrium effects at the high temperatures at which combustion occurs. The author has analyzed the Hottel charts to determine such values of k. Checking in the regions of high temperature and pressure, comparable with those existing in engines, values between 1.25 and 1.3 are obtained. Higher values of k would be obtained from the charts by extending the range downward to atmospheric conditions.

Due to variable specific heats alone k decreases with increases in temperature, and equilibrium effects just tend to make this decrease greater. However, it cannot within practical limits reach a value as low as 1.

Experiments on our universal test engine at the University of Michigan have indicated that the use of $k = 1.3$ for the calculation of the loss with detonation in an Otto-cycle engine gives results comparable with experimental results. In this connection, however, it must be remembered that the mass vibration of the gases in the engine produces a scrubbing action on the walls which offers an excellent opportunity, for heat transfer. The author is inclined to believe that the high radiation, reported by early experimenters who measured radiation through quartz windows in the combustion chamber, merely represented the increased temperature of the wall surfaces and not the increased gas radiation. We now know that temperatures with normal combustion may be as high or higher than those existing at any time in the detonating portions, so that the only factor which could contribute to the higher radiation would be the increased density of the gas. The heat loss, due to the scrubbing action of the gases on the cylinder walls resulting from the mass motion of the gases caused by the detonation, is attributable to the detonation.

The opinion has been expressed that these considerations are theoretical and some question has been raised as to their practicability. It is appreciated that this treatment is theoretical but, at the same time, it brings out certain fundamentals in the burning of the gases in engines which give a good indication of what is to be expected from the phenomenon called "combustion knock."

The writer has no experimental data to indicate to what extent the curves plotted in Fig. 8 are applicable for the Diesel cycle, but a check for the Otto cycle has already been cited. It may be pointed out that, in the work of Professor Vincent who has been concerned with the development of Diesel engines, it has been found that a slight amount of knock gives more efficient operation. This apparently is due to the increased turbulence in the combustion chamber, which helps to mix the fuel with the air.

As to Mr. Rosenberg's question regarding homogeneity, it is necessary to look at it from two standpoints. In the Otto cycle, it is questionable whether the incoming charge is thoroughly mixed with the products of combustion remaining from the previous cycle, so undoubtedly there is a certain amount of nonhomogeneity in the Otto-cycle engine. In the Diesel cycle, we know that it is necessary for the fuel vapor in infinitesimal portions to be associated with the oxygen within certain limiting ratios in order to secure combustion. As far as the infinitesimal portions are concerned, however, their behavior is much the same whether or not they burn in one flame front, as in the Otto cycle, or in one of the innumerable flame fronts existing in the Diesel cycle as combustion progresses. They undergo the same phenomena of compression prior to combustion, expansion during combustion, and compression following combustion, unless they burn during the detonating period in which period they have been assumed, in this study, to have no expansion during combustion. This is somewhat difficult to visualize, but the author trusts that it answers the question in regard to homogeneity.

Operation of Supercharged Engines in Pipe-Line Service

By J. B. HARSHMAN,[1] TULSA, OKLA.

This paper deals with some of the historical aspects of supercharging and the experiences of the Stanolind Pipe Line Company in the application of exhaust turbochargers, "Buchi" system, to four-cycle air-injection engines in pipe-line service.

History and Description of Supercharging Methods

THE ambition of engineers and designers of Diesel engines for many years has been to build an engine which would produce more horsepower from a given cylinder size. The limiting factor (brake mean effective pressure) could not be raised above a certain point without encountering excessive operating temperatures, resulting in inefficient operation and high maintenance costs. Since most four-cycle engines were designed against inertia forces and not combustion forces, anything which increases the engine capacity by utilizing these oversized parts is an economic accomplishment; therefore, it was only natural that consideration would be given to mechanical means of charging the cylinders with air at pressures above atmospheric.

Some of the methods used to accomplish this are as follows:

1 Mechanically driven air pumps, mounted and driven from the main shaft of the engine or driven by rocker arms from the main crosshead assembly.

2 Belt-driven blowers, either centrifugal or rotary type.

3 Mechanically driven rotary-type blowers mounted directly on the engine frame and driven from the main shaft by gearing or chain.

4 The "Wibu" system, invented by two Polish engineers, Wicenski and Bujak. This system makes use of special intake cams and a tuned intake-piping system. The inventors claim from 25 to 40 per cent increase in engine horsepower.

5 The "tuned intake-pipe system" which provides for an intake pipe of the proper length to produce a natural oscillation frequency to coincide with the intake-valve opening. Thus, a certain amount of kinetic energy is produced, giving a ramming effect of the air in the cylinder.

6 The exhaust turboblower.

Certain claims are made for all of these methods. If an increased amount of air is provided, some results in the form of increased horsepower are to be expected. However, certain disadvantages were encountered with most of the methods mentioned which were undesirable, either from an operating or from an economic point of view.

Practically all direct-driven supercharging equipment comes in a similar category, i.e., it possesses certain undesirable characteristics, such as:

(*a*) The volume of air cannot be controlled to conform with load variation.

(*b*) A system of supercharging, producing only 15 to 20 per cent net increase in engine horsepower, cannot be justified economically.

The Buchi System

The Buchi system consists of a centrifugal air blower which is mounted on the same shaft with a single-impulse turbine, driven by the exhaust gas of the engine. The turbine and blower are mounted in the same case or housing with a system of labyrinth seals to prevent leakage from one compartment to another. The mean pressure on the exhaust gases ahead of the turbine is generally from 2 to 3 psi above atmospheric. The charging air from the blower is from 3 to 4 psi above atmospheric pressure. Extra-wide exhaust and intake cams are provided so that both exhaust and intake valves are open simultaneously, giving an overlap of 120 crank-angle deg.

While both valves are open, the charging air passes over the top of the piston, then through the exhaust valve. Thus, the cylinder is scavenged of burnt gases. The large volume of comparatively cool air, in passing through, to some extent cools the piston head, valves, and upper cylinder walls, and reduces the exhaust temperature. As the piston moves from upper dead center downward on the intake stroke, the cylinder is thoroughly charged with fresh cool air at pressures exceeding atmospheric.

Engines with four cylinders and over have a system of multiple manifolding of the exhaust to permit complete scavenging of one cylinder before the exhaust valve opens on another cylinder. Thus, overlap in the exhaust manifold is avoided. At the same time, efficient fluctuations or pressure waves are made use of in the exhaust manifolds to assist in scavenging the cylinders.

This division of exhaust manifolds is carried from the cylinders to the inlet of the turbine. Figs. 1 and 2 show typical arrangements for manifolding four- and five-cylinder engines.

Other than the division of the exhaust manifolds and the installation of larger inlet and exhaust cams, very few changes in the engine are required. The fuel system is adjusted to give a longer period of injection, the increase in the amount of fuel being proportional to the extra horsepower to be developed. The compression space must also be increased because of the higher pressure of the air at the beginning of the compression stroke.

The Buchi turbocharger can be set into the piping at either end of the engine at the height of the exhaust manifold, or it may be set on the floor and the piping extended from the engine to interconnect with the turbocharger.

Early Supercharging Experiments

Some of the first experiments in supercharging were made in Europe nearly 30 years ago. However, it was not until 1928 or 1929, that American engineers began to realize the possibilities of increasing horsepower satisfactorily by this method. The first commercial installation in the United States, of which the author has record, was made in 1928 by an American manufacturer in a Western state. The elevation of the plant was 9000 ft above sea level, and the engine was supercharged with a belt-driven rotary blower to produce its normal sea-level rating.

During the year 1930, another prominent American Diesel-engine manufacturer placed in service, in Middle Western States,

[1] Stanolind Pipe Line Company.

Presented at the National Meeting of the Oil and Gas Power Division, Kansas City, Mo., June 11–14, 1941, of The American Society of Mechanical Engineers.

Note: Statements and opinions advanced in papers are to be understood as individual expressions of their authors, and not those of the Society.

two engines making use of belt-driven rotary-type blowers for supercharging. These engines were of the four-stroke-cycle single-acting type having a bore of 17½ in., a stroke of 25 in., operating at 225 rpm. Both engines were used to drive alternators in municipal-plant service. The horsepower increase by supercharging was approximately 15 per cent.

About 1935, American Diesel-engine builders became interested in the accomplishments of certain European engine builders in the use of exhaust turbochargers. Early in 1936, several exhaust-turbocharger units were imported to this country for experimental purposes.

Since that time, numerous installations of supercharged engines have been placed in service, making use of the Buchi system. The majority of these are in locomotive service where maximum horsepower with minimum weight and space requirements are factors. There are, however, several stationary installations in use, two of which are in service on a major pipe line.

In the early part of 1936, the Stanolind Pipe Line Company was faced with the problem of increasing the pumping capacity at one of its trunk-line stations. The capacity desired was not sufficient to justify installation of an additional large unit; therefore, consideration was given to the possibility of supercharging one of the existing engines in the plant and increasing the speed of the pump by the installation of new gears of a lower ratio. Since the Buchi system seemed to have greater possibilities than other methods considered, an order was placed with the engine manufacturer for the turbocharger. The manufacturer also took the responsibility for doing the necessary engineering work and supplying the new cams, exhaust manifolding, etc., for the complete installation.

Experiences in Supercharging Pipe-Line Engines

In October, 1936, the company placed in service its first supercharged engine. The engine was a four-cylinder four-cycle type, having a 16.5-in. bore and 24-in. stroke, rated 400 hp at 200 rpm. The turbocharger was purchased for an increase of 25 per cent in engine output. The increased horsepower was accomplished without difficulty as far as engine troubles were concerned. However, trouble was experienced from the start with the ball bearings in the turbocharger. This turbocharger was built to operate at a top speed of 20,000 rpm, and operated at 15,000 to 16,000 rpm when carrying 500 engine hp. Apparently, the design of the ball bearings was inadequate for the thrust load to which they were subjected, and it was found that their life varied from a few hours to a maximum of 2000 hr.

Table 1 gives a comparison of the engine operating conditions when carrying 400 hp unsupercharged, with conditions prevailing when supercharged and carrying a 25 per cent increased rating.

TABLE 1 COMPARISON OF 400-HP ENGINE UNSUPERCHARGED WITH SAME ENGINE SUPERCHARGED AND CARRYING 25 PER CENT INCREASED HORSEPOWER

	Engine unsupercharged	Engine supercharged
Exhaust pressure at turbine, psi	..	2.45
Air pressure at blower, psi	..	3.31
Air-inlet temperature, F	..	50
Air-discharge temperature, F	..	105
Supercharger speed, rpm	..	15075
Injection pressure, psi	1000	1000
Compression pressure, psi	500	515
Maximum pressure, psi:		
1 Cylinder	590	650
2 Cylinder	650	650
3 Cylinder	700	650
4 Cylinder	600	650
Exhaust temperature, F:		
1 Cylinder	690	565
2 Cylinder	730	560
3 Cylinder	640	530
4 Cylinder	715	560

After about a year and a half of operation of this unit under a serious handicap, caused by bearing troubles in the turbocharger, during which time it was once returned to Switzerland for repairs, it was decided to ship the machine to an American engine builder and have the ball bearings replaced with sleeve-type bearings. During the period of tests on the supercharged pipe-line engine, this engine builder had placed several supercharged Diesel locomotives in service and had encountered similar troubles with the ball bearings. Sleeve-type bearings were then developed for the turbocharger, which had proved very successful on the locomotive engines. The ball bearings were replaced, in the turbocharger owned by Stanolind, with bronze sleeve-type bearings, after which the machine was again placed in service. Lubrication difficulties were then experienced with the new sleeve bearings, one bearing failing after 19 hr of operation. The bearing was replaced, the lubrication problem was corrected, and another test was started.

Tests Made on Turbocharger at Increased Loads

A 25 per cent increase in engine horsepower was satisfactorily obtained. However, by this time, other American engine builders were becoming interested in the possibilities of supercharging, and some tests had been made in which 75 and 100 per cent increase in horsepower had been reached. Because of the expense involved in such an installation, it was decided that supercharging could not be economically justified for a 25 per cent increase in engine horsepower. After consulting the engine builder, a decision was made to conduct tests using the same turbocharger for a horsepower increase of 50 per cent. Certain changes were made in the nozzle rings of the turbocharger to prevent exceeding the 20,000 rpm speed limit. This test was a failure due to insufficient capacity of the turbocharger, and the machine was subsequently badly damaged from overloading and overheating.

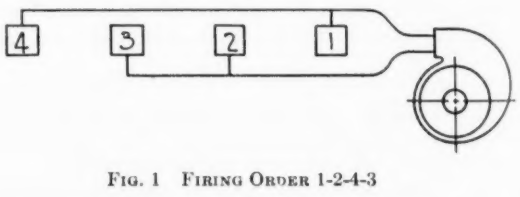


Fig. 1 Firing Order 1-2-4-3

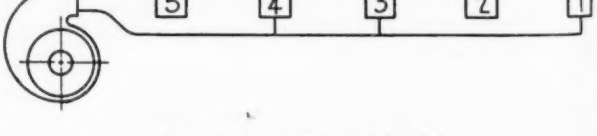


Fig. 2 Firing Order 1-3-5-4-2

Although many discouraging problems were encountered in the test of this first supercharged engine, sufficient information was obtained to convince all concerned of the practicability of supercharging, particularly by the Buchi method.

In August, 1940, the second supercharged engine was placed in service by Stanolind. This engine was of the four-cycle type with five 16¼-in. × 23½-in. cylinders, having a normal horsepower rating of 500 at 225 rpm. In October, 1940, another turbocharger was placed in service on a 500-hp, five-cylinder, 16¼-in. × 24-in. engine. The Buchi system was used on both of these installations; however, the turbochargers were much larger machines with a full-load speed of only 12,000 rpm. Both turbochargers were equipped with babbitt-lined sleeve-type bearings. This equipment was purchased with the idea of increasing the engine output 50 per cent, or from 500 to 750 hp. The gear ratio was changed on the pumps, increasing the pump speed from 47 to

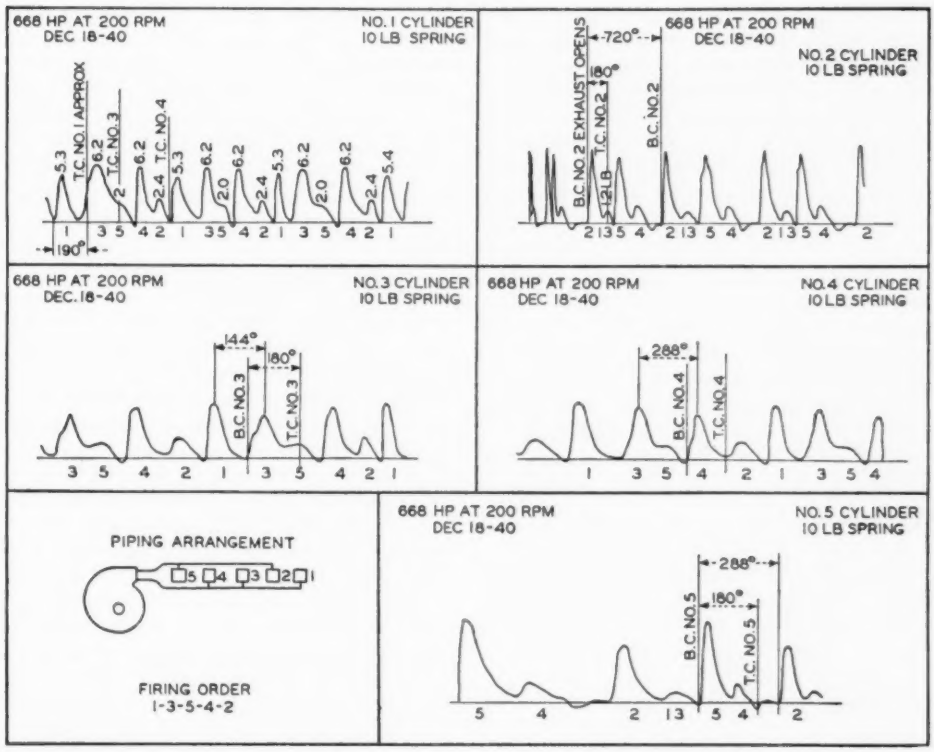


FIG. 3 WEAK-SPRING INDICATOR DIAGRAM TAKEN ON EXHAUST MANIFOLD; FIVE-CYLINDER ENGINE

55 rpm, in order to make full use of the increased horsepower. These units have been in continuous operation since that time. The only difficulty experienced is that the load balance cannot be maintained on the various cylinders of the engine because of overlap of the exhaust impulses in the three-cylinder manifold, as shown in Fig. 2.

Negotiations are now being carried on with the intention of developing a turbocharger with three openings in the exhaust-inlet casing for five-cylinder engines.

In Fig. 1, it will be noted that no two cylinders, exhausting into the same manifold, follow each other in firing sequence. In Fig. 2, showing the manifolding of a five-cylinder engine, it will be noted that Nos. 1 and 3 follow each other in firing order in the same manifold, which condition is unavoidable in a five-cylinder engine, unless three or more manifolds are used. Exhaust manifolds should be designed to prevent this condition; otherwise one of the cylinders affected by the overlap of the exhaust will not scavenge properly and will be overloaded.

Table 2 gives operating data on a five-cylinder, 500-hp, 16½ in. × 24-in. engine supercharged with a double-inlet turbocharger. Fig. 3 shows hand-pulled indicator cards, taken at the exhaust nozzle of each cylinder on this engine, and also indicates the reasons for disrupted scavenging and overloading of the No. 1 cylinder.

TABLE 2 OPERATING DATA FOR FIVE-CYLINDER SUPERCHARGED ENGINE, DEVELOPING 668 HP, AT 200 RPM AND 102 BMEP

Exhaust temperatures, [a] F				
No. 1 cyl	No. 2 cyl	No. 3 cyl	No. 4 cyl	No. 5 cyl
900	610	620	540	500
900	610	640	610	580
900	610	640	600	580
900	630	680	600	590
900	650	690	600	610

[a] Observed at different times during test.

From the measurements of weak-spring diagrams, shown in Fig. 3, it is reasonable to assume that the following back pressures at the middle of the scavenging period are approximately correct:

No. 1..... 4.5 Psi, with pressure increasing
No. 2..... 1.0 Psi, with pressure decreasing
No. 3..... 2.0 Psi, with pressure decreasing
No. 4..... 0.0 Psi, pressure curve level
No. 5.....—0.4 Psi, pressure curve level

Air pressure at 665 hp = 3 psi

Pressure (mean) in upper exhaust pipe, 1.4 psi
Pressure (mean) in lower exhaust pipe, 2.0 psi

CONCLUSION

Sufficient experience has been gained from the installations described to prove that increasing the horsepower of existing pipe-line pumping installations is not only practicable, but economically justifiable. For instance, a 250-hp increase can be obtained by supercharging a 500-hp engine for an investment of approximately $12,500, including the cost of new gears for increasing the speed of the pump. This is equivalent to $50 per installed horsepower, which is less than one half the cost per installed horsepower when purchasing additional pumping units.

The use of supercharging has other advantages which make it attractive for pipe-line service. For instance, it frequently becomes necessary to provide a temporary increase in horsepower and pumping capacity at trunk-line stations handling oil from flush fields, or for a temporary peak load to certain refineries. After this peak-load requirement no longer exists, an engine which involved a large investment is usually left idle or operating at low capacity. If this peak condition is met by supercharging, the turbocharger and other equipment used in its operation may be moved at a nominal cost to another station, where the additional capacity can be used to advantage.

The only disadvantage actually encountered in the operation of the last two installations has been the inability to operate

these units at loads below the original rated horsepower of the engine. Although the exhaust-driven turbine is supposed to compensate automatically for load variation, it appears that an excess amount of air is forced into the engine for the quantity of fuel consumed, which results in poor combustion. After operating at reduced loads for a few days, it is necessary to remove the turbine rotor and clean out the carbon accumulations.

Our experience in the operation of the three turbochargers on pipe-line pumping units indicates that the following improvements should be made for maximum success:

1 The proper method of manifolding to prevent overlapping of exhaust from different cylinders.

2 Provision for some method of regulation of air at low loads to insure proper combustion.

3 The design of the turbocharger should be such that it can be installed in different positions to simplify piping and to permit adaptation to existing piping. The general appearance of present installations indicates that little or no thought has been given to obtaining a uniform and workmanlike piping job.

Regardless of the difficulties experienced with the first installation and the undesirable features mentioned, we believe that supercharging of Diesel engines for increasing the capacity of existing installations in pipe-line service has tremendous possibilities, and that its use will become general throughout the industry.

Discussion

C. W. Smith.[2] There is little doubt that turbochargers will be used to an increasing extent in the future for industrial applications. Heretofore, they have been used almost exclusively in the United States in conjunction with military-aircraft engines.

Although the title of this paper does not so indicate it is obvious that the author had in mind only the supercharging of Diesel engines. There is no reason why turbosupercharging should not be used also with Otto engines, but it is to be expected that the operating conditions will be somewhat different and that experience acquired with the Diesel engine cannot necessarily be applied to the more common Otto engine.

For instance, the engines mentioned by the author operated at speeds in the vicinity of 200 rpm. For engine speeds in the vicinity of 1000 or 2000 rpm, or more, it is not certain that the Buchi method of dividing the exhaust manifold will, of itself, be sufficient to insure complete scavenging and to give the same large percentage increase of engine output obtained at very low engine speeds. It will be necessary to insist on the highest possible turbine and compressor efficiencies and perhaps to operate with a somewhat higher exhaust-gas temperature. It might be pointed out that the Buchi manifold would not be necessary even at low engine speeds if the over-all efficiency of the turbosupercharger were high enough.

Another method of avoiding the divided manifold would be the use of a geared or belted compressor in series with the turbine-driven compressor. In certain cases, this might result in somewhat less complication than the Buchi system.

The author mentioned the disadvantage encountered in operating at light loads. If this is caused by a disproportionately large air flow, it should be possible to correct the condition by changing the characteristics of the compressor, or of the turbine, or perhaps of both, with a resultant improved specific fuel consumption, as well as better mechanical operation.

It is ordinarily considered that, when engine output is increased by the method described in the paper, a gain in fuel economy should also result, since the fixed engine losses are increased much less than in proportion to the increase in brake horsepower. The author makes no mention of this, and it would be interesting to know whether his experience verifies this expectation.

E. S. Thompson.[3] Because of the fact that the title is rather general and might be interpreted to include turbosuperchargers applied to Otto-cycle engines, it seems to be desirable to add something to the history of superchargers, as presented in the paper.

The supercharger development was a by-product of an effort to develop a gas turbine, the modern turbosupercharger approaching that machine very closely. The gas turbine is an apparatus for obtaining power from products of combustion which directly operate a turbine wheel. This has been a dream of engineers since John Barber's British Patent of 1791, which shows most of the modern elements. The mechanical resources of that period could never have produced an operative apparatus, and so the idea lay dormant for a hundred years. Then the steam turbine and the internal-combustion engine, independently, became successful means for obtaining power; so beginning about 1890, many people thought of combining the two, most of them supposing that they themselves had invented the gas turbine.

The earliest extensive use of the supercharger was made to obtain sea-level power from an airplane engine when flying at an appreciable altitude. The density of the atmosphere decreases rapidly with the altitude and the weight of charge to the cylinder, and hence the engine power decreases proportionately. A supercharger compresses the altitude atmosphere so as to restore sea-level density within the cylinder, and thus, sea-level power. Such a use of superchargers to restore sea-level conditions at altitude was soon extended to give increase of power of an airplane engine at sea level, called "ground boost."[4]

Supercharger investigations were in progress by the Allies prior to the entry of the United States into the first world war, with most of the activity centering around the turbo or exhaust-gas-driven type of compressor, the investigations being under the direction of Professor Rateau of France. M. LeBlanc of France was also investigating the possibilities of supercharging with an engine-driven device. The Germans were reported to be doing considerable work along this line, with most activities centered around geared units. Upon entry of the United States into the conflict, such information as had been obtained by the Allies on superchargers was made available.

The American Expeditionary Force, under the direction of engineering officers, endeavored to construct a geared supercharger for use in conjunction with the Liberty engine. Mechanical details, however, appeared to preclude the possibilities of a satisfactory development along this line. The need for great altitude performance was paramount, and the problem of developing a suitable supercharger was undertaken by the engineering division of the Army Bureau of Aircraft Production, with every effort being made to expedite the development. Available information on superchargers was so limited that an analysis was decided upon to ascertain the most satisfactory type of drive-and-compressor assembly, in which rotary, reciprocating, geared-centrifugal, and exhaust-gas-driven compressors were considered.

At that time, some 15 years ago, to interconnect the geared-centrifugal compressor to the engine satisfactorily was believed to be impossible, since operating gearing and bearings at speeds required to provide efficient units was not believed possible. The rotary and reciprocating types were discarded because of their bulk. Therefore, the combination of the exhaust-gas

[2] General Electric Company, Lynn, Mass.

[3] General Electric Company, West Lynn, Mass.

[4] "Superchargers," by S. A. Moss, *Aeronautics*, vol. 7, 1941, p. 2341.

turbine and centrifugal compressor appeared to offer more possibilities than any other type because of its compactness, simplicity, flexibility, and the utilization of the energy available in the exhaust gases. This particular supercharger incorporates a centrifugal compressor which must rotate at high speed to be effective, thereby creating an application for which the turbine is ideally suited. Two projects were then started, one under the direction of S. A. Moss of the General Electric Company, and the other a series of designs by E. H. Sherbondy, which were more or less in accord with the practice of Rateau in using an entirely enclosed turbine wheel. Although the Sherbondy design was dropped after construction of three models, it had a number of ingenious details. Thereafter, all work was centered around the General Electric design.[5]

The use of turbosuperchargers for airplanes has advanced tremendously in the last few years, and it is not too great a stretch of the imagination to predict that all airplanes in the not distant future will be propelled by engines equipped with turbosuperchargers. Application of the turbosuperchargers to truck and automobile engines also offers attractive improvements in power and performance.

R. Tom Sawyer.[6] The advantage of the turbocharger is that it may be installed on practically any engine, although it works more efficiently on some engines than on others. It is, of course, better to have the engine and the turbocharger built as a unit, thus correcting certain minor faults which the author mentioned, as, for example, the piping.

The matter of time lag in the functioning of the turbocharger was not mentioned in this paper. When a load is applied to the engine, a certain time lag occurs before the turbocharger becomes effective. In locomotive practice when the throttle is closed, the engine is idling; when the throttle is opened quickly the engine comes up to speed, but the turbocharger does not respond instantaneously; there is a lag of 3 or 4 sec. Oddly enough, for locomotive operation, that lag is advantageous, since it gives a cushion effect.

Each year, the writer's company compiles a complete statement of the cost of operating its Diesel locomotives. We have two classes of switching locomotives. One is a 660-hp locomotive which consists of a six-cylinder engine; the other is a 1000-hp locomotive which consists of exactly the same engine except for a different camshaft and the turbocharger. Recent figures indicate that the maintenance cost of the 660-hp locomotives, from 1 to 4 years old, is 28 cents per hr. The cost of maintaining 1000-hp locomotives, in service from 1 to 4 years, comes to 29 cents per hr. Thus, for all practical purposes if the engines are adaptable to superchargers of the turbo type, we can be certain that the maintenance on the turbocharged engines will not be appreciably greater per year than on the same engine not turbocharged.

J. P. Stewart.[7] The writer would like to comment upon the author's three conclusions as follows:

1 The difficulty experienced with overlapping of exhausts from different cylinders was with five-cylinder engines. Present practice, in so far as Elliott-Buchi turbochargers are concerned, is expected to eliminate this difficulty by insuring that no two cylinders exhaust consecutively into any one individual exhaust pipe.

2 Not being familiar with the specific installations discussed, the writer will not attempt to explain the reasons for unsatisfactory combustion at low loads. However, one of the outstanding and well proved features of the Buchi system of turbocharging is the fact that charging-air flow is automatically adjusted on engine-load variations, as can be shown from numerous published performance curves on several makes of turbocharged engines.

3 The basic design of Elliott-Buchi turbochargers is such that they can be assembled in a number of different positions, to make them adaptable to widely varying installation conditions. Considerable thought is devoted to securing as neat and compact a piping installation as possible in each case. Naturally, it is somewhat easier to meet this requirement on new engines, which are designed specifically for turbocharging, although we can refer to a number of instances in which an eminently satisfactory piping arrangement has been worked out for engines of standard designs.

There are numerous distinct differences between turbochargers being built for aircraft gasoline engines and those for the Buchi system on Diesel engines. In aircraft applications, the turbine operates on constant pressure, as contrasted to the pulsating pressure with the Buchi system. Further, aircraft units operate on considerably higher exhaust temperature, and have a lightweight requirement, as well as a much shorter life expectancy. Turbochargers for Diesel engines need not be as lightly constructed and, for most heavy-duty services, should have a life comparable with that of the engine itself.

W. L. H. Doyle.[8] The author's experience involves large slow-running engines, having relatively fixed speed-range characteristics, and which are supercharged by the exhaust-gas-driven turboblower. In choosing supercharging equipment initially, he had available two other types: the mechanically driven centrifugal blower and the mechanically driven Roots-type blower. For his particular application, thinking in terms of the speed range involved, the supercharger equipment he selected has many advantages. Thinking in terms of faster running engines where wide speed ranges are involved, many factors enter which introduce the question as to the best type of supercharger equipment to use. That this is so is evidenced by the appreciable amount of thought being given to this subject, particularly among research engineers.

One point mentioned in the paper is that, for the author's type of equipment, the larger volume of comparatively cool air supplied by the turboblower is in part allowed to flow through the cylinder, serving to cool, to some extent, the piston head, valves, and upper cylinder walls. This is accomplished by delaying the exhaust-valve closing, in order to overlap the inlet-valve timing by a considerably greater angle than is usual for the nonsupercharged engine. This is a feature considered important to the operation of the exhaust-gas-turboblower scheme of supercharging.

For the mechanically driven type of superchargers, use of considerably less valve overlap seems advantageous, and, for "dry pistons," measurements of piston temperatures at high brake-mean-effective-pressure loads for values of overlap from 34 to 140 deg showed a negligibly small change in cooling effect on the piston head over this range. The advantage in blowing an excess of scavenging air through the cylinder during this overlap period for the mechanical-drive scheme apparently centers on the one factor of cooling the exhaust valve. Viewed in the light of these considerations, a certain amount of experimentation yet remains to define clearly good overlap practice, particularly as applied to the mechanically driven type of supercharging equipment.

[5] "The Turbosupercharger," by A. L. Berger and Opie Chenoweth, *Journal*, S.A.E., vol. 29, 1931, pp. 280–295.

[6] Sales Engineer, The American Locomotive Company, New York, N. Y. Mem. A.S.M.E.

[7] Manager, Superheater Department, Elliott Company, Jeannette, Pa. Mem. A.S.M.E.

[8] Research Engineer, Caterpillar Tractor Company, Peoria, Ill. Mem. A.S.M.E.

The author also points out that the fuel system is adjusted to give a longer period of injection. For the slow-running type of engine, particularly with the narrow speed range here involved, it is important to hold peak cylinder pressure to conservative values, primarily because of bearing limitations. Under these conditions, for increase in load, an increased injection period could be used. However, this introduces factors which tend toward limitations of power capacity and which are also reflected in less favorable fuel consumption.

In the data of test runs reported by the author, compression pressures under the nonsupercharged and supercharged conditions are shown as substantially the same value, indicating a reduction in compression ratio in the case of the supercharged-engine assembly. There is a definite tendency to adopt reduced compression ratios for supercharging. In wide-speed-range engines, speed and load have marked influence upon the compression pressures. In Table 3 of this discussion are shown test

TABLE 3 PART-LOAD TESTS ON EXPERIMENTAL SIX-CYLINDER 5¾-IN. × 8-IN. DIESEL WITH EXHAUST-GAS-DRIVEN TURBOBLOWER, STANDARD ENGINE COMPRESSION RATIO, AND VALVE TIMING

Engine speed, rpm	850	850	850	850	850
Brake horsepower	Idle	50.7	100.8	151.4	201
Brake mean effective pressure	0	37.9	75.5	113.4	150.4
Compression pressure, psi	560	625	645	690	775
Maximum pressure, psi	675	965	1050	1115	1175

data, taken about 2 years ago in connection with an experimental engine assembly, operating on part load at 850 rpm, and equipped with an exhaust-gas-driven turboblower supercharging unit. In the case of this particular experiment, standard or nonsupercharged engine valve timing was employed, and the supercharged air was passed through an aftercooler. Attention is called to the increase in compression pressure from idling to the 150-lb bmep load condition. It is also interesting to note the corresponding increase in maximum cylinder pressures under the special conditions of this test.

A maximum cylinder pressure of 850 lb is approximately correct for the standard line of engines. The conditions under which the special engine tests, shown in the tabulation, were run were appreciably different from any of the conventional engine conditions because of the supercharging situation.

The historical reference in the paper to altitude installations brings up another point. In most altitude applications, effort is made to regain sea-level power at the altitude. The term "normalizing" has recently been used in this connection, and is an expression which seems aptly fitted to describe these special conditions.

The writer would like to ask whether the supercharged engine, reported in Table 1, is an air-injection engine?

The author brings out a point, in connection with observed operating conditions, which is at variance with our experience, where he mentions difficulties experienced with his engines when operated at light loads, a condition he concludes as traceable to excess air. It seems more logical to attribute the cause for this difficulty to ignition and combustion factors involved in the use of crude oil, the effects of which are probably not aided by the less favorable atomization conditions inherent in the air injection, particularly at light load, than to consider the difficulties as being due to excess air or high air-fuel-ratio conditions.

Will the author supply information on changes in lubricating conditions as between the engines operating nonsupercharged and when operating supercharged?

E. J. Kates.[9] The question of satisfactory performance at partial loads is quite important. It would be even more important in some other fields of application than in pipe-line service. The latter is characterized by operation at constant load for long periods of time. Load changes are known in advance, and when once made, continue for quite a while. On the contrary, in certain other fields of application, such as electric generation, load changes come on so fast that supercharger control must be quick and automatic. Poor combustion, resulting from an excess amount of air delivered by the turboblower, might be quite troublesome. The writer's experience confirms the author's as to the bad effects of excess air. The resulting poor combustion should not be blamed on the fuel for it is inherent in the design of many engines. If turbocharging, as now employed, causes excessively high air-fuel ratios when the load is suddenly reduced, it is a fault which should be corrected before turbochargers are universally applied.

In presenting this paper, the author stated that he intended to experiment with supercharging produced by ramming and tuning effects in the air-intake system. This would be worth while, because if ramming will do the job, it will have many advantages over any mechanical apparatus attached to the engine as an accessory. Such ramming schemes hold promise, because even low-pressure scavenging greatly increases engine power, and much of the beneficial effect of supercharging comes merely from cleansing the spent gases out of the clearance space with fresh air. This is within the possibilities of a well-designed ramming system.

D. D. Cook.[10] The data previously submitted indicate that higher operating temperatures can be expected following the use of supercharging equipment. It would be interesting to know if the author's organization has encountered any new difficulties with piston rings, from the standpoint of increased cylinder wear, shorter ring life, etc. What combination of piston rings has rendered the most successful service in the Stanolind Company's supercharged engines?

R. D. Campbell.[11] Does the author's company follow the practice of selecting fuel from some particular batch of oil being handled, setting it aside in a tank to be used as fuel? That is a practice on some of the pipe lines.

G. F. Noltein.[12] About two years ago, the writer's company took an order for our first two supercharged engines for continuous 24-hr dredging service. The engines were eight- and six-cylinder units, 14½ in. × 20 in., of 1200 and 900 bhp, respectively. At that time, market conditions made it impossible to get exhaust turbochargers of the necessary size in the available time, so we used, in accordance with the rest of the equipment, Elliott centrifugal blowers driven by synchronous motors.

Our tests indicated at once that the exhaust temperatures as measured gave us no criterion as to the temperatures of various engine parts, such as pistons, valves, etc., as they would vary with the same load, but with different amounts of air passing through cylinders during the scavenging period and mixing with the exhaust gas.

More accurate investigations with the aid of built-in thermocouples convinced us that, whereas, the valves were actually considerably cooler than in an unsupercharged engine, since all the scavenging air has to pass by them, the piston, piston rings, liner, and spray-valve tip were hotter. Our company would not consider building supercharged engines for continuous duty without improved cooling and, particularly, without oil-cooled

[9] Consulting Engineer, New York, N. Y.

[10] Cooktite Ring Sales Company, Chicago, Ill.

[11] Shell Oil Company, Wood River, Ill.

[12] National Supply Company, Springfield, Ohio.

pistons (at least, if the engine is supercharged above 20 per cent of its original rating).

We also found that, if an engine is required to develop its full torque over a wide range of speed, a centrifugal blower mechanically connected to the engine or driven by a synchronous motor from the engine generator will not work out so well since with adverse exhaust conditions (pulsations), the impeller might more or less slip through the air, maintaining the pressure in the manifold which it is capable of developing at the respective speed, but without the assurance that the calculated amount of air is going to the engine. A metering device in the line would be necessary to indicate the exact amount of air going to the engine.

In this respect, a positive-displacement blower seems to be preferable, as it will automatically build up a pressure difference which will put all the air through the engine.

Although these engines have been in successful service about $1^1/_2$ years, it is felt that the investigations are far from finished and that we still have much to learn from them.

In view of our experience, the writer is not too certain whether or not his company would recommend exhaust-driven superchargers for such service as in dredges where full torque is required at variable speeds, in tugboats which have much maneuvering and accelerating to do, or in shovels, draglines, hoists, etc., unless definite provisions are made to restrict possible overloads lasting appreciable amounts of time at decreased engine speeds.

It has been mentioned that experiments for determining the best overlap on large engines are very expensive and require a long time to make. The writer's company has cut these items down considerably by using, in the test setup, special split cams in which one half can be displaced against the other to vary the resulting overlap as desired. This has permitted us to make up to four tests in one day.

Author's Closure

The first question brought up in the discussion concerns fuel economy. We do not have any information on the fuel economy of these supercharged engines. The author does not know whether all pipe-line companies follow the same practice. We have an abundant supply of fuel oil, for we burn the oil we pump. Therefore, we are not much concerned about fuel economy. There are no means available in our plants for making fuel-economy tests and, for that reason, the point was passed over. Our company is interested primarily in the possibility of getting additional horsepower at a reasonable price, to permit pumping more oil. The engines in question have a normal fuel economy of about 0.41 lb per bhp-hr. There is nothing to substantiate the claim, other than belief that the fuel economy is just as good supercharged, possibly a little better under full-load conditions, but much poorer under low-load conditions, which probably accounts for the carbon accumulations when operating at low loads.

Referring to Mr. Doyle's data, it is quite evident that the engine on which those tests were made does not lend itself very admirably to supercharging, since it operates with a high maximum cylinder pressure compared to low-speed engines. A maximum pressure of 850 lb is about 150 lb higher than the normal 225- or 300-rpm solid-injection engine. Most engines with which the writer is familiar carry about 700 lb maximum cylinder pressure. It is doubtful whether a supercharged engine carrying 1050 psi maximum pressure would operate satisfactorily.

Concerning the speed range of engines and the effect of speed variation on supercharging, that condition would be more pronounced in locomotive engines, dredge engines, and engines which require some maneuverability, but on a pipe-line engine, the speed is fairly constant. When there is occasion to change speed, it is done slowly, operation continuing at the same speed for several days. Normally, on pipe lines, the range of speed is from 25 to 30 per cent of the engine rated speed.

To the writer's knowledge, we have had no lubricating-oil problem other than on one particular job where oil was lost from the pressure system with which we lubricate the turbocharger bearings. As far as the writer knows, we have had no loss of oil from the engine system proper. We gain oil in the crankcases because oil is wiped downward from the cylinders.

In reply to Mr. Cook, we have experienced no trouble with piston rings. At the present time, 2 two-piece rings are fitted to each piston; the rest are standard miter-cut snap rings.

Mr. Noltein brought up the matter of excessive temperatures. We have suspected that there might be something to that also, but from some of the information brought out in the discussion, it would appear that others are operating at much higher brake mean effective pressures than we are which is reflected by higher exhaust-gas temperatures. We plan on supercharging about twelve more engines, most of them 500-hp units; and, eventually, unless unexpected trouble is experienced, probably three times that many. The temperatures on our supercharged engines are much lower than the temperatures which have been mentioned in the discussion, which, it is believed, is a much more desirable operating condition. For instance, in "Test Results With Under-Piston Supercharging,"[13] it is noted that the average exhaust temperature approached 1000 F. To the author this would seem to indicate they are not doing as good a job of supercharging as they think they are, for the simple reason that the exhaust temperature represents an overload caused by insufficient air. From the air pressure shown, the engines should have plenty of air, but the air temperature is such that the volumetric efficiency in the cylinders is greatly lowered. A great deal more supercharging could be done with one third the pressure, if the temperature were lower.

[13] Paper by E. S. Dennison and W. A. Morain, presented at the National Meeting of the Oil and Gas Power Division, Kansas City, Mo., June 11–14, 1941, of The American Society of Mechanical Engineers.

Pre-Exhaust-Gas-Pressure Measurements for Indicating Diesel-Engine Performance

By B. H. JENNINGS,[1] EVANSTON, ILL., AND T. E. JACKSON,[2] BETHLEHEM, PA.

The pressure existing just before exhaust in a Diesel engine is shown to be significant as a means of indicating load adjustments in a multicylinder engine. This paper explains the theory and method used in obtaining these pre-exhaust pressures, along with the supporting data from an extensive series of tests. These tests were conducted at Lehigh University on both two-stroke-cycle multicylinder engines and a four-stroke-cycle single-cylinder C.F.R. test engine. Under definite known conditions of injection, timing, and compression ratio it was found possible to evaluate both indicated and brake horsepower in terms of pre-exhaust pressure. Experimental work in progress shows that the same method is applicable to spark-ignition engines.

DETERMINATION of the distribution of load among the various cylinders of a multicylinder Diesel engine during operation has always been a difficult and tedious operation. Yet such information is vitally important when adjustments have to be made on the engine to enable it to develop its required power without overheating in any cylinder or when attempting to better poor operating economy. Such things as improper balance of fuel-pump quantity to each cylinder, variations in injection timing for each cylinder, and variations in spray-valve performance are items which should be under control of the operator at all times. Yet because suitable instruments for quickly indicating maladjustments have not been available, many engines do not operate even near their peak performance.

Various methods of gaging performance of Diesel engines during operation have been investigated over a number of years. With the slow-speed engine, conventional engine indicators have performed meritorious service but the time consumed in indicating a multicylinder engine was long and under quick load changes variations were often not even detected. Analysis of indicator diagrams themselves also led to inaccuracies as the necessarily high spring pressures produced cards of extremely small size. With the advent of higher-speed engines (even above 400 rpm) the conventional indicator was no longer satisfactory. Most indicating devices for high speeds, such as the carbon-pile or piezoelectric, each with its necessary recording or indicating device, represent relatively inflexible and expensive devices primarily suitable only for laboratory research. Balanced-diaphragm indicators are equally laboratory devices.

Methods available merely for equalizing loads among engine cylinders have been somewhat disappointing except for relatively crude adjustments in the field. When the indicator has not been used, comparisons of exhaust-gas temperatures and examination of exhaust color and appearance have been the most common methods.

The exhaust-gas-temperature method seems at first to have great possibilities, but does not seem nearly so satisfactory after being given deeper consideration. According to theory, the products of combustion will have a definite temperature after expanding during the working stroke of the piston, however, the actual temperature of the gases entering the exhaust will depend upon three things. The first of these is the amount of fuel and air burned together in the cylinder, where under balanced running conditions the exhaust-gas temperatures will all be the same. The second is the amount of scavenging air flowing into each cylinder of a two-cycle engine, particularly one having a reciprocating scavenging pump; this is not necessarily, and usually is not, the same in each cylinder. The uneven cooling of the thermal elements due to different quantities of scavenging air will unbalance the temperature readings haphazardly. The third factor affecting the exhaust temperature of any one cylinder is the location of its exhaust-gas opening into the manifold, with respect to the common outlet. The opening closest to the common outlet, having more hot gases flowing past it than the others, will definitely show a higher temperature. Any attempt, then, to balance the cylinders by this method may result in an overload on one or more cylinders.

The second method has more of the personal element embodied in it than the other one, as it consists merely of letting the exhaust gases escape into the atmosphere at the will of the operator. If the color of the gases, that is, the amount of visible smoke, is the same for each cylinder, the cylinders are assumed to be balanced. When these gases are almost colorless, the engine is assumed to be working under the best possible conditions. This method was the most popular among the older Diesel operators, but it is not very satisfactory even for balancing and gives no indication whatsoever of the power of the engine.

The use of the release pressure for indicating load conditions in the cylinders of internal-combustion engines was first proposed by Joseph C. Groff,[3] who devised an instrument that effectively operated on this principle. In this paper the principle is explained and developed and the experimental program and data corroborating the idea are presented.

Theory of Pre-Exhaust (Release) Pressure

Fig. 1 shows an idealized Diesel-cycle diagram drawn on the P-V plane. Here A to B represents compression, B to C combustion, C to D expansion, D to A the sudden drop in pressure when the burnt gases are released at start of scavenging. The pressure at D is here called release pressure or pre-exhaust pressure. Consider the cycle $ABC'D'$ in which less energy is developed, the release pressure D' is also correspondingly less than D. The problem involved becomes this: Does the variation in release pressure bear a commensurate relationship to either the brake or indicated mean effective pressure of the cycle? The answer to this question is definitely affirmative in terms of the indicated mean effective pressure of the theoretical air-standard cycle and the data hereinafter presented also show experimen-

[1] Professor of Mechanical Engineering, Northwestern Technological Institute. Mem. A.S.M.E.

[2] Instructor in Mechanical Engineering, Lehigh University. Jun. A.S.M.E.

Presented at the National Meeting of the Oil and Gas Power Division, Kansas City, Mo., June 11–14, 1941, of THE AMERICAN SOCIETY OF MECHANICAL ENGINEERS.

NOTE: Statements and opinions advanced in papers are to be understood as individual expressions of their authors and not those of the Society.

[3] U. S. Patent Reissue 20,303.

tally, under a variety of test conditions, that the relationship is definite and well defined in actual engines.

Carrying through a conventional air-standard analysis of the

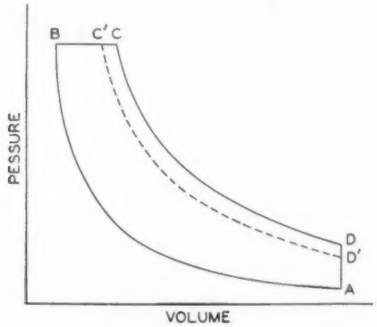


FIG. 1 TYPICAL THEORETICAL DIESEL DIAGRAM

cycle *ABCD* of Fig. 1 yields the following expression for the theoretical indicated mean effective pressure.

$$P_i = \frac{P_a r}{(r-1)(n-1)} \left\{ n r^{n-1} \left(\frac{P_d}{P_a}\right)^{\frac{1}{n}} - \frac{P_d}{P_a} + 1 - n r^{n-1} \right\} \ldots [1]$$

where P_a = suction pressure, psi
P_d = pre-exhaust (release) pressure, psi
r = compression ratio
n = polytropic coefficient of expansion or compression varying from 1.32 to 1.41 in value
P_i = indicated mean effective pressure, psi

This expression at first sight appears rather formidable but studied consideration shows that P_d is the only inherently variable term in the expression. The compression ratio r is fixed for a given engine, n is a function of cooling and scavenging conditions, and P_a, the suction pressure, is essentially constant for given engine and atmospheric conditions. Thus the release pressure is an index of mean effective pressure in this idealized analysis. If A, B, and C are constants for a given engine, Equation [1] can be written

$$P_i = A P_d \left\{ B \left(\frac{P_d}{P_a}\right)^{\frac{1}{n}} - \frac{P_d}{P_a} + C \right\} \ldots\ldots\ldots [2]$$

and in this form the relationship between P_i and P_d is more obvious.

That the air-standard Diesel cycle has pronounced limitations and does not represent any real cycle is realized by the authors but it does point to an existing relationship and indicates the feasibility of experimentally investigating the problem. This analysis also shows that the relationship will not be exactly linear between P_i and P_d but the actual release pressure will bear some definite relationship to the actual mean effective pressure.

EXPERIMENTAL ARRANGEMENT

The problem of experimentally measuring pre-exhaust pressure is the relatively simple matter of measuring the pressure which exists in an engine cylinder just before the exhaust valve opens in a four-stroke-cycle engine, or just before the exhaust ports are uncovered in a two-stroke-cycle engine. This merely involves making a connection through the water jacket, drilling a small hole through the cylinder wall, and tapping into place a connecting tubing to the outside. A typical design of a simple connection system which proved very satisfactory can be seen in Fig. 2, which is substantially similar to a conventional cylinder-lubricator connection.

It is also true that the position of the point of connection into the cylinder is not extremely critical. A study of Fig. 1 and of many actual indicator diagrams shows that just before D (or D') on the expansion stroke the pressure gradient per unit of piston displacement is rather small, consequently the point of placing the pressure tap can be moved up or down in the cylinder through the equivalent of an appreciable number of crank degrees without occasioning any significant change in the magnitude of the release-pressure values. It is only necessary that the tap point occur in the flattening portion of the expansion line reasonably ahead of the point of opening of the exhaust port in a two-stroke engine, or it must be uncovered by the piston in a four-stroke engine before the exhaust valve opens. In a given engine where relative evaluations of the output of each cylinder are significant, it is important that the tap points be placed at the same place in each respective cylinder.

To explain operation, as in Fig. 2, it can be seen that when the pressure in the cylinder is higher than in the pressure-gage chamber, a flow of gas passes through the check valve and a pressure build-up occurs while the tap is uncovered by the engine piston. After a few revolutions, the chamber pressure equals the then existing pressure in the cylinder during the period that the tap is uncovered, as the check valve keeps the chamber pressure from decreasing between impulses. To enable the release-pressure gage to follow decreases in load as the load and release pressure change on an engine, a slight leak-by opening is supplied. Thus, when the load decreases, the chamber pressure can fall until an equilibrium pressure comes into balance between the release pressure in the cylinder for that load and the pressure-chamber indication. This leak-by can be set to respond slowly or quickly and has been found to work satisfactorily for all conditions except very rapidly fluctuating loads.

This device was first tried out on a Bethlehem four-cylinder, single-acting, 8¼ × 12-in. two-stroke-cycle Diesel engine. The engine used mechanical injection of the fuel, with a separate

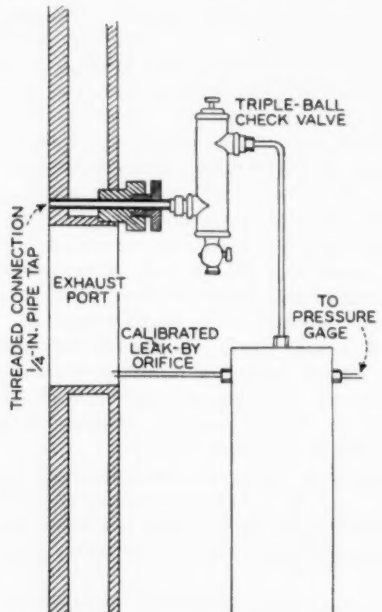


FIG. 2 ARRANGEMENT FOR MEASURING PRE-EXHAUST PRESSURE FOR A TWO-STROKE-CYCLE DIESEL ENGINE

pump element for each cylinder, and employed by-pass control in the fuel pump for load variation. A separate cylinder supplied scavenging air at about 3 psi into a common scavenging-air header. The rated capacity of the engine was 120 bhp at 400 rpm. The output of the engine on test was absorbed and measured on a direct-connected Froude hydraulic dynamometer. Fig. 3 shows the engine with the release-pressure gages in place above and behind the cylinders.

It was difficult to obtain good indicator diagrams on this engine but a series of carefully taken light-spring diagrams on each cylinder showed a very close agreement between the release-pressure-gage readings and the release pressures as scaled from the indicator diagrams. The agreement was well within the closeness to which the release-pressure gages could be read. These gages were Bourdon-type test gages, with 4-in. face and a range of 0–60 psi. Under operating conditions of engine vibration they could be read to within 1 psi anywhere in their range.

A series of tests was then run in which the balance between the cylinders was thrown out by altering settings on the fuel-pump units. In every case it was found that adjusting the fuel-pump elements until the release-pressure gages on each cylinder read essentially the same gave a close balance of load for each cylinder. These adjustments were corroborated by using supplementary methods such as measurements of exhaust temperature for each

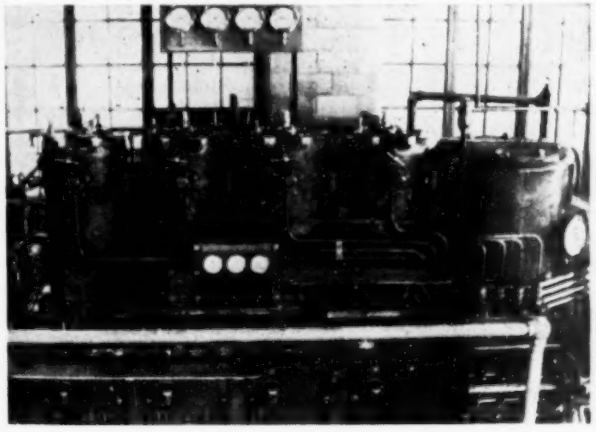


FIG. 3 BETHLEHEM DIESEL ENGINE WITH PRE-EXHAUST-PRESSURE GAGES

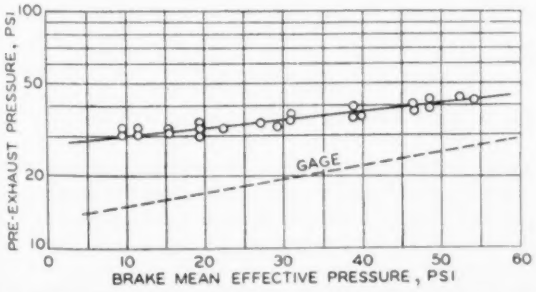


FIG. 4 PRE-EXHAUST-PRESSURE DATA—4-CYLINDER TWO-STROKE-CYCLE BETHLEHEM DIESEL ENGINE

cylinder by means of thermocouples; individual exhaust-color observations; measurements of jacket-water temperature; and, to a limited extent, by indicator diagrams. Over-all brake-horsepower tests, analyzed in terms of fuel economy with good and bad settings as indicated by the gages, also were indicative of the accuracy of this method for making adjustments.

It early became evident that a scientific analysis of release-pressure variations in terms of the variables of operation should be made on a one-cylinder engine so that individual effects could be singled out and evaluated. This was done, as is discussed later in this report, but certain of the data found on the four-cylinder engine also appear to be significant and are presented in Fig. 4. In this figure, the brake mean effective pressure is plotted against the release pressures averaged for the four cylinders. This shows a definite trend, as would be expected, but the points are more scattered than seems reasonable. The reason for this lies in faulty performance of the fuel-pump elements and of the injection system on this particular engine. Later investigation

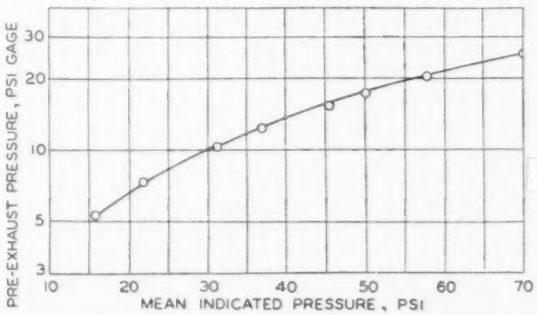


FIG. 5 PRE-EXHAUST PRESSURE DATA—WORTHINGTON TWO-CYLINDER TWO-STROKE-CYCLE DIESEL ENGINE

showed 6-deg variation on injection timing of this pump. During the running period of certain tests the individual pump units frequently changed their settings and threw the individual cylinders out of balance. This tended to overload some cylinders and underload others and, it is believed, accounts for much of the scattering apparent on this curve. On the basis of the average data of this graph the following empirical equation, relating brake mean effective pressure P_b (psi) with release pressure P_d (psi gage), was derived

$$P_b = 7.08(P_d - 12.8)^{0.747}$$

Such a particular equation or plot applies only to a particular engine or engine type but when once found some idea of power output at a given speed would readily be available from the readings of a single release-pressure gage or set of such gages.

The next series of tests was made on a Worthington two-cylinder $12^1/_2 \times 13^1/_4$-in. single-acting, crosshead-type, two-stroke-cycle engine. This engine used the under side of each piston for compressing the scavenging air. Rated horsepower was 100 at 325 rpm. For test, the engine was loaded on a Froude hydraulic dynamometer and equipped with release-pressure equipment and gages similar to those described for the previously tested four-cylinder engine. The main reason for using this second engine was to find whether the generalizations found would hold for any engine, and secondly to check release pressures against indicated-horsepower readings. On this latter engine it was possible to obtain reliable indicator diagrams using a well-built, conventional piston-and-drum-type engine indicator.

The system of balancing loads between cylinders by release pressures was found to be satisfactory and reliable for this two-cylinder engine also and here it was possible to get indicator diagrams to corroborate the accuracy of the adjustments. It might be mentioned here that adjustments were also made to balance loading between the two cylinders by means of measurements of pre-exhaust-gas temperatures as well as the conventional measurements of exhaust-gas temperatures. Careful checks against indicator diagrams showed that release-pressure values checked the diagram values of mean effective pressure very closely at every measured point, whereas the exhaust-gas temperatures,

which showed a good index at medium load, appeared quite unreliable at full load on the engine.

The averaged results of a series of carefully run tests on this engine using release pressures and indicator diagrams is shown in Fig. 5. The lower three points on this curve were not taken from indicator diagrams because of the difficulty of precise interpretation of the light-load diagrams, but were computed back from carefully measured brake-horsepower measurements made during the tests.

The tests on both of these engines point to the conclusion that pre-exhaust-gas pressures can be used to indicate brake or indicated mean effective pressures when a determination of mean effective pressures in terms of pre-exhaust pressures has been made. Knowing these values and the revolutions per minute, the brake horsepower or indicated horsepower developed also becomes determinate. These tests also showed that this method was effective in balancing the loading among the various cylinders of an engine whether there was any real interest in horsepower evaluation or not. This latter item was more conclusively proved in the third series of tests using a single-cylinder engine. Both of the two-stroke-cycle engines tested were early-design units of low mean effective pressure and specific capacity as well as moderately low speed, however, there is no reason to believe that modern high-capacity and high-speed units would not perform similarly and this was found to be the case on the small four-stroke-cycle unit used in the third series of tests up to 1200 rpm.

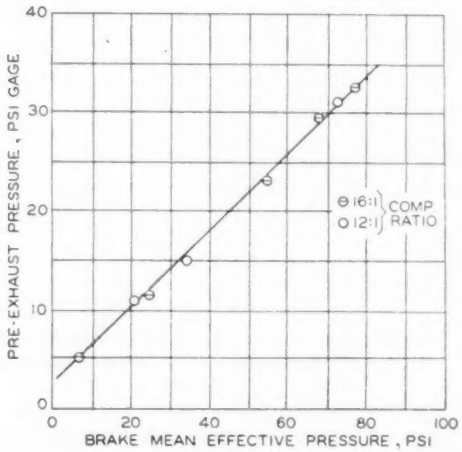


FIG. 6 PRE-EXHAUST PRESSURE WITH VARYING COMPRESSION RATIO

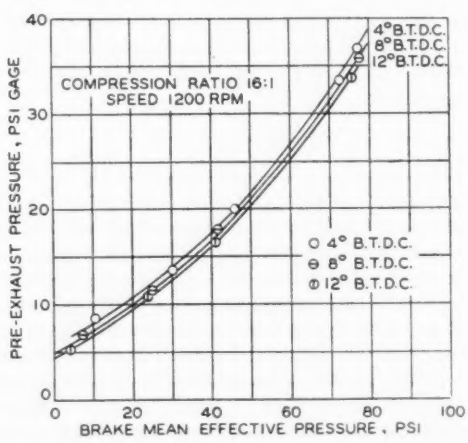


FIG. 7 PRE-EXHAUST PRESSURE WITH INJECTION TIMING VARIED

The third unit used in these release-pressure investigations was a Waukesha standard C.F.R. Diesel fuel-testing unit. This unit was a $3^1/_4 \times 4^1/_2$-in. single-cylinder, four-stroke-cycle engine with provision for changing the compression ratio over wide limits, roughly anywhere between 7 and 30 to 1. For fuel-rating work the engine speed is maintained essentially constant at 900 rpm by a V-belt connection to a synchronous-type induction motor. For release-pressure work, however, the V-belts were removed and instead the engine was directly coupled to a cradled electric dynamometer so that precise measurements, control of power output, and speed variations could be made. The release-pressure connection, $^1/_8$ in. diam, was drilled through the cylinder wall at a point equivalent to eight tenths of the stroke down from top-dead-center position of the piston. This position for the release-pressure drilling was uncovered by the top piston ring just ahead of the time of opening of the cam-operated exhaust valve. Similar to the arrangements on the other engines, a three-ball spring-loaded check valve was connected as close as possible to the engine cylinder and a 100-lb, 4-in. Bourdon gage attached. A stop-cock relief was attached so that the pressure could be relieved and then allowed to build up before all accurate test readings were taken.

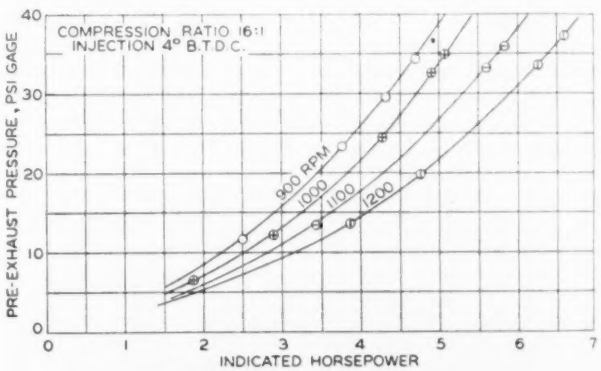


FIG. 8 PRE-EXHAUST PRESSURE VS. IHP AT VARYING SPEED

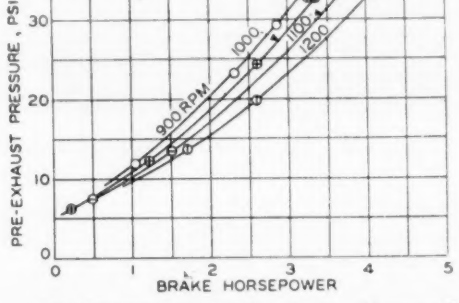


FIG. 9 PRE-EXHAUST PRESSURE VS. BHP AT VARYING SPEED

This unit has provisions for controlling and measuring both the quantity of fuel injected and also the time of injection. The cylinder-jacket water was kept at 212 F by evaporative cooling; and both lubricating-oil and air-supply temperatures were held constant within close limits. Indicator diagrams were not taken but numerous friction power tests were made by motoring the engine with the dynamometer, immediately following brake-horsepower tests and before thermal equilibrium had been lost by the engine.

Many tests were made on the engine in which speed, injection

advance, compression ratio, and fuel injection were varied. Space is available to record but a fraction of the data which were obtained and these are given in the curves of Figs. 6, 7, 8, and 9.

Fig. 6 shows a series of tests, in which the speed and injection timing were kept constant and the compression ratio varied. This series shows that for the range of compression ratios used, 12:1 and 16:1, the relationship of brake mean effective pressure and release pressure varies little with varying compression ratios, although for a given release pressure the value of brake mean effective pressure increases slightly with the higher compression ratios. This result was substantiated by additional tests at other speeds and compression ratios.

Fig. 7 shows the injection timing varied while compression ratio and speed are kept constant. Here, over the range investigated, for a given release pressure the brake mean effective pressure increases as the injection timing becomes further ahead of dead center. This trend also was confirmed at other speeds and compression ratios.

The effect of speed variations between the 900- and 1200-rpm ranges was found to be so small in relating brake mean effective pressure to release pressure that curves of this nature were not plotted. However, Figs. 8 and 9 are plotted to show release pressure in terms of indicated horsepower and brake horsepower with speed as the variable and with injection timing and compression ratio fixed.

Conclusions

All of these tests point to the fact that there is a definite value of release pressure which is related to the brake and indicated mean effective pressures being developed by an engine at a given time. In the case of two multicylinder engines it was also shown that using release-pressure readings as indexes for balancing and adjusting the load among the various cylinders was a simple yet effective method of control. The magnitude of release pressures in terms of brake or indicated mean effective pressures varies with each type engine, although these values should be the same for a given type of production engine. Three engines were tested, two of these were early-design two-stroke-cycle multicylinder Diesels and the third a single-cylinder four-stroke-cycle engine, of more recent design. Although release pressure showed a definite relation to brake mean effective pressure for each particular engine there is no relationship apparent between the three different engines. Maximum values for the three different engines showed 54 psi brake mep at 28.3 psi gage release pressure, 56 psi brake mep at 26.0 psi release pressure, and for the four-stroke engine, 80 psi brake mep at 35 psi release pressure. Even though release-pressure values did vary for these different engines, there is every reason to believe that this would not be true for a series of production engines but a given release pressure could be associated with a definite brake mean effective pressure, assuming that the gage attachments were properly made and operating conditions were essentially the same.

Discussion

C. B. Rosenberg.[4] Would the authors elaborate upon their description and function of the leak-by orifice which is incorporated into the instrument described? What effect would abnormal blow-by conditions have upon the results obtained with this instrument, that is, under conditions of instantaneously high blow-by rates at the time two or more piston-ring gaps are in line to allow leakage? Would the leak-by orifice compensate for such blow-by fluctuations? What effect would the presence of the increase in temperature, due to "hotter" blow-by gases gaining admittance into the "stabilizing" tank, have upon the gage reading?

E. J. Kates.[5] This method of measuring load conditions is interesting, and seems to have excellent possibilities. The writer would like to have the authors' opinions on the following questions:

(1) Is not this method subject to the same general faults as the method of checking load distribution by means of exhaust temperatures? In other words, if there are mechanical derangements of one kind or another in the individual cylinders, such as blow-by, do not the readings become unintelligible? One does not know whether a higher pre-exhaust pressure reading is caused by more load being carried in that cylinder, or by greater blow-by.

(2) What is the possibility of clogging occurring in the pipe lines which run from the cylinder connection through the tank and to the gage, due to oil and sludge accumulations getting into the lines?

(3) Has there been any trouble with corrosion of the gages due to the exhaust gases acting on the brass of the Bourdon tube?

Will the authors explain, if possible, the reason for the difference in curvature between the curves in Fig. 6 and Fig. 7 of the paper? Both charts seem to show pre-exhaust pressure plotted against mean effective pressure. In the case of the upper chart, Fig. 6, the relation seems to be that of a straight line, whereas the curves in Fig. 7 are all distinctly curved. Since the same relations are being plotted, why does the difference in curvature occur?

Referring to Fig. 5, it would be interesting to know, since this was a two-cylinder engine and the points plotted seem to be the average pressures of the two cylinders, what was the variation of the individual cylinder pressures? The curve of average pressures is quite smooth and the points seem to lie directly on it, but did the individual pressures of the two cylinders also come close to the same curve?

H. E. Degler.[6] Did the authors attempt to use pressure snubbers at the bottoms of the gages?

The writer is somewhat intrigued over the volume of the accumulator tank, as compared to the size of the orifice used, and as compared to the size of the connecting tube. Possibly, the word "volume" should be used for the connecting tube because the length is quite a factor, as well as the diameter, and also that other relation which, of course, would have to be the cylinder volume at the time this point is reached, as the piston moves downward. The writer believes there is some interrelationship between these volumes. This matter was not dealt with in the paper.

Do not speed of the engine and the inertia factors of the column of gas, as well as the possible, should we say, inefficiency of the check valve to function as effectively at all times and at all of these speeds, influence the curves given in the paper? Having a speed range of 400 to 1200 rpm, the writer believes there is something in that particular phase which might affect the curvature of the speed versus exhaust pressure and the mean effective pressure versus exhaust pressure. So it is his opinion that the insufficiency of the connecting device, as well as the column, etc., have something to do with the relationship of the quantities.

It would be of interest if the authors' experimental work could be continued on engines of higher than 1200 rpm, and also on engines with smaller cylinders; in other words, moving on into the more interesting and intricate range of speeds, smaller diameters, and,

[4] Pure Oil Company, Chicago, Ill.

[5] Consulting Engineer, New York, N. Y. Mem. A.S.M.E.

[6] Professor of Mechanical Engineering, University of Texas, Austin, Tex. Mem. A.S.M.E.

let us say, a greater variation of the adaptability of this very unusual method of pre-exhaust-pressure indication.

J. C. GROFF.[7] Having been indirectly associated with the authors in their work at Lehigh University in this new field, the writer appreciates what care and time were devoted by them to these tests and to the preparation of this paper and wishes to compliment them upon their presentation.

The writer's work on this development has been directed to the making of test installations on various types of engines operating under commercial conditions ashore and aboard ship. Naturally, this has involved considerable attention to detailed design for eliminating those "bugs" which always come into the picture.

To begin with, the apparatus involved in adapting this power-indicating principle has been termed "Load-I-Cator" for the reason that one of its chief functions is to indicate the "load balance" among the respective cylinders of a multicylinder engine. Now at last, internal-combustion-engine cylinder performance can be continuously gaged just as an electric motor is by a power meter. The instrument is designed to afford knowledge of instantaneous mean indicated pressure and mean effective pressure values indirectly by directly indicating "pre-exhaust pressure" or "pep," for short. Thus mean indicated pressure and mean effective pressure have acquired a new associate whose function it is to keep them balanced among the cylinders and so pep up their effectiveness by avoiding operation of inefficiently overloaded and underloaded cylinders.

Like many technical developments, this had its inception (in 1924) as the result of an engineer's laziness and desire for an easier way out. Being engaged on experimental and performance-test work ashore and as an operating engineer aboard various Diesel ships, one of the writer's jobs was to take a considerable number of indicator cards and then planimeter and figure them. Too often, this was done primarily to check the load balance, as indicated by the exhaust-gas pyrometers. This experience soon proved how unreliable pyrometers are for load balancing, and the work of indicating the engine was sufficiently bothersome and time-consuming to inspire developing something better.

From the thermodynamics involved, it seemed logical to suppose that there must be some reliable relationship between the amount of fuel injected, the amount of power developed, and the pressure to which the products of combustion are reduced at some single given point of piston travel, as indicated by a corresponding point on the expansion curve of the card.

Analysis of numerous indicator cards from various types of Diesel engines supported this supposition and showed that, subsequent to about 15 per cent of the power stroke, the pressure ordinate on the expansion curve varied in relationship with the mean indicated pressure developed at all corresponding single points of piston travel up to that of exhaust commencement. At from about 35 to 40 per cent of the power stroke, the corresponding cylinder pressure would almost indicate the mean indicated pressure directly in a 1-to-1 relationship. The next even relationship occurs at about 65 to 75 per cent of the power stroke where the cylinder pressures indicate about one half of the mean indicated pressure values in a 1-to-2 relationship.

As will be understood, the exact points of piston travel where the afore-mentioned even (mip/pep) relationships exist will vary with different types and sizes of engines, as well as with engine speed, due to correspondingly different heat losses which influence the shape of the expansion curve. However, once this point is determined from the indicator cards of a given engine, it remains practically fixed and can be used with reasonable accuracy for rapid checking of mean indicated pressure values from new cards. Also it is the same for all the cylinders of that engine. To so check new cards, it is only necessary to scale the pressure ordinates of the cards using a scale graduated in a 1-to-1 or 2-to-1 ratio to that of the particular indicator spring, depending upon which gaging point is used.

The next logical step was to so equip an engine that an indication of the cylinder pressure at some such point would be automatically and continuously available from each cylinder at all times. Doing this simply involves provision of a small port (i.e., $^1/_8$ to $^3/_{16}$ in. diam) in the side wall of the cylinder, to be uncovered by the top edge of the top piston ring at the proper point of piston travel, whereby the timing action is automatically taken care of. As described in the paper, the intermittent pressure pulses are translated into a self-adjusting sustained pressure, corresponding to that instantaneously existent in the power cylinder when the gaging port is uncovered, and this pressure is indicated by a conventional Bourdon-tube gage.

This led to the question as to where would be the most desirable point of piston travel for location of the Load-I-Cator gaging port. If the 1-to-1 ratio point were to be used, it would mean locating the port in the region of higher cylinder pressures and temperatures. Furthermore, the only advantage of so doing would be to obtain a 1-to-1 ratio so that the indicated cylinder pressures would read directly as mean indicated pressure values. Against this one dubious advantage were a number of compelling advantages in favor of locating the gaging port as near the exhaust point as practicable. These advantages have been proved valid from experience and are listed as follows, since they have an important bearing upon the successful operation of this scheme:

1 The nearer the exhaust point, the lower is the cylinder pressure and the temperature of the gases. This is of importance to avoid carbon formation in the gaging port, the check valve, and the connecting tubing.

2 The nearer the exhaust point, the more nearly does the expansion curve approach the horizontal and vice versa. Thus, near the exhaust point, reasonably small inaccuracies as to location of the gaging ports in the various respective cylinders of an engine have insignificant effect upon the accuracy of the cylinder-pressure indications. This will be apparent by merely comparing the slope of the expansion curve of any Diesel indicator card at about 35 per cent of the stroke with the slope near the exhaust point.

3 The nearer the exhaust point, the more nearly have the combustion gases expanded toward atmospheric pressure. Thus, at this point compression-ratio variations in the respective cylinders of an engine have the minimum effect on the cylinder-pressure indications.

The question has been asked whether difficulty has been experienced because of carbon formation in the cylinder-wall connection and the triple-ball check valve used. The answer is: None whatever; and the reasons will be more or less obvious when mentioned. To begin with, the teaching of the Load-I-Cator principle is to handle the cylinder gases near the exhaust point, where their pressures and temperatures are lowest; and, since the cylinder connection traverses the water jacket, near the comparatively cool water-inlet point, its temperature is such as to inhibit carbon formation. Furthermore, enough lubricating oil from the cylinder walls finds its way through the small bore of these cylinder connections to keep soot particles in a state of flocculent fluidity.

To anticipate the question which may occur to some readers, relative to the impairment of cylinder lubrication through the small loss of lubricating oil via these cylinder connections, as referred to, such doubts may be settled by repeating that the bore of these connections is only $^1/_8$ to $^3/_{16}$ in. ID. Thus, the amount

[7] Development Engineer, The Aldrich Pump Company, Allentown, Pa. Mem. A.S.M.E.

of cylinder oil to be lost thereby is insignificantly small compared to that lost through the much larger exhaust ports of two-cycle engines.

In the early stages, it was believed that an ordinary spring-loaded ball-check valve would be suitable for this purpose, but it was found that the spring superimposed a pressure-differential condition which produced erratic pressure indications under different engine speeds and load conditions. Using a free-ball check having a single ball, eliminated this condition; but occasionally, and too frequently for reliable results, a particle of soot would lodge between the ball and its seat and the pressure indication would gyrate. The solution arrived at was a triple-ball check valve with the idea in mind that the possibility of all three balls being so unseated at any one time would be highly remote. This has been proved in service.

Following the initial tests at Lehigh University and coincident with their subsequent test work, as covered in the paper, Load-I-Cator equipment was fitted to certain different types of two-cycle and four-cycle engines and subjected to continuous operation under actual service conditions for periods ranging up to more than 2 years to date. This was done to prove the principle and the ability of the equipment to operate successfully under nonlaboratory conditions, as must be faced in the field, before placing it on the market.

As a result of these tests at Lehigh and in the field, the apparatus has been developed and proved to the point described and illustrated.

The Load-I-Cator cylinder connection is much like a conventional cylinder-lubricator connection, in that it traverses a simple stuffing box screwed into the jacket wall and that its inner end is tapped into the liner wall (usually with a $^1/_8$-in. I.P.S. thread). The triple check valve is small in size and has a union connection with the cylinder connector. It is fitted with an inlet strainer which may be readily cleaned at periodic intervals by merely opening a pet cock while the engine is in operation. Incidentally, this pet cock affords the ideal method for obtaining true samples of exhaust gas for purposes of analysis.

Connected to the outlet from the check valve is a small pressure chamber. This vessel is mounted vertically and its upper portion serves as a receiver of sufficient volume to cushion the pulsating effects from the intermittent pressure pulses. The lower portion of this chamber is filled with a light grade of lubricating oil which serves as a seal between the corrosive gases and the Bourdon tubes of the pressure gages. The internal volume of this chamber is only about 4 cu in., which is sufficient for most engine speeds above about 350 rpm. For engine speeds below about 350 rpm, an auxiliary cushion chamber, having a volume of approximately 50 cu in. is interposed between the check valve and the afore-mentioned combination cushion-oil-seal chamber.

The question has been asked whether any special pressure-snubbing device is necessary to prevent the pressure gages from pulsating. The answer is yes; and a very simple snubbing device is incorporated in the aforesaid cushion chamber which eliminates all gage flutter.

A question has been asked as to the construction of the leak-by orifice, referred to in the paper, and provided for the purpose of equalizing automatically the pressure on the gages to that existent in the cylinder, in order to accommodate decreasing pressures for decreasing loads. This orifice is very simple and foolproof. As may be noted from its appearance, it consists merely of a stainless-steel pin located within a drilled hole, to provide an annular leak-off orifice of desirable small capacity yet without requiring a drilled hole of microscopic size. A glass-wool filter ahead of this orifice protects it against foreign matter and, should it become clogged, it is easily cleaned merely by moving the pin back and forth in its hole.

Since most stationary and marine Diesel engines are started by means of compressed air, the air pressure in each power cylinder, at the point where the Load-I-Cator gaging port is uncovered, may exceed the range of the pressure gages. Accordingly, to protect these gages from overpressure, each cushion chamber is equipped with a small spring-loaded relief valve. This valve may be so adjusted that it will relieve and whistle an alarm whenever the pre-exhaust pressure exceeds its normal full-load value. Thus, each cylinder is equipped with an overload safety alarm which will also indicate instantly the existence of piston-ring blow-by. For wholly automatic installations, this overload indicator may be used to actuate conventional safety controls to reduce the fuel supply, or to stop the engine just as do cooling-water-temperature and low-lubricating-oil-pressure safety devices.

With further reference to location of the pressure-gaging port, it will be obvious that the first requirement is that the top piston ring uncover it prior to commencement of exhaust. This means that the gaging port must be located above the top edge of the exhaust port on vertical two-cycle engines and ahead of the point of piston travel where the exhaust valve commences to open on four-cycle engines. The amount of lead or advance opening is governed largely by the engine stroke, speed and design of the piston as regards closeness of its fit in the cylinder, distance between the top ring and the top outer edge of the piston, etc. All of these factors have an important bearing and, for best results, the details of each prospective installation should be referred to the manufacturer of this patented equipment.

In order to minimize the pressure-build-up time in that part of the system, between the entrance to the gaging port and the triple check valve, it is made as compact in volume as possible. For this reason, the check valve is connected closely adjacent to the cylinder. As an example of how accurate the pressure indications are by this method, it may be mentioned that on a special test for this purpose the Load-I-Cator gage showed 23.0 psi, whereas scaling a light-spring pressure indicator card at the corresponding point of piston travel showed 23.3 psi, a difference of 0.3/23.0, or only 1.31 per cent.

Although not mentioned in the paper, being outside its scope, the Load-I-Cator performs another unique and important function in that it also affords a continuous check on the operating efficiency of the piston rings. This is done by indicating the existence of ring "blow-by" causing the pressure gages to read higher than normal. A gage reading which is somewhat higher than that proper for the maximum cylinder load indicates that the first or "fire" ring is stuck fast in its groove or otherwise improperly contacting the cylinder wall, to permit cylinder pressure to work down to the top of the second ring. Thus, under such conditions, the gaging port is uncovered earlier by the second ring and, in effect, at an earlier point of piston travel where the cylinder pressures are higher. Similarly, if the second ring is stuck or blowing-by, the gaging port is uncovered still earlier by the third ring and a still higher gage pressure shows up.

Since these pressure additions come in increments and since such overpressure can only result from ring blow-by, the indications can be relied upon. As an illustration of this, about 4 months after the first commercial installation went into operation, the engineer telephoned the writer to say that one of the Load-I-Cator gages on his two-cylinder engine showed an increase of about 25 psi since starting the engine following an overhaul. The answer to him was that the piston rings in that cylinder must have been changed and were not yet properly worn in to prevent blow-by. It required about 4 days of subsequent operation for the new rings to adjust themselves, during which time the high gage reading gradually came back to normal and stayed there.

In this connection, it is difficult to state which is the more important function of this device; its ability continuously to indicate accurate load balance, or its tell-tale indication of piston-ring blow-by, with the objectionable effects which are all too familiar. This would seem to be another of those "modern conveniences" which might be extolled at length without convincing one who is unfamiliar with it but which is quickly deemed invaluable by the operating engineer once he has it.

A. F. ROBERTSON.[8] The writer is not familiar with any work of a similar nature to that described in this paper. There is one point of concern, however, and that is the maximum pressures in the engine cylinder. The engine has to be designed to run under certain limits as to the maximum cylinder pressure, and, in order to meet government and other shipping regulations, these limits of maximum cylinder pressure must be maintained. So far as the writer knows, there is no reliable pressure indicator on the market which can be used as a maximum-pressure indicator by the average workman in the shop.

CARL A. JACOBSON.[9] Is the measurement of pressure at the pre-exhaust point relative rather than absolute? In other words, will this measurement, which is to be used as a means of determining the loading of different cylinders, have to be calibrated for each individual engine? Also, is it necessary to determine at which particular point ahead of the exhaust the orifice should be located?

V. L. MALEEV.[10] While not wishing to detract anything from the value of the research work done by the authors, the writer questions its practical value. It so happened that 14 years ago when the writer was employed by the Western Enterprise Engine Company of Los Angeles, we, not because we were lazy but because we were too busy, wanted to find a short cut for determining the horsepower developed by an engine under given operating conditions, when the engine was installed. We wanted to know whether the engine was operating with a normal load, an overload, or if the load could be yet further increased safely. At that time the writer conducted a little research. Five engines were available, ranging from 80 hp to 300 hp, with from three to six cylinders. With these engines a start was made in investigating the relationship between the brake mean effective pressure and the exhaust temperature. The results were incorporated in a paper presented before the Oil and Gas Power Division of this Society in 1927.

At that time the relationship developed between the five engines, which were all of the same type, could be covered very nicely by a curve which was almost a straight line similar to that shown in Fig. 6 of the paper, comparing brake mean effective pressure with exhaust temperatures. Since the authors probably wil continue their work, it would be very interesting if they would at the same time keep a close tabulation of the exhaust temperatures. They may find that this complication of taking pre-exhaust pressures is not necessary, that the temperature curve will be very close to their curves.

K. J. DEJUHASZ.[11] A reliable, simple, and accurate instrument for determining the distribution of load among the various cylinders of a multicylinder Diesel engine has been a long-standing engineering problem. Various indicators for maximum pressure, mean indicated pressure, and exhaust temperature have been proposed, tried, and found wanting. The basic objection is that all of these give inferential indications, based upon an assumed indicator diagram. The assumed interrelation is valid only as long as the indicator diagram obeys the assumed law. However as soon as the law of the indicator diagram changes, the simple relationship of these inferential instruments is upset, and the results become misleading.

These objections are fully valid against the method and instrument described by the authors. Incidentally, contrary to the statement of the authors, the broad idea itself is not new. About 20 years ago the writer was associated with a firm of indicator manufacturers in Germany in connection with the development of his phasing-valve indicator. Full consideration was at that time given to the possibility of keeping the phase of the opening of the indicating valve constant at a preselected phase of the engine cycle, and thereby obtaining a continuous indication of the load condition of the engine. A simplified device, using the engine piston itself as a phasing valve, in connection with a check valve, as described in this paper, was fully considered. A modification, using two check valves, one for the maximum and one for the minimum pressure occurring at the preselected travel of the engine piston, and measuring thereby the difference between the maximum and minimum pressures by means of a differential pressure gage, was also investigated and discarded. And probably even then the idea was not new; the German patent DRP 347,840 filed in 1919 by the Liebra Company shows tapped openings in the engine cylinders, bearing a close similarity to the method described by the authors.

Possibly the patent referred to by the authors does not claim the broad idea as such, and the question of novelty, in any case, is unimportant in this discussion. The important question is: Does the proposed method offer advantages in comparison with other differential methods? Let us make comparisons.

1 *Maximum-Pressure Gages.* Assuming a certain type of indicator diagram, a correlation formula can be developed or experimentally determined between the maximum pressure (Otto cycle, or mixed cycle) and the indicated mean pressure, the value of the maximum pressure being in itself of no significance. It can be objected that the maximum pressure puts greater demand on the ruggedness of the check valve; but these demands can be met by suitable design, construction, and materials.

2 *Mean-Pressure Indicators* (averaging the time integral of the cylinder pressures). Such an indicator is described in DRP 416,623 (1923) and DRP 540,803 (1929) issued to Geiger. The inferential relationship with the mean indicated pressure is closer in this case, because all the cylinder pressures have influence on the indication and not only that in one phase.

3 *Exhaust Pyrometer.* If such instruments are suitably designed and carefully mounted to minimize the influence of the other cylinders, and the heat conduction from the manifold walls, then the correlation appears to be about the same as with the pre-exhaust pressure gage. There is the advantage in favor of the pyrometers in that (1) they use wires which are easier to mount and connect, and (2) several thermocouples can be connected by switch to the same voltmeter and, therefore, accidental errors of calibration of the indicating instrument (in the case of pre-exhaust pressure, several pressure gages) cannot occur.

4 *Smoke-Density Meters.* Such meters have been mentioned by the authors. These instruments are intended to measure the completeness of combustion rather than the cylinder load. High smoke density can occur with both high and low load. Therefore, smoke meters are unsuited for gaging engine load and cannot be fairly compared with load-measuring instruments, apart from the fact that smoke meters proposed up till now are not suitable for use on each cylinder of a multicylinder engine.

---

[8] Fairbanks, Morse & Company, Beloit, Wis.

[9] Fairbanks, Morse & Company, Beloit, Wis. Jun. A.S.M.E.

[10] Research Professor of Mechanical Engineering, Oklahoma A.&M. College, Stillwater, Okla. Mem. A.S.M.E.

[11] Professor of Engineering Research, The Pennsylvania State College, State College Pa. Mem. A.S.M.E.

There are some factors which may influence the correlation of the pre-exhaust pressure with the same indicating pressure; namely, (1) if the uppermost ring is worn, and the next lower ring is not worn, or (2) if the uppermost ring gap happens to be at or near the tapped hole for the pressure-gage connection, then high pre-exhaust pressures will be shown even at low cylinder loads, giving an entirely erroneous indication.

From the foregoing consideration, it appears that the method and apparatus described by the authors is not superior to other existing inferential methods, but on the contrary, is open to serious objections.

These comments are not intended as an adverse criticism, and still less as a discouragement to further efforts. The problem is so important and so difficult that all efforts should be made to develop an ideal instrument which will be really useful to the operating engineer. From the description of the instrument, it is evident that considerable effort and technical skill went into its construction. Some aspects may have eluded the writer's attention which would make even the uncertain data supplied by this instrument of some help to the operating Diesel engineer in certain cases, in preference to no guide at all. However, the conclusion is inescapable that the quest toward a reliable, simple, and accurate instrument, as a substitute for the laborious procedure of indicating, for improving the operation of Diesel engines, is not ended.

Authors' Closure

The leak-by orifice consists of a small drilled hole in which a piece of stainless-steel wire fits snugly, but not tightly enough to prevent the desired outflow of gas. The wire may be moved back and forth by hand to clear the opening, if any deposition of soot should occur. The determination of the leak-by hole size is not very critical; if too small, the response is slow under rapidly varying pressures, and if too large, the pressure reading is somewhat low. When the engine stopped, in a period of about 3 min, the pressure reduced to zero. This was roughly the magnitude of the leak-by used.

Actually, in our experimental work, we were seeking to determine the definite pre-exhaust pressure existing at a given instant in the engine under test, and so the pressure was reduced by the release cock and then allowed to build up until we were certain that the correct value was indicated.

If there is excessive blow-by, the gage will indicate the existing maximum blow-by pressure. An indication would immediately be given that the engine operation was erratic. The high pressure would indicate sticking rings. The gage always indicates the maximum pressure at the measuring point, whether it is a pressure which occurred much earlier in the cylinder or not. However, in an engine under reasonable conditions, i.e., with rings free and worn in, that should not happen at all, and the true pre-exhaust pressure should appear. For example, another case where high pressures may exist is that of a large Diesel engine being started with compressed air. In that case, a small release valve somewhere on the chamber protects the gage.

The first question Mr. Kates asked was why this was better than taking the exhaust temperatures. In some cases perhaps it is not; in many cases it is. We were not especially interested in this method alone when we started the investigation, and tried using exhaust temperatures, which we found did not work well. The engine could be made to balance with exhaust temperatures at certain loads, while at other loads it would be out of balance. When considering scavenging air, the exhaust temperature for a given fuel-pump injection quantity of oil definitely will be affected by variations in quantity of scavenging and supply air. Although a slightly richer mixture would not necessarily affect the pressure, it may affect the temperature. Scavenging conditions in many multicylinder two-stroke-cycle engines are decidedly different among the different cylinders.

We did not experience any trouble from clogging or corrosion. The explanation probably is that in a two-stroke-cycle engine, when the piston gets to a point near the end of the stroke, it is in the cold part of the cylinder where the exhaust gases have cooled down to 800 to 1200 F. At this point, lubrication on the cylinder wall is relatively good. Thus, any oil coming through the pipe is of good quality. Let us assume that a certain amount of oil is coming through, which eventually would collect in the lower part of the chamber. If there is too much, it can be allowed to run out. All of our experience demonstrates the fact that the oil in the chamber is relatively clean. To protect the gage, instead of hooking it in at the high point, it was connected at a low level, thus the oil served to reduce or prevent corrosion of the gage. Sometimes the chamber would be filled with oil at the start of a test and never checked again during the entire series. No apparent trouble from clogging occurred. The fact that the connection is in the lower part of the chamber is a saving feature.

Mr. Kates questioned why a straight line is shown in Fig. 6, and why it is curved in Fig. 7. It can be seen from the plotted points that a curved line might have been produced in Fig. 6, as well as in Fig. 7, although it would not have as much curvature. In general, the tendency has been more toward the type of Fig. 7 than of Fig. 6. In happens that the points as plotted in Fig. 6 produced a "straight-line curve."

Individual readings for the two-cylinder Worthington engine were quite close since the pre-exhaust pressures were adjusted to read the same, the engine being balanced in that condition. It so happened that the indicated horsepower developed by each cylinder came into line. In no instance did it vary 10 per cent and in most cases was in the neighborhood of 3 to 4 per cent.

Prof. Degler's questions are of considerable interest. We did not use snubbers as such, but there was a steel- or glass-wool packing in each line which somewhat served the purpose. Many of the matters which Prof. Degler mentioned are still under investigation.

While we did not do so, the correct size of the chamber could have been determined by theoretical calculation. In the case of the larger low-speed engine, a piece of $2^1/_2$-in. pipe 8 in. long was welded on top and bottom and used for the chamber. In the case of the small high-speed engine, a casting was used as the chamber, the size being about 4 cu in., thus much smaller. Further work is planned for this phase of the study.

In reply to Mr. Jacobson, a pressure calibration should be made for each type of engine. For each type of engine under reasonably similar operating conditions the pressures should be the same. It is safe to say that for a given type of engine there is a certain value of pre-exhaust pressure which can be directly associated with brake mean effective pressure. For the three engines tested, adjustments were made in the pressure readings to allow for differences in the percentages of stroke at which the cylinders were tapped for the gage-pressure lines. The result of these adjustments to a common basis shows a remarkably close correlation in the values of pre-exhaust pressure indicated for each engine, and accounts for the deviations apparent from a casual reading of the curves. For purposes of record it may be mentioned that the engines were tapped in percentages of downstroke as follows: Bethlehem 60.4 per cent, Worthington 67 per cent, and Waukesha 80 per cent.

Replying to Mr. Jacobson's second question, when tests were first undertaken, an attempt was made to approach the actual release point closely; later it was found that it made no difference if we went farther up on the curve.

Prof. Maleev's comments are appreciated. The authors have used temperatures for years as a means of indicating load and

load balance, but with discouraging results. Definitely, the results have shown that the temperatures are not as reliable as this method of pre-exhaust-pressure measurements.

The possibility of measuring pre-exhaust temperatures was also considered. If at the bleeder point where the cylinders are tapped, we also tap the gases and measure the temperatures, we have an index which is fairly reliable, in fact about as reliable as the pre-exhaust pressures. However, a flow condition must be established in order to measure the temperatures, which is one of the difficulties with temperature measurement at that point.

Prof. DeJuhasz develops some interesting points, with many of which the authors are heartily in agreement. However, certain comments are so much at variance with the findings of the paper that some recapitulation seems desirable.

The present discussion does not deal with the measurement of heterogeneous pressures at any point in the engine stroke but with the specific measurement of pressure in the region just before exhaust where the pressure gradient per unit of piston travel has essentially reached its minimum value. In this region the often extreme fluctuations of the combustion process have been essentially smoothed out, and the pressure variations observed are less abrupt and apparently give an average more rational index of conditions than can be found in terms of pressure at any other point in the stroke. Whether or not the idea is new and whatever the status of the patent situation may be, are matters of no concern to the authors. However, in so far as could be ascertained, several years ago, when this project was first started, the only reference to the use of the pre-exhaust range for load indication was the one indicated in the paper, and no formal work was found in the literature. Since specific reference has been made to the German patent DRP 347,840, filed in 1919 by the "Liebra" Motorengesellschaft, it should be mentioned that the authors were familiar with this patent but completely failed to find therein any claims that the pressure obtained from any one single point of piston travel would indicate a relationship to the amount of power developed. On the other hand, the substance of the "Liebra" patent seems to apply wholly to an engine construction designed for the purpose of obtaining an indicator card by the "point-by-point" method, similar to that using a phase-changing indicator. Further, in the "Liebra" arrangement, the piston does not uncover the ports itself, as the timed uncovering is accomplished by a sleeve member interposed between the piston and the cylinder.

Maximum-pressure gages are indeed useful instruments, and correlation formulas for the indicated mean effective pressure in terms of the theoretical maximum pressure can be derived for some oil-engine cycles. However, for the actual engine cycle, how much confidence can be placed in the reading of maximum pressure as either an index of the load or load variation? In the authors' opinion and in the opinion of most of the Diesel operators with whom this question has been discussed, there can be none. The variations of the combustion process and slight changes in injection timing can appreciably change the maximum pressure, often with little change in mean effective pressure. In the case of a theoretical Diesel cycle, moreover, the load could change from zero to 100 per cent without any change in maximum pressure being indicated. Consequently, it is not surprising that the gage, reading the difference between maximum and minimum exhaust pressures, mentioned by Prof. DeJuhasz, was investigated and discarded.

A mean-pressure indicator, averaging the time integral of cylinder pressures, as a device for indicating developed load in an engine, represents what might be called an ideal. But it is an ideal not easy to attain, as such instruments are expensive and involve so many complications in installation and use that supplying and servicing a multicylinder engine with a set of such units practically falls back as the job for a laboratory technician and not that of an operating engineer.

The authors have no intention of minimizing the importance of the exhaust-temperature indicator as a device for indicating load balance among the cylinders of a Diesel engine. In many cases, this device performs meritorious and fine service. However, like anything else, it has its limitations and some of these are indicated in the paper. Scavenging-air variations with two-cycle engines, radiation, and conduction to or from the couple, can all affect the reading independently of load variations. In regard to ease of attachment, it is but slightly more difficult or expensive to run $^1/_4$-in. tubing than to run electric cable for the pyrometers. The cables themselves require careful soldering and adequate insulation against grounding. It is quite possible also to use a pressure-selector valve and one gage for a multicylinder engine, but the instantaneous picture of engine balance or nonbalance offered by a group of gages, indicating pre-exhuast pressures, eliminates the necessity of remembering all the other values as a selector is turned from point to point. The relatively low cost of gages makes the instantaneous picture feasible.

Professor DeJuhasz's comment as to the influence of the condition of the uppermost piston ring upon accuracy of the readings is well taken. Under such conditions, the pressure indication is sufficiently greater than normal to show that the piston ring is worn, stuck, or otherwise in need of attention or replacement. It is this very characteristic, in serving to indicate piston-ring performance, that makes the pre-exhaust-pressure method valuable to the engine operator.

The authors realize that this device is not the answer to all the Diesel operators' worries but feel the experimental data obtained have shown that the method is so reliable and useful as a load-indicating device that the research has been well worth while.

Design of Diesel-Engine Foundations

By KENNETH H. LARKIN,[1] KANSAS CITY, MO.

In this paper the author discusses all of the factors encountered in the layout, design, and construction of foundations for stationary Diesel engines of the vertical type. The factor requiring the greatest attention and consideration of designers is that of reducing or isolating the vibration of the engine. This matter is treated comprehensively. The author applies accepted theories and engineering principles to the problems. As in most engineering problems, the exercise of sound judgment enters to a large extent. The paper is presented in outline form, the subject matter following the sequence generally encountered in an actual design.

A PROPERLY designed engine foundation serves two purposes (1) it furnishes a place to set the engine, and (2) it acts to reduce and isolate the vibration of the engine due to the dynamic unbalance of its moving parts. The factors to be considered in fulfilling the first purpose of an engine foundation are technically simple, and satisfactory details have been fairly well standardized. The factors to be considered in fulfilling the second purpose are many and technically difficult because there are so many elements which cannot be treated analytically. However, by considering these factors in the light of accepted theories and engineering principles, with the exercise of sound engineering judgment, a satisfactory design may be assured. We sometimes hear of troublesome foundations but an inspection of each reveals a violation of some fundamental principle.

An engine foundation is a poor place to economize. Yet this is often done because of the failure of those handling the finances to realize the important part that an adequate foundation plays in the operation of the entire plant. The saving of a few hundred dollars in the cost of a foundation is little short of ridiculous if such saving jeopardizes the operation of the engine and risks the expenditure of several thousand dollars to rebuild the foundation adequately.

Consideration of Site of Operation

The first factor to be considered in the design of an engine foundation is the site of its operation. This includes the general features of the neighborhood (proximity, construction, and use of surrounding structures, possibility of interference with other operations in the same building, etc.) and characteristics of the subsoil on which the foundation will rest. If the engine is to be installed in a residential neighborhood, or within a hotel or apartment house, the foundation must be very efficient in isolating the engine vibration. If the installation is well removed from other structures or located in a manufacturing district, less attention need be given to this factor. At any location where the engine vibrations are likely to interfere with the activities or rights of others, this should be given thorough attention, because such interference may result in legal action prohibiting the operation of the engine. When the engines are operated in competition with electric utility companies, this factor must be given considerable attention because excessive engine vibration is a favorite basis for enjoining the operation of the competing equipment.

Subsoil. Some definite knowledge of the foundation soil is necessary. An auger boring extending at least 15 ft below the bottom of the foundation is generally adequate. A log of the boring should be made and samples of soil, taken at say 3-ft intervals, should be carefully inspected for general composition, moisture content, stability, etc. In granular soils it is important to take undisturbed samples and determine the percentage of voids by laboratory methods. Particular attention should be paid to the existence of ground water, noting the rise of water in the open hole. There is no point in making soil-loading tests, except possibly deflection tests as noted subsequently, because the static load of the engine and foundation can always be kept below 2000 lb per sq ft, and hence can be carried by practically any soil as far as its capacity for static load is concerned.

It is often desirable to know the natural vibration frequency of the elastic system, consisting of the engine, its foundation, and the subsoil, because the amplitude of the vibration is greatly increased if this natural frequency is very close to the forced frequency of the engine. The proof of this statement and an explanation of how this natural frequency can be determined is given in the following paragraphs.

It is pertinent to define some of the commonly used terminology of vibration engineering.

"Vibration" is a periodic motion which changes direction twice during a complete cycle and repeats itself after a certain interval of time.

"Period" is this interval of time (measured in seconds).

"Simple harmonic motion" is the simplest type of periodic motion. When the displacement is plotted against time, a pure sine curve is obtained.

"Cycle" is a complete movement of a vibrating body, measured from the time it passes through the equilibrium point until it again passes through this point, traveling in the same direction.

"Frequency" is the number of cycles of motion per unit time (measured in cycles per second f, or radians per second p, where $p = 2\pi f$).

"Amplitude" (A) is the magnitude of the vibratory motion measured from the equilibrium point to the extreme position (measured in inches).

"Natural frequency" (f in cycles per sec or p in radians per sec) is that frequency at which an elastic system will vibrate after having been displaced from the equilibrium position and then released.

"Forced frequency" (ω in radians per sec) is that frequency at which an elastic system will vibrate when acted upon by a periodic force of any frequency.

"Resonance" is that condition when the natural frequency is the same as the frequency of the periodic force.

"Damping" is the reduction of the amplitude of vibration due to natural forces as air, or liquid resistance, imperfect elasticity, etc., or artificial forces as dashpots, etc.

The theory of vibrations[2,3] shows that for the case of forced vibration with viscous damping

[1] Structural Engineer, Burns and McDonnell Engineering Company.

Presented at the National Meeting of the Oil and Gas Power Division, Kansas City, Mo., June 11–14, 1941, of The American Society of Mechanical Engineers.

Note: Statements and opinions advanced in papers are to be understood as individual expressions of their authors, and not those of the Society.

[2] "Mechanical Vibrations," by J. P. Den Hartog, McGraw-Hill Book Company, Inc., New York, N. Y., 1940, pp. 61–72.

[3] "Vibration Problems in Engineering," by S. Timoshenko, D. Van Nostrand Company, Inc., New York, N. Y., 1937, pp. 38–51.

$$A/\Delta = \frac{1}{\sqrt{(1 - \omega^2/p^2)^2 + (2C\cdot\omega/p)^2}} \quad \ldots\ldots [1]$$

where A = amplitude of forced vibration
Δ = deflection due to static load of same magnitude as unbalanced periodic force of engine
ω = frequency of unbalanced periodic force of engine
p = undamped natural frequency of elastic system
C = coefficient of damping; $C = 1$ is point of critical damping where damping is so great as to prevent vibration

The right-hand term in Equation [1] is often called the "magnification factor." If we draw curves for various values of C, we see that the curves in Fig. 1 all have a sharp peak near

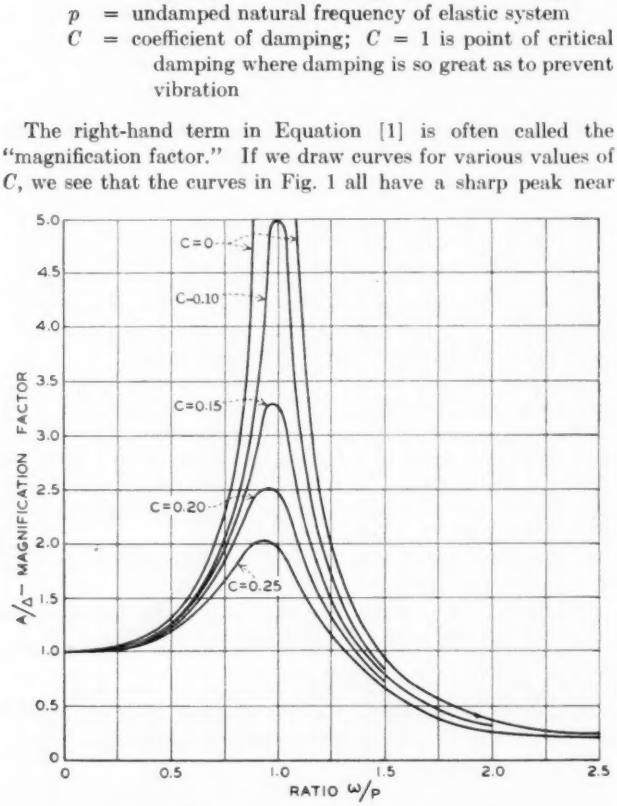


FIG. 1 CURVES OF COEFFICIENT OF DAMPING

$\omega/p = 1$ for all values of C. Note that when $C = 0$ the value of A/Δ approaches infinity for ω/p ratios near 1 and that for the larger values of C the peak of the curve corresponds to a ω/p ratio slightly less than 1, departing further from $\omega/p = 1$ as the values of C increase. Note, furthermore, that the curves are not greatly different for ω/p ratios outside the range 0.5 to 1.5.

This theoretical relation is approximately true for an engine foundation on an elastic subsoil. Its value lies not in determining the numerical value of the amplitude of vibration but in proving, as stated, "the amplitude of vibration is greatly increased if this natural frequency is very close to the forced frequency of the unbalanced forces of the engine" and in showing how such a condition can be avoided. The value of C will vary for different soils but, if we assume $C = 0.25$ as an average, we can see that if we avoid ω/p ratios between 0.5 and 1.25 the amplitude of vibration will not be greatly increased.

The theory of vibration[4] further shows that, for an elastic material conforming to Hooke's law

$$p = \sqrt{\frac{g}{\Delta}} \text{ or } f = 188\sqrt{\frac{1}{\Delta}} \text{ cycles per min} \quad \ldots\ldots [2]$$

where

g = acceleration of gravity
Δ = static deflection of elastic material

[4] Reference 2, p. 44.

This relationship is shown graphically in Fig. 2, and is approximately true for most soils. Thus, if we know the value of Δ we can predict the undamped natural frequency from Fig. 2, and the magnification factor from Fig. 1. The value of Δ should be determined in the field by static-load tests on the soil stratum at the bottom of the foundation. The static soil load, due to the engine and foundation, will be low, usually between 1000 to 2000 lb per sq ft and, by taking several readings within this range, the value of Δ for the actual load can be later interpolated. The undamped natural frequency for some typical soils is given in Table 1.

TABLE 1 UNDAMPED NATURAL FREQUENCY FOR TYPICAL SOILS

Material	Loading, lb per sq ft	Undamped natural frequency, cycles per min
Clay (wet)	2000	540
Clay (wet)	4000	380
Clay (dry, hard)	2000	660
Clay (dry, hard)	8000	330
Gravel	2000	1330
Gravel	8000	660
Sandstone	2000	4200
Sandstone	8000	2100

The author feels that the general features of the site as affecting the allowable vibration and the character of the subsoil to respond and transmit vibration should always be considered in the pur-

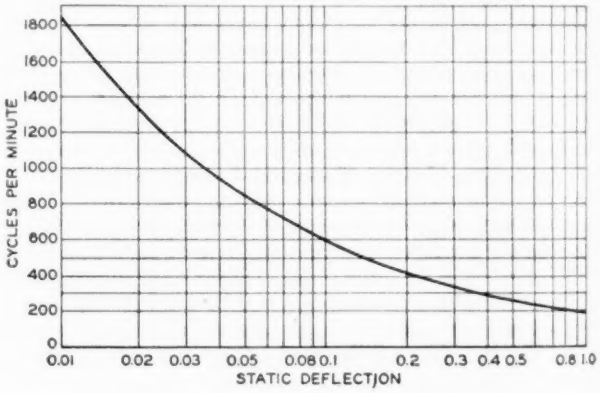


FIG. 2 UNDAMPED NATURAL FREQUENCY

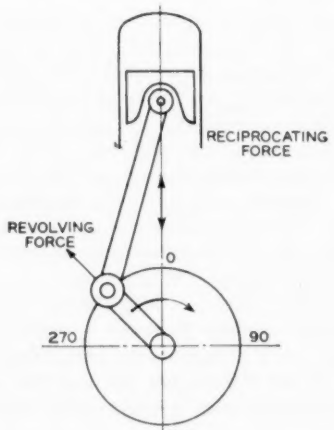


FIG. 3 ENGINE MECHANISM

chase of the engine. Of course, a foundation can be designed for any engine at any site, but if conditions are such that vibration of adjacent structures is undesirable, or if the subsoil is of a type to respond to and transmit the engine vibrations, then the pur-

chase of an unbalanced engine is poor judgment, because all the methods of foundation design and vibration isolation can never be a proper substitute for engine balance.

Cause of Vibration—Unbalanced Engines

Source of Unbalance. It is pertinent to consider the cause of unbalance in engines and the source of the forces which cause vibration of the engine and foundation. These forces are all inertia forces due to the change in motion of the moving parts of the engine, and are often called "free inertia forces" because they are not self-contained within the engine frame but are resisted only by the mass of the engine and foundation. The gas pressure in the cylinders causes no unbalanced forces outside the engine frame.

If we consider the forces acting in a one-cylinder vertical engine, Fig. 3, we observe that the mass of the crankshaft throw and pin revolves at uniform speed, causing a centrifugal inertia force, which has vertical and horizontal components varying in simple harmonic manner with a frequency equal to the engine speed. The mass of the piston reciprocates in a vertical line, reversing direction twice each cycle, causing vertical inertia forces. Because of the angularity of the connecting rod, the motion of the piston and, hence, the inertia force, is not of simple harmonic character, Fig. 4, but may be resolved[5] into two forces which vary in simple harmonic manner; one termed "primary force," having a frequency the same as the engine speed, and the other termed "secondary force," having a frequency twice the engine speed.

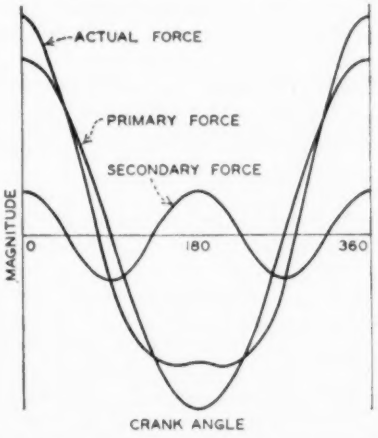


Fig. 4 Inertia Force of Reciprocating Mass

The connecting rod has a complex motion intermediate between that of the crankpin and the piston; the motion of the lower part resembling that of the crankpin and the motion of the upper part resembling that of the piston. However, the treatment of the connecting rod can be greatly simplified if we consider the mass of the rod distributed into two portions, one concentrated at the piston pin and one concentrated at the crankpin, such that the center of mass of the two portions coincides with the center of mass of the actual connecting rod. This involves no error whatever and, since the first mass has the same motion as the piston and the second mass has the same motion as the crankpin, we have not added any new forces but merely increased the inertia forces already considered by increasing the mass of the moving parts.

Summarizing, we have three inertia forces all varying in a simple harmonic manner, one a revolving force with horizontal and vertical components varying with a frequency the same as the engine speed, one a vertical force (primary) with frequency the same as the engine speed, and finally a vertical force (secondary) with a frequency twice the engine speed. The vertical component of the revolving force is in phase with the primary force at all positions. Hence, they can be added and considered as one force (the primary force as sometimes defined includes both these forces). The secondary force is in phase with the primary force only when the crank is at upper dead center.

Means of Balancing. Having determined the unbalanced forces normally existing in a one-cylinder engine, we are next interested in eliminating them or balancing the engine. The revolving force can be completely eliminated by counterweighting the crankshaft with an equal mass moment placed opposite the crank throw. This procedure is followed by most manufacturers. By further increasing the counterweight, we can reduce the primary vertical force or even make it zero. However, this additional counterweight (beyond that required to counterbalance the revolving force) introduces a horizontal unbalanced force. This horizontal unbalance is equal to the amount of reduction of the primary unbalance, the effect being that of turning part of the primary unbalanced force at 90 deg to its original direction. Because unbalanced horizontal forces are usually more serious than unbalanced vertical forces, there is not much to be accomplished in this manner. It is the practice of engine manufacturers to counterbalance not more than $^1/_3$ to $^1/_2$ of the primary vertical force.

Little can be done toward balancing the secondary force. The Lancaster balancer, a mechanism of two weights driven from the crankshaft at twice crankshaft speed, with weights revolving in opposite directions and so arranged that the vertical forces balance the secondary force and the horizontal forces balance each other, is 100 per cent effective. However, it is an expensive device and its use is seldom economical.

Multicylinder Engines. When we enter the field of multicylinder engines, we must consider the resultant at any instant of the unbalanced forces for each cylinder. In so doing, we find that by certain crank arrangements, the unbalanced forces of individual cylinders can be made to balance each other. We find, furthermore, that because the forces of the individual cylinders are not in the same transverse plane they sometimes cause unbalanced moments about a vertical or transverse axis even when the resultant of the forces for the entire engine is zero.

We have seen that the mass of the crank throw, pin, and lower part of the connecting rod produces a force revolving at engine speed. It can be shown[6] that the primary force can be represented as the vertical component of a vector revolving at engine speed and the secondary force as the vertical component of another vector revolving at twice engine speed. In the light of this, it is easy to study balance conditions of multicylinder engines by means of rotating vectors, the vectors being spaced apart by the same angles as the crank throws.

Consider a three-cylinder engine with cranks 120 deg apart. With No. 2 cylinder at upper dead center, No. 1 and No. 3 cylinders are in the positions shown in Fig. 5, and the revolving forces are balanced as shown in Fig. 6(*a*), except that the horizontal components of the forces 1 and 3 form an unbalanced rotating couple. This couple can be balanced by two weights *A* and *B* placed on the end crank throws, and counterweights on No. 2 crank throws are unnecessary.

Considering the primary forces, that of No. 2 cylinder is a maximum and will be represented as a vector directed upward, Fig. 7, the vector representing No. 3 cylinder had this location 120 deg of rotation previously and that of No. 1 cylinder will have

[5] Reference 2, p. 209.

[6] Reference 2, p. 215.

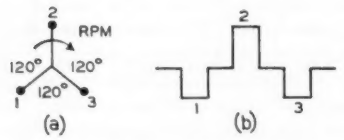


FIG. 5 CRANK ARRANGEMENT

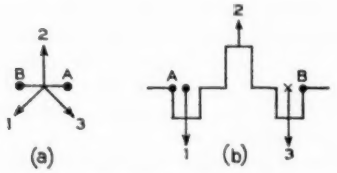


FIG. 6 REVOLVING FORCE

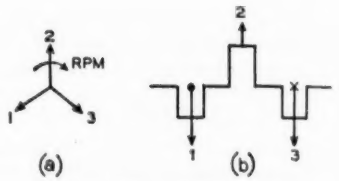


FIG. 7 VECTORS OF FORCES

FIG. 8 PRIMARY FORCES

FIG. 9 SECONDARY FORCES

this location 120 deg of rotation hence. Therefore, the revolving vectors representing these forces are as shown in Fig. 7, and are similar to the revolving forces of Fig. 6(*a*).

Because the primary forces being studied, Fig. 7, are the vertical components of these revolving vectors, it is obvious that the forces are balanced for all crank positions. However, there is an unbalanced moment, varying in simple harmonic manner with frequency equal to engine speed, due to the fact that forces 1 and 3 are not in the same plane as force 2 and the resultant of their moments about the center of No. 2 cylinder varies as the vectors revolve. This moment is passing through zero value for the crank position shown in Fig. 7(*a*), but consider its value as vectors revolve to crank position shown in Fig. 8. This moment is called the primary moment.

Considering the secondary forces, that of No. 2 cylinder is a maximum and will be represented as a vector directed upward. Then, since the secondary-force vectors are revolving at twice engine speed, they will have positions shown in Fig. 9. By reasoning similar to that for the primary forces, we see that the secondary forces are balanced for all crank positions, but that again there is an unbalanced moment varying in simple harmonic manner, only now with a frequency equal to twice engine speed. This is called the secondary moment.

In this manner the balance conditions of any multicylinder in-line engine can be investigated. The balance for some of the common crank arrangements for engines from three to eight cylinders is given in Table 2.

TABLE 2 ENGINE BALANCE

No. of cylinders	Crank sequence	Forces		Moments	
		Primary	Secondary	Primary	Secondary
3 (2 ~ or 4 ~)	120° Cranks 1-3-2	Balanced	Balanced	Unbalanced	Unbalanced
4 (2 ~)	90° Cranks 1-3-4-2	Balanced	Balanced	Unbalanced	Balanced
4 (4 ~)	180° Cranks 1-4, 2-3	Balanced	Full unbalance	Balanced	Balanced
5 (2 ~ or 4 ~)	72° Cranks 1-5-2-3-4	Balanced	Balanced	Small unbalance	Unbalanced
6 (2 ~)	60° Cranks 1-6-2-4-3-5	Balanced	Balanced	Balanced	Small unbalance
6 (4 ~)	120° Cranks 1-6, 3-4, 2-5	Balanced	Balanced	Balanced	Balanced
7 (2 ~ or 4 ~)	51°-26′ Cranks 1-6-5-3-2-7-4	Balanced	Balanced	Balanced	Unbalanced
8 (2 ~)	45° Cranks 1-8-6-2-4-5-7-3	Balanced	Balanced	Balanced	Balanced[a]
8 (2 ~ or 4 ~)	90° Cranks 1-8, 4-5, 2-7, 3-6	Balanced	Balanced	Balanced	Balanced

[a] Space between Nos. 4 and 5 cylinders increased to 1.828 regular spacing.

Mode, Frequency, and Magnitude of Vibration. It should be noted that unbalanced forces cause the engine to stamp up and down on its foundations, while unbalanced moments cause it to pitch fore and aft. Also, that the frequency of primary forces and moments is equal to engine speed, while that of the secondary forces and moments is equal to twice engine speed. The magnitudes of the primary and secondary forces are in the same ratio as

$$\frac{\text{Length of connecting rod}}{\text{Radius of crank}} \text{ (approximately 4 for average engine)}$$

In practice no perfectly balanced engines are constructed because the dissimilarity of parts for the different cylinders will cause some unbalanced forces and moments, both primary and secondary. Because the inertia forces due to unbalanced parts vary directly as the square of the speed, the higher the engine speed the greater attention is required to the engine balance.

DESIGN OF FOUNDATION

Manufacturer's Drawings. Having purchased the engine, the layout of the foundation can begin. The manufacturer will provide a "certified" foundation drawing. Do not be misled, "certified" merely means that the holes for the anchor bolts and general shape of the engine base will be as shown; the engine manufacturer will assume no responsibility for the design of a successful foundation, and it is not to be expected that he should. However, these drawings usually show over-all dimensions and give a recommended yardage of concrete for the foundation.

Foundation Yardage. A tabulation of the foundation yardage recommended by engine manufacturers gives the average values shown in Table 3. All of the foundations tabulated fell within 20 per cent of these average values and the large majority were within 10 per cent.

The data were taken from manufacturers' catalogues and bid strips, and cover many speeds and cylinder sizes. The engines were both 2-cycle and 4-cycle, the majority with speeds ranging from 225 to 327 rpm; most of the 2-cycle engines developing

TABLE 3 AVERAGE VALUES OF FOUNDATION YARDAGE

No. of cylinders	3	4	5	6	7	8
Foundation cubic yards per engine horsepower	0.141	0.120	0.108	0.100	0.096	0.091
No. of engines tabulated	7	10	20	20	14	14

from 75 to 360 hp per cylinder and the majority of 4-cycle engines developing from 75 to 130 hp per cylinder. The extreme limits of the tabulated engines were a 2-cycle engine running at 150 rpm developing 680 hp per cylinder available in 5, 6, 7, and 8 cylinders; a 4-cycle engine running at 400 rpm developing 83 hp per cylinder available in 5, 6, 7, and 8 cylinders; and a 4-cycle engine running at 327 rpm developing 55 hp per cylinder available in 3 and 4 cylinders.

The tabulation reveals no relation of foundation yardage either to engine speed or cylinder size; all of the extremes mentioned are within 10 per cent of the average values shown in Table 3.

This yardage of concrete is the result of experience with damping the engine vibration. Manufacturers generally state that it is based on a hard firm subsoil. Theoretically, the anchorage of an engine to a large mass of concrete is an application of the theory of mass damping which is based on the principle of using the small accelerations set up in a large mass to balance the large accelerations of a small mass (unbalanced engine parts). This may be expressed

$$P = Ma = M\omega^2 A \quad [3]$$

or

$$A = \frac{P}{M\omega^2} \quad [4]$$

where P = unbalanced periodic inertia force of engine
M = mass subject to vibration (engine, foundation block, and a part of subsoil)
a = acceleration
ω = frequency of periodic force
A = amplitude of vibration of foundation block

This relation, Equation [3], assumes the natural frequency of the foundation is infinitely large and that the magnification factor, Fig. 1, is unity. This is approximately true for ω/P ratios less than 0.5.

By means of this relation, we might determine the mass of the foundation block which would be required to limit the amplitude of vibration to any predetermined value, if we knew just how much of the subsoil should be included in the mass subject to vibration. However, this is so variable—depending upon the type of subsoil, unit loading, whether the foundation sets in or on the subsoil, and probably other factors—that the theory of mass damping cannot be accurately applied and, as stated, the mass of the foundation block is generally determined by experience.

Notwithstanding, this theory can be qualitatively applied, indicating that the amplitude of vibration will vary directly as the unbalanced inertia force and inversely as the mass subject to vibration. Therefore, it is clear that any means for increasing the mass of earth subject to vibration will reduce the amplitude of vibration. We might accomplish this by tamping the earth solidly around the foundation block, driving long piles into the subsoil, etc. In general, there is not much to be gained by increasing the size of the foundation block beyond the values shown in Table 3.

Miscellaneous Details. Having the certified drawing, the location of anchor bolts can be made, pits for the flywheel, generator, etc. can be provided, as well as openings for pipes, conduits, drains, etc.; in short, the entire upper part of the foundation can be laid out. The author recommends Fig. 10 as a standard anchor-bolt detail. It is economical, provides for inaccuracy of setting, and allows the withdrawal of the bolt during setting of the engine bed plates or in case of a broken bolt. The use of long anchor bolts is recommended as they stretch more under a given load, allowing a degree of resiliency and are not so apt to break because the unit stress is thereby lowered. Any pits in the foundation should be provided with a drain extending through the foundation.

The pit for the flywheel, generator, or other driven machine should be surrounded by a protecting handrail. A double pipe handrail of welded construction with top rail 30 to 36 in. above floor level is satisfactory as it is rugged, economical, and generally considered of adequate appearance. Safety laws of many states require that such pits be surrounded by curbs or steel kick plates. This feature is never costly and is always recommended.

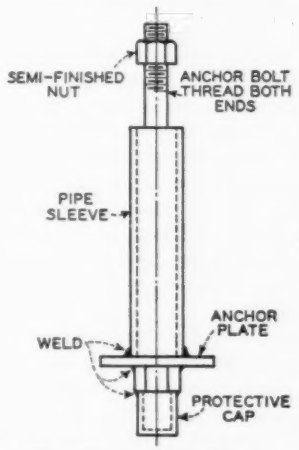


FIG. 10 ANCHOR BOLTS

The inclusion of pipes within the engine foundation is never desirable. Ample openings and chases should be provided for the necessary small piping at the engine end of the foundation and this piping should never be grouted in. Some makes of engines require that the intake-air pipe be encased in the foundation. When this is done the pipe should be wrapped with several layers of tarred felt or asbestos paper; this to allow movement of the pipe under temperature changes without stressing the concrete. The large area of concrete left void by this air piping should be replaced by an equivalent area of reinforcing steel, in order to avoid shrinkage cracks in the foundation. The inclusion of exhaust piping within the engine foundation is an open invitation to trouble unless extensive precautions are taken, as this piping is subject to large expansion due to temperature changes.

Consideration of Subsoil. There remains the design of the lower part of the foundation, the connection to the subsoil. The foundation should always rest on undisturbed soil at a level not higher than the foundations of the power-plant building. The depth of foundation should be not less than 4 to 5 times the stroke of the engine, with a minimum of 5 ft. The width of base should be at least equal to the vertical height from the bottom of the foundation to the center of the shaft and should be increased for engines having unbalanced horizontal forces. This can usually be done at little extra cost by using projecting cantilever footing slabs. The length of base is generally so large that no consideration is required in this direction, except that the length should be so adjusted that the center of gravity of the total weight on the subsoil (foundation, engine, flywheel, generator, etc.) coincides with the center of gravity of the area of contact with subsoil. All the rules cited are strictly empirical and, whenever necessary, should give way to more important considerations.

Where the foundation is to be set on rock, the considerations are few and simple. Practically any type of engine can be operated with a minimum of vibration. The foundation should be well keyed into the rock and often can be reduced in yardage below the limits recommended by the engine manufacturers, other factors permitting. Only in the case of engines installed

inside hotels or apartments is any kind of vibration insulation required with rock foundations. Processed cork slabs are recommended in this case, as the low-frequency vibrations will be absorbed by the rock; it is the higher-frequency vibrations approaching the sound range which have to be isolated.

Where the subsoil is soft, spongy, and water-bearing, the problem is complicated by many factors. First a well-balanced engine should be chosen. A definite attempt should be made to avoid synchronism between the forced frequency of any accidental unbalance of the engine and the natural frequency of the foundation and subsoil. Some compaction of the subsoil should be accomplished by driving piles or subsoil drainage. These efforts, including a conservatively designed foundation block, will usually reduce the vibrations to limits which are allowable in a power plant located at a reasonable distance from habitable structures. A further reduction of vibration will require the use of some vibration isolation, preferably springs.

Other conditions of the site, intermediate between the extreme conditions mentioned, may be satisfactorily solved by the use of intermediate measures. All of these combinations cannot be discussed here but remedies for some of the more critical conditions will be given.

Within limits, the "undamped natural frequency" of the engine, foundation, and subsoil is under the control of the foundation designer. Table 1 indicates that this frequency increases with decreased unit loading. Then, if larger footing areas are used, the natural frequency will be increased and vice versa. It is also evident that both drainage and compaction of the subsoil tend to increase the natural frequency. The removal of subsurface water is always desirable but generally expensive. The driving of closely spaced piles is probably the most effective method of compacting soft subsoils as far as engine foundations are concerned. Other advantages of the use of piling are given herein.

A study of Table 1 indicates that for the problem at hand the forced frequencies are so low that ω/p ratios will never be more than 1.5 and, because we must consider the frequency of both primary and secondary forces, the best procedure is to provide ω/p ratios of less than 0.5, Fig. 1. Considering the secondary forces of a 300-rpm engine, this would require a value of

$$p = 300 \times 2 \times 2 = 1200 \text{ cycles per min}$$

It should be noted that, because of the greater magnitude of primary forces and moments, it is more desirable to avoid resonance with them than with the secondary forces and moments. This is another reason for working on the left-hand side of the peak of the curves of Fig. 1.

Furthermore, it should be noted for firm dense soils the value of Δ will be very low, and the amplitude of vibration will not be very great regardless of the ω/p ratio. Hence, it is only in soft soils that this consideration of the undamped natural frequency becomes important.

At locations where a poorly consolidated granular subsoil is encountered, there is a definite possibility that the vibrations of the engine foundation may cause a rearrangement of the particles and a gradual consolidation. The resulting settlement may be considerable. Such conditions require a careful study of the natural density and effect of vibration thereon. In such locations, the use of piling is generally indicated. The piling will spread the vertical load to lower strata, and the vibration of driving will effect some consolidation. The use of vibration isolation might be considered, if other factors make the reduction of vibration desirable or necessary.

Vibration Isolation

In considering the use of vibration isolation, the first step is to understand the basic theory and then to determine the results which attend the use of various isolating materials.

Theory of Undamped Vibrations

Steel Springs. If we take the case of a weight W supported by a compression spring, Fig. 11, and consider only vibratory motion in the direction of the axis of the spring (an undamped linear system in vibration terminology), it can be shown[7] mathematically that

$$\text{Natural frequency } f = \frac{1}{2\pi}\sqrt{\frac{g}{\Delta}} \quad \ldots\ldots [5a]$$

$$p = \sqrt{\frac{g}{\Delta}} \quad \ldots\ldots [5b]$$

where Δ = statical deflection of spring due to W, in.
g = acceleration of gravity (32.2 fps per sec)

If the elastic system of Fig. 11, initially at rest, is acted upon by a periodic force $P \sin \omega t$, it can be shown[2,3] mathematically

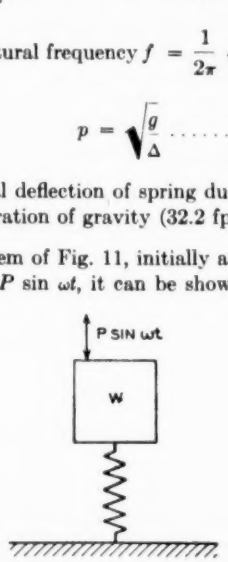


Fig. 11 Weight Supported by Compression Spring

that there is produced both forced vibrations of period ω and free vibrations of period p. In all practical systems, this latter vibration will be eliminated soon after starting due to various damping forces and only forced vibration, having the same frequency as the periodic force, will remain. For this condition it can be shown[2,3] that

$$A = \frac{P\Delta}{W}\left(\frac{1}{1 - \omega^2/p^2}\right) \quad \ldots\ldots [6]$$

If we draw a curve for the expression in the parentheses, Equation [6], plotting its value for various ω/p ratios (curve C = 0, Fig. 1), we see that it is always greater than 1 for ratios of ω/p between 0 and 1.41, but that for ratios of ω/p greater than 3, this factor is considerably reduced. Furthermore, at ratios of ω/p approaching 1, the value is very great becoming infinite for $\omega = p$.

Also we see (note Equation [5b]) that, with other factors remaining constant, the value of p and hence the amplitude of vibration A is reduced when Δ is increased. We note that this can be done by using a softer spring or heavier weight W or both. Furthermore, the amplitude of vibration is the deflection of the spring under the forced vibration, and the deflection of the spring multiplied by the spring constant gives the force transmitted to the foundation. The spring constant $K = W/\Delta$. Applying this value to Equation [6], we have

$$\text{Force on foundation } F = P\left(\frac{1}{1 - \omega^2/p^2}\right) \quad \ldots\ldots [7]$$

and the curve $C = 0$ of Fig. 1 gives directly the "magnification factor" to be used for various values of ω/p.

Use of Steel Springs. Interpreting this for our particular prob-

[7] Reference 2, p. 44.

lem, we see that, by putting suitable springs under a Diesel-engine foundation, we can reduce the amplitude of the vibrations transmitted to the subsoil and that, by a suitable combination of concrete engine block and supporting springs, we can keep the amplitude of engine vibration within allowable limits. Practically all engines of the type being considered will operate at a fairly constant speed and, by designing for a ω/p ratio of 3 or more, we can greatly reduce the amplitude of transmitted vibration.

However, the elastic system under consideration is of the simplest type and the practical case of vibration damping using springs is complicated by many factors not herein considered. For example, Diesel engines may have unbalanced forces acting in a lateral direction due to unbalanced revolving forces, torques acting to rock the engine in a transverse direction, and couples acting to rock the engine longitudinally. All of these act together on the springs and, under such conditions, the system may have six different modes of vibration each with its own frequency. The complete design of a system of springs for isolating a Diesel engine is quite beyond the scope of this paper, indeed beyond the ability of the average consulting engineer, and should be left to the vibration specialist.

Theory—Damped Vibrations

Cork, Hair Felt, Etc. The analysis as given neglects the effect of any damping forces. This is practically correct for steel springs, the damping effect of which is very small, but is not applicable for other resilient materials. Let us consider the case where cork, sponge rubber, hair felt, or similar resilient material is used for isolating a vibrating mass.

If we assume a material such that the damping is proportional to the velocity ("viscous damping" in vibration terminology), it can be shown [2,3] that

$$A = \frac{P\Delta}{W} \frac{1}{\sqrt{(1 - \omega^2/p^2) + (2C\cdot\omega/p)^2}} \quad \ldots\ldots [8]$$

where C = coefficient of damping, as in Equation [1].

Also

$$F = P \frac{1}{\sqrt{(1 - \omega^2/p^2)^2 + (2C\cdot\omega/p)^2}} \quad \ldots\ldots [9]$$

The curves for various values of C, shown in Fig. 1, indicate that the effect of damping is to reduce the peak amplitude and force transmitted at the point of resonance. This effect may be of practical importance in reducing the amplitude and transmitted force while the engine is passing through the critical speed.

Use of Cork, Etc. That isolating materials such as cork, hair felt, rubber, etc. conform closely to the relation, Equation [8], has been demonstrated by tests.[8] Thus, if we know the characteristics of these materials we can predict their efficiency as vibration isolators. Of these materials only cork has found much use as an isolating medium under Diesel-engine foundations.

TABLE 4 VIBRATION CHARACTERISTICS OF CORK

Material	Natural frequency, cycles per min	Loading, lb per sq ft	Source of data
Cork, 6 in. thick	420	14400	Anderson[9]
Cork, 1 in. thick	1080	14400	Anderson[9]
Cork, 5 in. thick	600	4000	Jackson[10]
Coarse-ground compressed cork, 2 in. thick	770	4130	Hull[8]
Natural cork, 1.35 in. thick	1450	4460	Hull[8]

The cork producers are either unwilling or unable to furnish any pertinent data on their product. However, certain data, given in Table 4, are available from independent sources.

Values of the damping coefficient $C = 0.11$ and 0.14 for compressed and natural cork, respectively, have been determined experimentally.[8]

Engines of the type under consideration are called medium-speed, say 200 to 400 rpm. Then, the frequency of the primary forces is 200 to 400 cycles per min and that of the secondary forces is 400 to 800 cycles per min. Then for a 400-rpm engine (the upper speed limit considered), the natural frequency of the isolating material must be less than $400/1.414 = 283$ cycles per min to effect any reduction of the vibration due to the primary force and less than $800/1.414 = 566$ cycles per min to effect any reduction of the vibration due to the secondary force. For slower-speed engines those limits would be proportionately lower.

Considering the data of Table 4, and the curve of Fig. 1, it is evident that, even if the natural frequency of cork can be brought to say 400 cycles per min by the use of a considerable thickness and heavy loading, the reduction of secondary forces is not very great and the primary forces may be actually increased. Thus, we see that this material, which has proved very effective in insulating sound and high-frequency mechanical vibrations, is not suited to the isolation of low-frequency mechanical vibrations, because its natural frequency is too high.

Effect of Subsoil. All the preceding theory of isolation considers that the subfoundation under the springs or isolating material is of unyielding character. If the subfoundation is of yielding character, both the amplitude of the forced vibration and the transmitted vibration are increased. There are too many variables to deal with this analytically and it is best handled by keeping the natural frequency of the subsoil as high as possible. Methods of improving the subsoil have already been discussed.

Use of Sand or Gravel Bed. There is one kind of vibration isolation which has not yet been considered. This is a layer of sand or gravel. Tests[11] indicate that these materials have some isolating value, reducing the amplitude of vibration approximately $1/2$ to $1/3$. This seems to be a surface effect, the particles acting much as a mass of ball bearings. The isolating value is greater for gravel than for sand and does not seem to vary appreciably with the depth of the material.

The author has no experience with this material, but the use of a 3-in. layer of sand topped by a 9-in. layer of gravel seems to follow the dictates of good judgment. The gravel should be well tamped into the sand layer in order to reduce the settlement.

Miscellaneous Isolation Details. There are certain degrees of isolation of the engine foundation which should be incorporated in every design. The floor slab surrounding the engine foundation should never be in direct contact with the foundation. When the floor is laid on earth it should abut the foundation. It should not be supported on a shoulder, and should be separated from the foundation by an expansion joint, preferably of the sponge-rubber type. When there is a basement surrounding the engine foundation, the operating floor is generally separated from the foundation by an air gap of $1/4$ in. The edges of this gap are generally protected against chipping by metal edge strips which are embedded in the concrete finish course after the engine is grouted. It is important that this floor also be supported independently of the engine foundation. Furthermore, it is desirable that any columns supporting this floor be placed as far as possible from the foundation mat. The author has used cantilever floor

[8] "Influence of Damping in the Elastic Mounting of Vibrating Machines," by E. H. Hull, Trans. A.S.M.E., vol. 53, 1931, paper APM-53-12.

[9] "Diesel Engineering," by J. W. Anderson, McGraw-Hill Book Company, Inc., New York, N. Y., 1938, p. 264.

[10] "Vibrations of Oil Engines," by P. Jackson, Papers of Diesel Engine Users' Association, Westminster, England, April 26, 1933.

[11] "Noise and Vibration Engineering," by S. E. Slocum, D. Van Nostrand Company, Inc., New York, N. Y., 1931, pp. 39–41.

slabs to good advantage in these locations. A cantilever slab of say 3 ft projection is constructed as part of the engine foundation and a similar slab extends out from the surrounding beams and columns. This construction is particularly advantageous where a group of engines are set in parallel positions, since the cantilever slabs can be extended from the foundations of adjacent engines, and basement columns in the aisle between engines are eliminated.

The maximum projection for a cantilever slab should be about 3 to 3½ ft and the slab should be of variable thickness, say 4 in. at the outside edge, and ⅛ of the projecting length at the inside edge.

It is often necessary to provide removable steel floor plates spanning between the permanent floor and the engine foundation. These plates are so flexible that it is necessary to support them from the engine foundation. The connection should allow lateral motion in all directions and yet hold the plate against a vertical vibration causing rattling. Joints in this floor plate should be bolted and stiffened against vibration. Large areas or long spans should be reinforced by welded stiffeners.

Concrete—Mix–Placing–Curing

Concrete for engine foundations should be low-volume-change, high-unit-weight material. Engine foundations are always massive, hence a low-volume-change concrete is necessary to prevent cracking of the foundation. Low volume change may be accomplished by the use of low cement factor (approximately 5 sacks per cu yd, maximum), and low water content (slump not exceeding 2 in.). The use of large maximum-size coarse aggregate, low ratio of sand to rock, and uniform grading of sand and rock are important items in attaining both of these objectives. The use of low-heat cement is advantageous for very large foundations. High unit weight is of course desirable; it can be attained by the use of heavy rock of large maximum size.

The use of high-early-strength cements for engine foundations is never advisable. This class of cements universally exhibits the properties of high shrinkage and high heat evolution which invite trouble from severe cracking.

A concrete meeting the foregoing requirements will easily exceed a minimum-strength specification of 2500 psi, providing it is properly placed in the forms and adequately cured. This dry, low-slump concrete must be thoroughly compacted. The use of internal vibrators is recommended. The strength gain of Portland-cement concrete requires a certain period of time in the presence of both temperature and moisture. The setting of the cement evolves a considerable quantity of heat and will maintain proper curing temperature under all except extreme temperatures. In very cold weather, the heating of the adjacent air to say 45 F is advisable, in order to provide curing temperatures for the concrete near the surface. Adequate moisture for curing concrete is present when it is placed in the forms. The conservation of this moisture by covering exposed surfaces and leaving the form in place as long as possible is a most effective curing method. There are several liquid curing membranes on the market which are effective in sealing the concrete surfaces. The use of these is advisable if early form removal is required.

Reinforcing. Construction of concrete engine foundations without reinforcing steel is never advisable. With the exception of cantilever-footing slab, there are no calculated stresses to be carried by this reinforcing steel, but its use in nominal quantities is necessary to eliminate serious cracking completely. Cracks which would cause no concern in ordinary concrete construction are often serious in engine foundations, because the severe vibration to which they are subjected may cause progressive cracking. The author's practice is to use deformed intermediate-grade steel reinforcing bars of ½ or ⅝-in. diam, spaced on 12-in. centers, extending both vertically and horizontally near all faces of the foundation block. The size of reinforcing bars may be varied to suit the general massiveness of the foundation.

In Diesel-electric sets where the generator is mounted on the same foundation as the engine and in similar installations, there is a large reduction in the cross-sectional area of the foundation block at the flywheel pit and generator pit. At these locations and all cross sections where the area is considerably reduced, additional reinforcing amounting to say 0.75 per cent of the reduction of area should be provided.

Grouting. The use of a nonshrink grout between the engine bed and the foundation is always desirable. The one factor causing shrinkage of cement and concrete is excess water. Some excess water is necessary in order to get the grout into place, but this should be held to a minimum. The sand must be well graded with a maximum size as large as can be worked into place. Add fine gravel if the depth of grout is more than 1½ in. This provides a minimum percentage of voids and reduces the amount of water-cement paste required. Never use a mix richer than 1:3. The addition of an expanding admix, as specially prepared powdered iron, is recommended to reduce the shrinkage further. Several brands of this material are on the market and the author feels that their cost is certainly justified.

The dry materials should be thoroughly mixed and water added slowly until the consistency becomes plastic but not soupy. It should then be placed with thorough puddling and ramming.

Vibrations Not Attributable to Faulty Foundations

Properly designed foundations are often blamed for vibrations that are actually air-borne, caused by the air columns set in motion by the engine intake and exhaust. Treatment of this subject is beyond the scope of this paper but it should always be considered in the design of a Diesel-engine installation. The use of adequate intake and exhaust silencers is the first step in eliminating this difficulty.

Locating large flimsy window areas, especially those with hinged ventilating sections, adjacent to the intake and exhaust is a practice always to be avoided. Furthermore, it is true of the entire power-plant building that the use of light flexible structural members is to be avoided. The author favors the use of rigid-frame bents instead of trusses and columns and, in general, the use of continuous construction wherever possible.

Discussion

R. D. Campbell.[12] Let us assume a case in which the ground has a fixed period of vibration, or natural frequency. On such a subsoil is placed an isolating material, springs or cork, having a period of vibration, or natural frequency, different from that of the subsoil or ground. If the engine or vibrating mass is then placed on this isolating material will the frequency of the subsoil or the frequency of the isolating material determine the effectiveness of the isolation, i.e., the amplitude and force of the transmitted vibrations?

A. F. Robertson.[13] What precautions actually have to be taken in the field when determining Δ, the deflection of the soil under static load, so that the equations given in the paper may be applied properly? Is the value of Δ determined from experience with past installations, or must static-deflection tests actually be made on the soil being used?

C. B. Rosenberg.[14] Inasmuch as most of the work cited in

[12] Shell Oil Company, Wood River, Ill. Mem. A.S.M.E.
[13] Fairbanks, Morse & Company, Beloit, Wis.
[14] The Pure Oil Company, Chicago, Ill.

the paper is based upon a consideration of the harmonics developed in multicylinder engines, the conclusions are not applicable to single-cylinder engines. What comments would the author care to make upon the installation of one-cylinder Diesel engines to minimize engine vibration?

A. L. Bayles.[15] In connection with the mounting of a single-cylinder compressor and engine on a common base for ship service, a damping effect had to be achieved. The compressor in question had a high ratio of moving mass to fixed mass. The matter was solved ultimately by creating a fictitious mass through the process of imposing dampers acting downward as well as upward. The installation was successful.

To elaborate, what we did was to assume that the entire mass, composed of engine, compressor, and subbase, weighed more than it actually did. (In this particular case, about 2000 lb.) We then designed the lower dampers for the compression of the actual plus the fictitious load, distributed over the dampers. The top dampers were then designed to impose a load of approximately 2000 lb more to make up the deficiency of the actual load.

Would the author's formula apply in the case of a damper imposed on top as well as below? He is presuming that there is no particular "jump." In this particular case, we had a very marked upward reaction. As a matter of fact, the isolation calculated by conventional methods was perfect, but the unit oscillated badly. In this case we could not resort to the expedient of additional mass because of limitations imposed by the capacity of the ship.

W. Exline.[16] Where direct-connected compressing units are coupled at 90 deg with the same crankshaft as the power cylinders, we have found that an unbalanced load exists. When the engines were originally set this condition caused them to move in a horizontal plane, setting up stresses in the crankcase, which caused the grouting corners to fracture and break. Are there any types of insulation which could be used on this type of engine construction, such as springs or insulating material, to eliminate this difficulty? The reference is to units used in gasoline plants and gas-compressor stations where this particular trouble has been experienced when setting the shafts of such engines.

E. J. Kates.[17] The author has done an excellent job in preparing this scientific treatise on a subject which has been permeated with empiricism and shrouded in mystery. A few questions come to mind. One concerns the use of cork isolation. The author concludes from theoretical considerations that cork isolation "has proved very effective in insulating sound and high-frequency mechanical vibrations, but is not suited to the isolation of low-frequency mechanical vibrations, because its natural frequency is too high." However, in actual use, cork seems to be a peculiar material that does not abide by the theories now applied. The writer has observed low-speed, low-frequency units installed years ago on cork foundations, which have proved entirely satisfactory although, according to the theories developed later, the isolation should have been a failure. However, the installations did prove successful. Therefore, too great reliance should not be placed on the present theory concerning cork isolation until, after further study, the theory is corrected and made to conform more closely with experience.

Confirming statements made relating to the use of springs above vibration isolators in order to simulate additional weight, the writer has witnessed such an application to a 4-cylinder vertical engine which bounced very badly on its foundation until such springs were installed. They were very stiff springs and caused the foundation to act as if it were heavier, thus reducing the bouncing motion.

What has the author found it advisable to do for side isolation of foundations, particularly in the case of horizontal engines? Of course, with vertical engines, the best side isolation is just air. In the case of horizontal engines, where there are heavy unbalanced forces in the horizontal direction, one cannot always isolate with air, otherwise the foundation may shift.

G. C. Boyer.[18] The author mentioned the fact that some things do not work out according to theory and that applies equally, it is believed, to horizontal engines on foundation blocks. The writer recalls an experience in Oklahoma where a group of horizontal engines were installed on a concrete boat set in a marsh. According to all the vibration theory known to any of us, that plant should have been down the river 2 or 3 miles within a couple of weeks. The plant is still running in the original location, and vibration troubles are unknown.

Bear this fact in mind. When the preparation of this paper was undertaken some months ago, the only information available in our office on the subject of foundation design was what we had obtained from some of the large engine manufacturers, and that was very meager. This is not intended as criticism; rather it is the result of the lack of progress in the science of foundation design.

Too often it has been the practice to place a block of concrete in the ground, set an engine on it and, because of the fact that the soil was good, and nothing of a delicate character was around to shake, the foundation was a success. When the installation of another foundation was required, the original drawings were used again. In this case, perhaps, the soil was not so good, and the result was excessive vibration. A third installation was required, so, remembering the sad experience in the second case and in order to be on the safe side, the designer increased the size of the foundation in the hope that the addition of mass would correct the evil. It appears to the writer that the evolution of foundation design has too often been one merely of increasing the mass of the concrete block under the engine without fully evaluating all of the items which enter into the design of a successful foundation for an internal-combustion engine.

There is much concerning the design of foundations which has not been covered in this paper, but it was prepared in the hope that it would stimulate more interest in this subject, which has had so little discussion in the past. It was hoped that enough interest would be aroused in the subject so that perhaps someday we can explain some of the vagaries cited in the discussion where theoretically a design was not supposed to work and it did work; a place where dry sand was not supposed to isolate the foundation but it did; a place where a foundation on mushy soil was supposed to vibrate but did not. There must be a reason for all these contrary facts. This paper may stimulate others to try and find out some of the reasons for these contrary experiences.

Author's Closure

In answer to Mr. Campbell, the predominating factor will be the isolating material. It will still be effective, but the general effect of very soft subsoils is to reduce the efficiency of vibration isolation. In other words, the material under the vibration isolation should be fairly firm for best results. This problem is completely covered by vibration theory but is rather complicated.

In answer to Mr. Robertson, the design problem would fall

[15] Hill Diesel Engine Company, Lansing, Mich.
[16] Exline Diesel Engine Works, Kipp, Kan.
[17] Consulting Engineer, New York, N. Y. Mem. A.S.M.E.
[18] Burns & McDonnell Engineering Company, Kansas City, Mo. Mem. A.S.M.E.

into one of three classifications upon visual inspection of the subsoil: (1) With a firm hard subsoil, vibration will not be an important factor and the design will be simplified; (2) with a soft subsoil the reduction of vibration will be a serious consideration and unusual care should be taken in the design; (3) with an intermediate subsoil condition, intermediate measures of design will be in order and the designer must exercise judgment in considering the various factors involved.

In the latter two cases the natural frequency of the engine and foundation will be an important factor. The natural frequency of an engine foundation can be predicted roughly from Table 1. In cases where vibration is objectionable and preliminary studies indicate an ω/p ratio greater than 0.5 the author would recommend a calculation of the natural frequency based on a field determination of Δ.

To begin with, the unit loading of the foundation on the subsoil will usually be between 1000 and 2000 lb per sq ft. If static deflections are taken for several loadings within this range, a curve can be drawn from which the deflection for the particular unit loading may be obtained. Another factor which must be taken into account is that the deflection is not the same for an area of 1 sq ft at 2000 lb load as it would be for a 200-sq-ft area loaded to 2000 lb per sq ft. However, static deflections may be taken for two or three different sized areas at the same unit loading, and the effect of the size of the area determined approximately. By the combination of these two relations, a reasonably good prediction of Δ and the natural frequency can be made.

In single-cylinder engines, as mentioned by Mr. Rosenberg there will be unbalanced forces and, in general, isolation will be quite a problem. By means of isolation, the vibration that is transmitted to surroundings may be reduced, but it is the author's belief that the unbalanced forces would be so great that the suspended foundation block would hop around considerably. Generally, in a location where vibration is very undesirable, a single-cylinder engine cannot be operated satisfactorily. If vibration is permissible to some extent, the best foundation which can be provided for a single-cylinder engine is as large a mass as can be used on a subsoil as firm and hard as can be produced.

Mr. Bayles' expedient of using springs both above and below an engine is a good one. Such an installation should behave exactly according to the formulas. The effect of the upper springs is to increase the static deflection and decrease the natural frequency.

Mr. Exline's problem is one of unbalanced horizontal forces, probably in the compressor. These forces produce a twisting moment about a vertical axis. Of course, the stress due to this moment is greatest at the corners of the foundation, and apparently, the corners were not strong enough to resist the stress. It is the author's belief that vibration isolation does not enter this problem at all.

The author has little faith in the efficiency of cork as an isolator for low-frequency vibration, although his conclusions are based mostly on theory. However, the theory is rather definitely confirmed by a number of experiments, notably those of reference 8, in the paper. Cork has been used on a number of foundation installations which probably would have worked as well without it, but the cork has received the credit.

The author has had but little experience with foundations for horizontal engines. However, it is believed that such a foundation could be very well isolated by the use of both horizontal and vertical springs. The horizontal springs should be compressed into place and would act much as those used both above and below the vertical engine cited by Mr. Bayles.

Instrumentation for Developing and Testing Diesel Engines

By C. R. MAXWELL[1] and K. M. BROWN,[1] PEORIA, ILL.

This paper gives a comprehensive idea of the range of Diesel-engine measurements essential to the design of efficient and successful types. Such measurements include accurate power determination, fuel consumption, lubricating-oil consumption, record of crankcase blow-by, exhaust-smoke measurement, all of which are items of performance. In addition, such informative items as pressures attained, rate of pressure rise, combustion analysis, flame duration, exhaust-gas analysis, functions of fuel-injection system, temperature measurements, vibration data, are all essential of determination. Descriptive details are given of the instruments and methods employed in one of the leading Diesel-engine testing laboratories of the country for the determination of these and other Diesel-engine design and operating factors.

ALTHOUGH Diesel engines are widely advertised as burning little or no fuel, having low peak pressures, running smoothly, and having other qualities, engines are bought and sold on a basis of power. Therefore the measurement of power is certainly of primary consideration. Great accuracy of power measurement may not be necessary for rating purposes or for endurance runs, but successful development of an engine is greatly facilitated by the use of accurate reliable power determinations.

Another factor of considerable importance to the buyer of a Diesel is fuel consumption. Because of its high expansion ratio, the Diesel engine converts fuel into power with a fair degree of efficiency. However, so many engine factors influence efficiency that really good fuel consumption can only be obtained as the result of considerable development. Without a good device for the measurement of fuel consumption, such development is impossible.

Due to the low fuel consumption of the Diesel engine and the considerable price differential between fuel oil and lubricating oil, oil consumption is a large factor in operating economy. Unfortunately, the rules for obtaining good oil consumption are general, at best. Consequently, oil consumption must be checked, particularly in a new design, even though the design has been based on the results of past experience. The length of time required for such tests is an inverse function of the accuracy of the measuring equipment.

As a criterion of the condition of pistons and rings, crankcase blow-by is unexcelled. No endurance test is complete without a record of blow-by. Crankcase blow-by, or more accurately piston-ring blow-by, has so many deleterious effects and so few good ones, it might easily be termed the ill wind that blows nobody good. Even an engine in excellent condition has some blow-by. In reducing this to a minimum, measuring equipment is essential.

Of late years, it would seem that everyone has become "smoke conscious." Cities are instituting smoke-prevention campaigns, legislative bodies are legislating about it, and the general public is complaining about smoke. For some time, the Diesel engineer has realized that smoke meant incomplete combustion, with consequent reduced efficiency and greater internal engine deposits. He thus finds it desirable to measure the amount of smoke given out by an engine, and particularly to be able to indicate small changes in the smoking tendency of an engine, so that he may know when he is making an improvement.

All the items that we have so far considered—power, fuel consumption, smoke—are what the engine does, or how it performs. However, to be able to improve an engine the engineer must know "why" it performs as it does. One of the most informative items that is reasonably easy of attainment is the pressure diagram or indicator card. In the old steam-engine days, the indicator card was a pressure-volume card, but the Diesel engineer finds that a pressure-time diagram gives him more information, particularly about the combustion period, which is his chief interest. One of the first things the indicator card tells him is about timing; whether combustion is starting too early or too late or is "just right." Of course, he is interested in the pressures attained, not only from the combustion standpoint, but also from the standpoint of loading on engine components, and he is particularly interested in the rate of pressure rise, which has a bearing on engine smoothness and knock. To an experienced Diesel engineer, the general shape of the card is most informative. Combustion analysis by means of logarithmic diagrams may be made from the card if desired. The card may also be used to determine indicated horsepower and turning-moment diagrams.

Another way the Diesel engineer has of determining the "why" of his engine is to observe flame duration. Also, an analysis of the exhaust gases gives him a clue as to the chemical changes going on in his engine.

The maximum usable output of a given engine depends directly on the rate of air consumption. Many engines have had their lack of performance traced directly to a deficiency in this respect. Here again, measuring equipment is essential.

It may be said that no Diesel engine is better than its fuel system. It may also be said that few engine parts or functions are more reluctant to give up their secrets. The injection of fuel is a complex phenomenon involving pressure, inertia, compressibility, wave motion, vibration, ballistics, and other factors, occurring in the space of a few milliseconds. Surely there are not many places where instrumentation may be employed to greater advantage than in the development of a fuel system.

The Diesel engine is a "heat" engine, so high temperatures are involved. The temperatures attained by certain parts may be a limiting factor in their life and performance. Particularly is this true of pistons and bearings, but these are the parts where temperatures are most difficult to measure.

Finally, we find that our engine sometimes has an unfortunate habit of shimmying and shaking more than we would like. Vibration is annoying to an operator or anyone near an engine, but it also can be the cause of excessive stresses in certain parts and result in failure of that part. One particular form of vibration which needs attention is valve-spring surge. Torsional vibra-

---

[1] Engineering Research Department, Caterpillar Tractor Company.

Presented at the National Meeting of the Oil and Gas Power Division, Kansas City, Mo., June 11–14, 1941, of THE AMERICAN SOCIETY OF MECHANICAL ENGINEERS.

NOTE: Statements and opinions advanced in papers are to be understood as individual expressions of their authors and not those of the Society.

tion of crankshafts is often the source of noise and sometimes even of failures.

Horsepower and Fuel Consumption

The measurement of the power of a Diesel engine is today relatively simple. Dynamometers of many types are available in a wide range of sizes. Probably the best dynamometer for general development work is the Sprague-type electric dynamometer, Fig. 1. These dynamometers are essentially d-c generators with

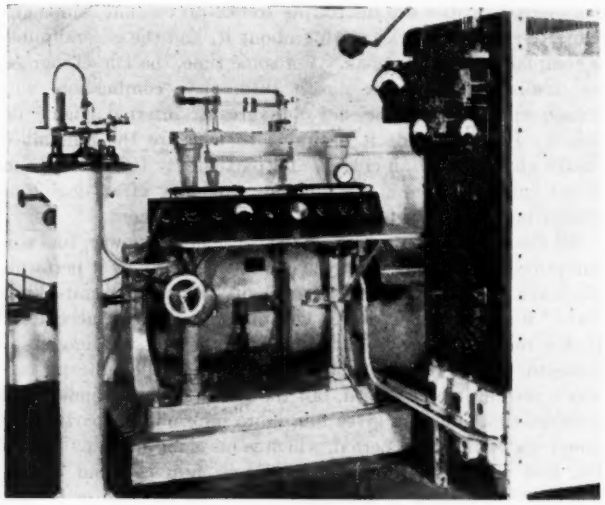


Fig. 1 Dynamometer and Fuel Scales

the stator mounted in bearings so that the torque reaction may be measured on scales. The power is absorbed by resistances or grids and dissipated as heat. Advantages over other types include ease of control and, most important, the possibility of using the dynamometer as a motor to measure friction torque directly.

A relatively new dynamometer which has gained considerable popularity in recent years is the eddy-current electric dynamometer. An iron or steel disk is rotated in a magnetic field, causing eddy currents in the disk. The power is thus converted to heat, which is carried off by a considerable flow of cooling water. The stator is cradle-mounted so that torque reaction is measured directly. These dynamometers are characterized by their large power-absorption capacity in small sizes, and simplicity of control. While they will not run as a motor, dynamometers are now available with cradle-mounted d-c motors connected in tandem for starting purposes and friction-torque measurements.

Most dynamometers measure torque directly. Horsepower being a function of torque and speed, no dynamometer can be more accurate than the means used for measuring revolutions per minute. Electric tachometers consisting of a permanent-magnet generator and voltmeter calibrated in rpm are quite reliable. Being readily adjustable, they are capable of giving accurate speed indication for years with a minimum of maintenance.

Stroboscopic devices are often used as speed indicators. By using constant-frequency alternating current for timing the flash and the proper number of equally spaced markings on a rotating engine part, a great many synchronous speeds may be obtained.

One of the earliest forms of speed-indicating devices is a revolution counter and stop watch. These two instruments have now been combined into one compact unit which automatically counts the revolutions for a given period of time and registers rpm. These have proved to be quite accurate.

An excellent device for speed measurements in engine testing is a revolution counter directly coupled to the dynamometer shaft through a solenoid-operated clutch, and an electrically operated stop watch, Fig. 2. Both are started and stopped simultaneously by a single button. The stop watch may be a solenoid-operated conventional stop watch, or some type of electric time clock. Although some maintenance may be required, results can be very satisfactory if the units are well designed.

A good counter and stop watch are essential for accurate fuel-consumption measurements. Volumetric fuel-consumption measurements may be quite easily made by installing a tee in the fuel line between the tank and engine with a valve between the tank and tee. A calibrated pipette is connected to the third branch of the tee with the overflow piped back to the tank. When the valve is shut off, the engine draws fuel from the pipette. As the fuel passes the calibration marks on the pipette a stop watch is



Fig. 2 Counter and Tachometer Drive

started and stopped. If horsepower is read at the same time, specific fuel consumption may be obtained.

Fuel consumption on a weight basis may be obtained by replacing the pipette with a small fuel container placed on one tray of a simple balance, with suitable weights on the other tray. The valve is shut off, causing the engine to draw fuel from the container. As fuel is drawn from the container the scale becomes unbalanced and trips an electrical contact which simultaneously starts the watch and counter. A weight is then removed from the scale and, when the scale again trips, the electrical contact stops the watch and counter. Thus time and total revolutions for the consumption of a given weight of fuel are obtained. If the torque is read, we have all the data necessary for a complete fuel-consumption reading. It may be of interest to point out that a specific fuel-consumption reading is not affected by watch accuracy, since it is a function of torque and total revolutions for a given weight of fuel. The watch is necessary only for rpm readings for brake-horsepower calculations.

Oil Consumption and Blow-By

Oil consumption has always been difficult to measure accurately in a short period of time. While the oil in circulation is substantially constant, the continued splash of oil being thrown from the rods and air currents set up by the whirling crankshaft, keeps the oil level in a state of extreme disturbance.

A method successfully used to overcome these difficulties is to drain the sump into an external reservoir. Oil is pumped from

this reservoir to the engine in the usual manner. The reservoir is placed on a platform scale and weighed at suitable intervals. Since the main portion of the oil is now removed from the major disturbing influences it is in a relatively quiet condition and rate of oil consumption may be determined in a few hours.

For the measurement of piston-ring blow-by, displacement meters are generally used, either the wet or dry type. Dry meters are usually preferred because of their smaller size for a given capacity. These are of the same general design as the ordinary home gas meter.

Occasionally it is desirable to read blow-by continuously so as to watch fluctuations more closely. For this purpose rate-of-flow meters are available. The most common type consists of a tapered glass tube through which the gas passes, causing a float to rise to a height determined by the rate of flow.

Smoke Measurement

The simplest method of measuring smoke is, of course, the visual method. The observer looks at the smoke and then rates it as clear, trace, light, medium, or heavy, according as his judgment dictates. It is obvious that a great personal factor enters into such a determination, and even an experienced observer has difficulty in judging smoke from one time to another because of changing light conditions, and because the nature of the background against which the smoke is observed influences what may be seen. In this connection, it may be noted that, when smoke is observed against a dark background, with light streaming across the column of smoke (thus viewing the smoke by reflected light), the smoke appears denser, and hence, smaller traces of smoke may be observed than when the smoke is observed by transmitted light.

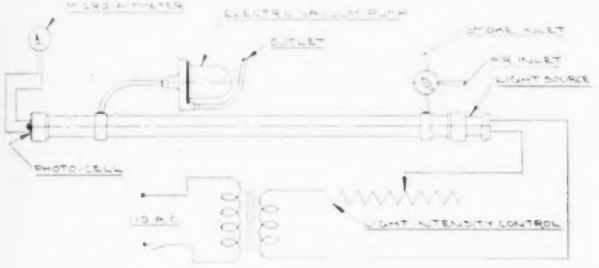


Fig. 3 Schematic Diagram of Smoke Meter

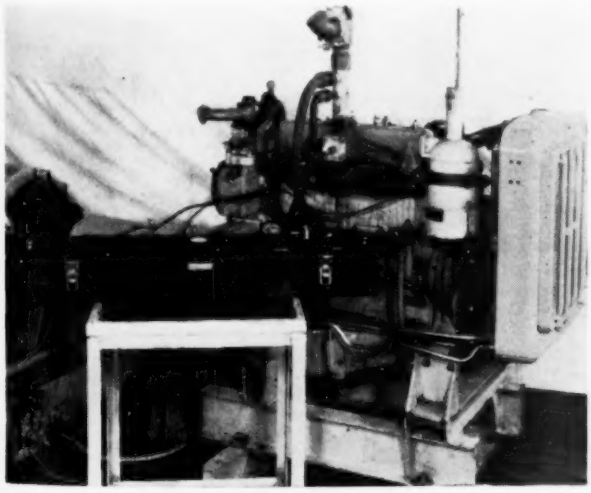


Fig. 4 Smoke Meter on Engine

A method of measuring smoke which is coming into considerable use is the sampling-type smoke meter, such as the one described in a recent paper[2] by K. M. Brown. This smoke meter, Fig. 3, consists essentially of a tube through which, by turning a two-way valve, either clean air or a continuous sample of the smoke may be drawn by means of an electric vacuum pump. At one end of the tube is a light source, the intensity of which may be controlled, and at the other end, a photoelectric cell. The method of use consists of turning the control handle so that clean air is drawn into the meter, and adjusting the light intensity so that a definite reading is obtained on the meter indicating the photoelectric-cell output. The control handle is then turned so that the sample of smoke is brought into the tube, thus causing the light falling on the photoelectric cell to diminish proportionally to the density of the smoke. Fig. 4 shows the smoke meter connected to an engine. These meters may be made very sensitive by increasing the length of the measuring tube.

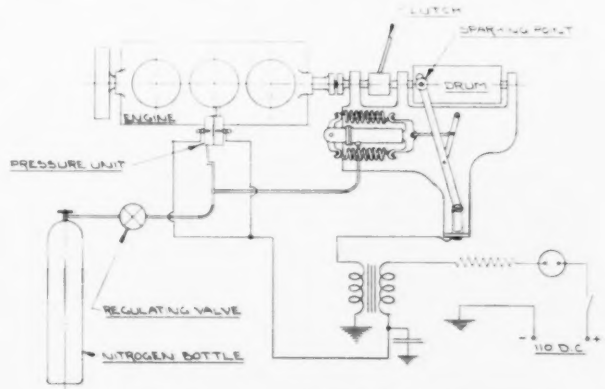


Fig. 5 Schematic Diagram of Farnboro Indicator

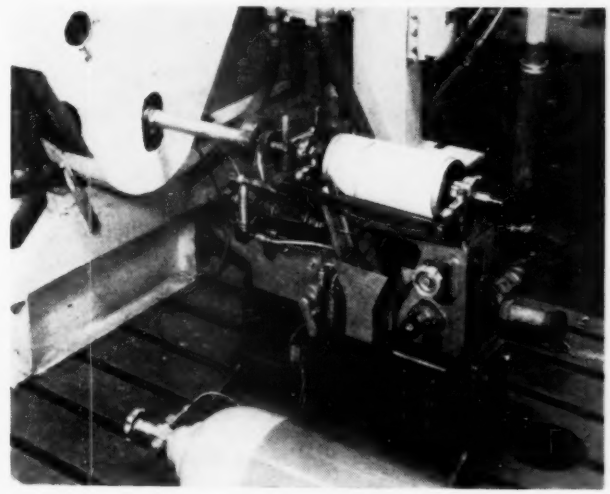


Fig. 6 Farnboro Indicator

Combustion Analysis

For slow-speed engines, the old steam-engine indicator was quite satisfactory but, for higher-speed engines, it is entirely inadequate, principally because of its excessive inertia. It has thus been necessary to develop other types of instruments to indicate cylinder pressures in medium- and high-speed Diesel en-

[2] "Requirements of a Smoke Meter," by K. M. Brown, *S.A.E. Journal*, vol. 48, no. 5, May, 1940, pp. 188–192.

gines. There are three general types now in use, i.e., the sampling type, the balanced-pressure type, and various electrical types.

The sampling type consists essentially of a mechanism similar to the old steam-engine indicator, but which may be mounted a short distance from the engine and subjected to engine-cylinder pressure through a sampling valve in the engine cylinder. The sampling valve is operated electrically and is open only for a few degrees of engine revolution. A contactor and phasing device, driven by the engine, successively open the sampling valve for a few degrees so that 720 deg of crankshaft rotation is finally covered. Thus one complete engine cycle is covered over a period of many revolutions, so that the resulting card is a composite card.

The balanced-pressure-type indicator, such as the Farnboro

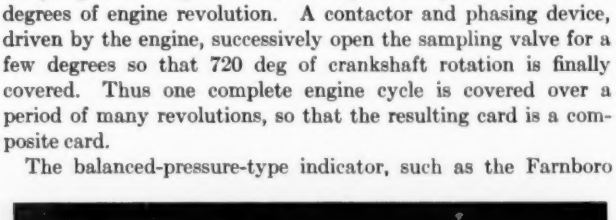


Fig. 7 Typical Farnboro Card

indicator, shown in Figs. 5 and 6, also yields a composite card but it is obtained in a somewhat different manner. The cylinder unit consists of a case containing a diaphragm which may be exposed to cylinder pressures on one side and to a controllable pressure derived from a nitrogen bottle on the other side. Electrical contacts are provided on both sides of the diaphragm. The controllable pressure is also applied to a calibrated spring-loaded piston which moves a sparking point parallel to the axis of a drum. The drum is rotated through a clutch from the engine shaft. The method of operation is as follows: Pressure is gradually applied from the nitrogen cylinder to the pressure unit and the piston operating the sparking point, causing the sparking point to move along the surface of the drum proportionally to the applied pressure. At the same time, when the cylinder pressure coming up on the compression stroke becomes greater than the applied pressure, the diaphragm in the pressure unit will move over, breaking one contact and making the other. The breaking of the contact causes a spark to jump from the sparking point to the drum, puncturing a hole in special paper which has previously been secured to the drum. When the cylinder pressure becomes just less than the applied pressure, the diaphragm moves the other way breaking the contact on the other side, so that a spark jumps to the drum at this instant. Thus, as the full range of pressures are covered, the crank angle at which the cylinder pressure equaled the applied pressure is recorded on the paper on the drum. By connecting the punctured holes, a pressure-time diagram may be drawn. Fig. 7 shows a typical diagram obtained on a Farnboro indicator.

This method is highly accurate, it gives a large-size diagram which may be easily scaled for the pressures, and is applicable to both low- and high-speed engines. It gives an average of a large number of cycles, which is an advantage if measurements from an average card are desired, but is a disadvantage if it is desired to see the cycle-to-cycle variation, or if one individual cycle is wanted. The method has one serious drawback which is that there is considerable volume in the pressure unit. In small Diesel engines, this volume is an appreciable proportion of the compression volume, so that these units cannot be applied to a small engine without changing the compression ratio.

In the last few years electrical pressure pickups of various types have come into considerable usage. They have the advantage that their inertia may be kept extremely low or negligible, so that they are usable at high frequencies. They show individual cycles and, particularly, with the advent of the cathode-ray oscillograph, they provide a quick and easily seen method of ascertaining what is going on within an engine cylinder. It is only necessary to screw the pressure pickup into its proper place in an engine cylinder, connect a few wires, and a good-size pressure diagram may be made visible on a screen. The electrical-type pickups have the common disadvantage in that they are difficult to calibrate successfully.

There are five general types of electrical pickups, i.e., the resistance type, the magnetic type, the condenser type, the piezoelectric type, and the photoelectric-cell type.

The resistance type depends upon changing the resistance of some element in an electric circuit proportionally to the change in the quantity desired to be measured. The capacity type similarly depends upon changing the capacity of a condenser.

In the magnetic type, the reluctance of a magnetic circuit is changed, thereby changing the reactance of the element, or a voltage is generated by moving a coil in a magnetic field, or changing or moving a magnetic field about a coil.

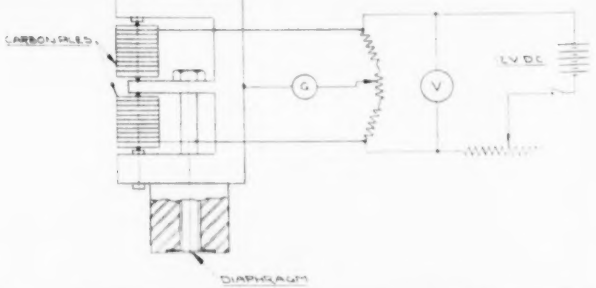


Fig. 8 Schematic Diagram of Carbon-Pile Pressure Unit

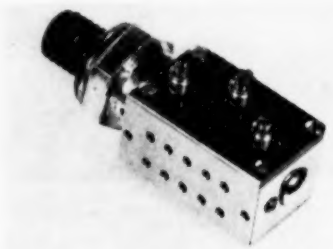


Fig. 9 Carbon-Pile Pressure Unit

The piezoelectric type depends upon the fact that changing the stress in certain crystals sets up an electrical charge on the crystal proportionally to the stress.

The photoelectric type depends upon varying the amount of light falling on a photoelectric cell proportionally to the pressure. One method of accomplishing this is by means of a diaphragm exposed to the cylinder pressures and used as a reflecting surface. As the curvature of the diaphragm changes with changes

in pressure, the amount of light falling on the photoelectric cell changes.

As an example of the resistance-type pressure pickup, the carbon-pile indicator, shown in Figs. 8 and 9, has been the most commonly used. It consists of two stacks of carbon disks placed as shown in Fig. 8 and loaded in the center by a cantilever beam. The cylinder pressures are communicated through a diaphragm and a rod to this cantilever beam. When the pressure increases, the compression on the upper stack of carbon disks is increased, thus lowering the resistance of this stack, while the compression in the lower stack is decreased, increasing its resistance. The two stacks are connected in an electrical circuit so as to form two legs of a Wheatsone bridge. The other two legs of the bridge are formed by fixed resistors with a variable resistor between them, so that the bridge may be initially balanced at atmospheric pressure. Thus, at atmospheric pressure, the resistances in the four legs of the bridge are proportional, so that the voltage across the center of the bridge is zero. When the pressure changes, the change in resistance in the two carbon-stack legs causes a voltage to appear across the center of the bridge, which may be measured by a galvanometer, or which may be applied to the grid of a radio tube and be amplified. Using the most sensitive galvanometers available suitable to the purpose only a small diagram may be obtained, so that if a large diagram is desired it is necessary to use an amplifier. The carbon-pile pickup is affected by temperature so that some cooling means must be employed. In the one shown, air is used for cooling.

Probably the most commonly used electric-type pressure pickup today is the piezoelectric type, shown in Figs. 10 and 11.

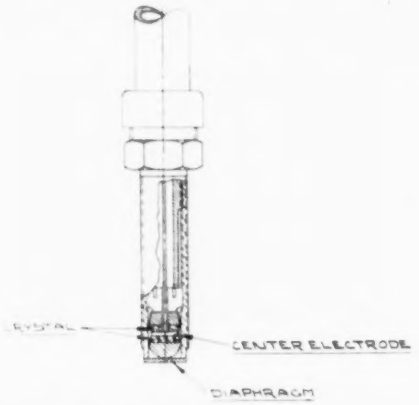


FIG. 10 SKETCH OF PIEZOELECTRIC PRESSURE UNIT



FIG. 11 PIEZOELECTRIC PRESSURE UNIT

It consists of a stainless-steel case with a diaphragm at the bottom which is exposed to the cylinder pressures. This pressure is communicated to two quartz crystals held within the case. A center electrode between the crystals makes the external electrical connection. The application of pressure to the crystals causes them to acquire a charge. The crystals are so oriented that the charges on the two crystals are additive. If precautions are taken to prevent this charge from leaking off, the charge appears as a voltage, directly proportional to the pressure, which may be amplified and indicated on an oscillograph.

Since it is impossible to obtain perfect insulation, the charge on the crystals will have a certain time rate of leakage, so that if the pressure cycles come at too low a frequency, a certain percentage of the charge will have time enough to leak off. This fact imposes a low-frequency limitation on this type of pickup. It is stated that the error due to this cause will be less than 5 per cent if the speed of the engine is greater than 1200 rpm for a four-cycle engine or 600 rpm for a two-cycle engine.

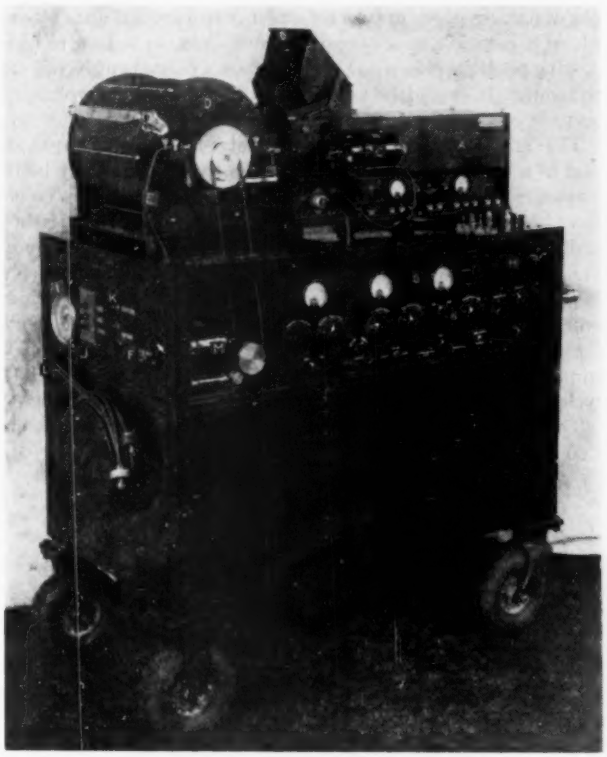


FIG. 12 GALVANOMETER-TYPE OSCILLOGRAPH

For practically all types of electrical pickups the voltage output is so low that it is necessary to amplify it to obtain sufficient output to operate an oscillograph. This fact calls for some type of electronic amplifier, which brings up the question of frequency limitations. The most commonly used amplifier for this type of work is the resistance-capacity-coupled. Amplifiers of this type are built with an essentially flat response from 2 to 15,000 cycles per sec. If it is desired to amplify zero frequency, it is necessary to resort to a so-called d-c amplifier, which is straight resistance-coupled. This type of amplifier has the disadvantage of tending to be unstable.

In engine work it must be remembered that a rather large range of frequencies is encountered. In the engine-cylinder-pressure diagram, there are sometimes quite steep pressure rises, which would correspond to a very high frequency. Also the pressure diagram is essentially flat between working strokes, which condition would correspond to a low frequency—lower than the number of engine cycles per second.

So far, we have converted our pressure changes in the cylinder into voltage changes, and have amplified the voltage change to a

workable quantity. In order to make this voltage change visible, so that we can see and measure our pressure diagram, we employ the electrical engineer's oscillograph. There are two general types of oscillographs, the older galvanometer-type, and the quite common one today, i.e., the cathode-ray.

The fundamental unit in the galvanometer-type oscillograph is the elementary galvanometer, which consists of a loop of wire in a magnetic field, supporting a small mirror. When a current is passed through the loop of wire, it is deflected so that the mirror is turned through an angle proportional to the current. From a source of light, a narrow beam is focused on the small mirror. The mirror reflects it back, either onto a rotating polygon of mirrors which in turn reflects it onto a ground-glass screen, where it is visible as a moving trace of light, or onto a piece of moving photographic paper or film where a permanent record can be made. It should be noted that this type oscillograph is essentially a current-measuring machine.

The advantages of the galvanometer-type oscillograph are that in a relatively small unit four or more elements may be incorporated so that four or more simultaneous events may be observed or permanently recorded. It is thus possible to measure, easily and accurately, intervals of time between any two events. This oscillograph also has the advantage in that it will indicate low frequencies, down to zero frequency, or direct current. However, it does have a high-frequency limitation, the limit depending upon the characteristics of the galvanometer. As an example, the response of one commonly used element is flat to 1000 cycles per sec, but falls off very rapidly beyond that.

The galvanometer oscillograph is a more delicate instrument

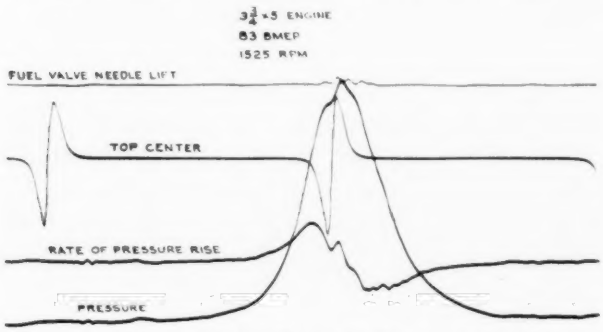


FIG. 13 TYPICAL RECORD TAKEN ON GALVANOMETER-TYPE OSCILLOGRAPH

than the cathode-ray oscillograph and requires an experienced operator for its successful use. For quick, visual observation of phenomena, it is not as convenient as the cathode-ray oscillograph.

The unit shown in Fig. 12 is a four-element galvanometer-type oscillograph. Phenomena may be observed in the viewing screen *B*, or may be recorded on the rotating film drum shown at *D*. This film drum yields a record 6 in. wide × 36 in. long, and film speeds up to 40 fps are possible. A carbon-arc lamp is normally used as a source of light for this unit. As may be seen, the oscillograph and film drum are mounted on a movable buggy, which contains all the amplifiers and controls for the unit that are required.

Fig. 13 shows a typical record taken with this machine. A pressure record, a rate-of-pressure-rise diagram (obtained by differentiating electrically the pressure record), a record of the fuel-valve-needle lift, and a timing record, comprising a top and bottom dead-center mark, are included on the one diagram. It may be seen that besides the usual analyses of each individual diagram, the injection lag, the ignition lag, and the duration of injection may be obtained from this record.

The introduction of the cathode-ray oscillograph has provided a relatively inexpensive and very convenient means of observing visually any phenomena which can be converted into electrical voltage. The basic element of this oscillograph is the cathode-ray tube, a glass envelope exhausted to a high vacuum, which contains a filament or cathode to supply a source of electrons, various grids to concentrate and focus the electrons into a beam and to control its intensity, a pair each of vertical and horizontal deflecting plates, and a fluorescent screen at the end of the tube which glows when the stream of electrons strikes it, thus making

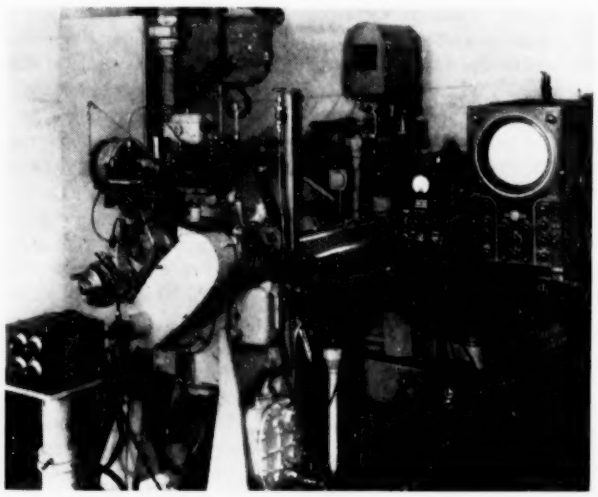


FIG. 14 CATHODE-RAY OSCILLOGRAPH

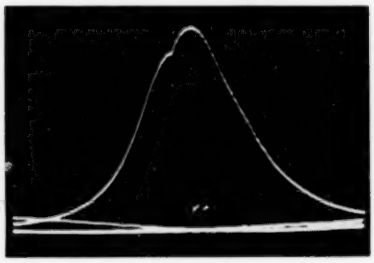


FIG. 15 DIAGRAM OBTAINED ON CATHODE-RAY OSCILLOGRAPH

their path visible. Applying suitable voltages to the deflecting plates deflects the beam of electrons proportionally to the voltages. Since a stream of electrons has extremely small inertia, the cathode-ray tube may be used at very high frequencies, considerably higher than any usually encountered in engine work.

The low-frequency limitation of the instrument depends upon the amplifiers used to secure sufficient voltage to operate the tube. Cathode-ray oscillographs are available, suitable for engine work, with screen diameters of 3 in., 5 in., and 9 in. The 9-in. screen provides a generous-size diagram, while the 5-in size is quite usable. Permanent records may be made of diagrams by photographing the screen with an ordinary camera. It also is possible to photograph the screen with a motion-picture camera, and thus obtain a succession of events. An arrangement has been made whereby several cathode-ray tubes have been focused on a rotating film drum, thereby obtaining simultaneous records similar to those obtained with the galvanometer oscillograph.

Fig. 14 shows a 9-in. cathode-ray oscillograph, along with an amplifier, mounted on a portable buggy, being used to obtain

pressure records from a single-cylinder test engine. Fig. 15 shows the diagram so obtained.

The advantages of the cathode-ray oscillograph are its relatively low cost, its wide frequency limits, its ease and convenience of use, and the fact that it is fairly foolproof and not easily damaged by misuse.

Its disadvantages are that it shows only a single event at a time without some rather elaborate equipment. Ordinarily it is not particularly suitable for d-c measurements, and the usual

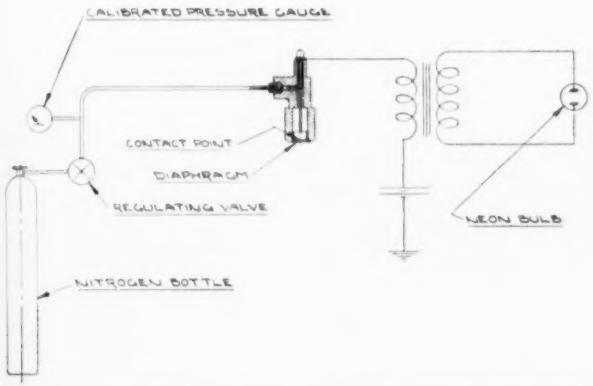


FIG. 16 SCHEMATIC DIAGRAM OF PEAK-PRESSURE INDICATOR

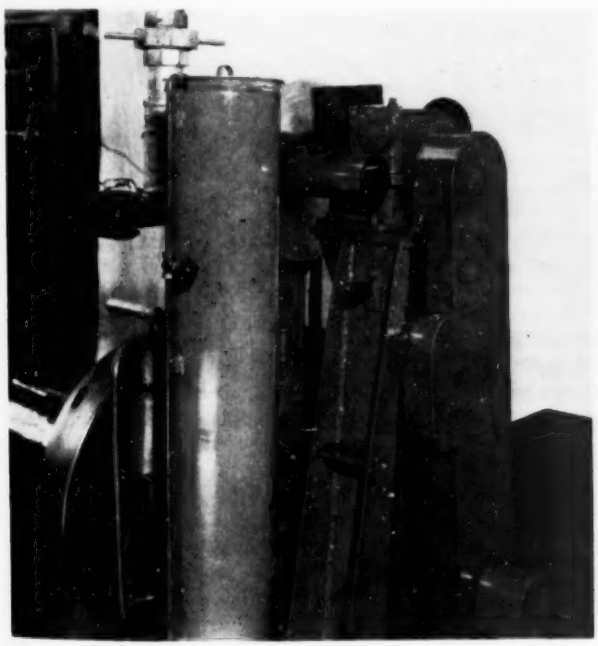


FIG. 17 FLAME-DURATION SETUP

photographic record obtained from it is not so usable as that obtained from the galvanometer-type oscillograph.

PEAK-PRESSURE INDICATOR

One disadvantage of all electrical-type pressure pickups, which has been noted, is the difficulty of obtaining a good calibration. For this reason, when it is desired to know the actual value of the pressures in an engine cylinder, resort has been made to a peak-pressure indicator which is quite accurate to give either peak compression pressures or peak explosion pressures. A device of this type is shown in Fig. 16. It is of the balanced-diaphragm type. A diaphragm is exposed on one side to the cylinder pressure and on the other side to a controllable pressure supplied from a nitrogen cylinder. A calibrated pressure gage is located in this line to measure accurately the applied pressure. There is one electrical contact in the pickup unit. When the cylinder pressure is less than the applied pressure, the diaphragm stays away from this contact. The instant the cylinder pressure becomes greater than the applied pressure, the diaphragm moves over, grounding the electrical contact, thus completing the circuit and inducing a voltage in a coil sufficient to make a neon lamp glow instantaneously. If the applied pressure is increased until it is just slightly more than the peak pressure in the cylinder, the diaphragm will not move over and the neon light will not glow. By noting the point at which a slight increase in applied pressure will cause the neon lamp to stop glowing, or a slight decrease in the pressure will just cause it to glow, the peak pressure may be quite accurately determined.

FLAME DURATION

Fig. 17 shows a setup that has been used to determine visually the flame duration in an engine. A quartz window is located in

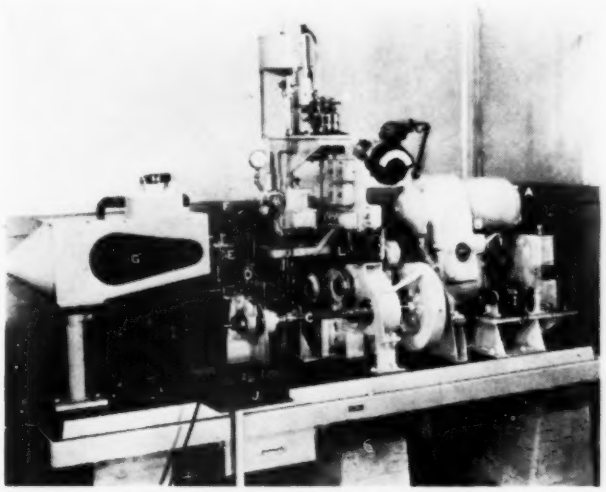


FIG. 18 SPRAY MACHINE

the engine head so that it looks into the combustion space. A stroboscopic shutter is driven from the engine crankshaft and fitted with a phase-changing device so that the quartz window may be observed for a few crankshaft degrees each cycle starting at any point in the cycle desired. A scale is provided to read the crank angle at which the shutter opens. By adjusting the phasing device so that the flame in the engine cylinder can just be seen to start, and then so it can just be seen to end, the duration of the flame may be determined.

A Diesel engine generally runs with more or less excess air, depending upon the load, or on a "lean" mixture. It has been demonstrated that most exhaust-gas analyzers are unsatisfactory at lean mixtures. For this reason, the conventional Orsat apparatus is believed to be the only satisfactory means at present of analyzing the exhaust gas of a Diesel engine.

Often in the course of engine development it becomes imperative to know the air consumption of an engine. The measurement of air flow presents so many problems that methods of measurement have been the subject of considerable discussion. Since we have no desire to precipitate further discussions on this subject, we will only say that the measurement of air flow by means of well-rounded nozzles has proved entirely satisfactory

for normal engine testing. If a few simple rules are followed, reliable results, if not hair-splitting accuracy, will be obtained.

Spray Machine

The development and testing of fuel-injection equipment is no such simple task. For this purpose a spray machine has been developed, Fig. 18. Fundamentally, this consists of a fuel cam driven by a motor and variable-speed pulleys at any speed between 15 rpm and 2400 rpm. Suitable mountings are provided for any fuel pump it is desired to test.

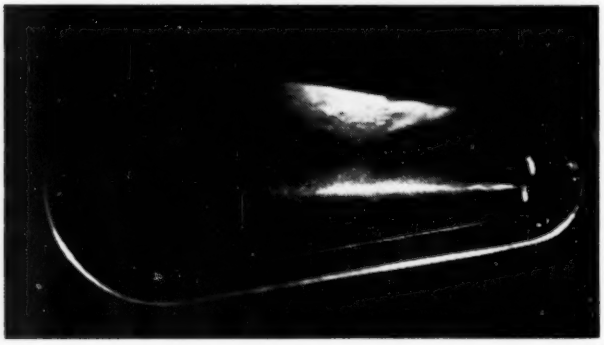


Fig. 19 Fuel Spray



Fig. 20 Rate-of-Discharge Machine

For visual inspection of the fuel spray, a spray box is provided, one end of which has an opening for a fuel valve, the other being connected to a spray collector. The light from a high-speed stroboscope is mounted in the top of the box and one side of the box is open for the inspection of the spray. The stroboscope used is of rather simple and completely reliable design. A large condenser is charged to a potential of several thousand volts and discharged across a gap and through a neon tube when the gap is broken down by a small priming current applied by a timed contactor. The resulting flash is extremely bright and has a duration of but a few millionths of a second. By properly timing the flash, the spray may be "stopped" and examined at any point in the cycle. For taking photographs, a larger condenser is provided which gives a light of such intensity that pictures may be taken of a single flash by a camera with an *f*4.5 opening using moderately fast film. Fig. 19 shows a spray photograph taken on this machine.

For rate-of-fuel-discharge determinations, there is an attachment consisting of a disk which holds a number of light aluminum cups. The machine is so arranged that the cups are placed before the fuel valve and automatically indexed every 50 pump strokes. Blotters are placed in the bottoms of the cups to catch the spray. The spray is discharged through a slot, 1 deg in width, in a second disk, which rotates at cam speed. A third disk, placed between the other two, rotates at 0.02 cam speed and blanks off the spray for 25 injections, remaining open for 25 injections. A phase-changing gear is provided to time the slotted disk to the proper cam angle. Fig. 20 shows the machine.

The sequence of operation is as follows: First the pump cam is rotated at the desired speed and the pump is turned on. The slotted disk is then set, by means of the phase-changing gear, so that fuel is just beginning to appear through the slot, and then backed off 1 deg. Next the cups are carefully weighed and installed, after which the whole machine is set in motion. Thus, a 1-deg increment of the fuel discharge is discharged into the first cup 25 times. Then the fuel spray is blanked off for 25 injections while the next cup is automatically placed before the fuel valve, and the slotted disk is manually indexed 1 deg. Twenty-five 1-deg increments are discharged into this cup and so on until the complete fuel cycle is finished. Then the cups are again weighed, the result being a point-by-point determination of the rate of fuel discharge.

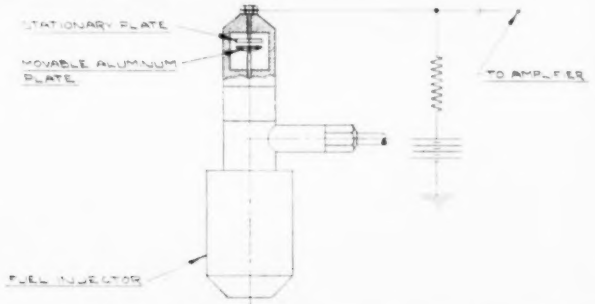


Fig. 21 Schematic Diagram of Fuel-Valve-Needle Lift Indicator

Sometimes information regarding the motion of the fuel-valve needle can be of great assistance in correcting the faults of a fuel-injection system. The simplest device for this purpose that has come to our attention is a small condenser mounted on the end of the fuel valve, Fig. 21. The plate is fixed and insulated from the fuel-valve body. The other plate is rigidly attached to the fuel-valve needle so that needle motion varies the distance between the two plates. A voltage is applied through a high resistance to the insulated plate which is connected to an amplifier having a high-impedance input circuit, the amplifier output going into an oscillograph. Since the capacity of a condenser varies inversely as the distance between the plates, and if current can be prevented from flowing in or out of the circuit, the voltage across a condenser varies inversely with the capacitance, then the voltage across the condenser will vary directly as the valve lift.

It has been found that these diagrams of fuel-valve-needle lift are very nearly proportional to the rate of fuel discharge through the valve, Fig. 22. This makes the fuel-valve lift indicator a very convenient tool for estimating fuel-discharge rate. It also has the advantage of showing differences in valve operation of successive cycles.

For the investigation of fuel-line pressure variations, a cathode-ray oscillograph using a piezoelectric pressure pickup may be used. The crystal pickup has the advantages of adding negligible volume to the fuel system and requiring minimum displacement for a given pressure indication. Its main disadvantage is its inability to register static pressures.

If it is necessary to obtain absolute values of pressure other

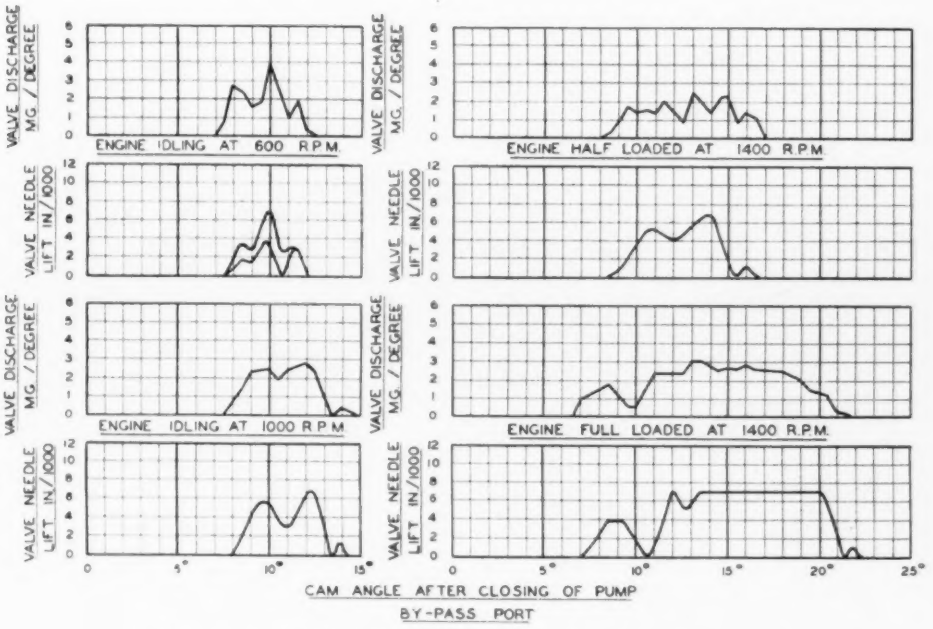


FIG. 22 FUEL-VALVE-NEEDLE LIFT AND RATE OF DISCHARGE

devices will have to be used. For the determination of residual fuel-line pressures a small lapped piston with a calibrated spring will give good results. The natural frequency of the spring-and-piston combination should be as high as is practical. A pin is fastened to the piston so that it extends outside the body of the instrument. The instantaneous displacement of the piston may be easily measured with a Brinnell microscope and a stroboscope. This device is hardly fast enough to register the rapid pressure variations which occur during injection, but is quite reliable for the measurement of residual pressure while the pump is not injecting fuel. The combination of these two instruments gives a very good picture of the pressures in a fuel line.

TEMPERATURES

It is desired to know the temperature at many points on a Diesel engine, and the use of thermometers and thermocouples for obtaining temperatures on stationary parts of the engine is well known. However, the determination of temperatures on movable parts such as pistons involves some difficulties. Two methods which have been used to determine piston temperature will be discussed; both use thermocouples to indicate the temperature. The problem lies in getting the reading out of the moving piston and into a stationary meter.

Fig. 23 shows a cable device for accomplishing this result. The cable consists of a strong central cord about which is wound spirally in a flat layer (1) one thermocouple wire, (2) a silk fish line of about the same diameter as the wire, (3) the second thermocouple wire, and (4) another fish line. Over this is wound a larger-diameter fly-line in the opposite direction, and the whole enameled in place. The cable is made of sufficient length to reach from the piston and out through the side of the crankcase. To support the cable, a linkage is provided which is pivoted on the wristpin and at a point on the crankcase, with a joint in between. This linkage is so designed as to reduce the bending of the cable to a minimum.

The second means of taking the reading out of the piston involves a set of contacts so located that the contacts are made at the bottom of the piston stroke. Fig. 24 shows one type of contact which has been used. This is an adaptation of a design developed at General Motors. Here, two small contact points, one for each thermocouple lead, are fastened to the piston. These slide into two stationary contact strips fastened to the crankcase. There is a slight spring action in the stationary contacts during the sliding. Contact is made for about 50 to 60 deg of crankshaft rotation at the bottom of the stroke. The con-

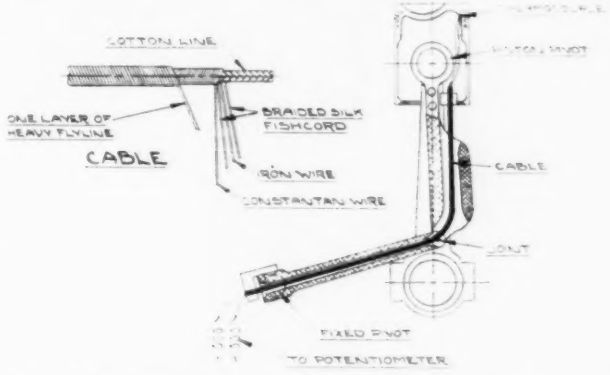


FIG. 23 SCHEMATIC DIAGRAM OF CABLE-TYPE PISTON-TEMPERATURE INDICATOR

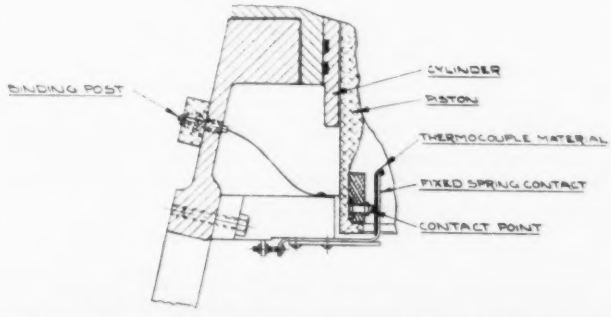


FIG. 24 SCHEMATIC DIAGRAM OF CONTACT-TYPE PISTON-TEMPERATURE PICKUP

tacts are covered with their respective thermocouple materials. The readings are taken with an ordinary potentiometer-type instrument. However, since the circuit is closed only about $^1/_6$ of the time, the sensitivity of the galvanometer is reduced. For this reason, it is desirable to substitute a more sensitive galvanometer for the standard instrument. If it is necessary that the contact be made for an even shorter period than this, it is possible

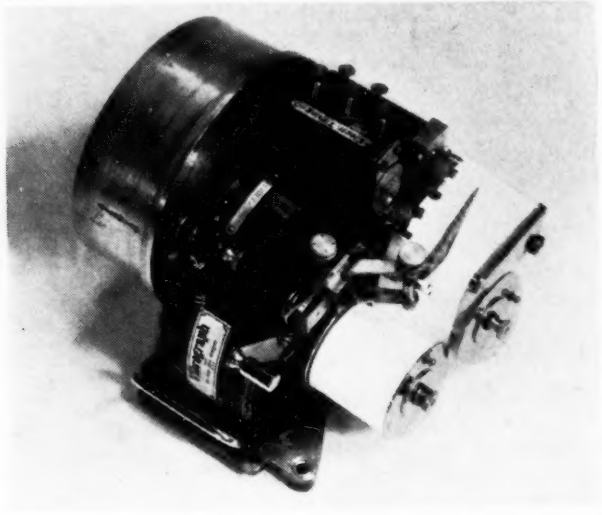


FIG. 25 GEIGER TORSIOGRAPH



FIG. 26 PIEZOELECTRIC VIBRATION PICKUP

to devise a circuit which will put in an adjustable compensating voltage during the open period of the contacts and to use an oscillograph to accomplish a balance between the thermocouple voltage and the compensating voltage.

VIBRATION

Instruments for measuring vibration, like those for pressures, may be divided into two types, mechanical and electrical. In both types there are two elements, i.e., the stationary or seismic part, and the moving part, which partakes of the motion of the vibrating body. It is then necessary to indicate the relative motion between the two parts. In the mechanical type there is a mechanical linkage between the two, which through a suitable lever system amplifies and indicates the relative motion.

Fig. 25 shows a Geiger torsiograph, used to indicate torsional vibration, which embodies these principles. A light aluminum pulley is driven from the engine crankshaft, usually by a belt, and partakes of the crankshaft motion. A relatively heavy flywheel rotates on the same shaft as the pulley and is driven from it through a light spring. The relative value of the mass and spring constant are such that the natural frequency of the system is quite low. This flywheel, then, is the seismic mass and attains the average velocity of the crankshaft. Between the pulley



FIG. 27 MAGNETIC-TYPE VIBRATION PICKUP

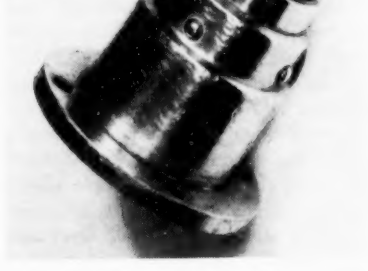


FIG. 28 MAGNETIC-TYPE TORSIONAL-VIBRATION PICKUP

and the flywheel there is a lever system, which amplifies any relative motion between the two and moves a recording pen across a moving tape driven by clockwork.

This instrument is most suitable for low-speed engines. With the older-type instruments, belt-driven, the results are questionable above a vibration frequency of 3000 cycles per min. With the most recent design, it is claimed to be good up to 5000 cycles per min.

In general, the electrical vibration pickups are of the same basic principles as the electric pressure pickups, and they can be classified into the same five general types, i.e., resistance, magnetic, condenser, piezoelectric, and photoelectric. A few of the most important commercially available types will be discussed.

Fig. 26 shows a piezoelectric vibration pickup. The prod on the case is held directly against the vibrating body, or the case may be fastened directly to the vibrating body. Inside the case is a Rochelle-salt crystal, supported at one edge. This type of mounting gives an inertia loading of the crystal; so the output of the pickup is proportional to the vibration acceleration. This output may be integrated to give the vibration velocity, or integrated twice to give the displacement. In the last case, unless the vibration is rather severe, there is apt to be not a great deal left of the output after two integrations. The output of this pickup is affected by temperature; in engine work, this fact may cause difficulties.

Fig. 27 shows a magnetic-type pickup for linear vibration. In this instance, the case is intended to be held stationary and the prod partakes of the motion of the vibrating body. The case contains a permanent magnet, while the prod actuates a small coil which is supported by light springs in the case. The movement of the coil in the magnetic field produces a voltage proportional to the vibration velocity. If displacement is desired, the output may be integrated once. To give linear response at low frequencies, the natural frequency of the coil assembly must be low. The pickup illustrated is supposed to be good down to 10 cycles per sec.

Fig. 28 shows a torsional-vibration pickup of the magnetic type. It is of the same fundamental principle as the linear magnetic-type pickup, but differs in the detailed construction. The case fastens directly onto the crankshaft and partakes of its motion. A permanent magnet is supported on a concentric shaft within the case, and acts as the seismic mass. The magnetic attraction of the magnet and pole pieces in the case act as the weak spring to drive the magnet mass. The coils are fastened in the case. The output is taken out through a brush in the center of the case. The output of this unit is again proportional to the vibration velocity, and if the displacement is desired, it must be integrated. This unit has been found very suitable for medium- and high-speed engines.

A resistance-type instrument, which is generally used as a strain gage, but may be used to indicate vibration, consists of a fine wire of special alloy embedded in a thin plastic. When fastened to a part that is strained, the slight elongation of the wire changes its resistance. By incorporating this in a suitable circuit the actual displacements may be indicated.

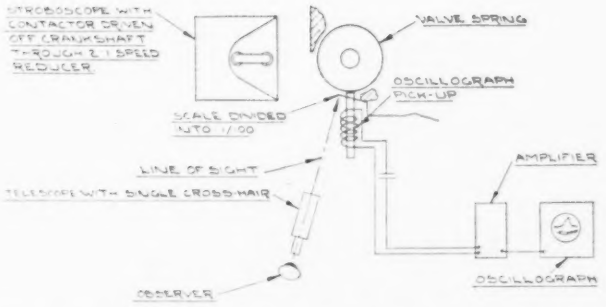


FIG. 29 SCHEMATIC DIAGRAM OF SETUP USED TO STUDY VALVE-SPRING SURGE

All of these electric vibration pickups require the same amplifiers and indicating means, such as the oscillographs discussed under the electric pressure pickups. However, if an average value of the magnitude of the vibration is all that is desired, an output meter may be substituted for the oscillograph. We generally use the oscillograph though, as it gives us more information, showing not only magnitude, but also frequency and wave form. It is also possible to determine phase angles with the oscillograph.

A setup to study the particular problem of valve-spring surge is illustrated in Fig. 29. In order to be able to pick out resonant speeds easily, a magnetic-type pickup was located close to the center of the valve spring. This was a very simple unit consisting only of a small permanent bar magnet, with a coil of wire wound around it. The output of this was amplified and indicated on a cathode-ray oscillograph. By watching the diagram on the screen of the oscillograph, it was very easy to pick out critical speeds. To measure actual displacements of the valve-spring vibration, a scale was set alongside the valve spring, and a stroboscopic light timed by the engine itself was flashed on the spring and scale. The crank angle at which the light flashed was under the control of the observer, who, looking through a telescope at the spring and scale, could pick out the point of maximum displacement and read it on the scale.

CONCLUSION

Undoubtedly, there are a great number of instruments of inestimable value, which have not been mentioned here. However, since the methods of developing Diesel engines are continually in a state of flux, we have thought it prudent to confine these observations to instrumentation in everyday use in one particular laboratory.

Internal-Combustion-Engine Casualty Experience

By H. J. VANDER EB,[1] HARTFORD, CONN.

THIS paper is based on a survey of accidental breakdowns of oil and gas engines, experienced by The Hartford Steam Boiler Inspection and Insurance Company during the years 1938, 1939, and 1940. The company specializes in power-plant insurance and breakdown prevention, and covers the great majority of insured oil and gas engines. It is hoped that the compilation of accident data in the tables may contribute in some degree toward efforts to lower the accident frequency on internal-combustion engines and thus further improve their reliability.

The three-year experience of 413 accidents compiled in Table 1 covers approximately 1450 engine-years.

Of the 413 accidental breakdowns, 65 were on gas and gasoline engines, 167 on two-stroke-cycle oil engines, and 181 on four-stroke-cycle oil engines. The total amount of losses in these accidental breakdowns was $142,400.

Table 2 is an analysis by type of accident with respect to the "initial part broken or damaged." In the summation of the "initial part broken" in Table 2, the actual number of such parts involved in each accident was not used. Instead of this, the numbers of the various items in Table 2 are the number of accidental-breakdown cases in which the "initial part broken" was the principal source of the trouble. For instance, the number opposite "main bearing" is the number of cases where one or more main bearings failed.

There has been a gradual improvement in the accident frequency during the last several years. It will be noted from the totals in Table 2 that the number of accidents decreased from year to year.

Table 3 gives the accident frequencies for 10 years. The figures in this table, such as 1:2.3, mean that there was one accidental breakdown for each 2.3 engines during the year.

As a comparison, it may be stated that for steam engines the accident frequency is about 1:11.

An accident to an internal-combustion engine is defined in the insurance policy as follows:

> Accident shall mean a sudden and accidental breaking, deforming, burning out, or rupturing of the object or any part thereof, which manifests itself at the time of its occurrence by immediately preventing continued operation or by immediately impairing the functions of the object and which necessitates repair or replacement before its operation can be resumed or its functions restored, but the breaking, deforming, burning, or rupturing of any exhaust valve, valve spring, gasket, or gland packing shall not constitute an accident, nor shall the depletion of material in any part of the object, due to pitting, corrosion, or wear, be construed as an accident.

From this definition it will be noted that any sudden breakdowns of the engine or its parts (with minor exceptions) are covered by insurance. It is not the intention to cover defects that are found by inspection, such as slow progressive cracks, although the affected part might, at that time or later, need replacement, or any troubles that are clearly of a maintenance character.

Referring to Table 2, the crankshaft breakdown cases are 2.2 per cent of the total number of accidents. This is quite favorable as compared with previous experience. During 1940 not a single crankshaft case occurred which is a record. This favorable crankshaft experience is, undoubtedly, to a large extent, the result of painstaking inspection by means of a strain gage designed by the company.

The bearing troubles, 31 per cent of the total, run fairly true to previous experience. For many years, the bearing-failure accidents in internal-combustion engines have roughly amounted to one in every three accidents. Practically, no improvement can be reported. The principal causes of bearing failures were improper attention to the lubricating systems and unduly rapid sludging of the oil. Overloading also appears to have been a considerable factor in the bearing failures. More than half of the bearing failures were on crank bearings.

The cases of cylinder heads, cylinders, and cylinder liners combined, amounted to 21.8 per cent of the total. This is a somewhat lower ratio than it has been formerly. The last previous survey showed 24.3 per cent for the combined cases of cylinder heads, cylinders, and cylinder liners. Also the piston cases, 14 per cent, are fewer as compared with previous accident surveys. The fuel-pump and spray-nozzle cases, 5.4 per cent, are slightly higher than formerly.

The connecting-rod and crank-bolt accidents, 1.9 per cent, are well below previous averages. In miscellaneous accidents, 13.5 per cent of the total, are included camshafts, gears, rocker arms, valves, flywheels, clutches, water pumps, and also such parts as give trouble very rarely.

A careful review of all the experience has clearly brought out the advantages of the dual-circuit type of closed cooling system as compared with the various types of open cooling systems. A much lower premium is charged (about 40 per cent less) for insuring engines with closed systems than for engines with open cooling systems. These lower premium rates have been in use for five years and the result has been that the ratio between numbers of insured engines with closed systems and those with open systems has changed, during the last three years alone, from 50–50 to 65–35.

This change to closed systems has been a big factor in the improved accidental-breakdown experience.

---

[1] Assistant Chief Engineer, Turbine and Engine Division, The Hartford Steam Boiler Inspection & Insurance Co.

Presented at the National Meeting of the Oil and Gas Power Division, Kansas City, Mo., June 11–14, 1941, of THE AMERICAN SOCIETY OF MECHANICAL ENGINEERS.

NOTE: Statements and opinions advanced in papers are to be understood as individual expressions of their authors and not those of the Society.

TABLE 1 INTERNAL-COMBUSTION-ENGINE ACCIDENTS

D-2-C.Sc. = Diesel, 2 cycle, crank case scavenging
SD-2-C.Sc. = Semi Diesel, 2 cycle, crank case scavenging
D-2 P.Sc. = Diesel, 2 cycle, pump or blower scavenging
D-4 = Diesel, 4 cycle
G-4 = Gas, 4 cycle
O = Open cooling system
Cl = Closed cooling system

An * after cost of damage denotes that indirect damage is included.

1938 No.	Rated Capacity Bhp.	Cylinder Bore, In.	TYPE	Rated Speed Rpm	Year Built	Type of Cooling System	Part that Failed	Cause	Cost of damage
1	165	13 1/2	G-4	277	'27	O	Piston	Valve dropped in	$ 190.
2	120	14	D-2-C.Sc.	257	'22	O	Crankshaft	Misalignment	1,626.*
3	120	13 1/4	D-4	277	'27	O	Intermediate gear	Foreign object	62.
4	240	14	D-2-C.Sc.	257	'26	O	Crank bearing	Oil supply plugged	48.
5	40	4 1/2	D-4	1200	'37	Cl	Lubricating oil pump	Fatigue failure	82.
6	400	11 1/2	D-4	400	'37	Cl	Crank bearing	Oil line plugged	99.
7	33	4 1/4	D-4	1200	'36	Cl	Intermediate gear	Undetermined	30.
8	40	12	D-4	100	'20	Cl	Crank bearing	Oil passage plugged	59.
9	400	16 1/2	D-4	200	'18	Cl	Main bearing	Oil ring stuck	405.*
10	400	16 1/2	D-4	200	'18	Cl	Main bearing	Improper oil ring	405.*
11	180	14	D-2-C.Sc.	257	'25	O	Crankshaft	Misalignment	3,435.*
12	230	17	D-4	200	'36	Cl	Main bearing	Babbitt cracked	193.
13	200	9	D-4	527	'34	Cl	Circulating pump	Fatigue failure	73.
14	165	13 1/2	G-4	277	'29	O	Pistons	Overload	105.
15	110	12	D-2-C.Sc.	360	'35	O	Rocker arm	Starting lever loose	58.
16	100	14	SD-2-C.Sc.	257	'20	O	Cyl. heads	Water pump stopped	281.
17	420	14	D-2-C.Sc.	300	'34	Cl	Wristpin bearing	Overload	91.
18	420	14	D-2-C.Sc.	300	'34	Cl	Wristpin bearing	Overload	161.
19	420	14	D-2-C.Sc.	300	'34	Cl	Wristpin bearing	Overload	222.
20	240	14	D-2-C.Sc.	257	'26	O	Crank bearing	Improper fit	46.
21	250	14	G-4	250	'21	Cl	Cylinder	Preignition	1,171.*
22	12	5	D-4	720	'37	Cl	Cylinder jacket	Frost	51.
23	420	14	D-2-C.Sc.	300	'34	O	Piston seized	Overloading	347.
24	420	14	D-2-C.Sc.	300	'34	O	Wristpin bearing	Overloading	88.
25	400	11 1/2	D-4	400	'37	Cl	Exhaust Manifold	Improper cooling	187.
26	120	10	D-2-C.Sc.	360	'26	O	Crankshaft	Misalignment	2,996.*
27	165	8	G-4	630	'37	Cl	Bearing studs	Undetermined	8.
28	100	14	SD-2-C.Sc.	257	'24	O	Wristpin bearing	Oil passage clogged	39.
29	33	4 1/4	D-4	1200	'36	Cl	All bearings	Inattention	307.
30	33	4 1/4	D-4	1200	'35	Cl	Starting engine	Preignition	119.
31	100	14	SD-2-C.Sc.	257	'24	O	Wristpin bearing	Improper fit	213.
32	240	14	D-2-C.Sc.	257	'26	O	Piston seized	Overloading	602.*
33	250	14	G-4	257	'24	Cl	Cylinder head	Overloading	110.
34	240	14	D-2-C.Sc.	257	'26	O	Crank bearing	Improper fit	73.
35	100	12 1/2	D-2-C.Sc.	260	'30	O	Air Camshaft	Fatigue failure	21.
36	230	17	G-4	200	'36	Cl	Piston rod	Seized compressor piston	197.
37	450	12 1/2	D-4	360	'35	O	Cylinder head	Insufficient water circuit	176.
38	35	8 3/4	G-4	400	'26	O	Connecting rod	Defective Material	195.
39	112 1/2	9 1/2	D-4	400	'33	Cl	Exhaust manifold	Improper Assembly	150.
40	240	14	D-2-C.Sc.	257	'26	O	Wristpin bearing	Overload	397.*
41	30	3 1/4	G-4	900	'28	O	Cylinder block	Scale in jacket	35.
42	165	12	G-4	257	'29	Cl	Inlet valve	Fatigue failure	19.
43	60	14	D-4	225	'18	O	Cylinder	Scale in jacket	598.
44	450	14	D-4	257	'31	Cl	Crank bearing	Oil passage clogged	245.
45	25	8 1/2	D-4	300	'24	O	Crank bearing	Oil line plugged	35.
46	165	8	G-4	630	'37	O	Cylinder head	Insufficient water circulation	84.
47	165	8	G-4	630	'37	O	Cylinder head	Insufficient water circulation	153.
48	1140	22	D-4	220	'34	Cl	Cylinder liner	Undetermined	543.
49	60	4 1/2	D-4	1000	'34	O	Crank bearing	Oil line plugged	180.
50	100	10	G-4	225	'28	Cl	Crank bearing	Oil line broken	17.
51	400	13 1/4	D-4	327	'35	Cl	Piston seized	Faulty cooling system	482.
52	240	14	D-2-C.Sc.	257	'27	Cl	Crank bearing	Overloading	80.
53	90	16	D-4	200	'23	O	Crank bearing	Babbitt cracked	244.*
54	200	9	D-4	527	'34	O	Cylinder block	Preignition	1,560.*
55	240	14	D-2-C.3c.	257	'27	Cl	Wristpin bearing	Oil passage closed	80.
56	163	14	SD-2-C.Sc.	257	'16	Cl	Piston	Improper fit	101.
57	450	12 1/2	D-4	360	'35	Cl	Cylinder	Insufficient water circulation	265.
58	110	12	D-2-C.Sc.	360	'35	Cl	Crank bearing	Oil line clogged	85.
59	85	16 3/8	D-4	250	'25	O	Cylinder	Scale in jacket	355.
60	140	11 3/4	D-4	327	'36	O	Crankshaft	Torsional vibration	3,377.
61	400	11 1/2	D-4	440	'37	Cl	Crank bearing	Inattention	101.
62	100	7 1/8	D-4	514	'36	O	Piston	Scale in jacket	239.
63	110	12	D-2-C.Sc.	360	'35	Cl	Wristpin bearing	Overloading	477.
64	240	14	D-2-C.Sc.	257	'27	Cl	Wristpin bearing	Oil passage clogged	88.
65	120	9	D-4	514	'36	Cl	Governor	Excessive wear	16.
66	18	4 1/2	D-4	1200	'33	Cl	Camshaft gear	Defective material	32.
67	60	6 1/2	D-4	720	'34	Cl	Crank bearing	Sludge	60.*
68	110	12	D-2-C.Sc.	360	'34	O	Piston seized	Mud in jackets	1,651.*
69	60	4 1/4	D-4	1200	'36	O	Governor	Ball bearing	15.
70	180	12	D-2-C.Sc.	360	'36	Cl	Main bearing	Oil ring stuck	98.
71	100	14	SD-2-C.Sc.	257	'24	O	Wristpin bearing	Oil passage clogged	289.
72	125	17 1/2	D-4	150	'14	O	Crosshead bolts	Fatigue failure	65.

TABLE 1 INTERNAL-COMBUSTION-ENGINE ACCIDENTS (*Continued*)

1938 No.	Rated Capacity Bhp.	Cylinder Bore, In.	TYPE	Rated Speed Rpm	Year Built	Type of Cooling System	Part that Failed	CAUSE	Cost of Damage
73	55	7 1/4	D-4	475	'29	O	Crankbolt	Fatigue failure	680.
74	60	8	D-4	400	'34	O	Camshaft	Undetermined	137.
75	240	14	D-2-C.Sc.	257	'27	C1	Cylinder head	Undetermined	138.
76	150	14	D-2-C.Sc.	300	'36	C1	Lubricating oil pump	Undetermined	18.
77	140	14	D-2-C.Sc.	300	'34	C1	Crank bearing	Oil line clogged	89.
78	180	14	D-2-C.Sc.	257	'29	O	Cylinder head	Scale in jackets	75.
79	60	4 1/4	D-4	1200	'35	O	Crank bearing	Lubricating oil pump leak	88.
80	100	14	SD-2-C.Sc.	257	'22	O	Piston	Oil line clogged	235.
81	240	14	D-2-C.Sc.	257	'27	C1	Cylinder head	Undetermined	137.
82	90	6 3/4	G-4	720	'34	C1	Crankbolts	Fatigue failure	792.*
83	200	13 1/4	D-4	327	'33	C1	Liner gasket	Neglect	64.
84	400	16 1/2	D-4	200	'18	C1	Wristpin bearing	Improper assembly	701.*
85	120	14	D-2-C.Sc.	257	'25	O	Wristpin bearing	Overload	135.
86	100	11	D-4	320	'32	O	Cylinder head	Scale in jackets	81.
87	120	14	D-2-C.Sc.	257	'25	O	Wristpin bearing	Overload	201.
88	100	18 1/2	SD-2-C.Sc.	225	'26	O	Flywheel hub	Preignition	586.
89	100	14	SD-2-C.Sc.	257	'17	O	Wristpin bearing	Misalignment	237.
90	165	8	D-4	825	'30	C1	Cylinder heads	Insufficient water circulation	212.*
91	120	13	SD-2-C.Sc.	400	'31	O	Crank bearing	Lubricator failed	75.
92	400	11 1/2	G-4	440	'37	C1	Piston	Defective Material	198.
93	120	14	D-2-C.Sc.	257	'26	C1	Crankcase cover	To stop overspeed	15.
94	900	17	D-4	225	'29	C1	Governor	Excessive wear	369.
95	120	14	D-2-C.Sc.	257	'25	O	Crankshaft	Misalignment	1,894.
96	110	8	G-4	440	'23	C1	Flywheel hub	Preignition	171.
97	160	12 3/4	G-4	300	'22	C1	Cylinder head	Undetermined	187.
98	160	12 3/4	G-4	300	'22	C1	Crank bearing	Improper adjustment	38.
99	150	8 1/4	G-4	550	'33	C1	Exhaust manifold	Overheating	54.
100	350	16 1/2	G-4	288	'38	O	Crank bearing	Sludge	48.
101	200	14	D-2-C.Sc.	277	'28	C1	Crank bearing	Improper adjustment	191.
102	135	12 1/2	SD-2-C.Sc.	250	'23	C1	Cylinder head	Undetermined	113.
103	100	14	SD-2-C.Sc.	257	'17	O	Crank bearing	Improper adjustment	56.
104	160	12 3/4	G-4	300	'22	C1	Cylinder head	Overheating	187.
105	100	14	SD-2-C.Sc.	257	'17	O	Crank bearing	Improper adjustment	53.
106	150	8	G-4	550	'33	C1	Rocker arm	Valve stuck	7.
107	120	14	D-2-C.Sc.	257	'26	C1	Main bearing	Oil ring stuck	85.
108	125	17 1/2	D-4	150	'14	O	Distance piece	Scale accumulation	226.*
109	85	12 1/2	SD-2-C.Sc.	300	'34	C1	Connecting rod	Improperly adjusted	166.
110	135	12 1/2	SD-2-C.Sc.	250	'23	C1	Governor	Undetermined	24.
111	200	10	D-4	514	'36	C1	Crankbolt	Loosening of nut	539.
112	100	14	SD-2-C.Sc.	257	'20	O	Cylinder head	Carelessness	73.
113	100	14	SD-2-C.Sc.	257	'20	O	Cylinder head	Carelessness	73.
114	120	14	D-2-C.Sc.	257	'26	O	Cylinder head	Overloading	115.
115	350	18	G-4	225	'17	C1	Piston	Lubricating oil line closed	677.
116	120	14	D-2-C.Sc.	257	'23	O	Cylinder head	Scale in jackets	67.
117	120	14	D-2-C.Sc.	257	'26	C1	Airvalve	Stuck open	8.
118	160	12 3/4	G-4	300	'22	C1	Crank bearing	Water in oil	34.
119	210	14	D-2-C.Sc.	300	'31	O	Cylinder cracked	Scale in jackets	386.
120	120	14	D-2-C.Sc.	257	'26	O	Cylinder head	Overload	127.
121	120	14	D-2-C.Sc.	257	'25	O	Piston	Overload	201.
122	120	14	D-2-C.Sc.	257	'26	O	Cylinder head	Overload	218.
123	290	10	D-4	600	'38	C1	All bearings	Oil pump stopped	1,406.*
124	180	14	D-2-C.Sc.	257	'26	O	Cylinder heads	Overload	218.
125	210	14	D-2-C.Sc.	300	'31	O	Piston	Overheating	304.
126	120	14	D-2-C.Sc.	257	'26	O	Cylinder head	Overload	176.
127	120	14	D-2-C.Sc.	257	'24	O	Cylinder head	Improper cooling	67.
128	200	9 1/2	D-4	400	'36	C1	Main bearing	Oil pump lost prime	54.
129	120	14	D-2-C.Sc.	257	'26	O	Cylinder heads	Overload	199.
130	115	9 1/4	D-4	400	'36	O	Cylinder head	Airbound jacket	170.
131	400	11 1/2	G-4	420	'36	O	Exhaust manifold	Circulating pump stopped	626.*
132	180	12 1/2	D-2-C.Sc.	257	'35	O	Cylinder head	Carelessness	69.
133	42	4 1/2	D-4	1200	'37	O	Exhaust manifold	Sudden cooling	45.
134	42	4 1/2	D-4	1200	'37	O	Cam	Fatigue failure	26.
135	400	13 1/4	D-4	327	'35	C1	Piston seized	Faulty cooling system	344.
136	75	4 1/2	D-4	1200	'38	C1	Oil cooler	Undetermined	22.
137	83	3 3/4	D-4	2600	'37	C1	Clutch	Fatigue failure	29.
138	30	10 1/2	SD-2-C.Sc.	400	'34	C1	Cylinder head	Overloading	183.
139	500	16 1/4	D-4	225	'30	C1	Air cylinder jacket	Air coil rupture	756.
140	80	9	D-4	400	'36	O	Cylinder head	Defective material	523.*
141	180	14	D-2-C.Sc.	257	'26	O	Cylinder head	Improper cooling system	187.
142	450	12 1/2	D-4	360	'35	C1	Cylinder head	Insufficient circulation	179.
143	150	14	SD-2-C.Sc.	257	'38	C1	Crank bearing	Improper repair	128.
144	120	14	D-2-C.Sc.	257	'27	O	Main bearing	Oil line clogged	451.
145	60	4 1/4	D-4	1200	'36	O	Cylinder head	Overheating	38.
1939									
1	100	17 1/2	D-4	200	'16	O	Crank bearing	Oil contaminated	$ 138.*
2	180	14	D-2-C.Sc.	257	'35	O	Crank bearing	Oil contaminated	220.*
3	280	14	D-2-C.Sc.	300	'32	O	Wrist pin bearing	Improper adjustment	94.
4	150	14	SD-2-C.Sc.	257	'16	C1	Crankshaft	Misalignment	1,079.
5	125	5 3/4	D-4	850	'38	C1	Water pump	Loosening of parts	6.
6	150	8 1/2	D-4	400	'29	O	Intermediate gear	Fatigue failure	58.

TABLE 1 INTERNAL-COMBUSTION-ENGINE ACCIDENTS (*Continued*)

1939 No.	Rated Capacity Bhp.	Cylinder Bore, In.	Type	Rated Speed Rpm	Year Built	Type of Cooling System	Part that Failed	Cause	Cost of Damage
7	100	14	SD-2-C.Sc.	257	'15	O	Wristpin bearing	Inattention	291.
8	120	14	D-2-C.Sc.	257	'26	O	Cylinder head	Scale in jackets	133.
9	450	14	D-4	257	'27	Cl	Piston seized	Water leakage	664.
10	100	4 1/2	D-4	1200	'36	Cl	Governor	Fatigue crack	97.*
11	110	12	D-2-C.Sc.	360	'35	Cl	Wristpin bearing	Oil contaminated	380.
12	80	12	D-2-C.Sc.	300	'30	Cl	Cylinder heads	Water valves closed	170.
13	240	14	D-2-C.Sc.	257	'27	Cl	Cylinder head	Previous cooling system	49.
14	60	10 1/2	SD-2-C.Sc.	400	'23	Cl	Piston	Overloading	832.
15	420	14	D-2-C.Sc.	300	'34	Cl	Piston seized	Metal spray flaked	241.
16	60	10 1/2	SD-2-C.Sc.	400	'23	Cl	Crankbearing	Overloading	513.
17	225	9 1/2	D-4	400	'36	O	Pistons	Overloading	918.*
18	115	9 1/4	D-4	400	'36	O	Cylinder head	Jacket Airbound	163.
19	10	5	D-4	720	'35	Cl	Rocker arm	Improper adjustment	70.
20	100	6	G-4	900	'37	Cl	Piston	Air in cooling system	144.
21	100	5 1/4	D-4	1200	'35	Cl	Crank bearing	Inattention	75.
22	1480	14	D-4	277	'37	Cl	Lubricating oil pump	Oil contaminated	538.
23	100	5 1/4	D-4	1200	'35	Cl	Crank bearing	Inattention	158.
24	120	9	G-4	514	'36	Cl	Governor spring	Fatigue failure	12.
25	110	9 1/4	D-4	300	'36	O	Cylinder head	Jacket airbound	70.
26	500	22	D-4	225	'30	Cl	Valve stems	Design	44.
27	40	4 1/4	D-4	1200	'36	Cl	Crank bolts	Fatigue failure	843.
28	60	4 1/4	D-4	1200	'36	O	Camshaft	Jamming	148.
29	180	14	D-2-C.Sc.	257	'29	O	Piston seized	Growth of cylinder wall	257.
30	450	14	D-4	257	'27	Cl	Cylinder head	Previous cooling system	93.
31	750	17	D-2-P.Sc.	277	'21	O	Piston	Loosening of parts	694.
32	365	11 1/2	D-4	400	'36	Cl	Crank bearing	Oil contamination	61.
33	60	14 1/4	SD-2-C.Sc.	300	'34	Cl	Ball bearing	Improper repair	9.
34	90	16	D-4	200	'16	O	Crankbearing	Improper adjustment	101.
35	319	11 1/2	G-4	420	'37	O	Piston scored	Mud in jackets	451.*
36	420	14	D-2-C.Sc.	300	'34	Cl	Governor	Fatigue failure	89.
37	200	14	D-2-C.Sc.	277	'27	Cl	Crankbearing	Defective Material	124.
38	400	11 1/2	D-G-4	400	'37	Cl	Fuel pump	Faulty lubrication	78.
39	100	13 1/4	D-2-C.Sc.	300	'35	Cl	Piston	Heat Cracks	189.
40	420	14	D-2-C.Sc.	300	'34	Cl	Pistons seized	Improper repair	18,966.*
41	185	14 5/8	D-2-C.Sc.	260	'27	Cl	Wristpin bearing	Overloading	4,004.*
42	1000	17 1/2	D-4	260	'35	Cl	Idler gear	Vibration	771.*
43	560	17	D-4	225	'26	O	Injector valve	Exploded	166.
44	600	17 3/4	D-4	240	'28	Cl	Lubricating oil pump	Defective material	192.
45	75	4 1/2	D-4	1200	'36	Cl	Governor shaft	Loosening of parts	120.
46	180	14	D-2-C.Sc.	257	'28	O	Main bearings	Oil contaminated	558.
47	400	15	D-4	300	'34	Cl	Spray valve	Fatigue failure	41.
48	400	11 1/2	D-G-4	400	'37	Cl	Fuel pump	Faulty lubrication	86.
49	120	8	G-4	475	'37	Cl	Oil line	Vibration	23.
50	210	14	D-2-C.Sc.	300	'35	Cl	Wristpin bearing	Oil line plugged	627.*
51	120	7	D-4	600	'32	Cl	Cylinder head	Overheating	96.
52	115	9 1/4	D-4	400	'36	O	Cylinder head	Jacket airbound	145.
53	400	11 1/2	G-4	400	'37	Cl	Fuel pump	Faulty lubrication	45.
54	120	14	D-2-C.Sc.	257	'26	O	Wristpin bearing	Overloading	378.
55	460	10	D-4	600	'37	Cl	Lubricating oil pump	Defective material	192.
56	1480	14	D-4	277	'37	Cl	Governor shaft	Fatigue failure	24.
57	600	17 3/4	D-4	240	'28	O	Piston	Overloading	906.
58	210	14	D-2-C.Sc.	257	'34	Cl	Wrist pin bearing	Improper adjustment	21.
59	60	14	D-2-C.Sc.	257	'29	O	Crankbearing	Oil contaminated	133.*
60	100	6	G-4	900	'37	Cl	Timing gears	Defective material	71.
61	85	8 1/2	D-4	375	'29	O	Fuel pump	Improper repair	13.
62	150	7 1/2	G-4	720	'29	Cl	Piston scored	Defective material	42.
63	150	7 1/2	G-4	720	'29	Cl	Piston scored	Improper repair	50.
64	120	14	D-2-C.Sc.	257	'30	O	Cylinder	Warping	384.
65	60	14 1/4	D-2-C.Sc.	300	'33	Cl	Ball bearing	Defective material	59.
66	300	17	D-4	145	'24	O	Piston	Defective material	318.
67	75	13 1/2	D-4	285	'28	O	Compressor shaft	Torsional crack	229.
68	35	6 3/8	G-4	405	'24	O	Main bearings	Faulty lubrication	491.
69	150	7 1/2	G-4	720	'29	Cl	Governor gears	Vibration	45.
70	400	15	D-4	300	'34	Cl	Cylinder liner	Undertermined	320.
71	100	4 1/4	D-4	1200	'36	Cl	Idler gear	Loosening of parts	186.*
72	365	11 1/2	D-4	400	'36	Cl	Crank bearing	Defective material	135.
73	125	5 1/2	D-4	1400	'35	Cl	Cylinder block	Inattention	111.
74	1000	17 1/2	D-4	260	'35	Cl	Piston seized	Improper adjustment	890.
75	460	10	D-4	600	'37	Cl	Main bearings	Inattention	673.
76	150	9 1/2	D-4	330	'27	Cl	Crank bearing	Failure of oil pump	150.*
77	150	9 1/2	D-4	330	'27	Cl	Crank bearing	Improper fit	26.
78	150	7 1/2	G-4	720	'29	Cl	Governor gears	Undetermined	36.
79	400	11 1/2	D-G-4	400	'37	Cl	Fuel pump drive	Undetermined	71.
80	165	14	D-2-C.Sc.	257	'21	Cl	Crankbearing	Oil contamination	79.
81	120	7 1/2	G-4	720	'29	Cl	Inlet valve	Improper adjustment	91.
82	120	7 1/2	G-4	720	'29	Cl	Inlet valve	Improper adjustment	50.
83	2250	21	D-2-P.Sc.	225	'37	Cl	Piston cracked	Undetermined	270.
84	400	11 1/2	D-G-4	400	'37	Cl	Piston	Defective material	62.
85	250	16	G-4	257	'21	Cl	Connecting rod	Fatigue failure	2,759.*
86	160	12 3/4	G-4	300	'22	Cl	Main bearing	Defective material	31.

TABLE 1 INTERNAL-COMBUSTION-ENGINE ACCIDENTS (*Continued*)

1939 No.	Rated Capacity Bhp.	Cylinder Bore In.	Type	Rated Speed Rpm	Year Built	Type of Cooling System	Part that Failed	Cause	Cost of Damage
87	140	14	D-2-C.Sc.	300	'34	C1	Wristpin bearing	Clogged oil passage	202.
88	375	14	D-2-C.Sc.	300	'37	C1	Crankbearing	Oil line clogged	50.
89	180	12	D-2-C.Sc.	360	'38	C1	Piston ring	Undertermined	3.
90	140	11 1/2	D-4	300	'35	O	Oil line	Vibration	108.
91	225	7	D-4	900	'39	C1	Main bearings	Insufficient oil cooling	908.*
92	600	13 1/4	D-4	300	'38	C1	Piston seized	Improper adjustment	541.*
93	800	14	D-4	300	'37	C1	Cylinder head	Undetermined	251.
94	360	14	D-2-C.Sc.	257	'28	C1	Piston seized	Overload	670.
95	120	12	D-2-C.Sc.	360	'38	C1	Cylinder	Defective casting	94.
96	1400	16	D-2-P.Sc.	300	'36	C1	Cylinder head	Defective casting	188.*
97	100	14	D-2-C.Sc.	257	'28	C1	Crank bearing	Overload	40.
98	180	14	D-2-C.Sc.	257	'25	C1	Crank bearing	Improper adjustment	144.
99	2250	21	D-2-P.Sc.	225	'37	C1	Cylinder heads	Design	542.
100	2250	21	D-2-P.Sc.	225	'37	C1	Piston cracked	Undetermined	193.
101	750	17	D-4	227	'31	C1	Piston seized	Lubricating oil pump failed	1,090.
102	2250	21	D-2-P.Sc.	225	'37	C1	Piston cracked	Undetermined	54.
103	10	5	D-4	720	'37	C1	Rocker arm	Design	8.
104	350	18	G-4	225	'17	C1	Rocker arm	Undetermined	88.
105	400	11 1/2	G-4	400	'37	C1	Exhaust valve seat	Undetermined	146.
106	400	11 1/2	G-4	400	'37	C1	Exhaust valve	Undetermined	165.
107	45	11	SD-2-C.Sc.	350	'33	O	Combustion chamber	Improper fuel	80.
108	262	9 1/2	D-4	410	'37	O	Piston	Inattention	151.
109	1140	22	D-4	220	'31	C1	Cylinder liner	Undetermined	200.
110	75	4 1/2	D-4	1200	'36	C1	Fuel pump gear	Loosening of parts	71.
111	375	14	D-2-C.Sc.	300	'37	C1	Fuel pump	Jammed	85.
112	365	11 1/2	D-4	375	'36	C1	Valve cage	Improper adjustment	6.
113	100	12 1/4	D-2-C.Sc.	327	'24	O	Fuel pump	Jammed	6.
114	200	14	SD-2-C.Sc.	257	'23	O	Crank bearing	Inattention	39.
115	400	15	D-4	300	'34	C1	Cylinder liner	Undetermined	310.
116	319	11 1/2	G-4	420	'37	C1	Cylinder heads	Faulty cooling	882.*
117	150	14	SD-2-C.Sc.	257	'18	C1	Crank bearing	Improper fit	39.
118	150	9	D-4	590	'37	O	Exhaust manifold	Mud accumulation	237.
119	180	12	D-2-C.Sc.	360	'38	C1	Wristpin bearing	Improper fit	210.
120	40	4 1/4	D-4	1200	'35	O	Crank bearing	Improper fit	308.
121	165	14	D-2-S.Sc.	257	'21	C1	Crankshaft	Misalignment	2,154.
122	45	4 1/4	D-2-P.Sc.	1200	'39	C1	Piston rings	Sludge in oil	62.
123	1140	22	D-4	220	'31	C1	Cylinder liner	Undetermined	178.
124	100	12	D-2-C.Sc.	360	'28	C1	Crank bearing	Inattention	36.
125	200	14	D-2-C.Sc.	277	'27	C1	Cylinder head	Overloading	70.
126	80	9	G-4	300	'37	C1	Magneto frame	Improper adjustment	19.
127	120	13 1/4	D-4	277	'27	O	Idler gear	Vibration	121.
128	100	4 1/2	D-4	1200	'36	C1	Governor shaft	Fatigue crack	128.
129	100	4 1/2	D-4	1200	'36	C1	Fuel pump gear	Undetermined	81.*
130	50	4 3/4	D-4	1200	'37	C1	All bearings	Inattention	139.
131	1140	22	D-4	200	'31	C1	Cylinder liner	Undetermined	178.
132	400	11 1/2	G-4	400	'36	C1	Exhaust manifold	Faulty cooling	24.
133	400	11 1/2	G-4	400	'36	C1	Exhaust manifold	Faulty cooling	16.
134	262	9 1/2	D-4	410	'37	O	Piston	Improper adjustment	169.
135	180	12	D-2-C.Sc.	360	'38	C1	Cylinder	Defective casting	21.
136	135	12 1/2	SD-2-C.Sc.	257	'23	C1	Crankbearing	Oil contamination	80.
137	80	12 1/4	D-2 C.Sc.	300	'27	O	Crankshaft	Misalignment	571.
1940									
1	300	16 1/4	D-4	225	'35	C1.	Fuel valve	Gasket blew out	277.*
2	100	9 1/2	D-4	360	'36	O	Cylinder head	Scale	138.
3	200	14	SD-2-C.Sc.	257	'23	O	Crank bearing	Overload	40.
4	40	12	D-4	110	'31	O	Cylinder head	Welding failure	150.
5	120	14	D-2-C.Sc.	257	'26	C1.	Cylinder head	Welding failure	120.
6	180	14	D-2-C.Sc.	257	'25	C1.	Cylinder heads	Frost	60.
7	100	12 1/2	D-4	277	'35	O	Clutch disk	Vibration	202.
8	1480	14	D-4	277	'37	C1	Fuel pump	Lint in fuel	29.
9	100	9	G-4	530	'35	C1	Cylinder liner	Cracked from distortion	136.
10	160	12 3/4	G-4	300	'22	C1	Crank bearing	Undetermined	43.
11	350	18	G-4	225	'17	C1	Crack in waterjacket	Undetermined	21.
12	400	15	D-4	300	'34	C1	Governor	Clogged oil passage	55.
13	100	4 1/2	D-4	1200	'36	C1	Fuel pump gear	Vibration	159.*
14	262	9 1/2	D-4	400	'37	O	3 cylinder heads	Circulating pump stopped	442.
15	290	10	D-4	600	'38	C1	Lubricating oil pump	Fatigue failure	654.*
16	600	13 1/4	D-4	300	'38	C1	Pistons	Overload	556.
17	350	18	G-4	225	'17	C1	Crack in waterjacket	Undetermined	433.*
18	30	10 1/2	D-2-C.Sc.	380	'28	C1	Wristpin bearing	Improper adjustment	35.
19	1450	17	D-4	257	'33	O	Cylinder block	Mud accumulation	3,643.
20	18	4 1/2	D-4	1000	'34	O	Crank bearing	Improper adjustment	46.
21	385	12 1/2	D-4	360	'36	C1	Cylinder head	Insufficient circulation	224.*
22	460	10	D-4	600	'37	C1	Lubricating oil pump	Loosening of parts	30.
23	600	13 1/4	D-4	300	'38	C1	Piston seized	Overload	141.*
24	600	13 1/4	D-4	300	'38	C1	Cylinder liner	Distortion	138.*
25	60	14	D-2-C.Sc.	257	'29	O	Wristpin bearing	Overloading	404.*
26	60	14	D-2-C.Sc.	257	'29	O	Lubricating oil pump	Fatigue failure	283.*
27	100	9 1/2	D-4	514	'35	C1	Valve spring	Fatigue failure	10.

TABLE 1 INTERNAL-COMBUSTION-ENGINE ACCIDENTS (*Continued*)

1940 No.	Rated Capacity Bhp.	Cylinder Bore In.	Type	Rated Speed Rpm	Year Built	Type of Cooling System	Part that Failed	Cause	Cost of Damage
28	120	14	D-2-C.Sc.	257	'26	Cl	Piston scored	Inattention	200.
29	115	9 1/2	D-4	400	'37	O	Exhaust manifolds	Airbound jackets	513.
30	600	13 1/4	D-4	300	'38	Cl	Pistons	Distortion	849.*
31	85	12 1/4	D-2-C.Sc.	300	'34	Cl	Piston seized	Distortion	107.*
32	60	14 1/4	D-2-C.Sc.	316	'35	Cl	Wrist pin bearing	Oil line clogged	88.
33	380	12 1/2	D-4	270	'35	O	Cylinder head	Overheating	173.
34	90	4 7/8	D-4	1500	'39	O	Fuel pump seized	Inattention	18.
35	2250	21	D-2-P.Sc.	225	'37	Cl	Spray nozzle hous'g	Undetermined	95.
36	100	6	G-4	1000	'37	Cl	Governor parts	Undue wear	30.
37	120	5 1/2	D-2-C.Sc.	1200	'36	Cl	Crank bearing	Failure of lubrication	55.
38	140	14	D-2-C.Sc.	257	'36	Cl.	Crank bearing	Oil contamination	71.
39	360	14	D-2-C.Sc.	257	'28	Cl.	Piston seized	Improper adjustment	238.
40	115	9 1/2	D-4	400	'37	O	Cylinder head	Air bound jacket	174.
41	40	12	D-4	110	'31	O	Main bearing	Loss of lubricating oil	71.
42	1200	14 1/2	D-4	340	'39	Cl	Crank case explosion	Overloading	113.*
43	750	17	D-4	277	'31	Cl	Piston seized	Inadequate cooling	815.
44	60	10	D-2-C.Sc.	500	'33	O	Crank bearing	Oil passage clogged	1,502.*
45	100	6	G-4	1000	'37	Cl	Push rod	Fatigue failure	5.
46	57	4 7/8	D-4	1200	'40	Cl	Clutch housing	Undetermined	228.
47	90	4 7/8	D-4	1500	'39	O	Cylinder liners	Insufficient circula.	149.*
48	360	14	D-2-C.Sc.	257	'27	Cl	Piston seized	Inattention	463.
49	450	14	D-2-C.Sc.	300	'37	Cl	Crank bearing	Overloading	59.
50	120	14	D-2-C.Sc.	257	'28	O	Wristpin bearing	Oil stoppage	654.
51	100	12 1/2	D-2-C.Sc.	260	'30	O	Governor	Defective material	82.*
52	180	12	D-2-C.Sc.	257	'38	O	Cylinder cracked	Mud accumulation	403.
53	55	12	D-2-C.Sc.	360	'34	Cl	Crankbearing	Loosening of bolts	1,100.
54	450	14	D-4	257	'31	Cl	Cylinder heads	Previous cooling syst.	350.
55	240	14	D-2-C.Sc.	257	'28	Cl	Main bearing	Undetermined	123.
56	180	12	D-2-C.Sc.	360	'38	Cl	Main bearing	Loose babbitt	35.
57	240	14	D-2-C.Sc.	257	'28	Cl	Crank bearing	Defective material	108.
58	85	8 1/2	D-4	360	'28	O	Pump plunger	Undue wear	16.*
59	85	8 1/2	D-4	360	'29	O	Fuel pump	Misalignment	9.*
60	100	9 1/4	D-4	360	'36	O	Oil pump	Fatigue failure	5.
61	380	12 1/2	D-4	270	'35	O	Fuel pump	Fatigue failure	36.
62	1200	14 1/2	D-4	340	'39	Cl	2 pistons seized	Overloading	2,647.*
63	600	14 1/2	D-4	300	'29	Cl	Cylinder head	Undetermined	236.
64	350	9	D-4	550	'37	Cl	Camshaft	Welding failure	38.
65	450	12 1/2	D-4	360	'35	Cl	Cylinder liner	Distortion	157.
66	2250	21	D-2-P.Sc.	257	'37	Cl	Cylinder head	Light design	275.
67	750	17	D-4	277	'31	Cl	Piston seized	Inadequate cooling	811.
68	100	6	G-4	1000	'37	Cl	Cylinder cracked	Previous open system	110.
69	300	14	D-2-C.Sc.	257	'28	Cl	Wristpin bearing	Oil scraper broke	25.
70	60	4 1/2	D-2-C.Sc.	1200	'35	O	Cylinder head	Defective casting	217.
71	150	7	G-4	720	'26	Cl	Piston cracked	Defective material	58.
72	280	8	G-4	720	'38	Cl	Exhaust valve stem	Overheating	450.
73	2,250	21	D-2-P.Sc.	257	'37	Cl	Fuel pump	Undetermined	92.
74	100	5 1/4	D-4	1200	'35	O	Piston	Overloading	1,152.
75	90	4 7/8	D-4	1500	'39	O	Crankbolt	Improper adjustment	39.
76	115	9 1/2	D-4	400	'37	Cl	Air starting pipe	Vibration	7.
77	55	4 7/8	D-4	1200	'40	Cl	Clutch gear	Undetermined	142.
78	60	6 1/2	G-4	720	'34	Cl	Governor shaft	Undue wear	150.
79	90	6 1/2	G-4	720	'35	Cl	Crank bearing	Oil line clogged	20.
80	80	6	G-4	600	'37	O	Crank bearing	Oil line clogged	27.
81	240	14	D-2-C.Sc.	257	'23	Cl	Crank bearing	Improper fit	49.
82	240	14	D-2-C.Sc.	257	'25	Cl	Crank bearing	Improper fit	48.
83	240	14	D-2-C.Sc.	257	'23	Cl	Wrist pin bearing	Worn cylinder well	30.
84	150	9 1/2	D-4	330	'28	Cl	Lubricating oil pump	Undue wear	195.*
85	2250	21	D-2-P.Sc.	257	'37	Cl	Fuel pump	Undetermined	92.
86	46	4 1/2	D-4	960	'37	Cl	Intake valve stem	Undetermined	139.
87	90	6 1/2	G-4	720	'35	Cl	Crankbolt	Overstrained	1,550.
88	80	7 1/2	D-4	525	'35	O	Lubricating oil pump	Foreign object	100.
89	180	14	SD-2-C.Sc.	257	'29	Cl	Crank bearing	Oil supply failed	108.
90	380	12 1/2	D-4	255	'37	Cl	Exhaust manifold	Inadequate circulation	450.
91	262	9 1/2	D-4	400	'37	O	Main bearing	Oil contaminated	164.
92	240	14	D-2-C.Sc.	257	'25	Cl	Crank bearing	Improper fit	51.
93	240	14	D-2-C.Sc.	257	'25	Cl	Crank bearing	Improper fit	45.
94	240	14	D-2-C.Sc.	257	'25	Cl	Crank bearing	Improper fit	106.
95	240	14	D-2-C.Sc.	257	'25	Cl	Crank bearing	Improper fit	65.
96	200	14	D-2-C.Sc.	257	'23	O	Crank bearing	Improper fit	49.
97	300	14	D-2-C.Sc.	300	'36	Cl	Piston seized	Overload	17.
98	450	12 1/2	D-4	360	'35	Cl	Cylinder head	Improper adjustment	141.
99	120	7	G-4	720	'24	Cl	Crank bearing	Undetermined	31.
100	400	16 1/2	D-4	200	'22	Cl	Wrist pin bearing	Oil passage clogged	185.*
101	400	16 1/2	D-4	200	'22	Cl	Wrist pin bearing	Oil contaminated	50.
102	30	5	D-4	1200	'39	Cl	Crank bearing	Listing of boat	466.
103	1140	22	D-4	220	'34	Cl	Cylinder liner	Improper adjustment	258.
104	735	14	D-2-C.Sc.	300	'27	O	Wristpin studs	Improper fit	382.
105	735	14	D-2-C.Sc.	300	'27	O	Wristpin studs	Improper fit	327.
106	350	9	D-4	625	'37	Cl	Exhaust manifold	Inadequate circulation	450.
107	400	15	D-4	300	'35	Cl	Governor	Undue wear	60.

TABLE 1 INTERNAL-COMBUSTION-ENGINE ACCIDENTS (*Continued*)

1940 No.	Rated Capacity Bhp.	Cylinder Bore In.	Type	Rated Speed Rpm	Year Built	Type of Cooling System	Part that Failed	Cause	Cost of Damage
108	400	17	D-4	225	'27	Cl	Piston	Defective spray nozzle	213.
109	60	7 1/4	G-4	720	'35	Cl	Crank bearing	Insufficient strength	38.
110	350	18	G-4	225	'17	Cl	Crack in water jacket	Undetermined	385.*
111	20	4 1/4	D-4	1200	'37	Cl	All bearings	Water in oil	116.
112	360	14	D-2-C.Sc.	257	'28	Cl	Piston seized	Overloading	428.
113	250	16	G-4	257	'20	Cl	Cylinder cracked	Fatigue failure	1,200.*
114	1000	17 1/2	D-4	252	'35	Cl	Idler gear	Vibration	387.
115	675	17	D-4	225	'28	Cl	Air coil	Vibration	92.
116	50	10	D-4	400	'38	Cl	Cylinder jacket	Frost	1,158.
117	180	14	D-2-C.Sc.	257	'24	Cl	Piston rings	Inattention	50.
118	875	16	D-2-P.Sc.	300	'39	Cl	Main bearings	Undetermined	1,500.
119	100	9 1/4	D-4	360	'36	O	Cylinder head	Scale in jacket	135.
120	200	14 1/4	D-2-C.Sc.	320	'36	Cl	Wristpin bearing	Improper adjustment	650
121	400	15	D-4	300	'35	Cl	Fuel pump	Grit in fuel	25.
122	660	17.	D-4	240	'29	O	Crankcase explosion	Improper adjustment	500.
123	80	12 1/4	G-4	277	'24	O	Exhaust valve	Fatigue failure	162.
124	150	7	G-4	720	'26	Cl	Piston cracked	Defective material	91.
125	450	14	D-2-C.Sc.	300	'35	O	Piston seized	Overload	1,114.
126	180	14	D-2-C.Sc.	257	'25	Cl	Crank bearing	Oil contamination	91.
127	800	15 1/2	D-4	270	'38	Cl	Connecting rod	Preignition	2,000.*
128	400	16 1/2	D-4	200	'22	Cl	Wristpin bearing	Overload	129.*
129	130	12 5/8	D-2-C.Sc.	275	'32	O	Wristpin bearing	Oil Supply Failed	718.*
130	130	12 5/8	D-2-C.Sc.	275	'32	O	Wristpin bearing	Improper adjustment	287.
131	180	14	D-2-C.Sc.	257	'29	Cl	Crank bearing	Cracked oil ring	144.

TABLE 2 INTERNAL-COMBUSTION-ENGINE ACCIDENTS—ANALYSIS OF ACCIDENTS

Initial part broken or damaged	1938	1939	1940	Total	% of Total
Crankshaft	5	4	0	9	2.2
Main bearing	9	6	6	21	5.1
Crankbearing	25	21	24	70	16.9
Wristpin bearing	16	9	12	37	9.
Bearing cases combined	50	36	42	128	31.
Cylinder head	30	14	14	58	14.
Cylinder liner	1	5	5	11	2.7
Cylinder & Cylinder block	9	4	8	21	5.1
Piston & Piston rings	14	26	18	58	14.
Exhaust manifold	5	3	3	11	2.7
Fuel pump & spray nozzles	0	11	11	22	5.4
Lub. oil pump & piping	3	5	6	14	3.4
Connecting rod & crankbolts	3	2	3	8	1.9
Governor	4	8	5	17	4.1
Miscellaneous	21	19	16	56	13.5
TOTALS	145	137	131	413	

TABLE 3 INTERNAL-COMBUSTION ENGINES—ACCIDENT FREQUENCIES

1931	*1932*	*1933*	*1934*	*1935*	*1936*	*1937*	*1938*	*1939*	*1940*
1:2.0	1:1.5	1:1.4	1:1.7	1:2.3	1:2.3	1:2.5	1:2.7	1:3.1	1:3.5

Discussion

H. S. KILBY.[2] Does the 40 per cent increase in premium on open systems apply where there is an adequate clean soft-water supply?

T. M. ROBIE.[3] No doubt the author will agree that accidents in steam plants, because of large capacity of steam under pressure, are likely to be much more serious, in so far as human life is concerned, than accidents with Diesel plants of similar sizes. Conceivably the monetary loss would also be greater in the case of the former.

In view of the accident-frequency ratio of 1 to 11 for steam plants versus 1 to 3.5 for Diesel, it would be informative if the author will supply the corresponding ratios of financial loss involved. The writer is familiar with many of the Diesel-engine accident cases cited by the author. It would be interesting to have him supply the case histories of typical accidents in order to demonstrate the things to avoid in making Diesel installations. In cases known to the writer, the fault was chargeable to improper installation and not in any degree to design or workmanship.

The author's reaction to the closed cooling system is gratifying to the writer, since his company has been a consistent advocate of the system. This opinion is also shared widely by other engine manufacturers. We now insist that closed-type cooling be incorporated in all of our installations.

The author might explain Table 3 somewhat more fully. The writer does not of course know how many engines were being insured in 1931, or their average age, but would guess that the average age of those insured in 1940 is considerably greater than those in 1931. Actually, greater improvements have been made in the design of newer engines than the ratio shown in the table would indicate. In other words, the assumption is being made,

[2] The Kansas Power Company, Great Bend, Kan.
[3] Fairbanks, Morse & Company, Chicago, Ill.

perhaps erroneously, that many of the engines which were insured in 1931 are still insured, 10 years later. Hence, a better operating record necessarily would have to be made by the newer engines to offset the greater age of the older ones.

H. S. CROSBY.[4] The writer's company operates a number of engines at various points in the Southwest, on which no insurance against mechanical failure is carried. That is definitely contrary to the policy of the company toward insurance in general. Several occasions have arisen in which we have checked the cost of insurance against our opinion as to our operating records and in each instance could form no justification for asking the company to pay the insurance premiums. We reached the conclusion that insurance coverage in the field of engine operation is in a different category from other types of insurance.

It occurred to us that what appeared to be an unusually high cost might be due either to lack of volume for the insurance companies in this field or to an unusually greater percentage of relatively poor risks. In this connection, it should be pointed out that we do not consider ourselves any better than average operators, and in many ways we are probably less successful than firms operating a larger amount of engine capacity.

Frankly, it would be desirable for our company to carry engine-breakdown insurance, and so we would be interested in determining whether there is any special approach to this problem which might lead to lower premiums. Possibly, there is some procedure in classifying types of risk with which we are not familiar. It has also occurred to us that there might be some possibility in using a relatively high deductible clause. Finally, we would be definitely interested in encouraging a larger volume of engine insurance if such an increased volume would lower the premium.

V. L. MALEEV.[5] What is the difference between rates in a low classification and the highest classification? Also, in each classification are the rates constant in each group or does the rate depend upon the size of the engine, that is, is there a sliding scale for larger engines and vice versa? The author remarked that his company does not encourage the use of electric welding for repairing crankshafts. What would be the attitude toward crankshafts made entirely by electric welding instead of forging? Such crankshafts are being made in Europe and possibly will soon be made here.

R. D. CAMPBELL.[6] An accident-frequency ratio of 1 to 11 for steam engines is mentioned in the paper, which presumably is for the engine alone. Is there a composite accident-frequency factor covering the engines, the boiler, and any other piece of the steam-plant equipment which might cause a shutdown? A Diesel engine is more or less a self-contained unit and may be treated as such. The composite factor in relation to steam plants is of importance, since it is believed that the boiler probably causes as many shutdowns as does the engine.

In connection with the cooling system, the author mentioned that in writing insurance a certain water quantity was required, presumably so many gallons per horsepower; also a certain limit is placed on temperature rise. Allowing a 20 F rise, is a rise of 150 to 170 F just as acceptable as a rise from 50 to 70 F?

E. J. KATES.[7] The writer questions whether the accident-frequency ratio of 1 to 3.5 in 1940, reported in the paper, is typical. Even though this ratio is a considerable improvement over those for 1932 and 1933, it would indicate, if typical, that the average engine is likely to suffer an accidental breakdown every $3\frac{1}{2}$ years. Such a performance record would be deemed far below average by most persons conversant with Diesel-engine operation. The cause of this inconsistency is probably that many well-run Diesel plants are not being insured; consequently, the accident-frequency ratio of the insured plants is not so good as the average. However, in the writer's opinion, the author's data are exceedingly useful.

E. C. COLE.[8] Does it make any difference whether or not an installation is fitted with alarm devices, such as are used in modern plants? Will the author also supply a definition for the term, "consequential damage?" For instance, a pin could shear off which might break the pump which in turn might burn the bearings out, which in turn might cause a complete collapse of the machine. Where does "consequential damage" stop?

AUTHOR'S CLOSURE

Diesel-engine risks with open cooling systems are rated regardless of the quality of the cooling water. The quality of the cooling water is a very important factor in the desirability of the risk on engines with open cooling systems. If the quality of the cooling water is such that an undue amount of scale is formed in the jackets, such engines may be found uninsurable. Aside from the quality of the cooling water, it has been found that the open system gives greater exposure to piston seizures and bearing failures, which apparently is due to the fact that a sudden considerable temperature drop of the inlet water is far more prevalent with the open system than with the closed system. The premium-rate differential between engines with open systems and those having closed systems is based upon loss experience.

The capacity of steam under pressure in steam-engine plants has its own peculiar hazard which is difficult to compare with the exposure to serious accidents in Diesel plants. Also, the comparative danger to human life is difficult to evaluate, in these two categories of plants. The explosion of the steam generator is to a considerable extent paralleled by the explosion of air systems and crankcase explosion in the Diesel plant. The author is not prepared to supply the corresponding financial losses. The results of Diesel-breakdown accidents, shown in the tables in the paper, speak for themselves. Unquestionably, many accidents are chargeable to faulty installation, particularly as regards the cooling system.

The average age of insured Diesel engines has not varied greatly from year to year. In 1931, the average age was approximately the same. With good inspection and maintenance (referred to later), the accident frequency of the older engines is not greatly different from that of the newer engines. While the author is of the opinion that progress in engine design has had its effect on reducing breakdown accidents, the improvement in the accident frequency, as given in Table 3 of the paper, has been mainly the result of the conversion from the open to the closed cooling system.

The accident frequency of 1:11 for steam engines, as mentioned in the paper, is for the engines alone. No composite accident frequency covering steam engines, boilers, and other steam-plant equipment is available.

The group of insured engines is a cross section of the best obtainable operating practices. Engines in poor condition or where the operating conditions are subnormal are not insurable. The insurance experience has been compared with the experience reported for a similar large group of engines which indicated a somewhat higher frequency of accident for the latter group. In

[4] General Mills, Inc., Minneapolis, Minn.
[5] Research Professor of Mechanical Engineering, Oklahoma A.&M. College, Stillwater, Okla. Mem. A.S.M.E.
[6] Shell Oil Company, Inc., Wood River, Ill. Mem. A.S.M.E.
[7] Consulting Engineer, New York, N. Y. Mem. A.S.M.E.
[8] Fairbanks, Morse & Company, Beloit, Wis.

judging the cost of Diesel-engine insurance, the fact is frequently overlooked that, in the payments of losses, there enters unavoidably a large amount of money that would ordinarily be charged to maintenance if the accidents had not happened. In other words when accidental breakdowns occur to insured engines the normal maintenance account is considerably helped out by the replacement with the new parts incident to the accidental occurrence.

Diesel-engine risks are grouped in four different industrial classifications, in accordance with the different exposures to breakdown in these groups. The cost of insurance in the lowest classification is approximately double that of the highest classification. The engines are rated by horsepower capacity. There is a provision for premium reduction under an agreed deductible amount for each accident.

In judging the reported accident frequency of 1:3.5, it must be remembered that the definition of accident is quite broad and it is not merely confined to the catastrophic type of accident, but covers sudden bearing failures and practically every sudden failure of or damage to small parts. As already pointed out, there is no basis for assuming that insured engines are of an inferior class or subject to poor operating conditions.

There is no experience in this country with crankshafts which are fabricated by fusion welding, such as were mentioned as being made in Europe. The reference to welding on crankshafts is based on adverse experience where worn shafts were built up with fusion welding. This, as a rule, causes crack formation in the built-up surfaces and ultimately complete breaking of the shaft.

The recommended minimum quantity of cooling water for Diesel engines is 20 gal per hp-hr. The recommended maximum temperature rise through the cooling jackets is 20 F. Obviously, a low temperature rise means that there is good circulation of water over the hot spots, such as around exhaust valves and exhaust ports. It is not recommended that one be guided entirely by a favorable low temperature rise because of the fact that this may be the result of a badly scaled-up cylinder jacket.

There is no differentiation in the cost of engine-breakdown insurance for the use of alarms or automatic shutdown devices. Such devices are very useful if they are kept in good reliable operating condition at all times. They are, therefore, strongly recommended, and in some installations their use is insisted upon.

Consequential damage insurance is a form of coverage having to do with spoilage of goods due to lack of power or refrigeration, caused by the breakdown of insured engines or other power-plant equipment. The direct-damage-insurance coverage comprises the complete damage resulting from an accidental occurrence, as given in the accident definition. It does not merely stop with the initial part broken, but takes care of all the subsequent damage to the engine resulting from the breakage of the initial broken part.

Earlier in this closure the matter of good maintenance practice was mentioned. The recommended maintenance routine should include the examination and overhaul of vital parts at intervals in accordance with the following schedule:

Parts involved:	Operating period, hr
Spray nozzles	1250
Pistons and piston rings in 2-cycle crankcase-scavenging engines	3000–3500
Checking of exhaust-port bridges and relieving of them in 2-cycle engines	3000–3500
Piston and piston rings in 2-cycle engines with scavenging pump, and in 4-cycle engines	5000–6000
Exhaust valves of 4-cycle engines	1600–2500
Fuel pumps and fuel systems	4000–5000
Lubricating-oil pumps and systems	4000–5000

In order to secure reasonably long life of pistons and piston rings, the recommended maximum exhaust temperature for full-load conditions on 2-cycle crankcase-scavenging engines is 400 F; for 2-cycle engines with scavenging pump or blower, 550 F; for 4 cycle engines, 750 F.

Hydraulic Characteristics of Fuel-Injection Nozzles

By O. F. ZAHN,[1] MARTINEZ, CALIF.

This paper makes use of both new and previously published material in studying the hydraulic actions and limitations of fuel-injection nozzles. The primary function, hydraulically, of such a nozzle is to inject all portions of the fuel at velocities above a certain minimum necessary for atomization. The most serious factor tending to prevent this is the wide range of speeds found in present small Diesel engines. It is found that the closed nozzle meets the requirements of speed flexibility better than the simple open type, and that the variable-area-orifice closed nozzle is a further improvement over the plain-hole closed nozzle. The effects on the rate of injection and minimum regular quantity of injection are noted.

THE high-speed Diesel engines of today have top speeds about 3 times those of 10 years ago, and their size has shrunk accordingly. As idling and cranking speeds, on the other hand, have increased little if at all, today's engine is far more flexible than formerly. It is this flexibility, rather than high speed in itself, which is the dominant problem facing the designer of fuel-injection equipment. Small size has resulted in idling quantities of less than 10 mm³ per injection being required; this too has made the requirements of injection more exacting than they were a decade ago. This paper attempts to discuss the newer problems of injection as they pertain to that part of the injection system called the nozzle or spray valve.

The basic hydraulic equation in injection design is that derived from the familiar Torricelli law

$$Q = A \times t \times V = c_d \times A \times t \sqrt{\frac{2g(EIP)}{d}}$$

in which

Q = quantity of injection
A = orifice area
t = time duration of injection
V = jet velocity
c_d = coefficient of discharge
EIP = effective injection pressure
d = specific weight of fuel

It has been demonstrated in rather classic tests by Lee (1)[2] that atomization depends primarily on V, and hence largely on pressure, Fig. 1, and also that it becomes finer with smaller orifice areas, Fig. 2. How are these factors affected by flexibility requirements?

Effect of Atomization on Flexibility

Let us take the case of a typical present-day Diesel engine which idles at 400 rpm and pulls peak power at 2400 rpm. Suppose that the coarsest permissible atomization corresponds to an *EIP* of 1400 psi, which is a workable minimum in most Diesels. Then, with the timed-pump system normally used on such an engine (common rail systems not being used commercially on engines having this speed range), the orifice area A must be small enough so that this pressure is obtained at 400 rpm if the nozzle is of the simple, open type. If then the *EIP* at 400 rpm is 1400 psi, what is the pressure at 2400 rpm? There are two alternatives:

1 If the compressibility of the system is negligible the velocity is 6 times as great and the *EIP* 36 times as great, or 50,400 psi. Thus, unit-injection systems, because of their low fuel volumes, are characterized by high top-speed pressures. In this case 50,400 psi is obviously higher than needed if only 1400 psi is sufficient at idling. The disadvantage of such a pressure is that a heavy, well-built system is required and the power used to drive the pump is considerable.

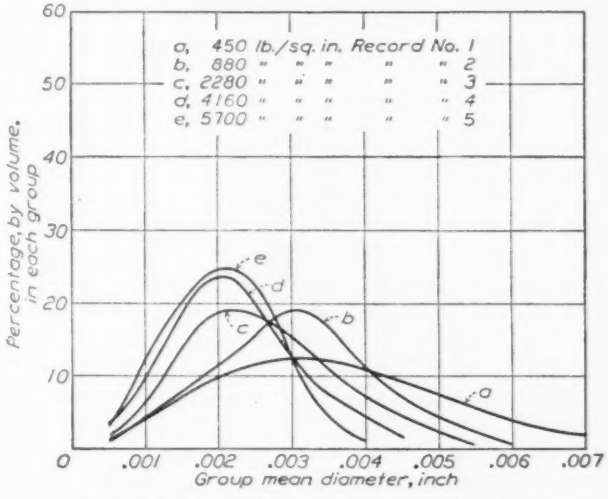


FIG. 1 EFFECT OF SPRAY VELOCITY ON DROP SIZE
(The velocity was varied by changing the mean pressure.)

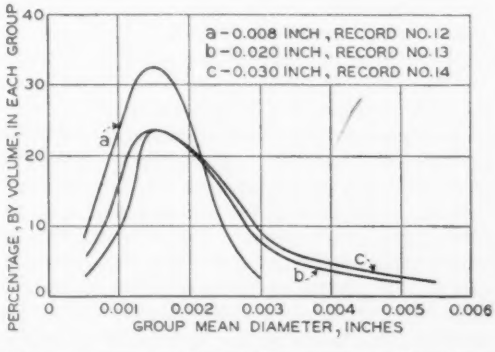


FIG. 2 EFFECT OF ORIFICE DIAMETER ON DROP SIZE

2 When compressibility is present, and of course it always is to some extent, the jet velocity at top speed is less than 6 times as great. This means that the time duration t is then greater than

[1] Diesel Engineer. Jun. A.S.M.E.

[2] Numbers in parentheses refer to the Bibliography at the end of the paper.

Presented at the National Meeting of the Oil and Gas Power Division, Kansas City, Mo., June 11–14, 1941, of THE AMERICAN SOCIETY OF MECHANICAL ENGINEERS.

NOTE: Statements and opinions advanced in papers are to be understood as individual expressions of their authors and not those of the Society.

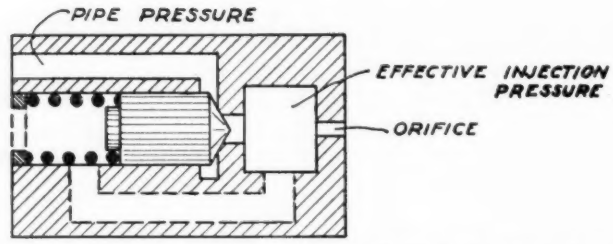


FIG. 3 DASHED LINES CHANGE CLOSED NOZZLE INTO OPEN-TYPE NOZZLE

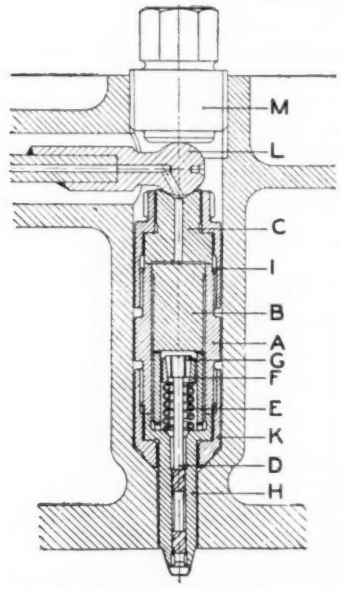


FIG. 4 SAURER "UMBRELLA-SPRAY" NOZZLE
(Variable-orifice closed nozzle with centrifugal spray; orifice and valve combined.)

1/6 for the same quantity, so that the angular duration of injection is longer at the higher speed. In such a case, the designer is confronted not with excessive pressures but excessive durations.

A closed nozzle, in which the *EIP* is determined not only by the orifice but also by a spring-loaded valve, tends to obviate both effects of changing speed. In the engine example such a nozzle might be used in which the orifice area is large enough to give a top-speed pressure of, say, only 4000 psi and no more than the desired duration, relying entirely upon the valve at low speeds. The "valve-closing pressure" (*VCP*) could be set at 1400 psi to maintain the minimum jet-velocity requirements at 400 rpm. A nozzle valve can do this, ideally, providing the nozzle is truly of the closed type and not an open nozzle with a check valve.

It is sometimes thought that valve differential is a distinguishing feature of the closed nozzle. The ratio of *VCP/VOP* in commercial closed nozzles varies from 0.6 to 0.9. Actually there are designs of open nozzles whose check valves also have differential. The basic criterion of a closed nozzle is that the fuel acts on its valve in only one direction. The nozzle shown diagrammatically in Fig. 3, without the dashed passage, is a closed nozzle. When the valve is open, the *EIP* is the full amount of the pipe pressure. If, however, the spring space is sealed to the outside and fuel is admitted through the dashed passage to this space, the valve becomes a check valve, and the nozzle an open one. A check valve is a pressure-reducing valve, and the *EIP* then becomes less than the pipe pressure by the amount of the *VCP* of the valve. The design of Fig. 4 is a closed nozzle even though it has no pressure-sealing lapped fits because here again pressure acts on the valve in only one direction.

When the *VCP* of a closed nozzle with fixed orifice area is higher than the *EIP* given by the Torricelli law, the instantaneous rate of injection is higher than the rate of delivery from the pump, so that the valve opens and closes more than once each injection. This action is shown in the lower curve of Fig. 5, from the work of Gelalles and Marsh (2). It is to be noted that the duration at both 215 and 470 rpm is practically the same but that at higher speeds, where the orifice area controls the pressure, the duration increases. Had the orifice been appreciably larger, the top-speed duration would have been shortened, and intermittent injection would have occurred up to a higher speed. There seems to be no evidence that such intermittent injection in itself is harmful to engine operation, but there is every indication that the accompanying valve action is detrimental to atomization.

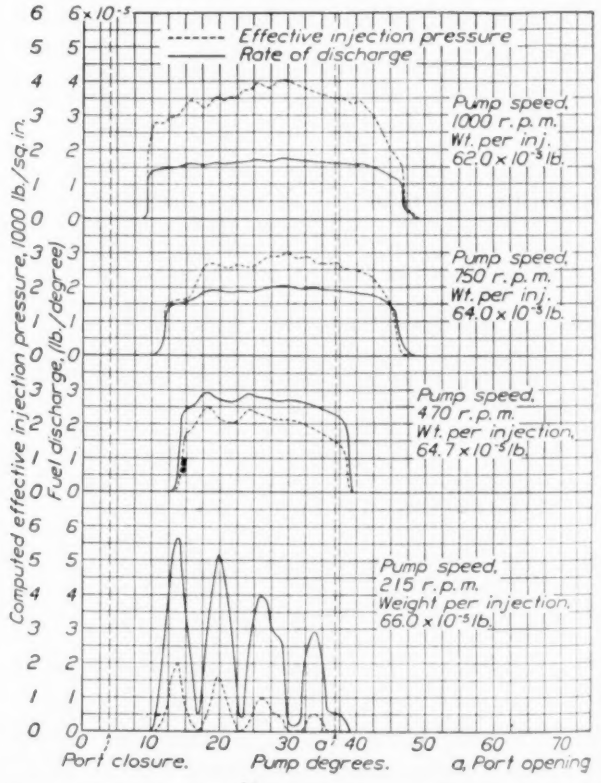


FIG. 5 EFFECT OF PUMP SPEED ON DURATION, RATE OF INJECTION, AND PRESSURE

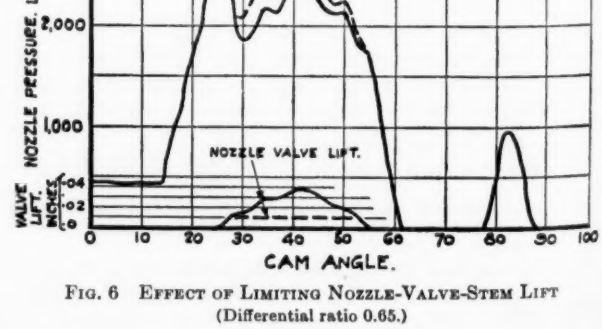


FIG. 6 EFFECT OF LIMITING NOZZLE-VALVE-STEM LIFT
(Differential ratio 0.65.)

One action of the valve is its displacement. Considering the closed design in Fig. 3, it is obvious that each time the stem lifts it reduces the *EIP* momentarily by increasing the volume of fuel under pressure. Fig. 6 is an interesting test reported by Davies and Rowe (3), showing how the reduced limit of the valve-stem lift increased the injection pressure in the pipe. To be noted is the sudden fall of pressure when the valve first started to lift. Stem displacement reduced the pressure, and limiting the displacement limited the reduction.

Another action of the valve is its throttling or "wire drawing" in which the pressure drop occurs across the valve instead of through the orifice. In the closed design in Fig. 3, it is clear that, up to a certain lift of the valve, its area is actually less than that of the orifice. A representation of the flow conditions in a closed

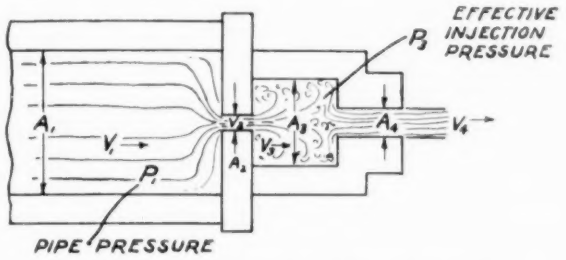


FIG. 7 VALVE THROTTLING IN CLOSED NOZZLE

nozzle when the valve is but partially open is shown in Fig. 7. Let A_1 be the area of the section ahead of the valve, A_2 the flow area between the valve seats, A_3 the area of the section below the valve, and A_4 the orifice area. The term P_1 is the pipe pressure and P_3 the *EIP* behind the orifice. With the valve slightly open, P_3 is still almost zero and the full pressure drop of P_1 occurs in the valve A_2. Expressed mathematically, and assuming that A_1 is large enough so that V_1 may be neglected, the equation is

$$V_2 = c_v \sqrt{\frac{2g(P_1 - P_3)}{d}} = c_v \sqrt{\frac{2gP_1}{d}}$$

This velocity is dissipated in frictional heat in section A_3. Term P_3 remains practically zero, the loss of pressure P_L being given by (4)

$$P_L = \frac{K(V_2 - V_3)^2 d}{2g}$$

where K is a factor near 1. Assuming that A_3 is large and V_3 is negligible, P_L then becomes P_1. Under such assumptions, all the pipe pressure is lost in valve throttling.

The smaller the orifice area, the less this loss will be. Since

$$V_2 A_2 = V_4 A_4$$

it is possible to reduce V_2 by reducing A_4, and this will reduce P_L in the preceding equation. This analysis explains why, in Fig. 2, the 0.008-in-diam orifice showed more small drops and fewer large ones, even though the calculated mean pressure acting on the over-all stem area was 3913 psi in all three curves.

Gelalles (5) has reported that there was no throttling apparent when the valve lift was 0.005 in., which with some orifices was a valve area of only twice the orifice area. In connection with Fig. 6, the investigators stated that there was throttling when the lift limit was decreased to 0.006 in. As previously shown, the greater the orifice area, the greater will be the lift below which throttling occurs but, moreover, the greater will be the number of openings and closings of the valve at low speeds. Thus, for reasons of throttling and stem displacement there is a practical maximum limit of the orifice area which may be advantageously used in a closed nozzle.

ORIFICE-AREA LIMITATIONS

There is some experimental evidence that orifice area influences the minimum regular quantity which can be regularly injected with a closed nozzle, as shown in Fig. 8. With a given *VOP*, *VCP*, and volume of high-pressure fuel, it thus seems of value to

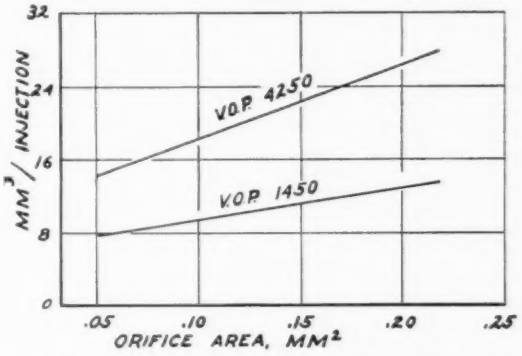


FIG. 8 MINIMUM REGULAR QUANTITY OF INJECTION INCREASES WITH ORIFICE AREA

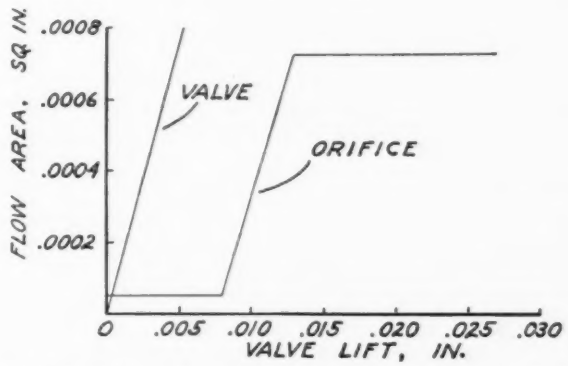


FIG. 9 VALVE AND ORIFICE AREAS AT VARIOUS LIFTS; PINTLE NOZZLE

keep the orifice area small for this reason if the minimum lies in or near the operating range of quantity of the engine.

These orifice-area limitations are largely overcome in the variable-area-orifice closed nozzle. Fig. 9 shows the valve-area-orifice-area relationship in a so-called "pintle" nozzle. In this particular design, the valve area is larger than the orifice area at lifts above 0.0005 in., whereas, if the orifice area were fixed at its maximum, this would be true only at lifts above 0.004 in. Hence, valve throttling is tremendously reduced with such a design. Such a nozzle also possesses an inherent damping action against valve fluctuation at low delivery rates since, as the valve tends to close, the orifice area grows smaller and the instantaneous rate of injection decreases. This tends to keep up the *EIP* and keep the valve open. A variable-area-orifice nozzle with a high differential ratio can be designed to give a continuous injection over a wide speed range quite impossible with a nozzle having a fixed orifice equal to the maximum area of the former.

A comparison of the atomizations of two such nozzles can be easily made on a hand pump. Let both nozzles have the same *VOP* and *VCP*, and let the plain-hole area be equal to the maximum area of the variable orifice. The pressure should be slowly raised and the sprays noted in strong crosslighting against a dark background, as in Fig. 10. Many more large drops, far ahead of

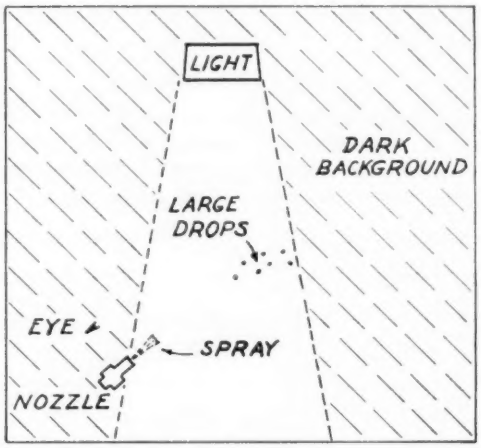


FIG. 10 SHOWING CORRECT LIGHTING FOR VISUAL DETECTION OF POOR ATOMIZATION

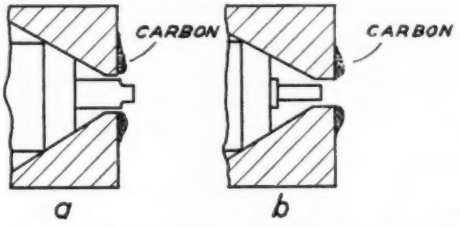


FIG. 11 SHOWING EQUAL CARBONIZATION IN TWO DESIGNS OF VARIABLE-ORIFICE NOZZLE

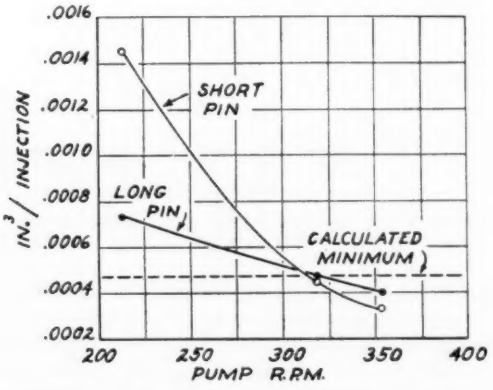


FIG. 12 EFFECT OF CHANGING ORIFICE-AREA-LIFT RELATIONSHIP ON MINIMUM REGULAR QUANTITY OF INJECTION (*VOP* 1700 psi; *VCP* 1150 psi.)

the spray tip, will be seen with the plain-hole orifice. The larger the orifices, the greater the differences will be. The same test, of course, may be applied in other cases to detect rather wide differences in the amount of low-pressure injection.

The ability of a variable-area-orifice type to reduce much of the low-pressure injection, or dribble, results in more of the jet shooting clear of the face of the nozzle. When connected to a pump running at slow speeds, a plain-hole closed nozzle will usually "wet its face" more than a variable-orifice type of the same maximum area. This is thought to be the reason why the pintle type is freer of carbon rather than the commonly accepted reason of mechanical-wiping action. One bit of supporting evidence for this theory was a series of tests run on the two variable-area-orifice designs of Fig. 11; nozzle (*a*) having wiping action and nozzle (*b*) none. Both had the same area-lift relationship and the same *VOP* and *VCP*. After a rather severe carbonization test, the carbon was as indicated, and the same in both. Other carbonizing runs confirmed the equal tendency of both designs toward carbonization. Another bit of evidence is that lowering the *VOP* of a pintle nozzle increases the amount of carbonization. In many engines, it is in fact this deposit which determines the minimum *VOP* required.

The minimum regular quantity for a nozzle of the design of Fig. 11 (*b*) is shown in Fig. 12. The variable areas were the same in both curves except that, in the case of the long pin, the stem had to lift 0.006 in. higher before the initial area changed to the maximum area. This tended to keep the orifice area small and so produced the more favorable curve. The dashed curve shows the minimum quantity calculated on the basis of compressibility. The variable-area design, by providing a small orifice when the duration (and quantity) is small, and by permitting the use of a higher differential ratio without valve throttling, makes possible the injection by a closed nozzle of smaller minimum quantities than otherwise.

COMPARISON OF THROTTLING AND NONTHROTTLING NOZZLES

One of the most interesting developments of the variable-area design is the so-called "throttling" type. This term refers to

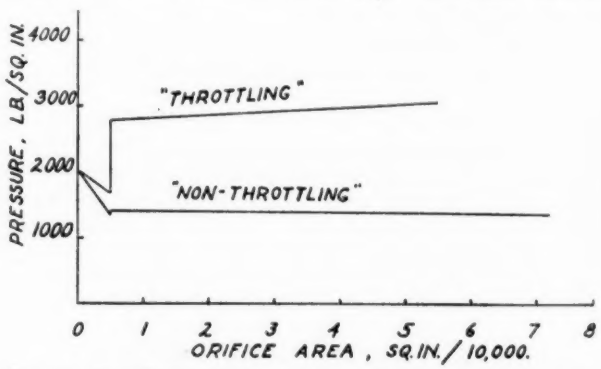


FIG. 13 PIPE-PRESSURE-ORIFICE-AREA CURVES FOR THROTTLING AND NONTHROTTLING PINTLE NOZZLES, BOTH SET AT 2000-PSI *VOP*

the slow rate of increase of area with pressure, and not to throttling in the usual hydraulic sense. The area-pressure relationships in a "throttling" and "nonthrottling" type, both of commercial design, are shown in Fig. 13. These curves have been calculated on the following assumptions:

1 The *VOP* is 2000 psi in each case.

2 The *EIP* is the full amount of the pipe pressure when the valve area equals the orifice area. In both cases this occurs when the areas are 0.00005 sq in.

3 Loss of pipe pressure at smaller valve areas varies indirectly with that area.

4 The change in effective stem area due to change in orifice area is negligible.

5 The effects of stem displacement and inertia can be neglected.

In these two designs the *VCP* of the nonthrottling type is then 1350 psi and that of the throttling type 1650 psi. This higher differential ratio, in conjunction with a higher spring rate and a more gradual shape of annulus pin, results in a much higher pressure being required in the throttling type to increase the orifice area to its maximum.

The advantage of such a design lies in the lower initial rate of injection, desirable in some combustion chambers.

Fig. 14 shows a comparison of the rate curves of a throttling and nonthrottling nozzle. Both nozzles had the same differ-

ential ratio, the orifices and springs alone making the differences. Test conditions were identical except that the pump timing was shifted 1 deg to give the same start of injection, and the quantity control was reset to give 53 mm³ per injection in each case.

The disadvantage, hydraulically, of the variable-area-orifice nozzle is its low coefficient of discharge. Reviewing this matter briefly, there are three jet coefficients to be considered. In Fig. 15, the ratio of the minimum area A_j of the jet to the orifice area is called the coefficient of contraction c_c. The jet velocity V_j in this section, divided by that given by the Torricelli law, gives the coefficient of velocity c_v. The coefficient of discharge is the product of these two $c_d = c_c \times c_v$. Term c_v is of importance since a low value means poor atomization and requires an increase in *EIP* to offset its effect, while a low c_c merely requires a larger orifice. Because of experimental difficulties, little has been done in fuel-injection research in measuring c_v. One of the few reporting such results is Schweitzer (6) who determined the mean

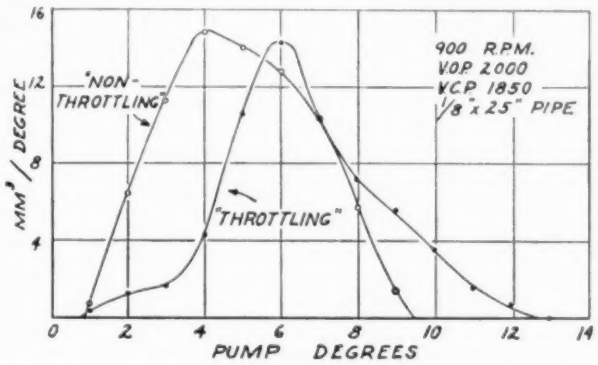


FIG. 14 RATE OF DISCHARGE OF THROTTLING AND NONTHROTTLING NOZZLES
(Start of injection is at left.)

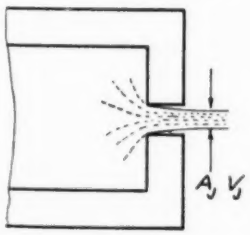


FIG. 15 JET FROM ORIFICE, SHOWING CONTRACTION

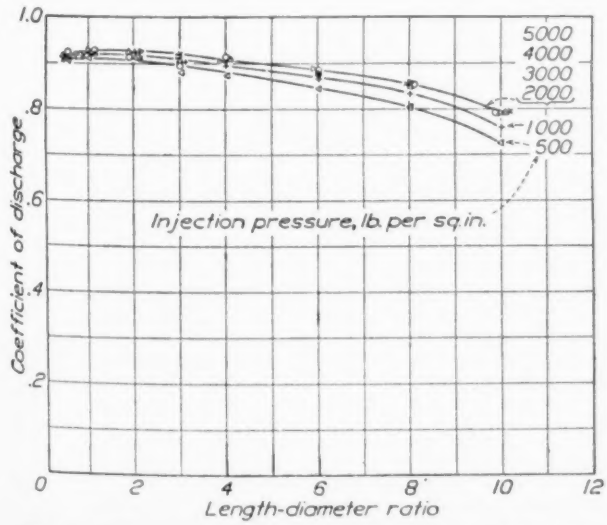


FIG. 16 EFFECT OF L/D RATIO ON COEFFICIENT OF DISCHARGE

spray velocity at the nozzle. Values of practically unity at 1000-psi pipe pressure down to 0.94 at 8000 psi were found.

It is quite possible to draw certain conclusions from the more exhaustive work done on c_d regarding c_v. For example, Fig. 16 from Gelalles (7) shows the effect of L/D ratio on c_d at several pressures. Since it is known in other hydraulic work that increasing the L/D ratio increases the friction and tends to reduce c_v, but tends to increase c_c, the evidence is that in this test c_v was falling at least as fast as c_d. In other words, long orifices reduce the jet velocity at least as much and probably more than the coefficient falls in Fig. 16.

In annular orifices, the L/D ratio is unfavorable. This is because the dimension D is the thickness of the annulus and not the total annulus diameter. In some commercial designs, this annulus thickness is a minimum, when the valve is seated, of only 0.0004 in., while the length is 0.0208 in., giving an L/D ratio maximum of 52:1. In the variable-area-orifice design of Fig. 4, in which the annulus is the valve itself, the ratio approaches infinity as the valve seats. In any case, the ratio becomes more favorable as the stem lifts and the orifice area increases, for the simple reason that every annulus must have a finite length. Table 1 shows the effect of orifice area on c_d in a variable-area-orifice nozzle. The low values of c_d at small lifts clearly show the effect of fluid friction in reducing the jet velocity. There is thus a minimum orifice area which may be advantageously used in the variable-orifice nozzle, the practical lesson being to make annular clearances as large as possible by keeping the annular diameters as small as possible The over-all effect, however, has generally been greatly to the advantage of the variable-area-orifice closed nozzle, wherever a wide range of speeds has been involved, and this largely accounts for the popularity of such designs in today's flexible Diesels.

TABLE 1 EFFECT OF ANNULAR-ORIFICE AREA ON COEFFICIENT OF DISCHARGE

Lift of stem, in.	Annulus area, sq in.	c_d
0.006	0.00024	0.26
0.010	0.00033	0.54
0.016	0.00046	0.70
0.018 (max)	0.00051	0.74

ACKNOWLEDGMENTS

The author wishes to express his appreciation to the Ex-Cell-O Corporation and the American Bosch Corporation for permission to publish the new test information given in this paper. Permission of the N.A.C.A. to reproduce Figs. 1, 2, 5, and 16, of the S.A.E. Journal for Fig. 4, and of the Institution of Automobile Engineers for Fig. 6, is gratefully acknowledged.

BIBLIOGRAPHY

1 "The Effect of Nozzle Design and Operating Conditions on the Atomization and Distribution of Fuel Sprays," by Dana W. Lee, U. S. N.A.C.A., Technical Report No. 425, 1932.

2 "Rates of Fuel Discharge as Affected by the Design of Fuel-Injection Systems for Internal-Combustion Engines," by A. G. Gelalles and E. T. Marsh, U. S. National Advisory Committee for Aeronautics, Technical Report No. 433, 1932.

3 "Processes in Oil-Engine Injection Systems With Spring-Loaded Nozzle-Valves," by S. J. Davies and A. W. Rowe, Proceedings of the Institution of Automobile Engineers, London, vol. 31, 1936, pp. 278–301.

4 "Hydraulics," by R. L. Daugherty, third edition, McGraw-Hill Book Company, Inc., New York, N. Y., 1925.

5 "Coefficients of Discharge of Fuel-Injection Nozzles for Compression-Ignition Engines," by A. G. Gelalles, U. S. National Advisory Committee for Aeronautics, Technical Report No. 373, 1931.

6 "Penetration of Oil Sprays," by P. H. Schweitzer, The Pennsylvania State College, State College, Pa., Engineering Experiment Station, Bulletin No. 46, 1937.

7 "Effect of Orifice Length-Diameter Ratio on Fuel Sprays for Compression-Ignition Engines," by A. G. Gelalles, U. S. N.A.C.A., Technical Report No. 402, 1932.

Variation in Shrinking and Swelling of Wood

By A. J. STAMM[1] and W. K. LOUGHBOROUGH,[2] MADISON, WIS.

The purpose of this paper is to point out that while the forces that cause wood to shrink and swell are chemical in nature, the factors which influence the degree of external dimension change are largely physical or mechanical. Orientation of the structural units, specific gravity or porosity of the wood, and the stresses set up by moisture gradients determine the change in external dimensions as the wood loses or gains moisture. Water-soluble extractives, because of their bulking effect, reduce the shrinkage of wood.

THE shrinking or swelling of the substance of which the cell walls of wood are composed is dependent upon the chemical nature of the wood. The extent to which this shrinking and swelling is transmitted to the external dimensions of the wood is also dependent upon (*a*) the orientation of the structural units, (*b*) the nature and extent of the gross capillary structure, and (*c*) the stresses set up in the wood due to moisture-content gradients or external forces.

Effect of Chemical Composition

The shrinking or swelling of the substance of which the cell walls of the wood are composed, except for a slight adsorption-compression correction (1, 2),[3] is equal to the volume of water lost or gained up to a saturation value known as the fiber-saturation point (3, 4). Values for the fiber-saturation point obtained by a number of different methods vary from about 27 to 33 per cent at room temperature (3). The shrinking and swelling of the wood substance of different species should thus not vary by more than about 20 per cent.

Wood is made up of cellulose, together with other carbohydrate materials, lignin, and extractives. Moisture content - relative vapor pressure data indicate that the holocellulose (the hemicellulose and cellulose in the wood) and lignin are about equally hygroscopic, that is, they have about equal fiber-saturation points (5). The stable cellulose portion of the holocellulose (the alpha cellulose) is somewhat less hygroscopic than the hemicellulose portion. This might account for the tendency for hardwoods (woods from broad-leaved deciduous trees) to have slightly higher fiber-saturation points than softwoods (woods from needle-bearing coniferous trees) as the former have somewhat higher hemicellulose contents than the latter.

The extractives of wood, which are not part of the fibrous structure but are merely infiltrated into the structure, may be divided into two groups: (*a*) Extractives which are soluble only in organic solvents and are deposited only in the coarser microscopically visible capillary structure; and (*b*) extractives which are soluble in water and, as a consequence, are distributed throughout both the free water in the coarse capillary structure and the bound water within the cell walls. The former have no effect upon the shrinking and swelling of wood, but they do affect the specific gravity of wood and, as a consequence, will affect the shrinkage - specific gravity relationship. The water-soluble extractives, however, have a definite effect upon the shrinking and swelling of the cell-wall structure, and, therefore, also affect the shrinking and swelling as transmitted to the external dimensions.

It has been demonstrated by Stamm (6) that water-soluble salts enter the bound water within the cell-wall structure and attain a concentration virtually equal to the concentration in the coarse capillary structure. When wood is dried, free water is first removed from the coarse capillary structure. The salt concentration thus increases in the coarse capillary structure and, as a consequence, salt diffuses into the bound water where the concentration is less. When the drying process is sufficiently slow and the solubility of the salt is sufficiently high so that all the salt within the wood structure will dissolve in the bound water, practically all the salt is finally transferred to the cell-wall structure when drying to the fiber-saturation point. During this process either an equal volume of water or a somewhat smaller volume of water than the volume of the salt taken up is displaced from the cell-wall structure (6, 7). The wood substance thus either retains its water-swollen dimensions or swells slightly, depending upon the nature of the salt (4, 6, 7). When the drying of the wood is continued to the oven-dry condition, the shrinkage is reduced below that which would have taken place if the wood contained only water by an amount equal to the volume of the salt within the cell-wall structure, as the salt is not evaporated. Hence, the reduction in shrinkage is equal to the volume of salt entrapped in the cell wall. This volume can be calculated from the partial specific volume of the salt in the solution when only enough solution is present to fill the transient cell-wall capillary structure (6).

Measurements were made on a series of thin cross sections of green redwood in order to determine the effect of the extractives on the shrinkage. Part of the sections were extracted for 2 weeks in frequently changed water at 60 C. At the end of that time no color appeared in the water after 1 day of soaking. The remainder of the sections were held in a sealed jar at the same temperature. The water-soluble extractive content of the sections was 14.5 per cent and the specific gravity of the extractives was about 1.5. The sections were then dried for 3 days at 90 per cent relative humidity, 2 days at 65 per cent, and 2 days at 30 per cent relative humidity, followed by oven drying for 1 day. The average shrinkage of area, which is practically equal to the volumetric shrinkage, of the extracted sections was 7.7 per cent and of the unextracted sections 6.2 per cent. The average dry weight - green volume specific gravity of the former sections was 0.313 and of the latter 0.353. The presence of the extractives reduced the shrinkage by 19.5 per cent. If the fiber-saturation point of the wood on a volume of water per unit weight of wood is 0.27, then $0.27 \times 0.195 = 0.0525$, which represents the volume of extractives within the cell-wall structure per unit weight of wood necessary to give the experimental reduction in shrinkage.

[1] Principal Chemist, Forest Products Laboratory, Forest Service, U. S. Department of Agriculture.

[2] Senior Engineer, Forest Products Laboratory, Forest Service, U. S. Department of Agriculture. (The Forest Products Laboratory is maintained in cooperation with the University of Wisconsin.)

[3] Numbers in parentheses refer to the Bibliography at the end of the paper.

Contributed by the Wood Industries Division and presented at the Fall Meeting, Louisville, Ky., October 12–15, 1941, of The American Society of Mechanical Engineers.

Note: Statements and opinions advanced in papers are to be understood as individual expressions of their authors and not those of the Society.

This is equivalent to an extractive content of 7.9 per cent of the weight of the dry wood, which is slightly more than one half of the actual amount of extractives present. The fact that only part of the extractive content is effective in reducing the shrinkage is quite logical, as it can be shown from microscopical observation that an appreciable part of the extractives is deposited within the coarse capillary structure, where it can have no effect upon shrinkage.

The data thus indicate that the shrinkage of redwood, which contains an appreciable amount of water-soluble extractives, is considerably lower than it would be if no extractives were present. It is largely for this reason that redwood and woods containing large amounts of water-soluble extractives shrink less than would be predicted on the basis of the shrinkage - specific gravity relationship to be considered later.

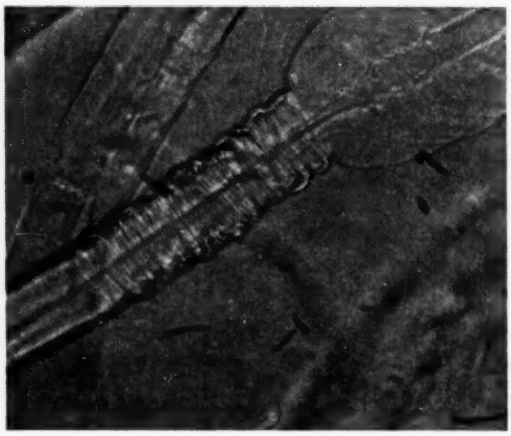


FIG. 1 PHOTOMICROGRAPH OF ISOLATED WOOD FIBER
(This shows outer fibril wrapping at right angles to fiber direction intact over part of fiber length, and ballooning of fiber where it has been removed; reference 9.)

EFFECT OF STRUCTURAL ORIENTATION

The differences in the shrinking and swelling of wood in the different structural directions are due to the highly organized orientation of the structural parts. This orientation also has a very definite effect upon the proportion of the dimension changes which are transmitted to the external dimensions.

The cell walls of wood are believed to be made up primarily of bundles of long threadlike submicroscopic molecules of cellulose, in which zones along the length of the threads are bunched into highly oriented bundles, with zones in between in which the orientation is less perfect. Molecular threads emerging from a single bundle may enter either of several adjacent bundles (8). The less perfectly oriented zones of cellulose threads are believed to be incrusted with hemicelluloses and probably some lignin. The microscopically visible fibrils into which the cell walls can be broken down are made up of large multiples of these submicroscopic threads. Most of the fibrils are oriented at only a slight angle to the length direction of the fibers (9). There is, however, an outer wrapping composed of fibrils which are oriented practically at right angles to the fibers (9). Fig. 1 shows a highly magnified photomicrograph of an isolated wood fiber taken from a report by Ritter (9) in which the outer fibril wrapping is clearly shown on part of the fiber. The ballooning of the fiber in the zone where the fibril wrapping has been removed will be considered later.

X-ray evidence indicates that the adsorbed water is taken up between the highly oriented bundles of threadlike molecules and within the zones of less perfect orientation to add its volume to the volume of the cell walls (10, 11). The dispersing of the structural units thus takes place almost entirely at right angles to the direction of the orientation of the threadlike units. That only a limited amount of water can be taken up within the cell wall is apparently due to the fact that the threadlike molecules which pass from one highly oriented bundle to another do so in such a random way as to tie all of the bundles together through chemical bonds.

Normal woods shrink and swell only about 1 to 2 per cent as much in the fiber direction as across the fibers. This is readily explainable on the basis of the fiber structure just given. The fact that the longitudinal shrinking and swelling is as large as it is, is due to deviations from a linear orientation of the structural units thus causing a slight component of the transverse-dimension changes to occur in the longitudinal direction.

It has been shown by X-ray means that the fibril orientation in compression wood deviates more than normal from the fiber direction (12). As a consequence, compression wood shrinks and swells more than normal woods in the fiber direction (13).

The cellulose fibers of wood are cemented together by a continuous middle lamella of lignin and hemicellulose. The shrinking and swelling of the middle lamella must conform largely to that of the fibers which it surrounds. If this were not the case, there would be evidence of the middle lamella breaking away from the cell wall as a result of shrinking or swelling. The middle lamella evidently possesses enough elasticity, due to molecular rearrangement under stress, to account for this as well as the flexibility of wood.

The shrinking and swelling of wood is from 1.5 to 3.5 times as great in the tangential direction (the direction of the annual rings) as in the radial direction (the direction of a plane through the diameter of the tree) (14). This was formerly believed to be due to ray cells restraining the dimension changes of the wood in the direction of their length, as a result of the assumed orientation of the threadlike units of which the ray cells are composed being in the length direction of the ray cells. It has been recently shown by Ritter and Mitchell (15), however, that the ray cells are made up almost entirely of structural units oriented in the lengthwise direction of the tree. Hence there can be no appreciable restraining action on the shrinking and swelling of wood in the radial direction by the ray cells. Ritter and Mitchell (15) have explained the difference between tangential and radial shrinking and swelling on the basis of the pits which are concentrated on the radial faces of the fibers. The structural units of the radial faces, in passing around the pits, are necessarily less perfectly oriented than on the tangential faces where there are few pits. Consequently, there is less of a transverse shrinking-and-swelling component in the radial than in the tangential direction. Frey-Wyssling (16) has recently come to a similar conclusion.

MOISTURE CONTENT - SHRINKAGE RELATIONSHIPS

The external shrinkage of practically all the softwoods and many of the hardwoods, in any one of the structural directions or combinations of directions, is approximately proportional to the moisture lost from the fiber-saturation point to the dry condition. Fig. 2 gives a typical set of curves for the volumetric shrinkage of loblolly pine boards ($8^1/_2 \times 5^1/_2 \times {}^7/_8$ in.) of different specific gravity, which illustrates this relationship (17). There is a tendency for the lines to have a slightly concave curvature toward the moisture-content axis. This can be accounted for on the basis of the adsorption compression of the bound water (1, 2). There is also a tendency for the lines to show a reverse curvature at moisture-content values just below the fiber-saturation point. This is in large part due to the fact that, in drying specimens of any appreciable dimensions, the outer part of the wood falls below the fiber-saturation point and tends to shrink,

while the average moisture content is still above the fiber-saturation point.

In the case of the normal woods, such as the loblolly pine, the break in the approximately linear relationship can be made to occur much nearer to the fiber-saturation point by very slowly drying thin cross sections of the wood, so as to minimize moisture gradients and resultant drying stresses (14). In the case of some of the hardwoods, notably Southern swamp oak, Fig. 3, the Australian eucalyptus species (14), and beech (18), there is a much more marked tendency for an appreciable shrinkage to occur above the normal fiber-saturation point. This type of shrinkage curve will be considered in more detail later.

When the external volumetric-shrinkage measurements are made on thin transverse wood sections less than 1 fiber length in thickness, which have been previously dried and resoaked, the extrapolation of the linear portion of the curve back to zero shrinkage gives moisture-content intercepts practically equal to the fiber-saturation point of the wood as obtained by other methods (3). The same is roughly true for the extrapolation of the tangential- and radial-shrinkage curves. The tangential- and radial-shrinkage curves, however, often give slightly different intercepts, the tangential usually being slightly higher than the radial (14). The deviation in intercepts can be explained either on the basis of the greater tangential than radial shrinkage causing a greater intensity of tangential than radial stresses and, consequently, a greater deviation from the theoretical stress-free shrinkage; or on the basis of a differential relief of stresses which exist in the green wood. The presence of such stresses is indicated by the fact that Koehler (19) found green wood to increase slightly in tangential dimensions and decrease in radial dimensions on boiling in water.

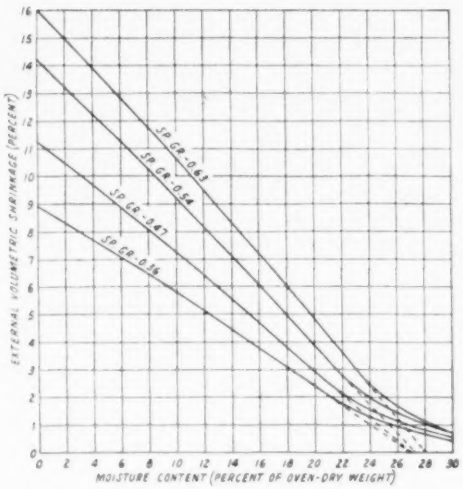


FIG. 2 EXTERNAL VOLUMETRIC SHRINKAGE - MOISTURE CONTENT RELATIONSHIP

(7/8-in. boards of loblolly pine with four different specific gravities; reference 17.)

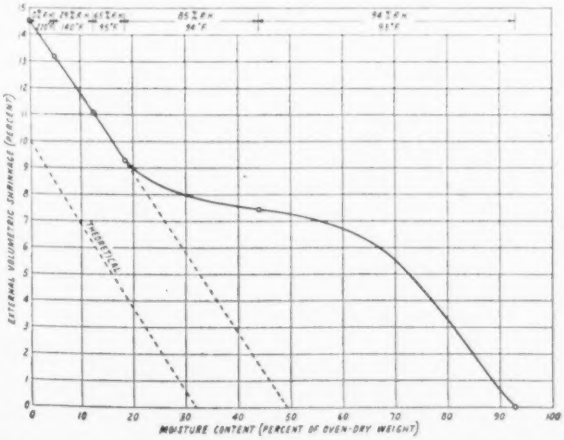


FIG. 3 AVERAGE TANGENTIAL SHRINKAGE - EQUILIBRIUM MOISTURE CONTENT RELATIONSHIP

(1-in. boards of Southern red oak with average specific gravity of 0.565, dry weight green volume basis. Relative humidity and drying temperature used to bring wood to various equilibrium conditions are given.)

The practically linear moisture content - shrinkage relationships would be expected to hold for wood substance, as the volume change would then be entirely due to the removal of bound water and should, in fact, be equal to the volume of bound water removed. The fact that the relationship holds, in general, for the externally manifested dimension changes of wood is due to the nature of the internal-dimension changes which will be considered in the next section.

EFFECT OF CAPILLARY STRUCTURE

Wood varies in specific gravity from about 0.25 to 1. The specific gravity of wood substance is practically constant for all species, the average value as determined in helium being 1.46 (2, 20). This means that the internal voids of wood, which contain either water or air, amount to 83 to 31 per cent of the overall volume. The question thus arises as to how this large void volume affects the shrinking and swelling of wood as transmitted to the external dimensions.

If wood were made up of an unoriented material like a gelatin jelly, the presence of capillary voids would not affect the shrinking and swelling as transmitted to the external dimensions, if the drying or soaking conditions were such as to avoid undue moisture-content gradients and resultant stresses. For example, a thin disk of gelatin jelly with a hole in the center will show the same external-dimension changes on shrinking or swelling as if no hole were present. This is due to the fact that the hole changes in dimensions by the same amount as the disk cut from the hole. If wood acted in a similar manner, the shrinking and swelling of wood would not vary with changes in specific gravity. The shrinking and swelling of wood, in general, increases with an increase in the specific gravity, Fig. 2. This can be accounted for on the basis of the fiber structure. If the cross section of a dry wood fiber is observed under the microscope, it appears like the gelatin disk with a hole through the middle. When a drop of water is placed on the slide near the fiber cross section, it swells at first in a similar manner to the gelatin disk. The diameter of the fiber cavity, as well as the external dimensions, increases. When the external swelling has progressed to the point where the outer wrappings at right angles to the fiber axis are taut, further swelling is forced to be internal and the fiber cavities then decrease in size. On the average, the fiber cavities change but slightly in size for most of the species between the swollen and the dry condition.

The restriction of the external swelling of an isolated wood fiber by the outer fibril wrapping is illustrated in Fig. 1. The lower part of the fiber, from which the outer wrapping has been removed, swells entirely in the external direction. The presence of the wrapper, however, forces a large part of the swelling to occur into the fiber cavity.

Schwalbe and Beiser (21) found, from an analysis of their data for the swelling of spruce, that the fiber-cavity dimensions are practically unchanged when assuming a fiber-saturation point of their wood of 30 per cent. Beiser (22) also has shown from microscopical studies of the cross sections of spruce and beech that the change in size of the fiber cavities resulting from shrink-

ing and swelling of the wood is small. He found that the fiber cavities of springwood increase in diameter slightly or do not change at all upon swelling of the wood, while the fiber cavities of summerwood actually decrease slightly in size. Stamm (23) has also shown, from data on the permeability of the fiber cavities to air of different relative vapor pressures, that the size of the fiber cavities of thin transverse sections of Western white pine and Western hemlock remain practically constant under different degrees of swelling.

The approximate constancy of the size of the fiber cavities between the swollen and the dry condition indicates that part of

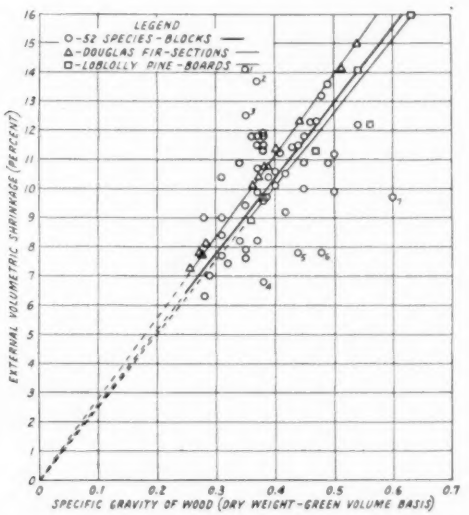


FIG. 4 AVERAGE EXTERNAL VOLUMETRIC SHRINKAGE OF 2 × 2 × 6-IN. SPECIMENS FOR EACH OF 52 DIFFERENT SPECIES OF SOFTWOODS FROM GREEN TO OVEN-DRY CONDITION, PLOTTED AGAINST AVERAGE DRY WEIGHT - GREEN VOLUME SPECIFIC GRAVITY

(Each point represents average of a number of specimens from 4 to 30 different trees; reference (24). Numbered points, which show maximum deviation from the relationship, are for 1 fir, Pacific silver, *Abies amabilis;* 2 spruce, white, *Picea glauca;* 3 fir, noble, *Abies nobilis;* 4 redwood, virgin, *Sequoia sempervirens;* 5 red cedar, eastern, *Juniperus virginiana;* 6 juniper, alligator, *Juniperus pachyphlaea;* 7 yew, Pacific, *Taxus brevifolia.* Similar shrinkage data for thin tangential sections of Douglas fir containing different proportions of springwood and summerwood and for average, maximum, and minimum specific gravity of 50 loblolly pine sapwood boards are also plotted.)

the dimension change occurs internally. This is fortunate for the wood user. If the structure were similar to that of the gelatin jelly, the shrinking and swelling of wood as manifested by external-dimension changes would be several times as great as it actually is.

Stamm (4) has shown that the external volumetric shrinkage of thin tangential sections of Douglas fir, containing different proportions of springwood and of summerwood, which were cut from a single specimen, increase linearly with an increase in the specific gravity of the wood, and that extrapolation of this linear relationship to zero specific gravity gives zero shrinkage, as is shown in Fig. 4. A similar linear relationship is shown for the loblolly pine boards of Fig 2. Other species give similar linear relationships but, in a number of cases, the moisture content-shrinkage regression lines of individual specimens deviate considerably from the mean line of the species.

This same relationship holds in a general way between the average external volumetric shrinkage and average specific gravity of a large number of species of both softwoods and hardwoods, as is shown in Figs. 4 and 5. These data of Markwardt and Wilson (24) are for 2 × 2 × 6-in. specimens of 52 different softwood species, Fig. 4, and of 106 different hardwood species, Fig. 5. Each point represents the average value for a number of specimens taken from 4 to 30 different trees. The slopes of the heavy lines give the mean ratios of the external volumetric shrinkage to the specific gravity for all the data. The mean ratio of the percentage external volumetric shrinkage to the specific gravity for the softwoods is 26 and for the hardwoods is 27. In the case of the softwoods, 50 per cent of the species show a deviation of less than 10 per cent from the mean value and 75 per cent of the species show a deviation of less than 19 per cent from the mean value. In the case of the hardwoods, 50 per cent of the species show a deviation of less than 11 per cent from the mean value, and 75 per cent of the species show a deviation of less than 22 per cent from the mean value. Greenhill (25) gives data for the shrinkage versus specific gravity of 170 different Australian species before reconditioning. The mean ratio of the percentage external volumetric shrinkage to specific gravity is about 27, in excellent agreement with the foregoing values. The deviations from the mean value are, however, somewhat greater in the case of the Australian woods, 50 per cent of the species showing a deviation of less than 21 per cent from the mean value and 75 per cent of the species showing a deviation of less than 33 per cent from the mean value.

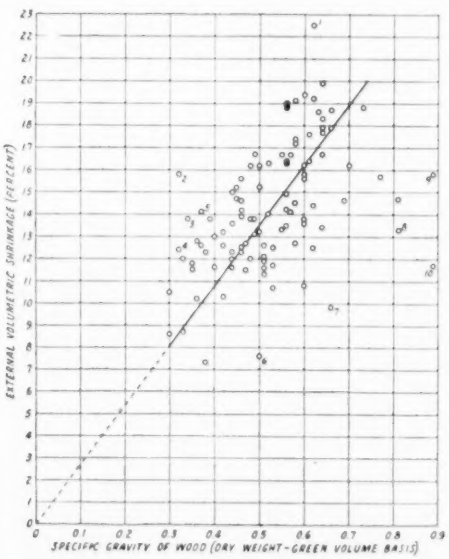


FIG. 5 AVERAGE EXTERNAL VOLUMETRIC SHRINKAGE OF 2 × 2 × 6-IN. SPECIMENS FOR EACH OF 106 DIFFERENT SPECIES OF HARDWOODS FROM THE GREEN TO THE OVEN-DRY CONDITION, PLOTTED AGAINST AVERAGE DRY WEIGHT - GREEN VOLUME SPECIFIC GRAVITY

(Each point represents average of a number of specimens from 4 to 30 different trees, reference (24). Numbered points, which show maximum deviations from the relationship, are for 1 gum, blue, *Eucalyptus globulus;* 2 basswood, *Tilia glabra;* 3 willow, black, *Salix nigra;* 4 cottonwood, northern black, *Populus trichocarpa hastata;* 5 cottonwood, eastern, *Populus deltoides;* 6 cascara, buckthorn, *Rhamnus purshiana;* 7 locust, black, *Robinia pseudoacacia;* 8 stopper, red, *Eugenia confusa;* 9 mangrove, *Rhizophora mangle;* 10 false-mastic, *Sideroxylon foetidissimum.*)

It is of interest that the mean percentage external volumetric shrinkage - specific gravity ratio is practically equal to the average fiber-saturation point of wood, expressed in terms of the volume of water held per 100 g of dry wood (4). Accordingly, the external volumetric shrinkage, S (in per cent), is, on the average, approximately equal to the dry weight - green volume specific gravity of the wood ρ, times the fiber-saturation point f, on a volume of water per unit weight of dry-wood basis (in per cent), thus

$$S = \rho f \longleftrightarrow \left(100\,\frac{l^3}{l^3} = \frac{w}{l^3} \times 100\,\frac{l^3}{w}\right)$$

The equation in parentheses, where l is a linear dimension and w is the weight, shows that the relationship is dimensionally sound.

When the proportionality constant f has a mean value equal to the fiber-saturation point on a volume-of-water basis, the fiber cavities of wood will not change in size when the wood shrinks and swells. This is further confirmation of the findings previously given that the fiber cavities of most woods tend to remain constant in size.

There are a few species, however, which are numbered and listed in Figs. 4 and 5, which shrink either considerably more or less than is compatible with the f value, which corresponds to constant fiber-cavity dimensions. It is of interest that the species having abnormally low shrinkage values are, in general, species which are rather high in water-soluble extractives. It has already been shown that the presence of extractives in redwood is largely if not entirely responsible for the low shrinkage. Removal of the water-soluble extractives shifted the f value for

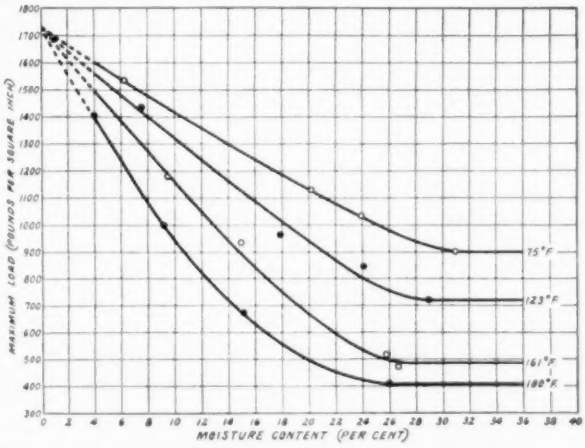


FIG. 6 RELATIONSHIP BETWEEN MAXIMUM LOAD IN TENSION PERPENDICULAR TO GRAIN AND MOISTURE CONTENT OF BEECH AT FOUR DIFFERENT TEMPERATURES

the specimens of redwood tested from the abnormally low value of 18 per cent to the practically normal value of 25 per cent.

EFFECT OF STRESSES

Deviations from the general shrinkage relationship, other than those due to extractives, are due to changes in the fiber-cavity dimensions. These changes result from externally imposed stresses or stresses resulting from moisture gradients, induced by either a process of moisture loss or moisture regain.

An extreme case in which the externally manifested shrinking and swelling can be shifted to internal-dimension changes has been demonstrated by Tiemann (26). A dry block of wood is clamped in a mechanical device so that its external dimensions cannot change. It is then placed in a water-saturated atmosphere or in water and allowed to come to equilibrium. When removed from the clamp and dried the external dimensional shrinkage is practically the same as if the block had previously swollen normally. If the block is again clamped in the mechanical device and allowed to absorb water, followed by drying, the block shrinks to yet smaller external dimensions than after the first drying. After ten such cycles Tiemann has shown that the volume of a block of wood can be reduced to about two thirds of its original value. Perkitny (27) has similarly shown that mechanical restraint in a single direction increases the shrinking and swelling in the other directions. In the case of plywood mechanical restraint practically eliminates both swelling and shrinking in the sheet directions. The actual swelling and shrinking is not reduced, however, but merely shifted to the thickness direction and internally into the fiber cavities.

It is thus evident that wood which is subjected to abnormally high compressive forces while drying will shrink more in external dimensions than normal and the fiber cavities will be reduced in size. Conversely, wood which is subjected to abnormally high tension forces while drying will shrink less in external dimensions than normal and the fiber cavities will be increased in size.

The effects due to drying stresses are somewhat more complicated than those due to externally applied forces, because both

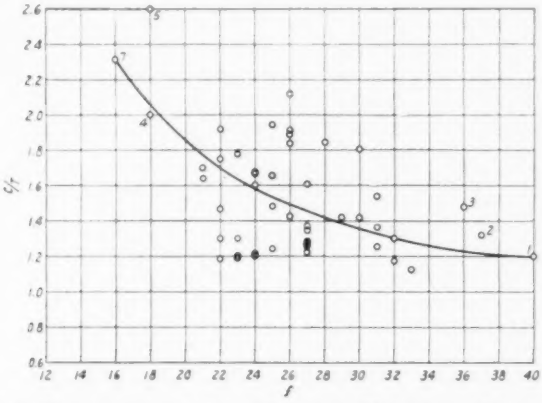


FIG. 7 VARIATIONS OF AVERAGE EXTERNAL VOLUMETRIC SHRINKAGE (IN PER CENT)—SPECIFIC GRAVITY (DRY WEIGHT - GREEN VOLUME) RATIO f, WITH RATIO OF AVERAGE COMPRESSIVE TO AVERAGE TENSILE STRENGTH PERPENDICULAR TO GRAIN FOR GREEN WOOD C/T, OF EACH OF 49 DIFFERENT SPECIES OF SOFTWOODS
(Numbered species are the same as in Fig. 4.)

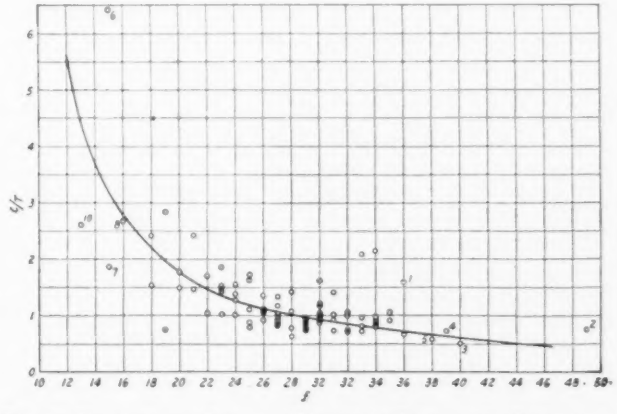


FIG. 8 VARIATION OF AVERAGE EXTERNAL VOLUMETRIC SHRINKAGE (IN PER CENT)—SPECIFIC GRAVITY (DRY WEIGHT - GREEN VOLUME) RATIO f, WITH RATIO OF AVERAGE COMPRESSIVE TO AVERAGE TENSILE STRENGTH PERPENDICULAR TO GRAIN FOR GREEN WOOD C/T, OF EACH OF 89 DIFFERENT SPECIES OF HARDWOODS
(Numbered species are the same as in Fig. 5.)

tension and compression stresses are set up in different parts of the wood at the same time. These stresses are always in balance because of the fact that they are autoapplied and self-contained. The neutral axis is constantly shifting as the wood dries. The surface fibers go from maximum tension in the early stages of drying to compression when the process is complete. Conversely, the central fibers are at first squeezed and in the final stages of drying they are stretched. Not only do the stresses vary as drying progresses, but also the resistance to the stresses, due to the fact that dry wood is stronger than wet wood, Fig. 6.

When a green board is exposed to a drying atmosphere the surface fibers soon attain a moisture content which is well below the fiber-saturation point. Thus, a moisture gradient is es-

tablished. As drying continues, the moisture distribution changes constantly. Successively lamina by lamina the number of fibers which have been dried below their fiber-saturation point increases and the number which are not dry enough to shrink decreases. As the normal shrinkage tendency is directly proportional to the moisture lost below the fiber-saturation point, there is a constantly shifting stress pattern which follows the changing moisture distribution.

If, as is usually the case, the tension stress set up in the surface lamina exceeds the elastic limit in tension perpendicular to the grain, the surface lamina becomes set in tension. If the tensile strength at maximum load is exceeded the piece fails, creating a surface check. If, on the other hand, the surface stresses are not relieved by face checking of the wood, they exert a compression upon the inner laminae which have not dried. If this compression exceeds the compressive strength of the wood, the fiber walls will collapse into the fiber cavities.

Collapse, occurring in the early stages of drying, has also been attributed by some investigators (14, 25, 28) to a liquid tension set up in the fiber cavities which are completely full of water. This tension results from the evaporation of water from the fiber cavities through pit membrane openings which are so small that they reduce the relative vapor pressure of the water by an amount such that the vapor tension exceeds the compressive strength of the cell walls. Such a tension can be set up only when the fiber cavities are completely full of water, since any contained air bubble, which has a greater diameter than the largest opening through which evaporation occurs, will expand under the tension and, as a consequence, relieve the stress on the cell wall. These conditions for liquid-tension collapse may be met by randomly distributed fibers in the case of some species. In practice, however, the collapsed fibers are not randomly distributed throughout the wood but are located in the central zone which is under compression. For this reason, and others which will be discussed later, it appears to the authors that collapse is more generally due to compression stresses set up during the drying process than to a liquid tension.

When wood is dried under controlled conditions, moisture-content gradients near the surface are not permitted to become sufficiently steep to cause face checking. If the wood is equally strong in compression and in tension perpendicular to the grain, the wood will normally not collapse. Under these conditions, the tension set up in the surface fibers will tend to keep the fibers stretched. As drying progresses, a zone a little farther into the wood will dry below the fiber-saturation point and change from a zone under compression to one under tension. Meanwhile, the outer zone under the influence of the tension stress becomes set in tension, that is, retains its dimensions, even though the tension stresses are relieved. Each lamina of the wood in to the center will successively be subject to a tension stress. Naturally, under these conditions, the shrinkage of the wood will be less than it would have been if drying stresses had been absent.

If, on the other hand, the compressive strength of the wood perpendicular to the grain is considerably less than the corresponding tensile strength, then a drying gradient which will avoid face checking of the wood may be sufficiently great to cause collapse within the inner part of the wood. The zone in which collapse occurs will collapse before that zone has fallen below the fiber-saturation point since any shrinkage in the zone will naturally relieve the compressive stress.

From this it appears that woods which have a high compressive strength relative to the tensile strength perpendicular to the grain will tend to shrink less than normal, whereas, woods which have a low compressive strength relative to the tensile strength perpendicular to the grain will tend to shrink more than normal. That this is the case is illustrated by the data of Figs. 7 and 8, in which the shrinkage - specific gravity ratio values of Figs. 4 and 5 are plotted against the ratio of the compressive to the tensile strength perpendicular to the grain for the green wood. A few of the species shown in Figs. 4 and 5 had to be omitted in Figs. 7 and 8 because of the lack of tensile-strength data, thus accounting for the fewer points. Although there is considerable spread among the points, the trend is obvious.

It should be pointed out that the strength values used (24) are those obtained for mechanical purposes and deviate somewhat from the values which should be used here. The compressive-strength values of Markwardt and Wilson include a shear factor around the edges of the plate causing the compression, so that they will be slightly higher than the desired compression values. The tension values, on the other hand, are probably a little low, due to a slight experimentally unavoidable bending moment. The ratios of compressive to tensile strength may thus be somewhat high but their relative values should be approximately correct.

In order to analyze comprehensively the effects of stresses on the shrinkage of wood, it would be necessary to know both the tensile and compressive strengths perpendicular to the grain both at different temperatures and for different moisture contents. A valuable start has been made by Greenhill (29) in obtaining such data. His investigation was confined entirely to the tensile-strength properties of beech perpendicular to the grain. The data show a decrease in the maximum load, Fig. 6, the load at elastic limit, and the modulus of elasticity both with an increase in temperature and an increase in moisture content. He also obtained a decrease in unit deformation at maximum load with a decrease in temperature for temperatures below 120 F, which seems to correspond to the temperature of maximum deformation.

It is highly probable that for some woods the decrease in compressive strength perpendicular to the grain with increases in temperature and moisture content will parallel the tensile-strength values, whereas in other cases the decrease in the compressive-strength values may appreciably exceed the decrease in tensile-strength values. This is indicated by the fact that white-pine specimens dried at winter air-drying temperatures and also at 170 F under several different relative-humidity conditions give practically the same shrinkage, presumably because the ratios of tensile- to compressive-strength values are about equal under the various conditions. White oak, on the other hand, gives a rather large increase in shrinkage with an increase in the drying temperature which indicates that the compressive strength perpendicular to the grain must decrease considerably more rapidly than the corresponding tensile strength as the temperature is raised. This would promote an increase in both forms of collapse with an increase in temperature.

Steaming of wood, after it is partially seasoned, results in a reduced shrinkage on subsequent drying (25, 28). The steaming raises the moisture content and causes swelling of the outer lamina to the point at which the normal drying stresses are reversed. The outer lamina is put under compression and the inner part of the wood under tension. This tension tends to relieve the previous compression of the inner part of the wood, resulting in an expansion of the wood as a whole. When the steamed wood is again dried it is normally subjected to a lower relative humidity than that at which drying was initially started, as the wood is less susceptible to face checking. This rapidly puts the outer lamina again in tension and results in a tension set which brings the center of the wood under further tension as drying progresses. The resultant is the setting up of a tension stress in the center of the wood, both during steaming and subsequent drying. The shrinkage is therefore reduced below the normal for normal wood and still more for wood which is subject

to either a compression collapse or collapse due to a liquid tension.

This method of reducing the shrinkage of wood by reconditioning with steam is extensively used in Australia on species of wood which shrink greatly (25). According to the data of Greenhill (25), the shrinkage of Australian timbers can, on the average, be reduced to about 70 per cent of the normal value by using this steaming process. That is to say, the average shrinkage - specific gravity ratio is reduced from the normal value of 27, as previously mentioned, to 19. Because of the fact that on the average the fiber cavities of the Australian woods did not change in size on normal drying and actually increased in size after reconditioning, the process is, in general, one of creating a tension set in normal wood rather than one of recovering collapsed wood from collapse. Although collapse undoubtedly took place in the case of the woods having abnormally high shrinkage - specific gravity ratios, the reduction in shrinkage by steaming does not indicate that collapse had necessarily taken place.

The peculiar moisture content - shrinkage curve, of Fig. 3, can be explained on the basis of drying stresses. The drying of the outer part of the wood caused a compression stress on the green inner zone which was sufficiently great to result in a collapse of the inner fibers. During the early stages of drying the inner part of the wood offered little resistance to the shrinkage of the surface fibers. The inner fibers, therefore, were squeezed. The over-all shrinkage was made possible by a decrease in the size of the cell cavities in the portion under compression. In due time when the compressed interior fibers began to lose hygroscopic moisture, the shrinkage of these fibers occurred so as to relieve the squeeze, rather than manifesting itself externally in the usual manner. When the elastic limit in compression of the wet fibers has not been exceeded, the cell cavities will gradually attain their original size as shrinking continues. On the other hand, if the elastic limit has been exceeded, the cell cavities will only partially regain their original size.

Regardless of whether the elastic limit has been exceeded or not, the space occupied by the compressed fibers will not become smaller until the compressive force has been neutralized by their shrinkage. This accounts for the relatively flat section of the moisture - shrinkage curve. In the early stages of drying, tension set in the outer zones of the wood developed tardily and only to a minor extent, due to the high relative humidities employed and to the plasticity of the core. For this reason the tension stress was not able to overcome the collapse completely. Normal shrinkage thus occurred during the last stages of drying. This is indicated by the approximate parallelism of the latter part of the shrinkage curve with the theoretical curve for wood of the same specific gravity.

When wood that gives a shrinkage - moisture content curve like that of Fig. 3 is commercially dried, it is subject to honeycombing. This occurs when the core has been stressed in compression beyond its elastic limit when green. Under these conditions, particularly at high temperatures, a high degree of tension set in the outer zone puts the collapsed fibers into tension which can only be relieved as they dry by internal rupture of the structure.

A moisture contents—hrinkage curve with a similar but much less pronounced hump to that in Fig. 3 was obtained by Stevens (18) for the drying of thin cross sections of beech only $^1/_8$ in. in the fiber direction. This indicates that drying stresses are still somewhat effective even in such thin transverse sections.

The size of the wood specimen will affect the shrinkage in so far as the size of the specimen affects drying stresses. Although the use of thin sections of wood cut across the fibers would be expected to minimize drying stresses appreciably, considerable evidence has been accumulated to indicate that these stresses are never completely eliminated. In the case of many woods these stresses are insufficient to affect the shrinkage appreciably. Presumably, these woods are the ones that have approximately equal tensile and compressive strengths perpendicular to the grain.

The shrinkage of $^1/_8$-in. cross sections of the numbered species in Figs. 4 and 5, which showed abnormally low and also abnormally high shrinkage values in larger specimens, continued to be both low and high, indicating that drying stresses were still present. These sections were initially dried at 90 per cent relative humidity. Because of the small size of the sections and the high relative humidity, very little tension set was obtained. Even under these conditions, drying of the tangential faces was not uniform because the edges dried a noticeable amount before the center of the faces. This exerted a dead-load squeeze on the inner zone, which was, naturally, accentuated by relative humidities that minimize tension set. For this reason all the sections shrunk slightly more than the larger blocks. It thus appears that the shrinkage of thin sections will tend to exceed the shrinkage of large specimens, regardless of whether the wood tends to shrink to an abnormally large or small extent. Although tension set can be largely avoided by carefully drying thin cross sections, compression and collapse apparently cannot be avoided.

If the abnormally high shrinkage of the numbered species of Figs. 4 and 5 were primarily due to a liquid-tension collapse, the use of thin transverse sections should have minimized this collapse because most of the fibers were cut across at least once, making it impossible for a liquid tension to be set up within these fiber cavities. It thus appears that the collapse at least of these particular woods is primarily due to a compression stress set up in drying rather than to a liquid tension.

Summary

The shrinking and swelling of wood substance has been shown to depend upon the chemical composition, being chiefly affected by water-soluble extractives which may reduce the shrinkage by 20 per cent or more. The shrinking and swelling, as transmitted to the external dimensions, has been shown to depend also upon (*a*) the orientation of the structural units; (*b*) the nature and extent of the gross capillary structure, and (*c*) the stresses set up in the wood by moisture gradients or external means. The directional shrinking and swelling is shown to be primarily due to structural orientation. There is a tendency for the fiber-cavity size to remain constant when the wood shrinks and swells. This makes the shrinkage tend to be equal to the specific gravity of the wood (dry weight - green volume basis) times the fiber-saturation point of the wood on a volume of water per unit weight of wood basis. Deviations from this relationship are caused by stresses and by water-soluble extractives.

When the compressive strength of the wood perpendicular to the grain is low relative to the tensile strength, the wood tends to collapse under drying stresses, and hence shrinks excessively. When the tensile strength of the wood perpendicular to the grain is low relative to the compressive strength, the wood tends to shrink less than normal under the drying stresses. In the authors' opinion, collapse is more generally due to compressive stresses than to a liquid tension.

BIBLIOGRAPHY

1 "Calculations of the Void Volume in Wood," by A. J. Stamm, *Industrial and Engineering Chemistry*, vol. 30, 1938, pp. 1280–1281.

2 "The Bonding Force of Cellulosic Materials for Water (From Specific Volume and Thermal Data)," by A. J. Stamm and L. A. Hansen, *Journal of Physical Chemistry*, vol. 41, 1937, pp. 1007–1016.

3 "The Fiber-Saturation Point of Wood as Obtained From Electrical Conductivity Measurements," by A. J. Stamm, *Industrial and Engineering Chemistry*, Analytical edition, vol. 1, 1929, pp. 94–97.

4 "Shrinking and Swelling of Wood," by A. J. Stamm, *Industrial and Engineering Chemistry*, vol. 27, 1935, pp. 401–406.

5 "Sorption of Water Vapor by Papermaking Materials," by C. O. Seborg, F. A. Simmonds, and P. K. Baird, *Industrial and Engineering Chemistry*, vol. 28, 1936, pp. 1245–1250.

6 "Effect of Inorganic Salts Upon the Swelling and the Shrinking of Wood," by A. J. Stamm, *Journal of the American Chemical Society*, vol. 56, 1934, pp. 1195–1204.

7 "Colloid Chemistry of Cellulosic Materials," by A. J. Stamm, U. S. Department of Agriculture, Miscellaneous Publication 240, 1936.

8 "Intermicellar Hole and Tube System in Fiber Structure," by H. Mark, *Journal of Physical Chemistry*, vol. 44, 1940, pp. 764–788.

9 "Structure of the Cell Wall of Wood Fibers," by George J. Ritter, *Paper Industry*, vol. 16, 1934, pp. 178–183.

10 "Das Problem der Quellung der Cellulose und ihrer Derwate," by J. R. Katz, *Cellulosechemie*, vol. 11, 1930, pp. 17–30.

11 "The Laws of Swelling," by J. R. Katz, Trans. Faraday Society, vol. 29, 1933, pp. 279–300.

12 "Cellulose as It Is Completely Revealed by X-Rays," by G. L. Clark, *Industrial and Engineering Chemistry*, vol. 22, 1930, p. 474.

13 "Structure, Occurrence, and Properties of Compression Wood," by M. Y. Pillow and R. F. Luxford, U. S. Department of Agriculture, Technical Bulletin 546, 1937.

14 "The Shrinkage of Australian Timbers—Part I," by W. L. Greenhill, Australian Council for Scientific and Industrial Research, Division of Forest Products, Technical Paper 21, Pamphlet 67, 1936.

15 "Crystal Arrangement and Swelling Properties of Fibers and Ray Cells in Basswood Holocellulose," by George J. Ritter and R. L. Mitchell, *Paper Trade Journal*, vol. 108, Feb. 9, 1939, pp. 33–37.

16 "Die Anisotropie des Schwindmasses aus der Holzquerschnitt," by A. Frey-Wyssling, *Holz als Roh u. Werkstoff*, vol. 3 (2), 1940, pp. 43–45.

17 "Shrinkage of Boards of Douglas Fir, Western Yellow Pine and the Southern Pines," by E. C. Peck, *American Lumberman*, July 14, 1928, pp. 52–54.

18 "The Shrinkage and Expansion of Wood," by W. D. Stevens, *Forestry*, vol. 12, 1938, pp. 38–43.

19 "Effect of Heating Wet Wood on Its Subsequent Dimensions," by A. Koehler, American Wood-Preservers' Association Proceedings, vol. 29, 1933, pp. 376–388.

20 "Density of Wood Substance, Adsorption by Wood, and Permeability of Wood," by A. J. Stamm, *Journal of Physical Chemistry*, vol. 33, 1929, pp. 398–414.

21 "Die Quellung von Holz durch Wasser und wässrige Lösungen," by C. G. Schwalbe and W. Beiser, *Papier-Fabrikant*, vol. 31, 1933, pp. 655–667.

22 "Mikrophotographische Quellungsuntersuchungen von Fichten- und Buchenholz an Mikrotomschnitten im durchfallenden Licht und an Holzklötzchen im auffallenden Licht," by W. Beiser, *Kolloid-Zeitschrift*, vol. 65, 1933, pp. 203–211.

23 "The Effect of Changes in the Equilibrium Relative Vapor Pressure Upon the Capillary Structure of Wood," by A. J. Stamm, *Physics*, vol. 6, 1935, pp. 334–342.

24 "Strength and Related Properties of Woods Grown in the United States," by L. J. Markwardt and T. R. C. Wilson, U. S. Department of Agriculture, Technical Bulletin 479, 1935.

25 "The Shrinkage of Australian Timbers—Part II," by W. L. Greenhill, Australian Council for Scientific and Industrial Research, Division of Forest Products, Technical Paper 35, Pamphlet 97, 1940.

26 "Does Paint Preserve Wood?" by H. D. Tiemann, *Scientific American*, vol. 130, 1924, pp. 314–315.

27 Über den Einfluss mechanischer Hindernisse auf Quellung und Schwindung von Kiefernholz," by T. Perkitny, *Holz als Roh u. Werkstoff*, vol. 1 (12), 1938, pp. 449–454.

28 "Lessons in Kiln Drying," by H. D. Tiemann, *Southern Lumberman*, Nashville, Tenn., 1938.

29 "Strength Tests Perpendicular to the Grain of Timber at Various Temperatures and Moisture Contents," by W. L. Greenhill, *Journal*, Australian Council for Scientific and Industrial Research, vol. 9, 1936, pp. 265–276.

Progress in Methods of Edge-Gluing Lumber and Veneers

By H. K. VON MALTITZ,[1] CHICAGO, ILL., and O. BOLLING,[2] MINNEAPOLIS, MINN.

Boards for lumber cores of plywood, for solid-dimension stock, such as chair seats, solid tops, etc., are still almost universally edge-glued together with conventional cold-setting glues, i.e., animal, vegetable, and casein. Veneers are still widely taped together and, when edge-glued without tape, are generally glued with prespread animal glue. This paper describes new methods and machines[3] for edge-gluing lumber and veneer with waterproof and water-resistant heat-setting adhesives, particularly urea-formaldehyde resin, and points out the advantages gained through adoption of these new methods.

WITHIN the last 5 years, the widespread adoption of synthetic-resin adhesives by the plywood and furniture industries has rendered obsolete the older conventional glues. To date, however, the resin adhesives have been limited chiefly to the gluing together of the laminations or plies of plywood. The older conventional glues are still in general use for edge-gluing of lumber-core stock for lumber-core plywood, solid-dimension stock for chair seats, solid tops, etc., and also for edge-gluing of veneers when tape is not used.

The ideal plywood panel, whether veneer core or lumber core, is one in which all edge joints, as well as the laminations or plies, are welded together with waterproof or water-resistant glue. In like manner, the ideal solid top is one in which the exposed joints are bonded with water- and mold-proof glue. Such edge joints prevent deterioration from exposure to moisture and mold. However, the glues commonly used for edge joints are subject to deterioration from these causes.

For the purpose of this discussion, the edge-gluing methods will be divided into two categories:

1 Lumber: boards or strips from 1/4 in. thickness up.

2 Veneers: rotary-cut, sliced, and sawed sheets from 1/4 in. thickness down.

Edge-Gluing of Lumber With Resin Adhesives

The conventional method of edge-gluing lumber in the United States is by means of clamping the stock in piling clamps or in revolving clamp carriers. The latter method in particular is widely employed throughout all of the wood industries. The most commonly used adhesive for this purpose is animal glue, while vegetable and casein glues are also used for this purpose, but to a lesser extent.

Within recent years, some work has been done in rather isolated instances with the use of urea-formaldehyde resins in clamp carriers. When a fast-acting cold-setting hardener or catalyst is used in the resin-glue mix, the work generally is left in the clamps for approximately 50 min at room temperature (70 to 75 F), or slightly less if the clamp carriers are hooded over and the surrounding air is heated to 110 to 140 F. Preheating the stock will also reduce the setting time. The most rapid gluing is obtained with this method when paint-on hardeners are used, whereby the resin mixed with a slower hardener is applied on one edge and the fast paint-on hardener is applied on the other edge of the pieces to be glued together. However, even with the fastest possible cold-setting resin glue, the clamping time is still approximately 20 to 30 min minimum. Thus, while the use of resin adhesives in the conventional clamping equipment brings about qualitative benefits, no particular advantages are gained from the standpoint of production increase.

Lumber-Core Continuous-Feed Presses

After years of research and thorough testing, a revolutionary new method and machine have been developed for gluing lumber cores and other types of glued-up lumber dimension stock. The purpose of this new machine, known as the lumber-core continuous-feed press, is threefold:

1 Cost reduction.

2 Straight-line production in lumber-core department, eliminating present drying interval necessary to remove glue moisture.

3 Better quality edge-glued joints, through use of waterproof urea-formaldehyde resin glue in place of the usual water-soluble glues. Quality is also enhanced by the prevention of sunken joints in finished veneered-lumber-core panels.

Advantages of New Lumber Edge-Gluing Method

In the conventional lumber-core process, the lumber strips or boards coming from the ripsaw or glue jointer are matched to width. In some instances this is done on a matching saw; in others right at the straight-line ripsaw. Instill other instances, accurate matching to width is not practiced. Instead, the boards for each core are laid up to approximate width only.

The prematched cores are then taken to the piling clamps or clamp carriers and are glued up.

With the lumber-core continuous-feed press, this matching operation is omitted in many cases, because the core or other product is glued up in an endless ribbon of stock and is automatically divided to width by an automatic cross-traveling rip saw, located at the outfeed end of the lumber-core machine. This elimination of the matching operation saves time, material, and labor.

The new lumber-core press further introduces the possibility of greatly increased production with thesame personnel. Ordinarily, one lumber-core machine has the capacity of two or more 40-section clamp carriers.

In some lumber edge-gluing operations, the cores are trimmed to length or are squared up after leaving the clamp carrier and before being veneered. This function can be performed by the lumber-core press in the same operation in which the stock is glued together, by means of end-trim saws, situated at the outfeed end of the machine.

Also to be considered is the fact that, under the conventional core-gluing methods, the cores are usually stick-piled after re-

---

[1] The Plycor Company, associated with the Mereen-Johnson Machine Company, and the Adamson Machine Company.

[2] Mereen-Johnson Machine Company.

[3] Application has been made for various United States patents, which are pending on the machines described and illustrated in this paper.

Contributed by the Wood Industries Division and presented at the Fall Meeting, Louisville, Ky., October 12–15, 1941, of The American Society of Mechanical Engineers.

Note: Statements and opinions advanced in papers are to be understood as individual expressions of their authors and not those of the Society.

moval from the clamps, and are then often kiln-dried for 48 hr or more until all glue moisture is dried out. Otherwise sunken joints would later develop. Animal glues, such as used in edge-gluing lumber, are frequently mixed in proportions of 1 part glue to 2¼ parts water. The liquid glue, therefore, contains approximately 70 per cent water. This glue is spread so that 65 lb or more of liquid glue covers 1000 sq ft of surface.

In contrast, the urea-resin mixture, employed in the new continuous-feed press, contains only approximately 30 per cent water. In addition, the resin glue is spread very thin, so that only about 30 to 32 lb of liquid glue cover 1000 sq ft of surface.

Therefore, it is quite obvious that the new edge-gluing method introduces only about one fourth the amount of moisture into the joint as that introduced by the conventional gluing method.

This great reduction in the amount of water introduced, plus the fact that the joints are subjected to heat in the core press, prevents the later development of sunken joints. At the same time, the stick-piling and kiln-drying operations are eliminated, as the slight amount of excess moisture introduced is quickly distributed through the stock. Also, the heating of the wood vaporizes a considerable portion of this moisture.

A further fact to be considered is that lumber-core joints, glued with animal or vegetable glues, often deteriorate greatly in strength when the cores are thereafter veneered in a hot-plate plywood press. The resin-bonded cores are in no way affected by this subsequent reheating.

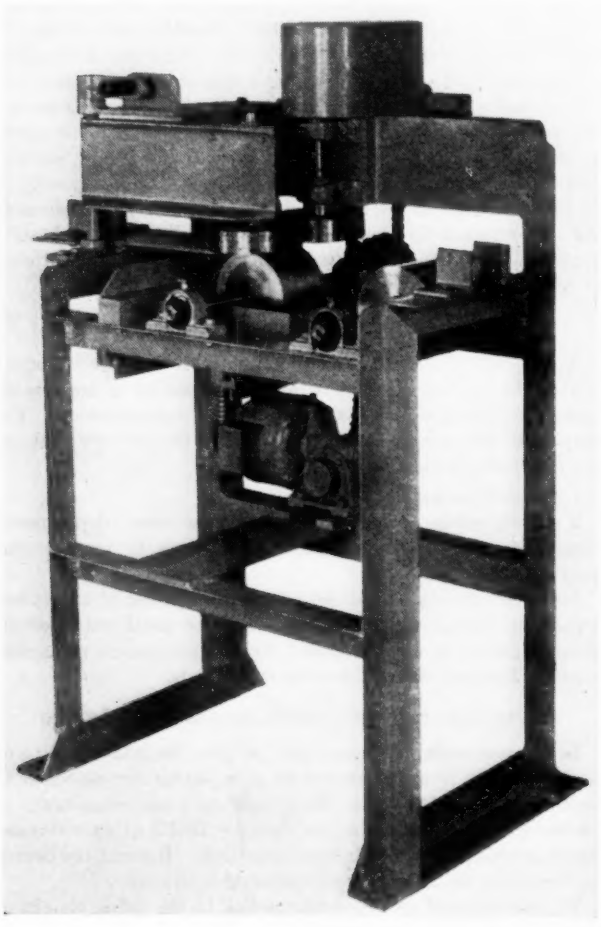


FIG. 1 HAND-FED CORE-EDGE GLUE SPREADER

SOME OPERATING DETAILS OF NEW LUMBER-CORE PRESS

The boards to be glued together can be brought directly from the ripsaw or glue jointer to the lumber-core press, without matching to width. The edges are then spread with urea-resin glue (one edge only of each board). This spreading is done by a power-feed core-edge glue spreader, which may be either hand-fed or hopper-fed, Figs. 1 and 2.

The operator feeding the lumber-core press takes the boards as they come out of the glue spreader and places them on the feed table of the core machine, Figs. 3 and 4. A reciprocating pusher plate feeds these boards or strips into and through the machine continuously.

A continuous ribbon of lumber core, chair seats, solid tops, etc., thus passes through the core press. In the machine, the boards are subjected to powerful edge pressure. This pressure establishes and maintains firm edge-to-edge contact and squeezes out surplus glue. As the boards then continue to move forward through the machine, they are subjected to heat from above and below, transmitted by top and bottom steam-heated hot plates. The glue is set in this hot zone to a sufficient depth from each surface to permit safe handling of the freshly glued cores. Due to the use of a cold-setting hardener in the resin, the cure of the glue continues after the cores are discharged from the machine. Generally, the resin will have set up all the way through the joint within 10 to 15 min after the core emerges from the core press, because of the effect of continued heating as the stock slowly cools.

The boards, as glued together, emerge from the lumber-core press in the form of an endless ribbon of stock. At the outfeed end of the machine, this endless ribbon of lumber is divided into

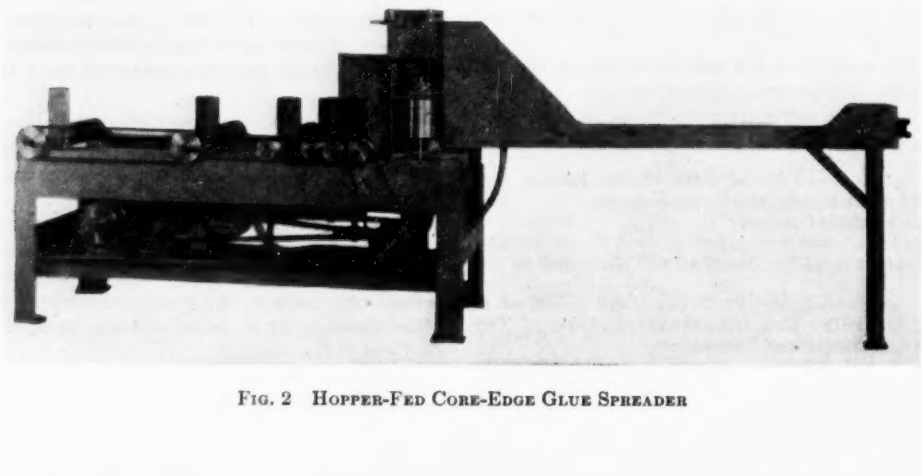


FIG. 2 HOPPER-FED CORE-EDGE GLUE SPREADER

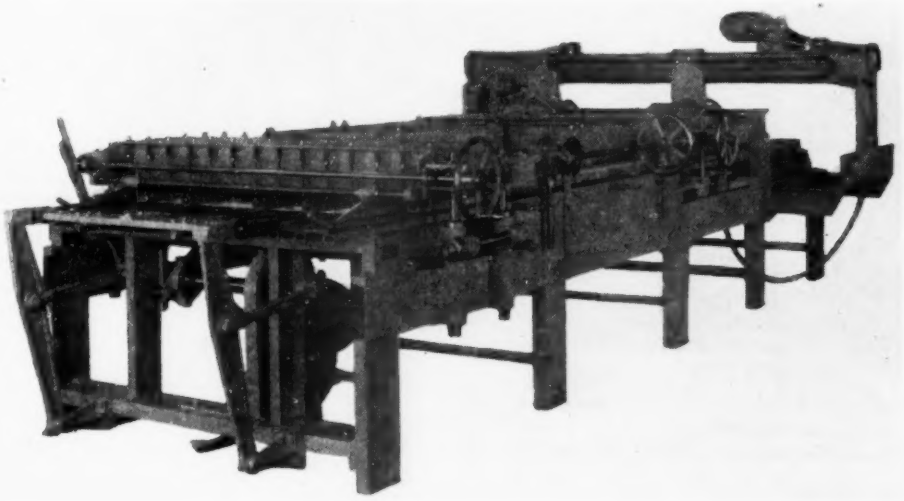


FIG. 4 LUMBER-CORE PRESS

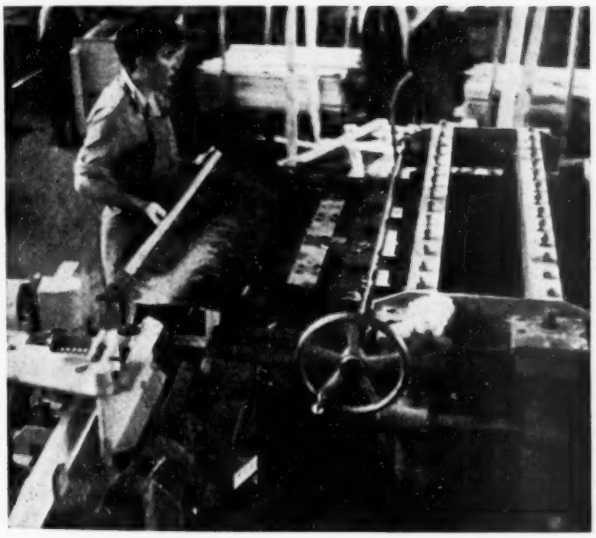


FIG. 3 OPERATOR FEEDING BOARDS AS THEY COME FROM THE GLUE SPREADER ONTO TABLE OF LUMBER-CORE PRESS

any desired width by an automatic cross-traveling ripsaw. The operation of this saw is started when the end of the core trips an adjustable trigger in the outfeed table of the machine.

The cores can also be divided to width periodically by leaving a dry joint in the assembly at the feed end. When this latter method is employed, it is generally necessary to match the cores or tops to width beforehand.

The core machine can also be equipped with one, two, or more end-trim saws. The purpose of these is to trim the cores to desired length, to square them up, or to divide them into shorter lengths if this latter is desired. Thus, it is seen that this new lumber-core continuous-feed press not only glues up the stock, but also dimensions the cores on all four sides; it even divides the stock into shorter lengths.

The lumber-core machines are generally built to handle any lumber from 1/2 to 1 1/2 in. thick. Stock as thin as 1/4 in. and thicker than 1 1/2 in. can also be handled in special machines. The greatest length of stock which can be handled in any given machine depends, of course, upon the size of the machine in question. These machines are built in a number of standard sizes. Naturally, there is no limit to the width of the cores which can be produced in any machine.

The machines can also be equipped to handle two or more rows of short stock. In that case, the stock is fed in two or more rows, side by side. This feature is of value not only for short lumber-core stock, but also for such products as solid chair seats, etc., which are relatively short in length. When feeding multiple lines of core, dividing to width is generally done by means of dry joints, unless the core strips in both lines are all of identical width.

The lumber-core presses will handle tapered stock, i.e., the two edges of each board do not have to be parallel. However, both edges must be straight. Joints suitable for this process can be made on a glue-joint ripsaw or on a glue jointer. Joints can be flat, or they can be tongue and groove. However, the core press eliminates one of the chief needs of tongue-and-groove joints, namely, holding the boards in alignment. The core press exerts such great flattening pressure that the need for tongue-and-groove joints is eliminated.

After the dimensioned cores are discharged from the lumber-core press, they are dead-piled (or stick-piled for faster cooling), and are then ready for surfacing in the planer. Cooling can be forced for yet quicker processing. If the factory layout permits, movement of the cores from the core press to the planers can be effected by means of conveyer, with cooling taking place en route.

The production of a lumber-core machine depends not so much upon the thickness of the core as it does upon the proficiency of the operator and upon the correct catalyst being used in the resin glue. Experience has shown that cores up to 1 in. thick can be fed through the machines at speeds averaging 4 to 5 linear ft per min. The actual feeding speed is higher, but the progression of the stock through the machine is "stop-start." These speeds can be exceeded under favorable conditions, and may also be less under unfavorable conditions.

Assuming cores 60 in. in length are being made, approximately 9600 to 12,000 sq ft of core or other glued stock can be produced in 8 hr, if the average feeding speeds of 4 to 5 linear ft per min are maintained. This is an enormous production when compared with the conventional lumber-edge-gluing methods.

Operation of one lumber-core machine requires from 2 to 3 men depending upon the type of glue spreader employed.

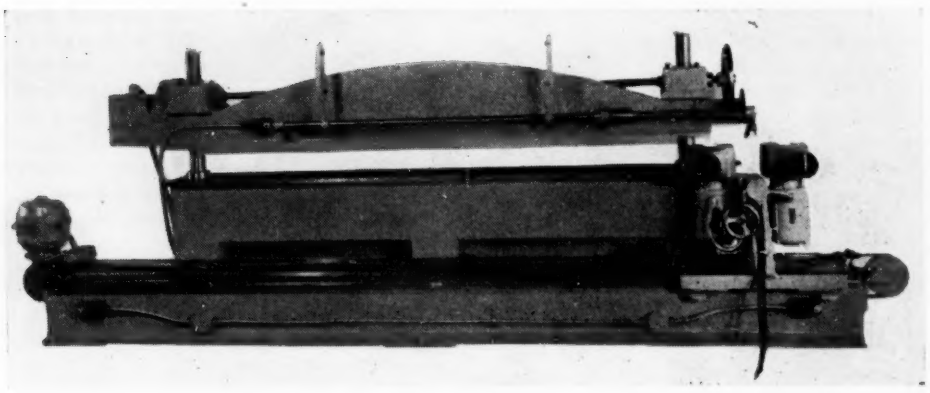


FIG. 5 VENEER JOINTER WITH GLUE-SPREADING ATTACHMENT

EDGE-GLUING OF VENEER WITH RESIN ADHESIVES

Prior to 1934, the standard method of joining veneers together in the United States was by means of paper tape. When veneers were to be edge-glued, the standard practice was to fold back the veneers after taping, spread the exposed joints with glue, unfold the veneers again, and then place them in a concave cradle until the glue had set. Taping of veneers is still the most widely used veneer-joining method.

In 1934, the first tapeless veneer-edge-gluing machines were introduced into this country. These first machines were of foreign manufacture. Several years ago, however, the manufacture of these machines was undertaken in this country. At first progress was slow with these tapeless veneer edge gluers, but today they are coming into more and more widespread use due to great improvements made in current models.

Until very recently, the conventional adhesive used with tapeless veneer edge gluers has been hide (animal) glue. The method of operation is as follows:

After the veneers are jointed, the veneer edges are spread with a light-colored hide glue. This glue application is done either manually with a brush or by mechanical means in the veneer jointer. Fig. 5 shows a veneer jointer with glue-spreading attachment. After being spread with glue, the pack of veneers is "fanned" apart and laid aside until the glue has dried.

Following this, the veneers with dried glue on their edges are fed into the tapeless veneer-edge-gluing machine. Driven rolls automatically draw the veneers into the machine, while the glue-spread edges are moistened automatically with a dilute formaldehyde solution. As the veneers pass through the machine, they are firmly pressed together, edge to edge, and simultaneously subjected to controlled electric heat transferred from top and bottom heating elements. This heat sets the animal glue almost instantly.

One make of tapeless veneer-edge gluer has a single wide bottom transport chain with toed-in pressure rolls on top. These rolls press the veneers tightly together. Another type of tapeless edge gluer has two converging transport chains with straight pressure rolls on top. In this machine, the chains pull the veneers firmly together. A modification of this latter machine has two parallel chains on top in place of the rolls.

The main drawback to the method of tapeless edge-gluing of veneer, as described, is the necessity for applying the glue in an operation separate from the edge-gluing operation itself. The piles of veneer, with prespread glue on the edges, have a tendency to stick together, sheet to sheet, due to the inherent "stick" of animal glue. This causes some loss of time and damage to the veneers as the operator separates the individual sheets of veneer. A secondary drawback is that the glue used does not have that

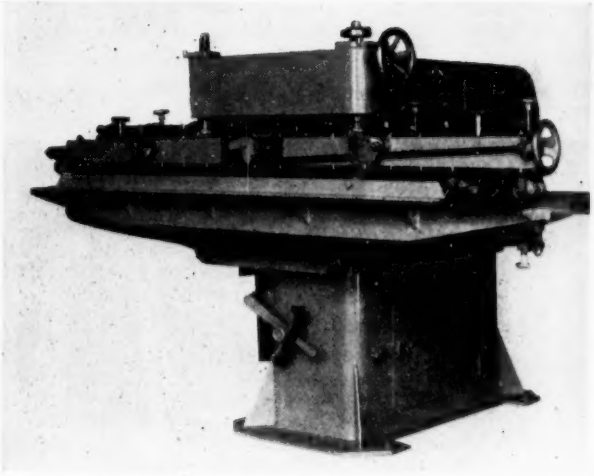


FIG. 6 TAPELESS VENEER-EDGE-GLUING MACHINE WITH AUTOMATIC GLUE-SPREADING DEVICE

degree of water resistance found in resin adhesives, although it must be pointed out that the application of the formaldehyde to the animal glue does render it water-resistant to some extent.

The ideal tapeless veneer-edge-gluing machine is one in which the glue is spread on the veneer edges as the stock is fed into the edge gluer. Attempts to produce such a machine have been made by several sources in the past. Only recently has the problem been solved successfully, to an extent where the method can now be employed on a regular production scale.

A tapeless veneer-edge-gluing machine with an automatic glue-spreading device is shown in Figs. 6 and 7. A urea-resin glue is placed in a glue tank which is located directly beneath the first pair of pressure rolls. A grooved thin glue wheel, operating between these pressure rolls, spreads the resin adhesive to the veneer edges as the veneers are fed into the machine. The veneers then progress onto the heated transport chain, while toed-in top-pressure rolls force the veneer edges tightly together. Heat is also applied from above through a pressure shoe located between the pairs of pressure rolls. This shoe also irons the veneer joint against the moving transport chain, thereby preventing overlapping. Special means are provided in this machine to keep the machine parts clean of squeezed-out glue. The resin is cured almost instantly under the heat, and the veneer sheets emerge from the discharge end of the machine ready for subsequent processing.

When edge-gluing relatively thick veneers, the glue-applying wheel is often removed so that the veneers will not be held apart



FIG. 7 OPERATORS FEEDING TAPELESS VENEER-EDGE-GLUING MACHINE

by this wheel. In such instances, the glue is applied to the veneer edges just before the veneers are fed into the machine. This can be done mechanically by a special spreader. Boards as thick as 1/2 in. are being edge-glued in this way on a production scale, using the method herein described.

Another type of veneer-edge-gluing machine is still under development as far as this country is concerned. This machine is known as a cross-feed tapeless veneer edge gluer. It is patterned generally after similar machines which have been widely used in Europe for over 20 years. The European machines all operate with prespread animal glue, whereas the American machine will employ urea resin, spread at the machine.

In general, the cross-feed edge gluer will be quite similar to the lumber-core continuous-feed press previously described. The main difference will be the method of feeding. Whereas, the lumber-core presses have pusher-bar feed, the cross-feed edge gluers will have roller feed. The veneers will emerge from this machine in a continuous ribbon, in a manner very similar to the way veneer comes from a rotary veneer lathe. An automatic veneer clipper at the outfeed end of the cross-feed edge gluer will clip the edge-glued veneers to desired width.

This cross-feed edge gluer is suitable chiefly for thicker veneers. It is not suitable for face veneers. Its purpose is to fill the gap between the edge-gluing machines first described, which are intended chiefly for thinner veneers, and the lumber-core presses which are for heavier board stock.

ADVANTAGES OF TAPELESS VENEER-EDGE-GLUING

Tapeless edge-gluing of veneer saves the cost of the tape. The cost of the glue used is very minor.

Sanding costs are greatly reduced, since there are no tape particles to clog the sandpaper. In many instances, the drum-sander operation, used to remove tape, is eliminated. The plywood is taken from the trim saws direct to the belt sander.

Edge-gluing also makes practical the utilization of narrow veneer strips for cores and crossbands, without having closely spaced lines of paper tape in the interior of the plywood to detract from quality of surface appearance or strength of the glue bond between the plies. Edge-glued crossbands are superior to one-piece crossbands in minimizing warpage of plywood.

The growing use of plywood in military and naval aircraft and boats makes tape-free joining of veneers of vital importance. The presence of tape on veneer cores or crossbands would destroy the waterproof glue bond at the points where the tape occurs, because paper separates under the action of moisture.

A further advantage of tapeless edge-gluing is the elimination of pressed-in tape in the case of plywood glued in a hot-plate plywood press. Such tape is often difficult to remove.

GLUES

To date urea-formaldehyde resins have had the most widespread use in the machines for edge-gluing lumber and veneer, as described in this paper. However, work is being done toward adapting other heat-setting adhesives for these purposes. Not only phenol-formaldehyde resins, but also such adhesives as blood albumen, casein, animal, and soybean glues can be set under heat and pressure, and many or all of them may well find important application in this field.

CONCLUSION

The development of fast heat-setting glues has made possible great forward strides not only in the machinery for gluing plywood (such as hot-plate plywood presses), but has also been a prime factor in instigating the development of new methods and machines for the edge-gluing of lumber and veneer. The mechanization of the wood industries is thereby increased, with the goal of true straight-line production ever nearer in sight.

Discussion

HENRY GRINSFELDER.[4] We have investigated the Plycor core machine from the "resin" angle and feel that three of our findings are worth disclosing at this time. We have made a study of the surface temperature of the exit wood and find that there is a variation from about 125 F to 190 F, depending upon the speed of the machine, the temperature of the steam-chest surface, and the degree of contact between the lumber cores and the steam chest. The depth to which the resin cures before leaving the machine is dependent upon the heat penetration. As the author has pointed out, it is desirable to have a resin bond at least 1/8 in. in depth from the top and bottom surfaces of the lumber cores before the cores are to be handled and subject to fracturing. If the bond is less than 1/8 in. in depth, the cores are liable to break apart when first handled. In a reasonable time, of course, these resin adhesives will set throughout the entire thickness of the core, so that the critical point of judging the quality of the bond is when the core stock is first moved from the Plycor core machine.

In our work, we have also investigated the quality of bond produced by various resins and catalysts, and our findings have been that, whereas a great many catalyst and resin mixtures will give a depth of cure of 1/2 in., the quality of the bond is not the same, depending upon the resin and catalyst. Some of the resins produce a very poor bond, others a very good bond, as evidenced by the strength necessary to break the joint open and the amount of wood failure.

H. S. JONES.[5] The development of the edge-gluing process

[4] The Resinous Products & Chemical Company, Inc., Philadelphia, Pa.

[5] Factory Manager, The Globe-Wernicke Company, Cincinnati, Ohio.

both for lumber and veneer is another step in the advancement of the woodworking industry. It not only makes a superior product but reduces the process time very materially. It is not uncommon for those who have edge-gluing equipment and a hot-plate press to make delivery of certain special runs in 24 hours. As these methods become more universally used, the writer sees the possibility of making deliveries of plywood in 48 hours a common practice. In other words, the plywood industry is rapidly approaching straight-line production when the veneers will be taken directly from the lathes into the driers, directly from the driers to the edge gluers, to the hot-plate presses, through the saws and sanders, and out. It certainly should reduce the amount of inventory required under the old methods.

Author's Closure

The depth to which the resin cures in the Plycor lumber-core press depends not entirely upon the heat penetration but also upon the type of catalyst or hardener used in the resin adhesive. Since writing this paper, further progress has been made in the development of special resin hardeners. As of December, 1941, it is possible to secure solid bonds all the way through a 1-in-thick lumber joint even at high feeding speeds.

Results of Laboratory Embrittlement Testing of Boiler Waters

By F. G. STRAUB,[1] URBANA, ILL.

This paper reports the results of laboratory embrittlement testing of boiler waters as part of an investigation conducted under a cooperative agreement between the Utilities Research Commission, Inc., Chicago, Ill., and the Engineering Experiment Station, University of Illinois. The data presented have been released by permission of both institutions. The author briefly describes the testing apparatus and procedure. He then presents, in the form of curves, results of 1300 laboratory tests on power-plant boiler waters, completing the paper with a general discussion of the results.

IN 1938, the author reported the results of tests which had been conducted at the University of Illinois in the embrittlement-testing units. The development of these units has been described in detail.[2] However, in order to facilitate the presentation of data in this paper, a brief description of the apparatus will be given.

Testing Equipment and Procedure

Fig. 1 shows a section of the testing unit. The test specimen is normally made of 1-in. round hot-rolled S.A.E. 1020 steel with the center bored out, but for special tests can be made of any desired steel. Inserted into the specimen is a small steel plunger or partial filler, the diameter of which at the top is several thousandths of an inch less than the inside diameter of the specimen, and is still further reduced below this top portion. The specimen is partially filled with the boiler water to be tested, the filler inserted, and the specimen, with a thin solid iron gasket on top, is screwed into the holder at the top. Iron and constantan thermocouples are peened into the side of the test specimen. Another holder, fitting into a sleeve around the specimen, is screwed on the bottom of the specimen, which is thus held so that, when the spring is compressed by screwing down on the top nut, a definite load is applied to the reduced section of the specimen. A small electric furnace, in which the test unit is placed, enables the specimen to be heated to any desired temperature. Fig. 2 shows two batteries of 48 test units with heating furnaces and temperature-control equipment.

In testing a sample of boiler water, 7 cc is put in a new specimen, a new oxidized filler inserted, and the unit assembled. The filler is oxidized prior to use in order to retard action of the boiler water on the unstressed filler, and thus concentrate the attack on the stressed walls of the test specimen. Without the filler no cracking will occur due to lack of capillary space where the boiler water might concentrate.

The assembled unit, without any stress being applied to the specimen, is then placed in the heating furnace and heated to the desired temperature for about 4 or 5 hr. At the end of that time, the spring is compressed, by using the equipment shown in Fig. 3, until the desired stress is applied. In standard tests, this is 40,000 psi on the area at the reduced section of the specimen, although some tests have been run at higher stresses. The temperature is held at the desired value.

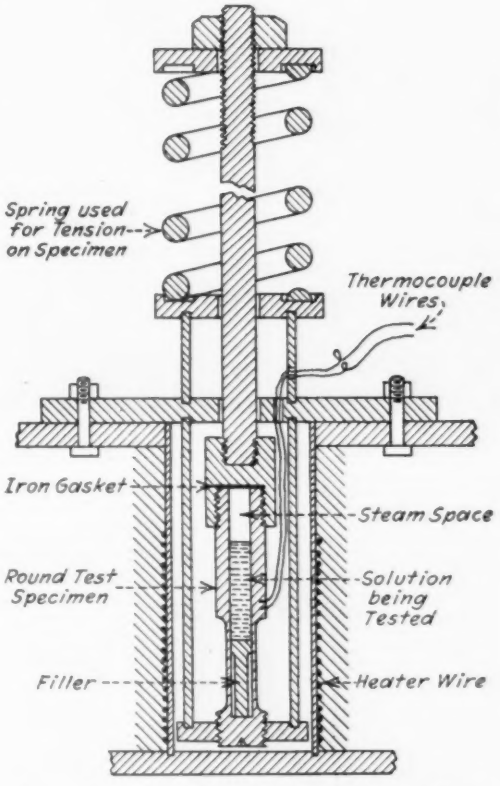


Fig. 1 Section of Embrittlement-Testing Unit

If the water is embrittling in nature, the specimen will break. The time in which a break occurs depends upon the type of water being tested. However, the fracture usually takes place within 24 hr. If no failure occurs, the test is continued for about 30 days, after which the specimen is removed, sectioned, and examined for any cracks. A water not causing failure or cracks in 30 days is classed as a nonembrittling type. Since, in each test, a new test specimen and filler are used, cracking or lack of cracking can be directly attributed to the water being tested. If a water is tested and found to cause failure, additional tests can be made after various chemicals have been added to the water to see what types of treatment would prevent failure.

Boiler-water samples from power-plant boilers have been submitted for testing by engineers interested in determining the condition of water being used. To date, we have tested 900 boiler waters, involving the running of 1300 tests in the laboratory test units. The results of these tests are plotted in Figs.

---

[1] Chemical Engineering Department, University of Illinois.

[2] "Boiler-Water Treatment—New Methods for Preventing Embrittlement," by F. G. Straub and T. A. Bradbury, *Mechanical Engineering*, vol. 60, 1938, pp. 371–376.

Contributed by the Joint Research Committee on Boiler Feedwater Studies and presented at the Annual Meeting, New York, N. Y., December 1–5, 1941, of The American Society of Mechanical Engineers.

Note: Statements and opinions advanced in papers are to be understood as individual expressions of their authors and not those of the Society.

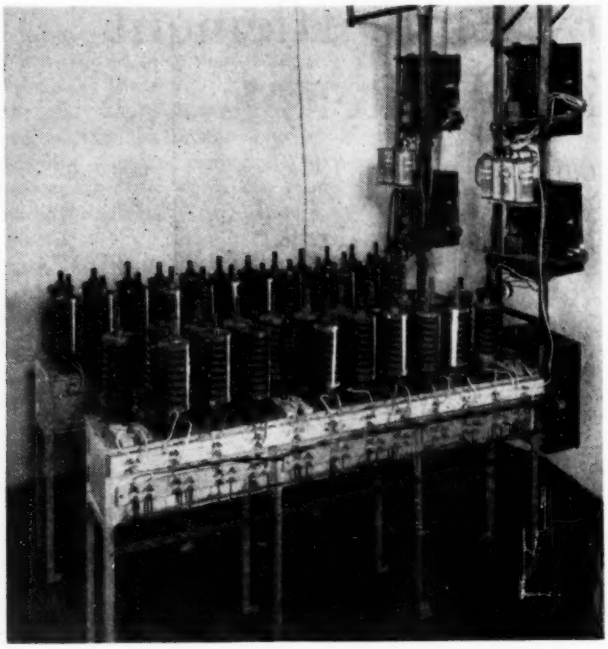


FIG. 2 TESTING UNITS, HEATING FURNACES, AND TEMPERATURE CONTROLLERS

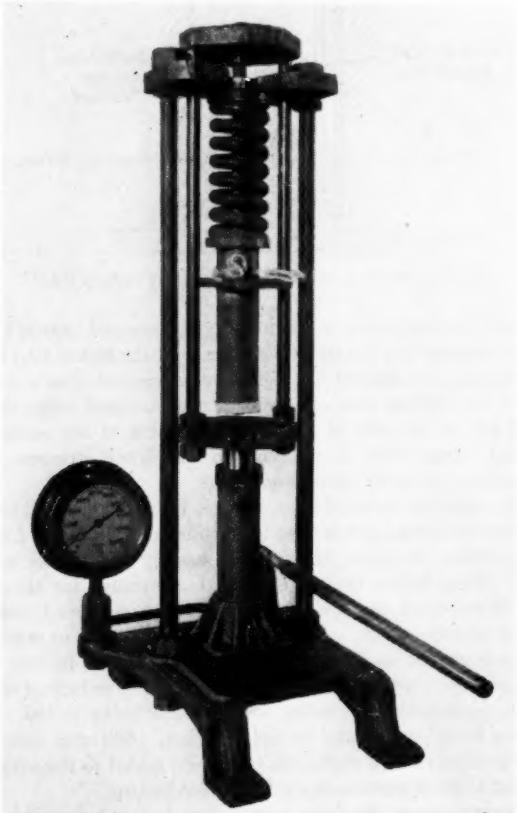


FIG. 3 HYDRAULIC PRESS USED FOR COMPRESSING SPRING

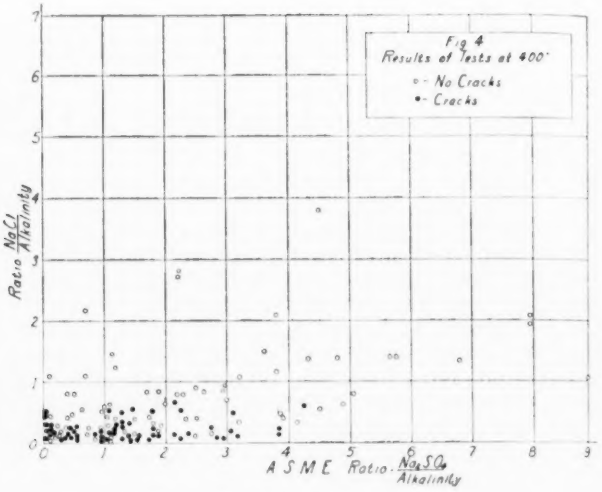


FIG. 4 RESULTS OF TESTS AT 400 F

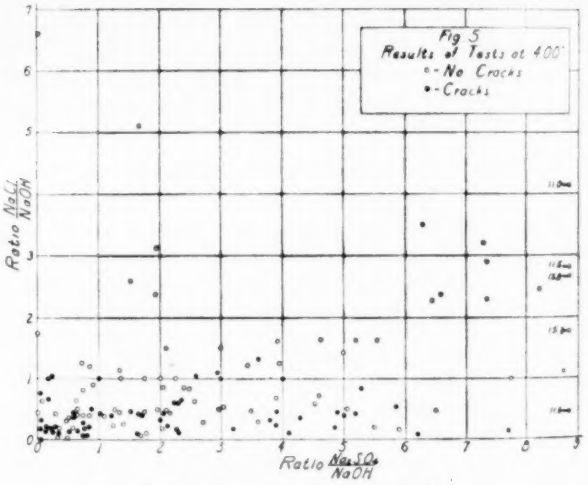


FIG. 5 RESULTS OF TESTS AT 400 F

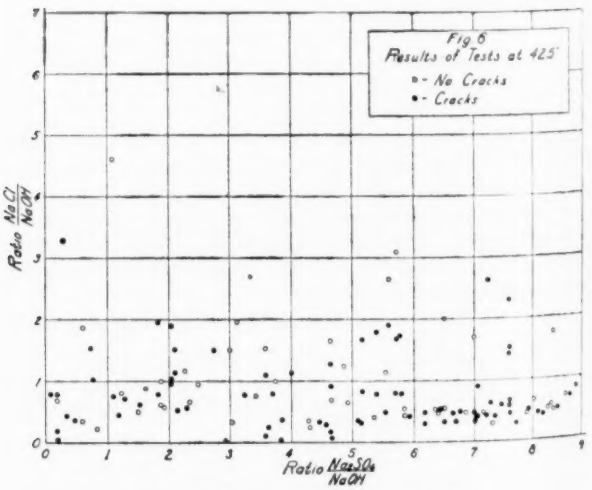


FIG. 6 RESULTS OF TESTS AT 425 F

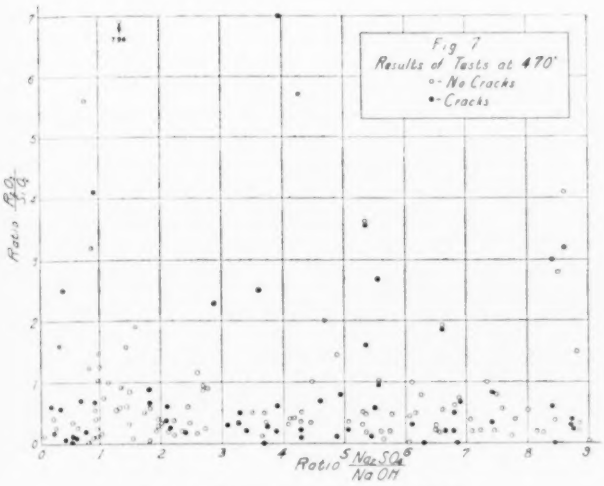


FIG. 7 RESULTS OF TESTS AT 470 F

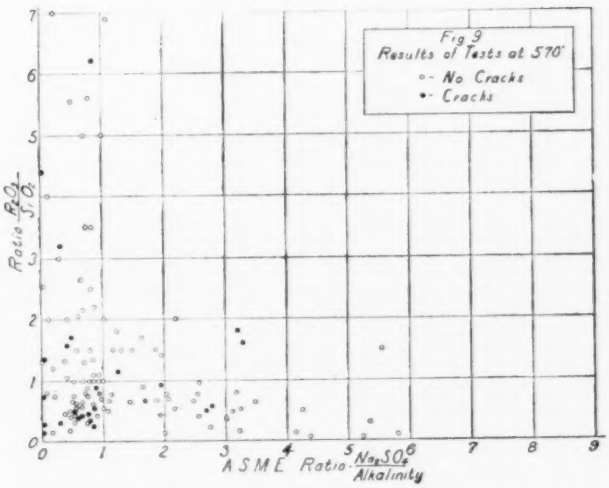


FIG. 9 RESULTS OF TESTS AT 570 F

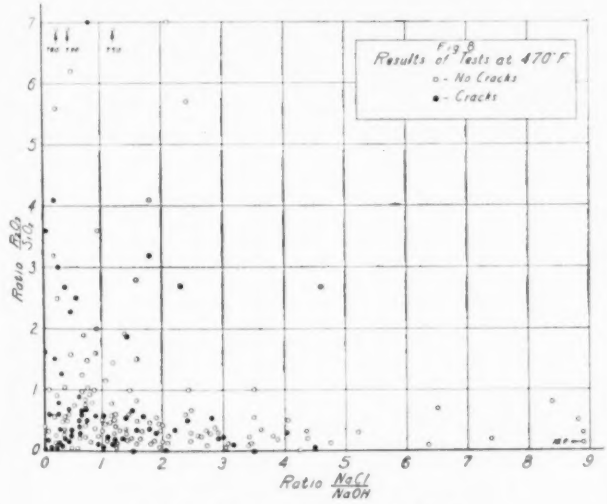


FIG. 8 RESULTS OF TESTS AT 470 F

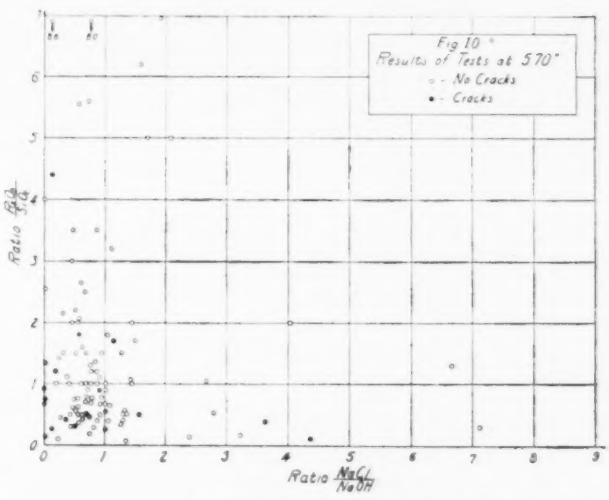


FIG. 10 RESULTS OF TESTS AT 570 F

4 to 10. Since many of the results fall close to other results, it has not been possible to plot all the results in these curves. However, since these results fall in the crowded area of the curves, their absence does not detract from the conclusions to be drawn.

The curves have been plotted several ways so as to allow comparison with those previously published, as well as with those to be presented by others.

In the tests conducted at 400 and 425 F, the ratios of the NaCl to the alkalinity and NaCl to NaOH are plotted against the A.S.M.E. ratio (Na_2SO_4 to alkalinity) and the Na_2SO_4 to NaOH.

At 470 and 570 F the ratios[3] of the R_2O_3/SiO_2 are plotted against the A.S.M.E. ratio and against the NaCl to NaOH.

RESULTS OF TESTS

The results of tests conducted at 400 F, shown in Figs. 4 and 5, indicate that with low NaCl content the sulphates do not appear to be effective in preventing failure of the test specimen. When the NaCl is greater than about 0.6 of the alkalinity or 1.0 of the sodium-hydroxide content, the combination of sulphate and chloride appears to be effective in preventing failure. There are many tests in which the chloride is low, but failure does not take place. Many of these waters have been treated with organic extracts, and no analyses have been made for the organic matter, nitrates, etc. In many waters having low chloride content and which produced failure in the laboratory tests, chlorides have been added, with the result that failure has been prevented.

At 425 F, in Fig. 6, there does not appear to be the correlation of high chlorides preventing failure, although in many cases the addition of chloride has stopped failure.

At 470 and 570 F, in Figs. 7 to 10, there appears to be a definite influence exerted by the R_2O_3 content in respect to that of the SiO_2. It has been noted that, when the chlorides are rather low, the failure occurs even when the R_2O_3 content is comparatively high. However, when the chloride is increased, the failures are prevented. This is shown in Figs. 8 and 9, where the ratios of the R_2O_3/SiO_2 are plotted against the NaCl/NaOH.

DISCUSSION OF RESULTS

It should be remembered that these results represent laboratory tests and are not the results of actual cracking in power-plant boilers. In order that a laboratory test may be of any real service to industrial operation, the test must be correlated with actual plant experience. The tests which have been conducted have been controlled so that conditions existing in the

[3] R_2O_3 means the iron and aluminum presence expressed as their oxides.

tests are similar to those existing in the stationary power boiler. The stress has been held around 40,000 psi on a steel of about 36,000 psi yield strength. This stress might be encountered as localized stresses around rivets, etc. It has been found that, if the stress is increased to around 50,000 to 55,000 psi, no reasonable combination of salts, either inorganic or organic, would prevent failure. Consequently, this lower stress has been set as the standard.

If the results of the laboratory tests do not agree with those obtained in actual operation, it is not logical to discard the operating data in favor of the laboratory tests. In such an instance, it appears to be necessary to modify the laboratory control tests so that the results will agree with actual operating results.

The power-plant data which have been submitted to the author indicate that sodium sulphate has been effective in preventing embrittlement in the stationary power boiler. We have made no study of the locomotive boiler, and very meager data have been published in respect to embrittlement in this type of boiler, consequently this statement is limited to the stationary boiler. Our tests indicate that sulphate is effective in preventing failure in the laboratory at the pressures where the greatest percentage of embrittlement failures has occurred in steam boilers. This appears to indicate definite correlation between the laboratory tests and actual operation.

Embrittlement of Boiler Steel—Experiences With the Schroeder Detector

By T. E. PURCELL[1] and S. F. WHIRL,[2] PITTSBURGH, PA.

In 1928 the authors were faced with the discovery that boilers of the authors' company were being attacked by so-called caustic embrittlement, and steps were taken to combat the evil. Experiences with this metal disease, since that time, are described. More specifically, however, the paper treats with results of 26 tests in which the Schroeder embrittlement detector was used on boilers, operating under varying conditions of water treatment, pressure, time, and specimen composition.

THE type of boiler-metal cracking, identified as caustic embrittlement, was first encountered on our system in 1928 at the Brunot Island Power Station (1).[3] Both intercrystalline and transcrystalline cracks were found in the flange of a mud-drum blowoff pad of a 195-psi Stirling-type boiler installed in 1919. In 1931, cracked and broken rivets were noted in a similar boiler placed in service at the same time. Examination revealed drum-metal failure at both the head and longitudinal seams. Detailed inspection of the other boilers disclosed cracks in the drum metal in all of the twenty-six Stirling-type boilers, twenty of which were damaged to the point that they were not considered fit for service. These units had been installed between 1914 and 1919. Typical failures, in which some of the cracks extended across the ligaments between the rivet holes, and representative examples of misalignment of rivets and poorly fitted butt straps are shown in Figs. 1, 2, and 3. Up to this time the boilers were not treated internally, and the ratio of sodium sulphate to total alkalinity as sodium carbonate, as recommended by this Society (2), was not maintained. The approximately 10 per cent make-up was Ohio River water, softened by the cold, intermittent, lime-soda-ash process, using ferrous sulphate as a coagulant.

At the Colfax Power Station, built in four stages between 1920 and 1927, no failures due to embrittlement have been experienced. It was intended that this station should be operated with evaporated make-up and without chemical treatment, but corrosion and scale early became major problems. In spite of pronounced efforts to reduce the oxygen content of the boiler feedwater by mechanical means, corrosion persisted until caustic-soda and oxygen scavengers were added to the boiler water. Trisodium phosphate, the first chemical used for internal treatment, eliminated scale but did not correct the corrosion difficulties. A detailed account of these experiences has been reported by Partridge and Hall (3).

Chemical treatment of the boiler water has been practiced at the James H. Reed Power Station since its initial operation in 1930. The make-up is provided by the evaporation of zeolite-softened Ohio River water. It is noteworthy that a scaling machine has never been used on these boilers and that corrosion has not been encountered.

Since 1931, the boilers at all stations have been treated with sodium sulphate, in keeping with the recommendations of this Society (2) for the protection of boilers against embrittlement. In view of the doubtful efficacy of this form of treatment, an extensive program was begun in 1938 to determine to what extent the boiler waters might be embrittling. The embrittlement detector, developed by Schroeder and his associates (4), has been used for this investigation.

Embrittlement-Detector Tests

The data relative to 26 tests made on boilers at three different stations are presented in Table 1 and shown graphically in Fig. 4. From the results of these tests, it is apparent that the maintenance of the A.S.M.E. ratio (2) does not afford protection against embrittlement of the specimens. Of particular interest are the tests at the Reed station, where a sodium chloride to total alkalinity ratio of 1.6, as well as the A.S.M.E. ratio (tests Nos. 102 to 104, inclusive), also failed to prevent embrittlement. The specimens did not fail, however, during three tests (Nos. 106 107A, and 107B), in which the alkalinity was maintained by the use of trisodium phosphate, there being no caustic alkalinity. It is particularly noteworthy that the last two of these tests, which were simultaneous, were concurrent with two tests (Nos. 201A and 201B) on an adjacent boiler using the same feedwater, in which specimen failures were experienced while maintaining the A.S.M.E. ratio.

In contrast, the four tests conducted at the Stanwix plant of the Allegheny County Steam Heating Company produced no specimen failures in spite of the fact that the last of these was 195 days in duration, approximately one heating season, and that internal treatment of the boilers was similar to that practiced at the two power stations. The reason for this seeming anomaly was not evident at the time; but it was found that a sample of water taken during the last test contained 22 ppm of sodium nitrate.[4] Subsequent analyses have shown that approximately 20 ppm of sodium nitrate are normally present in this boiler water. In view of present knowledge relative to the possible inhibiting effect of sodium nitrate, it is believed that its presence may be responsible for the noncracking of the specimens. Analyses at the Reed and Colfax stations have shown only negligible amounts of this salt.

Data obtained at the Colfax station, while comparable with those obtained at Reed, have not been as consistent. The time element is noted to be very important. It was found in a number of tests that, where no failure was evident at the end of 30 days, 60-day tests showed marked etching and checking of the specimens, and complete failure was experienced at the end of 90 days. Typical specimens as they appeared at the end of three different tests of 30, 60, and 90 days duration under similar conditions are shown in Fig. 5.

Operation of Detectors

The boilers selected for test purposes were chosen as being

[1] General Superintendent of Power Stations, Duquesne Light Company. Mem. A.S.M.E.

[2] Chief Chemist, Power Stations Department, Duquesne Light Company.

[3] Numbers in parentheses refer to the Bibliography at the end of the paper.

Contributed by the Joint Research Committee on Boiler Feedwater Studies and presented at the Annual Meeting, New York, N. Y., December 1–5, 1941, of The American Society of Mechanical Engineers.

Note: Statements and opinions advanced in papers are to be understood as individual expressions of their authors and not those of the Society.

[4] Analysis by W. C. Schroeder in connection with laboratory detector tests on a sample of this boiler water.

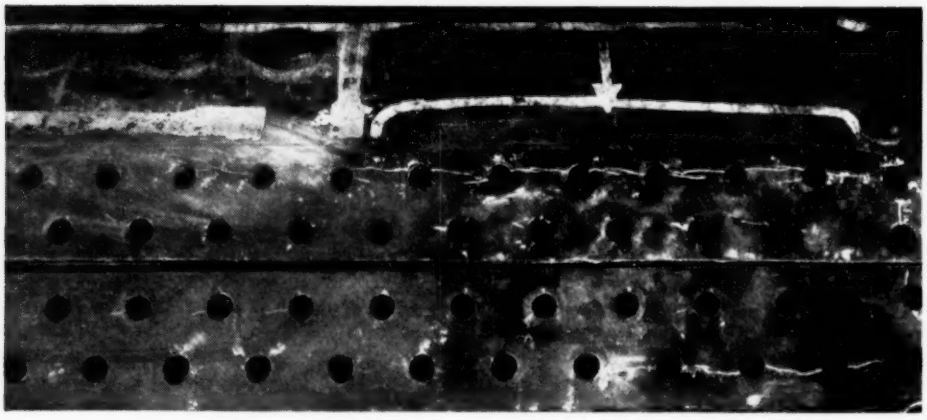


FIG. 1 CRACKS IN REAR LONGITUDINAL SEAM OF BOILER DRUM



FIG. 2 FAILED METAL IN A BOILER-DRUM-HEAD SEAM

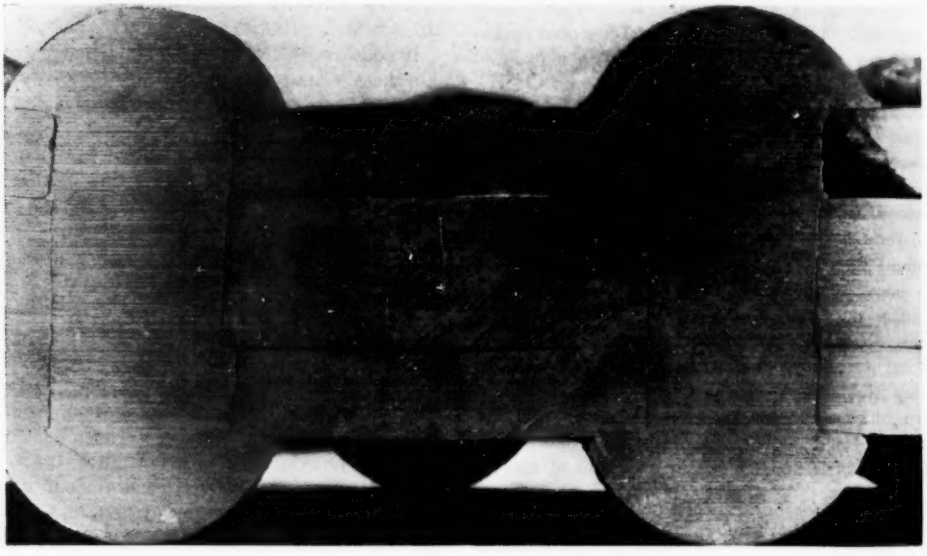


FIG. 3 CROSS SECTION THROUGH LONGITUDINAL SEAM OF BOILER DRUM AT SECOND ROW OF RIVETS

representative of conditions at the several stations with respect to pressure, make-up conditions, and internal treatment. Installation of the detectors was such that the boiler water was supplied from lines connected directly to the drums. In all cases the piping between the boiler and the detector inlet was lagged and the flow of water so controlled that the specimen temperature approximated that of saturation conditions within the boiler. The detectors were inspected daily, except Saturdays and Sundays, to assure the proper amount of steam leakage. Such tests were made by observing the amount of condensation occurring on a watch glass held in close proximity to the exposed end of the specimen. In most cases, adjustment was necessary approxi-

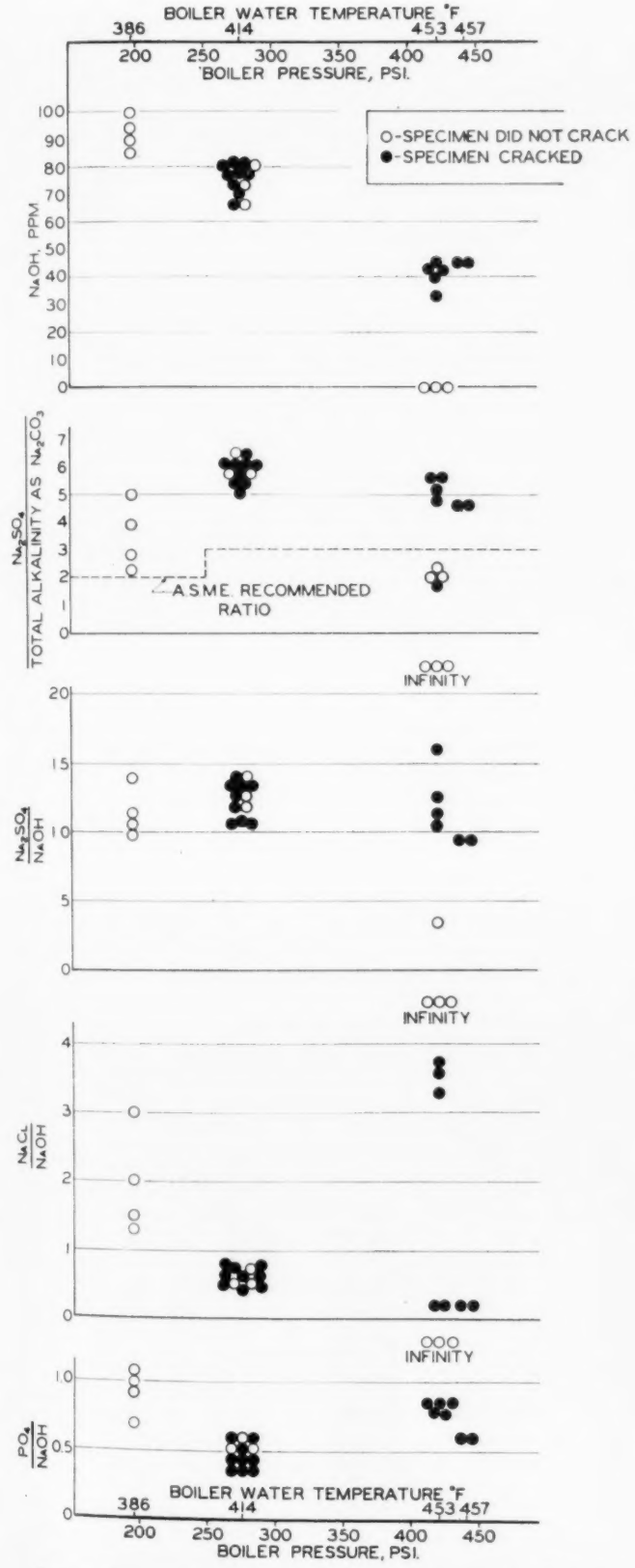


FIG. 4 DETECTOR-SPECIMEN BEHAVIOR WITH RESPECT TO VARIOUS FACTORS

TABLE 1 EMBRITTLEMENT-DETECTOR TEST DATA

Station	Boiler No.	Test No. (a)	Duration, days	Boiler Water Analysis: Oil(b) ppm.	CO_3(c)/A ppm.	PO_4 ppm.	SO_4 ppm.	Cl ppm.	SiO2 ppm.	Organic(d) ppm.	Na_2SO_4/Na_2CO_3(e)	Na_2SO_4/NaOH	NaCl/NaOH	PO_4/NaOH	Test Material (f)	Results (g)	Remarks
Reed (420 psi.)	5	101	34	18	25	39	29	456	10	10	35	6.7	10.0	0.4	0.9	C.R.	●●●●	One large, several small cracks.
		102	35	17	21	35	29	339	90	6	31	5.6	12.6	3.7	0.9	C.R.	●●●●	One large, several small cracks.
		103	61	15	20	32	31	301	85	5	24	4.9	10.6	3.3	0.6	H.R.	●●●●	Small crack at edge; cracking in stressed area.
		104	60	19	23	36	30	361	97	27	17	5.2	11.5	3.6	0.5	H.R.	●●●●	Several small cracks in stressed area.
		105	57	14	14	23	8	80	8	14	31	3.7	5.6	0.4	0.9	C.R.	●●●●	One large crack, 2/3 through specimen.
		106	67	0	45	65	5	123	11	7	7	8.3	∞	∞	∞	H.R.	○○○○	No cracks; slight etching.
		107A	91	0	27	64	3	84	6	5	9	2.6	∞	∞	∞	C.R.	○○○○	No cracks; slight etching.
		107B	90	0	27	64	3	84	6	5	9	2.6	∞	∞	∞	H.R.	○○○○	No cracks; slight etching.
Reed (440 psi.)	4	201A	92	19	17	28	27	281	12	8	9	4.7	9.2	0.4	0.6	C.R.	●●	One large, several small cracks.
		201B	94	19	17	28	27	281	12	8	9	4.7	9.2	0.4	0.6	H.R.	●●	One large, several small cracks.
Colfax (275 psi.)	18	301	32	28	30	39	(h)	507	26	11	18	6.3	13.4	0.7	0.6	C.R.	○●○●	Etching, but no cracks.
		302	60	23	29	40	(h)	480	25	14	11	5.1	10.6	0.6	0.6	C.R.	○●○●	Etching, slight cracking.
		303	62	31	34	40	(h)	606	22	17	10	5.8	12.5	0.5	0.5	C.R.	○●○●	Etching, but no cracks.
		304	92	35	34	40	(h)	603	30	11	11	6.1	12.5	0.6	0.5	C.R.	●●●●	One large, several small cracks.
		305	94	31	30	38	(h)	617	31	11	13	6.1	12.5	0.7	0.5	C.R.	●●●●	One large, several small cracks.
		306A	106	34	31	41	(h)	579	25	15	12	5.4	10.7	0.6	0.5	C.R.	●●●●	Several cracked.
		306B	106	34	31	41	(h)	579	26	15	12	5.4	10.7	0.6	0.5	H.R.	●●●●	Cracked.
Colfax (275 psi.)	11	401	62	34	34	41	40	646	25	13	14	5.8	11.9	0.5	0.5	C.R.	○●●●●	No cracks.
		402	63	30	32	40	41	577	27	12	19	5.7	11.0	0.6	0.6	C.R.	●●●●●	Slight checking of stressed area.
		403	92	34	33	43	45	710	21	8	12	6.5	13.3	0.4	0.5	C.R.	●●●●●	One large, several small cracks.
		404	106	34	32	40	43	680	28	10	12	6.2	12.6	0.6	0.5	C.R.	●●●●●	One large, several small cracks.
		405	91	33	31	46	42	644	30	19	13	6.1	12.2	0.6	0.6	H.R.	●●●●●	Several small cracks in stressed area.
Starwix (195 psi.)	2	601	36	42	72	89	(h)	764	122	46	121	2.3	14.1	2.0	0.9	C.R.	○○○○	No cracks.
		602	60	39	63	96	(h)	654	84	24	105	2.6	10.5	1.5	1.1	C.R.	○○○○	No cracks.
		603	89	36	61	87	(h)	609	66	10	95	4.0	10.1	1.3	1.0	C.R.	○○○○	No cracks.
		604	195	36	44	60	(h)	636	156	53	64	5.0	11.1	3.0	0.7	C.R.	○○○○	No cracks.

(a) Suffixes A and B indicate simultaneous tests on the same boiler. (b) By Winkler test except on tests Nos. 106, 107A, and 107B when $SrCl_2$ was substituted for $BaCl_2$ in this method. (c) By Winkler test. (d) Total organic content. (e) Total alkalinity as $NaCO_3$ (A.S.M.E. ratio). (f) C.R. indicates cold-rolled S.A.E. 1020 or 1112 steel specimen; H.R., a hot-rolled specimen of boiler-flange quality. (g) ● indicates cracked specimen; ○ a noncracked one. (h) $Fe(OH)_3$ is used as an oxygen scavenger by internal treatment with $FeSO_4$ and NaOH.

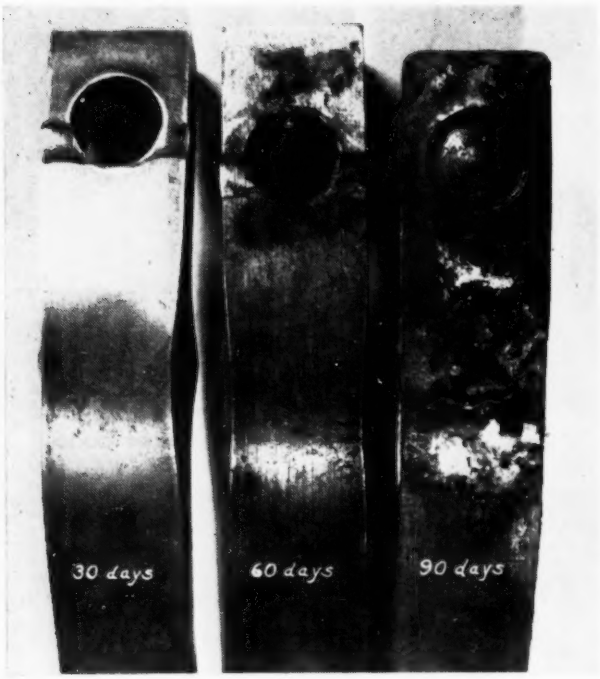


FIG. 5 EMBRITTLEMENT SPECIMENS AT END OF THREE DIFFERENT TESTS MADE UNDER SIMILAR CONDITIONS

mately once every 7 to 10 days. This was usually accomplished by adjusting the specimen setscrew approximately 1/8 turn. When this was not effective, the top bolts in the test block were loosened slightly.

It is interesting to note the change of shape of the specimen during the course of testing. Fig. 6 (*A*) shows the straight specimen before being placed in the detector; (*B*) indicates the shape of the specimen when in place at the start of the test; and (*C*) and (*D*) are, respectively, a failed specimen, and one which at the end of the test showed only slight checking on the test surface and was subsequently bent to determine whether or not cracking occurred.

A typical example of the type of specimen cracking encountered is shown in the photomicrographs in Fig. 7. It is to be noted that the cracks are principally intercrystalline. In general, it is difficult to obtain a good photomicrograph in the region of the principal crack due to distortion at the time of failure or while bending during subsequent study.

For those tests, where internal treatment of the boiler water was a departure from standard practice, the special treatment was initiated sufficiently in advance of placing the detector in service in order to permit the establishment of the desired conditions.

SPECIMEN COMPOSITION

In the initial tests of this investigation, cold-rolled S.A.E. 1020 or 1112 steel specimens were used. When repeated failures were experienced, hot-rolled specimens of boiler-flange quality were tried. With ten detectors now in service, six at Colfax and four at Reed, it is standard practice to make simultaneous tests on the same boiler using both materials. The detectors are installed in parallel with separate drain lines. The cold- and hot-rolled specimens are identified in the data, presented in Table 1, by the letters C.R. and H.R., respectively; the suffixes A and B following the test number indicate the simultaneous tests.

BOILER-WATER ANALYSIS

Except for the silica and organic contents, the boiler-water data, given in Table 1, are the average results of analyses made three times each week. The silica and organic contents were determined biweekly.

The analyses for silica were made in accordance with the A.P.H.A. gravimetric procedure (5). The method proposed by Hecht and Whirl (6) was used in the determination of organic matter. In the alkalinity titrations, the standard Winkler test (7) was followed, except in tests Nos. 106, 107A, and 107B, when the strontium-chloride modification (7) proposed by Schroeder and Partridge was employed. Other constituents were determined by accepted procedures for routine control work; these were checked periodically by referee methods.

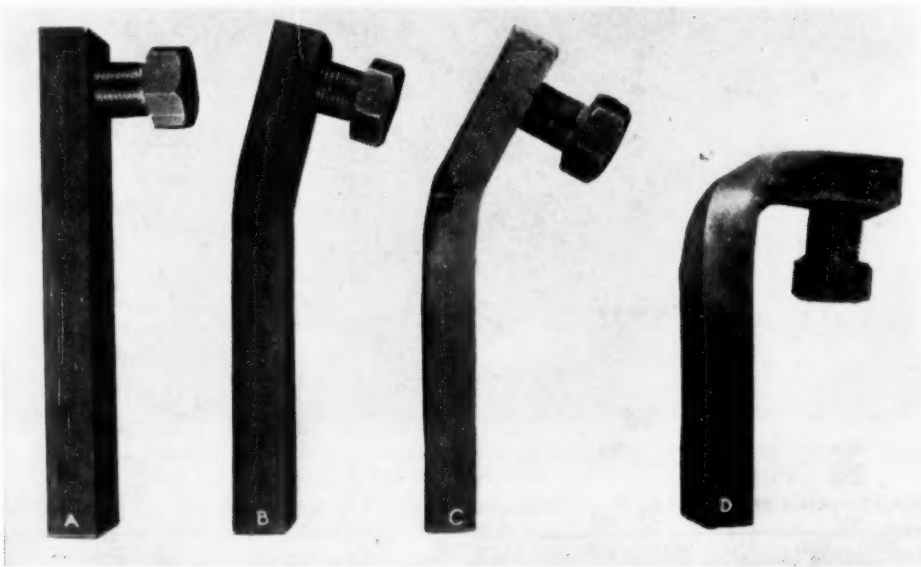
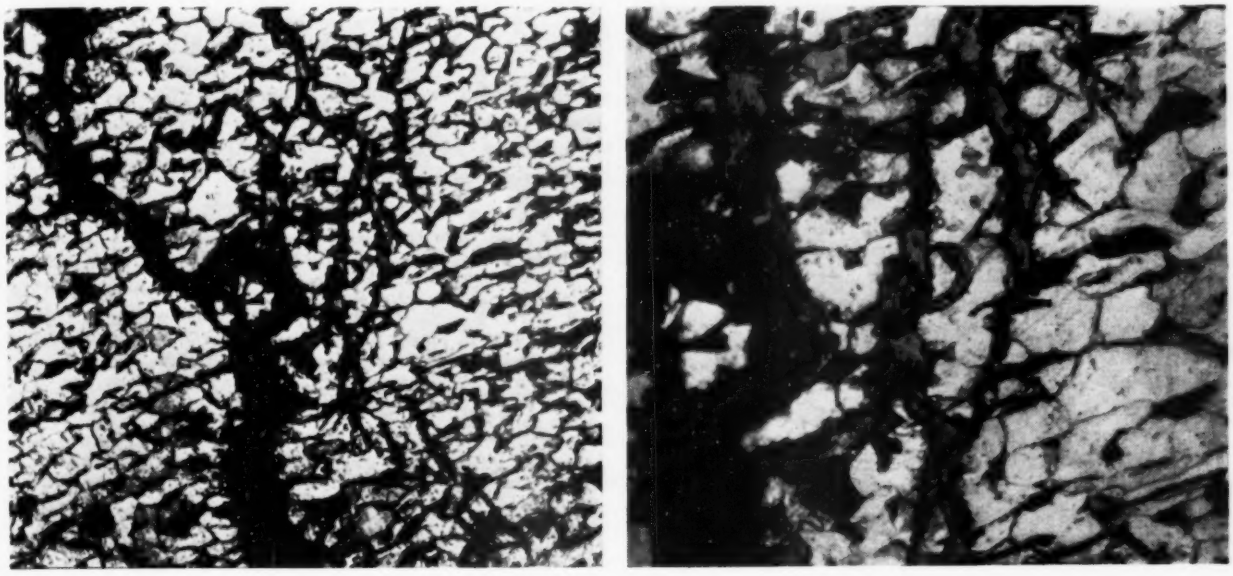


FIG. 6 APPEARANCE OF TEST SPECIMENS

(*A*, Ready for installation; *B*, after being clamped in test block; *C*, at end of test when failure was apparent; *D*, after further deformation when no cracks were evident.)



(*a*) (*b*)

FIG. 7 TYPICAL PHOTOMICROGRAPHS OF SPECIMEN FAILURE
(*a* Magnification, ×200; *b* magnification, ×500.)

DISCUSSION

When internal treatment of boiler water was initiated at the several stations, it was made to conform with the recommendations of this Society (2) for protection against embrittlement. From the data obtained with the Schroeder detectors, it has become apparent that boiler waters treated in this manner may produce embrittlement under certain conditions.

While the Schroeder detector simulates conditions existing in a leaking boiler seam, it must undoubtedly accelerate the action; otherwise, it would be difficult to understand how the specimens crack in such a short time. Experience has shown that boilers which leak may operate for many years without failure. The severity of the test is not believed to be a cause for undue criticism, however, since the development of a method of treatment which completely inhibits specimen cracking would offer increased assurance against failure of the drum metal itself.

In the operation of the embrittlement detector, evaporation of the boiler water to the atmosphere permits the solids to accumulate on and adjacent to the highly stressed specimen. A concentrated solution of the boiler water is thus obtained, which, if aggressive, will attack the specimen. Since caustic soda is the active chemical, there are two logical methods of affording protection against its action, namely (*a*) the control of alkalinity with chemicals, which on evaporation do not deposit caustic soda, and (*b*) the use of inhibitors. The tests made in this investigation include experiences with both methods. The use of trisodium phosphate alone in tests Nos. 106, 107A, and 107B is an example of the first; the presence of nitrates in the boiler water in tests Nos. 601 to 604, inclusive, illustrates the latter.

The fundamental principle in the use of trisodium phosphate as the only treating chemical in tests Nos. 106, 107A, and 107B was to produce a boiler water which on evaporation would yield a deposit containing no caustic soda and yet provide sufficient alkalinity for protection against corrosion. Due to variable feedwater quality, in some stations, the use of trisodium phosphate alone may not be feasible. An acid feedwater would require excessive amounts of this chemical for neutralization of the acid, resulting in high boiler-water salines; an alkaline feedwater would tend to defeat the purpose of the treatment by developing caustic alkalinity. In addition the use of oxygen scavengers may be absolutely essential in some cases.

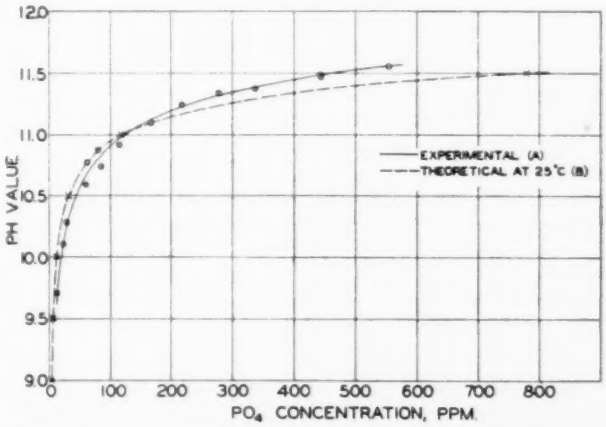


FIG. 8 RELATION OF pH TO TRISODIUM-PHOSPHATE CONCENTRATION EXPRESSED AS PO_4 ION
(*A* Determined by measurement at room temperature of the pH of known concentrations of C.P. trisodium phosphate with a hydrogen electrode pH meter. *B* Calculated according to method proposed by McKinney, ref. 8.)

It is possible, however, to adhere to the principle of the method of treatment by controlling the pH of the boiler water with the requisite amounts of either alkaline or acid chemicals, depending upon conditions. The relationship of pH and trisodium-phosphate concentration in pure water is shown in Fig. 8. As long as the pH and phosphate concentration conform with this curve, trisodium-phosphate salt will be obtained on evaporation; no caustic soda will be present. Should the pH be above that corresponding to the phosphate concentration, a mixture of trisodium phosphate and caustic soda would result. Therefore, to assure complete protection against embrittlement in accordance with the theory, the measured pH should never be above the curve. Should the pH of the boiler water fall below the curve value, acid-phosphate salts, which are not conducive to embrittlement, would be obtained. The optimum condition, therefore, with respect to embrittlement, corrosion protection, and boiler-water

salines is the maintenance of the pH value slightly below that on the curve corresponding to the desired phosphate concentration.

The testing program at Colfax and Reed has been expanded considerably. Tests are now under way at both stations to determine the effect of sodium nitrate. At Colfax, the influence of quebracho in one boiler and phosphate alkalinity control in another, in accordance with the curve in Fig. 8, is also being studied.

In experimenting with these new methods of treatment, the practice has been to make careful internal inspections of the boilers following each test. In addition to data on embrittlement, valuable information will be obtained concerning the influence of these types of treatment on other boiler conditions, such as boiler deposits, corrosion, and carry-over. It is noteworthy that no ill effects have been observed at Reed following the use of trisodium phosphate alone.

Conclusions

From the data obtained to date with the Schroeder detector, it is concluded that

1 Maintenance of the A.S.M.E. ratio of sodium sulphate to total alkalinity as sodium carbonate does not prevent embrittlement of the specimens.

2 A sodium-chloride to total-alkalinity ratio of 1.6 in conjunction with the A.S.M.E. ratio does not protect the specimens against failure at 420 psi.

3 Specimen cracking is not encountered in boiler waters in which the alkalinity is controlled on the basis of the pH value corresponding to the phosphate concentration, as shown in Fig. 8.

4 Sodium nitrate appears to offer possibilities as an inhibitor against embrittlement.

5 Under some conditions the duration of the test period is an important item.

BIBLIOGRAPHY

1 "Boiler Metal Cracking—a Case Study," by M. Hecht and D. S. McKinney, *Power*, vol. 70, 1929, pp. 633–636.

2 "Suggested Rules for the Care of Boilers," A.S.M.E. Boiler Construction Code, 1926, sec. 7, par. CA-5.

3 "Attack on Steel in High-Capacity Boilers as a Result of Overheating Due to Steam Blanketing," by E. P. Partridge and R. E. Hall, Trans. A.S.M.E., vol. 61, 1939, pp. 597–622.

4 "Intercrystalline Cracks in Locomotive Boilers," by W. C. Schroeder, A. A. Berk, and R. A. O'Brien, *Railway Age*, vol. 109, 1940, pp. 25–28.

5 "Standard Methods of Water Analysis," Eighth edition, American Public Health Association, 1936, pp. 77–78.

6 "The Estimation of Sodium in Water Supplies by an Indirect Method," by J. B. Romer, W. W. Cerno, and H. F. Hannum; discussion by M. Hecht and S. F. Whirl, Proc. A.S.T.M., vol. 38, part 2, 1938, pp. 638–646.

7 "Standard Methods of Water Analysis," Eighth edition, American Public Health Association, 1936, pp. 95–100.

8 "Calculation of Corrections to Conductivity Measurements for Dissolved Gases," by D. S. McKinney, A.S.T.M. Preprint No. 103, 1941.

Experience With Intercrystalline Cracking on Railroads

By R. C. BARDWELL,[1] RICHMOND, VA., AND H. M. LAUDEMANN,[2] HUNTINGTON, W. VA.

With 60 per cent of the steam-boiler horsepower of the United States in locomotives, which operate under widely diverse conditions and with waters of many compositions, this field offers extensive opportunity for the study of embrittlement cracking. The authors present a record of the experience of The Chesapeake & Ohio Railway with intercrystalline cracking as representative of the more recent work being done by the railroads to combat this form of metal deterioration. The paper deals with the investigation of various inhibitors, covering a period from 1933 to the present time, based on extensive testing with the embrittlement detector applied to locomotives in service. It was found that sodium sulphate does not prevent or even delay embrittlement cracking; that waste sulphite liquor will prevent cracking of detector specimens on many boiler waters, failing in but few cases; and that sodium nitrate has essentially eliminated cracking of detector specimens on the entire system of The Chesapeake & Ohio Railway.

IN THE report of the National Resources Committee, 1937, which was reviewed by Orrok (1)[3] before the American Society of Civil Engineers, Dean Potter scheduled 56,684,000 hp in steam plants at stationary power plants in the United States, as compared with 88,000,000 hp in steam locomotives. With 60 per cent of the steam-boiler horsepower in America embodied in approximately 42,000 locomotives normally in service on American railroads, consuming water of varying quality under widely diverse conditions, it would appear that this affords an excellent opportunity to observe and consider cases of intercrystalline-cracking, both from the standpoint of the number of boilers in service, as well as from the number that have been reported as cracked. A single large railroad may have several thousand locomotives under its jurisdiction operating over a large territory, which should permit consideration of this subject from a broader viewpoint than could be the case with isolated central power stations using one definite supply.

The history of intercrystalline cracking or "embrittlement" on the railroads is ordinarily dated from the "epidemic" of cracking on the Chicago & Northwestern lasting from 1912 through 1926. During and subsequent to this period, other railroads have had similar difficulties of a more or less acute nature. Study of such cases has yielded very interesting information, but the cracking on The Chesapeake & Ohio Railway is unique in several respects. It occurred during a period when the art of water conditioning was in an advanced state and when rapid, accurate, and complete methods of water analysis were available. It was paralleled by extensive investigation, especially by the U. S. Bureau of Mines, concerning the chemical and mechanical factors involved in intercrystalline cracking, the development of test equipment for determining the embrittlement characteristics of boiler water, and methods of treatment for preventing embrittlement. This situation led to rapid field application of laboratory findings to see if they would stand the test of practical operation. This study has been made as systematic and complete as is possible in railroad operation, and an enormous amount of data has been accumulated.

It might be well to review briefly the development of water treatment on railroads as affecting embrittlement cracking. Early in this century, it was found that, if waters were treated with soda ash or an equivalent chemical in amount to maintain the sodium alkalinity at least at 15 per cent of the dissolved solids in the boiler (2), the scaling matter would not adhere to the tubes and sheets and could be blown out readily as soft sludge, which fact was later developed more fully by Hall (3) at the Bureau of Mines and Carnegie Institute. Pitting and corrosion in locomotive boilers caused losses estimated to exceed $12,000,000 per annum, and, as limited clearances on locomotives prevent use of deaerating feedwater heaters to remove the oxygen, it was found necessary to increase the excess sodium alkalinity from 15 per cent of the total dissolved solids as recommended by McDonnell (4) to as high as 30 per cent in some cases, as found necessary by Seniff (5). Silica is usually present in railroad water supplies and, with this excess alkalinity which is required to offset scale, pitting, and corrosion, conditions resulted which were favorable to starting intercrystalline cracking where small apparently insignificant leaks caused a saturated solution of caustic soda to form in the capillary spaces against the stressed metal in riveted seams. Where the water is of an embrittling nature, cracking results.

In view of the interest which is still active in some quarters concerning the effect of sodium sulphate on cracking, the first section of this paper will be devoted to a brief discussion of experience with this salt. Extensive testing has been carried out with the embrittlement detector (6) to determine the usefulness and protective action of waste sulphite liquor, and of sodium nitrate in locomotive boilers. The results of this work will be presented in detail. Throughout the investigation, close contact has been maintained with the U. S. Bureau of Mines laboratory. Reports made to Subcommittee 6 of the Joint Research Committee on Boiler Feedwater studies have been made the basis of large-scale plant tests in the field.

Railroad Experience With Sodium Sulphate

In the early experience of the Chicago & Northwestern Railroad with embrittlement, it was noted that embrittlement cracking predominated on the divisions in which the sulphate was high. Strangely enough, certain western territories were free from this trouble, in spite of the fact that alkalinities were extremely high with comparatively small amounts of other inorganic salts in solution. It was later found that this was not necessarily due to the absence of the inorganic salts, but more probably to the use in these waters of an antifoam compound which contained waste sulphite liquor.

---

[1] Superintendent Water Supply, The Chesapeake & Ohio Railway.

[2] Chief Chemist, The Chesapeake & Ohio Railway.

[3] Numbers in parentheses refer to the Bibliography at the end of the paper.

Contributed by the Joint Research Committee on Boiler Feedwater Studies and presented at the Annual Meeting, New York, N. Y., December 1–5, 1941, of The American Society of Mechanical Engineers.

Note: Statements and opinions advanced in papers are to be understood as individual expressions of their authors and not those of the Society.

TABLE 1 YEARLY AVERAGE RATIOS FOR SWITCH ENGINES

Year	Number of analyses	Average $\frac{Na_2SO_4}{Na_2CO_3}$[a]
1933	65	2.9
1934	28	3.8
1935	10	5.2
1936	1	1.5
1937	20	3.0
1938	20	2.3
1939	32	2.7

[a] Total alkalinity as Na_2CO_3.

TABLE 2 CHRONOLOGICAL HISTORY OF SWITCH-ENGINE CRACKING AND REPAIRS[a]

Date	Engine	Repair
Nov., 1932	A	Second course renewed.
Jan., 1934	E	Circumferential seam patched between first and second course.
Feb., 1934	H	Second course renewed.
Sept., 1934	G	Circumferential seam patched between first and second course.
Nov., 1934	C	Butt straps replaced on second course.
May, 1936	B	Second course renewed; first course patched.
Oct., 1936	G	First and second courses renewed.
Nov., 1936	E	First and second courses renewed.
Dec., 1936	I	Second course renewed.
Jan., 1938	I	First and second courses renewed.
Jan., 1938	D	Second course renewed.
Aug., 1941	K	No cracks reported.
1941	F	No cracks reported.
1941	J	No cracks reported.

[a] Lignin treatment started February 12, 1938.
Sodium-nitrate treatment started January 14, 1941.

The experience of The Chesapeake & Ohio Railway with sodium sulphate parallels that of the Chicago & Northwestern. Through and east of the Allegheny Mountains, the waters contain but little sulphate, and the ratio of sodium sulphate to total alkalinity in the boilers rarely exceeded 1 to 1. In the Ohio River district and through Ohio and Indiana, the sulphates are higher and the sulphate-alkalinity ratio will average 1.5 to 1 or much higher. Out of 203 cases of intercrystalline cracking reported, 134 or 66 per cent were in the territory of the high sulphate ratios, while 69 or 34 per cent were in the territory of the low ratio. The number and types of power units involved were similar. This would indicate that, if this salt had any value in preventing embrittlement, the reverse of this situation should have existed.

More specific evidence concerning the action of sodium sulphate is available for 11 switch engines, operating at 180 psi gage. They were assigned to one city terminal, and took water from other sources only on infrequent trips to the shops for heavy repairs. Even then they were in territory in which the sulphate content of the water was quite high.

The average sulphate ratios for these engines for the years 1933 through 1939 are shown in Table 1. Since these locomotives used only treated well water and untreated city water throughout their life, the values shown should represent normal conditions. Table 2 shows that, in spite of the sulphate present, 8 of the 11 boilers had suffered embrittlement by 1938. This was all rivet-hole cracking in circumferential seams, or cracks in butt straps or drum metal of longitudinal seams.

The history of engine I is especially interesting, as the second course was renewed at the end of 1936, and again in the early part of 1938. During this interval the analysis showed fairly high sulphate values. These data offer no support for the idea that sodium sulphate will prevent embrittlement cracking in locomotive boilers.

The development of the embrittlement detector made available yet another means for testing the effect of sodium sulphate on cracking. In this equipment, the stress application and the arrangement of test surfaces are very similar and directly comparable with those existing in the riveted seams of a locomotive boiler. Concentrated boiler water is produced by slow leakage of water into the crevice under the stressed specimen, and diffusion of steam toward the atmosphere. Since it is well known that it is difficult to keep riveted seams in locomotive boilers tight against such minute leaks, this condition is one which may readily exist.

None of the tests with the embrittlement detector attached to the locomotive has shown that sodium sulphate has any influence on cracking of the specimens. This confirms laboratory work (6) and testing in stationary plants (7) with this equipment which have been reported already.

Use of Waste Sulphite Liquor to Prevent Embrittlement

Tests reported by the U. S. Bureau of Mines Laboratory in 1936 (8), and published in 1938, indicated that waste sulphite liquor[4] would inhibit embrittlement. Its use was started on The Chesapeake & Ohio Railway early in 1938. It was first noted that it caused and stabilized foam in the chemical vats, and it was suspected that it would engender similar difficulties in locomotive boilers. This did not prove to be the case, however, and no difficulties were reported. No extended search has been made for an explanation of this fact, but it seems logical to believe that the foam-stabilizing characteristics are destroyed by the elevated temperature in the boiler.

One of the most unsatisfactory factors, involved in the treatment with waste sulphite liquor during this early period, was the lack of a method for determining its concentration in the boiler water. It was simply added to the feedwater with the hope that it would reach the boiler and exist in the right concentration. This situation was greatly improved by the development in the U. S. Bureau of Mines Laboratory during 1938, of an approximate method of analysis (9), and the boiler waters showed concentrations much lower than had been anticipated. The losses apparently occurred through adsorption and coprecipitation with calcium-carbonate sludge in both the feedwater-treating tanks and in the boiler. The effect of the sludge in the water treatment was especially bad. Destruction by dissolved oxygen in the boiler was a second source of loss. The magnitude of this latter effect is unknown, although laboratory results would indicate that it might be large.

Loss of waste sulphite liquor in the feedwater could be prevented by introducing it after all softening operations had been completed. This procedure was followed, although it introduced some complications in the treatment. The loss in the boiler was taken care of simply by adding a sufficient excess to the feedwater.

The analysis afforded assurance regarding one point of the treatment, namely, that the inhibiting agent was actually in the boiler water. However, the vital point as to whether it would stop cracking in the riveted seams was still wide open to question. During the early part of 1939, the embrittlement detector was made available, which offered means of securing an immediate answer to this question.

[4] Waste product containing large amounts of lignin, obtained from the sulphite process of paper manufacturing. The material used in this investigation was furnished by the West Virginia Pulp and Paper Company in the form of a viscous liquid, containing about 50 per cent dissolved solids. An analysis shows approximately the following properties and constituents:

Specific gravity	1.32
Baumé	35.0
Ash	15.65
Fe	0.062
CaO	0.13
MgO	0.07
Na_2O	9.67
Sulphur	3.71
Total solids	54.6
Nontannin	40.1
Tannin	14.5
pH	10.6
Carbohydrate	6 3

Detector installations were made on switch engines, which normally take their feedwater from one source, in order that the effect of the treatment could be most accurately ascertained. The tests were started on six engines and the number was later increased to fifteen. Ordinarily, one detector was attached to the engine, although in two cases three units were used to permit simultaneous testing of three different steels. Fig. 1 shows three detectors attached to a boiler. These were bolted to a bracket which was in turn fastened to the side sheet, below and just forward of the cab. Water connections were tapped into the side sheets as shown; the bottom connection was high enough so that it did not clog with sludge. Both lines to the detectors were, of course, provided with valves so that the specimens could be removed and new ones put in at any time. The cooling of the solution as it passed through the detector blocks caused rapid circulation of the boiler water.

The detectors were examined and leakage adjusted once daily by shopmen at the various points on the road. The reason for the tests was explained to these men, and they were shown exactly how to install the specimens and adjust the steam flow. During

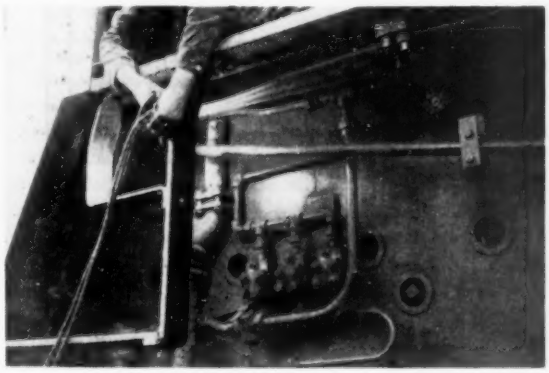


FIG. 1 BATTERY OF THREE EMBRITTLEMENT DETECTORS INSTALLED ON A LOCOMOTIVE

the first few tests on each engine, officials of the railroad were present during the removal of specimens and installation of new ones to insure continued interest and to eliminate any possible carelessness. The shopmen were very cooperative and took an active part in the study.

In general, it was necessary to adjust the steam leakage three or four times during the early part of the test, but it would then continue for long intervals without further adjustment. It appeared that the units needed less attention than is normally the case where they are used on stationary boilers. This is probably due to the effect of vibration and motion of the locomotive in preventing plugging of the leakage.

The results for the detector tests during the time waste sulphite liquor was in use are shown at the left in Fig. 2. The boiler water in each engine was usually analyzed from five to ten times during each experiment, the long-time tests requiring the greater number of analyses. The averages are plotted in Fig. 2. Alkalinity was determined by titration with phenolphthalein and methyl orange. The value for total alkalinity as NaOH was calculated from the methyl-orange end point. This normally runs from 300 to 600 ppm. Chloride was determined by titration with silver nitrate. Total solids were estimated by a calibrated conductivity measurement. Waste sulphite liquor was determined as previously indicated (9).

None of the specimens, tested at Peach Creek or Huntington, W. Va., Stevens or Russell, Ky., or Gladstone, Va., has cracked. These waters may have been nonembrittling, due to the presence of some naturally occurring inhibiting agent, or the maintenance of concentrations of waste sulphite liquor or sodium nitrate. The testing was not carried far enough to identify the inhibiting agent.

At Walbridge, Ohio, the first four specimens did not crack in periods up to 90 days, but when a substitute material, Glutrin,[5] which laboratory tests had shown to be inferior, was used in place of the West Virginia waste sulphite liquor, the last specimen cracked in 60 days.

At Parsons Yard, Ohio, the first specimen cracked with concentrations of waste sulphite liquor below 20 per cent,[6] but all of the remaining specimens were uncracked, even in periods up to 90 days, when the concentration was about 25 per cent, except the last two specimens when Glutrin was used.

At Peru, Ind., one specimen cracked, but an increase in waste sulphite liquor eliminated the cracking for periods up to 90 days.

At Newport News, Va., cracking was produced in the first specimen, which was eliminated by an increase in concentration of the waste sulphite liquor. In test No. 6, the waste sulphite liquor was purposely reduced and essentially eliminated from the feedwater, and cracking occurred. An increase in concentration of a protective agent again stopped the cracking. These tests seemed to demonstrate quite clearly the marked protective action of the treatment at Newport News.

At Fulton, Va., the first specimen cracked, but subsequent specimens, with much higher concentrations of waste sulphite liquor did not crack.

At Clifton Forge, Va., the first four specimens cracked, and it was necessary to reach concentrations of waste sulphite liquor near 70 per cent to secure any marked protective action. Even then, some slight cracking was encountered.

At Ashland, Ky., and Handley and Hinton, West Va., the cracking has little direct relation to the concentration of the inhibitor. It is possible that results at Hinton may be taken to indicate that a comparatively high concentration is effective, but this is not clearly demonstrated.

The results of the treatment at Charlottesville, Va., were quite unsatisfactory, and cracking of the specimens continued even though the concentration of waste sulphite liquor was raised nearly to 70 per cent.

These tests would indicate that waste sulphite liquor is satisfactory on many waters, but its protective action can fail in some cases. This result seems to be in qualitative agreement with the most recent laboratory studies, although the reasons for the differences are still obscure (6). In spite of these facts, however, the use of this inhibitor did bring a noticeable reduction in engine cracking over the 2-year period in which it was in use, and no cracked engines have been reported at the Parsons, Fulton, or Newport News terminals since this treatment was started in February, 1938, whereas, a number had occurred previously.

USE OF SODIUM NITRATE TO PREVENT EMBRITTLEMENT

During the latter part of 1940, the West Virginia Pulp and Paper Company changed its manufacturing process and waste sulphite liquor was no longer available from this source. Other supplies were investigated, but laboratory tests showed that the concentrations necessary to produce protection were somewhat higher, and some of the materials gave sticky sludges when they were used in conjunction with metaphosphate.

About this time, investigation[7] had indicated that the protective action of sodium nitrate was superior to that of waste sulphite liquor and less subject to interference from the presence of other

[5] Glutrin is a waste-sulphite-liquor product prepared at Erie, Pa.

[6] Twenty per cent of total alkalinity as NaOH; based on waste sulphite liquor containing 50 per cent dissolved solids.

[7] Private correspondence with the U. S. Bureau of Mines.

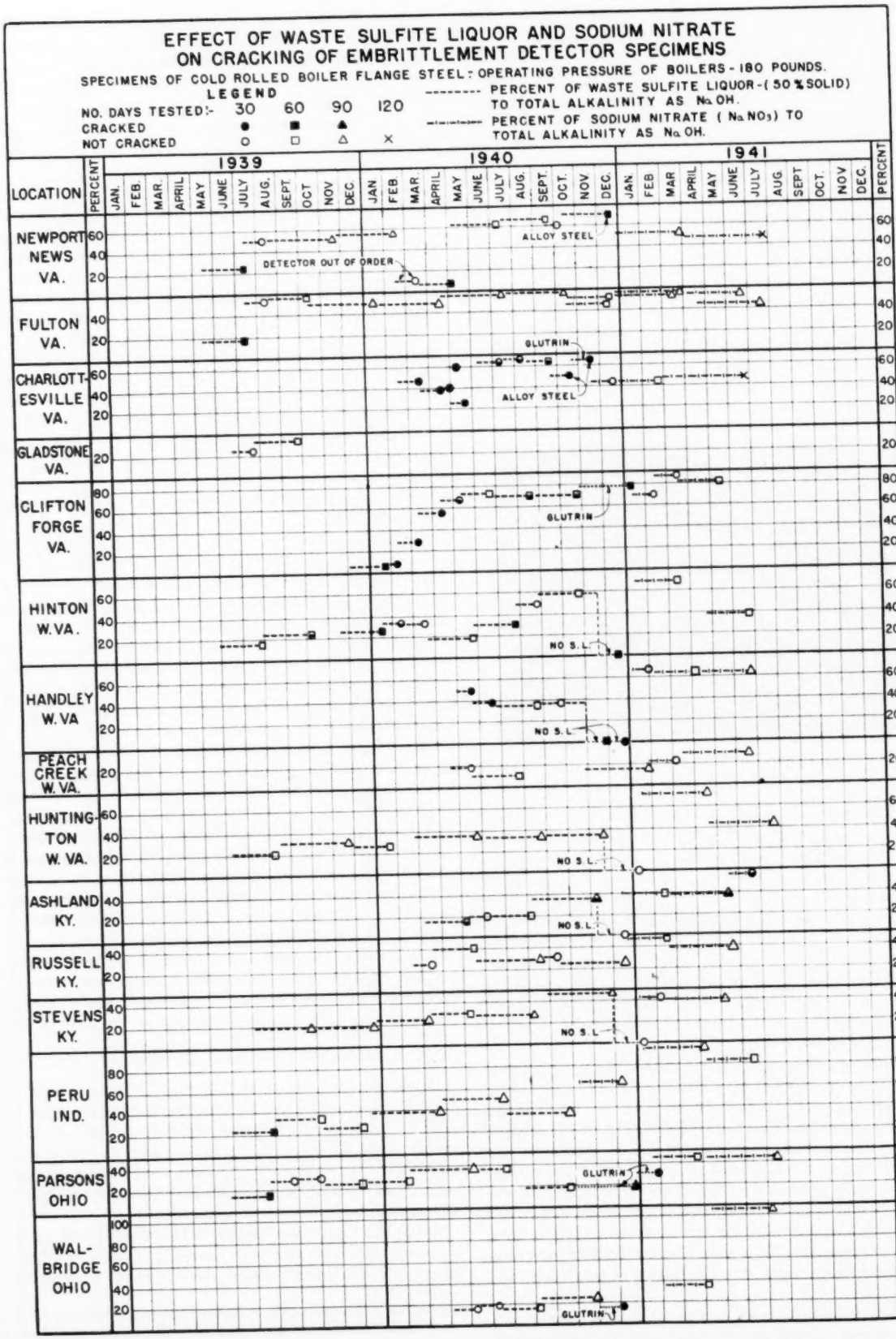


FIG. 2 CHART SHOWING EFFECT OF WASTE SULPHITE LIQUOR AND SODIUM NITRATE ON CRACKING OF EMBRITTLEMENT-DETECTOR SPECIMENS ON LOCOMOTIVES OF THE CHESAPEAKE & OHIO RAILWAY

substances in the boiler water. Sodium nitrate had other advantages, as follows:

1 It could be added at any point in the feedwater treatment without being lost.

2 It is not adsorbed or coprecipitated in the boiler.

3 It is not subject to oxidization. Our experience also shows that it does not decompose in a locomotive boiler.

4 It is an inorganic chemical of definite known composition which can be purchased from numerous sources.

5 Its concentration in the boiler water can be determined by accurate and precise analytical methods.[8]

The effect of sodium nitrate on the embrittlement-detector tests is shown at the right in Fig. 2. The operation of the detectors and the chemical analysis of the boiler waters were made in the same manner as described for waste sulphite liquor. The determination of waste sulphite liquor was omitted,[9] of course, and the nitrate determination made instead.

The use of sodium nitrate was first introduced at Charlottesville, and Fulton, Va. At Fulton, cracking was prevented for 90 days without difficulty. Results at Charlottesville were especially gratifying, and cracking was completely stopped for periods up to 120 days. If these results are compared with those shown at the left in Fig. 2, for waste sulphite liquor at this same location, it will be seen that the nitrate is by far the more effective inhibitor.

After the nitrate treatment had been in use about 3 months at these two locations, a thorough internal inspection was made of the engines for evidences of pitting and corrosion. The engine boilers were found to be in excellent condition and, so far as could be determined, the nitrate treatment had no undesirable effects.

Sodium-nitrate treatment was then introduced on the entire system and, as shown at the right in Fig. 2, cracking was eliminated in all tests with the exception of two specimens at Ashland, which were slightly cracked in 90 and 37 days. These results may have been due to an interval not picked up in the analysis, during which the nitrate concentration was low, or may indicate the requirement of constituents other than nitrate. No boilers have been reported cracked as yet at this terminal. The test is now being repeated with an increase in nitrate concentration, as well as more frequent analyses.

During the tests shown at the right in Fig. 2, it was desired to maintain a concentration of sodium nitrate equivalent to 40 per cent of the total alkalinity as sodium hydroxide. This was done with reasonable accuracy in most cases. At Clifton Forge, Handley, and Peru, however, higher concentrations have been held in order to protect road engines that subsequently take some feedwater which is not nitrate-treated.

[8] For the work reported in this paper, nitrogen was determined by distillation with Devarda's alloy essentially in accord with the Vamari-Mitscherlich-Devarda method for determination of nitric nitrogen in soil extracts, Wilfred W. Scott, "Standard Methods of Chemical Analysis," 1917 edition, pp. 304–305. A more rapid colorimetric method is now under investigation.

[9] In all cases the addition of waste sulphite liquor was discontinued when the nitrate treatment was started.

In view of the fact that most of the tests, shown at the right in Fig. 2, are for periods of 60 or 90 days, or even longer, the almost complete elimination of cracking is deemed quite satisfactory. The nitrate treatment has been very easy to use and does not have the objectionable features encountered with waste sulphite liquor.

Conclusions

Embrittlement-detector tests and railroad operating experience have shown that sodium sulphate does not prevent or even delay embrittlement cracking.

Waste sulphite liquor will prevent cracking of detector specimens on many boiler waters, but in a few cases its protective action fails.

Sodium nitrate has essentially eliminated cracking of detector specimens on the entire system of The Chesapeake & Ohio Railway. This treatment has been easy to apply and its use has not created any difficulty in the operation of the locomotive boiler. This chemical seems to be the most efficient treatment yet developed for counteracting intercrystalline cracking, but more information concerning its action is desirable.

Treatment with waste sulphite liquor and subsequent treatment with sodium nitrate have made a material reduction in the repairs required because of cracking in locomotive boilers. Repairs, which are still necessary where these materials are being used, appear to be due to cracks started before the treatment to prevent embrittlement was undertaken. Once these old cases have been eliminated, it is believed that further improvement will be noted.

BIBLIOGRAPHY

1 "Progress in Generation of Energy by Heat Engines," by George A. Orrok, Proc. American Society of Civil Engineers, vol. 63, 1937, pp. 1884–1892.

2 "Water Treatment and Boiler Troubles," by W. A. Pownall, Proceedings, Western Railway Club, vol. 24, 1912, pp. 217–238.

3 "A Physico-Chemical Study of Scale Formation and Boiler-Water Conditioning," by R. E. Hall, G. W. Smith, H. A. Jackson, J. A. Robb, H. S. Karch, and E. A. Hertzell, Carnegie Institute of Technology, Mining and Metallurgical Investigations, Bulletin 24, 1927.

4 "Pitting and Corrosion of Boiler Tubes and Sheets," by M. E. McDonnell, Proceedings, American Railway Engineering Association, vol. 25, 1925, pp. 377–379.

5 "Development of Water Treatment on the Alton Railroad," by R. W. Seniff, Proceedings, Master Boiler Makers' Association, 1939, pp. 42–53.

6 "Intercrystalline Cracking of Locomotive Boilers," by W. C. Schroeder, A. A. Berk, and R. A. O'Brien, Association of American Railroads, Circular D. V. 989, May, 1940; also "Intercrystalline Cracks in Locomotive Boilers," describing investigations sponsored by The Association of American Railroads, *Railway Age*, vol. 109, 1940, pp. 25–28.

7 "Embrittlement Detector Testing on Boilers," by W. C. Schroeder, A. A. Berk, and C. Kerby Stoddard, *Power Plant Engineering*, August, 1941, pp. 76–79.

8 "Protecting Steel Against Intercrystalline Attack in Aqueous Solution," by W. C. Schroeder, A. A. Berk, and R. A. O'Brien, Trans. A.S.M.E., vol. 60, 1938, pp. 35–42.

9 "Colorimetric Method for the Determination of Lignin," American Railway Engineering Association, vol. 40, no. 407, December, 1938, pp. 222–224.

Studies on the Cracking of Boiler Plate

By P. G. BIRD[1] and E. G. JOHNSON,[1] CHICAGO, ILL.

This paper reports a series of tests on the cracking of boiler steel, based upon the use of the Schroeder embrittlement detector. Two types of waters were employed, one consisting of synthetic solutions and the other of boiler waters. The results are reported in comprehensive tables which show the amount and kind of inhibitor added, the water analysis, the amount of organic matter as indicated by the Tyrosin test, and other pertinent data. The tests show that, of the inorganic substances used to inhibit cracking, sodium nitrate is one of the best when combined with organic matter. With a given feedwater, it was found that ever-increasing amounts of inhibitors are required as the number of concentrations increases. This unit should be used only by skilled operators.

THE cracking of steel in locomotive and stationary boilers has been a subject of interest for many years. Most investigators are in agreement as to the factors involved in the cracking of boiler plate. The essential conditions appear to be the presence of a high concentration of caustic with some silica in contact with steel under high tensile stress.

An example of how such stresses can be brought about is illustrated in Fig. 1. This shows an etched cross section of a locomotive-boiler seam which cracked close to a rivet. In this case calking was severe enough to separate the plates on both sides of the rivet. This put the section of the steel under the rivet head in high tension. Microscopic examination revealed both transcrystalline and intercrystalline cracks.

In order to reproduce in the laboratory conditions similar to those which are necessary to crack steel, the embrittlement detector, as developed by W. C. Schroeder, of the United States Bureau of Mines, was adopted, and the results embodied in this report were obtained by employing this device.

Fig. 2 is a general view of the laboratory used for this work. Each of the units has an insulated cover to minimize the loss of heat. These covers also help in obtaining more consistent results by maintaining constant conditions. There are thirty-four units, including two obtained from the Bureau of Mines, one of which is shown at the right in Fig. 2. A close-up view of an assembled unit is shown in Fig. 3. The unassembled test blocks, the clamping blocks, and specimens are shown in Fig. 4. These units were built to accommodate two test specimens instead of one. In all other respects, the units are like those designed by Dr. Schroeder.

Principle of Concentrating Boiler Waters

The principle employed in concentrating boiler waters is quite simple, although the adjustment required to maintain proper conditions must be expertly done. The connecting pipes from the test block to the autoclaves extend down nearly to the bottom inside of the autoclaves, so that, when the unit is heated up to boiler operating pressure, the water in the autoclave is forced upward and is circulated through the test block. The test specimens are laid in the grooved portions of the test block, and when clamped down in place, assume the curvature of the grooves. There is a small opening connecting the water space and the bottom of the groove. This opening is tight when the test specimen is clamped in place. A very small amount of boiler water is allowed to escape from this hole under the test specimen. Tightening or loosening the clamping blocks, together with proper setting of the adjusting screw, regulates the amount of boiler water escaping from this small hole. As the temperature of the head block is above 212 F, the escaping solution flashes into steam and leaves a deposit of the solids contained in the boiler water. This results in a highly concentrated solution in contact with the stressed metal specimens. These conditions provide for the physical and mechanical requirements to produce cracking.

The usual time of testing is 30 days. Fig. 5 shows the depth of cracking of one specimen after it had been removed from the block at the completion of the test. This specimen had been broken by placing it in a vise and tapping it with a hammer. The freshly broken portions, resulting from the hammer blow, are the light patches in the broken section. The dark patches show the penetration of corrosion through the metal.

When test specimens are subjected to an embrittling solution without inhibitors being present, they will generally crack in a period of 2 weeks; always in less than 3 weeks, but when distilled water only is in the bomb, no cracking is obtained on repeated 30-day tests. Thus, it is apparent that the chemicals in the solution are necessary for producing cracking in this device.

In operating this equipment the fundamentals required for cracking must be constantly observed. The operator must bear in mind that the solution under test must be concentrated to a high degree on the surface of the steel at a point where the steel is under high tensile stress. Obviously, if a concentrate is not obtained, or if the concentration takes place on metal not under high tensile stress, cracking cannot be expected, even with a highly embrittling boiler water.

Great care must be taken when making water-leakage adjustments on the embrittlement detector. Failure to do this may result in erroneous conclusions.

Test Procedure Followed

The following procedure has been found to yield reasonably good check results. This procedure was adopted because it seemed to insure a high tensile stress and would also maintain a high concentration of solution on this stressed surface.

Tension is first applied to the specimen when the unit is assembled for testing. The specimen, which has previously been polished to insure a smooth surface, is placed in the groove of the detector and the adjustment screw is turned into the specimen to a point where the end of the screw is flush with the bottom surface of the specimen, as shown in Fig. 6. After placing the specimen in the groove, it is clamped tightly in place. This puts the under surface of the test piece under tension, due to the curvature of the bottom of the groove.

Tension is also maintained on the under surface of the specimen during the water-leakage adjustments, which are made daily for the duration of the test. The initial adjustment is made in the following manner:

The adjustment screw is tightened by a fraction of a turn. Then the clamp is loosened just sufficiently to produce a small leak, after which the clamp is again tightened until the leak is just

---

[1] National Aluminate Corporation.

Contributed by the Joint Research Committee on Boiler Feedwater Studies and presented at the Annual Meeting, New York, N. Y., December 1–5, 1941, of The American Society of Mechanical Engineers.

Note: Statements and opinions advanced in papers are to be understood as individual expressions of their authors and not those of the Society.

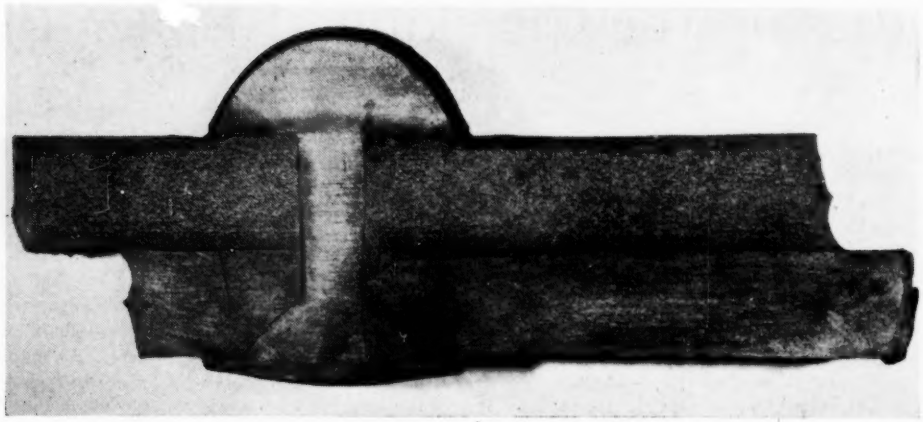


FIG. 1 CRACKED PLATE FROM A LOCOMOTIVE-BOILER SEAM

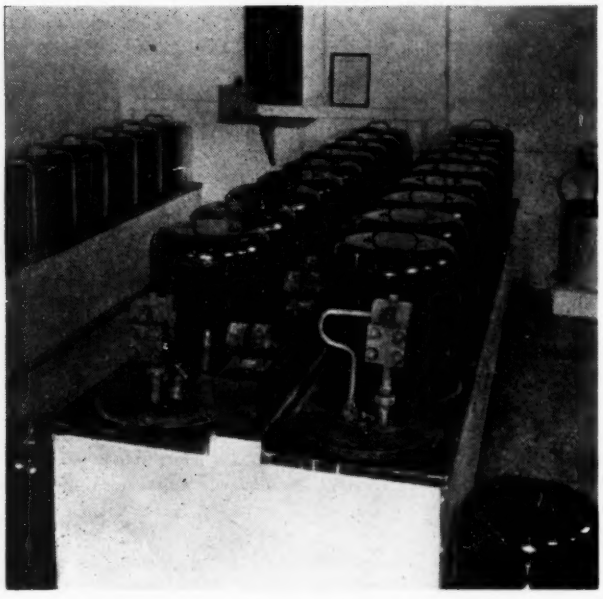


FIG. 2 GENERAL VIEW OF TESTING LABORATORY

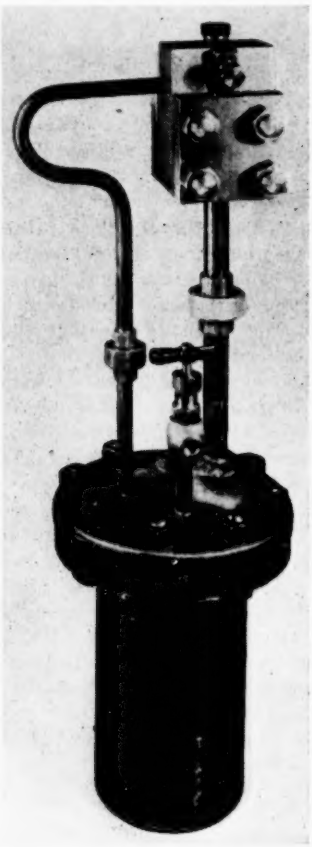


FIG. 3 ASSEMBLED DETECTOR UNIT

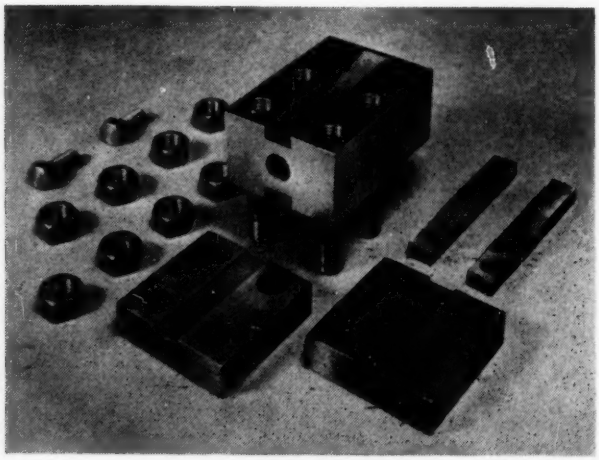


FIG. 4 DISASSEMBLED TEST BLOCK

stopped. The water leak is then regulated the desired amount by turning in the adjustment screw a fraction of a turn. Subsequent daily adjustments are made by releasing the clamping block slightly until a small leak is obtained, and then closing or nearly closing the leak by tightening the clamp. This is then followed by a sufficient turn on the adjusting screw to give the desired leakage. Care is taken while making adjustments to prevent excessive loss of water, which would wash away accumulated deposits.

When the specimen is originally clamped in place the under surface is put under tension. However, when the clamp is re-

leased ever so slightly, the under surface of the specimen is no longer under tension, and may even be in compression. As it is necessary to have this surface under tension, the clamp is again tightened to a point of little or no leakage, which may or may not put the under surface in tension. The desired leakage is obtained by turning in the adjustment screw which insures the under surface of the specimen being under high tension. Failure to have the under surface under tension will result in no cracking, even though a highly embrittling solution is employed.

Because of the careful adjustment required in the use of the detector, it is believed that results obtained by other than highly skilled operators are likely to be misleading. For example, if the specimen should crack, it may not mean that the boiler is in danger. Likewise, if the specimen does not crack, it does not necessarily mean that the boiler is not in danger. This does not mean, however, that the detector is not a valuable tool when operated by, and the results interpreted by, competent personnel. Indiscriminate usage of this instrument should be avoided.

Because of the fine adjustments required, all tests conducted

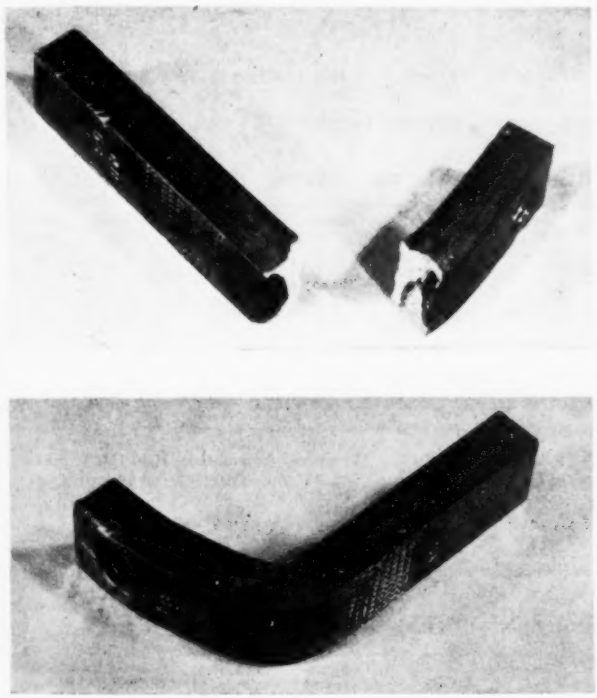


FIG. 5 CRACKED AND UNCRACKED DETECTOR SPECIMENS

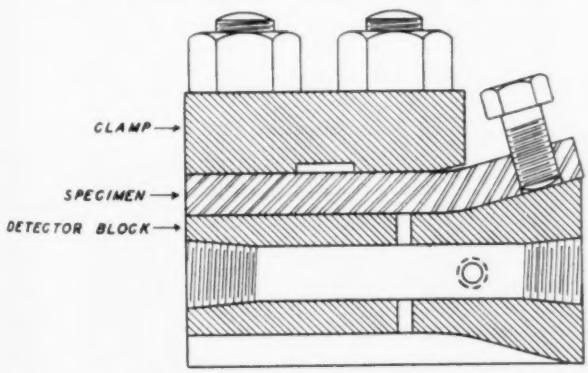


FIG. 6 CROSS SECTION OF DETECTOR ASSEMBLY

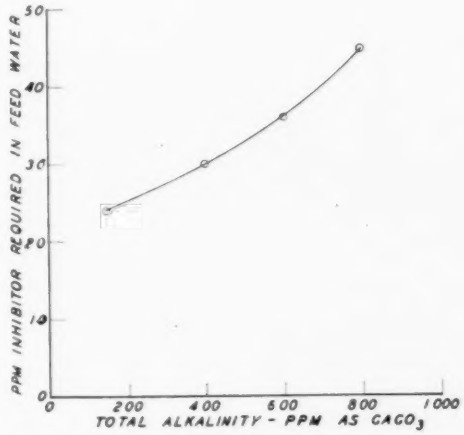


FIG. 7 INHIBITOR REQUIREMENTS VERSUS ALKALINITY

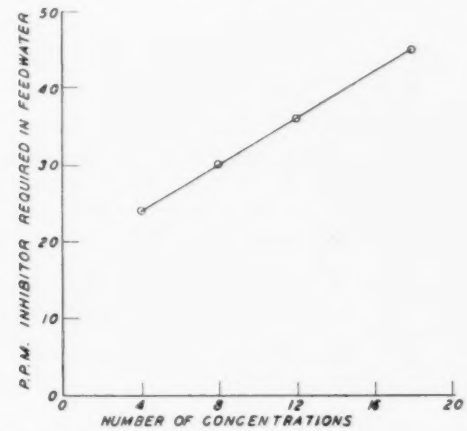


FIG. 8 INHIBITOR REQUIREMENTS VERSUS CONCENTRATION

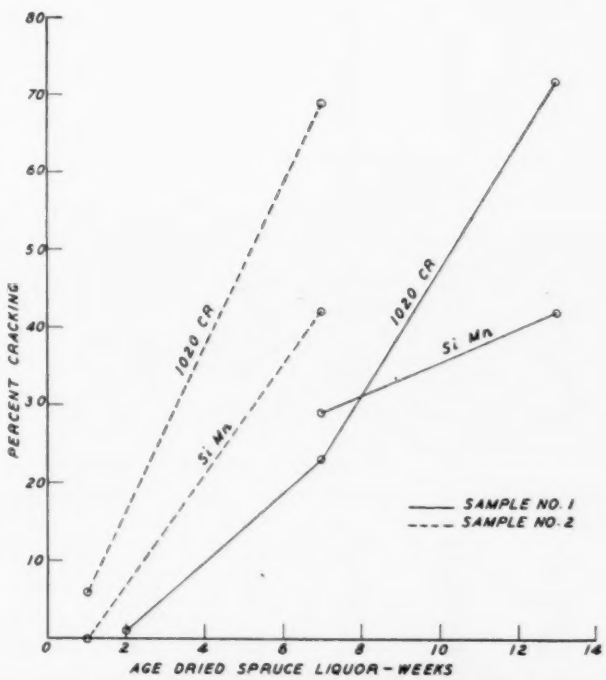


FIG. 9 EFFECT OF AGE ON SPRUCE LIQUOR

TABLE 1 PROCESSED LIGNIN SULPHONATE AND SODIUM NITRATE IN FEEDWATER

Inhibitor in feedwater, ppm	Boiler-water analysis, ppm										
	P	M	NaCl	Na_2SO_4	SiO_2	S.S.	D.S.	Organic (Tyrosin)	Inhibitor (calculated)	Per cent 1020 HR	Cracking nickel
0.0	335	398	314	1150	17.1	430	1930	5.1	0	38	64
1.5	350	410	314	1020	15.4	384	1860	14.5	12	35	35
3.0	308	370	311	1010	20.5	460	1860	25.6	24	31	16
7.5	308	362	308	940	21.2	1020	1780	49.5	60	25	53
10.0	287	346	308	940	21.2	342	1780	68.4	80	0	54
15.0	300	376	326	1025	8.5	318	2040	87.0	120	12	16

Inhibitor: 90 per cent lignin sulphonate after being subjected to high-pressure alkaline cook; 10 per cent sodium nitrate. Feedwater concentrated 8 times at 200 psi.

TABLE 2 LIGNIN RESIDUE AND SODIUM NITRATE IN FEEDWATER

Inhibitor in feedwater, ppm	Boiler-water analysis, ppm										
	P	M	NaCl	Na_2SO_4	SiO_2	S.S.	D.S.	Organic (Tyrosin)	Inhibitor (calculated)	Per cent 1020 HR	Cracking nickel
0.0	267	352	328	1150	27.4	462	1880	5.1	0	17	21
7.5	270	346	324	1150	20.5	625	1930	8.6	60	0	12
15.0	270	338	335	1200	25.8	700	1930	17.1	120	0	6
22.0	260	352	328	1080	25.8	371	1930	20.5	176	0	4
30.0	270	352	335	1150	25.5	419	1930	29.0	240	0	0

Inhibitor: 10 per cent sodium nitrate; 90 per cent lignin residue. Feedwater concentrated 8 times at 200 psi.

TABLE 3 LIGNIN RESIDUE AND SODIUM NITRATE IN FEEDWATER

Inhibitor in feedwater, ppm	Boiler-water analysis, ppm										
	P	M	NaCl	Na_2SO_4	SiO_2	S.S.	D.S.	Organic (Tyrosin)	Inhibitor (calculated)	Per cent nickel	Cracking Si-Mn
0.0	359	432	321	960	34.2	335	1760	1.7	0	52	42
7.5	342	424	326	990	29.1	370	1860	5.1	60	36	36
15.0	335	414	321	990	20.5	116	1090	12.0	120	21	27
22.0	321	411	321	1090	20.5	361	1840	25.6	176	23	13
30.0	325	421	326	1090	20.5	291	1990	32.5	240	0	0

Inhibitor: 22 per cent sodium nitrate; 78 per cent lignin residue. Feedwater concentrated 8 times at 200 psi.

TABLE 4 LIGNIN SULPHONATE AND SODIUM NITRATE IN FEEDWATER

Inhibitor in feedwater, ppm	Boiler-water analysis, ppm										
	P	M	NaCl	Na_2SO_4	SiO_2	S.S.	D.S.	Organic (Tyrosin)	Inhibitor (calculated)	Per cent 1020 HR	Cracking nickel
0.0	155	190	162	503	11.3	240	940	4.3	0	4	2
7.5	150	192	175	513	8.9	376	872	20.6	28	2	2
18.0	152	188	167	503	11.3	240	975	46.1	72	2	1
24.0	115	150	171	518	8.2	103	924	85.5	96	0	0
36.0	104	185	171	530	10.3	34	1040	137.0	144	0	0

Inhibitor: 90 per cent lignin sulphonate; 10 per cent sodium nitrate. Feedwater concentrated 4 times at 200 psi.

TABLE 5 LIGNIN SULPHONATE AND SODIUM NITRATE IN FEEDWATER

Inhibitor in feedwater, ppm	Boiler-water analysis, ppm										
	P	M	NaCl	Na_2SO_4	SiO_2	S.S.	D.S.	Organic (Tyrosin)	Inhibitor (calculated)	Per cent 1020 HR	Cracking nickel
0.0	316	362	328	958	6.8	1090	1675	6.8	0	41	57
9.0	287	356	322	958	7.5	790	1750	42.8	72	8	18
19.0	302	376	352	1024	20.6	291	1800	89.0	152	2	1
25.0	308	398	359	1180	18.1	240	2080	137.0	200	1	0
30.0	292	398	363	1210	17.8	342	2170	171.0	240	0	0
39.0	290	390	342	1195	17.8	102	2170	192.0	312	0	0
48.0	287	390	335	1180	18.1	102	2140	219.0	384	0	0

Inhibitor: 90 per cent lignin sulphonate; 10 per cent sodium nitrate. Feedwater concentrated 8 times at 200 psi.

TABLE 6 LIGNIN SULPHONATE AND SODIUM NITRATE IN FEEDWATER

Inhibitor in feedwater, ppm	Boiler-water analysis, ppm										
	P	M	NaCl	Na_2SO_4	SiO_2	S.S.	D.S.	Organic (Tyrosin)	Inhibitor (calculated)	Per cent 1020 HR	Cracking nickel
0.0	425	500	438	1490	11.3	256	2390	6.8	0	6	10
6.0	425	534	492	1610	11.3	480	2650	48.0	72	49	51
12.0	431	557	492	1610	11.3	720	2900	85.5	144	30	31
20.0	475	582	492	1440	17.1	239	2890	137.0	240	19	28
27.0	425	557	489	1540	10.2	395	2740	192.0	324	10	16
36.0	438	588	528	1780	5.5	1030	3140	248.0	432	0	0
48.0	396	547	503	1670	5.5	1280	3080	325.0	576	0	0

Inhibitor: 90 per cent lignin sulphonate; 10 per cent sodium nitrate. Feedwater concentrated 12 times at 200 psi.

TABLE 7 LIGNIN SULPHONATE AND SODIUM NITRATE IN FEEDWATER

Inhibitor n feedwater, ppm	Boiler-water analysis, ppm										
	P	M	NaCl	Na_2SO_4	SiO_2	S.S.	D.S.	Organic (Tyrosin)	Inhibitor (calculated)	Per cent 1020 HR	Cracking nickel
0.0	780	910	780	2460	15.4	1470	4350	10.3	0	100	73
4.0	745	773	774	2260	9.9	975	4130	53.0	72	49	49
8.0	752	872	759	2305	18.1	1280	4130	85.4	144	32	22
15.0	752	885	745	2305	18.1	495	4030	137.0	270	26	20
25.0	725	885	745	2305	19.5	410	4250	212.0	450	8	9
36.0	710	872	774	2305	17.1	1450	4390	266.0	648	0	10
42.0	653	826	774	2660	32.5	256	4870	333.0	756	1	2
45.0	622	800	763	2820	25.6	580	4790	359.0	10	0	0

Inhibitor: 90 per cent lignin sulphonate; 10 per cent sodium nitrate. Feedwater concentrated 18 times at 200 psi.

TABLE 8 EFFECT OF VARIOUS INORGANIC SALTS

Inorganic substance, ppm	NaCl, ppm	Na_2SO_4, ppm	Cracking, per cent 1020 CR	1020 HR	Si-Mn
100 Sodium nitrate	20	..	31	..	40
200 Sodium nitrate	20	..	0, 44, 2	..	6, 7
10 Sodium nitrate	500	1500	51	46	..
100 Sodium nitrate	500	1500	38	2	..
200 Sodium sulphite	20	..	22	..	63
100 Trisodium phosphate	20	..	20	..	..
125 Sodium carbonate	500	1500	85	100	..
200 Sodium chromate	500	1500	86	78	..
200 Potassium ferrocyanide	500	1500	21	13	..
200 Potassium ferricyanide	500	1500	27	4	..
No inhibitor	500	1500	60	41	57

NOTE: The solutions in this table contained 500 ppm of caustic soda; 50 ppm of sodium silicate and sodium chloride; and sodium sulphate as indicated.

TABLE 9 LIGNIN-BASE MATERIALS WITH SODIUM SULPHITE

Organic, ppm	Na_2SO_3, ppm	NaCl, ppm	Na_2SO_4, ppm	Cracking, per cent 1020 CR	Si-Mn
198 Lignin sulphonate	2	20	..	0, 1	4, 7
95 Lignin sulphonate	5	20	..	0	0
90 Lignin sulphonate	10	20	..	20, 42	0, 2
80 Lignin sulphonate	20	20	..	1, 15	0, 0
95 Lignin sulphonate	5	500	1500	..	4
90 Lignin sulphonate	10	500	1500	47	49
190 Processed lignin no. 1	10	20	..	0	0
95 Processed lignin no. 1	5	20	..	39	8
90 Processed lignin no. 2	10	20	..	0	3
90 Processed lignin no. 1	10	500	1500	63	32
90 Processed lignin no. 2	10	500	1500	3	0
160 Processed lignin no. 2	40	500	1500	57	28

NOTE: All the solutions in this table contained 500 ppm of caustic soda; 50 ppm of sodium silicate and sodium chloride; sodium sulphite and sodium sulphate, as indicated.

Processed lignin no. 1: Lignin sulphonate after high-pressure alkaline cook.

Processed lignin no. 2: Lignin sulphonate neutralized before drying.

TABLE 10 VARIOUS ORGANIC MATERIALS WITH SODIUM NITRATE

Organic, ppm	$NaNO_3$, ppm	TSP, ppm	Na_2CO_3, ppm	Cracking, per cent 1020 HR	1020 CR
200 Lignin sulphonate	..	..	..	16	20
90 Lignin sulphonate	10	..	..	0	0
95 Lignin sulphonate	5	..	..	0	0
99 Lignin sulphonate	1	..	..	22	27
90 Lignin sulphonate	10	100	500	2	58
90 Lignin sulphonate	10	..	500	0, 0	0, 0
90 Lignin sulphonate	10	100	..	0	0
200 Quebracho	..	..	..	5	3
90 Quebracho	10	..	..	0	0
90 Quebracho	10	100	500	0	0
200 Hemlock	..	..	..	..	20
90 Hemlock	10	..	..	0	0
90 Hemlock	10	100	500	0	6
200 Chestnut no. 1	..	..	..	15	8
90 Chestnut no. 1	10	..	..	0	0
90 Chestnut no. 1	10	100	500	16	0
90 Chestnut no. 2	10	..	..	0	0
95 Chestnut no. 2	5	..	..	0	0
90 Starch	10	..	..	0	0
90 Starch	10	100	500	3	20
300 Lignin residue	..	..	..	0	3
200 Lignin residue	..	..	..	16	12
100 Lignin residue	..	..	..	23	18
90 Lignin residue	10	..	..	0	0
90 Lignin residue	10	100	500	0, 0	0, 0
50 Processed lignin sulphonate no. 1	..	..	..	10	8
100 Processed lignin sulphonate no. 1	..	..	..	0	4
22.5 Processed lignin sulphonate no. 1	2.5	..	..	0	0
22.5 Processed lignin sulphonate no. 1	2.5	100	500	0	0
200 Processed lignin sulphonate no. 3	..	..	..	6	21
90 Processed lignin sulphonate no. 3	10	..	..	0	0
90 Processed lignin sulphonate no. 3	10	100	500	12	5
100 Myrobalans no. 1	..	..	..	23	15
200 Myrobalans no. 1	..	..	..	16	13
90 Myrobalans no. 1	10	..	..	0	0
90 Philippine cutch	10	..	..	0	0
No organic	..	..	..	41	60

NOTE: The solutions in this table contained 500 ppm caustic soda; 500 ppm sodium chloride; 50 ppm sodium silicate; 1500 ppm sodium sulphate and sodium nitrate; trisodium phosphate and sodium carbonate, as indicated.

Processed lignin sulphonate no. 1: Lignin sulphonate after high-pressure alkaline cook.

Processed lignin sulphonate no. 3: Lignin sulphonate after high-pressure alkaline cook in the presence of sodium sulphite.

TABLE 11 NITRATED-LIGNIN SUBSTANCES

Organic	TSP, ppm	Na_2CO_3, ppm	Cracking, per cent 1020 HR	1020 CR
Nitrated-lignin-sulphonate no. 1 sample	..	..	20	93
Nitrated-lignin-sulphonate no. 2 sample	..	..	35	54
Nitrated-lignin-sulphonate no. 1 sample	100	500	55	98
Nitrated-lignin-sulphonate no. 2 sample	100	500	50	91
Nitrated-lignin-residue no. 1 sample	..	..	6	8
Nitrated-lignin-residue no. 2 sample	..	..	0	3
Nitrated-lignin-residue no. 1 sample	100	500	43	68
Nitrated-lignin-residue no. 2 sample	100	500	31	41

NOTE: The solutions in this table contained 500 ppm caustic soda; 50 ppm sodium silicate; 500 ppm sodium chloride; 1500 ppm sodium sulphate and sodium carbonate; and trisodium phosphate, as indicated.

All solutions contained 100 ppm of the nitrated material.

TABLE 12 EFFECT OF AGE ON DRIED SPRUCE SULPHITE LIQUOR

Material, ppm	Age, weeks	NaCl, ppm	Na_2SO_4, ppm	Cracking, per cent 1020 CR	Si-Mn
100 Spruce no. 1 sample	2	20	..	1	..
100 Spruce no. 1 sample	7	20	..	23	29
100 Spruce no. 1 sample	13	20	..	72	42
100 Spruce no. 2 sample	1	500	1500	6	0
100 Spruce no. 2 sample	7	500	1500	69	42

NOTE: All the solutions in this table contained 500 ppm of caustic soda; 50 ppm of sodium silicate and sodium chloride; and sodium sulphate, as indicated.

TABLE 13 PRESSURE-COOKED LIGNIN SULPHONATE NO. 1

Lignin sulphonate, ppm	NaCl, ppm	Na_2SO_4, ppm	Cracking, per cent 1020 CR	1020 HR	Si-Mn
100	20	..	0, 2, 0	..	6, 0
50	500	1500	8	10	..
100	500	1500	4	0	..
200	500	1500	11	..	0

NOTE: The solutions used contained 500 ppm of caustic soda; 50 ppm of sodium silicate and sodium chloride; and sodium sulphate, as indicated.

Processed lignin no. 1: Lignin sulphonate after high-pressure alkaline cook.

TABLE 14 COMPARISON OF VARIOUS TANNINS

Tannin, ppm	Cracking, per cent 1020 CR	1020 HR
100 Quebracho	76	..
200 Quebracho	3	5
100 Myrobalans no. 1	15	23
200 Myrobalans no. 1	13	16
100 Myrobalans no. 2	59	38
200 Myrobalans no. 2	2	0
100 Liquid myrobalans	56	18
200 Liquid myrobalans	49	36
100 Quercitron	58	72
200 Quercitron	51	8
100 Equadorian cutch	80	45
200 Equadorian cutch	52	50
200 Logwood	42	36
100 Liquid sumac	56	18
200 Liquid sumac	15	4
200 Chestnut No. 1	8	15

NOTE: The solutions used contained 500 ppm of caustic soda; 50 ppm sodium silicate; 500 ppm sodium chloride; and 1500 ppm of sodium sulphate.

TABLE 15 VARIOUS LIGNIN-BASE MATERIALS

Lignin material, ppm	Cracking, per cent 20 Ppm NaCl 1020 CR	Si-Mn	500 Ppm NaCl 1500 ppm Na_2SO_4 1020 CR	1020 HR
100 Lignin sulphonate	..	68	..	..
200 Lignin sulphonate	23	19	27	9
50 Lignin residue	44	25	..	..
100 Lignin residue	..	..	18	23
200 Lignin residue	20	..	12	16
300 Lignin residue	0	0	3	0
200 Dried sulphite waste liquor	58	..	22	36
300 Dried sulphite waste liquor	55	45	..	..
200 Concentrated sulphite waste liquor	4	17	55, 78	8, 22
100 Dried hemlock sulphite liquor	24	42	..	..
300 Untreated sulphite liquor	44	57	..	..
200 Iron lignin sulphonate	..	..	12	8
100 Copper lignin sulphonate	..	..	14	58

NOTE: The solutions used contained 500 ppm of caustic soda; 50 ppm of sodium silicate and sodium chloride; and sodium sulphate, as indicated.

TABLE 16 ALKALINE DRIED CHESTNUT TANNIN

Chestnut tannin, ppm	pH of drying	NaCl, ppm	Na_2SO_4, ppm	Cracking, per cent 1020 CR	1020 HR	SiMn
200	9.8	20	0	0	..	0
100	9.8	500	1500	59, 69	16	..
200	9.0	500	1500	11, 38	2,28	..
100	7.62	500	1500	47	6	..
200	7.62	500	1500	0,3	1,0	..
100	11.8	500	1500	83	80	..
200	11.8	500	1500	48	4	..
200	Untreated	20	0	39	..	66

NOTE: The solutions contained 500 ppm of caustic soda; 50 ppm of sodium silicate and sodium chloride; and sodium sulphate, as indicated.

TABLE 17 TESTS OF VARIOUS STEELS

Steel no.	Designation	Cracking through 1/4-in. specimens, per cent
1	1020 HR	27
2	1020 CR	100
3	SiMn—0.69 per cent manganese, 0.27 per cent carbon, 0.018 per cent phosphorus, 0.025 per cent sulphur, 0.232 per cent silicon	16
16	Rimmed steel—0.10 per cent carbon	2
17	Semikilled steel—0.16 per cent	0
18	Killed steel—0.08 per cent carbon	0
19	Nickel steel—0.21 per cent carbon, 2.25 per cent nickel	2
20	0.5 per cent copper, 1 per cent nickel, 1 per cent chromium, 1 per cent phosphorus, 0.09 per cent carbon	4
21	Killed steel—0.19 per cent carbon	2
22	Firebox steel—0.10 per cent carbon	4
23	0.30 per cent chromium, 1.25 per cent manganese, 0.80 per cent silicon, 0.19 per cent carbon	2

NOTE: The solutions contained 500 ppm caustic soda; 50 ppm sodium silicate; 500 ppm sodium chloride; and 1500 ppm sodium sulphate.
Single specimens only were used in the tests given in this table.

TABLE 18 TESTS OF VARIOUS STEELS

Steel no.	Designation	Cracking through 1/2-in. specimens, per cent
1	1020 HR	45
2	1020 CR	60
3	SiMn—0.69 per cent manganese, 0.27 per cent carbon, 0.018 per cent phosphorus, 0.025 per cent sulphur, 0.232 per cent silicon	57 (one test)
4	Nickel steel	44
5	1.25 per cent manganese, 0.25 per cent vanadium, 0.17 per cent carbon	68 (one test)
6	0.50 per cent chromium, 0.12 per cent carbon	75 (one test)
7	0.50 per cent molybdenum, 0.15 per cent carbon	72
8	Plain low carbon, silicon-killed	38
9	Plain low carbon, low aluminum	5
10	Plain 0.20 per cent carbon, low aluminum	9
11	Plain 0.20 per cent carbon, 0.20 per cent aluminum	10
12	0.20 per cent carbon, 0.20 per cent aluminum, molybdenum	86
13	0.20 per cent carbon, 0.20 per cent titanium	9
14	0.20 per cent carbon, 0.20 per cent zirconium	3
15	0.20 per cent carbon, 0.20 per cent aluminum, 0.20 per cent titanium, 0.20 per cent zirconium, 0.20 per cent molybdenum	81

NOTE: The solutions used contained 500 ppm caustic soda; 50 ppm sodium silicate; 500 ppm sodium chloride; and 1500 ppm sodium sulphate.
All results are averages of two or more tests, except where indicated.
The No. 9 steel showed only a small amount of cracking. This is a very soft steel.

in the laboratory are carried out with utmost care and comparable tests are conducted as nearly alike as is humanly possible. By refining the technique of testing, it was found that the results obtained agreed fairly well on check tests. This led to a method of recording the results which may be referred to as being a semi-quantitative method. In this method all results are recorded in terms of per cent cracking. This term refers to the depth to which cracking penetrated through the metal. If the cracking penetrated 1/2 the thickness, the result is recorded as being cracked 50 per cent.

This method of recording the results is not to be interpreted quantitatively, that is, a record of 50 per cent cracking does not mean that the inhibitor was 50 per cent effective, or that 50 per cent of the total number of specimens cracked. Such records may be used in a qualitative manner to indicate in a general way the relative effectiveness of various inhibitors when all conditions of such tests are the same.

TYPES OF WATERS TESTED

In general, two types of waters were employed in this work. One type consisted of synthetic solutions, while the other type consisted of boiler waters. Included in the latter type were a number of experimental boiler waters which were tested to com-

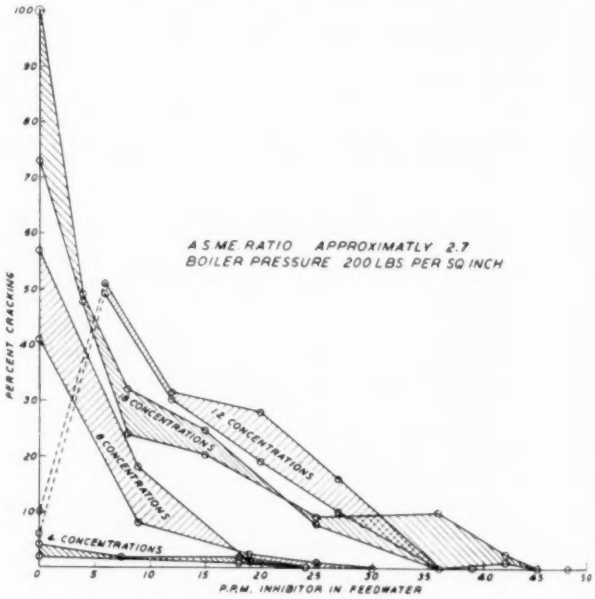


FIG. 10 EFFECT OF CONCENTRATION OF INHIBITOR

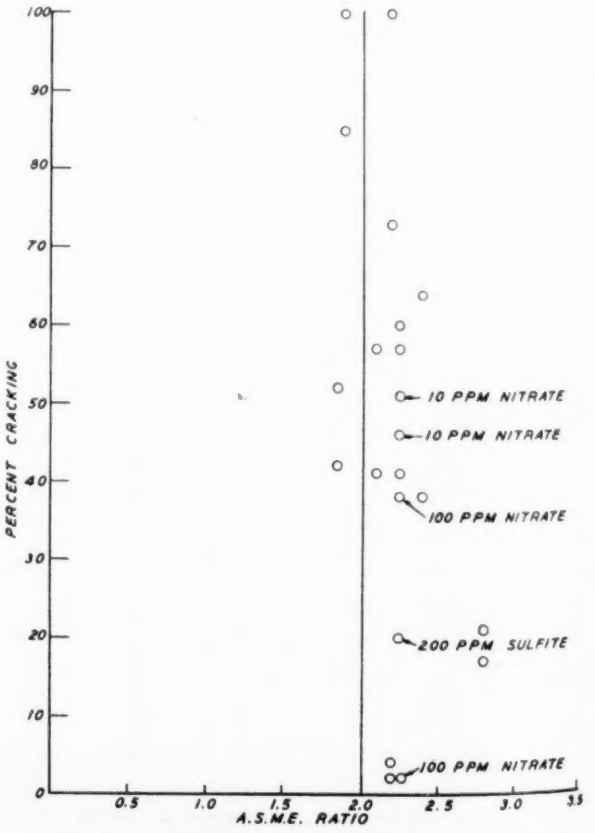


FIG. 11 PER CENT CRACKING VERSUS A.S.M.E. RATIO
(Pressure 200 psi; no inhibitors present.)

pare the effectiveness of inhibitors added to the feedwater against the addition to synthetic solutions.

The feedwater for all experimental boiler waters had an analysis of hardness as $CaCO_3$ of 120 ppm, alkalinity of 166 ppm, sulphates as Na_2SO_4 of 132 ppm, NaCl of 43 ppm, and SiO_2 of 4.5 ppm. The pressure was 200 psi gage, and no condensate was returned to the boiler.

The accompanying tables show the amount and kind of inhibitor added to the feedwater, the boiler-water analysis, and the results of the cracking tests. The amount of organic present as indicated by the Tyrosin test, and the amount of inhibitor calculated to be present from the amount known to be in the feedwater are also indicated.

It is much easier to protect steel against the action of synthetic solutions than against boiler waters. For example, 22.5 ppm of lignin, which had been pretreated, plus 2.5 ppm of sodium nitrate

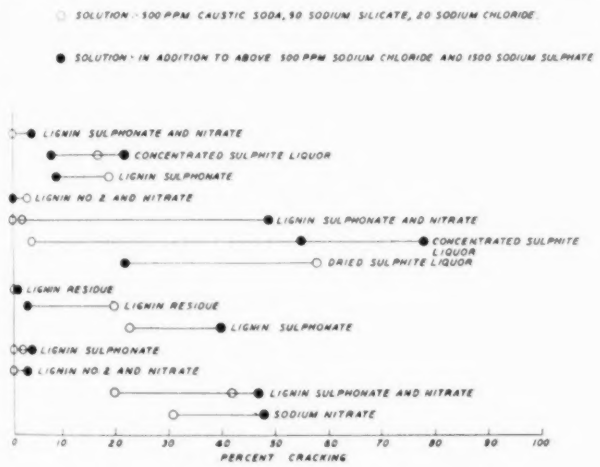


FIG. 12 EFFECT OF SALTS ON CRACKING

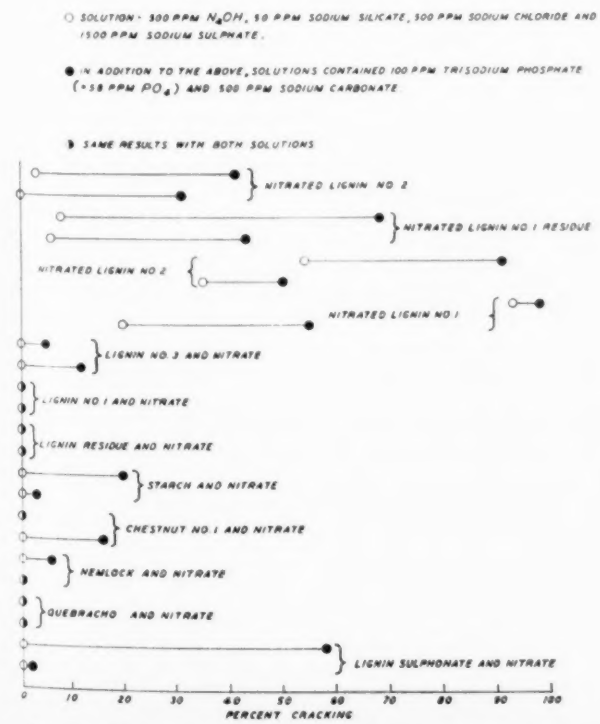


FIG. 13 EFFECT OF CARBONATES AND PHOSPHATE ON CRACKING

gave good protection on synthetic solutions containing a high salt content (Table 10), but much higher quantities failed to protect steel when this treatment was added to the feedwater, and the resulting boiler water tested (Table 1). This is also true of other inhibitors tested.

The explanation of this may be the fact that when synthetic solutions are used, it is customary to withdraw the excess air from the bomb before bringing it up to pressure, as most organic inhibitors have slight effect unless this is done. While this same procedure is followed with boiler waters, the feedwater in these tests was not deaerated, as such is not the common railroad practice. It would be interesting to see what effect predeaeration would have on the results with boiler waters.

The amounts of inhibitor indicated as being required by these boiler-water tests seem excessive, being calculated at about 240 ppm in the boiler when carrying only 8 concentrations of feedwater. This value is higher than is probably necessary, as the test is admittedly very severe. It would be an exceptional condition where boiler plate had undergone distortion as great as these steel specimens, and at the same time such ideal conditions for leakage were maintained.

These tests with boiler water show that in general, as the number of concentrations increases, increased organic matter is required for complete protection. As boiler waters are increased in concentration, the quantity of alkalinity often increases also. Figs. 7 and 8 indicate the amount of alkalinity present and the number of concentrations with respect to the amount of inhibitor required in the feedwater for complete protection in these tests.

EFFECT OF INORGANIC SALTS

The effect of the various inorganic salts commonly present in boiler waters is not great when these salts are tested in synthetic solutions. The addition of 500 ppm of sodium chloride and 1500 ppm of sodium sulphate has, in some instances, resulted in more cracking, and in others less.

The addition of trisodium phosphate and sodium carbonate has resulted in several cases of cracking where cracking was not obtained in their absence. However, there is no conclusive evidence that these salts are undesirable, as in some cases no cracking resulted when these salts were present.

The great discrepancy, therefore, between results obtained with synthetic solutions and boiler waters is due to factors other than the inorganic salts which are present.

Of the inorganic substances tested, sodium nitrate is one of the best. It is not nearly as effective alone as when combined with organic matter, as shown by the tests on synthetic waters.

Sodium nitrate in such tests is very effective in small amounts and greatly improves the inhibiting effect of all organics with which it was tested. These results are shown in Table 10.

Because of the uniformly better results with a mixture of nitrate and organic matter, some organic substances were nitrated and tested. The nitrated materials in general were not effective.

A number of the inhibitors listed in the accompanying tables should be described in some detail.

In some cases organic substances were secured from more than one source. Such materials are labeled, for example, myrobalans No. 1 and No. 2. The numbering of such samples is consistent throughout.

The substance, lignin sulphonate, is a purified product, and differs from sulphite liquors in that the solid content of the latter is approximately one half lignin sulphonate, the remainder being sugars and other substances. The lignin sulphonate used was a solid. The concentrated sulphite liquor used contained approximately 50 per cent solids.

Lignin residue is the product remaining after the cellulosic portion of wood has been converted and removed. The exact

nature of this substance is unknown, but is believed to be a partially oxidized form of lignin, which has the property of forming alkali-soluble salts.

Powders obtained by evaporating sulphite liquors from spruce wood were found to be unstable. Two samples of such powders were found to be very effective when fresh, but they were not effective after aging for a period of several weeks. Table 12 and Fig. 9 give the results. The age as indicated is the time at which the tests were started after the materials were manufactured. Further tests are under way to determine whether or not similar substances show a decrease in inhibiting properties with age.

There has been considerable discussion regarding more resistant steels than some which have been in use. Accordingly, a number of steels were tested without inhibitors present. A few of these steels were of $^1/_4$ in. thickness and are listed separately. The value of these data on various steels lies in the fact that steels are known which have greater resistance to cracking than some steels now in use for boiler shells. Whether or not any of these chemical crack-resistant steels would be suitable from the standpoint of other properties is outside the scope of this paper. Likewise, those steels which show low resistance in these tests should not be condemned for use in boiler parts not normally subject to caustic embrittlement, nor rejected solely on the basis of chemical analyses for use in boiler plate, as variations in rolling conditions, heat-treatment, etc., may so alter the physical properties of such steels that they would show high resistance to cracking. This, of course, is a subject for further investigation.

Conclusions

On the basis of tests on synthetic solutions and boiler waters there is no indication that inorganic salts ordinarily found in boiler waters exert a pronounced protective action. This is also true of sodium sulphate while operating well within the A.S.M.E. code recommendations. Some tests indicate that a high sulphate content may interfere with the protective action of organics, but this effect is not pronounced nor consistent enough to be used as a basis for drawing the conclusion that sulphates are harmful.

With a given feedwater, it was found that increasingly large amounts of inhibitors are required in the feedwater, as the number of concentrations increased. Whether this is due to a corresponding increase in the concentration of neutral salts or caustic soda, or whether it indicates deterioration of the inhibitor in the boiler water, has not been determined.

Highly effective inhibitors are known as indicated by tests on synthetic solutions.

The embrittlement detector is believed to be a valuable instrument in the study of cracking of boiler plate, but great care must be exercised in its use.

Field Data From the Embrittlement Detector

By E. P. PARTRIDGE,[1] C. E. KAUFMAN,[2] AND R. E. HALL[3]

This paper constitutes a progress report based on test data from 100 embrittlement detectors installed on operating boilers to ascertain the embrittling tendency of the respective boiler waters. Not until more than 10 years after the well-known sulphate-alkalinity ratios were formulated and published in the A.S.M.E. Boiler Code of 1926 were means devised whereby the tendency of an actual boiler water to cause cracking could be tested. Mention is made of the apparatus designed for laboratory use, developed by Straub and Bradbury, and the embrittlement detector of Schroeder and his associates for installation on an operating boiler. The tests reported by the authors were carried out by means of the latter. The procedure followed and the effects of various inhibitors used are given in some detail and the results are presented in the form of a series of graphs. The authors in conclusion suggest that boiler operators, faced with the problem of embrittlement cracking, take advantage of the testing methods now available, and determine the conditions which they can economically and effectively maintain in their boilers to minimize the difficulty.

INTERGRANULAR failure along riveted seams in steam boilers has now been a matter of concern for more than 30 years. Attempts during the first half of this period to correlate the incidence of cracking with various factors led, in Europe, to major emphasis upon methods of fabrication; in the United States, concurrently with efforts to improve boiler manufacture, attention was directed particularly toward control of boiler-water composition. The well-known ratios of sodium sulphate to total alkalinity as sodium carbonate, which first appeared in the A.S.M.E. Boiler Code in 1926, were the expression of the hope shared in common by the manufacturers and the operators of boilers that chemical control might obviate cracking.

When the sulphate-alkalinity ratios were formulated, no simple direct test of their efficacy was possible. The suggested values were based largely upon the limited information available concerning the composition of the water in low-pressure boilers which had cracked or had not cracked in service over a period of years. The data, which have never been made public, must necessarily have been rather sketchy, for few analyses of boiler waters were made prior to 1926. The sulphate-alkalinity ratios received some support from tests with highly concentrated synthetic solutions in the laboratory equipment of Parr and Straub (1),[4] but not for more than 10 years after 1926 were means devised whereby the tendency of an actual boiler water to cause cracking could be tested.

How thoroughly the sulphate-alkalinity ratios had been accepted in the meantime is attested by the initial program of a co-operative investigation undertaken in 1933, by the Joint Research Committee on Boiler Feedwater Studies and the Bureau of Mines. This program, initiated by one and directed for the first 2½ years by another of the authors of the present paper, had as its first objective the determination of the solubility of sodium sulphate in the saline solutions which would result from the excessive concentration of a boiler water in a riveted seam. The question at that time was not whether sodium sulphate would inhibit cracking but, instead, how much would be necessary under various conditions.

The rest of the story of the renaissance of research concerning cracking in riveted seams has been told in the technical papers published during the last few years (2–13). Much has been learned about the mechanism of intergranular cracking. In the opinion of the authors, however, the great achievement has been the development of devices, on the one hand by Straub and Bradbury (6, 7), and on the other by Schroeder, Berk, and O'Brien (11, 12, 13) for direct testing of the ability of a boiler water to cause cracking when the necessary mechanical conditions are provided.

While the apparatus of Straub and Bradbury was particularly intended for use in a central laboratory, the "embrittlement detector" of Schroeder and his associates was developed for installation on an operating boiler. The relative advantages of these two methods of approach to the problem of testing might be argued without end. Admittedly uniform procedure during the actual test is more probable if samples of boiler water from many plants are brought to the laboratory and run by specially trained personnel. On the other hand, the samples so tested may not properly represent the average compositions of the respective boiler waters over a period of time, and may be significantly altered in composition and behavior during sampling and transfer to the laboratory.

The alternative procedure of installing an embrittlement detector on an operating boiler automatically integrates the effect of fluctuations in the composition of the boiler water during any desired test period, but unavoidably introduces variation in the personal factor. That the latter is not serious has been demonstrated by the experience of the authors with approximately 100 plants which had carried out tests with the detector by August 1, 1941.

This field experience, over a period of approximately two years, constitutes the basis for the present progress report. In common with the other papers on this general subject, correlation—or lack of correlation—of cracking with boiler-water composition has been presented graphically in a series of figures based upon the tabulated data.[5] The results are offered, not as a basis for codification of recommendations for preventing intergranular cracking, but instead as an argument that each plant should determine by direct test what boiler-water conditions will most effectively and most economically safeguard it against this type of damage.

Significance of Data From Embrittlement Detector

Viewed against the background of knowledge accumulated since Stromeyer's first simple but suggestive experiment (14),

[1] Director of Research, Hall Laboratories, Inc., Pittsburgh, Pa.
[2] Research Engineer, Hall Laboratories, Inc., Pittsburgh, Pa.
[3] Director, Hall Laboratories, Inc., Pittsburgh, Pa. Mem. A.S.M.E.

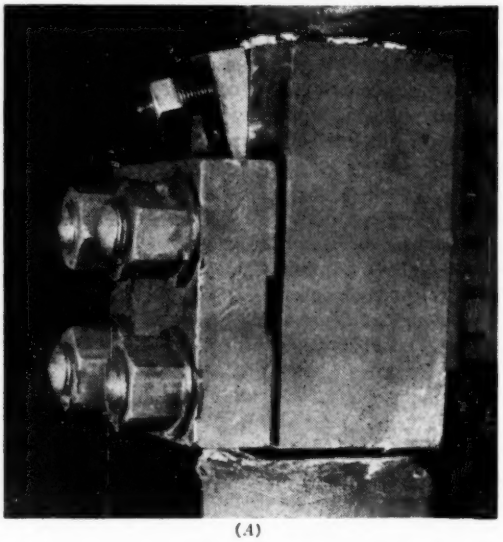
[4] Numbers in parentheses refer to the Bibliography at the end of the paper.

Contributed by the Joint Research Committee on Boiler Feedwater Studies and presented at the Annual Meeting, New York, N. Y., December 1–5, 1941, of THE AMERICAN SOCIETY OF MECHANICAL EGINEERS.

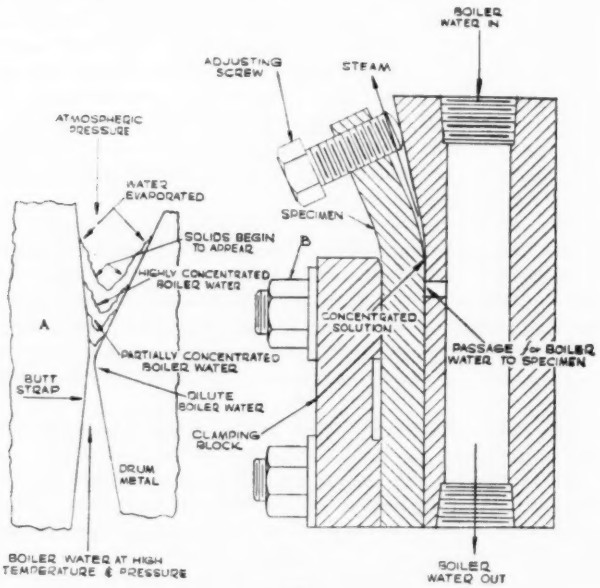
NOTE: Statements and opinions advanced in papers are to be understood as individual expressions of their authors, and not those of the Society.

[5] Space did not permit publication of tabulated data which resulted from the tests, but a complete set of these tables is on file at the Engineering Societies Library, 29 West 39th Street, New York, N. Y., for reference.

intergranular cracking of a riveted seam in a boiler is evidence of the co-operation of certain essential mechanical and chemical factors: Boiler water must have concentrated greatly, a hundred or a thousandfold; the concentrated solution must have been in contact with steel under high applied or residual stress; and the chemical composition of the concentrated solution must have been such as to lead to localized corrosion at grain boundaries, rather than general attack (15).



(*A*)



(*B*)

FIG. 1 EMBRITTLEMENT DETECTOR

(*A*, Photograph of detector installed on vertical blowdown line. *B*, Cross section of detector and schematic representation of concentration of boiler water by flashing through a capillary leak.)

The absence of cracking in a riveted seam might be due to the absence of any one of these factors. The seam might have been so tight as to obviate concentration of dissolved substances by flashing of vapor to the outside through a slow leak; concentration might have occurred, but not in contact with metal under sufficiently high stress; or some inhibitor of intergranular corrosion might have been present naturally in the water or have been added as a conditioning chemical. Uncracked seams in operating boilers can only then be adduced as evidence of the chemical protective effect of an inhibitor, if the basic assumption is made that every riveted seam is so constructed that it would crack in the absence of such an inhibitor.

Perhaps this is true; however, instead of wondering year after year whether it is true and whether his water really is safe because his boiler has not failed, the operator may now set up the mechanical factors for himself in the embrittlement detector. Then, if the specimen fails to crack, he will feel reassured; on the other hand, if it cracks, he can determine in successive tests the effect of various inhibitive treatments.

The operator must, of course, consider the question of adjustment of leakage in the detector. If no leakage occurs between the test specimen and the block of the detector, illustrated in Fig. 1, no concentration of boiler water can occur; on the other hand, if water leaks too freely through this space, little concentration may take place until the water has passed the region of high residual stress at the bend in the specimen. Emphasis is therefore placed upon adjustment of the detector until only the slightest haze of condensed moisture can be discerned on a cold

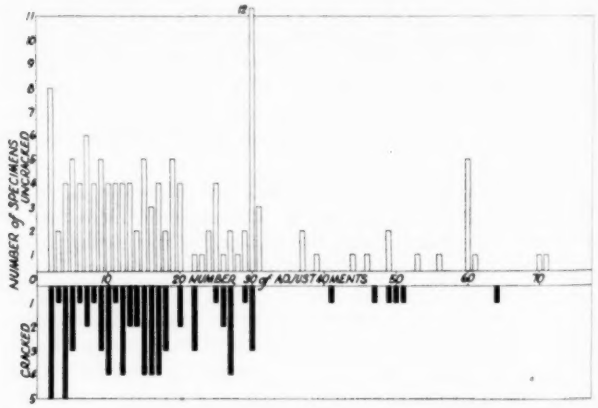


FIG. 2 LACK OF SIGNIFICANT RELATION BETWEEN NUMBER OF ADJUSTMENTS AND CRACKING OF SPECIMENS

(Repetition of stress on specimen as a result of adjustment apparently does not promote cracking.)

surface of glass or polished metal held directly over the end of the specimen.

Frequent adjustment is undesirable, because it increases the likelihood that a concentrated solution will be washed out by too wide an opening of the capillary space, and because it subjects the specimen to repeated changes in stress. That the number of adjustments is not, however, particularly significant is indicated by the lack of any consistent trend in Fig. 2, representing the experience with the nearly 250 specimens discussed in the present paper. The rather even distribution between cracked and uncracked specimens continues from the lowest to the highest number of adjustments.

From the viewpoint of the authors, cracking of a specimen during a properly conducted detector test means that the boiler water during that test would have been capable of promoting cracking at any point in a riveted seam where mechanical conditions of stress and concentration equivalent to those artificially created in the detector happened to exist. Since the opportunity for boiler water to concentrate to a high degree in contact with steel stressed as severely as the cold-rolled specimen may not actually exist in the boiler, cracking of the specimen does not necessarily mean that cracks have already developed or will develop in the boiler seams, but it is a warning signal that some corrective treatment might well be initiated. More severe chemical conditions are required in the laboratory to induce failure in

a hot-rolled than in a cold-rolled specimen; hence cracking of a hot-rolled specimen in a detector test is considered as a more emphatic warning of the embrittling character of the boiler water.

Correlation of Cracking of Detector Specimens With Boiler-Water Composition

Many substances have been mentioned as affecting intergranular failure. Of these, sodium hydroxide is regarded as the fundamental corroding agent, and silica as the agent which tends to accelerate failure by localizing the chemical attack at the grain boundaries. Of the various substances suggested as inhibitors, the greatest attention has been paid in recent years to sodium sulphate, chloride, phosphate, and nitrate, to alumina, and to organic products such as tannin and lignin. The relation between these chemical factors and the incidence of cracking is shown in Figs. 3 to 14. In most of the figures, a chemical factor such, for example, as the concentration of NaOH in Fig. 3, or the SiO_2/NaOH ratio in Fig. 4, is plotted against boiler pressure. Two ratios may also be plotted against each other to investigate interdependence or relative significance, as in Figs. 7, 12, and 13.

The values of the various chemical factors are based upon one or more samples of boiler water analyzed for this particular purpose during each test. The collection of composite samples over periods of 30, 60, or 90 days being impractical, it was necessary to rely on spot samples selected to reflect, as well as possible, the average conditions during a test. Comparison of many of the analyses with the daily plant-control records indicates that few of the points in the figures are likely to be significantly out of their proper places.

Each solid circle in a figure indicates that the detector specimen showed obvious cracks when removed from the detector, or contained cracks not visible to the eye, which opened up when the specimen was bent in a hydraulic press after removal. An open circle signifies the absence of such cracking even after bending, while a few borderline cases, in which only the slightest indica-

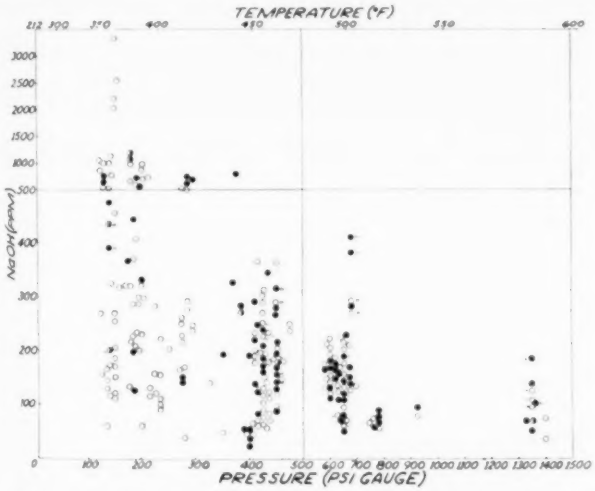


Fig. 3 Incidence of Cracking Related to Concentration of Sodium Hydroxide

(Cracking may occur with as little as 50 ppm, or may not occur with as much as 3000 ppm of NaOH.)

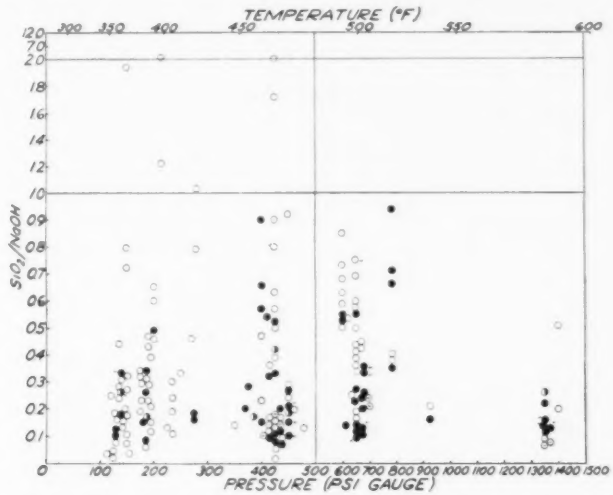


Fig. 4 Incidence of Cracking Related to Ratio of Silica to Sodium Hydroxide

(Cracking occurred with values of SiO_2/NaOH in the broad range from 0.1 to 1.)

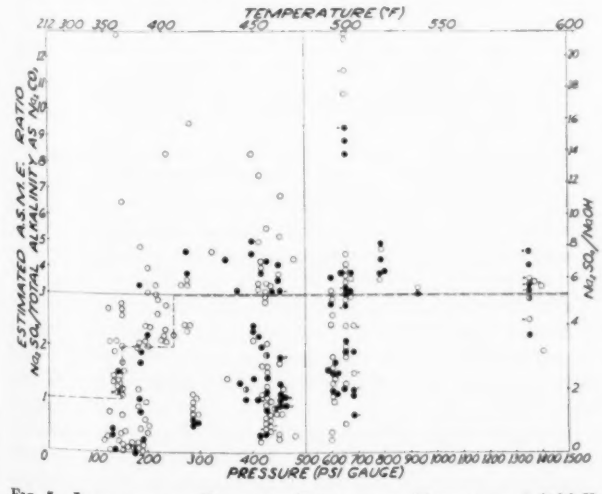


Fig. 5 Incidence of Cracking Related to Estimated A.S.M.E. Ratio of Sodium Sulphate to Total Alkalinity as Sodium Carbonate, and to Actual Ratio of Sodium Sulphate to Sodium Hydroxide

(Specimens cracked when A.S.M.E. ratio values were above as well as below the recommended levels indicated for the various pressure ranges by the broken line.)

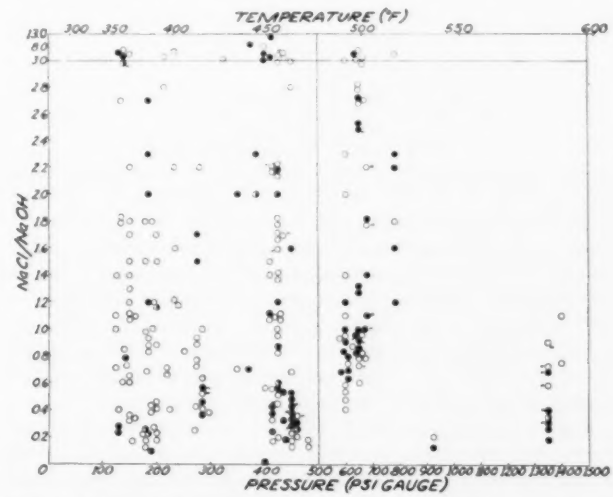


Fig. 6 Incidence of Cracking Related to Ratio of Sodium Chloride to Sodium Hydroxide

(No particular effect of sodium chloride is indicated.)

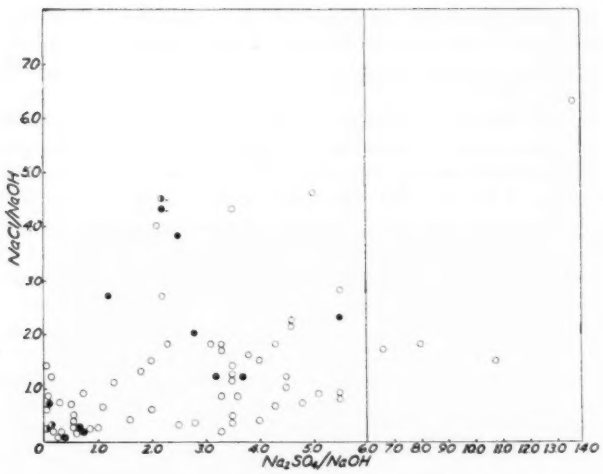


FIG. 7 INCIDENCE OF CRACKING RELATED TO RATIOS OF SODIUM SULPHATE TO SODIUM HYDROXIDE, AND OF SODIUM CHLORIDE TO SODIUM HYDROXIDE IN PRESSURE RANGE UP TO 250 PSI
(No combined protective effect of sulphate and chloride is apparent.)

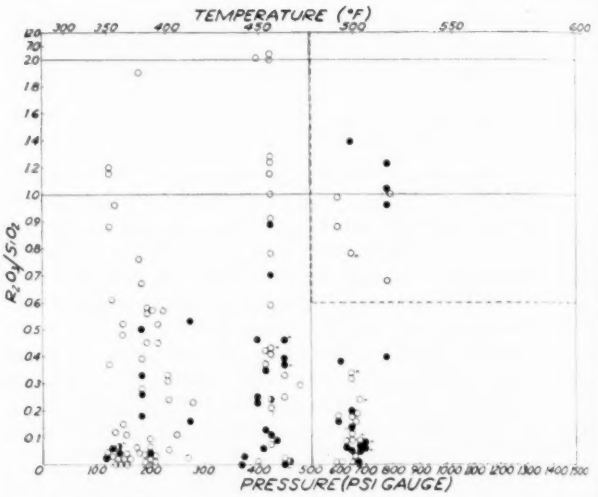


FIG. 8 INCIDENCE OF CRACKING RELATED TO RATIO OF IRON AND ALUMINUM OXIDES TO SILICA
(Cracking occurred in tests at pressures above 500 psi with values of ratio above level of 0.6 suggested as protective.)

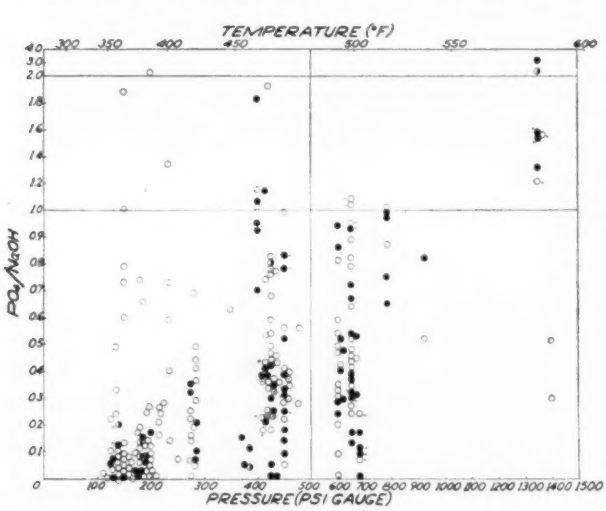


FIG. 9 INCIDENCE OF CRACKING RELATED TO RATIO OF PHOSPHATE TO SODIUM HYDROXIDE
(No inhibiting effect of phosphate is indicated over a wide range of ratio values.)

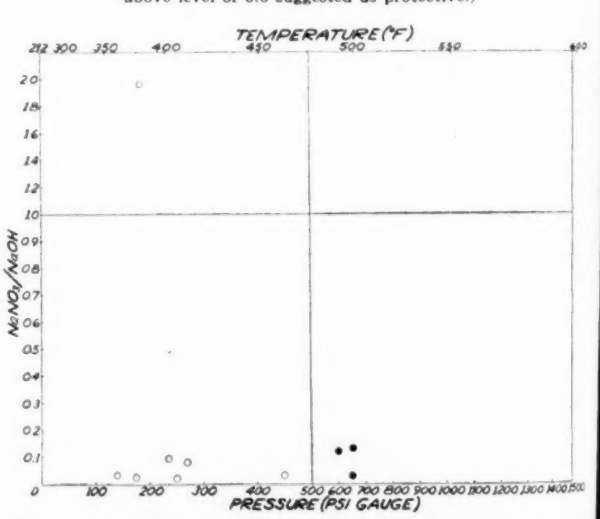


FIG. 10 INCIDENCE OF CRACKING RELATED TO RATIO OF SODIUM NITRATE TO SODIUM HYDROXIDE
(Values for nitrate have been determined only in most recent tests. No conclusion can be drawn from these few data.)

tion of checking of the surface was seen after bending, are represented by half-solid circles. Specimens of hot-rolled steel are indicated by the letter H adjacent to the circle.

By considering as a group the tests from each detector, one might characterize the boiler water in each plant as inherently capable or incapable of producing cracking. The character of the boiler water may, however, change from test to test as a result of natural variation in the water supply, as well as intentional modification of treatment. It has seemed best, therefore, to plot each test independently, even though this may throw disproportionate emphasis upon those boiler waters with which more tests have been run. Any real correlation should not be obscured, however, by this treatment of the data.

Concentration of Sodium Hydroxide. From Fig. 3, it appears that a high concentration of sodium hydroxide in the boiler water is not a prerequisite for cracking; a number of specimens failed with waters containing only from 50 to 100 ppm of NaOH. This is understandable, however, since, in the detector, as in the riveted seam it simulates, boiler water may be concentrated thousands of times, producing a film of strong caustic from the flashing of a boiler water with a normal low content of this constituent.

The number of cases in which abnormally high concentrations of sodium hydroxide failed to produce cracking may seem strange until it is remembered that naturally occurring or intentionally added inhibitors may have been present.

The tentative conclusions may be drawn from Fig. 3, that as little as 50 ppm of sodium hydroxide may be sufficient to cause cracking in the absence of an inhibitor, but that as much as 3000 ppm may not produce failure in the presence of sufficient inhibitor.

Ratio of Silica to Sodium Hydroxide. The profound effect of small amounts of silica in promoting the intergranular corrosion of steel by concentrated caustic solutions was reported simultaneously in 1936 by Straub and Bradbury (3) and by Schroeder and Berk (2). In the tests of the latter investigators, as little as 0.08 per cent of silica on the weight of the sodium hydroxide showed a definite effect. That no cracking is evident in Fig. 4 at a value lower than this for the $SiO_2/NaOH$ ratio is perhaps

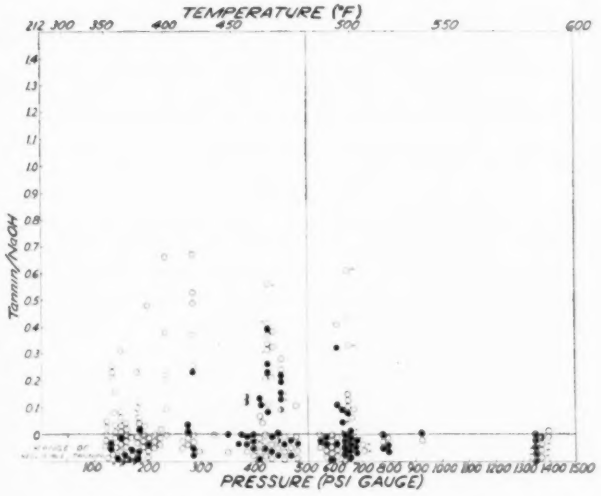


FIG. 11 INCIDENCE OF CRACKING RELATED TO RATIO OF TANNIN TO SODIUM HYDROXIDE

(Three quarters of cracked specimens came from boiler waters with negligible tannin content, while no cracking occurred when ratio value was above 0.4.)

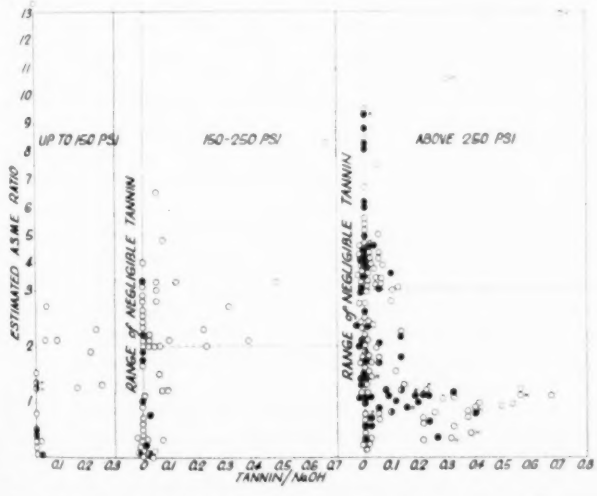


FIG. 13 COMPARATIVE INFLUENCE OF SULPHATE AND OF TANNIN UPON CRACKING IN ALL TESTS

(Cracking has occurred when the sulphate to alkalinity ratio exceeded 9, but not when the tannin to NaOH ratio exceeded 0.4.)

fortuitous, but nevertheless interesting. Most of the cracking seems to have been produced in the range from 0.1 to 1; still higher ratio values apparently tend to inhibit failure, although not enough data are available to justify a definite conclusion to this effect.

Ratio of Sodium Sulphate to Total Alkalinity Expressed as Sodium Carbonate. In boiler water containing carbonate, silicate, and phosphate, as well as hydroxide, "total alkalinity" has so little significance that it is not customarily measured by the authors' organization. In the past it has been observed that "total alkalinity as sodium carbonate" averaged approximately 5/3 times the sodium-hydroxide content of the boiler water. If the use of this factor in Fig. 5 seems arbitrary, it may be recalled that, since all evidence points to sodium hydroxide rather than to the alkaline buffer salts as the corroding agent, "total alkalinity," as the denominator of the A.S.M.E. ratios, rests actually upon no less arbitrary a basis.

While any individual point in Fig. 5 might lie at a somewhat

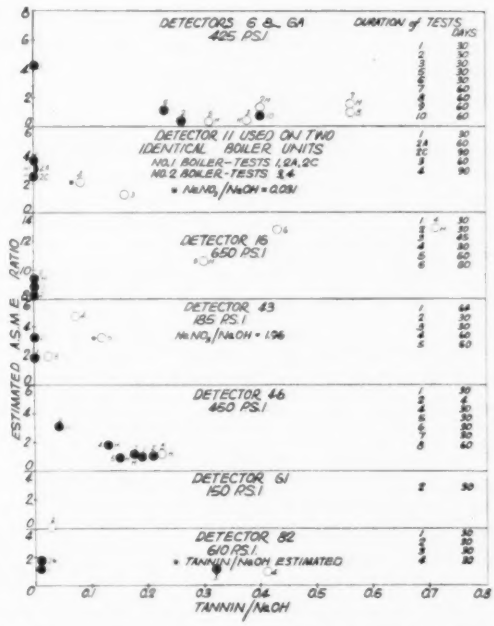


FIG. 12 COMPARATIVE INFLUENCE OF SULPHATE AND OF TANNIN UPON CRACKING IN SEVEN PLANTS

(In various plants, values of tannin to NaOH ranging from less than 0.1 to nearly 0.6 have been found to inhibit cracking more effectively than maintenance of the A.S.M.E. ratios.)

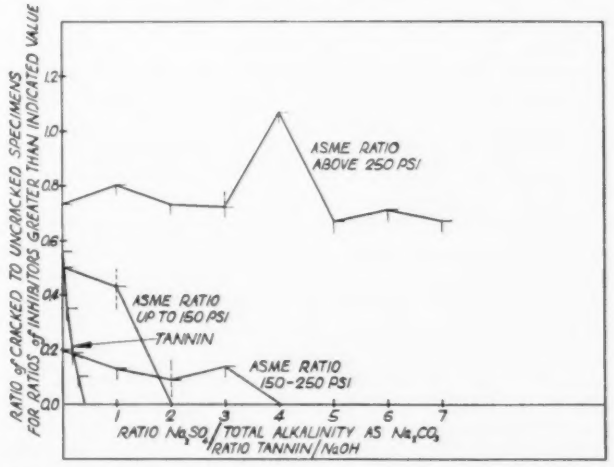


FIG. 14 TENTATIVE EXPRESSION OF CHANCE OF CRACKING A SPECIMEN WHEN A.S.M.E. RATIO OR TANNIN-TO-NAOH RATIO IS MAINTAINED ABOVE ANY SPECIFIED VALUE

(Maintenance of A.S.M.E. ratio recommended for each pressure range does not appreciably reduce chance of cracking over that in absence of sulphate; relatively low values of tannin to NaOH ratio seem to exert a protective effect.)

higher or somewhat lower value if the total alkalinity had been measured directly by titration rather than approximated from the value for sodium hydroxide, the general conclusion could scarcely be changed. This conclusion is obvious: Poor correlation is shown between the incidence of cracking and the sulphate-alkalinity ratio.

The right-hand vertical scale of Fig. 5 expresses the data directly in terms of the ratio of sodium sulphate to sodium hydroxide.

Ratio of Sodium Chloride to Sodium Hydroxide. Sodium chloride has been regarded both as an accelerator of intergranular attack (16, 5), and as a promoter of the reputed protective action of sodium sulphate (6, 7). From Fig. 6, it would appear that any

influence of sodium chloride is overshadowed by other factors, since cracking occurs in a random manner over a wide range of ratio values.

Combined Ratios for Pressures Up to 250 Psi. Straub has concluded from laboratory tests that, in the pressure range up to 250 psi, maintenance of ratios of Na_2SO_4 to total alkalinity, and NaCl to total alkalinity greater, respectively, than 1 and 0.6 will inhibit cracking (7).

While a plot of the Na_2SO_4/NaOH ratio against the NaCl /NaOH ratio is admittedly not identical with one in which values for total alkalinity are employed, considerable similarity would be expected. Fig. 7, however, shows a random occurrence of cracking, in no way dependent upon the relative concentrations of sodium sulphate, sodium chloride, and sodium hydroxide, for specimens tested in the pressure range up to 250 psi.

Ratios of R_2O_3 to Silica. It has been suggested by Straub (7), that the tendency of boiler water to cause cracking may be offset in the range of pressure above 500 psi by maintaining a value of 0.6 or above for the ratio of R_2O_3 to SiO_2. In a normal alkaline boiler water, the iron in solution will be so low that R_2O_3 virtually means aluminum oxide.

As a matter of general interest, values for the ratio of R_2O_3 to SiO_2 have been plotted in Fig. 8, for all tests for which data were available. In the range above 500 psi, it will be noted that four specimens cracked in spite of ratio values well above that recommended.

Ratio of Phosphate to Sodium Hydroxide. Although phosphate has been included among the possible inhibitors of cracking (17), there is little indication from Fig. 9 that maintenance of any particular ratio of phosphate to sodium hydroxide might prevent cracking. On the other hand, as suggested by Schroeder (13), phosphate conditioning may be so controlled as to yield a water which is moderately alkaline in the boiler, yet will not produce a concentrated caustic solution by flashing through a slow leak.

Control of the boiler water in the manner just noted would correspond to maintenance of a substantially infinite value for the ratio of phosphate to hydroxide in Fig. 9.

Ratio of Sodium Nitrate to Sodium Hydroxide. Although Parr and Straub reported eleven years ago[6] that sodium nitrate inhibited cracking in their tests with concentrated solutions, no attempt was made to employ this substance in boiler-water conditioning until very recently. Since nitrate was not considered as a factor in the prevention of cracking when the tests described in this paper were started, only the relatively few data plotted in Fig. 10 are available. Three specimens cracked, but the $NaNO_3$ /NaOH ratios in these cases, as well as in six of the seven cases of uncracked specimens, were considerably below the value of 0.4 suggested by Schroeder, Berk, and Stoddard (13). No conclusions could safely be drawn from this small number of tests.

Ratio of Tannin to Sodium Hydroxide. Lignin-containing materials, derived from sulphite-waste liquor, and various tannins have long been used in compounds for treating boiler water. While tannic acid was reported by Straub (17) to act as an inhibitor of cracking, lignin derivatives and tannins have only come into general intentional use for this purpose in the field since the further experimental work of Schroeder and his associates (5). Waters to which no lignin or tannin has been added during treatment may, however, carry significant amounts of these types of organic materials, derived either from the dumping of industrial wastes into streams or the natural decay of vegetation.

Fig. 11 must be regarded as an encouraging progress report concerning the efficacy of tannin, rather than as proof of universal ability to inhibit cracking. Approximately 75 per cent of the cracked specimens came from boilers in which the content of tannin was negligible, while no cracking was observed when the ratio of tannin, as determined by the tyrosin test (18),[7] to sodium hydroxide was more than 0.4. In only a few stubborn cases was it necessary to attain as high a value as this. Some of these individual cases are discussed in the following section.

[6] Bibliography (16), p. 80.

Cases Illustrating the Effectiveness of Tannin as an Inhibitor

Since individual discussion of every series of tests is not possible within the limitations of this paper, data from seven plants have been selected to represent the experiences with tannin as an inhibitor. The individual plots of Fig. 12 show the values of the A.S.M.E. sulphate-alkalinity ratio and of the ratio of tannin to sodium hydroxide for each test.

Tannin Used Primarily for Sludge Control. At the plant in which detectors 6 and 6A are installed on a welded-drum 425-psi boiler, quebracho tannin is used primarily as a dispersing agent in sludge control. Initially only one detector was installed; later two were connected in series so tests could be run simultaneously on specimens of both cold- and hot-rolled steel. The first test without feed of tannin, but with the A.S.M.E. ratio maintained, resulted in cracking. In subsequent runs, no attempt was made to hold the recommended value of 3 for this ratio. During tests in which the tannin content varied, cold-rolled specimens failed, with the exception of one trial in which a tannin-to-NaOH ratio of about 0.56 was reached. Hot-rolled specimens did not crack in tests where the tannin-to-NaOH value varied from about 0.31 to 0.56. The evidence indicates that this boiler water is mildly embrittling when the tannin concentration is low; cold-rolled specimens crack while hot-rolled bars do not. By maintaining a minimum value of tannin, which may vary with the season and the total boiler-water concentration, it seems possible to prevent all specimen cracking.

Comparative Tests on Low-Pressure Boilers. Detector No. 11 has been installed successively on two identical boiler units operating at about 140 psi. No tannin was added to No. 1 boiler; the results indicate a highly embrittling water, since even hot-rolled specimens cracked. On the other hand, on a comparison boiler running under substantially the same conditions except that tannin was added, two cold-rolled specimens failed to crack. At this low pressure, a relatively small tannin-to-NaOH ratio appears to be adequate. In all these runs, the A.S.M.E. ratio of 1 was maintained. A small quantity of nitrate was found in a sample drawn during test No. 4; this may have had some protective influence, although it is likely that nitrate was present to a similarly slight extent during the other tests.

Tannin Effective as Inhibitor at 650 Psi. Runs with detector No. 16, installed on a 650-psi boiler in a utility plant with evaporated make-up, provided a test of the efficacy of quebracho treatment at a higher pressure. Three initial runs were made with no tannin added. In each case, severe cracking resulted, even though one specimen was hot-rolled. During these and subsequent runs, the estimated sulphate-alkalinity ratio was very high, between 8.3 and 12.9, as a result of the conversion to sodium sulphate of sodium sulphite, added as an oxygen scavenger. After tannin feed was instituted, three specimens were tested; none cracked. Two of the unaffected bars were hot-rolled while the last was cold-rolled steel.

Nitrate Present With Tannin. The plant in which detector No. 43 is mounted on a 185-psi boiler draws its water from an impounded section of a river contaminated with sewage. Two specimens were cracked when no organic inhibitor was added. When quebracho was fed, even in amounts to yield a tannin-to-NaOH value of less than 0.1, three specimens remained uncracked. The sulphate-alkalinity ratio was met during prac-

[7] Refer to Appendix, section on "Tannin."

tically all of the testing program. However, there should be no hasty conclusion that tannin was the effective inhibitor in this case. Determinations made during the last run showed the presence of over 500 ppm of sodium nitrate in the boiler water. It is possible that this constituent, rather than the tannin, may account for the nonembrittling character of the boiler water during the later tests. If this is the case, the nitrate content during the first two runs presumably was considerably less.

Natural Organic Inhibitor Present. The water in the 150-psi boiler on which detector No. 61 is installed might be considered on the basis of its content of ordinarily determined constituents to be quite embrittling. Alkalinity is very high while sulphate is vanishingly small, hence the sulphate-alkalinity ratio is negligible; yet four specimens tested at this plant for periods up to 120 days did not crack. The inhibiting effect appears to be due to the naturally occurring organic material in the feed, which concentrates to an appreciable extent in the boiler water. A determination of this organic material made during test No. 2 (the only specimen plotted) yielded a value of 97 ppm on the basis of a quebracho standard. It is possible that the actual amount of organic substance present is greater, since it may react to a different extent than does tannin in the colorimetric test employed.

Higher Tannin-to-NaOH Ratio Required. Detector No. 46 takes water from a 450-psi boiler to which quebracho has been added from the beginning of the test program. During practically all this period the A.S.M.E. ratio was not met. Cracking of both hot- and cold-rolled specimens occurred despite the addition of tannin, until the last run made with a hot-rolled specimen, when the average concentration of quebracho was slightly higher than in previous tests. Further work will be required to define protective conditions more fully.

Detector No. 82 is attached to a closely controlled boiler operating at 610 psi, in which the A.S.M.E. ratio is not maintained. Two initial tests in the essential absence of tannin (a very small amount of naturally occurring material was present) resulted in pronounced cracking. Tannin was fed, but a third specimen failed, although less severely than the first two. During a fourth run, the quebracho content was increased somewhat. The result was no cracking. All four of these tests were for 30-day periods. It remains to be seen whether present conditions will inhibit failure over longer intervals.

Relative Effectiveness of Sulphate and of Tannin in Preventing Cracking

That tannin is more effective as an inhibitor of cracking than sulphate is indicated by the selected series of tests in Fig. 12. When all of the data are plotted similarly for the three pressure ranges of the A.S.M.E. ratio, as in Fig. 13, the same conclusion is reached. It is true that, in the range above 250 psi, a number of specimens cracked when the ratio of tannin to NaOH was above 0.2, ranging up to 0.4; comparison of Figs. 12 and 13 shows, however, that most of these specimens came from detectors Nos. 6, 46, and 82, with each of which an increase in the tannin-to-NaOH ratio apparently has lessened the tendency to crack. In contrast, among the waters containing negligible or low amounts of tannin, cracking has occurred with values of the sulphate-alkalinity ratio far above the suggested limits of 1, 2, and 3.

Even in the pressure range above 250 psi, the number of observations is scarcely large enough to justify statistical treatment; in either of the two lower ranges of pressure, the cracking of a single future specimen in a water with a high sulphate-alkalinity ratio would materially alter any conclusions which might now be attempted from a statistical viewpoint. Nevertheless, Fig. 14 is ventured as a tentative picture, subject to modification as data accumulate, of the relative effectiveness of sulphate and of tannin in preventing cracking.

In Fig. 14, the chance of cracking is represented by the vertical scale, expressing the ratio of cracked to uncracked specimens. This ratio has been determined for the group of specimens whose sulphate-to-alkalinity or tannin-to-NaOH ratios exceed each of various values on the horizontal scale. Looking first at the line representing the A.S.M.E. ratio for boilers operating at 250 psi or above, it is apparent that the chance of cracking was about the same whether the ratio value was 1 or 7, or any intermediate value; on the average, three specimens cracked for each four which did not.

In the pressure range from 150 to 250 psi, no specimen had cracked by August 1, 1941, when the A.S.M.E. ratio equaled or exceeded 4. The chance of cracking, therefore, is represented as zero at this value of the ratio, although at 3 or below one specimen cracked on the average for each seven which remained undamaged.

In a similar manner, the limited number of tests in the pressure range up to 150 psi might be interpreted to mean no chance of cracking when the A.S.M.E. ratio was 2 or above, although at lower values one specimen cracked for each two which did not. Test results on a 130-psi boiler have already been published by others (13), however, which, if included in Fig. 14, would greatly increase the indicated chance of cracking for any A.S.M.E. ratio value up to more than 8. The suspicion cannot be avoided that, as data accumulate from detectors on boilers in the two lower pressure ranges, the line representing the chance of cracking will tend to flatten out like the one now shown for the range above 250 psi. If this should happen, it would remove such slight evidence, as Fig. 14 now indicates that sulphate inhibits cracking.

Although the effectiveness of tannin can only be proved beyond doubt by many more tests, the manner in which the curve for tannin, in Fig. 14, plummets consistently downward until the chance of cracking becomes zero at a tannin-to-NaOH ratio exceeding 0.4 suggests it to be a real inhibitor.

A Practical Program to Obviate Cracking in Riveted Seams

It would be easy to find contradictions in the data presented in the preceding sections or to stress the uncertainties inherent in field testing conducted by many individuals. An enthusiast for any particular method of controlling cracking could at least cast doubt upon the efficacy of other methods, even if he could find little support for his own. Certain conclusions, however, seem justified to the authors:

1 Neither sulphate nor chloride, nor sulphate and chloride in combination show evidence of an inhibiting effect over the range of pressures above 250 psi. At pressures up to this level, some effect is indicated by the limited data of the authors, but contradicted by the published results of other detector tests.

2 R_2O_3 (alumina) has not proved effective as an inhibitor of cracking either in the suggested range above 500 psi, or at lower pressures.

3 Phosphate appears to be without effect as an inhibitor, even at a PO_4/NaOH ratio as high as 2. This does not deny, however, the possible utility of eliminating sodium hydroxide substantially from a boiler water containing phosphate by controlling the pH in the range below 11.

4 The experience of the authors with nitrate is not yet sufficiently extended to justify any conclusion concerning its effectiveness.

5 Tannin, as determined by the tyrosin test, seems effective as an inhibitor over the range up to 650 psi in which it has been used to date.

Starting with these conclusions, it would seem logical neither

to accept with blind faith the semiofficial sulphate-alkalinity ratios, nor with blind zeal to replace them with some other system of ratios based upon the effect of tannin or any other proposed inhibitor. Instead of the formulation of rules, the authors suggest instead that full advantage be taken of the testing methods now available, and that each operator determine, with the assistance of whatever coordinating agency he may choose, the conditions which he can most economically and effectively maintain in his own boilers to minimize the likelihood of cracking.

If he has no boilers with riveted seams, the operator may feel justified in ignoring the problem. He may still, however, wish to take precautions to avoid the admittedly rare possibility of intergranular cracking in tube ends. Along with the operator more directly concerned because of riveted construction, he can, by means of the embrittlement detector, first test his boiler water under existing operating conditions. If specimens crack in repeated tests, he can then explore, in a consistent manner, the effect of any changes in treatment. Experience to date indicates that he will be likely to find practical conditions under which the steel of the detector specimen will remain uncracked.

Having once achieved favorable conditions, there is then much to be said for using the detector as a continuous or semicontinuous indicator to be sure that some apparently unimportant change may not make the boiler water again capable of cracking steel. Once established, the routine of adjusting leakage is simple, requiring not more than five minutes attention per day, while the cost of the detector and of specimens is nominal. Altogether, the use of the embrittlement detector in this manner may prove as desirable as the measurement of carbon dioxide in the flue gas or of dissolved salts in the steam condensate.

Perhaps the answer in any particular case will lie in the use of tannin; on the other hand, nitrate may demonstrate its superiority, or the reduction of the sodium-hydroxide content of the boiler water substantially to zero by maintaining alkalinity with phosphate may prove satisfactory and desirable. The emphasis does not rightly belong upon any particular chemical means of inhibiting cracking; instead, the important fact to be realized is that the reinvestigation of boiler-metal cracking in recent years now has produced a means of measuring the elusive chemical factor in this type of failure. Even though the measurement be rough, the way has been opened to approach the problem of cracking, not by arguing as an advocate, but by testing as an engineer.

Acknowledgments

To the many men in the various plants who have cooperated wholeheartedly in the testing program; to Dr. Schroeder, Mr. Berk, and their assistants at the Eastern Experiment Station of the Bureau of Mines, who have examined all specimens and given helpful advice; to the field engineers of Hall Laboratories, Inc., who have assisted in checking test conditions in the detector units; and to their associates who have supplied the analytical data and otherwise assisted in the preparation of this paper, the authors express their sincere appreciation.

Appendix

Methods of Analysis

The following methods were employed in the analysis of the samples of boiler water taken during the various tests:

Silica. Gravimetric determinations were made on all samples.

R_2O_3. This was determined gravimetrically as aluminum (and iron) phosphates.

Hydroxide. After the addition of barium chloride in excess of the amount required to precipitate buffer salts such as carbonate and phosphate, the sample was titrated with standard acid to the end point of phenolphthalein.

Sulphate. Both the turbidimetric method devised by Hall (19) and the gravimetric method were utilized.

Phosphate. The method developed by Hall (20), in which the amount of the yellow precipitate of ammonium phosphomolybdate is estimated visually, was verified on a number of the samples by separation and titration of the yellow precipitate with standard alkali and acid, using phenolphthalein as an indicator.

Chloride. A sample was titrated with silver nitrate, using potassium chromate as an indicator.

Tannin. The analytical method suggested by Berk and Schroeder (21) depending upon the reducing or oxygen-absorbing power of tannins and lignins was employed. The tyrosin reagent of Folin and Denis (18) is reduced to give a blue solution of a color density which varies with the concentration of the tannin or lignin. The reagent is sensitive to small amounts and is, therefore, particularly suitable for boiler and feedwater analyses.

Solutions needed include the following:

1 Sodium tungstate-phosphomolybdic acid: 100 g of sodium tungstate, 20 g of phosphomolybdic acid, and 50 ml of 85 per cent phosphoric acid are dissolved in 750 ml of water. The liquid is boiled under reflux for 2 hr, cooled, and made up to 1 l.

2 Saturated sodium carbonate: Add enough sodium carbonate to 1 l of water to supersaturate the solution with respect to $Na_2CO_3 \cdot 10H_2O$ and allow excess to crystallize.

3 Comparison solution: This solution represents the "standard" for the method and should be made up with exactly the same organic material that is fed to the boiler. Weigh out a 10-g sample of the solid and dissolve in 1 l of water. Let this be solution *A*. Pipette out 10 ml of solution *A* and dilute to 1 l to form solution *B*. Tannin solutions are slightly acid. They should be especially guarded against alkaline contamination, since, in the presence of alkalinity, oxidation of the tannin will take place and poor results will be obtained. If after a period of use the purity of the solutions is in doubt, make up fresh reagents.

The procedure is as follows:

1 A 50-ml filtered, clear, and cooled sample of boiler or feedwater, containing less than 20 ppm of tannin or lignin, is put in a Nessler tube. If the water contains more than 20 ppm, a smaller sample should be taken and diluted to 50 ml.

2 Make up 2 or 3 similar samples from the comparison solution *B* to contain lower and higher concentration of tannin or lignin than the unknown sample. A definite amount of solution *B* is diluted to 50 ml with distilled water to form each standard, according to the following table

Preparation of tannin or lignin standards

Tannin or lignin, ppm	Solution B, ml
0	0
2	1
4	2
6	3
8	4
10	5
12	6
14	7
16	8
18	9
20	10

3 Treat each known and unknown with 2 ml of the sodium tungstate-phosphomolybdic acid solution. Stir and allow to stand 5 min. Add 10 ml of saturated sodium carbonate to each sample, stir it, and allow to stand 10 min.

4 Match the blue color of the unknown with the knowns to estimate the amount of tannin or lignin.

This method of analysis is free from interference by sulphate, silicate, chloride, phosphate, hydroxide, and sulphite, as well as most of the positive ions encountered in water samples. Ferrous iron will, however, cause interference. Fortunately, in most alkaline boiler waters, the concentration is too low to cause difficulty. If a small amount of iron is present, it may be desirable to allow the sample to settle for a few hours before an aliquot is taken for analysis. This will cause some oxidation of the iron and allow it to precipitate. The tannin or lignin itself will not suffer appreciable oxidation over a short period at room temperature.

The method of analysis suffers interference from some organic materials, especially phenolic compounds which might be present in some feedwater. A blank should be run on the feedwater if appreciable interference is suspected.

One ppm of tannin will produce as much color as 4 to 7 ppm of lignin. In general, it would seem undesirable to add tannins and lignins simultaneously to the boiler feed, since this would complicate the analysis.

BIBLIOGRAPHY

1 "Embrittlement of Boiler Steel," by S. W. Parr and F. G. Straub, University of Illinois Engineering Experiment Station, Bulletin 155, 1926, pp. 42–46.

2 "Action of Solutions of Sodium Silicate and Sodium Hydroxide at 250 C on Steel Under Stress," by W. C. Schroeder and A. A. Berk, American Institute of Mining and Metallurgical Engineers, Technical Publication 691, 1936; also, *Combustion*, vol. 7, 1936, pp. 29–33.

3 "New Laboratory Data Relative to Embrittlement in Steam Boilers," by F. G. Straub and T. A. Bradbury, *Power Plant Engineering*, vol. 40, 1936, pp. 104–105.

4 "Intercrystalline Cracking of Steel in Aqueous Solution," by W. C. Schroeder, A. A. Berk, and R. A. O'Brien, *Metals and Alloys*, vol. 8, 1937, pp. 320–330.

5 "Protecting Steel Against Intercrystalline Attack in Aqueous Solution," by W. C. Schroeder, A. A. Berk, and R. A. O'Brien, Trans. A.S.M.E., vol. 60, 1938, pp. 35–42.

6 "Boiler-Water Treatment. New Methods for Preventing Embrittlement," by F. G. Straub and T. A. Bradbury, *Mechanical Engineering*, vol. 60, 1938, pp. 371–376.

7 "A Method for the Embrittlement Testing of Boiler Waters," by F. G. Straub and T. A. Bradbury, Proc. A.S.T.M., vol. 38, 1938, pp. 602–615.

8 "Bureau of Mines Investigation of the Intercrystalline Cracking of Boiler Steel," by W. C. Schroeder, A. A. Berk, and R. A. O'Brien, American Railway Engineering Association, Bulletin 404, June-July, 1938.

9 "Intercrystalline Cracking in Boiler Steel," by W. C. Schroeder, A. A. Berk, and C. H. Fellows, *Journal*, American Water Works Association, vol. 30, 1938, pp. 679–694.

10 "What About Embrittlement?" by E. P. Partridge, *Blast Furnace and Steel Plant*, vol. 27, 1939, pp. 1056–1060, and 1076–1080.

11 "Intercrystalline Cracks in Locomotive Boilers," by W. C. Schroeder, A. A. Berk, and R. A. O'Brien, Association of American Railroads, Circular DV-989, 1940.

12 "Embrittlement Detector," by W. C. Schroeder, A. A. Berk, and R. A. O'Brien, *Combustion*, vol. 12, no. 2, 1940, pp. 19–21.

13 "Embrittlement Detector Testing on Boilers," by W. C. Schroeder, A. A. Berk, and C. K. Stoddard, *Power Plant Engineering*, vol. 45, no. 8, 1941, pp. 76–79.

14 "Memorandum by the Chief Engineer," by C. E. Stromeyer, Manchester Steam Users' Association, 1910, and 1917.

15 "Addenda to Par. CA-5 of Boiler Construction Code," *Mechanical Engineering*, vol. 62, 1940, pp. 249–252. Conclusions presented to the committee by J. H. Walker, p. 251.

16 "Embrittlement in Boilers," by F. G. Straub, University of Illinois Engineering Experiment Station, Bulletin 216, 1930, p. 71.

17 "Embrittlement of Boiler Plate," by S. W. Parr and F. G. Straub, University of Illinois Engineering Experiment Station, Bulletin 177, 1928, p. 44; also Bulletin 216, 1930, p. 79; and U. S. Patent 1,910,403, May 23, 1933.

18 "On Phosphotungstic-Phosphomolybdic Compounds as Color Reagents," by Otto Folin and W. Denis, *Journal of Biological Chemistry*, vol. 12, 1912, pp. 239–243.

19 "Method and Apparatus for the Determination of the Concentration of Turbid Suspensions," by R. E. Hall, U. S. Patent 1,681,339, August 21, 1928.

20 "Some Results of Boiler Water Conditioning," by R. E. Hall, *Iron and Steel Engineer*, vol. 6, 1929, pp. 380–389.

21 Paper presented before the Division of Water, Sewage, and Sanitation at the 102nd Meeting of the American Chemical Society at Atlantic City, N. J., Sept. 8–12, 1941. To be published.

Summary of Papers Composing the Symposium[1] on Embrittlement[2]

By W. C. SCHROEDER[3] AND A. A. BERK,[4] COLLEGE PARK, MD.

FOR over 30 years investigation and discussion of embrittlement have revolved around research from a few laboratories in the United States and in one or two foreign countries. The papers in this symposium advance the study into actual operation and show (*a*) how to determine that a boiler water is embrittling and (*b*) methods which may be followed to make it non-embrittling.

In this summary the results obtained by the contributors to the program are not treated separately; instead they are grouped to evaluate the protective action of tannins, lignins, sodium sulphate, sodium sulphate and sodium chloride, sodium phosphate, and sodium nitrate. Consideration of the combined data for individual chemicals clarifies the picture regarding their protective action and shows the degree of correlation existing between the results of various investigations.

Tannins

The work of Partridge, Kaufman, and Hall (5)[1] is the most extensive reported in this symposium on the use of tannins[5] as protective agents. The results show that these authors have been extremely successful in gaining the interest and co-operation of the plant personnel.

Their preliminary investigation of the effect of the number of adjustments on cracking has furnished the answer to a moot point concerning the embrittlement detector since it was first developed. Their Fig. 2 shows that this factor has no measurable influence on the results. Specimens cracked with as few as 2 or as many as 65 adjustments, and remained uncracked with over 70 adjustments.

Their statistical analysis of all their embrittlement-detector tests definitely shows a decrease in cracking of the specimens as the ratio of tannin to sodium hydroxide in the boiler water is increased. The effect appears to be extremely pronounced up to 250 psi, very low ratios preventing cracks. Above 250 psi, the ratio must in some cases be increased to about 0.4 to secure complete protection, but more data are desirable to establish this value accurately.

For any specific boiler water, these authors have developed a practical test program. If detector tests show that the water will cause cracking, inhibitor is added in progressively increasing amounts until the cracking is stopped. The satisfactory results secured in six illustrative cases, at pressures of 140 to 650 psi, indicate that, under the proper control, the tannin treatment should be generally effective. The authors also mention that this material is useful in sludge control, while Fager and Reynolds[6] have demonstrated its effectiveness in oxygen removal. These features should make it a valuable chemical in boiler-water treatment.

In most of their work, Partridge, Kaufman, and Hall have used quebracho tannins. Bird and Johnson (4) show a few tests with similar materials in their Table 10. Good protection was secured but they find that a small amount of sodium nitrate makes this material even more effective. This point should deserve further attention, although if the nitrate concentration becomes too high it may oxidize and destroy the quebracho so that no protective agent remains in the solution.

Lignins

Bird and Johnson (4) report extensive and systematic examination of the protective action of the lignin compounds. They are to be congratulated on their well-developed embrittlement-detector testing equipment and on the valuable data they have contributed to the symposium.

The lignin-sulphonate compounds which they investigated show definite protective action in most cases. Their observation that a small amount of nitrate greatly increases their effectiveness is an interesting one. In this combination, it would be anticipated that the nitrate would act as an oxidizing agent and largely disappear from the solution during the test. The increased protection may result from the slightly higher state of oxidation of the organic compound, or from the formation of an oxide film on the steel surface which may permit more tenacious adherence of the lignin film. The desirability for further investigation is obvious.

Bird and Johnson concentrated synthetic feedwaters in a small experimental boiler to prepare many of the samples for their detector tests. They show that, with constant alkalinity, more inhibitor must be added to the feedwater to prevent cracking of the detector specimens as the number of concentrations in the boiler increases. The solid line, in Fig. 1 of this summary, represents their data. They also give the concentrations[7] of organic inhibitor as well as the total alkalinity in the boiler water at the start of the embrittlement-detector tests. These values have been used to determine the position of the dotted line in Fig. 1, which indicates the ratio, as measured in the boiler water, of inhibitor to alkalinity required to prevent cracking. The value ranges between 0.42 and 0.58, but for boiler concentrations of 8,

[1] The five papers constituting the "Embrittlement Symposium," their authors, and location in this issue of the Transactions will be referred to throughout this summary and the subsequent discussion by numbers in parentheses as follows:

1 "Results of Laboratory Embrittlement Testing of Boiler Waters," by F. G. Straub, pp. 393–396.

2 "Embrittlement of Boiler Steel—Experiences With the Schroeder Detector," by T. E. Purcell and S. F. Whirl, pp. 397–402.

3 "Experience With Intercrystalline Cracking on Railroads," by R. C. Bardwell and H. M. Laudemann, pp. 403–407.

4 "Studies on the Cracking of Boiler Plate," by P. G. Bird and E. G. Johnson, pp. 409–416.

5 "Field Data From the Embrittlement Detector," by E. P. Partridge, C. E. Kaufman, and R. E. Hall, pp. 417–425.

[2] This summary is published by permission of the Director of the Bureau of Mines, U. S. Department of the Interior.

[3] Senior Chemical Engineer, Eastern Experiment Station, Bureau of Mines. Mem. A.S.M.E.

[4] Associate Chemist, Eastern Experiment Station, Bureau of Mines.

[5] Quebracho tannins were generally used.

Contributed by the Joint Research Committee on Boiler Feedwater Studies and presented at the Annual Meeting, New York, N. Y., December 1–5, 1941, of THE AMERICAN SOCIETY OF MECHANICAL ENGINEERS.

NOTE: Statements and opinions advanced in papers are to be understood as individual expressions of their authors and not those of the Society.

[6] "Adsorption of Oxygen by Alkaline Tannates," by E. P. Fager and A. H. Reynolds, *Industrial and Engineering Chemistry*, vol. 21, 1929, pp. 357–359.

[7] As measured by the tyrosine test, which is admittedly rough, but will do for a basis of comparison.

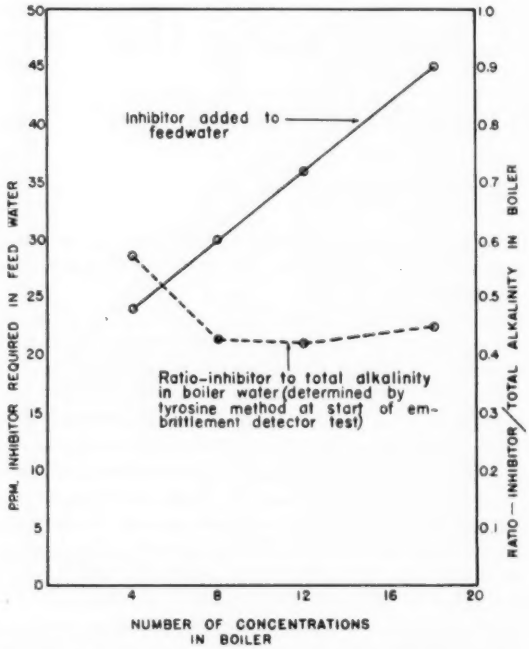


FIG. 1 INHIBITOR REQUIREMENTS VERSUS CONCENTRATION

12, and 18, the range is 0.42 to 0.45. From these data the protective action of the organic material (to which nitrate was added) appears to be independent of the number of concentrations in the boiler. Therefore, inhibitor must be lost between the feedwater and boiler water, and the effect becomes progressively greater as the number of concentrations increases. This might be due to adsorption on precipitating calcium salts, to thermal decomposition (an increased number of concentrations means longer exposures at high temperature), or to destruction by oxygen (the higher alkalinities resulting from increased concentrations would favor the reaction of the organic material with oxygen). *This work by Bird and Johnson emphasizes the necessity for basing treatment on analysis of the boiler water rather than on control of concentrations in the feedwater.*

Bird and Johnson obtained their results from laboratory testing and they have devoted major attention to lignin sulphonate. Bardwell and Laudemann (3), on the other hand, have investigated the use of waste sulphite liquor (which inhibits cracking largely because it contains lignin) in locomotive boilers. They show that this material was entirely effective at five or six locations on the railroad, but in three others the cracking had little direct relation to its concentration. The treatment was also unsatisfactory at Charlottesville, Va., even though the concentration of waste sulphite liquor was raised to nearly 70 per cent of the sodium-hydroxide alkalinity. *In these tests, sodium nitrate was not added* with the waste sulphite liquor, although some may have been naturally present in the feedwater supplies.

Bardwell and Laudemann (3) make the following statements concerning their work: "These tests would indicate that waste sulphite liquor is satisfactory on many waters, but its protective action can fail in some cases. This result seems to be in qualitative agreement with the most recent laboratory studies, although the reasons for the differences are still obscure.[8] In spite of these facts, however, the use of this inhibitor did bring a noticeable reduction in engine cracking over the 2-year period in which it was in use, and no cracked engines have been reported at Parsons, Fulton, or Newport News terminals since this treatment was started in February, 1938, whereas, a number had occurred previously."

This investigation by Bardwell and Laudemann strongly indicates the necessity for testing the action of the organic protective agents under operating conditions. It also shows that the embrittlement detector can be operated satisfactorily by the normal railroad personnel. Bird and Johnson would add greatly to the value of their results by a series of tests on operating boilers similar to those carried out by Bardwell and Laudemann.

SODIUM SULPHATE

Any discussion of the effect of sodium sulphate is usually based upon the arbitrary pressure ranges within which varying amounts of this substance are suggested by the A.S.M.E. Boiler Code. At pressures of 250 psi and above, the data from the entire symposium show that sodium sulphate will not stop cracking or failure of the test specimens. This agreement in results from five different investigations is gratifying, especially as the work covers the field from refined laboratory technique to tests on stationary and locomotive boilers over the entire United States. In the face of such evidence, the present recommendations for the use of this salt to prevent embrittlement lose their significance.

Below 250 psi, the studies by Bird and Johnson (4) show that sodium sulphate does not prevent cracking. The tentative correlation made by Partridge, Kaufman, and Hall (5), on the basis of what they are careful to describe as insufficient data, indicates, on the other hand, a possible protective action for this salt at these lower pressures. It should be noted, however, that these authors have included all the specimens in their statistical analyses and that the absence of cracking in any particular case does not necessarily indicate the effect of sulphate but, instead, *may show the protective action of tannin, nitrate, or other inhibitor.* In their Fig. 13 (5) it is possible to distinguish between the effect of the tannin and sulphate. *In all three pressure ranges cracking is found, in the absence of tannin, for A.S.M.E. ratios near the highest encountered in any of the boiler waters.* In direct contrast, a very small increase in the tannin ratio appears completely effective in stopping cracks in the two pressure ranges up to 250 psi. Above 250 psi, a higher ratio of tannin is necessary.

Partridge, Kaufman, and Hall have referred to published data

[8] "Intercrystalline Cracking of Locomotive Boilers," by W. C. Schroeder, A. A. Berk, and R. A. O'Brien, Association of American Railroads, Circular D. V. 989, May, 1940.

TABLE 1 SODIUM SULPHATE DOES NOT STOP CRACKING AT 130 PSI IN PLANT TESTS WITH THE EMBRITTLEMENT DETECTOR

		Average composition of boiler water, ppm									
Test no.	Steel[a]	Total alkalinity as NaOH	Total alkalinity as Na_2CO_3	Na_2SO_4	NaCl	Na_3PO_4	SiO_2	Na_2SO_4[b] / Na_2CO_3	NaCl[b] / Na_2CO_3	Length of test, days	Result
DZ-19	CR	280	371	1588	184	86	39	5.6	0.6	50	Cracked
DZ-20	CR	280	371	1588	184	86	39	5.6	0.6	50	Cracked
DZ-21	CR	143	190	1607	191	112	37	8.7	0.7	52	Cracked
DZ-22	CR	143	190	1607	191	112	37	8.7	0.7	52	Cracked
DY-1	HR	171	227	1323	196	64	32	6.1	0.9	50	Cracked
DY-2	HR	171	227	1323	196	4	9	6.1	0.9	50	Cracked
DY-3	HR	331	438	1507	301	79	31	4.4	0.9	50	Cracked
DY-4	HR	331	438	1507	301	79	31	4.4	0.9	50	Cracked

[a] CR, cold-rolled boiler-flange steel; HR, hot-rolled boiler-flange steel.
[b] Ratio values are averages of daily ratios. They are not calculated by dividing the average for sodium sulphate or sodium chloride by the average total alkalinity.

concerning the action of sodium sulphate in detector tests on a boiler operating at 130 psi. This work was carried out by The Detroit Edison Company, and the results are shown in Table 1 of this summary. Tests were run in duplicate and all eight specimens cracked in spite of the fact that the sulphate ratios were held very high.

Straub's plotted data (1) show cracking and failure of a number of specimens at 230 psi with sodium-sulphate to total-alkalinity ratios well above 2.

There is no consistent evidence from the combined data in this symposium that sodium sulphate will stop cracking of the specimens either at high or low boiler pressures.

Sodium Sulphate and Sodium Chloride

Several of the chemicals for preventing embrittlement, that have been investigated by some of the authors in this symposium, were originally suggested during Straub's early work on embrittlement.[9] As a result of investigation with a new type of testing equipment in 1938,[10] Straub expressed the belief that sodium sulphate and sodium chloride together would prevent cracking up to 250 psi. In the current symposium, he presents further data on the action of these salts (1). Several of the other papers in the symposium offer no support for the belief that these salts act as protective agents.

Above 250 psi, the data from the symposium are in agreement that these salts have no protective action.

Sodium Phosphate

Results obtained by Purcell and Whirl, and Bird and Johnson, as well as by Partridge, Kaufman, and Hall, all show that sodium phosphate will not prevent embrittlement cracking in the presence of appreciable concentrations of sodium hydroxide.

Purcell and Whirl (2), in their tests at Reed Station on a boiler operating at 450 psi, eliminated the embrittling tendencies of the water by the most direct method of all, i.e., elimination of all alkalies which will yield sodium hydroxide when the boiler water is concentrated. The desired pH was secured by the addition of sodium phosphate alone.[11] This treatment must not be confused with the unsuccessful method of using sodium phosphate as an inhibitor in the presence of sodium hydroxide.

The results reported by these authors (2) in their Table 1 show that their Reed Station boilers unfailingly cracked specimens in 30 or 60 days with free[12] sodium-hydroxide concentrations above 33 ppm (OH above 14 ppm); on the other hand, when this constituent was eliminated all cracking stopped for periods at least up to 90 days. The pH in the boiler water, in the absence of free[12] sodium hydroxide and with PO_4 concentrations between 60–70 ppm, was slightly above 10.5.

The unique method developed by these authors for controlling the phosphate treatment further enhances its value. Tricky chemical analyses that are difficult to interpret are avoided. It is only necessary to measure the pH value and the PO_4 concentration to estimate from their Fig. 8 if any free[12] hydroxide can be present.

The treatment used by Purcell and Whirl (2) has other advantages. In cases of steam blanketing, Partridge and Hall[13] have noted that high NaOH concentrations may increase the rate of attack on the metal. They can also increase carry-over and contribute to the stickiness of the solids with consequent turbine-blade fouling. Elimination of the sodium hydroxide may be advantageous in all of these respects.

Purcell and Whirl have conducted their tests in a skillful and thorough manner and have been willing to pioneer in new methods of water treatment.

Sodium Nitrate

Data have been published showing that sodium nitrate will prevent cracking of embrittlement-detector specimens at 210 psi.[14] The data in Fig. 10 of the Partridge, Kaufman, and Hall paper (5) are in satisfactory agreement with these published results at pressures below 450 psi. Low concentrations of sodium nitrate did not prevent cracking when the pressure exceeded 600 psi. Purcell and Whirl found that no cracking occurred at Stanwix (195 psi), where the nitrate averages about 20 per cent of the caustic alkalinity.

Bird and Johnson (4) find from their laboratory tests that nitrate is an effective inhibitor in some instances but not in others. Their reported concentrations of nitrate represent the amount added at the beginning of the test and not the amount found at the end. The present writers are inclined to believe that failure occurred where the protecting nitrate was destroyed during the test. This loss might be especially pronounced if the bomb surfaces were coated with organic materials from previous tests, as these would tend to reduce and decompose the nitrate.

Bardwell and Laudemann (3) have carried out extensive testing with sodium nitrate on the Chesapeake & Ohio Railway. This was done with embrittlement detectors attached directly to switch engines at various locations on the railroad. In this work they show that the detector can be operated by the normal railroad personnel to secure consistent results and they outline the method by which they insured the interest and co-operation of each individual engaged in the work. Their suggestions should not be difficult to follow on any railroad well organized for the treatment of boiler waters.

Their results show that sodium nitrate prevented cracking at all locations except one. At Ashland, Ky., Fig. 2 of paper (3), two specimens showed slight cracking, but even this minor trouble has been eliminated. At several locations, the nitrate has proved to be definitely superior to waste sulphite liquor as a protective agent.

Conclusions

Effective chemical inhibition of embrittlement presumably results from the reaction of the treating chemical with the steel surface to produce a protective film. In all laboratory tests reported up to the present time, the same solution has been used throughout the test period. Since it is in contact with a relatively large surface of hot metal, a continuous decrease in the concentration of inhibiting chemical generally occurs. On the other hand, in the tests on operating boilers, any desired amount of chemical, within reasonable limits, can be maintained in the boiler water and this is the solution which is circulating through the detector.

Experiments have already shown that this difference between laboratory and plant tests can profoundly influence the results. It is probably responsible for some of the differences which have been noted in this symposium. However, the results of embrittlement tests carried out on the boiler would more nearly represent the action of the water in the riveted seam than would the

[9] "Embrittlement in Boilers," by F. G. Straub, Engineering Experiment Station, University of Illinois, Urbana, Ill. Bulletin No. 216, 1930.

[10] "A Method for the Embrittlement Testing of Boiler Waters," by F. G. Straub and T. A. Bradbury, Proceedings of the American Society for Testing Materials, vol. 38, 1938, pp. 602–615.

[11] This method of treatment is most useful for boilers operating on evaporated make-up.

[12] As determined by the modified Winkler method.

[13] "Attack on Steel in High-Capacity Boilers as a Result of Overheating Due to Steam Blanketing," by E. P. Partridge and R. E. Hall. Trans. A.S.M.E., vol. 61, 1939, pp. 597–622.

[14] "Embrittlement Detector Testing on Boilers," by W. C. Schroeder, A. A. Berk, and C. Kerby Stoddard, *Power Plant Engineering*, vol. 45, 1941, pp. 76–79.

laboratory tests carried out on isolated samples of the boiler water.

The following conclusions concerning the effect of a number of chemicals in preventing embrittlement are based upon all the data that have been submitted in this symposium:

1 Certain tannins, especially those of the quebracho type, will retard embrittlement-cracking in test specimens. Relatively low concentrations are sufficient, even at the higher pressures. The protective action probably decreases around 500 psi, although the tannin has been successfully used in several cases at 650 psi.

2 Lignins will prevent cracking of test specimens in many boiler waters. In some instances, however, they are not satisfactory. One investigation has indicated that their protective action may be increased by the use of a small amount of sodium nitrate. This possibility needs further study.

3 The data in the symposium do not show that sodium sulphate will prevent embrittlement cracking in test specimens.

4 The data in the symposium are in agreement that sodium sulphate and sodium chloride do not prevent cracking at pressures above 250 psi. At lower pressures, the various authors are not in agreement concerning the action of these salts.

5 A boiler water containing sodium hydroxide in appreciable concentration cannot be treated with sodium phosphate to prevent cracking in specimens.

6 Embrittlement can be prevented by eliminating from the boiler water all alkalies which will yield sodium hydroxide when the water is concentrated. The pH in the boiler water is then maintained by the use of sodium phosphate. Simple chemical methods have been worked out for controlling this treatment.

7 Sodium nitrate appears to inhibit embrittlement in the detector tests at least up to 300 psi.

Final proof of the value of the embrittlement-detector method of testing has been provided by Bardwell and Laudemann on the Chesapeake & Ohio Railway. Their work was not a result of academic interest in the embrittlement problem, but instead was due to the pressing necessity for preventing cracks in 22 to 40 locomotive boilers each year. While this condition was unfortunate for the railroad, it furnished perhaps the only chance that will ever be available for determining the effect of protective chemicals in a number of operating boilers otherwise probably destined to crack. At the same time, direct correlation was possible between the action of the water on specimens in the embrittlement detector and in the cracking of locomotive boilers.

Fig. 2 of this summary represents the number of boilers found cracked during each 6 months since 1934. From this time

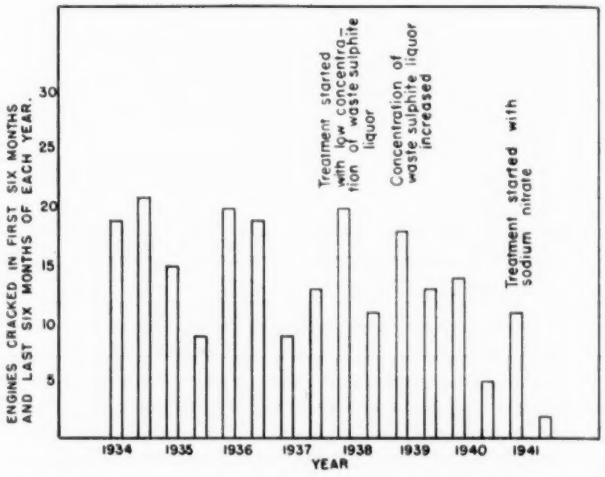


FIG. 2 EFFECT OF TREATMENT WITH WASTE SULPHITE LIQUOR AND THEN SODIUM NITRATE ON LOCOMOTIVE-BOILER CRACKING

through 1938, there were never less than 9 and a peak of 21 was reached.

During 1938 and 1939, treatment was started with waste sulphite liquor. No appreciable decrease in cracking was noted during 1939, nor was it expected, since old cracks in the boilers must be found and repaired, a process that would probably require a few years for completion. In 1940, the last 6 months showed a decrease in the number of cracked boilers. In 1941, cracking rose in the first 6 months but results for the last 6 months are extremely gratifying, for only two boilers were found cracked. This is particularly significant since the engine mileage during this period has been much greater than that for any similar period in the previous years which are shown. The results furnish strong evidence that this railroad is on its way to elimination of its embrittlement troubles.

The fact that the decrease in engine cracking follows the elimination of cracking in the detector specimens indicates that the establishment of nonembrittling conditions, according to this test, is a strong criterion that the water can be used in the boiler without danger. On the other hand, if the boiler water cracks the detector specimens, it will not necessarily crack the boiler, yet it is difficult to guarantee that conditions do not exist or will not arise in the boiler structure from which cracking may result.

Discussion—Symposium on Embrittlement

Comment on Paper by F. G. Straub (1)

T. C. Rathbone.[1] In his discussion of results, the author indicates the possible necessity of modifying the laboratory control tests to conform with actual operating results. It is suggested that some of the difficulty may be caused by unanticipated stresses in the test specimen.

The construction of the embrittlement-testing unit, as illustrated in Fig. 1 of the paper, would indicate the possibility of eccentric loading on the specimen walls in spite of any ordinary guides, by reason of the nonaxial reactions of the compression-spring coil ends on the rigid pull-rod assembly. If this is so, the combined tensile stress on one side of the specimen might become very appreciably greater than the stress arrived at by formal calculation.

The attempt is made to stress the specimens at 40,000 psi, or about 11 per cent above the yield strength, to provide comparable results in a reasonably short time. It was found that if the stress is increased above 50,000 psi, or about 40 per cent above the yield point, no reasonable combination of salts will prevent failure. Differences of a few thousand pounds pressure more or less are apparently critical. Yet the combined stresses possible with eccentric loading may introduce deviations of several thousand pounds.

With no data on the actual dimensions of the test unit at hand to venture calculation of possible eccentric stresses, the following dimensions were assumed by scaling the illustrations: Outside diameter at test section, 0.6 in.; inside diameter, 0.5 in; wall thickness, 0.05 in.; and mean diameter of spring, $2^1/_2$ in. Considerable variations from these assumptions will not materially affect the nature of the results.

Assume that the ground coil ends provide effective and uniform bearing over three quarters of the full circumference. The centroid of this loading would have an eccentricity of 0.3 radius, or 0.375 in. If the load centers of both ends are in line, this would be the moment arm of the eccentric load on the specimen and pull-rod assembly. The area of the tube section is 0.0865 sq. in. With a nominal stress of 40,000 psi, the actual spring load is 3450 lb. The bending moment on the specimen is therefore 1300 in-lb.

The moment of inertia of the section is 0.0033 in.[4] and extreme fiber distance, 0.3 in., from which the bending stress is $S = \frac{cM}{I} = \frac{0.3 \times 1300}{0.0033} = 118{,}000$ psi, to be added to the 40,000 psi direct stress on the tension side and subtracted from the opposite side. The stress on the inner wall will be only slightly less.

Obviously, with these assumed data, the guides must at least be partially effective, otherwise immediate failure would always occur. However, such guides cannot prevent all flexure and still leave the surfaces free to slide; also, the slightest amount of clearance would permit appreciable bending stresses. If the coil-end reaction centroids are diametrically opposite instead of being in line, the test-rod assembly will assume a compound flexural curve, and the guides, near the neutral point, will be still less effective in preventing lateral displacement.

The magnitude of these figures would indicate that even with guides, extraneous stresses of sufficient order to confound the test results may have existed.

The possibility of additional bending stresses can, of course, be explored with extensometers or, more simply, by applying the "stress-coat" method used by Professor de Forest, which consists

[1] Chief Engineer, Turbine and Machinery Division, The Fidelity and Casualty Company of New York, New York, N. Y., Mem. A.S.M.E.

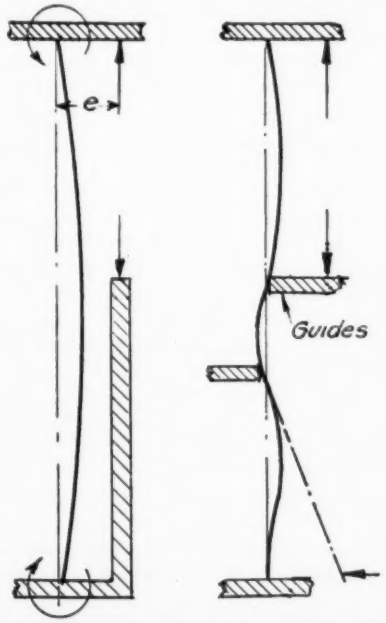


Fig. 1 Showing Possible Bending Stresses

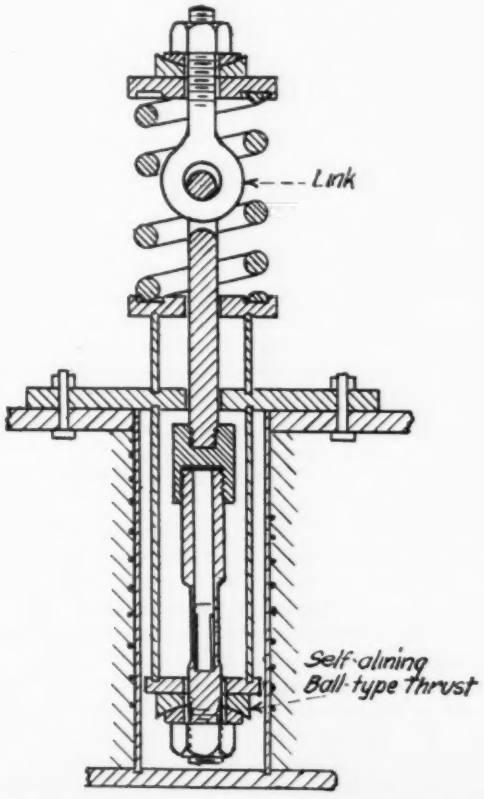


Fig. 2 Suggested Changes in Apparatus to Eliminate Stresses Caused by Both Misalignment and Eccentric Loading

in coating the surfaces with a special brittle lacquer and observing the cracking or "crazing" of this coating when the test piece is loaded. Rough approximations of stresses as low as 20,000 psi can be made. Any nonuniformity of stressing would instantly be exposed by the denser and more closely pitched cracking occurring on the more highly stressed side.

To avoid the possibility of imposing compound stresses on the specimen, either by misalignment or eccentric loading, it is suggested that links be interposed in the extension pull rod, and also that the rigid threaded connection at the bottom be replaced by a spherically seated ball-type thrust bearing.

It is presumed that the spring scale is such that the plastic yielding of the specimen will result in no appreciable change in the loading; that no residual torsional stresses can be imposed by tightening the nut; and that the stress due to the trapped steam pressure is negligible.

Comment on Paper by T. E. Purcell and S. F. Whirl (2)

H. E. Einert.[2] This paper (2) represents a distinct contribution to feedwater treatment and control, particularly for high-pressure boilers. We are primarily interested in pressures in excess of 1000 psi, at which pressure the use of nitrates or organic material such as quebracho and lignin is excluded.

We have found definite indications of cracking of the test bars by means of the Schroeder embrittling detector at 1400 psi, when the hydroxide content has been in the neighborhood of 30 to 50 ppm. Incidentally, the cracking has been identified as truly intercrystalline. On the basis of the curve, as suggested in Fig. 8 of the paper (2), if the pH value of the boiler water is maintained at 11, there must be a PO_4 concentration of approximately 115 ppm. This, of course, is much higher than we would normally recommend. From the standpoint of solids, the hydroxide concentration as determined by the strontium or barium procedure's being entirely eliminated, the solids concentration of the boiler water is increased, but not excessively. Whether the elimination of the hydroxide concentration with an appreciable increase in phosphate would have any effect on carry-over can only be conjectured. It would, however, be our opinion that there should not be any increase in the amount of carry-over.

At plants where corrosion has been experienced in floor tubes and which condition has been diagnosed as sluggish circulation, with the attendant "steam-binding," the pH value has been decreased in order to eliminate the OH radical. With the maintenance of 100 to 120 ppm of PO_4 in the boiler water, the complete elimination of the OH radical is possible, under which conditions the reduction in the pH value need not be made. We have always been opposed to lowering the pH value in the boiler whenever the PO_4 has been held at normal concentrations.

The authors indicate that adjustments of the embrittlement detector are made only once in 7 to 10 days. This is very interesting to us, as most of our clients find it necessary to make adjustments more frequently.

We note that some of the tests were conducted for periods ranging from 90 to 195 days. Certainly, this is a step in the right direction, for we feel that a 30- or 60-day test period is not sufficient, unless, of course, the bars are positive with respect to cracking. In our opinion, tests No. 107-A and B, which were run for 90 days, give conclusive evidence that cracking would not occur, regardless of the length of time the test might be run. The SiO_2 content reported for tests Nos. 106, 107-A, and 107-B are comparable to those tests reported for Nos. 102 and 103, and on this basis, we believe that the authors have eliminated one variable, namely, the silica concentration. The radical decrease in hydroxide concentration is striking and, under the conditions of the test, must certainly be a dominating factor.

No determinations of pH are recorded, but these would have been of interest in the paper. An additional test would have been worth while, in which the pH values were placed on a comparable basis for tests Nos. 101, 102, etc.

This, of course, would mean increasing the phosphate concentration to a value in excess of 100 ppm. On the basis of about 65 ppm of PO_4, we interpolate the pH value to be about 10.7. We do not believe that there would have been any difference in the cracking characteristics of the water if the phosphate concentration had been increased from about 65 to 110 ppm of PO_4.

For those plants that use sea water as cooling water and where the leakage would be predominantly noncarbonate hardness, the soluble PO_4 would be removed without liberating an equivalent sodium bicarbonate, which eventually would decompose into sodium hydroxide. The absence of the hydroxide would permit the control to be carried along much more readily than in plants where the carbonate hardness is relatively high when compared to the total.

Comment on Paper by R. C. Bardwell and H. M. Laudemann (3)

F. G. Straub.[3] In the chemical-engineering department of the University of Illinois, we are primarily interested in research. However, we realize that research, to be of real value to industry, must be at least partially correlated with industrial operation before the maximum industrial utilization of the results is possible. In the development of the embrittlement-testing unit, it was so designed as to give results which were apparently in agreement with available operating data.

The question is often asked: "Where and how have you obtained the operating data?" Early in our research, we contacted the power-plant operators with the purpose of obtaining as many data as possible. At that time many of our sources of information were of a confidential nature. We have summarized the data obtained and published them without revealing the source of the confidential information. Now for the first time since starting this work we find it necessary to betray this confidence placed in us and to reveal the source of part of our confidential information. We do this in the interest of the power-plant industry and only after the identity of the source of our information has been revealed by the authors of this paper (3). We would still hesitate to reveal the source of the data, if it were not for the fact that the authors state that certain data obtained from the same source are contradictory to the data furnished us in 1925 and 1926. The authors state, "In the early experience of the Chicago and Northwestern Railroad with embrittlement, it was noted that embrittlement cracking predominated on the divisions on which the sulphate was high." In his files, the writer finds the following memorandum: "January 29, 1926, I visited Chicago Northwestern Railroad and talked with Messrs. ——— and ——— at the Chicago shops. I was shown analyses of locomotive boilers at the time of washout of eight locomotives. Two were high in sodium carbonate and low in sulphates. One of the locomotives, from which the high-carbonate and low-sulphate water came, operated around Powers and Escanaba, Mich. This locomotive was in the shop with embrittled plates. I also received analyses from raw waters on the Green Bay Division in which this cracking predominated. All of these analyses showed low sulphates. The treatment given these locomotives was 1 lb of soda ash to 1000 gal of water. Such a treatment would produce a boiler water having low sulphates and high alkalinities."

[2] Cyrus Wm. Rice & Company, Inc., Pittsburgh, Pa.

[3] Research Professor of Chemical Engineering, University of Illinois, Urbana, Ill.

From these data, we were at that time led to believe that the experience of the Chicago and Northwestern Railroad showed definitely that their locomotive cracking was confined to boiler waters of low sulphate instead of high sulphate content, as stated by the authors. This being a fact, the writer wonders if the authors' statement that their experience on the Chesapeake & Ohio Railroad is similar to that of the Chicago and Northwestern Railroad might not lead one to conclude that their further statements, to the effect that high sulphates favor embrittlement, could also be reversed to show that their cracking has taken place on low-sulphate boiler waters.

A rather brief survey of the meager operating locomotive-boiler-water data, given in the paper, would indicate that the cracking they described has not occurred in locomotives having boiler waters with a high sulphate-to-alkalinity ratio. A breakdown of the summarized data given in Table 2 of the paper (3) gives data that definitely show that the A.S.M.E. ratios were not maintained in these locomotive boilers. From the data previously published, from which the summary in Table 1 is taken, it is found that, during 7 years, 176 analyses were made on water samples obtained from eleven engines. This amounts to less than $2^1/_2$ analyses per year per engine. A further examination of the analyses indicates that $28^1/_2$ per cent of the analyses have an A.S.M.E. ratio of less than 2; and 24 per cent have a ratio between 2.1 and 2.5. Thus, these analyses would indicate that the ratio had not been definitely maintained in the engines in question.

The authors state: "The history of engine I is especially interesting, as the second course was renewed at the end of 1936, and again in the early part of 1938. During this interval, the analyses showed fairly high sulphate values." A summary of their own analyses during this interval shows one analysis during 1936 with a ratio of 1.5. During 1937, twenty analyses are reported, although they do not state from what locomotives these analyses were taken. Of these twenty analyses, 35 per cent have a ratio less than 2; another 35 per cent have a ratio between 2 and $2^1/_2$; the final 30 per cent have a ratio between $2^1/_2$ and 8. During 1938, twenty analyses were also made, and these in turn have ratios almost identical with those reported for 1937. This analysis of the information given certainly does not indicate that the A.S.M.E. ratio was maintained in these boilers.

Data furnished by the authors indicate definitely that they did not maintain the A.S.M.E. ratio in the cracked boilers which they describe.

The results with the Bureau of Mines detector, which the authors report, relative to the effectiveness of the organic material in the nitrates in preventing failure, are extremely interesting. These results seem to agree with those which appeared in a bulletin[4] by the writer in 1930.

Comment on Paper by E. P. Partridge, C. E. Kaufman, and R. E. Hall (5)

F. R. Owens.[5] The writer is indebted to the authors for their contribution, and particularly for the statement of their conception of the research: "Even though the measurement be rough, the way has been opened to approach the problem of cracking, not by arguing as an advocate, but by testing as an engineer."

The writer can very readily subscribe to this brief and general statement and feels that an expansion of the thought in this discussion will, at least in part, present the authors' reasoning in arriving at the stated conclusion.

A review of the literature on intercrystalline cracking in boilers leads the lay mind and, in many instances, the professional one to confused uncertainties with respect to protective chemical methods. The writer has encountered this expressed criticism innumerable times from operating engineers.

It is obvious, at least to the writer, that the mechanical and chemical environment which promotes intercrystalline cracking is quite involved, and investigations to date have not successfully isolated all factors. In view of this, the controversial status of the subject is a natural sequence.

As the authors point out, even though the detectors developed by Straub[6] and Schroeder[7] and their associates have decided limitations, the fact remains that they have given us a laboratory and plant method for measuring effect. Furthermore, as the authors indicate, even though we may favor the use of a certain inhibitor, on the basis of our present-day knowledge, we can definitely eliminate the possibility of prejudice and determine the chemical environment which effects maximum protection for a specific operation.

The reproduction of existing chemical and mechanical environment in any plant is certainly an ambitious task. In fact, from the viewpoint of circulation; heat input and distribution; stress, applied or residual; the delivery and maintenance of protective materials in the film surface of the liquid; concentration of all salts, and their respective influence on each other; and many other factors, we face seemingly hopeless tasks at such reproduction. Hence, the Straub and Schroeder detectors offer real help in reducing the problem to a more factual basis. It behooves those of us engaged in this particular field of endeavor to encourage their use as additional assurance of safe operation of boilers.

From our experience with the Schroeder detector, we wish to discuss two factors, and suggest that both Straub and Schroeder investigate them, if possible. Our experience tends to indicate that the amount and nature of the precipitated products in the boiler concentrates may be a factor with respect to intergranular cracking.

Also, the solubility of ferrous hydroxide would appear to be pertinent. The work of Whitman, Russell, and Davis[8] showed definitely that a close relationship exists between the rate of corrosion and the solubility of ferrous hydroxide in the presence of certain salts of different concentrations. They further revealed that this is also true of alkalies. Their results demonstrated that, as the concentration of the solution increases, the solubility of ferrous hydroxide, formed in the film surface of the liquid, either increases or decreases. If the solubility of the ferrous hydroxide increases, corrosion increases, and conversely, if the solubility decreases, the rate of corrosion is lowered.

Therefore, it would appear to be feasible to check various inhibitors in boiler waters of various concentrations with the Straub and Schroeder detectors and to attempt, by means of them, to determine the effect and nature of precipitated products.

The authors are to be commended on their suggested use of embrittlement detectors as engineering instruments. Their approach to the problem may well be one which this Society can support, rather than the adoption of definite rules for the maintenance of specific ratios.

[The general discussion of the papers composing the Symposium on Embrittlement follows directly.]

---

[4] "Embrittlement in Boilers," by F. G. Straub, Engineering Experiment Station, University of Illinois, Urbana, Ill., Bulletin No. 216, 1930.

[5] Secretary, Cyrus Wm. Rice & Company, Inc., Pittsburgh, Crafton, Pa.

[6] "A Method for the Embrittlement Testing of Boiler Waters," by F. G. Straub and T. A. Bradbury, Proceedings of the American Society for Testing Materials, vol. 38, 1938, pp. 602-615.

[7] "Embrittlement Detector," by W. C. Schroeder, A. A. Berk, and R. A. O'Brien, *Combustion*, vol. 12, August, 1940, pp. 19–21.

[8] "The Solubility of Ferrous Hydroxide and Its Effect Upon Corrosion," by W. G. Whitman, R. P. Russell, and G. H. B. Davis, *Journal of the American Chemical Society*, vol. 47, 1925, pp. 70–79.

General Discussion

L. D. Betz.[9] The authors of all of the papers presented in this symposium are to be commended upon the details with which their data have been assembled. In the evaluation of these data, however, and in drawing conclusions from them, there are several points which might be clarified yet further.

For instance, in the paper presented by Partridge, Kaufman, and Hall (5), no statement is given to indicate the types of containers used in sampling the boiler waters. If the boiler waters, of an alkaline character, were obtained in glass, then there is a likelihood that the silica values may be high because of a pick-up of silica from the glass. The amount of silica picked up may not be sufficient to alter the general conclusions drawn, but in interpreting the data, it should be borne in mind that the silica values shown are slightly higher than the true values, provided glass sample containers were used.

In the same paper, it is noted that the authors employed the tyrosine method, proposed by Berk and Schroeder, for determining the tannin content of the boiler water. At this point, it is well to raise the question as to whether or not these tannin determinations were made at the plant immediately after collection of the boiler samples, or whether tannin determinations were made at a later period on samples forwarded to the laboratory. If the latter case is true, the values obtained will be considerably lower than were actually present in the boiler water at the time of sampling. Considerable work has been done in our laboratories, which indicates that there is an appreciable change in the tannin content, with an elapse of time, when determined by this method. This change is more pronounced in alkaline tannin solutions. The drop in active tannin is also dependent upon the initial tannin concentration. Such a drop, however, is of sufficient magnitude so that testing of a sample several days after it was drawn would present an entirely erroneous picture of the tannin content of the boiler water at the time of sampling.

A statement from the authors on these points will aid in the interpretation of the data presented.

In the paper by Bird and Johnson (4), covering the laboratory investigations of embrittling characteristics with the Schroeder detector, the authors present a wealth of valuable data and are to be complimented on the excellent manner in which this study was conducted and presented.

In our field experience with the Schroeder detector, many instances have occurred in which nitrates, naturally present in the make-up water, have appeared to be the factor preventing cracking of specimens, even with low concentrations of sulphate and extremely high alkalinity. It is possible that, when nitrate is naturally present, inhibitory properties are possessed by many waters used for make-up.

However, from our experience, we do not feel that it is a safe procedure to rely entirely upon the natural nitrate content of a make-up water for complete inhibition of embrittlement, without periodic checks for the nitrate concentration of the boiler water. We have found that the nitrate concentration present in many raw supplies is subject to considerable seasonal variation and while, at one season, it may be sufficient to prevent cracking of detector specimens, at other periods of the year, it may be reduced to a negligible value and thus afford no protection whatever.

Incidentally, nitrate determination is frequently overlooked in a water analysis. Many will be surprised to learn how often fairly large quantities of nitrate are present in a feedwater, especially if there is any opportunity for the raw supply to become contaminated with sewage.

We have been privileged to work with the Joint Research Committee on Boiler Feedwater Studies and have installed quite a few Schroeder detectors at various plants throughout the United States and Canada. We have not presented separate records of the results of these installations but have forwarded all data and results to Dr. Schroeder. No doubt, he has incorporated these records in his complete files on the subject and has probably included them in the data of his summary.

The subject of caustic embrittlement or intercrystalline cracking has been extensively treated in this symposium as has also the Schroeder detector. That this instrument provides a very greatly accelerated condition of caustic embrittlement is clearly evident. Apparently, specimens in this detector crack far in advance of any actual cracking of the boiler metal. Therefore, the question is raised: Is this acceleration increased to a point beyond that condition reached in the actual boiler metal? In short, does it necessarily follow that cracking of a specimen under the accelerated conditions in a Schroeder detector implies similar conditions to be expected in the boiler metal? Have any cases been recorded where a Schroeder detector showed failure and where the boiler metal showed a similar condition? These detectors have now been in use for a considerable period of time, and it is hardly likely that lack of sufficient time can be the cause for a negative answer to this question. True, anyone who finds cracking in a specimen of a Schroeder detector will waste no time in attempting to establish proper ratios to prevent this action for boilers are expensive equipment. Certainly no operator will deliberately permit a condition such as this to exist, if it can be prevented. But have we any records to indicate that the cracking of a sample in a Schroeder detector forecasts a condition of actual embrittlement in the boiler metal? Bardwell and Laudemann (3) have indicated the other side to this question by showing how embrittlement of the locomotive-boiler metal apparently ceased when failure of the specimen did not occur in the Schroeder detector.

C. B. Bryant.[10] It is noted that the papers, constituting this symposium, have not dealt with one phase of the intercrystalline-corrosion problem, namely, the economic justification of the various methods of embrittlement protection.

It has been clearly brought out that the development of intercrystalline corrosion is a consequence of the simultaneous occurrence of several factors: (*a*) the boiler metal must be highly stressed, (*b*) there must be leakage, (*c*) there must be such conditions that, as a consequence of the leakage, the dissolved solids in the boiler water become highly concentrated in contact with the boiler metal, and (*d*) the chemical characteristics of the dissolved solids must fulfill certain requirements. In other words, the existence of intercrystalline corrosion depends upon a chain of circumstances, hence the destruction of any link in this chain would prevent embrittlement.

It occurs to the writer that the prevention of embrittlement by chemical treatment of the water in the boiler may not be the most economical method of attacking this problem. If stress-relieving a boiler at the time of original construction will prevent the possibility of intercrystalline corrosion regardless of the water characteristics, then a single expenditure will settle the problem for the life of that particular unit. If, on the other hand, the development of embrittlement is prevented by treating the water, there is a continuing expense for the purchase and application of the treating chemicals which, conceivably, during the life of a boiler, might be much more expensive than the original heat-treatment which would accomplish the same end.

The tannins, used by different experimenters as embrittlement inhibitors, come from various sources, and, obviously, are not all

[9] General Manager, W. H. & L. D. Betz, Philadelphia, Pa. Assoc. A.S.M.E.

[10] Engineer of Tests, Southern Pacific Railway System, Alexandria, Va.

of the same chemical composition. It seems likely and has been suggested by some experimenters that there are definite active components of the mixtures we speak of as tannins, which, although present only in small quantity with respect to the total amount of tannin compound, are responsible for the beneficial effects. It seems worth while to suggest the attempt to determine what these active constituents might be, which would perhaps afford a means of better understanding the nature of the protective action, and might even result in lowering the cost of the protective treatment. This situation may be similar to the development of vitamin preparations from fish oils. A number of years ago children were fed a teaspoonful of cod-liver oil per day in order to provide the proper vitamin dosage. Later it was found that the useful and active constituent of cod-liver oil was present only in minute quantity and, by the preparation of concentrates of the beneficial and active constituents, the accuracy of dosage was greatly improved and the amount of material considerably reduced. If it could be shown similarly that certain definite chemical compounds, constituting only a small portion of the tannins used in boiler-water treatment, are responsible for the results secured, then the way might be pointed to better understanding and improvement of the practice as well as toward a reduction in the cost.

L. F. Collins.[11] After carefully explaining why in his test apparatus the metal specimens are stressed only at about 40,000 psi, Straub (1) makes the following statement: "It has been found that if the stress is increased to around 50,000 to 55,000 psi, no reasonable combination of salts, either inorganic or organic, would prevent failure."

The inference is that a "critical stress" exists, at which it is impossible to prevent intercrystalline failures, of the common types of boiler metal, by adding to otherwise embrittling waters chemical inhibitors in amounts commensurate with other boiler-operating considerations. This seems to be attested to by the data of Bird and Johnson (Tables 1 to 7, paper 4), obtained with Schroeder detectors, as summarized by their statement: "The amounts of inhibitors indicated as being required by these boiler-water tests seem excessive . . ."

If the foregoing is a valid outline of the situation, and keeping in mind the uncertainty of the stresses which may be present in various areas of an operating boiler, two important conclusions are unavoidable:

1 The boiler-water chemist has completed his portion of the job of solving the embrittlement problem, because he has disclosed the existence of a number of chemicals which prevent failures when the metal is stressed below the critical value.

2 The ultimate solution of the problem of intercrystalline boiler-metal cracking is not within the province of the water chemist but rather becomes the heritage of the engineer and/or the metallurgist.

In pursuing conclusion 1, it is indicated that in boilers such as, for example, locomotive boilers, which may be subjected to all types and degrees of stress, the use of optimum amounts of inhibitors would conspicuously reduce the number of failures but would not entirely eliminate them. The Bardwell and Laudemann paper (3) discloses precisely this situation.

D. K. French.[12] In the past, there has been some skepticism as to the possibility of tannins' being of value in inhibiting embrittlement. It is difficult for the writer to understand why, at times, there is so much opposition to certain methods of treatment. The use of tannins was given to the engineering public very nearly 15 years ago, and it is felt that Drs. Straub and Parr should be given some credit for this initial work. It might be interesting to state that, even as early as the summer of 1923, the writer was in correspondence with Dr. Parr regarding the use of tannins and endeavored to have explained some of the reasons of the inhibition which was being obtained by tannin treatment of definitely embrittling types of water.

Early in the summer of 1927, when the Boiler Code provisions for the use of sulphates was seriously handicapping the treatment of certain plants under the writer's observation, a meeting was arranged at the University of Illinois, with Drs. Parr and Straub. The difficulties being experienced were explained to Dr. Parr, and arrangements were made to carry out experimental work on three different types of treatment which the writer had recommended for high-alkali waters. It was agreed that samples of the water would be supplied but, in the meantime, because he has always been actively interested in the problem, Dr. Straub obtained some tannic acid from the University of Illinois stockroom and before the week was up had come to Chicago to tell the writer that it had been impossible to break any of the test bars. He was greatly excited over the results. The results of this work were made public.[13] In concluding that report Dr. Parr stated, "As result of the experimental work, new embrittlement-inhibiting agents have been developed." While the writer has used the results then reported as the basis of treatment and has never yet had a case of embrittlement develop, it was very difficult to obtain support for the procedure.

While Dr. Straub was willing to confirm the original results, he did not give them publicity because of the difficulty of determining the presence of tannins in the boiler water. It is quite possible that the work of the Bureau of Mines in developing such a method is responsible for the emphasis on this agent now. An interesting explanation of the action involved appears in a bulletin[14] by Dr. Straub, from which the following statement is taken:

"The action of the organic matter is apparently different from that of the sodium sulphate in preventing the deposits. There is apparently a chemical reaction between the organic matter and the sodium hydroxide in the superheater, which changes the hydroxide to carbonate. This reaction does not take place until the sodium hydroxide reaches a high concentration. Thus, in dilute solutions at boiler temperature, the sodium hydroxide remains as such in the presence of these organic materials. However, as the sodium hydroxide mixed with the organic matter concentrates in the superheater, the concentrated sodium hydroxide reacts with the organic matter to form sodium carbonate."

According to Dr Parr, sodium carbonate, as such, has inhibiting properties.

With reference to specific cases, the writer can mention two without identifying them at this time.

One is a mine in West Virginia, utilizing water, which apparently is collected after passing through a natural green-sand deposit, because it carries between 25 and 30 grains, or 500 ppm of free alkali as sodium carbonate, and practically no hardness. When the writer was first consulted on this plant, the operators were pleased with the nonscaling results obtained from the use of this water supply. The writer gave warning against embrittlement and a year later was retained to prevent it in the future because four out of six drums were then being replaced as the result

[11] The Detroit Edison Company, Detroit, Mich.

[12] President, Dudley K. French & Associate, Chicago, Ill. Mem. A.S.M.E.

[13] "Embrittlement of Boiler Plate," by S. W. Parr and F. G. Straub, Engineering Experiment Station, University of Illinois. Urbana, Ill., Bulletin 177, 1928.

[14] "The Cause and Prevention of Steam-Turbine Blade Deposits," by F. G. Straub, Engineering Experiment Station, University of Illinois, Urbana, Ill., Bulletin 282, 1936, p. 34.

of this trouble. The treatment supplied consisted of tannin extract and phosphoric acid, which was added to the water so that 1 part of tannin would be present to each 20 parts of alkali, or 1 part of organic matter of tannic origin to 10 parts of alkali.

The method of ascertaining the presence of tannin was an indirect one in which total alkali, total chloride, and total sulphate were determined and calculated as the soda scale and substracted from a carefully run and corrected solid residue. The difference could be nothing other than organic matter. Based upon this treatment, this plant has been supervised for nearly seven years up to the present time, without the slightest indication of any embrittlement cracking showing, although the boilers are carefully inspected—sometimes twice a year.

The other case is that of a laundry in Winnetka, Ill. In this plant, well water, which has been treated with an exchange silicate softener, supplies feedwater containing approximately 150 ppm of free alkali directly to the boiler. The use of this supply resulted in the replacement of one drum before the writer was called in to supervise the operating conditions. The condensate, collected in the supply lines on the laundry floor, was very highly alkaline, showing about 250 ppm total solids. Apparently it was quite corrosive. A treatment combining tannin, acid phosphate, and acetic acid was used, the tannin content being controlled by indirect methods of analysis just as in the previous case. Operations have improved so greatly that the writer's term of service is apparently an indefinite one.

It might be interesting at this time to comment on one feature of this treatment which, to be perfectly frank, the writer fails to understand himself. While the feedwater introduces its alkali entirely as carbonate and bicarbonate of soda, and while the boiler water shows approximately 75 to 80 per cent of caustic soda in the concentrated alkali, the condensate collected from the longest line on the laundry floor rarely shows in excess of 30 ppm total solids, sometimes a very faint trace of pink to phenolphthalein, and never less than a pH of 7.6.

It would seem that, as this boiler operates and breaks down the carbonate with the release of CO_2, we should find this in the steam. In that event, the condensate should be acid, but such is not the case, and the question arises whether there is any chance of chemical adsorption or reaction. That would remove CO_2 before it has an opportunity to go into the steam.

MAX HECHT.[15] In paper (5) of this symposium, the authors have presented some of their data graphically. Because of the success which has attended the use of the statistical method in evaluating the results of corrosion testing, when large numbers of tests are available, it would seem appropriate that consideration of such mathematical treatment be given to all available tests, using the Schroeder detector, as reported in papers (2, 3, 5). Therefore, the writer would suggest a method which would include (*a*) correlation analysis of the least variation in time of cracking which can be considered significant; (*b*) correlations between water composition and time of cracking, which at the moment appears to be in confusion; (*c*) correlation between concentration of both inhibiting and noninhibiting substances and time of cracking.

Such a statistical analysis might assume that the design of the Schroeder detector and its operation were constant for all data reported, that the composition of the test specimen was similar, and that a uniform stress was applied in all instances. It would be further assumed that the methods of analysis for water composition used by the various authors furnish relatively equivalent data. Thus, the variables under consideration might be operating pressures and temperatures and variation in both composition and concentration of the boiler water. The problem would be simplified if the composition of the water were to be expressed in a uniform manner for all test results reported. As a suggestion, these results preferably might be reported in ions, equivalents per million.[16] The study may show the necessity of labeling the results of the water composition as cracking or noncracking in terms other than a simple ratio, such as that of sodium sulphate to total alkalinity as sodium carbonate.

It is recognized that the statistical study would be an arduous task, but nevertheless the inclusion of the results of such a study with this symposium may produce a clear picture of the field tests. A similar mathematical treatment may also be given to the results reported by F. G. Straub, in paper (1).

The following point is worth consideration. Straub and Schroeder and their co-workers have discovered the beneficial effects of several materials such as nitrates, sulphite liquors, quebracho, etc., and the harmful effects of others such as hydroxide and silica. The statistical study may show that there exist in the water unknown substances of natural occurrence which have inhibiting or accelerating characteristics whose detection escapes routine analysis.[17]

Confirmation of such findings may be secured by comparing the results of laboratory embrittling tests, making parallel runs with the sample of boiler water and with synthetic water of the same nominal composition, but prepared from pure materials. If significant differences are found, a refined analysis of the boiler water may disclose the nature of the materials responsible for the effect. For example, a refined analysis was made on a sample of boiler water from the Stanwix plant, shown by Purcell and Whirl (2), which gave evidence of a sufficient amount of nitrates to prevent cracking of the test specimen.

J. W. NELSON.[18] The development of test equipment by Prof. F. G. Straub, Dr. W. C. Schroeder, and their associates, in which the intercrystalline cracking of boiler steel could be developed, using boiler waters of normal operating concentration, or synthetic solutions of similar concentration, has accelerated greatly the work on this important problem and added considerably to our knowledge and appreciation of this subject. The embrittlement-testing unit, described by Professor Straub, was intended for use under controlled conditions in his laboratory, and it has been possible in a relatively short period of time to test a large number of waters with this testing unit. The embrittlement detector, developed by Dr. Schroeder and his associates at the Bureau of Mines, is designed for use on operating boilers as well as in laboratory testing. Its wide distribution and utilization by engineers responsible for boiler maintenance, operation, design, and feedwater treatment is attested by the results reported.

The embrittlement-testing unit is a spring-loaded device, employing no loss of solution or steam during a test cycle. If it indicates a water to be embrittling in nature, it also gives information as to the time required to produce failure of the test specimen because the tension on the spring-loading arrangement is released when a specimen fails.

The embrittlement detector employs a solution leak past a test specimen maintained in a state of stress, and in most applications a test period of 30 days has been established. If no cracks develop on the specimen in the 30-day period, longer test periods are quite often employed, especially when the detector is being used on an operating boiler. Possible results of this extended test period have been shown by Messrs. Purcell and Whirl in their

[15] Pittsburgh, Pa.

[16] "Method for Reporting the Results of Analysis of Industrial Waters," A.S.T.M. Standard Method D596-41, A.S.T.M. Standards Supplement Part III, 1941, Non-Metallic General, p. 247.

[17] Ibid., Table 1.

[18] Research Chemical Engineer, Dearborn Chemical Company, Chicago, Ill.

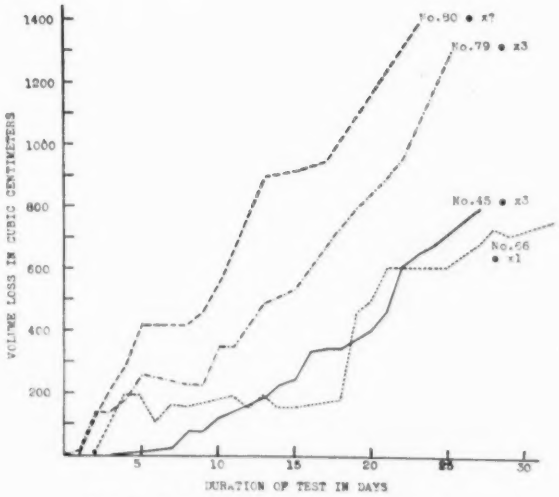


FIG. 3 BLANK TESTS; DAILY ADJUSTMENT

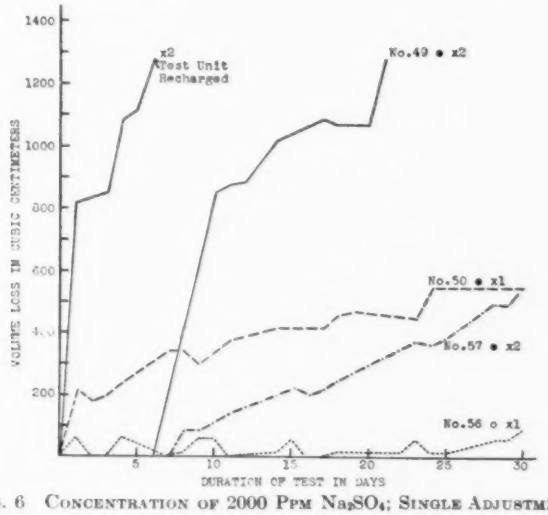


FIG. 6 CONCENTRATION OF 2000 PPM Na_2SO_4; SINGLE ADJUSTMENT

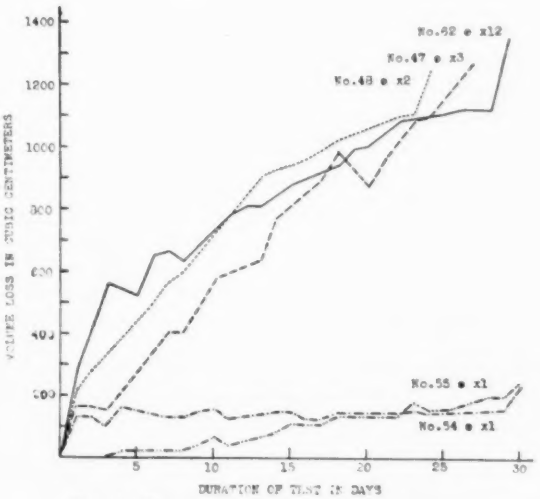


FIG. 4 BLANK TESTS; SINGLE ADJUSTMENT

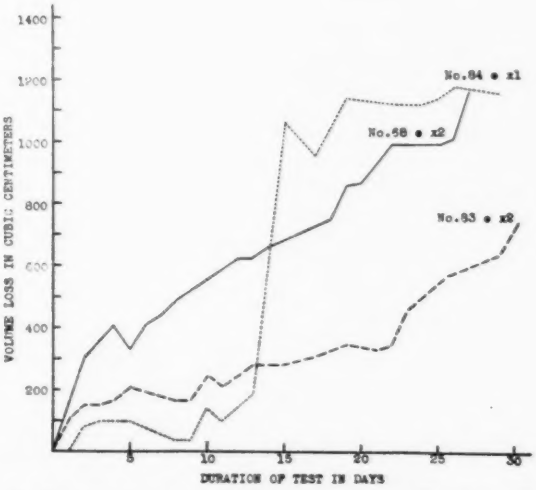


FIG. 7 CONCENTRATION OF 200 PPM QUEBRACHO EXTRACT; DAILY ADJUSTMENT

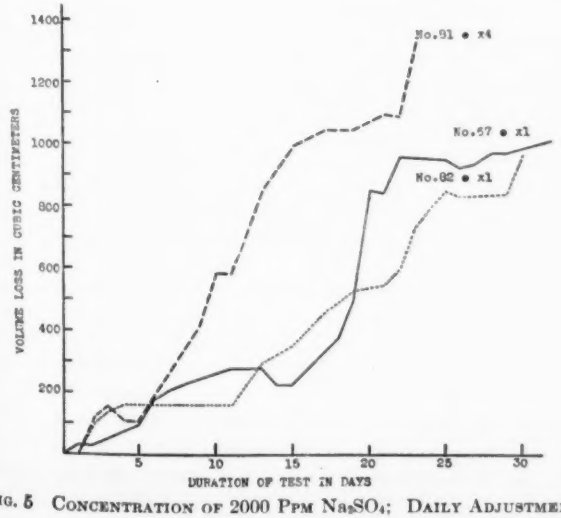


FIG. 5 CONCENTRATION OF 2000 PPM Na_2SO_4; DAILY ADJUSTMENT

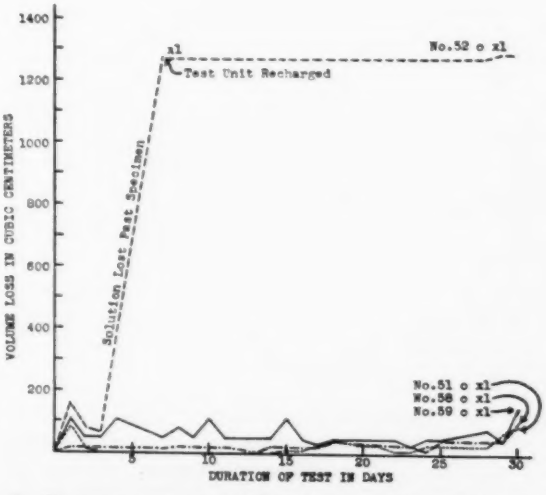


FIG. 8 CONCENTRATION OF 200 PPM QUEBRACHO EXTRACT; SINGLE ADJUSTMENT

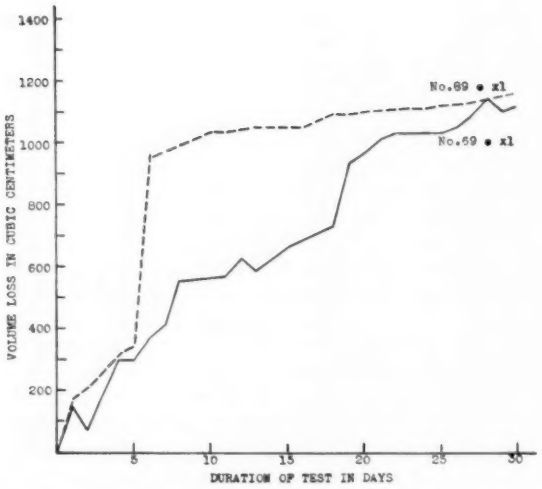


FIG. 9 CONCENTRATION OF 2000 PPM Na_2SO_4, 200 PPM QUEBRACHO EXTRACT; DAILY ADJUSTMENT

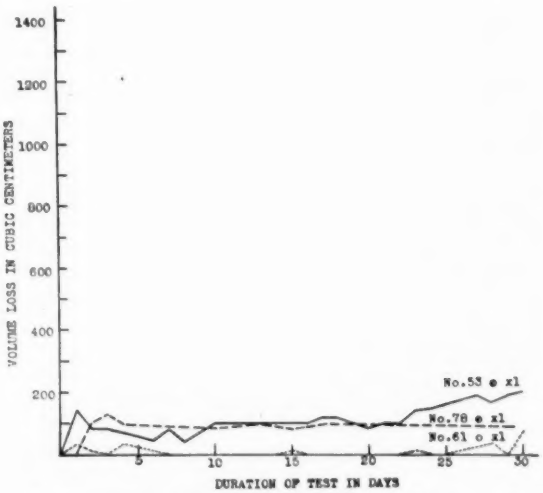


FIG. 12 CONCENTRATION OF 200 PPM WASTE SULPHITE LIQUOR; SINGLE ADJUSTMENT

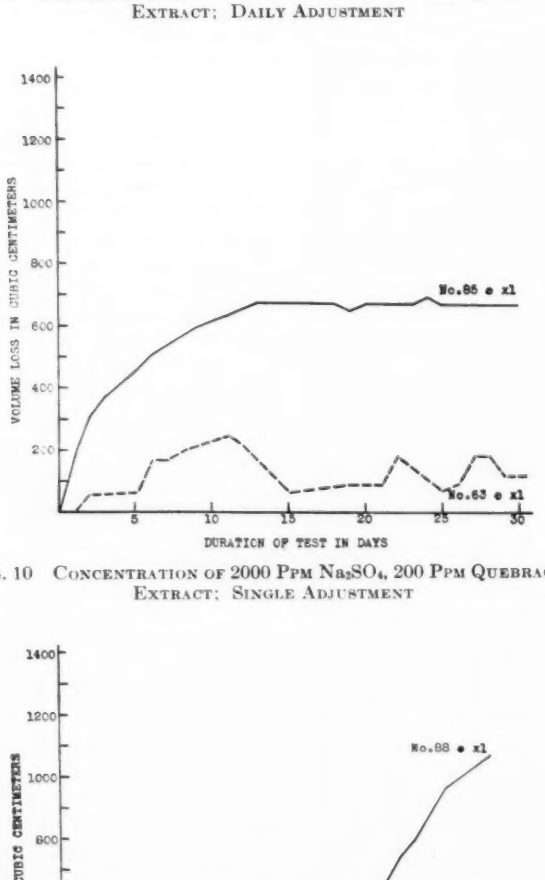


FIG. 10 CONCENTRATION OF 2000 PPM Na_2SO_4, 200 PPM QUEBRACHO EXTRACT; SINGLE ADJUSTMENT

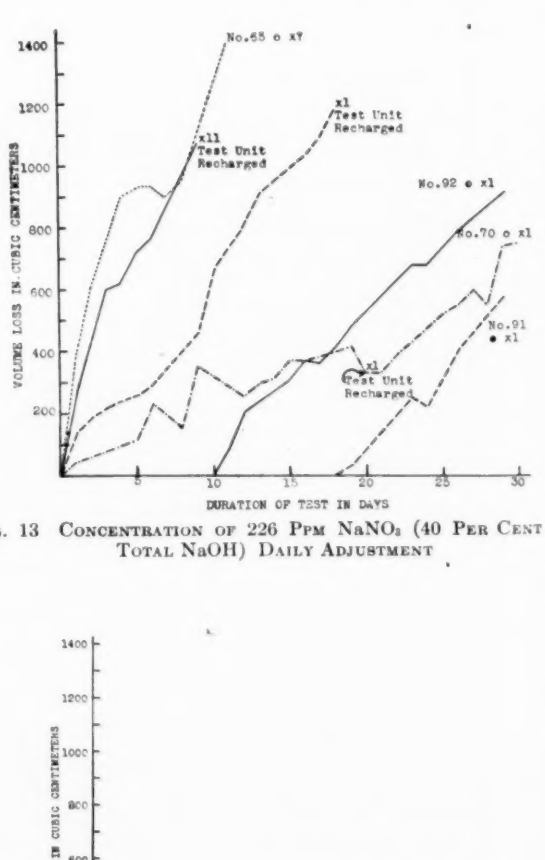


FIG. 13 CONCENTRATION OF 226 PPM $NaNO_3$ (40 PER CENT OF TOTAL NaOH) DAILY ADJUSTMENT

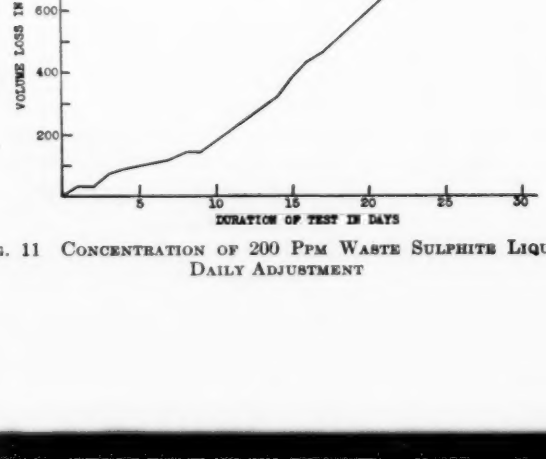


FIG. 11 CONCENTRATION OF 200 PPM WASTE SULPHITE LIQUOR; DAILY ADJUSTMENT

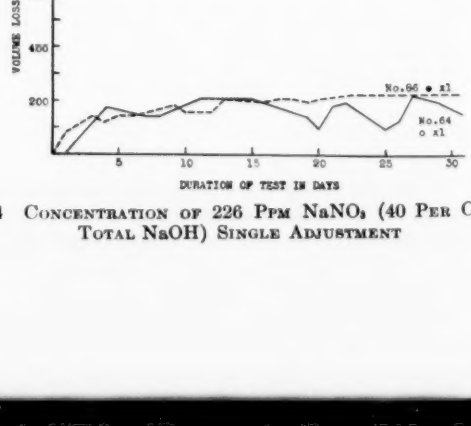


FIG. 14 CONCENTRATION OF 226 PPM $NaNO_3$ (40 PER CENT OF TOTAL NaOH) SINGLE ADJUSTMENT

report on tests run for periods of 30, 60, and 90 days under similar test conditions. Possible differences in the stress maintained on the test specimen should be considered along with the time of test. The effect of increased stress on the specimen under test has been reported by Professor Straub. In his test unit, no reasonable combination of salts would prevent failure at stresses of 10,000 psi over his established test stress of 40,000 psi.

The development of cracked specimens in any type of test equipment is necessarily dependent on maintained conditions that are favorable to such cracking. That these conditions are developed and maintained in both of the units, that have been devised, is attested by the fact that test specimens may be cracked in either type of equipment in a relatively short test period. That differences may develop in results obtained in the two test units and those obtained in operating boilers can be appreciated. A study of the results obtained in the embrittlement detector is the basis of the work to be herein reported.

Our laboratory equipment follows the general arrangement in which the detector is attached by pipes to a steel-trap body which serves as a reservoir and boiler for the solution under test. All of our equipment is electrically heated and temperatures are automatically controlled.

The personal factor involved in establishing a proper leak past the test specimen in the detector may have considerable effect on the results obtainable with this equipment. An effort to evaluate this effect lead to the development of a system for determining the solution level in the test unit at any time during the test period. This system employs an electrode consisting of a coil of resistance wire applied to the test units through a spark plug. A low-voltage alternating current is connected to this electrode and the electric circuit is completed through a milliammeter grounded to the test unit. We have found that the solution level in the units affects the current flow in the circuit and have calibrated our equipment accordingly. The current flow in the measuring circuit varies with the conductivity of the solution in the test unit, and this factor has been incorporated in our calibrations.

The use of our electrical system for solution-level determination makes it possible to construct graphs showing the rate of solution loss from the test units with respect to time. We believe that this rate of loss is an important factor in the embrittlement-detector test procedure. This knowledge of the rate of solution loss past the test specimens is particularly valuable in studying the extent of the plugging tendencies of various materials and their relation to embrittlement cracking in controlled tests. We have made a series of tests to demonstrate the importance of this factor, and the results obtained are herewith presented in graphical form.

Because of the many places where leaks may develop in the laboratory arrangement of the embrittlement detector, we have used a notation on our graphs to indicate concentration of the solution during the test procedure. Notation X-1 after a graph implies no concentration; X-2, concentrated to twice the concentration of the solution at the start of the test, etc. To minimize this factor and the resulting concentration in our tests, we have regularly tested our assembled units, when prepared for a new test, by immersing them totally in clear water, applying air pressure, and checking for leaks.

On our graphs an uncracked specimen is indicated by an open circle at the end of the graph. A cracked specimen is shown by a filled-in circle. Where a specimen exhibited slight cracks that appeared to be of the intercrystalline type, or where slight cracks were opened on bending the specimen in a hydraulic press, a half-filled circle is employed. Cold-rolled-steel specimens were used in all tests and the test pressure was 210 psi.

The accompanying volume-loss graphs, Figs. 3 to 14, are drawn as straight lines between volumes determined on successive days using the electrical measuring circuit. The indicated occasional increases in volume, shown on some of the graphs, were caused by loose wiring connections from the spark plugs on the trap bodies to the measuring panel. In later tests, all connections were soldered, and the curves obtained are much more presentable.

Fig. 3 of this discussion shows the results obtained from four blank tests where daily leakage adjustments were made in accordance with the standard embrittlement-detector test procedure. The necessity for adjustment was determined by daily inspection of the specimen leak, using a cold watch glass and checking the indication obtained with a medical-type stethoscope. By blank tests is meant tests on solutions containing 500 ppm NaOH and 100 ppm Na_2SiO_3 in distilled water. In the balance of the tests, this same basic solution was used, with additions of other materials made as indicated on the graphs. In all of the tests, a vacuum technic was employed, in filling the test units, to avoid the effect of trapped air on the test solutions. Air was eliminated from the test solutions by boiling, before the solutions were placed in the test units and before inhibitors were added.

The results shown for the blank tests indicate some plugging tendency in the single-adjustment tests, but these results are not sufficiently consistent to warrant any positive conclusions. We have found that, in starting all tests in the detector unit, it is necessary to check and adjust the specimen leak at least twice during the first day of the test. To avoid an excessively large adjustment of the leak on the so-called single-adjustment tests during the first day, these tests are checked and readjusted on the second and third days and are then allowed to continue with no further adjustment, but with a daily record of any evidence of leak past the specimen. From the data presented for the blank tests, it appears that a very slow but consistent leak past the specimen will cause positive cracking even though only 200 cc of test solution is lost past the specimen in the 30-day test period. A leak of about 150 cc during the first 5 days of a single-adjusted test, with no indicated further loss, will cause cracks to open when the test specimen is bent at the conclusion of the test.

Results using sodium sulphate are consistent with results reported by other investigators using this material in tests run in the detector unit. Except for one test, no plugging is indicated for this salt. It must be pointed out that, in our tests with sodium sulphate, we maintained the A.S.M.E. ratios, but we did not use sodium chloride, the addition of which is recommended by Professor Straub.

The results, using quebracho alone and quebracho plus sodium sulphate, indicate that very similar results are obtained in the regular or daily-adjusted tests. In the single-adjusted tests it appears that the plugging action of the straight quebracho protects the specimen; while the mixture with sulphate does not allow for effective plugging of the leak and permits the development of cracks that are intercrystalline in appearance. The sudden breaking of a plugged condition is demonstrated in tests Nos. 52, 84, and 89, and these results may indicate that a theory of embrittlement protection, based on plugging tendencies of the protective materials added, is tenable, providing conditions are not present which may serve to break such chemical plugs as are formed.

The use of waste sulphite liquor appears to provide effective sealing of leaks but, in the concentrations used in our tests, fails to prevent cracking even where relatively small amounts of liquid are lost past the specimen, and even if such loss occurs only during the first few days of the test.

The results obtained with sodium nitrate would indicate very little plugging tendency for this material. The protective action of this material is not indicated by the results we have obtained using an initial concentration of 40 per cent of the available alkalinity.

In the tests herein reported, no attempt was made to maintain a concentration of the inhibitor materials in the test solutions by a regular recharging of the test units with fresh solution. Our tests were carefully started with the desired amount of inhibitor materials added to test solutions which had been freed from air by boiling, and, unless excessive leakage during the test period made recharging of the units desirable, they were operated for the full 30-day period on their original charge of solution. Accordingly, in all of the tests using quebracho extract, an average loss of about 75 per cent of the extract was noted, but in no test was the remaining extract less than 25 ppm. Results of tests to determine possible losses of waste sulphite liquor were inconclusive. In the nitrate tests, it was found that cracking of the specimens could be attributed to there being no residual nitrate at the conclusion of the test period.

We do not consider that the results we have herein reported constitute conclusive evidence that the various materials employed to control the embrittling tendencies of the solutions tested are or are not beneficial in such control. We believe that the graphical evidence, which our equipment has made possible, is helpful in obtaining a better understanding of our results and we are hopeful that the continued use of our equipment will provide some assistance in the clarification of the embrittlement problem.

A. H. Reynolds.[19] It has been our belief, based upon published data and conversations which we have had with other investigators in the field, as well as upon results of tests that we have obtained, that the more practical type of test, as carried out by Dr. Partridge (5), is less severe than the strictly laboratory type of test, on which Dr. Bird (4) has reported.

In other words, we have had instances where specimens would show cracks in the laboratory when using the embrittlement detector, while a boiler operating on the waters tested, or a detector unit connected to the boiler using these waters, failed to show embrittlement cracking.

There are several possible explanations for this real or fancied difference in the results obtained between laboratory tests and the more practical tests where embrittlement detectors are applied directly to boilers in operation. The most logical reason, and one which will immediately be apparent to everyone, is the opportunity for a change to take place in the boiler water during transit to the laboratory. In this way certain salts may be precipitated from the boiler water and others changed decidedly because of coming in contact with oxygen or carbon dioxide.

However, there are at least two other factors which might explain in part the higher percentage of laboratory failures. The first of these possibilities is the much larger metal surface per unit volume of test solution in the laboratory equipment and the possible inhibiting or accelerating effect resulting from it. The second and probably the more important difference is the continued exposure of a limited amount of test solution to high temperature and pressure for periods of 30 days or more without any replenishment or replacement.

It is known that certain constituents of boiler water, particularly many of the organic treatments used in their conditioning, are subject to partial decomposition under the conditions of temperature and pressure used in the tests. Over a period of 30 days, this decomposition may become quite pronounced and may exert a marked influence upon the embrittling tendencies of the water tested, increasing these tendencies or decreasing them as the decomposition products are more effective or less effective inhibitors.

Having equipment and facilities available in our laboratory to investigate some of the factors referred to, a few months ago we undertook such a study. For this purpose, we connected two embrittlement detectors to a laboratory-size, electrically heated, fire-tube-type experimental boiler. The boiler is equipped with a blowdown condenser, a feedwater pump, and a Mercoid pressure regulator which regulates the electrical input to the boiler. Circulation through the detectors was assured by attaching a strip heater to one of the boiler lines. All lines to and from the detectors were heavily lagged.

The capacity of the experimental boiler, while in no way comparable with that of practical boilers, is large with respect to the capacity of the traps commonly used as solution reservoirs, or boilers in laboratory embrittlement equipment. In this type of test, the experimental boiler can be conveniently operated with 17 liters of test solution. In our tests, we proposed to blow the boiler down daily, leaving just sufficient water in it to cover the heating elements, and then to make up the blowdown volume with feedwater of the same composition as that in the boiler at the start of the test. No provision was made to take off steam, as this would introduce another variable into the test.

As a preliminary to running a series of tests to determine how various waters containing known inhibitors would show up under our modified test conditions, we decided to run one or two tests using a solution which Dr. Schroeder and his associates have used as a standard embrittling solution. This solution consists of 100 ppm of anhydrous sodium silicate and 500 ppm of sodium hydroxide in distilled water. During the running of the tests with the experimental boiler, corresponding duplicate tests were run as blanks using the same composition test solution in the small regular laboratory equipment.

The tests were run more or less in accordance with the accepted procedure. The leak past the specimens connected to the boiler and those attached to the individual units were adjusted daily, Monday through Friday. No provision was made to adjust the specimens on Saturdays or Sundays. Leakage past the specimens was determined by two methods, i.e., by sound, using a stethoscope, and visually on a cold watch glass. The experimental boiler was blown down each day, Monday through Friday, about 11 liters being removed from the boiler each time. The standard embrittling solution was used to replace the water removed by blowdown.

At the end of 30 days, the test specimens were removed from the test equipment. The two specimens, which had been attached to the experimental boiler and which had had fresh makeup water added five times a week, failed to show any evidence of embrittlement cracking, even when subsequently subjected to severe bending or microscopic examination.

Of the two specimens taken from the regular small laboratory equipment, one was badly cracked when removed from the detector and the other readily opened up cracks upon subsequent bending.

While showing that different results were obtained from the two types of equipment, the tests indicated that this difference existed to a much greater degree than we had anticipated. We questioned the accuracy of any conclusions which might be drawn from these results and immediately started repeat tests in both types of equipment. While the repeat tests were being run, we took temperature measurements of the detector units attached to the experimental boiler and of the units attached to the smaller test equipment.

Using an accurately checked thermocouple, we found the temperature of the detector blocks connected to the experimental boiler to be 265 F and the temperature of the actual specimens to be only 247 F. Similar measurements made on the smaller laboratory units showed the detector blocks to have a temperature of 335 F and the actual specimens a temperature of 320 F.

From these data, it appears that, while the detector units on

[19] Chief Chemist, Dearborn Chemical Company, Chicago, Ill.

both types of equipment were operated under a hydraulic pressure, corresponding to the 210 psi of steam pressure developed, the temperature in the detector units was very much lower than the 392 F which would correspond to this pressure. As a matter of fact, the temperatures found in the blocks and test specimens, where cracking did not take place, would correspond to only 24 and 14 psi of steam pressure, respectively. In the small units where cracking was obtained, the temperatures corresponded to 95 and 75 psi of steam pressure in the head and specimens, respectively.

The second set of tests which was run on the standard embrittling solution gave results which are substantially the same as those previously obtained.

We propose, by repiping the detectors to our boilers, or by the application of added external heat to the lines leading to the detectors, to obtain temperatures in the blocks and specimens attached to our experimental boiler which will be at least as high as those obtained in our laboratory units.

This may show that the temperature of the detector block and specimen is an unimportant factor in the results obtained by the use of this kind of testing device. It may be found, however, to be an important factor and if so would tend to explain some of the differences found between strictly laboratory tests and the more practical type of field tests, where the detectors are attached to the operating boilers. In the latter type of tests, and particularly in railroad practice, the detectors are usually mounted in exposed places, often with the feed and return lines to and from the units devoid of any lagging. In such cases the possibility for cooling through the detectors is more pronounced than it is in our equipment.

As soon as the effect of temperature of the detector units has been more clearly evaluated, we propose to investigate the factors originally considered, when we started our work, particularly the possibility of partial decomposition of certain constituents influencing the results obtained.

At any rate, regardless of whether or not subsequent results will show that detector tests on operating boilers are somewhat less severe than they might be, because of a drop in temperature through the detectors, or that tests in laboratory units are more severe than they should be, because of decomposition or other causes, there is nothing in the results obtained which would disprove in the least the statement made by Dr. Schroeder that any inhibitor which would prove entirely effective in laboratory detector tests would very probably be a satisfactory inhibitor of caustic embrittlement in operating equipment.

F. G. Straub.[20] A laboratory testing unit is of value to industry only as long as that unit is operated under conditions simulating operating conditions and, then, only when the laboratory data substantiate the operating data.

When this symposium was first suggested, the writer was under the impression that operating data were to be correlated with research data and paper (1) was so prepared as to furnish the research data, with the expectation that the operating engineers would furnish boiler data. However, it appears that the various authors and discussers have merely compared the results of two methods of laboratory testing, without the correlation of either unit with actual operating results.

Early in the development of the laboratory testing of boiler waters from the embrittlement viewpoint, we realized we were on dangerous ground, and we hesitated a long time before publishing our first paper on this method of testing. Realizing the limitations of our method of testing, we delayed placing it on the market as a universal method of testing. Many times we have been condemned for such action, but today we are inclined to believe that we followed the proper procedure. We have certainly prevented a great deal of confusion which would have resulted had we done otherwise.

The statement has been made that a laboratory embrittlement-testing unit should impose so severe a test that, if any inhibitor is found which will prevent failure under these conditions, it would serve as a universal inhibitor. We do not deny this premise; however, we question how such a test which is completely comparable with industrial operation may be devised and still give accelerated results. To obtain acceleration of the time factor, something must be sacrificed. The criticism of the Illinois embrittlement tester has been that it is not a severe enough test. The same critics state that the Bureau of Mines test unit, being a more severe test, should prove of more value. Granting this to be true, we find that the University of Illinois unit shows sulphates to have some protective values, whereas, the Bureau of Mines unit shows no protection. This condition is explained by the apparent severity of testing. The two units appear to agree when using certain organic materials and show evidence that these organic materials are of value even under the severe test conditions of the Bureau of Mines unit. When nitrates are tested, the reverse occurs. Nitrates protect the Bureau of Mines unit and do not protect the steel in the University of Illinois test unit. Is this explainable on the assumption that the University of Illinois

[20] Research Professor of Chemical Engineering, University of Illinois, Urbana, Ill.

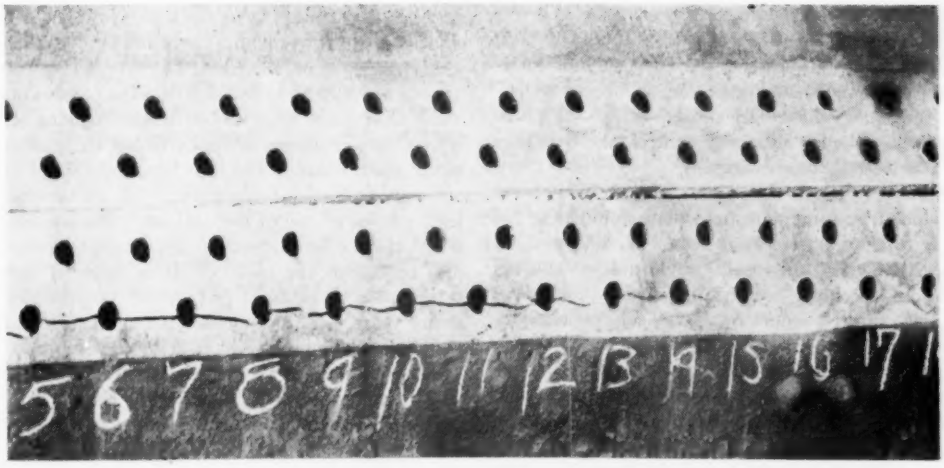


Fig. 15 Section of Cracked Boiler Showing Points of Boiler-Water Concentration

test is too severe on nitrates and not severe enough on the sulphates?

The writer has a different explanation for the results obtained, which the chemists may readily comprehend but which, it is feared, will further confuse the engineers.

Fig. 1 of the writer's paper (1) shows our test unit. The concentration takes place in the capillary space around the filler. Part of this concentration is caused by the reaction between H_2O and Fe to form Fe_2O_4 and H_2. This reaction is accelerated, and the concentration of the NaOH increases, continuing to increase as the reaction proceeds, due to the removal of H_2O by this reaction. If an alkaline nitrate solution is brought in contact with Fe and H_2 is generated, the nitrate is quantitatively reduced to NH_3. Thus, nitrates are reduced to a low value and have no protective value in these tests. Actual tests of nitrate solutions run on specimens not subjected to stress show the reduction of the NO_3 to a very low value.

Fig. 15, of this discussion, shows a section of a cracked boiler. The points of concentration are evident. How in these sections do we have the leak with subsequent concentration as explained by the Bureau of Mines unit? The University of Illinois test unit appears comparable to boiler operation.

Closures

Closure to Paper by F. G. Straub (1)

T. C. Rathbone raises the question of stress concentration caused by possible misalinement of the parts of the test unit. We realize that it is possible to have a stress higher than that actually calculated. However, there are other factors, such as the finish of the specimen, which cannot be definitely controlled.

Our purpose in developing this unit was to devise a test which would not be too complicated, and yet which would give reproducible results. We have had no difficulty in obtaining reproducible results with the unit. Consequently, we have not incorporated the finer points of refinement of construction which have been recommended.

Closure to Paper by T. E. Purcell and S. F. Whirl (2)

Mr. Einert, in his timely and constructive discussion, states that a knowledge of the pH value of the boiler water during tests Nos. 106, 107-A, and 107-B would be of interest. Such data were not deemed necessary when these tests were started and, consequently, only routine measurements were made using Hellige indicator and pH color disks. Irregularities in the alkalinity data of these tests led to the development of the curve of Fig. 8. For test No. 106, the average pH was 10.5; the corresponding value for tests Nos. 107-A and 107-B was pH 10.4. In general, these results are lower than the curve values corresponding to the phosphate concentrations and, in all probability, somewhat below the true values. In subsequent tests, where the curve has been the basis for alkalinity control, the Beckman high-resistance glass electrode has been used.

The authors doubt very much the value of the test suggested by Mr. Einert in which trisodium phosphate alone would be added to increase the pH to the value of tests Nos. 101, 102, etc. If practice conforms with theory, the results would not be expected to vary with trisodium-phosphate concentration, since, regardless of concentration, a saturated solution of this salt presumably exists at the stressed portion of the specimen.

A 90-day test recently completed indicates that some free hydroxide alkalinity can possibly be tolerated when present in conjunction with trisodium phosphate. During the test, the alkalinity was maintained at approximately 4 ppm OH ion, as measured by the modified Winkler method used for tests Nos. 106, 107-A, and 107-B in which strontium chloride was substituted for barium chloride. While both specimens developed cracks, they were not visible at 50-diam magnification until test pieces were severely distorted by cold bending.

At all times the pH was above the curve value for the corresponding trisodium-phosphate concentration. A testing program is now under way to determine the minimum hydroxide alkalinity which will produce failure under the established test conditions. Also in progress are tests to ascertain the effect of increased time.

Aside from the problem of protection against embrittlement, the method of alkalinity control, proposed by the authors, has certain other advantages worthy of mention. Mr. Einert emphasizes one of these in his discussion; namely, it offers a practical boiler-water treatment for those cases of corrosion due to faulty circulation. Instead of lowering the alkalinity to a dangerously low level, as has been practised, it is possible by this method to eliminate the aggressive agent, free OH alkalinity, without reducing the pH. This type of corrosion referred to as steam-blanketing, and so ably described by Partridge and Hall,[21] has been attributed to the chemical action of concentrated sodium hydroxide on hot boiler-tube metal. By the proposed method, the boiler water deposits trisodium phosphate alone on evaporation, sodium hydroxide being absent. Therefore, this type of metal attack is limited to the comparatively mild action of trisodium phosphate. Other advantages are simplification of the alkalinity control and the decreased blowdown, occasioned by notable reduction in boiler-water salines, as compared with the concentrations experienced when treatment complies with the recommendations of this Society. This latter condition, of course, applies strictly only when evaporated make-up is employed.

Closure to Paper by R. C. Bardwell and H. M. Laudemann (3)

The papers and discussions presented in this Symposium have been interesting, indeed, and afford a substantial contribution to the available knowledge on means for overcoming damage from intercrystalline corrosion in steam boilers. The remarks made by Professor Straub concerning the present paper would appear to require a reply.

In railroad operation, we are primarily interested in research, only to the extent that it directly affects our duties and responsibilities and is of assistance in helping actually to solve a working problem. We are not consultants and have no secrets to hide, confidences to betray, nor patents to exploit. The duties and responsibilities of ourselves and co-workers consist in obtaining and properly conditioning the water supply for 1428 locomotives and 78 steam power plants operating in nine states and 16 steamships operating on the Great Lakes and Hampton Roads, which affords a rather wide field for detailed observation. The records show that more than 44,000 water samples of widely varying quality are examined annually in our six laboratories, as well as many tests made in the field by ten full-time chemists who are specially trained for this work. All the reports are maintained in the office of one of the authors. We are constantly in touch with the boiler-inspection department concerning conditions and results in the boilers. It is believed that the correlated information thus developed, which is a matter of record over many years, is of considerable value in formulating opinions on the subject of embrittlement-cracking.

It is not claimed that the A.S.M.E. sulphate-alkalinity ratios were maintained in all locomotive boilers at all times. They were not so maintained and no effort was made to do so, as this

[21] "Attack on Steel in High-Capacity Boilers as a Result of Overheating Due to Steam-Blanketing," by E. P. Partridge and R. E. Hall, Trans. A.S.M.E., vol. 61, 1939, p. 597.

did not seem warranted because of the fact that none or much less cracking has been experienced in the same class of engines, operating at 200 psi or over, where the ratios are normally 0.5–1 to 1 than where they have been between 1.5–2 to 1.

The water used in the switch engines listed in Tables 1 and 2 of the paper (3), which is questioned by Professor Straub, is obtained from a deep well and is softened with lime and soda ash using sodium aluminate or alum as a coagulant. Tests are made at least twice daily, and the quality has been uniform since the plant was placed in service in 1923. The only other water used by these engines is raw city water, which is uniformly of such composition that it would lower the alkalinity and raise the sulphates. The sodium sulphate-alkalinity ratio in the boilers could not be below that in the treated well water for which semi-daily tests are available on which to base judgment. The fact remains that considerable cracking was experienced in these locomotive boilers and it has been eliminated, not by adding sodium sulphate and increasing the foaming troubles, but by treatment with a small amount of lignin and later with sodium nitrate, in accordance with recommendations made by the Bureau of Mines.

Similar results were experienced on the Chicago and Northwestern Railroad. One of the authors has examined several thousand boiler-water analyses on this railroad, which were made over the past 30 years, not merely the analyses for eight locomotives. He has also listened to the discussion of this trouble at a number of meetings of the American Railway Engineering Association Water Service Committee both while the trouble was in progress and since it has been eliminated. The conditions were essentially as noted, in that cracking took place on territories with relatively high sulphates, not necessarily up to or over the A.S.M.E. ratios but still relatively high, whereas no cracking was experienced in the same class of power in other districts using natural high-sodium-bicarbonate water with sulphate-alkalinity ratios of 0.05 to 1, instead of 2 to 1. The trouble has been practically eliminated since 1926, not by following the method advocated by Professor Straub and raising the sulphate content, thus suffering from foaming tendencies, but by adding a small amount of a lignin material which was one of the ingredients of an antifoam compound used in the territory of the high-bicarbonate waters.

It should be remembered that intercrystalline cracking, although troublesome and expensive at times, is one of the minor troubles to be corrected in conditioning water for locomotives and possibly ordinary power-plant boilers. In order of their importance, the real operating problems are (*a*) scale deposition, (*b*) pitting and corrosion, and (*c*) foaming. In locomotive practice, scale can be kept under control by maintaining the sodium alkalinity at 15 per cent or more of the total dissolved solids. The control of pitting and corrosion requires the maintenance of a higher alkalinity ratio, even up to 30 per cent, probably because of the high concentration of dissolved oxygen carried in with the feedwater. In controlling foaming, it is necessary to keep the total dissolved-solids concentration below the critical point for the respective type of power and local conditions. When it is necessary to maintain 30 per cent alkalinity to prevent pitting, it would be impossible, either mathematically or otherwise, to maintain a sodium sulphate-alkalinity ratio of 3 to 1 in 250-lb-pressure locomotive boilers of which there are many in service. If any appreciable amount of chlorides was present, it would be difficult to maintain a sulphate ratio of even 2 to 1. A more satisfactory remedy is needed to control intercrystalline cracking than the A.S.M.E. sulphate-alkalinity ratio, even if it is presumed that sodium sulphate will prevent cracking and the data presented in this Symposium offer no evidence to support this theory.

In our opinion and from our experience, it is felt that steam-power users owe a debt of gratitude to the Bureau of Mines and to Dr. Schroeder for determining and describing the fundamental causes for this trouble, as well as for developing a practical and workable means for controlling and eliminating the embrittling tendencies of various water supplies in boiler use. Our experience has shown us that, where boilers crack, detector specimens will crack and where the water is treated with a small amount of lignin or sodium nitrate, in accordance with the recommendation of the Bureau of Mines, cracking of the detector specimens is stopped and the cracking of boilers appears to be gradually eliminated.

Our paper was prepared and presented at the request of the Joint Research Committee on Boiler Feedwater Studies to afford a record of the extensive work which has been carried out on The Chesapeake and Ohio Railway to develop a practical solution of the troubles experienced with intercrystalline corrosion which would not interfere appreciably with operation. It is felt that much has been accomplished and, if these results are of benefit to others having similar problems, it is considered that the effort will have been worth while.

Closure to Paper by P. Partridge, C. E. Kaufman, and R. E. Hall (5)

Almost any boiler water contains enough silica to promote intergranular attack when the water is concentrated. As Mr. Betz has pointed out, any increase in silica content during shipment would scarcely alter the broad conclusions drawn concerning its effect. Routine samples of boiler water, in connection with plant detector tests, accordingly, are customarily shipped in glass containers. Wherever the silica content of a boiler water is considered to be of special significance, containers which cannot contribute silica to the water are naturally used.

Mr. Betz has also questioned the values obtained for tannin on samples of boiler water shipped in from a plant. To prevent appreciable change in the tannin concentration during shipment, a special sample of boiler water is filtered and acidified at the plant. As an example of the relative stability under alkaline and acid conditions, a boiler water containing approximately 260 ppm of NaOH and 20 ppm of tannin as determined by the tyrosin test at the time of sampling showed only 5 ppm after standing for 5 days, but a duplicate sample which had been acidified still showed 18 ppm of tannin.

It has been suggested by Mr. Owens that the process of intergranular cracking may be affected by whatever precipitates and the amount of it which does precipitate, as boiler water undergoes concentration in a capillary space. One can scarcely deny this possibility; indeed, the guess might be hazarded that many stationary boilers of the era when boiler scale was an inevitable nuisance may actually have been protected from embrittlement by the sealing of the riveted seams by calcium carbonate, calcium sulphate, or calcium silicate. It has been pointed out before that such sealing might easily be less perfect in the seams of a locomotive boiler subjected to the racking stresses of movement over the roadbed.

Turning to the embrittlement detector, it seems reasonable to assume that the daily adjustment to maintain the optimum slow rate of leakage may deliberately discount the possible protective effect of solids which might accumulate in an actual riveted seam in such a manner and to such an extent as to protect the steel. The answer to this, of course, is that anyone using the embrittlement detector deliberately desires to set up the worst possible combination of mechanical conditions so that, if failure does not develop, he may feel assured that the chemical factor in the process of intergranular corrosion has been thoroughly suppressed.

Considerable discussion has centered around the question of whether failure of a detector specimen means that the boiler in question has cracked or will crack. To the extent that the mechanical and chemical conditions in a riveted seam may duplicate those existing in the detector, one would expect the steel in the riveted seam to suffer damage as readily as the steel in the specimen. In few riveted seams, however, will all the necessary conditions be brought together as completely as in the detector. Many a boiler might, therefore, survive to a ripe old age even though the boiler water cracked a detector specimen in less than 30 days. The real significance of a cracked specimen is the mute but emphatic warning that the chemical factor has not been inhibited but is ready to go to work whenever the proper mechanical conditions exist.

Closure to Summary by W. C. Schroeder and A. A. Berk

The widespread interest in these papers, as evidenced by the variety and length of the discussion, has been most gratifying to the participants in the Symposium. A number of questions have arisen concerning the embrittlement detector, its operation, and the exact meaning of the results. The answers in general are provided in a recent Bureau of Mines publication[22] and cannot be repeated here without making this closure unduly long.

While complete agreement does not exist among all the papers, the Symposium shows surprising unanimity of opinion concerning methods which are satisfactory for preventing embrittlement. That the authors have arrived at their viewpoints by investigation in diverse fields, including laboratory research, testing on stationary and locomotive boilers, and actual observation of the sharp reduction in the cracking of locomotive boilers following the use of protective agents based on embrittlement-detector tests, lends strong practical proof of their validity. Nitrates and quebracho tannin have given satisfactory results in a considerable number of applications. The more direct method of controlling alkalinity on the basis of a phosphate-pH relationship offers a solution for the embrittlement problem at the higher pressures. A suitable inhibitor for embrittlement can now be designated for almost every boiler water and every operating pressure at which cracking has occurred.

[22] "Intercrystalline Cracking of Boiler Steel and Its Prevention," by W. C. Schroeder and A. A. Berk, Bulletin 443, Bureau of Mines, 1941.

Heat Conditions in Bearings

An Outline of Problems for Research

By MAYO D. HERSEY,[1] WORCESTER, MASS.

Offered as part of a symposium on temperature relations in bearings, this paper reviews briefly the older and newer research problems in that field.

Experimental data are needed on the over-all heat-transfer constants governing the relation of power loss to the temperature elevation in oil-film bearings. The effect of oil flow on load capacity should be further investigated. Better methods for measuring or calculating film temperature would be useful. Other problems are suggested in connection with the properties of lubricants and methods of bearing design.

The conclusion is reached that a new epoch in bearing design is approaching in which the assumption of constant viscosity must give place to a study of heat conditions. This situation is intensified by the increasing loads and speeds to be dealt with in meeting national-defense requirements.

Introduction

SPEEDING up the wheels of national defense makes the bearings run warmer. This applies literally to all forms of transportation and production. To conserve power, maintain performance standards, and reduce wear calls for improved design, better lubricants, and more intelligent control of operating conditions—accomplishments depending on lubrication education[2] and lubrication research.

Accordingly the Special Research Committee on Lubrication desired to place immediately before the Society for discussion a brief review of the recognized problems associated with heat effects and temperature rise. This has been done to provide a background for research, while reserving for later publication any critical review of the available numerical data. It is hoped that additional data may be contributed during the discussion.

The hydrodynamic theory of lubrication, reaching its most advanced form in the recent investigation by Professor Waters (59), presupposes a knowledge of the viscosity. The fact that the true film viscosity is usually in practice an unknown quantity constitutes one of the reasons why the Committee seeks to encourage research on temperature relations in bearings.

While the present survey is expressed in the language of thrust and journal bearings of the oil-film type, analogous problems are met in the lubrication of ball and roller bearings, gear teeth, cutting tools, engine cylinders, and other mechanical elements. We consider first the problem of steady running conditions, or thermal equilibrium, with special attention to heat transfer, friction loss, and load capacity. Then follow questions relating to transient conditions, nonuniform viscosity, thin-film lubrication, temperature measurement, and properties of lubricants; concluding with notes on bearing operation and bearing design from the standpoint of heat conditions.

Thermal Equilibrium

Under steady running conditions the mean temperature of the oil film in a bearing gradually reaches some maximum limiting value known as the equilibrium temperature. This remains constant as long as the ambient temperature, i.e., room temperature or temperature of the remote surroundings, remains unchanged. The corresponding temperature elevation, or difference between film temperature and ambient temperature, may be anywhere from a very few degrees, or even a fraction of one degree, up to 100 F or more, depending on a multitude of complex factors. Without some means for estimating the temperature elevation it is impossible to assign numerical values to the viscosity of the lubricant appearing in the hydrodynamic equations.

The temperature rise can frequently be estimated from previous experience with similar bearings. A more rational solution has, however, been found (4, 38, 47). This is based upon three simultaneous equations, the physical meanings of which are not difficult to understand.

The first of these equations will be some form of the classical relation expressing the power loss, H, as a function of the mean film viscosity, Z, thick-film lubrication being presupposed. Up to this point no innovation is involved except that we are to regard the speed, load, and all design factors as constants for the time being. We are starting with a single equation connecting two unknowns, H and Z. This equation will be a characteristic of the particular type of bearing.

The second relation needed is a characteristic equation for the cooling system. Such an equation will express the rate of heat transfer, H', from the lubricating film outward as a function of its temperature elevation, T, above the ambient, or room temperature. For the moment all other factors governing the rate of heat transfer are treated as constant, leaving a second equation connecting two unknown quantities, H' and T. Not only will the coefficients in this equation depend on the type of cooling system employed, but the general form of the equation may be quite different according as the bearing is air-cooled, water-cooled, or cooled by oil circulation. For the present purpose H' should be expressed in power units.

Our third relation is the characteristic viscosity-temperature equation for the lubricant, or the corresponding curve if graphical methods of solution are more convenient. The equation should be recast so as to express the viscosity, Z, as a function of the temperature elevation, T, rather than of the actual temperature, θ. This offers no difficulty since T is defined as θ minus room temperature, hence θ in the viscosity formula can be replaced by T plus a constant.

When thermal equilibrium has been reached, H' may be replaced by H since the rate of heat transfer is now exactly balanced by the rate of generating heat. This leaves only three unknowns, H, Z, and T, with three simultaneous equations available for their determination.

While there remain three equations with three unknowns in a physical sense, H can always be eliminated by equating the right-

---

[1] Consultant, National Research Council, Washington, D. C. Fellow A.S.M.E.

[2] Refer to Bibliography (48), and pp. 144–146 of Bibliography (38). Numbers in parentheses refer to the Bibliography at the end of the paper, in which references are listed chronologically by years, and alphabetically by authors within any one year.

Contributed by the Special Research Committee on Lubrication and presented at the Annual Meeting, New York, N. Y., December 1–5, 1941, of The American Society of Mechanical Engineers.

Note: Statements and opinions advanced in papers are to be understood as individual expressions of their authors and not those of the Society.

hand sides of the first two equations, leaving only two equations with two unknowns, Z and T, for the mathematical or graphical work in any particular application.

Heat Transfer

The foregoing outline provides a formal method of solution for temperature-rise and power-loss problems. Its practical use depends on the availability of heat-transfer data. Here lies one of the greatest fields for experimental research in the near future.

For air-cooled bearings with moderate temperature elevations, Newton's law of cooling may be accepted as a first approximation, according to which H' is directly proportional to T. The investigation reduces to the determination of a constant, which in turn depends on the shape and size of the bearing housing, and other factors. Values for thrust bearings have long been available (8) but are based upon bath temperature rather than film temperature. Tentative values for journal bearings have been given by Karelitz and others (15, 38). For geometrically similar bearings this constant may be taken as roughly proportional to the square of the diameter. It varies over a wide range depending on the degree of movement of the air.

With higher temperatures Lasche's law is often used (3). According to this relation the rate of heat transfer varies as the 1.3 power of the temperature elevation. Experimenting with automotive-type bearings in which air cooling was supplemented by forced lubrication, McKee found a variation nearly proportional to the 1.6 power (51).

Water-cooling by coils in the oil bath, or otherwise, is more effective than air-cooling. The rate of heat transfer depends on such factors as the speed of the shaft, shape and size of coil and housing, rate of flow, water inlet temperature, bath temperature, oil viscosity at bath temperature, and the viscosity index or temperature coefficient of viscosity. Test data should be analyzed by the method of dimensions, as in other heat-transmission problems. Little if any research work has been published in this field, though tables are available giving maximum speeds for air-cooled operation of thrust and journal bearings for any given load (8 *a* and *b*).

Forced lubrication with external cooling of the circulating oil is common practice for high-speed journal bearings in the larger sizes (14, 17, 58). The rate of heat transfer now depends on the temperature elevation of the film above the oil inlet, rather than above the room temperature, since air cooling may be neglected or dealt with separately as a small correction.

All three types of heat transfer in bearings—air cooling, water cooling, and oil circulation—require further investigation. In the meantime a slightly better foundation for thermal-equilibrium calculations may be hoped for if the existing data can be more fully collected and coordinated; in particular, data showing values of power loss and temperature elevation when running in a steady state.

Friction Loss

A formal procedure has been outlined above for calculating the temperature rise and friction loss in a bearing under equilibrium conditions when three characteristic expressions are given. These are, first, the friction function, which may be symbolized by $f_1(Z)$; second, the cooling function, $f_2(T)$; and third, the viscosity function, $f_3(T)$. Two simultaneous equations are then set up, one derived by equating $f_1(Z)$ to $f_2(T)$, the other by equating Z to $f_3(T)$. The values of the two unknowns Z and T that satisfy the two equations are the required equilibrium values. Solutions may be obtained analytically when the expressions are not too involved, otherwise graphically.

Generalizations have been proposed in two cases (48): First, when thermal expansion has a noticeable effect on the clearance and hence on the power loss; H will then depend directly on T as well as on Z. In this case an expression $F_1(Z, T)$ takes the place of $f_1(Z)$. Second, when the cooling function has a marked dependence on the viscosity of the lubricant. In this case a more general expression $F_2(T, Z)$ may be substituted for $f_2(T)$. A third generalization may be suggested for any case in which the viscosity-temperature relation cannot be explicitly solved for Z as a function of T, as in the case of Cragoe's "liquidity" function (25). If the relation is given in the form $F_3(Z, T)$ equals zero it may be used in that form, without attempting to solve for Z.

Among the illustrative examples that have been worked out (38, 47) mention may be made of an air-lubricated journal (2) and a 7-in. journal bearing with forced lubrication (44).

The simplest case usually described is that of a high-speed journal bearing following Petroff's law and Newton's law of cooling, for which an analytical solution is obtained (4). This solution is limited to a temperature range within which the viscosity relation may be expressed by a hyperbola. Other solutions have recently been obtained applicable to partial bearings, and to more exact viscosity formulas (48). The friction coefficient for the full journal bearing, when plotted against speed, is given by a curve approaching some fixed upper limit as the speed approaches infinity. The power-loss curve approaches a straight line through the origin. These results are not inconsistent with ZN/P requirements,[3] but imply an inverse variation of viscosity with speed.

Relations of this kind in which bearing performance is expressed in terms of speed, load, etc., not for a given viscosity but for a given lubricant, have been termed "working equations" (4). Such an equation is derived by eliminating the viscosity from the "characteristic" or hydrodynamic equation. This elimination is accomplished with the aid of the heat-transfer relationship; hence the importance of research on heat transfer in bearings.

Load Capacity

The definition of load capacity may be expressed in terms of film thickness, film stability, or temperature rise. These conceptions would seem to reflect the viewpoints of the designer, experimenter, and operator, respectively, though there is much ground in common.

The present-day bearing designer, accepting the hydrodynamic theory, visualizes conditions in terms of film thickness at the point of nearest approach. If rigidity and smooth finish are contemplated, he can allow a relatively low value for the safe limiting thickness (4, 19).

The experimentalist is more conscious of the transition from stable to unstable lubrication which occurs at the minimum point on the coefficient-of-friction diagram. Watching his instruments with increase of load or decrease of speed, he marks the moment when friction torque jumps rapidly up, followed by a sharp rise of temperature. This, to him, measures the ultimate load capacity, which must be avoided by assigning a factor of safety (11, 33, 50).

The operating engineer cannot see the oil film, or slow down to observe minimum points. But by touching the bearing with his hand and examining the outlet oil, he may form some judgment as to the permissible operating temperature (29, 46, 51). A limit of 50 C has been recommended by Thoma (43), while McKee advocates a combination of the minimum point and temperature requirements.

A clear setting forth of all advantages and interrelations of the several criteria would constitute, in itself, a research problem of

[3] Under thick-film conditions the coefficient of friction is fixed by ZN/P where Z denotes the mean film viscosity, N the speed in revolutions per unit time, and P the load per unit of projected area.

no slight magnitude and practical value. In particular, it should be noted that the film thickness and minimum friction criteria are not mutually equivalent, even though both are commonly expressed in terms of ZN/P. The film thickness is fixed uniquely by ZN/P, but the location of the minimum point depends somewhat on the values of the separate variables.

It is instructive to calculate load capacities from the film-thickness criterion under thermal-equilibrium conditions. An analytical solution has been given for the full journal bearing corresponding to the friction calculation described (4, 38). The resultant curve starts out from the origin with load capacity directly proportional to the speed. It then rapidly drops until, at higher speeds, the curve levels off and the load capacity remains constant. This is all on the assumption of a moderate change in viscosity with temperature. For aircraft-engine oils, having higher initial viscosities and steeper viscosity-temperature slopes, the load capacity, as shown by McKee (51), passes through a maximum and diminishes with further increase of speed.

The rated load capacities of thrust and journal bearings are generally (8 *a*, *b*) in fair accord with the analytical solution mentioned, though one catalogue (26) shows loads diminishing as the speed goes up.

The effect of oil flow on temperature rise and load capacity was investigated by Orloff (27, 34) using methods of calculation that appear to be in close agreement with Barnard's experiments (7). Here is an important problem for research on which only a beginning has been made.

Transient Conditions

The shape of the temperature-time curve is a matter of interest in connection with (*a*) heating and possible wiping of bearings when starting from rest under load; (*b*) temperature rise during momentary periods of overload; (*c*) estimating time required to approximate a steady state; and (*d*) predicting equilibrium temperature from observations during a short run.

Some progress has been made on the first two problems by the application of Kelvin's theorem for temperature rise due to a heat source distributed over the surface, with experimental confirmation (23, 28, 36, 37). Satisfactory solutions of the last two problems will require experimentation. It is to be hoped that the results of such tests can be extended to geometrically similar bearings of other sizes by the principle of similarity.[4]

Nonuniform Viscosity

The temperature cannot be strictly uniform in a lubricating film after reaching equilibrium, since the heat originating in the film can be removed only by convection and temperature gradients. It has been established that the temperature distribution across the film is approximately parabolic (5, 16), the principal deviation being due to the change in viscosity with temperature. This problem has been solved graphically and confirmed experimentally by Albert Kingsbury (23). An analytical solution by Donald Bratt will be found in the discussion of Kingsbury's paper. The problem remains of expressing the analytical solution in a more convenient form.

Boswall (12) allowed for temperature change in the direction of motion by assuming linear variation of viscosity. A more exact solution for the circumferential temperature distribution was derived by Hummel (10). It would be of value to compare this solution with the experimental findings of Nücker, Pearce, and others (21, 53) and to extend the hydrodynamic theory, if possible, to include the combined effects of temperature and pressure on viscosity.

Thin-Film Lubrication

When the load on a bearing is increased, and the speed or viscosity sufficiently decreased, the condition of operation changes from one of thick-film lubrication, governed by the hydrodynamic theory in its simpler form, to a mixed condition known as thin-film lubrication, in which the high spots on the two rubbing surfaces are beginning to experience boundary lubrication. With further increase of load and decrease in speed or viscosity, boundary lubrication predominates and finally gives way to an extreme condition of imperfect lubrication characterized by wear and seizure. Thick-film lubrication and pure boundary lubrication may be regarded as the two limiting cases of thin-film lubrication.

Wear and seizure phenomena have been investigated at great length, particularly in connection with cylinder lubrication, running-in, bearing metals, and the development of extreme-pressure lubricants (40, 46, 50, 54). These investigations have brought an increasing realization of temperature as a factor for consideration in future studies.

Relatively less has been done in the field of pure boundary lubrication (38, 50) because of the difficulty of isolating such phenomena and avoiding wear or contamination. Bowden has reported on the stick-slip phenomenon, correlating friction with surface-temperature measurements (37). Needs discovered such characteristics as directional rigidity and thixotropy in boundary films, taking care to avoid heat effects (52). It would be of interest to learn to what extent these useful, load-carrying characteristics persist in conjunction with heat effects at the higher speeds.

Thin-film lubrication embraces a variety of phenomena induced by surface irregularities, quite apart from the adsorption phenomena constituting boundary lubrication. Since these phenomena are physically simple, being complicated only in a geometrical sense, they offer inviting problems for dimensional analysis. For example, the heat generated locally by the rapid tangential motion of high spots on opposite sides of the film must have some effect on the total frictional resistance. This effect depends both on the heat capacity of the lubricant per unit volume, h, and its temperature coefficient of viscosity, a (the fractional change in viscosity per degree rise of temperature). Dimensional theory then shows that the coefficient of friction will be a function not only of ZN/P (in which Z represents the mean film viscosity) but also of h/aP (22). Thus the coefficient of friction for a given load and speed depends not only on the viscosity, Z, of the lubricant but also on the property h/a.

The same relationship was later pointed out by Vogelpohl, who found confirmation in the experiments by Voitländer (30, 45). This method of reasoning has been extended to include the effects of thermal conductivity and the pressure coefficient of viscosity (38). Further comparison of theory and experiment is therefore desirable in the field of thin-film lubrication.

Temperature Measurement

For research purposes the procedure of placing a mercurial thermometer in a drilled hole or in the oil bath or drain, is not always reliable. Thermocouple technique is now well standardized. Copper-constantan or similar couples with a direct-reading millivoltmeter of low range form a convenient setup. A vacuum flask is useful for the cold junction which may either be in melting ice, or in atmospheric air with a room-temperature thermometer attached. The hot junction may be brought close to the rubbing surface (21, 45), and thus an approximation to the bearing temperature is obtained.

[4] Thermally similar models are discussed on pp. 95–96, 119–120 of reference (38). In Equation [42], p. 95, H represents power loss per unit length; if defined as total loss, multiply left side by diameter, D.

Astonishing differences are often found when this method is substituted for older procedures, including the orthodox procedure of averaging the inlet- and outlet-oil temperatures (44, 58). It remains to correct for the temperature gradient across the film, discussed above, before the effective film temperature can be determined.

The film temperature may be estimated from observations of oil-bath temperature by formulas based upon the assumption that the oil is a perfect insulator, so that heat is removed from the film only by convection (43). When this method is applied to thrust bearings it is commonly assumed that the bearing metal remains at the bath temperature. From figures given by Michell it would appear, however, that in heavily loaded thrust bearings not more that 10 per cent of the heat is carried away by the oil, the remainder being conducted through the film into the bearing shoes (41). The two assumptions just mentioned cannot therefore be generally valid, and further research is required.

The difficulty of measuring film temperatures with perfect or imperfect lubrication has prompted the suggestion of novel methods. These range from the use of microscopic suspended particles of known melting points to the thermoelectric effect of dissimilar moving surfaces. The latter method had been suggested by Lyman J. Briggs (9, 28). When applied to large areas it involves an averaging effect recently studied by Emmons (49). In view of the widespread use that has been made of the thermoelectric method it might be of value to investigate its accuracy and methods of calibration for various applications, particularly for use under high pressure.

Properties of Lubricants

The physical properties of chief interest for lubrication in the present state of our knowledge are viscosity (regarded as a function of pressure and temperature); heat capacity per unit volume (product of density by specific heat); and thermal conductivity. If we understood better how to define and measure adhesion, wetting, and other surface properties, it is possible that significant differences between lubricants might be found and correlated with their performance.

Vogel's equation is generally accepted as an accurate expression for the viscosity-temperature relation (6) and has been used in developing the A.S.T.M. charts for kinematic viscosity (18). Similar charts for absolute viscosity are needed. Further mathematical studies of the viscosity-temperature relation have been conducted by Cragoe (13), Erk and Eck (29), Lederer (32), and Barr (35). In the meantime unpublished observations have been accumulating which could usefully be made available to extend the temperature range.

Viscosity-pressure relations have been formulated by Kiesskalt, Cragoe, Suge, and others (25, 31) while a general coordination of high-pressure data is in progress under a committee of The American Society of Mechanical Engineers. This line of experimentation has recently been extended to include preliminary studies of the consistency of oils undergoing apparent solidification under pressure (57). There is need for improvement in technique and extension of observations to higher temperatures.

A correlation of specific heat with density and temperature was given by Cragoe for petroleum lubricants (13). From these tables the heat capacity per unit volume at 100 F, in the case of an oil of specific gravity 0.90 at 60 F, may be taken equal to 136.7 in-lb per cu in. per deg F. To correct for temperature, add 0.7 per cent for every 10 deg above 100 F; and for specific gravity, 0.6 per cent for each 0.01 above 0.90.

The foregoing applies to oils of a medium V.I. (viscosity index). For 100 V.I. (low slope on viscosity-temperature diagram) add 2 per cent; for 0 V.I. (steep slope) subtract an equal amount. Cragoe's investigation is based on tests completed before 1929. Additional data have been published by Kraussold (20). An improved method of correlation has been proposed by Watson and Nelson (24). There is an opportunity for research in bringing heat-capacity values up to date, and extending them to other lubricants than straight petroleum oils.

Thermal-conductivity determinations on oils are difficult. Relatively few investigations have been reported (13, 23, 38). With increasing need for conductivity data, new determinations and correlations are in order.

To meet lubrication requirements of the near future, every encouragement must be given toward the development of improved lubricants having lower viscosity-temperature slopes, greater heat capacities per unit volume, and higher thermal conductivities.

Operating Troubles

Some bearing surfaces are expected to run warm because of heat from other sources, notably those of engine cylinders (40, 46) and steam-turbine bearings on the high-pressure side (42, 56). Others overheat from excessive friction, which in turn may be due to misalignment, eccentric loading, aeration or failure of the oil supply, and similar causes not anticipated by the designer (14, 42, 43, 55).

Graphite in some form is often recommended for high-temperature lubrication (39). Denton found that heavily loaded bearings, when overheated, ran cooler after throwing a liberal quantity of sand or emery into the lubricant (1). Possibly this combination may be regarded as the forerunner of modern E.P. lubricants (40).

While special lubricants may be necessary for gears and cutting tools, the rational treatment of bearing problems seems to lie in correct design, finish, adjustment, and selection of bearing metals (50, 54). Aircraft-engine bearings and roll-neck bearings are now designed to carry normal operating loads well above 3000 psi of projected area.[5] A good bond between bearing metal and backing, in fact good contact between all adjoining parts is essential to facilitate conduction.

Trouble analysis offers a starting point for research. The customer's plant makes an excellent laboratory if supplied with recording instruments and sufficient mutual understanding. There is constant need for coordination and intercomparison of theory, experiment, and field data on service performance.

Bearing Design

In the prehydrodynamic era, bearing design was governed by Thurston's rule according to which the load per unit area is taken inversely proportional to the surface speed. Interpreted on the assumption of imperfect lubrication with a constant coefficient of friction, this corresponds to a fixed rate of heat generation per unit area and a nearly constant upper limit of temperature. If two journal bearings of equal diameter were to be designed for different speeds, the faster one would be given the greater length.

Following the work of Reynolds it came in time to be realized that in well-lubricated bearings, the load corresponding to any fixed film thickness is proportional to the product of the viscosity by the speed (4). Thus if two bearings of the same diameter and operating at equal film viscosities are designed for different speeds, the faster one may be the shorter. Present-day methods of bearing design are based on these principles, and have been applied to a variety of problems on the assumption of a constant viscosity (19).

Length-diameter ratios have been reduced from 2 or 3 in the days of Thurston to as low as $^1/_2$ or $^3/_4$ in modern connecting-rod

[5] Reference (50), pp. 157–159, 214–215.

and roll-neck bearings. Determination of clearance-diameter ratios is more difficult, and hardly compatible with the constant-viscosity assumption, since a slight change of clearance may produce a marked difference in oil flow and temperature rise.

All signs point now to the arrival of a third epoch in bearing design, in which heat conditions must be explicitly considered (33, 43, 51). This situation can only be intensified during the national-defense period. It imposes two new requirements on bearing design, (*a*) more efficient lubricating and cooling systems, and (*b*) the calculation of film temperatures, load capacities, and other relations without assuming constant viscosity.

Recent patent literature on thrust and journal bearings shows increasing attention to cooling devices such as internal water circulation and even thermal contact between movable parts. Thus requirement (*a*) has clearly been foreseen. It is to be hoped that the necessary calculations will rapidly follow and be applied to such interesting problems as, for example, optimum clearances in journal bearings.

Conclusion

It has been predicted in this paper that with the increasing loads and speeds to be dealt with in bearing practice, a more systematic study of heat conditions will be required. Bearing design can no longer be approached as a problem in pure mechanics. Tentative methods of solution have been indicated, particularly in the case of thermal equilibrium, and some of the research problems that seem to lie just around the corner have been described.

Acknowledgment

Acknowledgment is made to the Kingsbury Machine Works, Inc., and the Morgan Construction Company for information and experience utilized in preparing the paper.

BIBLIOGRAPHY

1 "Special Experiments With Lubricants," by J. M. Denton, Trans. A.S.M.E., vol. 12, 1891, pp. 405–450.

2 "Experiments With an Air-Lubricated Journal," by Albert Kingsbury, *Journal*, American Society of Naval Engineers, vol. 9, 1897, pp. 267–292.

3 "Die Reibungsverhältnisse in Lagern mit höher Umfangsgeschwindigkeit" (Friction Relations in High-Speed Bearings), by O. Lasche, *V.D.I. Forschungsarbeiten*, Heft 9, 1903, pp. 1–59.

4 "On the Laws of Lubrication of Journal Bearings," by M. D. Hersey, Trans. A.S.M.E., vol. 37, 1915, pp. 167–202.

5 "Der Wärmeaustausch zwischen festen Körpern und Flüssigkeiten mit kleiner Reibung und kleiner Wärmeleitung" (Heat Transfer Between Solids and Fluids With Low Friction and Heat Conduction), by E. Polhausen, *Zeit. für angewandte Mathematik und Mechanik*, Band 1, 1921, pp. 115–121.

6 "Die Bedeutung der Temperature Abhängigkeit der Viskosität f. d. Beurteilung von ölen" (Significance of the Viscosity-Temperature Relation for Judging Oils), by H. Vogel, *Zeit. angewandte chemie*, Band 35, 1922, pp. 561–563.

7 "Oil Flow in Complete Journal Bearings," by D. P. Barnard, 4th, Trans. S.A.E., vol. 20, part 2, 1925, pp. 66–81.

8 "Kingsbury Thrust Bearings," Catalog C-1, Kingsbury Machine Works, Inc., Philadelphia, 1925, pp. 61–63; see also (*a*) Bulletin HV, 1931, pp. 11–13; (*b*) Bulletin S, 1932, pp. 22–25.

9 "Thermoelectric Measurement of Cutting Tool Temperature," by Henry Shore, *Journal*, Washington Academy of Sciences, vol. 15, 1925, pp. 85–88; see also (*a*) Proceedings of The Institution of Mechanical Engineers, London, 1926, p. 328.

10 "Kritische Drehzahlen als Folge der Nachgiebigkeit des Schmiermittels im Lager" (Critical Speeds Due to Yielding of the Lubricant in a Bearing), by C. Hummel, *V.D.I Forschungsarbeiten*, 287, 1926, 48 pp.

11 "The Lubrication of Surfaces Under High Loads and Temperatures," by T. E. Stanton, *Engineering*, vol. 124, 1927, pp. 312–313.

12 "The Theory of Film Lubrication," by R. O. Boswall, Longmans, London, 1928, p. 40.

13 "Thermal Properties of Petroleum Products," by C. S. Cragoe, Miscellaneous Publication M97, National Bureau of Standards, 1929.

14 "Journal Bearing Practice," by F. Hodgkinson, Proceedings of The Institution of Mechanical Engineers, London, 1929, pp. 843–904.

15 "Performance of Oil-Ring Bearings," by G. B. Karelitz, Trans. A.S.M.E., vol. 52, 1930, paper APM-52-5, pp. 57–70.

16 "A Possible Criterion for Bearing Temperature Stresses," by D. P. Barnard, 4th, *S.A.E. Journal*, vol. 30, 1932, pp. 192–197.

17 "The Film Lubrication of the Journal Bearing," by R. O. Boswall and J. C. Brierly, Proceedings of The Institution of Mechanical Engineers, London, vol. 122, 1932, pp. 423–569.

18 "Variation of Viscosity With Temperature," by J. C. Geniesse and T. G. Delbridge, Proceedings A.P.I., vol. 13M (III), 1932, pp. 56–58; see also (*a*) A.S.T.M. Standards for Petroleum Products and Lubricants, revised annually.

19 "Optimum Conditions in Journal Bearings," by Albert Kingsbury, Trans. A.S.M.E., vol. 54, 1932, paper RP-54-7, pp. 123–148.

20 "Die specifische Wärme von Mineralölen," by H. Kraussold, *Petroleum Zeitschrift*, vol. 28, 1932, pp. 1–7.

21 "Über den Schmiervorgang im Gleitlager" (On the Lubrication of Journal Bearings), by W. Nücker, *V.D.I. Forschungsheft*, 352, 1932, 24 pp.

22 "Thin Film Lubrication of Journal Bearings," by M. D. Hersey, *Journal*, Washington Academy of Sciences, vol. 23, 1933, pp. 297–305.

23 "Heat Effects in Lubricating Films," by Albert Kingsbury, *Mechanical Engineering*, vol. 55, 1933, pp. 685–688; vol. 56, 1934, pp. 120–121.

24 "Improved Methods for Approximating Critical and Thermal Properties of Petroleum Fractions," by K. M. Watson and E. F. Nelson, *Industrial and Engineering Chemistry*, vol. 25, 1933, pp. 880–887.

25 "Changes in the Viscosity of Liquids With Temperature, Pressure, and Composition," by C. S. Cragoe, Proceedings World Petroleum Congress, London, 1934, pp. 529–533.

26 "Nomy Bearings. Description—Dimensions—Loads," The Nomy Block Bearing Agency, 520 Grand Buildings, Trafalgar Sq., London, 1935, pp. 44, 46, 47, 80, 81.

27 "Coefficient of Friction, Oil Flow, and Heat Balance in a Complete Cylindrical Bearing" (in Russian), by P. I. Orloff, *Aeronautical Engineering*, Moscow, Jan., 1935, pp. 25–26.

28 "The Surface Temperature of Sliding Metals—The Temperature of Lubricated Surfaces," by F. P. Bowden and K. E. W. Ridler, Proceedings of The Royal Society of London, series A, vol. 154, 1936, pp. 364–367.

29 "Über die Temperaturabhängigkeit der Zähigkeit von Schmierölen" (Effect of Temperature on Viscosity of Lubricating Oils), by S. Erk and H. Eck, *Physikalische Zeitschrift*, Band 37, 1936, pp. 113–119.

30 "Hydrodynamische Lagertheorie und halbflüssige Reibung" (Hydrodynamic Theory and Semi-Fluid Friction), by G. Vogelpohl, *Zeit. für angewandte Mathematik und Mechanik*, Band 16, 1936, pp. 371–373; see also (*a*) *V.D.I. Forschungsheft*, 386, 1937.

31 "Collected Results on Viscosity of Lubicants Under Pressure, I—Fatty Oils," by M. D. Hersey and R. F. Hopkins, *Journal of Applied Physics*, vol. 8, 1937, pp. 560–566.

32 "Zur Kenntnis der Viskositäts-Temperature Funktion" (On the Viscosity-Temperature Function), by E. I. Lederer, *Petroleum Zeitschrift*, Band 33, 1937, pp. 2–7.

33 "Journal Bearing Design as Related to Maximum Loads, Speeds, and Operating Temperatures," by S. A. McKee, National Bureau of Standards, *Journal of Research*, vol. 19, 1937, RP 1037, pp. 457–465; Proc., G. D.,[6] vol. 1, 1938, pp. 179–186.

34 "Lubrication of Light Internal Combustion Engines" (in Russian), by P. I. Orloff; N. R. Brilling, Leningrad, 1937, pp. 125–141, 194–201.

35 "The Determination of the Viscosity of Oils at High Temperatures," by Guy Barr, Proc., G. D., vol. 2, 1938, pp. 217–221.

36 "Theoretical Study of Temperature Rise at Surfaces of Actual Contact Under Oiliness Conditions," by H. Blok, Proc., G. D., vol. 2, 1938, pp. 222–235.

37 "The Friction of Sliding Metals," by F. P. Bowden, Proc., G. D., vol. 2, 1938, pp. 236–240.

38 "Theory of Lubrication," by M. D. Hersey, John Wiley & Sons, Inc., New York, N. Y., Chapman & Hall, London, second printing, 1938.

39 "Lubrication Under High Temperature Conditions," by H. Higginbotham, Proc., G. D., vol. 1, 1938, pp. 480–486.

40 "General Discussion on Lubrication and Lubricants," Proceed-

[6] Proc., G. D., in references (33, 35), et seq., is an abbreviation for reference (40).

ings of The Institution of Mechanical Engineers, London, 1938, 2 vols.; (*a*) reprinted by A.S.M.E., New York, 1938, in one volume.

41 "Tilting Pad Bearings and Their Practical Limitations," by A. G. M. Michell, Proc., G. D., vol. 1, 1938, pp. 196–203.

42 "Bearing Problems of Large Steam Turbines and Generators," by C. R. Soderberg, Proc., G. D., vol. 1, 1938, pp. 285–296.

43 "Der Heisslauf der Gleitlager," by H. Thoma, *V.D.I. Forschung*, Band 9, 1938, pp. 149–158.

44 "Tests of a 7 by 10½ In. Bearing at 3600 Rpm," by L. M. Tickvinsky, Trans. A.S.M.E., vol. 60, 1938, pp. 393–397.

45 "Oiliness as a Result of the Heating of Lubricants," by G. Vogelpohl, Proc., G. D., vol. 2, 1938, pp. 442–451.

46 "Temperature Rise in Bearings of Automobile Engines and Its Influence on Durability," by C. G. Williams, Proc., G. D., vol. 1, 1938, pp. 336–342.

47 "Thermal Equilibrium in Journal Bearings," by M. D. Hersey, Proc. Fifth International Congress for Applied Mechanics, John Wiley & Sons, Inc., New York, N. Y., 1939, pp. 638–641.

48 "Teaching Lubrication," by L. J. Bradford, *Journal of Engineering Education*, vol. 30, 1940, pp. 870–886.

49 "Theory and Application of Extended Surface Thermocouples," by Howard Emmons, *Journal of The Franklin Institute*, vol. 229, 1940, pp. 29–52.

50 "Friction and Surface Finish," Proceedings Special Summer Conferences, Massachusetts Institute of Technology, Cambridge, Mass., 1940, pp. 157–159, 214–215.

51 "Friction and Temperature as Criteria for Safe Operation of Journal Bearings," by S. A. McKee, National Bureau of Standards, *Journal of Research*, vol. 24, 1940, RP 1925, pp. 490–508.

52 "Boundary Film Investigations," by S. J. Needs, Trans. A.S.M.E., vol. 62, 1940, pp. 331–345.

53 "Temperature Distribution and Sources in the Conventional Railway Journal Box," by E. S. Pearce, Trans. A.S.M.E., vol. 62, 1940, pp. 633–638.

54 "A Machine for Testing Bearings," by E. A. Ryder, *Metals & Alloys*, vol. 11, 1940, pp. 69–74.

55 "So You've Had Bearing Trouble," by H. L. Eberts, *Bus Transportation*, vol. 20, 1941, pp. 324–325.

56 "Temperaturuntersuchungen an hochdruckseitigen Turbinenlagern" (Temperature Investigations of Bearings on High Pressure Side of Turbine), by F. Hüttner and L. Hieble, *Archiv für Wärmewirtschaft*, Band 22, 1941, pp. 15–17.

57 "Flow Properties of Lubricants Under High Pressure," by A. E. Norton, M. J. Knott, and J. R. Muenger, Trans. A.S.M.E., vol. 63, 1941, pp. 631–643.

58 "Power Losses in High-Speed Journal Bearings," by F. C. Linn and D. E. Irons, Trans. A.S.M.E., vol. 63, 1941, pp. 617–629.

59 "Characteristics of Centrally Supported Journal Bearings," by E. O. Waters; preprinted for the Annual Meeting, New York, N. Y., December 1–5, 1941, of THE AMERICAN SOCIETY OF MECHANICAL ENGINEERS.

Discussion

A. L. BEALL.[7] It is not difficult to agree with the conclusions expressed in this paper in dealing with the type of practice for which there are no useful precedents. While heat conditions are extremely important, it is possible to design lubricant supplies to a bearing with a part of the lubricant directed to maintaining the film, while much of it is used only for cooling.

It is axiomatic that any design to provide extra cooling must insure the availability of an adequate supply of lubricant to maintain the film, and that the film supply is not subjected to a sufficiently high temperature to lower its viscosity dangerously.

Aircraft-engine bearings are now regularly designed to carry loads in excess of 8000 psi of projected area for limited periods of operation, and, in practice, frequently carry this load for extended periods. Major difficulties to overcome are eccentric loading and distortion of the material of the bearing, which are hardly legitimate lubrication problems but definitely come within the designer's province.

Highly loaded gear teeth do show the advantage of lubricants with extreme pressure properties under high-temperature operating conditions, but both in the case of gears and bearings the means of providing the lubricant, the material and finish of the surfaces exert a substantially greater effect than differences in the load-carrying ability of the lubricants thus far tested.

J. T. BURWELL.[8] The author has devoted a section of the paper to transient conditions, referring to occasions when the temperature is changing with time. The writer wishes to point out that there is another kind of transient condition, namely, when the geometry is changing with time, such as occurs during the running-in of bearings and other moving surfaces. Here the surface profile changes from the initially formed surface to the steady-state one, which is finally achieved when the run-in is complete. The mechanism is little understood, but it is known that the degree and efficacy of running-in is strongly dependent upon the temperature at which it takes place. Conversely, the amount of heat produced depends upon how well the surfaces are run in.

This question of change in surface profile brings us to the matter of surface finish per se. A great deal more work needs to be done on its effect on bearing performance. In the thin-film region, this means its effect upon the rate of heat production and tendency to gall.

Finally there is a class of phenomena which, while not related to the question of heat at all, should be mentioned because of their rather unexpected electrical nature and also because very little work has been done on them other than by the workers who postulated them. Kyropoulos[9] has suggested that a difference in dielectric constant will exist between the bulk of the lubricant in the film between moving surfaces, whose molecules are aligned by flow in the direction of motion, and the adsorbed layers of lubricant on the two surfaces, whose molecules are oriented essentially perpendicular to the direction of flow. The resulting electric field between these two regions will make dispersed solid particles in the oil stick to the surfaces, thus forming an artificial roughness which increases wear. He states that this trouble may be mitigated either by connecting the two surfaces electrically through an external circuit or by adding ionizing constituents to the oil.

Schnurmann[10] has suggested that among the many factors contributing to the phenomenon of dry solid friction should be included that of contact electrification. When two solids, one of which is a dielectric, are brought into contact and then separated, they develop residual electrostatic charges of opposite sign which can then attract each other, thus increasing the normal force holding the two together. He points out that this can become appreciable in the case of long strips of paper running over metal rolls during the course of manufacture.

The relative importance of these electrical phenomena under various conditions of friction should certainly be investigated further.

T. M. GUNN.[11] Most of us remember well the old rules of thumb used a short generation ago for the design of bearings and the rating of their loads. Their virtue consisted mainly in their simplicity, the ease with which one man could apply them as well as another. Then experimenters started work, and it was not long before the world knew that the old rules of thumb were inadequate and misleading. Technical papers galore show how misleading the old rules are, and in a spotty way begin to fill in the

[7] Research Engineer, Wright Aeronautical Corporation, Paterson, N. J. Mem. A.S.M.E.

[8] Department of Mechanical Engineering, Massachusetts Institute of Technology, Cambridge, Mass.

[9] "Experimental Studies on Non-Fluid Lubrication: Part 1, Wear Phenomena in Fluid Lubrication," by S. Kyropoulos, *Refiner and Natural Gas Manufacturer*, vol. 18, 1939, pp. 273–277.

[10] "The Mechanism of Static Friction," by R. Schnurmann, *Journal of Applied Physics*, vol. 11, 1940, pp. 624.

[11] Haddonfield, N. J.

information for new rules, new formulas, new charts. Today there are a few research workers, a few designing engineers, and still fewer operating engineers who are familiar enough with present knowledge to apply it to certain specific problems.

However, today as never before the situation demands immediate results. The pressure of these times necessitates drafting men from one field of effort to another where they have had little or no experience. Such men are forced to make decisions. Correct design is vital. The inexperienced engineer will have little time for study, and so his information must be reduced to the simplest form that will provide a safe basis for his work.

It may be said that this is a problem for technical writers. But who is the logical person to gather data, record it in useful form, correlate, plot, and show the extent to which extrapolation is safe? Does not this call for research methods and mentality? Is not this the time for investigators to review notebooks, and pick out such data as will bear on this subject; to offer the information with suggestions on correlation and methods of presentation? The results of such assembled facts and formulas should finally be drastically systematized and simplified, so that a publication will result that leads its user unfailingly to the best available answer to his problem by analysis as definite as the classification of a wildflower by reference to a book on systematic botany.

The last few years have seen the disclosure of much valuable information, but it is still arranged for the use of the research worker rather than for the practical user. The viewpoint of the latter, the ultimate consumer of this knowledge, must be kept in mind if research work of the last several years is to render its full service at this time when it is most needed.

A campaign of concerted effort along these lines will benefit all parties. The investigator will gain by the review. The mechanical designer will save time and will be able to avoid perilous guesswork. Machine operators may then determine correct operating conditions for their equipment, and even the lubricant manufacturer should find valuable information for his guidance.

J. H. Hitchcock.[12] Probably no one is better qualified than the author of this paper to point out the gaps in our present knowledge regarding the theory of lubrication, and the author has lived up to his qualifications admirably in this instance. He has outlined the phases of the problem which require further investigation, and he has simplified the task of future investigators by appending to his paper an excellent bibliography of sources on this subject.

With the present widespread use of oil-film bearings in enormous numbers, and in applications of the most varied character, and with the growing trend in this direction, resulting from the current congestion in production of antifriction bearings, it is important that effort be continued to fill in the missing parts of the lubrication picture. In the writer's opinion, the points which are in most urgent need of clarification are determination of the actual viscosity prevailing in the loaded oil film, as affected by local temperature and pressure, and evaluation of the optimum quantity of oil supply. Study of the conditions under which thin-film lubrication occurs, and determination of the friction loss and limiting load capacity with thin-film lubrication, are also essential items. It is hoped that the Special Research Committee on Lubrication will carry on its program relentlessly until workable solutions have been provided for all of these questions.

A. B. Lakey.[13] That the temperature rise in the oil film of a Kingsbury thrust bearing is proportional to the unit loading and independent of speed, in the absence of heat transfer from the film to the bearing surfaces, may be seen as follows:

The rate of oil flow in cubic inches per minute from n shoes is approximately

$$F = nhx(\pi D_m N/2) \quad [1]$$

where h is the film thickness, x the radial width of the shoe, and D_m the mean diameter of the bearing, all in inches, and N the revolutions per minute. From hydrodynamic theory

$$h = (0.0215\ \mu a D_m N/w)^{1/2}/K \quad [2]$$

where μ is the viscosity in pound-seconds per square inch, a the mean circumferential length of the shoe in inches, w the load in pounds per square inch, and K a side leakage factor equal to 1.6 for square shoes ($a = x$). Similarly the friction horsepower is given by

$$H = 3.29(10)^{-6} KA(\mu D_m^2 N^2 w/a)^{1/2} \quad [3]$$

where A denotes the total area nax, in square inches.

The ratio of the horsepower loss to the flow in gallons per minute is 231 H/F. The maximum temperature rise of the oil in passing from the leading to the trailing edge of the shoe will be 12.4 times this if we assume 12.4 hp per gpm, as the heat capacity of the oil per degree F. The mean temperature rise Δt_m may be taken equal to one half as much, or 1432 H/F. Substituting from the foregoing equations gives

$$\Delta t_m = 0.052\ w \quad [4]$$

i.e., the mean temperature rise in degrees F is equal to about one twentieth of the load in pounds per square inch under the conditions assumed.

Little information exists on the effect of suspended air under conditions of steady supply. In cases observed, the air content, although apparently high, was not enough to decrease the films to the point which caused actual bearing trouble while the supply was maintained. No means were available to trace the effect on bearing friction.

It has sometimes been assumed that the narrow entrance to the film in a thrust bearing would act as a sort of strainer for the bubbles, permitting only solid oil to enter. The throttling effect of the bubbles would probably in many cases prevent the entrance of sufficient oil to permit the film to attain its normal thickness.

We have occasionally used test tubes to trace the influence of various arrangements of baffles on aeration. We would immerse a tube in the bath permitting it to fill with the oil; then, keeping its mouth submerged, would shift it to an inverted position with the closed end above the bath. We have then noted the rate at which air has accummulated in the tube, displacing the oil. We have made point-to-point explorations of oil baths in this way and have derived some idea of the distribution of air bubbles, as affected by depth below the free surface and other circumstances.

Indirectly, aeration can be a definite cause for lubrication failure. Consider, for instance, an horizontal-shaft installation in which the nominal oil level is carried close up beneath the shaft. Then, especially if the free surface area of the oil in the system, whether in the bearing housings themselves or in reservoirs or sump tanks, is small, the introduction of air may cause an immediate rise in the oil levels, permitting the oil to touch the shaft, which will thrash up the bath into foam at a cumulative rate. Oil will be lost from the system, especially where the shafts pass out of the housings, and, if the equipment is shut down, the oil after giving up its air may end up at a dangerously

[12] Engineer, Morgan Construction Company, Worcester, Mass. Mem. A.S.M.E.

[13] Chief Engineer, Kingsbury Machine Works, Inc., Philadelphia, Pa. Mem. A.S.M.E.

low level. If this loss is not made up before the next start, there is danger of the bearings' not receiving their proper supply of oil on that run.

With the free-oil surface restricted as noted, there will be slight opportunity for the oil to give up its air in operation; hence, in such a situation, it is especially important to see that aeration cannot even start. This condition also implies that a small change in volume of the bath, whether due to aeration or other causes, will produce a large change in the elevation of the free surface of the baths.

Rapid oxidation of oil has sometimes been traced to aeration. Oxidation of bearing parts was noted in certain of these cases.

It is further true that aerated oil, especially if there is a little water present in the emulsion, will not readily give up its heat in the coolers, or indeed flow properly in piping or other passages.

M. Muskat.[14] The author has presented an excellent summary and review of the various factors involved in determining and controlling the heat and temperature conditions in bearings. He has outlined a method for calculating bearing temperatures by equating expressions for the frictional-heat generation to that for the heat-transfer dissipation, through the intermediary of an independently determined relation between the lubricant viscosity and its temperature. This method is physically sound. However, it involves the conception that the bearing or oil film has a so-called effective or average temperature. On the other hand, it requires a knowledge of heat-transfer constants and coefficients which are not readily obtainable directly. In fact, if there were a satisfactory method available for determining the bearing or lubricant-film temperature independently, the procedure suggested might perhaps be better used for the calculation of the effective heat-transfer constants.

In order to establish any theoretical procedure for calculating heat conditions in bearings it is necessary to compare the calculated temperatures with those determined by some other independent process. Such independent methods have been a subject of much consideration and the source of great difficulty in the past. Suggestions have been made that the bearing or film temperature be taken as a direct or weighted average of the inflow- and outflow-lubricant temperatures. Proposals have been made for, and some measurements reported on, the direct temperature-distribution determinations in actual bearing systems. These have involved the question as to how such bearing-temperature distributions should be averaged, and that of the relationship of the temperatures at or near the surface of the bearing to those within the lubricant film. Moreover, even if the latter could be directly measured, the problem would still remain of averaging these lubricant-film temperatures, since in all the theoretical methods for temperature calculation thus far suggested, such as the one outlined in the paper, the temperature is represented by a single parameter and hence must correspond to some type of average.

In view of these difficulties, it is proposed, at least for the purpose of establishing any general method of calculating bearing or film temperatures, and of obtaining data on actual effective or average temperatures in test bearings, that the procedures heretofore considered be reversed. That is, instead of adjusting the temperature so that the calculated heat dissipation by heat transfer should equal that generated by friction, it is proposed that the temperature be calculated directly from friction coefficients measured with the test bearings.

The basis for such a procedure lies in the observations that the Reynolds hydrodynamic theory of lubrication is strictly valid under thick-film conditions, and that there are now available satisfactory theoretical calculations for the friction performance of journal-bearing systems, even for large journal eccentricities. The former has been established quite conclusively by experiments with both journal bearings and thrust bearings,[15] which were found to give results in almost exact agreement with those predicted theoretically for the particular conditions obtaining in the experiments. It may therefore be concluded that the hydrodynamic theory can be "trusted," as it were, in the prediction of the numerical values of the friction coefficients of bearing systems operating under thick-film conditions.

The second observation refers to the extensive theoretical calculations for the friction coefficients of partial journal bearings of finite width recently reported by E. O. Waters.[16] By using Waters' results directly, or by simple extension to other partial bearings, or even to full journal bearings, we now have available means of predicting quantitatively what the friction coefficient of a particular journal-bearing system should be for a given journal speed, bearing load, and lubricant viscosity; and if the system be operated at high speeds or low loads, even the simple Petroff theory should be applicable.

In the light of this situation, the suggested procedure is essentially as follows: Quantitative friction-coefficient determinations should be made on journal-bearing systems under accurately controlled conditions and operating at speeds for which the temperature rise in the bearings may be anticipated to be comparable to those occurring in practice. For these same bearings, the theoretical friction coefficient versus Sommerfeld variable curves should be constructed. One should then simply adjust or choose the value for the lubricant viscosity entering the expression of the Sommerfeld variable to be such that the theoretically calculated friction coefficient will agree with that observed. Thus, an effective hydrodynamic average lubricant viscosity will be obtained. From the independently determined relation between the viscosity of the lubricant and its temperature, the corresponding effective hydrodynamic average film temperature will be readily obtained. By applying a heat balance one can then also determine the heat-transfer coefficients.

By this procedure one should obtain automatically the physically significant and appropriate average of the true temperature distribution of the lubricant film. The accuracy of such determinations naturally rests upon the accuracy of the measurements and the degree to which a journal bearing under ideal conditions would agree in performance with that calculated by the Reynolds equation. The latter question has already been discussed; the former is one inherent in all experimental work and should involve no greater difficulties here than generally encountered elsewhere. On the other hand, it may be noted that the errors in the calculation of the effective temperature may be significantly lower than those for the viscosity, because of the relative insensitivity of the lubricant temperature to its viscosity in the ranges normally encountered in practice in journal-bearing systems. Moreover, this method should be especially applicable to transient conditions where direct bearing temperatures would be even more susceptible to difficulties of interpretation than those for steady-state conditions.

It is, of course, realized that the method here suggested relates only to experimental test bearings. However, it is felt that it should serve to provide data, hitherto difficult to obtain satisfactorily, which may serve as a basis for developing suitable

[14] Gulf Research and Development Company, Pittsburgh, Pa.

[15] "Studies in Lubrication," by F. Morgan and M. Muskat, *Journal of Applied Physics*, vol. 10, 1939, pp. 327–334; also by F. Morgan, M. Muskat, and D. W. Reed, *Journal of Applied Physics*, vol. 11, 1940, pp. 541–548.

[16] "Characteristics of Centrally Supported Journal Bearings," by E. O. Waters, presented at Annual Meeting, A.S.M.E., New York, N. Y., December 1–5, 1941 (preprint no. 13); also "Studies in Lubrication," by M. Muskat and F. Morgan, *Journal of Applied Physics*, vol. 10, 1939, pp. 398–407.

methods for predicting film temperatures and heat conditions in bearings to be used in commercial practice.

S. J. NEEDS.[17] Referring to the author's statement that unpublished data on the viscosity-temperature relation have been accumulating, the absolute viscosities of several oils were measured over a considerable temperature range in Dr. Kingsbury's laboratory several years ago. These measurements were made with the tapered-plug viscosimeter, an instrument of the rotational type, described in a previous publication.[18] With this instrument, it is believed that the viscosity of an oil may be measured with an error not exceeding plus or minus 0.2 per cent.

Results of the the investigation mentioned are shown in Fig. 1 of this discussion, from which it appears that, for each of the oils tested, there is a linear relationship between logarithm of temperature and logarithm of viscosity over the temperature range from approximately 100 F to 225 F. In general, the measured viscosities are below the straight line at temperatures less than 100 F and above the line at temperatures greater than 225 F.

When an oil is raised to a high temperature, the lighter fractions are driven off and the viscosity increases. For this reason observations above 300 F were made as rapidly as possible. Nevertheless, it is probable that observed points above that temperature may be somewhat high. After the original observation at 300 F with Valvoline Edgewater cylinder oil, it was found that the viscosity at 100 F had increased 0.3 per cent. After the reading at 400 F the viscosity at 85 F had increased 4.9 per cent and after readings were completed at 562 F the viscosity at 85 F had increased 27.9 per cent. While this is an example of the instability of oils at high temperatures, it accounts for only a small part of the deviation from the straight-line law.

One interesting exception to the general rule that observed points on the viscosity curves (plotted as in Fig. 1) fall below the straight line at temperatures under 100 F was found in the case of Valvoline Edgewater cylinder oil. Here the viscosity began to rise above the line at 100 F and at 70 F the measured viscosity was 45 per cent above the point on the straight line. This unusual behavior was also observed by Fortsch and Wilson,[19] who found a sharp upturn in the curve for road oil at temperatures below 200 F. They suggested that this behavior was probably a colloidal phenomenon and due largely to adsorption of a film on the walls of their viscosimeter capillary at lower temperatures. In our case, this seems unlikely, since the formation of adsorbed films on the walls of the tapered-plug viscosimeter would quickly be detected by the resulting change in location of the zero film thickness. Possibly the upturn of the viscosity curve is due to the presence of an additive not in perfect solution at temperatures below 100 F.

E. A. RYDER.[20] It is stated in the paper that thermocouple technique is now well standardized. The author probably has in mind the use of thermocouples instead of glass thermometers. However, as to the actual technique of using thermocouples, there is need for much more precise methods than seem to be available at present. Under conditions at which temperature gradients in the metal parts are low, there is no great difficulty in getting accurate temperature measurements. However, where high gradients exist, there is very considerable difficulty.

We have done considerable work on the development of a thermocouple technique for measuring temperatures in the metal walls of a combustion chamber and cylinder barrel and this is equally applicable to measuring temperatures in bearings and their surrounding parts. We are now able to weld small wires to

[17] Service Manager, Kingsbury Machine Works, Inc., Philadelphia, Pa. Mem. A.S.M.E.

[18] "Heat Effects in Lubricating Films," by A. Kingsbury, *Mechanical Engineering*, vol. 55, 1933, p. 687.

[19] "The Viscosity of Oils at High Temperatures," by A. R. Fortsch and R. E. Wilson, *Industrial and Engineering Chemistry*, vol. 16, 1924, pp. 789–792.

[20] Consulting Engineer, Pratt & Whitney Aircraft, East Hartford, Conn.

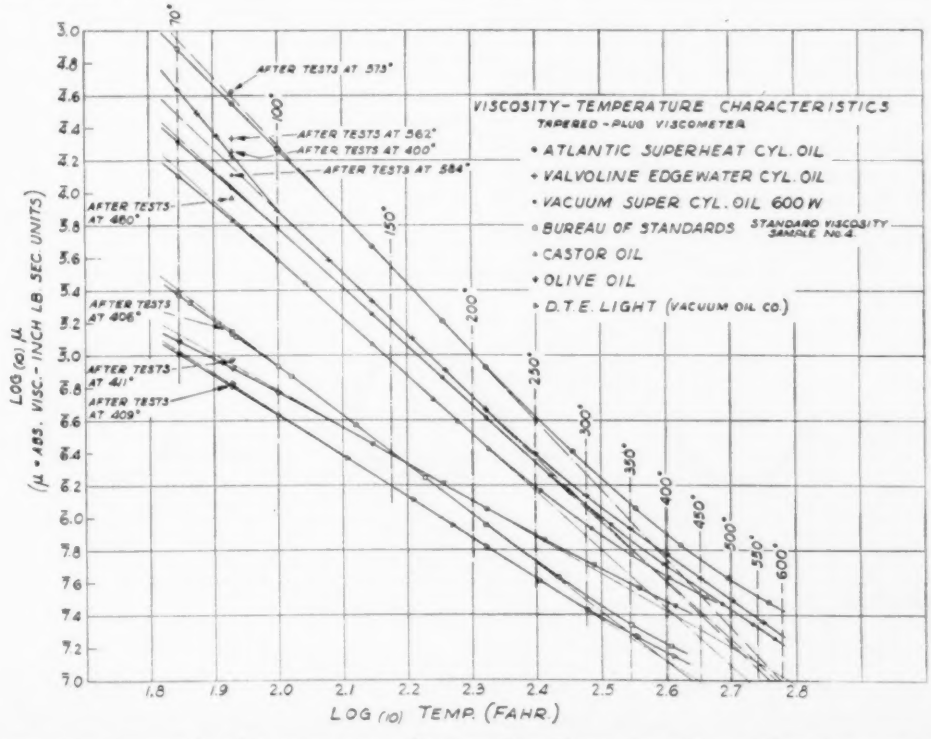


FIG 1 VISCOSITIES OF VARIOUS OILS MEASURED BY THE TAPERED-PLUG VISCOSIMETER OVER A WIDE RANGE OF TEMPERATURES

the bottom of small holes which may be drilled into the cylinder walls to any desired depth and feel that we can know the location where a certain indicated temperature exists to within 0.03 to 0.04 in. This is none too close when studying gradients in walls of only $^1/_8$ to $^1/_4$ in. thickness. It is fairly good for a cylinder-head wall which may be about 0.8 in. thick. We would like to know of some means for measuring spot temperatures to yet closer location. Stated another way, the problem is to know where the temperature exists which is read on the meter.

The author mentions as an operating trouble, excessive aeration of the oil supply. We would like to know what conditions were in mind in making this remark. We have made tests on engines in which air was introduced from the shop air line into the oil supplied to the main bearing and were never able to find much difference in the operation, that is, we could not cause bearing failure by introducing a considerable quantity of air into an otherwise satisfactory bearing.

L. M. Tichvinsky.[21] The author's outline of problems for research will undoubtedly be welcomed by everyone who works on bearing problems and on bearing design. It is hoped that bearing investigations, as outlined, will be carried on successfully and without undue duplication.

It seems to be appropriate to mention specific Diesel-engine-bearing problems. The performance of a Diesel engine is complicated because of several variables which are not encountered in stationary-power bearings.

The "rotating" load characteristic of a Diesel-engine bearing indicates that loads of various magnitudes might act along the entire circumference of the bearing. This is illustrated in Fig. 2 of this discussion, on which representative polar diagrams are given of a power bearing and of arbitrary Diesel-engine connecting-rod and main bearings.

The loading of a power bearing is produced by the weight of rotating masses and by such additional forces which might be due to gear reaction or steam force. The direction of the resultant load, therefore, varies along a relatively small angle spanning the lower bearing shell. The direction of the resultant force of Diesel-engine bearings varies during a working cycle along an arc of 360 deg. The magnitude and the direction of such resultant forces depend upon gas pressure, inertia forces of reciprocating masses, and on the resultant centrifugal force of rotating masses. The effect of gas and reciprocating forces is predominant in connecting-rod bearings of low- and medium-speed engines. The effect of centrifugal forces is usually predominant in main bearings. Unfortunately, the available literature on performance and experimentation of dynamically loaded bearings is meager and incomplete (60, 61, 62, 63, 64).[22]

Operating bearing temperatures of Diesel-engine bearings are considerably higher than of power bearings. It is difficult to cool Diesel-engine bearings efficiently in poorly ventilated crankcase space, using a low-heat-capacity lubricating oil as a coolant. Heat dissipation from small bearing housings to the crankcase ambient air takes place at a low rate.

All these unfavorable conditions are particularly aggravated in marine Diesel engines which are built to definite restricted weight and space diagrams (65).

Various types of lubricating oils used in Diesel engines might be contaminated by products of combustion. This, together with the effect of high operating temperatures endangers the satisfactory performances of bearings which are often subjected to prohibitive corrosion (66).

There is urgent need for more information pertaining to the performance of Diesel-engine bearings.

Author's Closure

Mr. Beall points out that eccentric loading and other factors may have greater effect than differences in lubricants. Attempts to take into account an eccentric load system of moment M seem to have been made in the testing machine of Fickel (67). To specify this condition dimensional analysis requires a new variable M/PD^3, where P is the resultant load per unit area and D the journal diameter, in addition to ZN/P.

Dr. Burwell discusses running-in and surface finish, and describes electrical phenomena that should be investigated.

Mr. Gunn may have put his finger on the Achilles' heel of our whole research situation, especially as applied to national defense. It is to be hoped that some codification and elucidation of results can be organized, and that in the meantime every encouragement may be given to those few teachers offering courses on lubrication in the engineering schools.

The program urged by Mr. Hitchcock should improve the efficiency of industrial bearings, and seems to call for a further development of field observations on film temperatures. The problem of optimum oil flow dovetails with optimum clearance, and might be advanced by combining Orloff's theory (27, 34) with that of Burwell (68).

[21] U. S. Naval Engineering Experiment Station, Annapolis, Md.

[22] Numbers in parentheses for (60 to 66), inclusive, refer to the Bibliography at the end of the closure.

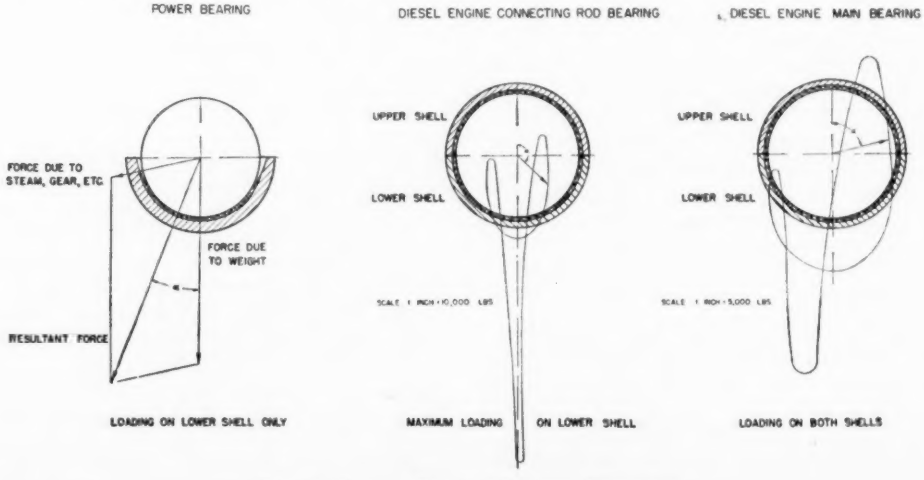


Fig. 2 Typical Bearing-Loading Diagrams

It is fortunate to have on record the derivation given by Mr. Lakey for temperature rise on the adiabatic assumption, thus providing a base for future inquiries into the effects of thermal conduction. The consequences of aeration are described in a way that should be of practical value.

Dr. Muskat offers a procedure for determining the effective film temperature in test bearings from torque observations. This procedure is logical and has something in common with the reasoning applied by Kingsbury in his study of temperature distribution across the film (23). Careful measurements of clearance are essential. It is to be hoped that these experiments may be carried through.

The viscosity-temperature data contributed by Mr. Needs were obtained with an absolute viscosimeter of unique design, and serve not only to extend the range of data available, but to reveal complications that should not be overlooked.

Our knowledge of thermocouple technique has been advanced by Mr. Ryder's discussion. It is reassuring to learn from tests that no serious aeration troubles need be feared in aircraft-engine bearings. The author had in mind conditions reported by steam-turbine operators and others (pp. 56, 69, 248, and 392–393 of Ref. 40, vol. 1). Further light is thrown upon this subject by Mr. Lakey's discussion. Experiments at Göttingen (69) show that the hydrodynamic theory gives correct results only when entry of air into the bearing is prevented.

Mr. Tichvinsky calls attention to the Diesel engine, where load diagrams are complicated and cooling arrangements restricted. A beginning has been made on the theory of fluctuating loads by Harrison (70) and Swift (71), but further study is required.

Among the problems outlined, those relating to optimum clearance and heat transfer have been discussed by Burwell (68) and Karelitz (72) in separate papers, while solutions for non-uniform viscosity due to the combined effects of pressure and temperature are given by Christopherson (73).

BIBLIOGRAPHY

60 "A Machine for Testing Bearings," by E. A. Ryder, *Metals and Alloys*, vol. 11, 1940, pp. 69–74.

61 "Lager-Prüfmaschine für Verschiedene Balastungsarten," by E. A. Cornelius and E. H. Barten, *Zeitschrift des Vereines deutscher Ingenieure*, vol. 83, 1939, pp. 1219–1221.

62 "Prüfung der Laufeigenschaften von Lagermetallen Unter Dynamischer Belastung," by H. O. Heyer, *Automobiltechnische Zeitschrift*, vol. 40, 1937, pp. 551–559.

63 "Film-Lubrication Theory and Engine Bearing Design," by E. S. Dennison, Trans. A.S.M.E., vol. 58, 1936, pp. 25–36.

64 Note the references (over 500) on general bearing performance in "Theory of Lubrication," by Mayo D. Hersey, John Wiley and Sons, Inc., New York, N. Y., 1938.

65 "Diesel Engines for the Navy," by Lieut. Commander Marshall M. Dana, U.S.N., presented at the Annual Meeting of the Society of Automotive Engineers, Detroit, Mich., January 6–10, 1941; excerpts in S.A.E. Journal, April, 1941, p. 137.

66 "Bearing Metals From the Point of View of Strategic Materials," by H. W. Gillett, H. W. Russell, and R. W. Dayton, *Metals and Alloys*, vol. 12, 1940, pp. 274–283; 445–463; 629–639; 749–758, and 768.

67 "Lagerprüfmaschine für verschiedene Belastungsarten," by E. Fickel, *Maschinenbau*, Band 19, 1940, p. 528.

68 "The Effect of Diametral Clearance on the Load Capacity of a Journal Bearing," by J. T. Burwell, Trans. A.S.M.E., vol. 64, 1942, pp. 457–461.

69 "Nachprüfung der hydrodynamischen Schmierungstheorie durch Versuche," by W. Frössel, *Forchung auf dem Gebiete des Ingenieurwesens*, Ausgabe B, Band 9, 1938, pp. 261–278.

70 "The Hydrodynamical Theory of the Lubrication of a Cylindrical Bearing Under Variable Load, and of a Pivot Bearing," by W. J. Harrison, Trans. Cambridge Philosophical Society, vol. 22, 1919, pp. 373–388.

71 "Fluctuating Loads in Sleeve Bearings," by H. W. Swift, *Journal of the Institution of Civil Engineers*, no. 4, 1937, pp. 161–195.

72 Heat Dissipation in Self-Contained Bearings," by G. B. Karelitz, Trans. A.S.M.E., vol. 64, 1942, pp. 463–464.

73 "A New Mathematical Method for the Solution of Film Lubrication Problems," by D. G. Christopherson, Proceedings of The Institution of Mechanical Engineers, January, 1942, pp. 126–135.

The Effect of Diametral Clearance on the Load Capacity of a Journal Bearing

By J. T. BURWELL,[1] CAMBRIDGE, MASS.

It has been found that there is an optimum value of the diameter-clearance ratio of a journal bearing for any given applied load. When the ratio has this value, operation is characterized by a minimum temperature rise in the bearing and a constant value of the Sommerfeld variable $\left(\frac{D}{C}\right)^2 \frac{\mu N}{P}$. These values of the diameter-clearance ratio, while considerably larger than those used in commercial practice, are quite possible of attainment by present machining methods. The use of these closer fits will result in increased load capacities and lower operating temperatures. The present paper is devoted to an investigation of the effect of D/C on the load capacity in a quantitative manner, considering both the hydrodynamic and thermodynamic aspects of bearing operation.

Introduction

IT HAS been shown by the use of dimensional analysis (1)[2] that when a journal bearing is operating hydrodynamically, the friction coefficient, the minimum film thickness, and other dependent operating variables of the system will depend upon the dimensionless products $\mu N/P$, D/C, and L/D, where μ is the viscosity of the lubricant, N the revolutions per unit time, P the load per unit projected area, D the diameter of the bearing, L the axial length of the bearing, and C the difference in diameters of shaft and bearing. If all the quantities are expressed in the same system of units, then the numerical values of the products are independent of the particular system used. If the heat balance in the bearing is taken into account, then, as we shall see later, the operation will also depend upon the thermal properties of the system. Furthermore, Sommerfeld's (2) work on the infinitely long bearing and the subsequent approximate treatment by Muskat and Morgan (3) of bearings of finite axial length make it seem fairly certain that operation of a bearing with a given axial length-to-diameter ratio L/D is determined by the composite expression $\left(\frac{D}{C}\right)^2 \frac{\mu N}{P}$ often called the Sommerfeld variable and denoted by S.

Indeed, numerous experiments have shown that bearing assemblies of a given type, i.e., made of the same materials, using the same oil, and having the same finish on the rubbing surfaces, will all be characterized by the same minimum value of $\left(\frac{D}{C}\right)^2 \frac{\mu N}{P}$ which marks the limit of safe operation of the assembly, and hence determines its load capacity. It would appear from the foregoing that it is necessary only to increase the ratio D/C indefinitely in order to carry any desired load and keep $\left(\frac{D}{C}\right)^2 \frac{\mu N}{P}$ above the minimum. On the other hand, the smaller clearance would result in higher rates of shear in the lubricant and, hence, higher temperatures with correspondingly lower viscosity so that the net result might even be a decrease in $\left(\frac{D}{C}\right)^2 \frac{\mu N}{P}$. It is the purpose of the present paper to investigate the question of the effect of D/C on the load capacity in a quantitative manner, considering both the hydrodynamic and thermodynamic aspects of bearing operation.

This question has now become of practical interest for two reasons, as follows:

1 Several trends in modern bearing design have been such as to favor the use of smaller clearances. These include the use of smaller axial length-to-diameter ratios which makes the effect of shaft deflection and misalignment much less important; the use of more accurate machine tools and techniques as applied to both shaft and bearing which makes better and closer fits possible; and finally the fact that the attention of both designers and builders has been attracted to the importance of controlling and improving the surface finish. Improvement in each of these three respects will render smaller clearances possible. It will be shown in the present work that the use of small clearances, smaller than are generally used at present, has very distinct advantages.

2 The question of the effect of the diameter-clearance ratio on operation becomes important in studying the mechanism of the running-in process. During the running-in of hard bearing materials it seems probable that the only change in geometry of the system is the smoothing of rough surfaces and local wear on isolated high spots but when softer bearing materials, notably babbitt, are run-in a momentary failure of the oil film may result in a wiping of the entire loaded side of the bearing by the shaft. As a result, the curvature of this portion of the bearing is appreciably changed and the diameter-clearance ratio becomes different. It is of great interest to know how this change will affect the operation of the bearing; to know whether it will be advantageous or detrimental. The application of the results to this type of running-in of soft bearing materials will be discussed.

Equations for Thermal Equilibrium

The treatment given here follows that outlined by Hersey[3] and employed by McKee (4) to determine the safe load capacity of a bearing as a function of the speed and other variables.

The rate of heat production in a journal bearing is given by the equation

$$H = fPLD \cdot \pi DN \quad [1]$$

where H is the rate of heat production, f is the friction coefficient, and the other symbols have their previously assigned meanings.

The rate of heat dissipation in bearings can be described (4, 5) by the equation

$$H' = B\pi LD(\Delta T)^a \quad [2]$$

Here ΔT is the rise in temperature of the bearing above its surroundings, and B and a are empirical constants, depending upon the type of housing and surroundings, but are roughly independent of the dimensions.

[1] Department of Mechanical Engineering, Massachusetts Institute of Technology.

[2] Numbers in parentheses refer to the Bibliography at the end of the paper.

Contributed by the Special Research Committee on Lubrication and presented at the Annual Meeting, New York, N. Y., December 1-5, 1941, of The American Society of Mechanical Engineers.

Note: Statements and opinions advanced in papers are to be understood as individual expressions of their authors and not those of the Society.

[3] Bibliography reference (1), chap. 5.

The condition for thermal equilibrium is given by equating H and H'

$$fPLD \cdot \pi DN = B\pi LD(\Delta T)^a \quad [3]$$

As previously stated, it is now well established that the friction coefficient is some function of $\left(\frac{D}{C}\right)^2 \frac{\mu N}{P}$ and $\frac{L}{D}$, and the relationship, as shown by the theoretical work of Sommerfeld (2) and Muskat and Morgan (3), is of the form

$$\frac{D}{C} f = \varphi\left[\left(\frac{D}{C}\right)^2 \frac{\mu N}{P}, \frac{L}{D}\right] \quad [4]$$

The explicit form of the function φ has never been derived from hydrodynamic theory, but the wealth of experiments on the Equation [4] relationship have produced a number of empirical expressions. Very careful experiments (6) indicate that Equation [4] can be described approximately by an equation of the form

$$\frac{D}{C} f = K_1 \left(\frac{D}{C}\right)^2 \frac{\mu N}{P} + K_2 \quad [5]$$

where K_1 and K_2 depend upon L/D and the length of the bearing arc, but are independent of D/C. There is some indication (3, 7) that, in cases where sufficiently low values of $\left(\frac{D}{C}\right)^2 \frac{\mu N}{P}$ can be attained, the friction-coefficient curves cease to be straight lines and curve downward toward the origin. Indeed, theory would indicate an intercept of unity on the D/C axis when the friction torque is measured on the shaft, and an intercept of zero when it is measured on the bearing. In this case, the exponent of $\left(\frac{D}{C}\right)^2 \frac{\mu N}{P}$ in Equation [5] should be less than unity.

Finally it is well known that the viscosity of a lubricant is strongly dependent upon both the temperature and pressure, and this furnishes us with the third necessary relation. It will be sufficiently accurate for our purposes to take this relationship in the form

$$\mu = \frac{\mu_0 e^{bP}}{(T_P + \Delta T)^m} \quad [6]$$

This form of the temperature dependence was first suggested by Slotte (8). Here μ_0, T_P, m, and b are constants for a given lubricant, and T_P may be considered the difference in temperature between the solidifying point of the oil and room temperature at atmospheric pressure. In this treatment the dependence of m on P and of b on T is neglected although they may be quite appreciable for the naphthenic oils (9).

Two Conditions for Stable Operation

We have the three Equations [3], [5], and [6] in the three quantities f, ΔT, and μ. Now there are two conditions which limit the practical operation of a journal bearing. The first is the hydrodynamic condition that $\left(\frac{D}{C}\right)^2 \frac{\mu N}{P}$ must always exceed a definite minimum value, say S_0, which is characteristic of the particular assembly and is dependent upon nonhydrodynamic properties of the system. Below this point metal-to-metal contact takes place between bearing and journal, and additional heat is produced, which in turn thins and reduces the carrying capacity of the supporting oil film, so that more metal-to-metal contact can take place. This is an unstable condition and automatically leads to seizure. Above this minimum value, operation is hydrodynamic and stable.

The second condition for safe operation is that the temperature rise in the bearing ΔT shall not exceed a certain amount, otherwise the oil deteriorates rapidly and the softer bearing materials may even melt and flow.

These two conditions lead to two different equations. First put

$$\left(\frac{D}{C}\right)^2 \frac{\mu N}{P} = S_0 \quad [7]$$

where S_0 is a constant. This determines a value of f by Equation [5]

$$\frac{D}{C} f = K_1 S_0 + K_2 \quad [8]$$

Substituting this value of f in Equation [3] and eliminating μ and ΔT between Equations [3], [6], and [7], we obtain, after rearrangement, the relation

$$e^{bP} \cdot bP = \frac{bS_0}{\mu_0 N} \cdot \left(\frac{P}{D/C}\right)^2 \cdot \left[\left(\frac{\{K_1 S_0 + K_2\} DN}{B}\right)^{1/a} \cdot \left(\frac{P}{D/C}\right)^{1/a} + T_P\right]^m \quad [9]$$

This form of the equation is chosen because it is convenient for calculation.

If next we set ΔT equal to a constant ΔT_0 in Equations [3] and [6], and then eliminate μ and f between Equations [3], [5], and [6], we obtain after rearrangement

$$e^{bP} \cdot bP = \frac{bK_2(T_P + \Delta T_0)^m}{K_1 \mu_0 N} \cdot \frac{P}{D/C} \cdot \left[\frac{B(\Delta T_0)^a}{K_2 DN} - \frac{P}{D/C}\right] \quad [10]$$

This equation also gives the load capacity as a function of the clearance ratio, but this time for a given temperature rise in the bearing.

In Figs. 1 to 5 we have chosen particular numerical values for the quantities occurring in Equations [9] and [10], and have plotted P as a function of D/C for values of S_0 equal to 0.005, 0.05, 0.267, and 0.5, and for values of the temperature rise of 170 F, 220 F, and 270 F. As an example, we have employed the dimensions and operating data of the friction-testing machine described elsewhere (7). It employs a partial bearing of 147-deg arc, and the friction-coefficient curves given in the reference can be best fitted with $K_1 = 7.5$ and $K_2 = 2$. The radius of the bearing is $2^1/_{16}$ in., and its axial length 1.08 in. Lasche (5) found experimentally that for the conventional type of bearing housing $a = 1.3$, while McKee (4) found $a = 1.65$. We have taken $a = 1.5$ in plotting these curves. Following Lasche, we have taken $B = 2.9$, when H is expressed in Btu per hour, L and D are in feet, and ΔT is in degrees F. The measured viscosities of both grades of oil considered over the temperature range from room temperature to 350 F are well represented by Equation [6], if m is taken as 3. In all the plots except Fig. 2, $b = 2 \times 10^{-4}$ sq in. per lb which from the data of Dow (9) is intermediate between a Pennsylvania and a California oil. In Fig. 2 the effect of neglecting the dependence of viscosity upon pressure, i.e., $b = 0$, is shown. Term T_P has been taken as 80 F. Calculations are made for three speeds, 500, 1500, and 2500 rpm, and two grades of oil, an S.A.E. 10 for which $\mu_0 = 0.096$ when the viscosity is expressed in lb-min per sq in., and the temperature in deg F, and an S.A.E. 30 oil for which $\mu_0 = 0.225$.

For large values of P the curves of constant S_0 bend toward the P axis as shown in Fig. 4 but for most of the range of practical interest, it can be said that the load capacity for a given S_0 increases as D/C increases.

The curves for a constant temperature rise show an increase in load capacity with increasing D/C up to a certain point after which it decreases again to zero. From this point of view there

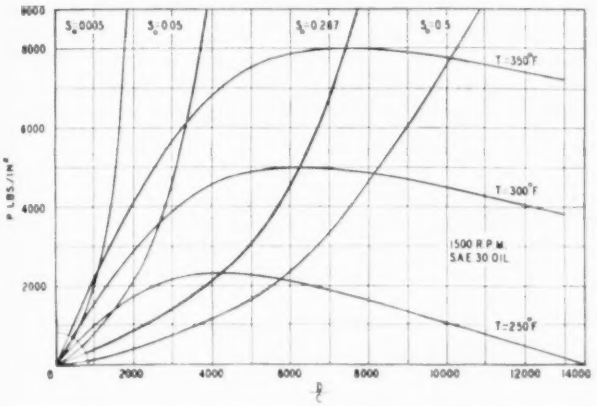


FIG. 1 DEPENDENCE OF LOAD ON DIAMETER-CLEARANCE RATIO FOR CONSTANT VALUES OF TEMPERATURE RISE AND CONSTANT VALUES OF SOMMERFELD VARIABLE
(Speed 1500 rpm; oil S.A.E. 30.)

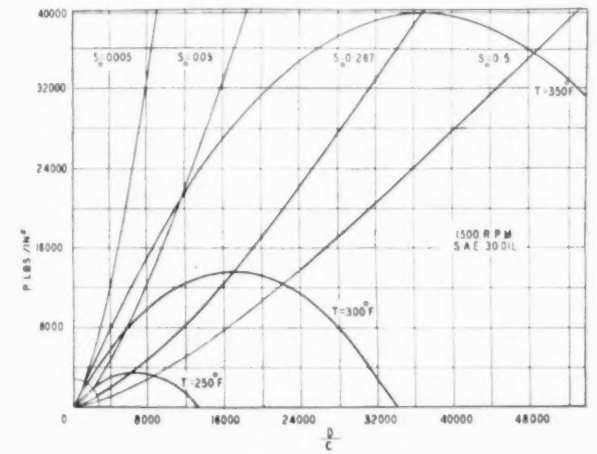


FIG. 2 DEPENDENCE OF LOAD ON DIAMETER-CLEARANCE RATIO FOR CONSTANT VALUES OF TEMPERATURE RISE AND CONSTANT VALUES OF SOMMERFELD VARIABLE, NEGLECTING DEPENDENCE OF VISCOSITY ON PRESSURE, I.E., $b = 0$
(Speed 1500 rpm; oil S.A.E. 30.)

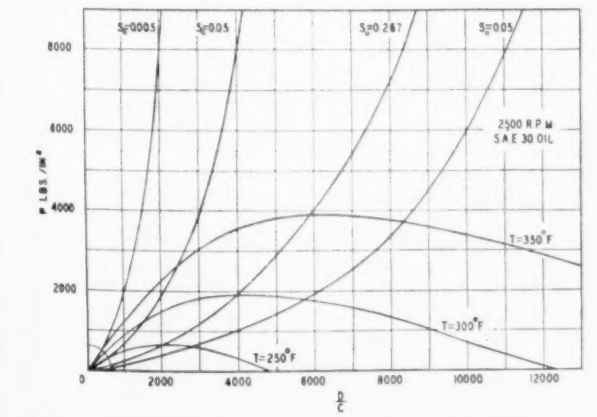


FIG. 3 DEPENDENCE OF LOAD ON DIAMETER-CLEARANCE RATIO FOR CONSTANT VALUES OF TEMPERATURE RISE AND CONSTANT VALUES OF SOMMERFELD VARIABLE
(Speed 2500 rpm; oil S.A.E. 30.)

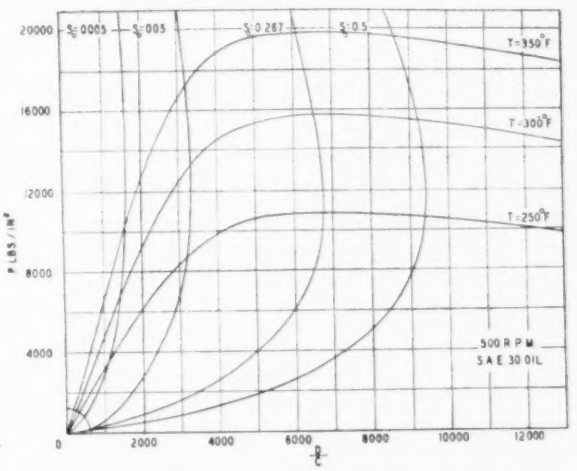


FIG. 4 DEPENDENCE OF LOAD ON DIAMETER-CLEARANCE RATIO FOR CONSTANT VALUES OF TEMPERATURE RISE AND CONSTANT VALUES OF SOMMERFELD VARIABLE
(Speed 500 rpm; oil S.A.E. 30.)

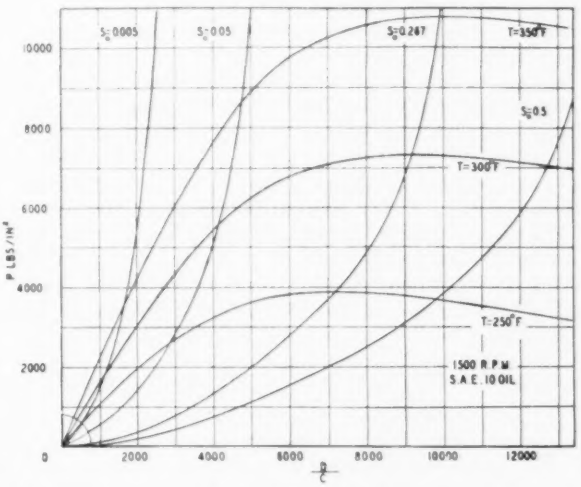


FIG. 5 DEPENDENCE OF LOAD ON DIAMETER-CLEARANCE RATIO FOR CONSTANT VALUES OF TEMPERATURE RISE AND CONSTANT VALUES OF SOMMERFELD VARIABLE
(Speed 1500 rpm; oil S.A.E. 10.)

is a limit as to how much it is desirable to increase D/C. It will be noted from Fig. 2 that when $b = 0$, these curves become parabolas.

The maxima of these curves are of interest. Since $e^{bP}bP$ is an increasing function of P for all positive values of P, then a maximum in the value of the function will yield a maximum value of P, hence

$$\frac{d}{d(D/C)}\left(e^{bP}\,bP\right) = \frac{bK_2(\Delta T_0 + T_P)^m}{K_1\mu_0 N}\cdot\left[\frac{B(\Delta T_0)^a}{K_2 DN} - 2\,\frac{P}{D/C}\right]\cdot \frac{\frac{D}{C}\cdot\frac{dP}{d(D/C)} - P}{(D/C)^2} = 0$$

At the maximum $\dfrac{dP}{d(D/C)}$ is also zero so that the only maximum occurring for positive values of P is characterized by the expression

$$\frac{D}{C} = \frac{2K_2DN}{B(\Delta T_0)^a}\cdot P_{max} \qquad [11]$$

Substituting this value of D/C into Equation [10], we obtain the expression for P_{max}

$$e^{bP_{max}} \cdot bP_{max} = \frac{bB^2(\Delta T_0)^{2c}(T_P + \Delta T_0)^m}{4K_1K_2\mu_0D^2N^2} \quad [12]$$

If Equations [11] and [12], together with Equation [6] for μ, are substituted into the expression $\left(\frac{D}{C}\right)^2 \frac{\mu N}{P}$, we find

$$\left(\frac{D}{C}\right)^2 \frac{\mu N}{P} = \frac{K_2}{K_1} \quad [13]$$

This is independent of the temperature rise and shows that the maximum load that can be carried for any temperature rise will always yield the same value of $\left(\frac{D}{C}\right)^2 \frac{\mu N}{P}$, namely, $\frac{K_2}{K_1}$. Hence, if the diameter-clearance ratio can be varied to obtain the maximum load capacity, the bearing should never have to operate below this value. It will be seen from the illustrations that the curve $S_0 = \frac{K_2}{K_1} = 0.267$ passes through the maxima of all three curves.

Discussion

Safe operation of the bearing requires that both criteria must be satisfied. This means that the region in Figs. 1 through 5 which lies below both the curve for the selected S_0 and that for the operating temperature, represents the region of safe operation, i.e., a bearing with a given D/C will safely carry a given load P if the point determined by these two values lies in this region. All the rest of the area of Figs. 1 through 5 represents a region of unsafe operation, one or both of the conditions being violated. It is seen that, in order to remain above the limiting value S_0, the clearance ratio should be increased as the load is increased but, for a given temperature rise in the bearing, there is a maximum load which cannot be exceeded no matter how the diameter-clearance ratio is varied.

The locus of these maxima is the curve $S_0 = \frac{K_2}{K_1}$ which is independent of the temperature rise. The axial length of the bearing does not appear explicitly in either Equation [9] or [10]; it does, however, enter implicitly through K_1 and K_2 which depend, not upon the absolute value of the axial length, but rather on its ratio to the diameter L/D. Term K_2/K_1 decreases as L/D increases and, although the exact functional relationship is unknown, Equation [5] being only an approximation, K_2/K_1 is rarely less than 0.05, so that it is generally possible to operate a bearing safely at this value of $\left(\frac{D}{C}\right)^2 \frac{\mu N}{P}$.

This being the case, we are now in a position to find the optimum value of the diameter-clearance ratio for any given set of conditions. If a bearing whose characteristics are known is required to carry a given load at a given speed using a given oil, then Equation [12] will give the temperature rise to be expected. Using this calculated temperature rise the correct value for the diameter-clearance ratio can be calculated from Equation [11]. This is the least temperature rise that can result from that load as far as variation in D/C is concerned; but if even that temperature is excessive, then a lighter oil will have to be used as shown by Equation [12].

It is evident from the illustrations that these optimum values of the ratio are considerably larger than those in common use today. However, these are quite possible of attainment with the more refined machining techniques at present available. In order to produce these closer fits, more and more accurate geometry is required, both as regards large-scale trueness and also small-scale roughness. For instance, at 1500 rpm, using an S.A.E. 30 oil, the bearing for which the graphs in Fig. 1 are calculated should have a diameter-clearance ratio of 1 part in 2300 to carry a load of 1000 psi, and a ratio of 1 part in 6250 to carry a load of 5000 psi. The bearing will in both cases operate at a value of $\left(\frac{D}{C}\right)^2 \frac{\mu N}{P}$ of 0.267.

It should be pointed out that Equations [9] and [10] are quite general and show the dependence of the load capacity not only on the diameter-clearance ratio, but also on the speed, the oil, and the characteristics of the bearings. Hence, for a bearing whose ratio has already been determined, it may be found from Equations [9] and [10] what grade of oil to use for a given load and speed. In this connection it is clear from Equation [9] that McKee's statement (4) that an increase in viscosity increases the load capacity for a given minimum value of $\left(\frac{D}{C}\right)^2 \frac{\mu N}{P}$ is only true if the change of viscosity with pressure is neglected. If the latter is taken into account, a lighter-grade oil can carry the load at the higher pressures. Equation [10] shows that this is definitely desirable from the point of view of minimizing the temperature rise. For example, an S.A.E. 10 oil at 5000 psi may have the same viscosity, and hence the same load capacity, as an S.A.E. 30 oil at atmospheric pressure and will run much cooler.

These results were obtained by assuming a particular form of the function φ in Equation [4] for the friction-coefficient curve although this form has been shown by numerous experiments to simulate actual operation closely. However, the general features of the plotted curves are preserved for a wide variety of assumed forms for φ so long as they approximate the experimental values. The general shape of the curves of constant S_0 do not depend upon the form of φ anyway, and it can be shown by minimizing the friction force $fPLD$ that the curves of constant temperature rise will always show a maximum provided that

$$\frac{\partial \varphi}{\partial S} = \frac{1}{2}\frac{\varphi}{S}$$

where $S = \left(\frac{D}{C}\right)^2 \frac{\mu N}{P}$. This condition will always be satisfied at some point on any curve having the same general shape as the experimental friction-coefficient curve. Hence, our conclusions about an optimum diameter-clearance ratio are not affected by the particular assumed form of φ.

As stated in the introduction, the running-in of soft bearing materials may, under high loads, produce a wiping of the bearing surface with a resultant change of curvature. This change is always in the direction of conforming more closely to the shaft, which means that the D/C ratio for the assembly has been increased. It is apparent from the accompanying illustrations that such a change will always increase the operating value of $\left(\frac{D}{C}\right)^2 \frac{\mu N}{P}$ which is in itself advantageous. Furthermore up to a certain point which is characterized by $S_0 = \frac{K_2}{K_1}$, it will decrease the bearing temperature, which is also advantageous; but beyond this point the temperature will rise again with accompanying thinning and increased deterioration of the oil. This will increase the tendency of the surfaces to wipe, thus producing an unstable condition leading to failure. This wiping may prove beneficial or it may prove detrimental. This will depend upon whether it takes place gradually so that when the optimum value of the diameter-clearance ratio is reached the bearing has an opportunity to operate stably, or whether the change takes place in one step producing a D/C far to the right of the optimum value, thus producing high temperatures and leading to failure. How-

ever, if the temperature rise for the given applied load is excessive even with the optimum clearance, then failure is bound to result and the only possibility is to use a lighter oil. It may be concluded then that under certain controlled conditions the change of curvature of a soft metal bearing surface during running-in may be beneficial.

Summary and Conclusions

The effect of the diameter-clearance ratio on the load capacity of a journal bearing has been investigated, considering both the hydrodynamic and thermodynamic aspects of its operation. It has been found that, from the point of view of remaining above a minimum value of $\left(\frac{D}{C}\right)^2 \frac{\mu N}{P}$, the ratio must be increased as the load is increased. It has also been found that for any given applied load there is a minimum temperature rise when the ratio has the proper value. This value can be calculated from the formulas given. It varies with the applied load, but the value of $\left(\frac{D}{C}\right)^2 \frac{\mu N}{P}$ at these points of minimum temperature is independent of all the variables except the axial length-to-diameter ratio of the bearing. The actual value of $\left(\frac{D}{C}\right)^2 \frac{\mu N}{P}$ is such that it is entirely feasible to operate bearings at these points of minimum temperature. The values of the diameter-clearance ratio thus required, while considerably larger than those used commercially today, are quite possible of attainment. The use of these closer fits should result in increased load capacities and lower operating temperatures.

From the formulas presented one can also determine the correct oil to be used for a given load and speed in a bearing whose diameter-clearance ratio has already been fixed.

BIBLIOGRAPHY

1 "Theory of Lubrication," by M. D. Hersey, John Wiley & Sons, Inc., New York, N. Y., chap. 4, 1938.

2 "Zur hydrodynamischen Theorie der Schmiermittelreibung," by A. Sommerfeld, *Zeitschrift für Mathematik und Physik*, vol. 50, 1904, pp. 97–153.

3 "Studies in Lubrication; Parts I, III, and V," by M. Muskat and F. Morgan, *Journal of Applied Physics*, vol. 9, 1938, pp. 393–409; vol. 10, 1939, pp. 46–61 and 398–407.

4 "Friction and Temperature as Criteria for Safe Operation of Journal Bearings," by S. A. McKee, U. S. National Bureau of Standards, *Journal of Research*, vol. 24, 1940, pp. 491–508.

5 "Die Reibungsverhältnisse in Lagern mit hoher Umfangsgeschwindigkeit," by O. Lasche, *Zeitschrift des Vereines deutscher Ingenieure*, vol. 46, 1902, pp. 1881–1890.

6 "Studies in Lubrication; Parts II and IV," by F. Morgan and M. Muskat, *Journal of Applied Physics*, vol. 9, 1938, pp. 539–546; vol. 10, 1939, pp. 327–334.

7 "Effects of Surface Finish," by J. T. Burwell, J. Kaye, D. W. van Nymegen, and D. A. Morgan, Journal of Applied Mechanics, June, 1941, p. A-49.

8 "Om den inre friktronen hos vätskor," by K. F. Slotte, Öfversigt af Finska Ventenskaps-Societetens Förhandlingar, Helsingfors, vol. 32, 1890, pp. 116–149.

9 "The Effects of Pressure and Temperature on the Viscosity of Lubricating Oils," by R. B. Dow, *Journal of Applied Physics*, vol. 8, 1937, pp. 367–372.

10 "Friction of Journal Bearings as Influenced by Clearance and Length," by S. A. McKee and T. R. McKee, Trans. A.S.M.E., vol. 51, 1929, paper AMP-51-15, pp. 161–171.

Discussion

B. L. Newkirk.[4] The author has not dealt with the question of stability of operation of bearings with large D/C ratios. If the journals ran more nearly concentric with these bearings than in ordinary bearings with smaller D/C ratios, we might question whether whirling might not develop at speeds well below twice the critical speed of the rotor. It is known that the speed at and above which whirling due to oil action occurs in bearings with smaller D/C ratios may be increased by increasing unit loading or by other measures which cause the journal to run farther from the bearing center. Conversely a lightly loaded journal will support whirling at lower speeds. If the theoretical possibilities of these large D/C ratios look attractive, it would seem that experimental studies should be made to throw light on the whirling characteristics of bearings of such proportions.

Author's Closure

The author agrees with Professor Newkirk that any experimental investigation of the performance of journal bearings with large D/C ratios should include a study of their stability with reference to oil whirl. It seems doubtful that whirling will develop at speeds appreciably below twice the critical since this is not observed even with vertical shafts in guide bearings where the shaft and bearing are most nearly concentric. The unusually small clearance may, however, be expected to affect this stability in two ways. First, the amplitude of the whirl will be small, and second, small displacements or deflections which bring the journal and bearing into contact might induce whirling in the reverse sense under the impulse of dry friction.

[4] Professor, Rensselaer Polytechnic Institute, Troy, N. Y. Mem. A.S.M.E.

Heat Dissipation in Self-Contained Bearings

By G. B. KARELITZ,[1] NEW YORK, N. Y.

Heat Dissipation

THE losses in self-contained bearings[2] are caused usually by the viscous friction in the fluid film separating the journal from the bearing. After a steady state of temperature has been reached (from 1 to 3 hr after starting the machine), the heat generated by friction is equal to that dissipated by the housing into the surrounding air, plus the heat conducted through the shaft, and through the pedestal to the foundation or bearing support.

The portion of the heat carried off by conduction is rather small. The thermal conductivity of the common structural metals is comparatively low, as shown in Table 1.

Furthermore, the temperature gradient along the shaft or along the pedestal is small, 1 or 2 deg F per in. (The pedestal is frequently separated from the machine by an air gap.) For instance, in a 5-in. bearing, with a loss of, say, 0.5 hp = 1273 Btu per hr, with a temperature gradient of, say, 1.5 deg F per in., the heat conducted through the steel shaft would be only $2[(\pi/4)\ 25]\ 1.5 = 58$ Btu per hr. In the first approximation, it can be assumed that the heat generated by friction is dissipated entirely through the housing surface.

TABLE 1 THERMAL CONDUCTIVITY OF COMMON STRUCTURAL METALS

Metal	Thermal conductivity: Calories, Sq cm × sec × deg C/cm	Thermal conductivity: Btu, Sq in. × hr × deg F/in.	Remarks; composition, per cent
Carbon steel	0.109	2.02	C-0.6
Nickel steel	0.074	1.38	Ni-5
Steel S.A.E. 4140	0.086	1.59	C-0.4, Mn-0.8, Cr-1, Mo-0.2
Gray cast iron	0.112	2.08	C-3
Gun metal	0.170	3.18	Cu-85, Sn-9, Zn-5, Pb-1
Bronze	0.118	2.20	Cu-88, Sn-10, Zn-2
Babbitt	0.075	1.40	Sn-85, Sb-10, Cu-5

The rate of dissipation was determined[3] for bearing housings of common finish by direct measurement of heat input and surface temperature

$$K = 0.0075 \frac{\text{Watt}}{\text{Sq in.} \times \text{deg C}} = 2.1 \frac{\text{Btu}}{\text{Hr} \times \text{sq ft} \times \text{deg F}}$$

in quiet air

$$K = 0.021 \frac{\text{Watt}}{\text{Sq in.} \times \text{deg C}} = 5.9 \frac{\text{Btu}}{\text{Hr} \times \text{sq ft} \times \text{deg F}}$$

in a draft of 500 fpm velocity

The values are in line with generally accepted heat-dissipation factors from metal surfaces. Within the temperatures encountered in bearings, the rate of heat dissipation is $H = KSt$, where S is the hot outside area of the pedestal or box, and t is the temperature rise of this outside surface above the ambient temperature.

Heat Transfer From Oil Film to Bearing Bushing

The source of heat in a bearing is the oil film between the rubbing surfaces. Since heat flows from this source outward, to be finally dissipated either through the housing surface or through the shaft, the oil film is the seat of the highest temperature in the bearing. An exception may be encountered, however, in improperly designed disk-lubricated bearings, where a substantial volume of oil is entrained at high speed and thrown off by centrifugal force against the housing, thus creating another parasitic source of heat.

In loaded bearings, the rate of heat generation is not uniform circumferentially. It is highest where the film is thinnest, at the point where the surfaces approach most closely to each other. In fact, this region predominates vastly the rest of the film as a source of heat. Now, one must differentiate between bearings which have a copious supply of lubricant (class 1), such as oil-ring-lubricated bearings, and those which are starved (class 2), such as drop-feed-lubricated machine-tool bearings, or waste-packed railway bearings. In class 1, the journal carries along a portion of the film circumferentially; hence the oil is brought in contact with the shell all around the circumference. Heat is brought to the bearing bushing at all points, and there is not much difference in temperature along the circumference of the bushing. On the other hand, in the bearings which are fed a drop of oil per minute, or even less, the bearing clearance is substantially empty, filled with air; not only is the heat generation more concentrated than in the bearings of class 1, but also the transmission of heat to the shell is localized to the pool of oil at the closest approach. Consequently, temperature differences, as great as 30 deg F, are observed between opposite circumferential points in bushings of class 2 bearings.[3]

This distinction also holds true axially. In class 1 bearings, oil flows axially through distribution grooves provided for this purpose, and the heat generation is approximately uniform along the entire axial width of the bearing. In class 2, the source of heat is localized, and an appreciable axial heat gradient may be observed in the bushing.

It may be mentioned that, since the heat generated in the "bulk" of the oil film must be transferred to the metal of the bearing (journal and bushing), a temperature gradient must exist from the middle of the film thickness toward the two metal surfaces. This gradient is, of course, small but not negligible. However this question is not under discussion here. It was indicated in its first approximation by A. Kingsbury.[4] Its further development, theoretical and experimental, would be of interest.

Temperature Drop From Bushing to Housing Surface

The heat generated in the film is carried away along three paths toward the surrounding atmosphere. In the first place, a part of the heat travels from the oil film through the shaft; this part, as mentioned previously, is small. Each point of the shaft surface sweeps the film once each revolution. Therefore, the temperature of the shaft is equal to the average temperature of the oil film.

Further, the two classes of bearings mentioned earlier must be considered separately. In class 1, the oil, flowing in bulk through

[1] Professor of Mechanical Engineering, Columbia University. Mem. A.S.M.E.

[2] Dissipating losses by conduction and convection, without water or oil cooling.

[3] "Lubrication of Waste-Packed Bearings," by G. B. Karelitz, Trans. A.S.M.E., vol. 48, 1926, p. 1165.
"Performance of Oil-Ring Bearings," by G. B. Karelitz, Trans. A.S.M.E., paper APM-52-5, 1930.

Sponsored by the Special Research Committee on Lubrication and presented at the Annual Meeting, New York, N. Y., December 1–5, 1941, of The American Society of Mechanical Engineers.

Note: Statements and opinions are to be understood as individual expressions of their authors and not those of the Society.

[4] "Heat Effects in Lubricating Films," by A. Kingsbury, *Mechanical Engineering*, vol. 55, 1933, p. 685.

TABLE 3 RELATION BETWEEN TEMPERATURE RISE OF WALL AND TEMPERATURE GRADIENT FROM SHELL TO HOUSING SURFACE

Average temperature rise, F		558 Rpm			372 Rpm			186 Rpm		
		Bushing	Wall	Temperature gradient	Bushing	Wall	Temperature gradient	Bushing	Wall	Temperature gradient
Still air	Oil bath	88.1	72.3	15.8	66.0	54.5	11.5	36.1	26.8	9.3
	Waste pack	146.3	59.6	86.7	107.5	41.4	66.1	60.8	22.6	38.2
Moving air	Oil bath	54.8	32.8	22.0	40.3	24.3	16.0	25.7	15.5	10.2
	Waste pack	128.3	26.0	102.3	93.1	18.6	74.5	56.1	12.3	43.8

or over the bushing or shell, carries away a substantial portion of the heat into the oil sump. There, the oil is agitated and mixed more or less vigorously. A good supply of cooler oil is carried by the oil ring, chain, or disk for lubricating the bearing. Furthermore, the agitation increases the transfer of heat to the sump wall, and through it to the surrounding air.

The transport of heat by the oil is rather effective. For instance, in the 5-in. bearing mentioned, the total heat loss was assumed to be 1273 Btu per hr = 0.5 hp. With oil-ring lubrication, the amount of oil carried over would be, say, 1/4 gpm, or 105 lb per hr. Assuming that the oil temperature rises approximately 10 F, while passing over the bearing bushing, the heat transported by the oil to the sump is $105 \times 10 \times 0.52 = 546$ Btu per hr, or nearly 40 per cent of the total heat generated. The greater proportion of the heat is transmitted through the body of the bearing by conduction.

In starved bearings of class 2, this mechanism of heat transfer does not exist. The total heat in bearings of class 2 must be transferred from the bushing to the heat-dissipating surface of the housing by conduction through the metal body of the bearing, or, in a small part, by radiation and convection through the air spaces between the shell and the housing. The thermal conductivity of the common metals used in the construction of bearings has been shown in Table 1 to be comparatively low. Furthermore, the bearing supports are frequently designed with a view to light weight, flexibility of supports, or economy in manufacture, without due consideration being given to good heat transfer. As a result, the temperature gradients between bushing or shell and housing surface are rather high, particularly in bearings of class 2.

There is but scant information available on the numerical values of these gradients for bearings of various designs of either class.

A numerical estimate of the gradient is hardly possible, in view of the complicated geometry of the path from bushing to housing surface. However, for a rational design of self-contained bearings, knowledge of the gradient is imperative. The losses depend in a calculable way upon the viscosity of the film, i.e., on its temperature, while the heat dissipation is governed by the temperature of the wall. The difference between the two temperatures dictates the thermal equilibrium of the bearing.

The author previously suggested[3] a table giving the approximate gradient as a function of the temperature rise of the wall above the ambient-temperature oil-ring-lubricated pedestal bearings.

However, Mr. Fast recently called attention to the fact that, in his bearings,[5] he had observed gradients considerably lower than given in Table 2. In view of this, it will be of interest to compare the values in the suggested table with the findings of E. S. Pearce[6] who experimented with a railway-journal-box bearing. On the suggestion of the Lubrication Committee, Mr. Pearce recorded the temperatures of the bearing under controlled conditions at more than 50 stations in the box, both at the bearing brass and box surface. The tests were made with a $5\frac{1}{2} \times 10$-in. bearing under a load of 20,000 lb, at speeds of 186, 372, and 558 rpm in still air, and with air blown against the housing, simulating surface conditions. The tests were made under two conditions of lubrication: (1) With the usual waste pack supplying oil to the journal; and (2) with the waste pack removed and the journal partly immersed in an oil bath. The temperature rise F at the various stations in the bearing above ambient temperature was tabulated and presented in one instructive graph. It may be mentioned that the experiments were run during the summer, so that the ambient temperature was near 90 F. An analysis of the data[7] is given in Table 3, in which the relations between the temperature rise of the wall and the temperature gradient from shell to housing surface are indicated.

TABLE 2 APPROXIMATE GRADIENT AS FUNCTION OF TEMPERATURE RISE

Temperature rise of housing wall, deg F	20	30	40	50
Temperature gradient between bushing and wall, deg F	30	42	54	65

[5] The Flexible-Sleeve Multiple-Oil-Film Radial Bearing, by G. Fast, Trans. A.S.M.E., vol. 63, 1941, pp. 725–733.

[6] "Temperature Distribution and Sources in the Conventional Railway Journal Box," by E. S. Pearce, Trans. A.S.M.E., vol. 62, 1940, pp. 633–638.

The data given in Tables 2 and 3 are plotted in Fig. 1. With the oil-bath lubrication, the agitation of the oil was very effective; transportation of heat from the shell to the box wall was very efficient. The temperature gradient was therefore low, very much lower than for the waste-packed bearing. The figures suggested in Table 2 may be too high for bearings working in still air; instead, the range indicated by shading might be suggested for use with oil-ring-lubricated bearings. It is of interest to note that the temperature rises of the wall are appreciably higher for the case of oil-bath lubrication. The difference was approximately 30 per cent, caused by the higher viscosity of the cooler oil. In moving air, the bearing temperatures were lower, the viscosity of the oil was higher; consequently, the bearing losses were also higher. The corresponding temperature gradients between the brass and box wall were considerably greater. A detailed analysis of the losses cannot be made, since the heat-transfer coefficient K for the case of moving air is not known; K depends upon the air velocity which was not recorded.

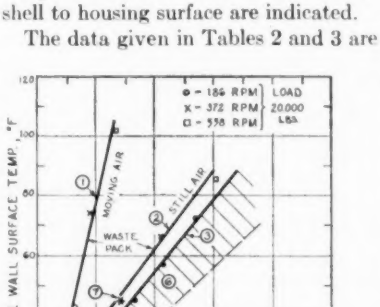


FIG. 1 PLOT OF DATA FROM TABLES 2 AND 3, SHOWING TEMPERATURE GRADIENTS AS FUNCTION OF TEMPERATURE RISE (1, 2, 4, 5, Tests by E. S. Pearce on railway journal box; 3, suggested by the author for oil-ring bearings in 1926; 6, suggested range for oil-ring bearings; 7, check point, waste-packed bearings, reference 2, by author in 1926.)

CONCLUSION

It is self-evident that considerable improvements could be made in the operation, wearing properties, and safety of self-contained bearings, simply by providing a better path for the heat from the source of generation to the surface of the bearing housing. As a first step in this direction, it may be hoped that further experiments will be undertaken to determine the temperature gradients and the rates of heat dissipation in self-contained bearings of various types, operating under a wide range of conditions.

[7] The analysis was made with the assistance of E. G. Fischer, gradute student, Columbia University.

Relaxation Resistance of Nickel-Alloy Springs

By B. B. BETTY,[1] E. C. MACQUEEN,[2] and CARL ROLLE[3]

As a result of a series of tests reported in this paper, stresses required to produce 2, 4, and 6 per cent load loss, or relaxation, in coil springs, held at constant height and constant temperature, have been determined by the authors for several alloys, namely, Monel,[4] "K"[4] Monel, "Z"[4] nickel, and Inconel.[4] Successive test temperatures from 300 F to 700 F were used. The range of temperature over which these several alloys can be used successfully, when load loss is a criterion, has been determined. "K" Monel, "Z" nickel, and Inconel have been found to be comparable, in this respect, to high-alloy spring steels, while Monel is more nearly comparable to low-alloy steels.

INASMUCH as the high-nickel alloys retain their strength to a considerable degree at elevated temperatures and resist oxidation and corrosion as well, they have been useful in many elevated-temperature spring applications. Unfortunately, quantitative data have been lacking on the extent to which coil springs of these materials would retain their load-carrying capacities. As a result of this situation, and in co-operation with the A.S.M.E. Special Research Committee on Mechanical Springs, the authors have undertaken to supply accurate laboratory data for Monel, "K" Monel, "Z" nickel, and Inconel.

Throughout this discourse the term "relaxation" will be used to denote load loss occurring, at constant height, in closely coiled helical compression springs. In this case elastic strain in the outer fibers of the wire, produced by the external load on the spring, is converted gradually to plastic strain, or permanent set. The amount of elastic, or recoverable strain is thereby reduced and there is a proportionate reduction in the load supported by the spring. The percentage loss from the original load is expressed as "per cent load loss" or "per cent relaxation."

The data and conclusions presented herein are based upon tests of springs loaded to a constant height. However, many applications involve the use of springs at constant load rather than constant height. It is felt that, within stress and temperature limits which would produce not more than about 10 per cent relaxation, these data could be applied to cases of constant-load service also. McKeown (1)[5] has discussed the case in which springs are subject to creep deformation under constant load at elevated temperatures.

Some previous load-loss data for Monel have been published in a paper by Zimmerli, Wood, and Wilson (2). The results of an outstanding experimental investigation of load loss, involving approximately 120,000 test springs, have been presented recently to this Society by Zimmerli (3).

[1] Huntington Works Laboratory, The International Nickel Company, Inc., Huntington, W. Va. Mem. A.S.M.E.

[2] Huntington Works Laboratory, The International Nickel Company, Inc., Huntington, W. Va.

[3] Development and Research Division, The International Nickel Company, Inc., New York, N. Y. Mem. A.S.M.E.

[4] Registered United States Patent Office.

[5] Numbers in parentheses refer to the Bibliography at the end of the paper.

Contributed by the Special Research Committee on Mechanical Springs and presented at the Annual Meeting, New York, N. Y., December 1–5, 1941, of The American Society of Mechanical Engineers.

Note: Statements and opinions advanced in papers are to be understood as individual expressions of their authors and not those of the Society.

Description of Test Springs

The springs tested were $1^1/_4$ in. OD, $2^3/_4$ in. free height and had $6^1/_4$ total coils and $4^1/_4$ active coils. The 0.148-in-diam wire was produced and cold-drawn by the Huntington, W. Va., works of the authors' company. Table 1 gives the chemical analyses of the various alloys and metals investigated. The specimens were coiled by the Barnes-Gibson-Raymond Division of the Associated Spring Corporation. After coiling, ends were ground flat for 270 deg.

All springs were given a thermal treatment before being tested. The two solid-solution alloys, Monel and Inconel, were given appropriate low-temperature stress-equalizing anneals, while the precipitation-hardenable alloys, "K" Monel and "Z" nickel, were heat-treated to take full advantage of that property. In the latter cases, the hardness and general mechanical properties produced in the wire by cold-drawing are augmented appreciably by the heat-treatment component.

On completion of a series of preliminary tests, it was found that optimum resistance to relaxation was produced in Monel by a 650 F stress-equalizing anneal for 1 hr, and in Inconel by a 900 F anneal for 1 hr. Further discussion of these tests will be given in Appendix 1. These stress-equalizing treatments were used on all Monel and Inconel springs involved in the main investigation.

All "K" Monel springs were given a heat-treatment of 1000 F for 6 hr, followed by 900 F for 16 hr. All "Z" nickel springs were aged at 900 F for 6 hr.

The influences of these thermal treatments upon the mechanical properties of the materials may be observed by inspection of Table 2. The data in this table were determined from wire samples which were given the same respective treatments as the coiled test springs.

Care was taken not to compress the springs beyond the height used during the test, thus the specimens received no benefit from cold-working prior to testing. Springs generally would be pressed solid as a manufacturing operation, but this operation was omitted since it is not universally used in practice. Actually some of the stresses used in testing were in excess of the elastic limit of the wire. However, in such cases any immediate relaxation taken by the spring automatically was included in the relaxation reported in this paper. The reason for this is that, as covered later under "Test Conditions and Procedure," the springs were loaded to the test height and then held there without making any allowance for set which may have taken place.

Test Conditions and Procedure

A second preliminary series of experiments was run to determine the necessary duration of exposure to insure that practically all the relaxation had occurred. It was found that a 7-day period was appropriate. Figs. 30 and 31, showing relaxation of Monel and Inconel, subjected to various stress-equalizing treatments, show also that there is no consistent difference in per cent relaxation experienced during 7-day and 10-day tests under identical conditions.

TABLE 1 CHEMICAL COMPOSITIONS, PER CENT

Material	Melt	C	Mn	Fe	S	Si	Cu	Ni	Al	Cr
Monel	M-4555-B	0.18	0.94	1.24	0.007	0.10	28.46	69.02	..	...
"K" Monel	M-1050-K	0.18	0.12	0.25	0.005	0.20	29.69	66.10	2.92	...
"Z" nickel	N-6840-Z	..	0.05	0.14	0.005	0.14	0.03	98.61	..	...
Inconel	NX-3530	0.06	0.16	5.77	0.010	0.22	0.04	80.65	..	13.07

TABLE 2 MECHANICAL PROPERTIES

			Tensile properties			Torsional properties			Hardness
Material	Per cent cold reduction	Heat-treatment	Tensile strength, psi	Elongation in 2 in., per cent	Reduction of area, per cent	Proportional limit, psi	Breaking strength, psi	Total twist in 10 in., turns	VHN, 10 kg
Monel	75	None	157000[a]	5[a]	59[a]	67800[a]	110000[a]	93[b]	284
		650 F-1 hr	160000[b]	10[b]	56[b]	64700[a]	104900[a]	95[b]	309
"K" Monel	50	None	163000[a]	3[a]	40[a]	68000[a]	107000[a]	18[b]	287
		1000 F-6 hr, 900 F-16 hr	197000[b]	7[b]	28[b]	74600[a]	137200[a]	7[b]	380
"Z" nickel	50	None	175000[a]	4[a]	40[a]	71000[a]	127000[a]	74[b]	330
		900 F-6 hr	225000[b]	10[b]	20[b]	76200[a]	159700[a]	10[b]	450
Inconel	65	None	172000[a]	4[a]	47[a]	74000[a]	115000[a]	75[b]	317
		900 F-1 hr	188000[b]	8[b]	47[b]	66600[a]	123900[a]	37[b]	366

[a] Average of two specimens.
[b] Average of five specimens.

As a result of these observations it was decided to employ a 7-day testing period for all springs used in the main investigation.

In the performance of these relaxation tests, the loads required to produce the desired stresses in the springs were first calculated. These calculated loads were applied to the springs in a weighing attachment mounted upon a Toledo scale, the sensitivity of which was 1 oz. The loaded length of each spring was measured to 0.001 in. by a caliper and micrometer. The spring then was compressed to the measured loaded length and held firmly to that length upon a special bolt and nut. The bolt was of $^7/_8$-in-diam Monel, so that no creep could be expected to occur in it during the course of the test. Washers, larger than the outside diameter of the test spring, were welded to the head of the bolt and to the nut. The faces of these washers were machined flat and parallel to facilitate length measurements.

The assembled bolts, nuts, and springs were placed inside a nickel box and into an electrically heated oven for the heating period. Sixty springs were tested simultaneously. A temperature uniformity of 3 F was observed to exist throughout the box, and temperature control within 5 F was maintained during each heating period.

After the 7-day heating period, the springs were removed from the furnace and cooled in air. After removal of the holding bolts, the springs were compressed to the original loaded length in the spring-weighing machine. The load supported after test was measured. The difference between the originally applied load and the load the spring supported after the heating period is the basis of the "load-loss" calculation.

Load and Stress Calculations

The loads applied to the springs, in order to impose the desired arbitrarily chosen values of maximum fiber stress, were calculated by the use of the formula

$$P_t = \frac{S_t \pi d^3}{8DK} \qquad [1]$$

where

P_t = load at test temperature, lb
S_t = maximum fiber stress at test temperature, psi
d = wire diameter, in.
D = mean coil diameter, in.
$c = \frac{D}{d}$
K = stress-correction factor, developed by A. M. Wahl (4)
$= \left(\frac{4c-1}{4c-4} + \frac{0.615}{c}\right)$

All maximum fiber stresses stated in connection with the results of this investigation are those prevailing at the test temperature. In order to convert values of P_t into load required for the same deflection at room temperature, a correction was applied for the change in torsional modulus of elasticity. The change in modulus, from room temperature to test temperature, produces a proportionate change in the calibration rate of the spring.

To effect this correction, therefore, the load obtained from Equation [1] was converted to room-temperature load by the formula

$$P_r = P_t \frac{G_r}{G_t} \qquad [2]$$

where

P_r = load at room temperature, lb
G_r = torsional modulus at room temperature, psi
G_t = torsional modulus at test temperature, psi

The value obtained for P_r was used in the initial loading of each spring.

A discussion of the method used for obtaining values of G_r and G_t is given in Appendix 2.

It should be noted that Zimmerli (3) stated his results in terms of stress on the spring at room temperature, although the method for adjusting these values was outlined. The correction used in this investigation results in reported stress values which are lower, for any given design and deflection, than if the correction had not been applied.

No attempt was made to correct the data for changes in the length of the springs and bolts due to thermal expansion. The maximum error involved occurs in the testing of Inconel at 700 F and in this case the difference between the computed expan-

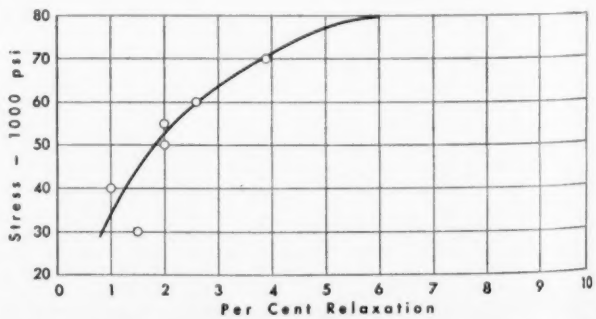


Fig. 1 Stress Versus Relaxation in 7 Days; Monel at 300 F

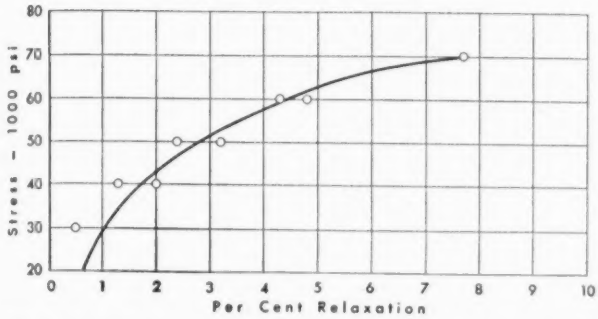


FIG. 2 STRESS VERSUS RELAXATION IN 7 DAYS; MONEL AT 400 F

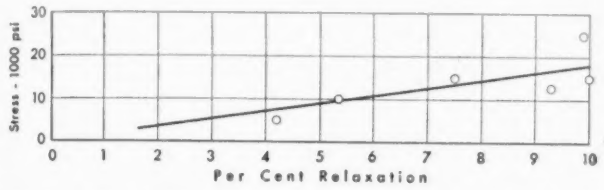


FIG. 4 STRESS VERSUS RELAXATION IN 7 DAYS; MONEL AT 500 F

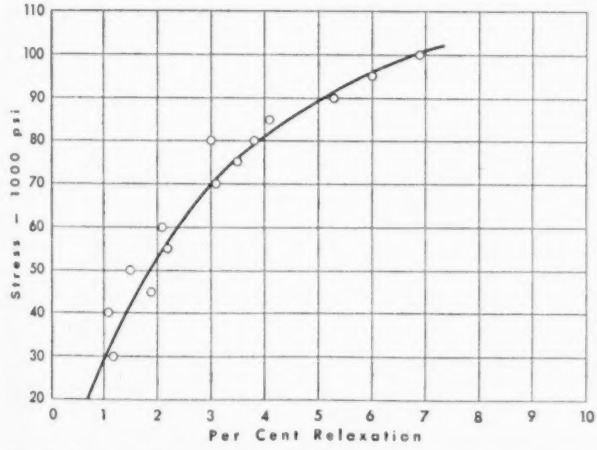


FIG. 6 STRESS VERSUS RELAXATION IN 7 DAYS; "K" MONEL AT 450 F

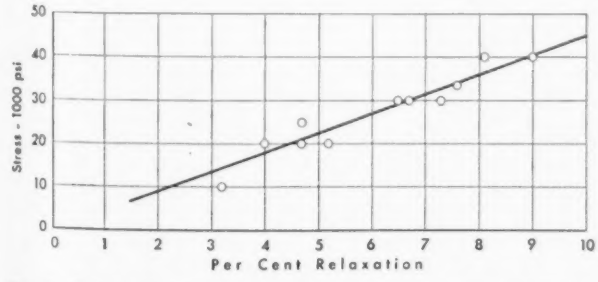


FIG. 8 STRESS VERSUS RELAXATION IN 7 DAYS; "K" MONEL AT 550 F



FIG. 9 STRESS VERSUS RELAXATION IN 7 DAYS; "K" MONEL AT 600 F

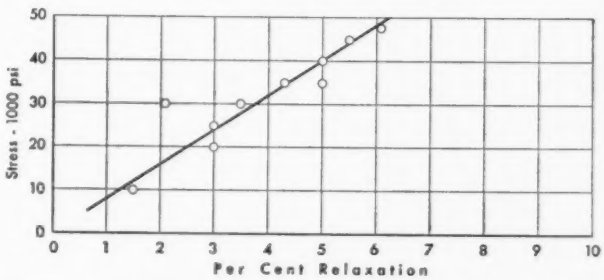


FIG. 3 STRESS VERSUS RELAXATION IN 7 DAYS; MONEL AT 450 F

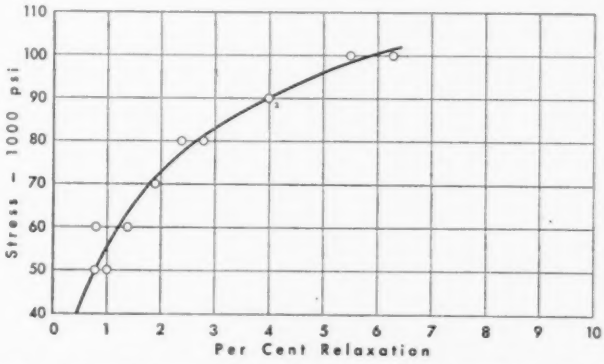


FIG. 5 STRESS VERSUS RELAXATION IN 7 DAYS; "K" MONEL AT 400 F

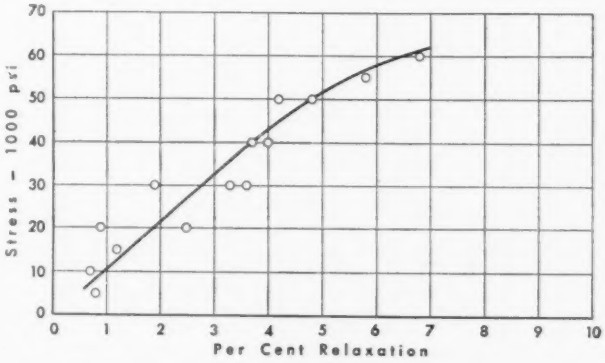


FIG. 7 STRESS VERSUS RELAXATION IN 7 DAYS; "K" MONEL AT 500 F

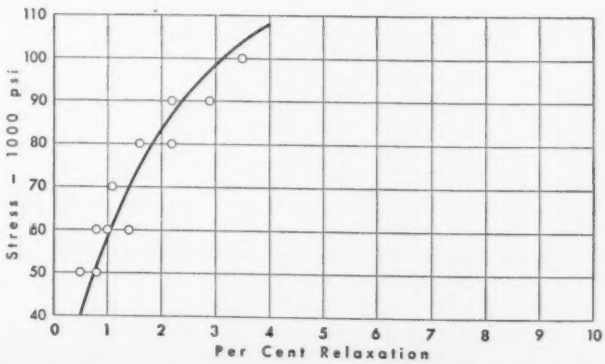


FIG. 10 STRESS VERSUS RELAXATION IN 7 DAYS; "Z" NICKEL AT 400 F

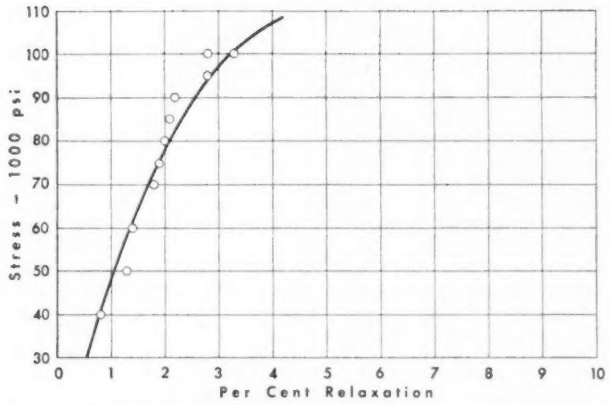


FIG. 11 STRESS VERSUS RELAXATION IN 7 DAYS; "Z" NICKEL AT 450 F

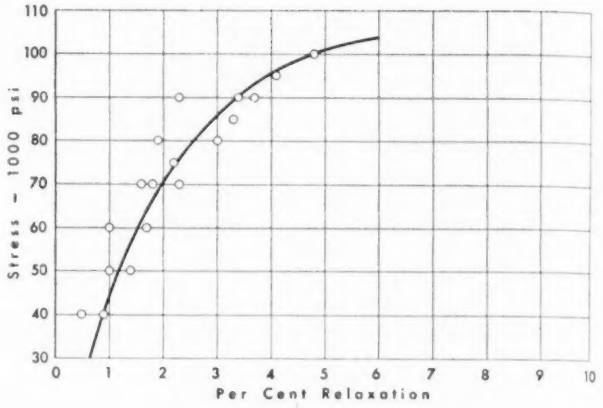


FIG. 12 STRESS VERSUS RELAXATION IN 7 DAYS; "Z" NICKEL AT 500 F

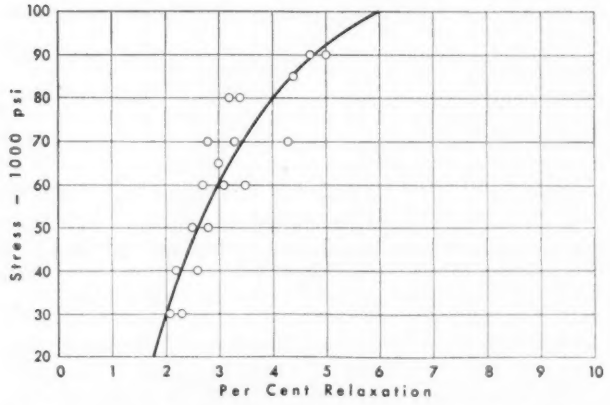


FIG. 13 STRESS VERSUS RELAXATION IN 7 DAYS; "Z" NICKEL AT 550 F

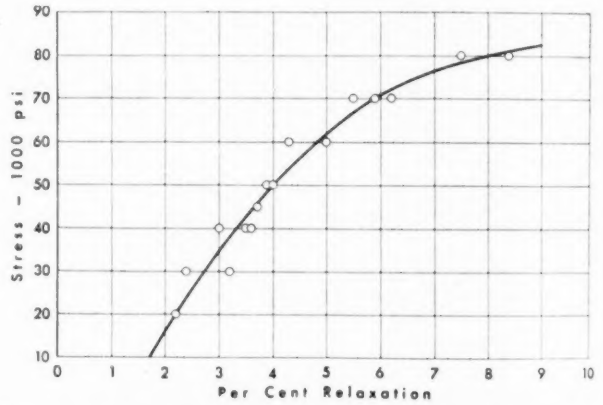


FIG. 14 STRESS VERSUS RELAXATION IN 7 DAYS; "Z" NICKEL AT 600 F

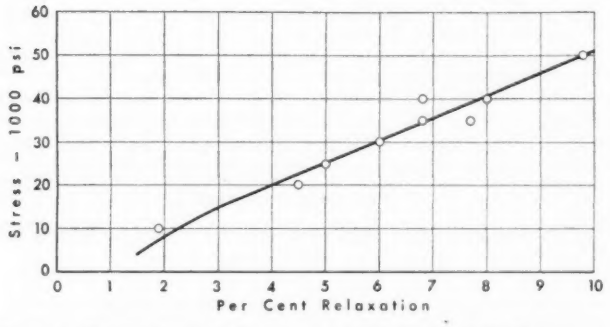


FIG. 15 STRESS VERSUS RELAXATION IN 7 DAYS; "Z" NICKEL AT 650 F

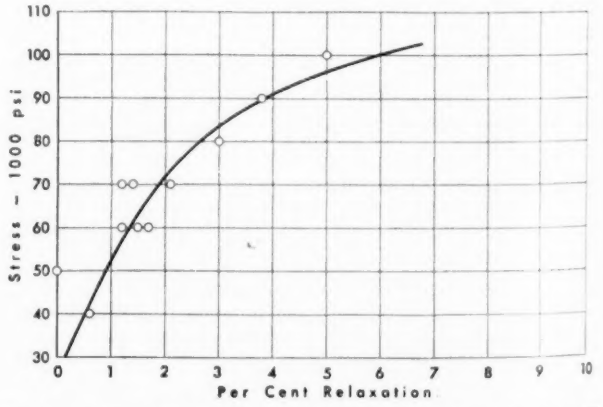


FIG. 16 STRESS VERSUS RELAXATION IN 7 DAYS; INCONEL AT 400 F

sions of the spring and the Monel bolt is only 0.0007 in. per in.; less than the probable accuracy of measurement.

DISCUSSION OF RESULTS

The experimental values of per cent relaxation from given initial stresses at various test temperatures are plotted in Figs. 1 to 22, inclusive. These figures represent the results, respectively, for Monel at 300 to 500 F; "K" Monel at 400 to 600 F; "Z" nickel at 400 to 650 F; and Inconel at 400 to 700 F.

Each test point plotted represents the average value observed for a set of three springs. The notation "2" which appears beside some points indicates that the averages for two independently tested sets fell at the same point. In drawing the curves through the test points, due consideration was given to the data obtained for the same material at temperatures immediately above and below that of the curve in question, so that a consistent family would be obtained if all curves for one material were assembled on a single sheet.

This group of charts indicates that even after averaging together the results on a set of three springs there exists a fair degree of scatter in the data. In many cases a single determination would be sufficiently inconsistent to "throw off" the average of three. The data are plotted in this manner, using a separate chart for each curve, so that the degree of scatter might readily

TABLE 3 INDICATED MAXIMUM FIBER STRESS TO PRODUCE GIVEN PERCENTAGES OF RELAXATION

(Stress in 1000 psi)

Temperature, F	Monel			"K" Monel			"Z" nickel			Inconel		
	2 Per cent	4 Per cent	6 Per cent	2 Per cent	4 Per cent	6 Per cent	2 Per cent	4 Per cent	6 Per cent	2 Per cent	4 Per cent	6 Per cent
300	52.5	70.5	80.0	..	..	...	..	..	...	..	..	..
400	43.0	57.5	65.5	73.0	90.0	100.5	83.0	108.0	...	72.0	91.0	100.0
450	16.0	32.5	48.0	53.0	81.0	96.0	78.0	107.0	...	68.0	86.5	93.0
500	4.0	7.5	11.0	21.5	43.0	58.0	70.0	95.5	104.0	61.0	81.0	91.5
550	..	..	..	9.0	18.0	27.0	30.0	80.0	100.0	55.0	77.0	88.0
600	..	..	..	3.5	7.0	11.0	16.0	50.0	71.0	44.0	68.0	83.0
650	..	..	..	..	..	...	8.0	20.0	30.5	31.0	55.0	74.0
700	..	..	..	..	..	...	..	...	...	..	4.5	27.0

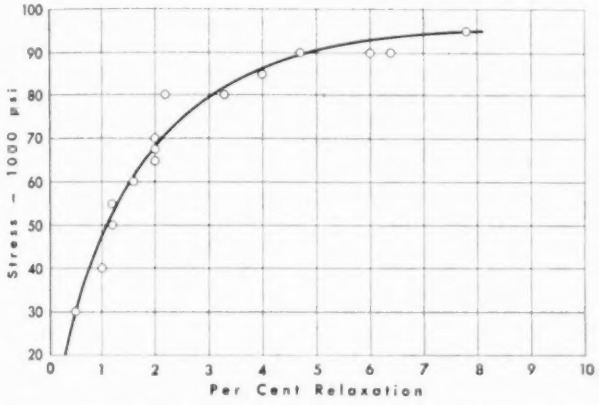


FIG. 17 STRESS VERSUS RELAXATION IN 7 DAYS; INCONEL AT 450 F

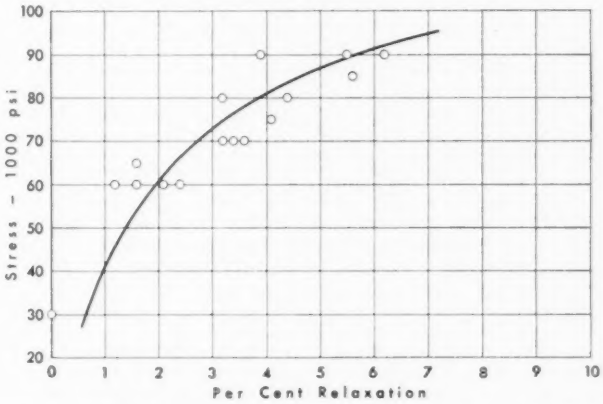


FIG. 18 STRESS VERSUS RELAXATION IN 7 DAYS; INCONEL AT 500 F

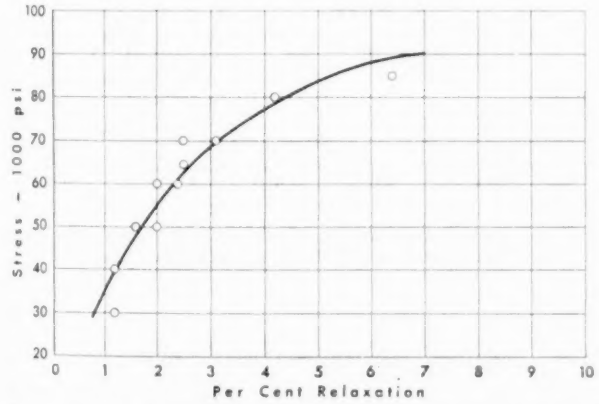


FIG. 19 STRESS VERSUS RELAXATION IN 7 DAYS; INCONEL AT 550 F

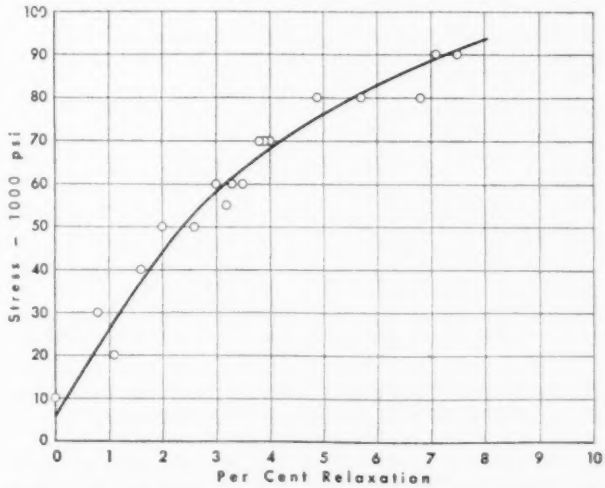


FIG. 20 STRESS VERSUS RELAXATION IN 7 DAYS; INCONEL AT 600 F

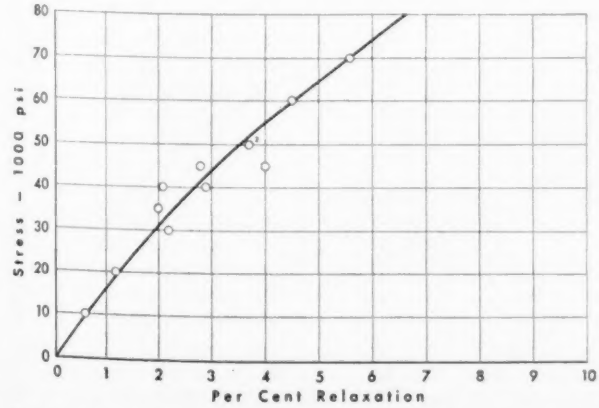


FIG. 21 STRESS VERSUS RELAXATION IN 7 DAYS; INCONEL AT 650 F

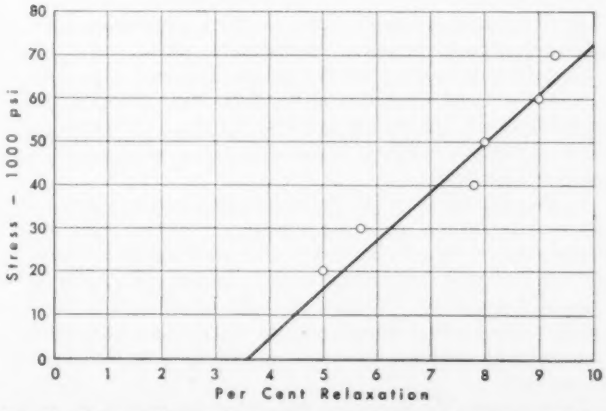


FIG. 22 STRESS VERSUS RELAXATION IN 7 DAYS; INCONEL AT 700 F

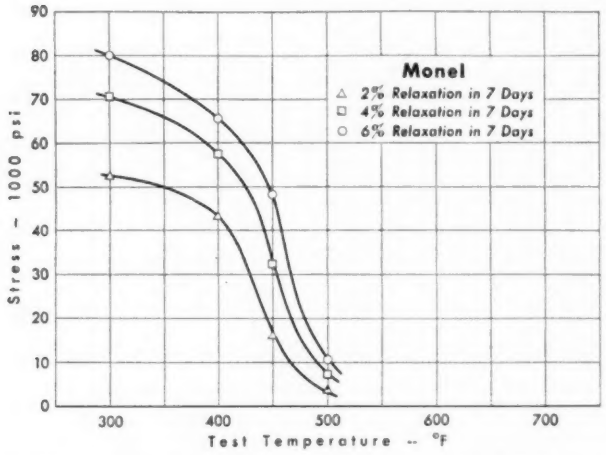


FIG. 23 STRESS REQUIRED TO PRODUCE 2, 4, AND 6 PER CENT RELAXATION OF MONEL SPRINGS IN 7 DAYS

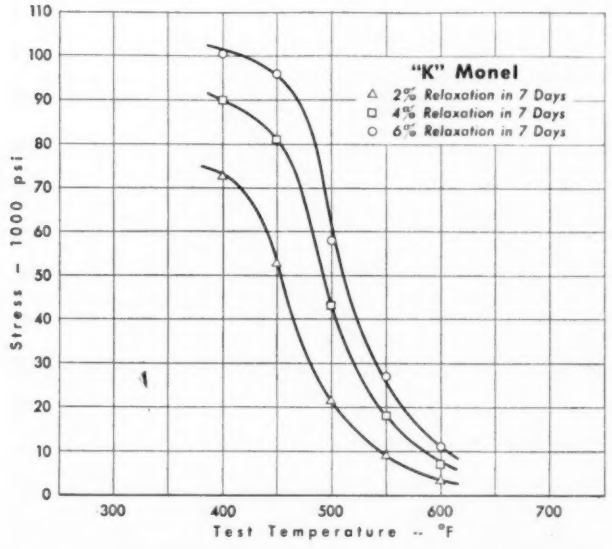


FIG. 24 STRESS REQUIRED TO PRODUCE 2, 4, AND 6 PER CENT RELAXATION OF "K" MONEL SPRINGS IN 7 DAYS

be observed and considered. It will be noted that the curves were drawn so as best to represent the entire group of data rather than to encompass the extreme points of low stress or high per cent relaxation.

In adapting these data to practical design, therefore, due consideration should be given to the scatter of results.

Compiled in Table 3 are the stresses required to produce 2, 4, and 6 per cent relaxation in the 7-day testing period, as obtained from the curves in the previous figures. It was not possible to determine, with any degree of accuracy, similar data for 0 per cent relaxation.

In Fig. 23, the stress values required to produce 2, 4, and 6 per cent relaxation in Monel springs are plotted against test temperature. Figs. 24, 25, and 26 are similar figures in which are plotted corresponding data for "K" Monel, "Z" nickel, and Inconel, respectively. This set of charts illustrates the fact that much higher working stresses may be used for any of these alloys when slightly higher percentages of relaxation or load loss are permissible.

By inspecting the respective values for torsional proportional limit given in Table 2, it will be noted that these values are exceeded considerably by the stresses required to produce only 2 per cent load loss at the lower temperatures. This follows the characteristic behavior of these alloys in that, when the proportional limit is exceeded, a sudden yielding does not take place. Instead, there is a considerable increase in load-carrying capacity with only a relatively small degree of permanent set.

The degree of flatness of the stress-temperature curve for any given percentage relaxation is, of course, governed by the degree to which each material retains its room-temperature properties at elevated temperatures.

Fig. 27 is a chart showing the stress required to produce 2 per cent relaxation plotted against test temperature for all the alloys discussed, while Figs. 28 and 29 are drawn in a similar manner to show 4 and 6 per cent relaxation, respectively. These figures

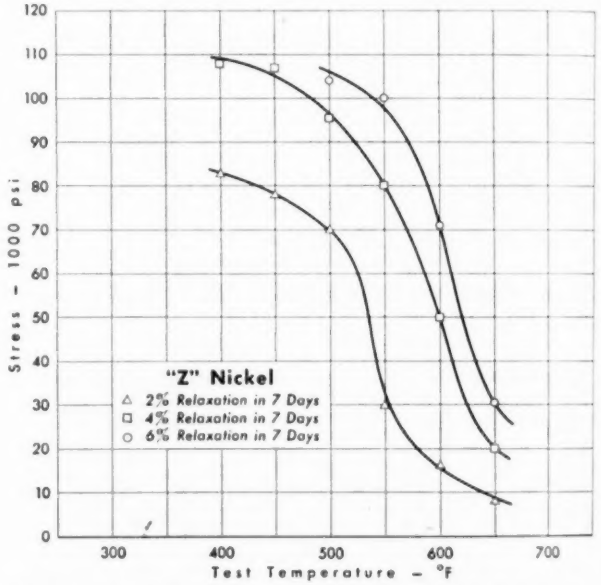


FIG. 25 STRESS REQUIRED TO PRODUCE 2, 4, AND 6 PER CENT RELAXATION OF "Z" NICKEL SPRINGS IN 7 DAYS

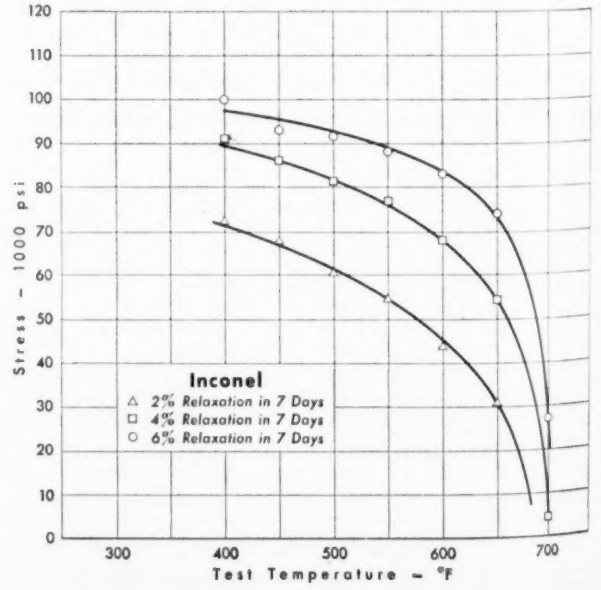


FIG. 26 STRESS REQUIRED TO PRODUCE 2, 4, AND 6 PER CENT RELAXATION OF INCONEL SPRINGS IN 7 DAYS

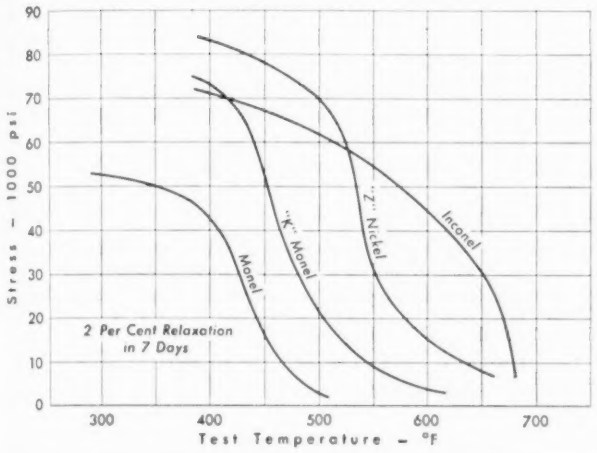


FIG. 27 STRESS REQUIRED TO PRODUCE 2 PER CENT RELAXATION OF MONEL, "K" MONEL, "Z" NICKEL, AND INCONEL SPRINGS IN 7 DAYS

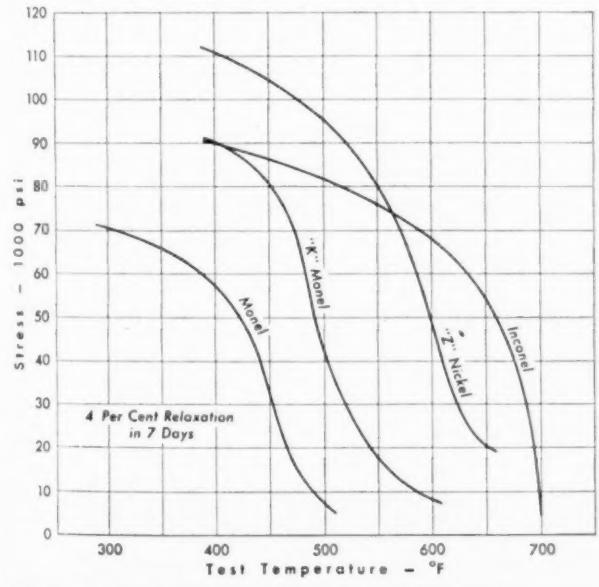


FIG. 28 STRESS REQUIRED TO PRODUCE 4 PER CENT RELAXATION OF MONEL, "K" MONEL, "Z" NICKEL, AND INCONEL SPRINGS IN 7 DAYS

illustrate the relative positions of the several alloys studied with respect to the stress and temperature scales.

It is evident that, at temperatures up to about 400 F and where severe stress conditions must be met, "K" Monel or "Z" nickel would be the choice, with "Z" nickel maintaining a preferred position up to about 550 F. At higher temperatures, however, where somewhat lower stresses would be necessary, Inconel would be preferable. Monel appears to be useful only up to about 400 F and then only at moderate stress levels.

In applying these data to design, the size and strength of the wire used in making the test springs should be borne in mind. While the tensile properties were typical of those obtained in 0.148-in-diam wires of these alloys, they cannot be assumed as minima. Furthermore, these materials, especially Monel and Inconel, show lower tensile strengths for larger diameters; hence, for any specific design problem, the wire size also should be considered. However, the data presented herein should be representative for all wire diameters up to about 0.148 in.

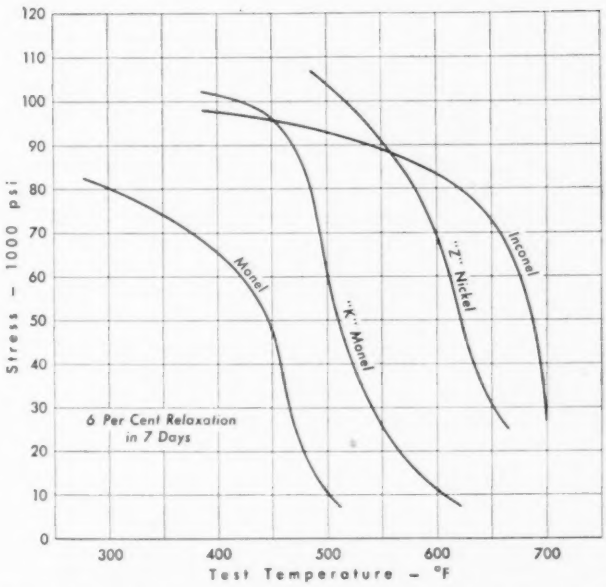


FIG. 29 STRESS REQUIRED TO PRODUCE 6 PER CENT RELAXATION OF MONEL, "K" MONEL, "Z" NICKEL, AND INCONEL SPRINGS IN 7 DAYS

CONCLUSIONS

1 Inconel resists relaxation up to high temperatures and may be used at high stresses up to 650 F. Above this temperature the stress must be lowered considerably and a slight degree of relaxation must be tolerated.

2 "Z" nickel and "K" Monel will withstand higher stresses than Inconel at the lower temperatures, consistent with their generally higher level of mechanical properties.

3 "Z" nickel may be used with high stress at temperatures up to 550 F and with reduced stress up to 600 F.

4 "K" Monel may be used with high stress up to 450 F and with reduced stress up to 500 F.

5 Where other factors such as corrosion resistance are involved, Monel offers possibilities as a spring material for temperatures up to about 400 F and at moderate stress levels.

6 Monel springs should be stress-equalized for 1 hr at 650 F where relaxation resistance is desired.

7 Inconel springs should be stress-equalized for 1 hr at 900 F for service at elevated temperatures.

Appendix 1

OPTIMUM STRESS-EQUALIZING TREATMENTS

Several series of tests at various stress levels and at various test temperatures were carried out on Monel and Inconel springs for the purpose of determining the optimum stress-equalizing treatments.

Fig. 30 shows the results of a typical series for Monel under test conditions of 40,000-psi stress, and 400 F. Each test point represents the average relaxation value for three springs. Tests were conducted for both 7 days' and 10 days' duration.

Fig. 31 shows the results of a similar series for Inconel at 65,000 psi, and 600 F.

In the case of Monel it was concluded that a treatment of 1 hr at 650 F would provide practically minimum relaxation under any test conditions suitable for the service of this material. A temperature of 650 F affords almost complete freedom from heat-tarnishing. Since this is a factor in some applications, and since 650 F produces essentially maximum relaxation resistance, higher temperatures are not suggested.

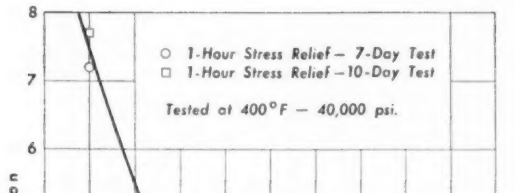


FIG. 30 EFFECT OF STRESS-EQUALIZING TEMPERATURE UPON RELAXATION OF MONEL SPRINGS IN 7 AND 10 DAYS
(Tests run at 400 F and 40,000-psi stress.)

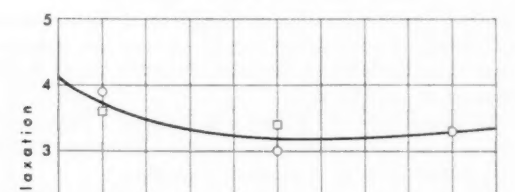


FIG. 31 EFFECT OF STRESS-EQUALIZING TEMPERATURE UPON THE RELAXATION OF INCONEL SPRINGS IN 7 AND 10 DAYS
(Tests run at 600 F and 65,000-psi stress.)

It is not possible even to approach maximum resistance to relaxation in Inconel and still prevent heat tarnishing. As is indicated by Fig. 31, the optimum heat-treatment conditions for this alloy would be 1 hr at 900 F. This treatment was used, therefore, in all subsequent work and is suggested for commercial practice.

Appendix 2

VARIATION OF MODULUS OF ELASTICITY

The question of variation of modulus of elasticity with temperature has received relatively little attention in the way of actual test determinations. Zimmerli, Wood, and Wilson (5) have obtained values of torsional modulus for a number of spring materials, including Monel.

Keulegan and Houseman (6) made determinations on a number of materials, including Monel, using only the temperature range —50 to +50 C. These data are particularly pertinent to precision spring work where modulus changes under ordinary atmospheric-temperature ranges are significant. They found a drop of 3.2 per cent in the torsional modulus of Monel with a temperature rise of 100 C.

Jasper (7) has reviewed this subject extensively and quotes the following formula as initially proposed by Sutherland (8)

$$\frac{G}{G_0} = 1 - \left(\frac{T}{T_m}\right)^2 \quad \ldots\ldots\ldots\ldots\ldots\ldots [3]$$

where

G = torsional modulus at any absolute temperature, psi
G_0 = torsional modulus at zero temperature absolute, psi
T = absolute temperature at which G is to be computed
T_m = absolute temperature of melting point of material

Equation [3] is checked excellently by data of nine investigators using eight different pure metals having a wide range of melting points. Jasper also quotes tests on several steels which provide an additional check on the formula.

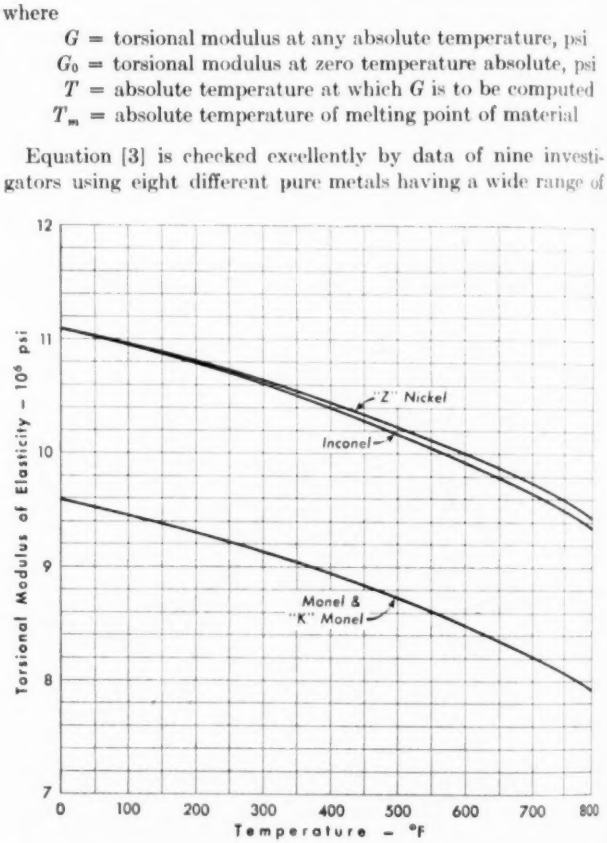


FIG. 32 TORSIONAL MODULUS OF ELASTICITY VERSUS TEMPERATURE FOR MONEL, "K" MONEL, "Z" NICKEL, AND INCONEL, ACCORDING TO SUTHERLAND'S EQUATION

The data for Monel obtained by Zimmerli, Wood, and Wilson, if plotted with G/G_0 as ordinate and T/T_m as abscissa, also provide a reasonable check. These latter data come generally higher than the curve plotted from Sutherland's equation. Thus corrections made according to Equation [3] and applied as explained under "Load and Stress Calculations" in this paper, would constitute overcorrection on the basis of the Zimmerli, Wood, and Wilson data. Such corrections, therefore, would be on the side of safety in that the fiber stress in the springs might actually have been slightly higher than the values reported herein.

Because of these considerations, therefore, values of G_r/G_i for use in Equation [2] were obtained from the curves in Fig. 32. These curves are plotted from known average values of G at 70 F for the materials, together with appropriate values of melting point.

It should be noted that it is not necessary to know the actual value of G for the specimens tested. The values of 11×10^6 for Inconel and "Z" nickel and of 9.5×10^6 for Monel and "K"

Monel are subject to variations of plus or minus approximately 0.3×10^6 from lot to lot. Whatever the value at room temperature for a given sample, the ratio G_r/G_t would not change and, hence, the correction from P_t to P_r by Equation [2] would not be affected.

BIBLIOGRAPHY

1 "The Creep of Metals—I," by J. McKeown, *Metal Industries* (British), vol. 56, 1940, pp. 325–328.

2 "Load Losses in Small Helical Springs at Elevated Temperatures," by F. P. Zimmerli, W. P. Wood, and G. D. Wilson, Trans. American Society for Steel Treating, vol. 21, 1933, pp. 796–806.

3 "Effect of Temperature on Coiled Steel Springs Under Various Loadings," by F. P. Zimmerli, Trans. A.S.M.E., vol. 63, May, 1941, pp. 363–368.

4 "Stress in Heavy Closely Coiled Helical Springs," by A. M. Wahl, Trans. A.S.M.E., vol. 51, part 1, 1929, p. 185.

5 "The Effect of Temperature Upon the Torsional Modulus of Spring Materials," by F. P. Zimmerli, W. P. Wood, and G. D. Wilson, Proceedings A.S.T.M., vol. 30, part 2, 1930, pp. 350–360.

6 "Temperature Coefficient of the Moduli of Metals and Alloys Used as Elastic Elements-RP531," by G. H. Keulegan and M. R. Houseman, U. S. Bureau of Standards, *Journal of Research*, vol. 10, January-June, 1933, pp. 289–320.

7 "The Value of the Energy Relation in the Testing of Ferrous Metals at Varying Ranges of Stress and at Intermediate and High Temperatures," by T. M. Jasper, *Philosophical Magazine*, series 6, vol. 46, 1923, pp. 609–627.

8 "Kinetic Theory of Solids," by Wm. Sutherland, *Philosophical Magazine*, series 5, vol. 32, 1891, part 2, pp. 31–43, 215–225, 524–553.

Discussion

A. NÁDAI.[6] The authors subject helical springs to an axial load while they maintain the lengths of the springs unchanged during a time of seven days. The springs are exposed to elevated temperatures during this time. The decrease of the load of these springs is measured by the change of the lengths of the springs. While, however, these are subjected to relaxation at elevated temperatures, all the measurements are made at room temperature. The authors are aware that this introduces the necessity of certain corrections containing unknown factors. They also restrict their observations to the statement of the drop of the load after a given time (one week). It would have been preferable to extend observations over a longer period of time and to record decrease of load as a function of time.

The writer introduced this method of testing many years ago for running relaxation tests and believes that it is necessary to plot load as a function of time for the purpose of being able to extrapolate such observation curves to the service times of the order of several years. If plots are recorded on semilogarithmic charts, it is comparatively simple to extrapolate readings so that the final drop of the load can be predicted for service conditions of several years' duration. An example of such a set of relaxation curves is given in Fig. 33 of this discussion, showing the drop of the load for a Cr-Mo-W steel at 500 C. Several such curves have recently been published in a paper by W. E. Trumpler.[7] That paper also contains reference to several other papers in which tests on the relaxation of steels have been reported, and various methods are suggested for observation and for the manner of recording such information. The writer wonders that the authors have not made more use in their work of these methods to test and to record the relaxation behavior of steels at high temperatures.

If a cylindrical bar is subjected to a tension load at an elevated temperature and the length of the bar cannot change, the load will decrease because of the creep of the material. There is an exchange between the elastic strain and the permanent strain, the latter increasing at the expense of the former one. After having seen a great number of such relaxation curves, in which the load is plotted as a function of the time, it seems probable that two phenomena combine in these relaxation curves: (*a*) There usually occurs a comparatively rapid drop of the load. This may be due to small plastic strains which were connected with the loading of the bar, or it may be due to the presence of large internal stresses. (*b*) After this first initial readjustment period has passed, which usually does not take a long time, the load further starts to drop and decreases continuously. This second period of the relaxation may be called the "steady readjustment period," or steady relaxation. It is due to the creep under stress and demonstrates the fact that any given stress must produce a certain rate of plastic flow. In some tests run with copper at room temperature, there was still observable this second or steady relaxation of the copper. Therefore, the

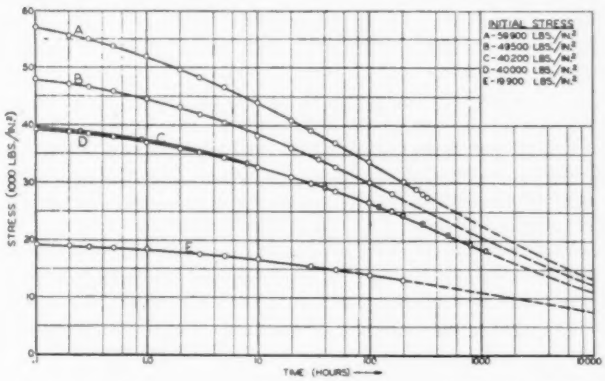


FIG. 33 RELAXATION OF CR-MO-W STEEL (2) AT 500 C

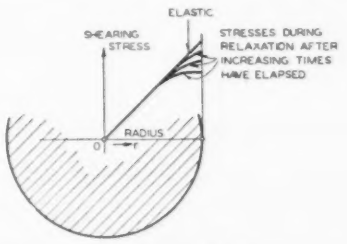


FIG. 34 RELAXATION OF SHEARING STRESSES IN A BAR UNDER TORSION

writer questions the usefulness of recording a drop of the load in a helical spring after a given time, such as 1 week. The most essential question which is not answered by the authors' tests is how will the load decrease under the second steady-relaxation period in the springs? This question cannot be answered without running the tests in the manner described and only after plotting load against time.

If the case of pure viscous flow is excluded, in which stress is proportional to the rate of flow, relaxation in a helical spring cannot take place without a disturbance in the distribution of the shearing stresses in the wire of the spring. Equation [1], used by the authors, can serve to compute the initial load, assuming a linear distribution of the shearing stresses with the radius from the center of the circular cross section of the spring; however, after relaxation has set in, this distribution must necessarily change gradually in a manner as shown in Fig. 34 of this discussion. It is not difficult to predict also the changes which will occur in the stress distribution during what has been termed

[6] Westinghouse Research Laboratories, East Pittsburgh, Pa. Mem. A.S.M.E.

[7] "Relaxation of Metals at High Temperatures," by W. E. Trumpler, *Journal of Applied Physics*, vol. 12, 1941, pp. 248–253.

previously as the second or the steady readjustment period, after taking into account the actual laws of creep which have been observed for many of the metals. Under the assumption of a purely speed-dependent flow, it is not difficult to compute such stress distributions during the relaxation in a spring. The writer believes that some such analysis is needed and, if more reliable and exact information should be gathered on the relaxation of helical springs Equation [1] must be modified correspondingly.

A formula was quoted for expressing the modulus of shear G as a function of the absolute temperature. The formula which the authors use is based on an assumption, namely, that at the melting point of the material the modulus of shear vanishes. This is highly improbable for theoretical and practical reasons. It is believed that sufficient experimental material is available to show the fallacy of such a formula. If the modulus of shear should vanish at the melting temperature, a piece of ice could not be deposited in an ice box, nor could a skater move on ice. There is an abrupt drop of the shearing modulus from a definite finite value at the melting temperature to the value zero at the liquid state. Thus, in the solid state, G cannot become zero at any temperature.

Authors' Closure

The authors wish to thank Dr. Nádai for his very interesting discussion of several points not particularly emphasized in the paper. One of these to which attention was called is that relaxation might well have been studied as a function of time. The technique suggested involves making an intensive and detailed study of a few specimens; whereas the authors chose to investigate many specimens with a simplified procedure already described. As a matter of fact, the procedure used was established by those who had conducted the very extensive studies of the relaxation of steel springs. The authors have provided data on nickel-alloy springs to supplement those for steel ones. A detailed study of the time-relaxation characteristics of a few specimens would make an interesting and illuminating supplement to the present observations.

The validity of the formula by which the shearing stress was calculated has been questioned on the ground that the stress distribution assumed by that formula does not prevail under conditions of relaxation. The authors recognized this from the outset of the work, but felt justified in using the formula inasmuch as this same formula will be used by the spring designer. Whatever error there might have been in the authors' use of this equation will be erased when the designer substitutes back in this same formula the safe working stresses which have been determined experimentally by the use of this formula.

Some comments were made on the use of Sutherland's formula for the variation of torsion modulus of elasticity with temperature. Emphasis was placed on the invalidity of Sutherland's assumption of zero modulus at the melting point. Inasmuch as the range of temperatures over which the formula was used was about 2000 F below the melting point for the nickel alloys it does not seem to be justifiable to attach undue importance to this objection. Furthermore, the authors showed that from the experiments of Zimmerli, Wood, and Wilson, the Sutherland formula is very nearly correct within the temperature range studied in this relaxation work and that the error is on the side of safety.

Dr. Nádai states that the most important question not answered by the experiments reported is: "How will the load decrease under the second steady relaxation period?" The authors recognize the importance of this question and are making this the subject of the next phase of their experimental investigation.

Symposium on Formulation of Code for Design of Helical Springs

In response to the evident need for the correlation of data on mechanical springs and the formulation of a standard code of design for helical springs, suggestions are made in this symposium by a group of spring specialists which will tend to crystallize the matter into early action. The papers presented cover the scope of the problem of formulating a practical working code, and then in detail discuss such matters as design stresses, preparation of spring tables, research work required, and the preparation and use of nomographic charts as a design method.

What Does the Practical Spring Designer Need?

By J. K. WOOD[1]

EIGHTEEN years ago the Special A.S.M.E. Research Committee was created for the purpose of correlating and expanding our knowledge of the functionally important art of spring design which at that time was in a more or less chaotic state. During the intervening time, the committee has sponsored many research projects and papers, those of its own and those of co-operative members, but the job still remains of correlating both the old and new knowledge in a compact and simplified form suitable for safe practical use.

Most of this research has been done in connection with helical springs, and the committee considers this the opportune time to correlate the accumulation of knowledge in this phase of spring design in the form of a code. This subject is so unusual in many respects that it is a problem as to how we should best proceed to formulate a code which will serve as a useful tool to the great mass of mechanical designers. Those participating in this symposium represent that very small group of men specializing in spring research. Therefore if we are to keep in mind the greater mass of practical designers, who are interested only in getting quick and effective results with the new tool, we will have to restrain ourselves from the natural inclination to wade in the deep waters of our pet hobby.

The purpose of this symposium is to discuss the formulation of a code of design for helical springs. A helical spring, in the unstressed state, is an elastic bar of constant cross section, the normal axis of which conforms to the helix or screw thread. This excludes other types of coil springs, the radius of curvature of which varies, such as "hourglass," conical, "barrel," and spiral springs.

When the load is applied along the axis of the helix (spring axis) in such a manner as to reduce the space between unstressed coils, the bar is stressed principally in torsion, and we have what is known as a "compression helical spring." When the load is applied in the reverse direction along the spring axis in a manner to increase the space between unstressed coils, the bar is also stressed principally in torsion, and we have what is known as an "extension helical spring." When the load is applied as a torque about the spring axis so as to increase the number of coils, the bar is stressed principally in flexure, and we have what is known as a "torsional helical spring." Therefore, consideration is to be given to these three types of springs, namely, compression, extension, and torsion helical springs.

When a load is applied to a straight bar along the normal axis of its cross section, as in "pure" tension or compression, every "fiber" is stressed equally. Using this type of stressed member as a standard of 100 per cent elastic efficiency, the compression and extension helical springs vary in elastic efficiency from 25 to 50 per cent, depending upon the spring index (curvature correction); and the torsion helical spring varies in elastic efficiency from 20 to 33 per cent, depending also upon the spring index (curvature correction). Springs are peculiar with respect to all other types of stressed elements in mechanical design in that the deflection component of the stored elastic energy is relatively very large. This fact makes it very important to consider the relation of any spring design, specifically its natural period of vibration, to the motion involved. It also gives rise to that general feeling among some practical men that springs are "temperamental."

The following brief topical outline is submitted as the scope of the proposed code:

1 *Service Requirements.*

(*a*) Load-deflection rate.
(*b*) Available space.
(*c*) Frequency and regularity of operation which have a bearing on resonance and fatigue.
(*d*) Temperature and atmospheric conditions during operation.
(*e*) Precision.
(*f*) Number of springs required in a given time, i.e., production.
(*g*) Purchase cost and liability in case of failure.

2 *Materials Available.*

(*a*) Shape: Rounds mostly for the compression and extension types, and both rounds and rectangulars for the torsion type.
(*b*) Size: Existing wire gages and formulation of a new single wire and bar gage with number of sizes reduced to minimum and progressive increases in size, arranged logically both from the manufacturers' and calculators' standpoints. Tabulation of available bar lengths.
(*c*) Composition: Ferrous, nonferrous, and nonmetallic.
(*d*) Physical properties: Ferrous, nonferrous, and nonmetallic.
(*e*) Tabulation of all important spring-material specifications in use.
(*f*) Tabulation of commercial variations in size, composition, and physical properties of some of the more important materials.

3 *Manufacture.*

(*a*) Effects on material and bar dimension when coiling cold with and without mandrel, and coiling hot on mandrel. Effect of spring index. Effect of surging compression springs.

---

[1] Vice-President and Chief Engineer, General Springs Corporation, New York, N. Y. Mem. A.S.M.E.

Papers presented at the Mechanical Springs Session of the Annual Meeting, New York, N. Y., December 1–5, 1941, of THE AMERICAN SOCIETY OF MECHANICAL ENGINEERS.

NOTE: Statements and opinions advanced in papers are to be understood as individual expressions of their authors and not those of the Society.

(*b*) Heat-treatment.
(*c*) Surface defects due to hot coiling and heat-treatment.
(*d*) Effects of plating on material.
(*e*) Control of quality by manufacturing specification; classification of springs according to maximum variations to be expected in spring dimensions.
(*f*) Shipping methods.
(*g*) Cost analysis.

4 *Design.*

It is proposed that the three following procedures of design be included in the code:

(*a*) General Engineering Procedure. The usual formulas supplemented by nomographic charts and tables, showing the relation of spring dimensions and ultimate spring constants (safe working stress and modulus of elasticity) to service requirements should be given here. The curvature correction factor, spring-end design, correction for initial tension in extension springs, and solid closure in compression springs, buckling criterion, elevated temperature, and natural period of vibration should also be included in this procedure.

(*b*) Scientific Procedure. In scientific research and in design of highly precise instruments, the usual spring formulas are inaccurate and incomplete. Formulas of a much more complicated kind, which take into account such factors as variation in modulus of elasticity with stress, eccentricity of loading, correction for pitch angle, hysteresis and creep effects, change of spring diameter with loading, change of dimensions due to thermal expansion, spring-end effects, and a number of others should be used in this instance. These formulas could conveniently be made an appendix to the code.

(*c*) Field Procedure. One of the greatest deterrents to popularizing the art of spring design among the great mass of practical designers has been the difficulty in applying the rather complicated types of formula associated with springs, including as they do terms raised to the 3rd, 4th, and 5th powers. Suppose Ohm's law instead of being the simple relation "current equals voltage divided by resistance" was "current equals voltage cubed divided by resistance raised to the fourth power," the effect on practical progress in the electrical art, while not serious, might have been sufficient to cause an appreciable lag.

Approximate Spring Determination for Field Work

We of course cannot change the laws underlying spring formulas, but we can provide a few simple relations that will permit a quick determination in the field of a spring that is approximately near the exact solution. Therefore it is proposed to supply the field engineer or mechanic, or in fact anyone who wants to make a quick exploratory survey, with a design procedure which might be called a field tool. This procedure will also serve to give a greater number of people a better mental picture of the apparently broad and complicated field of helical-spring design.

Referring to Fig. 1 and Table 1 of this presentation, a proposed field procedure has been developed for ordinary carbon-steel helical extension and compression springs in which the curvature correction factor has been taken into account, and a safe maximum stress of 80,000 psi and a torsional modulus of 11,500,000 psi have been assumed.

No matter what size wire or bar is assumed, the maximum percentage of compression or extension given in the second column of Table 1 should not be exceeded. To obtain the corresponding safe maximum loads, the constants given in the third column are simply multiplied by the square of the wire or bar diameter. For exploratory purposes diameters of 0.1, 0.2, 0.3 and so on up by tenths to 1 in. or more can be used to great advantage. Of course it should be borne in mind that this procedure should be used only for making a quick and preliminary solution of a spring problem, and that ultimately the "engineering" or "scientific" procedure should be resorted to.

TABLE 1 QUICK METHOD FOR GAGING LIMITATIONS IN HELICAL-SPRING DESIGN

Spring index	Maximum percentage,[a] compression or extension, F_m/H_l	Maximum load, P_m, lb	Maximum deflection, F_m, in.	Value P_m/F_m, d = 1 in. and H = 10 in.
4	22	5000 d^3	0.22 H	2273
5	39	4500 d^3	0.39 H	1154
6	60	4000 d^3	0.60 H	666
7	85.5	3600 d^3	0.855 H	421
8	115.5	3250 d^3	1.155 H	281

[a] In cases of initial tension in an extension spring and uneven solid closure in a compression spring, the percentages may be only 90 per cent of these values.

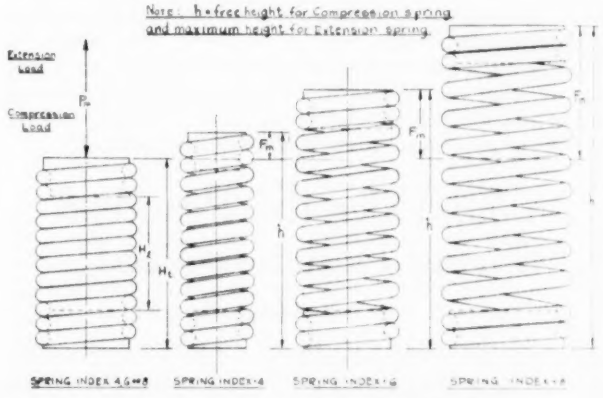


Fig. 1 Relative Safe Maximum Deflections Versus Spring Index in Helical-Spring Design

Summarizing, it is proposed by the writer that a tentative "Code for Design of Helical Springs," along the lines suggested, be drawn up by a subcommittee for submission to the whole committee for approval. It is further proposed that this subcommittee be made permanent in order to revitalize and improve the code from year to year in accordance with the experience gained from suggestions made by engineers using it and with new facts learned from future research projects.

Helical-Spring Design Stresses for a Standard Code

By A. M. WAHL[2]

Introduction

In choosing the design or working stresses for a proposed standard code of helical-spring design, it seems to the writer that one must be guided by the fact that it is clearly impossible in such a code to take into account all the variables which may arise in actual practice. In evaluating these design stresses it therefore seems advisable to use fairly large factors of safety; in other words, the stresses chosen should be quite conservative. This means that the code will be of value chiefly to engineers or designers who are occasionally faced with the problem of selecting a spring for a given application, but who do not have the time to make a complete study of all the limiting factors present. In cases where the number of springs required for a given application is large or the space available for the spring is limited, it is probable that a thorough study of the problem is justified. In such a case, higher working stresses than those given in the code may often be justified.

[2] Research Engineer, Westinghouse Electric & Manufacturing Company, East Pittsburgh, Pa. Mem. A.S.M.E.

Among the more important factors which influence the choice of working stress the following may be mentioned:

1 Material properties.
2 Condition of surface.
3 Kind of loading (static or fatigue).
4 Corrosion effects.
5 Creep or loss of load (static loads).
6 Temperature effects.
7 Surging or vibration effects.
8 Effects due to eccentricity of loading.
9 Completeness of knowledge regarding actual loads or deflections.
10 Seriousness of spring failure.
11 Method of stress calculation (i.e., whether curvature effects are included or not).

While most of these factors do have an effect on the allowable stress, they cannot all be accurately evaluated in a code simple enough for practical use. In addition, our knowledge concerning many of these factors (such as the fatigue properties of springs) is incomplete.

It is the primary purpose of this discussion to point out some of the fundamental principles involved in the choice of design stresses for a standard code and to suggest some values which may be used as a basis for further discussion.

For purposes of working-stress evaluation, spring applications may be grouped into two fundamental classes as follows:

1 Springs under static or infrequently repeated loading.
2 Springs under variable or fatigue loading.

Springs Under Static or Infrequently Repeated Loading

For springs which are subjected to a static load (or a load repeated but a relatively few times during the life of the spring), it is suggested that either the yield point or elastic limit in torsion be taken as a basis for choosing the working stress. Since the determination of elastic limit in torsion is subject to some variation depending upon the accuracy of the instruments used to measure torsional deflection, it is believed that the yield point of the material in torsion would probably be a better criterion for the present purpose than the elastic limit.[3] Since spring materials usually do not have a pronounced yield point, a satisfactory value may be taken as that point where the plastic strain is 0.2 per cent.[4]

If the yield point in torsion is not known, its value may be estimated by taking a figure of about 60 per cent of the tension yield point. This will usually give a fairly reasonable figure for most spring materials; however, figures based on actual torsion tests would be preferable.

In calculating the stress for helical springs under static loading, all evidence points to the fact that the stress augment, due to curvature of the bar or wire, may be considered as a condition of stress concentration since the peak stress is more or less localized near the inside of the coil. Such localized stresses may usually be neglected in so far as static loads are concerned. However, the stresses due to direct shear loading are not localized but are distributed over the cross section, and hence should be included in the stress calculation.[5] The working stress, figured in this way, would then be taken equal to the yield point in torsion divided by the factor of safety.

As an example of the use of this method consider an oil-tempered wire with a yield point in tension of 180,000 psi. The yield point in torsion would be about 60 per cent of this or 108,000 psi. Taking a factor of safety of 1.5 with respect to the yield point, this gives a working stress for static loading of 108,000/1.5 = 72,000 psi. If a factor of safety of 1.25 is used, the working stress would be 108,000/1.25 = 86,000 psi. (These stresses would be higher if the stress augment due to curvature were included.) Such values are in line with values frequently used in practice. (It should be noted that even when the yield point is reached in the outer fibers, the spring can still carry perhaps 30 per cent more load before complete yielding over the entire cross section occurs.) For purposes of a code where static loads and normal temperatures are involved, a factor of safety of around 1.5 on the torsional yield point is suggested as a basis for further discussion.

For higher temperatures, the effects of creep or relaxation (loss of load) must usually be considered. Not many data are available for springs under such conditions, and it is questionable whether the proposed code should provide for these situations. However, some limitation on the temperature at which ordinary steel springs may be used should be given.[6]

Variable or Fatigue Loading of Springs

Where springs are subjected to variable or fatigue loading (an example is the automotive valve spring), the most important quantity is the stress range, i.e., the difference between the maximum and minimum stresses. Since stress concentration affects the fatigue strength of materials, it is logical to include the stress augment due to curvature, in calculating the stress range of actual springs.[7] Usually this stress range will not vary a great deal as the mean stress increases, provided the elastic limit or yield point is not exceeded, so that, for purposes of the code, a minimum value of the range should probably be taken as a basis for design. Actually the endurance range will decrease somewhat as the mean stress increases but, if the value corresponding to the highest practical mean stress is taken as a basis, the design will be on the safe side.[8] The allowable stress range in the spring is then equal to the endurance range divided by the factor of safety.

In addition, to avoid excessive creep or loss in load, it should further be specified that the peak load for fatigue loading should not exceed the permissible value for static loading. The stresses due to this peak load may, however, be calculated by neglecting the curvature effect.

As an example of the method of choosing working stress for fatigue loading, assume that it is desired to determine working stresses for a music-wire spring of about 0.1-in. wire diam subject to a minimum stress of 20,000 psi (calculated with curvature correction). Tests show the endurance range of this material

---

[3] "Working Stresses," by C. R. Soderberg, Trans. A.S.M.E., vol. 55, 1933, paper APM-55-16, pp. 131–140.

[4] The use of this value for yield point was suggested by C. R. Soderberg, loc. cit.

[5] A more complete discussion of this is given in "Analysis of Effect of Wire Curvature on Allowable Stresses in Helical Springs," by A. M. Wahl, *Journal of Applied Mechanics*, Trans. A.S.M.E., vol. 61, 1939, p. A-25; also "Calculating Springs for Static Loading," by A. M. Wahl, *Machine Design*, June, 1941, pp. 66–71.

[6] A considerable number of data on load losses in springs under elevated temperature were given in the paper, "Effect of Temperature on Coiled Steel Springs Under Various Loadings," by F. P. Zimmerli, Trans. A.S.M.E., May, 1941, pp. 363–367.

[7] Because of lack of full sensitivity to stress concentration in actual materials, the use of the full curvature-correction factor may result in too high a calculated value for the stress range when compared to the results of fatigue tests. However, until further test data are at hand, it is believed that the full correction for curvature should be made for fatigue loading.

[8] See, for example, "Permissible Stress Range for Small Helical Springs," by F. P. Zimmerli, University of Michigan, Engineering Research Bulletin No. 26, 1934, for a number of endurance diagrams. A more accurate method would be to assume a variable stress range as a function of mean stress, but this complication would probably not be justified for use in the code.

to be 0–75,000 psi. Assuming a factor of safety of 1.5 on the stress range, this gives an allowable range of 75,000/1.5 = 50,000 psi. The peak stress would then be 20,000 + 50,000 = 70,000 psi (with curvature correction). If the spring index is 8, the calculated stress at the peak load, neglecting curvature effects, would be 63,000 psi, which is low compared to an estimated torsional yield point of around 130,000 psi for this material. Hence no loss in load due to creep would be expected.

Because of the fact that the fatigue strength of springs is greatly influenced by variations in surface condition, it may, however, be desirable when fatigue conditions are involved to use an even larger factor of safety than 1.5 in the proposed code.[9]

In calculating stresses for helical compression springs, it also seems advisable to take into account eccentricity of loading, particularly if the spring has relatively few turns. This might be done by using the formula given by Keysor.[10]

Examples From Practice

As an example of working stresses occurring in practice, the writer would like to mention the spring tables used as a basis for design by his company. These spring tables are based on the stresses shown in Table 2 of this discussion (curvature correction included). It is assumed that no corrosion is present and that temperature effects are not involved.

TABLE 2 WORKING STRESSES IN SHEAR: HELICAL COMPRESSION SPRINGS[a]

Wire diam, in.	Severe service, psi	Average service, psi	Light service, psi
Up to 0.085	60000	75000	93000
0.085– 0.185	55000	69000	85000
0.185– 0.32	48000	60000	74000
0.32 – 0.53	42000	52000	65000
0.53 – 0.97	36000	45000	56000
0.97 – 1.5	32000	40000	50000

[a] Made of good-quality steel such as music or oil-tempered wire. Curvature correction included.

Light service as indicated in Table 2 would correspond to statically loaded springs or those loaded infrequently. For most cases, the values given in the table are conservative and may frequently be increased. For springs of average index, the values for light service correspond roughly to a factor of safety of 1.5 with respect to the torsional yield point.

The values given in the table for severe service correspond to factors of safety of 1.5 to 2 on the estimated endurance range.

W. R. Berry in a paper before The Institution of Mechanical Engineers of Great Britain[11] suggests that, where fatigue conditions do not enter, springs be designed on the basis of a working stress of 70 per cent of the torsional elastic limit of the spring material, the curvature correction being considered. Since the yield point would be somewhat above the elastic limit, and since the effect of wire curvature is considered, this method would correspond to a factor of safety of somewhat more than 1.5 for springs of average index, based on the suggested method of calculation for static loading.

Values of stress equal to 100,000 psi (with curvature correction) are suggested for a good grade of steel wire by Wallace Barnes Company[12] for extension springs where excessive fatigue or corrosion are not factors. This would correspond to stresses of about 90,000 psi, figured by neglecting curvature effects for springs of average index. Assuming a yield point in torsion of around 120,000 psi for good-quality steel wire, this stress would correspond to a factor of safety of about 1.33.

From these figures it would appear that the suggested figure of 1.5 for factor of safety is not out of line with values in actual use.

Conclusions

In fixing design stresses for helical-spring applications at normal temperatures, and where the load is static or repeated a relatively few times, it appears reasonable to use the yield point of the material in torsion as a basis. For this type of loading the stress should be calculated by neglecting stress-concentration effects due to curvature (but including the stress augment due to direct shear). The design or working stress is then equal to the yield point divided by a factor of safety which is required to take into account unknown variables. To determine allowable stresses to be used in a standard code, this factor of safety should probably be taken slightly high, a figure of 1.5 being suggested as a basis for further discussion. This would be done with the reservation that after careful consideration higher stresses than those suggested in the code may be used in many cases.

For springs subjected to elevated temperatures, it seems difficult at present to fix on allowable working stresses until more data are at hand.

For helical springs, subjected to fatigue or repeated loading, it is suggested that that the range of stress (calculated with curvature correction) be taken as a basis for design. To obtain the allowable working-stress range to be used in the code the minimum endurance range of the material (assuming a peak stress below the yield point) is divided by a factor of safety. For purposes of the code, values of this factor of safety of 1.5 to 2 are suggested as a basis for discussion. To avoid excessive creep or loss in load, the peak stress (calculated by neglecting the stress augment due to curvature) should not exceed the allowable value as determined for static loading.

[9] A factor of safety of 1.25 to 1.5 on the stress range (figured with curvature correction) is suggested in "Die Federn," by S. Gross and E. Lehr, V.D.I. Verlag, Berlin, 1938.

[10] "Calculation of the Elastic Curve of a Helical Compression Spring," by H. C. Keysor, Trans. A.S.M.E., vol. 62, 1940, pp. 319–326.

[11] "Practical Problems in Spring Design," by W. R. Berry, Proceedings of The Institution of Mechanical Engineers, vol. 139, 1938, pp. 431–479.

[12] "The Mainspring," published by Wallace Barnes Co., June, 1940.

Helical-Spring Tables—Scope and Arrangement

By H. C. KEYSOR[13]

THE primary function of a spring table is to save time by eliminating formula calculations. For the accomplishment of this end, scope and arrangement are of vital importance.

As regards scope, the table should be extensive enough to cover the complete range of bar sizes and coil diameters with increments sufficiently small to include any reasonable design. The importance of this requirement will be appreciated by anyone who has had occasion to use a short table and has found that the design wanted was missing. While no table can be made to cover every design, the user has a right to expect coverage of all but some unusual cases which comprise a negligible proportion of the total. The actual time-saving possibilities of a spring table can be realized only when the designer has learned to turn to it with the feeling that the required entries are almost certain to be there. The following range of sizes is reasonably satisfactory according to the author's experience in hot-wound-spring design:

Bar diameters
- $\frac{3}{8}$ in. to $1\frac{1}{4}$ in., inclusive, by $\frac{1}{32}$-in. increments
- $1\frac{5}{16}$ in. to 2 in., inclusive, by $\frac{1}{16}$-in. increments
- $2\frac{1}{8}$ in. and $2\frac{1}{4}$ in.

[13] Mechanical Engineer, American Steel Foundries, Chicago, Ill.

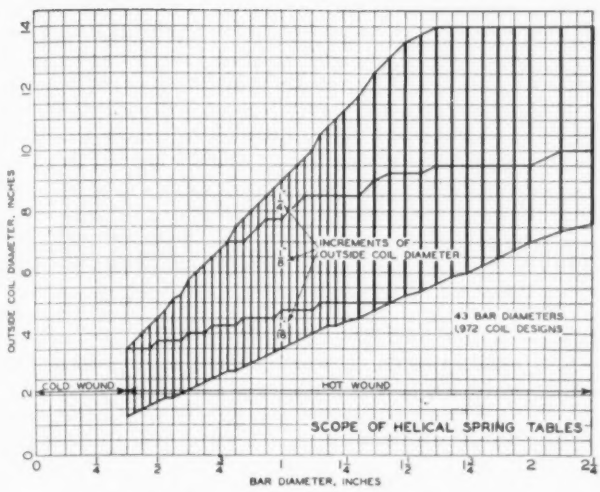


FIG. 2 SCOPE OF HELICAL-SPRING TABLES

Outside coil diameters { minimum $3^1/_2$ × bar diameter; maximum 9 to 10 × bar diameter up to 14 in. diam

Fig. 2 of this presentation shows the scope of the table, together with the increments in bar and coil diameters. The rather minute subdivisions of bar diameters are made necessary by the fact that the load rate of a spring varies directly as the fourth power of bar diameter. Thus, the change from a $1^3/_{16}$-in. bar to a $1^7/_{32}$-in. bar results in a load-rate increase of 10.3 per cent; changing from a $1^1/_4$ to a $1^3/_{16}$-in. bar, the rate increases 19 per cent. A load-rate differential of 10 per cent is small enough for most practical purposes, hence $1^7/_{32}$ in. represents the upper limit of $^1/_{32}$-in. increments of bar diameter. Naturally, the use of such an odd size as $1^7/_{32}$ in. would be avoided except where special load and space limitations required it. Sometimes an odd-size bar must be figured for other reasons, as in a recent case in the writer's experience, where it was necessary to use a $1^{15}/_{16}$-in. bar, because it was the only adequate size available for a rush job. The usual short table would not list such sizes, thus requiring a formula calculation—work that is time-consuming for the busy designer.

BAR DIAMETER 1⅞

COIL O.D.	SOLID H.→	SOLID LOAD AND FREE HEIGHT FOR 140,000 #/□" SOLID STRESS										
		3	4	5	6	7	8	10	12	16	20	30
—	—	—	—	—	—	—	—	—	—	—	—	—
—	—	—	—	—	—	—	—	—	—	—	—	—
5	LOAD	9,984	10,960	11,480	11,800	12,010	12,170	12,370	12,500	12,660	12,750	12,880
	FREE H.	3.390	4.688	5.992	7.299	8.607	9.917	12.534	15.153	20.392	25.631	38.739
⅛	LOAD	9,800	10,760	11,270	11,580	11,790	11,940	12,140	12,270	12,420	12,520	12,640
	FREE H.	3.421	4.743	6.071	7.403	8.735	10.068	12.735	15.404	20.739	26.082	39.433
¼	LOAD	9,614	10,560	11,060	11,360	11,570	11,720	11,910	12,040	12,190	12,280	12,400
	FREE H.	3.453	4.799	6.153	7.509	8.867	10.226	12.943	15.663	21.102	26.543	40.15
⅜	LOAD	9,437	10,360	10,850	11,150	11,350	11,500	11,690	11,820	11,970	12,060	12,170
	FREE H.	3.486	4.858	6.237	7.620	9.004	10.389	13.159	15.933	21.479	27.027	40.89
½	LOAD	9,264	10,170	10,660	10,950	11,150	11,290	11,480	11,600	11,750	11,840	11,950
	FREE H.	3.521	4.919	6.326	7.735	9.147	10.559	13.384	16.210	21.867	27.526	41.67
—	—	—	—	—	—	—	—	—	—	—	—	—
—	—	—	—	—	—	—	—	—	—	—	—	—

RANGE OF NUMBER OF TURNS: 2.667 TO 26.67

EXAMPLE: 5⅛ O.D. 7⅞ SOLID HEIGHT

SOLID LOAD = 11,350 + ⅞(11,500 − 11,350) = 11,440 LBS.

FREE HEIGHT = 9.004 + ⅞(10.389 − 9.004) = 9.870"

$$\text{LOAD RATE} = \frac{11{,}440}{9.870 - 7.625} = 5{,}096 \text{ LBS. PER INCH}$$

$$\text{STRESS RATE} = \frac{140{,}000}{9.870 - 7.625} = 62{,}360 \text{ PSI PER INCH}$$

FIG. 3 TYPICAL SPRING TABLE FOR USE IN DESIGNING AND CHECKING

The conventional spring table assumes axial loading and shows the load for a given stress and the deflection, at this load, for one active turn. Three supplementary numerical operations are required:

1 Determination of the total number of turns.

2 Deduction of the inactive end turns.

3 Multiplication of the number of active turns by the deflection per turn to obtain the total travel.

A fourth operation is necessary to find the stress augment due to load eccentricity which is present in compression springs, deflected between parallel planes. While this factor is usually omitted, it is of importance in short springs.

The elimination of this supplementary arithmetical work would be a distinct advantage. A table which gives results without recourse to formulas was made by the author five years ago and its practicability has been proved by daily use in designing and checking. The arrangement is shown in Fig. 3 of this discussion, the essential feature being that free heights and solid loads are given for a selected series of solid heights, interpolation being used for solid heights intermediate between tabular values. The basic solid stress is 140,000 psi, including Wahl's factor and an allowance for loading eccentricity. Each bar diameter occupies a separate page, various coil diameters are shown in the left-hand vertical column, and for each coil diameter there is a double horizontal row of figures, the top row being solid loads and the bottom row free heights, corresponding to the solid heights given at the top of the table. The range of solid heights corresponds to $2^3/_4$ to 30 turns, approximately.

This table possesses several advantages over the conventional type:

1 The deduction for inactive end turns is contained within the table by reason of free and solid heights being given. Therefore, it is not necessary for the designer to make this deduction or to know the number of turns, a marked advantage, especially for those users who are not familiar with spring calculation.

2 The effect of load eccentricity, in reducing capacity for any given stress, is also contained within the table by decreasing the solid load with decrease in the number of turns.

3 Since the use of formulas is eliminated, calculation is merely a matter of interpolation, just as in the familiar trigonometric tables. This feature reduces the chances for numerical error, as the tabular values are available for rapid mental checking of results.

4 When only load and loaded heights or free heights are given, as is often the case, the required bar diameter and solid height can be found approximately by inspection, thus avoiding much numerical work which would be necessary with the conventional table. This feature is especially helpful in designing double and triple coil springs.

5 Frequently load and space requirements are not closely restricted, which permits a satisfactory design to be taken directly from the table without any calculation.

Future Research Work Needed in Mechanical-Spring Problems

BY M. F. SAYRE[14]

IN 1924, the A.S.M.E. Research Committee on Mechanical Springs was organized. It had before it a large task, namely, that of establishing a foundation of technical information which would serve as the basis for improving the empirical methods of spring design which in essence were all that were available at that time. For 22 years previously, from 1902 to 1924, not one paper had been published in the Transactions of this Society, dealing closely enough with springs, to justify its inclusion in the index under that title. One paper was published in 1924, that by J. K. Wood, which helped in giving the impetus to the formation of the committee. For the 17 years since then, there are 65 papers in the index dealing with spring properties or spring design, most of them reporting research results of real importance.

There is a law of diminishing returns in research, which states that most fruitful results are likely to be obtained in a new unbroken field, and that after much work has been done the rewards of future work are likely to be less. This fact suggests that now may be a good time to survey what has been accomplished by the Committee on Mechanical Springs in its 17 years of existence, and what further need there is for its existence.

During these 17 years, major emphasis, possibly to too great a degree, has been directed to the design and use of helical extension or compression springs, in no less than 23 papers. In one direction, starting from the old-time simple formula $PR = S_s J/r$, these studies have introduced complexity, first in the form of the curvature correction formula, as brought over from German papers, simplified and experimentally proved by Wahl, then in the equations by Sayre and de Forest, showing deviation from uniform rate of elongation with load, and more recently in Keysor's excellent work which shows the impossibility of assuming the existence in compression springs of a centrally applied loading and a uniform rate of elongation per coil. The fatigue tests sponsored by Edgerton and by Zimmerli have aided materially in interpreting the rather confusing results given in the papers just mentioned, but much more work remains to be done. A complete list of topics covered in other papers on helical springs during this period would be too long to give here. Table 3 summarizes the record of publication of papers on mechanical springs.

TABLE 3 PAPERS ON OR REFERENCES TO MECHANICAL SPRINGS, A.S.M.E. TRANSACTIONS AND MECHANICAL ENGINEERING

	1883 to 1902	1921 to 1925	1926 to 1930	1931 to 1935	1936 to 1940	1941	Total since 1924
Helical springs	2	3	3	4	11	2	23
Flexural springs	..	..	..	..	1	..	1
Spiral springs	..	..	..	1	..	..	1
Disk and other special types of springs	..	..	3	..	2	..	5
General	3	4	3	..	..	..	7
Spring uses	3	2	1	1	3	..	7
Spring materials	1	..	3	2	..	..	5
Rubber	..	..	..	1	8	1	10
Vibration	..	..	..	2	5	..	7
							66

There have been five papers on disk springs, ring springs, and various other special types during this time. On the other hand, spiral springs have been the subject of but one paper and that is also true of the entire field of flexural springs, including leaf springs, surprising as it may seem. These have of course been touched upon to some extent in the seven papers which deal with the general topic of spring design, but these represent rather summations of existing knowledge than extensions of the field.

Five papers deal with fundamental properties of metallic materials for springs; and these have given us a fairly good background of knowledge of some but not all of the quirks which affect stress distribution in springs and their resulting behavior. The current paper, presented by D. J. McAdam, Jr.,[15] is another very important contribution to this field. Six papers deal with vibration problems as influenced by springs and seven with other spring uses.

Research Work Necessary

This leads up to the question of the type of research work which yet remains to be done. The writer can claim no right to speak with authority and so will only attempt to give suggestions which may serve as a foundation on which others may build a more satisfactory set of conclusions. With this limitation in mind, the following set of suggestions is offered:

1 In the present state of the art, an attempt to compute the so-called "true" maximum stress in a helical spring, particularly a compression helical spring, calls for use first of the Keysor formula, then of the Wahl formula, coupled with correction formulas to take into account the effect of combined stresses. Then, if we wish to be accurate, a correction must be made to allow for the effect of the initial stresses introduced by "surging" the spring. This combination is much too complex for ordinary use. Furthermore, we have as yet no truly satisfactory evidence as to what relation, if any, this so-called "true" stress may bear to the probable service life of the spring. Further studies, probably in the form of fatigue tests, are needed to develop this relationship.

2 In compression helical springs Keysor has developed equations indicating marked advantages from the use of certain specific angular relationships between the positions of point of first contact between coils at the two ends of a compression spring. Experimental results have also been given which leave this advantage apparently uncertain. In short springs the stress increments suggested by Keysor are great enough to suggest further study with a view to finding means of capitalizing on these theoretical advantages.

3 Spiral springs seem to have had but little study given to them. Their importance has of course been reduced in recent years by the substitution of electric motors in place of power springs in many applications. Furthermore, a good deal of research work has been done which has not reached the publications of this Society. Possibly the cure may lie in the form of encouraging future publications which will summarize some of this unpublished research work.

4 Leaf and other flexural springs remain of great importance. At a meeting of the committee a few years ago, a verbal report was given covering important research work carried on privately in this field. The writer expresses the hope that this work will be supplemented by published reports and by further investigation.

5 In recent years, there has been a rapidly increasing use of rubber as a spring material. The extent to which this material has forced its way into attention is in some measure indicated by the fact that since 1936 no less than nine papers have dealt with its properties or its engineering uses, as compared to only one paper in the preceding history of this Society. The properties of rubber are widely different from those of the metallic springs with which we have become familiar in the past, and further

[14] Professor of Applied Mechanics, Union College, Schenectady, N. Y. Mem. A.S.M.E.

[15] "Technical Cohesive Strength of Metals," by D. J. McAdam, Jr., *Journal of Applied Mechanics*, Trans. A.S.M.E., vol. 63, December, 1941, p. A-155.

study dealing with its properties and method of application would seem to be desirable.

The results obtained by the committee during its 17 years of existence have been very great. In the writer's opinion, the fields for its work in the near future should be somewhat different from those it has emphasized in the past. It is hoped that its future efforts will be equally fruitful.

BIBLIOGRAPHY

1 "Spiral Springs—Compressible and Tensile," by Oberlin Smith, Trans. A.S.M.E., vol. 4, 1883, pp. 335–340.

2 "Helical Springs," by J. W. Cloud, Trans. A.S.M.E., vol. 5, 1884, pp. 173–184.

3 "Speed of Operation of Springs (topical discussion)," Trans. A.S.M.E., vol. 6, 1885, pp. 866–871.

4 "Metal for Springs (topical discussion)," Trans. A.S.M.E., vol. 7, 1886, pp. 384–386.

5 "Length of Indicator Card," by J. B. Webb, Trans. A.S.M.E., vol. 11, 1890, pp. 941–950.

6 "Comparison of Mean Effective Pressures of Simultaneous Cards Taken by Different Indicators," by D. S. Jacobus, Trans. A.S.M.E., vol. 15, 1893–1894, pp. 277–305.

7 "Constants for Correcting Indicator Springs That Have Been Calibrated Cold," by R. C. Carpenter, L. S. Marks, and S. H. Barraclough, Trans. A.S.M.E., vol. 15, 1893–1894, pp. 454–487.

8 "Graphical Method of Designing Springs," by G. R. Henderson, Trans. A.S.M.E., vol. 16, 1894–1895, pp. 92–103.

9 "Spring Tables," by G. R. Henderson, Trans. A.S.M.E., vol. 17, 1896, pp. 340–358.

10 "Some Peculiarities of Springs. Spring Testing Machine (topical discussion)," Trans. A.S.M.E., vol. 23, 1902, pp. 277–290.

11 "Experiments on Spiral Springs," by C. H. Benjamin and R. A. French, Trans. A.S.M.E., vol. 23, 1902, pp. 298–302.

12 "Mechanical Springs," by J. K. Wood, Trans. A.S.M.E., vol. 46, 1924, pp. 915–925.

13 "Code of Design for Mechanical Springs," by J. K. Wood, Trans. A.S.M.E., vol. 47, 1925, pp. 33–56; also abridged, *Mechanical Engineering*, vol. 47, 1925, pp. 713–718.

14 "Phosphor-Bronze Helical Springs From Standpoint of Precision Instruments," by W. G. Brombacher, Trans. A.S.M.E., vol. 47, 1925, pp. 699–712; also *Mechanical Engineering*, vol. 48, 1926, pp. 488–491.

15 "Formulas for Design of Helical Springs of Square or Rectangular Steel," by C. T. Edgerton, Trans. A.S.M.E., vol. 47, 1925, pp. 717–729.

16 "Outline for Application of Fatigue and Elastic Results to Metal-Spring Design," by T. M. Jasper, Trans. A.S.M.E., vol. 47, 1925, pp. 731–739.

17 "Mechanical Springs," by J. K. Wood, *Mechanical Engineering*, vol. 47, 1925, pp. 258–260.

18 "Manufacture of Commercial Steel Helical Springs," by F. H. Brown, *Mechanical Engineering*, vol. 47, 1925, pp. 1053–1055.

19 "Characteristics of Weighing Springs," by J. W. Rockefeller, Jr., *Mechanical Engineering*, vol. 47, 1925, p. 1056.

20 "Springs for Electrical Measuring Instruments," by B. W. St. Clair, *Mechanical Engineering*, vol. 47, 1925, pp. 1057–1058.

21 "Specification and Control of Mechanical Springs," by J. K. Wood, Trans. A.S.M.E., vol. 48, 1926, pp. 91–117; also abridged, *Mechanical Engineering*, vol. 48, 1926, pp. 808–814.

22 "The Ring Spring," by O. R. Wikander, *Mechanical Engineering*, vol. 48, 1926, pp. 139–143.

23 "Formulas for Design of Helical Springs of Square or Rectangular Steel," by C. T. Edgerton, *Mechanical Engineering*, vol. 48, 1926, pp. 484–487.

24 "Factors of Design of Shock-Absorbing and Recuperating Steel Springs," by T. M. Jasper, *Mechanical Engineering*, vol. 48, 1926, pp. 487–488.

25 "Hysteresis Relative to Operation of Mechanical Springs," by J. K. Wood, *Mechanical Engineering*, vol. 49, 1927, pp. 561–569; also discussion, pp. 1203–1207.

26 "Tests on Belleville Spring by Ordnance Department, U. S. Army," by D. A. Gurney, Trans. A.S.M.E., vol. 51, 1929, paper APM-51-2, pp. 13–17.

27 "Fatigue and Corrosion Fatigue of Spring Material," by D. J. McAdam, Jr., Trans. A.S.M.E., vol. 51, 1929, paper APM-51-5, pp. 45–56.

28 "Telephone-Apparatus Springs," by J. R. Townsend, Trans. A.S.M.E., vol. 51, 1929, paper APM-51-8, pp. 81–83.

29 "Stresses in Heavy Closely Coiled Helical Springs," by A. M. Wahl, Trans. A.S.M.E., vol. 51, 1929, paper APM-51-17, pp. 185–193; also abridged, *Mechanical Engineering*, vol. 51, 1929, pp. 434–437; errata, Trans. vol. 51, 1929, APM, pp. 307–308.

30 "Stress Distribution and Hysteresis Losses in Springs," by M. F. Sayre and Anthony Hoadley, Trans. A.S.M.E., vol. 51, 1929, paper APM-51-24, pp. 287–303.

31 "Radially Tapered Disk Spring," by W. A. Brecht and A. M. Wahl, Trans. A.S.M.E., vol. 42, 1930, paper APM-52-4, pp. 45–53.

32 "Elastic and Inelastic Behavior in Spring Materials," by M. F. Sayre, abridged, *Mechanical Engineering*, vol. 51, 1929, pp. 915–916 and 970; also Trans. A.S.M.E., vol. 52, 1930, paper APM-52-9, pp. 105–109; and Trans. A.S.M.E., vol. 53, 1931, paper APM-53-8, pp. 99–103.

33 "Further Research on Helical Springs of Round and Square Wire," by A. M. Wahl, Trans. A.S.M.E., vol. 52, 1930, paper APM-52-18, pp. 217–224.

34 "Spiral Springs," by J. A. Van den Broek, Trans. A.S.M.E., vol. 53, 1931, paper APM-53-18, pp. 247–259.

35 "Forced Vibrations With Nonlinear Spring Constants," by J. P. Den Hartog and S. J. Mikina, Trans. A.S.M.E., vol. 54, 1932, paper APM-54-15, pp. 157–162.

36 "Design of Spring Gears for Exhaust-Turbine Installations," by J. Ormondroyd and T. C. Kuchler, Trans. A.S.M.E., vol. 54, 1932, paper APM-54-20, pp. 205–214.

37 "Design and Investigation of Spring in Which All Coils Nest Simultaneously," by J. B. Reynolds and O. B. Schier, Trans. A.S.M.E., vol. 54, 1932, paper RP-54-11, pp. 197–202.

38 "Design and Investigation of Conical Springs With Coils of Constant Slope," by J. B. Reynolds and O. B. Schier, Trans. A.S.M.E., vol. 54, 1932, paper RP-54-12, pp. 203–211.

39 "Number of Active Coils in Helical Springs," by R. F. Vogt, Trans. A.S.M.E., vol. 56, 1934, pp. 467–472; corrections, *Mechanical Engineering*, vol. 56, 1934, p. 566.

40 "Laws of Elastic Behavior in Metals," by M. F. Sayre, Trans. A.S.M.E., vol. 56, 1934, pp. 555–558.

41 "Correlation of Spring-Wire Bending and Torsion Fatigue Tests," by E. E. Weibel, Trans. A.S.M.E., vol. 57, 1935, pp. 501–516; also discussion, Trans. A.S.M.E., vol. 58, 1936, p. 331.

42 "Helical Compression and Tension Springs (Design Data)," by A. M. Wahl, *Journal of Applied Mechanics*, Trans. A.S.M.E., vol. 57, 1935, p. A-35.

(*a*) "Uniform Section Disk Spring," by J. O. Alman and A. Laszlo, Trans. A.S.M.E., vol. 58, 1936, pp. 305–314.

43 "New Spring Formulas and New Materials for Precision Spring Scales," M. F. Sayre and A. V. de Forest, Trans. A.S.M.E., vol. 58, 1936, pp. 379–387; discussion, Trans. A.S.M.E., vol. 59, 1937, pp. 339–341.

44 "Stress and Deflection of Helical Springs," by R. F. Vogt, Trans. A.S.M.E., vol. 58, 1936, pp. 467–475.

45 "Stress and Deflection of Circular Plates (Design Data)," by A. M. Wahl and Stewart Way, *Journal of Applied Mechanics*, Trans. A.S.M.E., vol. 58, 1936, p. A-28.

46 "Forced Vibration in Nonlinear Systems With Various Combinations of Linear Springs," by J. P. Den Hartog and R. M. Heiles, *Journal of Applied Mechanics*, Trans. A.S.M.E., vol. 58, 1936, p. A-127.

47 "Rubber Cushioning Devices," by C. F. Hirshfeld and E. H. Piron, Trans. A.S.M.E., vol. 59, 1937, pp. 471–491; also discussion, Trans. A.S.M.E., vol. 60, 1938, pp. 203–205.

48 "Abstract of Progress Report No. 3 on Heavy Helical Springs," by C. T. Edgerton, Trans. A.S.M.E., vol. 59, 1937, pp. 609–616.

49 "Load-Deflection Characteristics of Initially Curved Flexural Springs," by W. E. Johnson, *Journal of Applied Mechanics*, Trans. A.S.M.E., vol. 59, 1937, p. A-119.

50 "Rubber Springs," by W. C. Keys, *Mechanical Engineering*, vol. 59, 1937, pp. 345–349.

51 "Relation of Wahl Correction Factor to Fatigue Tests on Helical Compression Springs," by F. P. Zimmerli, Trans. A.S.M.E., vol. 60, 1938, pp. 43–44; also discussion, pp. 685–688.

52 "Mechanical Characteristics of Rubber," by F. L. Haushalter, Trans. A.S.M.E., vol. 61, 1939, pp. 149–158; also discussion, pp. 463–464.

53 "Deflection of Helical Springs Under Transverse Loadings," by W. E. Burdick, F. S. Chaplin, and W. L. Sheppard, Trans. A.S.M.E., vol. 61, 1939, pp. 623–630.

54 "Stresses in Helical Compression Springs—Present Status of Problem," by C. T. Edgerton, Trans. A.S.M.E., vol. 61, 1939, pp. 643–648.

55 "Analysis of Effect of Wire Curvature on Allowable Stresses in Helical Springs," by A. M. Wahl, *Journal of Applied Mechanics*, Trans. A.S.M.E., vol. 61, 1939, p. A-25; discussion, p. A-188.

56 "Spring Clutch," by C. F. Wiebusch, Trans. A.S.M.E., vol. 61, 1939, p. A-103; also discussion, *Journal of Applied Mechanics*, Trans. A.S.M.E., vol. 62, 1940, p. A-89.

57 "Vibration Problems (Design Data), Part II," by J. Ormondroyd, *Journal of Applied Mechanics*, Trans. A.S.M.E., vol. 61, 1939, p. A-127.

58 "Rubber Springs—Shear Loading," by J. F. D. Smith, *Journal of Applied Mechanics*, Trans. A.S.M.E., vol. 61, 1939, p. A-159.

VIBRATION MOUNTINGS

59 "Rubber in Airplane Construction," by C. Saurer, Trans. A.S.M.E., vol. 53, 1931, paper AER-53-4, pp. 41–43.

60 "Influence of Damping in Elastic Mounting of Vibrating Machines," by E. H. Hull, Trans. A.S.M.E., vol. 53, 1931, paper APM-53-12; pp. 155–163; also abridged, *Mechanical Engineering*, vol. 53, 1931, pp. 805–809.

61 "Use of Rubber in Vibration Isolation," by E. H. Hull, *Journal of Applied Mechanics*, Trans. A.S.M.E., vol. 59, 1937, p. A-109.

62 "Rubber Mountings," by J. F. D. Smith, *Journal of Applied Mechanics*, Trans. A.S.M.E., vol. 60, 1938, p. A-13.

63 "Theory of Elastic Engine Supports," by S. Rosenzweig, Trans. A.S.M.E.. vol. 61, 1939, pp. 31–36; also discussion, pp. 460–463.

64 "Mechanical Characteristics of Rubber," by F. L. Haushalter, Trans. A.S.M.E., vol. 61, 1939, pp. 149–158; discussion, pp. 463–464.

65 "Deflection of Helical Springs Under Transverse Loadings," by W. E. Burdick, F. S. Chaplin, and W. L. Sheppard, Trans. A.S.M.E., vol. 61, 1939, pp. 623–630.

SPRINGS, 1940

66 "Calculation of Helical Compression Springs," discussion of paper by H. C. Keysor, *Mechanical Engineering*, vol. 62, 1940, p. 755.

67 "Factors in the Fatigue of Helical Springs," by R. R. Tatnall, *Mechanical Engineering*, vol. 62, 1940, pp. 289–292; also discussion, pp. 752–755.

68 "Fundamental Development in Suspension and Construction for Railroad Cars," by P. K. Beemer, F. C. Lindvall, E. F. Stoner, and W. E. Van Dorn, *Mechanical Engineering*, vol. 62, 1940, pp. 779–784.

69 "Calculation of Elastic Curve of Helical Compression Spring," by H. C. Keysor, Trans. A.S.M.E., vol. 62, 1940, pp. 319–324.

70 "Helix Warping in Helical Compression Springs," by D. H. Pletta and F. J. Maher, Trans. A.S.M.E., vol. 62, 1940, pp. 327–329.

71 "Neoprene as a Spring Material," by F. L. Yerzley, Trans. A.S.M.E., vol. 62, 1940, pp. 469–474.

72 "Spring Clutch," by C. F. Wiebusch, *Journal of Applied Mechanics*, Trans. A.S.M.E., vol. 61, 1939, p. A-103; also discussion of paper, vol. 62, 1940, p. A-89.

73 "Vibration Problems, Part 3, Systems With One Degree of Freedom (design data)," by J. Ormondroyd, *Journal of Applied Mechanics*, Trans. A.S.M.E., vol. 62, 1940, p. A-34.

SPRINGS, 1941

74 "Rubber Springs Under Compression Loading," by J. F. D. Smith, *Mechanical Engineering*, vol. 63, 1941, pp. 273–277.

75 "Effect of Temperature on Coiled Steel Springs Under Various Loadings," by F. P. Zimmerli, Trans. A.S.M.E., vol. 63, 1941, pp. 363–367.

76 "Recommended Code of Procedure for Fatigue Testing of Hot-Wound Helical Compression Springs," by C. T. Edgerton, Trans. A.S.M.E., vol. 63, 1941, pp. 553–558.

Nomographic Charts

Advantages and Disadvantages

By L. C. PESKIN[16]

OF all the possible methods available to engineers for computing design formulas graphically with the greatest saving in labor and the maximum amount of precision, none has the advantages of the nomographic or alignment chart, i.e., (1) The chart uses very few lines, as will be readily seen later, and is thus extremely easy to read. (2) Any interpolation that is involved is made along a simple scale rather than between curves with a very definite gain in accuracy. (3) As compared to other graphical methods, the labor of construction of these charts is comparatively slight. (4) One of the most important advantages to the practical designer is the graphic way in which the chart indicates instantly the change in one of the variables due to changes in the other variables.

The fundamental principle involved in the construction of nomographic or alignment charts consists in the representation of an equation connecting three variables, $f(u, v, w) = 0$, by means of three scales along three straight lines (or curves) in such a manner that a straight line cuts the three scales in values of u, v, and w satisfying the equation. This procedure can be extended to take care of more than three variables, and examples of three- and four-variable charts are shown in the figures which follow.

Figs. 4 to 9, inclusive, of this presentation are devoted to the design of helical compression and extension springs. Figs. 4 and 5 permit the stress determination of a complete range of spring sizes and loads. Stress correction for curvature may be determined from Fig. 6, while Figs. 7 and 8 enable the deflections per coil for the same range of spring sizes and loads to be readily obtained. Fig. 9 provides a means for modifying the deflections so as to provide for the design of springs using a variety of materials. Figs. 10 to 15, inclusive, show a set of charts serving the same general design purposes in the case of torsion springs. Finally, Figs. 16 to 19, inclusive, provide the necessary means for designing the very smallest to the largest of flat spiral or motor springs. While not shown, there have been derived simple factors which may be applied to Figs. 4 to 15, so as to make them readily applicable to the design of springs using rectangular wire. We will not go into the detail of constructing these charts, except to state that they were originally laid out with extreme care on cardboard sheets 24 × 36 in. and subsequently reduced by photographing to an $8\frac{1}{2} \times 11$-in. size, in which form they will soon be issued as part of a new piece of spring-design literature which we have been preparing for some time.

So far as the advantages of these charts are concerned, the ease with which they may be read is at once obvious from the illustrations. With respect to accuracy, as long as the charts are not laid out on too small a scale completely satisfactory results are readily obtained by any user. It is more desirable to cover a full range of spring sizes on more than one chart than to sacrifice accuracy by trying to cover all with too condensed a scale. It is also important to note that the nomographic chart is fundamentally no more than a means for computing graphically some given analytical expression. In the design of springs, this expression may be any one of the many formulas available for determining stress deflection, load, etc. Consequently, the chart may, at its best, be expected to duplicate exactly the numerical results obtained by direct calculation from the original formula itself. If

[16] Director of Spring Mill Products, American Steel and Wire Company, Cleveland, Ohio.

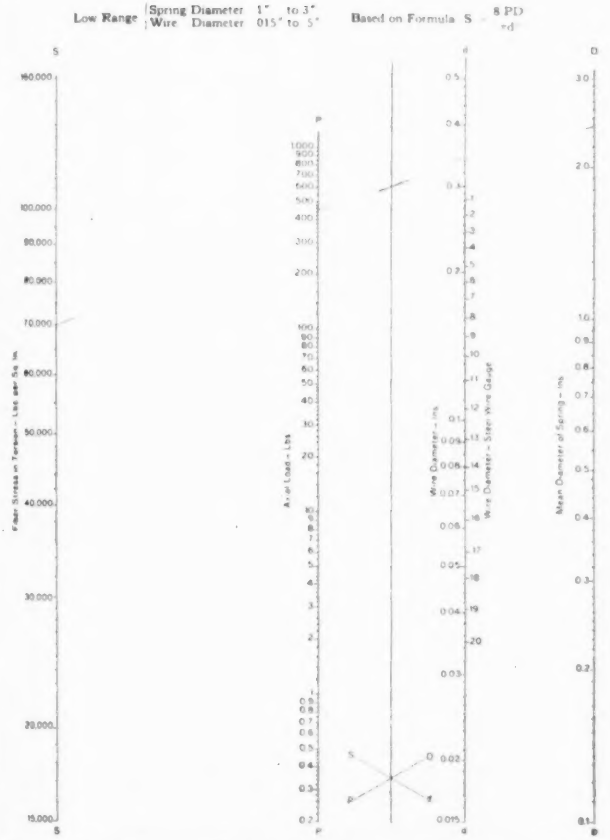


FIG. 4 FIBER STRESS, NOT CORRECTED FOR CURVATURE, VERSUS LOAD; HELICAL EXTENSION AND COMPRESSION SPRINGS

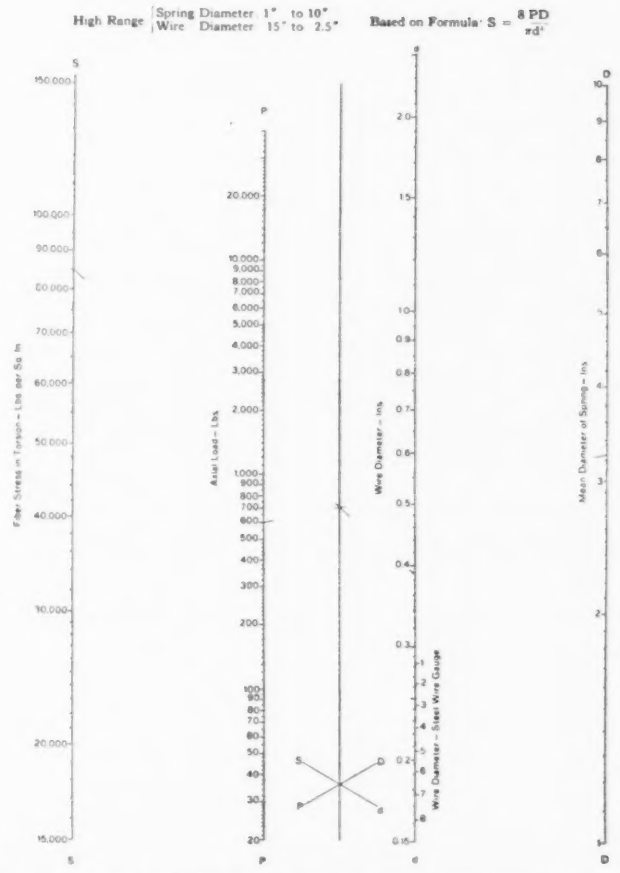


FIG. 5 FIBER STRESS, NOT CORRECTED FOR CURVATURE, VERSUS LOAD; HELICAL EXTENSION AND COMPRESSION SPRINGS

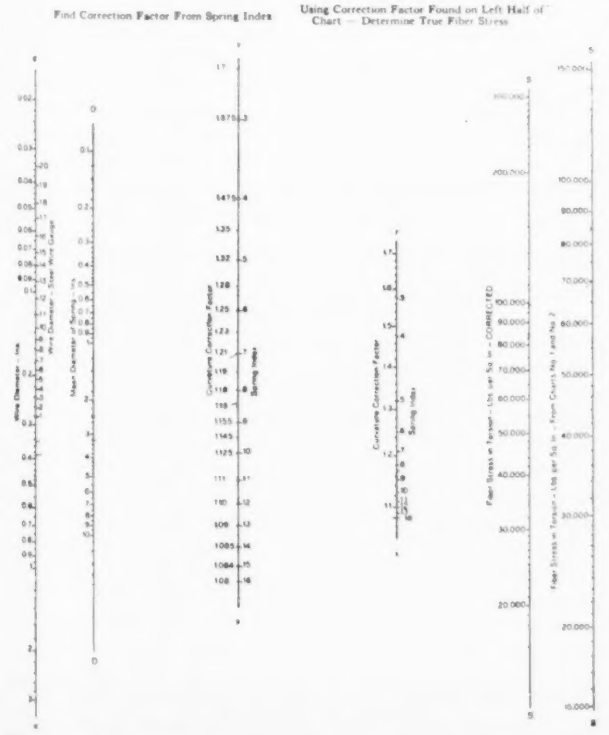


FIG. 6 FIBER-STRESS CORRECTION FOR CURVATURE; HELICAL EXTENSION AND COMPRESSION SPRINGS

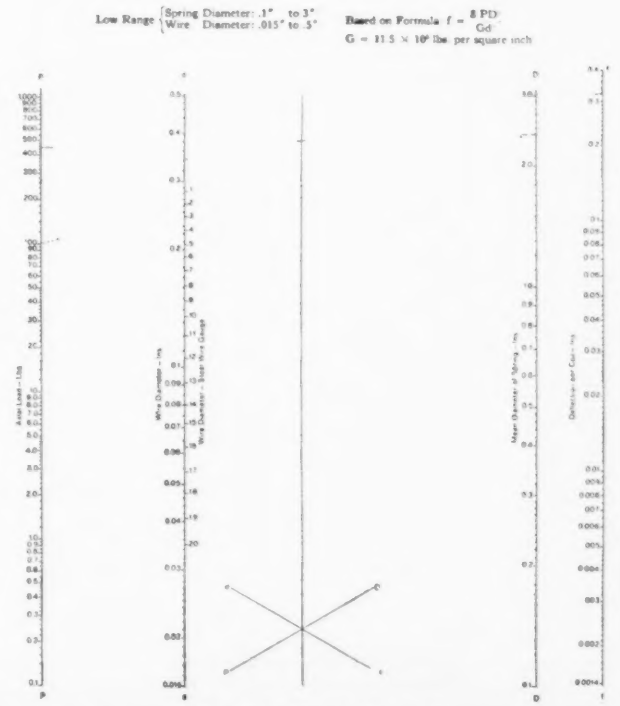


FIG. 7 DEFLECTION PER COIL VERSUS LOAD; HELICAL EXTENSION AND COMPRESSION SPRINGS

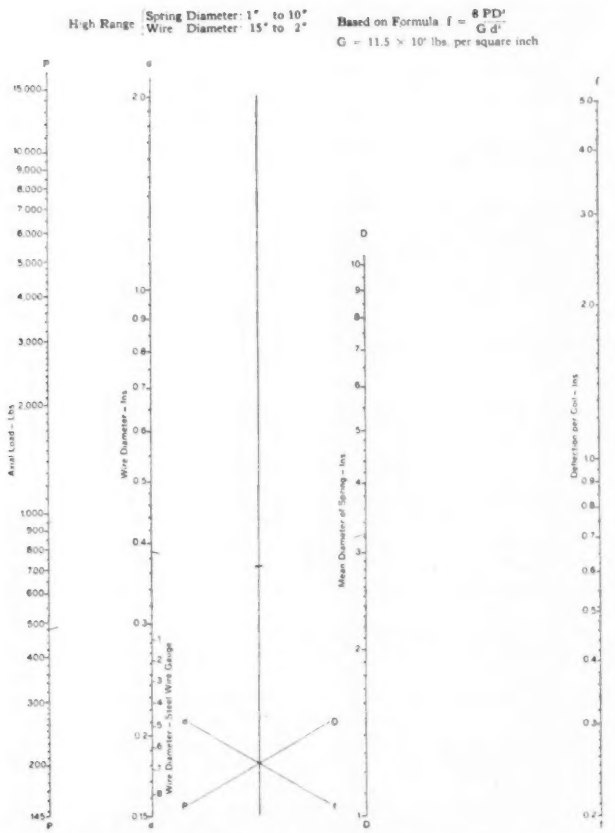


FIG. 8 DEFLECTION PER COIL VERSUS LOAD; HELICAL EXTENSION AND COMPRESSION SPRINGS

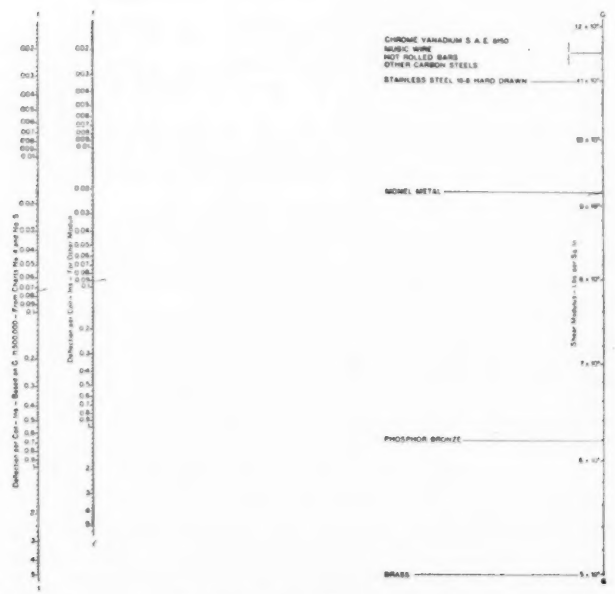


FIG. 9 DEFLECTION PER COIL
(Modulus, G, other than 11.5×10^6.)

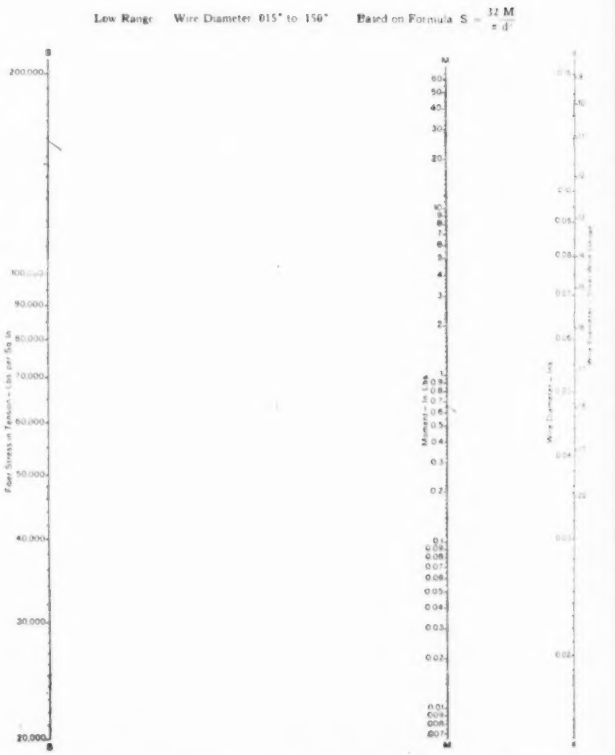


FIG. 10 FIBER STRESS, NOT CORRECTED FOR CURVATURE, VERSUS MOMENT; TORSION SPRINGS

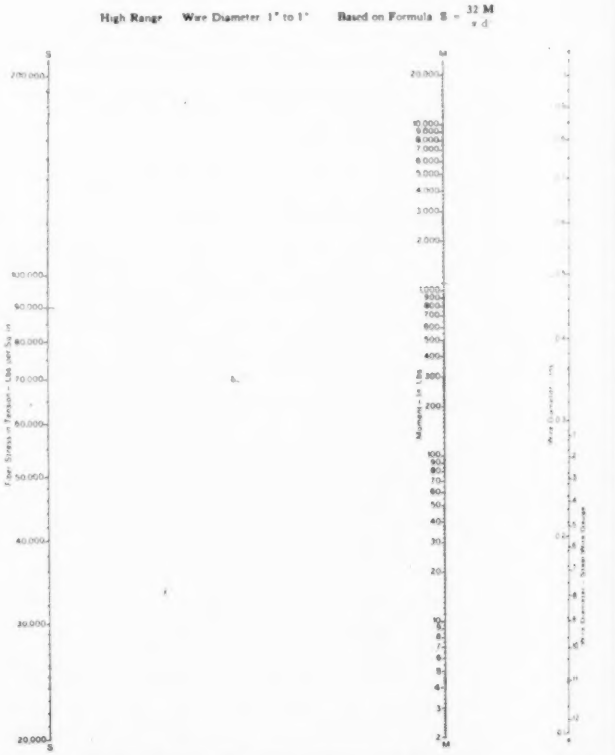


FIG. 11 FIBER STRESS, NOT CORRECTED FOR CURVATURE, VERSUS MOMENT; TORSION SPRINGS

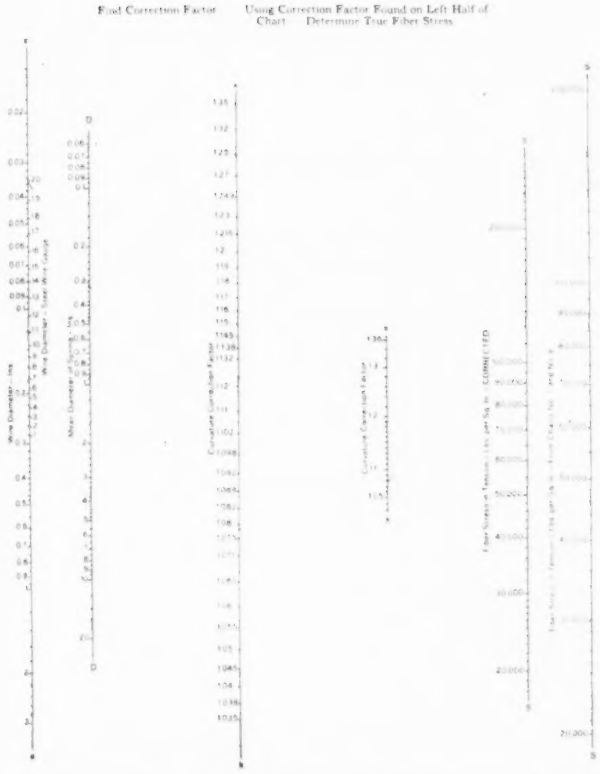


FIG. 12 FIBER-STRESS CORRECTION FOR CURVATURE; TORSION SPRINGS

the design formulas are approximate or even in error to begin with, the derived chart can only mirror these same departures in accuracy. Furthermore, the actual springs fabricated according to the design, no matter what procedure is used, will show in practice other deviations from the calculations as a result of unavoidable variations required by manufacturing tolerances. Hence, fair judgment of the accuracy of nomographic charts in spring design is therefore obtained, not alone when results determined thereby are compared to those obtained by direct calculation, but also when all of these results are compared to the actual performance of commercially made springs.

COMPARING SPRINGS MADE BY THREE DESIGN METHODS

Such a comparison was made and is illustrated in Figs. 20 and 21. Fig. 20 shows a typical extension-spring setup in the laboratory with two precision cathetometers arranged to read individual coil deflections. Fig. 21 is a similar experiment arranged for deflection measurements on a compression spring, and in Fig. 22 the results are plotted for nine different springs. The first eight springs are extension springs measured at two loads. Springs 1, 2, and 3 are duplicates, so far as design is concerned, selected at random from a large lot. Springs 6 and 7 are likewise design duplicates, and No. 9 is a compression spring, measured at three different loads. It will be noted that the three methods of design, logarithms, slide rule, and nomograph, in only one or two cases agree exactly with the measured results. These methods, however, for the most part substantiate each other as to relative accuracy. Logarithms and slide rule follow each other almost precisely, while at one time three observers read the nomographic charts with an average result less than 2 per cent away from the other design methods. As a matter of interest, it will be noted that springs of identical design deviated from one another on actual test over 3 per cent. Also, the springs, as commercially made, deviated in individual cases from the design, no matter what method was used, as much as 5 per cent. Since these results are found in all cases as both plus and minus deviations, it can be stated that on the average a lot of springs manufactured according to any one of the three methods of design illustrated will be in all respects commerically identical.

CONSTRUCTING NOMOGRAPHIC CHARTS

In commenting on the labor of constructing these charts, all we can say is that the work is neither difficult nor time-consuming but must be carried out with care on a sufficiently large scale. As to the charts showing graphically the effects of varying the different quantities involved in the design, this is a self-evident fact as will be noticed by the user at once. This has already proved a great boon to designers making trial calculations in a spring design. Finally, by actual experience, we have found it possible to place these charts in the hands of spring users and, with but few explanations, have them obtain entirely satisfactory spring designs.

Frankly, after having spent many long hours in practical spring design making tedious slide-rule calculations, struggling through spring-table interpolations, or finding a way through a maze of

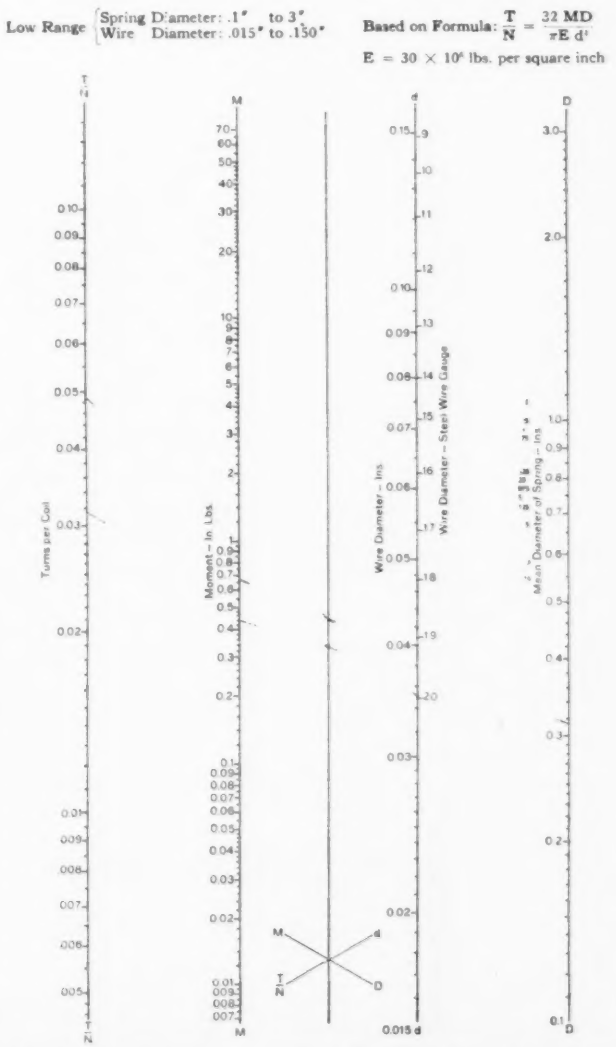


FIG. 13 TURNS SPRING WILL GIVE PER COIL VERSUS MOMENT; TORSION SPRINGS

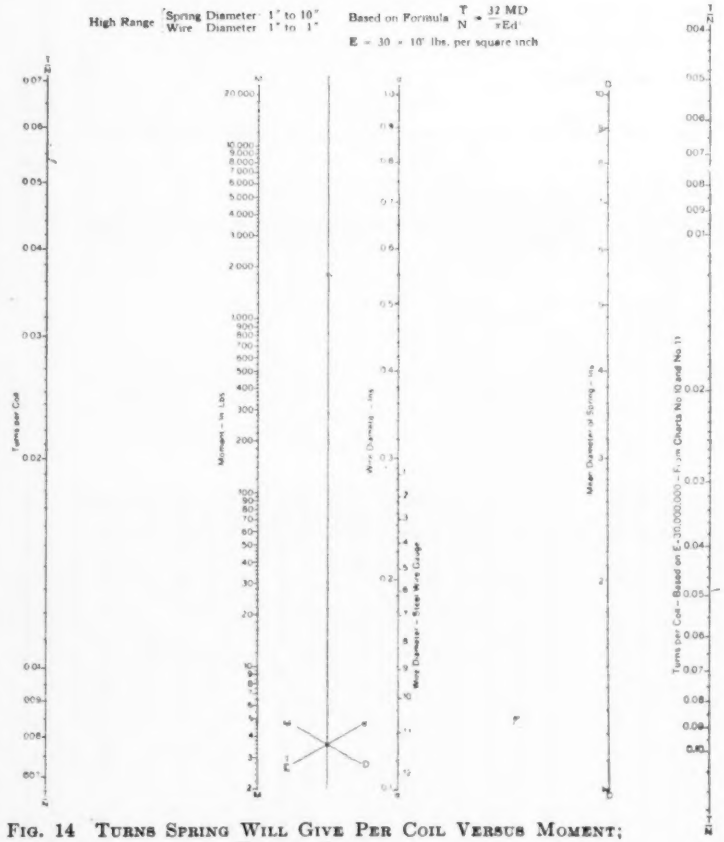


FIG. 14 TURNS SPRING WILL GIVE PER COIL VERSUS MOMENT; TORSION SPRINGS

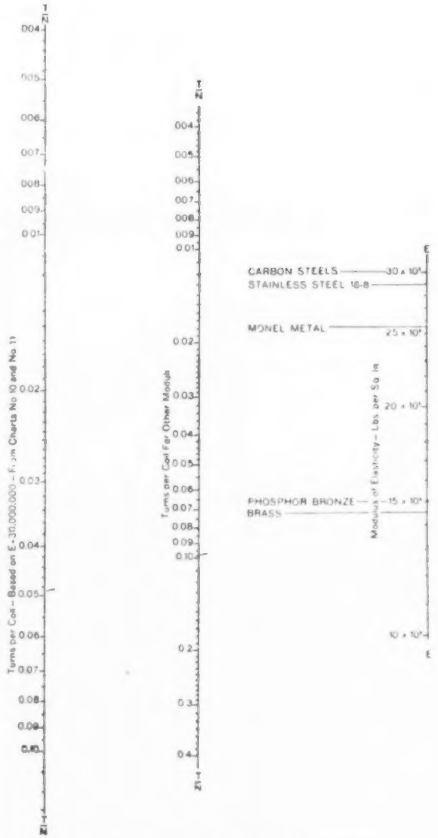


FIG. 15 TURNS SPRING WILL GIVE
(Modulus, E, other than 30×10^6.)

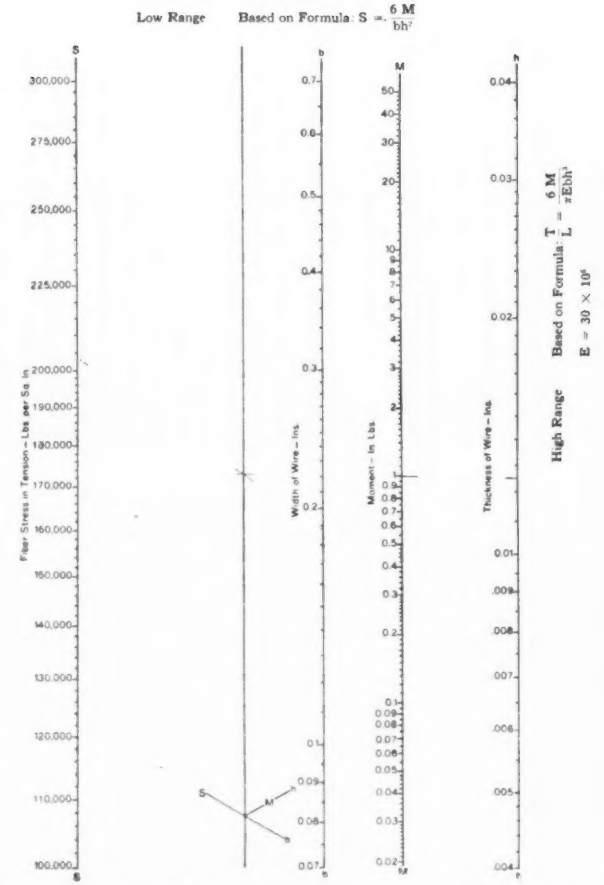


FIG. 16 FIBER STRESS VERSUS MOMENT; MOTOR OR CLOCK SPRINGS

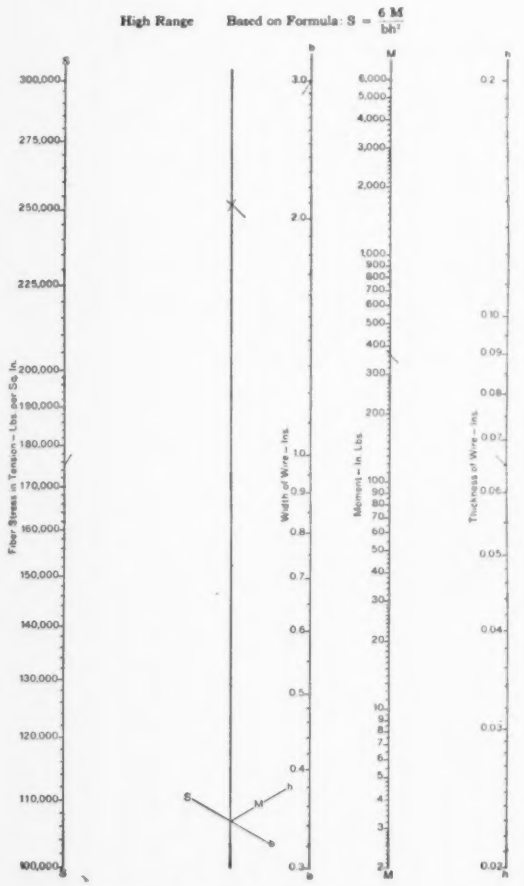


FIG. 17 FIBER STRESS VERSUS MOMENT; MOTOR OR CLOCK SPRINGS

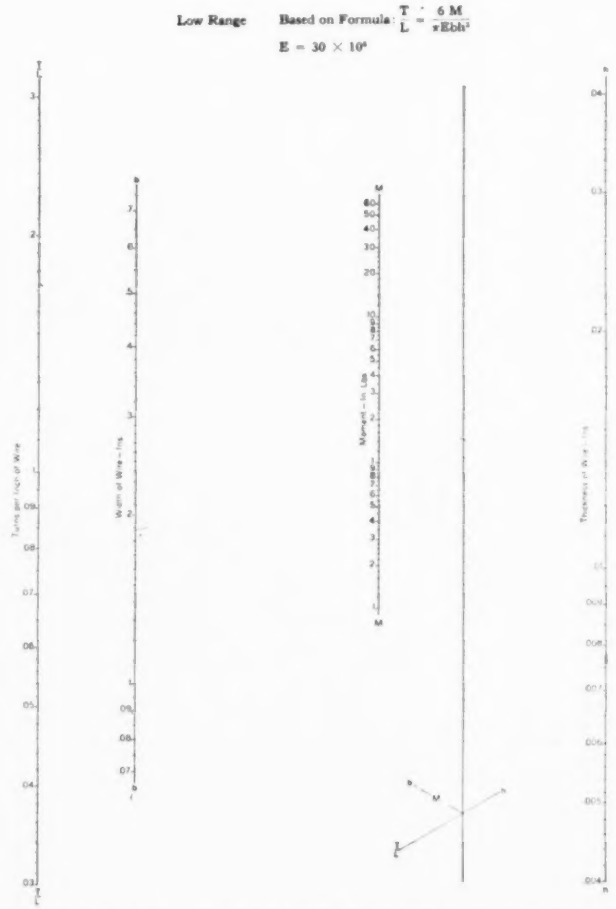


FIG. 18 TURNS PER INCH OF WIRE VERSUS MOMENT; MOTOR OR CLOCK SPRINGS

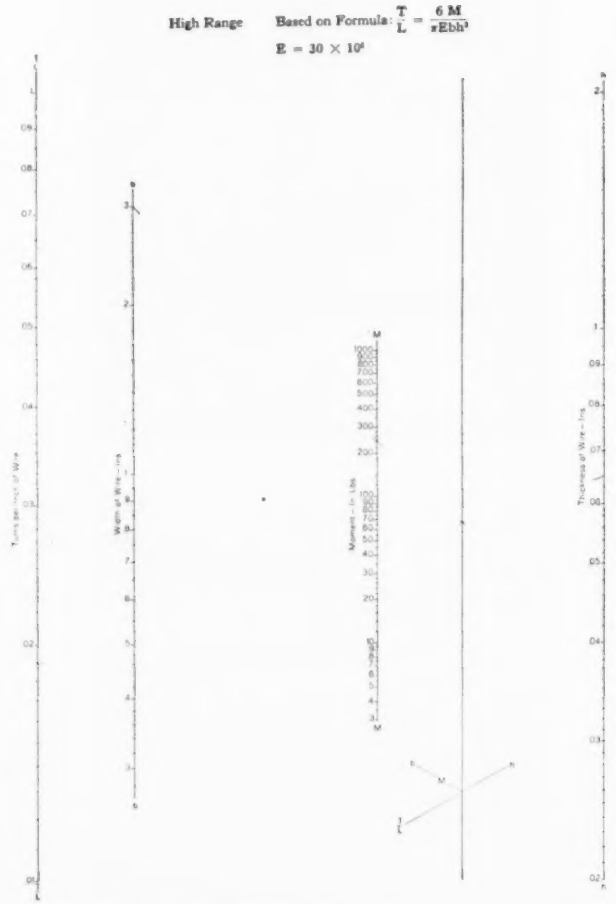


FIG. 19 TURNS PER INCH OF WIRE VERSUS MOMENT; MOTOR OR CLOCK SPRINGS

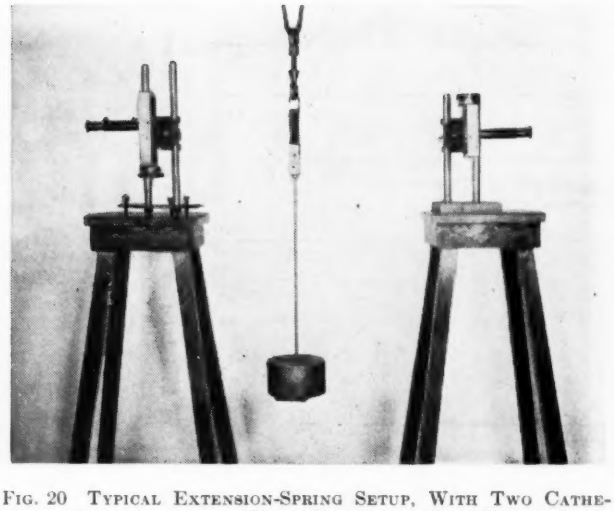


FIG. 20 TYPICAL EXTENSION-SPRING SETUP, WITH TWO CATHETOMETERS ARRANGED TO READ INDIVIDUAL COIL DEFLECTIONS



FIG. 21 COMPRESSION SPRING ARRANGED FOR DEFLECTION MEASUREMENTS

spring curves, the writer finds it difficult to cite a single disadvantage of the nomographic-chart method of design for springs. It may be said that constant use will disfigure these charts but this is also true of any set of spring curves. In the case of the nomographs, we have available not only the very large originals but also the $8^1/_2 \times 11$-in. electroplates with which the charts may be reproduced in any quantity whenever desired.

NOTE: Nomographic charts reproduced with this presentation are published through the courtesy of The American Steel & Wire Company. The charts are copyrighted by that company.

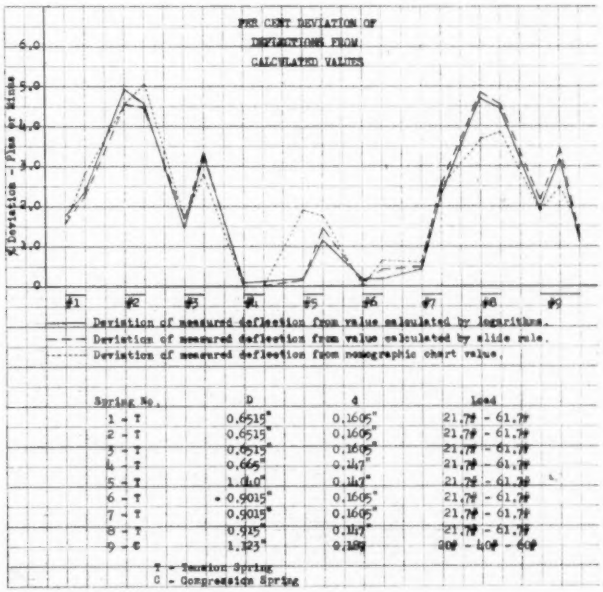


FIG. 22 PERCENTAGE DEVIATION OF DEFLECTIONS IN SPRINGS FROM CALCULATED VALUES

High-Performance Fins for Heat Transfer

By R. H. NORRIS[1] and W. A. SPOFFORD[2]

Earlier investigations have determined the forced-convection heat transfer of a single isolated plane or cylinder and of continuous parallel fins. This paper presents test results for groups of small discontinuous fins and pins. These results have been correlated on the basis of Reynolds number in order to show a common quantitative relationship. The heat-transfer coefficients are found to increase in substantially inverse proportion to the square root of the size, or perimeter of the surface element, and can be more than doubled, compared to continuous fins. The relationship between heat transfer and fluid friction is covered quantitatively. Tests of applications show that the data may be rationally applied with satisfactory results.

Introduction

FINS attached to tubes or other base surfaces are much used for transferring heat to or from forced-flow air. Uses include unit heaters, finned coils for air conditioning (evaporators and condensers), hot-air furnaces, "radiators" for liquid-cooled engines, etc.

Most fins for these uses may be called the "continuous" type, i.e., the fin extends in a continuous sheet for more than 1 in., and generally for several inches, as indicated in Fig. 1(*a*).

Much higher performance, i.e., higher heat-transfer coefficients, can be obtained, however, by splitting up a continuous fin into a multiplicity of discontinuous strips, as indicated in Fig. 1(*b*), or by using an array of small pins, as indicated by the cross section shown in Fig. 1(*c*).

To provide a basis for the design of these high-performance fins is the object of this paper. Results of tests of both heat transfer and pressure drop are presented for a considerable variety of these "strip fins" and "pin fins," and a simple, generalized correlation, based on the perimeter of the fin, is obtained.

The tests here reported are concerned primarily with smooth fins having their upstream edges substantially perpendicular to the direction of air flow. Another type of design in commercial use has spikes or strips projecting radially from a round tube. Examples of the latter type of design were also tested by the authors. They too were found to have higher heat-transfer coefficients than continuous fins, but not so high as designs with all the edges perpendicular to the flow (comparing the same size strip or pin for both types).

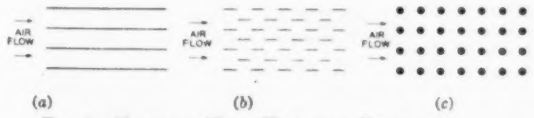


FIG. 1 TYPES OF HEAT-TRANSFER SURFACES
(*a* Continuous fins; *b* strip fins; *c* pin fins.)

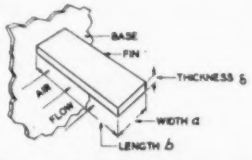


FIG. 2 FIN NOMENCLATURE

Terminology

The terms used in this paper to distinguish certain fin dimensions require definition to prevent ambiguity.

The terms "width" and "thickness" are illustrated in Fig. 2.

The fin "length" is measured from the base of the fin (where it is attached to the tube or other base surface) to the free end or to the mid-point of the fin extending between two walls.

"Depth" is the over-all dimension of the fin assembly, measured in the direction of air flow.

The fin "perimeter," denoted by ψ, is twice the sum of width and thickness for strip fins (see Fig. 2), and is the circumference of a pin fin.

"Short-perimeter" fins is the term used to denote strip fins and pin fins collectively, the perimeter being limited to a fraction of an inch.

Nomenclature

A = surface area of "effective" air-side heat-transfer surface (see Appendix), sq ft

A_c = minimum cross-sectional area open for air flow, sq ft

A_f = surface area of fins alone, on air side, sq ft

A_s, A_w = surface area of steam side (including fins there), and of wall, respectively, sq ft

a = width of strip fin or plane (see Fig. 2), ft

b = length of fin (see Fig. 2), ft

c = specific heat of air, Btu per deg F per lb

f = friction factor, defined by Equations [3] and [3*a*], dimensionless

$G = \rho V$ = mass velocity of air, lb per hr ft^2

g = acceleration of gravity = 4.17×10^8 ft per hr^2

h, h_s = surface heat-transfer coefficients* for air side, and steam side, respectively, Btu per hr ft^2 deg F

$j = \left(\frac{h}{cG}\right)\left(\frac{c\mu}{k}\right)^{2/3}$ = heat-transfer factor, dimensionless (for air below 300 F, $j = 3.30h/G$)

k, k_f, k_w = thermal conductivity of air, of fin material, and of wall material, respectively, Btu per hr ft^2 deg F per ft

Δp_f = pressure drop of air, due to "friction," psf

$R_\psi = \frac{G\psi}{\mu}$ = Reynolds number, based on perimeter ψ, dimensionless

Δt_{12} = temperature change of air from inlet to outlet, deg F

Δt_m = logarithmic-mean temperature difference from surface to air, deg F

U = over-all heat-transfer coefficient, steam-to-air, based on effective area A, Btu/(hr ft^2 deg F)

V = air velocity (at the free area A_c), ft per hr

δ, δ_w = thickness of fin (see Fig. 2) or wall, respectively, except that for pin fins, δ is radius, ft

* Referred to fin *average* surface temperature, not to temperature of the *base* of the fin. To refer to the latter, use ηh, as in Eq. [6].

[1] General Electric Company, Schenectady, N. Y. Jun. A.S.M.E.
[2] General Electric Company, Bloomfield, N. J.

Contributed by the Heat Transfer Professional Group and presented at the Annual Meeting, New York, N. Y., December 1–5, 1941, of THE AMERICAN SOCIETY OF MECHANICAL ENGINEERS.

NOTE: Statements and opinions advanced in papers are to be understood as individual expressions of their authors and not those of the Society.

η = effectiveness factor of fin (evaluated from Equation [7]), dimensionless
μ = viscosity of air (evaluated at average of air and surface temperatures), lb per hr ft
ψ = fin perimeter [$= 2(a + \delta)$ for strip fins], ft
ρ = density of air, lb per cu ft

Nature of Tests

Smooth copper fins (or pins) joining two parallel steam-heated copper walls, as shown, for example, in Fig. 9, were used to obtain the new test results here reported. The finned samples were placed in a duct through which air flowed, as indicated in Fig. 10.

The use of copper, the small "length" of the fin from the center to the wall (either 0.5 or 1 in.), and the fin thickness (0.01 or 0.02 in.) combined to keep the temperature gradient in the fin small enough so its effect could be calculated by well-established methods (1).[3]

The Appendix gives additional details regarding the tests.

Heat-Transfer Results

Choice of Correlation Basis. The correlation of data by the use of dimensionless groups of variables is a well-established method. In this paper, heat-transfer data will be correlated in terms of the dimensionless groups $[(h/cG)(c\mu/k)^{2/3}]$, which for air simplifies to $0.79h/cG$ or $3.3h/G$. This quantity will be denoted by j, called by Colburn (2) the "heat-transfer factor." One advantage of this dimensionless group is that it does not contain the size of the fin as a factor. Another advantage is that it gives a simple numerical measure of heat transfer for different fluids, e.g., air, hydrogen, or water.

The effect of size of the fin is represented in the dimensionless group known as "Reynolds number," $G\psi/\mu$, expressed in terms of the fin perimeter ψ. The perimeter is used instead of the fin width a, or the fin thickness δ, because, as shown later, it simplifies the correlation of strip fins and pin fins on the same basis. This definition of Reynolds number should be distinguished clearly from the Reynolds number based on diameter in some other applications. For pin fins the Reynolds number based on perimeter is π times as great as that based on diameter.

Single Plane Surface. As a standard of reference, consider heat transfer for a single isolated thin plane parallel to an air stream before considering the more complex case of groups of plane fins. The perimeter ψ here represents twice the width a, in the direction of flow, since the thickness may be considered negligible.

It has long been known (2) that for Reynolds numbers in the low range, corresponding to a laminar boundary layer, both theory (3) and test (4) give heat-transfer data for a flat plate which agree within ±5 per cent with the straight-line log-log plot denoted as curve *B-B* in Fig. 3. The equation of this line is

$$j = 0.94/\sqrt{R_\psi} \quad \ldots\ldots [1]$$

Single Cylinder. Usually heat-transfer data for a single cylinder, diameter D, transverse to an air stream have been correlated in terms of the Reynolds number (2), based on diameter, GD/μ.

Surprisingly close agreement with the data for a plane surface is obtained, however, when the perimeter Reynolds number, $G\psi/\mu$, is used, as shown by curve *C-C* in Fig. 3. There is increasing divergence with increasing Reynolds number, but it does not become large for Reynolds numbers R_ψ, up to 20,000, and higher values are not considered in the fin tests reported in this paper.

Even more surprising is the simplicity of the equation of the straight line *A-A*, in Fig. 3, which can be used as a reasonably close approximation for both a plane and a cylinder, for R_ψ up to 20,000. The equation of this line *A-A* is

$$j = 1/\sqrt{R_\psi} = \sqrt{\frac{\mu}{G\psi}} \quad \ldots\ldots [2]$$

These correlations for a plane and a cylinder show that the heat-transfer coefficient can be increased for a given mass velocity G, and given temperature conditions (which determine μ), inversely as the square root of the perimeter ψ. To transfer a reasonable amount of heat, however, many small planes or cylinders would have to be provided, and the effect of adjacent surfaces on the flow and temperature distribution would presumably require consideration.

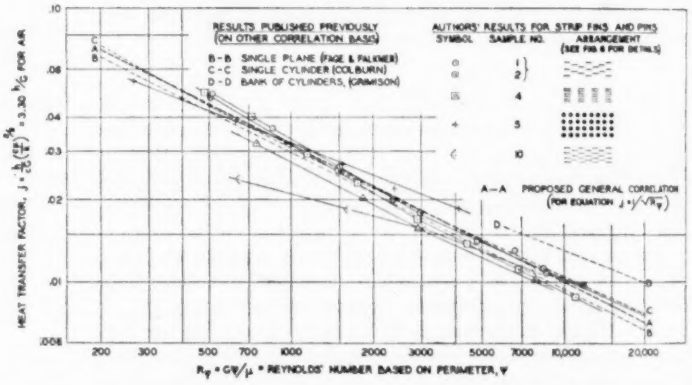


Fig. 3 Dimensionless Heat-Transfer Correlation for Surfaces of Various Shapes, Where Distance, Transverse to Flow, Between Surfaces Is not too Small Relative to the Perimeter; Generally not Less Than 0.1ψ

(For long, closely spaced planes or ducts, j becomes independent of ψ.)

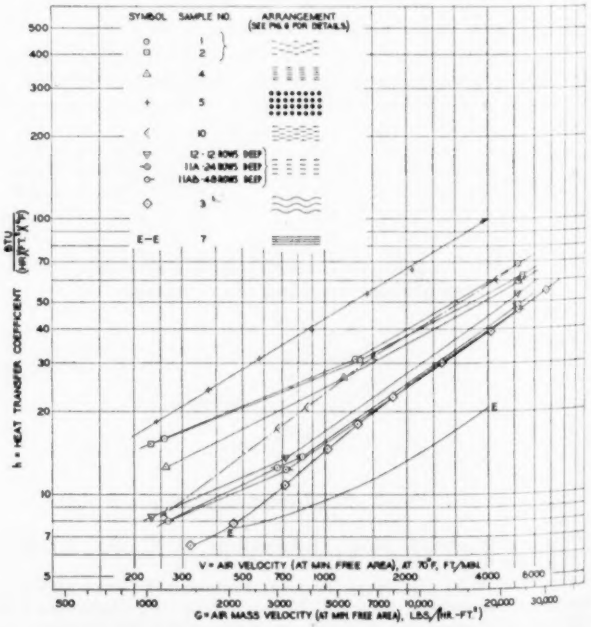


Fig. 4 Heat-Transfer Coefficients for Strip Fins 1/8-In. Wide and 0.04-In-Diam Pins, Compared With Continuous Surfaces for Air at Mean Temperature of 70 F

[3] Numbers in parentheses refer to the Bibliography at the end of the paper.

Accordingly, various arrangements and dimensions of groups of strip fins or pins were tested, with the results to be described.

Results for Strip Fins and Pins. Substantial agreement of results for several designs of strip fin with the basic correlation for a single plane is shown in Fig. 3, where the plotted test results for strip fins are denoted, as indicated in the legend. The results for one design of bank of small round pins are also shown in Fig. 3, which show like agreement, although a tendency to divergence is evident at the upper end of the range of Reynolds number considered, in accordance with the trend shown by line *D-D* for cylinders representative of boiler-tube sizes.

Not all arrangements of strip fins give equally good performance, however. Results for the various designs tested are compared in Fig. 4, and discussed under "General Conclusions."

Results, in Fig. 4, are presented in terms of heat-transfer coefficient as a function of air velocity, instead of in terms of dimensionless variables, in order to facilitate appreciation of the practical significance of the results, but these are restricted to the dimensions specified and to air at the mean temperature of 70 F.

Compared to continuous fins, an increase of over 2-to-1 ratio in the heat-transfer coefficient is obtainable from suitable designs of narrow ($^1/_8$-in-wide) strip fins, as shown by the results tabulated in Fig. 6 and by supplementary data in Table 1.

Air-Pressure-Drop Results

Choice of Correlation Basis. The air-pressure drop observed in a test sample does not by itself have immediately recognizable

TABLE 1 DATA ON SAMPLES TESTED[a]

Sample No.	Description	Ratio, fin-to-wall area	Heat-transfer area used	Ratio, a/δ	Fin-area to wall-area ratio usable for range
1	Strip fins staggered by threes	6.33	$A_f + {}^1/_{12}A_w$	12.5	4 to 10 with error < ±2 per cent
2	Same as sample No. 1 except for thickness	6.95	$A_f + {}^1/_{12}A_w$	25.0	4 to 10 with error < ± 2 per cent
4	Strip fins in line, close spacing	6.19	$A_f + {}^1/_{12}A_w$	12.5	4 to 10 with error < ±2 per cent
5	Pin fins	3.18	A_f only	..	2 to 6 with error < ±2 per cent
10	Strip fins staggered by twos	5.10	$A_f + {}^1/_{12}A_w$	12.5	3 to 10 with error < ±2.5 per cent
11A, 11AB	Strip fins in line, wide spacing	3.46	$A_f + {}^1/_{12}A_w$	12.5	3 to 10 with error < ±2.5 per cent
12	Strip fins in line, wide spacing	2.98	$A_f + {}^1/_{12}A_w$	12.5	3 to 10 with error < ±2.5 per cent

[a] Supplementing sketches in Fig. 6.

significance, for it will vary widely with the depth of the sample and the air velocity. There is, moreover, no customary measure of pressure drop per unit of surface area analogous to h, the measure of heat transfer per unit of surface area, and likewise relatively independent of depth of the sample.

There is, however, a dimensionless measure of pressure drop which is relatively independent of depth, and has significant advantages. This is the quantity called the generalized friction factor f, and defined by

$$\Delta p_f = f \cdot \frac{\rho V^2}{2g} \cdot \frac{A}{A_e} = f \frac{G^2}{2\rho g} \frac{A}{A_e} \quad \ldots\ldots [3]$$

This is a generalized form of the well-known Fanning equation for pressure drop of fluids in pipes.

For a single isolated plane or cylinder, drag, not pressure drop, is the measure of friction, so an alternative definition of f is required, namely

$$\text{Drag force, } F_D = f \frac{\rho V^2}{2g} A \quad \ldots\ldots [3a]$$

For a bank of cylinders, the f thus defined has the same value as the limit approached by the f defined by Equation [3], as the transverse spacing of the cylinders is increased toward infinity.

The ratio of heat transfer to pressure drop, not pressure drop alone, is really the most significant measure of merit of pressure-drop performance.

This ratio is here expressed by $j/(f/2)$, a ratio of the dimensionless measure of heat transfer to one half the dimensionless measure of pressure drop, as this ratio has significance and value which are found to be very convenient and relatively independent of the particular velocity or depth used in the tests.

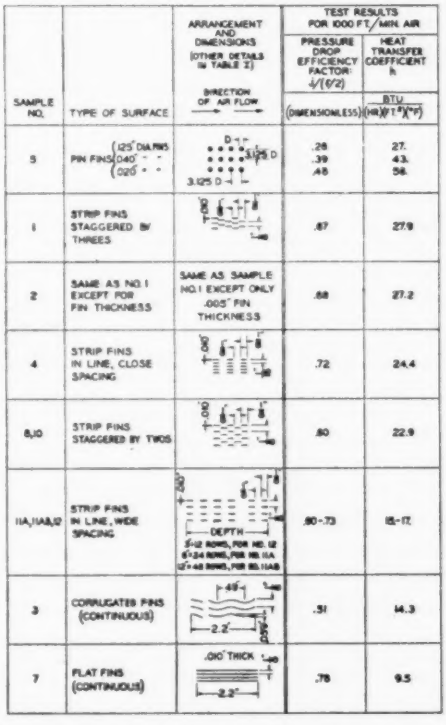


FIG. 6 ARRANGEMENTS, DIMENSIONS, AND RESULTS FOR 1000-FPM AIR VELOCITY FOR STRIP FINS $^1/_8$ IN. WIDE, AND FOR OTHER SURFACES AT MEAN TEMPERATURE OF 70 F

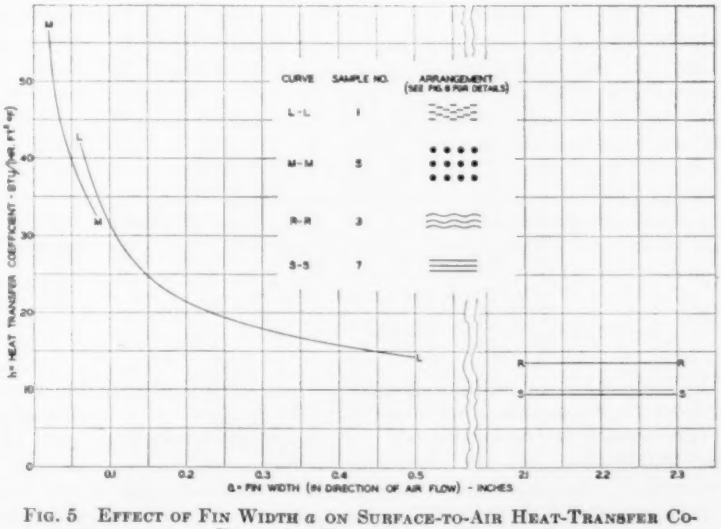


FIG. 5 EFFECT OF FIN WIDTH a ON SURFACE-TO-AIR HEAT-TRANSFER COEFFICIENTS FOR A FIXED AIR VELOCITY, AT MINIMUM FREE AREA OF 1000 FPM AT 70 F

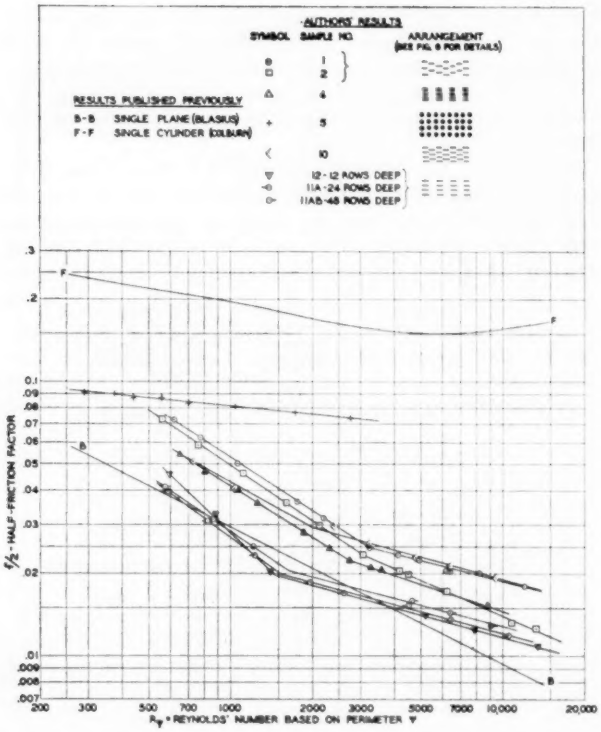


FIG. 7 HALF-FRICTION-FACTOR CORRELATION FOR STRIP FINS AND ROUND PINS

Unity may be considered as the ideal upper limit to the ratio $j/(f/2)$, which may accordingly be considered as a sort of pressure-drop efficiency, as explained in a previous paper (5). This significance of $j/(f/2)$ is indicated by the relation

$$\Delta p_f = \frac{\Delta p_0}{j/(f/2)} \quad \ldots\ldots [4]$$

where

$$\Delta p_0 = \frac{\rho V^2}{g} \frac{\Delta t_{12}}{\Delta t_m} \left(\frac{c\mu}{k}\right)^{2/3}$$

which may be considered as the minimum theoretically obtainable pressure drop, as explained in reference (5), and Δp_f is the actual friction pressure drop, higher than Δp_0 the more $j/(f/2)$ drops below unity. The test results are therefore presented in the form of $f/2$, and of the ratio $j/(f/2)$, plotted as functions of Reynolds number, as shown in Figs. 7 and 8.

Single Plane. Blasius' theoretical results, as quoted in reference (2), for the friction factor for a single thin smooth plane, parallel to an air stream, for Reynolds numbers up to 20,000, are represented, in the form of $f/2$, by the line *B-B* in Fig. 7, the equation of which is

$$\frac{f}{2} = 0.94/\sqrt{R_\psi} \quad \ldots\ldots [5]$$

This value of $f/2$ is thus the same as the value of j (see Equation [1] and Fig. 3), as pointed out by Colburn (2).

The value of $j/(f/2)$ for this case is therefore unity for R_ψ below 20,000 when f is based on Blasius' theoretical results. No values of f from test, to check Blasius' results, have been found for the values of R_ψ below 20,000 here considered.

Single Cylinder. For a single cylinder, transverse to an air stream, one half the friction factor, as quoted by Colburn (2) from test results in previous literature, is shown by curve *F-F* in Fig. 7. This curve is much higher than the corresponding heat-transfer curve *C-C* in Fig. 3. The value of $j/(f/2)$ is therefore much less than unity.

Strip Fins and Pins. The authors' test results for pressure drop of strip fins, and of banks of pins, are shown in Fig. 7. The values of the ratio $j/(f/2)$, obtained from combination of the test results in Figs. 3 and 7, are presented in Fig. 8.

The significance of these results is discussed later, under "General Conclusions—Pressure Drop."

PRACTICAL APPLICATIONS

The data presented permit an economic evaluation of changes in design detail without need for recourse to extensive tests for each new application. As has been shown, the heat-transfer performance may be increased without limit as the fin perimeter is made smaller. (Strictly speaking, only within the range of Reynolds number covered by tests.) This is true, even though some arrangements of fins are superior to others. The object of design is then to select an advantageous arrangement of surface elements made as small as possible consistent with practical design limitations. The design detail is dictated primarily by the method of manufacture, the material used, the strength or ruggedness required, and the conditions of operation.

Extended surfaces on round tubes are typical of construction for which the fin data cannot be applied without some compromise with the more ideal fin arrangements which have been tested. The necessity of having the air circulate around the tube prevents having the air move at uniform velocity at right angles to the fin element and thus prevents the attainment of the same performance reported for strip-fin tests. Even so, the data correlated in this paper have been applied satisfactorily to surfaces on round tubes

Since the trend of the heat-transfer coefficient with velocity, perimeter, and fin arrangement is known, an analysis can be made of the effects on cost and pressure drop of changing tube size and spacing, fin spacing and thickness, etc., in order to establish the most economical design of surface for the particular application. Tests then serve to confirm or rate the performance of the finished design.

The economic advantages of such a short perimeter surface are greater for applications using low air velocities. These surfaces occupy less space, in the direction of air flow, than conventional surfaces. For a given face area, the air pressure drop for a given heat transfer is about the same as for conventional surfaces. As with any surface, the pressure drop can be lowered by an increase in face area with an increase in surface area and cost.

In these surfaces the thermal conductivity of the fin material, which determines the temperature drop along the fin, has an important bearing on the suitability of the design, as an application that is good, when made with high-conductivity copper, may show small advantage over a conventional surface if made with a lower-conductivity metal.

GENERAL CONCLUSIONS

Heat Transfer

1 An increase of over 2-to-1 ratio in the heat-transfer coefficient is obtained by use of a multiplicity of 1/8-in-wide strip fins, suitably spaced, instead of continuous fins (see Fig. 6).

2 Still greater increase is obtained by yet smaller strip widths, or by pins of the order of 0.040 in. diam or less (see Figs. 5 and 6).

3 The heat-transfer coefficient increases inversely as the square root, approximately, of fin width or fin perimeter, for most of the strip-fin or pin arrangements tested (see Figs. 3 and 5).

4 A single simple curve (curve *A-A* in Fig. 3) suffices as an

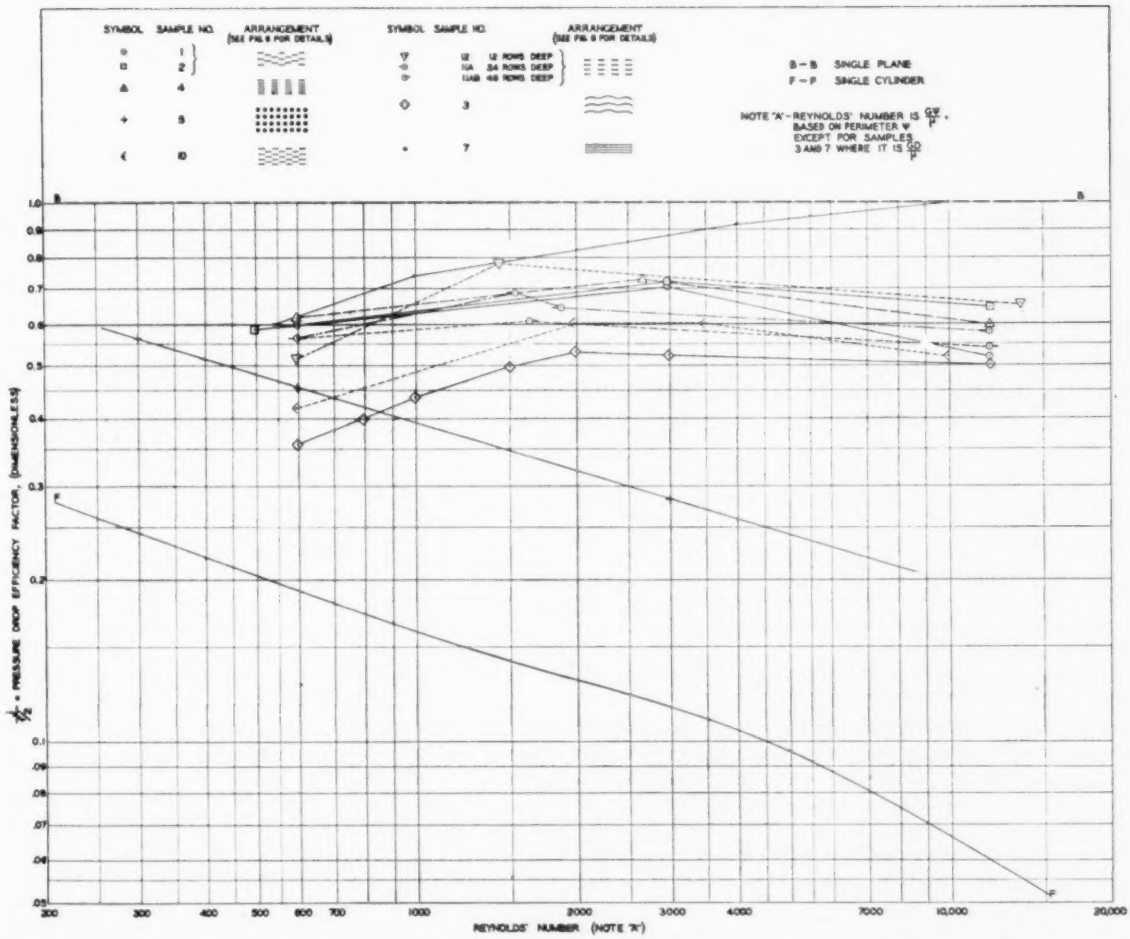


FIG. 8 PRESSURE-DROP EFFICIENCY FACTOR, RELATING HEAT TRANSFER AND PRESSURE DROP, FOR STRIP FINS, ROUND PINS, AND CONTINUOUS SURFACES

approximate correlation of heat transfer for the following variety of surfaces in the range of conditions considered:

(*a*) A single plane (parallel to the air flow).
(*b*) A single cylinder (transverse to the air flow).
(*c*) Strip fins of various designs (except for certain less favorable designs).
(*d*) Pin fins (at least for the one design tested).

5 The generality of this correlation curve permits heat-transfer predictions for strip- or pin-fin designs, differing from those tested both in size and arrangement (for limitations, see Conclusion 8).

6 Fin thickness has but slight effect on the heat-transfer coefficient of strip fins (when this coefficient is based upon the average fin temperature, not the temperature at the base of the fin). Halving the thickness (4 per cent instead of 8 per cent of fin width) decreased the coefficient only 4 to 12 per cent (samples Nos. 1 and 2).

7 The over-all "depth" (in the direction of air flow) of the fin assembly has only a slight effect on the heat-transfer coefficient. A fourfold increase in depth produced a decrease of less than 13 per cent in coefficient (samples 11AB and 12 in Fig. 4).

8 The spacings between strip-fin layers should be kept within a limited range; too great a spacing tends to decrease the heat transfer (compare sample No. 11A with samples Nos. 1, 4, and 10 in Fig. 6). The spacing of the layers should be less than one strip width (i.e., less than in sample No. 11A) and preferably one third of a strip width (as in sample No. 1, Fig. 6).

9 Whether the strips of one layer are in-line or whether they are staggered with respect to the strips of the adjacent layer has

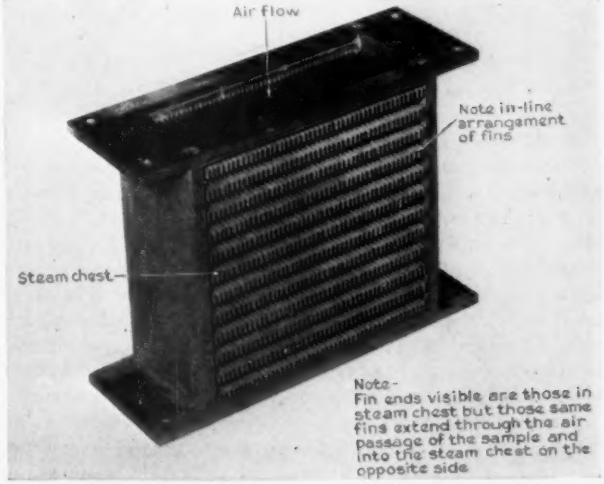


FIG. 9 STRIP-FIN HEAT-EXCHANGER SAMPLE NO. 4
(Steam-chest covers not shown.)

but slight effect on heat transfer (samples Nos. 4 and 10, Fig. 6).

10 The dimensionless correlation of results is substantially independent of the size of the sample chosen for test (e.g., sample No. 12 was made to twice the scale of sample No. 11A; for results, see Fig. 4).

Pressure Drop

Pressure drop is here discussed mostly in terms of the pressure-drop-efficiency factor, $j/(f/2)$, for reasons previously explained.

1 In general, the ratio $j/(f/2)$ for strip fins ranges from 0.5 to 0.7, for the considerable variety of designs tested (see Fig. 8).

2 This range of 0.5 to 0.7 for strip fins is close enough to the 0.7-to-1 range for continuous flat fins (see Fig. 8), so that the difference does not prevent utilization of the great heat-transfer advantages of strip fins (see Figs. 6 and 8).

3 Strip fins seem decidedly superior to corrugated continuous fins, since they give both higher heat-transfer coefficients and a higher $j/(f/2)$ ratio (see Figs. 6 and 8).

4 Smaller thickness helps to increase the $j/(f/2)$ ratio for strip fins. Decreasing the thickness from 8 per cent of strip width to 4 per cent increased $j/(f/2)$ by 1 to 19 per cent (samples Nos. 1 and 2, Fig. 8).

5 The over-all depth (in the direction of air flow) of the fin assembly does not have much effect on the pressure drop of strip fins per unit of depth. A 4-to-1 change in depth changes $f/2$ (a measure of pressure drop per unit of depth) by less than 10 per cent. The effect on $j/(f/2)$ is slightly more than on $f/2$ (Figs. 7 and 8).

6 For pin fins at low Reynolds numbers, the ratio $j/(f/2)$ is surprisingly good (around 0.5), considering the round, unstreamlined cross section (sample No. 5, Fig. 8). Values as low as 0.5 may be quite acceptable in consideration of the very high heat-transfer coefficients obtainable (sample No. 5, Fig. 6).

7 For pin fins, increasing the Reynolds number greatly decreases the ratio $j/(f/2)$, so large pins at high velocities do not appear attractive.

Practical Applications. In practical applications, the designer selects the minimum size of fin element that can be economically fabricated, or that will have sufficient strength in service, or that will satisfy special conditions of operation. As compared to less scientifically designed surfaces, the surface will have less weight and will occupy less space. It will have about the same air-pressure drop for a given heat transfer as a conventional surface, unless the performance gain is to be used to reduce pressure drop rather than to obtain maximum weight reduction.

Appendix

Test Equipment and Procedure

Air System. The air system is shown in Fig. 10.

The air flow was measured by the pressure drop across a square-edged orifice, several sizes being used to cover the different ranges of flow. The orifices were calibrated to $\frac{1}{2}$ per cent, using the same duct and vanes. The calibration was made by measured volumetric displacement of a 2200-cu-ft "gas-meter-prover" tank. The coefficients obtained were 1 to 1.9 per cent higher than the corresponding values given by the A.G.A.-A.S.M.E. standard tables. The calibration values, not the standard ones, were used, particularly as they seemed to give slightly less error in the heat balances (which were generally within 2 per cent).

The temperature and barometric pressure were taken into account. The water vapor in the air was considered in selecting the specific-heat value, and also in calculating the air flow from the orifice pressure drop.

A mixing chamber downstream from the test sample provided practically uniform temperature for measurement. This uniformity was confirmed with a movable thermocouple.

The air approaching the test sample was at substantially room temperature, so no insulation was needed there. The test sample and the duct system downstream from it were so well insulated that correction for the heat loss through the insulation was needed only at the lowest air flows, and was then very small.

Steam System. Dry steam, at substantially atmospheric pressure, and a superheat of 6 to 60 F, was supplied to both sides of the test sample. The condensate flowed from the sample through a water-cooled U-shaped trap, thermally insulated, into a beaker, and was weighed at regular intervals.

Scavenging of air from the steam chests was insured by a continual venting process, but check tests without venting (except prior to the test) showed that the amount of noncondensable

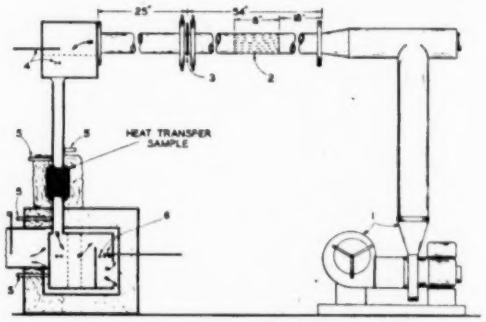


Fig. 10 Arrangement of Equipment for Tests of Heat Transfer

(1 Fans in series; 2 straightening vanes; 3 air-measuring orifice; 4 thermometers and thermocouples in air-inlet mixing box; 5 air-pressure connections; 6 thermometers and thermocouples in air-outlet mixing box.)

carried in by the steam was so small that it would reduce the heat transfer by less than 2 per cent per hr. To provide uniform distribution of steam flow, and thereby facilitate elimination of air, the steam was supplied to a header across the entire 6-in-wide top of the test sample. The presence of the ends of the fins, Fig. 9, or, in certain samples, other restrictions, provided uniformly distributed resistance to steam flow, so that withdrawal of steam from the header at the bottom would cause flow through the entire steam chest.

The rate of withdrawal of vent or "excess" steam was large before each test, and was then reduced to a relatively low value throughout the test to prevent entrainment of liquid water. To permit calculations of the heat obtained from superheat in the entering steam, the excess steam was measured by an orifice and assumed to leave dry at saturation temperature. No noticeable variation of results was obtained by variation of the excess steam flow up to 300 per cent of the amount condensed.

Temperature Measurements. Air temperatures were measured by copper Copnic thermocouples, which were calibrated, together with the potentiometer, to 0.2 deg F. The cold junctions were kept at 32 F. Thermometers, calibrated to 0.05 deg F, were used for check purposes. The accuracy of the outlet-air temperature was aided by the location of the six thermocouples beyond the air-mixing system previously mentioned, Fig. 10.

Steam-saturation temperature was obtained from the steam pressure (atmospheric plus a correction for water in the trap). Temperature of the superheated steam at the inlet was measured by a thermocouple with a long sheath.

Pressure-Drop Measurements. Pressure drop across the test sample was measured by use of draft gages connected to small holes flush with the duct walls, located as shown in Fig. 10. Two independent sets of pressure connections and gages were

used to eliminate danger of undetected leaks. A micromanometer was used when necessary.

From the pressure drop as thus measured, there was deducted the pressure drop of the duct itself, obtained for the same flow by clamping the inlet and outlet ducts together with the test sample removed.

Test Procedure. Each heat-transfer test run consisted of at least four consecutive sets of readings at 10-min intervals, after stable conditions were obtained.

For most pressure-drop tests, isothermal conditions were used, although tests with the sample heated gave substantially the same results after adjustment to the chosen standard conditions of 70 F and 14.7 psi abs.

The number of test runs for heat transfer could be fewer than for pressure drop, because it was found that the results as plotted consisted of two straight lines, the intersection of which could be estimated from the pressure drop.

Calculation of Results. The over-all heat-transfer coefficient U was obtained by dividing the total heat transferred (average of the values from air and from steam) by the "effective" surface area of the air-side surface and by the logarithmic-mean temperature difference between the air and the saturated steam.

The "effective" area was taken as the fin area (both sides of each fin) plus a suitable fraction of the wall area, as specified in Table 1, which also gives the range of ratios of fin to wall area for which use of this fraction of the wall area gives a specified accuracy.

The wall-to-air heat-transfer coefficient (ηh) was calculated by the equation

$$\frac{1}{(\eta h)} = \frac{1}{U} - \frac{1}{h_s}\frac{A}{A_s} - \frac{\delta_w}{k_w}\frac{A}{A_w} \quad \ldots\ldots\ldots\ldots [6]$$

The steam-side coefficient h_s was calculated on the assumption of film condensation, for which consistent results are available (6). The steam-side thermal resistance was, however, only a small fraction of the over-all resistance, being from $^1/_2$ to 3 per cent for all samples except No. 10, where it reached 15 per cent because the steam side in that instance had no fins.

The effectiveness factor η was calculated from the well-known (1) equation

$$\eta = \frac{\tanh\, b\sqrt{(2h/k_f\delta)}}{b\sqrt{(2h/k_f\delta)}} \quad \ldots\ldots\ldots\ldots [7]$$

Accuracy. Satisfactory accuracy is indicated by the agreement of the heat gain by the air with the heat loss by the steam which was generally within 2 per cent, except at the lowest air flows, where there was a slightly greater discrepancy. The closeness of the plotted results to a smooth curve and the agreement between results for similar samples also indicate good accuracy.

Acknowledgment

The authors gratefully acknowledge the large share of this investigation contributed by Mr. Stanford Neal, who built the test equipment and carried out most of the tests.

BIBLIOGRAPHY

1 "Mathematical Equations for Heat Conduction in the Fins of Air-Cooled Engines," by D. R. Harper, 3rd, and W. B. Brown, U. S. National Advisory Committee for Aeronautics, Technical Report No. 158, 1922.

2 "A Method of Correlating Forced-Convection Heat-Transfer Data and a Comparison With Fluid Friction," by A. P. Colburn, Trans. American Institute of Chemical Engineers, vol. 29, 1933, pp. 174–210.

3 "Der Wärmeaustausch zwischen festen Körpern und Flüssigkeiten mit kleiner Reibung und kleiner Wärmeleitung," by E. Pohlhausen, *Zeitschrift für angewandte Mathematik und Mechanik*, vol. 1, 1921, pp. 115–121.

4 "On the Relations Between Heat Transfer and Surface Friction for Laminar Flow," by A. Fage and V. M. Falkner, Great Britain Aeronautical Research Committee, Technical Report, vol. 39, 1931-1932, pp. 172–201; Reports and Memoranda No. 1408.

5 "Concepts of Efficiency of Heat-Transfer and Pressure-Drop Relations in Heat Exchangers," by R. H. Norris, Proceedings of 5th International Congress for Applied Mechanics, Cambridge, Mass., 1938, pp. 585–589.

6 "Heat Transfer by Condensing Vapor on Vertical Tubes," by C. G. Kirkbride, Trans. American Institute of Chemical Engineers, vol. 30, 1934, pp. 170–186.

Discussion

R. C. Martinelli,[4] M. Tribus,[5] and L. M. K. Boelter.[6] The results given in this paper are very interesting and useful. As pointed out by the authors the trend of the results can be predicted with some success by the approximate relation

$$j = \frac{f}{2} = 0.94\Big/\sqrt{R_\psi}$$

It should be emphasized, as a precaution to those who may apply the test results to larger fins, that all of the authors' data fall within the range of laminar flow along flat plates. In this type of flow, the unit thermal conductance varies inversely with the square root of the fin width a. With larger plates, however, the flow becomes turbulent.

For smooth flat plates, the drag coefficient in the turbulent region may be expressed[7] approximately as

$$\frac{f}{2} = \frac{0.074}{2}\left(\frac{\mu}{V\rho a}\right)^{0.20}$$

As a close approximation $j = f/2$. Substituting physical constants for air at 70 F yields

$$h = 6.06 \times 10^{-3}\left(\frac{V\rho}{a^{0.250}}\right)^{0.80}$$

[4] Instructor, Department of Mechanical Engineering, College of Engineering, University of California, Berkeley, Calif. Jun. A.S.M.E.

[5] Department of Mechanical Engineering, College of Engineering, University of California, Berkeley, Calif.

[6] Professor of Mechanical Engineering, University of California, Berkeley, Calif. Mem. A.S.M.E.

[7] "Modern Developments in Fluid Dynamics," composed by the Fluid Motion Panel, and edited by S. Goldstein, Great Britain, Air Ministry, Aeronautical Research Committee, Clarendon Press, Oxford, England, 1938, p. 362.

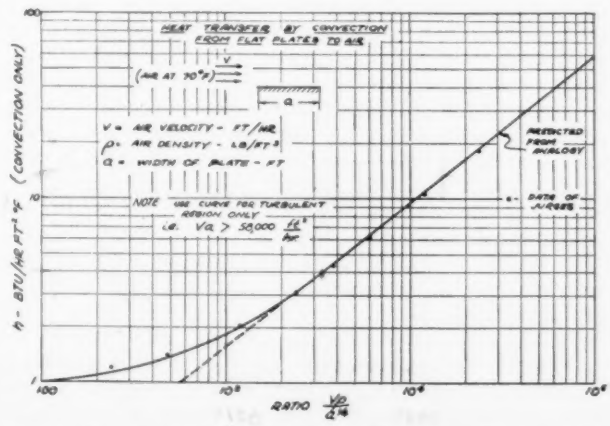


FIG. 11 HEAT TRANSFER BY CONVECTION FROM FLAT PLATES TO AIR

where h = unit thermal conductance from plate to air, Btu per hr ft² deg F; V = air velocity, fph; ρ = air density, lb per cu ft; and a = width of plate, ft.

A plot of this equation is shown in Fig. 11 of this discussion, together with points obtained from the data of Jurges.[8] At the low magnitudes of the mass velocity G, free convection becomes effective. It is noted that, for large plates in the turbulent region, the unit thermal conductance varies inversely with the $^1/_3$ power of the plate length, as contrasted with the $-^1/_2$ power in the viscous region.

Authors' Closure

The data for a large flat plate provided by Martinelli, Tribus, and Boelter furnishes a particularly convenient correlation for conditions of much practical interest. The rather unusual choice of the variable used for the abscissa in Fig. 11 has considerably simplified the graphical correlation. A less simple but more general correlation of substantially the same data, with j and $f/2$ plotted versus Reynolds number, will be found in reference (2) of the Bibliography of the paper.

The data in Fig. 11 do not necessarily apply, however, to a group of large plates, as distinguished from a single plate. The determination of the effect of different arrangements of the plates in a group, was, in fact, the major object of the authors' investigation, but only for small plates. For these small plates, or strips, the performance can change considerably with some changes in the arrangement, as shown in Fig. 6.

The distinction between laminar and turbulent flow here considered probably applies primarily to the boundary layer on the strips or plates, rather than to the rest of the stream. It seems doubtful that turbulence can be completely absent, for example, in the wake of each strip, for the entire Reynolds number range covered by the authors' tests. The sharp break in some of the curves in Fig. 7 and Fig. 8 may indicate the beginning of turbulence in some part of the stream.

In regard to data for closely spaced large plates, or flat narrow ducts, as represented by sample 7, the test results presented in this paper have been found to confirm, for low Reynolds number, the purely theoretical correlation for laminar flow given in a paper by R. H. Norris and D. D. Streid.[9] In fact, the data for sample 7 in terms of j versus Reynolds number, although purposely not included here, in Fig. 3, will be found in Fig. 5 of that earlier paper.[9]

[8] "Heat Transmission," by W. H. McAdams, McGraw-Hill Book Company, Inc., New York, N. Y., 1933, p. 237.

[9] "Laminar-Flow Heat-Transfer Coefficients for Ducts," by R. H. Norris and D. D. Streid, A.S.M.E. Transactions, August 1940, p. 525–533.

Combustion of Pulverized Fuel—Mechanism and Rate of Combustion of Low-Density Fractions of Certain Bituminous Coals

By A. A. ORNING,[1] PITTSBURGH, PA.

In the course of the investigation reported in this paper, individual particles of burning coal were studied, using all convenient means of observing the burning process and examining the residues which might be obtained. Using Pittsburgh seam coal and Pocahontas No. 3 seam coal, it was found that the particles were blown into cenospheres before they ignited. The exposures just required to make an impression on the photographic film were used to estimate the temperature history of individual particles. With the available furnace temperatures, less than 1000 C, the degree of combustion depended upon the ability of the particles to maintain themselves above about 1400 C. The degree of combustion increased with increasing furnace temperature in the region where the cenospheres were formed. Photographs of partially burned cenospheres and data on the relation of particle size to burning time were obtained.

THE use of pulverized fuel has developed largely as an engineering art. Furnace conditions, such as gas composition, temperature, radiant flux, dust loading, etc., have been determined (1),[2] but such information tells us very little about what happens to the individual coal particle.

The rate of burning of spheres of electrode carbon under forced-air convection is fairly well known. Mayers (2) has reviewed the earlier work, while Hottel and associates (3, 4, 5) have made important later contributions. However, it is neither safe to extrapolate from comparatively large spheres to dust particles, nor to assume that the burning coal particle resembles a sphere of electrode carbon. Coal particles under certain conditions are known to form cenospheres (6). Although such particles have been found in industrial furnaces, it has not been demonstrated that they are generally involved in the combustion of pulverized fuel.

Griffin, Adams, and Smith (7) have made photographic measurements of the time of incandescence of individual particles in a stream of closely sized coal falling into an electric furnace. For a given coal sample they found that the average time of incandescence, as measured on their photographs, increased with increasing furnace temperature throughout the range explored from 700 to 1000 C. However, they offered no experimental evidence either to establish the relation of incandescence time to burning time, or to show that complete combustion was obtained.

The present investigation was made to study the behavior of individual particles of burning fuel, using all convenient means of observing the burning particles and examining the residues which might be obtained. It has led to several interesting results such as the temperature history of an individual burning particle, and has also indicated that the previously reported negative temperature coefficient (7) may be explained on the basis of incomplete combustion. Ideally, a furnace should have been used which could reach temperatures even above those found in industrial furnaces, but the amount of exploratory work required made it advisable to set a limit at about 1000 C, until the results obtained indicated the type of equipment best suited to the higher-temperature region.

Any carbonaceous substance capable of being pulverized is a conceivable pulverized fuel, but the immediate interest has centered on the bituminous coals. A Pittsburgh seam coal was chosen for the preliminary work, while a Pocahontas No. 3 and an Illinois No. 6 coal were available for comparative tests. The work was confined to the low-density and, therefore, relatively low-ash fractions of these coals. The influence of ash should be the subject of a separate investigation.

Apparatus and Procedure

Figs. 1 and 2 show the furnace used. The main heating elements were supported in fused-quartz tubes placed behind silicon-carbide plates which enclosed a slot $^1/_2 \times 4 \times 24$ in. These elements, each made of about 13.5 ft of 14-gage Nichrome-V wire and operated at a maximum of about 150 w, were connected in a series-parallel arrangement suitable for operation at 220 v. Rheostats were placed across various sections of the furnace in order to obtain uniform temperature as indicated by a survey with a chromel-alumel thermocouple. The average temperature was controlled by means of another couple located near one of the heating elements and connected to a potentiometer-recorder controller.

A blower took air from behind the baffle plates in the dust receiver at the bottom of the furnace and returned it to the top of the window channels. Additional air was admitted through the preheater into a chamber in the top of the furnace. Radiation shields, which protected all but a $^3/_4$-in. strip of glass opposite the furnace slot, carried deflector plates which forced the air out of the channels into the furnace. By proper positioning of these plates and by control of the rate of air circulation, it was possible to maintain a fairly uniform downward air velocity, except for a noticeable increase at the bottom, which resulted from forcing nearly all the air to pass through a constricted space between the heater plates. The velocity of the air could be estimated from the photographic traces of burning particles. These particles were so light and small that they had low drift velocities. The velocity indicated by the slopes of their traces on the photographic record is essentially that of the air.

A rotary vibrator caused the coal sample to flow out of a glass funnel, around a spiral, and through a water-cooled tube into the top of the furnace. The intensity of vibration was kept as low as possible in order to avoid segregation and yet maintain a steady rate of flow. In some cases it was necessary to use a sampling tube which allowed only part of the flow from the spiral to pass on into the furnace.

[1] Coal Research Laboratory, Carnegie Institute of Technology.

[2] Numbers in parentheses refer to the Bibliography at the end of the paper.

Contributed by the Fuels Division and presented at the Annual Meeting, New York, N. Y., December 1–5, 1941, of The American Society of Mechanical Engineers.

Note: Statements and opinions advanced in papers are to be understood as individual expressions of their authors and not those of the Society.

The camera shown in Figs. 3 and 4 consisted of a disk shutter, rotated at 1800 rpm, placed between the lens and the film drum, which rotated at 10.5 rpm. The lens was a 107-mm F 3.7 Kodak Anastigmat Ektar. The film drum shown removed from its box had a $2^1/_2$-in. face which fitted standard 620 roll film. Several types of film were tested and Eastman Kodak Super-XX Panchromatic roll film was decided upon as being the most satisfactory. The drum in its box could be lifted off the camera and taken to the darkroom for loading. A variety of shutter disks was used; the one shown was of metal and had sector openings corresponding to exposure times of 0.0106, 0.0212, 0.0424, 0.0848, 0.170, and 0.68 millisec. Fig. 7 is a portion of a photographic record obtained with this shutter; each line of dots is the interrupted trace of a single burning particle. The longest exposure registered as a slightly elongated dot, while the others were short enough to "stop" the particles. The time of incandescence, in sixtieths of a second, could be determined by counting the heaviest dots, while the density and shape of the dots indicated the intensity and character of the combustion process. In some records the hot furnace walls appeared as a background of light vertical lines. In making these records, a cam on the axle of the film drum acting through a switch and a solenoid opened the lens shutter only during the passage of a desired sector of the film. In general, the records were single exposures showing only what was in the furnace at the one time.

The coal samples were sized between standard screens and separated into float and sink fractions on various mixtures of benzene and carbon tetrachloride. After removing the organic solvents some coals formed a caked mass which it was necessary to break up by rescreening. The treatment produced a fairly homogeneous sample both in chemical and physical character,

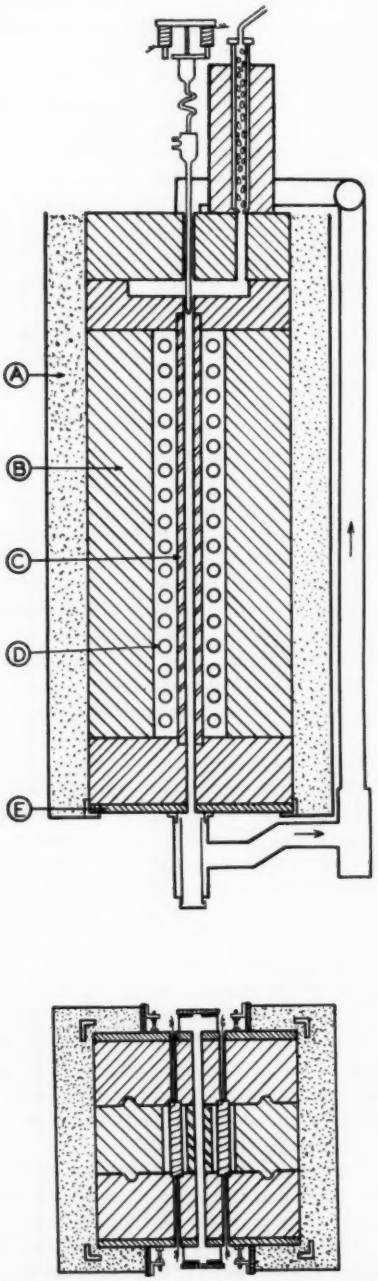


FIG. 1 SECTIONS OF THE COMBUSTION FURNACE
(*A*, Sil-o-Cel; *B*, insulating firebrick; *C*, silicon-carbide plate; *D*, fused-quartz tube; *E*, transite.)

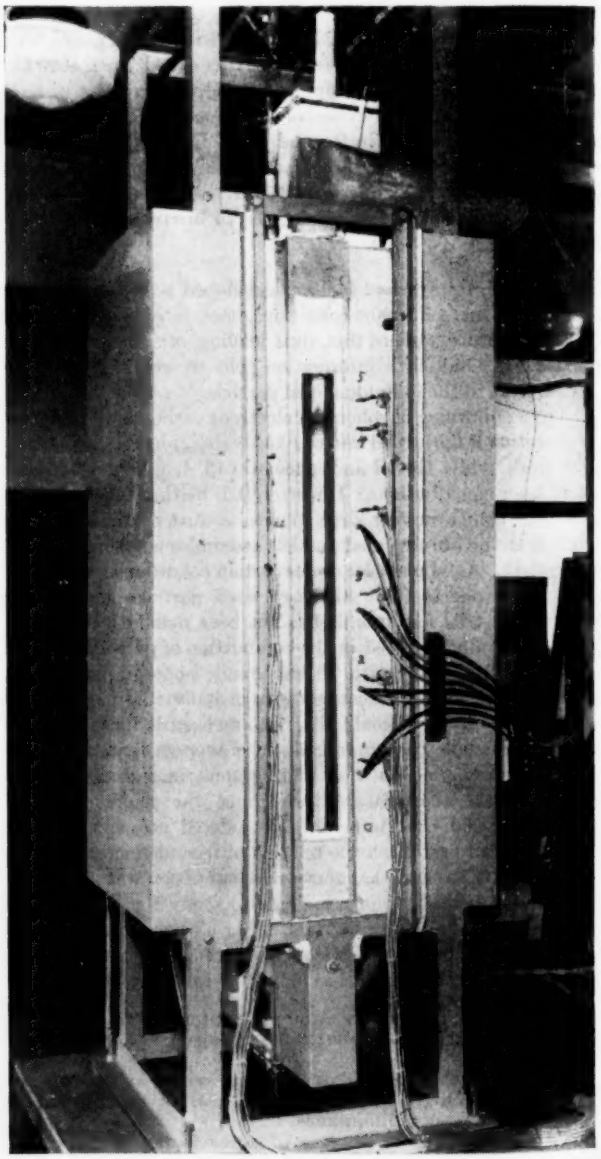


FIG. 2 COMBUSTION FURNACE

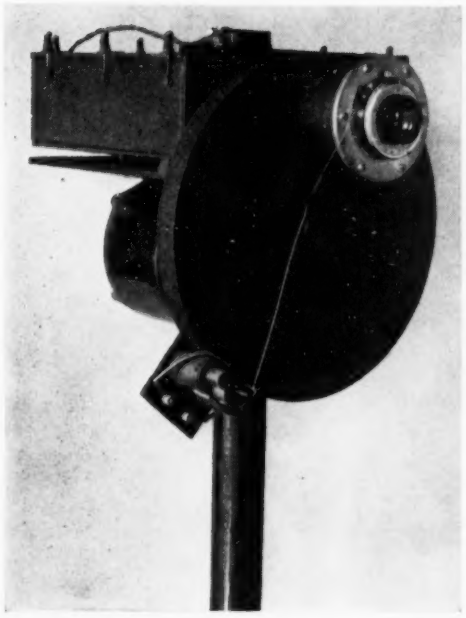


FIG. 3 CAMERA FOR PHOTOGRAPHING BURNING PARTICLES

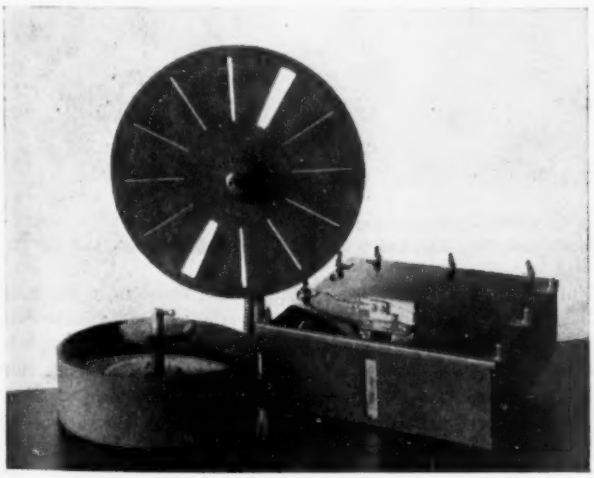


FIG. 4 PARTS OF CAMERA

as well as in performance in the furnace. Samples of too wide a density range contained particles which ignited at widely separated levels making it difficult to keep them all in the furnace during the incandescence period. Those density ranges which included nearly pure coal except for finely distributed ash were most uniform in behavior.

The proximate analyses of the coals used are given in Table 1. The volatile-matter contents, on an ash-and-moisture-free basis, and the ash contents for the samples as used are given in Table 2. The volatile-matter contents given in Table 2 were determined by a microanalytical procedure which was developed for the purpose of this investigation. This procedure gives about 10 per cent more volatile matter than is given by the standard A.S.T.M. test.

The principal effect of the density separation was to eliminate particles of high ash content. There was no apparent separation of the pure coal material of the Pittsburgh coal except for an observed concentration of fusain in the 1.35 sink fraction. However, the 1.35 float fraction of the Pocahontas coal was brighter in appearance than the sink fraction. It had a higher ratio of volatile matter to fixed carbon and formed a coke button in the determination of volatile matter, which was not obtained with the sink fraction. There was probably some separation into petrographic constituents with this coal.

MECHANISM OF IGNITION AND COMBUSTION

There were definite limitations on the types of fuel which could be ignited in the apparatus used. The controlling factor was the furnace temperature, which was limited to 950 C. For instance, when Pittsburgh seam coal was passed through the furnace, occasional particles of fusain in the residues showed no change in size and shape, although some etching occurred which intensified the fusain-like characteristics. Similarly, a sample of 170–200-mesh anthracite could not be uniformly ignited with the furnace set at 950 C. An occasional bright flash was seen and a few particles showed evidence of attack on thin layers of more reactive material.

The influence of temperature on the degree of combustion was most clearly demonstrated by an examination of the residues. Fig. 5 is a series of photographs showing the 60–80-mesh 1.29-float Pittsburgh coal and the residues obtained by passing it through the furnace at various temperatures. All these pictures were taken at the same enlargement, approximately 15 fold.

This coal began to show some melting, taking on a bright pitch-black surface, at 500 C. As the temperature was raised, the kernel sizes increased, and, on examination under the microscope, they were found to be somewhat irregular cenospheres. At temperatures up to 700 C there was no visible sign of ignition, but at 750 C short bright flashes were seen in the furnace, and the residues occasionally had a dull black coat of soot, but there was no attack on the kernels and the bright black surface could be found by brushing off the sooty coat. At 800 C some attack on the kernels occurred leaving lacy structures of bright graphitic sheen. As the temperature was further raised, the amount of attack in-

TABLE 2 ANALYSES OF COALS AS USED

Seam	Mesh size	Density	Ash, per cent	Volatile matter,[a] per cent
Pittsburgh.....	40–50	1.29 F	1.78	39.30
	60–80	1.29 F	1.84	39.20
Pocahontas No. 3....	60–80	1.35 F	2.37	18.83
	80–100	1.35 F	2.60	18.70
	100–140	1.35 F	2.24	19.48
	140–170	1.35 F	2.45	19.35

[a] On an ash-and-moisture-free basis, determined by a microprocedure, giving yields of volatile matter about 10 per cent higher than those given by the standard A.S.T.M. test.

TABLE 1 PROXIMATE ANALYSES OF THE COALS USED

Seam	Mine	County	Moisture, per cent	Volatile matter, per cent	Fixed carbon, per cent	Ash, per cent	Btu
Pittsburgh	Edenborn	Fayette, Pa.	1.9	33.6	57.0	7.5	13910
Pocahontas No. 3	Pinnacle	McDowell, W. Va.	0.8	15.3	78.3	5.6	14760
Illinois No. 6	Orient No. 1	Franklin, Ill.	6.7	33.9	50.3	9.1	12270
*	....	....	1.4	32.5	56.3	9.8	13260

* Kanawha gas coal from the Cabin Creek District of West Virginia. Used by Griffin, Adams, and Smith (7).

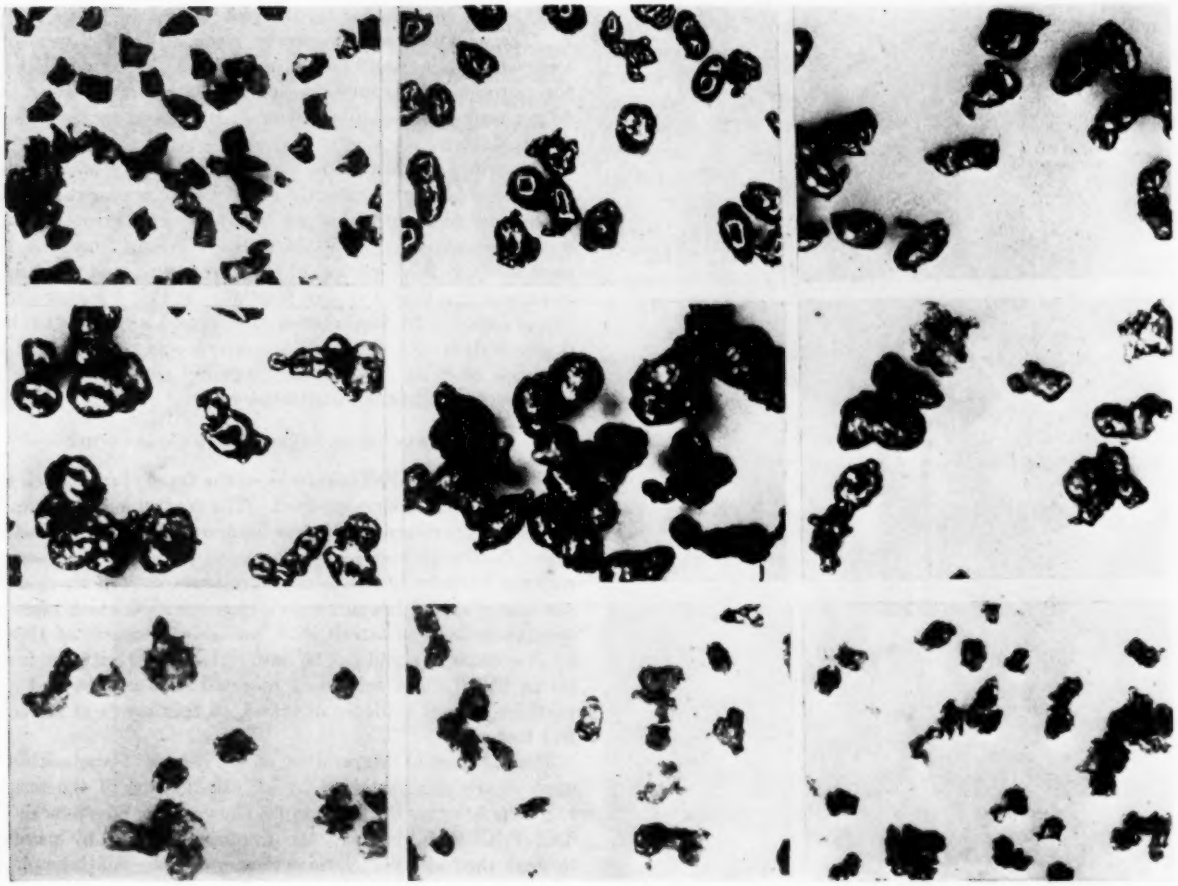


FIG. 5 PITTSBURGH SEAM COAL AND COMBUSTION RESIDUES; ×15
(Furnace temperatures, top row, left to right, original coal, 520, 600 C; middle row, 700, 750, and 800 C; bottom row, 850, 900, and 950 C.)

creased and the graphitic sheen turned to a dull gray. A point of special interest was the maximum in kernel size at about 750 C. The small cenospheres formed at the higher temperatures were very fragile and highly perforated. Their lacy structures followed the outline of typical cenospheres. Except for the elimination of nodules there was no indication that they had been formed by partial combustion of larger structures. The small nodules which appeared on most kernels were hollow. Their presence indicated that the surface had begun to harden while the interior was still fluid, the nodules being formed from fluid forced out through a point of rupture in the initial surface.

Fig. 6 is a similar series of photographs, showing the residues obtained from the 60–80-mesh 1.35-float Pocahontas coal. These showed characteristic differences from the Pittsburgh coal. At lower temperatures the cenospheres were wrinkled. They were neither so large at moderate temperatures nor so small at higher temperatures. No sooty particles were observed. Corresponding stages of combustion occurred at definitely higher temperatures, although this difference seemed to decrease as the temperature was increased.

Table 3 shows the analyses of residues which were duplicates of part of those shown in Fig. 6. The degree of combustion, the percentage completion of the combustion reaction, was calculated on the basis of ash contents. The volatile matter was not characterized. It may have been largely carbon dioxide and carbon monoxide.

Residues have also been obtained from the Illinois coal. On microscopic examination they were found to be cenospheres which were generally more irregular than those from the Pittsburgh coal. No evidence was found to indicate any fundamental difference in the behavior of the Illinois coal. It did appear to be more easily ignited than the other coals, but further work must be done to obtain quantitative information on its performance.

Microscopic examination of particles subjected to various furnace temperatures revealed delicate shadings of color and details of structure which are barely suggested in the illustrations. The unattacked cenospheres varied from a mat to a bright pitchy black, depending upon the character of the sample. The presence of perforations and lustrous graphitic sheens was a sensitive indicator of attack on the cenospheres. Delicate lacy structures and dull gray colors were signs of advanced stages of combustion. These differences in appearance offered convenient and convincing criteria for judging the degree of combusion. With the lighter fractions of the 60–80-mesh coals it was found that very few particles ignited below 750 C and that furnace temperatures in excess of about 850 C were necessary to obtain uniform ignition, while even 950 C was insufficient to ignite fusain or anthracite. Every sample that ignited at 900 C or lower showed evidence of increased combustion at 950 C.

Since the degree of combustion depended so strongly upon the furnace temperature, it was decided to investigate the character of the incandescence and its relation to the burning time at the highest available furnace temperature, 950 C. Fig. 7 is part of a record of burning 60–80-mesh 1.29-float Pittsburgh coal. The furnace was set at 950 C and the camera at F 3.7. Fig. 8 is part of a similar record for 60–80-mesh 1.35-float Pocahontas coal.

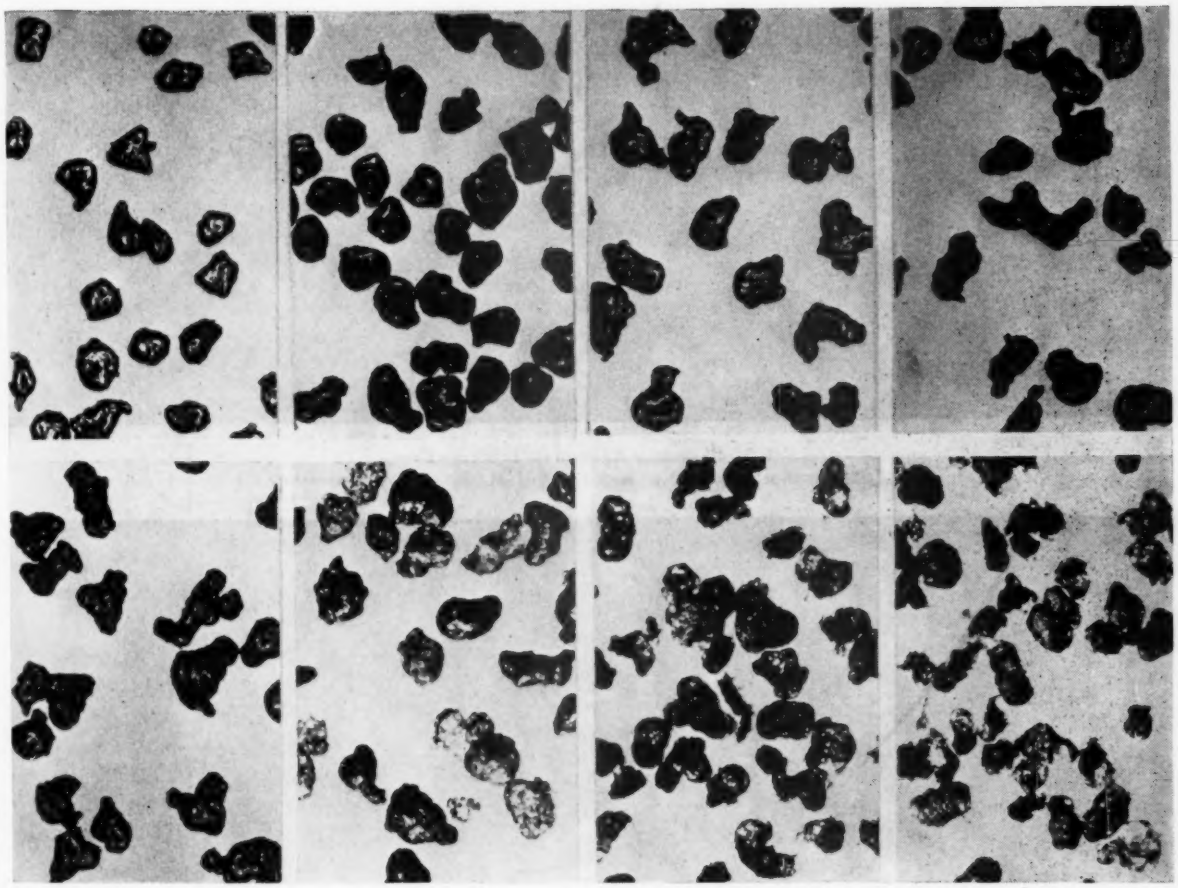


FIG. 6 RESIDUES FROM POCAHONTAS COAL; ×15
(Furnace temperatures, top row, left to right, 600, 650, 700, and 750 C; bottom row, 800, 850, 900, and 950 C.)

TABLE 3 ANALYSES OF RESIDUES[a]

Sample	Furnace temperature, F	Volatile matter, per cent	Ash, per cent	Degree of combustion
Original coal.....	...	18.83	2.37	...
Residues.....	800	12.57	3.12	24.7
	850	11.97	4.97	53.6
	900	4.32	11.63	81.6
	950	2.70	15.25	86.5

[a] Pocahontas No. 3 seam coal, 60–80 mesh 1.35 float.

The negatives for these records were intensified for the purpose of reproduction but are otherwise typical of many that were obtained. Other than in the apparent difference in radiant indensity, the Pittsburgh coal differed in that almost every particle ignited with a very intense flame which momentarily died out and then reached a second maximum. This effect, which was quite evident on microscopic examination of the original negatives, was better illustrated with coarser mesh sizes.

Figs. 9*a* and 9*b*, an enlargement of another portion of the same record, show a sample of 40–50-mesh 1.29-float Pittsburgh coal, burning in a furnace temperature of 950 C. The shutter disk used for this record had openings giving exposures of 0.021, 0.042, 0.085, and 3.18 millisec. This record is typical of many in which the brilliant portion of the traces had broad dashes which thinned out to a feathery top edge, while the dots took on a typical teardrop shape.

Using the same 40–50-mesh sample at 800 C furnace temperature it was very difficult to obtain satisfactory pictures. With high feed rates, there appeared to be a cooperative effect causing ignition at high levels in the furnace with considerable smoke. With lower feed rates it was difficult to maintain a steady flow of igniting particles. When the coal feed was so adjusted that the rate of flow of igniting particles was about one half the usual rate, the residues collected at four to five times the usual rate. It appeared that only an occasional particle was sufficiently reactive to ignite at or below 800 C. The brilliant portions of the photographic traces were frequently absent and when present were of short duration. Where they did occur there was usually an accidental grouping of two or more ignited particles.

It seemed quite evident that the brilliant portions of the traces were due to the combustion of volatile matter. This conclusion was also reached by Griffin, Adams, and Smith (7). The fact that the incandescence passed through a minimum indicated that combustible matter was still present, but it could not immediately be assumed that the remaining portion of the trace corresponded to the burning of the coke residue. In an attempt to determine the rate of the combustion process during the final portion of the incandescence period, a series of experiments was performed, using 40–50-mesh 1.29-float Pittsburgh coal, in which the particles were forced out of the furnace at various times after the point of ignition and before they had lost incandescence. It was supposed that the rapid cooling as the particle left the furnace would quench the combustion process.

Fig. 10 shows the results of these experiments. The percentage of the original combustible left in the residues, calculated on the basis of ash contents, is plotted against the time after ignition



FIG. 7 PART OF A RECORD OF BURNING COAL
(Pittsburgh seam coal, 60–80 mesh 1.29 float, at 950 C furnace temperature.)

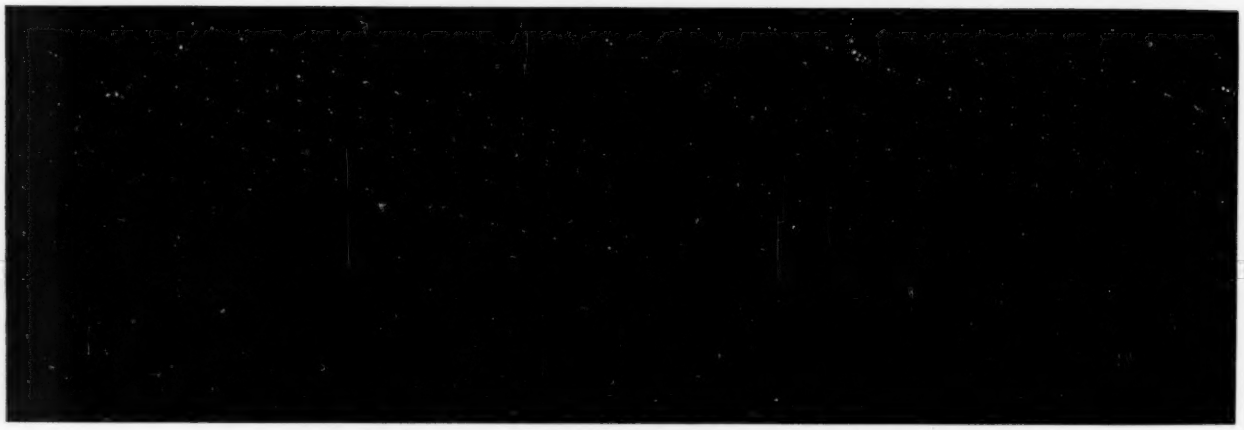


FIG. 8 PART OF A RECORD OF BURNING COAL
(Pocahontas No. 3 seam coal, 60–80 mesh 1.35 float, at 950 C furnace temperature.)

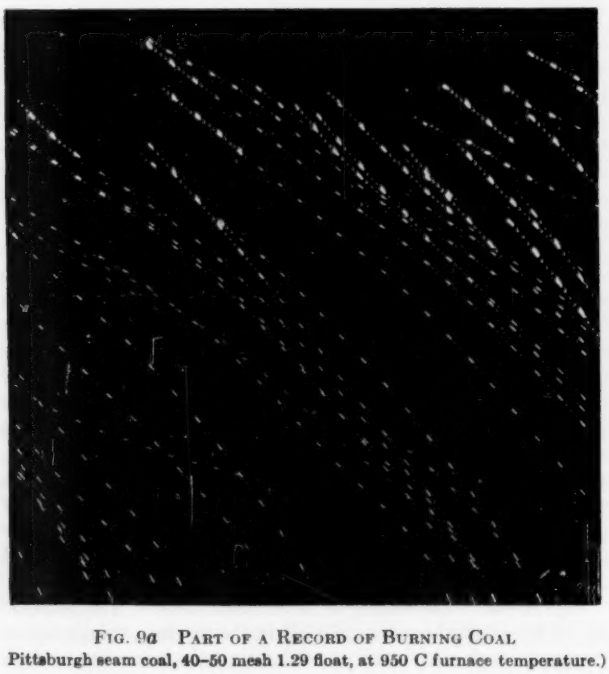


FIG. 9a PART OF A RECORD OF BURNING COAL
Pittsburgh seam coal, 40–50 mesh 1.29 float, at 950 C furnace temperature.)

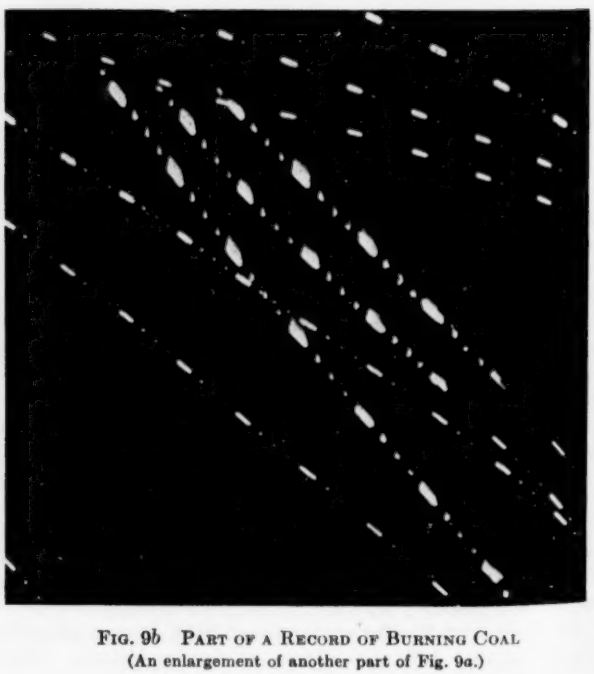


FIG. 9b PART OF A RECORD OF BURNING COAL
(An enlargement of another part of Fig. 9a.)

during which the average particle remained in the furnace. The total period of incandescence was estimated from later tests as 0.6 sec at 950 C and probably somewhat less at the lower temperatures. At 800 C ignition was not uniform. The increased degree of combustion at the higher time was probably due to an increased percentage of ignition as well as the effect of time on the evolution of volatile matter. At the higher temperatures the variations barely exceeded the limits of experimental accuracy.

The particles, after leaving the furnace, were in their latter stages of combustion where the rate might be expected to be comparatively slow. It is also possible that efficient quenching was not obtained. The particle temperatures, as will be shown

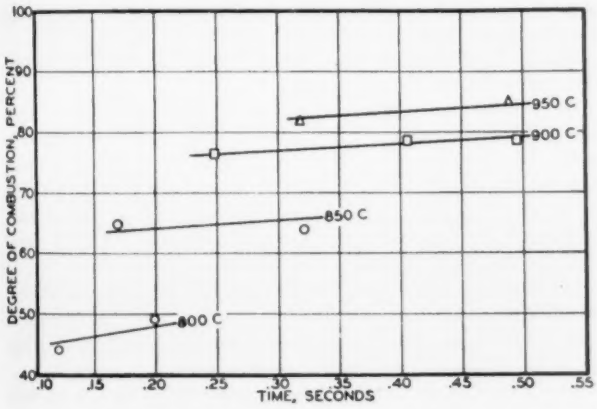


FIG. 10 DEGREE OF COMBUSTION AS FUNCTION OF TIME OF EXPOSURE TO FURNACE TEMPERATURE
(Pittsburgh seam coal, 40–50 mesh 1.29 float.)

later, were about 1500 C. Since radiation is proportional to the difference of the fourth powers of the absolute temperatures, substituting 25 C for the furnace temperature of 950 C would increase the rate of radiation by 29 per cent. Thermal conduction to surrounding gases, being controlled to a first order of approximation by the temperature difference, would be increased by 168 per cent. Wohlenberg and Wise (8), considering a theoretical furnace with angle factors to cold and refractory walls of 0.576 and 0.424, respectively, found that 71.1 per cent of the heat lost by the pulverized-coal flame was conducted directly to the surrounding gases. However, they were considering a coal pulverized 70 per cent through 200 mesh. Since the rate of conduction from a sphere contains the reciprocal radius as a factor, which is not involved in radiation, the portion of the heat lost by thermal conduction from the 40–50-mesh coal was probably less than that from their pulverized coal by a factor of four or five. Considering the differences in the two furnaces, it appeared reasonable to assume that substituting room temperature for 950 C would increase the rate of heat loss by 50 to 125 per cent, depending upon the mesh size in the range from 40 to 200 mesh. Since no criterion was available to determine the rate of heat loss required to cause quenching, the only conclusion that it was possible to draw from these experiments was that, although the degree of combustion depended strongly upon the furnace temperature, it was not significantly affected by forcing the particles out into colder surroundings before they had lost incandescence.

A study of the temperature history of individual particles was much more fruitful in interpreting the final portions of the photographic traces. It was assumed that the exposure just required to make an impression on the film depended only upon the amount of radiant energy available within the spectral-sensitivity range of the film. It was also assumed that the burning coal particle emitted true black-body radiation. According to Planck's law, the amount of energy in black-body radiation, dE, within the wave-length range $d\lambda$, is

$$dE = \frac{\sigma d\lambda}{\lambda^5(e^{c/\lambda T} - 1)}$$

where σ is the Stefan-Boltzmann radiation constant, T is the absolute temperature, and c is a constant depending upon the units of temperature and wave length used. By integrating over those wave lengths to which the film was sensitive, multiplying by the exposure time t, and dividing by the square of the relative lens aperture f, the following expression was obtained for the amount of energy reaching the film which was useful in forming an image

$$E' = \sigma t/f^2 \int_0^{\lambda} \frac{d\lambda}{\lambda^5(e^{c/\lambda T} - 1)}$$

The lower limit was taken as zero since the spectral sensitivity extended into the ultraviolet where the energy in black-body radiation, except for extremely high temperatures, becomes comparatively negligible. The upper limit was taken as 6500 Angstroms for super-XX film, which had a comparatively flat sensitivity curve extending from this point into the ultraviolet. If the integral had been taken from zero to infinity it would have

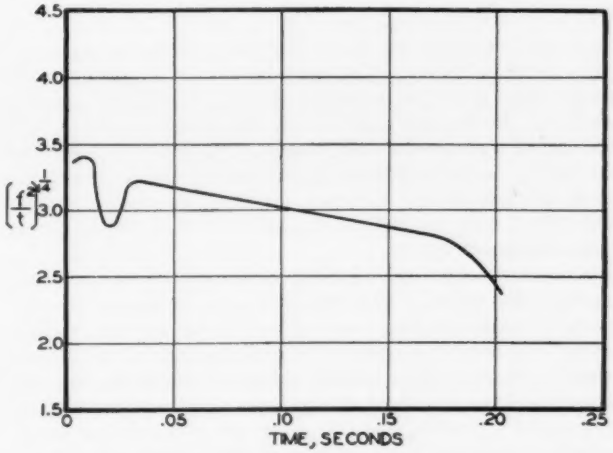


FIG. 11 TEMPERATURE HISTORY OF A BURNING PARTICLE
(Pittsburgh seam coal, 60–80 mesh 1.29 float. Temperature in arbitrary units estimated from relative lens aperture f, and exposure time in seconds t, just required to make an impression on the film.)

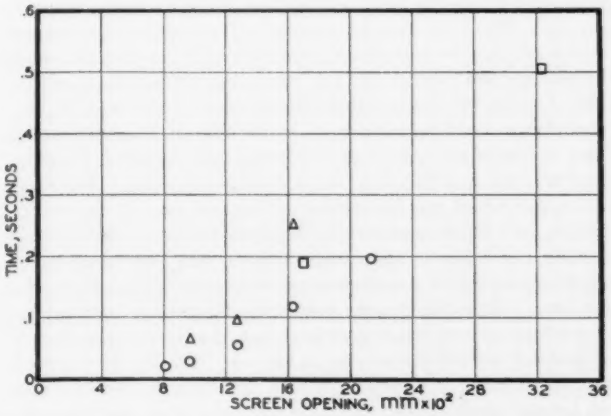


FIG. 12 BURNING TIME AS FUNCTION OF MEAN SCREEN OPENING
(○ 1.29-float Pittsburgh seam coal; △ 1.35-float Pocahontas seam coal; □ Kanawha gas coal, as reported by Griffin, Adams, and Smith, ref. 7.)

led to the familiar result that the rate of radiation was proportional to the fourth power of the absolute temperature. The partial integral could not be solved explicitly for T. However, numerical values for the integral were available (9). By plotting these values against T on a logarithmic scale, it was found that, within limits of accuracy sufficient for the purpose and in the neighborhood of 1500 C, the partial integral was proportional to the fourteenth power of the absolute temperature. By substituting this approximation for the integral and absorbing the constants of proportionality in an arbitrary unit of temperature, the foregoing expression became

$$T' = (f^2/t)^{1/14}$$

This permitted an estimation of the temperature history in terms of relative lens aperture and the exposure time in seconds.

In order to apply the latter equation it was necessary to find lens apertures at which pictures could be obtained with dots, corresponding to different exposure times, disappearing at various points along the traces. In general it was not possible to determine these points with a very high degree of accuracy, but a study of a number of pictures for 60–80-mesh 1.29-float Pittsburgh coal at 950 C furnace temperature led to the composite curve given in Fig. 11. This procedure for determining particle temperatures should be calibrated against sources of known temperature. Preliminary calibrations, involving pictures of the filament of a pyrometer bulb, placed at the same distance from the camera as the burning coal without any optical system between the camera and the bulb, led to an estimate of 1800 C and 1500 C as corresponding, respectively, to the first maximum and minimum of Fig. 11.

It is now possible to give a fairly complete interpretation of the photographic traces. When the coal particle entered the furnace, it was blown into a cenosphere by the escaping volatile matter. If there was sufficient volatile matter and the furnace temperature was high a brilliant flame of burning gas resulted. Since this flame consumed all the oxygen in the vicinity of the particle the temperature of the residue fell after the flame disappeared, until oxygen could again reach the particle. Whether or not the volatile matter ignited, the attack on the residue raised its temperature to a maximum, and then as the process continued, the temperature gradually fell. The residue was in the form of a cenosphere which was being etched and pitted by the combustion process. Thin wall sections, especially the nodules, disappeared or at least they were so fragile that it was impossible to collect the residues and observe any ash structures in the holes that were left. Except for the possible falling away of the nodules, the cenospheres could be considered as burning at constant radius. Since the inner surfaces were visible through the holes, the effective radiation area was at most decreasing very slowly. However, the oxygen, which was being consumed as rapidly as it reached the surface, and which was largely depleted before it could diffuse through the holes to the inner surfaces, was consumed on an effective area which was decreasing more rapidly than the radiation area. Since these areas controlled the rate of heat release by combustion and the rate of heat loss, the temperature had to fall in order to keep the process in balance. Finally the temperature began to fall at a very rapid rate, although the residues were still largely combustible. Starting with coal of about 2 per cent ash, the residues contained from 20 to 30 per cent ash at the highest furnace temperatures obtainable in the present apparatus.

Tu, Davis, and Hottel (3) found that the rate of burning of a sphere of electrode carbon, burning in air under forced convection, increased rapidly with increasing surface temperature up to about 1000 C, while above this temperature the rate increased very slowly. Parker and Hottel (4) found that above 1100 C the concentration of oxygen at the carbon surface approached zero, while at lower temperatures it rose rapidly to the normal concentration in the air. Their interpretation was that at low temperatures the rate of the surface-reaction was the controlling factor, while at high temperatures the oxygen was being consumed as rapidly as it could diffuse to the surface. Since surface-reaction rates generally have high temperature coefficients while those of diffusion processes are comparatively low, this explained their results. In applying their conclusions to the burning cenospheres it was necessary to consider that the cenospheres, being formed at temperatures probably on the order of 1800 C, were less reactive than the electrode carbon. This meant that as the temperature gradually fell, a point estimated at about 1400 C was finally reached where the rate of the surface reaction became a controlling factor and the high temperature coefficient of this reaction caused the final rapid fall in temperature.

The study of the mechanism of combustion has led to three important results as follows:

(*a*) During all of the incandescence period, except for a small part at the end, the rate of combustion was controlled by the rate of transport of oxygen to the surface. Since the cenosphere was burning at nearly constant radius, the effective surface could not have been decreasing rapidly, and the rate of combustion must have had the same order of magnitude, except for the very last portion of the incandescence period.

(*b*) The degree of combustion was not significantly reduced by forcing the particle out of the furnace while it was still incandescent, a major fraction of the normal incandescence period being spent in surroundings at room temperature.

(*c*) The degree of combustion increased with increasing furnace temperature.

These results indicated that the cenospheres burned at a rate which was independent of changes in the temperatures of their surroundings during the combustion period, until the rate suddenly decreased at a degree of combustion which depended strongly upon the temperature at which the process began. It was also shown, as illustrated in Figs. 5 and 6, that the residues were in the form of cenospheres even though the temperature was too low to cause ignition, while the size and shape of the cenospheres depended upon the temperature at which they were formed. The most plausible conclusion seems to be that the conditions ahead of the point of ignition, under which the cenospheres were formed, were the controlling factors.

Relation of Particle Size to Burning Time

Before making a study of the relation of particle size to burning time it was necessary to decide on a suitable definition of burning time. Obviously the period of incandescence, as determined by the photographic records, could not be used because it was found that this period depended upon the film and the lens aperture used. It was also necessary to consider that slow combustion processes occur even at room temperature. The study of particle temperatures indicated that the rate of combustion was decreasing slowly, until the surface reaction became a controlling factor causing the final rapid fall in temperature. During this final period the rate of combustion was probably so low that it would be of no importance in changing the degree of combustion attainable in the times available in any practical furnace. For these reasons, the time of combustion was defined as the time from the point of ignition to the beginning of the final rapid fall in temperature. Experimentally this time was determined by counting the dashes along a given trace until a point was reached at which two or more dots disappeared within a single timing cycle, $^1/_{60}$ sec. Since the ratio of exposure times for successive dots in each cycle was two to one, this meant that at this point more than a twofold increase in exposure time was required to compensate for the temperature fall within $^1/_{60}$ sec.

A series of experiments was made at 950 C to determine the relation of burning time to particle size. Fig. 12 shows the time in seconds plotted against the mean screen opening for each size fraction (60–80, 80–100, 100–140, 140–170, 170–200). These are provisional values subject to further confirmation. It must be emphasized that these were burning times at constant furnace temperature and not at constant degree of combustion. This was probably not a serious limitation because the degree of burning of the 60–80-mesh Pittsburgh coal was estimated from ash contents of the residues as approximately 94 per cent, while the finer sizes with which it was impossible to collect residues must have reached even higher degrees of combustion. The Pocahontas

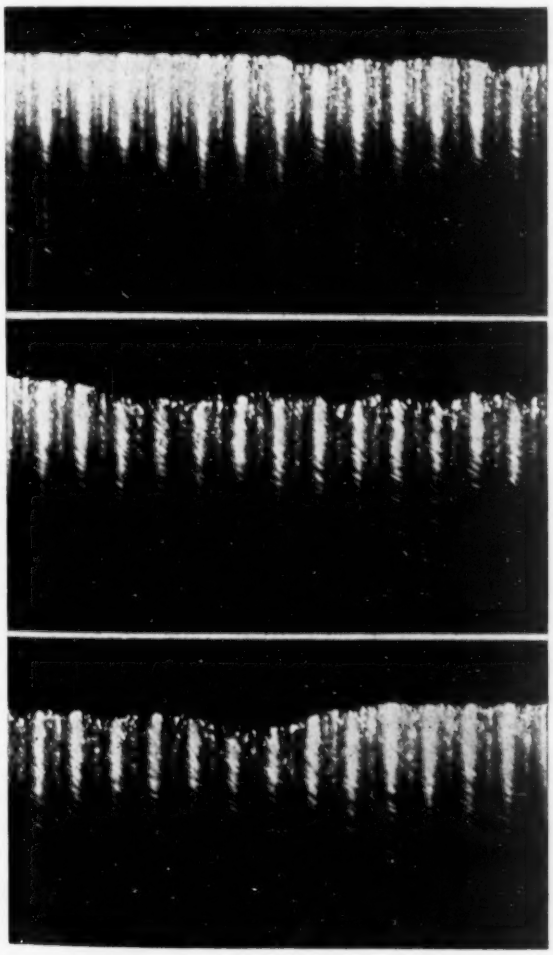


FIG. 13 FLAME OF PITTSBURGH SEAM COAL
(Minus 200-mesh coal at 950 C furnace temperature.)

coal showed the longer burning times although residues were collected even for the 140–170-mesh size which indicated a much lower degree of combustion than for the Pittsburgh coal. The two values shown for Kanawha gas coal are those reported by Griffin, Adams, and Smith (7). They used a recording paper for most of their work, but did get some data on panchromatic film. These materials being slow, as compared to Eastman super-XX roll film, it is possible that their traces may have died out before the particles entered the final period of rapidly falling temperature. On the other hand, if their traces had died out during the period of slowly falling temperature, the paper and the film, which had different speeds, should have indicated distinctly different times of incandescence. Since they reported almost no difference, their traces must have died out at or shortly after the beginning of the final rapid fall in temperature. This means that they were measuring approximately what has been defined previously as the burning time.

The burning times were obtained with rates of coal feed such that nearly infinite air supply could be assumed. With higher rates of feed, the burning time increases. This is clearly indicated in Fig. 13, which shows the flame of minus 200-mesh Pittsburgh coal at a furnace temperature of 950 C. Where the cloud was most dense, the incandescence time increased, but it was not possible to evaluate the density, except that in this case the formation of smoke indicated, at least in a part of the flame, that there was an actual deficiency of air. The increased burning time was probably due to the decreased excess-air supply, but it is possible that, at least in part, it was due to an increased degree of combustion with higher cloud densities. Aside from its influence on burning time, the cloud density had another very important effect. As the density was increased, the flame became steadier and occurred at a higher level in the furnace. The formation of well-defined and steady flame fronts depended critically upon the cloud density and was most easily obtained with the finer-mesh sizes of the higher-volatile coals. There appeared to be a co-operative effect causing a continuous-gas-phase flame front in the volatile matter which was driven out before ignition occurred.

GENERAL CONSIDERATIONS

In the present investigation, the available furnace temperatures were not, in general, sufficient to obtain complete combustion. Rapid combustion depended upon the ability of the individual particle to maintain itself considerably above the temperature of its surroundings. Whether the temperature required varied with particle size was not determined. However, an examination of the records which were obtained showed that the finer particles burned at approximately the same temperature as the 60–80-mesh sample, which was used in the quantitative studies, except that the onset of rapidly falling temperature was more sharply defined. Since the temperature required, above about 1400 C, was the same order as that found in industrial furnaces, it appeared probable that incomplete combustion would only occur with those particles that still contained combustible when they passed out of the high-temperature regions of the furnace. The experimental results have indicated that such particles would be able to maintain their temperature sufficiently above their surroundings to sustain active combustion, until a degree of combustion was reached which was determined by the character of the particle itself and only to a minor degree by its surroundings.

Furnace temperature was the variable subject to control but was not the variable which could be compared with conditions in a flame front. The important factor was probably the temperature history of the individual particle before ignition occurred. With the coals investigated it was shown that increasing furnace temperature, and therefore increasing rates of rise of particle temperature, influenced the size and form of the cenospheres. It has also been shown that the yield of volatile matter increases with the rate of rise of temperature (10, 11). It would seem reasonable to suppose that the tremendous rates of rise available in the flame front might have considerable effect on the yield of volatile matter. Since the degree of combustion and probably the percentage conversion to highly combustible volatile products both increased with increasing furnace temperature, it appears desirable that the rate of rise of particle temperature should be high. However, no evidence has been obtained to indicate how far it might be practical to go in this direction.

The appearance of the flame depended upon the cloud density. At low densities ignition occurred at random levels in the

furnace but, as the density was increased, a point was reached where a definite flame front appeared. This effect was probably due to propagation of a continuous gas flame in the volatile matter which was driven out before ignition occurred.

Any air in excess of that required in the region where volatile matter is burned would have to be consumed in the comparatively slow combustion of the residues. The amount of such excess air would have an effect on the temperature attained in this region, which in turn is most directly responsible for the rate of heating of the coal particle. These results indicated that the desirability of high rates of heating of the coal particle, as well as flame stability, are fundamental reasons for not admitting all the air required for combustion with the coal.

Information on the relation of burning time to particle size was also obtained. The numerical results must be interpreted with care. They were obtained at constant furnace temperature and not at constant degree of combustion. They must be corrected for the influence of limited excess air. This information is probably of greater value for comparison of different coals than it is for interpretation of furnace conditions.

Probably the most important result of the investigation has been that it has focused attention upon those changes in the coal particle which occurred before ignition. The indicated desirability of a limited primary-air supply, as a means of obtaining flame stability as well as high rates of heating the unignited coal, must be considered in relation to the fuel used. Delayed admission of secondary air requires considerable power for thorough mixing. It generally involves more expensive equipment. Such extra costs may not be justified except for fuels which are more difficult to ignite and burn.

Summary and Conclusions

1 The mechanism and time of burning of individual particles of coal have been determined using all convenient means of observing the burning coal particles and examining any residues that were obtained.

2 The investigation was limited to low ash fractions of Pittsburgh, Pocahontas No. 3, and Illinois No. 6 seam coals, but included particle sizes ranging from 40 to 200 mesh.

3 The residues obtained at various furnace temperatures showed nonuniform ignition at temperatures below about 850 C and an increasing degree of combustion with increasing temperature throughout the range explored up to 950 C.

4 The coal particles were blown into cenospheres by escaping volatile matter. The conditions under which this process occurred were found to be the controlling factors in the performance of the coals investigated. It is probable that the temperature, and therefore the rate of temperature rise, in the region just ahead of the zone of ignition should be maintained as high as possible.

5 Contrary to the assumption which has frequently been made in theoretical calculations, the coke residues were in the form of cenospheres which burned essentially at constant radius.

6 Probably the most important result of this investigation has been a demonstration of the fact that the changes, which occur before the particle of coal ignites, exert considerable influence upon the subsequent combustion process.

BIBLIOGRAPHY

1 "Burning Characteristics of Pulverized Coals and the Radiation From Their Flames," by Ralph A. Sherman, *Combustion*, vol. 5, December, 1933, pp. 30–38.

2 "The Combustion of Carbon," by Martin A. Mayers, *Chemical Reviews*, vol. 14, 1934, pp. 31–53.

3 "Combustion Rate of Carbon," by C. M. Tu, H. Davis, and H. C. Hottel, *Industrial and Engineering Chemistry*, vol. 26, 1934, pp. 749–757.

4 "Combustion Rate of Carbon," by Almon S. Parker and H. C. Hottel, *Industrial and Engineering Chemistry*, vol. 28, 1936, pp. 1334–1341.

5 "Combustion Rate of Carbon," by H. Davis and H. C. Hottel, *Industrial and Engineering Chemistry*, vol. 26, 1934, pp. 889–892.

6 "The Formation and Structure of Cenospheres," by F. S. Sinnatt, *Journal of The Society of Chemical Industry*, Transactions, vol. 47, pt. 1, 1928, pp. 151–155T.

7 "Rate of Burning of Individual Particles of Solid Fuel," by H. K. Griffin, J. R. Adams, and David F. Smith, *Industrial and Engineering Chemistry*, vol. 22, 1929, pp. 808–815.

8 "The Distribution of Energy in the Pulverized-Coal Furnace," by W. J. Wohlenberg and D. E. Wise, Trans. A.S.M.E., vol. 60, 1938, pp. 531–547.

9 "Tables of Planck's Radiation and Photon Functions," by A. N. Lowan and G. Blanch, *Journal of the Optical Society of America*, vol. 30, 1940, pp. 70–81.

10 "Carbonization of Coal," by William B. Warren, *Industrial and Engineering Chemistry*, vol. 27, 1935, pp. 72–77.

11 "Thermal Decomposition of a Coal in High Vacuum," by B. Juettner and H. C. Howard, Contribution No. 8, Coal Research Laboratory, Carnegie Institute of Technology, Pittsburgh, Pa., 1934.

Discussion

Henry Kreisinger.[3] The paper gives the results of an interesting laboratory investigation of combustion of pulverized coal and deserves a careful study and analysis. The furnace conditions under which the experiments were conducted should be carefully compared with the conditions existing in a commercial pulverized-coal furnace before any general conclusions can be reached.

In the paper the furnace temperature has not been defined. It is assumed to be the temperature of the two silicon-carbide plates which form the inner sides of the experimental furnace. Pulverized-coal particles were dropped into the space between these two plates and fell through the furnace. Air was circulated through the furnace in the same direction as the falling pulverized-coal particles. The paper does not state how hot this air was while flowing through the furnace, but it probably never reached the temperature of the two plates. The particles of coal falling through the furnace were heated mainly by radiation. The heating drove the gas from the particles and, when this gas reached certain concentration and temperature, it ignited.

The rate of heating depended upon the temperature of the plates and the size of the particles. The smaller particles had greater surface compared to their mass and were heated more quickly than large particles. When the temperature of the plates was low, the rate of heating of the coal particles was low, the gas was evolved from the coal particles slowly, and the particles formed almost perfect cenospheres. With high temperature of the plates, the coal particles were heated rapidly, and the gas was evolved faster, in most cases breaking the surface while cenospheres were being formed. This procedure in the formation of the cenospheres seems to be indicated by Fig. 5 of the paper, which shows the residue from Pittsburgh coal and furnace temperature, varying from 520 to 950 C. According to Fig. 5, the most perfect cenospheres were obtained with temperature of 700 to 750 C. With the lowest temperature, the coal particles did not get hot enough to form cenospheres; with high temperature the surface of the coal particle was broken before cenospheres were formed.

When the coal particles ignited, their temperature reached 1400 to 1500 C, which is several hundred degrees higher than the furnace temperature. The elevation of the temperature was the result of the heat generated by the combustion of the gas. The combustion took place at or near the surface of the particle, and the heat was contained in the small amount of combustible

[3] Engineer in Charge of Research and Development, Combustion Engineering Company, Inc., New York, N. Y. Mem. A.S.M.E.

and the oxygen which had combined. The heat from the products of combustion was then transmitted to the surrounding gas and to the silicon-carbide plates. The temperature of 1400 to 1500 C corresponds to the temperature obtained in a commercial furnace in the ignition zone. The particles of pulverized coal entering a commercial furnace are heated mostly by radiation from the coal already ignited, which is at a temperature of about 1500 C. Because of this very much higher temperature in a commercial furnace, the coal particles entering the furnace are heated quickly. Therefore, it is questionable whether under such rapid heating any cenospheres are formed.

Pulverized coal, as burned in commercial furnaces, contains a large percentage of superfines which heat and evolve gas very quickly. It is these superfines which start the ignition. With such rapid heating, it is likely that the evolution of the gas from the coal particles is so fast that it breaks the surface before any cenospheres can be formed. This is true of the average conditions under which pulverized coal is burned. If any cenospheres are formed, it is the large particles of certain coals which may go through the cenosphere stage when burned under unfavorable conditions.

The fineness of pulverized coal, burned in commercial furnaces, is about 70 per cent through a 200-mesh and 90 per cent through a 100-mesh screen. Large particles remaining on an 80-mesh screen, which include the size on which most of the experiments were made, may amount to 5 per cent. Inasmuch as this small amount of large particles is surrounded by a large amount of fine and superfine particles which ignite readily, these large particles are heated quickly by the heat generated by the combustion of the fine particles. Therefore, the large particles behave differently in commercial furnaces from what they did in the experimental furnace where they were burned by themselves without the influence of the heat from combustion of the fine particles. It is doubtful that satisfactory results could be obtained in a commercial furnace with pulverized coal from which all coal passing through an 80-mesh screen was removed.

When the experimental furnace was operated at the low temperatures, the heating of the particles was so slow that some of them passed out of the furnace before they ignited. If allowed to fall freely, they would stay in the furnace about $^1/_3$ sec. If the air moved faster than the falling particles, there was a drift and the coal particles stayed in the furnace less than $^1/_3$ sec.

In the experimental furnace, the furnace temperature controlled the rate of heating of the coal particles and the evolution of combustible gas, thereby controlling the ignition. With high furnace temperature, the ignition conditions were reached soon after the particles entered the furnace. Most of the time that the particles stayed in the furnace was available for combustion. At low furnace temperature, the heating of the coal particles was slow, and much of the time that the particles stayed in the furnace was used to bring them to ignition condition, and very little time was left for combustion. Some of the particles did not ignite, and therefore did not burn at all. When ignition occurred, the combustion proceeded at the temperature of the coal particles, which was always much higher than the furnace temperature.

The coal particles and the air in the furnace moved in the same direction with very little or no relative velocity between them. The products of combustion, after ignition had been established, formed an envelope around the coal particles and moved with them, thus preventing access of free oxygen to the surface of the coal particles, or to the combustible gas evolving from them. As a result of the formation and retention of this envelope of inert gas, the combustion quickly decreased and stopped, not because of drop of temperature, but because of lack of oxygen. The results would be different if the air moved in the opposite direction to the falling particles. The ignited particles would be continually moving out of the envelope of inert products of combustion and meeting free oxygen. Combustion would occur as fast as combustible made contact with free oxygen and the temperature at or near the surface of the particles would be maintained considerably above the furnace walls. In commercial furnaces, we often observe particles of burning coal puffed out through the observation doors continue to burn at bright red heat for 1 or 2 sec in the boiler room in spite of the low atmospheric temperature, because they meet plenty of free oxygen to support combustion.

Authors' Closure

It is gratifying to find that a laboratory investigation is sufficiently interesting to merit careful study and analysis in relation to conditions existing in a commercial pulverized-coal furnace. It is necessary, however, to examine carefully any conclusions that are made and to determine whether or not they are based on experimental evidence.

The aim of the investigation was to replace the uncontrolled surroundings of an individual particle burning in a flame by the controllable surroundings of an electric furnace, so that the variables could be individually studied. The temperature effect was studied to the limit of the present equipment. There was no indication that higher furnace temperatures would cause any changes except the continued decrease in cenosphere size and increase in degree of combustion.

Mr. Kreisinger's assumption as to the furnace temperature is incorrect. The furnace temperature was determined by an unprotected chromel-alumel thermocouple temporarily inserted into the air space between the heater plates. A temperature difference between the air and the heater plates may have existed, but the air temperature was not necessarily the lower. The air entering the top of the furnace was passed through a preheater minimizing such differences. The indicated temperature was a good approximation to that which brought about the ignition of the coal particles.

The supposition, that ignition occurs as soon as the gas being driven out of the particle has reached a sufficient concentration and temperature, has no foundation in the present experimental investigation nor has any experimental evidence for it been found in the literature. The identification of the brilliant streaks at the beginning of the photographic traces as the burning of volatile matter does not identify the ignition process. The ignition of the volatile matter may be brought about by previous localized heating of the particle surface due to oxidation reactions. Ignition of the volatile matter was not found to be essential to burning of the residue. At the lower furnace temperatures especially, many photographic traces were found without the initial brilliant traces. Experimental investigations on the ignition processes in solid-injection Diesel engines have indicated that combustion reactions at the surface of large oil drops, rather than the ignition of previously vaporized small oil droplets, were responsible for the initial pressure rise.[4]

There is need for a similar direct experimental investigation of the ignition processes in pulverized-coal flames.

Mr. Kreisinger's interpretation of Fig. 5 is not correct. With all the coals examined and at all furnace temperatures, including the highest, the residues were cenospheres. It is true that escaping volatile matter probably caused some breakage but, even under the microscope, evidence of breakage was obscured by the effects of combustion.

Undoubtedly the presence of unburned cenospheres in the resi-

[4] "Neuere Anschauungen über den Zündvorgang im Dieselmotor," by K. Zinner, *Zeitschrift des Vereins deutscher Ingenieure*, vol. 83, 1939, pp. 1073–1079.

dues from commercial furnaces is correlated with unfavorable furnace conditions. However, the absence of cenospheres in the residues, under more favorable conditions, does not indicate that cenospheres were not involved in the combustion process. An ash skeleton, containing a small percentage of carbon and at a temperature above its fusion point, could not be expected to retain the form of the carbonaceous particle from which it originated.

The relative velocity between particles and air was controlled by the acceleration of gravity and by inertia effects in regions of changing gas velocity. Any attempt to obtain higher relative velocities was considered impractical for experimental reasons. Further, it is improbable that appreciably higher relative velocities occur in commercial pulverized-coal furnaces. A large dense object when thrown into an air stream maintains its relative velocity for a considerable time. Small particles show this tendency to a comparatively negligible degree. The inertia effect, being controlled by the mass and hence the cube of a linear dimension, decreases much more rapidly than the flow resistance. The latter varies as the projected area at high velocities while in the region of Stokes' law, which probably applies in the present case, it varies as a linear dimension. Except in regions where opposing gas streams impinge, the added accelerating forces are probably small as compared to gravity. High relative velocities produced in such regions are quickly destroyed. In order to maintain such velocities throughout the burning period, strong and continuous accelerating forces, such as those found in cyclone separators, would have to be employed.

The slopes of the lines in Figs. 7, 8, and 9 are measures of the particle velocities. The particle velocity was the sum of the air velocity and the relative velocity between air and particle. The upward convexity in Figs. 7 and 8 indicates that one or both of these velocities were decreasing as the particles moved through the furnace. The downward convexity in Fig. 9 indicates the converse. The relative velocities may be estimated on the basis of the rate of fall of free particles in stagnant air. Since the particles were cenospheres of low apparent density and lost weight due to combustion with little decrease in projected area, the relative velocities were probably a small fraction of the total velocity and decreased strongly as combustion proceeded. The slight curvature indicates slow changes in velocity and correspondingly small inertia contributions to the relative velocity.

Depreciation Estimates in Appraisals of Manufacturing Equipment

By P. T. NORTON, JR.,[1] AND E. L. GRANT[2]

A replacement-cost appraisal should answer the question: "What could one afford to pay for this asset in comparison with the most economical new one?" The depreciation deduction from the cost of the most economical new asset should measure the value inferiority of the existing old asset. Depreciation estimated in this way may be very high even for comparatively new assets. General recognition of this in the manufacturing industries might well lead not only to a new concept of appraisals but also to a revision of depreciation-accounting policies and methods. The purpose of this paper is to outline briefly the theory which should govern measurements of value inferiority in appraisals, in other words measurements of appraisal depreciation.

CONVENTIONAL practice in commercial appraisals may result in misleading valuations because of the failure of the appraiser to understand clearly the theory which ought to govern appraisal depreciation. This may be illustrated by an example.

Shortly after the first World War, a manufacturing plant was appraised by a well-known appraisal organization as a basis for a loan. The major part of this plant consisted of several well-built brick buildings which had been constructed some years before. These were appraised on the basis of cost of reproduction less depreciation. The high cost of brick construction at this postwar date was naturally reflected in the reproduction-cost estimates. Because these buildings were so well built, the appraisers estimated a long life for them; hence straight-line depreciation deduction was but a small percentage of their reproduction cost.

On the basis of this high appraisal, the manufacturing company secured a substantial loan. Within a few years the company was unable to meet the interest and principal payments on this loan and went into receivership.

An important element in this company's failure was the high cost of materials handling. This high cost was due largely to the fact that electric overhead traveling cranes could not be used in these brick buildings. The lower-cost steel-frame mill-type buildings used by some competitors permitted this more economical method of handling materials. This fact had been given no consideration in the conventional "reproduction-cost less straight-line-depreciation" appraisal.

Appraisal Depreciation Should Measure Value Inferiority

Many such incidents could be cited where conventional appraisals have been misleading. The interpretation of a reproduction-cost-less-depreciation appraisal requires a clear understanding of the limited inferences which may be drawn from any appraisal based on replacement cost. It also requires an understanding of the theory which should govern the depreciation deduction from replacement cost. The clearest and most complete explanation of these matters which has come to the attention of the authors is by J. C. Bonbright.[3] Professor Bonbright summarizes his analysis as follows:

"A sharp distinction must be drawn between replacement cost in the sense of the cost of acquiring a substantially identical type of property, and replacement cost in the sense of the cost of constructing or buying the most desirable substitute. The former is never a measure of value unless it happens to approximate the latter. But even the cost of a different type of substitute cannot be used directly as a measure of value. Account must be taken of the likelihood that in some respects the substitute would be superior to the present property, while in other respects it would be inferior."

The most economical new substitute asset may have many advantages over an existing old asset, such as longer life expectancy, lower annual disbursements for operation and maintenance, increased receipts from sale of product or service. The depreciation deduction from the cost of the hypothetical new substitute asset should be a measure in money terms of all of these disadvantages of the existing old asset. Seldom, if ever, is the conventional depreciation deduction, based on the age of the old asset in combination with some formula (usually either straight-line or sinking-fund), a satisfactory measure of this value inferiority.

Four Examples of Measurement in Appraisal Depreciation

Before discussing the kind of forecasts which ideally should be made in order to measure this value inferiority, it will be helpful to consider four representative examples expressed in money terms. In all of these examples, the central question is how much could be paid for the existing old asset in order to realize annual costs exactly equal to those obtainable from the most economical new asset which could replace the service. Because equal services are assumed, the question of differences in annual receipts does not enter into any of these four examples. For the sake of simplicity, zero salvage values are assumed at all times in all four examples.

Example 1. The hypothetical new asset to be used as the valuation base is identical with the existing old asset. This implies that there have been no improvements in design and no changes in service requirements. The only difference is that the existing old asset has a shorter remaining life expectancy.

An old asset being appraised has a remaining life expectancy of 10 years. The identical new asset to be used as the valuation base has a first cost of $1000 and a life expectancy of 20 years. There are no other differences. The minimum prospective rate of return considered sufficient to justify such an investment is 7 per cent. In other words, this enterprise will not make such an investment unless an economy study indicates that the investment will be recovered plus at least 7 per cent interest. This means that all annual cost calculations should involve an interest rate of 7 per cent.

[1] Professor of Industrial Engineering, Virginia Polytechnic Institute, Blacksburg, Va. Mem. A.S.M.E.

[2] Professor of Economics of Engineering, Stanford University, Stanford University, Calif.

Contributed by the Management Division and presented at the Fall Meeting, Louisville, Ky., October 12–15, 1941, of THE AMERICAN SOCIETY OF MECHANICAL ENGINEERS.

NOTE: Statements and opinions advanced in papers are to b understood as individual expressions of their authors and not thos of the Society.

[3] "Valuation of Property," by J. C. Bonbright, McGraw-Hill Book Company, Inc., New York, N. Y., 1937; especially chapters 9 and 10.

Let X = the appraised value of the old asset which will give annual costs equal to those of the new asset.

The annual cost of capital recovery of P dollars in n years with interest rate i is P multiplied by the capital-recovery factor $\frac{i\ (1+i)^n}{(1+i)^n - 1}$. The derivation of this formula may be found in texts either on engineering economy or on the mathematics of finance.

As all other annual disbursements are the same, equal annual costs may be obtained by merely equating the annual capital-recovery costs for the two assets as follows:

$$X\ \frac{0.07\ (1.07)^{10}}{(1.07)^{10} - 1} = \$1000\ \frac{0.07\ (1.07)^{20}}{(1.07)^{20} - 1}$$

$$0.14238\ X = (0.09439)\ \$1000$$

$$X = \$663$$

The value inferiority of the old asset with the 10-year life expectancy to the new asset with the 20-year life expectancy is \$337, the difference between \$1000 and \$663. In other words, the appraisal depreciation is \$337.

Example 2. The hypothetical new asset is superior to the existing old asset not only in longer life expectancy but also in a uniform annual saving in disbursements for all purposes. This prospective saving might come from various causes, such as improved design or the better adaptation of the new asset to the present service.

An old asset being appraised has a remaining life expectancy of 10 years and prospective disbursements for all purposes of \$500 per year during this remaining life. The most economical new asset to perform the same service has a first cost of \$1000, a life expectancy of 20 years, and prospective disbursements for all purposes of \$450 per year during its life. Interest is at 7 per cent as before.

Let X = the appraised value of the old asset which will give annual costs equal to those of the new asset. Then

$$0.14238\ X + \$500 = 0.09439\ (\$1000) + \$450$$

$$X = \$312$$

Here the value inferiority or appraisal depreciation is \$688.

Example 3. As in example 1, the hypothetical new asset is identical with the existing old asset; there have been no improvements in the art or changes in service requirements. However, unlike example 1, the termination of the life of assets of this type occurs because of a progressive and steady increase in the cost of operation and maintenance. The old asset has two disadvantages as compared to the hypothetical new one, shorter life expectancy and higher annual disbursements for operation and maintenance.

A certain type of asset has a first cost of \$1000. Annual disbursements for all purposes are \$500 in the first year of its life, \$508 in the second year, \$516 in the third year, and increase by \$8 each year thereafter. A 10-year-old asset of this type is to be appraised at a figure which will give an equivalent uniform annual cost for its remaining life equal to the equivalent uniform annual cost over the life of a new asset. Interest is at 7 per cent.

Where disbursements vary from year to year, an equivalent uniform annual disbursement for any period may be determined by first finding the sum of the present worths of the respective annual disbursements during the period, and then multiplying this sum by the capital-recovery factor for the period. The present worth of each disbursement is obtained by multiplying the disbursement by the present-worth factor $\frac{1}{(1+i)^n}$. The sum of the present worths of annual disbursements for this asset for a 20-year period is as follows:

$$\begin{aligned}&\$500\ (0.9346) + \$508\ (0.8734) + \$516\ (0.8163) + \$524\ (0.7629) + \\ &\$532\ (0.7130) + \$540\ (0.6663) + \$548\ (0.6227) + \$556\ (0.5820) + \\ &\$564\ (0.5439) + \$572\ (0.5083) + \$580\ (0.4751) + \$588\ (0.4440) + \\ &\$596\ (0.4150) + \$604\ (0.3878) + \$612\ (0.3624) + \$620\ (0.3387) + \\ &\$628\ (0.3166) + \$636\ (0.2959) + \$644\ (0.2765) + \$652\ (0.2584) = \\ &\$5917\end{aligned}$$

The equivalent uniform annual disbursement is \$5917 (0.09439) = \$558.5. This, added to the annual capital-recovery cost of \$1000 (0.09439), gives an equivalent uniform annual cost of \$652.9 over a 20-year life. As the annual disbursement was \$652 in the twentieth year and will be \$660 in the twenty-first year, it is evident that the economic life of such an asset is 20 years.

A 10-year-old asset therefore has a remaining economic life of 10 years. The sum of the present worths (at age 10) of the annual disbursements during the final 10 years of its economic life is as follows:

$$\begin{aligned}&\$580\ (0.9346) + \$588\ (0.8734) + \$596\ (0.8163) + \$604\ (0.7629) + \\ &\$612\ (0.7130) + \$620\ (0.6663) + \$628\ (0.6227) + \$636\ (0.5820) \\ &\quad + \$644\ (0.5439) + \$652\ (0.5083) = \$4295\end{aligned}$$

The equivalent uniform annual disbursement during this final 10 years is \$4295 (0.14238) = \$611.5.

Let X = the appraised value of the 10-year-old asset which will give annual costs equal to those of a new asset. Then

$$0.14238\ X + \$611.5 = 0.09439\ (\$1000) + \$558.5$$

$$X = \$291$$

Here the value inferiority or appraisal depreciation is \$709.

Example 4. In this example the hypothetical new asset has the advantages described in examples 2 and 3. Both the old and new assets are subject to progressive and steady increases in the cost of operation and maintenance. However, the hypothetical new asset has an improved design, and its annual disbursements start at a lower level than would be possible with a new asset of the old design. Thus the old asset has disadvantages of shorter life expectancy, higher operation and maintenance costs, and obsolescence. These combine to create its value inferiority or appraisal depreciation.

The 10-year-old asset in this example is the same as the one described in example 3. The improved new asset in this example has a first cost of \$1000, and annual disbursements of \$450 in the first year of its life, \$458 in the second year, \$466 in the third year, and increasing \$8 each year thereafter.

If it is assumed that there will be no further improvements in design or changes in prices or service requirements, it may readily be shown that the economic life of the improved new asset will be 20 years, and that the equivalent uniform annual disbursements will be \$50 less than the \$558.5 calculated in example 3, or \$508.5. This, added to the annual capital-recovery cost of \$94.4, gives an equivalent uniform annual cost for the 20-year economic life of \$602.9.

The existing old asset requires annual disbursements next year of \$580, followed by annual disbursements of \$588, \$596, and \$604. It is evident that the remaining economic life of the old asset is only 3 years, as the disbursements of \$604 in the fourth year are higher than the expected equivalent uniform annual cost of \$602.9 over the anticipated life of the most economical new asset. The sum of the present worths of the annual disbursements, during this 3 years of life remaining, is \$580 (0.9346) + \$588 (0.8734) + \$596 (0.8163) = \$1542. The equivalent uniform annual disbursement is \$1542 multiplied by the 3-year capital-recovery factor, 0.38105. This product is \$587.6.

Let X = the appraised value of the old asset which will give annual costs equal to those of the improved new asset. Then

$$0.38105\ X + \$587.6 = 0.09439\ (\$1000) + \$508.5$$

$$X = \$40$$

Here the value inferiority or appraisal depreciation comes to $960.

Discussion of Examples

These four examples may seem somewhat theoretical in that they make use of more specific forecasts of future events than one usually can make with assurance. However, the point which they emphasize is a severely practical one. This point is that the question which a replacement-cost appraisal should answer is "what is the greatest amount one could afford to pay for an existing old asset in comparison with the most economical present method of performing its service?" The answer to this question may not be the appropriate value of the asset in an appraisal, but it usually should place an upper limit on any appraised "value." Moreover it should have its bearing on other important matters such as the choice of a depreciation-accounting policy and the determination of taxable income for income-tax purposes. Some of the implications of these four examples will, therefore, be explored further.

Few actual situations will be found like example 1, in which the only difference between the old and new asset was future life expectancy. This example implies that retirements are imperative at the end of a fixed number of years, rather than that they depend upon someone's decision that it is economical to make them because of obsolescence, inadequacy, increasing cost of operation and maintenance, or some combination of these causes. An example is a railroad crosstie which has no appreciable maintenance cost up to the time when it is retired because of wear or decay.

It is evident that, for the special type of situation considered in example 1, an asset with 10 years of prospective service is worth considerably more than one half as much as an asset with 20 years of prospective service. Because of the time value of money, service for 10 years starting now is worth more today than 10 years of similar service starting 10 years hence. It may readily be shown that the $337 appraisal depreciation found in example 1 is the depreciation obtainable by the so-called sinking-fund method for an age of 10 years and a total life of 20 years with interest at 7 per cent.

It will be recognized that most actual situations contain in some measure the reasons for value inferiority illustrated in examples 2, 3, and 4. In all such cases the appraisal depreciation will be greater than that given by the sinking-fund method. Although the magnitude of the appraisal depreciation in any individual case naturally depends upon the facts of that case, the authors believe that many situations in industry will be similar to examples 2, 3, and 4, in that appraisal depreciation will be much greater than would be estimated by the conventional straight-line method.

Data Needed for Replacement-Cost Appraisals

The facts and estimates required for a sound appraisal based on replacement cost are as follows:

1 The expected service to be performed. Because replacement-cost appraisals should be based on the cost of replacing a service, they have little meaning unless related to some specific service. The appraised value of an old asset for one service will differ from its appraised value for another service. In the appraisal of machinery, care must be taken not to base the appraisal on full rated capacity when this is greater than the expected service.

2 The most economical new asset to perform this service. This requires an engineering economy study to compare the various alternative ways of getting this service performed.

3 The remaining life expectancy of the old asset.

4 The life expectancy of the substitute new asset.

5 The minimum attractive return or interest rate to be used in the comparison.

6 The prospective difference in annual disbursements (and whenever applicable, in annual receipts) between the existing old asset and the most economical new asset.

Some Paradoxes

Many paradoxes arise in the application of this equal-annual-cost viewpoint to replacement-cost appraisals, for instance:

1 Often the appraised value of a plant as a whole should be less than the sum of the appraised values of its parts. The substitution of an entire new plant of radically different design may indicate many economies not possible in contemplating the most economical replacement asset for each part of the plant without any general change in the plant design or arrangement.

2 The more rapid the prospective future obsolescence, the more valuable may be the present obsolescent asset. Prospective improvements in design of new assets or prospective changes in service requirements may reduce the appraisal depreciation of existing old assets. For instance, in example 4 the prospect of further design improvements would reduce the expected life of the new asset below 20 years. This in turn would increase the equivalent uniform annual costs during the life of the new asset and would therefore increase the appraised value of the old asset.

3 In some cases, as time goes on, the appraisal depreciation of an old asset may become less as compared to a specific new one. If engineering ingenuity permits its better adaptation to the present service, the value of an old asset may increase with time even without price-level changes. For instance, developments in materials handling by lift trucks in the last 20 years served to decrease the value inferiority of the brick buildings to the mill-type steel-frame buildings in the factory previously described.

4 Appraisal depreciation may be negative, in other words, the appraised value of an old asset may be greater than the cost of the most economical substitute asset. For instance, if the most economical substitute is a new 18-in. pipe line, the lower pumping costs of an old 24-in. pipe line might give it a value superiority to the new pipe line.

5 Appraised values may be negative. The value inferiority of the old asset may be greater than the cost of the most economical substitute asset; for instance, in example 2, if the annual disbursements for the new substitute asset were $400 (instead of $450), the appraised value of the old asset would be negative. This simply means that it would pay to make an immediate replacement.

6 The less the contemplated service, the greater may be the appraised value. Although the most extreme instance of this seems to arise when appraising a plant used merely for stand-by purposes, it should be emphasized that the most economical plant for stand-by service may be quite different from that for regular operation.

Comments on Objections to Equal-Annual-Cost Appraisals

Objections of two sorts have been raised to replacement-cost appraisals made on the equal-annual-cost basis described:

1 Because it is the existing asset which is to be appraised, some objectors maintain that a different substitute asset should not be used as the basis of valuation. This objection is apt to be made by those who advocate "reproduction-cost" appraisals, based on the assumed replacement of the existing old asset with an identical new asset.

However, if replacement with a different substitute asset would be more economical, the cost of reproducing identically an existing old asset has no bearing on its value. This objection is therefore without merit.

2 Because there may be differences of opinion as to the most economical new asset to replace a service and as to the advantages of this new asset over an existing old one, it is even more difficult to reach agreement on appraised values in equal-annual-cost replacement appraisals than in the usual reproduction-cost appraisals with conventional depreciation deductions. There is no doubt that this difficulty of securing evidence is a very real one; value judgments which depend upon forecasts of future events are inevitably matters upon which opinions will differ. However, this difficulty in applying a method which is sound, although complicated, certainly does not justify the use of another complicated method (such as the conventional reproduction-cost method) which is fundamentally unsound.

Whenever it is likely that any complicated method of valuation may involve expensive and long-drawn-out litigation, practical considerations may dictate the use of a simple method. In such cases, definiteness may be more important than soundness of principle.

Examples and Limitations of Predetermined Depreciation Rates

Nearly 2000 years ago, Vitruvius[4] wrote as follows:

"No walls made of rubble and finished with delicate beauty—no such walls can escape ruin as time goes on. Hence, when arbitrators are chosen to set a valuation on party walls, they do not value them at what they cost to build, but look up the written contract in each case, and then, after deducting from the cost one eightieth for each year that the wall has been standing, decide that the remainder is the sum to be paid. Thus they in effect pronounce that such walls cannot last more than eighty years."

Vitruvius' use of a predetermined base (cost) and a predetermined depreciation deduction at any time finds a modern counterpart in a proposal made in the autumn of 1940, that a defense plant financed with government funds might be purchased from the government by the private operator at cost less a 5 per cent annual depreciation on buildings and a 12 per cent annual depreciation on heavy machinery. The following excerpt from a letter[5] to the editor of a business publication gives the viewpoint of a production man at the time of this proposal:

"Take the case of the typical plant manager—as of five years from now. By paying 'only' 75 cents on the dollar for buildings and 'only' 40 cents on the dollar for machinery, he then gets an equipped plant 'only' five years old. But what a five years! It's been a day-and-night operation—much of it seven days a week. Maintenance has been some problem because of the breakneck production pace. Inexperienced operators have taken their toll of the machine tools.

"And how about that 1945 dollar? Won't it buy a lot more than the 1940-1941 dollar did when it bought this stuff? Won't my 75 cents of 1945 pay for a new plant, built on 1945's labor and material market, instead of a five-year-old plant built on the bull market of 1940-1941?

"And isn't XYZ Machine Company offering me in 1945 some brand new milling machines for $4000 each, whereas, I paid (for the government) $5750 apiece for twenty almost identical ones five years ago in 1940? Let's see—40 per cent of $5750 amounts to $2300. For $2300 I can get one of these five-year-old machines that's kinda wheezy but will work okay as long as Jim Smith is around to run it (Jim knows its eccentricities). On the other hand, for $4000 I can get a new machine—it's faster and has all the latest attachments, and any good operator can handle it without difficulty. Put yourself in my place—What would you do?"

As this quotation shows, the question of the cost of replacing a service is always relevant in judgments regarding values which are made by a prospective purchaser of old assets.

Relationship of Appraisal Depreciation to Other Depreciation Concepts

"Depreciation" is a word with several meanings. This paper has discussed "appraisal" depreciation. To show the relationship of this paper to other depreciation problems, it is necessary to recognize three fundamentally different depreciation concepts:[6]

1 The appraisal concept of depreciation. As has been pointed out, this should mean the value inferiority at some particular date (the date of the appraisal) of one asset, the existing old one being appraised, to another asset, a hypothetical new one used as the basis of valuation. This concept implies two assets and the measurement of their values at one date.

2 The popular concept of depreciation is decrease in value. This involves subtracting from the value of an asset at an earlier date the value of the same asset at a later date. "Values" may be determined by appraisal, by market price, or in any other appropriate way. This concept involves one asset and the measurement of its value at two dates.

A common practice in the manufacturing industries illustrates a use of the popular concept of depreciation. Frequently, a manufacturer will refuse to install new machinery unless an engineering-economy study indicates that it will "pay for itself in 3 years" (or some other short time from 1 to 5 years). This requirement usually means that the manufacturer thinks it probable that machinery acquired now will have a very low value 3 years hence, as compared to the most economical machinery likely to be available then for meeting the service requirements which may exist at that time. That is, the manufacturer (perhaps unconsciously) applies the appraisal-depreciation viewpoint, outlined in this paper, to the valuation 3 years hence of the proposed machinery; he then applies the viewpoint of popular depreciation in his forecast that the decrease in value during the next 3 years of machinery purchased now will be nearly 100 per cent of his investment in it. This forecast is made despite his expectation that the final retirement of the machinery from his service may not take place for 10, 15, or 20 years.

3 The accounting concept of depreciation is the writing off or amortization of cost on the books of account. It should be emphasized that this relates to cost and does not relate to value at all. The definition of depreciation as "loss in value" which is so common in accounting literature is a misleading description of the actual practice of accountants.

The practical question in depreciation accounting is how rapidly cost should be written off. Occasional appraisals would help management answer this question. Such appraisals should be based on the principles outlined in this paper. However, appraisals could not be used as the sole basis of depreciation accounting, which for practical reasons must be based on some systematic procedure.

For many years, the manufacturing industries wrote off most machinery at a rate of 10 per cent per year. This arbitrary rate gave no consideration either to realized service lives or to the common experience that before a machine is many years old its value is quite low compared to the most economical substitute. Recently the U. S. Bureau of Internal Revenue has effected drastic reductions in depreciation allowances made on income-tax returns. The purpose has been to bring depreciation rates, for tax purposes, into line with available evidence that realized lives of most machines are more than 10 years. In many cases

[4] "Vitruvius, the Ten Books on Architecture," trans. by M. H. Morgan, Harvard University Press, Cambridge, Mass., 1914, Book II, chap. 8, par. 8.

[5] *Business Week*, Oct. 26, 1940, page 67.

[6] Adapted from a classification in "Valuation of Property,"[3] p. 183.

these reduced depreciation rates have also been adopted for corporate-accounting purposes.

It is the belief of the authors that a continued trend in corporate accounting toward lower depreciation rates is undesirable both for individual corporations and for the nation. Depreciation charges in corporate accounting have many indirect effects on the economic system through their influence on such matters as dividend policy, pricing policy, taxes, security issues, maintenance of stand-by plant, and the selection and replacement of machinery. Although space limitations prevent a discussion in this paper of the various consequences of inadequate depreciation charges, the authors believe that a more desirable development than the one now taking place would be toward high depreciation rates in the early years of the life of machinery followed by lower rates in subsequent years.

The primary purpose of this paper has been to emphasize the concept that appraisal depreciation should be a measurement of value inferiority. A second purpose—possibly more important in the long run—has been indicated in the last few paragraphs; it is to suggest that if a number of manufacturing concerns could be persuaded to make such value-inferiority studies of machines of various ages, this might serve as a basis for a critical review and possible modification of depreciation-accounting policies and methods. As the facts on which such studies would be made are essentially engineering facts, the lead in any such development must be taken by engineers.

Discussion

HARRY A. BULLIS.[7] The approach to the determination of values proposed by the authors, whereby the value assigned to properties is based on the most economical substitute, provides an apparently sound basis of valuation which should assist management from two viewpoints:

1 From the point of view of deciding upon the desirability of replacement of existing assets.

2 Possibly from the point of view of valuation for purposes of refinancing, or of purchase or sale of all or a substantial part of the properties and business of a company.

This theory provides a useful tool to management, but one which should be used carefully. Valuation obviously is an intangible process. Most of the factors upon which it depends lie in the minds of men and their judgment of the relative desirability of goods. Concepts of value depend largely upon the purposes for which the values are being determined. For example, the term "fair cash value," as used by insurance companies, has come to mean the cost to reproduce a particular asset in its condition at the time of loss. The element of cost to replace with the most economical new asset of a substantially different character has been, in the past, only a minor consideration in the settlement of insurance losses. Nevertheless, the theory of valuation, developed in the paper, is a real contribution to the science of valuation and, used restrictively for certain purposes, provides an index from which there will flow important managerial decisions relative to property replacements.

A few general observations are offered, not with the idea of criticism, but from the point of view of indicating the possible limitations:

1 Most appraisals are used for insurance purposes. The extreme flexibility of the proposed system presents a problem, in that the available types of insurance coverage are not designed with this approach in mind and are not sufficiently flexible. The benefits of this particular approach could probably be most fully realized only for properties which are 100 per cent self-insured.

2 It seems probable that the adoption of this policy would tend to decrease the value of outside appraisals for most manufacturing concerns. The "equal-annual-cost" theory depends largely upon engineering knowledge, research, and management opinion in arriving at values. Presumably, the best information and the best judgment in this field exist within the particular organization. It seems safe to say that there are few, if any, established appraisal companies which would be qualified to exercise this type of judgment except in a limited number of manufacturing fields, of which the utility field is probably outstanding.

3 The theory as presented tends to ignore the possible existence of an actual market for assets which might be at a substantially higher level than a low value arrived at from the equal-annual-cost approach. In the specific illustration given of the brick building which led to the bankruptcy of a company, because it was impossible to use therein a particular type of mechanical handling system, the value of this property presumably prior to the company's collapse would be zero. Yet it is entirely possible that this building would have a relatively high market value for some other manufacturing operation.

4 Along this same line, the theory seems to place little or no emphasis on the rather generally accepted idea of fixed property values. Values are approached from the point of view of earning power only. This may be entirely sound in studying specific replacements, but is it not possible that it might lead to an unfortunate situation if a company's earnings were abnormally low or even nonexistent because of improper management? Are we justified in reaching the conclusion that property values are actually decreased by poor management? This leads to a rather difficult consideration of the differences between real property values and earning values.

5 The application of this approach requires the combination under one centralized authority of several phases of business activity. These would be operations, engineering, research, cost accounting, and what might be termed management judgment in forecasting future trends. To wrap these all up in one package and arrive at a specific answer is a large degree of concentration, but it is realized that this is the information that management must have to make the most intelligent decisions.

These observations seem to be mostly in the nature of objections or difficulties which might be encountered in using this theory. It should be emphasized again that the approach seems to be basically sound and is very interesting. In general, it seems that it can be used with real value in connection with the conventional type of appraisal and with ample consideration of possible outside market values rather than as a replacement of either of these two accepted approaches.

E. C. CLARKE.[8] The purpose of this paper has been to emphasize the concept that appraisal depreciation should be a measurement of value inferiority. There can be no exceptions taken to this purpose. The basic concept of progress in our system of free enterprise is one of more goods at lower costs. The attainment of this progress requires the systematic obsolescence of both materials and processes; hence the systematic obsolescence of manufacturing equipment and the replacement of that which has been made obsolete. Cash is necessary for each replacement, and it is important that capital invested in facilities be recaptured in the selling price of the products of the facilities during the life of the facilities. In the cycle, appraisals of values are needed frequently and factually.

[7] Executive Vice-President of General Mills, Inc., Minneapolis, Minn.

[8] President, Chambersburg Engineering Company, Chambersburg, Pa. Mem. A.S.M.E.

The cycle of obsolescence is a shortening one, as the conclusions of our research laboratories are brought into practical uses. Thus, example 1 of the paper, the replacement of an asset with an identical one, is the exception rather than the rule, and additional emphasis is placed upon the importance of the stated purpose.

However, in the writer's opinion, the second purpose stated, i.e., that manufacturing concerns be persuaded to make more realistic appraisals of their assets, seems the more important one by far. This purpose would be strengthened were it to include provision for reversal by the Department of Internal Revenue of its policy of depressing depreciation allowances for tax purposes. Germany rebuilt her factories by a governmental relief from taxes, if new equipment were installed, and by this artificial means built productive facilities which exceeded those of her then potential enemies. One can agree with the results attained by Germany, although the method violated every sound theory of depreciation. If we are to compete in the postwar world, both management and government must realize that obsolescence is with us always and requires quick recognition of actualities of value in use, for cost purposes and for tax purposes. The quick are strong.

Hence, the writer must disagree with the concluding sentence of the paper, implying that the problem is one for engineers. Actually, it is one reflected in sales, distribution, costs, and all phases of demand and production and, hence, becomes a responsibility of management. Mayhap, the best conclusion might be that the subject of depreciation of one's assets is a painful one which requires a cold-eyed, realistic manager to see that the engineers face it without favor to their brain children of yesteryear, and that the comptrollers get more enthusiasm for lowered costs than for book values; in other words, better plans for tomorrow with less emphasis on today's valuation; or, less credence to the score of depreciation written in advance of realization.

The authors are to be congratulated on cementing a principle particularly applicable to evaluations, and it is hoped that they will continue their fruitful studies into broader fields.

A. R. COLBERT.[9] The authors emphasize that the value of an existing plant unit is the amount which could be paid for it in order to realize total annual costs, including operating expenses, depreciation, and return, equal to those obtainable from the most economical new unit which could replace the service. The difference between the value found for the existing asset and the cost of the new is called appraisal depreciation or value inferiority of the old unit, as compared with the new.

It should be noted that the appraisal depreciation found by the authors' method is not the deduction to be made from the cost of the old asset, but rather the deduction to be made from the cost of the new hypothetical asset to bring it to the value of the existing asset. The difference between the value so found and the cost of the old asset (assuming the cost represented value at the date acquired) would represent the total decline in value of the old asset between the date acquired and the date of the appraisal.

Unquestionably, the cost, new, and the annual costs of new equipment have an important effect upon the value of old equipment. The conclusion of the authors that the maximum value attributable to the old is that amount which would permit total annual costs to be no higher than if the most economical substitute were purchased seems sound, for the value of an existing asset can be no greater than the worth of what it will live to do.

The proposed method of estimating value would be particularly helpful in determining the most economical time to make replacements of property or in comparing the over-all costs of new equipment best suited for the desired function. Also, it may be useful for general appraisal purposes in some instances, particularly competitive commercial industries. However, considerable difficulty lies in the application of the valuation formula, especially where circumstances are those illustrated in examples 3 and 4. This becomes more apparent when the authors' formula is restated, as shown hereafter, in a manner to emphasize the extent to which estimates of the future are involved.

It can be shown mathematically that the following is equivalent to the equal-annual-cost formula, suggested by the authors:

The value of existing equipment equals a, the cost, new, of the substitute equipment, plus b, the present worth of operating expenses of the substitute equipment during its entire life, minus c, the present worth of operating expenses of the existing equipment during the remainder of its life, minus d, the present worth of operating expenses of the substitute equipment if installed at the end of the life of existing equipment for a period thereafter equal to the difference between the life of the substitute equipment and the remaining life of the existing equipment, minus e, the present worth of the cost, new, of the substitute equipment if installed at the end of the life of the existing equipment, plus f, the present worth of the value of the substitute equipment if installed at the end of the life of the existing equipment at a date in the future corresponding with the end of the life of the substitute equipment if it were installed now.

The formula in this form, although giving results identical with the equal-annual-cost application proposed by the authors, is not recommended for actual use, as it becomes quite involved. It illustrates, however, the extent to which estimates of the future are involved in the valuation method proposed; and, as stated in the paper, the difficulty of securing evidence regarding the future is a very real one. In fact, in many instances, the necessary estimates of future conditions might well be so uncertain as to detract substantially from the reliability of value determinations by the method suggested. However, the uncertainty of estimates of the future is present, in greater or lesser degree, in all valuations of physical property, and a method, which attempts to measure the worth of what a piece of equipment will live to do, has much to commend it, as compared with appraisal methods which ignore this important element of value.

It is interesting to note that the authors' method of measuring the value of old equipment indicates that the depreciation may be greater than the conventional straight-line method (refer to examples 2, 3, and 4). Perhaps this condition prompts the authors to favor higher depreciation rates in the early years of life of machinery, followed by lower rates in subsequent years.

The wisdom of such a procedure is questionable. Since income-tax rates are on the upgrade, additional taxes would be incurred in the future if high depreciation were taken now, followed by lower charges at a later date. Also, equipment is often installed which does not operate at capacity for some years, and the higher depreciation in the early years might be quite burdensome during a period of low earnings. Further, even if depreciation reserves higher than under the straight-line method are believed desirable, a company may retain part of its earnings in surplus and thus accomplish all of the financial benefits which a higher reserve would, although it must be admitted that, as long as a large surplus were shown, pressure for higher dividends might be brought.

On the other hand, low charges for depreciation initially followed by higher charges in later years (as is the case with the sinking-fund or compound-interest methods, considering both the annuity and the interest component) involve the danger inherent in postponing charges to the later years of life of property (the uncertain part of life estimates) when operating costs are

[9] Chief, Accounts and Finance Department, Public Service Commission of Wisconsin, Madison, Wis.

probably higher. As between these two extremes, it is the writer's belief that the straight-line method is the most satisfactory method of accounting for depreciation in most instances.

W. D. ENNIS.[10] Depreciation is too often and too seriously underestimated, and it is more than time to acknowledge the fact. Old tabulated life expectancies were too generally based on expected wear and tear alone. Obsolescence was recognized but dodged. Many of the tabulated expectancies, long in general use, are admittedly ridiculous in the light of later experience. Yet the Federal Bureau of Internal Revenue continues to assume and emphasize improbably long lives, for reasons which are obvious enough, but in defiance of engineering judgment.

Inadequate depreciation estimates are dangerous to the permanence of the enterprise, and misleading to investors.

The authors' thesis is (briefly) that, in an appraisal, the criterion of value is the cost of duplicating, not the plant, but the service rendered by the plant. Other engineers have sensed this and have in effect paralleled the Norton-Grant analysis. Some of the "paradoxes," the concept of negative value, for example, have been recognized before. The present authors now clear the atmosphere by suggesting, as a result from their thesis, that reproduction cost (as well as actual or historical cost) of the actual plant thus becomes a matter merely of academic interest. The value of the plant may depend, not on its characteristics, but on those of another plant capable of doing the same (or better) work. This is notable.

The "capital-recovery factor" is of course the annuity i, n, realized from a purchase price of 1.

H. B. FERNALD.[11] The writer concurs in the conclusions of this paper that "a continued trend in corporate accounting toward lower depreciation rates is undesirable," and that "a more desirable development than the one now taking place would be toward high depreciation rates in the early life of the machinery followed by lower rates is subsequent years." There is less concern with the theoretical question of what one could afford to pay for a present asset in comparison with the most economical new one or with questions of "value inferiority" than with the question of how much should be charged against costs each year to write off the cost of machinery ratably over its probable useful life, and the question of when machinery now in use should be replaced by new machinery.

The formula developed and the discussion given with the various examples seem appropriate, but the writer is not ready to condemn as of no value, or as never appropriate, the old-style appraisals based on reproduction cost. Probably they are more certain as to their factual basis than appraisals based on "value inferiority," as proposed in this paper, since that involves the appraiser's estimate of probable future operating costs and usefulness of one machine as compared with another, which may rapidly change from month to month, or day to day. However, there can be no question that replacement-cost appraisals do not serve to indicate how much should be written off each year in order that the cost of plant and equipment be recovered ratably out of operating profits during the useful life, nor do they answer the question whether existing plant and equipment should be displaced in favor of new. Such formulas as those here proposed undoubtedly are more indicative of what should be written off and when equipment should be replaced.

More important than the actual formulas are the various factors to which attention is here drawn; such as, the usefulness of present compared with other available equipment, relative costs of operation and of output, etc. The full and continual recognition of these factors is probably more important than the exact formulas by which their results may be expressed. The great problem of depreciation is obsolescence, due to changes in competitive conditions, in demands for product, in materials to be handled, in cost of materials or labor, in taxes and government controls, and the progress of the art as to machinery and materials; as this paper recognizes.

After many years of accounting practice, the writer is satisfied that the "straight-line" method of depreciation, which seems to be the generally accepted accounting basis (particularly under the impetus of income-tax regulations) is far from a satisfactory guide. Even if a machine might have a life of 20 years, it is doubtful whether its actual useful value in operations will be as great in the nineteenth and twentieth years as in the first and second years. Yet that is the assumption, if we write off 5 per cent depreciation each year. Generally, it probably would be better if we charged a relatively high rate of depreciation on the declining balance (cost less depreciation to date). An alternative would be to start with a relatively short estimated life and consequent high annual depreciation rate; then when, if, and as it appeared the machine would have a longer life, thereafter apply a reduced rate. Either of these plans would give depreciation charges more nearly in accord with the factual situation.

Of one thing the writer is sure, which is that the desirability of replacement or substitution is never to be determined by the amount at which plant and equipment are carried in the books. If we can look ahead and see that in the long run new equipment will pay for itself and leave us more dollars in hand than we would have from continuing the old machinery, there should be no hesitancy in making the change. The real question is the ultimate dollar result, and that should not be sacrificed because of any disinclination to write off the balance carried on the books for old machinery.

Of course, we should try to have our depreciation charges such that the equipment will have been fully depreciated when it becomes obsolete, but changes may come so swiftly they cannot be foreseen. That should be recognized so no one will feel that a charge-off of obsolete equipment is any reflection either on management or on accountants. Rather, if it is done in good faith, it is meritorious; certainly better than to retain machinery which ought to be replaced.

Whether or not in reaching the appropriate conclusions, we use the particular formulas here set forth, the writer feels that this paper is a material contribution to the thought on this subject.

M. R. SCHARFF[12] AND F. J. LEERBURGER.[13] The literature on the subject of depreciation is so voluminous and the discussions and arguments so extensive that it sometimes seems that little room remains for further contributions. It is heartening, therefore, to have the authors demonstrate so clear an understanding of the proper places of theory and practice in the solution of appraisal problems; and to have them bring the discussion back to the economic field, where it belongs, by relating value to the present worth of prospective return of and return on capital.

The writers have been particularly interested in the consideration of these problems as related to the public-utility industry, where their difficulty has been increased by the precedents established by the courts under the fair-value rule, based on conflicting legal, engineering, and accounting interpretations of

[10] Humphreys Professor of Economics of Engineering, Stevens Institute of Technology, Hoboken, N. J.

[11] Loomis, Suffern & Fernald, Certified Public Accountants, New York, N. Y.

[12] Consulting Engineer, 285 Madison Avenue, New York, N. Y.

[13] Consulting Engineer, 285 Madison Avenue, New York, N. Y. Mem. A.S.M.E.

Smyth vs. Ames,[14] and Knoxville vs. Knoxville Water Company.[15] It is their view, however, that the principles, suggested by the authors for the appraisal of manufacturing equipment on the basis of the present worth of the returns it will produce at competitive prices for its product, are equally valuable as a guide to the solution of the problem in the public-utility field.

The one criticism the writers would make of this paper is that the authors are too modest, and advance their sound proposals with too many reservations and qualifications. For example, they suggest that, "whenever it is likely that any complicated method of valuation may involve expensive and long-drawn-out litigation, practical considerations may dictate the use of a simple method. In such cases, definiteness may be more important than soundness of principle." This seems to be an unnecessary abandonment of the engineering point of view. A simple and direct method, if sound in principle, is, of course, always to be preferred to a complex one. Nevertheless, engineers properly reject analytical procedures, no matter how simple, when they fail to take cognizance of the facts. Apart from engineering considerations, it may also be stated that, for many businesses, including the public-utility industry, soundness of principle is far more important than simplicity.

With respect to the reference to long-drawn-out litigation, the highest court of the land has repeatedly shown a clear preference for presentation of facts bearing on loss in value in contrast to simple and direct mathematical calculations with no known relation to the facts. Public-utility rate regulation is generally considered as aiming to simulate competition. Loss in value caused by competitive forces is admittedly not usually capable of direct and simple measurement. However, utilization of economic theory as a guide to judgment, in estimating accrued and annual depreciation, has at least the advantage that it aims at the actual objective and not in the direction corresponding with an unrelated mathematical formula.

The paper points out the distinction between recorded book costs and value new, as well as between accounting for depreciation and loss in value or accrued actual depreciation. That such distinctions are customarily recognized, is clear enough; but they are not necessary distinctions. The writers suggest that there would be advantage in a reconciliation of ideas, in order to relate in a consistent manner, recorded book costs and recorded depreciation with value and loss in value. The fact that depreciation accounting is to be recorded in terms of book cost does not seem to be a sufficient argument to reject a recording of the facts of depreciation in favor of some systematic but unrealistic amortization program. It is true that much inertia must be overcome in order to direct depreciation accounting toward the recording of complex economic facts after so many years have been devoted to rule-of-thumb and oversimplified approximations. Governmental regulatory agencies are by their rules and decisions forcing a reconsideration of depreciation accounting and have indicated a preference for recorded book costs and estimates of actual depreciation in terms of these book costs. Again, the authors appear to have placed too many qualifications and limitations on their excellent paper, because, in the present state of knowledge, they have presented at least as good a guide as could be found to begin the study of how to make depreciation-accounting techniques reveal the realities of economic loss in value. Accounting, for most aspects of business activity, attempts to approximate facts, and it is only in the accounting for accrued and annual depreciation that oversimplified rules of practice, recognized as being divergent from the facts, have been accepted.

[14] 171 U.S., 361.
[15] 212 U.S., 1.

G. O. MAY.[16] The proposition which the authors of the paper advance seems to the writer to have a certain theoretical validity, and some, though only a limited, significance. The writer has regarded it as a legitimate and effective counterproposition to the crude replacement-cost theory of value, and so used it in an article,[17] in commenting on the majority decision in the Indianapolis Water Company case. In that case the Court had said:

"There is to be ascertained the value of the plant used to give the service and not the estimated cost of a different plant. Save under exceptional circumstances, the Court is not required to enter upon a comparison of the merits of different systems."

However, the objection to the crude form of the replacement-cost theory of value can be stated in more general terms; that it begs the whole question whether property is worth replacing as and where it is.

The authors suggest that the appraisers have failed to understand their point. It seems doubtful whether this is so. The position may rather be that the appraisers regard it as having less general application than the authors believe it to possess. It would seem to be directly relevant to the case of determining the postemergency value of emergency facilities. But the fact cannot be too strongly emphasized that it could not properly be applied to each item in the valuation of a normally constructed plant of average or more than average efficiency. In an imperfect world, an attempt to measure depreciation by reference to a constantly moving standard of perfection would be to ignore the way in which plants are constructed and to present a practically insoluble task of measuring the annual charge against operations. It would be open to the criticism which Mr. Justice Brandeis made of the "spot reproduction cost basis." It would not, it is believed, produce economically desirable results.

As a practicable procedure, the method of computation, which the authors propose, suffers from the defect that the results which it produces depend largely upon assumptions made as to the appropriate rate of return and the life expectancies of the existing units and of the potentially replacing units. Moreover, the elements of the problem are far more numerous and complex than the authors' examples suggest. For instance, the existing units are already installed; substitution of new units would entail cost for dismantlement and installation, and possibly a loss of production during the period of change.

The authors are perhaps correct in saying that in accounting, depreciation is not a value concept, though it might perhaps be argued that accountants merely take liberties with the word "value" and that every other profession does the same. The more one studies the problem the more convinced one becomes of the wisdom of accountants in declining to range over the uncertain ground that lies where the boundaries of law, engineering, economics, and finance meet in pursuit of that will-o-the-wisp. They prudently take their stand on the relatively firm ground of cost.

It is believed that the authors are correct in suggesting that present tax allowances for depreciation are inadequate. It is also agreed, that there is much to be said for writing off depreciation more liberally in the earlier than in the later days of use. However, since the authors apparently hold that interest or return on investment should enter into the computation of depreciation, they should recognize that the straight-line method does produce a higher charge in the earlier years. This point is clear from their own first example. Reference may be made to a defense of straight-line depreciation[18] suggested a few years ago.

[16] New York, N. Y.
[17] "Further Thoughts on Depreciation and the Rate Base," by G. O. May, *Quarterly Journal of Economics*, vol. 44, 1930, pp. 687-697.
[18] "A Defense of the Straight-Line Method," by Oliver May, *Journal of Accountancy*, vol 60, 1935, p. 282.

The treatment of depreciation seems to be one of those cases to which the authors refer, in which "practical considerations may dictate the use of a simpler method." Among the advantages of the straight-line method of depreciation is the fact that it is simpler, and that no one can be deceived into believing that it is scientifically precise or anything but a crude approximation. There is danger as well as absurdity in applying meticulous mathematical processes to assumptions which have no surer foundation than our highly precarious knowledge of the future and our subjective concepts on such questions as to what constitutes a reasonable rate of return in a given set of circumstances. Such processing cannot convert the raw material of guesswork into a finished product of statistics of a higher order of significance.

DUNDAS PEACOCK.[19] What is the purpose of the depreciation reserve provided upon the books of a company by charges against current operations? Is it intended that the reserve shall reflect the change in value of the assets through wear and tear, obsolescence, market value, etc., or is it a means of absorbing the cost of the asset as part of the cost of production during the period of the useful life of the asset?

The authors have pointed out that "the accounting concept of depreciation is the writing off or amortization of cost on the books of account. . . . . and does not relate to value at all." This is entirely true, for, obviously it would be impossible to evaluate the worth of existing assets annually or periodically and to attempt to reflect on the books of account the changes in value which have taken place, which values are dependent upon the condition and usefulness of the assets and changing economic conditions. Consequently, it follows that the depreciation-accounting policies are intended to result in the absorption of the cost of assets in operating costs during the useful life of the assets.

It does not seem logical, therefore, for the authors to suggest that appraisal depreciation should serve "as a basis for a critical review and possible modification of depreciation-accounting policies and methods." The theory of appraisal depreciation, as expounded in the paper, is intended to indicate the economic worth of an old asset, which worth could change rapidly, depending upon many factors, not least of which is prevailing or anticipated economic conditions. The accountant, realizing the impracticability of attempting to reflect such rapidly changing values on the balance sheet of a company, confines himself to showing the cost of the assets and the portion of the cost which has been recovered through charges against operations.

We may therefore assume that the authors' theories are worthy of consideration only for:

1 Determining the real value (as opposed to the book value) of the assets of a company upon sale of those assets to a willing buyer.

2 Determining the relationship of real value of the assets of a company to the book value.

3 Determining the desirability of continued use of an old asset or the replacement with a new asset.

The exception taken by the authors to the use of depreciated replacement values in commercial appraisals, when it is extremely doubtful if identical replacements would ever be made, is sound. However, to attempt to evaluate each of the assets of any company, other than a very small company, in accordance with their appraisal-depreciation theories, would be so lengthy as to be almost impractical. Furthermore, the sum total of the appraised values so determined would not represent the true worth of the assets, since allowance would have to be made for the cost of revisal of production methods which would undoubtedly be made if the hypothetical substitute assets, which formed the bases for the multitude of calculations, were actually acquired.

No appraisals of the value of the assets of any large or moderate-sized concern can ever be other than an estimate of doubtful worth, and should be looked upon, not as a guarantee of value, but as a starting point for determining the possible value.

It would seem, however, that the appraisal concept of depreciation is a sound policy to follow to determine the desirability of continuing to use old assets or groups of assets, or to replace those assets with new or more efficient assets.

M. E. PELOUBET.[20] This paper points out several basic considerations in depreciation and appraisals which are frequently lost sight of. It has often been said that facts are stubborn things. It is also true that unless they are properly understood and interpreted, they are useless things. As this paper points out so clearly, the mere reproduction cost of an identical building or facility, no matter how carefully proved and documented, is of no use in determining a fair sales price or value to the enterprise. Accountants quite properly do not attempt to deal in values, but the determination of values is the most important part of the appraiser's work. It is, perhaps, true that the determination of value or loss of value involves certain assumptions, but if these assumptions lead to an approximation of what the property is really worth to the company, they are of far more value than so-called facts which, while perfectly true as isolated statements, have no bearing on the present or future operations of the company.

The dependence on proper engineering data of any reasonably correct determination of depreciation or loss of value is well covered. One of the difficulties under which public accountants frequently have to labor is the assumption that, because the accountant is able to make proper entries and to set up proper accounts for depreciation, he must necessarily be able to determine a correct rate. Occasionally, this is possible by some more or less rule-of-thumb method derived from experience and observation but, in the long run, questions such as the life expectancy of new property, remaining life of the old, the additional amount of depreciation caused by accelerated production, and other questions of this sort, are ones which may well be raised by the accountant but which must be answered, if the answers are to be satisfactory, by the engineer. In saying that they must be answered by the engineer, it is also meant that they must be answered by the appraiser, as appraisal is essentially an engineering function.

There is a great deal in the paper which could well be expanded in rather more detail and with somewhat fuller examples. The conception of a negative appraised value is an interesting one and, although it seems paradoxical, should be of much assistance to management in working out replacement programs. The proposal that depreciation rates should be arranged so that greater amounts would be written off in the earlier years of the life of the property than in the later years is an interesting one. It is, of course, well known that this is the British practice, carried out by the use of the diminishing-balance method. It is also probable that in some cases the use of a method of depreciation based on production would have somewhat the same result.

It is certainly true that, as a rule, more of the value, if not the physical life of a machine, is exhausted in the first few years of its life than in the later years.

The paper is interesting, well thought out, and the writer is in hearty agreement with the principles developed in it. His only real criticism is that it covers rather too much ground in a very concentrated way and probably would be more valuable if it were expanded and more examples given.

[19] Elliott Company, Jeannette, Pa.

[20] Pogson, Peloubet & Company, New York, N. Y.

WALTER RAUTENSTRAUCH.[21] The authors have suggested several important matters which need to be taken into account for estimating the "value" of the machinery of manufacture and industrial equipment.

The procedure proposed in this paper for determining value depreciation on the basis of annual costs equal to those of a new machine or equipment is a much closer approximation to the fact of value in a competitive economy than is the method for determining present depreciated worth.[22]

The reliability of any method of value determination, as the authors recognize, depends upon the probable error of estimate. The authors point out, quite properly, that the results of calculations of "present depreciated worth" frequently have no relation to the value of an asset as a unit of competitive enterprise. No competent industrial engineer would advise an investment banker to loan money against the value of the building of a manufacturer without inquiring into the probability of success of the manufacturer's business. The first example cited in this paper is a good illustration of what happens when values are determined by formulas which do not provide for the significant variables. The paper also suggests that a piece of industrial property, whether buildings or machinery, cannot have its value correctly determined as an item by itself. These values are always relative. For example, a gasoline-condensing plant, connected to a natural-gas pipe line may have a very high value so long as the natural gas is flowing. When the gas well is exhausted, even though the plant may be only 1 year old, its value may decline 100 per cent. If the machinery of a manufacturing plant is not well balanced in relation to the processing needs of the business then, quite obviously, the total value of the property is not the sum of the values of the individual machines and buildings. This raises the question of procedure in determining the value of groups of assets, or the problem of determining the value of the "relationship" of assets to each other. This problem is implied by the authors in their statement under the heading, "Data needed for Replacement-Cost Appraisals" that "In the appraisal of machinery, care must be taken not to base the appraisal on full rated capacity when this is greater than the expected service." How is the probable average annual load factor on each machine to be estimated? If a group of machines are integrated into a production line, it is not difficult to determine the hourly output of the line and compare it with the maximum capacity of each machine. However, production lines are changed and new layouts are constantly being made, perhaps several times a year, for the manufacture of new models and new styles. How can we estimate the probable average annual load factor on any machine for the period of its life expectancy? Obviously, this problem is more easily solved in the case of plants of the process industries than of the mechanical manufacturing industries.

In fact, the relative values of some plants of the process industries may be compared when their outputs may be measured in terms of production rates of the same unit products. Sugar refineries are a good example, since their capacities may be measured in pounds of daily melting capacity. A study of six cane-sugar refineries shows that their approximate original investment costs divided by their daily melting capacities varied from a maximum of \$3.75 to a minimum of \$1.74 per lb daily melt capacity. The plant with the maximum investment cost per unit capacity cost \$6,000,000 to build, the other cost \$4,350,000. Assuming, two such plants were built in the same year and that their total annual costs except depreciation are the same (which of course is not likely to be the case, but is assumed for simplicity) and assuming that each has the same life expectancy, then, according to the equal-annual-cost method of appraisal it appears that the value of the \$6,000,000 plant should be written down to approximately \$3,840,000. But in the case of an automobile manufacturing plant, no unit of output, such as an automobile, is found and, hence, no comparison is possible as was made for the sugar refineries. When appraisals are made for the purpose of establishing a basis for a loan, the banker is interested in the probability of the value of the assets underlying the mortgage, for the period of the loan. If this should be a 10-year period, it is perfectly obvious that many factors must be taken into account other than the present depreciated worth of the physical assets as of a given date. The writer's experience indicates that sole reliance on values of physical assets made by any one of the several commonly used appraisal methods is largely a reliance on pure fiction. The real value of the property lies in the combination of the values of the physical assets, management, markets, and reserve margins of a business.

It is realized that this raises problems outside of the limits of presentation which the authors have set for themselves. It is hoped that the authors' suggestion to manufacturing concerns to make such value-inferiority studies of machines as this paper proposes will be carried out, for we need data from studies of this kind.

The writer suggests, that a symposium be held on the problem of methods for determining the comparative economic worths of entire industrial plants.

L. S. READY.[23] The writer's particular interest in depreciation estimates has largely had to do with appraisals of public-utility properties in rate and condemnation proceedings. This new treatise is helpful in such matters as well as in appraisals of manufacturing plants.

There is a very strong tendency in appraising public-utility properties, in connection with purchases and sales, and in condemnation proceedings, to estimate (1) the reproduction cost, new, of the units of property actually in existence and (2) the accrued depreciation thereon, either by general inspection or by the use of estimated lives and expectancies, disregarding all causes of removal which in the normal run of operations may be considered accidental, or not in any way a function of time.

In determining accrued depreciation, many appraisers ignore or refuse to give thought to the cost of constructing a modern up-to-date facility or system and, consequently, fail to take into account improvements in the art and in the design. The disregard of this important element invariably results in an estimate of the accrued depreciation which is lower than the actual loss in value. A recent example was the appraisal of a building more than 40 years of age, which was initially constructed for use as a steam-electric plant and later made over for use as a substation building. The accrued depreciation was determined at 5 per cent of the cost to reproduce the building new at the present time. Such a procedure ignores advances and changes in the design of substations during the last 40 years.

One additional point, not mentioned specifically in the paper, but of importance in determining accrued depreciation or "value inferiority," is the maintenance condition of old equipment, as compared with new, as of the time of appraisal. Although maintenance is not an item to be reckoned with under depreciation accounting, the condition of maintenance must be taken into account in appraising a property which is not new. As a simple example, the painting of a building which may be required once in 5 years, though charged to operating expenses, must be definitely considered in determining the depreciated value of the building at a given time. If the periodic painting is only due but

[21] Professor, Department of Industrial Engineering, Columbia University, New York, N. Y. Mem. A.S.M.E.

[22] Replacement of the identical machine at current prices less straight-line depreciation from date of purchase.

[23] Consulting Engineer, San Francisco, Calif.

not done, its cost should be a deduction from the depreciated value of the property determined on a strictly age-and-life basis, while if it has just been finished, no deduction or modification of the depreciation of the structure as a whole would be necessary. Likewise, periodic maintenance of equipment must also be given weight when determining its depreciated value.

Authors' Closure

The discussion has been very helpful in supplementing the points made in the original paper. The authors take this opportunity to thank the discussers for their participation. Because so many topics have been mentioned in more than one discussion, this closure is arranged by topics. It falls naturally into three main headings:

1 Depreciation estimates in actual appraisals.
2 Relationship of the concept of appraisal depreciation to depreciation accounting.
3 Relationship of the concept of appraisal depreciation to managerial decisions.

Actual Appraisals

Mr. Bullis suggests that the general acceptance of the viewpoint of this paper would tend to decrease the usefulness of outside appraisals. Although this might be a temporary result, the authors believe that in the long run, the usefulness of outside appraisals would be increased. Professional appraisers would become skilled in utilizing information secured from management by means of techniques which could be applied best by specialists in the appraisal field.

Several discussers have commented on the authors' point that there are difficulties in making value judgments which depend upon forecasts of future events. The influence of such forecasts upon appraised value is emphasized by Mr. Colbert's restatement of the equal-annual-cost method in terms of present worth. Mr. May correctly points out that "meticulous mathematical processes" can give results no better than the forecasts on which they are based. Mr. Peacock expresses doubt of the practicability of making such forecasts except in the case of small companies. In apparent contrast is the view emphasized by Messrs. Scharff and Leerburger that "soundness of principle is far more important than simplicity."

Complexities of two kinds may enter into any valuation process. One kind is the complexity involved in making the necessary forecasts and cost estimates; the other is the complexity involved in converting these forecasts into value. Basically, the complexity of forecasts emphasized by several discussers enters into any valuation; valuation methods which appear to be simple really involve implied forecasts even though the appraiser may not be conscious of making such forecasts. The forecasts and estimates required by the equal-annual-cost method are no more complex than those made by engineers of large industrial companies in connection with proposals for new plants or new processes. It should be emphasized that once the forecasts and estimates are made, the calculations of value required by the equal-annual-cost method are relatively simple. Moreover, the question of complexity should not be confused with the related question of definiteness. Some complex methods may be definite; other simpler methods may be indefinite.

Professor Rautenstrauch refers to a particular difficulty, that of forecasting future load factor when making equal-annual-cost appraisals. Clearly this is a difficult estimate to make. However, it is a necessary one for many other purposes, such as calculation of unit costs.

Messrs. Scharff, Leerburger, and Ready point out that the equal-annual-cost viewpoint of depreciation proposed for manufacturing industries is equally sound in public-utility appraisals. Apart from the many problems introduced by regulation, the differences between public utilities and manufacturing industries in this respect are less a matter of principle than of difference between the typical situations. The large value-inferiority of individual assets a few years old to new substitute assets, so common in manufacturing industries, seems less likely to exist in public utilities. An offsetting consideration is that the equal-annual-cost viewpoint in public utilities usually should be applied to combinations of assets rather than to individual assets; because of the piecemeal growth of most public utilities, the most economical substitute combination of assets to perform a service may differ even more from the present combination than in manufacturing industries.

Mr. Bullis suggests that the equal-annual-cost approach tends to ignore actual market values. Bonbright[24] as the very basis of his two-volume treatise on valuation, recognizes "two distinct though related major concepts of property value, the one referring to sale price, the other referring to value to a specific owner or group of owners." The equal-annual-cost viewpoint of depreciation obviously relates to the concept of "value to the owner," placing an upper limit on this value for some specific use. If the market price of an asset is higher than "value to the owner" for a specific purpose, the owner should either sell the asset at this price, or adapt it to another use which is associated with a higher value to him.

Mr. May points out that the equal-annual-cost method will be appropriate in postwar valuations of wartime facilities. Certainly the value of such facilities to their owners after the war cannot possibly be greater than a value calculated by this method. Many factors will combine to create low values for war plants at the close of the war, even if they can be adapted for postwar use. Different types of possible substitute plants may require consideration in making postwar appraisals. One type will be the new plant which might be built with the benefit of the newest methods and the careful economy studies which were not practicable in hastily constructed war plants. Another type of substitute will be the plant that might be constructed at low first cost using second-hand machinery from war plants that are dismantled.

As Mr. Bullis points out, equal-annual-cost appraisals could hardly be used for fire-insurance purposes under present insurance practices. This is evidently one of those situations in which definiteness is essential. However, in selecting the most economical type of insurance coverage, it often is desirable for management to estimate "value to the owner" as well as the "fair cash value," which latter will probably be applied by the insurance company in the event of a loss. Where industrial fire insurance is written with a co-insurance clause, the insured will not be completely covered for a partial loss unless the amount of the policy is a specified percentage of this "fair cash value." Where obsolescence or other causes make "value to the owner" substantially less than "fair cash value," it may be economical to carry less insurance, paying the higher premium rate which is required when there is no co-insurance clause.

Accounting Aspect

It is on the question of the relationship between appraisal depreciation and depreciation accounting that the issue is most sharply drawn among the discussers. Mr. Peacock states that it is illogical to suggest that appraisal depreciation should serve "as a basis for a critical review and possible modification of depreciation accounting policies and methods." Mr. May commends accountants for not ranging "over the uncertain ground" of value determination. Messrs. Colbert and May commend the conventional use of straight-line depreciation based on average

[24] See reference 3, particularly pp. 14 to 16.

life. In contrast, Messrs. Scharff and Leerburger favor a consistent relationship between "recorded book costs and recorded depreciation" on the one hand, and "value and loss in value" on the other.

The authors are in agreement with the position expressed by Mr. Fernald that "the full and continual recognition" of such factors as "the usefulness of present as compared with other available equipment" and "relative costs of operation and of output" is essential in judging how rapidly cost of fixed assets should be written off. When Mr. May states that accountants "prudently take their stand on the relatively firm ground of cost" and Mr. Peacock states that "the accountant. . . . confines himself to showing the cost of the assets and the portion of the cost which has been recovered through charges against operations," they are, the authors believe, begging the question of how rapidly cost ought to be written off, all things considered.

If past decrease in "value to the owner" of fixed assets has been substantially greater than the portion of their cost which has been written off in the accounts as depreciation, it is evident that the enterprise has not been as profitable to its owners as the accounts have indicated. Similarly in situations in which prospective decrease in "value to the owner" in the early years of life of assets is much greater than will be written off under conventional depreciation accounting, it is evident that profit figures based on such accounting will be, during this period, an overstatement of the profitableness of the enterprise to its owners. As already pointed out, this prospect exists with respect to much of our war industry. It was given recognition in 1940 in the sixty-month-amortization provision of the income-tax law. This provision was justified because of the probability that after a few years, the value of war plants to their owners would be very low, even though their physical lives might continue for many years thereafter.

The authors agree with Mr. Fernald that the recognition of such matters in depreciation accounting is the important thing, more important than the specific depreciation formulas by which they are recognized. This viewpoint is also clearly brought out by Mr. Peloubet.

The important and controversial question of depreciation allowances for income-tax purposes is intimately related to depreciation accounting. Comments on this question are made by Messrs. Clarke, Colbert, Ennis, Fernald, and May.

No tax system is ever completely free of inequities. The most important problem is not so much the possible inequity in a tax policy, as the effect of that policy on the social and economic system. In this instance, this relates to the effect of depreciation tax policy on the investment of private capital in depreciating assets.

Depreciation allowances on federal tax returns have long been a subject of controversy between taxpayers and the Bureau of Internal Revenue. However when corporate tax rates were at 13.75 per cent or thereabouts the fact that future depreciation allowances might seem inadequate did not deter new plant investments.

Today, March, 1942, with a present top effective rate of 72.4 per cent, and with the Treasury Department's proposal that this be increased to 88.75 per cent, the situation is very different. Under these circumstances, inadequate depreciation allowances may result in taxes higher than 100 per cent of true profits. Obviously, even the fear that this may happen will discourage new capital investment. It did in fact delay necessary expansion of defense plants during the critical summer of 1940 before the passage of the sixty-month-amortization provision.

This has a direct bearing on Mr. Colbert's statement that taxes are on the upgrade, and on his suggestion that high present depreciation allowances might result eventually in greater total taxes. His point was certainly valid a few years ago, but seems so no longer.

Professor Ennis refers to "improbably long lives" used by the Bureau of Internal Revenue in setting depreciation rates. Under orthodox straight-line depreciation accounting, the question of whether depreciation rates are consistent with past life experience is a matter of fact to be determined by statistical studies of past physical-property mortality. Unfortunately few manufacturing companies have plant ledger records adequate for such studies. Where such records exist, they may be used to support depreciation rates used in tax returns.

In all fairness to the Bureau of Internal Revenue, it should be pointed out that the Bureau's policies are consistent with the orthodox accounting view of basing straight-line depreciation on expected average lives. Several discussers agree with the authors that it might be well to have higher depreciation rates in the early years of life of much manufacturing equipment. However, the most elaborate statistical documentation of life estimates would not produce this result if combined with orthodox accounting methods. A necessary prerequisite to any change in tax policy is a considerable acceptance of the view that "value to the owner" may decrease more rapidly in the early years of life, and that depreciation accounting should be consistent with this decrease.

Relationship to Managerial Decisions

Messrs. Bullis, Colbert, Fernald, and Peacock suggest that measurements of value-inferiority of old assets to proposed new substitute assets might be used to determine whether proposed replacements are economical. Although this can be done, the methods of calculation outlined in this paper were not intended as a solution for this problem. Both authors have written elsewhere explaining simpler methods for such replacement economy studies.

One type of managerial decision already discussed is the decision regarding plant expansion when the prospect of high income-tax rates is associated with what management believes to be inadequate depreciation allowances for tax purposes. The reference by Mr. Clarke to postwar problems suggests that the period immediately following the war may be a critical one. It seems probable that a high rate of private capital investment in this period will be necessary to avoid a severe depression. It will be extremely unfortunate if at that time depreciation tax policy acts as a deterrent to this needed capital investment.

On Some of the Essentials of Control-Chart Analysis

By E. G. OLDS,[1] PITTSBURGH, PA.

In this paper the author indicates the possibility of a new approach to control-chart technique in connection with manufacturing processes. The advantages of quality control of product are widely recognized, and the principles pioneered by Walter A. Shewhart in 1924 have since that time been the object of intensive investigation. Primarily, the present paper is concerned with control with respect to a given standard. By analyzing hypothetical examples, illustrated graphically, the basis of the control-chart method is clarified. However, in exemplifying the control-chart technique, the author indicates a method of reversing the usual procedure, by creating uncontrolled conditions, and then noting whether the tests made locate the "assignable causes" which have been introduced in the experiments. The investigation is carried out with the aid of H. C. Tippett's tables of "Random Sampling Numbers."

IT IS generally recognized that any measurable quality characteristic varies from item to item in a manufacturing process. For example the measured tensile strength of steel bars changes from bar to bar. The desirability of reducing such variability to an economic minimum has long been recognized and the general problem has been and still is the subject of a great amount of investigation. Thus it seems unnecessary to record here the manifest advantages of a manufacturing process so controlled that uniformity in quality can be guaranteed.

The control-chart technique as pioneered by Walter A. Shewhart in 1924, and developed by him and many others over the period of the last 17 years, is now so well known as to need no detailed explanation. It has been the subject of a multitude of books and articles published both here and abroad. Within the year, the field of application has been reviewed by an Emergency Technical Committee[2] appointed by the American Standards Association upon request of the War Department. The findings of this committee have been published.[3]

Two uses of the control chart are given in a publication of the American Society for Testing Materials, namely, control with respect to a given standard and control when no standard is given. This paper is concerned with a discussion of some of the questions involved in the first of these two uses.[4]

[1] Associate Professor of Mathematics, Carnegie Institute of Technology.

[2] The membership of this committee was as follows: Chairman, H. F. Dodge, Bell Telephone Laboratories; A. G. Ashcroft, Alexander Smith and Sons Carpet Company; W. Edwards Deming, Bureau of the Census; Leslie E. Simon, Ordnance Department, U. S. Army; R. E. Wareham, General Electric Company; Secretary, John Gaillard, American Standards Association.

[3] "Guide for Quality Control and Control-Chart Method of Analyzing Data," American Defense Engineering Standards, Z 1.1 and Z 1.2, American Standards Association, New York, N. Y., 1941.

[4] "Manual on Presentation of Data," supplement B, American Society for Testing Materials, 1941, p. 48.

Contributed by the Management Division and presented at the Annual Meeting, New York, N. Y., December 1–5, 1941, of THE AMERICAN SOCIETY OF MECHANICAL ENGINEERS.

NOTE: Statements and opinions advanced in papers are to be understood as individual expressions of their authors and not those of the Society

CONTROL WITH RESPECT TO A GIVEN STANDARD

To make reasonably sure that our process remains in a state of control at the given standard, we take samples of items produced and examine the variation in their measured characteristics with the aid of statistical tests. We use tests to check on hypotheses. In this case our hypothesis could be that our process was in a state of control at the given standard with respect to a given quality characteristic at the time when the samples were taken.[5] Should the test, when applied to a set of measurements of individual items, indicate that variation could well be attributed to chance, then the conclusion would be drawn that the test gave no evidence to cast doubt on the truth of the hypothesis. But should the test indicate the presence of variation not attributable to chance, then the truth of the hypothesis would be in question and in practice the necessity for investigation of trouble indicated.

To clarify the foregoing statements without introducing too many technicalities let us consider the following hypothetical example:

Sixty per cent of the items from a manufacturing process have been receiving an A-1 grade. Forty per cent have been marked defective[6] and subjected to poorer classification.[6] A series of 50 samples each consisting of 20 items is drawn at random, and the percentage of defectives in each sample is computed. Does this set of results undermine the hypothesis that the process is controlled at the 60 per cent level of effectiveness?

An appropriate test[7] is the following:

If the per cent defective in one or more of the samples is greater than 73 or less than 7, reject the hypothesis, otherwise, accept the hypothesis.

Omitting a detailed exposition of the mathematical assumptions underlying this test, it is sufficient to state that, if the product is controlled at the standard level of quality assumed, and if a random sample of 20 items is drawn, then the probability that the percentage of defectives will fall between 7 and 73 is greater than 0.997. The occurrence of a value outside these limits is taken as an indication of the presence of an assignable cause of variability.

From a process producing 40 per cent of defectives, it is possible to get by chance a sample with no defectives or with as many as 100 per cent of defectives. Therefore, in common with all other tests of significance, this test may lead to the rejection of a true hypothesis.[8] Also, the test might lead to the acceptance of a false hypothesis, as will be exemplified later.

[5] In correspondence, W. A. Shewhart has suggested that the reader be duly forewarned of the difference between the formal statistical hypothesis and the control hypothesis. For a discussion of this distinction refer to "Statistical Method From the Viewpoint of Quality Control," by W. A. Shewhart and W. E. Deming, Graduate School of U. S. Dept. of Agriculture, Washington, D. C., 1939, chap. 1, in part, pp. 39–43.

[6] In using this high percentage, there is no implication that such would be tolerated in practice. Because it avoids certain technicalities, this percentage is convenient to use as an illustration of the principles involved.

[7] The limits have been set at $p \pm 3\sqrt{\frac{p(1-p)}{n}}$, where $p = 0.40$ and $n = 20$.

[8] "On the Use and Interpretation of Certain Test Criteria for Purposes of Statistical Inference," by J. Neyman and E. S. Pearson, *Biometrika*, vol. 28A, 1928, pp. 175–240.

TABLE 1 TEST DATA FOR CONTROL OF A QUALITY LEVEL

(*a*) Number and percentage of defectives in random samples of 20 from a population 40 per cent defective

Sample	Defective No.	Defective Per cent	Sample	Defective No.	Defective Per cent	Sample	Defective No.	Defective Per cent	Sample	Defective No.	Defective Per cent	Sample	Defective No.	Defective Per cent
1	7	35	11	6	30	21	6	30	31	8	40	41	5	25
2	11	55	12	7	35	22	11	55	32	10	50	42	9	45
3	8	40	13	9	45	23	11	55	33	9	45	43	7	35
4	8	40	14	11	55	24	6	30	34	9	45	44	8	40
5	8	40	15	7	35	25	5	25	35	7	35	45	8	40
6	9	45	16	9	45	26	9	45	36	6	30	46	7	35
7	6	30	17	9	45	27	6	30	37	14	70	47	5	25
8	10	50	18	11	55	28	8	40	38	11	55	48	9	45
9	8	40	19	9	45	29	7	35	39	8	40	49	13	65
10	9	45	20	8	40	30	10	50	40	9	45	50	7	35

(*b*) Number and percentage of defectives in random samples of 20, when samples 5, 10, 15, . . ., 50 are from a population 60 per cent defective, and the others are from a population 35 per cent defective

Sample	Defective No.	Defective Per cent	Sample	Defective No.	Defective Per cent	Sample	Defective No.	Defective Per cent	Sample	Defective No.	Defective Per cent	Sample	Defective No.	Defective Per cent
1	3	15	11	10	50	21	8	40	31	7	35	41	5	25
2	5	25	12	6	30	22	6	30	32	6	30	42	5	25
3	4	20	13	6	30	23	9	45	33	2	10	43	7	35
4	7	35	14	4	20	24	6	30	34	8	40	44	8	40
5	8	40	15	14	70	25	14	70	35	12	60	45	11	55
6	8	40	16	9	45	26	7	35	36	5	25	46	6	30
7	9	45	17	5	25	27	4	20	37	10	50	47	5	25
8	6	30	18	6	30	28	10	50	38	7	35	48	2	10
9	9	45	19	7	35	29	8	40	39	11	55	49	10	50
10	11	55	20	11	55	30	15	75	40	16	80	50	13	65

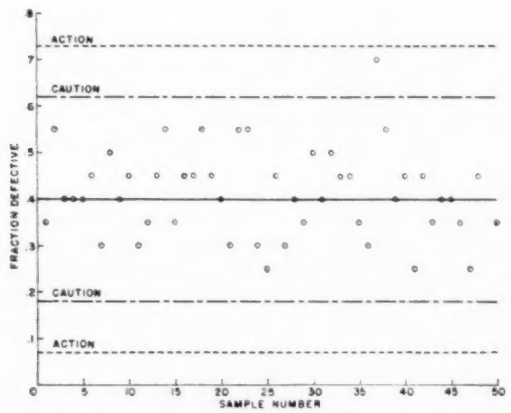


FIG. 1 TEST FOR CONTROL AT A QUALITY LEVEL OF 40 PER CENT DEFECTIVE. SAMPLES OF 20
[Data from Table 1 (*a*).]

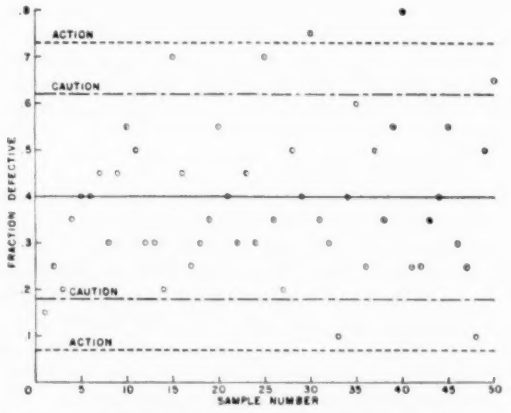
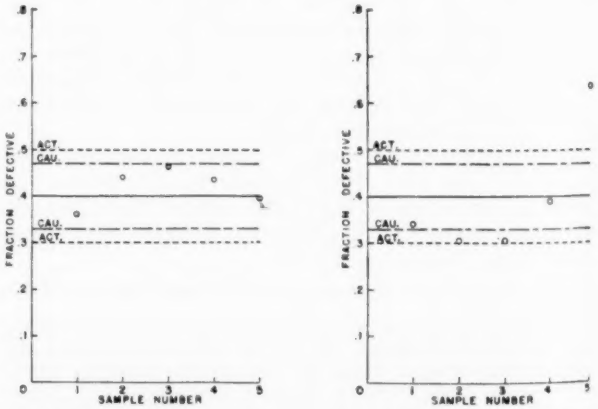


FIG. 2 TEST FOR CONTROL AT A QUALITY LEVEL OF 40 PER CENT DEFECTIVE. SAMPLES OF 20
[Data from Table 1 (*b*).]

Table 1(*a*) presents the data for one series of samples from the specified process and Fig. 1 exhibits the graphical application of the test. It should be noted that since no points fall outside the action lines the test gives us no cause to reject the hypothesis that the process is controlled at the given level.

Table 1(*b*) presents a second series of data to be tested, and Fig. 2 shows the test. Here we are forced to reject the hypothesis that the process is controlled at the given level. The rejection of the hypothesis is due to samples 30 and 40. We are forced to the consideration of one of two alternative hypotheses; either (1) the process is under control but at a different level, or (2) assignable causes of variation are present in the process.

The concept of "assignable" causes seems to have been introduced by W. A. Shewhart,[9] and has been developed by him in various books and articles. From an engineering point of view, assignable causes are those causes of variability which can be found and eliminated. Mathematically they might be defined as those causes whose effect on any individual item depends upon the position of the item in time or space and, therefore, prevent accurate prediction of the characteristics of items when the knowledge of the dependence and positions of individuals is absent. Another definition might be that assignable causes are those which tend to introduce heterogeneity. In any case, the



(*a*) Data from Table 1(*a*) (*b*) Data from Table 1(*b*)

FIG. 3 TESTS FOR CONTROL AT A QUALITY LEVEL OF 40 PER CENT DEFECTIVE. SAMPLES OF 200, FORMED BY RATIONAL SUBGROUPING

[9] "A Problem of Inspection Engineering," *Engineering Economics*, Bell Telephone Laboratories, 1926, pp. 16–20.

"Random Sampling," *American Mathematical Monthly*, vol. 38, 1931, pp. 245–270.

"Economic Control of Manufactured Product," D. Van Nostrand Company, Inc., New York, N. Y., 1931.

"Application of Statistical Methods to Manufacturing Problems," monograph B-1089, Bell Telephone System Technical Publications, 1937.

"Statistical Method From the Viewpoint of Quality Control," Graduate School of the U. S. Department of Agriculture, Washington, D. C., 1939.

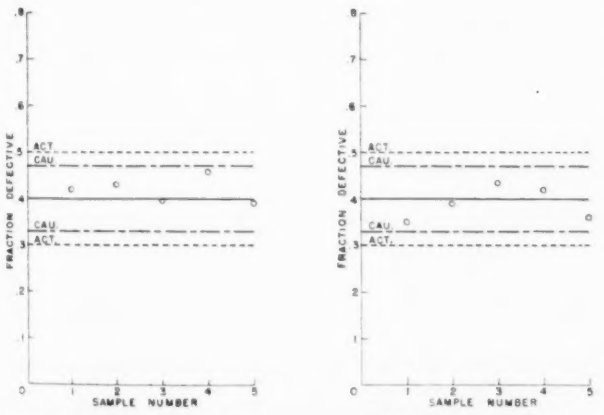
general effect of the presence of such causes is the prevention of the prediction of the behavior of quality characteristics in random samples.

The method proposed by Shewhart for the investigation of assignable causes is that of "rational subgrouping."[10] In Fig. 2 we note that points 30 and 40 are outside of the action lines. Taking this as evidence of lack of control, it is now the engineer's job to locate and eliminate the assignable causes whose presence is indicated. If there is available a careful description of the conditions under which each sample was taken, the engineer may note that some unusual condition, such as excessive humidity, was common to both of the bad samples. Combining engineering judgment with the statistical evidence, he may adopt the tentative hypothesis that excessive humidity is an assignable cause. Before taking long and expensive measures to eliminate excessive humidity, he is likely to desire further evidence. This may be obtained by dividing the data into subgroups on the basis of the suspected property.

[10] Reference (9), "Economic Control of Manufactured Product," p. 299.

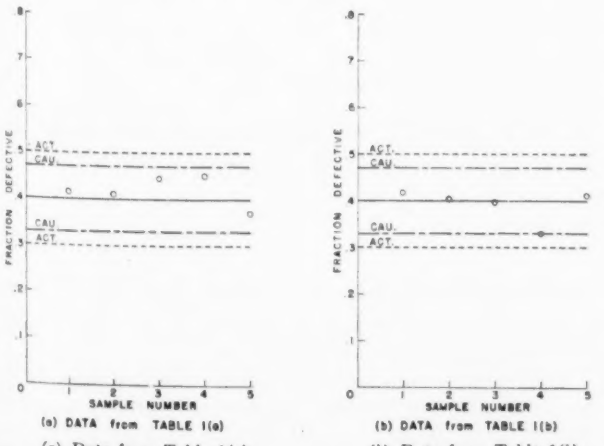
1373	1360	1012	3593	6309	0988	8901	8496
0490	5187	4604	8395	8890	8902	3369	2975
4852	6791	0630	3098	3605	5826	2605	3109
2358	5063	9889	8890	0631	2773	0629	9990
4088	1002	0360	2582	0990	0854	6420	1357
9150	4717	5063	6277	1366	3334	9888	9259
6434	3088	1099	3085	0495	5792	9024	3727
6940	8925	0136	4333	2976	6050	6926	2840
7667	9407	6049	4579	5567	6296	0505	7420
0495	5445	5297	2605	0260	4321	1741	8654
3224	7793	6556	0629	5174	1234	9654	3334
6052	7397	7026	6432	1088	6926	3223	5677
9888	5444	0517	1123	8903	0405	3568	9136
9250	6926	4108	4692	5938	1853	1360	9260
6311	2852	8890	6040	3953	1098	0483	4949

FIG. 4 ILLUSTRATING THE GENERAL APPEARANCE OF PART OF A PAGE OF TIPPETT'S "RANDOM SAMPLING NUMBERS"
(Reference 13; not a copy.)



(a) Data from Table 1(a) (b) Data from Table 1(b)

FIG. 5 TESTS FOR CONTROL AT A QUALITY LEVEL OF 40 PER CENT DEFECTIVE. SAMPLES OF 200, FORMED BY SERIAL SUBGROUPING



(a) Data from Table 1(a) (b) Data from Table 1(b)

FIG. 6 TESTS FOR CONTROL AT A QUALITY LEVEL OF 40 PER CENT DEFECTIVE. SAMPLES OF 200, FORMED BY RANDOM SUBGROUPING

The control chart for the new test is given in Fig. 3(*b*). Since the numbers in the samples are larger, the action lines are closer together. The fact that the fifth point falls outside the action lines gives support to the theory that every fifth sample came from a population significantly different from the population which produced the others.

Figs. 1 and 2 contain a second pair of lines which the author has chosen to call "caution lines." The position of these lines[11] is so chosen that the probability of finding a sample point outside is less than 0.05, when the process is controlled at the 40 per cent level. The appearance of a point between an upper caution line and an upper action line, or between the corresponding lower lines, is a signal that trouble may be approaching. It does not mean necessarily that investigation should start. If this were the case, we should be looking for trouble in 5 per cent of the controlled situations. Occasionally this might be desirable, but usually it seems to be uneconomical.[12]

In the case under consideration, sample points 15, 25, and 50 fall above the upper caution line. Also, points 10, 20, 35, and 45 fall above the mean. It is the combination of these facts which suggests grouping the multiples of 5.

CREATING UNCONTROLLED CONDITIONS

In exemplifying the control-chart technique, it has been customary to take a manufacturing process, apply a test for control, state what assignable causes were found and eliminated, and then apply the test again in order to show that control has been achieved. Examples of this sort are of the greatest value, and it is to be fervently hoped that many more of them will find their way into print. The author, however, has found considerable interest in endeavoring to reverse the process, and the remainder of this paper will be concerned with the results of a few simple experiments in creating uncontrolled conditions. Rather than moving into control, we shall see how to get out of control, and then note whether or not our tests locate the assignable causes we have introduced into the situation.

[11] The lines are set at $p \pm 2\sqrt{\frac{p(1-p)}{n}}$, where $p = 0.40$ and $n = 20$.

[12] L. E. Simon, in "An Engineers' Manual of Statistical Methods," John Wiley & Sons, Inc., New York, N. Y., 1941, has suggested the use of two sets of control lines, together with supplementary tests designed to appraise the significance of the number of points falling outside either set. His control lines, however, are differently located.

The table of "Random Sampling Numbers,"[13] prepared by L. H. C. Tippett, contains 41,600 four-digit numbers obtained by taking 40,000 digits "at random"[14] from census reports and combining them by fours. On each page, the numbers are arranged in 8 columns of blocks of 5, 10 blocks to a column.

Using this table it is possible to set up many kinds of distributions and draw long series of samples without excessive labor. For example, if one wishes the number of heads resulting from 10 tosses of a coin, he need only turn at random to some page of the table, read the first digits of each of 10 numbers in a column, let the digits 0 to 4, inclusive, represent heads, and count their number. If we were to use the first digits of the numbers of Fig. 4, we could count 6 heads (corresponding to 1, 0, 4, 2, 4, and 0).

A satisfactory model of a controlled process may be obtained by regarding certain digits as representing defective items. Then we have a model of control at the level of 40 per cent defective. Considering each block as a sample of 20, it is quick and easy to draw 50 samples. The data of Table 1(*a*) were obtained by this method.

To obtain data like that of Table 1(*b*) we may proceed as follows: For samples 1, 2, 3, 4; 6, 7, 8, 9; 11, 12, 13, 14; . . ., let the digits 0, 1, 2, and the 3's in the first two columns of each block represent defectives. For samples 5, 10, 15, . . ., let the digits 0, 1, 2, 3 represent good items. Then the probability for a defective item is 0.35 for the one set of samples and 0.60 for the other set. For the total set the expected percentage of defects is still 40. We now have a model of an uncontrolled process which we can compare with the model of a process controlled at the same expected value.

As shown in Fig. 2, our test rejects the hypothesis of control at the 40 per cent level. It is interesting to note that the probability that a single sample point of the 35 per cent set will fall outside is 0.005, and the probability for one or more of the 40 points is 0.18. For the 60 per cent set we have a probability of 0.12 for a single point and 0.72 for one or more of the 10 points. For the 50 points, the probability for one or more points outside the action lines is 0.77, so that the chances are greater than 3 to 1 that the presence of assignable causes of variability will be suspected.

The rational subgrouping of the data of Table 1(*b*) has been explained and the result exhibited graphically in Fig. 3(*b*). The result of similar subgrouping for the data of Table 1 is exhibited in Fig. 3(*a*). As expected, no lack of control is indicated. Of course, for this controlled situation we should not expect any kind of subgrouping to indicate the presence of assignable causes of variability.

One method of subgrouping the data of Table 1(*b*) strengthens our belief in the presence of assignable causes. How about other methods? It is fairly clear that, if the hypothetical basis for rational subgrouping is false, the new set of samples will be expected to behave like a set formed at random and may give an indication of control.

As a first illustration of the foregoing statement, let us form 5 samples of 200 by combining the samples 1–10, 11–20, 21–30, 31–40, and 41–50 of Table 1(*b*). The result for this is shown in Fig. 5(*b*). The result for a similar treatment of the data of Table 1(*a*) is shown in Fig. 5(*a*).

As a second illustration, let us consider 5 samples formed at random as follows: Write down one half of each of the even two-digit numbers in pairs of columns of Fig. 4, starting with the first column, omitting duplications, and continuing until 40 numbers are obtained.[15] The first 10 of these indicate which samples to combine into the first sample of 200. The next 10 indicate the parts of the second large sample, and the third and fourth sets of 10 give the third and fourth samples. The remaining small samples are combined for the fifth sample of 200. Figs. 6(*a*) and 6(*b*) show the results of applying this procedure to the data of Tables 1(*a*) and 1(*b*), respectively.

Measuring Quality Characteristics

Up to this point we have been focusing our attention on the control-chart technique for fraction defective. Much of the time, however, we are not content with sorting items into just two categories, good and bad, but we are rightly concerned with actual measurements of the quality characteristic under consideration.

The situation as regards control immediately becomes quite complex because of the variety of functional forms useful in describing controlled characteristics and the number of constants contained in these forms. Even the notation becomes complicated.

Let us assume that the measurement of a quality characteristic is denoted by the continuous variable x. Further assume that, for an infinite collection of items, the percentage of the items with quality between $x = \alpha$ and $x = \beta$ is given by the relation

$$P(\alpha \leq x \leq \beta) = \int_{\alpha}^{\beta} f(x)dx$$

It follows then, that

$$P(-\infty < x < \infty) = \int_{-\infty}^{\infty} f(x)dx = 1$$

Further let $\bar{x} = \int_{-\infty}^{\infty} xf(x)dx$ give the mean or average value of x, and let $u_n = \int_{-\infty}^{\infty} (x - \bar{x})^n f(x)dx$ give the nth moment about $\bar{x}$.

In particular, we shall call the second moment μ_2 the variance, and the square root of μ_2 the standard deviation. We denote the standard deviation by σ and mention that it is a measure of the dispersion of the individual measurements from the mean.

In case $f(x)$ is of the form

$$\frac{1}{\theta_2\sqrt{2\pi}} e^{-\frac{(x-\theta_1)^2}{2\theta_2^2}}$$

we call it "normal." It is well known and easily verified that $\bar{x} = \theta_1$, and $\sigma = \theta_2$ for this function. Also the transformation

$$t = \frac{x - \theta_1}{\theta_2}$$

reduces the function of x to the t function $\frac{1}{\sqrt{2\pi}} e^{-t^2/2}$. The integral of this latter function for the limits 0 to t, or $-\infty$ to t, is available in many handbooks and sets of tables.

Judging from both written and oral testimony many of the frequency distributions met in engineering practice are approxi-

[13] "Tracts for Computers," No. XV, Cambridge University Press, London, 1927.

[14] The question of the "randomness" of these numbers is discussed in the following papers: "Randomness and Random Sampling Numbers," by M. J. Kendall and B. Babington-Smith; *Journal*, Royal Statistical Society, vol. 101, 1938, pp. 147–166; "Second Paper on Random Sampling Numbers," by M. J. Kendall and B. Babington-Smith, Supplement to *Journal*, Royal Statistical Society, vol. 6, no. 1, 1939, pp. 51–61; "A Test of Tippett's Random Sampling Numbers," by G. U. Yule, *Journal*, Royal Statistical Society, vol. 101, 1938, pp. 167–172. For a discussion of the general concept of "randomness," see W. A. Shewhart and W. E. Deming, reference (5), pp. 12–17.

[15] The numbers are: 2, 24, 20, 32, 38, 45, 26, 29, 44, 25—17, 16, 30, 49, 46, 5, 12, 1, 15, 47—27, 14, 22, 13, 6, 18, 35, 28, 4, 40—41, 31, 3, 23, 33, 37, 19, 48, 9, 10.

mately normal.[16] While the condition seems by no means to be necessary, the sufficient condition for a controlled process is the condition that it behave as though its items were normally distributed.

The method of setting up a working model for a normal distribution, and, therefore, for a controlled process, will now be described.

Working Model for a Controlled Process

Tippett's table[17] provides careful instructions for the construction of a finite frequency distribution whose difference from a normal distribution is due, in the main, to its finiteness. Using his general method but not his result, we set up the numerical correspondence given in Table 2. This finite distribution is approximately normal. It has a mean of 10 and a standard deviation of 2.5. From our knowledge of the Tippett numbers we have reason to believe that the 41,600 numbers will serve as a satisfactory model of a normal distribution, provided the numbers are renamed, as indicated in Table 2.

TABLE 2 TRANSFORMATION FROM A RECTANGULAR DISTRIBUTION TO A NORMAL DISTRIBUTION WITH A MEAN OF 10 AND A STANDARD DEVIATION OF 2.5

The integers	Correspond to	Relative frequencies
0000	0	0.0001
0001–0002	1	0.0002
0003–0012	2	0.0010
0013–0046	3	0.0034
0047–0138	4	0.0092
0139–0358	5	0.0220
0359–0807	6	0.0449
0808–1586	7	0.0779
1587–2741	8	0.1155
2742–4206	9	0.1465
4207–5792	10	0.1586
5793–7257	11	0.1465
7258–8412	12	0.1155
8413–9191	13	0.0779
9192–9640	14	0.0449
9641–9860	15	0.0220
9861–9952	16	0.0092
9953–9986	17	0.0034
9987–9996	18	0.0010
9997–9998	19	0.0002
9999	20	0.0001

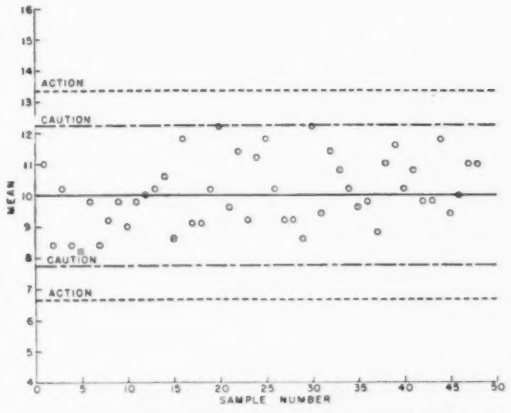


FIG. 7 MEANS OF SAMPLES OF 5 FROM A PROCESS CONTROLLED AT A MEAN OF 10 AND A STANDARD DEVIATION OF 2.5
(Data from Table 3.)

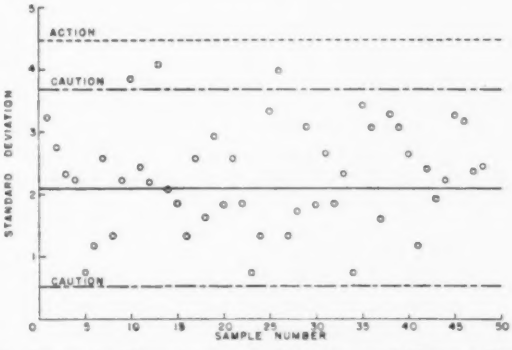


FIG. 8 STANDARD DEVIATIONS OF SAMPLES OF 5 FROM A PROCESS CONTROLLED AT A MEAN OF 10 AND A STANDARD DEVIATION OF 2.5
(Data from Table 3.)

Using Fig. 4 as a substitute, we can draw a sample from a

[16] It is not always clear what this implies. Usually it seems to mean that a normal curve has been fitted to observational data and some test of "goodness of fit" has been applied.

[17] Reference (13), pp. iv, v.

TABLE 3 SAMPLES OF 5 FROM A NORMAL DISTRIBUTION WITH A MEAN OF 10 AND A STANDARD DEVIATION OF 2.5

Shift	Time	Day	Sample	Mean	Standard Deviation
			(Material A used for period)		
I	9	Mon.	11,10,16,12,6	11.0	3.22
	11		6,9,11,12,3	8.4	2.76
	1		7,14,11,10,9	10.2	2.32
	3		6,6,9,12,9	8.4	2.24
II	5	Mon.	7,9,9,8,8	8.2	0.75
	7		11,9,8,11,10	9.8	1.17
	9		4,9,12,9,8	8.4	2.58
	11		10,9,11,9,7	9.2	1.33
III	1	Tues.	8,12,8,13,8	9.8	2.23
	3		11,11,8,2,13	9.0	3.85
	5		10,12,10,6,11	9.8	2.44
	7		13,8,11,7,11	10.0	2.19
			(Material B used for period)		
I	9	Tues.	11,15,5,14,6	10.2	4.07
	11		12,13,11,10.7	10.6	2.06
	1		10,9,7.11,6	8.6	1.85
	3		12,14,12,11,10	11.8	1.33
II	5	Tues.	9,9,6,6,13	8.6	2.58
	7		7,8,11,10,7	8.6	1.62
	9		9,14,6,13,9	10.2	2.93
	11		9,14,12,14,12	12.2	1.83
III	1	Wed.	8,6,12,13,9	9.6	2.58
	3		14,10,9,13,11	11.4	1.85
	5		9,10,9,10,8	9.2	0.75
	7		11,11,12,9,13	11.2	1.33
			(Material C used for period)		
I	9	Wed.	13,16,11,13,6	11.8	3.31
	11		5,10,17,8,11	10.2	3.97
	1		9,7,9,10,11	9.2	1.33
	3		8,12,9,7,10	9.2	1.72
II	5	Wed.	10,9,3,12,9	8.6	3.07
	7		9,14,12,14,12	12.2	1.83
	9		8,6,12,13,8	9.4	2.65
	11		14,10,9,13,11	11.4	1.85
III	1	Thurs.	10,14,11,7,12	10.8	2.32
	3		9,11,10,10,11	10.2	0.75
	5		4,8,14,10,12	9.6	3.44
	7		11,11,14,5,8	9.8	3.06
			(Material D used for period)		
I	9	Thurs.	10,7,7,11,9	8.8	1.60
	11		12,9,9,17,8	11.0	3.29
	1		10,15,15,11,7	11.6	3.07
	3		15,9,7,10,10	10.2	2.64
II	5	Thurs.	12,9,10,12,11	10.8	1.17
	7		12,12,6,8,11	9.8	2.40
	9		8,11,9,13,8	9.8	1.94
	11		14,11,14,12,8	11.8	2.23
III	1	Fri.	12,14,9,5,7	9.4	3.26
	3		5,11,8,12,14	10.0	3.16
	5		12,10,8,10,15	11.0	2.37
	7		9,8,11,15,12	11.0	2.45

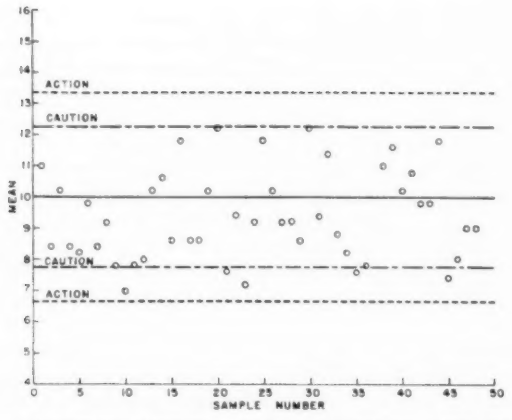


FIG. 9 MEANS OF SAMPLES OF 5 FROM A PROCESS WITH TROUBLE INTRODUCED

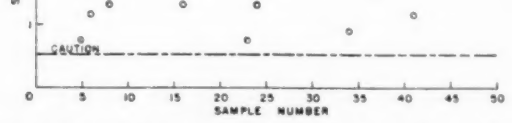
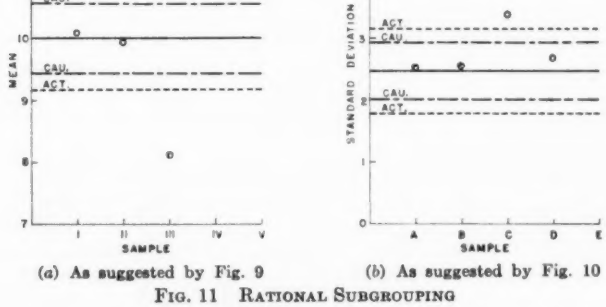


FIG. 10 STANDARD DEVIATIONS OF SAMPLES OF 5 FROM A PROCESS WITH TROUBLE INTRODUCED



(*a*) As suggested by Fig. 9 (*b*) As suggested by Fig. 10

FIG. 11 RATIONAL SUBGROUPING

normally distributed population. If we take the upper left-hand block and transform the numbers

1373 becomes 7
0490 becomes 6
4852 becomes 10
2358 becomes 8
4088 becomes 9

If we replace integration by summation in our formulas for the mean and standard deviation and compute these statistical quantities for our sample, we find that $\bar{x} = 8.0$ and $\sigma = 1.4$.

While we might test single items, it is better practice to test small groups of items. Both the mean and standard deviation will be considered.

The hypothesis to be tested is that the process is controlled at a mean of 10 and a standard deviation of 2.5 If the hypothesis is true then (with certain approximations):

1 The probability is greater than 0.997 that the mean of a sample of 5 items will fall between 6.65 and 13.35.[18]

2 The probability is greater than 0.997 that the standard deviation of a sample of 5 items will be less than 4.47.[19] Failure to satisfy either condition clouds the hypothesis.

Suppose we have an item in mass production by three 8-hr shifts, with four different lots of material being used, one lot for each three shifts. Furthermore, let us suppose that samples of 5 items are taken at 2-hr intervals. Using Tippett's table,[13] as explained, we can set up a model for a controlled process and draw an experimental set of samples. Such a set of samples is given in Table 3, together with their means and standard deviations.

Figs. 7 and 8 give the control charts for the means and the standard deviations of these samples, respectively. As expected, both tests are passed so no lack of control is indicated.

As in the case of fraction defective, let us see what happens when the process goes out of control. Fig. 9 shows the situation when the samples for the third shift come from a model with a mean reduced 20 per cent, but the standard deviation is unchanged. Our test fails to indicate the presence of assignable causes, although we now find three points between the two lower control lines. If, however, we were to group our data into rational subgroups on the basis of shifts, we would get the condition pictured in Fig. 11(*a*). Here the point for the third shift is far outside the action lines.

Now let us look at the effect of an increase in the variability of material C. If the mean is unchanged but the standard deviation is increased 20 per cent, we have the situation shown in Fig. 10. The one sample point outside the action lines gives an indication of lack of control, and the presence of several points between the two upper control lines lends support. When we group on the basis of material and draw Fig. 11(*b*), the change in variability of material C becomes very apparent.[20]

CONCLUSIONS

The elimination of assignable causes is a problem for the engineer. The principal service of the statistician is in the application of tests designed to reveal the existence of such causes and, in many cases, to give some clue as to their general character. In addition to the tests outlined in this paper, there are many others which rest on sound assumptions and have important applications. In particular, it should be noted that the entire group of tests, which must be used before control has been established and the standard determined, has been omitted. The author has neither the space nor the confidence to give an adequate treatment of this larger problem. However, its omission should not minimize its great importance.[21]

Our principal purpose has been that of setting up models of controlled processes and of showing a few ways of throwing them out of control. As has been indicated, samples can be drawn

[18] The limits are set at $\bar{x} \pm \frac{3\sigma}{\sqrt{n}}$, where $\bar{x} = 10$, $\sigma = 2.25$, and $n = 5$.

[19] The limits are set at zero and $0.84\,\sigma + \frac{3\sigma}{\sqrt{2n}}$, where $\sigma = 2.5$ and $n = 5$. If $0.84\,\sigma - \frac{3\sigma}{\sqrt{2n}}$ were greater than zero, it would have been used as the lower limit.

[20] This situation presents an excellent opportunity for the analysis of variance. Discussion of such a method of attack is outside the scope of the present paper.

[21] For a discussion of some of the difficulties see W. A. Shewhart and W. E. Deming, reference (5), chap. 2; and "Determination of Sample Sizes for Setting Tolerance Limits," by S. S. Wilks, *The Annals of Mathematical Statistics*, vol. 12, no. 1, 1941, pp. 91–96.

with ease and their nature quickly analyzed. Sometimes our simple tests failed at first to give a clear indication of the presence of assignable causes. This was to be expected, since from their very nature, statistical tests occasionally reject true hypotheses or fail to reject false ones. One of our great problems is to adjust significance levels so that both types of errors are reduced to an economic minimum.

In each of the cases considered the use of rational subgrouping provided samples which revealed the presence of the trouble introduced. Wherever chance subgrouping was applied, results were obtained which were easily explainable on the basis of chance. This was a matter of good luck, as there was some probability, as previously noted, that the reverse situation might have eventuated.

In conclusion, the hope is expressed that the methods outlined in this paper may prove of some slight help in increasing the general understanding of statistical methods for the control of quality. Although many of our larger companies have been using these methods with beneficial results, some organizations have been hesitant to try them until their engineers could examine the theory more closely and gain more knowledge of its operation. Perhaps this discussion will be of assistance in that direction.

Discussion

G. J. Meyers, Jr.[22] The question was asked in connection with this paper why statistics were used to show things which would have in any case become observable in the course of the normal use of common sense. This question seemed to the writer to be quite in order, since it is one being asked many places by manufacturing people who are being told about statistical methods of quality control. The reason behind the question is that, in describing statistical methods, it is often necessary to use conditions which are sufficiently extreme to enable the average person to see the gain made by the use of statistics. In actual use, statistical methods are applied to borderline cases where the answers are not as obvious as in those cases which are only used as examples of statistical methods.

Statistical methods serve as landmarks which point to further improvement beyond that deemed obtainable by experienced manufacturing men. Hence, after all obvious correctives have been exhausted and all normal logic indicates no further gain is to be made, statistical methods still point toward a reasonable chance for yet further gains; thereby giving the man who is doing trouble shooting sufficient courage of his convictions to cause him to continue to the ultimate gain, in spite of expressed opinion on all sides that no such gain exists.

Author's Closure

Mr. Meyers reports that the question was asked why statistics were used to show things which would have in any case become observable in the course of the normal use of common sense. In so far as I understand the question, I quite agree with the answer he has suggested. However, a certain amount of clarification of the question and amplification of the answer seems to be in order.

I am not clear as to what is meant by "common sense" or the "normal use" of it. If this is translated as being the ordinary use of good judgment, then I must assert that, in my opinion, any judgment, to be good, must be arrived at by the collection and correct interpretation of pertinent facts. But the science of statistics is concerned with the collection, classification, and interpretation of numerical data. It would seem, then, that good judgment about quantitative matters must be based on statistics of some sort. As to the amount and type of the arithmetical calculations necessary, this seems to depend somewhat on the relation of its cost to the value of increased precision in discrimination between possible decisions.

Let us look at the data given in Table 1 (*b*) of the paper. Without any statistical theory, how can we decide whether or not it came from a controlled process? We are restricted from assuming that the samples in any way represent the lots from which they were taken; we cannot compute any measure of central tendency or dispersion; we cannot even think about any expected number of defects in samples of size twenty. With these aids to jugment ruled out, I doubt that we can reach any decision in which we would have much confidence.

Judging from past experience, I suspect that the real point at issue is not the desirability of the use of some statistical principles and techniques but of the use of such elaborate ones. "If the process has been averaging 8 defects out of 20 pieces, cannot anyone see, without a control chart, that something must be wrong when there are 16 defects in a sample of 20?" is the usual question.

It would seem that the proper rejoinder would be the following interrogations:

1 Just what chain of reasoning leads to the inescapable conclusion that something must be wrong?

2 Would you say that something was wrong if there were 15 defects? How about 14 or 13 or 12? Where would you draw the line, and why?

3 Would 16 defects out of 20, 8 defects out of 10, or 4 out of 5 give you equal assurance that something was wrong? Why or why not?

Anyone who gives careful consideration to these question should begin to perceive that one needs to have some systematic knowledge of the kind of samples different sorts of lots are likely to produce. Having such knowledge, he is likely to agree that the methods of control-chart analysis provide efficient application of it. And, since many industrial organizations have been able to save money and material by the use of these methods, it would seem to be uncommonly bad common sense not to try them.

[22] General Engineering, General Electric Company, West Lynn, Mass.

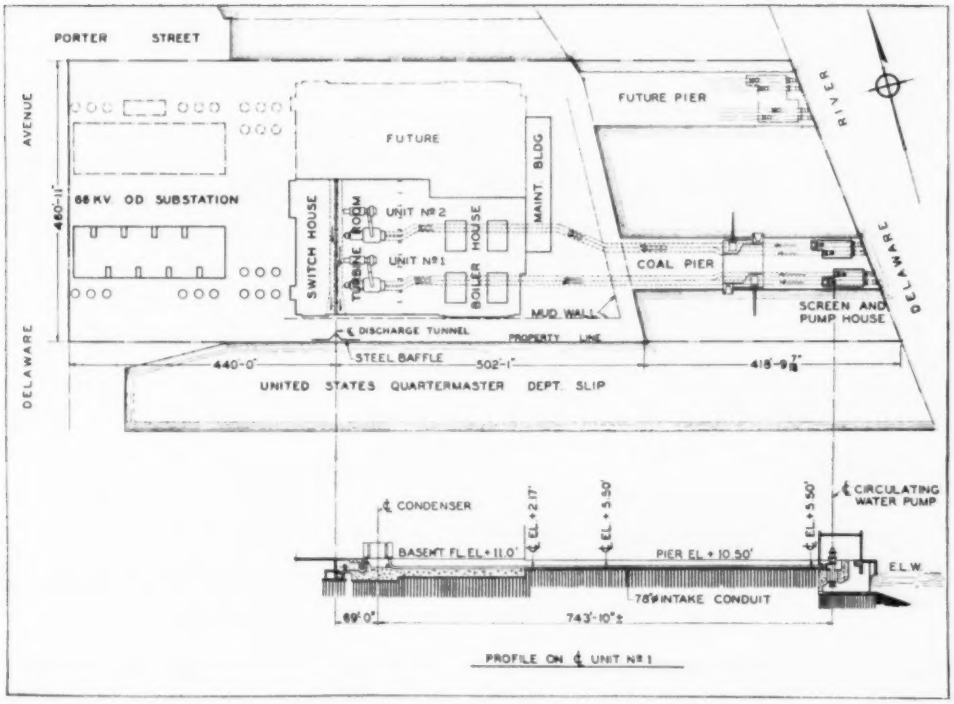


FIG. 1 PLOT PLAN AND ELEVATION OF SOUTHWARK STATION

Hydraulic-Engineering Problems at Southwark Generating Station

BY S. LOGAN KERR[1] AND STANLEY MOYER,[2] PHILADELPHIA, PA.

This paper discusses the hydraulic-engineering features of the Philadelphia Electric Company's Southwark Station, the latest addition to its chain of generating stations along the Delaware River. Problems in the design and selection of major equipment centered around (*a*) the location of the intake and discharge passages for condenser circulating water; (*b*) the prevention of recirculation of warm discharge water from condensers; (*c*) operating head on pumps under various river-level conditions; (*d*) size, type, and arrangement of pumps and conduits. A comprehensive model-test program was carried out to solve certain pump, circulating-water-discharge, and condenser problems, the results of which are reported.

THE latest addition to the Philadelphia Electric Company's chain of generating stations along the Delaware River in the Philadelphia area will be Southwark Station located at Delaware Avenue and Porter Street in South Philadelphia. Fig. 1 shows the plot plan of the site and the general arrangement of the major items of equipment, both for the initial development and for the ultimate project.

[1] United Engineers & Constructors Inc. Mem. A.S.M.E.

[2] Engineer, Mechanical Engineering Division, Philadelphia Electric Company. Mem. A.S.M.E.

Contributed by the Power Division and presented at the Annual Meeting, New York, N. Y., December 1–5, 1941, of THE AMERICAN SOCIETY OF MECHANICAL ENGINEERS.

NOTE: Statements and opinions advanced in papers are to be understood as individual expressions of their authors and not those of the Society.

DESCRIPTION OF INITIAL INSTALLATION

The initial installation will consist of two 168,750-kw 90 per cent power factor units of the cross-compound two-cylinder type. The 3600-rpm, single-flow, high-pressure turbine element drives an 81,250-kva generator. The low-pressure element operates at 1800 rpm double flow and drives a 106,250-kva generator. These ratings are continuous at normal hydrogen pressure. The turbine elements together are capable of developing 187,500 kw. Each low-pressure unit condenser has a total surface of 77,000 sq ft.

Steam is supplied by four 850,000-lb-per-hour, two-drum, open-pass, direct-pulverized-coal-fired, continuous-slag-tap boilers at 925 psi and 900 F total temperature. Each main unit is arranged to be completely independent, a pair of boilers serving a single turbo-generator without cross connection.

HYDRAULIC-ENGINEERING FEATURES

The design and selection of many of the major items of equipment for this station depended upon a satisfactory solution of certain hydraulic-engineering problems, as follows:

1 The location of the intake and discharge passages for condenser circulating water, and their effect on adjoining structures.

2 The prevention of recirculation of warm discharge water from condensers.

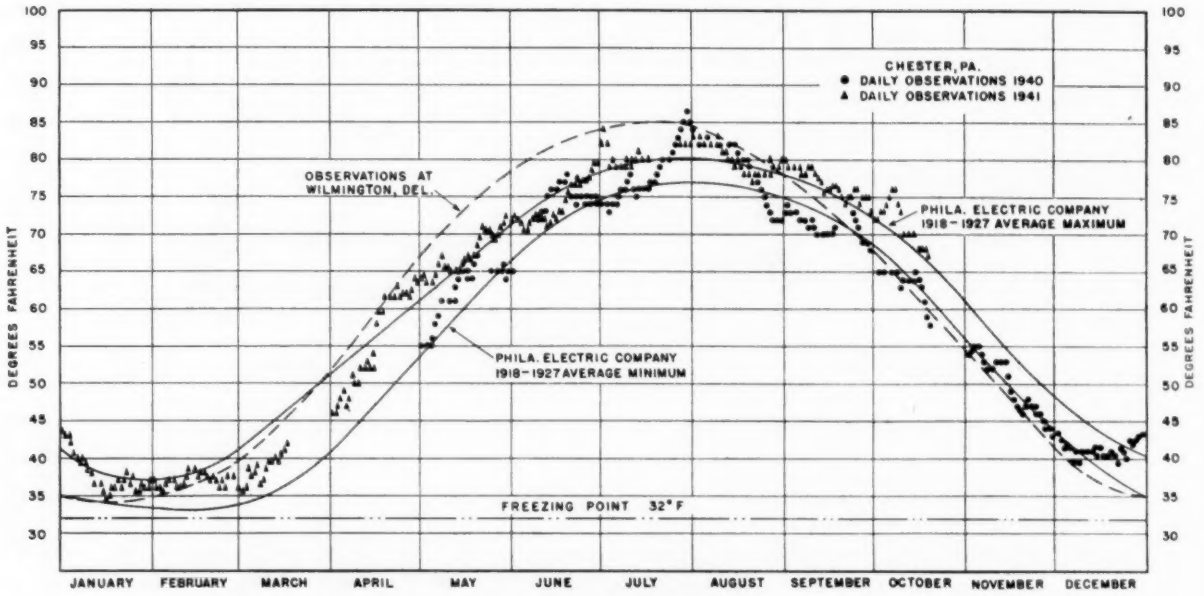


FIG. 2 DELAWARE RIVER WATER TEMPERATURES IN THE VICINITY OF PHILADELPHIA

3 The operating head on the pumps under various river level and flow conditions.

4 The size, type, and arrangement of the pumps and conduits.

Since the site is new and no existing structures other than a marginal wharf are to be used in the station, it was possible to approach the solution of these hydraulic problems without restriction.

CONDENSER-WATER REQUIREMENTS

The total water requirement for condensing alone was set at 146,000 gpm for each unit. An additional 6000 gpm per machine is needed to supply the hydrogen and turbine-bearing-oil coolers. An allowable water velocity of 8 fps was decided upon, and the maximum river-water temperature for design purposes was taken as 85 F. Fig. 2 shows the temperature records at several locations on the Delaware River over long periods of time.

To guard against a complete shutdown of a turbogenerator because of the failure of a single circulating pump, it has long been the practice of the Philadelphia Electric Company to provide two pumps for each condenser, each pump providing about half of the cooling water required under peak conditions. Such an arrangement allows a substantial portion of rated load to be carried on the turbine with one pump out of service.

Studies were made of the effect of condenser vacuum upon the coal rate. A potential saving of about 0.6 per cent of the coal used would result from an increase in vacuum of $^1/_{10}$ in. At half load this would be about 300 lb of coal per hr, and at full load, about 700 lb per hr.

LOCATION OF INTAKE

The first study of the site as shown on the plot plan, Fig. 1, indicated a number of possible locations for the circulating-water intake from the river, i.e., navigable slips on both sides of the property, frontage on the river along the established bulkhead line, or the piers constructed for coal-handling purposes.

The conventional design, calling for intake and discharge tunnels under the turbine room with the pumps located adjacent to the condensers, would have necessitated a substantial lowering of the substructure. Since the entire station is to be built on piling, depressing the elevation of the top of the piles was considered undesirable.

Both slips have some undesirable features for an intake. The upriver slip would have required bulkheading and backfilling, and extensive dredging would be necessary to provide and maintain a satisfactory depth of intake canal from the river. The water here is contaminated by inflow from several city sewers, making it a still less favorable location.

The plan of development called for the installation of two units on the downriver or south side of the site; hence if the pumping station were located on the north side of the site, it would be separated at some distance from the initial development and would have required considerable additional construction work not otherwise needed for the first two units.

The downriver slip in the adjacent dock is in constant use for loading and unloading ocean-going ships. An intake located in this area might at times be blocked or restricted by vessels tied up at the marginal wharf. The yard area between buildings and the downriver edge of the wharf is to be used for railroad tracks over which emergency rail deliveries of coal will be handled. Interference with this layout by an intake structure was considered undesirable.

With four units installed ultimately, an outlet tunnel carried through the structure could be arranged to discharge into either the upriver or downriver slip. This plan had many advantages and eliminated either slip as an intake channel.

If the intake were located at the bulkhead line, interference with flow would be experienced from the piers and from barges moored at the coal-handling equipment.

After a review of these conditions, another alternative was considered, namely, locating the intake on the end of the coal piers which extend out from the bulkhead line some 450 ft into the river to the established pierhead line adjoining the ship channel on the Pennsylvania side of the river. The ship channel maintained by the government is now 35 ft deep and is being developed to a depth of 37 ft as a part of the improvements to the Port of Philadelphia.

A usual design would call for long submerged intake conduits leading to the circulating pumps located close to the condenser. Extreme low water at the site is about $9^1/_2$ ft below mean high water, and about 15.35 ft below flood. To provide ample submergence for such intake tunnels would require laying of sub-

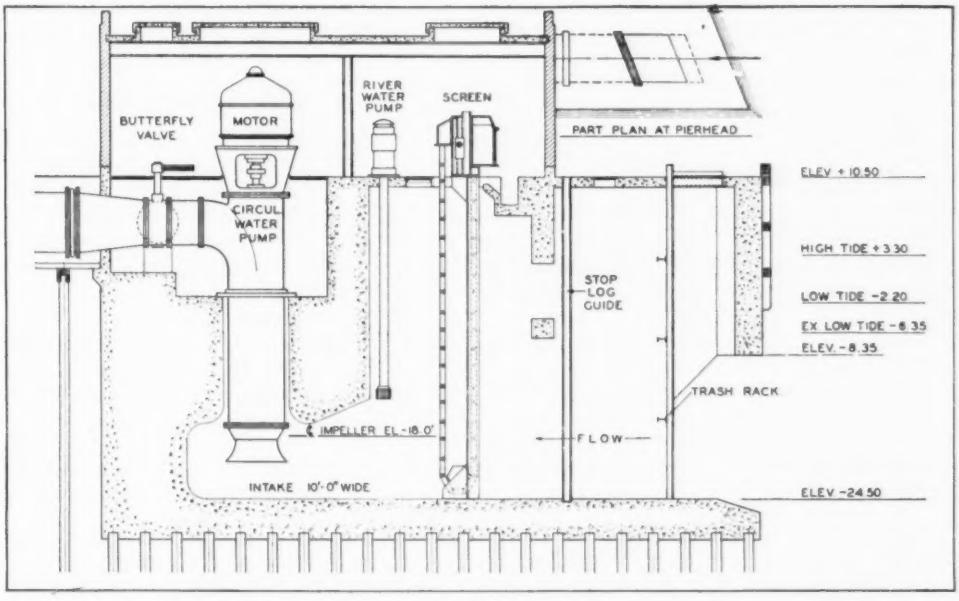


FIG. 3 ARRANGEMENT OF INTAKE AND PUMPING UNITS

aqueous pipe or construction of a cast-in-place conduit inside a long and costly sheet-pile cofferdam. Subaqueous pipe was ruled out early in the design stages because of the closely spaced pile construction necessary for supporting the pier itself.

The cost of a cofferdam in which to construct cast-in-place conduits appeared so high that an alternate method was sought. After a careful study of pumping heads, reliability of long pressure conduits, and the co-ordination of pump and condenser operation, a scheme was developed locating pumps at the pierhead connected to the condensers through pressure conduits 650 ft in length. Estimated construction costs were so greatly in favor of the latter design, with operating cost and reliability so little affected, that it was immediately adopted. The conduits are to be placed on the relieving platforms of the pier and wharves under the coal-handling machinery and tracks. In the yard and below the floor of the boilerhouse and turbine hall, the conduits are carried on pile-supported cradles. General excavation in the building area was not substantially increased and much subaqueous work was eliminated.

Two coal piers, shown in Fig. 1, are required in the ultimate development, although only one pier is planned for the initial project. With a pair of pumps for each generating unit, two such installations could be placed at the end of each pier and thus conform to the general plan of development. A general arrangement of the pumps and intake passages is shown in Fig. 3.

The intake racks are arranged so that they present a uniform, smooth face, parallel to the pierhead line. At Southwark Station, the pierhead line and the bulkhead line are at an angle to the center line of the piers. This construction requires the rack bars to be skewed, making the clear face of the intake structure parallel to the channel of the river where the high-velocity tidal currents should assist in keeping the racks free from trash.

The concrete deck of the pier is carried out beyond the intake and forms a skimmer wall to fend off floating debris and ice. The construction is rugged and provides sufficient strength to withstand forces exerted by mooring barges and other vessels. Mechanical rack-raking and cleaning devices are provided to remove trash from the racks. Disposal channels are provided where this refuse can be discharged or removed. A vertical traveling intake screen 8 ft wide and 35 ft deep is provided ahead of each pump.

Vertical-shaft high-speed-type pumps are placed in separate intake channels. Each pump is connected to an individual discharge conduit, and an automatic check valve of the butterfly type is located between the pump-discharge flange and a taper section leading to the pressure conduit.

It was possible to segregate each pair of pumps serving one condenser in a separate pump house and intake structure. No cross connection of the pump-discharge lines occurs except at the condenser-inlet water box where two separate circular connections are made. Rubber expansion joints are included at both ends of each conduit.

OUTLET CHANNELS

Returning the circulating water to the river introduced additional problems due to conditions peculiar to the Southwark site. The marginal wharf and the bulkhead on the downriver portion of the site are on Philadelphia Electric Company property, but are owned by the United States Government and constitute an easement on the Southwark site.

The discharge of 300,000 gpm or more into this navigable slip had to be carefully studied. The effect on the existing marginal wharf on the Southwark site, upon docking and unloading of ocean-going vessels in the slip, upon the existing Quartermaster pier structures, and upon the silting of the slip between the Southwark wharf and the Quartermaster pier, all had to be considered.

Two series of model tests, described later, were undertaken, the first to establish the means of dissipating the energy in the discharge water; the second to extend such studies to the detailed design features, to the problem of distributing the discharge in the adjoining slip, avoiding heavy local currents, and to the effect of this discharge upon the existing silting problem in the slip.

RECIRCULATION STUDIES

A further study was required of the possible recirculation of warm condenser-discharge water back into the intake on the ends of the piers. The structures on the shore side of the bulkhead line are of solid construction, with the exception of the marginal wharf on either side of the Quartermaster slip. This portion is of open piling construction, but only 40 ft inshore from the edge of

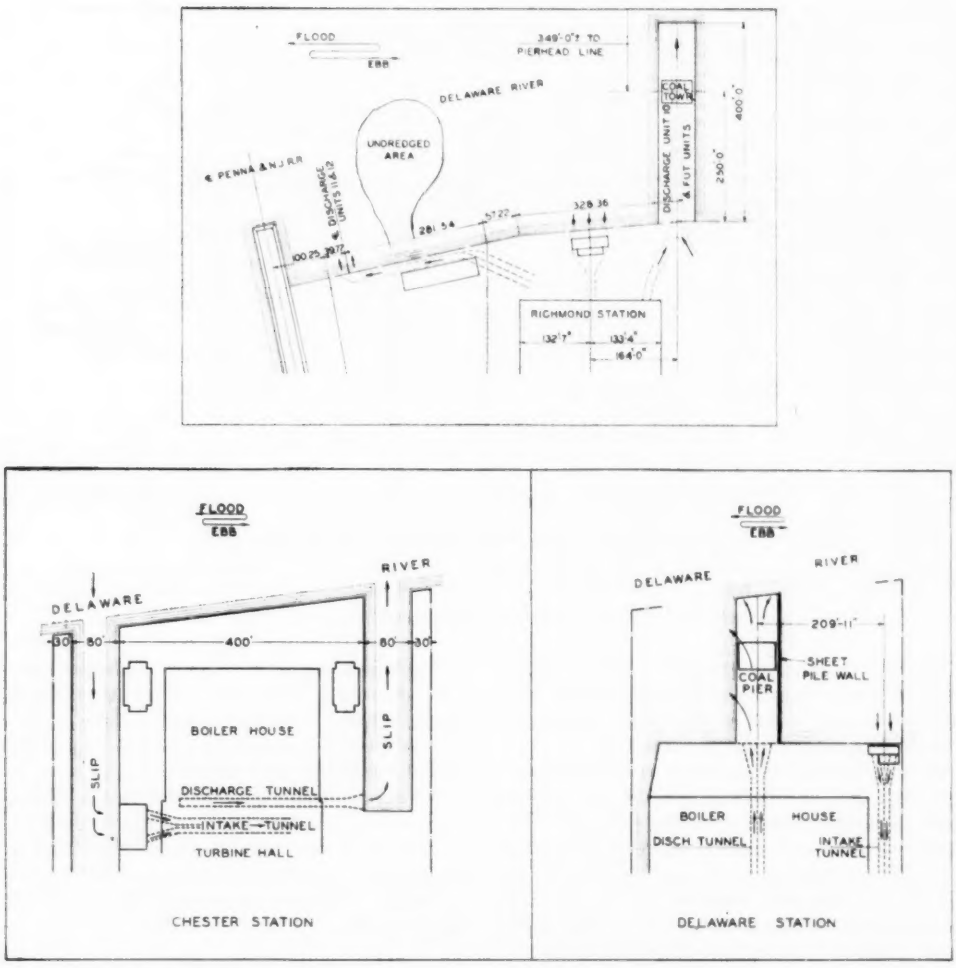


FIG. 4 GENERAL ARRANGEMENT OF CIRCULATING-WATER SYSTEMS AT RICHMOND, DELAWARE, AND CHESTER STATIONS

the wharf. The rest of the property is filled land cut off from any river flow. Riverward of the bulkhead line, the new coal piers and the Quartermaster pier are of open construction, as required by the United States Engineer Office, to reduce the silting effect and avoid local high velocities adjacent to the pierhead.

Referring to the circulating-water conditions at the Richmond, Delaware, and Chester Stations, each has a different physical arrangement of the intake and discharge works, Fig. 4. Operating records of the three stations were studied in relation to total output, condenser vacuum, river-water temperature, and tide conditions. At Richmond Station there is evidence of some recirculation, and the condenser-inlet water on downriver tides showed an increase of several degrees above the mean river-water temperature. There is a corresponding decrease in condenser vacuum, and while there is no impairment in station capacity, it is evident that some slight reduction in economy takes place during certain tide conditions.

At Delaware Station, the discharge is carried under the coal pier. The downriver side of this pier has been bulkheaded off with steel sheet piling to prevent recirculation of warm water back into the intake located on the bulkhead downriver from the discharge tunnel. The analysis of Delaware Station performance shows that there is some slight recirculation, but negligible in amount, as compared with the conditions at Richmond.

At the Chester generating station the intake water is drawn rom the upriver side, carried through and discharged on the downriver side of the station. Both intake and discharge channels act as slips for handling coal barges and are physically separated a distance of 400 ft. The water must travel in from the river about 300 ft to reach the intake, and on the discharge side it must go slightly more than 300 ft before it reaches the main river. The observations on this station show that there is no measurable recirculation.

Various theories were advanced with regard to the behavior of the water in the Delaware River. A study of the tide conditions and tidal currents[3] indicated that while the fresh-water discharge in the Delaware River averaged about 12,000 to 14,000 cfs, the maximum upriver flow, due to tide, reached about 150,000 cfs. The downriver flow, due to tide and fresh-water discharge, is about 130,000 cfs maximum, but is of a longer duration. A maximum channel velocity of about 2 fps upriver or downriver can be expected at times of mean tide.

The surveys made by the United States Engineer Office in Philadelphia over an extended time, at different periods of the year, under different weather, wind, and tide conditions, showed that these velocities were sufficient to cause a thorough mixing of the water in or near the channel. In the many thousand observations taken, the measured difference in temperature between the surface and the bottom of the channel rarely exceeded one degree F, and except for occasional isolated instances, never exceeded

[3] "Tidal Hydraulics," by Brig. Gen. George E. Pillsbury, U.S.A. (retired), published by Corps of Engineers, U. S. Army, 1940.

two degrees F. This showed clearly that there was no stratification of the water in the Delaware in the vicinity of Philadelphia and adjacent to the channel.

Field Temperature Measurements

Further investigation was needed to determine the behavior of warm water discharged from the condensers and to fix the distance required for this water to travel before it blended completely with the main flow of the river. The Chester Station offered the best opportunity to investigate this matter, since it simulates to some degree the proposed design of the discharge channels at Southwark.

It was decided to make temperature measurements in the discharge channel and the area in the river beyond the bulkhead line. Observations were made at intervals of about one hundred feet in this area on traverse lines, as shown in Figs. 5 and 6.

Special thermocouples were prepared to give temperature readings at different elevations, and check readings were made with a separate thermometer held one foot below the surface, against which the thermocouples could be given an approximate calibration at every station where measurements were made.

Fig. 5 shows the differences between mean river-water temperature and the temperature measured at various depths on an incoming tide. Fig. 6 shows another analysis of these same relations on an outgoing tide. The cross-section views demonstrate that the warm water has a very definite tendency to rise to the surface and spread out in a thin layer which gradually merges with the river flow.

These tests were run between July 28 and August 5, 1941, when the Delaware River temperatures were between 82 and 84 F. It will be noticed that the discharge-water temperature is approximately 8 to 10 degrees above the intake temperature. The air temperature on July 28 reached a maximum of 102.5 F and on July 29, a low of approximately 78 F. It is interesting to note that the river-water-temperature observations shown in Fig. 2 reach a maximum of 80 to 85 F during the latter part of July and the first part of August, and that they go as low as 35 F in December or January. The tests made at Chester were, therefore, comparable to the mean high-temperature conditions to be expected on the river.

The observations showed conclusively that the warm water

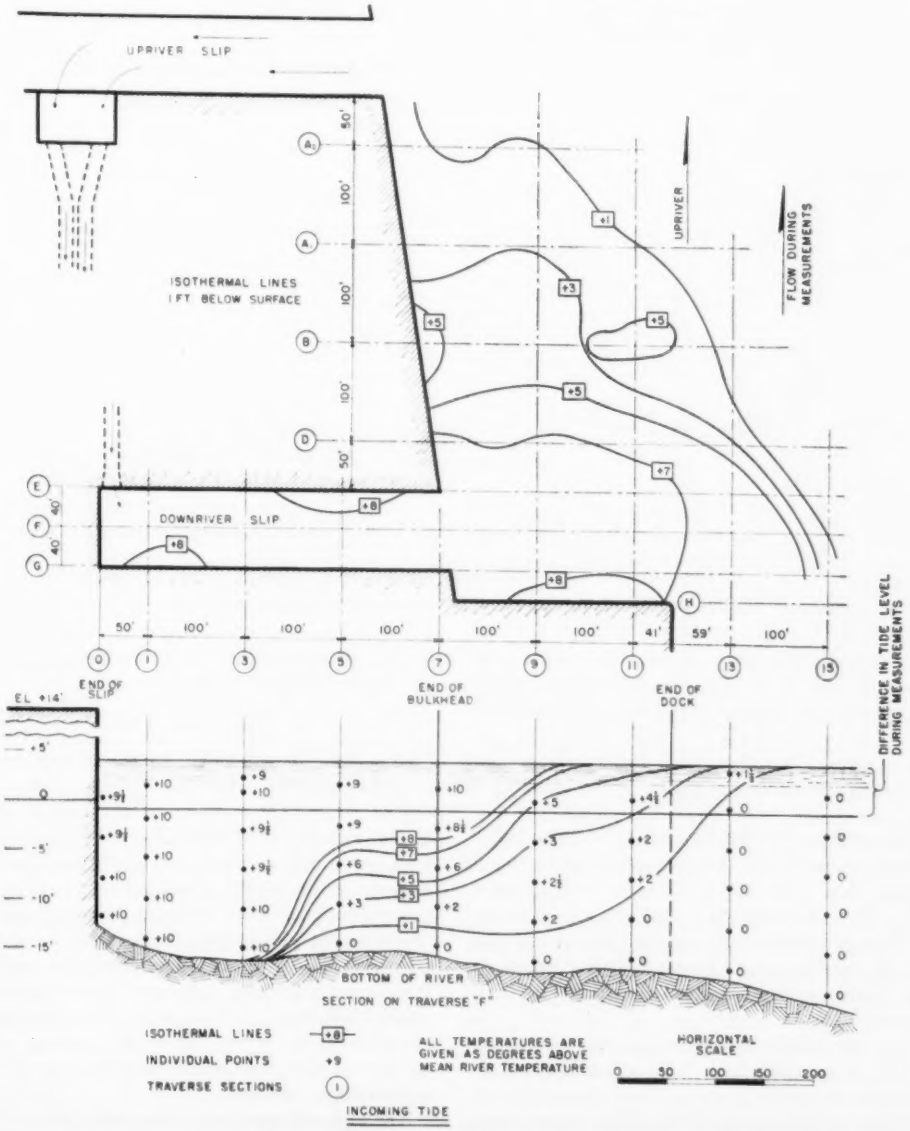


Fig. 5 Temperature Measurements at Chester Station on an Incoming Tide

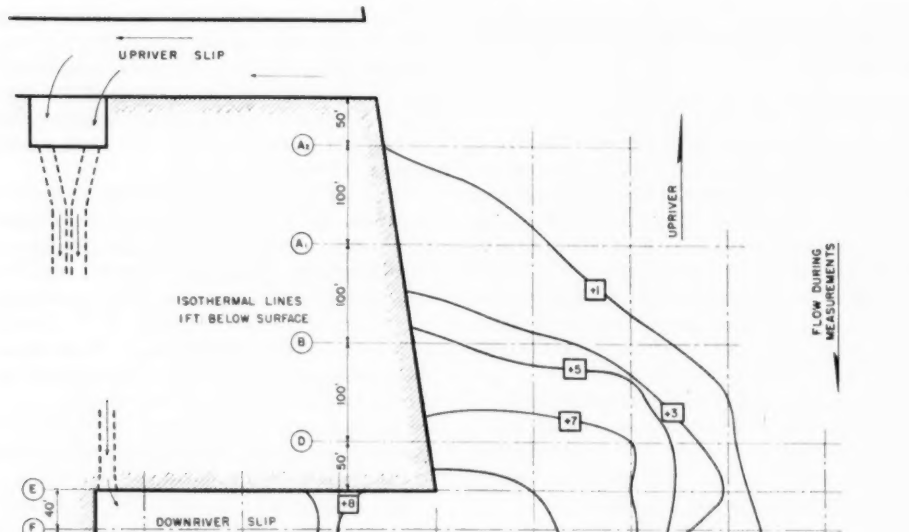


FIG. 6 TEMPERATURE MEASUREMENTS AT CHESTER STATION ON AN OUTGOING TIDE

rises to the surface within 300 ft from the tunnel outlet, and by the time it was 400 ft beyond the bulkhead line, it approached the mean river-water temperature and only a thin surface layer remained.

Based on standard tables, the difference in density of the water in the temperature range observed at Chester is less than 0.1 lb per cu ft.

Relating these observations to the Southwark Station design, it is felt that the warm water will rise to the surface by the time it reaches the bulkhead line, some 450 ft from the tunnel outlet. The thin layer of warm water extending out in the river should pass through the open pile construction of the piers at low tide, or be deflected into the upriver or downriver flows well above the deep intake for the circulating pumps, located at the ends of the piers near the ship channel.

As a result of these investigations, the final arrangement was fixed as shown in Fig. 3, with the floor of the intake located approximately 22 ft below mean low water. From this point out, the river bottom takes a gradual slope to the 35-ft-channel depth. The discharge of the condenser-outlet water into the slip adjoining the Quartermaster pier could then be considered independently of the recirculating problem.

PUMP OPERATING CONDITIONS

Once the general design of the station was determined, the operating conditions for the circulating-water system could be investigated in detail. As previously outlined, the Delaware River in the vicinity of Philadelphia is really a tidal estuary. The fresh-water flow under normal conditions amounts to less than 10 per cent of the tidal flow, and hence, can be neglected in so far as the relative location of intake and discharge passages is concerned. The water at Philadelphia is free from sea-water contamination. Occasionally during the summer months and with extreme low fresh-water inflow, the water at Chester (approximately 15 miles below Philadelphia) shows a brackish tendency but can still be classed as fresh water. Materials suitable for fresh-water applications can therefore be used and the more expensive marine-type construction avoided.

The high and low fresh-water inflow does not cause more than one to two feet variation in the Delaware River levels at Phila-

delphia. The principal influences are due to tidal flow and to wind conditions in combination with the tide. A study of the river-level variation was made on the basis of information secured from the United States Engineer Office in Philadelphia, as well as from company records and referred to the United States Coast and Geodetic Survey Datum being used in the design and construction of the station.

The total variation between maximum and minimum water level is 15.35 ft. Normal variation is approximately 5.4 ft, corresponding to the difference between mean high tide and mean low tide. The extreme flood level recorded was elevation plus 9.0. The mean high tide is elevation plus 3.2. Extreme low tide is minus 6.35.

The center line of the pump-discharge conduits was set at elevation plus 5.5, placing the bottom of the conduit at about mean tide level. The surface of the pier is at elevation plus 10.5, but the walls, doors, and other entrances to the pumping station and to the station itself are held slightly higher.

An unusual factor, influencing the elevation of the floor levels in the station, was the location of the New York Shipbuilding Company directly across the river. A recording gage installed at the Southwark site was in operation during the launching of the U.S.S. *South Dakota*, June 7, 1941, and showed a reading of approximately two ft above high-tide level due to waves set up by this large battleship.

The intake and screen losses were established for various discharges, based upon manufacturers' guarantees and upon the operating experience of the Philadelphia Electric Company. The conduit between the pumping units and the condensers was analyzed for head loss. An estimate was prepared on the use of two conduits, each 78 in. ID, with a normal velocity of 5 fps.

The head loss through the condenser was taken from the manufacturers' guarantees and checked against experience with other types of condensers for large generating units. The outlet from the condensers was studied in relation to the arrangement of the equipment in the generating room, the floor levels, and also the foundation conditions under the generating station.

It was found desirable to raise the condenser sufficiently to maintain a single floor level at elevation plus 11.0 in the generating room. Due to the very large capacity of these units and the size of the condenser, the top of the condenser-outlet water box extended a considerable distance above extreme low water.

With outlet temperatures which could be expected during summer months, calculations showed that the free water surface should be not more than 27.5 ft below the top of the discharge water box of the condenser. This introduced a definite head loss at all times when the tide level was below the elevation corresponding to this free water surface. It was also necessary to provide some sort of a seal which would prevent breaking the water column in the downpipe of the condenser, and yet not impose an excessive head loss when the tide elevation approached the normal free water surface.

Head-Duration Curves

To arrive at an economic design, a study was made of the net effective head available on the pumps at all conditions of tide. Curves and data, Fig. 7, were secured from the United States Engineer Department on the variation of water level for mean, spring, and neap tides. The occurrence or frequency curves for the various tide ranges were also related to time. In this manner, a static-head-duration curve, Fig. 8, was derived which indicated that the condenser could be raised substantially without any excessive increase in pumping costs throughout the year.

With the friction-head values already determined for the intake, the conduit, the condenser, and the discharge passages, a series of head-discharge curves was prepared for the various general conditions, namely, maximum head, minimum head, normal annual average, and normal maximum head. These are shown in Fig. 9. The intersection of these curves with the desired value of 152,000 gpm determined the estimated range in head at rated discharge and gave a nominal rating for each pump of 76,000 gpm at 25 ft total head. Due to the tide variations and other conditions, the normal daily variation with two pumps in operation is expected to range from 21 ft up to 27 ft. Under extreme low-water conditions where the static-head loss at the outlet of the condenser will be a maximum, the pumps will have to operate under a head

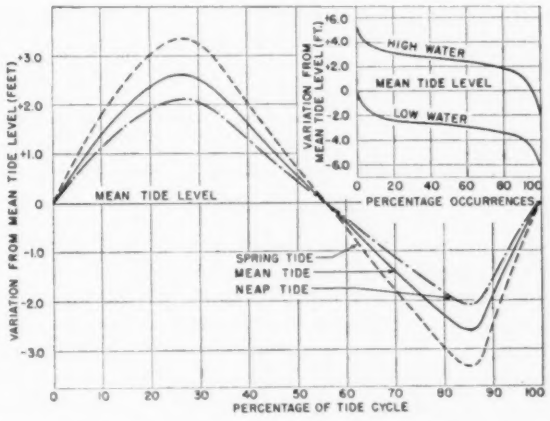


Fig. 7 Tide Variations and Occurrences at Philadelphia

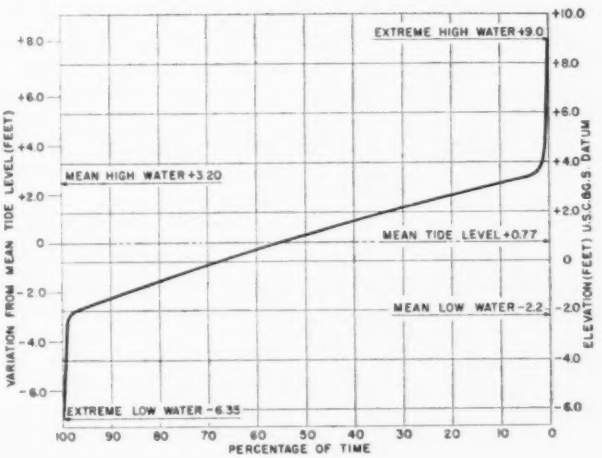


Fig. 8 Static-Head-Duration Curve

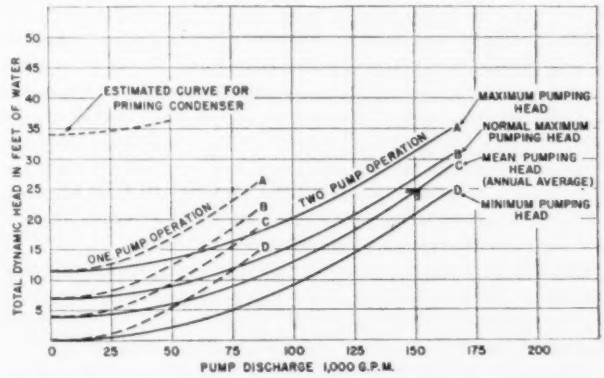


Fig. 9 Head-Discharge Curves for Circulating-Water System

of 31.5 ft. The records available in the City of Philadelphia and the United States Engineer Office showed that extreme low water could be expected to occur less than 0.5 per cent of the time, and the normal maximum head of 27 ft is not expected to be exceeded for more than 2.5 per cent of the time. The minimum head which occurs when the tide is sufficiently high to submerge the sealing weir will probably not occur more than 1 or 2 per cent of the time.

Pump Characteristics

Due to the location of the pumping units at the end of the coal piers and immediately adjacent to the deep-water channel, it was possible to arrange the structure to utilize the full value of submergence of the pump impellers and thus permit the use of high-speed pumps. The normal submergence obtainable at mean tide level is approximately 18 ft. Even at extreme low tide the submergence will be on the order of 11 to 12 ft. This gives an additional safety margin against the possibility of excessive accumulation of trash on the intake racks and screens, as a drawdown in the suction chamber of as much as 6 or 8 ft will still give a substantial seal over the suction of the pump.

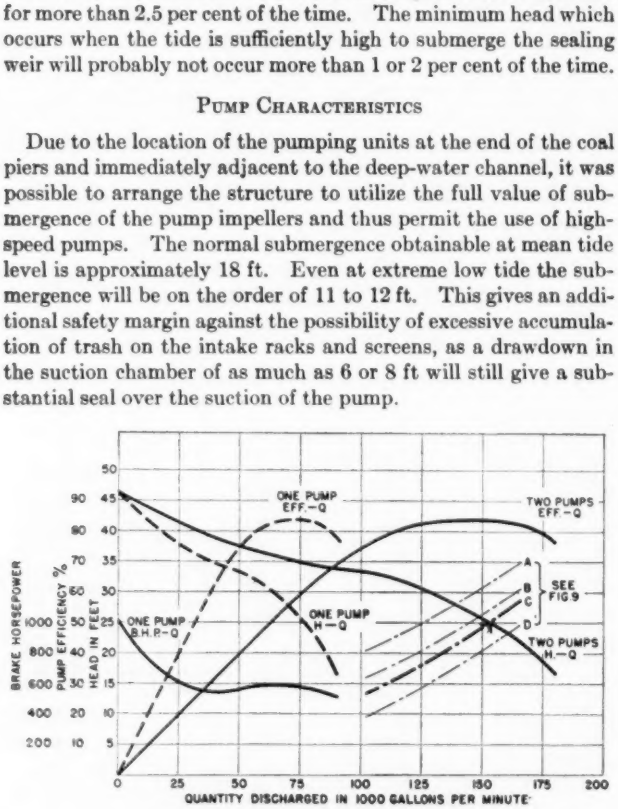


Fig. 10 Pump Characteristic Curves

Advantage has been taken of design improvements to insure against difficulties with the pumping units by providing for ample width of water passage and sufficient submergence to have the pumps operate well above the cavitation limit.

A preliminary investigation was made with the co-operation of the various pump manufacturers, the individual practice of each pump builder being studied prior to the issuance of the specifications. The maximum and minimum widths of water passages, the distance from the bottom of the suction bell to the bottom of the intake, the relation of the bell to the walls of the passage, and the degree of submergence desired were all studied.

It was finally decided to set up limits of width, depth, and submergence which would impose no penalty on any of the manufacturers. Almost without exception, it was possible to allow more liberal dimensions than they required, and, under all tide levels, a substantial margin of safety against cavitation was indicated.

Since intake conditions have a very marked effect upon the performance of propeller pumps, as well as axial-flow and centrifugal pumps, it was decided to require, as part of the pump contract, that the manufacturer conduct complete model tests, in his own experimental laboratory, on a unit similar to the full-scale unit and under all conditions of head, discharge, and inlet level.

It was further decided to insure that all features of the hydraulic design of the intake and of the pumping unit were suitable for Southwark conditions by requiring the completion of the model tests and their approval by the power company before the manufacturer can proceed with the fabrication of the main pumping units.

These pumps will be connected to long conduits, and water measurements can be made with a high degree of accuracy. The right was retained by the power company to make final acceptance tests in the field, even though the model tests should indicate that the performance of the unit would meet the contractual requirements.

To prime the condenser automatically without the necessity of using an ejector or other similar device, it was assumed that a discharge of about one third of the normal flow would sweep out the air in the discharge water box and establish the siphon effect. This was confirmed from the experience at the existing stations of the Philadelphia Electric Company system. An approximate water-requirement curve for priming was included in the pump specifications.

The pump characteristics proposed by the successful bidder are shown in Fig. 10.

Cavitation

Impeller submergence becomes increasingly important as the specific speed of the pump is increased, particularly where wide fluctuations in suction levels exist. The research work, carried out on pumps and turbines recently, has shown that the relation between the suction lift or positive suction head and the total effective head of the pump can be set up in the simple relation, known as "sigma," in

$$\sigma = \frac{(H_b - H_{vp}) - H_s}{H_0}$$

where

σ = cavitation factor
H_b = barometric head, in feet of water
H_s = static head, measured from center line of impeller to free-water surface or its equivalent
H_{vp} = vapor pressure of water at maximum temperature to be expected in intake
H_0 = normal effective head on pump

Cavitation tests on a model pump can be made through varying the suction and discharge pressures simultaneously by the same increment of head, thus giving the effect of raising or lowering the pump with respect to the suction level. So long as the pump impeller is submerged sufficiently to maintain the required absolute pressure on the under side of the blades, the water will remain against the blades and there will be little or no change in the pump performance. As the cavitation limit is approached, the water tends to depart from the blade, causing local areas to be alternately filled with water vapor or to collapse. The pump characteristics will then change and, as the condition is aggravated, will cause excessive loss of efficiency and discharge.

This critical "sigma" value, representing the point at which the water passing through the pump impeller departs radically from its normal flow pattern, is the value to be used in fixing the suction lift of the pump or in determining the required submergence of the impeller below suction level.

In selecting the pumps, it was found in many instances pumping units were specified for the maximum possible head conditions. With centrifugal pumps of low specific speed, a change in head would have only a small effect on the discharge. The efficiency curve is flat and the loss of efficiency, due to operation at substantially lower heads, does not impose an excessive penalty.

With high-speed pumps of the axial-flow or propeller type, the shape of the efficiency curve is much steeper than with centrifugal pumps, and the range of high efficiency is much narrower. The head curve tends to be flatter and, since the total head is low, a small change in head usually amounts to a substantial proportion of the total pumping head and causes impairment in

discharge. It may also cause the pump to operate at a point far beyond the maximum efficiency. The loss of efficiency alone is important but it is also most desirable to avoid running such pumps beyond their best efficiency, since the tendency toward local cavitation, vibration, and other difficulties becomes more pronounced.

By giving the manufacturer complete information on the expected operating requirements, the range in discharge and range in head for normal conditions, and by requiring sufficient experimental work to prove out the proposed designs, it is hoped to have as complete freedom from operating difficulties from this source as possible.

Check Valves

Between the pumping units and the conduit it is necessary to have some form of shutoff valve. After a study of the operating requirements, it was decided to install hydraulically operated butterfly or pivot valves, which could be opened or closed sufficiently fast to permit them to operate as check valves. This avoids the necessity of draining and refilling the discharge lines each time the power is cut off from the pumps or during emergencies. The butterfly valves will be arranged with a separate oil-pressure system and an accumulator tank which will have a sufficient supply of power fluid to close the valves upon a power failure, hold them closed, and reopen them upon the restarting of the pumps. Such controls are quite common in waterworks and hydroelectric practice and have been utilized in all parts of the country with very low maintenance requirements.

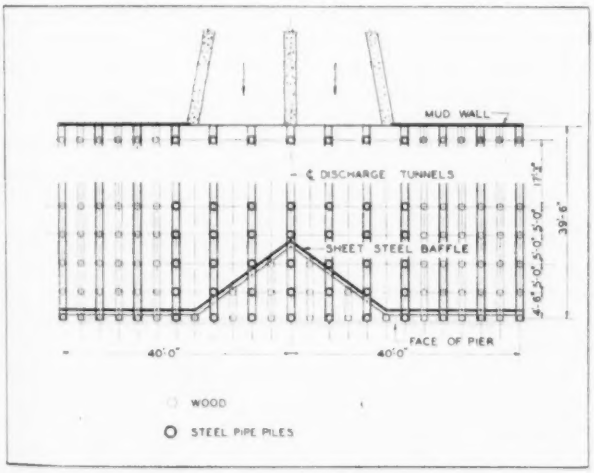


Fig. 11 Preliminary Design of Outlet Baffle

The practice of rating the circulating pumps as a function of the diameter of the discharge elbow tends to be misleading. With the pumps selected for this project, the outlet diameter was reduced to 54 in. and the butterfly valve connected directly to the pump discharge. Between the pump discharge and the 78-in. conduit an expanding tapered section is provided which has a total angle of flare not exceeding 10 deg to insure the recovery of approximately 80 per cent of the velocity at the throat of the valve.

The controls for these valves will be interconnected with the controls for the pumps. Induction-type motors are being used for driving the pumps and liberal torque allowances have been made for starting the unit. It is not expected that it will be necessary to open the check valve in advance of starting the pump.

On shutting down the pump, the check valve will be closed automatically, making the first part of its travel at a rapid rate and the last part at a much slower rate. This will provide against excessive backward flow through the pump and will retain most of the water in the conduit. The check valve itself will act to relieve any surge due to water hammer, and timing adjustments can be made to permit the valve to go through each part of the closing stroke at any desired rate.

Pump-Discharge Conduits

In selecting the type of pipe for the conduit between the pumps and the condenser, consideration was given first of all to steel pipe which could be encased solidly in concrete. The superimposed load of the railroad tracks and other equipment would be carried by this reinforced concrete to the foundation piles.

Alternative plans were studied, using steel pipe with flexible couplings laid in a concrete trench and backfilled. Wrought-iron pipe and cast-iron pipe were also considered, as well as reinforced-concrete pressure pipe of the "lock-joint" type used for many years in water-supply practice.

The friction head losses for each type of conduit were carefully reviewed, and it was found that the differences were not in excess of 0.5 ft at maximum discharge. An analysis made of the installed cost showed for Southwark conditions that reinforced-concrete pressure pipe was the least expensive. Consideration

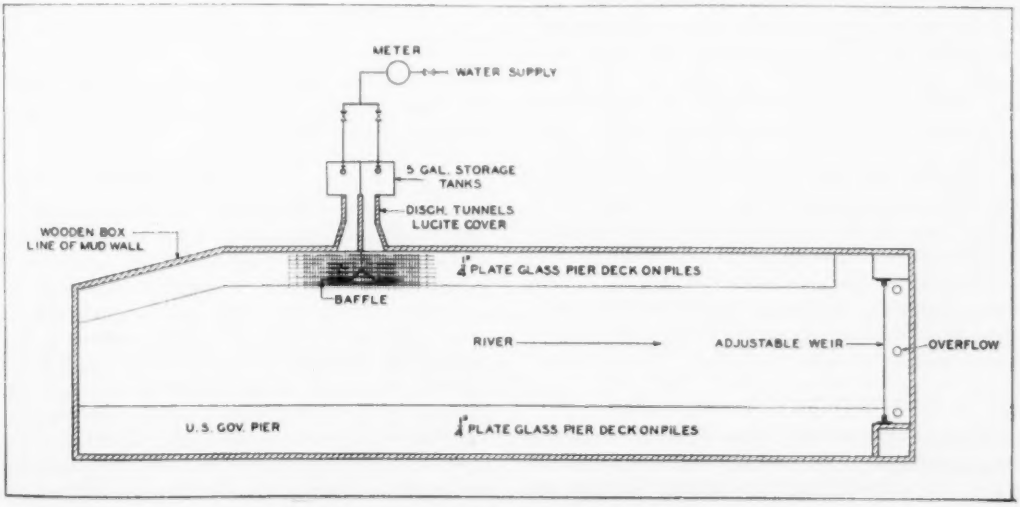


Fig. 12 Model of Outlet Works and Navigation Slip

was given as well to the relative difficulty of securing various types of material as a result of the defense program.

It was decided to use reinforced-concrete pressure pipe since it required a minimum of steel and prompt deliveries could be secured in the particular sizes needed. The fabrication of the pipe will be carried out on company property, a short distance away from the site. Each of the four individual conduits is 78 in. ID, arranged with access manholes at either end and with an air-release valve at the invert beyond the coal-handling tower. The pipe has a wall thickness of 7 in. throughout and has a nominal pressure rating of 50 ft. A steel reinforcing cage is cast in each section, as the continuous steel membrane used to seal high-pressure pipe was not considered necessary. Each line is approximately 650 ft in length and two such conduits are needed for each generating unit.

Outlet Model Test Program

The first part of the model-test program was devoted to the design of the outlet passage into the Quartermaster slip. The first model constructed for this study was to $^1/_{24}$ scale and consisted of an outlet tunnel, and the piling and deck immediately adjacent to it. It was found that the presence of the piles alone was not sufficient to break up high-velocity currents, but that a deflecting baffle, Fig. 11, would divide the flow and turn it through 90 deg in such a way that it was diffused through a longer length of piling, its velocity cut down to less than 1 fps, and the energy in the water at the tunnel outlet dissipated, so that no heavy currents were found beyond the face of the wharf. Following these tests, it was possible to secure the necessary government permission for rebuilding the bulkhead and marginal wharf.

A second model to $^1/_{100}$ scale, Fig. 12, was constructed to develop the final details of the design of this baffle and its relation to the silting problem in the adjoining slip, as well as to fix the limits beyond the tunnel outlet itself that must be paved or otherwise protected against wash from the discharge currents.

This second model-testing program has not yet been completed, but a description of the model itself may be of interest. The space between the two cutoff walls, adjoining the slip and the marginal wharves on both sides of the slip, is reproduced in detail. The piling has been included to scale for a distance equivalent to more than 100 ft on either side of the condenser outlet, and the outside line of fender piles on the full perimeter of the slip have been used to support the plate-glass cover corresponding to the pier deck.

The model is constructed of wood with the piles made of $^1/_8$-in-diam dowels. A weir has been located at a point beyond the bulkhead line and centered on the axis of the slip. The crest of the weir is adjustable to give the equivalent of either high-tide or low-tide conditions. The discharge tunnels have been reproduced to scale and are connected to separate sources of water supply, which can be regulated individually and give the equivalent of from one to four units in operation at any one time and with any combination of units in the respective channels. Since the design contemplates the connection of alternate units to the divided tunnel sections, the model can be operated at any condition which might be encountered in the ultimate development. Photographic recording of the test is planned, together with studies of the silting of the basin and the effect of the discharge upon the present filled section under the wharves.

Condenser Model

The design of the condenser water boxes is also the subject of an experimental investigation, particularly with respect to the outlet water box. In order to lead the discharge down to the sealing pool below the main floor at elevation plus 11.0, a design was proposed which would split the stream into two parts and carry them down to a common rectangular discharge opening at the bottom of the water box. The tube sheet is sealed by a U-shaped wall, and the discharge water flows over the top of the legs of the U.

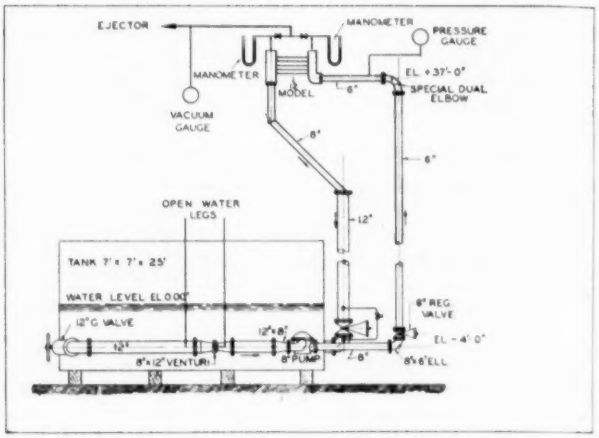


Fig. 13 Model of Condenser

A model of the condenser was constructed and set up for tests under conditions of temperature and vacuum corresponding to those encountered in actual service. Arrangements were made to determine the distribution of water flow in the various sections of the condenser by utilizing large-diameter tubes, each of which is equivalent to a number of smaller condenser tubes. An orifice piece is arranged in each tube to simulate the frictional resistance of the full-scale condenser tubes, and also to act as a measuring device to determine whether or not any wide variations in flow occur in the different portions of the condenser.

The model is constructed with transparent end covers and the flow can be observed through these windows. The complete series of tests had not yet been finished at the time that this paper was written, but the results will be made available at some later time.

The engineering design for the Southwark Station is being carried out by the Philadelphia Electric Company, with such assistance as they may desire from United Engineers & Constructors Inc., or other consultants on specific problems. The construction work is being done by United Engineers & Constructors Inc.

Appendix

Research Program

At the time the paper was written, portions of the research program had not been completed. It is now possible to release the results of these investigations.

Condenser Model

Tests made at the manufacturer's laboratory in co-operation with the Philadelphia Electric Company disclosed that the split-stream design for the outlet water box could not be used satisfactorily in this project. The width of passage needed to turn the water through 180 deg without inducing cavitation required more lateral space than was available in the plant. The larger mass of water contained in this water box, as compared with the more usual design, tended to introduce higher eccentric loadings on the turbogenerator than were considered desirable. The final arrangement for the outlet water box and also the down pipe, the barometric sealing weir, and the connection to the outlet tunnels is shown in Fig. 14. Some additional tests are scheduled to develop the final design of the connections to the inlet water box and to reduce the turbulence and air inclusion at this point to a minimum.

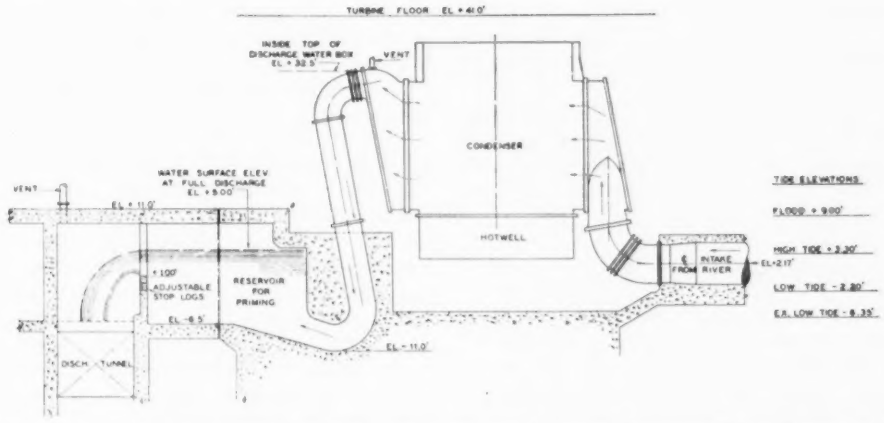


FIG. 14 GENERAL ARRANGEMENT OF CONDENSER AND BAROMETRIC SEALING CHAMBER, INCLUDING FINAL DESIGN OF OUTLET WATER BOX

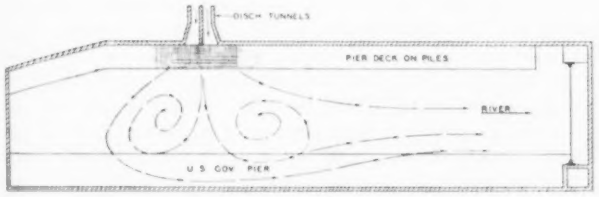


FIG. 15 FLOW PATTERN RESULTING FROM DIFFUSING SECTION IN TUNNEL AND USE OF PILING TO BREAK UP FLOW

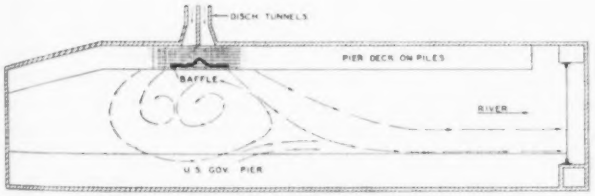


FIG. 16 FLOW PATTERN WITH V-SHAPED BAFFLE AS PROPOSED IN FIG. 11 OF ORIGINAL PAPER

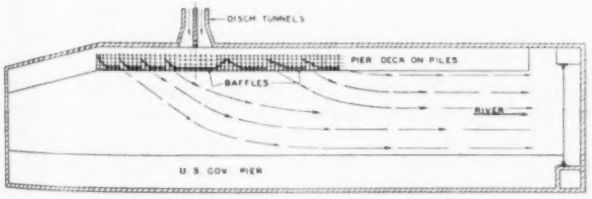


FIG. 17 FLOW PATTERN USING FINAL DESIGN AS SHOWN IN FIG. 18

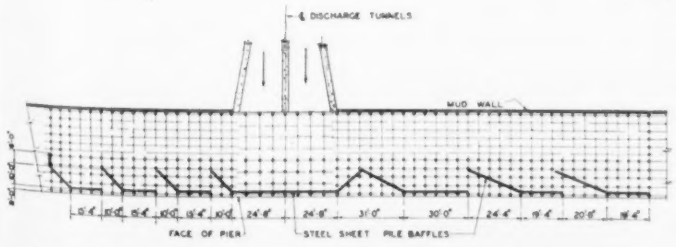


FIG. 18 DETAILS OF FINAL BAFFLE ARRANGEMENT FOR DIFFUSING FLOW FROM CONDENSER-TUNNEL OUTLET

INTAKE AND PUMP TESTS

The model tests in the pump manufacturer's laboratory have been completed in so far as the intake and physical setting of the pump are concerned. The original design with the bottom of the bell located 4 ft above the floor (approximately 0.65 times the bell diameter and about equal to the impeller diameter) proved superior to a greater distance (1 bell diameter) and gave a more stable performance curve, and from 1 to 2 per cent better efficiency in the operating range. The model tests also showed that the design based on a gradually accelerating velocity, with the water carefully guided into the pump suction, gave the best results. There was complete freedom from cavitation in the model throughout the required operating range. The final design closely approximates that shown in Fig. 3 of the paper.

TUNNEL-OUTLET MODEL

The tunnel-outlet model proved that practically all the original ideas concerning the behavior of the water in the Quartermaster slip were in error. Tests with the diffusing section alone and with dependence placed upon the piling to break up any heavy concentrations of flow showed that this scheme was most ineffective. Fig. 15 is a simplified diagram of the flow pattern with this first arrangement. Heavy currents swept across the slip and cut under the government pier.

The second series of tests was based upon the design shown in Fig. 11 of the paper. There was some reduction in the intensity of the flow concentrations, and the high-velocity currents under the government pier were not as pronounced. There was a very large primary and secondary eddy, as indicated in Fig. 16, which would have caused heavy depositions of silt in the navigable section of the slip.

The final design, adopted after more than 40 separate experiments, gave the flow pattern shown in Fig. 17. There were no heavy currents across the slip under simulated high- or low-tide conditions and the outflow water was distributed uniformly across the 270 ft of length needed for the baffle section. The design is indicated in greater detail in Fig. 18. The baffles are to be of interlocking steel sheet piling driven in the pattern shown. The section opposite the tunnel outlet is closed off completely and the water made to pass under the wharf platform. In this manner much of the energy of the water is dissipated, because of the turbulence caused by the wood piles and the inward projecting wings of the baffle.

Color moving pictures were taken of the three basic proposals at simulated high- and low-tide conditions with

exaggerated velocities and with the flow scaled down to maintain a constant Froude number. Dye was injected into the tunnel sections and the progressive development of the flow pattern could thus be recorded.

All tests of the final design showed a most satisfactory distribution of flow, as well as complete elimination of concentrated eddies and heavy currents. Formal approval was secured from the governmental agencies concerned and construction of these deflecting baffles is now under way.

Discussion

W. E. Caldwell.[4] The dual-pump arrangement described by the authors is very commendable in that it affords service reliability and high availability for the main unit, in addition to other advantages of an operating nature. In some plants with this arrangement and divided condenser water boxes, alternate halves of the condenser may be cleaned with the units in service. The high summer water temperature probably accounts for the large pump capacity installed, as this factor is an important influence in choosing the size of the condensing plant. However, for a number of months during the year, the circulating water is cold, and the flow may be materially reduced without appreciably impairing the vacuum in the condenser.

It is common practice in some installations to provide variable-speed (or two-speed) drives on the circulating pumps in order to save pumping power during the cold weather. No mention was made of variable-speed operation in this installation, and it may be possible that such provision has been made. The height of the condenser and water-box discharge, with respect to low water, handicaps low-speed considerations, since the occasional low tides, with incomplete siphon recovery, would necessitate undue operating vigilance by the pump attendants to avoid loss of circulating water. While it may be possible to operate one pump on the whole condenser with some saving in power, it is a less attractive method, since the change in head-volume relations results in operation at an unfavorable point on the efficiency curve. Furthermore, reliability is sacrificed, since the entire machine is dependent upon the single pumping unit.

Experience indicates that with the water-temperature conditions reported in the paper, there is economic justification for reduced-flow operation, at least 4000 hr per year.

With induction-motor drive, the choice of the low speed depends upon the winter water temperature and the number of poles required for high-speed operation. With water temperatures indicated in the paper and favorable hydraulic circuit, economic considerations would probably establish the low speed at about 60 per cent of summer speed. At 60 per cent speed, the head on the pump drops to 9 ft, assuming full siphon recovery, resulting in a saving in pumping power of about 700 hp per unit.

There would be a slight reduction in vacuum during part of this time which would be largely offset by increased condensate temperature for the entire period which, combined with the inability of the turbine to profitably utilize extremely high vacuum, practically amounts to a thermal standoff. Aside from the large power saving, resulting from reduced-speed operation during the cold-water season, lower maintenance on pump and condenser tubes follows the reduction in water velocity.

The large capital value of the power-saving possibilities with reduced-speed operation would seem sufficient to exceed the cost of correcting almost any foundation problem necessary to permit more complete siphon recovery.

Authors' Closure

In reply to Mr. Caldwell, the circulating pumps at Southwark Station will not be connected to variable-speed drives. Consideration was given in the design of the circulating-water system to the possible use of variable-speed drives, or adjustable-blade propeller-type pumps. Of the two methods for varying circulating-water discharge, the latter appeared to be the more advantageous. Both schemes, however, were discarded when investigation indicated that operating savings were insufficient to pay an adequate return on the added investment.

The low-pressure turbines at Southwark Station are of the double-flow type. The blading in the last stages has been carefully designed to eliminate crowding. These machines will, we believe, profitably utilize the extremely high vacuum, made possible by the use of large quantities of cold river water during the winter months. Rather than level off the vacuum at a point obtained by two-pump operation and summer water temperatures, the saving in the coal rate together with the elimination of a comparatively costly variable-speed drive and control will, viewing the situation broadly, more than compensate for the additional power used at the pumps. Increased condensate temperature is, of course, only obtained at the sacrifice of working the turbine against a higher back pressure with the resultant drop in over-all efficiency.

As has been indicated, it will be possible to carry a substantial load on the turbogenerator with one circulating pump. Under these conditions, it is true that the pump is working to the right of and below the best point on the efficiency curve. However, one-pump operation will be resorted to only in the event of pump failure, which with this type of equipment is a remote possibility.

[4] Mechanical Plant Engineer, Consolidated Edison Company of New York, Inc., New York, N. Y. Mem. A.S.M.E.

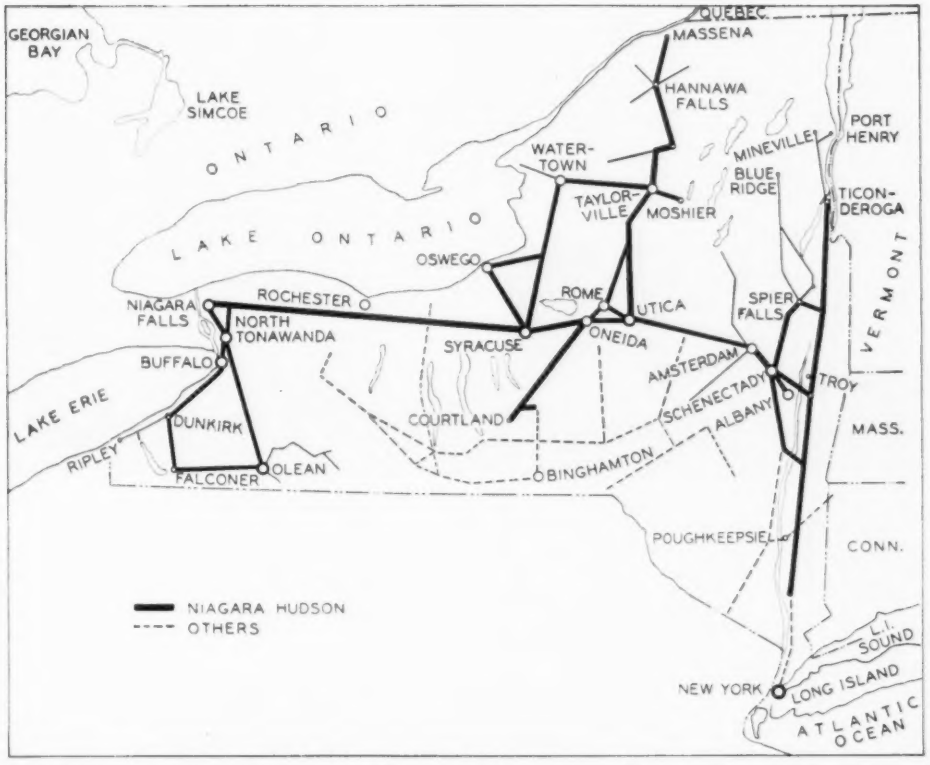


FIG. 1 MAP SHOWING CENTRAL LOCATION OF OSWEGO STEAM STATION ON NIAGARA HUDSON TRANSMISSION SYSTEM

Advanced Design—Original Features Embodied in New 160,000-Kw Oswego Steam Station

BY N. R. GIBSON[1] AND H. M. CUSHING,[2] BUFFALO, N. Y.

Advanced design is the keynote of the new 160,000-kw Oswego Station of the Niagara Hudson Power System. In the present paper, the many outstanding and original features incorporated in this two-unit, one-boiler-per-turbine plant are described and illustrated. Among these are the 80,000-kw single-spindle condensing turbine for 1250-psi 900-F steam; soot blowers which use 250-lb compressed air for the blowing medium to save 1250-lb steam, and which operate automatically in succession on a preselected schedule; electric couplings of the eddy-current type for control of fan speeds; pilot operation of boiler safety valves for obtaining better protection and reduced maintenance; acceleration of the main generator for synchronous-condenser operation by motorizing its direct-connected exciter.

THE normal growth of the Niagara Hudson System is in the order of 40,000 kw per year. Its annual peak is in excess of 1,500,000 kw. About two thirds of the energy used is generated by hydro and one third by steam. Its high-voltage transmission lines extend from Buffalo to New York City through the industrial sections of New York State, as shown in Fig. 1. The System is operated as three divisions, Eastern, Central, and Western. The yearly growth of the 60-cycle loads is about equal in the three divisions. To provide for growth and to maintain adequate reserves, it was decided to add 80,000-kw steam-generating units, one for operation in 1940, one in 1941, and a third unit in 1942.

SELECTING A SITE FOR THE NEW STATION

Load studies showed that the first two units should be installed

[1] Vice-President of the Niagara Hudson Power Corporation, in charge of Engineering. Mem. A.S.M.E.

[2] Consulting Engineer of the Niagara Hudson Power System. Mem. A.S.M.E.

Contributed by the Power Division, and presented at the Annual Meeting, New York, N. Y., December 1–5, 1941, of THE AMERICAN SOCIETY OF MECHANICAL ENGINEERS.

NOTE: Statements and opinions advanced in papers are to be understood as individual expressions of their authors and not those of the Society.

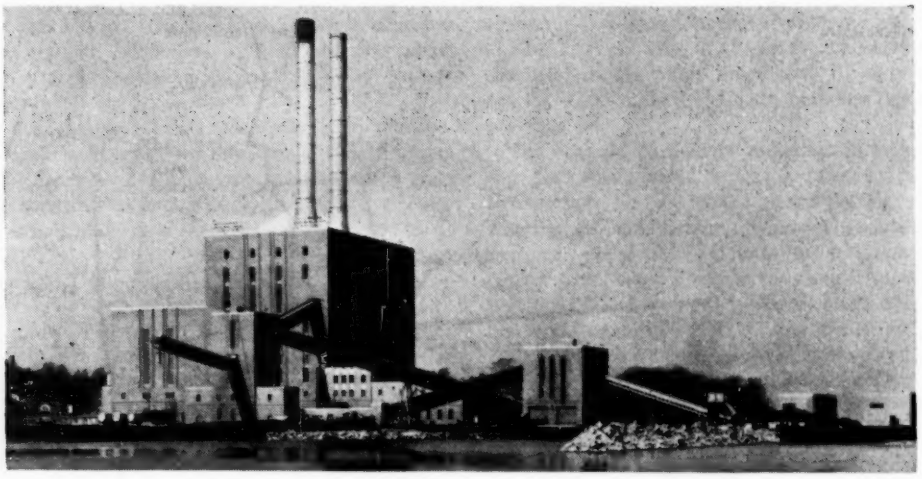


FIG. 2 STEAM STATION VIEWED FROM OSWEGO HARBOR
(Gatehouse, screenhouse, and coal breaker house on right, with outdoor electrical structures at extreme left.)

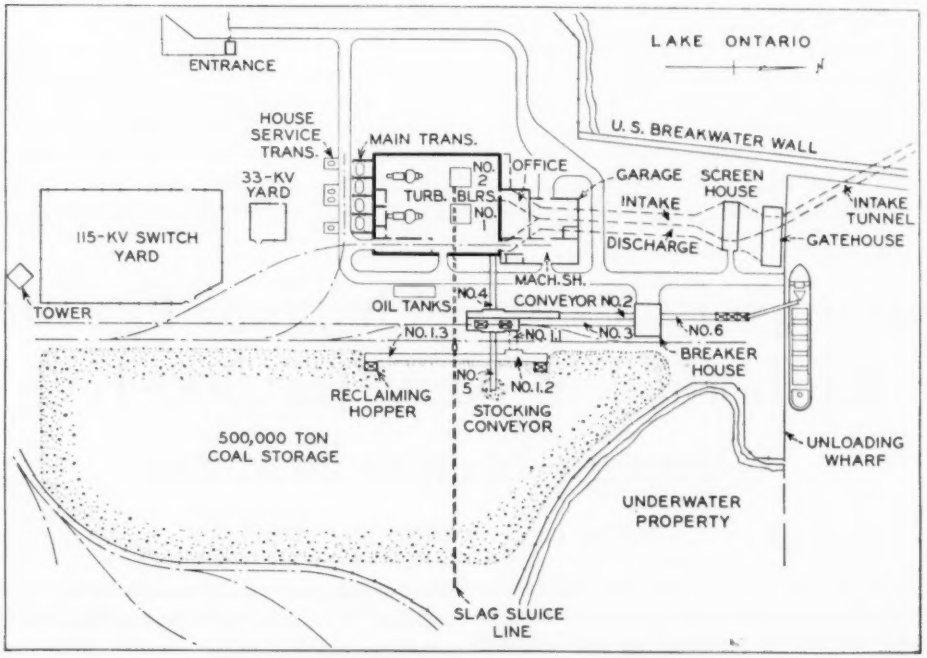


FIG. 3 PLOT PLAN OF OSWEGO STEAM STATION

in the Central Division and the third unit in the Western Division. Sixteen possible powerhouse sites (twelve lake and four river locations) were studied before the present site at the west end of the Oswego harbor was selected for the location of the first two units. This new station is designed for an ultimate capacity of 400,000 kw. An unlimited supply of clean cool condensing water is available from Lake Ontario. Rail and water facilities already existed for bringing in the coal. This site has excellent foundation conditions, and it was possible to work in the open while constructing the foundations, intake and discharge canals, and the intake tunnel. Fig. 2 shows the steam plant as it is viewed from the harbor, and a plot plan, Fig. 3, shows its location on the property. Circulating water for condensing purposes is normally drawn from the lake through a 550-ft-long rock excavated tunnel under the west end of the breakwater wall and discharged into the harbor. The circulation can be reversed to meet storm and ice conditions, or it can take place wholly within the harbor, or be partially recirculated.

Service conditions required that the plant be built for maximum flexibility of operation, i.e., for maximum load during low flow at the hydroplants, minimum load of 4000 kw per turbine on stand-by, and rapidly varying load on frequency control. The generator may readily be disconnected from the turbine for operation as a synchronous condenser during maximum flow of the hydroplants. Each 80,000-kw turbogenerator is supplied by a single steam generator, having a capacity of 900,000 lb of steam per hour. This capacity of the unit is about five per cent of the system's peak load.

The reasons for selecting a one-boiler-per-turbine plant were recognition of the reliability of modern boilers, simplification in the station design, and lowest capital, maintenance, and operating costs.

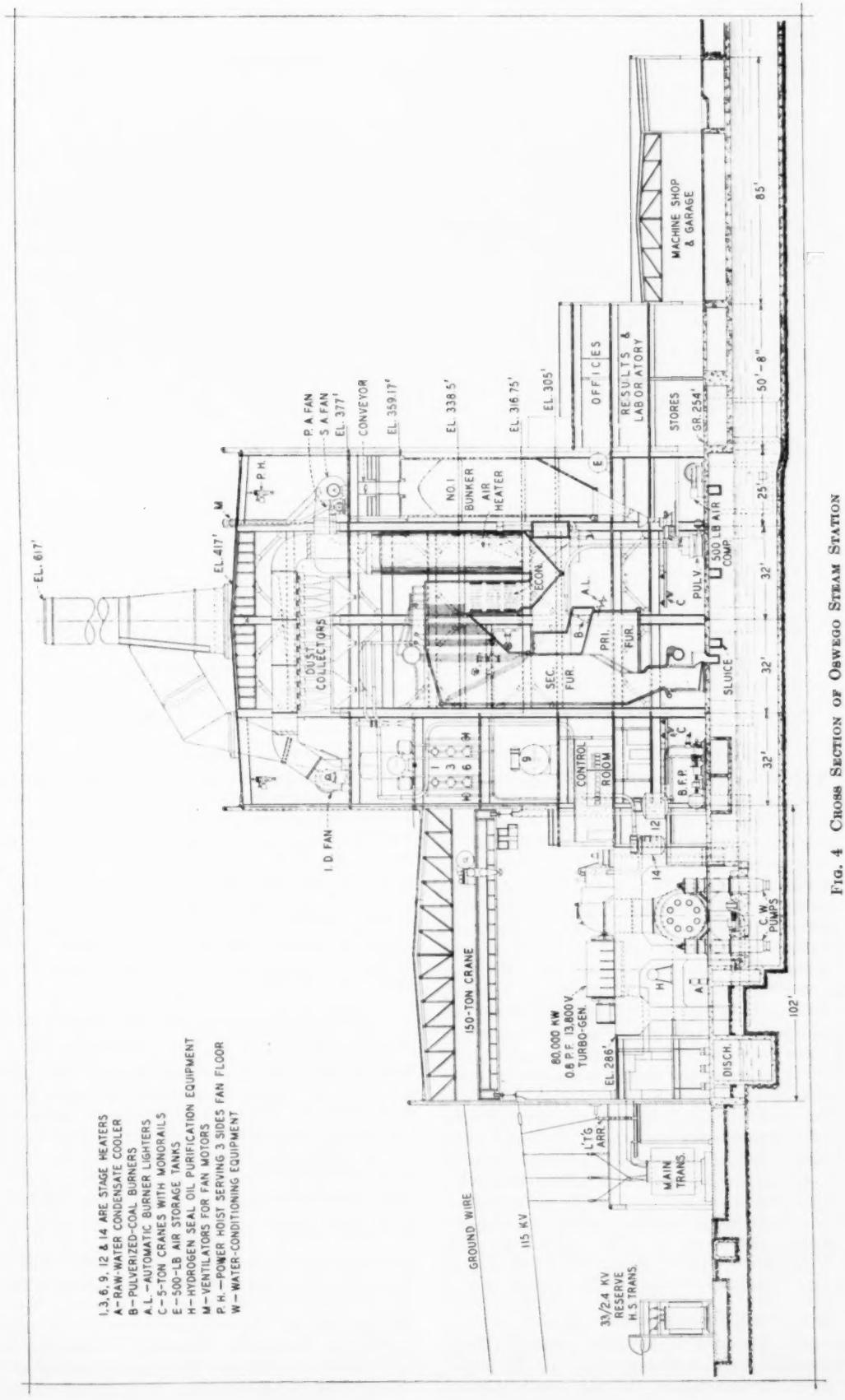


FIG. 4 CROSS SECTION OF OSWEGO STEAM STATION

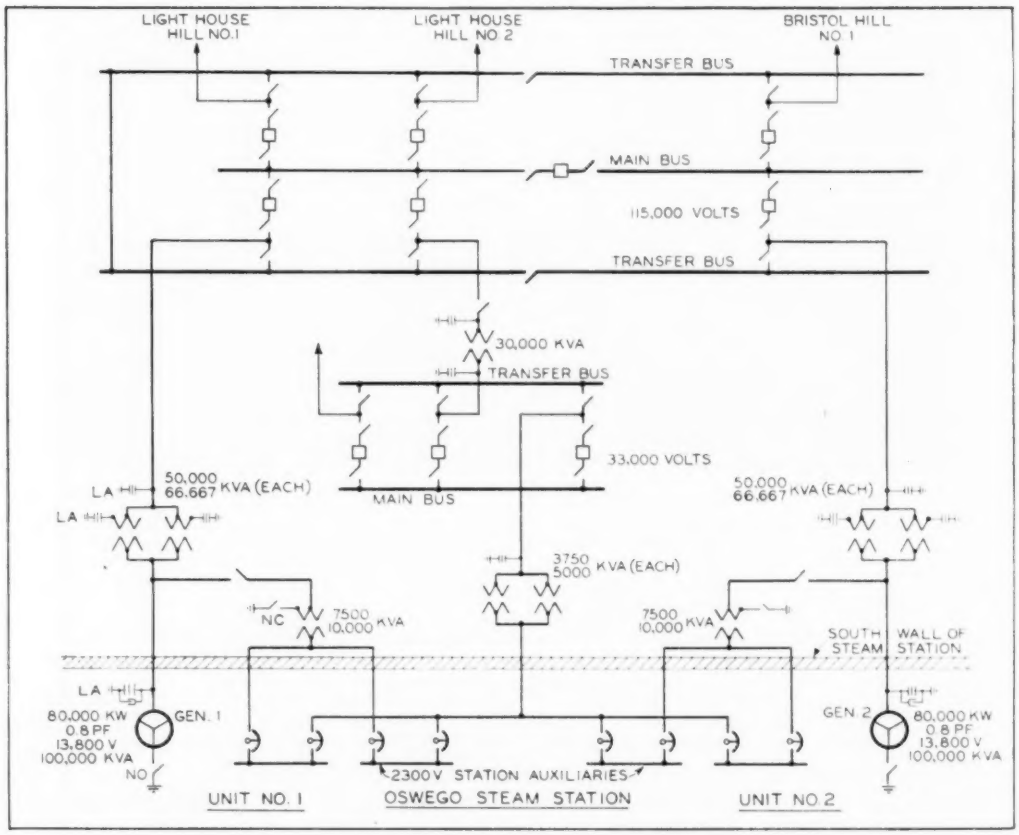


FIG. 5 SCHEMATIC DIAGRAM OF MAIN ELECTRICAL CONNECTIONS

COAL HANDLING

Standard road-building equipment is used for storing, compacting, and reclaiming the coal. Diesel-powered tractors of 113 hp, having a bulldozer attachment, either push the coal to its position or pull a 23-cu-yd-capacity wagon which can be loaded or emptied when in motion by the tractor operator. The coal is stored in a layer and compacted, as the next layer is being deposited, to prevent spontaneous combustion. Thus there is no limit to the height to which the coal can be stored. Space was available for storing 500,000 tons of coal and additional space will be made available by filling the underwater section of the property with slag from the plant. Coal is delivered in 4000-ton-capacity self-unloading vessels which discharge at the rate of 800 tons per hr. Two hopper-bottom railroad cars can be unloaded simultaneously over track hoppers. Rubber-lined canvas belts 42 in. wide of 600 tons capacity per hour (400 fpm) transport the boat- and rail-delivered coal to the bunkers or to the initial pile for storage. The same belts carry the coal from the reclaiming hoppers in the storage yard to the bunkers. A Bradford breaker is in the circuit mainly for cleaning but will also be used for crushing lump coal. A test sample of coal for the laboratory is taken automatically from the stream of coal as it discharges from one of the belts. All coal is weighed on a weightometer as it passes over No. 3 belt en route to the bunkers or to the yard storage. This weightometer is equipped with a master register for all the coal passing over it and a subregister for each of three delivery points.

BUILDING EQUIPMENT AND STACKS

The mechanical equipment of the building consists of (1) two automatic push-button-operated elevators, one in the service building and one in the boilerhouse; (2) two 100-hp oil-fired heating boilers; (3) one 150-ton 100-ft-span turbine-room crane with a 15-ton auxiliary hoist; (4) three 15-ton cranes with power hoists, one for the machine shop, one for the gatehouse, one with a monorail attachment on the top floor of the boilerhouse; (5) two 5-ton hand-operated cranes with monorail attachments to move material from the track bay lengthwise of the plant to the pulverizers and boiler feed pumps, respectively, with a crosswise monorail at each of the equipment locations. All of these devices were used extensively during construction. There are two stacks each 16 ft in diam, fabricated of steel sheets butt-welded, lined with 2 in. of gunite, which extend 200 ft above the powerhouse roof.

TURBOGENERATORS AND ELECTRICAL CONNECTIONS

The turbine generators are rated 80,000 kw, 0.8 pf, 13.8 kv, 3 phase, 60 cycle, 1800 rpm, 1250 lb, 900 F, 17 stage, single cylinder, and each is supplied by a 900,000-lb steam per hr radiant steam generator. The first unit was placed in regular service on December 1, 1940, and the second unit on August 1, 1941. These two generating units, their auxiliaries, and three 115-kv and one 33-kv transmission lines are controlled from one centrally located control room shown in Fig. 4. The station is connected to the main, east-west, 115-kv bulk-power system and also to the local 33-kv system. The 33-kv system is supplied normally by a number of near-by hydrostations and becomes, therefore, a reliable alternative source of power for starting up the steam-station auxiliaries. The connections of the station to the high-voltage transmission system are shown in Fig. 5. Two 3-phase, 50,000-kva (66,667-kva fan-cooled), delta-wye, 13.2/115-kv transformers are connected solidly to the leads of each generator without intervening switching. A main and a transfer 115-kv

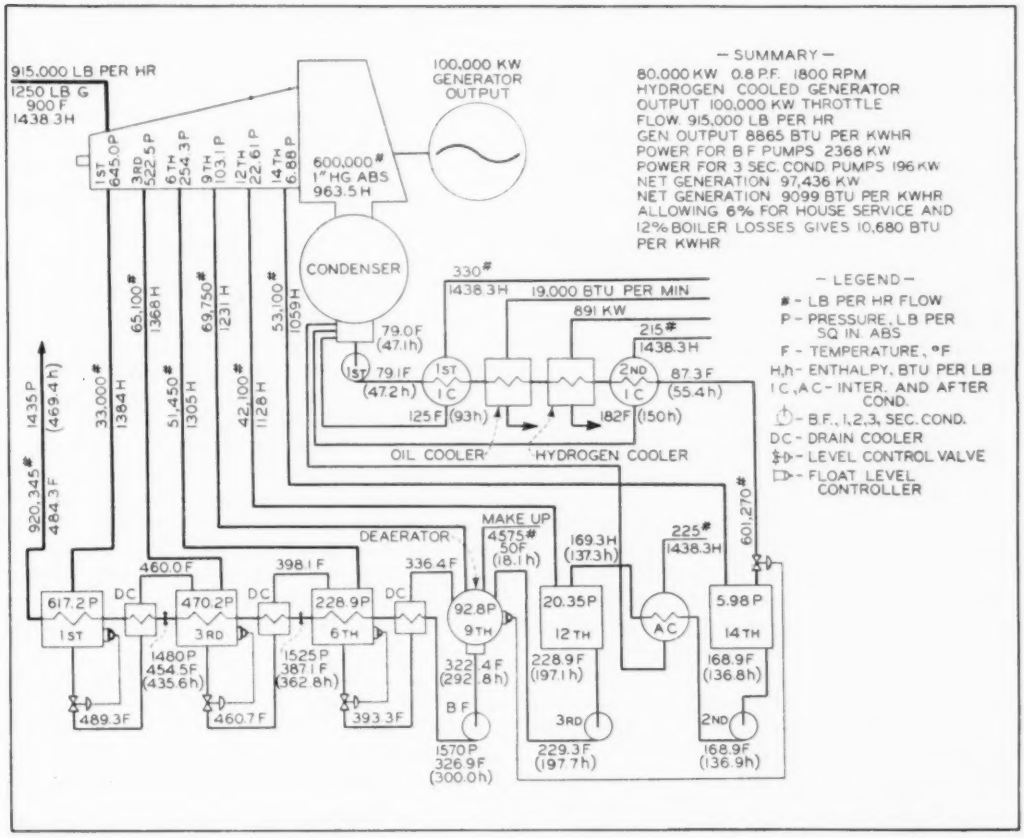


FIG. 6 HEAT-BALANCE DIAGRAM FOR 100,000-KW UNITY-POWER-FACTOR OUTPUT FROM OSWEGO TURBOGENERATOR

bus are provided. The 33-kv local system is connected to the 115-kv station bus through one 30,000-kva, 33/115-kv, wye-delta bank of three single-phase transformers which were rewound for this service. Phase-to-ground current of a generator fault is limited by the impedance of the 7500-kva station-service transformer which is connected solidly to the generator leads. The turbogenerator is hydrogen-cooled and has 250-v excitation from a 300-kw, direct-connected, shunt-wound exciter with a 4-kw, 250-v, direct-connected pilot exciter. The main exciter is used as a starting motor to accelerate the generator (when it is disconnected from the turbine) for synchronous-condenser operation. A 500-kw motor generator set supplies the accelerating power. Automatic frequency control has been provided to enable this station to assist in the regulation of system frequency when the units are not operating at their maximum or minimum capacity.

Lightning protection is provided for all of the transformers by arresters and gaps, and for the generators by arresters and capacitors. The outdoor switching stations are protected from direct strokes by the station stacks, supplemented by extensions to the outdoor steel structures to form lightning rods. An extensive grounding grid was installed underneath the entire powerhouse and outdoor stations.

TURBINES

Each turbine is so designed that all the steam passes through the first-stage nozzles and the first-stage wheel. Ten normal operating valves, five in the upper valve chest and five in the lower, admit steam to different sections of the first-stage wheel, and four overload valves by-pass the second- and third-stage wheels. The turbine will pass 956,000 lb of steam per hr with 1250-lb 900-F steam and $2^1/_2$-in-abs Hg back pressure when operating with full extraction from its six bleed points. A motor-operated turning device is used to keep the turbine shaft straight during cooling.

The turbine-generator unit has been provided with a complete set of electronic-tube-operated supervisory instruments whose respective functions are:

1 The eccentricity recorder indicates and records in mils the eccentricity of the front end of the turbine shaft.

2 The vibration-amplitude recorder indicates and records in mils the transverse vibrations occurring at the four turbine-generator bearings.

3 The interference detector serves as an electric listening rod with a loud-speaker. It is of greatest service during starting and may be switched on or off at will.

4 The expansion recorder gives a continuous graphic record of the axial movement of the head end of the turbine, caused by the expansion of the shell.

5 The speed and camshaft-position recording equipment provides a continuous graphic record of the speed of the turbine during starting and shutting-down periods. When the turbogenerator is synchronized an auxiliary switch on the main circuit breaker cuts out the speed recorder and connects in the camshaft-position device which indicates the amount of valve opening, as a measure of the turbine loading.

The solid coupling between the turbine and generator has been designed so that it can be easily and quickly disconnected when the generator is to be used for synchronous-condenser operation. The turbine-exhaust shell and condenser casing are protected against excessive pressures by a vacuum relay, which will trip the turbine stop valve only on rising pressure, should the casing pressure rise above predetermined values. It is now set to op-

erate at 20-in- and 10-in-abs Hg. As a backup protection a copper diaphragm in the exhaust casing will rupture at 18 lb abs.

All oil pumps and the twin oil coolers are located in the main oil tank which is installed below the basement floor level. The main lubricating-oil pump of 430-gpm capacity is driven from the main turbine shaft through worm gears and extended shaft drive. Three motor-driven pumps are installed, one full-capacity a-c-driven, one half-capacity a-c-driven for synchronous-condenser operation, or when the unit is on the turning gear, and one half-capacity pump operated from the 250-v station battery for back-up protection. All pressure oil lines are carried through the return lines in an all-welded construction. The main hydraulic-control mechanism is located in the turbine standard from which the oil drainage is conducted down the main-pump drive-shaft chute to the oil tank.

Heat Balance

The turbine is provided with six bleed points of which three supply direct-contact heaters and three supply surface heaters. Two independent constant-speed motor-driven condensate pumps are installed, each of which is built in three sections, incorporated in a common shell. One pump is normally in service, the other a stand-by. The flow of condensate through the three pump sections, the fourteenth-stage jet-type, the twelfth-stage tray-type contact heaters, and the ninth-stage deaerating tray-type storage heater (43,600 lb capacity) is shown on the heat-balance diagram, Fig. 6. The water level in this ninth-stage heater is automatically regulated by a three-element control which operates a diaphragm-type control valve located in the condensate line supplying the fourteenth-stage heater. As shown in the diagram, the condensate picks up heat from the inter- and aftercooled condensers of the air-removal equipment, from the lubricating-oil and hydrogen coolers, as well as from the heaters supplied from the six bleed points on the turbine. The throttle flow to the turbine for 100,000 kw gross generation is expected to be 915,000 lb of 1250-psi gage 900-F steam which makes the throttle heat rate 8865 Btu per kwhr of gross generation. The total house-service power for the station, including that used for lighting, miscellaneous power, and coal handling, has been running less than 6 per cent of the gross generation.

Auxiliary Power

The auxiliary power is supplied normally from two 3-phase, 7500-kva (10,000-kva fan-cooled), wye-delta, 13.2/2.4-kv outdoor transformers (one connected to each generator) and, for starting up and reserve, from two 3-phase, 3750-kva (5000-kva fan-cooled), wye-delta, 33/2.4-kv outdoor transformers, operated as a single bank. There are no steam-driven auxiliaries.

All motors of 150 hp and larger are supplied at 2.3 kv, those smaller at 575 v. Both the 2.3-kv and 575-v station-service supply is divided into two sections. All auxiliary service is supplied by at least two motor-driven devices, i.e., there are two boiler fans of each type, two condenser-circulating-water pumps, two hot-well pumps, etc., connected to opposite sections of their respective buses. As shown in the schematic diagram for the electrical auxiliaries, Fig. 7, each unit normally supplies its own auxiliaries with a backup from the 33-kv system. In case of a voltage failure to a 2.3-kv bus, it will be automatically transferred to the reserve supply. The numeral at the arrow, which indicates a feeder, designates the number of feeders of that type which are connected to that section of the bus. The house-service transformers, stepping down to 2.3 kv, are oil-filled, whereas, those

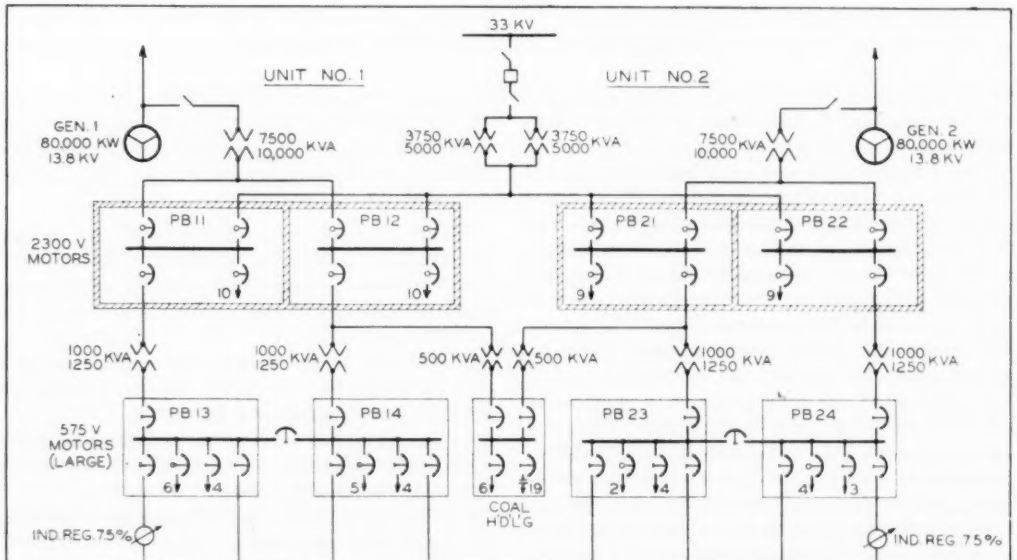


Fig. 7 Schematic Diagram of Electrical Connections for Auxiliary Power

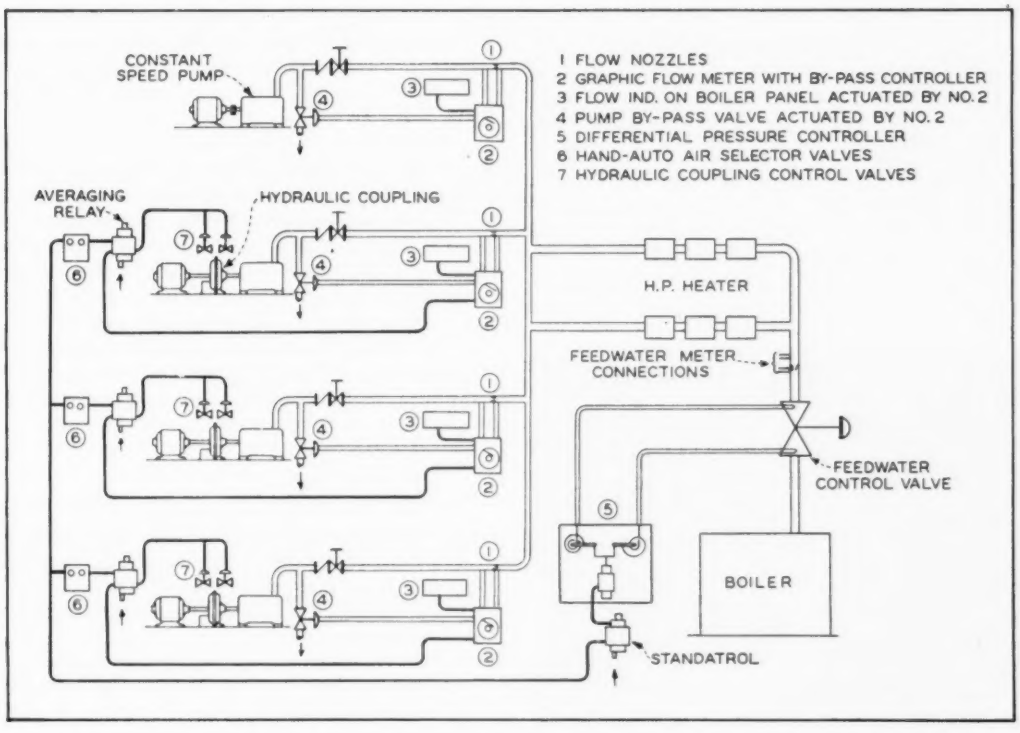


FIG. 8 CONTROLS FOR BOILER FEED PUMPS WITH VARIABLE-SPEED DRIVES FOR THE THREE LARGE PUMPS

stepping down from 2.3 kv to 575 v are pyranol-filled and are located in the boilerhouse adjacent to the 575-v power boards.

MAIN CONDENSERS

Each 58,600-sq-ft single-pass surface condenser will maintain 1.5 in. Hg abs pressure at the turbine exhaust when 588,000 lb per hr of 974.4-H heat-value steam is being condensed with 83,500 gpm of 70 F circulating water. It has $^{7}/_{8}$-in. diam admiralty-metal condenser tubes 29 ft, $8^{1}/_{2}$ in. long, and muntz-metal tube sheets and is bolted to the turbine-exhaust shell with part of the weight taken by spring supports. The condenser has a steel shell, which was shop-welded in four sections to facilitate transportation, and bolted together in the field. The cast-iron water boxes have vertical partitions to permit one side of the condenser to be cleaned with the turbine operating at reduced capacity. A sectionalizing gate valve in the inlet-water-box partition, together with a gate valve between each 59,000-gpm vertical-shaft circulating-water pump and the condenser, makes it possible for either pump to supply both sides of the condenser at times of light load. The air-removal apparatus consists of one set of 15-cfm and two sets of 25-cfm three-stage steam ejectors which are supplied with steam at 225 lb, obtained by throttling the 1250-lb 900-F steam by means of a "Flo-control" valve. The inter- and aftercoolers are cooled with condensate.

BOILER FEED PUMPS AND THEIR CONTROLS

Three 550,000-lb per hr, 8-stage, 3600-rpm and one 220,000-lb per hr, nine-stage, 3600-rpm boiler feed pumps are installed for each boiler with no feedwater connections to the other unit. Each of the larger pumps is driven by a constant-speed, 1800-rpm, induction motor through a variable-speed, 1800-rpm, hydraulic coupling and a 1-to-2 step-up herringbone gear. The smaller pump is for use at light loads and is driven at a constant speed by a 3600-rpm motor.

The boiler feed piping is welded throughout from the flange at the outlet of the boiler feed pumps to and including the inlet to the economizer. The main carbon-moly steam pipe is also welded throughout, with only one flange in the line between the boiler and the turbine and that is located at the connection to the top turbine valve chest. This chest is integral with top half of turbine and must be raised for turbine inspection.

The pump control is illustrated diagrammatically in Fig. 8. This system is designed to save power by operating feed pumps at the minimum speed required to maintain the desired excess pressure across the three-element feedwater-control valve, and also to regulate automatically the speed of each individual pump so that it carries its share of feedwater. This share may be the same or different from that carried by the other pumps and it may be varied by the operators. Another function of this control is to protect the high-pressure pumps from overheating should feedwater requirements be reduced below the minimum allowable rate of flow. If such a condition occurs, a by-pass valve automatically opens so that the pump circulates at least the minimum allowable flow. The ratio of pressure at the inlet to that at the outlet of the feedwater-control valve is measured by two Bourdon tubes which operate a pilot valve through a ratio linkage. The air loading pressure established by this pilot represents the required feedwater-header pressure. As such, it is transmitted to each pump. Here by means of an averaging relay it is combined with the loading pressure established by a flow controller in the outlet line. In this manner a final control pressure embodying the feedwater-header-pressure requirement as well as the individual pump-speed requirement is established by the averaging relay. The final control pressure for each pump regulates the speed of that pump by means of a variable-speed hydraulic coupling. A constant-speed pump is also installed, and the feedwater flow is controlled only by the boiler feed valve. This pump is intended to operate by itself at times of light load.

Steam Generators

The steam generators are of the radiant type, rated to deliver 900,000 lb of 1320-lb 900-F steam with a furnace heat release of one billion Btu per hr. The boiler has a 66-in-ID top drum and a 30-in-ID bottom drum and is suspended from the building steel 111 ft above the basement floor. It expands downward $4^3/_8$ in. from cold to hot. It has a primary and secondary furnace, two nondraining superheaters having a total heating surface of 25,300 sq ft, one 26,900-sq-ft steaming economizer, and two tubular air heaters having a total heating surface of 147,500 sq ft. The primary furnace has a volume of 9900 cu ft and is lined with partially studded tubes, while the secondary furnace has a volume

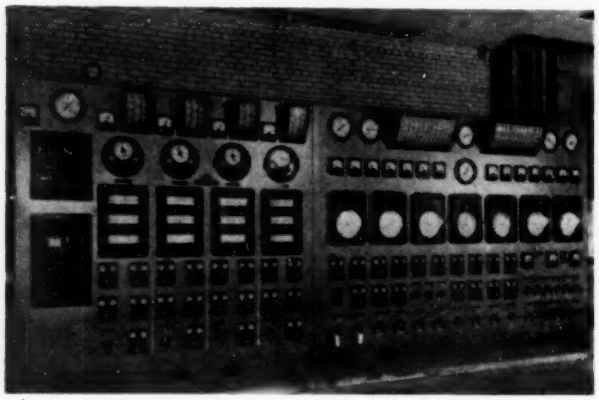


Fig. 9 View of Boiler- and Turbine-Control Board for Unit No. 1

This room is air-conditioned and contains the control boards for both units including the main electrical control board.)

of 33,620 cu ft and is surrounded on three sides and the roof with closely spaced bare tubes. The energy of discharge of the water entering the drum is put to useful work by the cyclones in the drum to separate the water from the steam as the mixture of steam and water rush into the drum from the generating tubes. The water recirculated amounts to 15 times the output of steam from the boiler at its rated capacity, and a higher proportional value at lower loads. A damper in the center gas by-pass between the two superheaters provides a means of controlling the superheat temperature, and dampers in the exit-gas circuit from each superheater afford means for equalizing the temperatures at the outlet of each superheater. Their operation is effective in keeping the temperatures together under all operating conditions, including that of one pulverizer carrying two thirds of the rated boiler capacity. No metal covering is provided over the heat insulation of the boiler and furnace.

The furnace is of the continuous-tap design and the slag drains through two openings in the screen tubes between the primary and secondary furnaces into a water-filled compartment from which it is periodically sluiced to the yard. The boiler controls, located in the control room, occupy the left-hand two thirds of the control board shown in Fig. 9, the turbine controls occupying the remaining third. Four type E56 pulverizers, each with a pair of vertical intertube burners, have been provided. Three of these are guaranteed to operate the boiler at 900,000 lb of steam per hr when grinding 60-grindability, 8 per cent ash, 13,000-Btu coal to a fineness of 70 per cent through a 200-mesh sieve. A load of 600,000 lb of steam per hr has been carried for one hour by one pulverizer grinding 55,000 lb per hr of 90-grindability, 8 per cent ash coal with power input to the pulverizer motor of 72 kw.

The most highly prized accessories to the pulverized-coal-firing equipment are the fuel-oil lighters. The push of an electric button on the boiler panel starts the fuel-oil pump. The oil pressure injects the lighter into the furnace and an electric spark ignites the oil. Within seconds a fat oil flame is burning beneath each pulverized-fuel burner, resulting in positive ignition of pulverized coal as soon as it appears in the furnace. The lighters are used each time a new burner is brought into service whether or not there is coal flame in the furnace from other burners. There never has been even a minor puff in the furnace.

The following special metering equipment has been provided to indicate and record the condition of feedwater, boiler water, and flue gases: (1) Ohmmeters to give the conductivity of the condensate from the main and evaporator condensers; (2) steam-purity meters to give in microhms the purity of the steam entering and leaving the superheater; (3) a meter with degasifying equipment to show the hydrogen emitted with the steam; and (4) also an oxygen-analyzing equipment to record the percentage of oxygen in the flue gases.

Safety Valves

All drum and superheater safety valves are provided with actuating cylinders which enable the valves to be popped by air from a centrally located control station on the operating floor or by steam from pilot safety valves. These pilot-actuator safety valves are installed, one on the boiler drum and two on the steam lines at the turbine stop valve. These give added protection to the superheater and turbine because of the big drop in pressure in the superheater and steam mains, Fig. 10. Gate valves, installed under the pilot valves, permit them to be maintained without a boiler outage, because the main valves provide the boiler-code requirements. The advantages of the scheme are: (1) It reduces the wear on the main valves by forcing them to have a

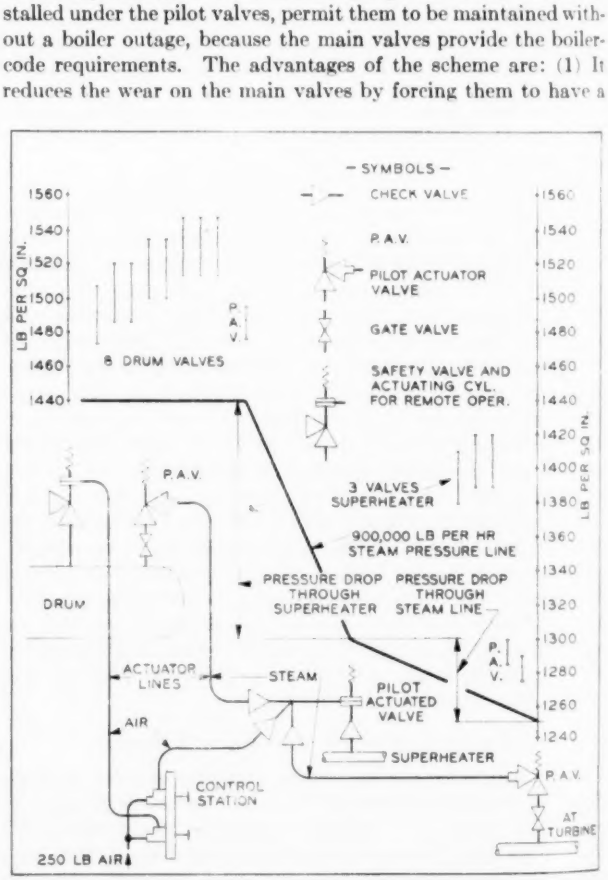


Fig. 10 Safety-Valve Arrangement Which Provides Added Protection to Turbine and Increased Operating Continuity of Boiler by the Use of Actuating Cylinders on Main Valves, Together With Pilot Safety Valves With Actuating Lines

sharp opening and closing; (2) most of the wear is taken on small valves which are easier and less expensive to repair; (3) it reduces the boiler outages required to repair safety valves; and (4) more effective protection is afforded the superheater and turbine.

Soot Blowing

The conventional method of cleaning boilers has been to use steam as the blowing medium but this becomes less desirable as higher steam pressures are used. The decision was made to use 250-lb air, after carefully considering four means of obtaining steam. The studies show that air-blowing takes no more energy from the coal pile, takes no water from the boiler, eliminates the expansion and warming-up problems of the steam-blower piping, lends itself admirably to automatic control, and is more suitable to combine with water than steam with water, should the blowing conditions call for water. Four 500-cfm 500-lb compressors, with storage tanks and pressure-reducing valves, supply a 250-lb tank from which the air for blowing is obtained. With the operating conditions obtaining to date, the blowers are actually taking about one half the air provided for blowing and are doing an excellent job. Poorer coals and worn tube surfaces will require more air. The automatic program board is at the extreme left of the boiler panel, shown in Fig. 9.

The advantages of this automatic soot-blowing system are as follows:

1 Preselected sequential automatic operation from a central point reduces labor and operating costs; assures a definite time duration for operation of each unit, each time it is blown, without the attention of the operator; gives direct control of boiler cleanliness independent of the human element; enables the operator to tell at a glance which group is then operating, and which groups have completed their operation.

2 The blower grouping sectionalizes the heating surface into zones so that normal heat absorption can be maintained in each zone by the frequency of group operation.

3 Puff operation on units provides automatic rotation of the soot blowers with a minimum amount of air.

4 The use of nozzles of the mass-blowing type provides greater bank penetration and does not require maintaining accurate alignment with the tube lanes.

5 Retracting units are used in all locations where equipment permanently installed in gas flow may not give satisfactory life.

6 Intermittent blowing is employed on the traveling-frame air-heater blowers to save air and to avoid impingement on the tube sheets.

7 The telescopic blowers are projected into the boiler at twice the retracting or normal cleaning speed to save 25 per cent of the air required for a complete cycle at normal speed.

8 No blower can start operation unless the air pressure is up to a predetermined value, thereby assuring effective cleaning.

Control features for protection of the automatic equipment are:

1 Alarm system both visible and audible indicates motor overload. It is arranged to show the same percentage of load regardless of different motor sizes.

2 The air-control valves to the telescopic blowers have electrically operated latches to prevent their closing should current fail. This assures cooling air for the blowers until the primary-air receivers are exhausted. When current is restored, the blowers automatically return to their retracted positions even though they had been moving forward when current failed.

Automatic Combustion Control

The combustion-control system is based on the correct proportioning of the coal and the air to each pulverizer and its burners. The premeasuring system, as originally developed by R. C. Roe, has been modified to increase the speed of response to provide for rapid changes in load. As previously stated, each turbine is supplied by one boiler having a complement of two primary-air fans, two forced-draft fans, two induced-draft fans, and four type

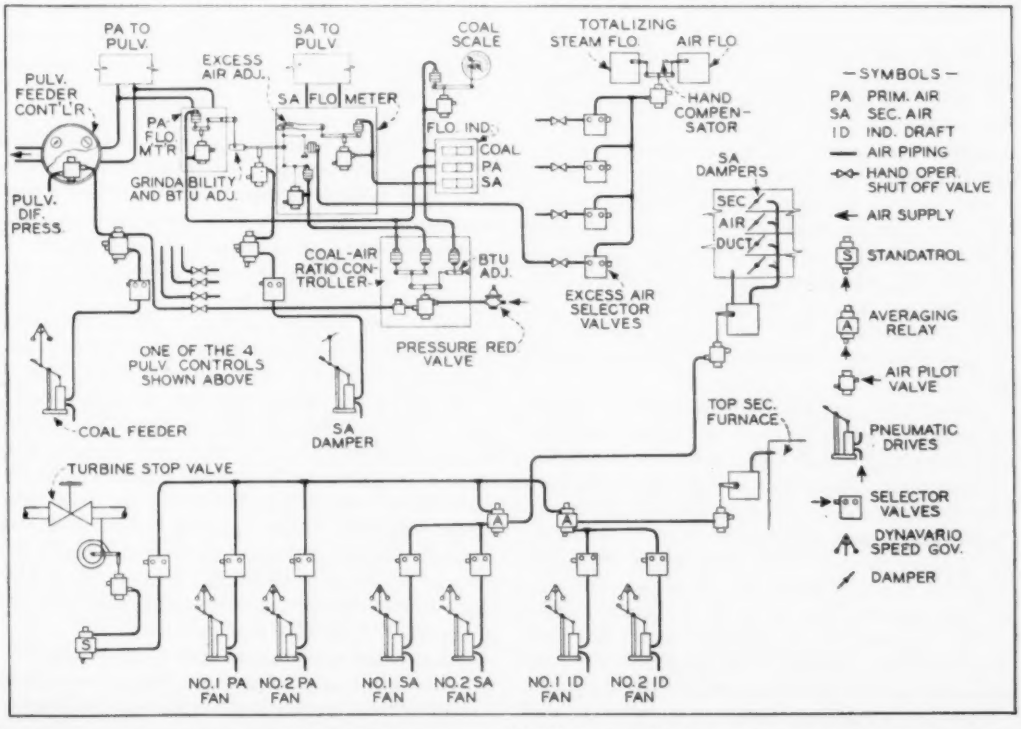


Fig. 11 Automatic-Combustion-Control System for 900,000-Lb per Hr Steam Generator, Using Compressed Air as Control Medium

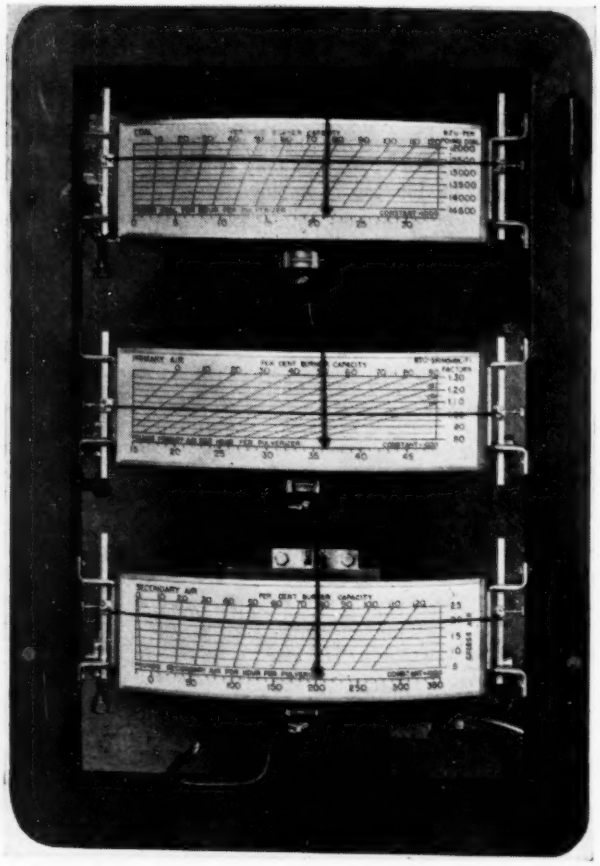


FIG. 12 FURNACE-FLOW INDICATOR, ONE FOR EACH PULVERIZER, SHOWING POUNDS PER HOUR OF COAL, PRIMARY AIR, AND SECONDARY AIR TO EACH PAIR OF BURNERS

E pulverizers, each with its coal scale and raw-coal feeder. Each pulverizer supplies two burners. The fans and raw-coal feeders are individually driven by constant-speed motors through variable-speed eddy-current couplings. The coupling speed in each case is controlled by a built-in Dynavario governor whose setting is positioned by a pneumatic-drive unit. The primary air and secondary air, and the coal for each pulverizer and its burners, are measured in the manner shown in Fig. 11. The air-measuring elements are equipped with automatic temperature compensators. These meters supply flow indicators, Fig. 12, which indicate the rate of flow in pounds per hour of the coal, of the primary air, and of the secondary air being delivered to each pulverizer and its pair of burners. These indicators are located on the control panels as shown in Fig. 9.

The control is actuated by a master steam-pressure controller connected to maintain constant pressure at the turbine stop valve. The control medium is compressed air supplied by compressors with carbon rings, aftercoolers, and filters which keep the air supply free from oil, water, and dirt. The steam-pressure controller sends air loading pressure simultaneously to the pneumatic drives which adjust the speed of the primary air, secondary air, and induced-draft fans. Changes in primary-air flow immediately affect the pressure drop across the pulverizer. This change in pressure drop calls for adjustments in the fuel feed through the action of the pulverizer-feeder controller, whose pilot valve sends a loading pressure to the coal-feeder pneumatic-control drive. Therefore, a loading pressure set up by the master pressure controller increases or decreases the speed of the primary, secondary, and induced-draft fans and also the speed of the raw-coal feeders, as required by variations in steam pressure. The induced-draft and the secondary pneumatic-control drives are further modified from other control points by means of averaging relays in the air circuits, i.e., the induced-draft-fan speeds are readjusted to maintain 0.3 in. water suction at the top of the secondary furnace, and the secondary-air-fan speeds are readjusted to maintain a predetermined minimum pressure drop across the control dampers in the secondary-air ducts. While these operations are taking place, the premeasuring control equipment is readjusting the fuel and air conditions to each individual pulverizer and its pair of burners, for the purpose of maintaining the proper relation between the primary air and the secondary air, and the proper relation between the coal feed and the sum of the primary and secondary air.

A common method of automatic combustion control is based on the assumption that the volumetric products of combustion as they leave the furnace or pass by the boiler heating surface are a true index of the amount of air required for combustion. This assumption is not correct, and at best the index is only an approximation. The volume of the gas, consisting of the products of combustion, in relation to its weight, varies with changes of both pressure and temperature and also varies to some degree due to different proportioning of the constituent elements of the products of combustion. The volumetric measurement referred to is generally taken across some portions of the heating surface of the boiler or its appurtenances. Inasmuch as draft loss (and hence the pressure of gas at the point where the measurement is taken) varies both with the rating of the boiler and with the cleanliness of the heating surfaces, and inasmuch as the temperature of the gas at the point where the measurement is taken also varies both with the rating of the boiler and the cleanliness of the heating surface preceding the point of measurement, it is readily seen that a volumetric measurement is not a true indication of the weight of the products of combustion. It has been claimed that these volumetric measurements repeat themselves for the same steam-flow conditions from the boiler. However, this too is not a fact because the cleanliness of the boiler affects both heat transfer and draft losses; and draft losses, of course, affect pressure. Therefore an adjustment of the meter to give air quantities based on volumetric measurement of flow of the products of combustion is in essence a reasonably accurate adjustment only for the conditions existing at the time the adjustment was made and may vary with other conditions of cleanliness, or with a change of fuel, or with other changes in basic conditions which were not present at the time the adjustments were made. Further, the assumption that a volumetric measurement of the products of combustion is equivalent to weight is based on complete combustion, which may or may not be the case.

It is further pointed out that, with installations using two or more pulverizers, the fuel and air ratio for each pulverizer with its burners may vary widely from the ideal ratio, although the total fuel bears a correct relation to the total air entering the furnace. In other words, the burners supplied by one pulverizer may be operating with too large an amount of air and those supplied by another pulverizer may have a deficiency of air resulting in unburned carbon. Therefore, while the totals are correct, the combustion in the furnace may be badly unbalanced. With the system installed at Oswego, the correct amount of fuel and air is supplied to each combination of pulverizer and burners. It is expected that this premeasuring scheme will result in a coal saving in the order of one half of one per cent.

In order that a comparison may be made between the two systems of control, i.e., the premeasuring unit system and the post-measuring total system, a steam flow-air flow controller was also provided so that the combustion-control system may be operated either on the premeasurement basis of coal and air to each pul-

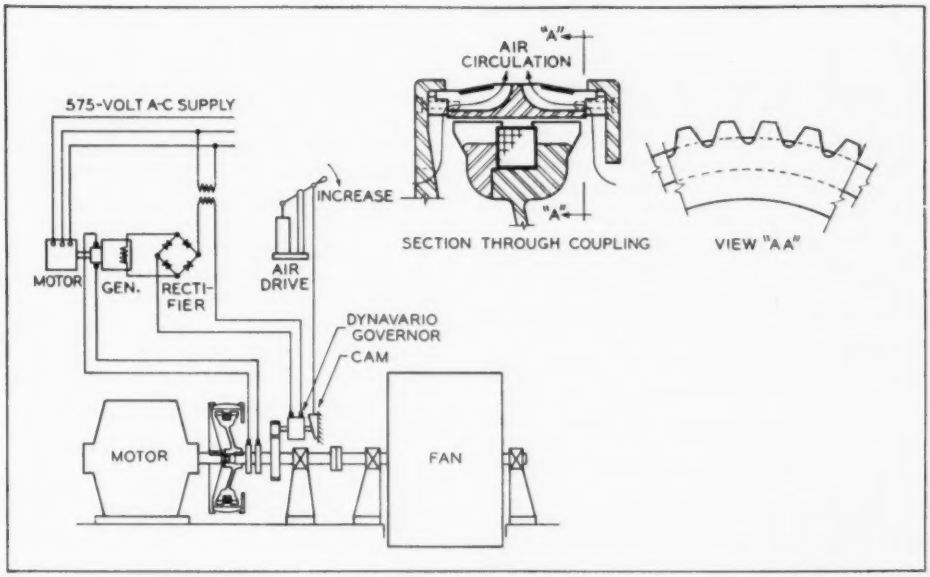


FIG. 13 VARIABLE-SPEED EDDY-CURRENT COUPLING FOR 1250-HP INDUCED-DRAFT FAN

verizer or by proportioning the total products of combustion to the total fuel.

The rate of coal feed supplied to each pulverizer is measured by a coal-conveyer-and-scale assembly, which consists of a synchronous-motor-driven conveyer mounted on a Toledo scale so that the actual quantity of coal on the conveyer is measured by the scale at all times. The readings of the scale are pneumatically transmitted to the indicator located on the boiler panel. The coal feed is readjusted to give the correct coal-air ratio to each pulverizer by the individual coal-air-ratio controllers.

The secondary-air control dampers are used for proportioning secondary to primary air for each pulverizer unit. The secondary-air flow to the burners corresponding to each pulverizer is measured and maintained in a definite relation to the primary-air flow by means of primary-air-flow–secondary-air-flow ratio controllers.

Individual shutoff dampers with pneumatic-control drives, for the induced-draft, secondary- and primary-air fans, are provided and so connected as to be actuated by the differential pressure across the dampers, in order to insure maintaining the capacity of any fan of a pair when its mate fails. Pressure connections are made into the duct in such a manner as to obtain the benefit of the velocity effect when the dampers are in a wide-open position at which time the differential pressure across them would be exceptionally small. Thus, whenever a fan is started up, the differential pressure acts in such a way as to open up the corresponding dampers. In case this fan should fail during operation and the slightest amount of recirculation should occur, the dampers would automatically close. The primary ducts to the pulverizers, being supplied from a common plenum chamber, are provided with pneumatically operated shutoff dampers, which serve also as a means of dividing the load between the pulverizers and for cutting them in or out of service. The ten pneumatic damper controls mentioned herein are not shown in the diagram as they are not a part of the automatic combustion controls.

VARIABLE SPEED FOR FANS

Because of the loading conditions on the plant, it was very de-

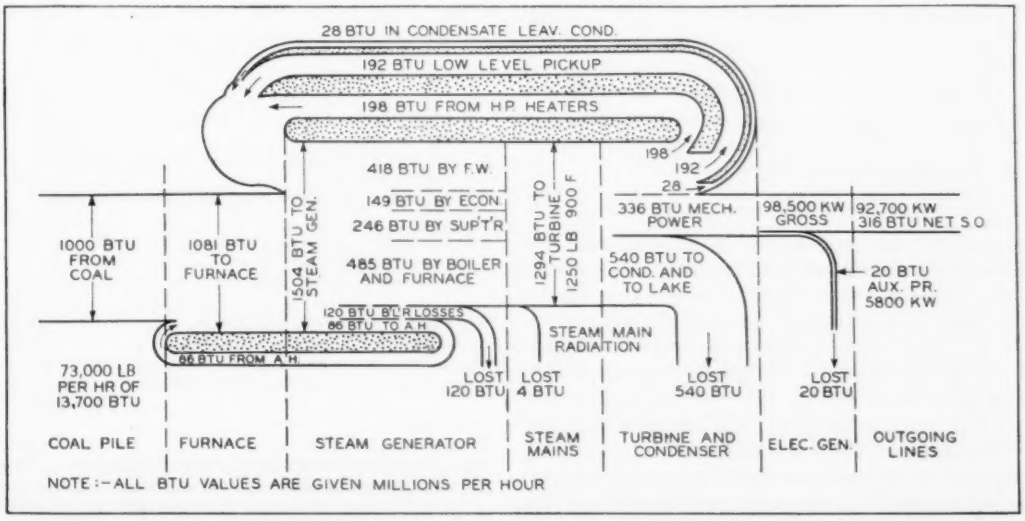


FIG. 14 HEAT-FLOW DIAGRAM FOR 900,000-LB PER HR OUTPUT FROM OSWEGO STEAM GENERATOR

sirable to select fan drives that would permit a wide range in speed adjustment. After careful consideration of the various types of drives and methods available, it was decided to install electric couplings of the eddy-current type for the induced-draft, secondary-air, and primary-air fans. Some of their outstanding advantages are: (1) No large quantities of oil are required; (2) speed reductions up to 90 per cent are obtainable by simple means; (3) an infinite number of speed points are available; (4) response is practically instantaneous; (5) the heat is generated in the constant-speed drum and dissipated by the fan action of the coupling itself; (6) permit the use of a single motor of the squirrel-cage type; and (7) the governor is designed for linear speed characteristic of the fan, i.e., fan speed directly proportional to control air pressure.

Reference to Fig. 13 will show the elements of a 1250-hp coupling on an induced-draft fan and the pneumatic drive for adjusting the position of the governor. The speed of the fan can be varied from maximum speed down to 10 per cent of maximum speed. At maximum speed, the slip of the coupling is 2.5 per cent of the motor speed and the excitation power is 2500 w. At Oswego, motor generator sets supply the excitation of all the large couplings, except those on the primary-air fans where copper-oxide rectifiers are used.

The variable-speed drives for the raw-coal feeders also contain eddy-current couplings. These drives are rated 2 hp and derive their excitation from selenium rectifiers.

The largest eddy-current coupling built at the time the order was placed for the first Oswego couplings was 150-hp capacity and on that account the first 1250-hp coupling was rushed to completion, installed with its regular motor and fan, and given extensive field tests before the work was released on the other five couplings. The same design of couplings was ordered for the second unit at Oswego and similar couplings for a new unit in the C. R. Huntley Station.

Automatic Controls

In addition to the automatic controls previously described, float-controlled air-actuated valves control the water levels in the high-pressure heaters, and in the hot wells of the main and evaporator condensers. For the main condenser, a second air-operated valve admits water from the open condensate storage tank in case of low water. The superheat temperature at the turbine throttle is controlled by a two-element type of air control, initially positioned by steam flow and readjusted by the steam temperature, which actuates a damper in the gas by-pass around the superheater. The hydrogen is normally cooled by heat exchangers mounted in the turbogenerator frame, but in case the cooling is insufficient because of hot condensate (or new condensate not available in the case of synchronous-condenser operation) the temperature control positions a butterfly valve in a raw-water supply to a special heat exchanger, which is always in the condensate circuit ahead of the hydrogen coolers.

Heat-Flow Diagram

The flow of Btu's through the station when the steam generator is delivering 900,000 lb of steam per hour requiring a heat release in the furnace of one billion heat units per hour is shown in Fig. 14. The heat above 32 F in the air to the forced-draft fans and primary blowers is omitted in order not to complicate the diagram further. The heat which circulates through the steam generator, when operating at its rated capacity, is 50 per cent greater than the heat in the fuel that is being fired. The heat flowing in any part of the circuit, expressed as a percentage of the heat in the fuel fired, is obtained by dropping one digit, for example, the condenser loss of 540 million Btu is 54 per cent of the energy in the fuel.

Fire Protection

Very complete protection against fire hazard is being installed. Fixed water-spray systems are provided for all of the oil-filled power transformers, the oil-filled hydraulic couplings in the boiler feed pumps, turbine-oil tanks and piping, turbine-oil storage room, turbine-oil treatment equipment, repair pit in the turbine room, and the coal-handling conveyer galleries. Some of these systems are automatic in operation and others manual. Fixed hose racks and hose lines with adjustable-spray nozzles are provided throughout the powerhouse in an arrangement whereby any fire can be fought simultaneously by two hose lines. Hose houses were built near the outdoor switching structures which contain hose lines with "poweron" nozzles, and CO_2 and carbontetrachloride portable equipment. Portable devices of various types and sizes, including large "foam generators," are strategically placed throughout the property.

Acknowledgment

The authors gratefully acknowledge the assistance of J. M. Geiger of the Buffalo Niagara Electric Corporation.

Appendix

Equipment Data for Oswego Power Station

Plant Capacity:

Initial capacity ..... 160,000 kw
Ultimate capacity ..... 400,000 kw

Coal and Ash Handling:

Coal-storing capacity ..... 500,000 tons
Coal is received in hopper-bottom railroad cars and in 4000-ton-capacity self-unloading freighters
Belt-conveying equipment for transporting coal to the bunkers or into or out of storage on 42-in. belts at the rate of 600 tons per hr, complete with lump breakers and pan conveyers under the reclaiming hoppers, automatic coal sampler with "Ridler" conveyer, also a Knittle crusher ..... Stephens-Adamson Manufacturing Co.
Herringbone-gear speed reducers for drives on coal-handling equipment ..... Farrel-Birmingham Co.
Rubber-lined 6-ply 32-oz 42-in-width canvas belts ..... Hewitt Rubber Co.
Weightometer with master and three individual delivery-point registers ..... Merrick Scale Manufacturing Co.
Bradford-Hammermill, 12 ft × 19 ft ..... Pennsylvania Crusher Co.
3 Model D-8 113-hp Caterpillar Diesel tractors with Model CK-8 LeTourneau angle dozers and two Model W, 23-cu-yd Carryall scrapers ..... Syracuse Supply Co.

Boilers and Furnaces With Auxiliaries:

2 boilers, each rated 900,000 lb of steam per hr continuous at 1320 lb pressure 903 F total temperature, and each with 66-in-ID upper drum and 30-in-ID lower drum, containing 7307 sq ft boiler heating surface; 9779 sq ft of heating surface in primary and secondary furnace walls; 43,520 cu ft furnace volume; armored blocks for primary furnace floor and secondary furnace sidewall observation lanes ..... Babcock & Wilcox Co.
4 pendant-type (2 per boiler) 12,650 sq ft superheaters with a gas passage between ..... Babcock & Wilcox Co.
2 (1 per boiler) 26,900-sq-ft steaming economizers ..... Babcock & Wilcox Co.
4 (2 per boiler) 73,750-sq-ft-tubular air heaters for primary and secondary air to furnace with dampers to by-pass the second and third air passes to control minimum exit-gas temperatures ..... Babcock & Wilcox Co.
Superheater refractory side walls ..... M. W. Detrick Co.
Boiler and furnace heat insulation ..... Johns-Manville Co.
Smoke breechings and ducts ..... Connery Construction Co.
Steel stacks, 200 ft high, all-welded construction ..... Chicago Bridge & Iron Co
Stack linings ..... Cement Gun Co
Gage glasses (Bi-color) ..... Diamond Power Specialty Co.
Three-element feedwater control of drum level ..... Bailey Meter Co.
Air soot blowers, preselected automatic blowing ..... Diamond Power Specialty Co.
8 pulverizers, 12.5 tons per hr capacity ..... Babcock & Wilcox Co.

8 raw-coal feeders.....Babcock & Wilcox Co.
8 coal-feed drives (10-to-1 variable-speed a-c motors)..Louis Allis Co.
4 induced-draft, 4 secondary-air, and 4 primary-air fans.....Buffalo Forge Co.
12 variable-speed couplings for fan drives.....Dynamatic Corp.
Dust catchers (multicyclone type).....Prat-Daniel Corp.
Hydrojet system of dust removal.....Allen-Sherman Hoff Co.
Slag hoppers and slag-handling equipment...Allen-Sherman Hoff Co.
Coal hoppers; extensions to concrete bunkers...Chicago Bridge Co.
Valves in raw-coal spouts.....Stock Engineering Co.
2 two-stage hot-process lime-soda water-conditioning system, with integral deaerating heaters arranged for phosphate feed into second stage; capacity 30,000 lb per hr.....Cochrane Corp.
2 evaporators with evaporator condensers; capacity each, 30,000 lb per hr.....Griscom-Russell Co.
Heat exchangers for evaporators.....Alberger Heater Co.

Turbines and Auxiliaries:

2 turbine generators 80,000 kw, 0.8 pf, single cylinder, 17 stage, 1250 lb, 900 F, 3 phase, 60 cycle, 13.8 kv with 1$^1/_2$ rpm turning gear and hydrogen cooling for generator, 300-kw, 250-v, direct-driven exciter and 4-kw pilot exciter.....General Electric Co.
2 single-pass steel-shell condensers mounted on springs and bolted solid to turbine exhaust; 58,600 sq ft of surface. Condensers have $^7/_8$-in-OD admiralty tubes, divided water boxes, reheating hot wells, and steam-jet air-removal equipment with inter-, after-, and tertiary condensate-cooled condensers.....Worthington Pump & Machinery Corp.
2 sets (1 per turbine) of direct-contact heaters, with vent condensers for fourteenth-, twelfth-, and ninth-stage bleed points of turbine..Foster Wheeler Corp.
4 sets (2 per turbine) of high-pressure horizontal heaters, with hairpin tubes and subcoolers for sixth-, third-, and first-stage bleed points of turbine; capacity 457,000 lb per hr, each..Griscom-Russell Co.
2 raw-water coolers for condensate for synchronous-condenser operation.....Ross-Heater Corp.

Pumps:

4 vertical-shaft (2 per unit), 59,000-gpm, 400-rpm, circulating-water pumps with rubber guide bearings.....Worthington Pump & Machinery Corp.
4 (2 per unit) three-section condensate pumps to deliver condensate to the direct-contact heaters.....Foster Wheeler Corp.
6 (3 per unit) 550,000-lb-per-hr (2000 lb at shutoff), 8-stage, 3600-rpm, horizontally split casing boiler feed pumps.Ingersoll-Rand Co.
6 herringbone 1750 hp, 1-to-2 step-up gears for boiler feed pumps...DeLaval Steam Turbine Company
6 variable-speed hydraulic couplings, 1750 hp 1800 rpm to give 22 per cent speed reduction for boiler feed pumps.....American Blower Co.
2 nine-stage, 3600-rpm, constant-speed, boiler feed pumps; capacity 220,000 lb per hr, each.....Ingersoll-Rand Co.
2 "Hydroseal," 1000-gpm, horizontal-shaft, slag-handling pumps with adjustable-speed V-belt drive.....Allen-Sherman Hoff Co.
2 horizontal-shaft slag-sluicing pumps; capacity each 750 gpm at 518 ft total head.....Buffalo Pumps, Inc.
1 horizontal-shaft house-service pump; capacity 750 gpm at 200 ft total head.....Morris Machine Co.
3 horizontal-shaft low-service pumps; capacity 1200 gpm at 115 ft total head.....Morris Machine Co.
2 pumps of 1700 gpm capacity, 25 ft head, supplying raw water to auxiliary coolers.....Morris Machine Co.
4 condensate-circulator pumps; capacity 700 gpm at 25 ft head....Ingersoll-Rand Co.
3 screenhouse washing pumps; capacity 350 gpm at 200 ft head....Worthington Pump & Machinery Corp.
2 vertical-shaft sump pumps for hot-well pit; capacity 300 gpm at 20 ft head.....Buffalo Pumps, Inc.
2 evaporator-condenser distillate pumps; capacity 150 gpm at 143 ft head.....Ingersoll-Rand Co.
2 No. 1$^1/_2$ rotary Aroclor pumps.....Worthington Pump & Machinery Corp.
2 rotary fuel-oil pumps, 2-in. size, for burner lighters.....Worthington Pump & Machinery Corp.
7 vertical sump pumps, three 60 gpm 15 ft head, three 30 gpm 30 ft head, and one 30 gpm 15 ft head.....Taber Pump Co.
2 sewage sump pumps, 7$^1/_2$ hp.....Yeoman Brothers Co.

Air Compressors:

4 cross-compound air compressors, 500 cfm 500 lb, direct-connected to 200-hp synchronous motors for soot blowing.Ingersoll-Rand Co.
3 carbon-ring air compressors, 125 cfm 100 lb, for meter service and automatic controls.....Worthington Pump & Machinery Corp.

Pipe Fitting and Valves:

Carbon steel 0.5 per cent moly, steam piping welded throughout, high-pressure and low-pressure condensate piping, and miscellaneous piping.....M. W. Kellogg Company
Cast-iron piping for circulating water.....Wetherly Foundry & Machine Co.
High-pressure traps.....Atwood & Morrill
Low-pressure traps.....Strong, Carlisle & Hammond; Wright Austin Co.
Strainers.....Andale Co.; Elliott Co.
Bleeder nonreturn valves.....Atwood & Morrill
Boiler blowdown valves (tandem assembly).....Yarnall Waring Co.
Boiler nonreturn 14-in. angle stop valves (motor-operated).....Schutte & Koerting Co.
Check valves, tilting-disk type..Chapman Valve Manufacturing Co.
Chemical feed pumps to boilers.....Hills McCanna Co.
Circulating-water gate valves, 48-in. hydraulically operated.....Rensselaer Valve Co.
Forged-steel valves.....Henry Vogt Co.
Foot valves.....Buffalo Pumps, Inc.
Gate valves for high-pressure steam and feedwater.....The William Powell Co.
2 motor-operated globe valves, 8 in. 2000 lb, for feed line to boiler...The William Powell Co.
Globe valves for high-pressure steam and miscellaneous services....The Lunkenheimer Co.
Gate valves for 250- and 125-lb miscellaneous services.....The Lunkenheimer Co.
Relief valves for water pressure....Crosby Steam Gage & Valve Co.
Safety valves with actuating cylinders and pilot-actuator safety valves.....Crosby Steam Gage & Valve Co.
Drainer valves, pilot-operated float-controlled.....Bailey Meter Co.
Heat insulation for pipes, flues, and ducts.....Union Asbestos & Rubber Co.
Rubber expansion joints.....U. S. Rubber Co.

Meters and Controls:

Remote-operated pulverized-coal-burner lighters.....Babcock & Wilcox Co.
Automatic combustion controls, premeasuring type.Bailey Meter Co.
Automatic superheater-temperature control.....Bailey Meter Co.
Automatic water-level controls.....Bailey Meter Co.
Automatic control of hydrogen temperature.....Bailey Meter Co.
Condensate-flow control.....Bailey Meter Co.
Soot-blower preselecting-program panel.....Autocall Co.
Manometers.....Meriam Co.
Degasifier for detection of hydrogen in steam.....Cochrane Corp.
Recording ohmmeters for condensate purity.....Esterline-Angus Co.
Turbine supervisory instruments.....General Electric Co.
Conductivity recorder for steam purity.....Leeds & Northrup Co.
Boiler and turbine control panels.....Bailey Meter Co.

Electrical Equipment:

4 main generator transformers, 50,000 kva (66,667 fan-cooled), 13.2/115 kv 60 cycle.....General Electric Co.
Lightning arresters.....General Electric Co.
Oil circuit breakers, 33 and 115 kv....Westinghouse Elec. & Mfg. Co.
2 auxiliary transformers, 7500 kva (10,000 fan-cooled).....General Electric Co.
2 auxiliary transformers, 3750 kva (50,000 fan-cooled).....General Electric Co.
4 pyranol-filled auxiliary transformers, 1000 kva (1250 fan-cooled)..General Electric Co.
Outdoor disconnecting switches 33 and 115 kv.....Hi-Voltage Equipment Co.
Control and relay boards.....General Electric Co.
Automatic frequency controls.....General Electric Co.
Generator voltage, automatic regulators.....General Electric Co.
Auxiliary power boards with 575 and 2300-v air-break switches.....I.T.E. Circuit Breaker Co; General Electric Co.
250-v battery-charging motor-generator set....Electric Products Co.
250-v 480-amp-hr storage battery.....Gould Battery Co.
Electric motors 575 and 2300 v.....General Electric Co.
300-kw and 500-kw motor-generator sets for reserve exciter and starting unit.....General Electric Co.
4 motor-operated "limit torque" valve mechanisms.....Philadelphia Gear Works

Miscellaneous:

Oil-storage and purifying equipment.....Turbine Equipment Co.
Powerhouse elevator, 6000 lb capacity, 100 fpm....Otis Elevator Co.

Passenger elevator, 2500 lb capacity, 200 fpm; service building.... Westinghouse Elec. & Mfg. Co.
Stairways and platforms.....Syracuse Stair & Iron Works
Structural steel for powerhouse building.....Bethlehem Steel Co.
Structural steel for coal galleries..Lackawanna Steel Construction Co.
Structural steel for switchyard..Lackawanna Steel Construction Co.
Traveling water screens.....Chain Belt Co.
Turbine-room crane, 150 ton....Shepard-Niles Crane & Hoist Corp.
Flue-dust catchers (multicyclone).....Prat-Daniel Corp.
Heating boilers, two 100 hp 125 psi.....Ames Iron Works
Chemical laboratory furniture.....Kewaunee Manufacturing Co.
Coal grindability machine.....Babcock & Wilcox Co.
1 machine-shop crane, 15 ton.....Shaw-Box Crane & Hoist Co.
1 crane for gatehouse, 15 ton....Shepard-Niles Crane & Hoist Corp.
1 transfer crane and hoist for fan floor, 7½ ton.....Shepard-Niles Crane & Hoist Corp.
2 transfer cranes and hoists, 5 ton.....Chisholm-Moore Corp.
All-welded rectangular condensate surge tank for 29.5 in. Hg vacuum .....Chicago Bridge Co.
Thearle portable dynamic-balancing equipment..General Electric Co.
2 mill seal D-4 blowers.....Allen Billmyre Co.

Discussion

J. R. Baker.[3] It is obvious that the designers of a new station to serve a system which stretches the length and breadth of the State of New York could look to the ultimate in size of individual generating units. The choice of 100,000-kw electric units, however, does not reflect such an approach but rather the selection of the maximum capacity of the simplest type of turbogenerator to operate on the highest proved steam conditions, the steam to be obtained from the smallest number of the largest boilers that have indicated feasibility. A single-cylinder condensing turbine operating at 1800 rpm is probably the least complicated turbogenerator yet devised for operation with high-pressure and high-temperature steam; previous units of large capacity have generally utilized a tandem or cross-compound arrangement with double flow in the low-pressure section, and sometimes with reheating of the steam between sections of the turbine. It appears that the commercial maximum sizes in the selected types of electric and steam generating units also fit into the system requirements with respect to operating flexibility. Thus, the design seems to embody or to approach closely the present-day peak of thermal efficiency combined with the minimum of capital costs.

It is believed that the analysis which led to the adoption of an 1800-rpm single-spindle condensing turbine of 100,000-kw capacity to operate on steam of 1250 psi and 900 F, and to the discarding of possible alternatives in capacity, speed, and arrangement, portrays the basic advance in design represented by the station, and far overshadows the development of the comparatively minor items such as automatic soot blowers and pilot safety valves, useful as they may be. The authors have been too modest in setting forth their real achievement.

The thermal efficiencies, indicated in Figs. 6 and 14 of the paper, of 10,680 Btu per kwhr and 31.6 per cent, respectively, appear to correspond to full load on the turbine. Is it expected that the point of best loading will decrease the thermal rate? What is the expected thermal rate on a yearly basis, reflecting operation under stand-by conditions? The thermal rates mentioned in the paper are partly explained by the authors' statement: "The heat which circulates through the steam generator, when operating at its rated capacity, is 50 per cent greater than the heat in the fuel that is being fired." Perhaps the influence upon thermal efficiency of the six bleeder heaters and the oil and hydrogen coolers could be more directly stated by pointing out that, of the heat going to the turbine, 26 per cent is converted to power, 32 per cent is returned to the boilers, and 42 per cent only is lost to the circulating water. The heat contributed to the steam generator by the air heaters amounts only to between 8 and 9 per cent of the heat in the fuel fired, as contrasted to 42 per cent brought in by the feedwater.

Returning to the main emphasis in the paper, that of automatic control and supervision of equipment, no one can question the desirability of seeking the utmost in continuous reliability of essential equipment for the full operation of the station and of the large savings possible in capital cost by the elimination of duplicate equipment the only function of which is that of replacement for equipment in trouble. Automatic control can also contribute to fuel and labor savings by maintaining operation at a predetermined level of efficiency and by eliminating manual attendance for many repetitive procedures. In fact, the modern-steam-plant operator, in contrast to his progenitors, has in recent years become largely the handmaid of automatic-control equipment. Until the Oswego Station was designed, such jobs as soot-blowing had, however, been left to the personal attention of operators. The authors now find that this innovation will pay its way.

Apparently, coal and ash handling, perhaps the control of boiler-water conditions, and certain starting and stopping procedures comprise the only manual functions expected of operators, although in certain cases of starting and stopping, the equipment is so interlocked as to compel the proper routine. In connection with the starting of the boilers and turbines, a description of the steps required in bringing the equipment into operation from a cold condition, together with the time required, would be of interest. It has been reported that a half day or more has been required in other stations of similar characteristics. This period would seem critical and appears to present the only condition for which some automatic-control equipment has not been specifically mentioned in the paper. Instruments for noting the starting conditions of the turbines have of course been provided, and the juxtaposition of the boiler, turbine, and electrical control boards in a central location between the turbines and boilers should facilitate the starting procedures. The question might be asked if the controls of the condensate, boiler feedwater, and circulating-water pumps are also located in this control room. What is the organization of personnel in the control room; that is, does one operator manipulate all controls, or is there a segregation of duties according to the basic divisions of the station?

C. H. Delany[4] and V. F. Estcourt.[4] In this paper the authors give some interesting details covering the design of a modern steam plant intended for quick pickup operation in connection with a large hydroelectric system.

For the last ten years we have been operating a 1250-lb steam-turbine plant containing two 50,000 kw vertical compound units operating at 750-deg steam temperature with the steam reheated to the same temperature before entering the low-pressure turbine. This station is operated as a stand-by station. Some of the results of emergency load pickup at this station were described in a paper by V. F. Estcourt.[5] Operation of this plant has been entirely satisfactory and there have been no important troubles that can be ascribed to the high pressure.

One advantage of a high-pressure plant which is not usually recognized is the fact that steadier boiler operation is obtained due to the greater density of the steam at high pressure than at low pressure. This results in less fluctuation of water level in

[3] Assistant to president, Pennsylvania Water & Power Company, Baltimore, Md. Mem. A.S.M.E.

[4] Assistant Engineers of Operation, Pacific Gas & Electric Co., San Francisco, Calif. Mems. A.S.M.E.

[5] "Design and Operating Problems with Gas- and Oil-Fired Boilers for Stand-By Steam-Electric Stations," by V. F. Estcourt, Trans. A.S.M.E., vol. 59, 1937, paper FSP-59-1, p. 7.

boilers, which is of special advantage where sudden load pickups occur.

Maintenance has not proved a serious matter in the high-pressure plants. The advent of high temperatures and pressures has forced a marked improvement in the design and construction of valves and flanges, as well as the development of more suitable alloys. Thus the frequency of maintenance work is no more than in a low-pressure plant. Some difficulty has occurred in valves in the feedwater line because of water getting under the threaded seats, but this has occurred as much on the 600-lb pressure line as on the 1400-lb line. On the newer jobs this trouble has been prevented by the use of welded seats on all valves.

It is stated in the authors' paper that the Oswego station contains two units with one boiler per turbine. It is not stated whether there is any interconnection between the boilers and turbines of the two units. We have found that for quick pickup there should be available about 40 per cent more boiler capacity than is required for operating at full load. This being the case, interconnection between boilers of the separate units is very desirable, as it makes possible an instantaneous pickup of full load on one turbine as long as both boilers are in operation.

It is also stated that one of the reasons for the selection of one boiler per turbine was the recognition of the reliability of modern boilers. However, the availability of boilers cannot be considered equal to that of turbines and therefore some turbine shutdowns must be charged against forced boiler outages in a one-boiler one-turbine installation. Whether or not this is an acceptable condition will depend upon whether system conditions as a whole justify carrying the additional reserve in turbines necessary in order to allow a certain number of turbine outages chargeable against boiler outages. This statement of course would not apply to the Oswego installation, if interconnection between the two boilers has been provided with sufficient reserve capacity in each boiler to carry some additional load on the second turbine.

The use of 250-lb air for soot blowing is noted. Since, with certain types of fuels, deposits on boiler heating surfaces is a serious problem which has not been entirely solved by means of steam soot blowers, more detailed information on the actual operating performance of this installation would be of interest, both from the standpoint of soot-blower and air-compressor operation and maintenance, and also the results obtained in deposit removal as compared with steam.

In some cases a plant of high efficiency may be justified even for stand-by operation, because of the fact that it may later be used as a base-load plant; and furthermore the more efficient the plant, the smaller the boiler capacity and the condenser capacity required. The condenser equipment is smaller not only because less steam is required at the throttle but also because of more extraction points, resulting in much less steam going to the condenser. This results in less cost of circulating water intake and discharge tunnels and tends to offset the extra cost of the high-temperature, high-pressure equipment. In this connection, it is noted that the Oswego turbines have six extraction points, which is more than would normally be used in a plant designed for lower pressure.

In deciding upon the operating pressure, the size of the unit will also be a factor. For example, in so far as the turbine is concerned, there is an optimum size for maximum turbine efficiency based on the two factors of size and steam pressure. If too high an operating pressure is selected for a small-sized unit, a sacrifice in efficiency must be made due partly to the small bucket sizes required in the first-stage wheel.

J. C. Hobbs.[6] It would appear that this station is the result of the combination of long years of actual experience, including the pioneering of "high pressures" in the C. R. Huntley plant, and the many subsequent power developments originating in the Buffalo General Electric plants. The best theory and practice made available by committees and individuals of the A.S.M.E. and by public-utility organizations were utilized in this development.

This paper indicates very clearly that a great deal of attention to details, and successful solutions to many problems, were required to obtain the proper functioning of the component parts of a power station of such large size. Not only does the equipment appear to be designed to function properly, but the instrumentation appears to be such that the operators, many of whom cannot be trained technical men, because of their scarcity, are furnished at all times with sufficient information so that they can obtain the desired economical result.

Years ago the central station which contained a condensate- or a coal-weighing system which could be used for making periodic tests was the envy of those built without such features, but today (and this station appears to represent the best) a station is on continuous test and the operator knows at all times whether the equipment is performing properly and, if not, what is necessary to make it function. Air was once considered a free component of combustion but this station includes air meters. The entire installation seems to be built to give the operating staff complete information so that they will have an opportunity to obtain creditable performance.

It is interesting to note that today's practice, as represented in this station, includes bank-balance methods of accounting for all items of value. At the same time, it is observed that modern banks now use electrical devices for accounting for the dollars and pennies which they handle. It was formerly customary for concerns, even public utilities, to place under bond the petty-cash clerk, who handled only a few dollars, in order to make certain that every penny was accounted for. These same companies employed firemen who might not even be able to speak the English language, whose job it was to handle thousands of dollars worth of fuel—many times recklessly. No provision was made for instrumentation to determine how much unburned fuel was being discharged through the stack or shipped out in the ash cars.

The adoption of 1250 lb pressure for a condensing plant is another step in the right direction. At first thought the 1250 lb now appears to be so relatively low that its significance is not realized. There are many reasons for the adoption of the 1250 lb which should not be forgotten just because the present-day practice has not reached this standard. Each improvement advancing the power art has been criticized. Pulverized-coal and water-cooled furnaces got their share.

High pressure, in spite of a considerable number of topping plants, operating at 1200 lb and above, is not appreciated in proportion to its merit. There seems to be an antipathy for high pressures by those who have not had actual operating experience. In one plant containing equipment operating at 700, 800, and 2200 lb, the operators much prefer the high-pressure apparatus even though, before it actually went into service, they were literally "scared stiff," as the expression goes.

A few fundamental reasons should not be overlooked:

1 That fewer pounds of steam are required to produce a kilowatthour with high pressure than with low pressure at the same temperature.

2 Considerably less heat or coal is required to make a pound of steam at high pressure than at low pressure.

3 Equipment such as piping, pumps, valves, and even turbine parts are much smaller when using high pressure than the relatively "low" pressure formerly considered standard. It is

[6] Vice-President, Diamond Alkali Company, Painesville, Ohio. Fellow A.S.M.E.

true that some of this equipment, such as valves, has not been commercially developed to take full advantage of increases in reliability and decreases in weight; but all in all, because of lower total steam consumption and the smaller piping, turbines, and condensers, the cost of a plant around 2000 to 2500 lb can actually be less than for the low-pressure plants of less than 1000 lb.

Another factor which should not be overlooked is that, because of the smaller piping and smaller valves, differential temperature stresses are less than they are in large equipment where greater temperature ranges may occur with correspondingly greater stresses and probability of expansion failures.

Commendation is due the designers for going to a 1250-lb straight-condensing plant. If any criticism were to be offered, it would be because they did not make full use of the opportunities offered at pressures of 2000 lb and above.

SABIN CROCKER.[7] The A.S.M.E., and particularly its contingent of central-station engineers, is indebted to the authors for a thoroughgoing factual account of what equipment went into the Oswego Steam Station. Where pioneering work is being done, as in this case, it is a great help to others in keeping abreast of new developments to have those responsible take the time and make the effort to set forth the facts. Although steam conditions of 1250 psi g and 900 F have been used for some time in superposing new equipment on old plants, this is one of the few instances where these conditions have been used for a wholly new plant built for straight-through condensing operation.

It would be of interest to have the authors say something about the economic analysis which led them to adopt 1250 lb at 900 F for the straight regenerative cycle in preference to the 800 to 850 lb at 900 F which has been used in a number of other recent condensing installations. In the case of topping units, the reason for using as high a pressure as is commensurate with a 900 F throttle temperature is apparent, since greater installed capacity is made available thereby as well as improved heat rate. Under these circumstances the presumed higher first cost of 1250-lb equipment over 800- to 850-lb equipment will be defrayed on two counts, whereas, with new condensing plants, the higher pressure probably has to pay its way out of fuel saving alone.

The installation described by the authors will afford a valuable proving ground for demonstrating whether the actual performance results in such a plant are up to theoretical expectations for the cycle. It is interesting to note that six stages of feedwater heating are used at Oswego, and that the ejector condenser, oil cooler, and hydrogen cooler are used as heat traps besides. This results in an unusually high final feedwater temperature, which in turn dictates a small economizer and a correspondingly larger air heater. On first impressions, these refinements would seem to involve a considerable capital outlay of an optional nature which would need to be supported by the high plant factor associated with base-load operation. Yet, it would seem from the paper that Oswego is intended as steam stand-by for existing hydroplants.

Hence, the writer is puzzled why the pressure adopted for Oswego is 1250 lb, whereas, economic studies in his own company have led to the use of 815 lb at 900 F for new condensing equipment having a normal plant factor. These remarks are not offered in a critical vein, but are voiced in the hope that the authors will feel disposed to discuss why they chose 1250-lb steam pressure and used what might seem to be a multiplicity of extraction stages and heat traps. Perhaps, a brief exposition of some concepts held by the writer will help the authors in trying to clear up certain points for his benefit and that of others interested.

[7] Senior Engineer, Engineering Division, The Detroit Edison Company, Detroit, Mich. Mem. A.S.M.E.

Fig. 15 of this discussion serves to show the trend of net heat rates with increasing pressure, as taken from typical figures for existing plants. The lower curve represents the best performance to be expected of a plant under ideal conditions at something approaching full load on the turbines, or possibly under steady base-load conditions. The point for 1250 lb is the net plant heat rate for ideal conditions at Oswego, as computed from

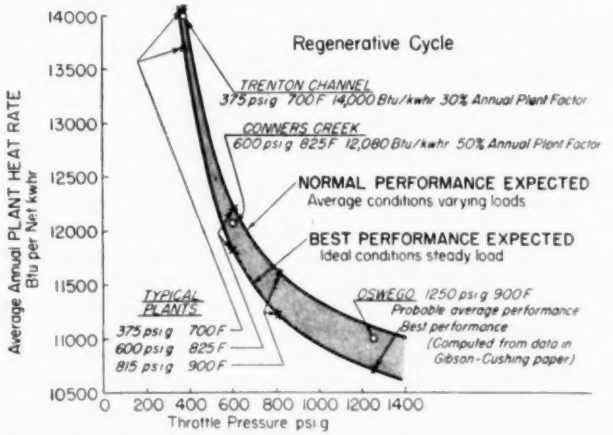


FIG. 15 TREND OF PLANT HEAT RATES WITH THROTTLE PRESSURE

the throttle heat rate and auxiliary-power requirements given in the paper, and with an assumed boiler efficiency of 88 per cent. The upper curve, which simulates average annual plant performance, shows the effect of varying load, banking losses, condensing-water temperature variation giving back pressures higher than nominal, and similar factors of an adverse nature. Both curves serve to point to the possibility that the 1250-lb 900 F regenerating plant may be in the region of diminishing returns because the thermal gains due to increased pressure have tended to flatten out. That this might be true is indicated by the fact that the heat saving, shown for the 435-lb step from 815 to 1250 psi is less than for the 215-lb step from 600 to 815 psi.

The extent to which the adoption of optional refinements of the plant cycle is warranted hinges in a large measure upon whether the turbogenerators can be kept loaded to somewhere near capacity most of the time. In other words, if optional refinements are to pay for themselves out of fuel savings, the savings have to be realized on a large output of kwhr. The index commonly employed to express the use made of generating capacity throughout the year is termed "annual plant factor," which is the ratio of actual kwhr turned out by a unit or plant to the number of kwhr it could have turned out if it had been fully loaded to rated capacity throughout the whole year. With base-loaded units, the annual plant factor may be as high as 70 or 80 per cent, or perhaps 90 per cent in rare cases. Such favorable plant factors usually are short-lived, since, with the subsequent addition of still newer equipment, the once-favored units are apt to be relegated to system-average service. Many plants, particularly those connected with rapidly expanding systems, never get a chance at base-load service.

The graph of annual plant factors covering 16 years since starting such a plant is presented in Fig. 16 of this discussion, which was plotted from the records of the Trenton Channel Station of The Detroit Edison Company. During this period nearly 14 billion kwhr have been generated, which represent an average annual plant factor of 36 per cent. The straight dash line through the 36 per cent point placed above the one-half-age ordinate is merely the writer's personal guess as to a likely trend in plant factor with time in this particular case.

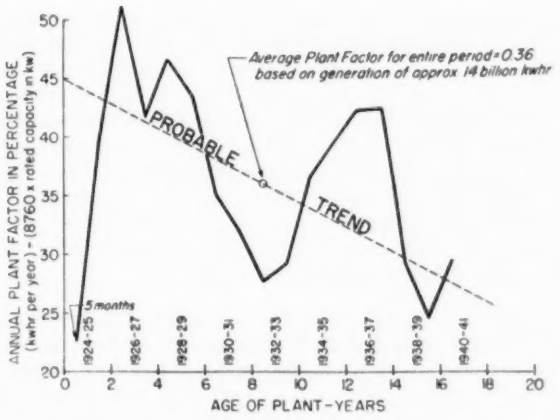


FIG. 16 ANNUAL PLANT FACTOR 1924–1940; TRENTON CHANNEL POWER PLANT

From reading this paper, the writer infers that Oswego is more in the nature of a stand-by than a base-load plant. If this is correct, the expected annual plant factors for Oswego hardly can be better than shown by the graph for Trenton Channel. It would be of interest for the authors to state what sort of annual plant factors over a period of years they would deem necessary to justify selecting 1250 lb steam pressure for a condensing plant over, say, 815 lb pressure, and what the investment differential would be.

F. P. FAIRCHILD.[8] In many ways the new Oswego Station reflects recent progress in steam-station design, and the authors are to be congratulated for their vision and courage in adopting many new and heretofore untried features, including the following:

1 One boiler per turbine for units having a maximum output of 100,000 kw.

2 Single-shaft turbine for this size and 1250-psi 900 F operation.

3 Three-phase transformers for the main unit.

4 Omission of the usual unloading tower for water-borne coal, depending entirely upon self-unloading vessels.

5 Use of electric couplings for forced- and induced-draft-fan speed variation.

6 Automatic soot blowing, using air as the blowing medium.

Operating records of these new features will be watched with great interest by all those concerned with steam-station design.

The choice of 1250 psi is also interesting. During the period of 1935 to 1938, equipment for this pressure was developed to a high degree of perfection in connection with superposed plants, for which it is justified by additional capacity obtained, as well as by better efficiency. At the time the Oswego Station was designed, it is probable that, for a condensing plant, the theoretically most economical pressure was 800 to 900 psi by a small margin. The economical pressure does not, however, remain fixed, experience in the past indicating that it is continually changing toward higher pressures. In deciding on the steam conditions for a new station, such as Oswego, which probably will not be completed for many years, it is important to keep this factor in mind.

G. B. WARREN.[9] This paper has been paralleled in recent months by several other papers in the technical press describing other new and outstanding power-station designs. In some cases, these design papers have been followed or supplemented by detailed reports of the operating results. A more common agreement as to what represents the best practice in all of the various phases of power-plant design should come from such an interchange of information by outstanding engineers as to their various design ideas, and by a frank discussion later of the results obtained. As a result, we should get power plants of even greater simplicity lower initial cost, higher efficiency, and greater reliability.

Although the steam conditions of 1250 psi pressure and 900 F temperature represent advanced and modern steam conditions, they are not so high as to present, at this time, a hazard to good operation. Boilers and turbines have now been operating commercially at 1000 to 1200 psi pressure in this country for somewhat over 15 years. According to the 1939 turbine-operating records in the latest Edison Electric Institute publications, the original turbines, and it is assumed the original boilers, for these conditions are still operating at load factors which closely approach those for modern machines. Since that time several million kilowatts of plant capacity have been installed to operate at this pressure or above.

The first station to operate commercially in this country at 900 F went into operation about 5 years ago and has been followed since that time by just under 3,000,000 kw, now installed and operating at this or higher temperatures, and by more than 3,000,000 kw now on order. So far as the writer can ascertain, no failure in service has occurred as a result of these high temperatures, which testifies to the thoroughness with which the metallurgists, the steel manufacturers, the equipment builders, as well as the power-plant designers have studied the problems of the effect of higher temperature on their materials and their machines and so have anticipated the difficulties which might arise and have guarded against them.

We who have been closely associated with turbine design over the last 20 years or so feel that, fortified with the additional knowledge we now have as to the performance of metals at high temperatures, we can design for these conditions more conservatively than we designed 15 or 20 years ago for the lower temperatures then in use. This was because of our deficiency in knowledge at that time as to the behavior of the materials which we were then using at those lower temperatures. Probably, the same is true of the design of all of the other parts of the equipment in the power plant which operate at relatively high temperatures.

The sincere efforts which have been expended to make this station outstandingly economical from the fuel-consumption standpoint no doubt have been inspired by what the writer believes may be the correct long-range viewpoint, namely: (1) Fuel prices in the future are apt to increase relatively to other prices; and (2) a station which is designed and built now for high economy may not have its load factor depreciated as rapidly in the years to come as one which does not have such a good fuel economy, or as has the average plant with which we have had experience over the last few years.

The salient features of the turbines have been described in this paper, and the detailed internal construction was further described in a paper[10] presented by the writer.

The turbines, Fig. 17 of this discussion, are of the popular and rugged single-cylinder, single-flow condensing type, with numerous special features which have been incorporated in order to

[8] Chief Engineer, Electric Engineering Department, Public Service Electric and Gas Company, Newark, N. J. Mem. A.S.M.E.

[9] Designing Engineer, Turbine Engineering Department, General Electric Company, Schenectady, N. Y. Mem. A.S.M.E.

[10] "Progress in Design and Performance of Modern Large Steam Turbines for Generator Drive," by G. B. Warren, Trans. A.S.M.E., vol. 63, 1941, pp. 49–79.

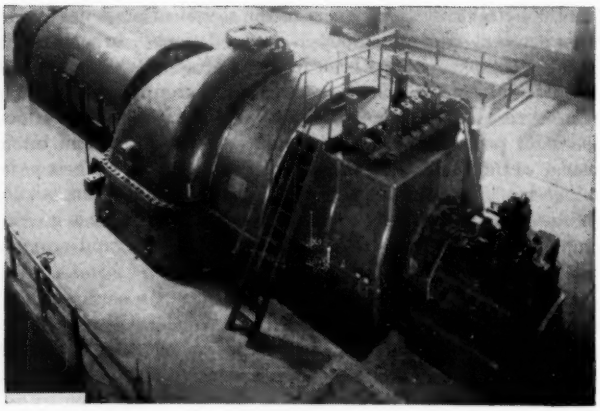


FIG. 17 SINGLE-CYLINDER, SINGLE-FLOW, CONDENSING-TYPE TURBINE AT OSWEGO STEAM STATION

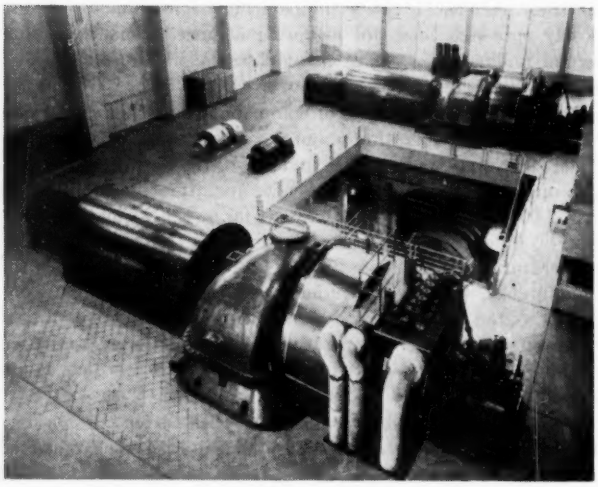


FIG. 18 SINGLE-CYLINDER TURBINE PREFERRED BECAUSE GREATER CAPACITY THAN TANDEM-COMPOUND-TYPE TURBINES

adapt this type of turbine to the high-pressure and temperature conditions at which they operate.

There seems to be an almost universal preference for such single-cylinder machines on the part of turbine-operating men.

On the other hand, because of the inherent limitations as to the number of wheels which can be put between two bearings, and because of the necessarily large shaft which such turbines require, it is sometimes impractical to make the economy of such a machine under normal load quite as good as it may be possible to obtain in a tandem-compound or a cross-compound turbine of similar excellence of design. This was discussed in the paper[10] by the writer previously referred to and in a companion paper presented in collaboration with P. H. Knowlton.[11] This difference, however, in a machine of this capacity and for these conditions is not great, and, where prospective turbine purchasers have been offered the alternatives of such compound turbines and single-cylinder turbines with the necessary differences in price and economy, by far the larger number have chosen the single-cylinder turbines where conditions of capacity, steam conditions, and speed permit such a design.

The single-cylinder turbine, Fig. 18 of this discussion, has been preferred by many over the tandem-compound type of turbine because of its generally shorter length with resultant lower station costs, or because installations of greater capacity have been permitted within the limitations of existing stations. It has also been preferred by many over the cross-compound type of turbine because of the simpler foundation structures, the simpler switch gear, and the simpler operation resulting.

In this matter as in many others with respect to power plants the opinions of competent engineers differ, and for this reason turbines of different designs continue to be built. Out of such experience the final best design will emerge.

E. KLAFSTAD.[12] Since details of the safety-valve arrangement used by the authors may be of some general interest, the main points of valve arrangement and construction will be presented. The arrangement is a new idea designed to improve upon the established uses of spring-loaded safety valves without sacrificing safe practices, also to add to the flexibility, foolproofness, and general all-around adaptability.

The subject installation makes use of the required spring-loaded code valves (of which eight are located on the drum and three at the superheater outlet) to a decided advantage.

In addition to the eleven code valves (all 3-in. size) there are three pilot valves (also spring-loaded safety valves) of purposely low-capacity ratings, one of which is located on the drum and two on the steam line at the turbine stop valve. The pilot valve on the drum actuates two of the valves at the superheater outlet, one on either side of the divided superheater. These same two superheater valves are also actuated by the highest-set pilot valve at the turbine throttle. The lowest-set pilot valve at the turbine throttle actuates the third valve at the superheater outlet. The pilot valve on the drum, being set at a pressure lower than the drum valves, gives positive assurance that a demand for steam through the superheater will be created before any drum valve opens. The pilot valves at the turbine stop valve prevent the pressure at the turbine, under normal operating conditions, from rising above a safe maximum. Thus it is seen that protection is afforded to both the superheater and the turbine.

The advantages of this arrangement have been covered by the authors.

The pilot valves, also referred to as "actuator" valves, are, as stated, spring-loaded safety valves of small size and low capacity. They are not included in the required safety-valve setup in relation to aggregate capacity requirement but are in addition to the code valves and can therefore be placed on gate valves for maintenance removal without boiler outage. The pilot (actuator) valve is so designed that, when it pops, the body pressure created by the discharging steam is transmitted, through a separate vent at the side of the body, to a line which in turn is connected to a pressure chamber in the superheater (actuated) valve. The pressure acts on the underside of a piston fastened to the spindle of the superheater valve, thereby overcoming the spring load which holds this valve closed. The valve remains open until the pilot valve closes, then reseats immediately. The time lag on opening and closing between the two valves is less than 3 sec when the pilot valve is 150 ft away, as in the case of the turbine pilots, and less than 1 sec when the distance is 50 ft or less, as in the case of the drum pilot in the subject installation.

As the superheater (actuated) valves are in themselves recognized spring-loaded code safety valves, they can be adjusted to any desired self-actuating set pressure up to within a reasonable range below the lowest-set drum valve and, thereby, allow the pressure at the superheater header to be raised during opera-

[11] "Relative 'Engine Efficiencies' Realizable From Large Modern Steam-Turbine Generator Units," by G. B. Warren and P. H. Knowlton, Trans. A.S.M.E., vol. 63, 1941, pp. 125–135.

[12] Chief Engineer, Crosby Steam Gage & Valve Company, Boston, Mass. Mem. A.S.M.E.

tion without inadvertent popping of the superheater valves. There is added assurance, during "overfiring" conditions, when the pressure rises nearly an equal amount over the system without change in the rate of flow, that a positive demand will be created at the superheater outlet, because pilot valves are located at both ends of the system and will therefore respond before the drum valves under all operating conditions.

If and when "overload" conditions occur, with higher than normal pressure drops, again protection is provided from inadvertent popping of the actuated superheater-outlet valves, because of the higher than normal set pressure of these valves.

M. D. Engle.[13] The designers of the Oswego Station are to be congratulated upon the courageous manner in which they have proceeded with the design of this new generating station. They have apparently endeavored to utilize the results of their own experience in their other stations, where economical to do so, but have not hesitated to depart from their past practice, where experience elsewhere has indicated the wisdom of such a change, or where their own experience and the experience of others has not produced a satisfactory answer.

To mention only a few items: They have continued with the use of the slag-tap furnace which was largely developed in their own plants and which has proved satisfactory for the fuels which they customarily burn.

They have adopted the higher steam pressures and temperatures which have been proved reliable and economical in many other stations. As a result of this foresight, it is probable that this station will have a longer useful life than if more moderate pressures and temperatures had been used. Because of present world conditions resulting in greater than normal demands on all modern power-generating facilities, it is probable that the adoption of the higher pressure and temperature will show up more advantageously than expected.

They have pioneered with equipment of new design for the operation of boiler feed pumps, induced-draft fans, and soot blowers, because neither they nor anyone else has found an economical and thoroughly satisfactory solution.

The adoption of the unit construction of one boiler for each turbine should result in lower cost of construction and operation and has sufficient operating background to be justified for their system even though it required a boiler of abnormally large size.

The heat-balance arrangement adopted appears to many of us to be more complicated and expensive than is warranted. However, heat-balance arrangements have been for years almost as personal as one's religion, and certainly we should not criticize too severely when few of us ever put in two units with the same arrangement.

It would appear, however, that if high thermal efficiency was desired, as indicated by the heat-balance arrangement, a regenerative reheat cycle with a simpler heat-balance arrangement would have given better station economy and would not have been any more complicated.

The use of high-pressure air for soot blowing is indeed a novel experiment which will be watched with interest. To some of us, it would appear to be unduly expensive; it would add to the usefulness of the paper if the authors could explain how they were able to reach the conclusion that it was cheaper than steam soot blowers. Also how they will be able to take care of the deslagging blowers which may require higher pressures than provided for with the air compressors mentioned in the paper.

Some will also question the need for the greater complication in the combustion-control system, which endeavors to proportion accurately the air to coal from each pulverizer. It will be interesting to learn after several years of operation whether or not the additional first cost and maintenance costs have been justified. If it proves economical, the industry will again be indebted to this company for having pioneered for our benefit.

The use of road-building equipment for stocking and reclaiming coal in large quantities appears logical and economical. Such equipment is built for more rugged service than will be required for coal handling and should have a long life. Its low comparative cost and its flexibility should prove very attractive. Many of us will no doubt follow their lead in this innovation.

E. H. Krieg.[14] Good judgment has been shown by the selection of 900,000-lb per hr boilers and 80,000-kw turbine generators which are really good for 100,000 kw. Units of this size appear to be approximately correct for a 1,500,000-kw-peak system. The selection of a 1250-lb 900 F cycle, unusual for the anticipated wide load range of 4000 to 100,000 kw, is doubtless justified and gives an economical cycle which may permit base-loading in the future, since load conditions are bound to differ somewhat from the original estimates. No doubt the war has already changed the original expectations.

Some amplification of the following points would be appreciated:

1 Is it economical to install two 100-hp oil-fired heating boilers in contrast to the usual practice of using bleed steam for heating? It has not proved difficult to avoid contamination of condensate.

2 Cannot the variable-speed boiler feed pumps go down to 220,000 lb per hr? Or is efficiency at that point so poor that the 220,000-lb per hr boiler feed pumps are financially justified?

3 What is the function of the raw-water condensate cooler, labeled *A*, in Fig. 4? Were any objections found to the usual practice of recirculating condensate?

4 Would it not be somewhat better to place the deaerator, part 9 in Fig. 4, on elevation 377 floor rather than the 305 floor, particularly since it is built for 90 psi abs? We rather like to have as much static head on the feed-pump suction as possible to minimize difficulties resulting from changes in bleed pressure. What is the oxygen guarantee of these deaerators?

5 Why use direct-contact heaters on the two lowest-stage heaters? The accumulator effect of such heaters requires extra-safe nonreturn valves, with an appreciable pressure drop. Would not closed-type heaters give just as close, if not a closer, terminal difference if no nonreturn valves were installed? We have pointed out on several occasions that nonreturn (or check) valves are usually not required on the lowest-pressure closed-bleed heaters, since the available energy in the low-pressure steam is seldom great enough to overspeed the turbine. The steam also passes through relatively few turbine stages. Such valves were omitted at the Windsor, Atlantic City, Philo, and Cabin Creek plants.

6 Is automatic water-level control for the ninth or deaerating heater advisable? In the event of sudden load loss, the ninth-stage bleed steam pressure would probably have a much faster rate of change than the condensate flow into the heater. In such a case, does not the heater pressure drop too rapidly, making it possible to lose the necessary positive feed-pump suction pressure? The same effect might result from a broken boiler tube, causing a proportionately greater feedwater flow than usual for a given load or bleed pressure. What would be the objection to an uncontrolled level? On several deaerators, having 1,000,000-lb per hr flows, we have experienced no difficulty under any operating condition.

[13] Assistant Superintendent of Engineering, Boston Edison Company, Boston, Mass. Mem. A.S.M.E.

[14] Engineering Department, American Gas and Electric Service Corporation, New York, N. Y. Mem. A.S.M.E.

We agree that with an adequate outside power source, there is no need for turbine-driven auxiliaries. The latter practice was formerly required, but many engineers have found that steam-driven auxiliaries are not needed for plants which need not be self-starting. However, turbine drives are still very attractive for most superposed or topping stations.

W. P. Thomas.[15] The automatic sequentially operated compressed-air soot-blower system, outlined in the paper, has created so much interest that it is believed an elaboration of this subject will be of interest.

One of the most important problems encountered in the design of this plant was that of feedwater. The following sources of steam for soot blowing were investigated:

1 Directly from the boiler drum or superheater header, using soot blowers designed for full boiler pressure.
2 From the boiler drum or superheater header reduced to 600 psi through a reducing valve.
3 Bleeding from an intermediate stage of the turbine.
4 From the evaporators.
5 From a separately fired boiler.

All of these sources had definite drawbacks. The simplest method was installing a reducing valve on a saturated drum outlet. The reduction in pressure from 1250 to 200 psi required on the soot-blower nozzles would result in wet steam. In order to eliminate the possibility of trouble caused by wet steam, it was decided to study the use of compressed air blowing on the air heater and the economizer. The economy of air over steam indicated by this study warranted expanding the study to cover the entire boiler, including the furnace walls.

Experience with soot blowers on a boiler of similar construction indicated that an air pressure of 200 psi on the nozzles would be required for removing the soot and fine ash from the superheater, economizer, and the tubular air heater with tubes 50 ft long. Since this boiler would be fired with a larger variety of coals than on other boilers of this same construction with which we were familiar, it was impossible to predict whether or not this pressure would suffice for slag removal from the waterwalls. In order to provide a margin of safety, it was decided to make provision for mixing water with the air and also to have a source of higher air pressure available. Comparisons of 350 psi and 500 psi costs were made. All things considered, the higher pressure appeared more favorable.

With the air demand and pressure determined, a study of the duty cycle showed that two 500-cfm compressors feeding four 500-psi receivers of 500 cu ft capacity each would provide an excess air capacity of 20 per cent. Allowance of 50 psi drop through the pipe, valves, and soot-blower heads, plus the change in receiver pressure during blowing, determined the reducing valve required for dropping the pressure in the main receivers to that in the 100-cu ft ballast or low-pressure receiver.

The study of relative costs of steam versus air blowing showed that the increased initial cost for the air equipment would be offset in the first year of operation without taking into consideration the intangible value of the make-up water.

The use of compressed air as a soot-blowing medium was not new. It had been recognized as offering certain advantages over steam for nearly 20 years. In the early days, air-operated blowers proved uneconomical because of uncertain cleaning results (low air pressure was used), and because of the high capital investment required for large compressors and receivers. Both of these deficiencies arose from the lack of automatic controls. We had been working on this control problem for several years in our research department and had developed a comparatively simple control system. In the case of Oswego, however, automatic control fitted ideally into the picture because the entire station would be monitored from a central control room.

All the soot-blower units and air-control valves are actuated either by air pistons or electric motors. Air operation is used on the conventional rotating units installed within the boiler settings because it provides automatic operation at minimum cost.

The piping is of welded-header construction. Connection to the furnace-wall units is designed for 500 psi pressure, and all other connections are suitable for 250 psi pressure. All automatic valves are of the "Thrustor" flanged type. They were chosen for this particular service because of their quick opening and closing characteristics. These valves are all backed by hand-operated emergency valves to facilitate regrinding.

The electrical control was assembled from standard equipment, grouped to meet our specific requirements. The Oswego installation was made unusually complicated to provide for emergencies which never arose. Subsequent experience in the plant indicates that future installations can be simplified without sacrificing foolproof operation of every unit.

Very little trouble developed in over a year of operation. Long strap-type standing bearings bolted to lugs welded to the top of the economizer tubes in the by-pass section broke loose from the lugs and permitted the element to warp and sag. Changes had to be made in the Thrustor valves to make them satisfactory for this particular service. Both of these troubles have been eliminated. Contact trouble due to high resistance developed in the electrical control; it is believed this trouble can be eliminated by substituting different contact material. The method of making contact will be changed in future installations.

The use of air as a cleaning medium in soot blowers has been demonstrated to be economically sound in nearly 100 installations on low-pressure boilers, where the soot-blower equipment was entirely automatic. This Oswego installation is the first utility project where air has been used as a cleaning medium in soot-blowing equipment which is entirely automatic. After more than a year of operation, it appears that the economies figured by the engineers, in labor saving and maintenance of piping and equipment, as well as operation, have been fully justified.

R. C. Roe.[16] The writer's organization has enjoyed working with the authors and their associates as consultants during the design of this station.

There are several features of the station which perhaps deserve more comment than appears in the paper. One of these is the boilers. Inasmuch as the turbines were each to be served by a single boiler, and inasmuch as the capacity of the turbines was large and, hence, the effect of the loss of a unit on the system was great, the boiler designs were scrutinized with exceptional care by all those concerned, to the end that the maximum reliability and availability would be provided.

The hydraulic circuits are particularly noteworthy and are believed to have furnished an example which has been incorporated in designs following later. The arrangement of furnace surface and screen tubes to cool the gas before entering the tube banks has been very successful in operation, with the result that the tube banks are free from slag accumulations and are easy to keep clean under continuous service at high ratings. The operating record of the boilers has fully come up to expectation, both as to reliability and availability.

The use of high-pressure air for blowing soot automatically with a predetermined sequence is a step in advance for large

[15] President, Diamond Power Specialty Corporation, Detroit, Mich. Mem. A.S.M.E.

[16] Burns & Roe, Inc., New York, N. Y. Mem. A.S.M.E.

stationary high-pressure boilers. This method not only saves some fuel on a Btu basis, but also has a tendency to maintain a much cleaner boiler, to contribute less to corrosion in the air heater, to clean surfaces subject to slag accumulations more effectively, and to improve the reliability and availability of the boiler.

The use of an automatic premeasuring combustion-control system is a fundamental step in the right direction.

The use of electric couplings of the eddy-current type for the control of fan speed is believed to be the first use of such coupling for such service, at least on central-station steam boilers. When it is realized that these couplings, at the time they were built, were several times as large as any similar couplings then in existence, it is readily seen that the engineers had faith in the fundamental soundness of the design or they would not have used such a device in a place where the entire station depended upon its successful operation.

The use of a six-point regenerative cycle with three points using closed heaters having integral drip coolers and three points with direct-contact heaters is not only a fine design thermodynamically, but also sound from an operating viewpoint.

The direct-contact-heater system, with its multisection heater pumps, the last two sections of which pump a mixture of steam and water in the form of a fluid of lower density than would be the case if the fluid were solid water, was the largest direct-contact-heater system yet built. It has been very successful in operation and free from any serious difficulties.

Taken as a whole the Oswego Steam Station is one of the most progressive yet safe and conservative designs that has come to our attention.

A. T. Hutchins.[17] This paper is replete with descriptions of interesting design features which include one of the most complete systems of automatic control that has come to our notice. A brief analysis of the turbine performance indicates that, in addition to the gain by carrying the feed-heating cycle to six stages and a final feedwater temperature of 485 F, there is a gain in turbine efficiency due to the increase in flow to the throttle while, at the same time, the exhaust losses are kept reasonably low, because of the reduced quantity of steam flowing to the condenser.

Possibly, one of the boldest features of this design is the requirement that a generating unit swing from full load to 4000-kw load almost instantaneously. In order that this might be possible on a single-cylinder unit of this size with steam conditions of 1250 psi and 900 F, the manufacturer has designed and built these units so that all the steam at any load passes through the first-stage nozzles and first-stage wheel. This results in limiting the high temperature to the steam chest and the first-stage nozzles and first-stage blades.

The arrangement of pilot pop valves to secure a predetermined pattern of steam release and so protect the turbine steam chest from excessive pressures is well worked out and should give excellent results. One of the important results from this arrangement is the positive protection of the superheater.

A unit arrangement of boiler and turbine invites close control of every feature of operation, and the accessories, provided in this design for giving the operator an indication of the performance of every piece of equipment in respect to any feature of opesation, deserve special attention. The devices chosen for such indications and records should give the required information as to the performance of all the important equipment.

In regard to combustion control, the size of the steam-generating unit warrants as complete control as may be desired, provided only that the operation of such control secures the result intended, that the control equipment does not become too complicated for quick and accurate manipulation, and that the maintenance does not require more attention than it saves in operation.

The writer is of the opinion that the maintenance of the proper steam-flow – gas-flow ratio, with the fuel supply to the burners closely following the heat demand, is more easily secured and gives better results than any other method of control in use. This statement is made because of the fact that a change in the heat content of the coal going to the mills will cause a much greater error in the ratios required for good combustion, when an attempt is made to maintain a fuel-air ratio than will normally occur due to sudden changes in the physical elements used in securing the steam-flow – gas-flow ratio.

As an example, a change of moisture in the coal, as weighed, from 3 to 10 per cent will disturb the fuel-air ratio approximately 7 per cent, while it will affect the steam flow – gas flow ratio by only a fraction of this amount, or approximately 0.9 per cent. We are pleased to note that the combustion control at Oswego is set up so that, under actual operating conditions, the relative value of these two methods of control can be determined for the range of fuel fired.

F. A. Allner.[18] In an earlier publication,[19] one of the authors had reported on design and economic features of Huntley Station No. 2. The data on capital investment of that station established a most enviable record for the author as a designer of low-cost steam plants. Similar cost data on this recent Oswego project, if and when such information is available, would be received with great interest by many engineers and would be a timely and pertinent supplement to this excellent paper.

S. M. Arnow.[20] This paper describes a plant where few possibilities for heat recovery were overlooked. Six stages of bleeding, three direct-contact heaters, variable-speed drives for boiler feed pumps, subcooling of drains, and recovery of bearing and generator losses leave little chance for any noticeable heat-unit losses.

No doubt the individual economies of the various pieces of apparatus have been carefully considered and proved for this plant; however, some of the heat-recovery schemes rather complicate the piping and are expensive when compared with the benefits obtained, hence they may not be applicable in all cases. As an example, the rise in feedwater temperature between the condenser and the 14-stage heater is 8.2 F. This represents approximately 5,000,000 Btu of which 700,000 are recovered by the air-ejector condensers, which are essential for the proper operation of the ejectors. The remaining heat recovery equipment results in a reduction of about 10 Btu per kwhr and at best would be justifiable only in a plant having a very high load factor.

While the authors do not include the expected duration curve for this plant, they mention a minimum load of 4000 kw during the period of high hydrocapacity, full load during droughts, also rapidly changing load conditions, so that this plant will have periods of very light as well as very heavy loads.

Using condensate for hydrogen and oil-cooling presents the possibility of losing hydrogen during light-load and low-vacuum operation and low oil temperature during high-vacuum high-load periods. Because of the location of the oil coolers and the

[17] Commonwealth & Southern Corporation, Birmingham, Ala.

[18] President, Safe Harbor Water Power Corporation, Baltimore, Md. Mem. A.S.M.E.

[19] "Design and Operation of Huntley Station No. 2," by H. M. Cushing, Trans. A.I.E.E., vol. 54, 1935, pp. 632–645.

[20] Division of Mechanical Engineering, Philadelphia Electric Company, Philadelphia, Pa. Mem. A.S.M.E.

air ejectors in the basement, and the hydrogen coolers on the operating floor, a somewhat complicated piping system must result. There is also present the possibility of condensate contamination by oil. For these reasons, the value of this part of the heat-recovery scheme is somewhat open to question.

Inasmuch as a 6-stage bleeding machine is somewhat uncommon, an evaluation of the economies of the first-stage heater is interesting. At the load, shown in Fig. 6 of the paper, the installation of the top heater results in a saving of about 5,000,000 Btu per hr, which represents a reduction of about 60 Btu in the heat rate. If this heater were left off and a 5-stage bleeding machine giving the same final feedwater temperature were used, the increase in the heat rate would only be approximately 40 Btu per kwhr. Assuming coal at $5 per ton, 60 Btu on the heat rate represents a saving of about 90 cents per hr. Assuming further that the average saving would be 50 cents per hr for 7000 hr of operation, the total saving would be $3500 a year. A 40-Btu saving in heat would reduce this figure to approximately $2500 a year. It is questionable whether such savings will be attractive when balanced against the cost of the two high-pressure heaters, drain controllers, piping, and valves.

Fig. 4 seems to be inconsistent, as it shows the drain coolers after the drain-control valves, while in the list of equipment integral subcoolers are indicated.

While in general the desirability of variable-speed drives for boiler feed pumps depends upon the loading conditions, for the Oswego plant, where the pumps take their suction from a direct-contact heater, reduction in load results in reduced suction pressure, which would appear to reduce somewhat the gain attributable to the variable-speed operation.

Authors' Closure

It is true, as Mr. Baker says, that the very simplest design of turbogenerator was selected for Oswego, i.e., a single-shell turbine where all of the steam passes through the first-stage nozzles and the first-stage wheel. In this design, rapid changes in the turbine loading will produce the minimum of temperature and pressure stresses in the turbine rotor and its casing because of a large reduction in the temperature and the pressure of the steam as it passes through the first-stage nozzles. In fact, the stresses are lower than exist under similar load changes in the 250-psi, 750 F, 75,000-kw Huntley turbines of the conventional design installed in 1928 and 1930.

The station heat rates, given in Figs. 6 and 14 of the paper, apply to loads of 100,000 kw. A loading of 70,000 kw on a boiler-turbine unit will produce about 2 per cent lower values. It would be very difficult to predict the yearly thermal rate for a steam unit operating on the Niagara-Hudson system, because the monthly as well as the yearly loading for the unit depends upon an unpredictable value, i.e., the rainfall on the watersheds of the hydroplants.

An unusual feature, which has been introduced in the starting up and shutting down of the steam generators, is the practice of having the boiler drum full of water to minimize the difference in temperature of the various parts of the drum during the heating-up and cooling-down periods. The following starting procedure is based on keeping the rate of change of drum-metal temperature to within 100 F per hr.

Normally the drum is filled with 80 F condensate up to the drum vents. The superheater may have been left partially filled with condensate from the last cooling-down period or be entirely full from a hydrostatic test. While starting the steam generator, the turbine is being turned slowly by means of a turning gear. With boiler and turbine steam-line stop valves open and all of the drum, steam-line, and superheater drains and free-blows open, the automatic lighters are started and pulverized coal is introduced into the furnace from one pulverizer through one burner at the minimum rate of coal feed (approximately 5000 lb per hr). This firing is continued on a 10-minute-on and 10-minute-off schedule until the drum pressure reaches 35 psi gage. The water in the drum is dropped to normal operating level; the drum and main steam-line vents closed; continuous firing of pulverized coal is then established and the rate of rise of the drum pressure is controlled by the amount of steam drawn from the superheater-outlet drains. At 300 psi, the rate of coal feed is increased to about 10,000 lb per hr, and the hogging steam jet opened to bring up vacuum on the turbine. At 500 psi and 15 in. Hg vacuum, the turbine is started with steam and brought up to 300 rpm. The rate of rise of the steam temperature is controlled by adjusting the superheater by-pass dampers which had been closed up to this time.

Fig. 19 of this closure shows the time required for starting the

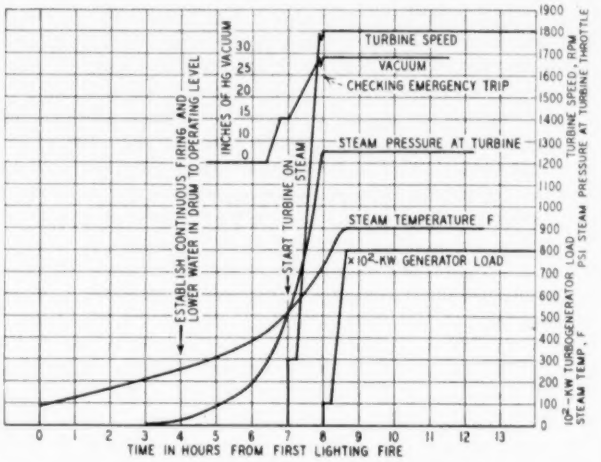


Fig. 19 Depicting Rate of Change of Boiler Temperature, Steam Pressure, Vacuum, Turbine Speed, and Loading for a Cold Start of Boiler-Turbine Unit

(Rate-of-speed change and loading of turbine-generator is censored by indications of supervising instruments.)

boiler and turbine and the rate at which steam pressure, steam temperature, vacuum, and turbine speeds are changed during this period. To aid in starting up and cooling down, rate-of-change templates have been carefully prepared for use in tracing the rate-of-change values onto the boiler and turbine control-meter charts. The fuel-firing controls, gas dampers, and superheater-outlet-drain valves are then so operated that the control-meter pens will retrace these template markings. The total elapsed time from the first lighting of the fire to the synchronizing of the generator is normally $8^1/_2$ hours.

The automatic level controls of condensate in the hot well, the deaerating heater, and the subcooling sections of the high-pressure heaters are in service during the starting period; but the automatic combustion controls are not put in service until the turbine is carrying load. Condensate and circulating-water pumps, pulverizers, and boiler fans are operated from the central control room. Boiler feed, house-service, slag, and sluice pumps and air compressors are operated from positions adjacent to the equipment.

Based on some 10 years of operating experience with 1250-psi condensing turbine generators, Messrs. DeLany and Estcourt bring out in the discussion and in the paper[5] to which they refer the many advantages to be gained by the use of 1250 psi steam pressure for a peak-load stand-by station, i.e., greater heat-storage capacity in the boiler and steadier boiler operation for sudden load pickups. Also, that maintenance has not proved a

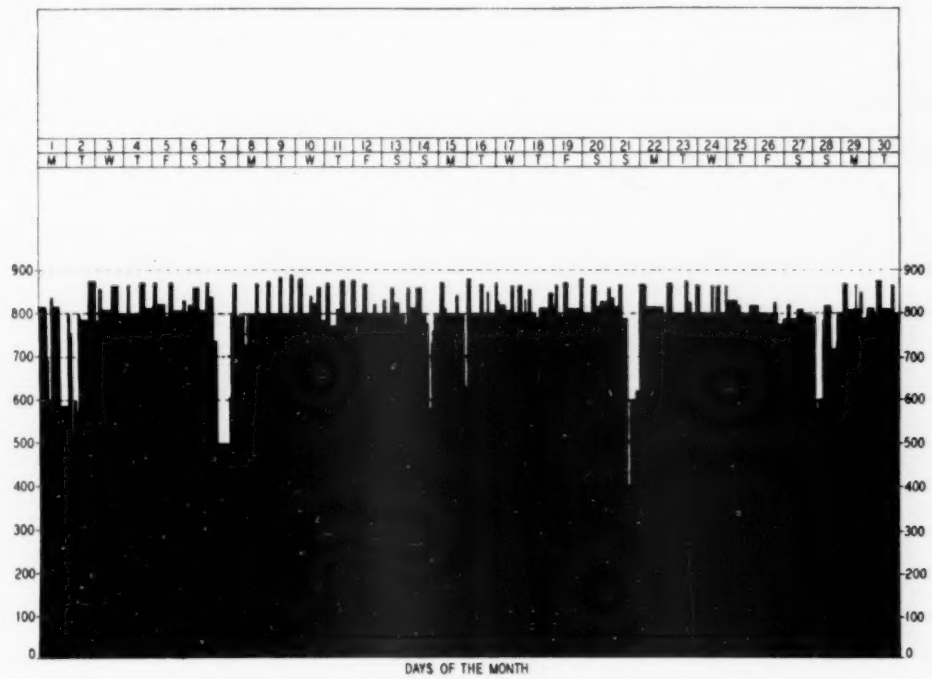


FIG. 20 OUTPUT CHART, NO. 1 BOILER UNIT, FOR 900,000-LB PER HR STEAM GENERATOR
(Net output, 56,402,000 kwhr.)

serious matter nor required more frequent attention than in low-pressure stations. The advantages of 1250 psi steam pressure for base-load stations are unquestionable.

There are no steam or feedwater interconnections between the two one-turbine one-boiler units. The extra-large capacity of the pulverizers has enabled the firing rate to be increased at the rate of 10,000 kw per min, thus making another source of steam unnecessary for quick turbine pickups.

Considerable time and effort have been fruitfully expended by the engineers of our company, the consultant, and the boiler manufacturer, in studying and modifying those features of the equipment where a change would add to the reliability and the availability of the steam generators and their auxiliaries.

The excellent condition of the waterwalls and gas passages of No. 1 steam generator, which was recently out for annual overhauling, convinces the designers of the soundness of the decision to use 250-lb air for soot blowing. Up to the present, this equipment has required very little maintenance. The operating department estimates that the maintenance cost of the air soot-blowing equipment, including the air compressors, will be less than on steam-blowing equipment.

As Mr. DeLany points out, there is an optimum size of turbine for maximum turbine efficiency which should be considered in the choice of steam pressure; e.g., a 10,000-kw condensing unit would be too small to use 1250 psi efficiently because of the resistance loss in its small steam passages.

Mr. Hobbs, from the wealth of his operating experience, outlines some of the fundamental advantages of high steam pressures and suggests reasons why these high pressures have been avoided by some engineers. It is interesting to note his prediction that we need not necessarily expect 2000-psi steam stations to be more expensive than those built for 1200-psi conditions.

The authors are sorry they led Mr. Crocker to believe that Oswego is more of a stand-by than a base-load plant. The station is designed for both purposes, to operate as "spinning reserve," stand-by service during seasons of high flow at the water power plants, and also to operate as base-load during seasons of low flow. This dual-service feature characterizes the steam station which operates on a generating system supplied largely by water power, in distinction to the steam station which is just another unit on a system supplied mainly by steam.

Instead of Oswego being one of the few stations built for 1200 psi steam pressure and straight-through-condensing operation, it represents only two of forty-three such units which are operating or are now being built for 1200 lb or higher steam pressure.

Fig. 20 of this closure, which shows the load carried by No. 1 boiler in September 1941, is an example of the base-loading for which this station is designed. During the first 6 months of operation, after No. 2 unit was started, the station generated 624,477,000 kwhr, equal to a capacity factor of 89 per cent. The amount of energy used by the auxiliaries, coal handling, miscellaneous power, and station lighting amounts to 6 per cent of that generated. It is expected that as the operating personnel become more experienced and greater attention is paid to the small savings here and there, this percentage will be reduced. There are no steam-driven auxiliaries.

Fig. 16 of Mr. Crocker's discussion was given to illustrate how the plant factor varies with the age of a steam station which is a generating unit on a system supplied mainly by steam. This curve has been reproduced in Fig. 21 of this closure and shows, in addition, how the plant factor of the two-unit 160,000-kw Huntley Station No. 2, a steam-generating unit of a system supplied mainly by water-power generation, has varied since it was first put in service in October, 1930. Note that, whereas the trend of plant factor for the 16-year old Trenton Channel Station has been downward from its high of 51 per cent plant factor in its third year of service, the trend of the plant factor of the 425-psi 750 F Huntley Station has been upward, reaching 74 per cent in 1941, its eleventh full year of service. These facts are offered to explain why it was necessary to design Oswego for both stand-by and peak-load operation.

Mr. Crocker asks what led to the adoption of 1250-psi 900 F

steam for the straight regenerative cycle at Oswego in preference to 850 psi 900 F which a number of recent installations have used.

Many of the advantages of 1250 psi steam, as compared to the lower pressures, have been brought out in other discussions.

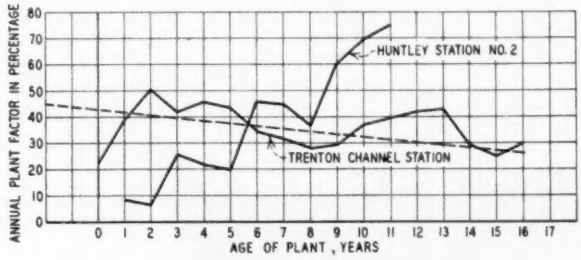


FIG. 21 COMPARISONS OF ANNUAL PLANT FACTORS

It does not appear that those items most affected by pressure are relatively large in the following table showing how the Oswego costs were divided:

	Per cent
Land	1.0
Wharf, yard, and channel improvements	2.6
Rock tunnel, intake and discharge flumes with enclosing buildings for gates and screens	4.7
Main powerhouse buildings and foundations	13.2
Coal galleries and coal-handling equipment	5.5
33- and 115-kv switchyard and transformers	5.4
Turbogenerators and condensers	21.1
Boilerhouse equipment	22.5
Piping for high-pressure steam, bleed lines, boiler feed, condensate, house service, and instruments	5.6
Accessory electrical equipment	5.0
Miscellaneous powerhouse equipment	1.3
Construction expense and overheads	12.1
	100.0

From an economic viewpoint, construction costs come into the picture. Construction costs are only slightly affected by pressure but are greatly affected by design in its relation to pressure. To illustrate, in the Oswego Station the differential construction cost was minimized because the quantity and number of valves, fittings, and the length of the pipe in the high-pressure installation were reduced by the use of one boiler per turbine and no interconnections between units. If interconnections were provided or if any piping arrangement except one of Spartan simplicity were used, then the differential in cost would increase because piping is one of the big items affecting differentials in cost.

As was brought out in the reply to another discussion, condensate was used in the ejector condensers, oil coolers, and hydrogen coolers to keep the heat-transfer rates as nearly as possible to their design values and to save cleaning expense of the coolers, as well as to recover some Btu's. An appreciable amount of the pumping power and piping costs would have been required even though raw water had been used for this cooling service.

In regard to Mr. Fairchild's comments that it is a bit unusual to adopt 1250-psi steam conditions for condensing turbines, it is interesting to note that there are now in service or on order some 43 condensing turbine-generators in sizes from 20,000-kw to 150,000-kw, designed for 1200-psi or higher steam pressures.

As Mr. Fairchild points out, the theoretically most economic steam pressure does not remain fixed and is continually changing to higher pressures. Since 1780, when steam pressure of 15 psi was first used for steam engines, the discussion has been raging as to the comparative merits of higher steam pressures. Our engineers received more criticism for adopting 250-psi 700 F steam conditions in 1916 for the Huntley Station than appears at this time when 1250-psi 900 F steam conditions were adopted for the Oswego Station.

Mr. Warren's comments should allay the fears of the engineer who thinks of the 1250-psi steam conditions as entering far into the field of the unknown, when he points out that the metallurgical knowledge and the operating experience now available enable the engineer to design more conservatively for 1250-psi steam conditions than was possible for the low-pressure turbines some 15 or 20 years ago and that boilers and turbines have been operating at pressures of 1000 psi to 1250 psi for more than 15 years.

Mr. Klafstad explains the details of safety-valve construction, which makes possible this new safety-valve arrangement, designed to reduce boiler outages and give greater protection to the turbine.

As Mr. Engle mentions, the slag-tap furnace was developed by Niagara-Hudson engineers—this was in 1925. With the addition of the Oswego Station, the steaming capacity of the slag-tap furnaces on the system exceeds 7,000,000 lb per hr.

It is gratifying to hear one so intimately associated with the first 1200-psi steam-turbine installation mention the proved reliability of high steam pressure and predict that the adoption of these higher steam conditions for Oswego will probably give the station a longer useful life.

Although Mr. Engle speaks of these boilers, generating 900,000 lb of steam per hour, as being abnormally large, one boiler represents only about 5 per cent of the generating capacity in operation on the system. There are now 17 steam generators in this high-capacity class in operation and on order in this country.

The straight regenerative steam cycle was used in preference to the regenerative reheat cycle because of the simplicity of turbine design.

The authors did not intend to convey the impression that air soot blowing was cheaper in first cost than steam soot blowing with steam direct from the boiler; however, they believe that it does require fewer Btu from the coal pile. Steam soot blowing requires considerable quantities of steam to warm the lines before each blow. Experience with 250-psi compressed air for boiler cleaning indicates that higher pressures will not be required. The present system does a splendid job of cleaning the furnace walls and boiler passages.

The adaptation of road-building equipment to coal handling was first tried at the Huntley Station in 1931 when additional coal-storing equipment was required upon short notice in the middle of the coal-storing season.

Replying to Mr. Krieg's questions by number:

1 In regard to the installation of heating boilers, they paid for themselves during the first season by facilitating the erection of machinery during the winter months. The winters are long and cold. The heating boilers are of the fire-tube type. They were installed on permanent foundations in a wood enclosure before the service section of the station was built around them.

2 The small constant-speed boiler feed pump was provided because a wider range of speed was not then available in the 1800-rpm coupling to enable the large pumps to handle the small loads efficiently during the long hours that the station would be operating as a spinning reserve. These couplings were the first 1800-rpm units of a new high-speed line of hydraulic couplings. A greater speed range is being provided and the small pump omitted for the boiler feed pumps on a similar generating unit now being installed at Huntley Station.

3 The raw-water condensate cooler *A* in Fig. 4 of the original paper is required for cooling the hydrogen when the generator is operating as a synchronous condenser disconnected from the turbine. Extra cooling may also be required in the summer time because of high circulating-water temperatures occasioned by a

protracted period of wind blowing from the lake, piling up warm water along the shore.

4 There is no objection to placing the deaerating heater at a higher level. At its present level, it furnishes the suction head specified by the boiler-feed-pump manufacturer and provides the best arrangement of the equipment.

5 In regard to the use of the direct-contact instead of closed-type heaters in the two lower stages, our engineers believe that a direct-contact heater is a more rugged device, therefore needs no provision for by-passing, and provides some additional deaerating of the feedwater. The use of closed heaters would not eliminate the need for nonreturn valves as they would then be required to protect the turbine against a ruptured heater tube.

6 In the event of a sudden loss in load, the drop in pressure in the 9th-stage heater would be accompanied by a corresponding drop in temperature. The authors do not agree with the principle of using an uncontrolled water level above the pump suction.

Mr. Thomas gives some of the additional reasons leading up to the adoption of compressed air for soot blowing. The evaporators, which were mentioned in his item 4, as a means of obtaining steam for soot blowing, were separate and distinct units from those supplying the boiler make-up water. Pressure switches prevent the starting of the blowing units until full air pressure is available.

Mr. DeLany said that the availability of boilers was not equal to that of turbines. Mr. Roe's comments explain what was done in connection with the Oswego Station to improve this situation by using exceptional care in scrutinizing boiler designs. The wholehearted co-operation given by the manufacturers in discussing design details has accomplished much to improve the availability factor of the Oswego steam generators and their appurtenances.

The continuous and simultaneous premeasuring of coal and air to each pulverizer and its pair of burners should do much to lessen the likelihood of operating with a reducing atmosphere in contact with the furnace walls. Reducing atmospheres in contact with 900 F metal of the wall-tube surface, together with the presence of sodium sulphide (which can exist only in a reducing atmosphere) are now thought to be responsible for the wasting away of the tube metal.

Engineers from other operating companies who have inspected No. 1 steam generator after $1^1/_2$ years of service expressed surprise at the thoroughness with which air blowing has done its work. No hand-lancing has been used or has been required at any time. The 250-psi air does the job very satisfactorily.

While, as Mr. Hutchins points out, the carrying of 4000-kw load on 80,000-kw turbine-generators is an unusual feature, this practice has been followed at the Huntley steam stations for years. This low-load operation really became attractive with the advent of the multiple-admission type of steam turbine which gives a relatively flat efficiency curve through a wider range of loading than was practical with the earlier design of turbine, the "best-point machine."

As Mr. Hutchins states, the automatic combustion controls have been set up so that the relative merits of the steam-flow–air-flow postmeasuring total system of controls can be compared in actual service with the premeasuring unit system. One advantage of the one-boiler-per-turbine arrangement that is often overlooked is that the heating and cooling strains in the boiler and turbine are more easily controlled when the two are operating as a unit without interconnections to other units.

Mr. Allner asks about the relative cost of this station compared with Huntley No. 2, both built to house two 80,000-kw steam-generating units. With rock only a few feet below basement-floor grade, the Oswego steam station cost 35.8 cents per cu ft of volume for the powerhouse and service buildings with their foundations, whereas, Huntley No. 2 Station, built on steel caissons with rock about 40 ft lower, cost $36^1/_2$ cents per cu ft. The spacing of the equipment at Oswego was made liberal in order not to put space limitations on the future units. The station contains 12 per cent more volume than Huntley although it has no electrical bay, the 33- and 115-kv structures being located outdoors. Of the Oswego volume, 2,000,000 cu ft, or 34.7 per cent of the total, is in the service building and track bay which will serve the ultimate development of five units.

Volumetric comparisons in thousands of cu ft are given in the following table:

	Huntley No. 2, M cu ft	Oswego, M cu ft
Turbine bay	1500	1790
Boiler bay	3005	3460
Service building and machine shop	...	600
Electric bay and control room	708	...
Total—main powerhouse buildings	5213	5850

Mr. Arnow and others have commented on the use of six-stage bleeding and the use of condensate for cooling the hydrogen, the lubricating oil, and condensing the steam from the air-removal equipment, implying that the only advantage of so doing was to increase the cycle efficiency. There are other advantages, for example: A liberal bleeding of the turbine in the low-pressure stages assists in removing water from the turbine with the resultant effect of increased life of the turbine blades; the first-stage, the highest-temperature-bleed point, tends to reduce the temperature fluctuations of the feedwater due to load changes, thus reducing thermal strains on the equipment; the use of condensate instead of raw water for cooling reduces the cleaning problem to nil, lessens maintenance, and keeps the heat-transfer rate to a maximum in the hydrogen- and air-removal steam condenser and does not materially add to the piping cost. We have experienced no tendency toward the increased loss of hydrogen during light-load operation. Mr. Arnow is correct in assuming that the drain coolers of the three high-pressure heaters are an integral part of these heaters, and the level-control valves should have been shown after the drain-cooler sections, instead of as indicated in Fig. 6 of the paper.

Energy Transfer Between a Fluid and a Rotor for Pump and Turbine Machinery

By SANFORD A. MOSS,[1] CHESTER W. SMITH,[2] AND WILLIAM R. FOOTE[3]

The paper presents an analytical treatment of the energy transfer between a working fluid and a rotor for pump and turbine machinery, which affords means for selection of the particular sort of vane angles and general arrangements best for a machine for a particular service, and for determination of the detailed dimensions of a machine for particular pressure conditions. A single general formula is given which applies to every sort of machine and which is reduced to a particular form for every particular machine.

In the analytical study a kinematic treatment of rotor energy is first given, which is followed by a hydraulic and thermodynamic treatment of fluid energy. The relations set forth are then applied to pumps and turbines of the axial-flow and of the radial inward- and outward-flow types.

Some of the matter here set forth has been given before, in discussion of particular machines; some of this old matter is here presented in a new way. However, it is doubtful if there has hitherto been presented a general expression for energy transfer correlated with its various applications and physical interpretations. It is the primary purpose of this paper to give such a presentation from many years of practical experience of the authors. In order to give an orderly presentation, the new and old matter are so intermingled to form a complete whole that it is difficult to make distinction and to give reference for the old matter.

THE transfer of energy between a working fluid and a rotor is fundamental in the study of a wide variety of machines. Such machines are steam and water turbines, centrifugal pumps, fan blowers, and centrifugal compressors; and the fluids involved may be water, steam, air, or others. An analytical treatment of this energy transfer is here made. This gives means for selection of the particular sort of vane angles and general arrangements best for a machine for a particular service, and for determination of the detailed dimensions of a machine for particular pressure conditions. There is given a single general formula which applies to every sort of machine and which is reduced to a particular form for every particular machine. This gives a perspective and elegance not existing when the particular formula is independently deduced for every particular machine. The general and particular formulas are analyzed so as to display the physical actions which occur, so as to show what really makes each sort of machine operate.

In the analytical study, first, there is given a kinematic treatment of rotor energy. Expressions are derived for the energy transfer between rotor and fluid in terms of the fluid velocities and directions at the entrance and exit of the rotor, together with the rotor velocities at these places. Such expressions for the energy transfer are true regardless of losses that may occur while the fluid is passing through the rotor, the pressure differences that may exist across the rotor, or the path of the fluid through the rotor. They do not include the rotation loss due to the fluid friction on the sides of the rotor. It is not usually realized that these expressions in terms of the velocities are exact. This energy transfer between the fluid and the rotor, in foot-pounds per pound of fluid flowing, derived kinematically in terms of the fluid and rotor velocities, is here called the rotor energy, E.

Second, there is given a hydraulic and thermodynamic treatment of fluid energy. Expressions are collected for the energy transfer between rotor and fluid in terms of the changes of the fluid temperature and pressure through the machine. By taking the case of an incompressible fluid, or different compressible fluid processes, isothermal, adiabatic, or hyperadiabatic, a wide variety of such energy expressions is possible. The energy obtained in this way, in foot-pounds per pound of fluid flowing, is here called the fluid energy, w.

In pump machinery, because of losses, the fluid energy is less than the rotor energy. Thus a practical coefficient, called the hydraulic efficiency, is defined by $\eta = w/E$. On the other hand in turbine machinery the fluid energy is greater than the rotor energy so that the hydraulic efficiency is then defined as $\eta = E/w$.

Historical Résumé

The history of theoretical work on energy transfer between a fluid and a rotor properly begins in 1750 when Segner (1)[4] of Göttingen invented a hydraulic turbine which operated on the reaction principle. Various types of lift pumps and water wheels had been made from earliest times, but this was the first to attract the attention of the scientific world. Segner attempted to explain the operation of his turbine, but it was the mathematician Euler (2) who set down the laws of flow. However, this work was neglected for many years until it was resurrected by Combes (3), who in 1843 presented a two-dimensional theory of flow. The attempt was made to apply this two-dimensional theory to cases of three-dimensional flow with the result that the theory contributed little to the design of hydraulic machinery. Instead, machines were built according to the ideas of the engineers who invented them, with the help of experience only. The clear presentation of the theory of turbines and centrifugal pumps was not made until 1899 when Zeuner (4) published his work, "Theorie der Turbinen," which included not only hydraulic apparatus but steam turbines as well. The basic theory laid down by Zeuner is the filament or streamline theory of uniform flow that is largely used today and is here presented and enlarged upon. There have been some more recent developments in considering the pressure and velocity distributions around rotor blades by means of the hydro- and aerodynamic quantity circulation. Such items contribute refinements to the basic theory but are outside the scope of this paper.

Some of the matter here set forth has been given before in

[1] General Electric Company, West Lynn, Mass. Fellow A.S.M.E.
[2] General Electric Company, West Lynn, Mass.
[3] General Electric Company, West Lynn, Mass. Jun. A.S.M.E.

Contributed by the Aviation, Hydraulic, and Power Divisions and presented at the Annual Meeting, New York, N. Y., Dec. 1–5, 1941, of The American Society of Mechanical Engineers.

Note: Statements and opinions advanced in papers are individual expressions of their authors and not those of the Society.

[4] Numbers in parentheses refer to Bibliography at end of paper.

discussion of particular machines; some of this old matter is here presented in a new way. However, it is doubtful if there has hitherto been presented a general expression for energy transfer correlated with its various applications and physical interpretations. It is the primary purpose of this paper to give such a presentation from many years of practical experience of the authors. In order to give an orderly presentation, the new and old matter are so intermingled to form a complete whole, that it is difficult to make distinction and to give reference for the old matter. Diagrams are given to illustrate the equations, accompanied in most cases by illustrations of typical machines culled from past publications, to assist in visualization.

Assumptions Regarding Rotor Energy

The theory to be presented makes various assumptions, given in what follows, most of which were originally mentioned by Zeuner. While it is realized that no actual machine operates exactly under the conditions imposed by these assumptions, it is necessary to make some such assumptions in order to construct a basic theory. In practice there may be deviations from these assumptions to a greater or lesser degree, as may be found by comparing the performance and characteristics of actual machines with those predicted from the theory herein.

The following assumptions are made in order to compute the rotor energy. The assumptions necessary for the various thermodynamical expressions will be indicated later when these expressions are introduced.

First, only steady-state operation is treated. There are transient phenomena occurring whenever a machine is started up or undergoes a change of load, but these are generally of short duration and do not greatly affect the general characteristics. With steady-state operation it follows that the flow of fluid, the speed and torque of the rotor, and the energy transfer between the fluid and the rotor are all constant with time.

Secondly, it is assumed that the flow of the fluid through the rotor is perfectly uniform. By uniform it is meant that every filament of fluid has a similar entrance to and a similar exit from the rotor. Thus the fluid in two different filaments will have the same velocity at entrance to the rotor and the same direction with respect to the radius vector. Similar conditions hold at exit. Of course there are actual departures from this ideal flow, which must be taken account of by practical coefficients.

This assumption of uniformity is most easily explained further by a discussion of blading, which is the chief cause of nonuniformity. In the region between blades the fluid velocity may be greater and in a different direction from that just along the edge of a blade. Furthermore, all blades tend to act as airfoils and set up pressure and velocity distributions around them. These distributions affect the uniformity of flow and also cause the fluid to leave the blade with a relative velocity in a direction different from that of the blade exit angle. This phenomenon is known as slip, and this is greater the fewer blades there are on the rotor. However, in the theory to be presented it is assumed that the flow is uniform and that there is no slip. As sometimes stated, this assumes a rotor having an infinite number of blades, each with an infinitesimal thickness. This assumption of uniformity applies only to fluid at entrance and exit. Conditions of flow along the rotor between these two points are matters of indifference.

Since flow is assumed to be uniform there can generally be found some average circumference along which it may be considered to take place. Thus in an axial-flow turbine the entire flow may be considered to take place at a pitch diameter. Herein, this pitch diameter is taken as the root mean square of the inner and outer diameters, so that there are equal flow areas on either side.

The assumption of uniform flow obviates a difficulty that occurs if nonuniform flow is dealt with. This is, that with nonuniform flow the mean velocity upon which the flow depends cannot be used to determine the kinetic energy of the fluid, since this depends on the square of the velocity.

In many rotors there is continuous uniform flow. This means that the flow at inlet or exit extends continuously throughout some area. In this case there is a continuous enveloping surface at inlet or exit which includes the rotor blade tips. Flow takes place with the same velocity through all parts of this surface, and the individual filaments of fluid are similar. In this case the volume rate of flow, Q, is given by

$$Q = AV \quad [1]$$

Here A is the area of the enveloping surface which includes the rotor blade tips, and V is the component of the fluid velocity normal to this surface. A steam turbine with full arc admission is a machine in which this type of flow is approximated.

If reasonably close approximations to the fluid inlet and exit velocities can be found, so that uniform flow may be assumed, then noncontinuous flow is covered by the theory herein presented. Two such sorts of noncontinuous uniform flow may be mentioned. The first type occurs when the flow does not completely fill the passageways provided for it. An example of this is the exit of a centrifugal-compressor impeller. Here the fluid crowds against the forward side of the blades and separates from the back side. Hence the exit flow is in a series of jets even though the area provided for the flow is practically continuous. In this case the equation $Q = AV$ cannot be used since the area through which flow actually takes place is not known. However, this crowding effect usually is not very great and continuous uniform flow may be assumed and the effect of any departure thrown into the hydraulic efficiency.

The second type of noncontinuous uniform flow is that in which there are gaps in the surface through which flow may take place. Examples of this are the Pelton water wheel, Barker's mill, and a certain type of centrifugal-compressor impeller in which the discharge is through a series of nozzle-like openings. In the two latter machines the flow practically fills the nozzles, and the equation $Q = AV$ still holds provided A in this case is the area of the nozzles or openings.

It should be emphasized that existence of continuous flow merely determines whether the fluid velocity can be found from the volume rate of flow. The equations to be discussed later merely assume that the flow is uniform, regardless of whether it is continuous or not.

Finally, all losses that take place outside of the rotor are neglected. These losses are the loss due to by-passed fluid and the rotation loss. In any machine there is generally some fluid that by-passes, short-circuits, or leaks past the rotor, and hence contributes nothing to the energy transfer. This is neglected by considering only the fluid that actually passes through the rotor. The rotation loss arises from the friction of the fluid on the sides of the rotor, since the rotor is generally enclosed in an atmosphere of the working fluid. However, this loss is not here included, and the only energy considered is that transferred between the rotor and the fluid as it passes through. Thus in the case of a compressor the rotor energy is the shaft work minus the rotation loss, and in the case of a turbine the rotor energy is the sum of the shaft work and rotation loss.

Kinematic Treatment of Rotor Energy

The basic equation for the energy transfer between a fluid and a rotor will now be discussed. In Fig. 1 is shown a rotor revolving at constant angular velocity about an axis XX, with uniform flow through the rotor. The torque about the axis of the shaft

is constant. A fluid, compressible or incompressible, passes over or through the rotor, and the generality of its path should be emphasized. The fluid may enter the rotor at the center, at the rim, or at any intermediate point, and it may likewise leave at any radius. It enters at any velocity in any direction, passes through or around the rotor by any path whatever, and may leave on the same side or the opposite side from which it entered. The velocity of the fluid may stay constant during its passage through the rotor, or it may change because of change in flow area, or because of expansion or compression in the rotor passages. The rotor may be in a casing as is a steam-turbine rotor, or the casing may be unnecessary, as for a Pelton water wheel.

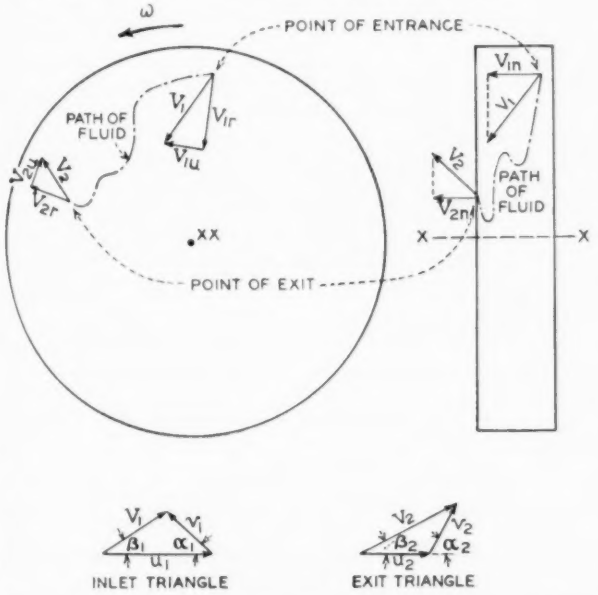


FIG. 1 GENERAL DIAGRAM SHOWING HOW FLUID ENTERS WHEEL WITH ABSOLUTE VELOCITY V_1, PASSES THROUGH BY ANY PATH WHATEVER, AND LEAVES WITH ABSOLUTE VELOCITY V_2. SUBSCRIPTS r, u, AND n DESIGNATE RADIAL, TANGENTIAL, AND AXIAL DIRECTIONS RESPECTIVELY

The notation which is to be used is defined at the end of this paper, but it is helpful to repeat some of it here and to explain the system that is used in defining the velocities. The absolute velocity of the fluid is denoted by V, the relative velocity with respect to the rotor by v, and the tangential velocity of the rotor at any radius by u. In addition, various subscripts are used. Subscript $_1$ refers to entrance to the rotor, and subscript $_2$ refers to exit. While the rotor velocity is always in the tangential direction, the fluid velocity may be in any direction, the only restriction being that the flow is uniform. Hence the fluid velocity has three components, a tangential component denoted by subscript $_u$, a radial component denoted by subscript $_r$, and an axial component denoted by subscript $_n$. The subscripts denoting the components are added to those denoting entrance or exit. Thus V_{1_u} is the tangential component of the inlet absolute velocity of the fluid, and v_2 is the total relative velocity of the fluid at exit. The components of the absolute fluid velocity are shown in Fig. 1.

By the application of Newton's laws of motion to the fluid, it is shown in Appendix 1 that for any rotor whatever, under all of the varying circumstances discussed, as shown diagrammatically in Fig. 1, the rotor energy is the very simple expression

$$E = \frac{1}{g}(u_2V_{2_u} - u_1V_{1_u}) \quad [2]$$

In this equation E is the rotor energy in foot-pounds per pound of fluid passing through the rotor; E (as well as the fluid energy w) is positive if the energy transfer is from the rotor to the fluid as in a compressor, and negative if the transfer is from the fluid to the rotor as in a turbine. This equation is one of several alternate forms of the basic equation for the rotor energy that will follow. There are some features which may be pointed out.

First, the only fluid characteristics that are involved are the tangential components of the fluid velocities at inlet and exit. The equation is derived on the basis of the fluid entering and leaving with velocities in any direction, but it is only the tangential component of velocity that affects the energy transfer. The change in the axial component produces thrust on the rotor, and the change in the radial component produces stresses in the rotor, but neither change directly affects the energy transfer.

Since the equation involves no fluid properties except the fluid velocities, it follows that it is true regardless of the compressibility of the fluid or the pressure changes across the rotor. Of course both of these items, compressibility and pressure change, may affect the value of the exit velocity, but if the fluid velocities are known, then the equation gives the energy transfer regardless of compressibility and pressure change.

The equation as derived involves only the fluid conditions at entrance and exit. Hence it is independent of losses that may occur while the fluid is passing through the rotor. In particular it is independent of shock losses, losses due to friction against the rotor blades, or losses due to heat transfer between the fluid and the rotor. These losses affect the value of the exit velocity of the fluid and in this way are implicitly involved in the equation, but no term explicitly represents them.

Finally, it may be noted that the equation does not involve the blading except as the blading may affect the exit velocity. This is important from two standpoints. First, the change of tangential velocity of the fluid is a measure of the amount of turning or bending that the fluid undergoes while passing through the rotor. On this basis the equation shows that it is only the net amount of bending that influences the energy transfer. Machines have been invented in which the fluid entering the rotor is bent once, and then without leaving the rotor is bent again in the reverse direction in an attempt to get an increase in the energy transfer. Such a procedure is useless, since the rotor energy is independent of the path of the fluid through the rotor. Secondly, there is the matter of using airfoil sections as blades. With a rotor made up of airfoil sections attached to a drum, there are various velocity and pressure distributions which take place while the fluid is passing through the rotor, giving a change of pressure and hence a lift on each blade. However, regardless of this, the rotor energy is given by the tangential velocities at inlet and exit, always supposed uniform. The airfoil sections or any special blade may give a smooth passage for the fluid through the rotor and in this way affect the losses and the exit velocity, but there is no added effect due to the use of airfoil sections or any other special blade form beyond the effect on the losses and the exit velocity.

It is shown in Appendix 1 that Equation [2] may be put in a slightly different form

$$E = \frac{\omega}{g}(r_2V_{2_u} - r_1V_{1_u}) \quad [3]$$

by the introduction of the rotor angular velocity and the radii at inlet and exit. In this form the energy transfer is seen to depend on the quantities $r_2V_{2_u}$ and $r_1V_{1_u}$. This quantity, rV_u, is known as the "whirl" of the fluid, so that the rotor energy is directly proportional to the change in whirl. Whirl, an important concept in hydro- and aerodynamics, is related to the concept of circulation, but is outside the scope of this paper.

Finally, it is found to be convenient to express the rotor energy as

$$E = \frac{Ku^2}{g} \quad [4]$$

In such a form K is a function of the ratios and angles of the velocity diagrams. The value u is the rotor velocity at inlet or at exit, depending on which is greater. K is a characteristic of conditions and is a convenient quantity by which various rotors may be compared. Expressions for K for various particular rotors are given later. Machines which differ in scale but have the same arrangement and angles, and similar velocity diagrams, are said to be similar machines operating under similar conditions, or to have similarity. Machines thus having similarity have the same K.

Hydraulic and Thermodynamic Treatment of Fluid Energy

Before proceeding further with the kinematic treatment of rotor energy, it seems best to consider the changes that occur in the fluid as it passes through the machine. In the case of a pump or compressor the fluid absorbs energy, whereas in turbine apparatus the fluid gives up energy. In any case the energy that the fluid gains or loses is evidenced by change of pressure and temperature. Usually there are also changes in kinetic energy and elevation. Generally, it is only the pressure that is of interest, since this is the useful portion of the energy. Then the fluid energy will be defined as the energy required for the pressure change of the fluid, with conventions on signs as given for Equation [2]. In general this is not the total energy the fluid receives from or gives to the shaft because of the losses represented by η and the rotation losses. Instead of the rotor entrance and exit, the machine entrance and exit will be used, since it is the pressure and fluid energy at these points that are of chief interest. These points will be denoted by subscripts $_0$ and $_3$ respectively. As will be shown, this bunches inlet- and exit-passage losses with fluid losses on the rotor to give the total fluid losses in the machine. In these passages, except for losses, there is conversion of static pressure and velocity head, with no change of total pressure or energy. All of the energy change occurs on the rotor.

For a liquid or incompressible fluid, the fluid energy is

$$w = (Z_3 - Z_0) + \frac{p_3 - p_0}{\rho} + \frac{1}{2g}(V_3^2 - V_0^2) \quad [5]$$

This is merely Bernoulli's expression for the ideal energy change. In this expression the pressures are static pressures. The equation may be rearranged as

$$w = (Z_3 - Z_0) + \left(\frac{p_3}{\rho} + \frac{V_3^2}{2g}\right) - \left(\frac{p_0}{\rho} + \frac{V_0^2}{2g}\right) \quad [6]$$

Here it can be seen that the fluid energy is defined as the change in vertical height $(Z_3 - Z_0)$ plus the change in dynamic or total head as given by the readings of impact tubes. We have already defined the hydraulic efficiency η. For a pump $w = \eta E$ and for a turbine $E = \eta w$.

In the case of a gas the matter is somewhat complicated by the fact that the pressures are dependent upon the temperatures, which may be given by various idealized processes such as isothermal, adiabatic, or hyperadiabatic. These matters have been treated in another paper (5), but may be briefly reviewed here. In case of a compressor there is compression of a given volume of fluid, and this volume depends on the heat lost or gained with respect to the surroundings and the friction losses within the compressor. Both of these items are reflected as change of temperature. An increased temperature increases the volume of the gas, which in turn makes it harder to compress. Thus, thermodynamically the gas undergoes an irreversible process with heat transfer. The fluid may be assumed to follow a law $pv^n = c$ as it is compressed. As a fair standard of comparison there may be used the theoretical work of compressing a gas with the existing pressures and temperatures given by an actual n. This is called the "hyperadiabatic energy" and is

$$w_n = \int v dp = \frac{nRT_0}{n-1}\left[\left(\frac{p_{3i}}{p_{0i}}\right)^{(n-1)/n} - 1\right] \quad [7]$$

In this equation p_{0i} and p_{3i} are the total pressures at the entrance and the exit of the machine. The value of n is found from the relation

$$\frac{T_3}{T_0} = \left(\frac{p_{3i}}{p_{0i}}\right)^{\frac{n-1}{n}} \quad [8]$$

The value of Equation [7] is called the work of hyperadiabatic compression and takes account of the heat transfer. As stated, it is a theoretical value and represents the mechanical energy needed for compression with temperatures as they actually exist. For an ideal compressor with no losses or heat transfer this reduces to the isentropic work. Complete details are given in reference (5).

The energy given by Equation [7] may be compared with the rotor energy. In Equation [4] this was expressed as $\frac{Ku_2^2}{g}$. As before, a practical coefficient η, called the hydraulic efficiency, may be defined by the equation

$$w_n = \eta\left(\frac{Ku_2^2}{g}\right) \quad [9]$$

Such a hydraulic efficiency may be found from experimental work and then this value may be used in further design work.

The hyperadiabatic energy of Equation [7] is sometimes inconvenient to work with because of the variations of the value of n in machines of different types. For machines of a single type, the isentropic work is often used instead. Thus

$$w_k = \frac{kRT_0}{k-1}\left[\left(\frac{p_{3i}}{p_{0i}}\right)^{\frac{k-1}{k}} - 1\right] \quad [10]$$

This is treated in full in the reference (6). By the introduction of the factor X, defined as

$$X = \left(\frac{p_{3i}}{p_{0i}}\right)^{\frac{k-1}{k}} - 1 \quad [11]$$

the previous equation may be reduced to

$$w_k = \frac{kRXT_0}{k-1} \quad [12]$$

As before, this value of the isentropic fluid energy may be compared with the rotor energy, and we may define

$$\text{Pressure coefficient} = \frac{w_k}{Ku_3^2/g} \quad [13]$$

This pressure coefficient is used in work on that type of supercharger which is a high-speed centrifugal compressor. For these, the pressure coefficient varies from 65 per cent to 75 per cent with a value of about 70 per cent being quite common.

Finally, in the case of steam or other vapor for turbines and the like, the fluid energy is the isentropic change in enthalpy

or total heat from the initial temperature and pressure to the final pressure. Thus

$$w = J(h_3 - h_0) \quad [14]$$

Multistage Compressors and Turbines

The preceding relations, as well as most of the matters treated in this paper, apply primarily to a single stage. In many cases, such as with reheaters between turbine stages or intercoolers between compressor stages, a multistage machine must be treated as successive individual stages. However, in the absence of heaters or coolers between stages, a multistage machine or a group of stages having similiarity may be treated as a whole. For every stage there must be geometrical similiarity, similar velocity diagrams, and consequently the same K. In the case of a multistage turbine, some of the losses of one stage are available in the following stages because of reheat. For an entire turbine or group of stages this reheated energy would be used as the fluid energy Σw_r. In the case of a multistage compressor, the hyperadiabatic energy Σw_a is the proper value for a group of similar stages. In the case of hydraulic pumps and turbines with groups of stages having similiarity, there are no thermodynamic complications, and Σw_a and Σw_r become simply the total energy for a group. For groups of similar stages for pumps or turbines, respectively, Equation [4] gives the following expressions which show equivalence of various combinations of stage diameters and peripheral speeds

$$\Sigma w_a = \frac{\eta K}{g} \Sigma u^2$$

$$\frac{K}{g} \Sigma u^2 = \eta \Sigma w_r$$

In the latter case, for steam turbines, a special form of Σu^2 is in use

$$\lambda = \sum \left(\frac{Dn}{1000}\right)^2 = 0.05253 \Sigma u^2$$

Here D is the diameter in inches and n is the speed in rpm.

Alternate Form for the Rotor Energy

With this brief treatment of the fluid energy, the rotor energy may be discussed further. It is shown in Appendix 1 that Equations [2] and [3] may be put in the form

$$E = \frac{1}{2g} [(V_2^2 - V_1^2) + (u_2^2 - u_1^2) + (v_1^2 - v_2^2)] \quad [15]$$

In this form the equation shows the nature of the energy changes that take place as the fluid passes through the rotor. This equation is as general as are the other expressions for the rotor energy. The rotor velocity is necessarily tangential, but the fluid velocities may be in any direction provided only that the flow at entrance and at exit is uniform. This equation has a physical meaning, probably never before given, which it is quite desirable to understand. In this discussion the passage of an incompressible fluid through a centrifugal pump is treated for simplicity. A similar physical interpretation can be given to the passage of any fluid through any rotor. To simplify the treatment it is assumed that all parts of the pump have the same efficiency η.

The first item in the equation, $\frac{1}{2g}(V_2^2 - V_1^2)$, is obviously the change in the kinetic energy of the fluid as it passes through the rotor. If the fluid enters at an absolute velocity V_1, and leaves with a different absolute velocity V_2, it has experienced a change in kinetic energy, and this energy comes from the rotor.

The term $\frac{1}{2g}(V_2^2 - V_1^2)$, the change in the kinetic energy of the fluid that takes place as the fluid flows through the rotor, is converted into the pressure change that takes place in the machine other than across the rotor. Thus, if there is no friction in the inlet passage to the pump

$$\frac{p_{0i}}{\rho} = \frac{p_1}{\rho} + \frac{V_1^2}{2g} \quad [16]$$

In other words the velocity energy $V_1^2/2g$ was obtained by conversion of pressure energy, and the inlet conditions to the rotor may be taken as those at the inlet to the machine since the total pressures are the same. In case there is not perfect conversion of the pressure energy into velocity energy, the efficiency, supposed constant throughout, may be introduced. Thus, if V_1 is the theoretical velocity

$$\eta \frac{V_1^2}{2g} = \frac{p_{0i} - p_1}{\rho} \quad [17]$$

Such an expression may be written for the entrance passage to the rotor of any pumping machine using any fluid. It is here done for an incompressible fluid for the sake of simplicity, but similar relations hold for a vapor or a perfect gas.

Similar to this is the diffuser and discharge passage from a centrifugal pump. In this case the fluid leaves the rotor with a high velocity which is largely converted into pressure at the exit of the machine. However, this conversion is not perfect, so that the efficiency is introduced. Thus

$$\frac{\eta V_2^2}{2g} = \frac{p_{2i} - p_2}{\rho} \quad [18]$$

Hence the velocity term $V_2^2/2g$ represents pressure change in the discharge passage leading from the rotor to the exit of the machine. If Equations [17] and [18] are combined, then

$$\eta \left(\frac{V_2^2}{2g} - \frac{V_1^2}{2g}\right) = \frac{p_{2i} - p_2}{\rho} + \frac{p_1 - p_{0i}}{\rho} \quad [19]$$

Thus these velocity terms represent the change in pressure that occurs other than in the rotor, by conversion of the kinetic energy. If inlet or discharge take place in a large region, with negligible velocity, p_{0i} and p_{2i} are static pressures. In any case they are total pressures.

The kinetic-energy terms of Equation [15] have been discussed. The other terms

$$\frac{1}{2g} [(u_2^2 - u_1^2) + (v_1^2 - v_2^2)]$$

remain. Together these will be shown to represent the static pressure change that takes place across the rotor. The term $(u_2^2 - u_1^2)/2g$ is a centrifugal effect. The values u_2 and u_1 are the rotor speeds at inlet and exit, respectively, and if they are different, the fluid flows radially and experiences a change of centrifugal force. This in turn gives rise to pressure differences. To clarify this, consider a body of fluid in a hollow cylinder, rotating at the speed of the cylinder. In order to force the fluid at any radius to rotate in a circular path a centripetal force is necessary, and this force can only be furnished by an increased pressure of all fluid at greater radii. Conversely, the fluid at any radius may be considered to exert a centrifugal force on all the fluid at greater radii, resulting in an increase of static pressure from the center of the cylinder to the circumference. If a pound of fluid is taken from a radius where the velocity is u_1 to a greater radius where the velocity is u_2, then

work of amount $(u_2^2 - u_1^2)/2g$ must be done on this pound of fluid. The situation in a radial-flow machine is complicated by the flow. However, the derivation of Equation [15] shows that this centrifugal effect exists with the other effects of flow superposed upon it, and the energy involved in this effect is additive to the energy involved in the effects of flow. This centrifugal effect is, of course, absent in axial-flow machines.

The final term in Equation [15] is $(v_1^2 - v_2^2)/2g$. This term is due to the change in the relative velocity of the fluid as it passes through the rotor. If there were no centrifugal effect this term would give the change in static pressure across the rotor. Thus in a pump there is generally a decrease of relative velocity of the fluid, and this corresponds to an increase of pressure. This is the same action that takes place in a stationary diffuser, and for this reason this action is known as the diffuser or velocity-conversion effect. In a reaction turbine there is an increase in the relative velocity accompanied by a drop in pressure across the rotor. This increase in relative velocity gives the kickback or reaction that helps drive the turbine.

It has been said that the centrifugal and the diffuser or reaction effects combined give the pressure change across the rotor. Thus

$$\frac{\eta}{2g}\left[(u_2^2 - u_1^2) + (v_1^2 - v_2^2)\right] = \frac{p_2 - p_1}{\rho} \quad \ldots\ldots [20]$$

where η is introduced since the change is not ideal but involves losses, such as friction losses, shock losses, eddy losses, or others. If Equation [20] is compared with Equation [19] it will be seen that the terms of Equation [20] involve the pressure and energy changes across the rotor while the terms of Equation [19] involve the pressure and energy changes that take place elsewhere. If these equations are added, then

$$\frac{\eta}{2g}\left[(V_2^2 - V_1^2) + (u_2^2 - u_1^2) + (v_1^2 - v_2^2)\right] = \frac{p_{02} - p_{01}}{\rho} \quad [21]$$

In other words the rotor energy for pumps, multiplied by an efficiency factor, results in the fluid energy as found by total pressures at entrance and exit of the machine.

In this section an incompressible fluid has been used throughout. This has been done only for simplicity. Similar treatments may be given vapors and compressible gases. Furthermore, the efficiency η has been taken as a constant for each part of the machine. Actually this efficiency varies widely, and in Equation [21] each term should be multiplied by its own efficiency factor and the sum taken to give the change in pressure across the machine. This was not done in this section in order to simplify the presentation. The only result here desired is the physical interpretation of Equation [15].

In this section only compressor or pump apparatus was treated, for which $\eta E = w$. A similar treatment can be given to turbine apparatus for which $E = \eta w$. The physical interpretation of Equation [15] would be the same, except that in this case it is the pressure terms rather than the velocity terms that are to be multiplied by an efficiency.

TABLE 1 CLASSIFICATION OF TYPES OF APPARATUS

		Radial flow		Axial flow
		Inward	Outward	
Pumps		.....	Centrifugal fan, pump, or compressor, Figs. 2 and 3	Axial-flow fan, blower, or compressor, Fig. 6
Turbines	Hydraulic	Francis turbine, Fig. 7	Fourneyron turbine, Fig. 8 Barker's mill, Fig. 14	Pelton water wheel, Fig. 13 Impulse turbine, Fig. 9
	Gas or steam	.....	Ljungström turbine	Reaction turbine, Fig. 11

Types of Apparatus

Now that the general expressions for the rotor energy and the fluid energy have been presented, it remains to apply these to various types of apparatus. The apparatus to be treated is classified in Table 1.

As may be seen, the apparatus is divided first into pump apparatus or turbine apparatus, depending on whether the energy transfer is from the rotor to the fluid (pump) or from

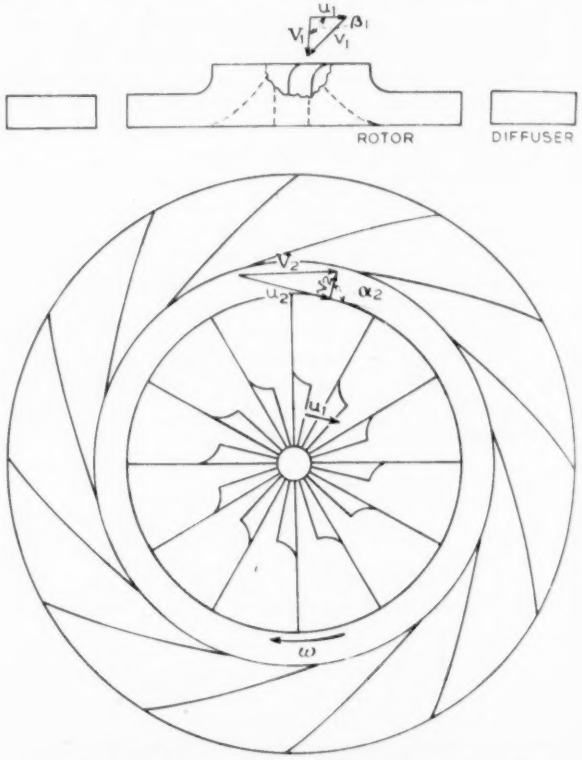


FIG. 2 CENTRIFUGAL PUMP OR COMPRESSOR, AXIAL INLET

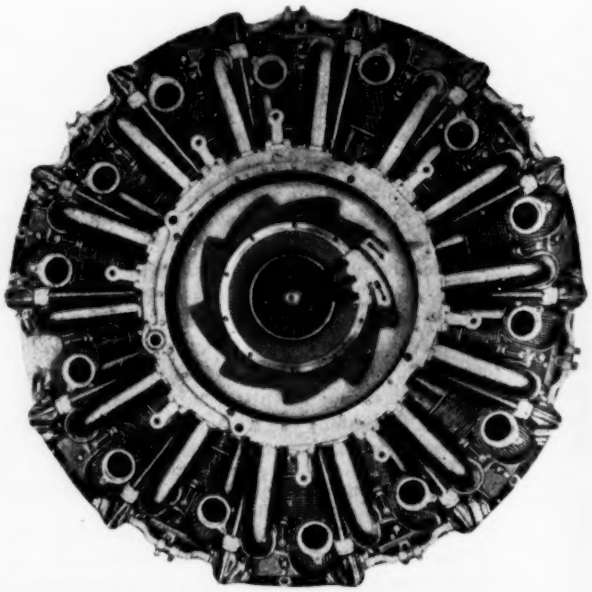


FIG. 2a DIAGRAM OF CENTRIFUGAL COMPRESSOR USED AS SUPERCHARGER OF AN AIRPLANE ENGINE

the fluid to the rotor (turbine). The apparatus is further divided into radial flow and axial flow. In the treatment to follow the pump apparatus is considered first and the turbine apparatus later. In the treatment of the turbine apparatus the foregoing order is not followed, but the Pelton water wheel and Barker's mill, being somewhat different from the other apparatus, are treated last.

Centrifugal Fans, Compressors, and Pumps

Centrifugal fans, compressors, and pumps are shown in Figs. 2, 2*a*, 3, and 3*a*. The fluid enters the rotor, which is generally known as an impeller, in an axial or radial direction. This entrance may take place through a set of stationary guide vanes, or these may be unnecessary. During passage through the rotor, the flow may be changed from the axial direction to the radial direction. At exit the fluid passes from the impeller to a diffuser, which converts velocity energy into pressure energy. The diffuser may have guide vanes on it, or these may be lacking. Fig. 2*a* is a diagram of the sort of centrifugal compressor used as a supercharger for an airplane engine.

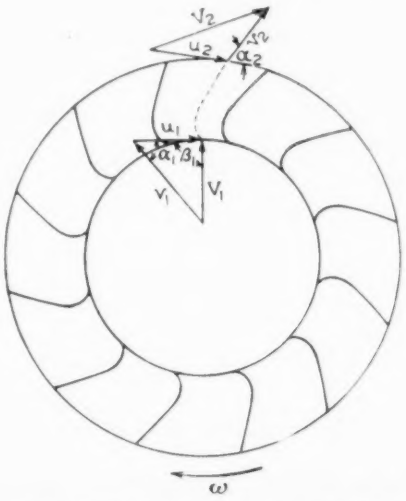


Fig. 3 Centrifugal Pump or Compressor, Radial Inlet

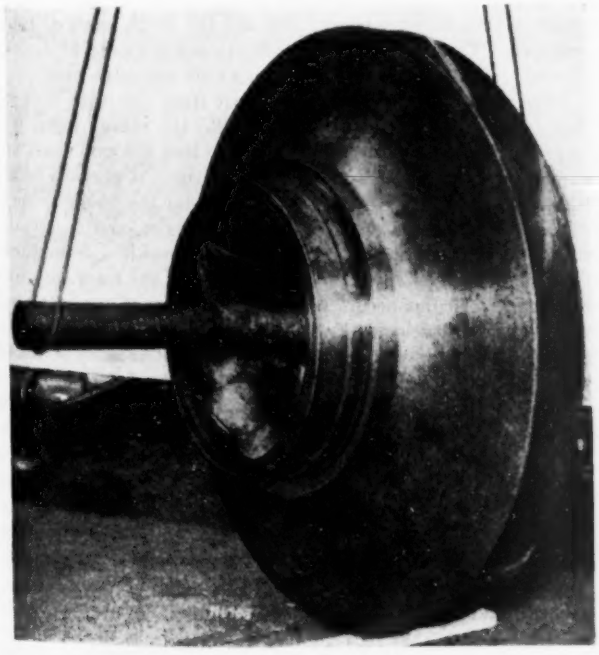


Fig. 3*a* Centrifugal Pump Impeller

Recalling the previous discussion on the energy transfer between rotor and fluid, there appear several theoretical reasons for designing such a rotor with outward flow. First and foremost, outward flow takes advantage of the centrifugal effect due to the discharge of the fluid at the greater radius, and the pressure rise caused by it. Secondly, there is the effect of outward flow on the absolute velocity and hence on the change in kinetic energy of the fluid. At entrance to a centrifugal compressor or pump rotor there is no very good method of obtaining an appreciable fluid velocity, and hence it is desirable that the rotor velocity likewise be small. However, at exit a larger absolute velocity of the fluid is possible and can be utilized, so that a comparable rotor velocity is desirable. Hence with outward flow there is an increase in absolute velocity of the fluid as it passes through the rotor, and this contributes to the energy transfer. Finally, outward flow, with increasing area for flow at larger radii, permits a decrease in the relative velocity of the fluid as it passes through the rotor, and this introduces a desirable velocity-conversion effect.

Centrifugal Pump or Compressor With Normal Absolute Inlet and Radial Relative Impeller Discharge

Perhaps the simplest construction for a centrifugal compressor or centrifugal pump is that in which there are no inlet guide vanes. It is an experimental fact, probably for a theoretical reason, that the absolute velocity at a rotor inlet is normal to an enveloping surface which includes the rotor blade inlet tips. This enveloping surface is a radial plane for an axial flow inlet such as Fig. 2, and the surface of a short cylinder for a radial inlet such as Fig. 3. Sometimes the inlet tips are inclined and the enveloping surface is conical. If the inlet is axial, as in Fig. 2, the inlet velocity is purely axial at the inlet tips of the vanes, and has no other components. In particular, there are no tangential components, so that $V_1 = V_{1a}$ and $V_{1u} = 0$. If the inlet is radial, as in Fig. 3, the inlet velocity is purely radial at the rotor blade inlet tips, and again there are no tangential components, so that $V_1 = V_{1r}$ and again $V_{1u} = 0$. Similarly, there is no tangential component with a conical inlet. Thus it follows from Equation [2] that the rotor energy is

$$E = \frac{u_2 V_{2u}}{g} \qquad [22]$$

In this case the rotor energy depends neither on the inlet velocities nor on the inlet diameter. If in addition to normal inlet the fluid leaves the rotor with a relative velocity in the radial direction, then $u_2 = V_{2u}$, and the value of the rotor energy is

$$E = \frac{u_2^2}{g} \qquad [23]$$

In the general relation of Equation [4], $E = Ku_2^2/g$, K is 1.00 for this case of normal inlet and relative radial discharge. The condition under which this equation holds in practice is that the exit blades of the rotor are radial and there are a sufficient number of them so that there is no slip of the fluid at exit.

The rotor energy has been found to be independent of the inlet conditions if the inlet is normal. It is of interest to note how the centrifugal and velocity-conversion effects change as the inlet diameter of the rotor is varied. Take the case that V_1 is constant and v_2 is kept constant or is negligible. This

implies constant inlet area as dimensions change. Then from the inlet velocity diagram, Fig. 3

$$v_1^2 = V_1^2 + u_1^2 \quad \ldots\ldots\ldots\ldots\ldots\ldots [24]$$

This may be changed algebraically to

$$V_1^2 + u_2^2 - v_2^2 = (v_1^2 - v_2^2) + (u_2^2 - u_1^2) \quad \ldots\ldots [25]$$

For a constant rotational speed, the left-hand side of this equation is constant. It follows that the sum of the centrifugal and velocity-conversion effects is a constant. Hence, as the inlet diameter is increased the centrifugal effect is reduced and the velocity-conversion effect is increased. This can also be seen from the inlet-velocity diagram, Fig. 3. As u_1 increases while V_1 remains constant, v_1 must also increase, indicating an increase in the velocity-conversion effect. In the Sirocco blower this interchange is carried to a great degree by a very large inlet diameter.

By means of Equation [23] where $K = 1.00$, a simple analysis can be made of the proportion in which the various items of energy are added which make up the total rotor energy. To do this it is assumed that the relative velocity of the fluid at exit, v_2, is negligible, which is a common situation. Then $u_2 = V_2$ and the kinetic energy of the fluid at exit is $u_2^2/2g$, which is just half of the total rotor energy. Thus half of the pressure rise that theoretically occurs, that due to the centrifugal effect and velocity-conversion effect, takes place in the rotor, and the other half of the pressure rise, which is that due to the conversion of this velocity head $u_2^2/2g$, into pressure, takes place in a diffuser. This consideration of energy division is important. A hasty analysis might possibly lead to the conclusion that the kinetic energy is the only energy input to the fluid (7), whereas the analysis here shows that the kinetic energy is approximately half of the total input.

A diffuser is needed to convert the velocity head of the fluid from the rotor into pressure. Several types of diffusers are used. One of these is the scroll diffuser, which collects the fluid from the rotor at velocity V_2 and at the same time expands this area to reduce fluid velocity. A second type is the Venturi-meter diffuser, which is merely an expanding pipe section. If this is used, a collecting ring is necessary to collect the fluid from the rotor at the rotor exit absolute velocity. A third arrangement is a combination of the scroll and Venturi where the scroll collects the fluid and diffuses it partially and the Venturi completes the process. A somewhat different type is the vaneless diffuser with parallel walls. These parallel walls are radial planes between which the fluid diffuses in a free vortex. Such a diffuser has a large exit diameter. A variation of this is the Moss-Robinson short-path diffuser (8) in which the distance between the walls changes with radius. The first change is a reduction that takes place as the fluid leaves the impeller, for the purpose of giving the fluid velocity a larger radial component. The second change in the distance between the walls is an increase near the outer diameter of the diffuser for the purpose of reducing the radial component of the fluid velocity, thus making it easy to collect the fluid in a collecting ring. This diffuser also has a large outer diameter. A final type is the vaned diffuser. This is similar to the two preceding ones except that vanes are introduced to effect the diffusion in a smaller space than would otherwise be required. Any combination of these types is possible.

Inlet Guide Vanes and Rotor Exit Angles

The directions of the fluid at entrance and at exit have an important effect on the amount of energy transferred to the fluid. Referring to Fig. 1, the important angles involved in this respect are the absolute angle of stationary inlet guide vanes, β_1, and the blade angle at exit from the rotor, α_2. The blade angle at entrance to the rotor is based upon the velocity diagram. To investigate the effect of these angles Equation [15] may be put in the form

$$E = \frac{1}{g}(u_2^2 + u_2 v_2 \cos \alpha_2 - V_1 u_1 \cos \beta_1) \quad \ldots\ldots [26]$$

as shown in Appendix 1. In this equation the angles β_1 and α_2 are acute if the inlet guide vanes and the rotor exit vanes direct the fluid forward in the direction of rotation.

If β_1 is less than 90 deg, that is, forward inlet guides, the greater the value of V_1 the less the rotor energy. The inevitable increase of friction with increased V_1 and inlet guides would further reduce the rotor energy. Since this is undesirable, inlet guide vanes turned forward are rarely, if ever, used.

If, however, the inlet guide vanes are turned backward so that β_1 is greater than 90 deg, $\cos \beta_1$ is negative, and the term involving it becomes positive. Then the greater V_1 is, the greater the energy addition becomes. This statement would seem to contradict a conclusion from Equation [15] from which it would appear that a decrease of V_1 would be beneficial. However, from the velocity diagram, Fig. 3, it may be seen that an increase of V_1 effects an increase in v_1 also. Hence, by turning the inlet guide vanes backward the velocity conversion effect is increased, while the kinetic energy effect is decreased, but the

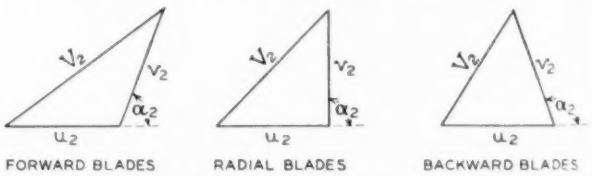


Fig. 4 Velocity Diagrams for Various Exit Angles

quantity $(v_1^2 - V_1^2)$ increases, thus giving a net increase in the rotor energy. However, this increase in energy input is usually not great if the rotor inlet diameter is small, and the little increase that is possible is accomplished by increases of V_1 and v_1, which in turn increase the friction and the shock losses at rotor entrance. There is also the complexity of the guides to be considered. For these reasons inlet guides are not often used.

Next, the effect of the angle at exit from the rotor may be considered. According to Equation [26] the energy input will be greatest when α_2 is an acute angle, so that the exit vanes are turned forward. However, in this case there is another factor to be considered. The velocity diagrams for the fluid leaving a rotor with forward-curved blades, radial blades, and backward-curved blades are shown in Fig. 4. It is evident from these that the greater energy input to the fluid for the rotor with forward-curved blades occurs principally because of the increased value of the exit velocity V_2. The purpose of a compressor is to give an increased pressure, and the greater exit velocity obtained with forward-curved blades can be useful only if the passage of the fluid through the rotor is followed by a passage through an efficient diffuser. It is well known that diffusers are often inefficient, so that a large exit velocity from a rotor cannot always be used to best advantage in a compressor. In some fans or blowers, the purpose of which is principally to deliver a large quantity of fluid at a low pressure, a high exit velocity may be useful, and forward-curved blades may be used to advantage, but compressors with vanes turned forward at exit are rare.

If the blades of a blower or compressor rotor are turned backward at exit so that in Equation [26] $\cos \alpha_2$ is negative, the energy added to the fluid is decreased, principally because of the decrease in the value of V_2. In other words, a rotor with

blades turned backward at exit transfers less energy to the fluid passing through it than does a rotor with radial or forward-curved blades, and hence it produces a smaller pressure rise. Since V_2 is thus smaller, such a rotor gives the best efficiency in machines such as blowers, where there is no opportunity for conversion of $V_2^2/2g$ by a good diffuser.

However, the design of a rotor to be used with a diffuser must take account of the inefficient use of the high exit velocities produced by a rotor with forward-curved blades and the lower rotor energy produced by the use of backward-curved blades. As a compromise the rotor with radial blades is frequently used. This has the obvious advantage of being by far the simplest in construction and also the sturdiest. The equations for the rotor energy for this case have already been presented in Equations [22] and [23]. It may be recalled here that in this case the kinetic energy of the fluid at exit is roughly half of the total energy input, the rest of the energy input resulting in pressure rise in the rotor.

The theoretical effect of stationary inlet guide vanes and of bending the exit rotor blades is shown graphically in Figs. 5*a* and 5*b*. To do this the rotor energy of Equation [26] is compared with that of a rotor with no stationary inlet guide vanes and with radial blades at the rotor exit. For this case the rotor energy has already been found in Equation [23] to be

$$E = \frac{u_2^2}{g} \quad \ldots\ldots\ldots\ldots\ldots\ldots [23]$$

and this will be taken as a reference. The rotor energy when the effects of inlet guides and variable rotor exit angles are considered is given by Equation [26]. The value of K is defined so that this rotor energy is Ku_2^2/g, as in Equation [4]. Thus

$$\frac{Ku_2^2}{g} = \frac{1}{g}(u_2^2 + u_2 v_2 \cos \alpha_2 - V_1 u_1 \cos \beta_1) \ldots\ldots [27]$$

or

$$K = 1 + \frac{v_2 \cos \alpha_2}{u_2} - \frac{V_1 u_1 \cos \beta_1}{u_2^2} \quad \ldots\ldots\ldots [28]$$

Now, as the angles α_2 and β_1 may be supposed to change, it is convenient for purposes of comparison to keep the rotor speed and the flow constant. The flow at inlet to the rotor is normal to a surface which envelops the rotor blade inlet tips. We suppose that the area of this enveloping surface remains constant if inlet guides are used. The volume flow at entrance is this area multiplied by the component of velocity normal to this surface. This velocity component, as may be seen from Fig. 1, is $V_1 \sin \beta_1$, and this value is to remain constant as β_1 is varied. Thus the factor

$$x_1 = \frac{V_1 \sin \beta_1}{u_1} \quad \ldots\ldots\ldots\ldots\ldots [29]$$

is introduced, and the constancy of this at constant u_1 assures constant flow. Similarly at exit the factor

$$x_2 = \frac{V_2 \sin \beta_2}{u_2} = \frac{v_2 \sin \alpha_2}{u_2} \quad \ldots\ldots\ldots\ldots [30]$$

is used. The constancy of this likewise assures constant volume flow at exit at constant u_2, with constant enveloping surface of rotor blade exit tips. Thus x_1 and x_2 are factors constant with constant flow, constant rotor speed, and constant enveloping surfaces. If these factors are substituted in Equation [28], then

$$K = 1 + x_2 \cot \alpha_2 - x_1 \left(\frac{r_1}{r_2}\right)^2 \cot \beta_1 \quad \ldots\ldots\ldots [31]$$

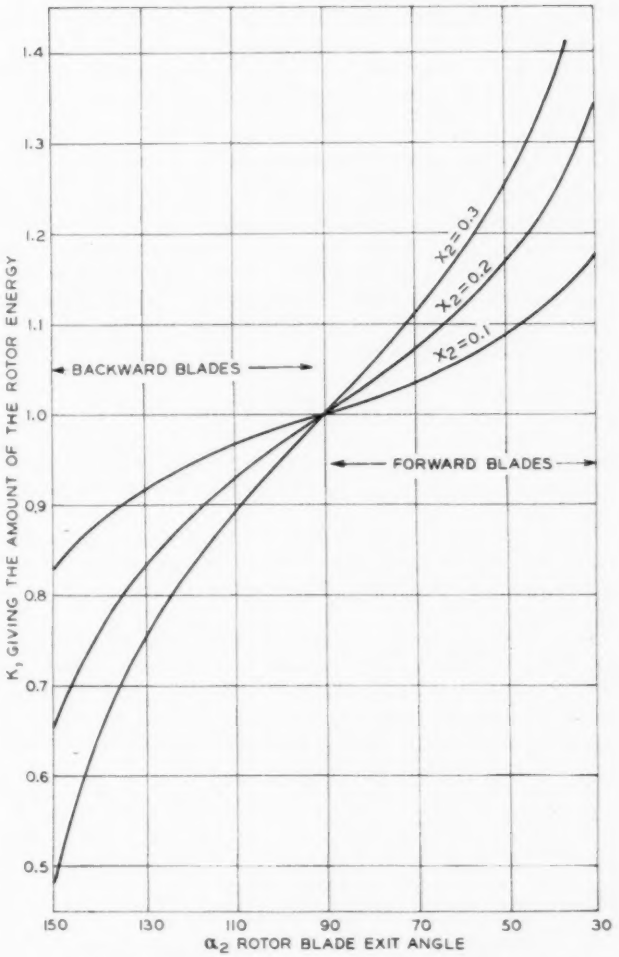


FIG. 5*a* EFFECT OF VARIATION OF EXIT BLADE ANGLES

(Values of $K = 1 + x_2 \cot \alpha_2$, with varying rotor blade exit angle, α_2, and no inlet guide vanes. $x_2 = \frac{V_2 \sin \beta_2}{u_2}$ is a factor constant with constant flow, constant rotor speed, and constant exit-tip enveloping surface.)

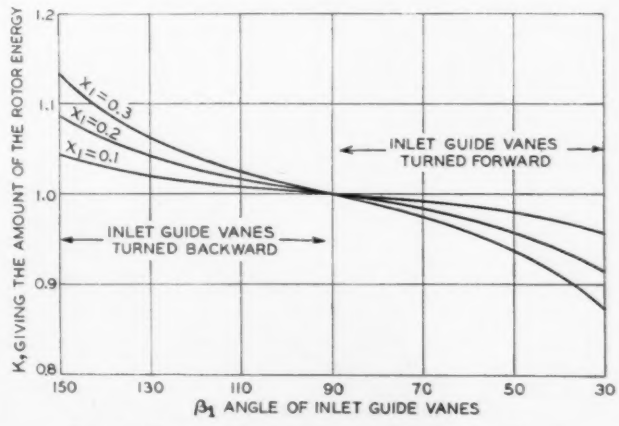


FIG. 5*b* EFFECT OF VARIATION OF INLET GUIDE VANES

(Values of $K = 1 - x_1 \left(\frac{r_1}{r_2}\right)^2 \cot \beta_1$ with varying inlet guide vanes, where the rotor blades at exit are radial and $\frac{r_1}{r_2} = 1/2$. $x_1 = \frac{V_1 \sin \beta_1}{u_1}$ is a factor constant with constant flow, constant rotor speed, and constant inlet-tip enveloping surface.)

This equation is plotted in Figs. 5*a* and 5*b* to show what gain is possible by variation of the angles. It is evident that the possible gain in rotor energy for a given u by the use of inlet guide vanes is less than that from bending the exit rotor blades forward.

Axial-Flow Fans, Blowers, and Compressors

Axial-flow fans, blowers, and compressors, Figs. 6 and 6*a*, are generally used for the movement of fluid rather than for the production of a large pressure rise. With axial flow the centrifugal effect for producing pressure rise is absent, but the change in kinetic energy and the velocity conversion effect are both present. Equation [15], without the centrifugal term, holds in this case. Hence, the rotor energy is

$$E = \frac{1}{2g}\left[(V_2^2 - V_1^2) + (v_1^2 - v_2^2)\right] \ldots\ldots [32]$$

Details of the transformation of this equation, and application to the actual case of the axial-flow compressor, are not further discussed.

In radial-flow compressors the centrifugal effect is quite important in producing pressure rise, and because of the absence of a centrifugal effect in axial-flow machines, these usually have a number of stages.

Stationary inlet guide vanes and diffusers can be used with axial-flow machines as with radial-flow machines but their use is less frequent. It can be shown that Equation [26] still holds for axial-flow machines so that for maximum rotor energy, inlet guide vanes should be turned backward, and the blade at exit from the rotor should be turned forward. However, blades with airfoil sections usually are used as these give the fluid a smooth passage through the rotor and result in a machine of high efficiency. Then it is not feasible to turn the rotor blades forward.

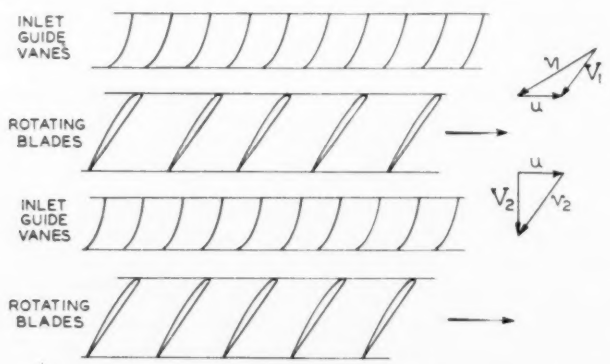


Fig. 6 Axial-Flow Fan, Blower, or Compressor

There is a feature of diffusers that should be mentioned. In radial-flow machines the diffuser takes fluid from the rotor exit through a passage at a greater radius. By the law of conservation of angular momentum it follows that any diffuser with radial flow, even an empty annular space, usually effects some pressure recovery. However, this is not the case with a diffuser on axial-flow machines, and it is possible for the entire kinetic energy associated with the tangential component of absolute velocity at exit from the fan to be lost in friction and eddying.

Some axial-flow machines present some practical deviations from the assumptions made that should be mentioned. These are made with so few blades that their characteristics can hardly be approximated by a rotor having an infinite number of blades. Furthermore, the blades may take up such a large portion of the face of the actual rotor that it would be hard to say at just what radius the various velocities and angles should be measured. Finally, the only cases that can be treated here are those in which the flow is uniform. Hence propellers such as may be used to drive airplanes or ships, Kaplan turbines, and propeller pumps must be excluded. In these applications the flow through the rotor must be determined from hydrodynamic considerations.

Radial-Flow Turbines—Francis Turbine

The subject of compressors, blowers, fans, and such machines in which the flow of energy is from the rotor to the fluid has been treated. Now machines will be discussed in which the flow of energy is from the fluid to the rotor, which is the general class of turbine machinery. Aside from the fact that turbines are the reverse of compressors there is one practical difference between the two which may be mentioned. In compressor machinery it is impractical to obtain a very great fluid velocity except at exit from the rotor, and a diffuser to convert velocity energy into pressure energy is comparatively inefficient. On the other hand, in turbine machinery an appreciable velocity may be obtained by passage of the fluid through a set of nozzles, which is an efficient process.

Because of the differences in properties of liquids and vapors, hydraulic and steam turbines are quite dissimilar. A vapor is highly compressible, and generally a number of stages are required to extract the energy from it efficiently. This staging is done in the simplest fashion in axial-flow machines. The Ljungström

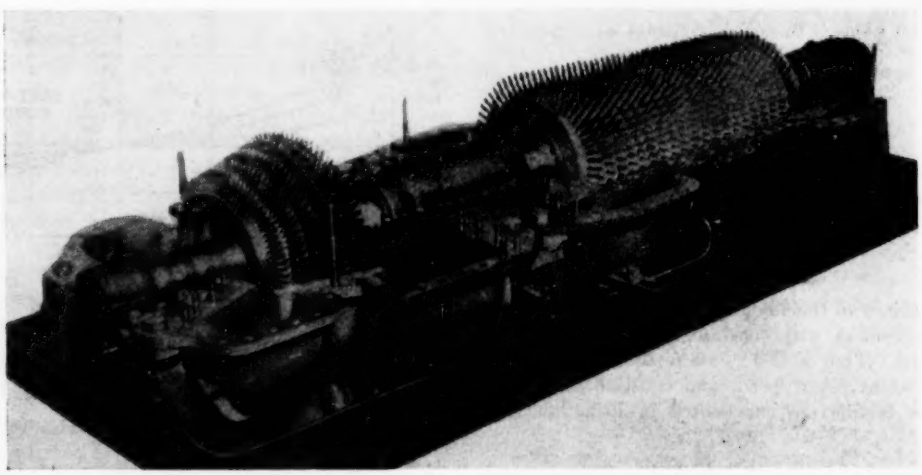
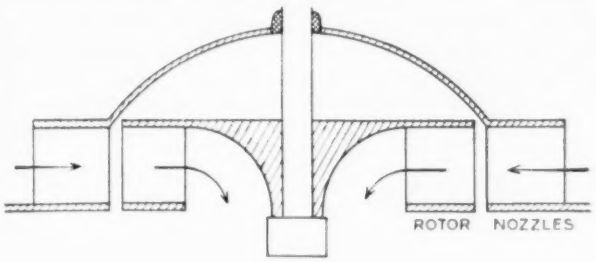


Fig. 6*a* Gas-Turbine Unit With Top Removed, Showing an Axial-Flow Turbine Driving an Axial-Flow Compressor (Brown Boveri & Co., Ltd., Switzerland, and Allis-Chalmers Manufacturing Co., Milwaukee, Wis.)

turbine is the only well-known radial-flow steam turbine. In this the successive radial stages rotate in opposite directions. Flow is outward to allow for the expansion of the steam as it passes through the turbine. The general equations of energy transfer apply to each stage of the turbine, but since this turbine is rarely found in this country, nothing further will be said about it here.



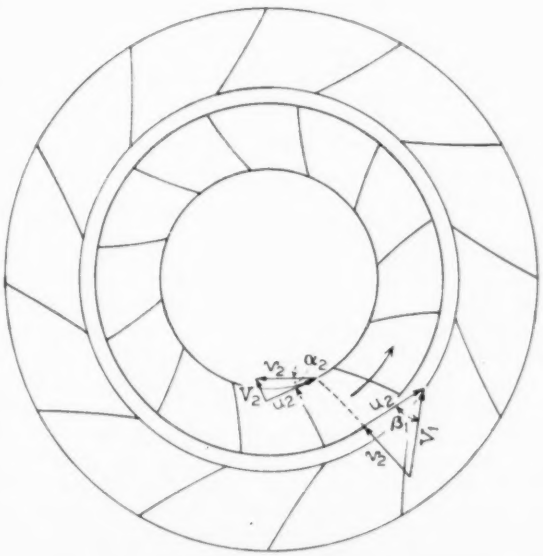


FIG. 7 FRANCIS TURBINE

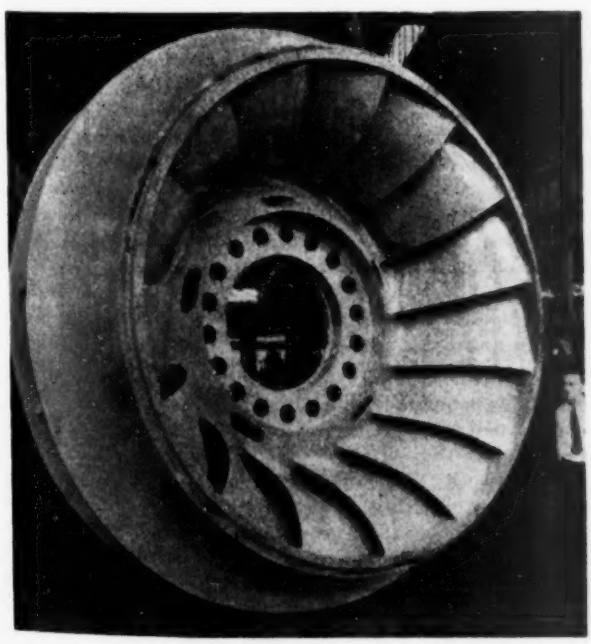
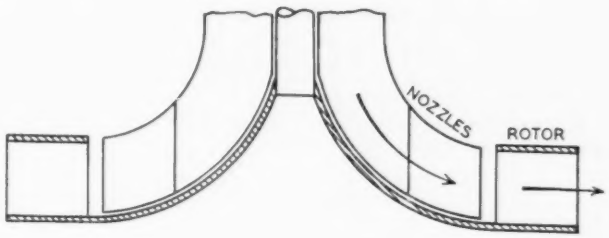


FIG. 7a RUNNER OF FRANCIS TURBINE



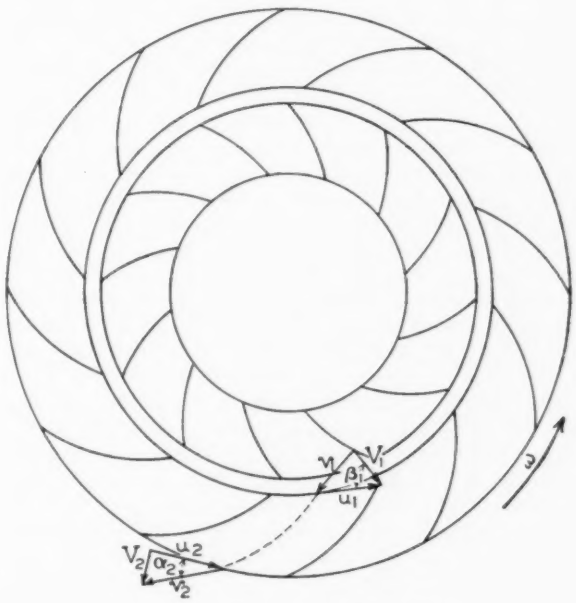


FIG. 8 FOURNEYRON TURBINE

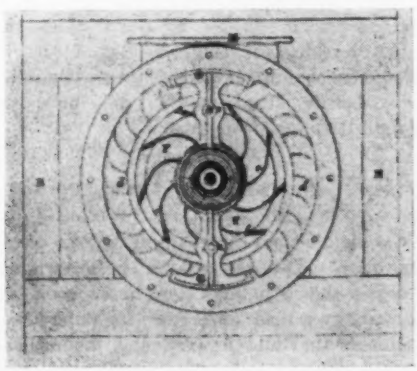


FIG. 8a FOURNEYRON TURBINE OF 1834

Hydraulic turbines sometimes have a restriction not present in steam turbines. This is that at times the available heads are so small that angles and other conditions must be selected which give a small value of K. However, in some hydraulic and all steam turbines a large value of K is sought to lower the rotor speed.

The most common hydraulic turbine that has its flow primarily radial is the Francis water wheel. This is shown diagrammatically in Figs. 7 and 7a. Water flows radially inward

through nozzles or guide vanes at the outer periphery, passes through a rotor, called a runner, and leaves with as low a velocity as is practical. Thus the Francis water wheel is to some extent a centrifugal pump in reverse.

The general Equation [15] of energy transfer between fluid and rotor is applicable here. This is

$$-E = \frac{1}{2g}\left[(V_1^2 - V_2^2) + (u_1^2 - u_2^2) + (v_2^2 - v_1^2)\right] \quad [33]$$

where subscript 1 refers to entrance of the fluid, subscript 2 to exit, and E is negative, since energy transfer in this case is from the fluid to the rotor. The terms have the same physical meaning here as they do for pumps and compressors. The term $(V_1^2 - V_2^2)/2g$, arising from the change of absolute velocity of the fluid, represents the change in kinetic energy of the fluid. Likewise the term $(u_1^2 - u_2^2)/2g$ indicates a centrifugal effect. Since $u_1 = r_1\omega$ and $u_2 = r_2\omega$, it is readily seen that if this term is to represent energy transfer from the fluid to the rotor then $r_1 > r_2$. In other words, a radial turbine must have inward flow if it is to utilize the centrifugal effect, just as a centrifugal pump must have outward flow for the same reason. Finally, the term $(v_2^2 - v_1^2)/2g$ represents a reaction effect, or a drop in pressure due to the increased velocity relative to the rotor. The equivalent of this reaction effect in a centrifugal compressor is the velocity-conversion effect. This reaction will be discussed in greater detail in the treatment of axial-flow turbines.

In years past a hydraulic turbine, the Fourneyron turbine, Figs. 8 and 8*a*, was made with radial outward flow. This may be compared with the Francis turbine. It has already been shown that a Francis turbine with its inward flow takes advantage of each of the items of rotor energy as given in Equation [33]. On the other hand, it is obvious that in the Fourneyron turbine both the centrifugal effect and the reaction effect are negative and so reduce the rotor energy. Thus in the Francis turbine the rotor energy is comparatively high and these turbines are suitable for high heads. On the other hand, in the Fourneyron turbine the rotor energy is low, and these turbines are suitable for low heads and high speeds. In recent years the Kaplan turbine has been largely used for low heads.

The subject of inlet and exit angles for a radial-flow turbine may be treated briefly. Equation [26] may be shown to hold for this case as it does for a compressor

$$-E = \frac{1}{g}(V_1 u_1 \cos\beta_1 - u_2^2 + v_2 u_2 \cos\alpha_2) \quad [34]$$

In this case the signs have been changed to take account of the present application. The angles have been chosen as acute when they are as shown in Fig. 7. The equation shows that the maximum energy is abstracted from the fluid when the inlet guide vanes direct the fluid forward and the rotor exit vane angle directs the fluid backward. The exit angle is such that the fluid leaves the rotor with as small an absolute velocity as is possible; for the Francis rotor shown this is a purely radial velocity. The actual form of the blades varies somewhat. Generally in hydraulic turbines the rotor velocity at inlet is as large or larger than the absolute fluid velocity. This gives a blade which varies from a radial entrance to the backward entrance that is shown in Fig. 7, rather than a blade with a large curvature as is commonly found in steam turbines. This condition arises from two reasons. First, the absolute velocity of the fluid at entrance to a Francis rotor is limited by the head available, which is often quite small, and it is desirable to make the rotor speed as high as possible to reduce the size of the turbine. Secondly, a blade with a large curvature causes large differences of velocity in the space between blades, and this gives rise to cavitation difficulties. For these reasons the backward blade is used.

With the aid of Equation [34] a value of K may be found similar to that found for centrifugal compressors. Only the case where the absolute velocity at exit is radial will be considered here. This represents the condition of minimum leaving loss. For this condition, as may be seen from the exit velocity triangle of Fig. 7

$$\cos\alpha_2 = \frac{u_2}{v_2} \quad [35]$$

Equation [34] becomes

$$-E = \frac{1}{g}(V_1 u_1 \cos\beta_1) \quad [36]$$

The value of K is defined in Equation [4], which for turbine apparatus becomes

$$-E = K\frac{u^2}{g} \quad [37]$$

Thus by comparison with Equation [36]

$$K = \frac{V_1 \cos\beta_1}{u_1} \quad [38]$$

In other words K is determined by the ratio of the tangential component of the inlet velocity to the inlet rotor velocity.

It is possible to treat this case as the centrifugal compressors were treated and to find the variation of K with β_1 at constant speed and constant flow. However, for hydraulic turbines, such a treatment has little meaning. The velocity V_1 is limited by the available head, which is often small. The flow is also usually fixed for a particular application. It follows that the nozzle angle β_1 is fixed by the size of the rotor and the application to which the machine is to be put and is not a quantity the designer varies at will as is the case with the centrifugal compressors. The quantity that the designer does vary, however, is the rotor speed. The variation of K with rotor speed u is obvious.

Specific Speed

The use of the factor K in the discussion of hydraulic apparatus is an important item of the present paper. However, hydraulic rotors of different types often are distinguished by a quantity known as the specific speed. The specific speed is defined as the speed at which a rotor, similar to the given one and operating under conditions such that its velocity triangles are geometrically similar to those of the given rotor, would run if it takes one horsepower at a head of one foot, assuming that the influence of Reynolds' number can be neglected. In books on hydraulics (9, 10) the specific speed is given as

$$n_s = \frac{n\sqrt{P}}{H^{5/4}} \quad [39]$$

Here P is the horsepower. The quantity H is the energy of the fluid, and is numerically equal to w, discussed previously. Both P and H are usually measured at the condition of maximum efficiency.

Machines with geometrically similar dimensions operating under similar conditions (having similar velocity triangles) are said to have similarity. This similarity is with respect to both machine dimensions and velocity triangles. Effects of compressibility and Reynolds' number may be ignored. Machines with complete similarity, or with similar velocity triangles and therefore the same K but with dissimilar dimensions, or with geometrical similarity and different velocity triangles, may be

designated, compared with, and distinguished from each other by a factor known as the quantity constant. One expression for this is Q/nD^3 where Q is the volume flow and D is the rotor diameter.

If two rotors are similar and operate under similar conditions, they have the same K and the same quantity constant. They also have the same specific speed. A relation exists between the specific speed, the factor K, and the quantity constant. This may be found as follows. The horsepower required by a machine is

$$P = \frac{\rho Q E}{550} \quad [40]$$

The head delivered by a pump is

$$H = w = \eta E = \frac{\eta K u^2}{g} \quad [41]$$

For the rotor speed u there may be substituted the quantity $\pi nD/60$. Upon combining Equations [40] and [41] with the specific speed in Equation [39] there results

$$n_s^4 = 5.34 \times 10^6 \left(\frac{\rho^2}{\eta^5}\right)\left(\frac{1}{K^3}\right)\left(\frac{Q}{nD^3}\right)^2 \quad [42a]$$

Thus the specific speed for pump apparatus is found to be a function of two separate items, K and the quantity constant. In pump apparatus these two items are varied independently. Thus K is varied by change of angles on the rotor or guide vanes; and the quantity constant is varied by changing the flow, rotor speed, or rotor diameter. The specific speed shows the combined effect of variation of all of these items.

An expression similar to Equation [42a] can be found for turbine apparatus. Thus

$$n_s^4 = 5.34 \times 10^6 \rho^2 \eta^5 \left(\frac{1}{K^3}\right)\left(\frac{Q}{nD^3}\right)^2 \quad [42b]$$

However, in this case the angles are fixed by conditions under which the turbine is to operate, so that K is not a factor that the designer varies at will. Equation [42b] then shows that the specific speed depends primarily on the quantity constant.

Axial-Flow Turbines

The axial-flow turbines that are to be discussed here are the steam turbines in common use. Both the impulse and the reaction turbines will be treated. Figs. 9a and 6a show typical machines. Such turbines, especially those of large capacity, generally have a number of pressure stages; such turbines are made with axial flow because this makes the mechanical construction simpler. However, in spite of staging and its importance, only a single stage will be discussed here.

In general, the fluid passing through an axial-flow machine leaves the rotor at the same radius at which it entered. Hence the rotor velocities at inlet and exit are the same, and may be designated as u. Thus Equation [2] takes the form

$$-E = \frac{u}{g}(V_{1u} - V_{2u}) \quad [43]$$

This shows that the rotor energy depends only on the rotor velocity and the change in the tangential component of the fluid velocity. This equation is merely a statement of the fact that in this case the rotor energy is the force on the wheel multiplied by the rotor velocity, the force on the wheel being given by the change in tangential momentum. It is worth while to show the meaning of this equation on the velocity diagram, Fig. 9. The tangential component of the inlet velocity is AD. The tangential component of the exit velocity is BC. The difference between AD and BC is the net change in tangential velocity, which gives the force on the wheel.

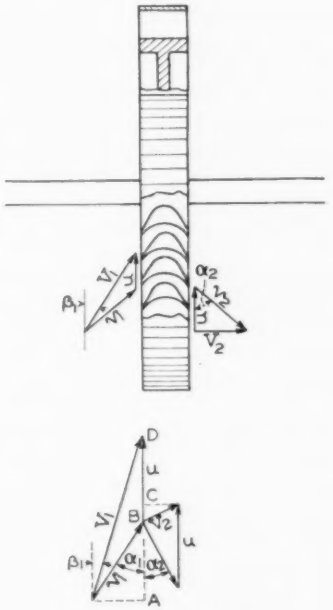


Fig. 9 Impulse Turbine

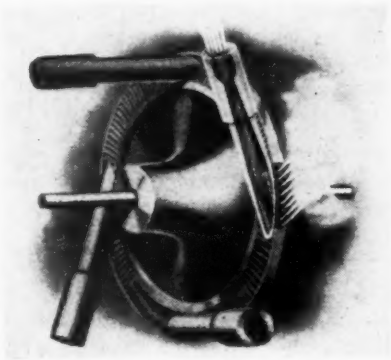


Fig. 9a Original Representation of an Impulse Turbine Used by the DeLaval Co.

From the velocity diagram the following relations are apparent, in which β_1 is the nozzle angle and α_1 and α_2 are the blade angles at entrance and exit respectively

$$V_{1u} = V_1 \cos \beta_1 = v_1 \cos \alpha_1 + u \quad [44]$$
$$V_{2u} = -v_2 \cos \alpha_2 + u$$

By substitution of these relations in Equation [43] there results

$$-E = \frac{u}{g}[V_1 \cos \beta_1 + v_2 \cos \alpha_2 - u] \quad [44a]$$

$$-E = \frac{u}{g}[v_1 \cos \alpha_1 + v_2 \cos \alpha_2] \quad [44b]$$

Equation [44b] is interesting in regard to the velocity diagram. It shows that the change in the tangential velocity of the fluid in passing through the rotor is equal to the sum of the projections of the relative velocities.

A final form for the equation of rotor energy may be found from Equation [15], where the centrifugal effect may be neg-

lected since the entrance and exit are at the same radius. Then

$$-E = \frac{1}{2g}\left[(V_1^2 - V_2^2) + (v_2^2 - v_1^2)\right] \quad [45]$$

which shows that the energy change depends only on the change in kinetic energy and the reaction effect. In particular it shows that the exit velocity V_2 should be as small as possible unless it can be used efficiently in the following stage. Generally this is known as the leaving loss and is unavoidable at the last stage of the turbine.

The foregoing equations next will be applied to an impulse turbine, in which there is no pressure change across the rotor. Under ideal conditions this stipulation would mean that the relative velocity remains constant while the fluid passes through the rotor. However, because of friction and other losses the relative velocity decreases, and this may be taken account of conveniently by introducing a factor C_b, less than unity, such that

$$v_2 = C_b v_1 \quad [46]$$

If C_b is substituted in Equation [44a] there results

$$-E = \frac{u}{g}\left[V_1 \cos \beta_1 + C_b v_1 \cos \alpha_2 - u\right] \quad [47]$$

It is evident from this equation that the nozzle angle β_1 should be as small as possible for the greatest rotor energy.

Sometimes the bucket angles α_1 and α_2 are made equal, and any actual impulse buckets do not depart far from this condition. By making the assumption that the bucket angles are equal a number of relations can be found which are approximately true for all impulse buckets. Thus from Fig. 9 if $\alpha_1 = \alpha_2$ then

$$v_1 \cos \alpha_2 = v_1 \cos \alpha_1 = V_1 \cos \beta_1 - u \quad [48]$$

and Equation [47] may be written as

$$-E = \frac{u}{g}(1 + C_b)(V_1 \cos \beta_1 - u) \quad [49]$$

This expression may be differentiated with respect to u, and the speed at which the rotor energy is a maximum is found to be

$$u = \frac{V_1 \cos \beta_1}{2} \quad [50]$$

Since β_1 is usually rather small, it can be seen that for the maximum rotor energy the rotor velocity is about half the steam velocity. The factor is about $^1/_2$ in some cases.

The fact that the rotor speed for maximum rotor energy is half the tangential component of the entrance velocity can be given a physical explanation for the ideal case where there are no losses in the bucket. Referring to Fig. 9, it can be seen that under these conditions the tangential component AB of the inlet relative velocity is equal to the rotor speed. Since v_1 is assumed equal to v_2, the same is true at exit. It follows that the velocity V_2 is purely axial and hence is a minimum. Thus with no bucket losses, Equation [50] gives the rotor speed such that the leaving loss is a minimum.

The efficiency may now be treated. The input to the wheel is the kinetic energy $V_1^2/2g$, since there is no pressure drop across the rotor. However, this kinetic energy is produced by a drop in pressure through the nozzles, and this is accompanied by a friction loss. Thus the velocity V_1 is less than the ideal velocity V_0 that would be produced by an isentropic pressure drop, and this may be taken account of by introducing a factor C_n such that

$$V_1 = C_n V_0 \quad [51]$$

Thus the input to the stage is $\frac{V_0^2}{2g}$. The output is given by Equation [49] which, with the introduction of the factor C_n, reduces to

$$-E = \frac{u}{g}(1 + C_b)(C_n V_0 \cos \beta_1 - u)$$

The efficiency of the stage is the ratio of this quantity to the input, or

$$\eta = 2\left(\frac{u}{V_0}\right)(1 + C_b)\left(C_n \cos \beta_1 - \frac{u}{V_0}\right) \quad [52]$$

This efficiency is known as the nozzle and bucket efficiency. It is a function of the velocity ratio u/V_0, and is so plotted in Fig. 10 for the representative values $C_b = 0.85$, $C_n = 0.97$, and $\beta_1 = 12$ deg.

In this discussion, nozzle coefficients and bucket coefficients

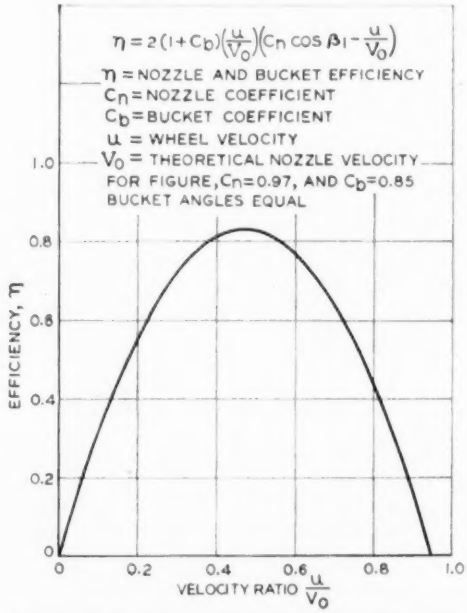


FIG. 10 EFFICIENCY OF IMPULSE STAGE OF TURBINE

have been introduced to find the nozzle and bucket efficiency. It is found that such coefficients are useful in drawing velocity diagrams and finding nozzle and bucket angles. However, the nozzle and bucket efficiency of Equation [52] is of somewhat limited utility. The action between nozzle and bucket is quite complex, and some degree of reaction may be present. For these reasons the nozzle and bucket efficiency may be determined from experiment; the rotor energy is then

$$-E = \eta w$$

where w is the isentropic drop in enthalpy. Such a procedure often results in greater accuracy.

Finally, if a factor K is desired, this may be found from Equation [49] by comparing this quantity with Ku^2/g. Thus

$$K = (1 + C_b)\left(\frac{C_n V_0}{u} \cos \beta_1 - 1\right) \quad [53]$$

The effort is usually made to make the nozzle angle β_1 as small as possible. Thus K is determined by the ratio u/V_0. For the condition of best efficiency as given in Equation [50]

$$K = (1 + C_b) \quad [54]$$

which is close to the value 2. Thus the ideal rotor energy for an impulse stage is close to

$$-E = 2u^2/g \quad [55]$$

The impulse stage just discussed is characterized by the pressure equality across the rotor. Ideally the entire drop in enthalpy occurs across the stator nozzles, with no drop across the rotor. On the other hand, a reaction stage has a drop in enthalpy across the rotor with a corresponding drop in pressure. Fig. 6*a* shows on the left a reaction turbine driven by combustion gases. A reaction steam turbine is similar. Stages may be designated by the proportion of the drop in enthalpy which takes place across the rotor. Thus a turbine with 0 per cent drop in rotor would be one in which there is no drop in enthalpy across the rotor—in other words an impulse turbine. A turbine with 50 per cent drop in rotor would be one in which the drop in enthalpy across the rotor is equal to that across the stator. A turbine with 100 per cent drop in rotor would be one in which the entire drop in enthalpy takes place across the rotor. In this case the stator would merely change the direction of the velocity of the fluid coming from the preceding stage without causing any increase of its velocity.

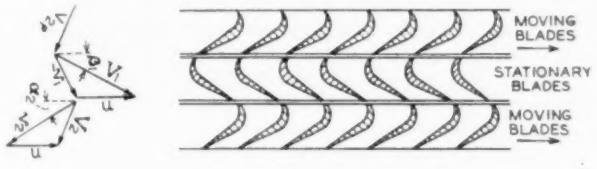


FIG. 11 REACTION TURBINE

A drop in enthalpy across the rotor of a turbine causes an increase of the relative velocity of the fluid. The acceleration of the fluid requires a force from the rotor, and the reaction or recoil of this is the force which drives the rotor.

For a 50 per cent drop in the rotor the use of stator blade and rotor blade with the same angles is common. The velocity diagram for this case is shown in Fig. 11, and it can be seen from this that the stator blade section is the same as the rotor section. Such a construction has obvious advantages in manufacture.

With the aid of Fig. 11, it may be shown that in the absence of friction losses the equal angle arrangement has 50 per cent drop in rotor, assuming the blade height varies directly as the specific volume of the fluid. The converse is also true. The stator angle, β_1, is equal to the rotor angle α_2. The velocity V_{2p} is the velocity of the fluid coming from the previous stage. From Fig. 11 the following relations are apparent

$$V_1 = v_2 \quad [56]$$

$$v_1 = V_2 = V_{2p} \quad [57]$$

The fluid velocity is obtained by a drop in enthalpy. Thus if subscript $_s$ denotes the stator and subscript $_r$ the rotor, the following equations may be written

$$\Delta h_s = \frac{1}{2gJ}(V_1^2 - V_{2p}^2) = \frac{1}{2gJ}(V_1^2 - V_2^2) \quad [58]$$

$$\Delta h_r = \frac{1}{2gJ}(v_2^2 - v_1^2) = \frac{1}{2gJ}(V_1^2 - V_2^2) \quad [59]$$

Thus half of the total drop in enthalpy takes place in the rotor so that the stage has 50 per cent drop in rotor.

Because of the various degrees of reaction that can be used and the compressibility of the fluid, no ideal analysis of a reaction stage, such as was made for an impulse stage, is given here, since in general the exit conditions are not defined by the inlet conditions. However, a few features may be pointed out. In many reaction turbines the rotor angle at inlet is close to 90 deg rather than the small angle found in impulse stages. This 90-deg rotor inlet angle corresponds to the condition

$$u = V_1 \cos \beta_1 \quad [60]$$

which is found to be approximately the velocity at which maximum efficiency occurs. If this is combined with the condition that the absolute exit velocity from the bucket is axial then the maximum energy transfer for a reaction stage with 90-deg bucket inlet angle can be found from Equation [43] as

$$-E = \frac{u^2}{g} \quad [61]$$

In this case, the inlet angles of the stator and rotor are the same, although exit angles may be different. However, if exit angles also are the same this becomes a particular case of the 50 per cent drop in the rotor.

There may be made some rough comparisons between the ideal impulse stage and the reaction stage in which nearly all the pressure drop takes place across the rotor. Upon comparing Equations [50] and [60] it is apparent that for a given fluid velocity, the stage with usual reaction has a rotor velocity twice that of the impulse stage. In other words, a reaction machine is inherently a higher-speed machine than the impulse machine. Upon comparing Equations [55] and [61] it is apparent that the ideal impulse stage extracts twice as much energy as the stage with usual reaction. Put in another way, in order to extract equal amounts of energy the usual reaction stage must have a rotor speed equal to $\sqrt{2}$ times the speed of the impulse stage, or about 40 per cent greater. However, both of these comparisons may be changed somewhat in practice.

Comparison of Axial- and Radial-Flow Turbines

In the study of centrifugal compressors it was emphasized that there were three important divisions of the energy transfer from the rotor to the fluid. These were the change in kinetic energy of the fluid passing through the rotor, the centrifugal effect due to the fluid's leaving the rotor at a radius different from that at which it entered, and a diffusion effect due to a reduction of the relative velocity of the fluid as it passes through the rotor. The centrifugal effect is of the greatest importance, since a diffuser to convert velocity energy into pressure energy is in practice a comparatively inefficient device, and a rotary compressor which does not make use of the centrifugal effect would be impractical. On the other hand, the turbines studied have been chiefly axial-flow machines in which there is no centrifugal effect. It is thus of interest to compare axial turbines and radial turbines with inward and outward flow and to obtain mathematically relations that are well known from experience.

To compare radial- and axial-flow turbines all losses will be neglected and it will be assumed that the fluid enters the rotor tangentially, i.e., with zero entrance angle, and that it leaves at zero absolute velocity. In other words the turbines will be compared at 100 per cent efficiency. It is, of course, impossible to satisfy these conditions and still have fluid flow through the rotor, but the expressions for energy are simplified by these assumptions without being radically changed in value. Under these conditions the rotor energy as found from Equation [2] is

$$-E = u_1 V_1/g \quad [62]$$

Two new variables are introduced. One is V_θ, which is the velocity the fluid would have at the entrance to the rotor if the

entire pressure drop that takes place across the machine took place in the stator blades. Thus the definition of V_0 is

$$-E = V_0^2/2g \quad [63]$$

The quantity V_0 is the nozzle velocity of the ideal impulse turbine. Thus $(V_0^2 - V_1^2)/2g$ is the energy that is derived from a drop in pressure across the rotor. Of this energy a portion

$$\frac{C}{2g}(V_0^2 - V_1^2) = \frac{1}{2g}(u_1^2 - u_2^2) \quad [64]$$

may be attributed to the centrifugal effect if present. Thus $C = 1$ represents a radial-flow turbine with no reaction effect and $C = 0$ represents an axial-flow turbine in which there is no centrifugal effect.

By combining Equations [62] and [63] with [64] there results

$$\left(\frac{u_2}{V_0}\right)^2 = C\left[\frac{1}{4\left(\frac{u_1}{V_0}\right)^2} - 1\right] + \left(\frac{u_1}{V_0}\right)^2 \quad [65]$$

In this equation u_1 and u_2 are the rotor velocities, and these depend upon the inlet and exit radii. Thus the dimensionless factors u_2/V_0 and u_1/V_0 form convenient measures of these radii. These quantities may be used as co-ordinates on which to plot lines of constant C as in Fig. 12, and on the basis of this figure, various types of turbines may be compared. The co-ordinates chosen seem particularly appropriate, since they are dimensionless and V_0 is a measure of the total energy transfer that takes place in a stage.

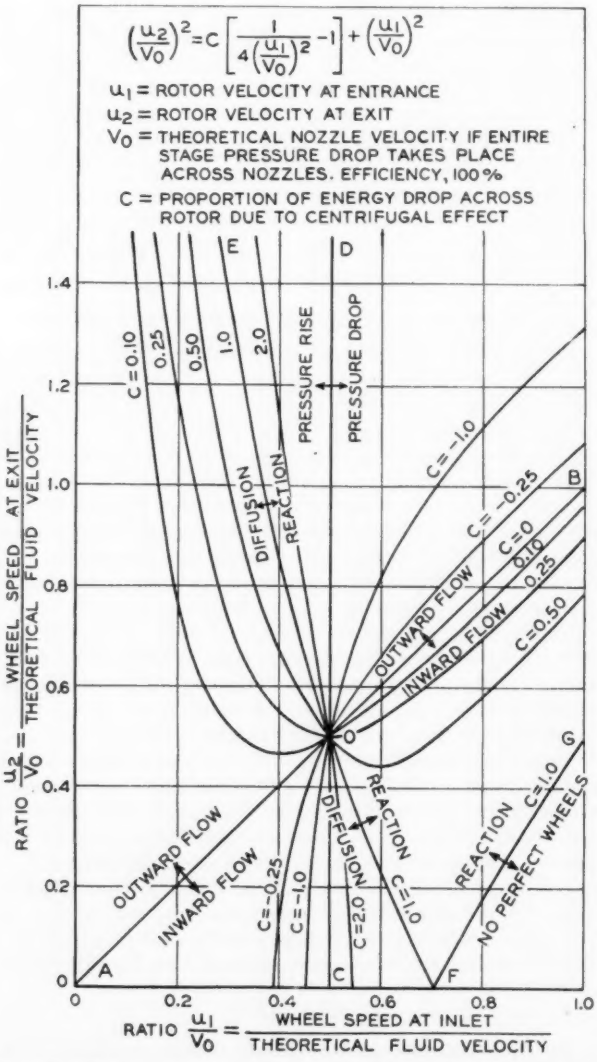


FIG. 12 COMPARISON OF AXIAL- AND RADIAL-FLOW TURBINES

In Fig. 12 the diagonal line AB represents axial-flow turbines. To the right of AB are inward-flow turbines, and to the left are outward-flow turbines. On this line $C = 0$, since there is no centrifugal effect.

On the line CD are found rotors with no pressure change, or $V_1 = V_0$. In other words, either the reaction effect and the centrifugal effect balance each other or each is zero. At the point 0 is the axial-flow impulse turbine. To the right of CD are represented rotors for which $V_1 < V_0$; this indicates a pressure drop across the rotor. On the other hand, in the region to the left of CD are represented rotors for which $V_1 > V_0$; this means that the fluid is overexpanded in the nozzles and there is a pressure rise across the rotor.

Finally, the broken line $EOFG$ is the plot of $C = 1$, or the locus of turbines in which there is no velocity-conversion effect or reaction. Along this line the entire pressure change across the rotor is utilized in producing the centrifugal effect. In the region to the right of EOF are located rotors with reaction effect, and to the left of EOF are located rotors with diffuser effect, i.e., the relative velocity at exit from the rotor is less than the relative velocity at entrance. In the region to the right of FG there are no perfect turbine rotors.

By means of Fig. 12 an investigation may be made as to which type of rotor gives the smallest outside diameter. All of the rotors which lie in the region $V_1 < V_0$, i.e., to the right of the line CD, have their larger diameter greater than that of a pure impulse rotor. The inward-flow rotors of this region with C between $^1/_4$ and 1 have their inner diameters first decrease and then increase as V_1/V_0 decreases. The rotors in the region COF have diminishing inner diameters as V_1/V_0 decreases. These are diffuser rotors. The reduction of the inner diameter causes such an excess of centrifugal action that the relative velocity has to decrease along the rotor in order to counterbalance it. All other rotors in the region $V_1/V_0 < 1$ have an increasing exit diameter as V_1/V_0 diminishes. Moreover, they call for a considerable expansion, especially in the outward-flow type, because in this case the pressure difference between inlet and outlet has to balance not only the reaction effect, but the centrifugal effect as well. The investigation so far indicates that none of the rotors working under the condition $V_1/V_0 < 1$ has characteristics that would make them preferable to pure impulse rotors.

The rotors represented along the line CO have their greater diameter the same as that of a pure impulse rotor. The nearer alike the inlet and exit diameters are, the less is the diffuser action required in them. The rotors along OD are outward flow, but have their exit diameter greater than that of an impulse rotor. Hence, none of these rotors is desirable.

Finally, the region to the left of CD may be considered. For this region $V_1/V_0 > 1$, and the rotors have a pressure rise across them. This makes them of particular interest, as they have not yet been used in practice. The following rotors have their large diameter less than that of a pure impulse rotor: The inward-flow rotor in the space AOC; the axial-flow wheels along the line AO; and the outward-flow wheels on the space between AO and the curve $C = ^1/_4$. Of these three possibilities for a given value of V_1/V_0 the outward-flow wheel has its larger diameter greater than that of an axial-flow rotor, but with less diffusion; the inward-flow rotor has its larger diameter equal to that of an axial-flow, but with more diffusion. The rest of the

rotors in the region $V_1/V_0 > 1$ have their larger diameter greater than that of an impulse wheel.

Of all the types of rotors discussed it is only those with outward flow and with $C < 1/4$ that seem to offer any advantage over the impulse rotor. All of these have a diffusion effect. They have not yet been made in practice and it may be that the diffusion may counterbalance the inherent advantage they seem to have.

Before leaving this discussion it would be well to recall the assumptions under which it was made. In the first place it was assumed that the fluid entered the rotor with its absolute velocity tangential. This is approximately true for an impulse turbine, but less so for a reaction stage. However, for a turbine like the Francis water wheel this is even further from the truth.

The other assumption made was that the fluid leaves the rotor at zero velocity. This was done for simplicity. However, in multistage machines an effort is made in practice to utilize as much as possible of the leaving velocity from one stage in the following stage of the turbine. If this is done, the condition of zero leaving loss is closely approximated.

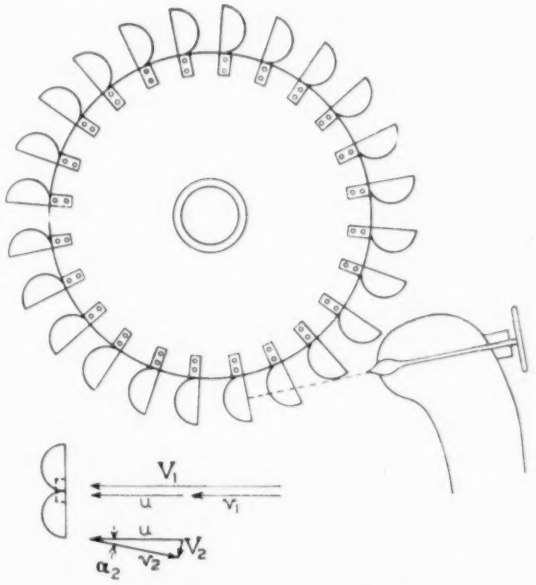


FIG. 13 PELTON WATER WHEEL

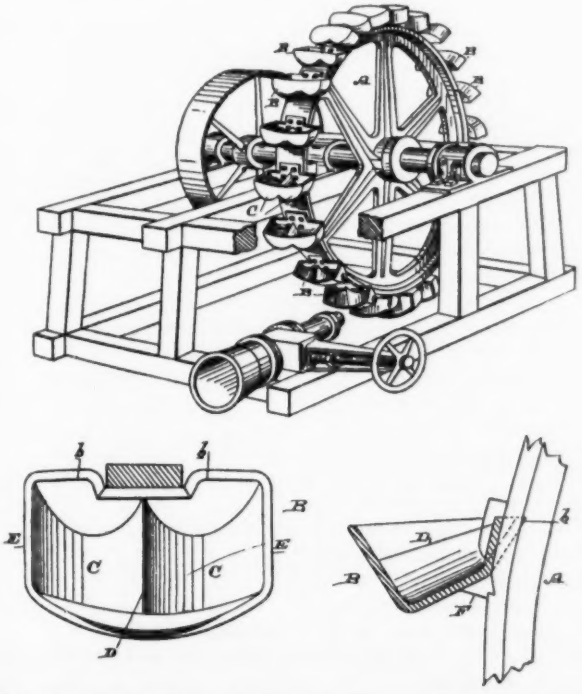


FIG. 13a PELTON WATER WHEEL, AS GIVEN IN PELTON'S PATENT OF 1889, BUT TYPICAL OF ALL PELTON WHEELS

THE PELTON WATER WHEEL

The Pelton water wheel was one of the earliest impulse machines used. This differs from the machines already discussed since the fluid does not completely fill the flow passages. For this reason greater outputs from a rotor of this kind may be obtained by increasing the flow without causing much change in efficiency. In fact the Pelton water wheel maintains its efficiency under changing flow better than most other turbine machines.

A Pelton wheel is shown schematically in Figs. 13 and 13*a* The flow is quite different from that in the other machines considered. So far, a continuous flow around an entire circumference has been considered. As opposed to this the flow at entrance to a Pelton rotor is through one or more nozzles, resulting in a few jets impinging on the rotor. However, each filament of fluid in the jet has approximately similar paths as regards velocities and directions, so that the flow may be regarded as uniform. There is a periodic change as the jet changes from one bucket to the next, but the slight effect of this will be disregarded.

As shown in Fig. 13 the flow of fluid enters the buckets essentially tangentially. The rotor is usually designed so that this is possible without the buckets greatly interfering with the flow into adjacent buckets. During passage through the buckets the direction of flow is practically reversed. The relative velocity of flow at exit is at a small angle α_2 with the direction of the bucket velocity so that the leaving fluid is cleared out of the way without interfering with the following buckets.

The fundamental Equation [2] is applied to this case as well as to the other cases considered.

$$-E = \frac{1}{g}(u_1 V_{1u} - u_2 V_{2u}) \quad [2]$$

In this case the rotor velocities u_1 and u_2 are equal and may be designated by u. The inlet velocity triangle degenerates into a straight line so that

$$V_1 = v_1 + u \quad [66]$$

At exit evidently

$$-V_{2u} = v_2 \cos \alpha_2 - u \quad [67]$$

Hence

$$-E = \frac{u}{g}(v_1 + v_2 \cos \alpha_2) \quad [68]$$

This equation is true regardless of the losses that take place while the fluid is passing through the rotor. A Pelton wheel by nature is an impulse machine. Because of the open passageways, it is impossible to maintain any pressure drop between entrance to the rotor and exit. Hence in an ideal rotor in which there are no losses v_1 and v_2 are equal. If this condition together with [66] be substituted in [68], there results

$$-E = \frac{u}{g}(V_1 - u)(1 + \cos \alpha_2) \quad [69]$$

This may readily be shown to be a maximum if

$$u = \frac{1}{2} V_1 \quad [70]$$

and in this case the maximum rotor energy is

$$-E = \frac{V_1^2}{4g} (1 + \cos \alpha_2) \quad [71]$$

The physical reason behind the existence of this condition for maximum energy transfer is similar to that for the impulse turbine. In Fig. 13, if the rotor velocity is half the fluid absolute velocity, then the relative velocity of the fluid at entrance and the velocity of the rotor are equal. If there are no losses as the fluid passes through the bucket, then at exit likewise the relative velocity of the fluid and the velocity of the rotor are equal. If the exit angle were zero, then the absolute fluid velocity at exit would be zero, and it is clear that this would be the condition for maximum energy transfer between the fluid and the rotor. Since

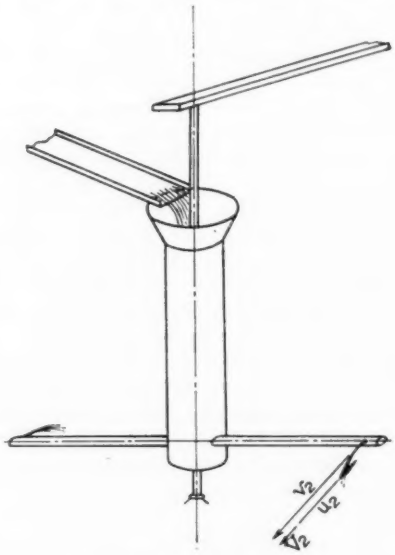


FIG. 14 BARKER'S MILL

the exit angle of the rotor α_2 is not zero, there is a small exit velocity, but the same condition for maximum energy transfer holds.

Equation [71] also throws light on another matter. The Pelton wheel bends the fluid, and at times this bending may be practically 180 deg. The impulse turbine also bends the fluid, but not as much as this. For this reason, the Pelton wheel can effect a greater energy transfer than the impulse turbine.

The action of the fluid on the buckets of a Pelton wheel is fairly complicated and further mathematical work on this subject is useless. The development of the Pelton wheel has been advanced more by systematic experimentation than by mathematical analysis.

BARKER'S MILL

As a final machine for discussion, Barker's mill will be treated. This machine is no longer of much practical importance, but it was one of the early reaction machines and gives another illustration of the application of the fundamental equations for the rotor energy. Moreover, unlike the axial-flow reaction turbine, some ideal conditions may be assumed for Barker's mill so that at least an approximate value of the best speed may be found.

Barker's mill is shown schematically in Fig. 14. It will be seen that this is similar to a common form of lawn sprinkler. The fluid, generally water, enters at the axis of rotation, from which it proceeds out along the arms of the mill. At the far radius of the arms the flow is bent practically to the tangential direction. Thus at the outer radius it follows that

$$V_{2u} = V_2 = v_2 - u_2 \quad [72]$$

The fluid enters at the axis so that $u_1 = 0$. Hence by Equation [2] the rotor energy may be found as

$$-E = \frac{u_2 (v_2 - u_2)}{g} \quad [73]$$

Now assume an ideal mill. In this case the only loss is the kinetic energy of the fluid at exit. This kinetic energy is

$$\frac{V_2^2}{2g} = \frac{(v_2 - u_2)^2}{2g} \quad [74]$$

The total energy input is

$$-E + \frac{V_2^2}{2g} = \frac{1}{2g} (v_2^2 - u_2^2) \quad [75]$$

Thus the ideal efficiency is

$$\eta' = \frac{\frac{u_2}{g} (v_2 - u_2)}{\frac{1}{2g} (v_2^2 - u_2^2)} = \frac{2u_2}{v_2 + u_2} \quad [76]$$

According to Equation [73] the relative velocity v_2 must be greater than the rotor velocity u_2 if the mill is to deliver energy. Hence it follows from Equation [76] that the efficiency increases as the rotor speed increases and can only reach unity at infinite speed. Practically, of course, this effect is offset by frictional losses at the greater rotor speeds. However, this ideal maximum efficiency of Barker's mill contrasts with that of the impulse turbine which has its maximum efficiency when the rotor velocity is half the fluid jet velocity.

NOMENCLATURE

A = area for flow, sq ft
Q = flow, cu ft per sec
E = rotor energy, ft-lb per lb of fluid
V = absolute velocity of fluid, ft per sec
v = relative velocity of fluid
u = absolute tangential velocity of rotor, ft per sec
ω = angular velocity of rotor, radians per sec
r = radius, ft
g = acceleration due to gravity, ft per sec^2
J = mechanical equivalent of heat, ft-lb per Btu
c_p = specific heat at constant pressure, Btu per lb per deg F
c_v = specific heat at constant volume, Btu per lb per deg F
k = c_p/c_v = specific-heat ratio
T = temperature, deg abs F
h = enthalpy or total heat, Btu per lb
Z = vertical height of fluid, ft
ρ = density, lb per cu ft
R = gas constant, ft-lb per lb per deg F
n = hyperadiabatic constant in $pv^n = c$
p = static pressure, lb per sq ft
p_t = total pressure, lb per sq ft
α = angle between rotor blade and tangential direction
β = angle between absolute velocity of fluid and the tangential direction
K = constant by which u_2^2/g is multiplied to obtain the rotor energy for rotors with different angles

$x_1 = \dfrac{V_1 \sin \beta_1}{u_1}$ introduced in Equation [29]

$x_2 = \dfrac{V_2 \sin \beta_2}{u_2}$ introduced in Equation [30]

w = energy received per pound of fluid as it passes through a machine—the fluid energy

w_a = theoretical work of hyperadiabatic compression; $dw_a = vdp$ if $pv^n = c$ where v is specific volume

w_k = theoretical work of isentropic compression

η = hydraulic efficiency, $w = \eta(Ku_2^2/g)$ in Equation [9]

η' = ideal efficiency, where the only loss considered is the leaving loss

V_0 = defined by Equation [63]

C = defined by Equation [64]

M = torque exerted by rotor on fluid, ft-lb

P = power transferred from rotor to fluid, ft-lb per sec

W = total quantity of matter passing through rotor, lb

n = speed of rotation, rpm

n_s = specific speed

D = diameter, ft

Subscripts

1 indicates rotor entrance

2 indicates rotor exit

0 indicates machine entrance

3 indicates machine exit

u indicates tangential direction

r indicates radial direction

n indicates axial direction

APPENDIX 1

Derivation of the Equations for Rotor Energy

The general equations for the rotor energy have been given and discussed for various applications in this paper. This rotor energy is the theoretical energy that the rotor transfers to the fluid as determined kinematically. The derivation of these relations will now be given.

The assumptions and conditions for the validity of the expressions for the rotor energy have already been given. They involve principally a steady-state flow of fluid to and from a rotor which is turning about a fixed axis at constant angular velocity. The fluid enters and leaves the rotor at any radius, at any velocity, and in any direction, provided only that the flow is uniform. The meaning of the assumption of uniformity is that all filaments of fluid enter the rotor with the same velocity in the same direction with respect to the radius vector, and likewise all filaments of fluid leave the rotor with the same velocity and similar directions.

The physical principle involved in the derivation comes from Newton's laws of motion. These state that the time rate of change of angular momentum of a particle about an axis is equal to the moment of the applied force. Consider the rotor during a short time dt. A quantity of fluid dW at radius r_1 and velocity V_1 is taken into the rotor. The angular momentum of this fluid is $dW(r_1V_{1u})/g$. In the same short time dt an equal quantity of fluid dW leaves the rotor radius r_2 with velocity V_2. Its angular momentum is $dW(r_2V_{2u})/g$. Since the flow is steady the quantity discharged is equal to the quantity taken in. Hence the change in angular momentum in time dt is

$$\frac{dW}{g}(r_2V_{2u} - r_1V_{1u})$$

and

$$M = \frac{1}{g}\frac{dW}{dt}(r_2V_{2u} - r_1V_{1u}) \quad \ldots\ldots [77]$$

where dW/dt is the quantity of matter flowing per unit of time. Thus the power is

$$P = M\omega = \frac{\omega}{g}\frac{dW}{dt}(r_2V_{2u} - r_1V_{1u}) \quad \ldots\ldots [78]$$

The energy transfer per pound of fluid is

$$E = \frac{\omega}{g}(r_2V_{2u} - r_1V_{1u}) \quad \ldots\ldots [79]$$

By use of the relations $u_2 = \omega r_2$ and $u_1 = \omega r_1$ it follows that

$$E = \frac{1}{g}(u_2V_{2u} - u_1V_{1u}) \quad \ldots\ldots [80]$$

Equations [80] and [79] are identical with Equations [2] and [3] for the rotor energy.

Fig. 1 will be referred to now. In general, the entrance flow is a conical sheet. The rotor velocity, the absolute fluid velocity, and the relative fluid velocity may be shown by vectors in any plane tangent to this cone. As shown in the velocity diagram β_1 is the angle between the absolute fluid velocity and the rotor velocity and hence is the angle at which stationary inlet guide vanes direct the fluid against the rotor. Likewise α_1 is the angle between the relative fluid velocity and the rotor velocity and hence is the angle the rotor blades should have at entrance if the fluid is to enter the rotor without shock. The exit velocity diagram may be explained similarly. Thus

$$V_{1u} = V_1 \cos \beta_1 \quad \ldots\ldots [81]$$

$$V_{2u} = u_2 + v_2 \cos \alpha_2 \quad \ldots\ldots [82]$$

From the law of cosines

$$v_1^2 = u_1^2 + V_1^2 - 2u_1(V_1 \cos \beta_1) = u_1^2 + V_1^2 - 2u_1V_{1u}$$

so that

$$-u_1V_{1u} = \frac{1}{2}(-V_1^2 - u_1^2 + v_1^2) \quad \ldots\ldots [83]$$

Also

$$V_2^2 = v_2^2 + u_2^2 + 2u_2v_2 \cos \alpha_2$$

$$V_2^2 = v_2^2 - u_2^2 + 2u_2(u_2 + v_2 \cos \alpha_2)$$

$$V_2^2 = v_2^2 - u_2^2 + 2u_2V_{2u}$$

whence

$$u_2V_{2u} = \frac{1}{2}(V_2^2 + u_2^2 - v_2^2) \quad \ldots\ldots [84]$$

By the substitution of Equation [83] and [84] in Equation [80] there results Equation [15]

$$E = \frac{1}{2g}[(V_2^2 - V_1^2) + (u_2^2 - u_1^2) + (v_1^2 - v_2^2)] \ldots [15]$$

Also, by the substitution of Equation [81] and [82] in [80], there results Equation [26]

$$E = \frac{1}{g}(u_2^2 + u_2v_2 \cos \alpha_2 - V_1u_1 \cos \beta_1) \quad \ldots\ldots [26]$$

The derivation of the other equations is indicated at the place where they are discussed.

BIBLIOGRAPHY

1 "Theoria machinae cujusdam hydraulicae at computatio formae atque virum hydraulicae nuper descriptae," by M. Segner, Gottingae, 1750.

2 "Recherches sur l'effet d'une machine hydraulique proposee par M. Segner a Gottingue," by Euler. Koeniglich Preussische Akademie, p. 311, Histoire de l'Academie Royale, Berlin, année 1750. Other papers, année 1754, p. 2275, année 1755, pp. 217, 274, 316.

3 "Recherches théoriques et experimentales sur les roues a reaction ou a tuyaux," by Combes, Paris, 1843.
4 "Theorie der Turbinen," by G. Zeuner, Leipzig, 1899.
5 "Air Compression With Temperatures Above Adiabatic, With Special Reference to Airplane Superchargers," by S. A. Moss, Trans. A.S.M.E., vol. 50, 1932, paper AER-55-5.
6 "Engineering Computations for Air and Gases," by S. A. Moss and C. W. Smith, Trans. A.S.M.E., vol. 52, 1930, paper APM-52-8.
7 "New Theory for the Centrifugal Pump," by A. F. Sherzer, Proceedings A.S.C.E., Oct., 1927, p. 1775. Also, Trans. A.S.C.E., vol. 93, 1929, paper 1697.
8 U. S. Patent No. 1,617,133.
9 "Centrifugal Pumps, Turbines, and Propellers," by Wilhelm Spannhake, The Technology Press, Massachusetts Institute of Technology, 1934.
10 "A Textbook of Applied Hydraulics," by Herbert Addison, John Wiley & Sons, Inc., New York, N. Y., 1938.

Discussion

C. H. BERRY.[4] The authors have presented an informative discussion of an important detail of fluid engineering and have done the profession a service in emphasizing the generality of the fundamental equation for the work transfer between fluid and impeller, and in bringing together a well-chosen set of examples.

On several points the writer has communicated his comments to the authors privately. He wishes to mention here a few points that seem to have general interest.

At several points, the paper asserts that the equations apply only to an incompressible fluid. The writer believes that this supports a widespread misconception that the Bernoulli equation in the form given in Equation [5] of the paper is inapplicable to the flow of gaseous fluids. This is not the case. The criterion is not whether the fluid might be compressed, but whether it is in fact compressed in the process considered. It would, he believes, be better to say "uncompressed" instead of "incompressible."

The physical interpretation of the Euler equation in terms of three parts, into which it can be broken down, is illuminating, as the writer can testify from his experience in attempting to make the situation clear to students, who find that this breakdown somewhat dispels the seeming abstraction of the simple Euler equation.

The Euler equation, which appears as Equation [3] of the paper, asserts that the work transfer between fluid and impeller is determined by the change in value of the product of radius multiplied by the tangential component of the absolute velocity of the fluid, together with the rotative speed of the impeller.

This equation is easy enough to accept as applied to impellers that receive fluid at one radius and discharge it at another, especially if the fluid passages through the impeller lie in a plane perpendicular to the shaft. We can readily picture the fluid as rotating within the impeller, and it is no shock to think of the rotational velocity of the fluid as changing, as in centrifugal pumps, or some types of water wheels.

But there is a large class of so-called "axial-flow impellers," such as ship or airplane propellers, the propeller type of fan, the screw type of pump, or the Kaplan water wheel. For these, the conclusion seems far from evident. Some people stoutly deny its validity. We picture each streamline of fluid entering and leaving such an impeller at the same radial distance from the shaft. For this situation, our mathematics tells us that there can be no transfer of work between fluid and impeller unless the rotational velocity of the fluid is changed. The fluid must receive a twist to receive work, and must receive a negative twist to develop work.

Moreover, the work transfer is computed in terms of this change in rotational velocity. In the case of an airplane or ship propeller, this seems artificial. One has a feeling that the real work is done by the thrust force. If, however, we look at the impeller from the standpoint of the driving engine or motor, this objection seems less serious.

It may be helpful to consider the situation in connection with a common analogy that is sometimes cited to prove (so it is alleged) that a change in rotational velocity is not necessary. The analogy pictures the screw impeller driving a fluid stream much as a screw would drive a nut. Certainly a screw can drive a nonrotating nut. Why cannot a propeller drive a nonrotating stream of fluid? Let us consider this screw analogy in some detail.

First, consider a vertical shaft fitted with a shoulder upon which rests a collar, Fig. 15 of this discussion. The contact is

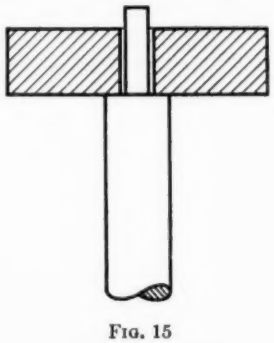


FIG. 15

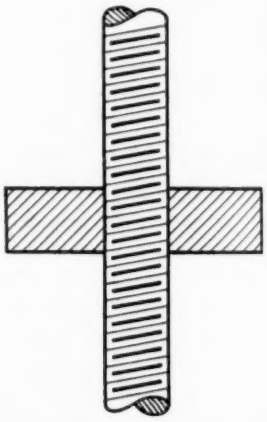


FIG. 16 (RIGHT)

frictionless. Everything is at rest. Now start rotating the shaft. What does the collar do? Nothing. No force acts on the collar, wherefore it remains at rest. In particular, it does not rotate.

Now consider a screw fitted with a nut, Fig. 16. Again the contact is frictionless. Starting from a position of rest, set the screw rotating. Offhand, it appears that, like the previous collar, the nut will not rotate, because friction is absent, whereupon the nonrotating nut will be driven upward by the rotating screw. But this is not correct. We assume the nut free to rotate.

If the nut does not rotate, there can be no torque acting on the nut. If no torque acts upon the nut, there can be no torque resisting the rotation of the screw. Accordingly, no work is expended in driving the screw. But the nut is lifted, so that work is done against gravity. This is then a machine that gives a finite work output for zero input. Impossible!



FIG. 17

Look more carefully at the screw. Friction being absent, the force acting between the nut and the thread of the screw must be normal to the thread. It is not parallel to the axis. This force has two components, Fig. 17, one axial, one tangential. The axial component tends to lift the nut and imposes a thrust upon the screw. The tangential component tends to rotate the nut and imposes a torque on the screw.

The axial force does work on the nut, lifting it, but merely imposes thrust on the

[4] Gordon McKay Professor of Mechanical Engineering, The Graduate School of Engineering, Harvard University, Pierce Hall, Cambridge, Mass. Mem. A.S.M.E.

screw, entailing no work transfer (friction being absent). The torque alone involves a work transfer to the screw, and yet all that the torque does to the nut is to give it a useless rotational acceleration.

What really happens then is somewhat as follows: As the screw is put into rotation, the nut is subject to a lifting force and to a torque. The nut moves upward and also rotates in the same direction as the screw. Moreover since torque is continuously imposed on the nut, its rotation is accelerating continuously (variable acceleration, to be sure, but nonetheless continuously applied). The rotational velocity of the nut increases unremittingly. At the same time, of course, the nut moves upward with a variable vertical velocity.

Ultimately the rotational velocity of the nut will rise to equal the rotational velocity of the screw (which is assumed to be constant), when the nut will cease rising. But the rotational torque and the rotational acceleration continue, so that the nut thereafter rotates faster than the screw, and hence moves downward. At last it will reach a steady state of downward motion, characterized by constant accelerations, vertical and rotational. It is not our present purpose to analyze this analogy beyond the immediate application. Accordingly, we shall confine our attention to the nut during its upward motion.

At any instant, the screw is rotating with velocity ω_s = constant, and the nut is rotating with velocity $\omega_n < \omega_s$.

The rate of rise of the nut is equal to the relative rotational velocity of the screw in the nut $(\omega_s - \omega_n)$ multiplied by the advance of the screw thread per radian of rotation, which is the pitch p of the screw (the advance per revolution), divided by 2π. If V_n denotes the vertical velocity of the nut

$$V_n = (\omega_s - \omega_n)\frac{p}{2\pi}$$

The vertical acceleration of the nut is found by differentiation.

$$\frac{dV_n}{dt} = -\frac{d\omega_n}{dt}\frac{p}{2\pi}$$

since ω_s and p are constants.

The torque acting upon the nut is the product of its angular acceleration and its moment of inertia, J. It also equals the tangential force component multiplied by the pitch radius of the screw.

$$T = \frac{Jd\omega_n}{dt} = F_t r$$

whence the tangential force component can be formulated as

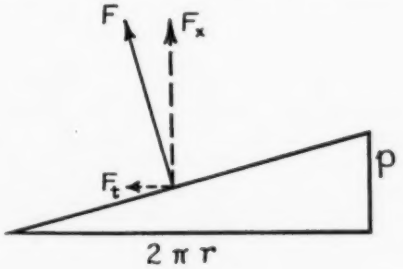


FIG. 18

$$F_t = \frac{J}{r}\frac{d\omega_n}{dt}$$

From the geometry of the screw thread, Fig. 18, the axial force component must be

$$F_x = F_t\frac{2\pi r}{p} = \frac{J}{r}\frac{d\omega_n}{dt}\frac{2\pi r}{p} = \frac{2\pi J}{p}\frac{d\omega_n}{dt}$$

The rate at which work is done upon the nut by the axial force component and by the torque can now be formulated.

$$\frac{dW_x}{dt} = V_n F_x = (\omega_s - \omega_n)\frac{p}{2\pi}\frac{2\pi J}{p}\frac{d\omega_n}{dt} = J(\omega_s - \omega_n)\frac{d\omega_n}{dt}$$

$$\frac{dW_t}{dt} = T\omega_n = J\omega_n\frac{d\omega_n}{dt}$$

Adding these two work rates, we find the total rate at which work is being done upon the nut

$$\frac{dW_n}{dt} = J\omega_s\frac{d\omega_n}{dt}$$

This equation, it will be observed, is closely analogous to the work Equation [3] of the paper. (In that equation, let the two radii be equal and note that $V_i = r\omega_f$, where ω_f is the rotational velocity of the fluid.)

The total power delivered to the nut depends upon the moment of inertia of the nut, the rotational acceleration of the nut, and the rotational velocity of the screw. If the nut has no rotational acceleration, it can receive no work.

Now consider the power required to drive the screw. By the axial component of the force, F_x, no work is done. This force merely produces a thrust in the screw.

By the torque work is done equal to the torque multiplied by the angular velocity of the screw.

$$\frac{dW_s}{dt} = T\omega_s = J\omega_s\frac{d\omega_n}{dt}$$

This is the total rate of work delivery to the screw; it equals the total rate of work delivery to the nut.

$\frac{dW_s}{dt} = J\omega_s\frac{d\omega_n}{dt}$ The power delivered to the screw has two ultimate destinations:

$\frac{dW_t}{dt} = J\omega_n\frac{d\omega_n}{dt}$ part of it is devoted to accelerating the nut rotationally. If the primary object is to lift the nut, this power is wasted, save in the sense that without it the lifting could not occur.

$\frac{dW_x}{dt} = J\omega_s\frac{d\omega_n}{dt} - \frac{dW_t}{dt}$ part of it is devoted to lifting the nut vertically (with a negative acceleration).

The total power required to drive the screw is the product of the moment of inertia of the nut, times the rotational acceleration of the nut, times the rotational velocity of the screw. Not a word about the upward velocity of the nut, notwithstanding the principal purpose of this mechanism is presumably to lift the nut.

The nut must have rotational acceleration if the screw is to absorb any work from the driving mechanism.

This study of the screw analogy may somewhat allay the incredulity with which some receive the statement that the work required to drive a propeller can be formulated in terms of the rotational velocity of the propeller and the change in the product of radius times rotational velocity of the fluid.

It would be interesting to study further the screw and nut, but it would be irrelevant to the present purpose and must be left to those interested in mechanics. A few aspects will be mentioned.

Consider the process of starting from rest, with the nut at the

lower end of the screw. The screw is abruptly set into rotation. Obviously a case of impact.

Consider the nut partially restrained from rotation by a frictional drag. This may perhaps be analogous to a propeller driving a viscous fluid through a duct.

Let the nut be positively restrained from rotating by frictionless guides.

Friction in the screw thread, between screw and nut, will introduce an additional torque and alter the allocation of power.

Finally, it is interesting to study the downward course of the nut after it has reached a rotational velocity exceeding that of the screw, and to formulate the final constant accelerations of the nut, vertical and angular.

Examination of the power allocation just developed indicates how the effectiveness of this screw mechanism can be improved. It is desired to increase the power devoted to lifting without increasing that devoted to rotational acceleration of the nut. Clearly, the one thing that will do this is to drive the screw at a high rotational speed, ω_s.

For analogous reasons, a propeller fan must operate at high rotational speed.

D. J. Bloomberg.[5] Those of us who are actively participating in developmental design work on turbines for different types of applications appreciate the need of this analytical treatment of the transfer of energy between a working fluid and a rotor, as presented by the authors.

Any practical turbine design for a given application embodies compromises in respect to the ideal turbine design because of the limitation of the designer's knowledge of the art, the manufacturing methods and facilities, and also the economic considerations.

When a new turbine design is called for to meet new operating requirements or new manufacturing methods, it is highly essential, in order to avoid pyramiding the compromises required on previous designs with those required by the new conditions, to go back to fundamentals in choosing the proper design combination to meet the new conditions.

The more thoroughly this procedure is followed, the shorter will be the developmental time period in arriving at a satisfactory design.

As pointed out in the paper, the transfer of energy between the fluid and the rotor is a function of the fluid and rotor velocities at the rotor entrance and exit.

The performance of any type of turbine design can be calculated by means of the velocity diagram with a reasonable degree of precision.

If this were more generally known, a considerable amount of well-intentioned but wasted efforts in designing and developing some new types of turbine could be avoided by a few comparatively simple calculations.

In other words, the first test any turbine design should be subjected to is that of a rational calculation system, based on the velocity diagram.

That portion of the paper covering the relation between rotor and fluid velocities for ideal energy transfer between fluid and rotor is of particular interest in respect to choosing a design combination to fit specific application requirements.

The number of design combinations for the hypothetical ideal energy transfer between the fluid and rotor, as shown in Fig. 12 of the paper, are innumerable, but certain portions of the field can be eliminated at the start as impractical.

For given ranges of fluid flow volume the problems involved in the size of the flow-path parts, stresses, rotation losses, etc., will still further narrow down the field of possible combinations. Even then, as is indicated by the different types of turbines being manufactured for the same general field of application, the choice of combinations is comparatively large.

In general practice, practical considerations, such as the desire to specialize on one general type of design and manufacturing facilities, usually are predominant.

In this connection, a comparatively small percentage of the effort normally spent on developmental work could be well spent on graphical analysis similar to that shown in Fig. 12, covering theoretical velocity-diagram performance data for definite ranges of fluid flow volume.

However, under the present world conditions, with the rapid development of new manufacturing methods, materials, etc., and with the newer fields of applications for which the turbine drives are suitable, it is well to re-examine the field of design combinations in order to reduce to a minimum that costly development period usually devoted to new design applications.

In the paper a brief mention is made of the opposed-rotation type of turbine; the comparison data for the ideal turbine-fluid and rotor-velocity relations, as shown in Fig. 12, do not include this type of turbine.

Although this type of turbine has not been widely adopted in this country, there is still the possibility that new fields of turbine applications and new manufacturing methods may offer a place for this turbine type.

K. A. Browne.[6] The authors have presented the complete basic theory of rotating machines in a remarkably clear and concise manner. The use of a simple general expression for energy transfer for all the various types of fluid flow creates a truly enlightened viewpoint on the fundamental operation of pumps and turbines.

Aircraft-engine supercharging is being accomplished solely by the radial-vane impeller, shown in Fig. 2 of the paper, and the writer's comments will be confined to this design. Vaned diffusers are used primarily to reduce the diameter of the compressor, a factor becoming more critical with every step forward in engine performance. In the last 10 years, aircraft engines have quadrupled in power output for the same diameter or head area; compressor design has kept in step by not requiring more than its same proportion of space. Now the emphasis is on altitude performance, up to 40,000 ft, where the volume to handle is 4 times that at sea level and the total pressure ratio around 8. Based on conventional practice, the size and weight of the necessary compressors increase prohibitively.

In spite of the basic advantages of the centrifugal type, serious consideration is being given the axial-flow compressor primarily because of its high Q/nD^3 and secondarily, because of its high efficiency, even though its capacity range is severely limited. There appears to be nothing in the theory of the radial type which penalizes the use of an entrance diameter equal to the rim diameter, yet practice shows that restrictive losses develop when the entrance substantially exceeds one half the rim diameter, because effective velocity conversion does not take place in the conventional rotor inlet. If we disallow any theoretical inlet diffusion ($v_1^2 = 0$, in Equation [25] of the paper) yet maintain the assumption of uniform V_1, an obviously incompatible condition, the portion of rotor energy theoretically available for conversion to pressure

$$= 1 - \frac{(r_1/r_2)^2 + (r_h/r_2)^2}{2}$$

With a hub radius r_h of 0.22 r_2, this factor is as follows:

[5] Research Engineer, Steam Turbines, General Electric Company, River Works, Lynn, Mass. Mem. A.S.M.E.

[6] Research Engineer, Wright Aeronautical Corporation, Paterson, N. J.

0.85 for inlet to rotor diam ratio of 0.5, avg optimum Q/nD^3 of 0.13
0.73 for inlet to rotor diam ratio of 0.7, avg optimum Q/nD^3 of 0.286
0.65 for inlet to rotor diam ratio of 0.8, avg optimum Q/nD^3 of 0.383
0.57 for inlet to rotor diam ratio of 0.9, avg optimum Q/nD^3 of 0.495

It is obvious that high volume capacity is obtained at the expense of efficiency, unless effective velocity conversion is obtained at the entrance. No one would consider making the diffuser vanes as short and sharply bent as the entry hooks on the usual supercharger blades, yet the diffusion problem is very similar for both parts. The authors call attention to the relative inefficiency of the diffusion process for creating pressure, yet actual tests do not show the impeller part of a compressor substantially better than the diffuser, thus indicating a large entry loss. Mr. Planiol has used airfoil-blade fans in the entrance with some degree of success toward improving efficiency. Further development on the impeller entrance is essential to allow higher specific capacity called for by high-altitude conditions.

Steady-flow tests of compressor-diffuser passages indicate a very high recovery, therefore, the poor recovery during operation must result from nonuniformity of flow, or departure from the theoretical assumptions. Good velocity conversion at the entrance will materially improve the axial-flow distribution. Incidentally, the slight gain in pressure, mentioned as desirable in the expanding impeller passage, can well be expended in choking the exit to obtain more uniform radial flow in both axial and tangential directions, but real gains in performance will not be forthcoming until efficient velocity conversion is obtained at the impeller entrance.

KENNETH CAMPBELL.[7] Of general interest these years is the application of rotor fluid energy-transfer relations to the supercharging of aircraft engines. In this great field of application, the position of Dr. Moss of the General Electric Company is unique. During the last 7 years, the activities of the engine companies and the larger laboratories of the country on supercharger research have increased until today there is a great flood of effort in this direction. Dozens of engineers with scores of thousands of dollars worth of equipment are investigating the field in detail. All this follows as a logical result of the foresight, enthusiasm, and contribution of Dr. Moss's work, extending continuously from the last war to the present day.

Referring to Equation [15] of the paper, the authors have made a simplified and most effective explanation of the three important components of energy imparted to the fluid by the rotor of a centrifugal compressor. A few years ago, our investigations indicated that, in the case of radial-blade centrifugal superchargers to meet the modern requirements of high pressure ratio, there is a substantial net advantage in foregoing much of the pressure regain offered by the third component of the equation. This component represents the reduction of velocity and the resulting conversion to pressure within the impeller itself.

At the high angular velocities (up to 26,000 rpm) necessary to obtain high tip speeds with impellers of limited diameter, the eddy losses in the expanding impeller passages reduce the efficiency to a low value, which defeats the purpose of the high speed. Therefore, we have been designing our impeller passages so that the expansion ratio is in the neighborhood of 1. Of course, there is still a considerable velocity reduction because of increasing density along the path; nevertheless, by this design, the radial component at the impeller exit is made appreciable, rather than zero as assumed for simplicity in the paper, and more than one half of the rotor energy, instead of exactly one half, is represented by total velocity imparted to the fluid. This in turn places a premium on diffuser efficiency in aircraft-engine superchargers.

[7] Project Engineer, Wright Aeronautical Corporation, Paterson, N. J.

With regard to the design of vaneless diffusers, fewer velocity changes are encountered by keeping up the value of the radial component in the impeller rather than increasing it again in the diffuser after it has been reduced in the impeller. As the authors point out, however, the vaned diffuser provides the same diffusion in a smaller space and, as space is paramount in an aircraft engine, at least some form of vaning is necessary.

Rational design of vaned diffusers for comparative testing is accomplished by assuming that, as the fluid moves outward from the tips, the fronts of equal pressure across the diffuser path lie approximately on circles concentric about the main supercharger axis, as in the case of a vaneless diffuser. This conception fits in with pressure-gradient surveys which show most of the velocity-pressure conversion occurring before the so-called throat, normal to the path at the tip of the following vane.

R. EKSERGIAN.[8] This paper is of value in the presentation of over-all generalizations that hold for all types of turbines and pumps. While a considerable part of the analysis is a recapitulation of well-known theory, such a presentation is useful in showing the applications of first principles, namely, those of momentum and energy, to a variety of equipments.

The term "rotor energy" appears somewhat misleading. This would imply the kinetic energy stored up in the rotor, whereas, the authors mean the energy transfer between the fluid and rotor. This energy transfer has two aspects. When considering the fluid flow, it is the work of the moving blades reacting on the flow. When considering the rotor, it is the work on the rotor due to the reaction of the fluid. The rate of this energy transfer is measured either by the tangential reaction component, due to the interaction between fluid and rotor, times the peripheral velocity of the rotor, or more generally by the torque times the angular velocity of the rotor.

The torque interaction between fluid and rotor is equal to the rate of change of the angular momentum of the fluid due to this interaction and is, therefore, the change in angular momentum of the fluid from the entrance to the exit sides or vice versa. The entrance angular momentum is determined by the tangential velocity from the stationary blades, whereas, the exit angular momentum is determined by the absolute whirl velocity from the moving blades. When the entrance angular momentum to the moving blades exceeds the exit angular momentum, the torque reaction of the rotor opposes the flow, while the action on the rotor drives the rotor, and the energy transfer corresponds to that of a turbine. When the exit angular momentum exceeds the entrance, work is done on the flow, with a corresponding resistance to the motion of the rotor. In this case we have a pump.

Using the authors' nomenclature and referring to Fig. 9 of the paper, the torque reaction Φ and the rate of energy transfer E between fluid and rotor are

$$\Phi_{\text{turbine}} = \frac{1}{g}\left[V_1 \cos \beta_1 \cdot r_1 - (u_2 - v_2 \cos \alpha_2) r_2\right] \text{ (per pound of flow)}$$

and since $E = \Phi \omega$, where $\omega = \frac{u_1}{r_1} = \frac{u_2}{r_2}$

$$E_{\text{turbine}} = \frac{1}{g}\left[V_1 u_1 \cos \beta_1 - u_2^2 + u_2 v_2 \cos \alpha_2\right] \text{ (per pound of flow)}$$

while the terms are interchanged for a pump. The latter is the authors' Equation [26].

It is important to note, however, that Equation [26] of the paper represents only the energy transferred between the rotor and the fluid. It does not represent the change in energy between

[8] Edward G. Budd Manufacturing Company, Philadelphia, Pa. Fellow A.S.M.E.

the entrance and exit sections to the rotor (as was the case in considering the change in angular momentum), because entrance-shock losses occur as well as friction losses through the rotor itself.

Now in general the relative velocity at entrance, i.e., the vector difference $\bar{V}_1 - \bar{u}_1$ does not coincide with the blade angle α_1. Therefore, Equations [44] and [44*b*] hold only for one specific speed. The same objections apply to Equations [46] to [49]. If C_b is to cover all losses, when $\alpha_1 = \alpha_2 = \alpha$ it would be preferable to replace Equation [46] by $v_2 \cos \alpha = C_b\ [V_1 \cos \beta_1 - u_1]$ and then Equation [49] retains its previous form. This interpretation of Equation [49] is necessary since the authors use it to discuss the form of the efficiency curve with speed, which, therefore, includes the very shock losses just discussed.

Referring to the alternate form for the energy transfer, given in Equation [15] of the paper, it is again important to note that the entrance relative velocity v_1 is obtained from the vector relation $\bar{v}_1 = \bar{V}_1 - \bar{u}_1$, which is not the authors' relative velocity.

It is difficult to concur with the authors' thermodynamic treatment of the fluid-energy relations through the turbine. The authors' statement cannot be sustained, i. e., that the energy that the fluid gains or loses is in the form of change of pressure and temperature, and that only pressure is of interest, since this is the only useful portion of the energy. The authors mean that only the energy changes, expressed in terms of pressure and temperature, are of interest. Neglecting kinetic energy and head as small, the energy per pound of fluid, associated with a given pressure and temperature at any section of the flow, is given by the relation

$$h = Apv + u - u_0$$

where $A = 1/J$, v = specific volume, u = intrinsic energy per pound of fluid, and h = the total heat, or better, the enthalpy of the fluid.

The authors' Equations [7] to [12] can be regarded as a specialized case, applicable to the flow of gases, whereas, a more generalized relation should be stated.

Therefore the fundamental energy equation of the fluid across the turbine is

$$Q_{12} - AP + H_1 - H_2 = \frac{AW}{2g}(V_2^2 - V_1^2)$$

$$\text{and } E = \Phi\,\omega \qquad J = 1/A = 778$$

where

P = rate of energy transfer between fluid and rotor, (ft-lb/sec)
W = fluid flowing across a section, lb per sec
(This W is not W as used in Appendix 1)
V_1 and V_2 = terminal absolute velocities, (ft/sec)
$H_1 - H_2 = W\,[A(p_1v_1 - p_2v_2) + u_1 - u_2]$ = total heat drop
Q_{12} = total external heat transmitted to fluid per sec, (Btu/sec).

While the kinetic-energy term across the entire turbine can usually be neglected, on the other hand, it cannot be neglected when considering the flow across the rotor. When $Q_{12} = 0$, we have an adiabatic change in the flow.

In the case of a pump, the energy transfer to the fluid across the rotor E increases the enthalpy at section 2 over that at section 1, so that

$$AP - Q_{12} = H_2 - H_1 + \frac{AW}{2g}(V_2^2 - V_1^2)$$

where Q_{12} is now the external heat lost by the fluid. Since the change in intrinsic energy of a gas from state 1 to state 2 is

$$u_2 - u_1 = A\left[\frac{p_2v_2 - p_1v_1}{k-1}\right]$$

then, for an adiabatic compression $Q_{12} = 0$; and since $h = Apv + u$, and $H = Wh$

$$P = \frac{kW}{k-1}\,[p_2v_2 - p_1v_1] + \frac{W}{2g}(V_2^2 - V_1^2)$$

It is important to point out the fact that this relation holds irrespective of friction, shock, and throttling losses and is equal to the energy-transfer rate between fluid and rotor.

In the case of an ideal adiabatic isentropic (constant entropy) compression $pv^k = C$ then

$$P = \frac{kWRT_1}{k-1}\left[\left(\frac{p_2}{p_1}\right)^{(k-1)/k} - 1\right] + \frac{W}{2g}(V_2^2 - V_1^2)$$

This is an ideal adiabatic reversible compression. Actually, however, the compression is irreversible with external heat transfer, and $pv^n = C$ is assumed for the pressure–volume relation in the compression. In this case, the expression for the energy relation is

$$P - J\,Q_{12} = \frac{kWRT_1}{k-1}\left[\left(\frac{p_2}{p_1}\right)^{(n-1)/n} - 1\right] + \frac{W}{2g}(V_2^2 - V_1^2)$$

so that, knowing the pressure limits, measuring P and Q_{12} through the jacket water, n can be calculated.

Relative to Equation [14] of the paper, the interpretation is somewhat confusing. If the authors mean the actual change in enthalpy from the initial to the final conditions, the change is not isentropic, due to the internal losses. In this case, we should write $P = J\,(H_2 - H_0)$, since E is the actual energy-transfer rate across the rotor and H_2 and H_0 are the terminal-section enthalpies. With this interpretation, the losses do not have to be taken care of by an efficiency factor. If an efficiency factor is used, i.e., $P' = \frac{1}{\eta}P = J(H_2 - H_0')$, then we may assume an ideal isentropic adiabatic heat drop for the same pressure and temperature limits but H'_0 is not the actual enthalpy at the lower terminal section.

It is just this point that requires the statement of an additional relation which the authors have not included in their flow analysis. This is the heat equation, which gives the thermodynamic relation for the changes of state of the fluid at the terminal sections. We can always measure the actual changes of state which occur through an irreversible process, by a reversible path. The heat transferred to the fluid for the reversible path is the total heat, both externally and internally transferred to the fluid between the terminal sections. The internal-heat component is due to the various mechanical losses, regenerated within the fluid into heat. If Q_{12} and Q_R are the external and internal heat transferred to the fluid, then

$$Q_r = Q_{12} + Q_R = W\,[u_2 - u_1 + 1/J \int_1^2 p\,dv]$$

$$= H_2 - H_1 - W/J \int_1^2 v\,dp$$

where the corresponding change in entropy (per pound of fluid) is

$$\phi_2 - \phi_1 = \frac{1}{W}\int_1^2 \frac{d(Q_{12} + Q_R)}{T}$$

For an adiabatic flow, $\phi_2 - \phi_1 = \frac{1}{W}\int_1^2 \frac{dQ_R}{T}$

We may write the adiabatic-energy equation for the fluid, as

$$(H_1 - WT_0\,\phi_1) - (H_2 - WT_0\,\phi_2) - WT_0\,(\phi_2 - \phi_1) = \frac{1}{J}P$$

which reduces to

$$H_1 - H_2' - WT_0\,(\phi_2 - \phi_1) = \frac{1}{J}\,P$$

where T_0 = the lowest available temperature of the system; in this case $T_0 = T_2$ and $H_2' = H_2 - WT_2\,(\phi_2 - \phi_1)$ = the enthalpy, assuming an isentropic heat drop, at the lower terminal section. We note, $H_1 - H_2'$ = the isentropic adiabatic heat drop, and

$$WT_2\,(\phi_2 - \phi_1) = T_2 \int_1^2 \frac{dQ_R}{T} = \text{increase of unavailable energy}$$

due to throttling, etc.

In other words, the isentropic heat drop minus the increase of unavailable energy, resulting from throttling, etc., and measured by the increase of entropy, is equal to the work performed. In this case, the turbine efficiency referred to in the authors' Equation [14] is

$$\eta = \frac{P}{J(H_3 - H_0')}$$

where

$$H_0' = H_0 - WT_0\,(\phi_0 - \phi_3)$$

J. H. Marchant.[9] In this paper, the authors have attempted to generalize the very complicated field of jet-and-vane machinery, probably with the idea of giving the reader a better perspective of this whole problem. Such an objective is certainly praiseworthy, but it seems as though the many simplifying assumptions, which the authors have been forced to make, tend to promote intangibility.

Regarding the centrifugal supercharger itself, the writer would like to comment more specifically. This piece of equipment, like other jet and vane machinery handling compressible fluids, is not susceptible to the simple analysis given by the authors. In this case, hyperadiabatic work has little significance, except possibly to mask the complication of its internal workings. Furthermore, is it not impractical for the authors to assume that one half of the pressure rise occurs in the impeller? Generally speaking, none of these simple relations stated by the authors have actual significance unless they may have in mind being able to alter the machine to fit their formulas; and, judging from the performance of the most modern centrifugal aircraft-engine superchargers, this cannot be done quite yet.

A look at what actually may be taking place in the modern centrifugal aircraft-engine supercharger will serve to illustrate the limitations of any such generalizations. Suppose that it has an axial inlet with no inlet guide vanes, as the authors assume; the air enters axially for no particular theoretical reason (as the authors state) except that, among others, it is trying to obey Newton's first law. It enters the impeller generally with rather large impact losses, except probably over one very narrow range of $Q/(ND^3)$, at which it seldom is operated in practice. Immediately, flow separation develops in the impeller, generally beginning at the inlet-vane tips, and by the time the air leaves the impeller that passage is running perhaps not over one third full. The circumferential velocity traverse of the air in any one passage is probably a weird-looking thing, with air flowing radially outward near the high-pressure side of the blade and radially inward near the low-pressure side of the next adjacent blade. Besides all of this, most of the air crowds to the back wall of the impeller. What now will the authors use for A (area) or V (velocity) in their Equation [1]? Next, the air leaves the impeller with the usual large leaving losses, the vortices, which are produced by each blade tip, being dragged around in the clearance space between the impeller and the diffuser at the rate of approximately 25,000 rpm.

It is obvious that no simple steady-flow equation applies here, since the flow is probably about as unsteady as it could be made conveniently. Then the air enters the diffuser, with unknown impact losses, with a stream velocity which is probably supersonic, and the diffuser vanes, which are curved airfoil sections usually cast and rough, stall; flow separation occurs, and compression shock may develop from each rough spot; and no one knows what comes out of it into the collector case.

Generally speaking, the air stream is so completely garbled that it would be difficult to interpret the significance of readings of the instruments which might be installed to measure component performance. There is also some question in the writer's mind as to whether or not the instruments themselves even would know what to indicate, due to induced instabilities.

Thus, the supercharger is no simple piece of equipment. Even the authors, competent as they are, would find it difficult to make it conform to the simple laws which they would like to have us believe it obeys.

The bibliography of this paper is high-lighted by the absence of the name of Prof. A. Stodola, who some time ago pointed out the practical limitations of the Euler equations, the generality of which the authors have undertaken to expound.

In closing, the writer wishes to commend the authors on their purpose in presenting this paper. The useful information in this field is scattered and in some cases certainly difficult to ferret out. Such a general compilation as the authors have undertaken is needed and could be very useful. Unfortunately, however, any such comprehensive survey is difficult and vulnerable to all sorts of criticisms; since generalities inevitably lead to exceptions.

R. D. Madison.[10] Without detracting in any way from the valuable aspects of this paper, the writer wishes to comment on certain parts that may be of special interest. The paper as a whole brings to the reader a very clear picture of the energy transfer between a fluid and a rotor. However, one should be on the alert to remember that in many cases the chief purpose is not to effect the greatest energy transfer. Frequently, a smaller energy transfer can be effected under more favorable conditions of efficiency.

In this connection, in discussing inlet guide vanes, the authors say: "The inevitable increase of friction with increased V_1 and inlet guides would further reduce the rotor energy. Since this is undesirable, inlet guide vanes turned forward are rarely, if ever, used." Stationary inlet guide vanes have been used on both high-speed high-duty centrifugal fans, as well as on ventilating fans for many years, and in ever-increasing quantities. It is true that there is an increase in V_1 and a decrease in v_1 and to obtain the same pressure and air delivery, the fan must be operated at somewhat higher speeds. In doing so $(u_2^2 - u_1^2)$ becomes greater and there is a larger percentage of static-pressure rise across the rotor, a form of pressure development more efficient than is possible in velocity-pressure conversion in the usual commercial-fan volutes.

Then the authors admit that in the case of inlet guide vanes turned backward (against wheel rotation) an increase of v_1 increases the shock loss at entrance to the rotor. By the same reasoning, a decrease of v_1 (in the case of the forward inlet vane) reduces the shock loss and, in many cases, this is more desirable than increase of energy transfer.

In the most approved form of the stationary inlet guide vane,

[9] Engineer, Pratt & Whitney Aircraft, East Hartford, Conn. Mem. A.S.M.E.

[10] Research Engineer, Buffalo Forge Company, Buffalo, N. Y. Mem. A.S.M.E.

the curvature varies from the center of the inlet outward, that is, the air is guided forward in the direction of wheel rotation, but the amount of spin is small near the shaft center and large near the outer diameter of the fan inlet. In terms of the values in the paper, β_1 near the shaft center is substantially 90 deg, but at the largest radius, β_1 becomes as small as 30 or even 20 deg. It is also interesting to observe the flow between the vane and rotor inlet. The fluid near the shaft center takes a long sweeping curve to meet the rotor entrance. The air passing through the guide vane farthest from the shaft center is first curved forward in the direction of wheel rotation and then outward through the rotor vane with an absolute velocity approximately at right angles to the initial flow. The latter type of flow is very much less power-consuming than would appear at first thought. Tests[11] on compound elbows with turns in planes at 90 deg have shown this to be the case.

The advantages of inlet guide vanes turned forward may be summarized as follows:

1 Fan efficiency is increased when the rotor-blade shape is backward-curved at the exit.

2 A self-limiting horsepower curve is produced which greatly facilitates good motor selection without danger of overloading.

3 Fan noise is reduced for a given amount of air and pressure, in spite of higher rotative speeds. This lowered noise is observable both in the space surrounding the fan housing, as well as in the air stream itself as measured near the duct outlet.

The disadvantage lies solely in the fact that for very high pressures the extra speed required may be beyond the strength of materials of construction, and other expedients must be employed.

The use of variable-inlet vanes (forward-curved) is another example having wide present-day acceptance as a means of throttling fan capacity and lowering the power transfer between rotor and fluid. In this case, over-all fan efficiency may not be high at part load, but it can be made appreciably higher than by straight dampering at the fan outlet and, hence, its usefulness.

An interesting use may be made of Equation [15] of the paper, in plotting characteristic horsepower curves of fans with forward-, radial, and backward-curved rotor blades at their tip. These will show curves concave upward, straight inclined, and concave downward, respectively, for the cases mentioned. Obviously, these are somewhat modified by friction on the outside of the rotor surface and therefore the actual curves do not pass through the origin. However, the characteristic shape of the horsepower curve remains and is valuable in the study of fan types.

In conclusion, the writer wishes to emphasize the value of this paper and to urge its study by all interested in the subject. The authors have repeatedly warned against assumptions based on nonuniform continuous flow. Many complications are thus introduced and sometimes it is difficult to know of their presence. In spite of this, many present-day misconceptions of what transpires when a fluid passes through a rotor can be cleared up by applying the fundamental principles, as outlined in the paper.

A. F. Sherzer.[12] Early in the paper, the authors state: "In pump machinery, because of losses, the fluid energy is less than the rotor energy. Thus a practical coefficient, called the hydraulic efficiency is defined by $\eta = W/E$." It should be pointed out that the value of η thus obtained is usually less than the actual work efficiency of the pump or $\frac{\text{output horsepower}}{\text{input horsepower}}$ If this is true, it must be clear that η is not the real hydraulic efficiency. The actual efficiency of a pump is the product of two other efficiencies, one mechanical and the other hydraulic, and either must, of course, be greater than the actual efficiency since all values are less than 100 per cent. This is frequently pointed out in texts, and a more accurate term such as "manometric constant," etc., is used.

In the writer's opinion, the reason for this numerical discrepancy can be traced to a misunderstanding of the fundamental theory involved.

Later it is stated: "Generally, it is only the pressure that is of interest, since this is the useful portion of the energy. Then the fluid energy will be defined as the energy required for the pressure change of the fluid, with conventions on signs as given for Equation [2]." When this statement is applied to a centrifugal pump through which is passing a fluid whose compressibility is neglected, it just does not make sense. The writer hopes the authors in their closure will fully explain just how energy may be stored in a fluid by changing the pressure without a resulting change in volume.

An inelastic vessel filled with an incompressible fluid contains no energy no matter what the internal pressure may be, in so far as the pressure itself is concerned. The term "pressure energy" is incorrect when referring to a substance so slightly compressible as water.

Pressure may be used to measure potential or kinetic energy, but when so doing it should be kept in mind that the pressure is only a convenient means of measuring other forms of energy and is not energy of itself, so long as no change in volume takes place.

If an inelastic vessel were to be lowered 231 ft below the surface of a lake, it could be filled with water at a pressure of 100 psi. If the vessel be closed and raised to the surface, there would be water contained in it at a pressure of 100 psi, but, of course, little or no energy due to that pressure. It should be clear that the pressure of 100 psi was only the measure of the potential energy of 231 ft of water column above it.

Would the authors claim that there was an energy equivalent of $H = 231$ ft $+ (P/\gamma = 100$ lb $= 231$ ft) or a total of 462 ft available head? That claim seems to be repeated several times in their paper. For example, refer to statement at the beginning of page 6.

"However, the derivation of Equation [15] shows that this centrifugal effect exists with the other effects of flow superposed upon it, and the energy involved in this effect is additive to the energy involved in the effects of flow."

The substance of much of the paper is to the effect that, when the equations are applied to a centrifugal pump, the pressure produced by centrifugal force is added to the velocity which produced it. Expressed in terms of energy, the pressure produced by centrifugal force is approximately $u_2^2/2g$, and the kinetic energy of the water discharged $V_2^2/2g$ is also approximately $u_2^2/2g$ for small rates of flow, regardless of the vane angles. Hence, the total energy $= E$ is claimed to be $\frac{V_2^2}{2g} + \frac{V_2^2}{2g} = \frac{V_2^2}{g}$ or nearly that. This is only approximately true but it is close enough to illustrate the point.

The fallacy of this is not hard to show as follows: Suppose a known mass were revolved at the end of a string of known radius and at a known angular velocity. From these data, using the well-known formula for centrifugal force, it is possible to compute the tension in the string, as well as the kinetic energy of the mass. Consider now the fundamentals of the problem. What is the energy of the rotating mass? Clearly, it is only the kinetic

[11] "Pressure Losses in Rectangular Elbows," by R. D. Madison and J. R. Parker, Trans. A.S.M.E., vol. 58, 1936, paper AER-58-2, p. 175.

[12] Professor of Mechanical Engineering, University of Michigan, Ann Arbor, Mich.

energy of the mass ($^1/_2\ MU^2$) (neglecting the mass of the string). Would the authors suggest that to this should be added the tension in the string? Probably not in this case, yet that is exactly what has been done several times in their paper.

The tension developed in the string and the pressure developed in a rotating impeller are both manifestations of the same centrifugal force, and both are computed by the same general law. Whether the mass extends to the center or nearly so, or is located at the end of the string, is only a numerical difference and does not in any way affect the principles involved.

Centrifugal force is not and never was kinetic energy, or any other kind of energy when dealing with incompressible fluids; although it may be used to measure the kinetic energy present if sufficient data are available.

The writer would take exception to the authors' statement that a diffuser is needed to convert the velocity into pressure. This is surely not borne out by present-day designs. Velocity can more efficiently be converted into pressure through the action of centrifugal force, in which case the efficiency is nearly if not 100 per cent. In the case of a revolving water paraboloid $H = U_2^2/2g$ with mathematical accuracy.

However, to add the pressure head, so produced by the velocity, to the velocity which produced it would be like eating your cake and having it too. Most centrifugal pumps give a shutoff head of $U_2^2/2g$ for the reason that that is all the head there is. If there is no flow, there can be no losses, and what would become of the other $U_2^2/2g$? Careful power measurements will account for only $U_2^2/2g$ and, if more were put in, the dynamometer would have to show it, which it does not.

It is quite possible to build a form of pump which will give a total E of U_2^2/g, or even $2U_2^2/g$ and the writer has done so, but no one would call it the equivalent of a modern centrifugal pump.

The authors claim that, in a radial inward flow (Fourneyron) turbine, the rotor energy is reduced by the effect of centrifugal force. This is the same old fallacy and leads to the idea that this is an inefficient form of turbine, which is not the case. The idea regarding the effect of head on the application of the Fourneyron turbine is most unusual. One of the early, if not the first, installations of turbines at Niagara Falls was of that type, and surely that would not be called a low-head plant. There were other reasons for not using the Fourneyron turbines on either high or low heads.

Equation [41] states: The head delivered by a pump is $H = \eta KU^2/g$.

Assuming that this refers to a centrifugal pump, it should be known that the head developed by such a pump varies with the rate of flow and is by no means the fixed value that Equation [41] would imply. This equation could be applied to a rotating impeller without a casing, in which case the head and rate of flow would both be fixed, but at present centrifugal pumps are not built that way.

Finally, it was stated that the physical meaning of Equation [15] had never before been explained. Equation [15] is the usual one found in texts. The writer gave substantially the same explanation as the authors in a paper[13] presented in 1926 and was criticized for it. This explanation was commonly used by some European writers and is not claimed to be original by the writer, but it has often been given before.

R. B. Smith.[14] The authors are to be commended for their broad exposition of the application of Euler's equation, or perhaps more rigorously of Newton's laws, to rotating power machinery. Expositions of this type have been presented to the Society before, notably by Spannhake (11),[15] but in view of the grandeur such a fundamental treatment discloses, repetition is healthy.

The Euler equation is a powerful basic tool, but it is not entirely free of shortcomings. For instance the authors' Equation [2], while correct, cannot be solved until one is able to ascertain the magnitude of V_2u and of V_1u. These quantities depend upon the angles at which the fluid enters and leaves the rotor; they are not the geometric angles of the blading or of the impeller. The difference between average geometric and actual angles depends upon the nature of the flow and the strength of the circulation around the impeller or turbine blades.

For turbines, the flow in the channel is generally an accelerated one with contact losses at the walls minimized, and the fluid follows reasonably well the geometric contour of the passage, providing the blades are closely spaced and the lift is not abnormally large. Compressors, where the flow is taking place in such a way that the velocity of the fluid is being decelerated, are subject to very serious contact losses at the walls. Furthermore, the lift desired per blade in most centrifugal blowers is large in relation to the blade pitch, with the result that a divergence between the geometric and the actual angle of efflux exists.

It has often been said that Euler's law applies only to those cases in which perfect guidance of the stream is possible, i.e., to impellers with an infinite number of blades. Actually Euler's equation is always applicable, but in order to effect its solution one must know something of the character of the flow and particularly of the circulation. Stodola (12) was one of the first to consider the effect circulation within the impeller passage might have on the flow; and the work has been taken up and extended more recently by Eck (13), Pfleiderer (14) and Kearton (15). The effect of circulation is not minor; in a centrifugal impeller it diminishes the exit whirl component V_2u by from 10 to 25 per cent, depending upon the number of blades and the wheel configuration; it accounts for the fact that at reduced flow the stream breaks away from the back side of the impeller blade and not the front side as was long supposed; and further, it precludes the possibility of a flow, as stated by the authors, which is "normal to the enveloping surface" at the inlet, although at this point, the effect of circulation is slight.

In the authors' Equation [4], the value of K cannot be determined from the geometric angles of the impeller, unless account is taken of the magnitude of the circulation and the number of blades. While it may seem convenient to accept K as a function of the geometric angles and incorporate the circulation effect as an efficiency correction after the fashion of Equation [9], it frequently leads to erroneous conclusions. The fact that K is diminished by the circulation is not an indication of an energy loss, it means instead that less energy was transferred to the fluid from the rotor, and is in no way a reflection on the efficiency of the machine. Experimental determination of the values of K are possible on a well-insulated blower through temperature measurements at the inlet and discharge.

Generally the internal efficiency of a well-designed supercharger, with tip velocities in the region of 60 per cent of the acoustic velocity, can be between 80 and 85 per cent. For higher tip speeds, the efficiency will fall, largely as a result of acoustic-shock waves created at localized points. Analysis of the losses in the blower confirm the authors' conclusion that the diffuser losses are generally the largest single item. The diffuser design has a marked effect upon the performance of the machine in that one may achieve by suitable changes either a pronounced

[13] "New Theory for the Centrifugal Pump," by A. F. Sherzer, Trans. A.S.C.E., vol. 93, 1929, pp. 1–29.

[14] Assistant Chief Engineer, Elliott Company, Jeannette, Pa. Mem. A.S.M.E.

[15] Numbers in parentheses from (11) to (16), inclusive, refer to the Bibliography at the end of this discussion.

sloping or a very flat performance characteristic. Vaneless diffusers are the most attractive from the standpoint of efficiency and surging characteristic, but least attractive in view of their size. The authors' reference to the advantages of the Moss-Robinson diffuser is slightly obscure. A diverging-wall vaneless diffuser would seem to offer little that is desirable, since the tangential-velocity component, which is much greater than the radial, is unaffected by the divergence. In general, the object of a vaned diffuser is to reduce in the minimum length the tangential-velocity component.

In discussing typical applications of Euler's theorem, it may be of interest to mention the Schict (16) axial-flow blower. This machine is designed for a constant velocity in the blade passages and with all the pressure increase developed in the diffuser. The most attractive feature of this design is that values of K approaching 2 can be achieved in a single stage. This is about 3 times as great a coefficient as a conventional airfoil stage produces.

The authors have discussed the basic operation of an impulse steam-turbine stage and have represented the result by the simple expression of Equation [52]. An equally simple relation is possible for the 50 per cent reaction-turbine stage. Assuming that the reaction blades are so proportioned that the velocity triangles from row to row are identical and that each stage utilizes the leaving velocity from the preceding stage, then the work done per rotating row is, with the notation of Fig. 11 of the paper

$$\text{Work} = 2\frac{v_1^2}{2g}\left(2\frac{u}{v_1}\cos\beta_1 - \frac{u^2}{v_1^2}\right)$$

The term in parentheses is frequently called the diagram factor and is defined as

$$\epsilon = \frac{u}{v_1}\left(2\cos\beta_1 - \frac{u}{v_1}\right)$$

Since, under these conditions, the enthalpy drop per stage is

$$A\,\Delta H = \frac{v_1^2}{g}\left(\frac{1}{C_n^2} - (1-\epsilon)\right)$$

the efficiency of the stage is

$$\eta = C_n^2\left(\frac{\epsilon}{1 - C_n^2(1-\epsilon)}\right)$$

For reasonably high value of C_n, as all reaction blades possess, the parenthetical term may be neglected, and the efficiency of the stage at its ideal velocity ratio is thus equal to the square of the nozzle-velocity coefficient. For the usual value of $C_n = 0.96$ to 0.97 the result is a stage efficiency in excess of 92 per cent.

BIBLIOGRAPHY

11 "Problems of Modern Pump and Turbine Design," by W. Spannhake, Trans. A.S.M.E., vol. 56, 1934, pp. 225–245.

12 "Steam and Gas Turbines," vol. 2, by A. Stodola, McGraw-Hill Book Company, Inc., New York, N. Y., 1927, p. 1255.

13 "Ventilatoren," by Bruno Eck, Julius Springer, Berlin, 1937.

14 "Die Kreiselpumpen," by C. Pfleiderer, second edition, Julius Springer, Berlin, 1932.

15 "The Influence of the Number of Impeller Blades on the Pressure Generated in a Centrifugal Compressor, and on Its General Performance," by W. J. Kearton, Proceedings of The Institution of Mechanical Engineers, vol. 124, 1933, pp. 481–540.

16 "Gleichdruckgebläse," by E. Sorensen, *Zeitschrift des Vereines deutscher Ingenieure*, vol. 83, 1939, pp. 925–931.

Authors' Closure

The authors wish to express their thanks and appreciation to those who have discussed the paper. There is evidence that a number of people have thought it worth while to spend a great deal of time on the study of the details presented. A number of discussers point out that some of the individual fundamental principles presented in the paper can be found at various places in previous publications. However, the discussion indicates that the present paper may serve a worth-while purpose in gathering and generalizing the facts and in showing their meaning and application in a way useful to modern designers.

We emphasize the meaning of the term "rotor energy" because of the remarks of Mr. Eksergian and others. We do not mean the kinetic energy of the rotor as a revolving body but do mean the flow of energy between rotor and fluid. A graphical summary of all the mathematics connected with rotor energy is given in Figs. 19, 20, and 21, which are self-explanatory.

The senior author of the paper has been working on standardization of symbols for many years, and his face is therefore very red because Professor Daugherty has privately pointed out that the velocity diagrams in the paper reverse α and β of the American Standard Letter Symbols for Hydraulics, ASA Z-10.2–1942, where α is the angle between the tangent to the rotor and the absolute fluid velocity, and β is the angle between the tangent to the rotor and the relative fluid velocity. Obviously all authors, including the authors of the present paper, need to be very careful to see that they use standard symbols.

Professor Berry's analogies are both instructive and amusing. He gives some fundamental reasons why rotors with few blades—such as airplane propellers or Kaplan water wheels—are covered by the principal equations of the paper. However, the paper considers primarily rotors with so many blades that all fluid filaments at entrance and exit theoretically have uniform velocity. This does not occur with rotors having few blades, and additional items which are not within the scope of the paper must be brought in. The details of "lift" with blades of airfoil shape also are outside the scope of the present paper.

We agree with Professor Berry that it would have been more accurate if we had used the term "uncompressed" rather than "incompressible."

Mr. Bloomberg has given some practical comments. The authors believe, with him, that the theoretical possibilities and limitations of a new turbine design should be investigated before much work of a practical nature is attempted.

In connection with the discussion of Mr. Browne, it is to be remarked that one of the mathematical purposes of the paper is fulfilled when it is pointed out that for a centrifugal pump or compressor there is usually a rather high relative inlet velocity, v_1, which is decreased along the rotor to a lower relative exit velocity, v_2. So far as mathematics is concerned, there is a conversion of velocity into pressure energy corresponding to $(v_1^2 - v_2^2)/2g$. But we agree with Mr. Browne that the mathematical assumption of this conversion and its accomplishment on an actual rotor are two quite different things. As Mr. Browne remarks, "entry hooks on the usual supercharger blades" do not make a very good diffuser for converting $(v_1^2 - v_2^2)/2g$ into pressure energy. The practical achievement of some better conversion passage along the rotor is therefore highly desirable. The alternative mentioned both by Mr. Browne and Mr. Campbell, of maintaining the high relative rotor velocity from inlet to exit, has a disadvantage of large friction loss. However, a supercharger engineer can take some comfort from the fact that these "entrance hooks," crude diffuser though they may be, do result in a perceptible gain as compared with having no bend at all at the entrance, which is periodically proposed as a method of reducing impeller costs.

Mr. Browne talks about steady flow tests of diffuser passages, and possibly he means tests of a straight passage such as a Venturi meter tail. In such a test there would be practically uniform conditions in a plane perpendicular to the passage axis. On the

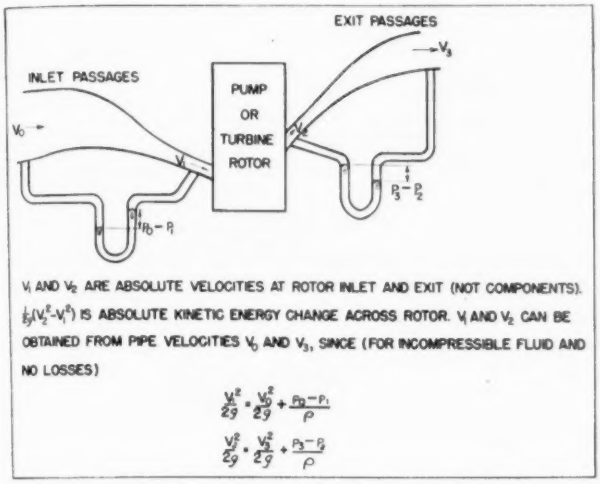


FIG. 19 DIAGRAM OF KINETIC ENERGY EFFECT

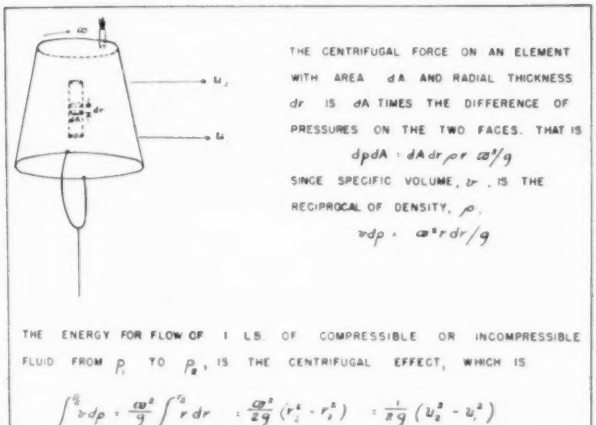


FIG. 20 DIAGRAM OF CENTRIFUGAL EFFECT

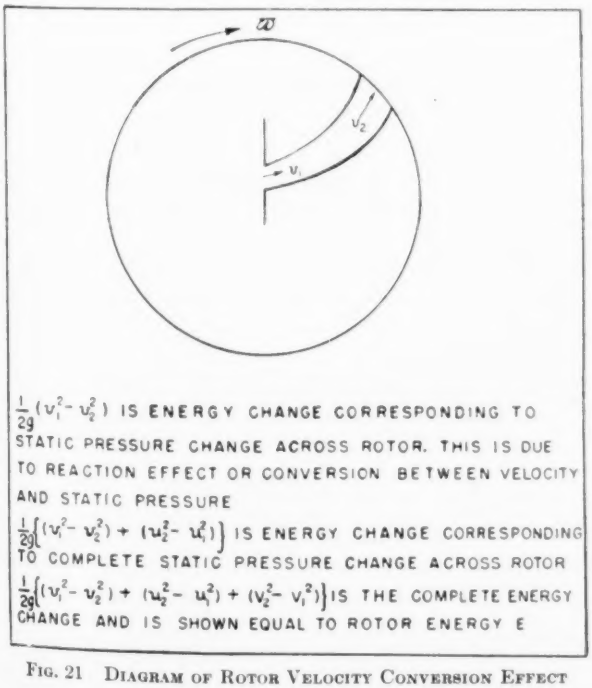


FIG. 21 DIAGRAM OF ROTOR VELOCITY CONVERSION EFFECT

other hand, Mr. Campbell assumes that fronts of equal pressure are approximately concentric with the axis. Finally, Dr. Marchant talks about the "weird-looking" results of an impeller passage velocity traverse where, instead of the simple steady state, "the flow is probably about as unsteady as it could be made." Probably the velocities in an actual diffuser passage are just as weird and unsteady. Therefore, as Dr. Marchant rightly points out, the actual occurrences in any practical machine differ from the simplified ones given by Messrs. Browne or Campbell or by the equations of the paper. But we have to start somewhere, and one of the purposes of the paper is to propose that this start be made with the particular mathematical methods given. These must be corrected either by purely empirical coefficients or by theoretical corrections such as the effect of circulation which Mr. Smith mentions. We certainly are not going to say that the actual actions are so weird-looking and unsteady that we can't at least start their analysis by the ideal equations of the paper. And we do not understand that Dr. Marchant proposes any other method of attack.

The reference to Professor Stodola that Dr. Marchant mentions is (12) in the bibliographical references added by Mr. Smith.

Mr. Eksergian speaks of "change in energy between entrance and exit sections to the rotor" and "entrance shock losses." We reiterate the statement, made in the second paragraph of the paper, that the fluid velocity and direction just preceding entrance to the rotor and following exit from the rotor, together with the rotor velocities, give the energy transferred between the rotor and fluid. Shock losses at entrance and exit occur on the rotor so far as this fundamental principle is concerned, and the C_h of Equations [46] to [53] is on this basis. C_h is found to vary but little with usual changes in the velocity ratio, u/V_0. Mr. Eksergian's substituted equations do not change this situation.

Mr. Eksergian calls attention to the fact that the fluid angle at entrance to any blade may not be the same as the angle of the blade itself. If the blade inlet angle, or better still, the angle corresponding to the effective passage between the blades, does not match the fluid angle at any given speed, there is a shock loss.

In spite of Mr. Eksergian's remarks about external heat transfer, we do not think his equations differ from ours in any essential particular. His group of equations has a kinetic-energy term. If this is appreciable, it is equivalent to the use in our own equations of total pressure, such as would be given by an impact tube.

With regard to heat transfer mentioned by Mr. Eksergian, we did not propose to give expressions for fluid energy for every possible case. Each one of the expressions we do give is for an explicit case, and each such case implies a thermodynamic process which the inlet temperature and the change of pressure completely measure. In our equations for a liquid or uncompressed fluid, changes in total pressure give the entire fluid energy. The losses are taken care of by the hydraulic efficiency, η, whether they appear wholly as liquid temperature rise, or with the usual very small percentage of external heat transfer. In the case of compression or expansion of a gas with exponent n, as stated in bibliographical reference (5), n takes full account of the temperature changes, even if rotor losses and rotation losses are added, and whether or not there is external heat transfer by radiation from the casing or by means of a water jacket.

With regard to our Equation [14], given as a general expression for the fluid energy of a single turbine stage, we are following usual practice. That is, the efficiency of the stage is based on isentropic drop of enthalpy as a standard. On this conventional basis, the efficiency multiplied by the isentropic drop gives the rotor energy. In all turbines of appreciable size and with the usual casing lagging, the external heat loss is negligible. It is true that a precise analysis will take account of the fact that the

enthalpy drop is not isentropic because of the losses which occur.

The final equations which Mr. Eksergian gives no doubt theoretically take care of all the heat transfer, but they are not in form useful to designers. The actual values of the external and internal heat transfer seldom are known, whereas for every kind of actual machine there are experimentally determined coefficients which enable the fluid energy to be calculated from the pressures involved.

In connection with the discussion of Mr. Madison, the authors have overlooked the special uses of inlet guides and agree with all of the points he has made. A complete mathematical analysis based on the fundamental equations of the paper and the particular cases which Mr. Madison mentions would be a useful contribution.

Referring to the discussion of Professor Sherzer, the authors



❀ 284 ❀

PROBLEME XI.

CX. *Une telle Machine hydraulique étant conſtruite pour une chûte & dépenſe d'eau donnée, trouver le moment de la reaction de l'eau, & l'effet de la machine lorsqu'elle eſt tournée autour de l'axe avec une viteſſe donnée.*

SOLUTION.

Soit comme jusqu'ici D la quantité d'eau, que le reſervoir peut fournir par ſeconde; h la hauteur de la chute entiere; a la hauteur du vaiſſeau tournant BBFF; b la diſtance des embouchures F, F, à l'axe; ff la ſomme de toutes ces embouchures; ζ l'angle que la direction des embouchures fait avec la direction de leur mouvement de rotation; Vu la viteſſe de ce mouvement; Vv la viteſſe reſpective dont l'eau ſort par ces embouchures; c la diſtance moyenne des orifices ſupérieurs E, E, à l'axe; ee leur amplitude totale unie dans l'eſpace annulaire E, E, E, &c.; ii la ſomme des embouchures des canaux Ji, Ji, par leſquels l'eau deſcend du réſervoir immobile DDJJ dans le vaiſſeau mobile BBFF; & g la hauteur de la chute pendant une ſeconde, qu'on ſait être de 15½ pieds de Rhin. Cela poſé, il faut qu'on ait ſatisfait à ces quatre équations:

I. $a = h - \frac{DD}{4gii}$;

II. $\frac{cc}{bb} = \frac{DD}{4gu}\left(\frac{1}{ii} - \frac{1}{ee}\right)$;

III. $v = h + u - \frac{DD}{2g}\left(\frac{1}{ii} - \frac{1}{ee}\right) = h + u - \frac{2cc}{bb}u$;

IV. $ff = \frac{DD}{4gv} = \frac{DDbb}{4g\{bbh + (bb - 2cc)u\}}$

& de plus les canaux Ji doivent être tellement inclinés à l'horizon, que le ſinus de leur inclinaiſon ſoit $= \frac{ii}{ee}$, & il faut que ee ſoit conſidérablement plus grand que ff, & que ee ne ſurpaſſe point cc. Main-

FIG. 22 EULER'S FIRST PAPER ON ENERGY TRANSFER, 1750

agree with him that the existence of a given quantity of compressed or uncompressed fluid at a given pressure involves no energy transfer. But a flow of fluid from a place of low pressure to a place of high pressure does involve energy transfer. In Fig. 20, the fluid in the rotating bucket is at a high pressure because of centrifugal force. As Professor Sherzer points out, the mere existence of this fluid at the centrifugal pressure is no evidence of energy transfer. So long as the bucket rotates at the end of the string with the same quantity of fluid in it, no power is required to keep the bucket rotating (except, of course, for atmospheric friction). But if fluid is passing from atmospheric pressure through the bucket, so that there is continuous flow from its outer radius at a pressure corresponding to the centrifugal pressure, then an energy transfer is involved. If the fluid is a

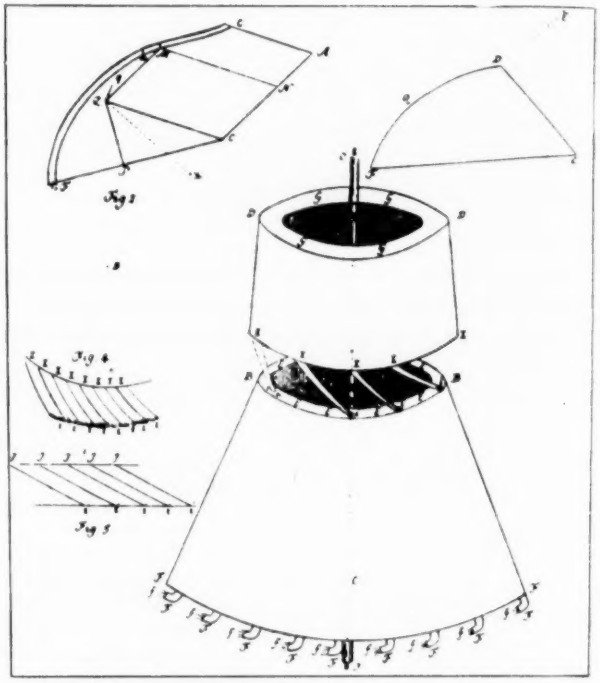
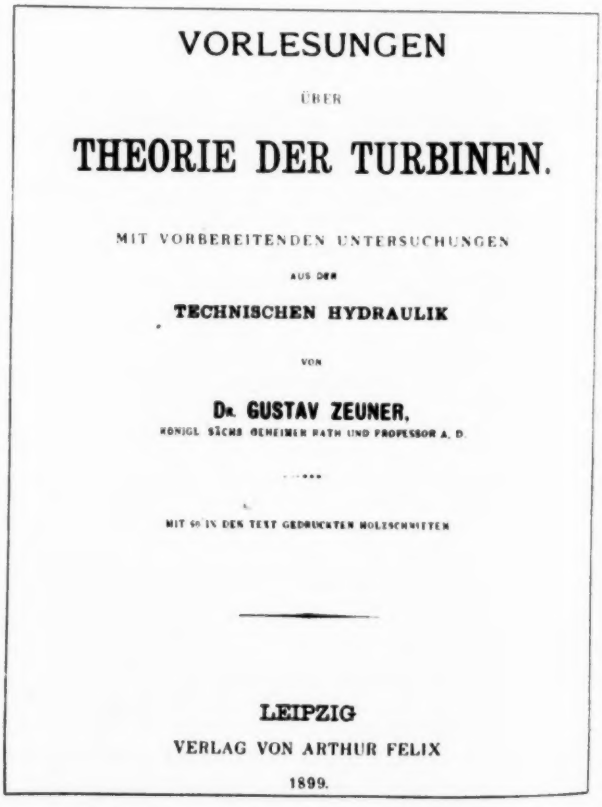


FIG. 23 EULER'S TURBINE PICTURE



VORLESUNGEN

ÜBER

THEORIE DER TURBINEN.

MIT VORBEREITENDEN UNTERSUCHUNGEN

AUS DER

TECHNISCHEN HYDRAULIK

VON

Dr. GUSTAV ZEUNER,

KÖNIGL. SÄCHS. GEHEIMER RATH UND PROFESSOR A. D.

MIT 69 IN DEN TEXT GEDRUCKTEN HOLZSCHNITTEN

LEIPZIG

VERLAG VON ARTHUR FELIX

1899.

FIG. 24 ZEUNER'S BOOK GIVING ENERGY TRANSFER

liquid, this energy transfer is equal to $(p_1 - p_0)/\rho$ foot-pounds per pound of liquid flowing. In the general case, it is equal to $\int v dp$, where v is the specific volume of the fluid. Our interest is always with machines operating at normal flow, and not with the abnormal condition of no load, where the equations of the paper do not apply. Bibliographical reference number (7) indicates a fundamental disagreement between Professor Sherzer and other writers on this subject, including the present authors. As Professor Sherzer points out, the physical interpretation of Equation [15] is not original with the authors.

We quite agree with Mr. Smith that the equations of the paper are concerned with actual fluid angles, and that these are not necessarily the same as the blade angles. Any theories of circulation, lift, and the like, which permit a better knowledge of actual angles of fluid flow, would be important additions to the general theory.

The brilliant scientist Euler, in the course of his scientific work in Berlin at the court of Frederick the Great, seems to have been the first to expound the mathematical theories enlarged upon in this paper. Figs. 22 and 23 show excerpts from his contribution to the Transactions of the Prussian Royal Academy, 1750. Fig. 24 shows the title page of Zeuner's book of 1899, which has been used frequently in the engineering careers of the senior authors. But Euler, the Prussian Royal Academy, and Zeuner probably did not have the faintest conception of the kinds of pumps and turbines to which these theories are applied in modern times. Steam and water turbines of 100,000 to 200,000 kilowatts capacity could not have been imagined in their wildest dreams. And they had no idea that the mathematics which they originated would lead to machines like the turbosupercharger, operating at 1500 F and 25,000 rpm in the *Flying Fortress* and other high-altitude airplanes.

Comparative Characteristics of Fixed- and Adjustable-Blade Axial-Flow Pumps

By J. D. SCOVILLE,[1] YORK, PA.

This paper compares the hydraulic characteristics of the fixed- and adjustable-blade type of pump. Certain advantages of the adjustable-blade design are enumerated. In it is described a large unit installed in the Traicao pumping plant of the Sao Paulo Tramway, Light and Power Company. The method used in making model cavitation tests is outlined.

THE comparison between the adjustable-blade pump and the fixed-blade axial-flow type is quite similar to the comparison between the Kaplan and the propeller turbines. The Kaplan turbine can deliver power at high efficiency over a wide range of discharge at normal heads; while at low heads, its output can be substantially increased over that of the propeller turbine by opening its blades. The propeller unit is at a considerable disadvantage in efficiency at variable flow. With the adjustable-blade pump operating at constant head, its discharge may be reduced by decreasing the blade pitch, maintaining high efficiency, and proportionately reducing the power input and, at low head, increased discharge is possible up to the motor capacity by an opposite change in blade angle. With a fixed-vane constant-speed propeller pump, a variable quantity at constant head can be delivered only by means of throttling on the discharge side, with the result that the horsepower input is no less than at full discharge, and often is substantially more. At reduced head, the discharge of the fixed-blade pump is determined by its inherent characteristics and cannot be increased as can that of the adjustable-blade type.

Blade Adjusting Mechanism

The mechanism by which the blades are adjusted is identical with that of the Kaplan turbine. Trunnions on which the blades rotate are a part of the vane castings. The bearings in which they turn are a part of the impeller hub. Levers are keyed to the trunnions and are connected by links to a common crosshead. Axial motion of the crosshead thereby changes the pitch of the impeller blades. This axial motion may be produced by a hand wheel mounted on top of the motor, through a thrust bearing to a draw rod passing through the hollow motor and pump shaft to the crosshead. This method is suitable only for small pumps. For medium-sized pumps, the same purpose can be accomplished by a motor in the shaft which produces axial motion of the draw rod by a reducing gear and a slowly rotating nut. On large pumps, it is advantageous to use a servomotor in the pump shaft, actuated by means of oil under pressure which is admitted through the hollow motor shaft and controlled by a valve located on top of the motor. This valve may be moved manually or may be float-operated, so as to keep a constant suction level with varying flow. Fig. 1 illustrates the scheme of operation, using an oil servomotor in the shaft.

[1] Assistant Chief Engineer, S. Morgan Smith Company. Mem. A.S.M.E.

Contributed by the Hydraulic Division and presented at the Annual Meeting, New York, N. Y., December 1–5, 1941, of The American Society of Mechanical Engineers.

Note: Statements and opinions advanced in papers are to be understood as individual expressions of their authors and not those of the Society.

Fig. 2 shows the comparative performance of a fixed- and an adjustable-blade impeller of the same diameter and speed. Their specific speed is 14,000 on a gpm basis. This curve illustrates that, for a constant head, the power requirement for the adjustable-blade design decreases as the flow diminishes. In order to pump less than rated capacity with the fixed-blade pump, the discharge must be throttled, thereby increasing the head on the pump as, for instance to 295 per cent, at 20 per cent Q. The motor horsepower goes up to about 220 per cent. If a mixed-flow pump of about one half the specific speed were used, the head at 20 per cent Q would be about 160 per cent, and the horsepower requirement 105 per cent. The adjustable-blade pump has a decided advantage at low flow over both types, about 25 per cent horsepower being required at 20 per cent Q.

At low heads, it is possible to obtain higher discharge than with the fixed-blade design, as indicated, 19 per cent more at 25 per cent head, and yet keep within the motor rating. At normal head, more than rated discharge is possible temporarily, by overloading the motor.

Pumps of this new type have been used in handling pulp stock

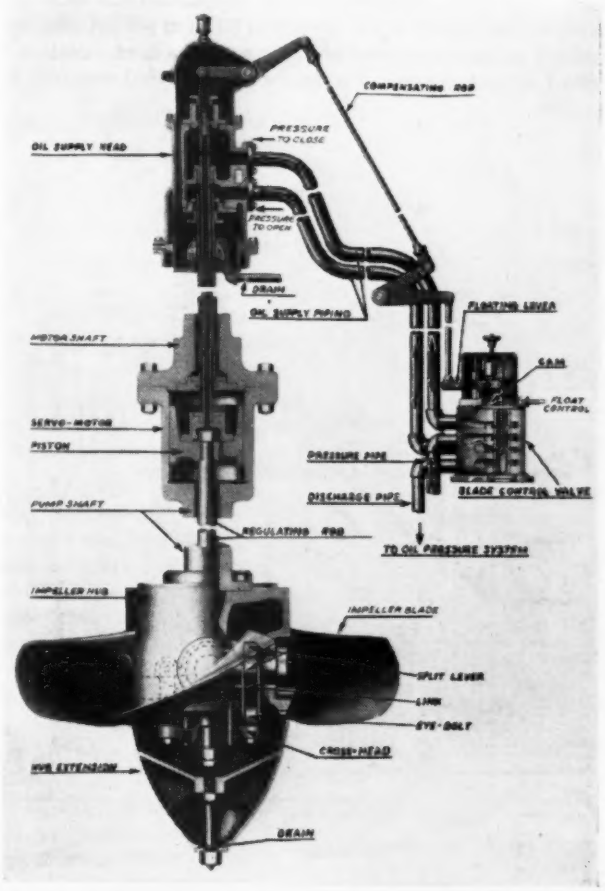


Fig. 1 Arrangement of Adjustable-Blade-Pump Mechanism

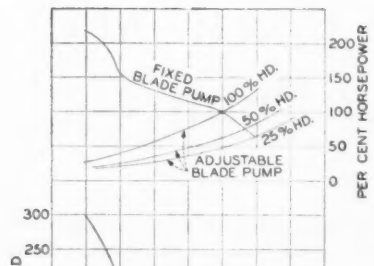


FIG. 2 COMPARISON OF FIXED AND ADJUSTABLE-BLADE PUMPS OF 14,000 N_S AT 100 PER CENT Q AND H

in paper mills, pumping condenser cooling water for steam turbines, and for flood-control work. Of special interest is a unit built for the Traicao plant of the Sao Paulo Tramway, Light and Power Company in Brazil.

PUMP UNIT AT TRAICAO PLANT

This plant is located on the outskirts of the City of Sao Paulo. It was designed and the machinery purchased by the Canadian and General Finance Company, Limited, of Toronto, Ontario. It is one of two plants in series, with a total lift of about 100 ft. Their purpose is to impound additional water for the Serra power plant, a large high-head station having a number of impulse turbines operating at about 2400 ft head; and further to provide flood control by transferring water from one shed to another.

The Traicao plant now has one unit, but will ultimately have four. The pump installed is of the adjustable-blade axial-flow type, having a guaranteed capacity of 50 cu m per sec discharge under 7 m maximum head at 150 rpm. The head variation is from 7 down to 4.5 m. The blades are controlled manually by means of a valve on top of the motor which admits oil under pressure to the servomotor in the pump shaft, thereby moving the blades to the desired pitch.

The general arrangement of the pump is shown in Fig. 3. The water enters the suction tube, passes through the impeller, and through a set of warped guide vanes to the discharge tube. Figs. 4 and 5 are shop views of the assembled impeller and shaft, and of the warped guide-case section, together with part of the hollow tube which surrounds the shaft. The impeller and the guide-vane assembly are removable through the motor stator. It will be seen that the discharge tube acts as a siphon, the lower part of the invert being slightly above the maximum-discharge water level. Two air valves are provided to break the siphon automatically when the pump shuts down.

This pump is driven by a 6600-hp, 3-phase, 60-cycle, 150-rpm synchronous motor with a pressure-lubricated thrust bearing for easy starting.

MODEL TEST OF PUMP

The size and the required service of the pump were such that it was deemed necessary to make a complete model test to determine its hydraulic characteristics. The prototype size is 138 in., and the model was made 10 in. diam. Tests were conducted in the laboratory to determine the efficiency variation with pitch change and head, cavitation limits under varying head and tail-water level, discharge, hydraulic thrust, torque variation during the starting cycle, and the maximum reverse speed in case of power failure.

Curves A, B, and C, Fig. 6 show the model efficiency plotted against prototype discharge in English units with the quantity in cubic feet per second, and the head in feet, corresponding to 7.5, 6, and 4.5 m net head. Curves A', B', and C' show the discharge horsepower and the expected discharge-efficiency performance of the prototype, the latter stepped up in accordance with the well-known Moody formula. In computing this efficiency differential, an exponent of 0.20 was used for the diameter ratio in the formula, as suggested by W. S. Pardoe in his discussion (1)[2] of a paper by L. M. Davis.

Of special interest is the large capacity of this unit, namely, 2780 cfs at 24.6 ft head, and 3070 cfs at 14.8 ft head. These figures correspond to 15,000 specific speed at the high head and 23,000 at the low head. However, the horsepower capacity of the motor limits the available output of the pump. Herein is one of the advantages of the adjustable-blade design. Due to possible casting variation, a fixed-blade impeller could not safely be made for more than 6400 hp or 1910 cfs at 24.6 ft head for a 6600-hp motor. At 14.8 ft head, the discharge would be about 2190 cfs. With an adjustable-blade impeller, the pump can be operated within the motor capacity of 6600 hp at both heads and deliver 1960 cfs and 2560 cfs,

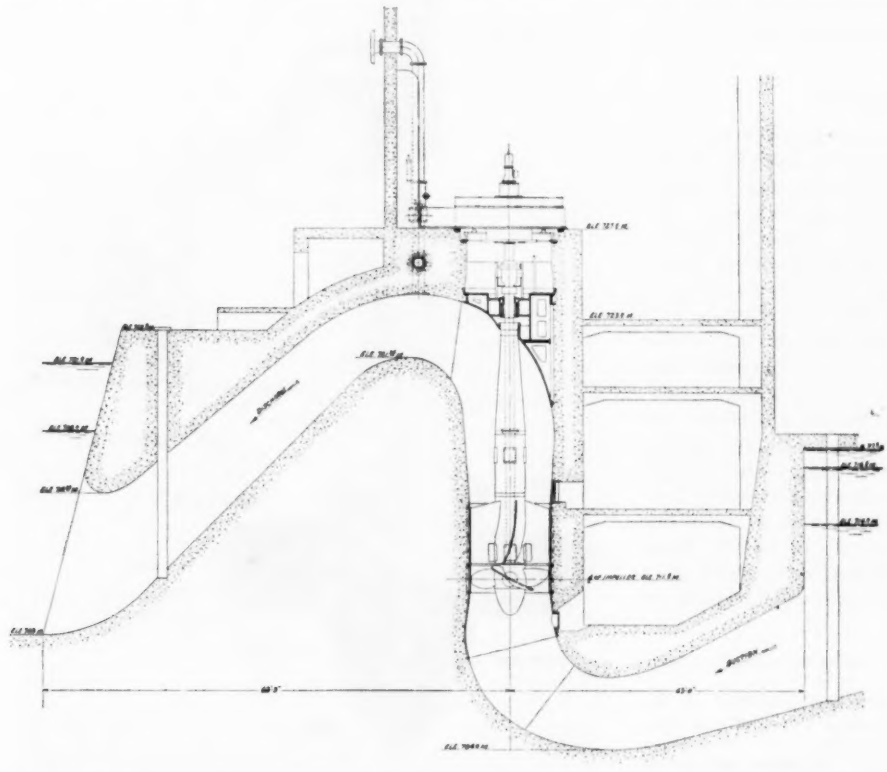


FIG. 3 GENERAL ARRANGEMENT OF ADJUSTABLE-BLADE AXIAL-FLOW PUMP AT TRAICAO PLANT, SAO PAULO

[2] Numbers in parentheses refer to the Bibliography at the end of the paper.

respectively. The latter is an increase in discharge of 17 per cent, as compared with the fixed-blade design. It will be noted that the cavitation-limit curve, shown in Fig. 6, is well above the 6600-hp motor capacity.

Fig. 7 shows the head-speed relationship, and also the torque variation during the starting cycle, neglecting the torque required for acceleration. Characteristic curves for both fixed- and adjustable-blade impellers are indicated. They show that, with this particular design of pump, if the blades are fixed at such an angle as to give the required discharge, the impeller produces its rated head at about one-half speed, the torque having risen rapidly up to this point. Beyond this, discharge starts and the torque rises more slowly. At synchronous speed, the full-load torque of the motor is reached. During the starting period of the adjustable-blade pump, the blades are held in the flat position. At synchronous speed, maximum head has not been reached and the maximum torque is only about 19 per cent of the fixed-blade-impeller torque at normal speed. After the circuit breaker has been closed, the blades may be opened slowly to the required setting. This results in less shock to the system and permits a somewhat cheaper motor, having less pull-in torque than for the fixed-blade design. Full-voltage starting is used.

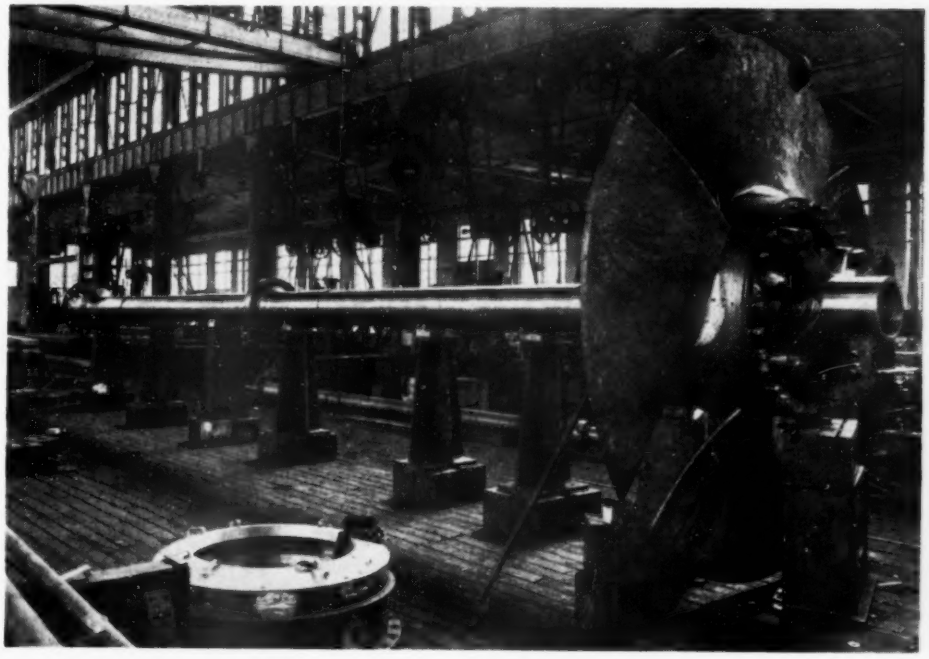


FIG. 4 SHOP VIEW OF TRAICAO UNIT IMPELLER-AND-SHAFT ASSEMBLY

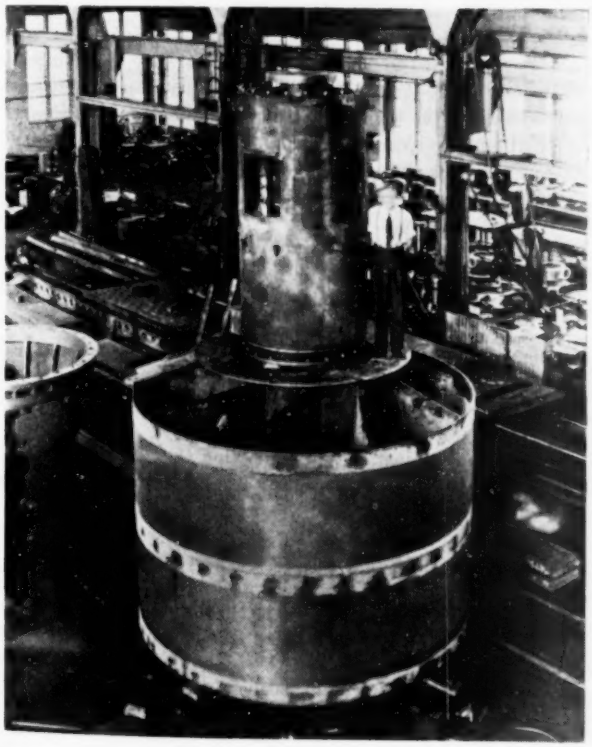


FIG. 5 WARPED GUIDE-CASE SECTION OF TRAICAO UNIT SET UP IN THE SHOP

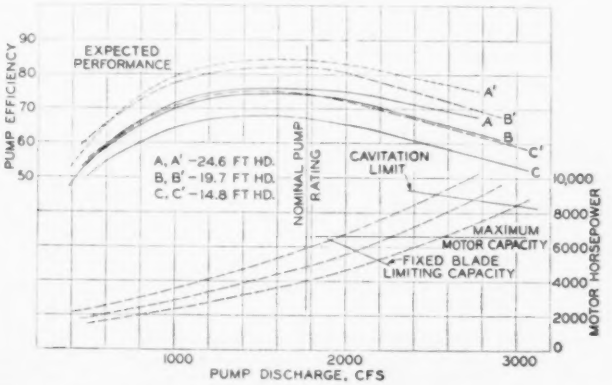


FIG. 6 EFFICIENCY CURVES OF MODEL PUMP AND CURVES OF EXPECTED PERFORMANCE OF PROTOTYPE

The behavior of the pump during shutdown is of interest. The blades may be slowly closed and the breaker opened when the load on the motor is a minimum. At this time, the solenoid-operated air valves at the top of the invert of the discharge tube open and break the vacuum, thus pre-

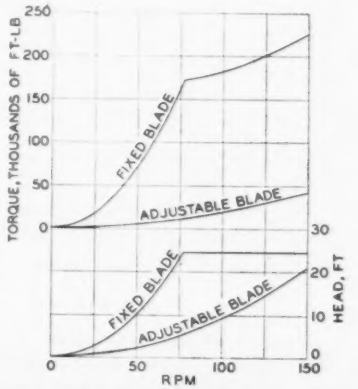


FIG. 7 TORQUE-SPEED RELATIONSHIP OF FIXED-BLADE AND ADJUSTABLE-BLADE PUMPS

venting backflow. In the event of power failure during full load, the air-valve capacity is sufficient to break the vacuum and bring the speed to zero. Tests made in the field show that 7 sec were required for the pump to reverse its direction, 13 sec to reach its maximum runaway speed of 225 rpm, and 7 sec to reach normal speed again after opening the air valves manually. When the air valves are operated automatically at the opening of the circuit breaker, the unit comes to rest in about 5 sec.

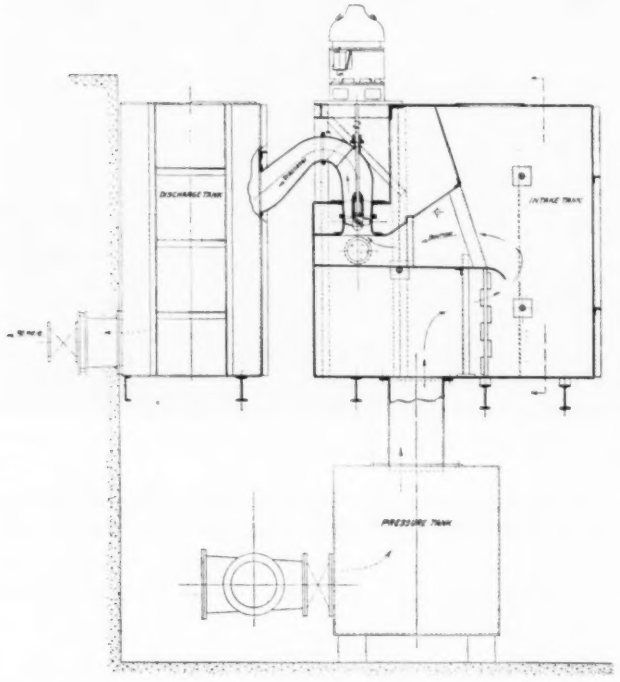


FIG 8 LABORATORY ARRANGEMENT FOR PUMP CAVITATION TESTING

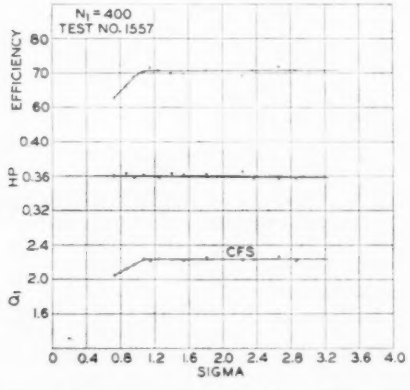


FIG. 9 TYPICAL CAVITATION TEST FOR ONE N_1 AND BLADE ANGLE

The pump has been in operation in the field, but as yet to a very limited extent, and not over the entire range of head it was intended for. Its showing so far, however, has been satisfactory.

PROBLEM OF CAVITATION

As with the Kaplan turbine, the high specific speed and unit discharge introduce special problems with regard to cavitation. In order to attack a problem involving adjustable-blade pumps, cavitation tests are required.

The method of obtaining cavitation limits in the laboratory for hydraulic turbines has been described recently by L. M. Davis (2) and R. E. B. Sharp (3). The same system is used for pumps. Fig. 8 shows the laboratory setup for this type of test. The pump is operated at constant speed and head, but with variable intake and discharge pressures. The discharge and suction heads are decreased equally until cavitation progressively reduces the efficiency. Fig. 9 shows a typical test for one N_1 and blade angle.

$$\sigma = \frac{H_B - V_P - H_S}{H}$$

N_1 = rpm of model under 1 ft head
H_B = barometric pressure
V_P = vapor pressure
H_S = suction lift
H = total head

The term σ is the ratio of velocity head at some point within the impeller plus the remaining pressure safety, to the total head. Critical σ is reached when this remaining pressure safety is reduced to zero, thus starting cavitation.

It is this cavitation which causes the loss in efficiency shown in Fig. 9. The critical σ values must be determined experimentally for the entire range of N_1 (or head) and blade angle of a given design of pump, in order properly to locate the impeller with reference to the suction level, and predict a safe value of pump discharge. During cavitation tests, observations made through windows in the suction tube, with a stroboscope, gave valuable information on the location of critical parts of the impeller blade and the magnitude of the cavitation.

CONCLUSION

In this paper, the author has endeavored to point out certain advantages of the adjustable-blade type of pump, which are:

1 High speed combined with a flat efficiency curve.
2 Extra capacity in an emergency and at low heads.
3 Easy starting characteristics and the elimination of a valve to control discharge.
4 Possible operation of pump under abnormal suction conditions by adjusting the blade position to eliminate cavitation.
5 Flexibility; not available in a fixed-blade design.

It has the disadvantage of increased cost, but as with the Kaplan turbine, this can be offset by the use of fewer and larger pumps. It is perhaps significant that most low-head-turbine installations suitable for high-speed propellers are now being made with the Kaplan type of runner.

Possibly many installations involving the pumping of a variable quantity under low heads can use the adjustable-blade type of pump at a net saving in cost.

ACKNOWLEDGMENT

Acknowledgment is made to Mr. Rolfe Sahle who was in charge of the pump tests conducted in the S. Morgan Smith Company's laboratory, and to the Canadian and General Finance Company, Toronto, Ontario, with whose permission the information on the Traicao pumping plant has been released.

BIBLIOGRAPHY

1 "Model and Prototype Tests," by L. M. Davis, Proceedings, A.S.C.E., vol. 65, 1939, pp. 1575–1589; discussion by W. S. Pardoe, ibid., vol. 66, 1940, pp. 179–180.
2 "Cavitation Laboratory Practice," by L. M. Davis, *Civil Engineering*, March, 1941, pp. 148–149.
3 "Cavitation of Hydraulic Turbine Runners," by R. E. B. Sharp, Trans. A.S.M.E., vol. 62, 1940, pp. 567–575.
4 "Adjustable-Blade Propeller-Type Pumps," by R. E. B. Sharp, *Power*, vol. 77, 1933, pp. 242–243.
5 "The World's Oddest Hydro Development," *Power Plant Engineering*, August, 1941, pp. 54–57.

Discussion

R. W. Angus.[3] If for no other reason than its flexibility, the pump referred to in this paper has a very definite field of service. Many years ago when the writer was in Germany, he visited an outdoor river-flow laboratory near Berlin, in which the water used was supplied by this type of pump. Running at constant speed the discharge could be varied from a mere trickle to a very large volume by adjusting the impeller blades by hand. For low heads, the axial-flow pump permits the use of a high-speed motor which usually may be direct-connected without gears.

A pump with fixed impeller blades, however, has the unfortunate characteristic that maximum driving power is required for minimum flow, and this power decreases as the flow increases, as has been pointed out by the author.

The mechanism for operating the blades is fairly costly, and it would be instructive if the author could give some indication of the minimum capacity for which this type of unit is economical. When so much expense has been put into adjusting the impeller blades, it would seem that considerable efficiency is being sacrificed by leaving the guide-ring vanes stationary. The writer wishes to ask if any development work has been done on variable guide vanes, and what success has been achieved.

The quarter turn in the suction pipe, Fig. 3 of the paper, is not generally approved in centrifugal-pump work, as it has a general tendency to reduce the capacity. Some of the earlier axial-flow pumps used entry guides in front of the impeller. Has the author had any experience with these?

Only one view of the author's laboratory is given in Fig. 8, and in it there is an apparent difference between the suction arrangement and that shown in Fig. 3, already referred to. The laboratory setup indicates more nearly axial entry to the suction pipe with slight tendency for whirling and probably with less danger of cavitation. It would be interesting to know what the effect of the quarter turn in the suction pipe would be on the limiting sigma, as found from the setup of Fig. 8.

The value of the paper would be greatly increased if actual test curves from the model were shown. The writer hopes that the author may yet be able to add test curves from the actual Traicao pump.

W. S. Pardoe.[4] The author has used Professor Moody's step-up formula for turbines, adopting the writer's suggestion of 0.2 as exponent of the model scale. It might be well to bear in mind the source of this exponent, coming as it does from the following expression for the coefficients of 56 cast-iron Herschel-type Venturi meters with finished bronze throats

$$C = \sqrt{\frac{1 - \left(\frac{d_2}{d_1}\right)^4}{1 - \left(\frac{d_2}{d_1}\right)^4 + \frac{0.045}{d_2^{0.23}}}}$$

$\frac{0.045}{d_2^{0.23}}$ is a coefficient of $\frac{V_2^2}{2g}$ giving the lost head, including such change as takes place in the pipe factors. The writer reduced this exponent to 0.2 as some of the turbine losses vary as V^2. Note that the Venturi meters were all of the same physical roughness. Hence, both model and prototype turbines should have surfaces of the same physical roughness. No attempt should be made to get the same proportional roughness (whatever that means). It would seem reasonable, if both model and prototype were very smooth, for the exponent to approach Professor Moody's 0.25. If model and prototype have the physical roughness of sand-cast pipe, the exponent might approach 0.15 as in the Williams and Hazen formula

$$V = cd^{0.63}S^{0.54} \text{ or } h = \left(\frac{V}{c}\right)^{1.85}\frac{L}{d} \times \frac{1}{d^{0.15}} \alpha \frac{1}{d^{0.15}}$$

The writer's suggestion of 0.2 was a mean between these values and was intended for the step up of turbine efficiencies. The author and others have used it for centrifugal pumps—unwisely, the writer believes. He uses it for the upstream section of the Venturi meter with its converging boundaries, but would hesitate to use it to step down the loss in the downstream section with its diverging boundaries, where losses vary as V^2.

If the model centrifugal pump is very smooth and the prototype pump rough, we may get no step up and a probable step down in efficiency.

C. B. Spellman.[5] This paper is of particular interest to the Baldwin-Southwark division of Baldwin Locomotive Works. The I. P. Morris department of this division, in its capacity of builders of large hydraulic machinery, has conducted numerous and extensive tests on models of turbines and pumps. During 1940, I. P. Morris tested a four-bladed axial-flow propeller-type pump, of approximately 11 in. throat diam and having adjustable impeller blades. The results obtained, if stepped up to 138 in. diam and 150 rpm, would essentially duplicate the performance data shown in the author's Fig. 6. The maximum efficiency obtained from this model was 77.5 per cent, when tested at a speed of approximately 1350 rpm, under a normal head of about 10½ ft, measured from suction water level to discharge water level. As in the case of the S. Morgan Smith model, the pump was placed in a cavitation-laboratory setting.

The writer realizes the manifold advantages of the usual adjustable-blade axial-flow pump. Nevertheless, it is believed that there is a possibility, not generally recognized, of still further improvement which might prove to be advantageous in cases where operating economy is of prime importance. In such cases, it would be highly desirable to operate on the envelope of the efficiency curves for the various blade positions. That this cannot be done with the usual adjustable-blade axial-flow pump against a constant head can be seen by a brief study of a typical characteristic chart for such a pump.

In Fig. 10 of this discussion, the *H-Q* curves represent pump-performance curves of head versus quantity at constant speed for various fixed positions of the adjustable-blade pump. Points of equal efficiency are shown by the customary contour lines. The characteristics of this type of pump are such that the locus of the best efficiency for the various blade angles is a sloping line, as L_E. This is the *H-Q* curve on which the pump must operate in order to attain its maximum efficiency. In other words, this line corresponds to the envelope efficiency curve E_E. Now, since L_E is a sloping line, it follows that pump operation against a constant head, denoted by the horizontal line H_C, can be on the envelope curve only at the point of intersection E_M. At any other point on the line H_C, the efficiency will be below the envelope of maximum efficiency. Hence the maximum efficiency actually obtainable for constant-head operation becomes a curve, such as shown by the dotted line E_A, tangent to the envelope at one point only.

It is the writer's opinion that the envelope shown by the test could be more nearly approached, for any given head, if the pump

[3] Professor of Mechanical Engineering, University of Toronto, Toronto, Ontario, Canada. Honorary Member A.S.M.E.

[4] Civil Engineering Department, University of Pennsylvania, Philadelphia, Pa.

[5] Sales Engineer, Baldwin-Southwark Division, Baldwin Locomotive Works (I. P. Morris Department), Philadelphia, Pa. Mem. A.S.M.E.

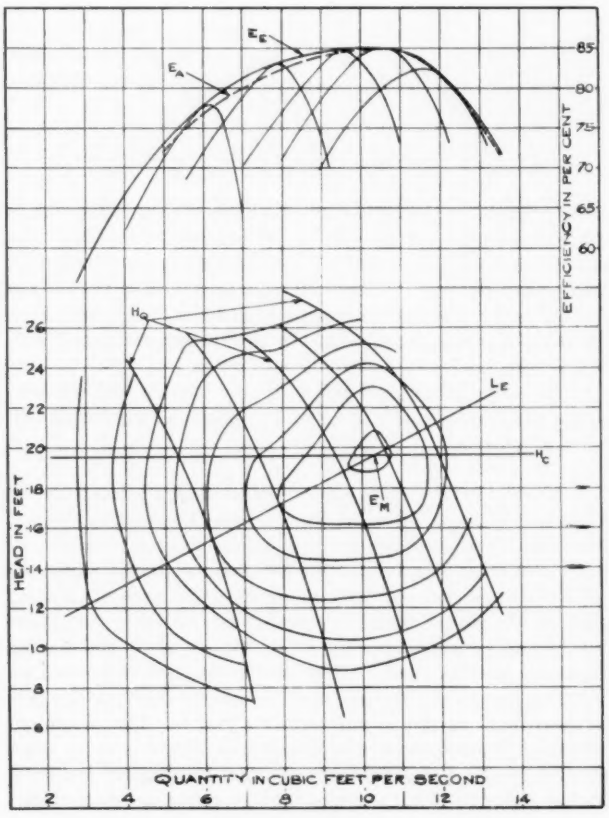


FIG. 10 TYPICAL CHARACTERISTIC CHART FOR ADJUSTABLE-BLADE AXIAL-FLOW PUMP

were supplied with movable guide vanes, instead of fixed guide vanes at the discharge side of the impeller. Such vanes should be positioned in relation to the impeller-blade position, to minimize the hydraulic losses as the water enters the guide case. Thus, instead of attaining performance analogous to that of an adjustable-blade turbine with fixed guide vanes, it would be logical to expect performance analogous to that of the full Kaplan turbine, where the guide vanes and runner blades are both adjusted to their proper relative positions. However, the gain in efficiency which could be realized by the use of such movable guide vanes at the entrance to the guide case might be too small to warrant the increase in cost.

The author also mentions the runaway speed of the Traicao pump in the reverse direction. It is not clear from the context whether this speed was obtained with the pump blades in the full-open position. It is the writer's thought that the maximum speed in the reverse direction would probably be attained with the impeller blades in an intermediate position. It would be interesting to know whether the S. Morgan Smith tests over the full range of blade positions have been such as to confirm this thought.

AUTHOR'S CLOSURE

As stated by Professor Angus, the adjustable-blade pump has considerable merit because of its flexibility. It is this feature which has justified the construction of pumps having a capacity as low as 5000 gpm for handling pulp stock for paper mills.

Professor Angus points out that the adjusting mechanism is costly. True, but there are certain types of installations where the extra cost is more than compensated for by other savings. For instance, a dry-dock pump must operate over a 100 per cent head range. For such an installation, an adjustable-blade pump permits a smaller size, running at higher speed, requiring a smaller motor of a cheaper design than for a fixed-blade design. The starting characteristics of the adjustable-blade pump allow the use of a synchronous motor at a considerable saving in cost, as compared with the induction motor which is customarily used on the fixed-blade design.

Both Professor Angus and Mr. Spellman suggest the desirability of using movable guide vanes above the impeller. Because of practical limitations, it is questionable whether this would result in better efficiency. A rather expensive construction would be required. It is possible that fixed axial vanes below the impeller, and the elimination of vanes above, with the substitution of a volute casing at the discharge, would accomplish equal improvement.

It is felt that the use of an accelerating velocity elbow suction tube is preferable to the common bellmouth. However, comparative efficiency and cavitation tests made recently on the two types of intake tubes showed no difference in performance, at least for that particular pump.

The curves *A*, *B*, and *C* in Fig. 6 of the paper are the actual model performance stepped up mathematically to prototype size and head with no efficiency correction. There is no field test available for the Traicao installation.

The author appreciates Professor Pardoe's discussion of the Moody formula. It is regrettable that there is not more information on the efficiency step up for size on pumps. In Table 4 of a paper[6] before this Society, Professor Angus supplies tests on four pumps for the City of Toronto and shows that on the average the efficiencies check with those computed from the model test using an exponent of 0.25.

The author cannot present any confirming data on pumps but can do so on Kaplan turbines. Fig. 11 of this closure shows the

[6] "An Improved Technique for Centrifugal Pumps—Efficiency Measurements," by R. W. Angus, Trans. A.S.M.E., vol. 63, 1941, pp. 13–19.

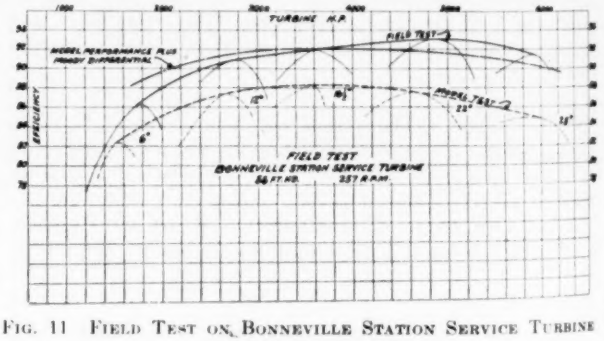


FIG. 11 FIELD TEST ON BONNEVILLE STATION SERVICE TURBINE (56-ft head; 257 rpm.)

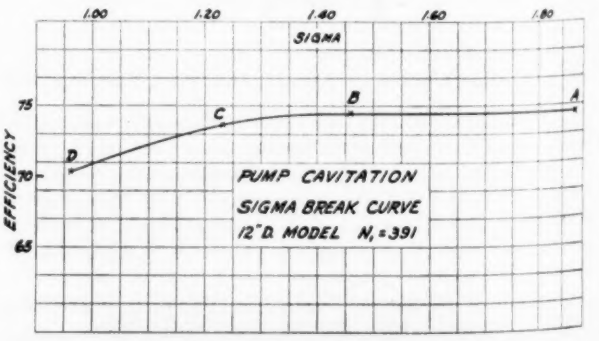


FIG. 13 PUMP CAVIATION SIGMA-BREAK CURVE (12-in-diam model; $N_1 = 391$.)

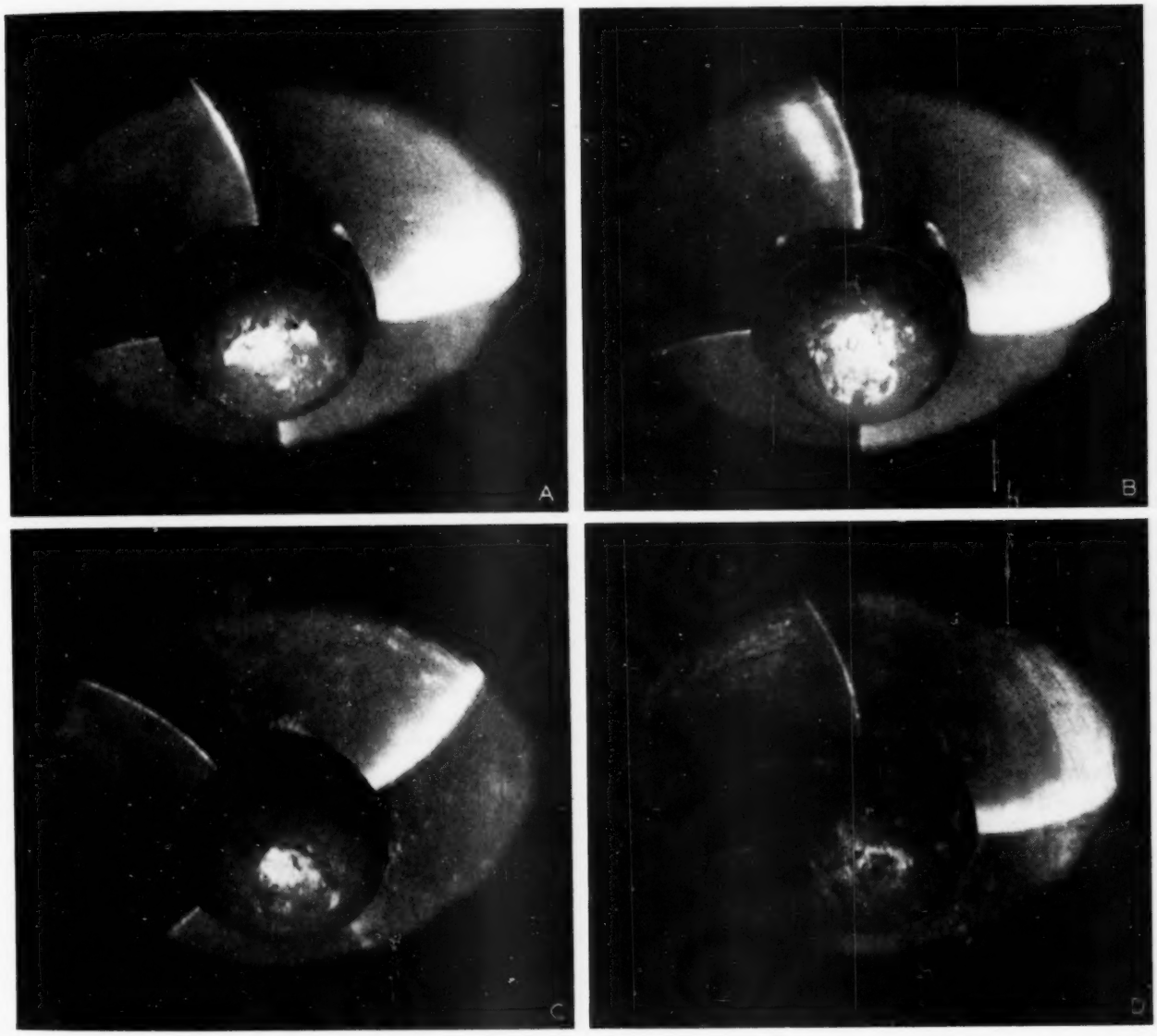


FIG. 12 HIGH-SPEED STUDIES OF CAVITATION

field test of the Bonneville service unit compared with the model test and the computed performance using the Moody efficiency step up. The model diameter was 16 in. and the prototype 81 in. It is logical that the efficiency displacement is upward and to the right, indicating that the efficiency increase resulted in larger output. This shift is confirmed by about 25 or more index tests on Kaplan turbines where relative efficiency was obtained without making an actual water measurement. Therefore, it would be reasonable to expect the increased efficiency in a pump to result in larger discharge from the same horsepower input.

The S. Morgan Smith tests on the Traicao model show that the maximum reverse speed on the adjustable-blade pump occurs when the blades are about half open. This answers Mr. Spellman's question.

Fig. 12 (*A* to *D*) of this closure shows cavitation on the lower side of the runner blades at various stages. The original photographs were taken under the direction of Rolfe Sahle using a 4 × 5 Graphic View camera having a Zeiss Tessar 4.5 lens. The pump speed was 1200 rpm, and the motion was stopped by the use of a Speedotron lamp with a flash duration of about 0.00003 sec.

Fig. 13 shows the sigma-break curve of the pump, the points *A* to *D* corresponding to the views *A* to *D* of Fig. 12. The illustrations show progressive increase of cavitation as sigma is lowered, and there is a change in efficiency corresponding to the progression in cavitation.

Some Problems in the Selection and Operation of Centrifugal Pumps for Oil and Gasoline Pipe Lines

By A. HOLLANDER,[1] LOS ANGELES, CALIF.

During the 15 years since they were first introduced, high-pressure motor-driven centrifugal pumps have been adopted to an ever greater extent in crude-oil trunk lines. Since the inception of gasoline trunk lines six years ago, centrifugal pumps have been exclusively used in this service. This paper deals with the basic principles of developing pumping stations of suitable capacity under present conditions and mentions future improvements contemplated. Today, trunk-line centrifugal pumps include units having capacities from 5000 to 125,000 bbl per day, working against pressures of 300 to 1100 psi, driven by two-pole induction motors of 200 to 900 hp. Units proposed for the National Defense Pipe Line will have 250,000 bbl per day capacity against 775 psi, operating three single-stage pumps in series, each driven by a 1300-hp motor. The procedure followed by the pump designer in developing units to meet given requirements is outlined, together with details of the resulting characteristics. Discussion of trunk-line operating schedules is included, and finally a method is given for solving pipe-line-pumping problems.

SINCE their first introduction some 15 years ago in pipe-line service (1),[2] high-pressure centrifugal pumps have found ever wider acceptance for crude-oil trunk lines, until today reciprocating pumps are considered only in exceptional cases. The lower viscosity of gasoline served as a further factor in favor of centrifugal pumps, and for gasoline trunk lines starting about six years later (2), centrifugal units were initially employed and have been used exclusively ever since.

With low-cost and reliable electric power supplied from great interconnected networks close to the pumping stations, the high-speed, two-pole induction motors, direct-connected to light multistage centrifugal pumps, constitute an irreducible minimum in pumping machinery and material, with the least building and foundation requirement.

Even though oil is available at low cost from the pipe line, the more expensive oil engines, driving centrifugal pumps through speed-increasing gears, are seldom used today in preference to the direct-connected electric-motor drives. The use of electric-motor-drive centrifugal pumps was further advanced by automatic, or at least semiautomatic operation, which practice is becoming more and more general.

It is fortunate that the electric-centrifugal pipe-line station can be considered as proved and economically sound. Otherwise, the great defense trunk-line projects, now under consideration, or in process of construction, would not have been feasible.

The engineering staffs of the pipe-line and oil companies design the pipe-line systems. These staffs are fully conversant with all the numerous elements involved and in close touch with the manufacturers thereof. Based on some assumed loading of the line, the staff determines by successive approximations, among a great many other details, the final specifications of the pipe, its size, thickness, and material, the number and location of stations, and of their pumping units, which call for definite capacities, pressures, and horsepower, arrived at through some previous consultations with the manufacturers of the equipment. It is this last phase of the problem, describing the main factors determining the pump design and its implications for future developments, which is the subject of this paper, with some operating possibilities and diagrams that might be of interest.

Present Practice and Future Improvements

The trunk-line centrifugal pumps include units having capacities of 5000 to 125,000 bbl per day, working against pressures of 300 to 1100 psi and driven by two-pole motors of 200 to 900 hp. The final pressure is obtained either with a single multistage pump or by operating two units in series. The pumps are built in two to eight stages, three to six stages being the most common. Gathering pumps are similar but smaller, coming down in capacity to about 1000 bbl per day.

It is noted that the units proposed for the National Defense Pipe Line are quite exceptional, as the requirements indicate pumps of 250,000 bbl per day capacity against 775 psi, operating three single-stage units in series, each driven by a 1300-hp motor. The pump designer uses as the unit of the flow rate or capacity q gallons per minute, and as the unit of the head per stage h feet; with these units, he defines the pump type of one stage by the specific speed n_s.

$$n_s = \frac{q^{1/2}\ \text{rpm}}{h^{3/4}} \qquad [1]$$

This varies for pipe-line pumps from about 500 to 2000, and, within this range, the optimum efficiency is reasonably well established (3). Optimum efficiency is defined as the best obtainable efficiency under the most favorable suction conditions of a single-stage pump, pumping cold water and built in a sufficiently large size, so that any further increase in its size will make only a negligible improvement.

The second factor which will have a major effect on the pipe-line-pump efficiency is the pump size, which is determined by the flow rate of the pump divided by a characteristic velocity, e.g., $\sqrt{2gh}$, of which every velocity through the pump is a function.

As the flow rate divided by a velocity gives an area, to get a linear dimension, the square root of this figure is taken. Omitting constants, the characteristic size s is defined

$$s = \sqrt{\frac{q}{\sqrt{h}}} = q^{1/2}/h^{1/4} \qquad [2]$$

[1] Consulting Engineer, Bryon Jackson Company, Mem. A.S.M.E.

[2] Numbers in parentheses refer to the Bibliography at the end of the paper.

Contributed by the Hydraulic Division and presented at the Annual Meeting, New York, N. Y., December 1–5, 1941, of The American Society of Mechanical Engineers.

Note: Statements and opinions advanced in papers are to be understood as individual expressions of their authors and not those of the Society.

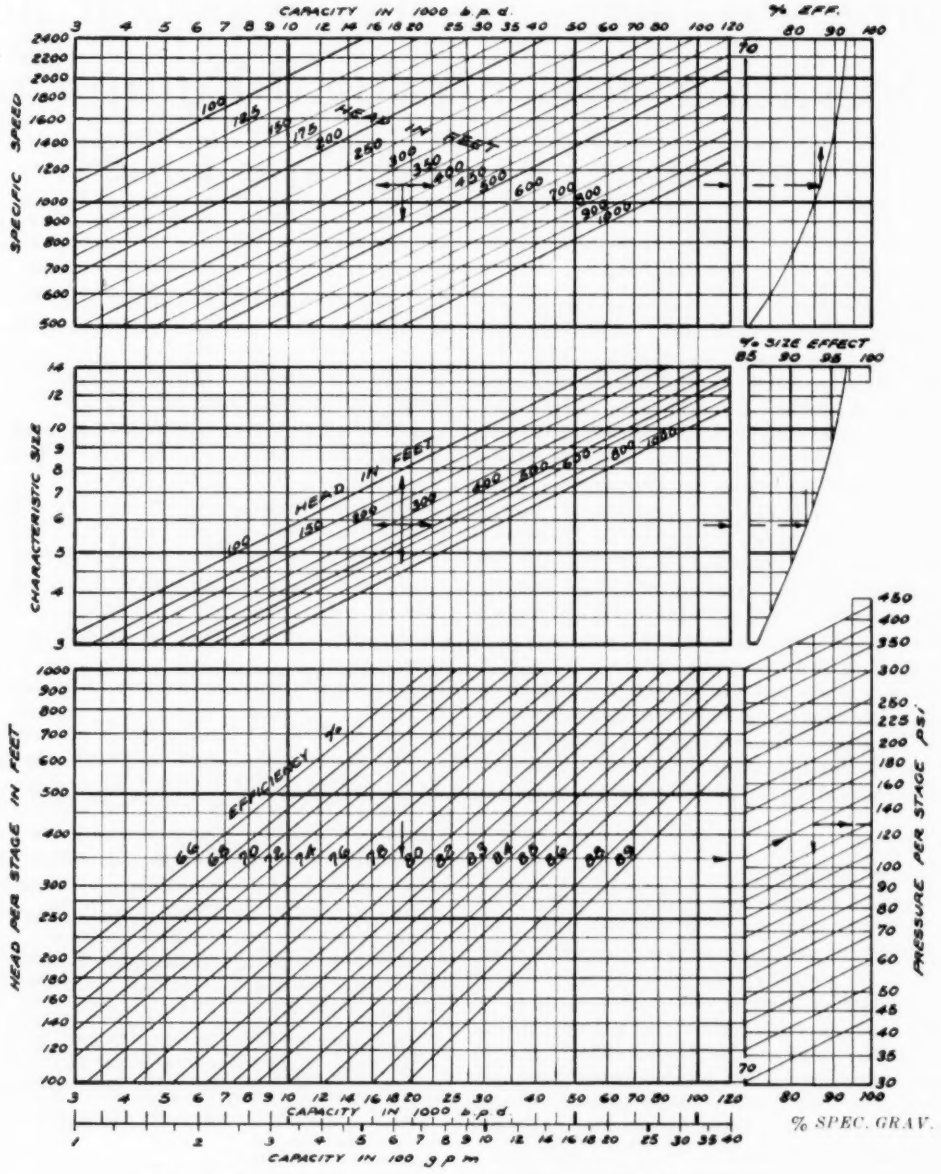


FIG. 1 DETERMINATION OF IDEAL EFFICIENCY FOR PIPE-LINE PUMPS

This varies from about 3 to 14, and the efficiency variation, due to this size factor, is also fairly well established.

It is noted, that using these two factors, the affinity law, according to which the efficiency e remains substantially constant for different speeds for a constant value of the characteristic size, is fully complied with, so that this term is more suitable for the size definition than the capacity. This conception is not novel in so far as it is the application of the model law (4) for units of the same type and different size, but it limits the range of types and sets the absolute value of the characteristic sizes.

The approach, however, is just the opposite in so far as it starts from an optimum and reduces this with the size decrease; the very assumption of an optimum is contradictory to the turbine-model laws which assume that the losses in per cent $(1 - e)$ will decrease *ad infinitum* the same way, i.e., if the doubling of the model diameter reduces the losses 13 per cent, a similar percentile reduction will take place by doubling the size of the units, e.g., from 20 to 40 times that of the model. This means an efficiency increase of an 80 per cent model to 82.6 or 2.6 points for a double-sized model; a 20 times to 40 times model size will give efficiencies of 87.8 per cent and 89.4 per cent, respectively, or show a 1.6 point increase with a model law, according to which the losses are proportional to the fifth root of the size ratio.

For the small sizes and narrow range of types, experience with the pipe-line pumps indicates that the change of efficiency with size is rather independent of the type, and this is how Fig. 1 is laid out. It is noted that the values indicated are only estimates and in some cases economically impractical.

The great effect of viscosity, particularly for heavy crude, is not considered in this paper, but it should not be neglected when the absolute maximum of obtainable efficiency is to be determined for oils of different viscosities. This effect is subject to further exploration, some of which is being carried through at present. The reduction of efficiency, due to viscosity, is greater for the lower specific speeds; therefore any conclusions which call for

higher-specific-speed types are even more valid for viscous than for nonviscous oils.

The important factor of cavitation may be overlooked for the newer pipe-line systems, because they are designed to give ample positive suction head to avoid cavitation even at the starting station, while for the successive stations pressure regulators on the suctions provide sufficient inlet pressure. On the first station, or in those with tank farms, if the static head provided is insufficient, auxiliary pumps furnish the required suction pressure. Furthermore, the pumps being multistage, only the first stage would have to be changed to reduce cavitation tendencies so that the total effect would be rather small.

Secondary effects, due to the larger shaft required by a great many stages or higher or lower stuffing-box pressures, also may be taken into account, but the general picture developed in this paper will not change materially if they are neglected.

Operating at a single given speed of 3550 rpm, a nomogram, Fig. 1, was constructed from which the best efficiency for a given capacity and head per stage may be determined. The nomogram consists of three sections, the abscissa showing the capacity in barrels per day and gallons per minute being the same for all of them.

In the uppermost section, from the capacity and the slanting head lines, the type or the specific speed, shown as an ordinate, is determined, and at the right the corresponding optimum efficiency is given.

Similarly in the middle section, the characteristic size, as defined by Equation [2], is determined, and at the right the corresponding size effect or the reduction of efficiency is given. By multiplying the optimum efficiency with the size effect, for a given capacity and head per stage, the best efficiency for the unit may be figured.

While the values of the specific speed and size are designated, they could be omitted and only the corresponding efficiencies marked, thus avoiding these terms altogether; however, they are given because, by their continued use, a certain "feel" of the pumps may be obtained, e.g., the ratio of impeller width to its diameter by the specific-speed term, or linear dimension of the volute outlet within the pump, by the size term. The discharge-nozzle diameter, which is used in the trade to differentiate pump sizes, is far from being a characteristic figure and was adopted because it is an easily measurable dimension.

In the third and lowest section, the ordinate is the head per stage and the constant-efficiency lines, obtained from the two upper sections, are shown. This section alone gives the final values directly, so that the others could have been omitted. On the other hand, further developments and later modifications to include such important effects as viscosity should be made by alterations of either or both of the first two steps, thus making such changes easily comparable with the data herein outlined.

Looking over the optimum-efficiency curve, it is found to be going up with the specific speed toward a maximum for the full range. On the other hand, for a given capacity, higher specific speed means less head per stage, or more stages for a given pressure; it is evident that the gain beyond $n_s = 1500$, with an optimum efficiency of 90 per cent, is very slight and slow, so that there is not much reason to go beyond this point. Contrasted with this, at a lower range of specific speeds, there is a gain of 10 points or 13 per cent from 500 to about 800, which is certainly worth while.

Similar statements can be made of the change of efficiency as a function of size, which also shows much greater effect at its lower end, although it is less pronounced.

It should also be noted that by doubling the number of stages the specific speed or type number is increased to 168 per cent of its former value, there being simultaneous increase in the characteristic-size term, which increases to 119 per cent of its former value; both are advantageous from an efficiency standpoint, and particularly effective for low capacities.

The efficiencies, obtained in the third section from the two sections above it, are straight lines for constant efficiency; the equation of the uppermost, 66 per cent efficiency line, is $q = 0.04\ h^{1.25}$ and that of the lowest, 89 per cent efficiency line, is $q = 0.2h$.

These compared with the constant specific-speed lines, the equation of which is $q/h^{1.5} =$ constant (not shown), indicate that the greatest deviation from them is at small sizes and low specific speeds, as expected.

The head per stage is also given in psi with a specific-gravity correction scale to get it from the foot per stage on which the diagram is based.

Pipe-line pumps of today are proved and satisfactory machines. For capacities of 10,000 bbl per day and over, they are built as horizontal machines. They are axially and radially well-balanced units, as illustrated in Figs. 2, 3, and 4.

The pump cases are of the volute type without diffusers and with external crossovers from stage to stage. Cases are axially split, bolted together with heavy bolts, permitting the assembling of the complete rotating element and mounting it in the case as a unit.

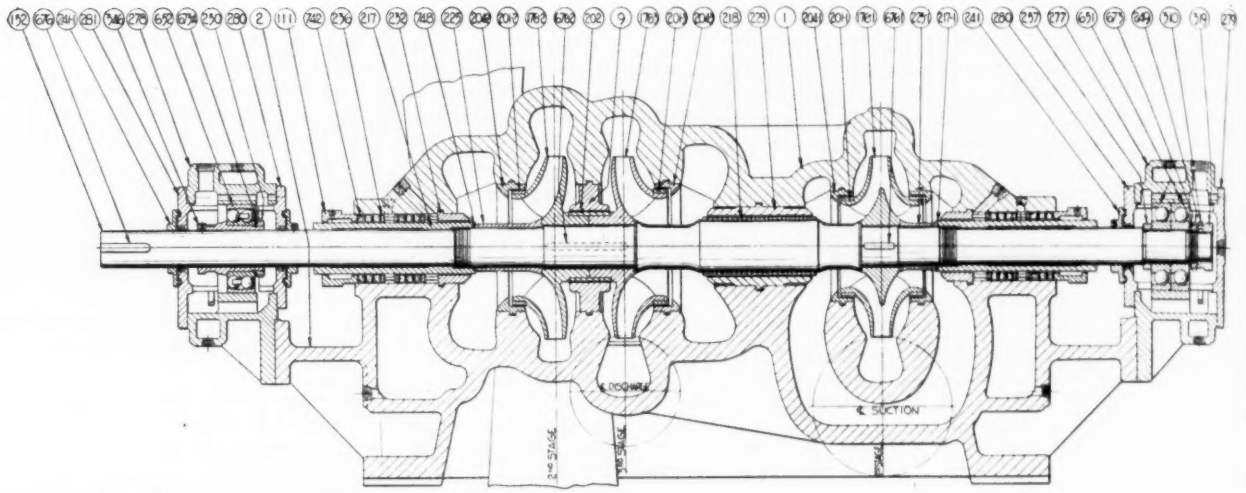
For different conditions, two complete rotating elements can be furnished for any one pump. By initially furnishing large-diameter runners and later reducing such diameters, lower volumes and pressures are obtained. Lately this practice has been extended by suitable design to provide for a change in impellers to secure larger volumes and increased pressures. Optimum efficiencies with full- and reduced-diameter impellers are practically unimpaired.

As an example of this practice, the Plantation Pipe Line Company (5) pumps are to be started with a capacity of 60,000 bbl per day which later on is to be extended to 90,000 bbl per day, doubling the resistance of the line and the number of stations. The first pumps are provided with low-capacity impellers, but have also been tested with the future high-capacity impellers, so that all the units can be used for the final conditions, requiring only that the impellers be changed. Fig. 5 shows the performances, which indicate only a slight sacrifice for the starting conditions. The explosion-proof motors at the start will have fans for 600 hp, later to be changed to fans of greater volume for 900 hp, which is the electrical design load of the units.

The electric motors for centrifugal pipe-line pumps are of high efficiency and lately, as a rule, of explosion-proof type. If explosion-proof motors are not used, the pump and motor are usually separated by a fire wall. The motor drives the pump by means of a shaft operating in a stuffing box in the fire wall. The stuffing box prevents the passage of flame from one room to the other. In both cases the motor is air-cooled.

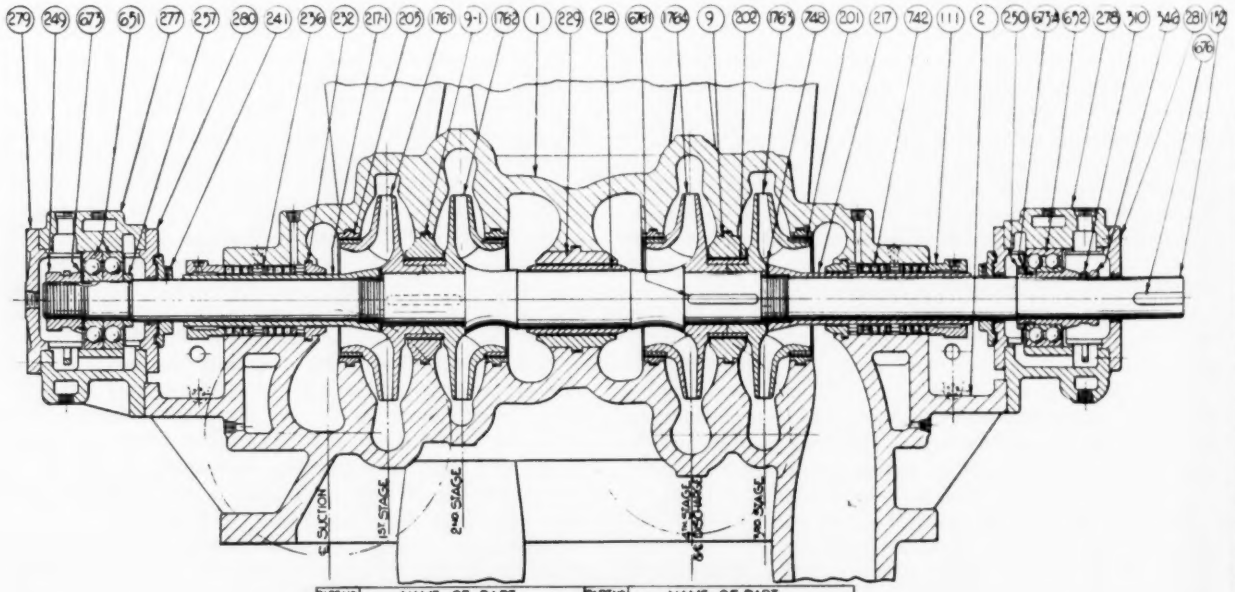
Precautions are taken to minimize dust entering the motor room, even though considerable air is needed for cooling the large motors. It seems that cooling by the pumped liquid would be more rational. Pumping units called by their inventors the Rannett type, with the motor cooled by the pumped liquid, were built for one gasoline line and were quite successful Their price is high because of various special structural features, including a fluid jacket, which surrounds the stator of the motor, to take away the heat, and which jacket has to stand the full line pressure. Such a unit is illustrated in Fig. 6.

To obtain good efficiency with small-capacity pumps, the specific speed and the characteristic size have to be increased, which means low head per stage and many stages. The first objection to many stages is the critical speed. This was serious until pumps were made to run below the first critical; however,



PART NO.	NAME OF PART	PART NO.	NAME OF PART	PART NO.	NAME OF PART
1	CASE - UPPER HALF	217	SHAFT SLEEVE-HIGH PRESSURE	279	COVER-CLOSED END BEARING
2	CASE - LOWER HALF	217-1	SHAFT SLEEVE - SUCTION	280	COVER - INSIDE BEARING
9	STAGE PIECE	218	SHAFT SLEEVE - INNER	281	COVER - COUPLING END
111	GLAND	229	SPACER SLEEVE-HIGH PRESSURE	310	OIL RING
152	SHAFT	229-1	SPACER SLEEVE - SUCTION	319	OIL RING RETAINER
176-1	IMPELLER - 1ST. STAGE	239	BUSHING - CENTER	346	SLEEVE - RADIAL BEARING
176-2	IMPELLER - 2ND STAGE	232	THROAT BUSHING	651	BALL BEARING - THRUST
176-3	IMPELLER - 3RD STAGE	236	CAGE RING	652	BALL BEARING-RADIAL
201-1	IMPELLER WEAR RING- 1ST STAGE	241	DEFLECTOR - INBOARD	673	LOCK - THRUST BEARING
201-2	IMPELLER WEAR RING-2ND STAGE	241-1	DEFLECTOR - OUTBOARD	673-A	LOCK - RADIAL BEARING
201-3	IMPELLER WEAR RING - 3RD STAGE	249	THRUST BEARING NUT	676	KEY - COUPLING
202	IMPELLER HUB WEAR RING	250	RADIAL BEARING NUT	676-1	KEY - IMPELLER - 1ST STAGE
204-1	CASE WEAR RING - 1ST STAGE	257	SHAFT LOCATING RING	676-2	KEY - IMPELLER-2ND & 3RD STAGES
204-2	CASE WEAR RING - 2ND STAGE	277	HOUSING-THRUST BALL BEARING	742	PACKING
204-3	CASE WEAR RING - 3RD STAGE	278	HOUSING-RADIAL BALL BEARING	748	GASKET - SHAFT SLEEVE

FIG. 2 TYPICAL SECTIONAL ELEVATION OF THREE-STAGE OIL-PIPE-LINE PUMP



PART NO.	NAME OF PART	PART NO.	NAME OF PART
1	CASE - UPPER HALF	241	DEFLECTOR
2	CASE - LOWER HALF	249	THRUST BEARING NUT
9	STAGE PIECE - 3RD & 4TH STAGES	250	RADIAL BEARING NUT
9-1	STAGE PIECE - 1ST & 2ND STAGES	257	SHAFT LOCATING RING
111	GLAND	277	HOUSING-THRUST BALL BEARING
152	SHAFT	278	HOUSING-RADIAL BALL BEARING
176-1	IMPELLER - 1ST. STAGE	279	COVER-CLOSED END BEARING
176-2	IMPELLER - 2ND STAGE	280	COVER - INSIDE BEARING
176-3	IMPELLER - 3RD STAGE	281	COVER - COUPLING END BEARING
176-4	IMPELLER - 4TH. STAGE	310	OIL RING
201	IMPELLER WEAR RING	346	RADIAL BALL BEARING SLEEVE
202	IMPELLER HUB WEAR RING	651	THRUST BALL BEARING
205	CASE WEAR RING	652	RADIAL BALL BEARING
217	SHAFT SLEEVE-HIGH PRESSURE	673	LOCK - THRUST BEARING
217-1	SHAFT SLEEVE- SUCTION	673-A	LOCK - RADIAL BEARING
218	SHAFT SLEEVE - INNER	676	KEY - COUPLING
229	BUSHING - CENTER	676-1	KEY - IMPELLER
232	THROAT BUSHING	742	PACKING
236	CAGE RING	748	GASKET - SHAFT SLEEVE

FIG. 3 TYPICAL SECTIONAL ELEVATION OF FOUR-STAGE OIL-PIPE-LINE PUMP

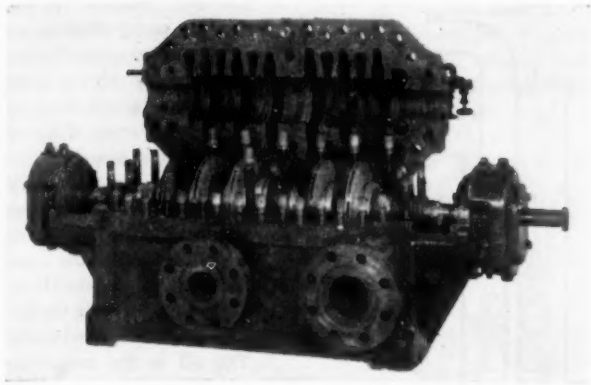


FIG. 4 SPLIT-CASE FEATURES COMMON TO ALL PIPE-LINE PUMPING EQUIPMENT BUILT BY UNITED STATES MANUFACTURERS

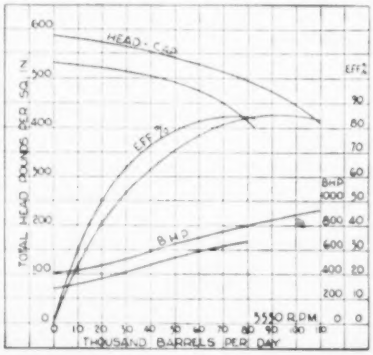
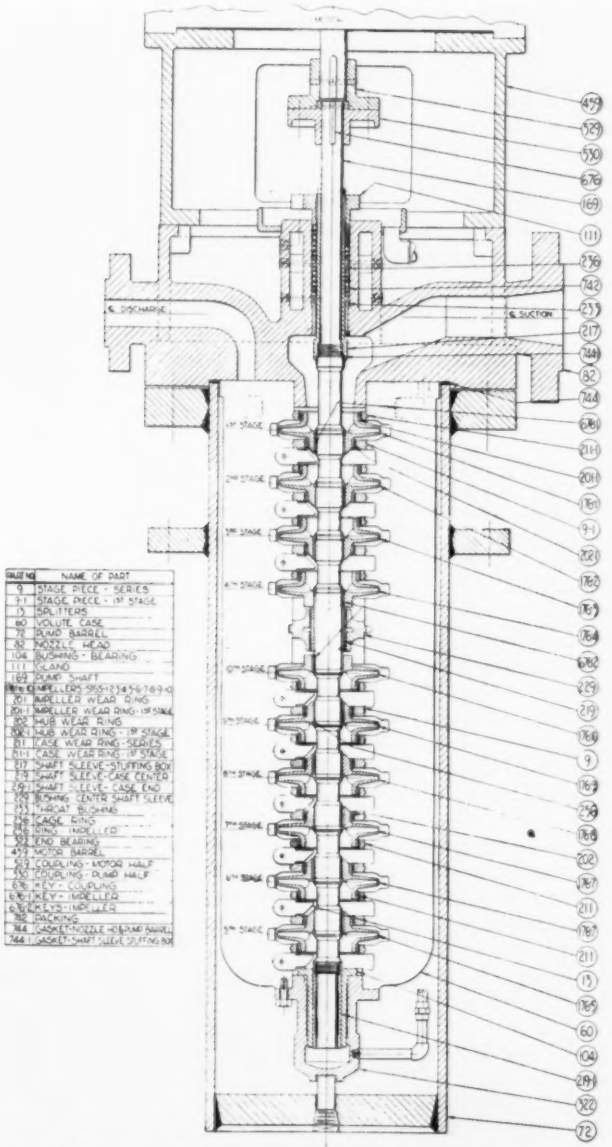


FIG. 5 PERFORMANCE CURVES OF 8-IN. BY 10-IN. THREE-STAGE PIPE-LINE PUMP WITH HIGH- AND LOW-CAPACITY IMPELLERS FOR PLANTATION PIPE LINE COMPANY



FIG. 8 PARTIALLY DISMANTLED VERTICAL-SHAFT DOUBLE-CASE MULTISTAGE OIL-LINE PUMP, SHOWING INNER SPLIT-CASE PUMPING ELEMENT PULLED FROM ITS OUTER-CASE ENCLOSURE



PART NO.	NAME OF PART
9	STAGE PIECE - SERIES
9-1	STAGE PIECE - 1ST STAGE
15	SPLITTERS
60	VOLUTE CASE
72	DIAM BARREL
82	NOZZLE HEAD
104	BUSHING - BEARING
111	GLAND
169	DIAM SHAFT
169-A	IMPELLERS 9RS-1-2-3-4-5-6-7-8-9-10
201	IMPELLER WEAR RING
201-1	IMPELLER WEAR RING-1ST STAGE
202	HUB WEAR RING
202-1	HUB WEAR RING - 1ST STAGE
211	FACE WEAR RING - SERIES
211-1	CASE WEAR RING - 1ST STAGE
217	SHAFT SLEEVE-STUFFING BOX
239	SHAFT SLEEVE-CASE CENTER
240	SHAFT SLEEVE-CASE END
242	BUSHING CENTER SHAFT SLEEVE
253	THROAT BUSHING
259	STAGE RING
269	RING - IMPELLER
522	END BEARING
492	MOTOR BARREL
523	COUPLING - MOTOR HALF
530	COUPLING - PUMP HALF
676	KEY - COUPLING
676-1	KEY - IMPELLER
676-2	KEYS - IMPELLER
782	PACKING
784	GASKET-NOZZLE HEAD-DIAM BARREL
744-1	GASKET-SHAFT SLEEVE-STUFFING BOX

FIG. 7½ SECTIONAL ELEVATION OF VERTICAL-SHAFT DOUBLE-CASE MULTISTAGE OIL-PIPE-LINE PUMP

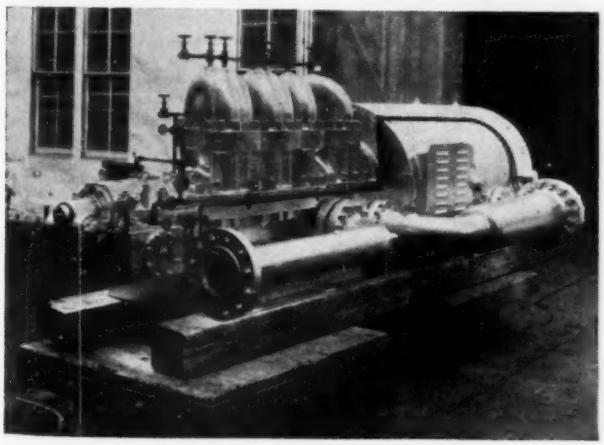


FIG. 6 RANNETT MULTISTAGE OIL-PIPE-LINE PUMP WITH MOTOR COOLED BY PUMPED LIQUID

today they are made to run between the first and second critical, so that the unit has to be quite long to come near to the latter. This requirement in most cases is not a serious limitation. The initial bending, due to the weight of the rotating element, for small horizontal units can be eliminated by making them vertical. Such a vertical unit is illustrated in Figs. 7 and 8. These vertical units have a single stuffing box and a solid coupling between pump and motor, which latter carries any slight thrust of the pump. While horizontal units are as a rule limited to eight stages, vertical units have practically no limitations, but there is no object in going above the specific speed of about 1200, as for small capacities the head would become impractically low.

Special consideration must be given to the stuffing-box pressures in selecting centrifugal pumps for pipe-line duty. When centrifugal pumps were first used in pipe-line work, frequently two separate pumps were operated in series. This meant that the second-unit stuffing boxes were subjected to high pressures. Generally, the crude oils handled were reasonably good lubricants and wear on the well-lubricated packing was satisfactorily low.

Stuffing boxes are made with or without pressure-breakdown bushings and bleeder lantern rings. Pressures on the external packing may be reduced by providing a leak-off to the first suction.

Gasoline pumps, from which leakage constitutes an important loss and because gasoline is a rather poor lubricant, were first made in a single unit for the whole pressure, so that there were only two stuffing boxes, both of which were under low pressure. Later on, with improved shaft-sleeve materials, such as stellited chrome steel, and increased size of the pumps, the gasoline as well as the crude-oil pumps were separated into two units operated in series, the second unit having high pressure on the stuffing boxes, the leakage being bled back to points of lower pressure. Like all stuffing boxes, they are a nuisance, as special pumps have to be provided to pump the leakage back to the line from an underground tank, which stores this leakage until it is repumped.

No matter how good the stuffing box, it is an anomaly and the final solution of the pipe-line pump stuffing box will be its complete elimination. While this goal is not yet fully attained, there are a number of units of the so-called stuffing-boxless type in service, pumping light fractions and gasoline, where both the pump and motor are submerged in the liquid pumped. The stuffing-boxless units now in the field are using an oil-filled motor. The oil in the motor and the pumped liquid are separated by a mercury seal with a balance line equalizing the pressure on both sides of the seal. This unit, which is built in a vertical type and has no stuffing box, is independent of the system pressure, so that a combination of units for any pressure or volume is easily possible. The advantages, of course, are a much greater variation in capacity with good efficiency for the line, the good efficiency being obtained because of the lack of throttling which is possible with the use of a number of units.

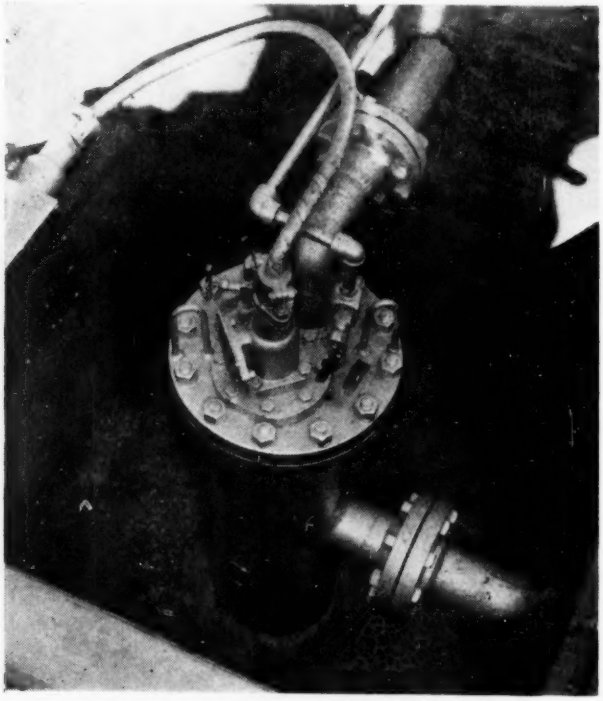


FIG. 9 TYPICAL STUFFING-BOXLESS INSTALLATION

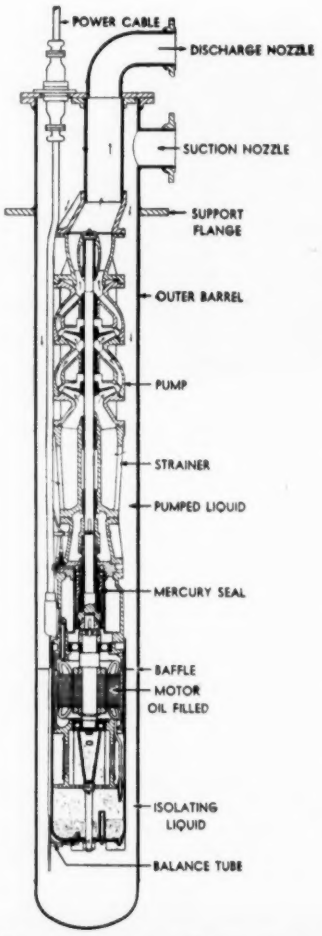


FIG. 10 SECTIONAL ELEVATION OF STUFFING-BOXLESS PUMP REVEALS CONSTRUCTION PRINCIPLE AND WORKING ELEMENTS

The automatic or semi-automatic stations which are becoming more and more general would become very simple with the use of stuffing-boxless units, inasmuch as the pump house would be eliminated, and only a control chamber required.

At present, units up to about 50 hp are fully developed. These have some limitations, e.g., that the pumped oil can contain but little sulphur, in order not to create an emulsion with the mercury in the seal.

As the stuffing-boxless pump and motor are put in a single barrel, with the suction and discharge nozzles and the cable connection in the cover of the barrel, a subterranean pit is all that is needed to serve as a pump and motor room for the head of the pump, the control panel being located some distance away. Stations built in this manner, can be readily made bombproof. These units are more suitable for automatic operation, as the number of control items is materially reduced by the elimination of the stuffing box. Furthermore, not having a stuffing box makes the automatic separation of the units from the line, when the unit is not working, unnecessary. It seems that the ultimate design of pipe-line stations will use such units as soon as they are fully developed and proved.

Figs. 9 and 10 show a stand-by plant pumping butane (6). Figs. 11 and 12 illustrate a proposition covering pipe-line pumps for a foreign government (7).

OPERATING SCHEDULES FOR PIPE LINES

Under this heading, it may be well to mention the great advance

made in keeping the pipe lines clean, when they are laid, and thus saving the pumps from being "shot" right at the start. After all, high efficiencies are obtained with close clearances, and these can only be maintained with clean liquids. Any precaution in this direction will pay for itself many times in power and maintenance costs.

The other great advance is the cathodic protection of the pipe lines from corrosion, and the maintenance of clean inner surfaces by scrapers, which may be run through without interruption of the flow.

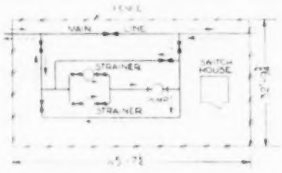


FIG. 11 STUFFING-BOXLESS STATION FOR PROJECTED GASOLINE PIPE LINE (7)

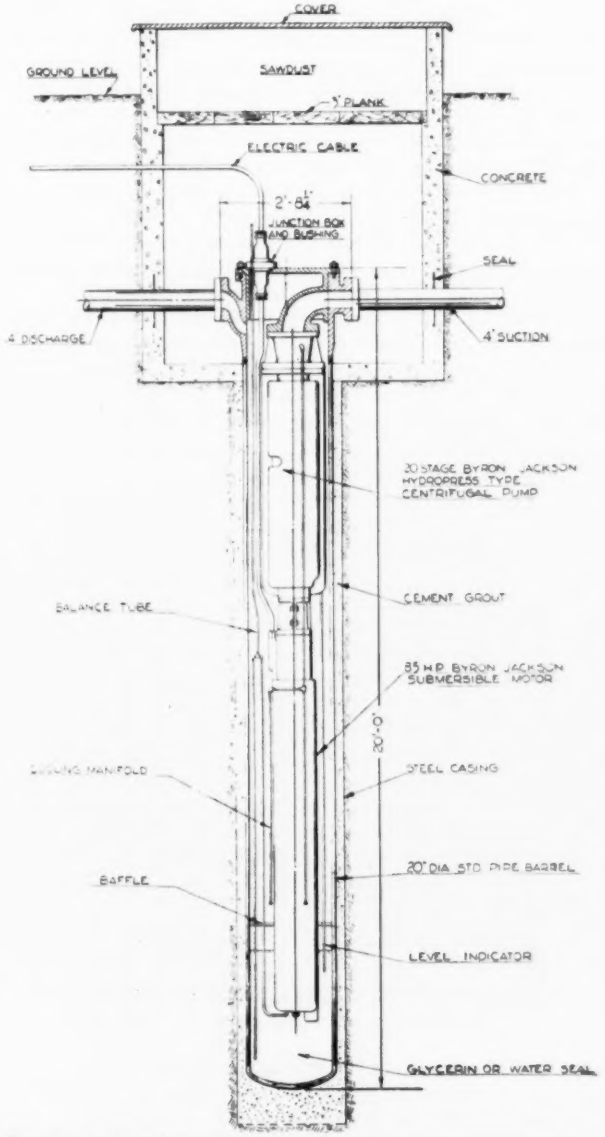


FIG. 12 CROSS SECTION OF MAIN-LINE PUMP FOR PROPOSED STATION SHOWN IN FIG. 11

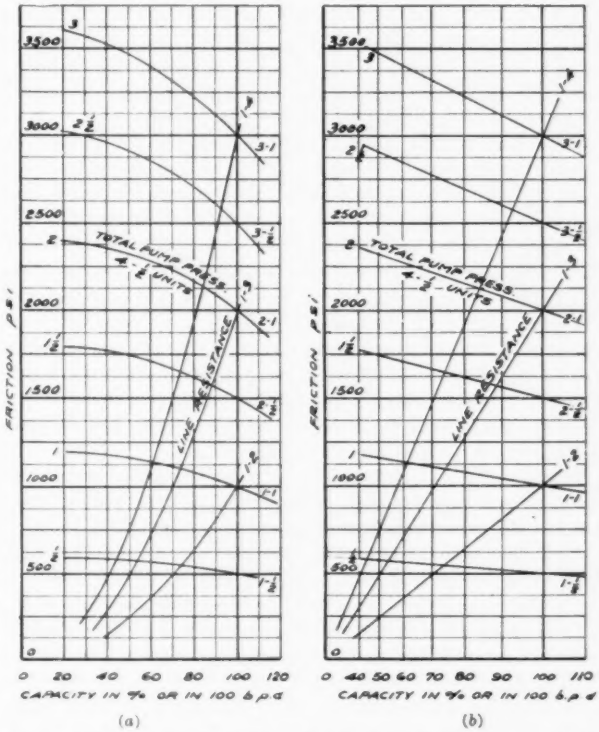


FIG. 13 PIPE-LINE FRICTION LINES AND PUMP-PERFORMANCE CURVES FOR PIPE LINE WITH THREE STATIONS AT SAME ELEVATION, EACH WITH TWO IDENTICAL HALF UNITS

Operating schedules of a pipe-line system pumping a single crude, gasoline, or other products are quite complicated problems, particularly if there are many pumping stations, which are also take-off points for given percentages of the oil pumped in definite time intervals. As the line friction is increasing approximately with the 1.75 power of the capacity, the lowest rate of pumping to get the required total for a definite period is the most economical, even if the pumps do not work at their best efficiency. As half pressure means close to three-quarters capacity, and a third pressure more than one-half capacity, the power saving by pumping at low rates is very large. It is a surprise to outsiders to find how small is the total quantity actually pumped, compared with the maximum possible for continuous operation, 24 hr, 365 days a year (8).

It is, of course, understood that the pipe line would earn more by continuous full-load operation and, like the railroads, tries to get all the load which it can handle, but seemingly the full load, at least in the past, was not available.

Many limitations are to be considered in these schedules for partial loading, among them the maximum permissible pressure on the line, the minimum inlet pressure to the pumps, the minimum gradient between stations that goes over the local peaks and the changed loading after each take-off, etc. All these are automatically satisfied at full rate of pumping, for which the line is designed, and also at any lower capacity, if that is obtained by throttling. The problem is to obtain the lower rate of flow with as little throttling as possible. As the dispatcher must have an immediate answer to all conditions, the most economical schedules had to be worked out in advance taking into account all the bottlenecks.

A late development hardly mentioned in the literature is the transformation of some lines designed for a single product to transport many products of different character, as a number of grades of gasoline, kerosene, furnace oil, etc. The scheduling of

such lines, with plugs of different oils of various lengths in the line is even more complicated, as the increased number of take-offs at each station, because of the different products, leads to many more combinations, and because the contamination plugs between the products have to be specially handled.

The charting of a simple constant-diameter line with three stations at the same elevation and an equal distance from one another, each operating with two identical pumps in series (called one unit) at full load, is shown as an example in Fig. 13. For simplicity's sake, the friction lines are shown as second-degree parabolas, Fig. 13*a*. The diagram shows that operating one-half unit at the first station will give 45 per cent capacity, one full unit 61 per cent, one and a half units 72 per cent, two units 83 per cent, and, of course, three full units 100 per cent capacity.

It is proposed to simplify this charting by making the capacity scale a power scale, corresponding to the exponent of the capacity as function of the head, in this case 2, but it could just as well be 1.85 or any other figure.

This is fully justified, particularly for gasoline and heavier products, and even for most of the crude lines, because in practice the Stanton Pannell friction-coefficient line as a function of Reynolds number is shown as a line, flattening out only at high Reynolds number, and elongated as a matter of safety until it meets the viscous-flow line, thus avoiding the uncertain range (9, 10). Flow rates in the viscous range are, as a rule, excluded. To have a single power, that is, substituting a straight line for this coefficient in a logarithmic scale, means that the friction head may be expressed as a power below 2 of the flow rate, thus taking account of the variation of the friction coefficient for the different capacities.

For different oils, different scales may be made, but in most cases this will be unnecessary; it will be sufficient to change the friction-loss figure to agree with the actual test or expected value for a given capacity and use the same capacity scale.

If the ordinate representing the pressure remains linear, the former parabolic or exponential functions will be straight lines, which can be easily drawn. Furthermore, if the pump performance curves are plotted in this scale, they will be found to be remarkably close to a straight line, thus also determined by two points. Fig. 13*a* is repeated in Fig. 13*b* illustrating the simplicity of the method.

Static-head differences are taken care of by drawing a line parallel to the friction lines, at a distance of the elevation difference refigured in psi. Different distances between stations mean a proportional reduction of friction at a given capacity, therefore are also determined by one point. Different pump performances are characterized by two pressure points, e.g., those at one-half and full capacity; they are just as easily added as identical ones. When the number of stations is great and all these factors are varying, the saving of work with this method will be appreciable. Some other applications of this method are illustrated by a few different problems.

Problems of Looping Lines, Equivalent Length, and Take-Offs

(*a*) A problem very often encountered is the looping of the line. As a concrete example of this, a pipe line 30 miles in length, with a friction resistance of 800 psi at 10,000 bbl per day capacity, is to be looped with a line of the same size, so that its capacity is increased to 12,000 bbl per day without changing its resistance The question is what is the length of the loop. The solution is shown in Fig. 14, which has a capacity scale with 1.85 exponent.

Line *OA* represents the original friction line, H_3 the pressure at 100 per cent capacity. Elongating this line to the 120 per cent capacity (point *B*) we see that without looping it would have 1110 psi friction (H_1). Looping the line with the same size of pipe means that at any pressure the capacity is doubled. Taking the 50 per cent capacity line, the friction pressure will be *CD*, which will prevail for a looped line at 100 per cent capacity (point *E*). Line *OE* represents the friction characteristics of a looped line for the full length which, elongated to 120 per cent capacity, will give point *F* and the corresponding pressure H_2. The requirement is that the pressure H_3 be maintained. If the loop length is x per cent of the full length, then the friction at 120 per cent capacity can be expressed as xH_2 for the looped

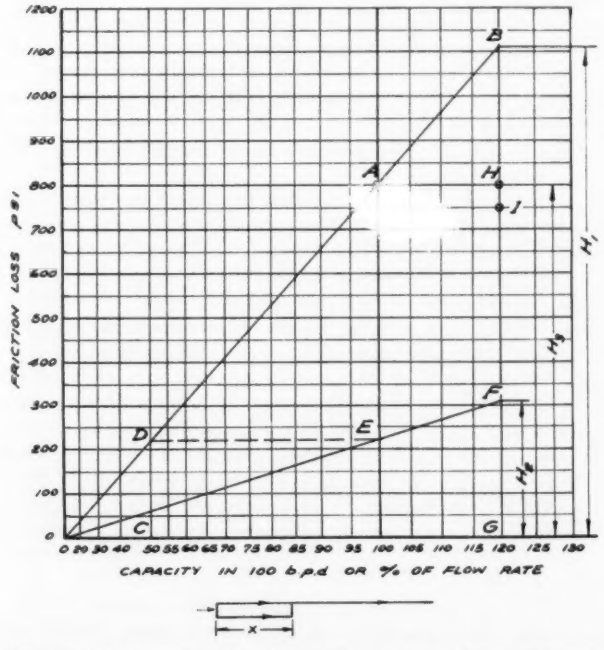


Fig. 14 Determining Length of Loop x for Given Pressure Drop at Given Capacity

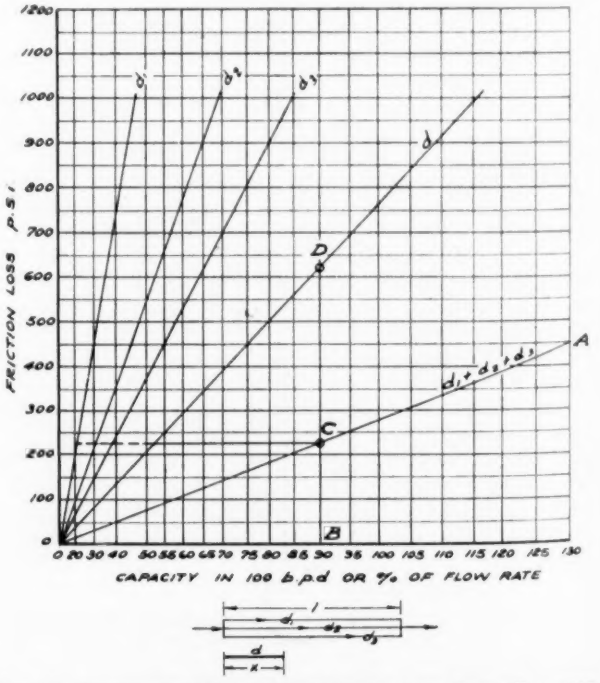


Fig. 15 Determining Equivalent Length x for Given Diameter d of Looped Line of Three Members at a Definite Flow Rate

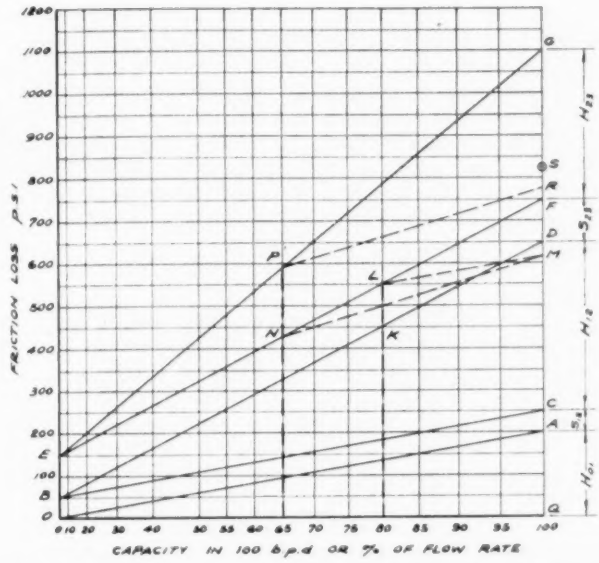


FIG. 16 LINE PRESSURE FOR PIPE LINE HAVING THREE DEPOTS, WITH SPECIFIED SIMULTANEOUS TAKE-OFF CAPACITIES

length and $(1—x)H_1$ for the single line remaining, the sum of these being equal to the total pressure H_3

$$H_3 = xH_2 + (1 - x)H_1$$

and from this

$$x = \frac{H_1 - H_3}{H_1 - H_2} = \frac{310}{800} = 38.7 \text{ per cent or } 4.65 \text{ miles}$$

If the problem required a reduction of the line pressure to 750 psi, the looped length would be

$$x = \frac{1110 - 750}{1110 - 310} = \frac{360}{800} = 45 \text{ per cent or } 5.4 \text{ miles}$$

Similarly, if the pipe size were different, it would mean only adding a different capacity at the same pressure for the determination of point E and proceeding the same way. It is the proportionality of the friction with the length which makes the solution so simple.

(*b*) A problem solved the same way is the substitution of a single line for a looped line, and finding the equivalent length which gives the same resistance for a given capacity.

Assuming that there are three lines in parallel of the same length and of d_1, d_2, and d_3 diameters with the friction characteristics as shown in Fig. 15; the equivalent length of a line of d diameter with known friction characteristics is to be determined. Fig. 15 shows the capacities of the lines composing the loop at 450 lb to be 3000, 4500, and 5500 bbl per day, respectively, so that the total capacity is 13,000 bbl per day (line OA). If the equivalent length of d diameter at a flow rate of 9000 bbl per day is wanted, the line BD is drawn, this being the resistance of line D for the full length. The resistance of the looped line is BC; therefore, the length of line d, to have the same resistance, has to be reduced in the proportion of BC:BD. If the full length is 10 miles, the reduced length will be $L = \frac{225}{625} 10 = 3.6$ miles for a flow of 9000 bbl per day.

The equivalent length for any other capacity can be similarly determined by a single line in place of the laborious calculations formerly used (8). The flow rates in the different members of the loop may be read off and checked to assure that they do not come into the viscous range.

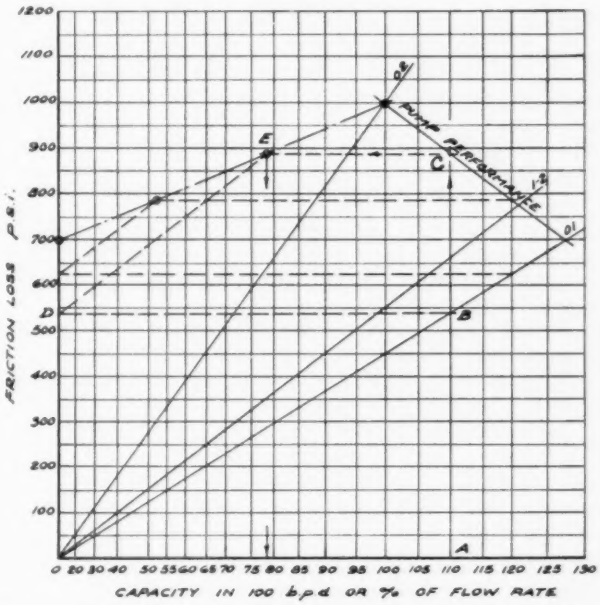


FIG. 17 LINE PRESSURE FOR GIVEN PUMP PERFORMANCE WITH SPECIFIED FLOW RATES AT END OF PIPE LINE, WHICH HAS AN INTERMEDIATE TAKE-OFF

(*c*) A line with intermediate depots and take-offs is the third problem. Suppose the line length to the first depot is 20 miles, from the first depot to the second, 40 miles, and from the second to the last, 35 miles. The corresponding friction resistance at 10,000 bbl per day flow are 200, 400, and 350 psi, respectively, so that the total friction resistance to the end is 950 psi. There is also an elevation difference between the first depot and the second which is equal to 50 psi, and between the second and third, equal to 100 psi.

The question is: If 2000 bbl per day are taken off at the first depot and 1500 bbl per day at the second, what pressure is needed at the pumping station to get 50 psi at the last depot?

The line friction characteristics for the oil pumped are such that the friction varies with the 1.75 power of the flow rate, and the abscissa is laid out accordingly, Fig. 16; H_{01} being the friction for the first section, at 10,000-bbl per day flow rate, line OA being the friction line.

The static-elevation difference between 1 and 2 is S_{12}, while BC is a corresponding line parallel to OA.

The friction from the first to the second depot at 10,000 bbl per day is H_{12}, and BD is the corresponding friction line measured from BC.

Similarly, S_{23}, H_{23}, and lines EF and EG are the corresponding terms between the second and third depots.

The flow to the first depot is 10,000 bbl per day, the resistance being H_{01} = 200 psi. Going to the second depot, the static difference is added, giving a total of 250 psi. Taking off 20 per cent, the flow continues at the rate of 8000 bbl per day; the intersection of a vertical at this capacity with BC and BD is the friction of the second section, which is added to BC by drawing a parallel to BC from K. As the next static head is to be added immediately, the parallel is drawn only from point L, leading to a pressure QM.

The flow from this point on is at a rate of 6500 bbl per day, 1500 bbl per day having been taken off. The friction is given by the intersection of a vertical at this rate, with lines EF and EG; that is, NP. It is added to QM by connecting M with N and drawing a parallel to it from P. The line PR is the pressure at the start with zero pressure at the end. However, as a pressure of

50 psi is wanted there, this is added to QR, giving QS = 825 psi as the required pumping pressure, the answer to the problem.

(*d*) As a final example: Determine the capacity and pressure at which a pump of a given performance will operate, pumping into a line of known friction characteristics with one take-off. The rate requirements at the end station are given, and the difference between them and the pump capacity is taken off at the intermediate depot, Fig. 17.

This problem is solved by assuming a pumping rate and determining how much of it will arrive at the end station; the few points so determined are then connected to give an immediate answer for any rate.

The friction is, for a flow of 10,000 bbl per day, from the pump to the take-off 450 psi, from there to the end 550 psi, a total of 1000 psi, at which the total capacity is pumped to the final depot, this being an intersection point with the pump characteristics.

The intersection of the first-section friction with the pump characteristics gives another point where the total pump capacity, this time 12,750 bbl per day, is taken off at the first depot.

At the rate of 11,000 bbl per day, the first section will have a friction of OB which is projected horizontally over to D, from whence a line is drawn parallel with the second-section friction line. This will intersect the horizontal line drawn from the pump performance curve and total-friction point C at a point E. Reading it below this tells that, out of 11,000 bbl per day pumped, 7800 will get to the end, therefore 3200 bbl per day has to be taken off in the middle.

A similar determination of another point for 12,000 bbl per day is plotted and the four points connected. The line turns out to be straight enough so that the connection of the two end points with a straight line gives a close approximation.

BIBLIOGRAPHY

1 "One Example of Centrifugal Pumps for Petroleum Transportation," by F. E. Warterfield, Jr., Trans. A.S.M.E., vol. 50, 1928, paper PET-50-7.

2 "A 100-Mile Natural-Gasoline Transmission Line," by F. B. Simms, *Western Gas Journal*, April, 1927, pp. 20.

3 "Hydraulics," by R. L. Daugherty, McGraw-Hill Book Company, Inc., New York, N. Y., 1937, Fig. 316, p. 444.

4 "Model and Prototype Tests," by L. M. Davis, Proceedings, American Society of Civil Engineers, vol. 65, 1939, pp. 1575–1589; discussion by W. S. Pardoe; ibid., vol. 66, 1940, pp. 179–180.

5 "Pipe Line Progress in '41," by Paul Reed, *Oil and Gas Journal*, vol. 40, 1941, pp. 57–58.

6 "Use of Pumps Without Stuffing Boxes for Highly Volatile Liquids," by W. A. Sawdon, *The Petroleum Engineer*, vol. 12, 1940, pp. 102 and 104.

7 "Sweden's Projected Gasoline Pipe Line," by H. W. Wickstrom, *World Petroleum*, vol. 11, 1940, pp. 24–26.

8 "Operating-Cost Analysis of Electrified Oil Lines," by W. H. Stueve, Trans. A.S.M.E., vol. 59, 1937, pp. 247–252; discussion Trans. A.S.M.E., vol. 60, 1938, pp. 90–91.

9 "Flow Formulas Used for Design of Gasoline Pipe Lines," by W. E. Rea, *Oil and Gas Journal*, vol. 39, 1941, pp. 38, 40, 45, and 47.

10 "The Design of Oil Trunk Pipe Lines," by Oscar Wolf, *Oil and Gas Journal*, vol. 23, 1929, p. T-166.

Discussion

A. J. Stepanoff.[3] The writer has studied certain phases of this subject in considerable detail, one of which, dealing with the determination of a composite-pipe-line characteristic and location of the operating point on the centrifugal-pump head-capacity curve has been the subject of a recently published paper.[4]

[3] Engineer, Cameron Engineering Department, Ingersoll-Rand Company, Phillipsburg, N. J. Mem. A.S.M.E.

[4] "Determining Operating Points of Centrifugal Pumps Working on Pipe Lines," by A. J. Stepanoff, *Oil and Gas Journal*, vol. 40, Dec. 4, 1941, p. 45.

Although the United States leads in pipe-line construction and establishes standards in this field for the rest of the world, the literature on this subject is very scant so that this paper is a welcome contribution to the published information on this subject.

It is interesting to mention that, when Russia decided to build pipe lines, a group of engineers was sent to this country to learn all they could about our pipe-line practice. Upon returning home, one of these engineers, Professor Pritula at the Moscow Engineering School, wrote a two-volume book on the subject of pipe lines,[5] based entirely on American practice. A one-year course was also started by Pritula at the University of Moscow on petroleum transportation.

A new term "size factor" not commonly used is introduced in the paper. Mathematically it is the square root of the "unit capacity," more widely known. There is one feature about "size factor" which does not appeal to the writer, that is, if the number of stages to get the same head is increased, or less head is developed per stage, the "size factor" will increase, while the actual impeller diameter, and hence the pump over-all dimensions per stage, will decrease.

The question of cavitation in pipe-line pumps still presents a problem. There are many stations which do not carry suction pressures high enough to assure freedom from cavitation. Such stations have floating tanks on the line, the level in these tanks determining the suction pressure on the pumps. Such an arrangement has advantages from the operating point of view. The effect of cavitation under such conditions may appear only in a slight drop of the pump head-capacity curve and efficiency. No vane pitting, noise, or sudden breakoff of the head-capacity curve are observed.

The question of relationship between the pump type or specific speed and efficiency is brought up frequently not only among the pump manufacturers but also by the users and operators of centrifugal pumps. The writer has studied this problem from a different point of view from that presented in the paper. The writer has attempted to demonstrate the reasons for efficiency variation with the specific speed. It can be shown that disk-friction and leakage losses increase very rapidly when the specific speeds of pumps are decreased.

The discussion of the stuffing-box problem is incomplete without mentioning mechanical seals. There are many centrifugal pumps in pipe-line service which have given satisfactory operation for several years, pumping crude, gasoline, and propane with suction pressures of 200 to 400 psi, without injection of lubricant or coolant into the stuffing box.

It is possible that there is a definite field for application of small stuffing-boxless pumps described in the paper. Essentially, however, it is not a pipe-line pump. To the writer's knowledge, no vertical pump, such as shown in Figs. 7 to 12 of the paper, was ever employed for pipe-line service as such. The experience with the Rannett pumps, referred to in the paper, shows that, while the pump house is not necessary for the pump protection when in operation, a building around pipe-line pumps is indispensable for servicing pumps, such as dismantling pumps for replacing parts, storage of spare parts and tools. There are many motor-coupled pumps in the refineries installed in the open air without any weather protection. In such cases, repair-shop facilities are available for servicing pumps. The motor protection and stuffing-box care are not the only problems to be considered when deciding upon the automatic pipe-line pumping stations; maintaining the proper suction pressures on individual stations, when the capacity of the pipe line is varied, is only one of them, a satisfactory solution for which is not yet available.

[5] "Oil Transportation," by A. F. and B. A. Pritula, U.S.S.R. State Publication, 1934; in Russian.

Author's Closure

The foregoing discussion brings out quite properly, that the United States leads in pipe-line construction; and in this connection the author would like to add that the standard pipe-line pumps are a distinctive American product, simpler in design, better in efficiency and reliability, and easier to assemble because of the split-case volute construction than the competing European pumps.

For his preference of the term "unit capacity" in place of the author's "size factor," Mr. Stepanoff gives as a reason that a pump of "larger dimensions" will have a smaller size factor. It is to correct the natural expectation that the larger pump should be also hydraulically bigger as, for example, a pipe would be, that the author used the "size" term which designates true size in hydraulic terms and gives warning that the larger-diameter unit for a given capacity and speed is hydraulically smaller.

Contrary to Mr. Stepanoff's statement that floating tanks on the incoming lines have advantages from the operating point of view, their elimination and the establishment of a closed line is considered as one of the greatest advances in pipe-line operation. This step, besides eliminating the evaporation loss of these tanks, permitted a much greater flexibility of operation of long lines, as it made high pressure on the incoming line possible, instead of limiting it to the height of the floating tank.

As an example, if the three-station pipe line, shown in Fig. 13*b*, is a closed line, it could operate at a flow rate of 83 per cent of normal without any throttling with four half units, two in the first station and one half each in the second and third stations; the suction pressure would be about 370 psi at the second and about 200 psi at the third station. It could also operate at about 88 per cent of the normal flow rate with five half units (two each in the first and second and one in the third station) by throttling 250 psi at the second station.

With floating-tank operation, in both cases six half units would have to be used, thus increasing the power consumption by 50 per cent for the 83 per cent operation and by 20 per cent for the 88 per cent operation. In the first case, a total of 1000 psi, in the second, 750 psi would have to be destroyed by throttling in the second and third stations. Such operations at partial capacities close to normal are quite common on long lines with many stations, whenever smaller take-offs are required at intermediate points.

On closed lines, the maximum pressure on the outgoing line and the minimum pressure on the incoming line is limited by pressure regulators on these lines, set for a predetermined maximum and minimum, respectively, and actuating the throttle valve on the outgoing line from the station. Provision is made that, whenever the pressure on the incoming line rises to half the maximum line pressure, if two pumps are in operation one will shut down. Mr. Stepanoff's statement, that for the maintenance of proper suction pressures on individual stations, when the capacity of the pipe line is varied, no satisfactory solution is yet available, may have been true years ago, but for some time a full line of standard valves and auxiliaries have been available from the best manufacturers and are actually installed on a number of pipe lines.

Concerning vertical double-case pumps with a stuffing box as shown in Figs. 7 and 8, Mr. Stepanoff's statement, "no vertical pump was ever employed for pipe-line service as such," was correct up to six months ago. However, there have been several 150-hp units furnished for the Plantation Pipe Line, chosen on the basis of their long satisfactory performance in similar refinery service and their general application in other fields for ten years.

The author is grateful to Mr. Stepanoff for bringing up the mechanical seals which should have been described as one kind of stuffing box, even though they are not mentioned in any pump manufacturer's catalogue. They rely on the contact or throttling by means of one or two small rotating disks running against stationary surfaces; thus unlike the conventional stuffing box, their failure, because of their short leakage path, is very dangerous particularly for lighter hydrocarbons and high suction pressures. For this reason they may be applicable for clean crudes with some lubricating quality even in automatic stations, but for gasoline and propane, especially without auxiliary lubricating feed, they would not be considered in any station without constant attendance.

It is the elimination of this limitation which makes the stuffing-boxless unit especially attractive as a pipe-line pump for an automatic station. The greater subdivision of the station into smaller units, without limitation of suction pressure, permits more efficient operation at partial capacities without throttling, by simply taking one or more units off the line or putting them on as required. The excellent record of the present pipe-line pumps and motors, contrary to Mr. Stepanoff's opinion, certainly would not call for a building to maintain them. The buildings are there, either because the station has to have a constant attendance, or because of the auxiliaries and complicated control of the automatic stations. With the simplified control of the stuffing-boxless units and no auxiliaries, there may be a structure housing the controls, but the pumping units would require none. The possibilities are indicated by the experience of Byron Jackson Company, builders of these units, with a 20-hp propane loading pump, similar to Fig. 12, located 10 miles from the loading station without any building. This unit has been in operation for three years up to the present time, without any servicing or attendance. The development of large units, already under way but interrupted by the war, will constitute a great advance in the realization of a simple and reliable automatic station.

Test Stand for Centrifugal and Propeller Pumps

By G. F. WISLICENUS,[1] HARRISON, N. J.

This paper describes a new test stand for experimental investigations on centrifugal- or propeller-type pumps, as well as on pump installations. The test stand is particularly suited for a complete determination of the cavitation characteristics of the test pump and for reliable control of the flow conditions at the pump inlet.

THE test stand which will be described in this paper is located at the Harrison Works of the Worthington Pump and Machinery Corporation. It was developed for the purpose of experimental investigations and model studies on pumps of the centrifugal and propeller type. Beyond this general purpose, the design of the test stand is intended to satisfy the following specific requirements:

1 To offer means for a reliable determination of the hydraulic operating characteristics of radial-flow, mixed-flow, or axial-flow pumps up to 150 hp, with particular attention to the cavitation characteristics of these machines. The test pumps are subjected to certain limitations regarding size and mechanical construction, since it is not intended that this equipment be used for routine tests on commercial pumps with widely varying mechanical arrangements.

2 To provide sufficient space for modeling, not only the pump, but also the entire pump installation; in particular, the inlet structure.

3 To prevent the throttle valve or any other part of the test circuit from having any disturbing influence on the flow conditions at the inlet of the test pump.

Figs. 1 and 2 show the general arrangement of the test stand.

The Test Circuit

For convenient observation of the cavitation behavior of a pump, it is desirable to vary the inlet and discharge pressures of the test pump simultaneously in such a manner that the difference between these two pressures remains essentially unaltered. In this way, it is possible to study the effect of changes in the inlet head on the pump performance without changing the other operating conditions of the pump. Such simultaneous variations in the inlet and discharge pressures of the test pump can be obtained most simply by the use of a closed test circuit, i.e., a test circuit which at no place is open to atmospheric pressure. The most important pump test stand with closed circuit, so far discussed in the technical literature, is that of the hydraulic machinery laboratory of the California Institute of Technology.[2] The hydraulic-turbine test stand of the Baldwin Southwark Corporation is of the same type.[3] Since Worthington engineers have been in intimate and prolonged contact with the hydraulic machinery laboratory of the California Institute of Technology and were permitted to study the test stand of the Baldwin Southwark Corporation, it is natural that the design of the new test stand was considerably influenced by these two laboratories. On the other hand, the special requirements listed previously lead to an entirely new form of design, borrowing merely a number of general principles from the laboratories just mentioned.

The test circuit of the new test stand, Fig. 1, consists of the test pump, the discharge-pipe system of the test pump, the Venturi meter, the main throttle valve, the stilling tank, and the inlet tank.

The test pump, in all cases, has a vertical shaft. This arrangement was chosen for the following reasons:

1 An ever-increasing number of important pump installations are being built with vertical shafts.

2 Vertical-shaft installations are more likely to require model studies of the inlet structure than pump installations with horizontal shafts.

3 The vertical-shaft arrangement seems to permit a simpler and less expensive mechanical construction of the test pump.

4 It was felt that a vertical-shaft driver offered certain advantages as a dynamometer.

5 It is possible to investigate the hydraulic characteristics of horizontal-shaft pumps by means of model pumps with vertical shafts, excepting extremely large units and installations where an inlet structure with a free water surface has to be included in the model.

Fig. 1 shows an axial-flow test pump, because up to the present the test stand has been used chiefly for investigations on this type of pump. By changing the pump-discharge line, it is possible to test axial-flow pumps of different lengths, as well as mixed-flow or radial-flow (centrifugal) pumps. The test pump is located either on the upper deck of the inlet tank, as shown, or inside of the suction tank with the discharge pipe passing through an opening in the tank wall opposite the stilling tank.

The pump shaft is guided in two bearings with water and grease lubrication. The upper bearing serves as a shaft seal. The small basin on top of the upper bearing collects the leakage if the pump-discharge pressure is above the atmospheric. For discharge pressures below the atmospheric, this basin provides an airtight water seal, using an outside water supply. The test pump does not need to have any thrust bearing. The pump thrust can be transmitted by a special coupling (see discussion of dynamometer) to the dynamometer motor. This arrangement simplifies the mechanical construction of the test pump and eliminates to some extent the uncertain element of stuffing-box friction.

The pump-discharge line above the Venturi-meter vane elbow should be considered rather as part of the particular pump on test than as a part of the permanent test equipment and has to be changed in accordance with the varying requirements of the test pump.

---

[1] Hydraulic Engineer, Worthington Pump & Machinery Corporation. Mem. A.S.M.E.

[2] "Hydraulic Machinery Laboratory at the California Institute of Technology," by R. T. Knapp, Trans. A.S.M.E., vol. 58, 1936, pp. 663–676.

[3] "Cavitation of Hydraulic-Turbine Runners," by R. E. B. Sharp, Trans. A.S.M.E., vol. 62, 1940, p. 567.

"Cavitation," by L. F. Moody, *Baldwin Southwark*, third quarter, 1938, pp. 14–21; and "Cavitation Study," by K. W. Beattie, *Baldwin Southwark*, September, 1940, pp. 20–24.

Contributed by the Hydraulic Division and presented at the Annual Meeting, New York, N. Y., December 1–5, 1941, of The American Society of Mechanical Engineers.

Note: Statements and opinions advanced in papers are to be understood as individual expressions of their authors and not those of the Society.

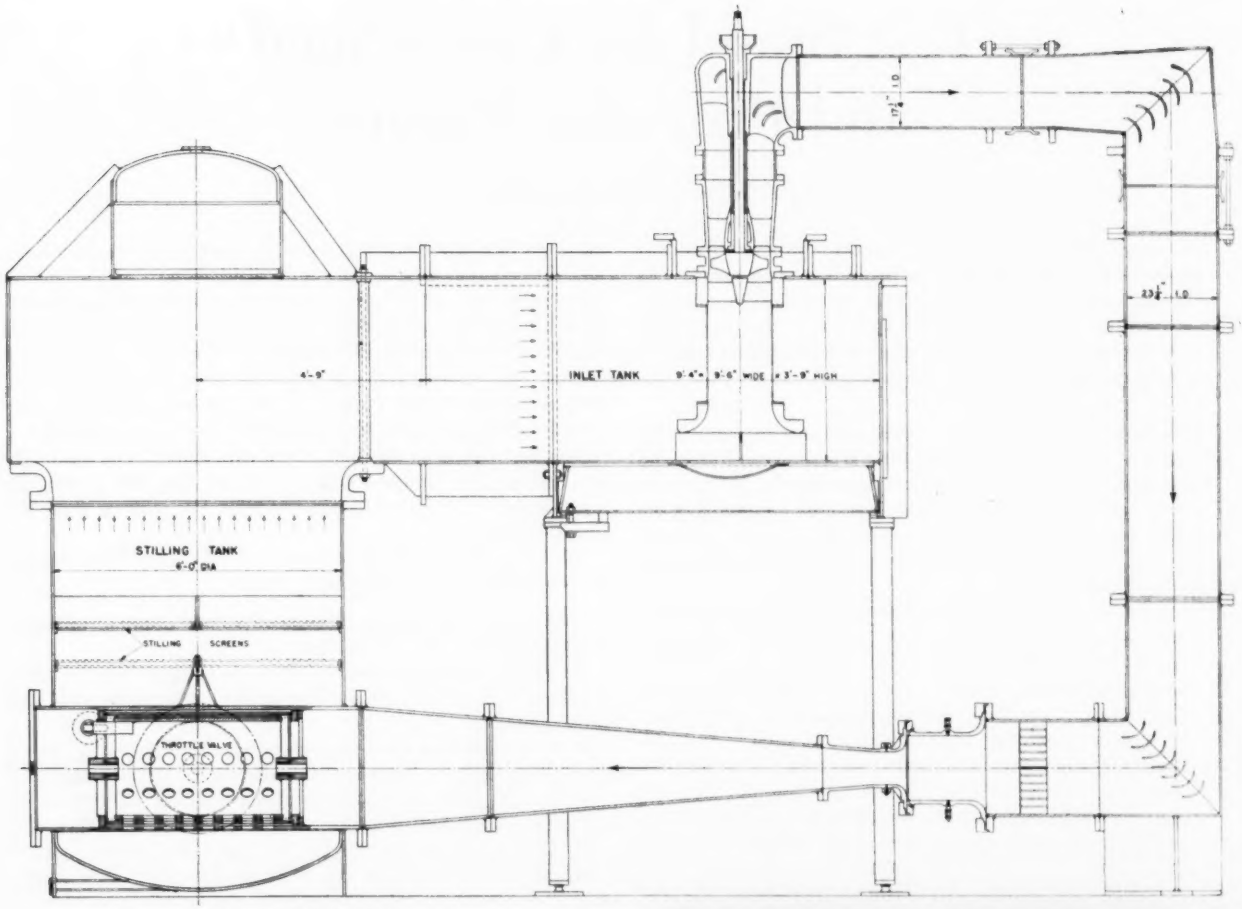


FIG. 1 TEST CIRCUIT

The Venturi meter has so far been used without calibration, since the present investigations require comparative results rather than absolute accuracy. The calculated coefficient can hardly differ more than 1 per cent from its true value, but an exact calibration will be made as soon as the general test program will permit this interruption.

It is seen from Fig. 1 that the approach to the meter is carefully guarded by vanes and a honeycomb. In order further to reduce any influence from irregularities in the approaching stream, the conduit has been given a contraction immediately in front of the first measuring station. (This method has been used before in the laboratory of the California Institute of Technology.) The Venturi-meter throat is easily removable so that throats of different diameters can be inserted to cover various ranges in capacity. Four throats from $4^1/_2$ to $10^1/_2$ in. diam are available. (Fig. 2 shows one of these Venturi throats standing on the ground floor.)

The main throttle valve, Figs. 1, 3, and 4, is located in the lower part of the stilling tank at the end of the long discharge cone of the Venturi meter. The throttle valve consists of four concentric cylinders with 64 radial $2^7/_8$-in-diam holes and a number of smaller holes, Figs. 3 and 4. The first and the third cylinder, counting from the inside, can be rotated by about one half the angle between two successive longitudinal rows of $2^7/_8$-in. holes. With the holes of the different cylinders in line, the throttle valve is open. The smaller holes flatten out the throttling effect as the 64 large holes are being pinched off, so that it is easy to adjust for small throttle-valve openings. The movable cylinders are rotated by a tangential link- and-screw arrangement

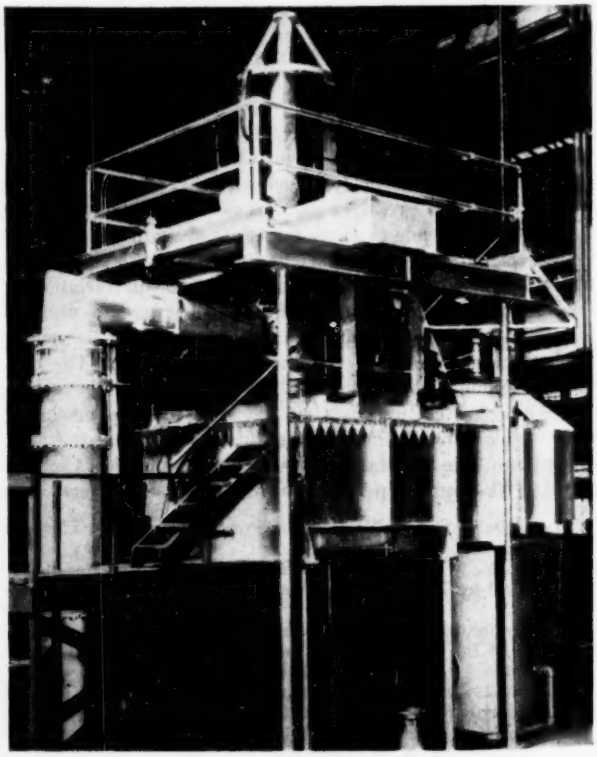


FIG. 2 TEST STAND

operated by a two-speed electric drive and controlled by a corresponding switch on the control desk. The housing and opening through which the moving mechanism reaches into the outer throttle-valve cylinder is visible in Fig. 3. The outer throttle-valve cylinder is welded permanently into the stilling tank, Fig. 3, while the other cylinders, Fig. 4, are assembled outside of the tank and are inserted as a unit.

The purpose of this design is, of course, the breaking up of the unavoidable disturbance caused by the throttling action into a number of smaller disturbances which require a correspondingly smaller distance for their dissipation into heat. Furthermore, by using, between the four cylinders, three points of throttling in series, the local intensity and destructive effect of the individual disturbances are correspondingly reduced.

So far this throttle valve has been found to operate according to expectations.

The space around the throttle valve is separated from the upper part of *the stilling tank* by four screens made from $^1/_8$-in-thick steel sheets with $^1/_8$-in-diam closely spaced perforations. Thereby the remaining disturbances are further reduced in size, so that it is safe to assume that they will have practically vanished before reaching the inlet tank.[4] The resistance of the stilling screens tends to distribute the flow evenly over the 6-ft-diam stilling tank, although the average value of this resistance will seldom exceed 1 ft of water. The mean velocity in the upper part of the stilling tank usually stays below 1 ft per sec.

The transition piece between the stilling tank and the inlet tank is approximately semicircular in shape when viewed in a vertical direction. Four stay bolts near the periphery of the stilling tank support the top of the transition piece at the open side of the latter. A dome on the top of the transition piece aids in removing the air from the system if desired. The flow from the stilling tank to the inlet tank, of course, may be guided by suitable vanes which can easily be fastened to the stay bolts previously mentioned. Such vanes, however, should be considered as part of a particular test setup, rather than as a permanent element of the test stand.

The inlet tank is of rectangular shape. Its flat walls are sufficiently stiffened by outside ribs to withstand a high vacuum, as well as an internal pressure of at least 36 ft above atmospheric pressure. No internal supports are used here, so that the inside of the inlet tank is left entirely free for the construction of a model inlet structure. The upper deck of the inlet tank is composed of individual steel panels which are bolted together and are readily removable. The panel which carries the test pump is specially reinforced for mechanical stiffness and may be shifted to various places along the top of the inlet tank. In the lateral direction, the test pump may be displaced by cutting a new opening into the pump support panel. For the investigation of pump-interference problems, it is possible to arrange an auxiliary connection between the desired point in the inlet tank and an opening already provided in the side of the stilling tank outside of the throttle valve and below the stilling screens. A circulating pump has to be placed into this connection. By such an arrangement, it becomes possible to study the effect of a neighboring pump or of a flow past the pump intake on the operation of the test pump.

Arrangement for Cavitation Tests

Control of the inlet pressure is obtained by means of a pressure-control circuit, following essentially the same principle as that used in the laboratory of the California Institute of Technology.

For cavitation tests with a completely filled test circuit, a certain amount of water is withdrawn continuously from the highest point of the dome on top of the stilling tank. The water is being pumped to an open tank of about 60 cu ft content which is located approximately 25 ft above the inlet tank of the main test circuit. From the open tank, the water is returned by gravity through a throttle valve to the low-pressure side of the test circuit. This auxiliary throttle valve is located within sight of the inlet-pressure gage and is used for coarse adjustments of this pressure. Fine regulation is obtained by changing the pump speed in the pressure-control circuit. The field rheostat used for this purpose is located within convenient reach of the observer of the inlet pressure. The pump of the pressure-control circuit is a small centrifugal unit of about 100 gpm capacity and good suction characteristics. It is located on the ground floor about 12 ft below the test pump. This arrangement permits very low inlet pressures for the test pump. Any air which might come out of solution in the test circuit is carried away by the flow through the pressure-control circuit without noticeably disturbing the operation of the pressure-control pump.

The pressure-control circuit just described is not used for

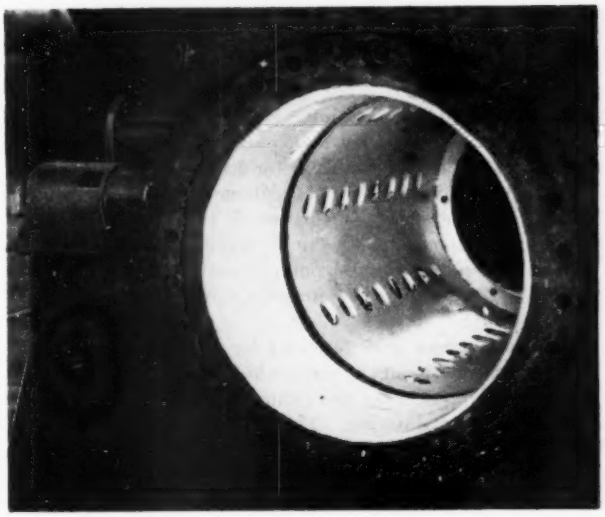


Fig. 3 Outer Throttle-Valve Cylinder in Stilling Tank

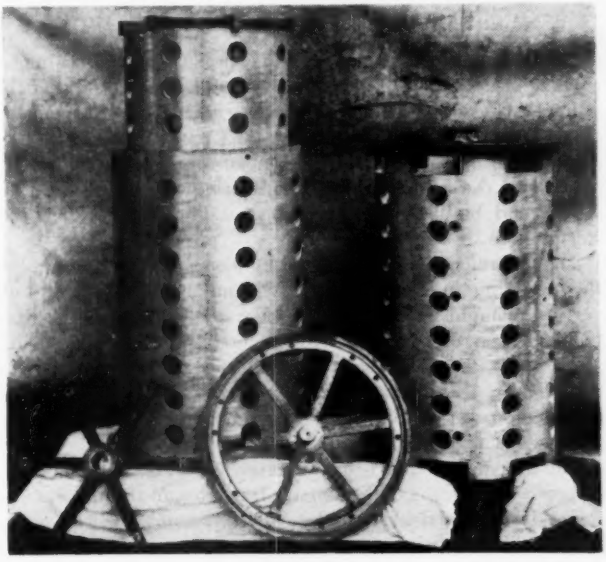


Fig. 4 Removable Parts of Main Throttle Valve

[4] "Beitrag zum Turbulenz Symposium," by L. Prandtl, Proceedings, Fifth International Congress for Applied Mechanics, Cambridge, Mass., 1938, p. 344.

maintaining a high and constant inlet pressure. For this purpose, a very small stream of plant-service water is admitted continuously to the test circuit and is discharged from the highest point of the dome above the stilling tank to a simple overflow about 36 ft above the test pump.

Finally, for extremely low inlet pressures, for tests with a free water surface in the inlet tank, or for deaerating the water in the test circuit, the highest point of the dome can be connected to an ordinary steam ejector. In this way it is possible to bring the pressure in the inlet tank close to the vapor pressure of the water. The inlet pressure of the test pump, therefore, can be varied between this lower limit and a pressure about 36 ft above atmospheric pressure.

No special means were provided for cooling the test circuit. The temperature rise of the water which is due to the absorption of the energy input to the test pump was found not to exceed 10 deg F during normal testing. This change in temperature cannot be expected to have any noticeable influence on the test results, provided proper corrections are made for the corresponding changes in density and vapor pressure. This means that the effect of such variations in temperature on the Reynolds number of the pump flow is being neglected.

The Dynamometer

The test pump is driven by a vertical dynamometer motor capable of developing 150 hp for 2 hr. The motor speed at full voltage (230 v direct current) can be varied between 850 rpm and 2000 rpm. The motor was built by the Crocker Wheeler Electric Manufacturing Company, while the surrounding dynamometer frame and the complete torque-measuring equipment were designed and built by the Worthington Pump and Machinery Corporation.

The dynamometer is supported by a separate platform above the test pump, as shown in Fig. 2. The platform rests on four vertical columns and is braced laterally against the existing building structure. The dynamometer rests on a bridge which spans the frame of the platform. By moving this bridge along the platform and by moving the dynamometer along the bridge, it becomes possible to bring the dynamometer over any desired point of the inlet tank.

The dynamometer is shown in Figs. 5 and 6. The motor is suspended inside the dynamometer frame by means of a suspension rod which carries the total weight of the motor as well as any thrust which is being transmitted from the test pump to the motor thrust bearing. The suspension rod is fluted to reduce its torsional rigidity.

The motor is guided in the dynamometer frame by two bearings shown in Fig. 6. These bearings do not carry any vertical load and only a small horizontal load, resulting from the fact that the measuring torque cannot be applied always as a perfect couple. This horizontal bearing load seldom exceeds 50 lb. With this arrangement it becomes unnecessary to use the customary method of eliminating the friction torque by rotating the outer bearing races continuously in opposite directions. The friction torque was found not to exceed $^1/_{20}$ ft-lb, including the friction of the weight pulleys and all other parts of the torque-measuring apparatus.

The sensitivity of the dynamometer bearings is maintained by means of a special frictionless seal against any dirt carried by the atmosphere. The bearings can be flooded with oil without removing or opening the bearing housing. After draining the bearing, there remains a ring of oil standing in the upper and lower labyrinth of each bearing, forming a hermetic seal against the atmosphere. The pressure inside of the bearing housing is kept in equilibrium with the atmosphere by means of a dustproof breather.

The bearing housings also may be rotated by hand, in order to bring new parts of the bearing races into contact with the balls.

Torque-Measuring Mechanism

Usually the greater part of the dynamometer torque is measured by means of a number of 50-lb weights suspended on steel tapes which are wrapped around the dynamometer motor and pass over four pulleys from a horizontal to a vertical direction. This part of the torque balance is similar to that used at the laboratory of the Baldwin Southwark Corporation. The difference between the moment of the 50-lb weights and the actual dynamometer torque is measured by an oil piston in a rotating cylinder. The use of a hydraulic balance for torque measurements is, of course, not new. The present arrangement differs from earlier applications,[2] and an arrangement proposed by Dr. W. M. White, principally by the fact that it depends clearly on a calibration. This calibration is obtained by placing known weights on the weight pans opposing the oil-hydraulic piston. By recording the corresponding readings of a mercury manometer which measures the oil pressure behind the piston, a calibration may be obtained, not only of the torque-measuring device, but also of all other influencing factors such as pull in the electric cables, any residual torque of the suspension rod, and the like. This calibration has the added advantage of permitting far greater movements of the dynamometer motor than would otherwise be acceptable, avoiding the delicacy of more closely controlled systems or the use of a restoring mechanism.

In the present case, the allowable movements of the dynamometer are restricted only by the limits of elastic response of the

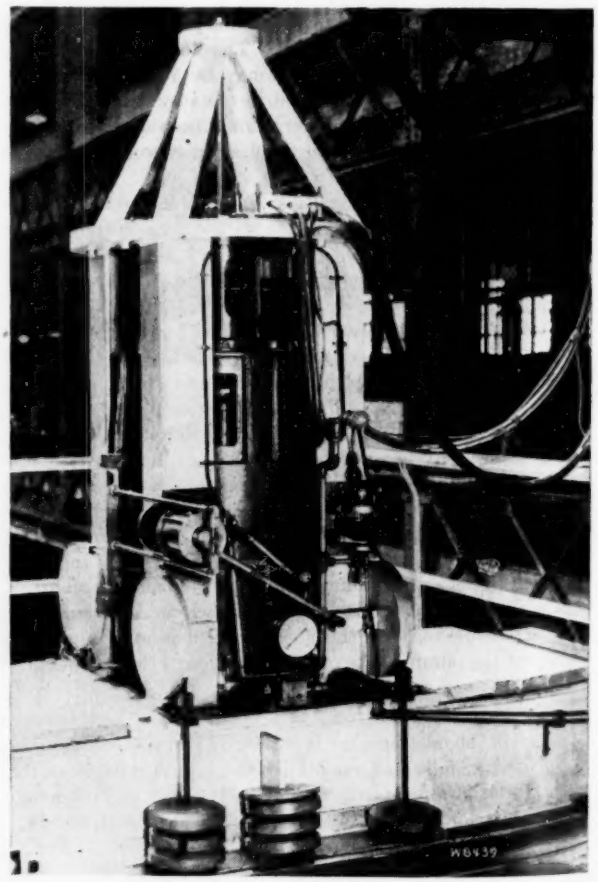


Fig. 5 Dynamometer

electric cables and other influencing factors, and by the mass effect of the motor. Adherence to the former limits can be checked by the calibration while the mass effect was not found to be disturbing in any way, since the peripheral movements of the dynamometer motor seldom exceed $^1/_{32}$ in. during actual operation.

It should be noted that the dial gage, visible in Fig. 5, is not used for measurements but only for crude observations on the dynamometer platform. The measuring manometer is located on the ground floor in a common manometer rack, together with all other manometers of the test stand. The free leg of the torque-measuring manometer is connected to an oil-filled pipe line reaching back to the elevation of the measuring piston at the dynamometer. The free level on top of this return line is visible in the glass bowl, shown in Fig. 5. In this way, any disturbing influences from the long leads of the torque manometer are eliminated.

Dynamometer Speed-Measuring Device

The speed of the dynamometer is measured by means of a Westinghouse precision tachometer generator which is connected to one end of the horizontal shaft above the upper end of the motor shaft. This tachometer generator produces alternating current which controls a dial indicating instrument having a precision of 0.25 per cent. For closer measurements or for calibration of the indicating instrument, it is possible to compare the generator frequency with the frequency of a precision tuning fork by means of a cathode-ray oscillograph. The latter method of speed control was found to be easier for the observer and by far more accurate so that it is used almost exclusively. In this case the speed of the dynamometer motor is held by means of a vernier field rheostat at a speed at which the tachometer frequency has a simple ratio to the frequency of the tuning fork, giving a steady figure on the target of the oscillograph. Such synchronous speeds are available in steps of 100 to 200 rpm, without any mechanical changes in the speed ratios between the dynamometer and the tachometer generator.

Coupling and Instruments

The dynamometer motor and the test pump are connected by means

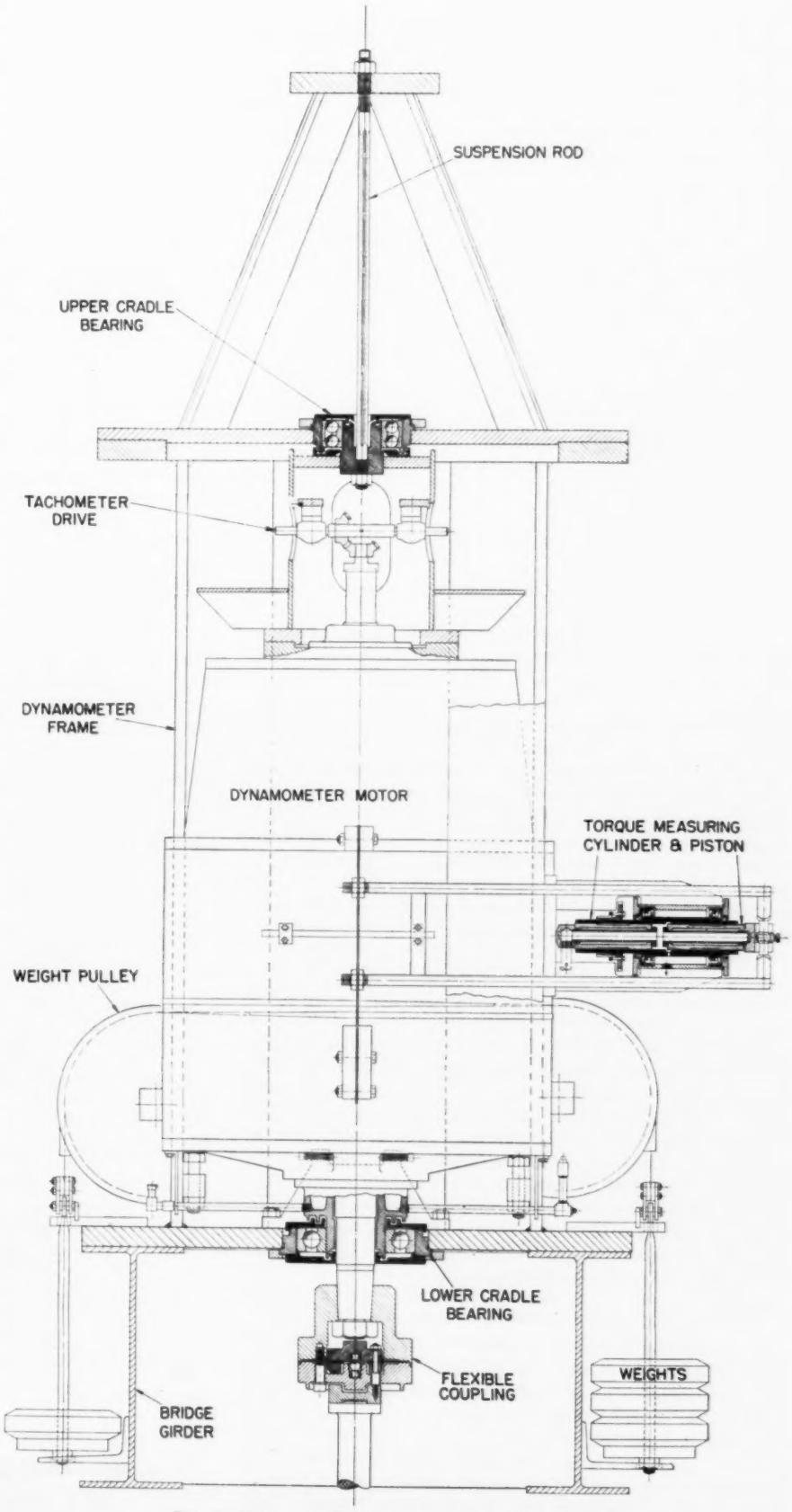


Fig. 6 Sectional Elevation of the Dynamometer

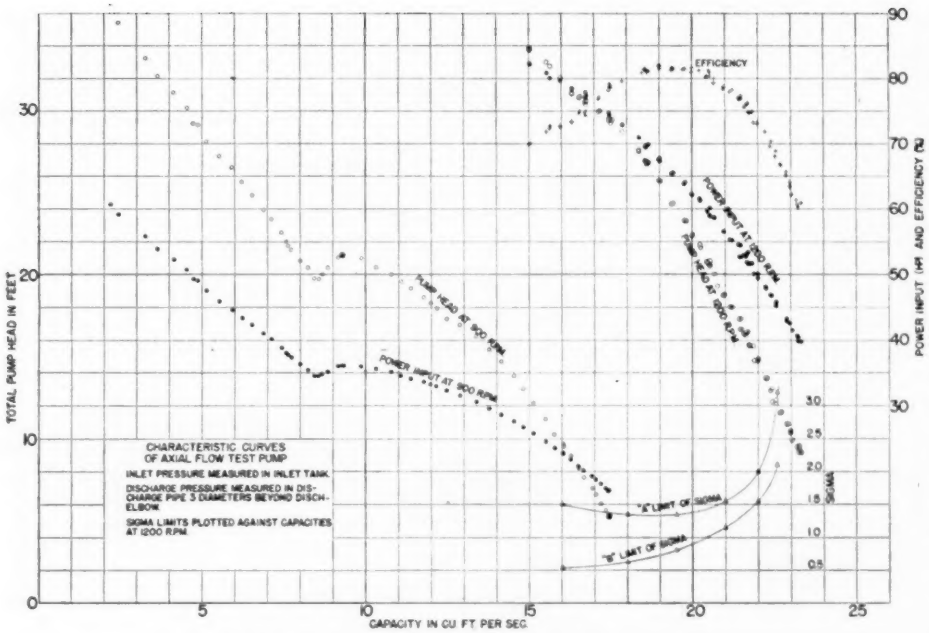


FIG. 7 TYPICAL PROPELLER-PUMP CHARACTERISTICS

resulting changes in pump head and power input indicate the effect of cavitation on the performance of the pump. The scatter of the cavitation-test points is partly due to the steepness of the head and power versus capacity characteristics of this type of pump. For instance, a change of 0.25 per cent in capacity will cause from 0.5 to more than 1 per cent change in head and power. In spite of this inherent difficulty, it has been possible to derive from these tests surprisingly consistent conclusions regarding the cavitation limits of the test pump. This is demonstrated by the derived cavitation-limit curves in Fig. 7, showing the σ values at the beginning of cavitation A and at the breakdown B, plotted against the capacity. The limits A and B are indicated by the corresponding arrows in Fig. 8.

of a special flexible coupling which is capable of transmitting the pump thrust to the dynamometer. The coupling consists of two parts of identical design connected by a simple spool piece. The length of the spool piece is determined by the distance between the motor and pump shaft of the particular test setup. In each half of the coupling, the torque is transmitted through an elastic diaphragm, while the thrust is carried in compression over a steel ball in the center of the coupling.

As indicated before, all measuring instruments and controls are grouped closely together on the ground floor permitting simultaneous observations and easy adjustments. All pressures or pressure differences are measured by mercury manometers. The throttle valve and the speed controls are within easy reach while observing the corresponding instruments.

Operating Range of the Test Stand

The test stand may be used up to approximately 30 cu ft per second for test pumps of very high specific speeds. For pumps of lower specific speeds, the capacity has to be correspondingly reduced to stay within the speed (850 to 2000 rpm) and power (150 hp) limitations of the dynamometer. For testing low-head pumps, it is significant that the residual resistance of the test circuit with the throttle valve completely open is relatively low, making it possible to subject the test pump at, for instance, 20 cu ft per sec to a head difference as low as 7 ft without requiring the use of a booster pump. Furthermore, by reversing the Venturi meter and adding a suitable booster pump in a large by-pass around the throttle valve, the test pump may also be subject to reversed-flow conditions (turbine operation).

Typical Test Results

The test stand has been in almost uninterrupted operation since the beginning of 1941. As mentioned previously, most of this test work has been devoted to pumps of the propeller type. A typical set of characteristic curves selected at random from these tests is shown in Fig. 7, while some typical cavitation-test results are given in Fig. 8. The latter results are obtained by the well-known procedure of reducing the inlet head step by step, while the capacity is being kept as constant as possible. The

Acknowledgments

The importance of improved facilities for experimental test work is generally recognized. Messrs. M. Spillmann, B. R. McBath, and F. Fritscher were among those advocating the construction of the new test stand on this basis. Prof. L. F. Moody contributed to practically every phase of its development and operation. Mr. O. H. Dorer influenced the design by pointing to the possibility of a misleading effect of a throttle valve in a closed test circuit. Mr. F. C. Gilman assisted effectively in the development of the test stand. The test work has been in the hands of Messrs. T. A. Herman and C. Collar. Thanks are due to the Baldwin Southwark Corporation and to their Mr. K. W. Beattie for the opportunity to study their turbine laboratory.

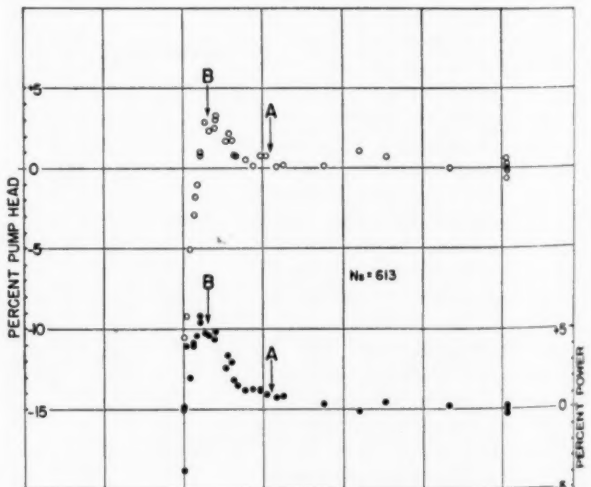


FIG. 8 TYPICAL CAVITATION TEST RESULT

The Mercury-Vapor Process

By A. R. SMITH[1] and E. S. THOMPSON,[2] SCHENECTADY, N. Y.

This paper is a brief history of the development of the mercury-vapor process from the first tube tested in 1912 to the latest 20,000-kw unit at the Kearny Station of the Public Service Electric & Gas Company. A typical cycle and a temperature-entropy diagram show how a better efficiency is obtained by raising the boiling temperature of the working substance. Operating results are given for the installations at the Dutch Point Station and at the South Meadow Station of The Hartford Electric Light Company, the outdoor power plant at the Schenectady Works of the General Electric Company, two small units at the Lynn and Pittsfield plants of the General Electric Company, respectively, the original unit at the Kearny Station of the Public Service Electric & Gas Company and the new boiler at Kearny which replaced the original boiler. This latter unit as shown by test is very efficient and reliable. The main reasons for this better reliability are better design, better shaft packings, better welding which results in extremely low air leakage, the use of alloy-steel tubes and the use of chemical treatment of the mercury which wets the interior surfaces of the tubes and insures a maximum heat transfer to the mercury at all times.

THE mercury-vapor process is a binary system for producing power from fuel with greater thermal economy than is possible with the steam cycle alone. The mercury cycle can also be considered as a steam producer in which, for a given amount of fuel, nearly as much steam is produced as in a steam cycle and, in addition, the by-product power from the mercury turbine generator is obtained at nearly the mechanical equivalent of the thermal energy. A typical cycle is illustrated in Fig. 1 in the temperature-entropy diagram.

In this process mercury is vaporized in a boiler at comparatively low pressure and passes through a mercury turbine which drives a generator. The vapor from the turbine is exhausted to a condenser boiler where its latent heat is transferred to water, which vaporizes at any desired pressure. The steam formed in the condenser boiler is superheated in coils located in the gas passages of the mercury boiler and is then used in steam turbines or for process work. The process is illustrated diagrammatically in Fig. 2. It should be noted that the mercury condenser boiler is in effect an evaporator which permits the use of poorer water than can be tolerated in a superposed steam turbine.

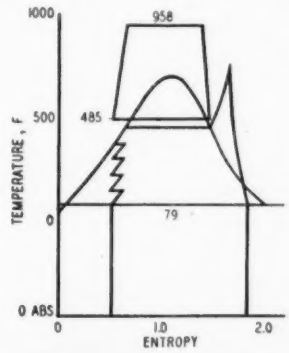


FIG. 1 TEMPERATURE-ENTROPY DIAGRAM

Mercury, 125 psi gage; 958 F; 3 in. back pressure
Steam, 400 lb gage; 750 F; 1 in. back pressure
Over-all heat rate, 8960 Btu per kwhr
Turbine heat rate, 7365 Btu per kwhr
Boiler, 85 per cent; mercury turbine, 72.5 per cent; steam turbine, 80 per cent
Feed pump, 0.5 per cent; auxiliaries, 2.9 per cent

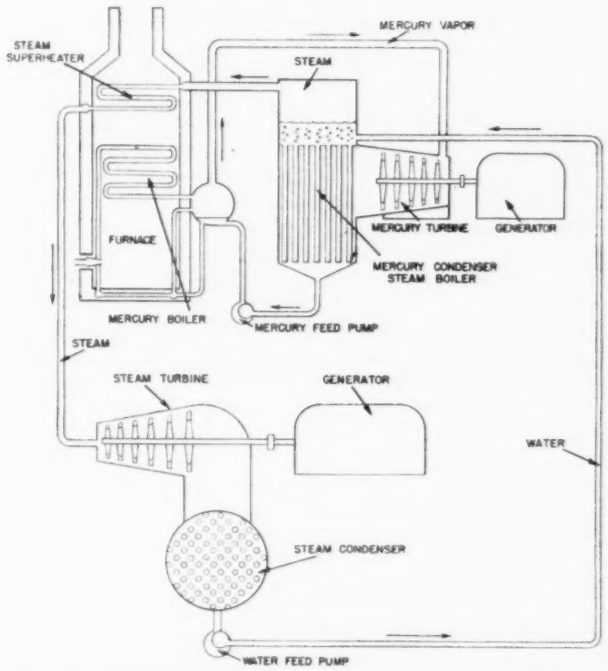


FIG. 2 MERCURY-VAPOR-STEAM-ELECTRIC GENERATING SYSTEM

In general, the efficiency of a power cycle is determined by the temperature range through which it operates; the greater the temperature range, the higher the efficiency. The lower temperature limit is rather definitely set by the cooling medium available and, as this is usually river, lake, or sea water, the lower temperature of the condensed steam is in the range of 50 to 100 F. To improve the efficiency it is necessary to increase the initial temperature to the limit allowable by the materials available. It makes considerable difference, however, whether the high temperature is obtained by increasing the pressure or by superheating the vapor. The energy required to superheat vapor to a certain temperature is only a fraction of that necessary to obtain the same temperature by increasing the pressure and maintaining the vapor in a dry and saturated state.

Steam is the best medium available for use as the lower-temperature fluid in a binary cycle. Certain other fluids such as ammonia, methyl chloride, ethyl chloride, sodium dioxide, and ethyl bromide have been investigated but no commercial success has yet been obtained.[3]

[1] Turbine Engineering Department, General Electric Co. Mem. A.S.M.E.

[2] Turbine Engineering Department, General Electric Co. Jun. A.S.M.E.

Contributed by the Power Division and presented at the Annual Meeting New York, N. Y., December 1–5, 1941, of THE AMERICAN SOCIETY OF MECHANICAL ENGINEERS. Also presented at a Meeting of the Metropolitan Section of the Society, New York, N. Y., March 19, 1941.

[3] "La Turbina A Vapore Ed I Cicli Binari Con Fluidi Diversi Dall'Acqua Fra Le Isoterme Inferiori," by Luigi D'Amelio, *L'Elettrotecnica*, May 10, 1936, vol. 23, p. 250.

All known fluids for use as the top fluid in the binary cycle have been investigated and, with the exception of mercury, have been found lacking in some of the fundamental requirements.

Mercury has many advantages as a thermodynamic fluid for use in power production. Its vapor pressure is low at high temperatures, being 140 psi gage at 975 F and 300 psi gage at 1100 F. Mercury is an element and is stable at temperatures well above the limit imposed by materials now available for boiler tubes, pipes, and turbine nozzles. Its critical temperature is about 2240 F.[4] There is no danger of solidifying in the tubes, as with many other top fluids, for the freezing point of mercury is —37.97 F.

Very little power is required to maintain vacuum in the condenser boiler because air leakage is very low and the absolute pressure is relatively high. With a 25 F terminal difference a mercury pressure of 6.07 psi abs will produce 1200 psi abs steam, and a mercury condenser pressure of 1.20 psi abs will produce 400 psi abs steam.

The specific heat of the liquid is only one thirtieth of that of water at 80 F and one sixty-sixth of that of water at 650 F. This means a steep liquid line on the temperature-entropy diagram so that nearly ideal conditions are inherent in the cycle and no regenerative feed heating is required. Its relatively high density at condensing pressures simplifies the turbine-design problem of providing sufficient length for the last-stage nozzles and buckets. Spouting velocities and available energies for given pressure ratios are much lower than for steam, so mercury turbine speeds are low.

Known world deposits of mercury are large. The yearly production has varied from 2150 metric tons to 5650 metric tons,[5] and there is no reason to suppose this annual production cannot be increased. An increase of 3000 tons per year, which is no more than the ordinary variation, would make available for mercury plants about 1,000,000 kw in combined mercury-steam plants which could be installed each year, and this mercury is not used up as in many industrial processes but would be used year after year. At the time this article is written the market for mercury, as with other metals or commodities which have strategical value, is affected by war conditions. However, studies indicate that in normal times all the mercury necessary will be available for power production without dislocating the market.

[4] "The Possibilities of Mercury as a Working Substance for Binary-Fluid Turbines," by W. J. Kearton, Proceedings of The Institution of Mechanical Engineers, London, England, Nov. 16, 1923.

[5] Minerals Yearbook, 1930 to 1940, inclusive, United States Department of the Interior, Bureau of Mines.

History of the Development—Schenectady Tests

The mercury-vapor process was introduced by Dr. W. LeR. Emmet in a paper before the American Institute of Electrical Engineers, Dec. 16, 1913.[6] The first mercury boiler, as shown in Fig. 3, was a single tube containing a solid core with a small clearance between the core and the tube. A central hole in the core provided the down circulation of the liquid. The multiplying lever on the top of the "drum" was connected through a packing to a rod extending through the central core to the bottom of the tube. The average difference in temperature between the outer heated walls and the liquid in contact with the rod was accurately measured with this device. The complete test apparatus is shown on the right in Fig. 3. The funnel on the left was for filling the boiler and the column at the right was the condenser.

Some of the fundamental requirements for mercury boilers were discovered with this apparatus. Further tests with boiling mercury between concentric glass tubes confirmed the fact that very free circulation of the liquid must be provided if large amounts of heat were to be absorbed with small differences in temperature between the liquid and the heated surface. Since the mercury did not wet the heating surface, there was a tend-

[6] "Power From Mercury Vapor," by W. LeR. Emmet, Transactions of the A.I.E.E., vol. 32, Dec. 16, 1913, pp. 2133–2149.

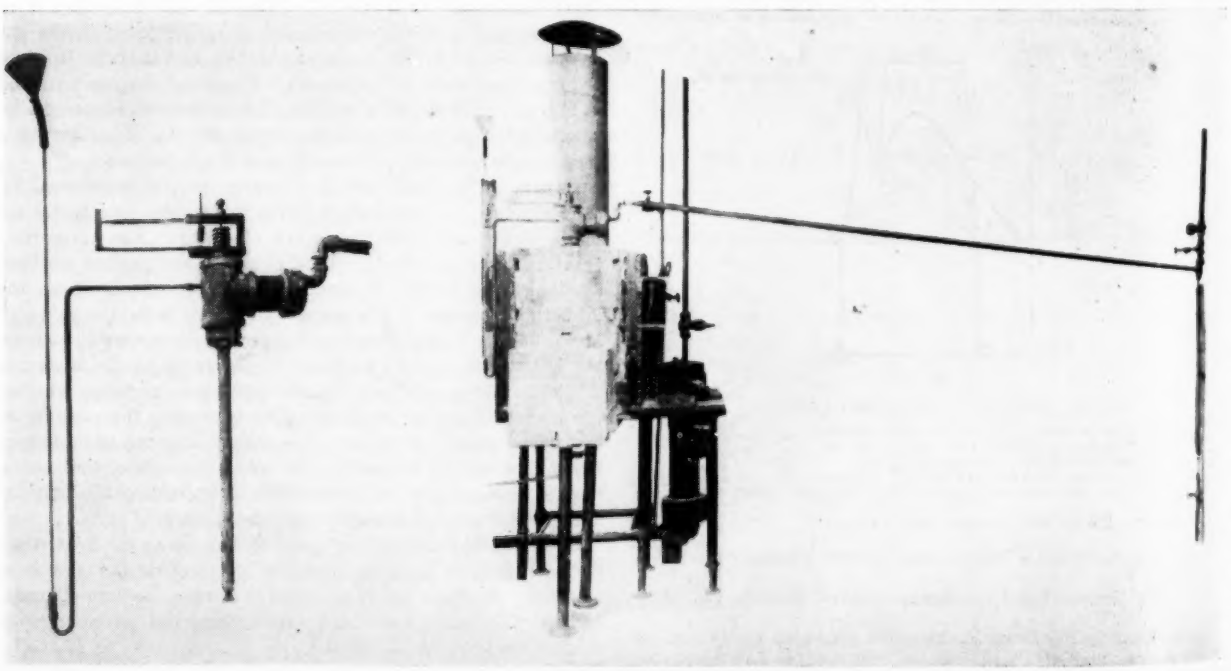


Fig. 3 First Mercury Boiler, Operated in 1912
(View showing element at left, and element encased in brick setting at right.)

ency for the vapor to form a film at the tube surface, thus preventing good heat transfer to the liquid. To prevent this condition high circulation ratios had to be maintained so that very little vapor would be formed until the heated liquid reached the upper parts of the tube where the pressure was relieved, thus allowing the stored heat to form vapor. Many years were to pass before a way was found to make mercury wet the tube surface, thereby increasing the heat-transfer rate with lower circulation ratios.

High temperatures made it impossible to maintain tight expanded joints in the tube sheet so it was necessary to resort to a boiler consisting of flattened tubes bent into an arc and welded to two headers which were connected by a return pipe. Several boilers of similar type and various capacities were tested in Schenectady, N. Y., and one unit successfully produced 1000 kw from the mercury turbine generator. The results were encouraging for the economy expected from the process was realized even though many mechanical difficulties had still to be overcome.

Hartford Electric Light Company, Dutch Point Station

The results obtained at Schenectady through the ten-year

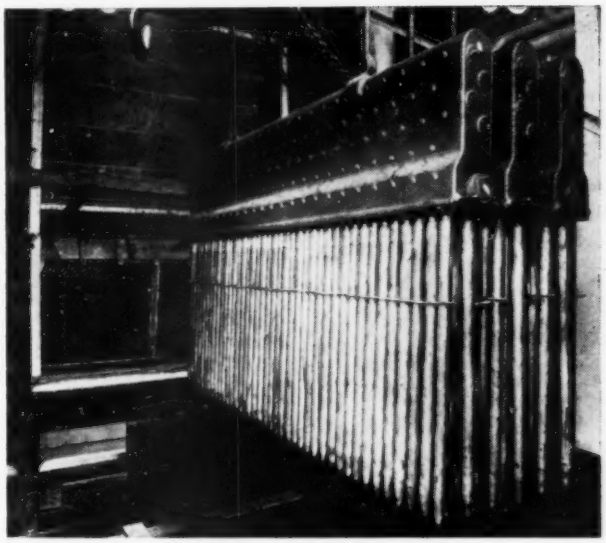


Fig. 5 Mercury Boiler Units With Porcupine Tubes During Erection at the Dutch Point Station of The Hartford Electric Light Company, Hartford, Conn., 1925

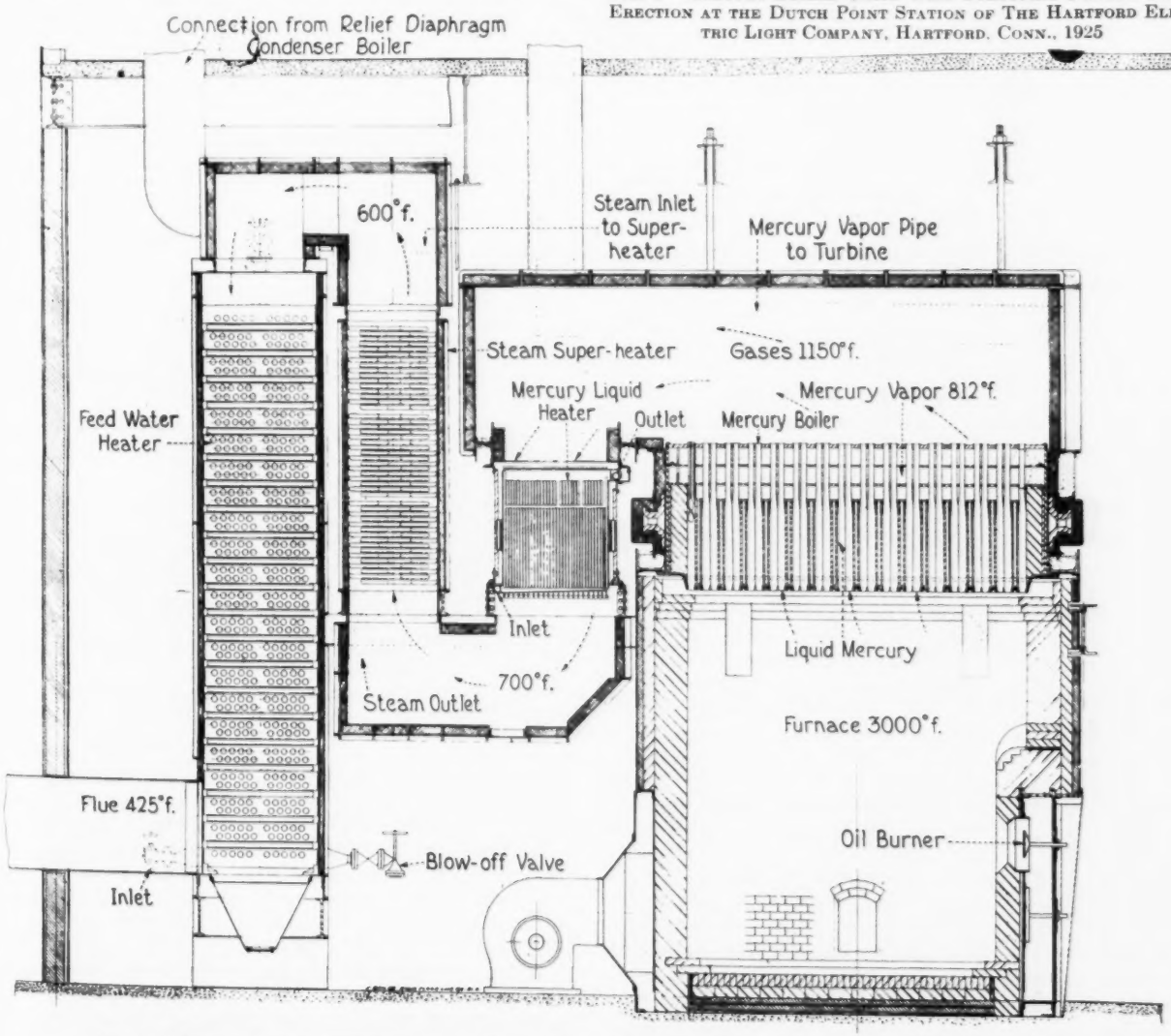


Fig. 4 Mercury Boiler Installed at the Dutch Point Station of The Hartford Electric Light Company, Hartford, Conn., 1922

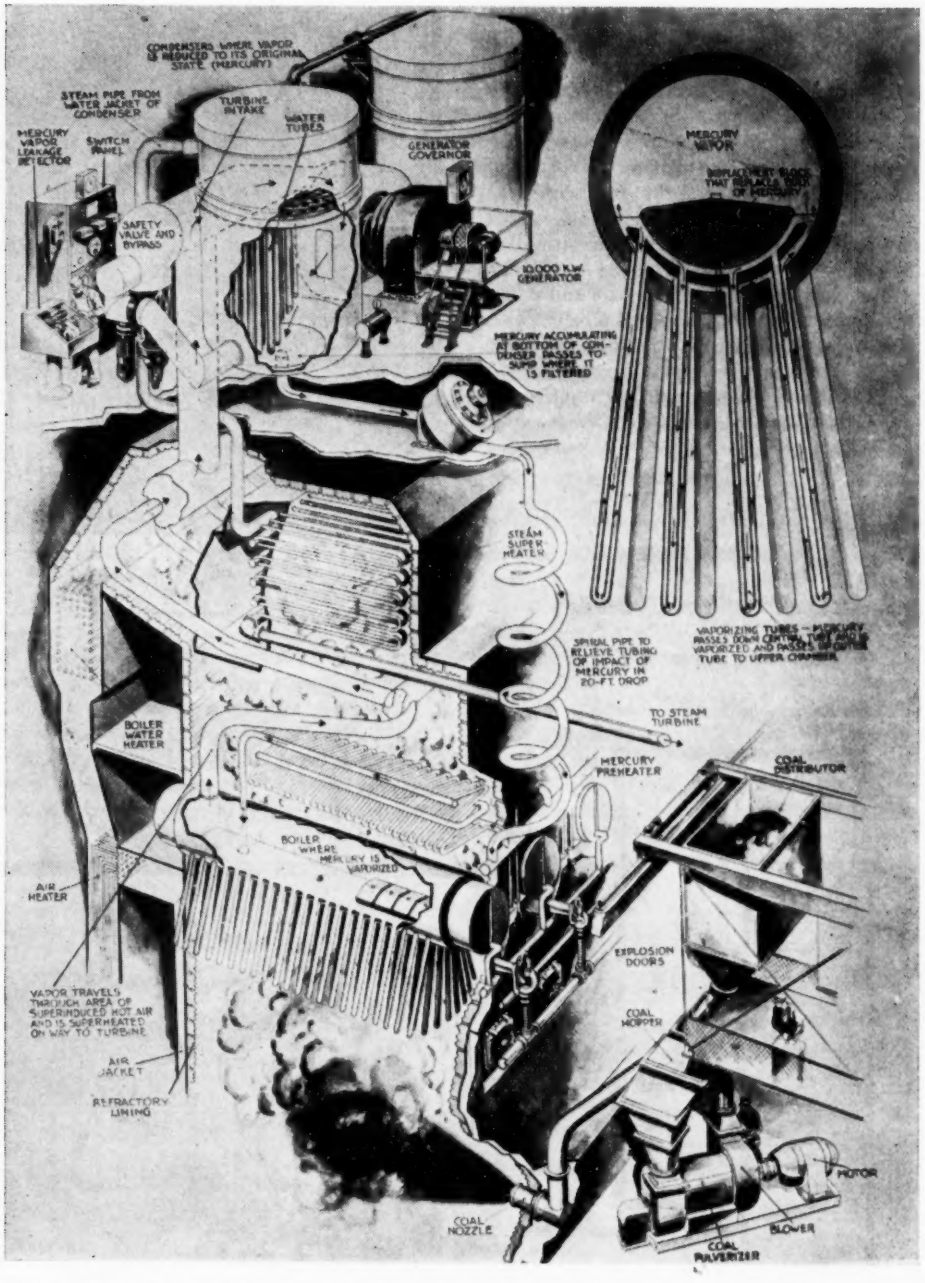


FIG. 6 MERCURY-VAPOR POWER-STATION EQUIPMENT. INSTALLED AT SOUTH MEADOW STATION OF THE HARTFORD ELECTRIC LIGHT COMPANY, HARTFORD, CONN., 1928

(Photograph of drawing by courtesy of *Popular Science Monthly*.)

period prior to 1922 convinced the executives of the Hartford Company that the binary cycle had sufficient promise to justify the necessary expenditures for proving it on a commercial operating basis.[7]

The first installation at the Dutch Point Station was designed to deliver 1800 kw from the mercury turbine generator and to produce 40,000 lb per hr of steam at 200 psi gage and 100 F superheat. The boiler was a new design employing the fire-tube principle and operated at 35 psi gage mercury pressure. A sectional view of the boiler, Fig. 4, shows the furnace, mercury boiler, liquid heater, steam superheater, and economizer. The boiler looked like a honeycomb with the center cell of each group of seven sealed over to make a return tube for the other six.

Inadequate provision for expansion of adjacent tubes and inaccessibility for cleaning made it necessary to replace this boiler in 1925 with one made up of suspended "porcupine" tubes similar to the tube used in the early experiments. There were four headers each having 160 porcupine tubes. Short coils were also provided above the headers to function as mercury superheater elements. This boiler, partially assembled, is shown in Fig. 5. The operating pressure of the new boiler was increased to 70 psi gage.

The 1800-kw 1800-rpm turbine and generator and the con-

[7] "Experiences With the Mercury Boiler and Turbine," by Samuel Ferguson, *Journal of The Franklin Institute*, vol. 220, no. 6, December, 1935, pp. 687–717.

denser boiler were installed on a deck above the boiler. This arrangement allowed the condensed liquid to flow back by gravity through the sump and liquid heater to the boiler drum. The turbine was originally a single-stage unit but, at the time the boiler was replaced, the turbine was rebuilt as a three-stage machine with the rotor overhung from the generator. The condenser boiler tubes were dead-ended with a center strip inside to aid circulation from the large steam drum at the top.

The first unit produced a total of 2,423,500 kwhr and 54,427,000 lb of steam while the second unit produced 2,056,500 kwhr and 33,817,000 lb of steam. The improvement in efficiency of the second unit can be noted from the greatly increased electrical output per pound of steam produced.

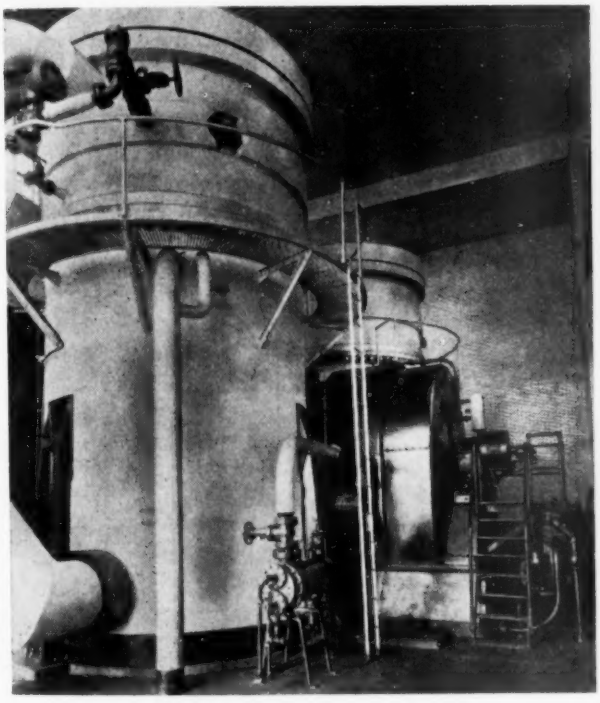


FIG. 7 10,000-KW MERCURY TURBINE GENERATOR UNIT
(View of generator end, showing generator and condenser boilers. South Meadow Station, The Hartford Electric Light Company, Hartford, Conn.)

During 1927 plans were being perfected for the next step which was to install a unit of much larger size.

TABLE 1 PERFORMANCE RECORD OF 10,000-KW MERCURY PLANT AT SOUTH MEADOW STATION OF THE HARTFORD ELECTRIC LIGHT COMPANY

Year	Kwhr mercury only at approximately 4000 Btu	Kwhr total mercury and steam (net)	Btu per kwhr	Hours run
1928	2,900,000	5,700,000	....	429
1929	5,600,000	11,700,000	11,200	993
1930	52,500,000	121,000,000	10,300	6157
1931	5,400,000	12,700,000	11,300	651
1932	49,400,000	110,000,000	10,600	6516
1933	43,000,000	102,000,000	10,500	6753
1934	51,773,000	124,283,533	10,889	7596
1935	49,190,000	122,096,850	10,250	7212
1936	52,725,000	129,261,710	10,210	7309
1937	49,979,000	125,737,275	10,120	7729
1938	47,646,000	123,023,058	10,000	7684
1939	50,240,000	131,122,000	10,000	8140
(1940 to 9–25–40)	27,712,000	74,897,000	10,250	5162
Total	488,065,000	1,193,521,426		72,331

NOTES:
Data through 1933 from "Experiences With the Mercury Boiler and Turbine," by Samuel Ferguson, *Journal of The Franklin Institute*, vol. 220, no. 6, Dec., 1935, p. 713.
Data 1934 to present from station records.

HARTFORD ELECTRIC LIGHT COMPANY—SOUTH MEADOW STATION

The mercury plant now operating at the South Meadow Station was installed in 1928. An isometric section, Fig. 6,[8] of the plant shows the path of the fuel, gas, mercury, and steam throughout the system. The mercury boiler, which operates at 85 psi gage and 908 F, has seven drums 37 in. OD × 30 in. ID, 21 ft, 6 in. long. Suspended from each drum are 440 porcupine tubes 5 ft, 6 in. long × 3¹/₈ in. OD. The circulation path in these tubes is shown in the sectional view in the upper right-hand corner of Fig. 6.

The 720-rpm turbine has five impulse stages on the rotor which is overhung from the generator. Enclosing the inlet end in this manner eliminates the high-pressure packing.

The condenser boilers supply steam to the superheater from which it is delivered at 375 psi gage and 700 F, to the station mains. The turbine floor assembly, Fig. 7, shows the two condenser boilers and the 10,000 kw generator.

The mercury turbine generator output, the total output from mercury and steam, the net plant heat rate, and the hours run are shown in Table 1. Up to, and including 1934, a steam-turbine water rate of 10 lb per kwhr was used. From 1935 to September 25, 1940, the steam was used in a better turbine, so a turbine water rate of 9.5 lb per kwhr was used.

SCHENECTADY WORKS STATION OF GENERAL ELECTRIC COMPANY

Two plants were built in 1932, one for the Schenectady Works of the General Electric Company and the other for the Kearny Station of the Public Service Electric and Gas Company of New Jersey. The capacity of these plants was double that of the Hartford plant and the mercury-boiler pressure and temperature were increased to 140 psi gage and 975 F.

The boiler shown in Figs. 8 and 9 has seven drums and the same type porcupine tubes as the Hartford boiler but much better utilization of the radiant heat was obtained by lining the upper furnace walls with mercury vaporizing surface and the lower part of the furnace walls with steaming tubes. The mercury wall tubes were made by embedding three tubes in copper in a frame to obtain more uniform heat transfer around the periphery of each tube. The feed for these wall-tube sections is obtained from outside downcomers at each end of each drum. The wall tubes and underside of the porcupine tubes are shown in Fig. 10. The waterwalls in the lower part of the furnace function as a standard 400-lb-pressure steam boiler with the steam drums located on each side of the furnace as may be seen in Figs. 8 and 9.

The Schenectady plant differs from all previous plants in that the turbine generator and condenser boilers are not placed above the boiler. Condensed mercury liquid is returned to the boiler by means of a centrifugal pump. This pump requires only 8 hp per 1000 kw of mercury-turbine capacity.

The mercury turbine shown in Fig. 11 is rated 20,000 kw, 5-stage double-flow, 900 rpm. Vapor enters the center annular chamber and flows in both directions to the exhaust openings and to the two condenser boilers. Projection of the shaft through the turbine casing is in the vacuum space so two packings to prevent leakage of air into the condensers are used but no high-pressure packing is required.

The total steam output from the condenser boilers and waterwalls is superheated and then is added to the output of a steam boiler and flows at 450 psi gage and 750 F to a 6000-kw 3600-rpm back pressure steam turbine. The steam from the exhaust of this turbine at 225 psi gage and 647 F flows to the Schenectady Works where it is used in various industrial processes.

The Schenectady plant is an outdoor station. It has passed through several severe winters without any operating difficulties.

[8] Courtesy of *Popular Science Monthly*.

TABLE 2 MERCURY PLANT—SCHENECTADY WORKS OF GENERAL ELECTRIC COMPANY

Year	Kwhr mercury turbine generator	Pounds of steam produced	Hours run
1933	2,537,000	53,317,000	425
1934	52,136,000	1,088,411,000	4,921
1935	31,304,000	687,040,000	3,203
1936	28,248,100	693,597,000	3,671
1937	17,066,800	567,209,000	3,375
1938	36,752,100	1,136,689,000	7,225
1939	47,345,200	1,169,399,000	6,384
(1940 to 9–1–40)	36,464,900	870,830,000	4,555
Total	251,854,100	6,266,492,000	33,759

The mercury turbine generator, condenser boilers, steam turbine generator, feedwater heaters, and evaporators are exposed to the elements but very infrequent attention to these units by the operators is required. The control panels, firing aisles, pumps, pulverizers, and other equipment are under cover.

Power or heating plants for industry generally grow over a long period during which time styles and sizes of apparatus change so materially as to make the original building plan quite unsuitable for contemplated new equipment. Furthermore, buildings are especially designed to suit the original equipment and it seems unwise to construct a special building good for a life of seventy-five years to house apparatus which may have to be replaced in twenty-five years.[9]

A section through the plant, Fig. 12, gives a clear picture of the heat-flow path from coal car to stack. An airplane view of the completed plant is shown in Fig. 13.

This plant runs at reduced loads over week ends so that high capacity factors are not obtainable. The output since the start in 1933 is shown in Table 2.

The only changes made in the seven-year period have been the replacement of the liquid heater by a mercury convection surface above the drums and a change to the condenser boiler tubes in which adjacent dead-ended tubes were connected to improve circulation.

Kearny Generating Station of the Public Service Electric and Gas Company of New Jersey

The original mercury plant installed in the Kearny generating

[9] "Co-Ordinated Production of Industrial Steam and Utility Power," by A. R. Smith, Trans. 1933, World Power Conference (Sectional Meeting, Scandinavia), vol. 4, pp. 251–273; also *General Electric Review*, vol. 36, no. 7, July, 1933, pp. 300–309.

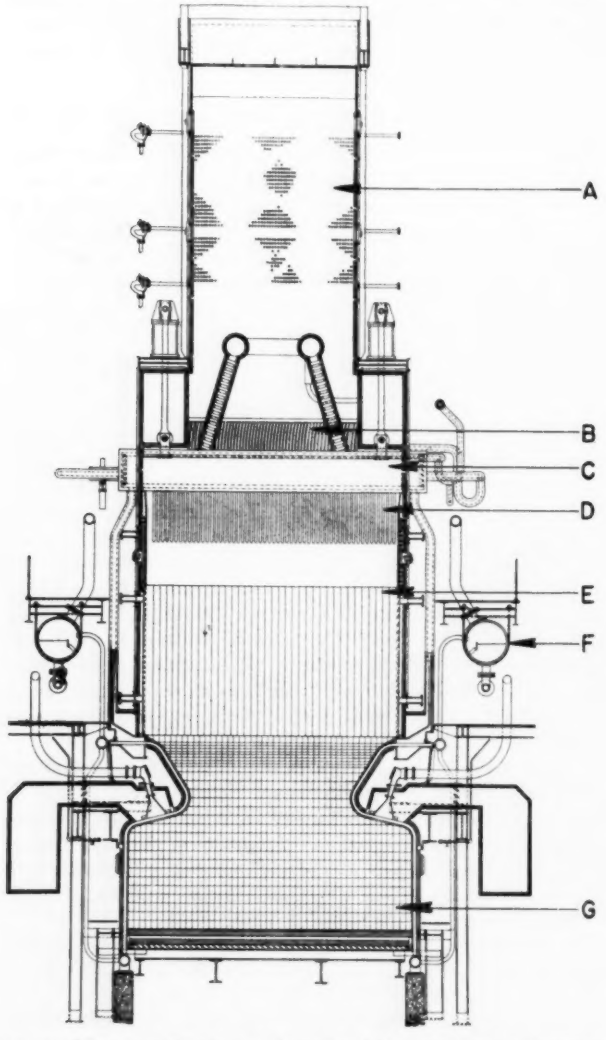


Fig. 8 Mercury Boiler in Outdoor Mercury-Steam-Electric Power Station, Schenectady Works, General Electric Company

A Steam superheater
B Mercury liquid heater
C Mercury drum
D Porcupine tubes
E Mercury walls
F Steam drum for waterwalls
G Waterwalls

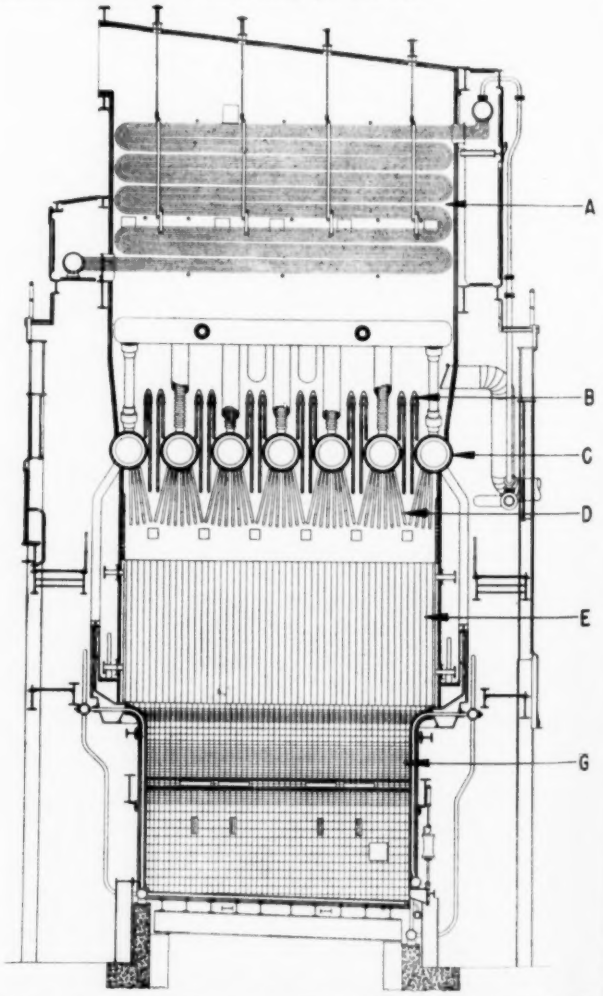


Fig. 9 Mercury Boiler in Outdoor Mercury-Steam-Electric Power Station, Schenectady Works, General Electric Company

A Steam superheater
B Mercury liquid heater
C Mercury drum
D Porcupine tubes
E Mercury walls
G Waterwalls

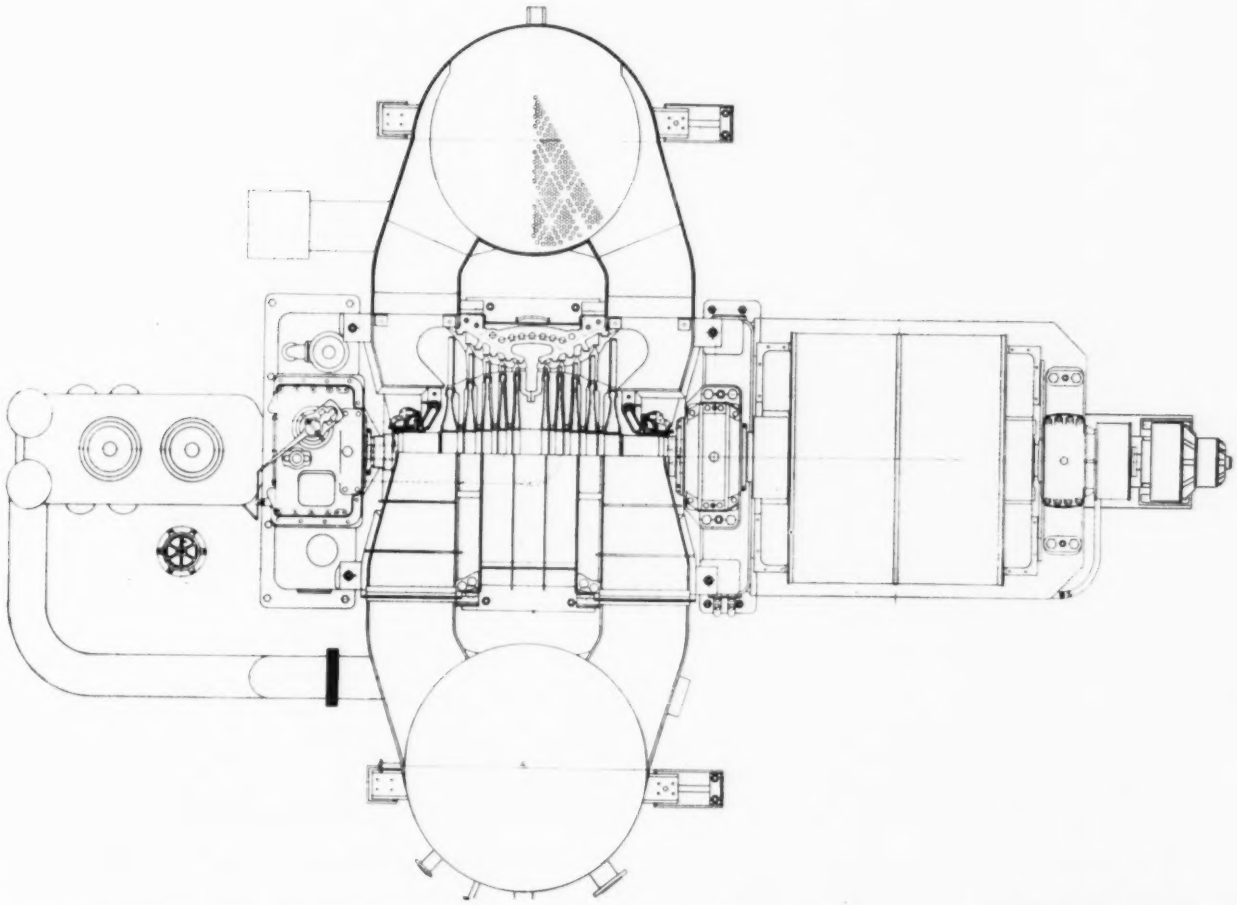


FIG. 11 MERCURY TURBINE GENERATOR SET, 20,000 KW, 900 RPM, OUTDOOR MERCURY-STEAM-ELECTRIC POWER STATION, SCHENECTADY WORKS, GENERAL ELECTRIC CO.

station was first operated in March, 1933. The boiler, turbine generator, and condenser boilers were duplicates of those at Schenectady but the mercury-boiler feed is returned by the gravity system as at Hartford. Floor-space limitation was a major factor in this decision.

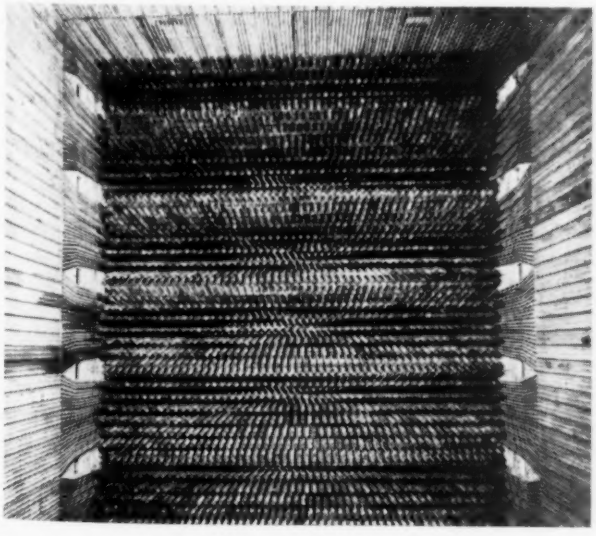


FIG. 10 MERCURY BOILER IN OUTDOOR MERCURY-STEAM-ELECTRIC POWER STATION, SCHENECTADY WORKS, GENERAL ELECTRIC CO.
(Interior view upward showing tubes and walls of No. 1 mercury unit, 20,000 kw.)

The first boiler was operated until September, 1938, when it was removed to make way for a new one of advanced design, which will be described later. The plant production from 1933 to 1938 is shown in Table 3.

TABLE 3

Year	Kwhr mercury turbine generator	Pounds of steam produced
1933	51,153,000	1,032,673,200
1934	46,028,000	1,013,240,400
1935	72,485,000	1,542,618,900
1936	36,679,000	877,970,600
1937	42,604,000	913,522,500
1938 to Sept. 1	28,924,000	655,783,300
Total	277,873,000	6,035,808,900

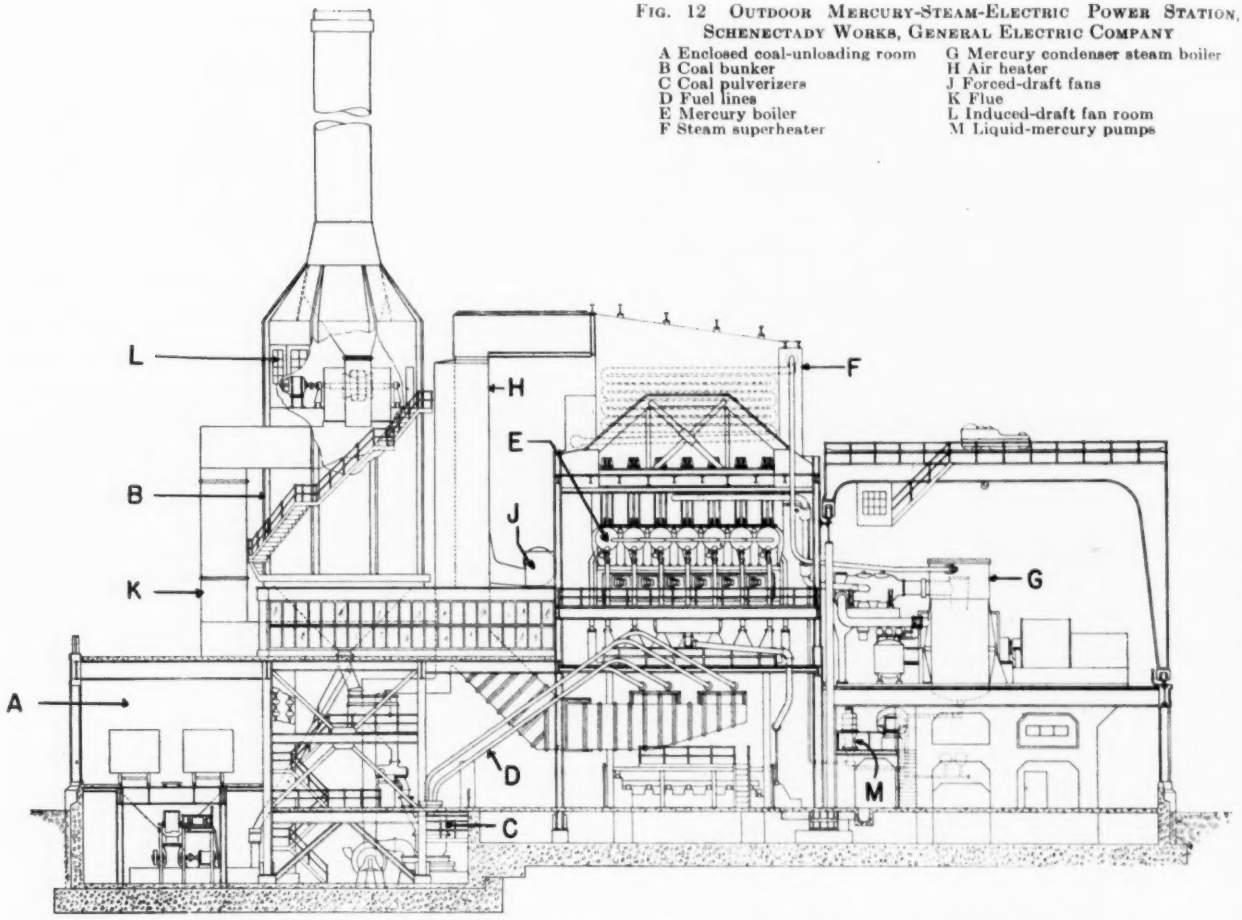
FORCED-CIRCULATION BOILER

An interesting development in the process was a 1000-kw forced-circulation boiler which was tested in Schenectady. The firebox was formed of helically wound tubes forming a cylindrical combustion chamber. For a short distance above the bottom of the firebox, the tubes were open-spaced to allow the gas to pass out and up through a concentric mercury-liquid heater and steam superheater. After leaving the steam superheater the gas passed through a two-pass air preheater to the stack.

Mercury liquid was pumped into a distributing chamber at the bottom of the boiler and then through the radiation tubes to a ring header at the top which discharged to the separator. The separator contained nozzles in which the vapor was formed

FIG. 12 OUTDOOR MERCURY-STEAM-ELECTRIC POWER STATION, SCHENECTADY WORKS, GENERAL ELECTRIC COMPANY

A Enclosed coal-unloading room
B Coal bunker
C Coal pulverizers
D Fuel lines
E Mercury boiler
F Steam superheater
G Mercury condenser steam boiler
H Air heater
J Forced-draft fans
K Flue
L Induced-draft fan room
M Liquid-mercury pumps



by flashing due to release of pressure. To prevent any vaporization in the boiler surfaces a circulation ratio of 35 to 1 was maintained. A circulating pump, fed directly from the liquid outlet of the separator, pumped 35 lb of liquid through the boiler for each pound of vapor formed. Liquid return from the condenser boiler was forced by a feed pump through the liquid heater to the separator. The two pumps had mercury centered bearings which functioned quite satisfactorily. Test data and experience obtained from this installation led to the design of the unit for the River Works.

UNIT POWER PLANT AT THE RIVER WORKS OF THE GENERAL ELECTRIC COMPANY AT LYNN, MASS.

The power plant installed in 1937 at the River Works of the General Electric Company in Lynn, Massachusetts, was composed of elements which could be completely assembled in the factory, thus requiring a minimum of expense for field erection.

The forced-circulation mercury boiler, Fig. 14, is similar in design to the 1000-kw boiler but of increased rating. It delivers sufficient mercury vapor at 165 lb gage and 1000 F, dry and saturated to produce 1000 kw from the mercury turbine generator and 12,650 lb per hr of steam at 180 lb gage and 150 F superheat. The radiation tubes, convection tubes, liquid heater, and steam-superheater assembly is lowered into the casing as a unit as shown in Fig. 15. The casing is formed of two thin concentric sheets which form a narrow air space through which air is forced on its way to the air preheater, the top of which can be seen at the upper left in the photograph. This air-cooled jacket takes the place of the usual lagging on the exterior of boiler casings.

The mercury turbine generator and condenser boiler are so arranged that the generator and turbine can be moved back out of the condenser boiler so as to expose the turbine for inspection or repair as shown in Fig. 16. This was the first 3600-rpm mercury turbine. It is overhung from the generator and operates above the critical speed.

The condenser boiler was built with two drums and outside downcomers to assure positive and adequate circulation of the boiling water.

The steam-driven circulating pump recirculates the mercury from the separator through the boiler at a flow of 4,750,000 lb per hr at a head of 45 ft of mercury when operating at 1200 rpm. The steam from the superheater at 380 lb gage and 645 F is reduced to 180 lb gage and 150 F superheat in passing through the high-speed single-stage turbine which drives the pump through a reduction gear. The mercury centered pump bearing is supplied with mercury from the feed-pump discharge.

The unit could be started and stopped very rapidly with no danger of unequal heating of tubes. It operated successfully for 6000 hr during which time it produced 4,480,000 kwhr from the mercury turbine generator and the equivalent of 4,000,000 kwhr from the steam produced in the condenser boiler. It carried full load without difficulty and, when sufficient experience was gained with this type of boiler, the plant was shut down in August, 1939.

An advantage of the forced-circulation type of boiler appears to be the possibility of conforming the firebox and tube circuits to confined spaces such as are encountered on ships and locomotives.

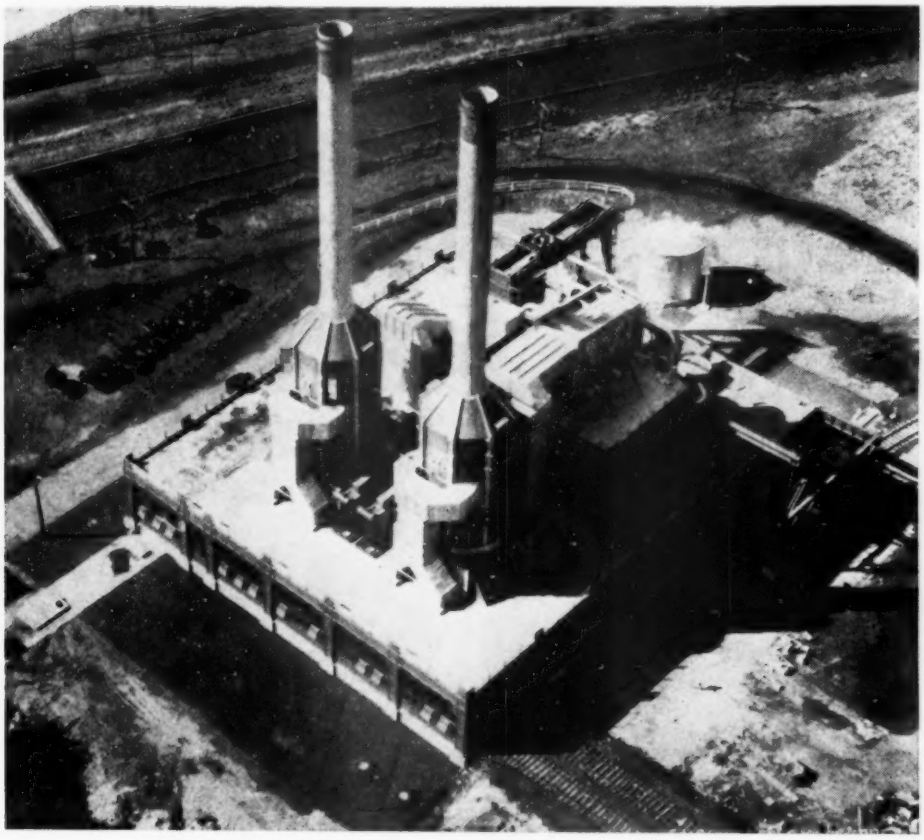


FIG. 13 OUTDOOR MERCURY-STEAM-ELECTRIC POWER STATION, SCHENECTADY WORKS, GENERAL ELECTRIC COMPANY

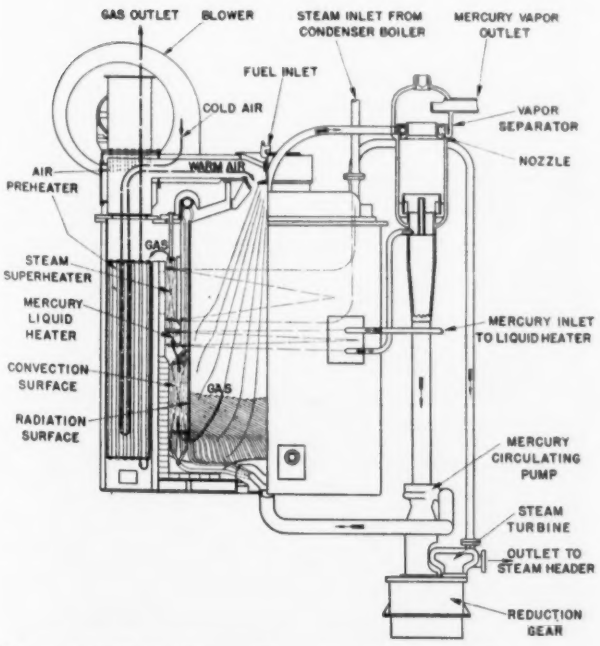


FIG. 14 OIL-FIRED FORCED-CIRCULATION MERCURY BOILER, FOR UNIT POWER PLANT, 1900 KW, RIVER WORKS, GENERAL ELECTRIC COMPANY, WEST LYNN, MASS.

TEST BOILER AT PITTSFIELD WORKS OF THE GENERAL ELECTRIC COMPANY

A small boiler was installed at the Pittsfield, Mass., works of the General Electric Company in 1937 to study the action of a unit composed of relatively high vertical wall tubes with natural, or thermal, circulation. This was also the unit in which most of the advances in treatment of the mercury were made. The tubes were arranged to form a cylindrical firebox and brought together into a short horizontal drum as shown in Fig. 17. The burner for oil firing was at the bottom and the gas was directed out by two baffles at the top to a liquid heater, steam superheater, and air preheater.

The remainder of the equipment, including the generator, mercury turbine, valves, and condenser boiler, was used originally in the Dutch Point installation twenty years before, but it performed admirably during the two-year testing period at Pittsfield.

The unit produced 4,931,000 kwhr from the mercury turbine generator and 82,000,000 lb of steam at 185 psi gage and 650 F during the test operation.

NEW MERCURY BOILER AT KEARNY

The new mercury boiler at the Kearny Station of the Public Service Electric and Gas Company of New Jersey began operation on May 5, 1940. It produces 20,000 kw from the mercury turbine generator and 300,000 lb per hr of steam at 365 psi gage and 750 F.

The new boiler, shown in Figs. 18 and 19, occupies the same space as the old boiler. The furnace is of octagonal shape in plan, for the purpose of conserving mercury and better to equalize the heat absorbed by all the furnace tubes. The burners are located on each of the eight sides. A uniformly distributed flame can be carried by proper selection of burners throughout the load range. The burners are so constructed that either coal or oil may be used.

The furnace walls are completely covered with mercury tubes, which are practically contiguous, having a minimum inside diameter of $^{13}/_{16}$ in. at the bottom and 1 in. at the top of the vertical run. At the beginning of the arch at the top of the vertical run the tubes are supported by hangers, Fig. 20, so they hang vertically and, in turn, partially support the bottom which is formed as a unit with a structural-steel frame. Large coil springs on the underside aid in supporting the bottom. In order that no single tube may be overstressed by this hanging load, they are attached through small springs to the structural bottom which allows for a reasonably individual motion consistent with possible temperature differences between tubes. The expansion of the tubes downward at full load is $2^{13}/_{16}$ in.

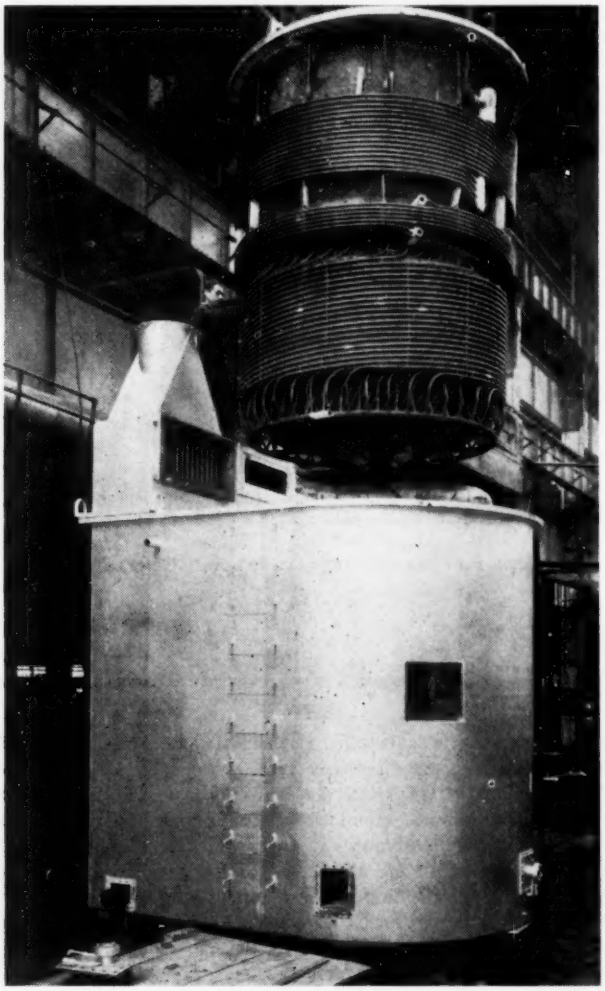


FIG. 15 MERCURY BOILER, 1900 KW, FOR GENERAL ELECTRIC MERCURY-VAPOR-STEAM UNIT POWER PLANT
View of firebox, convection tubes, liquid heater, and steam superheater before lowering into casing; outlet of air preheater at upper left.)

Insufficient experience was available at the time the original Kearny boiler was built in regard to the pumping, or circulating ability, of high vertical furnace wall tubes. The Hartford boiler was the first large boiler and it had no mercury wall tubes. The next large boilers at Kearny and Schenectady had mercury wall tubes over the upper half of the firebox and waterwalls forming the lower half. The new Kearny boiler completes the evolution and the tubular lined firebox is now quite similar to those of modern waterwalled steam boilers as may be seen from the interior view of one wall, Fig. 21.

The experience to justify the new design was obtained from

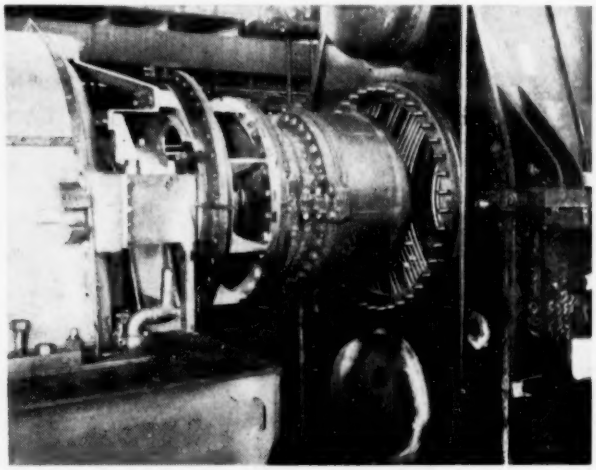


FIG. 16 MERCURY TURBINE BEING PUSHED INTO CONDENSER BOILER OF MERCURY-VAPOR-STEAM-ELECTRIC POWER PLANT, 1900 KW, RIVER WORKS, GENERAL ELECTRIC COMPANY AT WEST LYNN, MASS.

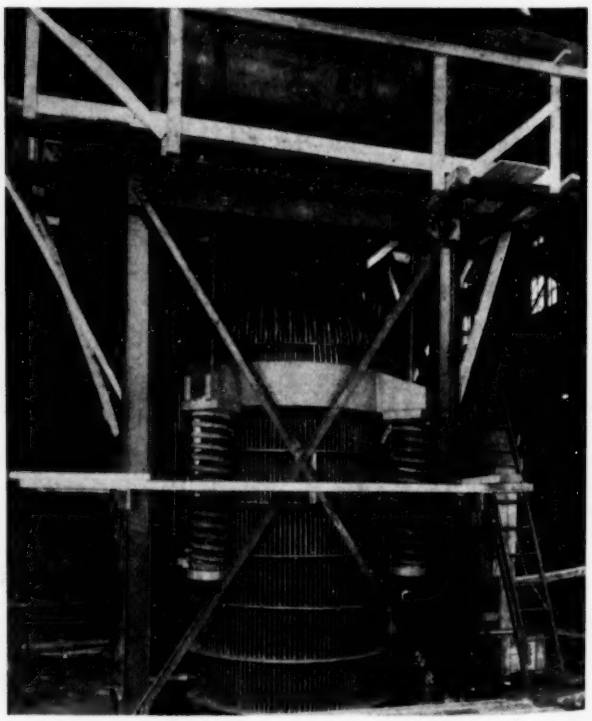


FIG. 17 TUBE ASSEMBLY FOR MERCURY BOILER, PITTSFIELD WORKS, GENERAL ELECTRIC COMPANY

the Pittsfield boiler tests, and from tests in Schenectady of typical full-size tube circuits. Every new design detail of this boiler was adopted only after exhaustive tests on full-scale models with water-air mixtures, mercury-air mixtures, and under actual fired conditions, with mercury vapor being formed. This care has resulted in the excellent performance of the equipment from the first day of operation to the present.

The porcupine tubes used for many years in mercury boilers were ingenious in design and functioned quite well, but the small passages were a potential source of plugging by foreign material and they were hard to clean and expensive to manufacture, so they were not used in the new boiler. By substituting wall tubes for the former porcupine-tube surface it became possible to remove the complication of seven drums which involved equalizing difficulties and other disadvantageous features. The new boiler has a single drum of 54 in. ID with $4^1/_2$-in-thick walls, 30 ft long, weighing 90,000 lb. A section through the drum, Fig. 22, shows the arrangement of baffles which are functioning so well that there is no measurable moisture carry-over. In fact, the pressure drop from the drum to the turbine produces about 30 F superheat in the vapor. The air-water test on a full-

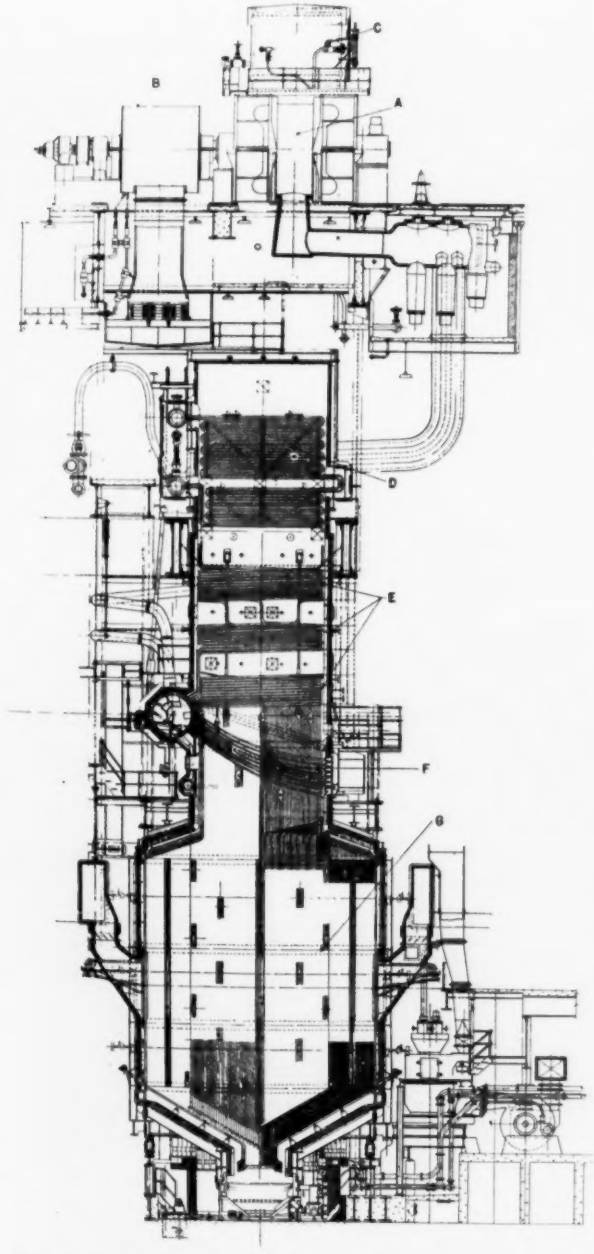


FIG. 18 GENERAL ELECTRIC MERCURY BOILER INSTALLED AT THE KEARNY STATION OF THE PUBLIC SERVICE ELECTRIC AND COMPANY OF NEW JERSEY, 1940

A Mercury turbine
B Generator
C Mercury condenser steam boiler
D Steam superheater
E Convection surface
F Slag screen
G Furnace

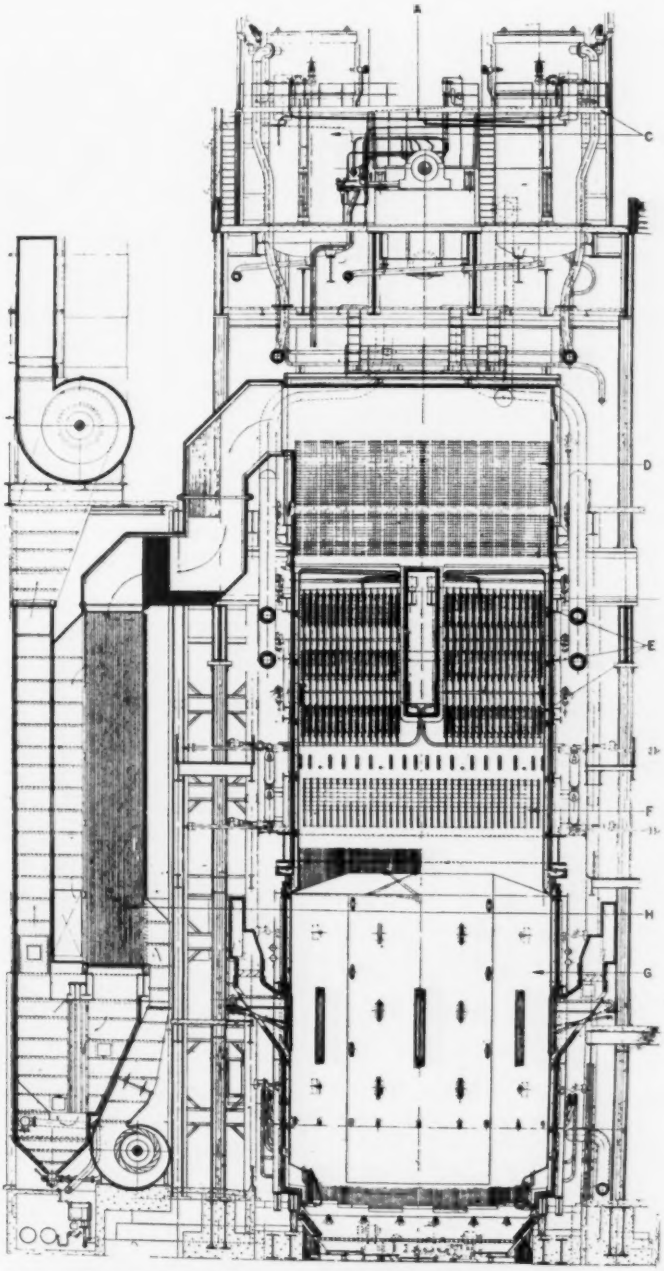


FIG. 19 GENERAL ELECTRIC MERCURY BOILER INSTALLED AT THE KEARNY STATION OF THE PUBLIC SERVICE ELECTRIC AND GAS COMPANY OF NEW JERSEY, 1940

A Mercury turbine
C Mercury condenser steam boiler
D Steam superheater
E Convection surface
F Slag screen
G Furnace
H Air heater

size model of the drum baffles showed a maximum moisture carry-over on a mercury basis of seven parts per million, or only 0.007 per cent by weight, and the solids about one two-hundredth of this value.

To form the slag screen, shown in Fig. 23 (which is a view upward from below), 288 of the furnace wall tubes are continued across the reduced section or neck of the furnace, being attached at one end to a movable panel, Fig. 24, and at the other end to the drum. The $1^{11}/_{16}$-in. OD × $1^{1}/_{8}$-in. ID tubes are arranged in 36 sections, 8 tubes high on $8^{3}/_{4}$-in. horizontal centers. The catenary shape helps to keep the stresses low and the movable panel, which is moved by the expansion of four tubular columns which are heated by circulating boiler mercury, maintains a low stress for all temperature conditions, including those encountered during starting and shutting down the boiler.

The convection surface consists of the six bundles of tubes above the drum. They are separated for soot blowers and for accessibility. The tubes are individually supported by vertical tube supports cooled by water circulating thermally from the condenser boiler drums on the floor above.

The mercury convection tubes are $2^{3}/_{8}$ in. OD × $1^{7}/_{8}$ in. ID in the lower bank and $2^{1}/_{4}$ in. OD × $2^{1}/_{4}$ in. ID in the two upper banks. They are fed from 180 of the furnace wall tubes at the top of the upper bundles and at the top of the lower bundles. The middle bundles are in series with the upper bundles. During

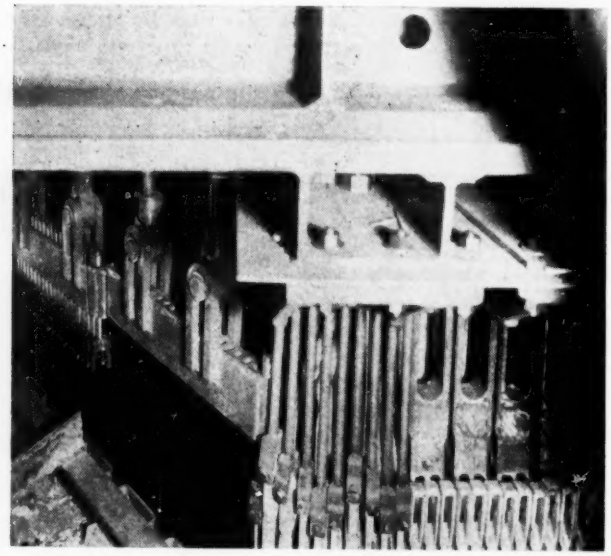


FIG. 20 GENERAL ELECTRIC MERCURY BOILER
(View showing furnace wall tube suspension at arch, during construction. In mercury-steam-electric power station of the Public Service Electric and Gas Company at Kearny, N. J.)

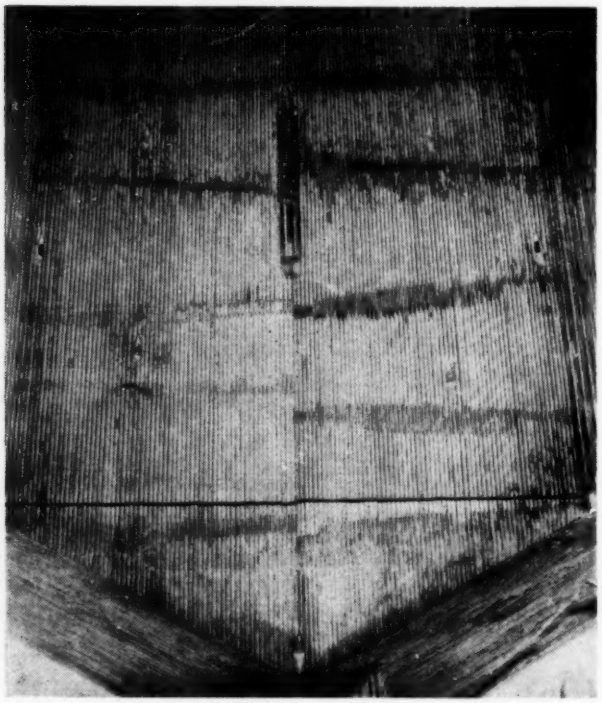


FIG. 21 GENERAL ELECTRIC MERCURY BOILER
(View showing east side furnace wall with burner in the middle. In mercury-steam-electric power station of the Public Service Electric and Gas Company at Kearny, N. J.)

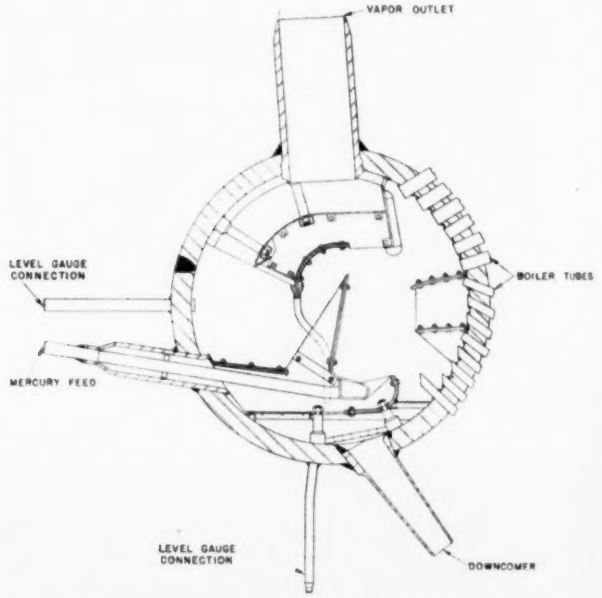


FIG. 22 SECTION THROUGH MERCURY-BOILER DRUM SHOWING BAFFLING TO ASSURE DRY VAPOR

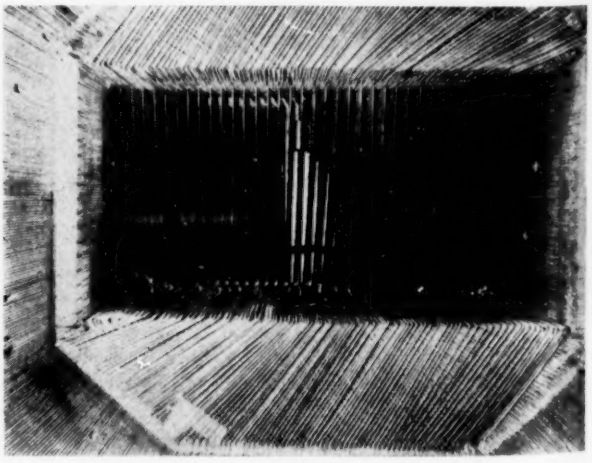


FIG. 23 GENERAL ELECTRIC MERCURY BOILER
(View showing slag screen and arch, from below, in mercury-steam-electric power station of the Public Service Electric and Gas Company at Kearny, N. J.)

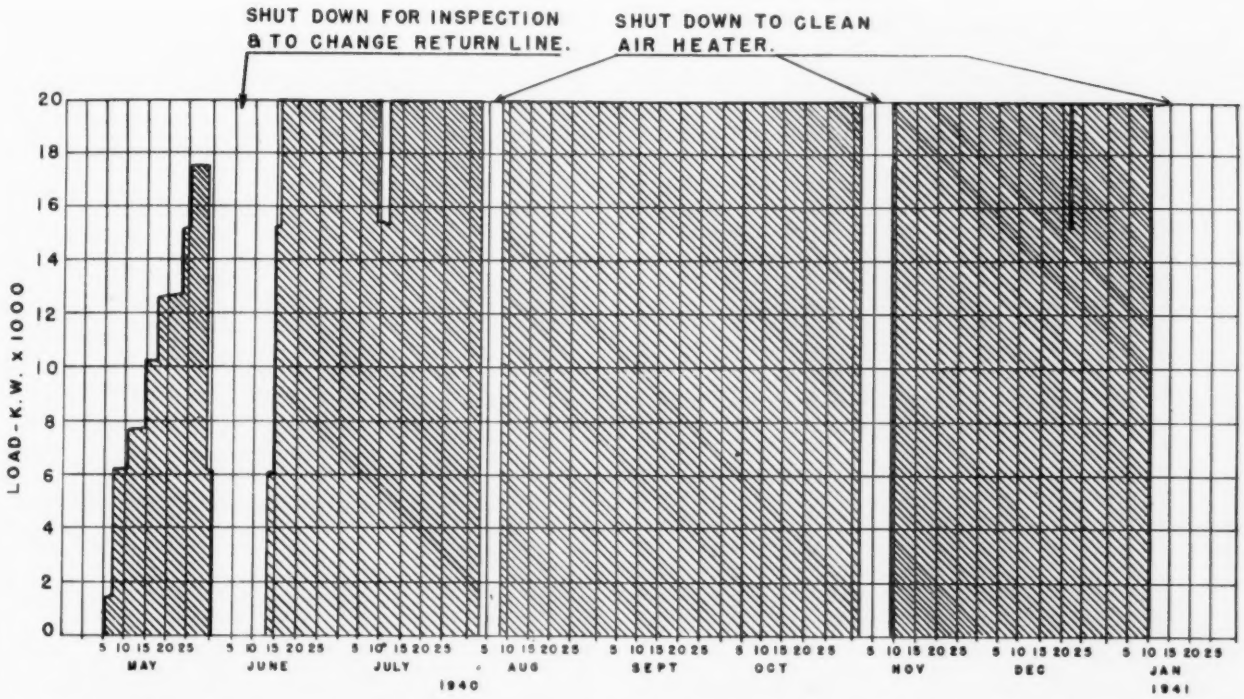


FIG. 25 LOAD CHART—GENERAL ELECTRIC MERCURY TURBINE, KEARNY GENERATING STATION, THE PUBLIC SERVICE ELECTRIC AND GAS COMPANY OF N. J. (COMPLETE RECORD TO JAN. 10, 1941)

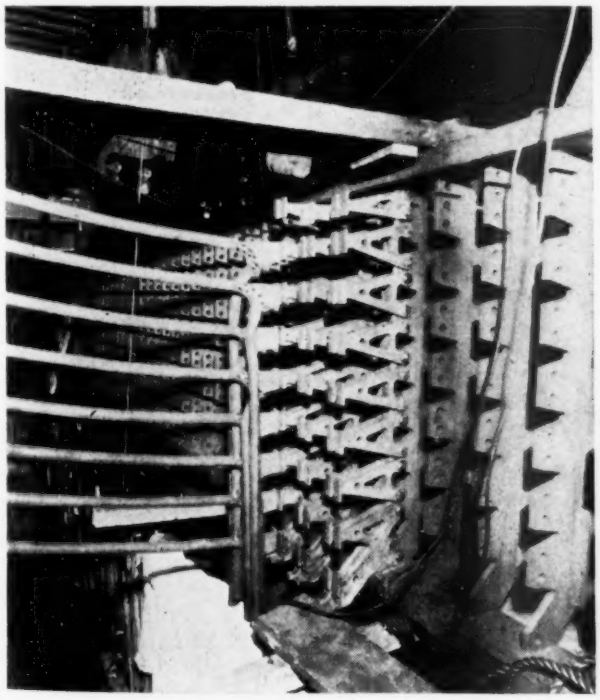


FIG. 24 GENERAL ELECTRIC MERCURY BOILER
(View showing connection of slag screen tubes to floating support, during construction in mercury-steam-electric power station of the Public Service Electric and Gas Company at Kearny, N. J.)

operation the thermal circulating action lifts the mixture of liquid and vapor to the top of the tube banks and from this point it flows back to the drum by means of a combination of pressure drop and gravity head. When the boiler is cold all the mercury, normally in the convection tube bank when operating, drains back into the drum because of the constant hydraulic grade from the top to the bottom.

The steam superheater, located above the fog bank, is of standard design and is the one originally installed in 1933.

The air preheater is the single-pass tubular type which was installed in 1933.

The Kearny boiler contains 392,000 lb of mercury. The heat developed suffices for the generation of 20,000 kw in the mercury turbine and 30,000 kw from the steam generated in the condenser boiler. Since auxiliary equipment requires 1200 kw, the total mercury in the boiler amounts to 8.0 lb per net kw.

The convection surface is empty when cold but, in service, is filled with a mixture of liquid and vapor, mostly vapor. It is believed that an extension of this principle of mixture-filled tubes to the hotter parts of the furnace would materially reduce the amount of mercury needed in future designs so that its cost and obtainability would be less important factors.

The design of this boiler in so far as the functioning of the mercury is concerned was by General Electric Company. The mechanical design, combustion facilities, and building and erection were done by The Babcock & Wilcox Company.

Between May 6, 1941, and Feb. 1, 1941, the new plant has produced 103,540,000 kwhr from the mercury turbine generator and 1,505,232,000 lb of steam. There are approximately five thousand field and factory welds in the boiler and no leaks were found in the hydrostatic test or during operation.

Operation has been excellent and practically all the time at full load. (See load chart, Fig. 25.) Firing has been with oil for the most part. Because of the unusual boiler design and the temperatures at which the tubes work, it was thought advisable to try out coal firing to find the nature and location of slag deposits before installing soot blowers.

Mercury Turbine and Auxiliary Equipment

The good condition of the mercury-turbine rotor and dia-

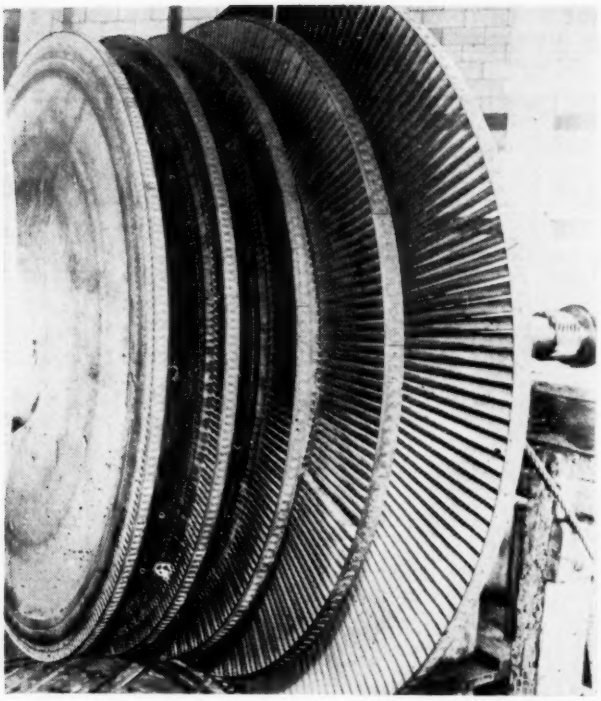


FIG. 26 ROTOR (HALF) FOR GENERAL ELECTRIC DOUBLE-FLOW MERCURY TURBINE, 20,000 KW, 900 RPM, 5-STAGE. IN MERCURY-STEAM-ELECTRIC POWER STATION OF THE PUBLIC SERVICE ELECTRIC AND GAS COMPANY AT KEARNY, N. J.

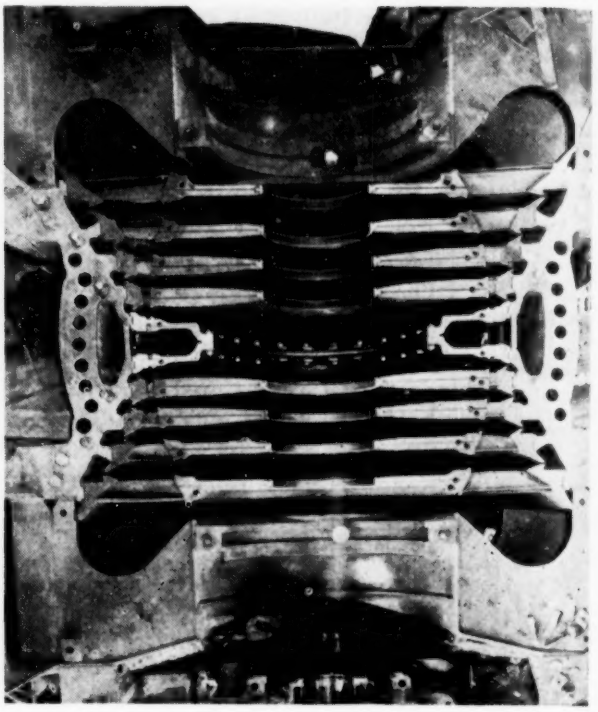


FIG. 27 SHELL: LOWER HALF WITH DIAPHRAGMS FOR GENERAL ELECTRIC DOUBLE-FLOW MERCURY TURBINE, 20,000 KW, 900 RPM, 5-STAGE. IN MERCURY-STEAM-ELECTRIC POWER STATION OF THE PUBLIC SERVICE ELECTRIC AND GAS COMPANY AT KEARNY, N. J.

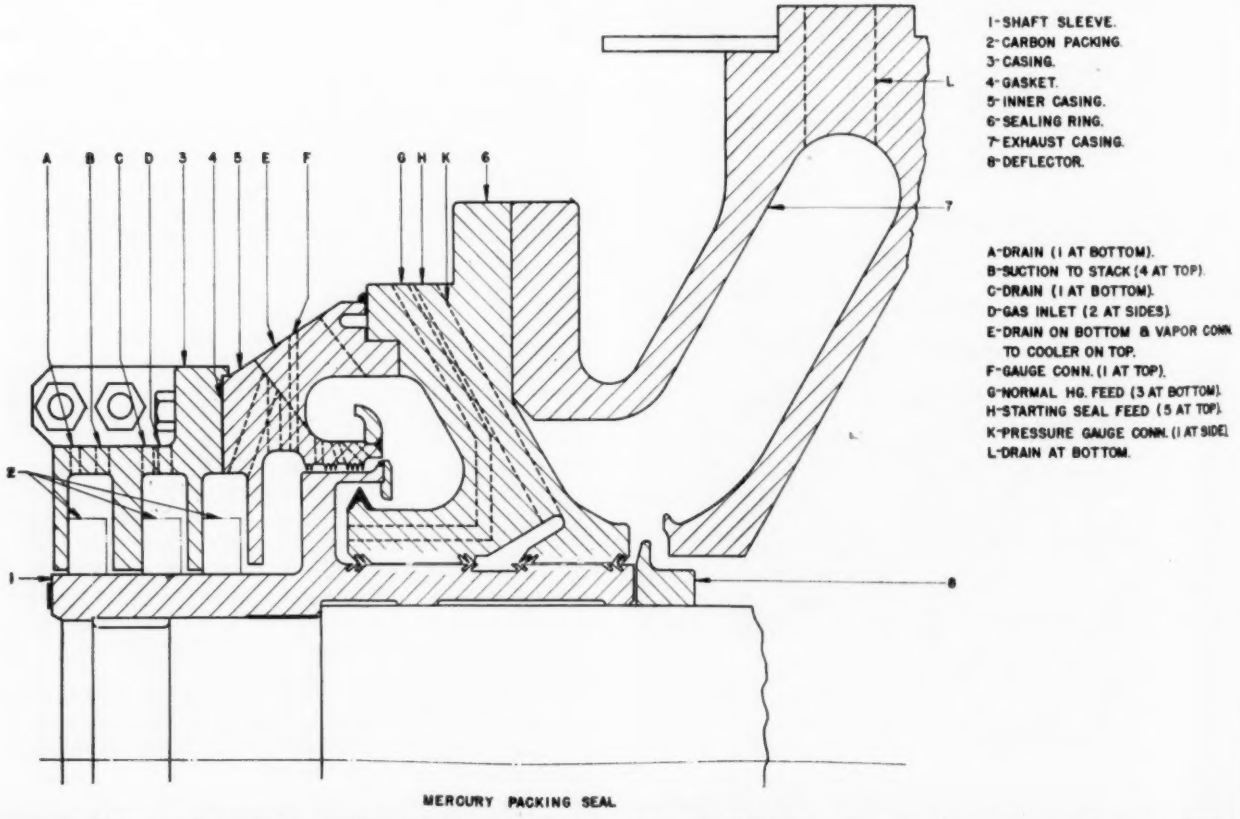


FIG. 28 MERCURY PACKING SEAL FOR GENERAL ELECTRIC MERCURY TURBINE, 20,000 KW. VERTICAL SECTION ALONG SHAFT OF UPPER HALF. FOR THE PUBLIC SERVICE ELECTRIC AND GAS COMPANY, KEARNY, N. J.

phragms after five years' service can be seen in Figs. 26 and 27. One of the shaft packings, which prevent leakage of air into the turbine, is shown in section in Fig. 28. It is a liquid-seal packing in which the seal is maintained by mercury liquid being whirled by the rotating cup which is part of the shaft sleeve. Mercury overflowing from the cup, as well as mercury from the inner casing, drains by gravity to a cooler, in which the cooling is done by a water-filled coil, and is then drawn back into the rotating cup by the vacuum on the condenser side of the seal. A drain to the condenser ahead of the outside carbon packing ring prevents any escape of mercury. Neutral gas is supplied to the middle carbon ring box and the excess, together with any air which leaks past the outside carbon ring, is sucked off to the stack from the outside packing box. The small amount of make-up liquid required is obtained from that which is condensed in the air-removal coolers on the condenser boilers.

It is desirable to remove the air from the entire system and to have a vacuum of about 0.4 in. Hg abs before firing the boiler. The turbine shaft when idle, or operating below normal speed, is sealed by pumping a sufficient quantity of mercury liquid through the packing so that the shaft is submerged. The pump has a capacity of 1,800,000 lb per hr at 60 ft head, which is far in excess of normal requirements unless the labyrinth teeth on the packing are seriously damaged. This pump is mounted in a small tank containing a cooler so that the liquid for starting is in a closed circuit. The mercury from the tank can be returned to the boiler after normal speed on the turbine is reached.

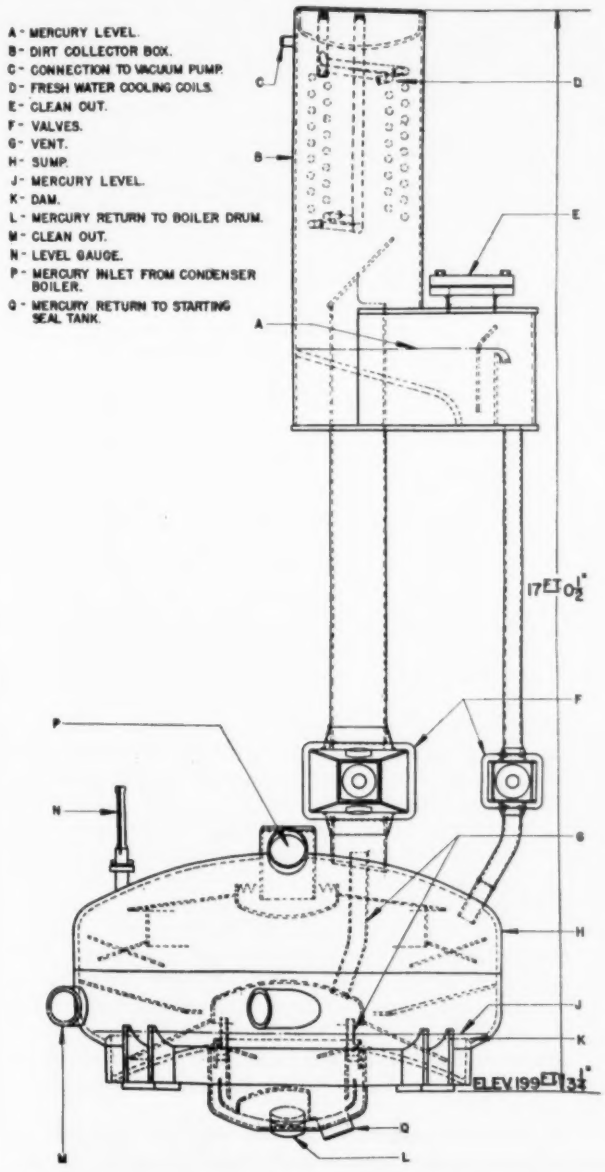


FIG. 29 MERCURY IMPACT CLEANER. FOR THE PUBLIC SERVICE ELECTRIC AND GAS CO., KEARNY, N. J.

Mercury Impact Cleaner

The mercury impact cleaner for removing dirt and solids from the mercury consists of a sump and dirt-collector tank with interconnecting pipes and valves as shown in Fig. 29. Condensed mercury from the two condenser boilers flows by gravity to the sump where it is cleaned and flows back to the boiler drum by gravity.

A vacuum of about $^1/_2$ in. of mercury higher than that in the condenser boiler is maintained in the dirt-collector box by means of the vacuum pump. Mercury liquid cascading down over the shelves in the sump tends to break up into fine particles and the dirt-bearing liquid is flashed, or reboiled, because of the reduced pressure, and carried up to the dirt-collector box. Here the vapor is condensed by the water-cooling coils and then returns over the baffles and through the small pipe to the sump. The fine dirt remains on the surface of the pool in the dirt-collector box and at infrequent intervals during operation the two connecting valves can be closed and the flange cover removed for cleaning.

Any heavy foreign material, such as welding beads, will be washed and held behind the dam around the inside of the sump. At a regular plant-inspection period this dirt can be removed through the openings provided. The sealing arrangement at the bottom maintains the vacuum in the sump and prevents vortexing of the outflowing liquid.

Air Removal and Vacuum System

An air-removal cooler is provided for each condenser boiler. The cooling coil passes all the feedwater entering the condenser boiler steam drum. Air and other noncondensable gases are drawn from the condenser shell into the air-removal cooler and then through a secondary cooler to the vacuum pump. Mercury condensed in the air-removal coolers is used as make-up for the shaft seal packings and any excess is drained directly back to the condenser. Mercury condensed in the secondary cooler is drained to the sump.

Steam-jet air ejectors are used for rapidly reducing the pressure in the system before starting. During operation a Kinney vacuum pump is used. The air leakage has been maintained below 0.4 cu ft per hr.

Boiler Filling and Draining System

A tank in the basement will store the 392,000 pounds of mercury in the system if it becomes necessary to drain the boiler. In the event of a leak two emergency drain valves can be opened which allow the mercury to rapidly drain through a cooler to the tank. A small pump in this tank will return the mercury to the boiler drum.

Mercury Tube Temperature Recorder

In order to have complete knowledge of the action of this boiler during the initial operation, a thermocouple was attached to the back of each of the 764 tubes surrounding the firebox. A temperature recorder is attached to the couples from 78 typical tubes and a record is automatically made of each of these tem-

peratures, as well as the mercury saturation temperature, every thirty minutes. The recorder is mounted on the boiler instrument panel and has been accepted by the operators as a real aid in operation. A sample section from the recorder chart is seen in Fig. 30. The other thermocouples are attached to portable recorders and temperatures were measured during the starting period.

Mercury Detector

The first reliable mercury detector depended upon the action of mercury vapor on selenium-sulphide coated paper. Samples from the flues were continuously blown on a slowly rotating chart and the chart was scanned by a photoelectric cell which would actuate an alarm if the paper darkened due to the presence of mercury vapor in the gas. Selenium sulphide is extremely reactive toward mercury vapor, black compounds of mercury sulphide and mercury selenide being formed. This instrument can detect one part per million of mercury vapor in the flue gas.

The latest mercury detector is of the optical type and its operation depends upon the opacity of mercury vapor to ultraviolet light of a certain wave length. A flue-gas sample is continuously passed through a chamber at one end of which is an ultraviolet lamp and at the other end a photoelectric tube. Through proper amplification the photoelectric tube records the vapor concentration on a meter located on the boiler instrument panel. This detector will accurately detect a concentration of one part per hundred million. The normal test consists of throwing one cubic centimeter of mercury into the fire which gives full scale reading on the concentration meter.

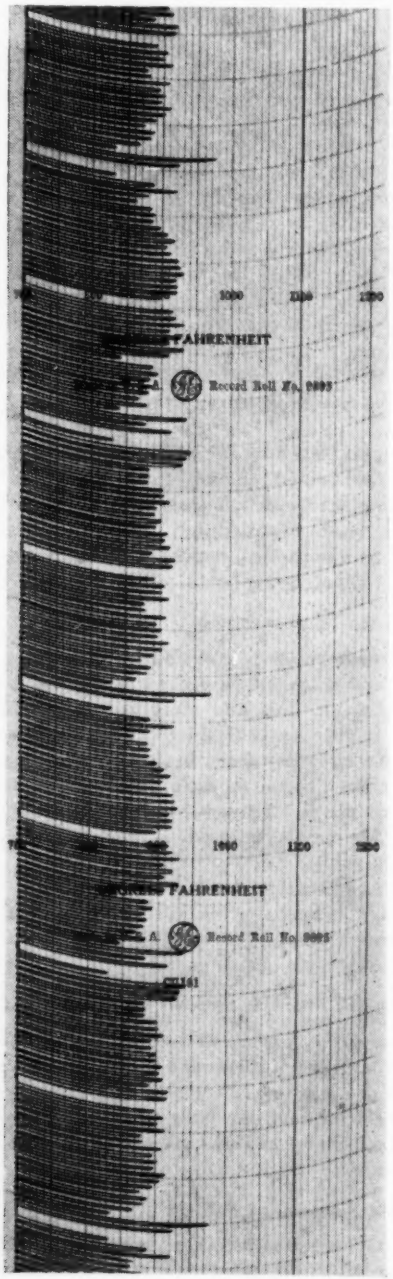


FIG. 30 REPEATING TEMPERATURE RECORD OF 80 THERMOCOUPLES ON GENERAL ELECTRIC MERCURY BOILER. THE PUBLIC SERVICE ELECTRIC AND GAS CO., KEARNY, N. J.

Tube Material

Up to the time of the Lynn boiler which had chrome-molybdenum-steel tubes, all previous mercury boilers were made of ordinary low-carbon steel, and in most cases were calorized by the dip method and heat-treated. This was done before there was any knowledge of the rupture strength of such material at high temperature for extended periods of time. In 1937 test machines were started to study the long-time rupture strength under temperature of carbon steel and many kinds of alloy steels. The General Electric Company now has seven such furnaces in operation at different temperatures, each holding twelve samples.

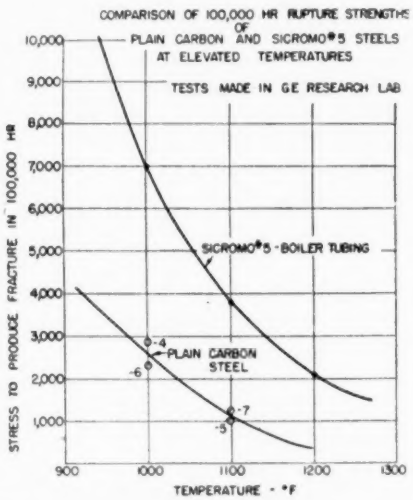


FIG. 31 COMPARISON OF 100,000-HR RUPTURE STRENGTHS OF PLAIN CARBON AND SICROMO 5 STEELS AT ELEVATED TEMPERATURES

(The steel originally known as Sicromo 5 is now known as Sicromo 5S.)

The results of these rupture tests, together with other considerations mentioned later, led to the selection of an alloy called Sicromo 5S (formerly known as Sicromo 5) for the Kearny boiler tubes. This alloy contains 0.12 per cent carbon, 0.50 per cent molybdenum, 5.0 per cent chromium, and 1.5 per cent silicon. Fig. 31 shows that 3000 psi is the 100,000-hour rupture strength of carbon steel at 975 F, whereas the Sicromo 5S is equally good at 1140 F.

The particular composition selected for these tubes contains sufficient chromium and silicon to resist oxidation at the operating temperature and with the usual character of coal or oil ash. In the cooler passes of the boiler Croloy 3, used for the lower bundles

of the fog bank, and Croloy 2, used for the upper bundles of the fog bank, will give equal protection.

Solubility of Iron in Mercury

The solubility of iron in mercury at high temperature has been a fundamental obstacle in the development of the mercury cycle. This action reduced the thickness of the metal, and the disintegrated iron and iron oxide were deposited in some places on the heating surfaces in the lower-temperature regions, frequently restricting or stopping the flow of mercury or vapor.

How far this solubility is retarded by the use of Sicromo 5S steel can be seen from Table 4, which shows the rate of solubility per year expressed in mils. The carbon steel is the material used in Hartford, Schenectady, Pittsfield, and the old Kearny boilers. The 5 per cent chrome steel was used in Lynn. The new Kearny boiler and slag-screen tubes are made of Sicromo 5S.

TABLE 4 SOLUBILITY OF STEEL IN MERCURY IN MILS PER YEAR

Temperature, deg F	Carbon steel	5 per cent chrome	Sicromo No. 5S
900	4	2	0.2
1000	9	4	0.5
1100	22	10	1.1
1200	53	25	2.5

While these tests, which were carried on over a period of five years, showed a possibility of extending the period between cleanings 20 times, or the possibility of using higher temperatures with the same period between cleanings, a parallel investigation was made to find some element which could be added to the mercury to inhibit solubility of the steel. Zirconium and titanium were found to be the most promising, the latter being preferred because of its ease of application. The present indications are that a low percentage of titanium maintained in the mercury completely stops solubility of the steel. The amount of solubility is readily detectable by measuring the deposit on tubes and by analyzing the solids in the sump and pipe lines. The amount of titanium required is a function of the temperature with a spread of 0.0001 per cent for 850 F up to 0.001 per cent, or ten parts per million, for 1000 F saturation mercury temperature.

Wetting and Dewetting

Steel surfaces, even though slightly oxidized, can be wetted by mercury alone with time and patience. But such surfaces will not remain wetted if more oxygen is introduced. In other words, mercury is a poor deoxidizing agent. As the result of a comprehensive search for suitable deoxidizing and wetting agents, the combination of magnesium and titanium has been found to hold the boiler tubes in a properly wetted condition unless the air infiltration is excessive. In combination with the titanium concentration previously mentioned it is necessary to maintain 0.002 per cent metal magnesium in solution in the boiler. It appears that magnesium is essential to maintain the titanium active, and that titanium assists in wetting the steel.

Oxides

The formation of oxides formerly caused considerable trouble in the mercury cycle. These difficulties appeared as dewetting, causing poor heat transfer, and mercury-oxide and iron-oxide deposits in tubes, sumps, and pipes. The possible sources of oxygen are air infiltration through the turbine and condenser casings operating below atmospheric pressure, the turbine shaft packings, air in the boiler when starting up, and water leaks in the condenser boilers or coolers.

TABLE 5

Test No.	1	2	3	4	5	6	7	8
Date, 1940	5-9	5-11	5-16	5-20	5-23	5-27	6-17	6-18
Mercury turbine generator output, kw	6250	7763	10188	12712	15333	17683	20213	20175
Steam flow, 1000 lb per hr	125.7	140.9	178.4	211.7	239.9	271.9	306.6	306.7
Steam pressure, lb per sq in. gage	351.6	355.6	355.4	356.6	356.8	359.7	358.1	359.4
Steam temperature, F	666	689	708	682	700	688	711	706
Feedwater temperature, F	375	306.7	375.3	374.2	370.7	367	374	374
Equivalent steam-turbine output, kw	11863	13497	17290	20223	23141	26185	29790	29713
Total gross output, kw	18113	21260	27478	32935	38474	43868	50003	49888
Auxiliary power (calc), kw	396	466	610	743	887	1034	1212	1208
Total net output, kw	17717	20794	26868	32192	37587	42834	48791	48680
Fuel oil, lb per hr	9481	11464	14346	16672	19029	21760	24626	24518
Stack temperature, F	310	368	369	370	358	373	382	374
Calorific value of fuel (as fired), Btu per lb	18276	18276	18276	18276	18272	18272	18268	18202
Net plant heat rate, Btu per kwhr	9780	10076	9758	9465	9250	9282	9220	9168
Net plant heat rate corrected to 370 F stack temperature, Btu per kwhr	9948	10082	9761	9465	9282	9274	9189	9158

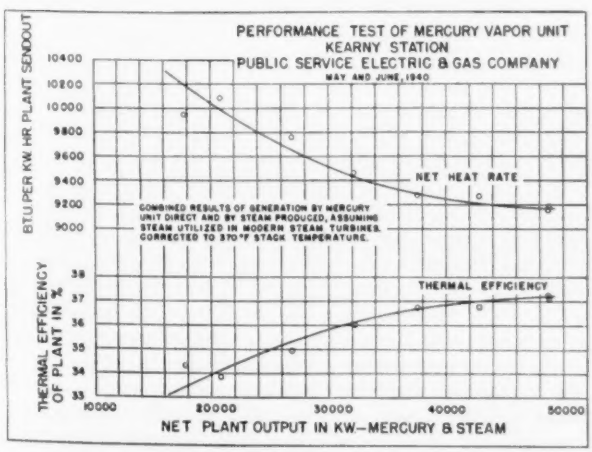


FIG. 32 PERFORMANCE TEST OF GENERAL ELECTRIC MERCURY-VAPOR UNIT, KEARNY STATION, THE PUBLIC SERVICE ELECTRIC AND GAS COMPANY OF NEW JERSEY. MAY AND JUNE, 1940

Excessive oxygen means loss of the titanium and magnesium and the production of solids. To prevent air leakage the new-type mercury shaft packing was developed, and valve stems operating under vacuum were covered with metal caps. These precautions have reduced the air leakage at Kearny from 300 cu ft per hr to less than 0.4 cu ft. An operating rule for all the mercury plants is to investigate any leakage greater than 1 cu ft per hr.

With this slight amount of air which still infiltrates into the system it is relatively easy to absorb all the oxygen with the magnesium, forming magnesium oxide which is easily cleaned out.

When shutting down a plant, nitrogen is bled into the system until the temperature is so low that the rate of oxidation is negligible. When starting up a plant, it is pumped down to a reasonable vacuum before the fires are lighted.

KEARNY TEST RESULTS

During the months of May and June, 1940, tests of the mercury plant at Kearny were conducted by the General Electric

Company with the assistance of The Babcock & Wilcox Company and the Public Service Electric and Gas Company of New Jersey. Eight-hour tests at 37½, 50, 62½, 75, 87½, and 100 per cent load were made, allowing at least 48 hr at each load before making the test. A test at 30 per cent load was run for two hours.

The generator terminal output was obtained from the station totalizing wattmeter which is periodically checked by the Public Service Company. The steam flow from each condenser boiler and the steam superheater was measured by calibrated steam flowmeters. The total flow from the steam superheater closely checked the sum of the flows from the condenser boilers. The fuel-oil flow was measured by an accurately calibrated oil flowmeter. All pressure gages, thermocouples, and thermometers were calibrated before the test.

The steam from the superheater was delivered to the station mains. As no particular steam turbine was driven by the steam produced in the mercury plant it was necessary to make a calculation of the total plant auxiliary power, which was deducted in order to arrive at a net plant heat rate. The equivalent power from the steam is based on the assumption that the steam made in the mercury plant was being used in modern steam turbines from which steam was extracted to heat the feedwater to the temperatures prevailing during the tests.

At reduced loads corrections to the steam-turbine water rates were made for reduced temperature and pressure but no correction was made for increased water rate due to reduced flow. In other words, it was assumed that the steam produced was mixed with the station steam and credit was taken only for the power which would be generated by the steam produced in the mercury plant. With only one steam turbine receiving all its steam from the mercury plant, which would be the case with a mercury-vapor-steam condensing plant, the plant heat rate would be somewhat higher at light loads than those shown, because of the increased steam-turbine water rate at reduced load.

The test results are shown in Table 5 and the net plant heat rate is shown in Fig. 32. The full-load heat rate of 9175 Btu per kwhr, or 37.19 per cent thermal efficiency, means that a kilowatthour is being produced for 0.502 lb of 18,275 Btu per lb bunker C fuel oil.

Applications

All the mercury equipments built so far have been "topping" units. This is the field for the widest application of the process, as any steam plant, no matter what its operating temperature and pressure, can be given a new lease on economic life if mercury equipment is added.

With mercury superposed over 600 lb gage and 730 F steam, 7250 kw may be generated per 100,000 lb per hr of steam produced in the condenser boiler, whereas a superposed steam turbine at 1200 psi gage and 925 F can generate 1960 kw per 100,000 lb per hr steam flow. Even when such a steam turbine is superposed over low-pressure turbines operating at 350 psi gage and 635 F, the power generated by the high pressure is only 3330 kw per 100,000 lb per hr steam flow. Looking into the future, mercury might be superposed on modern 1200 psi gage and 925 F steam and in this case 5650 kw would still be generated per 100,000 lb per hr of 1200 psi gage steam. This illustrates the large amount of by-product power which can be produced by superposing the mercury cycle over a fixed amount of steam flow.

As time goes on there will, no doubt, be applications for superposition over higher existing steam pressures and superposing still greater capacities over moderate steam pressures.

Industries requiring steam for process work at any pressure and temperature will find the mercury plant furnishes an economical means of supplying the steam, with greater amounts of by-product power available than can be furnished by any other power cycle.

The mercury process, because of its better fuel economy, should be well suited for ship propulsion. The savings in fuel would result in an increase in pay load for merchant ships, or an increase in cruising radius of naval vessels.

A mercury-vapor steam-turbine electric locomotive could be built with the steam turbine exhausting at atmospheric pressure, thus decreasing the size of the air-cooled condenser. Even with high exhaust pressure, considerable savings in fuel would be realized.

The mercury cycle offers an extremely simple and profitable means for producing power and is especially adaptable to any case where cheap power is desired.

Discussion

Perry Cassidy.[10] The boiler manufacturer has generally kept pace with the prime-mover manufacturer with respect to the pressures and temperatures required. Probably he, as well as the turbine manufacturer, has been somewhat ahead in his readiness to build beyond the economic operating limits demanded by the user. Steam boilers have been built for pressures approaching the critical, and superheaters for average steam temperatures over 950 F, and with maximum steam temperatures above 1000 F in individual elements due to imperfect distribution of steam and gas flow. Carbon steel constitutes the principal material for steam-boiler pressure parts, with a tendency toward higher tensility but with no need for alloys, except for higher-temperature superheaters. Since we are not limited by available materials, we are ready to produce steam boilers which meet the further requirements of the turbine design and operating engineers.

When asked by the General Electric engineers to co-operate with them in the design and to build the second mercury boiler for Kearny, we were able to draw upon our experience with steam boilers and superheaters, but we were not limited by ideas and practice entirely applicable to steam. It was necessary to change the basis of design from maximum temperatures of 600 to 650 F inside the generating tubes, the usual maximum limit for steam, to a range of 975 to 1070 F for mercury. Only the hot end of the highest-temperature superheaters had approached such temperatures. Even with the best commercial alloys available for generating tubes, the minimum as well as maximum temperatures in the second Kearny mercury boiler are well within the range where creep limits the design stress. The maximum calculated tube temperature in this boiler is such that even the best available commercial alloy steel will require operating experience to determine its limitations and usefulness.

Both the earlier mercury units and the high-pressure steam units have brought about a realization of the factors involved in thermal gradients through thick pressure members, such as drums, and tube connections. Thermal sleeves and other means of keeping temperature gradients within suitable stress limits have been developed for all purposes required. Fig. 22 of the paper shows such a thermal sleeve at the mercury-feed connection. This same factor is also involved in the rate of bringing up a unit with thick drums and other pressure parts where stresses due to temperature gradient must be respected.

One of the most important factors in connection with the construction of the Kearny rebuilt unit is the tube welding, both shop and field. The assembly and construction of such a unit, without adequate knowledge of welding and heat-treating of

[10] Executive Assistant, The Babcock & Wilcox Company, New York, N. Y. Mem. A.S.M.E.

many welds in alloy steels throughout this unit, would be impossible. Many long circuitous tubes without headers or junction boxes are being used in steam boilers as well, which demonstrates that any development in a given field involves certain problems which, when solved, apply to other similar problems. The development of the steam unit helps mercury, and vice versa.

The early designs and construction of mercury boilers were quite complicated and involved expensive fabricating operations. The attempt to utilize plain-carbon-steel pressure parts and the difficulties involved in keeping the tubes wetted by the mercury without the stoppage of some of the circuits by deposits of solids in the tubes resulted in continued complication. Until the time of the design and installation of the present new Kearny unit, this condition became worse rather than better. In the Kearny boiler the best available alloys were used and, in addition, every detail of design was carefully studied in order to produce as safe and conservative an operating unit as possible, with the consideration of cost as secondary.

In developing newer boiler designs, the General Electric Company has considered lower-head units with less spread between the drum pressure and that at which boiling begins, which is probably where the highest tube temperature occurs. This permits higher drum pressures with higher thermal efficiency of the cycle, or the use of less expensive alloy tubes, or a higher factor of safety on tube temperatures for the same alloy.

Wider tube spacing in the furnace and higher heat-release rates per square foot of furnace surface and furnace volume tend to make boiler costs still lower, particularly by reducing the mercury content of the boiler.

It is likely that the ultimate economic limits of temperature will be established by the rate of oxidation of the outside of the tube subjected to the hot gases of combustion. This may also be the limit in temperature of steam-superheater elements, affecting the choice of alloys and their costs and establishing the ultimate economics of the unit.

Progress toward simplicity applies to the condenser boiler also. The use of alloys in this case is not a factor. The application of the principles of steam-boiler design to the design of condenser boilers does not present any special difficulties. The boiler casing must be designed to stand the full vacuum on the condenser and of course all-welded construction is necessary.

The solution of the wetting problem in the mercury tubes by the General Electric engineers, in the development of chemical treatment with minute quantities of titanium and magnesium is, in our opinion, an outstanding example of the application of the highest type of engineering. We wish to pay tribute to the work of those men whose labors have contributed to this accomplishment.

We are of the opinion that engineers responsible for the installation of power equipment should be aware and fully informed as to the possibilities of mercury power generation.

The development of the mercury-power cycle may proceed from this time with increasing rapidity and, even though power engineers may not find mercury justifiable at present, they should not necessarily assume that this will be true in later years as the art progresses.

B. P. Coulson, Jr.[11] Throughout the development of the Emmet mercury-vapor process, the mercury boiler design has been the outstanding problem. In the early experiments with mercury boilers, the overheating of tube surfaces was not understood, and it was not until later years that the importance of wetting by mercury was fully appreciated. Methods to insure adequate wetting of heating surfaces were not developed until recent years by the General Electric Company.

In some of the early experiments, it was observed that the boiler surfaces did not become overheated in the liquid regions of the tubes but, where vapor started to form, the heat transfer became uncertain. From these observations, it was considered important for the hottest gases first to pass over that portion of all the tubes containing liquid and thus apply a less intense heat where vapor is formed. Also, to insure against overheating, a vigorous circulation was considered necessary. On this principle the honeycomb type of boiler, shown in Fig. 4 of the paper, was designed. The gases in this boiler entered all of the tubes at the bottom, in the region of the liquid mercury. The radiant heat from the furnace is absorbed also by the liquid circulating in the lower ends of all the tubes.

This boiler had an additional feature for providing dry vapor by allowing the vapor to cross over the upper portion of the tubes between baffles before leaving the boiler. This boiler was, however, abandoned because of insufficient provision for unequal expansion of the tubes, which caused leaks to develop through the welds at the bottoms of the tubes. To provide for free expansion of tubes, a dependent porcupine-tube boiler was adopted, as shown in Fig. 5 of the paper. Some years before this boiler was installed at Hartford, a porcupine-tube mercury boiler was made having tubes attached to a single upper header, the gas flow being across the tubes. At that time, the principle of applying the hottest gases at the bottom of all the tubes in the region of the liquid was not known, thus the tubes became overheated on the sides where vapor was formed. The gas flow over the boiler tubes, shown in Fig. 5, was parallel with the tubes in an upward direction, and the four headers were spaced to allow the gases to pass between them.

A further development of this boiler was the adoption of round headers, thus eliminating objectionable stay bolts. Three features of this boiler which at that time were of great importance were as follows:

1 When repairs were made to the boiler the mercury could be left in the tubes, and thus the interior surfaces were not exposed to oxidizing air which might impair the heat transfer.

2 The boiler tubes could be easily calorized by the dip method.

3 In case mercury leaks developed in any one of the tubes, the maximum loss of mercury could not be excessive.

In the early days of this development several minor mercury leaks developed in the boiler tubes.

When designing the new replacement boiler for Kearny, the all-important problem of coal-slag accumulation on heating surfaces was given the utmost consideration.

When slag screens were first proposed for mercury boilers, some doubt was felt for their safety, as they are exposed to both radiant and convection heat. To make sure of this a slag-screen tube was suspended across the furnace of the mercury boiler in the Schenectady Works of the General Electric Company, and its operation was observed for several weeks. These slag screens not only screen out some of the slag from the gases but also shield the slag particles which go through the screens from the radiant heat of the furnace. Thus, the slag particles assume the temperature of the gases and enter the convection surface in a dry condition.

In addition to slag screens to insure against slag accumulation on convection surfaces, the furnace-wall surfaces were designed with liberal proportions, thus the heat absorption from the furnace is high and so further reduces the temperature of slag particles both entering the convection surface and in the furnace proper.

This liberally proportioned furnace also insures good combus-

[11] Consulting Engineer, General Electric Company, Schenectady, N. Y.

tion, which in turn insures more complete oxidation of the iron in the slag, thus elevating the fusing temperature of the ash.

The mercury boiler at Kearny has now been operating at overloads for many months burning coal, and the slag conditions are most satisfactory.

It is now believed that the success of the Emmet mercury-vapor process is assured, the only requirements being to put into production an inexpensive boiler requiring only a small quantity of mercury.

W. LeR. EMMET.[12] The writer is very glad that this paper has been written. It gives a brief but nearly complete outline of the long history of this process, shows the very high degrees of fuel economy which it affords, and demonstrates that such results are not merely matters of theory but have been reduced to actual practice in recent months in the plant at Kearny, N. J.

The new knowledge, which, in spite of many setbacks, has developed step by step through experience with this process, has caused abandonment of methods which were at first considered practicable. In such things, every change of plan is likely to mean long delay.

If the mercury process does not come to the full commercial success which the writer knows that it deserves, it will be the first engineering failure that he was ever connected with. Naturally, there is a strong personal interest, since success with it would be more important than anything that the writer was ever able to accomplish, even his steam-turbine work.

The mercury installation, which has been operating at Hartford for many years, has been uniformly successful in all respects, except in the matter of the mercury boiler which, while still commercially available at a somewhat reduced load, has long since shown limitations which convinced the writer that a very much better and cheaper type of boiler must be devised, if this process were ever to come to its proper development. It has been mainly to the boiler problem that the writer has devoted such means as he could command in the last 7 or 8 years of his retirement.

Papers[13] have been presented before this Society and the Society of Naval Architects and Marine Engineers in which a new type of mercury boiler is described, which has been developed as a result of the studies and experiments of the writer.

Two definite aims were in mind in designing this new type of boiler: (1) To make a boiler of which every part of the interior is readily accessible for cleaning; and (2) to develop a mercury boiler in which the cost for construction and for mercury required is sufficiently low to give this process advantages over others with which it must compete. Experience has taught the lesson that first cost is vital, if it is desired to make a progressive move in the power industry. In these days of governmental expenditures of billions, the writer's ideas may seem small, but they may appeal to some of the practical men who attend meetings of this Society.

In his work in the power industry, whether electrical or mechanical, the writer has long used a rough rule as a basis of comparison and that is that, if we can save 1 per cent of the fuel, we can afford to spend a dollar a kilowatt to do so. This means that, if we could build a plant which did not require fuel at all, we could, in many cases, not add more than $100 per kilowatt to that cost without getting into difficulties in the matter of fixed charges.

Whether the exact rate here stated is or is not correct, the rule is valuable and applies to added parts which are expected to give improvements, as well as to complete plants.

The type of mercury boiler, which the writer has designed, is the only one so far proposed which in his opinion meets the two requirements that have been stated. Incidentally, it has shown another very valuable advantage, namely, that the chemical treatment of mercury mentioned in the paper under discussion has acted effectively in the one boiler of this type which has been commercially operated. Reference is made to the boiler at Pittsfield, shown in Fig. 17 of the paper. In other boilers known to the writer, conditions have appeared with this treatment which are considered dangerous.

It is hoped that what the writer has presented to the published record during his recent years of retirement may lead others to use the principles which he has demonstrated.

H. N. HACKETT.[14] The rebuilt Kearny mercury boiler is a success. The plant operates at full output continuously except for minor outages for cleaning and repairs. The availability of the rebuilt mercury plant to date has rarely, if ever, been equaled by steam units of like size. We believe this record can be duplicated over and over again in new installations.

The heat rate of the Kearny mercury unit is approximately 9200 Btu per net kwhr, which is better than originally expected. Heat rates of less than 9000 Btu are now attainable, and who can predict what the final figures will be when the steel producers make it possible radically to increase the temperature and pressure at the mercury turbine. A mercury unit, operating at 500 psi and 1500 F, superposed over the best steam cycle, should approach 7500 Btu per kwhr.

Kearny is successful. The development engineers have progressed sufficiently far to produce predicted results, and the operators are securing high availability from the equipment.

If the second book of "The Story of Mercury" is to be written, the principal text must come from the vast laboratories of the power industry, as the future of mercury unquestionably lies in that field. Expansion and commercial development can only come through increased use.

The leaders of this industry must again show the same courage and determination demonstrated while writing "The Story of Steam."

The search for higher and higher efficiencies, along with the relative simplicity of mercury operation, will most certainly provide the incentive for carrying this great development to its conclusion; thereby opening a new era of power generation that is destined to be as gigantic as the one we now enjoy.

H. E. MELTON.[15] The development of turbines, boilers, and related equipment for the utilization of mercury vapor under pressure has been one of the engineering achievements of the last few years. The progress made since the early experiments at Schenectady has been very clearly described by the authors.

The engineers of the General Electric Company are justified in being proud of the latest installation. This is an outstanding accomplishment of engineering design, construction, and performance. Great credit is due them, not only for having pioneered this highly efficient thermal process, but also for having at the same time put it on the successful commercial basis demonstrated at Schenectady, Hartford, and Kearny.

There are enormous possibilities for the application of mercury

[12] Deceased since the discussion was presented on March 19, 1941. Inventor of the Mercury-Vapor Process of power generation; formerly Consulting Engineer, General Electric Company, Schenectady, N. Y. Mem. A.S.M.E., and A.S.M.E. Medalist, 1929.

[13] "Mercury Vapor for Central-Station Power," by W. LeR. Emmet, *Mechanical Engineering*, May, 1941, pp. 351–356; also "A Mercury Propelled Cargo Ship," by W. LeR. Emmet, Trans. the Society of Naval Architects and Marine Engineers, vol. 48, 1940, pp. 371–379.

[14] Construction Engineering Department, General Electric Company, Schenectady, N. Y. Mem. A.S.M.E.

[15] Sun Oil Company, Marcus Hook, Pa.

vapor as a heating medium in many industrial processes. There are at present several mercury boilers operating in widely divergent fields. Perhaps the best examples of these are in the Marcus Hook Refinery of the Sun Oil Company. Sun Oil was the first to take advantage of mercury vapor for extremely close control of a large-scale manufacturing process.

The authors have described the 1925 porcupine-tube boiler at Dutch Point, the first commercial unit. This was known to the builders, The Babcock & Wilcox Company, as HgB1.

The next unit, HgB2, was put into service in April, 1926, at Sun Oil Company. This boiler was not so hard to sell, perhaps, as was the first one at Hartford, since the Sun Oil Engineering and Development Department had, at that time, just perfected a process for the continuous vaporization of oil using mercury vapor as a heating medium. This process will be described only briefly here, as it has been widely discussed. Essentially, it is the same as a double boiler on a stove, with a layer of oil in the upper part and mercury vapor underneath. If one can conceive of a series of double boilers connected together and inclined slightly downward with oil flowing by gravity continuously from one to the next, with a certain proportion of the oil stream being vaporized off in each step, he will have a good idea of how the plant functions and how products of different viscosities are obtained by means of a heating medium held at a constant temperature within 1 or 2 deg F.

The oil heaters are overhead, and condensed mercury returns by gravity through rundown lines to the boiler. The entire system is welded, and the mercury side operates under pressure. The oil vapors are distilled over to towers where side cuts are made through condensers and coolers to products tanks.

Mercury does not come in contact with the oil.

The advantages of such a system, compared to the old separately fired batch still, are obvious. One of these is the fact that the mercury plants have an "on-stream" factor of 95 per cent. Closely controlled production of lubricants and specialty oils, ranging from the lightest to the heaviest, is carried on for months at a time without forming coke, due to "burning" of the oil. The heating surfaces over which the oil flows are only a few degrees hotter than the oil being heated and no hot spots exist. As a result, the transfer rates remain high, the charge to the plant in barrels per hour can be held uniform and the specifications of any particular product can be duplicated at any time.

Since 1926, six additional boilers have been put in operation at Sun Oil. Thus, out of a total of seventeen mercury boilers built to date, Sun Oil has taken seven.

The latest boiler dates from January, 1938, and is of the twisted-tube or catenary type. The unit comprises a main boiler bank, convection bank, and air heater, and is rated at 30,000,000 Btu per hr absorbed. Boiler tubes are of carbon-molybdenum steel and are calorized. The fuel is dry gas, a by-product from stills in the refinery.

This unit, containing 55,000 lb of mercury, has comparatively small-bore tubes and natural circulation. It carries the load of one of the lubricating-oil plants which was formerly carried by two dead-end-tube-type boilers, each containing 45,000 lb of mercury. These two older boilers are now stand-bys for the newer boiler. This last unit has operated continuously for 3 years with the exception of four scheduled shutdowns per year for cleaning the oil side of the plant and one forced outage caused by the equivalent of a case of low water, due to a holdup in the gravity-return system.

The characteristics of this unit are as follows:

Design pressure, psi	100
Mercury content, lb	55,000
Gas temperature entering tubes, F	2400
Gas temperature to convection bank, F	1250
Gas to air heater, F	750
Gas to stack, F	500
Air to burners, F	500
Fuel fired, cu ft of gas per hr	22,000
Heat units absorbed per hour, Btu	27,000,000
Mercury vapor per hour, lb	210,000

Until 1938, Sun Oil's experiences closely paralleled those of General Electric in the matter of solubility of iron in hot mercury and the consequent restriction of vapor passages in the tubes with redeposited metal. To take care of this difficulty, it was the practice to pickle each boiler once every 2 years, an operation requiring about 3 days per boiler. In 1938, chemical treatment was started under the direction of General Electric chemical engineers, using magnesium and titanium. This has overcome the dissolution of metal, the surfaces being free of oxides and completely wetted by mercury. The experiences with chemical treatment have likewise closely paralleled theirs, except that, with the closed system, no air-leakage or moisture problems exist while operating, and the limits are therefore much easier to maintain.

The removal of accumulated oxides and "dirt" from the Kearny system is accomplished by means of a flash sump. At Sun Oil, this material is trapped out in a submerged horizontal section of the return line. The area at this location is such that the liquid velocity is decreased to the point at which the material floats out. For the quantities of mercury flowing, 6-month cleaning periods suffice to keep any oxides from carrying back into the boiler.

Of the total of seven mercury boilers installed at Marcus Hook, three have become obsolete. None of the seven can be compared in size or capacity with the General Electric, Hartford, or Kearny installations, but back of them is a record of 15 years of sucessful operation in the manufacture of lubricating oils. This is conclusive proof that the adaptation of mercury vapors to process work is fundamentally sound and highly advantageous.

R. C. Muir.[16] The writer has followed this development closely for the last 10 years, being first impressed with its possibility for great simplicity in design, aside from its great promise as an efficient cycle. In many respects, it is simpler in principle than the closed cycle of the sealed household refrigerator.

The difficulty experienced in its development has been the lack of suitable high-temperature materials and the unknown behavior of high-temperature mercury in steel enclosures.

The metallurgists have now given us suitable materials, with the promise of still better materials, and the chemists have supplied simple treatments for the mercury so that it will behave properly in steel containers. The designers and engineers can now proceed with continuing improvement in the simplicity of design. The writer is confident that the mercury-vapor process for power production will assume an important place in the future.

T. H. Soren.[17] The mercury boiler at the Dutch Point Station was placed in operation on September 7, 1923. This was the first installation in which welding was used for mechanical strength, particularly on piping.

The present mercury boiler at the South Meadow Station is in regular operation, carrying about 6000 kw 24 hr a day. The availability of the mercury equipment is about 90 per cent for the year.

The mercury boiler at South Meadow is operating in every essential exactly as it was laid out by its inventor W. LeR. Emmet. There have been no fundamental changes in operation

[16] Vice-President in Charge of Engineering, General Electric Company, Schenectady, N. Y. Fellow A.S.M.E.

[17] Vice-President, The Hartford Electric Light Company, Hartford, Conn.

and no material changes in the original equipment. We are not using any chemical beyond illuminating gas on the vacuum side of the unit.

The reason for the reduced capacity at which the unit operates is that, with higher capacity, it is necessary to boil out the accumulation of iron and mercury oxides in the boiler tubes with acid every 2 or 3 months. At lower capacity, the unit can operate from 12 to 15 months without cleaning.

The entire unit was built of low-carbon steel, and the bottoms of the boiler tubes are beginning to show some hair cracks on the inside, indicating that there is a definite life to the carbon steel at high temperatures.

It is not practical to retube this boiler for the reason that the ligaments in the boiler drum between tubes are about $^5/_8$ in. and would not stand a complete retubing of 3080 tubes. It is the intention at some later date to replace this boiler with one of a later design. The mercury turbine is in good condition. Some of the last-stage buckets show signs of erosion. This probably would mean rebucketing one stage and possibly two.

It has been necessary to increase our capacity twice in the last few years. The first increase was 40,000 kw, and the present one, 45,000 kw. At the time of the first increase, the General Electric Company was not in a position to offer a mercury unit of sufficient size to take care of our additional load.

The present increase of 45,000 kw will go into operation in 1942 and is required for the tremendous increase in war load at the United Aircraft Company, Colt's Patent Fire Arms Manufacturing Company, and in the other local machine shops.

This 10,000-kw unit was started in 1928, and it was limited in operation for three of the first 6 years of its operation. The other 3 years produced 334,000,000 kwhr. It was on the line 75 per cent of the time. Total operation has produced 1,346,598,000 kwhr, and for the last 8 years it has been on the line 90 per cent of the time. The per cent of the time out has been due to repairs on the furnace and steam auxiliaries, as well as mercury.

G. B. WARREN.[18] In connection with the consideration of the mercury boiler and mercury turbine which has been so ably presented, it might be worth while to emphasize the possibilities of one particular application, that is, the application, in the near future, of the mercury cycle as a superposed cycle over present highly efficient steam plants. It may be that for some time the mercury-vapor-steam plant will cost slightly more than a corresponding steam plant. Experience in the power-plant field, today, indicates that a somewhat more costly but more efficient cycle can be justified as a superposed cycle than can be justified as a straight-condensing cycle. The economics back of this situation seems to be sound. To a great extent this is due to the greater capacity which the more efficient cycle will permit in the superposed plant when superposed over a given existing plant capacity.

The present mercury plants have largely been superposed over 250- to 400-psi steam plants. A careful study of the situation indicates that the over-all economy may be slightly improved if the mercury cycle is installed over a high-pressure high-temperature, or high-pressure resuperheated steam plant; and, further, when so applied, the cost and size of the mercury-vapor turbine is considerably reduced. In addition, the total kilowatts which can be developed from a given mercury boiler is also increased.

All of these considerations point to the possibility that one of the big applications for the mercury-vapor cycle may be as superposed capacity over the 600-lb and 1200-lb stations of which 2,000,000 kw were installed during the period from 1925 to 1932. Such superposition will probably be on the base-load sections of these plants, in which a considerable portion of the boiler depreciation has undoubtedly already been taken.

[18] Designing Engineer, Turbine Engineering Department, General Electric Company, Schenectady, N. Y. Mem. A.S.M.E.

NOTE: A joint discussion by P. H. Hartung of this paper and the paper, "Mercury for the Generation of Light, Heat, and Power," by H. N. Hackett, appears on page 653 of this issue of the Transactions.

AUTHORS' CLOSURE

The cost of mercury depends upon supply and demand and the amount mined depends upon the price. The result is that the price has fluctuated from $50 to $250 a flask of 76 lb. If the mining and refining operations were put on an economical basis for a good regular output per year, it is believed that the cost of mercury can be brought down to from 35 to 50 cents a pound.

The mercury content can be reduced in a moderate-sized boiler to 2 lb per kw which would include the kilowatts generated by the steam, as well as the mercury. A plant costing $100 per kw, and mercury 50 cents per lb, the mercury cost would represent 1 per cent.

The condenser boiler is not an expensive piece of equipment. The temperature difference between the mercury vapor and the water is low and fixed, and a tube cannot burn out from overheating.

The mercury cycle has a large volume flow, and, where the volume flow is large, the turbine is generally inexpensive for small-capacity units. On the other hand, a large volume flow makes the large-capacity turbines more expensive.

Mercury losses can be figured like depreciation. If the Hartford, Schenectady, and Kearny units pooled their losses for all the years the plants have been operated, the loss would represent about 1 per cent depreciation.

With 140 psi in the drum, the pressure at the boiling point in the Kearny boiler is 260 lb, so that every pound of mercury vaporized at the 260-lb pressure will be expanded in the boiler down to 140 lb upon reaching the drum, thus making an efficient heat pump. Such mercury liquid as is vaporized at some pressure between 140 lb and 260 lb will have that much less heat head as a pump. The transport of heat is done by the vapor and the circulation of an excess amount of liquid is ineffective work. Therefore, if the drum is lowered, the amount of liquid circulated becomes less, and the velocity of the mercury becomes greater.

It is recalled that the Dow Chemical Company admitted some years ago that diphenyl oxide dissociated above 750 F, and that it had no advantage over a steam cycle which is capable of using higher temperatures. This fluid seems to be most successful as a heat-transfer medium at moderate temperatures.

Mercury for the Generation of Light, Heat, and Power

By H. N. HACKETT,[1] SCHENECTADY, N. Y.

This paper outlines the principles upon which the mercury boiler was first developed and tested in a small unit in 1912. Many difficulties were experienced in units built in succeeding years, the full importance of which was not apparent until the two 20,000-kw units at Schenectady and Kearny were placed in operation in 1932 and 1933, respectively. The major problem from then on was the elimination of mercury attack on the steel tubes, which after short periods of operation became plugged with an iron crystalline deposit. As a result of extensive research, a mercury-sodium-titanium amalgam was discovered which solved the problem of dissolution of the steel. This development combined with the exclusion of oxygen from the boiler, piping, and valves greatly improved the situation. The final solution came in the redesign of the Schenectady plant in 1937 and the construction of an entirely new mercury-vapor unit at Marcus Hook in 1939, in which magnesium and titanium were used in the boiler mercury. Details are also given of the more recently rebuilt plant at Kearny, incorporating all known improvements. This unit, producing 21,000 kw per hr from the mercury turbine and 30,000 kw per hr from by-product steam, operates on 0.5 lb of fuel oil per kwhr. During more than 15 months of operation, this boiler has carried an average hourly load of 205 per cent of the national average for steam-generating units for 1940.

MERCURY, the only metallic element that is liquid at atmospheric temperatures, has been known and used by man for centuries. It occurs in nature chiefly in the form of red sulphide HgS, called "cinnabar," which as a rule is accompanied by more or less of the reguline metal and is found in formations of all ages. It has been found in both sedimentary and eruptive rocks of the most varied character.

The normal world production of mercury is about 120,000 flasks per year, but at the present time it is estimated to be in the order of 160,000 flasks per year. Of this amount, approximately 50,000 flasks are being produced by the United States, Canadian, and Mexican mines and the remainder by Spain and Italy. The United States yields about 34,000 flasks from approximately 100 mines.

Uses of Mercury

Industry, medicine, and the arts consume approximately 85 per cent of the world's production in the form of mercury compounds. The following statement from a recent article[2] gives some of its many uses:

"Vermilion, used for paint and cosmetics (an ancient use) is the sulphide. Mercurochrome is one-quarter mercury; calomel, a seed disinfectant as well as a medicine, is 85 per cent mercury; and corrosive sublimate is 74 per cent mercury. Compounds of the metal are used as catalysts in making acetic acid, caustic soda, and chlorine. Ships may be protected with a mercury anti-barnacle paint. The dentist may use vermilion to color his plates to match the gums, and mercury amalgam (formerly much used in smelting gold and silver) in making fillings. Mercury goes into electric arcs and lamps for signs. Even the felt-hat industry depends on mercury. The process of making fur into felt uses mercuric nitrate.

"As an out-and-out war material, mercury is used as a detonating agent, in the form of mercury fulminate, invented in 1799. Before that time muskets were fired with the famous flint and steel. To make fulminates, mercury is treated with nitric acid and alcohol."

Power Generation With Mercury

For the generation of power, a binary cycle employs the latent heat of boiling mercury to convert the heat of the fuel to electrical energy with greater thermal efficiency than with the steam cycle alone. The power from the mercury-turbine-driven generator is produced at nearly theoretical mechanical equivalent of the thermal energy; the heat wasted being recovered by producing steam, in a condenser boiler, and using it in an ordinary steam turbine. The economy of such a process is plain when it is considered that the power is generated in two turbines with only the same boiler waste and condenser loss that is accepted with a steam turbine alone, Fig. 1.

The use of mercury for generating power and making lubricating oils has had very little effect on world consumption, as in over a quarter of a century only about 21,000 flasks have been used for these purposes.

Mercury, as a medium for the generation of light, heat, and power, was first experimentally tested by General Electric in 1912, on a small mercury boiler. Observations of the boiling fluid were made by looking down the open end of the pipe in which the mercury was being heated.

In 1912, mercury was considered to be a coherent mobile liquid that would actively amalgamate with such metals as gold, silver, copper, or tin, but would not wet glass, iron and steel, or objects placed in it. When heated, the metal expands uniformly and vaporizes at 458 F at 29 in. vacuum, and at 975 F at 140 psi gage pressure. The vapor is colorless. The heat of the liquid is low, being only 0.033 Btu per lb per deg temperature rise. Likewise, the heat of vaporization is much less than for steam, being about 125 Btu per lb. Because of the greater available energy throughout any temperature range, the binary mercury cycle produces power with less heat loss than can be done with steam alone, with resulting thermal efficiencies above 37 per cent. Future applications of the cycle may exceed 50 per cent thermal efficiency.

Early experiments with the mercury-vapor-steam cycle on a 100-hp boiler and later on a 1500-kw unit, operating at 10 psi

---

[1] Construction Engineering Department, General Electric Company. Mem. A.S.M.E.

[2] "The Many Uses of Mercury," *Mechanical Engineering*, vol. 61, 1939, pp. 920–921.

Contributed by the Power Division and presented at the Annual Meeting, New York, N. Y., December 1–5, 1941, of The American Society of Mechanical Engineers.

Note: Statements and opinions advanced in papers are to be understood as individual expressions of their authors and not those of the Society.

gage and 730 F vapor temperature, indicated that mercury was practically inactive to iron or steel.

In fact, the affinity of iron for mercury was so slight that considerable difficulty was experienced in securing suitable heat transfer from the steel-tube walls to the boiling mercury. Relatively long periods of operation at low rates of heat application were necessary to "break in" a boiler properly, before expected outputs could be secured.

As time went on and larger boilers were built burning greater

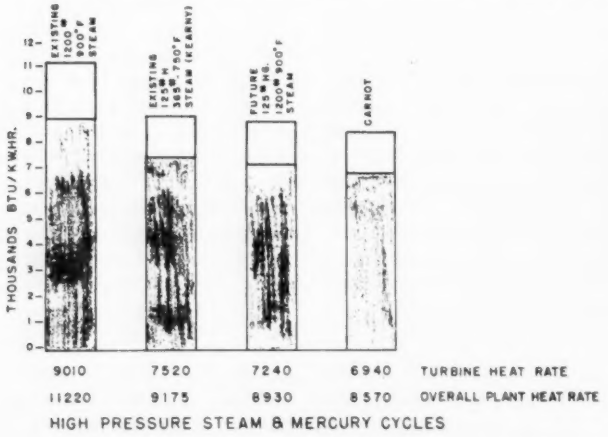


FIG. 1 HIGH-PRESSURE STEAM AND MERCURY CYCLES

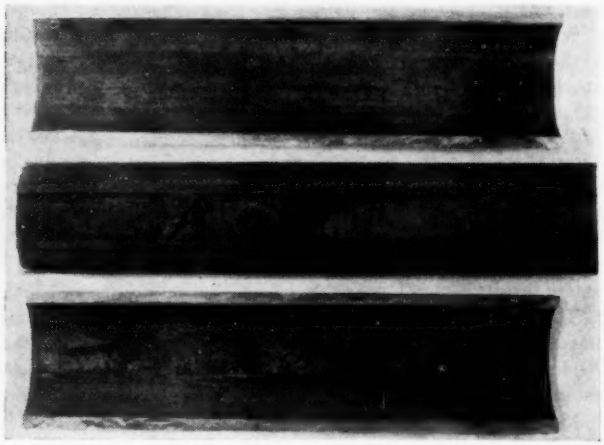


FIG. 2 BOILER TUBE REMOVED FROM HARTFORD 10,000-KW UNIT, SHOWING DEPOSITS OF PREVIOUSLY DISSOLVED TUBE METAL RESULTING IN RESTRICTION OF MERCURY CIRCULATION

quantities of fuel, it was discovered that the heat-absorbing ability of a tube filled with mercury was not only uncertain but unpredictable to such a degree that pronounced overheating and actual damage to the boiler tubes occurred. Furthermore, mercury did cause disintegration of the steel to such a degree, by dissolving slowly great quantities of iron from the inside walls of the tubes and redepositing it in the cooler regions, that the tubes became plugged at their upper ends. Overheating occurred, due to restriction of mercury circulation, Fig. 2.

MERCURY ATTACK ON TUBE STEEL

The full importance of these difficulties was not appreciated until after the two 20,000-kw units—one installed in the Schenectady Works of the General Electric Company, and the other in the Kearny Generating Station of the Public Service Electric & Gas Company of Newark, N. J.—were placed in service in 1932 and 1933, respectively. However, the first positive results of mercury attack on the tube steel were evident after nine months of operation of the 10,000-kw mercury unit in the South Meadow Station of The Hartford Electric Light Company in 1930. Because of incorrect diagnosis, nothing of a fundamental nature was done to correct the trouble.

The deposits of iron in the Hartford tubes were thought to be from mechanical erosion of certain cast-iron filler pieces in the drums and were removed by means of acid pickle. Even though this operation required the use of some 10,000 gal of 20 per cent

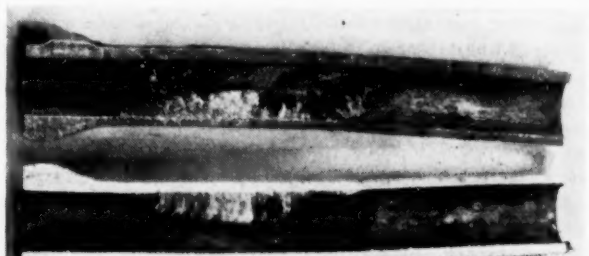


FIG. 3 SECTION OF MERCURY WALL TUBE SHOWING MERCURY-IRON-OXIDE DEPOSIT
(Tube taken from Kearny mercury-boiler unit.)

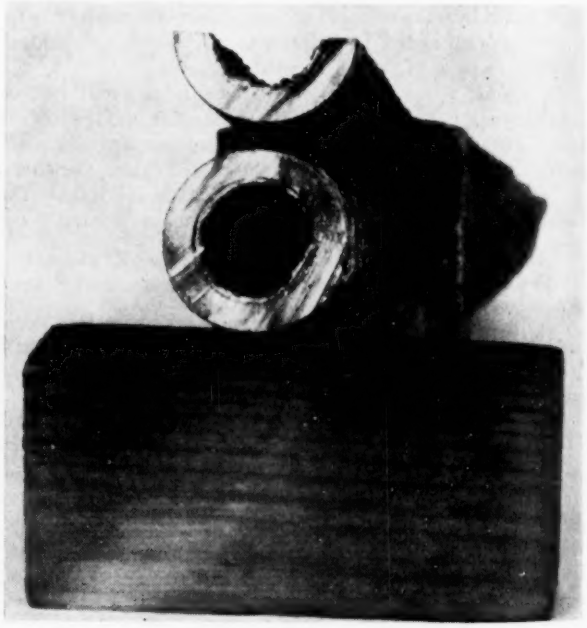


FIG. 4 RISER FROM DRUM NO. 7, KEARNY MERCURY-BOILER UNIT: SECTION AT DISTRIBUTION BOX
(Removed March 2, 1936.)

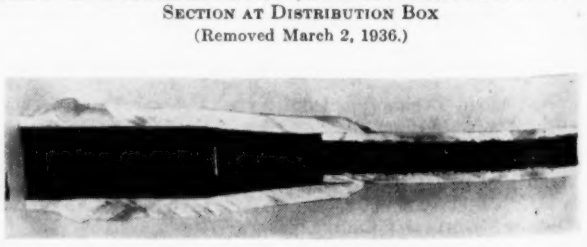


FIG. 5 RISER DISTRIBUTION BOX FROM DRUM NO. 7, KEARNY UNIT
(Removed March 2, 1936.)

concentration hydrochloric acid to clean the 25,000 sq ft of inside drum and tube surfaces, the results seemed sufficiently satisfactory to proceed with the building of the Schenectady and Kearny units.

Shortly after the Kearny unit had been placed in operation, examination of the external surfaces of the tubes indicated that overheating had occurred, as certain of the mercury-filled furnace-wall tubes were distorted and bent, and several hundred of the porcupine boiler tubes had increased in diameter at their lower ends. Internal examination of the porcupine tubes disclosed the same iron-crystalline deposit at the upper end, as was previously found at Hartford, and the upper ends of the $^{7}/_{8}$-in-diam furnace tubes were likewise plugged with similar material, Figs. 3, 4, and 5.

This could not be attributed to mechanical erosion, as was first thought at Hartford, since the lower portions of the furnace tubes showed actual loss of metal of a measurable amount. The deposits were principally iron oxide, mechanically combined with mercury particles. The inside surface of the tubes was believed to be nonwetted, because of formation of oxide films on the surface.

It soon became evident that these two problems had to be solved if full-load operation was to be attained, as the boiler at Hartford had to be cleaned again some ten months after the first experience. It was necessary to pickle the units to continue operation. This practice existed for many months at Schenectady and Kearny, until suitable correctives were found. It is still followed at Hartford. Some loss of iron occurred with each pickling operation, which necessitated the addition of equal volumes of mercury so that correct operating levels could be maintained.

The rapid dissolving of the iron from the lower tube surfaces with the subsequent redepositing of the metals, as either iron or iron oxide at the top, and the unexpected overheating of the tubes were both problems for which no immediate answers were available.

It was believed that, if the dissolving of the iron could be stopped, the operation of a mercury boiler would be satisfactory, as relatively long intervals between pickling operations would not be objectionable. To accomplish this desirable result, three general lines of attack were followed.

Steel specifications were altered and various alloys were developed in an effort to find a material that would reduce or, if possible, entirely eliminate the loss of metal by dissolving. Some success was attained, as certain alloys showed definite improvement.

An all-liquid boiler using alloy tubes, in which the mercury-liquid temperature continuously increased throughout the heating circuit, was built and thoroughly tested in the belief that the dissolved metal would not be released in the tube circuit, but in a large receiver or flash chamber where flashing of the heated liquid occurred. These hopes were only partially realized, as some dissolving of the tube material, as well as appreciable deposits of oxidized metal, did occur after a few months of operation.

Overheating of the mercury-filled tubes was not cured entirely by either of these two procedures, although considerable improvement did occur with the all-liquid boiler.

Research on Effect of Mercury on Steel

Ultimate and complete success was realized, however, as the result of an extremely active research program in which the metallurgical and chemical properties of mercury, combined with other metals, were thoroughly studied by the scientists and chemists of the General Electric Laboratory.

Hundreds of small "harp" boilers, in which were placed small test pieces of polished and weighed steel on which the experiments were to be made, were operated many hours at temperatures of 1200 to 1300 F to accelerate the results. The mercury in each of the test boilers contained small quantities of one or more of the known elements and metals, such as tin, lead, sodium, magnesium, silver, titanium, or zirconium. Sometimes combinations of these several metals were used together and in varying amounts to study the effects.

After more than 300 tests, in which mercury, titanium, and sodium were used, one harp boiler produced startling results. The test piece of steel showed no dissolving; it was perfectly silvered or "wetted," and when cleaned of all adhering mercury, weighed exactly the same as when it was placed in the boiler many hours before. Repeated successes with identical harp boilers indicated that a satisfactory method had been discovered

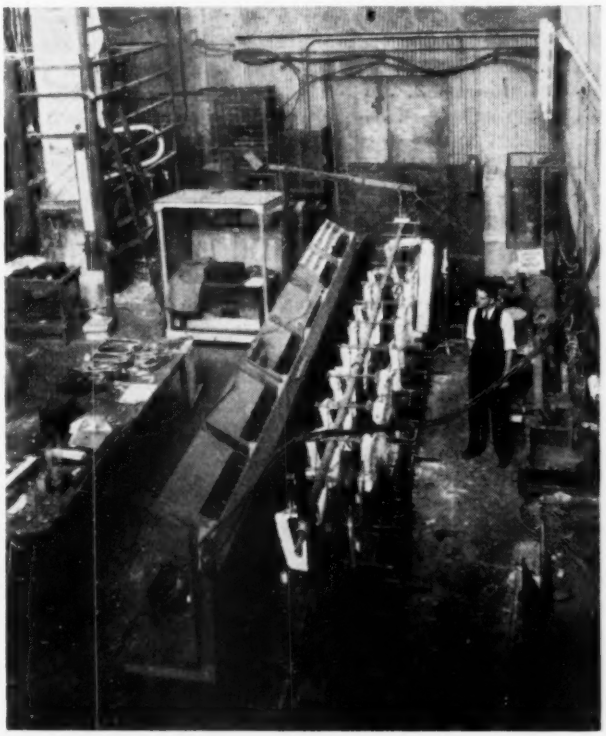


Fig. 6 Harp Boilers Used for Testing Effect of Mercury Amalgams on Steel

which would not only control but apparently stop the dissolving of the iron in the boiler mercury. The steel maintained its original weight and size with no loss of metal. The mercury-filled tube became a suitable and reliable absorber of heat at unbelievably high rates. Plugging and overheating of test boilers had been eliminated. Apparently only minute quantities of these elements were sufficient, only a few parts per million by weight of mercury, Fig. 6.

What chemical or metallurgical effects had been performed by the simple combination of these well-known metals, operating in heated mercury-boiler tubes, was not known. Microscopic examination of the treated mercury-coated surfaces and careful chemical analysis of the treated mercury brought to light the phenomena which are believed to be responsible for the successful results.

Mercury-Sodium-Titanium Amalgam Solves Problem

The steel was found to be perfectly wetted with the dilute mercury-sodium-titanium amalgam to such a degree that intimate

and positive contact occurred between the steel and the mercury. The spheroidal properties of the mercury were entirely gone, and the liquid spread over the tube surface to form a tenacious layer almost impossible to wipe away.

Sodium was believed to be the wetting agent, causing a breakdown and removal of oxides on the surface of the steel and in the mercury, thereby allowing actual intimate contact of the mercury and the steel. The sodium was also thought to reverse the meniscus of the mercury, thereby causing it to spread uniformly over the tube surface to produce the effect of wetting.

Titanium was found as a thin microscopic layer deposited on the surface of the steel, as well as a eutectic compound with iron in the mercury. It was not known whether the surface deposits of the iron-titanium alloy functioned to inhibit the dissolving of the iron, but that this occurred was certain.

Could this information be applied to the large power boilers in use in Hartford, Schenectady, and Kearny? To apply the meager knowledge gained from the laboratory test boilers, weighing only a few pounds, to the great power units, weighing more than 6,000,000 lb each, offered many problems.

Treatment of Boiler Mercury at Kearny

For certain reasons, Kearny was chosen for the first application of what is now known as "treatment of boiler mercury." During the night of March 4, 1934, sufficient metallic sodium in the form of a 25 per cent sodium-mercury amalgam was added to the boiler mercury to bring the sodium concentration to 100 ppm by weight of mercury. No titanium was added as yet. The immediate results were astounding, as the boiler at the time the sodium-mercury amalgam was added could only carry 20 per cent of full rating without overheating the boiler tubes. Immediately after the injection of the amalgam, the fire was increased to produce one-half capacity. The following day, the load was increased to full rated output of the boiler and was subsequently operated continuously for three months. During this period, efforts to add titanium to the mercury were ineffectual. Various appliers were used, but to no avail, as the titanium refused to dissolve in the boiler mercury. However, the boiler appeared to operate satisfactorily with no overheating of the furnace tubes.

These results were very gratifying, but actual success was only partial, as stoppage occurred in certain furnace tubes of the mercury boiler. This time, however, the effect was different as the plugging was not at the top of the tube but at the bottom, caused by a ball of hard material which, when analyzed by the chemists, was found to be a mechanical mixture of mercury and sodium ferrite.

The elimination of sodium ferrite, $Na_2OFe_2O_3$, the end point of a chemical reaction between sodium, iron oxide, and oxygen, was believed to be a difficult problem. Further tests were conducted which proved conclusively that oxygen was the principal offender and would have to be eliminated.

Just how this was to be done was not known. The problem involved a great power unit weighing millions of pounds, having thousands of square feet of steel surfaces exposed to air and mercury, containing hundreds of pounds of oxygen-bearing iron rust and scale. This vast unit must be made free and kept free of oxygen.

Improvements Made in System

The turbine shaft rotating at high speed in shells in which high vacuum is maintained must be perfectly sealed. Many feet of welded and bolted joints must be made absolutely tight, as well as

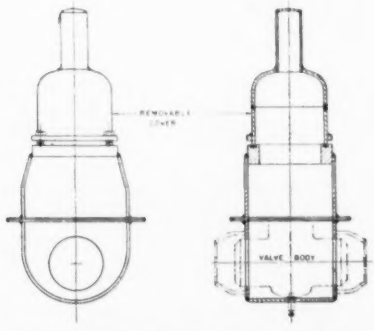


Fig. 8 Airtight Enclosed Vacuum Valve
(End elevation, left; vertical section, right.)

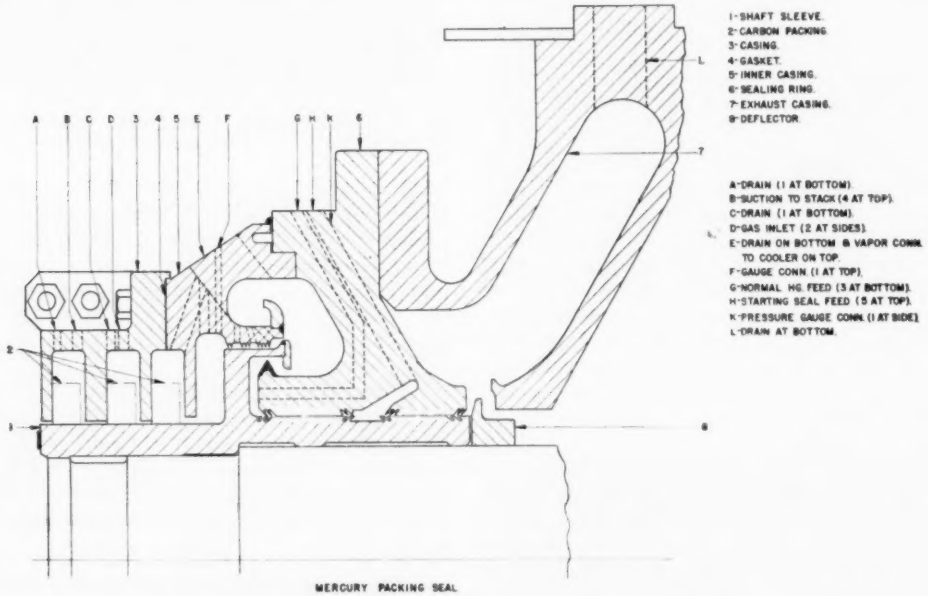


Fig. 7 Mercury-Packing Seal for 20,000-Kw Mercury Turbine
(Vertical section along shaft of upper half with key for numbered parts; Kearny unit.)

the stems of leaking valves. None of these things were required in steam plants of like size.

New and effective shaft seals were built, Fig. 7, using the centrifugal force of a revolving cup of liquid mercury to form the seal; designs were altered; the best technique of welding was employed for making welded joints tight; flanges and valve stems were sealed by special means, Fig. 8. Air infiltration was reduced from 500 cu ft per hr to less than 1 cu ft per hr.

Further laboratory and field tests discovered that magnesium and titanium had all the desirable wetting features of sodium and titanium and none of the undesirable ones, so magnesium replaced sodium in the boiler mercury. It was found that magnesium did not form the hard dangerous balls when reaction between the metallic magnesium and iron oxide or free oxygen took place in the boiler mercury. The final products of the reaction were, instead, a very fine, dry, harmless powder consisting of free iron and magnesium oxide, easily removed from the boiler mercury.

All the known improvements were made on the Schenectady unit in 1937, with immediate and unqualified success. No difficulties or unexpected results from the mercury or its ingredients developed, and the equipment operated at satisfactory output 93 per cent of the time for the next 18 months, when further alterations were made to the plant to increase its capacity.

This success was duplicated in a 1000-kw test boiler of simple design in Pittsfield in 1938.

An entirely new boiler, embodying all the developments so painstakingly discovered, was built and placed in operation in the Marcus Hook Refinery by The Babcock & Wilcox Company for the Sun Oil Company in early 1939, for the purpose of producing

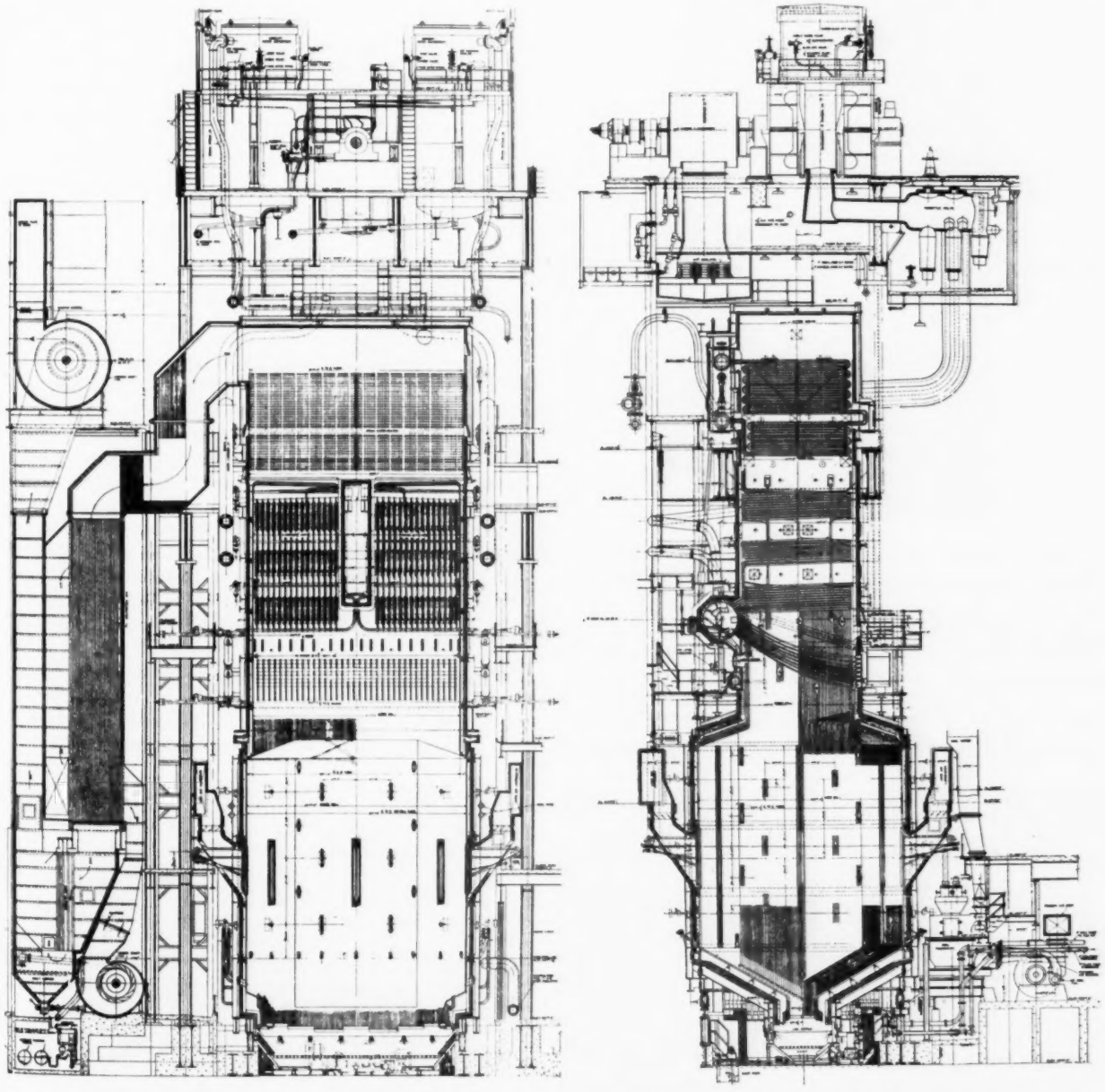


FIG. 9 VERTICAL SECTIONS THROUGH MERCURY BOILER AND TURBINE-GENERATING SET; KEARNY STATION OF PUBLIC SERVICE ELECTRIC & GAS COMPANY OF NEW JERSEY

lubricating oils. Its complete success as a new venture, designed and planned to incorporate all the known facts, made it appear that sufficient knowledge was at last available to expect predicted results.

Operating results from Schenectady, Marcus Hook, and Pittsfield indicated unquestionably that our chemical and metallurgical data were sufficiently correct to warrant the building of a replacement boiler for Kearny, capable of carrying rated output

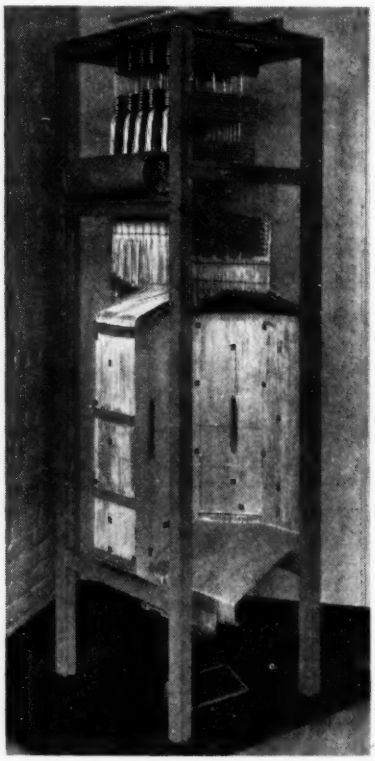


FIG. 10 MODEL OF MERCURY BOILER FOR KEARNY STATION
(Right-side section of tubes shown; scale 1 in. = 1 ft. Constructed by The Babcock & Wilcox Company.)

continuously. It would be necessary to apply accurately all the available knowledge of mercury, chemistry, metallurgy, and engineering to do the job successfully.

REBUILT MERCURY BOILER FOR KEARNY PLANT

The Kearny unit was rebuilt with complete success, Figs. 9 and 10, and its record of operation has rarely, if ever, been equaled by steam units of similar size. The new mercury boiler followed conventional steam-boiler designs and employed all the facts so carefully learned at Schenectady, Marcus Hook, and Pittsfield. Simple through-flow mercury circuits were employed, using fog-type convection surface to the limit of existing experience with the result that, of the 24,407 sq ft of mercury heating surface, 17,400 sq ft, or 71 per cent, was of the fog type, which is empty of liquid mercury at starting. The only liquid-filled tubes are those below the center line of the mercury drum, Fig. 9.

The octagonal furnace is approximately 26 × 28 1/3 ft × 50 ft high inside the furnace, having a sloping bottom and a top covered by wide-spaced slag-screen tubes. The over-all height of the boiler is approximately 67 ft to the top of the fog tubes and 100 ft to the top of the steam superheater, Figs. 9 and 10.

All the furnace tubes are relatively small, varying from 7/8 in. ID × 1 7/16 in. OD to 1 1/8 in. OD × 1 11/16 in. ID in the slag screen, in order to reduce the mercury content of the boiler. Because these tubes must operate at metal temperatures of from 1050 to 1180 F and pressures of from 140 psi gage at the drum to 395 psi gage at the lower header, Croloy 5 MSi, a ductile chrome-alloy steel, was chosen as the best material from which to make the furnace and slag-screen tubes. Because of the lower metal temperature encountered in the 1 7/8-in-ID fog convection tubes, Croloy 3 was used in the lower bank and Croloy 2 in the upper two banks of the 2 1/4-in-ID tubes.

The 4-in-thick 54-in-ID carbon-molybdenum drum is 35 ft 6 in. long and operates at 150 psi gage, 985 F mercury temperature, as do the downcomers and vapor piping which also were made of the same material.

Of the 310,000 lb of mercury in the boiler, which is all below a 4-in. drum liquid level at starting, 41,000 lb ultimately is flowing through the fog tubes as a finely divided mixture of liquid and mercury vapor when the boiler is at full output or less. The fog surface only requires approximately 1/20 of the mercury per square foot as the liquid region, indicating its great economic value. A boiler using all liquid-filled surface might be prohibitive in mercury cost.

Even though a boiler of like dimensions and operating temperatures had never before been built, using such quantities of alloy metals, assembled throughout by perfect welding, the unit went into service in May, 1940, and has operated almost continuously since at 20,000 to 21,000 kw either coal- or oil-fired, generating power at 9200 Btu per kwhr, the lowest Btu rate per kwhr in history, with only two short outages due to equipment failures, Fig. 11. The normal rated output of the unit is 21,000 kw per hr from the mercury-turbine generator and approximately 30,000 kw per hr from the by-product 365-psi-gage steam produced.

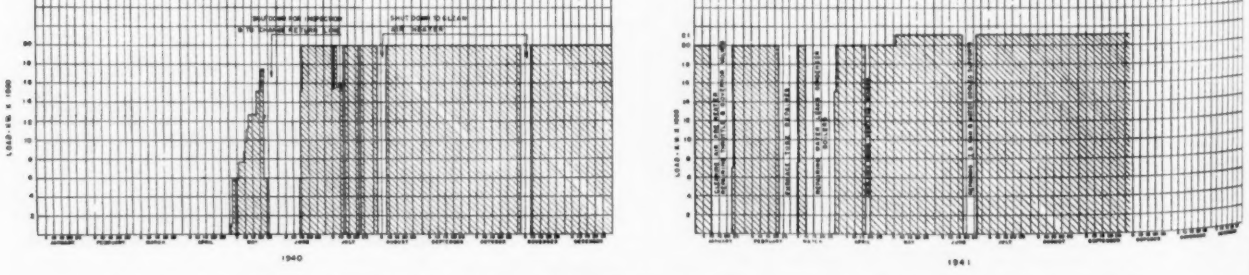


FIG. 11 LOAD CHART, MERCURY TURBINE, KEARNY GENERATING STATION OF THE PUBLIC SERVICE ELECTRIC & GAS COMPANY OF NEW JERSEY

Operating the New Unit

The operation of the new unit is extremely simple, requiring no more attention from the "operators" than similar steam equipment. Because of its high availability, the mercury-vapor plant has proved to be the most reliable generating equipment in the system. During more than 15 months of operation it has carried an average hourly load of 205 per cent of the national average for steam-generating units for 1940.

The scientists, chemists, and engineers can now produce predicted results. The successes at Schenectady, Marcus Hook, and Kearny can be duplicated over and over again, with ever-improving efficiencies. Mercury at Kearny now produces 1 net kwhr for 0.5 lb of fuel oil. If a new plant were built of similar capacity, the fuel burned to generate the same amount of power would be still less. If, in the future, mercury were used at 500 lb pressure and 1500 F temperature, the power could be produced at a fuel consumption of only 0.41 lb of oil per kwhr.

Because of a very valuable and somewhat unexpected development, resulting from the use of chemicals in the mercury, it is possible to design and build low-mercury-content boilers for any desired capacity at reasonable cost.

A Development Which Reduces Cost of Mercury Boiler

A tube surface properly wetted with treated mercury is coated with a tenacious film which because of high surface tension can be superheated considerably above its normal saturation temperature before becoming destroyed due to heat application, as long as the film is continuously supplied with other treated mercury as fast as loss is sustained by evaporation from the surface of the heated film. Such thermal action makes possible the use of large-diameter tubes, fed by relatively low-density mixtures, or a fog of mercury vapor and mercury droplets of the order of 5 parts of liquid to 1 part of vapor or less, by weight, with complete safety at high rates of heat input. As long as reasonable mixture velocities are maintained, the tubes may be operated in any position, flat, sloping upward or downward, or vertically in either direction, with no apparent limitation of size, shape, or length of the heated circuits.

About 71 per cent of the heating surface of the new Kearny boiler is of this type. It is believed possible to use upward of 90 per cent in future boilers with complete safety.

By taking full advantage of these new principles of boiler design, utilizing maximum rates of heat absorption throughout the boiler, made possible by the definitely controllable heat-absorbing properties of properly treated mercury in the boiler circuits, the mercury-vapor cycle offers an exceptionally economic and reliable method of generating light, heat, and power when and where it is needed.

Discussion

P. H. Hartung.[3] The writer's discussion of this paper and that by A. R. Smith and E. S. Thompson[4] deals entirely with the new mercury boiler at the Kearny generating station of the Public Service Electric & Gas Company.

The performance of the mercury unit to date has been most satisfactory. This is clearly shown in Fig. 11 of the paper. To complete the load chart, it should be extended at 21,000 kw to October 27, 1941. From May 5, 1940, the initial starting date, to October 27, 1941, the unit was in service 83.6 per cent of the time. During that time the average hourly load was 19,700 kw and the capacity factor 82.3 per cent.

The run from March 27 to October 27 is particularly noteworthy, for during that time the unit was in service 4786 hr of the total 5139 hr or 93.1 per cent, and carried an average load of 20,770 kw. In this span of 7 months, continuous operation was interrupted only twice, once because of bearing trouble on the forced-draft fan; and again to repair the induced-draft fan and make burner changes in the furnace. The last run was 121 days long with an average hourly load of 21,040 kw.

Since October 27, the unit has been out of service to make changes in the superheater to increase the steam temperature, to install rotary classifiers in the pulverizers, to continue with the removal of the bottom spacer plate in the condenser boilers, to install an automatic tube-temperature recorder, and to investigate the cause of an increase in the temperature of one tube. These changes were all designed to improve the performance of the unit as a whole and had been planned well in advance.

Up to March 7, 1941, the unit was oil-fired, with the exception of a few days in July, 1940, when the coal-firing pulverizing equipment was tried out. At that time it became clearly evident that it was impractical to attempt to fire coal until mechanical cleaning equipment was installed. The boiler is so constructed that it is impossible to clean it with hand lances; and it was thought that continuous firing with coal at full load would soon result in a shutdown for external cleaning.

Since the completion of the soot-blower installation in March, 1941, the boiler has been coal-fired exclusively with the exception of starting-up periods and the times when a pulverizer was out of service for cleaning or repairs. When coal firing was first started, it was thought that the boiler would slag up quickly and a very elaborate soot-blowing schedule was initially set up. However, for the first time, the boiler failed to come up to expectations and before long many of the blowers had been tagged out as unnecessary while others were operated only as conditions required. It was found, in fact, that until some slag has built up on the walls, coal firing is somewhat unstable even at full load. It is felt that changes made during the last outage will go far toward eliminating this instability and greatly improve coal-firing performance. It is interesting to note that since going over to coal firing, we have experienced no trouble whatsoever with plugging in the air preheater. During the first outage after coal firing was started, the preheater was washed but that was not considered necessary. Since then no effort has been made to clean the preheater.

The mercury unit while in operation must be checked regularly for magnesium and titanium concentrations in the mercury, the component elements of the gas evacuated from the condenser boilers, as well as the regular analysis of the water in the condenser boilers. The gas analysis, together with the rate of discharge, gives a constant check on the tightness of the negative-pressure side of the mercury system and, at the same time, gives a valuable lead in the location of possible sources of leakage. For instance, within certain limits, an increase in gas discharge, accompanied by an increase in oxygen content, indicates a leak external to the mercury system, i.e., in the air-removal system; whereas an increase in gas discharge without the oxygen showing up probably indicates leakage into the condenser boiler. The former does not present any hazard to operation. The latter, however, is quite serious as it can have a direct bearing on the concentrations of chemicals in the mercury and consequent wetting of the tubes. It is interesting to note that during the last run the average air leakage was 0.20 cfh.

The most important factor in operation is the control of the concentrations of magnesium and titanium in the boiler. Without proper concentrations, the tubes are in grave danger of overheating. During the starting-up period, analyses are made every

[3] Superintendent, Kearny Generating Station, Electric Generation Department, Public Service Electric & Gas Company, Kearny, N. J.

[4] This is a joint discussion of the present paper and the paper, "The Mercury-Vapor Process," by A. R. Smith and E. S. Thompson, appearing on page 625 of this issue of the Transactions.

4 hours, until the concentrations tend to level out, when the frequency is decreased. After a stable condition has been attained, analyses are made twice a day, i.e., one in the morning, and the other the last thing in the afternoon. The fact that the unit has been operating in a most satisfactory manner for some time does not warrant any relaxation of vigilance in this work. Three occasions have been experienced when, for no apparent reason, the magnesium concentration was sharply reduced to a value which would have made continued operation at full load hazardous to the equipment. The reason for these changes in concentration is not definitely known, but it is quite possible that they may be due to changes in furnace conditions which produced sudden changes in circulation rates, with an attendant stirring up of some oxides which had settled out. Fortunately, these decreases were detected early and were carefully followed by increasing the frequency of analysis. The addition of large dosages of magnesium in each case corrected the trouble. It may seem that a considerable amount of chemical work is involved, but the tests are relatively short and simple, and the normal routine can be easily handled by one man.

It has been very forcefully brought out that the operation of the boiler without knowledge of the temperature of the individual tubes in the furnace wall is most hazardous. When the unit first started up, readings of the thermocouples attached to the back of each of the tubes were made at $^1/_2$-hr intervals and served as an indication of the speed with which wetting took place. When stable conditions had been established, these readings were discontinued and we relied solely upon the automatic temperature recorder, which reads the temperature of one tube in every ten and gives an excellent indication of general conditions in the furnace wall. The failure of a wall tube through overheating demonstrated the need for regular readings of the temperature of all the tubes, and these have been taken manually, while automatic equipment was being developed. This equipment has now been installed but, because of the short period it has been in service, the writer is unable to say anything about its performance except that to date it has been successful.

The elapsed time from lighting a cold boiler to full load is approximately 16 hr. This time is divided roughly as follows:

To bring the boiler-drum pressure up to 75 psi, $6^1/_4$ hr.
To bring the machine up to speed and synchronize, $1^3/_4$ hr.
To raise the load to 6000 kw, 1 hr.
At the rate of 2000 kw per hr., to attain full load, 7 hr.

The reason for the rapid initial loading is to bring the convection surfaces, or "fog banks" as they are called, into action as soon as possible. Sufficient pumping does not take place under 6000 kw to keep these surfaces cool.

Although the station personnel has operated the mercury unit since its installation, it has only recently had the responsibility of the entire maintenance of the unit as well. Based on our experience to date, and that includes a wide range of items, several of which we hope will not require attention in the future, we do not believe that the mercury-unit maintenance is more difficult than that of a steam unit, or that it presents problems which a well-trained crew is not thoroughly capable of handling.

In the 18 months of operation of the new unit, it has been subjected to three severe operating disturbances, more than its predecessor experienced in its lifetime. The first of these occurred in July, 1940, when, during a severe lightning storm, the throttle tripped on overspeed while the unit was carrying full load. This electrical disturbance also took out the mercury-unit auxiliaries. Notwithstanding, the machine was back in service in 49 min. The second instance came 12 days later when a switchboard operator tripped out the field of the mercury generator instead of the steam-driven machine which was coming out of service. The mercury generator had been carrying full load, and the consequent by-passing of the high-pressure mercury vapor into one condenser boiler caused overheating which required about 3 hours to rectify. This shutdown served to indicate some weak points in our operating setup which were immediately corrected. The writer is confident that, were the same thing to happen now, the unit would be synchronized in a very short time. The last instance occurred in February, 1941, when a piece of steel lodged across the entrance of a wall tube and so restricted the flow of mercury to the tube that it burned thin and finally ruptured. To reduce the loss of mercury through the failed tube, the boiler was drained as far as possible through the emergency coolers into the main storage tank. The boiler which had been carrying full load was shut down and drained in 30 minutes.

No operating man wants emergency shutdowns but, in this case, they had a most beneficial effect. They proved that the boiler could "take it" and, together with its excellent performance and operating record, have created in the operating personnel a feeling of great confidence in the mercury unit.

H. J. Kerr.[5] Mr. Hackett's paper tells in a few simple words of the successful completion of a job which has required some thirty years of hard work by his organization, in which he has played a prominent part.

With the fact established that the mercury cycle was materially more efficient than the simple steam cycle, it remained to develop the apparatus that would make the utilization of this method possible.

One of the obstacles was the cost of mercury. Because of this factor, efforts were directed from the beginning to decreasing the internal volume of the boiler. Some of the early boilers, which were built by the company with which I am connected, were fitted with annular spaces for the mercury to pass through, $^1/_{16}$ in. wide. As the paper describes, an entirely new approach has been made to this problem, and the Kearny boiler is fitted with tubes having a minimum ID of $^3/_4$ in. In accomplishing this, the General Electric Company engineers have violated one of the most sacred traditions of boilermakers, in other words; they are deliberately designing a boiler to be operated with low water (i.e., low mercury), and with this condition they are operating the boilers successfully and without a mechanical pump.

Another obstacle was the solution of the steel of the boiler. The rate of solution at lower temperatures was not so rapid, but as the temperature increased so did the rate. Not only did this become serious from the standpoint of the loss of steel, but the resulting iron sludge led to overheated tubes and general interference with circulation. This situation can be appreciated when the size of the annular spaces of the older boilers is considered.

A third major obstacle was failure of the mercury to wet the tube surface, except when it happened to be in the humor to do it. A mercury tube would be tested one day and show a temperature differential of 25 deg, then a few days later, a similar test would show a differential of 200 deg. The overcoming of these two obstacles by treating the mercury with minute quantities of magnesium and titanium is an accomplishment that has made the mercury power cycle practical.

While in the past steel quality was a problem for the high temperatures required, satisfactory alloy steels are today available which have been proved. The Kearny unit is evidence of this fact.

After the years of effort and engineering research which have been expended on this method of making power, the company and the engineers who have made this possible are to be congratulated on their accomplishment.

[5] Executive Assistant, The Babcock and Wilcox Company, New York, N. Y. Mem. A.S.M.E.

While the paper in most part deals with mercury vapor as a means of making power, the advancements described are equally applicable to the use of mercury for process work, in which field it has already proved its value as a means of obtaining constant high-temperature conditions at low pressure.

H. E. MELTON.[6] The author has outlined very clearly the necessity for developing a special chemical treatment for mercury boilers. That some treatment would be required to enable these units to operate successfully at high ratings became evident only after the mercury boiler was well established in the power and process industries. The effort expended by the General Electric Company in search of the answer has been of tremendous importance not only to company engineers, but to operators of the large power-generating units and to those utilizing mercury vapor as a heating medium in numerous processes.

Originally, we had the idea that the mercury boiler was the ultimate answer to the wish for a boiler that would be forever free from cleaning, scale troubles, and the necessity for chemical treatment. This idea had a rude awakening after about one year of operation at Hartford, and possibly two years after the first large process boiler was put into service at the Marcus Hook Refinery of the Sun Oil Company.

Experience at Marcus Hook with the Emmet porcupine-tube-type boiler closely paralleled that at Hartford. After approximately a year of service at relatively high temperatures, the heating surfaces in contact with hot liquid mercury would become free of oxides to the extent that at least partial wetting of the steel occurred. When this stage was reached, it was felt that the ideal was being approached.

Following this, however, there came, at more or less frequent intervals, certain tube failures which could not be attributed to any particular cause, unless it were poor circulation. In those days it was customary to blame circulation when steam boilers were in trouble, so at least in this respect we were being consistent with steam-boiler practice.

After several such failures, it became evident from inspection that the direct cause was restriction of vapor passages due to accumulation of an amalgam of oxides, pure iron, and mercury. It was found that metal from the lower portion of the tubes was being dissolved by the hot liquid. This metal, together with suspended oxides, was being redeposited near the upper end of the tubes. This accumulation would finally restrict circulation; the resultant overheating of the lower end of the tube would cause cracking, and a leak would develop.

The original attempt to clean a boiler mechanically, after removing liquid mercury, was such a task that subsequent cleanings were carried out by boiling the mercury off through a condenser to storage tanks and then pickling the unit with a hydrochloric-acid solution.

Until the inauguration of chemical treatment in 1938, each boiler was thus cleaned by pickling at intervals of $1\frac{1}{2}$ to 2 years.

Chemical treatment of the latest-design twisted-tube-type boiler, installed by The Babcock & Wilcox Company, which went into service in January, 1938, consists of introducing magnesium and titanium, as required to maintain an excess of a few parts per million in the boiler liquid. The capacity of the boiler and the amounts of chemicals used are small, as compared to Kearny or Schenectady. The heating surfaces under liquid are "silvered" and entirely wet by the mercury. The treatment apparently completely inhibits the dissolution of boiler metal by hot mercury.

The product of this treatment is a gray amalgam of mercury and magnesium-titanium oxides. As formerly was the case with the amalgam of mercury and iron, this would accumulate in the boiler, except for the fact that it is evidently being continually carried along as a dust with the vapors throughout the system, and is then washed back through the return lines with the mercury condensate. One portion of the return system is submerged below the mercury level in the boiler so that the line runs full of mercury. In this section, the velocity is quite low so that the entrained oxides separate out of the stream as a sludge and are trapped for periodic removal. This part of the mercury system is practically the only one that is ever opened at present. Cleanouts and traps which formerly were cleaned during each shutdown are now free of any accumulation.

The mercury side of the lubricating-oil plant at Marcus Hook is of all-welded construction, except for a few flanged cleanouts; there are very few valves and the system operates under pressure. There are no shaft seals to contend with as in a turbine installation and the problem of oxygen leakage, therefore, does not exist. Whenever the plant is shut down, the mercury side is allowed to cool, and it is then filled with nitrogen before any part is opened. In this way oxidation of chemicals, mercury, and equipment is kept to a minimum.

A. J. NERAD.[7] The development of the mercury-vapor process for power generation, as the author in his interesting paper has shown, is full of many puzzling problems. The difficulty in discovering that mercury dissolves steel lay in the very slow rate of surface attack, about 2.5 mils per year at the mercury temperature of 500 C in the Hartford mercury-boiler tubes. This rate increases 5 times for every 100 C. The use of pickling agents for cleansing the mercury-boiler tubes before operation tended to mask the effect of the dissolving by the mercury. However, early in 1932, by microscopic examination of the surface of a piece of a core from a Hartford mercury-boiler-tube unit, dissolving of the steel by mercury was discovered.

Laboratory tests followed quickly. In a few months, an inhibitor had been found, the rates of dissolution of ordinary steel for temperatures up to 800 C had been established, and the somewhat limited increase in resistance to dissolution of some alloy steels observed. From that time on, the application of wetting agents and inhibitors to large mercury boilers was studied, until the very satisfactory magnesium-and-titanium addition to the mercury was developed. The success of this chemistry on mercury boilers is largely due to the efficient efforts of the engineers who obtained in commercial units conditions comparable to those obtained in the near-test-tube-size laboratory boilers holding approximately $1/100{,}000$ of the mercury of a large unit.

AUTHOR'S CLOSURE

The control of air and water leakage into the vacuum spaces of the mercury turbines and condenser boilers is essential for proper control of the magnesium and titanium used for mercury treatments. In the two large plants in Schenectady and Kearny, the consumption of magnesium metal is at a rate of about 1 lb every 200 hr, with the titanium usage varying from 2 lb per day at Kearny to 2 lb per week in Schenectady.

Both metals are applied to the boiler mercury through a simple "locking" device by the mercury condensate from the condenser boiler. The magnesium metal dissolves readily in the mercury condensate, which is at a temperature of approximately 450 F. The titanium metal dissolves in the magnesium-treated mercury in the boiler.

The ultimate efficiency of the binary mercury cycle cannot be predicted, as it depends largely upon metallurgical developments to produce steels capable of operating at temperatures in the order of 1500 F and pressures of 500 psi or more. However, with

[6] Sun Oil Company, Marcus Hook, Pa.

[7] Research Laboratory, General Electric Company, Schenectady, N. Y. Mem. A.S.M.E.

existing materials and operating experience, large power units can be built having approximately 41 per cent thermal efficiency.

Wear and erosion of the turbine parts are negligible, giving long life and good reliability, as is borne out by operation in all the mercury plants. The 10,000-kw Hartford turbine has operated some 80,000 hr since it was last opened for inspection, and the Schenectady turbine has not been taken down for inspection since the summer of 1935, with some 47,000 hr of operation in that period. No bucket replacements have been made since its installation in 1932. The Kearny turbine was opened in 1938 for alterations to increase its capacity, but no replacement parts were required.

The Flow of a Flashing Mixture of Water and Steam Through Pipes

By M. W. BENJAMIN[1] and J. G. MILLER,[2] DETROIT, MICH.

This paper presents a method of designing piping to carry a flashing mixture of water and steam. An example of such piping is the cascade drain lines between feedwater heaters. The flow formula is based on a thermodynamic analysis of the problem, and the necessary coefficients of friction have been determined from tests. Calculations indicate the possibility of a critical-pressure condition at the end of a pipe carrying a flashing mixture. Each of the drain lines included in the study exhibited this phenomenon. The paper also includes a discussion of erosion of elbows in pipe lines carrying a flashing mixture, and suggests designs for minimizing or preventing failures from this cause. A criterion for predicting the comparative life of different sizes of pipes for a given line carrying a flashing mixture is set up on the basis of the total force on the elbows due to the momentum of the flowing fluid. An example of the application of the proposed flow formula to an actual design case is given in the Appendix.

DURING recent years power-plant engineers have become more and more interested in the flow of a flashing mixture of water and steam through pipes in connection with the design of cascade drain lines between extraction feedwater heaters. Several such lines, designed by the rule-of-thumb methods that have been used heretofore either have caused trouble with erosion in the elbows or have been unnecessarily large and expensive.

The case of fluid flow, involving a flashing mixture of water and steam, can readily be analyzed on the basis of thermodynamic equilibrium. However, to derive a usable formula for design purposes, it was necessary to obtain test data from which coefficients of friction could be determined. Since it was thought such tests might well include the friction effect of elbows, valves, and tees, it was decided to conduct an experimental investigation using existing cascade drain lines, particularly those in which trouble with erosion was being experienced.

While the data presented in this paper are not complete, sufficient information is given to be of assistance in the design of pipe lines to carry a flashing mixture of water and steam. An analysis is made of the flow in several cascade drain lines in order to learn why some have failed because of erosion while others have not. Several other factors of particular interest in designing pipe lines to carry water and steam are also discussed.

More complete results could have been obtained by means of special equipment, but the extra cost was not considered warranted by the amount of data which could be obtained by such equipment over that which could be obtained from tests of the existing drain lines.

[1] Engineer, Engineering Division, The Detroit Edison Company. Mem. A.S.M.E.

[2] Engineer, Engineering Division, The Detroit Edison Company. Jun. A.S.M.E.

Contributed by the Power Division and presented at the Annual Meeting, New York, N. Y., December 1–5, 1941, of The American Society of Mechanical Engineers.

Note: Statements and opinions advanced in papers are to be understood as individual expressions of their authors and not those of the Society.

In this paper the term "flashing mixture of water and steam" is used in preference to "boiling water" as used by earlier writers since it is considered to be more definite and possibly more accurate. It is used to denote a mixture of saturated water and steam in which additional steam is continually being formed at the expense of the sensible heat in the water, made available as a result of the continuing reduction in pressure as the mixture flows down the pipe.

Flow of a Flashing Mixture of Water and Steam Through Pipes

When saturated water flows from a receiver at one pressure through a throttling valve (or an orifice) and pipe to a receiver at a lower pressure, the following changes take place:

(*a*) As the pressure decreases the saturation temperature also decreases, and the enthalpy of that part of the fluid that remains liquid water is reduced in proportion to the drop in temperature.

(*b*) The heat liberated by the reduction in enthalpy of the water is all absorbed as latent heat in evaporating part of the water.

(*c*) The specific volume of the mixture of water and steam increases rapidly as steam is produced.

(*d*) The energy which becomes available with the decrease in pressure is expended in accelerating the mixture of water and steam and thus increasing its kinetic energy.

For example, if saturated water flows from receiver *A*, Fig. 1, through the throttling valve and the pipe into the lower-pressure



Fig. 1 Schematic Diagram Illustrating Flow of Flashing Mixture of Steam and Water Through a Pipe Connecting High- and Low-Pressure Receivers

receiver *B*, some of the water will flash into steam immediately following the valve at point 1, and an increasing amount of water will flash into steam as the mixture flows toward receiver *B*. The amount of steam flashed at point 1 in the pipe depends upon the initial temperature in *A* and the pressure P_1. Pressures P_1 and P_2 (at points 1 and 2) are functions of the initial saturation temperature in *A*, the weight of mixture flowing through the pipe, the size and length of the pipe, and in some cases the pressure in *B*.

Equations of Flow. According to the continuity equation

$$V = \frac{wv}{A} \qquad [1]$$

where V is the velocity in ft per sec; v the specific volume in cu ft per lb; w the weight flowing in lb per sec; and A the cross-sectional area of the pipe in sq ft.

Since w/A is constant for flow through a pipe, the velocity and, therefore, the kinetic energy at any point along the pipe during expansion depend upon the specific volume of the mix-

ture. The rate of increase of the velocity and kinetic energy during the expansion is a function of the rate at which the specific volume increases. Fig. 2 shows an example of the increase in specific volume of a flashing mixture of water and steam for an isentropic expansion from an initial pressure of 15 psi abs. This curve shows that, if saturated water flowing through a pipe expands from 15 psi abs to 3 psi abs, the velocity at the end of the pipe, due to the increase in specific volume of the flashing mixture, would be 475 times the velocity of the water at the entrance.

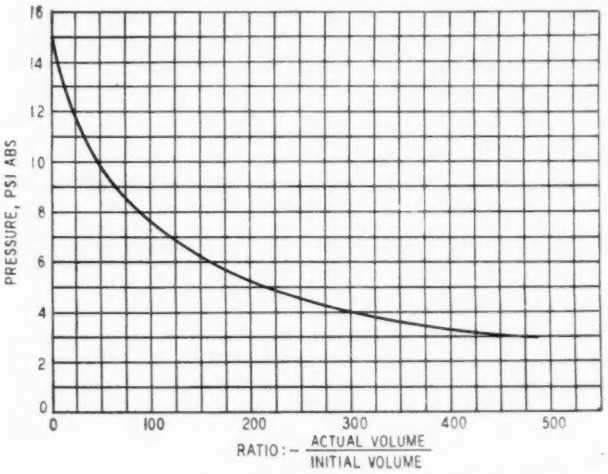


FIG. 2 INCREASE IN VOLUME OF FLASHING MIXTURE OF WATER AND STEAM DURING ISENTROPIC EXPANSION FROM SATURATED WATER AT 15 PSI ABS

A mixture of saturated water and steam in which additional steam is continually being flashed is not strictly an elastic fluid, although it is believed to behave in much the same way and will, therefore, be treated accordingly. The general energy equation for the flow of fluids can be expressed in the form

$$\bar{v}dP + \frac{VdV}{g} + \frac{KV^2}{2gD}\,dx = 0 \qquad [2]$$

in which v is the specific volume in cu ft per lb; P the pressure in lb per sq ft; V the velocity in ft per sec; D the diameter of the pipe in feet; K the friction factor; and x the distance in ft through which the mixture flows. This equation may be derived either from the energy relation as given by Goodenough[3] or by using Bernoulli's theorem.

From Equation [1] $(w/A)v$ can be substituted for V in Equation [2] to give

$$vdP + \left(\frac{w}{A}\right)^2 \frac{vdv}{g} + \frac{K}{D}\left(\frac{w}{A}\right)^2 \frac{v^2}{2g}\,dx = 0$$

or

$$\frac{1}{v}\,dP + \left(\frac{w}{A}\right)^2 \frac{1}{g}\,\frac{dv}{v} + \frac{K}{D}\left(\frac{w}{A}\right)^2 \frac{1}{2g}\,dx = 0$$

substituting ρ for $1/v$ and integrating

$$\int_{P_1}^{P_2} \rho dP - \left(\frac{w}{A}\right)^2 \frac{1}{g}\int_{\rho_1}^{\rho_2} \frac{d\rho}{\rho} + \left(\frac{w}{A}\right)^2 \frac{1}{2g}\,\frac{K}{D}\int_0^L dx = 0$$

or

$$\int_{P_1}^{P_2} \rho dP + \left(\frac{w}{A}\right)^2 \frac{1}{2g}\log_e\left(\frac{\rho_1}{\rho_2}\right)^2 + \left(\frac{w}{A}\right)^2 \frac{1}{2g}\,\frac{KL}{D} = 0 \qquad [3]$$

The density (or specific volume) used in Equation [3] is determined by assuming isentropic expansion in the pipe. In the actual expansion, the fluid friction and pipe friction impose a throttling action which causes the expansion to depart to some extent from the isentropic. However, in the usual case, the density of the mixture will be very nearly the same whether an isentropic expansion or a constant-enthalpy expansion is assumed.

No attempt has been made in developing Equation [3] to in-

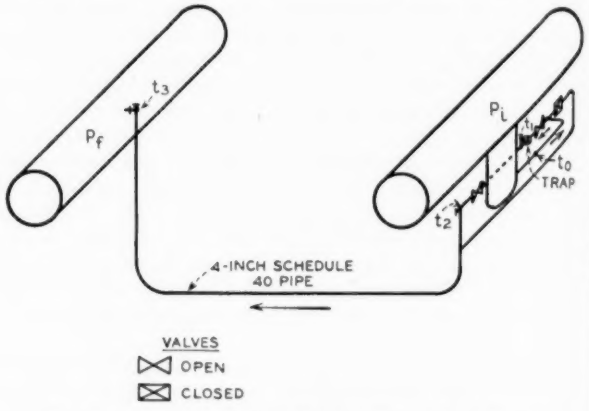


FIG. 3 DIAGRAM OF FIRST HEATER DRAIN LINE TESTED
(Refer to Table 1 for results of test.)

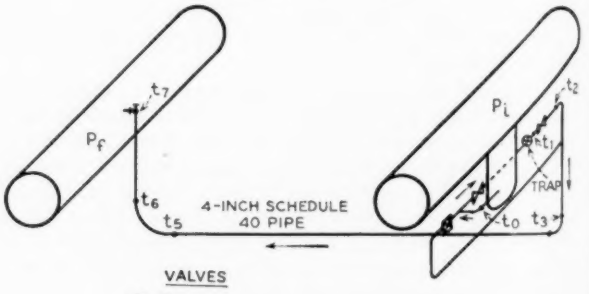


FIG. 4 DIAGRAM OF SECOND HEATER DRAIN LINE TESTED
(Refer to Table 2 for results of test.)

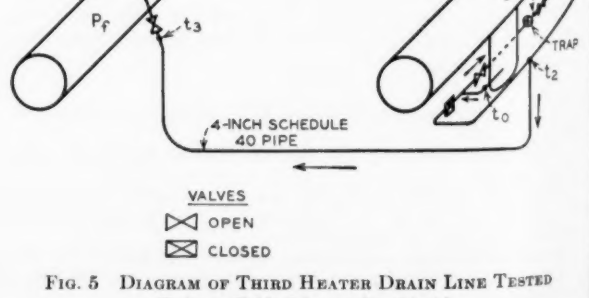


FIG. 5 DIAGRAM OF THIRD HEATER DRAIN LINE TESTED
(Refer to Table 3 for results of test.)

[3] "Principles of Thermodynamics," by G. A. Goodenough, second and third editions, Henry Holt and Company, New York, N. Y., 1912, 1920, respectively.

TABLE 1 RESULTS OF TEST OF DRAIN LINE SHOWN IN FIG. 3[a]

Run number	1	2	3	4
Duration of test, hr	1/2	1/2	1/2	1/2
Flow through pipe, lb per sec	18.22[b]	13.05[b]	10.25[b]	7.29[b]
Initial pressure, p_i, psi abs	37.2	29.8	23.9	18.2
Final pressure, p_f, psi abs	8.0	6.5	5.1	3.8
Friction factor, K	0.0095	0.0162	0.0097	0.0106

		Temperatures and Corresponding Saturation Pressures						
		Run No. 1		Run No. 2		Run No. 3		Run No. 4	
Temperature-measuring point	Distance from trap (equivalent length), ft	Temp, F	Saturation pressure, psi abs	Temp, F	Saturation pressure, psi abs	Temp, F	Saturation pressure, psi abs	Temp, F	Saturation pressure, psi abs
t_5 (Saturation temp)	..	263	37.0	250	29.8	238	23.9	223	18.2
t_1[c]	0	..	27.0	..	20.0	..	15.0	..	10.7
t_2	15	241	25.6	225	18.8	210	14.2	194	10.1
t_3 (End of pipe)	58	223	18.2	207	13.2	195	10.6	175	6.7

[a] This test was of a preliminary nature to determine if a critical-pressure condition existed at end of pipe.
[b] Estimated from previous test data.
[c] Extrapolated.

TABLE 2 RESULTS OF TEST OF DRAIN LINE SHOWN IN FIG. 4

Run number	1	2	3	4
Duration of test, hr	1	1	1	1
Flow through pipe, lb per sec	25.3	21.1	17.5	13.9
Initial pressure, p_i, psi abs	48.9	41.9	35.6	30.8
Final pressure, p_f, psi abs	10.46	9.02	7.64	6.47
Friction factor, K	0.0119	0.0118	0.0131	0.0119

		Temperatures and Corresponding Saturation Pressures							
		Run No. 1		Run No. 2		Run No. 3		Run No. 4	
Temperature-measuring point	Distance from trap (equivalent length), ft	Temp, F	Saturation pressure, psi abs	Temp, F	Saturation pressure, psi abs	Temp, F	Saturation pressure, psi abs	Temp, F	Saturation pressure, psi abs
t_5 (Saturation temp)	..	271	42.8	265	38.2	253	32.5	245	27.4
t_1[a]	0	..	35.8	..	30.5	..	25.5	..	20.0
t_2	5.0	261	35.8	251	30.5	241	25.3	227	19.8
t_3	16.2	259	34.6	250	29.6	239	24.5	226	19.3
t_4	22.0	257	33.5	249	29.2	237	23.7	225	18.9
t_5	34.2	251	30.4	243	26.3	231	21.2	219	16.9
t_6	42.6	251	30.4	243	26.2	231	21.1	219	16.8
t_7 (End of pipe)	48.9	245	27.4	236	23.0	225	18.8	211	14.5

[a] Extrapolated.

TABLE 3 RESULTS OF TEST OF DRAIN LINE SHOWN IN FIG. 5[a]

Flow through pipe, lb per sec	22.2
Initial pressure, p_i, psi abs	43.4
Final pressure, p_f, psi abs	8.4
Friction factor, K	0.0116

		Temperature and corresponding saturation pressure	
Temperature-measuring point	Distance from trap (equivalent length), ft	Temp, F	Saturation pressure, psi abs
t_5 (Saturation temp)	...	269	41.4
t_1[b]	0	..	35.0
t_2	40	256	33.0
t_3	82.5	244	26.8
t_4 (End of pipe)[b]	90.3	..	22.0

[a] This line was tested because of trouble with trap.
[b] Extrapolated.

clude the effect of a static head due to a vertical section of pipe. In most of the heater drain lines encountered by power-plant engineers, a major part of the pipe is horizontal; therefore the effect of the static head is of secondary importance compared to the thermodynamic head.

Before Equation [3] can be used, values for the friction factor K must be determined experimentally. All of the other quantities in the equation will be given for each design case under consideration.

Experimental Investigation of Flow of a Flashing Mixture of Saturated Water and Steam Through Pipes

The experimental work was carried out on some of the heater drain lines on 30,000-kw and 60,000-kw steam turbines at the Connors Creek Power Plant. Schematic sketches of the drain lines tested are shown in Figs. 3, 4, and 5.

During each test, temperature measurements were taken at various points along the drain-line piping, as shown in the sketches and, since the flashing mixture in the pipe was a mixture of saturated water and steam, the pressures at the various points were obtained from steam tables.[4] The quantity of drains flow-

[4] "Thermodynamic Properties of Steam," by J. H. Keenan and F. G. Keyes, John Wiley & Sons, Inc., New York, N. Y., 1936.

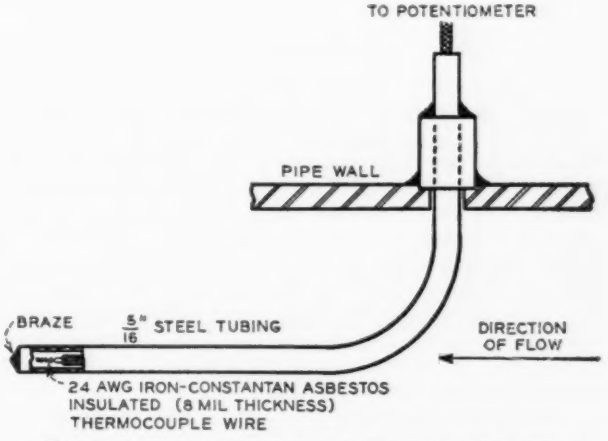


FIG. 6 DESIGN OF THERMOCOUPLE WELL USED IN TESTS

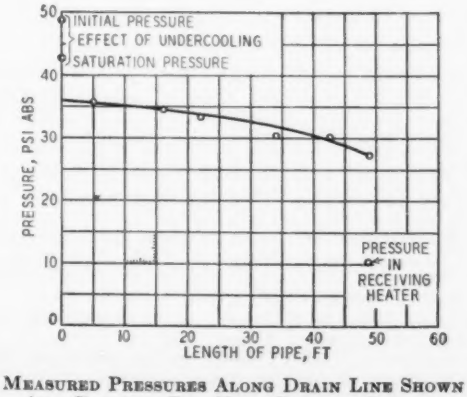


FIG. 7 MEASURED PRESSURES ALONG DRAIN LINE SHOWN IN FIG. 4, AS FOUND IN RUN NO. 1 GIVEN IN TABLE 2

ing through the line was determined by heat-balance calculation.

All temperatures were determined with iron-constantan thermocouples and a temperature indicator of the potentiometer type. It is believed that the measured temperatures are in error by no more than ±1 F. The design of the thermocouple well is shown in Fig. 6.

Test Results

Included in the results of the tests are the pressures at various points along the drain lines, the weight flowing through the pipe, and the values for the friction coefficient K from Equation [3]. In determining the values for K, the length of pipe used in Equation [3] was the equivalent length determined by use of data from various sources.[5]

Table 1 gives the results of a test of the drain line illustrated in Fig. 3. This test was conducted primarily to verify the existence of a critical-pressure condition in the end of the pipe or at the entrance to the low-pressure receiver. The weight of mixture flowing through the pipe was estimated from previous test data, and the values determined for K have been given here mainly for the record.

Table 2 gives the results of a test of the drain line illustrated in Fig. 4. This test was conducted to determine the friction factor K. Fig. 7 shows the pressures at the various points along the pipe for run No. 1 plotted against the equivalent length.

Table 3 shows the results of a test of the drain line illustrated in Fig. 5. This drain line, which operates with about the same initial and final pressures and quantity of mixture flowing as the one illustrated in Fig. 4, but which is somewhat different in piping arrangement, was investigated because of trouble with the float-operated drainer trap.

Analysis of Results

As far as the authors know only two other writers[6,7] have discussed the subject of the flow of a flashing mixture of water and steam through pipes and only one of them offered any test results.[7] His investigation consisted of a single test, and it was felt that additional test data were needed to establish a basis for design. As previously stated, the results of the tests given by the authors in this paper are not complete; however, they do include data that apparently are not available elsewhere, and it is for this reason that this paper has been written. These data offer assistance in designing piping to carry a flashing mixture of water and steam, and it is hoped that other investigators will publish such information as they may have on the subject to provide a still better basis for design work.

Critical Pressure at End of Pipe. It has been known for some time that when an elastic fluid flows through a pipe a critical pressure will occur at the end of the pipe when the ratio of the velocity to the specific volume is a maximum. This critical pressure with an elastic fluid, such as steam, occurs when its velocity equals the velocity of sound in the fluid.

It is interesting to note that a critical-pressure condition can also occur when a flashing mixture of water and steam flows through a pipe, as shown by the test results in Tables 1, 2, and 3. Since the velocity of sound in a mixture of steam and water is not known, it is impossible to state whether or not the velocity attained by the mixture when the critical-pressure condition occurs is that of sound. It may be stated, however, that the critical pressure in the end of the pipe is reached when the increase in energy made available by an increment drop in pressure balances the resulting increase in kinetic energy and the increase in friction. From Equation [3], this relation can be expressed

$$\left(\frac{w}{A}\right)^2 \frac{1}{2g} \log_e \left(\frac{\rho_1}{\rho_2}\right)^2 + \left(\frac{w}{A}\right)^2 \frac{1}{2g} \frac{KL}{D} = 144 \int_{p_1}^{p_2} -\rho dp$$

or

$$\left(\frac{w}{A}\right)^2 \frac{1}{2g} \times \frac{1}{144} = \frac{\int_{p_1}^{p_2} -\rho dp}{\log_e \left(\frac{\rho_1}{\rho_2}\right)^2 + \frac{KL}{D}} \quad \ldots\ldots [4]$$

in which $(p \times 144)$ has been substituted for P in Equation [3].

Fig. 8 is a graph of solutions of Equation [4] for various downstream-end pressures, assuming a fixed initial pressure of 35 psi abs. As shown by the curve, the maximum value of $\left(\frac{w}{A}\right)^2 \frac{1}{2g} \times \frac{1}{144}$ and therefore the maximum capacity of the pipe is reached when the downstream-end pressure is about 22 psi abs. From

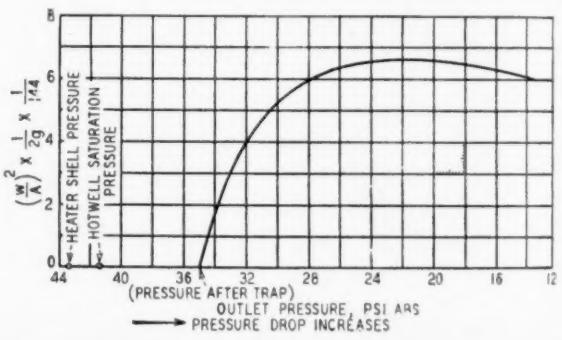


Fig. 8 Illustration of Graphical Method Used in Connection With Equation [4] to Determine Pressure After Trap and End, or Critical Pressure, in a Pipe Carrying Flashing Mixture of Steam and Water

(The pipe size in this case is 4 in., and the equivalent length following the trap is 90.3 ft. The value of K is considered as 0.0120 and w equal to 22.2 lb per sec.)

Table 3 and Fig. 5, it is seen that the 22-psi-abs downstream-end pressure is the critical pressure found on test at the end of the line, and the 35-psi-abs upstream pressure is that found on test near the outlet of the trap, while the flow of 22.2 lb per sec through a 4-in. pipe corresponds to the maximum value of 6.65 shown in Fig. 8, for $\left(\frac{w}{A}\right)^2 \frac{1}{2g} \times \frac{1}{144}$. In this calculation, which is given in detail in the Appendix, the equivalent length was 90.3 ft and the value for K was taken as 0.0120. From this example, it is seen that, when the saturation temperature, quantity of the water, and length and diameter of the pipe are known, it is possible by use of Equation [4] to determine the critical pressure at the end of the pipe, and the initial pressure following the throttling valve or orifice. Also Equation [4] can be used to determine the best pipe size when the saturation temperature, quantity of saturated water, and the length of the line are known.

Friction Factor, K. The friction factor for the flow of a mixture of water and steam through a pipe in which a critical-pressure condition exists at the end of the pipe was found to vary from 0.0116 to 0.0131, see Tables 2 and 3. In his test Bottomley[7] found the friction factor to be 0.0120 which compares favorably with the values found by the authors.

[5] "Engineering Data on Flow of Fluids in Pipes, and Heat Transmission," Crane Company, Chicago, Ill., 1935. "Piping Handbook," by J. H. Walker and S. Crocker, third edition, McGraw-Hill Book Company, Inc., New York, N. Y., 1939.

[6] "Discharge Capacity of Traps," by A. E. Kittredge and E. S. Dougherty, *Combustion*, vol. 6, Sept., 1934, pp. 14–19.

[7] "Flow of Boiling Water Through Orifices and Pipes," by W. T. Bottomley, Trans. North East Coast Institution of Engineers and Shipbuilders, vol. 53, 1936–1937, pp. 65–100.

TABLE 4 RESULTS OF STUDY OF FLOW CHARACTERISTICS THROUGH SEVERAL EXISTING CASCADE DRAIN LINES

No. of line	Nominal diam of pipe, in.	Pressure—Receiver—High (sat), psi abs	Pressure—Receiver—Low, psi abs	Pressure—End of line, psi abs	Specific volume at end of line (v), cu ft per lb	Density at end of line (ρ), lb per cu ft	Flow (w), lb per sec	Velocity of mixture (V), fps	Momentum ($1.414MV$), lb	Kinetic energy $\left(w\frac{V^2}{2g}\right)$ ft-lb	Density × velocity head $\rho\frac{V^2}{2g}$, psf	Lines having elbows replaced
1[a]	4	152.0	45.8	47.2	0.800	1.25	14.00	127	78	3500	310	X
2[a]	4	42.8	10.5	27.3	0.426	2.35	25.30	122	136	5870	545	X
3	3	208.8	93.8	93.8	0.340	2.94	5.98	40	11	150	73	
4	4	93.8	36.2	36.2	0.800	1.25	11.30	102	51	1830	200	
5[a]	4	37.0	6.5	18.2	0.900	1.11	18.20	185	148	9700	590	X
6	3	108.8	37.9	37.9	0.821	1.22	10.72	171	81	4870	555	X
7	4	37.9	13.0	19.3	0.833	1.20	19.13	180	151	9630	605	X
8	6	13.0	2.8	10.4	0.427	2.34	29.90	64	84	1870	145	X
9	4	236.0	108.0	108.0	0.312	3.20	13.64	48	29	4910	115	
10	6	108.0	37.7	37.7	0.834	1.20	26.60	110	128	5000	225	
11	6	11.3	2.5	4.1	3.900	0.256	7.70	150	51	2700	90	
12	4	25.1	7.2	7.4	3.030	0.330	6.94	238	73	6100	290	
13	6	7.2	2.2	4.6	1.500	0.667	13.08	98	56	1950	100	
14[a]	4	41.4	8.4	22.0	0.704	1.42	22.2	177	172	10,800	690	

[a] Test results; all others are calculated.

In studying these results it is important to keep in mind that all the tests were conducted with existing installations of 4-in. pipe and for a limited number of pressure combinations. To obtain complete information concerning the friction factor for the flow of a flashing mixture of water and steam through pipes, it would be necessary to investigate the flow through several sizes of pipes, with several pressures in the low-pressure receiver for each of a large number of initial pressures in the high-pressure receiver, and with various quantities for each pipe size and each pressure combination. To conduct such a test, it would have been necessary to build special test equipment involving the expenditure of more time and money than was believed warranted by the importance of the authors' particular problem. A value of 0.0120 for the friction factor will give results that are sufficiently accurate for many design purposes.

Design of Pipe Lines to Carry a Flashing Mixture of Water and Steam

Past practice in the design of pipe lines to carry a flashing mixture of water and steam has depended more upon the judgment of the designer than upon any actual information. For instance, some designers have chosen pipe sizes to give a certain water velocity, neglecting the effect of steam forming in the line, while others have gone to the opposite extreme and chosen excessively large pipes. A line designed by the latter would usually be unnecessarily expensive, while one designed by the former would be liable to troubles with erosion in the elbows and in some cases operating difficulties with float-operated drainers.

Erosion in Drain-Line Piping. The results of a study of the flow characteristics through several existing cascade drain lines are given in Table 4. It should be noted that not all of these lines have a critical pressure at the end of the line, and neither have all the lines had an elbow replaced. The cause of erosion in some drain lines has not definitely been determined; however, there is some indication that it is the result of cavitation which occurs at the elbows due to the momentum of the flowing mixture. For instance, when a saturated mixture of water and steam flows around a bend, the increase in pressure at the outer wall, which results from the change in direction of flow, will cause steam bubbles to collapse, constituting the cavitation condition.

For design purposes it is important to be able to determine in advance whether a line carrying a mixture of water and steam will have a satisfactory life or whether it will wear out in a short time due to erosion. Three methods for correlating experience with erosion have been investigated, namely, (a) force on elbows due to the momentum of the flowing mixture $\left(1.414\frac{wv}{g}\right)$, ($b$) kinetic energy $\left(\frac{wV^2}{2g}\right)$, ($c$) the product of the velocity head and the density $\left(\rho\frac{V^2}{2g}\right)$. Of these ($a$) seems to give the most consistent results based on experience with existing lines, as shown by the data given in Table 4. For example, all the lines except three, having a force on the elbow at the end of the line of 75 lb or more, have had at least one elbow replaced. Two of the exceptions have been in service only a short time, while the other is subject to corrosion. All of the lines with a force below 75 lb have not as yet failed by erosion. The methods (b) and (c) do not give results that are consistent in all cases with experience, as the reader can observe by comparing the values for lines Nos. 4 and 8 in Table 4.

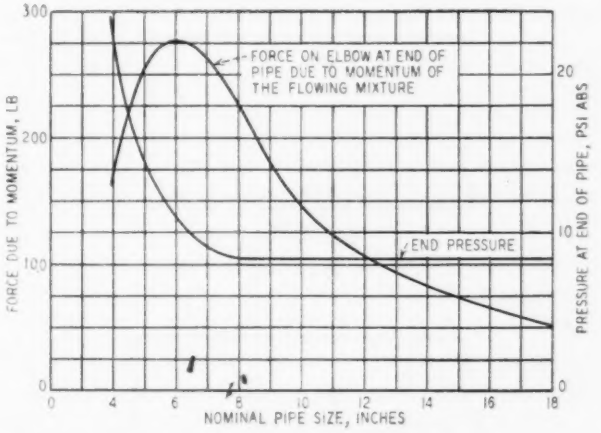


FIG. 9 CURVES SHOWING RELATION BETWEEN DOWNSTREAM-END OR CRITICAL PRESSURE, FORCE DUE TO MOMENTUM, AND PIPE SIZE FOR PARTICULAR DESIGN

(Case in which the weight of flashing mixture flowing is 22.2 lb per sec, and the initial saturation pressure of the water is 41.4 psi abs.)

It is important to note that in some cases increasing the pipe size will not always result in a lower velocity at the end of the line. As an example, take line No. 14 in Table 4, for which test data are given in Table 3. If the pipe in this line is increased from a 4-in. to a 6-in. size, the pressure at the end of the line will be about 11 psi abs or 2.5 to 3 psi above the pressure in the low-pressure receiver. The specific volume then is 2.56 cu ft per lb, the velocity is 285 fps, and the force due to the momentum of the flowing mixture at the end of the line is 277 lb.

Fig. 9 shows how the force due to momentum varies for different pipe sizes, as well as the pressures at the end of the line. From the standpoint of this force, it is seen that the 4-in. pipe is better than either the 6-in. or 8-in. pipe. Also in order to get the value of the force due to momentum down to about 75 lb it would be necessary to use a 14-in. pipe, as shown in Fig. 9. It

is probable, however, that the larger sizes of pipes, because of the greater projected area at the elbows, will stand a considerably greater total force than pipes ranging up to 8 in. diam. For this particular line, it would probably be necessary to use at least a 10-in. pipe to reduce the erosion to the point where it would not be objectionable.

In many lines it is desirable to use the smaller-size pipe and to resort to various schemes for retarding erosion. One scheme, which has been tried with only partial success, is to install tees in place of elbows in such a manner that the momentum of the flowing mixture will be partially dissipated against a blind flange. Another scheme is the installation of elbows with extra-heavy walls. In line with this it should be pointed out that cast-iron elbows, because of thicker walls, last longer than steel elbows. To avoid a forced shutdown of a turbine, telltales can be installed on the elbows to indicate by a leak when the wall is getting thin. Each telltale should be equipped with a valve which can be closed to permit the elbow or tee to be replaced at a convenient time.

Another scheme for minimizing erosion which has been considered is to separate the trap from its usual direct connection to the float operator, and move the trap proper to the downstream end of the drain line. The trap would then be actuated by the remote float through a mechanical or hydraulic linkage. This remote-control arrangement was not favored, however, because it would complicate the heater layout with additional control lines.

Whenever feasible the use of orifices[8] in place of float-operated traps for draining feedwater heaters offers another solution to the erosion problem. By installing the orifice near the end of the drain line so it will discharge into the low-pressure heater through a tee, as shown in Fig. 10, the erosion can be concentrated on the blind flange and in the tee, which can be examined and replaced if necessary whenever the turbine is down for inspection. This scheme has the additional advantage that smaller-size pipe can be used than would be possible if the orifice (or trap) were located at the beginning of the line.

[8] "The Flow of Saturated Water Through Throttling Orifices," by M. W. Benjamin and J. G. Miller, Trans. A.S.M.E., vol. 63, July, 1941, pp. 419–426.

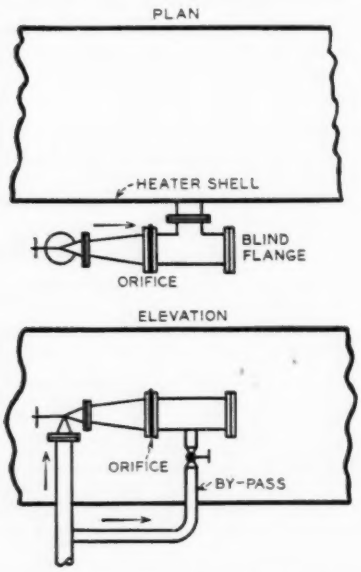


FIG. 10 SKETCH SHOWING INSTALLATION OF AN ORIFICE NEAR END OF DRAIN LINE DISCHARGING INTO LOW-PRESSURE-HEATER SHELL THROUGH TEE

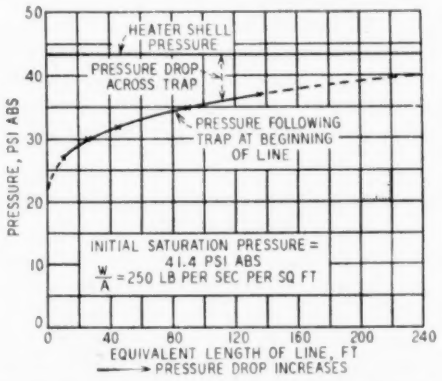


FIG. 12 CURVES SHOWING RELATION BETWEEN LENGTH OF DRAIN LINE AND PRESSURE DROP ACROSS TRAP FOR ACTUAL DESIGN CASE

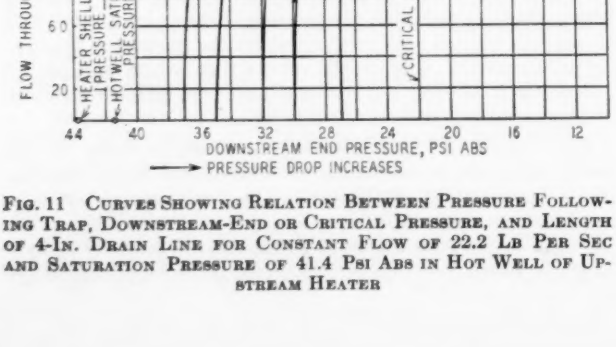


FIG. 11 CURVES SHOWING RELATION BETWEEN PRESSURE FOLLOWING TRAP, DOWNSTREAM-END OR CRITICAL PRESSURE, AND LENGTH OF 4-IN. DRAIN LINE FOR CONSTANT FLOW OF 22.2 LB PER SEC AND SATURATION PRESSURE OF 41.4 PSI ABS IN HOT WELL OF UPSTREAM HEATER

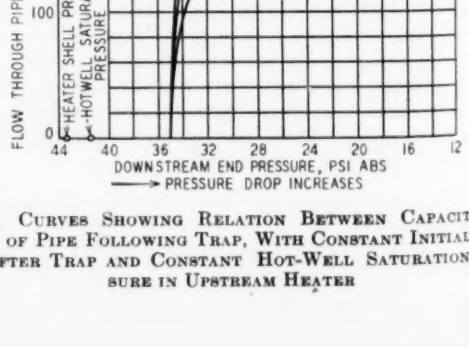


FIG. 13 CURVES SHOWING RELATION BETWEEN CAPACITY AND LENGTH OF PIPE FOLLOWING TRAP, WITH CONSTANT INITIAL PRESSURE AFTER TRAP AND CONSTANT HOT-WELL SATURATION PRESSURE IN UPSTREAM HEATER

Effect of a Variation in Length on Flow Through Pipes. The effect on the flow characteristics of varying the length of pipe is mainly of interest in lines where the combination of flow and initial temperature is such that a critical-pressure condition will exist at the end of the line. If for example several lengths are assumed for the drain line, shown in Fig. 5 (No. 14, Table 4) while maintaining a constant flow of 22.2 lb per sec it is seen in Fig. 11 that the critical pressure is constant, but the pressure at the beginning of the line (immediately following the trap) varies from 27 psi abs for a length of 10 ft to 37 psi abs for a length of 135.5 ft. This variation of initial pressure with length is also shown in Fig. 12 along with the pressure drop available for forcing the water through the trap. For instance, for a length of 90 ft, which is the installed equivalent length of this line, the available drop is 8.4 psi. The trap as originally installed did not function properly at high loads on the turbine. An investigation showed that, because of the head required to push the water from the heater hot well to the trap, the float chamber on the trap was only half-full, or the trap valve was only half-opened, when the heater flooded, and the available pressure differential of 8.4 psi was not great enough to overcome the friction in the half-opened valve. This trouble was overcome by connecting the float chamber directly to the hot well of the heater, thus making the float respond directly to the water level in the hot well. There were two other possible solutions to this problem, however. One was the readjustment of the linkage between the float and the valve so that when the float chamber was half full of water the valve would be wide open. This solution was discarded mainly because it necessitated the installation of a stop to prevent the valve from lifting out of the seat. The other solution was to install 6-in. pipe or larger in place of the 4-in. pipe. With a 6-in. pipe the pressure following the trap valve would be about 19 psi abs, giving a pressure drop across the valve of approximately 25 psi. However, this scheme has the disadvantage of being subject to even more severe erosion than exists in the 4-in. pipe, as shown in Fig. 9.

If the initial temperature of the saturated water and the pressure of the mixture immediately following the trap are held constant, an increase in length of pipe results in a decrease in capacity and critical pressure. This relationship is illustrated in Fig. 13, for the drain line shown in Fig. 5 (No. 14, Table 4). It is interesting to note that the curves in Fig. 13, are similar to those for steam, showing the relationship between pressure drop, length of pipe, and weight of steam flow.[9]

[9] "How to Design Steam Piping for Maximum Capacity and High-Pressure Drop," by M. W. Benjamin, *Heating-Piping and Air Conditioning*, vol. 8, 1936, pp. 475–478. "Steam and Gas Turbines," by A. Stodola, vol. 1, 1927 ed., McGraw-Hill Book Company, Inc., New York, N. Y., p. 63.

Conclusions

For practical purposes a flashing mixture of water and steam flowing through a pipe can be treated as an elastic fluid. The results of tests show that a critical-pressure condition can exist in the end of a pipe carrying a mixture of water and steam, which is similar to the critical-pressure condition that will exist in a line carrying steam (or any other elastic fluid), in which the pressure drop in the pipe is sufficient to produce an acoustic velocity. Whether or not the velocity of a mixture flowing through a pipe having a critical-pressure condition is the acoustic velocity is a question that cannot be answered until more is known about the velocity of sound through a mixture of a liquid and vapor. The existence of a critical-pressure condition in a pipe carrying a mixture of water and steam depends upon the combination of the following factors: (*a*) The initial saturation temperature of the water leaving the high-pressure receiver; (*b*) the quantity flowing; (*c*) the size and length of the pipe; (*d*) the pressure of the receiver into which the pipe discharges.

It is important to keep in mind that the data presented in this paper are not complete, and the authors hope that other investigators who have the proper testing facilities will be encouraged to gather more information concerning this subject. The data obtained in the authors' tests, however, are useful in making calculations from which pipe lines carrying a flashing mixture of water and steam can be designed to minimize erosion in the elbows, while avoiding the use of unnecessarily large pipe. Similarly, the data are helpful in determining the loss of pressure in the piping adjacent to an orifice or float-operated trap, so that a proper size of orifice can be provided, or so that sufficient pressure differential across the trap is assured.

While the data presented in this paper concern only the flow of a flashing mixture of water and steam, it seems probable that the analysis given here would be applicable to the flow of any flashing mixture of a liquid and its vapor. For the latter, however, it might be necessary to determine new values for the friction coefficient.

Acknowledgment

The authors gratefully acknowledge the encouragement and help of Messrs. P. W. Thompson, Sabin Crocker, and W. A. Carter in preparing this paper; and of Mr. A. C. Pasini and the technical staff at the Connors Creek Power Plant in collecting the test data.

Appendix

Nomenclature

A = cross-sectional area of pipe, sq ft
D = diameter of pipe, ft
g = acceleration due to gravity, 32.2 fps per sec
K = friction coefficient
L = over-all length, ft
P = pressure, psf abs
p = pressure, psi abs
q = quality of steam
t = temperature, F
v = specific volume, cu ft per lb
v_m = specific volume of mixture of water and steam, cu ft per lb
V = velocity, fps
w = flow of mixture of water and steam, lb per sec
x = distance to any point along pipe, ft
ρ = density, lb per cu ft

Keenan and Keyes Steam Table nomenclature for Table 5.

Example to Illustrate the Solution of Equation [4]

In order to solve the equation

$$\left(\frac{w}{A}\right)^2 \times \frac{1}{2g} \times \frac{1}{144} = \frac{\int_{p_1}^{p_2} -\rho dp}{\log_e\left(\frac{\rho_1}{\rho_2}\right)^2 + \frac{KL}{D}}$$

the densities of the mixture for various pressures must first be determined. Table 5 shows the method of calculating the densities for constant-entropy expansion for an initial temperature 269.3 F, or saturation pressure of 41.4 psi abs (see Table 3). Fig. 14 shows how these densities vary as the pressure decreases.

The integral $\int_{p_1}^{p_2} -\rho dp$ can best be evaluated arithmetically, since, to integrate directly, it would be necessary to find the equation of the curve in Fig. 14. The arithmetical integration is shown in Table 6, together with the solution of Equation [4]. This shows that, for an initial pressure, following the trap, of 35 psi abs and a downstream-end pressure of 22 psi abs, the value of $\left(\frac{w}{A}\right)^2 \times \frac{1}{2g} \times \frac{1}{144}$ is 6.64 (see also Fig. 8), which corresponds to a flow of 22.2 lb per sec through a 4-in. pipe.

It should be pointed out that it usually requires at least three trials to find a solution. For instance if the initial pressure p_1 had been chosen as 36 psi abs the maximum value of $\left(\frac{w}{A}\right)^2 \times \frac{1}{2g} \times \frac{1}{144}$ would have been greater than the required value of 6.64.

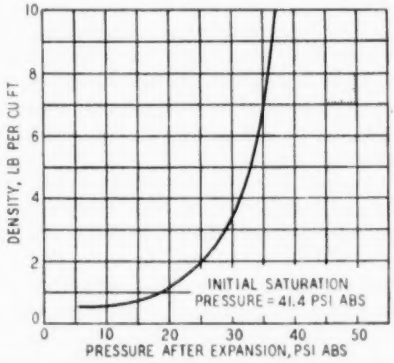


FIG. 14 CURVE GIVING DENSITIES OF MIXTURE OF WATER AND STEAM WHEN SATURATED WATER IS EXPANDED ISENTROPICALLY FROM INITIAL SATURATION PRESSURE OF 41.4 PSI ABS

TABLE 5 CALCULATION OF DENSITIES OF MIXTURE OF STEAM AND WATER FOR CONSTANT-ENTROPY EXPANSION

p	41.4	36	32	28	24	20	16	8.4
S_1	0.3948							
S_2	.....	0.3831	0.3733	0.3623	0.3500	0.3356	0.3184	0.2708
$S_f q$	.....	1.3017	1.3209	1.3425	1.3672	1.3962	1.4313	1.5312
$(S_1 - S_2)$	.....	0.0117	0.0215	0.0325	0.0448	0.0592	0.0764	0.1240
$q = \frac{S_1 - S_2}{S_f q}$	.....	0.0090	0.0163	0.0242	0.0328	0.0424	0.0534	0.0810
$(1 - q)$	.....	0.9910	0.9837	0.9758	0.9672	0.9576	0.9466	0.9190
v_f	0.01716	0.01709	0.01704	0.01698	0.01691	0.01683	0.01674	0.01654
v_g	.....	11.588	12.940	14.663	16.938	20.089	24.75	45.25
$(1 - q)v_f$	.....	0.0169	0.0168	0.0166	0.0164	0.0161	0.0158	0.0152
$(q)v_g$	.....	0.1043	0.2109	0.3548	0.5556	0.8518	1.3217	3.6653
v_m	.....	0.1212	0.2277	0.3714	0.5720	0.8679	1.3375	3.6805
ρ	58.3	8.25	4.39	2.69	1.75	1.15	0.75	0.27

TABLE 6 ILLUSTRATION OF METHOD OF SOLVING EQUATION [4]

p_1	35																
p_2	34	33	32	31	30	29	28	27	26	25	24	23	22	21	20	19	18
d_p	1	1	1	1	1	1	1	1	1	1	1	1	1	1	1	1	1
ρ_1	6.85																
ρ_2	5.85	5.05	4.39	3.87	3.41	3.01	2.69	2.40	2.16	1.94	1.76	1.57	1.42	1.27	1.15	1.03	0.93
ρ_a	6.35	5.45	4.72	4.13	3.64	3.21	2.85	2.55	2.28	2.05	1.85	1.66	1.49	1.34	1.21	1.09	0.98
$\rho a dp$																	
$\Sigma \rho a dp$	6.35	11.80	16.52	20.65	24.29	27.50	30.35	32.90	35.18	37.23	39.08	40.74	42.23	43.57	44.78	45.87	46.85
ρ_1/ρ_2	1.17	1.35	1.56	1.77	2.01	2.28	2.55	2.86	3.17	3.53	3.89	4.36	4.78	5.39	5.95	6.65	7.37
$(\rho_1/\rho_2)^2$	1.37	1.83	2.43	3.13	4.04	5.20	6.55	8.19	10.05	12.45	15.10	19.00	22.80	29.00	35.40	44.20	54.30
$\log_e (\rho_1/\rho_2)^2$	0.32	0.60	0.89	1.14	1.40	1.65	1.88	2.10	2.30	2.52	2.71	2.92	3.13	3.37	3.57	3.79	3.99
$\frac{KL}{D} = \frac{0.012 \times 90.3}{0.3355}$	3.23	3.23	3.23	3.23	3.23	3.23	3.23	3.23	3.23	3.23	3.23	3.23	3.23	3.23	3.23	3.23	3.23
$\log_e (\rho_1/\rho_2)^2 + KL/D$	3.55	3.83	4.12	4.37	4.63	4.88	5.11	5.33	5.53	5.75	5.94	6.15	6.36	6.60	6.80	7.02	7.22
$\frac{\Sigma \rho a dp}{\log_e (\rho_1/\rho_2)^2 + KL/D}$	1.79	3.08	4.01	4.72	5.25	5.64	5.93	6.17	6.40	6.47	6.58	6.63	6.64	6.61	6.59	6.54	6.49

Discussion

W. T. BOTTOMLEY.[10] The Society has granted the writer permission to discuss, in conjunction with this current paper, a paper[11] which the authors previously presented.

Dealing first with their previous paper, the authors do not appear to have fully understood the data which the writer gave in his paper,[7] or they would have realized that their inference, that there is no evidence of a critical pressure in sharp-edged orifices when passing saturated water, is probably not correct.

The orifice the writer used was not sharp-edged but was a converging nozzle, having a cold-water discharge coefficient of nearly unity and was formed by drilling a hole in a $^1/_2$-in. plate, forming a well-rounded entry.

The pressure at the discharge side of the orifice, as measured by the temperature of the water, was not atmospheric pressure but was about 45 to 50 per cent of the initial saturation pressure.[12] Although the final discharge pressure at the other side of the heat exchanger was atmospheric pressure, the resistance through the heater, because of the large volume of flashing steam and water, accounted for the high back pressure at the nozzle discharge.

The writer did not assume that there was a critical pressure at the throat but deduced the fact from the results of the experiments. The last line in Table 1 of the writer's paper[7] gives the estimated throat pressure calculated from the discharge rate, assuming no vaporization before the throat and shows that the throat pressure was well above the pressure on the discharge side. The initial pressures were 48 to 64 psi abs, and the calculated critical pressure at the throat was about 67 per cent of the initial pressure.

Although these conditions were different from those of the authors', yet Fig. 2, of their paper, shows that the maximum discharge rates are in agreement; but for the sharp-edged orifice, it was necessary to drop the back pressure to zero to obtain the maximum discharge; whereas, with a nozzle the maximum discharge was obtained with a much higher back pressure.

At first sight, it may appear that the agreement of the maximum flow of saturated water through converging nozzles, with the maximum flow through sharp-edged orifices, is a coincidence, but the writer proposes to show that it is an indication there is a

[10] Merz and McLellan, Carliol House, Newcastle-on-Tyne, England.

[11] "The Flow of Saturated Water Through Throttling Orifices," by M. W. Benjamin and J. G. Miller, Trans. A.S.M.E., vol. 63, 1941, pp. 419–426.

[12] Second, third, and last lines of Table 1, reference 7.

critical pressure at the throat of the flow through the sharp-edged orifice.

The authors point out that, when the back pressure on the discharge side of the sharp-edged orifice is nil, the illustrations in Fig. 11 indicate that flashing occurs close to the downstream face. From this it may be inferred that no vena contracta is formed and therefore the discharge coefficient of the orifice under these conditions is practically unity. From the flows given in Fig. 7 for different initial pressures, when the back pressure is nil, the critical pressure at the throat can be calculated by Equation [1], assuming unity discharge coefficient, and is found to be from 63 to 69 per cent of the initial pressure, and is the same as that obtained at the throat of the nozzle.

The same argument applies to the flow of steam through sharp-edged orifices and nozzles, as shown in Fig. 12 of the authors' first paper.[11] It is not a coincidence that the maximum discharge is the same, but it indicates the same critical pressure at the throats.

If there is a critical pressure in the flow through sharp-edged orifices, the formulas in Equation [2] for the flow and the discharge coefficient, shown in Fig. 13, do not apply when the back pressure is below the critical pressure.

It was suggested in the writer's paper[7] that the excessive flow obtained, compared with the flow indicated by theory assuming thermal equilibrium, was due to the effect of surface tension, and that the critical pressure obtained indicated that the size of the bubbles which form at the throat is of the order of 0.001 mm.

It is interesting to note that the additional experimental data given in the present paper agree with the test data which the writer gave and confirm the fact that the flow through pipes can be calculated from the theory, assuming thermal equilibrium, and assuming an average resistance coefficient of about 0.012. The theory indicates the presence of a critical pressure at the pipe discharge when the receiver pressure is low enough, which incidentally has no connection with the critical pressure at the throats of orifices.

The authors have not given general curves showing the sizes of pipes required on the discharge side of orifices, such as are shown in Fig. 11 of the writer's paper.[7] It is necessary to note that the pipe sizes, shown in Fig. 11, apply to the pipes on the discharge side of orifices in the form of nozzles. For practical purposes, orifices with well-rounded entry are preferable to sharp-edged orifices, because they simplify the design of the layout.

Since the writer's paper[7] was presented in 1936, several power stations have been erected in this (England) and other countries which are operating satisfactorily with nozzle plates instead of traps in the feed-heater drains. These nozzle plates are generally about $1^1/_2$ to 2 in. thick, and the throat areas are made large so that they are capable of passing double the designed quantity of water at maximum output.

Only one case is known to the writer where erosion has occurred in elbow pipes, and this was at a bend immediately after the orifice. In this case, the orifice was lightly loaded and was above the receiver; the bend was in a downward direction close to the discharge side of the orifice.

In general, we have avoided erosion troubles at bends after orifices by placing the orifice below the receiver, so that the discharge side of the orifice is submerged. The water lying in the discharge pipe forms an effective buffer which dissipates the kinetic energy of the mixture issuing from the orifice.

The authors appear to be more concerned with erosion at the elbow near the pipe discharge. So far, we have not experienced this trouble. On checking the pipe sizes given in Table 4 of the present paper with those which we would have installed, based on Fig. 11 of the writer's paper,[7] it is discovered that pipe lines Nos. 2, 5, 7, 8, and 14 in Table 4 are too small to be used after nozzle plates.

Pipe line No. 6 is on the border line and we would have made it larger. Except, therefore, for pipe line No. 1, we would consider all those pipe lines, having replaced elbows, in Table 4 to be too small, and it is possible that this may account for our freedom from erosion trouble at the discharge elbow.

Pipe line No. 1 is a common condition in this country and, as we have not experienced trouble with it, the writer is unable to account for the erosion experienced by the authors. The authors say that the data for pipe line No. 1 were obtained from test results; but the writer cannot find these test results in Tables 1 to 3 and shall be glad if the authors will give a diagrammatic sketch of it similar to Fig. 5.

The writer is not satisfied with the authors' suggestion that the criterion for erosion is the total momentum force on the elbow and would expect the erosion to depend upon the intensity of the force on the surface area at the bend, in which case, it should depend rather upon the velocity head multiplied by the density either of the mixture or of the solid water.

It is to be noted that the arrangement shown in Fig. 10 of the paper can only operate when the water level in the previous receiver is above the orifice, in order to provide sufficient gravity head to overcome the resistance in the connecting pipe. The gravity head is necessary because the pressure in front of the orifice will be the same as the vapor pressure in the previous receiver.

A. G. Christie.[13] It was the writer's privilege to design some of the earlier drainage systems for bleeder heaters. These were designed on the basis of solid water flow with a liberal allowance for velocity and were generally large. When these did not function properly, larger pipes were used. In the early days, difficulties would frequently arise with the drainage traps; some of which troubles were quite unexplainable with the knowledge then at hand. These were remedied by cut-and-try methods.

The first suggestion that flashing of the water in the trap and piping might be the cause of the trouble was made by one of the officials of C. A. Parsons & Co., England, who were having trouble with heater drainage. It is understood that this company at a later date made some tests on this problem but, other than the paper by Bottomley,[7] none of these tests were made public.

The tests reported by the authors furnish the first concrete data on this rather baffling problem. The method for determining the critical pressure as presented by the authors is complicated and time-consuming. Probably some mathematician can develop a simpler method. It would also be of interest to determine whether this critical pressure at the end of the pipe corresponded to the acoustic velocity of the water-steam mixture.

The authors conclude that the momentum of the mixture causes the erosion at the elbows. The use of tees with blank flanges is recommended to enable easy replacement. The mass of steam and water must enter the lower pressure heater at high velocity and considerable momentum, which would cause erosion of the baffle that may be placed in this heater. Few heaters are designed with provision for the renewal of this baffle should such erosion occur.

Quite aside from the value of this paper in fixing conditions in piping from bleeder heaters, there is the suggestion that similar phenomena subject to the same analytical methods may exist in the side wall tubes of boiler furnaces. Certainly, similar flashing of water into steam will obtain in the blowoff pipes of boilers. While erosion has not been serious in either of these

[13] Professor of Mechanical Engineering, Johns Hopkins University, Baltimore, Md. Past-President A.S.M.E.

cases, the remedies proposed in this paper may find application in plants where there have been erosion troubles.

The authors suggest that further data should be secured by other observers. Let us hope that such data are soon made available. An interesting phenomenon has been carefully studied and the authors have made a notable contribution to our technical knowledge.

G. M. DUSINBERRE.[14] The suggestion has been made that the solution of the authors' problem would be simplified by the use of a suitable chart. The writer has constructed such a chart, Fig. 15, with a range covering several of the authors' examples. Similar charts could be made for higher and lower pressure ranges.

The best co-ordinates appear to be entropy versus specific volume. A uniform volume scale simplifies the construction, as the constant-pressure lines become straight. However, there are many advantages in using a logarithmic volume scale: (1) The chart is contracted and slide-rule accuracy is obtained throughout. The volume scale can be laid off conveniently directly from a slide rule. (2) If a density scale is desired, it need not be calculated but may be laid off by reversing the slide rule. (3) The logarithmic scale simplifies the authors' process of step-by-step integration. The quantity $\log_e(\rho_1/\rho_x)^2$ has to be evaluated a great number of times. With the use of Fig. 14, this is done as follows:

1 With dividers step off the horizontal intercept between the state points 1 and x.

2 Apply this on the scale of natural logarithms to obtain $\log_e(\rho_1/\rho_x)$.

3 Double this to obtain $\log_e(\rho_1/\rho_x)^2$.

The authors have measured condensate temperatures and then have expressed the data in terms of the corresponding saturation pressures. This seems an unnecessary complication. The saturation pressure does not exist in the system, except at some point in the drainer valve; nor is it used in the calculations except to determine the point on the liquid line at which the expansion process starts. For this purpose, the directly measured temperature serves as well. In design, the temperature would be estimated from the assumed heater shell pressure and the probable amount of subcooling. In the writer's Fig. 15, temperatures are shown on the liquid line.

The actual shell pressure must not be neglected since it is this, and not the saturation pressure, which determines the pressure ahead of the drainer valve. Hydrostatic pressure is often an appreciable factor.

The authors point out the fact, rather surprising at first thought, that there is little difference between the isentropic and the constant-enthalpy expansions in this situation. The writer has shown one constant-enthalpy line in Fig. 15 for comparison. The isentropic represents the limiting case of zero friction, and the constant-enthalpy line the limiting case of zero increase of kinetic energy. Neither of these conditions exists, and the actual expansion lies between.

H. W. EMMONS.[15] In order to interpret their test results, the authors have set up a simple theory of what happens to water-steam mixtures as they pass through pipes. Before any reliance can be placed on the theory, and hence on the interpretation of the experiments, several of the authors' assumptions must be checked by test.

1 It was assumed that the water and steam were in equilibrium, having properties as given in the wet region of the steam tables. Such properties only apply for equilibrium when a plane interface exists between the water and steam. If the water is finely divided, as it may well be after the specific volume has increased 100- or 200-fold, the surface energy cannot be neglected, even if equilibrium exists. The authors missed an opportunity to shed a little light on this important question by failing to make simple pressure measurements at the same time they were making temperature measurements. If the pressure measurements had not agreed with the steam-table saturation pressures, the difference would have given an indication of what deviation from the simple equilibrium must be considered.

2 It was assumed that the water and steam were distributed uniformly over the pipe cross section and moved with the same velocity. Of course, this is approximately true only if the water occurs in very fine droplets. Note that assumptions 1 and 2 are mutually exclusive, that is, the equilibrium cannot be for a plane liquid-vapor interface and for fine droplets at the same time. If assumption 2 is not correct there are several alternative possibilities. The water may be finely divided but not moving with the same velocity as the steam. The water may be segregated in one portion of the pipe, say, the bottom, moving with a velocity probably different from that of the steam.

The analysis, to be correct, must be modified if either assumption 1 or 2 is not admissible. It might be argued that the quantities used in the theory represent "average" quantities. If the quantities vary considerably across the pipe cross section, these averages become very inaccurate. For example, the continuity equation requires the use of the "flow average velocity," while the energy equation requires the "flow average of the velocity cubed," which may differ considerably.

Before closing this discussion, it might be well to note the effect of two extreme water-steam distributions on the cause for a critical-flow condition. If it is correct to make the authors' assumption that the distribution is uniform then, by thermodynamics, it can be shown that the

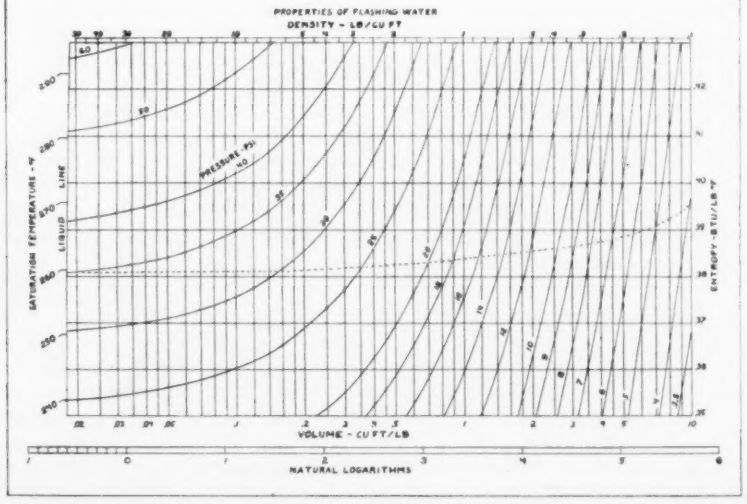


FIG. 15

[14] Assistant Professor of Mechanical Engineering, Virginia Polytechnic Institute, Blacksburg, Va.; at present on duty at U. S. Naval Academy, Annapolis, Md. Mem. A.S.M.E.

[15] Graduate School of Engineering, Harvard University, Cambridge, Mass. Jun. A.S.M.E.

velocity at the end of the pipe must be equal to or smaller than

$$V = \left(\frac{\partial p}{\partial \rho}\right)^{1/2} = v\left(-\frac{\partial p}{\partial v}\right)^{1/2}$$

This is the speed of sound in the mixture. This velocity is easily found by calculating the slope of a p-v diagram for the change of state which actually occurs. For example, the square root of minus the slope of the authors' curve, Fig. 2, multiplied by the abscissa gives the maximum velocity for each state assuming an isentropic-equilibrium change of state. On the other hand, if the water is flowing essentially along the bottom of the pipe, the critical condition would occur, for a steam velocity equal to the speed of sound in the steam, and a water velocity equal to the maximum velocity in streaming.

In closing, the writer wishes to compliment the authors for the care with which they have stated their assumptions. It is certainly excusable, in the solution of a practical problem needing immediate attention, to make whatever assumptions seem adequate. To make such work useful to others, however, it is important that the assumptions be stated as clearly as possible.

G. T. Hutchison.[16] Previous papers have developed the theory that, when saturated water passes from one pressure to a region of lower pressure, the rate of flow through a restriction is governed by the increase in volume due to flashing of the liquid and the acceleration of the mass resulting from the reduction in pressure. It has also been established that the rate of flow increases with a reduction in the lower pressure to an optimum point, beyond which any decrease in pressure has no effect upon the rate of flow. This point is called the critical pressure and has been defined by the authors as being reached when the increase in energy made available by an increment drop in pressure balances the resulting increase in kinetic energy and the increase in friction. In their work, reported in a previous paper,[11] the authors found that no critical-pressure condition existed when using a thin-plate orifice as a throttling device. Tests run by the writer's company in 1934 and 1938, upon a nozzle with a rounded approach, and an approximate ratio of length to diameter of 8 to 1, definitely showed critical pressures to exist at the throat of the nozzle, as determined by pressure measurements. Additional tests, run by the company within the last 3 months, on a $^1/_2$-in. inverted bucket trap proved definitely the existence of a critical pressure, since variation of the back pressure below a certain point had no effect upon the capacity of the trap with constant initial conditions.

The existence of a critical pressure at the downstream end of a pipe, handling a mixture of saturated water and its vapor, is shown clearly by the authors' tests. Had these tests been run with the length of pipe as the only restriction to flow, and water at the saturation temperature supplied to the inlet of the pipe, rather than a mixture of vapor and water, the authors would also have found that a critical-pressure condition exists at the outlet end of the pipe.

It is also interesting to note that various tests indicate different critical pressures for identical initial conditions, depending upon the design of throttling device tested.

The logical deductions from the test data at hand may be enumerated as follows:

1 Design of the throttling device determines the order of a lower pressure which regulates the amount of flow from the initial conditions. For saturated water, the head available for producing flow varies approximately as the square root of the pressure differential in one extreme design, when the throttling device is a thin-plate orifice with no other factors to influence the flow. In the other extreme, where the design is such as to produce a critical pressure, the flow varies approximately directly with the first power of the absolute pressure, providing, of course, the back pressure is below the critical pressure in that design of throttling device.

2 Properties of the fluid considered, which might affect the order of the critical pressure for any particular design of throttling device, are surface tension, viscosity, and the thermodynamic properties of the fluid.

3 Characteristics of the throttling device affecting the order of the critical pressure are:

(*a*) Any features producing turbulence in the flow stream which aid in overcoming the resistances to a change in phase. This effect may be produced by irregularities in castings in traps, change in the direction of flow in pipe fittings and trap bodies, and simple wall friction, as may be found in a nozzle, or length of pipe.

(*b*) Time elements involved in passage through a throttling device.

Consideration must be given to each of these deductions in any attempt to anticipate the flow of a saturated fluid through a throttling device.

Future experimental work might well be directed toward determining the factors affecting the critical pressure in the design of throttling devices when handling saturated water. It is suggested that tests be run on a small-diameter nozzle of appreciable length to determine capacity and order of critical pressure, and shorten the nozzle in subsequent tests until it becomes a thin-plate orifice. An analysis of results may show useful relationships to exist between initial conditions, critical pressure, flow, length, hydraulic diameter, nozzle wall friction, time, and such properties of the fluid as may affect the transition from the liquid to the vapor state. In test work of this nature, it would be more accurate to determine pressures by actual pressure measurements, rather than temperature readings converted to pressures, since the absence of a critical pressure, when an orifice is the throttling device, indicates the possibility of a state of nonequilibrium.

The authors have developed a rather complete formula for flow of flashing liquids through pipes, which is based on the premise that flashing fluids behave much the same way as an elastic fluid. In applying Bernoulli's theorem or Goodenough's energy relation to the flow of flashing liquids, the authors have indicated the differential-friction head as varying directly as the square of the velocity. The variation in friction in a pipe line, handling a mixture of this nature, is sufficient material for considerable research and several papers. Future experimental work may indicate that the differential-friction drop varies as some function of the fluid density, as well as the velocity squared, since friction of both gas or turbulent liquids flowing in pipes is affected by the density. As the flow is turbulent during its passage through the piping tested, it would be expected that it would follow the laws of turbulent flow.

The authors reached the conclusion that a critical pressure can exist at the end of a pipe line draining saturated water. The test results and analysis made here prove conclusively that a critical pressure will always exist at the end of the line as long as the receiver pressure is below that critical pressure.

A. A. Markson.[17] The authors state that obtaining complete information concerning the friction factor would have necessitated the expenditure of more time and money than was believed warranted by their particular problem. This is often the case in engineering. The thermodynamics of this particular

[16] Cochrane Corporation, Philadelphia, Pa. Jun. A.S.M.E.

[17] Research Engineer, Consolidated Edison Company of New York, New York, N. Y. Mem. A.S.M.E.

problem presents some extraordinary difficulties which are not lessened by any means by the fact that they are dealing with a two-phase mixture. Therefore, it would be captious to criticize the thermodynamics of this paper from an engineering point of view. The writer believes it would have been better if the authors had restricted the generality of their friction factor to its use in the particular method of integration which they found to be convenient in solving this problem. Further, another series of tests not requiring a great amount of time or expense should be run on both solid water and saturated steam flowing through their lines so that the relationship, of the coefficients which they found to the isothermal friction coefficients usually considered, could be seen. The coefficients they report are of the form $4f$, where f is the conventional way of basing the coefficients on mean hydraulic radius. The magnitude of their coefficient is somewhat below anything predicted for isothermal friction in ordinary pipes. Therefore, the test on water is very necessary to be sure whether the difference is due to the method of integration employed or to a different friction mechanism.

It is to be noted that there is apparently no systematic treatment of inlet and exit losses in such a system and the authors should clarify this point.

The method of computation of the state of the mixture is cumbersome, which is no fault of the authors, simply because there are no adequate diagrams such as the Mollier or Ellenwood which cover the wet-vapor region. It is to be hoped that this deficiency in a field of increasing technical importance will be remedied by those whose function is the production of graphical charts of steam properties. For a constant-enthalpy expansion this has been partially done[18] in a series of charts giving the enthalpy volume and pressure for very wet steam. It should also be done for the isentropic.

What is most important is that to engineers this paper represents a practical way of solving a theoretically complex problem. Their refusal to misrepresent the "scientific" rigor of their solution warrants a special word of commendation.

Authors' Closure

In preparing this paper for publication, the authors hoped to stimulate interest in the study of the flow of a flashing mixture of a liquid and its vapor and are therefore pleased with the discussions contributed and the interest which is thereby indicated to exist among engineers. The authors are particularly pleased to have a discussion from W. T. Bottomley; his paper offered considerable assistance to the authors in their work.

The first part of Mr. Bottomley's discussion refers to the authors' earlier paper,[11] and the comments immediately following apply to this part of his discussion.

With reference to Mr. Bottomley's remarks concerning critical pressures in the orifice, the authors would first like to state that in their opinion the terms "orifice" and "nozzle" are too loosely applied. For instance, there have been found several references to flow through nozzles when the so-called "nozzles" were either orifices or short tubes. Also short tubes are often called orifices. Actually, there may be considerable difference in the way these two devices perform.

Whether or not a critical-pressure condition can actually exist in a sharp-edged orifice, the authors are not prepared to say. However, it seems that before this question can definitely be settled, many data will have to be obtained from very carefully conducted tests. For all practical purposes saturated water flowing through sharp-edged orifices follows the same law as cold water; and the illustrations for all cases except those with high pressure differentials show that the saturated water did not flash until it was through the orifice. Sometimes it was as much as 6 in., or more, from the orifice downstream face before flashing. For these cases the authors believe that no critical-pressure condition existed. So long as a decrease in back pressure with a fixed initial pressure results in an increase in flow, as Fig. 7 of the previous paper[11] indicates is the case for saturated water flowing through sharp-edged orifices, Equation [2] of that paper, together with the coefficients given in Fig. 13, applies equally well for the complete range of back pressures. It seems to the authors that this is also an indication that no critical-pressure condition exists in the throat of the orifices, since such a condition is essentially one of a maximum flow. This is not saying, however, that a critical pressure will not exist in nozzles or short tubes. In fact, the authors would expect such a condition to exist in the case of the latter devices, and the discussion by Mr. Hutchison supports this opinion.

The following remarks apply to Mr. Bottomley's discussion of the authors' present paper.

Because of the number of variables involved, the authors have not attempted to formulate any general curves to be used in the design of heater drain lines. Each drain line is an independent problem and should be treated accordingly. In the authors' opinion, the generalization that would be required in making up design curves might well make the problem appear more difficult than it really is. This does not say, however, that a simpler method of calculating flow through heater drain lines cannot be developed.

Three methods for correlating experience with erosion in heater drain lines are suggested in the paper. Among these three is the method $\left(\rho \frac{v^2}{2g}\right)$, suggested by Mr. Bottomley. It is pointed out in the paper under "Erosion in Drain-Line Piping" and in Table 4 that, of the three methods, the total momentum force seems to give the most consistent results based on experience.

Regarding Mr. Bottomley's remarks about the use of orifices for draining feedwater heaters, particularly the design shown in Fig. 10 of the paper, the authors would like to state that at present there are seven turbogenerator units in the authors' company utilizing orifices for controlling the drains from the feedwater heaters. On six of these units, the orifices are installed as shown in the design given in Fig. 10 and, contrary to Mr. Bottomley's belief, the water level in the upstream heater is not required to be above the orifice. These orifices are sized initially from heater performance data and finally sized in the field for some definite load (usually overload) on the turbine. At the maximum load for which the orifice is sized, the water level will be in the upstream heater hot well. For loads less than maximum, no water level will show in the upstream heater hot well, which means that a small quantity of steam is probably blowing through the drain line with the water. Heat-balance calculations indicate that the effect on cycle efficiency of by-passing this steam is slight. At Connors Creek, where orifices have replaced traps on four of the six modern units, no noticeable change in the plant efficiency can be ascertained.

As pointed out in the paper, the design of heater drain lines, given in Fig. 10, makes possible the use of smaller pipe. This has proved to be a distinct advantage in plants where the space available for feedwater heaters is limited. The orifice plates used so far in this design have been 1/4 in. thick. In the later installations, the orifices are simply holes drilled in the center of the plate.

In response to Professor Christie's suggestion that the baffle would be eroded by the steam and water entering the low-pressure heater, the authors would like to point out that the condition of the mixture is practically the same with an orifice at the end of the line as it is with a trap at the beginning, because the end conditions in the heaters are the same in either case. The authors know of only one case where trouble with erosion was found inside

[18] Lefax Data Sheet, No. 41-11.

the heater, and this was due to faulty design of the baffle. It is believed that, if the mixture is permitted free expansion in all directions inside the heater shell and does not enter the shell near a tube support plate, little trouble will be experienced with erosion.

Professor Christie is quite right in suggesting that the same phenomena that exist in a heater drain line will also exist in a boiler blowoff line. The essential difference between these two types of lines is that in the latter the water does not go through a throttling device at the beginning of the line if all blowoff valves are wide open as they should be with intermittent blowdown. For continuous-blowoff lines, however, where the line may be throttled to get a given rate of blowdown, the condition is similar to the heater drain line. It should be pointed out here that the friction factor 0.012 given in the paper was determined from tests of heater drain lines which have normally much lower pressures and are comparatively larger than most blowoff lines. Whether this friction factor applies equally well in blowoff lines the authors are not prepared to say. However, the use of Equation [4] with $K = 0.012$ for designing boiler-blowoff lines probably is justified until more accurate data are obtained from actual tests of blowoff lines.

The authors are grateful to Professor Dusinberre for developing the chart in Fig. 15 accompanying his discussion. It is hoped that he or someone else may have time to prepare charts for the complete range of pressures in use today.

Professor Dusinberre's statement that the actual heater shell pressure must not be neglected is correct, but it should be pointed out that the amount of flashing in the line depends on the initial saturation pressure. The pressure drop across the trap, as shown in Fig. 12 of the paper, is the difference between the heater shell pressure and the pressure after the trap. The latter pressure and the amount of flashing, however, depend on the temperature (or saturation pressure) of the water entering the trap, which may be less than the saturation temperature corresponding to the heater shell pressure.

Regarding the discussion by Mr. Emmons, the authors would first like to point out that, at best, tests conducted on the heater drain lines of an actual turbine-generator unit leave much to be desired in so far as the testing procedure is concerned. The tests are only incidental to the operation of the unit and, therefore, must be made to a very great extent to fit the conditions as they exist. It is believed, however, that information obtained from such tests is much better than no information at all. The authors are well aware of the possible refinements pointed out by Mr. Emmons. It was hoped that the second and third paragraphs of the paper would indicate that no claims were being made beyond the fact that the data in the paper would be of assistance in the design of heater drain lines.

In the authors' tests for determining the flow of saturated water through throttling orifices,[11] both pressure and temperature measurements were taken in a line carrying a flashing mixture of water and steam. In all cases the saturation pressure corresponding to the temperature measurements checked the actual pressure measurements within 0.5 psi, which is well within the expected accuracy of the readings to be obtained on a commercial-size setup. While a rigorous scientific analysis might be derived from a delicate laboratory installation, it is questionable whether the laboratory results could be translated into actual practice with any greater satisfaction than is possible from the authors' tests.

The authors appreciate Mr. Hutchison's contribution to their paper and, in general, are in agreement with what he has said. It is hoped that he will find it convenient soon to publish the results of the tests by his company of flow of saturated water through nozzles.

With reference to Mr. Markson's suggestion that cold-water tests should have been carried out on the heater drain lines in question, the authors would like to say that this would have been impossible. The remarks about the friction factor are quite true and, because of this fact, the symbol K was used instead of the symbol f which is ordinarily used. No attempt was made to treat inlet and exit losses because, as already pointed out, all tests were conducted on drain lines of operating turbine-generator units and not on pipe lines which were especially designed for the tests.

The lack of suitable diagrams or curves for use in calculation has been partially taken care of by Professor Dusinberre.

In conclusion, the authors wish to express their appreciation to all the discussers for their interesting additions to the paper. It is hoped that further and more rigorous experimental investigations will be made and reported to the Society.



FIG. 1 SITE OF RIVERSIDE GENERATING STATION
(Scale 1 in. = 2215 ft.)

Wind-Tunnel Tests to Establish Stack Height for Riverside Generating Station

BY H. L. VON HOHENLEITEN[1] AND E. F. WOLF,[1] BALTIMORE, MD.

Because of its proximity to a residential area and to the municipal airport, the Consolidated Gas Electric Light and Power Company of Baltimore, in the construction of its new Riverside Generating Station, found it necessary to give careful consideration to the flue-gas problem and the height of stacks. The problem resolved itself into three distinct phases: (*a*) to establish the wind and weather conditions which would produce the most serious smoke annoyance; (*b*) to determine the effect of adding units to the plant; (*c*) to investigate all possible means for improving dissipation of flue gases. The model-test procedure followed, in studying these elements, in the wind tunnel of the Allied Aviation Corporation, the results attained in comparison with known data from the Westport Plant of the company, and the decisions reached in designing and arranging stacks at Riverside are thoroughly discussed.

THE Consolidated Gas Electric Light and Power Company is now engaged in the construction of its new Riverside steam-electric generating station on a site along the Patapsco River near Baltimore, between the Dundalk residential community and the Sparrows Point steel center. Work on the first 50,000-kw condensing unit is now in progress and the installation of a second unit of equal size has been authorized. Because of the proximity to the municipal airport, Fig. 1, height of structures was an important consideration in the design of this station. By careful study of mechanical arrangement, the height of the building itself was eliminated as a critical factor, and the stack remained as the sole point upon which a decision of height must be reached. The desired stack height, which had been de-

[1] Consolidated Gas Electric Light and Power Company of Baltimore.

Contributed by the Power Division and presented at the Annual Meeting, New York, N. Y., December 1–5, 1941, of THE AMERICAN SOCIETY OF MECHANICAL ENGINEERS.

NOTE: Statements and opinions advanced in papers are to be understood as individual expressions of their authors and not those of the Society.



FIG. 2 WIND TUNNEL, LOOKING DOWNWIND

termined on the basis of past experience, was in excess of elevations suitable for this location.

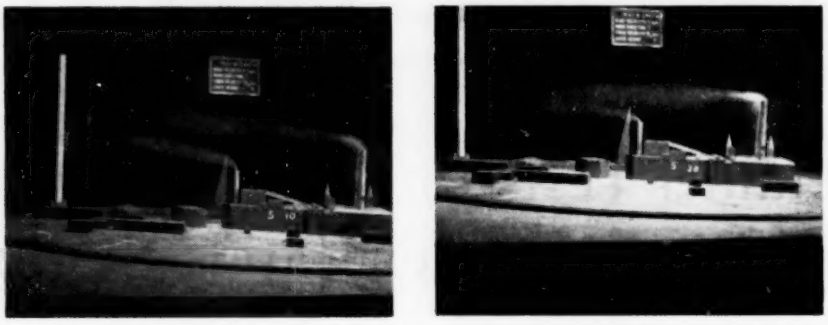
There are several factors in the design of the Riverside stacks which are different from the usual problem. On account of the induced-draft-fan system, height is not required to produce draft, and with the Cottrell precipitator, the dissipation of flue gases rather than "smoke" is the primary consideration. It is usually desirable to have a stack sufficiently high to be free from smoke troubles under all normal wind conditions. At Riverside, it was necessary to select a stack height consistent with company requirements for reasonable dissipation of flue gases and yet satisfactory from the viewpoint of air navigation. It was concluded that the proper point of compromise between these contradictory requirements could be found only through the study of models in a wind tunnel.

ELEMENTS OF THE PROBLEM

Three distinct phases of this problem had to be analyzed: (*a*) It was necessary to establish what wind or weather conditions would produce the most serious smoke annoyance at this station, and, under these conditions, to determine the required stack height; (*b*) the effect of the addition of successive units to the plant had to be considered; (*c*) due to stack-height limitations, it was necessary to investigate all possible means of improving the dissipation of flue gases, such as stack design or arrangement, shielding of the stack or building, and increase of stack velocity.

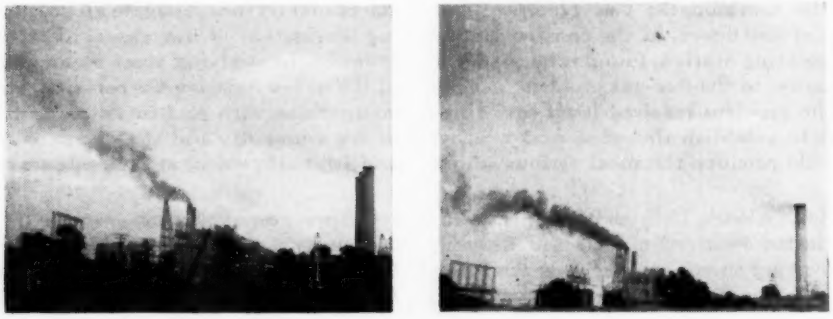
Available Information. Prior to these tests, a study was made of available engineering information on the subject. Published reports of work carried on in England (1),[2] and to some extent in this country, on stacks with low-velocity output, indicate that a stack height 2.5 times the height of the building is desirable. There were no satisfactory data on height of stacks with high-velocity output directly applicable to the problem. However, it is known that the company's high-velocity Westport stacks which extend approximately 60 ft above the boilerhouse (or 1.46 times the height of the building) are sufficiently high to prevent troublesome downdraft at that location (Fig. 3). At Riverside, it was necessary to limit the stack height to an elevation less than that of the Westport stacks, but it was not known to what extent this

[2] Numbers in parentheses refer to the Bibliography at the end of the paper.



10 Mph 20 Mph

Westport model; wind direction south; wind velocity as noted



Note tip vortexes as shown by parting of smoke path — Note smoke on head tower

Westport Plant, Nos. 1, 3, 4, and 5 units; prevailing wind velocity, 15 mph; prevailing wind direction, south; June 28, 1941

FIG. 3 COMPARISON OF WESTPORT MODEL AND PROTOTYPE

(Momentary emission of smoke for test purposes.)

height could be reduced without experiencing smoke troubles.

Wind Tunnel. The wind tunnel in the plant now owned by the Allied Aviation Corporation at Dundalk, Md., was used for a 4-month period for this investigation. The tunnel, fan motor, and control equipment are installed in a separate brick structure. The tunnel is the recirculating type with double return paths from the discharge side of the fan to the intake end of the throat. A grid of vanes at the inlet end of the tunnel serves to straighten the air flow. The throat of the tunnel is 7 ft in diam. The open test space is 7 ft 6 in. long.

Air is circulated by a 12-ft-diam four-bladed wooden propeller fan, driven by a 175-hp variable-speed d-c motor at the downwind end of the tunnel, Fig. 2. Wind velocities from 5 to 100 mph are obtainable. The velocity is indicated by a pitot tube at the upwind end of the working space. Preliminary surveys showed that the uniformity of air flow within the test space was satisfactory.

Model Theory. Careful consideration was given to the reliability of model tests for smoke problems. Previous investigators have found that models satisfactorily predict the path of smoke from the prototype, provided the wind and flue-gas velocities are kept actual (2, 3, 4). This procedure was adhered to in the present experiments. In a Bureau of Standards report of 1926 (5, 6), it was stated that there is no error due to scale effect with sharp-edged models and this point now seems to be generally accepted. It was further stated, however, that there is some error due to scale effect with spherical, cylindrical, and streamlined models. With such curved objects, there is a critical value of the Reynolds number at which a change takes place in the flow phenomena. The model stacks used in these tests have a Reynolds number (17,000 at 20 mph) below the critical range, whereas, the actual stack will have a Reynolds number (2,040,000 at 20 mph) well above the critical range at normal wind velocities. Accordingly, there is a somewhat different partial vacuum distribution on the downwind side of the model stack than on the actual stack. This may cause slightly greater downdraft immediately back of the model stack. However, available data indicate that this should not produce a large experimental error.

Verification of Model Theory. Although theoretical considerations and previous work indicated that model investigations should produce sufficiently reliable results for predetermining required stack height, it seemed desirable to establish further proof of the validity of such tests. Accordingly, a simplified model of this company's Westport Station and surrounding property was tested to observe the relationship between the model smoke patterns and the actual smoke patterns of a familiar existing structure. It is the opinion of independent observers that the model satisfactorily reproduced the actual path of smoke from the Westport stacks. A comparison of the actual and model smoke paths under typical conditions is shown in Fig. 3.

The Westport model (scale 1 in. = 20 ft) showed no downdraft of smoke around the buildings or adjacent properties at 20 mph wind velocity in any direction, which is in accord with practical experience. A limited number of tests were conducted to determine the effect of low stack heights at this location for comparison with the Riverside model tests. When the No. 1 stack was lowered from 60 ft to 30 ft above the roof, objectionable downdrafts were observed. The downdraft from the "low" Westport stack was comparable with the downdraft from Riverside model stacks of equivalent height above the adjacent boiler room.

Tests on Riverside Models

Three models of the Riverside generating-station development were tested, namely, a single-unit, a three-unit, and a six-unit model. The last was regarded as the probable ultimate development at this location. The models were designed for maximum flexibility of operation so that desired test conditions could be obtained readily for the study or demonstration of the effect of any required variable. The models, constructed of wood, were placed on a turntable on a platform erected between the throat and bell of the tunnel. The platform was placed so that the horizontal diameter of the tunnel bisected the height of the models. The forward end of the platform was streamlined to minimize the disturbance of air flow.

The 1-in-ID brass-tube miniature stacks were adjustable in height and were equipped for variable discharge of air up to 70 fps. For the single unit, the "flue gas" was supplied through a 1-in-diam rubber hose from a blower, driven by a variable-speed d-c motor. The multiunit stacks were fed through a large plenum chamber. The velocity of discharge was controlled by individual supply-line valves. A scale of 1 in. = 10 ft was selected for convenience of size and ease of interpreting results. The six-unit model to this scale was in reasonable proportion to the diameter of the tunnel throat.

Procedure and Technique. In other investigations of smoke dissipation, it has been found that wind velocity and wind direction are the only meteorological phenomena which appreciably affect the downwash of smoke. Consequently, such factors as humidity, air temperature, and barometric pressure could be disregarded. It has also been found that stack-gas temperature has only a minor influence on the downwash for a given stack velocity (1, 2, 3). Therefore, this variable also was omitted, and the effect of elevated temperature was regarded as a small factor of safety.

For a complete analysis of this problem, it was felt that it would be necessary to make tests with each of the three models in the eight principal wind directions, at four wind speeds, five different stack heights, and three flue-gas velocities. If all combinations of variables were checked, this alone would have resulted in 1440 individual observations on the three models. This number of tests, together with the necessary preliminary work and special scheduled tests, was excessive. It was, therefore, imperative to determine how many of these individual observations could be safely eliminated. It was felt that a study of the turbulence produced by the models would enable differentiation between critical and noncritical variables.

Study of Turbulence. Previous work (2, 3) had indicated that, if downwash of smoke is to be avoided, smoke must be discharged at a sufficiently high elevation, or at a sufficiently high velocity, to be carried above the turbulent area set up by the structure. This consideration, together with the necessity of establishing the critical variables, led to a thorough study of the turbulence patterns.

When an obstruction is placed in the path of the wind, the flow of air is diverted in part around the sides of such obstruction and in part over the top. On account of this constriction of flow, the velocity of the wind immediately around and over the top of the building is increased. Since the pressure energy plus the velocity energy must remain constant (Bernoulli's theorem), the pressure is reduced in the high-velocity region on the top, sides, and back of the building and increased in the more or less dead air space directly in front of the structure. Vortexes are set up in the low-pressure areas immediately over the top, sides, and rear of the structure (6, 7). The nature of the vortexes or turbulent areas depends upon the configuration of the building, the wind direction, and the wind velocity. If the smoke stream is carried into one of these turbulent areas, it is dispersed and may be brought down to earth, Fig. 4. The stack also causes a disturbance. A cylindrical stack is known to set up two types of vortexes, namely, trailing vortexes and tip vortexes. Trailing vortexes of cylindrical shape with vertical axes originate along the vertical sides of the stack cylinder. These vortexes break off from the opposite sides

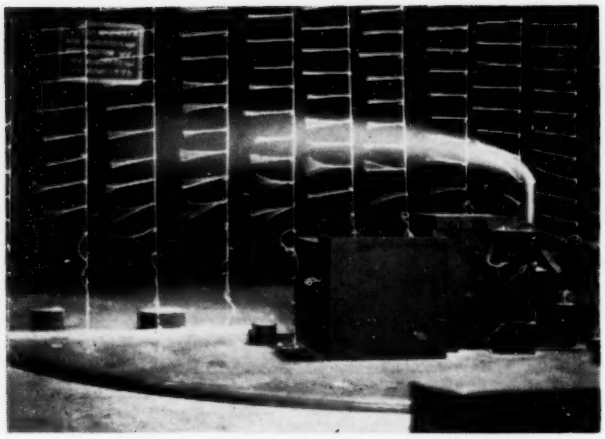


FIG. 4 TURBULENCE PATTERN OF SINGLE-UNIT MODEL
(20-Mph west wind.)

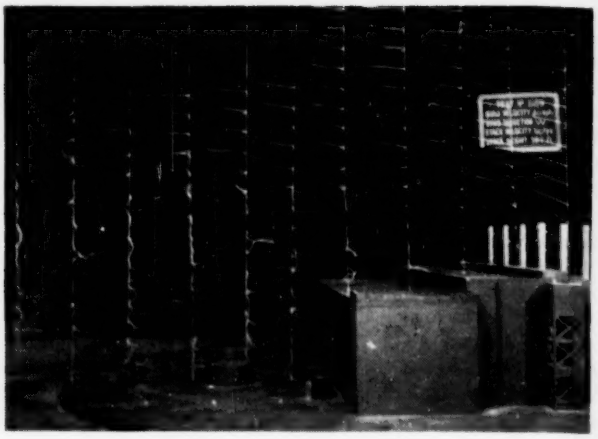


FIG. 5 TURBULENCE PATTERN OF SIX-UNIT MODEL
(20-Mph west wind.)

and travel downwind (Kármán's trail). The tip vortexes with horizontal axes in the direction of the wind form at the opposite sides of the top of the stack. These cone-shaped vortexes have a downward sense of rotation outside of the wake and an upward sense within the wake.[3] The effect of these tip vortexes may be seen in Fig. 3, where the smoke is leaving the stack in two separate cones. In high-velocity winds, these two types of vortexes tend to disperse the smoke and carry it downward, unless the discharge gas velocity is sufficiently high to overcome their effect.

Turbulence was studied by means of threads. Taut, vertical strings were set up at 6-in. intervals in line with the stack in a plane parallel to the wind direction. White silk threads, 5 in. long, were used as streamers tied at one end to the vertical strings at 2-in. spacings. The length and spacing were selected after a considerable amount of experimental work to determine the most suitable type and arrangement of threads which would follow the path of the wind. Photographs were taken of these string patterns, Figs. 4 and 5.

The area around the building was also explored by means of a fine silk thread on the end of an exploring rod. Flake mica (Christmas-tree snow) was distributed at points around the building. The path of the particles of mica showed the regions of turbulence, the direction of flow, and the character of the vortexes. The turbulence areas were also investigated by means of droplets of titanium tetrachloride placed at spots around the model. On the basis of the fixed and exploratory indicators, charts were plotted to show the turbulence patterns produced in line with the stacks.

Figs. 17 and 18 illustrate the effect of wind direction and wind velocity on the turbulence. The wind velocity affected the area of the turbulent zone to some extent, but did not in general affect the character of the turbulence pattern. The wind direction very markedly affected the area as well as the character of turbulence. The relative proportions of the building in the three planes is a vital factor. The surface of the single-unit building, exposed to north or south winds, is much greater than to east or west winds and, consequently, the turbulent zone extends higher with the north or south winds than with the east or west winds. Under the worst conditions, this turbulent zone extends as much as 70 ft higher than the building. In the six-unit plant, the proportions of the building are reversed and, consequently, the turbulence patterns are quite different. With a 20-mph west wind, the six-unit model set up a turbulent zone equivalent to 120 ft above the building, Fig. 5.

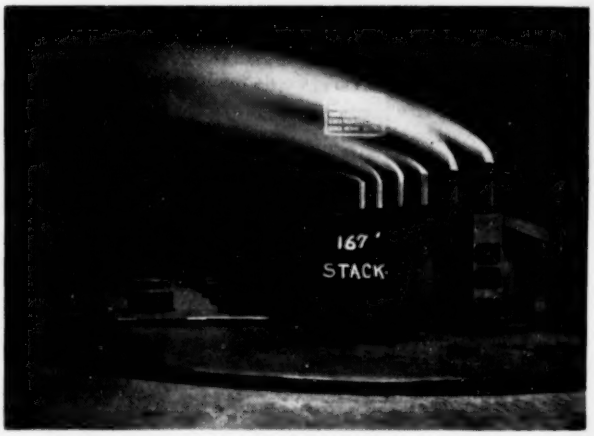


FIG. 6 SMOKE PATTERN OF SIX-UNIT MODEL
(20-Mph west wind.)

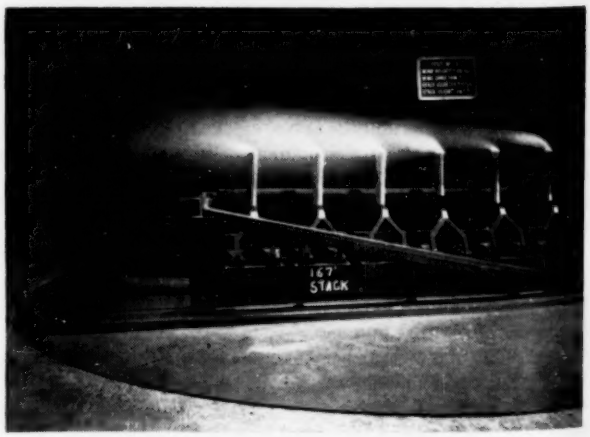
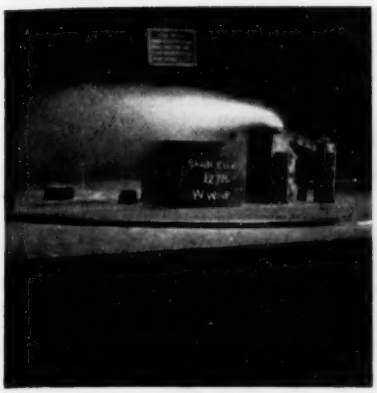


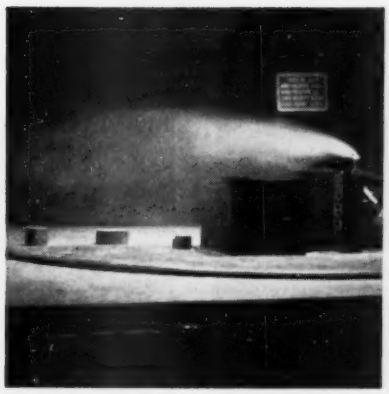
FIG. 7 DOWNDRAFT CAUSED BY WIND IN LINE WITH STACKS

Smoke-Pattern Technique. In the Sherlock and Stalker investigation of the smoke problem for the Crawford Avenue Station, Chicago (2, 3), hydrogen sulphide was discharged from the model stacks and chemical indicators were used to detect the

[3] The sense of direction reported here is opposite to that reported by Sherlock and Stalker (2, 3), and was demonstrated by direction of rotation of threads in the wind-tunnel tests, and confirmed by field observations.



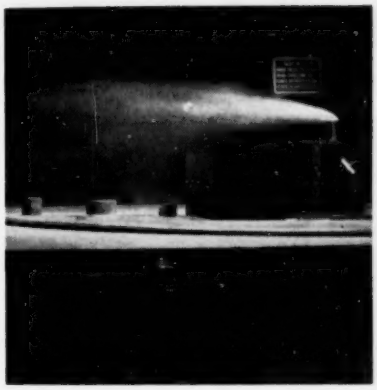
127 Ft



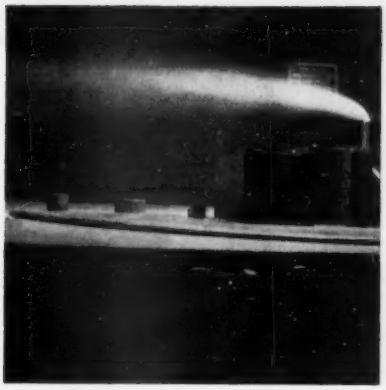
139 Ft



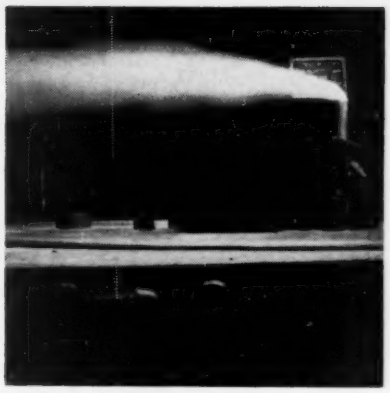
147 Ft



157 Ft



167 Ft



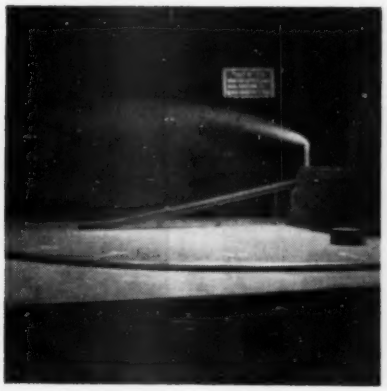
175 Ft

FIG. 8 ONE UNIT; EFFECT OF STACK HEIGHT

(Wind direction, west; wind velocity, 20 mph; stack height, as noted; stack velocity, 50 fps; No. 2 monitor roof. In all figures, stack height is expressed as elevation above mean low tide. Ground level is at elevation plus 10.)



10 Mph



20 Mph



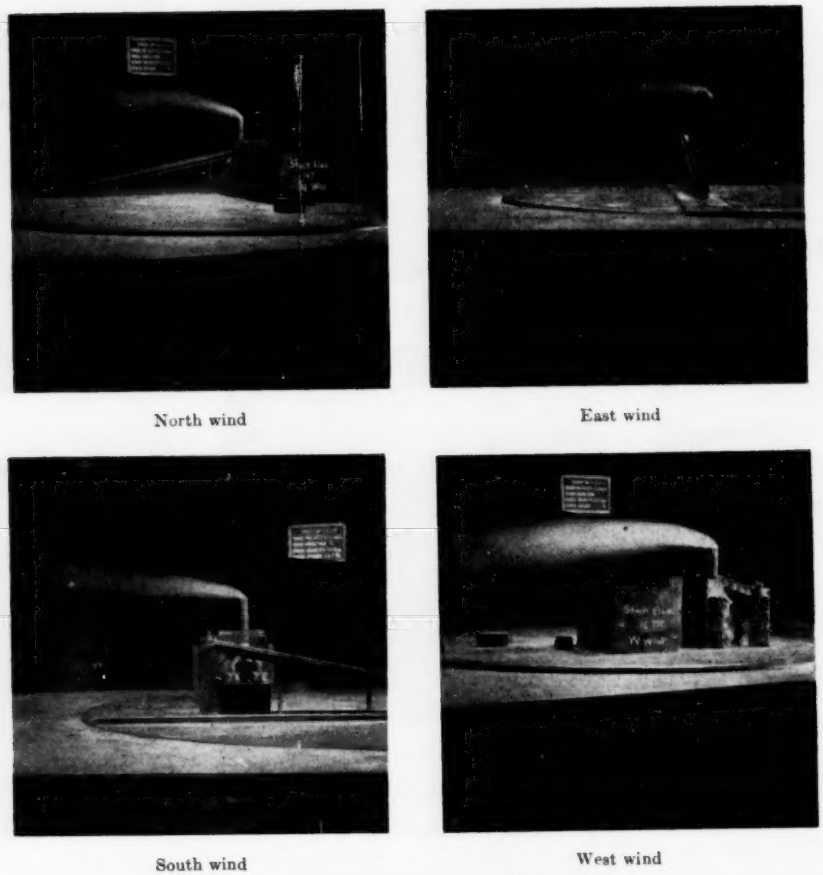
30 Mph



40 Mph

FIG. 9 ONE UNIT; EFFECT OF WIND VELOCITY

(Wind direction, north; wind velocity, as noted; stack height, 167 ft; stack velocity, 50 fps; No. 2 monitor roof.)



North wind East wind

South wind West wind

FIG. 10 ONE UNIT; EFFECT OF WIND DIRECTION
(Wind direction, as noted; wind velocity, 20 mph; stack height, 167 ft; stack velocity, 50 fps; No. 2 monitor roof.)



15 Fps 50 Fps

FIG. 11 ONE UNIT; EFFECT OF STACK VELOCITY
Wind direction, east; wind velocity, 10 mph; stack height, 167 ft; stack velocity, as noted; flat roof.)

path of the gas discharge. This method was tried but found to be unsuitable in the present case. Since the working space in the tunnel was open, the exposure of the operator to the toxic hydrogen sulphide was objectionable. Furthermore, the indicators were not adapted to detecting the path of the smoke in more than one plane. Rapid evaporation of the chemical indicator made accurate recording difficult at the higher wind velocities. The same objection applied to the discharge of ammonia and other gases from the model stack.

Consequently, a technique was developed for the discharge of a dense white smoke from the stacks. Ammonium chloride was used for this purpose because of its relatively low toxicity and corrosiveness, high degree of visibility, and freedom from fire or explosion hazards. The ammonium-chloride smoke was found to

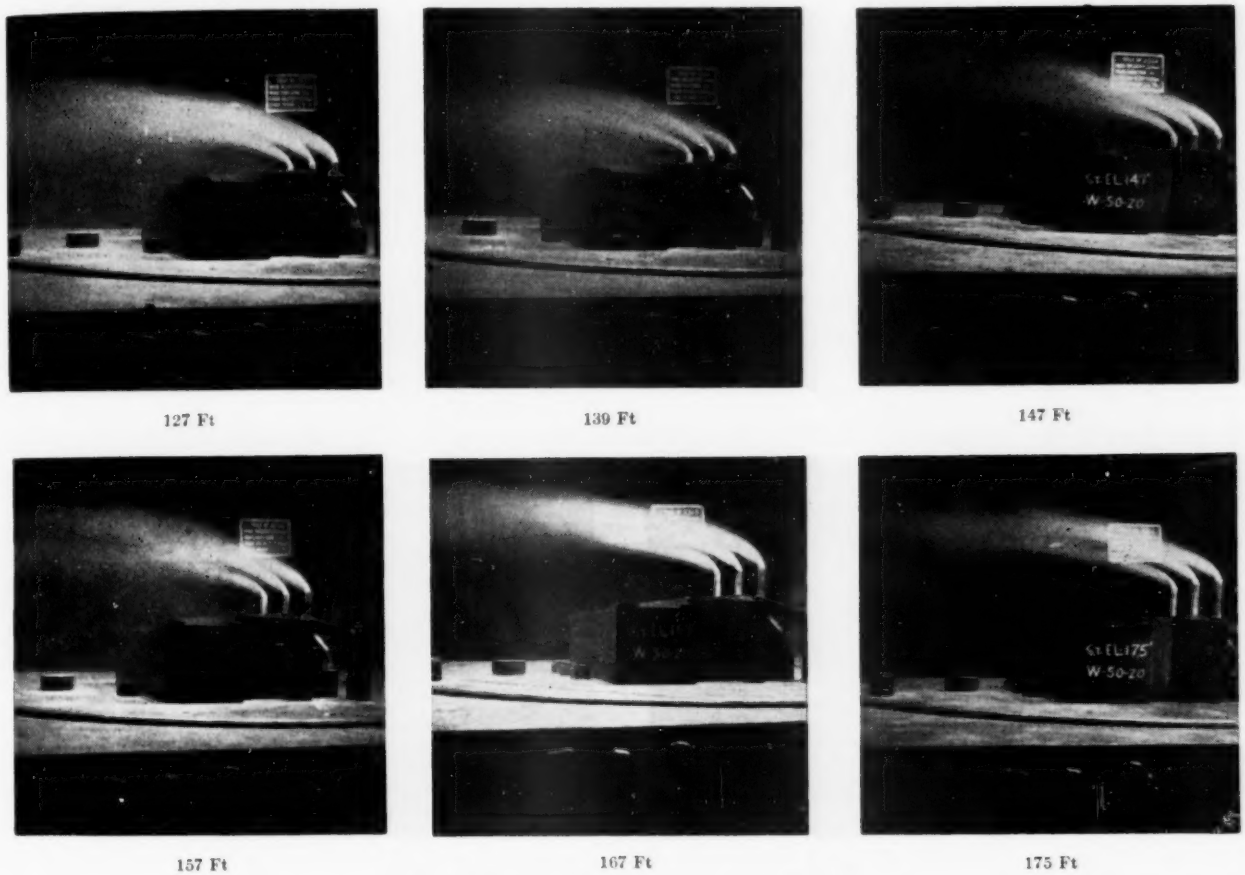


FIG. 12 THREE UNITS; EFFECT OF STACK HEIGHT
(Wind direction, west; wind velocity, 20 mph; stack height, as noted; stack velocity, 50 fps; No. 2 monitor roof.)

be quite satisfactory since it was possible to observe the path of the smoke in three planes and to see the vortexes around the building and stack structures. A satisfactory procedure was developed for making still and motion pictures of the smoke, which was generated by passing air from a compressed-air line through half-filled 1-gal bottles of concentrated ammonium hydroxide, and then neutralizing the ammonia-saturated air by passage through bottles of hydrochloric acid in a partially closed wooden box. The cloud of white smoke emanating from the hydrochloric-acid bottles was fed to the intake side of the blowers which supplied the stacks.

The smoke technique was found to be very useful, however, there are certain limitations in that some trouble is experienced from clogging of model stacks smaller than $^1/_2$ in. diam, or stacks with very low velocities.

RESULTS OF INVESTIGATION

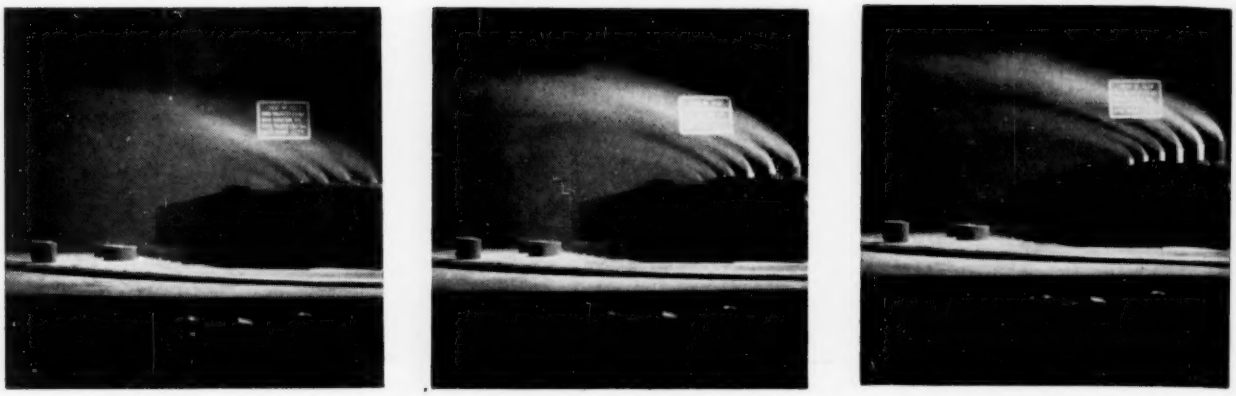
Wind Velocity. The effect of wind velocity was investigated in the range of 5 to 40 mph. The tests brought out two conditions which may cause troublesome flue-gas concentration in the immediate vicinity of the plant, namely, extreme calm and moderately high wind velocities. In the almost complete absence of air movement, the stack-discharge gases rise more or less vertically from the stack and form a cloud over the building. This large mass of discharge gas tends to diffuse gradually downward. With wind velocities from 5 to 10 mph and stack velocities of the order of 50 fps, the discharge gases are carried in a gently curved arc upward clear of the surrounding property, with moderate stack heights, Figs. 9, 14, 21. From a practical consideration, wind velocities in the neighborhood of 20 mph cause the most concern. Winds in this range occur with considerable frequency in the Baltimore area, Table 1. With increasing velocity, the path of the smoke is carried lower. However, the rate of dissipation of smoke increases in proportion to the wind velocity, according to the investigation of Pearson, Nonhebel, and Ulander (1). Our own observations show that, at high winds, in the neighborhood of 30 to 40 mph, the downwash becomes very pronounced, but that the smoke is rapidly diluted. Although these higher velocities are relatively infrequent and the rate of smoke dissipation is also in our favor, we believe that with the stack heights under consideration, there will be some annoyance from smoke when these higher wind velocities do occur.

Wind Direction. The seriousness of the downdraft of smoke is very markedly affected by the wind direction, as indicated in the charts and photographs, Figs. 10 and 20. With the single unit, the north and south directions present a large area of building surface to the wind and create a particularly serious downdraft problem.

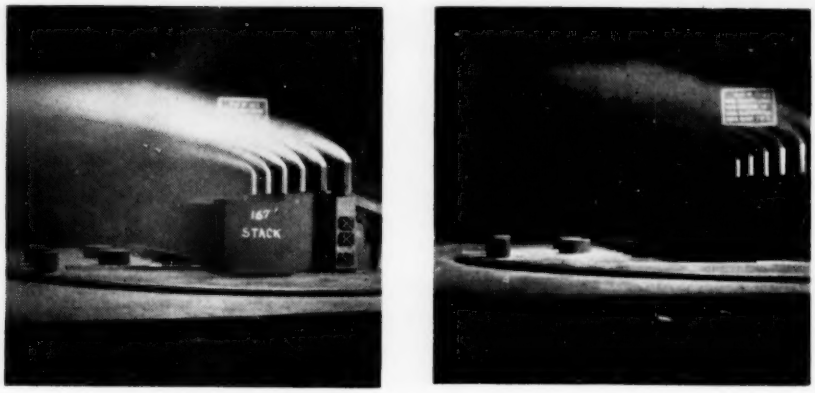
TABLE 1 WIND-VELOCITY DATA FOR BALTIMORE
(For the one-year period, from July 1, 1940, to June 30, 1941)

Maximum wind velocity for 5-min period, during any one day, mph	Number of days
Less than 8	0
8–13	32
13–18	141
18–23	100
23–28	47
28–33	36
33–38	6
38–43	3
Over 43	0

Average velocity for year = 10.2 mph



127 Ft 139 Ft 157 Ft



167 Ft 175 Ft

FIG. 13 SIX UNITS; EFFECT OF STACK HEIGHT
(Wind direction, west; wind velocity, 20 mph; stack height, as noted; stack velocity, 50 fps; No. 2 monitor roof.)

With a south southeast wind, there exist the combined effects of the large southern exposure of the building and the complicated turbulence patterns created by the partial exposure of the stack-and-breeching structure to the wind. This tends to cause a downwash around the induced-draft-fan structure.

With the three-unit and six-unit models, cumulative disturbances are set up when the wind is blowing directly in line with the stacks. The smoke is brought lower and lower with each successive stack, Fig. 7. With a south southeast wind, there is also a troublesome condition with the multiunit models. The successive disturbances of the stacks and the disturbance of the building itself combine to create a serious downdraft.

Stack Velocity. The path of the smoke as it emerges into the atmosphere is determined by both stack velocity and wind velocity. However, it should be pointed out that, at equal stack velocities and wind velocities, the smoke does not emerge at a 45-deg angle, as might be anticipated from a simple application of resultant forces. The problem is much more complicated and has been treated theoretically in the technical literature (8).

Under average weather conditions, high flue-gas velocity is decidedly beneficial in carrying the smoke upward, Fig. 11. A small-diameter stack creates less disturbance and high velocity tends to carry the smoke above the disturbed area. Under the conditions of Fig. 22, an increase in stack velocity from 15 to 50 fps raises the upper limit of the smoke path about 50 ft at the rear of the building. At wind velocities of the order of 30 to 40 mph, the effect of stack velocity is less pronounced. With wind velocities of approximately 20 mph and with low stack velocity, there is a very pronounced downdraft of smoke immediately along the downwind side of the stack. This phenomenon can be observed very readily on any windy day with the usual low-velocity industrial stacks.

Stack Height. As would be expected, the seriousness of the downwash of gas decreases with increased stack height, Figs. 8, 12, 13, 19. With a 127-ft stack elevation, which is approximately

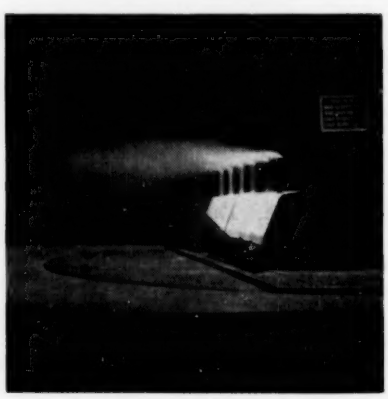
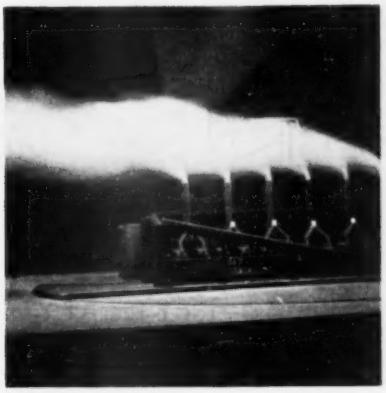


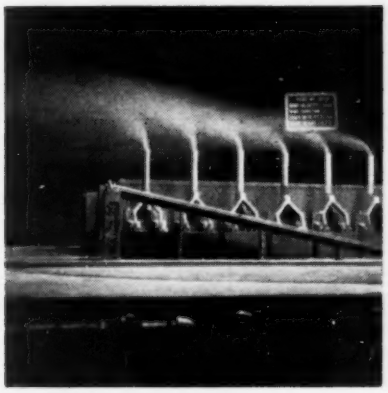
FIG. 15 SIX UNITS; EFFECT OF BREECHING SHIELD
(Wind direction, east; wind velocity, 20 mph; stack height, 167 ft; stack velocity, 50 fps; No. 2 monitor roof.)



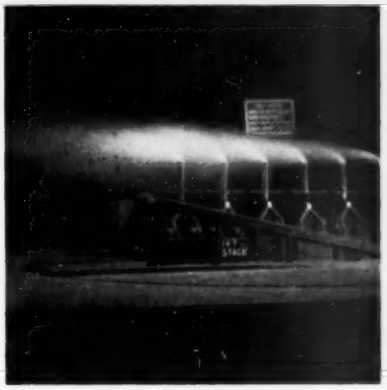
5 Mph



10 Mph



20 Mph



30 Mph

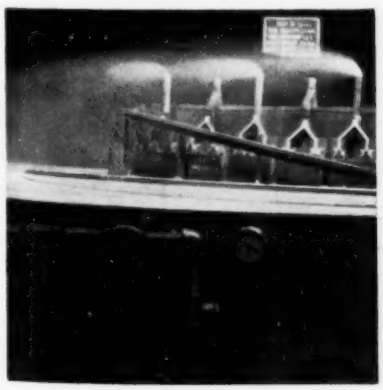


40 Mph

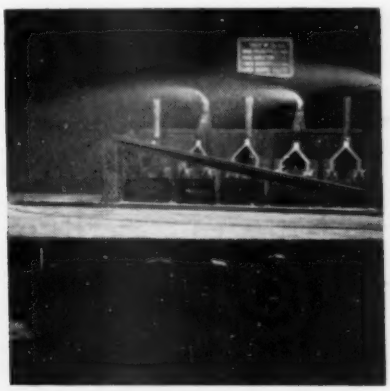
FIG. 14 SIX UNITS; EFFECT OF WIND VELOCITY
(Wind direction, south; wind velocity, as noted; stack height, 167 ft; stack velocity, 50 fps; No. 2 monitor roof.)

equal in height to the boiler-room monitor, the lower portion of the smoke path sweeps over the model roof or swirls over near-by ground under a wide range of wind conditions. With a 139-ft stack, the smoke path is approximately the same, but the concentration appears to be somewhat less dense near the ground. With a 147-ft stack, the smoke path is raised somewhat but continues to swirl to the ground. At 157 ft, the downwash is still pronounced, even at a 10-mph wind velocity in some directions. Consequently, at this stack height smoke annoyance would be anticipated on a large number of days each year. At 167 ft, downwash is present within limited angles of wind direction at 20 mph, and quite general at 30 mph. It is the authors' opinion that this is the minimum height at which the smoke downwash would not be entirely excessive.

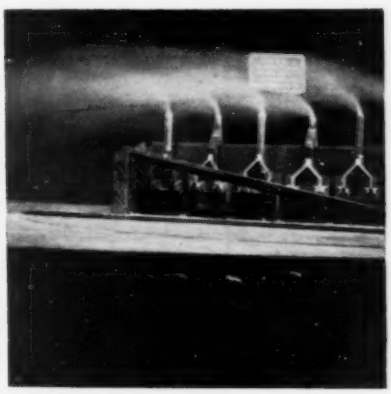
Even at the maximum elevation of 175 ft, set for this group of experiments, some smoke is carried downward close to the base of the model with unfavorable wind directions at the higher wind velocities.



Straight stacks alone



Staggered stacks alone



Combination of both, known as six staggered stacks

FIG. 16 COMPARISON OF EFFECT OF STRAIGHT AND STAGGERED STACKS ON THE SIX-STAGGERED-STACKS MODEL
(Wind direction, south-southeast; wind velocity, 20 mph; stack height, 167 ft; stack velocity, 50 fps.)

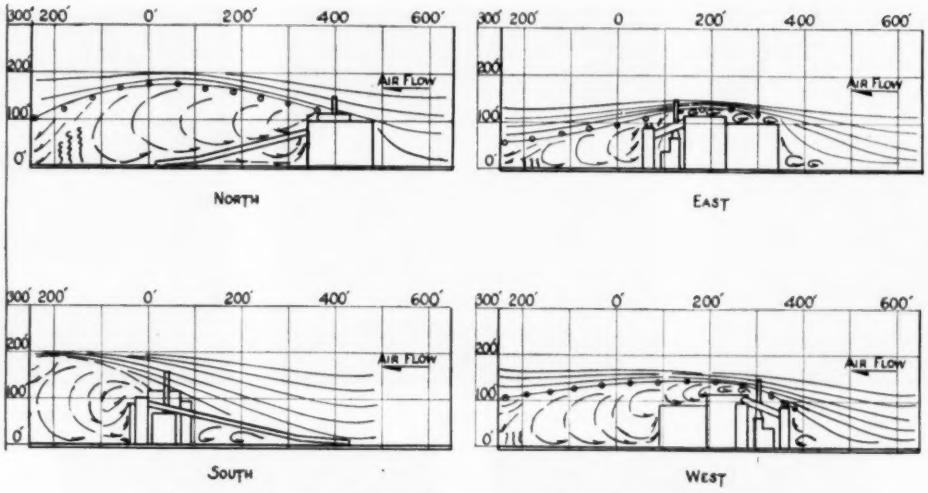


FIG. 17 EFFECT OF WIND DIRECTION ON TURBULENCE PATTERNS
(One unit Riverside model; stack elevation, 167 ft; wind velocity, 20 mph; flat roof.)

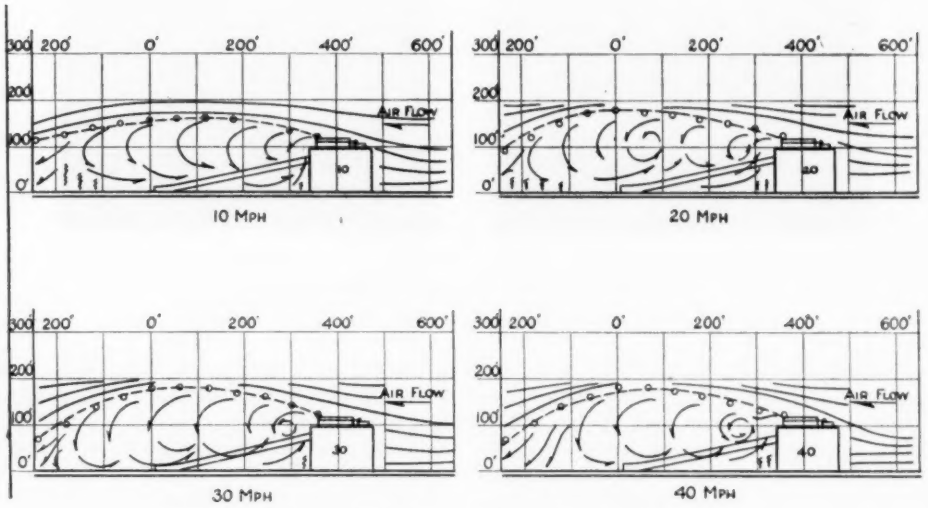


FIG. 18 EFFECT OF WIND VELOCITY ON TURBULENCE PATTERNS
(One unit Riverside model; stack elevation, 127 ft; north wind; flat roof.)

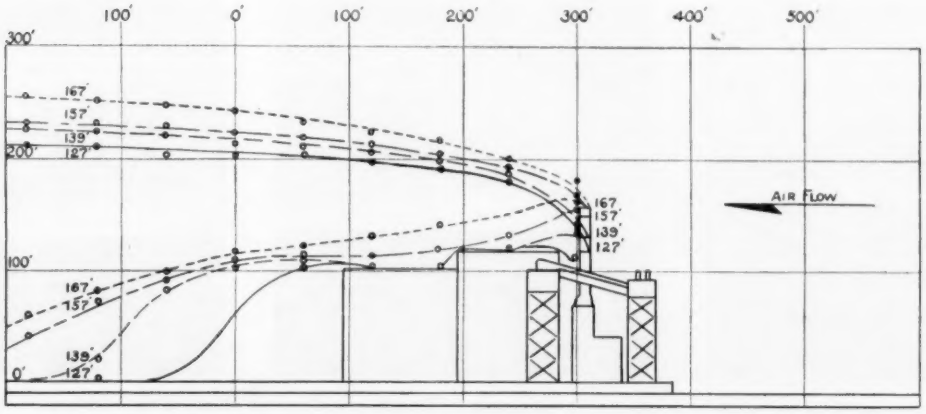


FIG. 19 UPPER AND LOWER OUTLINES OF SMOKE PATH; EFFECT OF STACK HEIGHT
(One unit Riverside model; 20 mph west wind; stack velocity, 50 fps; flat roof.)

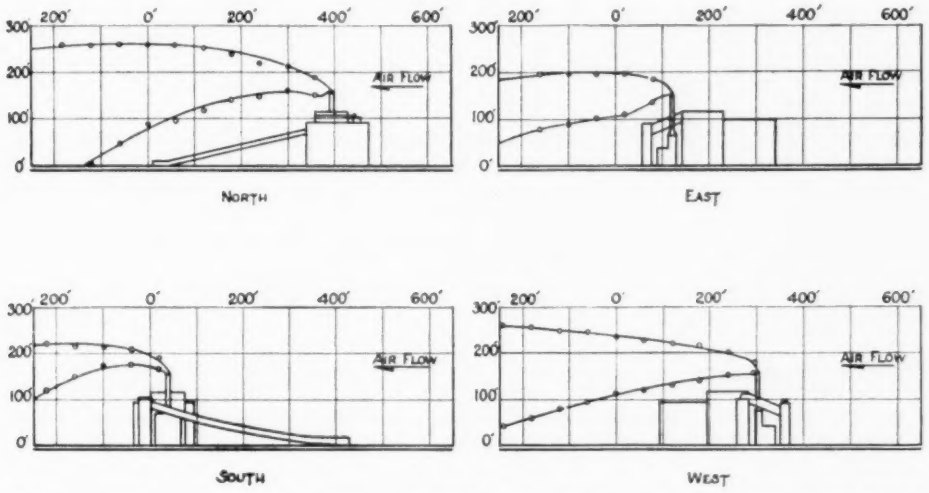


FIG. 20 UPPER AND LOWER OUTLINES OF SMOKE PATH; EFFECT OF WIND DIRECTION ON SMOKE PATTERN

(One unit Riverside model; flat roof; wind velocity, 20 mph; stack velocity, 50 fps; stack elevation, 167 ft.)

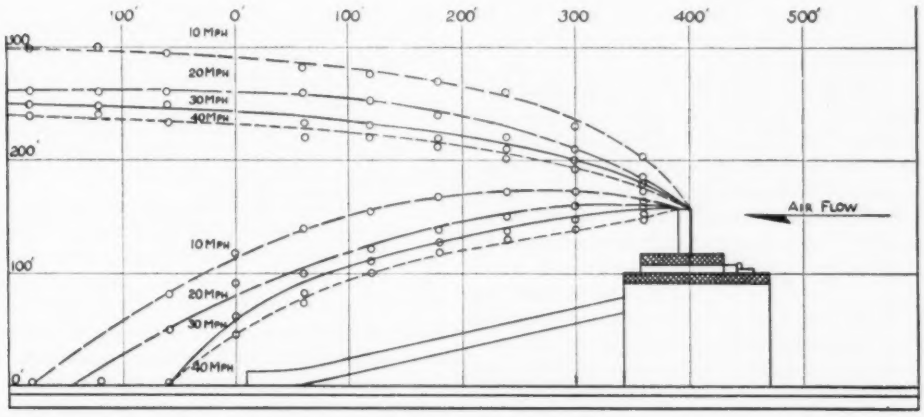


FIG. 21 UPPER AND LOWER OUTLINES OF SMOKE PATH; EFFECT OF WIND VELOCITY ON SMOKE PATTERN

(One unit Riverside model; flat roof; north wind; stack elevation, 167 ft; stack velocity, 50 fps.)

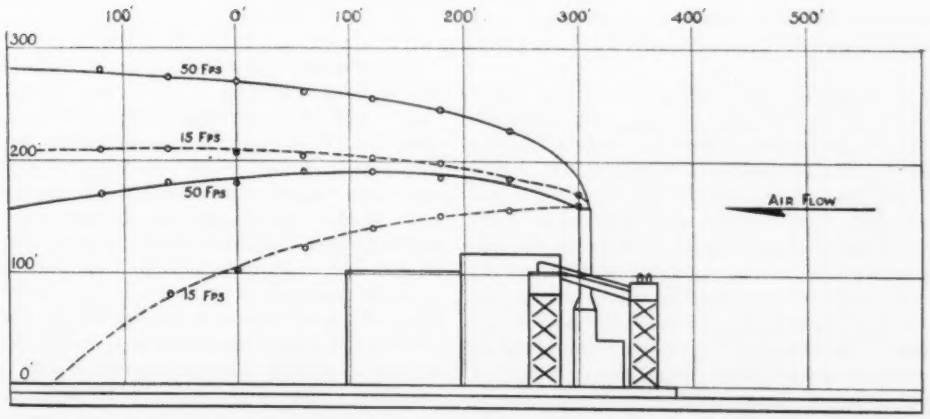


FIG. 22 UPPER AND LOWER OUTLINES OF SMOKE PATH; EFFECT OF STACK VELOCITY ON SMOKE PATTERN

(One unit Riverside model; 10 mph west wind; stack elevation, 167 ft; flat roof.)

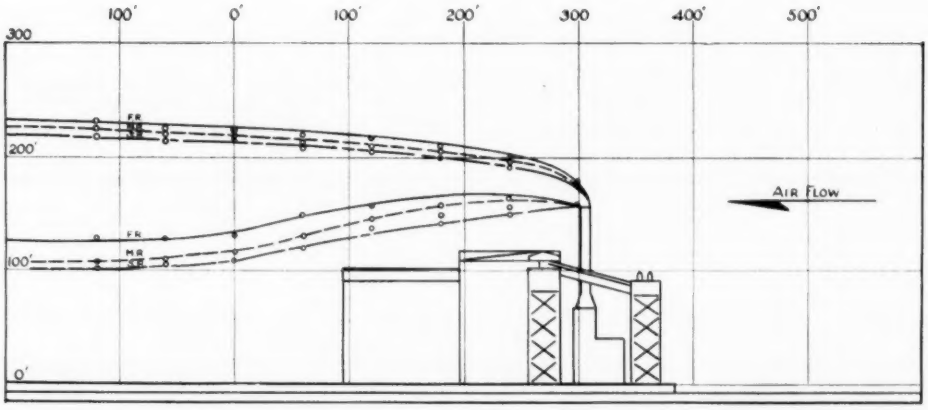


FIG. 23 UPPER AND LOWER OUTLINES OF SMOKE PATH: EFFECT OF ROOF DESIGN ON SMOKE PATTERN

[One unit Riverside model; 20 mph west wind (flat roof); stack elevation, 167 ft (monitor roof); stack velocity 50 fps (sloping roof).]

SPECIAL STRUCTURAL TREATMENTS

Roof. No appreciable improvement could be obtained by variation in roof design within practical limitations. Several types of monitor roofs, flat roofs, and sloping roofs, all with the same maximum elevation, were studied. There was not sufficient difference in the smoke dispersion for this to be a deciding factor in the selection of the alternate roof plans.

Stack Arrangement and Design. One of the troublesome conditions which appeared with the three-unit and six-unit models has been mentioned previously. When the wind direction is approximately parallel to the line of the stacks, a disturbance originates at the first stack and is amplified by each successive stack which causes an increasing degree of downdraft. Tests were made to determine if a staggered arrangement would improve this condition. Since the stack, precipitator, and coal-conveyer structures are located comparatively close to the waterfront, there are practical limitations in the possible arrangement of the staggered stacks. The only available space for the location of the alternate stacks would have been on top of the boiler-room roof over the monitor. Stacks were arranged in this manner for tests, Fig. 16. Observations indicated that there are advantages in staggering, if it can be done in an ideal manner. However, with the arrangement which is possible at the Riverside location, there are no advantages. The stacks over the boiler-room roof produce especially troublesome downdraft of smoke. This test indicated that stacks which are placed directly on top of a building must be somewhat higher than stacks which are placed away from the main structure if the same degree of smoke dissipation is to be maintained.

Since the flow of smoke was not entirely satisfactory within the height limitations set for these experiments, considerable efforts were made to test all possible devices that might improve discharge conditions. A large number of stack nozzles, venturi jets, external flat-disk shields, streamlined shields, and flat and spiral vanes were tested. These devices were designed in an attempt to increase the gas-discharge velocity, break up the disturbance created by the stack, create a natural updraft outside the stack, or interfere with the downdraft of smoke back of the stack. The constricting nozzles, which increased the stack velocity, definitely raised the smoke path, but there are limitations to the use of such devices on account of the energy losses. Several of the shields produced improvement with critical adjustments under specific wind velocities and directions. Under other conditions, however, these devices not only failed to produce improvement but created new troubles.

Shielding. At the Riverside location, there are no other large structures near-by to create the effect of a streamlined approach to the plant. Consequently, the structure presents a somewhat abrupt exposure to the wind. The effect of streamlined shielding created by the coal pile was studied. Consideration was also given to the effect of long rows of trees along the property boundaries. Such shielding is beneficial to a limited extent only.

An effort was made to break up the very pronounced turbulent areas around the breechings and induced-draft-fan structures, Fig. 15. Such shields help to break up this local turbulence, but give no material aid in eliminating the smoke downdraft under most conditions.

Smoke-Dilution Analyses. An attempt was made to determine the degree of dilution of discharge gases. Samples were taken in a number of places on the roof and ground where there was visible downdraft of smoke. For this purpose, sulphur-dioxide gas in concentrations equivalent to the actual flue gases was discharged from the model stacks. Analyses for SO_2 content of the samples disclosed that even with low stack height, the dilution of flue gas was in excess of a hundredfold on the roof or ground. Studies elsewhere have shown that flue-gas dilutions of the order of a thousandfold are necessary to eliminate objectionable SO_2 odors (1). Since the tunnel was of the recirculating type, the entire atmosphere became permeated with traces of SO_2 rather rapidly. It was, therefore, impractical to measure greater dilutions than 1 part of flue gas per 100 parts of air in the stream of discharged smoke.

CONCLUSIONS

1 Following tests of the model of the Westport Plant, frequent observations were made of the smoke discharge from the actual plant. The model was found to reproduce actual conditions satisfactorily. These observations add further evidence that model tests furnish a reliable basis for judgment in predetermining necessary stack height for the dissipation of discharge gases.

2 Since it was necessary in this case to select a stack height consistent with requirements dictated by the proximity of the airport, and, at the same time, to insure reasonable freedom from a smoke nuisance, a compromise had to be reached. From practical considerations, it was felt that the performance at wind velocities of approximately 20 mph should govern. The reason for this selection is the large number of days during which wind velocities in the neighborhood of 20 mph occur. Velocities in excess of 20 mph will definitely produce a greater degree of downdraft, but these stronger winds occur with diminishing frequency.

3 With very low stacks, smoke is carried down around the

model and close to the ground at the prevailing average wind velocities. As would be expected, the amount of downdraft diminishes with increasing stack height. The model tests indicate that it is necessary to have a stack height of approximately 157 ft above ground (elevation 167 ft or 1.31 times the height of the boiler-room monitor) to reduce smoke nuisance to reasonable limits with a 20-mph wind. Even at this stack height, there is noticeable downdraft of smoke around the model within limited angles of wind direction. Also at this height, some annoyance from SO_2 can be expected on the days when very high wind velocities occur.

4 The benefits from high stack velocities are found to be distinctly worth while for flue-gas dissipation. The tests indicate that a stack velocity of 60 fps is desirable at this plant.

5 The annoyance from downdraft may be expected to increase somewhat with the addition of each unit.

6 None of the large number of special stack designs or shields showed sufficient merit to justify its use at this plant.

7 It is well to point out that the results obtained by model tests apply specifically only to that prototype for which the model is designed. The influence of surrounding structures greatly changes the turbulence pattern. Therefore, considerable care should be exercised in applying the results of one set of tests to other structures.

Acknowledgments

This investigation was carried out under the general direction of Mr. A. L. Penniman, Jr., general superintendent of the authors' company.

The authors wish to express their appreciation for the valuable comments which were made by the large number of engineers who witnessed the tests. Dr. P. L. Betz gave especially valuable assistance in developing special apparatus and test technique. Capt. L. M. Rawlins, Jr., and Mr. W. W. Pagon gave valued help in the investigation of special stack designs, and in developing additional methods of studying flow phenomena around stacks. A large part of the actual test work covered by this paper was carried out by Messrs. F. L. Griffith, Jr., and J. E. Goeller.

BIBLIOGRAPHY

1 "The Removal of Smoke and Acid Constituents From Flue Gases by a Non-Effluent Water Process," by J. L. Pearson, G. Nonhebel, and P. H. N. Ulander, *Journal*, The Institution of Electrical Engineers, vol. 77, 1935, pp. 1–48; also *Journal*, Institute of Fuel, vol. 8, 1935, pp. 119–156.

2 "A Study of Flow Phenomena in the Wake of Smoke Stacks," by R. H. Sherlock and E. A. Stalker, University of Michigan, Department of Engineering Research, Engineering Research Bulletin No. 29, Ann Arbor, Mich., March, 1941.

3 "The Control of Gases in the Wake of Smoke Stacks," by R. H. Sherlock and E. A. Stalker, *Mechanical Engineering*, vol. 52, 1940, pp. 455–458.

4 "Air Resistance of Railroad Equipment," by A. I. Lipetz, Trans. A.S.M.E., paper RR-59-4, vol. 59, 1937, pp. 617–640.

5 "Wind Pressures on Structures," by H. L. Dryden and G. C. Hill, Scientific Papers of the U. S. Bureau of Standards, vol. 20, no. 523, 1926, pp. 697–732.

6 "Wind Pressure on Circular Cylinders and Chimneys," by H. L. Dryden and G. C. Hill, U. S. Bureau of Standards, *Journal of Research*, vol. 5, RP-221, 1930, pp. 653–693.

7 "Modern Development in Fluid Dynamics," by G. Goldstein, composed by the Fluid Motion Panel of the Aeronautical Research Committee, Clarenden Press, London, England, 1938 (2 vols.).

8 "Spread of Smoke and Gases From Chimneys," by C. H. Bosanquet and J. L. Pearson, Faraday Transactions Society, vol. 132, 1936, pp. 1249–1264.



FIG. 1 AERIAL VIEW OF PARKCHESTER

Problems in Water-Steam Cycle of Central Steam-Generating and Decentralized Control Systems, Parkchester

BY S. T. POWELL[1] AND J. A. DONDERO[2]

Parkchester, located in the Bronx, New York City, is the largest apartment community in the world, having 58 buildings, containing 12,273 apartments, which eventually will accommodate nearly 40,000 persons. The entire group of buildings is heated by a central steam-generating plant, and all condensate is collected at individual groups of buildings and returned to the central plant in an ingenious and novel collection system. To avoid corrosion of the distribution and condensate-return lines required the generation of steam of the highest quality. Numerous engineering problems were encountered and had to be economically solved in the basic design of the various structures. The project is now completed and the period of initial operation has demonstrated the soundness of the development. This paper presents a general discussion of certain problems which occurred in this development, emphasis being placed on the engineering aspects.

[1] Consulting Chemical Engineer, Baltimore, Md. Mem. A.S.M.E.
[2] Chief Engineer, Parkchester, Bronx, N. Y.

Contributed by the Power Division and presented at the Annual Meeting, New York, N. Y., December 1–5, 1941, of THE AMERICAN SOCIETY OF MECHANICAL ENGINEERS.

NOTE: Statements and opinions advanced in papers are to be understood as individual expressions of their authors and not those of the Society.

INTRODUCTION

PARKCHESTER, located in the Borough of the Bronx, New York City, about four miles east of the George Washington Bridge, is the largest apartment community in the world. Its magnitude is indicated by the aerial view, Fig. 1, and by data given in Table 1. The development was conceived and financed wholly by the Metropolitan Life Insurance Com-

TABLE 1 STATISTICAL DATA—PARKCHESTER APARTMENT COMMUNITY

(Owned and operated by Metropolitan Life Insurance Company, New York, N. Y.)

Area, acres	129	Cost	$50,000,000
Buildings		Ultimate population	40,000
7 to 13 stories high	58		
Apartments			
2 to 5 rooms	12,273		

pany. Ground was broken in August 1938, and 3 years were required to complete the project. The last building was turned over to the operating management of the company on August 27, 1941.

This paper relates primarily to certain problems involved in the design, construction, and initial operation of the steam-heating system. The problems encountered with respect to corrosion and allied matters will be discussed under two major headings: (1) the selection of proper materials and equipment, and (2) the operating procedure followed for the control of water and steam quality.

Description of the Steam-Heating System

It will be noted in Fig. 2 that the Parkchester heating system consists of a single steam-generating plant from which feeder mains diverge underground to supply the various buildings. Steam at boiler pressure is distributed to 29 heat-control rooms strategically located throughout the development. Each of these control rooms houses a pressure-reducing station, duplicate hot-water generators, various pumps, and control equipment which automatically regulates the flow of steam throughout the building or buildings served by that particular control room.

The steam-generating plant houses four Foster Wheeler D-type boilers and auxiliary equipment. Each boiler has a normal rated capacity of 100,000 and a maximum capacity of 135,000 lb of steam per hr. Electricity is supplied to the entire project by the public utility; however, should future economic conditions warrant, turbogenerators may be installed, as necessary space has been provided for this purpose. The boilers have been designed to operate at a pressure of 500 psi, and provisions were incorporated to facilitate equipping them with superheaters. At present the boiler pressure has been limited to 95 psi. In addition, the station has been so laid out that coal bunkers can be erected and pulverized-coal preparation and burning equipment installed, should conditions necessitate a change of fuel. The boilers are oil-fired at present and are equipped with waterwalls and air preheaters.

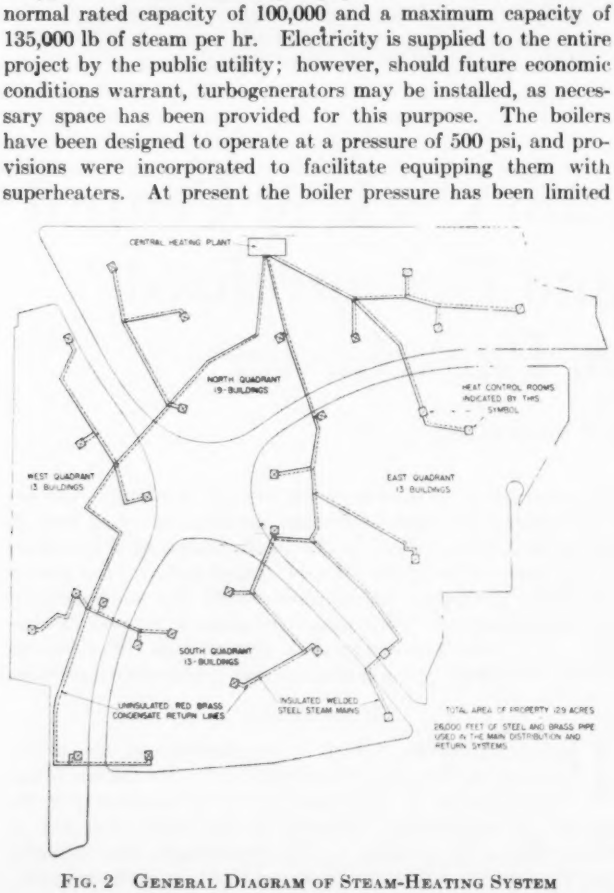


FIG. 2 GENERAL DIAGRAM OF STEAM-HEATING SYSTEM

Operation of the boilers and auxiliaries is handled through a central panel board and automatic combustion control has been incorporated in line with modern practice.

The steam, at boiler pressure, is distributed through three transmission lines, two of which are 16 in. and one 14 in. in diameter. They are of welded steel construction, have packless stainless-steel bellow-type expansion joints, and are insulated with magnesia block, bound with copper sheathing. The condensate-return piping is of red brass connected by sweated fittings and provided with packed-type expansion joints. Approximately 13,000 ft of steel pipe and the same amount of red-brass pipe were required for the distribution and return mains.

Aside from the actual monetary value of the pipe involved, the relative inaccessibility of these underground mains would make replacement, in whole or part, a costly procedure and the protection of this portion of the heating system was the primary object that motivated the control measures adopted for the prevention of corrosion and deposition of solids.

The steam enters the control room at 80 lb pressure, allowing for a reduction of about 10 to 15 lb because of losses, passes through two reducing valves in series where the pressure is reduced to 5 lb, after which it is discharged to a low-pressure header for distribution. One line supplies two hot-water generators which are thermostatically controlled, maintaining the hot-water supply at 140 F.

These generators are copper-clad steel tanks with a copper-loop steam-heating element. As the water pressure is greater than the steam pressure, these generators must be regarded as potential sources of condensate contamination, although no actual cases of city water leakage into condensate have occurred to date.

The steam required for apartment heating next passes through an automatic electrically operated control valve, and the quantity admitted to the heating system is dependent upon two factors, i.e., the outside temperature and the amount of heat in the building.

In the radiation system[3] which was specially designed, the steam travels up bare pipe risers located in kitchens and bathrooms, heating these smaller rooms, and crosses over at the top floor of the building into adjacent downcoming banks of small cast-iron finned heat convectors. All condensed steam drains by gravity to the horizontal condensate-return line in the building basement where traps (one to each vertical convector bank) remove it from the radiation system proper.

The condensate is discharged through an accumulator tank to the vacuum pump, where the entrained noncondensable gases are evacuated, and the water is then delivered into the return mains leading to the storage tank in the heating plant.

The Water and Steam Cycle

Design and Installation Phase. It will be noted from the foregoing description of the mechanical aspects of the heating system and the diagram, Fig. 3, that the water-and-steam cycle is essentially a closed circuit. When designing the system it was estimated that the maximum loss of water and steam from this circuit would not exceed 3 per cent of the total steam output. The boiler feedwater would therefore consist of 97 per cent condensate returns and 3 per cent make-up.

The make-up supply, which is New York City water, consisting of either Catskill or a combination of Catskill and Croton

[3] Patented.

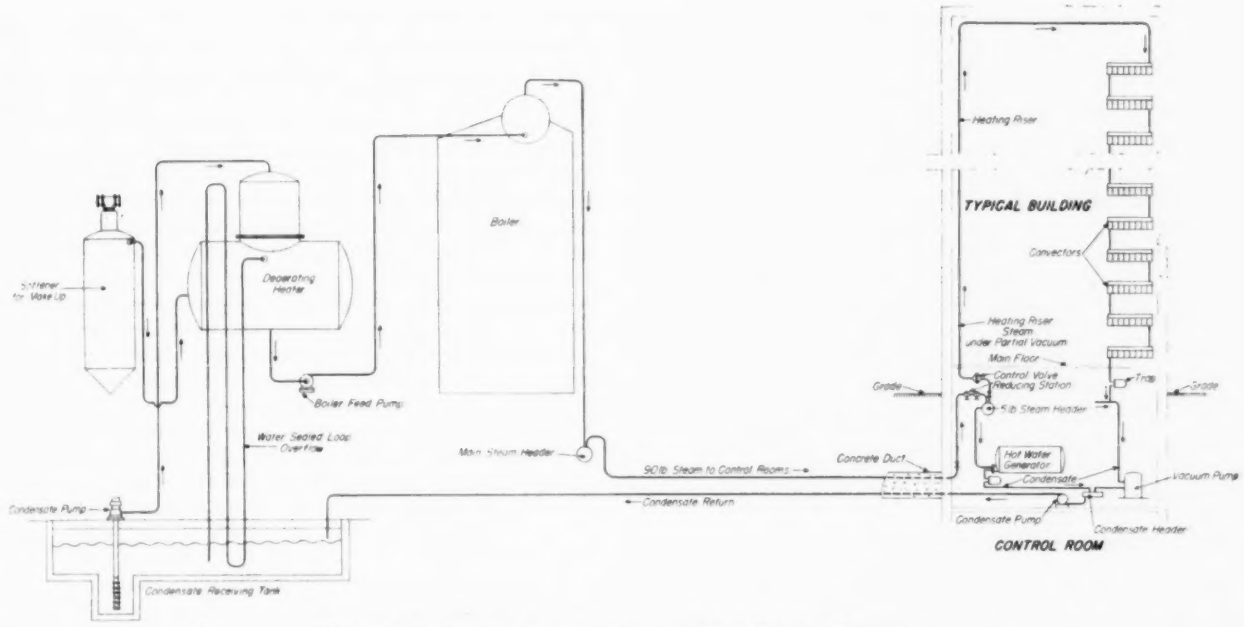


FIG. 3 MECHANICAL ARRANGEMENT OF STEAM-HEATING SYSTEM

water, is deaerated and treated in a hot-process softener using phosphates. The softener effluent is discharged into the storage tank of the feedwater heater where it mixes with the deaerated condensate. This method of treatment was selected by the designing engineers primarily to keep to a minimum carbon dioxide in the steam delivered from the boilers. A further design precaution was the inclusion of steam-purifying devices in the boilers in order to provide steam of a low total-solids content.

To protect the entire system, it was necessary to adopt additional measures, particularly with regard to corrosion. Since the heating system proper operates under high vacuum most of the time, slight leakage of air into that portion of the system is inevitable, and the condensate may actually take into solution oxygen and other gases. These gases will not be completely removed at the vacuum pump. Further, the condensate is exposed to pollution with air in the return lines, between the condensate pumps and the receiving tank in the plant, as the greater portion of the return piping is only partially filled with water and is under atmospheric pressure; hence the use of red brass to resist corrosion from these gases in the underground condensate return lines.

Careful consideration was given also to positive drainage of all piping, avoiding couples of dissimilar metals wherever practicable, and introducing numerous scale pockets to catch mill scale and debris left in pipe during construction.

Initial Operation. Steam generation began November 15, 1939, during the construction period, before the water-treating equipment was installed, which deficiency necessitated the use of untreated city water for a short period. An emergency chemical feeding system was hastily provided for protecting the boilers, the steam-distribution system, and the condensate lines against scale and corrosion.

It was originally planned to turn steam on the first buildings requiring heat and to flush the piping system to eliminate mill scale, dirt, and oil, which were known to be present to some extent in the system. After these lines had been cleaned, it was proposed to return the condensate to the boiler plant to be reused as feedwater. During the first flushing-out period, the boiler feedwater was to consist of 100 per cent make-up; subsequent flushing-out operations progressively reducing the percentage of make-up required. Considerable delay was encountered in putting this plan into effect because of the fact that the condensate receiving tank was not completed until sometime after the plant was placed in operation.

The most aggravating operating problems encountered during the first few months of operation were the clogging of the steam-washer elements with solids and corrosive attack on steel nipples on the inlet manifold of the washer. The deterioration of these nipples was distinctly a case of oxygen corrosion due to lack of proper deaeration because of the unavailability of the deaerating heater. Although these problems were troublesome, they were of no greater magnitude than would usually occur in starting up a plant before construction had been completed and caused no permanent damage to the system as a whole.

Correction of Carry-Over. The boilers as originally installed were equipped with steam purifiers of the wet type, which provided for washing the steam with feedwater to lower the solids in the saturated steam. Difficulty occurred from deposition of solids in the washer elements because of the use of phosphate-treated feedwater. It was found necessary to replace the equipment with dry purifiers. This change effected a marked improvement in steam quality delivered from the boilers. The efficiency of the dry-type purifier over the wet type is shown in Fig. 4.

To provide an accurate check on steam quality, a permanent conductivity-recording assembly, embodying vacuum degasification of the sample was installed. This assembly consists of a combination condenser and tempering coil, a sample temper-

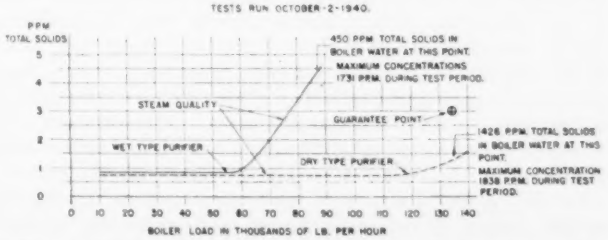


FIG. 4 GRAPH COMPARING PERFORMANCE OF STEAM PURIFIERS
(Tests obtained with both indicating and recording conductivity apparatus.

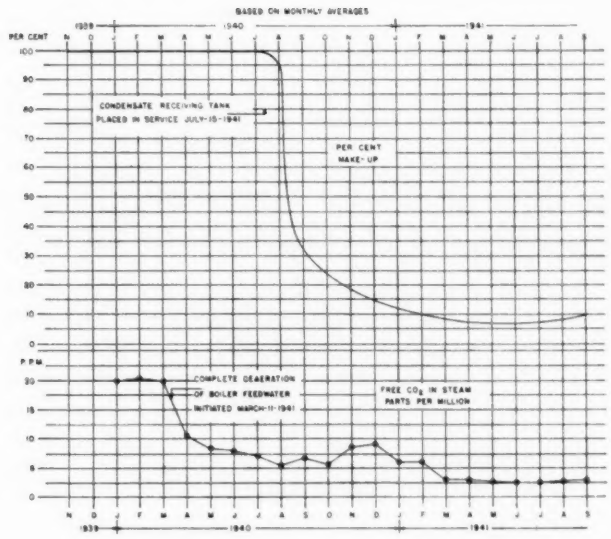


FIG. 5 GRAPH OF CO_2 CONTENT OF STEAM

ature-control device, a Pyrex flow vessel, two water-jet-type aspirators, and a Leeds and Northrup conductivity cell and recorder. Undesirable conditions, such as abrupt and sizable load increases and excessive concentration of solids in boiler salines, will be reflected on the chart by a rise in conductivity thus indicating a decrease in steam quality. One year of operation disclosed that the quality of the steam delivered into the main ranged from 0.6 to 1.5 ppm of total solids.

Reclamation of Condensate. Delayed condensate reclamation, enforcing the use of untreated city water introduced several undesirable factors; viz., the presence of free carbon dioxide in steam, high boiler-water turbidity, and slight deposition in parts of the feedwater cycle. However, most of these conditions have been either wholly or partially corrected.

The progressive reduction from amounts on the order of 20 to 30 ppm of CO_2 in the steam, which prevailed during the first four months of operation, to current values of 0.5 to 2.0 ppm is traceable in part to reductions in the amount of untreated make-up admitted to the system during the earlier stage of operation. The first reduction from over 20 ppm to about 10 ppm was due to better feedwater-heater performance. Most of the untreated city water was admitted to the boiler-feed system through the feedwater heater, therefore, the increased deaeration had an immediate effect on the carbon-dioxide content of the steam. These occurrences are illustrated graphically in Fig. 5.

One of the most troublesome factors still encountered in condensate reclamation has been the high turbidities that occur in the condensate over the first week or two of the heating season and recur to a somewhat lesser degree during the intermittent heating at the end of the season. When this condition arises the condensate is diverted to the sewer until it has cleared. Most of the suspended matter is undoubtedly rust, accumulating during extended periods of no flow, which, although present in minor amounts in the individual lines, collectively, over so large a system, imparts an appreciable turbidity to the condensate for a short period upon resumption of heating. This remains as one of the problems requiring solution, and as an initial step toward correction of the condition, a piping change is contemplated which will permit diversion of the condensate from the heating system proper to the sewer during start-up periods without affecting normal return of condensate from hot-water generators and other sources. It is estimated that in this manner from 20,000 to 40,000 lb of 130 F water can be saved per hour during these initial flushing periods.

Feed-Line Deposition. Difficulty was experienced from deposits which accumulated in the control valve of the Copes feedwater regulator. The analyses of these deposits showed them to consist largely of calcium and magnesium phosphates, some iron, and a small amount of copper. These deposits, which were quite hard, accumulated slowly during the period when it was necessary to use fairly large amounts of make-up, and although the mixture of condensate and treated water resulted in a relatively low hardness in the feedwater, still these deposits persisted. It was necessary to dismantle the equipment at intervals and remove the deposits manually.

These deposits occurred because of the presence of small amounts of calcium and magnesium phosphates which tend to precipitate as hard crystalline formations at pH values about 8.5 when the temperature of the water is moderately elevated. It is expected that by maintaining the pH value of the feedwater at 8 to 8.5, and by the use of a low percentage of treated make-up, the accumulation of such deposits can be greatly minimized.

INSPECTION AND MAINTENANCE OF THE HEATING SYSTEM

In so extensive a steam-distribution and condensate return system, periodic inspection and overhauling of certain portions of the equipment are essential to efficient and economical operation. During the summer all condensate traps are removed, cleaned, and tested. Necessary replacements of parts are made at this time. Scale pockets are opened and cleaned. Whether this operation will be necessary every 12 months can only be ascertained by future experience. It is quite probable that after all mill scale and debris have been removed from the system, some of the work will be required at less frequent intervals.

This maintenance program has provided an excellent means to ascertain the condition of the metal surfaces in the system and the last annual inspection, which covered about one half of the property, disclosed that out of a total of 2200 condensate traps, less than 0.5 per cent required replacement of parts due to deterioration incidental to normal operation.

The last inspection also disclosed that many of the scale pockets were entirely filled with mill scale and other dirt. Analysis of a sample of deposit (see Table 2) indicates that it consists of

TABLE 2 ANALYSIS OF MATERIAL REMOVED FROM HEATER-HEADER DRIP TRAP, NO. 4 GARAGE

Constituent	Expressed as	Per cent
Silica	(SiO_2)	49.79
Iron	(Fe_2O_3)	30.14
Aluminum	(Al_2O_3)	10.96
Calcium	(CaO)	1.26
Magnesium	(MgO)	1.29
Phosphates	(P_2O_5)	0.50
Sulphates	(SO_3)	None
Copper	(Cu)	None
Zinc	(Zn)	None
Lead	(Pb)	None

NOTE: Analysis made on the dried sample which contained 36.60 per cent of water before drying.

mill scale and silica-bearing construction debris, with traces of calcium and magnesium phosphates. The latter contamination occurred during the tuning up of the steam plant. Some of these scale pockets had been cleaned previously, which leads to the conclusion that purging of the piping still continued to a marked degree during the 1940-1941 heating season.

Examination of steel piping adjacent to scale pockets and traps revealed only a small amount of general oxidation, adjudged by the condition of the metal and the presence of mere traces of red-iron-oxide film. From our observation metal deterioration has been practically absent in the steel pipe.

Additional evidence as to the apparent freedom from corrosion

in the building system was the excellent condition of the metal in one of the cast-iron convector elements. This element was taken from the bottom of a vertical convector bank, a point subject to maximum contact with hot condensate, after it had been in service 16 months.

Some general corrosion, indicated by a rust coating, has occurred in the 2-in. steel lines connecting the condensate pumps to the brass return lines. The total length of line which is so affected is relatively small. However, this point in the system is probably the most susceptible to attack because of the contact of condensate with air. It is probable that most of the rust which fouls the condensate returns during intermittent heating periods originates at these locations. It is interesting to note, however, that pitting has not occurred, and these deposits, when once formed, appear to be acting as an impervious coating retarding further aggressive attack. These points are being carefully observed, and should the condition warrant the pipe will be replaced with brass or other nonferrous material. In order to detect corrosion or deposition in steam-distributing mains and condensate return lines, the use of spool pieces as routine observation specimens is resorted to.

Idle Equipment

Experience in numerous boiler plants has demonstrated that serious corrosion is encountered during periods when equipment is idle. Heating plants are particularly subject to such action on account of the low steam demand during warm weather. At Parkchester three boilers are idle, one of which must be kept filled with water for stand-by service. Also considerable changing of boilers from active to idle or stand-by status is necessary in the summer on account of maintenance work.

To avoid corrosion, current practice is to keep the pH of the water in idle boilers at 10.8 or over, by addition of caustic soda, and also to maintain a sodium-sulphite residual of approximately 100 ppm to combine with any dissolved oxygen. Whenever practicable, idle boilers are filled to the vents, expelling all free air, the vents then being closed, and hydrostatic pressure of about 50 psi imposed to eliminate seepage of air into the unit.

Aside from boilers, consideration is being given to the problem of corrosion prevention in steel accumulator and vacuum-pump tanks. Just how far these protective measures should be extended we are unable to say at present.

Treatment of Make-Up

Supplementary Treatment. It was apparent from the period of initial operation that chemical deaeration utilizing sodium sulphite would be incorporated with the water-treating system as designed to assure the removal of traces of dissolved oxygen. The probablility of pH adjustment with caustic soda was also recognized, but subsequent experience with the hot-phosphate softener disclosed that this apparently would not be required.

Laboratory Control. To facilitate proper control of treatment in the water-steam cycle and to ascertain conditions in the various parts of the entire system, a chemical laboratory completely equipped for this type of work has been provided. Routine analyses are conducted which embrace samples and determinations, as given in Table 3.

TABLE 3 SAMPLING POINTS THROUGHOUT WATER-STEAM CYCLE WITH ROUTINE TESTS INDICATED FOR EACH POINT

Sampling points	Determinations
City water	Free CO_2, pH, total alkalinity, chloride, hardness
Softener discharge	pH, hydroxide and total alkalinity, chloride, hardness, turbidity
Condensate storage	Free CO_2, pH, hardness, phosphate, copper, iron
Boiler feed	pH, hydroxide and total alkalinity, chloride, hardness, phosphate, copper, iron
Boiler salines	pH, hydroxide and total alkalinity, chloride, hardness, phosphate, sodium sulphite, sodium sulphate, turbidity, estimated solids, copper, iron
Steam	Recorded total solids by electrical conductivity, free CO_2, pH, phosphate, copper, iron

Summary

Two years of operating experience and close observation of the entire heating system have demonstrated the foresightedness of the management and their designing engineers in the selection and use of materials for reducing corrosion of metals, and for preventing the deposition of solids, sometimes encountered in large-scale heating systems.

Acknowledgment

The authors desire to acknowledge the co-operation of the management in making available the necessary facilities for the preparation of this paper.

Radiation Configuration Factors Using Light in Furnace Models

By FRED ENGLAND[1] and H. O. CROFT[2]

In problems involving the exchange of heat energy by radiation between bodies, it becomes necessary to know what areas of the bodies in question "see each other." Those factors expressing mutual visibilities are known as "configuration factors." Configuration factors have usually been determined either by mathematical analysis and computation, or by actual experiment with bodies radiating heat energy. This paper introduces an experimental method of determining configuration factors by employing models of furnace cavities and utilizing the exchange of "light" energy instead of "heat" energy.

Nomenclature

The following nomenclature is used in the paper:

A = area, sq ft
B = correction factor for illumination, which is measured by a photoelectric cell when the angle of incidence is greater than zero (no units)
B_{am} = arithmetic-mean correction factor (no units)
B_{cm} = cosine-mean correction factor (no units)
B_{tm} = true-mean correction factor (no units)
e = emissivity of a body (no units)
E_A = normal intensity of light, ft-c
E_p = intensity of light, ft-c
E/E_w = intensity factor; ratio of intensity of light at a point on furnace wall to average intensity of light from base of furnace (no units)
F_c = configuration factor (no units)
F_e = emissivity factor (no units)
k = conversion factor of lumens to Btu per hr (5.1×10^{-3} Btu per hr per l)
n = adjacent side of a right triangle whose angle with the hypotenuse is θ, the angle of incidence, ft
q = energy transferred per unit of time, Btu per hr
q_A = light energy in transit, l
R = intensity of other forms of energy than light which cause photoelectric cell to respond, ft-c
r = distance between centers of two radiating surfaces, ft
T = absolute temperature of a system, deg R
X = ratio of length of side of parallel planes to their distance apart (no units)
Y = ratio of length of unique side on which heat-transfer equation is based to length of common side (no units)
Z = ratio of length of unique side of other rectangle to the length of the common side (no units)
θ = angle of incidence, deg
λ = wave length of electromagnetic phenomenon, mu
σ = Stefan-Boltzmann constant (0.173×10^{-8} Btu per sq ft per deg R^4 per hr)

Introduction

Since "the phenomena of light are inherently the same as those of radiant heat, although the wave lengths are of different frequencies,"[3] the possibility of the use of light in lieu of radiant heat for the determination of configuration factors for radiation in furnace models is discussed.

A great amount of work has been done on configuration factors from a theoretical viewpoint, involving certain assumptions which may not be strictly valid. Very little work has been done from the practical side, however, because of the difficulty of measuring the high temperatures usually involved in radiation, and because of the difficulty of obtaining equilibrium conditions.

This investigation involves measuring the intensity of light in various parts of furnace models which have a constant light source instead of a radiant-heat source, and, from the intensities of light, calculating the configuration factors which might be used in industrial-furnace design.

Furthermore, it was desired to compare the configuration factors determined experimentally with some determined by purely mathematical means.

When heat is transferred by radiation from a completely enclosed body to the enclosing body, the Stefan-Boltzmann equation is used in its usual form

$$q = \sigma A(T_1^4 - T_2^4) \quad \ldots\ldots [1]$$

where q is the heat transferred per unit time, σ is the Stefan-Boltzmann constant, A is the area of the enclosed body, T_1 is the absolute temperature of the enclosed body, and T_2 is the absolute temperature of the enclosing body.

In many cases of heat transmission by radiation, one body is not enclosed by another; thus all of the radiation from one body is not intercepted by the other body, except in the case of infinite parallel planes. Therefore, for radiant-heat transfer between two black bodies which do not directly intercept all of the radiation of each other, another term F_c, the configuration or shape factor, must be placed in the Stefan-Boltzmann equation, which then takes the form

$$q = \sigma A F_c(T_1^4 - T_2^4) \quad \ldots\ldots [2]$$

The configuration factor is simply a constant, never greater than unity, which represents the fraction of the areas of the bodies, involved in the transfer of heat, that are "seen" by each other.[4]

Configuration factors have been determined geometrically by use of the principles of illumination. If radiation takes place between two infinitesimal surfaces dA_1 and dA_2, which are small in

[1] Department of Chemical Engineering, Massachusetts Institute of Technology, Cambridge, Mass.

[2] Head of Department of Mechanical Engineering, University of Iowa, Iowa City, Iowa. Mem. A.S.M.E.

Contributed by the Heat Transfer Professional Group and presented at the Annual Meeting, New York, N. Y., December 1–5, 1941, of The American Society of Mechanical Engineers.

Note: Statements and opinions advanced in papers are to be understood as individual expressions of their authors and not those of the Society.

[3] "Light, Photometry, and Illumination," by W. E. Barrows, McGraw-Hill Book Company, Inc., New York, N. Y., 1925, p. 1.

[4] "Thermodynamics, Fluid Flow, and Heat Transmission," by H. O. Croft, McGraw-Hill Book Company, Inc., New York, N. Y., 1938, p. 196.

comparison to their distance apart, the configuration factor can be determined by assuming the Lambert cosine law and the square-of-the-distance law to hold. The Lambert cosine law states that the radiation from a given area in a direction at an angle to the normal to the surface is proportional to the cosine of the angle. The square-of-the-distance law states that the intensity of radiation from a point source decreases with the square of the distance from the point source. Referring to Fig. 1, it is

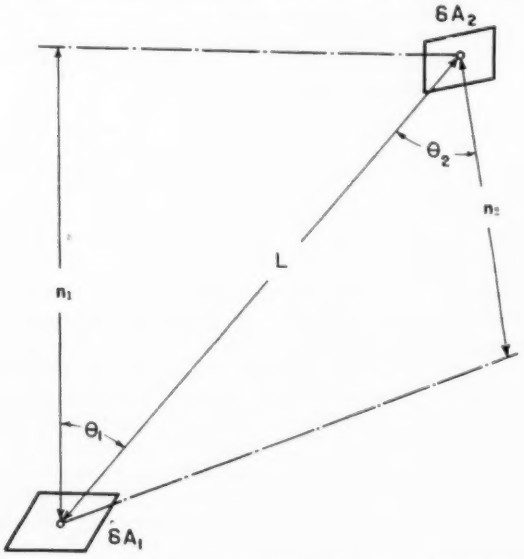


FIG. 1 RADIATION BETWEEN SURFACES SMALL IN COMPARISON TO THEIR DISTANCES APART

seen that the black-body radiation between dA_1 and dA_2 will follow the equation

$$q = i(dA_1 \cos \theta_1)(dA_2 \cos \theta_2)/L^2 \quad [3]$$

where q is the heat transferred between the infinitesimal elements of areas dA_1 and dA_2, i is the normal intensity of radiation, $dA_1 \cos \theta_1$ is the area of the surface dA_1 which is "seen" by dA_2, $dA_2 \cos \theta_2$ is the area of the surface dA_2 which is seen by dA_1, and L is the distance between the centers of dA_1 and dA_2. Since $\cos \theta_1$ may be written as n_1/L and $\cos \theta_2$ as n_2/L, Equation [3] may be written

$$q = i dA_1 dA_2 (n_1 n_2)/L^4 \quad [4]$$

where, as shown in Fig. 1, n_1 is the perpendicular distance from dA_1 to a plane through the center of dA_2 parallel to dA_1, and n_2 is the perpendicular distance from dA_2. Since πi, the total forward radiation from a surface, is equal to σT^4, Equation [3] may be rewritten

$$q = \sigma dA_1 \cos \theta_1 dA_2 \cos \theta_2 (T_1^4 - T_2^4)/\pi L^2 \quad [5]$$

Therefore, if Equation [5] is based on surface dA_1, the configuration factor is

$$F_c = dA_2 \cos \theta_1 \cos \theta_2 / \pi L^2 \quad [6]$$

Hottel[5] has derived equations for the configuration factors for radiant-heat transfer between rectangles in perpendicular and parallel planes. Hottel and Keller[6] determined mathematically and proved experimentally the effect of reradiation on heat transmission in furnaces and through openings. In their mathematical derivations, they assumed reradiating nonconducting walls which emitted as black bodies, and they determined the fraction of the radiation given off by one surface which is received by a parallel surface when the two surfaces are connected by nonconducting reradiating walls.

When the surfaces are not black bodies, another term F_e must be inserted in the Stefan-Boltzmann equation, which assumes the form

$$q = \sigma A F_c F_e (T_1^4 - T_2^4) \quad [7]$$

The term F_e depends upon the emissivity e of both bodies involved. In the case where one body is small in comparison to the distance to the other body, F_e is equal to $e_1 e_2$. Since the emissivity is equal to the absorptivity, the assumptions can be made that the emission from the first surface is e_1 times as much as that from a black body, and that the absorption of the second surface is e_2 times as much as that of a black body. Therefore, the amount of radiation $(1 - e_2)$ will be reflected in all directions from the second body, and a negligible fraction of this will reach the first body. For cases where a large amount of $(1 - e_2)$ is intercepted by the first body, F_e is not equal to $e_1 e_2$. Hottel has shown that for infinite parallel planes

$$F_e = (e_1^{-1} + e_2^{-1} - 1)^{-1} \quad [8]$$

For concentric spheres and concentric infinite cylinders, Hottel has proved that

$$F_e = [e_1^{-1} + A_1 A_2^{-1}(e_2^{-1} - 1)]^{-1} \quad [9]$$

where A_1 is the area of the enclosed body, and A_2 is the area of the enclosing body.

ANALOGY BETWEEN LIGHT AND RADIANT HEAT

An interesting analogy between radiant heat and light can be drawn by comparing the properties of each. Temperature is an intensive property of heat which tells the direction of the flow of heat, while the foot-candle is an intensive property of light. A foot-candle is the intensity of illumination upon a surface at a point which is 1 ft from a source of 1 c of standard light intensity, the surface being perpendicular to the light rays at that point. The quantity of the flow of heat is the British thermal unit per hour, which is the quantity of heat required to raise the temperature of 1 lb of water from 39 to 40 F in 1 hr, whereas, the extensive unit of light is the lumen, which is the quantity of light falling on a surface which has an area of 1 sq ft when every point of the surface is 1 ft from a point source of light of 1 c.

If a perfectly diffusing body, which absorbs none of the light energy coming to it, is reflecting this energy, then

$$q_A = E_A dA \quad [10]$$

represents the amount of energy coming to and diffusing from the body. In Equation [10], term q_A is the energy in lumens, E_A is the normal intensity in foot-candles of the light energy diffusing from the body, and dA is a small element of area in square feet.

If a black body is radiating the same amount of energy as this perfectly diffusing reflector, then

$$q_B = \sigma T_B^4 dA = k q_A = k E_A dA \quad [11]$$

where q_B is the energy radiating from the black body in British thermal units per hour, σ is the Stefan-Boltzmann constant, T_B is the absolute temperature of the black body, and k is the factor for the conversion of lumens to British thermal units per hour.

[5] "Radiant Heat Transmission Between Surfaces Separated by Nonabsorbing Media," by H. C. Hottel, Trans. A.S.M.E., vol. 53, 1931, paper FSP-53-19b, p. 270.

[6] "Effect of Reradiation on Heat Transmission in Furnaces and Through Openings," by H. C. Hottel and J. D. Keller, Trans. A.S.M.E., vol. 55, 1933, paper IS-55-6, p. 39.

the numerical value of which is 5.1×10^{-8} Btu per hr per l. Thus it is seen that

$$E_A = \left(\frac{\sigma}{k}\right) T_B^4 \ldots\ldots\ldots\ldots\ldots\ldots [12]$$

In other words, if a perfectly diffusing nonabsorbing body is reflecting the same amount of energy as a black body is emitting, then the intensity of the light energy coming to or diffusing from the reflector is proportional to the fourth power of the absolute temperature of a black body which is emitting the same amount of energy.

A hot body gives off radiations of different wave lengths. Those waves which produce heating effects are called heat waves, and those which are sufficiently short to affect the optic nerve are called light waves.[7] Fig. 2 compares the relative sensitivity to various wave lengths of the eye and of the Type 1 Weston Photronic cell.[8] From this illustration, it can be seen that the photoelectric cell is more sensitive than the eye to nearly all wave lengths of visible light, and also responds to some wave lengths which do not affect the optic nerve. Therefore, the photoelectric cell measures not only light but also other forms of energy. Thus, if a photoelectric cell is used to measure the energy coming to and diffusing from the nonabsorbing perfectly diffusing reflector, Equation [12] must be rewritten as follows

$$(E_A + R) = \left(\frac{\sigma}{k}\right) T_B^4 \ldots\ldots\ldots\ldots\ldots\ldots [13]$$

where the term $(E_A + R)$ is the intensity of the light and other

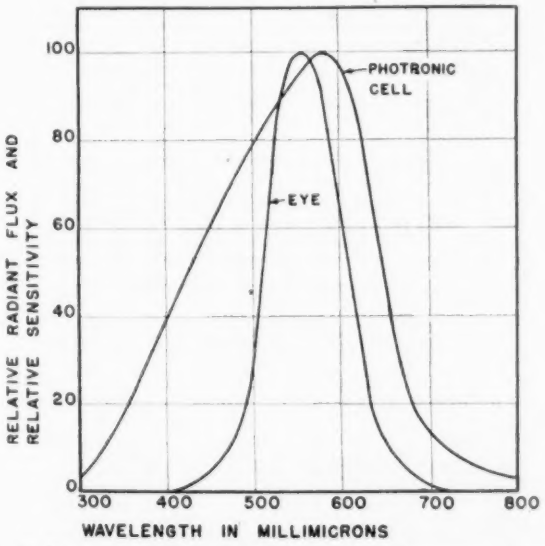


FIG. 2 RELATIVE SPECTRAL SENSITIVITY OF PHOTRONIC TYPE 1 CELL AND AVERAGE EYE

forms of energy which cause a response on the photoelectric cell. If this term is replaced by E_p, then the equation may be written

$$E_p = \left(\frac{\sigma}{k}\right) T_B^4 \ldots\ldots\ldots\ldots\ldots\ldots [14]$$

Rather than invent a name for E_p, the intensity of radiation from a light source as determined by a photoelectric cell, it seemed more expedient to redefine light as that form of energy to which the photoelectric cell responds.

Referring to Fig. 2 again, and assuming the square-of-the-distance law to be strictly valid, it is seen that doubling the distance from the source of the light for which the curve for the photoelectric cell is plotted causes the intensity for all wave lengths to be one fourth as great. Therefore, since the area under the curve is the total amount of energy received by the cell from the source of light, this area, and therefore the energy received when the distance is doubled, will be one fourth as great.

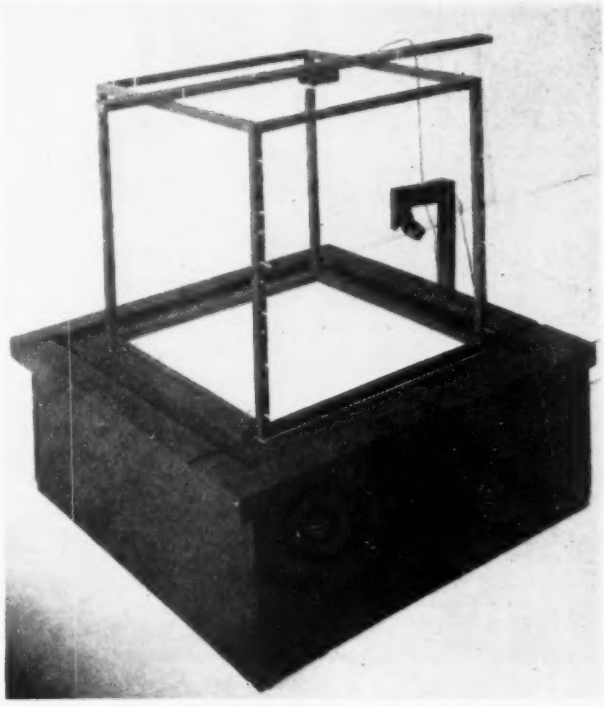


FIG. 3 MODEL FURNACE NO. 1 AND CONSTANT LIGHT SOURCE ENCLOSURE

EXPERIMENTAL APPARATUS

The apparatus consisted of a constant light source, a specially mounted photoelectric cell, a standard photoelectric cell, a potentiometer, four model furnaces, a darkroom, a Weston illumination meter, and a standard reflector of magnesium carbonate.

The source of light was nine bulbs mounted in a box. The box was 3 ft wide, 3 ft long, and 1 ft high, and was made of 1-in. white pine. It was painted with flat white paint on the inside and flat black paint on the outside as shown in Fig. 3. The cover of the box was movable and was also painted with flat black paint. In the center of the cover was a piece of pure white opal glass, $^1/_8$ in. thick, 2 ft long, and 2 ft wide.

A Weston Photronic cell, No. 594, Type 1, was used as a standard cell to check the intensity of light from the constant light source. It was placed in a convenient position with respect to the light source. In Fig. 3 the standard cell is seen on the side of the light source, while, in Fig. 4, it is seen above both the model furnace and the light source.

Fig. 3 is an illustration of furnace No. 1 on the constant light source. It is a frame without any walls and represents a furnace with total-absorbing walls. The frame was constructed from $^3/_4$-in. $\times$ $^3/_4$-in. white pine; it has a square base 24 in. $\times$ 24 in. and is $23^1/_4$ in. high. Thus, the inside of this frame is a $22^1/_2$-in.

[7] "The Elements of Physics," by A. W. Smith, McGraw-Hill Book Company, Inc., New York, N. Y., 1927, p. 444.

[8] "Technical Data Bulletin," No. D-18-A, Weston Electric Instrument Corporation, Newark, N. J.

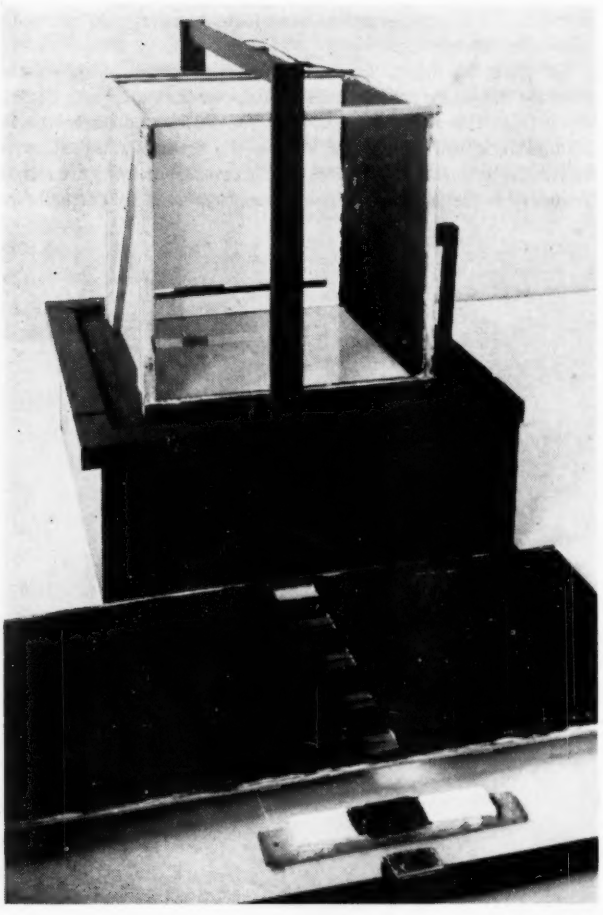


FIG. 4 MODEL FURNACE NO. 2 ON CONSTANT LIGHT SOURCE ENCLOSURE

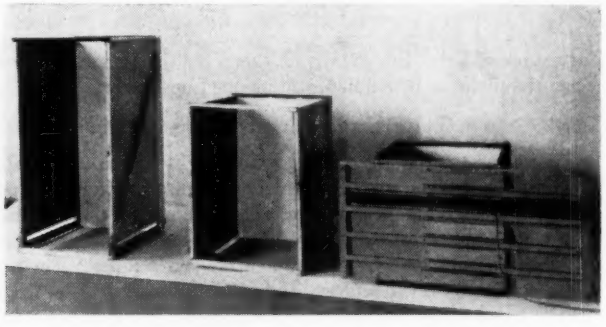


FIG. 5 MODEL FURNACES NOS. 4, 3, AND 2

cube. As shown in Fig. 3, stud bolts were used to fasten the traversing bar, holding the measuring cell in the correct positions. This frame was painted with flat black paint, which absorbs 95 per cent of the light. Model furnace No. 1, Fig. 3, corresponds to a furnace with total-absorbing walls and top.

Model furnace No. 2 is shown in Figs. 4 and 5. It has four walls, no top, and is made of $^1/_4$-in. plywood. The inside of this furnace is a 2-ft cube. The front wall is 4 ft long and may be slid horizontally to the desired position. In the front wall are five holes with templates; thus the cell may be placed into the desired hole for traversing the side wall.

Model furnaces Nos. 3 and 4, Fig. 5, are identical with model furnace No. 2, except for the fact that they are, respectively, 1.4 times and 2 times as high as No. 2. The inner dimensions of No. 3 are 24 in. × 24 in. × 33$^3/_8$ in., while those of No. 4 are 24 in. × 24 in. × 48 in. Furnace No. 3 has seven holes in its sliding front wall, while furnace No. 4 has ten.

METHOD OF CONDUCTING EXPERIMENTS

The photoelectric cell used for measurements was calibrated in the following manner: A 200-w bulb in a lamp with no reflector and 1 ft 6 in. high was placed in the circuit used by the constant light source, described in the previous section. This lamp was placed in the darkroom, and the standard photoelectric cell was placed in a position near and to the rear of the lamp. The standard cell was kept at a constant reading on the potentiometer. The temperature of the room was maintained at 82 F, since the current of photoelectric cells is a function of temperature. The "measuring" cell was fastened to the front of furnace No. 1, so that it faced the lamp and was at the same height as the bulb in the lamp. To make sure that the cell was parallel to the lamp at all times, a string was hung horizontally across the darkroom at a height of 1 in. above both the lamp and the photoelectric cell. Thus, since the cell was attached to the front part of the furnace,

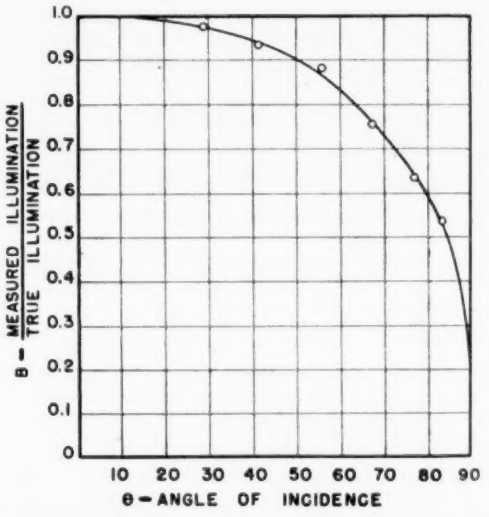


FIG. 6 EFFECT OF LIGHT INCIDENCE ON ILLUMINATION OF SPECIAL PHOTOELECTRIC CELL AT CONSTANT ILLUMINATION

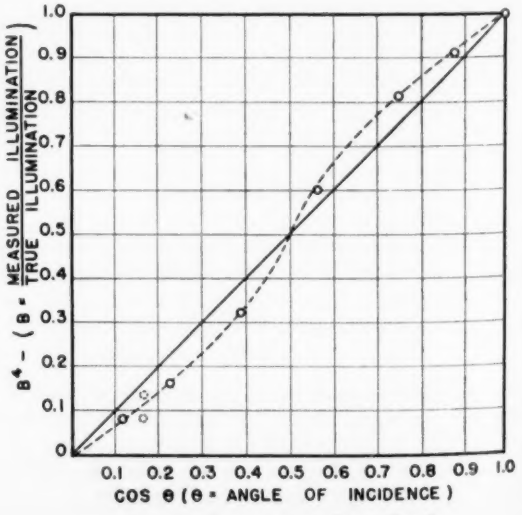


FIG. 7 RELATION OF B' TO COS θ

the cell was perpendicular to the light rays when this suspended string extended over the lamp, the photoelectric cell, and a point on the rear of the furnace, corresponding to the position of the cell on the front part of the furnace.

When the lamp had sufficient time to reach its equilibrium temperature, the current in the measuring cell was determined, while the current in the standard cell was held constant by keeping the illumination from the light source constant by means of the rheostats. When the readings for the current in the measuring cell became constant, this value in microamperes was recorded. Then the distance of this cell from the lamp was measured. The illumination at this cell was next found by means of a Weston illumination meter. This procedure was repeated for various distances of the photoelectric cell from the lamp.

Fig. 6 is a curve showing the relation of the correction factor to the angle of incident light. An interesting relation between the fourth power of the correction factor and the cosine of the angle of incident light is shown in Fig. 7.

Procedure for Model Furnace No. 1[9]

The distribution of illumination on the sides of model furnace No. 1 was determined in the following manner: The light in the light source was turned on, and the room temperature was held at 82 F for 2 hours prior to conducting the experiment, to insure equilibrium conditions.

The current generated in the measuring cell, when it was placed in the center of each of the thirty-six equal areas into which the top of the furnace was divided, was measured. Before and after determining the current in the cell at each point, the illumination from the constant light source was checked by means of the standard cell. Then readings were taken for each of the centers of the thirty-six equal areas of the side of the furnace. Because the thickness of the opal glass on the constant light source varied slightly, the sides of the furnace received slightly different amounts of light. Therefore, readings were taken alternately for the thirty-six points on the top and the thirty-six points on the side for each of the four sides. This procedure was repeated for five furnaces, similar to model furnace No. 1, except for the fact that their heights were from $^1/_6$ to $^5/_6$ times as great as the height of model furnace No. 1.

[9] Corresponding to a furnace with total-absorbing walls and top, Fig. 3.

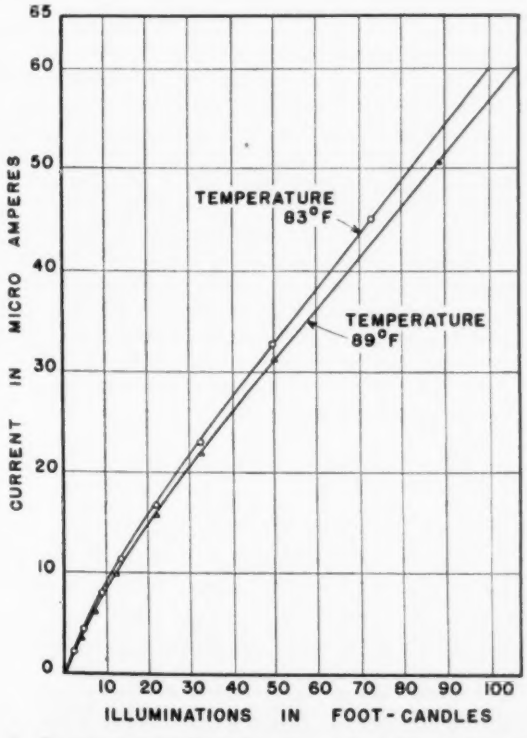


Fig. 8 Calibration of Photoelectric Cell Used With Model Furnaces Nos. 2, 3, and 4

Model Furnace No. 2, Procedure With Varied Absorption on Walls

Experiments were next conducted using model furnace No. 2, Figs. 4 and 5. A different light-sensitive element was used in the measuring cell and was calibrated in the same manner as before for temperatures of 83 and 89 F, as shown in Fig. 8. The sides of the furnace were first painted with flat black paint. A similar run was conducted as that described for model furnace No. 1. The intensity of the light was measured over the top and, by use of the sliding wall, on the front side of the furnace. To correct for the nonuniformity of the opal glass of the constant light source, it was found more convenient here to turn the opal glass clockwise 90 deg, and to take measurements for the top and the side four times. Then the four readings for each corresponding point were averaged and converted to foot-candles by means of Fig. 8. Next, the furnace was repainted with two coats of a flat paint containing 50 per cent flat white paint and 50 per cent flat black paint. The procedure described was repeated and the furnace repainted. The ten shades of paint which are shown in Fig. 9 varying from flat black paint to flat white paint were used.

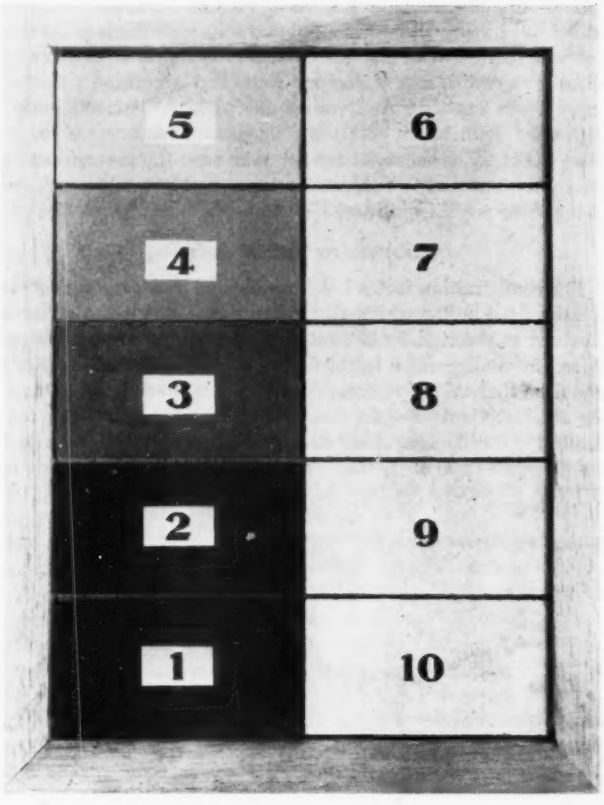


Fig. 9 Various Shades of Paint Used on Model Furnace No. 2

The absorption of light on each of the paints was determined

by a method of Barrows[10] as follows: A flat block of c.p. magnesium carbonate was placed vertically a few inches away from the measuring cell. The current generated in the cell, when the light from a lamp trained upon the block was reflected to the cell, was read on the potentiometer. Then the current was measured when the magnesium carbonate was replaced by a piece of plywood painted with the desired paint. Since the reflection coefficient of light on magnesium carbonate is known to be 0.98, the product of the ratio of the light reflected from the paint to that reflected from the magnesium carbonate and 0.98 gives the reflection coefficient of the paint. The difference between unity and this value is the absorption coefficient of the paint. The data for the various paints are given in Table 3.

Procedure for Furnaces Nos. 2, 3, and 4

The next experiment consisted of runs on furnaces Nos. 2, 3, and 4, all having three walls painted with flat black paint and one wall painted with flat white paint to simulate a furnace with three waterwalls, one refractory wall, and absorbing tubes on top. These experiments were conducted in a manner identical with that described in the previous section for furnace No. 2, except that, since the walls are not alike as in the previous cases, a complete run had to be made having the white wall in each one of the three possible positions.

Results of Experiments

The configuration factor has been defined as a constant, never greater than unity, which represents the fraction of the areas involved in the transfer of heat that are "seen" by each other. Thus, the configuration factor for the top of model furnace No. 1 would be the ratio of the amount of light received by the top to the total amount of light received by the sides and the top. Similarly, the configuration factor for the side of this furnace would be the ratio of the amount of light received by the side to the total amount of light received by all sides and the top. These two cases constitute directly opposed parallel planes and adjacent perpendicular planes, respectively. The configuration factors determined for these two cases are shown in column 4 of Table 1, together with the values (column 3) calculated from Hottel's equations which were discussed previously.

Light striking the photoelectric cell at an angle of incidence greater than zero does not have as great an effect per unit of "effective" area (that area calculated from Lambert's law) as does light normal to the cell on the current generated in the cell. Therefore, to obtain the correct value for the illumination at each of the thirty-six points on the top and each of the thirty-six points on the side, it is necessary to use a correction factor for each point. Fig. 6, which was discussed previously, shows the relation of the correction factor B to the angle of the incident light. The light-emitting surface was divided up into thirty-six equal areas, and the angle of incidence from each of these thirty-six equal areas to each of the thirty-six equal areas on the top and to each of the equal areas on the side (the number of which depended upon the height of the furnace) was found and used.

From Fig. 6 the correction factor B for each of these angles of incident light was determined. Thus, each point on the top and each point on the side had thirty-six correction factors, for which factors it was necessary to find a correct mean. Since it is usually assumed that light intensity varies inversely with the square of the distance from its source, it is obvious that the light, coming from points closer to the point under consideration, should have more influence in determining the true-mean correction factor than points which are further away. Therefore, the true-mean correction factor, based upon the true-mean values B_{tm}, is expressed by the following equation

$$B_{tm} = \frac{(B_1/L_1^2 + B_2/L_2^2 + \ldots + B_{35}/L_{35}^2 + B_{36}/L_{36}^2)}{(1/L_1^2 + 1/L_2^2 + \ldots + 1/L_{35}^2 + 1/L_{36}^2)} \quad [15]$$

where B_1, B_2, etc., are the correction factors, read from Fig. 6, for each of the angles of incidence of each of the thirty-six points on the light-emitting surface to the point under consideration, and where L_1, L_2, etc., are the distances from each of the thirty-six points on the light-emitting surface to the point under consideration. There are six dissimilar points on the top surface and eighteen dissimilar points on the side surface of model furnace No. 1. Both the true mean $B(B_{tm})$ and the arithmetic mean $B(B_{am})$ were determined for each point on the top and each point on the side of model furnaces 1a, 1b, 1c, 1d, 1e, and 1f, which furnaces have the following values for Z (the ratio of the height of the furnace to the length of the square base): 1, 5/6, 2/3, 1/2, 1/3, and 1/6, respectively, Table 2. Fig. 7, which is a plot of the relation of B^4 to the cosine of the angle of incident light, shows an S curve which approaches a straight line. Another mean value of $B(B_{cm})$ was found by assuming B to be equal to $\cos^{1/4}\theta$ as in Equation [16].

[10] Reference 3, p. 110.

TABLE 1 SUMMARY OF CONFIGURATION FACTORS FOR FIVE MODEL FURNACES

For parallel planes

1 Model furnace, no.	2 D/L	3 F_c calculated	4 F_c experimental, with no B	5 F_c experimental, with B_{tm}	6 F_c experimental, with B_{am}
1a	1.0	0.198	0.237	0.224	0.231
1b	1.2	0.266	0.285	0.273	0.285
1c	1.5	0.321	0.337	0.342	0.351
1d	2.0	0.414	0.450	0.441	0.461
1e	3.0	0.540	0.596	0.606	0.624
1f	6.0	0.737	0.771	0.791	0.817

For perpendicular adjacent planes

Model furnace, no.	Z	F_c calculated	F_c experimental, with no B	F_c experimental, with B_{tm}	F_c experimental, with B_{am}
1a	1.000	0.201	0.191	0.194	0.192
1b	0.833	0.190	0.179	0.182	0.171
1c	0.667	0.170	0.162	0.165	0.162
1d	0.500	0.147	0.138	0.138	0.135
1e	0.333	0.115	0.101	0.0986	0.0940
1f	0.167	0.0657	0.0574	0.0523	0.0459

TABLE 2 RATIO OF HEIGHT OF MODEL FURNACE TO LENGTH OF ITS BASE (Z)

Model, furnace, no.	Z
1a	1
1b	5/6
1c	2/3
1d	1/2
1e	1/3
1f	1/6
2	1
3	1 1/3
4	2

TABLE 3 SUMMARY OF RUNS 1 TO 10 FOR MODEL FURNACE NO. 2

Run no.	1	2	3	4	5	6	7	8	9	10
Black paint, per cent	100.00	50.00	25.00	12.50	6.25	1.56	0.78	0.50	0.20	00.00
White paint, per cent	0.00	50.00	75.00	87.50	93.75	98.44	99.22	99.50	99.80	100.00
Reflection coefficient	0.052	0.069	0.100	0.221	0.292	0.455	0.523	0.640	0.804	0.906
Absorption coefficient	0.948	0.931	0.900	0.779	0.708	0.545	0.477	0.360	0.196	0.094
F_c for top	0.262	0.276	0.274	0.300	0.332	0.369	0.396	0.467	0.610	0.758
F_c for sides	0.738	0.724	0.726	0.700	0.668	0.631	0.604	0.533	0.390	0.242
E_w/E for the following relative heights:										
0.833	0.004	0.005	0.008	0.019	0.028	0.050	0.065	0.101	0.136	0.228
0.667	0.006	0.008	0.012	0.028	0.039	0.075	0.097	0.145	0.200	0.310
0.500	0.008	0.011	0.018	0.040	0.065	0.104	0.122	0.196	0 265	0.409
0.333	0.013	0.017	0.027	0.057	0.093	0.145	0.164	0.254	0.336	0.509
0.167	0.018	0.022	0.036	0.077	0.124	0.194	0.220	0.324	0.424	0.597

$$B_{cm} = \frac{(\cos^{1/4}\theta_1/L_1^2 + \cos^{1/4}\theta_2/L_2^2 + \ldots + \cos^{1/4}\theta_{36}/L_{36}^2)}{(1/L_1^2 + 1/L_2^2 + \ldots + 1/L_{36}^2)} \quad [16]$$

The results indicate that the average B_{am} is 3.71 per cent larger than the average B_{tm}, whereas, the average B_{cm} is only 0.618 per cent larger. The difference between the B_{am} and the B_{tm} is that the coefficient of each B in the equation for the arithmetic mean is 1, whereas, the coefficient for each B in the equation for the true mean is $1/L^2$, and in both cases the divisor is the sum of the coefficients, which is 36 in the first case and

$$\sum_{L=L_1}^{L=L_{36}} 1/L^2 \text{ in the second.}$$

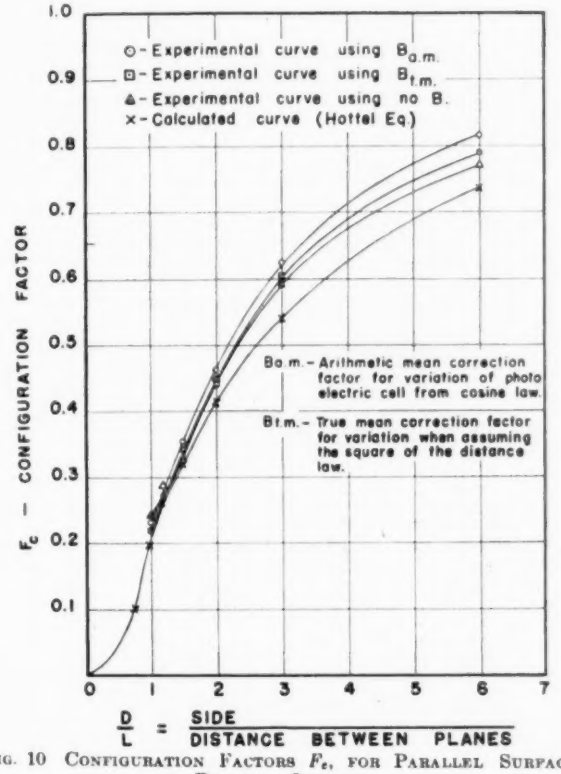


FIG. 10 CONFIGURATION FACTORS F_c, FOR PARALLEL SURFACES DIRECTLY OPPOSED

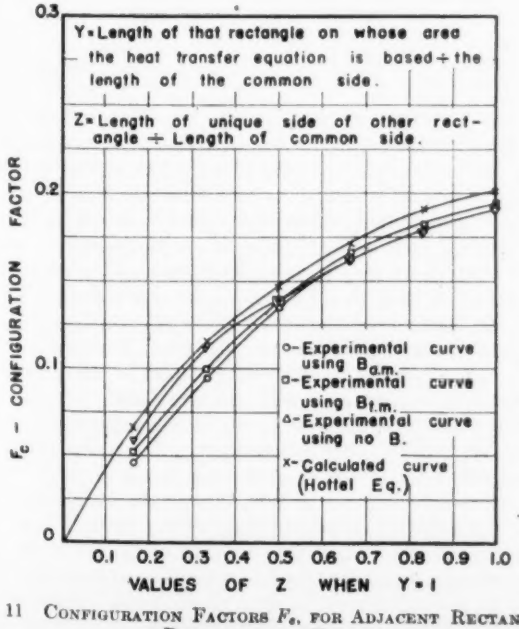


FIG. 11 CONFIGURATION FACTORS F_c, FOR ADJACENT RECTANGLES IN PERPENDICULAR PLANES

New configuration factors were, therefore, redetermined for model furnaces Nos. 1a, 1b, 1c, 1d, 1e, and 1f, using B_{tm} and B_{am}. To find the correct illumination at the points on the side or on the top, the values were divided by the appropriate correction, in order to obtain the correct illumination. Configuration factors were redetermined as described and are given in columns 5 and 6 of Table 1. Figs. 10 and 11 show the relation of the configuration factors F_c to Z (the ratio of the height of the furnace to the length of the square base) for both the top and the sides of model furnaces Nos. 1a, 1b, 1c, 1d, 1e, and 1f. The curves in Fig. 10, relating the configuration factor for directly opposed parallel planes to the ratio of the height of the side to the distance between the planes, show that the experimental values of the configuration factors are in all cases higher than those predicted by Hottel's equation. The curves in Fig. 11, for the configuration factors of adjacent rectangles in perpendicular planes, show lower values than those predicted by Hottel's equation.

DEVIATION FROM SQUARE-OF-THE DISTANCE LAW

It is known that the square-of-the-distance law is not strictly valid, unless the distance between the emitting and the absorbing bodies is great in comparison with the size of the bodies. Schack[11] states: "The intensity of radiation from sources that are neither points nor can be considered as infinitely extended surfaces varies with a power of the distance ranging from zero to two, depending upon the size of the source of radiation relative to the distance r." Thus, since Hottel has assumed the square-of-the-distance law in his derivations, it might be that his values for the configuration factors for parallel planes are lower than the true values, and that his configuration factors for adjacent perpendicular planes are higher than the true values. If the square-of-the-distance law were strictly valid, the curves, using the true mean correction factor B, should be the same as the curves calculated from Hottel's equations. The curve using the arithmetic-mean correction factor does not assume the square-of-the-distance law, i.e., it assumes that the intensity of the light is independent of the distance from the source. Thus, according to Schack's statement, the true configuration factors should lie somewhere between the experimental curve, using the arithmetic-mean correction factor, and the curve, using the true-mean correction factor. It is also probable that, where the parallel planes are far apart, or where the adjacent perpendicular plane is large in comparison to the energy-emitting plane, the experimental curves, using true-mean correction factors, are approached. Conversely, when the parallel planes are close together, or when the adjacent perpendicular plane is small in comparison to the energy-emitting plane, the experimental curves, using the arithmetic-mean correction factor, are approached.

DEVIATION FROM LAMBERT'S COSINE PRINCIPLE

Hottel and Keller[12] state: "An assumption implicit in the basic equation is the validity of Lambert's cosine principle. Actually, the intensity of radiation from all surfaces in directions at large angles from the normal is different from that required by the cosine principle. The data that are yet available as to the

[11] "Industrial Heat Transfer," by A. Schack, translation by Hans Goldschmidt and E. P. Partridge, John Wiley & Sons, Inc., New York, N. Y., 1933, p. 178.

[12] Reference 6, p. 41.

deviation, however, indicate that the over-all error introduced by assuming the correctness of the cosine principle is not great." Therefore, unless the departure of the radiation, from the surfaces involved in the radiant-heat transfer, from Lambert's law is known as a function of the angle of incidence, the experimental curves in Figs. 10 and 11, using no correction factor, are probably the best to use.

Configuration Factors for Furnaces With Radiating Walls

The definition of the configuration factor, as given early in this paper, has to be modified when reradiating walls are involved, and might read as follows: The configuration factor is a constant, never greater than unity, which represents the fraction of the areas involved in the transfer of heat that are "directly or indirectly seen" by each other. Thus when a furnace has reradiating walls, part of the heat from the base of the furnace is absorbed by the walls and reradiated to the top of the furnace, and part of the heat is radiated directly from the base of the furnace to the top. That part of the energy, which is intercepted directly by the absorbing top, divided by the net amount of radiation given off by the bottom of the furnace, is the fraction of the top and of the bottom areas of the furnace which are directly seen by each other. That part of the energy which is reradiated by the walls to the top of the furnace, divided by the net amount of energy given off from the bottom of the furnace, is the fraction of the top and of the bottom areas which are seen indirectly by each other.

Determination of Configuration Factor for Model Furnace With Total-Absorbing Top and Partial-Absorbing Walls

To simulate a furnace with reradiating walls, it was found convenient to paint the walls of model furnace No. 2 with flat paints possessing a range of absorption coefficients as described in Table 3, and displayed in Fig. 9. Thus, the assumption was made that diffuse reflection was identical with reradiation. Therefore, the configuration factor for the top of a furnace, having a total absorbing top and partially absorbing walls, would be the ratio of the light absorbed by the top to the light absorbed by all of the walls and the top. Since none of the light coming to the top was reflected, all of it was absorbed, and, since the absorption coefficient for the paint on the walls was known, the amount of light absorbed by the walls was the product of the amount of light coming to the walls and the absorption coefficient of the paint. Hence, the configuration factor for the top is the ratio of the light absorbed by the top to the light absorbed by the walls and the top. The configuration factor for the walls is the ratio of the light absorbed by the walls to the light absorbed by the top and the walls. Configuration factors, found for both the top and the sides, are given in Table 3, and plotted in Figs. 12 and 13.

The intensity factor (E_w/E) is the ratio of the light intensity at any point on the furnace wall to the average intensity of the base of the furnace. The light intensity at any point on the furnace wall is the product of the reflection coefficient for the wall and the intensity of light received by the point. Thus, to find the intensity factor, the average intensity for each row for the sides is multiplied by the reflection coefficient of the wall and is divided by the average intensity of light from the base. The intensity factors (E_w/E) for the five points on the wall of model furnace No. 2 are given in Table 3, and are plotted in Figs. 14 and 15.

Discussion of Results

It will be noticed that the extrapolation of the curve of Fig. 12

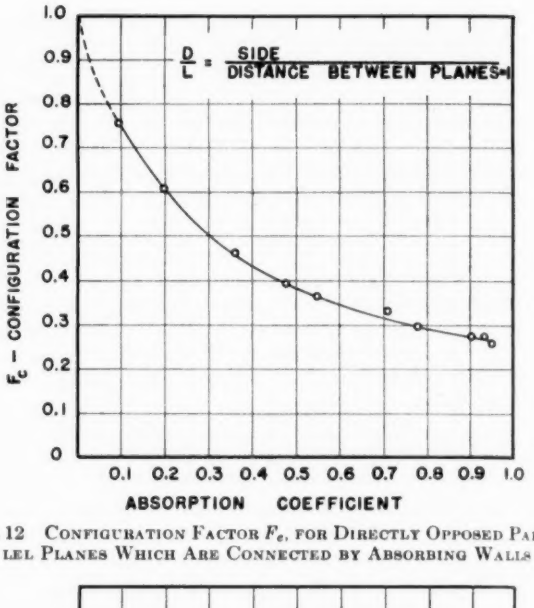


Fig. 12 Configuration Factor F_c, for Directly Opposed Parallel Planes Which Are Connected by Absorbing Walls

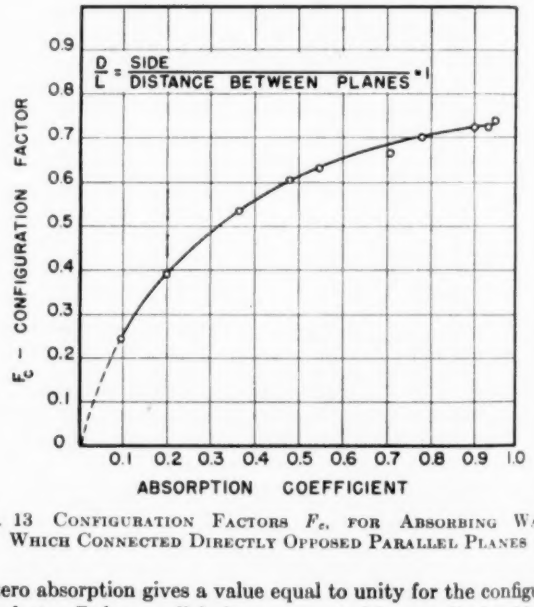


Fig. 13 Configuration Factors F_c, for Absorbing Walls Which Connected Directly Opposed Parallel Planes

to zero absorption gives a value equal to unity for the configuration factor F_c for parallel planes separated by reradiating black-body walls (diffusely reflecting walls). The Hottel and Keller value for a furnace similar to model furnace No. 2 with nonconducting reradiating black-body walls is 0.535. Also, from Fig. 12, it can be seen that a furnace with a configuration factor of 0.535 would have to possess walls which absorb 26 per cent of the energy coming to them. As previously stated, it was assumed in this investigation, that diffuse reflection from the walls is comparable to reradiation from the walls. For example, if two planes are separated by diffusely reflecting walls, part of the energy from the energy source will strike the wall and be reflected equally to all points in an enclosing hemisphere; if the two planes are separated by nonconducting reradiating black-body walls, part of the energy from the energy source will strike the wall, be absorbed by the wall, and be reradiated in its entirety, since the walls are nonconducting. Thus, in both cases, the energy absorbed by the wall is returned to the system in an almost identical manner. Hence, it seems logical that since all of the energy, which is received by a nonabsorbing diffusely reflecting wall or a nonconducting reradiating wall, is given back to the

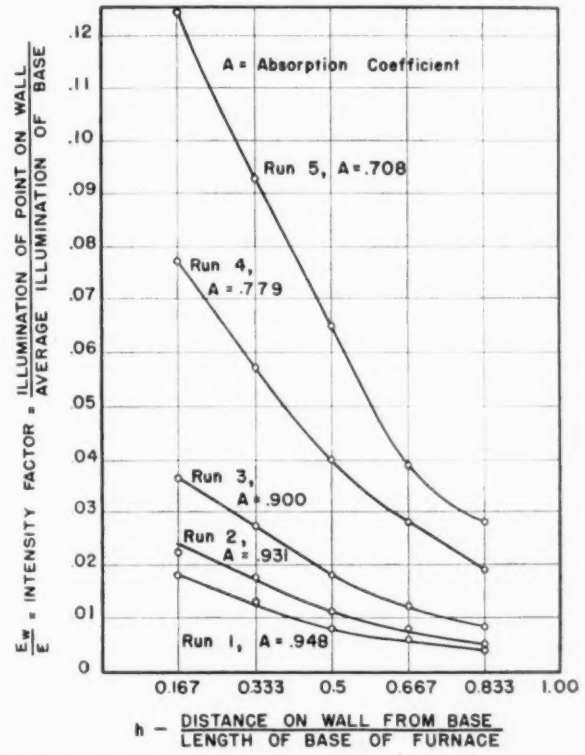


FIG. 14 RELATION OF INTENSITY FACTOR TO DISTANCE FROM BASE OF CUBICAL FURNACE

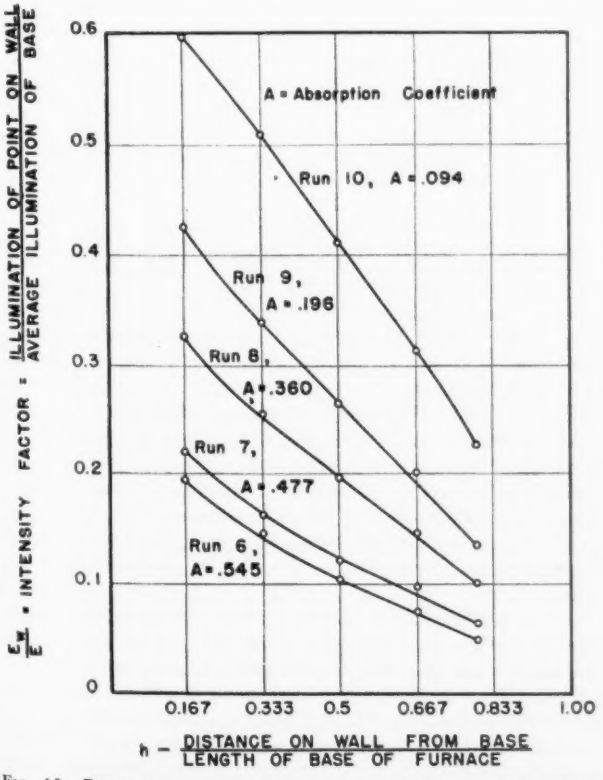


FIG. 15 RELATION OF INTENSITY FACTOR TO DISTANCE FROM BASE OF CUBICAL FURNACE

system and is finally absorbed by the top, the configuration factor for the top should be unity, and the configuration factor for the sides should be zero, as extrapolated from the curves in Figs. 12 and 13.

The amount of light reflected from the walls is a function of the amount of light they receive and of the reflection coefficient. Thus, since that part of the wall which is closer to the energy source receives more light, it should reflect more. It has been shown that, if a perfectly diffusing nonabsorbing body is reflecting the same amount of energy as a black body is emitting, then the intensity of the energy coming to or from the reflector is proportional to the fourth power of the absolute temperature of a black body which is emitting the same amount of energy. Therefore, the intensity factor E_w/E, where E_w is the intensity of light leaving the wall at any point, and E is the average intensity of light leaving the light source, should be the same as T_w^4/T^4,

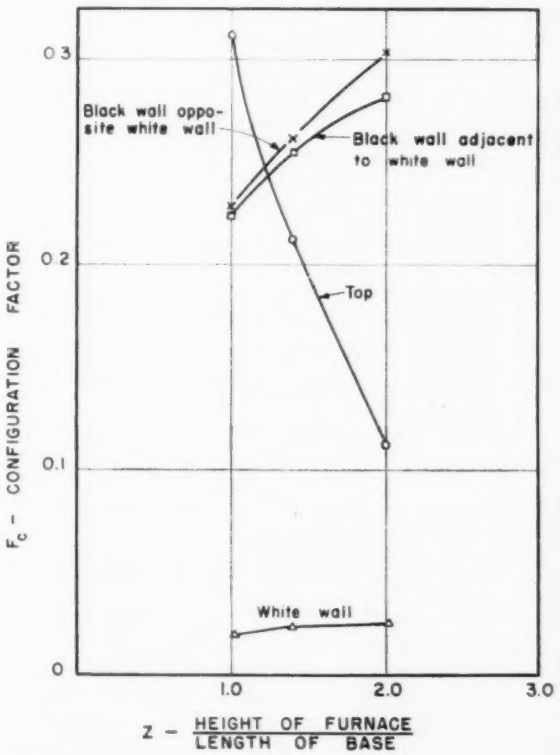


FIG. 16 CONFIGURATION FACTORS F_c, FOR DIRECTLY OPPOSED PARALLEL SURFACE WITH A TOTAL-ABSORBING TOP, THREE CONNECTING BLACK WALLS, REPRESENTING WATERWALLS, AND ONE CONNECTING WHITE WALL, REPRESENTING A REFRACTORY WALL, AND CONFIGURATION FACTORS FOR THE VARIOUS WALLS

where T_w is the absolute temperature of the furnace wall at any point, and T is the average absolute temperature of the base of the furnace.

Inspection of Figs. 14 and 15 makes it obvious that, for every different absorption coefficient, a different series of E_w/E or T_w^4/T^4 will be obtained on the wall. Thus, as the absorption coefficient becomes greater, the E_w/E becomes smaller, and the slope of the line decreases. Hottel and Keller[13] give a curve, derived for the radiation loss through a round hole in a furnace wall, assumed to be a nonconducting reradiating black body. Their curve falls just above the curve given in Fig. 13 for an absorption coefficient of 0.094. Their curve has a slope of —0.5, whereas, the curve cited from Fig. 13 has a slope of —0.6. If

[13] Reference 6, p. 46.

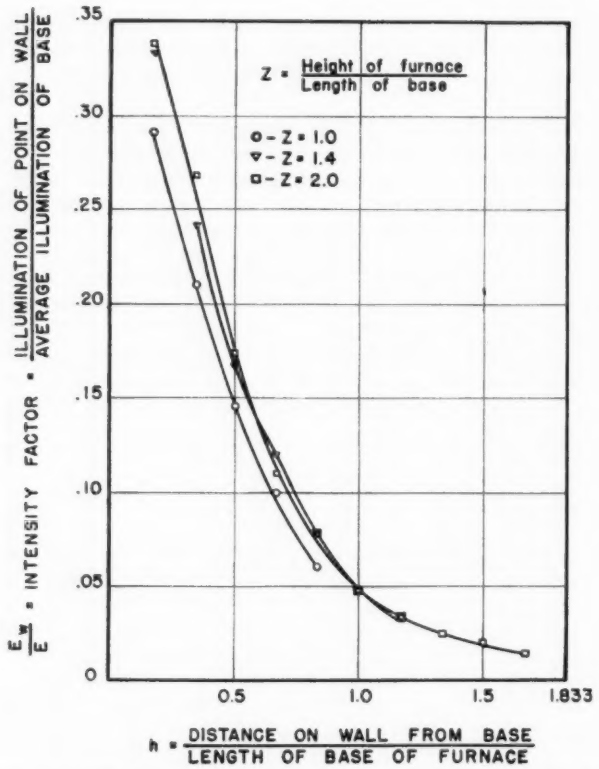


FIG. 17 RELATION OF INTENSITY FACTOR FOR WHITE WALL TO DISTANCE FROM BASE OF FURNACE WITH THREE BLACK WALLS AND ONE WHITE WALL

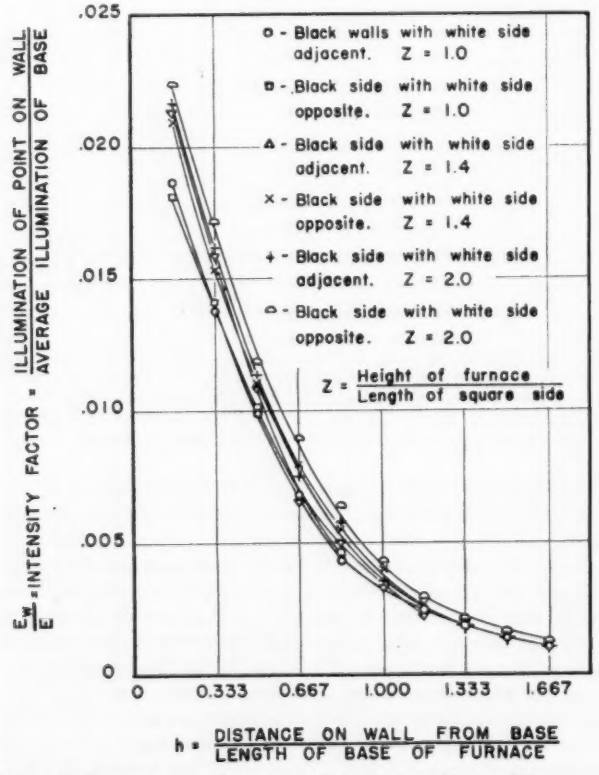


FIG. 18 RELATION OF INTENSITY FACTOR FOR BLACK WALLS TO DISTANCE FROM SQUARE BASE OF FURNACES WITH THREE BLACK WALLS AND ONE WHITE WALL

it were possible to use a flat paint which has an absorption coefficient of zero on the walls of model furnace No. 2, the other curves indicate that its slope would have a greater negative value than —0.6.

Model furnaces Nos. 2, 3, and 4, with three black walls and one white wall, represented furnaces with total-absorbing tubes on top, three completely exposed waterwall sides, and one refractory wall. Since the flat black paint on the walls absorbed 95 per cent of the light coming to them, the completely exposed tubes which they represent would probably be slagged up to such an extent as to reradiate 5 per cent of the energy coming to them. Since the flat white paint on the diffusely reflecting wall absorbs about 10 per cent of the light coming to it, the refractory wall which it represents would probably have some unexposed waterwall in it, or be not as thick as the usual furnace wall, so that more heat would be lost by conduction through the wall. The configuration factors were calculated for the white wall, for the black wall adjacent to the white wall, for the black wall opposite the white wall, and for the top of model furnaces 2, 3, and 4 in a manner identical with that described for the model furnace with total-absorbing top and partial-absorbing walls. These factors are plotted against Z (the ratio of the height of the furnace to the length of the base) in Fig. 16.

The intensity factors for the walls of each model furnace were also determined in the same manner as that described for the model furnace just mentioned. These are plotted against the ratio of the distance of the point from the base of the furnace to the length of the base of the furnace in Figs. 17 and 18. Since the intensity factor E_w/E for any point on the wall is equal to T_w^4/T^4 (the ratio of the absolute temperature for any point on the furnace wall to the average absolute temperature of the energy-emitting source), the temperature for any point on the wall of a furnace similar to one of the model furnaces can be found. Of course, this assumes that there is no heat transfer by convection or conduction to the wall. This also assumes that there is no radiation from luminous gases, nonluminous gases, or from particles of any kind. In most actual furnaces, these other heat-transfer agencies will be present, and each will have to be treated separately. However, in many actual cases, one of the means of heat transfer predominates to such an extent that the others may be allowed for or ignored without affecting the final result materially.

EFFECT OF RERADIATION

After the completion of the first portion of the experimental work, it was decided to determine, if possible, the reasons for the differences in the values for the configuration factors for a furnace with nonconducting reradiating walls, as determined experimentally, and as derived mathematically by Hottel and Keller. The experimental value for the configuration factor for this case was found to be unity, whereas the theoretical value as determined by Hottel and Keller, is 0.535. Since the walls of the furnace model are nonconducting and reradiating, no heat is absorbed by the furnace walls that is not emitted again; therefore the configuration factor for the walls of such a furnace must be zero. Since the sum of all configuration factors in a system must be equal to unity, it appears as though the experimental value is correct.

It was noticed during the experimental work that, in cases where a small portion of the light coming to the walls of the furnace model was absorbed, the amount of light given off by the bottom of the furnace was greater than that absorbed by the top and all of the sides. This difference resulted because part of the light which struck the walls of the furnace model was returned to the bottom of the furnace and was again given off by the bottom. Thus, the less absorbent the walls were, the brighter

was the light-emitting surface on the bottom of the furnace model. Therefore, the net amount of light given off by the bottom was the amount of light given off when no light was reflected back to the bottom, and the gross amount of light given off by the bottom was the amount given off when the furnace model had reflecting walls which reflected part of the light they received back to the bottom. It is seen that the amount of light absorbed by the sides and the top of the furnace model should be less than the gross amount of light given off from the bottom when all of the light received by the walls of the furnace model was not absorbed by them. Therefore, for furnaces with reradiating walls, it is necessary to include another term, the reradiation factor F_R, in the Stefan-Boltzmann equation

$$q = \sigma F_e F_c F_R A(T_1^4 - T_2^4) \quad [17]$$

The reradiation factor is the ratio of the net amount of energy given off by the energy-emitting surface to the gross amount of energy given off by this same surface.

Reradiation factors and configuration factors were determined in the following manner: Furnace model No. 2 was painted, and

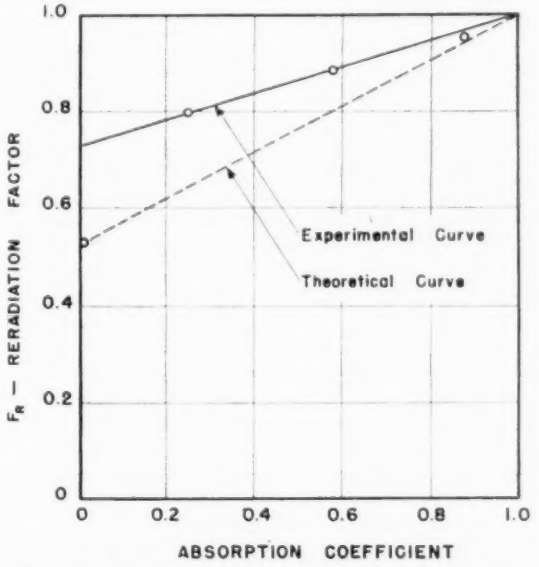


FIG. 19 RELATION OF RERADIATION FACTOR TO ABSORPTION COEFFICIENT OF WALLS OF A CUBICAL FURNACE WITH A TOTAL-ABSORBING TOP

the absorption coefficient of the paint was determined as previously described. Then the illumination was measured on the top and the sides of the furnace. From these data, the configuration factor for the top was calculated. The photoelectric cell was next turned face upward, and the amount of light coming back from the walls to the bottom of the furnace model was measured. Then the furnace model was removed, and the illumination was measured at the center of each of twenty-five equal areas at a distance of 2 in. from the light-emitting surface. All of these measurements were taken in the darkroom, and the light from the light source was maintained constant, as previously described. Thus, the net amount of light emitted by the light source was that measured in the absence of the reflecting walls, and the gross amount of light given off was the sum of that measured in the absence of the reflecting walls and that measured with the cell facing upward. This procedure was followed using gray paints with the following absorption coefficients: 0.247, 0.581, and 0.878. Fig. 19 is a graph on which the experimentally determined reradiation factors are plotted against the absorption coefficients of the paints used on the walls of the furnace model.

Reradiation factors were determined only for furnace model No. 2, since in the case of furnace model No. 1 the walls were total-absorbing and therefore did not reradiate. In the case of furnace models Nos. 2, 3, and 4, in which three walls were painted black and one wall was painted white, the reradiation factor would be close to unity since only one wall reflected light back to the source, i.e., the average absorption coefficient here would be about 0.75 and, from Fig. 19, the reradiation factor would be 0.93. However, the value of the reradiation factor might be expected to be somewhat greater than 0.93, since the light reflected from the white wall to the black walls would less likely be reflected back to the light source than in the case where all the walls had an average absorption coefficient of 0.75.

Hottel and Keller determined a total radiation factor which corresponds to the product of the configuration factor F_c and the reradiation factor F_R as used in this work. Their total radiation factor was the sum of a direct radiation factor and a reradiation factor. Their direct radiation factor is the configuration factor F_c determined for directly opposed parallel planes; their reradiation factor, which was determined mathematically, represents the increase in the configuration factor, due to the presence of nonconducting reradiating walls. The dotted line, in Fig. 19, is an extrapolation from Hottel's value of 0.535 for the total radiation factor for a cubical furnace with nonconducting reradiating walls. Thus, it is seen that the product of the configuration factor and the reradiation factor, as determined in this investigation, is about 35 per cent greater than the total radiation factor, as determined by Hottel and Keller.

Hottel and Keller state: "If the walls were perfectly reflecting (or absorb none of the radiation), the total radiation factor would be increased to unity for all openings, and the opening would be equivalent to a freely exposed diaphragm."[8] This statement is correct if the reflection is perfectly specular; however, this work shows that, with perfectly diffuse reflection, the total radiation factor would not be unity. Thus, with diffusely reflecting nonabsorbing walls, part of the radiation from the warmer (or brighter) surface is returned to it by the walls, thereby keeping it at a higher energy-emitting level than the cooler (or less bright) surface.

POSSIBLE SOURCES OF ERROR

It was assumed that the light from all parts of the constant light source was equal, however, the measurement of the intensities of light at a distance of 2 in. above the light source shows that the average intensity of light in the outer perimeter is about 3 per cent less than the over-all average intensity. However, this error is small and would have slight effect on furnaces, the sides of which are so close to the energy-emitting source that the intensity of light is independent of the distance from the source.

In the data for model furnace No. 1f, only six readings were taken to find the average illumination for the side of that furnace. These values might not represent the true-mean values if the light intensity varies with some function of the distance. However, since the light intensity at these points probably varies with some function considerably less than the square-of-distance function, the error here likely would be small.

In the experiments with model furnaces Nos. 2, 3, and 4, it was assumed that the reflection from the flat paints was perfectly diffuse. Barrows[14] has shown that for glossy surfaces specular reflection takes place, and for nonglossy and flat-painted surfaces perfectly diffuse reflection is approached. Thus, since the reflection from the flat paints was not perfectly diffuse, a certain amount of specular reflection took place. This specular reflection

[14] Reference 3, p. 11.

simulates the reflection which takes place from a non-black body, the emissivity e of which is less than 1. The diffusely reflected part of the light from the painted surfaces was probably about 90 per cent, which corresponds to an emissivity of 0.9 for the actual heat-transfer surfaces which the painted surfaces represent. No calculations for model furnaces Nos. 2, 3, and 4, were made for the variance of the illumination due to the effect of the angle of incident light on the photoelectric cell, because actual surfaces are known to vary also. Thus, it is thought that the configuration factors, given in Figs. 12, 13, and 16, approach the true values of those required in practice.

Conclusions

1 A new method was devised for determining configuration factors for radiation by the use of light energy instead of radiant heat.

2 Configuration factors for radiation between directly opposed parallel planes, Fig. 10, and for radiation between perpendicular adjacent planes, Fig. 11, have been determined and are found to conform fairly well with the theoretical values obtained by mathematical derivation.

3 Configuration factors have been determined for model furnaces with diffusely reflecting walls (reradiating walls). The data indicate that a furnace, with nonconducting reradiating black-body walls, would have a configuration factor for the top of the furnace of unity, Figs. 12 and 13.

4 Configuration factors have been determined for model furnaces having three black walls (waterwalls), one white wall (refractory wall), and a total-absorbing top (exposed tubes), Fig. 16.

5 Intensity factors have been found for the walls of model furnaces having various absorption coefficients, and for model furnaces having three black walls and one white wall, Figs. 14, 15, 17, and 18.

6 Another term F_R, the reradiation factor, has been inserted into the Stefan-Boltzmann equation, namely, Equation [17]. The reradiation factor corrects the Stefan-Boltzmann equation for discrepancies due to reradiation from the furnace walls to the energy source, Fig. 19.

Discussion

V. Paschkis.[15] The authors of this paper have developed a very interesting technique. It has, however, one difficulty in common with the mathematical analysis by H. C. Hottel, quoted by the authors, namely, the necessity of assuming a wall of nonconducting material.

This simplification will in some cases be undesirable. Therefore an electric-analogy method, previously published[16] might be of interest. In that method, the thermal conduction in the structures emitting and receiving heat can be duly considered. The method consists briefly in the breaking up of the total radiation in a number of radiation paths, each of which is represented by a resistor. The resistance of each element is so adjusted that it is true to the Stefan-Boltzmann law.

The geometry of small elements of the radiating areas is so simple that the radiation can easily be calculated for each element. Conduction in the radiating material is represented by additional fixed resistors.

---

[15] Research Associate, Department of Mechanical Engineering, Columbia University, New York, N. Y.

[16] "Elektrisches Modell zur Verfolgung von Wärmestrahlungsvorgaengen, insbesondere in elektrischen Oefen," by V. Paschkis, *Elektrotechnik und Maschinenbau*, vol. 54, 1936, no. 52.

Correlation of Coefficient of Friction With Drilling Torque and Thrust for Different Types of Cutting Fluids

By A. O. SCHMIDT,[1] W. W. GILBERT,[2] AND O. W. BOSTON[3]

The authors report results of a series of tests made to determine the lubricating effects of a wide variety of cutting fluids on the forces involved in drilling. The investigation was conducted in the metal processing laboratories of the University of Michigan. Torque and thrust, from which the coefficient of friction was obtained, were measured on a special lubrication dynamometer and recorded graphically. Brief specifications are given for the cutting fluids used. The technique for carrying out lubrication tests and the results obtained are discussed, as well as those for the drilling tests. A comprehensive series of graphs showing test results accompanies the paper, and clearly defined conclusions are drawn from the investigation.

IN ORDER to determine the lubricating effect of cutting fluids on the forces involved in drilling, a series of tests was conducted for the purpose of investigating this quality in cutting fluids of a wide variety of types. The coefficient of friction of these oils was obtained when they were operating under conditions of lubrication and seizure. Values of torque and thrust were recorded, as the load, applied to a special type of dynamometer, was periodically increased in uniform increments. The results of these friction tests are correlated with values of torque and thrust obtained from drilling tests in a manner to show how cutting fluids act and where they are most beneficial in actual metal cutting. Torque and thrust under cutting conditions were determined by drilling in such a way that their values could be determined for the drill point as a whole, the cutting edges, the margin, and the chisel-edge point, each independently.

The Lubrication Tests

Torque and thrust, from which the coefficient of friction was obtained, were measured on a special lubrication dynamometer. This friction device, shown in Fig. 1, was designed to simulate the sliding of a ductile chip over the face of a single-point tool cutting continuously. The torque and thrust were recorded graphically on a sheet mounted on a slide moving with the spindle. A typical graph is shown in Fig. 2. A test plate was held on the top of the dynamometer inside of a cup. The test plate, made of S.A.E. 2340 steel normalized and annealed, was surface-ground before each test in order to eliminate any previous seizure marks. It was submerged in the cutting fluid. Bearing on the plate were three high-speed-steel pins having a diameter of 0.125 in. at their rubbing ends. The area of contact of the pin-end rubbing surfaces was kept small in order that high unit pressures might be obtained. These pins were mounted axially in a body connected to the driving Morse-taper shank by means of a universal joint. They were spaced 120 deg apart on a circle having a radius of 1 in. In operation, the test pins were first run over a flat abrasive stone, and then on fine emery paper to insure their being flat and smooth. The spindle of the drill press was rotated at 225 rpm to give a rubbing speed of the lower ends of the pins on the upper ground face of the plate of 118 fpm, similar to normal metal-cutting speeds. Pressure was applied on the pins through the spindle of the drill press. The thrust was kept low enough at the start of the tests so that no seizure occurred. It was increased in steps until seizure was obtained, or until the capacity of the dynamometer was reached. The coefficient of friction was then computed as follows

$$\text{Coefficient of friction} = \frac{\text{Force of friction}}{\text{Normal force}} = \frac{12\ \text{Torque}}{r \times \text{Thrust}} = \frac{12\ \text{Torque}}{\text{Thrust}}$$

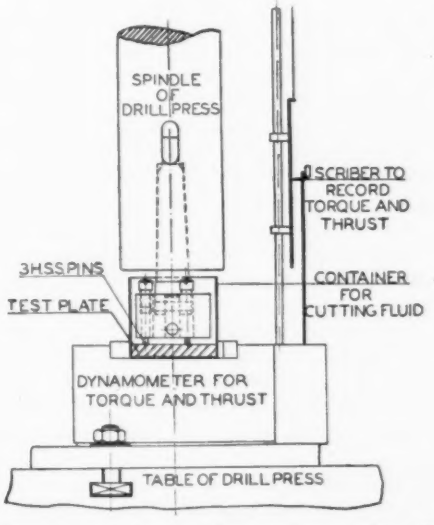


FIG. 1 TORQUE AND THRUST DYNAMOMETER WITH THREE-PIN FRICTION DEVICE AS SET UP ON A DRILL PRESS

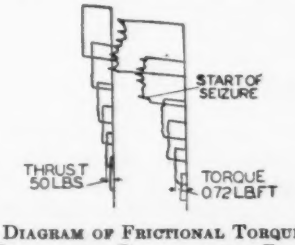


FIG. 2 TYPICAL DIAGRAM OF FRICTIONAL TORQUE AND THRUST AS MADE ON THE DYNAMOMETER, FIG. 1

[1] Assistant Professor of Mechanical Engineering, Colorado State College of Agriculture and Mechanic Arts, Fort Collins, Colo.

[2] Assistant Professor of Metal Processing, University of Michigan. Ann Arbor, Mich. Jun. A.S.M.E.

[3] Professor of Metal Processing, Chairman of Department, University of Michigan. Mem. A.S.M.E.

Contributed by the Special Research Committee on Cutting of Metals and presented at the Annual Meeting, New York, N. Y., December 1-5, 1941, of THE AMERICAN SOCIETY OF MECHANICAL ENGINEERS.

NOTE: Statements and opinions advanced in papers are to be understood as individual expressions of their authors and not those of the Society.

As r, the working radius of the rubbing pins, was 1 in., the torque is in pound-feet, and the thrust is in pounds. These results are then plotted against the thrust or load in pounds per square inch for analysis.

Cutting Fluids Used

Distilled water, two plain mineral oils, five sulphurized mineral-lard oils, and two emulsions containing sulphur were used, as follows:

Oil sample *A*	100 per cent Gulf coast pale mineral oil of 150 viscosity at 100 F, with 0.15 per cent natural sulphur
Oil sample *B*	100 per cent mid-continent mineral oil of 165 viscosity at 100 F, with 0.2 per cent natural sulphur
Oil sample *C*	96 per cent mineral oil, plus 1 per cent fatty oil and 3.5 per cent sulphur; viscosity 135 at 100 F
Oil sample *D*	95 per cent mineral oil, plus 0.5 per cent fatty oil and 3.6 per cent sulphur; viscosity 155 at 100 F
Oil sample *E*	45 per cent mineral oil, plus 47 per cent lard oil (sulphurized), and 7.7 per cent sulphur; viscosity 180 at 100 F
Oil sample *F*	77 per cent mineral oil, plus 19 per cent lard and tallow oils and 4 per cent sulphur; viscosity 130 at 100 F
Oil sample *G*	83 per cent mineral oil, plus 17 per cent lard and tallow oils and 1.33 per cent dissolved sulphur; viscosity 175 at 100 F
Emulsion 1:50	1 part sulphurized soluble oil to 50 parts water
Emulsion 1:10	1 part sulphurized soluble oil to 10 parts water

Results of Lubrication Tests

When light thrusts were applied there was no seizure. However, as the thrust was increased, seizure marks became visible on the test plate. In the case of dry cutting, or when using water or plain mineral oils, a further increase in thrust would induce seizure, and metal to a depth of 0.005 in. would actually be removed through the heavy rubbing action of the pins. The thrust or load in pounds as read from the chart, Fig. 2, was divided by the combined area of the three rubbing pins to give the applied pressure in pounds per square inch. The coefficient of friction is plotted over these pressures in Figs. 3 to 5, inclusive.

The range of seizure for a variety of the cutting fluids is indicated in Fig. 3. When seizure occurred, there was an appreciable increase in the coefficient of friction and a change in surface quality of the rubbing surfaces. The friction tests on the various types of cutting fluids of Fig. 3 proved that cutting dry, or with water, or mineral oil *A*, allowed seizure under relatively light pressures and caused actual metal removal with very high values of coefficient of friction. The compounded oil *E*, which is a sulphurized mineral oil plus a fatty oil, had a low coefficient of friction under both nonseizure and seizure conditions. When slight seizure occurred, this oil had a smoothing or nonwelding characteristic which prevented further seizure, and also any further increase in the coefficient of friction. The emulsions which contained a sulphurized soluble oil also exhibited these smoothing characteristics. There was only slight increase in coefficient of friction during the range of seizure. It was noticed that the emulsions formed a strong oil film on the plate where the pins were rubbing, which actually gave a decrease of the friction coefficient under pressures between 1500 and 7500 psi. The pressure at seizure was approximately 500 psi for dry cutting, 1200 to 1300 psi for water and mineral oil, 5000 to 6000 psi for the 1:50 emulsion, 8000 to 10,000 psi for the 1:10 emulsion, and 11,000 to 13,000 psi for the compounded sulphurized oil *E*.

The effect of sulphurizing the cutting oils is indicated in Fig. 4. The 3.5 per cent sulphur in mineral oil *C* gave a marked decrease in the coefficient of friction. The pins began to leave seizure marks on the plate at a pressure of about 5800 psi. Lower coefficients of friction were obtained with oil *D*, which contained 3.6 per cent sulphur where seizure marks became visible at 8750 psi.

The friction tests comparing the sulphurized and the sulphur-

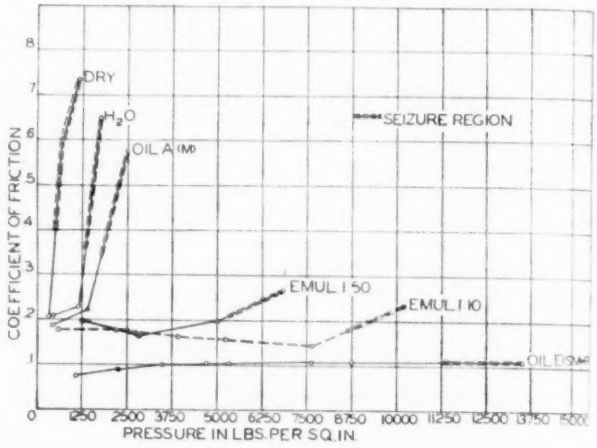


Fig. 3 Friction Tests of Various Fluids

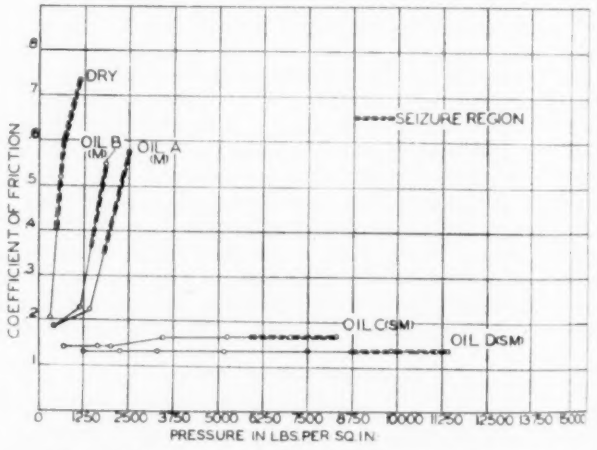


Fig. 4 Friction Tests, Showing Effect of Sulphur

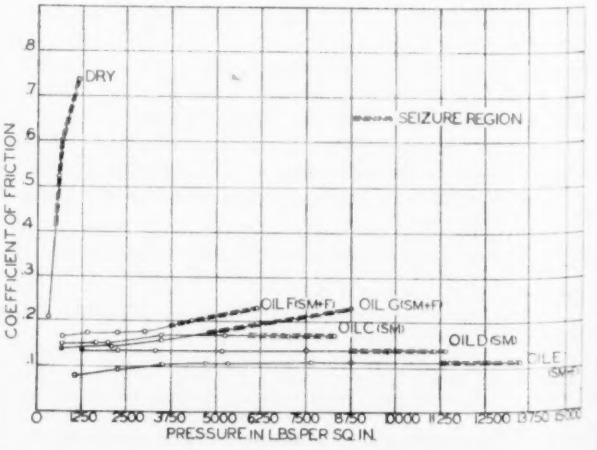


Fig. 5 Friction Tests, Comparing Sulphurized and Sulphurized Fatty Oils

ized fatty oils are reported in Fig. 5. All the oils, *C*, *D*, *E*, *F*, and *G*, gave a low coefficient of friction, but the lowest was obtained with oil *E* which had the highest sulphur content of 7.7 per cent, and a lard-oil content of 47 per cent. With oil *E*, pressures up to 11,000 psi left no seizure marks on the test plate, and even at 13,500 psi seizure marks were only 0.0005 in. deep. The other oils produced seizure marks varying in depth between 0.001 and 0.003 in.

The coefficient of friction divided by the pressure at the beginning of seizure gives a value representing the performance of the oils just prior to seizure. Fig. 6 brings out clearly the poor performance of the dry tests, the reduction of friction by water and pure mineral oils, and the very marked frictional decrease of the oils and emulsions which contain sulphur and lard oil.

Drilling Tests

To check the behavior of these different cutting fluids under actual cutting conditions, a series of drilling tests was carried out

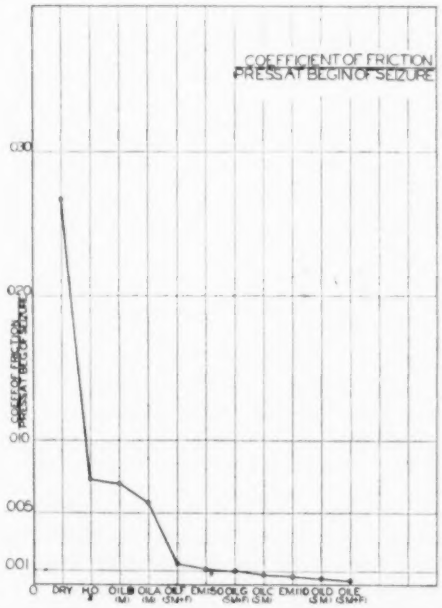


Fig. 6 Rating of Cutting Fluids in Friction Tests
(Values were obtained by dividing the coefficient of friction by the pressure in pounds per square inch at the beginning of seizure.)

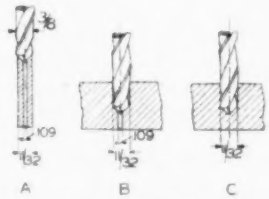


Fig. 7 Test Bars for Drill Tests

on a drill press. The procedure followed in the drilling tests was to use essentially the same test equipment, shown in Fig. 1, except that the friction pins and the test plate were replaced by a twist drill and screw stock, as shown in Fig. 7. The material drilled was S.A.E. 1120 cold-finished steel. The drills used were of high-speed steel having a helix angle of 28 deg 30 min, a point angle of 118 deg, chisel-edge angle of 120 deg, and a relief angle of 12 deg. These drills had a web thickness of 0.062 in., but it was necessary to use a pilot drill of 0.109 in. diam for conditions *A* and *B* of Fig. 7 to remove the effective working area of the chisel edge. The drill and work were completely flooded with cutting fluids during the tests. A preliminary test was made by varying the cutting speeds of the drill, and it was found that the cutting fluids were most effective at slow cutting speeds. Therefore the tests were run at 143 rpm or 13 fpm with feeds of 0.004 and 0.006 in. per revolution.

Fig. 7 shows how these tests were made. At *A* is shown the cylindrical test bar of $^{11}/_{32}$ in. diam with a pilot hole in the center.

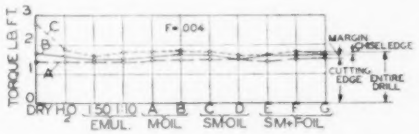


Fig. 8 Effect of Cutting Fluids on Drilling Torque
(Material, S.A.E. 1120 cold-finished steel; speed, 143 rpm; feed, 0.004 in. per revolution.)

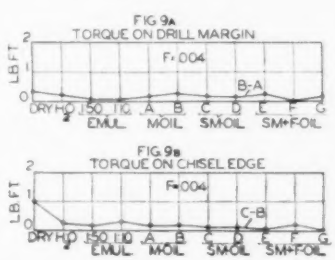


Fig. 9 Torque Caused by Friction on Drill at Feed of 0.004 In. per Revolution

When drilling the test bar with a $^{3}/_{8}$-in. drill, cutting was confined to the cutting edges. This eliminated the effect of the chisel-edge point and the margin of the drill. At *B*, the pilot hole was drilled in a test bar, and then a larger hole was cut of the same diameter ($^{11}/_{32}$ in.) as the test bar at *A*. This eliminated the forces on the chisel-edge point. The third cutting condition illustrated at *C* consisted of drilling a hole $^{11}/_{32}$ in. diam into the solid material, in which the whole drill was in action. By subtracting the test results of *A* from *B*, it was possible to show the frictional piloting action of the margin; by subtracting *B* from *C*, it was possible to isolate the action of the chisel-edge point.

These three zones may react differently under the influence of cutting fluids. The actual cutting edge on the lip of the drill is heavily stressed, and the chip pressures are so high that lubricants have but little effect. The margin on the drill, which is the cylindrical portion forming the outside diameter, actually does no cutting, but merely pilots the drill due to its rubbing on the side of the hole drilled. The bearing pressures are low when the drill is properly ground, but may become quite high if the drill operates off-center. The chisel edge acts as a blunt cutting edge with negative relief. The stress is so high that under normal conditions approximately 60 per cent of the thrust on the drill is localized at this point, and bearing pressures are very high.

Fig. 8 shows the effect of the various cutting fluids on the value of torque at a feed of 0.004 in. The graph for the whole drill, line *C*, shows that the torque was highest for dry cutting, that water and mineral oil reduced the torque somewhat, but that the emulsions and the sulphurized oils produced the lowest values. In test *B*, in which the effect of the chisel-edge point was eliminated, there was less friction and, therefore, less variation due to the cutting fluids. However, all the cutting fluids produced a decrease in torque. In test *A*, in which only the cutting edge of

the drill works, there was practically no difference between dry cutting and the cutting operations with cutting fluids.

In Fig. 9(*a*), only the amount of torque caused by friction on the margin is shown for the various cutting fluids; and in Fig. 9(*b*), only the amount of torque developed at the chisel edge is shown. The decrease in torque on the chisel edge, produced with the emulsions and oils, from that when drilling dry is very conspicuous.

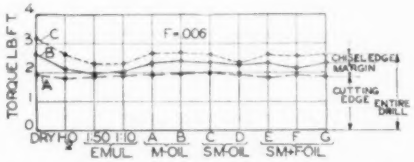


FIG. 10 EFFECT OF CUTTING FLUIDS ON DRILLING TORQUE AT 0.006 IN. PER REVOLUTION FEED

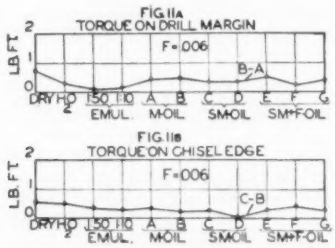


FIG. 11 TORQUE ON DRILL FOR VARIOUS CUTTING FLUIDS AT FEED OF 0.006

A graphical representation of the torque developed during the drilling tests with a feed of 0.006 in. per revolution is shown in Fig. 10. There is a pronounced variation in torque for the different fluids in test *C*, where the entire drill point is involved. Test *B*, in which the chisel edge is eliminated, also produces considerable variation, but test *A*, involving only the lips, shows very little variation.

The torque on the drill margin with a feed of 0.006 in. per revolution is shown for the various cutting fluids in Fig. 11(*a*). A decrease of torque is effected by the use of liquids as against dry cutting. The sulphurized emulsions give the lowest values. Fig. 11(*b*) shows values of torque on the chisel edge. That for dry cutting is highest, while the cutting liquids reduce the amount of torque slightly. Sulphurized mineral oil *D* gives the lowest value. The torque usually can be reduced 25 per cent by using an appropriate cutting fluid. This reduction takes place only at the margin and chisel edge as there is no appreciable reduction on the cutting edges themselves.

The effect of the cutting fluids on thrust is graphically represented in Fig. 12. With a feed of 0.004 in. per revolution, the thrust was highest when cutting dry. The sulphurized emulsions

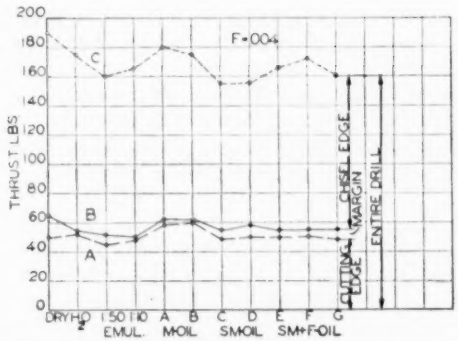


FIG. 12 EFFECT OF CUTTING FLUIDS ON DRILLING THRUST AT 0.004 IN. PER REVOLUTION FEED

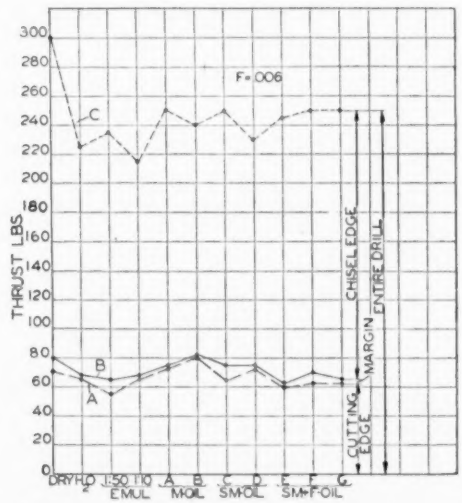


FIG. 13 EFFECT OF CUTTING FLUIDS ON DRILLING THRUST AT 0.006 IN. PER REVOLUTION FEED

and sulphurized mineral oils show the highest degree of reduction for the drill point as a whole. Water is even better than the oils. The thrust for condition *B* was highest for dry cutting, and slightly less for the plain mineral oils. The thrust for test *A*, involving only the cutting edges, shows much less variation for the cutting fluids because of less effect on the cutting edges. Most conspicuous are the values for the plain mineral oils, which in this case give values even higher than dry cutting. The chisel edge is shown to account for about 60 per cent of the total thrust. The sulphurized emulsions and oils effect the greatest reduction.

Fig. 13 shows the values of thrust from the drilling tests at a feed of 0.006 in. per revolution. For the entire drill, there is a decided decrease in thrust produced by all of the liquids, as com-

TABLE 1 RELATIVE VALUES AND DISTRIBUTION OF TORQUE, WHEN DRILLING 11/32-IN-DIAM HOLE INTO S.A.E. 1120 STEEL

	Feed 0.004 in. per revolution				Feed 0.006 in. per revolution			
	Dry	Emulsion 1:10	Mineral oil *B*	Sulphurized oil *G*	Dry	Emulsion 1:10	Mineral oil *B*	Sulphurized oil *G*
Entire drill	100	65	68	60	100	72	85	82
Cutting edge	50	50	52	52	62	60	63	58
Chisel edge	40	10	7	7	18	8	10	10
Margin	10	5	9	1	20	4	12	14

LE 2 RELATIVE VALUES AND DISTRIBUTION OF THRUST, WHEN DRILLING 11/32-IN-DIAM HOLE INTO S.A.E. 1120 STEEL

	Feed 0.004 in. per revolution				Feed 0.006 in. per revolution			
	Dry	Emulsion 1:10	Mineral oil *B*	Sulphurized oil *G*	Dry	Emulsion 1:10	Mineral oil *B*	Sulphurized oil *G*
Entire drill	100	88	92	85	100	67	80	84
Cutting edge	25	25	31	25	24	22	26	21
Chisel edge	67	61	60	56	73	44	53	62
Margin	8	2	1	4	3	1	1	1

pared to dry cutting. The most effective liquid, in this case, is the sulphurized emulsion of 1:10. In the tests involving only the cutting edges, there was very little difference between dry cutting and cutting with fluids. The cutting fluids had little effect upon the *B* tests, involving the cutting edges and margin. These graphs also show that the greatest proportion of the thrust is produced at the chisel edge.

Conclusions

1 The results of the friction tests show that under conditions of seizure, mineral oils and water produce approximately the same high coefficient of friction at relatively low pressures, and that considerable metal is displaced. When sulphurized oils are used under conditions of seizure, the coefficient of friction is greatly reduced, and there is very little metal displacement or seizure even at very high pressures. Emulsions containing active sulphur also reduce the coefficient of friction between the friction surfaces in the same manner as that produced by the sulphurized oils. Only at very high pressures was the sulphurized-oil film ruptured to permit metal-to-metal contact and seizure.

2 Cutting fluids, even those which possess high sulphur content, high antiseizure properties, and low coefficient of friction in the friction tests, will not decrease the cutting forces unless there is rubbing friction on noncutting surfaces where the antiseizure properties become effective.

3 When drilling a hole of $^{11}/_{32}$ in. diam into S.A.E. 1120 at a speed of 143 rpm, the relative values and distribution of torque are as given in Table 1, taking dry cutting as 100 per cent.

4 When drilling a hole of $^{11}/_{32}$ in. diam into S.A.E. 1120 at a speed of 143 rpm, the relative values and distribution of thrust are as given in Table 2, taking dry cutting as 100 per cent.

Acknowledgments

The lubrication dynamometer used in these tests was originally designed and made by Mr. Charles E. Kraus, a student assistant and later instructor in the department of metal processing, for experimental work to determine lubricating properties of cutting fluids. It has since that time been modified.

The work covered in this paper was done by Mr. A. O. Schmidt as a partial requirement for the degree of master of science in engineering (mechanical engineering) in the metal processing laboratories, under the supervision of Professors Gilbert and Boston.

Discussion

Hans Ernst.[4] This paper is of particular interest in that it represents a further attempt to correlate the results of tests in the field of friction with tests in the field of metal cutting.

In the friction tests (authors' Fig. 3), it is interesting to note the sharp rise toward high values for the coefficient of friction, under increase of load, in the case of the dry test and with water and plain mineral oil.

In an investigation of static friction made in the research laboratory of the Cincinnati Milling Machine Company, and reported in part in a paper[5] presented before the National Metals Congress in October, 1940, it was found that the coefficient of friction between extraordinarily clean surfaces of high-speed steel and S.A.E. 3145 at room temperature was approximately 1.0. With high-speed steel in contact with FM 18-8 stainless steel, the coefficient of friction was 0.92, while with S.A.E. 1112 it was 0.73. In view of these results and the theoretical analysis presented in the paper mentioned, it would seem likely that all of the curves of the authors' Fig. 3 would have reached limiting values in the neighborhood of 1.0, if the apparent pressures had been increased to sufficiently high values.

In stating that a rubbing speed for the pins of 118 fpm is "similar to normal metal-cutting speeds," the authors may have overlooked the fact that the rubbing speed of a chip on the face of a cutting tool is usually on the order of $^1/_3$ to $^1/_4$ of the speed of the tool relative to the work surface. Thus a chip rubbing speed of 118 fpm would normally correspond to a cutting speed of about 400 fpm, which is, in general, far too high for use with a high-speed-steel tool.

In view of the fact that the avowed purpose of this paper is the correlation of coefficient of friction with drilling torque and thrust, it is regrettable that the actual values of coefficient of friction were not calculated, where possible, from the data gathered in the torque and thrust tests. If this had been done, the small effect of the cutting fluids in reducing the coefficient of friction on the actual cutting edge of the drill would have been brought out even more clearly.

Referring to Fig. 14 of this discussion, which shows condition *A* of the authors' paper, it will be seen that the force perpendicular both to the cutting edge and to its path is

$$F_v = \frac{T}{2 \cos 31^\circ} = 0.584\ T$$

where T is the thrust on the drill. Making the approximation, mean torque radius (R_m) equals mean cutting radius, then

$$R_m = \frac{0.109 + 0.343}{4} = 0.113 \text{ in.}$$

and thus the cutting force F_c, perpendicular to the cutting edge and tangential to its path, is equal to

$$F_c = \frac{\text{Torque (in lb-ft)} \times 12}{2 \times 0.113} = 53.1 \times \text{torque}$$

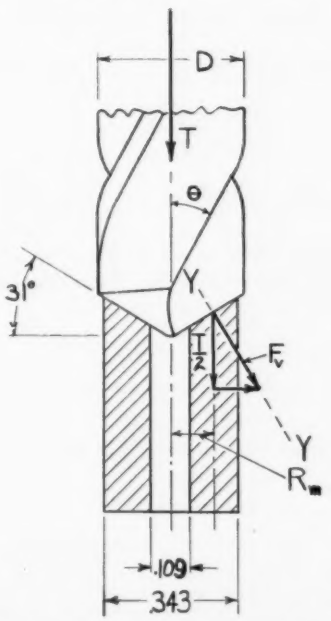


Fig. 14 Detail Showing Condition *A*, Fig. 7 of Authors' Paper

[4] Research Director, The Cincinnati Milling Machine Company, Cincinnati, Ohio. Mem. A.S.M.E.

[5] "Chip Formation, Friction, and High Quality Machined Surfaces," by H. Ernst and M. E. Merchant: "Symposium on Surface Treatment of Metals," American Society for Metals, Cleveland, Ohio, 1941, pp. 299–335.

As the mean true rake angle is very nearly equal to the true rake angle (α) at the mean cutting radius, then

$$\tan \alpha = \frac{2R_m \cdot \tan \theta}{D} \cdot \cos 31°$$

where θ is the helix angle of the drill, and D is the outside diameter.

For the dimensions given in Fig. 14, therefore

$$\tan \alpha = 0.281 \text{ and } \alpha = 15° 42'$$

From Fig. 15 of this discussion (which is a reproduction of Fig. 8 of the aforementioned paper,[5] and which may be considered as a cross section through the line Y-Y of Fig. 14), it will be seen that the previously determined forces F_v and F_c form mutually perpendicular components of the resultant force R between the tool point and the work which, for simplification, is used to replace the distributed load on the tool face. This resultant force R may also be resolved into the mutually perpendicular components F and N which are, respectively, the friction force acting along the face of the tool and the force normal thereto.

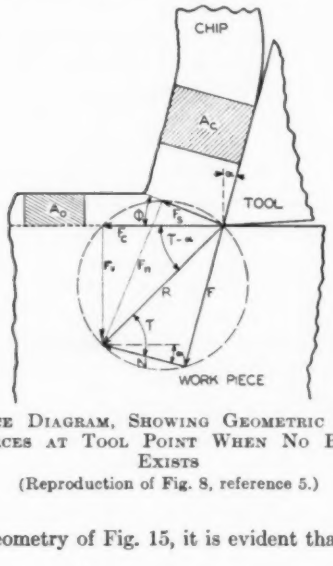


FIG. 15 FORCE DIAGRAM, SHOWING GEOMETRIC RELATIONSHIPS BETWEEN FORCES AT TOOL POINT WHEN NO BUILT-UP EDGE EXISTS
(Reproduction of Fig. 8, reference 5.)

From the geometry of Fig. 15, it is evident that

$$\frac{F_v}{F_c} = \tan (\tau - \alpha)$$

and that the coefficient of friction $= \mu = \frac{F}{N} = \tan \tau$

From the authors' data for condition A, when cutting dry at 0.004-in. feed, the thrust is 48 lb and the torque 1.4 lb-ft. From the relationships thus determined

$$F_v = 0.584 \times 48 = 28 \text{ lb}$$

and

$$F_c = 53.1 \times 1.4 = 74.3 \text{ lb}$$

$$\tan (\tau - \alpha) = \frac{28}{74.3} = 0.377$$

and

$$\tau - \alpha = 20° 40'$$

but

$$\alpha = 15° 42' \therefore \tau = 36° 22'$$

and

$$\tan \tau = \mu = 0.74$$

Similarly, for the worst case (mineral oil B), at 0.004-in. feed, where the thrust was 59 lb, and the torque 1.45 lb-ft, we find

$$\tan (\tau - \alpha) = 0.448$$

whence

$$\tau = 39° 50' \text{ and } \mu = 0.83$$

For the best case (1:50 emulsion) at 0.004-in. feed, the thrust was 45 lb, and the torque was 1.4 lb-ft. Consequently

$$\tan (\tau - \alpha) = 0.353$$

whence

$$\tau = 35° 09' \quad \text{and} \quad \mu = 0.70$$

It is interesting to note that the coefficient of friction with mineral oil B is even higher than for the case of dry cutting, where the "cutting fluid" is of course, air. This is not inconsistent with previous findings and may be due to the exclusion of air by the oil, thus preventing the formation of oxide or nitride films on the tool face and permitting even more intimate contact of chip and tool.

The fact that the coefficient of friction with even the "best" fluid was only slightly less than when cutting dry (0.70 as against 0.74, as contrasted with large differences found in the authors' friction tests) again indicates the extreme difficulty encountered by a cutting fluid in reaching the chip-tool interface. This should further dispose of the false idea, still widely held, that a crack normally precedes the nose of the cutting tool, thus permitting the cutting fluid to enter and form a wedge film against the tool face. Actually no such crack exists, and thus a substantial reduction of friction between chip and tool face can only be obtained by means of highly active fluids such as carbon tetrachloride which can, to some extent, penetrate the labyrinth of microscopic passageways separating the actual contact points of chip and tool, and react with the freshly ruptured chip material to form stable compounds of low shear strength. This is a mechanism quite remote from that of a lubricant in a common journal bearing, and thus it is evident that the term "cutting lubricant" (which is still often used in the shop) is a misnomer. Except for the questionable term "lubrication dynamometer," and the casual reference in the paragraph opposite Fig. 7, the authors have carefully and correctly refrained from associating the word "lubrication" with the reduction of friction between chip and tool through the use of cutting fluids.

H. L. MOIR.[6] There are one or two points which might be suggested to help make a better understanding of the friction curves of the paper, particularly those which have been run with the sulphurized oils. It would be well to determine the ratio of active to inactive sulphur in these oils, instead of simply presenting the total sulphur content. It is believed that this information will help to explain the long seizure region of oil *G* in Fig. 5, as compared with the relatively short seizure region of oil *E*. We have found generally that active sulphur has the apparent effect of prolonging the seizure region by alternately healing and seizing, while a combined sulphur has a twofold effect both of lowering friction and producing a region of new seizure considerably in excess of active sulphur at higher loads. It might be well to have some qualitative means of determining the effect of the different cutting fluids upon these seizure regions at the same load, or at different loads, by weighing the small pins to determine the loss of metal due to abrasion.

The writer would like to comment upon some remarks[7] made by C. G. Williams, concerning tipped tools from an oil man's standpoint. There seems to be considerable confusion existing

[6] Asst. Chief Products Engineer, Pure Oil Mechanical Laboratory, Winnetka, Ill.

[7] "Oil for Carbides," by C. G. Williams, *American Machinist*, vol. 85, 1941, p. 1124.

in the industry at present as regards the so-called "vulnerability" of tipped tools when used with a sulphurized oil as a cutting fluid. This situation is quite analogous to the confusion which existed in the minds of many for a long time regarding the lubrication of hypoid gears when they were introduced in large-scale production in 1937. Apparently, the year 1937 was to many the date of the invention of the hypoid gear, in spite of the fact that the petroleum industry had successfully been lubricating many other automobiles which were equipped with hypoid gears prior to that time.

It is easy to understand the confusion which exists in the mind of an oil salesman when he is contronted with a turret operation which may have, for example, four tools in the head. Two of these tools may be tipped tools, while the other two may be solid tools, e.g., a drill and a tap. It is obvious that the best cutting-oil recommendation for the tap and drill will be a sulphurized oil. However, if the recommendation to use nonsulphurized oils or coolants, because of the tipped tool, is followed, the cutting speed for all of the tools will be governed by the safe cutting speed for the solid tool. In this manner it is easy to see that all of the advantages which tipped tools have will be nullified if a restriction is based upon the operation of tools which do not cut efficiently with certain cutting fluids, for example, soluble oils. The writer believes that this situation should be clarified promptly since a solution would be of threefold benefit; namely, to the user of tools and cutting fluids, to the tool manufacturer, and to the oil manufacturer.

Authors' Closure

The comments of the various discussers are greatly appreciated. Mr. Ernst has shown that the coefficient of friction, calculated from the torque and thrust loads, is greatest for the mineral oil and smallest for the sulphurized mineral oil and the emulsion. As shown in Table 3 of this closure, the coefficient of friction, determined from the torque and thrust drilling tests, has a maximum variation from 0.67 for the 1:50 emulsion to 0.84 for the mineral oil. This variation is exceedingly small when compared with the computed coefficients of friction of from 0.1 to 0.2, obtained with the three-pin friction device operating under nonseizure loads, as shown in Figs 3, 4, and 5 of the paper. It is thus seen that metal cutting must be considered to be in the seizure region of dry cutting, and therefore the general conception of cutting fluids, acting as lubricants between the tool face and chip, must be changed. However, as pointed out in the conclusions, some of the cutting fluids are effective in reducing cutting forces when they act on noncutting surfaces such as the margin or chisel edge of the drill, or on the outside surface of a continuous chip formed by turning. In turning, there is little change in cutting force for various types of cutting fluids.

TABLE 3 COEFFICIENT OF FRICTION WHEN DRILL IS CUTTING ON CUTTING EDGES ONLY

	Coefficient-of-friction feed in I.P.R.	
Cutting Fluid	0.004	0.006
Dry	0.76	0.77
H_2O	0.80	0.77
1:50	0.71	0.67
1:10	0.74	0.74
A (M)	0.82	0.80
B (M)	0.84	0.84
C (SM)	0.81	0.72
D (SM)	0.73	0.79
E (SM + F)	0.76	0.72
F (SM + F)	0.72	0.70
G (SM + F)	0.71	0.72

Mr. Moir's suggestions that the tests be continued, and that quantitative results be obtained by weighing the loss of metal due to abrasion, are very timely. It is felt that these tests should be run under conditions of greater pressure so that actual metal would be abraded from the test plate even when the sulphurized oils are used.

C. G. Williams[7] has questioned the use of sulphurized oils as cutting fluids for cemented-carbide tools. This objection is heard from many different sources, and is discussed by Mr. Moir. General commercial practice as to the use of emulsions on carbide tools varies. When high cutting speeds are used, the chips may prevent the coolant from functioning continuously, and as a result the tool is alternately hot and cold and, therefore, becomes cracked or damaged. If the flow on the tool cannot be maintained uniformly, it is better to cut dry.

Mr. Lange stated that 80 per cent of the carbide-tipped tools on Warner and Swasey turret lathes are cooled with emulsions. At high speeds sulphurized oils cause too much smoke. Mr. Lucht also added that emulsions are preferred to cool carbide turning tools.

Characteristics of Centrally Supported Journal Bearings

By E. O. WATERS,[1] NEW HAVEN, CONN.

The primary purpose of the study reported in this paper is to determine the load capacity and friction of journal bearings having arcs of contact of 80 to 120 deg, eccentricity ratios ranging from zero to unity, length-width ratios ranging from zero to infinity, and central support. Essentially, it is a continuation of the work published by Needs,[2] which covered the range of eccentricities from 0 to 0.8, but with two important differences, i.e., (1) the results have been obtained by mathematical, rather than experimental, solution of the Reynolds equation for two-dimensional viscous flow in a thin channel; (2) the matter of negative pressures has been dealt with in the manner advocated by Swift.[3] In other respects, the treatment of the fundamental variables is akin to that which is found in the majority of journal-bearing- and fluid-film-lubrication papers, published by the Society, e.g., the journal radius, journal velocity, mean clearance, eccentricity ratio, and oil viscosity are assumed constant for any given bearing, and the oil channel is of rectangular plan form.

Nomenclature

THE following nomenclature, in addition to other notations,[4] is used in this paper:

B' = angle between line joining centers of bearing and journal (line of centers) and trailing edge of extended bearing
F_0 = friction force per unit width of bearing, in an infinite-width bearing
m_n = characteristic number in solution of homogeneous form of Reynolds equation, associated with the nth order solution
$\bar{p}$ = pressure per unit of bearing area, averaged over the bearing width
p_s = pressure per unit of bearing area in a bearing of infinite width
Q_A = volumetric flow of oil into bearing at entering edge, per unit of time
Q_B = volumetric flow of oil out of bearing at trailing edge, per unit of time
Q_s = volumetric flow of oil out of bearing at one side, per unit of time
q = pressure drop per unit of bearing area, due to side leakage in a finite-width bearing
$\bar{q}$ = pressure drop per unit of bearing area, due to side leakage, averaged over the bearing width
r = ratio of bearing length to bearing width, in a terminal or preterminal bearing
r' = ratio of bearing length to bearing width, in an extended bearing
W_0 = load capacity per unit width of bearing, for an infinite-width bearing
z = co-ordinate of oil channel, perpendicular to x and parallel to axis of journal
β' = arc length of extended bearing
ϵ = arc increment of extended bearing; $\epsilon = \beta' - \beta$
ξ = modified angular co-ordinate of bearing, advancing from 0 at entering edge to π radians at trailing edge; $\xi = (\theta - A)\pi/\beta$

Introduction

If a bearing is specified by giving arbitrary values to the variables, journal radius, journal velocity, mean clearance, eccentricity ratio, and oil viscosity, it is possible to compute the local pressure at any point by direct solution of the Reynolds equation. Then, as a second step, the total capacity, coefficient of friction, and the direction of the resultant load line can be directly obtained by integration. However, if the direction of the load line is specified, with respect to the entering and leaving angles, while these angles themselves are unknown, it does not appear feasible to make a direct computation of the load capacity. This is certainly the case for infinite-width bearings, the properties of which are now well known, and is therefore all the more true when the bearing width is finite. Accordingly, the method adopted in this paper has been to find the properties of a field of bearings having specified entering and leaving angles, to compute the capacity and load-line direction of each, and then, by interpolation, to find the properties of those bearings whose arcs of contact are 80, 100, and 120 deg, and whose load lines come midway between the angle of entrance and the angle of exit. The chief disadvantage of this method is that a large number of individual cases must be computed, but this is balanced by the fact that, from the original cases, it is possible to make interpolation not only for centrally supported, but for offset bearings as well.

General Computation of Load Capacity, Friction, and Oil Flow of Partial Bearings

Calculations have been completed on 108 different bearings, having eccentricity ratios, entering and leaving angles, and length-width ratios as specified in Table 1. These are referred to in subsequent portions of the paper as "fundamental" bearings. The pressure distribution in each bearing has been computed by the method previously described by the author[5] and need not be repeated here. Briefly, this method employs, instead of the actual pressure p, a pressure function, equal to p multiplied by an arbitrary power of h, which can be developed in a convergent trigonometric series from $\theta = A$ to $\theta = B$.[4] Such a development

[1] Associate Professor, Mechanical Engineering, Mason Laboratory, Yale University. Mem. A.S.M.E.

[2] "Effects of Side Leakage in 120-Degree Centrally Supported Journal Bearings," by S. J. Needs, Trans. A.S.M.E., vol. 56, 1934, pp. 721–732.

[3] "The Stability of Lubricating Films in Journal Bearings," by H. E. Swift, Proceedings of The Institution of Civil Engineers, vol. 233, 1931-1932, pp. 267–322.

[4] Besides the symbols peculiar to this paper, the notations used correspond as far as possible to those used by Kingsbury, Howarth, and Needs in previous papers published by this Society.

Contributed by the Special Research Committee on Lubrication and presented at the Annual Meeting, New York, N. Y., December 1–5, 1941, of The American Society of Mechanical Engineers.

Note: Statements and opinions advanced in papers are to be understood as individual expressions of their authors and not those of the Society.

[5] "Theoretical Pressure Distribution in Journal Bearings," by E. O. Waters, Proceedings of the Fifth International Congress for Applied Mechanics, John Wiley & Sons, Inc., New York, N. Y., 1939.

TABLE 1 PROPERTIES OF FUNDAMENTAL BEARINGS

e	β, deg.	A, deg.	B, deg.	r	d/β	$W/\frac{\mu U a^2}{h^2}$	$F/\frac{\mu U a}{h}$	Volumetric Flow $\frac{U a h}{2}$ at A	at B	c sides	error, %	Side leakage factors W/W_o	F/F_o	$\lambda/\frac{h}{a}$
0.6	80	90	170	0	.5693	1.9326	2.7409	.2626 w/a	.2626 w/a	.0000	0.0	1.0000	1.0000	1.4182
				1	.5749	.9144	2.5254	.5491	.3249	.1947	5.7	.4731	.9214	2.7618
				2	.5746	.3883	2.4158	.3144	.1523	.1412	7.1	.2009	.8814	6.2215
				3	.5867	.2065	2.3771	.2198	.0988	.1113	4.6	.1069	.8673	11.5114
				4	.5902	.1241	2.3601	.1634	.0731	.0880	4.5	.0642	.8611	19.0177
0.6	80	110	190	0	.5186	1.9944	3.0954	.2302 w/a	.2302 w/a	.0000	0.0	1.0000	1.0000	1.5520
				1	.5019	.9060	2.9450	.4427	.3002	.1149	6.6	.4543	.9514	3.2506
				2	.4770	.3746	2.8691	.2488	.1447	.0878	7.0	.1378	.9269	7.6991
				3	.4582	.1883	2.8408	.1737	.0988	.0667	4.9	.0944	.9178	15.0866
				4	.4462	.1109	2.8285	.1333	.0715	.0531	7.0	.0556	.9138	25.5050
0.6	80	130	210	0	.3491	.9102	3.2089	.2195 w/a	.2195 w/a	.0000	0.0	1.0000	1.0000	3.5254
				1	.2531	.4222	3.1691	.3625	.3149	.0388	2.5	.4639	.9876	7.5062
				2	.1327	.1898	3.1424	.1944	.1593	.0307	2.2	.2085	.9793	16.5562
				3	.0485	.1017	3.1282	.1344	.1077	.0238	2.1	.1117	.9749	30.7594
				4	-.0020	.0625	3.1206	.1028	.0816	.0191	2.0	.0686	.9725	49.9301
0.6	100	80	180	0	.5753	3.1998	3.5672	.2512 w/a	.2512 w/a	.0000	0.0	1.0000	1.0000	1.1148
				1	.5773	1.6428	3.2653	.6931	.3975	.3137	2.6	.5134	.9154	1.9877
				2	.5804	.7686	3.0881	.4139	.1864	.2501	5.5	.2402	.8657	4.0178
				3	.5827	.4102	3.0158	.2951	.1208	.1932	6.4	.1282	.8454	7.3519
				4	.5841	.2486	2.9834	.2283	.0893	.1543	6.7	.0777	.8363	12.0008
0.6	100	90	190	0	.5482	3.1788	3.7503	.2381 w/a	.2381 w/a	.0000	0.0	1.0000	1.0000	1.1798
				1	.5419	1.6222	3.4857	.6353	.3868	.2417	1.1	.5103	.9294	2.1487
				2	.5324	.7333	3.3326	.3752	.1841	.1923	0.3	.2307	.8886	4.5447
				3	.5240	.3822	3.2709	.2671	.1205	.1459	0.2	.1202	.8722	8.5580
				4	.5188	.2296	3.2433	.2066	.0898	.1187	1.0	.0719	.8648	14.1375
0.6	100	100	200	0	.5055	2.8812	3.8561	.2308 w/a	.2308 w/a	.0000	0.0	1.0000	1.0000	1.3384
				1	.4862	1.4289	3.6557	.5809	.3875	.1747	3.3	.4959	.9480	2.5584
				2	.4607	.6850	3.5385	.3369	.1882	.1393	2.9	.2169	.9176	5.6616
				3	.4233	.3195	3.4897	.2391	.1250	.1079	2.7	.1109	.9050	10.9224
				4	.4042	.1838	3.4672	.1849	.0939	.0863	2.6	.0695	.8991	18.3645
0.6	120	70	190	0	.5740	4.3020	4.3670	.2441 w/a	.2441 w/a	.0000	0.0	1.0000	1.0000	1.0151
				1	.5690	2.2271	3.9628	.8714	.4722	.3858	1.9	.5177	.9074	1.7794
				2	.5739	1.0089	3.7172	.5333	.2233	.3046	1.0	.2345	.8512	3.6845
				3	.5733	.5316	3.6232	.3825	.1455	.2344	0.7	.1236	.8297	6.8157
				4	.5704	.3191	3.5816	.2966	.1081	.1869	0.5	.0742	.8202	11.2241
0.6	120	80	200	0	.5377	4.1358	4.5015	.2367 w/a	.2367 w/a	.0000	0.0	1.0000	1.0000	1.0884
				1	.5271	2.1358	4.1649	.7993	.4735	.3091	2.1	.5165	.9252	1.9500
				2	.5104	.9669	3.9630	.4835	.2279	.2467	2.1	.2338	.8804	4.0987
				3	.4942	.5066	3.8906	.3476	.1504	.1939	0.9	.1225	.8621	7.6601
				4	.4823	.2997	3.8418	.2702	.1127	.1557	0.7	.0725	.8535	12.8187
0.6	120	90	210	0	.4833	3.5838	4.5676	.2333 w/a	.2333 w/a	.0000	0.0	1.0000	1.0000	1.2745
				1	.4614	1.8596	4.3215	.7312	.4936	.2321	0.75	.5189	.9461	2.3239
				2	.4085	.8640	4.1638	.4352	.2385	.1898	1.62	.2355	.9116	4.9354
				3	.3671	.4383	4.0923	.3130	.1600	.1486	1.37	.1223	.8959	9.3366
				4	.3180	.2751	4.0627	.2436	.1211	.1188	1.55	.0768	.8895	14.7670
0.8	80	90	170	0	.6356	5.348	4.6587	.1477 w/a	.1477 w/a	.0000	0.0	1.0000	1.0000	.8711
				1	.6181	2.875	4.9181	.1694	.1802	.2519	8.6	.5376	.8625	1.3976
				2	.6657	1.403	3.6436	.2975	.0830	.1962	6.6	.2624	.7821	2.5970
				3	.6781	.7767	3.4894	.2143	.0530	.1492	6.0	.1452	.7490	4.4926
*				4	.6863	.4835	3.4191	.1661	.0388	.1182	5.8	.0904	.7339	7.0716
0.8	80	110	190	0	.5720	7.350	5.8178	.1295 w/a	.1295 w/a	.0000	0.0	1.0000	1.0000	.7915
				1	.5655	3.960	5.2739	.3280	.1535	.1600	4.6	.5388	.9065	1.3318
				2	.5553	1.867	4.9330	.2070	.1211	.0761	5.0	.2540	.8479	2.6422
				3	.5462	.9876	4.7856	.1510	.0950	.0498	4.3	.1344	.8226	4.6857
*				4	.5389	.5920	4.7176	.1180	.0764	.0373	3.9	.0805	.8109	7.9690
0.8	80	130	210	0	.3126	3.719	6.0527	.1235 w/a	.1235 w/a	.0000	0.0	1.0000	1.0000	1.6275
				1	.2591	2.097	5.8344	.2377	.1835	.0455	3.8	.5638	.9639	2.7822
				2	.1590	1.020	5.6713	.1387	.0952	.0398	2.8	.2742	.9370	5.5601
				3	.0906	.5576	5.5756	.1002	.0657	.0320	2.6	.1409	.9212	9.9993
*				4	.0507	.3487	5.5245	.0783	.0505	.0260	2.4	.0938	.9127	15.8431
0.8	100	80	180	0	.6488	8.532	6.2904	.1317 w/a	.1317 w/a	.0000	0.0	1.0000	1.0000	.7373
				1	.6572	4.841	5.4175	.6076	.2088	.3623	6.4	.5674	.8612	1.1191
				2	.6753	2.524	4.8689	.4048	.0971	.3006	1.8	.2958	.7740	1.9290
				3	.6861	1.433	4.6255	.2972	.0622	.2225	4.4	.1680	.7353	3.2278
				4	.6927	.9016	4.5112	.2322	.0456	.1786	3.5	.1057	.7171	5.0035
0.8	100	90	190	0	.6125	9.522	6.8509	.1226 w/a	.1226 w/a	.0000	0.0	1.0000	1.0000	.7195
				1	.6136	5.472	6.0680	.5205	.2045	.2834	6.7	.5747	.8857	1.1089
				2	.6148	2.754	5.5452	.3476	.0968	.2353	4.7	.2892	.8094	2.0135
				3	.6134	1.514	5.3095	.2573	.0629	.1840	4.2	.1590	.7750	3.5069
				4	.6110	.9266	5.1982	.2022	.0467	.1477	4.0	.0973	.7588	5.6100
0.8	100	100	200	0	.5455	8.964	7.1377	.1202 w/a	.1202 w/a	.0000	0.0	1.0000	1.0000	.7963
				1	.5268	5.059	6.5263	.4478	.2131	.2086	6.2	.5644	.9143	1.2900
				2	.5049	2.505	6.0910	.2936	.1039	.1769	4.6	.2795	.8534	2.4315
				3	.4782	1.333	5.8814	.2186	.0692	.1409	4.0	.1487	.8260	4.4121
				4	.4492	.7787	5.7764	.1726	.0522	.1136	4.1	.0869	.8093	7.4180
0.8	120	70	190	0	.6451	11.124	7.7235	.1240 w/a	.1240 w/a	.0000	0.0	1.0000	1.0000	.6943
				1	.6512	6.760	6.7545	.7600	.2484	.4835	3.7	.6076	.8745	.9958
				2	.6581	3.662	6.0823	.5275	.1177	.3995	2.0	.3291	.7875	1.6609
				3	.6609	2.102	5.7564	.3933	.0762	.3116	1.4	.1889	.7453	2.7385
				4	.6605	1.315	5.5961	.3092	.0563	.2492	1.2	.1181	.7246	4.2556
0.8	120	80	200	0	.5887	10.986	8.0902	.1217 w/a	.1217 w/a	.0000	0.0	1.0000	1.0000	.7405
				1	.5812	6.534	7.2656	.6580	.2582	.3769	3.6	.5980	.8981	1.1120
				2	.5688	3.420	6.6686	.4650	.1252	.3199	2.2	.3130	.8243	1.9499
				3	.5521	1.890	6.3687	.3429	.0828	.2541	1.8	.1730	.7872	3.3697
				4	.5354	1.150	6.2175	.2715	.0623	.2050	1.6	.1053	.7685	5.4065
0.8	120	90	210	0	.4994	9.366	8.2983	.1224 w/a	.1224 w/a	.0000	0.0	1.0000	1.0000	.8660
				1	.4731	5.596	7.6471	.5719	.2772	.2764	3.3	.5975	.9215	1.3665
				2	.4268	2.856	7.1360	.3883	.1397	.2408	2.0	.3049	.8599	2.4986
				3	.3805	1.581	6.8625	.2947	.0953	.1948	1.6	.1686	.8270	4.3406
				4	.3407	.9671	6.7129	.2349	.0732	.1584	1.4	.1033	.8089	6.9412

TABLE 1 PROPERTIES OF FUNDAMENTAL BEARINGS (*continued*)

c	β, deg.	A, deg.	B, deg.	r	d/β	W/(μUa²/h²)	F/(μUa/h)	Volumetric Flow U a h_c / A	at B	2 sides	error, %	Side leakage factors W/W₀	F/F₀	λ/λ_c
0.9	80	90	170	0	.6961	11.076	7.3116	.0841 w/a	.0841 w/a	.0000	0.0	1.0000	1.0000	.6601
				1	.7096	6.668	6.1453	.3820	.1062	.2782	0.6	.6020	.8405	.9216
				2	.7490	3.897	5.3798	.2734	.0491	.2216	1.0	.3518	.7358	1.3805
				3	.7687	2.859	5.0107	.2028	.0310	.1690	1.4	.2040	.6853	2.2181
				4	.7604	1.491	4.8279	.1598	.0225	.1338	2.3	.1346	.6603	3.2380
0.9	80	100	180	0	.6834	16.907	9.2377	.0662 w/a	.0662 w/a	.0000	0.0	1.0000	1.0000	.5464
				1	.6961	10.504	7.9285	.3025	.0849	.2153	0.8	.6213	.8583	.7548
				2	.7217	5.856	6.9811	.2178	.0396	.1765	0.8	.3464	.7557	1.1921
				3	.7236	3.509	6.5771	.1651	.0253	.1374	1.4	.2075	.7120	1.8743
				4	.7310	2.271	6.3576	.1309	.0185	.1101	1.8	.1343	.6882	2.7995
0.9	80	110	190	0	.6256	19.638	10.1422	.0609 w/a	.0609 w/a	.0000	0.0	1.0000	1.0000	.5317
				1	.6500	12.202	9.2680	.2315	.0800	.1529	0.6	.6213	.8876	.7596
				2	.6288	6.585	8.4253	.1680	.0384	.1305	0.5	.3353	.8068	1.2795
				3	.6249	3.730	8.0005	.1292	.0251	.1046	0.1	.1899	.7662	2.1449
				4	.6247	2.349	7.7881	.1035	.0187	.0841	0.7	.1196	.7458	3.3155
0.9	100	80	180	0	.7180	19.020	10.3797	.0667 w/a	.0667 w/a	.0000	0.0	1.0000	1.0000	.5466
				1	.7295	11.696	8.7362	.5362	.1076	.4274	0.2	.6149	.8417	.7469
				2	.7549	7.166	7.6727	.3910	.0504	.3386	0.5	.3768	.7392	1.0707
				3	.7684	4.488	7.1290	.2920	.0322	.2573	0.9	.2360	.6968	1.5885
				4	.7770	3.007	6.8482	.2292	.0235	.2029	1.2	.1574	.6598	2.2774
0.9	100	90	190	0	.6717	22.500	11.7719	.0614 w/a	.0614 w/a	.0000	0.0	1.0000	1.0000	.5232
				1	.6770	14.530	10.3251	.4097	.1013	.3141	1.4	.6458	.8771	.7106
				2	.6819	8.395	9.2481	.3101	.0484	.2684	2.2	.3731	.7856	1.1016
				3	.6823	5.021	8.6819	.2393	.0316	.2151	3.1	.2232	.7375	1.7291
				4	.6798	3.198	8.3837	.1912	.0235	.1746	3.6	.1425	.7122	2.6216
0.9	100	100	200	0	.5711	20.208	12.5272	.0617 w/a	.0617 w/a	.0000	0.0	1.0000	1.0000	.6159
				1	.5604	12.998	11.3649	.3191	.1074	.2232	3.6	.6432	.9072	.8744
				2	.5408	7.303	10.4261	.2413	.0540	.1976	4.3	.3614	.8323	1.4277
				3	.5145	4.185	9.8865	.1905	.0368	.1620	4.4	.2071	.7894	2.3631
				4	.4897	2.603	9.5934	.1549	.0283	.1338	4.6	.1288	.7658	3.6855
0.9	120	50	170	0	.7468	13.812	9.0824	.0856 w/a	.0856 w/a	.0000	0.0	1.0000	1.0000	.6576
				1	.7662	10.118	7.8507	.8812	.1713	.8085	11.2	.7326	.8643	.7754
				2	.7836	7.209	6.9520	.6539	.0816	.6537	12.4	.5219	.7654	.9644
				3	.8140	4.997	6.2490	.4852	.0520	.4837	10.4	.3618	.6880	1.2505
				4	.8278	3.642	5.8826	.3766	.0376	.3469	12.2	.2637	.6477	1.6152
0.9	120	60	180	0	.7445	20.448	11.2955	.0670 w/a	.0670 w/a	.0000	0.0	1.0000	1.0000	.5524
				1	.7678	14.331	9.6166	.7292	.1496	.6384	8.1	.7008	.8514	.6710
				2	.8002	9.691	8.3753	.5526	.0796	.5275	9.7	.4740	.7415	.8642
				3	.8307	7.024	7.7005	.4193	.0540	.4115	11.0	.3435	.6817	1.0963
				4	.8568	5.511	7.3360	.3504	.0413	.3288	12.0	.2695	.6495	1.3311
0.9	120	70	190	0	.7116	24.222	12.6868	.0616 w/a	.0616 w/a	.0000	0.0	1.0000	1.0000	.5238
				1	.7149	16.474	11.1886	.6574	.1218	.5121	3.7	.6801	.8319	.6792
				2	.7199	10.081	9.9560	.5086	.0581	.4294	4.3	.4141	.7848	.9025
				3	.7188	6.151	9.2627	.4010	.0375	.3365	7.2	.2539	.7301	1.5059
				4	.7206	4.069	8.8740	.3102	.0280	.2677	4.9	.1680	.6999	2.1321

is desirable for fitting the boundary conditions of the particular solution of Reynolds equation (infinite-width case) to the boundary conditions of the homogeneous form of the equation, and overcomes the stumbling block encountered by Reynolds, who tried unsuccessfully to express the pressure in trigonometric series form for high eccentricity ratios. Once this pressure function has been evaluated, the remaining data (capacity, attitude, etc.) can be found by simple quadratures, which may be performed by the available formulas of integral calculus or by Simpson's rule, whichever is more convenient.

The Appendix contains an outline of the computations for a specimen bearing, for the benefit of those who wish to examine the application of this method in detail. Attention is called to Fig. 8, in this Appendix, in which $\bar{p}\Big/\frac{\mu Ua}{\eta^2}$, the factor of mean pressure with respect to bearing width, is plotted against the bearing angle θ and the modified bearing angle ξ, for length-width ratios $r = 0, 1, 2, 3, 4$, $A = 70$ deg, $B = 190$ deg, and $c = 0.8$; compare the curve for $r = 0$ with the dotted curve, which is proportional to the mean-pressure function $\bar{p}h^2/\eta$ for the same value of r, and note the absence of prominent harmonics in the latter.

The final results which were obtained for these 108 bearings are assembled in Table 1, and represent the bulk of the arithmetical work. From the side-leakage factors in this table, graphical interpolations were made, from which Table 2 was constructed. The material in Table 2 affords a direct comparison with Needs's results for $c = 0.6$ and 0.8, $\beta = 120$ deg, $\alpha = 60$ deg, and may be used as a basis for determining bearing performance on the assumption that theoretical negative pressures may be neglected.

The values of oil flow in Table 1 furnish a convenient index of the accuracy of the boundary-value solutions obtained for the homogeneous form of Reynolds equation. Where the discrepancy between computed inflow and outflow is fairly large, it is believed that the error may be ascribed to two causes, i.e.

TABLE 2 SIDE-LEAKAGE FACTORS FOR CENTRALLY SUPPORTED BEARINGS, NEGLECTING NEGATIVE PRESSURES

c	β deg.	A deg.	B deg.	r	Side leakage factors: Load	Friction
0.6	80	114.0	194.0	0	1.000	1.000
		110.2	190.2	1	.464	.952
		106.7	186.7	2	.188	.919
		105.2	185.2	3	.095	.905
		104.1	184.1	4	.056	.898
0.6	100	101.1	201.1	0	1.000	1.000
		97.7	197.7	1	.500	.943
		94.3	194.3	2	.226	.901
		92.7	192.7	3	.119	.881
		91.7	191.7	4	.070	.871
0.6	120	87.3	207.3	0	1.000	1.000
		84.0	204.0	1	.515	.933
		81.1	201.1	2	.235	.884
		79.4	199.4	3	.122	.861
		78.4	198.4	4	.075	.848
0.8	80	118.9	198.9	0	1.000	1.000
		117.1	197.1	1	.545	.965
		114.9	194.9	2	.256	.867
		113.8	193.8	3	.136	.839
		112.8	192.8	4	.081	.823
0.8	100	104.7	204.7	0	1.000	1.000
		102.5	202.5	1	.558	.929
		100.6	200.6	2	.277	.856
		98.7	198.7	3	.150	.816
		97.5	197.5	4	.088	.794
0.8	120	89.7	209.7	0	1.000	1.000
		87.9	207.9	1	.596	.916
		85.3	205.3	2	.309	.843
		83.6	203.6	3	.170	.801
		82.4	202.4	4	.103	.779

0.9 extrapolation from Table 1 is unreliable

(1) an insufficient number of iterations in arriving at the accepted value of the solution; (2) an inherent error in expressing the film thickness h, together with its reciprocal and derivatives, as a cosine series in ξ. Actually, h is a function of θ which is not a multiple or divisor of ξ, and accuracy, at least at the end points, requires the use of a complete sine-cosine series. In addition, the oil-flow data are of course obtained by a differentiation of p, which tends to magnify any errors already present in the solution for p. Terms W and F, on the other hand, are obtained by integration, which tends to minimize the effects of these same errors.

Interpolation for Terminal Bearings

The data in Table 1 furnish the raw material for determining the properties of centrally supported bearings. First, however,

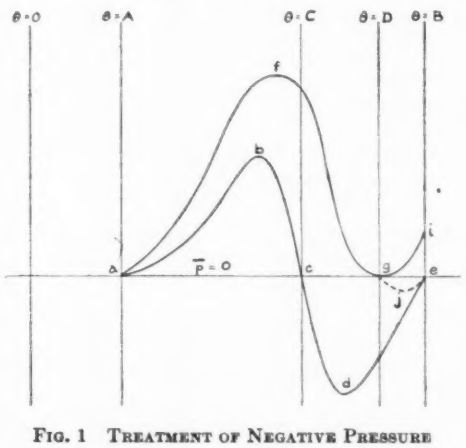


Fig. 1 Treatment of Negative Pressure

it is necessary to settle the matter of negative pressures, which appear in many of the computed cases where $B > 180$ deg. At least two ways of doing this have been proposed. Let us assume that a bearing extends in the lengthwise direction from $\theta = A$ to $\theta = B$, Fig. 1. Then, according to the first method, we take as our boundary conditions $p = 0$ at $\theta = A$, $p = 0$ at $\theta = B$, and obtain for $\bar{p}$ a curve such as *abcde*. Either we use this curve as it stands, on the assumption that the negative portion has little effect, or else we neglect the negative portion *cde* as being physically impossible, and determine the load capacity of the bearing, direction of the resultant line of support, friction, and oil flow, solely from the curve *abc*.

According to the second method, we first find whether $d\bar{p}/d\theta$ is positive or negative at $\theta = B$, on the basis of the same boundary conditions as for the first method. If negative, the pressure curve lies above the zero axis for the entire length of the bearing, and no consideration of negative pressure is necessary. If positive, we arbitrarily reduce the leaving angle until a value is found, say $\theta = D$, at which $d\bar{p}/d\theta = p = 0$. Then, using the boundary conditions $p = 0$ at $\theta = A$, $p = 0$ at $\theta = D$, we obtain the pressure curve *afgi* and, neglecting the portion *gi*, use the portion *afg* to determine the properties of the bearing.

This latter method for the treatment of negative-pressure cases has been advocated by Swift[3] and, after studying the relative merits, has been adopted by the author for the present paper. Swift's line of reasoning will be found fully expounded in his own paper; the following independent analysis, based on considerations of oil flow for an infinite-width bearing, may also be enlightening. First, assume that a bearing extending from $\theta = A$ to $\theta = B$, Fig. 1, by formal integration gives the pressure curve *abcde*. The same result is obtained by assuming that two bearings exist in tandem, and by performing separate integrations from $\theta = A$ to $\theta = C$ and from $\theta = C$ to $\theta = B$. Assume further that actual running conditions are represented by neglecting the theoretical pressure in bearing $C - B$, so that the effective pressure line is *abcge*. The oil discharge at the leaving end of bearing $A - C$ is then determined by the thickness of the clearance space and the negative pressure gradient at C. Since bearing $C - B$ is assumed to have the same clearance space at C, but no negative pressure gradient, it is unable to take the full volume of oil discharged by bearing $A - C$.

On the other hand, assume that formal integration gives the pressure curve *afgi*, g being located by Swift's criterion, this is equivalent to two bearings $A - D$ and $D - B$ in tandem, the first of which discharges at zero pressure, while the second discharges against a terminal pressure *ie*. But, obviously, there is no terminal pressure, which simply means that bearing $D - B$ is fully capable of taking all the oil, or more, that is supplied by bearing $A - D$. The pressure line in this case is theoretically *gje* for the full volume of oil that bearing $D - B$ is capable of handling, being negative because of the divergence of the clearance space, but in reality the pressure is maintained at zero by cavitation in the oil film. The hydrodynamic equations are satisfied by taking constant mass flow rather than volumetric flow for the oil film in bearing $D - B$, i.e., mass flow per unit time per unit width of bearing $= \left(\frac{Uh}{2} - \frac{h^3}{12}\frac{dp}{\mu dx}\right)\rho = \text{constant}$, assuming that the density ρ decreases according to the law $\rho = \rho_0 h_0/h$, where ρ_0 and h_0 are, respectively, the oil density and the clearance at $\theta = D$. The same line of reasoning may be extended to bearings of finite width.

If a bearing of constant eccentricity ratio c and constant length $a\beta$, with $p > 0$ throughout, is given an increasing entering angle A, the pressure gradient at the leaving edge first increases from a negative value to zero. A further increase in A is no longer accompanied by an equal increase in the leaving angle of the effective film, even though the length of the bearing shell is maintained constant, and the pressure curve takes the form of line *afge*, Fig. 1. In this paper, all cases where the mean pressure gradient at the leaving edge of the bearing is zero are designated "terminal bearings." The local values of dp/dx across the bearing width need not equal zero for the same value of x; that is to say, the leaving edge of a terminal bearing may be a curve, rather than a straight line, but this possibility has been neglected as being of minor importance. In Fig. 1 bearing $A - D$ is a terminal bearing. All cases in which the entering angle is so great as to cause the point of zero pressure gradient to recede toward the entering edge, as from e toward or beyond g in Fig. 1, are designated "extended bearings." Actually, they consist of a terminal bearing, followed in tandem by a bearing ($D - B$, Fig. 1), which contributes nothing to load capacity, but doubtless adds a share to the velocity term of the friction. This extension also affects the attitude of the complete bearing with respect to the load line; if this is α/β for the terminal bearing, it will be $\alpha/(\beta + \epsilon)$ for the extended bearing, ϵ being the angular length of the inert extension.

Experience shows that the majority of centrally supported bearings with eccentricity of 0.6 or more lie in the extended range; hence it is desirable to know the properties of terminal bearings. This is done by first ascertaining the exit angle B, and then interpolating between values of the properties of those fundamental bearings having the same length, width, and eccentricity ratio as the terminal bearing in question. For example

$$\left.\frac{d\bar{p}}{d\theta}\right]_B = \left.\frac{dp_s}{d\theta}\right]_B - \left.\frac{d\bar{q}}{d\theta}\right]_B = 0 \text{ for terminal bearing}$$

$$\frac{6\mu Ua}{\eta^2}\left[\frac{1}{(1+c\cos B)^2}+\frac{C_1}{(1+c\cos B)^3}\right]-\left[\frac{d\bar{q}}{d\theta}\right]_B=0$$

$$1+c\cos B=-C_1+\frac{\eta^2}{6\mu Ua}$$

$$(1+c\cos B)^3\left[\frac{d\bar{q}}{d\theta}\right]_B=f(B)$$

Draw a curve for the left side of this equation versus B; and, using points calculated from a group of fundamental bearings, having a given c, β, and r (usually three in number), plot a curve for the right side of the equation. The intersection gives the value of B for the associated terminal bearing; the results, for the three series of bearing lengths, are shown in Fig. 2. As the eccentricity approaches unity, it becomes rather difficult to locate these terminal bearings by three-point interpolation, due to the suddenness with which the value of $dp/d\theta$ changes over a small range of B in the neighborhood of 180 deg. For this reason the curves in Fig. 2 have been faired without attempting to intersect plotted points, where these were obviously out of line.

The α/β values and side-leakage factors of all fundamental bearings in each group having the same c, β, and r were plotted simultaneously versus B. By using appropriate values of B from Fig. 2, the properties of the terminal bear-

TABLE 3 PROPERTIES OF TERMINAL BEARINGS

c	β deg.	r	B	α/β	W/W_0 for B in col. 3	P/P_0 for B in col. 3	Factor for W_0 for B in col. 3	Factor for P_0 for B in col. 3	Side leakage factors for terminal bearings of same span. load	friction
.6	80	0	202.3	.444	1.0000	1.0000	1.4599	3.1937	1.000	1.000
		1	196.3	.453	.457	.973	1.7794	3.1571	.557	.962
		2	190.5	.472	.190	.925	1.9819	3.1012	.258	.901
		3	188.0	.477	.094	.912	2.0369	3.0708	.131	.877
		4	186.5	.478	.056	.904	2.0606	3.0508	.079	.863
.8	80	0	197.0	.518	1.0000	1.0000	6.7200	6.0051	1.000	1.000
		1	192.7	.541	.540	.914	7.1887	5.9035	.578	.897
		2	188.8	.563	.255	.844	7.3887	5.7743	.280	.812
		3	187.0	.572	.135	.810	7.4088	5.7028	.149	.768
		4	185.6	.578	.080	.792	7.3928	5.6421	.088	.743
.9	80	0	192.0	.607	1.0000	1.0000	19.812	10.5965	1.000	1.000
		1	189.9	.630	.621	.888	19.626	10.4377	.615	.876
		2	187.7	.660	.388	.790	19.284	10.2290	.329	.763
		3	186.3	.672	.197	.742	18.989	10.0806	.189	.706
		4	184.9	.694	.128	.711	18.633	9.9181	.120	.665
1.0	80	all values except		180.0	1.000		∞	∞		
.6	100	0	205.3	.470	1.000	1.000	2.5753	3.8810	1.000	1.000
		1	198.7	.495	.498	.946	2.9405	3.8468	.569	.938
		2	193.0	.510	.228	.897	3.1279	3.7902	.277	.876
		3	189.3	.529	.121	.871	3.1859	3.7450	.150	.839
		4	187.3	.540	.073	.856	3.1965	3.7084	.091	.818
.8	100	0	198.3	.560	1.000	1.000	9.168	7.1084	1.000	1.000
		1	194.5	.580	.569	.899	9.463	7.0139	.587	.876
		2	190.5	.608	.286	.811	9.531	6.8718	.297	.785
		3	187.7	.635	.160	.764	9.431	6.7162	.165	.725
		4	186.3	.648	.100	.742	9.336	6.6754	.102	.697
.9	100	0	192.8	.653	1.000	1.000	22.140	12.0476	1.000	1.000
		1	190.5	.673	.645	.878	22.522	11.8248	.647	.861
		2	188.3	.695	.374	.778	22.316	11.5802	.372	.747
		3	186.6	.716	.227	.720	21.965	11.3700	.222	.679
		4	185.6	.730	.148	.689	21.680	11.2377	.143	.643
1.0	100	all values except		180.0	1.000		∞	∞		
.6	120	0	207.5	.498	1.000	1.000	3.758	4.5575	1.000	1.000
		1	201.4	.518	.518	.941	4.082	4.5149	.562	.933
		2	195.1	.542	.235	.885	4.265	4.4441	.267	.862
		3	191.0	.562	.123	.846	4.303	4.3836	.141	.813
		4	188.6	.570	.074	.810	4.295	4.3427	.085	.771
.8	120	0	199.0	.594	1.000	1.000	11.007	8.0607	1.000	1.000
		1	195.1	.618	.600	.886	11.193	7.9304	.610	.872
		2	191.6	.649	.326	.793	11.184	7.7929	.331	.767
		3	189.1	.667	.192	.741	11.075	7.6828	.193	.706
		4	187.0	.684	.125	.709	11.018	7.5826	.125	.666
.9	120	0	192.9	.688	1.000	1.000	24.781	12.9368	1.000	1.000
		1	190.5	.710	.682	.838	24.335	12.7350	.659	.874
		2	188.5	.735	.424	.769	23.838	12.5223	.408	.744
		3	187.1	.770	.290	.706	23.423	12.3680	.274	.674
		4	186.0	.800	.222	.671	23.056	12.2289	.206	.634
1.0	120	all values except		180.0	1.000		∞	∞		

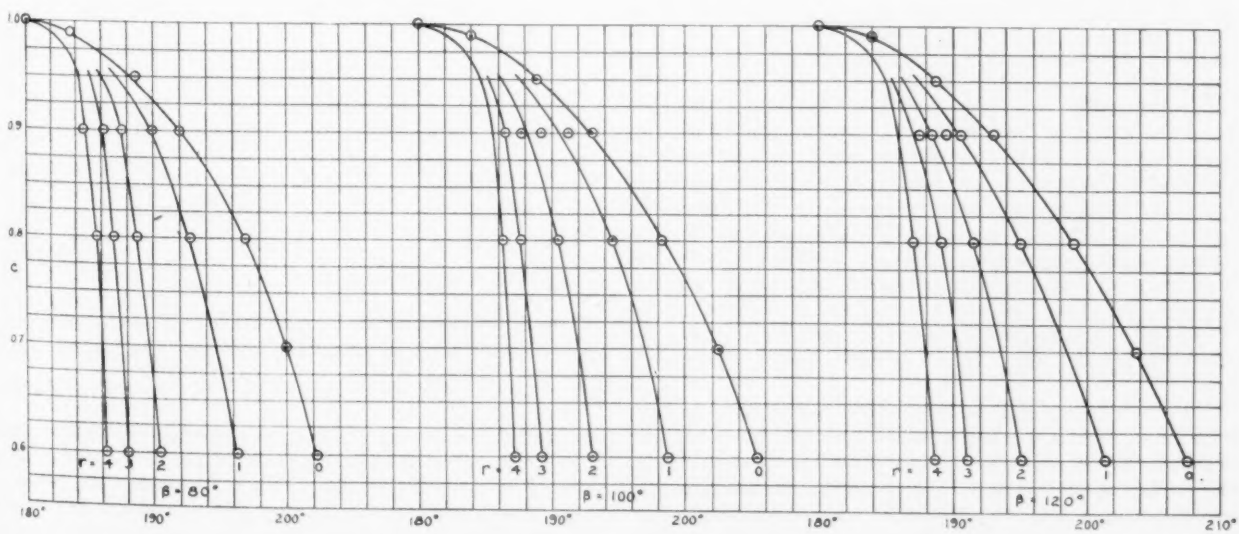


FIG. 2 EXIT ANGLE FOR TERMINAL BEARINGS

TABLE 4 PROPERTIES OF CENTRALLY SUPPORTED BEARINGS, HAVING NO NEGATIVE PRESSURE: WIDTH INFINITE

c	β', deg.	A, deg.	$W/\frac{\mu Ua^2}{h_2^2}$	$F/\frac{\mu Ua}{h_2}$	$\lambda/\frac{h_2}{a}$	
0.6	80	114.0	1.87	3.14	1.679	based directly on fundamental bearings.
	100	101.1	2.83	3.86	1.364	
	120	87.3	3.77	4.56	1.210	
	140	72.8•	4.67•	5.25•	1.124•	
0.6	80	115.6	1.91	3.47	1.817	based on fictitious terminal bearings.
	100	101.1	2.85	4.04	1.418	
	120	87.3	3.76	4.57	1.217	
	140	74.0•	4.45•	5.07•	1.141•	
0.8	80	118.6	6.36	5.87	.923	
	100	106.2	8.32	6.68	.803	
	120	93.3	9.69	7.37	.761	
	140	80.7	10.85	7.99	.737	
0.9	80	118.7•	17.92•	9.66•	.539•	
	100	109.4	20.06	10.75	.536	
	120	98.9	21.69	11.65	.537	
	140	87.5	23.10	12.36	.535	

• Uncertain, due to extrapolation.

ing pertaining to each of these groups were obtained by interpolation and entered in Table 3. Consider for example line 10 in Table 3; this represents the terminal bearing of eccentricity ratio 0.8, 80-deg span and length-width ratio 4:1, and was derived from the three starred lines in Table 1. The three B values in these lines of Table 1 are 170, 190, and 210 deg; from Fig. 2, B for the terminal bearing is 185.6 deg, which gives the interpolation interval. Accordingly, the three α/β values in Table 1, which are 0.6863, 0.5389, and 0.0507 give $\alpha/\beta = 0.578$ for Table 3. Similarly, the W/W_0 and F/F_0 values in Table 3, respectively, 0.08 and 0.792, are interpolated from the six side-leakage factors in the starred lines of Table 1.

Terms W/W_0 and F/F_0 in Table 3 are not true side-leakage factors for terminal bearings, since the value 0.08, for example, means that the capacity of a terminal bearing of length-width factor 4 is 0.08 that of an infinite-width bearing whose entering and exit angles are the same as those of the finite-width bearing, and such an infinite-width bearing is not terminal. To find the true side-leakage factor for load, 0.080 must first be multiplied by the load capacity for an 80-deg infinite-width bearing whose exit angle is 185.6 deg, and then be divided by the load capacity of an 80-deg infinite-width terminal bearing, i.e., $0.080 \times 7.3928 / 6.7200 = 0.088$. For the friction side-leakage factor, $0.792 \times 5.6421/6.0051 = 0.743$. The W_0 and F_0 factors, used in this corrective process, are interpolated from the appropriate values of $W \Big/ \left(\frac{\mu Ua^2}{\eta^2}\right)$ and $F \Big/ \left(\frac{\mu Ua}{\eta}\right)$ in Table 1.

The exit angles, α/β values, and load and friction factors entered in Table 3 for the case of $c = 1$, are in harmony with the negative-pressure theory adopted in this paper. According to this theory, the load line and line of centers become coincident in this limiting case, and pass through the leaving edge of the bearing, regardless of the value of the entering angle A. Obviously, any terminal bearing having $c = 1$ may be extended into a centrally supported bearing merely by doubling the length of the shell; all of the pressure in the oil film is developed in the convergent half, approaching infinity at the point of contact between journal and shell. In the divergent half, the pressure is zero.

No values for side-leakage factors have been entered in Table 3 for $c = 1$. When negative pressures are neglected, it has been customary to assume unity for both these factors, as well as for the coefficient of friction. However, with the interpretation here placed upon negative pressures, it is suspected that the side-leakage factors approach values lying between 0 and 1, and that the friction coefficient approaches zero. The author is at present making a detailed study of this region and expects to report his findings at a later date. Fortunately, this uncertainty does not appear to have a vital effect upon the determination of optimum bearings, at least in the range of minimum film thickness ordinarily used.

Properties of Centrally Supported Bearings

Ignoring for the present the terminal bearings with $c = 0.6$, most of which have, according to Table 3, noncentral support with $\alpha/\beta < 0.5$, it is possible to convert all the remaining examples into centrally supported bearings simply by adding an arc ϵ at the leaving edge of the shell, such that $\epsilon = (2\alpha/\beta - 1)\beta$.

TABLE 5 PROPERTIES OF CENTRALLY SUPPORTED BEARINGS HAVING NO NEGATIVE PRESSURE: WIDTH FINITE

c	β' deg.	r	A, deg.	Side leakage factor for load	Side leakage factor for friction	r'
0.6	80	1	110.2	.464	.936	1.00
		2	106.8	.206	.692	2.00
		3	105.2	.105	.873	3.00
		4	104.0	.061	.860	4.00
	100	1	97.0	.527	.954	1.00
		2	94.2	.279	.885	2.05
		3	93.0	.151	.853	3.12
		4	92.6	.090	.857	4.20
	120	1	84.1	.563	.933	1.02
		2	81.5	.272	.866	2.12
		3	80.4	.148	.825	3.28
		4	80.1	.091	.800	4.41
	140	1	69.6•	.551•	.932•	1.05•
		2	69.0•	.259•	.859•	2.21•
		3	67.9•	.138•	.809•	3.39•
		4	66.2	.082	.765	4.57
0.8	80	1	117.0	.577	.903	1.07
		2	115.0	.278	.823	2.19
		3	113.3	.166	.793	3.25
		4	111.8	.084	.764	4.32
	100	1	104.3	.581	.882	1.12
		2	102.9	.284	.803	2.33
		3	102.4	.152	.755	3.55
		4	101.7	.090	.736	4.78
	120	1	92.0	.589	.676	1.17
		2	91.4	.295	.788	2.46
		3	91.5	.161	.732	3.70
		4	91.2	.096	.707	5.13
	140	1	80.1	.605	.873	1.22
		2	80.3	.314	.775	2.55
		3	80.4	.175	.716	3.90
		4	80.4	.108	.666	5.28
0.9	80	1	121.9•	.594•	.895•	1.21•
		2	122.8•	.284•	.788•	2.52•
		3	122.0•	.171•	.701•	3.80•
		4	123.4•	.111•	.695•	5.30•
	100	1	110.3	.614	.876	1.26
		2	111.0	.316	.768	2.61
		3	110.6	.181	.716	3.97
		4	111.5	.116	.676	5.48
	120	1	96.7	.634	.866	1.31
		2	99.2	.348	.754	2.70
		3	99.2	.200	.693	4.18
		4	99.6	.125	.658	5.81
	140	1	87.5	.651	.860	1.36
		2	87.7	.373	.747	2.79
		3	88.3	.219	.679	4.43
		4	88.7	.138	.612	6.27

• Uncertain due to extrapolation.

The complete bearing arc is then $\beta + \epsilon = \beta'$, and $\alpha/\beta' = 0.5$. At the same time, the length-width factor changes, becoming $r' = 2\alpha r/\beta$. The load factor $W \Big/ \left(\frac{\mu Uh^2}{a^2}\right)$ is unaffected by this addition to the bearing arc, since, as previously explained, the oil film which carries the load maintains the same arc β as before. The effect upon the friction factor is uncertain; the pressure term is zero, and the velocity term is indeterminate, due to the discontinuous nature of the oil in the portion of the bearing represented by arc ϵ. It has been assumed that this term is small

n comparison with the corresponding term for the load-carrying part of the bearing, and may be neglected.

Consider, as an example, the three infinite-width terminal bearings with $c = 0.8$ in Table 3, all of which have $\alpha/\beta > 0.5$. These may be extended into centrally supported bearings with $\alpha/\beta' = 0.5$, as follows

B, deg	A, deg	ϵ, deg	β', deg	$W\Big/\left(\frac{\mu Ua^2}{\eta^2}\right)$	$F\Big/\left(\frac{\mu Ua}{\eta}\right)$
197.0	117.0	2.88	82.9	6.7200	6.0051
198.3	98.3	12.00	112.0	9.168	7.1084
199.0	79.0	22.56	142.6	11.007	8.0607

Note that the load and friction factors have not been altered by the addition of ϵ to the bearing arc. Now, by interpolating between these three rows of figures, the properties of any centrally supported bearing having $c = 0.8$, and a bearing arc in the range of 80 to 145 deg, may be ascertained. The interpolation is practically straight-line for all of the cases investigated, so that good accuracy is assured. The results are given in Table 4, and Table 5 contains similar data for finite-width bearings, with the inclusion of the corrected length-width factor r' and the substitution of side-leakage factors for load and friction factors.

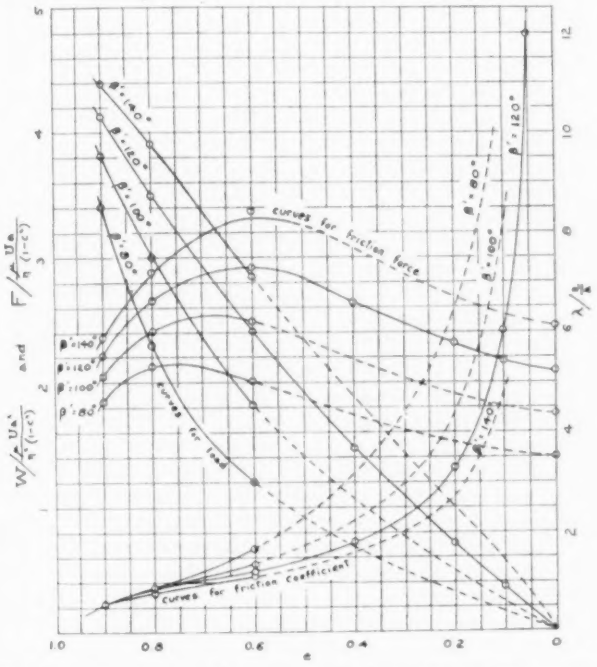


FIG. 3 CAPACITY AND FRICTION OF INFINITE-WIDTH CENTRALLY SUPPORTED BEARINGS

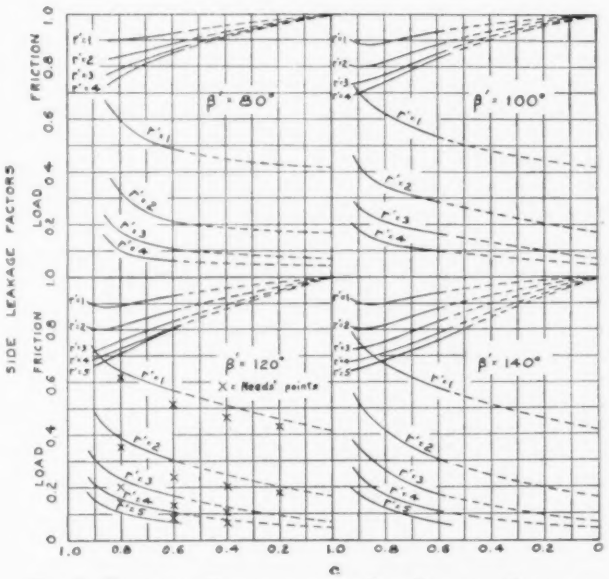


FIG. 5 EFFECT OF ECCENTRICITY ON SIDE-LEAKAGE FACTORS

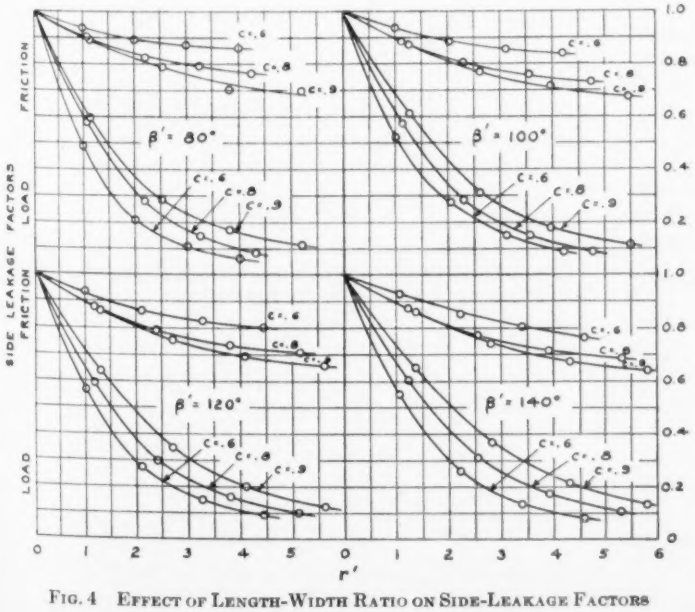


FIG. 4 EFFECT OF LENGTH-WIDTH RATIO ON SIDE-LEAKAGE FACTORS

Fig. 3 shows the load capacity, friction force, and coefficient of friction of infinite-width centrally supported bearings. The values for $c < 0.6$, $\beta = 120$ deg, have been taken from Needs's paper,[2] since in this range, there is no question of negative pressures; above $c = 0.6$, the load and friction factors tend toward infinity, and the coefficient of friction apparently tends toward zero. Fig. 4 shows the variation of side-leakage factors with length-width ratio, according to the data in Table 5, and Fig. 5 presents the same data as variation of side-leakage factors with eccentricity.

If crossplots are made to show the effect of varying the bearing length, the curves are slightly irregular at some points, showing the need of additional data to verify the interpolations. There is, however, a small but consistent increase in the side-leakage factor for load, and decrease in the factor for friction, with increasing bearing length, for all values of length-width ratio that were investigated. This can be seen by comparing the adjacent sections of Figs. 4 and 5.

If the mean clearance η is replaced by the minimum

clearance $h_0 = \eta(1 - c)$, Kingsbury[6] has shown that the load capacity and friction coefficient attain definite maxima and minima for any given value of h_0, bearing size, speed, and viscosity. Bearings operating at such points are said to be running under optimum conditions. Hitherto, this analysis has been based on the conventional neglect of negative pressures, and it would seem to be a matter of some interest to find what effect, if any, is produced by the principle of the exclusion of negative pressures, as contrasted with their neglect. Accordingly, Figs. 6 and 7 have

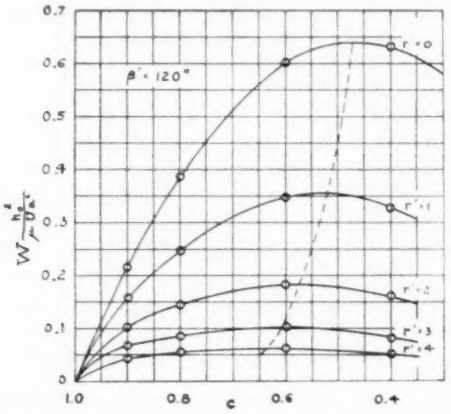


FIG. 6 OPTIMUM CONDITION FOR LOAD, 120-DEG BEARINGS

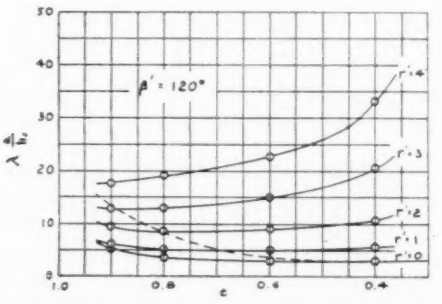


FIG. 7 OPTIMUM CONDITION FOR FRICTION, 120-DEG BEARINGS

been plotted from the data for 120-deg bearings. For $c < 0.6$, the curves for $r = 0$ were taken directly from Needs's paper[2] and the curves for $r = 1, 2, 3, 4$ were then obtained by using the tentative side-leakage factors given by dotted lines in Fig. 5 for this region.

COMMENTS AND GENERAL CONCLUSIONS

Table 2 indicates that the author's method of solution for the fundamental bearings gives results of the same order of magnitude as those previously obtained by experimental integrations, but the factors for load and friction both decrease more rapidly as the length-width ratio increases above unity. When $r = 4$, $c = 0.6$, $\beta = 120$ deg, the values are respectively 10.7 and 4 per cent lower, making the friction coefficient 6.6 per cent higher. When the criterion of bearings without negative pressure is introduced, there is no effect upon infinite-width bearings in the approximate range $0 < c < 0.6$; beyond this, the film arc β has to be reduced to eliminate the negative-pressure region, and the entering angle A has to be increased to maintain $\alpha/\beta = 0.5$. The resulting bearings are offset in the sense that their point of support is not at the center of the oil film, but actually they are centrally supported, due to the effect of the nonloaded portion of the bearing shell. In the limiting case of a 120-deg bearing, with $c = 1$, β has shrunk to 60 deg, $A = 120$ deg, and the line of centers bisects the bearing arc. The entering half of the bearing then carries the entire load. The effect of these shifts is to increase $W \Big/ \left(\frac{\mu U a^2}{\eta^2}\right)$ and decrease $F \Big/ \left(\frac{\mu U a}{\eta}\right)$ in relation to the conventionally accepted values.

The side-leakage factors in Table 1 are all based on a comparison of the properties of a finite-width bearing with those of an infinite-width bearing with the same values of entering and exit angles. When the basis of comparison is altered to that of terminal bearings, having the same span, then the line of centers for each finite-width bearing undergoes a definite shift, and this has a decided effect upon load capacity in the range of eccentricities covered by the present paper. This explains the main reason for the discrepancy between the author's curves in Fig. 5 and the points determined by Needs[2] who considered it unnecessary to correct the side-leakage factors for shift of centerline angle. The terminal points of these curves, at $c = 0$, were computed by a simplified mathematical analysis for centrally supported bearings of small eccentricity, in which the expression for clearance, $h = \eta(1 + c \cos \theta)$, is expanded in ascending powers of c, and all terms of order higher than unity are neglected. According to this analysis, the side-leakage factor for load equals, to a first approximation, $1 - [(\tanh \pi/2r)/(\pi/2r)]$. The results agree exactly with those extrapolated from Needs's experimental points.

Figs. 5 and 6 indicate the existence of a definite relation between eccentricity and length-width ratio for maximum-capacity or minimum-friction coefficient on the basis of a fixed minimum clearance. However, the general flatness of the curves indicates that the eccentricity may be varied over a considerable range without much effect on capacity or friction. As r increases, the divergence between the eccentricity for greatest load and that for least friction becomes much more pronounced than is apparent from the work of Needs. A set of points for $c = 0.95$ is desirable for establishing this relationship definitely.

ACKNOWLEDGMENT

In conclusion, the author wishes to acknowledge his thanks for the very material aid that he has received from the Society's Special Research Committee on Lubrication.

[6] "Optimum Conditions in Journal Bearings," by A. Kingsbury, Trans. A.S.M.E., vol. 54, 1932, pp. 123-148.

Appendix

Outline Solution for Typical Fundamental Bearing

(1) Solution of Reynolds' equation

$$\frac{\partial}{\partial\theta}\left(\frac{h^3}{\mu}\frac{\partial p}{\partial\theta}\right)+a^2\frac{\partial}{\partial z}\left(\frac{h^3}{\mu}\frac{\partial p}{\partial z}\right)=6U_a\frac{dh}{d\theta} \tag{1}$$

$p=p_s-q$, where p_s is a particular solution of

$$\frac{d}{d\theta}\left(\frac{h^3}{\mu}\frac{dp_s}{d\theta}\right)=6U_a\frac{dh}{d\theta} \tag{2}$$

q is a general solution of the homogeneous equation

$$\frac{\partial}{\partial\theta}\left(\frac{h^3}{\mu}\frac{\partial q}{\partial\theta}\right)+a^2\frac{\partial}{\partial z}\left(\frac{h^3}{\mu}\frac{\partial q}{\partial z}\right)=0 \tag{3}$$

Boundary conditions: $p=0$ when $\theta=\theta_1$ and θ_2, for all values of z; $p=0$ when $z=\pm l$, for all values of θ.

Eccentricity ratio: $c=0.6$

Pressure function: $p\left(h/\eta\right)^{3/2}$

$$p_s(h/\eta)^{3/2}=(0.08323\sin\theta+0.003248\sin2\theta+0.0005583\sin3\theta+0.001690\sin4\theta-0.0006310\sin5\theta+0.0005756\sin6\theta)\frac{6\mu U_a}{\eta^2(1-c^2)^{3/2}} \tag{4}$$

by 6-ordinate harmonic analysis of conventional solution.

Let $q=\sum A_n\left[\frac{X}{\left(h/\eta\right)^{3/2}}\right]Z_n$, X and Z being functions respectively of θ and z only. Then, by separating the variables in (3),

$$\frac{d^2X}{d\theta^2}+\left[m^2-\frac{3}{2}\frac{d^2h/d\theta^2}{h}-\frac{3}{4}\left(\frac{dh/d\theta}{h}\right)^2\right]X=0 \quad\text{or}$$

$$\frac{d^2X}{d\beta^2}+\left[\frac{4}{9}m^2-1.3476+1.3814\cos\beta+0.1568\cos2\beta-0.05126\cos3\beta+0.01857\cos4\beta-0.006684\cos5\beta+0.0024\cos6\beta\right]X=0 \tag{5}$$

by Fourier theorem for cosine series.

Also

$$\frac{d^2Z}{dz^2}-\left(\frac{m}{h}\right)^2Z=0 \tag{6}$$

The first six solutions for $q\left(h/\eta\right)^{3/2}$ are (by method of successive approximation):

	$\sin\beta$	$\sin2\beta$	$\sin3\beta$	$\sin4\beta$	$\sin5\beta$	$\sin6\beta$	
$q_1(h/\eta)^{3/2}=(A_1\cosh\frac{m_1z}{h})[$	$+1$	$+.2326$	$+.02913$	$+.0003687$	$-.0005943$	$-.0003807$	$]$
$q_2(h/\eta)^{3/2}=(A_2\cosh\frac{m_2z}{h})[$	$-.3417$	$+1$	$+.1386$	$+.01752$	$-.0005453$	$-.0003871$	$]$
$q_3(h/\eta)^{3/2}=(A_3\cosh\frac{m_3z}{h})[$	$+.004015$	$-.1383$	$+1$	$+.09815$	$+.003397$	$-.0005852$	$]$
$q_4(h/\eta)^{3/2}=(A_4\cosh\frac{m_4z}{h})[$	$+.002216$	$-.003348$	$-.09878$	$+1$	$+.07633$	$+.006696$	$]$
$q_5(h/\eta)^{3/2}=(A_5\cosh\frac{m_5z}{h})[$	$-.0002439$	$+.001625$	$-.001536$	$-.07684$	$+1$	$+.06231$	$]$
$q_6(h/\eta)^{3/2}=(A_6\cosh\frac{m_6z}{h})[$	$+.0001048$	$-.0003339$	$+.001138$	$-.007774$	$-.06230$	$+1$	$]$
	$m_1=2.3522$	$m_2=3.4357$	$m_3=4.8329$	$m_4=6.2503$	$m_5=7.2910$	$m_6=9.1743$	

(7)

$p_s=q=p=0$ at $z=w/2$; hence, equating to zero the coefficients of terms in (4) and (7) having the same multiple of β in $\sin\beta$, and letting $A_n\cosh\frac{m_nz}{h}=B_n$ when $z=w/2$, also $\eta_1^3=\eta^3(1-c^2)^{3/2}$,

$$\begin{aligned}
&\frac{\eta_1^3}{6\mu U_a}\left(B_1-.2415B_1+.004015B_3+.002216B_4-.0002439B_5+.0001048B_6\right)=0.08323\\
&\frac{\eta_1^3}{6\mu U_a}\left(.2326B_1+B_2-.1383B_3-.003348B_4+.001625B_5-.0003339B_6\right)=0.003248\\
&\frac{\eta_1^3}{6\mu U_a}\left(.02913B_1+.1386B_2+B_3-.09878B_4-.001536B_5+.001138B_6\right)=0.0005583\\
&\frac{\eta_1^3}{6\mu U_a}\left(.0003687B_1+.01752B_2+.09815B_3+B_4-.07684B_5-.001774B_6\right)=0.001690\\
&\frac{\eta_1^3}{6\mu U_a}\left(-.0005943B_1-.0005453B_2+.003397B_3+.07633B_4+B_5-.06230B_6\right)=-0.0006310\\
&\frac{\eta_1^3}{6\mu U_a}\left(-.0003807B_1-.0003871B_2-.0005852B_3+.006696B_4+.06231B_5+B_6\right)=0.0005756
\end{aligned} \tag{8}$$

Solving (8), $B_1=0.07955\left(\frac{6\mu U_a}{\eta_1^3}\right)$ $\quad B_4=-0.01518\left(\frac{6\mu U_a}{\eta_1^3}\right)$

$B_2=0.0005150\left(\frac{6\mu U_a}{\eta_1^3}\right)$ $\quad B_5=0.001796\left(\frac{6\mu U_a}{\eta_1^3}\right)$

$B_3=-0.0007350\left(\frac{6\mu U_a}{\eta_1^3}\right)$ $\quad B_6=0.0006068\left(\frac{6\mu U_a}{\eta_1^3}\right)$

Since $\overline{q}_n=q_n\frac{\left(\tanh\frac{m_nw/2a}{2}\right)}{m_nw/2a}$ and $r=l/w=2$, we have

$$\begin{aligned}
&\overline{q}_1=q_1\left(\tanh\tfrac{1}{2}m_1\right)/\tfrac{1}{2}m_1=0.7015\,q_1, \quad \overline{q}_2=0.5190\,q_2, \quad \overline{q}_3=0.3902\,q_3\\
&\overline{q}_4=0.3047\,q_4, \quad \overline{q}_5=0.2478\,q_5, \quad \overline{q}_6=0.2082\,q_6
\end{aligned} \tag{9}$$

Combining (7), (8) and (9), $\overline{q}=\sum\overline{q}_n=$

$$(0.05771\sin\theta+0.005573\sin2\theta+0.000682\sin3\theta+0.000472\sin4\theta-0.000147\sin5\theta+0.000120\sin6\theta)(z/h)(6\mu U_a/\eta_1^3) \tag{10}$$

Subtracting (10) from (4),

$$\overline{p}\left(h/\eta\right)^{3/2}=(0.01552\sin\theta-0.001825\sin2\theta-0.000126\sin3\theta+0.001318\sin4\theta-0.000484\sin5\theta+0.000456\sin6\theta)(\mu U_a/\eta_1^3) \tag{11}$$

$$\left.\begin{aligned}W_u&=a\int_A^B\overline{p}\cos\theta\,d\theta=-3.1383(\mu U_a/\eta_1^3)\\ W_v&=a\int_A^B\overline{p}\sin\theta\,d\theta=1.8877(\mu U_a/\eta_1^3)\end{aligned}\right\}\text{ from (11) by Simpson's rule for 12 equal intervals}$$

$\phi=\tan^{-1}\left(\frac{W_v}{W_u}\right)=-0.6015=148°58'$

$\alpha/\beta=(148°58'-70°)/120°=0.6581$

$W=W_u\sqrt{(W_v/W_u)^2+1}=3.662(\mu U_a/\eta_1^3)$

See Fig. 8 for graph of $\overline{p}$, p_s and $p_s(h/\eta)^{3/2}$

(2) Friction computation. $F=\int_A^B\frac{\mu U_a}{h}d\theta+\int_A^B\frac{h}{2}\frac{d\overline{p}}{d\theta}d\theta$

$=F_1+F_2$

$F_1=5.3273\,\mu U_a/\eta$ $\quad F_2=\frac{1}{2}\int_{\overline{p}_A}^{\overline{p}_B}h\,d\overline{p}=\frac{1}{2}h\overline{p}\Big]_{\overline{p}_A}^{\overline{p}_B}-\frac{1}{2}\int_{\overline{p}_A}^{\overline{p}_B}\overline{p}\,dh$

$=0-\frac{1}{2}\int_A^B\overline{p}\frac{dh}{d\theta}d\theta$

$=\frac{\pi c}{4}\int_A^B\overline{p}\sin\theta\,d\theta=\frac{\pi c}{4a}W_v$

$=0.7550\,\mu U_a/\eta$

$F=6.0823\,\mu U_a/\eta$ $\quad \lambda=F/W=1.6603\,\eta/a$

(3) Oil flow computation. $\left.\frac{\partial q/\partial z}{q_n}\right]_{z=l}=\frac{m_n}{h}\tanh\frac{m_nw}{2a}$,

and $\frac{q_n}{\overline{q}_n}\Big]_{z=l}=\frac{m_nw/2a}{\tanh\frac{m_nw}{2a}}$, hence $\partial q_n/\partial z\big]_{z=l}=\frac{m_n^2w}{2a^2}\overline{q}_n$

Combining this with (7), (8) and (9) gives $\partial q/\partial z\big]_{z=l}=\sum\partial q_n/\partial z\big]_{z=l}=$

$$(0.3066\sin\theta-0.03108\sin2\theta-0.002470\sin3\theta+0.02130\sin4\theta-0.008735\sin5\theta+0.01013\sin6\theta)\left(\frac{w}{2a}\right)(\eta/h)^{3/2}\left(\frac{6\mu U_a}{\eta_1^3}\right) \tag{12}$$

$$Q_z=-\int_A^B\frac{h^3}{12\mu}\frac{\partial p}{\partial z}\Big]_{z=l}d\theta=\int_A^B\frac{h^3}{12\mu}\frac{\partial q}{\partial z}\Big]_{z=l}d\theta$$

$=0.1998\,\overline{U}a\eta$, from (12), by Simpson's rule for 12 equal intervals.

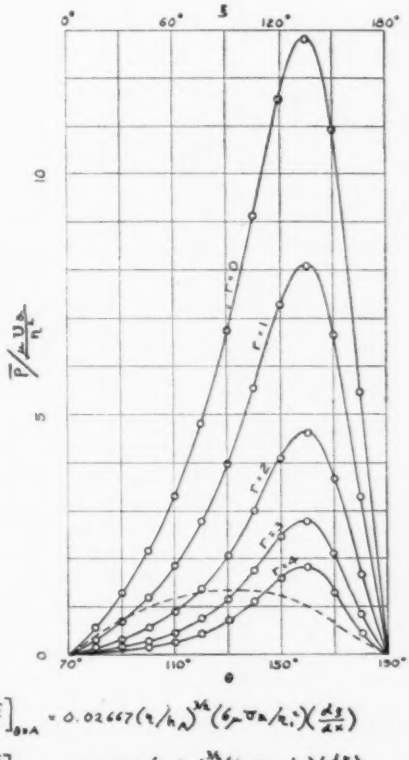


Fig. 8 Mean Pressure Distribution in a Typical Bearing

From (11), $\left.\frac{d\overline{p}}{dx}\right]_{\theta=A}=0.02667(\eta/h_A)^{3/2}(6\mu U_a/\eta_1^2)(\frac{dh}{dx})$

$\left.\frac{d\overline{p}}{dx}\right]_{\theta=B}=-0.01876\,(\eta/h_B)^{3/2}(6\mu U_a/\eta_1^2)(\frac{dh}{dx})$

$$Q_A=w\left[\frac{Uh}{2}-\frac{h^3}{12\mu}\frac{d\overline{p}}{dx}\right]_{\theta=A}=\left(\frac{ph}{2}\right)\left(\frac{U_2}{2}\right)(1+0.8\cos70°)-\left(\frac{ph}{2}\right)\frac{(1+0.8\cos70°)^{3/2}}{12\mu(1-c^2)^{3/2}}\left(0.02667\times6\mu U_a\eta\right)\frac{\pi}{4p}$$

$=0.5275\,\overline{U}a\eta$

Substituting -0.01876 for 0.02667, and $190°$ for $70°$, in the foregoing, gives

$$Q_B=0.1177\,\overline{U}a\eta$$

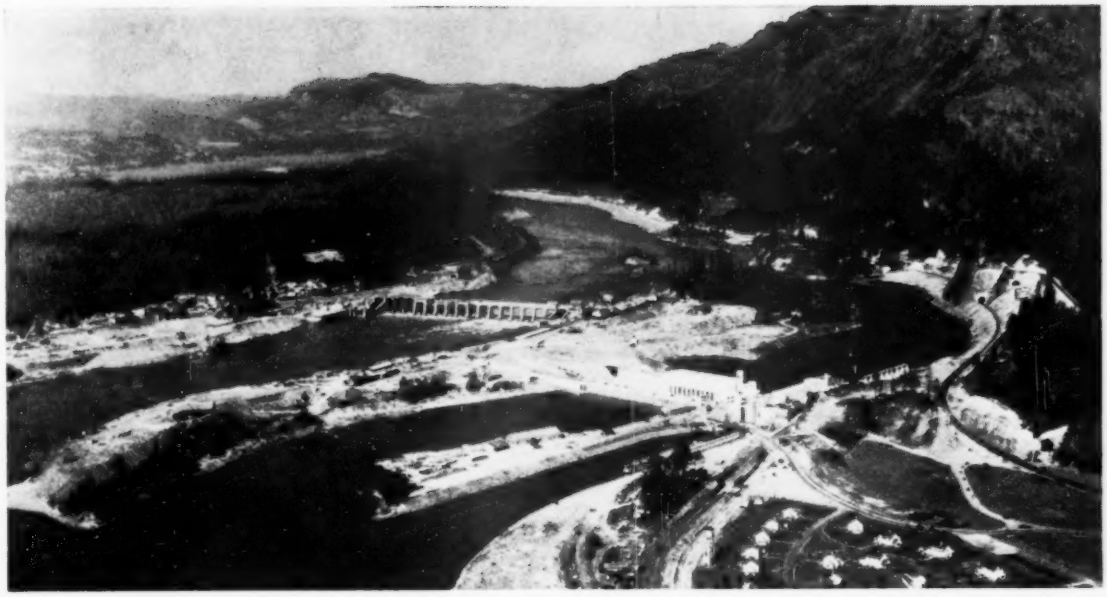


FIG. 1 PANORAMIC VIEW OF BONNEVILLE PROJECT

(This view shows the unfinished north half of the spillway. Some of the gates are in place, and one gantry on the south half. The Columbia Construction Company's gigantic high line can be seen with the fixed tower dominating North Bonneville. Fish ladders are at each end of the dam, with the south fishway meeting the one from the powerhouse in the form of a Y, leading to the pool between Bradford Island and the Oregon shore.)

Structural-Steel Tolerances at Bonneville

BY T. M. OBER,[1] BREMERTON, WASH.

This paper describes features of the Bonneville Project, which have attracted widespread interest. Noteworthy among these are the eighteen 225-ton vertical-lift spillway-dam gates, each of two sections, operated by two 350-ton gantry cranes; and the variety and number of fishways requiring numerous gates and lifts. The great size of steel units involved in the construction required unusual care in erection. Close tolerances were maintained in the setting of embedded steel. The methods of erection employed and the limits within which the work was carried out are dealt with at some length. The author deals quite extensively with the matter of selecting personnel for the structural-steel inspection staff for a project of this magnitude. Also, in the text, he refers quite extensively to drawing numbers, and specification page numbers, in order that those who so desire may be enabled to refer directly to the original plans and specifications of the project.

ON September 30, 1933, the Federal Administrator of Public Works authorized the construction of the Bonneville Power-Navigation Project as Federal Project No. 28, under the provisions of the National Industrial Recovery Act. The sum of $32,200,000 was allocated for this purpose. The dam was to be constructed under the supervision of the Corps of Engineers, U. S. Army.

The Bonneville Power-Navigation Project is located at tidewater on the Columbia River approximately 140 miles from its mouth and 42 miles east of Portland, Ore. At this point, the river flows in a general westerly direction in two channels which are separated by Bradford Island. The center of the north channel is the boundary line between the states of Oregon and Washington. The spillway dam, approximately 1250 ft in length, was constructed across the north or main channel and the powerhouse and navigation lock were located in the south channel with the lock on the Oregon shore. A levee on Bradford Island connects the dam and the powerhouse.

The lock chamber is 76 ft wide, 500 ft long, and has a depth of 26 ft over the lower sill at low water. The vertical lift at extreme low water is 66 ft, the greatest of any lock yet built. At normal river stage the lift is 59 ft; at extreme high water about 30 ft.

The existing project for the improvement of the Columbia River between Vancouver and Bonneville was adopted by Congress on August 26, 1937, with an estimated cost of $2,649,000 for new work and $200,000 annually for maintenance. This project provides for a channel 300 ft wide and 27 ft deep at low water, which depth conforms with the minimum clearwater of 26 ft over the lower sill of the Bonneville locks, and the depth of 30 ft in the river stretch above Bonneville.[2]

The spillway design was based on the record flow of 1,170,000 sec-ft which occurred in 1894. The design provides for a maxi-

[1] Mechanical Engineer, Puget Sound Navy Yard. Formerly of the U.S.E.D., Ohio River Division Office, Cincinnati, Ohio, and Head of Mechanical and Structural Steel Section, Bonneville Spillway Dam and Fishways. Mem. A.S.M.E.

Contributed by the Hydraulic Division and presented at the Annual Meeting, New York, N. Y., December 1–5, 1941, of THE AMERICAN SOCIETY OF MECHANICAL ENGINEERS.

NOTE: Statements and opinions advanced in papers are to be understood as individual expressions of their authors, and not those of the Society.

[2] "The Columbia River Between Vancouver and the Dalles," by Major T. D. Weaver, *The Military Engineer*, March-April, 1939, pp. 91–95.

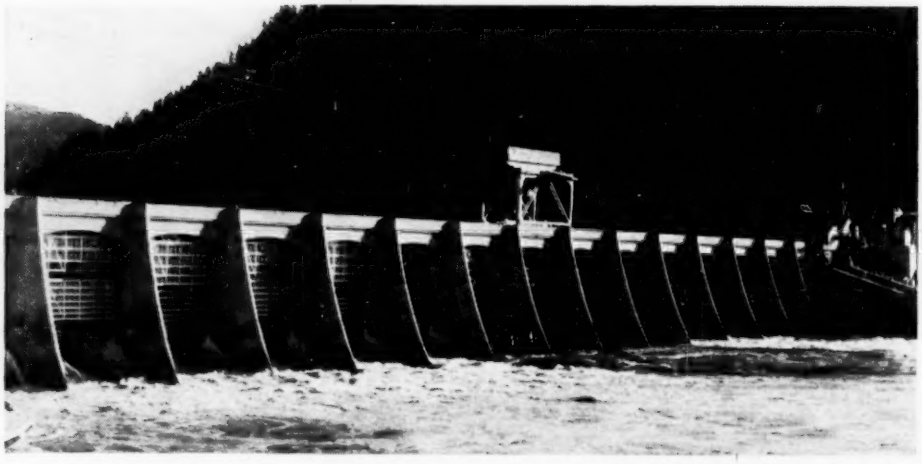


FIG. 2 VIEW OF SPILLWAY, SHOWING GATES AND CRANE IN OPERATION

mum flow of 1,600,000 sec-ft (an estimated 1 in 10,000 year flood) and a minimum of 40,000 sec-ft. Although both navigation and power are provided by the Bonneville Dam, navigation requirements at the dam or in the river will not affect operation of the power plant. There is no seasonal storage available in the Bonneville pool, but daily load fluctuations can readily be accommodated with 3 ft or less of drawdown.

The size of the turbines was given careful consideration. The units are about as large as is practicable under existing shop conditions. As finally designed, the turbines have a rating of 66,000 hp under 50 ft head. They are the largest Kaplans in this country, the highest Kaplans ever built, and the generators they drive are the largest in physical dimensions so far constructed. Normal headwater elevation at minimum flow was provided to be at elevation +72 with tailwater at +14. With normal maximum flow of 600,000 sec-ft, the headwater is raised to +82.5 to develop the full power of the turbines.[3]

The magnitude of the Corps of Engineers' project at Bonneville prevents discussion here of any save spillway and fishway features.

SPILLWAY-GATE DESIGN

The fish industry in Oregon and Washington, valued at $10,000,000 annually, influenced the gate and dam design. The fish ladders and collecting systems at each end of the dam required the complete closure of the three end gates. The straight-lift-type gate, made in two sections because of the height and the necessity for raising them clear of the water during high flows, was required for a depth of flow of 50 to 60 ft and a width of 50 ft. Accordingly six gates were built with a height of 60 ft for the end bays and twelve with a height of 50 ft 9 in. The twelve center gates were provided with a skimmer section 8 ft high and 42 ft long. The headwater elevation above the dam is regulated by the operation of the spillway-dam gates by means of two 350-ton gantry cranes. An allowable pool-operating range of $^1/_2$ ft above or below the desired level was assumed as reasonable.

Therefore, it was concluded that, because of the large reservoir capacity above the dam amounting to 20,000 acre-ft per ft of depth at elevation 72, neither rapid nor refined gate operation would be required. Provision of a rack bar, enabling each gate to be raised in 2-ft steps, was considered adequate from the standpoint of regulation.

Twenty gates and two gantry cranes were contracted to the Columbia Steel Corporation for approximately $1,200,000. The

[3] "The Kaplan Turbines at Bonneville," by P. L. Heslop and G. A. Jessop, Trans. A.S.M.E., vol. 61, 1939, pp. 97–108.

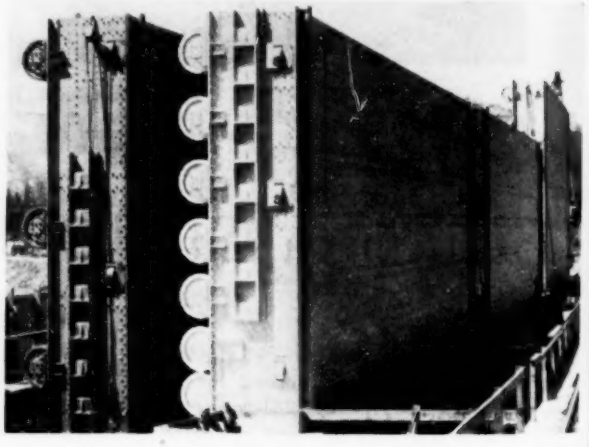


FIG. 3 SPILLWAY GATES BEING PAINTED
(The near gate section with the seven wheels showing is a bottom section, the other near gate at the left is a top section.)

gantry cranes were built by the Morgan Engineering Company, Alliance, Ohio, and the gates by the American Bridge Company. The general contractor, Columbia Construction Company, placed the embedded steel, which cost approximately $1,000,000 in addition, for both fishways and dam. Gantry cranes were selected for handling the gates on account of the necessity for transferring the upper gate sections from the downstream to the upstream slots; the ease of handling spare gates in case repairs are required; and their considerably lower first cost over fixed hoists. Each crane is supplied with a Climax driven generator for emergency use.

This paper is principally concerned with steel tolerances, but some details of the gate construction and accessories will be related for clarity.

SPECIFICATIONS FOR REINFORCED-RUBBER SEALING STRIPS

The side and intermediate seals for the gates are similar to a J-type used on previous work, but, it is believed, the bottom seal is an innovation. The side seals were specified as follows:

Tread Stock. The tread stock shall consist of high-grade stock containing 60 per cent by weight of new plantation rubber free from reclaim, silica, and other coarse material, balanced to permit thorough cure. Tensile strength shall be not less than 3000 psi, and elasticity not less than 600 per cent.

Cushion Stock. The cushion stock shall consist of high-grade stock, containing not less than 80 per cent by weight of new plantation rubber, free from reclaim, silica, and other coarse material, balanced in compound to permit thorough cure. Tensile strength shall be not less than 2500 psi; elasticity not less than 700 per cent.

Reinforcement. Two-ply 13-oz Karded Peeler tire cord, frictioned both sides and skimmed one side to a gage of 0.047 in., shall be used for reinforcement.

General Notes. The different elements shall be well cured and well bonded together, so as to withstand a friction pull, between the plies of fabric, of 26 lb per in. of width, and shall be cured in a mold. The provisions of Federal Specifications ZZ-R-601 and CCC-T-191 shall apply.

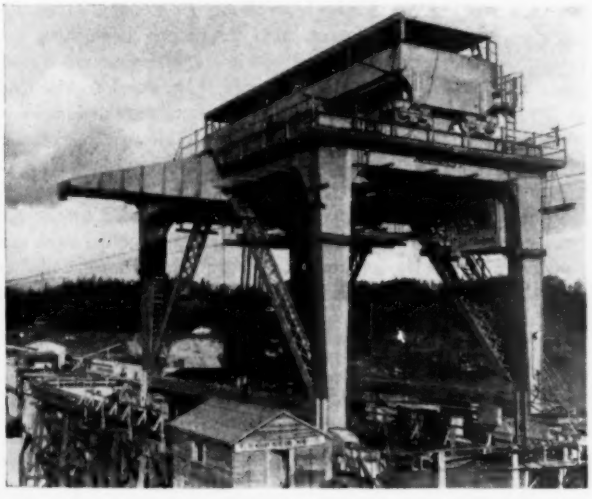


FIG. 4 THE FIRST OF TWO 350-TON GANTRY CRANES NEARING COMPLETION

Length. The rubber seal of above cross section shall be fabricated in unbroken lengths as required.

Aging Test. After samples cut from the various stocks have been subjected to an accelerated aging test in air for 7 days at 158 F, the tensile strength shall be not less than 75 per cent of the original value.

The bottom seal shall consist of tread stock, reinforced by two layers of six-ply 28- or 32-oz cotton canvas duck.

GATE MECHANISM

Gates were provided with 27-in-diam wheels and with SKF self-aligning roller-bearing mountings, similar to a number of previous installations. The wheels are mounted on finished flange plates on the gates, and are assembled with corrugated-steel springs and shims to secure an accuracy of alignment on each row of wheels equaling 0.001 in. per ft of distance, when the springs are compressed with a load of 20,000 to 30,000 lb. Gate wheels and mountings were designed to be suitable for carrying the load, due to the pressure of the water against the gates, under the maximum head, and to allow vertical travel of the gates without excessive friction. To assure even bearing of the wheel treads against the gate guide track plates, under varying deflections of the gates, spherical roller bearings were provided. By means of oval shaft bushings contacting cylindrically bored bearing covers, a maximum movement of 1 deg was allowed the wheels from a vertical plane normal to the track, to compensate for gate deflection, and a maximum movement of only 0.1 deg from a horizontal plane, normal to the track, so that the wheels could not "wander" from the track.

To avoid overloading of individual gate-wheel units, caused by unavoidable track irregularities, both pedestals of each unit were mounted upon a pair of transversely corrugated spring plates to permit an elastic displacement of each of the units. Springs were formed as shown in Fig. 6. Twist or warp in any one spring was not to exceed an amount which would prevent full transverse bearing at all bearing planes, when the spring was subjected to a total load of 10,000 lb.

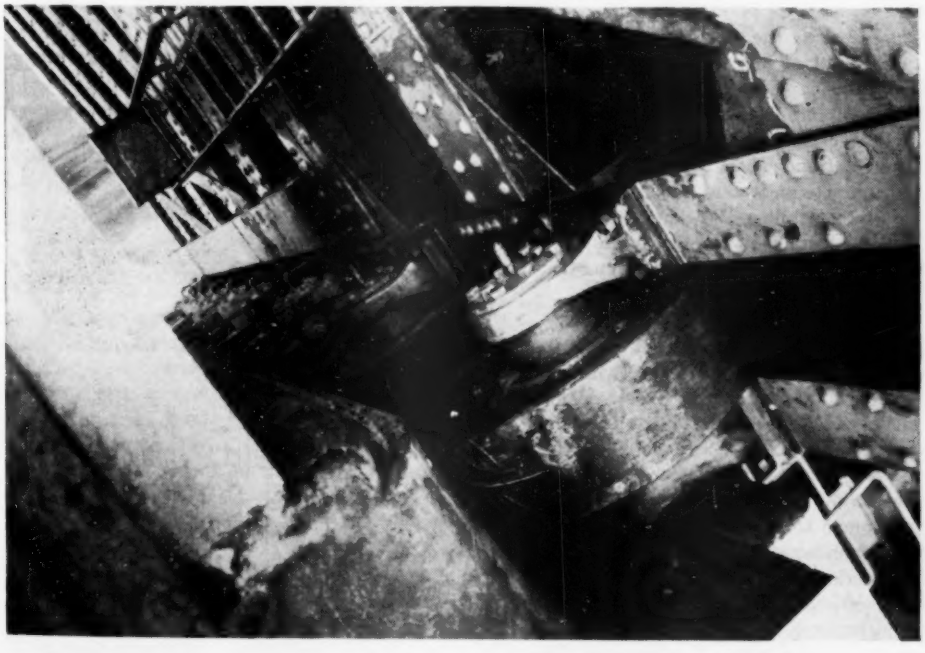


FIG. 5 VIEW LOOKING DOWN GATE SLOT

(This view shows large size of wheels with pedestal mountings; the water can be seen rushing by underneath.)

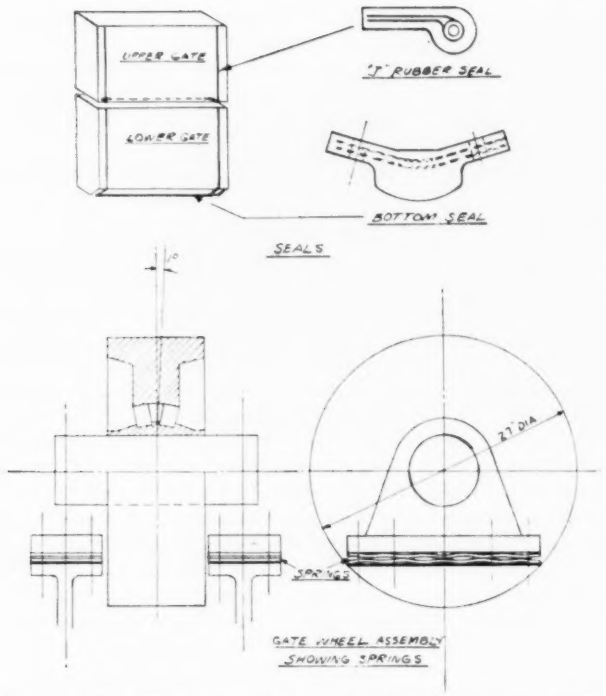


FIG. 6 ARRANGEMENT AND SECTIONS OF RUBBER SEALS AT TOP; BELOW ARE MAIN WHEEL ASSEMBLIES AND CORRUGATED SPRINGS

To permit the bearing surfaces of the wheels to be brought into a common plane, suitable shims, fabricated from corrosion-resistant steel, were placed between the spring plates and the gates. Shims had a minimum thickness of 18 gage. They were supplied in such total thickness that unit stresses in spring plates in no case varied from that resulting from a minimum load of 5000 lb and a maximum load of 10,000 lb, applied at each pedestal mounting at the time specified tolerance conditions of wheel alignment were met.

The wheels are spaced along the gate end girders so that each wheel carries a radial load of approximately 210,000 lb with perfect alignment of track and wheels. The permitted tolerances would cause a maximum load on any wheel not exceeding 265,000 lb. Errors in track and wheel alignment, the deflection and flexibility of the gate, and wheel assembly and loading on the track beams and concrete piers were factors requiring careful study. The tolerances controlling the placing of the various embedded structural members were maintained at considerable expense both to the contractor and to the government.

FIELD PERSONNEL

It was concluded, after 6 months of trial, that the construction-survey crews were best qualified to check steel alignments of embedded gates, guides, and structural members. A few of the better-class machinists, who were capable of making sketches and reading construction blueprints, were successful on this work, but their services were obtained only after many difficulties. It is believed the reason for this is that the construction-survey crews are more accustomed to climbing forms at various elevations. Also, they are familiar with making close measurements with tapes, and are experienced in the use of micrometer adjustments on instruments and leveling rods, thus being able to use the machinist's inside micrometer. Mechanical inspectors usually advance from the grade of machinist. It is not only difficult to obtain them for this work, but, as a general rule, they are not as adaptable, since construction is an entirely new world to them. This faculty of adaptability is generally lacking in the case of structural inspectors, who advance from the grade of ironworker. These men are unable to make close measurements requiring micrometers. Of course, some notable exceptions were found in all groups. However the survey crews are recommended as being most readily available and most generally useful.

The dam was built in three steps. The south half was first constructed, with the crest and gate guides at elevation —10. The north half was built inside its cofferdam, as the second step, with crests at elevation +24; later the south-half crests were raised to elevation +24. The completion of the top of the first half and start of the second half were carried on simultaneously.

The maximum number of inspectors and machinists were employed checking steel at this time, the total being thirty-seven men in the section. In addition to the section head, this number included one junior engineer, replaced later by a surveyman (chief of party), as assistant, nine inspectors, twenty-one machinists and helpers, one master mechanic, and four crane operators. The machinists were gradually transferred to the shop, as the work decreased, and two survey crews were used to check spillway-gate steel, with other crews available to give points as needed. The inspectors continued to do individual checking before and after concrete pours. This large staff was required because of the extent of operations, which included fishways on both sides of the river. A great variety of embedded steel, gate guides, anchor bolts, and machinery supports were installed on the fishways, which included two fish ladders, four fish lifts, and

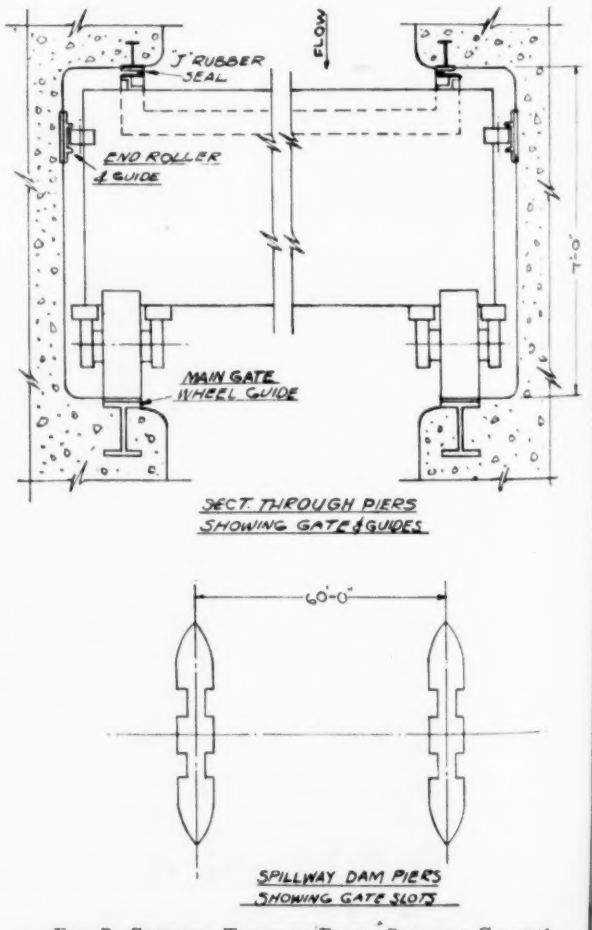


FIG. 7 SECTIONS THROUGH PIERS, SHOWING GENERAL ARRANGEMENT OF CONCRETE PIERS, GATE, AND GATE GUIDES

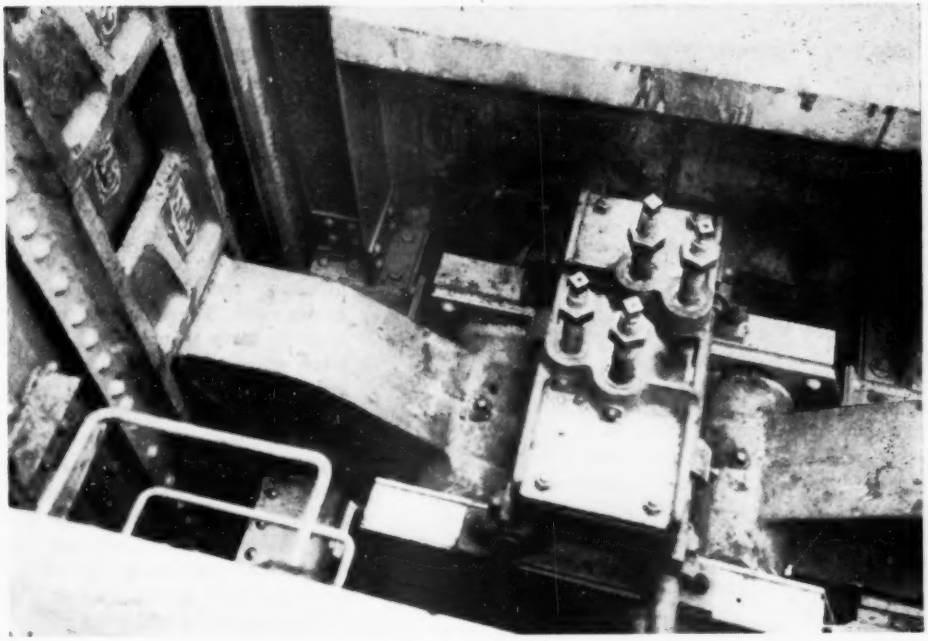


FIG. 8 VIEW OF UPPER LATCH-OPERATING MECHANISM

collection bays at the spillway dam. Othe. fishways were provided at the powerhouse and ship lock.

FIELD INSPECTION AT SPILLWAY DAM

Eighteen bays are included in the dam construction, with concrete piers 10 ft wide. Two sets of gate slots are provided—operating slots (downstream) and emergency slots (upstream). During extreme floods, when it is necessary to raise the gates clear of the water, the top sections are transferred to the upstream slots and latched in position above the water level by means of latches provided in the piers. The lower sections are then raised and similarly latched in the downstream slots. In emergency or for repairs to the operating slots, a spare gate is provided for regulating flow in the upstream slot, or to stop off the headwater as required. When this gate is in place, a small slide gate is dropped in front of the latch opening on the opposite side of the pier. Repair and storage pits are provided in two bays located in the northern approach to the dam.

The gate guides and latch-rack frames are attached to steel towers embedded in the piers. As the gates are in two sections, an upper and a lower latch frame are required to support either or both gate sections, if it is desired to do so during operation. It was a fairly easy matter to control placement of the towers which were set on bedplates and embedded anchor bolts. This placement was checked by transits and heavy weights suspended from piano wires. Control points were first established by the government survey parties at the base of each pier on welded steel frames. These points were carried up as the concrete was poured, by using 100-lb weights suspended from piano wires. Three guide beams are located in each slot to guide the gates and transfer the water-pressure loads from gate to piers. These guides are shown in Figs. 7 and 10.

The track beam consists of a heavy 10-in-width flange beam, having a finished flange, faced with a finished 1-in. × 12-in. 3.5 per cent nickel steel track plate. The plate is secured to the beam flange with $^{3}/_{4}$-in. round-head cap screws, countersunk in the plate. This track beam and plate are shown in Fig. 5. Special steel tapes, only slightly affected by temperature, were

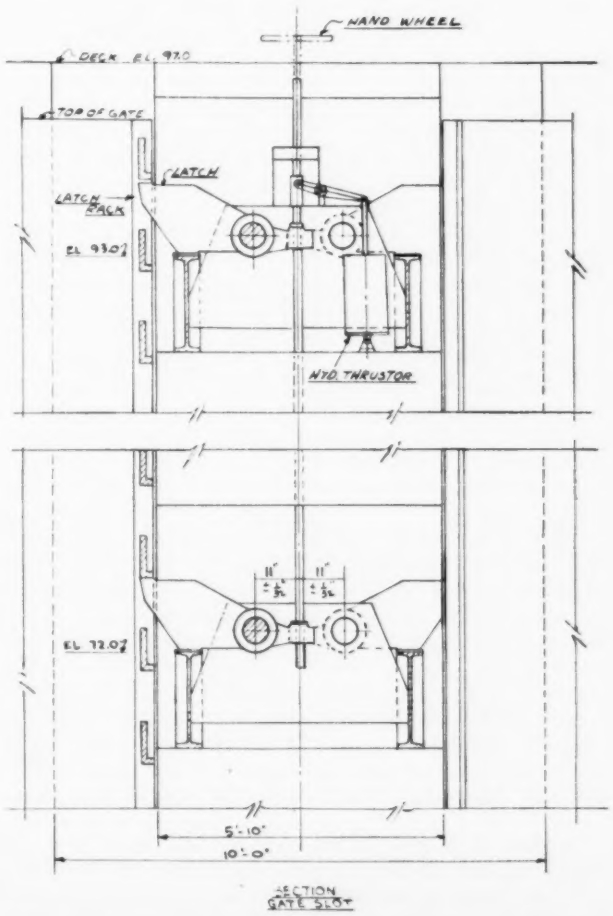


FIG. 9 SECTION THROUGH PIERS, SHOWING GATE-LATCHING MECHANISM

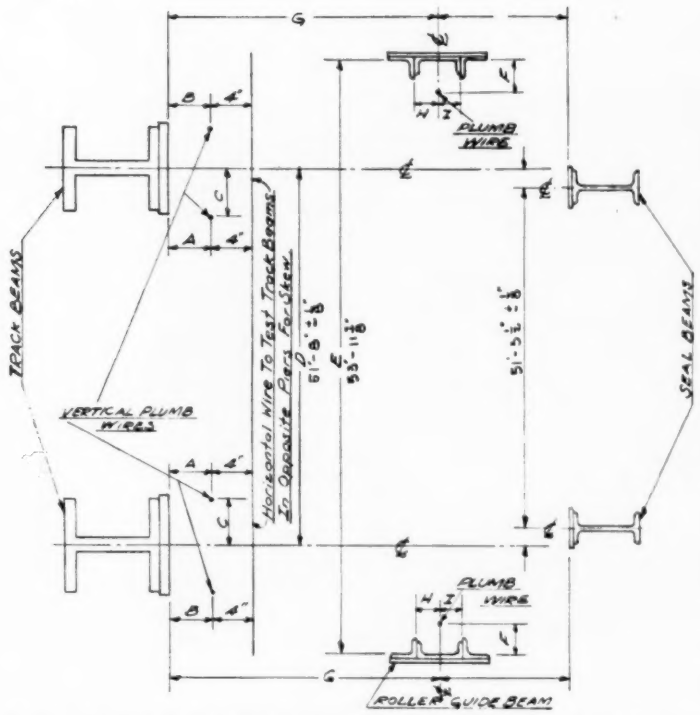


FIG. 10 SKETCH OF GATE GUIDES SHOWING METHOD OF USING PIANO WIRES FOR CONTROL OF PLACEMENT

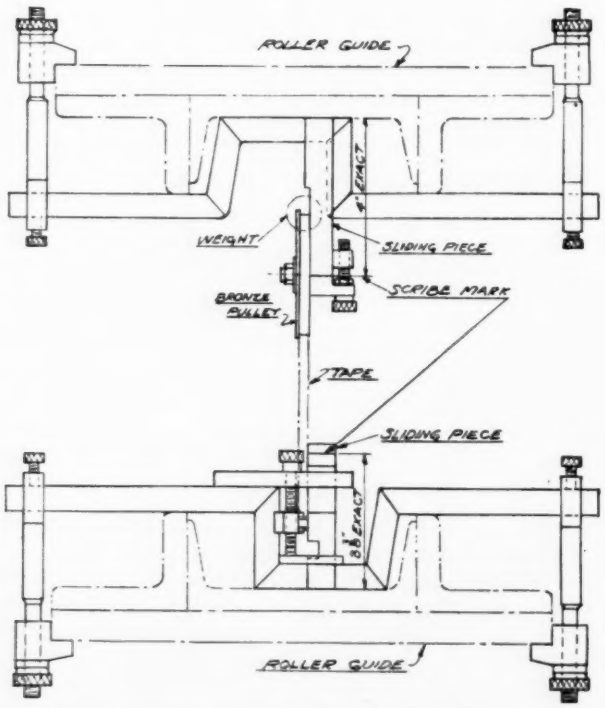


FIG. 11 MEASURING ATTACHMENTS FOR END ROLLER GUIDES

so marked as to give known measurements, when used with measuring attachments, such as those shown in Fig. 11.

These measuring attachments were used to facilitate handling the steel tape across bays on the end roller guides. The sliding pieces were brought into contact with the guides by an operator on each scaffold, then the screw was adjusted bringing the mark on the tape to the 3³/₈-in. mark on the lower device. The correction if any was then read on the other device as the distance between the mark on the sliding bar and the mark on the tape. A clamp was arranged to fit over the legs of the angles for the final check after grouting. The clamp was attached to the device shown.

A similar set of attachments was used on the track beams to control the distance between centers, as shown by *D* in Fig. 10; the tolerance is ±¹/₈ in. as given on the diagram. The track roller and seal beams were "boxed out" in the forms of the piers in order to leave them free to be moved and grouted in later, after completion of the piers. To locate these guides, the contractors used piano wires and tapes. Machinists then checked before grouting, and checked a second time after the grouting was completed. The track and roller and seal beams were checked by government employees who were in reality a three-man survey crew. The checking of the guides by the inspectors followed the usual procedure already outlined, except that the seal beam was checked to the track and roller guides by means of an aluminum gage.

The method of using the piano wires is outlined in Fig. 10. The tolerances in thousandths of an inch for track beams were obtained by the use of inside micrometers, measuring between guide and piano wire. Small screw jacks, welded to the backs of beams, were used for adjustments. Guides, found to be out of tolerance after embedding, were ground with portable electric grinders. Due to the severe weather conditions in the Columbia River gorge, which included sleet storms, scaffolding covered with plywood sheets was used. The enclosures were heated during January and February, enabling the contractor to make the same progress in cold weather as in warm weather.

REASONS FOR CLOSE TOLERANCE

The design notes to be given indicate the excessive wheel concentrations on the main gate guides of the spillway dam. The author will also analyze the increase of normal concentrations, as affected by the unevenness in gate guides. It is intended to demonstrate the fact that it was imperative to follow specifications in erecting these members. It is thought that this information may be helpful to other structural-steel-erection departments in the future.

As designed, one complete 50-ft gate weighs approximately 450,000 lb, and the horizontal hydraulic pressure against it is 4,190,000 lb. One complete 60-ft gate weighs approximately 560,000 lb, and the horizontal pressure is 5,800,000 lb.

The following wheel loads are figured by elastic analysis, assuming maximum permitted inaccuracy of guide beam by the specifications, which are as follows:

Gate Guides, Section 710 *a* of specifications: Contract No. W69eng 575, Change Order D, "* * * tolerance of inaccuracy not to exceed ¹/₁₀₀ of an inch on any 5 feet of length."

The specification of tolerance of inaccuracy of the line of gate wheels from a true line as given on Sheet 12 of M-4-30- is ¹/₁₀₀₀ of an inch per foot.

The combination of these tolerances gives a tolerance of 0.015 in. per 5 ft, or 0.003 in. per ft. Applying 0.002 in. per ft tolerance, conditions for a basis of stress analysis are obtained, Fig. 12.

Considering cases 1 and 2, in Fig. 12, the wheel points are taken as points on a deflection curve for the end girder of the gate.

computing the loads at the several points which would produce a deflection curve passing through these points. The important reactions for these cases are as follows

For case 1—R_a = 472,000 lb
For case 2—R_a = 395,000 lb
} for tolerance of 0.002 in. per ft

These reactions add directly to the normal wheel loads. Case 1 reaction may be neglected because of other effects not considered in this study, tending to relieve some of the stress.

The maximum wheel load, neglecting track yield and deformation of the wheel, bearings, and local deformation of the end-gate girder, would be as follows

Normal wheel load	220,000 lb
Increase due to high point on track beam	395,000 lb
Total	615,000 lb

The strain in wheel and track at point of contact is about 0.0015 in. for the normal wheel load. For twice that load, it

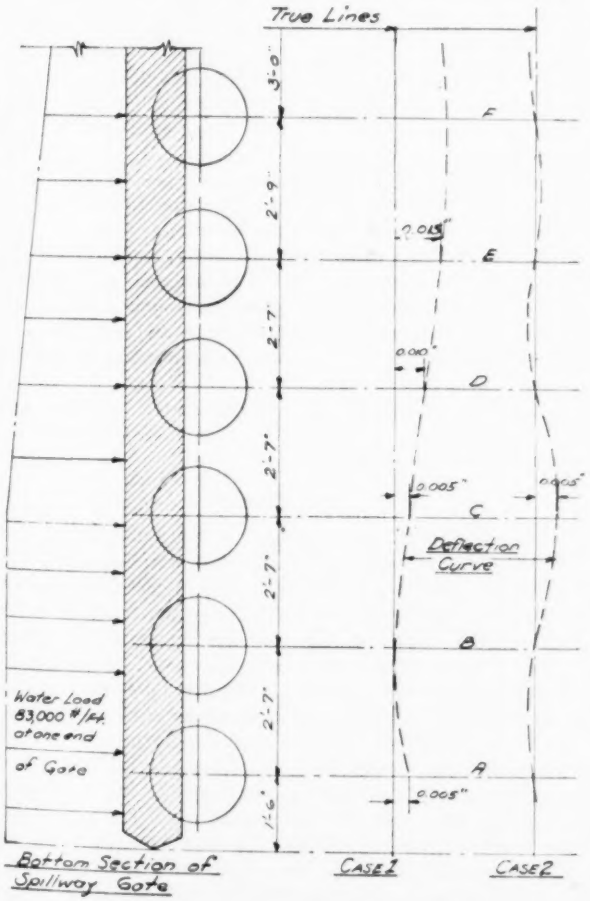


FIG. 12 STRESS ANALYSIS IN MAIN GATE GUIDE OF SPILLWAY DAM

would be about 0.002 in. The strain in bearings and in the girder around the bearing connection, not considered elsewhere in the analysis, would be approximately 0.0005 in., thus making a total relieving strain of approximately 0.0025 in., which is one half of the assumed track unevenness, Fig. 12.

The effect of this yielding is to reduce the increased wheel load, due to the track irregularity. Assume the yielding of adjacent loads to be 0.0005 in. (total), then the net effective yield would be 0.002 in. The resulting wheel-load reduction would be

$$\frac{0.002}{0.005}(395{,}000) = 160{,}000 \text{ lb}$$

The net maximum possible wheel load which could be anticipated from conditions as specified could be

615,000 lb
—160,000 lb
455,000 lb

or 207 per cent of normal wheel load. By applying the Timoshenko method of using the Hertz equations, the wheel load of 455,000 lb will produce a stress in the track plate under the wheel of approximately 175,000 psi, which is approaching the elastic limit for this type of stress.

Due to limiting the wheel diameter, the design is limited by the condition of contact stress, even if it were possible to design the wheels themselves for greater loads, which in itself would be well-nigh impossible. Therefore, it becomes necessary to obtain the degree of accuracy, required by the specifications, to insure safe operation of the gates.

To prove the sufficiency of the design of the wheel, bearings, and supports, two full-size experimental wheel assemblies, complete with SKF No. 22336, having two rows of fourteen rollers each, shaft diameter 7.0866 in., outer-race diameter 14.9606 in., rollers 1.772 in. long × 2.165 in. diam, and rated capacity in equivalent radial load 425,000 lb, were tested on a 600,000-lb Southwark-Emery testing machine at Oregon State College.

A special base was provided for the assembly which was to occupy the lower position in the testing machine. Between this base and the assembly was a set of flat springs, also a subject of these tests. The upper assembly, carried by the movable head of the testing machine, was provided with an auxiliary cast-steel block attached without springs.

A section of track plate 12 in. wide, 1 in. thick, and 5 ft long reciprocated under load between the adjacent wheel faces at a speed of 2 fpm. It was the purpose in these tests to simulate as nearly as possible actual conditions of use, except that it was not practicable to arrange for side thrust; instead, equivalent radial loads were computed and applied.

Under section IV in paragraph 416 of the specifications for gate wheels, it was required: "The normal static radial capacity per bearing shall be 210,000 pounds combined with a thrust load of 50,000 pounds and, under a load 75 per cent in excess of this load, the bearings should show no signs of permanent deformation either measurable or microscopically visible." The equivalent radial load for the proposed bearing satisfying this specification is 425,000 lb.

A flat-plate spring with machined loading pads, as well as two types which could be drop-forged or hot-pressed, were tested. Type 1 was a flat-plate spring with machined loading pads. Type 2 was a flat spring with forged loading pads. Type 3 was the corrugated plate spring, shown in Fig. 6. Bakelite models were made of these three types for photoelastic study.

Type 1 showed high stress concentration adjacent to the machined loading pads. Types 2 and 3 proved to be better designed with less stress concentration. They avoid the danger of hardening cracks, due to abrupt changes in section. Type 3 was chosen because of its being slightly more elastic, giving a greater deflection for the same load.

SPECIFICATIONS COVERING ERECTION OF GATE GUIDES AND SEAL BEAMS

Lower sections of towers, gate and roller guides, and seal beams to be set on anchor bolts, truly plumbed, braced and guyed

firmly and held rigidly. Dependence must not be made on anchor bolts or connections to sole plates to resist overturning. Sections to be shimmed and welded or riveted or bolted, as detailed. Plumbing to be observed and to be corrected when necessary.

Gate-guide-beam and seal-beam sections to be plumbed by means of the shims, and welding for guide beams to be performed at the thrust frames just in advance of the pouring of concrete. After each pour, the contracting officer to check plumbness in both directions, and necessary corrections to be made.

Face of gate guides shall not be covered with forms during concreting operations. Tolerance of inaccuracy, shown in Fig. 10, of face of guides shall be maintained during concreting operations without vibration, and access provided for measurement by the contracting officer of this face in two directions. Structural-steel connecting members, composing tower structure, shall be so stayed as to prevent movement of guide members during this period. Face of guide flanges to be milled to a plane surface having a variation not to exceed 0.01 in. in 5 ft of length. This same degree of accuracy to apply when erected. Particular care shall be given to the alignment of gate guides in plane of axis of dam. This alignment shall be based on a true plane surface passing through the milled surfaces of the gate-guide track plates, which in turn shall be parallel to the vertical longitudinal axis of the dam. The method of erection to achieve this result will be submitted to the contracting officer and his approval secured before erection shall be undertaken.

Gate and roller guides and seal beams when erected shall conform with the diagram of tolerances, as given. Axes must be truly at angles of 90 deg, and acceptance or rejection of this work by the contracting officer will be based on obtaining results in accordance with these requirements.

Note: For outside and center girders all construction loads shall be hung at panel points only.

The latch frames must be set to the exact position shown on the plans. The center lines of the pinholes must be in the same horizontal planes. The tops of the 24-in. I-beams must be in the same horizontal planes. The frames must be supported and fastened sufficiently as to prevent displacement during placing of concrete.

Gate-Guide Tolerances. As finally determined the gate-guide tolerances are as shown in Fig. 10, and are as follows:

A tolerance of $\pm 1/8$ in. was allowed across bays between seal beams and also track beams. The end roller guides were held to an exact dimension on print M-4-29, sheet 2, the pertinent data of which are shown in Fig. 10. A variation of $+1/8$ in. was allowed on end roller guides, in the field, but no minus tolerance. The following vertical tolerances were specified for track beams:

From elevation 24 to 56, a tolerance of 0.010 in. in 5 ft of height; from elevation 56 to 72, a tolerance of 0.015 in. in 5 ft of height; and from elevation 72 to top, a tolerance of 0.030 in. was allowed by letter instructions. By M-4-29, sheet 2, seal beams in any 60 ft of height were required to be within a tolerance of $1/4$ in. away from gate, of $1/8$ in. toward gate, and, in any 5 ft of height, not over $1/16$ in. The face sides of seal beams were required to have a mill tolerance of $1/16$ in. This meant that the plane of the flange of the seal beam in its width could not be more than $1/16$ in. out of parallel with the axis of the dam. On the south half of the dam, where crests were poured in two steps for elevations below 21, a tolerance of 0.020 in. in 5 ft of height was allowed. In storage pits, the end roller guides had the following tolerances: "They must not have sweep over $1/8$ in. in 16 ft, straight to tolerance of $1/16$ in. to 5 ft, with camber not more than $3/16$ in. for individual pieces," as specified on sheet 41 of M-4-29.

Latch-Frame Tolerances. The embedded latch frames to support the latch dogs and mechanism, as shown in Figs. 8 and 9, were first designed to be held to an exact dimension. This was found to be too exacting before embedding and impossible to hold while the piers were being poured. Therefore, as in the case of the track beams, a method was devised whereby adjustments might be made after the main part of the steel was embedded. Rivets on part of the steel frame were cut loose and bolted later after the "boxing out" and grouting operation, as in the case of the gate guides. A tolerance of $\pm 1/8$ across bays was allowed between latch pins, and a tolerance of $\pm 1/4$ from the axis of the dam to the latch frame. Due to the clearance of the latch and rack, the $\pm 1/8$ tolerance could have been $\pm 1/4$ in. An elevation tolerance of $\pm 1/8$ in. was also allowed.

Steel tubing of the size of the latch shaft was placed in the holes provided. These holes were bored to a close tolerance, which facilitated the method used to obtain close erection measurements. A piano wire was drawn through a small hole, drilled through the exact center of the tube. The wire was strung across bays, allowing a measurement to be taken to the track beam. This method of control was followed on the gate erection in that measurements were taken from the face of the rollers to the center line of the latch racks on the ends of the gates. The distance from the face of the end roller guide to the latch shaft gave a control or check on the distance between shafts across the bays, as the roller guides were held to a tolerance of $+1/8$ in. across bays.

Roadway-Girder Tolerances. The spillway-dam main truss girders, designed to support the gantry cranes and the roadway which is 30 ft wide, were held to the following:

Steel was required to be free from kinks, bends, and winds, which produce excessive stresses. The tolerance was 1 in 1000, which amounted to 0.6 in. End posts were required to be plumb before grouting; base plates and girder shoes and sole plates were machined for bearing fit. The over-all length tolerance was $\pm 1/4$ in.

There were two side trusses and one center steel truss, embedded in concrete. Concrete deck panels were placed across these to make the roadway.

Fishways

As previously mentioned, two fish lifts are provided at each end of the spillway dam and two at the powerhouse. As the name implies, these are merely elevators. A gate is closed when the chamber is filled with fish, and a platform is raised by means of hoists. The water in the chambers is controlled through exit and entrance passage leading to the bottom of the lifts by the use of radial gates. Four fish ladders are provided, namely, one on each end of the dam, one from in front of the powerhouse, connecting with the one from the south end of the dam, and the last starting from Tanner Creek below the site. This last fishway passes behind the white houses, shown in Fig. 1, then up through the south side of the ship-lock cut. The ladders are simply a series of pools regulated with weirs made of stop logs on top of a concrete wall. The lower pools are referred to here as diffusion chambers. They are provided with additional water, regulated by radial gates and sluice gates coming into the bottom of the pools through a grid of concrete and wood.

The fish-ladder and fish-lock steel caused considerable trouble principally because it was embedded at the time of the pour and not boxed out and grouted later. Where a steel frame for support could be welded across the gate openings, the guides were held to close tolerances but this could not be done in the larger openings of the elevators. These guides were out of plumb as much as $5/8$ in. and the concrete 2 in. in 70 ft, due to the poor placing of forms. The fishway-steel tolerances in general were as follows:

Diffusion-Chamber Gates. These are rectangular, similar to a number of sluice gates on the market. The sealing surface between the gate and the frame was held to a total leakage-orifice area of not more than $^1/_2$ sq in. and an orifice not wider than $^1/_{64}$ in.

Weir Stop Logs and Gate Guides. Maximum crack between log and concrete $^1/_4$ in. Minimum horizontal end play in guides $^1/_4$ in. Minimum side play in guides $^1/_4$ in. Minimum clearance between bottom of latching pin and top of notched end of timber log $^1/_4$ in.

A tolerance of $\pm^1/_4$ in. was specified for the length and width of openings for steel guides for the stop logs: Emergency, regulating, and segmental gates for all fishway gates, including fish-lock stop logs. Fish-lock roller-guide openings had a tolerance of $\pm^1/_2$ in., and segmental gates $\pm^1/_8$ in. A tolerance of not under 90 deg was required for corner end plates for the last two gates mentioned. A tolerance of $^1/_8$ in. at the outside end of these plates over 90 deg was allowed. All guides, except those for fish-lock entrance and exit gates were required to be held to not more than $^3/_8$ in. out of plumb for the entire vertical height, or more than $^1/_8$ in. out of plumb for any 10 ft of height. Fish-lock exit- and entrance-gate guides were required to be not more than $^1/_8$ in. out of plumb for the entire vertical height, or $^1/_{16}$ in. out of plumb for any 5 ft of height. Tolerances for horizontal dimensions were as discussed and were taken from T-3-117 sheets 1 and 2.

Tainter Valve (Radial Gate). Finished seals were specified to have an opening tolerance of $\pm^1/_{32}$ in. top to bottom and $+^1/_{32}$ in. from side to center line of the valve on the sides. The embedded-steel tolerance was generally $+^3/_{16}$ in. The bottom finished seal was required to be level. The top finished seal was required to be plumb and not more than $^3/_{16}$ in. from parallel for the entire width to the center line of the trunnion pin. It was difficult to hold these dimensions, and the finished seals were placed to valve after installation.

Conclusions

1 Where close tolerances on embedded structural steel are required, the best method to employ is that of the so-called "grouting system." This method requires setting the steel after the main body of concrete has been poured. Recesses are made by using box forms with reinforcing bars or ties for the structural steel left exposed. After all forms have been stripped, the structural steel can then be placed, lined up by means of piano wires and other devices, and cement grout placed around it.

2 The construction survey party makes the ideal structural-steel inspection crew for large installations, requiring close measurements, provided the individual members have had some college or engineering training in construction plans and specifications. These men have less difficulty in adapting themselves to making measurements with the special attachments provided than is the case with machinists who ordinarily are not accustomed to working in the field on construction projects. Of course, the regular structural-steel inspector is of value on riveting and welding work.

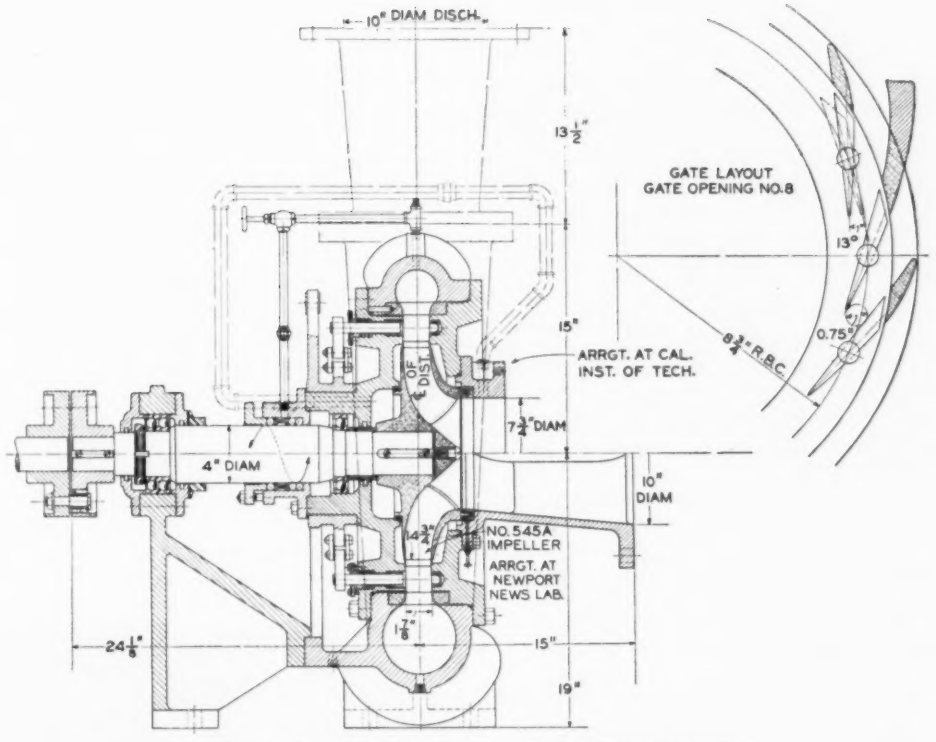


FIG. 1 SECTIONAL ELEVATION OF PUMP-TURBINE MODEL

Test Characteristics of a Combined Pump-Turbine Model With Wicket Gates

BY R. V. TERRY[1] AND F. E. JASKI,[2] NEWPORT NEWS, VA.

Tests of a wicket-gate pump-turbine model at the Newport News hydraulic laboratory and at the California Institute of Technology are described in this paper. The model was one of a series used in a study of pumps suitable for Grand Coulee. Characteristic curves both as a pump and turbine are illustrated, and expected-performance curves for a prototype stepped up to Grand Coulee conditions are developed from the tests. In conclusion, a summary is given of the advantages of the wicket-gate pump-turbine.

DURING recent years considerable study and experimental work have been devoted to the development of combination hydraulic machines with wicket gates which would be suitable for operation either as centrifugal pumps or as hydraulic turbines for peak-load storage development. Certain test characteristics of such a combination machine, and characteristics of wicket-gate pumps have been given in many articles in the technical press (1 to 9).[3]

However, it does not appear that the complete test characteristics of any one combination machine have been presented to this Society or published elsewhere.

The model described by the authors was one of a series of machines tested at the Newport News hydraulic laboratory in connection with the development of combination machines. It

TABLE 1 MAIN PARTICULARS OF WICKET-GATE PUMP-TURBINE MODEL

Impeller, diameter, in.	14.75 (progressively cut to 12 in.)
Eye diameter, in.	7.75
Number of vanes	8
Entrance angle at band, deg.	20
Entrance angle at hub, deg.	34
Discharge angle, deg.	30
Discharge height, in.	1.875
Number of wicket gates	16
Diameter of gate circle, in.	17.5
Outside diameter of speed-ring vanes, in.	21
Diameter of suction pipe, in.	10 (7⅜ in. diam at California Tech.)
Throat diameter of casing, in.	6⅞ in. (flaring to 10 in. discharge diam; flaring to 8 in. diam at California Tech.)
Offset of casing throat to center line, in.	13.5
Designed gate opening, in.	0.75 (gate 8)
Maximum gate opening, in.	0.95 (gate 10)

[1] Assistant Chief Engineer, Newport News Shipbuilding and Dry Dock Company. Mem. A.S.M.E.

[2] Hydraulic Division, Newport News Shipbuilding and Dry Dock Company.

Contributed by the Hydraulic Division and presented at the Annual Meeting, New York, N. Y., December 1–5, 1941, of THE AMERICAN SOCIETY OF MECHANICAL ENGINEERS.

NOTE: Statements and opinions advanced in papers are to be understood as individual expressions of their authors and not those of the Society.

[3] Numbers in parentheses refer to the Bibliography at the end of the paper.

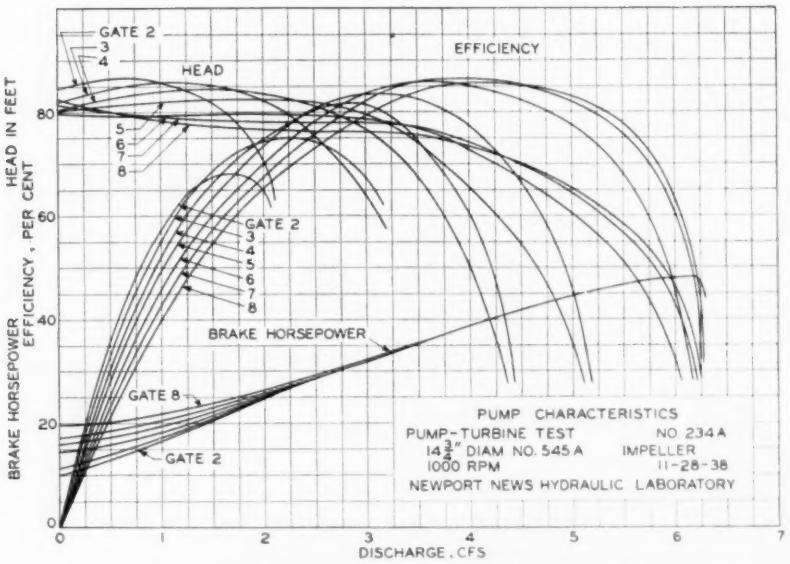


FIG. 2 PUMP CHARACTERISTICS, NEWPORT NEWS TEST

was a single-suction machine of a somewhat low-specific-speed type, its specific speed as a pump at best efficiency being about 1750 by the usual formula $N_s = \frac{N\sqrt{\text{gpm}}}{H^{3/4}}$ and its specific speed as a turbine at best speed and at 95 per cent of its full-gate power being about 25.

The model was designed to be used in a study of pumps of various types, including volute and double-volute types, which would be suitable for the proposed conditions at the Grand Coulee pumping plant. It is expected that the Grand Coulee pumps will operate under the following range of conditions and at a speed of not less than 150 rpm:

Dynamic head, ft	Discharge, cfs	Inlet head, ft
295 (rated)	1600	+80
367 (maximum)	1000 (approx.)	+ 5

Some of the characteristics of pump models with volute, double-volute, and with fixed diffuser vanes are given in a paper by R. T. Knapp (12).

DESCRIPTION OF MODEL

The model was of the horizontal single-suction type, as shown in Fig. 1. The principal particulars of the model are given in Table 1.

The wicket gates were in line with the fixed stay vanes or speed-ring vanes at 0.75 in. gate opening. At that opening, the angle of the center line of the gate tips was 9 deg with the tangent.

The impeller diameter of 14.75 in. selected was intermediate between that for a normal design of turbine and for a normal design of volute pump. The diameter was about 22 per cent larger than required for a normal turbine and about 5 per cent smaller than for a volute pump. The eye design was dictated by the pump requirements for high efficiency and was somewhat smaller than for a normal turbine.

Throughout the design, its functions as a pump were favored because of the somewhat critical conditions imposed by deceleration in the water passages, as opposed to acceleration in a turbine which is not as critical. Many previous studies by the author and others had shown that the usual proportions of pumps would result in fairly satisfactory turbine performance but that the usual proportions of turbines would not make satisfactory pumps.



FIG. 3 CASING WITH IMPELLER REMOVED

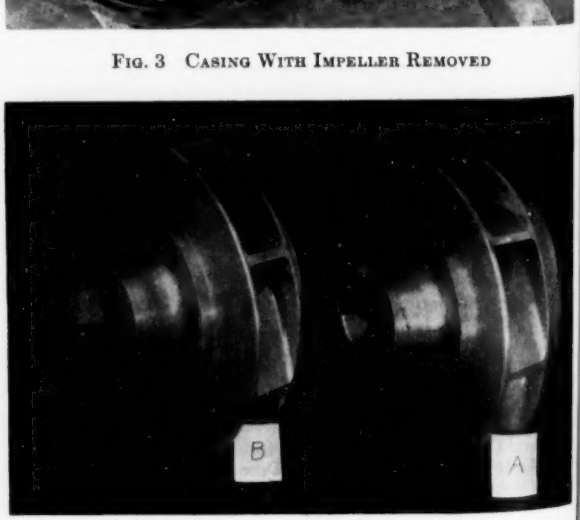


FIG. 4 IMPELLERS (*A*) AND (*B*)

Two impellers were built to the same design and are designated in the paper as impellers (*A*) and (*B*). The second impeller was necessary in order to make tests under different combinations of proportions, as will be described.

Tests at Newport News

The model was first tested at the Newport News hydraulic laboratory, the following tests being made:

Test no.	Impeller, in.	Type test	Speed, rpm	Head
1	14.75 (*A*)	Pump	1000	Variable
2	14.75 (*B*)	Pump	1000	Variable
3	14.00 (*B*)	Pump	1000	Variable
4	14.75 (*A*)	Turbine	450 to 1000	Abt. 45 ft

No cavitation tests were made at Newport News on these particular impellers.

Fig. 2 shows the complete pump characteristics for test No. 1 with 14.75-in. impeller (*A*). The results with impeller (*B*) were practically identical, except that the discharges were a little higher, the impeller measurements showing about 4 per cent larger suction vent openings than impeller (*A*). Fig. 3 shows the casing without impellers, and Fig. 4 the impellers.

In the Newport News tests a 65-hp, d-c electric dynamometer was used to measure the torque. A revolution counter, engaged and disengaged by a program machine and a master clock, was used to obtain the speed. The water was measured by a battery of 10-in. and 6-in. Venturi meters, calibrated volumetrically in place in both directions of flow. The inlet and discharge heads were measured by mercury manometers.

The Newport News hydraulic laboratory has been described in a paper previously presented to the Society (13). Tests made in this laboratory are accurate to within about 0.5 per cent.

Tests at California Institute of Technology

By arrangement with the Bureau of Reclamation, the complete model with impellers (*A*) and (*B*) was rather extensively tested at the California Institute of Technology. The measurement and control of speed, torque, head, and discharge was made in accordance with the regular practice of that laboratory (14). The pump tests were made principally at 2000 rpm, twice the speed and four times the head for the Newport News tests, corresponding with approximately the full-field-head conditions for the specific speed of the model. The turbine tests were made at constant speeds, principally at 1500 and 1800 rpm, the latter being the practical limit of the laboratory equipment for testing a turbine model of this size. Variation of unit speed was accomplished by variation of head. Turbine-discharge and pump-suction pressures were taken from a single orifice connection at a distance of 1 diam from the model. Turbine-inlet and pump-discharge pressures were taken with a single orifice connection about 6.75 ft from the model. A computed allowance was made for pipe friction.

The gate mechanism was calibrated at ten gate-opening positions, as follows:

Gate position no.	Gate opening, average, in.
1	0.092
2	0.181
3	0.275
4	0.370
5	0.465
6	0.560
7	0.655
8	0.750
9	0.850
10	0.950

Sixty test runs were made and plotted, fifteen as a turbine and forty-five as a pump. Nineteen of the pump runs were made for cavitation studies. It was not possible to test the model for cavitation as a turbine, because of its specific speed, but this was not necessary, since it is well known that, for a combination machine, the cavitation conditions when operating as a pump are critical and controlling. All of the turbine tests were made with impeller (*A*); while 37 of the pump runs were made with impeller (*A*) and 7 with impeller (*B*).

The regular tests for pump characteristics were run with a positive inlet head of 80 ft, measured from the center line of the model.

The diameter of the impeller (*A*) was progressively cut from $14^3/_4$ to 14, 13.5, 13, 12.5, and 12 in. In some cases, only the tips of the vanes were cut, leaving the shrouds extended, while in others the shrouds were cut back with the vanes. Impeller (*B*) was first tested at 14 in. diam, and progressively cut to 13.5 and 13 in., vanes and shrouds being cut at the same time.

For operation under 2000 rpm, it was found that the design of the bearings and seals was not adequate. Some trouble was experienced with heating and failure of bearings. The impeller seals were rather narrow axially and the average clearance on diam of 0.019 in. was exceptionally large for this size of model. Leakage past the crown seal ring was measured frequently and found to be 0.075 cfs at 295 ft head, corresponding to a leakage loss of about 2 per cent of the rated discharge for the two seals. This loss could readily be reduced to 1 per cent with a better seal design. However, the test results given in this paper are for the seals as tested, no allowance being made for the excess leakage in either the Newport News or California tests.

Figs. 5 and 6 show the model as installed in the laboratory of the California Institute of Technology.

Results of California Tests

Fig. 7 shows the complete characteristics of the model as a pump with 14.75-in. (designed diameter) impeller (*A*), and Fig. 8 shows its corresponding characteristics as a turbine.

The following will be noted from the pump characteristics, Fig. 7: (*a*) The curves at each gate opening above gate No. 3 show a discontinuity at about 4.8 cfs similar to that reported by Gongwer and Knapp (11, 12). Discontinuity at the same speed and discharge was also found from tests at the reduced impeller diameters. The discontinuity point occurred at a slightly higher discharge with impeller (*B*), corresponding with its increased vent openings previously mentioned. (*b*) At each gate position, the head at zero discharge is slightly lower than at an intermediate discharge; but, for the enveloping head curve, the highest head occurs at zero discharge. (*c*) Above a discharge of about 7 cfs, the power input at a given discharge is constant over a wide range of gate opening and head. (*d*) The shutoff power, required to drive the pump up to speed with the gates closed or nearly closed, is a small fraction of the shutoff power at the most efficient opening (gate No. 7), and is equal to about 16 per cent of the maximum power. (*e*) The best unit speed as a pump for the best gate openings is as follows:

Gate	Best N_1
6	$2000 \div \sqrt{307} = 114.0$
7	$2000 \div \sqrt{295} = 116.5$ (maximum efficiency)
8	$2000 \div \sqrt{285} = 118.5$

From Fig. 8, the following will be noted: (*a*) The full gate as a turbine is larger than the full gate as a pump, gate No. 10 versus gate No. 8. (*b*) The unit power P_1 and unit discharge Q_1 reduce rather rapidly as the unit speed is increased. This corresponds with the usual characteristics of low-specific-speed turbines and is

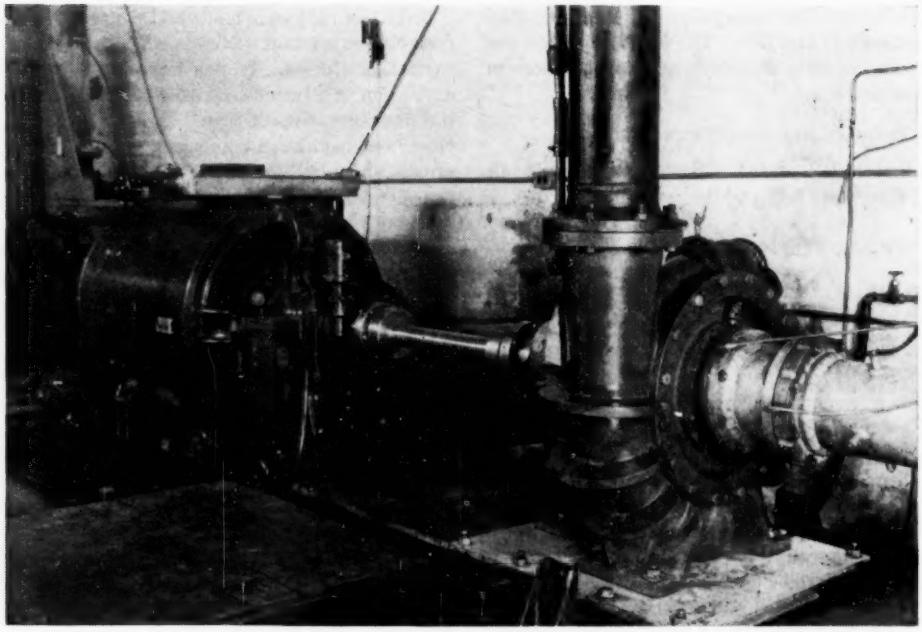


FIG. 5 PUMP SETUP FOR TEST AT CALIFORNIA INSTITUTE OF TECHNOLOGY LABORATORY

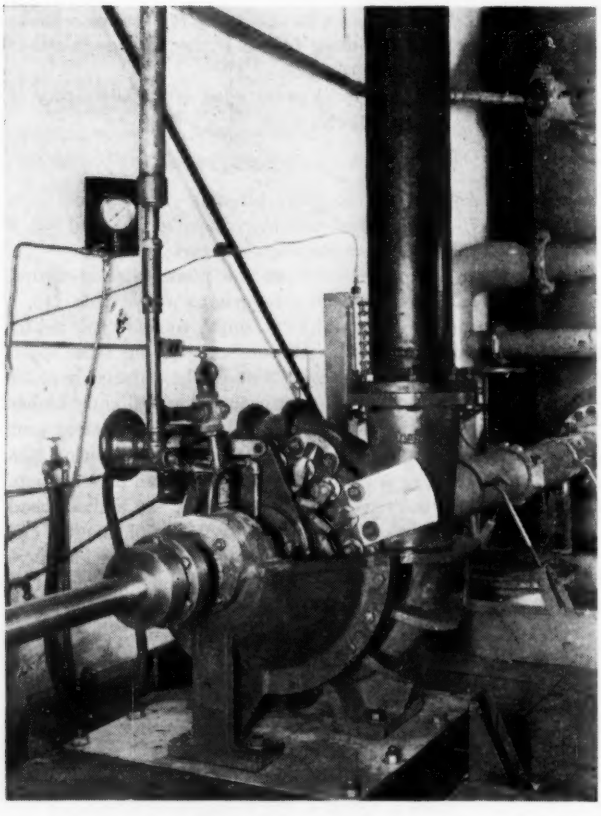


FIG. 6 VIEW OF OPERATING SIDE OF PUMP AT CALIFORNIA INSTITUTE OF TECHNOLOGY LABORATORY

attributable to the bucking effect on the head created by centrifugal force at the higher speed. In the case of the combination machine, since the impeller diameter is considerably larger than for the usual turbine, the centrifugal effect is more pronounced. (*c*) The best unit speed N_1 as a turbine is about 105. Since this is lower than the best unit speed as a pump, the use of a combination machine at constant speed and head would involve some sacrifice in efficiency. However, in a case like that at Grand Coulee where most of the pumped water would be used for irrigation, the unit would be operated as a turbine only at the higher heads which would reduce the unit speed as a turbine to a high efficiency value.

The several cavitation tests made as a pump brought out the following facts:

1 For a given discharge and speed, the limiting and critical inlet heads are the same for different gate openings, and are also the same for the different impeller diameters. This shows that the conditions surrounding the periphery of the impeller have no effect on the cavitation characteristics, which are determined solely by the proportions of the eye and suction edge of the vanes. This was found to be true over the entire cavitation-test range from 3 to 8.5 cfs at 2000 rpm, rather complete tests being made at 3.0, 6.0, and 8.5 cfs.

2 The efficiency as either a pump or turbine was not affected until the runner was cut to below 13 in. diam.

3 Cutting the discharge tips of the impeller vanes, while leaving the shrouds extended, lowered the efficiency both as a turbine and as a pump. However, the extended shrouds had an effect in increasing the head as a pump as would be expected. The head at 13 in. diam, with shrouds at 14.75 in. diam, was about 2 per cent greater than with the shrouds cut back to 13 in.

The cavitation characteristics of impellers (*A*) and (*B*) were at first found to be somewhat different. The inlet edges of the (*A*) impeller were found to be somewhat more irregular and more blunt than in impeller (*B*). After this was corrected, the results agreed very closely with those of impeller (*B*).

COMPARISON OF NEWPORT NEWS AND CALIFORNIA TESTS

In Fig. 9, the envelopes of the head and efficiency curves for the California tests at various gate openings at 2000 rpm, are reproduced from Fig. 7. The corresponding curves, stepped up from the Newport News tests of Fig. 2, are also shown. There is a slight increase in efficiency for the California tests under the higher head.

The break in the head curve in the California test occurs at a smaller discharge than in the Newport News test. This was

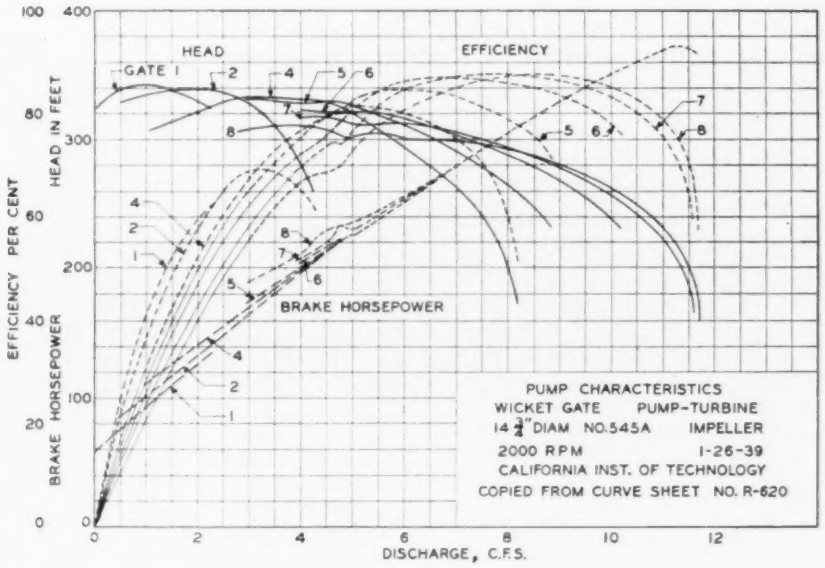


FIG. 7 PUMP CHARACTERISTICS, CALIFORNIA TESTS

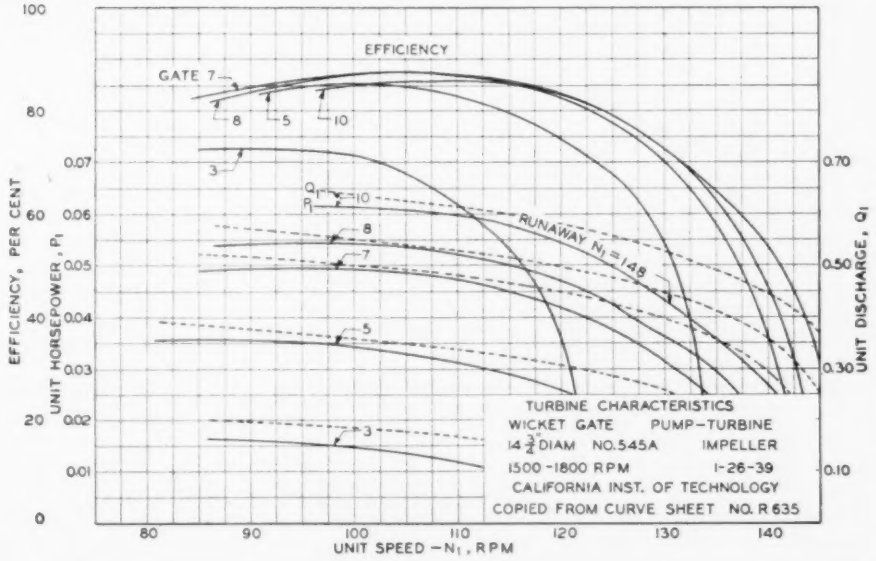


FIG. 8 TURBINE CHARACTERISTICS, CALIFORNIA TESTS

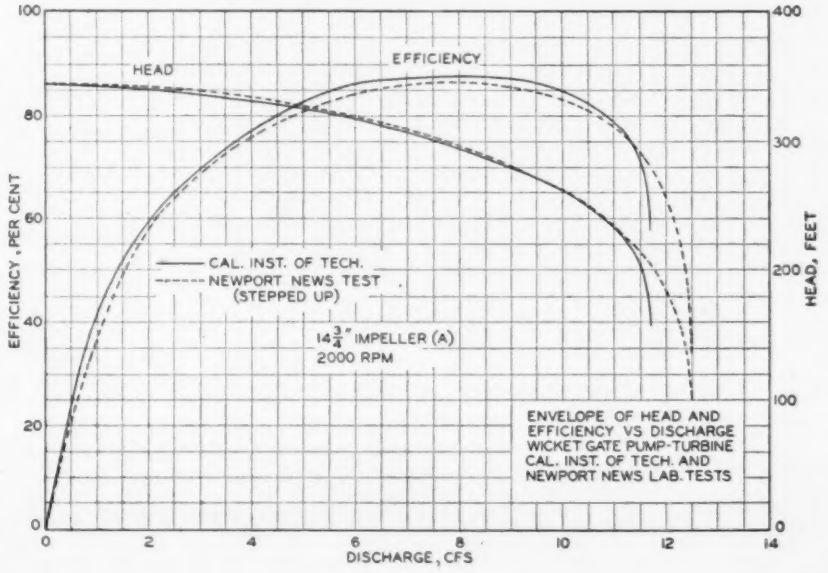


FIG. 9 COMPARISON OF CALIFORNIA AND NEWPORT NEWS PUMP-TEST CURVES

apparently due to the size of the suction pipe ($7^{5}/_{8}$ in. diam) used in the California tests. The entrance loss and friction loss in this pipe were the controlling factors which determined the cutoff point in the California test.

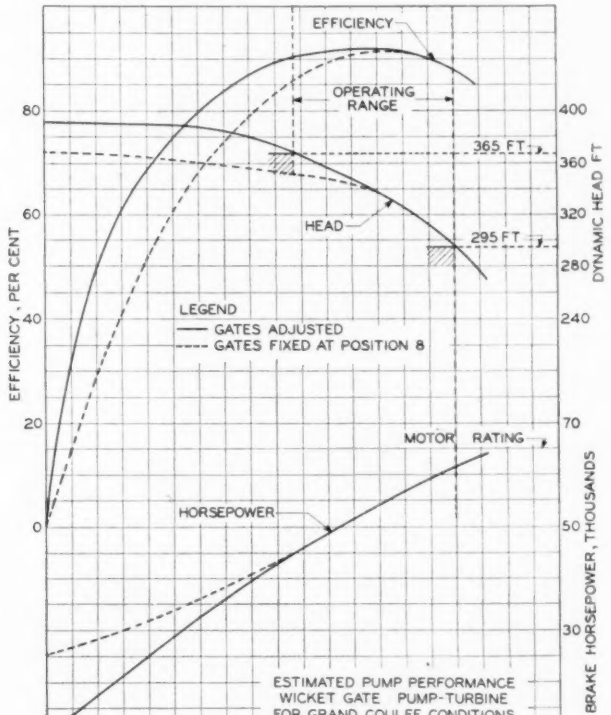


FIG. 11 EXPECTED-PERFORMANCE CURVES FOR PROTOTYPE, UNDER GRAND COULEE CONDITIONS, AS A PUMP

COMPARISON OF SPEED CHARACTERISTICS, PUMP VERSUS TURBINE OPERATION

Fig. 10 shows curves of efficiency versus unit speed, for turbine and pump operation, deduced from the tests at the California Institute of Technology. It will be noted that the best unit speed for pump operation is 11 per cent higher than for turbine operation. Thus, if the unit were operated as a turbine at a speed corresponding to an N_1 of 105, which is the best N_1 for turbine operation, it would have to run at 11 per cent higher speed when operated as a pump to obtain optimum performance under the same head.

Fig. 10 also shows the corresponding model unit speeds for a unit suitable for the proposed Grand Coulee pumping-plant conditions with a 14.75-ft-diam runner, operating at a constant speed

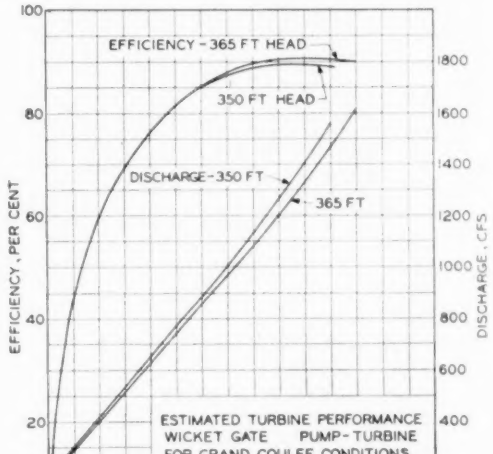


FIG. 12 EXPECTED-PERFORMANCE CURVES FOR PROTOTYPE, UNDER GRAND COULEE CONDITIONS, AS A TURBINE

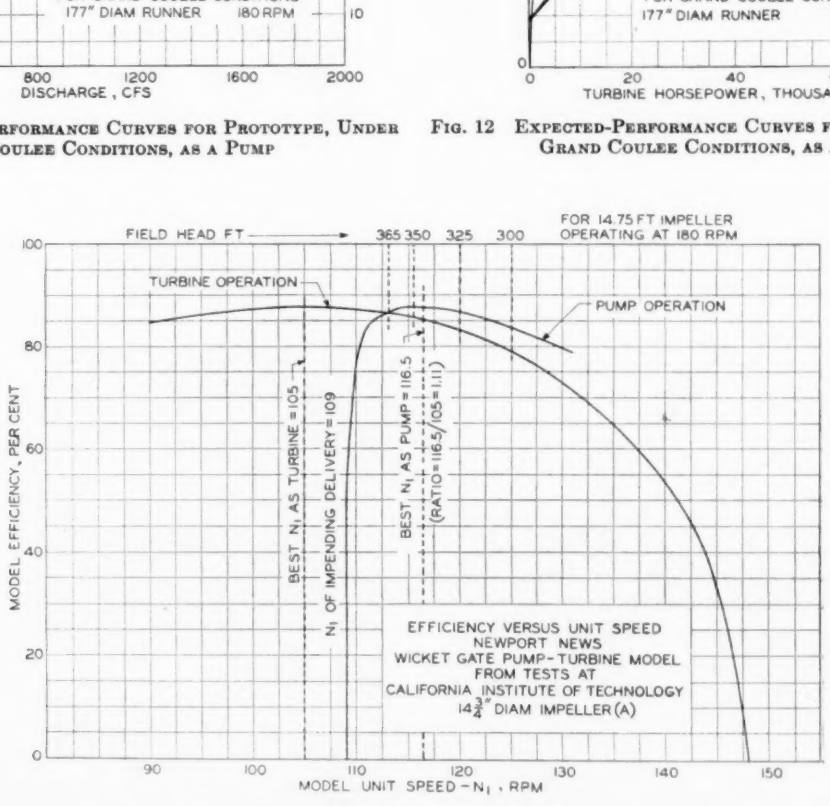


FIG. 10 EFFICIENCY VERSUS N_1 FOR TURBINE AND PUMP OPERATION

of 180 rpm under heads varying from 300 to 365 ft. If the unit were to be operated at the same speed of 180 rpm both as a turbine and as a pump, there would only be a small sacrifice in efficiency as a turbine over the range of heads from 350 to 365 ft, which would be the approximate head range prevailing when it is desired to generate power.

Estimated Performance of Unit for Grand Coulee Conditions

Fig. 11 shows the estimated pump-performance curves for Grand Coulee conditions deduced from the model tests at the California Institute of Technology. The head curve with adjustable wicket gates is much steeper than with gates fixed at best gate position. The brake-horsepower input to the pump is much lower for the adjusted gates at the lower discharges, and the horsepower at shutoff is less than one half of that required with fixed guide vanes. The gain in efficiency over the lower discharges is as much as 20 per cent with adjusted gates. Over the operating range, the gain in efficiency is mainly due to the higher head obtained with adjustable gates.

Fig. 12 shows the corresponding estimated turbine-performance curves for Grand Coulee conditions, deduced from the California tests. Over the range of heads from 350 to 365 ft, an output of 55,000 to 60,000 hp would be obtained when operating the unit as a turbine.

Advantages of Wicket-Gate-Type Pump-Turbine

The advantages of wicket gates for turbine operation are well known and will not be discussed. Some of the advantages for pumps are as follows:

1 Smaller shutoff power required to bring pump up to speed.

2 Flatter efficiency-discharge curves, resulting in higher efficiency over a wide range of discharge.

3 Steeper head curves, resulting in smaller variations in discharge with head changes.

4 More discharge overload capacity at lower heads, unless affected by cavitation.

5 Wicket gates take the place of a shutoff valve, and their use also forms an excellent means of controlling the discharge at constant speed and head.

6 Smaller impeller diameter, about 95 per cent of the diameter of a volute pump.

7 The use of stay vanes in the casing opposite the wicket gates gives a satisfactory casing construction without excessive deflection.

BIBLIOGRAPHY

1 "Economic Aspects of Water Power," by F. A. Allner, Trans. A.I.E.E., vol. 52, March, 1933, pp. 156–168.

2 "Problems of Modern Pump and Turbine Design," by Wilhelm Spannhake, Trans. A.S.M.E., vol. 56, 1934, p. 225.

3 "Hydraulic Practice in Europe," by R. W. Angus, Trans. A.S.M.E., vol. 54, 1932, Fig. 19 (showing test curves on small model of Herdecke pump), p. 133.

4 "Hydraulic Turbine and Pump Combined in a Single Unit," by F. A. Allner, *Power*, vol. 76, 1932, pp. 266–267.

5 "Pumped Storage Hydro-Electric Plants," by F. A. Annett, *Power*, vol. 78, 1934, pp. 20–24.

6 "Herdecke: The Largest Pumped Storage Hydro-Electric Plant," by Walter Netoliczka, *Power*, vol. 76, 1932, pp. 160–163.

7 "Turbines and Pumps for Pump-Fed Power Storage Plants," by A. Maas, *Escher-Wyss News*, vol. 3, 1930, pp. 52–62.

8 "Current Practice and Research in Hydro Development," *Electrical West*, vol. 68, 1932, p. 377.

9 "Trend in Hydraulic Turbine Practice—a Symposium; Economic Principles in Design," by I. A. Winter, Proceedings A.S.C.E., vol. 65, 1939, pp. 1554–1574; discussion by Lewis F. Moody and R. E. B. Sharp, Proceedings A.S.C.E., March, 1940.

10 "Cavitation Characteristics of Centrifugal Pumps Described by Similarity Considerations," by G. F. Wislicenus, R. M. Watson, and I. J. Karassik, Trans. A.S.M.E., vol. 61, 1939, pp. 17–24.

11 "A Theory of Cavitation Flow in Centrifugal-Pump Impellers," by A. Gongwer, Trans. A.S.M.E., vol. 63, 1941, pp. 29–40.

12 "Centrifugal-Pump Performance as Affected by Design Features," by R. T. Knapp, Trans. A.S.M.E., vol. 63, April, 1941, pp. 251–260.

13 "American Hydraulic Laboratory Practice," by L. J. Hooper, Trans. A.S.M.E., vol. 58, 1936, pp. 577–588.

14 "The Hydraulic Machinery Laboratory at the California Institute of Technology," by R. T. Knapp, Trans. A.S.M.E., vol. 58, 1936, pp. 663–676.

Discussion

R. W. Angus.[4] This paper presents valuable data on an interesting hydraulic machine. Pumped storage plants have been extensively used in Europe, where there are over fifty in operation, while a few have been installed in the United States and in South America,[5] a list being given by F. A. Annett. In a number of those visited by the writer, the turbine, pump, and electrical machine were installed as a unit, while in other plants the pumps and turbines have separate electrical machines.

Frequently, the electrical machine is placed in the center with the pump on one side of it and the turbine on the other; while the turbine is left permanently coupled, a clutch must be used on the pump so that the latter may remain stationary when the turbine is generating power. A unit so built is expensive and requires special gates for the draft tubes in order that the air in the turbines may be rarified when the pumps are running. Thus, the advantage of the dual-purpose hydraulic unit is obvious.

There are some features of the paper on which the writer would comment. The curves, Figs. 7, 8, and 9, are drawn to a somewhat small scale and in reading them the writer may have fallen into certain errors. From the turbine characteristics, for gate No. 8, given in Fig. 8, we find that the quantities corresponding to unit speed $N_1 = 118.5$ rpm are as follows: Unit discharge Q_1 = slightly in excess of 0.50 cfs; unit power $P_1 = 0.048$ hp, and efficiency 84.5 per cent. Calculating from these, the results at a head of 285 ft are: $N = 2000$ rpm, $Q = 8.50$ cfs, $P = 231$ hp. Presumably the efficiency would be unchanged, since the pump and turbine tests were made at nearly the same speed. Actually, however, the turbine speed was the lower, which should probably give an efficiency below 84.5 per cent at the speed of 2000 rpm.

Referring to Fig. 7, for the pump characteristics, it is seen that at $Q = 8.50$ cfs, an efficiency of 88 per cent is obtained, the head being 285 ft, and the power required being 315 hp, corresponding to the foregoing data. This agrees quite closely with the 231 hp from the turbine, if the efficiencies of 84.5 per cent and 88 per cent are allowed for. Thus, it appears that, for this unit speed at least, the machine has the same discharge of 8.5 cfs under a 285-ft head at 2000 rpm, whether running as a turbine or as a pump.

In order to examine this condition, let E_T and E_P represent the efficiencies of the turbine and pump, respectively, while M_T and M_P represent their corresponding mechanical efficiencies, and E_{HT} and E_{HP} their hydraulic efficiencies. Further, let L_T and L_P represent the losses in feet in the turbine and in the pump, respectively, when working under head H, then obviously

$$E_T = M_T \frac{H - L_T}{H} \quad \text{and} \quad E_P = M_P \frac{H}{H + L_P}$$

But, since the machine is assumed running at the speed of 2000 rpm in each case, it would be fair to take $M_T = M_P = M$. In the

[4] Professor of Mechanical Engineering, University of Toronto, Toronto, Ontario, Canada. Hon. Mem. A.S.M.E.

[5] For a list of plants, refer to "Experience Story of the Safe Harbor Plant, Part 1," by F. A. Annett, *Power*, vol. 78, 1934, p. 338.

case being examined $E_T = 0.845$, $H = 285$ ft, and $E_P = 0.88$. Substituting these values in the foregoing equations

$$0.845 = M\,\frac{285 - L_T}{285} \quad \text{and} \quad 0.880 = M\,\frac{285}{285 + L_P}$$

or

$$L_T = 285 - \frac{240.82}{M} \quad \text{and} \quad L_P = 323.90\,M - 285$$

The following table may then be constructed:

M	1	0.98	0.96	0.94	0.92	0.90	0.88
L_T ft	44.2	39.3	34.2	28.8	23.2	17.4	11.4
L_P ft	38.9	32.4	25.9	19.4	12.9	6.5	0
$(L_T - L_P)$ ft	5.3	6.9	8.3	9.4	10.3	10.9	11.4

Evidently M exceeds 88 per cent and in all probability is over 90 per cent. The difference $(L_T - L_P)$ must be due to shock, since the water velocities are the same in both cases; it would appear that the shock losses should also be similar in the two cases. It would tend to confirm the generally accepted view that the water passages in the impeller are not completely filled, so that the distributor setting for maximum efficiency must be changed when the flow is reversed.

At this same unit speed of $N_1 = 118.5$, with $Q = 8.5$ cfs, the velocity in the $7^3/_4$-in. suction pipe is 25.9 fps, with a corresponding velocity head of 10.4 ft, which is high for such a unit. However, the writer checked out the conditions at the rim of the impeller and, taking the distributor-guide angle of 9 deg stated in the paper and the impeller discharge angle as 30 deg also as given in the paper, found that these corresponded to best efficiency, assuming that the metal in the impeller vanes occupies 11.5 per cent of the total area, which seems reasonable.

The question of cavitation in such a unit is of great importance, and serious trouble has been experienced in some of the plants in operation. Hence, a valuable addition to the paper would be the results of further study on this phase of the work. Attention might also be called to the fact that this dual-purpose unit is confined to the case where a single-stage pump suffices, because the multistage turbine has not, so far, proved attractive.

The writer raises a mild protest against the practice of stating specific speeds of pumps in terms of gallons per minute, instead of cubic feet per second. The latter is the logical unit and makes it easier to compare results of machines in general.

R. L. Daugherty.[6] This paper is a clear presentation of the characteristics of a centrifugal pump when equipped with movable diffuser vanes; and it also shows the performance of the same pump when used as a reaction turbine. There are certain cases where such dual operation may be very desirable.

In Fig. 9, the authors show the efficiency curve for this pump as obtained at the California Institute of Technology with the pump being operated at 2000 rpm. They also show an efficiency curve obtained by them in the Newport News laboratory with a pump speed of 1000 rpm, but with the test results stepped up to 2000 rpm. The agreement between the two curves is very close. It is not to be expected that the two curves should coincide.

In general, the efficiency of any centrifugal pump will increase slightly with an increase in speed, until incipient cavitation or some other factor causes it to begin to decline with further increase in speed. This is shown in Fig. 13 of this discussion, in which the writer has plotted maximum efficiencies as a function of speed for four stock centrifugal pumps which were tested at the California Institute of Technology. An inspection of this figure will show that, for an increase in pump speed from 1000 rpm to 2000 rpm, the difference of about 1 per cent in efficiency, shown by Fig. 9 of the paper, is entirely reasonable.

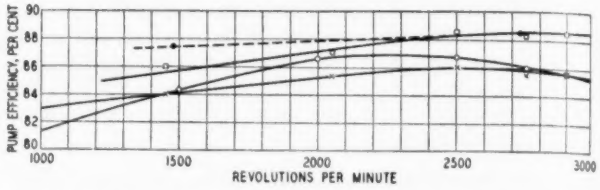


Fig. 13 Variation of Maximum Efficiencies of Four Centrifugal Pumps With Speed

The authors state that the difference in the point where the break occurs in the head curve is caused by the fact that the intake pipes in the two laboratories were not of the same size. The method of computing the head would seem to make the size of the intake pipe of no importance, but what will influence the break in the head curve is the beginning of cavitation. Cavitation is a function of a factor defined by the equation

$$\sigma = \frac{b - p - h_f - L}{H}$$

where b is the barometric pressure, p is the vapor pressure, h_f is the friction loss in the intake pipe, L is the static suction lift, and H is the total head developed by the pump per stage. If the water is supplied to the pump by gravity then the sign of L would be positive. Cavitation begins at the same value of σ regardless of other external conditions.

A. Hollander.[7] It is only a short time ago since it was realized that efficient pumps may serve also as efficient turbines. The historical review is given in Professor Knapp's paper,[8] which also first presented the circle diagram suggested by Prof. Th. von Kármán. This diagram, with ordinates of speed and flow rate in the positive and negative directions, and constant head and torque lines, covers all possible operating conditions of the machine which the authors call the pump-turbine, including, besides the normal pump and turbine operation, the abnormal pump and turbine operation when the units are running in the direction opposite to the normal, and showing besides these four sectors of energy dissipation. Consideration of this pump-turbine as a machine equally adapted for both purposes, and going over the full circle with all possible ways of its operation, would give a better and more complete picture of its nature. In colleges, the deduction of the energy formulas and the description of velocity diagrams, on this general basis, would constitute an advance compared with present teaching methods.

It was Dr. Knapp's paper, showing for the first time these results with good pumps of about 4-in. size and 80 per cent efficiency which induced the Metropolitan Water District of Southern California to install a modern hydraulic laboratory at the California Institute of Technology,[9] in order to establish specifications and later conduct the model tests for the large pumps of 4000 to 12,000 hp, required for the Metropolitan Aqueduct of Southern California.[10]

[6] Professor of Mechanical Engineering, California Institute of Technology, Pasadena, Calif. Former vice-president, and Fellow A.S.M.E.

[7] Consulting Engineer, Byron Jackson Company, Los Angeles, Calif. Mem. A.S.M.E.

[8] "Complete Characteristics of Centrifugal Pumps and Their Use in the Prediction of Transient Behavior," by Robert T. Knapp, Preprinted Papers, A.S.M.E., Aeronautic and Hydraulic Divisions Summer Meeting, June, 1934, pp. 60–64; available at Engineering Societies' Library as A.S.M.E. Miscellaneous paper 1-N, 1934.

[9] "The Hydraulic Machinery Laboratory at the California Institute of Technology," by R. T. Knapp, Trans. A.S.M.E., vol. 55, 1936, pp. 663–676.

[10] "Centrifugal Pumps for the Colorado River Aqueduct," by R. L. Daugherty, *Mechanical Engineering*, vol. 60, 1938, pp. 295–299.

The Reclamation Bureau used the results of this laboratory with 8-in. pumps of 300 to 500 hp and continued the work for the proposed 60,000-hp pumps for Grand Coulee. The results published by Dr. Knapp (12) are further elaborated and extended by the authors. The authors are to be congratulated that they gave not only performances but most of the physical dimensions. The interest of the turbine builders in these pumps is fully justified because of the large size of some of these units, particularly for hydroelectric-storage developments. Such pumps are more in line with the turbine manufacturers' facilities than with those of most pump builders. The developments, based mainly on the California Institute of Technology tests, will certainly permit us to make our hydroelectric storage projects a great deal simpler and less costly than those in Germany, which in a number of cases could have used the same machine as pump and turbine instead of having independent units with a great number of auxiliary connections, clutching and declutching apparatus, etc.

We missed the list of the disadvantages of the wicket-gate pump-turbine, as compared with the simple volute pump-turbine, without a wicket gate, and possibly a valve to regulate flow. Undoubtedly, for some purposes, particularly for widely varying flows, the wicket-gate pump-turbine has some justification. On the other hand, such units and especially their volute cases, due to the increase in diameter by the diffuser, are of very much greater over-all dimensions than plain single or double volutes. Thus, in the end probably they will be a great deal more expensive than volute-case pumps. For applications where the levels do not change very much, it seems that the plain volute will have its place even for hydroelectric storage units and, undoubtedly, in most cases where pumping is the only application.

It seems that, for the discussion of the Grand Coulee units, members of the staff of the California Institute of Technology, which conducted all the tests of the different types and makes of models, are best qualified; having all the test results at their disposal their contribution would complete and round out the very instructive paper of the authors.

R. T. KNAPP[11] and J. W. DAILY.[12] The following discussion is based primarily upon the results of the test program carried out in the hydraulic-machinery laboratory of the California Institute of Technology to investigate the pumping problems involved in the Grand Coulee installation for the U. S. Bureau of Reclamation. This program was conducted under the immediate direction of Profs. T. H. von Kármán, R. L. Daugherty, and R. T. Knapp, with J. W. Daily in charge of the technical staff.

The information contained in this paper makes it possible to complete the set of comparative studies previously presented by R. T. Knapp (12) in which the performance characteristics of single-volute, double-volute, and fixed-vane diffuser pumps were compared and discussed. The pumps involved were units purchased by the hydraulic-machinery laboratory for the study referred to. The performance of the wicket-gate pump, described by the authors, was not included in this comparison because, although it was designed to meet the same specifications, it was not a part of the test program. However, during the program it was tested for the Newport News Shipbuilding and Dry Dock Company, under special arrangements made with the Bureau of Reclamation. Therefore, the writers did not feel free to use the performance of this pump at the time the former paper was prepared.

This group of pumps presents a unique opportunity for a comparison of the performance characteristics of these different types of casings, since all of the units were designed for the same head and capacity and the same range of inlet heads. Two series of units were procured, one having a specific speed corresponding to 150-rpm operation of the Grand Coulee units, and the other having a specific speed corresponding to 180-rpm operation. The wicket-gate pump described in the present paper belongs to the first series. These test units represent the most modern design practice of some of the leading hydraulic-machinery manufacturers in the country. They are comparatively large machines, having discharge nozzles of 8 in. diam and requiring over 300 hp to drive them at normal capacity. It is seen that these units are considerably larger than the average commercial pump. Therefore, it is felt that the conclusions which can be drawn from the comparison of the performance of the different units must carry considerable weight.

Before the specific comparisons of the performance of the wicket-gate pump with the other test units are presented, the writers have a few miscellaneous comments on points brought out in the paper.

1 In describing the range of conditions under which it is expected that the Grand Coulee pumps will operate, the authors state that, at the maximum dynamic head of 367 ft, the discharge will be approximately 1000 cfs. Actually, this figure is best considered to be a minimum acceptable value. In the Grand Coulee operation the more water that can be pumped at maximum head the better, since this condition occurs at the beginning of the irrigation season. Thus, the capacity at the maximum head is limited only by the obtainable steepness of the pump characteristic.

2 In the description of the tests at the California Institute of Technology, the statement was made that turbine tests were limited to a maximum of 1800 rpm for units of this size by the laboratory equipment. Actually, the limitation is one of capacity and not of speed, since speeds of better than 4000 rpm are well within the range of the test equipment.

3 In discussing Fig. 7, the authors state that for an envelope head curve the highest head occurs at zero discharge. This must be thought of as a statement of idealized conditions, because in the actual test some droop of the head curve was always encountered as zero discharge was approached due to the impracticability of obtaining complete closure of the gates.

4 In discussing Fig. 8, as compared to Fig. 7, it is concluded that a full gate as a turbine is larger than a full gate as a pump, i.e., gate No. 10 versus gate No. 8. As the writers remember the situation, preliminary tests of the pump show that, for gates Nos. 9 and 10, the maximum efficiency was lower than for gates Nos. 7 and 8, and therefore the final test gates Nos. 9 and 10 were not run. In the turbine test a run was taken at gate No. 10, but as will be noted the maximum efficiency is again lower than for gates Nos. 7 and 8. Therefore, the writers have difficulty in understanding the conclusions of the authors.

5 In discussing these same two figures, it is pointed out that the best unit speed for the machine operating as a turbine is lower than the best unit speed as a pump. It is concluded from this that "the use of a combination machine at constant speed and head would involve some sacrifice in efficiency." It is felt by the writers that this generalization is not justified. The statement is certainly true as applied to the specific unit. However, if a different design point were used it would be possible to obtain equal efficiencies for both modes of operation. For example, this point is excellently illustrated by use of Fig. 14 of this discussion, which is a reproduction of Fig. 15 of the paper (12) previously mentioned. It will be seen from this diagram that a turbine operating at 100 per cent speed and normal head would have an efficiency about 3 per cent lower than the same unit operating as a pump at the same head and speed. However, if operating conditions are chosen with normal head and 96 per cent normal speed

[11] Associate Professor of Hydraulic Engineering, California Institute of Technology. Mem. A.S.M.E.

[12] Instructor, Mechanical Engineering, California Institute of Technology. Jun. A.S.M.E.

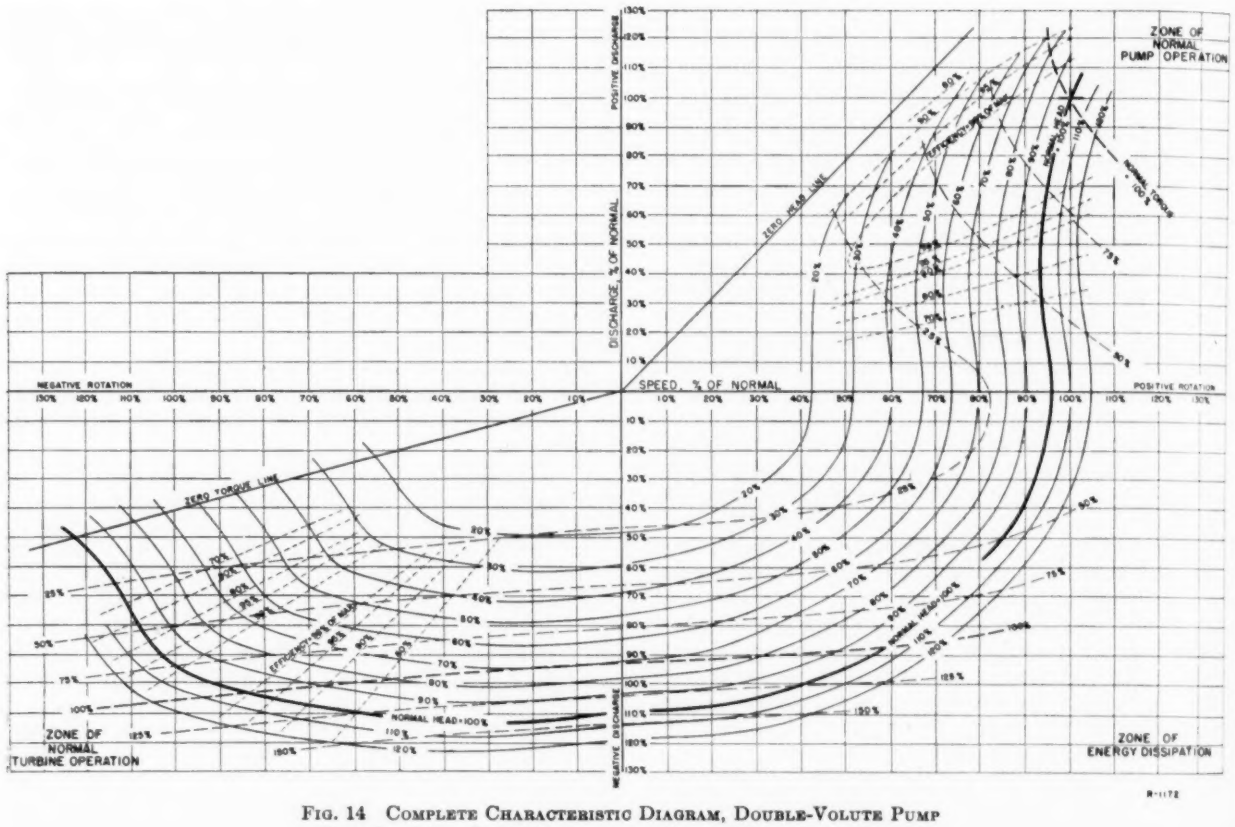


FIG. 14 COMPLETE CHARACTERISTIC DIAGRAM, DOUBLE-VOLUTE PUMP
(Reproduced from R. T. Knapp paper, authors' Bibliography 12, Fig. 15.)

both as a pump and a turbine, it will be seen that the maximum possible efficiency is obtained from both units. On the other hand, if operating conditions as pump and turbine had been chosen as normal head and 110 per cent normal speed, the diagram shows that the pump would still be operating within 3 per cent of its maximum efficiency, whereas the turbines would have dropped off about 25 per cent.

6 In presenting some of the general results of the California tests, the authors called attention to the fact that the efficiency as either a pump or a turbine was not affected until the impeller was cut below 13 in. in diameter, whereas cutting the discharge tips of the impeller vanes while leaving the shrouds extended lowered the efficiency. The writers feel that this test result has interesting implications, i.e., that the close clearance between the runner and the gate vanes generally incorporated in turbine design may not be necessary, and that there might be advantage in the pump practice of using large axial and radial clearances at the periphery of the wheel.

7 In comparing the Newport News and California tests, as illustrated in Fig. 9, the authors explain the smaller discharge at which the break in the head curve occurs in the California test by the small size of the suction pipe used. They say "the entrance loss and friction loss in this pipe were the factors which determined the cutoff point in the California test." However, in the California tests, the total dynamic inlet head was measured at a point only one diameter upstream from the impeller eye, so that the effect of any inlet-piping loss on the calculated inlet or net head produced was eliminated. It is probable that the discrepancy observed in the shutoff point is due to cavitation caused by a difference in the relative submergence at which the two tests were run. The California tests were made with an 80-ft submergence. This corresponds to a lift of 4.7 ft under the conditions of the test at Newport News. If the Newport News tests were run with an inlet pressure greater than this, the cutoff point would be expected to occur at a correspondingly higher capacity.

8 In preparing Fig. 11, the authors apparently stepped up the model efficiency to the expected prototype values by the use of the normal turbine step-up formulas. Thus the maximum model efficiency of 87.6 per cent has been increased to an expected prototype efficiency of 92 per cent. At this point it should be noted that it is the practice of the hydraulic-machinery laboratory of the California Institute of Technology to test the units at full prototype heads and velocities. In the case of the present units, this means that the Reynolds number of the flow in the suction and discharge nozzles is in the neighborhood of 2,000,000. Thus, comparatively little change in relative losses can be expected for any possible increase in the size of the units. This conclusion is borne out by the few comparisons between model and prototype test efficiencies in which models were tested at full prototype heads and velocities. Of the 4½ per cent step-up assumed, 1 per cent is justified, as the authors point out, by the excessive leakage found in the model tests. The writers feel that the remaining 3½ per cent is much too great a step-up to be warranted with the present knowledge.

Figs. 15 and 16 of this discussion show the comparative performances of the double-volute pump, the fixed-vane diffuser pump, and the adjustable wicket-gate pump. Fig. 15 is plotted on the basis of 150 rpm prototype operation, while Fig. 16 is calculated for the same machines but operating at a speed corresponding to 180 rpm prototype operation. Capacities and heads are represented in percentage of normal in accordance with the convention used in the previous paper (12). However, actual efficiencies of the test pumps are plotted in the place of relative efficiencies formerly used. The first point that is observed

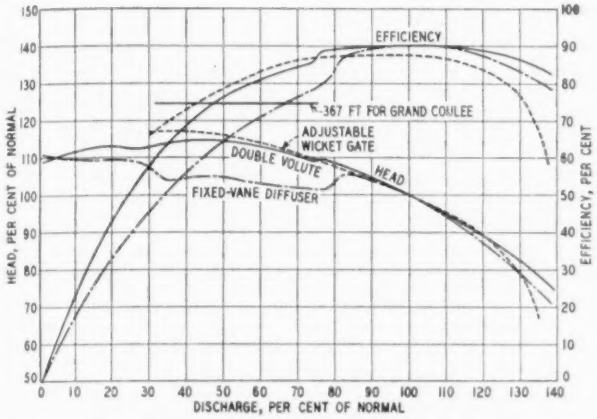


FIG. 15 COMPARISON OF CASING EFFECTS ON CHARACTERISTICS; DOUBLE-VOLUTE, FIXED-VANE DIFFUSER, AND ADJUSTABLE WICKET-GATE PUMPS
(Prototype speed, 150 rpm.)

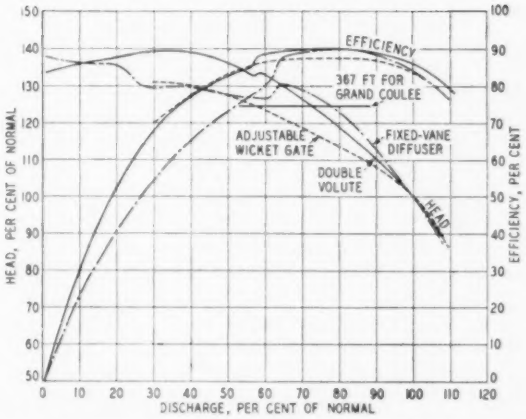


FIG. 16 COMPARISON OF CASING EFFECTS ON CHARACTERISTICS; DOUBLE-VOLUTE, FIXED-VANE DIFFUSER, AND ADJUSTABLE WICKET-GATE PUMPS
(Prototype speed, 180 rpm.)

in Fig. 15 is that none of the pumps when operated at the design speed would develop sufficient head to deliver against the maximum head encountered in the Grand Coulee installation. The second point of interest is that, over a surprisingly wide range, the double-volute and the wicket-gate pumps have nearly identical capacity-head curves. A comparison of the efficiency curves shows that both the double-volute and the fixed-vane diffuser pumps have maximum efficiencies about 3 per cent higher than the wicket-gate machine. Of this difference, 1 per cent is undoubtedly due to the excessive leakage loss previously mentioned, but the remaining 2 per cent is probably chargeable to the additional amount of friction surface in the high velocity flow.

The broad range of high-efficiency operation of both the wicket-gate and double-volute pumps is very apparent. Calculation shows that a range of capacity of approximately 61 per cent of the normal is covered with an efficiency within 5 per cent of the maximum by the wicket-gate machine, whereas, the corresponding value for the double-volute is about 58 per cent and for the fixed-vane diffuser about 43 per cent. The adjustable wicket-gate pump has a noticeably higher efficiency for all discharges below 60 per cent of the normal.

If Fig. 16 is now examined, it will be seen that the situation is changed. In the first place, all three pumps now are able to meet the required range of head when operated at 180 rpm. However, the relative steepness of the head curves is no longer the same. The fixed-vane diffuser case shows the best performance, giving a delivery of 78 per cent of normal capacity at the maximum head. The double-volute pump is next with 73 per cent, whereas, the adjustable wicket-gate pump delivers only 58 per cent. At this higher operating speed, the double-volute case shows a considerably wider range of high-efficiency operation than does either of the other two. The adjustable wicket-gate unit still shows a 3 per cent lower maximum efficiency and, in addition, no longer shows a better efficiency for the lower capacities. These conclusions are somewhat surprising when it is remembered that the curve shown here for the wicket-gate pump is the envelope for the different gate positions.

In the concluding paragraph of the paper, the authors give seven advantages of the wicket-gate construction over the non-adjustable cases. Figs. 15 and 16, of this discussion, offer a concrete means of evaluating these items as follows:

1 While the power curves for the three cases are not shown in either of these figures, it is recognized that the shutoff power for the wicket-gate pump is definitely lower, provided,of course, that the flow is controlled by closing the wicket gates themselves.

2, 3 These depend upon the speed selected for making the comparison. As was shown in the discussion of Figs. 15 and 16, the difference is small for the 150-rpm operation, but for the 180-rpm operation the double-volute case shows a flatter efficiency discharge curve, and both it and the fixed-vane diffuser case show steeper head curves.

4 Neither Fig. 15 nor Fig. 16 shows an appreciable increase in discharge-overload capacity in the lower heads. This is surprising for the 180-rpm operation, because of the flatter head curve of the wicket-gate pump. Here the lack of overload capacity is probably due, as the authors suggest, to cavitation.

5 It is certainly true that wicket gates form an excellent means of controlling discharge at constant speed and head.

6 The adjustable wicket-gate pump had a smaller impeller diameter when compared on a prototype basis. For the three pumps shown in Figs. 15 and 16, the adjustable wicket-gate pump would have an impeller diameter of 16.7 ft, the double-volute pump 16.95 ft, and the fixed-vane diffuser 17.1 ft. For this particular group, this represents a range of 2.4 per cent. However, this is not the entire story. The figure which best characterizes the casing sizes is the one given by the authors in Table 1, as "offset of casing throat to center line." Again, on the basis of 150 rpm prototype speed, this distance would be $15^1/_4$ ft for the adjustable wicket-gate pump, $13^1/_2$ ft for the double-volute pump, and $14^1/_2$ ft for the fixed-vane diffuser. Thus it is seen that, while the adjustable wicket-gate machine has the smallest impeller diameter, it has the greatest over-all case diameter. The cross-sectional areas of the spiral case surrounding the wicket gates and stay vanes will be larger also since the effect of the adjustable wicket gates is to reduce case velocities.

7 In units of this size, the structural design of a single-volute case is quite difficult. The introduction of a second volute overcomes a large part of this disadvantage. On the other hand, the stay vanes used in both the fixed-vane-diffuser and the adjustable wicket-gate pumps make possible a very satisfactory structural design.

In conclusion, the writers would like to make a few comments regarding the operation of these units as turbines. In the light of the comparison of the pump characteristics, it would appear that the chief advantage to be gained by the use of the adjustable wicket-gate case lies in the region of turbine operation and that, therefore, the whole discussion must be on a basis of the combined operation both as pump and as turbine. If, when the unit is operated as a turbine, the system conditions are such that

it must be governor-controlled, then the wicket-gate construction offers advantages which cannot be obtained with the other cases. However, if the system conditions permit the utilization of the unit to supply a block load, then governor-controlled operation is not necessary. For this condition, any of the case types gives satisfactory operation. For the three units under comparison, both the fixed-vane diffuser and the double-volute type show higher efficiencies as turbines than does the adjustable wicket gate. The wicket gate, however, does have the one advantage in that a wider range of power output can be obtained for a given head for the same relative variation of efficiency. For the non-adjustable type case, unless a throttle valve is incorporated in the system, there is only one output. For a multiple-unit installation this seems to offer no disadvantage.

It should be emphasized that the writers have been as objective as possible in making comparisons, limiting statements to the results which were substantiated by the tests. The laboratory staff feels that each of the different casing types has its own field of application and, therefore, few generalizations are justified. The present comparisons have as a background the Grand Coulee requirements. Other installations, which have entirely different operating conditions, would result in a completely different order of desirability of casing requirements.

R. E. B. Sharp.[13] Discussions of the performance of pump-turbines are in order, in view of the fact that the present capacity demand has recently awakened decided interest in pumped-storage projects.

For comparison with the authors' tests, Baldwin-Southwark Model Runner 115, tested during July, 1931, and Model Runner 117, tested during July, 1933, may be of interest.[14] Model 115 was designed for peak-load storage plants with relatively high heads, and Model 117 for medium heads. The specific speed of Model 115, when pumping, at best efficiency, is 1970, as compared to the authors' 1750; and when generating is 26, as compared to the authors' 25. Runner 117 has a specific speed of 2700 when pumping and 41 when generating. These tests were made under low-head conditions (3 to 4 ft).

While the resulting Reynolds number is low, it has been demonstrated as being sufficiently high to be well within the turbulent region of flow and to form a reliable comparison with prototype performance and with model tests under higher heads. The discharge was measured by a calibrated weir, and the power by electric dynamometer. The head, acting both for pumping and generating, was considered as the vertical difference between headwater and tailwater levels. The tests were made with vertical shafts, with the volute casing submerged, and with draft elbows of usual turbine design. The draft-tube losses are charged against the pump-turbine for both cycles of operation.

Figs. 17 and 18 of this discussion show characteristics, in general, similar to the authors'. The same tendency for irregularity in the curves to the left of the maximum-efficiency point was encountered.

The practical utilization of pump-turbines, in virtually all cases, requires that the head when pumping be somewhat greater than when generating, due to the friction losses both ways in the penstock. The pumping operation, although occurring at times of low system load, requires for its justification the minimum expenditure of energy. Therefore, both the pumping and generating cycle should be at the most efficient condition.

In Fig. 17, the performance of model 115 as a pump has been stepped up to 1000 rpm, the head at best efficiency being 111 ft. In Fig. 19, the performance of this model as a turbine has been plotted when operating at the same head of 111 ft. The curves for two speeds are shown, the lower efficiency curve being for 1000 rpm, and the higher efficiency and output for a speed of 868 rpm. It will be noted that the loss in efficiency for uniform speed of operation during both cycles is about 5 per cent. Therefore, in practice, two speeds are necessary, the indicated loss with uniform speeds being aggravated by the pumping head being in excess of the generating head. As an alternative, a booster pump in series with the pump-turbine can be utilized to reduce the pumping head on the pump-turbine so that maximum efficiency will be attained at a uniform speed.

In Fig. 18 of this discussion, the performance of model 117, as a pump, has been stepped to 1000 rpm, the head at best efficiency being 86.75 ft. In Fig. 20, the performance of this model as a turbine has been plotted, when operating at the same head (86.75 ft). In this case also, the curves for two speeds are shown, the lower one being for 1000 rpm; the higher curve is for 900 rpm. It is interesting to note that, for this higher-specific-speed

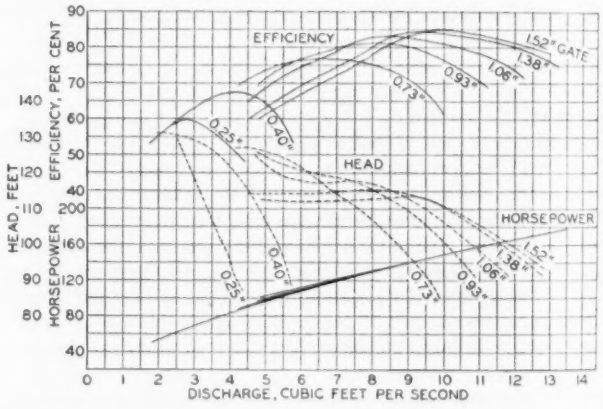


Fig. 17 Baldwin-Southwark Runner No. 115, Operating as a Pump
(Diameter of runner, 18 in.; speed, 1000 rpm.)

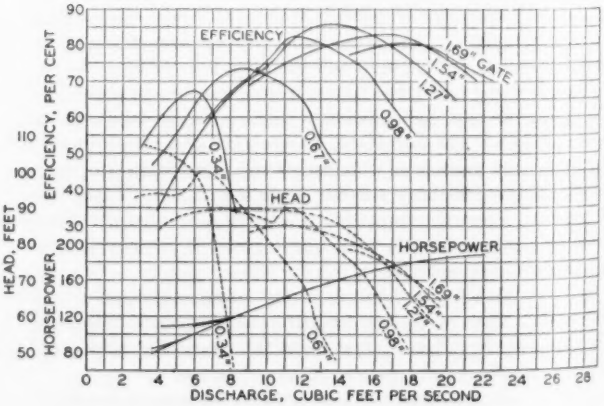


Fig. 18 Baldwin-Southwark Runner No. 117, Operating as a Pump
(Diameter of runner 16³/₁₆ in.; speed 1000 rpm.)

[13] Chief Engineer, I. P. Morris Department, Baldwin-Southwark Division, Baldwin Locomotive Works, Philadelphia, Pa. Mem. A.S.M.E.

[14] Note the following pertinent patents: No. 1,494,008, issued May 13, 1924, Method and Means for Converting Energy, by Forrest Nagler, assigned to Allis-Chalmers Manufacturing Company; No. 1,919,376, Reversible Pump-Turbine, by L. F. Moody; No. 1,941,361, Air Inlet Control and Method of Operating a Pump-Turbine, by L. F. Moody; No. 2,010,555, Hydraulically Reversible Pump-Turbine, by L. F. Moody; No. 2,246,472, Hydraulic Power Accumulation System, by R. E. B. Sharp, assigned to Baldwin Locomotive Works.

model, the loss in efficiency at uniform speed is distinctly less than for runner No. 115, of lower specific speed; that is, a two-speed unit, or the provision of a booster pump, is more essential for high-head units (400 to 600 ft) than for lower heads. The pumping efficiency of the pump-turbine models tested to date does not compare well with the best pumping efficiency obtainable without movable guide vanes surrounding the runner. Also the efficiency when operating as turbines of some conventional pumps has been found to be excellent. However, movable guide vanes on pump-turbines appear to be essential for operation as turbines, to obtain the best efficiency and maximum power possible under this cycle of operation. Pump-turbine research is still in its early stages and improvement in performance, particularly when pumping, can be effected.

A. J. Stepanoff.[15] The authors should be commended for publishing the design data as well as the tests and description of the pump. This permitted a critical examination of the test data. In the writer's opinion, some of the advantages claimed by the authors for the pump with adjustable diffusion-casing vanes are not sufficiently corroborated by their test data.

Considering that the double-volute pump, previously described by R. T. Knapp (12), had a maximum efficiency of 90 per cent, the authors envelope of efficiency curves lies below the double-volute-pump efficiency curve for capacities between 50 to 125 per cent of the rated capacity. It is only at capacities lower than 50 per cent that the authors' efficiency envelope passes above the double-volute-pump efficiency curve.

[15] Ingersoll Rand Company, Phillipsburg, N. J. Mem. A.S.M.E.

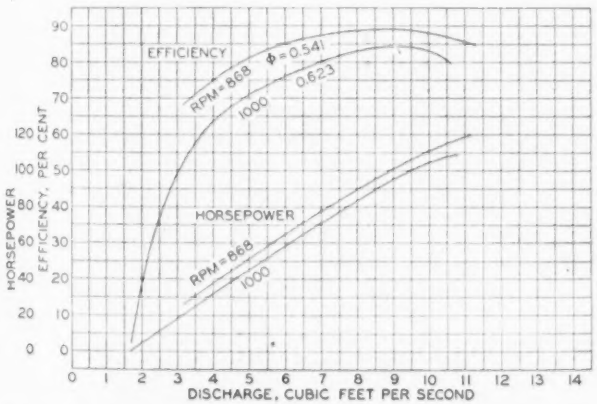


Fig. 19 Baldwin-Southwark Runner No. 115, Operating as a Turbine
(Head, 111 ft; diameter of runner 18 in.

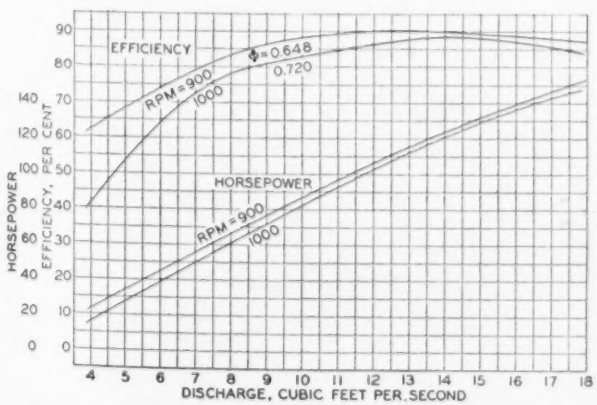


Fig. 20 Baldwin-Southwark Runner No. 117, Operating as a Turbine
(Head, 86.75 ft; diameter of runner 16 9/16 in.)

Since the double-volute-pump head at overload capacity is the same as that of the authors' pump, and the efficiency is probably better, the overload capacity of the double-volute pump at lower heads is essentially the same as that of the authors' pump.

A smaller impeller diameter of the authors' pump resulted from the use of a high discharge vane angle of 30 deg rather than any special feature of the adjustable-vane casing. The over-all dimensions of the authors' pump casing will be greater than those of the volute pumps by the space occupied by adjustable vanes.

It is believed that the double-volute design will result in a casing which will be rigid enough even when built in the size proposed for the Grand Coulee project.

The authors' mechanical design deviates from the orthodox construction in that they have placed the inboard ball bearing inside the pump casing between the stuffing box and the impeller. The writer wonders whether this was the bearing which caused trouble during testing mentioned in the paper. The casing is heavily ribbed, which is hardly necessary for this size of pump and pressures involved.

The writer is grateful to the authors for the published information, which enabled him to study the test results and be benefited by the authors' experience.

G. F. Wislicenus.[16] The paper presents an unusually complete account of the test results as well as the design characteristics of a pump-turbine model with wicket gates, and so represents a most valuable contribution to the literature on pumping machinery.

The comparison between pumps with adjustable wicket gates and pumps with a fixed-casing design might be slightly misleading, in so far as the characteristics of a fixed-casing machine may be somewhat more favorable than the characteristics of an adjustable-gate machine at a fixed-gate setting. For this comparison, the material presented by R. T. Knapp (12) will be found helpful and instructive.

The value of adjustable wicket gates for controlling the unit during turbine operation is so well established that the use of adjustable gates for pump-turbine units is almost a necessity wherever a close control of the power output during turbine operation is required. In designing such units, it is necessary to take into account the fact that the flow conditions at the gates during pump operation are such that increased and possibly pulsating forces on the gates can be expected which would not exist during turbine operation. This expectation is based on the fact that the accelerated flow through the gates during turbine operation is probably smoother and more stable than the outward flow during pump operation. Some experience gained with pump-turbine operation seems to bear out this reasoning.

In hydroelectric power plants where the units will be operated as pumps and as turbines, it may be possible to eliminate the necessity of using adjustable gates on the pump-turbine units if the plant contains, besides the pump-turbine units, at least one

[16] Engineer, Design, Worthington Pump and Machinery Corporation, Harrison, N. J. Mem. A.S.M.E.

water-turbine of standard design which would not be operated as a pump. In this case, the pump-turbine units could be used to carry the base load, while the load fluctuations are taken up by the standard control mechanism of the turbine. This arrangement is the more likely to be acceptable, since, for most hydroelectric storage plants, the turbine capacity has to be greater than the pump capacity in order to take care of peak loads.

Authors' Closure

The authors obtained both benefit and satisfaction from the large number and extensive discussions presented on this paper. In view of the great amount of material presented and the thorough analysis of the subject brought out in these discussions, the authors feel that they can hardly contribute much more in reply.

To Professor Angus we might add, that when the model was operated under a head of 365 ft, cavitation was not apparent until there was a suction lift of about 7 or 8 ft. On the prototype when operating under this head there would be a positive suction head of about 5 ft. When the model was operated at 295 ft head, cavitation set in at a suction head (positive) of about 13 to 14 ft. On the prototype there would be a positive suction head of 80 ft when operating under this condition. The sigma for the first condition is about 0.07, and for the latter condition about 0.15.

Professor Daugherty suggests that the cutoff point on the H-Q curve would not be influenced by the size of the suction pipe. The authors feel that not only the size of the suction pipe but also the kind of entrance piece used on the suction pipe would effect the cutoff point. These would determine the friction head loss h_f in the intake pipe and would thus be reflected in the sigma as illustrated in his discussion.

Professor Knapp and Mr. Daily question the conclusion that for turbine operation, as shown in Fig. 8, gate 10 is accepted as full gate, and for pump operation, shown in Fig. 7, gate 8 is considered as maximum.

In Fig. 7 it will be seen that the H-Q curves for gates 7 and 8 rapidly approach each other at the larger discharges. If gates 9 and 10 had been plotted it would be seen that there would not be much further gain in discharge for a given head at these larger discharges than is obtained with gate 8, and the efficiency would be lower. However, when operating as a turbine, as seen in Fig. 8, there is considerable gain in power at gate 10 over that obtained at gate 8, and the efficiency is still only about 3 per cent lower. Therefore, it may be concluded that for the pump, when operating at gates 9 and 10, it would be overgated, while when operating as a turbine, gate 10 could be used to considerable advantage.

The authors wish to thank all of the discussers for their valuable contributions and hope that the description of the model and its performance characteristics will be accepted only as another step in the development of the combined pump-turbine.

The Foren Mill for Rolling Seamless Tubes Achieves Virtually Continuous Production

By E. W. WRAGE,[1] MILWAUKEE, WIS.

This paper deals with the development of the Foren tube-rolling process, details of the first experimental unit, and the problems which required solution in making it commercially practicable. Operation of the present unit, which is based on straight-line production methods, is described. Automatic controls for practically all operations have been developed, which makes possible the reduction of personnel to a minimum.

THE production of seamless tubes had its inception about 1885, when two German engineers developed a cross-rolling method for manufacturing seamless hollow billets. Subsequently, the process came to be known as the Mannesman piercing method which is in use today with practically no changes other than refinements in machine design. This method is illustrated diagrammatically in Fig. 1.

One of the best known methods developed to improve upon the crude hollow billets, produced by the early machines, is the plug-type tube-rolling unit, which today produces the largest tonnage of seamless tubing in the industry. A typical cross section of this machine is shown in Fig. 2.

In this illustration it will be noted that the hollow pierced billet is forced between two large rolls, each of which is grooved to the correct dimension required to produce a predetermined tube size, in conjunction with a rolling mandrel or plug on the inside of the hollow pierced billet, supported on the end of a mandrel bar. As the tube is passed between the revolving mill rolls and the plug, it is rolled for approximately 60 per cent of two sections of its periphery, directly opposite each other, to a determined diameter and wall thickness. Upon completion of this cycle, the upper roll is raised to permit the return of the rolled billet to its original position by the stripper, or return rolls, which are located directly behind the forming rolls. The hollow billet or tube is then turned 90 deg from its original pass to permit working the roll and mandrel on this new axis. This turning operation is repeated with each pass until the required tube diameter, as well as the wall thickness, has been developed. Thereafter the tube is passed to the next operation for further processing.

Since the roll setting must be changed in accordance with the passes required, a great deal depends upon the skill of the operators in the production of tubes of uniform diameter and wall thickness.

Until recent years, this seamless-tube-rolling method was universally used throughout the industry, and but slight progress had been made toward perfecting a better one. Then several improved methods were devised, including the Pilger mill, the Assel mill, and the Diescher mill, all of which have a definite place in their several fields, and are being used to advantage for tube production.

Development of the Foren Mill

During the same period as these developments were taking place, P. A. Foren, a Swedish engineer in the employ of the author's company, conceived the idea that rolling a pierced billet over a solid bar on the inside, and through a series of successive passes, should produce a tube of better inside and outside finish, with a closer wall tolerance than is practicable on the conventional plug-type mill. He began his experiments about 1927, using

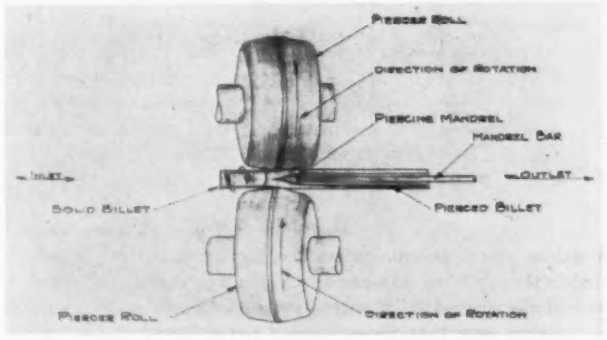


FIG. 1 CROSS-ROLLING METHOD FOR MANUFACTURING SEAMLESS HOLLOW BILLETS
(Diagram shows billet passing through piercing machine.)

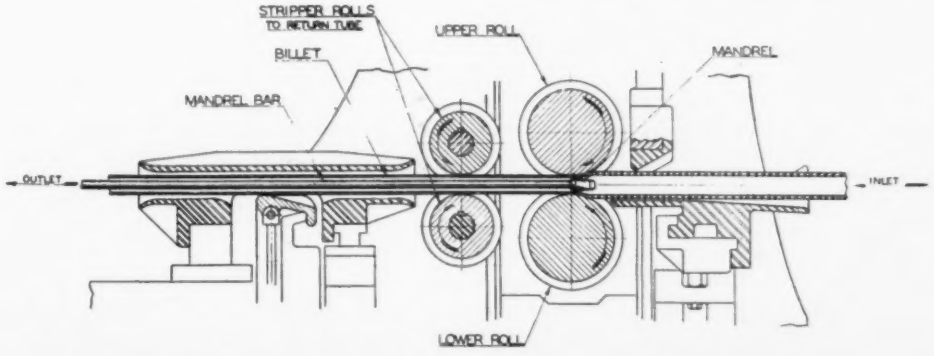


FIG. 2 BILLET PASSING THROUGH ROLLING MILL OF STANDARD SINGLE-STAND TYPE

[1] Chief Engineer, Globe Steel Tubes Co.

Contributed by the Metals Engineering Division and presented at the Annual Meeting, New York, N. Y., December 1–5, 1941, of THE AMERICAN SOCIETY OF MECHANICAL ENGINEERS.

NOTE: Statements and opinions advanced in papers are to be understood as individual expressions of their authors and not those of the Society.

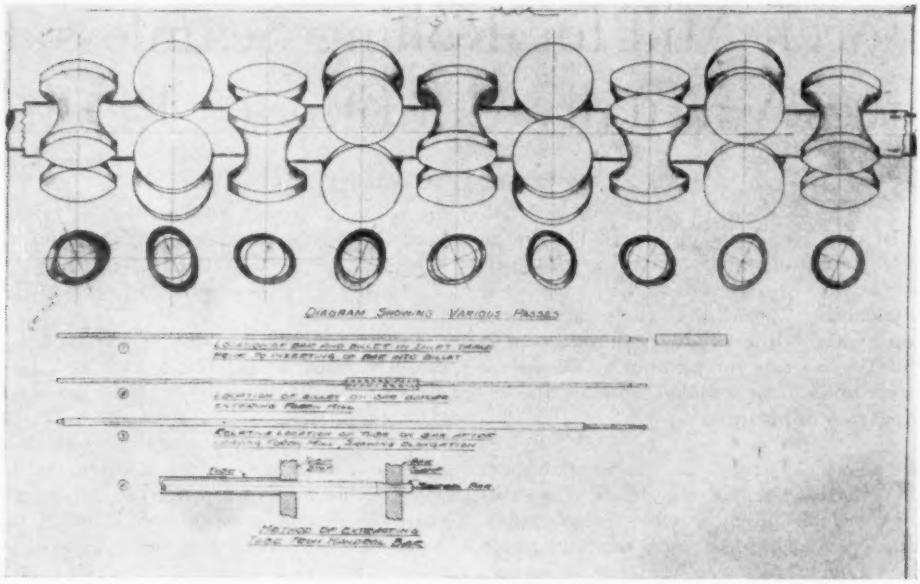


FIG. 3 DIAGRAM SHOWING VARIOUS PASSES AND DETAILS OF RELATION BETWEEN MANDREL BAR AND BILLET AT DIFFERENT STAGES OF PROCESS

mandrel bars in tubes produced on the plug mill and passing them through what is known as reducing or sizing mills. His experiments resulted in obtaining records of elongation, reduction per pass, and power consumption. Crude as it was, this procedure furnished sufficient information upon which to base the detailed development of the present-day Foren tube-rolling unit. In 1928 his ideas had advanced to a point where a patent covering this method of tube rolling was applied for and subsequently granted.[1]

However, there were still many unknown factors which required determination before a commercial unit could be designed and built, i.e., permissible speeds, roll pressures, impact angles, groove clearances, power consumption, and proper rolling temperatures. The development of motors to give a constant predetermined roll speed constituted a new problem for the motor builders.

In designing the mill twenty-one roll stands were selected, based on a certain contemplated reduction per pass. Realizing that in the use of twenty-one successive rolls considerable elongation of the pierced billet as well as reduction in diameter would materialize, and that the roll speed for each set of rolls would have to be of corresponding revolutions for a given tube diameter, a motor speed would naturally have to be developed for each different tube diameter and wall thickness. With this in mind, it was obvious that each roll set, or stand, would have to be independently driven, inasmuch as it was not practicable to design a gear train with such flexible ratios that all speeds could be obtained from a single drive.

The next step in the design of this mill was positioning the roll stands with respect to the pass line of the mill. The advantage of engaging the hollow billet by the rolls at as many angles as possible, in order to cover the entire circumference, was recognized.

To illustrate this point more clearly, let us assume that the first set of two rolls is placed on the horizontal plane with a groove of such design that both the upper roll and the lower roll will engage the billet for 50 deg of its circumference. In the first pass, the billet will be rolled at two sections by this set of rolls for 100 deg of its circumference. The following set of rolls, performing an equal amount of work on the billet, is placed at a 90-deg angle with the first roll set, or in a vertical plane. Hence, the billet, having passed through the first and second set of rolls, each set engaging it for an equal amount of its circumference, has received rolling by two sets of rolls to a total of 200 deg, in four sections of its circumference. In order to perform work on the billet over its entire circumference, the next two sets of rolls are placed in the same relation to each other, except that their axis is placed at a 45-deg angle with that of the first two sets. By this arrangement the billet having passed through four sets of rolls has received work over its entire circumference; a small overlap is also provided for each pass.

It should be noted that the groove design in each roll set is not a true radius. The billet, passing through each roll set with the mandrel bar on the inside, does not emerge from the pass perfectly round but is slightly oval in form, for reasons which will be explained. Obviously, the billet, having gone through four passes, is reduced in diameter as well as in wall thickness and is irregular in cross section, Fig. 3.

The billet then passes into the next set of rolls which have grooves so designed as to restore its circular cross section. The foregoing procedure is descriptive of a complete rolling cycle. In succeeding rolling cycles the operations are repeated, continuing to reduce both billet diameter and wall thickness, which results in elongation of the billet. After the billet has passed through the ninth set of rolls, it is again restored to a circular cross section, thus accounting for ten roll stands.

Passing through an additional eight sets of rolls, placed at alternating angles as previously, the billet is further reduced both in diameter and in wall thickness. The remaining three passes of the original twenty-one sets of roll stands perform the function of freeing the billet from the mandrel bar and, at the same time, of sizing the outside diameter, the wall thickness having been fixed by the previous passes.

SELECTING THE MOTOR DRIVE

Having determined the arrangement of the rolling cycle, as well as the angular location of the rolls, suitable drives had to be provided. In order to simplify the gear drives and their respective locations, the following arrangement was adopted:

[1] U. S. Patent No. 1,858,990, assigned to Globe Steel Tubes Co.

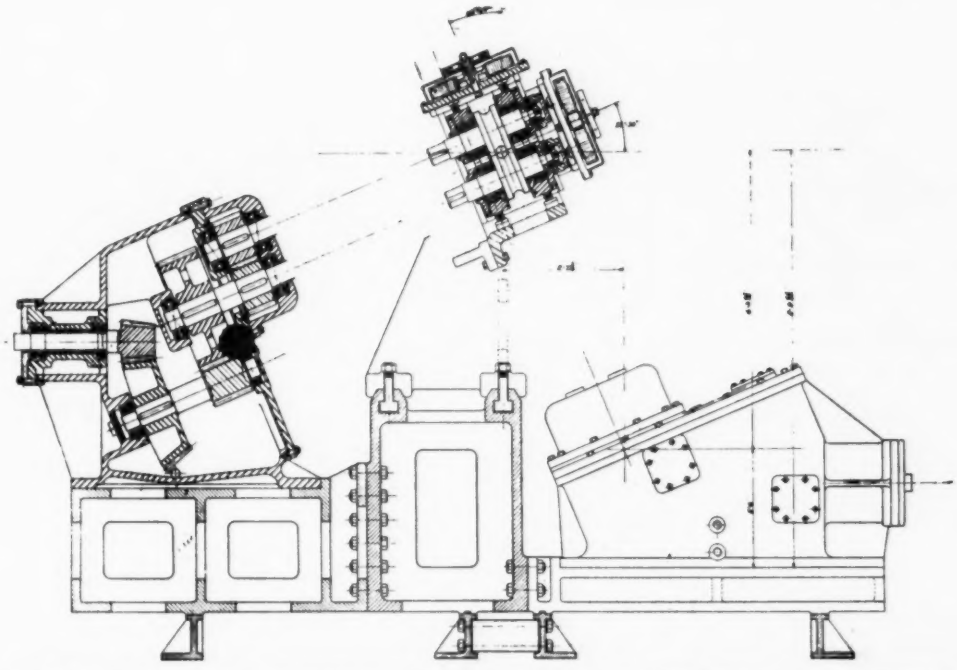


FIG. 4 TYPICAL ROLL STAND GIVING 45-DEG ANGULAR CONTACT BETWEEN ROLLS, ALSO SHOWING CROSS SECTION THROUGH GEAR DRIVE DESIGNED FOR 22-DEG 30-MIN ANGLE

The first set of rolls was set at an angle of 22 deg 30 min with one side of the vertical center line of the mill, followed by the second set of rolls, placed at an angle of 67 deg 30 min with the vertical center line but opposite to the first set, thus giving a total angular distance of 90 deg between roll stands Nos. 1 and 2. The following two sets of rolls were arranged as before, with this difference, that the third set of rolls was placed at 22 deg 30 min with the vertical center line on the side of the second roll stand which was placed at 67 deg 30 min. Pass No. 4 placed at 90 deg from pass No. 3 would then be located 67 deg 30 min on the opposite side from the vertical center line. In studying this arrangement it will be seen that the axes of the several sets of rolls throughout the mill are at an angle of 22 deg 30 min with each other, making it feasible to engage a billet to be rolled with a 45-deg angular contact between rolls. This is better illustrated in Fig. 4 which also shows a typical cross section through one of the gear drives designed for the 22-deg 30-min angle. This arrangement of gear drives with motors for each roll simplifies the design of the subbase as well as the angular drive spindle connection between gear unit and roll necks.

EXPERIMENTAL PERIOD

The first Foren mill, as described, together with its auxiliary equipment and electrical controls, was installed in a separate building and operated on an experimental basis for some time before it was placed in the production line. During the experimental period considerable data concerning its operation were developed and many difficulties were corrected. Some of the problems solved in this way involved such matters as determination of the maximum reduction per roll set; the correct elongation, resulting from each pass; the necessary increase in roll speed from one pass to the next; groove contours to provide for the free flow of metal; rolling tension between passes; power consumption per pass; generator loading for the entire unit; bar requirements; rolling temperatures; coefficient of friction between hot metal on a cold bar surface; and other essential data.

As already mentioned each set of rolls had to have a very flexible speed control. This was accomplished by driving each set of rolls through reduction gears by means of a direct-current motor with variable voltage and speed. All of the motors were in turn connected to a single motor generator set, having a voltage range from 230 to 375. A speed range of 2 to 1 was built into each motor at all voltages. This speed range plus the voltage variation for the motors furnished the flexible speed requirements. Each motor was equipped with an electric tachometer which indicated the correct motor revolutions. The motor speeds in turn were set by means of a coarse and fine rheostat in the motor field circuits. Automatic voltage regulation on the generator eliminated wide fluctuations.

After months of experiment, during which time a number of adjustments and changes were made in the mill drive, the unit was placed in the production line-up. The results were very encouraging, but it became apparent that additional study was required to develop the full potentialities of this rolling unit. Fig. 5 is a plan view of the mill as it was originally installed.

Fig. 6 is a diagrammatic arrangement of the rolls in their respective locations showing the reductions per pass throughout the mill to the final finish of the rolled billet, or tube, prior to the extraction of the mandrel bar.

Fig. 7 is a general layout of the entire Foren tube-rolling process from billet-heating furnace to the cooling table. This arrangement is being used today except for modifications and changes on the mill proper and on some of its auxiliary equipment.

DEVELOPMENT OF PRESENT MILL AND ITS OPERATION

The original mill having been in the production line for several years under constant observation by the engineering department, it became apparent that increased reductions per roll stand would result not only in a better product but also in increased production, chiefly through conservation of the heat in the pierced billet. After thorough study of the situation, the mill was changed from twenty-one sets of rolls to thirteen sets, which

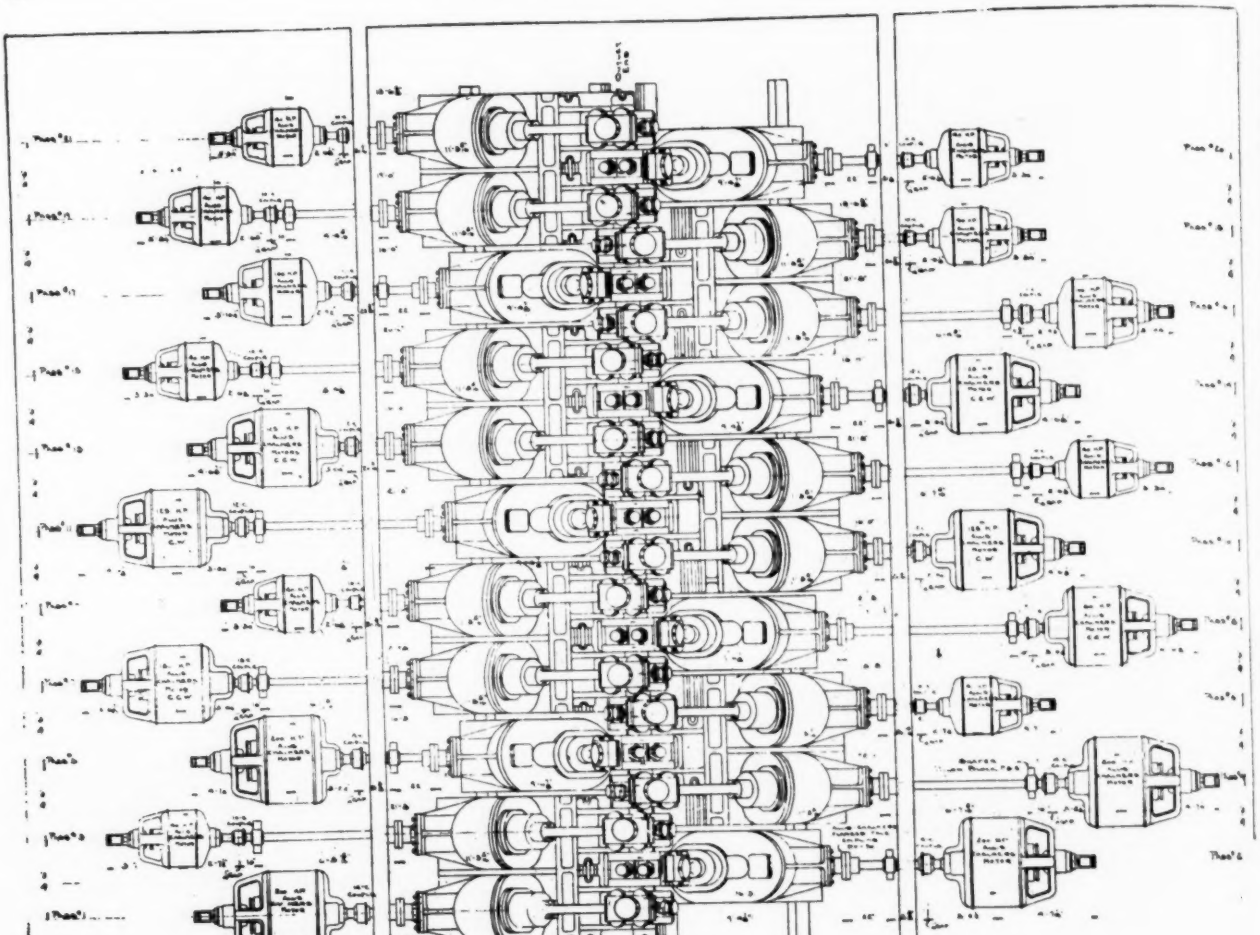


FIG. 5 PLAN VIEW OF MILL AS ORIGINALLY INSTALLED

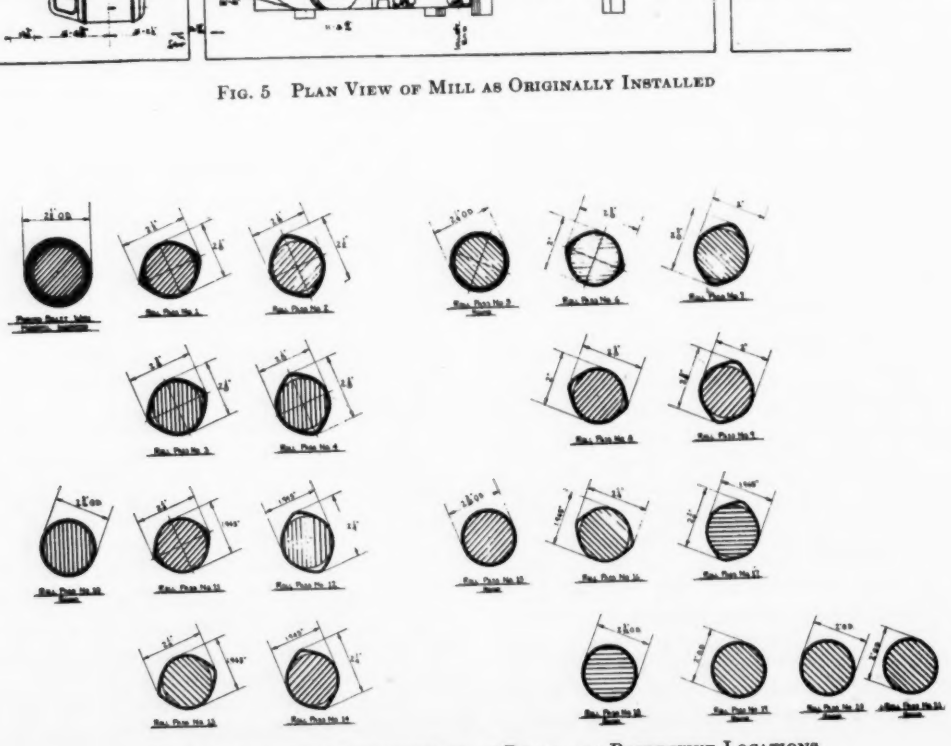


FIG. 6 SCHEMATIC ARRANGEMENT OF ROLLS AND RESPECTIVE LOCATIONS

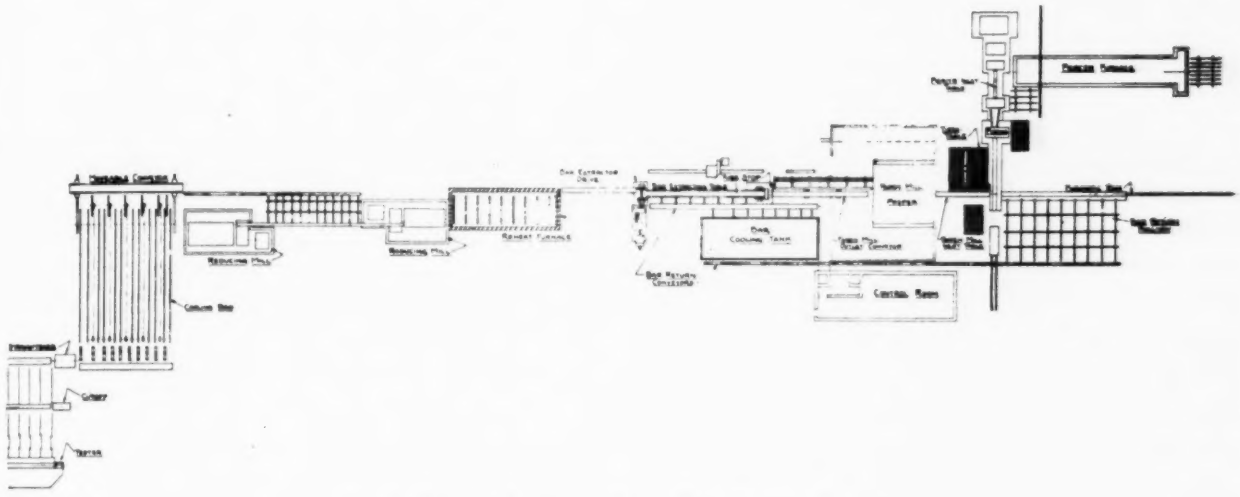


FIG. 7 GENERAL LAYOUT OF FOREN TUBE-ROLLING PROCESS

would appear to be a rather large reduction in the number of passes. However, it was possible to accomplish this change by installing larger motors in some of the mill stands which were called upon to take heavy reductions on the pierced billet. Motors were equipped with flywheels which provided against a drop in speed due to the impact loading on the rolls. The WR^2 built up in the flywheel, plus the gear reduction, plus constant voltage, resulted in a close regulation of the roll speed. From observation it was further determined that proper lubrication on the rolling mandrel was essential, as this has a direct bearing on the flow of the metal in each pass. The cycle of events on the thirteen mill stands, as they are now being operated with entirely satisfactory results, is as follows:

Upon inserting the mandrel bar into the pierced billet, the first two sets of roll stands reduce it to a diameter with which the inside of the billet is engaging the mandrel bar. The next eight sets of rolls, their angular positions remaining the same as in the original setup, perform the entire operation of reducing the diameter and wall thickness of the pierced billet. This is followed by a rounding-up pass, the remaining two passes then functioning as a means of freeing the billet from the mandrel bar and, at the same time, of acting as a sizing roll for the tube diameter. This arrangement achieves conservation of heat because of increased roll speeds and fewer passes.

To illustrate the results obtained by this mill, Fig. 8 incorporates a table of certain popular sizes which gives the billet size prior to piercing, the pierced-billet dimensions, the pierced-billet length, as well as the billet length leaving the mill. From this table, the elongation of the billet can be determined. It also gives a micrometer reading on the cross section of a certain tube size, illustrating the variations throughout the circumference of the tube at ten different positions of the circumference. This table also shows a graph of reduction in area, per cent of elongation, and roll speeds in feet per minute.

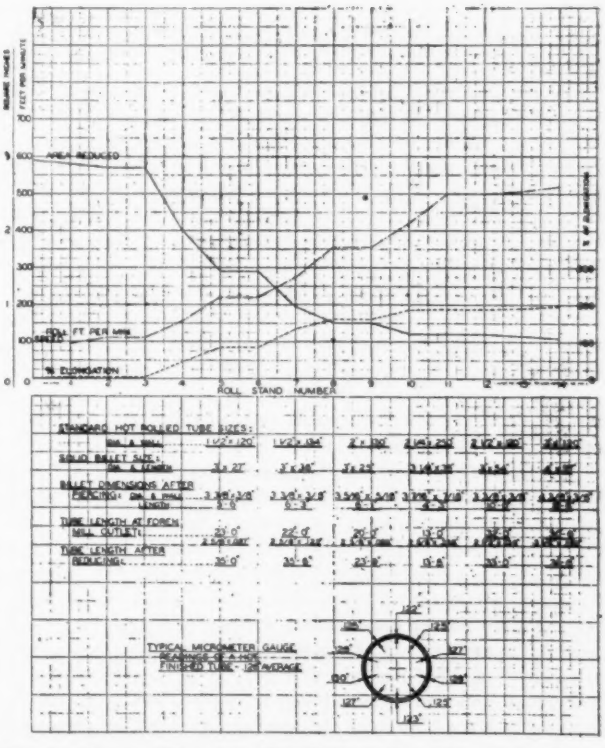


FIG. 8 WORKING TABLE OF HOT-ROLLED TUBE SIZES, AND GRAPH OF REDUCTION IN AREA, PER CENT OF ELONGATION, AND ROLL SPEEDS

RESULTS ACHIEVED

The results obtained have been gratifying because seamless tubes have been produced with walls as thin as 16 gage, which has not been accomplished by any other hot-rolling method.

All of the rolls can be completely changed from one groove diameter to another groove diameter in 4 hr, including the checking of all passes. To make a change in the wall gage requires only 15 min, as this involves changing only mandrel bars and speeds.

The capacity of this rolling unit together with its auxiliary equipment, including reducing mills, ranges from $1^1/_2$ in. OD to $4^1/_4$ in. OD in various gages. The process is not confined to rolling low-carbon steels, but will handle all alloys and stainless steels that can be successfully converted into tube stock.

From the standpoint of hot finish, tube-stock tubes produced on this mill are superior to those produced on the conventional plug-type rolling mill. By using a mandrel bar instead of a plug on the inside of the tube, a smooth inside diameter is assured. In general all tubing eventually becomes a container either for liquids or gases; hence a smooth interior finish is important. Another important advantage of smooth inside walls as well as a

smooth exterior is appreciated when this stock is to be used for further processing such as cold drawing. It has been found that reduction in diameter, as well as in wall thickness, can be increased and the die and mandrel life extended which results in better draw-bench capacity.

Tube lengths made on this type of mill are restricted only by the length of the mandrel bar providing all other auxiliary equipment is arranged for long lengths.

Production of Seamless Tubes on Present Foren Mill

In order to obtain a better understanding of this rolling unit and its auxiliary equipment, let us again refer to Fig. 7 showing the entire arrangement of the mill. The predetermined billet lengths of the proper grade of steel are stored in a yard which has been equipped with a chain conveyer to move the billets individually to a loading station. At this point the billet is automatically removed from the conveyer to a chain-driven billet elevator which conveys the steel to the inlet or charging end of the billet-heating furnace. This furnace is designed with an inclined hearth, which permits the billets to pass from the charging end to the discharge end by gravity. This oil-fired billet-heating furnace has a hearth 10 ft wide by 80 ft long, and is so arranged with heating zones that the steel will be heated to its required temperature gradually, thus assuring uniform temperature throughout.

At the discharge end of the furnace an automatic billet extractor, or pusher, is installed which is motor-operated and controlled by automatic timing. This extractor discharges each billet onto an inclined rollway from which it rolls into the inlet guide, or trough, to the Mannesman piercer. The inlet trough to the piercing mill is equipped with a pneumatic billet-inserting ram which forces the billet between the rolls of the piercing mill. The piercing mill engages the heated billet, passing it between the two rolls and the upper and lower guides and over the piercing mandrel, on through to the piercing-mill-outlet table, whereupon the piercing mandrel and its supporting bar are withdrawn pneumatically. No operator is required at the piercing mill, because the piercing mandrel, of patented design, does not require replacement and will pierce from 1000 to 1200 billets in normal operation without changing.

A pneumatically operated kickout conveys the hollow pierced billet to a table upon which is located a gate that turns the pierced billet through an arc of 90 deg. Again the pierced billet rolls onto an inclined table which conveys it to the entering table, or trough, immediately in front of the rolling unit. This entering trough is in line with a table on which the mandrel bar is conveyed. The bar is then moved forward through the pierced billet by a pneumatically operated ram. The movement is automatically controlled by limit switches, so arranged that the bar is inserted into the pierced billet to a predetermined position. In order that the friction of the inserting operation may not force a pierced billet into the entering rolls of the mill, a gate is installed at the mill entrance to restrict the movement of the billet and mandrel until the proper relative positions of billet and bar have been obtained. The gate is thereafter withdrawn by an air cylinder, equipped with automatic control, and both billet and mandrel bar enter the first set of rolls.

Having passed through the mill, the rolled billet, with the mandrel bar still inserted, is conveyed to the bar-extracting table. This table is designed to perform several operations. The tube and mandrel bar come to rest in their longitudinal travel just sufficiently long for a plier to engage the protruding end of the mandrel bar. At the moment this extracting plier engages and firmly grips the mandrel bar, a gate is simultaneously set in motion which holds the tube in place while the extracting plier withdraws the bar. Having withdrawn the bar from the tube the plier is immediately disengaged, whereupon the mandrel bar is automatically ejected from the conveyer rolls in the extracting table onto another conveyer which returns it to a point where it is loaded onto a transverse conveyer, which submerges it in a tank filled with cooling water. The moment that the mandrel bar has cleared the extracting table, the gate holding the tube is automatically released and the tube proceeds to travel longitudinally into a reheating furnace.

In the reheating furnace the temperature of the rolled tube is raised to a point which may be required for further processing. After the tube has acquired its proper temperature, it is extracted from the reheat furnace on conveyer rolls and enters a reducing mill having thirteen sets of roll stands. If the reduction in diameter through the first reducing mill is not sufficient, the tube is then conveyed to a second reducing mill capable of reducing the diameter to a minimum of $1^1/_2$ in. However, if the desired diameter is obtained in the first reducing mill, rollways and conveyers are so arranged that the tube can by-pass the second reducing mill, in which case it is deposited on a cooling table equipped with conveyer chains of such slow travel that it has sufficient time to cool before being conveyed to the inlet table of a straightening machine.

After the tube has passed through the straightening machine it is automatically ejected from the outlet table of the straightener and rolls onto inclined tables which carry it to the cutoff machines where it is cut to length and passed to the next operation which is the hydraulic test. Each tube is tested to a hydrostatic pressure of 1000 psi, carefully drained, and thereafter passed to the inspection tables for the last checkup of surface quality, wall gage, and other requirements for hot-finished tube material.

The rolling unit is not only used for hot-finished material, but a very large percentage of its output is further processed by the cold-drawing method to obtain small diameters and light gages. With the close hot-finish tolerances that are feasible, the advantage is marked when close tolerances and hot finish are required by the cold-drawing method.

After the mandrel bar has passed through the cooling tank with its temperature now reduced to normal, it is returned by a conveyer line to the storage rack parallel with the mandrel-bar-inserting table. In order that no delay may occur in the tube-rolling process, a sufficient number of mandrel bars are employed in order to maintain a supply of at least four at the inserting table.

Control of the Bar-Extracting Table

The numerous operations of the bar-extracting table have been so carefully interlocked by limit switches and pneumatic valves that no manual operations are required. In order to appreciate the complicated control thus involved let us consider the time required for the operations previously outlined. A billet with its mandrel bar, having a length of 40 ft, passes through the mill in 7 sec. Under normal operating conditions, a billet and mandrel bar enter the mill the moment the preceding billet and mandrel bar have cleared the mill. This means that the time is very short indeed in which the extracting plier must engage the bar and extract it from the tube, after which the bar must clear the extracting table, the tube must pass over it to the furnace, and the plier return to its original position ready to engage the next bar. These various operations are timed in fractions of a second and, being fully automatic, no manual labor is required. However, a technician is stationed at an extracting-table control desk on which are mounted all of the automatic controls, as well as independent push-button controls, so that he can perform any operation by individual control should an interruption in the rolling cycle occur.

The various operations of this mill have been carefully studied

and reduced to tabular form for use by the rolling-mill foreman. From these data he can adjust his cycles in accordance with the billet lengths, i.e., if a certain billet length requires the processing of four per minute without any lost time, he has a device at his desk which automatically controls the billet-extracting mechanism in the furnace. If he sets this timing device at four billets per minute, all that is required of the furnace operators is to have the heated billets at the inlet to the extractor, and the balance of the operations are fully automatic.

Operating Personnel

The operating force required for this rolling unit is very nominal. Three men are stationed at the billet-heating furnace. The next operator is on the control platform located at the junction of the piercing-mill-outlet table and the bar-inserting table. This operator manipulates push buttons and pneumatic valves which control the operations mentioned. Next in order is the technician stationed at the stripper table followed by two men at the reheating furnace. The reducing mills are in charge of two men. From the time it is discharged to the cooling table from the rolling mills, until it is conveyed to further processing operations, the tube is in the hands of the inspectors.

Thus the total operating force required on the rolling unit from the billet-heating furnace to delivery on the cooling bed consists of twelve men. In addition there is one man in charge of the lubricating systems on the various units, as well as general maintenance man who looks after details on the rolling unit should an interruption occur.

Controlling the Rolling-Mill Motors

In describing the Foren mill proper it was pointed out that each roll set is operated by an individual direct-current motor, connected to a motor generator set. This set and the controls for the motor and switch gear are located in a separate enclosure, in charge of an electrician. The electrician receives instructions from the rolling-mill foreman as to the size billet and tube to be rolled; from tables which have been computed from experience, he can then set the motor speeds required for the rolling operations. During normal periods after all motor speeds have been set, the operator is able to devote his time to the maintenance of all control equipment and other miscellaneous work on the various automatic controls built into the rolling unit. Thus whenever an interruption occurs because of failure of either electrical or mechanical equipment, skilled technicians are always on hand to correct the difficulties in the shortest possible time.

Conclusion

It will be obvious from the description given of this rolling unit that the entire layout is so designed that all of its operations come within the requirements of straight-line production. There is no movement of material which entails any backtracking. hence the process achieves virtually continuous tube production,

The Analysis of a Continuous Process by a Discontinuous Step Method

By J. A. HRONES,[1] CAMBRIDGE, MASS.

In this paper an attempt is made to predict the dynamic behavior of a simple heat exchanger by means of the hydraulic-thermal analog. The heat exchanger was subjected to a known input-temperature disturbance, and the resulting dynamic response of the output temperature was calculated and also measured. It was assumed that the physical conditions in the actual system could be approximated by considering the heat-exchanger tube to be divided into a number of sections; in the example carried through, three equal sections were considered. For purposes of calculation, the heat exchanger is represented by a hydraulic analog, in which the weight of fluid in a tank corresponds to the quantity of heat in an element of the system, the difference in pressure head is analogous to temperature difference, and the resistance of restrictions to fluid flow corresponds to resistance to heat flow in the thermal system.

THE material presented in this paper is in the nature of a progress report of research being carried on as an extension of the program initiated by the papers of C. E. Mason, G. Philbrick, and A. Spitzglass.[2] In the work to be described, the hydraulic-thermal analog is used in an attempt to predict the dynamic behavior of a simple heat exchanger. Theoretical results based on the analog are compared with experimental observations.

The heat exchanger employed is shown in Fig. 1. It consisted of a glass coil immersed in a constant-temperature bath. Liquid of specific heat c flows at a constant rate of w pounds per minute through the coil, the entering temperature T_i being held at a constant value. When steady-state conditions are reached, w pounds per minute of the liquid leave at a constant exit temperature T. In the first trial it was assumed that the heat capacity of the glass tubing was so small that one half of it could be lumped with the capacity of the water in the exchanger tube and the other half lumped with the capacity of the bath. The enclosing container was very large relative to the tube, the contents of which were stirred during the process to produce a uniform temperature T_s throughout the bath. Thus the heat capacity of the bath could be considered to be infinite.

The exchanger described was subjected to a known input-temperature disturbance and the resulting dynamic response of the output temperature was calculated and also measured.

The exchanger may be represented as shown in Fig. 2. The variation in temperature along the tube would follow some curve similar to A, Fig. 2, for a constant input temperature T_a. For a

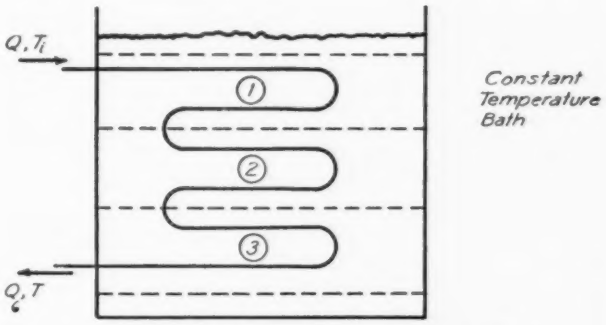


FIG. 1 TYPE OF HEAT EXCHANGER EMPLOYED

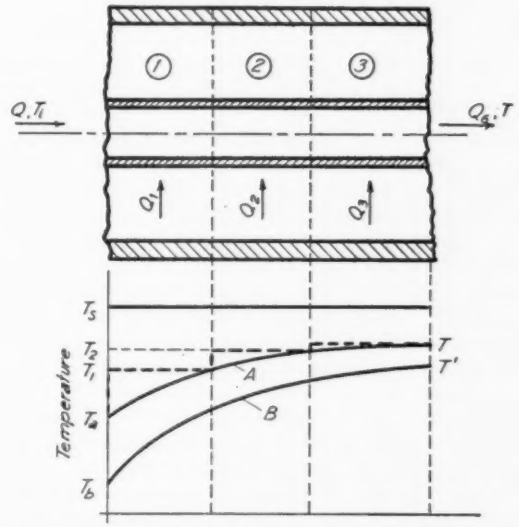


FIG. 2 REPRESENTATION OF HEAT-EXCHANGER AND TEMPERATURE CURVES

constant input temperature T_b the steady-state temperature distribution would be represented by a curve similar to B of Fig. 2. If input and output temperatures are measured, the steady-state temperature distribution may readily be calculated by the well-established principles of heat transfer.

DETERMINING OUTPUT TEMPERATURE VERSUS TIME RELATION

For a known input-temperature disturbance T_i, it is desired to determine the corresponding output temperature versus time relation. To demonstrate the method it was assumed that the physical conditions prevailing in the actual system could be approximated by considering the tube to be divided into a number of sections. As an example of the method, three equal sections will be considered, see Figs. 1 and 2.

In addition it was assumed that the temperature of the fluid in section (1) was T_1 throughout, that the temperature of the fluid in section (2) was T_2, and that the temperature of the fluid in section (3) was T throughout. This assumption means that

---

[1] Massachusetts Institute of Technology. Jun. A.S.M.E.

[2] "Automatic Control in the Presence of Process Lags," by C. E. Mason and G. A. Philbrick, Trans. A.S.M.E., vol. 62, 1940, pp. 295–308.

"Quantitative Analysis of Single-Capacity Processes," by A. F. Spitzglass, Trans. A.S.M.E., vol. 60, 1938, pp. 665–674.

Contributed by the Committee on Industrial Instruments and Regulators of the Process Industries Division and presented at the Annual Meeting, New York, N. Y., December 1–5, 1941, of THE AMERICAN SOCIETY OF MECHANICAL ENGINEERS.

NOTE: Statements and opinions advanced in papers are understood to be individual expressions of their authors and not those of the Society.

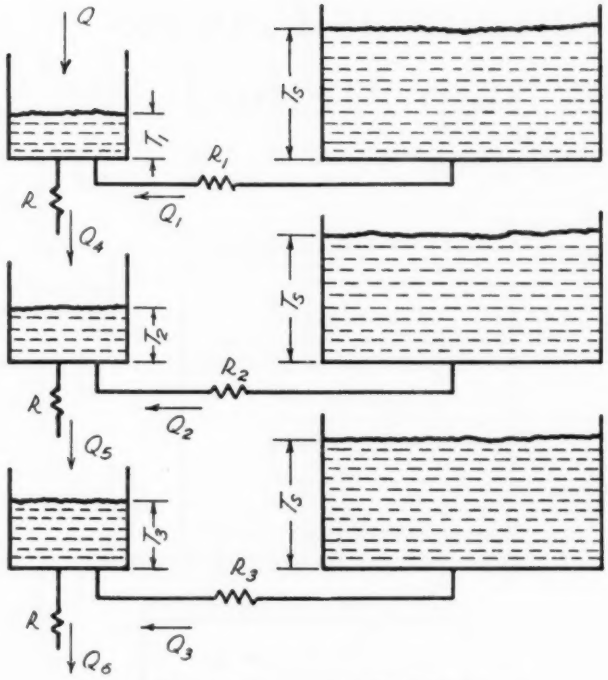


FIG. 3 HYDRAULIC ANALOG OF HEAT EXCHANGER

step jumps in temperature will occur at the ends of each section. This situation is inconsistent with the actual physical conditions. Nevertheless, the problem was solved on this basis with the results which are reported.

Under the foregoing assumptions, the heat exchanger may be represented by the hydraulic analog shown in Fig. 3, in which the weight of fluid in a tank corresponds to the quantity of heat in an element of the system, the difference in pressure head is analogous to temperature difference, and the resistance of restrictions to fluid flow corresponds to resistance to heat flow in the thermal system.

S represents a large storage reservoir with a constant pressure head T_s. This is the hydraulic equivalent of the thermal energy stored in the constant-temperature bath.

Tanks (1), (2), and (3) are small with respect to S and are fed from the main storage tank through restrictions having the resistances R_1, R_2, and R_3, respectively. For clarity of presentation the large storage tank is represented as three separate units, all having the same pressure head T_s. The weight of water contained in tank (1) corresponds to the heat-energy content of the water in section (1) of the heat exchanger. The pressure head of tank (1) is analogous to the temperature of section (1). Tanks (2) and (3) hold similar positions in the analogy with respect to sections (2) and (3). The resistance R_1 corresponds to the over-all thermal resistance of section (1) between the liquid of the bath and that flowing through the exchanger tube. R_2 and R_3 have the same significance with respect to sections (2) and (3). The resistance R determines the flow of thermal energy from one section to the following section and is a function of the rate of flow through the tube.

To make the analogy complete a linear relationship between rate of flow and pressure difference was assumed. Thus

$$Q_1 = \frac{T_s - T_1}{R_1}$$

where Q_1 is the flow per unit time from the storage tank (1). Under the assumptions previously mentioned the areas of the tanks (1), (2), and (3) were considered equal to the thermal capacity of the water in each section (Wc) plus one half of the thermal capacity of the glass wall of the section.

From a consideration of the rate of flow to and from tank (1), (2), and (3), the following equations can be written

$$a_1 \frac{dT_1}{dt} + \left(\frac{1}{R_1} + \frac{1}{R}\right) T_1 = \frac{T_i}{R} + \frac{T_s}{R_1} \quad \ldots\ldots [1]$$

where $a_1 \frac{dT_1}{dt}$ = rate of change of fluid within tank (1)

$\frac{Ti}{R}$ = rate of flow of fluid into tank (1) from source

$\frac{T_s - T_1}{R_1}$ = rate of fluid flow from storage tank

$\frac{T_1}{R}$ = rate of fluid flow into following tank (2)

Similar quantities with subscripts 2 and 3 represent corresponding quantities for the other tanks as follows

$$a_2 \frac{dT_2}{dt} + \left(\frac{1}{R_2} + \frac{1}{R}\right) T_2 - \frac{T_1}{R} = \frac{T_s}{R_2} \quad \ldots\ldots [2]$$

$$a_3 \frac{dT_3}{dt} + \left(\frac{1}{R_3} + \frac{1}{R}\right) T - \frac{T_2}{R} = \frac{T_s}{R_3} \quad \ldots\ldots [3]$$

If these three equations are solved for T, the following third-order differential equation is obtained

$$\frac{d^3T}{dt^3} + A\frac{d^2T}{dt^2} + B\frac{dT}{dt} + HT = D\frac{d^2T_s}{dt^2} + E\frac{dT_s}{dt} + FT_s + GT_i \quad \ldots\ldots [4]$$

where T_i is the input temperature. The complete solution for Equation [4], together with the values for the coefficients, is included in the Appendix.

The general solution of Equation [4] is

$$T = T_{ss} + K_1 e^{-t/\tau_1} + K_2 e^{-t/\tau_2} + K_3 e^{-t/\tau_3} + C_4 \Delta T_i \quad \ldots [5]$$

Where T_{ss} is the steady-state exit temperature and ΔT_i is a function of time and represents the difference between the steady-state value of input temperature and the input temperature at any time t. τ_1, τ_2, and τ_3 are the characteristic times of sections (1), (2), and (3), respectively, and are given by the following equations

$$\frac{1}{\tau_1} = + \frac{1}{a_1}\left[\frac{1}{R_1} + \frac{1}{R}\right] \quad \ldots\ldots [6]$$

$$\frac{1}{\tau_2} = + \frac{1}{a_2}\left[\frac{1}{R_2} + \frac{1}{R}\right] \quad \ldots\ldots [7]$$

$$\frac{1}{\tau_3} = + \frac{1}{a_3}\left[\frac{1}{R_3} + \frac{1}{R}\right] \quad \ldots\ldots [8]$$

If, as assumed, all sections are equal, then the characteristic times are equal and Equation [5] takes the following form

$$T = T_{ss} + C_4 \Delta T_i + (K_1 + K_2 t + K_3 t^2) e^{-t/\tau_1} \quad \ldots\ldots [9]$$

When steady-state conditions are reached, Equation [4] becomes

$$T_{ss} = \frac{F}{H} T_s + \frac{G}{H} T_i \quad \ldots\ldots [10]$$

$$\text{where } \left\{ \begin{array}{l} \dfrac{G}{H} = \left(\dfrac{\dfrac{1}{R}}{\dfrac{1}{R_1} + \dfrac{1}{R}} \right)^3 \\ \dfrac{F}{H} = 1 - \dfrac{G}{H} \end{array} \right\} \text{ for case where } R_1 = R_2 = R_3$$

T_s is the bath temperature; T_{if} is the steady-state input temperature. If all sections are assumed equal and the over-all resistance per unit length of the tube does not vary substantially over the temperature range involved, then $R_1 = R_2 = R_3$. It should also be observed that any transfer of heat between particles of the liquid flowing through the tube is neglected.

The values of T_{ss}, T_s, and T_{if} were observed and R_1 was calculated from Equation [10]. An attempt was then made to impose a step jump in input temperature to the heat exchanger. However, due to experimental difficulties this was temporarily given up and the actual input temperature–time relation given by a quick opening three-way valve was measured. The observed data were closely fitted by the following equation

$$T_i = T_{if} - (T_{if} - T_{i0})e^{-t/\tau_F} \quad \ldots\ldots [11]$$

Where T_{i0} is the steady-state value of input temperature at time $t < 0$. τ_F is the characteristic time of the input-temperature disturbance.

If Equation [11] is substituted in Equation [4] and a solution for T is obtained (see Appendix) the result is

$$T = T_{ss} + C_4 e^{-t/\tau_F} + e^{-t/\tau_1}[K_1 + K_2 t + K_3 t^2] \quad \ldots [12]$$

The coefficients may be determined by using the relations when $t = 0$

$$\left. \begin{array}{l} T_0 = T_{ss} + K_1 + C_4 \\ \dfrac{dT}{dt} = 0 \\ \dfrac{d^2T}{dt^2} = 0 \end{array} \right\} \quad \ldots\ldots [13]$$

Thus

$$K_1 = T_0 - T_{ss} - C_4$$

$$K_2 = + \left(\frac{C_4}{\tau_F} + \frac{K_1}{\tau_1} \right)$$

$$K_3 = - \frac{C_4 \left(\dfrac{1}{\tau_F} \right)^2 + K_1 \left(\dfrac{1}{\tau_1} \right)^2 - 2K_2 \left(\dfrac{1}{\tau_1} \right)}{2}$$

$$C_4 = \left[\frac{1}{a_1 R \left(\dfrac{1}{\tau_1} - \dfrac{1}{\tau_F} \right)} \right]^3 [T_{i0} - T_{if}]$$

where $\dfrac{1}{R} = wc$ Btu per deg F per min. The result of this analysis is shown as curve B, Fig. 4, and was obtained from Equation [13a].

$$T = 64 + 274e^{-11t} - [224 + 2720t + 12{,}580t^2]e^{-25.6t} \quad \ldots\ldots [13a]$$

Curve C, Fig. 4, is a plot of the observed output behavior. Similar calculations were carried out for one, two, and four equal sections, the results of which are shown in Fig. 5. Expressions for any number of equal sections n were also derived and are presented as follows:

$$T = T_{ss} + C_4 e^{-t/\tau_F} + (K_1 + K_2 t + K_3 t^2 + \ldots K_n t^{n-1})e^{-t/\tau_1} \quad \ldots [14]$$

$$C_4 = \left[\frac{1}{aR \left(\dfrac{1}{\tau_F} - \dfrac{1}{\tau_1} \right)} \right]^n [T_{i0} - T_{if}] \quad \ldots\ldots [15]$$

$$\frac{1}{R_1} = \frac{1}{R} \left[1 - \left(\frac{T_{ss} - T_s}{T_{if} - T_s} \right)^{1/n} \right] \quad \ldots\ldots [16]$$

$$\frac{1}{\tau_1} = -\frac{1}{a_1} \left(\frac{1}{R_1} + \frac{1}{R} \right) \quad \ldots\ldots [17]$$

$$K_1 = T_0 - T_{ss} - C_4 \quad \ldots\ldots [18]$$

$$K_n = -\left[\frac{C_4 \left(-\dfrac{1}{\tau_F} \right)^{n-1} + K_1 \left(-\dfrac{1}{\tau_1} \right)^{n-1}}{(n-1)!} + \frac{\left(-\dfrac{1}{\tau_1} \right)^{n-2}}{(n-2)!} K_2 + \frac{\left(-\dfrac{1}{\tau_F} \right)^{n-3}}{(n-3)!} K_3 + \ldots\ldots \left(-\frac{1}{\tau_1} \right) K_{n-1} \right] \quad \ldots [19]$$

Conclusions

For the case of the three equal sections, curve B, Fig. 4, is the calculated result. There are marked deviations from the experimental results shown by curve C. Although the general outline is reasonably well matched, the sharpness of the initial lag is not accurately predicted. The time to reach substantially steady-state exit-temperature conditions is accurately shown although the calculated response between 0.15 and 0.5 min is in considerable error. The sharpness of the initial effect on the output temperature or the lag is more accurately predicted as more sections are used in the solution. To show the trend of results as more sections are employed additional calculations were made for one, two, and four equal sections. The results are plotted in Fig. 5 where the experimental data are again reproduced as curve A. Increasingly better prediction of the lag is obtained as more sections are used. The improvement in the latter part of the response is small.

The failure of the calculated results to match experimentally determined values could be caused by a combination of the following reasons:

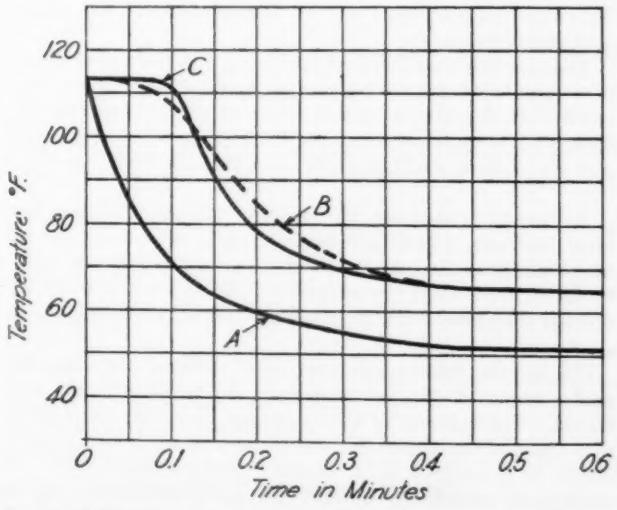


Fig. 4 Observed Output Behavior for Case of Three Equal Sections

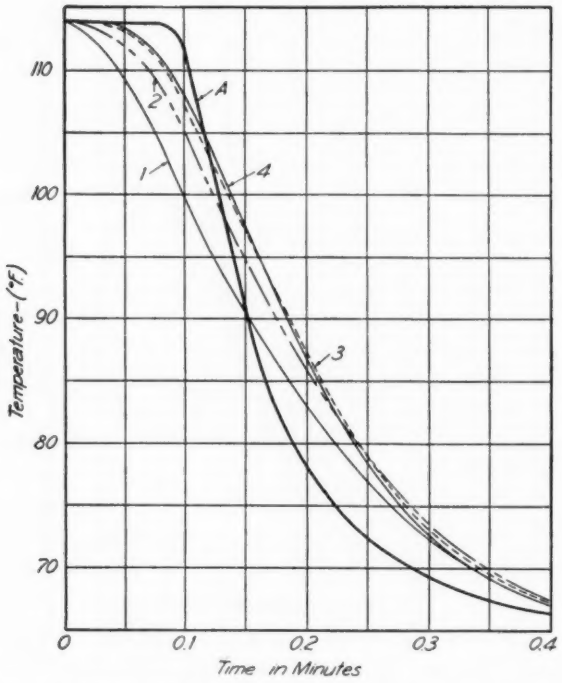


FIG. 5 CURVES FOR ONE, TWO, AND FOUR EQUAL SECTIONS

1 Instrument lag and errors.
2 Errors in making observations of temperature and time.
3 The choice of an insufficient number of sections.
4 Improper choice of the size of the sections.
5 The simplified analogy is not representative of the actual system.

The response of the temperature-measuring system to a step function is substantially exponential. The characteristic time was about 1.25 sec. This means that transient effects from a step function should become negligible in an interval between 3 and 4 sec. A forced response delay would be present after the transient is over. However, in the present case, instrument errors would have changed the observed effects in a fashion to improve the agreement between experimental and theoretical results. It is reasonable to conclude that the discrepancy was not due to instrument errors.

The time intervals involved were small and the rate of change of temperature rapid. A series of readings on identical runs indicated that the error at points where the curve was changing rapidly could be as great as 4 deg F. The plotted results are the average of three readings where the maximum deviation was 4 deg.

As already pointed out, the choice of a larger number of sections produces increasingly better results. However, the net improvement in the second half of the dynamic-response prediction is small and there is considerable doubt that even a very large number of sections would produce the accuracy that might be desired.

Finally, the inaccuracies may result because the simplified analog employed does not represent the process as closely as it should. The capacity of the exchanger tube wall was lumped with those of the section and the storage tank. If this wall capacity is introduced as a separate energy-storage tank, the analogy for section (1) becomes the one illustrated in Fig. 6. The storage capacity of the tube wall is represented by the tank w having an area a_w which corresponds to the heat capacity of

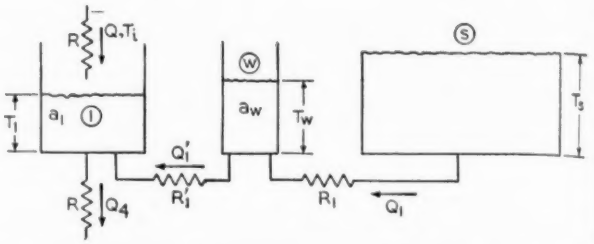


FIG. 6 ANALOGY FOR SECTION (1) WHEN WALL CAPACITY IS INTRODUCED AS SEPARATE ENERGY-STORAGE TANK

the tube wall per deg F. T_w represents the temperature of the tube wall. Thus each section of the tube would now be described by a differential equation of second order instead of the first-order one used in the former analogy. This will increase the difficulty of solution but the exit-temperature response may be readily calculated by first solving equations for T_1.

$$\left.\begin{aligned} a_1 \frac{dT_1}{dt} &= \frac{T_i}{R} + \frac{T_w - T_1}{R_1'} - \frac{T_1}{R} \\ a_w \frac{dT_w}{dt} &= \frac{T_s - T_w}{R_1} - \frac{T_w - T_1}{R_1'} \end{aligned}\right\} \quad \ldots\ldots [19a]$$

T_1 may then be used as a forcing function for section (2) and the procedure repeated for each section used.

It is hoped that the results of such calculations will soon be available.

Appendix

NOMENCLATURE

c = specific heat, Btu per lb per deg F
w = rate of flow through exchanger, lb per min
T_i = entering temperature at time t, deg F
T = exit temperature at time t, deg F
T_s = temperature of bath, deg F
T_1, T_2, T_3 = temperature of water in sections (1), (2), and (3), respectively, deg F
R_1, R_2, R_3 = over-all thermal resistances of sections (1), (2) and (3), respectively, $\frac{\text{min, deg F}}{\text{Btu}}$
$R = \frac{1}{wc}$ equivalent thermal resistance between the sections $\frac{\text{min, deg F}}{\text{Btu}}$
W = weight of water in each section, lb
a_1, a_2, a_3 = thermal capacities of sections (1), (2), and (3), respectively, Btu per deg F
T_{s_s} = steady-state output temperature, deg F, when $t > 0$
T_0 = steady-state output temperature, deg F, when $t < 0$
τ_1, τ_2, τ_3 = characteristic times for sections (1), (2), and (3), respectively, min
T_{i_f} = steady-state input temperature, deg F, when $t > 0$
T_{i_0} = steady-state input temperature, deg F, when $t < 0$
τ_p = characteristic time of input-temperature disturbance, min

Calculation of Results

The Equations [1] to [3], inclusive, are rewritten using the operator p to represent $\frac{d}{dt}$.

$$\left(a_1p + \frac{1}{R_1} + \frac{1}{R}\right) T_1 = \frac{T_s}{R_1} + \frac{T_i}{R} \quad \ldots\ldots [20]$$

$$\left(a_2p + \frac{1}{R_2} + \frac{1}{R}\right) T_2 - \frac{T_1}{R} = \frac{T_s}{R_2} \quad \ldots\ldots [21]$$

$$\left(a_3p + \frac{1}{R_3} + \frac{1}{R}\right) T - \frac{T_2}{R} = \frac{T_s}{R_3} \quad \ldots\ldots [22]$$

Using the method of determinants, the solution for T is readily found

$$T = \frac{\Delta_2}{\Delta_1} \quad \ldots\ldots [23]$$

where

$$\Delta_2 = \begin{vmatrix} \left(a_1p + \frac{1}{R_1} + \frac{1}{R}\right) & 0 & \left(\frac{T_i}{R} + \frac{T_s}{R_1}\right) \\ -\frac{1}{R} & \left(a_2p + \frac{1}{R_2} + \frac{1}{R}\right) & \frac{T_s}{R_2} \\ 0 & -\frac{1}{R} & \frac{T_s}{R_3} \end{vmatrix}$$

$$\Delta_1 = \begin{vmatrix} \left(a_1p + \frac{1}{R} + \frac{1}{R}\right) & 0 & 0 \\ -\frac{1}{R} & \left(a_2p + \frac{1}{R_2} + \frac{1}{R}\right) & 0 \\ 0 & -\frac{1}{R} & \left(a_3p + \frac{1}{R_3} + \frac{1}{R}\right) \end{vmatrix}$$

therefore

$$T = \frac{\frac{1}{a_1a_2a_3}\Delta_2}{\left[p + \frac{1}{a_1}\left(\frac{1}{R_1} + \frac{1}{R}\right)\right]\left[p + \frac{1}{a_2}\left(\frac{1}{R_2} + \frac{1}{R}\right)\right]\left[p + \frac{1}{a_3}\left(\frac{1}{R_3} + \frac{1}{R}\right)\right]} \quad \ldots\ldots [24]$$

The denominator of Equation [24] is the characteristic equation of the process and has the roots $-\frac{1}{\tau_1}$, $-\frac{1}{\tau_2}$, and $-\frac{1}{\tau_3}$ given in Equations [6], [7], and [8]. The expansion of Equation [24] gives

$$\frac{d^3T}{dt^3} + A\frac{d^2T}{dt^2} + B\frac{dT}{dt} + HT = D\frac{d^2T_s}{dt^2} + E\frac{dT_s}{dt} + FT_s + GT_i \quad \ldots\ldots [25]$$

The coefficients are

$$A = +\left(\frac{1}{\tau_1} + \frac{1}{\tau_2} + \frac{1}{\tau_3}\right) \quad \ldots\ldots [26]$$

$$B = \frac{1}{\tau_1\tau_2} + \frac{1}{\tau_2\tau_3} + \frac{1}{\tau_3\tau_1} \quad \ldots\ldots [27]$$

$$H = +\frac{1}{\tau_1\tau_2\tau_3} \quad \ldots\ldots [28]$$

$$D = \frac{1}{a_3R_3} \quad \ldots\ldots [29]$$

$$E = \frac{1}{a_2a_3R_2R} + \frac{1}{a_3R_3}\left[\frac{1}{\tau_1} + \frac{1}{\tau_2}\right] \quad \ldots\ldots [30]$$

$$F = \frac{1}{a_3R_3\tau_1\tau_2} + \frac{1}{\tau_1a_2a_3RR_2} + \frac{1}{a_1a_2a_3R^2R_1} \quad \ldots\ldots [31]$$

$$G = \frac{1}{a_1a_2a_3R^3} \quad \ldots\ldots [32]$$

The bath temperature is constant

$$\therefore \frac{d^2T_s}{dt} = \frac{dT_s}{dt} = 0$$

Thus the solution for Equation [25] becomes

$$T = T_{ss} + K_1e^{-t/\tau_1} + K_2e^{-t/\tau_2} + K_3e^{-t/\tau_3} + C_4\Delta T_i \quad \ldots [33]$$

If equal sections are used, the characteristic times τ_1, τ_2, and τ_3 become equal and the solution is

$$T = T_{ss} + C_4e^{-t/\tau_F} + [K_1 + K_2t + K_3t^2]e^{-t/\tau_1} \quad \ldots\ldots [34]$$

where the initial conditions are

$$T_0 = T_{ss} + K_1 + K_4$$

$$\frac{dT}{dt} = 0$$

$$\frac{d^2T}{dt} = 0$$

The coefficients are found to be

$$K_1 = T_0 - T_{ss} - C_4 \quad \ldots\ldots [35]$$

$$K_2 = \frac{C_4}{\tau_F} + \frac{K_1}{\tau_1} \quad \ldots\ldots [36]$$

$$K_3 = -\frac{\frac{C_4}{\tau_F^2} + \frac{K_1}{\tau_1^2} - 2\frac{K_2}{\tau_1}}{2} \quad \ldots\ldots [37]$$

$$C_4 = \left[\frac{1}{a_1R\left(\frac{1}{\tau_1} - \frac{1}{\tau_F}\right)}\right]^3 [T_{i0} - T_{if}] \quad \ldots\ldots [38]$$

If the foregoing procedure is repeated for n equal sections, the general Equations [14] to [19] are obtained.

Heat-Exchanger Data

Length of tube, in.	32
Inside diameter of glass tube, mm	9
Outside diameter of glass tube, mm	12
Temperature of bath (T_s), deg F	114
Steady-state input temperature (T_{if}), deg F	50.5
Steady-state input temperature (T_{i0}), deg F, $t < 0$	114
Rate of water flow through exchanger (w), lb per min	0.965
Steady-state output temperature (T_{ss}), deg F	64
Input temperature–time function (T_i)	$50.5 + 63.5e^{-11t}$

For these data:

$$T = 64 + 274e^{-11t} - (224 + 2720t + 12{,}580t^2)e^{-22.4t}$$

The values of coefficients for one, two, three, and four equal sections are listed in Table 1.

TABLE 1 SUMMARY OF CALCULATED RESULTS

Number equal sections chosen	Capacity of each section, Btu per deg F	Resistance of section, Btu per deg F per min	Root of characteristic equation, (1/min)	C_4	K_1	K_2	K_3	K_4
1	0.1215	3.85	−10.1	−558.5	+608.5	....	.....	.....
2	0.0608	9.10	−17.7	+354.0	−304.0	−1490	.....	.....
3	0.0405	13.62	−25.6	+274.0	−224.0	−2720	−12580	.....
4	0.0304	17.88	−33.6	+246.0	−196.0	−3380	−34590	−158000

Discussion

J. J. GREBE.[3] The work done by the author, both experimentally and mathematically, is very much worth reporting and should not be apologized for. It has shown that the lag due to transferring materials or energy through a resistance or a series of resistances and capacities results in a response curve of the familiar *S*-curve shape. What is more, it shows that this transfer or head lag can easily be resolved into an equivalent amount of velocity-distance lag, or dead time and a straight storage or capacity lag.

The fact that the theoretical curves, based on incomplete assumptions, do not exactly check the experimental data does not detract from the fact that the analysis accounts for the major portion of the observed function. A maintenance man should be able to operate a heat-interchange system from the observations on the response curves. He should be able to tell how much fouling of the surfaces there might be.

G. A. PHILBRICK.[4] It may add to the utility of the author's fine exposition to add an extension of the method used by him to model systems having a somewhat larger number of sections. While it might seem that an exact method, using a continuous model, would be preferable to the use of a large number of "lumps," this is not the case when simulating machinery of the discontinuous variety is available.

If a model with n sections is considered, the generic-level equation for the jth and kth sections, using the symbols of the paper, may be written operationally as

$$T_k = \frac{R}{R + R_k} T_s + \left[\frac{R + R_k}{R_k} + aRp\right]^{-1} \cdot T_j$$

Passing to the over-all relationship and applying the external conditions considered, yields with the aid of the shifting rule

$$T_n = T = T_s + (T_{if} - T_{i0})[\alpha^n(1 + \alpha\gamma p)^{-n} - \beta^n \epsilon^{-t/\tau_f}(1 + \beta\gamma p)^{-n}] \cdot I(t)$$

where

$$\alpha = \frac{R_k}{R + R_k};\ \beta = 1\Big/\left[\frac{1}{\alpha} - \frac{\gamma}{\tau_f}\right];\ \gamma = aR;\ I(t) = \text{unit step-function.}$$

Computation of the result involves evaluation of a pair of definite integrals of the form

$$\int_0^t \frac{i}{(n-i)!} \frac{t^{n-i}}{(\alpha\gamma)^n} \epsilon^{-\left(\frac{t}{\alpha\gamma}\right)} dt$$

which is formidable if attacked straightforwardly. If, however, the integrand itself is evaluated (as a function of time), and a simple Simpson integration performed, the work is not great.

[3] Director, Physical Research Laboratory, The Dow Chemical Company, Midland, Mich. Mem. A.S.M.E.

[4] Research and Development, The Foxboro Company, Foxboro, Mass. (On leave with National Defense Research Committee.) Jun. A.S.M.E

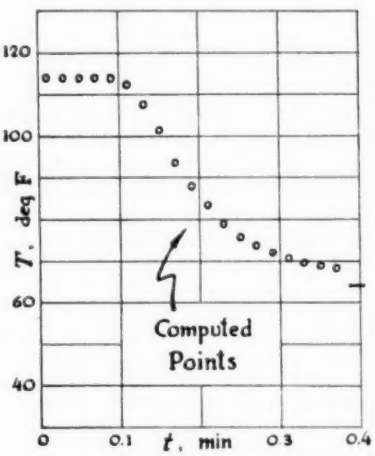


FIG. 7 OPERATIONAL RESULT FOR TWENTY-ONE EQUAL SECTIONS

Such a solution has been carried out for $n = 21$ (21 sections), and the response is shown in Fig. 7 of this discussion. A corresponding solution by classical methods would be enormously more tedious.

As is evident in Fig. 7, and by comparison with the experimental curve shown in the paper, the initial delay in the response of the output temperature is reproduced rather faithfully. The divergence from the experimental curve is very nearly representable as a stretching of the time dimension, and this could be accounted for by irregularities in the data which were not as consequential in the $n = 4$ solution.

AUTHOR'S CLOSURE

Mr. Grebe's discussion indicates the industrial usefulness of the results obtained. It is hoped that further correlation of the results of simplified mathematical analyses and empirical data will lead to a wider application of the rational mathematical solution of control problems.

Mr. Philbrick's extension of the mathematics of the paper is a very interesting and valuable one. In order to render comparison easier, the results obtained by dividing the heat exchanger into twenty-one sections by Mr. Philbrick have been reproduced in Fig. 8 together with observed empirical results and calculated values for four equal sections. The calculated response based on twenty-one equal sections follows the observed data, curve *A*, rather closely. The initial lag is very closely reproduced. The divergence at higher time values is more marked. However, it will be noted that while the curve based on twenty-one equal sections predicts the observed result during the initial stages with considerably more accuracy than the calculations based on four equal sections, little improvement results at higher time values.

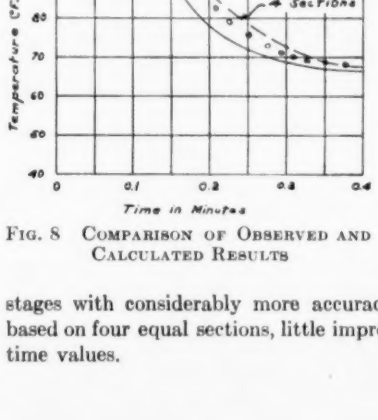


FIG. 8 COMPARISON OF OBSERVED AND CALCULATED RESULTS

Optimum Settings for Automatic Controllers

By J. G. ZIEGLER[1] and N. B. NICHOLS,[2] ROCHESTER, N. Y.

In this paper, the three principal control effects found in present controllers are examined and practical names and units of measurement are proposed for each effect. Corresponding units are proposed for a classification of industrial processes in terms of the two principal characteristics affecting their controllability. Formulas are given which enable the controller settings to be determined from the experimental or calculated values of the lag and unit reaction rate of the process to be controlled. These units form the basis of a quick method for adjusting a controller on the job. The effect of varying each controller setting is shown in a series of chart records. It is believed that the conceptions of control presented in this paper will be of assistance in the adjustment of existing controller applications and in the design of new installations.

A PURELY mathematical approach to the study of automatic control is certainly the most desirable course from a standpoint of accuracy and brevity. Unfortunately, however, the mathematics of control involves such a bewildering assortment of exponential and trigonometric functions that the average engineer cannot afford the time necessary to plow through them to a solution of his current problem.

It is the purpose of this paper to examine the action of the three principal control effects found in present-day instruments, assign practical values to each effect, see what adjustment of each does to the final control, and give a method for arriving quickly at the optimum settings of each control effect. The paper will thus first endeavor to answer the question: "How can the proper controller adjustments be quickly determined on any control application?" After that a new method will be presented which makes possible a reasonably accurate answer to the question: "How can the setting of a controller be determined before it is installed on an existing application?"

Except for a single illustrative example, no attempt will be made to present laboratory and field data, to develop mathematical relations, or to make acknowledgment of material from published literature. A paper covering the mathematical derivations would be quite lengthy as would also a paper covering laboratory and field-test results. Work on these phases of the subject is still under way, and it is expected that the results will be published at a later time when convenient. It is believed advisable to publish the present paper without delay in order to make the information available for use by the many persons interested in the application of automatic-control instruments. To these persons the present subject matter is of much greater interest than the other phases of the study which are being omitted.

To simplify terminology we will take the most common type of control circuit in which a controller interprets the movement of its recording pen into a need for corrective action, and, by varying its output air pressure, repositions a diaphragm-operated valve. The controller may be measuring temperature, pressure, level, or any other variable, but we will completely divorce the measurement portion of the control circuit and speak only of the pen movement in inches; 1 in. of pen movement might represent 1 or 1000 deg F, or a flow of 1 or 1000 gpm. The actual graduation will be of no moment in a study of control.

Our controller will translate pen behavior into behavior of a valve; the relation between the two behavior patterns is determined by the setting of each control effect. The term valve covers any similar device, i.e., a damper or rheostat which must be operated by the controller in order to maintain correct process conditions.

Proportional Response

In spite of the multitude of air, liquid, and electrically operated controllers on the market, all are similar in that they incorporate one, two, or at most three quite simple control effects. These three can be called "proportional," "automatic reset," and "pre-act."

Proportional Response. By far the most common effect is "proportional response," found in practically all controllers. It gives a valve movement proportional to the pen movement, that is, a 2-degree pen movement gives twice as much valve movement as a 1-degree pen movement. Simple spring-loaded pressure-reducing valves are really proportional-response controllers in that, over a short range of pressure, the valve is moved proportionally from one extreme to the other.

Sensitivity. The measure of proportional response is called "sensitivity" or "throttling range;" the former being valve movement per pen movement, the latter its reciprocal or the pen movement necessary to give full valve movement. Either sensitivity or throttling range describes the magnitude of proportional response, though in this paper each response will be measured in units which increase as the relative valve action per pen action increases. In the case of proportional response, the unit will accordingly be called "sensitivity."

Proportional-response sensitivity in some controllers is not adjustable; in most, however, it may be adjusted either continuously or in steps over a considerable range. If we define sensitivity as the output pressure change per inch of pen travel, it is apparent that the limits would be from zero (manual control) to infinitely high (on-off control). Perhaps the widest range of adjustment is found in one controller with sensitivity continuously variable from 1000 to 1 psi per in. A sensitivity of 1000 gives 1 psi output change for each 0.001 in. of pen travel.

Sensitivity adjustment is necessary if optimum control stability is to be attained. It is common knowledge that control with infinitely high proportional response is always unstable, oscillating continuously. True, on certain applications the oscillation may be of such small magnitude that it is not objectionable and, if the surges in supply are not serious in their effect on other portions of the process, the control obtained may be entirely acceptable.

Industry generally demands control of the "throttling" type rather than "on-off" since a proportional-response controller, set in any sensitivity below some maximum, will produce a damped oscillation and eventually straight-line control.

Amplitude Ratio. Sensitivity adjustment affects primarily the stability of control. On any application there is a definite and

---

[1] Sales Engineering Department, Taylor Instrument Companies.

[2] Engineering Research Department, Taylor Instrument Companies.

Contributed by the Committee on Industrial Instruments and Regulators of the Process Industries Division and presented at the Annual Meeting, New York, N. Y., December 1–5, 1941, of The American Society of Mechanical Engineers.

Note: Statements and opinions advanced in papers are to be understood as individual expressions of their authors and not those of the Society.

easily determined point called the "ultimate sensitivity" (S_u), above which any oscillation will increase to some maximum amplitude, and below which an oscillation of any size will diminish to straight-line control. Stability may be measured in terms of "amplitude ratio," the relative amplitude of any wave to that of the wave which preceded it. A controller set at the ultimate sensitivity gives an oscillation with an amplitude ratio

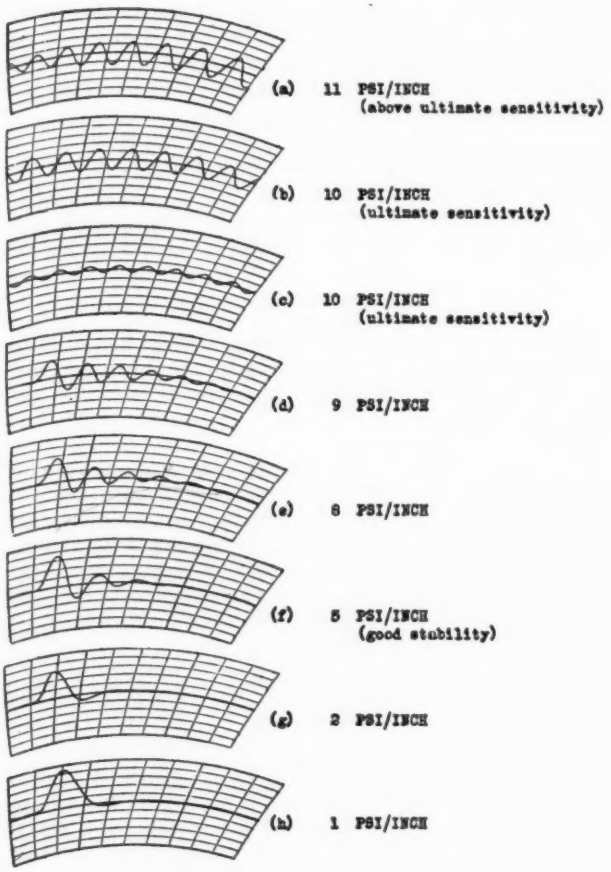


FIG. 1 AMPLITUDE RATIO VERSUS SENSITIVITY
(Effect of disturbance.)

of 1; above the ultimate sensitivity, an amplitude ratio greater than 1; and below the ultimate, an amplitude ratio less than 1.

Amplitude Ratio Versus Sensitivity. Fig. 1 shows the effect of sensitivity adjustment on a typical application. The oscillation was started by a momentary change in valve position. Curves (*b*) and (*c*) were produced at the ultimate sensitivity, which in this case was 10 psi per in. Curve (*a*) was produced at a sensitivity of 11 psi per in. (110 per cent of S_u). Curves (*d*) to (*h*) show the successively smaller amplitude ratios produced as the sensitivity was lowered to 90, 80, 50, 20, and 10 per cent of the ultimate (9, 8, 5, 2, and 1 psi per in.).

In Fig. 1 and succeeding charts, each division is 0.1 in. and each time interval represents 0.625 min.

Regardless of the ultimate sensitivity of any control application, the relationship between amplitude ratio and sensitivity, given as per cent of ultimate sensitivity, remains about as shown in Fig. 2. The ultimate sensitivity thus appears to be a good common point for consideration of sensitivity adjustment on most control applications.

Offset and Load Change. In considering the curves of Fig. 1, the most desirable setting from a stability standpoint would be (*h*), produced at quite a low sensitivity (10 per cent of ultimate). It should be noted in passing, however, that as sensitivity is reduced the period of oscillation increases slightly, which in itself is undesirable. The real drawback of using sensitivity settings a great deal lower than the ultimate value stems from the limitation of proportional response, e.g., that only one valve position can be maintained when the pen is at the desired set point. A "load change," any disturbance in the process requiring a sustained alteration of valve position, will cause the pen to shift away from the set point far enough to give the required valve movement. The magnitude of this shift or "offset" varies inversely with the sensitivity setting used and directly with the required change in

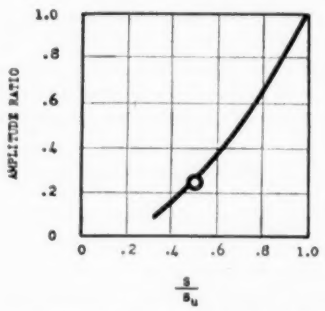


FIG. 2 AMPLITUDE RATIO VERSUS SENSITIVITY

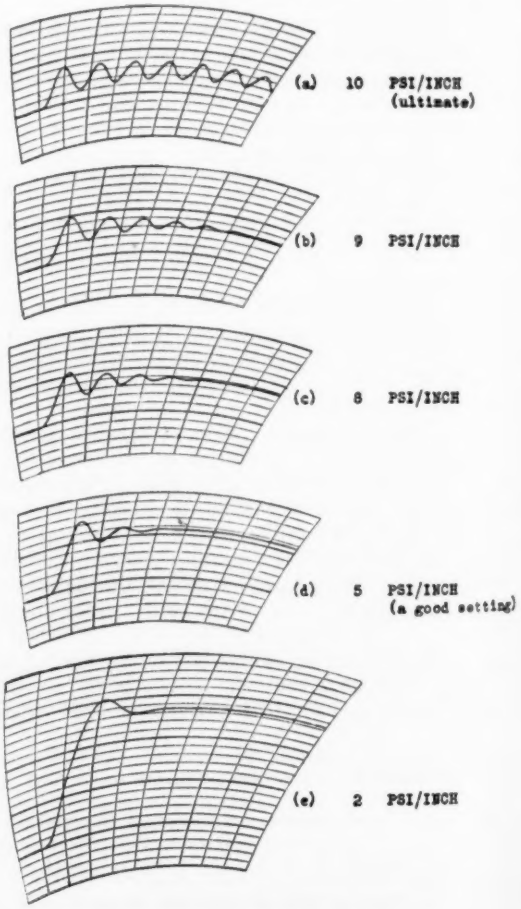


FIG. 3 OFFSET VERSUS SENSITIVITY
(Effect of load change.)

valve position. Fig. 3, curves (*a*) to (*e*), illustrates this point. Curve (*a*) shows the offset caused by a load change requiring a 2.8 psi change in output pressure with sensitivity at 10 psi per in. Since this is the ultimate setting, an amplitude ratio of 1 results and a lower setting is indicated. As the sensitivity is decreased to 9, 8, 5, and then 2 psi per in., the offset from this load change increases and the amplitude ratio decreases.

Amplitude Ratio Versus Offset. The rational adjustment of proportional-response sensitivity is then simply a matter of balancing the two evils of offset and amplitude ratio. For most applications a good compromise is the sensitivity which gives an amplitude ratio of 25 per cent. This sensitivity will be very nearly one half that of the ultimate sensitivity, as shown in Fig. 2. An excellent and rapid method of sensitivity adjustment is to find the ultimate sensitivity and then simply cut it in half. Fig. 1, curve (*f*), shows that an amplitude ratio of 25 per cent is achieved by this setting on the application under test. Fig. 3, curve (*d*), shows the result of a load change requiring a 2.8 psi change in controller output pressure. The sensitivity setting of 5 psi per in. allows an offset of 2.8/5 or 0.56 in. with a 25 per cent amplitude ratio.

On most air-operated controllers, the sensitivity adjustment is calibrated either in terms of sensitivity or throttling range. On such instruments the trick of halving the sensitivity to obtain a good setting is quite simple; on those calibrated in throttling range the setting should be doubled, since this unit is the reciprocal of sensitivity. The sensitivity of older instruments with arbitrary adjustment scales may be easily found by moving the pen a definite distance and noting the resulting output-pressure change. This test run at a few points will enable the user to plot a sensitivity-conversion scale.

The statement that a sensitivity setting of one half the ultimate with attendant 25 per cent amplitude ratio gives optimum control must be modified in some cases. At times a lower sensitivity is preferable. For example, the actual level maintained by a liquid-level controller might not be nearly as important as the effect of sudden valve movements on further portions of the process. In this case the sensitivity should be lowered to reduce the amplitude ratio even though the offset is increased by so doing. On the other hand, a pressure-control application giving oscillations with very short period could be set to give an 80 or 90 per cent amplitude ratio. Due to the short period, a disturbance would die out in a reasonable time, even though there were quite a few oscillations. The offset would be reduced somewhat though it should be kept in mind that it can never be reduced to less than one half of the amount given at our previously defined optimum sensitivity of one half the ultimate.

On processes involving wide changes in load, one condition is often encountered which must be considered here. A controller perfectly adjusted for one load condition may start oscillating under another load. If the ultimate sensitivity is checked at the new more difficult load, it will be found lower than at the original easy load condition. Consequently, the sensitivity must always be adjusted so that the correct stability is achieved under the most difficult load condition. Obviously the amplitude ratio will then be lower at the easy load.

Automatic-Reset Response

The second most common response found in modern controllers is "automatic reset." Its only purpose is to eliminate offset. In action it detects any disparity between pen and set point and gives a slow continuous valve movement in the proper direction to correct the offset. Furthermore, the rate of valve movement is proportional to the distance between pen and set point. Automatic reset then may be defined as a response giving valve velocity proportional to pen displacement from set point.

Some controllers give a constant valve velocity with the direction depending upon whether the pen is above or below the set point. This is a special case and will not be considered further. Neither will those controllers having automatic reset alone (floating response) be considered in this paper. It appears that the floating response controller is most useful on partially "self-controlling" processes.

Reset Rate. As sensitivity was the measure of proportional response, "reset rate" becomes the corresponding measure of automatic-reset response. The units of reset rate are minutes^{-1} or the number of times per minute that automatic reset duplicates the proportional-response correction caused by the disparity between pen and set point.

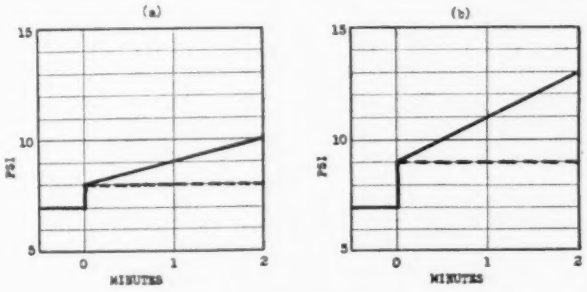


Fig. 4 Reset Rate
(Reset rate = 1 per min.)

Fig. 4(*a*) and (*b*) shows the course of output pressure with time for a reset rate of 1 per min. The dotted lines show the corresponding proportional response pressure. In Fig. 4(*a*), the pen was moved and held far enough from the set point to give a 1 psi change in proportional response. The reset proceeds at the rate of 1 psi per min per 1 psi original change. Fig. 4, curve (*b*), shows a reset rate of 2 psi per min per 2 psi original change. In both cases the reset rate is 1 per min.

In most controllers using automatic reset, some adjustment of the reset rate is provided, though continuous adjustment appears in only a few. In one, the reset rate is adjustable from zero to 20 per min. In order to determine reset rates on an instrument without a calibrated dial, it is only necessary to move the pen away from the set pointer far enough to cause a 1 psi output change and note the additional output-pressure change per minute. The same value can be put on the reset adjustment in controllers other than those of the air-operated type, by making a sustained pen change from the set point, noting the altered valve position which results from proportional response and the additional travel at the end of 1 min from automatic reset. The reset rate is the travel from reset divided by the travel from proportional.

Optimum Reset Rate. Fig. 5(*a*) to (*e*) shows the effect of reset-rate adjustment on control. Fig. 5, curve (*a*), resulted from a load change equivalent to 2.8 psi output pressure with a reset rate of zero, in other words, only proportional response. This curve is the same as Fig. 2(*d*) except that the sensitivity is reduced from 50 per cent of ultimate to 45 per cent of ultimate. A reset rate of 0.5 per min gives the slow return toward the set point shown in Fig. 5(*b*). As the reset rate is increased to 1, to 1.5, and to 2, in Fig. 5(*c*), (*d*), and (*e*), the return becomes more and more rapid. At the same time, instability and period of oscillation increase. In general, curve (*d*) of Fig. 5 would be considered the optimum in that it gives reasonably rapid return without excessive loss of stability or excessive increase in period.

Optimum Reset-Rate Adjustment. The actual reset rate which gives a recovery curve similar to Fig. 5(*d*) varies widely on different control applications. As will be pointed out later, the reset

rate appears to vary inversely as the time lag of the application. At present, however, we are more interested in finding a simple method for determining the correct setting.

It has been found that the period of oscillation (P_u) produced at the ultimate sensitivity (S_u) is a good index of required reset-rate adjustment. This period should be measured when the

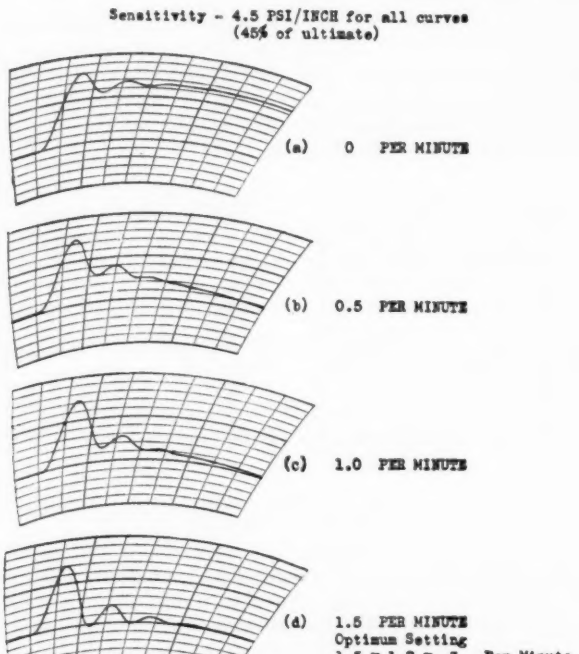


FIG. 5 RESET RATE VERSUS RECOVERY
(Load change.)

amplitude of oscillation is quite small, such as on curve (*c*) of Fig. 1, where the period is about 0.8 min. The optimum setting of reset rate, that which produces a recovery curve similar to Fig. 5(*d*), is usually about $1.2/P_u$. On the process being tested, the reset rate of 1.2/0.8 or 1.5 was used for curve Fig. 5(*d*).

In adjusting a controller with proportional and automatic-reset responses, the sensitivity which just gives a small sustained oscillation should be determined (S_u), and the period of oscillation (P_u) in minutes noted. Optimum controller settings will then be approximately

$$\text{Sensitivity} = 0.45S_u$$
$$\text{Reset rate} = 1.2/P_u$$

Note that the recommended sensitivity has been reduced from $0.5S_u$ to $0.45S_u$. Were this not done, the addition of automatic reset would have increased markedly the amplitude ratio. This tendency of automatic reset to decrease stability is one of its bad features; the other is its tendency to increase the period of oscillation.

While a reset rate of $1.2/P_u$ is generally recommended, recovery curves with the same amplitude ratio may be obtained at a higher reset rate and lower sensitivity. In general, however, this procedure results in recovery curves with longer period and greater initial deviation, both of which are detrimental.

PRE-ACT RESPONSE

The latest control effect made its appearance under the trade name "Pre-Act." On some control applications the addition of pre-act response made such a remarkable improvement that it appeared to be an embodiment of mythical "anticipatory" controllers. On other applications it appeared to be worse than useless. Only the difficulty of predicting the usefulness and adjustment of this response has kept it from being more widely used.

This pre-act effect is as distinct a response as proportional and automatic reset. Pre-act simply gives an additional valve movement proportional to the rate of pen movement. It is used only in conjunction with proportional response.

Pre-Act Time. Since pre-act response is an additional output pressure change per rate of pen movement, its unit is the "pre-act time" in minutes

(psi) per (psi per min) = min

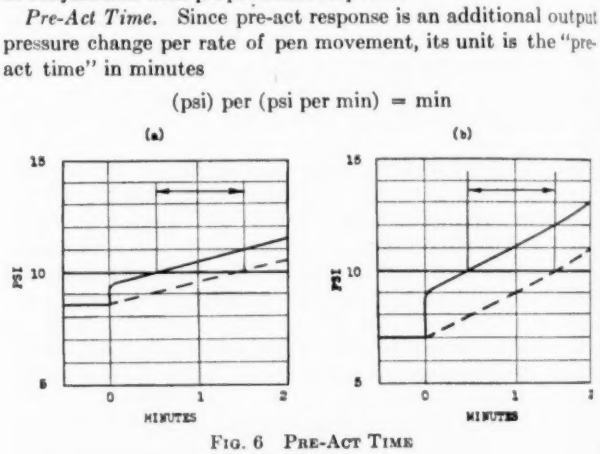


FIG. 6 PRE-ACT TIME
(Pre-act time = 1 min.)

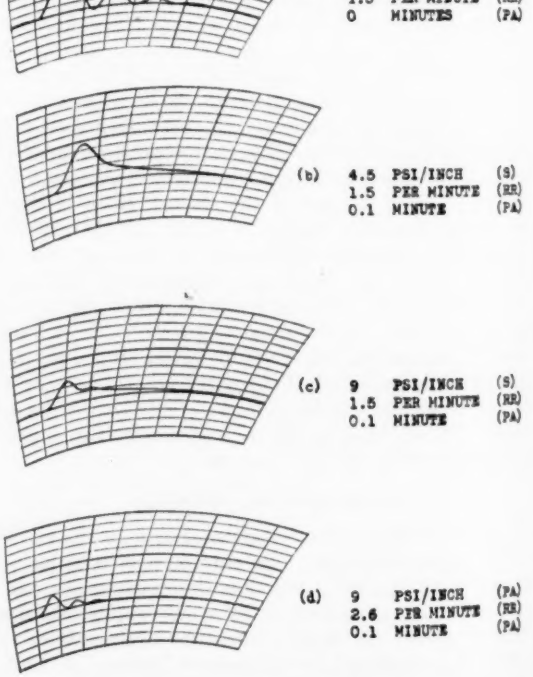


FIG. 7 CONTROL WITH PRE-ACT
(Load change.)

To visualize this unit, assume a controller pen moving away from the set point at such a rate that a proportional-response output change of 1 psi per min results (dotted line of Fig. 6(*a*)). Addition of 1 min pre-act time will cause the controller output to follow the solid line 1 psi higher, i.e., the pre-act response is 1 psi additional for 1 psi per min proportional-response change. Without altering the pre-act setting, a pen velocity twice as great would give 2 psi additional pressure, as shown in Fig. 6(*b*). The time by which the solid line of Fig. 6(*a*) and (*b*) leads the dotted line is the pre-act time, in this case 1 min.

Recently, several industrial instrument companies have made this control effect available in a more or less adjustable form. In one, the dial is calibrated in terms of pre-act time over a range of 0.2 to 10 min.

Use of Pre-Act Response. Pre-act response has been successfully used on applications which give a period of oscillation greater than about 0.4 min. It is not generally useful on pressure- or flow-control applications and rarely on control of liquid level, though this is not a hard and fast rule. To date, it has been used most widely on temperature-control applications.

The effect of pre-act on control is shown in Fig. 7. Fig. 7 curve (*a*) repeats curve (*d*) of Fig. 5, which represented about the optimum control obtainable with proportional and reset responses only. Without altering these settings, the addition of 0.1 min pre-act time changes the recovery curve for the same 2.8 psi load change to that shown at (*b*). The increased stability is an indication that a higher sensitivity may be used, so it is accordingly increased to 9 psi per in. The resulting curve (*c*) shows a much smaller initial deviation without excessive amplitude ratio, but an excessively slow return toward the set point, indicating that a faster reset rate is needed. (Compare with Fig. 5(*b*).) Increasing the reset rate to 2.6 per min produced the curve Fig. 7(*d*), representing approximately optimum control using the three responses.

A comparison of curves, Fig. 7(*a*) and (*d*), discloses that the pre-act response has improved control in several respects. Maximum deviation from the set point has been cut 71 per cent, period of oscillation has been reduced 43 per cent, and the time required for the oscillation to die out has been halved.

Pre-act response does not replace automatic-reset response since it ceases to act when the pen becomes stationary. However, while reset increases period of oscillation and decreases stability, the effect of pre-act is just the opposite. On the debit side for pre-act lies only the increased difficulty of adjusting three responses instead of two, but the use of the basic unit, pre-act time, allows the setting to be determined from the period of oscillation.

Optimum Pre-Act Time Adjustment. It has been found that, for a wide range of control applications, the optimum pre-act time depends directly upon the period of oscillation used to determine the adjustment of the reset rate. In fact the pre-act time should be about $^1/_8$ of the period of a small-amplitude oscillation at the ultimate sensitivity.

To adjust a controller with proportional, automatic reset, and pre-act responses, determine the ultimate sensitivity (S_u) and note the period (P_u) of a small-amplitude oscillation at this sensitivity. The optimum settings will then be approximately

$$\begin{aligned} \text{Sensitivity} &= 0.6S_u \\ \text{Reset rate} &= 2/P_u \text{ per min} \\ \text{Pre-act time} &= P_u/8 \text{ min} \end{aligned}$$

On some applications, the sensitivity with pre-act can be greater than $0.6S_u$. This is illustrated by the test application which allowed a sensitivity of $0.9S_u$ (Fig. 7(*d*)). We have found that the setting is generally between $0.6S_u$ and $1S_u$; in many applications, a sensitivity of $0.6S_u$ will be sufficiently near the optimum setting.

If, at these settings, the amplitude ratio is too high, each adjustment should be reduced slightly. When using the system of units proposed in this paper, a decrease in the setting of any response increases stability. (Actually pre-act increases stability up to its optimum setting and, above that, again gives less stability.) In general, oscillations with a period approximately the same as those occurring at the ultimate sensitivity are due to too high a sensitivity; automatic reset gives longer periods and pre-act shorter periods.

Process-Reaction Curves

A control circuit consists of a controller and a process, the valve being considered a portion of the latter. Pen movement

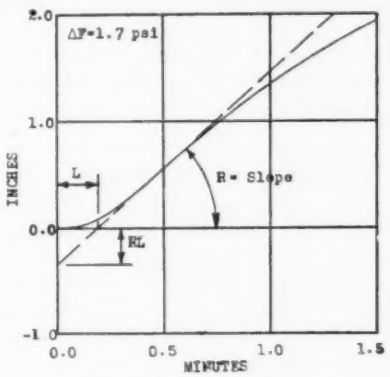


Fig. 8 Reaction Curve

gives an output-pressure change, which affects the process, which in turn affects the pen. So far, we have considered control effects, the portion of the control circuit tying pen movement to output-pressure-behavior pattern. We have also considered the effect of altering this pattern on the entire control circuit, taking as evidence the pen recovery from disturbances and load changes.

We will now eliminate the controller from the circuit, make certain output-pressure changes, and show how the resulting pen behavior can be used to evaluate controllability of the process and predict optimum controller settings.

Process-Reaction Curve. In any control circuit, there are several time lags. The lag of inflating the valve is present in all. Some time lag occurs in the measuring portion between a change at the thermometer bulb or pressure connection and the indication of that change at the pen. Added to these two may be series of lags in the apparatus under control.

The difficulty of dealing mathematically with processes involving a series of lags or even of applying values to the various lags and adding them is very great indeed. However, having a process, a pen, and a means of controlling the process (a valve), it becomes possible to get the summation of all the lags by simply altering the valve position and analyzing the resulting curve traced by the pen.

To be more explicit, suppose that we have an application with a controller installed and cut the air line connecting the controller to the diaphragm valve. Then, if we connect an air-reducing valve to the diaphragm-operated control valve, it will be possible to apply the air pressure necessary to hold the control valve in any position. We will thus be able to make a change in the pressure applied to the control valve in the same manner as the controller would do it (this can still be called an output pressure because its effect will be the same as though it came from the controller) and note the resulting pen behavior.

With a control circuit so arranged, we may, by applying the

correct pressure to the control valve, first bring the recording pen to the desired point on the chart. If then a sudden sustained change in pressure on the control valve of ΔF psi is made, the pen will trace an S-shaped curve which we will call a "reaction curve." Fig. 8 shows a reaction curve for the process which we have been considering.

While Fig. 8 represents a typical reaction curve, an infinite number of variations are possible. On some applications, notably liquid-level control, the curve may come to a maximum slope and continue indefinitely (or until the tank runs over). This type of process is not "self-controlling." On others a definite dead period or velocity-distance lag exists, and the reaction curve shows no pen movement for a finite time after the change in valve position; it then either starts at the maximum rate or builds up to the maximum.

In discussing optimum controller settings, when using pre-act response, we noted that a sensitivity between $0.6S_u$ and $1S_u$ could be used. The best value appears to depend upon the shape of the reaction curve prior to the maximum slope; a lag predominantly of the dead-period type calls for sensitivities toward $0.6\ S_u$.

Optimum Settings From Reaction Curve

Two characteristics of the reaction curve are used to fix the proportional-response sensitivity. The "reaction rate" (R), i.e., the maximum rate at which the pen moves occurs at the point of inflection in the reaction curve. A line drawn tangent to this point intersects the initial pen position a certain length of time after the change in valve position. This time we will call the "lag" (L) of our control circuit. The optimum setting of sensitivity for a controller is inversely related to the product of R and L, determined from the reaction curve. If the tangent line is projected until it intersects the vertical axis, the product RL is graphically determined, as shown in Fig. 8. Good control is generally obtained when proportional-response sensitivity is so adjusted that a pen movement of RL in. gives a pressure change of ΔF psi.

On the reaction curve of Fig. 8, a 1.7 psi valve change was made so the optimum sensitivity setting is approximately

$$\text{Sensitivity} = \frac{\Delta F}{RL} \text{ psi per in.}$$

where

$$R = 1.7 \text{ in. per min}$$
$$L = 0.2 \text{ min}$$
$$RL = 0.34 \text{ in.}$$
$$\Delta F = 1.7 \text{ psi}$$

The predicted sensitivity of 1.7/0.34 or 5 psi per in. gave curves Fig. 1(f) and Fig. 3(d). These curves were previously selected as giving good stability, that is, an amplitude ratio of approximately 0.25.

Unit Reaction Rate. No justification has been given for calling the distance L on the reaction curve the lag of the process, but there appears to be a good reason. On most processes, reaction curves, caused by different valve-pressure changes ΔF, are similar in shape, differing only in the value of R, that is, the reaction rate caused by a 1 psi change is about twice as great as that from a 0.5 psi change, but the intersected distance L remains constant regardless of ΔF.

When taking a reaction curve, it is sometimes necessary to make ΔF quite small, in order to prevent undue disturbance to the process being tested. The resulting reaction rate is then converted to a "unit reaction rate" (R_1), that which would be caused by 1 psi pressure change on the control valve. This is done by dividing the reaction rate found by ΔF

$$R_1 = \frac{R}{\Delta F} \frac{\text{in. per min}}{\text{psi}}$$

The formula for a good sensitivity setting may then be written

$$\text{Sensitivity} = \frac{1}{R_1 L} \text{ psi per in.}$$

The ultimate sensitivity will be about twice as great

$$S_u = \frac{2}{R_1 L} \text{ psi per in.}$$

At the ultimate sensitivity, the period of oscillation is about $4L$ min, increasing to about $4.6L$ as the sensitivity is lowered to one half the ultimate.

An approximate description of the characteristics of a process is given by values of the two quantities, unit reaction rate and lag. True, these two are only a rough measure of the entire reaction curve, telling nothing about its shape before and after the point of inflection, but they give enough of the story to allow a prediction not only of optimum sensitivity and period of oscillation but of optimum reset rate and pre-act time settings as well.

It should be kept clearly in mind that the controller settings are determined from the reaction curve caused by an output-pressure change (control-valve-position change) and not by the reaction curve which is caused by a load change.

Reset-Rate Determination From Reaction Curve. Since the period of oscillation at the ultimate sensitivity proves to be 4 times the lag, a substitution of $4L$ for P_u in previous equations for optimum reset rate gives an equation expressing this reset rate in terms of lag. For a controller with proportional and automatic-reset responses, the optimum settings become

$$\text{Sensitivity} = \frac{0.9}{R_1 L} \text{ psi per in.}$$

$$\text{Reset rate} = \frac{0.3}{L} \text{ per min}$$

At these settings the period will be about $5.7L$, having been increased by both the lowering of sensitivity and the addition of automatic reset.

Pre-Act Time Determination From Reaction Curve. Using again the relationship between L and P_u, we find that the optimum pre-act time depends directly upon the lag and is normally equal to $L/2$. This tells us that pre-act will not normally be used on applications in which the reaction curve shows a lag smaller than 0.2 min, since the minimum pre-act time available on industrial controllers is about 0.1 min. It will be useful on all applications with lags greater than 0.2 min.

The optimum settings determined previously for all three control effects, when expressed in terms of unit reaction rate and lag, appear as follows

$$\text{Sensitivity} = \frac{1.2}{R_1 L} \text{ to } \frac{2}{R_1 L} \text{ psi per in.}$$

$$\text{Reset rate} = \frac{0.5}{L} \text{ per min}$$

$$\text{Pre-act time} = 0.5L \text{ min}$$

Control-Valve Characteristics

In general, any change of a control circuit which allows a higher controller sensitivity and faster reset rate to be used will improve the control results obtained. We have seen that the addition of pre-act response gives both of these improvements

At times certain changes in the process can be made which allow a higher sensitivity and reset rate.

Any decrease in the lag of a process permits an increase in reset rate and attendant reduction in period of oscillation, since the reset rate is inversely related to lag and the period directly related. Any decrease in the lag of a process if it is not attended by an increase in reaction rate permits an increase in sensitivity since the sensitivity is inversely related to the lag. Any decrease in the unit reaction rate of a process, if not attended by an increase in lag, allows higher sensitivities, since sensitivity is inversely related to reaction rate.

Stated more concisely, any decrease in the value of R_1L increases the optimum sensitivity, and any decrease in L increases the optimum reset rate. Also any decrease in L decreases the period of oscillation.

Some applications, as we have already noted, call for widely different sensitivity settings at different load conditions. In these cases, we have said the sensitivity must be set low enough to give stability at the most difficult load even though the control is penalized at easy load conditions. This phenomenon is due to the fact that the unit reaction rate generally changes with load. The lag normally remains about constant. Control valves with special flow-lift characteristics have been used in an attempt to correct for this change in unit reaction rate with load. The optimum characteristics vary with the application under control and are not always "logarithmic" or "equal percentage" as is commonly thought.

Process Classification

Since either the ultimate sensitivity and attendant period or the unit reaction rate and the lag may be used to determine optimum controller settings, it follows that the latter values may be determined from the former. This suggests that, without running a reaction curve on a process, values of R_1 and L may be determined during adjustment of the controller.

Knowing the ultimate sensitivity (S_u) and the period at this sensitivity (P_u), a rearrangement of preceding equations shows how these values may be converted into L and R_1.

$$L = P_u/4 \text{ min}$$

$$R_1 = \frac{8}{P_u S_u} \frac{\text{in. per min}}{\text{psi}}$$

Classification of processes in terms of their unit reaction rates and lags would appear to be a decided improvement over present arbitrary methods.

Conclusions

We have proposed a system of units for measuring the control effects which are now in common use. When using these units, the values of the sensitivity, reset rate, and pre-act time all increase as the relative valve action per pen action increases.

The lag and unit reaction rate have been introduced as a quantitative measure of the controllability of processes, and we believe they form a good basis for a classification of processes.

Formulas have been presented which enable the controller settings to be obtained from an analysis of the process-reaction curves (that is, unit reaction rate and lag).

We have presented a simple method for adjusting the controller when it is installed on an application, making use of the ultimate sensitivity and period. Having shown that the controller settings can be obtained from the reaction curve, it will be possible for the equipment designer to calculate an approximate reaction curve for certain applications and thus determine the controller settings even before the equipment is built.

The usefulness of each particular control effect has been shown by examining its effect on the quality of control.

It has been pointed out that valve characteristics should be matched to each process so that a constant unit reaction rate prevails at all loads. This incidentally gives a rational explanation for the use of valves with special flow-lift characteristics.

Examination of pre-act response has shown that it improves control by increasing stability, reducing period, and allowing larger settings for the other responses. The relation between the pre-act setting and lag (or ultimate period) has simplified its adjustment. A summary of control effects is given in Table 1.

TABLE 1 SUMMARY OF CONTROL EFFECTS

Response	Action	Measure	Unit
Proportional	$\frac{\text{Valve movement}}{\text{Pen movement}}$	Sensitivity	Psi per in.
Automatic reset	$\frac{\text{Valve velocity}}{\text{Pen movement}}$	Reset rate	Per min
Pre-act	$\frac{\text{Valve movement}}{\text{Pen velocity}}$	Pre-act time	Min

Note that proportional response action may also be expressed as a valve velocity per pen velocity.

Summary of Controller Adjustments

Determine the ultimate sensitivity (S_u) and period (P_u), or the unit reaction rate R_1 and lag L. For the three types of controllers the optimum settings are as follows:

Proportional

$$\text{Sensitivity} = 0.5S_u = \frac{1}{R_1L}$$

Proportional plus reset

$$\text{Sensitivity} = 0.45S_u = \frac{0.9}{R_1L}$$

$$\text{Reset rate} = \frac{1.2}{P_u} = \frac{0.3}{L}$$

Proportional plus reset plus pre-act

$$\text{Sensitivity} = 0.6S_u = \frac{1.2}{R_1L}$$

$$\text{Reset rate} = \frac{2.0}{P_u} = \frac{0.5}{L}$$

$$\text{Pre-act time} = \frac{P_u}{8} = 0.5L$$

Discussion

E. S. Bristol.[3] The authors have presented a procedure for analyzing control and process characteristics which is logical, comparatively simple, and avoids the use of involved mathematics. The paper thus constitutes a worth-while contribution to the literature sponsored by the Committee on Industrial Instruments and Regulators in its endeavors to formulate standardized methods of approaching automatic-control problems.

Some of the terms and relations employed by the authors can be modified to advantage, in order to make the treatment more general in scope. From this point of view, it is believed preferable to express control action in terms of valve travel rather than in terms of actuating pressure on a diaphragm-operated valve. The latter procedure affords a basis for direct comparison of re-

[3] In charge, Combustion Control Division, Engineering Department, Leeds & Northrup Company, Philadelphia, Pa. Mem. A.S.M.E.

sults only for fluid-operated control valves having the same working pressure range. On the other hand, measurement of control action in percentage of full valve travel would apply to electrically operated, as well as fluid-operated power elements, regardless of the range or mode of application of the actuating media, and should not result in complicating the terminology. As a corollary of such a change the authors' "unit reaction rate," or rate of change resulting from 1 psi at the valve diaphragm, would be expressed as rate of change corresponding to full valve travel or to a stated fraction of full valve travel.

While it may be desirable in studying a controller mechanism to consider merely the action resulting from a pen movement measured in inches, this simplification presents difficulties when applied to any specific installation. Thus, on a temperature-control application, the significant characteristic is actual temperature variation and not the resultant pen motion of the particular recorder employed, which motion would vary with the individual scale range without reference to the inherent characteristics of the process. Possibly it is the authors' intention that the actual scale interval equivalent to 1 in. of pen travel be substituted in their relations, when dealing with any specific application.

It is noted that the authors' relation "reaction rate" multiplied by "lag" or RL is actually equivalent to the pen deviation that would occur in time L, with the pen moving at rate R. In other words, control sensitivity is found to be inherently related to the reciprocal of a hypothetical pen deviation. Attention is called to the fact that a simple manual simulation of two-position control can be imposed upon a process to investigate its reaction rate and lag characteristics. This can be done by watching a recorder measuring the variable to be controlled and manually opening or closing the valve whenever the pen crosses an arbitrarily selected control point. The slope of the resultant oscillating record where it crosses the control point constitutes a significant reaction rate. Also, the period of the resultant oscillation is related to the time required for valve change to affect the controlled variable. The product of the rate of change and the period as thus obtained constitutes another hypothetical pen deviation which can be used for a basis of correlation with the optimum throttling range or control sensitivity. The width of the pen band, obtained on a two-position test of this nature, is related to the rate of pen motion at the control point, and the period of oscillation, so that the pen band in itself is also a significant term for correlation with the optimum throttling range. The two-position test method for field checks is believed to be a particularly simple means for obtaining an indication of the response characteristics of a process.

G. A. PHILBRICK.[4] The authors exhibit the response given by the proportional-control action, on the one hand, when augmented by a differentiation, "pre-act," and on the other, when augmented by an integration, "reset." While such responses serve graphically to define these characteristics, it is striking that different generating functions are used in the two cases. Cannot these various classical control actions be better compared on the basis of some common impressed condition? To dispel the illusion of subterfuge, it is suggested that the authors exhibit in their closure the response of both sets of control actions when both varieties of change are imposed; or more simply, perhaps, the composite response of the three-term characteristic itself, for typical values of the three adjustables, when a sudden deviation occurs.

P. W. KEPPLER.[5] The authors have made a much-needed and highly useful contribution to the problem of setting regulators. However, in connection with the type of optimum transient curve recommended, it should be kept in mind that requirements vary over a wide range regarding uniformity of controlled flow, maximum deviation, average deviation, and stability. For example, any oscillation though damped may be hazardous if resonance can be set up by some other regulator connected to the same process.

The authors have also made a valuable comparison of control functions. To complete this comparison we should consider control based on measurement of the independent energy flow that causes the disturbance. This control function is widely used, generally by proportioning the controlled flow in some exact manner with the independent disturbing flow, and has therefore been called "exact correction."

While of course countless modifications are possible for this control function, in this exact form it requires no adjustment whatever and cannot possibly support any oscillation. It makes the admittedly undesirable "automatic reset" function unnecessary.

To illustrate "exact correction," a specific example is necessary, although it is universally applicable. For this purpose the writer has chosen a single-capacity process with dead time (velocity-distance) lag. In Fig. 9 of this discussion regulator E controls temperature T_4 of tank G, which is kept uniform by mixer H. Regulator E varies temperature T_3 entering pump F by moving gates C and D. Tanks A and B are assumed kept full with fluid at temperatures T_1 and T_2. Pump F maintains constant mass flow through the long pipe line M that introduces dead time lag. The manually operated gate K produces the independent energy flow that causes the disturbance. Float-controlled gate I keeps tank G full, but the constant temperature T_5 is below T_4. Tem-

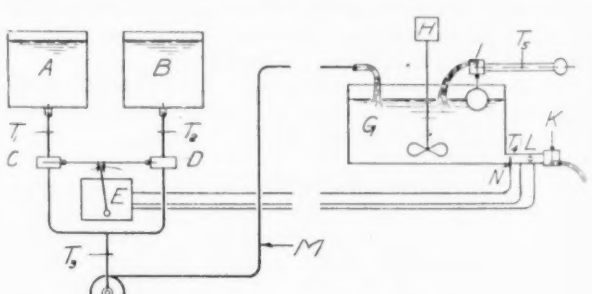


FIG. 9 SINGLE-CAPACITY PROCESS WITH VELOCITY-DISTANCE LAG TO DEMONSTRATE "EXACT CORRECTION"

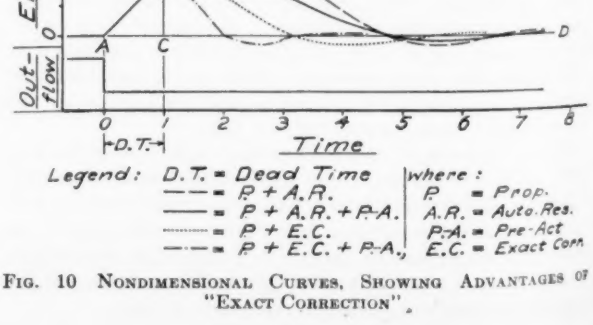


FIG. 10 NONDIMENSIONAL CURVES, SHOWING ADVANTAGES OF "EXACT CORRECTION"

[4] Research and Development, The Foxboro Company, Foxboro, Mass. Jun. A.S.M.E.

[5] Engineer, Sanderson & Porter, New York, N. Y. Mem. A.S.M.E.

perature T_4 is transmitted to regulator E by bulb N for proportional and other control functions, and "exact correction" is obtained by suitably connecting E with the orifice L. This control function keeps the heat flow at E equal to the difference between that at K (neglecting variations in outlet temperature) and that at I. It is also assumed that T_4 must be measured so closely that the effect of self-regulation of T_4 is negligible.

The nondimensional curves, shown in Fig. 10 of this discussion, obtained by graphical step-by-step integration, demonstrate the advantage of "exact correction" for any single-capacity process having dead time lag and lacking self-regulation. The unit of time is the dead time of the process, and the unit of error is the error at time 1. The disturbance is the indicated drop in outflow, and the ideal accuracy obtainable is the broken line *A-B-C-D*.

The curves shown give very nearly the minimum average error obtainable from the control function of each curve. The regulators containing exact correction are not only shown to give much better accuracy, but they are also much easier to adjust since they contain fewer adjustments.

The added cost of orifice, etc., is of course a disadvantage, but there are ways of overcoming this, so that in many cases a marked reduction in first cost results from exact correction.

J. J. GREBE.[6] This paper gives the simple rules for adjusting the control constants of commercial instruments to have the proper characteristics for any one plant. These rules have been checked in actual plant operations on many types of instruments made by different manufacturers and one homemade unit that the writer described in 1933. The much disputed assertion that a good automatic control system using deviation, rate of change, and second-derivative responses, which are also called reset, proportional, and third response or pre-act, should be able to bring about a new balance in the system, within less than twice the elapsed time of the velocity distance lag or the dead time, has been proved by the work of the present authors.

The third response, which in general is a damped second-derivative function so as to fade out at the time when the second derivative works against good control, serves to counteract the effect of the dead time or the velocity-distance lag called L in Fig. 8 of the paper. Contrary to the opinions of some individuals, such lags are quite common, especially in the chemical industry where long dead times up to several minutes are encountered in processes where considerable time is required to make a change felt through chemically resistant but poor thermal conductors, or where it takes considerable time for solid reagents such as lime slurry to come to equilibrium with the solution.

For this reason, the importance of the third response cannot be overemphasized. In fact, if one were to build a universal instrument suitable for any application, it would be better to have a wide range of adjustment on the third response and reduce the flexibility of adjustment of the second, the proportional-position response. In other words, with a good third-response element, the throttling range can be quite narrow for almost any condition.

Let us hope that the authors may continue to develop the art and improve the maintenance and operation of control installations by following up this good work.

AUTHORS' CLOSURE

Mr. Bristol's suggestion that valve travel replace pressure on a diaphragm-operated valve is sound and should be further considered. In the opinion of the authors, it stems from a universal desire to express sensitivity in terms of a dimensionless unit or at least in terms of a unit applicable to all types of controllers. For this paper "psi per inch" was chosen rather than "per cent valve travel per per cent pen travel" principally because the latter did not appear to be a very euphonious combination. In addition, the "per cent per per cent" unit gives the false impression of being dimensionless. One disadvantage of using percentage of full valve travel is that limiting the stroke of a control valve would alter the sensitivity given in that unit but would not change the sensitivity given as psi per inch.

Inches of pen movement was used rather than per cent of scale range or degrees Fahrenheit since the former was thought to be a more general unit. Degrees Fahrenheit would be a good basis for comparing temperature-control applications, but there would be no analogy between that and the feet of water change in liquid level on another application.

The search for a dimensionless sensitivity ratio is not new. Ivanoff[7] had one in his "Over-All Sensitivity," the ratio of uncontrolled or potential deviation to controlled deviation. In the language of this paper, that would be the final deviation in inches of a reaction curve for a one psi pressure change divided by the reciprocal of controller sensitivity or the inches of pen movement necessary to give a one psi change in output. Ivanoff, however, was dealing with "self-controlling" processes which had a definite potential deviation for each valve opening. On some processes, valve movement determines only the reaction rate and the reaction curve never levels out. The potential deviation on these processes is infinite and Ivanoff's over-all sensitivity is infinite regardless of the controller sensitivity setting and hence meaningless. Even on this type of process, however, the authors' value of R_1L is finite and their ultimate sensitivity a definite value. It appears that controller sensitivity settings can be more universally referred to either ultimate sensitivity or R_1L than to potential deviations. In fact, a controller setting given as "per cent of ultimate sensitivity or as sensitivity $\times$ R_1L is dimensionless and is possibly the answer to the problem.

Another clue in the search for a sensitivity yardstick comes from a scrutiny of control quality. The area under curves such as Fig. 5(*d*) might be taken as a measure of poorness of control on either a temperature or liquid-level control application. This area in inch-minutes, easily convertible to either "feet-of-water minutes" or "degrees-Fahrenheit minutes" will be directly related to the product of R_1L, L, and ΔF, where ΔF is the difference in output pressure before and after the largest sudden load change to which the process will be subjected. On any process, a load change will give an area under the recovery curve of (K) (ΔF) (R_1) (L^2), where K is a constant determined by the point in the process at which the load change occurs and by the dimensionless quantities of controller settings, namely, sensitivity $\times$ R_1L; reset rate $\times$ L; and pre-act time/L. It can be seen that any valve-motion unit may be selected for use in R_1, ΔF, and sensitivity as long as it is used consistently in all three.

A method of interpreting the oscillating record obtained by impressed two-position control would certainly be a worthwhile contribution to the study of automatic control. It is hoped that Mr. Bristol will soon publish a detailed method of quantitatively determining application data by such a test. It would be extremely useful if small valve movements giving a record like Fig. 1, curve (*c*) could be accurately interpreted. Generally industrial processes cannot be disturbed by making large valve movements.

The old concept of pre-act response as a "kicker" may have

[6] Director, Physical Research Laboratory, The Dow Chemical Company, Midland, Mich. Mem. A.S.M.E.

[7] "Theoretical Foundations of the Automatic Regulation of Temperature," by A. Ivanoff, *Journal of the Institute of Fuel*, Vol. 7, no. 33, Feb., 1934.

prompted Mr. Philbrick's request for showing its response to a sudden pen movement. In the interest of clarity the authors used a sustained pen deviation to show reset rate and a constant rate of pen movement to illustrate pre-act time. The course of output pressure from a controller with proportional plus automatic reset responses for a constant rate of pen movement would be as shown in Fig. 11. The proportional response is 2 psi per minute as in Fig. 6(*b*) and the reset rate one per minute. At any instant the output pressure from automatic reset is rising at a rate equal to the proportional-response output change times the reset rate. The addition of pre-act response will give an additional output pressure equal to the rate of output pressure change due to the proportional response times the pre-act time.

Analysis of pre-act response from an impressed sudden pen

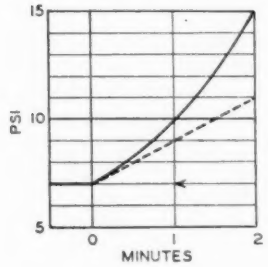


FIG. 11

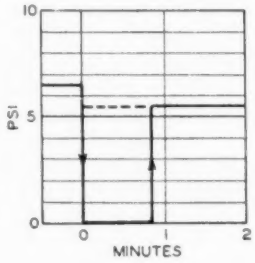


FIG. 12

movement is purely hypothetical because instantaneous pen movements are not met with in practice. A true derivative mechanism would give, for such a pen action, an infinite output change. Actually air-operated controllers do not give an output pressure lower than atmospheric nor higher than their supply pressure. A controller with proportional and pre-act responses would give an output pressure change as shown in Fig. 12 if a sudden pen motion were impressed equivalent to 1 psi proportional-response change. The pre-act time in Fig. 12 is 5 min.

As Mr. Keppler points out, control requirements on certain applications may be so strict that the improvement given by pre-act response may still not hold a pen within the tolerance required. In these cases it is necessary to cast about for another variable upon which a separate or related response may be based. While the study of these multiple controller systems is beyond the scope of this paper, it may be said that they are commonly used and are often very necessary to achieve desired control results. Grebe[8] has called this "metered control."

The type of multiple controller system shown by Mr. Keppler makes use of a separate flow measurement as an indication of demand, to reset the temperature controller. This removes the need for an automatic-reset response working on a basis of temperature pen deviation. The elimination of automatic reset in the temperature controller, however, would allow an offset if any other load change came into the system, for example, a change in temperature of one of the three incoming flows. Also, it would be rather difficult mechanically to convert the reading of flow into an exact mixed liquid temperature unless gates *C* and *D* reproduced flows exactly.

The more common multiple controller system is one in which one controller calls, not for a valve opening, but for a set point change on another controller capable of correcting for the major load change from a measurement at a point of favorable lag. Explaining this from Fig. 9, if the major load change in the system were not the position of gate *K* but temperature T_1, the control system would consist of two temperature controllers. One temperature controller would measure T_3 and operate gates *C* and *D* to maintain T_3. The second controller measuring T_4 would call for the required T_3 necessary to maintain T_4. The first controller would quickly correct for changes in T_1 and T_2 or partial clogging of gates *C* and *D*. The second controller would raise or lower T_3 to correct for the minor load changes such as temperature T_5 or flow through *I*.

[8] "Elements of Automatic Control," by John J. Grebe, *Industrial and Engineering Chemistry*, vol. 29, Nov., 1937, p. 1225.

Report on Tubular Creep Tests

By F. H. NORTON[1] AND C. R. SODERBERG,[2] CAMBRIDGE, MASS.

This report comprises the results obtained on tubular specimens tested under internal pressure as measured for circumferential and longitudinal creep. In addition, tensile-test specimens of the same material were run as a comparison. This work follows closely an investigation[3] reported upon previously. The apparatus and method of testing are exactly as described in that report. Preliminary reports[4,5] were presented at the 1940 Annual Meeting.

1—SUMMARY OF TEST RESULTS

Specimens

SEVEN tubular specimens, which were made up for this test by The Babcock & Wilcox Company, consisted of tubes 4 in. OD, having either a $^3/_8$-in. or $^1/_8$-in. wall, with hemispherical ends welded in place. The specimens were turned out of thick tubes of carbon-molybdenum steel of the composition reported in the previous test.[3]

Scope of the Test

In this program seven tubular specimens and four tensile specimens were tested. The pressure in the tubes was computed by Professor Soderberg to give stresses equivalent to those obtained in the tensile specimens. Five of the seven tests have been completed and two are to be allowed to run for another period of six or eight months.

Results on Tensile-Test Specimens

These specimens, which were cut from the wall of the tubes from which the tubular specimens were formed, were run in the regular creep-testing apparatus, using a 10-in. gage length. The temperature distribution over the gage length was kept within ±1 deg F, and the temperature of the specimen did not vary more than 1 deg F during the test. The elongation of the specimen was measured by telescopes with a precision of 3 parts in 1,000,000. The elongation curves of these four specimens are shown in Figs. 1 to 4, inclusive. It will be noted that the total period of approximately 16,000 hr gives a stable rate on all but the specimen at 1050 F and 8000 psi load. This specimen toward the end of the test showed an increase in rate and would undoubtedly break if sufficient time were allowed. It should be noted that in the illustrations it was possible to plot only every fifth experimental point on the curves. In Table 1 is shown the average creep rate for various time intervals.

Creep of Tubular Test Specimens

The elongation curves of these specimens, both circumferential and longitudinal, are shown in Figs. 5 to 11, inclusive. Here

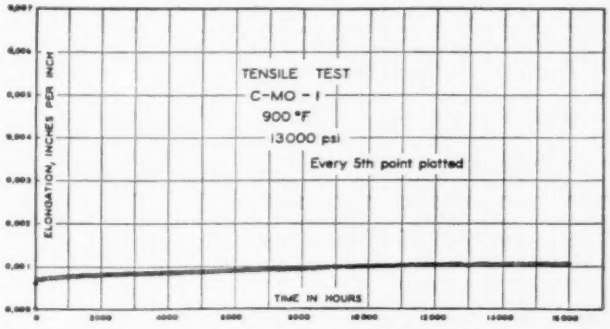


FIG. 1 CREEP OF CARBON-MOLYBDENUM TENSILE SPECIMEN AT 900 F; 13,000 PSI

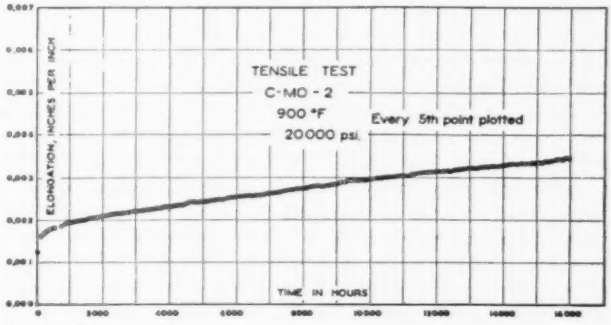


FIG. 2 CREEP OF CARBON-MOLYBDENUM TENSILE SPECIMEN AT 900 F; 20,000 PSI

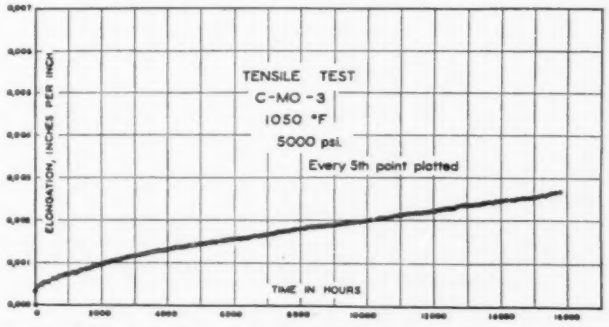


FIG. 3 CREEP OF CARBON-MOLYBDENUM TENSILE SPECIMEN AT 1050 F; 5000 PSI

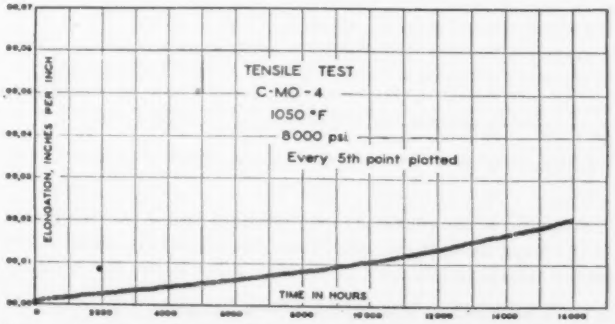


FIG. 4 CREEP OF CARBON-MOLYBDENUM TENSILE SPECIMEN AT 1050 F; 8000 PSI

[1] Associate Professor of Ceramics, Department of Metallurgy, Massachusetts Institute of Technology.

[2] Professor of Applied Mechanics, Massachusetts Institute of Technology. Mem. A.S.M.E.

[3] "Creep in Tubular Pressure Vessels," by F. H. Norton, Trans. A.S.M.E., vol. 61, 1939, p. 239.

[4] "Progress Report on Tubular Creep Tests," by F. H. Norton, Trans. A.S.M.E., vol. 63, 1941, pp. 735–736.

[5] "Interpretation of Creep Tests on Tubes," by C. R. Soderberg, Trans. A.S.M.E., vol. 63, 1941, pp. 737–740.

Presented at a meeting of the A.S.M.E. Joint Research Committee on the Effect of Temperature on the Properties of Metals, held at New York, N. Y., December 2, 1941.

NOTE: Statements and opinions advanced in papers are to be understood as individual expressions of their authors and not those of the Society.

TABLE 1 CREEP OF TENSION SPECIMENS

Test	Temperature, F	Stress, psi	Time elongation, Fig. no.	Creep rates, per cent in 100,000 hr: 0 to 1000	1000 to 2000	2000 to 3000	3000 to 4000	4000 to 5000	5000 to 6000	6000 to 8000	8000 to 10000	10000 to 12000	12000 to 14000	14000 to 16000
T-1	900	13000	1	0.3	0.3	0.27	0.24	0.22	0.2	0.2	0.2	0.2	0.2	0.2
T-2	900	20000	2	3.0	1.6	1.1	1.1	1.1	1.1	1.1	1.0	0.9	0.8	0.9 to 1.2
T-3	1050	5000	3	3.2	2.3	1.6	1.4	1.3	1.3	1.2	1.2	1.1	1.1	1.1
T-4	1050	8000	4	12.0	9.0	8.0	10.0	11.0	11.0	11.0	13.0	15.0 to 16.0	16.0	18.0 to 21.0

TABLE 2 CREEP OF TUBULAR SPECIMENS

Test	Temperature, F	Nominal thickness, in.	Internal pressure, psi	Time elongation, Fig. no.	Creep rates on outside diameter, per cent in 100,000 hr: 0 to 1000	1000 to 2000	2000 to 3000	3000 to 4000	5000 to 6000	6000 to 9000	Remarks
F-10	900	1/8	968	5	0.3	0.2 to 0.4	0.2 to 0.4	0.3–0.5	0.3–0.5	0.3–0.5	Concluded; no axial creep
F-7	900	3/8	3110	6	0.4	0.2 to 0.4	0.2 to 0.4	.....	.....	.....	Concluded; no axial creep
F-8	900	1/8	1490	7	2.5	1.2 to 1.8	0.9 to 1.1	.....	.....	.....	Concluded; no axial creep
F-5	900	3/8	4777	8	2.8	1.0 to 1.5	0.7 to 1.2	.....	.....	.....	Concluded; no axial creep
F-11	1050	1/8	372	9	3.7	1.7 to 2.0	1.3 to 1.8	0.9 to 1.3	0.9 to 1.3	0.9 to 1.3	Concluded; small axial creep
F-9	1050	1/8	596	10	10.7	9.3	9.3	.....	.....	.....	Concluded; no axial creep
F-6	1050	3/8	1911	11	8.5	7.0	6.5	.....	.....	.....	Concluded; no axial creep

again it will be seen that in most cases we have apparently reached a fairly stable rate of flow, and this is particularly true on the specimen which has been run 9000 hr. It should be realized that the creep rate as determined on the 4-in. diam has less than one half the precision of the tensile-test specimens, because of the shorter gage length. In all cases the longitudinal creep is substantially zero, although it will be noted that there is in some cases very small but definite creep over the entire period of time, sometimes positive and sometimes negative. This longitudinal creep is probably due to directional effects in the metal itself. It should be noted that one of the specimens at 1050 F and 1911 psi pressure developed a leak and had to be shut off at a period of 2200 hr. The specimen at 900 F and 4780 psi pressure had to be shut off for the same reason at 2700 hr. A description of the cause of these leaks was discussed in the previous progress report[4] because they seem of practical interest

ture and at an internal pressure determined by $p = 2/\sqrt{3} \cdot st/R$, where R and t are mean radius and wall thickness in inches, respectively.

3 At this pressure, the predicted tangential creep rate, expressed as change in mean radius, is $\sqrt{3}/2 \cdot u$, while the predicted axial creep rate is zero.

4 The measured creep rate at the mean radius is obtained by increasing the measured creep rate at the outside radius in the square of the ratio of the radii, or $\left(1 + \frac{t}{2R}\right)^2$.

The creep rates thus calculated from the tension tests are given in Table 3 for the three time intervals 1000 to 2000 hr, 2000 to 3000 hr, and 3000 to 9000 hr. Upon completion of this test the tubular specimens were sectioned and the actual wall thicknesses measured. To allow for the slight difference between

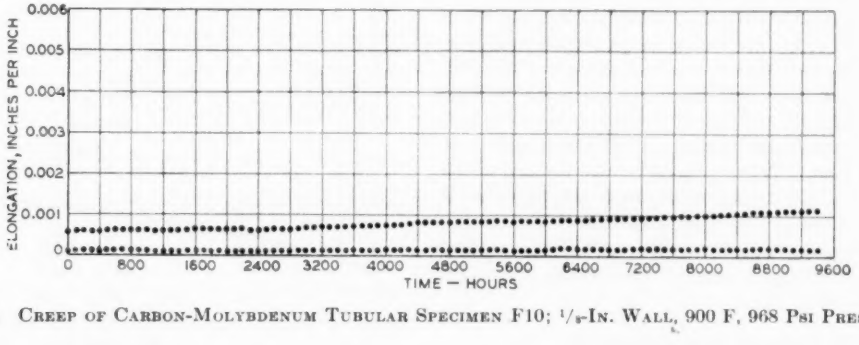


FIG. 5 CREEP OF CARBON-MOLYBDENUM TUBULAR SPECIMEN F10; 1/8-IN. WALL, 900 F, 968 PSI PRESSURE

in the design of tubular pressure vessels. In Table 2 are shown the average flow rates for various intervals of time.

A complete discussion of the microstructure as well as a series of photomicrographs are included in Appendix 1 of this report.

2—COMPARISON OF TEST RESULTS WITH THEORY

CALCULATION OF TUBULAR CREEP RATES FROM TENSION CREEP RATES

As shown in the previous report on these tests,[5] the calculation of the creep rates of the tubes from the creep rates obtained by tensile tests is as follows:

1 A tension test is available which has given the creep rate u at the stress s.

2 A tube of the same material is tested at the same tempera-

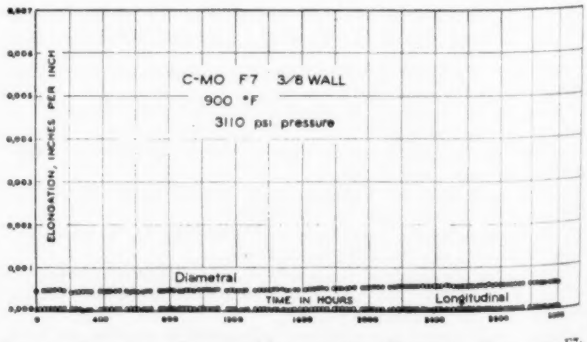


FIG. 6 CREEP OF CARBON-MOLYBDENUM TUBULAR SPECIMEN F7; 3/8-IN. WALL, 900 F, 3110 PSI PRESSURE

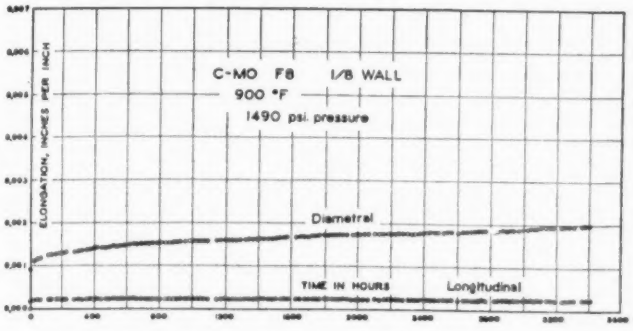


FIG. 7 CREEP OF CARBON-MOLYBDENUM TUBULAR SPECIMEN F8; 1/8-IN. WALL, 900 F, 1490 PSI PRESSURE

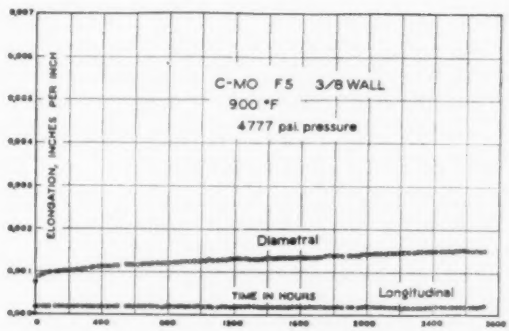


FIG. 8 CREEP OF CARBON-MOLYBDENUM TUBULAR SPECIMEN F5; 3/8-IN. WALL, 900 F, 4777 PSI PRESSURE

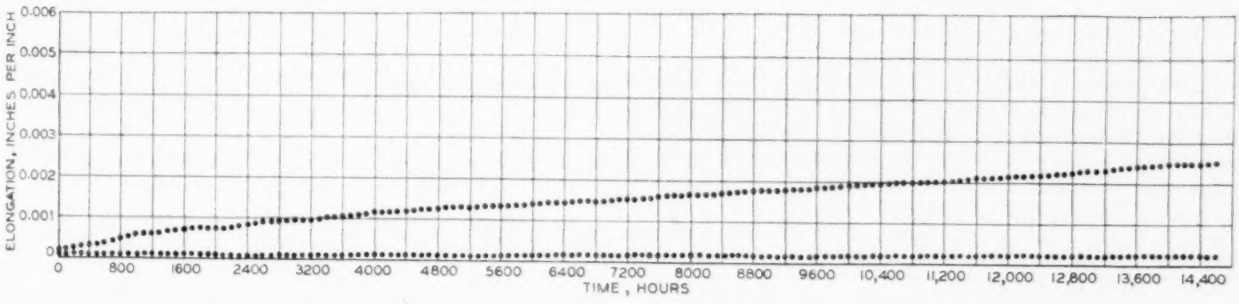


FIG. 9 CREEP OF CARBON-MOLYBDENUM TUBULAR SPECIMEN F11; 1/8-IN. WALL, 1050 F, 372 PSI PRESSURE

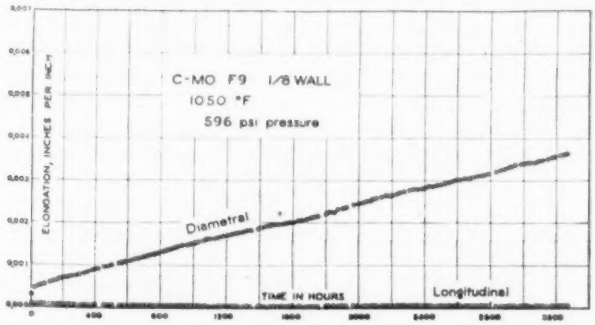


FIG. 10 CREEP OF CARBON-MOLYBDENUM TUBULAR SPECIMEN F6; 3/8-IN. WALL, 1050 F, 1911 PSI PRESSURE

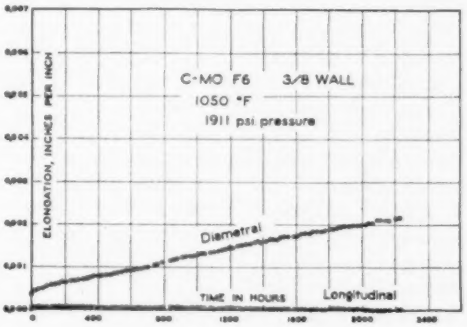


FIG. 11 CREEP OF CARBON-MOLYBDENUM TUBULAR SPECIMEN F9; 1/8-IN. WALL, 1050 F, 596 PSI PRESSURE

TABLE 3 SUMMARY OF TENSION TESTS AND PREDICTED TUBE PERFORMANCE

	Tensile tests				Predicted tube performance									
		Creep rates, per cent in 100,000 hr							Calculated creep rates at mean radius, per cent in 100,000 hr					
					Tube thickness, in.				1000 to 2000 hr		2000 to 3000 hr		3000 to 9000 hr	
Temperature, F	Stress, psi	1000 to 2000 hr	2000 to 3000 hr	3000 to 9000 hr	Nominal	Actual	Actual test pressure, p-i	Circumferential stress formula,[b] PR/t	Nominal thickness	Actual thickness	Nominal thickness	Actual thickness	Nominal thickness	Actual thickness
900	13000	0.3	0.3	0.27	1/8	0.124[a]	968	15140	0.26	0.27	0.26	0.27	0.23	0.24
					3/8	0.373	3110	15130	0.26	0.26	0.26	0.26	0.26	0.26
	20000	1.6	1.1	1.1	1/8	0.121	1490	23640	1.38	1.57	0.95	1.08	0.95	1.08
					3/8	0.374	4777	23240	1.38	1.38	0.95	0.95	0.95	0.95
1050	5000	2.3	1.6	1.2	1/8	0.124[a]	372	5800	2.0	2.1	1.38	1.43	1.04	1.08
					1/8	0.122	596	9490	7.8	9.1	7.8	9.1	9.5	11.1
	8000	9.0	9.0	11.0	3/8	0.374	1911	9280	7.8	7.8	7.8	7.8	9.5	9.5

[a] Based on tube measured before test.
[b] Circumferential stress = PR/t, where P = internal pressure, psi; R = mean radius; t = average wall thickness.

TABLE 4 COMPARISON OF MEASURED AND PREDICTED CREEP RATES

Temperature, F	Nominal stress intensity at mean radius, psi	Tube thickness, in. Nominal	Tube thickness, in. Actual	Actual test pressure, psi	Comparison of calculated and measured creep rates, per cent in 100,000 hr: 1000 to 2000 hr — Measured at outside radius	1000 to 2000 hr — Corrected to mean radius	1000 to 2000 hr — Calculated	2000 to 3000 hr — Measured at outside radius	2000 to 3000 hr — Corrected to mean radius	2000 to 3000 hr — Calculated	3000 to 9000 hr — Measured at outside radius	3000 to 9000 hr — Corrected to mean radius	3000 to 9000 hr — Calculated
900	13000	1/8	0.124	968	0.2 to 0.4	0.2 to 0.4	0.27	0.2 to 0.4	0.2 to 0.4	0.27	.....	.....	0.24
		3/8	0.373	3110	0.2 to 0.4	0.2 to 0.5	0.26	0.2 to 0.4	0.2 to 0.5	0.26	.....	.....	0.26
	20000	1/8	0.122	1490	1.2 to 1.8	1.3 to 1.9	1.57	0.9 to 1.1	1.0 to 1.2	1.08	.....	.....	1.08
		3/8	0.373	4777	1.0 to 1.5	1.2 to 1.8	1.38	0.7 to 1.2	0.9 to 1.5	0.95	.....	.....	0.95
1050	5000	1/8	0.124	372	1.7 to 2.0	1.8 to 2.1	2.1	1.3 to 1.8	1.4 to 1.9	1.43	0.9 to 1.3	1.0 to 1.4	1.08
		1/8	0.122	596	9.3	9.9	9.1	9.3	9.9	9.1	.....	.....	11.1
	8000	3/8	0.373	1911	7.0	8.5	7.8	6.5	7.9	7.8	.....	.....	9.5

the nominal and actual thickness, the actual stress intensity was determined from the dimensions of the tube; the tension creep rate was determined by extrapolation in the log-log plot, and the corrected tangential creep rate based on this new value of the tension creep rate. The correction in stress is small, but the greatest increase in creep rate is of the order of 17 per cent.

Comparison of Measured and Calculated Creep Rates

Table 4 shows the results of the comparisons which are available thus far. In reviewing these results, it should be kept in mind that the lower creep rates are quite uncertain, and a considerable range of values must be considered as equally probable. To avoid giving an erroneous impression of the relative accuracy of the results, it has been considered necessary to give a probable range of these values. The values presented have been obtained by a careful study of Prof. Norton's original plots. In some instances slight deviations will be found between these results and those previously presented[4,5] but the changes do not affect the general trend of the results.

The comparative creep rates have been listed for the three time intervals 1000 to 2000 hr, 2000 to 3000 hr, and 3000 to 9000 hr. With the exception of the 1/8-in. tube tested at 1050 F and 372 psi, the time interval 2000 to 3000 hr carries the greatest significance. It should be noted that the transition to the steady state does not necessarily run parallel in time for the tension tests and the tubes, but too little is known about this aspect of the problem to make any other interpretation possible.

On the whole, it is apparent that the agreement between measured and calculated creep rates is as good as can be expected, at least for the higher creep rates, where the accuracy of measurement is reasonably satisfactory. The tendency toward higher creep rates in the thin tubes, which was suggested in the previous results[4,5] can now be explained by the fact that the 1/8-in. tubes were slightly under thickness.

If the results presented in Table 3 are taken at their face value, it is possible to read into them a tendency toward somewhat higher observed rates than those calculated by the present theory. At the high creep rates, the difference is probably less than 10 per cent while, for the lower creep rates, larger differences may exist. However, the measured values are too uncertain to make a closer estimate of this difference possible. As already noted, the axial creep rates were zero in most cases, the only exception to this rule being the 1/8-in-thick tube at 1050 F and 372 psi, where a small axial creep was found.

It may be stated in conclusion, therefore, that the test program thus far has generally verified the present theory of creep under triaxial stress systems.

Approximation Involved for Large Wall Thickness

As already indicated, the test results available at the time of our last report suggested a systematic difference between the thick and the thin tubes, the latter having a larger creep rate than that demanded by the theory. It was suggested by Mr. Clinedinst, in the discussion[6] to the original paper, that this difference might be due to the fact that the thin-tube theory, when applied to the 3/8-in-thick tubes, involved some approximation.

While the correction for deviations from the nominal size has largely eliminated this systematic difference in the test results, it is of interest to clarify this question. In the following discussion, a solution is given which may be applied to thick tubes.[7]

In the steady state of flow, it is assumed that cross sections of the tube remain plane, reducing the problem to one of plane strain, for which $\sigma_3 = {}^1/_2\,(\sigma_1 + \sigma_2)$. This reduces the intensity of stress at any radius to $s = \sqrt{3}/2\,(\sigma_1 - \sigma_2)$. The creep rates at any radius then become by Equation [9] of the previous paper[5]

$$u_1 = \frac{\sqrt{3}}{2}\,u\,(s);\quad u_2 = -\frac{\sqrt{3}}{2}\,u\,(s);\quad u_3 = 0 \ldots\ldots [1]$$

To maintain the cross sections plane it is necessary that the radial displacement at any point of the tube vary inversely as the radius; that is, the tangential-creep rate must vary inversely as the square of the radius. If the creep rate also varies as the nth power of the stress intensity, it is evidently necessary to have

$$s = s_0\left(\frac{R}{r}\right)^{2/n} \ldots\ldots [2]$$

where s_0 is the intensity of stress at the mean radius r.

The condition of equilibrium also demands that $\sigma_1 - \sigma_2 = r\,\frac{d\sigma_2}{dr}$ so that

$$s = \frac{\sqrt{3}}{2}\,r\,\frac{d\sigma_2}{dr} \ldots\ldots [3]$$

Equating [2] and [3] and integrating, we obtain for σ_2

$$\sigma_2 = -\frac{n}{\sqrt{3}}\,s_0\left(\frac{R}{r}\right)^{2/n} + \text{const} \ldots\ldots [4]$$

At the inner radius $r = r_1$, $\sigma_2 = -p$; at the outer radius $r = r_2$, $\sigma_2 = 0$. The latter condition gives

$$\sigma_2 = -\frac{n}{\sqrt{3}}\,s_0\left[\left(\frac{R}{r}\right)^{2/n} - \left(\frac{R}{r_2}\right)^{2/n}\right] \ldots\ldots [5]$$

and in order to fulfill the first condition

$$s_0 = \frac{\sqrt{3}}{n}\,p\,\frac{1}{\left(\frac{R}{r_1}\right)^{2/n} - \left(\frac{R}{r_2}\right)^{2/n}} \ldots\ldots [6]$$

Introducing $r_1 = R - \frac{t}{2}$, $r_2 = R + \frac{t}{2}$ and expanding in terms of $t/2R$ this gives

$$s_0 = \frac{\sqrt{3}}{2}\,p\,\frac{R}{t}\left[1 - \left(\frac{t}{2R}\right)^2\right]^{2/n} \ldots\ldots [7]$$

[6] Discussion of paper, reference 3, by W. O. Clinedinst appeared in *Mechanical Engineering*, vol. 61, 1939, p. 757.

[7] The nomenclature in the following discussion is the same as that used in reference 5.

showing that in the thick tube the mean stress s_0 is slightly smaller than demanded by the theory of thin tubes.

It may be expected, therefore, that the deviation from the thin-tube solution should appear in the form of a factor

$$\left[1-\left(\frac{t}{2R}\right)^2\right]^2$$

to be applied to the creep rate at the mean radius. The values of this factor for the two tube thicknesses are as follows:

t	R	$\frac{t}{2R}$	$\left[1-\left(\frac{t}{2R}\right)^2\right]^2$
1/8	31/16	1/31	.998
3/8	29/16	3/29	.979

showing that the approximation involved for the 3/8-in-thick tube is of the order of 2 per cent.

This result is essentially the same as that presented by Mr. Clinedinst in the discussion[8] to the 1940 papers. It may be concluded that no appreciable systematic difference in creep rates can be expected from this cause.

ADDENDA

Since the tests reported herein, tubular specimens F-10 and F-11 have been continued under test, with the results as shown in Appendix 5.

These long-time tests tend to substantiate the report as made prior to these tests.

APPENDIX 1

Microstructure

The carbon-molybdenum bottles and tensile coupons, referred to in the main body of this report, were made from one heat of steel, namely, No. 37239. This heat was rolled into 5-in. rounds and then pierced to form 4-in-OD × 1/4-in-minimum-wall seamless tubes.

All of the material used for making tubular-creep coupons and standard tensile-creep coupons were made from two of these tubes as follows.

Tube No. 37239-B4

Tube No. 37239-B4 was used to prepare the following material:

Four carbon-molybdenum cylinders for tubular creep. These were marked F-1, F-2, F-3, and F-4.

Four tensional creep coupons marked T-1, T-2, T-3, and T-4.

Tubular creep coupons F-1 and F-4 were tested at 800 F.

Tubular creep coupons F-2 and F-3 were tested at 1050 F.

These four coupons were not cut for microexamination, either as part of the report previously published,[8] or as part of this Appendix. The microstructure of the four tensile coupons is being reported herewith.

Tube No. 37239-B3

Seven tubular creep coupons, F-5 to F-11, inclusive, were cut from this tube, and the microstructure of the original tube as well as five of the coupons at the end of the tests are being reported herewith.

Photomicrographs

The photomicrographs, Figs. 12 to 21, accompanying this report, and the comments appearing with them, were prepared by Mr. H. D. Newell of The Babcock & Wilcox Tube Company, Beaver Falls, Pa.

[8] Discussion of papers, references 4 and 5, by W. O. Clinedinst appeared in Trans. A.S.M.E., vol. 63, 1941, pp. 740–741.

Two photomicrographs for each specimen are designated by a single figure number. In all cases, the specimens were etched with 4 per cent nital prior to examination and photographing. In each case the photomicrograph at the top is at 100 diameters and the one below at 2000 diameters.

General Comments

A study of the microstructure of the four tensile coupons, Figs. 13 to 16 inclusive, indicates that there has been very little, if any, microstructural change at 900 F. This is true irrespective of the load, whereas, at 1050 F, the effect of temperature has been to bring about partial spheroidization with some diffusion in the tensile coupons.

In the case of the tubular-creep coupons Figs. 17 to 21, inclusive, the same remarks apply in general, although it would appear that the degree of spheroidization might be a little greater at 1050 F in coupon F-6, Fig. 18. The 1/8-in-wall tubular specimen F-9, Fig. 21, appears to show some recrystallization of the ferrite

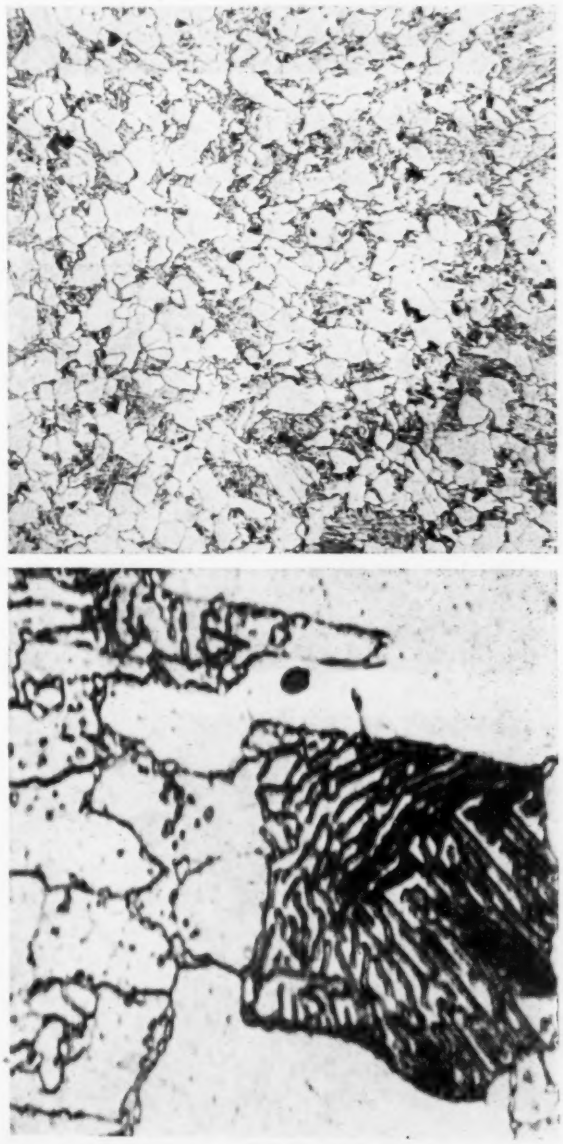


Fig. 12 Original Tube, No. 37239-B3; Ferrite-Pearlite Structure; Top, ×100, Bottom, ×2000

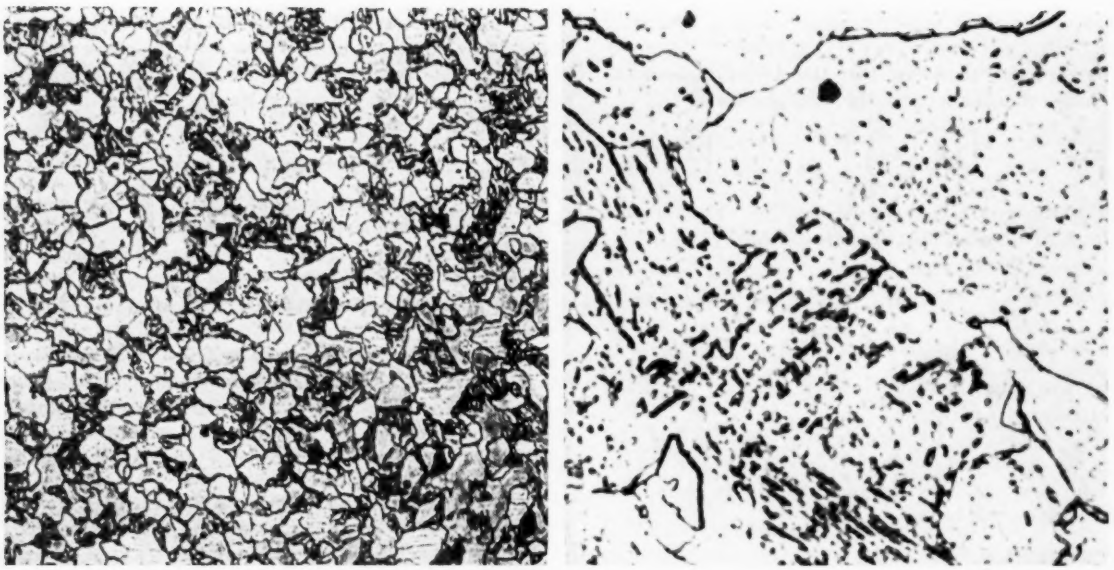


FIG. 15 TENSILE COUPON T-3; 1050 F, 5000 PSI; TOP, ×100, BOTTOM, ×2000
(Ferrite-pearlite structure partially spheroidized and diffused; some showed precipitation.)

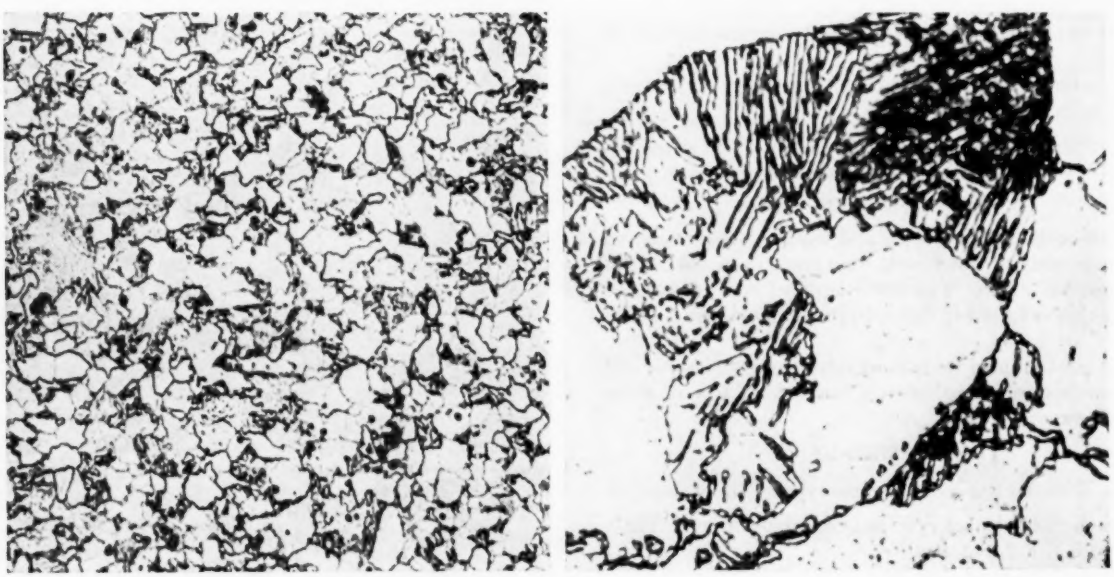


FIG. 14 TENSILE COUPON T-2; 900 F, 20,000 PSI; TOP, ×100, BOTTOM, ×2000
(Ferrite-pearlite structure.)

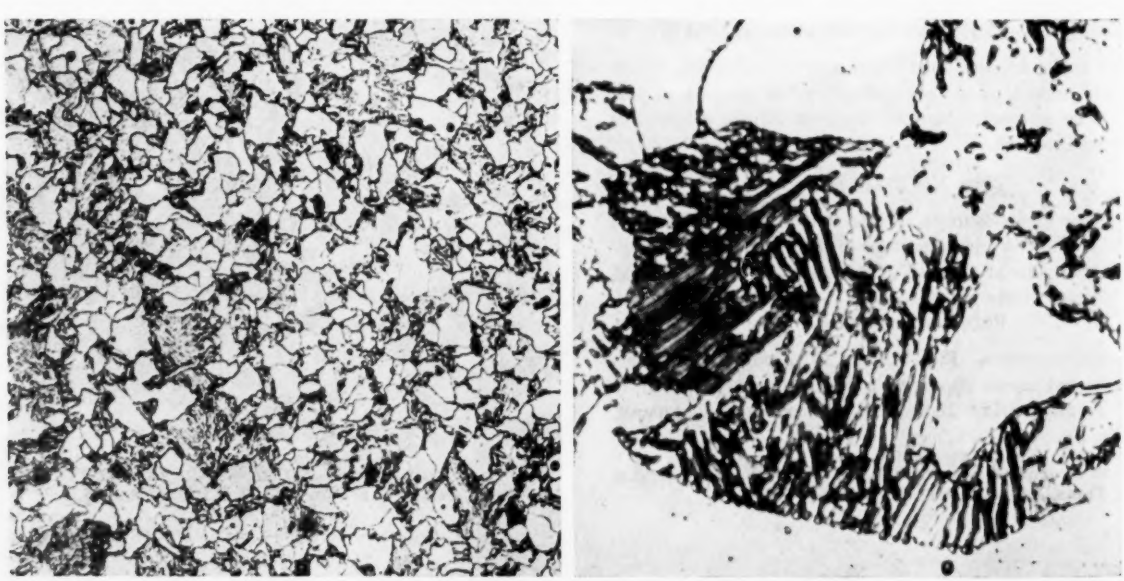


FIG. 13 TENSILE COUPON T-1; 900 F, 13,000 PSI; TOP, ×100, BOTTOM, ×2000
(Ferrite-pearlite; traces of incipient spheroidization.)

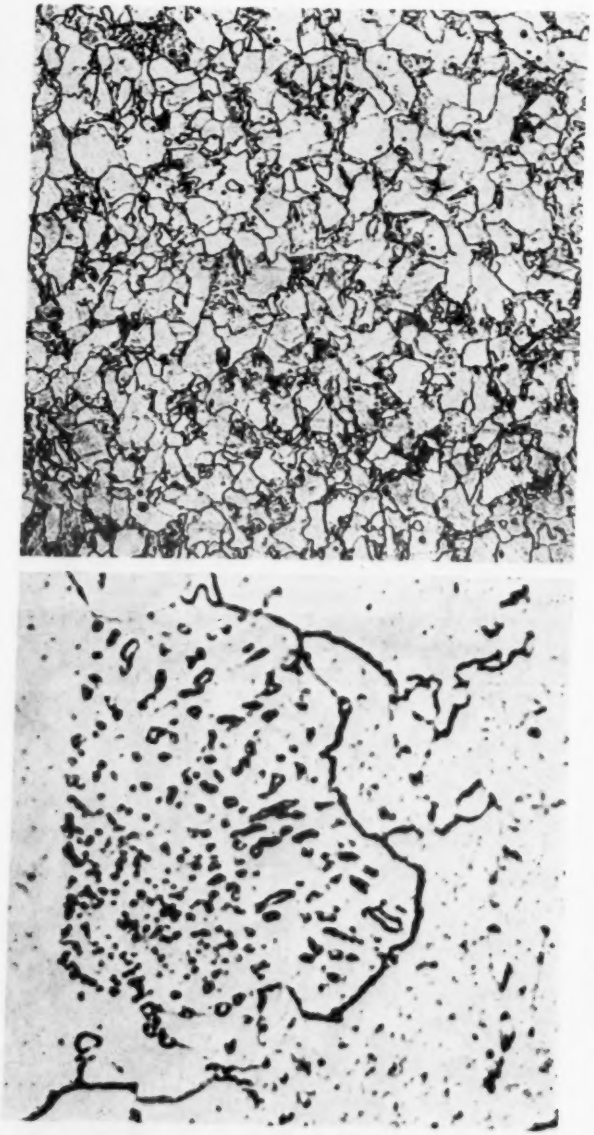


FIG. 16 TENSILE COUPON T4; 1050 F, 8000 PSI; TOP, ×100, BOTTOM, ×2000

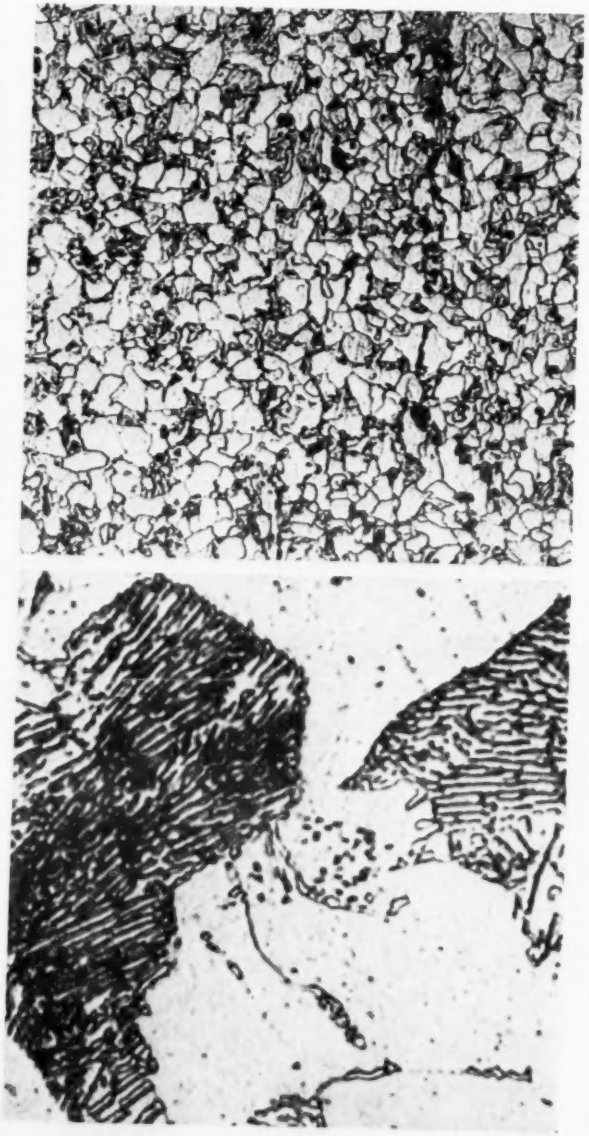


FIG. 17 TUBULAR COUPON F5; 3/8-IN. WALL, 900 F, 4777 PSI; TOP, ×100, BOTTOM, ×2000
Ferrite-pearlite structure.)

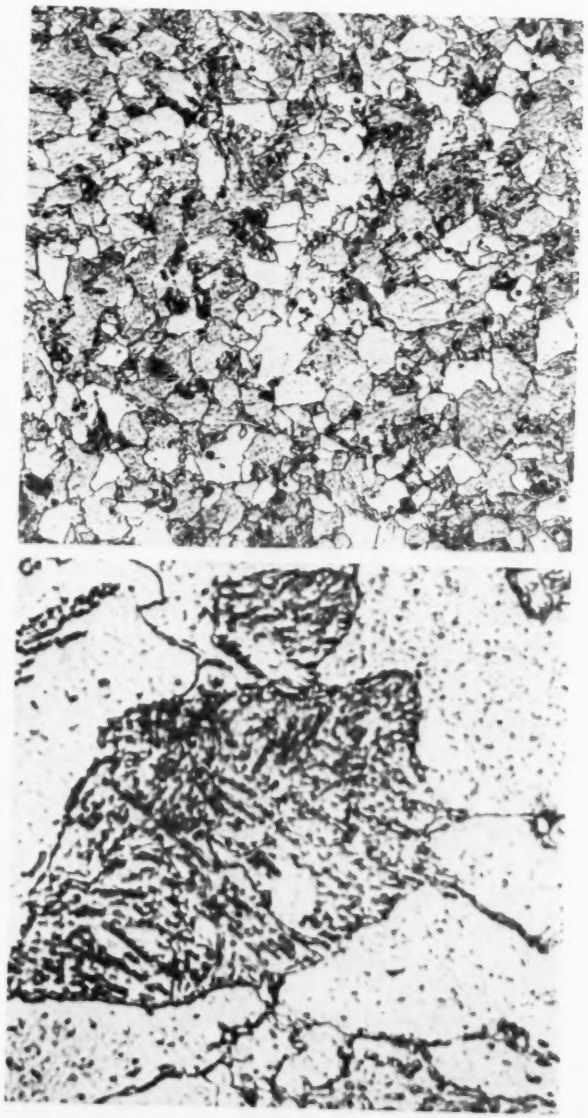


FIG. 18 TUBULAR COUPON F6; 3/8-IN. WALL, 1050 F, 1911 PSI; TOP, ×100, BOTTOM, ×2000
(Ferrite-diffused pearlite with spheroidization; slight precipitation in ground mass.)

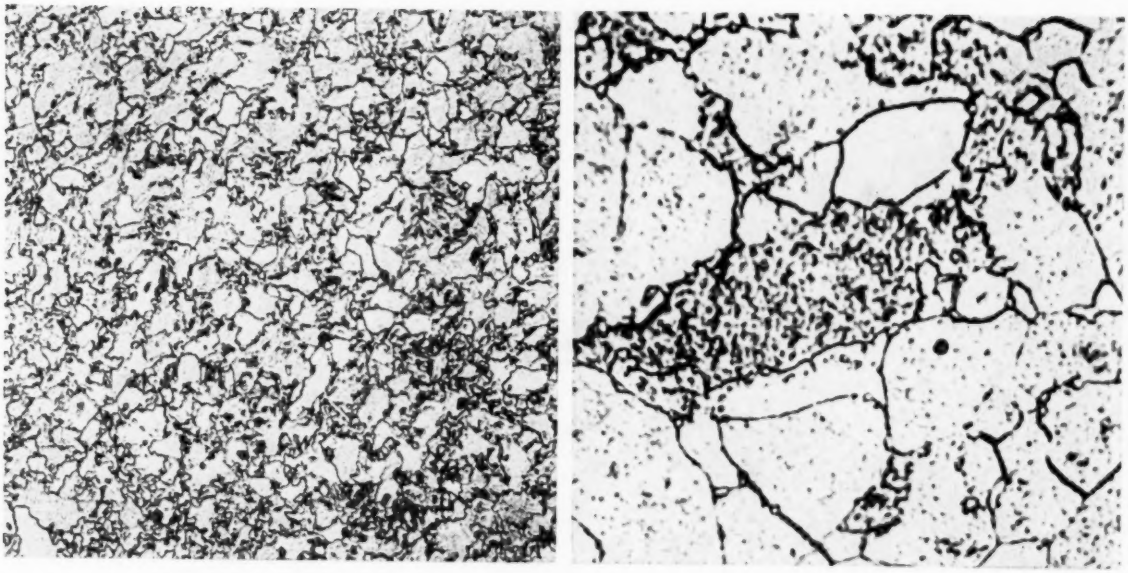


FIG. 21 TUBULAR COUPON F9; 1/4-IN. WALL, 1050 F, 596 PSI; TOP, ×100, BOTTOM, ×2000
(Ferrite partially recrystallized with grain-size contrast, finer grains than other specimens. Carbides spheroidized and diffused.)

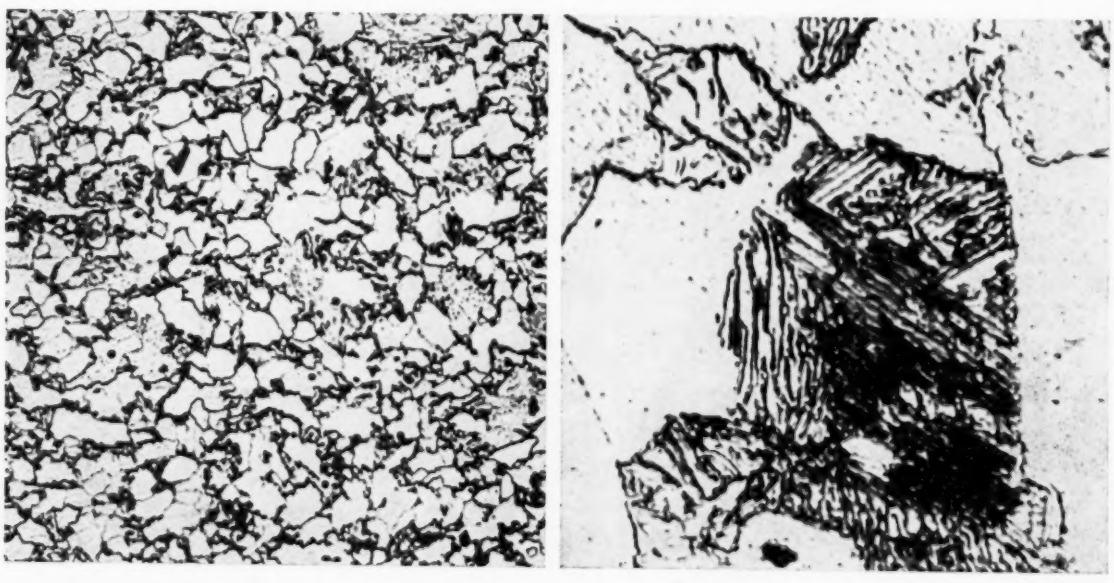


FIG. 20 TUBULAR COUPON F8; 1/4-IN. WALL, 900 F, 1490 PSI; TOP, ×100, BOTTOM, ×2000
Ferrite-pearlite structure.

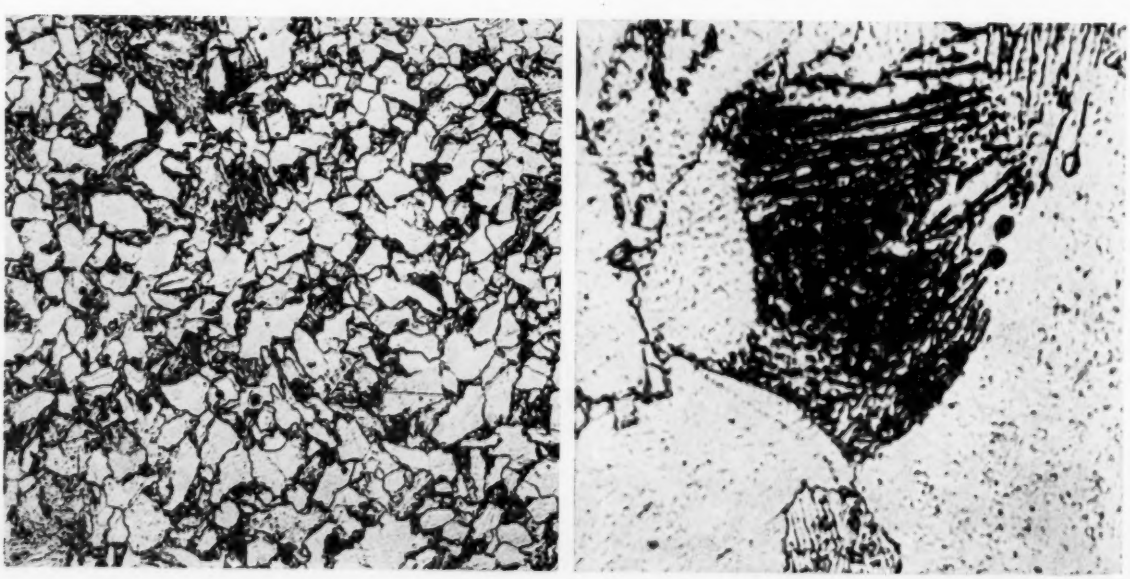


FIG. 19 TUBULAR COUPON F7; 1/4-IN. WALL, 900 F, 3110 PSI; TOP, ×100, BOTTOM, ×2000
(Ferrite-pearlite structure.)

and is finer in grain size than the other specimens with the carbides both spheroidized and diffused.

Appendix 2

METHOD OF MEASURING TUBULAR SPECIMENS

Serial No.—

Wall —Nominal wall thickness

Internal pressure —Pressure during test, psi gage.

Average OD —Average of 6 points on A axis and 6 points on B axis; A and B 90 deg apart
Two points each on axes at center line
Two points each on axes 1 in. from center line
Two points each on axes 2 in. from center line

Average ID —Measured in same manner as OD

Mean radius —Average of averaged OR and IR

$$OR = \frac{OD}{2}$$

$$\text{Average wall} = \frac{OD - ID}{2}$$

$$\text{Stress} = \frac{PR}{t} \text{ where } P = \text{pressure; } R = \text{mean radius; } t = \text{average wall}$$

Deviation, per cent—The stress at each measured transverse plane was first calculated and then averaged; this value given in previous column as stress. The maximum deviation, at any plane, from the average was calculated in terms of per cent of average. With two exceptions, the average and mean stress were the same. For the two exceptions, both the plus and minus maximum deviations are shown.

Appendix 4

RESULTS OF ALL TENSILE CREEP TESTS

Serial no.		Load, psi	Rate, per cent, 100,000 hr	Time interval for measured rate
		Carbon–Molybdenum		
		800 F		
C-10	0.505	17230	0.3	400–2300
A-9	0.505	39170	22.0	800–1500
		900 F		
T-1	0.505	13000	0.2	5000–16000
T-2	0.505	20000	1.0[a]	2000–16000
		1050 F		
T-3	0.505	5000	1.2[a]	4000–16000
B-10	0.505	6970	4.8	600– 2100
T-4	0.505	8000	16.0[a]	10000–14000
C-9	0.505	13930	195.0	800– 1200
		4–6 Chrome Molybdenum		
		1200 F		
A-10	0.505	2820	46.0	400–1000
B-9	0.505	3980	137.0	1000–1800

[a] Slowly changing, see Table 1.

Appendix 3

RESULTS OF ALL TUBULAR SPECIMENS WHICH HAVE BEEN TESTED

Serial no.	Wall	Internal pressure, psi	Average OD, in.	Average ID, in.	Mean radius, in.	Average wall, in.	Stress, $\frac{PR}{t}$	Deviation, per cent	Length of test, hr
				Carbon Molybdenum					
				800 F					
F-1	3/8	4000	4.0050	3.2499	1.8137	0.3775	19216	0.08	150
F-4	3/8	9240	3.9987	3.2509	1.8124	0.3739	44788	0.12	400
				900 F					
F-10	1/8	968	3.9981	3.7504	1.9370	0.1238	15143	{0.24 {0.45	3000+
F-7	3/8	3110	3.9988	3.2533	1.8131	0.3727	15127	0.13	3000
F-8	1/8	1490	3.9973	3.7529	1.9376	0.1221	23644	{0.84 {1.66	300
F-5	3/8	4777*	3.9984	3.2532	1.8129	0.3726	23241	0.24	3000
				1050 F					
F-11	1/8	372	3.9987	3.7503	1.9372	0.1242	5800	0.78	9000+
F-3	3/8	1620	4.0042	3.2501	1.8135	0.3770	7793	0.05	3000
F-9	1/8	596	3.9965	3.7531	1.9371	0.1216	9494	0.64	3000
F-6	3/8	1911	3.9974	3.2512	1.8121	0.3731	9280	0.16	3000
F-2	3/8	3230	4.0046	3.2511	1.8139	0.3768	15549	0.05	800
				4–6 Chrome Molybdenum					
				1200 F					
F-2	3/8	650	4.0004	3.2503	1.8126	0.3751	3141	0.10	800
F-1	3/8	920	4.0053	3.2505	1.8139	0.3774	4424	0.08	1100

Appendix 5

JOINT HIGH TEMPERATURE COMMITTEE, CREEP PROGRESS REPORT

Creep no.	Temp, F	Load, psi	Rate, per cent, 100,000 hr	Time interval	Inches per inch—Initial extension	Inches per inch—Total extension to date
	Circumferential					
C-Mo-F-10	900	968 Press.	15.0	0–100	.....	.....
			0.5	100–2600	.....	.....
			0.6	2600–6600	.....	.....
			0.8	6600–8200	.....	.....
			0.5	8200–9030	0.00042	0.00114
	Longitudinal					
	900	968 Press.	0.1	0–9030	0.00009	0.00020
	Circumferential					
C-Mo-F-11	1050	372 Press.	3.6	0–1200	.....	.....
			1.5	1290–3800	.....	.....
			1.2	3800–14230	0.00019	0.00242
	Longitudinal					
	1050	372 Press.	0.1	0–14230	0.00005	0.00020

A Review of Heat-Transfer Coefficients and Friction Factors for Tubular Heat Exchangers

By B. E. SHORT,[1] AUSTIN, TEXAS

This paper presents a summary of experimental and analytical work carried out on heat-transfer rate and pressure drop on the shell side of shell-and-tube exchangers. A comparison is made between the different methods which have been used in correlating the data, with the conclusion that no rational base has been established, except in so far as the fluid properties, fluid velocity, and dimensions of the exchangers are involved. However, an attempt is made to show that the effective velocity as used has a rational foundation.

Nomenclature

The following nomenclature is used in this paper:

A_a = net area of annular space at baffle of disk-and-doughnut baffles, sq ft
A_b = net area at baffle of half-moon baffles, sq ft
A_h = net area of hole in baffle of disk-and-doughnut baffles, sq ft
A_o = total annular area of clearance between baffle holes and tubes of orifice baffles, sq ft
A_s = cross-sectional area of shell minus total cross-sectional area of tubes, sq ft
B_h = height of half-moon baffle, ft
c = specific heat at constant pressure for shell fluid at mean stream temperature, Btu per deg F per lb
c_i = specific heat at constant pressure for tube fluid at mean stream temperature
D = inside diameter of tube, ft
D_o = diameter of holes in orifice baffles, ft
D_s = inside diameter of shell, ft
D_t = outside diameter of tube, ft
f = friction factor in Fanning equation, dimensionless
F = friction and roughness factor obtained from Fig. 6 for particular baffle type, dimensionless
g = acceleration due to gravitational force = 32.2 ft per sec per sec
G = mass velocity of the tube fluid, lb per sq ft per hr
G_a = velocity through annular space of disk-and-doughnut baffles, lb per sq ft per hr
G_b = velocity through opening at half-moon baffle, lb per sq ft per hr
G_h = velocity through hole in disk-and-doughnut baffle, lb per sq ft per hr
G_o = velocity through annular spaces of orifice baffle, lb per sq ft per hr
G_p = velocity perpendicular to tubes between baffles of half-moon baffles, lb per sq ft per hr
G_r = velocity perpendicular to tubes, radially, in disk-and-doughnut baffles, lb per sq ft per hr
G_s = velocity between baffles parallel to tubes of orifice baffles, lb per sq ft
G_x = effective velocity, lb per sq ft per hr
h_o = film coefficient for outside of tubes, Btu per deg F per sq ft per hr
h_i = film coefficient for inside of tube, Btu per deg F per sq ft per hr
k = thermal conductivity of shell fluid at mean stream temperature, Btu per deg F per sq ft per hr
k_i = thermal conductivity of tube fluid at mean stream temperature, Btu per deg F per sq ft per hr
L = heated or cooled length of exchanger, ft
μ = absolute viscosity of shell fluid at mean stream temperature, lb per ft per hr
μ_i = absolute viscosity of tube fluid at mean stream temperature, lb per ft per hr
N_b = number of baffles
Δp = pressure drop across shell side of exchanger, psf
P = center to center distance of tubes, ft
S = baffle spacing, ft
ρ = specific weight of the shell side fluid, lb per cu ft

Introduction

In the field of heat transmission by forced convection from one fluid to another across a separating wall is the general case of baffled tubular heat exchangers. This type of exchanger generally consists of a tube bundle with one fluid flowing through the tubes and the other fluid flowing across or along, or both across and along the tubes. Quite frequently, the rate of flow of one of the fluids is much less than the other, so that its film coefficient of heat transfer would be considerably lower than that of the other fluid, if the two were flowing at the same linear velocity. Also, quite frequently, the properties of one fluid are such as to cause a much lower transfer rate if the two fluids have the same linear velocity; or one may need to be lowered or raised through a much greater temperature range than the other. The designer has found that he can compensate for these differences and obtain a more economical design by using turbulence-promoting devices on the outside of the tubes in a shell-and-tube-type exchanger; he can increase the area of contact for the fluid which has the lower unit transfer rate; or he can increase the number of times that one fluid flows across or along the second fluid. The first scheme is that of using baffles of different kinds, the second scheme is the one of using fins or extended surfaces, and the third scheme results in the multipass exchanger.

Because of the complexity of the flow conditions on the outside of the tubes in the baffled exchanger, this paper is presented in an effort to review certain phases of the work that has been done on this type of unit, to compare the different methods that have been used in correlating the data, and to make a further examination of the possibilities of a rational correlation of the data on such units.

[1] Professor of Mechanical Engineering, The University of Texas. Mem. A.S.M.E.

Contributed by the Heat Transfer Division and presented at the Spring Meeting, Houston, Texas, March 23–25, 1942, of The American Society of Mechanical Engineers.

Note: Statements and opinions advanced in papers are to be understood as individual expressions of their authors and not those of the Society.

A detailed discussion is presented in which the factors the author used in correlating the data that he obtained in a series (11)[2] of experiments with different baffle types, baffle sizes, tube spacings, tube sizes, and rates of flow for the shell-and-tube exchanger, are critically examined.

Baffle Types

The more common baffles used in these exchangers are the orifice, half-moon, and disk-and-doughnut types, shown in Fig. 1.

The tube holes in orifice-type baffles are large enough to allow the fluid to flow parallel to the tube through the annular space between the tube and the edge of the tube hole in the baffle. Between the baffles, the flow is likewise generally parallel to the tubes.

In the case of half-moon baffles, the flow at the baffles is through the segmental opening between the shell and the flat edge of the baffle. From this opening, the fluid flows diagonally across the tubes to the segmental opening at the next baffle.

For disk-and-doughnut baffles, the flow at the "doughnut" baffle is parallel to the tubes through the circular opening in the baffle, then diagonally and radially to the annular space at the disk baffle. This annular space is formed by the shell and the edge of the disk baffle. The flow through this annular space is approximately parallel to the tubes.

Factors Affecting Transfer Rate and Pressure Drop

Variations in the construction of a shell-and-tube exchanger which affect the heat-transfer rate and the drop in pressure are tube size, tube spacing, baffle type, baffle spacing, baffle size length of exchanger, and diameter of the exchanger shell.

[2] Numbers in parentheses refer to the Bibliography at the end of the paper.

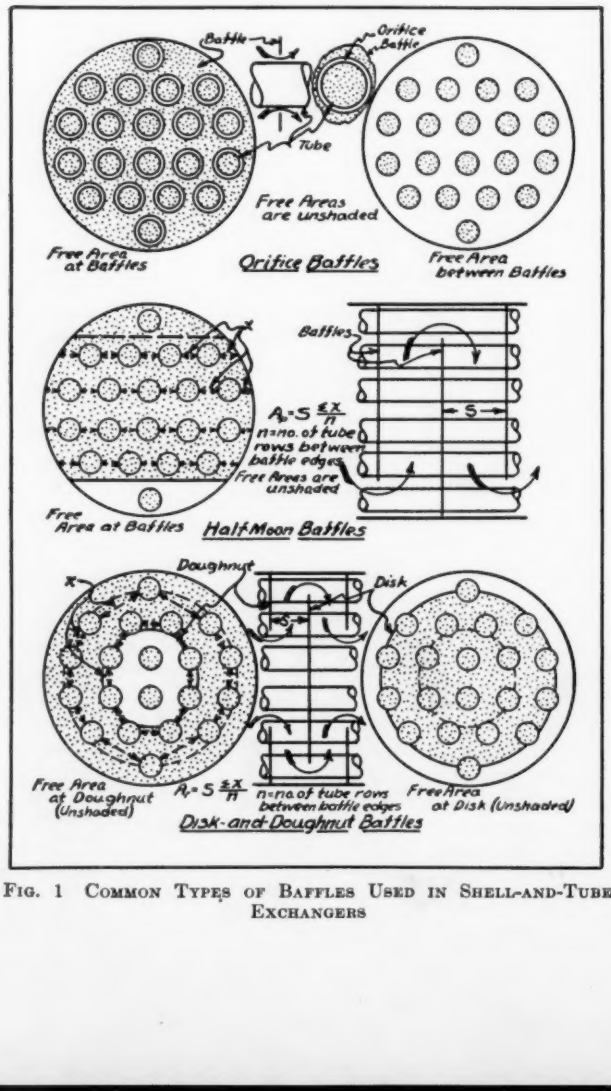


Fig. 1 Common Types of Baffles Used in Shell-and-Tube Exchangers

The size of the tube affects the pressure drop and transfer rate since the turbulent condition on the trailing side of the tube is affected directly by the width of the tube. In the case of heat transfer, the smaller tube gives a higher transfer rate than the larger tube since the fluid sweeps the back side of the tube more completely for the same fluid and same velocity. For the pressure drop, the reverse is true as the larger tube presents a greater frontal area for the fluid.

A variation in the spacing causes a variation in the transfer rate since a wider tube spacing increases the thickness of the stream flowing between the tubes and also allows a longer time for the mixing of the fluid after it has passed over the tube surface. The increased width of the fluid stream causes a decrease in the transfer rate but this is more than offset by the increased mixing on the trailing side of the tube, thus causing the transfer rate to increase with increases in the tube spacing. The pressure drop is increased by a decrease in the tube spacing because the number of changes in direction are increased per unit length of the path of flow.

The same transfer rate can be obtained with one baffle type as with another; but the pressure drop is greater with the orifice-type baffle for the same transfer rate than is true for either of the other two forms which have been named. This is shown graphically in Fig. 2.

An increase in the baffle spacing for a given exchanger length, if orifice baffles are used, increases the mixing time following flow through the baffle but this effect is not as great as the effect of the decrease in number of baffles resulting from this increase in spacing, and the net result is a lowering of the transfer rate with increase in baffle spacing. An optimum baffle spacing for the orifice baffle would be roughly 4 times the effective flow diameter of the region between the baffles. This optimum baffle spacing is nearly approached in the case of the orifice baffles shown in Fig. 3.

An increase in baffle spacing for either half-moon or disk-and-doughnut baffles decreases the velocity of the fluid across the tubes between the baffles and thus tends to decrease the transfer rate. This increase in spacing, however, allows a longer mixing time following the flow of the fluid through the opening at the baffle and this tends to increase the transfer rate, but a decrease in the baffle spacing produces a sharper turning of the fluid over or through the baffle which results in a better sweeping of the transfer surfaces. Since this decrease in spacing also increases the velocity of flow across the tubes between the baffles, the net result is an increase in the transfer rate with decreased baffle spacing. This decrease in baffle spacing also increases the pressure drop because of the increased velocity and increased turbulence.

The larger baffle heights for the half-moon baffles and smaller openings for the disk-and-doughnut baffles increase the velocity at the baffle and the distance that the fluid moves outward toward the next baffle. The net result is a general increase in the transfer rate even though it decreases the transfer surface in the baffle opening for the same tube spacing, which would tend to decrease the over-all transfer rate. For the orifice-type baffle, a decrease in orifice size increases the transfer rate, as is true for the other two types, since the velocity of the fluid at the baffle is so much greater than that between the baffles. The general effect is to increase the average velocity through the exchanger. Also, the thickness of the stream over the tube through the orifice is decreased with decreases in the orifice size for a given tube size. The drop in pressure is increased by anything that increases the average velocity and, of course, a decrease in the size of the openings at the baffles increases the restriction to the flow of the fluid as is true for any orifice. The effect of baffle spacing and

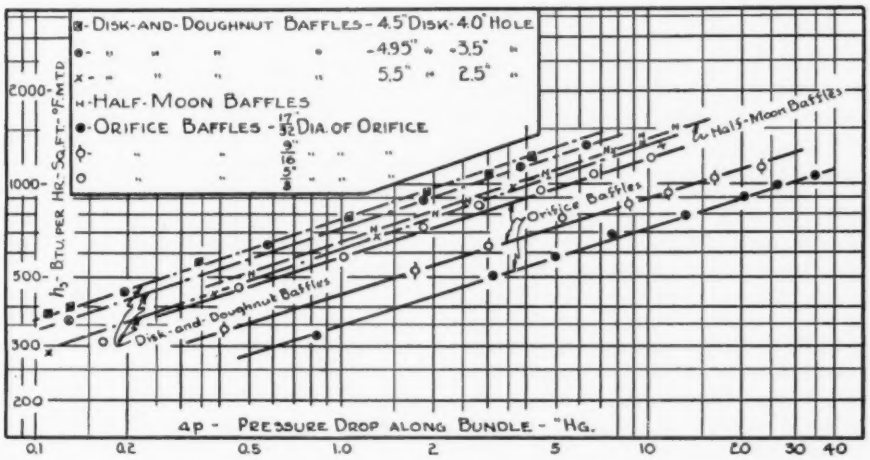


FIG. 2 COMPARISON OF RELATION BETWEEN TRANSFER RATE AND PRESSURE DROP FOR DIFFERENT BAFFLE TYPES FOR A BAFFLE SPACING OF 2.39 IN.

baffle size on the transfer rate and pressure drop are shown graphically in Figs. 2 and 3.

The length and diameter of the exchanger shell affect the general flow pattern of the fluid and their effects are those of increased or decreased times of mixing either for longitudinal or cross flow. More specifically, the longer shell length for the same baffle spacing increases the number of turns in the fluid stream and thus increases the mixing rate, whereas, the larger shell diameter for the same tube spacing and baffle spacing decreases the number of turns in the fluid stream per unit of heat-transfer surface.

POSSIBILITIES OF RATIONAL DETERMINATION OF AVERAGE VELOCITY

The flow pattern on the outside of the tubes for this shell-and-tube heat exchanger is quite complex and difficult to analyze rationally. The increased number of turns in the path of flow, which would be occasioned by an increased number of baffles for a unit length of exchanger, produces a more effective mixing of the fluid as it flows over the transfer surface, both as a result of the inertial effect of the fluid and as a result of the rotational effect produced by the turn in the fluid stream.

The orifice effect produced by the baffle, whether disk-and-doughnut, half-moon, or orifice type, on the flow pattern immediately following the restriction is one of the easiest to picture; yet, as a result of the internal boundary that is formed by the tube over which the fluid flows and the number of individual obstructions in the path, this effect is difficult to estimate rationally.

If the flow across the tubes, in between the baffles, was always perpendicular to the tubes for half-moon and disk-and-doughnut baffles the average velocity in this region could be obtained, but the shortness of the path in this direction causes very little of the flow to be perpendicular to the tubes. Some have shown a condition in this region which would indicate the flow pattern to be one that extends diagonally from one baffle opening to the next.

The periodic dividing of the flowing stream as it strikes one tube and then another also minimizes the possibility of describing the flow pattern in a rational manner.

In connection with a discussion of these direct effects on the flow pattern, it should be stated that some of the factors affecting the heat transfer and pressure drop, as discussed previously, indirectly affect the flow pattern and, therefore, the effective or average velocity. It is difficult, for example, to say that the diameter and length of the exchanger shell affect the average velocity. It is certainly evident that these two factors do not affect the velocity at any one point in the fluid path, unless the total number of turns around the baffle edges increases the rotational motion of the fluid, but each can have its effect on the average velocity for the entire exchanger. For a given baffle opening and tube spacing, an increase in the shell diameter will increase the length of the path of flow across the tubes and thus decrease the effect of the velocity at the baffle, that is, a "weighted" average would show a smaller effect for this baffle velocity. On the other hand, an increase in the shell length for a particular shell size, baffle spacing, and baffle height would increase the total transfer surface without affecting the crossflow

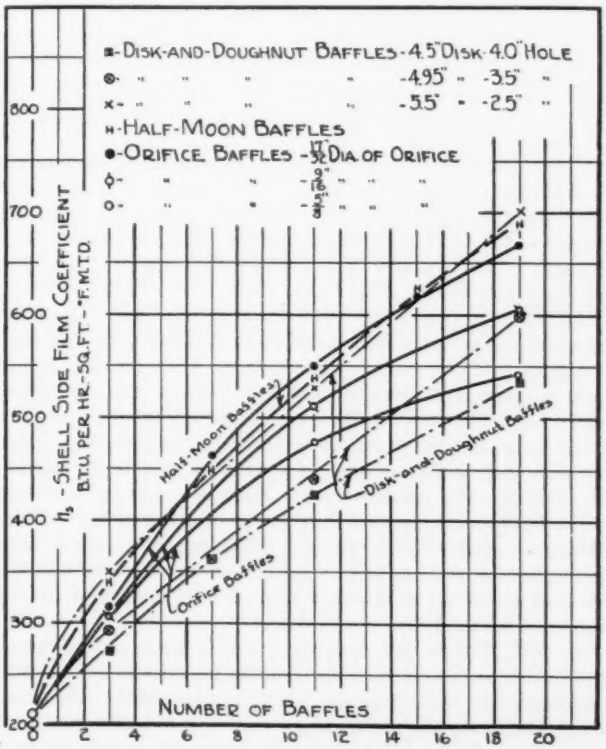


FIG. 3 COMPARISON OF h_o FOR ALL BAFFLE TYPES FOR 1/2-IN. TUBE, 25/32-IN-PITCH TUBE BUNDLE AT A SHELL FLUID (WATER) RATE OF 10,000 LB PER HR

velocity and this could, as indicated previously, increase the rotational effect on the fluid. For longer shell lengths, the effect at entrance to and exit from the exchanger shell would be less than for the shorter lengths and would thus have, approximately, the same effect as the flow inside of pipes in the viscous and critical-flow regions.

Previous Analysis for Shell-and-Tube Exchanger

From the standpoint of the designer, it has appeared simpler to use the velocity at some particular point in the exchanger or to use a velocity that would exist if a particular type of construction were used. For example, the writer and M. M. Heller (1), in 1931, published the results of a series of tests on a shell-and-tube exchanger in which the flow was assumed to be parallel to the tubes in correlating the results. This flow was assumed to be parallel to the tubes through an area equal to the cross-sectional area of the shell minus the cross-sectional area of all of the tubes. To correlate the data of these tests with those of McAdams and Frost (2) and Morris and Whitman (3), for flow through tubes, an equivalent diameter was used which was equal to the diameter of a circle with the same area as the "free" area given previously. The exchanger, however, which was used in these tests did not have cross baffles.

In 1933, McAdams (4) presented results of tests on several heat exchangers. The exchangers on which these tests were made had half-moon, orifice, and disk-and-doughnut baffles. To present these results, he used the same velocity that would be obtained if there were no baffles and the flow was entirely parallel to the tubes. Even though commercial exchangers are designed so that corresponding velocities in the different sections are in about the same ratio in different-sized units, McAdams found as much as 500 per cent variation in the transfer rate when based on this velocity.

Heinrich (5) performed some tests on small vertical heat exchangers in 1914, and Stückle presented these results in 1925, but the tube-fluid velocities were too low to permit accurate determination of the shell-side coefficients. A study of the effect of different relative movements of the oil and water in the exchangers on the over-all transfer rate seemed to be Stückle's primary object in his correlation.

Colburn (6) showed, in 1933, that transfer coefficients for the flow across the outside of tubes in a tube bank could be correlated by using the maximum velocity of flow across the tube banks. Sieder and Scott (7), in 1932, used this same velocity for the correlation of the pressure drop across tube banks with the flow perpendicular to the tubes.

In 1934, the author and T. F. Stack (8) published the results of a series of pressure-drop tests on tube bundles which had half-moon baffles. In making this study, an attempt was made to use an equivalent diameter with the velocity that McAdams had used. This method did not prove satisfactory and the data were correlated by means of an empirical combination of the velocity at the baffle and the average maximum velocity between the baffles. The combination of these two rates of flow was arrived at by assuming that the pressure drop was proportional to the square of the effective velocity, which velocity squared, when multiplied by the exchanger length, was equal to the distance through which the fluid flowed at each rate, multiplied by the square of its respective rate of flow.

In 1935, Perrone (9), with data from a series of half-moon-baffled exchangers, used a scheme similar to that which the author and Stack had used. Perrone, however, assumed that the cross-flow distance for the pass between each pair of baffles was from the center of gravity of the segment-shaped opening for flow at one baffle to the center of gravity of the corresponding opening for the next baffle. For the relatively narrow range of variables covered by the data Perrone used, his results showed close correlation.

Bowman (10), in 1935, published his correlation of a series of tests on shell-and-tube exchangers with half-moon baffles. These data covered several sizes of exchangers, several different ratios of baffle heights to shell diameter, several different tube diameters, and several different tube spacings. Bowman used a velocity equal to that obtained with the fluid flowing across all tubes during each pass, in conjunction with an arbitrarily assumed leakage factor. He found that his data followed closely Colburn's curve under these conditions.

The author presented a correlation (11) in 1935–1936 of data which covered tests on exchangers that were equipped with half-moon, orifice, and disk-and-doughnut baffles. These exchangers covered a wide range of tube spacings and tube sizes, as well as several sizes of disk-and-doughnut and orifice baffles. The author assumed that the most usable method of correlation would be one based on a combination of the velocity at the baffles and the velocity between the baffles in a manner that would show the effect of the different variables of the exchanger except the effect of the tube spacing, which effect was shown in the general transfer equation. It was found that the results from the empirical combination of these rates of flow correlated closely for all baffle types and that they were relatively close to Colburn's curve for tube banks and those of other investigators for single tubes. These results also showed a fair correlation with most of Bowman's data, as well as that of two other sources on orifice-baffled exchangers.

Grimison (12), in the fall of 1936, presented a correlation of the data of Huge and Pierson on the flow of air across tube banks, which covered a wide range of tube spacings and tube sizes. Grimison used the same effective velocity that Colburn had used and accounted for the variation in the physical dimensions of the apparatus from which his data were obtained by making use of an arrangement or correlating factor that gave the ratio of the film coefficient for a particular unit to that of the reference unit.

The author recorrelated (13) his own data in 1939, using the same method of approach that he had used in 1935–1936, but keeping the factors on a dimensionless-ratio basis since it was found that his earlier results did not apply very closely to exchangers differing widely in size from the ones which he had originally used. In order to make this new correlation, the author made use of Bowman's data as well as other data supplied by the Foster Wheeler Corporation and the Ross Heater and Manufacturing Company. In this last correlation, a series of equations was also presented which made use of the velocity that McAdams had used. These equations presented, in addition to the velocity effect, the effects of the tube spacing, tube size, shell diameter and length, baffle spacing, and baffle size.

Discussion of Heat-Transfer Correlation

To obtain the film coefficient of heat transfer (11) in this 1939 correlation on the outside of the tubes, the coefficient on the inside of the tubes was determined by the author by means of the equation

$$\frac{h_i D}{k_i} = 0.0225 \left(1 + \frac{50D}{L}\right) \left(\frac{c_i \mu_i}{k_i}\right)^{0.4} \left(\frac{DG}{\mu_i}\right)^{0.8} \quad \ldots\ldots [1]$$

It was found, in the earlier (11) correlation, that the tube-side coefficients, when calculated by an equation similar to Equation [1] without allowance for the end effects, were lower than would be expected for the values of Reynolds number obtained, and that the shell-side coefficients were abnormally high. It was also found that the shell-side coefficients thus obtained were not

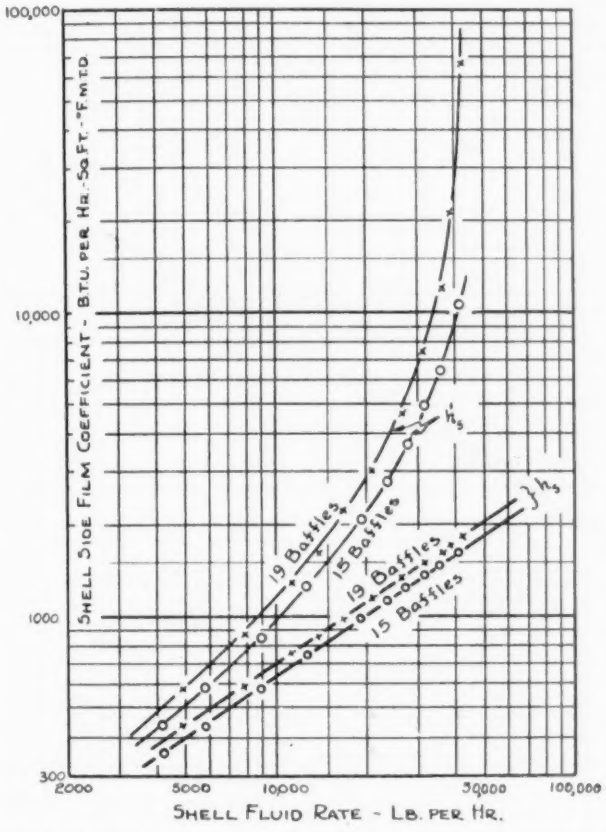


FIG. 4 EFFECT OF INTRODUCTION OF $\phi(D/L)$ INTO COMPUTATION OF h_i WHICH IS USED TO COMPUTE h_s

simple exponential functions of the rate of flow but varied in a rather complex manner. Fig. 4 shows a plot of the shell-side coefficients obtained when using the term $\left(1 + \frac{50D}{L}\right)$ in the tube-side-coefficient equation as contrasted with that obtained when it was omitted; h_s' being the shell-side coefficient obtained without this factor, and h_s being the one obtained when it was used. Results similar to those without the end effects being considered are obtained if Sieder and Tate's (14) curve for heating and cooling of petroleum oils inside of tubes is used.

In so far as the data are concerned on which this study was made, the difficulty discussed may be avoided by using a larger constant in the equation than 0.0225. Hinton's (15) work as well as that of Purday (16) justifies an increase in this constant, but to do this would require a constant that would suit the larger tube sizes which were used, and this did not appear justifiable. A constant could have been selected that would change with tube diameter without being affected by the tube length. Work done by W. A. Randle (17) in 1940 indicates that the end effects are more noticeable at higher Reynolds numbers for the flow through tubes of tube bundles than is true for single tubes. With these two things as a basis, the author feels justified in using the relation given by Equation [1].

The over-all transfer coefficients which were obtained from the test data and from which the shell-side coefficients were calculated were determined by the use of the logarithmic-mean temperature difference. In this correlation, the principal data were from exchangers which had single-pass flow for both the tube fluid and shell fluid. A few tests were used where the tube fluid made two passes with the shell fluid making a single pass through the exchanger. The results from these last tests were close enough to the single-pass tube-fluid results to ignore the effect on the mean temperature difference. The effect of crossflow between the baffles in the half-moon- and disk-and-doughnut-baffled exchangers was such as to cause the true temperature difference to be between the arithmetic mean and the logarithmic mean but with counterflow, as in these tests, and with the closeness of the terminal differences, the difference between the arithmetic and logarithmic means was not greater than 2 per cent as Perrone pointed out.

The fluid properties, as used in the correlation, were evaluated at the mean stream temperature because the properties evaluated at the mean temperature of the wall surface and stream did not improve the correlation. Since the tube-wall temperatures could not be measured accurately, these temperatures had to be determined by a trial-and-error method, and it was considered that the greater ease in using the mean stream temperature outweighed the use of the more rational film temperature.

The effective velocity used in this correlation for each of the three types of baffles is given by the following equations

Orifice baffles

$$G_z = G_s\left(\frac{L}{S}\right)^{0.55}\left[\frac{(D_s - D_t)D_t}{PD_s}\right]^{0.82} + G_s\left(\frac{L}{S}\right)^{0.55}\left(\frac{D_t^2}{A_o}\right)^{0.43} \quad \ldots\ldots [2]$$

Half-moon baffles

$$G_z = G_b\left(\frac{L}{S}\right)^{0.5}\left(\frac{A_b}{A_s}\right)^{0.8}\left[37.1\left(\frac{D_t}{D_s}\right)^2\right] + G_p\left(\frac{S}{L}\right)^{0.5}\left(\frac{A_s}{A_b}\right)^{0.8} \quad \ldots\ldots [3]$$

Disk-and-doughnut baffles

$$G_z = G_h\left(\frac{L}{S}\right)^{0.5}\left(\frac{A_h}{A_s}\right)^{0.6}\left(\frac{D_t}{D_s}\right)^{0.86} + G_a\left(\frac{L}{S}\right)^{0.5}\left(\frac{A_a}{A_s}\right)^{0.5}\left(\frac{D_t}{D_s}\right)^{0.86} + G_r\left(\frac{S}{L}\right)^{0.5}\left(\frac{A_h}{A_s}\right)^{0.1}\left[50\left(\frac{D_t}{D_s}\right)^{1.17}\right] \quad \ldots\ldots [4]$$

The film coefficient for the shell-side fluid is given by the equation

$$\frac{h_s D_t}{k} = 0.37\left(\frac{P - D_t}{P}\right)^{0.5}\left(\frac{c\mu}{k}\right)^{0.32}\left(\frac{D_t G_z}{\mu}\right)^{0.6} \quad \ldots\ldots [5]$$

If the velocity, which would be obtained for a shell and its tube bundle without baffles, is used to determine the heat-transfer rate, the following equations show the resulting correlation

Orifice baffles

$$\frac{h_s D_t}{k} = 2.5\left(\frac{c\mu}{k}\right)^{0.32}\left(\frac{P - D_t}{P}\right)^{0.5}\left[\frac{D_t G_s}{\mu}\left(\frac{L}{S}\right)^n\left(\frac{D_t}{D_s}\right)^{1.5}\right]^{0.6} \quad \ldots [6]$$

where

$$n = \frac{0.3}{\left[\frac{(D_o - D_t)D_t}{P^2}\right]^{0.25}} \quad \ldots\ldots [7]$$

Half-moon baffles

$$\frac{h_s D_t}{k} = 15.8\left(\frac{c\mu}{k}\right)^{0.32}\left(\frac{P - D_t}{P}\right)^{0.5}\left[\frac{D_t G_s}{\mu}\left(\frac{B_h}{L}\right)^{1.72}\left(\frac{D_t}{D_s}\right)^{0.86}\left(\frac{L}{S}\right)^{0.55}\right]^{0.6} \quad \ldots\ldots [8]$$

Disk-and-doughnut baffles

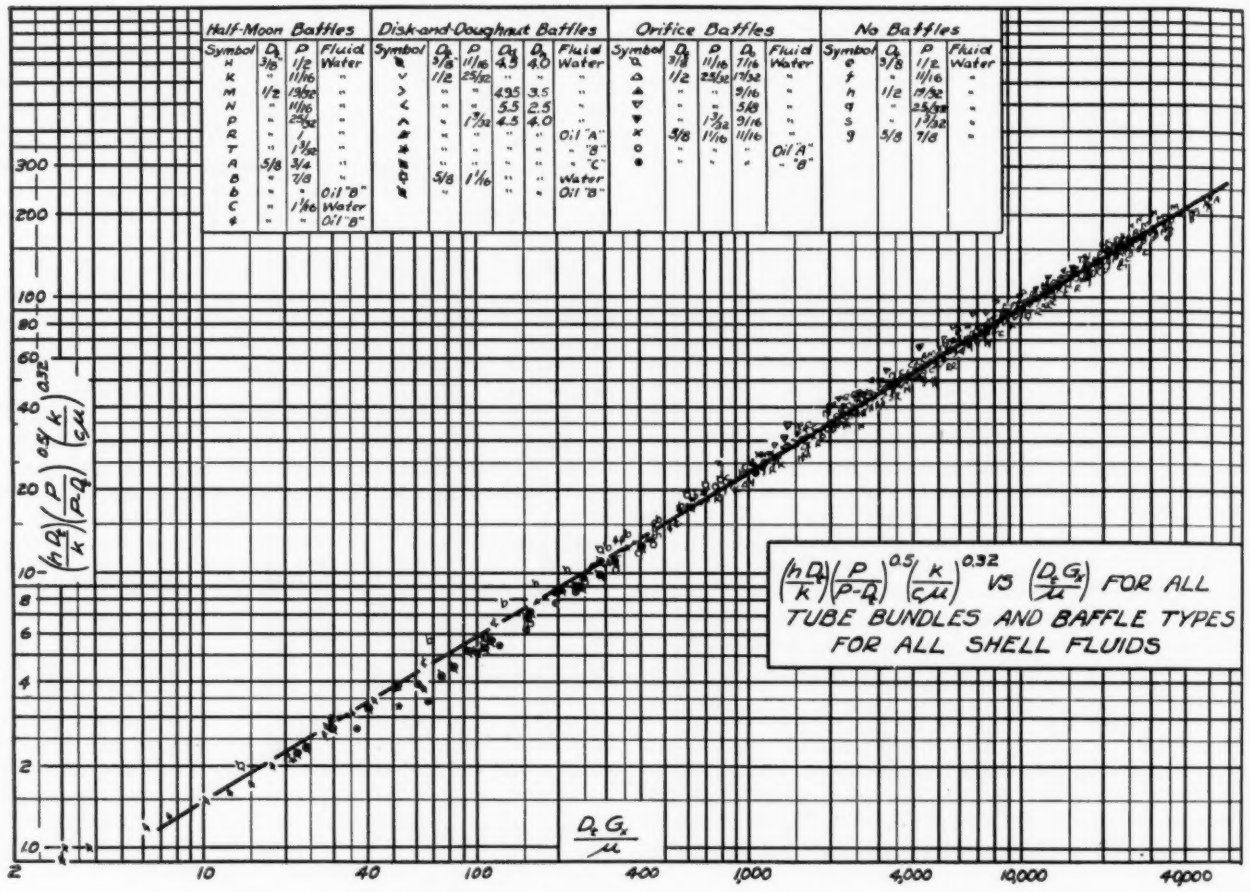


FIG. 5 DATA FROM TESTS USED IN ORIGINAL CORRELATION

$$\frac{h_oD_t}{k} = 0.45\left(\frac{c\mu}{k}\right)^{0.32}\left(\frac{P-D_t}{P}\right)^{0.5}\left[\frac{D_tG_s}{\mu}\left(\frac{L}{S}\right)^{0.5}\left(\frac{A_s}{A_b}\right)^{0.48}\left(\frac{D_t}{D_s}\right)^{0.6}\right]^{0.6} \quad \text{.....[9]}$$

In these equations, the symbols have the same meaning as in Equations [2 to 5].

From the standpoint of design, as was mentioned previously, Equations [6 to 9] have a greater utility than Equations [2 to 5] but these equations cannot be expected to approximate a rational basis. The effective velocity as given by Equations [2], [3], and [4] represents an empirical combination of two types of flow in the exchanger. It could be said that the two "components" of flow involved are those that would be found in an ideal exchanger of this type. That is, basically, in an exchanger, for example, with half-moon baffles, it would be expected that the flow would be parallel to the tubes at the baffles and perpendicular across the tubes between the baffles. In the actual exchanger, the fluid would cut diagonally across from one baffle opening to the next and would flow parallel to the tubes only at the outer edge of the turn around the baffle. Consequently, in the actual exchanger, the height of the baffle or the shell diameter, the distance from one baffle to the next, the size of the opening for flow at the baffle, the tube size and spacing, and the shell length would affect the actual stream path and, in that way, the cross-sectional area of the stream path and hence the effective velocity. The total length of the exchanger would, as has been mentioned previously, control the total number of turns around the baffle edge, with a given baffle spacing, thus affecting the rotation of the fluid stream.

The effect of the length on the velocity for the orifice type can be justified only as an end effect, which effect should decrease as the length of the exchanger is increased. In this correlation, however, it was assumed that the over-all transfer coefficient was constant for the entire transfer surface, but with petroleum oils with an appreciable change in temperature this is not true. For a cooling of the shell fluid, a decrease would take place in the over-all transfer coefficient. This change in the over-all transfer coefficient would increase with the length of the exchanger and, since this correlation was made from the basis of the heat-transfer rate, the length would enter into the resulting relations. This length effect is shown, by Equation [2] for the effective velocity and Equation [6] for the heat-transfer coefficient with G_s, to cause an increase in the effective velocity or the heat-transfer rate, respectively, approximately as a square-root function of the length.

The data which were used in the orifice-baffle correlation were obtained from exchangers that had lengths of 5, 10, and 19.6 ft, respectively, all other factors being relatively the same for these units. Part of this variation with length may be a result of the method of calculating the coefficient for the tube side, since the longer exchangers would have a calculated tube-side coefficient lower than the shorter ones. Other conditions being the same, the resultant shell-side coefficient would be higher. The experimental data, however, show an increase of only 3.5 and 9 per cent, respectively, for the 10- and 19.6-ft-length exchangers when the tube length is omitted from the calculations for the tube-side

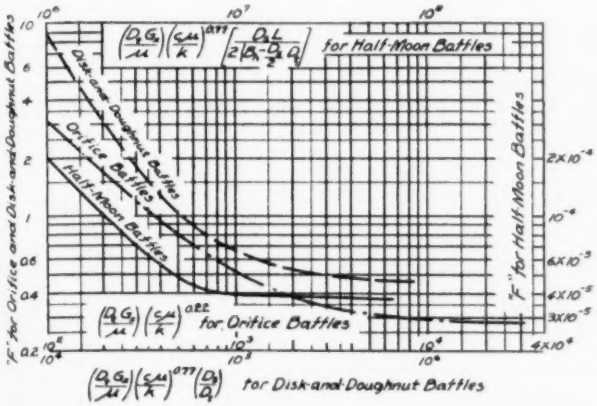


FIG. 6 FRICTION FACTOR-ROUGHNESS CURVES FOR SHELL-AND-TUBE HEAT EXCHANGERS

[For the correlation of data for the curves in Fig. 6, see pp. 29, 31, and 32 of reference (13).]

coefficient, as compared with the coefficient calculated with the tube length in the equation.

Fig. 5 shows all of the data from the tests used in the original correlation, plotted with the use of the effective velocity given by Equations [2], [3], and [4].

PRESSURE-DROP RELATIONS

The drop in pressure through the shell side of these exchangers may be obtained by means of the Fanning equation and the curves of Fig. 6, that is, the pressure drop is given by Equation [10], if the friction factor has been obtained for the particular baffle type from Fig. 6 and Equations [11], [12], and [13].

$$\Delta p = \frac{f L G_s^2}{2(3600)^2\, \rho g D_i} \qquad [10]$$

Orifice baffles

$$f = \left(\frac{P - D_i}{P}\right)^2 \left(\frac{D_s}{D_s - D_i}\right) \frac{F}{(N_b - 2.5)^{0.15}} \qquad [11]$$

Half-moon baffles

$$f = \left(\frac{D_s}{S}\right)^{0.7} \left[20 + \left(\frac{P - D_i}{P}\right)\left(\frac{D_s}{D_i}\right)\right]^{2.87} F \qquad [12]$$

where

$$(S/D_s)^{0.7} = 0.795 \text{ for } S \gtrless 0.36 \text{ ft}$$

Disk-and-doughnut baffles

$$f = \left(\frac{P - D_i}{P}\right)\left(\frac{A_s}{A_h}\right)^{0.8} F \qquad [13]$$

Rather than have individual curves for each exchanger design and arrangement, which would be normal when compared to the different degrees of roughness in a pipe, and also in order to allow for the orifice effects as a roughness factor, all of the factors which appear to affect the flow resistance in any way are used as a roughness effect and introduced as a correction to the friction factor. Likewise, the effect of heating and cooling is shown by the Prandtl number function by which the Reynolds number is multiplied.

GENERAL CONCLUSIONS

The author has attempted to present a résumé of most of the experimental and analytical work which has been done on the heat-transfer rate and pressure drop on the shell side of the tubes of shell-and-tube exchangers, pointing out, in a more or less progressive manner, the factors which affect the heat transfer and pressure drop, and how these factors could affect these quantities. The correlations presented are not rationally based, except in so far as the fluid properties, fluid velocity, and dimensions of the exchanger are involved, but an attempt has been made to show that the effective velocity as used has a rational foundation. If a fluid flows through an irregular-shaped passage so that its velocity changes periodically, the average velocity will be an average of the instantaneous rates at different points and it may be necessary to make use of the physical dimensions of the passage to obtain the weighted average. The basic error involved in this correlation, as the author sees it, is that the heat-transfer coefficient was used as the governing indicator of what factors caused a variation in the velocity and thus determined what things should be used to determine what weight should be placed on the velocity in each repeating section.

BIBLIOGRAPHY

1 "Heat Transfer in a Commercial Exchanger," by B. E. Short and M. M. Heller, Bulletin No. 3128, The University of Texas, 1931.

2 "Heat Transfer for Water Flowing Inside Pipes," by W. H. McAdams and T. H. Frost, *Refrigerating Engineering*, vol. 10, 1924, pp. 323–332.

3 "Heat Transfer for Oils and Water in Pipes," by F. H. Morris and W. G. Whitman, *Industrial and Engineering Chemistry*, vol. 30, 1928, pp. 234–240.

4 "Heat Transmission," by W. H. McAdams, McGraw-Hill Book Company, Inc., New York, N. Y., 1933, pp. 228–232.

5 "Wärmeübergang von Öl an Wasser," by E. Heinrich and R. Stückle, V.D.I. *Forschungsarbeiten*, no. 271, 1925.

6 "A Method of Correlating Forced Convection Heat Transfer Data and a Comparison With Fluid Friction," by A. P. Colburn, Trans. American Institute of Chemical Engineers, vol. 29, 1933, pp. 174–209.

7 "Fluid Friction at Parallel and Right Angles to Tubes and Tube Bundles," by E. N. Sieder and N. A. Scott, Jr., A.S.M.E. unpublished papers, no. 83, 1932.

8 "Effect of Diameter Spacing, Etc., on Pressure Drop Around Tubes of Shell Type Heat Exchanger," by B. E. Short and T. F. Stack, *Oil and Gas Journal*, vol. 32, May 10, 1934, pp. 115, 116, 118, 120.

9 "Pressure Drop and Heat Transfer in Exchangers," by S. A. Perrone, *Oil and Gas Journal*, vol. 33, March 28, 1935, pp. 71, 72, and 75, 76.

10 "Investigation of Heat Transfer Rates on the External Surface of Baffled Tube Banks," by R. A. Bowman, in "Heat Transfer," A.S.M.E. unpublished papers, no. 28, 1936, pp. 75–81.

11 "Heat Transfer and Pressure Drop in Heat Exchangers," by Byron E. Short, The University of Texas, Bulletin No. 3819, May, 1938.

12 "Correlation and Utilization of New Data on Flow Resistance and Heat Transfer for Crossflow of Gases Over Tube Banks," by E. D. Grimison, Trans. A.S.M.E., vol. 59, 1937, pp. 583–594.

13 "Heat Transfer Coefficients and Friction Factors for Heat Exchangers," by B. E. Short, Thesis, Cornell University, Sept., 1939; abstract published by Cornell University Press, 1939.

14 "Heat Transfer and Pressure Drop of Liquids in Tubes," by E. N. Sieder and G. E. Tate, *Industrial and Engineering Chemistry*, vol. 28, 1936, pp. 1429–1435.

15 "Technical Data on Fuels," by A. G. Hinton, quoted by H. M. Spiers, World Power Conference Report, London, 1928, pp. 101–103.

16 "Convection of Heat in Fluid Flow Through Tubes," by H. F. P. Purday, *Nature*, vol. 119, 1927, p. 527.

17 "Experimental Work for Thesis," by W. A. Randle, University of Texas, 1940.

18 "Mean Temperature Differences in Multipass Heat Exchangers," by W. M. Nagle, *Industrial and Engineering Chemistry*, vol. 25, 1933, pp. 604–609.

19 "Mean Temperature Difference in Design," by R. A. Bowman, A. C. Mueller, and W. M. Nagle, Trans. A.S.M.E., vol. 62, 1940, pp 283–294.

Condensation of Saturated Freon-12 Vapor on a Bank of Horizontal Tubes

By F. L. YOUNG,[1] QUINCY, MASS., AND W. J. WOHLENBERG,[2] NEW HAVEN, CONN.

The condensate film formed on tubes below the top tube, in a vertical bank of horizontal tubes, differs from that formed on the top tube because condensate formed on higher tubes drops or runs off to lower tubes, thus affecting the rate of heat transfer at the lower tubes. This paper includes the results of an experimental investigation of such effects on the heat transfer when saturated Freon-12 vapor condenses on the outsides of such a bank of tubes. The result as to film coefficient is correlated with Nusselt's number for condensation and reasonably good agreement is found with the results deduced from Nusselt's theory of condensation in so far as trends are concerned.

Nomenclature

The following nomenclature is used in the paper:

- A = area of heat-transfer surface, sq ft
- D = outside diameter of tube, ft
- Γ = weight rate of condensate flow per unit perimeter, lb per ft per hr
- g = acceleration due to gravity, 4.18×10^8 ft per hr per hr
- h = film coefficient of heat transfer, Btu per sq ft per deg F per hr
- k = thermal conductivity, Btu per sq ft per deg F per ft per hr
- μ = viscosity of condensate, lb per ft per hr
- n = number of pipes high in horizontal condenser
- N_u = Nusselt's number for condensation $\dfrac{r\rho^2 k^3 g}{D\mu\,\Delta t}$
- ρ = specific weight, lb per cu ft
- r = latent heat, Btu per lb
- t_g = temperature of saturated gas in condenser, deg F
- t_p = temperature corresponding to condenser pressure, deg F
- t_s = temperature of tube surface, deg F
- Δt = temperature difference between gas and tube surface $(t_g - t_s)$, deg F
- W = average weight of water flowing through each condenser tube, lb per min

Introduction

Much information has been published about the condensation of vapor upon a single horizontal tube. This applies to the performance of the top tubes in a condenser but, in the lower tubes in a bank, the rate of condensation decreases because of the fact that condensate falling from above increases the film thickness on the lower tubes and thus increases their resistance to heat flow. For the condition in the lower tubes of a bank, adequate experimental results have not been available. In lieu of this, Nusselt's (1)[3] theoretical approach to the problem may be employed. The results of his theory show the variation in heat-transfer coefficient from tube to tube in a vertical bank of horizontal tubes. One object of the present investigation is to compare Nusselt's theoretical results with those from experiment.

Because few data have been published for condensing Freon-12 (dichlorodifluoromethane), which is widely used in the refrigeration and air-conditioning industries, the experiment was performed with this fluid. Thus, the experimental results add to the information on heat transfer for a single tube, as well as furnish the data necessary for a check on Nusselt's theory for a bank of tubes.

Apparatus

The experimental work was conducted with a horizontal condenser, Fig. 1, consisting of 5 copper tubes, $^3/_4$ in. OD, 41 in. long, with axes in a vertical plane. The shell was composed of a piece of 10-in. pipe with welded heads. A 4-in. flanged side outlet was provided at the center to permit observation of the central portion of all the tubes through a $2^1/_2$-in. sight glass during operation. This outlet facilitated assembly and furnished a convenient space for the glands through which insulated thermocouple leads were brought out.

The tubes were fastened into the heads with tubing fittings. To insure accurate alignment and spacing of the tubes, holes for the fittings were bored and tapped on a horizontal boring machine.

Thermocouples were installed on the outer surface of the tubes to indicate surface temperature and inside the tube to indicate the temperature of the cooling water. The condenser and all gas pipes were insulated with 2 in. of hair felt.

Cooling water was supplied to the tubes from a header. Low velocities of flow were used to obtain satisfactory temperature rise of the cooling water between the thermocouple stations within the tubes. Swirl strips were inserted through the full length of tubes in order to agitate the water. This insured that the thermo-

[3] Numbers in parentheses refer to the Bibliography at the end of the paper.

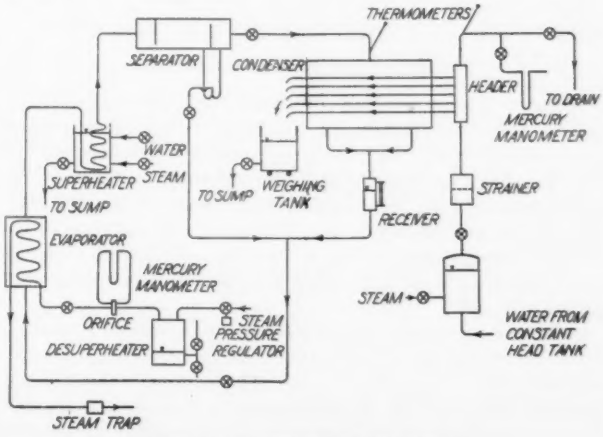


Fig. 1 Diagram of Apparatus

[1] Bethlehem Steel Company, Shipbuilding Division, Fore River Yard, Quincy, Mass.

[2] Professor of Mechanical Engineering, Yale School of Engineering, Yale University. Mem. A.S.M.E.

Contributed by the Heat Transfer Division and presented at the Spring Meeting, Houston, Texas, March 23–25, 1942, of The American Society of Mechanical Engineers.

Note: Statements and opinions advanced in papers are to be understood as individual expressions of their authors and not those of the Society.

couples would indicate the average temperature rather than the core temperature of the water.

To provide steady operating conditions and to prevent contamination of the Freon-12, a closed circuit operating at one pressure was employed. This consisted of the condenser, a small receiver, a steam-heated evaporator, a gas heater, and a separator. The general features of this system had previously been employed by the York Ice Machinery Corporation, York, Pa., in experiments on Freon. The particular arrangement employed in these tests is shown diagrammatically in Fig. 1.

The evaporator was placed at the bottom of the Freon circuit. The gas from the evaporator flowed through the superheater into the separator, where entrained liquid was removed, and then into the condenser shell. Condensate passed through the receiver and returned to the evaporator by gravity. The water temperature in the superheater was controlled by injecting steam into it.

A steady flow of condenser cooling water was obtained by using a large constant-head tank, which discharged into a mixing chamber, where the water could be steam-heated to any desired temperature. A calibrated orifice was placed in each of the tubes at the header to insure equal distribution of cooling water among the tubes.

Tube-Surface Temperature Measurement

Since this was an investigation of only the film coefficient and not the over-all coefficient for condensing Freon-12, it was important to measure surface temperatures as accurately as possible. This was done by means of copper-constantan thermocouples installed in the manner employed by Colburn and Hougen (2). Three slots, 1 in. long, 0.025 in. deep, and 12 in. apart, were milled into the central section of each tube. The thermocouples were butt-welded so that they could fit into the slots. The junctions were soldered into the centers of the grooves and the leads wrapped with thread and pressed into a litharge-glycerine compound, one lead running in each end of the slot. The soldered junctions were filed flush with the tube wall. This construction left the condensing surface practically unaltered and offered thermal contact for the leads, hence heat flowing along the wire from the hot gas was transferred to the tube rather than to the junction. Also, the leads were electrically insulated from the tubes so that the surface temperature at the junction rather than an average temperature was measured.

Baker and Mueller (3) have found that on a horizontal condenser tube, the average surface temperature is found on the side near a point 90 deg from the vertical. Since it was important to measure average temperature, and because the least mechanical difficulties would be encountered in this position, the thermocouples were placed in the tube wall 90 deg from the vertical.

Water-Temperature Measurement

Water temperatures were measured by traveling thermocouples supported inside the condenser tubes by $^3/_{16}$-in-OD stainless-steel tubes. Two thermocouples were carried in the end of each. These extended slightly beyond and to the side of the end of the supporting tube, so that the distance between the junctions was approximately $^3/_8$ in. The end of each tube was fitted with two fingers which guided it through a slot in the center of each swirl strip, thus preventing the thermocouples from contacting the strip.

In order to overcome end effects, the thermocouples were inserted approximately 6 in., so that a 24-in. test section was established in the center of each tube. The location of these almost coincided with the wall thermocouples, so that the surface and water temperatures could be measured at the beginning and end of each test section.

Calibration of Thermocouples

The tube-wall thermocouples were calibrated in place on the tubes before and after installation in the shell, and curves were drawn.

The water thermocouples were wired to the switchboard and then calibrated together. A single curve sufficed for these. There were 37 thermocouples in the apparatus. To avoid interconnection and current flow along the tube, each hot junction had its own cold junction in an oil bath kept at 32 deg F. Double-pole copper switches were connected with a potentiometer which was accurate to 0.3 deg F.

Other Measuring Instruments

The condenser pressure was measured by a 300-lb test gage, graduated in 1-lb intervals. Two thermometers with 1-deg divisions were placed in shielded wells 6 in. from each end of the shell to measure gas temperature. Two thermocouples inside the shell also measured gas temperature. The temperature of the gas at the condenser inlet was measured by a thermometer with 1-deg divisions.

Charging the System

Before charging, the system was evacuated with a laboratory pump capable of reducing the pressure to 10^{-3} in. of mercury. The system was then charged with Freon gas until the pressure rose to 10 psi. After standing for 24 hr, the system was again evacuated and then charged with 85 lb of commercially pure Freon-12.

Experimental Procedure

In operating the system, the condenser pressure was controlled by regulating the steam flow to the evaporator. Surface temperature of the tubes was controlled by varying both the initial temperature and velocity of the cooling water. In order to insure mixing, the rate of water flow through each tube was kept above 4 lb per min. At the same time, conditions were controlled so that there was at least a 5-deg temperature rise of the water flowing through each test section.

After test conditions had been established, the system was allowed to run for one hour before data were taken. Then the following measurements were made; three temperatures on each tube wall, two water temperatures at the inlet and outlet of each test section, four condenser-gas temperatures, the temperature of the gas entering the condenser, condenser pressure, total weight of water flowing through all the tubes, and the weight of water flowing through each individual tube. A run consisted of taking three complete sets of these data. Check runs were also made, but only two sets of data were taken during these.

After the bank of five tubes had been tested, the consistency of the data was investigated by blanking off the top tubes, one at a time, and operating this smaller number of tubes over the range of test conditions. For example, the first tube in the bank was plugged so that no cooling water ran through it, thus making it inactive as a condensing surface. Hence, there were only four tubes in the bank, the original second tube now becoming the first. This process was carried on until banks of five, four, three, and two tubes had been tested. In this manner, each tube was tested in a number of relative positions in the tube bank. During these later investigations, observations were made frequently to be certain that the inactive top tubes were not condensing gas.

Experimental Results

A total of 73 runs was made with saturated Freon-12 vapor at condensing temperatures varying according to the following schedule:

Saturation temperature, F	Mean temperature difference ($t_g - t_s$)
85	10
95	10, 15
105	10, 15, 20
115	15, 20, 25, 30
125	30

In order to insure reasonable accuracy in the determination of temperature differences, the apparatus was operated so that the temperature difference between the gas and the tube walls exceeded 10 deg F; the cooling-water temperature rise in the test sections was at least 5 deg F; the cooling-water flow rate was 4 or more pounds per minute to insure turbulence; and the measured condenser-gas temperature was within ± 1 deg F of t_g.

Characteristics of Film

Observation of the tube through the sight glass showed that, under all conditions and rate of condensation, a very quiet, streamline film formed on the first tube in the bank. At the bottom of the tube, the liquid formed drops which fell to the second tube. These did not always fall from the same point; at times the point of origin of each moved back and forth along the tube. At high rates of condensation, these drops became small streams.

The films on all the tubes below the first in the bank were definitely disturbed at all rates of condensation. Their characteristics are best illustrated by conditions existing when condensation started. A quiet, streamline film formed on all the tubes. A drop falling from above struck a tube and fell down over the top of the existing smooth film. This formed a rivulet approximately 1/4 in. wide which increased the film thickness around that part of the tube. As the rate of condensation increased, the number of rivulets became greater until all but the first tube exhibited a rapidly moving, rippled film. For all but the lowest rates of condensation, the liquid fell off the bottom of each of the lower tubes in steady streams. Condensate drained vertically down each tube wall and, upon reaching the bottom, immediately dropped off, thus showing that all the tubes were horizontal. Under no conditions was any liquid seen to break away from the film and drop off the tube before reaching the bottom.

End Effects

Several tests were made to determine end effects. This was done by including a greater length of the tube as a test section than the usual 24-in. length employed in the run of tests. With tube-wall temperatures of 95 deg F, among the highest used in testing, average values of h were only slightly different from those found in the regular runs. It was concluded that whatever end effects did exist were small.

Comparison of Results

In order to compare Freon-12 with other fluids, all test results are given in terms of heat-transfer coefficient, h, and Nusselt's number, N_c. This also simplifies the analysis and permits all data to be plotted against only two variables, since Nusselt's number takes into account the slight changes in physical properties of the fluid in this temperature range. In computing the data, the total surface of each 24-in. test section was used as the area for heat transfer. The heat flow through it was computed by multiplying the cooling-water rate by the water-temperature rise. The mean temperature difference between the gas and the tube wall was obtained by plotting the three wall temperatures and the gas temperature and then integrating the plot with a planimeter. In evaluating Nusselt's number, the physical properties of the fluid were taken at an average between the wall and the gas temperatures.

Experimental results for a bank of five tubes are given in Table 1. Results of the tests upon banks of four, three, and two tubes are summarized in Tables 2, 3, and 4. Tubes are designated A to E, going from the top to the bottom of the bank. Relative positions in the bank are numbered from 1 to 5, counting from the top tube. For example, tubes B, C, D, and E were in relative position 2 during the tests upon banks of five, four, three, and two tubes, respectively.

The data are plotted in Figs. 2 to 7, inclusive. A straight line with the theoretical slope of Nusselt's equation is drawn through each set of points. This is justified by McAdams' (4) correlation

TABLE 1 SUMMARY OF RESULTS FOR CONDENSING SATURATED FREON-12 ON A BANK OF FIVE TUBES

Run no.	t_c, deg F	Film coefficient, h, for tube no. 1	2	3	4	5	Δt for tube no. 1	2	3	4	5	$Nc \times 10^{-10}$, Nusselt's number for tube no. 1	2	3	4	5	W
37	85.9	180	316	274	248	177	8.2	9.7	9.1	11.0	10.9	6.45	5.45	5.8	4.84	4.89	3.7
42	95	190	302	276	218	200	11.3	12.3	12.2	12.6	13.8	4.29	3.94	3.98	3.89	3.54	3.9
36	96	204	287	235	205	164	12.8	14.2	13.9	14.8	16.8	3.78	3.41	3.48	3.27	2.91	4.0
41	95	165	216	236	188	180	13.5	15.8	16.1	16.7	17.5	3.62	3.14	3.08	2.98	2.84	3.9
35	96	186	232	244	192	191	14.1	16.5	15.8	17.1	17.8	3.44	2.97	3.09	2.86	2.78	4.0
29	104.5	259	301	272	254	197	9.2	9.6	9.3	9.9	11.6	4.69	4.54	4.64	4.3	3.76	4.8
31	104.7	260	228	246	205	160	9.8	11.3	10.3	11.6	13.0	4.4	3.86	4.21	3.74	3.37	4.7
30	104.3	264	263	253	232	213	12.8	13.7	13.2	14.0	15.6	3.44	3.21	3.31	3.14	2.86	4.8
46	106	218	226	232	197	186	15.3	17.0	16.2	18.0	19.0	2.86	2.58	2.71	2.45	2.34	4.6
13	104.5	261	302	252	181	...	15.6	16.8	15.9	16.7	...	2.83	2.65	2.8	2.66	...	4.0
45	106	190	250	243	199	192	19.3	21.2	21.0	22.9	24.0	2.29	2.12	2.14	1.98	1.90	4.6
34	106	183	232	238	190	176	19.7	21.8	21.4	22.8	23.4	2.26	2.06	2.09	1.99	1.93	5.2
33	105.7	208	256	244	225	206	20.5	22.7	22.7	23.4	24.5	2.18	1.99	1.99	1.94	1.86	5.2
12	105.6	241	209	210	179	...	21.1	22.1	21.5	22.3	...	2.14	2.04	2.10	2.02	...	5.4
32	106	172	232	214	183	177	22.2	24.1	23.7	24.5	25.9	2.02	1.89	1.92	1.85	1.76	5.2
8	116.4	228	277	272	190	...	17.3	19	17.4	20.9	...	2.26	2.08	2.25	1.91	...	3.4
48	114.7	184	210	234	174	165	20.4	23	22.7	24	24.9	1.97	1.76	1.78	1.70	1.64	4.4
49	114.4	161	226	224	190	191	23	24.6	24.6	26.6	27.4	1.77	1.66	1.66	1.55	1.51	4.3
47	117	163	218	219	183	178	28.9	30.8	30.2	31.7	32.9	1.4	1.32	1.35	1.29	1.25	5.9

TABLE 2 SUMMARY OF RESULTS FOR CONDENSING SATURATED FREON-12 ON A BANK OF FOUR TUBES

Run no.	t_c, deg F	Film coefficient, h, for tube no. 1	2	3	4	Δt for tube no. 1	2	3	4	$Nc \times 10^{-10}$, Nusselt's number for tube no. 1	2	3	4	W
53	106.7	290	262	180	170	12.2	12.4	14.7	15.6	3.46	3.41	2.92	2.77	3.8
25	103.8	254	260	189	188	15.7	16	16.7	18.7	2.84	2.74	2.7	2.43	3.8
51	106	238	264	192	166	16	15.7	18.4	19.7	2.74	2.79	2.4	2.16	4.2
52	105.1	296	283	229	208	19.2	19.3	22.3	23.1	2.34	2.33	2.04	1.97	5.0
61	107.5	244	258	199	180	19.8	20.2	22.1	23.8	2.21	2.16	2.0	1.85	4.8
50	106.3	289	286	240	208	20.2	20.3	23.1	24.4	2.19	2.18	1.94	1.85	5.2
59	115.8	210	234	174	180	17.1	16.7	19.9	20.2	2.28	2.34	1.98	1.95	5.1
60	117.4	236	250	195	188	18.1	18	20.4	21.6	2.12	2.14	1.91	1.80	5.0
54	114.8	240	232	198	159	20.7	20.4	23.6	24.6	1.94	1.97	1.72	1.66	5.5
57	117	241	254	188	177	22.5	22.6	25.9	26.7	1.74	1.73	1.54	1.49	5.0
58	118	248	260	190	204	22.7	22.8	26	26.6	1.71	1.70	1.51	1.47	5.0
55	116.2	236	232	180	159	25.2	25.3	28.3	29.7	1.59	1.59	1.43	1.38	5.4
56	115.5	204	220	183	174	25.8	25.9	28.7	29.8	1.58	1.57	1.43	1.38	5.9

TABLE 3 SUMMARY OF RESULTS FOR CONDENSING SATURATED FREON-12 ON A BANK OF THREE TUBES

Run no.	t_c, deg F	Film coefficient, h, for tube no. 1	2	3	Δt for tube no. 1	2	3	$N_c \times 10^{-10}$, Nusselt's number for tube no. 1	2	3	W
68	94.3	348	274	215	10.6	12.5	14.5	4.58	3.92	3.4	4.1
63	105.2	324	222	200	11	13.7	14.5	3.94	3.19	3.02	5.0
62	105.5	288	228	195	18.1	20.8	22.4	2.46	2.16	2.02	5.4
65	115.5	301	224	204	15.9	18.9	20.4	2.46	2.08	1.94	5.3
66	116.4	323	226	211	19.2	22.1	24.2	2.04	1.78	1.65	5.3
67	115.4	294	248	220	23.4	26.3	28.6	1.72	1.54	1.44	6.0
64	116.8	271	181	175	23.6	27	29.5	1.68	1.5	1.38	5.4

TABLE 4 SUMMARY OF RESULTS FOR CONDENSING SATURATED FREON-12 ON A BANK OF TWO TUBES

Run no.	t_c, deg F	Film coefficient, h, for tube no. 1	2	Δt for tube no. 1	2	$N_c \times 10^{-10}$, Nusselt's number for tube no. 1	2	W
69	93.8	296	222	11.4	12.7	4.3	3.87	4.1
71	104	246	190	13.5	15.5	3.27	2.88	5.1
70	106.6	236	181	18.6	20.5	2.35	2.16	5.0
72	113.9	195	177	20.6	23.4	1.96	1.75	4.9

of condensation data, which shows that Nusselt's curve gives a fairly good correlation throughout the range of N_c.

To obtain the curve for any one tube position, data for all the individual tubes in that position are plotted and averaged. This is done by drawing the curve so that the sum of the differences between the curve and the points above the line is equal to a similar sum below the line. Thus, results from tubes B, C, and D are combined to obtain the curve for No. 1 tube in the bank. The data show quite a deviation from the average, but this is small in comparison with the wide spread of most experimental data.

While the variation in film coefficient, h, with tube position, as shown in Fig. 8, is similar to that predicted by Nusselt, it is not so great. This may be explained by the fact that Nusselt developed his theory by assuming streamline conditions, while in the actual case the condensate film on the lower tubes is rippled and disturbed by drops from the upper tubes. These ripples produce convection as well as conduction in the condensate layer, thus increasing the rate of heat flow through the film. Furthermore, as shown by Nagle and Drew (5), the presence of ripples on the tubes can account for these higher rates, because thermal resistance is reduced more by a trough than it is increased by a crest.

From these curves, the following set of equations for the film coefficient, h, on the gas side of a horizontal multitubular condenser are given. The experimental values are compared with theoretical values predicted by Nusselt and by McAdams. The equations are as follows:

This experiment	Nusselt	McAdams
Tube 1 $h = 0.655 \sqrt[4]{N_c}$	$0.725 \sqrt[4]{N_c}$	$0.725 \sqrt[4]{N_c}$
Tube 2 $h = 0.576 \sqrt[4]{N_c}$	$0.493 \sqrt[4]{N_c}$	$0.61 \sqrt[4]{N_c}$
Tube 3 $h = 0.551 \sqrt[4]{N_c}$	$0.436 \sqrt[4]{N_c}$	$0.551 \sqrt[4]{N_c}$
Tube 4 $h = 0.498 \sqrt[4]{N_c}$	$0.401 \sqrt[4]{N_c}$	$0.513 \sqrt[4]{N_c}$
Tube 5 $h = 0.464 \sqrt[4]{N_c}$	$0.375 \sqrt[4]{N_c}$	$0.485 \sqrt[4]{N_c}$

An attempt was made to correlate the total weight of condensate flowing over each tube with Reynolds number $4\Gamma/\mu$, but no relationship could be established.

Variation of Δt in the Tube Bank

Cooling water entered all tubes at the same temperature; however, the wall temperature decreased going down the tube bank. Therefore, the temperature difference $(t_g - t_s)$, increased as the tube was placed lower in the bank. This variation is shown in Fig. 9, which indicates that the change in Δt is affected by condensing temperature. This is explained by the fact that an increase in temperature will decrease the thermal conductivity of the liquid. At the same time, the latent heat decreases, thus allowing more vapor to condense for a given rate of heat flow. This increased condensation will counteract the tendency of the film to become thinner due to a decrease in viscosity, hence the decrease in thermal conductivity will create a greater temperature drop across the condensate film.

Acknowledgment

The authors wish to express their appreciation to Prof. M. L. Wiedmann for his most helpful assistance in the design and construction of the apparatus, and for his many suggestions and interest while the experimental work was in progress.

Bibliography

1 "Die Oberflächenkondensation des Wasserdampfes," by W. Nusselt, *Zeitschrift des Vereines deutscher Ingenieure*, vol. 60, 1916, pp. 541–546, and 569–575.

2 "Studies in Heat Transmission," by A. P. Colburn and O. A. Hougen, Engineering Experiment Station, University of Wisconsin, Bulletin 70, 1930, p. 69.

3 "Condensation of Vapors on a Horizontal Tube," by E. M. Baker and A. C. Mueller, Trans. American Institute of Chemical Engineers, vol. 33, 1937, pp. 531–558.

4 "Heat Transmission," by W. H. McAdams, McGraw-Hill Book Company, Inc., New York, N. Y., p. 260.

5 "The Dropwise Condensation of Steam," by W. M. Nagle and T. B. Drew, Trans. American Institute of Chemical Engineers, vol. 30, 1933–1934, pp. 217–255.

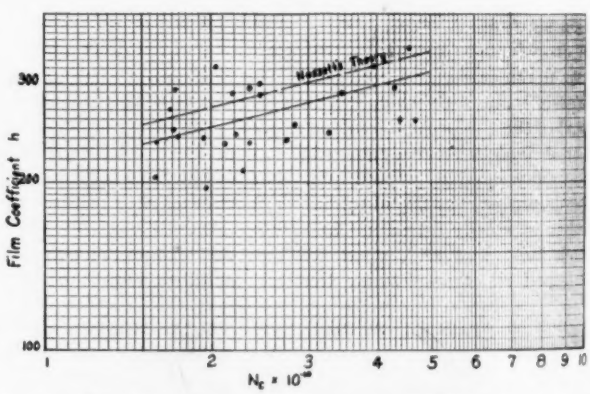


FIG. 2 FILM COEFFICIENT FOR CONDENSATION UPON FIRST TUBE IN BANK

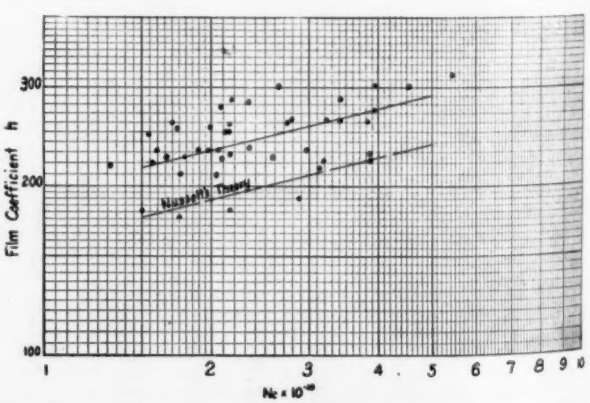


FIG. 3 FILM COEFFICIENT FOR CONDENSATION UPON SECOND TUBE IN BANK

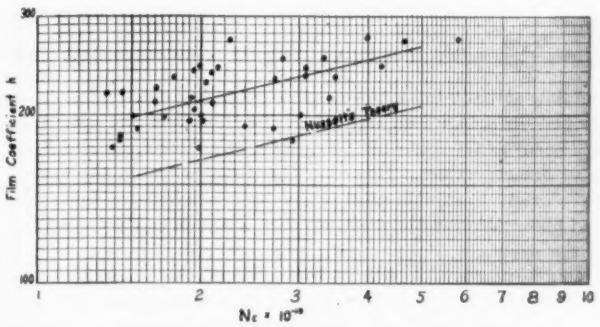


FIG. 4 FILM COEFFICIENT FOR CONDENSATION UPON THIRD TUBE IN BANK

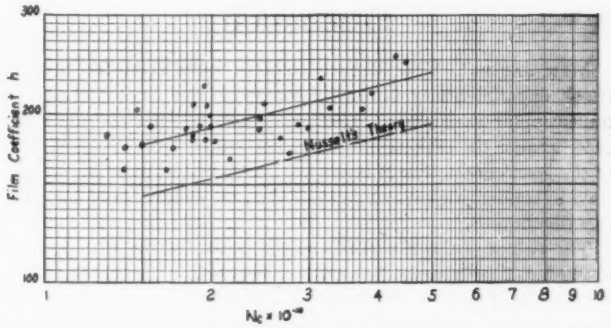


FIG. 5 FILM COEFFICIENT FOR CONDENSATION UPON FOURTH TUBE IN BANK

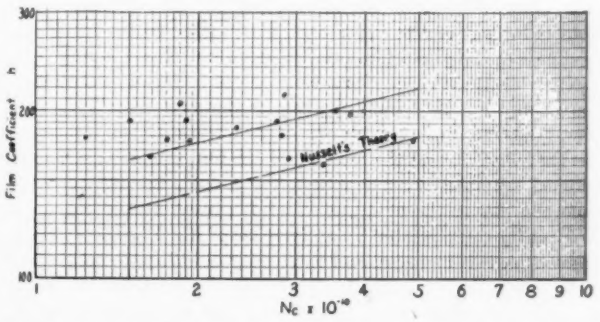


FIG. 6 FILM COEFFICIENT FOR CONDENSATION UPON FIFTH TUBE IN BANK

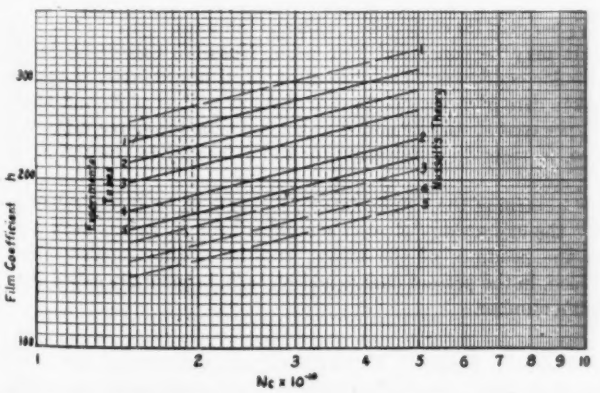


FIG. 7 FILM COEFFICIENT FOR CONDENSATION UPON A BANK OF FIVE HORIZONTAL TUBES

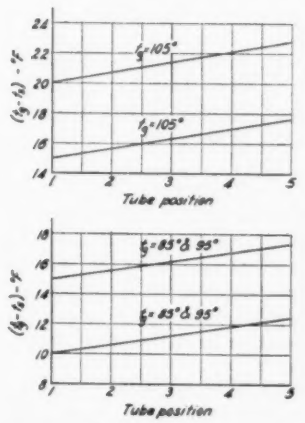


FIG. 9 VARIATION OF $(t_g - t_s)$ WITH RELATIVE POSITION OF TUBE IN BANK

(Entering water temperature same for all tubes.)

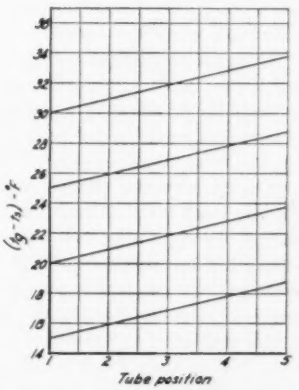


FIG. 10 VARIATION OF $(t_g - t_s)$ WITH RELATIVE POSITION OF TUBE IN BANK

(Entering water temperature same for all tubes; t_g 115 F.)

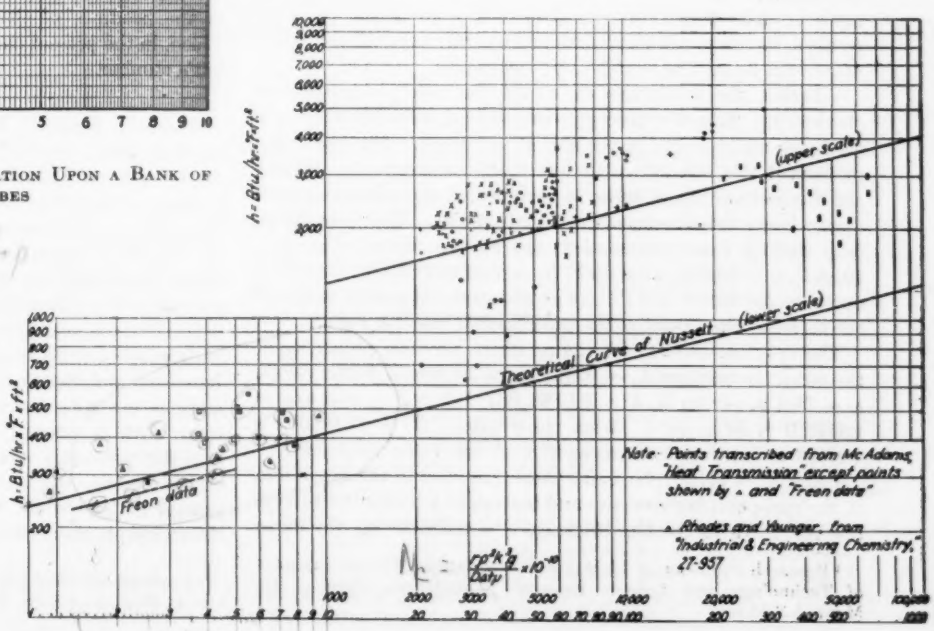


FIG. 8 CORRELATION OF DATA FOR CONDENSING VAPORS ON SINGLE HORIZONTAL TUBES

Discussion

MAX JAKOB.[4] The authors seem to have been the first to check experimentally Nusselt's theory of the heat transfer in multitubular condensers. Their contribution is particularly valuable because the experiments were performed with Freon-12, one of the least conducting of liquids, whereas water, most frequently used in condensing experiments, is the best conductor of the nonmetallic liquids.

The values of the film coefficient h, measured on tube A, were discarded, their average being 25 per cent below that of the values for the three other tubes when each of them was used as the uppermost in the condenser. The maximum deviations of the latter values from the adopted mean lines were of the order of ± 20 per cent, whereas the averages of the deviations were well in the range of ± 10 per cent. This is not excessive compared with the results of similar experiments. The lines, according to Nusselt's theory shown in Fig. 7 of the paper, deviate by 10 to 20 per cent from the adopted experimental lines. Thus the agreement as an average is quite satisfactory.

However, the differences between the experimental and theoretical values have a systematical trend which may be explained. It seems to be due mostly to an apparent deficiency in Nusselt's theory and partly to a difference of the present experimental conditions from those supposed in the theory.

The questionable point in the theory is that it leads to an infinitely thick layer of liquid on the top line of any horizontal tube except the uppermost one. The same holds for the bottom line of each tube, but this does not greatly affect the result; for, even so close to the bottom as $^1/_{50}$ of the circumference, the film is not appreciably thicker than at any place around the tube, and drops on the bottom have practically the same insulating effect which an infinitely thick layer would have.

It is different at the top line. There, an infinitely thick layer would not be stable, but the liquid falling upon the top of the tube will cause a considerable heat transfer under impact conditions spread over a somewhat extended region at the top of the tube. This holds whether drops or streams hit the tube. In the former case, however, the film will be very thin between the spots hit by drops, so that in these regions the heat transfer will be as good as on the top of the first tube. On the places upon which drops fall, turbulent flow must start as observed by the authors. This, however, may turn into streamline flow even in the observed rivulets, for these can be maintained by differences in the thickness of the liquid film as well as by turbulence.

Whether the conditions of turbulence will persist can be checked by Nusselt's theory, which includes formulas for the thickness and velocity of the film at any place. The writer has performed this calculation for the middle between the top line and the bottom line of tubes in position No. 2, under the conditions which existed in runs Nos. 30, 51, and 71. These runs differ only slightly from one another, the average data being t_g = 104.8 F, t_s = 89.8 F, Δt = 15 F, $N_c = 2.94\,(10^{10})\,\mathrm{B^4hr^{-4}\,ft^{-8}\,F^{-4}}$, and h = 258 $\mathrm{Bhr^{-1}\,ft^{-2}\,F^{-1}}$, in good agreement with $h \approx 254$ at the corresponding point of the experimental line 2 in Fig. 7.

The best known data for the pertinent physical properties at the mean temperature t_m = 97.3 seem to be r = 57.6 Btu per lb, ρ = 79.8 lb per cu ft, $k = 0.0483\ \mathrm{Bhr^{-1}\,ft^{-1}\,F^{-1}}$, and $\mu/g = 1.417(10^{-9})$ lb hr $\mathrm{ft^{-2}}$. With these values, $N_c = 3.10(10^{10})$ is derived in satisfactory agreement with the value mentioned.

Using $N_c = 3(10^{10})$, Nusselt's theory, applied to the liquid film at the mid-point between top and bottom of a horizontal tube in row No. 2, yields the film thickness s = 0.000194 ft; the mean liquid velocity v_m = 702 ft per hr, and the Reynolds number $\mathrm{R} = \frac{4v_m s\rho}{\mu} = 75$. The latter being far below its critical value, the flow actually tends to become streamlined again after the described disturbance on the top of the tube, and the same thing will occur in the following tubes although there s, v_m, and R will have greater values. However, the disturbance on the top will be sufficient to explain most of the difference between calculation and observation in the positions Nos. 2 and 5, as shown in Fig. 7 of the paper.

In addition to this, it must be considered that Nusselt's theory is based on the assumption of a constant temperature difference Δt all over the tube bank. In the present experiments, however, according to the tables and Figs. 9 and 10, Δt increases between the first and fifth row by about 20 per cent of its original value. This is due to the decrease of the temperature drop between the inner tube surface and the cooling water. This decrease comes from reduction of the radial heat flow, owing to the increase in thickness of the liquid film between positions Nos. 1 and 5.

Nusselt's theory includes a constant of integration C which is increasing by 3.4278 from one row to the next one. This, however, holds only for Δt = const. If Δt increases, then C increases less than 3.4278, and the increase of the film thickness is likewise reduced. By this in the equation $h = K\sqrt[4]{N_c}$, the decrease of N_c from one row to the next one which is caused by the increase of Δt is partly compensated by an increase of K. The theory allows calculating this increase, and the writer did it approximately for tube positions Nos. 2 and 3. It was found that K for the second row is to be increased by $^3/_4$ per cent and for the third row by 2 per cent. The writer estimates that for the fourth and fifth rows of the bank K will increase by $3^1/_2$ and $5^1/_2$ per cent, respectively. This means that h, as represented in Fig. 7 of the paper by dotted lines Nos. 2 to 5, should be raised by $^3/_4$ to $5^1/_2$ per cent for comparison with the full lines.

It may be concluded that using Nusselt's theory for multitubular condensers, the change of Δt, if appreciable, should be taken care of in the calculation of N_c as well as of K, and about 10 per cent should be added to h at all tube rows except the first one, in order to compensate for the deficiency in the theory, as explained.

Concerning the nomenclature, it seems to be inconvenient to use the expression "Nusselt's number" for N_c as has been done in the headings of the tables, because a dimensionless group which, in the present case would be hs/k, is generally called Nusselt's number.

BYRON E. SHORT.[5] The authors state that several tests were made to determine the "end effects." As understood, this would imply that a change in diameter of the tubes, using the same length, would not increase or decrease the transfer rate either on the inside or on the outside. Present published work shows that the end effects become negligible as soon as the Reynolds number values reach 5000 to 6000. The analyses that have been presented are based largely on the correlation of the data of different experimenters and, in many cases, on results which were obtained with calming sections ahead of the heating or cooling section. Lawrence and Sherwood's work was performed without calming sections but with the use of thermocouples on the surfaces of tubes with condensing steam. Moynihan and Jeffrey showed that thermocouples on tube surfaces with condensing steam gave erratic results, and Lawrence and Sherwood's results show no general pattern which is explained by them as a result of the thermocouple usage. So, in the case of the present paper, it seems

[4] Research Professor of Mechanical Engineering, Illinois Institute of Technology and Armour Research Foundation, Chicago, Ill. Mem. A.S.M.E

[5] Professor of Mechanical Engineering, University of Texas, University Station, Austin, Tex. Mem. A.S.M.E.

that the authors are not entirely justified in saying that the end effects were not noticeable, since they used thermocouples on the surfaces with a condensing substance and obtained somewhat erratic results.

In connection with Fig. 7 of the paper, it would appear that the decrease in rate of heat transfer for tubes at lower and yet lower levels in a tube bank should become less, as indicated by Nusselt, and eventually reach a constant value. It seems that a limit should be reached to the thickness of the condensate film formed on the tubes, as lower ones in the bank are reached, since the gravitational and cohesion forces should arrive at a point of equilibrium. Then too, with the increased rate falling from above, the condensate film should move at a higher velocity and thus place a limit on the minimum value of the heat-transfer film. The author's values in Fig. 7, are contrary to this point of view.

S. P. Soling.[6] In presenting data for condensation of saturated Freon-12 vapor on a bank of horizontal tubes, the authors have performed a service of double value. The information on Freon-12 is a welcome addition to the literature. The data on the performance of tubes other than the top tube are also of great value.

There are, however, a number of points that appear to the writer to be questionable, or at least controversial. The clarification of these points would aid in the understanding of the results presented by the authors.

The first, and most important point involves the question of temperature difference. The authors cite the work of Baker and Mueller (3) to justify the use of a point 90 deg away from the vertical, as giving an average temperature. However, in the paper referred to, Baker and Mueller point out in their conclusions,[7] "the assumption that the position of the thermocouple halfway between the top and bottom will give the average temperature is erroneous." They further state, "there is no location for the thermocouple that can be depended upon to give correct average readings for the tube temperature."

Baker and Mueller's statements appear justified in the case of the present work and apparently explain the erratic behavior of the (Δt)'s tabulated in Table 1. Variations in water quantities through the different tubes would also account for the behavior. The lines drawn by the authors in Figs. 9 and 10 would not give the trend of various runs, as No. 37 for example.

The second point also involves the temperature difference. Nusselt presented equations for determining the coefficient for any tube in a multitube bank. The equation for the nth tube in a bank involved the condensate from the $(n-1)$ tubes above the one in question and was assumed by Nusselt to be the theoretical amount determined by the equations he proposed. He also assumed that the temperature difference was the same for all tubes. If, therefore, the condensation rate for the first tube is considerably below the theoretical value, then the amount of condensate dropping onto the second tube would be considerably less than the theoretical amount that would justify the use of Nusselt's equation for the second tube. For this case, the film on the second tube would be too thin, and the actual coefficient obtained could readily be much greater than that obtained from Nusselt's equation without the need of an explanation regarding turbulence.

Considering run No. 37 in this light, the coefficient for the first tube should theoretically be (using N_c for the second tube)

$$h = 0.725 \sqrt[4]{5.45 \times 10^{10}} = 350$$

and it is apparent that the amount of condensate is $\frac{180 \times 8.2}{350 \times 9.7} =$ 43.5 per cent of the theoretical amount required to make the use of Nusselt's equation for the second tube valid.

By the use of the material contained in Nusselt's paper, it is possible to make the correction, but the process is laborious, requiring graphical integration. A possible method of correcting for this will be suggested.

Before dealing with this method, it should be observed that the values attributed to McAdams are numerically correct but do not apply as given. The McAdams' values give the average coefficient for n tubes and not for the nth tube. This relation between the author's theoretical values of Nusselt and McAdams may be checked as follows:

The average coefficient for five tubes would be (from Nusselt's values)

$$h = \frac{0.725 + 0.493 + 0.436 + 0.401 + 0.375}{5} \sqrt[4]{N_c}$$

$$= 0.486 \sqrt[4]{N_c}$$

McAdams value is given as $0.485 \sqrt[4]{N_c}$.

This relation may be found for any of the other values supplied by the authors.

Since the values given by McAdams are readily obtained, depending upon the following equation

$$\text{Average coefficient } h = \frac{0.725}{n^{1/4}} \sqrt[4]{N_c}$$

it can be shown that the coefficient for the nth tube of a bank may be written

$$h \text{ for } n\text{th tube} = 0.725 \sqrt[4]{N_c} \left\{ n^{3/4} - (n-1)^{3/4} \right\}$$

This then suggests a means of dealing with the condensation on a tube when the condensate coming down from the tubes above differs from the theoretical amount. The first four tubes of a bank might conceivably condense as much liquid as would six tubes following Nusselt's equations. The fifth tube in the bank would act only in accordance with the amount of condensate it received and its own temperature difference. If any comparison with theoretical values be made, it is apparent that the comparison should be made with theoretical values for the seventh tube.

Returning now for further consideration of run No. 37, the coefficient for the first tube should be (to permit comparison of actual and theoretical values for the second tube)

$$h = 0.725 \sqrt[4]{5.45 \times 10^{10}} = 350$$

$$\text{Btu per sq ft per hr} = 350 \times 9.7 = 3390$$

$$\text{Actual Btu per sq ft per hr} = 180 \times 8.2 = 1475$$

Since only the condensate corresponding to 1475 Btu per sq ft per hr would reach the second tube, 0.33 tube would produce the same result, if it behaved in the theoretical manner at $\Delta t = 9.7$. This would then make the second tube the same as $n = 1.33$, and therefore

$$h = 0.725 \sqrt[4]{5.45 \times 10^{10}} \left[1.33^{3/4} - 0.33^{3/4} \right]$$

$$= 350 \times 0.803 = 281$$

The actual coefficient is 316, or 112 per cent of the theoretical. If no consideration be given to the amount of condensate reaching the tube, then the actual coefficient is 132 per cent of the theoretical value.

From this, it should be apparent that consideration of the nth tube by itself is not sufficient. Corrections should be made for deviations of the amount of condensate from that which would theoretically be produced by $(n-1)$ tubes.

The writer attempted to correlate the coefficient against Rey-

[6] Mechanical Engineering Department, York Ice Machinery Corporation, York, Pa. Jun. A.S.M.E.

[7] Bibliography reference (3), p. 537.

nolds number before realizing that this cannot be done for the individual tube coefficients in a multitube bank, at least not in the laminar-flow region.

Authors' Closure

The authors are indebted to Messrs. Jakob, Soling, and Short for pointing out certain discrepancies and for including additional analyses which aid in the interpretation of the experimental results.

Dr. Jakob points out some of the inadequacies of Nusselt's theory when attempts are made to apply it to experimental information, such as this, when factors considered constant by Nusselt actually varied in the experiment. If the Nusselt, constant C referred to by Jakob had been corrected for the deviation of the actual condensate flow from the theoretical, then corrections noted by Jakob might have been somewhat smaller.

The method for correcting Nusselt's coefficients given by Mr. Soling is actually quite similar to that of Jakob. However, Mr. Soling would consider the variation of actual flow from the theoretical, rather than merely correct for change in Δt. Mr. Soling's choice of example is unfortunate because data for tube 1 in Table 1 of the paper were discarded due to experimental difficulties.

Regarding Mr. Jakob's remark on nomenclature, the authors are attempting to compromise by calling N_c "Nusselt's number for condensation." Since the parameter commonly called the condensation number is not the same as N_c, a name had to be coined. It is hoped this will not be confused with the group hD/k called "Nusselt's number."

In reply to Mr. Soling's remarks on tube-temperature measurement, the authors have realized that the best they could hope for was a temperature that would not deviate far from the average. Baker and Mueller data show that the average wall temperature is found somewhere near the 90-deg position. Their data for a single tube show the highest temperature at the top of the tube, the lowest at the bottom. This is to be expected from the film thickness around the tube predicted by Nusselt's equations. In multitubular condensers, it is quite possible that the temperature distribution around the lower tubes is not quite the same as in the first, but since the variation of heat-transfer coefficient around the lower tubes is nearly the same as in the top tube, the location of the point of average temperature is probably near the 90-deg spot. As a practical matter, the tubes could not be rotated to discover this temperature distribution, and the thermocouple leads had to be carried off at 90 deg in order to interfere least with the condensate film. The authors believe that the erratic behavior of the Δt terms is due to the thermocouple behavior and not to variations in water quantity through the individual tubes. This variation was so small that it can almost be neglected.

The end effects were determined by pulling the traveling water-side thermocouples toward the ends of the tubes, thus lengthening the test section. Since the rate of heat transfer per unit area remained unchanged, it was assumed that a negligible amount of heat was flowing along the tube walls.

Mr. Short's comment on the possibility of a lower limit for the value of h would be more nearly true of steam than of a poor conductor such as Freon-12. Such a limit would probably be a function of Reynolds number.

Heat Transfer, Pressure Drop, and Fouling Rates of Liquids for Continuous and Noncontinuous Longitudinal Fins

By A. Y. GUNTER[1] and W. A. SHAW,[2] NEW YORK, N. Y.

This paper contains test data on continuous and noncontinuous fins for liquids in the laminar-flow region. The data indicate that for longitudinal fin-tube "pipe-within-pipe" type heat exchangers, the transition range begins near $R_h = 200$. Correlation with earlier investigations on air with short longitudinal fins, for $R_h > 600$, indicates fair agreement with the authors' results, when length of fin and inlet turbulence are taken into consideration. Noncontinuous fins promote turbulence in the laminar-flow region and increase fin-side heat-transfer coefficients up to 100 per cent, in the range of $L = 10$ ft. The theoretical aspects of fouling on fin tubes versus bare tubes are graphically illustrated, and actual semi-plant-scale fouling rates are plotted. These data show that fin tubes are affected less by fouling than bare tubes, because the effectiveness of the fin increases when fouling becomes greater.

Nomenclature

THE following nomenclature is used in this paper:

$A = (A_f + A_t)$ = total "exposed" fin-side surface area, sq ft
A_c = net free cross-sectional area for flow on the fin side, sq ft
A_f = surface area of fins only, sq ft
A_i = inside surface area of tube sq ft
A_t = outside surface area of tube only, sq ft
b = height of fin (see Fig. 1*b*), ft
c = specific heat of fluid, Btu per deg F per lb
$D_h = \frac{4A_c}{\psi_h}$ = equivalent hydraulic diameter, for determination of heat-transfer coefficient, ft
$D_p = \frac{4A_c}{\psi_p}$ = equivalent hydraulic diameter, for determination of pressure drop, ft
f = friction factor, defined by Equation [9], dimensionless
$G = \rho V$ = mass velocity of fluid, lb per sq ft per hr
g = acceleration of gravity = 4.17×10^8 ft per hr per hr
h_d = fouling (or deposit) factor, for fin-side fluid, Btu per sq ft per deg F per hr
h_f = fin-side film coefficient (clean), based on A, Btu per sq ft per deg F per hr
h_{fd} = fin-side film coefficient (fouled), (see Fig. 4), Btu per sq ft per deg F per hr
h_i = fin-side film coefficient (h_f), referred to A_i, by correction for effectiveness and tube-wall resistance (see Fig. 4), Btu per sq ft per deg F per hr
h_{id} = fin-side film coefficient (h_{fd}), referred to A_i, by correction for effectiveness and tube-wall resistance (see Fig. 4), Btu per sq ft per deg F per hr
h_i = tube-side film coefficient, Btu per sq ft per deg F per hr
h_w = reciprocal of tube-wall resistance (see Fig. 4), Btu per sq ft per deg F per hr
$J_S = \frac{h_f}{k}\frac{D_h}{}\left(\frac{c\mu}{k}\right)^{-1/3}\left(\frac{\mu}{\mu_w}\right)^{-0.14}$ = heat-transfer factor, according to Sieder and Tate (1),[3] dimensionless
$J_A = \frac{h_f}{cG}\left(\frac{c\mu}{k}\right)^{2/3}\left(\frac{\mu}{\mu_w}\right)^{-0.14}$ = heat-transfer factor, according to Colburn (2) with Sieder (1) viscosity correction, dimensionless
k, k_f, k_w = thermal conductivity of fin-side fluid, of fin material, and of wall material, respectively, Btu per sq ft per deg F per hr per ft
L = length of fin section (see Fig. 2), ft
Δ_p = pressure drop of fin-side fluid, due to "friction," psf
$R_h = \frac{D_h G}{\mu}$ = Reynolds number, based on equivalent hydraulic diameter for heat-transfer coefficient, dimensionless
$R_p = \frac{D_p G}{\mu}$ = Reynolds number based on equivalent hydraulic diameter for pressure drop, dimensionless
U_c = over-all heat-transfer coefficient (clean), steam to fin-side fluid, based on A_i, Btu per sq ft per deg F—log *MTD* per hr
U_d = over-all heat-transfer coefficient (fouled), steam to fin-side fluid, based on A_i, Btu per sq ft per deg F—log *MTD* per hr
V = linear velocity of fin-side fluid (at A_c), fph
δ = thickness of fin (see Fig. 1*b*), ft
η = effectiveness factor of fin (see Fig. 4), dimensionless
η' = total surface effectiveness (see Fig. 4), dimensionless
μ = viscosity of fin-side fluid (evaluated at average fluid temperature), lb per hr per ft
μ_w = viscosity of fin-side fluid (evaluated at tube-wall temperature), lb per hr per ft
ψ_h = total wetted perimeter of heat-transfer surface (fins plus outside of tube), for heat-transfer coefficient only, ft
ψ_p = total wetted perimeter of heat-transfer surface (fins plus outside of tube, plus inner surface of sleeve), for pressure drop only, ft
ρ = density of fin-side fluid, lb per cu ft

Introduction

Tubes with longitudinal fins cast, welded, or mechanically bonded thereon, have been used industrially for a number of years. These tubes have, in most cases, been manufactured in "continuous" lengths up to 22 ft. Their main application has been for heat-exchange duties covering light fluids such as gaso-

[1] American Locomotive Company, Alco Products Division.
[2] American Locomotive Company, Alco Products Division.
Jun. A.S.M.E.
Contributed by the Heat Transfer Division and presented at the Spring Meeting, Houston, Tex., March 23–25 1942, of The American Society of Mechanical Engineers.
Note: Statements and opinions advanced in papers are to be understood as individual expressions of their authors and not those of the Society.

[3] Numbers in parentheses refer to the Bibliography at the end of the paper.

line, down to the heaviest tars and asphalts. In air heating and cooling, longitudinal fins of much shorter length, 6 in. and less, are quite often used. The heat-transfer coefficients for air, using very short fin lengths, have been obtained, correlated and analyzed by R. H. Norris and W. A. Spofford (3).

Since longitudinal fins for liquids are nearly always used with $L/D_h > 156$, and their structural shapes are somewhat equivalent to flat ducts, the data reported in this paper are more nearly equivalent to Norris and Streid (4).

The data herein reported refer to pipe-within-pipe-type units and are not strictly applicable to other types of fin-tube units.

The present paper has three objectives, as follows:

1 To furnish test data on liquids in laminar flow for long continuous fins, correlated with published data and theoretical curves for air (3, 4).

2 To indicate the advantages of noncontinous longitudinal fins over long continuous fins for liquids.

3 To present analysis of the theoretical aspects of fouling on fin tubes, as compared with bare tubes, together with a presentation of actual fouling rates encountered in intermittent semi-plant-scale operations.

It must be remembered that the plant-scale conditions of using various fluids from 10,000-bbl storage tanks made it impossible to control inlet temperatures from day to day, and prevented keeping μ constant for the various sets of tests; nor are the conditions of constant surface temperature or constant heat input per unit of length fulfilled, as called for by Norris and Streid (4).

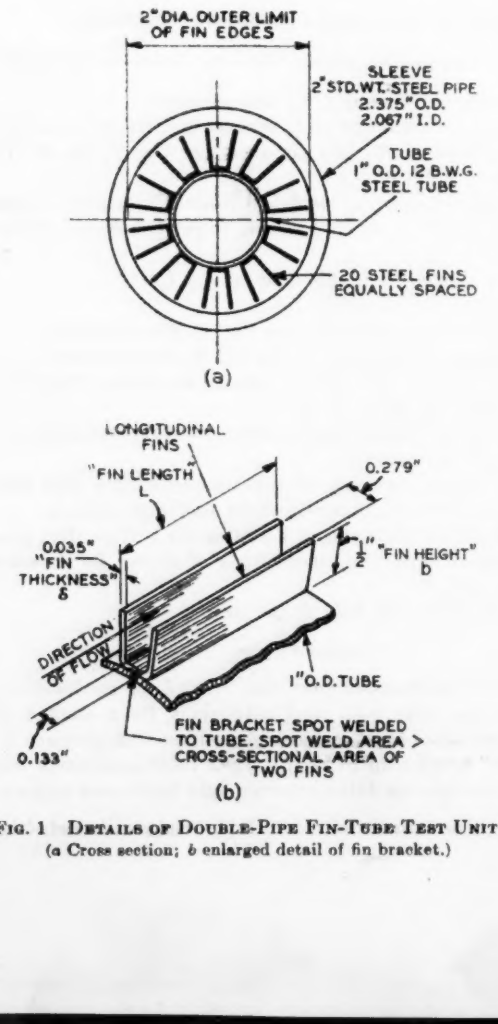


FIG. 1 DETAILS OF DOUBLE-PIPE FIN-TUBE TEST UNIT
(a Cross section; b enlarged detail of fin bracket.)

FIN SAMPLE DESIGNATION	TYPE OF FIN SURFACE AND L/D_h-RATIOS	FIN ARRANGEMENT AND DIMENSIONS (SEE ALSO FIG. 1) DIRECTION OF FLOW →	AVG. TEST RESULTS HEAT TRANS. FACTOR J_A @ R_h=30	FRICTION FACTOR f @ R_D = 23.4	PRESS. DROP EFF. FACTOR $J_A(f/2)$
		ALL DIMENSIONLESS			
A-1	CONTINUOUS: L=10' (L/D_h=313)	L	0.028	0.66	0.085
A-2	CONTINUOUS. L=5' (L/D_h=156)	L	0.035	0.69	0.101
A-3	NON-CONTINUOUS: L=2.45' (L/D_h=76.8)	L, 3/4", 10'-0"	0.039	0.77	0.101
A-4	NON-CONTINUOUS L=2.45' (FIN ENDS BENT) (L/D_h=76.8)	L, 3/4", 10'-0"	0.044	0.87	0.101
A-5	NON-CONTINUOUS: L=1.2' (FIN ENDS BENT) (L/D_h=37.6)	L, 3/4", 10'-0"	0.056	0.95	0.118
A-6	NON-CONTINUOUS: L=4.97' (SEGMENT TWISTED) (L/D_h=156)	L, 3/4", 10'-0"	0.035	0.70	0.10
A-7	NON-CONTINUOUS: L=2.45' (SEGMENT TWISTED) (L/D_h=76.8)	L, 3/4", 10'-0"	0.044	0.88	0.10
A-8	NON-CONTINUOUS: L=2.45' (FIN ENDS BENT, SEG. TWISTED) (L/D_h=76.8)	L, 3/4", 10'-0"	0.044	0.88	0.10
A-9	NON-CONTINUOUS: L=1.2' (FIN ENDS BENT, SEG. TWISTED) (L/D_h=37.6)	L, 3/4", 10'-0"	0.056	0.99	0.113
N-7	[THEORETICAL EXTRAPOLATION] "FLAT FINS"-CONTINUOUS (L/D_h=11.1)	L, 6", 0.311", 0.010" THICK FINS	@ R_h=30 0.082	@ R_D=30 0.867	0.189

FIG. 2 TABULATION OF HEAT-TRANSFER, FRICTION, AND PRESSURE-DROP EFFICIENCY FACTORS FOR FLUIDS

TERMINOLOGY

The terms "fin height" and "fin thickness," as used in this paper are illustrated in Fig. 1. The "fin length," L, is also indicated, but it should be pointed out that on the noncontinuous fins, the term fin length, L, is the continuous length between the cut sections, as shown in Fig. 2, and may consist of two, four, or more sections; however, only the length of each section is considered in the L/D_h ratio.

RÉSUMÉ OF TESTS

The majority of the tests made utilized the size and type of fin tube and sleeve illustrated in Fig. 1. Other tests were run utilizing fin tubes up to 4 in. diam with varying fin spacing, and 3/4 in. fin height, which are not reported in this paper. As indicated in Fig. 1, steel fins 1/2 in. in height and 0.035 in. in thickness were used from which fin effectiveness could be readily calculated by the method presented by Harper and Brown (5) (see Fig. 4).

The scope of the 300 tests herein reported is shown in Table 1.

TABLE 1 RANGE OF VARIABLES COVERED IN TESTS

Fluid characteristics	See Table 5
Steam temperatures, F	250 to 325
Average oil temperatures, F	115 to 235
Linear velocity, fps	0.3 to 10
$\left(\frac{\mu}{\mu_w}\right)^{0.14}$	0.85 to 1.9
$\frac{c\mu}{k}$	5 to 5000
L/D_h	37.6 to 313

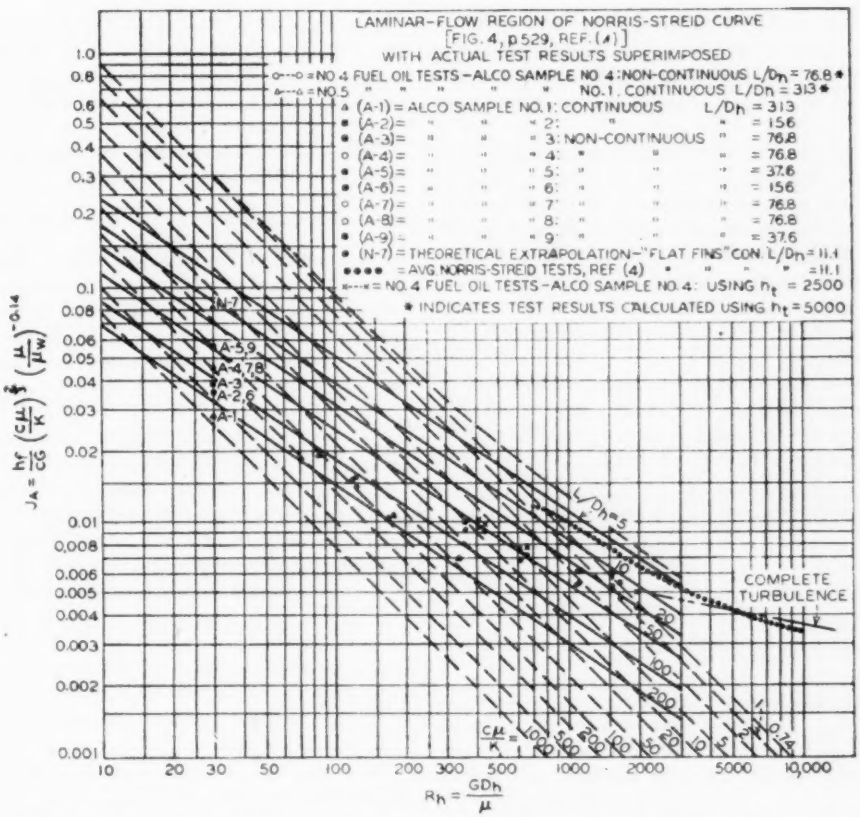


FIG. 3 CORRELATION OF TEST DATA WITH NORRIS AND STREID'S SUGGESTED CURVE
(Reference 4, Fig. 4, p. 529.)

CORRELATION OF HEAT-TRANSFER DATA

The original choice of correlation was based on

$$J_S = \frac{h_f D_h}{k}\left(\frac{c\mu}{k}\right)^{-1/3}\left(\frac{\mu}{\mu_w}\right)^{-0.14} \quad \ldots\ldots\ldots\ldots [1]$$

according to Sieder and Tate (1) for the following reasons:

1 This method would give one curve for both heating and cooling using L/D_h parameters.

2 From a practical rating standpoint, it provided the most convenient form for everyday use.

Therefore, all original data were calculated on this basis, using h_i = 5000 for the steam-film coefficient. This procedure introduced a factor of safety for h_f on an average of approximately 8 per cent. This is shown in Fig. 3, as a replot for No. 4 fuel oil.

For the purpose of correlating data reported in this paper with Norris and Streid (4), the ordinate expression

$$J_A = \frac{h_f}{cG}\left(\frac{c\mu}{k}\right)^{2/3}\left(\frac{\mu}{\mu_w}\right)^{-0.14} \quad \ldots\ldots\ldots\ldots [2]$$

was used, and these values are shown in Figs. 2 and 3.

As stated in the introduction, the tests on liquids herein reported are governed by L/D_h parameters, since all exceed the limiting values given by Equations [27] and [28] in reference (4). However, to correlate tests on liquids at various temperatures and linear velocities, it is necessary to use the $\left(\frac{\mu}{\mu_w}\right)^{0.14}$ ratio as outlined by Sieder and Tate (1). Further, to compare test results from different tubular units with different fluids, resort must be made to the Grashof number corrections as outlined by Colburn (2) and Sieder and Tate (1).

Fig. 2 has been set up from averages of actual test results to indicate the advantage of changing a long continuous fin tube into a long tube with short noncontinuous sections and turbulence promoters separating the sections. It will be noted that J_A increases up to 100 per cent with the L/D_h ratio decrease, and that $J_A/(f/2)$ of reference (3) remains substantially constant.

The J_A value for sample N-7 is the theoretical value at R_h = 30 for L/D_h taken from Fig. 4, reference (4) as there are no test data for air at this Reynolds number. There is no difference in R_h = 30 and R_p = 23.4, for D_h and D_p definitions give different wetted perimeters for heat transfer and pressure drop as shown in the nomenclature.

The choice of R_h = 30 for the tabulation was predicated on the fact that, between R_h = 100 and 200, the authors' test results indicate the transition range between laminar and turbulent flow begins. Numerous repeat tests were made to check this point, all giving materially the same result. This fact was believed to be due to the shape of the passages between the fins. Close inspection of Fig. 1 will show that the flow area of the test exchanger is an annular space divided into twenty small trapezoids (depth to width ratio = 0.41) by the fins. Therefore, better correlation was anticipated with published test data for flat or noncircular ducts.

Davies and White (6) have investigated the isothermal flow of fluids in tubes of various shapes. They found that, in the turbulent-flow region, the friction factors for all shapes were in substantial agreement. However, in the laminar-flow region, for shapes other than circular, they point out that the slope of the curve may not be 45 deg, and the friction factors in general are higher. Further, it was determined that the transition range between laminar and turbulent flow might begin as low as R_h = 200 for noncircular shapes.

Since the heat-transfer coefficient h_f normally increases with the increase of friction factor f, it would be expected, in view of Davies and White's data (6), that the test results herein reported would show higher J_A values and the transition range beginning well below $R_h = 2100$.

The results, as plotted in Fig. 3, indicate surprising agreement with this hypothesis. It is not intended, in this paper, to cover the entire range of tests in the laminar-flow region, nor to draw final conclusions as to the proper correction for shape factor in Equations [1] or [2], as these items are being reserved for further study. It is sufficient at this time to state that the L/D_h parameter curves, in Fig. 4 of reference (4), are conservative for liquids in the range of $R_h = 150$ to 2100, for the test unit described in Figs. 1 and 6 of this paper.

In considering the economic aspects of normal heat-exchanger design for liquids in the laminar-flow region, it will be found that for, say, steam heaters, the Reynolds number spread of 1 to 2100 covers a number of liquids as shown in Table 2.

TABLE 2 DATA SHOWING REYNOLDS NUMBERS VERSUS TYPES OF OILS NORMALLY ENCOUNTERED IN STEAM HEATERS

Type of oil	Reynolds number range
Gasoline, kerosene	>2300
Light burning oils (1, 3, and 4)	200 to 8000
Medium fuel oils (No. 5)	80 to 300
Heavy fuel oils and asphalts	<100

NOTE: Limiting range—temperature 80 to 350 F; linear velocity 0.3 to 8 fps.

To indicate this condition from test results and to show the shift in transition range, Fig. 3 has been included, which plots average values for Fig. 2 (pr. still resid. and asphalt) and test results for Nos. 4 and 5 fuel oils. The pr. still resid. and asphalt tests (Fig. 2) were run at average values, $\left(\frac{\mu}{\mu_w}\right)^{0.14} = 1.5$ to 1.9, $\frac{c\mu}{k} = 2000$ to 5000. The Nos. 4 and 5 fuel-oil average test values were $\left(\frac{\mu}{\mu_w}\right)^{0.14} = 1.1$ and 1.26; $\frac{c\mu}{k} = 61$ and 333, respectively. Linear velocities ranged from 0.3 to 5 fps, in all cases.

In addition, Fig. 3 shows a plot of Norris and Spofford's (3) actual test results for sample N-7. It will be noted that the J_A values are above the $L/D_h = 11$ parameter line. The tests in this paper do not cover an L/D_h value as low as 11, although extrapolation from the values between $L/D_h = 313$ and 37.6, to $L/D_h = 11$, indicates agreement within 10 per cent.

Colburn (2) suggested the use of the Grashof number as a correction to the equation of the empirical line for viscous flow as follows:

$$\psi = 1.5 \left(\frac{\mu}{\mu_f}\right)^{1/3} (1 + 0.015\, Gr^{1/3}) \quad [3]$$

(where μ_f is viscosity at film temperature).

Sieder and Tate (1) suggest the correction of h_f by a modified form of Equation [3] when dealing with gases or light liquids. (Here μ in the Grashof number is taken at average stream temperature):

$$(0.8 + 0.012\, Gr^{1/3})\, h_f \quad [4]$$

A brief check using Equations [3] and [4] with air at 70 F and $R_h = 700$ shows that the test unit for sample N-7 should give approximately a 10 per cent higher J_A value than the test unit in this paper, assuming L/D_h values are equal. This point is more or less academic since neither unit was tested on both liquids and air.

The equation for J_A in the laminar-flow region, as indicated in Fig. 3, where L/D_h parameters are controlling, is

$$J_A = 1.85\, (L/D_h)^{-1/3}\, (R_h)^{-1/3} \quad [5]$$

This equation is conservative in the range $R_h > 100$ and may be as much as 40 per cent low at $R_h = 2000$ with $L/D_h = 313$ for the test unit herein described. As stated earlier in this paper, the final solution of the foregoing variation must await further study of the data accumulated.

In view of the preceding points, it is obvious that the thermal engineer must be careful, in selecting h_f, to give critical consideration to such factors as $\left(\frac{\mu}{\mu_w}\right)$; the shape and alignment of fins; the geometry of fin passages; etc. These factors may tend toward cumulative effects which would radically modify theoretical analysis or extrapolations of test results. Fortunately, the use of Fig. 4, reference (4), is on the conservative side for liquids and can be used with safety in ordinary cases.

PRACTICAL APPLICATIONS

The data herein presented give an indication of the improvement that can be expected in the laminar-flow region for liquids by taking tubes with long continuous fins and altering the latter to relatively short noncontinuous sections. This procedure still maintains the economic advantage of long heat-exchanger shell construction with increases in over-all rates up to 100 per cent; it also preserves the desirable feature of ease of cleaning.

FOULING RATES

General Considerations. Published data on fouling rates for fin tubes are negligible at present. The data in this paper cover the theoretical aspects, together with actual results of semi-plant-scale operations.

As it happens, most longitudinally finned tube services cover the use of a relatively clean fluid (such as steam or water) on the inside of the tube, or the use of a dirtier fluid at linear velocities near or above the scouring range.

Therefore, in comparing longitudinal fin tubes with bare tubes, the main concern is with the fouling rate and its effects on the fin side, or in the case of bare tubes, on the outside surface.

Theoretical Considerations. Sieder (7) gives a very good résumé and proposed method for calculating fouling rates for bare tubes, which has been used in this paper.

The generalized equation for flow of heat from one fluid to another for bare tubes, with tube-wall and fouling resistance ignored is

$$\frac{1}{U_c} = \frac{1}{h_f} + \frac{1}{h_i} \quad [6]$$

In commercial practice, a fouling factor is applied and the equation becomes

$$\frac{1}{U_d} = \frac{1}{h_f} + \frac{1}{h_i} + \frac{1}{h_d} \quad [7]$$

However, in the case of fin tubes, the additional factor of fin effectiveness must be considered. Further, because of the high ratio of $\frac{A}{A_i}$, the tube-wall resistance to the flow of heat is appreciable and cannot be ignored. The equation then becomes

$$\frac{1}{U_d} = \frac{1}{h_{id}} + \frac{1}{h_{id}} \quad [8]$$

where

$$h_{id} = \frac{h_{fd}\, \eta' \frac{A}{A_i} \cdot h_w}{h_{fd}\, \eta' \frac{A}{A_i} + h_w}$$

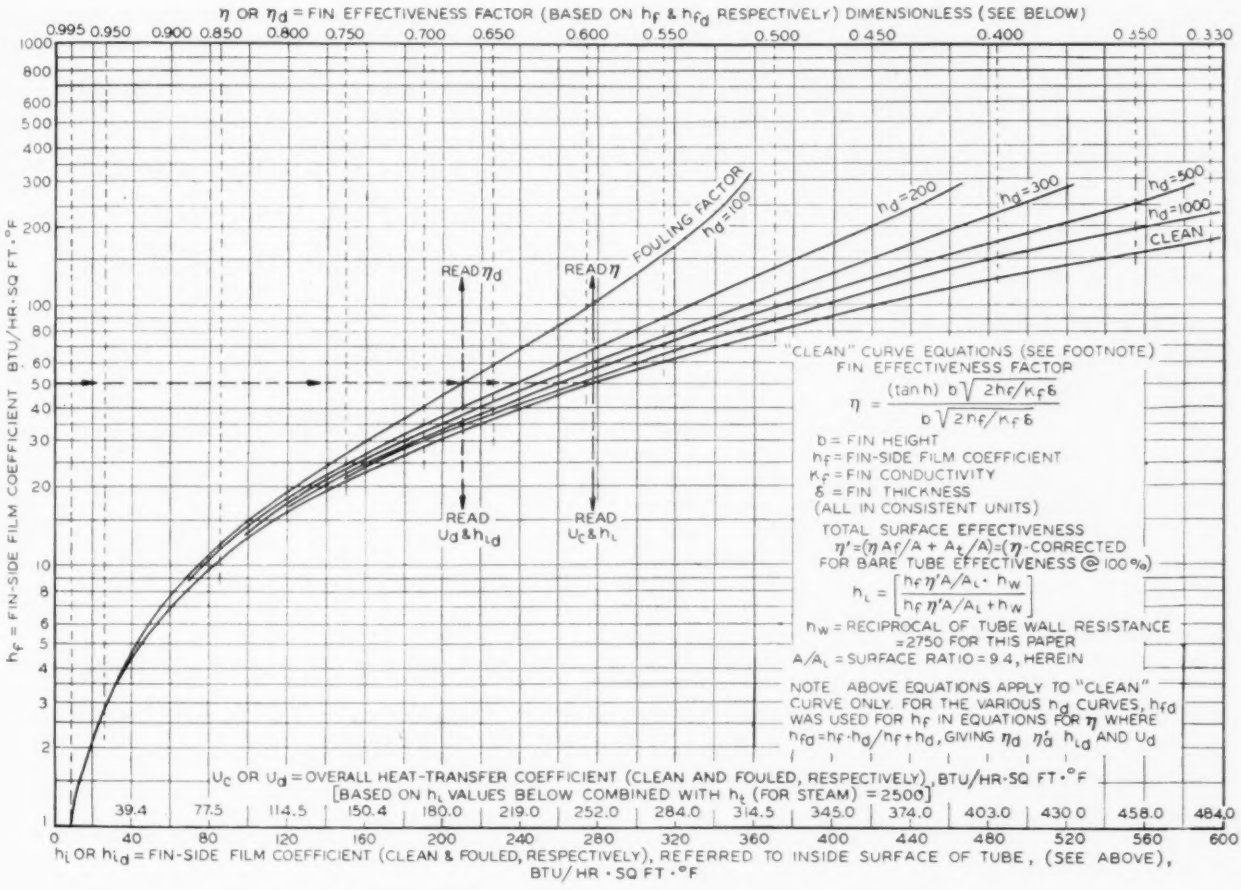


FIG. 4 THEORETICAL EFFECTS OF FOULING RATES ON LONGITUDINAL FIN TUBE
(1 In. OD, 12 BWG steel with 20 steel fins, 1/2 in. high by 0.035 in. thick attached.)

The fin effectiveness factor η of reference (5) and total surface effectiveness factor η' are described in Fig. 4.

Fig. 4 has been prepared for the tube in Fig. 1, based on the equations noted therein, and plots h_f versus h_i versus U versus η with various fouling factors applied. From a study of Fig. 4, it is immediately evident that fouling affects the fin effectiveness factor η appreciably, always increasing the effectiveness. This gives the fin tube a decided advantage over bare tubes when fouling is considered.

As an example, a point $h_f = 50$ with $h_d = 100$ is indicated in Fig. 4, in heavy black lines. This gives $U_c = 250$ and $U_d = 192$, or the decrease due to fouling effect on U was 23 per cent. The fin effectiveness factor η was 0.598 at $h_f = 50$ and 0.67 fouled, or a 12 per cent increase. For a bare tube at the same h_f and h_d, using Equations [6] and [7], it is found that $U_c = 49$ and $U_d = 33$, or the decrease due to fouling was 33 per cent. Thus, it is seen that fouling has less effect on fin tubes, as compared to bare tubes, when considering outside surface. In addition, it is obvious that the increase in the fin effectiveness factor η when fouling occurs, is the factor responsible for the advantage.

The increase in η due to fouling is less at lower values of h_f and varies as the hyperbolic tangent with variations in h_f or h_d.

Another inherent advantage in fin tubes is that, in heating liquids which have a tendency to coke or form heavy polymers, the fin-surface temperatures are lower than with bare tubes due to η, with consequent less fouling. Conversely, in cooling, the fin surfaces are at higher temperatures with less tendency to deposit tars, etc.

Test Results. Fig. 5 is a plot of actual test results from intermittent semi-plant-scale test runs reported in this paper (see Appendix, "Test Procedure"). The test shown for the commercial fin-tube tank-suction heater was on a 24-in-diam unit, in bunker "C" fuel-oil service at a major oil company's plant.

It is well known that intermittent operation increases fouling rates above continuous operation, because of oxidation, stagnant-fluid conditions, etc. For this reason, the data, shown in Fig. 5, should be considered as on the high side. However, it does indicate that, for most fuel-oil heaters with steam temperatures not greater than 350 F, an applied fouling rate of $h_d = 200$ to h_f, should result in at least 1 year of operation without cleaning.

In Fig. 5, a semi-Navy-type fouling test is indicated (Δ), which consisted of leaving the unit full of pr. still resid. for 18 hr, with 80-psi steam inside the tube. Test runs before and after the fouling period gave the fouling factor noted. A dotted line over to the average plot curve shows this test approximating a 1-year operating period for fuel-oil service without cleaning.

It should be pointed out that the tendency for fuel oils to break down with time and elevated temperatures varies considerably. The fuel oil used for the semi-Navy-type test was a 6° API pr. still resid. from cracking operations at 900 F, which should be comparable to most bunker "C" fuel oils on the market.

On the lighter oils, very little fouling was encountered beyond that expected for intermittent operations.

Standard Fouling Factors. The Tubular Exchanger Manufacturers Association (T.E.M.A.) (8) has set up standard fouling factors, based on actual plant experience, over a period of many

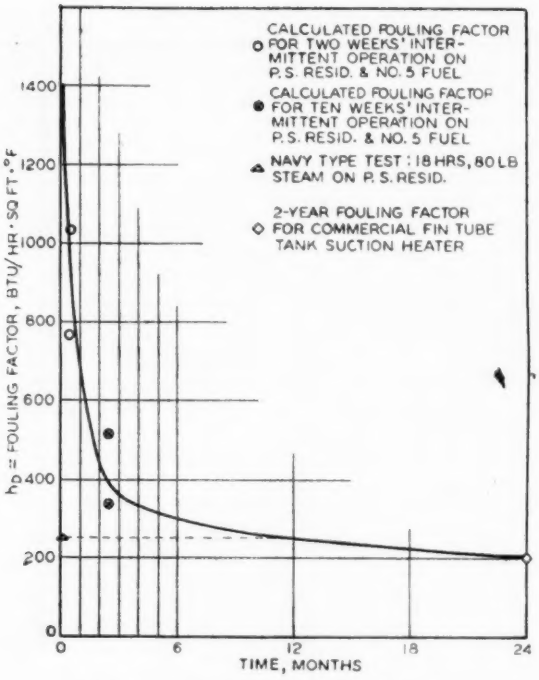


FIG. 5 TEST DATA ON FOULING RATES

years. The fouling factors which are applicable to data reported in this paper have been excerpted from reference (8) and are

TABLE 3 EXCERPT OF FOULING COEFFICIENTS FROM STANDARDS OF T.E.M.A. FOR VARIOUS FLUIDS USED IN THIS PAPER

Fluid	Fouling coefficient, h_d
Industrial fuel oil	200
Residual bottoms, less than 25° API	200
Distillate bottoms, 25° API or above	500
Side stream cuts (Nos. 1, 2, 3, and 4, fuel oils) atmospheric dist. units	770
Steam (non-oil-bearing)	0
Steam, exhaust (oil-bearing, from reciprocating engines)	1000

shown in Table 3. It will be noted that the test data check well in line with the T.E.M.A. Standards.

CORRELATION OF PRESSURE-DROP DATA

All the original pressure-drop test data covered in this paper were evaluated by use of the modified form of the general Fanning equation, as outlined by Sieder and Tate (1), who introduced the function $\left(\frac{\mu}{\mu_w}\right)^{0.25}$ to make it applicable to all fluids.

For purposes of correlation with data presented by Norris and Spofford (3), the generalized Fanning equation was used with $\left(\frac{\mu}{\mu_w}\right)^{0.25}$ function added

$$f = \frac{gD_p \Delta P}{2\rho V^2 L} \left(\frac{\mu}{\mu_w}\right)^{0.25} \quad \ldots\ldots\ldots\ldots\ldots\ldots [9]$$

The pressure-drop results are shown in Fig. 2, based on both f and $J_A/(f/2)$.

It will be noted that, for any given fluid, the efficiency factor $J_A/(f/2)$ is substantially a constant when $L > 1$ ft and < 10 ft. This means that a long continuous longitudinal fin can be divided into relatively short sections without increasing the total pressure drop beyond that to be expected with the increased heat transfer.

The f value, for sample N-7 in Fig. 2, is a theoretical value based on Equation [9] and modified for $L = 0.5$ ft in ratio to tests in this paper for short lengths. This procedure was necessary since no test data were available at this point.

Under "Correlation of Heat-Transfer Data," reference was made to Davies and White's report (6) on friction factors covering isothermal flow for pipes of various shapes. They found that noncircular shapes caused disturbances to flow in the laminar-flow region and, in some cases, the transition range might begin at a value as low as $R_p = 200$.

To correlate friction factors for the test unit samples A-1, A-9, and N-7 with the Hagen-Poiseuille friction-factor curve for circular shape, and Davies and White's (6) findings, Table 4 is presented.

TABLE 4 CORRELATION OF FRICTION FACTORS IN LAMINAR-FLOW REGION

Reynolds number, (R_p)	Sample no. and L/D_h ratio	Friction factor, f: Hagen-Poiseuille curve	Rectangular ducts per Davies and White (6): Sample A-1	Rectangular ducts per Davies and White (6): Sample N-7	Authors' tests[a] plotted, per Eq. [9]	Norris and Spofford N-7 tests (3)	Davies and White,[b] max test values
30	...	0.537	Does not apply		.....	....	0.537
	A-1; 313	....	....	....	0.511[c]	....	...
	A-9; 37.6	....	....	....	0.727[c]	....	...
	N-7; 11.1	....	....	....	.....	....	...
600	...	0.0265	0.0272	0.0332	.....	....	0.037
	A-1; 313	....	....	....	0.0402[c]	....	...
	A-9; 37.6	....	....	....	0.0471[c]	....	...
	N-7; 11.1	....	....	....	.....	0.040[c]	...
800	...	0.0198	0.0204	0.0249	.....	....	0.031
	A-1; 313	....	....	....	.....	....	...
	A-9; 37.6	....	....	....	.....	....	...
	N-7; 11.1	....	....	....	.....	0.036[c]	...
1000	...	0.0158	0.0163	0.0199	.....	....	0.0265
	A-1; 313	....	....	....	.....	....	...
	A-9; 37.6	....	....	....	.....	....	...
	N-7; 11.1	....	....	....	.....	0.030[c]	...

[a] Authors' tests include end losses.
[b] Davies and White maximum test values, from reference (6), Fig. 2, p. 70.
[c] Average test results.

Sieder and Tate (1) found that circular-tube friction factors for liquids in nonisothermal flow, in the laminar-flow region, would fall on the isothermal f curve when multiplied by 1.1 $\left(\frac{\mu}{\mu_w}\right)^{0.25}$. The evaluations of test data shown in Table 4 have not been corrected by the factor 1.1, as suggested by Sieder and Tate (1).

The Davies and White (6) f values, shown in columns 4 and 5 of Table 4, are based on rectangular shapes for ratio of depth to width. (The ratios were: A-1 = 0.41; N-7 = 0.156.) It will be noted that sample N-7 correlates better with Davies' (6) maximum limits for shape effects, or with parallel plates, rather than with rectangular shapes. Sample A-1 gave values well above the theoretical rectangular shape effect expected, and more nearly in line with an annular ring or parallel plates. It was originally believed that A-1 would correlate as a rectangle, since its flow area consisted of twenty small trapezoids.

Test data for pressure drop not shown in this paper indicate that the transition range begins somewhere near $R = 200$, which is in agreement with Davies and White's (6) conclusions.

Sample A-9, f values cannot be compared with samples A-1 or N-7, as it has twisted fins which offer additional resistance to flow.

GENERAL CONCLUSIONS

Heat Transfer.

1 The use of noncontinuous fin sections instead of long continuous fins increases h_f in the ratio of 2 to 1, where $L = 1.2$ to 10 ft.

2 Correlation of test data for liquids in this paper, where L/D_h is controlling, indicates the curves shown in Norris and Streid's (4) Fig. 4, are conservative above $R_h = 200$, because

present test results show the transition range beginning at about this point.

3 The dimensionless function $\left(\frac{\mu}{\mu_w}\right)^{0.14}$ should be included in the J_A value when correlating viscous liquids.

Pressure Drop.

1 The pressure-drop efficiency factor for noncontinuous fins is comparable to that on long continuous fins where L = 1 to 10 ft.

2 Correlation of test data on pressure drop in this paper with Norris and Spofford (3) gives fair agreement in the range of R_p = 700 to 2000 for sample N-7.

Fouling Rates.

1 From a theoretical viewpoint, fouling has less effect on fin tubes than on bare tubes, for as fouling increases, the fin effectiveness increases, tending to offset the fouling effect.

2 A fouling factor of 200 for longitudinal fin tubes in heavy-fuel-oil service, with steam temperatures not above 350 F, will normally assure at least 1 year of service without cleaning. Intermittent operations or operations at less than design throughputs may shorten this period.

Appendix

Test Equipment and Procedure

The essential items of the test setup for the work reported in this paper (and their general arrangement) are shown schematically in Fig. 6, as they were installed in the oil refinery where the tests were run.

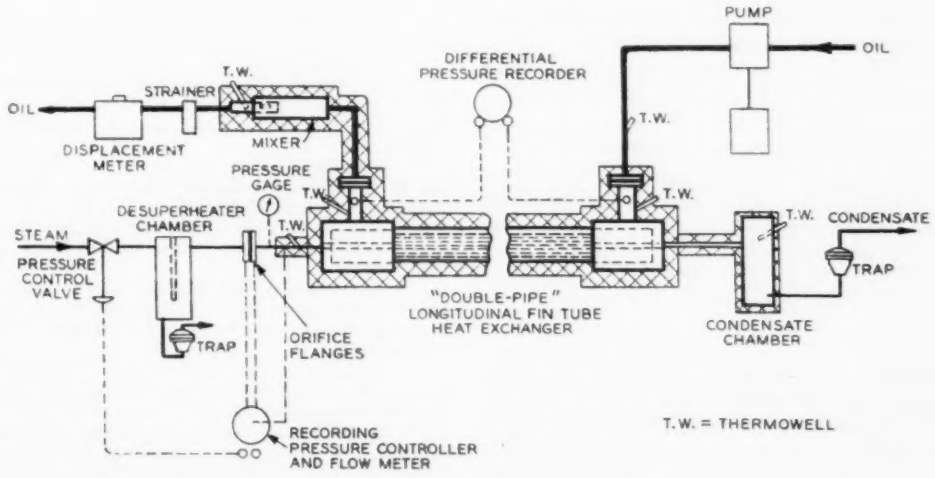


Fig. 6 Test-Unit Arrangement

Fin-Side Fluid Circuit. As previously mentioned, the fin-tube exchanger on which the test runs herein reported were made was of the "double-pipe" design (pipe-within-pipe type, see Fig. 1). The various fin-side fluids were drawn from refinery tankage (5 to 10,000-bbl capacity) and pumped through the annular space between the outside of the fin tube and the inside of the confining outer sleeve. Leaving the unit, the fluid then passed through a mixing chamber, which insured thorough commingling of the fluid particles for accurate outlet-temperature readings. Thermowells were provided as shown to give double checks on both entering and leaving fluid temperatures. Standard industrial-type glass thermometers were immersed in oil in these wells for the readings. These thermometers were check-calibrated against known standard ones in the refinery laboratory to establish their accuracy. Also, they were interchanged from time to time during the tests as a further check.

From the mixer, the fluid next went through a strainer and displacement meter (of the nutating-piston type), where the rates of flow were measured in conjunction with a standard laboratory timer clock, which was check-calibrated occasionally during the progress of the tests. Two sizes of meters were used in the tests to cover the wide range of flow rates run, and these instruments were check-calibrated from time to time during the course of the work to insure their accuracy. Upon leaving the metering device, the fluid then passed into the return piping system to refinery tankage.

Pressure drops across the test unit were measured by a differential-pressure recorder (of the mercury-manometer type). The location of the pressure taps in the inlet and outlet nozzles of the test unit, Fig. 6, meant that end losses were included in the pressure drops recorded. It should be pointed out, however, that, since the net free area of the end chambers below the nozzles was essentially equal to that of the nozzle pipes, these end losses therefore were kept to a nominal figure. Further, it must be noted that no calming section was provided to minimize inlet turbulence, since it was desired to approximate an actual commercial installation as closely as possible.

Fluids of various inlet temperatures were used in the work, and the manifold rates of flow which were run resulted in a considerable range of outlet temperatures. To insure further the accuracy of the temperature readings, the essential thermal apparatus was thoroughly insulated as shown. Standard pipe insulation (1-in-thick magnesia-asbestos) was used for the purpose, since this type readily suited dimensional and test-condition requirements. Tests for the magnitude of heat leakage through this material were not made, since, for the relatively low temperatures of the test operations, it was known that the possible error from this source would not be greater than 2 or 3 per cent.

Steam Circuit. Steam, at various pressures, was used as the heating medium inside of the fin tube. Live steam at refinery boiler-room conditions was taken from the mains and brought to the desired test-pressure requirements by means of the automatic air-actuated diaphragm control valve. The latter was connected to the recording pressure controller and flow-meter instrument, where manual setting of the desired test conditions was effected. A pair of orifice flanges, in conjunction with several interchangeable plates of different orifice sizes, were installed in the meter

system to cover the required test range. Suitable piping lengths, as required by the meter-installation manual, were strictly adhered to for correct and accurate operation of the meter system. An internally baffled desuperheater chamber was provided as shown, to insure the delivery of substantially dry, saturated steam to the test unit. A Bourdon-type pressure gage also was installed as shown, to give a double check on steam-meter-pressure readings. A trap at the bottom of the desuperheater chamber discharged the water removed from the steam, and this feature, together with observation of the pressure and temperature readings, assured that the desired steam conditions (freedom from superheat and wetness) were reasonably maintained.

At the steam outlet of the unit, it was found necessary to provide the condensate chamber shown, to guard against the possibility of flooding, by backing up condensate within the fin tube. An industrial-type steam trap was installed at the bottom of this compartment to discharge the condensate collected. Occasional blowdowns were made between tests to ascertain that the trap was operating correctly. Standard industrial-type glass thermometers (previously check-calibrated) in suitable thermowells were used for the temperature readings on the steam side.

Test Procedure. On any particular oil, tests were run at 3, 6, 12, 18, 24, and 30 gpm rate, with check tests going back down the scale 30, 24, 18, etc. Each test consisted of four consecutive sets of readings during a 10-min period after stable conditions were attained. The lower limit of oil throughput was set at 3 gpm, since it was found that any rates of flow below this value gave erratic readings which could not be measured accurately with the existing equipment.

For determining fouling rates, the first set of tests run, when the fin tube was new, were repeated at intervals. The difference between the original and repeat values of h_f were then recorded as fouling rates. The tubes used were of the bright annealed type and very little fouling occurred on the inside surface.

Average samples of the oil flowing through the unit were taken and tested in the plant laboratories for gravity and viscosity.

TABLE 5 CHARACTERISTICS OF FLUIDS TESTED

Fluid	Gravity, °API	Viscosity 70 F SSU	100 F SSU	130 F SSU	210 F SSU	77 F SSF	122 F SSF
Naphtha	46.2	..	29	..	...	...	...
No. 2 burning oil	35.5	..	34	..	...	...	...
No. 4 burning oil	27.1	61	47	..	...	...	...
No. 5 fuel	21.5	..	126	72	...	...	...
Pr. still resid	7.3	..	...	..	77	...	74
Heavy pr. still resid.	4.4	..	...	..	126	...	159
Cut-back asphalt	18.1	..	681	..	...	149	...

Calculation of Results. Since steam was used inside the tube, for which consistent results are available, the fin side coefficient h_f could be easily calculated, utilizing fin effectiveness curves based on (5), and shown in Fig. 4. The over-all heat-transfer coefficient used was obtained by dividing the total heat transfer by the total surface of the inside of the tube, using the log *MTD* between the fin-side fluid and the steam.

Since the data from these tests were to be set up for rating purposes, it was decided to use h_i of 5000 instead of 2500, to provide a factor of safety in the rating curves and yet not affect the consistency of the plot. Fig. 3 shows a plot of the No. 4 fuel-oil test results as calculated, using $h_i = 5000$ (o) and $h_i = 2500$ (x). The discrepancy introduced in the plot of these data relative to the other results shown is thus graphically illustrated. As stated previously, this introduced the desired factor of safety in the company standard rating curves. The foregoing assumption for the steam-side coefficient h_i, is in line with the film concept of condensation, as presented by Jakob (9). Verification of this point was established as well as could be accomplished with the existing setup, by passing steam through the unit at a linear velocity considerably in excess of 50 fps, and noting no apparent change in the outlet temperature of the oil.

Fluid characteristics were taken from the following sources:

c = specific heat; Standards of T.E.M.A., Fig. 20, ref. (8)
k = thermal conductivity; Bureau of Standards Miscellaneous Publications, No. 97
μ = absolute viscosity conversions; A.S.T.M. Tentative Standard D-341-32T viscosity-temperature chart.

Accuracy. Approximately 5 per cent of the plotted results did not give satisfactory agreement and consequently were discarded as being erroneous. The remaining 95 per cent were in substantial agreement, the variation being approximately ±6 per cent from the average. Further, heat balances made during the earlier part of the work (until oil-temperature results were verified satisfactorily) showed variations from 1 to 10 per cent, the oil-side duty always showing lower than the tube-side duty.

ACKNOWLEDGMENT

The authors wish to take this opportunity to express appreciation for the contribution to this work made by Mr. A. S. Denton in carrying out part of the tests and subsequent calculation of results. Credit is also due Messrs. S. Kopp and T. F. Fitzgerald for their many helpful suggestions during the test program. Appreciation of the co-operation of Mr. R. H. Norris in making available certain additional data not published in his reference papers and his valuable criticism and comments during the preparation of the present paper, is also hereby expressed. Further, the courtesy of the Tubular Exchanger Manufacturers Association, Inc. in giving permission to quote from its "Standards" is also gratefully acknowledged.

BIBLIOGRAPHY

1 "Heat Transfer and Pressure Drop of Liquids in Tubes," by E. N. Sieder and G. E. Tate, *Industrial and Engineering Chemistry*, vol. 28, 1936, pp. 1429–1435.

2 "A Method of Correlating Forced-Convection Heat-Transfer Data and a Comparison With Fluid Friction," by A. P. Colburn, Trans. American Institute of Chemical Engineers, vol. 29, 1933, pp. 174–210.

3 "High-Performance Fins for Heat Transfer," by R. H. Norris and W. A. Spofford, presented at A.S.M.E. Annual Meeting, New York, N. Y., December 2, 1941.

4 "Laminar-Flow Heat-Transfer Coefficients for Ducts," by R. H. Norris and D. D. Streid, Trans. A.S.M.E., vol. 62, 1940, pp. 525–533.

5 "Mathematical Equations for Heat Conduction in the Fins of Air-Cooled Engines," by D. R. Harper, 3rd, and W. B. Brown, U. S. Technical Report No. 158, National Advisory Committee for Aeronautics, 1922.

6 "A Review of Flow in Pipes and Channels," by S. J. Davies and C. M. White, *Engineering*, July 19, 26, and August 2, 1929 (specific reference: P. 70, including footnotes).

7 "Application of Fouling Factors in the Design of Heat Exchangers," by E. N. Sieder, A.S.M.E. miscellaneous paper, 1936; included in "Heat Transfer," by the Heat Transfer Committee of the Process Industries Division, A.S.M.E., pp. 82–86.

8 "Standards of Tubular Exchanger Manufacturers Association," 1941 edition, published by T.E.M.A., Inc., 366 Madison Avenue, New York, N. Y.

9 "Heat Transfer in Evaporation and Condensation, Part II," by Max Jakob, *Mechanical Engineering*, vol. 58, 1936, pp. 729–739.

Discussion

T. R. HEYCK.[4] One of the specified objectives of this paper is to indicate the advantages of noncontinuous longitudinal fins over long continuous fins for liquids. In Fig. 2 of the paper, for example, the fin sample designated as A-9, consisting of short noncontinuous sections 1.2 ft in length separated 3/4 in. by turbulence promoters, showed a heat-transfer factor of 0.056, with

[4] The Griscom-Russell Company, Houston, Texas.

a pressure-drop efficiency factor of 0.113. This suggests the conclusion that fin sample A-9 should be used instead of, say, fin sample A-1 which shows a heat-transfer factor of 0.028, with a pressure-drop efficiency factor of 0.085.

In considering other aspects of this subject, however, the writer is inclined to doubt the advantages of noncontinuous longitudinal fins. It is likely that structure A-9 would foul more rapidly, and serious difficulty might be encountered in attempting to clean it. A simpler structure, more readily accessible for cleaning, might give better over-all results than a more complicated structure, which will show improved transfer rates initially, but which will drop off rapidly in performance on fouling service and be difficult to clean.

Referring again to fin samples A-1 and A-9, the latter indicates a friction-factor increase of 50 per cent. If a unit were provided with continuous fins, indicated as fin sample A-1 and arranged so that the total over-all average pressure drop between reasonable cleaning periods would be the same as the total over-all average pressure drop for a unit provided with fins similar to sample A-9 for the same period of operation, it is believed that the increased fluid velocity which could be used through the first unit would compensate to a considerable extent for the artificial turbulence created by the noncontinuous structure. The higher velocity in a straight passage is much less liable to foul. The authors' comments on this point would be greatly appreciated.

B. E. Short.[5] Referring to Fig. 5 of the paper, would it not be better to show the resistance to heat flow, caused by fouling, rather than a heat-transfer factor similar to the convection transfer coefficients? This is merely a matter of personal opinion, but each time the writer has examined Fig. 5, he has gained the impression that it shows the decrease in the film coefficient on the finned side of the tubes with time rather than the separate coefficient for the fouling substance. It is not known why the standards of T.E.M.A. have been changed in this respect, as indicated by Table 3, from the original form of fouling resistances issued by the Heat Transfer Institute, but it seems that the resistance factors are much easier to apply.

Why would it not be better to follow the aeronautical scheme for Reynolds number in the case of these finned surfaces and consider a dimension in the direction of flow? This would tend to make the lines, as shown in Fig. 3, for different L/D_h values fall within a single field rather than spread apart.

In regard to the use of the J_A factor in Fig. 3, for the correlation of the data, it seems that some caution should be used. As a means of correlating the heat-transfer data it appears to the writer to be equally as useful as the other combinations using the Nusselt number. According to Osborne Reynolds, however, a direct relation between heat transfer and pressure drop is true only for similar passages, and Taylor, Prandtl, and von Kármán have not shown reasons in their analyses, since Osborne Reynolds' papers, to disagree with his statements. Consequently, it seems that the use of the J_A factor to establish an apparent relationship between the friction factor and the heat-transfer factor should be applied with care for flow outside of tubes with such dissimilar-shaped passages.

E. N. Sieder.[6] The effect of discontinuous longitudinal fins on heat transfer and pressure drop is most interesting and should prove of commercial value in saving scarce and strategic materials.

It is unfortunate that the authors did not show more detailed plots of the original data, particularly in the transitional region between laminar and turbulent flow. The writer was somewhat surprised at the authors' statement that this transitional region starts at a Reynolds number as low as 200.

The writer has conducted a number of pressure-drop and heat-transfer tests on longitudinal-fin tubes of the same type as used by the authors and has found no indication of a definite break in the nature of flow for Reynolds numbers as low as 200. As a matter of fact, heat-transfer and pressure-drop tests, taken on a tube of the same size as that used by the authors but having only 12 fins instead of 20, indicated that the break in heat transfer and pressure drop occurred at or close to a Reynolds number of 2000.

However, it might be pointed out that the shape of the trapezoidal duct, comprising the elemental-flow area, more nearly approached the shape of a square for the tube having 12 fins when compared with the one having 20 fins, as used by the authors. We also found that heat-transfer and pressure-drop values could be accurately predicted by the use of the curves recommended by Tate and the writer in an earlier paper.[7]

Tests taken with a greater number of longer fins, giving elemental-flow areas nearly approaching the effect of parallel plates, indicate that the transitional point may be lower than 2000 but certainly not lower than 1000.

Authors' Closure

Mr. Heyck's conclusion that fin sample A-9 is to be recommended over A-1 is partly correct. However, it has been found more economical to produce sample A-7 with $L = 1.2$ ft and still achieve the results obtained with sample A-9. While it may be noted that these results compare favorably with those of sample A-5 from a heat-transfer standpoint, it must be pointed out that sample A-7 ($L = 1.2$ ft) represents the simpler construction from the production angle; and in addition, has the desirable advantage of not sacrificing any of the extended surface as is the case with sample A-5.

As to the matter of cleaning, it can only be stated that from actual experience on heavy pr. still resid. service, it has been found that this problem is of no greater consequence with noncontinuous than with continuous longitudinal fins. It should be realized that the arrangement sketches of Fig. 2 of the paper are, of necessity, not drawn to scale, and in the particular instance of sample A-9, this fact may tend to mislead the reader into visualizing a rather complicated structure. Actually, the straight sections of fin are over 1 ft in length, interrupted by relatively short oblique segments. The turbulence and intermixing produced at these points, it is found, tend to scour these fin segments and to minimize the cleaning problem here.

The suggestion that continuous fins can be made as efficient as noncontinuous fins by increasing the fluid velocity with the former fin arrangement within allowable over-all pressure-drop limitations warrants detailed consideration.

From Equation [9] of the paper, it will be seen that pressure drop (ΔP) normally varies as the square of the linear velocity V. Further, the slope of the (L/D_h) lines in Fig. 3 is $-2/3$, whence it can be said that h_f varies as $V^{-2/3}$ (since $V = G/\rho$ in the abscissa; $R_h = GD_h/\mu = V\rho D_h/\mu$), referring to Equation [5].

Taking $R_h = 30$ (in Fig. 3), for example, we find $J_A = 0.028$ for a 10-ft length of continuous fins (sample A-1), as against $J_A = 0.056$ for a similar length on a noncontinuous basis (sample A-9); also, $\Delta P_{A-9} = 1.5\,\Delta P_{A-1}$, from Fig. 2. The foregoing, then, for a given condition, represents a 100 per cent increase in h_f with only a 50 per cent increase in ΔP, for noncontinuous (A-9) versus continuous (A-1) longitudinal fins.

Since $\Delta P_{A-9} = 1.5\,\Delta P_{A-1}$ from Fig. 2, V for A — 1 can be increased only 23 per cent to stay within equivalent pressure-drop limitations. The increase in h_f from this would be less than 10

[5] Professor of Mechanical Engineering, University of Texas, University Station, Austin, Texas. Mem. A.S.M.E.

[6] Foster Wheeler Corporation, New York, N. Y.

[7] "Heat Transfer and Pressure Drop of Liquids in Tubes," by G. E. Tate and E. N. Sieder, *Industrial and Engineering Chemistry*, vol. 28, 1936, pp. 1429–1435.

per cent and the effect on fouling rate from, say 5 up to 5.5 fps would not be appreciable.

Professor Short's comments are of interest. The confusion with respect to the use of fouling factors in Fig. 5 as reciprocals of fouling resistances is natural if one is accustomed to the use of the resistance forms. However, from practical everyday rating experience in the heat-transfer engineering industry, the authors have found the coefficient form of fouling factors a more convenient system with which to work.

The suggested use of Reynolds numbers incorporating a dimension in the direction of flow was considered when preparation of the paper was begun. However, since the preliminary work had been carried well along on the conventional basis before any thought of publication existed, dead-line limitations did not permit of a transposition to the suggested form of presentation, and this work was necessarily left for study at some more opportune time.

The authors are in complete agreement with Professor Short's precautionary remarks on the free use of data from tests with odd-shaped flow passages. As pointed out in the paper, various factors exist to which careful consideration must be given in applying test data to actual use outside the range of the original work. It must be stated that $J_A'/(f/2)$ relationships were included in the present paper reservedly, merely to indicate the comparison of the results of this investigation with previously published data.

Mr. Sieder's discussion is most timely. The savings in scarce and strategic materials through the use of noncontinuous fins is well worth while, since increases in over-all rate up to 100 per cent, after applying nominal fouling factors of $h_D = 200$, are achieved. The value of these factors is readily obvious on new installations. On continuous-fin double-pipe equipment already in service, noncontinuous-fin tubes could be installed and, depending upon service conditions, up to one half of the units in the original battery could be released for other work.

It is regretted that certain restrictions prohibited a more detailed presentation of the original test results. However, it was felt that sufficient data were included to indicate generally the conclusions arrived at through this investigation.

The apparent shift in the start of the transition region, as indicated by this work and suggested by the earlier data of Davies and White (6), was revealed primarily for the record and not as a final conclusive fact. As noted in the paper, the tests were made to simulate plant-scale conditions, with no calming sections and greater temperature rises in most cases than the usual 2-4 F used in normal laboratory work.

These factors no doubt are partly responsible for the shifting of the transition zone, as observed. However, since this work was undertaken for the essential purpose of producing practical rating curves, and since the aforementioned factors are normally present in actual operations of plant-scale equipment, the use of the data established by these tests as against the more theoretical values from laboratory-scale experiments should result in ratings which more nearly approach the desired plant-equipment performance.

Protecting Buried Metals Against Corrosion

By STARR THAYER,[1] HOUSTON, TEXAS

The author mentions briefly the various types of corrosion from the standpoint of methods used to combat it. His main concern, however, is with underground structures, such as pipe lines, which suffer a corrosion loss of upward of $100,000,000 yearly. Protective coatings have been developed which constitute a long step toward elimination of pipe-line corrosion, when applied to new pipe. Older lines can be protected by a cathodic process, based on correcting the galvanic differences in potential between small sections of the pipe wall, or changes in soil conditions. The process of making the pipe cathodic to the surrounding soil is described, illustrations of the practical effects of the method being given.

Introduction

PROBABLY there is no way of knowing actually how much we as a nation pay annually as tribute to corrosion. It has been estimated by some that one half of all of the iron mined is used to replace that lost through corrosion. One reliable estimate places this loss for the pipe-line industry alone in excess of $100,000,000 per year. This much is certain; we know that it is a very great national loss, larger than our losses from either floods or fires. There is nothing spectacular about a piece of rusty iron so it has received practically no national prominence. Perhaps an "anticorrosion week" would be as appropriate as our "fire-prevention week."

The elimination of these losses is an important undertaking at any time. During this time of national emergency, when all metals are so vitally needed in industry, it should be apparent that this work is of utmost importance.

Types of Corrosion

For convenience, we may separate the different kinds of corrosion into classes having to do with methods of prevention rather than with causes. Thus, we would have loss of metal from above-ground structures, or atmospheric corrosion, corrosion of industrial equipment, and corrosion of buried or submerged structures. The first two classes are approached from an entirely different angle from the third. Atmospheric corrosion is almost always combated with paints or a selection of materials such as copper for roofing material, and galvanizing for sheet iron and pipes. Industrial corrosion is generally combated to some extent with paints, but more often with a selection of materials. There are so many examples of this type of corrosion that only a few can be discussed here. Heat exchangers have come in for considerable attention. To date, the only practical method of reducing corrosion in such equipment is by the selection of special metals for the tubes. Losses in brine lines may be mitigated by confining the construction to only one kind of metal. If the line is constructed of steel, then all valves and fittings should be of the same material. Galvanic couples will be created if this is not done and one metal will suffer.

The elimination of corrosion in the case of buried or submerged structures, which is the principal topic of this paper, will be discussed more fully.

Underground Corrosion

The one single type of construction most exposed to underground corrosion is the pipe line. Probably more effort has been made to eliminate corrosion on these lines than in any other industry. With more than 130,000 miles of lines well scattered throughout most of the country, it is only natural that corrosion has become a serious problem. In most instances, the methods used in combating this corrosion can be applied to other underground or submerged structures, such as steel piping for other purposes, sheet piling, underground tanks, etc. This problem may be attacked by one or more of the following methods.

Selection of Materials. Some success has been had with the use of materials other than steel in eliminating underground losses. Copper pipe has been used with success in small sizes. Lead has been used as a covering for cables, with a minimum of trouble. Ceramic materials have lately been used for water lines and apparently will be satisfactory. However, pressures are limited with all of these. It is still necessary to use iron or steel when large volumes or high pressures are involved. At this time, there is nothing to indicate that a corrosion-resisting ferrous material will soon be available. Therefore the problem is reduced to making the iron or steel last as long as possible.

Selection of Right of Way. In laying pipe lines, it is sometimes possible to avoid known corrosive areas by selecting a more favorable location for the line. Swampy areas are sometimes avoided by going around them. Often, lines are built on trestle work to avoid laying them in a bad soil. It is the author's opinion, however, that these measures are not justified if any extra expense is incurred, and if it is done merely to avoid corrosive soils.

Protective Coatings. When corrosion is even suspected, it is common practice now, with most pipe-line companies, to apply a protective coating to the pipe. A few companies make it a practice to coat all lines. In the early days of pipe-line construction not much was known about coatings; for that reason, almost every conceivable material that was suspected of having protective qualities was used.

Within the last few years, worth-while progress has been made in the manufacture and application of coatings. The American Petroleum Institute, co-operating with the pipe-line industry and several coating manufacturers, began a study of this subject about 12 years ago. At about that time, Dr. Gordon Scott was employed to work on this subject, as well as on other phases of pipe-line corrosion. At the same time, the American Gas Association employed Dr. Scott Ewing for this purpose. Both of these experts in the field collaborated with the National Bureau of Standards.

One of the first undertakings of this group was to commence the study of the different types of coating materials and shields. Through the co-operation of coating manufacturers and pipe-line companies, sections of pipe were coated with the several materials in many widely scattered areas. These pipes were examined at intervals and detailed reports were made of their condition. The last and final inspection was made in 1940. At that time, the tests were 10 years old.

Space does not permit elaboration on the methods of making these examinations. It may be said, however, that a study of these reports will very clearly indicate the merits of the different

---

[1] Consulting Engineer.

Contributed by the Petroleum Division and presented at the Spring Meeting, Houston, Texas, March 23–25, 1942, of The American Society of Mechanical Engineers.

Note: Statements and opinions advanced in papers are to be understood as individual expressions of their authors and not those of the Society.

classes of materials. In summing up the data from these reports, we may draw the following conclusions:

1 The material must adhere to the pipe.
2 It must be of high dielectric strength.
3 It must be impervious to moisture.
4 It must resist soil stress. This may be accomplished with the addition of a shield.
5 It must retain these qualities over a long period.
6 It must be practical to apply.
7 Its cost must be reasonable.

It is evident that the best of coatings would be of little value if improperly applied. For some time, it has been possible to have pipe coated in stationary plants, with the assurance that an almost perfect application will result. In these plants, pipes are coated up to very large diameters, and are lined with a coating if necessary.

Often, lines are built and then coated. Sometimes the pipe is coated in stationary plants and then hauled to the line. The joints are coated by hand methods. However, a large part of the lines constructed now are completely coated after the welding has been done. Not so long ago, this was done by hand methods, which procedure resulted in an excessive waste of material, a good application being almost impossible. During recent years, machines have been developed which travel on the pipe and apply the coating and shield very satisfactorily. These machines waste very little material and will coat several miles per day if it is necessary.

It is now common practice to test lines electrically for possible faults in the coating before laying them in the ditch. With the use of detectors and all other available equipment it is possible to apply protective coatings economically, with the assurance that practically a perfect application is being secured.

Nearly all of the foregoing has reference to prevention and precautions to be taken in the design of new lines or structures. However, it is on the older lines, built some years ago, that the effects of corrosion are most serious. It is on these lines that the engineer has been able to accomplish the most good.

Cathodic Protection

Theory of Cathodic Protection. The theory of cathodic protection is rather simple. It is assumed that corrosion is electrolytic in action. Because of galvanic differences in potential between small sections of the pipe wall, or due to changes in soil conditions, or both, small batteries are created. Sometimes, these soil changes may be some distance apart and still cause trouble. Now, if the pipe lies in contact with a soil that is a conductor of electricity, small currents will be generated. Loss of metal will occur at the points of discharge from the pipe. This is illustrated

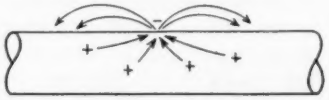


Fig. 1 Electrolytic Action on Pipe in Contact With Soil Which Acts as an Electrical Conductor

in Fig. 1. If the pipe is made cathodic to the surrounding soil, these currents can be prevented from leaving the pipe and there will be no loss of metal.

Application of Cathodic Protection. The application of this protection to a line or other structure is best illustrated by a rather simple electrical circuit, as shown in Fig. 2. As seen, the negative terminal of a source of direct current is connected to the pipe line or structure to be protected. The positive terminal is connected to a mass of scrap metal which is buried in the soil some distance from the line. In practice, we refer to the power supply as the "unit," the scrap metal as the "ground bed," and the connecting wire as the "ground-bed line." When the unit is turned on, current is forced from the ground bed, through the soil, and onto the pipe wall which carries it back to the unit.

Power Units. Naturally, the first and most important problem which arises in applying the protection is to secure a source of direct current. If commercial power lines are available, rectifiers can be used. Such units are now manufactured by several companies. They are available in almost any required size and come

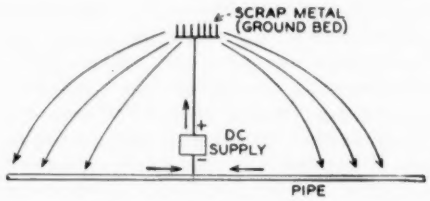


Fig. 2 Diagram Showing Application of Cathodic Protection to Pipe Line

complete, ready to put in use. Where power lines are not available, wind-driven units have been used with considerable success in some localities. Gas companies have used engine-driven units. In this case, fuel is taken from the pipe line. Some attempts have been made to use zinc anodes as the source of power. In this case, the driving force is the difference in potential between zinc and steel. This may be practical where the current requirements are comparatively small.

Ground Beds. The construction of the ground bed often becomes rather difficult. The purpose of this bed is to provide a path of low resistance for the current to enter the soil. It is necessary, therefore, to select the most favorable location. This is determined by securing the lowest soil resistance possible. The amount of metal to be buried, its distance from the pipe line, and the material to be used for the bed are factors which require consideration. Not only must the bed provide a low-resistance path, but it also must contain sufficient material to last for some time. Graphite or carbon anodes are available for this purpose and have been used to a considerable extent, especially when the bed is to be submerged in sea water.

Practical Application. In designing protection for a line or other structure, many factors must be considered. If engines are used, extensive protection will be secured from one unit. These units are not practical in small sizes. Wind units are limited in size and must be spaced on the line according to current requirements. Rectifiers may be large or small according to current requirements and location of power lines.

The amount of current necessary to protect a pipe line varies over a wide range. The factors that control this element are the size of the pipe, the condition of the soil surrounding the pipe, and the condition of the coating on the pipe, if any has been used. The last item is by far the most important factor. As an example of this, not long ago the author applied such protection to a line that had been coated by the most modern method. It took but 3 amperes to protect 20 miles of this line. Another line in the same type of soil and of the same size required 60 amperes per mile. This line is practically bare of any coating. The comparison is given as an example merely to show the variables encountered in the work.

Testing. As stated previously, the purpose of this system is to make the pipe cathodic to the soil. However, it must be more than just negative to stop the corrosion. By laboratory methods and by actual experience, we have found that the pipe must be at least 0.3 v negative to the soil to arrest the corrosion completely.

After a unit has been installed, the engineer measures the potential between the pipe and soil to determine its effectiveness. In

making these measurements, special equipment is used. First, it is necessary to have a contactor with the soil that will remain constant. A copper-sulphate plug is most commonly used for this purpose. The potential between this plug and the pipe is measured either with a high-resistance voltmeter or with a potentiometer.

If additional proof of the effectiveness is needed, coupons may be attached to the line. However, care must be exercised in doing this. Pilot coupons should also be placed unconnected in the same locality. In this instance, some time is required to get the information needed.

When the line is tested by means of the potential method, the readings may be plotted. When soil and coating conditions are uniform, a curve somewhat similar to the one shown in Fig. 3

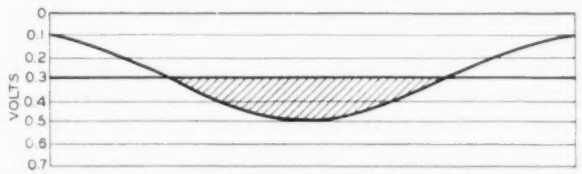


FIG. 3 TYPICAL CURVE DERIVED BY POTENTIAL METHOD WHEN SOIL AND PIPE-COATING CONDITIONS ARE UNIFORM

(The horizontal distance covered in this graph, as well as in Fig. 4, might be almost any distance. In some cases, it is as much as 16 miles and in other cases as little as 0.5 mile.)

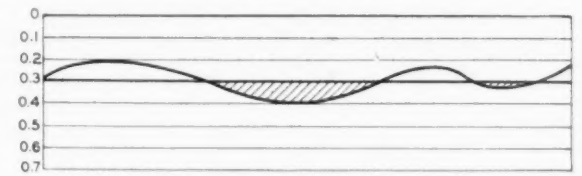


FIG. 4 VARIATIONS IN SOIL OR PIPE-COATING CONDITIONS PRODUCE A NONUNIFORM CURVE

would result. That part of the curve which shows a potential below the 0.3-v line would be protected. That part above this line but below the zero line would be protected but to a lesser extent. Any negative potential will prolong the life of the pipe.

It seldom occurs that a uniform curve, as shown in Fig. 3, is obtained. More often it will look something like the one shown in Fig. 4. These variations are due to changes in soil or coating condition.

Effectiveness of Cathodic Protection. Naturally, the question arises as to how effective this protection is. A few illustrations will demonstrate the value of this method. As far back as 10 years ago, the author applied this protection to two different lines that were in such bad condition and leak repairs were so frequent that their replacement was being considered. Cathodic protection was applied, with the result that both of these lines are still in service, no replacements having been necessary, and no further leaks have developed. Others have had similar experiences. On one section of the pipe line of an important company, a record of leak repairs was kept and plotted, as shown in Fig. 5. In 1936, cathodic protection was applied. The effectiveness of the method is shown by the curve obtained thereafter, as compared to what would have occurred had the protection not been applied. The prospective user may be assured that his corrosion losses will cease if this protection is properly applied.

Application to Structures Other Than Pipe Lines. Life can be prolonged on almost all underground or submerged metallic structures. Examples for treatment would be casings for water and oil wells, steel piling, underground cables, the inside walls of tanks, etc. Many large tank farms have applied this protection to the tank bottoms and connecting lines. Some work has been done in

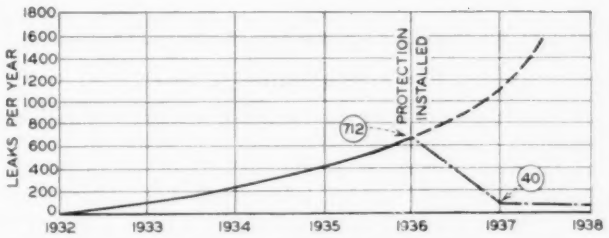


FIG. 5 CURVE SHOWING LEAK REPAIRS BEFORE AND AFTER CATHODIC PROTECTION WAS APPLIED

the protection of heat exchangers and condensers from corrosion. In at least one instance, the water jackets of an internal-combustion engine have been so protected.

Often, these structures are quite difficult to protect. As an example, one engineer applied this method of protection to a line consisting of 24 parallel pipes. In this case, large units were spaced but a few hundred feet apart, as against some miles apart on a pipe line.

CONCLUSION

It can no longer be said that the use of cathodic protection is an experiment. There are many hundreds of miles of lines now so protected and more are being added each year. Very few companies now replace corroded pipe, especially if any quantity is involved.

It is not likely that all corrosion can be eliminated. However, it is entirely incorrect to admit that corrosion is a necessary evil and must be tolerated. Probably most corrosion troubles can at least be mitigated.

Discussion

J. J. KING.[2] The subject of protection of buried metals, particularly pipe lines, is one of vital interest to those connected with the oil-and-gas industry. The same may be said for many other industries, though perhaps to a lesser degree because of the lesser amounts of buried lines involved. As operating pressures on oil, gas, and gasoline pipe lines are such that only steel pipe can be safely used in most cases, the problem of protecting such lines properly is becoming more important as additional miles of pipe are put underground.

Many different methods of coating pipe lines are employed in the oil-and-gas industry with such factors as the nature of the soil through which the line will pass, the degree of protection desired, and funds available for coating determining the type to be used. As brought out by the author, the use of cathodic protection for buried metals does not remove the necessity for coatings. As a matter of fact, it can safely be said that the more nearly perfect the coating, the more satisfactory the results from cathodic protection.

In the early days of the application of cathodic protection to pipe lines, scrap steel was almost universally used for ground beds, but in recent years carbon rods have been used as a substitute for scrap metal in some instances, with complete success. As scrap steel is not so available now as in previous years, it would have been timely for the author to mention the relative merits of metal and carbon rods for ground beds.

Recently, experimental work has been carried out in connection with the use of magnesium rods for the protection of pipe lines by burying cylindrical sections of this metal alongside of the pipe. In so far as the writer knows, very little has been published on

[2] Engineer, Producing Department, The Texas Company, Houston, Texas. Mem. A.S.M.E.

this work. If the author would care to comment upon the matter in the closure to his paper, his readers would be grateful.

Author's Closure

Fig. 2 of the paper illustrates the circuit that is used in cathodic protection. As shown, a mass of scrap metal is buried some distance from the pipe line to be protected. In the past it has been almost the universal custom to use scrap pipe for this ground bed. The exception has been when carbon, or graphite anodes were used.

The advantages of the scrap metal are (1) it generally has been readily available in the past; (2) its cost has been very small; (3) it is easily installed. The disadvantage of using this metal is that it has a very much shorter life than the carbon would have. Also, at this time, scrap metal may be more vital to our country than carbon.

As explained in the paper, one of the requirements of this ground bed is to provide a low-resistance path for the current to pass off into the soil. Often this is possible only by having a large anode surface in contact with the soil. In that case the cost of the carbon anode could possibly make its use prohibitive.

When the ground bed can be installed in sea water or in a soil of extremely low resistance, the use of carbon anodes would be preferable. Under such conditions, a small area would be required and a much longer life would result than with the use of metal.

It has been estimated that with the same current density on the discharge surface the graphite anode will last about 20 times as long as iron.

It is not probable that any set rule may be established as to which material should be used. There are so many factors involved that each installation should be engineered.

Some efforts have been made in the past to use a ground bed of such a material that an anodic condition would be created on the ground bed with the pipe line cathodic. This can be accomplished to a limited extent by the use of aluminum, zinc, or magnesium. In using this method, the circuit is the same as that shown in Fig. 2, with the exception that no generating unit is used.

It is easily seen that the driving force or difference in potential between the anode and the pipe line is very small. For that reason it is not possible to obtain any appreciable flow of current. Generally this current is measured in fractions of an ampere.

However, there is a place for this type of installation. Often it is necessary to protect a very limited area of small pipe or a larger but well-coated pipe. In such cases it is frequently not possible to install a power unit economically.

The advantage of the magnesium over zinc or aluminum for this purpose is that the difference in potential between this metal and the pipe is higher and the current flow is greater. Also, it is possible to protect a line completely with the magnesium, while the others only slow down the corrosion.

The disadvantage of this metal is that it is so unstable. It loses weight when buried in a soil and at a rapid rate whether connected in a circuit or not.

It is not probable that any of these metals will find a wide application since, at present, they are all on the critical list. It may be that other methods may be devised whereby the galvanic difference in potentials can be utilized.

The Application of Cathodic Protection for Corrosion Prevention

By R. J. SULLIVAN,[1] HOUSTON, TEXAS

The application of cathodic protection for the prevention of corrosion, either as the primary protective agent or in conjunction with external coatings, has been successfully and economically utilized on a variety of types of buried or submerged metal structures. This paper presents a short review of the subject of corrosion in general. However, it is devoted principally to the practical application of cathodic protection to numerous metallic structures. Sections are included covering the various types of equipment, the method of testing and keeping records in checking the operation of cathodic-protection installations, ground beds, preliminary survey methods, and illustrated descriptions of certain installations, such as pipe lines and oil-storage-tank farms.

A REVIEW of the published literature on corrosion will show that the result of a great amount of research, laboratory, and field work has been published on corrosion in general; that the effectiveness of pipe coatings has been tested in the field; and that cathodic protection has been found both practical and economical, either as a supplement to the coating, or as the primary protection for the submerged structures. Much has yet to be learned, however, about the proper application of cathodic protection.

The need for further research arises from the fact that the requirements for complete protection have not been agreed upon by all workers in this field, that better methods of predetermining the power requirements are needed, as well as further studies into the economics of the various types and combination of types of corrosion control. At the present time, the American Petroleum Institute (A.P.I.) is conducting an investigation on the effectiveness of resistance bonds.

Since we do not have the results of any research to report, this paper will be devoted to a short review of corrosion in general and methods of control. Principally, the discussion will deal with the equipment involved, various tests conducted, and records necessary to check the operation of cathodic protection units. Details of several electrolysis protection systems which are in service will also be included.

General Corrosion

Corrosion can be described as the disintegration or wearing away of metals by certain external agencies. This action can then be reclassified as caused by chemical or electrochemical attack or mechanical erosion. Often, corrosion and erosion operate together, promoting each other, and in practice may be difficult to distinguish. Evans (1)[2] of King's College, England, very aptly describes corrosion of a metal as "essentially the reverse process to the production of that metal from its ore. Metals occur in nature as oxide or sulphides; sometimes as normal or basic sulphates, chlorides, or carbonates which are reduced to the elementary condition by the smelting process; but when exposed in service, the metals sometimes return to the state of oxide sulphide, normal or basic sulphate, chloride or carbonate." Evans further states the interesting contrast "the study of metallurgy—the making of metals, appeals directly to a comparatively limited number of persons, but the study of corrosion—the unmaking of metals, has an interest for all who use metals, a far larger class."

Literature pertaining to corrosion indicates that, in general, there are two methods by which the disintegration of metals can take place. The first of these may be called direct chemical action and is typified by what happens when the metallic iron is exposed to the atmosphere at elevated temperatures. Under these circumstances, the iron reacts with and combines directly with the oxygen in the atmosphere to form the product which is commonly known as "mill scale," and which has essentially the same chemical composition as the naturally occuring iron ore called "magnetite." Other metals, when exposed to the same environment, behave in a similar manner to form a whole series of metallic oxides.

The second method by which disintegration of metal proceeds is called galvanic or electrochemical corrosion. This method differs from the first in that it is the result of the displacement of one element in one phase (usually in an aqueous solution) by another element originally present in another phase (in the solid form as a metal or alloy). Since this displacement of one element by another is invariably accompanied by a flow of electric current, this form of corrosion is broadly termed electrochemical. An excellent treatise on the accepted electrochemical theory of corrosion is presented by Speller (2).

Methods for Lessening and Preventing Corrosion

Various methods which have been successfully utilized in the protection of metals against corrosion, under a great variety of circumstances, are briefly as follows:

(*a*) Judicious selection of materials, which are immune to the corroding environment, is probably the most important means of preventing corrosion if the equipment involved is not too large. Various metals and alloys exhibit definite well-known properties when subjected to corrosive agents under certain conditions. Usually, the formation of a protective continuous film by interaction of the metallic substance with the corroding agent is the factor governing the suitability of the metal for the service. Because of this effect, lead is commonly used for exposure to sulphuric acid, the protective effect of the insoluble lead-sulphate coating keeping the attack low. Where the reaction of a considered material and a corroding agent is unknown, or questionable, corrosion tests can be made to judge their behavior, but these tests must be interpreted with caution, as aeration, temperature, movement of solution, etc., sometimes overbalance other factors. Kay and Worthington (3) offer a thorough discussion of the foregoing factors, and various alloy manufacturers (4) present tables listing materials and their suitability for different corroding agents. This method of preventing corrosion is widely used in condenser tubes, pipe, and the like. Special material is not usually adaptable for pipe lines because of the large tonnage

[1] Chief Engineer, Natural Gas and Gasoline Department, Humble Oil & Refining Company.

[2] Numbers in parentheses refer to the Bibliography.

Contributed by the Petroleum Division and presented at the Spring Meeting, Houston, Texas, March 23–25, 1942, of The American Society of Mechanical Engineers.

Note: Statements and opinions advanced in papers are to be understood as individual expressions of their authors and not those of the Society.

of steel involved, since a 1-mile section of 10-in. pipe line is composed of approximately 100 tons of steel.

(*b*) The mechanical application of impervious protective coatings such as paint and bituminous combinations, concrete mortar, and others, is very widely utilized and is ably discussed by Ewing (5), Larson (6), and Evans (1). An exhaustive series of pipe-coating tests has been conducted by the American Petroleum Institute for a period of 10 years, and the final report by Logan (7) has recently been published.

(*c*) The mechanical elimination of certain corroding constituents, i.e., oxygen and, to a lesser degree, carbon dioxide, have a pronounced effect on the corrosion of metals exposed to water. In many instances, the removal of these gases has successfully solved water-corrosion problems.

It is a well-established fact that oxygen in solutions combines with the hydrogen liberated as iron passes into solution during corrosion, thereby permitting the reaction to continue until the oxygen is used up. Oxygen also combines with the freshly dissolved iron to form an entirely new compound, an oxide of iron, and, in this manner, accelerates a concentration-cell pit, once it has started. Free carbon dioxide causes a lowered alkalinity in solutions, which increases the tendency for iron to pass into solution. For certain installations, where it is practical to remove these gases, corrosion can often be completely arrested. Both mechanical and chemical methods and combinations have been successful. Hammerschmidt (8) corrects the corrosive action of an engine cooling-water system by deaerating the water by means of natural gas which is passed countercurrent to the water through a novel contacting tower, after which the gas is utilized as engine fuel.

A notable example of mechanical deaeration has been described by Powell and Burns (9). A pipe line, designed to carry 4,000,000 gal per day of Mississippi River water a distance of 9 miles, suffered a rapid loss of capacity due to oxygen corrosion. The economic solution of this corrosion problem was obtained by a combination of physical and chemical deaeration. Ninety-five per cent of the dissolved oxygen was removed by passing the water through a slat-packed vacuum tower, operated at an absolute pressure of 1.5 in. Hg. The residual 5 per cent oxygen was removed by the addition of sodium sulphite, which combines with oxygen to form sodium sulphate. This deaeration plant has operated successfully since 1935.

(*d*) The chemical treatment of aqueous solutions by the addition of protective-film-forming agents, or the addition of oxygen-scavenging chemicals.

This subject is very broad, since each method of treatment is in itself a topic for lengthy discussion. The various types of waters encountered are susceptible to only certain chemical treatments. A judicious selection of chemicals is necessary since certain compounds will inhibit corrosion, but accelerate scaling, etc. The inhibitors generally used are sodium dichromate, sodium silicate, sodium hexametaphosphate, other phosphate salts of sodium, soda ash, caustic soda, lime, and various organic combinations. An example of this method is the treatment of boiler feedwater and cooling water for condensing and cooling systems with chemical inhibitors.

(*e*) The application of a counter electromotive force to reverse the natural electrochemical action taking place during the process of corrosion. This method is termed cathodic protection and will be discussed in the remainder of this paper.

Cathodic Protection

Cathodic protection is known as the process by means of which an electromotive force is applied to a corroding metallic structure in a manner such as to nullify or reverse the electrochemical reactions which take place during the natural corrosion of the metal. This method consists of making the structural metal the electrode which receives current from the corroding solution in an electrochemical cell. The structural-metal electrode in this case is called the cathode in a protective system. The other electrode from which the current enters the solution is called the anode. The cathode and the anode are connected externally by a suitable metallic circuit. When the current is supplied by a generator or a battery in the external circuit, the arrangement is called one of impressed-voltage cathodic protection. If the current is supplied by the natural galvanic action of two dissimilar metals used for anode and cathode, the arrangement is called galvanic cathodic protection. In both cases, the protection of the cathode structure is at the expense of the anode metal which corrodes in proportion to the protective current produced.

Galvanic cathodic protection has been used in protecting pipe lines, as well as small structures. A few years ago, a group of engineers experimented with various anode materials. However, at present the scarcity of suitable metals prohibits the use of this type of cathodic protection, and consequently will not be discussed.

The use of cathodic protection of underground structures probably developed through the practice of bonding these structures to the return circuits of electric railways for the prevention of stray-current electrolysis. It was soon observed that, in addition to stopping the leaks, caused by stray currents, there was a lessening of natural corrosion in the vicinity of the bonds. This suggested the possibility of preventing corrosion by impressing a negative potential on the pipe.

The potential difference between metallic structures and the surrounding solution necessary for protection has been reported by several investigators (10, 11, 12, 13, 14), and has been found to vary from 0.8 to 1 v when measured with a copper-sulphate electrode.

The amount of current entering the surface of a bare-metal structure, or the current density necessary to produce a protective potential depends upon the nature of the solution in contact with the metal. Laboratory investigators (15, 16, 12) have indicated that the required current density varies from 1.2 to over 30 ma per sq ft for various solutions. For well-coated lines or structures, the current density will be very small, since it is only necessary to protect the "holidays" or small uncoated areas.

The question of the possible damage done by a cathodic-protection installation to an adjacent nonprotected metallic structure and the proper method of preventing any damage have never been agreed upon. However, at the present time, the A.P.I. is conducting a research on this problem. Since most of the pipe-line companies are participating in the investigation, a satisfactory solution is likely to be obtained.

Results Obtained With Cathodic Protection

Hough (17) reviewed the results obtained by ten pipe-line companies at a meeting of the American Gas Association in Houston, in 1940. Nealy (18) and Miller (19) presented papers at the 1941 mid-year meeting of the A.P.I. on the application of cathodic protection to refinery equipment. These papers could be summarized as follows: That positive beneficial results were obtained; that there was no serious difficulty in maintaining cathodic protection; that the cost of applying cathodic protection is less than reconditioning and/or repairing the equipment; and that there is yet much to be learned about the proper application to secure the necessary protection with a minimum investment and power consumption.

Equipment

The essential equipment for constructing a cathodic-protection installation, as mentioned, are the anode (or ground bed), a source

of direct current, and the necessary electrical connections between the ground bed, source of direct current, and the cathode or the structure being protected. The selection of proper material is a problem similar to that of other engineering projects. There is an economic medium between the first cost and operating cost which should govern the selection of the equipment. Some very helpful information on the equipment available has been published by Ewing (5) and others (20).

Fig. 1 illustrates a typical cathodic-protection installation.

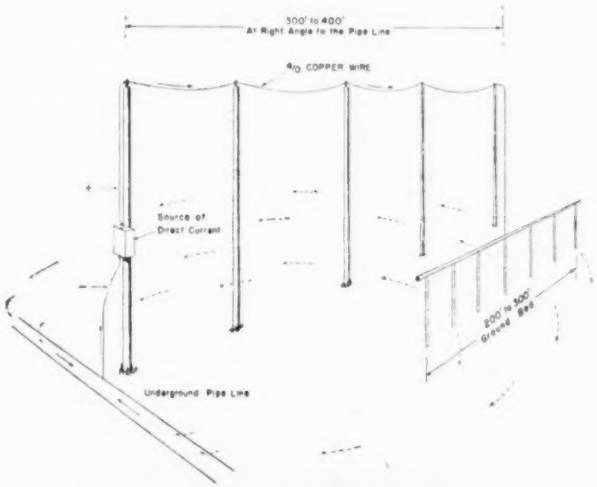


FIG. 1 TYPICAL CATHODIC-PROTECTION INSTALLATION

Since the direct-current voltage is generally low (less than 15 v), it is obvious that large conductors must be used. Conductor lines of copper are generally used; however, in some instances, old steel cables have been utilized.

The anode (or ground bed) should preferably have low resistance, sufficient volume to last several years, and current spread.

To secure low resistance, it is necessary to locate the ground bed in a low-resistance soil, and also to provide a sufficiently large area of exposed anode surface. At times it is also necessary to add salt and sometimes water to the ground-bed soil to lower the resistance. The life of the bed can be estimated from the weight of metal installed, its electrochemical equivalent, the amount of current flowing, and an assumed efficiency. The efficiency of ground beds under different arrangements has been reported by Rogers (21) and McAnneny (22). For the best distribution of current over the entire structure, it is advisable to have ground beds distributed at several points along or around the structure, since it takes a definite amount of current to protect a unit area; if the current is concentrated more than is necessary, the excess is wasted. An exception would be in the case of a well-coated line or structure where it would probably be more economical to install a small number of large units, as the resistance offered by the protective coating prevents high current densities in the vicinity of the ground bed. The high metal-to-ground potential does not indicate a waste of power. It should be further stated that conditions, such as cheap power, size of the structure, and the like, might make it more economical to install large units even on bare structures.

The most commonly used material for ground beds is junk pipe, old castings, scrap iron or steel, and carbon or graphite rods. Some experimental chemical ground beds have been reported by McAnneny (22). While chemical ground beds have not been used to date, the present scarcity of junk pipe and other suitable materials will encourage their development.

The majority of ground-bed installations consist of junk pipe because it is reasonably cheap, easy to install, and provides a better current distribution per pound of metal than other forms of scrap iron. This pipe is installed either vertically or horizontally, depending upon such conditions as the space available, type of soil, and depth of low-resistance soil. The location of the ground bed will be influenced by the size and surface condition of the structure being protected.

The requirements of an apparatus for producing a suitable direct current are (*a*) reliability, so as to require little attention; (*b*) ability to produce large direct currents at low voltages; and (*c*) economy of operation. Four methods of producing direct current are in general use, i.e., the alternating-current rectifier, the motor generator, the gas-engine-driven generator, and wind-driven generator.

The alternating-current rectifier is the most widely used method for providing a source of direct current where the output is less than 3000 w. The advantages of the rectifier are simplicity of installation; low maintenance, since there are no moving parts (except the cooling fan in some models); over-all efficiency of between 55 and 65 per cent, depending upon the size and the source of alternating-current power available; and initial cost, which is comparable with the motor generator set.

Motor generator sets may be used if a source of alternating-current power is available as with the rectifier, and are generally used where the output is above 3000 w. The over-all efficiency is approximately 65 per cent. The current of a motor generator is constant and may be varied to any desired output. This set must have some attention because of the moving parts and is, therefore, more suited for tank-farm and station-protection installations than for use on pipe lines and isolated areas.

Gas-engine-driven generator sets of various sizes are being manufactured. Such units produce a constant source of direct current, but because of the inherent nature of the gas engine, they require frequent servicing and repair.

The windmill or wind-driven generator, while picturesque, is not a very dependable source of direct current, since the output of the generator depends upon power derived from the wind; thus, during a calm period, no current is generated. These units are available in sizes from 20 to 2000 w, and their principal use is in isolated locations where there is sufficient wind for their operation.

The majority of installations for pipe lines, tank farms, and station equipment utilize rectifiers, with the motor generator and gas-engine generator as second and third choice, respectively. The wind-driven generator is seldom used except in isolated places. In some cases, two wind-driven generator units are installed; one to protect the pipe line, and the other to charge a battery which will discharge to the electrolysis system during periods of no wind.

Ewing (5) and others (21) have presented analytical methods of determining the number of units and the size most suitable for protecting pipe lines and similar structures, by taking into consideration the condition of the coating and the soil resistivity, which is known or determined experimentally.

Another method for determining the current and number of units required for protecting well-coated lines has been to install a temporary unit for experimental purposes. The installation consists of a ground bed of four or five 4-in. carbon rods or four 10-ft pieces of 4-in. or 6-in. pipe in a shallow well-salted trench about 100 ft from the pipe line. For a source of power, either six or eight regular storage batteries are used. The pipe line, batteries, and ground bed are connected with No. 2 insulated copper wire. By the proper arrangement of the batteries in series and parallel, it is possible to obtain a suitable unit output.

After this equipment has been installed and adjusted, pipe-to-ground potentials are taken in each direction to determine how much pipe is being protected. At each end of the section where

the pipe-to-ground potential is 0.8 v (referred to a copper-sulphate electrode), the current flowing is determined. The sum of these readings deducted from the total drained from the line will indicate the amount of current required to protect that particular section. By measuring the length of line protected, the current per mile necessary for protection can be determined. From these data, the size and location of the units can be made.

The procedure for determining the current required for protecting poorly coated or bare lines is the same as that just outlined, except a larger ground bed is usually installed, and a welding-machine or similar direct-current generator is required in place of the storage batteries.

Cathodic-Protection Methods Employed by Author's Company

The natural-gas department of the author's company has applied cathodic protection on approximately 120 miles of 10-in. line, and on another 60 miles of line, ranging in size from 3 to 8 in. Some of these lines pass through developed suburban territory, and at places they cross and are parallel to other pipe lines, oil-field, and refinery equipment.

Cathodic protection was installed as a preventive measure, there having been no leaks to date. The oldest section of line was laid about 10 years ago and was provided with a protective coating of a cold asphalt application without a wrapper. The other lines are all 5 years old or less and were protected from external corrosion by the application of a primer, two coats of petroleum asphalt enamel, and an asbestos-felt wrapper. The exception to this procedure was river or swamp crossings, at which areas an additional coat of enamel and Osnaburg was also applied.

For cathodic protection on these lines, it was found most practical to locate the units at points within ready access to electric power and most suitable for ground beds.

The lines mentioned are protected with eight units, four of which supply some protection to the Humble Pipe Line Company. The lines of the Humble Pipe Line Company are new and have coatings equal to the natural gas department lines.

It has been assumed that the metal is protected when the pipe line is 0.8 v negative to the soil, the pipe-to-ground potentials being determined by means of a potentiometer and a copper-sulphate electrode. Some coupons were attached to the pipe and, to date, no pitting has been observed.

The following procedure has been adopted for routine tests. When the first cathodic-protection unit was installed, a few complete pipe-to-ground surveys of the protected area were made and were found to have the same trend each time. Then the practice of making a complete survey was dropped, and only a few readings are made at the present time at permanent test locations.

After a new unit is installed a pipe-to-ground-potential survey is made to determine the limits of protection from the unit or the point of lowest potential between the unit and adjacent units.

Permanent test stations are then made at convenient points. These are located at or near the end of the section protected and near the rectifier unit. At each of these locations, a permanent weatherproof insulated copper wire is soldered onto the pipe, after which the other end is made fast to a fencepost or the concrete pipe-line marker at the side of the road. Potential readings are made between this wire and a copper-sulphate electrode which is placed over the pipe line and 1 ft away from the lead-wire connection. Potentials are determined with a Rhodes potentiometer.

Routine checks over the whole system are made each month by measuring the pipe-to-ground potentials at the permanent test station, and by checking the rectified voltage and current. Field data are recorded in a civil-engineer's notebook as it is taken, after which the original sheets are removed and made into a permanent file. From these data, the system potential map and also the unit data sheets are kept up to date. The potential map is a map of the entire system which is provided with blank spaces near each test station and a unit for recording the measured potentials and unit output. The unit data sheets contain information on unit output in volts and the current drained from each line; the ground-bed resistance; the power bill for the month, and remarks. This potential map and the unit data sheets afford a quick check of the entire system with reference to potentials and condition of equipment. The system can be checked by one operator in less than 3 days.

Cathodic Protection of an Oil-Storage-Tank Farm

The Humble Pipe Line Company has applied cathodic protection on a large oil-storage-tank farm and pump station in the Gulf Coast area, where the soil is fairly corrosive.

This farm consists of 62 storage tanks, 115 ft diam, with the auxiliary connecting lines, pumps, and station equipment. About 28 miles of buried pipe are involved in sizes varying from 2-in. to 16-in., the majority being 8-, 10-, and 12-in-diam pipe. In addition, various large-diameter incoming and outgoing lines are involved. Some of the lines have been coated and others are bare.

A number of tank bottoms have required replacement due to a combination of internal and external corrosion. Pit-hole leaks caused by external corrosion were also occurring on the oil lines at such a rate that maintenance required the expenditure of several thousand dollars a year. A cathodic-protection system was, therefore, installed and placed in operation in May, 1941.

The equipment consisted of a total of nine copper-oxide recti-

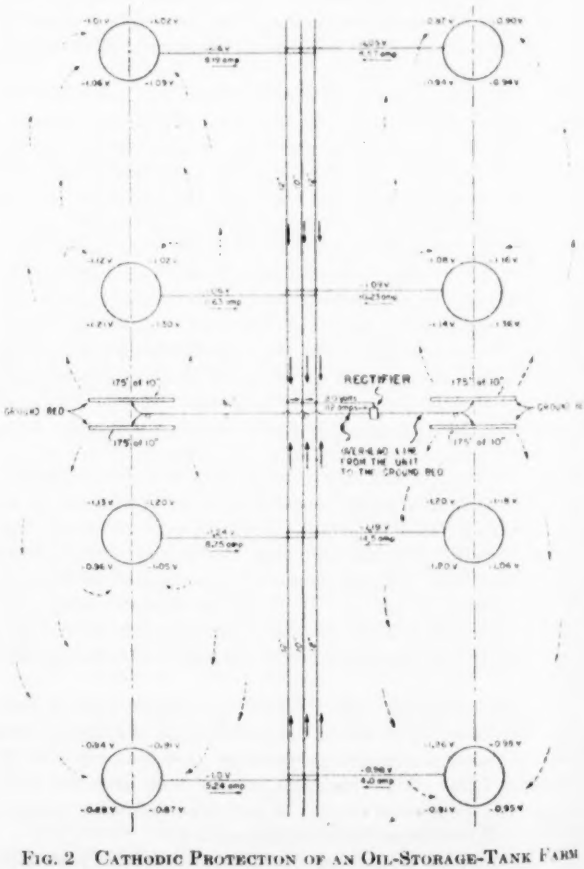


Fig. 2 Cathodic Protection of an Oil-Storage-Tank Farm

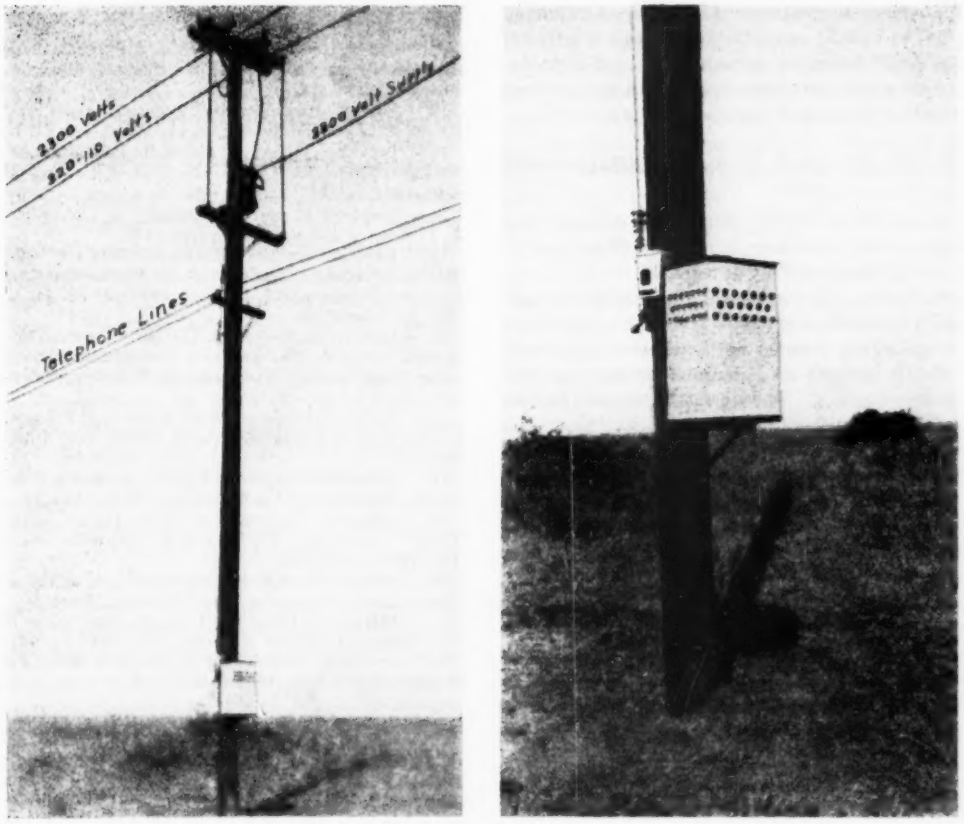


FIG. 3.—CATHODIC-PROTECTION INSTALLATION USING SMALL CLOSELY SPACED UNITS WITH POWER AND TELEPHONE LINES ON SAME POLES

fiers with the necessary ground beds, alternating-current power lines and transformers, and direct-current drainage and feeder lines. Seven rectifiers were 10-v, 120-a units, manufactured by Westinghouse, and two units were $10^1/_2$ v, 130 a, manufactured by General Electric.

The arrangement of the rectifiers and ground beds for one of the units with respect to the tanks and lines is illustrated in Fig. 2; this unit is typical for the combined system. It was possible in most cases to achieve a symmetrical arrangement of the rectifiers and ground beds so that one unit was centrally located with respect to eight tanks and the pipe lines serving them.

The ground-bed arrangement, shown in Fig. 2, has been particularly effective and consists of approximately 20,000 lb of junk pipe of 8, 10, and 12 in. diam, which is expected to serve for about 10 years. The ground-bed pipe is buried horizontally about 5 ft deep. Four sections of pipe are used in each dual ground bed which is arranged as shown with parallel sections 20 ft apart. A 6-in. riser pipe is welded into the middle of each section to which are connected the positive terminals of the unit. The risers extend above the ground and are left open so that water can be poured in if necessary to lower the resistance. This represents an external resistance of $^1/_{18}$ ohm, and in no case was the resistance greater than $^1/_{10}$ ohm for a ground bed of this type. Additional metal is now being added to three less efficiently arranged ground beds to improve their configuration.

Results achieved in eliminating or reducing corrosion cannot be accurately estimated at present because of the short period of time the system has been in operation. A survey is being made, however, which will indicate the metal-to-earth potential of the various structures, and of the amount of current being collected by the various portions of the tank and pipe-line system which will theoretically indicate the degree of protection.

The metal-to-earth potential values are shown in Fig. 2 for four points around each of the tanks, as well as the potentials of the pipe lines leading to the tanks, and the current being drained from each tank. The lowest potential value was found to be 0.87 v which indicates that all structures in this portion of the tank farm are receiving adequate protection. It may be noted that both potential and current drainage are somewhat affected by proximity of the structures to the ground beds. In the case of one tank, satisfactory potentials are obtained with a drainage of 4 a. The drainage from another tank is $14^1/_2$ a, but the negative potentials of the metal to earth are unnecessarily high. This suggests that a more even distribution of potential at a lower power consumption might have been obtained with a yet wider distribution of the ground-bed anodes, or by a system of negative connections which would permit the introduction of resistances into the drainage connections to structures close to the ground beds. In this case, however, it is doubtful whether the saving in power from such changes would justify the cost of making them.

The best measure of the effectiveness of such a system of protection is the stoppage of failures due to corrosion. While the time the system has been in operation is too short for positive conclusions to be drawn, there has been an apparent reduction in the number of failures. From the beginning of 1938, through the third quarter of 1941, leaks occurred on the lines at this station at the average rate of six a month. During the last quarter of 1941, only three leaks occurred, or an average of one a month. A much longer time will naturally be required to observe any change in rate of failure of the tank bottoms.

It is believed that this system of protection, which cost the company about $13,000 to install, and which involves a yearly expenditure of about $3000 for power, maintenance, and depreciation, will prove to be much more economical than the previous maintenance methods, consisting of repairs and renewals.

Cathodic Protection on Large Bare or Poorly Coated Lines

A very practical and unique method of applying cathodic protection by one large pipe-line company in the Gulf Coast area on large and poorly coated lines is worthy of mention.

The telephone-line poles, which are located alongside the pipe line, were changed by replacing every third pole with a power pole on which was strung a 2300-v primary line and a 110-v secondary line. The pipe line is utilized as a common return for both primary and secondary circuits. The small rectifiers are located on these power poles and utilize the 110-v circuit. About ten rectifiers and ground beds are used per mile of pipe. By a judicious selection of material, it was possible to make a very flexible and economical installation.

The economy of the purchased power for such an installation is well illustrated by the following readings which were taken on a section of a coated line, part of which was protected with the small units just described, and part protected with a large unit. The large unit protected 2.6 miles of line with a direct-current output of 20 v and 40 a, or 800 w. On an equal and adjacent length of line, 26 small units had an average direct-current output of 30 v and 2.7 a, or 210 w. Views of this installation are shown in Fig. 3.

Conclusion

It is concluded that cathodic protection will prove the most economical means of preventing external corrosion for pipe lines and similar structures, and we are using it in addition to external protective coatings. At present, the author's company has protection on several hundred miles of pipe lines, part of which are in salt-water marshes and bays, as well as on oil-storage-tank farms. In closing, it should be restated that a great deal is yet to be learned about the proper application of this form of protection.

Acknowledgment

The writer wishes to thank the Humble Oil & Refining Company, for permission to publish the data contained in this paper, and Mr. E. O. Staffel and Mr. R. A. Brannon for their help in preparing it.

BIBLIOGRAPHY

1 "Metallic Corrosion Passivity and Protection," by U. R. Evans, Edward Arnold and Company, London, England, 1938.

2 "Corrosion—Causes and Prevention," by F. N. Speller, second edition, McGraw-Hill Book Company, Inc., New York, N. Y., 1935.

3 "Corrosion Resistance of Metals and Alloys," by R. J. Kay and R. Worthington, Reinhold Publishing Corporation, New York, N. Y., 1936.

4 "Combating Corrosion in Industrial Process Piping," by L. G. Vaude Bogart, Technical Paper No. 408, Crane Company, Chicago, Ill., May, 1936.

5 "Soil Corrosion and Pipe Line Protection," by Scott Ewing, American Gas Association, New York, N. Y., 1938.

6 "Pipe Corrosion and Coating, Parts 19–28," by Erick Larson, *American Gas Journal*, New York, N. Y., vols. 148 and 149, 1938.

7 "Pipe Coating Tests—Final Report," by K. H. Logan, Proceedings A.P.I., section 4, "Production," 1940, pp. 32–69.

8 "Prevention of Corrosion in Water Cooling Systems," by E. G. Hammerschmidt, *Petroleum Engineer*, vol. 12, Nov., 1940, pp. 44, 46, 48.

9 "Vacuum Deaeration Combats Cold Water Corrosion," by S. T. Powell and H. S. Burns, *Chemical and Metallurgical Engineering*, vol. 43, 1936, pp. 180–184.

10 "Pipe Corrosion and Coatings," by Erick Larson, with chapter in "Cathodic Protection," by Geo. I. Rhodes, American Gas Association, New York, N. Y., 1938.

11 "Current and Voltage Needs for the Cathodic Protection for Steel Submarine Pipe Lines," by H. J. Keeling, *Gas*, vol. 15, Sept., 1939, pp. 31–32.

12 "Some Current Density Potential Curves for Steel," by W. F. Rogers, *Petroleum Industry Electrical News*, vol. 11, Dec., 1941, p. 27.

13 "Laboratory Tests of Cathodic Protection of Steel in Various Corrosive Solutions," by W. H. Hill, *Petroleum Engineer*, vol. 12, Sept., 1941, pp. 45–52 and 55–57.

14 "Relation of Current Density to Cathodic Protection," by W. F. Rogers, *Petroleum Engineer*, 1940.

15 "Determining the Minimum Current Required to Provide Adequate Cathodic Protection," by Dave Harrell and Milton Clerc, *Petroleum Engineer*, vol. 11, Oct., 1939, pp. 38, 41, and 44; and Jan., 1940, pp. 64 and 66.

16 "Determination of the Current Required for Cathodic Protection," by Scott Ewing, A.G.A. Distribution Conference, Houston, Texas, May, 1940. Published by American Gas Association, New York, N. Y.

17 "Results Obtained With Cathodic Protection," by F. A. Hough, American Gas Association Conference, Houston, Texas, May, 1940.

18 "Cathodic Protection," by V. L. Nealy, Proceedings, A.P.I., vol. 22, Midyear, Section 3, Refining, May, 1941, pp. 96–97.

19 "Cathodic Protection of Open Tank Condenser," by N. A. Miller, Proceedings, A.P.I., vol. 22, Midyear, Section 3, Refining, May, 1941, pp. 84–89.

20 "Trends in Cathodic Protection," compiled and published by Brance-Krachy Company, Inc., Houston, Texas.

21 "Method of Designing Cathodic Protection Installations," by W. F. Rogers, *Petroleum Engineer*, Jan., 1941, pp. 42, 44, 46, and 48.

22 "Insoluble Anodes," by A. W. McAnneny, *Petroleum Industry Electrical News*, July, 1941, p. 11.

Discussion

R. W. Warner.[3] Corrosion is a relentless enemy and one that knows no quarter. It is possible that fundamentally all metals are subject to this process of reverting back to their original state unless prevented by some natural or man-applied means. Our most useful metal, iron, is particularly subject to the ravages of corrosion especially when combined with other metals or compounds for the purpose of improving its commercial characteristics.

The author has presented an exceedingly interesting paper on some of the methods used by his company in combating corrosion of pipe lines and storage tanks. General acceptance of the electrolytic theory of corrosion at once suggested the feasibility of an electrolytic preventative. As he points out this is relatively simple in theory but more difficult in application because of the tremendous variety of conditions in the field.

Electrolytic corrosion is accompanied by the flow of electrical current in response to natural potentials which become established between a metal and a surrounding electrolyte which may be soil, a salt-brine solution, plain water, or any other medium capable of conducting electric current. The arrangement becomes a natural electrolytic cell. An ordinary dry battery is a common example of such a cell in commercial form.

The amount of voltage developed in such a natural battery is not large, in fact usually well under one volt. It depends upon a wide variety of conditions, such as the kind of metal present, the purity of the metal, the presence of unrelieved strains in the metal, the temperature gradient between parts of the metal, and upon the electrolyte itself. In the case of pipe lines buried in the earth this voltage also depends upon the chemical characteristics of the soil. Even though only a small voltage is developed, the natural battery thus formed is short-circuited through the body of the metal itself so that an electric current flows constantly. The amount of this current also is small but the cumulative action over a period of months or years is enormous.

[3] Professor of Electrical Engineering, The University of Texas, Austin, Texas.

Decomposition occurs only at points where the current leaves the metal. Wherever it enters no harm is done. The metal or electrode from which current flows into an electrolyte is known as the anode while that by means of which the same current leaves the electrolyte is called the cathode. Corrosion does not take place at the cathode. In order, then, to prevent corrosion which takes place as a result of the natural potentials mentioned it is necessary only to prevent the flow of the electric current, or to be on the safe side, to force it to flow in the opposite direction. The metal it is desired to protect is thus forced to become a cathode. Some other piece of metal, the corrosion of which will be harmless, is placed in the electric circuit as the anode. All the corrosion is centered at the anode. This, in the case of a pipe line or storage tank to be protected, is the ground bed. The best method of application and the amount of protective current required depend entirely upon the local conditions; and the author has given the upper and lower limits of the current needed.

It has been observed in many cases that a film or coating is deposited on metals that are being protected as cathodes. This film of itself possesses a certain protective value against corrosion just as do paint, asphalt, and other coatings. Its composition depends upon the electrolyte and the material of the anode. With metals in a salt-brine solution a chunk of zinc may effectively be used as the anode. A protective film consisting of a complex compound of zinc, oxygen, and chlorine is formed on the surface of the cathode. Its presence is a visual indication that the protective scheme is functioning. The film is soluble but will furnish complete protection for some time after the protective current is removed. To form such a film on steel, a current density of approximately 5 ma per sq ft of surface to be protected is necessary. This value falls well within the limits of current density given by the author for the protection of pipe lines and storage tanks.

When cathodic protection is applied to metals buried in the earth a similar coating is formed on the metal. It consists of compounds taken from the soil and deposited electrolytically upon the metal; without doubt it possesses protective characteristics. It would be interesting to know how long this coating would furnish protection if the current were to be removed. This might materially affect the cost of protection.

It is believed that the nonrusting characteristic of stainless steel is due to the presence of a natural protective film perhaps only one molecule in thickness. It is possible that an exhaustive study of protective films in general would furnish valuable information about corrosion.

Pipe lines buried in the earth frequently lie in the path of natural stray earth currents. Not a great deal is known about these wandering currents—as to what causes them, where they originate, or where they end—other than that they circulate constantly through the surface of the earth in widely varying amounts, sometimes in one direction and then reversing and flowing in the opposite direction. They undoubtedly follow pipe lines and contribute to their decomposition. A study of these natural currents would no doubt yield valuable and interesting information.

The author mentions the economic phase of cathodic protection and while the economics are certainly in favor of protection it would be extremely interesting to know more about the amount of annual savings that can be expected. This would form excellent material for a subsequent paper. Also, it would be interesting to know about the effectiveness of this method of protection, after a period of perhaps ten years of operation.

Effect of Variable Viscosity on Boundary Layers, With a Discussion of Drag Measurements

By J. G. BRAINERD,[1] PHILADELPHIA, PA., AND H. W. EMMONS,[2] CAMBRIDGE, MASS.

This work extends a previously reported investigation of the boundary-layer problem associated with the steady laminar flow of a perfect gas along a thin flat insulated plate. In the earlier study the viscosity was assumed constant and the distributions of velocity and temperature were obtained for a wide range of conditions. Part I of the present paper shows, for Prandtl number 0.733 (air) and Mach number of the undisturbed stream 2, the velocity and temperature distributions in the boundary layer under various assumed viscosity variations. Part II gives the distributions for various Prandtl numbers and Mach numbers, assuming the same viscosity functions as used by von Kármán and Tsien. Part III is devoted to a discussion of the method of interpretation of traverse tests of the efficiency and flow coefficients of nozzles or other passages. The results of Part I show that the variation of viscosity with temperature does not alter the equilibrium temperature of the plate, and hence the reading of a plate thermometer. This result is extended in Part II where it is shown that θ at the plate wall is equal to the same quantity when μ is taken constant to within 1 per cent in all cases studied. Furthermore, $\varphi U'$ at the plate wall does not vary greatly, so that the drag coefficient C_D is equal to $1.28/(\mathrm{Re})^{1/2}$ to within 5 per cent for most of the cases investigated. In Part III a passage efficiency as usually calculated is found to be subject to two errors, one of which reduces and the other of which increases the test result. The net effect is to cause the standard traverse test to give a conservative estimate of the efficiency. The flow coefficient as determined by traverse tests is somewhat higher than the correct one.

Nomenclature

a, a_1 = see note on subscripts at the end of the list
$b = (\gamma - 1)M_1^2$ = compressibility number
B = breadth of plate
c_v = constant-volume specific heat
c_p = constant-pressure specific heat
C_d, C_s = see Table 3
C_D = drag coefficient
E = internal energy per unit mass
$\boldsymbol{F}$ = vector body force per unit mass
h = enthalpy
k = thermal conductivity
L = length of plate
M_1 = Mach number of undisturbed stream = u_1/(acoustic velocity in undisturbed stream)
p = pressure
$\mathrm{Pr} = c_p\mu_1/k_1$ = Prandtl number
$\mathrm{Re} = u_1L\rho_1/\mu_1$ = Reynolds number
R = gas constant
s = entropy
t = time
T = absolute temperature
u = velocity component in X direction, along plate
$U = u/u_1$ = dimensionless velocity along plate
v = velocity component in Y direction, perpendicular to plate
$\boldsymbol{v}$ = vector velocity with rectangular components u, v, w
$V = v(x/\nu_1u_1)^{1/2}$ = dimensionless variable containing velocity perpendicular to plate
X, Y, Z = rectangular co-ordinate axes
x, y, z = rectangular co-ordinates of a point
$\gamma = c_p/c_v$
δ_u = thickness of velocity boundary layer
δ_T = thickness of temperature boundary layer
ϵ, ϵ_1, ϵ_2 see Table 3
$\eta = y(u_1/\nu_1x)^{1/2}$ = dimensionless variable, proportional to distance from plate wall at a fixed x
$\theta = T/T_1$
μ = absolute viscosity
$\nu = \mu/\rho$ = kinematic viscosity
$\xi = \eta U - 2V$ = velocity variable
ρ = mass density
τ = shear stress
φ_B, φ_C, φ_K, φ_S see Equation [16]
$\boldsymbol{\psi}$ = stress dyadic

Subscripts and primes: Subscripts 0 and 1 denote conditions at the plate wall ($\eta = 0$) and in the undisturbed stream, respectively; subscript a indicates an isentropic stagnation condition and a_1 the isentropic stagnation condition in the undisturbed stream. A prime denotes differentiation with respect to η.

The General Problem

In a previous paper (1),[3] assuming μ and k constant, the velocity and temperature distributions in the boundary layer adjacent to a thin flat insulated plate lying parallel to the undisturbed direction of a gas stream were given for a wide range of conditions. The present investigation extends those results by taking into account the dependence of μ and k on T. For the sake of brevity the mathematical basis of this investigation will be outlined in compact form; greater detail for the more-or-less parallel theory of the first study is given in the earlier report (1).

[1] Moore School of Electrical Engineering, University of Pennsylvania.

[2] Graduate School of Engineering, Harvard University. Mem. A.S.M.E.

Presented at the National Meeting of the Applied Mechanics Division, Philadelphia, Pa., June 20–21, 1941, of The American Society of Mechanical Engineers.

Discussion of this paper should be addressed to the Secretary, A.S.M.E., 29 West 39th Street, New York, N. Y., and will be accepted until April 10, 1942, for publication at a later date. Discussion received after the closing date will be returned.

Note: Statements and opinions advanced in papers are to be understood as individual expressions of their authors, and not those of the Society.

[3] Numbers in parentheses refer to the Bibliography.

The basic equations are, in the Gibbs vector notation

$$\nabla\cdot(\rho\boldsymbol{v}) + \partial\rho/\partial t = 0 \quad [1]$$

$$\rho\partial\boldsymbol{v}/\partial t + \rho\boldsymbol{v}\cdot\nabla\boldsymbol{v} = \rho\boldsymbol{F} - \nabla\cdot\psi = \rho\boldsymbol{F} - \nabla p - (^2/_3)\nabla\cdot(\mu\nabla\cdot\boldsymbol{v}) + \nabla\cdot(\mu\Phi) \quad [2]$$

where

$$\Phi = \nabla\boldsymbol{v} + (\nabla\boldsymbol{v})_{\text{conjugate}}$$

$$\nabla\cdot(E\rho\boldsymbol{v}) = (\psi\,\nabla)\cdot\boldsymbol{v} + \nabla\cdot(k\nabla T) \quad [3]$$

$$p = RT \text{ and } E = c_v T \text{ (perfect gas)} \quad [4a,b]$$

For a gas streaming in the $+X$ direction along a thin flat insulated plate, of indefinite extent in the $+X$ and $\pm Z$ directions and with the Z axis for its edge, these equations state that in the boundary layer the following relations hold closely under the conditions and assumptions previously used (1), and with $\mu = \mu_1\varphi$; $k = k_1\varphi$ (see Part I)

$$\theta(\xi' - U) = \theta'\xi \quad [5]$$

$$\xi + \frac{2\theta}{U'}\frac{d}{d\eta}(\varphi U') = 0 \quad [6]$$

$$\xi' - U + \frac{2}{\Pr}\frac{d}{d\eta}(\varphi\theta') + 2b\theta U'^2 = 0 \quad [7]$$

subject to the boundary conditions $U = V = \theta' = 0$ when $\eta = 0$ (i.e., when $y = 0$) and $U = \theta = 1$ when $\eta \to \infty$ (i.e., when $y \to \infty$).

The equations yield

$$\theta = -\frac{1}{2}U/\frac{d}{d\eta}\left[\varphi\frac{d}{d\eta}\log(\varphi U')\right] \quad [8]$$

$$\xi = -\frac{2\theta}{U'}\frac{d}{d\eta}(\varphi U') \quad [9]$$

$$\theta'' - (\Pr U''/U')\theta' + b\Pr U'^2 + \theta'(1-\Pr)\,d\log\varphi/d\eta = 0 \quad [10]$$

Equation [8] gives θ in terms of μ and U; Equation [9] then yields ξ (hence V) in terms of μ and U. Equation [10] is a different form of the relationship between θ and μ, U. For the special case $\Pr = 1$ which has been studied by von Kármán and Tsien (2), the term containing μ drops out and after some manipulations there is obtained

$$2(\theta - 1) = b(1 - U^2) \quad [11]$$

At the plate wall, where $U = 0$, the temperature ratio $\theta_0 = (b/2) + 1$.

Now (1)

$$b = (\gamma - 1)M_1^2 = 2(\theta_{a1} - 1) \quad [12]$$

hence, for $\Pr = 1$

$$(\theta - 1)/(\theta_{a1} - 1) = 1 - U^2 = (\theta - 1)/(b/2) \quad [13]$$

The last quantity is used as ordinate on some of the curves of Parts I and II, although $\Pr \neq 1$ for any of them.

The drag coefficient for a thin plate (two sides) of length L in the X direction and breadth B in the Z direction, assuming that L and B are not too small and that end effects may be neglected, is

$$C_D = 4\varphi_0 U_0'/(\mathrm{Re})^{1/2} \quad [14]$$

For the case of constant viscosity, Equations [8], [9], [10], and [14] reduce to

$$\left.\begin{aligned} &\theta(\xi' - U) = \theta' \\ &2\theta U'' + \xi U' = 0 \\ &(2/\Pr)\theta'' + \xi' - U + 2bU'^2 = 0 \\ &C_D = 4U_0'/(\mathrm{Re})^{1/2} \end{aligned}\right\} \quad [15]$$

which are the equations on which the previous study was based (1).

I—VARIOUS TYPES OF VISCOSITY VARIATION

There are numerous approximations for the dependence of μ on T. To determine the relative effect, on θ, θ', U, U', and V, of taking different μ variations, the particular case $\Pr = 0.733$ (air) and $b = 1.6$ (Mach number of undisturbed stream 2) was studied for 6 μ's

$$\left.\begin{aligned} &\mu = \mu_1 \quad = \mu_1\varphi_C \\ &\mu = \mu_1\theta^{1/2} \quad = \mu_1\varphi_B \\ &\mu = \mu_1\theta^{0.768} = \mu_1\varphi_K \\ &\mu = \mu_1\left(\frac{T}{T_1}\right)^{3/2}\frac{T_1 + 114}{T + 114} = \mu_1\varphi_S \\ &T_1 = 175, 273, 375\ \mathrm{C} \end{aligned}\right\} \quad [16]$$

where μ_1 is the value of μ in the undisturbed stream, and φ denotes the temperature function μ/μ_1. Thus φ_C is 1, $\varphi_B = \theta^{1/2}$ gives[4] μ/μ_1 as required by elementary kinetic theory, $\varphi_K = \theta^{0.768}$ is μ/μ_1 as used[5] by von Kármán and Tsien, φ_{S175} is μ/μ_1 as required[6] by the Sutherland formula (4) with $T_1 = 175$ C, and φ_{S273} and φ_{S375} are similar. Fig. 1 shows the variations of the φ's with θ.

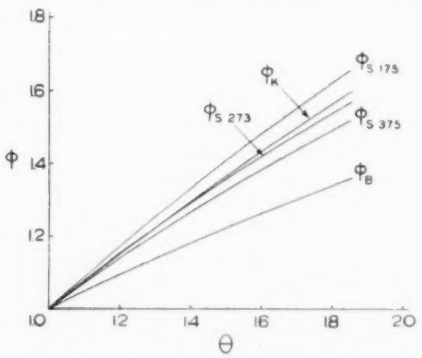


FIG. 1 VARIATION OF φ'S WITH θ ($\mu = \mu_1\varphi$ AND $k = k_1\varphi$; THE DIFFERENT φ'S ARE DEFINED IN EQUATIONS [16])

The kinetic theory of interacting spherical molecules indicates that the Prandtl number varies only slightly with the temperature. Experimental results on this point are meager but tend to confirm the theoretical prediction and suggest the empirical rule that Pr is constant in any range of the temperature in which c_p is constant. The specific heat c_p does not vary rapidly with the temperature and will be assumed constant in this paper. From the definition of Pr it then follows that k is the same function of T that μ is. Thus, corresponding to each of the six μ functions there is a relation

$$k = k_1\varphi \quad [17]$$

where φ is φ_C, φ_B, φ_K, φ_{S175}, φ_{S273}, or φ_{S375} as required, and k_1 is the value of k in the undisturbed stream.

Figs. 2, 3, and 4 show the distribution of θ, $\varphi\theta'$, U, $\varphi U'$, V for $\Pr = 0.733$ and $b = 1.6$, according to the various φ's. The noteworthy fact is that all the curves in a given group, except the φ_C and φ_B curves, fall very near to one another. The use of φ_K has certain practical advantages over the Sutherland formula, e.g.,

[4] Used by Busemann (3), who gave a few special solutions of the present problem for $\Pr = 1$.

[5] von Kármán and Tsien (2) have given for $\Pr = 1$ a much more comprehensive set of solutions than Buscmann's.

[6] The Sutherland constant 114 in Sutherland's formula is for air in the range 0–300 C. It has been used here for the case $T_1 = 175$ C as well as for $T_1 = 273$ C and $T_1 = 375$ C.

it is independent of the value of T_1 and contains no constant corresponding to the Sutherland constant. In consequence of these practical advantages and the results shown in the curves, $\varphi_K = \theta^{0.768}$ has been chosen as the temperature function $\mu/\mu_1 (= k/k_1)$ to be used in the sequel. The exponent 0.768 fits the experimental data for air quite well. All the data in or near the range 0–100 C reviewed by Chapman and Cowling (4) give an average value of 0.84 with an extreme variation of ±0.20. The viscosity of steam requires exponents from 1.1 to 0.25 for different pressures from 0 to 1500 psi. The exponent 0.768 corresponds to a pressure of about 200 psi. Table 1 summarizes in numerical form certain of the results.

TABLE 1

Pr = 0.733 and b = 1.6

Viscosity ratio μ/μ_1	θ_0	φ_0	U_0'	$CD(\mathrm{Re})^{1/2} = 4\varphi_0 U_0'$	V (At main stream)
φ_C	1.67	1.000	0.274	1.096	1.37
φ_B	1.66	1.290	0.234	1.208	1.53
φ_K	1.66	1.480	0.215	1.273	1.645
φ_{S175}	1.66	1.538	0.211	1.300	1.66
φ_{S273}	1.66	1.468	0.217	1.274	1.63
φ_{S375}	1.655	1.430	0.221	1.264	1.60

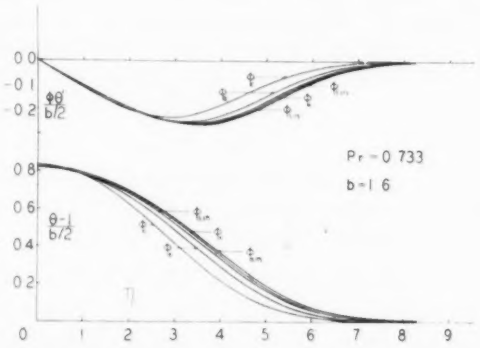


FIG. 2 VARIATION OF θ AND $\varphi\theta'$ FOR VARIOUS φ'S WHEN PR = 0.733 AND b = 1.6

(Curves for φ_{S273} are in each case very close to, and give smaller absolute values than, the φ_K curves.)

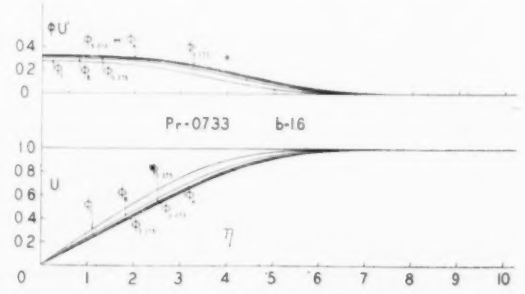


FIG. 3 VARIATION OF U AND $\varphi U'$ FOR VARIOUS φ'S WHEN PR = 0.733 AND b = 1.6

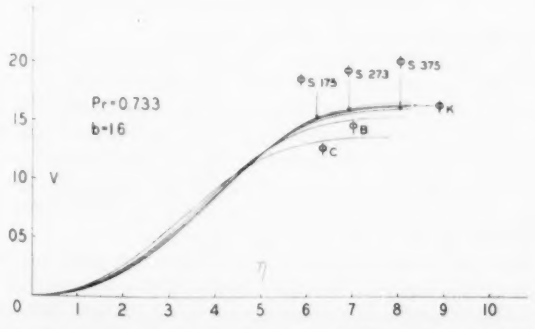


FIG. 4 VARIATION OF V FOR VARIOUS φ'S WHEN PR = 0.733 AND b = 1.6

II—DISTRIBUTIONS FOR $\mu/\mu_1 = \varphi_K$

In this part (II) all results are for $\mu/\mu_1 = \varphi_K$. Figs. 5*a* and 5*b*

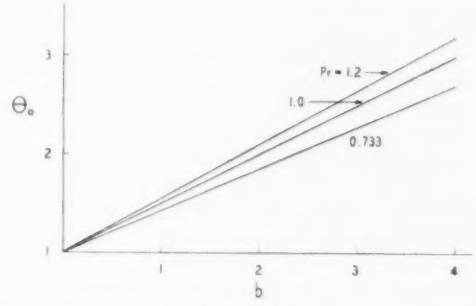


FIG. 5*a* VARIATION OF θ_0 WITH b FOR VARIOUS VALUES OF PR

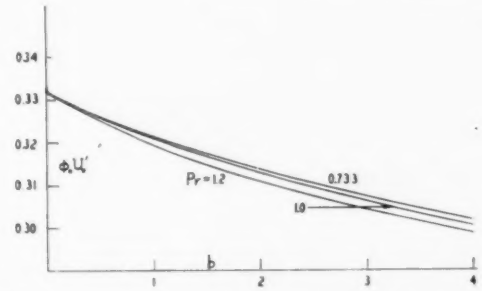


FIG. 5*b* VARIATION OF $\varphi_0 U_0'$ WITH b FOR VARIOUS VALUES OF PR ($\varphi_0 = \varphi_K$ AT PLATE WALL, $\eta = 0$.)

show conditions at the plate wall for various Pr's and b in the range $0 \leq b \leq 4$. It is noteworthy that $\varphi_0 U_0'$ varies little, and θ_0 is very closely a linear function of b. Since $\varphi_0 U_0'$ has such small variation, it is possible to write

$$C_D(\mathrm{Re})^{1/2} = 1.26 \quad \ldots\ldots [18]$$

as an approximation holding to within 5 per cent for all the points represented. For $b < 2$

$$C_D(\mathrm{Re})^{1/2} = 1.28 \quad \ldots\ldots [19]$$

is a better approximation, good to within 3 per cent. Table 2 gives data for the plate wall and, in the case of V, at the "boundary" between boundary layer and the main stream. The values of $C_D\,(\mathrm{Re})^{1/2}$ for Pr = 1.00 check those of other investigators (2) to well within 1 per cent.

Figs. 6, 7, and 8 show the distributions for Pr = 0.733, with b as the parameter. A comparison with similar curves for $\mu/\mu_1 = \varphi_C$ shows that the spread of the curves is appreciably greater,

TABLE 2

	b	θ_0	$\mu_0/\mu_1 = \varphi_0 = \theta_0^{0.768}$	$C_D(\mathrm{Re})^{1/2} = 4\varphi_0 U_0'$
Pr = All values	0	1.000	1.000	1.327
Pr = 0.733	0.1	1.042	1.032	1.319
	0.4	1.170	1.128	1.308
	0.9	1.380	1.280	1.289
	1.6	1.675	1.486	1.269
	4.0	2.705	2.147	1.209
Pr = 1.00	0.1	1.050	1.038	1.318
	0.4	1.198	1.149	1.308
	0.9	1.445	1.327	1.288
	1.6	1.793	1.566	1.264
	4.0	2.991	2.320	1.204
Pr = 1.20	0.1	1.053	1.041	1.320
	0.4	1.215	1.161	1.305
	0.9	1.484	1.354	1.284
	1.6	1.876	1.621	1.256
	4.0	3.186	2.435	1.196

indicating that the variation of μ markedly accentuates the dependence of the distributions on b. This is particularly interesting in the case of θ, since the value θ_0 of θ at the plate wall is, for all cases shown, within 1 per cent of the value for μ constant. It may also be noted that the thicknesses of the boundary layer δ_v for velocity and of the boundary layer δ_T for temperature have changed from the φ_C case.

Fig. 8 shows how V builds up from the plate wall to the main stream. It is important to distinguish here the "main stream" and the "undisturbed stream." Until the velocity component v corresponding to V at the beginning of the main stream has been returned to zero, the undisturbed stream is not reached. Thus adjacent to the boundary layer is another region in which the v readjustment takes place. However, since $v = (\nu_1 u_1/x)^{1/2} V$, the greater x the less v, other things being equal, and at any large distance from the edge of the plate ($x = 0$) the velocity component v is practically zero.

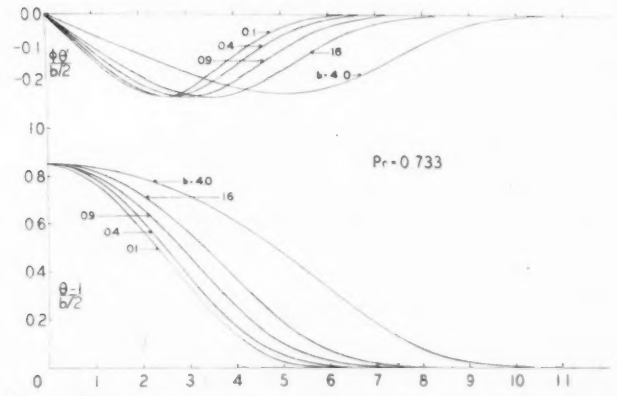


FIG. 6 VARIATION, FOR PR = 0.733, OF θ AND $\varphi\theta'$ IN BOUNDARY LAYER

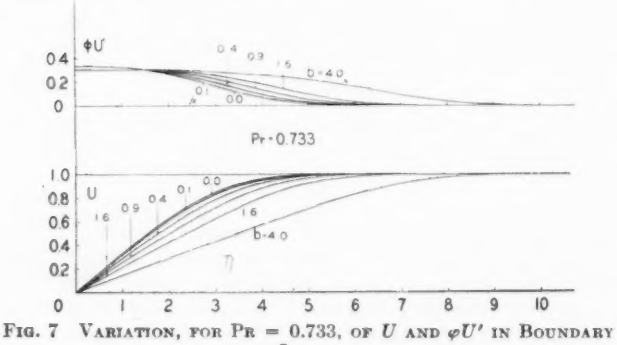


FIG. 7 VARIATION, FOR PR = 0.733, OF U AND $\varphi U'$ IN BOUNDARY LAYER

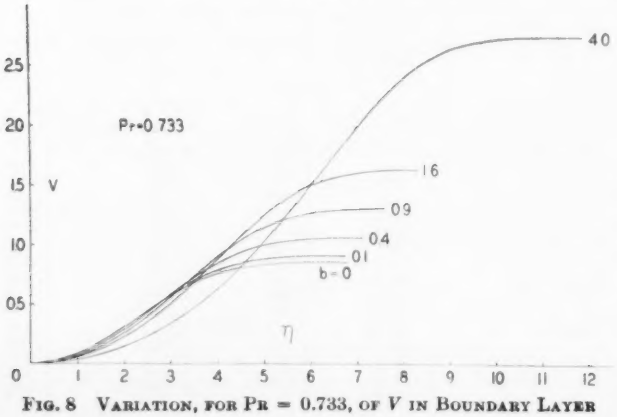


FIG. 8 VARIATION, FOR PR = 0.733, OF V IN BOUNDARY LAYER

The time rate of transfer of thermal energy across unit area perpendicular to the Y direction is

$$-k\frac{\partial T}{\partial y} = -\left[k_1 T_1 \left(\frac{u_1}{\nu_1 x}\right)^{1/2}\right]\varphi\theta' \quad [20]$$

and thus is proportional to $\varphi\theta'$ as given in Fig. 6. Likewise the shear stress τ through the boundary layer is given by

$$\tau = \mu\frac{\partial u}{\partial y} = \left[\mu_1 u_1 \left(\frac{u_1}{\nu_1 x}\right)^{1/2}\right]\varphi U' \quad [21]$$

and consequently is proportional to $\varphi U'$ as given in Fig. 7. It is for these reasons that $\varphi\theta'$ and $\varphi U'$ have been plotted rather than θ' and U'.

III—THE EFFICIENCIES AND FLOW COEFFICIENTS OF A PASSAGE

In the previous parts of this paper the variations of the temperature and velocity components through the boundary layer have been considered. These, together with the fact that the pressure is taken constant throughout the whole flow field, completely determine all other properties. For example the density ρ is calculated from

$$\rho/\rho_1 = 1/\theta \quad [22]$$

If the flow along a wall were to be measured, impact and static pressure measurements would be made and the corresponding fluid velocity would be calculated from the formula

$$u^2 = 2(h_a - h) = 2c_p T_a\left[1 - (p/p_a)^{(\gamma-1)/\gamma}\right] \quad [23]$$

Here u^2 is written instead of $u^2 + v^2$ since $v = V(\nu_1 u_1/x)^{1/2}$ and is therefore very small. The temperature T_a is the temperature reached by the fluid at any point in the stream when its velocity is destroyed isentropically. In engineering practice it is customary to assume that T_a is equal to the isentropic stagnation temperature of the undisturbed stream, T_{a1}. In general, however

$$\frac{T_a}{T_{a1}} = \frac{T + (u^2/2c_p)}{T_1 + (u_1^2/2c_p)} = \frac{\theta + (U^2 b/2)}{1 + b/2} \quad [24]$$

and thus T_a/T_{a1} varies from $\dfrac{\theta_0}{1 + b/2}$ at the wall to 1 outside the boundary layer. At the wall therefore T_a/T_{a1} is less than, equal to, or greater than 1 according as Pr is less than, equal to, or greater than 1. The temperature T_a is constant and equal to T_{a1} throughout the boundary layer for a fluid with Pr = 1, as can be seen from Equation [11]. If Pr $\neq$ 1, T_a varies from its value at the wall, passes through 1 somewhere in the boundary layer, and then approaches 1 from the opposite side. This variation is required by the fact that the enthalpy plus kinetic energy of the whole stream must remain constant in steady flow in the absence of external heat or work transfers.

Fig. 9 shows the variation through the boundary layer of the isentropic stagnation temperature T_a, the actual fluid temperature T, and the impact pressure p_a for the special case Pr = 0.733, b = 0.4, i.e., air flowing at the speed of sound. The variations of properties through the boundary layer in this special case are further pictured on a dimensionless Mollier chart, Fig. 10. The lines representing flow per unit area are modified through the boundary layer because of the heat transfers.

Since the isentropic stagnation temperature does not remain constant throughout the boundary layer, it is natural to inquire what error is made in efficiency and flow calculations by assuming it so. Consider the special case of a two-dimensional nozzle with a parallel throat 4 in. long and 1¼ in. wide, see Fig. 11. As-

sume that air flows at the speed of sound through this nozzle. The efficiency of such a passage is defined as the kinetic energy carried out of the nozzle per unit time divided by that which would have been carried out by the same fluid had the flow been isentropic. The efficiency for this case with a boundary layer at each wall is

$$\epsilon = \frac{\int (\rho/2)u^3 dA}{(u_1^3/2)\int \rho u dA} = \frac{\int^\eta (U^3/\theta)d\eta}{\int_0^\eta (U/\theta)d\eta} \quad \ldots\ldots [25]$$

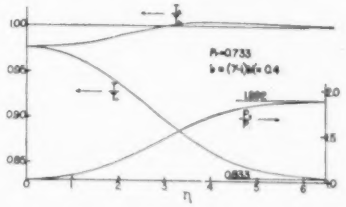


FIG. 9 VARIATION, FOR PR = 0.733 AND b = 0.4, OF T, T_a, AND p_a IN BOUNDARY LAYER

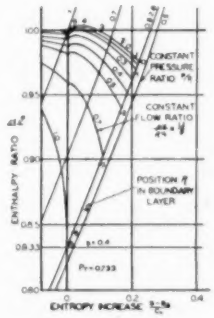


FIG. 10 VARIATION, FOR PR = 0.733 AND b = 0.4, OF FLUID PROPERTIES IN BOUNDARY LAYER

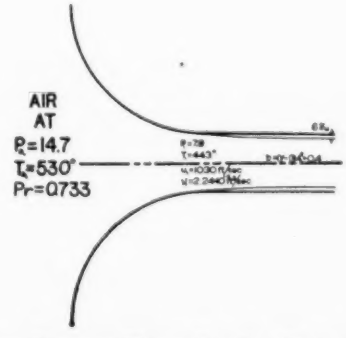


FIG. 11 NOZZLE THROUGH WHICH CRITICAL FLOW OF AIR OCCURS UNDER CONDITIONS SHOWN

in which A, the cross-sectional area, is assumed directly proportional to η. The integration must be carried out numerically through the boundary layer, to $\eta = 6$ for the case under consideration. Beyond $\eta = 6$, $U = 1$ and $\theta = 1$ so that the efficiency becomes

$$\epsilon = \frac{\int_0^6 (U^3/\theta)d\eta + \eta - 6}{\int_0^6 (U/\theta)d\eta + \eta - 6} \quad \ldots\ldots [25a]$$

For convenience in the interpretation of traverse tests of nozzles, the efficiency is commonly defined as the area mean kinetic energy per unit mass divided by the corresponding quantity for frictionless flow. The kinetic energy is determined at each point by measurements of impact and static pressure and the use of Equation [23] with T_{a1} used for T_a.

$$\epsilon_1 = \frac{\int c_p T_{a1}[1 - (p/p_a)^{(\gamma-1)/\gamma}]\, dA}{u_1^2 A/2} = \frac{\int_0^\eta U^2(T_{a1}/T_a)d\eta}{\eta} \quad [26]$$

$$= \frac{\int_0^6 U^2(T_{a1}/T_a)d\eta + \eta - 6}{\eta}$$

These efficiencies differ for two reasons:

1 The flow per unit area in the boundary layer has been reduced by the friction. The over-all efficiency of a machine containing a nozzle indicates how well the machine uses the fluid which actually flows through it. The static test efficiency should do the same. Thus a flow mean kinetic energy should be used instead of an area mean.

2 The isentropic stagnation temperature T_a was assumed equal to the isentropic stagnation temperature T_{a1} of the undisturbed stream.

To separate these two effects another efficiency is defined making the first assumption but not the second

$$\epsilon_2 = \frac{\int (u^3/2)dA}{u_1^2 A/2} = \frac{\int c_p T_a[1 - (p/p_a)^{(\gamma-1)/\gamma}]\, dA}{u_1^2 A/2} = \frac{\int_0^\eta U^3 d\eta}{\eta}$$

$$= \frac{\int_0^6 U^3 d\eta + \eta - 6}{\eta} \quad \ldots [27]$$

For the special case of Fig. 11, the boundary-layer thickness at the end of the passage, assuming zero thickness at the beginning of the passage, is

$$\delta_u = (\nu_1 L/u_1)^{1/2} = 0.0102 \text{ in.}$$

Half the width of the passage expressed in terms of η is therefore

$$\eta = y/\delta_u = 0.875/0.0102 = 85.8$$

TABLE 3

ϵ	$= \frac{\text{Actual kinetic energy}}{\text{Kinetic energy of same fluid if frictionless flow}}$	= 98.3 per cent
ϵ_1	$= \frac{\text{Area mean kinetic energy per unit mass } (T_a = T_{a1})}{\text{Kinetic energy per unit mass if frictionless flow}}$	= 97.3 per cent
ϵ_2	$= \frac{\text{Area mean kinetic energy per unit mass } [T_a = T_a(\eta)]}{\text{Kinetic energy per unit mass if frictionless flow}}$	= 97.0 per cent
C_d	$= \frac{\text{Actual flow}}{\text{Flow if frictionless}}$	= 97.8 per cent
C_u	$= \frac{\text{Area mean velocity assuming } T_a = T_{a1}}{\text{Velocity if frictionless flow}}$	= 98.3 per cent

of which $\eta = 6$ is boundary layer. Thus about 7 per cent of the area of the stream is affected by the boundary layer.

When the integrals in the efficiency expressions are evaluated, there results the comparison as shown in Table 3.

The actual efficiency of energy transformation is about one per cent better than that indicated by a traverse of the passage for the special case here studied. The major portion of the error arises in neglecting the reduction in flow per unit area in the boundary layer.

The flow coefficient of a passage is defined as the actual flow through the passage divided by the flow that would pass through the passage if it were frictionless and the pressure drop remained the same. In terms of the present notation

$$C_d = \frac{\int \rho u dA}{\rho_1 u_1 A} = \frac{1}{\eta}\int_0^\eta (U/\theta)d\eta = \frac{\int_0^6 (U/\theta)d\eta + \eta - 6}{\eta} \quad [28]$$

If the velocity were calculated from the measured pressures and

the assumption that $T_s = T_{s1}$, the velocity coefficient would be calculated from

$$C_s = \frac{\int 2c_p T_{s1}[1 - (p/p_s)^{(\gamma-1)/\gamma}]^{1/2}\, dA}{u_1 A} = \frac{1}{\eta}\int^{\eta} U \frac{T_{s1}}{T_s}\, d\eta = \frac{\int_0^6 U(T_{s1}/T_s)d\eta + \eta - 6}{\eta} \quad [29]$$

The velocity coefficients and the flow coefficients are the same for incompressible fluids and are sometimes erroneously assumed so for compressible fluids. The flow coefficient and velocity coefficient are shown in Table 3.

It is often supposed that the velocity coefficient squared is equal to the efficiency of the nozzle. The magnitude of the error made by assuming that the mean velocity squared is the square of the mean velocity is evident by the comparison

$$\epsilon_1 = 97.3 \text{ per cent}, \quad C_s^2 = 96.6 \text{ per cent}$$

For accuracy of ±1 per cent or better, a careful distinction should be made between the various definable energy, flow, and velocity coefficients.

The foregoing calculations are poor approximations to the coefficients for nozzles but do serve the purpose of showing the differences between the various definitions.

BIBLIOGRAPHY

1 "Temperature Effects in a Laminar Compressible-Fluid Boundary Layer Along a Flat Plate," by H. W. Emmons and J. G. Brainerd. Presented at A.S.M.E. Annual Meeting, New York, N. Y., Dec. 2–6, 1940.

2 "Boundary Layer in Compressible Fluids," by Th. von Kármán and H. S. Tsien, *Journal of the Aeronautical Sciences*, vol. 5, 1938, pp. 227–232.

3 "Gasströmung mit laminarer Grenzschicht entlang einer Platte," by A. Busemann, *Zeitschrift für angewandte Mathematik und Mechanik*, vol. 15, 1935, pp. 23–25.

4 "The Mathematical Theory of Non-Uniform Gases," by Sydney Chapman and T. G. Cowling, Cambridge University Press, London, England, and New York, N. Y., 1939, p. 224.

5 "Grenzschichten in Flüssigkeiten mit kleiner Reibung," by H. Blasius, *Zeitschrift für Mathematik und Physik*, vol. 56, 1908, pp. 1–37.

Buckling of the Circular Plate Beyond the Critical Thrust

By K. O. FRIEDRICHS[1] and J. J. STOKER,[2] NEW YORK, N. Y.

In this paper a complete mathematical solution of the problem of the buckling with large deflections of a thin circular plate under uniform radial pressure is given, assuming radial symmetry. Buckling takes place as soon as the prescribed thrust p_e at the edge reaches a certain critical value p_E. Thin plates do not, however, fail if the thrust p_e is increased beyond p_E. It is of importance, then, to determine the stresses when the ratio $\Lambda = p_e/p_E$ becomes greater than unity. This problem, which is a nonlinear one, is solved by two methods for finite values of Λ; also an asymptotic solution is given for the limit state when Λ tends to infinity. The most notable single result is that the membrane stresses for large values of Λ become tensions in the interior of the plate and change abruptly to compressions in a narrow "boundary layer" at the edge of the plate. Curves showing the behavior of the deflection and the stresses are given for a series of values of Λ. Such curves show clearly, in particular, that the limit state is approached quite closely for relatively small values of Λ, i.e., $\Lambda > 5$. In closing, the authors discuss the relation between their results and von Kármán's theory of effective width for the buckling of rectangular plates.

Notation

x, y = rectangular coordinates
r = distance from center
R = radius of plate
h = thickness of plate
E = Young's modulus
ν = Poisson's ratio
$\gamma = [12(1 - \nu^2)]^{-1/2}$
$\eta = \gamma h/R$ slenderness ratio
w = deflection of the middle surface
$q = -Rr^{-1}dw/dr$
q_e = slope of the middle surface at the edge
φ = Airy's stress function
$-p$ = radial membrane stress
$-p_c$ = circumferential membrane stress
σ_b = radial bending stress at the upper surface
σ_{cb} = circumferential bending stress at the upper surface
τ_b = shearing stress due to bending at the upper surface
p_0, p_{c0}, σ_{b0} = values of stresses at the center of the plate
p_e, p_{ce}, σ_{be} = values of stresses at the edge of the plate
p_E = critical value of p_e
$\Lambda = p_e/p_E$

If a straight slender column is subjected to gradually increasing thrusts applied at its ends, it will become instable and buckle when a certain critical value of the thrust is reached. If the thrust is increased a small amount beyond the critical value, the column will generally collapse completely. The behavior of a thin flat plate subjected to compressive forces at its edges and in its plane is quite different. The plate will become instable when the compressive forces reach certain critical values, but the forces can be increased considerably above such values without causing a collapse of the plate. The fundamental reason for this experimentally well-established difference in the behavior of column and plate is that a straight line (the axis of the column) can be bent into a curve without changing its length, while a plane surface, the edge of which is restrained, cannot be deformed without stretching the surface. Thus, when the plate buckles, the stretch which results relieves the central part of the plate of a portion of the compressive stresses and as a consequence the plate is relatively much stiffer than the column.

It is a matter of practical importance to determine the strength of thin plates when subjected to loads greater than those at which buckling begins, because such thin-walled structures are used extensively, for example, in aircraft, where lightness combined with maximum strength is desired and where buckling is permissible as long as it does not result in failure.

A formula for the design of rectangular plates for thrusts beyond the lowest buckling thrust has been developed by von Kármán. It is based on the assumption that the compressive stresses tend to become concentrated in a strip near the edge of the plate. Such an edge effect has been observed, in fact, by a number of experimenters (2, 3, 9, 12, 13, 18, 19).[3]

The purpose of this investigation is to give a complete mathematical solution for the case of the circular plate with simply supported edges, buckled with radial symmetry under the action of a uniformly distributed edge thrust. The results include, in particular, an explanation and discussion of an edge effect which is found here as a natural part of the solution. Important and interesting conclusions can be drawn which retain at least qualitative significance for the case of the rectangular plate—the case of more immediate practical importance.

The mathematical formulation of the problem of the buckled plate involves a pair of nonlinear differential equations derived by von Kármán for the bending of thin plates with large deflections (8). Various writers (6, 10, 11, 12, 13, 14, 16, 20, 24) have solved these equations using the perturbation and energy methods in order to obtain solutions valid at least for a limited range of the ratio Λ of applied pressure p_e to the lowest buckling pressure p_E. Such solutions deal in the main with the rectangular plate. An exact solution for the rectangular plate valid for an unlimited range of the ratio Λ presents seemingly insurmountable difficulties; for the circular plate,[4] however, the authors obtain

[1] Associate Professor of Applied Mathematics, Graduate School, New York University.

[2] Assistant Professor of Mathematics, College of Engineering, New York University.

Presented at the National Meeting of the Applied Mechanics Division, Philadelphia, Pa., June 20–21, 1941, of The American Society of Mechanical Engineers.

Discussion of this paper should be addressed to the Secretary, A.S.M.E., 29 West 39th Street, New York, N. Y., and will be accepted until April 10, 1942, for publication at a later date. Discussion received after the closing date will be returned.

Note: Statements and opinions advanced in papers are to be understood as individual expressions of their authors and not those of the Society.

[3] Numbers in parentheses refer to the Bibliography.

[4] The problem of the bending of a circular plate under lateral pressure and edge moment has been solved by Way (22) by an exact method for a rather large range of applied load.

Federhofer (24) has solved the problem of the buckling of the circular plate for simply supported and clamped edges. In the former case, which is the same as that treated here, the method of Federhofer yields accurate results up to about $\Lambda = 1.25$.

rigorous solutions valid for an unlimited range of Λ. The existence of an edge effect can then be derived by an asymptotic treatment for $\Lambda \to \infty$, which presents some mathematical analogy with the Prandtl boundary-layer theory for the flow of a viscous fluid around an obstacle (15). It is possible, as will be shown, to design plates for arbitrarily large values of Λ without exceeding given limits for the maximum stresses and without violating the assumptions upon which the von Kármán equations rest.

In the present paper are given the results of an investigation together with an outline of the mathematical methods. A detailed explanation, with proofs, of the mathematical methods will be given in a forthcoming paper (26).[5]

1—Mathematical Formulation

Consider a plane circular plate with radius R and thickness h subjected to a constant radial thrust at the edge; assume the plate simply supported, i.e., that deflection and radial bending moment vanish at the edge. Further, assume that the deflection w of the middle surface depends only upon the distance r from the center of the plate; a consequence of this assumption is that the radial and circumferential stresses also depend only upon r. Quantities which carry the subscript e or 0 refer to their values at the edge ($r = R$) or center ($r = 0$) respectively.

The von Kármán equations in Cartesian coordinates x and y are

$$E^{-1}\nabla^4\varphi = \left(\frac{\partial^2 w}{\partial x\,\partial y}\right)^2 - \frac{\partial^2 w}{\partial x^2}\frac{\partial^2 w}{\partial y^2} \quad \ldots\ldots [1]$$

$$\gamma^2 h^2 E \nabla^4 w = \frac{\partial^2\varphi}{\partial y^2}\frac{\partial^2 w}{\partial x^2} - 2\frac{\partial^2\varphi}{\partial x\,\partial y}\frac{\partial^2 w}{\partial x\,\partial y} + \frac{\partial^2\varphi}{\partial x^2}\frac{\partial^2 w}{\partial y^2} \quad \ldots\ldots [2]$$

where φ is the Airy stress function, E the modulus of elasticity, and $\gamma = [12(1 - \nu^2)]^{-1/2}$, where ν is Poisson's ratio. These equations imply that the stresses in the plate are given by combination of two stress systems, the bending stresses and the "membrane" stresses.

For the case of the circular plate with radial symmetry these nonlinear equations can be greatly simplified. Since φ and w depend only on r, the operation ∇^2 reduces to

$$\nabla^2 = \frac{d^2}{dr^2} + r^{-1}\frac{d}{dr} = r^{-1}\frac{d}{dr}\,r\,\frac{d}{dr} \quad \ldots\ldots [3][6]$$

and the von Kármán equations assume the form

$$E^{-1}r^{-1}\frac{d}{dr}\,r\,\frac{d}{dr}\,r^{-1}\frac{d}{dr}\,r\,\frac{dw}{dr} = -\frac{d^2 w}{dr^2}\,r^{-1}\frac{dw}{dr} \quad \ldots\ldots [4]$$

$$\gamma^2 h^2 E r^{-1}\frac{d}{dr}\,r\,\frac{d}{dr}\,r^{-1}\frac{d}{dr}\,r\,\frac{d\varphi}{dr} = \frac{d^2\varphi}{dr^2}\,r^{-1}\frac{dw}{dr} + r^{-1}\frac{d\varphi}{dr}\frac{d^2 w}{dr^2} \quad \ldots [5]$$

The right members here can be written in the form

$$-\frac{1}{2}\,r^{-1}\frac{d}{dr}\left(\frac{dw}{dr}\right)^2 \quad \text{and} \quad r^{-1}\frac{d}{dr}\left(\frac{d\varphi}{dr}\frac{dw}{dr}\right);$$

hence the equations can be integrated

$$E^{-1}r\frac{d}{dr}\,r^{-1}\frac{d}{dr}\,r\,\frac{dw}{dr} = -\frac{1}{2}\left(\frac{dw}{dr}\right)^2 + \text{const} \quad \ldots\ldots [6]$$

$$h^2 E r\frac{d}{dr}\,r^{-1}\frac{d}{dr}\,r\,\frac{d\varphi}{dr} = \frac{d\varphi}{dr}\frac{dw}{dr} + \text{const} \quad \ldots\ldots [7]$$

Since the left members and also dw/dr vanish for $r = 0$, the constants are zero. The equations are further simplified by introducing the quantities

$$p = -r^{-1}\,d\varphi/dr, \quad q = -Rr^{-1}\,dw/dr$$

the operation

$$\Gamma = R^{-2}r^{-1}\frac{d}{dr}\,r^{-1}\frac{d}{dr}\,r^{-2} = R^{-2}r^{-3}\frac{d}{dr}\,r^3\frac{d}{dr}$$

and the constant

$$\eta = \gamma h/R$$

which may be called the "slenderness ratio." Then the equations assume the form

$$E^{-1}\Gamma p = q^2/2 \quad \ldots\ldots [8]$$

$$E\Gamma q + pq = 0 \quad \ldots\ldots [9]$$

The quantity $-p$ is the radial membrane stress; the authors prefer to denote a membrane stress by $-p$ rather than by σ since it is a compression when buckling begins, i.e., p is then positive. The significance of the quantity q is that $(r/R)q$ is the slope of the deflected plate; in particular, q_e, the value of q at the edge, is the slope at the edge; the quantity $-q/R = r^{-1}dw/dr$ could also be interpreted as the circumferential curvature of the deflected plate.

The boundary conditions to be satisfied at the edge ($r = R$) in terms of p and q are

$$rdq/dr + (1 + \nu)q = 0 \quad \ldots\ldots [10]$$

and

$$p = p_e \quad \ldots\ldots [11]$$

The important quantity p_e is the prescribed radial compression at the edge. Equation [10] states that the bending moment at the edge vanishes. The conditions for $r = 0$ are

$$dp/dr = 0, \quad dq/dr = 0 \quad \ldots\ldots [12, 13]$$

which, on account of symmetry, imply regularity of p and q at the center of the plate.

Of the constants R, h, E, ν, p_e, which characterize the problem, only two, ν and $p_e/E\eta^2$, are essential in the sense that deflection and stresses in two plates having the same values of these ratios differ only by constant multipliers. This can be seen by introducing r/R, $p/E\eta^2$, q/η as new variables; the formulation of the problem obtained in this way contains only ν and $p_e/\eta^2 E$ as parameters.

Once p and q have been determined, the circumferential membrane stress $-p_c$ and the radial bending stress σ_b at the upper surface of the plate are given by

$$p_c = rdp/dr + p \quad \ldots\ldots [14]$$

and

$$\sigma_b = 6\gamma\eta[(rdq/dr) + (1 + \nu)q] \quad \ldots\ldots [15]$$

The deflection w is given by

$$w = R^{-1}\int^R qr^{-1}dr \quad \ldots\ldots [16]$$

thus $w(R) = 0$.

For sufficiently small values of $p_e/\eta^2 E$ there will be no buckling of the plate—corresponding to the fact that the mathematical problem has then as sole solution $q \equiv 0$, $p \equiv$ const. At a certain value p_E of p_e buckling will begin; for $p_e > p_E$ there will

[5] For a preliminary report, see reference (5).

[6] Cf., e.g., reference (21).

be two stable buckled states[7] differing only in the sign of w, while the state $w \equiv 0$, which continues to be a possible state of equilibrium, is instable. The critical value p_E of p_e is given by $p_E/\eta^2 E = 4.24$ when the value 0.318 is taken[8] for Poisson's ratio ν. This value of the critical or "Euler" pressure p_E is obtained from Equation [9] by assuming p to be constant, that is, by the standard linear treatment of the buckling problem. Cf. reference (26).

Instead of using $p_e/\eta^2 E$ as essential parameter, the authors prefer to use the ratio $\Lambda = p_e/p_E = p_e/4.24\eta^2 E$ in what follows.

2—Methods of Solution

There are at least two methods available for solving this problem: the perturbation and the power-series methods. Both methods are presented. The perturbation method is found to be manageable only for a rather low range of values of the ratio Λ. This fact is in itself of interest since the perturbation method has been used extensively in the case of the rectangular plate, where an analogue of the power-series method is not available. The power-series method can be used successfully for a much higher range of values of Λ if solutions for a low range of values of Λ have been obtained by some other means, for example by the perturbation method. In general, the authors recommend the power-series method for problems similar to the present one, and for this reason it will be explained in some detail. However, the power-series method also becomes cumbersome as Λ increases, and eventually one is forced to turn to an asymptotic treatment.

3—Perturbation Method

This method consists in a development of p and q with respect to a parameter ϵ, which may be chosen, for example, as $\epsilon = \sqrt{(\Lambda - 1)}$:

$$p = p^{(0)} + \epsilon^2 p^{(2)} + \epsilon^4 p^{(4)} + \ldots\ldots\ldots\ldots [17]$$

$$q = \epsilon q^{(1)} + \epsilon^3 q^{(3)} + \ldots\ldots\ldots\ldots\ldots [18]$$

Upon substituting in the original differential equations and equating coefficients of like powers of ϵ, one obtains a sequence of linear differential equations for $p^{(0)}$, $q^{(1)}$, $p^{(2)}$, $q^{(3)}$, ..., which can be solved successively, though with great labor. The quantity $p^{(0)}$ proves to be a constant identical with the lowest value p_E of p_e for which buckling begins and is the same as that obtained by the linear theory (26); its value, as stated previously, is $p^{(0)} = p_E = 4.24\eta^2 E$.

The authors have computed $q^{(1)}$ to $q^{(5)}$ and $p^{(0)}$ to $p^{(6)}$. The convergence is satisfactory only for a small range of values of $\Lambda = p_e/p_E$, namely, for q up to $\Lambda = 1.2, 1.8, 2.5$ if terms of the first, third, and fifth orders respectively are included; and for p up to $\Lambda = 1.4, 2.2, 2.8$ for terms of the second, fourth, and sixth orders respectively. For the other stresses the convergence is not quite as good. Nevertheless, even for these low values of Λ, some distinctive and rather surprising qualitative phenomena of the buckling are found. See section 5.

In Fig. 1 curves are shown which indicate the accuracy of the successive approximations. For this purpose it was chosen to plot $\sigma_b/p_e\sqrt{\Lambda}$ as a function of r/R for $\Lambda = 2.5$. This appears to be the least accurately obtained stress. The figure shows the curves obtained by taking successively terms up to first, third, and fifth orders in ϵ, together with the curve obtained by an exact solution to be discussed in the next section. The curve obtained by taking terms up to fifth order would give for the stress σ_b values in error by as much as 10 per cent.[9]

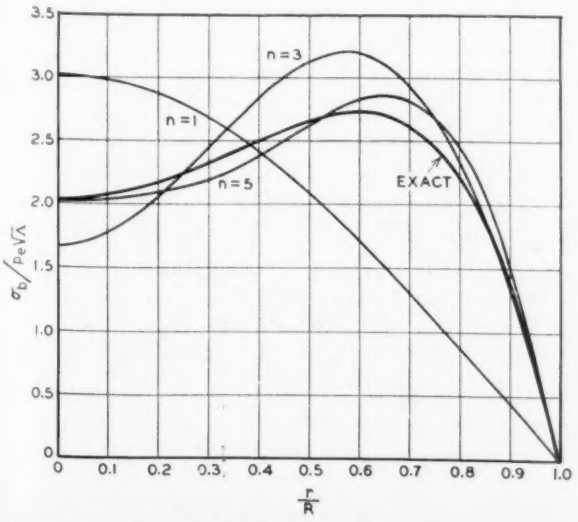


Fig. 1 Convergence of Perturbation Method for $\Lambda = 2.5$

4—Power-Series Method

The power-series method was used by Way (22) for solving the von Kármán equations as applied to the bending of circular plates under lateral loads and edge moment. See also reference (7). The method consists in setting up series for p and q in powers of r, with assumed values for the first coefficient of each series, i.e., for the values of p and q at the center of the plate.

Here are introduced a new independent variable

$$\alpha = AR^{-1}r, \quad 0 \leq \alpha \leq A \ldots\ldots\ldots\ldots [19]$$

and the new functions to replace p and q

$$\pi = A^{-2}p/\eta^2 E, \quad \kappa = A^{-2}q/\eta \ldots\ldots\ldots\ldots [20]$$

Differential Equations [8] and [9] assume the form

$$\alpha^{-3}\frac{d}{d\alpha}\left(\alpha^3\frac{d\pi}{d\alpha}\right) = \frac{1}{2}\kappa^2 \ldots\ldots\ldots\ldots [21]$$

$$\alpha^{-3}\frac{d}{d\alpha}\left(\alpha^3\frac{d\kappa}{d\alpha}\right) + \pi\kappa = 0 \ldots\ldots\ldots\ldots [22]$$

with boundary conditions

$$\frac{d\pi}{d\alpha} = 0, \quad \frac{d\kappa}{d\alpha} = 0 \quad \text{for} \quad \alpha = 0 \ldots\ldots\ldots [23]$$

$$B(\alpha) \equiv \alpha\frac{d\kappa}{d\alpha} + (1+\nu)\kappa = 0 \quad \text{for} \quad \alpha = A \ldots [24]$$

$$\pi = \pi_e \quad \text{for} \quad \alpha = A \ldots\ldots\ldots\ldots [25]$$

Instead of prescribing π_e and A, which would be equivalent to the

[7] That the equations have only two solutions is a consequence of their nonlinearity; linear theories of buckling always yield infinitely many buckled states differing only by constant factors.

[8] This value for ν, a typical value for aluminum alloy, was taken to facilitate calculation of p_E and was also used throughout the calculations.

[9] Marguerre (13) mentions that his solutions for the rectangular plate, which implied two perturbations, may perhaps be valid up to $\Lambda = 20$; Timoshenko (20) applies his Ritz method with three constants for $\Lambda = 59.7$ and mentions that an additional constant would be necessary only for $\Lambda > 50$. In the simpler case of the circular plate it is found that values of Λ of these magnitudes cannot be treated with three perturbations. In fact such values of Λ lead to solutions already well in the asymptotic range. See section 6.

The method of Federhofer (24), see also footnote,[4] corresponds to the determination of $q^{(1)}$ and $p^{(2)}$ by the Galerkin method. Federhofer's numerical results coincide with the authors' quite well up to $\Lambda = 1.2$; they deviate from them by 10 per cent for $\Lambda = 1.5$.

original formulation, one proceeds as follows: $\pi(0)$ and $\kappa(0)$ are chosen, A is determined by solving Equation [24], and π_e is calculated from Equation [25]; p and q are then determined from Equation [20].

It is easily seen that power series for π and κ contain only even powers of α

$$\pi = \sum_{k=0}^{\infty} \pi_k \alpha^{2k}, \quad \kappa = \sum_{k=0}^{\infty} \kappa_k \alpha^{2k} \ldots\ldots [26]$$

Upon insertion of these power series into Equations [21] and [22] one obtains the following recursion formulas for π_k and κ_k

$$\left.\begin{aligned} 2k(2k+2)\pi_k &= \frac{1}{2}\sum_{n+m=k-1} \kappa_m \kappa_n \\ 2k(2k+2)\kappa_k &= -\sum_{m+n=k-1} \pi_m \kappa_n \end{aligned}\right\} \ldots\ldots [27]$$

After having chosen $\pi(0) = \pi_0$ and $\kappa(0) = \kappa_0$ the successive coefficients are calculated from these formulas. Equation [24] becomes

$$B(\alpha) \equiv \sum_{k=0}^{\infty} (2k + 1 + \nu)\kappa_k \alpha^{2k} = 0 \ldots\ldots [28]$$

It must be solved for its lowest root $\alpha = A$.

One of the principal difficulties encountered in working with the power-series method consists in solving Equation [28]. Unless $A \sim 1$, the amount of labor involved in its solution is excessive. One reason for this is that otherwise one has no means of knowing the accuracy with which π_k and κ_k need be calculated and also the number of such coefficients necessary for reasonable accuracy. It might also be noted that the left side of Equation [28] changes rapidly with changes in α, and hence it is difficult to find the root A if no advance estimate of its value is available. What is evidently required for this purpose is a good estimate for π_0 and κ_0. This is, of course, also necessary if the solution is desired for a given value of Λ. One of the main purposes of this paper is to give solutions over a considerable range of values of Λ and with a fairly even distribution of such values.[10] For this objective it was found that solutions by the perturbation method were very helpful as a starting point.

As an example, the calculations are presented which yielded the solution for $\Lambda = 14.7$ (the highest value of Λ for which the power-series method was used). What was desired was the solution for $\Lambda = 15$; by extrapolation from previously calculated solutions,[11] which included values of Λ up to 7.3, it was found that $\kappa_0 = 7.0$ and $\pi_0 = -44.0$ were reasonable values for the first coefficients in the series. Equations [27] then lead to the coefficients π_k and κ_k given in Table 1.

TABLE 1

k	π_k	κ_k	k	π_k	κ_k
0	−44.00	7.00	16	2.71	0.86
1	3.06	38.50	17	1.99	−0.96
2	11.23	69.69	18	1.02	−1.75
3	25.60	59.79	19	0.18	−1.71
4	38.77	22.57	20	−0.35	−1.21
5	40.74	−10.25	21	−0.55	−0.59
6	29.55	−28.29	22	−0.51	−0.08
7	12.36	−33.37	23	−0.35	0.23
8	− 2.39	−28.56	24	−0.16	0.34
9	−10.60	−17.79	25	−0.01	0.30
10	−12.44	− 5.86	26	0.08	0.20
11	−10.03	3.30	27	0.10	0.09
12	− 5.79	8.00	28	0.09	0.00
13	− 1.64	8.62	29	0.06	−0.05
14	1.29	6.61	30	0.02	−0.06
15	2.65	3.60			

In order to solve Equation [28] $B(1)$ was calculated and found to be −155.0 instead of zero. To apply Newton's method $\alpha dB/d\alpha$ was calculated for $\alpha = 1$ and found to be −7800. The resulting new value for A, replacing the value 1, is then $A = 0.98$. Whence $B(0.98) = -9.14$. Repeating this process once more, $A = 0.978$, $B(A) = +2.16$. The value 2.16 for $B(A)$ is of the same order as the values of the last terms in the series for $B(\alpha)$; therefore further improvement in the value of A is not possible using these coefficients. With this value of A, the quantity π_e was calculated from Equation [25] and value of $\Lambda = \pi_e A^2 \eta^2 E/p_E$ was found to be 14.7 instead of 15.

The number of coefficients necessary for sufficient accuracy increases with Λ. For $\Lambda = 14.7$, as we have seen, 30 terms are needed; 23 terms suffice for $\Lambda = 7.3$.

The authors recommend a similar procedure for problems of this type involving circular plates with radial symmetry.

5—Discussion of Results

Curves are given showing the behavior of the deflection w, the slope $-dw/dr = rq/R$, the radial membrane stress p, the circumferential membrane stress p_c, and the radial bending stress σ_b. Actually, these quantities are multiplied by appropriate factors, so chosen that all remain finite as Λ tends to infinity, and are plotted with Λ as variable. Table 2 gives the calculated values from which the curves were obtained. Graphs are also given, for various fixed values of Λ, with r/R as variable.

TABLE 2

Fig.	2	6	6	6	8	8
		p_{ce}	σ_{be}	σ_{bmax}	q_e	w_0
Λ	p_0/p_e	$p_e\sqrt{\Lambda}$	$p_e\sqrt{\Lambda}$	$p_e\sqrt{\Lambda}$	$\sqrt{(p_e\Lambda/E)}$	$\gamma_k\sqrt{\Lambda}$
1.00	1.00	1.00	0	0	0	0
1.016	0.959	1.06	1.17	1.17	0.57	....
1.065	0.823	1.21	2.15	2.15	1.09	1.58
1.145	0.634	1.42	2.83	2.83	1.55	....
1.26	0.416	1.67	3.18	3.18	1.93	2.92
1.40	0.195	1.90	3.25	3.25	2.22	....
1.57	0	2.11	3.13	3.13	2.44	3.91
1.78	−0.182	2.30	2.88	....	2.63	....
2.01	−0.326	2.46	2.59	2.87	2.77	4.65
2.49	−0.519	2.64	2.03	2.75	2.91	5.15
3.76	−0.714	2.88	1.14	....	3.08	....
4.08	−0.730	2.92	1.00	....	3.09	....
5.12	−0.758	3.00	0.68	2.58	3.15	6.10
7.31	−0.750	3.09	0.35	....	3.20	....
14.74	−0.673	3.20	0.07	2.49	3.27	6.65
∞	−0.473	3.33	0	2.29	3.33	6.78

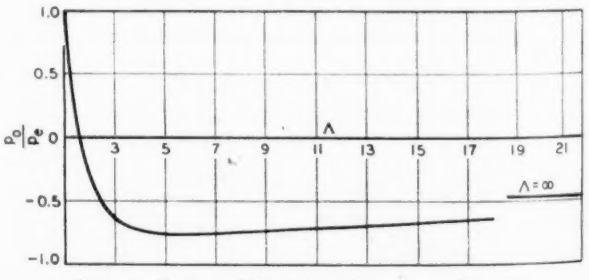


Fig. 2 Radial Membrane Stress at Center

It is convenient to discuss here limit situations for $\Lambda \to \infty$ and plot limit values of all quantities, though the mathematical discussion of these matters is given in the next section.[12]

Radial Membrane Stress. In Fig. 2 the curve for the quantity p_0/p_e is given to show the behavior of the radial membrane stress p_0 at the center of the plate in its dependence on Λ. The plate

[10] It is impractical for two reasons to choose values of π_0 and κ_0 more or less at random: After lengthy computations it can appear that two different choices for π_0 and κ_0 lead to nearly the same solution; the values of π_0 and κ_0 change with increasing Λ in rather unexpected ways, for example, π_0 changes sign, and κ_0 starts at zero for $\Lambda = 1$ and tends again to zero for large values of Λ.

[11] Figs. 2 and 6 give values of p_0/p_e and $\sigma_{b0}/p_e\sqrt{\Lambda}$. From these one derives the values $\pi_0 = (p_E/\eta^2 E)\Lambda p_0/p_e$ and $\kappa_0 = C\Lambda^{3/2}\sigma_{b0}/p_e\sqrt{\Lambda}$, where $C = (p_E/\eta^2 E)/6\gamma(1+\nu) = 1.76$ and $(p_E/\eta^2 E) = 4.24$.

[12] The earlier ones were obtained from the perturbation method. For $\Lambda = 1.57$ identical results were obtained using the power-series method.

is in a state of hydrostatic compression for $\Lambda = 1$, at which buckling just begins. With increase of Λ one expects p_0/p_e to decrease because of the buckling and consequent stretch of the middle surface. From the figure it is seen that p_0/p_e decreases rapidly and, what is surprising, eventually becomes negative,

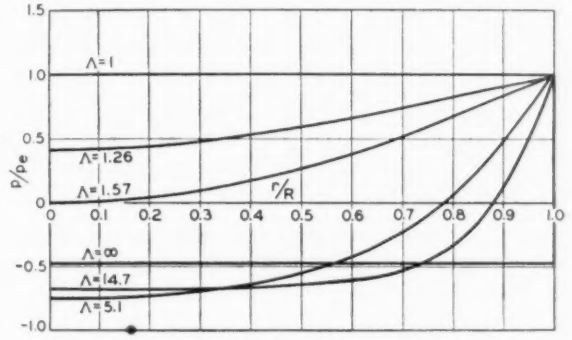


FIG. 3 RADIAL MEMBRANE STRESSES

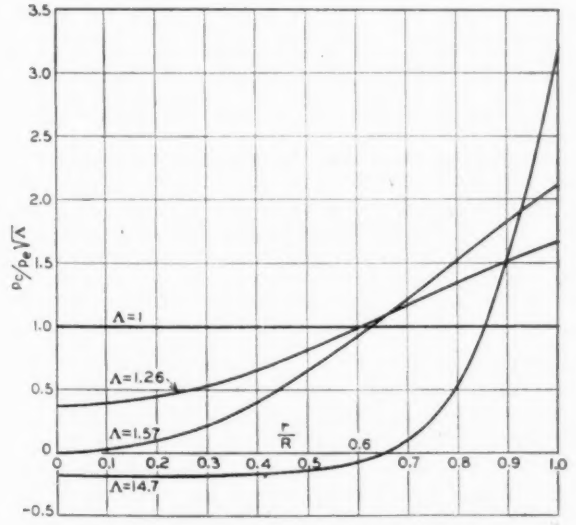


FIG. 4 CIRCUMFERENTIAL MEMBRANE STRESS

i.e., p_0 becomes a tensile stress. The transition occurs for the quite low value $\Lambda = 1.57$. For $\Lambda \sim 5.5$ the quantity p_0/p_e has an absolute minimum (—0.76); from this point on it increases slowly and attains the value —0.67 for $\Lambda = 14.7$. The asymptotic value for $\Lambda \to \infty$ is —0.47.

Fig. 3 shows curves for p/p_e as a function of r/R for various fixed values of Λ. The main feature of these curves is that for the higher values of Λ this quantity tends to become a negative constant over the central portion of the plate and then to rise rapidly to positive values in a strip near the edge. As will be shown in the next section, the width of this "boundary layer" tends to zero with increasing Λ. The curve marked $\Lambda = \infty$ indicates the limit curve for $\Lambda \to \infty$.

Maximum Stresses. Fig. 4 depicts the circumferential membrane stress p_c as a function of r/R for various fixed values of Λ. The values of p_c and of the radial membrane stress p are the same at the center of the plate (i.e., $p_{c0} = p_0$) because of symmetry, hence p_{c0} becomes negative beyond $\Lambda = 1.57$. The stress p_c increases much more rapidly than p toward the edge of the plate and for all values of Λ retains its maximum at the edge. These maxima (p_{c_e}) increase with Λ in higher degree than the maxima p_e of p: It was hence convenient to plot $p_c/p_e\sqrt{\Lambda}$ rather than p_c/p_e. For high values of Λ the curves indicate that p_c/p_e tends to become constant over an increasingly large portion of the plate. Since $p_{c0} = p_0$, it is clear that p_{c0}/p_e has the limit value —0.47.

Curves for the radial bending stress σ_b (actually $\sigma_b/p_e\sqrt{\Lambda}$) as a function of r/R for various values of Λ are shown by Fig. 5. For $\Lambda = 1$, when buckling just begins, $\sigma_b \equiv 0$. The maximum of σ_b is attained at the center until $\Lambda = 1.57$; up to this point the curves present no striking features. When Λ increases beyond 1.57, however, the point where p_b attains its maximum is no longer at the center, but shifts toward the edge of the plate. When $\Lambda = 2.01$, for example, the maximum is already beyond $r/R = 0.5$; for $\Lambda = 14.7$ the maximum occurs at $r/R = 0.87$. For large values of Λ, $\sigma_b/p_e\sqrt{\Lambda}$ at the center of the plate decreases rapidly and tends to zero as $\Lambda \to \infty$; it might be mentioned that the same is also true of the quantity σ_b/p_e at the center. With increasing Λ the high values of σ_b tend to be concentrated in a boundary layer.

The variation of $p_{c_e}/p_e\sqrt{\Lambda}$, $\sigma_{b0}/p_e\sqrt{\Lambda}$, and $\sigma_b \max/p_e\sqrt{\Lambda}$ with Λ is shown in Fig. 6. The limit values obtained by the asymptotic

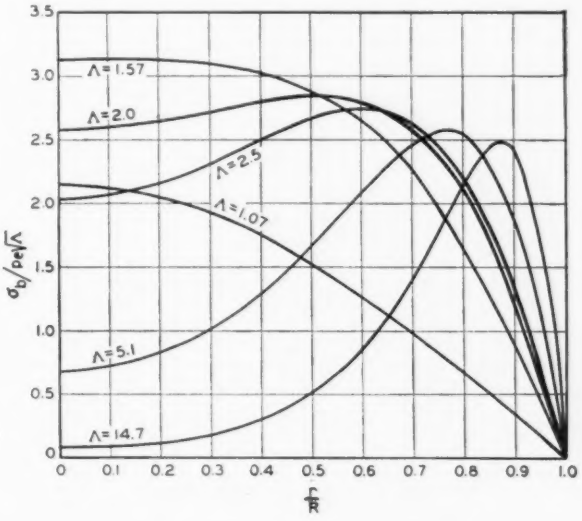


FIG. 5 RADIAL BENDING STRESS

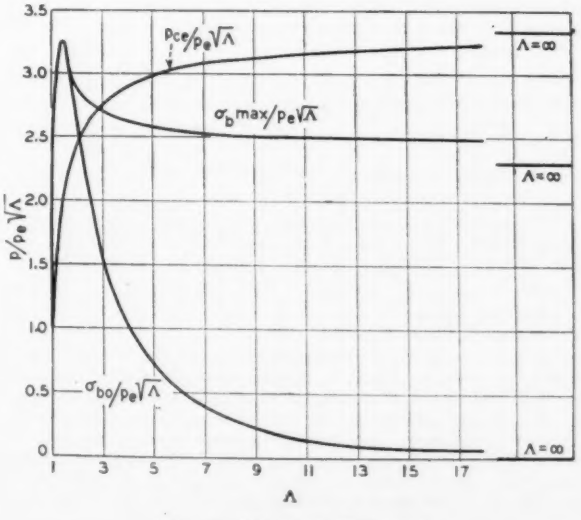


FIG. 6 MAXIMUM STRESSES

theory are also shown and the curves indicate clearly that these quantities really do tend to the limit values.

The circumferential bending stress σ_{bc} is not shown.[13] Its maximum is attained at the center and is the same as that of σ_b at this point up to $\Lambda = 1.57$; beyond this value of Λ, the maximum point also shifts toward the edge but the maximum value is always less than that of σ_b. Asymptotically $\sigma_{bc} = \nu\sigma_b$. Further, the maximum of the radial membrane stress p is always less than that of p_c. Hence, for design purposes, if the maximum-stress theory is used, only the stresses σ_b and p_c need be considered.[14] From $\Lambda = 3$ on, the circumferential membrane stress p_{cs} dominates.[15]

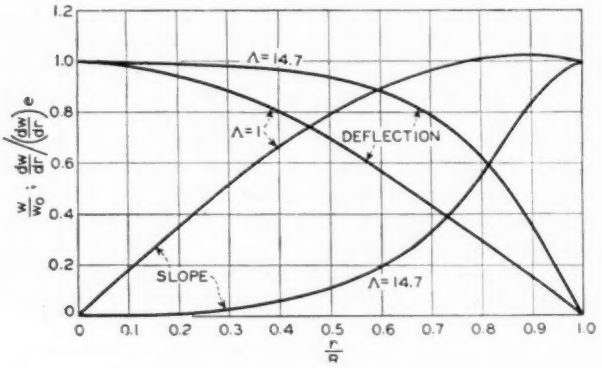


FIG. 7 SLOPE AND DEFLECTION

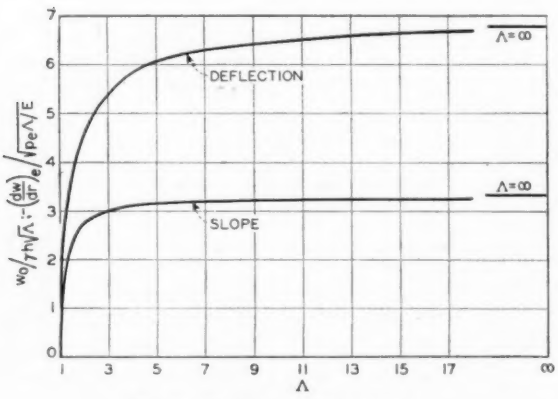


FIG. 8 SLOPE AND DEFLECTION

Slope and Deflection. In Figs. 7 and 8 the deflection w and the slope dw/dr are shown. In Fig. 7 the ratio of w and dw/dr to their maxima, i.e., w/w_0 and $(dw/dr)/(dw/dr)_e = rq/Rq_e$, are given as functions of r/R for the values $\Lambda = 1$ and $\Lambda = 14.7$. There is a quite perceptible flattening of the deflection curve for the higher values of Λ, accompanied by a tendency of the slope to approach zero in the central portion of the plate. Asymptotically the curve for w/w_0 would consist of two segments: a horizontal straight line up to the edge ($r/R = 1$) of the plate and a vertical line from it down to zero. Fig. 8 shows a rapid approach of the quantities $w_0/\gamma h\sqrt{\Lambda}$ and $-(dw/dr)_e/\sqrt{(p_e\Lambda/E)} = q_e/\sqrt{(p_e\Lambda/E)}$ to their asymptotic values.

Asymptotic Range. It is seen from the curves that the solutions from about $\Lambda = 5$ on do not change qualitatively; even quantitatively there is little change. Hence, for the range $\Lambda > 5$, which might be called the "asymptotic range," the solutions are at least roughly approximated by the asymptotic solution.

6—Limit State and Asymptotic Solution

As is seen from the curves, the deflection and stresses are nearly constant over a large portion of the plate when Λ becomes large and abrupt changes in all quantities occur in a narrow strip near the edge of the plate. In addition, the quantities p_0/p_e, $p_{ce}/p_e\sqrt{\Lambda}$, $\sigma_{be}/p_e\sqrt{\Lambda}$, etc., appear to approach finite limit values as Λ tends to infinity. It is possible to give a mathematical treatment of this limit process and obtain from it the limit values.

An asymptotic treatment of laterally loaded plates has been given by Hencky following A. Föppl (7, 4). Cf. also (1). It consists in omitting the terms referring to bending in the von Kármán equations (i.e., the left member of Equation [2]). One is tempted to apply an analogous treatment to the present problem, but this would lead to incorrect results. The procedure analogous to Hencky's would be as follows: Since $\Lambda = p_e/4.24\eta^2E$ it is clear that $\Lambda \to \infty$ if the slenderness ratio η tends to zero while p_e is held fixed. Upon allowing $\eta \to 0$ in the differential equations [8] and [9] one obtains

$$E^{-1}\Gamma p = q^2/2, \quad pq = 0 \ldots\ldots\ldots [29, 30]$$

the only nonsingular solution of which is $q \equiv 0$, $p \equiv$ const. If, then, this constant were identified with the edge value p_e, one would obtain as limit state a hydrostatic compression, which would clearly be wrong since the limit state appears rather to be one of constant tension. See Fig. 3. The error does not lie in the solution $q \equiv 0$, $p \equiv$ const but in the manner of fixing the constant. The sudden change in p from tension to compression that takes place across the boundary layer must be considered; the value of the constant under discussion is to be identified with the limit value of p at the inner edge of the boundary layer. Hence it can be found in this case only by an independent treatment of the boundary layer.[16]

The essential feature in the mathematical treatment of the boundary layer (as is also the case with Prandtl's boundary-layer theory for viscous flow) consists in stretching the scale with increasing Λ in such a way that the width of the boundary layer (measured in the new scale) does not shrink to zero. This can be done by introducing the new variable

$$\beta = (1 - r/R)\lambda, \quad 0 \leq \beta \leq \lambda, \text{ where } \lambda = (p_e/E)^{1/2}/\eta$$

It is necessary also to introduce new dependent variables which remain finite as $\Lambda \to \infty$. Such variables are found to be $P = p/p_e$ and $Q = q/\gamma\sqrt{(p_e/E)}$. Introducing the new variables into the differential Equations [8] and [9] and then allowing λ to tend to infinity, gives the differential equations

$$\frac{d^2P}{d\beta^2} = \frac{1}{2}Q^2, \quad \frac{d^2Q}{d\beta^2} + PQ = 0 \ldots\ldots [31, 32]$$

[13] The stress σ_{bc} is given by the formula

$$\sigma_{bc} = 6\gamma\eta E[\nu r q_r + (1 + \nu)q]$$

[14] The relative magnitudes of the stresses are here given for the case $\Lambda = 14.7$. The stresses at the edge ($r/R = 1$) where p_c is maximum, and at r/R where σ_b is maximum, are as follows

r/R	$p/p_e\sqrt{\Lambda}$	$\sigma_b/p_e\sqrt{\Lambda}$	$p_c/p_e\sqrt{\Lambda}$	$\sigma_{bc}/p_e\sqrt{\Lambda}$	$\tau_b/p_e\sqrt{\Lambda}$
1.0	0.3	0	3.2	0.7	1.8
0.87	0	2.5	1.2	1.4	1.2

The quantity τ_b is the horizontal shear stress due to bending. (τ_b is, as one expects, small and it vanishes asymptotically.) It is clear that the stress p should be combined with σ_b and the stress p_c with σ_{bc}. But, in any case, the stress p_c at the edge governs for $\Lambda = 14.7$.

[15] This is, however, not true in the case of the clamped plate, where the maximum of σ_b as well as of p_c is always attained at the edge. The authors have solved the asymptotic problem for this case and have found that in the limit $\sigma_{bs}/p_{cs} = 6\gamma = 1.8$; hence the bending stress governs.

[16] Hencky's method is, however, legitimate in his case where neither edge *compression* nor edge moment is prescribed.

The range of the variable β is obviously $0 \leq \beta \leq \infty$, where $\beta = 0$, $\beta = \infty$ correspond to the outer and inner edges of the boundary layer respectively. The boundary conditions become

$$P = 1, \quad dQ/d\beta = 0 \text{ for } \beta = 0$$

and regularity for $\beta = \infty$.

The authors have solved this nonlinear boundary-value problem and proved that its solution gives the limit values correctly (26).[17,18] From the functions P and Q thus obtained finite limit values were also found for all quantities discussed in the preceding section. In particular, $P(\infty) = -0.47$, which is the limit value for p/p_e at the inner edge of the boundary layer. Hence the constant $-0.47\ p_e$ is the one needed to complete the solution by the method of Hencky. Consequently it is proper to take -0.47 as the limit value for the ratio p_0/p_e, which refers to the value of p/p_e at the center of the plate.

Mathematically there is only one passage to the limit characterized by

$$\Lambda \to \infty \text{ or } p_e/\eta^2 E = p_e R^2/\gamma^2 h^2 E \to \infty \quad \ldots\ldots [33]$$

For a fixed plate (R and h fixed), this would require $p_e \to \infty$, implying infinitely high stress. If p_e is held fixed, one might consider a series of plates for which the slenderness ratio $\eta \to 0$; for example the radius R might be held fixed and the thickness h allowed to approach zero. In this case the governing stresses would tend to become infinite, as one sees from the limit relation

$$p_{c_e} \sim (3.33)p_e\sqrt{\Lambda} = 3.33\, p_e^{2/3}/(4.24)^{1/3}\eta E^{1/3} \to \infty \quad \ldots\ldots [34]$$

However, for a value of Λ as large as one pleases, plates could be designed for which stress and slope would be as small as necessary to insure the validity of the von Kármán equations. In order to see this let η and p_e tend to zero in such a way that $p_e/\eta^2 E \to \infty$ while $p_e/\eta E = \sqrt{(4.24\Lambda p_e/E)}$ remains sufficiently small; then it follows from the asymptotic formula $p_{c_e} \sim (3.33)p_e\sqrt{\Lambda}$ for the greatest stress and the formula $q_e \sim (3.33)\sqrt{(p_e\Lambda/E)}$ for the greatest slope (see Table 2), that p_{c_e} and q_e can be made as small as desired.

A valid objection on physical grounds to the application of our formulas for high values of Λ may well be raised: It is likely that there is a value of Λ for which the buckled state in its turn becomes unstable, and what might be called a "second buckling" sets in; such a second buckling would not, of course, possess the radial symmetry of the first buckled state. Rough calculations indicate, however, that the second buckling will probably not begin until Λ is somewhere in the asymptotic range ($\Lambda > 5$).

If one were to pursue the second buckling into its nonlinear range, it is likely that it would eventually also become instable and a "third buckling" ensue, and so on; that is, more and more wrinkles would appear at the edge of the plate. Various experimenters, working with rectangular plates, have found that the plates do become wrinkled near the edges (2, 3, 8, 12, 13, 18, 19). The authors feel that such wrinkles are to be explained as the result of a buckling of order higher than the first.

It is of interest to indicate the relation[19] between the authors' asymptotic results and the notion of effective width introduced by von Kármán for the rectangular plate which is simply supported on two opposite sides and subjected to a thrust at the other two sides. In spite of the obvious difference between the present case and that of von Kármán, it is nevertheless true that these results throw some light on the latter case and contribute to substantiate certain assumptions on which von Kármán bases the derivation of his formula. These assumptions concerning the stress distribution for high values of the thrust (or for small thickness) are as follows: 1 The stresses will be concentrated in a strip along the simply supported edge; and 2 the membrane stress on an element perpendicular to this strip rather than the bending stress will be the maximum stress. The same properties of the stress distribution are found mathematically for the present case of the simply supported circular plate with radial symmetry. It may be mentioned, however, that the stress distribution in the circular plate will not conform to property 2 if the plate is clamped.[15]

Von Kármán's formula can be considered as a relation between maximum and average value of the membrane stress on an element perpendicular to the boundary strip. In the present case the stress on an element perpendicular to the boundary strip is the circumferential membrane stress p_c. Its average value $\bar{p}_e$ is given by

$$\bar{p}_e = R^{-1}\int_0^R p_c dr = R^{-1}\int_0^R \frac{d}{dr}(rp)dr = p_e \quad \ldots\ldots [35]$$

From the asymptotic formula

$$p_{c_e}/p_e\sqrt{\Lambda} \to 3.3 \quad \ldots\ldots [36]$$

there results

$$(\bar{p}_c/\eta^2)/(p_{c_e}/\eta^2)^{2/3} \to 0.728 \quad \ldots\ldots [37][20]$$

In von Kármán's formula the power 1/2 takes the place of the power 2/3. A strong discrepancy was to be expected owing to the different shape of the plate, the different way in which the thrust is applied, and the different wave pattern that is assumed. The authors think it likely that the discrepancy is caused mostly by the different wave pattern. The wave pattern assumed in von Kármán's case probably corresponds to buckling of higher order than the first.

[17] In much the same manner the asymptotic solutions for the buckling of the clamped plate and the plate under edge moment were obtained. It may be of interest to note that the boundary-layer phenomenon occurs in these cases also.

[18] It is possible to apply a perturbation method in the neighborhood of $\lambda = \infty$ by expansions in powers of $1/\lambda$. The foregoing solution would constitute the first step in such a procedure. The authors have carried out the second step also (26).

[19] This relation is also discussed by von Kármán (25).

[20] This number was given incorrectly in (5). See reference (26).

BIBLIOGRAPHY

1 "The Clamped Square Sheet," by D. G. Bourgin, *American Journal of Mathematics*, vol. 61, 1939, p. 418.

2 "Summary of the Present State of Knowledge Regarding Sheet-Metal Construction," by H. L. Cox, Aeronautical Research Committee Report No. 1553, 1933, His Majesty's Stationery Office, London, England, pp. 1–20.

3 "Buckling of Thin Plates in Compression," by H. L. Cox, Aeronautical Research Committee Report 1554, 1933, His Majesty's Stationery Office, London.

4 "Vorlesungen über technische Mechanik," by August Föppl, B. G. Teubner, Leipzig, Germany, 1907, vol. 5, section 24, p. 139.

5 "The Non-Linear Boundary Value Problem of the Buckled Plate," by K. O. Friedrichs and J. J. Stoker, Proceedings of the National Academy of Sciences, vol. 25, 1939, p. 535.

6 "Sur la rigidité de la tôle flambée," by A. Grzedzielski and W. Billewicz, *Sprawozdania Instytut Techniczny Lotnictwa*, vol. 10, 1937, p. 5.

7 "Über den Spannungszustand in kreisrunden Platten mit verschwindender Biegungssteifigkeit," by H. Hencky, *Zeitschrift für Mathematik und Physik*, vol. 63, 1915, p. 311.

"Die Berechnung dünner rechteckiger Platten mit verschwindender Biegungssteifigkeit," *Zeitschrift für angewandte Mathematik und Mechanik*, vol. 1, 1921, pp. 81, 423.

8 "Festigkeitsprobleme im Maschinenbau," by Th. von Kármán, *Enzyklopädie der mathematischen Wissenschaften*, vol. 4, 1910, article 27.8, p. 348.

9 "The Strength of Thin Plates in Compression," by Th. von Kármán, E. E. Sechler, and L. H. Donnell, Trans. A.S.M.E., vol. 54, 1932, paper APM-54-5.

10 "Die über die Ausbeulgrenze belastete Platte. Energieansatz und Differentialgleichungen," by K. Marguerre, *Zeitschrift für angewandte Mathematik und Mechanik*, vol. 16, 1936, p. 353.

11 "Über die Tragfähigkeit eines längsbelasteten Plattenstreifens nach Überschreiten der Beullast," by K. Marguerre and E. Trefftz, *Zeitschrift für angewandte Mathematik und Mechanik*, vol. 17, 1937, p. 85.

12 "Die mittragende Breite der gedrückten Platte," by K. Marguerre, *Luftfahrtforschung*, vol. 14, 1937, p. 121.

13 "Verhalten eines von Schub- und Druckkräften beanspruchen Plattenstreifens oberhalb der Beulgrenze," by A. Kromm and K. Marguerre, *Luftfahrtforschung*, vol. 14, 1937, p. 627.

14 "Zum Problem der Plattenstabilität," by P. Polubarinova-Kotschina, *Applied Mathematics and Mechanics*, vol. 3, 1936, p. 16.

15 "The Mechanics of Viscous Fluids," by L. Prandtl, "Aerodynamic Theory," vol. 3, Julius Springer, Berlin, Germany, 1935, sec. 13, 14, pp. 80–90.

16 "Applied Elasticity," by John Prescott, Longmans, Green and Co., London, England, 1924, p. 496.

17 "Die Überschreitung der Knickgrenze bei dünnen Platten," by G. Schnadel, Proceedings, Third International Congress of Applied Mechanics, vol. 3, 1930, p. 73.

18 "Strength of Rectangular Flat Plates Under Edge Compression," by Louis Schuman and Goldie Back, National Advisory Committee for Aeronautics, Technical Report No. 356, 1930, Superintendent of Documents, Washington, D. C.

19 "Stress Distribution in Stiffened Panels Under Compression," by E. E. Sechler, *Journal of the Aeronautical Sciences*, vol. 4, 1937, p. 320.

20 "Theory of Elastic Stability," by S. Timoshenko, McGraw-Hill Book Co., Inc., New York, N. Y., First edition, 1936, pp. 321–323, 390–395.

21 "Theory of Elasticity," by S. Timoshenko, McGraw-Hill Book Co., Inc., New York, N. Y., First edition, 1934, chapter 3, section 21.

22 "Bending of Circular Plates With Large Deflection," by Stewart Way, Trans. A.S.M.E., vol. 56, 1934, p. 627.

23 "Buckling and Failure of Thin Rectangular Plates in Compression," by M. Yamamoto and K. Kondo, Tokyo Imperial University, Aeronautical Research Institute, Report No. 119, 1935.

24 "Tragfähigkeit der über die Beulgrenze belasteten Kreisplatte," by K. Federhofer, *Forschung auf dem Gebiet des Ingenieurwesens*, vol. 11, 1940, p. 97.

25 "The Engineer Grapples With Nonlinear Problems," by Th. von Kármán, *Bulletin of the American Mathematical Society*, vol. 46, 1940, p. 631.

26 "The Nonlinear Boundary Value Problem of the Buckled Plate," by K. O. Friedrichs and J. J. Stoker. To be published in the *American Journal of Mathematics*.

A Short-Gage-Length Extensometer and Its Application to the Study of Crankshaft Stresses

By C. W. GADD[1] and T. C. VAN DEGRIFT,[2] DETROIT, MICH.

The mathematical methods of determining elastic stresses in machine elements, particularly those of irregular contour, may be excessively complex, so resort is frequently made to approximate calculations, which tend to lose accuracy while achieving simplicity. As a result a constant effort is made to supplement the mathematical treatment with experimental methods of studying stress. In this paper, the authors describe a short-gage-length extensometer and explain its application in the determination of crankshaft stresses. This instrument meets the requirement of convenience in operation, which is so essential in assuring that it will be used for the study of localized stresses.

Introduction

A CONSIDERATION of the elastic stresses which a machine element is likely to encounter under operation is recognized as an important factor in its design. However, it is a task which, in the case of parts of irregular contour, may require mathematical methods of excessive complexity, and is therefore often attempted by inadequate approximate calculations which lose accuracy while achieving simplicity. Errors of considerable importance can thus result, particularly if the design is entirely new; and little or no background exists upon which to check theoretical calculations or build empirical ones. Furthermore, with the necessity in certain fields, for example, that of aircraft engines, of arriving as closely as possible at the ideal design, from the standpoint of employing a minimum of material consistent with adequate strength, it becomes increasingly important to determine stresses as accurately as possible.

Thus, there is a constant effort to supplement mathematical with experimental methods of studying stresses. In order to be of practical value in industry, however, the latter must be sufficiently convenient in operation that the engineer will actually use them in preference to a simplified calculation, or even a trial-and-error method. This requirement has seriously limited the use of measuring instruments designed for the study of localized stresses. An instrument is described in this paper which, it is felt, does to a great extent meet such a requirement.

Ordinarily no experimental method, short of actual service tests, can give the ultimate answer as to whether the strength of a newly designed part will be adequate, particularly if only a low factor of safety is desired. It is generally realized that other factors such as the condition of the surface, the material, residual stresses, and others, in addition to the actual shape of the part, influence importantly its strength. An instrument which can aid in the study of stress distribution due to shape of the part can, however, be of definite value in the following ways:

1 It can reduce the uncertainty in an original design by performing one step, namely, that of ascertaining stress distribution from assumed loads on the part.

2 It can provide a check upon the relative merit in alternate designs, when it is desired that a part, which has been failing, be improved.

The foregoing of course presupposes some knowledge of the nature of working loads imposed upon the part. These, if complex, may provide the source of greatest error in any stress investigation, whether mathematical or experimental. In checking alternative designs, however, it has usually been found possible to learn enough of the nature of actual loads to permit a valid check as to whether the alternate design is superior to the original, although the exact degree of improvement may be uncertain.

A program of stress investigation with the aid of the extensometer has usually been as follows:

1 The external loads on, or distortions of, the part in question are first estimated as accurately as possible by theoretical methods or, where feasible, by study of similar parts under operation with available instrumentation.

2 Static-loading devices are set up and stress-distribution traverses are made. It has been found desirable to employ "Stresscoat" strain-indicating lacquer in conjunction with the extensometer, both for the purpose of localizing quickly the analysis in the more dangerously stressed regions, and for determining the directions of the principal strains at these regions.

3 If it is desired that actual operating stresses be checked, as an aid in further study, after a model of the engine or other mechanism containing the part in question is in operation, this may be done by placing a dynamic strain gage at certain accessible points on the part, thus establishing a "scale" for the complete stress-distribution curves found statically.

Description of Extensometer

Principle of Operation. Operation of the gage is by means of

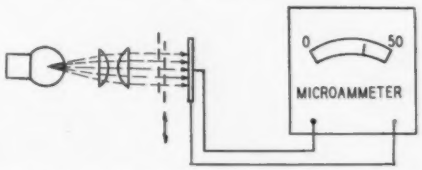


Fig. 1 Operation of Extensometer Optical System

(1) a simple mechanical lever integral with one of the gage points, and (2) a pair of gratings of alternate transparent and opaque bands, which intercept a collimated beam of light rays directed on a photocell. The mechanical stage is coupled directly to one of

[1] Research Engineer, Research Division, General Motors Corporation. Jun. A.S.M.E.

[2] Department Head, Mechanical Engineering No. 6, Research Division, General Motors Corporation.

Presented at the Annual Meeting, New York, N. Y., December 1–5, 1941, of The American Society of Mechanical Engineers.

Discussion of this paper should be addressed to the Secretary, A.S.M.E., 29 West 39th Street, New York, N. Y., and will be accepted until April 10, 1942, for publication at a later date. Discussion received after the closing date will be returned.

Note: Statements and opinions advanced in papers are to be understood as individual expressions of their authors, and not those of the Society.

the gratings, while the other remains fixed, except when making necessary adjustments prior to applying the load to the specimen and checking a stress. Thus, when the specimen is strained, the gratings move relative to one another in such a manner that light falling on the cell varies in proportion to the strain.

The variation in current generated by the cell is, in turn, indicated on a microammeter connected directly with the cell. Other data pertaining to the instrument are as follows:

Height, in	$2^1/_4$
Weight, oz	$^1/_2$
Gage lengths used (separate instruments), in	$^1/_{16}$, $^1/_8$, and $^1/_4$
Magnification:	
Mechanical	25:1
Optical	1200:1
Over-all	30,000:1
Strain-indicating scale	50-Mu-a ammeter with $6^1/_4$-in. scale. (Usable or linear range of gage output approximately 20 mu-a)
Power source for lamp	Voltage-regulating circuit connected in 110-v a-c line, for furnishing power to the 3.8-v extensometer lamp
Method of calibration	Standard tensile specimen mounted in testing machine

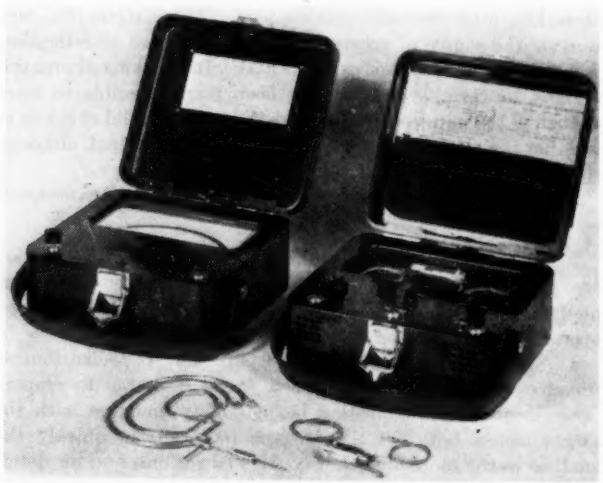


FIG. 2 MICROAMMETER, POWER UNIT, CLAMPS, AND EXTENSOMETER

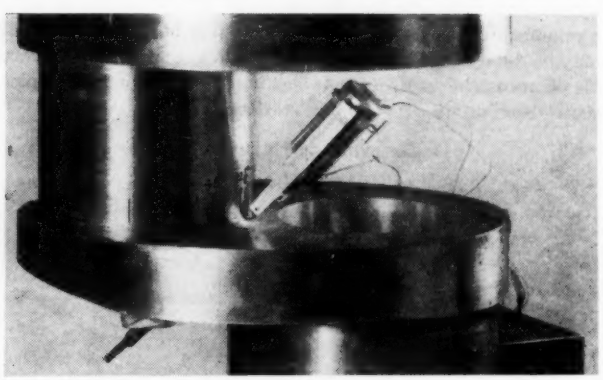


FIG. 3 EXTENSOMETER MOUNTED IN CRANKPIN FILLET

The 30,000:1 magnification cited, which results from the use of gratings of 120 lines per in. and the $6^1/_4$-in. microammeter scale, has been found satisfactory for all work done with the gages thus far.

Mounting the Gage. The gage is pivoted midway between the points, and mounted by one of the two methods shown in Fig. 4. The C-clamps are made of stock which can be bent with the fingers to various shapes. The second method is used where access cannot be had to the opposite side of the work.

No prick-punch marks are used with the gage. The force of approximately 1 lb required to hold the gage against the work provides a frictional force at the points sufficiently great to operate the gage.

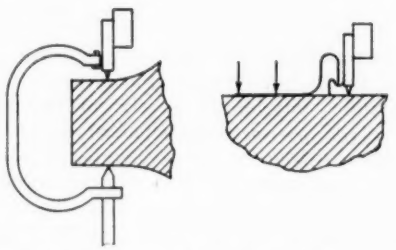


FIG. 4 METHODS OF MOUNTING THE INSTRUMENT

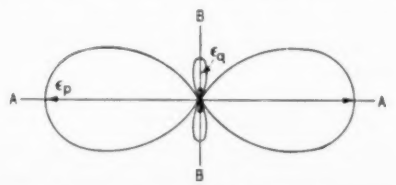


FIG. 5 STRAIN DIAGRAM IN POLAR CO-ORDINATES

Interpretation of Measurements. This phase of the work is considered in detail elsewhere in the literature; it will suffice here only to point out a variation from ordinary procedure, necessary when a short gage length is employed. Whereas, with a long gage length, a complete determination of the state of surface stress may be obtained by making measurements at a minimum of three known angles, this procedure is inadvisable if maximum accuracy is to be assured with a $^1/_{16}$-in. gage length, due to inaccurate maintenance of the angular relationship of the measurements. The alternative method for eliminating this inaccuracy consists, first, in making a sufficient number of checks in the general direction of AA, Fig. 5, to establish as accurately as is desired the value of the maximum principal strain ϵ_p. (Usually its direction may be estimated approximately before making any measurements.) Second, checks are made in the direction BB, at right angles to AA, for obtaining the minimum principal strain ϵ_q. Knowing the two principal strains, the formulas

$$\sigma_p = \frac{E}{1 - \mu^2}(\epsilon_p + \mu\epsilon_q)$$

$$\sigma_q = \frac{E}{1 - \mu^2}(\epsilon_q + \mu\epsilon_p)$$

for converting to stress are applied, where E = modulus of elasticity; σ_p and σ_q = principal stresses; ϵ_p and ϵ_q = principal strains; μ = Poisson's ratio.

To eliminate the foregoing computation for each point, however, a uniform-scale-alignment chart may be employed.

CRANKSHAFT-STRESS MEASUREMENTS

As an example of a practical application of the strain gage, an analysis of certain phases of the problem of crankshaft stresses will be given. It should be emphasized that this analysis is not complete, but that it is rather an attempt to learn the effect upon the magnitude of stress concentration in a shaft of only a

few of the design variables. A partial analysis of this kind has been found useful in two ways (1) as a method of improving an existing design, and (2) as an indication of the trends of shaft strength as functions of certain variables which are taken into consideration in an original design.

Torsional Stress

Critical Regions in Crank Throw. The critical region for a crank throw in torsion ordinarily occurs in the crankpin fillet, somewhat below center, as shown at *A*, Fig. 6, and with the principal planes oriented at approximately 45 deg with the fillet. A similar critical region also exists in the journal fillet which, however, is not usually as dangerous as the former, because of the heavier construction customarily employed in the journal. When the crank throw is left solid, high stresses are confined to these regions.

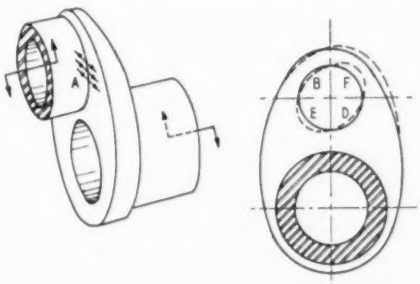


Fig. 6 Location of Critical Torsional Stress, and Distortion of Hollow Crankpin Under Torsion



Fig. 7 Crankpin Arrangement

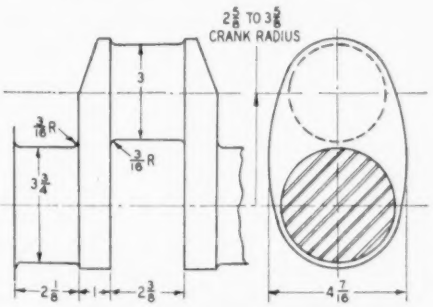


Fig. 8 Dimensions of Crank Throw

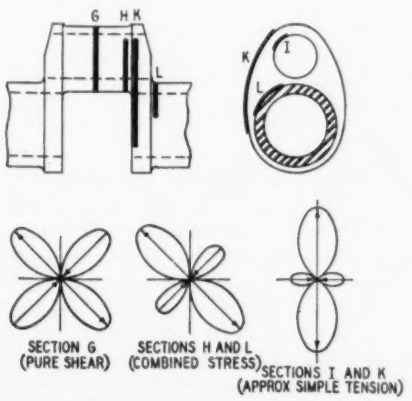


Fig. 9 Location of Torsional Strain Traverses, and Typical Strain Rosettes

If, in addition, the crankpins and journals are bored (for the purpose of lightening the shaft), a partial collapse of the ends of the pins and journals occurs, as shown, which produces concentrations of tensile stress at *B* and *D*, and compressive stress at *E* and *F*, with the principal stress oriented parallel to the edge of the lightening hole. (At the opposite end of the throw, distortion of the cheek is in the opposite direction, and points of tension and compression are consequently reversed.) Again, if heavier construction is employed in the journal, stresses are greater in the pin than in the journal, and are greater at *B* than at *D*.

In the case of hollow shafts, although stresses in the crankpin fillets ordinarily are more dangerous than at the edge of the lightening holes, it is possible, if the holes are enlarged sufficiently, to obtain stresses at their edges which are more severe than those in the fillets.

Method of Loading the Shafts in Torsion. All torsional measurements were made on 6-throw 7-main-bearing shafts, with the conventional 120-deg crank arrangement shown in Fig. 7. Dimensions of the throw are given in Fig. 8. The shafts were mounted on rollers 3 in. diam × ¾ in. wide, three of which contacted the shaft at each journal. In turn, these were mounted with a rigidity such that they partially constrained the journals from transverse motion as the torque was applied. The degree of constraint imposed upon the shaft by the crankcase of course influences the state of stress in the shaft, and, as in any experimental stress investigation, the location of most severely stressed points in the laboratory model should, wherever possible, be checked against the location of nuclei of field failures, if there is any question as to the validity of method of loading the model in the laboratory.

Stress-distribution traverses were made at sections *G*, *H*, *I*, *K*, and *L* of the crank throws, as shown in Fig. 9. At the mid-section of the crankpin, section *G*, contraflexure occurred, and the strain rosettes were those of pure shear, such as would be found in a straight shaft in torsion. At points around sections *H* or *L* in the pin and journal fillets, respectively, the strain patterns indicated shear, combined with a varying amount of normal stress, but with the principal planes still at approximately 45 deg. Strain along sections *K* and *I*, the edges of the cheek and crankpin lightening hole, respectively, approximated simple tension.

Strains were predominantly tensile on one side of the cheek (the forward side of the left-hand illustration in Fig. 6) and compressive on the other, but reversed when the direction of the torque was reversed.

Preliminary measurements on several shafts in torsion indicated two sources of scatter of the results:

1 A variation, usually no greater than 6 per cent, existed between results at identical points on different shafts of the same design. This was considered normal, and due to variations in material, machining, or measurement.

2 However, a type of scatter of much larger proportions was found in the stress-concentration values at identical critical regions of different cheeks of the same shaft, and at opposite sides of the same cheeks. Apparently stress concentration in torsion was a function of orientation of the crank throws adjacent to the one under consideration. This latter scatter reached approximately 30 per cent in the shear stress at the points of maximum crankpin-fillet concentration (point *A*, Fig. 6). An inspection of this scatter indicated that, of the twenty-four such critical localities on the 6-throw shaft, eight of these, situated such that the adjacent throw was at 240 deg (for example, the left side of the first cheek of throw No. 2, Fig. 7) were consistently more highly stressed than the others. The least highly stressed cheeks

were the middle ones, which are located at 0 deg relative to one another.

The stress-concentration factor in torsion in a conventional crankshaft, employing identical crank throws and symmetrical cheeks, therefore, cannot be stated as a constant for a given crank-throw design, but is in addition a function of crank arrangement. Stress-distribution curves, given subsequently, were taken from the right-hand side of the second cheek of throw No. 2,

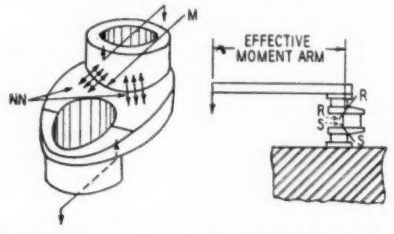


FIG. 10 LOCATION OF CRITICAL BENDING STRESSES

FIG. 11 METHOD OF APPLYING BENDING MOMENT

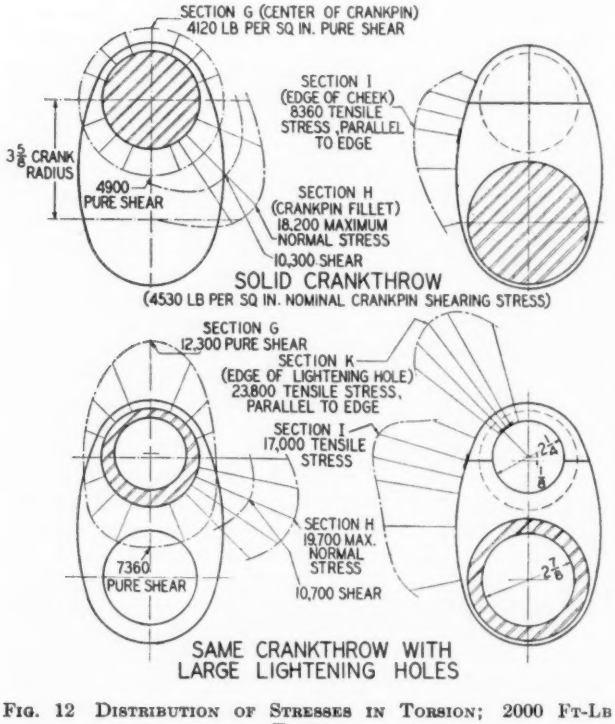


FIG. 12 DISTRIBUTION OF STRESSES IN TORSION; 2000 FT-LB TORQUE

in Fig. 7, which was one of the eight more highly stressed areas in the shaft.

BENDING STRESS

Only distortion of the type ordinarily encountered when resonant bending vibration is present, or when an overhung load exerts a reversed bending couple at the end of the shaft, will be considered. Distortion of this type was simulated by bending a single throw, flanged at the ends, with a beam as shown in Fig. 11. Greatest deflection, and highest stresses, for a given moment, were found to occur when the bending moment was applied in the plane of the crank throw.

As would be expected, the abrupt change in section at the journal and pin fillets, at sections *RR* and *SS*, resulted in highest concentrations of stress here. However, the nature of these concentrations depended in a large measure upon whether or not lightening holes were present. If journals and pins were solid, stress reached a maximum at the center, point *M*, Fig. 10, whereas if they were bored, stress at the center receded and a pair of peaks *NN* formed.

Bending throughout the short cheek section between pin and journal was found to differ from that of a simple beam, in that the constraint of the pin and journal annulled anticlastic curvature of the cheek, with the result that strain laterally was very nearly zero, and the principal stress in the direction shown in Fig. 10 was larger by the factor $1/(1 - \mu^2)$ than would be the case of simple bending. This condition held at the points of highest stress in both journal and crankpin fillets.

STRESS-DISTRIBUTION CURVES

In Figs. 12 and 13 are plotted sample distribution curves taken on solid crank throws of the dimensions shown in Fig. 8, before and after boring large lightening holes in the crankpin and journals. Included with both sets are nominal calculated stress values upon which stress-concentration factors may be based. In torsion, stress is calculated assuming the crankpin as a shaft in simple torsion. In bending, the calculation assumes a beam of the same cross section as the cheek, subjected to simple bending

EFFECT OF DESIGN VARIATIONS

(*a*) Crank Radius:

Holding other dimensions constant, the crank radius of the crank throw, shown in Fig. 8, was varied from $2^5/_8$ to $3^5/_8$ in. in three steps. This range covered typical degrees of "overlap" between journal and pin normally employed in practice.

As seen in Fig. 15 the solid shaft is strengthened considerably for a given bending load by overlapping the journal and crankpin. In the direction of increasing crank radius, stress concentrations approach constant values, because the pin and journal become isolated from one another and each is stressed independently of the other.

In torsion the trend is similar, but the percentage of variation in stress concentration is much less.

Although both in bending and in torsion, the use of a larger crank radius tends to weaken a solid crank throw, this trend does not necessarily obtain in particular designs of hollow crank throws, since, as will be made clear later, the proximity of a lightening hole to the region of high fillet stress constitutes another variable which can also exert an important influence upon the degree of stress concentration.

(*b*) Lightening Holes in Journal and Crankpin:

Stress Due to Bending. Concentration of stress in the fillets, resulting from a bending moment, is affected by the presence of lightening holes in two ways. Considering the critical journal-fillet stress, its value will rise according to curve *T*, Fig. 16, as the journal bore is enlarged, while holding the crankpin bore at an arbitrary diameter. On the other hand, if the journal bore is held, while varying the crankpin bore, the journal-fillet stress, will, instead of rising continuously, pass through a minimum or optimum value at a particular diameter of crankpin bore, as indicated by curve *U*. This minimum value occurs as the stress at the center of the cheek, point *M*, Fig. 10, is relieved by the crankpin lightening hole, and two points of concentration *NN* at either side appear in its place. If both pin and journal bores are enlarged simultaneously, curve *V* will result, with the optimum value still appearing with the same diameter of crankpin bore.

These same general trends hold for crankpin-fillet stress.

As a specific illustration of these trends, the results of measurements on the same three throws previously used, with each of the

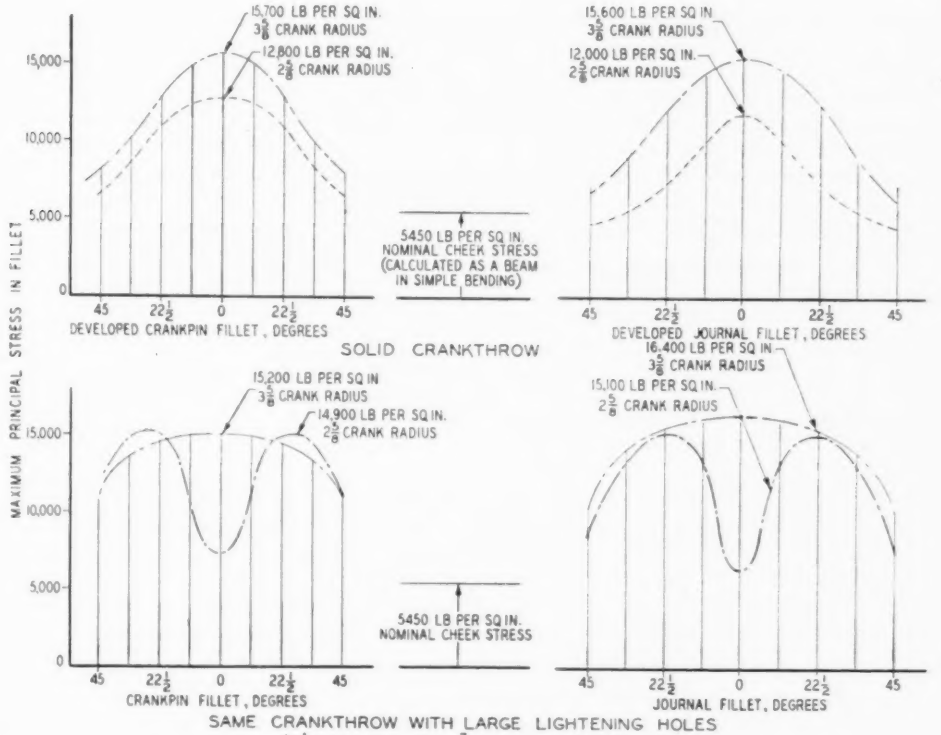


FIG. 13 DISTRIBUTION OF STRESSES IN BENDING; 336-FT-LB COUPLE APPLIED AS SHOWN IN FIG. 11

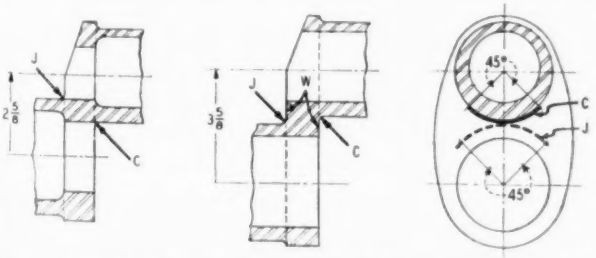


FIG. 14 SECTIONS SHOWING LOCATION OF BENDING-STRESS MEASUREMENTS ON THROWS OF 2⅜ IN. AND 3⅜ IN. CRANK RADIUS
(*C* = crankpin-fillet traverses; *J* = journal-fillet traverses.)

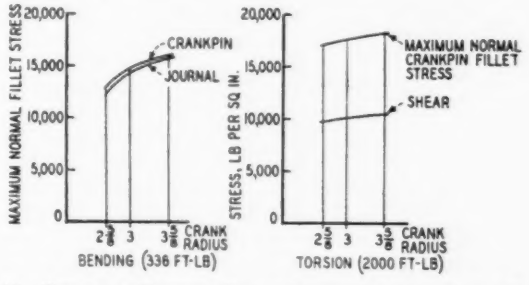


FIG. 15 EFFECT OF VARYING CRANK RADIUS OF SOLID CRANK THROW

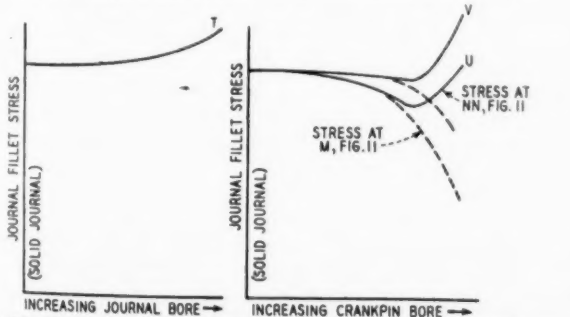


FIG. 16 EFFECT OF LIGHTENING HOLES ON JOURNAL-FILLET STRESS CONCENTRATION IN BENDING

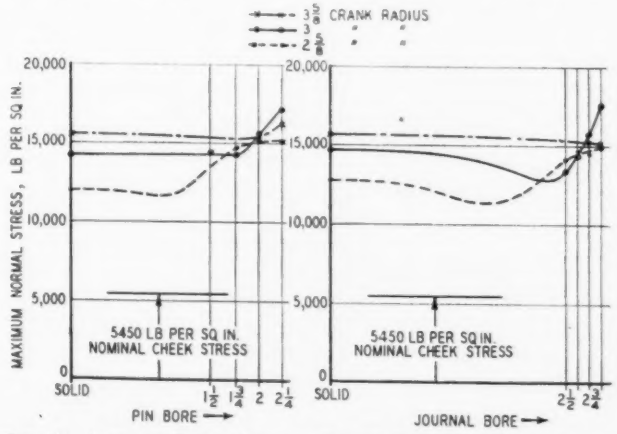


FIG. 17 JOURNAL-FILLET STRESS IN BENDING VERSUS LIGHTENING-HOLE SIZE; 336 FT-LB

FIG. 18 CRANKPIN-FILLET STRESS IN BENDING VERSUS LIGHTENING-HOLE SIZE; 336 FT-LB

following stages of lightening hole enlargement, will be given:

Stage No. 1; solid journal and solid crankpin
Stage No. 2; 2½ journal bore, 1½ crankpin bore
Stage No. 3; 2⅝ journal bore, 1¾ crankpin bore
Stage No. 4; 2¾ journal bore, 2 crankpin bore
Stage No. 5; 2⅞ journal bore, 2¼ crankpin bore

In each case, crankpin bores were located ⅛ in. outside concentricity with the outside diameter of the pin. In boring the throw of 2⅝ in. radius, straight bores were used until interference occurred with the bearing surfaces; from here on shoulders were left, as shown in Fig. 14.

Stresses due to bending for each of these stages are plotted in Figs. 17 and 18. In the case of the throw having the largest crank radius ($3^5/_8$ in.), it is seen that the lightening holes could not be enlarged sufficiently to affect bending stress in the fillets appreciably. Accomplishment of the latter would require removal of metal closer to the fillets, as at W, Fig. 14.[3]

Stress Due to Torsion. The influence of lightening holes upon torsional stresses is illustrated in the following two figures. Here again, stresses in the solid throws of shortest radius are least, but, with the introduction of lightening holes, the trend reverses. Furthermore, it is again possible, with the exception this time of the throw of shortest radius, to use an optimum lightening-hole size, such that a deviation either way aggravates the fillet stress.

[3] Mention is made of the expedient of removing metal, in effect, to produce a larger fillet radius in "Spannungsverteilung in Konstruktionselementen," by E. Lehr, V.D.I. Verlag, Berlin, 1934, p. 56.

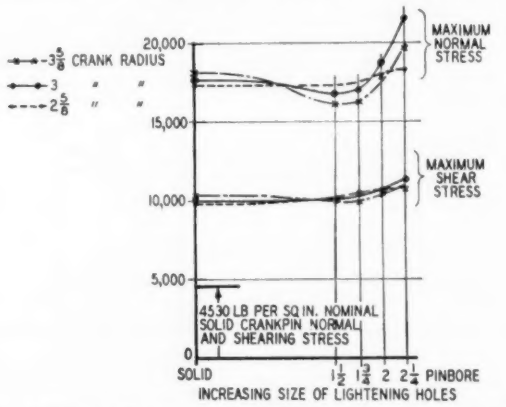


FIG. 19 CRANKPIN-FILLET STRESS IN TORSION VERSUS LIGHTENING-HOLE SIZE; 2000 LB TORQUE

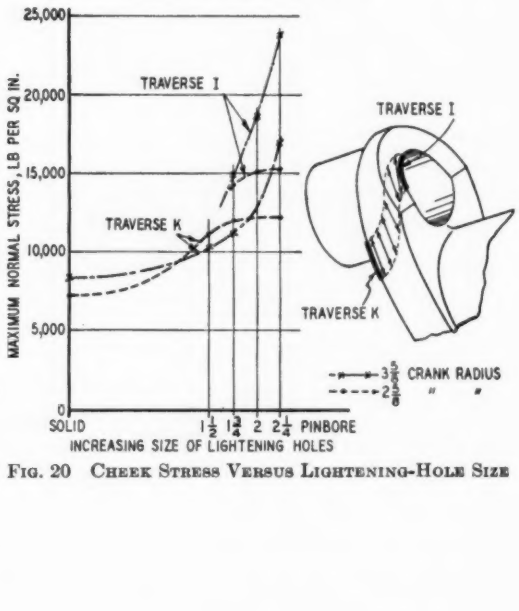


FIG. 20 CHEEK STRESS VERSUS LIGHTENING-HOLE SIZE

Fig. 20 illustrates another observation which can be made from the torsional measurements. Here are plotted the trends of maximum cheek stress against lightening-hole size. It is seen that, in contrast to fillet stress, the cheek stresses rise rapidly as the lightening holes are enlarged. As this is done, resulting distortion of the cheek produces a region of high tensile stress, extending around the cheek as shown, but with highest stresses at the edges I and K. If the crankpin lightening hole is enlarged sufficiently, stress at its edge I can become more severe than in the fillet. Thus, while it is not necessary to exercise care in providing fatigue-resisting cheek surfaces in manufacturing a heavy shaft, as in automotive practice, such a precaution becomes important in a lightweight, hollow one.

(*c*) Effect of Shoulders in Lightening Holes:

As was mentioned previously, shoulders were left in the lightening holes of the throw having a crank radius of $2^5/_8$ in., as illustrated in Fig. 14, in enlarging them beyond the point of interference with the bearing surfaces. As soon as this is done, the curves of critical stresses versus increasing lightening-hole diameter are seen to level off. Thus the leaving of a shoulder at the ends of the hole (sometimes used in aircraft practice), constitutes a means of preserving optimum design where it is needed while removing excess metal where it is not needed.

COMBINED STRESS

No attempt has been made in this analysis to combine bending with torsional loads. Thus far, it has been considered advisable to deal with each separately, according to the requirements of a particular problem, and, if both are critical, to look for design changes which do not increase bending strength at the expense of torsional strength, or vice versa.

CONVERSION CONSTANTS

Constants for conversion of the strain measurements into stresses were determined from strain measurements, made with the $^1/_{16}$-in. extensometer, on A.S.T.M. tensile-test specimens cut from the forged steel from which the shafts were made. These were as follows:

Modulus of elasticity = 29,500,000
Poisson's ratio = 0.300

All measurements were taken with the $^1/_{16}$-in-gage-length extensometer. In making fillet measurements, the gage was placed at several inclinations with respect to the crankshaft axis at every location, in order to determine the most severe stresses present.

Measurement of Latent Heat by the Gas-Current Method

By J. A. GOFF[1] and J. B. HUNTER,[2] PHILADELPHIA, PA.

The gas-current method of measuring latent heat appears to possess important advantages over other calorimetric methods. Preliminary results have been derived from a co-operative investigation carried out by the American Society of Heating and Ventilating Engineers and the Towne Scientific School, University of Pennsylvania, in which sufficiently reliable values of the interaction constant for air-and-water-vapor mixtures have been determined to permit an adequate thermodynamic analysis of the gas-current method. The present paper is devoted to the development of this analysis and its application to the reduction of certain experimental data recently obtained by one of the authors. The apparatus and method of conducting the experiments are also described.

Introduction

IN THE gas-current method of measuring latent heat, a steady stream of an indifferent gas is bubbled through, or passed over, the liquid to be investigated in an adiabatic calorimeter. Energy is supplied electrically at a constant measured rate in order to compensate the drop in temperature which would otherwise occur due to evaporation. The gas stream is brought to the temperature of the liquid before being admitted into the calorimeter. The rate of flow is continuously adjusted during test to maintain the temperature of the liquid constant and as nearly as possible equal to that of the surrounding bath. This not only eliminates heat leak into or out of the calorimeter, but also insures that the gas stream leaves the calorimeter with the same temperature as that of the liquid. The gas stream leaving the calorimeter contains vapor of the liquid. This is subsequently removed, usually by chemical means, over a measured period of time, and accurately weighed. Consequently, since the rate at which energy is supplied to the calorimeter is accurately known, the ratio of energy supplied to liquid evaporated, under conditions of constant temperature and constant total pressure, is easily computed.

The gas-current method appears to possess important advantages over other calorimetric methods. In the first place, it permits investigation over a range of temperature below the normal boiling point of the liquid, without requiring operation below atmospheric pressure. Thus the method permits measurements of latent heat at, or near, atmospheric temperature and atmospheric pressure (conditions most favorable to accurate calorimetry) in the case of liquids the normal boiling points of which may be well above atmospheric temperature. In the second place, the apparatus is comparatively simple and inexpensive, since glass construction can be used throughout. The method is particularly suitable for measurements on aqueous solutions of nonvolatile solutes.

The gas-current method seems to have been first employed successfully by A. W. Smith (1)[3] for measurement of the latent heat of pure water at five temperatures below 100 C. While Smith's experimental procedure is open to criticism in several important respects, and his results do not exhibit a high degree of consistency and reproducibility, nevertheless, his average values are lower than the values of latent heat recently reported by the National Bureau of Standards (2), as they should be for a reason which it is the principal object of this paper to explain. A completely satisfactory explanation must take into account the effect of intermolecular forces, particularly those of interaction between air and water vapor. Until recently no reliable data on the extent of this interaction have been available.

Preliminary results of the co-operative investigation between the American Society of Heating and Ventilating Engineers and the Towne Scientific School, University of Pennsylvania, have recently yielded sufficiently reliable values of the interaction constant for air-and-water-vapor mixtures to permit an adequate thermodynamic analysis of the gas-current method, at any rate as it applies to aqueous solutions of nonvolatile solutes in which the indifferent gas is dry carbon-dioxide-free air. These results are to be published shortly (3), and are described in more detail in the doctoral dissertation of A. C. Bates (4), on file in the Towne Scientific School library. The principal objective of the present paper is to develop the thermodynamic analysis and apply it to the reduction of certain experimental data recently obtained by one of the authors and which will form the basis of a dissertation to be submitted to the faculty of the Graduate School of Arts and Sciences, University of Pennsylvania, in partial fulfillment of the requirements for the doctorate in chemical engineering.

Thermodynamic Theory

Fig. 1 shows the flow diagram to which the following thermodynamic analysis applies. It is assumed from the start that:

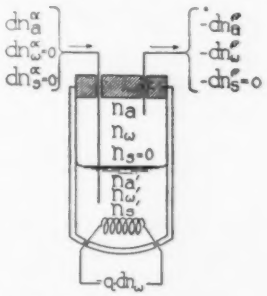


FIG. 1 FLOW DIAGRAM

1 The entering gas stream is dry CO_2-free air (subscript a) containing no water ($dn_\omega^\alpha = 0$) and no salt ($dn_s^\alpha = 0$).

[1] Dean, Towne Scientific School, University of Pennsylvania. Mem. A.S.M.E.

[2] Assistant Instructor in Chemistry and Chemical Engineering, Towne Scientific School, University of Pennsylvania.

Presented at the National Meeting of the Applied Mechanics Division, Philadelphia, Pa., June 20–21, 1941, of THE AMERICAN SOCIETY OF MECHANICAL ENGINEERS.

Discussion of this paper should be addressed to the Secretary, A.S.M.E., 29 West 39th Street, New York, N. Y., and will be accepted until April 10, 1942, for publication at a later date. Discussion received after the closing date will be returned.

NOTE: Statements and opinions advanced in papers are to be understood as individual expressions of their authors, and not those of the Society.

[3] Numbers in parentheses refer to the Bibliography at the end of the paper.

2 Concentration of salt in the vapor phase is entirely negligible ($n_s = 0$) and there is none in the leaving gas stream ($dn_s^\beta = 0$).

3 The temperatures of entering and leaving streams are the same and equal to that of the calorimeter contents which is constant.

4 The pressure is uniform throughout and constant.

5 The quantity of water evaporated and the consequent change in relative composition of the calorimeter contents are so small as to justify the use of mean values for partial molal volumes, energies, and enthalpies.

With the foregoing assumptions, the equations expressing conservation of matter are

for the air

$$dn_a^\alpha + dn_a' + dn_a + dn_a^\beta = 0; \quad [1a]$$

for the water

$$0 + dn_w' + dn_w + dn_w^\beta = 0; \quad [1b]$$

for the salt

$$0 + dn_s' + 0 + 0 = 0. \quad [1c]$$

The equation expressing constancy of the calorimeter volume is

$$\bar{V}_a' \cdot dn_a' + \bar{V}_w' \cdot dn_w' + \bar{V}_s' \cdot dn_s' + \bar{V}_a \cdot dn_a + \bar{V}_w \cdot dn_w = 0 \quad [2]$$

where the bar denotes differentiation with respect to the component designated by the subscript, at constant temperature, constant pressure, and constant weights of all other components. In other words, the bar specifies partial molal quantities for which mean values are to be taken in accordance with assumption 5. Finally, the equation expressing conservation of energy (no heat leak) is

$$h_a^\alpha dn_a^\alpha + \bar{H}_a^\beta dn_a^\beta + (\bar{H}_w^\beta - q) dn_w^\beta + \bar{U}_a' dn_a' + \bar{U}_w' dn_w' + \bar{U}_s' dn_s' + \bar{U}_a \cdot dn_a + \bar{U}_w \cdot dn_w = 0 \quad [3]$$

where h_a^α denotes the specific enthalpy of the entering air stream, and where it is to be noticed that q denotes the energy supplied electrically to the calorimeter per mol of water evaporated.

In the foregoing five equations, there appear eight differentials of type dn which must be eliminated, if a relation involving only thermodynamic properties is to be derived. For this purpose, therefore, three additional equations are required. One is obtained by assuming no appreciable accumulation of air in the liquid phase; that is

$$dn_a' = 0 \quad [4]$$

and two more are obtained by assuming that the relative composition of the vapor phase is constant and equal to that of the leaving stream; that is

$$\frac{dn_a}{dn_w} = \frac{n_a}{n_w} = \frac{dn_a^\beta}{dn_w^\beta} \quad [5]$$

However, with temperature, pressure, and relative composition the same in the vapor phase within the calorimeter as in the leaving stream, the following relations must hold

$$\bar{H}_a^\beta = \bar{H}_a \text{ and } \bar{H}_w^\beta = \bar{H}_w \quad [6]$$

Carrying out the desired elimination and, at the same time, eliminating internal energies in favor of enthalpies by means of the defining equation $H = U + PV$, the final result is

$$\bar{H}_w - \bar{H}_w' = q + (h_a^\alpha - \bar{H}_a) \frac{n_a}{n_w} - \frac{n_w \bar{V}_w'}{(n_a + n_w)v} \cdot q \quad [7]$$

where v denotes the specific volume of the vapor phase. It is by means of Equation [7] that data obtained by the gas-current method are to be reduced. The equation applies equally well to aqueous solutions of nonvolatile solutes and to pure liquids.

Pure Water

The data to be reported in this paper are on pure water. Although the ultimate objective of the experiments was information regarding certain aqueous solutions, pure water was used for calibrating the apparatus, since accurate values of the latent heat of water are available for comparison (2).

In the case of pure water, the partial molal quantities $\bar{H}_w'$, $\bar{V}_w'$ differ negligibly from the corresponding specific quantities h_w', v_w' since the concentration of dissolved air in the liquid phase is so small as to make it behave like an ideal solution (5). Thus, the application of Equation [7] reduces to the evaluation of the partial molal quanties $\bar{H}_w$, $\bar{H}_a$ and the specific volume v of the vapor phase, taking into account the effect of intermolecular forces which, though small, are nevertheless significant.

The starting point is the prediction of statistical mechanics (6) that at sufficiently low pressures

$$Pv = RT - [A_{aa}x^2 + 2A_{aw}x(1-x) + A_{ww}(1-x)^2]P \quad [8]$$

where

P = observed pressure
v = specific volume (volume per mol)
A_{aa} = second virial coefficient for air, a known temperature function
A_{ww} = second virial coefficient for water vapor, a known temperature function
A_{aw} = interaction constant, provisional values of which are now available
x = mol-fraction of dry air; namely, $n_a/(n_a + n_w)$

From Equation [8] may first be derived expressions for the partial molal enthalpies, although in this derivation a further prediction of statistical mechanics must also be used; namely, that at zero pressure the total enthalpy is the sum of separate contributions from the two constituents. The desired expressions are

$$\bar{H}_w = h_w^0 + [x^2 B - B_{ww}]P \quad [9a]$$

$$\bar{H}_a = h_a^0 + [(1-x)^2 B - B_{aa}]P \quad [9b]$$

where

$$B = B_{aa} - 2B_{aw} + B_{ww} \quad [9c]$$

and h_w^0, h_a^0 denote zero-pressure specific enthalpies; also where, for example

$$B_{aw} = -T^2 \frac{d(A_{aw}/T)}{dT} \quad [9d]$$

Introducing the saturation pressure of pure water p_s, a known temperature function, Equation [9a] becomes

$$\bar{H}_w = h_w^{sat} - B_{ww}(P - p_s) + x^2 B \cdot P \quad [10a]$$

while, applying Equation [9b] to air alone for the purpose of eliminating h_a^0

$$\bar{H}_a = h_a^\alpha + (1-x)^2 B \cdot P \quad [10b]$$

Finally, putting Equations [10a] and [10b] into Equation [7] this becomes

$$r - q = B_{ww}(P - p_s) - x \cdot B \cdot P - (1-x)\frac{v_w'}{v} \cdot q \quad [11]$$

where r denotes the latent heat of pure water.

TABLE 1 TEMPERATURE FUNCTIONS IN EQUATIONS [8] AND [9]

deg C	A_{aa}/RT (cm³ per kg)	B_{aa}/RT (cm³ per kg)	A_{ww}/RT (cm³ per kg)	B_{ww}/RT (cm³ per kg)	B/RT (cm³ per kg)
0	0.000578	0.00334	0.09005	0.6149	0.5719
5	0.000519	0.00317	0.07964	0.5356	0.4983
10	0.000464	0.00301	0.07072	0.4679	0.4356
15	0.000412	0.00287	0.06305	0.4101	0.3820
20	0.000364	0.00273	0.05642	0.3604	0.3359
25	0.000319	0.00260	0.05070	0.3178	0.2964
30	0.000277	0.00247	0.04573	0.2811	0.2623

In writing r for $h_w^{sat} - \overline{H}_w'$ and v_w for $\overline{V}_w'$ it has been assumed that the concentration of dissolved air in the liquid phase is so small that this behaves like an ideal solution. Reduction of test data by the gas-current method to obtain values of latent heat is accomplished by means of Equation [11].

Interaction Constant A_{aw}

The second virial coefficients A_{aa}, A_{ww} are known temperature functions, values of which are listed in Table 1. According to the prediction of statistical mechanics the interaction constant A_{aw} is also a temperature function, but until recently no experimental data have been available. In discussing these data it is convenient to introduce the ratio

$$\lambda(T) = \frac{2A_{aw}}{A_{aa} + A_{ww}} \quad \ldots\ldots\ldots\ldots\ldots\ldots [12]$$

as a dimensionless interaction constant. Preliminary results from the co-operative investigation referred to previously in-

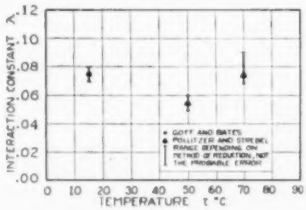


Fig. 2 Variation of λ With Temperature

dicate that, at 15 C, $\lambda = 0.075 \pm 0.005$. These results were obtained by use of a saturation-isotherm method in which a steady stream of dry CO_2-free air is saturated first at high pressure P_1, then dried, then resaturated at low pressure P_2, but at the same temperature as before, then dried again. The two pressures, the common temperature, and the two weights of water collected in the two driers over the same period of time suffice for the determination of the interaction constant λ. Of course, a theory of saturation is also required, but this is easily developed from Equation [8] together with appropriate assumptions regarding the liquid phase.

Evidence of complete saturation, complete drying, and satisfactory performance of the apparatus is obtained by changing the two pressures, by changing the rate of flow, by preliminary saturation at a temperature above or below that of final saturation, and by weighing the dry air. The average deviation of the measured weight of air from that calculated from the measured interaction constant is —0.08 per cent, equivalent to a temperature error of only 0.012 C.

In order to anticipate the probable variation of λ with temperature, certain data, obtained by Pollitzer and Strebel (7), at 50 C and 70 C were reduced. Fig. 2 shows the results and is self-explanatory. These results suggest that, for the purpose of the present paper, a constant value of λ may be taken. The value chosen is $\lambda = 0.075$. Table 1 lists values of the coefficients appearing in Equations [8] and [11]. In this table values of A_{aa}/RT and B_{aa}/RT were computed from the equation of Beattie-Bridgeman (8); values of A_{ww}/RT and of B_{ww}/RT were computed from the equation of Keyes (9); values of B/RT were computed according to Equation [9c], taking $\lambda = 0.075$ as previously explained.

Description of Apparatus

The apparatus is best described with reference to Fig. 3. A detailed description will not be attempted here, but will be in-

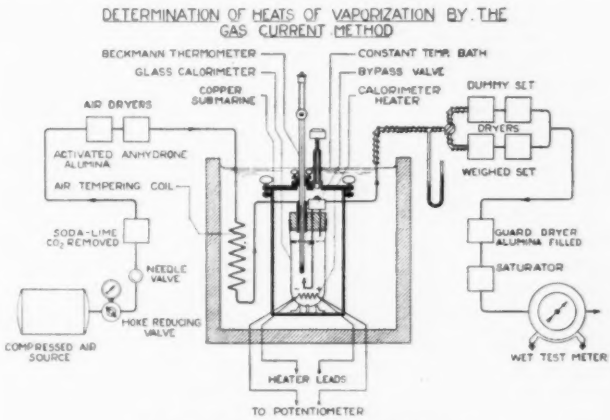


Fig. 3 Experimental Apparatus

cluded in the doctoral dissertation of one of the authors, a copy of which will be kept on file in the Towne Scientific School library.

The source of air is a large tank in which the pressure is maintained at about 63 psi (gage) by automatic control of a laboratory compressor. This pressure is reduced to about 1.5 psi (gage) by means of a Hoke valve, followed by a needle valve for fine regulation. Pressure fluctuations are effectively damped out by passing the air through several large bottles in series. The air is then passed through several large towers filled with soda lime and activated alumina to remove CO_2 and water vapor. Before being admitted to the tempering coil, it passes through a Midvale tower filled with Anhydrone, the drying agent used in the weighed towers following the calorimeter, to insure the same degree of dryness.

The calorimeter proper consists of a single-walled glass vessel 3 in. diam and about 8¾ in. long, closed at the top by a ground-to-fit hard-rubber plug through which extend the air-inlet and outlet tubes, and two additional tubes carrying the heater leads. After being brought to the temperature of the bath by passing through the tempering coil immersed in it, the air enters the inlet tube. In the lower end of this tube is constructed a small jet pump which enables the air to entrap slugs of liquid and carry them upward through the heater and then downward through a long glass spiral intended to prolong intimate contact. The air discharges near the bottom of the calorimeter whence it bubbles upward into the vapor space, entering the outlet tube through an entrainment separator. The upper part of the outlet tube itself is packed with glass wool. The heater is a double-walled glass tube with Nichrome wire wound around the inner tube, the annular space being completely filled with a suitable heat-transfer fluid (Aroclor). The ends of the wire are sealed

TABLE 2 TEST DATA ON PURE WATER AT 30 C

Test	26-A	26-B	27-A	27-B	28-A	29-A	31-A	32-A
Duration, sec	3602.1	3602.1	3602.1	3602.1	7204.0	7204.0	7204.0	7204.0
Heater voltage	0.67683	0.67704	0.67315	0.67315	0.67314	0.67400	0.66000	0.66000
Standard resistance voltage	0.65359	0.65386	0.65013	0.65013	0.65012	0.65090	0.63747	0.63750
Water collected, g	1.4707	1.4693	1.4588	1.4563	2.9100	2.9187	2.7987	2.7965
Wet-test meter, cu ft	.....	.....	1.7200	.....	.....	3.4600	3.3120	3.3390
Wet-test meter, F	73	73	76	74	73	78	78	77
Calorimeter pressure, cm Hg	78.6	78.6	79.0	79.0	79.2	78.4	77.8	78.9

through the outer tube into vertical tubes filled to the liquid level with mercury, but extending on upward through the hard-rubber plug. Also extending through the plug is a Beckmann thermometer the bulb of which is immersed in the liquid.

A submarine encloses the calorimeter which rests on four thin bakelite supports to minimize thermal conduction. Several concentric cylinders of aluminum foil are placed between the calorimeter and the submarine wall to minimize convection and radiation. The inner surface of the submarine wall is lined with several layers of this foil with paper backing. Near the top of the submarine is located a four-way valve, by means of which the air stream can be made to by-pass the calorimeter. Copper tubing leads from this valve through the wall of the opposite sides, one connecting to the tempering coil, and one to the glass tube leading to the driers. The remaining two openings into the four-way valve are connected to the air-inlet and outlet tubes of the calorimeter. All connections are made with rubber tubing. The top of the submarine is removable, but is screwed down watertight against a suitable gasket. Projecting through the top are two small hollow copper tubes, each carrying an insulated potential-lead wire inside. These tubes dip into the mercury leads from the heater. At or very near the liquid level in the calorimeter, they are joined with the potential lead wires in order to insure that only the energy supplied to the liquid is measured. In addition, the submarine top carries a device for manipulating the four-way valve from outside, and a watertight sleeve through which the stem of the Beckmann thermometer passes. A water bath surrounds the submarine, support for the latter being designed to insure complete submergence and to minimize heat conduction. Temperature regulation is accomplished in the usual manner by means of a glass thermoregulator filled with alcohol over mercury, a Cenco supersensitive relay, and a suitable resistance heater. A cooling coil is included for operation below room temperature. Temperature regulation to ± 0.001 C was easily maintained.

The glass tubing leading to the driers was wound with Nichrome wire heated from a small current transformer to prevent condensation. After leaving the driers, the air passes through a guard tower filled with saturated alumina, then through a saturator, and finally through a wet-test meter. The driers consist of two Midvale towers in series filled with Anhydrone. In parallel with the main driers is a similar set through which the air is passed before and after the test run.

The heater circuit consists of the heater itself, two small control rheostats in parallel, a standard resistance, and two 6-v storage cells connected in parallel. The standard resistance is a Manganin coil having a resistance of 0.4465 ± 0.0001 international ohms as certified by the National Bureau of Standards. In order to maintain constant voltage, the storage cells are continuously charged during test, as nearly as possible, at the same rate at which they discharge to the heater.

Voltage measurements across the heating coil (including the mercury leads) and across the standard resistance are made with a type K potentiometer, a Weston standard cell, and a suitable galvanometer.

Since only the time rate of supplying electrical energy to the calorimeter is measured it is necessary to determine accurately the time over which the water is collected in the driers. For this purpose a good laboratory stop watch is used, after comparing it with an electric clock over a number of 2-hour periods.

Experimental Procedure

The practice has been adopted of preconditioning the drying towers before each run by blowing them for about 1 hr with the air stream by-passing the calorimeter. The driers are then placed in a desiccator for several hours before being weighed and returned to their place in the apparatus. A prerun of about 1-hr duration is then used for the purpose of obtaining steady-flow conditions, as indicated by stationary readings of the Beckmann thermometer and of the voltage drop across the heater. These conditions are obtained by adjusting the rate of flow and the rate of charging the storage cells. During the prerun, the air by-passes the weighed driers through dummy driers having approximately equal flow resistance. It is generally possible in this manner so to balance the apparatus that the voltage drop across the heater does not vary more than ± 0.00005 v, and the temperature of the liquid does not change, nor differ from that of the bath, by more than ± 0.001 C during test.

The test is started at the instant the sweep hand of the wet-test meter crosses the zero mark. At this instant the air stream is switched to the weighed driers and the stop watch started simultaneously. After approximately 2 hr, the test is ended at the instant the sweep hand of the wet-test meter again crosses the zero mark when the watch is stopped and the air stream switched back to the dummy driers simultaneously. The driers are reweighed, after standing over night in the desiccator. Other precautions are followed in the use of the apparatus, but these need not be described in detail.

The procedure described was not followed exactly in early runs. For instance, some of these were of only 1 hr duration, and the tests were started and stopped by the watch instead of the wet-test meter. Table 2 gives test data covering eight runs with pure water at 30 C.

Reduction of Test Data

Sample calculations for test 29-A will explain the method of reducing the data in Table 2.

(a) $q/RT =$

$$\frac{\underset{\text{int.v}}{0.67400} \times \underset{\text{int.v}}{0.65090} \times \underset{\text{sec}}{7204.0} \times \underset{\text{abs j/int.j}}{1.00019} \times \underset{\text{g/kg}}{1000} \times \underset{\text{kg/k mol}}{18.0154}}{\underset{\text{int.ohm}}{0.4465} \times \underset{\text{mkg/kmol °K}}{847.88} \times \underset{\text{°K}}{303.16} \times \underset{\text{abs j/mkg}}{9.80665} \times \underset{\text{g}}{2.9187}} = 17.336$$

(b) $n_a/n_w = \dfrac{\underset{\text{ft}^3}{3.4600} \times \underset{\text{g/lb}}{453.5924} \times \underset{\text{lb/mol}}{18.0154}}{\underset{\text{ft}^3\text{/lb dry air}}{13.89} \times \underset{\text{g}}{2.9187} \times \underset{\text{lb/mol}}{28.963}} = 24.078;\ x = 0.9601$

(c) $P = \dfrac{78.4}{73.5559} = 1.066$ kg per cm^2; $p_s = 0.043254$ kg per cm^2

(d) $\dfrac{B_{ww}(P - p_s)}{RT} = 0.2811 \times 1.023 = 0.2875$

(e) $\dfrac{xBP}{RT} = 0.9601 \times 0.2623 \times 1.066 = 0.2685$

TABLE 3 REDUCTION OF TEST DATA

Test	26-A	26-B	27-A	27-B	28-A	29-A	31-A	32-A
q/RT	17.346	17.375	17.300	17.330	17.344	17.336	17.338	17.352
$x = n_a/(n_a + n_w)$	0.96[a]	0.96[a]	0.9598	0.96[a]	0.96[a]	0.9601	0.9601	0.9602
$B_{ww}(P - p_s)/RT$	0.2882	0.2882	0.2897	0.2897	0.2905	0.2875	0.2851	0.2894
xBP/RT	0.2691	0.2691	0.2704	0.2704	0.2711	0.2685	0.2664	0.2702
$(1-x)\frac{v'_w}{v}\frac{q}{RT}$	0.0005	0.0005	0.0005	0.0005	0.0005	0.0005	0.0005	0.0005
r/RT	17.365	17.394	17.319	17.349	17.363	17.355	17.356	17.371

[a] Reading of the wet-test meter not recorded.

TABLE 4 SUMMARY

	q/RT	r/RT	r, (int j/g)
Average of 2-hr runs	17.342 ± 0.0056	17.361 ± 0.0058	2428.7 ± 0.8
Weighted average of all runs	17.341 ± 0.0056	17.360 ± 0.0058	2428.6 ± 0.8
Bureau of Standards	.....	17.367	2429.6

$$(f)\ (1-x)\frac{v'_w}{v}\frac{q}{RT} = \frac{1.00442 \times 17.336}{32{,}929} = 0.0005$$

$$(g)\ \frac{r-q}{RT} = 0.2875 - 0.2685 - 0.0005 = 0.0185$$

$$(h)\ \frac{r}{RT} = 17.336 + 0.0185 = 17.355$$

By way of further explanation; in item (b) the volume of saturated air per pound of dry air at the temperature of the wet-test meter is read directly from Table 6, reference (6), there being no point in extreme accuracy; in item (f) the ratio $v/(1-x)$ is replaced by the specific volume of saturated steam, this being sufficiently accurate.

Table 3 is instructive as showing the relative magnitude of the various terms appearing in Equation [11].

In Table 4, the probable errors are estimated from the following information:

(a) The voltage readings are limited by the sensitivity of the galvanometer to 1 part in 20,000.

(b) There may be a residual error in the time measurements of about 1 part in 7200.

(c) The weighings are probably accurate to 1 part in 5600.

(d) The probable error in the resistance of the standard coil is 1 part in 4000.

(e) The value of λ is uncertain by about 1 part in 15.

The method of weighting individual runs is to weight each in proportion to its duration.

Conclusions

The following conclusions are drawn:

1 The present apparatus is capable of an high degree of consistency and reproductibility.

2 Direct measurements by the gas-current method require reduction to account for the effect of intermolecular forces in the vapor phase.

3 This reduction is now possible since data on the interaction constant for moist air have recently been made available.

4 After reduction, the data on the latent heat of pure water at 30 C are in satisfactory accord with recent values from the National Bureau of Standards.

5 Higher precision not only in the data of the gas-current method itself but also in the knowledge of latent heat from independent sources would be required to make the method suitable for the measurement of the interaction constant.

BIBLIOGRAPHY

1 "Heat of Evaporation of Water," by A. W. Smith, *Physical Review*, vol. 25, 1907, pp. 145–170; vol. 33, 1911, pp. 173–183.

2 "Measurements of Heat Capacity and Heat of Vaporization of Water in the Range 0° to 100° C," by N. S. Osborne, H. F. Stimson, and D. C. Ginnings, U. S. National Bureau of Standards, *Journal of Research*, Research Paper R. P. 1228, vol. 23, 1939, pp. 197–260.

3 "The Interaction Constant for Moist Air," by J. A. Goff and A. C. Bates, *Heating, Piping and Air Conditioning*, July, 1941, pp. 442–449.

4 "Measurement of the Interaction Constant for Moist Air by the Saturation Isotherm Method," by A. C. Bates, Doctoral Dissertation, University of Pennsylvania, 1941.

5 "Modern Thermodynamics," by E. A. Guggenheim, Methuen & Company, London, 1933.

6 "Heating, Ventilating, Air Conditioning Guide," American Society of Heating and Ventilating Engineers, New York, N. Y., 1941, chap. 1.

7 "Über den Einfluss indifferenter Gase auf die Sättigungs-Dampfkonzentration von Flüssigkeiten," by F. Pollitzer and E. Strebel, *Zeitschrift für physikalische Chemie*, vol. 110, 1924, pp. 768–785.

8 "A New Equation of State for Fluids," by J. A. Beattie and O. C. Bridgeman, Proceedings of the American Academy of Arts and Sciences, vol. 63, 1928, pp. 229–308.

9 "Comments on the Enthalpy of Saturated Steam From 0 to 100 C and Other Steam Properties," by F. G. Keyes, Trans. A.S.M.E., vol. 62, 1940, p. A-22.

Note on Plane Strain

By W. R. OSGOOD,[1] WASHINGTON, D. C.

THE strain in an elastic body is called plane strain if it permits choosing a rectangular co-ordinate system in the body, such that the displacements normal to one of the co-ordinate axes are independent of the value of that co-ordinate, and the component of linear strain parallel to that axis is constant.

In general, except in the case of bodies of cylindrical (in its general sense, including prismatic) shape and of homogeneous and isotropic material, the distribution of surface and body forces necessary to set up a state of plane strain is very complicated. For this reason discussions of plane strain are usually limited to strains in bodies of cylindrical shape, and it is common to characterize plane strain by some such statement as, "if a long, cylindrical or prismatic, elastic body of uniform and isotropic material is loaded by forces which are perpendicular to the longitudinal elements and which do not vary along the length of the body, then, except possibly in the immediate neighborhood of the ends, the body will remain cylindrical, and plane cross sections will remain plane." This, however, is not an adequate characterization. A long rectangular plate loaded along the long edges by equal and opposite uniformly distributed couples with axes parallel to the long dimension, is a simple example in which these conditions of loading are met, and yet the body does not remain cylindrical at a distance from the ends. Consequently, the strain is not plane strain.

It is well known that under the action of such couples the surface of the plate becomes an anticlastic surface with uniform principal curvatures[2]—it is nowhere cylindrical. If the problem is analyzed as a problem in plane strain, the analysis will show that the boundary conditions require, in addition, forces along the short edges to maintain a cylindrical shape for the deformed plate. The stresses on cross sections parallel to the long edges are unaffected by the forces acting on the short edges. It is easy to see in this example what is going on, but now let us consider another case of loading.

Suppose that the long rectangular plate is held fixed along one long edge and loaded like a cantilever beam by a uniformly distributed force along the opposite edge. If the problem is analyzed as a problem in plane strain, one finds the shearing stress τ_{xy} given by

$$\tau_{xy} = \frac{P}{2I}(b^2 - y^2)$$

where the origin of co-ordinates is taken at the free long edge, at the mid-plane; the axis of x is taken in the mid-plane, at right angles to and positive toward the fixed edge; the axis of y is taken normal to the mid-plane; P is the total load on the free long edge; I is the least moment of inertia of a cross section parallel to a long edge; and b is one half the thickness of the plate. Here again, the problem considered as one in plane strain will require forces to be acting along the short edges. Unless they do, the plate is nowhere cylindrical, and[3]

$$\tau_{xy} = \frac{1}{1+\nu}\frac{P}{2I}(b^2 - y^2)$$

where ν is Poisson's ratio. In this case the forces required at the ends (short edges) by the plane-strain solution alter the picture radically, and their effects are felt at any distance from the ends (short edges). Evidently the statement in the second paragraph of this note is not sufficient to characterize a state of plane strain. The applied forces there mentioned must not only be perpendicular to the longitudinal elements and must not vary along the length of the body, but in addition, they must give rise to displacements such that the body remains cylindrical. With the axis of z taken along the centroidal axis of the body (cylinder), the applied forces will give rise to the required displacements if they result in normal components of stress σ_x and σ_y such that

$$\int\int_A (\sigma_x + \sigma_y)\, x dA = \int\int_A (\sigma_x + \sigma_y)\, y dA = 0$$

where A is the cross-sectional area of the body. This condition merely states that the body is not bent about any transverse axis.

[1] National Bureau of Standards.

[2] "Theory of Elasticity," by S. Timoshenko, McGraw-Hill Book Company, Inc., New York, N. Y., 1934, p. 226.

Presented at the Annual Meeting, New York, N. Y., December 1–5, 1941, of THE AMERICAN SOCIETY OF MECHANICAL ENGINEERS.

Discussion of this paper should be addressed to the Secretary, A.S.M.E., 29 West 39th Street, New York, N. Y., and will be accepted until April 10, 1942, for publication at a later date. Discussion received after the closing date will be returned.

NOTE: Statements and opinions advanced in papers are to be understood as individual expressions of their authors and not those of the Society.

[3] Footnote[2], p. 296.

Determining Critical States of Equilibrium of Plates and Shells Under Initial Stress

By H. HENCKY,[1] MAINZ, GERMANY

The purpose of this paper is to show that Rayleigh's energy method, used by Timoshenko for the determination of critical loads in plates and shells, is capable of an important generalization.[2] The work involved is a direct continuation of the energy method of Timoshenko and is based on the principle of virtual work. According to this principle the variation of the work of the outer forces together with the variation of the kinetic energy is equal to the variation of the elastic energy stored up in the body. The author develops a series of formulas, by means of which the stability of a cylindrical shell under various conditions of stress may be determined. The practical applications of these formulas, requiring only a fundamental knowledge of the mathematics of engineering, are illustrated by suitable examples.

IF a virtual displacement is applied to a stressed body, a certain amount of elastic energy is stored up and at the same time the stresses, acting in the body and on the boundary, perform work during this virtual displacement. When the elastic energy is just equal to this work, we have the case of indifferent equilibrium; when it is greater, equilibrium is not possible, and the body vibrates about a middle position. If the elastic energy is smaller, the disturbing forces will prevail and the body is in a state of unstable equilibrium.

Though much has been written concerning this problem, it must be concluded that there is no simple method of analysis of unstable equilibrium in curved plates and shells. Therefore, this paper is being devoted to the explanation of a method which can be readily applied. Although some mathematical analysis is necessary to deduce this method, its practical application does not require a more extensive knowledge of mathematics than that with which an able student of engineering is familiar.

This work is a direct continuation of the work of Timoshenko, who applied the energy method in solving numerous practical problems in stability. However, in applying his method to problems of curved shells, we become aware that there are some things to be desired: (1) The question arises: What are the conditions at the free but stressed boundaries? (2) Since there can exist an arbitrary system of initial stresses varying from point to point, how can we determine the question of stability? To answer these questions we begin with the most general principle of mechanics, i.e., the principle of virtual work.

The Generalized Principle of Virtual Work

According to the principle of virtual work, the variation of the work of the outer forces together with the variation of the kinetic energy is equal to the variation of the elastic energy stored up in the body. In order to apply this principle to our problem, we consider the following three states of the body:

State 1 is the state of rest under the boundary stresses P_x, P_y, P_z, the inner stresses σ_x, σ_y, σ_z, T_x, T_y, T_z, and the body forces X, Y, Z.

State 2 is not necessarily a state of rest. In state 1 we apply the displacements Δu, Δv, Δw leading to state 2 and accompanied by the stresses $\sigma_x + \Delta\sigma_x$, ... $T_x + \Delta T_x$, ... and boundary stresses $P_x + \Delta P_x$, ... The displacements Δu, ... are so small that the second powers of the strains are to be neglected as compared with the first, but they are not infinitely small.

State 3 is the state of the body when we apply, moreover, infinitely small displacements $\delta\Delta u$, $\delta\Delta v$, $\delta\Delta w$.

Now we must bear in mind that all the quantities entering in the equation of virtual work are functions of a system of coordinates fixed in the body in state 1 but the equation of virtual work must be written for state 2. The general problem would be a very complicated one[3] but, since we are dealing only with bodies having at least one quite small dimension such as bars and thin shells, we know that the strains are much smaller than the rotations of the elements of the body. We may therefore neglect the strains entirely as compared with the rotations provided we are dealing with sufficiently thin shells.

It is known from the theory of elasticity that if Δu, Δv, Δw are the displacements of particles of a deformed body the rotations are given by three equations of the type

$$\Delta\omega_x = \frac{1}{2}\left(\frac{\partial\Delta w}{\partial y} - \frac{\partial\Delta v}{\partial z}\right) \quad \ldots\ldots\ldots\ldots [1]$$

and strains by

$$\left.\begin{aligned} \Delta e_x &= \frac{\partial\Delta u}{\partial x} \quad \ldots\ldots\ldots\ldots \\ \Delta\gamma_x &= \frac{1}{2}\left(\frac{\partial\Delta w}{\partial y} + \frac{\partial\Delta v}{\partial z}\right) \quad \ldots\ldots\ldots\ldots \end{aligned}\right\} \quad \ldots\ldots [2]$$

The equation of virtual work written for state 1 is

$$\begin{aligned} &\int\int dO(P_x\delta\Delta u + P_y\delta\Delta v + P_z\delta\Delta w) \\ &= \int\int\int dV\left(\sigma_x\frac{\partial\delta\Delta u}{\partial x} + T_z\frac{\partial\delta\Delta u}{\partial y} + T_y\frac{\partial\delta\Delta u}{\partial z} + T_z\frac{\partial\delta\Delta v}{\partial x}\right. \\ &\left. + \sigma_y\frac{\partial\delta\Delta v}{\partial y} + T_x\frac{\partial\delta\Delta v}{\partial z} + T_y\frac{\partial\delta\Delta w}{\partial x} + T_z\frac{\partial\delta\Delta w}{\partial y} + \sigma_z\frac{\partial\delta\Delta w}{\partial z}\right) \\ &\quad - \int\int\int dV(X\delta\Delta u + Y\delta\Delta v + Z\delta\Delta w) \quad \ldots\ldots [3] \end{aligned}$$

Integrating by parts we find

$$\int\int dO\left[\{P_x - \sigma_x\cos(nx) - T_z\cos(ny) - T_y\cos(nz)\}\delta\Delta u\right.$$

[1] Mechanical Engineer.

[2] "The Mathematical Theory of Elasticity," by A. E. H. Love, Fourth edition, Cambridge University Press, London, 1927, p. 512. "Statik und Dynamik der Schalen," by W. Flügge, Berlin, J. Springer, 1934, pp. 184–189.

Presented at the National Meeting of the Applied Mechanics Division, Philadelphia, Pa., June 20–21, 1941, of The American Society of Mechanical Engineers.

Discussion of this paper should be addressed to the Secretary, A.S.M.E., 29 West 39th Street, New York, N. Y., and will be accepted until April 10, 1942, for publication at a later date. Discussion received after the closing date will be returned.

Note: Statements and opinions advanced in papers are to be understood as individual expressions of their authors and not those of the Society.

[3] "The General Theory of Elastic Stability, Parts 1 and 2," by C. B. Biezeno and H. Hencky, Proceedings Koninklijke Akademie van wetenschappen te Amsterdam, vol. 31, no. 6, 1928, pp. 569–578, and 579–592.

$$+ \{P_y - T_z \cos(nx) - \sigma_y \cos(ny) - T_x \cos(nz)\}\delta\Delta v$$
$$+ \{P_z - T_y \cos(nx) - T_x \cos(ny) - \sigma_z \cos(nz)\}\delta\Delta w]$$
$$+ \int\int\int dV \left\{\left(\frac{\partial\sigma_x}{\partial x} + \frac{\partial T_z}{\partial y} + \frac{\partial T_y}{\partial z} + X\right)\delta\Delta u\right.$$
$$+ \left(\frac{\partial T_z}{\partial x} + \frac{\partial\sigma_y}{\partial y} + \frac{\partial T_y}{\partial z} + Y\right)\delta\Delta v$$
$$\left. + \left(\frac{\partial T_y}{\partial x} + \frac{\partial T_x}{\partial y} + \frac{\partial\sigma_z}{\partial z} + Z\right)\delta\Delta w\right\} = 0$$

Since the displacements $\delta\Delta u \ldots$ are perfectly arbitrary, we conclude that the coefficients of these quantities must vanish, but it is not our aim now to obtain the differential equations of the problem. We wish rather to retain the integral form, and we shall see presently that in so doing we reach a new and practically important statement.

Though the foregoing integral could be written for state 1, we will now introduce the small displacements $\Delta u, \ldots$ leading from state 1 to state 2, and then write the equation of virtual work for state 2. During these displacements, the stresses $\sigma_x, \ldots, T_x, \ldots$ acting on an element of the body change to $\sigma_x + \Delta\sigma_x, \ldots, T_x + \Delta T_x, \ldots$, while the element of the body is rotated through the angles $\Delta\omega_x, \ldots$. The strains which accompany these displacements $\Delta u, \ldots$ are neglected for the reasons mentioned.

Referring the rotated element of the body with stresses $\sigma_x + \Delta\sigma_x, \ldots, T_x + \Delta T_x, \ldots$, acting on it to coordinate axes fixed in the body in state 1, we obtain the nine components of stress

$$X_x = \sigma_x + \Delta\sigma_x + T_y\Delta\omega_y - T_z\Delta\omega_z$$
$$Y_x = T_z + \Delta T_z + \sigma_x\Delta\omega_z - T_y\Delta\omega_x$$
$$Z_x = T_y + \Delta T_y + T_z\Delta\omega_x - \sigma_x\Delta\omega_y$$

with similar expressions for $X_y, \ldots, X_z, \ldots$.

Similarly the three boundary stresses in the direction of the x, y, and z axes are of the type

$$P_x + \Delta P_x + P_z\Delta\omega_y - P_y\Delta\omega_z, \text{ etc.}$$

It is to be noted that $\Delta P_x, \ldots$ are increments of boundary force per unit area which causes the body to pass from state 1 into state 2. If a body is in a state of indifferent equilibrium, no increments $\Delta P_x, \ldots$ are required to cause collapse. Thus the condition that a body is in the state of indifferent equilibrium is that $\Delta P_x = 0;\ \Delta P_y = 0;\ \Delta P_z = 0$.

If we write the equation of virtual work for state 2 for the general case that state 2 is not a state of equilibrium, then subtract from it Equation [3], and put ΔP_x, ΔP_y, ΔP_z equal to zero, we find

$$\int\int dO\{(P_z\Delta\omega_y - P_y\Delta\omega_z)\delta\Delta u + (P_x\Delta\omega_z - P_z\Delta\omega_x)\delta\Delta v$$
$$+ (P_y\Delta\omega_x - P_x\Delta\omega_y)\delta\Delta w\} + \int\int\int dV\,\frac{\mu}{2}\,\delta\left\{\left(\frac{\partial\Delta u}{\partial t}\right)^2\right.$$
$$\left. + \left(\frac{\partial\Delta v}{\partial t}\right)^2 + \left(\frac{\partial\Delta w}{\partial t}\right)^2\right\} = \int\int\int dV\left\{\Delta\sigma_x\frac{\partial\delta\Delta u}{\partial x}\right.$$
$$+ \Delta\sigma_y\frac{\partial\delta\Delta v}{\partial y} + \Delta\sigma_z\frac{\partial\delta\Delta w}{\partial z} + \Delta T_x\left(\frac{\partial\delta\Delta w}{\partial y} + \frac{\partial\delta\Delta v}{\partial z}\right)$$
$$+ \Delta T_y\left(\frac{\partial\delta\Delta u}{\partial z} + \frac{\partial\delta\Delta w}{\partial x}\right) + \Delta T_z\left(\frac{\partial\delta\Delta v}{\partial x} + \frac{\partial\delta\Delta u}{\partial y}\right)\Big\}$$
$$+ \int\int\int dV\left\{(T_y\Delta\omega_y - T_z\Delta\omega_z)\frac{\partial\delta\Delta u}{\partial x}\right.$$
$$+ (T_x\Delta\omega_y - \sigma_y\Delta\omega_z)\frac{\partial\delta\Delta u}{\partial y} + (\sigma_z\Delta\omega_y - T_x\Delta\omega_z)\frac{\partial\delta\Delta u}{\partial z}$$
$$+ (\sigma_x\Delta\omega_z - T_y\Delta\omega_x)\frac{\partial\delta\Delta v}{\partial x} + (T_z\Delta\omega_z - T_x\Delta\omega_x)\frac{\partial\delta\Delta v}{\partial y}$$
$$+ (T_y\Delta\omega_z - \sigma_z\Delta\omega_x)\frac{\partial\delta\Delta v}{\partial z} + (T_z\Delta\omega_z - \sigma_z\Delta\omega_y)\frac{\partial\delta\Delta w}{\partial x}$$
$$\left. + (\sigma_y\Delta\omega_x - T_z\Delta\omega_y)\frac{\partial\delta\Delta w}{\partial y} + (T_x\Delta\omega_x - T_y\Delta\omega_y)\frac{\partial\delta\Delta w}{\partial z}\right\}$$

Introducing here the relations

$$\delta\Delta\omega_x + \delta\Delta\gamma_x = \frac{\partial\delta\Delta w}{\partial y}, \quad \delta\Delta\omega_y + \delta\Delta\gamma_y = \frac{\partial\delta\Delta u}{\partial z},$$
$$\delta\Delta\omega_z + \delta\Delta\gamma_z = \frac{\partial\delta\Delta v}{\partial x}$$
$$\delta\Delta\gamma_x - \delta\Delta\omega_x = \frac{\partial\delta\Delta v}{\partial z}, \quad \delta\Delta\gamma_y - \delta\Delta\omega_y = \frac{\partial\delta\Delta w}{\partial x},$$
$$\delta\Delta\gamma_z - \delta\Delta\omega_z = \frac{\partial\delta\Delta u}{\partial y}$$

and neglecting the components of strain, $\Delta e_x, \ldots, \Delta\gamma_x, \ldots$ as compared with the rotations, we find

$$\int\int dO\{(P_z\Delta\omega_y - P_y\Delta\omega_z)\delta\Delta u + (P_x\Delta\omega_z - P_z\Delta\omega_x)\delta\Delta v$$
$$+ (P_y\Delta\omega_x - P_x\Delta\omega_y)\delta\Delta w\} + \delta\Delta T + \int\int\int dV\{-(\sigma_y$$
$$+ \sigma_z)\Delta\omega_x + T_z\Delta\omega_y + T_y\Delta\omega_z\}\,\delta\Delta\omega_x + \{T_z\Delta\omega_x - (\sigma_z$$
$$+ \sigma_x)\Delta\omega_y + T_x\Delta\omega_z\}\,\delta\Delta\omega_y + \{T_y\Delta\omega_x + T_x\Delta\omega_y - (\sigma_x$$
$$+ \sigma_y)\Delta\omega_z\}\,\delta\Delta\omega_z = \delta\Delta A$$

where δT is the variation of the kinetic energy and δA is the variation of the elastic energy.

We are now able to draw our final conclusion by specializing the virtual displacement. We assume that $\delta\Delta u$ is the differential of Δu and that $\Delta u, \ldots$ are so small that the higher powers of $\Delta\omega_x, \ldots$ may be neglected. Under these circumstances, we can integrate the preceding equation, introducing the factor $^1/_2$ because $\Delta u, \ldots$ increase from zero to their final values.

Thus the final equation of virtual work will be

$$\frac{1}{2}\int\int dO\{(P_z\Delta\omega_y - P_y\Delta\omega_z)\Delta u + (P_x\Delta\omega_z - P_z\Delta\omega_x)\Delta v$$
$$+ (P_y\Delta\omega_x - P_x\Delta\omega_y)\Delta w\} + \Delta T + \frac{1}{2}\int\int\int dV$$
$$\{-\sigma_x(\Delta\omega_y^2 + \Delta\omega_z^2) - \sigma_y(\Delta\omega_x^2 + \Delta\omega_z^2) - \sigma_z(\Delta\omega_x^2 + \Delta\omega_y^2)$$
$$+ 2T_x\Delta\omega_y\Delta\omega_z + 2T_y\Delta\omega_x\Delta\omega_z + 2T_z\Delta\omega_x\Delta\omega_y\} = \Delta A \quad \ldots [4a]$$

where

$$\Delta T = \int\int\int \frac{\mu}{2}\left\{\left(\frac{\partial\Delta u}{\partial t}\right)^2 + \left(\frac{\partial\Delta v}{\partial t}\right)^2 + \left(\frac{\partial\Delta w}{\partial t}\right)^2\right\} dV \quad \ldots [4b]$$

and

$$\delta\Delta A = \int\int\int dV\{\Delta\sigma_x\delta\Delta e_x + \Delta\sigma_y\delta\Delta e_y + \Delta\sigma_z\delta\Delta e_z$$
$$+ 2\Delta T_x\delta\Delta\gamma_x + 2\Delta T_y\delta\Delta\gamma_y + 2\Delta T_z\delta\Delta\gamma_z\} \quad \ldots [4c]$$

The relation between the stresses $\Delta\sigma_x, \ldots, \Delta T_x, \ldots$ and the boundary stresses $\Delta P_x, \ldots$ is the same as for the stresses in state 1, that is

$$\Delta P_x = \Delta\sigma_x \cos(nx) + \Delta T_z \cos(ny) + \Delta T_y \cos(nz) \ldots [4d]$$

with similar expressions for ΔP_y and ΔP_z.

We conclude from these equations that the only term in which the strains have to be considered is the term ΔA. We assume the usual linear relationship between stress and strain components.

Taking the x direction as the direction of the normal to the plate or shell, we now introduce a device by which we can avoid the complicated theory of curved shells. If we let the displacements of the middle surface of the shell be given by Δu_0, Δv_0, Δw_0, then we can express the displacements of a point not on the middle surface by Δu_0, ... and linear functions of the distance of the point from the middle surface. Thus, we have a plate or shell subjected to plane stress. The stresses $\Delta\sigma_x$, ΔT_y, ΔT_z are statically determined and the stresses $\Delta\sigma_y$, $\Delta\sigma_z$, ΔT_x are connected with the strains Δe_y, Δe_z, $\Delta\gamma_x$ by a linear law. For an isotropic body, this law can be written[4]

$$\left.\begin{aligned} \Delta\sigma_y &= 2G\left\{\Delta e_y + \frac{1}{m-1}(\Delta e_y + \Delta e_z)\right\} \\ \Delta\sigma_z &= 2G\left\{\Delta e_z + \frac{1}{m-1}(\Delta e_y + \Delta e_z)\right\} \\ \Delta T_x &= 2G\,\Delta\gamma_x \end{aligned}\right\} \ldots\ldots [5a]$$

where m is the reciprocal of Poisson's ratio. The strains Δe_x, $\Delta\gamma_y$, $\Delta\gamma_z$ disappear as a consequence of our assumptions concerning the displacements Δu, ... With the aid of Equations [5a] we can integrate Equation [4c] with δ as a differential and we find

$$\Delta A = G\left\{\Delta e_y^2 + \Delta e_z^2 + 2\Delta\gamma_x^2 + \frac{1}{m-1}(\Delta e_y^2 + \Delta e_z^2 + 2\Delta e_y \Delta e_z)\right\} \ldots [5b]$$

Having Equations [4a], [4b], and [5b], the solution of our problem is completed. To illustrate the practical application of our equations, we shall now consider some simple examples.

Stability of a Cylindrical Shell Under Various Conditions

There are, of course, many ways in which a shell can collapse, but in most cases the form of the virtual displacement leading to destruction is known. Our method determines whether the assumed displacement of the middle surface causes the body to become unstable.

We take the x co-ordinate in the radial direction, the y co-ordinate in the direction of the tangent and the z co-ordinate in the direction of the axis of the cylindrical shell. To remove the dimensional quantities from the differentials we put

$$r = a\rho; \quad z = l\zeta$$

Taking the displacements of the middle surface as Δu_0, Δv_0, Δw_0, we obtain for the displacement of an arbitrary point, which is assumed to remain on the normal to the middle surface, the following equations

$$\left.\begin{aligned} \Delta u &= \Delta u_0 \\ \Delta v &= \rho\,\Delta v_0 - (\rho-1)\frac{\partial \Delta u_0}{\partial\phi} \\ \Delta w &= \Delta w_0 - \frac{a}{l}(\rho-1)\frac{\partial \Delta u_0}{\partial\zeta} \end{aligned}\right\} \ldots\ldots [6]$$

The rotations are given by the following equations in the cylindrical system of co-ordinates

$$\left.\begin{aligned} 2\Delta w_r &= \frac{1}{r}\frac{\partial \Delta w}{\partial\phi} - \frac{\partial \Delta v}{\partial z} \\ 2\Delta\omega_\phi &= \frac{\partial \Delta u}{\partial z} - \frac{\partial \Delta w}{\partial r} \\ 2\Delta\omega_z &= \frac{1}{r}\frac{\partial(r\Delta v)}{\partial r} - \frac{1}{r}\frac{\partial \Delta u}{\partial\phi} \end{aligned}\right\} \ldots\ldots [7a]$$

and the strains become

$$\left.\begin{aligned} \Delta e_\phi &= \frac{1}{r}\frac{\partial \Delta v}{\partial\phi} + \frac{\Delta u}{r} \\ \Delta e_z &= \frac{\partial \Delta w}{\partial z} \\ 2\Delta\gamma_r &= \frac{1}{r}\frac{\partial \Delta w}{\partial\phi} + \frac{\partial \Delta v}{\partial z} \end{aligned}\right\} \ldots\ldots [7b]$$

Substituting Equation [6] into Equations [7a] and [7b] we find

$$\left.\begin{aligned} \Delta\omega_r &= -\frac{1}{2l}\frac{\partial \Delta v_0}{\partial\zeta} + \frac{1}{2a}\frac{\partial \Delta w_0}{\partial\phi} \\ \Delta\omega_\phi &= \frac{1}{l}\frac{\partial \Delta u_0}{\partial\zeta} \\ \Delta\omega_z &= \frac{1}{a}\left(\Delta v_0 - \frac{\partial \Delta u_0}{\partial\phi}\right) \end{aligned}\right\} \ldots\ldots [8a]$$

$$\left.\begin{aligned} \Delta e_\phi &= \frac{1}{a}\left\{\frac{\partial \Delta v_0}{\partial\phi} + \frac{\Delta u_0}{\rho} - \left(1-\frac{1}{\rho}\right)\frac{\partial^2 \Delta u_0}{\partial\phi^2}\right\} \\ \Delta e_z &= \frac{1}{l}\frac{\partial \Delta w_0}{\partial\zeta} - (\rho-1)\frac{a}{l^2}\frac{\partial^2 \Delta u_0}{\partial\zeta^2} \\ 2\Delta\gamma &= \frac{1}{a\rho}\frac{\partial \Delta w_0}{\partial\phi} + \frac{1}{l}\left\{\rho\frac{\partial \Delta v_0}{\partial\zeta} - \left(\rho-\frac{1}{\rho}\right)\frac{\partial^2 \Delta u_0}{\partial\phi\,\partial\zeta}\right\} \end{aligned}\right\} \ldots\ldots [8b]$$

Using Equation [5a], we obtain the stresses

$$\left.\begin{aligned} \Delta\sigma_\phi &= 2G\frac{m}{m-1}\left\{\frac{\partial \Delta v_0}{\partial\phi} + \frac{\Delta u_0}{\rho} - \left(1-\frac{1}{\rho}\right)\frac{\partial^2 \Delta u_0}{\partial\phi^2}\right\} \\ &\quad + \frac{2G}{l(m-1)}\left\{\frac{\partial \Delta w_0}{\partial\zeta} - \frac{a}{l}(\rho-1)\frac{\partial^2 \Delta u_0}{\partial\zeta^2}\right\} \\ \Delta\sigma_z &= 2G\frac{m}{m-1}\frac{1}{l}\left\{\frac{\partial \Delta w_0}{\partial\zeta} - (\rho-1)\frac{a}{l}\frac{\partial^2 \Delta u_0}{\partial\zeta^2}\right\} \\ &\quad + \frac{2G}{m-1}\frac{1}{a}\left\{\frac{\partial \Delta v_0}{\partial\phi} + \frac{\Delta u_0}{\rho} - \left(1-\frac{1}{\rho}\right)\frac{\partial^2 \Delta u_0}{\partial\phi^2}\right\} \\ \Delta T &= \frac{G}{a}\left\{\frac{1}{\rho}\frac{\partial \Delta w_0}{\partial\phi} + \frac{a}{l}\rho\frac{\partial \Delta v_0}{\partial\zeta} - \frac{a}{l}\left(\rho-\frac{1}{\rho}\right)\frac{\partial^2 \Delta v_0}{\partial\phi\,\partial\zeta}\right\} \end{aligned}\right\} \ldots [9]$$

We shall now investigate the displacements of the middle surface taken in the form

$$\left.\begin{aligned} \Delta u_0 &= 2Bf(\zeta)\cos 2\phi \\ \Delta v_0 &= -Bf(\zeta)\sin 2\phi \\ \Delta w_0 &= 0 \end{aligned}\right\} \ldots\ldots [10]$$

where B is a perfectly arbitrary amplitude and f is an arbitrary function. Using Equations [8a] and [8b] we find

$$\left.\begin{aligned} \Delta\omega_r &= \frac{B}{2l}f'\sin 2\phi \\ \Delta\omega_\phi &= \frac{2B}{l}f'\cos 2\phi \\ \Delta\omega_z &= \frac{3B}{a}f\sin 2\phi \end{aligned}\right\} \ldots\ldots [11a]$$

[4] A. E. H. Love, ref. (2), pp. 207–208.

$$\left.\begin{aligned} \Delta e_\phi &= 6\frac{Bf}{a}\left(1-\frac{1}{\rho}\right)\cos 2\phi \\ \Delta e_z &= -\frac{2aBf''}{l^2}(\rho-1)\cos 2\phi \\ \Delta\gamma &= \frac{B}{2l}f'\left(3\rho-\frac{4}{\rho}\right)\sin 2\phi \end{aligned}\right\} \quad \ldots\ldots\ldots [11b]$$

1 For a free cylinder under outer pressure, $f = 1$ and Equations [11a] and [11b] become

$$\Delta\omega_r = 0;\quad \Delta\omega_\phi = 0;\quad \Delta\omega_z = \frac{3B}{a}\sin 2\phi$$

$$\Delta e_\phi = 6\frac{B}{a}\left(1-\frac{1}{\rho}\right)\cos 2\phi;\quad \Delta e_z = 0;\quad \Delta\gamma = 0$$

also

$$\int\int dO\,\Delta\omega_z\,\Delta v_0 = -3\pi l B^2$$

$$\int\int\int dV\,\Delta\omega_z{}^2 = 9\pi l B^2\left(\frac{h}{a}\right)$$

$$\int\int\int dV\,\Delta e_\phi{}^2 = 3\pi l B^2\left(\frac{h}{a}\right)^3$$

Substituting into Equation [4a] we have

$$\frac{p}{2}\pi B^2 l(3+9) = G\pi l B^2\left(\frac{h}{a}\right)^3\left(3+\frac{3}{m-1}\right)$$

from which we find the well-known equation

$$p_{\text{critical}} = \frac{3D}{a^3}$$

where D is the flexural rigidity of the shell.

2 For the case of the cylindrical vessel with rigid covers under uniform external pressure, we take

$$\begin{aligned} f(\zeta) &= 1+\cos\pi\zeta \\ f'(\zeta) &= -\pi\sin\pi\zeta \\ f''(\zeta) &= -\pi^2\cos\pi\zeta \end{aligned}$$

At the boundaries

$$\zeta = \pm 1$$

so that f and f' will disappear. From Equations [11a] and [11b] we find

$$\begin{aligned} \Delta\omega_r &= \frac{f'}{2l}B\sin 2\phi \\ \Delta\omega_\phi &= \frac{2B}{l}f'\cos 2\phi \\ \Delta\omega_z &= \frac{3B}{a}f\sin 2\phi \\ \Delta e_\phi &= \frac{6B}{a}f\left(1-\frac{1}{\rho}\right)\cos 2\phi \\ \Delta e_z &= -\frac{2aB}{l^2}f''(\rho-1)\cos 2\phi \\ \Delta\gamma &= \frac{B}{2l}f'\left(3\rho-\frac{4}{\rho}\right)\sin 2\phi \end{aligned}$$

The initial stresses are

$$\sigma_r \cong 0$$

$$\sigma_\phi = -p\frac{a}{h}$$

$$\sigma_z = -\frac{p}{2}\frac{a}{h}$$

Using Equations [4a] and [5b] and taking $m = 4$ we find

$$\frac{p_{(\text{crit})}}{2G} = \frac{\frac{h}{a}\frac{\pi^2}{4}\left(\frac{a}{l}\right)^2+\left(\frac{h}{a}\right)^3\left\{6+\frac{59}{48}\pi^2\left(\frac{a}{l}\right)^2+\frac{2}{9}\pi^4\left(\frac{a}{l}\right)^4\right\}}{18+\frac{19}{16}\pi^2\left(\frac{a}{l}\right)^2}$$

The critical load will always have the form

$$\frac{p_{(\text{crit})}}{2G} = A_{\text{extensional}}\left(\frac{h}{a}\right)+A_{\text{bending}}\left(\frac{h}{a}\right)^3$$

Since arbitrarily we have assumed the virtual displacements for our problem, it will be useful in studying the validity of our result to examine the last equation in some detail. The critical load is seen to be the sum of two terms which are related to an energy. The first term is the result of potential energy of strain of the middle surface, while the second term gives the influence of the energy of bending. When the first term gives such values of the critical load that the corresponding stress reaches the yield point, we must conclude that the assumed virtual displacement is not the correct one. It has been proved that a closed shell cannot undergo a deformation in which the extensional strains disappear. That means the term linear in h/a is always present and we must choose our virtual displacements in order to make the value of A_{ext} very small.

When the problem admits a solution in trigonometrical series, it is easy to do so. Putting, for instance

$$\Delta u_0 = 2B\{1+\cos(2m+1)\pi\zeta\}\cos n\phi$$

$$\Delta v_0 = -B\{1+\cos(2m+1)\pi\zeta\}\sin n\phi$$

$$\Delta w_0 = 0$$

we have a solution satisfying the same boundary conditions previously considered and having two parameters m and n which can be so chosen that the extensional energy is as small as possible. Timoshenko and Westergaard have shown[5] how in this way not only approximations but exact solutions can be obtained.

We wish to emphasize that it is not necessary to consider the three stress couples and the three stress resultants dealt with in the classical theory of elasticity. The stresses needed are given by Equations [9]. In the present method, we consider as unknowns only the displacements of the middle surface, and determine the displacements of points of the shell not on the middle surface from the assumption that the normals remain normals and that the distance from the middle surface does not change.

Although the general Equations [4a] and [5b] are written in Cartesian co-ordinates, only the components of vectors and tensors occur so that the transition to any curvilinear system of co-ordinates is not difficult.

---

[5] "Sur la Stabilité des Systémes Elastiques," by S. Timoshenko, *Annales des Ponts et Chaussées*, Mémories, Jan.-June, 1913, pp. 496–566.

"Buckling of Elastic Structures," by H. M. Westergaard, Proceedings American Society of Civil Engineers, vol. 47, 1921, pp. 455–533; discussion by G. Paaswell, Ibid., vol. 48, 1922, p. 103.

The Mechanism of Cavitation Erosion

By T. C. POULTER,[1] CHICAGO, ILL.

After pointing out the interrelation between corrosion resistance, caustic embrittlement, fatigue, creep, and other phenomena of metals, the author cites the results of experiments on glass and quartz rods, subjected to high liquid pressures, as indicative of the action which probably occurs in cavitation erosion. To demonstrate the mechanism of cavitation on this basis, an investigation was conducted, in which tests were made on gray-cast-iron specimens in water, alcohol, glycerin, and paraffin oil, using a magnetostriction oscillator as the source of energy. The results of the tests which are reported bear out the theory. Materials and protective coatings which reduce cavitation erosion greatly, and the effect of the presence of hydrogen in the liquid are discussed.

CORROSION resistance, caustic embrittlement, steam erosion, cavitation erosion, gun-barrel erosion, wire drawing, fatigue, penetration of gases into metals, penetration of liquids into metals, and creep of metals are phenomena which are so completely interrelated that it is impossible to arrive at a proper explanation of one without at the same time shedding considerable light upon the others. The differences between the various phenomena referred to likely fall into two classes: (1) Difference in the ratio of the chemical to the physical nature of the phenomena; and (2) the order in which these take place. The fact that in some cases the fatigue resistance of a metal can be varied as much as tenfold by surrounding the test sample with a different gas indicates that fatigue is not entirely a physical phenomenon. Cavitation erosion has been considered somewhat of an isolated phenomenon, but a study of it has led to interesting information which may throw light upon other of these effects.

Investigation of Properties of Glass and Fused Quartz Under Liquid Pressure

In the course of certain investigations, being conducted in the field of extreme-pressure research, it became necessary to study the properties of glass and fused quartz when surrounded by liquids at high pressures. Differences in the behavior of various liquids on pressure windows had suggested that in some cases liquids were penetrating the glass or quartz of the windows.[2] It was found that pressure windows would withstand several times as much pressure if oil or glycerin were used to transmit the pressure, than they would if water, ether, or alcohol were employed. Windows surrounded by water, ether, or alcohol would frequently break on lowering the pressure, even though they had previously withstood much greater pressures.

A series of tests was undertaken in which pieces of glass or fused-quartz rod, 3 to 4 mm in diam and about 15 mm long, were placed in a piece of rubber tubing 5 cm long, and 6 mm ID. This tube was filled with the desired liquid and stoppered at both ends. It was then placed in a pressure cylinder, surrounded by oil, and the pressure applied.

If the pressure were built up to 15,000 atm or higher and immediately released, the glass or quartz rod would not be affected, even though surrounded by any one of the five liquids in question. In all cases, 30 sec were required to reach the maximum pressure and about 5 sec to reduce it to zero. It was found that if instead of dropping the pressure immediately, it is maintained for 5 min and then rapidly dropped to zero, the glass or quartz rods which are surrounded by alcohol, ether, or water will be broken up into short plates, whereas, those rods surrounded by paraffin, oil, or glycerin are unaffected. Now, if the pressure is maintained for 20 min instead of 5 min, and then rapidly dropped to zero, instead of forming smooth plates, the rod is shattered in all directions forming small irregular pieces. If the pressure is built up as before but allowed to go down very slowly (over a period of several hours), the specimens will not be affected regardless of the liquid surrounding them. The results of these experiments are shown in Fig. 1, in which the actual specimens were laid out on a chart and photographed.

Several glass and quartz disks were then cut from flat stock 4 mm thick. One of these disks was placed in the middle of the

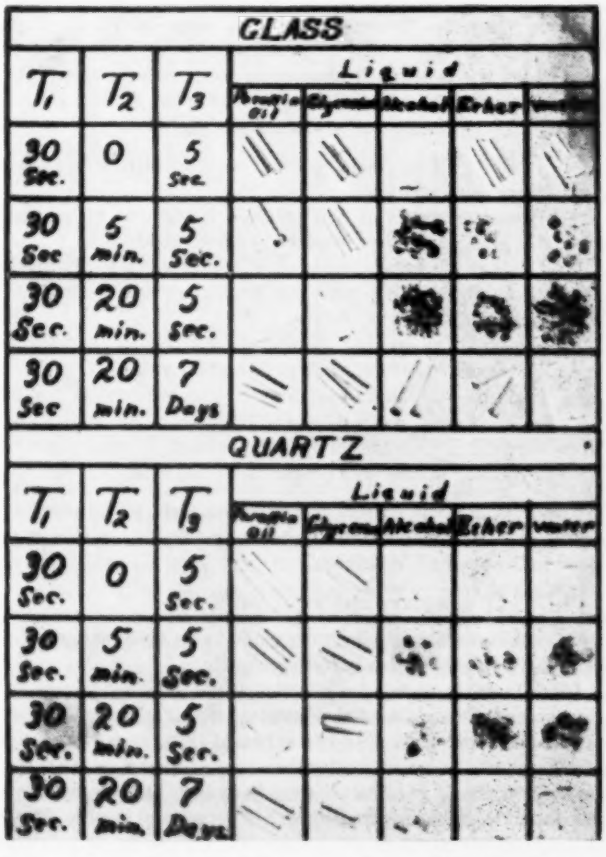


FIG. 1 CHART SHOWING RESULTS OF LIQUID-PRESSURE EXPERIMENTS ON SPECIMENS OF GLASS AND QUARTZ RODS

[1] Scientific Director, Armour Research Foundation.

[2] "Permeability of Glass and Fused Quartz to Ether, Alcohol, and Water at High Pressure," by T. C. Poulter and R. O. Wilson, *Physical Review*, vol. 40, no. 5, June 1, 1932, pp. 877–880.

Contributed by the Applied Mechanics Division, and presented at the Annual Meeting, New York, N. Y., December 1–5, 1941, of THE AMERICAN SOCIETY OF MECHANICAL ENGINEERS.

Discussion of this paper should be addressed to the Secretary, A.S.M.E., 29 West 39th Street, New York, N. Y., and will be accepted until April 10, 1942, for publication at a later date. Discussion received after the closing date will be returned.

NOTE: Statements and opinions advanced in papers are to be understood as individual expressions of their authors and not those of the Society.

rubber tube so that different liquids could be used on opposite sides of the glass. The results with these disks were similar to those with the glass rod, i.e., the side of a disk in contact with water, ether, or alcohol is shattered, unless the pressure is dropped immediately or allowed to subside very slowly; whereas, the side in contact with paraffin, oil, or glycerin remains intact in all cases. This fracturing cannot be explained on the basis of the rather large temperature change in the liquid in contact with the specimen accompanying the changes in pressure, for if that were the case, we would expect only the glass to be affected. Neither can it be explained on the basis of a differential compressibility of the solid modification of water and the glass or quartz, for no solid modification is known for alcohol or ether at these pressures and temperatures.

The fact that in cases where the glass or quartz has water on one side and oil on the other, only the side in contact with water is shattered, eliminates the possibility of the fracturing being due to a compressibility hysteresis effect of the glass or quartz being under extreme pressures. This is further demonstrated by the fact that, if glass or quartz pressure windows 4 mm thick and 12 mm in diam are mounted over a 6-mm-diam opening and subjected to a very high pressure, say, of 125,000 to 500,000 psi, they can be bent to a radius of curvature of 11 cm and returned without fracturing. This has been done with glass as many as 10 times with a single window, and with quartz as many as 4 times.

The most probable explanation of the fracturing of these materials, after having been subjected to pressures while surrounded by water, ether, or alcohol, is that the liquid, while compressed, actually penetrates the glass or quartz; then, as the pressure is released, the cohesive forces of the glass or quartz are not great enough to retain the liquid under the compressed condition. In the case where the pressure is dropped immediately, the liquid has not had sufficient time to penetrate the surface, and in the case where the pressure is allowed to go down very slowly, the liquid escapes without producing undue strain in the glass or quartz. These results can be summarized as follows:

(*a*) Little or no breakage occurs if insufficient time is allowed for the liquids to penetrate.

(*b*) Breakage occurs as the pressure is released rather than when it is being built up or retained at a high pressure.

(*c*) Little or no breakage occurs if the pressure is allowed to drop slowly enough to permit the gradual escape of the liquid which has penetrated the surface.

(*d*) No breakage occurs if liquids of relatively large molecules or a high viscosity are used, such as oil and glycerin.

(*e*) Fracturing is determined by the type of liquid in contact with the specimens and not by the pressure alone, as is shown when different liquids are on opposite sides of the same piece of glass or quartz; in this case pressures are obviously the same.

The results of the present investigation seem to indicate very clearly that the phenomenon of cavitation erosion is closely related to the one just described.

Studies on Cavitation Erosion

Cavitation-erosion studies were made using a magnetostriction oscillator and gray-cast-iron test specimens.

If cavitation erosion is a result of the penetration of liquids into the pores of the metal and their subsequent escape carrying some of the metal with it, it would be expected that the erosive action of water would be much greater than that of alcohol or ether, and that glycerin and paraffin oil would produce little or no effect. It is found that this is in accord with experimental results. Now, if the cavitation-erosion action were due primarily to a fatigue effect of the metal surface as a result of its being repeatedly stressed it would be expected that mercury would have a very large erosive effect since the forces involved would be much greater than in the cases of the other liquids, whereas, at moderate amplitudes it produces less erosion than water.



Fig. 2 Slightly Eroded Surface of Gray-Cast-Iron Specimen, Also Showing Fatigue Cracks; Vibrations Applied Perpendicular to Surface

In the case of cavitation erosion of iron samples by means of water, the iron that is removed from the surface of the test piece is found in the water as iron hydroxide. In an attempt to determine whether this hydrolysis of the finely divided particles of iron takes place as a part of the cavitation-erosion process or whether it takes place after the particles of iron have been dispersed in the water, experiments were run in which absolute alcohol was substituted for water. In this case the iron was found present in the alcohol in the form of finely divided metallic iron rather than the hydroxide. This, of course, does not prove that in the case of water, the hydrolysis does not take place on the surface of the metal but it does provide an eroded metal surface which is free from iron hydroxide. In addition to the normal erosion of the surface of a slightly eroded specimen, numerous cracks can be seen in the photomicrograph of the eroded surface, Fig. 2. These are probably fatigue cracks which have started to develop. It is possible that this method will give a means of determining the extent to which fatigue enters into cavitation erosion of this type.

Experiments With Magnetostriction Oscillator

Gray-cast-iron specimens were subjected to three different sets of conditions, in all cases using the magnetostriction oscillator as the source of energy. A nickel tube about 1 ft in length was used to give a normal frequency of 8000 cycles per sec.

Condition 1 The specimens under investigation were vibrated in a direction perpendicular to the surface being studied. A typical eroded surface is shown in Fig. 2.

Condition 2 The specimens under investigation were vibrated

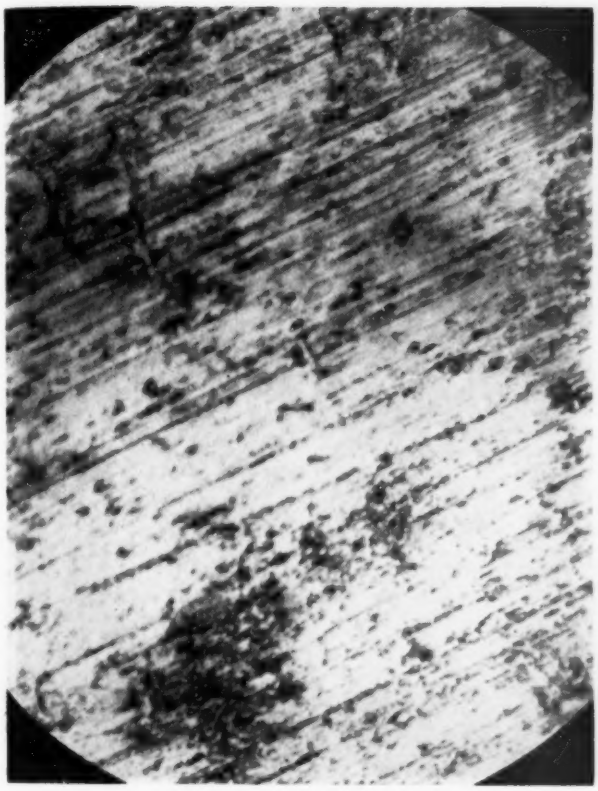


FIG. 3 ETCHED SPECIMEN AFTER HAVING BEEN VIBRATED IN A DIRECTION PARALLEL WITH SURFACE BEING STUDIED

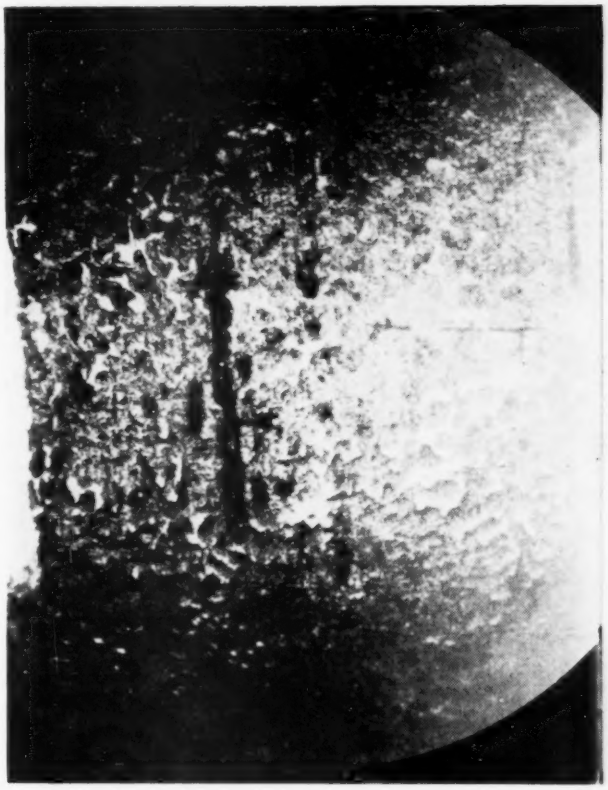


FIG. 4 ETCHED SPECIMEN OF GRAY-CAST-IRON TUBE AFTER BEING SUBJECTED ALTERNATELY TO COMPRESSION AND TENSION FORCES ACTING PARALLEL WITH THE SURFACE

parallel with the surface being studied. The results, Fig. 3, were very similar to those obtained under condition 1.

Condition 3 The specimen was stationary but was subjected to compression and tension forces acting parallel to the surface being studied. This was accomplished by silver-soldering a section of gray-cast-iron tube in at the center of the nickel tube so that, as the tube vibrated longitudinally, the iron specimen formed its node.

Under these conditions, there is still a very marked erosion of the surface, but in this case a more general erosion of the surface is produced rather than a concentration of the effect in deep cavities, Fig. 4.

An examination of the surface of the vibrating specimen under condition 1 was made with a microscope, illuminating the specimen with a stroboscopic light source. Under these conditions, the formation and collapse of small cavities in the water near the metal surface could be observed. These cavities seemed to reform in the same place on the surface of the metal rather than assuming a different random distribution for each cycle.

In all cases where attempts were made to detect the presence of supersonic or near-supersonic vibrations in the liquid producing cavitation erosion, they have been found to be very intense.

What the magnitude of the maximum tension or compression force is, which can be produced in a compression wave, depends upon the medium through which the wave is passing. This maximum also depends upon the wave form or, in other words, the distribution of energy among the various frequency constituents composing the wave.

For a gas, it is apparent that the average pressure over a complete cycle must be equal to the measured pressure of the gas. There seems to be no theoretical limit to the maximum pressure, but it would seem that the minimum pressure would be zero and that it could never be negative in value. In solids it would appear that the maximum pressure is theoretically unlimited and that the greatest negative pressure would be the tensile strength of the material.

However, there is considerable experimental evidence to indicate that the maximum negative pressure or tension is a function of the frequency, or a function of the rate at which the tension is applied; and that it may exceed the normal tensile strength of the material, the high values being associated with the high rate of application.

In liquids, the situation is even more complicated than it is in either gases or solids. It is largely this difference that makes possible the phenomenon of cavitation erosion. The maximum pressure for liquids is more closely related to that of solids, while the minimum or negative pressure resembles that of a solid up to a certain point; from then on it is similar to a gas. This sharp transition is the point at which the continuity of the liquid is broken and a cavity is formed. It takes place not at a zero pressure but at a negative pressure or tension which might correctly be called the tensile strength of the liquid; frequently, this may be several kilograms per square centimeter. Some experiments have indicated a tensile strength for water of several hundred kilograms per square centimeter.

In suggesting that the maximum pressure for compression waves theoretically may be infinitely large, the author is mindful of course that it would be practically impossible to produce an infinite pressure. However, illustrations of actual compression waves can be cited in all three physical states where these maximum pressures exceed 1,000,000 psi at the source of the disturbance. This is true notwithstanding the fact that the example for gas occurs, even though the average pressure is only a small frac-

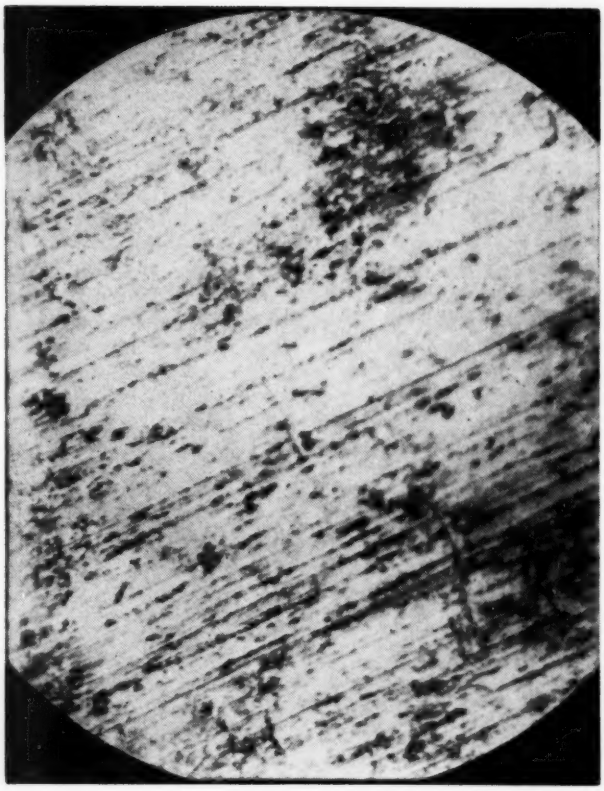


FIG. 5 SURFACE OF IRON SPECIMEN, SHOWING WIDESPREAD EROSION, AFTER BEING SUSPENDED IN WATER AND SUBJECTED TO COMPRESSION WAVE HAVING A FREQUENCY OF 8000 CYCLES PER SEC



FIG. 6 RESULT OF TREATING ONE HALF OF AN IRON SPECIMEN WITH OIL FILM TO PREVENT CAVITATION EROSION

tion of a millimeter of mercury. Reference is made to the compression wave set up, as particles of meteoric matter traveling with a velocity of 30 mps strike the very light upper atmosphere. At an altitude of about 100 miles, the gas pressure built up ahead of these tiny particles is in excess of 1,000,000 psi. Perhaps the nearest approach to those pressures, producing sound waves that are commonly heard by man, are developed by electrical discharges, such as lightning or discharges in the laboratory.

In the case of solids, pressures in excess of 1,000,000 psi are produced by such common things as striking two files together; the diamond of an emery-wheel dresser striking the grains of the wheel; or a high-powered-rifle bullet striking a hard object. Perhaps the most common example of liquid pressures approaching or exceeding 1,000,000 psi occurs when a cavity in a liquid is collapsed rapidly. Hence, this is the fundamental source of energy responsible for cavitation erosion.

FORCES PRODUCED DURING CAVITATION

Let us assume that we have a spherical cavity in water and that, due to the pressure on the water, this cavity is being collapsed.

Now, regardless of the size of the cavity or the rate at which it is being collapsed, if the water were incompressible the impact velocity of the walls of the cavity when they meet at the center would be infinity, therefore, the pressure produced would be infinitely great.

Since the water is not incompressible this is of course not true. There are two limiting factors: (1) The compressibility of the water produces some cushioning effect; (2) a thermal effect results from the compression. These two factors act in opposite directions and tend to offset one another. These effects are not

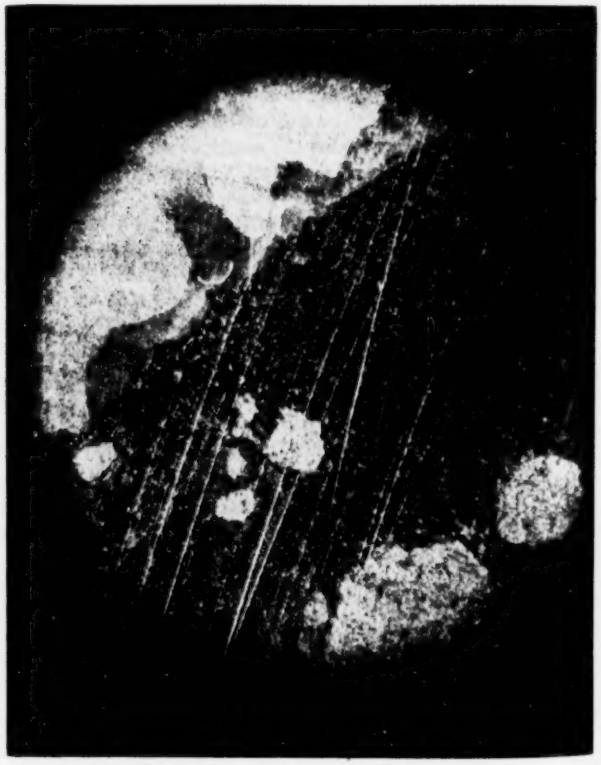


FIG. 7 WITH PARAFFIN OIL AS PROTECTIVE COATING, MANY SPOTS SHOW WHERE FILM WAS PENETRATED ALLOWING EROSION TO OCCUR

excessively large until a pressure of about 8500 atm is reached. At that pressure, if the temperature did not rise, the water would compress to about 60 per cent of its original volume and the water would change to a solid known as "ice six." Ice six has a melting point of 70 F at 8500 atm. Due to the sudden development of an extremely high pressure, it would be expected that a very high temperature would be developed. The elapsed time during which this extremely high pressure is being built up and again reduced probably does not exceed 10μ sec, but it may be repeated more than 10,000 times per sec at the same point.

Such conditions are effective in producing cavitation erosion only when they take place at the surface of the metal. However, the collapse of such a cavity out in the body of a liquid sets up a supersonic or near-supersonic compression wave in the water which travels with a velocity of about 5000 fps. If the amplitude of this compression wave as it strikes the walls of the containers is very large, a number of cavities will be formed at the metal-water interface.

Experimental Evidence of Cavitation Forces

In order to test this experimentally, an iron specimen was suspended in water and a compression wave, having a frequency of 8000 cycles per sec, was introduced into the water by means of a magnetostriction oscillator. The erosion produced on this specimen, as shown in Fig. 5, was widespread over the entire surface of the specimen.

If this is the correct mechanism of cavitation erosion, it would be expected in general that the more porous materials would be most readily affected. This in general is found to be the case, but the brittleness of the material cannot be overlooked. It will be recalled that, in the case of fracturing the glass or quartz specimens by subjecting them to a high hydrostatic pressure and subsequently releasing that pressure, water was most effective, ether next, alcohol next, glycerin producing fractures but rarely, and paraffin oil not at all. A careful examination of these results will show that both molecular size and viscosity play an important part. Water having the smallest molecule produces the greatest effect; the ether molecule, being considerably larger, produces a much less marked effect than water but somewhat greater than alcohol. Glycerin and ether were selected because of their relative molecular sizes and viscosities, the ether molecule being the larger, but having the lower viscosity. In spite of ether having the larger molecule, it is much more effective in producing fracture of the glass or quartz than is glycerin which has a smaller molecule but has a much greater viscosity. This, therefore indicates that the pores are relatively large as compared with these molecular dimensions, and that the glycerin does not enter because of its greater viscosity.

Also in the experiments on glass and fused quartz, it was found that, if a specimen had previously been subjected to pressure while immersed in paraffin oil, subsequent treatment in water

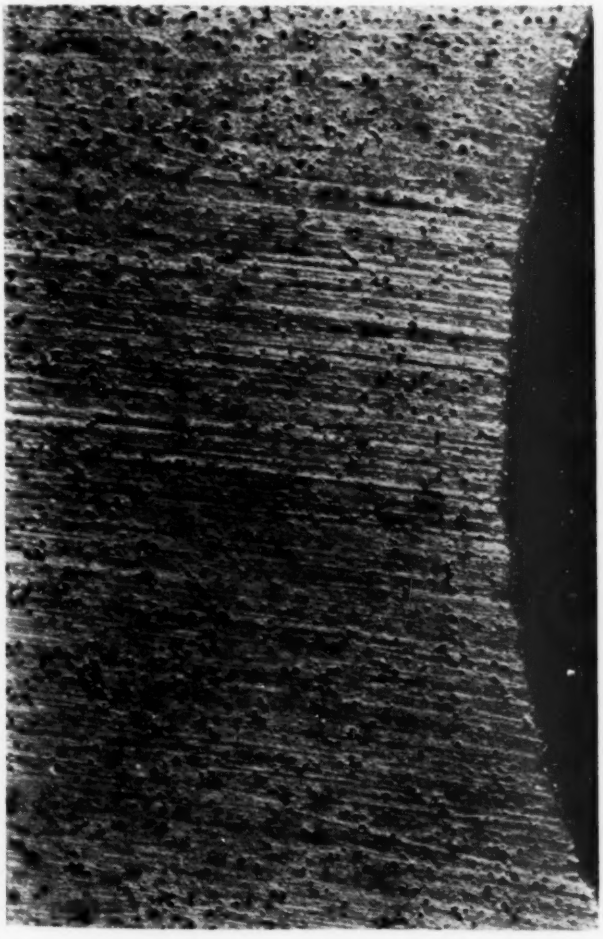


Fig. 8 Specimen From Pressure Cylinder Which Contained Oil Only, After Several Months of Intermittent Use

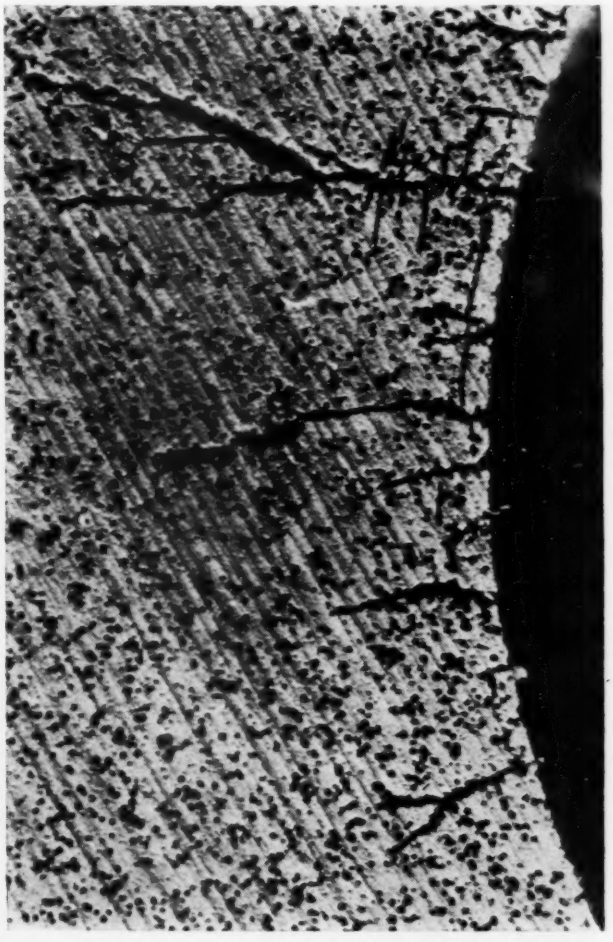


Fig. 9 Specimen From Pressure Cylinder Which Contained Oil, and in Addition Small Amounts of Hydrogen, After Two Hours' Use Under Pressure

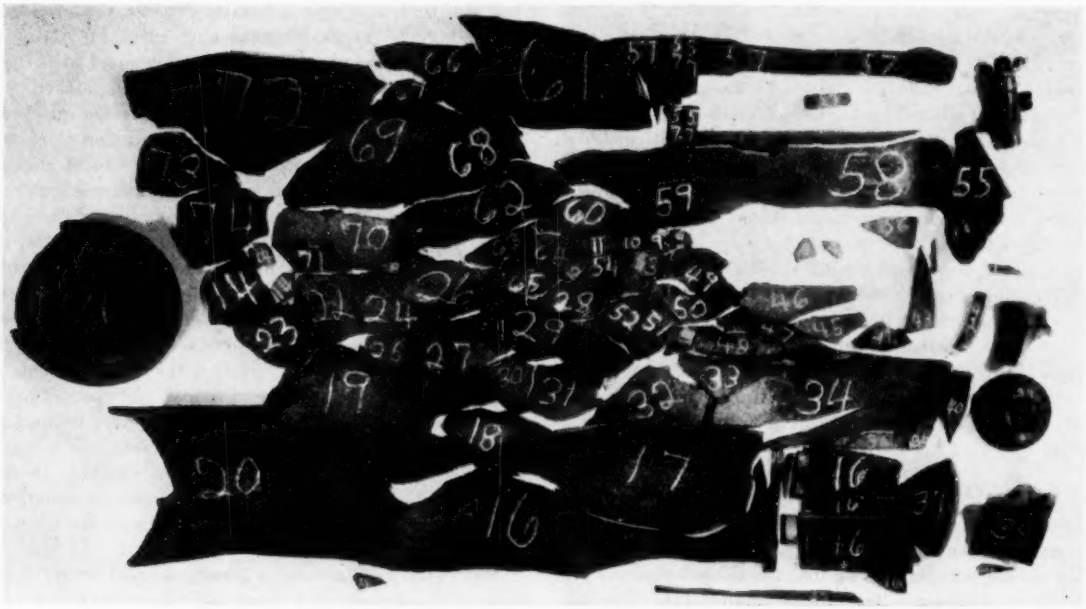


FIG. 10 HYDROGEN CYLINDER OF 200-CU-FT CAPACITY WHICH FAILED AFTER 25 YEARS OF SERVICE

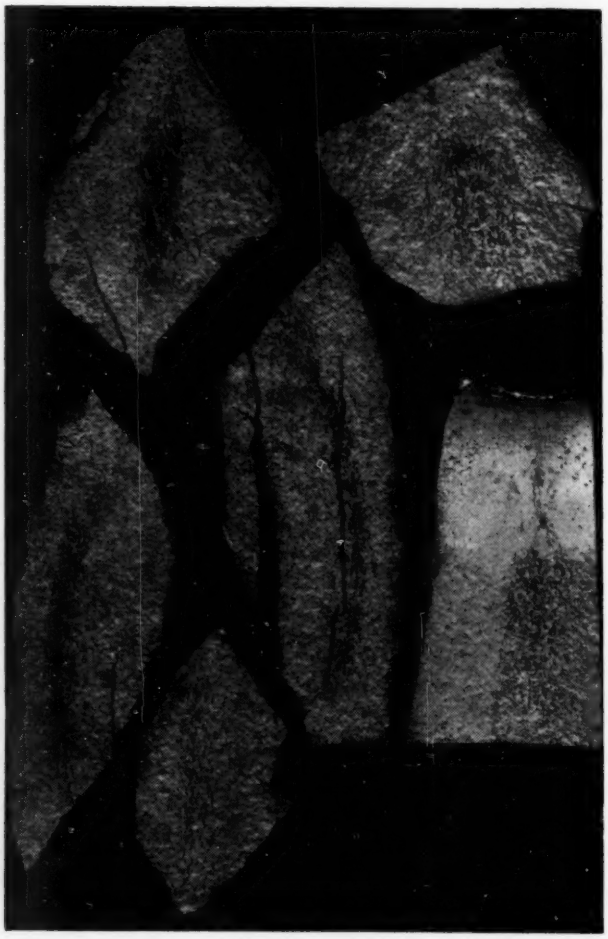


FIG. 11 SIX FRAGMENTS FROM HYDROGEN CYLINDER UNDERGOING MAGNAFLUX EXAMINATION

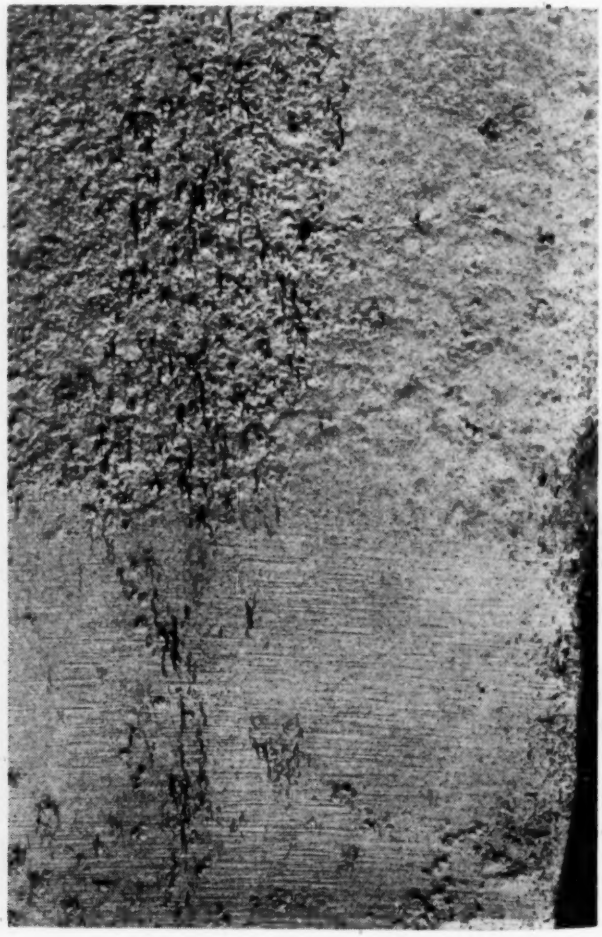


FIG. 12 ENLARGED VIEW OF ONE OF THE FRAGMENTS FROM THE HYDROGEN CYLINDER

would usually be less effective in producing fracture. It was therefore considered possible in some way to seal or fill the pores of the metal surface so as to prevent the cavitation-erosion action of water upon the surface, even though all other necessary conditions were present for producing erosion. Two identical specimens were prepared and one of them treated with a material which produces an absorbed molecular layer on the surface of the metal. This film produced a noticeable reduction in the erosion of the specimen. Another specimen was then prepared and one half of the specimen treated and the other half left in its original condition. In this case the oil film was somewhat thicker than on the previous specimen. The treated half of the specimen seemed to be completely protected against cavitation erosion for the duration of the experiment which was for 24 hr, or 500,000,000 cycles, whereas the other half of the specimen was quite badly eroded, Fig. 6. A similar series of tests were made in which paraffin oil was used as a protective coating instead of the film-forming material. The protection was found to be very much inferior to the first material. The protective coating in this case was penetrated at many points producing numerous eroded spots, Fig. 7.

Effect of Hydrogen on Cavitation Erosion

It is, of course, well known that a cylinder designed to withstand extremely high pressures will fail at a very much lower pressure, if, in addition to the liquid pressure, it contains considerable hydrogen. If a steel tube is filled at one end with water and at the other end with oil, and sufficient pressure applied, the failure will usually occur in the end of the tube containing the water, even though the pressure is applied through the end containing the oil.

Two pressure cylinders were constructed from the same bar of steel and received the same heat-treatment. Both cylinders were repeatedly subjected to pressures of approximately 400,000 psi. In one case, the cylinder contained only oil; and in the other case, a small rubber capsule containing zinc and sulphuric acid was suspended in the oil to generate hydrogen. Both cylinders were used under these conditions until they failed. The cylinder containing the hydrogen failed after it had maintained a pressure for a total time of less than 2 hr; whereas, the one containing no hydrogen had a service life of several months, during which time it was probably under pressure the equivalent of several days. After failure, these two cylinders were sectioned and deep-etched; Fig. 8 showing the one which contained no hydrogen, and Fig. 9 showing extensive cracks radiating from the inside surface of the cylinder which contained hydrogen. Subsequent experiments indicated that these hydrogen cracks may penetrate as much as $^1/_8$ in. into the cylinder wall in a few minutes with a pressure of only 30,000 psi, and that a similar effect takes place very slowly, even with gaseous hydrogen pressures of approximately 2000 psi.

Fig. 10 shows a 200-cu-ft hydrogen cylinder which failed after being in service for about 25 years. A careful examination of the walls of this cylinder shows that the inside surface is covered with small cracks, some of which extend as much as 25 per cent of the way through the cylinder wall. Fig. 11 shows six of these fragments undergoing magnaflux examination. Fig. 12 is an enlargement of one of the pieces. Hydrogen cylinders were then selected which had been in service about the same length of time, but which had not failed. Examination showed the inside surfaces to be in approximately the same condition as the one that failed, whereas, cylinders made at the same time and from the same batch of steel, but which had been in nitrogen service, were still in good condition.

In 1937, Fred R. Venton of the research testing laboratory, Crane Company, Chicago, reported results[3] on steam erosion of various alloys. Cavitation-erosion tests were run on a similar series of alloys with strikingly comparable results. In these results, it was found that a face-centered-crystal lattice offers very much greater resistance to steam erosion and cavitation erosion, and that there seems to be no correlation between hardness and erosion resistance. If the energy is not too great, lead and rubber resist cavitation erosion almost indefinitely, whereas glass, cast iron, and carboalloys are quite rapidly eroded.

[3] "New Method of Studying Erosion Aids Selection of Valve Seat Materials," by F. R. Venton, *Heating, Piping and Air Conditioning*, vol. 9, Jan., 1937, pp. 34–38.

Design Data

It is important that the data contained in technical papers be made readily available to designing engineers. In order to satisfy these needs of industry, this section of the JOURNAL will include a concise presentation of data and information drawn chiefly from papers previously published by the Applied Mechanics Division of The American Society of Mechanical Engineers.

The data are prepared by a subcommittee of the Applied Mechanics Division under the guidance of S. Timoshenko. This article contains data on the design of pipe.

Expansion of Formulas for Calculating Loads, Rotation, and Deflections of Quarter Bends and Tangents of Pipes

By A. S. McCORMICK,[1] SCHENECTADY, N. Y.

IN calculating the forces and moments due to thermal expansion on a run of pipe in three planes, made up of tangents and quarter bends, the greater part of the time consumed in the calculation has heretofore been spent in determining the correct direction of the various rotations and deflections. This was found to be especially true of the Karelitz-Marchant method, as previously published,[2] and other methods using the formulas of Hovgaard, Crocker, and McCutcheon.

These formulas are presented herewith in graphic form to show every possible position of quarter bend and tangent with respect to the axes X, Y, and Z, under the different loading conditions. This reduces possible error to a minimum inasmuch as, in working out the direction of rotation and deflection for the different loading conditions, it has been possible to check one condition against another. In the use of the formulas, it is merely necessary to locate the desired condition on the plates and copy the formulas so that the compilation of rotations and deflections, from one end of a pipe run to the other, becomes a more or less mechanical process.

Using this set of tables, it has been possible to reduce the calculation of a three-plane pipe problem from a task of several days to one of approximately a day and a half, a calculating-machine operator doing the arithmetical work.

The accompanying illustrations show the different cases in perspective. At the top of each panel, covering a loading condition, the formulas for rotation and deflection are given, the formulas in each case being numbered. The direction of rotation is given for each case, referred to the positive ends of the axes of the plane in which it occurs, followed by the number of the formula for the numerical value. The deflection of each case is given with respect to the axis along which it occurs, followed by the number of the formula for the numerical value and a letter denoting direction on the axis along which it occurs. Each section of each panel covers four cases; the tangents and quarter bends are assumed to be anchored at the intersection of the axes X, Y, and Z.

Direction of deflection

B = back ..... } ΔY
F = forward .. }

R = right .... } ΔX
L = left ..... }

U = up ..... } ΔZ
D = down .... }

X, Y, Z = rectangular axes through fixed end of quarter bend or tangent

F = force acting on free end of tangent or quarter bend

M_b = bending moment acting on free end of tangent or quarter bend

M_t = turning moment acting on free end of tangent or quarter bend

I = moment of inertia of pipe section

E = modulus of elasticity of material, corrected for working temperature, according to equation

$$E_t = E_{32}\left[1 - \left(\frac{T - 32}{1700}\right)^2\right]$$

where

E_t = modulus of elasticity at T deg F

E_{32} = modulus of elasticity at 32 F

K = rigidity multiplication factor $= \dfrac{1 + 12\,h^2}{10 + 12\,h^2}$

where

$$h = \frac{tR}{r^2}$$

t = thickness of pipe wall

R = mean radius of pipe bend

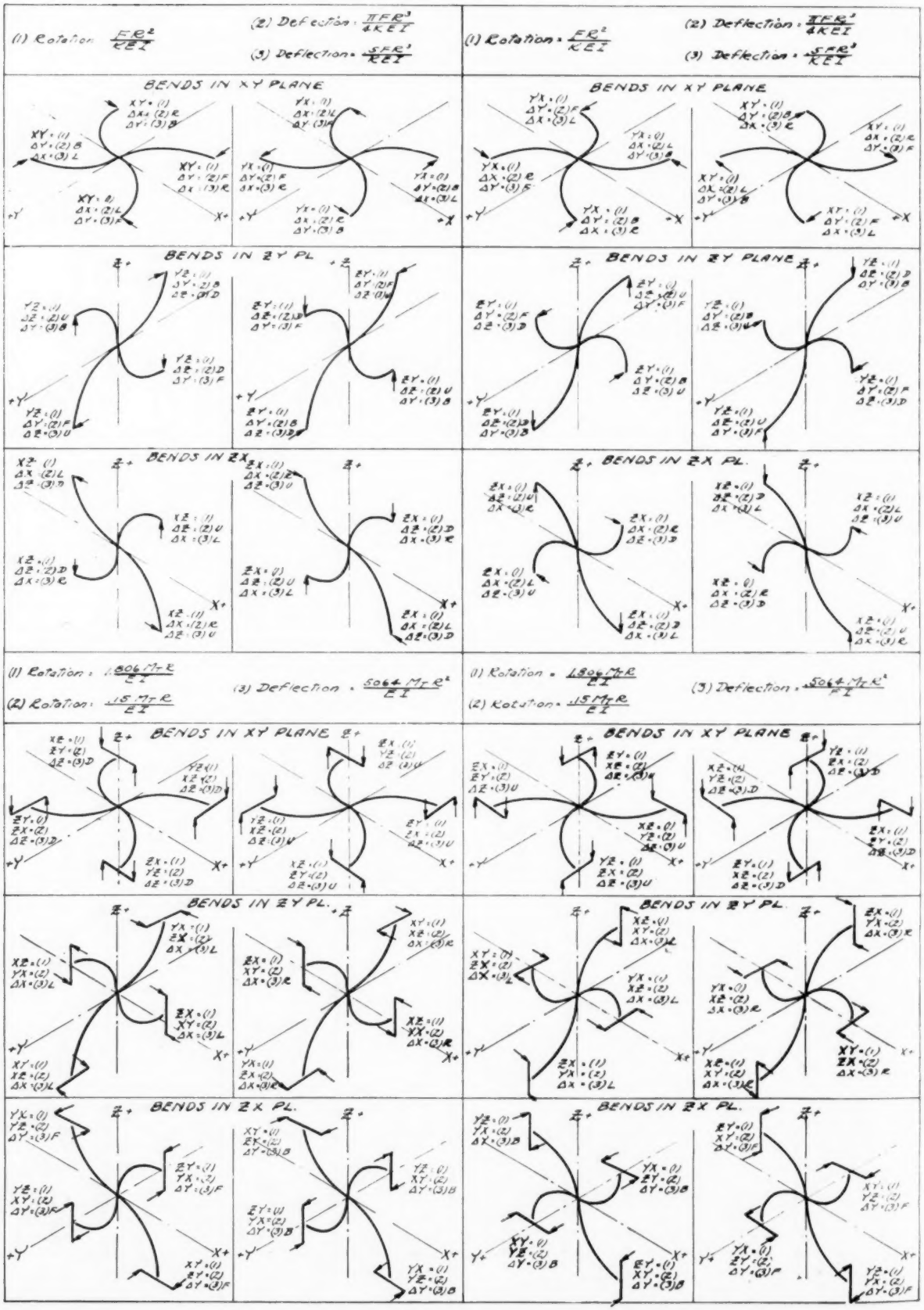
r = mean radius of pipe wall

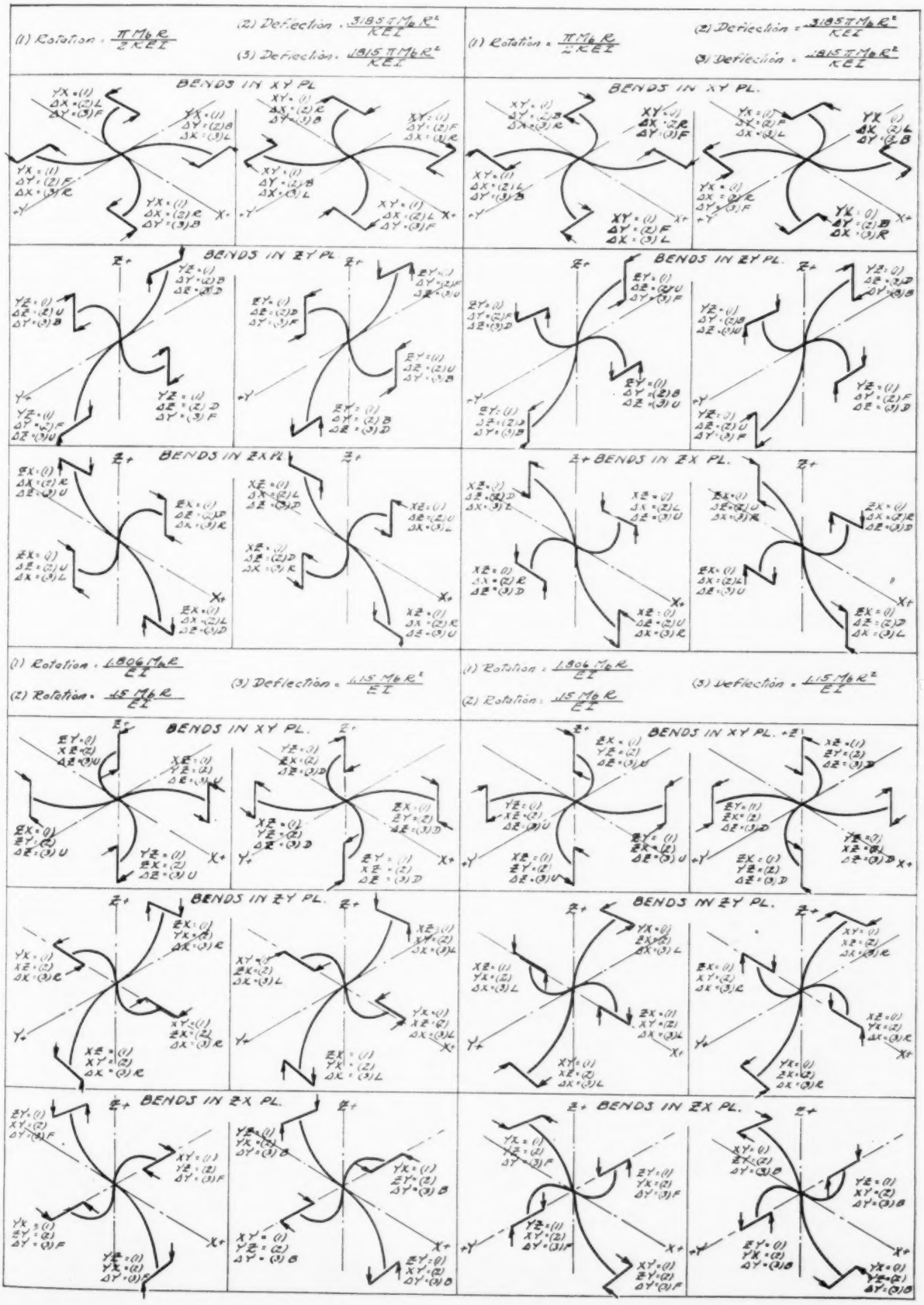
No basic change has been made in any of the formulas presented in the article cited.[2] Well-known formulas have merely been expanded to facilitate their use and to reduce labor and probability of error as much as possible.

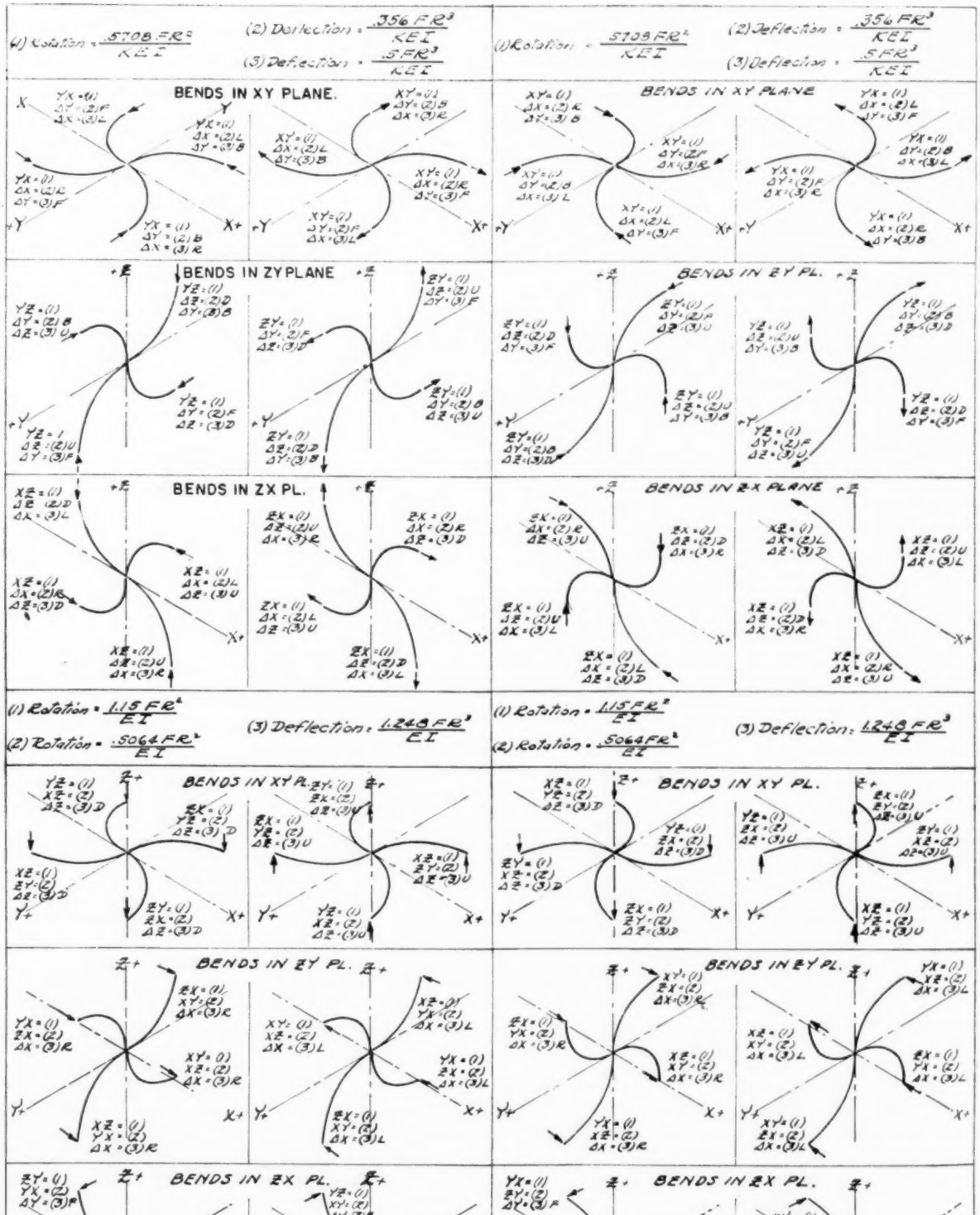
[1] Turbine Engineering Department, General Electric Co.

[2] "Data Sheets for Design of Piping," by H. E. Mayrose, JOURNAL OF APPLIED MECHANICS, Trans. A.S.M.E., vol. 59, 1937, p. A-89. A complete bibliography of the subject is incorporated in this paper.

	(1) Rotation = $\frac{FL^2}{2EI}$ (2) Deflection = $\frac{FL^3}{3EI}$
	TANGENTS IN XY PLANE
	Z+ TANGENTS IN ZY PL. Z+
	Z+ TANGENTS IN ZX PL. Z+
(1) Rotation = $\frac{MbL}{EI}$ (2) Deflection = $\frac{MbL^2}{2EI}$	(1) Rotation = $\frac{13}{24}\frac{M_cL}{EI}$ (2) Deflection = 0
TANGENTS IN XY PL.	Z+ TANGENTS IN XY PL. Z+
Z+ TANGENTS IN ZY PL Z+	Z+ TANGENTS IN ZY PL. Z+
Z+ TANGENTS IN ZX PL Z+	Z+ TANGENTS IN ZX PL. Z+


(1) Rotation = FR²/KEI
(2) Deflection = πFR³/4KEI
(3) Deflection = SFR³/KEI
BENDS IN XY PLANE
BENDS IN ZY PL.
BENDS IN ZY PLANE
BENDS IN ZX PL.
(1) Rotation = 1.806 MtR/EI
(2) Rotation = .15 MtR/EI
(3) Deflection = .5064 MtR²/EI
BENDS IN XY PLANE
BENDS IN ZY PL.
BENDS IN ZX PL.


(1) Rotation = $\frac{\pi M_b R}{2KEI}$
(2) Deflection = $\frac{3.185\pi M_b R^2}{KEI}$
(3) Deflection = $\frac{1.815\pi M_b R^2}{KEI}$
BENDS IN XY PL
BENDS IN ZY PL
BENDS IN ZX PL
(1) Rotation = $\frac{1.806 M_b R}{EI}$
(2) Rotation = $\frac{.45 M_b R}{EI}$
(3) Deflection = $\frac{.415 M_b R^2}{EI}$


(1) Rotation = 5708 FR²/KEI (2) Deflection = 356 FR³/KEI (3) Deflection = 5FR³/KEI
BENDS IN XY PLANE.
BENDS IN XY PLANE
BENDS IN ZY PLANE
BENDS IN ZY PL.
BENDS IN ZX PL.
BENDS IN ZX PLANE
(1) Rotation = 1.15 FR²/EI (2) Rotation = 5064 FR²/EI (3) Deflection = 1248 FR³/EI
BENDS IN XY PL.
BENDS IN ZY PL.
BENDS IN ZX PL.

Discussion

Effects of Surface Finish on Journal Bearing Performance[1]

C. R. Lewis.[2] Work on the subject matter of this paper is being done in the laboratories of the Chrysler Corporation which confirms in general the results of the research at the Massachusetts Institute of Technology. However, this work has brought out several points which the authors do not mention and which indicate some new reasons for his results.

The Chrysler work has indicated that, when surfaces of dissimilar roughness are run together, the results tend to be characteristic of the rough surface. This result throws some light on the observation in the paper that comparatively little increase in load-carrying ability is found below 15 microinches, as the babbitt bearings were reported to measure from 6 to 10 microinches.

It has also been found that the minimum of the friction curve tends to be much more sharply defined for smoother surfaces. Some indication of this condition is found in Fig. 6 of the paper. It is more evident when harder materials are used, as the soft babbitt tends to flow either plastically or due to melting when the oil film fails. This flow may change either the surface smoothness or the clearance ratio, and may, as the authors found, produce a succession of minima in the friction curve. In less definite cases, it produces a broadness in the minimum of this curve. The broadening of the minimum, because of surface roughness, is believed due to the introduction of turbulence in the oil film before actual rupture takes place. The hydrodynamic analyses, predicting the dependence of the friction coefficient on the quantity $S = ZN/P$, are based on the assumption that the oil in the lubricant film is in a condition of streamline flow at all times. It seems reasonable that skin friction of the oil against a rough surface would disturb this streamline flow, so as to give a more gradual departure from full hydrodynamic lubrication than in the case of a smooth surface. This effect is found in curves A, B, and M of Fig. 6 of the paper.

A preliminary investigation of the effect of surface finish on oil-film thickness has been made in the Chrysler Laboratories. In this work, the bearing surfaces were a stationary-plane pivoted slider and a revolving-plane disk. The film thickness was calculated from a measurement of the electrical capacity between the slider and the disk. The results are shown in Fig. 1 of this discussion. Both the rough (30-microinch) and the smooth (2-microinch) surfaces gave film thickness agreeing well with those predicted from a formula given by Professor Karelitz.[3]

Confirming results of the second part of the authors' paper, we found momentary metallic contacts even at quite light loads of about 50 psi. The frequency of these contacts increased with load until, with the highest load used on the smooth surface, the surfaces were touching about 30 per cent of the time. The fact that these contacts are related to surface imperfections is indicated by the observation that most of them were confined to a 90-deg segment of the disk.

At the maximum load shown for the rough surface (150 psi), the surfaces were in contact about 40 per cent of the time. An attempt to increase the load caused the surfaces to seize. At this point, the measured thickness of the oil film was about 7 times the height of the surface irregularities expected on each surface from a profilometer reading of 30 microinches. However, this measured thickness was an average value for the entire surface and does not indicate the minimum thickness. At the highest load available for the smooth surface, the measured film thickness was some 30 times the height of the surface irregularities, and no signs of failure were observed. These preliminary tests indicate that, when rupture of the oil film occurs due to surface imperfections, the thickness of the oil film is roughly of the same order of magnitude as the height of the surface irregularities. This result suggests the mechanism by which the surface finish affects the load-carrying ability of a bearing.

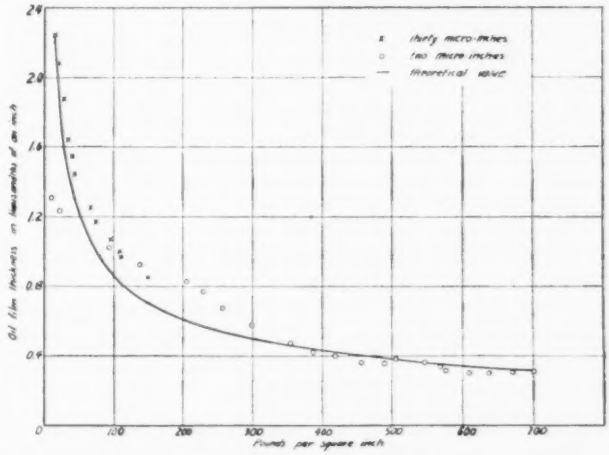


Fig. 1 Oil-Film Thickness Calculated From Measurement of Electrical Capacity Between Bearing Surfaces, Consisting of Stationary-Plane Pivoted Slider and Revolving-Plane Disk

L. M. Tichvinsky.[4] The fact that the authors determine the D/C ratio indirectly by measuring of μ, N, and P on the testing machine indicates that utmost precision has to be followed during such experimentation.

It is known that a ground surface may be wavy and at the same time very smooth. The waviness depends upon several factors such as the speed of the ground object and the grinding wheel, the feed, type of mounting, the bearing oil-film uniformity and carrying capacity, and also the skill of the operator. In this connection, it will be of interest to learn whether or not any waviness is being obtained when a superfinish method is applied.

The results of further investigations of this kind will be quite useful to bearing designers. Surface-friction relationships in the boundary region at loads encountered in industrial machines when starting or stopping are still unavailable.

Authors' Closure

Mr. Lewis' conclusion that the reason for the comparatively small increase in load-carrying capacity below 15 microinches is the roughness of the babbitt bearings themselves is interesting

[1] By J. T. Burwell, J. Kaye, D. W. van Nymegen, and D. A. Morgan, published in the June, 1941, issue of the Journal of Applied Mechanics, Trans. A.S.M.E., vol. 63, p. A-49.

[2] Engineering Division, Chrysler Corporation, Detroit, Mich.

[3] "Current Practice in Pressures, Speeds, Clearances, and Lubrication of Oil-Film Bearings," by H. A. S. Howarth; discussion by G. B. Karelitz, Trans. A.S.M.E., vol. 57, 1935, p. 357.

[4] U. S. Naval Engineering Experiment Station, Annapolis, Md.

but does not seem very probable. When metal-to-metal contact first occurs, the shaft wipes the much softer babbitt and imparts to it a surface having the same roughness as the shaft. Subsequent performance and ultimate seizure will be governed by this final roughness rather than the initial one. This effect may possibly be responsible for the fluctuating character of the minimum of the friction coefficient curve I in Fig. 7 of the original paper, although we are more inclined to attribute it to the change produced in the D/C ratio. The suggestion that the broadening of the minimum of the curves for rough surfaces is due to turbulence is an interesting and novel one. A further investigation of this idea should be undertaken.

Mr. Lewis' measurements of the oil-film thickness for a hydrodynamically lubricated plane slider show good agreement with the theoretical curve. From these results, he concludes that the rupture of the oil film, and hence the limit of stable bearing operation, occurs when the thickness of the oil film is of the same order of magnitude as the height of the surface irregularities. This conclusion is most important in substantiating the already postulated mechanism of what occurs when the limiting value of $\mu N/p$ is exceeded, namely, that metal-to-metal contact of the high spots on the two surfaces takes place with resultant failure of the oil film.

In answer to Mr. Tichvinsky's question, it is quite unusual to obtain any sort of waviness from a superfinishing operation, and waviness on a previously ground surface is generally removed. This is due to the small inertia and relatively large cutting area of the superfinishing stones. We agree that it is important to distinguish waviness from roughness, and this difference may be very significant in the region of boundary lubrication.

An Eddy-Current Method of Flaw Detection in Nonmagnetic Metals[1]

S. L. Burgwin.[2] The writer's limited experience in detecting flaws in nonmagnetic materials has indicated some of the possibilities of the eddy-current method of flaw detection, so it is with considerable interest that the present paper has been studied.

When the author claims a type of search unit which is universal, presumably he means universal in the sense that it can be used with almost any conducting material, not in the sense that it can be used for all sizes and shapes of metallic objects. The writer has in mind a particular problem which came up some years ago, wherein it was desired to check small contacts made up of two materials to be sure that they would not split apart. An eddy-current method of test was devised which has since operated very successfully. However, the size and shape of these contacts were such that it would be impractical to use the type of instrument developed by the author.

In other applications his device could be used successfully although, for production applications, practical use would probably require some modification of the design of the test unit for each application. Some years ago the writer developed a search unit of somewhat different design but having approximately the same underlying principle which was used to detect flaws in sheets. The device was successful enough, but scanning large sheets by hand was found to be rather slow and tedious. The successful use of such apparatus on large objects for other than trouble shooting would probably depend upon whether the scanning could be made automatic.

As to the practical use of the unit described in the paper, there are several points of interest which it is believed were not covered in the paper. For instance, if the axis of the search unit is not kept normal to the surface of the test material, as may occur when the surface of the test material is wavy or dirty or when testing objects with rough or uneven surfaces, would a voltage not be generated in the pick-up coil? If so, how serious is this effect? In the paper some mention was made of the rapidity of scanning. Could the author give some concrete idea of how long it would take to scan a sheet of stainless steel 3 ft square and perhaps $^1/_2$ in. thick?

H. J. Roast.[3] A paper such as this, which assists us in the discovery of latent flaws in metal articles, is of considerable value. The writer wishes to inquire whether or not this method will indicate the following: (*a*) Internal dross areas occluded in metal castings; (*b*) Gas holes occluded in metal castings.

The writer is a metallurgist dealing primarily with the manufacture of castings, rather than a physicist whose interest lies in physical phenomena of all kinds. The question from this point of view is whether the lack of continuity of a dross area or gas hole would prevent its reacting to the magnetic field in a manner similar to that of a continuous crack.

We have recently had bronze castings, weighing about $^1/_4$ lb, X-rayed. At the moment, the requirement is for each casting to be X-rayed and the price quoted is $5 each. This is mentioned because it will be obvious that any method which would definitely show up dross areas or gas holes in a more economical way would be highly desirable.

The metal in question is manganese bronze, essentially 60 per cent copper, 40 per cent zinc, with displacement of the zinc of 1 per cent of aluminum, iron, and manganese.

If the method is applicable to the points raised, would it be possible to locate roughly the areas in regard to the various configurations of the casting?

Author's Closure

Many practical matters must be considered in applying the eddy-current method to the location of flaws in a group of identical metallic objects. In general, a jig is employed to hold the exploring head in a suitable and reproducible manner so that the scanning process may proceed regularly and automatically. Full attention can then be directed to reading the indicator if automatic recording is not employed, or if the detection of gross flaws alone is desired. The use of a jig maintains a proper position of the head, and a slightly wavy or dirty surface produces no systematic indication. The scanning rate with apparatus, operating on commercial frequencies, is low, but not so low as to limit its usefulness. The area examined in a given time depends, of course, upon the size of the exploring head, the exciting frequency, and the degree of overlap. It is easily possible to examine 9 sq ft of $^1/_{32}$-in. stainless steel and make a permanent record of the test in less than 4 min.

Our tests of the method show that it may easily be adapted to the location of voids or dross areas in a casting if these are within $^1/_2$ in. of the surface, and if the casting is not too complicated. By employing properly designed scanning jigs and actual records of the electric currents, it is believed that much could be learned about moderately complicated castings.

Although the basic principles outlined in this paper are still employed, various improvements have been adopted recently which add considerably to the usefulness and convenience of the method.

---

[1] By Ross Gunn, published in the March, 1941, issue of the Journal of Applied Mechanics, Trans. A.S.M.E., p. A-22.

[2] Westinghouse Electric & Manufacturing Company, East Pittsburgh, Pa.

[3] Vice-President, Canadian Bronze Company, Ltd., Montreal, Canada.

High-Speed Tension Tests at Elevated Temperatures—II and III[1]

W. N. FINDLEY.[2] The authors have used an ingenious method of recording the stress-strain curve from a high-speed tensile impact machine, and it is interesting to note the oscillations resulting from the impact. In connection with this disturbance the writer would like to describe a high-speed testing machine which he designed to avoid the oscillations resulting from impact loading. This machine was built while the writer was a McMullen research scholar under the direction of T. R. Cuyken-

[1] By A. Nâdai and M. J. Manjoine, published in the June, 1941, issue of the JOURNAL OF APPLIED MECHANICS, Trans. A.S.M.E., vol. 62, p. A-77.

[2] Instructor in Theoretical and Applied Mechanics, College of Engineering, University of Illinois, Urbana, Ill. Jun. A.S.M.E.

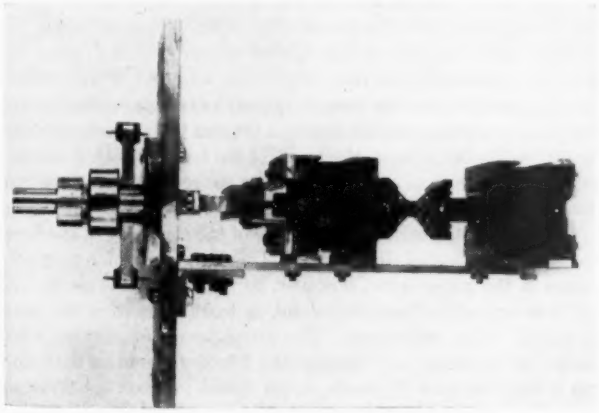


FIG. 1 CAM FOLLOWER AND ACTUATING SOLENOIDS OF HIGH-SPEED TESTING MACHINE

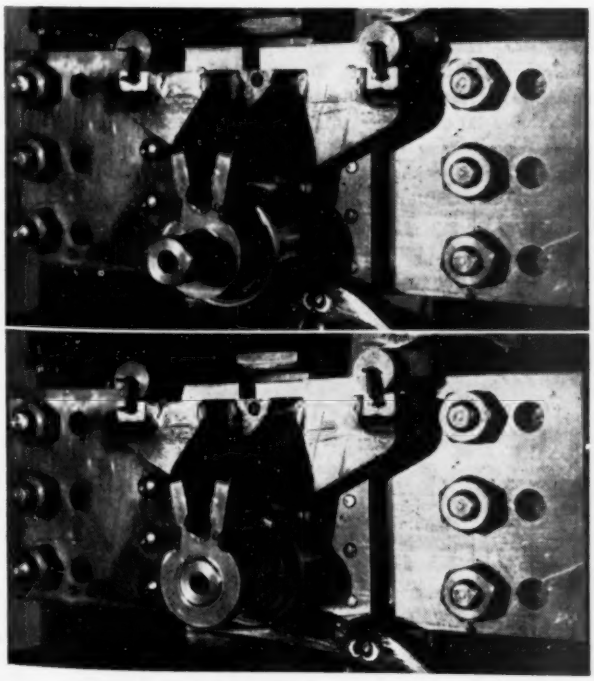


FIG. 2 LOADING HEAD OF TESTING MACHINE
(*a above*, Cam follower in running position; *b below*, cam follower in operating position.)

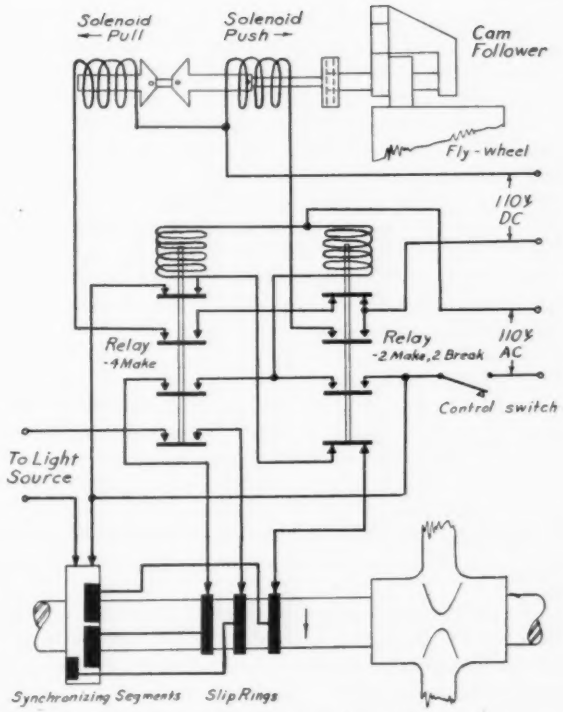


FIG. 3 SYNCHRONIZING APPARATUS

dall in the College of Engineering, Cornell University, and used in connection with a study of the photoelastic properties of Bakelite BT61893 under high-speed loading.[3] As used for this work the machine was designed to produce pure bending of a bar of the transparent material, but it could equally well be designed for tension or compression. The loading time obtained by this machine was of the same order of magnitude as that obtained by the authors. Oscillations resulting from impact or other nonuniform motion were avoided by using constant acceleration instead of constant velocity of crosshead motion.

The mechanism used to produce constant acceleration of the crosshead consisted of a plate cam, Fig. 2, mounted on the cylindrical surface of a 25-in-diam flywheel. A roller follower, Fig. 2, transmitted the motion of the cam to the specimen. The cam was formed in such a way that a constant velocity of the flywheel would produce a constant acceleration of the moving head. The cam follower consisted of a double row enclosed ball bearing which could be moved axially by two solenoids (electric magnets) Fig. 1. The outer race of the bearing was in rolling contact with the cam, Fig. 2.

The motion caused by the cam was transmitted through the roller follower and its shaft to a yoke which was fastened to the moving head of the machine. The unit consisting of the moving head, the roller follower, and its shaft was mounted in sliding ways which permitted vertical motion only.

Several revolutions of the flywheel were required to bring it up to speed. During this time the roller follower was in the outer extreme position in the yoke, Fig. 2*a*. In this position the cam passed under the follower shaft but the follower did not touch the cam. When it was desired to test the specimen the control circuit, Fig. 3, was closed, and by means of synchronizing segments and relays a solenoid was caused to pull the cam follower into

[3] "The Fundamentals of Photoelastic Stress Analysis Applied to Dynamic Stresses," by W. N. Findley, Ninth Semi-Annual Meeting of the Eastern Photoelasticity Conference, held at Cornell University, May 13, 1939; published by the College of Engineering, Cornell University, Ithaca, N. Y.

the operating position, Fig. 2*b*, and the test was performed. Immediately after the cam performed its function another solenoid pushed the cam follower back into the running position before the cam came around a second time. The horizontal motion of the follower shaft was controlled by the solenoids through a sliding finger so as not to interfere with the vertical motion of the loading head, Fig. 1. The circuit diagram, Fig. 3, shows provision for synchronizing other apparatus with the test such as a high-speed camera as in the case in which the apparatus was used.

L. H. Fry.[4] Study of this paper leads to a question as to the method used for measuring the strains in the so-called constant-strain-rate machine shown in Figs. 2 and 3 of the paper. These illustrations indicate that the strain is recorded by the rotation of the drum H which is turned by a string drive I. This string drive is shown to be attached to the heads of the testing machine and not to the test specimen itself. Under these conditions, the rotation of the drum measures the separation of the jaws of the machine, but there is no assurance that the separation of the jaws is directly proportional to the increase in the gage length of the specimen. This may be the case during plastic extension, but is almost certainly not so during the elastic stretch of the bar.

The writer has shown[5] that, during the plastic stage of a tension test with the testing-machine crosshead moving at a constant speed, the gage length of the specimen is stretched at a continually increasing rate. That is to say, the ratio of strain of specimen to crosshead travel increases rapidly until the yield point is reached. Therefore, it follows that, in the elastic range, the measurement of the crosshead travel cannot be used as a means of determining the rate of strain of the specimen.

The authors are mainly concerned with ultimate strengths, and it is probable that rate of travel of the head and rate of strain are more nearly equal at the end of the plastic stage than they are in the early period of the elastic stage. However, in all specifications of Committee A1 of the A.S.T.M. where an extensometer is used, it is required to be attached to the specimen and not to the head of the testing machine.

C. W. MacGregor.[6] This paper is particularly important since it represents a major extension of our knowledge in several directions. The range of testing speeds has been increased over those formerly reported and, at the same time, a very complete picture is given of the effects of temperature over this wide velocity range. The marked increase of the ultimate strength of copper at 1000 C of about 1000 per cent in a speed range of 10^8:1, as compared to 25 per cent at room temperature for the same increase in testing speed shows the great importance of strain velocities at elevated temperatures.

The writer is especially interested in Part III of the paper in which attempts are made to predict the shape of the necked-down tensile-test bar using various assumed stress-speed laws, such as the viscous and power function speed expressions. With certain modifications, it would appear possible also to predict the shape of the necked-down bar at room temperature. The writer would like to ask if any attempts were made to apply Ludwik's logarithmic speed law $\sigma = \sigma_0 + a \log V/V_0$, which holds at room temperature, to the problem of predicting the shape of the necked-down bar under these conditions?

[4] Railway Engineer, Edgewater Steel Company, Pittsburgh, Pa. Mem. A.S.M.E.

[5] "Speed in Tension Testing and Its Influence on Yield-Point Values," by L. H. Fry, Proceedings of the American Society for Testing Materials, vol. 40, 1940, p. 634.

[6] Associate Professor of Applied Mechanics, the Massachusetts Institute of Technology, Cambridge, Mass. Mem. A.S.M.E.

Authors' Closure

The suggestion made by Mr. Findley is appreciated. While it seems attractive when used in cases in which the displacement between the two heads of the test specimen is essentially an elastic one, it must somewhat be questioned whether the method suggested by Mr. Findley has similar advantages when used in cases in which, on the contrary, this distortion is of the plastic nature. It should be noted that the dynamic system with which Mr. Findley is concerned in his rapid photoelastic tests, made with bakelite or celluloid in the elastic range, is far simpler than the one which presents itself in the tests described by the authors. It must be remembered that in these tests the system consists of a combination in series of a very stiff elastic spring (the force-measuring bar) and of a plastic system, namely, the test bar. In the first case, the resistance is known to be proportional to its own extension. However, the inner resistance in the test bar is not only unknown, but it is known to depend at low temperatures both on the strain and the rate of plastic strain, and at high temperatures on the rate of plastic strain. Since this latter is admittedly the most important variable, it was deemed advantageous to run our tests so that in a first approximation this variable was kept constant during a tension test. In other words, it was preferable to move the heads of the test bar with a constant velocity rather than, as Mr. Findley suggests, with a constant acceleration. Admittedly, this procedure had the disadvantage of exciting elastic oscillations because of the elasticity of the force-measuring bar and of the test bar. The diagrams which were published in the paper seem, however, to prove that the oscillations did not seriously affect the results, at least not within the limits of speeds which were used. The consequence of running a test under the condition specified by Mr. Findley would be that, during a test, the rate of plastic strain would increase continuously with the time or with the extension of the test piece.

While it is believed that the simple string device to which Mr. Fry refers was sufficiently accurate for recording plastic strains, its use is considered objectionable when exact records of small strains of the order of magnitude of the elastic strains are to be observed. For the intended comparison of the plastic rates of stretching at large strains, however, this primitive method for measuring strains is entirely satisfactory. It must be noted that an error of 20 or 30 per cent in the strain rate would shift the curve representing the speed law in the semilogarithmic plots (such as the ones shown in Figs. 9 to 11, 13, and 15 of the paper) by an insignificant amount considering the enormous range of the speeds.[7]

Since Mr. Fry brought up this point in his discussion, it is perhaps in order to add one or two remarks concerning what has been called in the paper "a constant-strain-rate test." If the length l between the shoulders of a test bar increases uniformly with time t, the true rate of straining within the cylindrical length l

$$\frac{d\bar{\epsilon}}{dt} = \frac{1}{l}\cdot\frac{dl}{dt} = \frac{d}{dt}\log_e\frac{l}{l_0} = \frac{d}{dt}\log_e(1+\epsilon) = \frac{1}{(1+\epsilon)}\cdot\frac{d\epsilon}{dt}$$

must decrease if dl/dt = constant in the same proportion as l increases. However, the curve for the speed law is changed to a very minor degree when instead of $d\bar{\epsilon}/dt$, $d\epsilon/dt$ is maintained constant during the tests.

[7] By measuring the changes in length by various independent methods, it was ascertained that errors in the strain measurements were of the order of 1 to 2 per cent. Since the string device records the relative displacement between the reinforced portions beyond the shoulders of the specimens for obtaining the value of the strain ϵ in the cylindrical portion of the test bar, a correction factor had to be introduced which was found by calibration for each of the investigated metals.

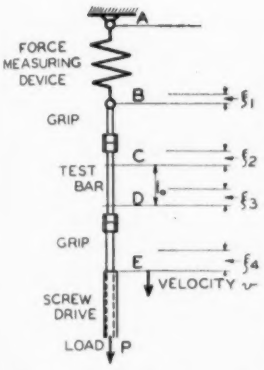


FIG. 4 TENSION MACHINE

With reference to Fig. 4 of this closure, which is a sketch of a mechanism for pulling a test bar, we wish to investigate the relation connecting the strain rate $d\epsilon/dt$ as measured in the gage length l_0 of the cylindrical test bar and the velocity v with which the lower head of the machine moves. The mechanism of a screw-driven tension machine was assumed, similar to the one described in the paper (Figs. 2 and 3), AB representing the force-measuring device, BC the upper grips, including the head of the test bar, CD the cylindrical portion of the test bar, and DE the lower grips. Assuming that the displacements of the points A, B, C, D, and E are 0, ξ_1, ξ_2, ξ_3, and ξ_4, respectively, we have for the increases of the lengths[a] the following:

In the force-measuring device (Fig. 5).....	$\xi_1 = g_1(P)$
In the upper grip.....	$\xi_2 - \xi_1 = g_2(P)$
In the gage length.....	$\xi_3 - \xi_2 = G(P)$
In the lower grip.....	$\xi_4 - \xi_3 = g_3(P)$
For the motion of the lower head.....	$\xi_4 = vt$

where the expression $g(P)$ designates functions of the load P, and t is the time. By adding these equations we obtain

$$vt = g_1(P) + g_2(P) + g_3(P) + G(P) \quad [1]$$

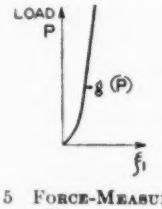


FIG. 5 FORCE-MEASURING DEVICE

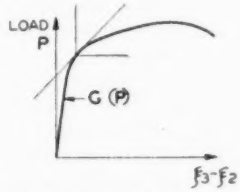


FIG. 6 STRESS-STRAIN CURVE

Since the strain is defined by

$$\epsilon = \frac{\xi_3 - \xi_2}{l_0} = \frac{G(P)}{l_0} \quad [2]$$

where $G(P)$ represents the conventional stress-strain diagram (Fig. 6 of this closure) of the material of the test bar, we have for the rate of strain

$$\frac{d\epsilon}{dt} = \frac{1}{l_0} \cdot \frac{dG}{dP} \cdot \frac{dP}{dt} \quad [3]$$

which equation connects the strain rate $d\epsilon/dt$ with the rate of loading dP/dt. Expression $dG/dP = G'(P)$ represents the slope of the stress-stain curve, Fig. 6. After differentiating Equation [1] with respect to the time t, and after eliminating dP/dt, we find that

$$\frac{d\epsilon}{dt} = \frac{v}{l_0} \cdot \frac{1}{\left[1 + \dfrac{(g_1' + g_2' = g_3')}{G'}\right]} \quad [4]$$

From this expression, the rate of strain $d\epsilon/dt$ can be computed for a given velocity v of the lower head of the testing machine provided sufficient observations were made for obtaining the values of the three functions g_1', g_2', and g_3'. Equation [4] is valid for uniform stretching, but not for discontinuous yielding, since in this latter case ϵ is not completely defined by means of Equation [3]. The g' terms are the derivatives dg/dP, i.e., the slopes in the curves $\xi_n - \xi_{n-1} = g_n(P)$. Some care should be exercised in their evaluation in the case when slipping occurs in the wedges or in the grips.

We can conclude from Equation [4] that while the looseness in the grips is gradually taken up under small loads the rate of strain $d\epsilon/dt$ cannot yet remain constant at a head velocity v = constant. The same is true due to slipping of the wedges or when gradually an elastic contact is established in the grips. However, in a machine with a strictly linear and stiff characteristic, such as the one described in the paper we have g_1' = constant. After the grips have become tight $d\epsilon/dt$ soon tends to become a constant, while the head of the machine moves with a constant velocity v. In other words, this device can well serve for running a constant-strain-rate test with a rate of stretching which for the larger strains is proportional to the velocity v of the head.

Dr. MacGregor mentions the possibility of further practical applications of the theory of the necking of bars to cases frequently observed. The few examples treated in the paper were selected with a view to describing simultaneous stretching and contracting of bars having variable cross sections, under the simplest assumption which could be made, namely, that stress would depend only upon the rate of strain. At low temperatures (room temperatures), it is not yet clear whether such a dependence would be sufficient for describing the necking in bars, since, at low temperatures, stress is a function of the plastic strain and of the rate of strain, which fact probably complicates the analysis further.

[a] The authors are indebted to P. G. McVetty for having called attention to the fact that the late Prof. T. Hammond Smith had separated the relative motions in the moving parts of a testing machine in a similar manner by plotting the ξ_1, ξ_2 . . . . in function of the time t; refer to "The Rate of Elongation in Tension Tests," by T. H. Smith, Proceedings of the American Society for Testing Materials, vol. 27, 1927, pp. 507–519.

Note on Calculation of Influence Surfaces in Plates by Use of Difference Equations[1]

V. P. JENSEN.[2] The author's theorem is a definite contribution to the literature on the engineering uses of difference equations. It materially extends the field of practical application of difference equations by making possible a rapid determination of the effect of moving loads on a slab.

The writer has applied the theorem to the problem of determining live-load moments at various points on skew-slab highway bridges with curbs.[3] Truck-wheel loads and spacings for the design of such bridges are specified by the American Association of State Highway Officials.[4] Since the positions of the wheel loads on the bridge will not coincide with the nodal points of the network used in the analysis, the advantages of an influence surface become apparent.

As an illustration of the practical application of the theorem, consider the bridge, shown in Fig. 1 of this discussion. A convenient network for the analysis of this bridge is shown in Fig. 2. The equation for the bending moment in the curb at point 4 is

$$(M_{curb})_4 = \frac{EI}{\lambda^2} (2w_4 - w_2 - w_7)$$

[1] By N. M. Newmark, published in the June, 1941, issue of the JOURNAL OF APPLIED MECHANICS, Trans. A.S.M.E., vol. 63, p. A-92.

[2] Special Research Assistant Professor of Theoretical and Applied Mechanics, University of Illinois, Urbana, Ill.

[3] "Analyses of Skew Slabs," by Vernon P. Jensen, Bulletin 332, University of Illinois Engineering Experiment Station, 1941.

[4] "Specifications for the Design of Highway Bridges," American Association of State Highway Officials, 1935.

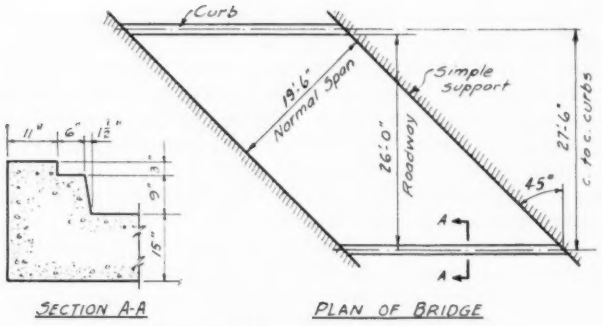


FIG. 1 SKEW-SLAB-BRIDGE DETAILS

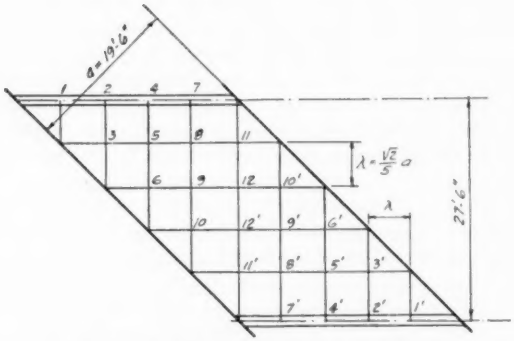


FIG. 2 NETWORK FOR ANALYSIS

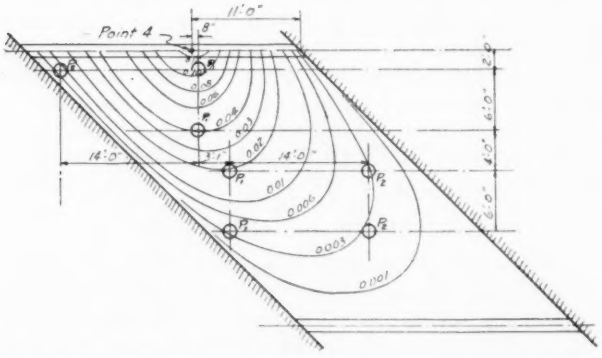


FIG. 3 INFLUENCE SURFACE FOR MOMENT IN CURB AT POINT 4

wherein EI designates the "stiffness" of the curb, λ is the distance between successive points of the network, and w designates deflection. By Newmark's theorem the influence surface for moment at point 4 will, therefore, be given by the deflection of the slab due to loads

$$P_4 = \frac{2EI}{\lambda^2} \qquad P_2 = P_7 = -\frac{EI}{\lambda^2}$$

Determination of the deflection of the slab loaded in this manner yields an influence ordinate at each point of the network.[3] Contours of the influence surface having these ordinates are shown in Fig. 3.

With the influence surface known, it becomes possible to determine the effect of truck-wheel loads for various positions on the lanes of traffic. Because the distances of the traffic lanes from the curb are specified, it is a simple matter to determine graphically the maximum moment in the curb due to each set of truck-wheel loads. The final position of the loads for maximum moment in the curb is shown in Fig. 3, when the rear-wheel loads P_1 are 4 times as great as the front-wheel loads P_2.

The Effect of Foundation Stiffness on the Resonant Frequencies of Rotating Machines[1]

T. C. RATHBONE.[2] The status of the vibration problem as affected by foundations is still far from satisfactory, hence this paper, describing a somewhat different method of attack, is a most welcome contribution. It is evident from the author's results that a great amount of valuable information can be obtained readily and simply by means of nonrotating prototypes.

In addition to those mentioned in the paper, some practical observations occur to the writer, which are offered as supplementary to the text, having to do principally with disparities of a secondary nature between the nonrotating model and the actual installation.

The transit of nodes in the "rotor" across the "bearings" with varying speeds, as so well illustrated in the diagrams, has amply been borne out by actual experience on large installations. No better exposure of the futility of attempting field balancing by the "horse-and-buggy" method of scribing the shaft to locate the balance correction could be asked for. Obviously, the scribed "high spot" will practically reverse itself as the node passes from one side of the scribed location (usually between the bearing and the gland or end-bell) to the other, with no change in the initial unbalance. Quite recently, the writer was assured that a turbine, still obviously vibrating badly, had been satisfactorily balanced, because the scribed mark showed all around the shaft! A node probably occurred at the scribed location.

Phase relationships have an additional meaning with the rotor actually rotating. Directional characteristics are absent with the linearly vibrating nonrotating member; the point on the generating circle for the harmonic motion in the vertical plane can be considered as rotating in either direction, while on the actual machine, the exciting forces together with the indexes are rotating in a fixed direction. On large units, the vibration characteristics can exhibit considerable differences between clockwise and counterclockwise rotation. This sounds paradoxical, but is inherently true.

The difference is brought about by the intercommunication of vibratory disturbances from one bearing to another through the foundation and stationary parts and by the time lag which depends upon the velocity of sound (impulse transmission) through the structure, during which lag the high-speed rotor can turn through a considerable angle. For example, with a modern, large 3600-rpm unit, having a distance of, say, 45 ft between the No. 1 and the outboard bearing, the rotor will turn through about 60 deg before a disturbance emanating from one bearing reaches the other. As the vibration at each bearing is a composite of the disturbances coming from the entire unit, the vector additions will give different resultants for the two directions of rotation. By the same token, if the assumed concentrated unbalance at one end of the rotor leads that of the other end by 90 deg, the vibration of the unit will not be the same as when it lags 90 deg.[3]

Another seeming paradox appears when exploring the relation between the phase of the bearing vibration, as referred to a datum on the rotor, and the speed. On actual tests on a large rotor, contrary to the expected shift from zero to 180 deg, the angle changed through over 700 deg, nearly two complete rota-

[1] By E. H. Hull, published in the September, 1941, issue of the JOURNAL OF APPLIED MECHANICS, Trans. A.S.M.E., vol. 62, p. A-121.

[2] Chief Engineer, Turbine and Machinery Division, The Fidelity and Casualty Company of New York, New York, N. Y. Mem. A.S.M.E.

[3] For experimental development, refer to "Turbine Vibration and Balancing," by T. C. Rathbone, Trans. A.S.M.E., vol. 51, 1929, paper APM-51-23, pp. 272–273.

tions, between rest and about 1900 rpm, and at a fairly uniform rate. This observation was made on the bearing, not on the shaft. Parallel data obtained on the shaft would furnish the relative motion between bearing and shaft by vectorial subtraction.[4]

The influence of the mat and ambient soil may introduce another variant from the prototype that may warrant recognition. Professor Bernhard has shown the effect of the vibrating mass of soil on the over-all dynamic characteristics of the installation.[5] Earth vibration from 1800-rpm turbines at a distance of several hundred feet has been observed and measured. In such cases, the mass and elasticity of the probably damp soil might have considerable influence. K. H. Larkin[6] gives data on the natural frequencies of soils in connection with Diesel-engine foundations, which indicate that the frequency increases as the unit loading decreases, and proposes that resonances with engine impulses can be avoided by selecting appropriate bearing area for the base.

Even though the nonrotating prototypes cannot duplicate all the full-size rotating characteristics, the informative data already obtained by the author in such a simple and inexpensive manner warrants extending this work to embrace a third system, representing the mat and its elastic support, and also the two-rotor three-bearing system with solid coupling.

H. D. Taylor.[7] This paper should be of special interest to all persons concerned with the mechanical operation of high-speed machinery, particularly turbine-generators. It indicates definitely that resonant speeds, at which unbalances may produce peaks of vibration, depend quite as much upon foundation stiffness as upon the conventional critical speeds of the rotor, calculated on the usual tacit assumption of rigid support at the bearings. A uniform shaft has the familiar series of critical speeds, for 1-, 2-, 3-, and 4-loop forms of vibration, in the ratio of 1, 4, 9, 16, as closely approximated in the tests reported in the paper, and shown in Figs. 4 and 5. A turbine-generator-type rotor, however, indicates relative speeds of about 1.0, 2.9, 6.4, 8.7, as illustrated in Fig. 16. The difference is due to the stepped diameters of the generator-type rotor, as shown in Fig. 14 of the paper. This type of rotor, assembled with its heavy stator, and mounted on a foundation of appreciable flexibility (i.e., any practical foundation for a large machine), will have all of its "criticals" depressed appreciably, the higher orders probably more, relatively, than the lower ones, as shown in Fig. 15 of the paper. In the examples tabulated by the author, the resonant speeds may be expressed as ratios based upon the fundamental critical speed of 2400, as follows:

Form	Rigid foundation	Elastic foundation — Vertical	Elastic foundation — Horizontal
1 loop	1.00	0.634	0.208
2 loops	2.94	1.087	0.337
3 loops	6.41	1.117	1.063
4 loops	8.74	3.00	3.00

In Figs. 15 and 16 of the paper, it is not quite clear that series B is derived from the basic form 3; that is, curve B approaches and merges with form 3 as the foundation stiffness is increased. Likewise, series D is derived from basic form 4. These relationships were shown in Fig. 7, as an extrapolation of the observations on a uniform shaft, but they apply definitely to the generator-type rotor also. They may be shown in another manner, perhaps more readily grasped, by plotting the test curves against foundation flexibility rather than stiffness. This permits the curves to start with zero flexibility which, of course, cannot be included in the present diagrams because it corresponds to infinite stiffness. The curves, in effect, would be reversed. The depression of all the criticals with increasing flexibility of the foundation can be shown clearly, starting from the familiar values as calculated for a rigid foundation.

The information given in this paper should be of material value in the development of the technique of refining the balance of turbine-generators and other high-speed machinery. In this connection, however, the writer would like to propose an amendment to the author's statement that "in most actual systems, all forms of resonance are excited by a single force, irrespective of position." This does apply to the type of laboratory test setup employed, having very little damping and being therefore very sensitive to properly tuned frequencies. However in work with rotating equipment, it has been the writer's experience that the arrangement or distribution of unbalances has a major effect on the roughness encountered at the various resonant speeds. "Static" unbalance brings out primarily the fundamental 1-loop form, and also in many cases the 3-loop form, but not the 2-loop or 4-loop forms; whereas, "dynamic unbalance," or a "couple," produces 2-loop or 4-loop vibration, but not the 1-loop or 3-loop varieties. These statements are based upon work with rotors which are symmetrical along their length, and may not hold for seriously unsymmetrical cases.

Referring again to Fig. 15, curve D indicates a resonance at 7200 vibrations per min which speed was almost constant, for the particular combination of rotor and stator, over a wide range of foundation stiffness. It might be expected that, if an actual 3600-rpm generator were built to the same proportions, it would be likely to get into trouble from the twice-per-revolution gravity deflection of the rotor. However, the gravity deflection is essentially a 1-loop phenomenon, like static unbalance, except for the double frequency; and the form of vibration required for this 7200-vibrations-per-min resonance is a 2-loop pattern (as shown at point 18 of Fig. 16) which should be responsive only to "dynamic" or couple-type stimulation. Therefore, it seems to the writer that this disturbance would not ordinarily appear. Such trouble might be encountered, however, if the rotor-deflection curve happened to be considerably unsymmetrical along its length, or if the machine proportions were such that either the 1-loop or 3-loop type of resonance, shown as series B and E in Fig. 15 (actually depressed 3-loop and 5-loop criticals), should happen to come at 7200 vibrations per minute.

The existence of a large number of resonant speeds or depressed "criticals," within the running range of high-speed turbine-generators has been perhaps not generally recognized, and might be viewed with some alarm. There should be no great concern about this, however, as it is common experience that refined balancing by modern methods takes care of them. In general, balancing work can be expedited if the resonant characteristics of the setup are understood. Here, it is believed, the author has made a significant contribution to the art.

Author's Closure

The author is indebted to Mr. Rathbone for adding his observations on full-scale machines, which confirm and enlarge the model data. There are of course many effects due to rotation which cannot be shown with a nonrotating model.

When we can work again on this project, there are several phases which can be studied by means of nonrotating models, such as, foundation mats and three-bearing sets, as suggested by Mr. Rathbone, as well as the effect of elastically supported stators in two-pole generators, on which some model work has already been done.

[4] Footnote[3], Figs. 10 and 26.

[5] "Geophysical Study of Soil Mechanics," by R. K. Bernhard, A.I.M.E. Technical Publication No. 834, 1938.

[6] "Design of Diesel Engine Foundations," by K. H. Larkin, presented at Semi-Annual Meeting, Kansas City, Mo., June 16–19, 1941, of The American Society of Mechanical Engineers.

[7] General Electric Company, Schenectady, N. Y.

Mr. Taylor has contributed several valuable ideas in his discussion, in addition to those made previously during the course of this work.

As Mr. Taylor indicates, series B has not taken on form 3 within the stiffness range of these experiments. As the foundation becomes more rigid, series B approaches form 3 by bringing the two nodes inside the bearings closer together. At the same time, a node appears outside each bearing, which progresses inward, arriving at the bearings when the foundation is rigid, giving form 3. The latter behavior is seen in series C.

It would be instructive to plot these model data as a function of flexibility rather than stiffness. Stiffness was used from selfish motives, the author having visualized the phenomena in that way.

Book Reviews

Mechanics Applied to Vibrations and Balancing

MECHANICS APPLIED TO VIBRATIONS AND BALANCING. By D. Laugharne Thornton. John Wiley & Sons, Inc., New York, N. Y., 1940. Cloth, 9¾ × 6 in., xii and 529 pp., 180 figs., $7.50.

REVIEWED BY J. ORMONDROYD[1]

BOOKS on mechanical vibrations have become numerous enough so that a newcomer in the field is eyed very critically. The content of this book and its treatment differ sufficiently from the content and treatment in other books on the same subject to justify its appearance.

The book gives an account of vibration theory and its applications which would appear to be practical to a mathematical physicist. It probably will seem rather mathematical and "theoretical" to the practicing engineer. The mathematics used is, of course, no more difficult or abstruse than that which must necessarily appear in any good work on the subject—but the physical introduction to the equations is curt and abbreviated—after the fashion of publishing physicists who assume they are speaking to their peers. To one already skilled in the art of vibration analysis, the work will be useful and stimulating. To a novice in the field it will not be so helpful. The very points over which the struggling engineer would stumble and hesitate are passed over by the author with a mere wave of the hand and the inevitable "it can readily be seen." Although the book is learned, it is not systematic enough in treatment and, in many respects, it is too superficial to be used by an engineer who lacks extensive training or interest in physics and mathematics.

To those who have already struggled successfully through the fundamental, elementary aspects of the subject the book has much to offer. Although practically all the problems treated can be found scattered through many existing treatises and papers, the combination put together by the author is somewhat unique. Chapters 1 and 2 give a more complete graphical and analytical treatment of reciprocating engine balancing than can usually be found in one place. Chapter 4 on the propagation of stress in elastic materials gathers together material which is of extreme practical interest to engineers today. Impactive or explosive loadings in metals, concrete, fluids, and air are coming more and more to the attention of design engineers. This chapter gives the concepts and procedures necessary for intelligent treatment of problems of this nature. Chapter 6 on rotating shafts and disks goes into the dynamics of these widely used elements of machinery more fundamentally and extensively than most treatments of this subject. Chapter 3 on the theory of vibrations besides giving the usual elementary and more sophisticated development of the subject contains three interesting sections on the vibrations of structural frames and buildings—a subject too much neglected by civil engineers, considering its practical importance.

The author illustrates the application of all the theory treated by means of numerous worked examples of a practical nature. In these examples he shows a knowledge of real problems in widely diversified fields. The book is primarily a practical treatise written from the outlook and background of a mathematical physicist. If the treatment causes bewilderment to the engineer, it is to be charged against his academic training and interests rather than against the author. Present-day trends in purely technical fields are such that physicists with mathematical training may soon displace engineers with the usual training in all the fields where really interesting and important developments are taking place. "Statics" has become the humble servant—"dynamics" has mounted the throne.

"Mechanics Applied to Vibrations and Balancing" is a book which has significance because of this fact.

[1] Professor of Engineering Mechanics, University of Michigan, Ann Arbor, Mich. Mem. A.S.M.E.

Kinetic Theory of Gases

AN INTRODUCTION TO THE KINETIC THEORY OF GASES. By Sir James Jeans. Cambridge University Press, London, England; The Macmillan Company, New York, N. Y., 1940. Cloth, 5½ × 8½ in., 311 pages, $3.50.

REVIEWED BY JOSEPH HENRY KEENAN[2]

IN his preface the author sets forth his purpose as follows: "I have intended that the present book shall provide such knowledge of the Kinetic Theory as is required by the average serious student of physics and physical chemistry. . . . . the book covers a good deal of the same ground as my earlier book, 'The Dynamical Theory of Gases' but it is covered in a simpler and more physical manner. Primarily, I have kept before me the physicist's need for clearness and directness of treatment rather than the mathematician's need for rigorous general proofs."

When one reads a classic work of rigor like "The Dynamical Theory of Gases," one is inclined to speculate whether the author ever thinks in terms of examples that are concrete, though crude, and graphic, though approximate. Here is evidence that at least one such author can match the most pictorial-minded in the explanation of complex concepts.

Any engineer with a little analytical experience will be able to follow most of the arguments. In the earlier chapters the reader finds himself taken by the hand and led by slow steps to those slight eminences from which some of the vistas of Kinetic Theory begin to unfold. Later the going becomes heavier, but nothing in this little book of 300 pages should be too formidable to one versed in mechanics.

There is frequent reference to thermodynamics in these pages, but there is no exposition of the principles of thermodynamics.

[2] Professor of Mechanical Engineering, Massachusetts Institute of Technology, Cambridge, Mass. Mem. A.S.M.E.

On at least one occasion the thermodynamic treatment is inadequate. The reader should bring his own thermodynamics and not expect to find it provided for him.

There are simple and readable explanations of the experimental verification of Maxwell's Law of Distribution, of the reasons why viscosity is independent of density (and when it is not), of Brownian movements, the relation between electrical and thermal conductivity, the distinction between liquid and vapor phases, and many other things.

It is not popular science; it is good science in a form that should appeal to the engineer.

Relaxation Methods in Engineering Science

RELAXATION METHODS IN ENGINEERING SCIENCE—A Treatise on Approximate Compution. By R. V. Southwell. Oxford University Press, New York, N. Y., 1940. Cloth 6 × 9½ in., vi plus 252 pp., $6.

REVIEWED BY HARDY CROSS[3]

THE author of this book, who is professor of engineering science at Oxford, has brought together work done during the last five years by himself and others in England. Of the twelve chapters, four deal with stress analysis in frames, five with vibrations and buckling, the others with miscellaneous problems including flow in distribution systems and adjustment of errors in surveys. The methods used are those of successive approximation, which are here called "relaxation methods."

For more than a decade there has been much interest in this country in methods of successive approximation—"methods of convergence," "iteration," "distribution procedures." Some books, various papers, and many important unpublished theses, memoranda, and lectures have treated the problems included in this book and have extended the study to other problems not here treated. Much of this American work has apparently not come to the attention of the author.

The term "relaxation" originates from the physical concept of step-by-step relief of artificial restraints imagined for purposes of analysis to restrict deformation of structural frames; general use of the term does not, however, seem especially apt. Various specialized terms appear throughout the book—"liquidation" of restraints, "block relaxation," "unit problem," "gyrostatic systems." The author brushes aside much terminology, methodology, and symbolism that has obscured the palm in "classical" mechanics. Scholarly chariots usually stir up a good deal of dust on the road to knowledge; by comparison, the author's material is relatively unclouded by complications. Most of the solutions are, as the title indicates, those of "engineering science" rather than of engineering, so far as this distinction has validity. Thus in continuous frames, the problem, as here treated, is to find the stresses rather than to discuss the dependability or importance of these as elements in stability.

The subtitle of the book seems somewhat misleading; this is not a general treatise on methods of successive approximation nor should methods of successive approximation be confused with approximate methods. American students will find interest in this contribution to what the author calls the "new mathematics," which makes it easier for the engineer to "take account of the unavoidable uncertainty of physical data." Methods of successive approximation are not "new," but methods of direct solution without symbolism are very powerful for the engineer, as this scholar explains.

[3] Professor of Civil Engineering, Yale University. New Haven, Conn.

Strength of Materials

STRENGTH OF MATERIALS. By S. Timoshenko. Second Edition. D. Van Nostrand Company, Inc., New York, N. Y., 1941. Cloth, 6 × 9 in., Part I. Elementary Theory and Problems. vii and 359 pp., figs., $4.50. Part II. Advanced Theory and Problems, xiii and 510 pp., figs., $4.50.

REVIEWED BY C. RICHARD SODERBERG[4]

THE appearance of a new edition of the two volumes of "Strength of Materials" by Professor Timoshenko is welcomed warmly by many engineers and teachers, who have become accustomed to look to this treatise for the solution of many important strength problems.

Although the scope of the new edition follows very closely that of the first, which appeared 11 years ago, there have been many changes, all of them enhancing the utility of the volumes for teaching purposes. The first volume has been rearranged to include less material of an advanced nature, which has in turn permitted the expansion of certain chapters. Chapter 2, covering the analysis of stress and strain, has been rewritten, and chapter 8, covering combined bending and tension, now contains a valuable introductory discussion of column theory.

In the second volume the principal changes occur in chapters 3, 8, and 9. Chapter 3 presents a treatment of thin plates and shells, which within the limited space allotted succeeds in giving a remarkably complete discussion of this important subject. Chapter 7, covering deformations beyond the elastic limit, gives a much more extensive treatment of this subject than that of the first edition. Chapter 9, on mechanical properties of materials, is much expanded, giving a considerable amount of an experimental nature which has become available since the publication of the first edition. Both volumes contain a large number of problems and practical applications which bear testimony to the author's wide experience.

The new edition has lost nothing of Professor Timoshenko's lucid style and clear reasoning, so familiar to those of us who have had the privilege of working with him. It seems presumptuous to advance even minor criticisms to a work of such outstanding merit, but certain aspects of the first edition which have not been fully corrected in the second edition seem worthy of note.

The analysis of stress and strain at a point, while adequate for the first volume, seems too brief and sketchy for much of the material of the second volume. This is certainly true when the book is used as reference in a more advanced course on strength of materials. The tensor nature of stress and strain is a fact worthy of attention, at least to those who expect to follow the studies of the subject into the more general theory of elasticity. A modest expansion of this point would also serve to lay a firmer basis for the subsequent treatment of yielding, particularly with reference to creep. The conventions which serve as a basis for Mohr's circle are not much clearer than those of the first edition, which in the past has been one of the objections to this part of the book.

The considerable extent to which the strain-energy method is used in the second volume would seem to justify a fuller treatment of the foundation upon which the basic theorems are based than that presented in chapter 10 of the first volume. The conventional proof of the theorem of Castigliano is not convincing, and usually leads to a stereotyped form of application which obscures the real possibilities of the strain-energy method. In fairness it should be conceded, however, that very few treatises do more with this subject than what is presented here.

While chapters 8 and 9 of the second volume, on deformations

[4] Professor of Applied Mechanics, Massachusetts Institute of Technology, Cambridge, Mass. Mem. A.S.M.E.

beyond the elastic limit and mechanical properties of materials, give an excellent summary of the subject, its treatment of plastic flow and creep could justify some extension. In the modern power industry creep plays a very important role, and a great deal of confusion exists with regard to the possibility of predicting flow under two- or three-dimensional stress from the information obtained through tensile tests. A book of this kind could perform a very useful service in clarifying these phenomena, on which a great deal of information is now available. Creep of boiler tubes, as an example, seems to the reviewer to be a far more important subject than the results which are presented for plastic deformations above the yield strength at room temperature.

The reviewer hastens to add that these points, some of which may be regarded as matters of taste, do not detract from the outstanding merit of "Strength of Materials." It will continue to remain a standard reference and textbook for a long time to come.

Statistical Mechanics

STATISTICAL MECHANICS. By Joseph Edward Mayer and Maria Goeppert Mayer. John Wiley & Sons, Inc., 1940. Cloth, 6 × 9¼ in., xi and 495 pp., illustrations, $5.50.

REVIEWED BY JOHN A. GOFF[5]

As van der Waals so clearly pointed out, the laws of thermodynamics themselves lead only to a series of identical relations between mechanical properties such as pressure, volume, temperature, and composition on the one hand, and calorimetric properties such as internal energy, entropy, and so on, on the other. The very fact that these relations enjoy the most general validity means that they are incapable of giving specific information regarding any particular substance. Hence it is absolutely necessary to implement the laws of thermodynamics in some way or other if they are to be given practical usefulness.

The perfect gas laws represent the earliest implementation of the laws of thermodynamics. While these laws were suggested by the experimental findings of Boyle, Charles, Gay-Lussac, and Regnault, nevertheless, subsequent more refined measurements have shown them to be strictly applicable to no known substance. They must, therefore, be regarded as purely hypothetical however useful they may be as such. In the development of our present accurate and comprehensive body of knowledge regarding the thermodynamic properties of water, all temptations to hypothesize were scrupulously avoided and direct experimental data insisted upon. But even in steam research, it soon appeared that the accuracy of and confidence in the final formulation could be greatly enhanced by utilizing the predictions of modern statistical mechanics based upon quantum mechanical interpretation of the spectrum of the water molecule.

Thus, within comparatively recent times, the science of statistical mechanics has been developed into a powerful method of implementing thermodynamics. For example, its quantitative predictions regarding the zero-pressure properties of gases are now generally regarded as more accurate and trustworthy than values inferred from direct calorimetric measurements. Moreover, its qualitative predictions form an invaluable guide to thermodynamic research and have greatly enhanced our understanding of the fundamental concepts of thermodynamics and their limitations. The result has been to make of what was formerly regarded as the plaything of the physicist an effective tool for the engineer. Obviously, therefore, it has become important for the engineer to comprehend the fundamentals of statistical mechanics in order that he may judge for himself the accuracy of its predictions. The present book must be regarded as one of the most significant aids toward this comprehension which has yet appeared.

The aim of the book, according to the authors, is to present the subject in as simple a manner as possible without sacrifice of rigor. Care has been taken to make the book suitable for reference by summarizing and tabulating final equations and making individual chapters complete in themselves. Written primarily for graduate students in physics, its scope and practical treatment will appeal to the engineer also.

The first chapter gives an illustration of the possibility of statistical methods by reviewing its application to the perfect monatomic gas in which the only mode of motion is that of translation. The concept of mean free path is introduced and its use in the treatment of transport phenomena, viscosity, heat conduction, and diffusion is briefly sketched. No fundamental assumptions except the validity of the laws of mechanics are introduced.

Chapter 2 is entitled, "Mechanical and Quantum-Mechanical Preliminaries." It describes the use of generalized co-ordinates in terms of which the Heisenberg Uncertainty Principle, the concept of quantum states, and the law of equal probability of single states find their most general expressions. The differential equation defining the wave function is written down and, by application to such simple systems as a point particle moving in field-free space, the harmonic oscillator, and the symmetrical top, it is shown how this function predicts discrete energy levels. Perhaps an important defect of this chapter is its failure to emphasize the postulatory character of the wave equation. The prediction of discrete energy levels is so startling to a reader not too easily converted from the classical point of view that he must leave the chapter with a feeling of skepticism.

In chapter 4 are derived the laws of thermodynamics with a discussion of their limits of validity. Special interest attaches to the discussion of the so-called Third Law of thermodynamics. It is pointed out that the general statement of the law has no great value to the experimental thermodynamist; for, though it is highly probable that it is true, nevertheless so many anomalies may occur in the range of inaccessibly low temperatures that no general directions for its application in purely experimental terms can be given. Still, confirmation of the law has been indicated in many cases where such anomalies either do not occur or can be delineated by the expert in quantum mechanics. Hence, the value of the law in illuminating the region of very low temperatures and thereby clearing away many misconceptions of classical thermodynamics must not be underestimated.

In subsequent chapters, it is shown how the equations for the energy levels of monatomic, diatomic, and polyatomic perfect gases can be used in interpreting spectra to obtain the necessary data for the calculation of thermodynamic properties of actual gases at zero-pressure. In chapter 13 is given an account of present progress toward predictions of the properties at finite pressures where an analysis of the effect of intermolecular forces must be made. No account seems to be given of the theory of gas mixtures, a subject of increasing practical importance in which confusion is rife and the need for help from statistical mechanics is especially urgent.

Space, and other obvious considerations, will not permit enumeration of all of the applications treated; suffice it to say that the book gives remarkably wide coverage. It is believed that the book will find favor with the physicist who has need of a reliable reference to aid in making practical use of the theory and with the engineer who wishes an insight into the fundamental theory and some comprehension of the nature and scope of its predictions.

[5] Dean, Towne Scientific School, University of Pennsylvania, Philadelphia, Pa. Mem. A.S.M.E.

von Kármán Anniversary Volume

THEODORE VON KÁRMÁN ANNIVERSARY VOLUME. Contribution to Applied Mechanics and Related Subjects. By the Friends of Theodore von Kármán on His Sixtieth Birthday. California Institute of Technology, Pasadena, Calif., May 11, 1941, 8½ × 11 in., xv and 337 pp., $3.75.

REVIEWED BY ALBERT E. HEINS[6]

ON the sixtieth birthday of Theodore von Kármán, twenty-three scholars in the United States and Canada, who are former pupils or friends of his, have dedicated an anniversary volume to him. Because of the present world crisis, scholars abroad have been prevented from contributing to this volume. The name von Kármán needs no introduction to the engineer, applied mathematician, or physicist. Clark Millikan, the editor of this volume, has summed up adequately in the foreword the many accomplishments of von Kármán in the fields of elasticity, hydrodynamics, aerodynamics, and applied mathematics. The central theme of this volume is mechanics, and it is particularly appropriate since von Kármán has made so many fundamental contributions to the various phases of mechanics. In addition to the twenty-three scientific papers, there is a short biography of Theodore von Kármán and a bibliography of his papers. From the table of contents:

H. Bateman: "Some Definite Integrals in Aerodynamics"
Max M. Munk: "On the Geometry of Streamlining"
J. C. Hunsaker: "Dimensional Analysis and Similitude in Mechanics"
Th. Thedorsen: "Impulse and Momentum in an Infinite Fluid"
Boris Bakhmeteff: "Coriolis and the Energy Principle in Hydraulics"
H. U. Sverdrup: "The Influence of Bottom Topography on Ocean Currents"
W. F. Durand: "Ionization as a Factor in Fluid Mechanics"
Hugh L. Dryden: "Isotropic Turbulence in Theory and Experiment"
J. L. Synge and W. Z. Chien: "The Intrinsic Theory of Elastic Shells and Plates"
Francis D. Murnaghan: "The Compressibility of Solids Under Extreme Pressures"
F. Zwicky: "Hydrodynamics and Structure of Stellar System"
H. M. Westergaard: "On the Elastic Distortion of a Cylindrical Hole by a Localized Hydrostatic Pressure"
Paul S. Epstein: "On the Absorption of Sound Waves in Suspensions and Emulsions"
R. Courant: "Method for Solution of Boundary Value Problems"
Karl Arnstein: "Engineering Treatment of Ring or Wheel Problems"
A. Einstein, V. Bragmann, and P. G. Bergmann: "On the Five Dimensional Representation of Gravitation and Electricity"
S. Timoshenko: "The Forced Vibrations of Tie Rods"
Th. Troller: "Effect of Wind-Tunnel Size on Pitching-Moments"
A. Nádai: "Creep of Metals Under Various Stress Conditions"
K. O. Friedrichs: "Minimum Buckling Load for Spherical Shells"
William Bollay: "Theory of Flow Through Centrifugal Pumps"
F. L. Wattendorf: "Ideal Performance of Curved Lattice Fans"
L. H. Donnell: "Stress Concentrations Due to Elliptical Discontinuities in Plates Under Edge Forces"
Hans Reissner: "On Lubrication Flow With Periodic Distribution Between Prescribed Boundaries"
R. von Mises: "Some Remarks on the Laws of Turbulent Motion in Tubes"
Wolfgang B. Klemperer: "Stress Pattern Grazing."

[6] Assistant Professor of Mathematics, Purdue University, Lafayette, Indiana.

Theory of Plates and Shells

THEORY OF PLATES AND SHELLS. By S. Timoshenko. Engineering Societies Monographs. First Edition, McGraw-Hill Book Company, Inc., New York, N. Y., 1940. Cloth, 6 × 9 in., xii and 492 pp., 189 figs.

REVIEWED BY A. NÁDAI[7]

THIS book is concerned with the discussion of the distortion of elastic bodies in which one dimension is small compared with the other dimensions. Problems concerning disk-shaped plane bodies stressed in their middle plane are excluded. Three hundred fifty pages are devoted to the bending theory of thin plates and one hundred thirty-two pages to the deformation of curved shells. The content of the first chapter carrying the title "the bending of long rectangular plates to a cylindrical surface" may be summarized by stating that it essentially still belongs to the elementary bending theory of slender bars under a lateral and axial load. The second chapter entitled "pure bending" contains the formulas for the slopes, curvatures, and bending moments of uniformly bent plates for different directions; the third chapter, the bending of circular plates having a rotational symmetric distortion; the fourth "small deflections of laterally loaded plates" including a discussion of the boundary conditions for plates. The following four boundary conditions are considered: the built-in, the simply supported, the free edge, and the elastically supported edge. Using rectangular coordinates x, y the simply supported edge is defined as follows: "if the edge $y = 0$ of the plate is simply supported the deflection w along this edge must be zero. At the same time this edge can rotate freely with respect to the axis, i.e., there are no bending moments M_y along this edge." The two conditions are given as

$$y = 0, \quad w = 0, \quad \frac{\partial^2 w}{\partial y^2} + \nu \frac{\partial^2 w}{\partial x^2} = 0$$

(ν Poissons ratio). If the condition $w = 0$ is essential for a simply supported edge, and since a straight edge is assumed, in the expression for the second boundary condition the term $\partial^2 w/\partial x^2 = 0$ and this condition should have been written simpler as $\partial^2 w/\partial y^2 = 0$. This "simply supported edge" is illustrated in Fig. 49, p. 89, showing a wedge-shaped edge hinged in a corresponding obtuse angle. For a plate carrying a *lateral* load such a support could not well be used. It seems that more justice could have been done to the practical sense of the reader (and to those who have previously discussed the same case) by admitting that what in textbooks including the present one has generally been considered to represent the conditions of a freely supported plate edge is a mathematical definition. When the author on the other hand introduces the expression $\frac{\partial^2 w}{\partial y^2} + \nu \frac{\partial^2 w}{\partial x^2} = 0$ despite the fact that each of the two terms in it are to be taken equal to zero, he had in mind that this was one of the two necessary conditions to be satisified for a simply or freely supported plate edge, with which the reviewer agrees. The trouble comes from the preceding condition and an unwarranted assumption that along a simply supported edge the deflection of the plate "must be zero." The experiments of C. Bach and of M. Bergstraesser have shown that a rectangular plate carrying transversal forces (weight) can rest freely on a smooth rigid edge situated in a plane but the deflections will be zero only in certain points along the edge. What makes the integration of the plate equation $\Delta \Delta w = f(x, y)$ possible using trigonometric and hyperbolic functions is really the fact that the conditions $w = 0$ and $\partial^2 w/\partial x^2 = 0$ or $\partial^2 w/\partial y^2 = 0$, respectively, for a rectangular plate are a special case of the two bound-

[7] Consulting Mechanical Engineer, Westinghouse Research Laboratories, East Pittsburgh, Pa. Mem. A.S.M.E.

ary conditions $w = 0$ and $\Delta w = \partial^2 w/\partial x^2 + \partial^2 w/\partial y^2 = 0$ which permit a double periodical development of the elastic surfaces w and Δw with an analytical continuation around the four corners of the plate. (The reviewer called them the boundary conditions of Navier.) If the student of the plate theory uses them with advantage, he should be aware that they are of a mathematic nature and that he should satisfy himself with a futher investigation of what happens also to the transversal shearing forces along the edges of the plate.

When reading paragraph 25 which is entitled "exact theory of plates" readers will conclude that the theory of the plate equation $\Delta\Delta w = f(x, y)$ to which the preceding and most of the following chapters of the book are devoted is less exact. This distinction between a "rigorous" and a less exact theory of plates which is also to be found in Love's treatise is somewhat misleading. It is shown when $\Delta w = \text{const}$, i.e., the shearing forces vanish or the stresses $\tau_{xz} = \tau_{yz} = 0$ that both theories (the Kirchhoff and the rigorous theory) are really identical. Now if Δw is not a constant or zero the case is essentially not much different as long as one of the fundamental assumptions on which the Kirchhoff theory rests has not been given up, namely, that h/a (h plate thickness and a a dimension in the plate) remains small. The second or correction terms in Equation (s), p. 111, referring to the exact theory are insignificant since the terms containing z have a factor h^2 and those of order z^3 are negligible compared to z. There is only one apparent exception to the rule. It refers to the formulas for the maximum stresses for plates under a concentrated force. When a singularity in the solution of a differential equation occurs of such a nature that one or more of the derivatives become infinite, for which the solutions are established, the corresponding expressions fail. This is not a weakness of the theory, but a consequence of a mathematic abstraction (concentration of a force in a mathematic point) which must then be modified.[8]

After the introductory chapters a large number of special cases are reported in detail such as rectangular plates with various end conditions, plates with various shapes, stretched and bent plates, and those with large deflections. The last three chapters of the book deal with the deformation of shells without and with bending including the theory of cylindrical and spherical shells.

Photoelasticity

PHOTOELASTICITY. By Max Mark Frocht. Vol. 1. John Wiley & Sons, Inc., New York, N. Y., 1941. Cloth, 6 × 9 in., xi and 401 pp., illustrated, $6.

REVIEWED BY W. M. MURRAY[9]

THIS book is a welcome addition to the available literature on photoelasticity. It brings together in one volume the fundamentals of the photoelastic method of stress analysis and the results of the investigations of an outstanding authority in the field. In volume one the author has confined his attention to the basic theory of photoelasticity and the interpretation of the information which can be obtained from observations with the polariscope. This is supplemented with information on the laboratory technique of the method.

In the initial chapter a rather comprehensive review of two-dimensional stress and strain with their respective relations is taken up even to the point of including information on strain rosettes.

A chapter is devoted to the development of the equations of equilibrium for plane stress in Cartesian, polar, and curvilinear co-ordinates. The equations are developed both in terms of the stress trajectories and the lines of maximum shear stress.

The nature of light and a consideration of elementary optics are taken up in two chapters. In this section are included such topics as reflection, refraction, simple harmonic motion, wave theory, polarization, and double refraction. Space is devoted to items such as dispersion, color, interference, intensity of illumination, and the mechanism of operation of different arrangements for polariscopes.

The actual interpretation of the photoelastic phenomena is commenced in the fifth chapter where various methods of calibration of material and determination of the difference between the principal stresses are taken up in detail. This is followed by a chapter dealing with the determination of the isoclinic lines and stress trajectories from observations with the polariscope. This is rather complete and includes information dealing with various kinds of isotropic points and the layout of the trajectories in their locations.

The following three chapters are devoted to the separation of the principal stresses within the model or the determination of the normal and shearing stress components across a given section. Several examples are solved using the slope-equilibrium method for sections of symmetry, the shear-difference method for arithmetic integration along an arbitrarily chosen straight line, and the graphical-integration method of Filon for working into the interior of the model along a stress trajectory.

A very welcome departure from most other texts on this subject is to be found in the last two chapters where the author gives a discussion of photoelastic materials and their properties. This is supplemented with useful comments on the preparation of the models and the actual laboratory and photographic technique. Some space is devoted to the general features of photoelastic equipment including polariscopes, testing machines, cameras, and light sources.

The book contains a great many diagrams to illustrate the text and a large number of photographs of stress patterns. The latter deserve special mention, as many of them are used in numerical examples which are worked out in detail to show the various methods of interpreting the laboratory observations. Although this work is not nearly so comprehensive as the "Treatise on Photoelasticity" by Coker and Filon, to whom it is dedicated, it provides sufficient material to be somewhat more than an engineers' manual and, at the same time, it retains the simplicity which makes it a suitable text for students of senior or graduate grade. To this end the author has included a number of problems and exercises which should be of considerable assistance for classroom use. The first volume does not contain a discussion of the auxiliary methods of analysis which have helped to make photoelasticity such a convenient engineering tool and it is hoped that these will be included in the second volume.

Volume one is a monument to the personal investigations of the author and the laboratory technique which he has successfully developed. The numerical checks which he has obtained from his calculations will do much to dispel, from minds of the skeptical, the idea that photoelasticity is only a qualitative tool. To the publishers must be given credit for the splendid presentation and printing of the book which contains so many illustrations a few of which are in color.

[8] It must by the way be questioned in some applications whether one is better off by taking resource to the formulas of the exact theory if the ratio a/h becomes too small, say, for example $h/a = 0.6$ (a case which is quoted in the book on p. 78 showing in Fig. 44 the corrected deflection line for a "thick" circular plate for a center load). The nearness of those portions along the periphery of the plate in which the reactions are transmitted to the central portion upsets the assumptions of the exact theory about the distribution of the transversal shearing stresses.

[9] Assistant Professor of Mechanical Engineering, Massachusetts Institute of Technology.

Steady Flow in the Transition Length of a Straight Tube[1]

By HENRY L. LANGHAAR,[2] LAFAYETTE, IND.

By means of a linearizing approximation, the Navier-Stokes equations are solved for the case of steady flow in the transition length of a straight tube. The family of velocity profiles is defined by Bessel functions, and the parameter of this family is tabulated against the axial co-ordinate in a dimensionless form. Hence, the length of transition is obtained. The curves give a comparison of the author's calculations of the velocity field with those of other investigators,[3,4,5] and with the experimental data of Nikuradse.[6] The pressure function is derived from the computed velocity field by means of the energy equation, and the pressure drop in the transition length is defined by a dimensionless constant *m*, which is computed to be 2.28. A discussion of this constant is given in the conclusions.

Notation

x, y, z = rectangular coordinates of a point. The center line of the tube is on the z axis, with the inlet at $z = 0$

r, θ, z = cylindrical co-ordinates of the point x, y, z

ω = cross-sectional area of the tube

a = radius of the tube

$q = r/a$ = dimensionless radial co-ordinate

u, v, w = x, y, z components of the velocity field

w_0 = velocity on the center line of the tube

c = mean velocity in the tube

$\lambda = w/c$ = dimensionless axial velocity

$\lambda_0 = w_0/c$ = dimensionless velocity on the center line of the tube

ρ = mass-density of the liquid

ν = kinematic coefficient of viscosity

$\mu = \rho\nu$ coefficient of viscosity

$R = ca/\nu$ = Reynolds number

$\sigma = z/aR$ = dimensionless axial co-ordinate

σ' = value of σ corresponding to $\lambda_0 = 1.98$

g_3 = the z component of the acceleration of gravity

p = static pressure at the point x, y, z

p_0 = static pressure at the inlet section $z = 0$

Δp = pressure drop between the still liquid in the supply reservoir and the section z

m = dimensionless constant which defines the pressure drop in the transition length

α, β = certain parameters which are functions of z alone

$\gamma = \beta a$ = dimensionless parameter

$I_n(x) = i^{-n}J_n(ix)$, where $i = \sqrt{-1}$, and J_n is the nth-order Bessel function.[7] Throughout this paper the argument of the I functions is γ if not otherwise indicated

The Family of Velocity Profiles

The Navier-Stokes equation for w is

$$dw/dt = g_3 - (1/\rho)(\partial p/\partial z) + \nu(w_{xx} + w_{yy} + w_{zz}) \quad [1]$$

The following three approximations, which are common to the theories of Boussinesq, Schiller, and Atkinson-Goldstein, will be employed in the present theory:

1 Over the inlet section $z = 0$, the velocity component w is constant and equal to the mean velocity c. Nikuradse's[6] test curves thoroughly justify this assumption for the case of tubes which are provided with short bell-shaped mouths.

2 The pressure gradient $-\partial p/\partial z$ is a function of z alone.

3 The term νw_{zz} may be neglected in Equation [1]. This is tantamount to the assumption that the derivative of the normal stress $\partial\sigma_z/\partial_z$ is the same as the pressure gradient $-\partial p/\partial z$.

In addition to these assumptions, there is introduced the fourth condition

$$dw/dt = \nu\beta^2 w \quad [2]$$

where β is a function of z alone. The purpose of this approximation is to reduce Equation [1] to a linear form. It can be partially justified on theoretical grounds. In the first place, Equation [2] is satisfied by $\beta = 0$ in the permanent regime beyond the transition length. Also, this equation is satisfied, irrespective of the value of β, at all points on the wall of the tube, since w and dw/dt both vanish there. Furthermore, if it is assumed with Schiller[4] and Atkinson-Goldstein[5] that the laminar state is attained by the development of a boundary layer in the transition length, then the conclusion is reached that Equation [2] is satisfied at all points in the undisturbed central core of fluid. This conclusion emerges from the fact that the derivatives w_x and w_y vanish over the flat central portions of the velocity profiles, and accordingly the acceleration $dw/dt = uw_x + vw_y + ww_z$ reduces to $dw/dt = ww_z$. Since w is a function of z alone in the central core, w_z is likewise a function of z alone in that region, and it follows that Equation [2] is there satisfied by $\nu\beta^2 = w_z$. Finally, it may be concluded from this that Equation [2] is satisfied at all points of the inlet section $z = 0$, since the depth of the boundary layer there reduces to zero. Thus, Equation [2] is justified, except for those points which lie within the boundary layer. Of

[1] Summary of a doctoral dissertation presented to Lehigh University.

[2] Instructor in Mathematics, Purdue University, Lafayette, Indiana.

[3] "Hydrodynamique," by J. Boussinesq, Comptes Rendus, vol. 110, 1890, pp. 1160, 1238; vol. 113, 1891, pp. 9, 49.

[4] "Die Entwicklung der laminaren Geschwindigkeitsverteilung und ihre Bedeutung für Zähigkeitsmessungen," by L. Schiller, *Zeitschrift für angewandte Mathematik und Mechanik*, vol. 2, 1922, p. 96.

[5] "Modern Developments in Fluid Dynamics," edited by S. Goldstein, Oxford University Press, London, England, and New York, N. Y., 1938, vol. 1, Atkinson-Goldstein, p. 304.

[6] "Applied Hydro- and Aeromechanics," by L. Prandtl and O. G. Tietjens, McGraw-Hill Book Co., Inc., New York, N. Y., first edition, 1934. Nikuradse's curves are reproduced from Fig. 13, p. 27. Seemingly a more detailed account of Nikuradse's tests has not been published.

Presented at the National Meeting of the Applied Mechanics Division, Philadelphia, Pa., June 20–21, 1941, of The American Society of Mechanical Engineers.

Discussion of this paper should be addressed to the Secretary, A.S.M.E., 29 West 39th Street, New York, N. Y., and will be accepted until July 10, 1942, for publication at a later date. Discussion received after the closing date will be returned.

Note: Statements and opinions advanced in papers are to be understood as individual expressions of their authors, and not those of the Society.

[7] For tables of the I functions see, for example, "Theory of Bessel Functions," by G. N. Watson, Cambridge University Press, London, England, 1922. "Bessel Functions," by Andrew Gray, G. B. Mathews, and T. M. MacRobert, Macmillan and Co., Ltd., London, England, second edition, 1922.

course, in the latter part of the transition length, a true boundary layer does not exist, since the central parts of the velocity profiles are appreciably rounded. However, in that region, the flow approaches the laminar state for which Equation [2] remains valid.

With the foregoing assumptions, Equation [1] reduces to the form

$$w_{zz} + w_{yy} - \beta^2 w = \alpha \quad [3]$$

where α and β are functions of z alone. This equation will apply for a cylindrical tube of any cross section, but the present discussion is restricted to the circular cross section.

A particular solution of Equation [3] is

$$w = -\alpha/\beta^2 \quad [4]$$

It then suffices to solve the complementary equation

$$V_{zz} + V_{yy} - \beta^2 V = 0 \quad [5]$$

In cylindrical co-ordinates, this reduces to Bessel's equation of order zero

$$V_{rr} + \frac{1}{r} V_r - \beta^2 V = 0 \quad [6]$$

The only solution which is finite for $r = 0$ is $V = KI_0(\beta r)$. Hence

$$w = KI_0(\beta r) - \alpha/\beta^2 \quad [7]$$

The quantities α and K may be eliminated from this equation by means of the boundary condition $w = 0$, and the continuity equation

$$\int_0^a rw dr = (1/2)a^2 c \quad [8]$$

Introducing the dimensionless notation $q = r/a$, $\lambda = w/c$, $\gamma = \beta a$, gives

$$\lambda = [I_0(\gamma) - I_0(\gamma q)]/I_2(\gamma) \quad [9]$$

This is the equation of the family of velocity profiles. It remains to express the parameter γ of this family of curves as a function of z.

The Function $\gamma(z)$

The problem of expressing the parameter of a known family of velocity profiles as a function of the axial co-ordinate is treated in the paper by Schiller.[4] In fact, Schiller assumes the velocity profiles to be straight-line segments terminated by parabolic arcs, and he obtains the parameter of this family as a function of z by applying the momentum equation to the whole body of fluid, and Bernoulli's equation to the central core. Essentially the same treatment is given here but, instead of using the simple Bernoulli equation, the two viscosity terms νw_{zz} and νw_{yy} in the Navier-Stokes equation are retained, since they are important for the latter part of the transition length. These terms are irrelevant in Schiller's treatment, since, by his hypotheses, they vanish.

The momentum equation, which can be obtained by integrating the Navier-Stokes equation over the cross section, is

$$2\nu \int_0^a (rw_{rr} + w_r)dr + a^2 g_3 - \frac{a^2}{\rho}\frac{dp}{dz} = 2\frac{d}{dz}\int_0^a w^2 r dr \quad [10]$$

By means of Equation [9], the first integral may be evaluated, giving

$$-\frac{2\nu c\gamma I_1(\gamma)}{I_2(\gamma)} + a^2\left(g_3 - \frac{1}{\rho}\frac{dp}{dz}\right) = 2\frac{d}{dz}\int_0^a w^2 r dr \quad [11]$$

The term $g_3 - (1/\rho)dp/dz$ may be eliminated by means of the Navier-Stokes equation[5]

$$g_3 - \frac{1}{\rho}\frac{dp}{dz} = w_0\frac{dw_0}{dz} - \nu(w_{rr} + \frac{1}{r}w_r)_0 \quad [12]$$

where the subscript zero refers to the central axis. Equations [9] and [12] yield

$$g_3 - \frac{1}{\rho}\frac{dp}{dz} = w_0\frac{dw_0}{dz} + \frac{\nu c\gamma^2}{a^2 I_2(\gamma)} \quad [13]$$

Substituting this relation in Equation [11] gives an equation which may be expressed in the following dimensionless form

$$\frac{2\gamma I_1(\gamma) - \gamma^2}{I_2(\gamma)} = \frac{d}{d\sigma}\int_0^1 (\lambda_0^2 - 2\lambda^2)q\, dq \quad [14]$$

Also, by Equation [9]

$$\int_0^1 (\lambda_0^2 - 2\lambda^2)qdq = \frac{(I_0 - 1)^2 - 4I_0 I_2 + 2I_1^2}{2I_2^2} \quad [15]$$

in which the argument of the I's is γ. It is convenient to use the abbreviations

$$\left.\begin{aligned} f(\gamma) &= [4I_0 I_2 - (I_0 - 1)^2 - 2I_1^2]/2I_2^2 \\ g(\gamma) &= I_2/(2\gamma I_1 - \gamma^2) \end{aligned}\right\} \quad [16]$$

Equation [14] then may be expressed

$$1/g(\gamma) = -f'(\gamma)d\gamma/d\sigma \quad [17]$$

This is a differential equation which determines γ as a function of σ.

By means of the asymptotic formula

$$I_n(x) = \frac{e^x}{(2\pi x)^{1/2}}[1 + \epsilon_n(x)], \quad \lim_{x\to\infty}\epsilon_n(x) = 0 \quad [18]$$

there results from Equation [9] $\lim_{\gamma\to\infty}\lambda = 1$. Since $\lambda = 1$ at the inlet section $z = 0$, then $\lim_{\gamma\to\infty} z(\gamma) = 0$. Hence, Equation [17] yields

$$\sigma = \int_\gamma^\infty g(\gamma)f'(\gamma)d\gamma = \int_\gamma^\infty g(\gamma)df(\gamma) \quad [19]$$

For the numerical integration of this equation, make the change of variables

$$X = f(\gamma), \quad Y = g(\gamma) \quad [20]$$

By the power series and the asymptotic series for the I functions the following limits are established

$$\left.\begin{aligned} X &\to 1/2,\ Y \to 0 \text{ as } \gamma \to \infty \\ X &\to -2/3,\ Y \to \infty \text{ as } \gamma \to 0 \end{aligned}\right\} \quad [21]$$

Equation [19] may then be expressed

$$\sigma = \int_X^{1/2} Y dX \quad [22]$$

Equation [20] may be regarded as the parametric equations of a curve, and Equation [22] shows that the function $\sigma(\gamma)$ is represented by the area under this curve in the interval $(X, 1/2)$. By assigning a set of values to γ, a table of points on the curve may be computed, which gives, by numerical integration, the corresponding values of σ. The values of σ in Table 1 are computed

[5] Schiller here employed the Bernoulli equation. This is obtained from Equation [12] by dropping the viscosity terms.

TABLE 1

γ	100.00	30.00	20.00	16.00	14.50	13.00	12.00
σ	0.000026	0.000334	0.000820	0.00137	0.00172	0.00222	0.00269
λ_0	1.0203	1.0701	1.1079	1.1377	1.1535	1.1734	1.1898
γ	11.00	10.00	9.00	8.00	7.00	6.50	6.00
σ	0.00332	0.00418	0.00541	0.00722	0.00997	0.01188	0.0143
λ_0	1.2095	1.2337	1.2638	1.3021	1.3514	1.3814	1.4157
γ	5.50	5.00	4.50	4.00	3.50	3.25	3.00
σ	0.0174	0.0214	0.0267	0.0335	0.0426	0.0483	0.0549
λ_0	1.4547	1.4989	1.5488	1.6041	1.6645	1.6961	1.7285
γ	2.75	2.50	2.25	2.00	1.85	1.70	1.55
σ	0.0625	0.0715	0.0821	0.0947	0.1034	0.1132	0.1241
λ_0	1.7612	1.7939	1.8261	1.8573	1.8753	1.8926	1.9090
γ	1.40	1.30	1.20	1.10	1.00	0.90	0.80
σ	0.1365	0.1459	0.1560	0.1671	0.1795	0.1934	0.2091
λ_0	1.9245	1.9342	1.9434	1.9520	1.9600	1.9673	1.9740
γ	0.70	0.60	0.50	0.40	0.00	....	....
σ	0.2270	0.2479	0.2730	0.3040	∞	....	....
λ_0	1.9800	1.9852	1.9897	1.9934	2.0000	....	....

in this way. The values of λ_0 are computed directly from Equation [9].

This table, with Equation [9], completely defines the velocity field in the transition length. The value $\sigma = \sigma'$, corresponding to $\lambda_0 = 1.98$, was called by Boussinesq the "length of transition." From Table 1 it follows $\sigma' = 0.23$.

The Pressure Drop

In the transition length, the pressure gradient $-dp/dz$ is higher than in a region of laminar flow, not only because of the increased frictional loss, but also because the kinetic energy of the liquid increases as it passes downstream. To evaluate the pressure drop, consider the energy equation. The power which is dissipated by fluid friction in the interval $z = 0$ to $z = z$ is[9]

$$E = \mu \int_0^z dz \int_\omega [2(u_x^2 + v_y^2 + w_z^2) + (w_y + v_z)^2 + (u_z + w_x)^2 + (v_x + u_y)^2] d\omega \quad \ldots [23]$$

It is assumed that the lateral velocity components u and v may be neglected in this equation. Then the continuity equation $u_x + v_y + w_z = 0$ shows that consistently the term w_z may be neglected, so that the preceding equation reduces to

$$E = \mu \int_0^z dz \int_\omega (w_x^2 + w_y^2) d\omega \quad \ldots [24]$$

By a theorem of Helmholtz,[10] the laminar velocity distribution furnishes a minimum to the integral [24], and accordingly the friction loss is always higher in the transition length than it is in the permanent regime further downstream.

During a time interval dt, the net work of pressure on the body of fluid in the interval $z = 0$ to $z = z$ is $c\omega(p_0 - p)dt$. The work of friction on this body of fluid is $-Edt$, where E is given by Equation [24]. It is assumed that the tube is horizontal, so that the work of body force is zero. Then, equating the work of all forces to the change in kinetic energy gives the energy equation

$$c\omega(p_0 - p) = \mu \int_0^z dz \int_\omega (w_x^2 + w_y^2) d\omega + (1/2)\rho \int_\omega (w^2 - c^2) d\omega \quad \ldots [25]$$

For the circular cross section, this may be expressed

$$\frac{p_0 - p}{(1/2)\rho c^2} = 2 \int_0^1 (\lambda^3 - 1) q \, dq + 4 \int_0^\sigma d\sigma \int_0^1 \lambda_q^2 q \, dq \quad \ldots [26]$$

By Bernoulli's equation, the pressure drop that occurs in the mouth of the tube is $(1/2)\rho c^2$. Accordingly, the total drop Δp between the supply reservoir and the section z is $(1/2)\rho c^2 + (p_0 - p)$. Equations [9] and [26] then give

$$\frac{\Delta p}{(1/2)\rho c^2} = 1 + 2 \int_0^1 (\lambda^3 - 1) q dq + 2 \int_0^\sigma \frac{\gamma^2}{I_2^2} (I_1^2 - I_0 I_2) d\sigma \quad \ldots [27]$$

[9] "Hydrodynamics," by Horace Lamb, Cambridge University Press, London, England, sixth edition, 1932, par. 329, p. 580.

[10] See footnote,[9] par. 344, pp. 617, 618.

TABLE 2

γ	σ	$\int_0^1 (\lambda^3 - 1) q \, dq$	$\int_0^\sigma \phi(\gamma) d\sigma$	$\Delta p/(1/2)\rho c^2$
20.0	0.00082	0.0677	0.0384	1.2122
11.0	0.00332	0.1112	0.0821	1.3866
8.0	0.00722	0.1540	0.1326	1.5732
6.0	0.0143	0.2055	0.2095	1.8300
5.0	0.0214	0.2433	0.2788	2.0442
4.0	0.0335	0.2923	0.3884	2.3614
3.0	0.0549	0.3531	0.5706	2.8474
2.5	0.0715	0.3867	0.7082	3.1898
2.0	0.0947	0.4210	0.8967	3.6354
1.4	0.1365	0.4588	1.2332	4.3840
1.0	0.1795	0.4796	1.5777	5.1146
0.6	0.2479	0.4912	2.1251	6.2326
0.4	0.3040	0.5000	2.5739	7.1478

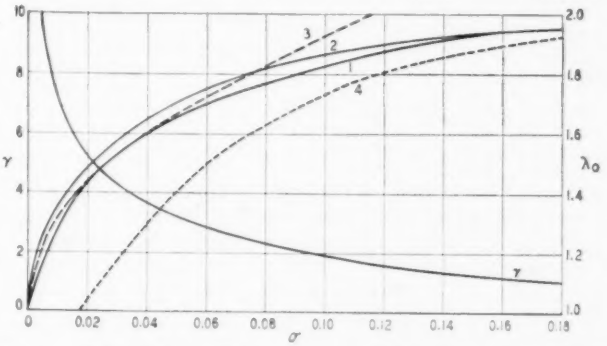


FIG. 1 CENTER-LINE VELOCITIES AS COMPUTED BY VARIOUS THEORIES

Curve 1—Observed by Nikuradse
Curve 2—Plotted from Table 2
Curve 3—Calculated by Schiller's formula
Curve 4—Calculated by Boussinesq's formula

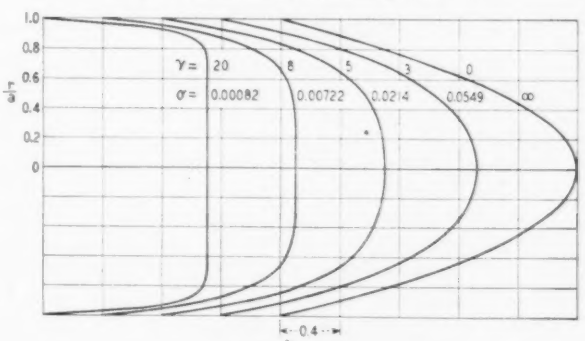


FIG. 2 VELOCITY PROFILES
(Computed by Equation [9] and Table 1.)

It is convenient to denote the integrand $(\gamma^2/I_2^2)(I_1^2 - I_0 I_2)$ by $\phi(\gamma)$. The evaluation of the integral of this function involves a difficulty, due to the fact that the integrand becomes infinite when $\sigma \to 0$. However, the relation $\lim_{\gamma \to \infty} \gamma^2\sigma = 1/4$ (which may be derived from Equation [19]), and the asymptotic formula

$$\phi(\gamma) \sim \gamma + 3 + \frac{5}{\gamma} + \frac{7}{\gamma^2} + \ldots \quad [28]$$

gives $$\int_0^{0.0426} \phi(\gamma)d\sigma = 0.00518 \quad [29]$$

($\sigma = 0.000026$ corresponds to $\gamma = 100$).

Hence

$$\int_0^{\sigma} \phi(\gamma)d\sigma = 0.00518 + \int_{0.0426}^{\sigma} \phi(\gamma)d\sigma \quad [30]$$

Since $\int_{0.0426}^{\sigma} \phi(\gamma)d\sigma$ is a proper integral, it may be evaluated by numerical methods. Also, the integral $\int_0^1 (\lambda^3 - 1)qdq$ may be calculated by Simpson's rule from Equation [9]. With Equation [27], Table 2 is then obtained.

From this table we may plot a curve of $\Delta p/(1/2)\rho c^2$ against σ. This curve determines the pressure drop Δp as a function of z. The slope of the curve is

$$-\frac{dp/d\sigma}{(1/2)\rho c^2} = -\frac{a^2}{(1/2)\rho v c}\frac{dp}{dz} \quad [31]$$

In the region of laminar flow, $dp/dz = -8c\rho\nu/a^2$. Consequently, the curve is asymptotic to a line with slope 16.

If a value σ_1 is chosen somewhat greater than the length of transition σ', and if $\sigma > \sigma_1$, Equation [27] may be expressed in the form

$$\frac{\Delta p}{(1/2)\rho c^2} = 1 + 2\int_0^1 (\lambda^3 - 1)qdq + 2\int_0^{\sigma_1} \phi(\gamma)d\sigma + 2\int_{\sigma_1}^{\sigma} \phi(\gamma)d\sigma \quad [32]$$

But, for $\sigma > \sigma_1$, $\lambda = 2(1 - q^2)$ (Poiseuille flow), and consequently $\int_0^1 (\lambda^3 - 1)q\,dq = 1/2$. Also, from the power series for the I functions, $\gamma^2/I_2 \to 8$ and $(I_1^2/I_2) - I_0 \to 1$ as $\gamma \to 0$. Since $\gamma \to 0$ as $z \to \infty$, it follows

$$\int_{\sigma_1}^{\sigma} \phi(\gamma)d\sigma = 8(\sigma - \sigma_1) \quad [33]$$

Hence, setting $\int_0^{\sigma_1} \phi(\gamma)d\sigma = K$, gives

$$\Delta p/(1/2)\rho c^2 = 16\sigma + 2K + 2 - 16\sigma_1 \quad [34]$$

Setting $2K + 2 - 16\sigma_1 = m$, this equation may be expressed in the form

$$\Delta p = \frac{8\mu cz}{a^2} + (1/2)m\rho c^2 \quad [35]$$

This is a fundamental equation in the theory of tube-type viscosimeters. If $\sigma_1 = 0.304$, Table 2 shows $K = 2.574$. Hence

$$m = 2.28 \quad [36]$$

Conclusions

The velocity field in the transition length is completely defined by Equation [9] and Table 1. The curves of Fig. 1 give a comparison of the center-line velocities as computed by this theory, and by the theories of Boussinesq[3] and Schiller,[4] and as observed by Nikuradse.[6] From Nikuradse's curve, the computed length of transition $\sigma' = 0.23$, appears to be in close agreement with experiment. A few of the computed velocity profiles are shown in Fig. 2.

The pressure function in the transition length is defined by Table 2. However, if the coordinate z is greater than the length of transition, the pressure drop Δp is given by Equation [35], in which, according to the present theory, $m = 2.28$. The most suitable value for this constant has not been well established by experiment. Schiller computed $m = 2.16$, but he says that this value seems to be too low. In four runs, he obtained the experimental values 2.115, 2.35, 2.36, and 2.45—average 2.32.[11] Other experimental results have been given by Riemann,[12] who obtained values ranging from 2.220 to 2.268—average 2.248 ± 0.012. Accordingly, he recommends for viscosimetry practice the value 2.24, which was computed by Boussinesq. Atkinson and Goldstein[5] computed $m = 2.41$, but this value appears to be high.

[11] "Handbuch der Experimentalphysik, IV, 4 Teil, Hydro- und Aerodynamik," by Ludwig Schiller, Akademische Verlagsgesellschaft M. B. H., Leipzig, Germany, 1932, p. 57.

[12] "The Value of the Hagenbach Factor in the Determination of Viscosity by the Efflux Method," by William Riemann, 3rd, *Journal of the American Chemical Society*, vol. 50, 1928, p. 46.

Model Tests of Two Types of Vibration Dampers

By C. A. MEYER[1] and H. B. SALDIN,[2] PHILADELPHIA, PA.

This paper deals with the construction and tests of two types of vibration dampers, selected from a number of original proposals, designed to damp out the vibration in steam-turbine impulse blades. These dampers were tested using models constructed of such size and physical dimensions as to simulate the conditions of operation in the actual turbine blade. Test results show that if a properly designed damper is attached to a freely vibrating system having 26 times the mass of the damper, it will reduce an initial deflection of the vibrating system to 4 per cent of its value in 10 cycles.

Nomenclature

The following nomenclature is used in the paper:

A = initial amplitude ratio $= x_0/D$
D = $2R$ = diameter of cylinder or hemispherical cup
d = $2r$ = diameter of roller or sphere
F = frequency of main system
f = frequency of damper $= \frac{1}{2\pi}\sqrt{C\,\frac{G}{(R-r)}\left(1-\frac{\rho}{\gamma}\frac{h}{D}\right)}$
($C = {}^2/_3$ for cylindrical, $C = {}^5/_7$ for spherical damper)
G = acceleration due to force field
= centrifugal acceleration in a rotating system
g = acceleration of gravity
H = fluid depth ratio $= h/D$
h = height of fluid in chamber
L = aspect ratio $= l/D$
l = length of roller
M = mass of main system (effective)
m = mass of damper
N = viscosity number $= \nu\sqrt{\frac{1}{GD^3}}$
n = number of cycles
P = density ratio $= \frac{\rho}{\gamma}$
R = groove-size number $= r_m/D$
r_m = $\frac{\text{cross-section area of groove}}{\text{wetted perimeter}}$ = hydraulic radius of groove
X = amplitude ratio $= x/x_0$
x_0 = initial amplitude of vibration
x = amplitude of vibration after n cycles; double amplitude $= 2x$
γ = density of roller or ball material
δ = logarithmic decrement of main system without damper
μ = absolute viscosity
$\nu = \frac{\mu}{\rho}$ = kinematic viscosity
ρ = density of fluid
Φ = mass ratio $= M/m$
ψ = frequency ratio $= f/F$
Ω = frequency number $= F\sqrt{D/G}$

Introduction

Two principal problems are considered in this paper. The first is concerned with the development of a method of testing blade-vibration dampers. The second has to do with the actual testing of the performance of two types of dampers. Due to the obvious difficulties which are encountered in testing the dampers in a rotating turbine blade, it appears attractive to investigate the fundamental behavior of the different dampers in a nonrotating test setup. In order to accomplish this, the methods of dimensional analysis have been applied to insure similarity between the conditions of operation of the dampers in the rotating turbine blade and those in a nonrotating model.

The two types of dampers described in the paper operate on the same principle. These dampers are intended to act as damped-vibration absorbers.[3] They consist fundamentally in connecting an auxiliary vibration system (the damper) to the main vibration system (for instance, the turbine blade), which we desire to be free from vibration.

For best operation, it has been found by means of theoretical calculations that the auxiliary system should be arranged to have a natural frequency of vibration very nearly equal to that of the main system. Also, it has been found that by introducing a proper amount of damping between the auxiliary and main systems, the combined system will become less affected by variations of the frequency of the exciting force. These characteristics of the damped-vibration absorber are well known and are shown more clearly by Den Hartog.[4]

The foregoing characteristics have been obtained through the theoretical calculation of the system consisting of an absorber attached to a main vibrating system which is *continuously excited*. The calculation of an absorber-vibration system which is *freely vibrating* is mathematically cumbersome. Therefore, no general characteristics have so far been obtained for the nonsteady vibration. However, we might expect that the best damper performance for the freely vibrating system would be obtained for some optimum tuning between the damper and the blade and also for some optimum value of damping between the auxiliary and main system. Thus, the principal purpose of testing the dampers has been to determine for the freely vibrating system:

1 The rate of vibration decay for the different damper constructions.

---

[1] Research Engineer, Westinghouse Electric & Manufacturing Company, South Philadelphia Works. Jun. A.S.M.E.

[2] Industrial Turbine Department, Westinghouse Electric & Manufacturing Company, South Philadelphia Works. Jun. A.S.M.E.

Presented at the National Meeting of the Applied Mechanics Division, Philadelphia, Pa., June 20–21, 1941, of The American Society of Mechanical Engineers.

Discussion of this paper should be addressed to the Secretary, A.S.M.E., 29 West 39th Street, New York, N. Y., and will be accepted until July 10, 1942, for publication at a later date. Discussion received after the closing date will be returned.

Note: Statements and opinions advanced in papers are to be understood as individual expressions of their authors, and not those of the Society.

[3] "Mechanical Vibrations," by J. P. Den Hartog, McGraw-Hill Book Company, Inc., New York, N. Y., 1934, p. 103.

[4] Ibid., Fig. 79.

2 The optimum damping between the main and auxiliary vibration systems.

3 The optimum tuning of the auxiliary system.

Vibration Dampers

Fig. 1 is a sketch of the so-called spherical damper. This damper consists of a spherical ball *a* which is placed in a capsule *b*. The capsule has a hemispherical end *c*, which has a slightly larger radius than the ball. A small amount of fluid is placed in the capsule and then the capsule is suitably sealed. The capsule is finally fastened in the blade shroud *d*. Under the action

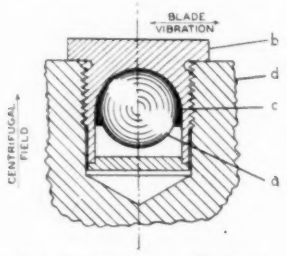


Fig. 1 Spherical Damper

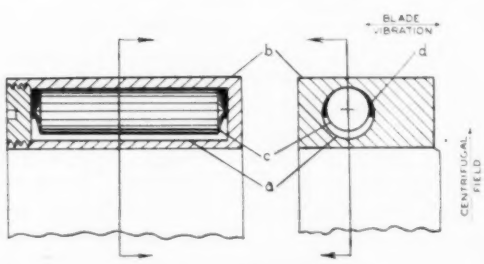


Fig. 2 Cylindrical Damper

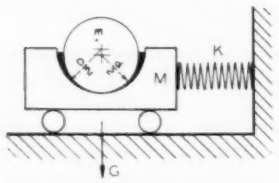


Fig. 3 Vibration Damper
(See Appendix 1.)

of the centrifugal field, due to the rotation of the blade, the spherical ball and the damping fluid are forced against the cup-shaped end of the capsule. The ball in this position will then have a natural frequency of vibration in the cup. In fact, by selecting suitably the radii of the ball and the cup, the natural frequency of the ball vibrating in the cup can be made to match the natural frequency of the blade. Thus, the ball in its cup acts as an auxiliary vibration system attached to the turbine blade. The fluid surrounding the ball supplies the damping between the auxiliary system (the ball) and the main system (the blade). It is further to be noted that the spring or restoring force of the auxiliary system is really supplied by the mass forces acting on the ball rather than by an actual spring. This fact eliminates one disadvantage of dynamic-vibration absorbers, namely, the large stresses which usually occur in the spring of the auxiliary system.

Fig. 2 is a sketch of a cylindrical damper which performs in the same manner as the spherical damper. In this case, a cylindrical roller in a cylindrical hole is used in place of a ball in a cup. This damper is constructed by drilling a hole *a* in the blade shroud *b*. The roller *c*, and a small amount of damping fluid *d*, is suitably sealed in the hole. Using this construction, a damper having a larger mass can be placed in a given available space. However, this damper is effective against vibration in only one direction. During the tests of the cylindrical damper, it was found that by cutting grooves in the surface of the roller a better performance could be obtained. Thus the grooved cylindrical roller was developed.

Theory Used in Constructing Damper Models

The actual size and frequency of the damper models have been obtained after first deciding on the variables on which the damper performance principally depends. The variables chosen to represent the damper performance have been obtained by means of the dimensional analysis in Appendix 1. The analysis shows that, within the accuracy desired, there exists a relation between the variables, represented as follows

$$\text{A function of } [X, n, \Omega, N, \Phi, \psi, L, R, \delta] = 0 \quad \ldots [1]$$

where the variables are defined in the nomenclature. The relation Equation [1] simply states that the dimensionless amplitude X principally depends upon the number of cycles of vibration, after release n, the dimensionless frequency of the main system Ω, the dimensionless viscosity of the damping fluid N, the ratio of the mass of the main system to that of the damper Φ, the ratio of the natural frequencies of the auxiliary and main vibrating systems ψ, the ratio of length to diameter of the damper roller L, the dimensionless groove size R, and the logarithmic decrement δ of the main system without the damper.

If we test a model using values of the dimensionless variables which are the full-scale values, the relation, for instance, between the dimensionless amplitude $X = (x/x_0)$ and the number of cycles n obtained in the model test, should be the same[5] as that for the full-scale damper. For instance, it is possible to test the model with the full-scale value of the dimensionless frequency term $\Omega = F\sqrt{D/G}$. Since the value of G in the turbine damper is roughly 5000 times that in the model, we can suitably adjust the size D and the frequency F to obtain the full-scale value of $\Omega = F\sqrt{D/G}$. The model size and frequency have been chosen so that there will not be too great a difference between the viscosity ν in the model and in the full-scale damper. An examination of the definition of the dimensionless viscosity number N should clarify this point.

The tests of the dampers were carried out with a few values of the dimensionless frequency term Ω which approximate the full-scale value. Several values of the dimensionless viscosity term N were tested in order to obtain the optimum value of this term for each of three values of tuning $\psi = (f/F)$. The tested values of $\Phi = (M/m)$, $L = (l/D)$, $A = (x_0/D)$ were approximately the full-scale values. The damping δ of the main system could not be controlled. However, the best damping curve for each type

TABLE 1 RANGE OF VALUES OF DIMENSIONLESS VARIABLES FOR TURBINE DAMPER

Dimensionless variable	Approximate range in turbine	Tested range, spherical damper	Tested range, cylindrical damper
$\Omega = F\sqrt{D/G}$	0.58– 2.1	0.835– 1.27	0.657– 0.877
$N \times 10^3 = \left(\nu\sqrt{\frac{1}{GD^3}}\right) \times 10^3$	[a]	1.45 –12.70	1.47 –29.4
$\Phi = (M/m)$	50 –10	23.2 –19.2	28.4 –24.2
$\psi = (f/F)$	0.7 – 1.3	0.58 – 1.26	0.85 – 1.14
$A \times 10^3 = \left(\frac{x_0}{D}\right) \times 10^3$	4 –20	8.19 – 9.17	8.34 –11.1
$R = (r_m/D)$	.....	.....	0 – 0.02

[a] The value of this term should be the optimum value determined by the model test.

[5] This statement is true if no important variable has been overlooked in writing Equation [1*a*], Appendix 1.

of damper was later corrected for the damping in the main system to give a comparison of the dampers for the case when the main system has no damping. Table 1 gives the approximate range of the values of the dimensionless variables for a damper in a turbine, together with the range of values covered by the tests.

Test Method

The method of testing the different dampers consisted principally in mounting them on a vibration system composed of a mass supported on four flat cantilever springs as shown in Fig. 4. The vibration system was deflected to a given amplitude and then released by a trigger *E*, Fig. 4. The variation of the amplitude of vibration with the number of cycles was measured using one of the following methods:

1 An arc light reflecting from a mirror *C*, Fig. 4, mounted on the center of a flat strip of metal, one end of which was held stationary, the other end being attached to the vibrating system. The reflection from the mirror was focused on a moving photographic film in an oscillograph.

2 A recording stylus connected to the vibrating system and recording on moving wax paper *F*, Fig. 4.

The cup *A*, Fig. 4, is the model of the spherical damper. The bottom of this cylindrical cup is made hemispherical. The steel

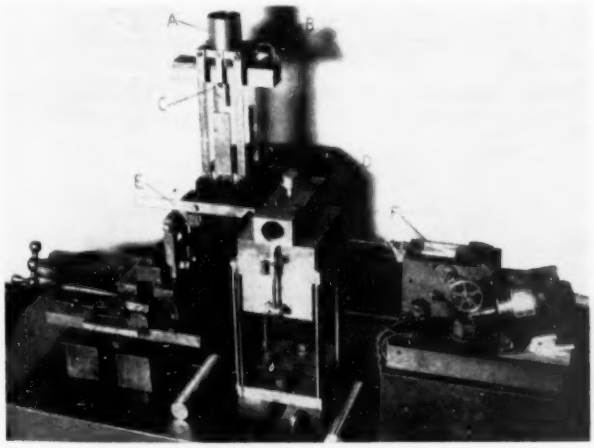


Fig. 4 Model-Test Arrangement

ball shown in the illustration is placed in this cup together with the damping fluid. The mirror *C* was used, together with a spotlight and a rotating photographic film to record the vibration decay. The weights, upon which the spherical ball rests in Fig. 4, were used to adjust the mass ratio of the vibrating system.

The arrangement *D* in Fig. 4 is the model of the cylindrical damper. The two cylindrical rollers (smooth and grooved) together with one of the two caps used to close off the ends of the cylindrical hole can be seen in the foreground. Three different groove sizes were tested. During the tests of the cylindrical damper, the recording system *F* was employed. This system was used in place of the photographic method in order to avoid the delay involved in developing films. This recording system consisted of a scriber arm mounted on an elastic hinge. The record was taken on wax paper driven over a flat surface by means of the motor gear mechanism shown.

The damping fluids used in the model tests were mixtures of kerosene and oil or oil and mineral spirits, in varying proportions, depending upon the viscosity desired. Acetone was also used in some of the tests.

The dampers were thoroughly cleaned with ether or carbon

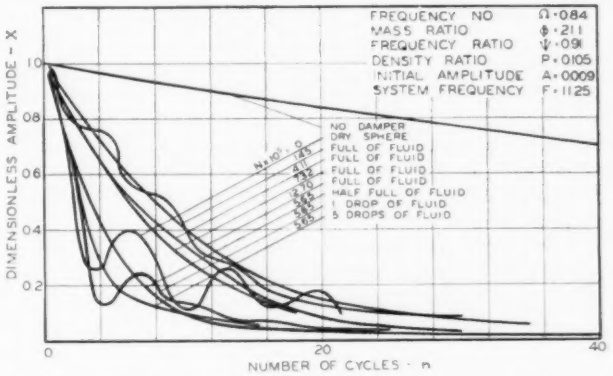


Fig. 5 Typical Curves of Vibration Amplitude of Spherical Damper

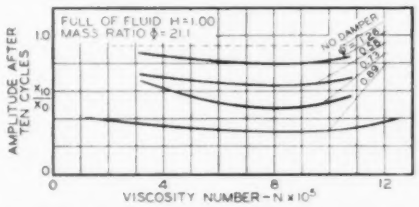


Fig. 6 Spherical Damper: Effect of Fluid Viscosity on Amplitude for Various Frequency Ratios

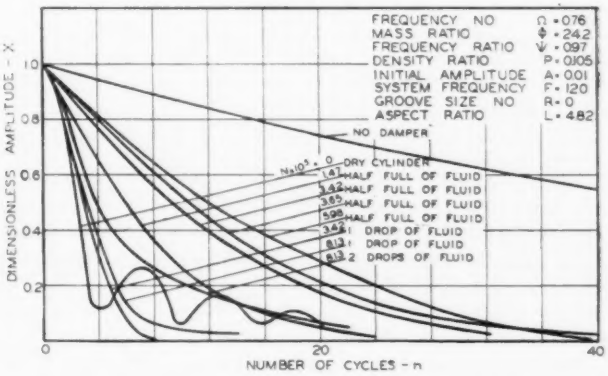


Fig. 7 Typical Curves of Vibration Amplitude of Cylindrical Damper

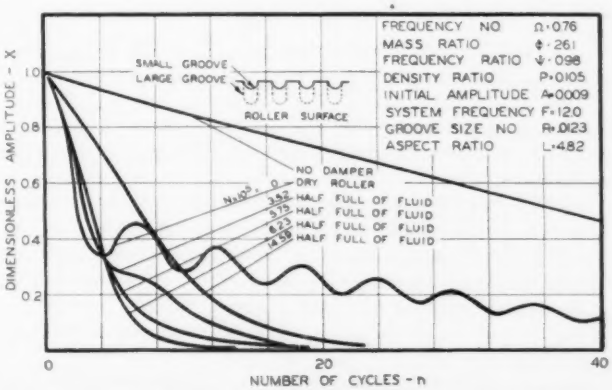


Fig. 8 Typical Curves of Vibration Amplitude of Grooved Cylindrical Damper

tetrachloride whenever the fluid was changed. Also the fluids were filtered before being used in the dampers. These precautions were found necessary in order to duplicate test results. The fluid viscosities were obtained by means of a rotating-disk viscosimeter. The frequency of the vibrating system was determined by means of a strobotac or by a timing wave on the recording tape.

Results of Model Tests

The curves shown in Figs. 5, 7, and 8 are typical curves obtained from the model tests. On these curves, the envelope of the vibration record has been plotted against the number of cycles of vibration after release. Originally it was the authors' intention to calculate the logarithmic decrement from the tests of the dampers. However, the decrement was found to vary so widely with amplitude (or number of cycles) that it appeared more instructive to plot the envelope of the vibration record against the number of cycles.

Fig. 5 shows typical vibration-record envelopes obtained from the tests of the spherical damper for one value of tuning ($\psi = 0.91$) and for different values of fluid viscosity N. On this curve is also shown the results of tests when the cup is half-filled with fluid ($H = 0.5$), and also using 1 or 5 drops of fluid. The difference between the performance when the sphere is covered with fluid and when using 1 or 5 drops of fluid is surprising.

Fig. 6 is a cross-plot of several curves similar to those of Fig. 5. The cross-plots were arbitrarily taken at 10 cycles. The curves, Fig. 6, show that the optimum value of the viscosity number is not very critical, e.g., a considerable variation in viscosity number is permissible in order to obtain optimum performance. In Fig. 10 is a cross-plot of Fig. 6, taken at the point of optimum viscosity number N. This curve shows the effect of tuning on the amplitude ratio at 10 cycles. The optimum tuning occurs for $\psi = 1$ which is similar to that for the steady-state operation of a tuned dynamic-vibration absorber. It is also seen from this curve that the damper is effective over a wide range of frequency ratios, ψ.

Typical curves obtained from the tests of the cylindrical-damper model are given in Fig. 7. A study of these curves reveals that, with the damper half-full of fluid, there is too much damping of the roller even when the lightest (least viscous) fluid available (acetone) is used. Further, the best performance of the damper occurs, as is the case with the spherical dampers, when using a small amount of fluid (1 drop).

After examining the curves in Fig. 7 together with other curves showing the damper performance at different tuning ratios ψ, it was suggested to groove the roller so that optimum performance might possibly be obtained with the roller half-covered with fluid and also while using a fluid having a greater viscosity than acetone.

An example of some of the records obtained with the grooved cylindrical roller is given in Fig. 8. Here, with the roller half covered with fluid, it was possible to determine the optimum viscosity number N with the fluids available for test. It is also to be noted that, with the smaller viscosities, beats occurred in the vibration record.

Fig. 9 shows a typical cross-plot taken arbitrarily at 10 cycles from five groups of curves similar to Fig. 8; the five groups of curves being the results of tests with five different tuning ratios ψ, and for one value of groove size ($R = 0.02$). The curves, Fig. 11, have been obtained from a set of four curves similar to those of Fig. 9, each set of curves representing tests with a different groove size, R.

Referring to Fig. 9, for instance, the optimum viscosity has been taken as the viscosity giving the minimum amplitude ratio (x/x_0) at 10 cycles. The curves, Fig. 11, show as might be

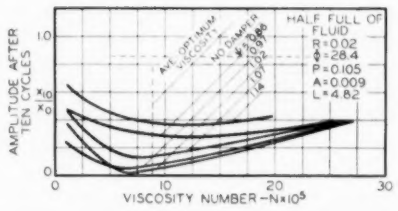


Fig. 9 Cylindrical Damper: Effect of Fluid Viscosity on Amplitude for Various Frequency Ratios

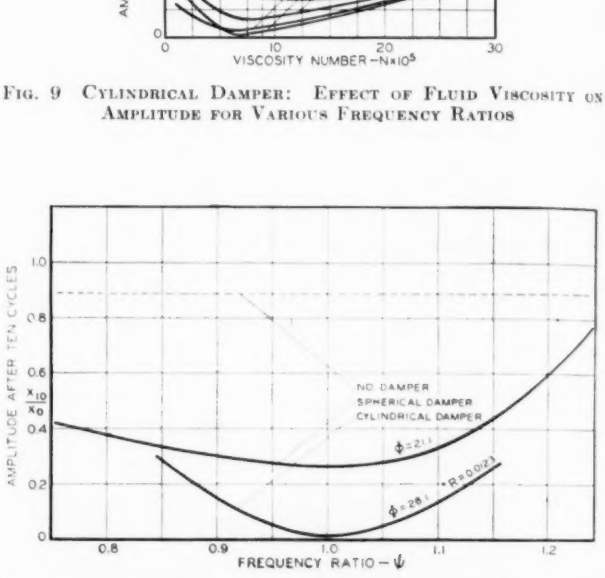


Fig. 10 Spherical and Cylindrical Dampers: Effect of Tuning on Amplitude With Fluid Having Optimum Viscosity

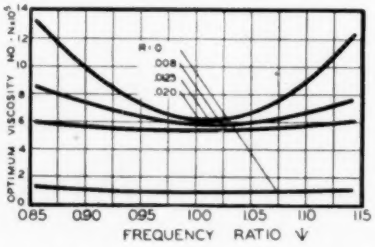


Fig. 11 Cylindrical Damper: Variation of Optimum Viscosity With Tuning and Groove Size

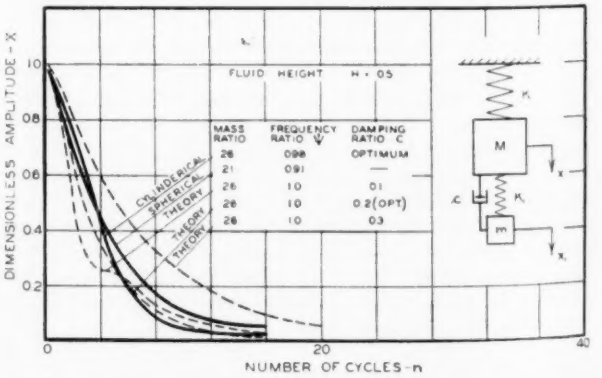


Fig. 12 Spherical and Cylindrical Dampers: Test Curves for Optimum Conditions After Correcting for Inherent Damping of Main System, and Theoretical Curves for the System Shown

expected that the larger the groove size the greater the optimum viscosity. Also, when the damper is not tuned ($\psi \neq 1$), a greater fluid viscosity is required for optimum damper performance. The lower curve in Fig. 10 is a typical curve for the grooved roller, showing the effect of varying the tuning ratio ψ on performance. The fact that the two curves in Fig. 10 are relatively flat is helpful when it is considered that some uncertainty may exist in predicting the natural frequency of the main system to which the dampers are attached.

The best tested performances of the spherical and cylindrical dampers are given in Fig. 12. These curves have been obtained by correcting the actual test results for the damping which was inherent in the main vibration system of the models. A step-by-step graphical integration was carried out, in which the actual vibration record was corrected for the energy absorbed in the main vibration system. The energy absorbed by the main system was determined from a vibration record of the main system without the damper.

The curve, Fig. 12, shows that if a cylindrical damper is placed in a vibrating system having 26 times the mass of the damper, it will reduce an initial deflection of the vibrating system to 4 per cent of its value in 10 cycles.

The dashed-line curves, Fig. 12, have been calculated for an assumed vibration system shown in Fig. 12. The method of calculating these curves is outlined in Appendix 2.

Acknowledgment

The authors wish to express their appreciation for the valuable assistance given them by Mr. R. P. Kroon in the various phases of this work.

Appendix 1

Dimensional Analysis

The purpose of the dimensional analysis is to determine what conditions must be met if we are to test the dampers described, using models which are subjected to terrestrial gravity g, as compared to the high centrifugal field which the dampers would experience in the rotating turbine blade.

Let us assume that we have the system, shown in Fig. 3, p. A-60, consisting of a mass M and spring system K (representing the blade) and a roller or ball m, in a cup or cylinder (representing the damper).

The entire system is in a gravity field expressed by acceleration G. Suppose the mass M is held to one side of the equilibrium position and then suddenly released. Upon what factors does the amplitude of vibration principally depend?

We can say that the amplitude will be some function of the variables, represented as follows

$$x = f\,(G, D, d, M, m, F, \mu, \rho, \gamma, x_0, n, \delta) \ldots\ldots [1a]$$

where the variables are as defined in the nomenclature.

By applying the methods of dimensional analysis[6] it is possible to replace the relation Equation [1a] by another relation containing a smaller number of dimensionless variables.

The theory of dimensional analysis also permits the selection of many different forms for the dimensionless variables. In the present case, we have selected the following forms of the variables and write the relation

$$\text{A function of}\left[X, n, \Omega, N, \Phi, P, A, \left(\frac{m}{\rho D^3}\right), \left(\frac{d}{D}\right), \delta\right] = 0 \ldots [2]$$

which replaces relation Equation [1a] and which is equally as valid as that relation, although it contains three less variables.

In order to determine completely the performance of the tuned dampers previously described, we must find the functional relation Equation [2] for the particular damper, either by calculation or by test.

Obviously, it is impossible to test in a reasonable time the effect of wide variations of all the variables in Equation [2]. For this reason an attempt is made to alter or eliminate some of the variables in Equation [2] by using some other information or assumptions.

The theoretical natural frequency of a sphere in a cup (or a cylinder in a cylindrical hole) without fluid is given by

$$f = \frac{1}{2\pi}\sqrt{C\frac{2G}{D-d}} = \frac{1}{2\pi}\sqrt{\frac{G}{D}}\sqrt{\frac{2C}{1-(d/D)}} \ldots\ldots [3]$$

where

$C = 5/7$ for a sphere

$= 2/3$ for a cylinder

since $F\sqrt{(D/G)} \equiv \Omega$

we write

$$(f/F) = \frac{1}{2\pi\Omega}\sqrt{\frac{2C}{1-(d/D)}} = \text{a function of } \Omega \text{ and } (d/D) \ldots [4]$$

by means of Equation [4], we can replace (d/D) in Equation [2] by (f/F). Further, the dimensionless variable $m/(\rho D^3)$ which is related to the loss of weight of the sphere or cylinder due to floating in the damping fluid is eliminated by noticing that for the sphere

$$m = \frac{4}{3}\pi(d/2)^3 \times \gamma$$

and

$$m/(\rho D^3) = \frac{\pi}{6}(d/D)^3\,(\gamma/\rho)$$

Since from Equation [4] (d/D) is a function of (f/F) and Ω we can write

$$m/(\rho D^3) = \text{a function of } (f/F), \Omega, \text{ and } (\rho/\gamma) \ldots\ldots [5]$$

By means of this relation, we can eliminate $m/(\rho D^3)$ from Equation [2].

For the cylindrical damper a procedure similar to the foregoing is easily carried out giving

$$m/(\rho D^3) = \text{a function of } (f/F), \Omega, (\rho/\gamma), \text{ and } (l/D)$$

where l is the length of the roller.

The term (l/D) together with any other geometrical dimensionless variable should also be incorporated in Equation [2]. With these substitutions we thus obtain the variables

$$\text{A function of } [X, n, \Omega, N, \Phi, \psi, P, A, L,^* \delta] = 0 \ldots [2a]$$

A further simplification has been introduced into Equation [2a] by assuming that the only effect of the term $(\rho/\gamma) = P$ on the damper performance is to change the frequency of the damper due to the floating of the sphere or cylinder. Accordingly, we have changed the definition of f to that given in Equation [6]. It is thought that this would introduce slight error, especially as (ρ/γ) for the model is approximately the full-scale value.

$$f = \frac{1}{2\pi}\sqrt{C\frac{2G[1-(\rho/\gamma)\,(h/D)]}{(D-d)}} \ldots\ldots\ldots [6]$$

[6] "Model Experiments and Forms of Empirical Equations," by E. Buckingham, Trans. A.S.M.E., vol. 37, 1915, p. 263; also, "Dimensional Analysis," by P. W. Bridgeman, Yale University Press, New Haven, Conn., 1931.

* This term is used only for the cylindrical damper.

The term (h/D) in Equation [6] has been introduced to take into account the case where the cylindrical or spherical dampers are not completely filled with fluid.

During the tests of the cylindrical damper, it was found that grooving the roller was necessary in order to obtain optimum damping with the fluid viscosities available for test.

The additional term $R = (r_m/D)$ was then added to the list of variables in Equation [2a]. The quantity r_m is the hydraulic radius of the groove cross section.

After introducing these assumptions, Equation [2a] becomes finally

$$\text{A function of}[X, n, \Omega, N, \Phi, \psi, A, L, R, \delta] = 0 \ldots [2b]$$

Appendix 2

Theoretical Calculation of Damper Performance

The differential equations of motion for the vibration system, shown in Fig. 12, are

$$\left.\begin{aligned} M\ddot{x} + kx + k_1(x - x_1) + c(\dot{x} - \dot{x}_1) &= 0 \\ m\ddot{x}_1 + c(\dot{x}_1 - \dot{x}) + k_1(x_1 - x) &= 0 \end{aligned}\right\} \ldots\ldots [7]$$

where x, x_1 = amplitudes of main and auxiliary systems
k, k_1 = spring constants, Fig. 12
c = damping constant of auxiliary system

Numerical solutions of the differential Equations [7] have been found[7] by first assuming the solution to be of the form

$$\left.\begin{aligned} x &= ae^{st} \\ x_1 &= a_1e^{st} \end{aligned}\right\} \ldots\ldots [8]$$

where a, a_1, and s are constants to be determined, and t = time.

Substituting the relations Equations 8 into Equations [7] and also introducing dimensionless variables, we obtain the frequency equation

$$y^4 + 2C\psi\left(1 + \frac{1}{\Phi}\right)y^3 + (1 + \psi^2)y^2 + 2C\psi\left(1 - \frac{\psi^2}{\Phi}\right)y + \psi^2\left(1 - \frac{\psi^2}{\Phi}\right) = 0 \ldots\ldots [9]$$

where $y = (s/\Gamma)$, $C = c/c_c$, $\psi = \dfrac{\omega}{\Gamma}$

$$\Gamma = \sqrt{\frac{k + k_1}{M}} = \text{frequency of main system}$$

$$\omega = \sqrt{\frac{k_1}{m}} = \text{frequency of auxiliary system}$$

$$c_c = 2\pi\omega = \text{critical damping of auxiliary system}$$

The numerical values of the roots of the frequency Equation [9] have been found using Graeffe's root-squaring method. The roots thus obtained are in the form

$$\left.\begin{aligned} y_1 &= -u_1 \pm iv_1 \\ y_2 &= -u_2 \pm iv_2 \end{aligned}\right\} \ldots\ldots [10]$$

A substitution of the roots into Equations [8] yields the expression for the motion of the main system

$$X = e^{-u_1\Gamma t}[A\cos(v_1\Gamma t) + B\sin(v_1\Gamma t)] + e^{-u_2\Gamma t}[D\cos(v_2\Gamma t) + E\sin(v_2\Gamma t)]$$

where $X = x/x_0$ = amplitude ratio of main system, and A, B, D, E are functions of u_1, v_1, u_2, v_2.

Numerical solutions have been carried out using the method outlined with an assumed value of mass ratio Φ of 26 and a value of tuning ratio ψ of unity. The calculations were carried out for each of three values of the damping ratio C.

One assumed value of the damping ratio C was taken as the value which gives optimum damping of the main system, the other two values give a smaller damping of the main system.

The results of the calculations are plotted in Fig. 12. The calculated curves are seen to check closely the tested curves. These curves also show that there is a tendency for beats to occur in the vibration record when the damping of the auxiliary system is less than the optimum value. This same effect has been found by the tests (refer, for instance, to Figs. 5 and 8).

[7] "Mathematical Methods in Engineering," by Th. von Kármán and M. A. Biot, McGraw-Hill Book Company, Inc., New York, N. Y., 1940, p. 166.

Self-Excited Oscillations in Dynamical Systems Possessing Retarded Actions

By NICHOLAS MINORSKY,[1] CARDEROCK, MD.

There exists a variety of dynamical systems, possessing retarded actions, which are not entirely describable in terms of differential equations of a finite order. The differential equations of such systems are sometimes designated as hysterodifferential equations. An important particular case of such equations, encountered in practice, is when the original differential equation for unretarded quantities is a linear equation with constant coefficients and the time lags are constant. The characteristic equation, corresponding to the hysterodifferential equation for retarded quantities in such a case, has a series of subsequent high-derivative terms which generally converge. It is possible to develop a simple graphical interpretation for this equation. Such systems with retarded actions are capable of self-excitation. Self-excited oscillations of this character are generally undesirable in practice and it is to this phase of the subject that the present paper is devoted.

Introduction

THE forces, or moments, considered in dynamics as functions of parameters, which determine them, are assumed to be instantaneously in phase with these parameters.

For example, a pendulum is acted upon by a couple of gravity $C = mgl \sin \theta$, where θ is the variable parameter, i.e., the angle. The couple C is thus in phase with $\sin \theta$, or θ, for small angles. The differential equations in all such cases are either ordinary differential equations or partial differential equations, as the case may be, but of a finite order.

There exists, however, a rather restricted class of phenomena of the so-called hereditary type, in which the condition of a system at a given instant is determined not only by forces acting at that instant, but depends upon the entire history either of the preceding motion, or the preceding states of the system in general.

V. Volterra has shown that such phenomena can be described mathematically in terms of "integrodifferential equations."

Another variety of systems not entirely describable in terms of differential equations of a finite order are systems possessing "retarded actions." Such systems, designated sometimes as being of a "hysteresis" type, are characterized by the fact that these retarded actions do not depend upon the entire previous history of motion, but merely reproduce variations of corresponding nonretarded actions, or forces, with a certain time lag. The differential equations of such systems are of an infinitely high order. They are designated sometimes as "hysterodifferential equations." So far no general theory for these equations has been developed.

An important particular case of hysterodifferential equations encountered in practical applications is when the original differential equation for unretarded quantities is a linear equation with constant coefficients and the time lags are constant. The characteristic equation, corresponding to the hysterodifferential equation for retarded quantities in such a case, has a series of subsequent high-derivative terms which generally converge. This permits replacing the infinite series of high-derivative terms by its limit which introduces transcendental functions in its expression. Under such circumstances, it becomes possible to give a simple graphical interpretation to this equation.

The most interesting feature of such systems with retarded actions is the fact that they are capable of self-excitation with a theoretically infinite number of frequencies which are determined not only by the parameters of the dynamical system, but also by the parameter of the retarded action, i.e., its time lag.

Such self-excited oscillations are generally undesirable in practice; they are sometimes referred to as "parasitic oscillations" or "hunt."

These oscillations are investigated in this paper.

Systems With a Retarded Action

Retarded actions are generally present in any control system. In fact, a control system B is generally intended to maintain a certain state or level (e.g., of pressure, temperature, voltage, direction in space, rate of motion, etc.) of the system A to be controlled.

A departure of A from its normal state of equilibrium causes B to operate so as to eliminate this initial departure. During this "return-trip" transmission of action (from A to B) and reaction

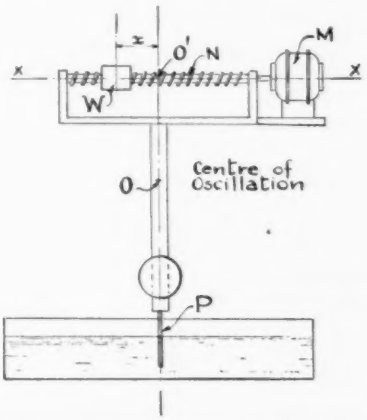


Fig. 1 System of Physical Pendulum in Which Occur Self-Excited Oscillations

(from B to A), a certain time interval Δt elapses, so that the control action, arriving back at A at a certain instant t, does not correspond to the condition of A at this instant but relates to the condition which A had in the past, i.e., at the instant $(t - \Delta t)$.

As an example of a system in which such self-excited oscillation was originally observed, consider a physical pendulum shown in Fig. 1. The differential equation of motion of the pendulum

[1] The David Taylor Model Basin, Bureau of Ships, United States Navy Department.

Presented at the National Meeting of the Applied Mechanics Division, Philadelphia, Pa., June 20–21, 1941, of The American Society of Mechanical Engineers.

Discusson of this paper should be addressed to the Secretary, A.S.M.E., 29 West 39th Street, New York, N. Y., and will be accepted until July 10, 1942, for publication at a later date. Discussion received after the closing date will be returned.

Note: Statements and opinions advanced in papers are to be understood as individual expressions of their authors, and not those of the Society.

with velocity damping (e.g., produced by a paddle P moving in viscous fluid) is

$$J\ddot{\theta} + B\dot{\theta} + C\theta = 0 \quad [1']$$

where θ is the angle of oscillation and J, B, C are the moment of inertia, the coefficient of the damping, and the "effective spring constant" of the pendulum, respectively.

Assume now that, in addition to the natural damping $B\dot{\theta}$, an artificially produced damping is provided, e.g., a weight w is displaced for that purpose along the axis x-x perpendicular to the axis of the pendulum at O, by means of a motor M acting through a worm N. If the motion of the weight is so controlled[2] that its distance x from the middle point O' is proportional to angular velocity $\dot{\theta}$ of the pendulum, it is clear that the moment of the weight w applied to the pendulum is $wx = S\dot{\theta}$, so that the differential equation of the pendulum is now

$$J\ddot{\theta} + B\dot{\theta} \pm S\dot{\theta} + C\theta = 0 \quad [1]$$

The double sign before $S\dot{\theta}$ means that there are two ways of connecting the control to produce the moment of that kind. If the control is so connected as to increase the damping, the sign + must be taken and the equation in this case becomes

$$J\ddot{\theta} + (B + S)\dot{\theta} + C\theta = 0 \quad [2]$$

It may be seen from the form of Equation [2] that the action of the weight so controlled will merely increase the natural coefficient B of damping of the oscillating system.

However, in addition to this expected behavior, the pendulum, under certain conditions, begins to oscillate spontaneously with a much higher frequency than that corresponding to its own damped period, or to that of an externally applied disturbing moment. For example, a pendulum having a natural period of about 7 sec was found to oscillate with a period of less than 1 sec with amplitude of a fraction of a degree. This particular case will be studied in this paper as a typical case of self-excitation caused by a retarded-action phenomenon.

Hysterodifferential Equation of Motion

In the foregoing simplified treatment of the problem, it was tacitly assumed that the control system acts with an infinite rapidity, i.e., with a zero time lag. In reality, the term $S\bar{\theta}$ is a retarded quantity (in the following treatment, the bar above a symbol designates that the corresponding quantity is retarded). In the arrangement described, this means that, whereas an ideal control should introduce a lever arm x corresponding to the present instant t of motion, the real control introduces x which relates to a past instant $(t - \Delta t)$ where Δt is the time lag.

Since the angular velocity $\dot{\theta}(t)$, considered as a function of time, is a continuous function with continuous derivatives under the normal conditions (absence of impulsive forces) it can be expanded in Taylor's series

$$\bar{\dot{\theta}} = \dot{\theta} - \Delta t\ddot{\theta} + \frac{\Delta t^2}{2!}\dddot{\theta} - \frac{\Delta t^3}{3!}\theta^{IV} + \dots \quad [3]$$

Equation [3] expresses the retarded value $\bar{\dot{\theta}}$ of angular velocity in terms of nonretarded values of $\dot{\theta}$ and its higher derivatives.

Substituting $\bar{\dot{\theta}}$ into the differential equation

$$J\ddot{\theta} + B\dot{\theta} + S\bar{\dot{\theta}} + C\theta = 0 \quad [4]$$

[2] There are several ways of accomplishing this; one of the simplest consists in mounting a small constrained gyroscope on the pendulum so that it will not interfere with the motion. This gyro can control through a vacuum-tube system the speed of the motor in proportion to $\dot{\theta}$. By providing a follow-up arrangement between the excursion of the weight and the control current, the couple of the form $S\dot{\theta}$ can be produced.

Using Equation [3]

$$S\left[\dots(-1)^n\frac{\Delta t^n}{n!}\theta^{(n+1)} + \dots - \frac{\Delta t^3}{3!}\theta^{IV} + \frac{\Delta t^2}{2!}\ddot{\theta} - \Delta t\cdot\dddot{\theta} + \ddot{\theta}\right] + J\ddot{\theta} + B\dot{\theta} + C\theta = 0 \quad [5]$$

Equation [5] is a hysterodifferential equation of motion of the pendulum. It is seen that this is an equation of an infinitely high order, with absolute values of higher-order terms decreasing with the increasing order.

It is to be noted that the new equation is still linear; there appear therefore new frequencies corresponding to an infinite number of roots of its characteristic equation.

One could proceed by limiting the number of terms of the higher order to some finite number and investigating the equation in this manner. Such procedure is generally complicated and there is no certainty as to whether the effect of terms of the higher order is negligible or not.

It is preferable for that purpose to transform this equation to a different form, owing to the fact that the series of terms of a gradually increasing order is always convergent.

Asymptotic Form of the Hysterodifferential Equation

Equation [3] can be written

$$\bar{\dot{\theta}} = \dot{\theta}\left[1 - \Delta t\frac{\ddot{\theta}}{\dot{\theta}} + \frac{\Delta t^2}{2!}\frac{\dddot{\theta}}{\dot{\theta}} - \frac{\Delta t^3}{3!}\frac{\theta^{IV}}{\dot{\theta}} + \dots\right] \quad [6]$$

Since the original hysterodifferential Equation [5] is linear with constant coefficients, it is satisfied by a solution $\theta = \theta e^{zt}$ where $z = (\alpha + i\omega)$; $(i = \sqrt{-1})$.

Forming the subsequent derivatives entering into the ratios $\ddot{\theta}/\dot{\theta}$, $\dddot{\theta}/\dot{\theta}$, ..., one finds that these ratios are z, z^2, z^3 ... so that Equation [6] becomes

$$\bar{\dot{\theta}} = \dot{\theta}\left(1 - \Delta tz + \frac{\Delta t^2}{2!}z^2 - \frac{\Delta t^3}{3!}z^3 + \dots\right) = \dot{\theta}e^{-\sigma} \quad [7]$$

where $\sigma = \Delta t\cdot z = \alpha\cdot\Delta t + i\omega\cdot\Delta t = \gamma + i\varphi$, putting $\alpha\cdot\Delta t = \gamma$ and $\omega\cdot\Delta t = \varphi$.

Substituting $\bar{\dot{\theta}} = \dot{\theta}e^{-\sigma}$ into Equation [4]

$$J\ddot{\theta} + (B + Se^{-\sigma})\dot{\theta} + C\theta = 0 \quad [8]$$

This is another form of the hysterodifferential Equation [5] in which the infinite series of higher time derivatives arising from Taylor's expansion has been replaced by its sum, $Se^{-\sigma}\cdot\dot{\theta}$.

Substituting $\theta = \theta_0 e^{zt}$ into Equation [8]

$$[Jz^2 + (B + Se^{-\sigma})z + C]\theta_0 e^{zt} = 0 \quad [9]$$

In order to have solutions other than trivial ones $\theta_0 = 0$, it is necessary to equate the bracket to zero, since $e^{zt} \neq 0$; this gives

$$Jz^2 + (B + Se^{-\sigma})z + C = 0 \quad [10]$$

For self-excitation it is necessary to make $\alpha > 0$ initially. In fact, in such a case, being given a small departure θ_0 initially, the process of self-excitation will be started according to the law $\theta = \theta_0 e^{\alpha t}e^{i\omega t}$.

As regards ω, the angular frequency, it is always a positive quantity. The solution of the problem is thus reduced to that of Equation [10].

Substituting $z = (\alpha + i\omega)$

$$J(\alpha + i\omega)^2 + (B + Se^{-\gamma}e^{-i\varphi})(\alpha + i\omega) + C = 0$$

Since $e^{-i\varphi} = \cos\varphi - i\sin\varphi$, this gives rise to two equations obtained by putting separately the real and the imaginary parts equal to zero

$$\left.\begin{aligned} J(\alpha^2 - \omega^2) + B\alpha + Se^{-\gamma}(\alpha\cos\varphi + \omega\sin\varphi) + C = 0 \\ 2J\alpha\omega + B\omega + Se^{-\gamma}(\omega\cos\varphi - \alpha\sin\varphi) = 0 \end{aligned}\right\} \ldots [11]$$

Transferring terms with $Se^{-\gamma}$ on one side of Equations [11] and dividing them out (which eliminates $Se^{-\gamma}$), finally upon rearranging the terms according to the power of α

$$(J\sin\varphi)\alpha^3 + (B\sin\varphi + J\omega\cos\varphi)\alpha^2 + [(J\omega^2 + C)\sin\varphi]\alpha + \omega[(J\omega^2 - C)\cos\varphi + B\omega\sin\varphi] = 0 \ldots [12]$$

Equation [12] arranged according to the powers of ω is

$$(J\cos\varphi)\omega^3 + [(J\alpha + B)\sin\varphi]\omega^2 + [(J\alpha^2 - C)\cos\varphi]\omega + [(C + B\alpha + J\alpha^2)\alpha\sin\varphi] = 0 \ldots [13]$$

Conditions of self-excitation are fulfilled in the domain where both α and ω are real and positive.

Dividing both equations by $\cos\varphi$

$$(J\tan\varphi)\alpha^3 + (B\tan\varphi + J\omega)\alpha^2 + [(J\omega^2 + C)\tan\varphi]\alpha + \omega[(J\omega^2 - C) + B\omega\tan\varphi] = 0 \ldots [14]$$

$$J\omega^3 + [(J\alpha + B)\tan\varphi]\omega^2 + (J\alpha^2 - C)\omega + \alpha(C + B\alpha + J\alpha^2)\tan\varphi = 0 \ldots [15]$$

Zones of Self-Excitation

Taking $\tan\varphi$ as a factor in the preceding equations

$$\tan\varphi = -\frac{\omega[J\alpha^2 + (J\omega^2 - C)]}{J\alpha^3 + B\alpha^2 + (C + J\omega^2)\alpha + B\omega^2} \ldots [16]$$

Since the observed self-oscillations are generally above the synchronism $(J\omega^2 - C) > 0$ and because $\alpha > 0$, $\tan\varphi < 0$ during the transient period of self-excitation; that is $\pi/2 < \varphi < \pi$, or $3\pi/2 < \varphi < 2\pi$.

The self-excited process eventually reaches a stable condition when $\alpha = 0$. Equation [16] shows that in this case

$$\tan\varphi_0 = -\frac{J\omega^2 - C}{B\omega} \ldots [17]$$

On the basis of Equation [16], it cannot be determined whether the self-excitation is possible below the synchronism $(J\omega^2 - C) < 0$. It will be shown in the following that only the oversynchronous case of self-excitation is possible.

During the transient period when the amplitudes are still increasing $(\alpha > 0)$, $\tan\varphi > \tan\varphi_0$; this can be seen by putting $\alpha = \infty$ in Equation [16], which gives $\tan\varphi = -0$. The self-excitation starts thus in the region of $\varphi = \pi - \epsilon$ (ϵ being a small quantity) and approaches the value of φ_0 given by Equation [17] for a steady state.

An Alternative Method

Dividing Equation [14] by $\tan\varphi$

$$J\alpha^3 + (B + J\omega\operatorname{cotan}\varphi)\alpha^2 + (J\omega^2 + C)\alpha + \omega[(J\omega^2 - C)\operatorname{cotan}\varphi + B\omega] = 0 \ldots [18]$$

In this form, the first term of the equation is positive; the equation being of an odd degree in α has certainly one real root, this root is positive, as required by the condition of self-excitation if the last term is negative. Since $\omega > 0$, this condition is equivalent to

$$(J\omega^2 - C)\operatorname{cotan}\varphi + B\omega < 0$$

whence

$$\tan\varphi > -\frac{J\omega^2 - C}{B\omega}$$

Designating the absolute value of $\tan\varphi$ by $|\tan\varphi|$ this gives

$$|\tan\varphi| < \frac{J\omega^2 - C}{B\omega}$$

For a stable state of self-excitation $\alpha = 0$; in this case the last term of Equation [18] vanishes, which gives $|\tan\varphi_0| = \dfrac{J\omega^2 - C}{B\omega}$ as previously found. Therefore, the condition for an oversynchronous excitation is

$$|\tan\varphi| \leq \frac{J\omega^2 - C}{B\omega} \ldots [19]$$

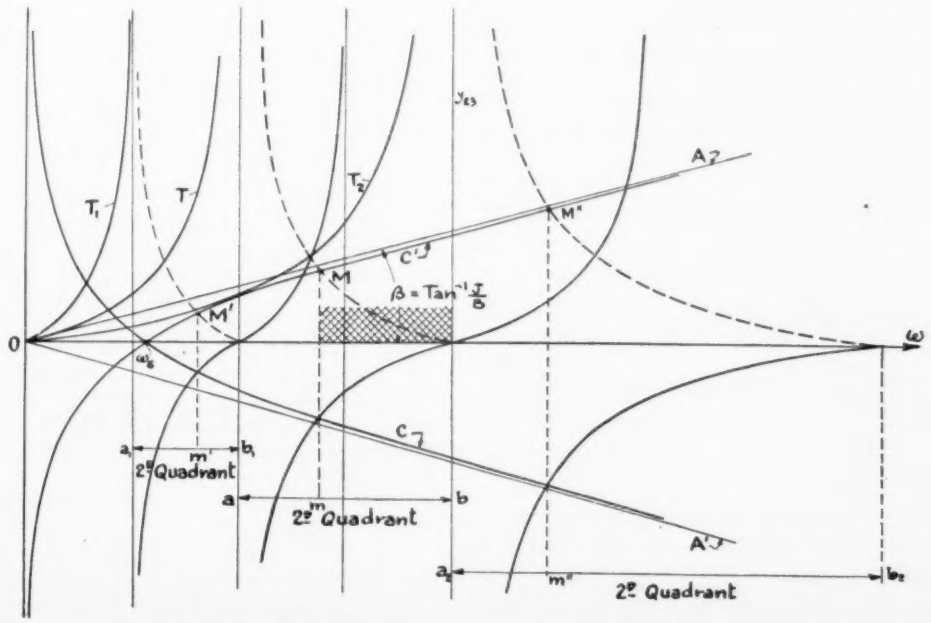


FIG. 2 GRAPHICAL REPRESENTATION OF CONDITIONS OF SELF-EXCITATION

the sign $<$ holds for the transient condition and $=$, for the steady state.

Graphic Interpretation

These conditions of self-excitation are represented graphically in Fig. 2 in which $\tan \varphi = \tan (\omega \Delta t)$ is plotted against ω as curve T. Tan φ undergoes discontinuities for $\varphi = \omega \Delta t = n\pi/2$ ($n = 1, 3, 5, \ldots$). Absolute values of tan φ are also plotted in dotted lines in even quadrants where $\tan \varphi < 0$.

Straight lines OA and OA' have angular coefficients respectively equal to $+J/B$ and $-J/B$; the curves B and B' are hyperbolas $+ C/B\omega$ and $-C/B\omega$ referred to the axes y and ω as asymptotes; these curves B, B' are omitted in Fig. 2.

By adding algebraically the ordinates of curves B and A' and those of curves B' and A, curves C and C' are obtained. Curve C has for its equation, $y_c = \dfrac{C}{B\omega} - \dfrac{J}{B}\omega = -\dfrac{J\omega^2 - C}{B\omega}$, and the equation for curve C' is

$$y_c' = -\frac{C}{B\omega} + \frac{J\omega}{B} = \frac{J\omega^2 - C}{B\omega}$$

Both curves intersect the abscissa axis at the point $\omega_s = \sqrt{C/J}$ which corresponds to the undamped synchronism of the system.

Condition of self-excitation of parasitic oscillations, given by the criterion, Equation [19], is found in the diagram, Fig. 2, between the ordinate y_{23} separating the second and the third quadrants and the abscissa of the point M, which is the intersection of curves C' and $|\tan \varphi|$. Within this range the inequality of Equation [19] is, in fact, satisfied.

The limit frequency is at the point m, the abscissa of M. The shaded area indicates the range of frequencies within which the self-excitation occurs in a transient state ($\alpha > 0$).

Vector Diagrams

The foregoing criteria show that the self-excitation above synchronism is possible in the second as well as in the fourth quadrants which means that these two oscillations may be of two different frequencies.

A further restriction to this multiplicity of possible frequencies is obtained from a consideration of conditions of dynamical equilibrium of moments applied to the dynamical system.

In view of the fact that this question resembles closely a similar question encountered in the theory of alternating currents, a parallel study of both problems is useful.

The differential equation of an electric circuit, containing an inductance L, resistance R, and capacity C, in series, and acted upon by electromotive force $E = E_0 e^{j\omega t}$ is[3]

$$L\frac{di}{dt} + Ri + \frac{1}{C}\int i\,dt = E_0 e^{j\omega t}$$

Differentiating this equation

$$L\frac{d^2i}{dt^2} + R\frac{di}{dt} + \frac{1}{C}i = E_0 j\omega e^{j\omega t} \quad \ldots\ldots\ldots [20]$$

The differential equation of a pendulum acted upon by an external moment $D = D_0 e^{j\omega t}$ is

$$J\frac{d^2\theta}{dt^2} + B\frac{d\theta}{dt} + C\theta = D_0 e^{j\omega t} \quad \ldots\ldots\ldots\ldots [21]$$

It is seen that the differential Equations [20] and [21] are identical in form, with the exception that the right side of the electrical equation figures the derivative of $E_0 e^{j\omega t}$, whereas, in the dynamical equation appears the nondifferentiated quantity $D_0 e^{j\omega t}$.

As the result of this, the real and the imaginary axes are inverted in electrical and mechanical vector diagrams. For example, the vector representing Rdi/dt is along the real axis in the electrical diagram, whereas, the vector $Bd\theta/dt$, representing an analogous physical quantity (the dissipation of energy), is along the imaginary axis in the mechanical diagram.

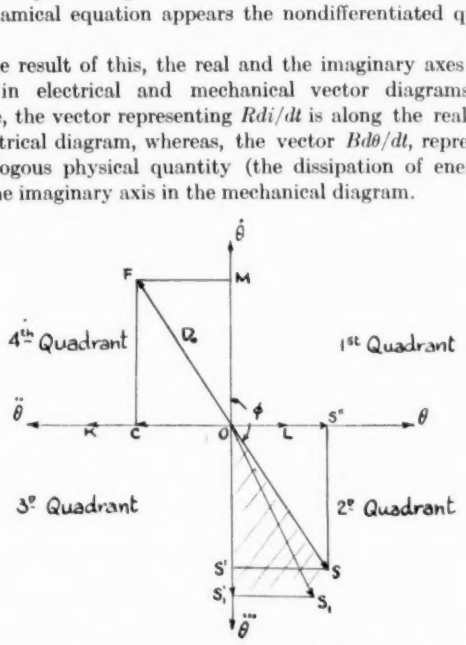


Fig. 3 Dynamical-Vector Diagram of Steady State of Self-Excitation

With this change of a formal character, the dynamical vector diagram of the steady state of self-excitation is shown in Fig. 3.

Vector $OL = C\theta_0$ is in phase with the angle θ

Vector $OM = jB\omega\theta_0$ is in phase with the angular velocity $\dot\theta$

Vector $OK = -J\omega^2\theta_0$ is in phase with the angular acceleration $\ddot\theta$

Vector $OC = OK + OL = (C - J\omega^2)\theta_0$

The vector sum $OC + CF = OC + OM = [(C - J\omega^2) + jB\omega]\theta_0$ clearly represents the left side of Equation [21] upon substituting $\theta = \theta_0 e^{j\omega t}$. Hence, OF represents the amplitude D_0 of the external moment with its phase relatively to θ.

When the self-excitation exists, the external moment D is absent. Since for dynamical equilibrium the polygon OCF is to be closed, a vector OS equal and opposite is necessary for this purpose. Thus, vector OS represents the retarded action, lagging behind the vector OM from which it is derived by an angle φ ($\pi/2 < \varphi < \pi$). This vector OS is in the second quadrant as previously found by another method. Tan φ is therefore negative and its absolute value is $|\tan \varphi| = OC/OM = \dfrac{J\omega^2 - C}{B\omega}$, as found previously, Equation [19].

The vectors in the diagram represent the moments acting on the system. If they are multiplied by ω they are capable of representing the power. It is seen from the diagram Fig. 3 that the conditions of self-excitation can be formulated as follows: (1) $OM = OS'$ and (2) $OC = OS''$.

The first condition states that the power output from the system caused by the dissipation of energy $B\dot\theta$ must be equal to the power input into the system through the component $OS' = OS \cos \varphi$ of the retarded action OS. This latter component figures therefore on the same basis as a negative-resistance effect in an electric circuit; it is well known that in an electric circuit no self-excitation is possible without a negative-resistance element's being present in the circuit.

The second condition $OC = OS''$, that is, $\theta_0(J\omega^2 - C) = OS \sin \varphi$ merely fixes the frequency of self-excitation.

Since OM is always directed along the imaginary axis upward, the vector OS' being equal and opposite to it, is always

[3] In order to avoid confusion in the following equations, j designates $\sqrt{-1}$ and i the electric current in this section on "Vector Diagrams."

directed along the same axis downward. This means that the vector OS can only be either in the second or in the third quadrant. In the first case, the self-excitation is above synchronism and in the second below it.

Thus, the retarded action OS can never be either in the first or in the fourth quadrants, if the self-excitation is to occur at all.

The condition of self-excitation previously found $|\tan \varphi| \leqslant \frac{J\omega^2 - C}{B\omega}$ has a simple significance in the vector diagram. In fact, since φ is contained between the limits $\frac{\pi}{2} < \varphi < \pi$ the previous condition means that the vector OS must be either somewhere inside the shaded area (during transient condition) or along the line OS. In the first case when it is, say, at OS_1 its projection is $OS_1' > OM$. In other words, in order to start the self-excitation, it is necessary to have the initial input of energy into the system greater than its dissipation. But as soon as the self-excitation is established, S_1 comes to S and $OS' = OM$, which corresponds to the steady state $\left(\tan \varphi = \frac{J\omega^2 - C}{B\omega}\right)$, as seen from the diagram; in such a case, the energy input through the retarded action $S\bar{\theta}$ is equal to its dissipation $B\dot{\theta}$.

Theoretically, if the self-excitation occurs in the second quadrant, it must also occur in the sixth, tenth, etc., quadrants, by adding $2\pi n$ (n being an integer). Such higher-order self-excitations correspond however to much higher frequencies and cannot be observed in practice; the only quadrant of interest from the standpoint of self-excitation is therefore the second quadrant.

Effect of Time Lag on Self-Excitation

If the time lag is made smaller, the spacing of quadrants for $\tan \varphi$ curves becomes wider for the same frequency scale on the abscissa axis (curves T_2 in Fig. 2); for larger time lags the spacing of quadrants becomes more crowded (curves T_1).

Curves C, C', and, hence, the synchronous frequency of the system remain the same, since they do not depend upon the time lag.

Time lags, assumed in the construction of Fig. 2, are half the size for the curve T_2 and twice as large for T_1, than the time lag adopted for curve T. For this latter case, the stable frequency is at the point m. For smaller time lag (curve T_2), it is at the point m'' and for a larger lag (curve T_1) it is at m'. All three points m, m', m'' are in the second quadrants of their respective frequencies (ab, a_1b_1, and a_2b_2).

Thus, it can be seen that the frequency of self-excitation decreases with an increasing time lag and vice versa. This is generally observed in practice.

Within the frequency range a_2b_2 of the second quadrant and small time lag, the self-excited frequency m'' is nearer to the point a_2 than to the point b_2. For large time lag m' approaches the end b_1 of its frequency range a_1b_1.

Thus, with a sufficiently small time lag, the point m'' may come so close to the point a_2 that the self-excitation may disappear entirely. This will happen when the vertical projection OS' of OS (Fig. 3) will become smaller than the vector OM. At this point, the energy input into the self-excitation process becomes smaller than the losses inherent in its maintenance. It is a well-known fact that systems with very small time lags behave practically in a "dead-beat" manner.

Conversely, for a large time lag, the point m' comes closer to the point b_1 in the second quadrant (Fig. 2). In the diagram Fig. 3, the vector OS representing the retarded action approaches the downward position. In such a case the conditions for the maintenance of the hunt are the most favorable. In fact, it is usually observed that a relatively low-frequency hunt, due to large time lags, is very persistent.

Effect of Fixed Parameters on Self-Excitation

If the time lag is small, the frequency of self-excitation is relatively high and the difference of ordinates of the curve C', Fig. 2, and its asymptote A is negligible. The angular coefficient of the asymptote A is J/B. The point of intersection M of the curve C' with the curve $|\tan \varphi|$ becomes practically identical with that of A with the same curve $|\tan \varphi|$.

The greater this ratio J/B, the nearer comes the frequency m to the critical value $\pi/2\Delta t$ at which the self-excitation ceases. The self-excited frequency thus decreases with an increasing inertia J and decreasing damping B.

Conversely, if this ratio decreases, the asymptote A rotates clockwise and the point M moves along the curve $|\tan \varphi|$ toward the point $\omega = \pi/\Delta t$ in the frequency range; the self-excited frequency increases in this case.

Thus, at a constant inertia, an increase of damping increases the frequency of the parasitic oscillation. In view of the fact that the amplitude of the parasitic oscillation is generally very small, it is difficult to provide an efficient damping.

As regards the parameter C, the spring constant of the system, it enters into the determination of the curve C' and not of its asymptote A. If, on the other hand, the time lag is small enough, the difference of ordinates between the curve C' and its asymptote A is negligible. This shows that the effect of C is also negligible, as compared to the other two factors, i.e., inertia J and damping B.

Effect of the Variable Parameter S on Self-Excitation

Parameter S, characterizing the intensity of self-excitation, that is, of the retarded action, does not appear in the preceding equations. This is due to the fact that Equations [11] were divided out so as to eliminate $Se^{-\gamma}$.

In order to be able to take into account the influence of this factor on self-excitation, Equation [10] must be studied directly. Since the determination of the regions in which the self-excitation is possible has been made already, the study can be simplified by putting $\alpha = 0$.

The condition for the existence of a steady self-excited oscillation is $\theta = \theta_0 e^{i\omega t}$, where i again designates $\sqrt{-1}$.

Putting $\sigma = i\omega\Delta t = i\varphi$ in Equation [8]

$$J\ddot{\theta} + (B + Se^{-i\varphi})\dot{\theta} + C\theta = 0 \quad \ldots\ldots\ldots\ldots [22]$$

Since $e^{-i\varphi} = \cos \varphi - i \sin \varphi$, this equation becomes

$$J\ddot{\theta} + (B + S\cos\varphi)\dot{\theta} - iS\sin\varphi \cdot \dot{\theta} + C\theta = 0 \quad \ldots\ldots [22a]$$

For a harmonic oscillation $\theta = \theta_0 e^{i\omega t}$, $\dot{\theta} = i\omega\theta$, whence $-i\dot{\theta} = \omega\theta$. This gives

$$J\ddot{\theta} + (B + S\cos\varphi)\dot{\theta} + (C + S\omega\sin\varphi)\theta = 0 \quad \ldots\ldots\ldots [23]$$

For a steady state of self-excitation, clearly $B + S\cos\varphi = 0$, whereas, during the transient state ($\alpha > 0$), $(B + S\cos\varphi) < 0$; thus in general $B + S\cos\varphi \leqslant 0$; that is, $\cos\varphi \leqslant -B/S$.

Since both B and S are positive, φ is in the second quadrant; as to the fourth quadrant, it is ruled out as was previously explained.

Furthermore, since $\cos\varphi < 1$, $S > B$; that is, the self-excitation of oscillations cannot occur if the coefficient of intensity of the retarded action is smaller than the coefficient B of damping.

This is obvious from a physical consideration, since $S\dot{\theta}$ and $B\dot{\theta}$ are proportional to the energy input into the system and its dissipation, respectively. Clearly, the self-excitation becomes impossible if the average energy input into the system is less than its dissipation.

For a steady state of self-excitation $J\bar{\theta} + (C + S\omega \sin \varphi)\theta = 0$ and, since $\sin \varphi = \sqrt{1 - (B/S)^2}$ this gives

$$J\bar{\theta} + (C + \omega\sqrt{S^2 - B^2})\theta = 0 \quad \ldots\ldots\ldots [24]$$

The steady frequency of self-excitation is thus given by the positive root of the quadratic equation

$$J\omega^2 - \omega\sqrt{S^2 - B^2} - C = 0$$

that is

$$\omega = \omega_1 + \sqrt{\omega_1^2 + \omega_0^2} \quad \ldots\ldots\ldots [24a]$$

where $\omega_1 = \sqrt{S^2 - B^2}/2J$ and $\omega_0 = \sqrt{C/J}$.

For $S = B$, $\omega = \omega_0$; the self-excitation cannot occur below this value for S.

Thus, no self-excitation is possible below the synchronism which rules out the possibility of self-excitation in the third quadrant.

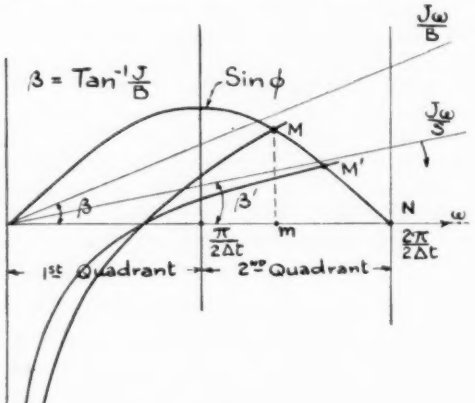


FIG. 4 GRAPHICAL CONSTRUCTION SHOWING SELF-EXCITATION RESULTING FROM INTRODUCTION OF SIN φ

The self-excitation is thus possible only in the second quadrant ($\pi/2 < \varphi < \pi$). If S is increased, Equation [24] shows that the self-excited frequency increases as long as it remains within the range in which the self-excitation is possible, as previously investigated.

In order to be able to show how the self-excited frequency changes with S, the diagram of Fig. 2 must be changed so as to introduce this factor. Arranging the first Equation [11] according to the powers of α

$$J\alpha^2 + (B + Se^{-\gamma} \cos \varphi)\alpha + [(C - J\omega^2) + Se^{-\gamma}\omega \sin \varphi] = 0$$

The condition for $\alpha \geqslant 0$ is $[(C - J\omega^2) + Se^{-\gamma}\omega \sin \varphi] < 0$; that is

$$\sin \varphi \leqslant \frac{J\omega^2 - C}{\omega} \frac{1}{Se^{-\gamma}} \quad \ldots\ldots\ldots [25]$$

From the second Equation [11]

$$\alpha = -\frac{\omega[B + Se^{-\gamma} \cos \varphi]}{2J\omega - Se^{-\gamma} \sin \varphi} \quad \ldots\ldots\ldots [26]$$

Since $B + Se^{-\gamma} \cos \varphi \leqslant 0$, from Equation [26] for $\alpha > 0$, it follows that $2J\omega - Se^{-\gamma} \sin \varphi \geqslant 0$, that is

$$\sin \varphi \leqslant \frac{2J\omega^2}{\omega Se^{-\gamma}} \quad \ldots\ldots\ldots [27]$$

Comparing inequalities of Equations [25] and [27], it is observed that the first dominates the second, because if the first is satisfied, the second is satisfied eo ipso; hence, only the inequality, Equation [25], is of interest.

For a steady state $e^{-\gamma} = 1$ and we have

$$\sin \varphi = \frac{J\omega^2 - C}{S\omega} \text{ and } \cos \varphi = -\frac{B}{S} = -\frac{B\omega}{S\omega}$$

Thus, it is seen that, although both $\sin \varphi$ and $\cos \varphi$ depend upon S, this factor was eliminated in the expression for $\tan \varphi$, with which the previous formulas were established.

If now $\sin \varphi$ is introduced into the graphical construction of Fig. 4, instead of $\tan \varphi$, this dependence upon S will appear. This is shown in Fig. 4.

The essential difference between the two diagrams is in the fact that the angular coefficient of the asymptote is now J/S (S being a variable quantity) and not J/B as it was in the case of Fig. 2. The limit frequency is reached as soon as S reaches the value B. The point M represents this limiting frequency m. It is obtained by the intersection of curves $\sin \varphi$ and $\dfrac{J\omega^2 - C}{B\omega}$.

If S is increased, the representative point comes to M' (intersection of curves $\sin \varphi$ and $\dfrac{J\omega^2 - C}{S\omega}$, with $S > B$). With S increasing, the asymptote turns in the direction of the arrow and the stable frequency approaches the limit N at which the self-excitation disappears.

In fact, it is generally observed that, for a sufficiently intense coupling S, the parasitic oscillations disappear and the system becomes "dead beat."

GENERALIZATION

Although the preceding study relates to a rather particular case of self-excitation, a further generalization of this theory does not present any difficulties.

It must be noted that, in establishing the preceding relations, a number of simplifying hypotheses were tacitly assumed:

1 The retarded moment is a linear function of the corresponding parameter. For example, in the analysis, this function was simply $S\bar{\theta}$, where S is a constant.

2 The dynamical system is governed by a linear differential equation with constant coefficients.

3 Time lag Δt is constant.

The first condition means that the retarded moment reproduces the retarded element of motion $(\bar{\theta}, \dot{\bar{\theta}}, \ddot{\bar{\theta}})$ without any distortion.

The second condition permits of applying the principle of superposition of component motions arising from the infinity of roots of the characteristic equation of the original Equation [5]. This, in turn, permits reducing that equation to its asymptotic form Equation [8], since the original equation is satisfied by the solution of the form $\theta_0 e^{zt}$ under such circumstances.

The last condition merely specifies the definiteness of Taylor's expansion, introduced into the problem.

These conditions introduce a certain idealization of real problems. By waiving them, the problems become more complicated, or even impossible to solve.

On the other hand, as was mentioned on several occasions, the conclusions derived from such an idealized formulation of the problem, seem to be in a fairly good agreement with the observed facts.

It is possible, under such assumptions, to extend the preceding theory to a greater variety of cases, by introducing the retarded moment $S_1\bar{\theta}^k$ into the original differential Equation [1']. The index k in this notation refers to the order of the corresponding derivative; the retarded moment previously investigated in accordance with this notation is $S_1\bar{\theta}$, in so far as it is obtained from the first derivative.

It is possible, in this manner, to investigate the effect of other retarded couples, such as $S_0\bar{\theta}$ (retarded angle), $S_2\bar{\ddot{\theta}}$ (retarded acceleration), etc., which may appear in different problems.

The following hysterodifferential equations are written in the asymptotic form:

$$J\ddot{\theta} + B\dot{\theta} + (C + S_0\epsilon^{-\sigma})\theta = 0 \quad \text{[I]}$$

$$J\ddot{\theta} + (B + S_1\epsilon^{-\sigma})\dot{\theta} + C\theta = 0 \quad \text{[II]}$$

$$(J + S_2\epsilon^{-\sigma})\ddot{\theta} + B\dot{\theta} + C\theta = 0 \quad \text{[III]}$$

$$S_2\epsilon^{-\sigma}\ddot{\theta} + J\ddot{\theta} + B\dot{\theta} + C\theta = 0 \quad \text{[IV]}$$

Equation [II] was studied in detail in the preceding sections. Equation [I] is obtained, if the moment of the weight w in the dynamical model, shown in Fig. 1, is so timed as to be in phase with the angle θ. In Equation [III] this timing must be in phase with $\ddot{\theta}$ and, in Equation [IV], in phase with $\bar{\theta}$, and so on.

In all these cases, as well as in combinations of such cases, the procedure is the same as that previously explained in connection with Equation [II]:

1 To substitute a solution $\theta = \theta_0\epsilon^{zt}$ which leads to the characteristic equation in asymptotic form, Equation [8].

2 To expand the characteristic equation by substituting $z = \alpha + i\omega$. In this manner, by equating separately the real and the imaginary parts to zero, two equations are obtained.

3 By eliminating $S\epsilon^{-\sigma}$ between these two equations one equation is obtained which is arranged according to the powers of α. These equations are of a gradually increasing order in terms of α, e.g., quadratic for Equation [I], cubic for Equation [II], quartic for Equation [III], etc.

4 The next step is to establish the conditions for existence of at least one positive real root for α, which determines the zones within which the self-excitation is possible.

5 The limit of self-excitation is obtained by putting $\alpha = 0$ in the equation for α.

The angle φ, obtained in this manner, always designates the lag of the retarded quantity with respect to the quantity from which it derives.

The interesting feature obtained from a comparison of different hysterodifferential Equations [I] to [IV] is that, in the vector diagram, the retarded vector $S_k\theta^k$ is always in the second quadrant as specified in Fig. 3. This is due to the fact that the vector diagram imposes two additional conditions for self-excitation, i.e., the energy input into the system must be equal to its dissipation and the self-excited frequency is always above synchronism.

It was shown in connection with Equation [II], in which the retarded moment is of the form $S_1\bar{\dot{\theta}}$, this angle φ_1 is contained between the limits $\pi/2 < \varphi_1 < \pi$, which brings the retarded vector in the second quadrant.

On the other hand, if a similar calculation is reproduced in connection with Equation [I], it is found that $0 < \varphi_0 < \pi/2$; but, since θ lags by $\pi/2$ behind $\dot{\theta}$, the retarded vector $S_0\bar{\theta}$ in this case is still in the second quadrant.

Thus the following important conclusions are reached:

1 The self-excitation can appear in any case, whether the retarded action is introduced through $\bar{\theta}$, $\bar{\dot{\theta}}$, or $\bar{\ddot{\theta}}$, etc. But, once it is established, the retarded vector (either $S_0\bar{\theta}$ or $S_1\bar{\dot{\theta}}$, or $S_2\bar{\ddot{\theta}}$) must be necessarily in the second quadrant, Fig. 3. This requires that the self-excitation must occur with such a frequency as will give $0 < \varphi < \pi/2$ in the first case ($S_0\bar{\theta}$), or $\pi/2 < \varphi_1 < \pi$ in the second case ($S_1\bar{\dot{\theta}}$), or $\pi < \varphi_2 < 3\pi/2$ in the third case ($S_2\bar{\ddot{\theta}}$), etc.

In other words the relative phase angle φ between the retarded and nonretarded quantities constitutes an additional degree of freedom of the phenomenon, by which the retarded vector $S_k\bar{\theta}^k$ can maintain itself in the second quadrant as required by the condition of the balance of energy, by which the energy input into the system is equal to its dissipation.

2 From a formal standpoint, the hysterodifferential equations are characterized by the fact that at least one of their coefficients is complex. The reduction of this coefficient to the real quantities introduces additional terms in the coefficient of the next order (higher or lower) and this gives the conditions of self-excitation analytically.

3 There exist an infinite number of frequencies of self-excitation forming a discrete spectrum, corresponding to the infinity of roots of the characteristic equation. In practice, generally only one first frequency is observed if the time lag is small enough, the other frequencies cannot be observed on account of the smallness of their amplitudes.

Conclusion

Although the preceding analysis was made in connection with a pendulum of a particular type, the results obtained are quite general.

In fact, in all control systems (dynamical, electrodynamical, electrical, hydraulic, thermal, etc.), there always exists a time lag Δt in the cyclic process of their operation. A mathematical description of such a process in terms of a hysterodifferential equation simplifies the commonly established procedure of introducing "couplings" between the different parts of the system which generally lead to ordinary differential equations of a relatively high order; this usually involves considerable difficulties if one attempts to discuss the characteristic equation algebraically. Furthermore, the nature of coupling very frequently remains unknown, particularly in dynamical problems.

On the other hand, in establishing a hysterodifferential equation of a retarded control, one must know only the over-all time lag Δt, without the necessity of knowing the intermediate links in the system. Whenever this time lag is known, the application of the foregoing method is very simple.

Conversely, in a given system in which self-excited parasitic oscillations are observed, it is possible to determine the time lag from the frequency of oscillations and known parameters of the system.

It can also be shown that the self-excitation of electric oscillations (e.g., thermionic-vacuum-tube generator) can be reduced to a retarded-action phenomenon, that is, it can be expressed in terms of a hysterodifferential equation. The only difference in the case of mechanical oscillations studied is in the fact that the phase angle φ, governing the condition of self-excitation in the electrical problem, is determined by the parameters of the electric circuit (L, C, R, M) and not by the time lag Δt directly. The criteria of self-excitation are practically the same in both cases.

It is possible that the condition of self-excitation of oscillations both in electrical and mechanical systems can be better generalized on the basis of retarded-action effect common to both problems than by studying each problem, so to speak, in its own plane.

The benefit of analogies between similar problems of different engineering professions is too well known to need any additional emphasis here.

Acknowledgment

The writer is indebted to Prof. Sheffer, of the mathematics Department, The Pennsylvania State College, for valuable assistance during the preliminary discussion of this problem.

Torsion of Multiconnected Thin-Walled Cylinders

By F. M. BARON,[1] NEW HAVEN, CONN.

The author develops an arithmetical procedure for the analysis of problems of torsion. The method of analysis presented is one of successive approximations. The solution to a problem is guessed at and successively corrected until the controlling conditions of static equilibrium and of continuity of deformation are satisfied. The convergence is reasonably rapid but may be hastened with a little judicious guessing. The problem under immediate discussion is a straight hollow member with constant cross section subject to a torque about the longitudinal axis of the member. Other applications and extensions of the method presented are suggested at the end of the paper. The arithmetical procedure is illustrated by an example.

Introduction

THE problem of torsion of multiconnected thin-walled cylinders may occur in the design of structural or machine members, but particularly in the design of frames of ships, floating dry docks, and airplane wings.

It is usually desired to determine the magnitude of the stresses on a cross section and, perhaps, the angle of twist per unit of length of the member. If the total torque and the distribution of stresses on the cross section are known, the magnitude of the stresses may be computed by arithmetic. The distribution of the stresses is controlled by the conditions of static equilibrium and of continuity of deformation. The two sets of conditions are interrelated through the defined properties of the material. The problem, then, is to determine the distribution of the stresses on a cross section.

In general, the analysis of complicated members by the use of stress functions or by formal algebraic procedures is either difficult or inconvenient. There are limitations and objections to the use of models in studying the problem.

H. M. Westergaard has suggested[2] that an arithmetical procedure may be developed for analyzing problems of torsion. The arithmetical procedure presented here is similar to that developed by Hardy Cross for the analysis of flow in networks of conduits.[3]

Conditions of Static Equilibrium and of Continuity

The properties of the member dealt with in the present and succeeding sections will now be defined. The member is shown in Fig. 1.

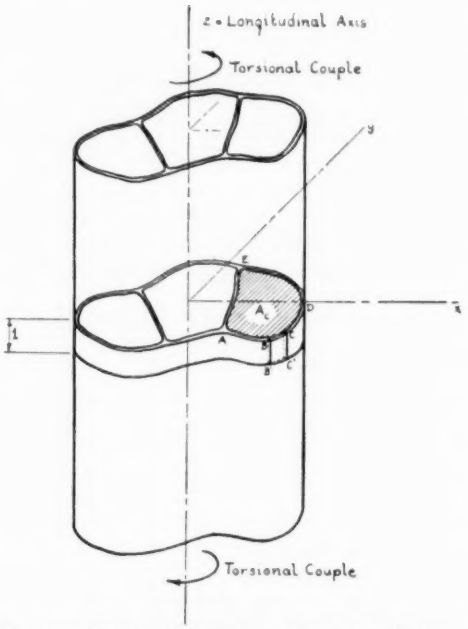


Fig. 1 Straight Hollow Member of Constant Cross Section Subject to a Torque About Its Longitudinal Axis

1 The member is straight, of constant cross section, and of homogeneous, elastic, isotropic material.

2 All the elements of a cross section rotate through the same angle. The angle is proportional to the longitudinal co-ordinate of the cross section and the constant α measuring the angle of twist per unit of length.

3 The displacement of any element of any cross section in the direction of the longitudinal axis is a function of the transverse co-ordinates only.

4 The member is hollow with walls so thin in proportion to the important transverse dimension that the shearing stresses may be assumed uniformly distributed across the thicknesses of the walls.

It is recognized that this paper does not discuss the instability of exceedingly thin walls, nor the problem of torsion when plane sections remain plane after deformation. The ordinary theory of torsion as presented first by Barré de Saint Venant is based on assumptions 1, 2, and 3. The derivations of the fundamental equations of the theory are available in a number of places in the literature.[4] It is sufficient here to summarize the relations necessary for the present work.

Consider a horizontal slice through the member shown in Fig. 1. Let the height of the slice be one unit, this unit being assumed small. Let a total force f be transferred across the thickness t of the wall at section B. The unit shear at section B is the force f divided by the thickness t. The equilibrium conditions of the element $BB'CC'$ require a total force f to be transferred across

---

[1] Assistant Professor of Civil Engineering, Department of Civil Engineering, Yale University.

[2] In a lecture at Harvard University, Graduate School of Engineering, March 2, 1937.

[3] "Analysis of Flow in Networks of Conduits or Conductors," by Hardy Cross, University of Illinois Engineering Experiment Station, Bulletin No. 286, 1936.

Presented at the Annual Meeting, New York, N. Y., December 1–5, 1941, of The American Society of Mechanical Engineers.

Discussion of this paper should be addressed to the Secretary, A.S.M.E., 29 West 39th Street, New York, N. Y., and will be accepted until July 10, 1942, for publcation at a later date. Discussion received after the closing date will be returned.

Note: Statements and opinions advanced in papers are to be understood as individual expressions of their authors and not those of the Society.

[4] "Theory of Elasticity," by S. Timoshenko, McGraw-Hill Book Company, Inc., New York, N. Y., 1934, pp. 228–284; particularly pp. 241 and 267–270.

the thickness of the wall at section C. Then, at any junction of walls, the condition of static equilibrium requires that the quantity of force f "flowing" into a junction must equal the quantity of force f "flowing" away from a junction.

Continuity of the deformations along a closed path such as $ADEA$ requires that the algebraic sum along the closed path of the relative displacements in the direction of the longitudinal axis must be zero. This requirement plus assumptions 1, 2, and 3 lead to Bredt's formula

$$\oint \frac{f}{t}\,dL = 2G\alpha A_c$$

that is, the product of the constant $2G\alpha$ and the area A_c within a closed circuit must equal the algebraic sum of the products of the unit shears $\frac{f}{t}$ and the increments of length along the closed circuit.[4] The constant G is the modulus of elasticity in shear.

Analysis of Torsion by Successive Approximations

The method of analysis presented here is a method of successive approximations. The solution to a problem is guessed at and approximately corrected. The revised answer is treated as a new guess and successively corrected until a reasonable degree of precision is obtained. The convergence is reasonably rapid and the method is useful. With some experience and judicious guessing, the convergence may be speeded up.

The method of analysis proposed always satisfies the condition of statics and successively corrects the errors in continuity of deformation until the condition of continuity is also satisfied. Other orders of procedure have been tried by the author but the foregoing is recommended for its simplicity.

The order of computations made in the method of successive approximations is as follows:

1 Assume a distribution of forces f along the walls satisfying the condition of statics.

2 Compute the following:

(*a*) The area A_c within each elementary closed circuit.

(*b*) The quantity $\frac{\text{Length } L}{\text{Thickness } t}$ for each wall.

(*c*) The quantity $\frac{1}{\Sigma L/t}$ for each elementary closed circuit.

3 Compute the algebraic sum $\Sigma f\frac{L}{t}$ for each closed circuit with due attention to the circulation ↻ or ↺ of the forces in the circuit.

4 Choose a constant $2G\alpha$ for the section, making the product of $2G\alpha$ and the area A_c within each elementary closed circuit approximately equal to the quantity $\Sigma f\frac{L}{t}$ of the circuit.

5 For each closed circuit, compute the correction $\Delta\Sigma f\frac{L}{t}$ needed to make the resultant quantity $\Sigma f\frac{L}{t}$ equal to $2G\alpha A_c$.

6 For each wall of each closed circuit multiply the corrections $\Delta\Sigma f\frac{L}{t}$ by the corresponding factors $\frac{1}{\Sigma\frac{L}{t}}$ of the circuits. Write the result Δf by the wall with due attention to the circulation of the correcting forces.

7 Compute the revised forces.

Treat the revised forces as new guesses and repeat steps 3, 5, 6, and 7 to any desired precision.

The method proposed has the advantage in that errors are not cumulative and, if made, are ultimately eliminated. It has also the desirable characteristic that an approximation to the relative distribution of forces is quickly seen.

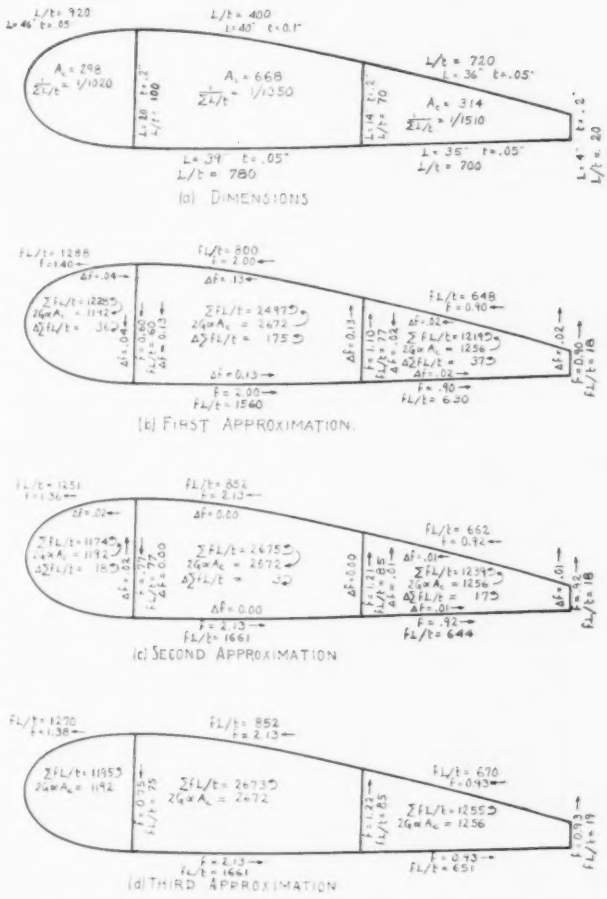


FIG. 2 COMPUTATIONS FOR SUCCESSIVE APPROXIMATIONS

The computations may be shortened by making the procedure one of successive corrections instead of successive approximations. Instead of computing the revised forces after each correction, it may be expedient to "carry over" the excessive or deficient circulation from the adjacent closed circuits. For the procedure of successive corrections, the first five computations are identical to those outlined for successive approximations. The succeeding computations are then as follows:

6 Compute the quantity $\frac{L/t}{\Sigma L/t}$ for each wall of each closed circuit.

7 For each wall of each closed circuit multiply the correction $\Delta\Sigma fL/t$ by the factor $\frac{L/t}{\Sigma L/t}$ of the wall. Write the result $\Delta fL/t$ by the wall with due attention to the circulation of the correcting flow.

8 For each closed circuit compute only the circulation "carried over" from the adjacent closed circuits. Distribute an equal but opposite circulation to each wall of the circuit according to the multiplier $\frac{L/t}{\Sigma L/t}$ of the wall. Repeat the procedure to any desired precision.

9 To compute the total correction force Δf in each wall, add up the total amount of $\Delta fL/t$ in the wall and multiply by t/L of the wall.

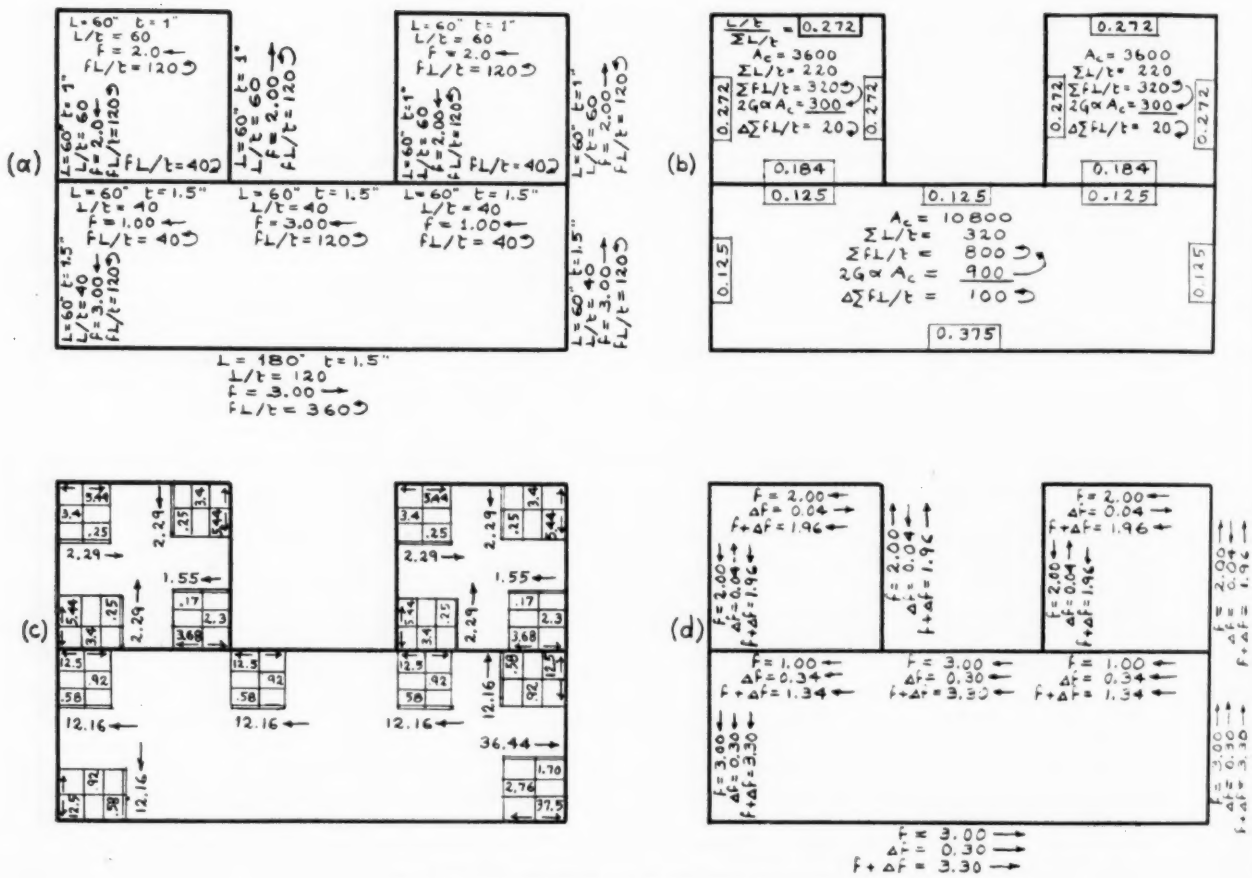


FIG. 3 COMPUTATIONS FOR SUCCESSIVE CORRECTIONS

The arrangements of computations suggested for the procedures outlined are illustrated in Figs. 2 and 3, respectively. Along each wall write the quantity L/t, the assumed force f with its direction, and the value fL/t with its direction. Write the quantity $\Sigma L/t$ inside each elementary closed circuit, and the quantities $\frac{L/t}{\Sigma L/t}$ of each wall along the wall and inside the circuit considered. Write in each elementary circuit the value of the area A_e, the value $\Sigma fL/t$ with its circulation ↻ or ↺, and the selected value of $2G\alpha A_e$. Put a curved arrow pointing to the smaller of the last two values. The arrow will show the circulation of the first correction $\Delta\Sigma fL/t$. The difference between the values of $\Sigma fL/t$ and $2G\alpha A_e$ is the magnitude of the first correction $\Delta\Sigma fL/t$. For the procedure of successive corrections, with due attention to the circulation of the corrections, write in columns perpendicular to each wall and inside each circuit the products of the corrections $\Delta\Sigma fL/t$ and the factor $\frac{L/t}{\Sigma L/t}$ of the wall.

CONCLUSIONS

The solution of the problem is correct when the conditions of static equilibrium and of continuity are satisfied. The convergence is apparently rapid but may be improved with a little judicious guessing. It is possible to get any reasonable degree of precision but, if a greater degree is wanted, considerable increase in computation is required. The method of successive approximations is recommended for its simplicity, rapidity of convergence, and generality. The answers to some problems of torsion may be obtained by successive guesses instead of successive approximations. Obviously the technique used in recording the computations depends upon the particular problem. The order and arrangements of computations may be simplified in cases of members with simple cross sections.

This paper deals directly only with straight hollow members with constant cross section. Members with a solid cross section may be studied by dividing the section into a network or grid. Clearly the related problems of fluid flow, current flow, membranes, and stress functions may be solved in the same way.

A Simple Air Ejector

By J. H. KEENAN[1] and E. P. NEUMANN,[2] CAMBRIDGE, MASS.

This paper reports the results of an investigation in which the authors studied the performance of the simplest form of ejector which would function in a useful manner. An attempt was made to analyze the data as nearly independent of other work on ejectors as possible, and to compare the performance with that predicted analytically. The primary purpose of the study was to test the utility and validity of a method of analysis, and not to devise a new type of ejector.

Previous Studies

THE many analyses that appear in the literature of ejectors may be classified into three groups: (*a*) Those that analyze only the essentially reversible processes at the entrance to and the exit from the mixing tube; (*b*) those that simplify the mixing process by assuming it to occur at constant pressure; and (*c*) those that simplify the mixing process by assuming it to occur at constant cross-sectional area.

Type (*a*) is too conventional to justify citing references. Type (*b*) is well exemplified by the work of Stodola[3] and of Bosnjakovíc.[4] The latter shows that if wall friction is neglected, the maximum ratio of secondary flow to primary flow is obtained if the mixing occurs at zero pressure. Of course, when wall friction is considered there will result a best pressure for mixing for any one apparatus.

It appears that the type (*c*) analysis has been published only by Flügel.[5] In fact, Flügel generalized his analysis so that mixing could take place partly at constant pressure and partly at constant cross-sectional area. He concluded, however, that it was best to have all mixing occur at constant area. He compares his analytical results based on this assumption with experimental data for a single ejector and finds excellent agreement. The agreement is to a minor degree the result of judicious selection of values for empirical coefficients in his analysis, but it is nevertheless striking.

Object of Present Investigation

The object of the investigation reported in this paper, was to select the simplest form of ejector which would perform in useful fashion, to analyze its performance as nearly independently of data on ejectors as possible, and to compare the actual performance with that predicted analytically. The objective is not to devise an ejector which is new or excellent, but rather to test the utility and the validity of a method of analysis.

The ejector chosen consists of a cylindrical tube (the mixing tube) with a rounded converging entrance, Fig. 1. A nozzle, which is fed with fluid at high pressure, discharges into the entrance to this tube. The stream for this nozzle entrains fluid in the tube and causes a secondary flow from a supply chamber surrounding the nozzle. The primary and secondary streams mix and issue from the tube into the atmosphere.

A better ejector can be devised by attaching a diffuser to the exit end of the mixing tube. However, since this device introduces a new independent variable (namely, the pressure at the exit of the mixing tube), it was not employed. It is hoped that analysis and experiments for an ejector with a diffuser can be presented later.

Reasons for Mixing at Constant Area

The design of the ejector is such that, when the primary nozzle discharges into the throat of the secondary nozzle, mixing of the two streams occurs at constant total cross-sectional area, Fig. 1. In the analysis, results of which are compared with experiment in the various figures, it is assumed that all mixing occurs at

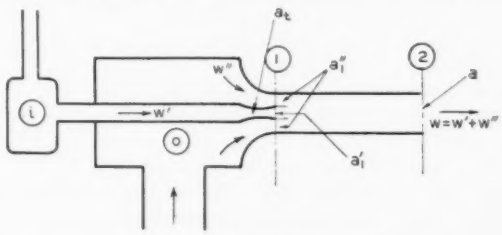


Fig. 1 The Simple Ejector

constant cross-sectional area. The reasons for this emphasis on mixing at constant area are as follows:

1 An ejector of this type can pump secondary fluid into an exhaust space at a pressure, p_2, higher than the pressure in the secondary chamber, p_0. If mixing occurs at constant pressure instead of at constant area, the pressure at the exit of the mixing tube cannot exceed the pressure in the secondary supply chamber. This means that in the absence of a diffuser a constant-pressure type of ejector can serve only as a blower and not as a pump.

2 Even when the ejector is serving as a blower, i.e., delivering air at the pressure of the secondary supply chamber, constant-area mixing gives higher secondary flows for a given exit area than constant-pressure mixing. Indeed, as shown by Fig. 2,[6] constant-area mixing gives higher secondary flows than any combination of constant-area and constant-pressure mixing.

Exception can be taken to these last two statements only at very small ratios of the area of the mixing tube to the area of the primary nozzle. Further consideration of small area ratios is given in the Appendix and in Fig. 18.

Analysis

Assume (*a*) that the primary fluid expands reversibly and adiabatically from a chamber *i* (Fig. 1) where its velocity is zero to a section 1 where it issues from the primary nozzle. This sec-

[1] Professor, Mechanical Engineering, Massachusetts Institute of Technology. Mem. A.S.M.E.

[2] Massachusetts Institute of Technology.

[3] "Steam and Gas Turbines," by A. Stodola, McGraw-Hill Book Company, Inc., New York, N. Y., vol. 2, 1927, p. 927.

[4] "Über Dampfstrahlgebläse," by Bosnjakovíc, *Zeitschrift für die Gesamte Kälte-Industrie*, vol. 43, 1936, pp. 229–233.

[5] "Berechnung von Strahlapparaten," by G. Flügel, *V.D.I. Forschungsheft*, no. 395, Berlin, 1939; also *Zeitschrift des Vereines deutscher Ingenieure*, vol. 83, 1939, pp. 1065–1069.

Presented at the Annual Meeting, New York, N. Y., December 1–5, 1941, of The American Society of Mechanical Engineers.

Discussion of this paper should be addressed to the Secretary, A.S.M.E., 29 West 39th Street, New York, N. Y., and will be accepted until July 10, 1942, for publication at a later date. Discussion received after the closing date will be returned.

Note: Statements and opinions advanced in papers are to be understood as individual expressions of their authors, and not those of the Society.

[6] See Appendix for the analysis on which Fig. 2 is based.

tion 1 is also the entrance to the mixing tube. Using subscripts to denote the locations indicated in Fig. 1, we may write

$$V_1' = \sqrt{2gRT_i \frac{k}{k-1}\left[1 - \left(\frac{p_1}{p_i}\right)^{\frac{k-1}{k}}\right]} \quad \ldots\ldots [1]$$

and

$$a_1' = \frac{w'v_1'}{V_1'} = \frac{w'v_i'}{V_1'}\left(\frac{p_i}{p_1}\right)^{\frac{1}{k}} \quad \ldots\ldots [2]$$

where V denotes velocity, T temperature, R the gas constant, k the isentropic exponent, a the cross-sectional area of the stream,

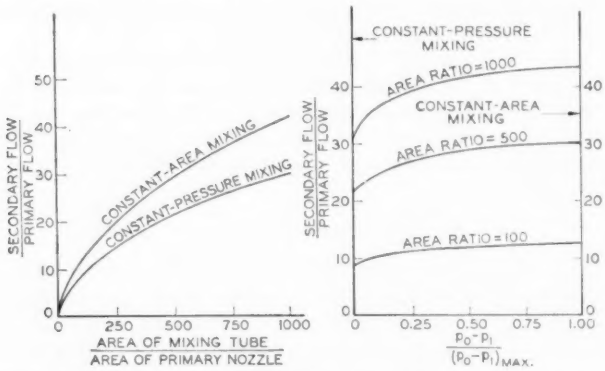


FIG. 2 PERFORMANCE OF EJECTOR FOR VARIOUS DEGREES OF MIXING AT CONSTANT PRESSURE
(The fluid is assumed incompressible. For analysis see Appendix.)

v the specific volume, and g the acceleration given to unit mass (the pound) by unit force (the pound). The superscript $'$ is used here to refer to the primary stream and the superscript $''$ is used later to refer to the secondary stream.

Assume (*b*) that the secondary fluid expands reversibly and adiabatically from a chamber 0 where its velocity is zero to the section 1 at the entrance to the mixing tube. Then we may write

$$V_1'' = \sqrt{2gRT_0 \frac{k}{k-1}\left[1 - \left(\frac{p_1}{p_0}\right)^{\frac{k-1}{k}}\right]} \quad \ldots\ldots [3]$$

and

$$a_1'' = \frac{w''v_1''}{V_1''} = \frac{w''v_0}{V_1''}\left(\frac{(p_0)}{(p_1)}\right)^{\frac{1}{k}} \quad \ldots\ldots [4]$$

Assume (*c*) that the primary and secondary streams mix as they pass adiabatically through a tube of constant area. The streams enter this tube at section 1 and leave at uniform velocity at section 2. It is assumed that the frictional forces applied by the stream on the walls of the tube are negligible. Nevertheless the process is highly irreversible because the condition of uniform velocity at 2 can only be realized through irreversible mixing of the two streams.

For the process 1–2, we may write the continuity equation

$$w = w' + w'' \quad \ldots\ldots [5]$$

the momentum equation

$$\frac{w'}{g}V_1' + \frac{w''}{g}V_1'' + p_1 a = \frac{w}{g}V_2 + p_2 a \quad \ldots\ldots [6]$$

and the energy equation

$$w'h_i + w''h_0 = w\left(h_2 + \frac{V_2^2}{2g}\right) \quad \ldots\ldots [7]$$

where w and a denote, respectively, the flow and the cross-sectional area at section 2, and h denotes enthalpy per unit mass of fluid.

We shall assume that the initial temperatures of the two streams are identical, that is, $T_i = T_0$. It follows that $h_i = h_0$. By virtue of this relation and Equation [5], Equation [7] becomes $h_i = h_2 + \frac{V_2^2}{2g}$. Noting that the change in enthalpy is equal to the specific heat multiplied by the change in temperature and that the velocity V_2 may be expressed in terms of the flow, area, and specific volume at 2, we get

$$c_p T_i = \frac{k}{k-1}p_2 v_2 + \left(\frac{w}{a_2}\right)^2 \frac{v_2^2}{2g} \quad \ldots\ldots [8]$$

This is a relation between v_2 and w/a_2 for given values of T_i and p_2.

METHOD OF SOLUTION

The method of solving the foregoing equations is one of successive approximations. First, let the throat area of the primary nozzle, a_i, be unity. Then select values for a, T_i, p_i, p_0, and p_2. For these selected values we must find the magnitudes of p_1 and w''/w'. We proceed as follows: Compute w' from the usual expression for isentropic flow through a throat of unit area from given initial conditions. Assume a value for p_1, compute V_1' from Equation [1], a_1' from Equation [2], and V_1'' from Equation [3]. Then $a_1'' = a - a_1'$ and w'' may be found from Equation [4]. Next compute w from Equation [5] and calculate w/a. Using this latter value in Equation [8], we may solve for v_2. Now we find a value for V_2 from $V_2 = \frac{wv_2}{a}$. Thus we have values for all the quantities in Equation [6]. If Equation [6] is not satisfied, a new value for p_1 is assumed, and the procedure outlined is repeated. By this method the calculated curves of Figs. 9, 11, 12, 13, 14, and 15 were found.

EXPERIMENTAL APPARATUS

The arrangement of the experimental apparatus is shown in Fig. 3. The primary stream of air passes through a strainer and

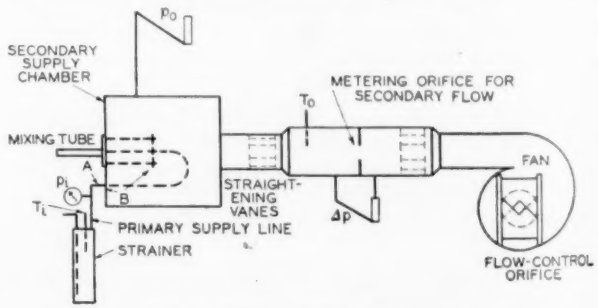


FIG. 3 EXPERIMENTAL APPARATUS

the tube A on its way to the primary nozzle at the entrance to the mixing tube. The initial pressure of the primary stream p_i is measured by a Bourdon-tube gage. The effect of friction between the gage and the nozzle was negligible except, perhaps, for the largest nozzle.

The secondary stream enters the mixing tube from a large chamber, which is supplied with air by a fan. The pressure in the chamber is controlled by means of a variable orifice at the entrance to the fan. A sharp-edged orifice is provided for measuring the secondary flow. The pressure drop across the orifice is measured by an inclined water manometer. Straightening vanes precede and follow the metering orifice.

The position of the primary nozzle relative to the entrance to the mixing tube is varied by moving the tube A in and out through guides B.

Details of the mixing tube are shown in Fig. 4. The converging entrance is $1^{5}/_{16}$ in. long. This part of the passage is referred to hereafter as the "secondary nozzle." The "throat" of the secondary nozzle is the cross section at the downstream end of the convergence. It is also the entrance to the parallel (constant-area) portion of the mixing tube. The pressure in the throat was measured at the pressure tap shown in Fig. 4. The length of the mixing tube was varied by attaching extensions as indicated.

Details of the primary nozzles are shown in Fig. 5. The nozzles

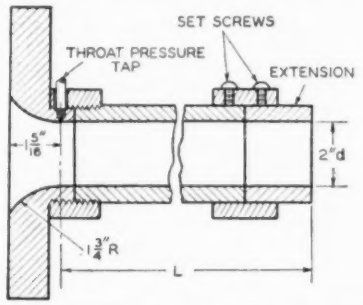
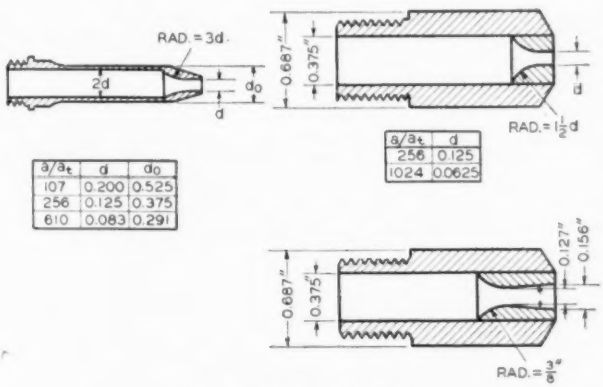


FIG. 4 SECONDARY NOZZLE AND MIXING TUBE



a/at	d	d0
107	0.200	0.525
256	0.125	0.375
610	0.083	0.291

a/at	d
256	0.125
1024	0.0625

FIG. 5 PRIMARY NOZZLES

used in the earlier tests were blunt-ended with thick walls. A nozzle with the same size throat as the largest of these (0.125 in. diam) was made with thin walls tapered toward the outlet to cause as little interference as possible with the secondary stream. No difference was found between the performance of the blunt nozzle and that of the tapered nozzle. Nevertheless, all subsequent tests were made with tapered nozzles.

Only one converging-diverging nozzle was used. Converging nozzles were used in general, because a single nozzle could be used over a wide range of initial pressures of the primary stream. However, the analysis was based on the assumption that the primary nozzle was always of the proper ratio of exit area to throat area. The tests with the single converging-diverging nozzle show distinctly better agreement with the analysis.

MEASUREMENT OF FLOWS

The secondary flow was measured by means of the metering orifice shown in Fig. 3. Coefficients for this orifice were obtained from A.S.M.E. data.[7]

The primary nozzles were calibrated by means of a gasometer. Each primary nozzle was then used as the metering nozzle for its own flow.

The flow through the primary nozzle was calculated from the usual expression for isentropic flow, namely

$$0.531\, a_t \frac{p_i}{\sqrt{T_i}}$$

where a_t denotes the throat area of the nozzle. This area was at first found from measurements of the diameter of the nozzle throat. After calibrations were made, the magnitude of a_t was altered for two nozzles, in order to bring the calculated flow into agreement with the flow as measured by the gasometer. For the other four nozzles, the change indicated was so small that it could be neglected. Table 1 shows for each nozzle the diameter as measured directly, the effective diameter as found from measurements with the gasometer, and the diameter employed to calculate primary flows. It is probable that the uncertainty in the flows is about ±1 per cent. The flow ratio is uncertain to slightly more than 1 per cent.

TABLE 1 NOZZLE DATA

Diameters, in., Measured	effective	Used	Type
0.0625	0.0625	0.0625[a]	Converging, thick wall
0.081	0.0805	0.0810[b]	Converging, thin wall
0.125	0.125	0.125	Converging, thick wall
0.125	0.125	0.125	Converging, thin wall
0.127	0.128	0.128[a]	Converging-diverging
0.200	0.193	0.193[b]	Converging, thin wall

[a] Measured by Thomas McElrath, Jr., reported in master's thesis, Massachusetts Institute of Technology, Cambridge, Mass., 1941.
[b] Measured by Dr. Joseph Kaye.

RESULTS OF EXPERIMENTS

Tests were made to determine the effect of variation in the position of the nozzle exit relative to the throat of the secondary nozzle. The pressure rise across the mixing tube ($p_2 - p_0$) was zero for these tests.

Fig. 6, showing the flow ratio plotted against the position of the

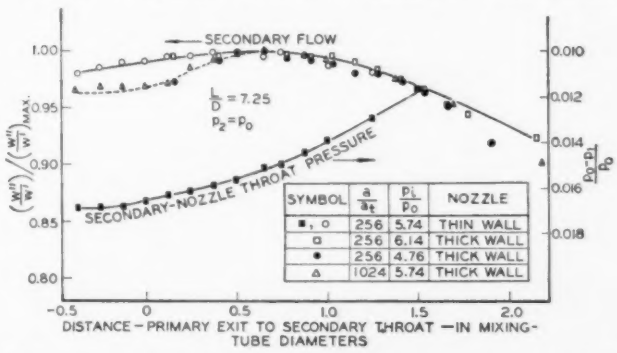


FIG. 6 EFFECT OF POSITION OF PRIMARY NOZZLE ON THROAT PRESSURE AND FLOW RATES

nozzle exit, indicates that the highest flow ratio is attained when the nozzle exit is slightly more than one half a mixing-tube diameter upstream from the throat of the secondary nozzle. The analysis given in the Appendix demonstrates that the best position for the nozzle exit is in the throat of the secondary nozzle. Some discrepancy from the analytical result is to be expected in view of the assumptions that the nozzle is properly diverged, that the secondary flow experiences no friction on the surfaces with which it comes in contact, and that the plane of the secondary-nozzle throat is one of uniform pressure. However, it should be noted that, if the exit of the primary nozzle is placed in the throat of the secondary nozzle, the flow ratio is only 1 to 3 per cent less than the maximum value.

[7] "Fluid Meters, Their Theory and Application," fourth edition, Trans. A.S.M.E., vol. 59, 1937.

The experimental data of Fig. 6 show that the best position of the primary nozzle is independent of the ratio (p_i/p_0) of the two initial pressures. Moreover, it is the same for an area ratio of 256 as for an area ratio of 1024.

In Fig. 6 is shown the variation of pressure in the throat of the secondary nozzle with the position of the primary nozzle. In accordance with the analysis, the pressure in the throat is virtually

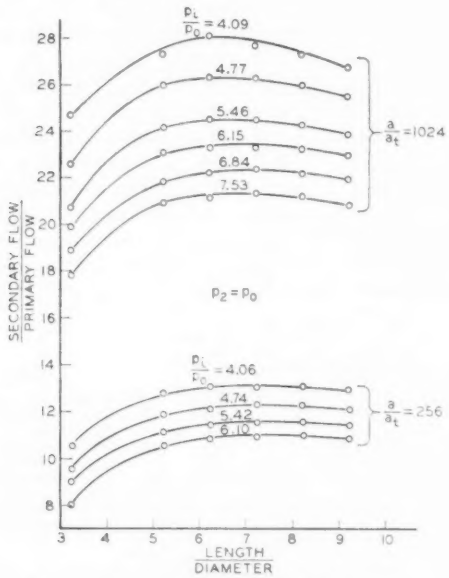


FIG. 7 EFFECT OF LENGTH OF MIXING TUBE
(Primary nozzle exit at entrance to secondary nozzle.)

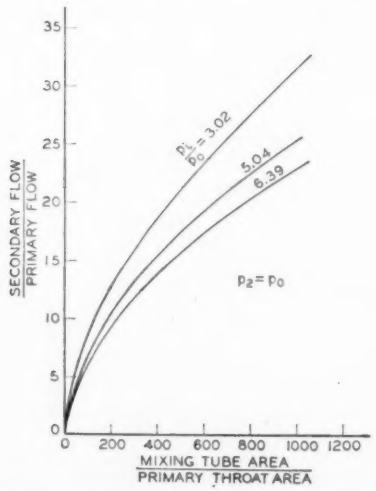


FIG. 8 EXPERIMENTAL CURVES SHOWING EFFECT OF AREA RATIO AND RATIO OF SUPPLY PRESSURES FOR BEST LENGTH OF MIXING TUBE AND BEST POSITION OF NOZZLE

at a minimum when the primary nozzle discharges into the throat of the secondary nozzle. In this instance, the flow ratio is also within a fraction of 1 per cent of its maximum value. The small effect at this area ratio (256) of thickness of the walls of the primary nozzle is indicated by the agreement between the results for two nozzles having the same throat diameter but different external dimensions.

The effect of the length of the mixing tube on the flow ratio for zero pressure rise across the mixing tube is shown in Fig. 7. The primary nozzle is placed at the best position, as indicated by the data of Fig. 6. In this instance, there is some evidence that the best length increases with increase in the ratio of the initial pressures p_i/p_0 and with increase in the relative size of the nozzle. Nevertheless, a value of L/D of 7 will give nearly the best performance throughout the range of conditions investigated.

The effect of area ratio on the flow ratio is shown by the experimental curves of Fig. 8. The data corresponding to these curves are compared with the results of analysis in Fig. 9.

COMPARISON OF EXPERIMENTAL VALUES WITH ANALYTICAL VALUES

In Fig. 9 are shown experimental and analytical values of the flow ratio for four different area ratios. The pressure rise across

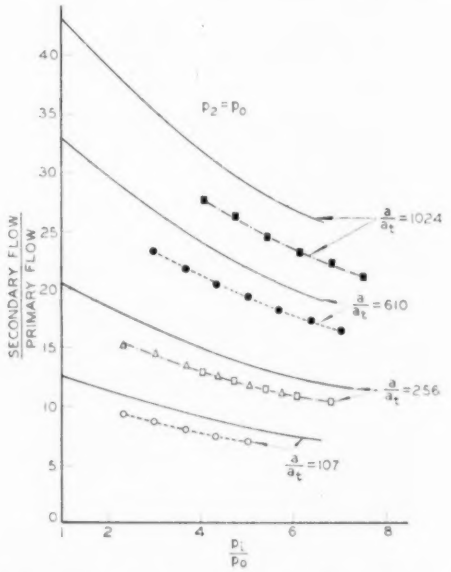


FIG. 9 COMPARISON OF MEASURED AND CALCULATED VALUES OF FLOW RATIO
(Solid lines indicate calculated values; broken lines, measured values.)

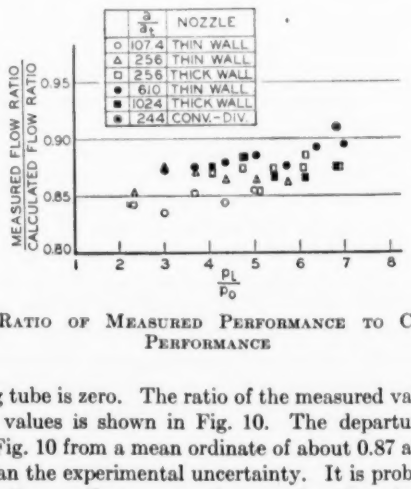


FIG. 10 RATIO OF MEASURED PERFORMANCE TO CALCULATED PERFORMANCE

the mixing tube is zero. The ratio of the measured values to the analytical values is shown in Fig. 10. The departures of the points of Fig. 10 from a mean ordinate of about 0.87 are scarcely greater than the experimental uncertainty. It is probable, however, that the smallest area ratio, namely, 107, gives slightly lower values of the ordinate than the others. It is also probable that the high value of the ordinate for the converging-diverging nozzle is significant.

Measured values of the pressure in the throat of the secondary nozzle are compared with analytical values in Fig. 11. The pres-

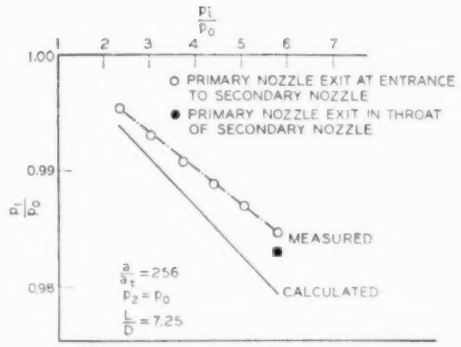


FIG. 11 COMPARISON OF MEASURED AND CALCULATED VALUES OF PRESSURE IN THROAT OF MIXING TUBE

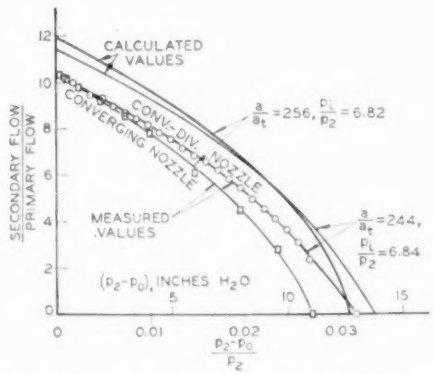


FIG. 12 COMPARISON OF MEASURED AND CALCULATED PERFORMANCE WITH VARIATION IN PRESSURE RISE ACROSS SECONDARY STREAM

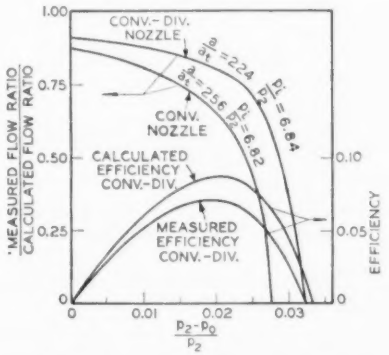


FIG. 13 EFFECT OF VARIATION IN PRESSURE RISE ACROSS SECONDARY STREAM

sure rise across the secondary stream is zero. The measured curve could be obtained from the analytical one by multiplying values of 1 minus the ordinate by 0.75. If the primary-nozzle exit is in the throat of the secondary nozzle, the multiplier is 0.83.

When the ejector is used as a pump to raise the pressure of the secondary stream through a finite range, the flow ratio decreases with increasing pressure rise ($p_2 - p_0$) for the secondary stream. Fig. 12 shows the measured and calculated performance for an ejector with a converging nozzle and with a converging-diverging nozzle having a divergence ratio appropriate to the conditions of the test. The performance with the converging-diverging nozzle is only slightly better when the pressure rise is small, but it is much better when the pressure rise is large. For the pressure rise at which the converging nozzle gives zero secondary flow, the converging-diverging nozzle gives a flow ratio of 2.5. The characteristics of the experimental and analytical curves are similar.

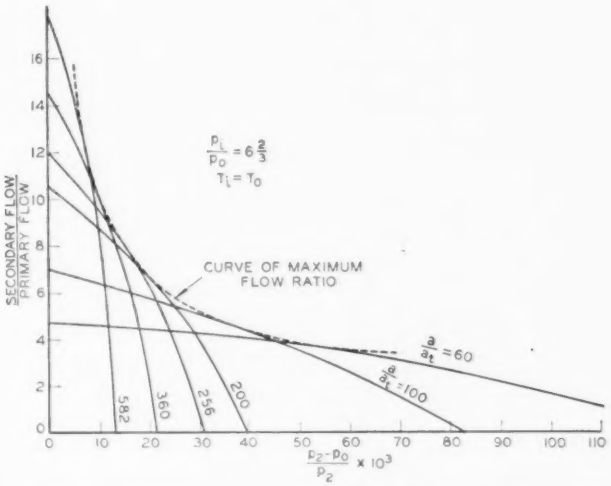


FIG. 14 CALCULATED PERFORMANCE OF THE SIMPLE EJECTOR

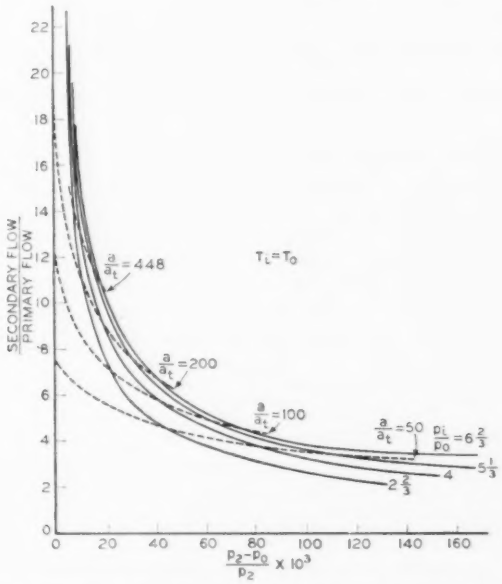


FIG. 15 CURVES OF MAXIMUM FLOW RATIO FOR SIMPLE EJECTOR AT DIFFERENT PRESSURE RATIOS

The ratio of the measured flow ratio to the calculated flow ratio for the tests of Fig. 12 is shown in Fig. 13. Since the analytical value for the pressure rise at zero secondary flow is not realized with either type of nozzle, the values of the ordinate of Fig. 13 must go to zero when the secondary flow goes to zero. Nevertheless, the ordinate holds up remarkably well over most of the range. For the converging nozzle it falls from 0.87 to 0.8 as the pressure rise increases to one third its maximum value; for the converging-diverging nozzle it falls from 0.89 to 0.8 only after the pressure rise increases to two thirds its maximum value.

This extraordinarily good agreement between experimental and analytical results justifies the computation of curves such as those of Figs. 14 and 15, to serve as guides in the design of ejectors. Fig. 14 shows that, for fixed values of the inlet and outlet pressures, there is a best area ratio. The calculated performance, corresponding to these best area ratios, is shown in Fig. 15.

Calculated and measured values of the efficiency of an ejector

with a converging-diverging primary nozzle are shown in Fig. 13. The efficiency, which credits the ejector with none of the leaving kinetic energy, is defined as the ratio of the isentropic increase in the enthalpy of the secondary stream between inlet and p_2 to the isentropic decrease in the enthalpy of the primary stream between inlet and p_2.

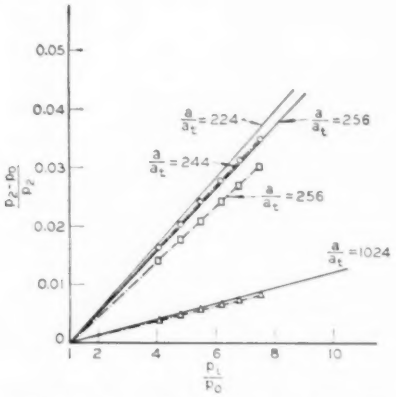


FIG. 16 PRESSURE RISE ACROSS MIXING TUBE FOR ZERO SECONDARY FLOW

(Solid lines indicate calculated values; broken lines indicate measured values.)

When the secondary flow is zero the analysis is that for a sudden enlargement of a passage. The corresponding values of the pressure rise across the mixing tube for various area ratios are compared in Fig. 16 with the measured values. Again, experimental and analytical curves are alike in characteristics; in fact the experimental curves for converging nozzles can be obtained quite accurately by multiplying the ordinates of the analytical curves by 0.9, and those for converging-diverging nozzles by multiplying by 0.95.

SUMMARY

1 In a simple ejector consisting of a primary nozzle and a cylindrical mixing tube with rounded entrance, constant-area mixing is better than constant-pressure mixing except for area ratios less than 10 (where some combination of the two is better than either one).

2 The performance of the simple ejector can be calculated from the conditions imposed by conservation of matter, conservation of energy, and the laws of motion.

3 Experiments on the simple ejector show that (*a*) the best position of the exit of the primary nozzle is only a short distance upstream from the throat of the secondary nozzle, and that a position in the throat of the secondary nozzle is practically as good; (*b*) the best length of the mixing tube is slightly greater than 7 diam; (*c*) the ratio of secondary flow to primary flow increases rapidly with the ratio of mixing-tube area to nozzle-throat area, and decreases with increase in the ratio of primary-supply pressure to secondary-supply pressure.

4 For zero pressure rise across the secondary stream (*a*) the experimental flow ratio is approximately 87 per cent of the calculated flow ratio for a converging primary nozzle, and approximately 91 per cent for a converging-diverging nozzle; (*b*) the pressure in the throat of the secondary nozzle is less than the secondary-supply pressure by 83 per cent of the calculated amount, when the exit of the primary nozzle is in the throat of the secondary nozzle.

5 The pressure rise in the secondary passage for zero secondary flow is 90 per cent of the calculated value for a converging nozzle, and 95 per cent for a converging-diverging nozzle.

Appendix

Consider the ejector shown in Fig. 17. Assume the following conditions: (*a*) Primary and secondary fluids are identical and incompressible; (*b*) the process (i-x) in the primary stream between the primary supply chamber and the exit of the primary nozzle is reversible; (*c*) the corresponding process (0-x) in the secondary stream is also reversible; (*d*) between sections x and 1 the two streams mix at constant pressure without wall friction, but mixing is, in general, incomplete at section 1; (*e*) between sections 1 and 2, mixing proceeds at constant cross-sectional area without wall friction; (*f*) the velocity of the fluid is uniform across section 2.

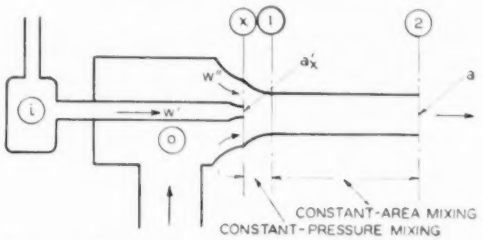


FIG. 17 EJECTOR DIAGRAM USED FOR ANALYSIS

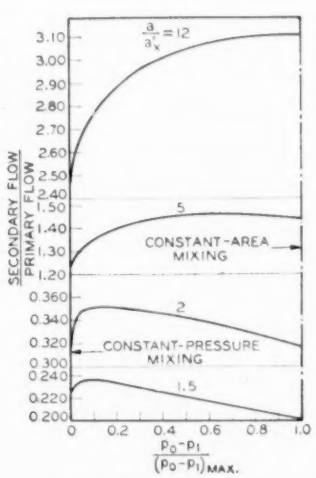


FIG. 18 PERFORMANCE OF EJECTOR FOR VARIOUS DEGREES OF MIXING AT CONSTANT PRESSURE

Using superscripts $'$ and $''$ for primary and secondary streams, respectively, and subscripts 0, x, and 2 to denote corresponding sections in Fig. 2, we may write the momentum equation between sections x and 2 in the form

$$\frac{w}{g} V_2 + p_2 a = \frac{w'}{g} V_x' + \frac{w''}{g} V_x'' + p_x a \quad \ldots\ldots [9]$$

where the symbols have the same connotation as in Equations [1] to [6]. Using the relations

$$V = \frac{wv}{a}, \quad V_x' = \frac{w'v}{a'_x}, \quad V_x'' = \frac{w''v}{a_x''}$$

we get Equation [9] in the form

$$\frac{w^2 v}{ga} + p_2 a = \frac{w'^2 v}{g a_x'} + \frac{w''^2 v}{g a_x''} + p_x a \quad \ldots\ldots [10]$$

Let $\omega = \frac{w''}{w'}$, $\alpha = \frac{a}{a_x'}$, and $\alpha'' = \frac{a}{a_x''}$. Noting that $w = (1 + \omega)w'$

we get from Equation [10]

$$1 + 2\omega + \omega^2 - \alpha - \alpha''\omega^2 + (p_2 - p_x)\left(\frac{a}{w'}\right)^2 \frac{g}{v} = 0 \ldots [11]$$

Let us restrict the problem to zero pressure rise across the secondary stream, that is, to $p_2 = p_0$. Then $p_2 - p_x = p_0 - p_x$, and, by assumption (*c*)

$$(p_2 - p_x) = \frac{V_x''^2}{2gv} = \left[\frac{\omega w' \alpha''}{\alpha}\right]^2 \frac{v}{2g}$$

Substituting this into Equation [11], we get

$$\left(1 - \alpha'' + \frac{\alpha''^2}{2}\right)\omega^2 + 2\omega + 1 - \alpha = 0 \ldots\ldots [12]$$

If we fix values for the area ratios α and α'', then Equation [12] is a quadratic in ω which may be readily solved. When sections x and 0 coincide then α'' is zero. Moreover, since $p_x - p_0 = 0$, it follows that, $p_2 - p_1 = 0$, and, therefore, no mixing occurs at constant area. Thus, sections 1 and 2 must coincide. This is the case of complete mixing at constant pressure for which Equation [12] becomes

$$\omega^2 + 2\omega + 1 - \alpha = 0 \ldots\ldots\ldots\ldots [13]$$

When sections x and 1 coincide, then $a = a_x' + a_x''$ and $\alpha'' = \frac{\alpha}{\alpha - 1}$. This is the case of complete mixing at constant area, for which Equation [12] becomes

$$\left[1 - \frac{\alpha}{\alpha - 1} + \frac{1}{2}\left(\frac{\alpha}{\alpha - 1}\right)^2\right]\omega^2 + 2\omega + 1 - \alpha = 0 \ldots [14]$$

Fig. 2 shows ω as a function of α corresponding to Equations [13] and [14]. In the same figure is shown ω as computed from Equation [12] as a function of the pressure rise $(p_2 - p_1)$ or $(p_0 - p_1)$ divided by the pressure rise $(p_0 - p_1)_{max}$ corresponding to complete mixing. It is easily seen from the foregoing analysis that

$$\left[\frac{p_0 - p_1}{(p_0 - p_1)_{max}}\right] = \left[\frac{\alpha''(\alpha - 1)}{\alpha}\right]^2$$

Although Fig. 2 indicates that the best performance is obtained for a given area ratio α with complete mixing at constant area, there is an exception to this rule, as shown by Fig. 18. For area ratios less than about 5, the best performance is obtained with more or less mixing at constant pressure. It appears that, for very small area ratios, it is desirable to discharge the primary nozzle outside the throat of the secondary nozzle, even under the idealized conditions of the analysis.

Graphical Solution of Fluid-Friction Problems

By E. S. DENNISON,[1] GROTON, CONN.

It is customary to present fluid-friction data in the form of a diagram to log scale in which friction coefficient appears as a function of Reynolds number. Such data are widely applicable to physical circumstances other than those which pertained to the original experiments. The present paper describes a graphical procedure for utilizing data of this character, where analytical methods are not practicable, and resort is made to trial-and-error methods. Similar methods to that described may be found useful in other fields than that of fluid friction, provided the experimental data are capable of being represented in nondimensional form.

THE data in any general case of fluid friction are commonly presented in the form of a diagram in which friction coefficient appears as a function of Reynolds number, both to log scales. This nondimensional method of plotting serves to identify all states of flow for which the dynamical conditions are similar. As a result, the data can be applied to physical circumstances which may be widely different from those of the original experiments.

In making use of friction data in this form, it is frequently required to find a solution in terms of some variable, for example velocity, which appears both in the friction-coefficient group ($= \psi$) and in the Reynolds-number group ($= R$). In the laminar region there is an explicit relation between ψ and R, and the analytical solution is simple. At higher values of R, the ψ-R relation is empirical and irregular. No analytical solution is practicable, and it is usually necessary to resort to a trial-and-error method. This is a time-consuming process.

The purpose of this paper is to describe a graphical procedure which can be used to solve the ψ-R equation directly in terms of the required variable. The method is simple in application, and introduces no error beyond what is common to graphical constructions. It will be explained by discussing certain common cases having to do, respectively, with terminal speed of a falling sphere and flow in a pipe. Similar methods may prove useful in other fields than that of fluid friction, provided that the experimental data are capable of being represented in nondimensional form.

Terminal Speed of a Falling Sphere

Resistance to motion of a sphere in a fluid medium is given by

$$r = \psi\rho \frac{v^2}{2} \cdot \frac{\pi}{4} d^2 \quad \ldots\ldots [1]$$

in which r = resisting force
ψ = coefficient of resistance, a number
ρ = density of fluid medium
v = velocity of motion
d = diameter of sphere

At terminal speed, resistance r equals the net gravitational force acting upon the sphere

$$r = \frac{\pi}{6} d^3(\sigma - \rho)g \quad \ldots\ldots [2]$$

in which σ = density of sphere
g = acceleration of gravity

From Equation [1]

$$\psi = \frac{8r}{\pi\rho v^2 d^2} \quad \ldots\ldots [1a]$$

Combining with Equation [2]

$$\psi = \frac{4}{3} g \left(\frac{\sigma - \rho}{\rho}\right) \frac{d}{v^2} \quad \ldots\ldots [3]$$

It is known that the coefficient ψ is a function of the Reynolds number, defined as

$$R = \frac{dv\rho}{\mu} \quad \ldots\ldots [4]$$

in which μ is the viscosity of the fluid. Stokes's law is valid in the laminar region and there $\psi = 24/R$, but this expression ceases to be accurate above $R = 0.5$. Fig. 1 represents $\log \psi$ as a function of $\log R$ over the extensive range for which data are available (1, 2).[2] Except in the narrow laminar region, the function cannot be expressed algebraically.

Technical application of the theory of terminal speeds, with special reference to spherical particles, leads to the following two cases (1):

I Given particle diameter and other necessary data, to compute terminal velocity.

II Given terminal velocity and other necessary data, to compute particle diameter.

In each case the variable sought appears in both ψ and R. What is required is the solution of two simultaneous equations. Graphical methods for effecting this result will be described in the following sections.

I *Computation of Terminal Velocity.* The curve in Fig. 1 represents the equation

$$\log \psi = f(\log R) \quad \ldots\ldots [5]$$

or

$$\log \left[\frac{4}{3} g \left(\frac{\sigma - \rho}{\rho}\right) \frac{d}{v^2}\right] = f\left[\log \left(\frac{dv\rho}{\mu}\right)\right] \quad \ldots\ldots [5a]$$

Let

$$x_v = \log \left(\frac{d\rho}{\mu}\right) \quad \ldots\ldots [6]$$

$$= \log R - \log v \quad \ldots\ldots [6a]$$

and

$$y_v = \log \left[\frac{4}{3} g \left(\frac{\sigma - \rho}{\rho}\right) d\right] \quad \ldots\ldots [7]$$

$$= \log \psi + 2 \log v \quad \ldots\ldots [7a]$$

Then Equation [5] may be written

$$(y_v - 2 \log v) = f(x_v + \log v) \quad \ldots\ldots [8]$$

---

[1] Engineer in Charge of Development, Electric Boat Company. Mem. A.S.M.E.

Presented at the Annual Meeting, New York, N. Y., December 1–5, 1941, of The American Society of Mechanical Engineers.

Discussion of this paper should be addressed to the Secretary, A.S.M.E., 29 West 39th Street, New York, N. Y., and will be accepted until July 10, 1942, for publication at a later date. Discussion received after the closing date will be returned.

Note: Statements and opinions advanced in papers are to be understood as individual expressions of their authors and not those of the Society.

[2] Numbers in parentheses refer to the Bibliography at the end of the paper.

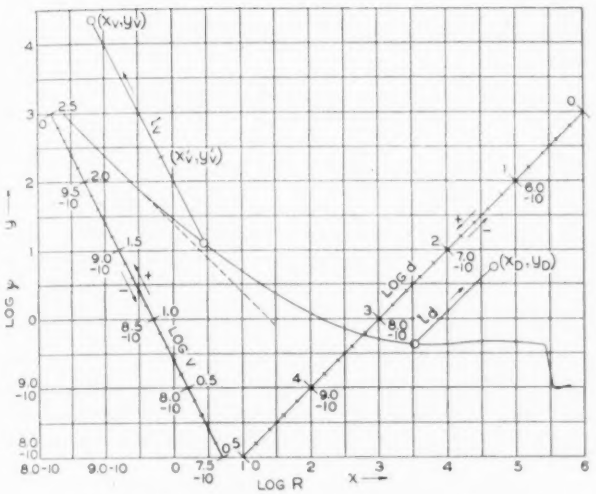


FIG. 1 TERMINAL SPEED OF A SPHERICAL PARTICLE

As a special case, when $v = 1$ (using any homogeneous system of units), $x_v = \log R$ and $y_v = \log \psi$. Then Equation [8] becomes numerically identical with Equation [5], and is represented by the curve in Fig. 1.

In general, a point (x_v, y_v) is displaced from the corresponding point (R, ψ) on the curve by the amounts $\Delta x = -\log v$ and $\Delta y = +2 \log v$. Therefore, all points corresponding to a state of flow (R, ψ) lie in a line passing through that point and having the slope -2. Furthermore, the distance l_v measured diagonally from (R, ψ) to (x_v, y_v) is $\sqrt{2^2 + 1} \log v = \sqrt{5} \log v$.

The data for a problem of type I permit x_v and y_v to be computed. An axis for $\log v$, having the proper slope and suitably graduated, has been added to Fig. 1. It is only necessary to locate (x_v, y_v) on the diagram and pass a line through it parallel to the $\log v$ axis. This line will intersect the curve at some point (R, ψ). The Reynolds number and resistance coefficient for the case in question are thus fixed at once. Velocity is found by laying off length l_v on the $\log v$ scale. If (x_v, y_v) lies above the curve, $v > 1$ (i.e., $\log v$ is positive); if below, $v < 1$.

In the foregoing, it will be noticed that a second diagram, the co-ordinates of which are dimensional in $\log v$, has in effect been superposed on the original nondimensional diagram. The geometrical construction is made in the dimensional plane. Displacements are measured from the data curve where $\log v = 0$.

The construction for a possible pair of values (x_v, y_v) is included in the diagram by way of illustration. Any consistent set of units may be used, and with a change in the unit of velocity, point (x_v, y_v) will merely shift up or down the same sloping line. Should (x_v, y_v) be found to lie outside the limits of the diagram, this can be adjusted by an arbitrary change of units. For example, plot $x'_v = x_v + 1$ and $y'_v = y_v - 2$, as in the figure. Velocity is then measured in a new unit 10 times as large as the original.

II *Computation of Diameter.* The reasoning is similar to that just outlined. In this case

$$x_d = \log\left(\frac{\rho v}{\mu}\right) \quad [9]$$

$$= \log R - \log d \quad [9a]$$

and

$$y_d = \log\left[\frac{4}{3}\frac{g}{v^2}\left(\frac{\sigma - \rho}{\rho}\right)\right] \quad [10]$$

$$= \log \psi - \log d \quad [10a]$$

Equation [5] becomes

$$(y_d + \log d) = f(x_d + \log d) \quad [11]$$

All points (x_d, y_d), for which R and ψ are constant, lie in a line having the slope $+1$. The distance $l_d = \sqrt{2} \log d$. Fig. 1 includes an axis for $\log d$, suitably graduated. In the region above and to the right of the curve $d < 1$; below and to the left $d > 1$. The procedure in case II parallels that given for case I. The construction is illustrated by an example.

FLOW IN A CIRCULAR PIPE

One form of the equation for frictional loss in a long straight circular pipe is

$$\Delta p = \lambda \rho \frac{u^2}{2} \frac{L}{D} \quad [12]$$

in which
- Δp = pressure loss due to fluid friction
- λ = pipe-friction coefficient, a number
- ρ = density of fluid
- u = mean velocity of flow
- L = pipe length
- D = pipe diameter

It is known that the coefficient λ is a function of the Reynolds number, $R = Du\rho/\mu$. In the laminar region $\lambda = 64/R$. At and above the critical range (R = 1200–2400) no simple algebraic relation exists, although for the turbulent region approximate expressions such as $\lambda = \text{const} \cdot R^n$ have been used. Frictional resistance varies with the relative roughness of the pipe wall, hence a number of curves representing $\lambda = f(R)$ are required. Fig. 2 includes a series of such curves as given by Pigott (3), although several have been omitted to avoid crowding. The reference should be consulted regarding the type of conduit to which each numbered curve applies. Of the two extremes, 18 represents "entirely rough" pipe ($\lambda = 0.054$) and 19, "lowest values for drawn brass tube." Many other sources of friction data are available (2, 4).

Two pipe-flow problems in which the graphical method can be used to advantage will be discussed. Both of these represent cases frequently encountered in practice.

III Given properties of the fluid, length and diameter of pipe, and pressure drop, to compute flow velocity.

IV Given properties of the fluid, volume rate of flow, length of pipe, and permissible pressure drop, to compute the requisite diameter of pipe. This is typical of the case where a pipe size is to be selected in order to meet a design specification.

III *Computation of Flow Velocity.* From Equation [12]

$$\lambda = \frac{2D \cdot \Delta p}{\rho u^2 L} \quad [12a]$$

Since

$$\log \lambda = f(\log R) \quad [13]$$

$$\log\left(\frac{2D \cdot \Delta p}{\rho u^2 L}\right) = f\left[\log\left(\frac{Du\rho}{\mu}\right)\right] \quad [13a]$$

Let

$$x_u = \log \frac{D\rho}{\mu} \quad [14]$$

$$= \log R - \log u \quad [14a]$$

and

$$y_u = \log\left(\frac{2D \cdot \Delta p}{\rho L}\right) \quad [15]$$

$$= \log \lambda + 2 \log u \quad [15a]$$

Equation [13] becomes

$$(y_u - 2 \log u) = f(x_u + \log u) \quad [16]$$

The data of the problem permit x_u and y_u to be computed.

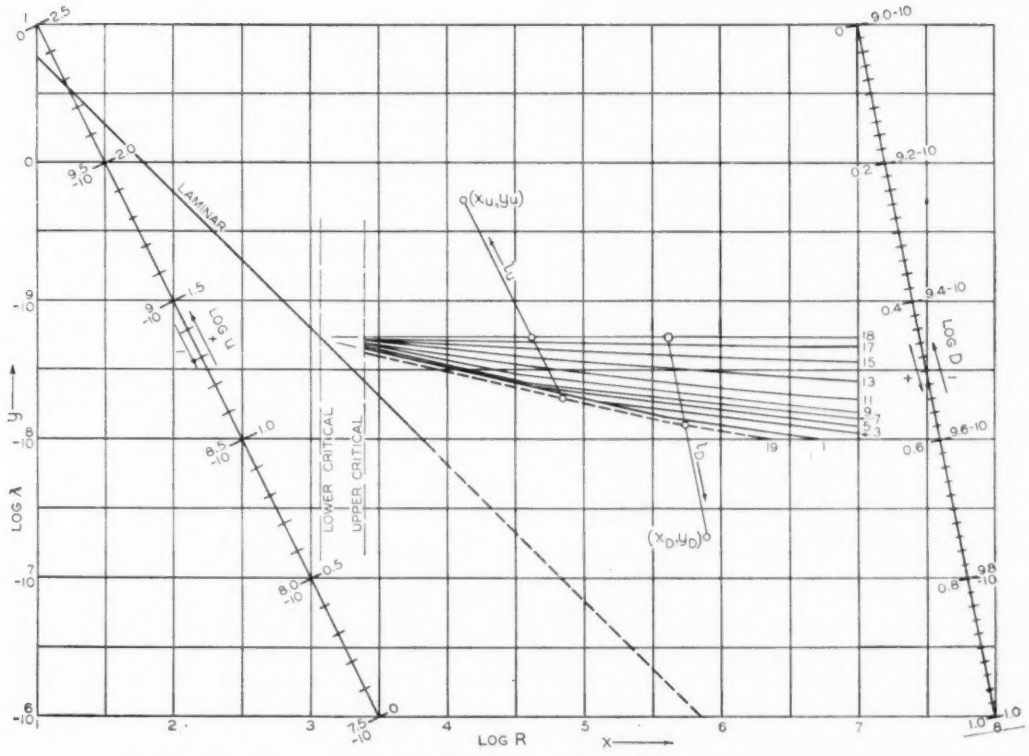


FIG. 2 FLOW IN A CIRCULAR PIPE

The point being plotted in the diagram, Fig. 2, will be displaced from the point (R, λ), representing the state of flow, by the amounts $\Delta x = -\log u$ and $\Delta y = +2 \log u$. As in case I, all such points lie in a line having the slope —2. The diagonal length l_u from (R, λ) to (x_u, y_u) is equal to $\sqrt{5} \log u$.

A graduated axis for log u, of proper slope, is given in Fig. 2. In the region above the curve, $u > 1$; below it $u < 1$. The construction is illustrated.

A useful feature of the graphical solution, in this case and in case IV, is that a single construction gives the result for each grade of pipe which the designer may wish to consider.

IV *Computation of Pipe Diameter.* Let Q = volume rate of discharge. Then in a circular pipe

$$u = 4Q/\pi D^2 \quad [17]$$

Substituting in Equation [12*a*]

$$\lambda = \frac{\pi^2 D^5 \cdot \Delta p}{8\rho L Q^2} \quad [18]$$

Also
$$R = \frac{Du\rho}{\mu} = \frac{4Q\rho}{\pi D\mu} \quad [19]$$

Then
$$\log\left(\frac{\pi^2 D^5 \cdot \Delta p}{8\rho L Q^2}\right) = f\left[\log\left(\frac{4Q\rho}{\pi D\mu}\right)\right] \quad [13b]$$

Let
$$x_D = \log\left(\frac{4Q\rho}{\pi\mu}\right) \quad [20]$$

$$= \log R + \log D \quad [21]$$

Also
$$y_D = \log\left(\frac{\pi^2 \cdot \Delta p}{8\rho L Q^2}\right) \quad [22]$$

$$= \log \lambda - 5 \log D \quad [23]$$

Equation [13] then becomes

$$(y_D + 5 \log D) = f(x_D - \log D) \quad [24]$$

Computing x_D and y_D from the data, the plotted point will be displaced by $\Delta x = \log D$ and $\Delta y = -5 \log D$ from the corresponding flow point (R, λ). Such points lie in a line whose slope is —5. The diagonal distance l_D is $\sqrt{5^2 + 1} \log D = \sqrt{26} \log D$. A graduated axis of proper slope has been added to the diagram and the construction is illustrated. Below the curve, $D > 1$; above it $D < 1$.

The solution yields directly the diameter of pipe required, together with the Reynolds number and friction coefficient at which it will operate. Results are found simultaneously for each grade of pipe represented in the diagram.

CONCLUSION

The graphical methods described in the paper are based upon the use of a simple mathematical device. In the problems discussed, the effect is to substitute a direct and rapid solution in place of a trial-and-error solution. It is possible that similar methods may be found useful in other instances, where experimental data have been assembled in nondimensional form.

BIBLIOGRAPHY

1 "Calculation of Terminal Speeds," *Engineering*, London, vol. 150, 1940, pp. 441–444; also discussion by E. S. Dennison, vol. 151, 1941, p. 294.

2 "Applied Hydro- and Aero-Dynamics," by L. Prandtl and O. G. Tietjens, McGraw-Hill Book Company, Inc., New York, N. Y., 1934.

3 "The Flow of Fluids in Closed Conduits," by R. J. S. Pigott, *Mechanical Engineering*, vol. 55, 1933, p. 497.

4 "The Mechanics of Turbulent Flow," by B. A. Bakhmeteff, Princeton University Press, 1936.

Correlation of Residual Stresses in the Fatigue Strength of Axles

By O. J. HORGER[1] and H. R. NEIFERT,[2] CANTON, OHIO

The object of this paper is to present a correlation between residual stresses, obtained by heat-treatment, with fatigue values, determined from an investigation of full-size railroad axles. The axles tested were of both solid and tubular design and represent members which could be used under a car in actual service. It was found from these tests that high axle fatigue strength is associated with high surface residual compressive stresses, and lowest axle strength values with surface residual tensile stresses.

Introduction

THERE is some question on the part of engineers as to the proper manner of evaluating residual stresses in their influence upon the fatigue strength of members subjected to a nonuniform distribution of stresses, such as are produced by bending or torsional loading. It is often felt that residual stresses obtained by heat-treatment are deleterious or have little effect upon fatigue strength; on the other hand, it is occasionally considered that certain kinds of residual stresses are favorable and other kinds unfavorable. This divergence of opinion may be explained by the small amount of experimental evidence available regarding fatigue strength, where the influence of residual stresses has been isolated from other factors. Often, changes in microstructure accompany any variation made in residual stresses, so that many fatigue investigations show the influence of both residual stresses and microstructure.

The comprehensive review of this subject by Barrett (1)[3] mentions, among other factors besides residual stresses involved in the results of reported investigations, (*a*) homogenization during the stress-relieving anneal; (*b*) possible "cushioning" effect of retained austenite; (*c*) microscopic stresses. Investigations have been reported by Gough (2), Gillett and Mack (3), French (4), Sachs (5, 6), and Becker and Phillips (7), showing that internal stresses may be controlled so as to be helpful or harmful. Unfortunately, these references give little correlating data between the magnitude of the internal stresses and the fatigue values; seldom were residual stresses isolated from other factors. Residual surface compressive stresses, obtained by cold-working, are known to increase greatly the fatigue strength of specimens over that for those not cold-worked. Here again, there is a difference of opinion as to whether residual stresses or the accompanying changes in the material are responsible for this increase in fatigue strength. The investigation, reported in this paper, however, is concerned only with residual stresses due to some form of heat-treatment.

Correlation of residual stresses with reversed-bending endurance values was obtained by Bühler and Buchholtz (8) on plain specimens about 0.71 and 1.07 in. diam. Their results represent the best quantitative analysis available and, for this reason, a diagrammatic summary of their findings is given in Figs. 1 and 2. Residual stresses were determined by Sachs's boring-out method (9). Their data indicate that (*a*) the endurance limit can be increased 15 to 20 per cent by high compressive stresses at the boundary, produced by quenching from a temperature below the A_1 point, without change in tensile properties; (*b*) the endurance limit can be decreased by about 15 per cent by high tensile stresses at the boundary (less than about 28,000 psi residual tensile stress did not have a damaging effect on the fatigue strength); (*c*) during the fatigue test, the magnitude of residual stresses at the surface leveled off (in one case the initial residual tensile stresses at the surface were reversed into residual compressive stresses by the alternating stress without damaging the fatigue strength); (*d*) measurable residual stresses at the boundary can be produced by alternating loading below or even at the endurance limit (a partial explanation for the well-known favorable effect of understressing).

In order to obtain residual stresses, it is necessary that plastic deformations of unlike magnitude occur in different zones of the member. Residual stresses may arise in cooling from (*a*) unequal contraction through pure thermal stresses, or (*b*) change in volume in passing through the transformation point. The hypothesis for the effectiveness of surface residual compressive stresses in these tests is that the zero-to-maximum fatigue strength of the steel is greater with compressive loading than with tensile loading. The presence of internal stresses is also manifested by the Bauschinger effect (10) and modification of damping capacity but these effects are not discussed here.

No correlation similar to that mentioned is known to exist for the case of members having stress concentration. The fatigue tests and associated determinations of residual stresses reported in this paper attempt partially to fill this gap. The tests reported on the solid axles and type A tubular axles were made under the auspices of the Mechanical Division of the Association of American Railroads, and through the direction of an axle committee under the chairmanship of W. I. Cantley, mechanical engineer (11). Type B tubular axles were investigated as a separate project by the authors' company in order to contribute additional data pertaining to the fatigue strength of axles.

Axle and Wheel Assemblies Tested

Three different designs of axles were investigated as indicated in Fig. 3. Two of these designs were tubular axles, designated as types A and B, and the third was a solid axle of conventional design. An equivalent wheel was pressed on each test axle, as shown in Fig. 3 (*c*), in accordance with the usual mounting practice of railroad shops.

Processing details as to rolling, forging, heat-treatment, and machining of the solid and tubular axles were previously published (12).

Material. Axles from five different materials were tested, in

[1] In charge of Railway Engineering and Research, The Timken Roller Bearing Company. Mem. A.S.M.E.

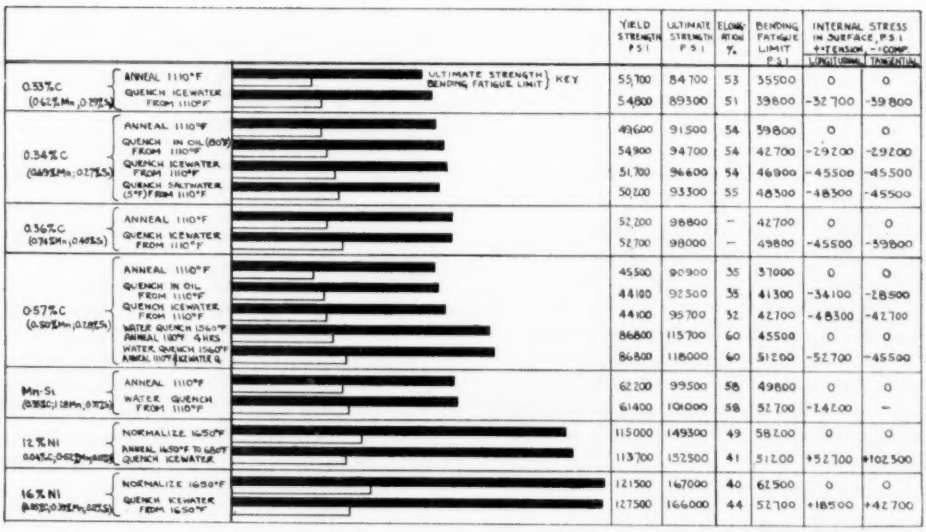
[2] Engineer, Research Laboratory, The Timken Roller Bearing Company.

[3] Numbers in parentheses refer to the Bibliography at the end of the paper.

Presented at the Annual Meeting, New York, N. Y., December 1–5, 1941, of The American Society of Mechanical Engineers.

Discussion of this paper should be addressed to the Secretary, A.S.M.E., 29 West 39th Street, New York, N. Y., and will be accepted until July 10, 1942, for publication at a later date. Discussion received after the closing date will be returned.

Note: Statements and opinions advanced in papers are to be understood as individual expressions of their authors and not those of the Society.



		YIELD STRENGTH P.S.I.	ULTIMATE STRENGTH P.S.I.	ELONGATION %	BENDING FATIGUE LIMIT P.S.I.	INTERNAL STRESS IN SURFACE, P.S.I. +TENSION, −COMP. LONGITUDINAL	TANGENTIAL
0.33% C (0.62% Mn, 0.19% Si)	ANNEAL 1110°F	55,700	84,700	53	35500	0	0
	QUENCH ICEWATER FROM 1110°F	54800	89300	51	39800	-32,700	-39,800
0.34% C (0.49% Mn, 0.27% Si)	ANNEAL 1110°F	49600	91500	54	39800	0	0
	QUENCH IN OIL (80°F) FROM 1110°F	54900	94700	54	42,700	-29,200	-29,200
	QUENCH ICEWATER FROM 1110°F	51,700	96600	54	46900	-45500	-45,500
	QUENCH SALTWATER (5%) FROM 1110°F	50,200	93300	55	48300	-48300	-45500
0.36% C (0.74% Mn, 0.46% Si)	ANNEAL 1110°F	52,200	98800	–	42,700	0	0
	QUENCH ICEWATER FROM 1110°F	52,700	98000	–	49800	-45500	-39800
0.57% C (0.50% Mn, 0.28% Si)	ANNEAL 1110°F	45500	90900	35	37000	0	0
	QUENCH IN OIL FROM 1110°F	44100	92300	35	41300	-34,100	-28,500
	QUENCH ICEWATER FROM 1110°F	44100	95700	32	42,700	-48300	-42,700
	WATER QUENCH 1560°F ANNEAL 1107°F 4 HRS	86800	115,700	60	45500	0	0
	WATER QUENCH 1560°F ANNEAL 1107°F ICEWATER Q.	86800	118000	60	51200	-52,700	-45500
Mn-Si (0.35% C, 1.28% Mn, 0.32% Si)	ANNEAL 1110°F	62,200	99500	58	49800	0	0
	WATER QUENCH FROM 1110°F	61400	101,000	58	52,700	-24,200	–
1.2% NI (0.04% C, 0.62% Mn, 0.18% Si)	NORMALIZE 1650°F	115000	149300	49	58200	0	0
	ANNEAL 1650°F TO 680°F QUENCH ICEWATER	113,700	152,500	41	51200	+52,700	+102,300
1.6% NI (0.35% C, 0.31% Mn, 0.21% Si)	NORMALIZE 1650°F	121500	167000	40	61,500	0	0
	QUENCH ICEWATER FROM 1650°F	127500	166000	44	52,700	+18500	+42,700

FIG. 1 CORRELATION OF RESIDUAL STRESSES WITH FATIGUE STRENGTH IN ROTATING BENDING FOR VARIOUS STEELS AND HEAT-TREATMENTS
(Bühler and Buchholtz, reference 8.)

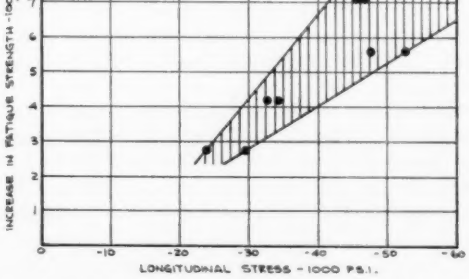


FIG. 2 INCREASE IN BENDING FATIGUE STRENGTH BY RESIDUAL SURFACE COMPRESSIVE STRESSES
(Bühler and Buchholtz, reference 8.)

which the analysis conformed essentially to S.A.E. 1040 and 1045 steels as shown in Table 1. The physical properties given in Table 2 represent minimum and maximum values obtained from a large number of specimens machined from the test axles. The disks, representing wheels pressed on these axles, were in accordance with A.A.R. Specification M-107-36 for "Multiple-Wear Wrought Steel Wheels." The scleroscopic hardness of these wheels was 35 to 37, as measured on the end of the hub face midway between the bore and outside diameter of the hub.

FATIGUE-TEST METHOD

These axles were tested on large double-end rotating cantilever-beam fatigue machines (12). The axle is supported in the test machine by bolting the rim of the wheel to a rotating head of the fatigue machine which operates at 800 to 1500 rpm. A constant spring load is applied on the opposite axle journal. This

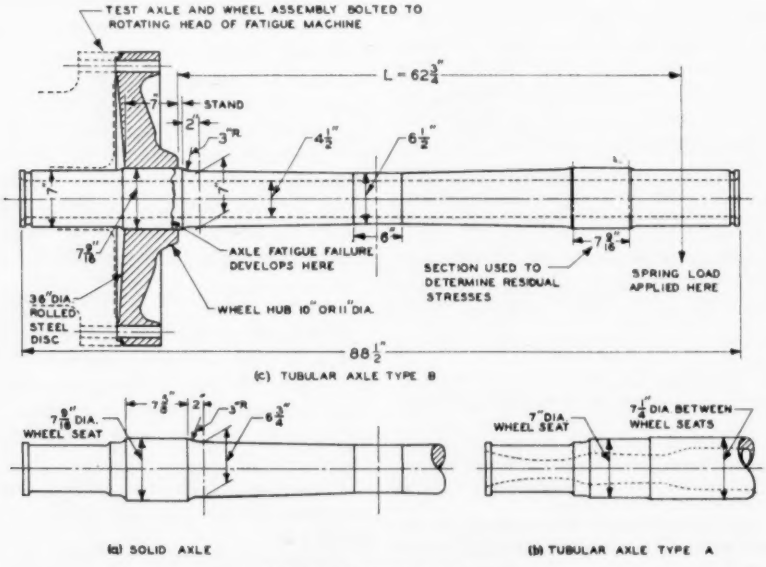


FIG. 3 DESIGNS OF AXLES

TABLE 1 CHEMICAL COMPOSITION OF AXLE MATERIAL

STEEL	KIND OF AXLE	CHEMICAL COMPOSITION, PER CENT						
		CARBON	MANGANESE	PHOSPHORUS	NICKEL	CHROMIUM	SULFUR	SILICON
C	Solid Axle - As Forged	0.39-0.43	0.54	0.016	- -	- -	0.028	0.22
D	Solid Axle - Norm. & Temp.	0.52-0.53	0.90	0.018	- -	- -	0.028	0.25
E	Tubular Axle - Type A	0.37	0.80	0.018	0.09	0.04	0.020	0.26
F	Tubular Axle - Type B	0.50	0.73	0.017	0.25	0.13	0.015	0.27

method of loading, shown in Fig. 3 (*c*), applies a bending moment on the axle of the same shape as that used by the designer when calculating a combination of vertical and lateral forces (Reuleaux method) to determine axle size.

The stress expressed here refers to the nominally calculated axle-bending stress at the end of the wheel fit. This is shown diagrammatically in Fig. 3 (*c*), where the bending moment is equal to *PL* and this product is divided by the section modulus of the axle to obtain the bending stress. For convenience of comparisons made later, the allowable bending stress for the tubular axles is given as the equivalent stress on a solid axle of the same wheel-seat diameter. This procedure is logical if we assume the axle forces produced in service to be the same whether a hollow or solid axle is used. In this manner the load-carrying capacity of the solid and tubular axles of the same wheel-seat diameter may be compared directly from the endurance-limit values, without considering how the section modulus is altered by the presence of the hole.

Endurance-limit values are based on a test of at least 84,300,000 axle revolutions which corresponds to an equivalent of 150,000 miles on 36-in-diam wheels.

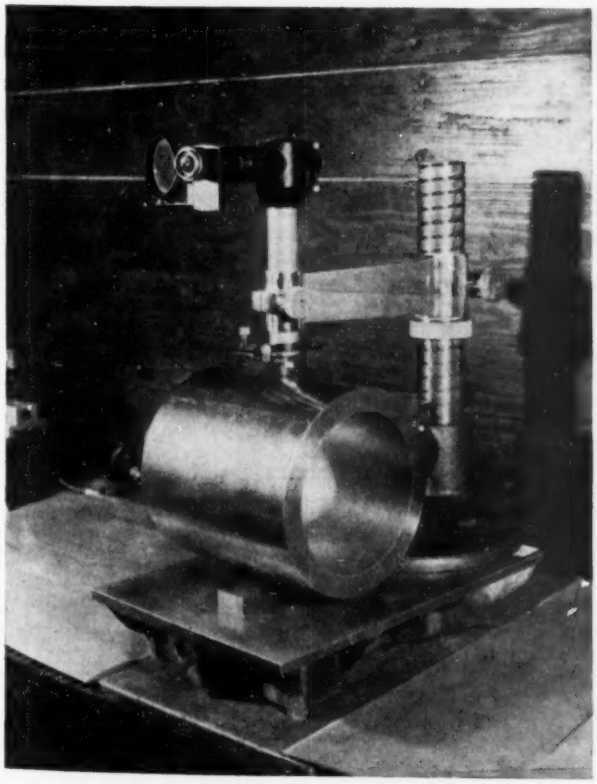


FIG. 4 METHOD OF MEASURING DIAMETER CHANGES WITH ZEISS OPTIMETER

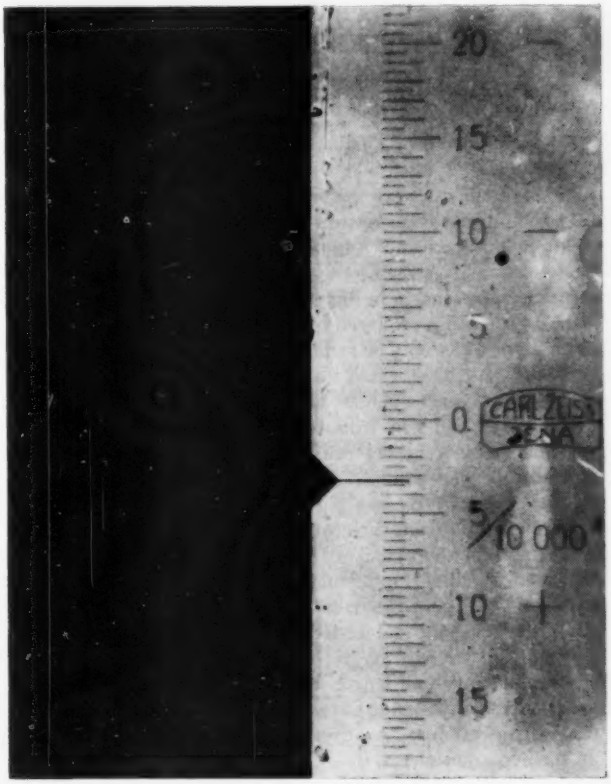


FIG. 5 REPRODUCTION OF SCALE IN ZEISS OPTIMETER TO SHOW ACCURACY OF MEASUREMENTS

DETERMINING RESIDUAL STRESSES

It was desired to determine the residual stresses in the axle wheel seat so that this portion (Fig. 3c) was machined from one full-size axle of each of the various types which had not been subjected to a fatigue test. These sections were ground on the outside diameter and ends with an extremely smooth finish to permit accurate measurements. Dimensions of these cylinders ranged from 7 to $7^{9}/_{16}$ in. diam by $7^{9}/_{16}$ in. length, and the hollow members had a $3^{1}/_{2}$-in-diam hole in type A, and $4^{7}/_{16}$-in. hole in type B axles.

Each cylinder was successively bored out on an engine lathe in accordance with Sachs's method (9, 13, 14) and the changes in cylinder length and outside diameter were determined after each removal of 5 to 10 per cent of the cross-section area. The solid cylinders were first bored with a $1^{3}/_{4}$-in. hole. In order to minimize the effects of heating and machining stresses, a very small amount of metal was removed in each boring, using a coolant. A series of cuts was required for each 5 to 10 per cent removal of cross-section area. An effective means of preventing deep boring cuts was employed by clamping the cylinder endwise against the face plate on the lathe and using no radial clamping force on

TABLE 2 PHYSICAL PROPERTIES OF AXLE MATERIAL

	SOLID AXLE SPECIMENS ½" DIA. X 2" GAGE LENGTH FROM WHEEL SEAT O. DIAMETER.		TUBULAR AXLE TYPE A SUB-SIZE SPECIMENS ½" DIA. X 1" GAGE LENGTH CUT FROM		TUBULAR AXLE TYPE B SPECIMENS ½" DIA. X 2" GAGE LENGTH CUT FROM CENTER OF WALL THICKNESS.	
STEEL	C	D	E		F	
Yield Strength, psi.[a]	36000–48000	52500–61000	82700–93900	73600–87700	61000–63500	72000–81000
Tensile Strength	79800–84500	101000–103500	113000–115100	109100–113100	103500–106000	119000–120000
Red. of Area, in %	41.9–46.6	23.0–45.5	40.8–42.8	42.9–45.0	41.9–42.2	47.2–50.6
Elongation, in %	26.0–30.0	17.0–26.0	19.0–20.0	20.0–21.0	22.0–23.0	20.5–21.5
Brinell Hardness[b]	156–167	187–207	229–253	223–235	183–192	217–223
Izod Impact, ft-lb.	11–24	9–21	- - -	- - -	13–16	17–23

[a] Determined by drop-of-beam method.
[b] Hardness measurements made on end of tensile specimen.

the cylinder. Too deep a cut would loosen or move the cylinder on the face plate.

All measurements were made on the cylinders after they had reached equilibrium temperature conditions in a gage room which was air-conditioned and the temperature and humidity maintained constant. A Zeiss optimeter was employed to make all measurements as shown in Fig. 4. The accuracy of measurement is indicated in the reproduced optimeter scale in Fig. 5, showing that direct readings may be made to 0.0001 in. and estimated with no difficulty to 0.000025 in.

Diameters of each cylinder were measured at three sections, i.e., the center, and 1 in. from either end. Maximum and minimum diameters were determined so that an average of six measurements was obtained between each series of boring-out operations. Length measurements were made every 90 deg and at each 90-deg position three measurements were made through the thickness of the cylinder. Twelve measurements were obtained in this manner by having one end of the cylinder rest on the base of the gage. The cylinder was then turned upside down so that the opposite end rested on the base of the gage, and other similar twelve length measurements were obtained. Then these twenty-four length measurements permitted drawing contour curves of the ends of the cylinder between each series of boring-out operations. An average length change was deduced from such contour curves.

This procedure of measuring, while tedious, was believed to be necessary because of the fact that the cylinder diameter and length were of about the same magnitude. In this manner any end effect[4] would be detected by distortion from a uniform cylinder to one which was larger or smaller in diameter at the ends than in the middle. Also, the ends of the cylinder would become concave or convex. It would have been desirable to have the cylinder length at least three times the diameter but the axle design did not permit this. The ratio used introduces some end effect and error in the residual stresses determined.

A comparison of the length and diameter changes as well as the calculated residual stresses for all cylinders is shown in Fig. 6. It will be noted that it was necessary to extrapolate the length and diameter changes to the surface of the specimens after the wall thickness was reduced to about $^3/_{16}$ in. This procedure is not desirable because some types of stress gradients near the surface could produce deformations deviating considerably from the extrapolated values. For this reason, future research is being directed toward turning off the outer layers and measuring changes in inside diameter and length. The same accuracy of measurements can be obtained as used in the boring-out method. Since the surface stresses are believed to be the most important on solid members, this latter method would not require the determination of the entire internal-stress distribution. Therefore, the number of layers to be machined away would be reduced as well

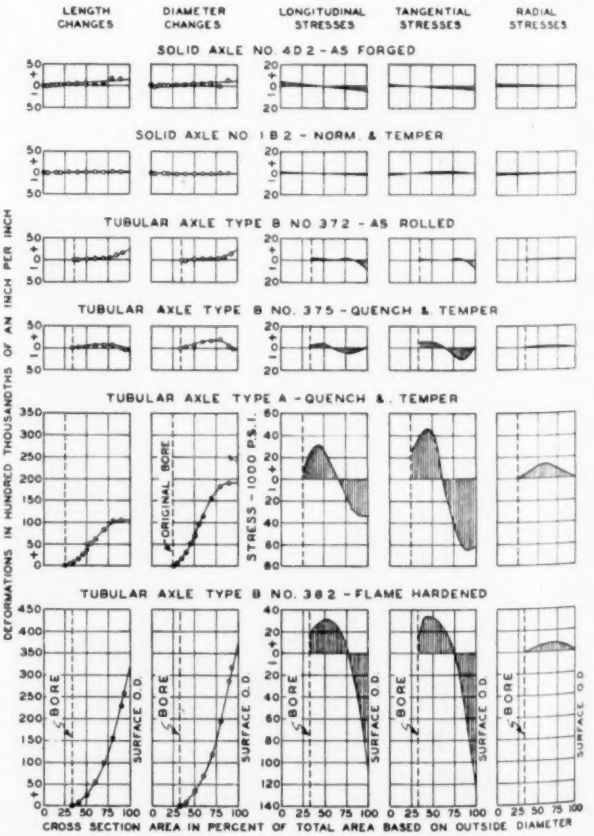


FIG. 6 COMPARISON OF RESIDUAL STRESSES AND DEFORMATIONS IN VARIOUS SOLID AND TUBULAR AXLES

[4] Treatment of end effect is discussed on page 355 of reference (14) for a solid cylinder, indicating that appreciable error in residual-stress determinations may be introduced by using a ratio of cylinder length to diameter of 1. Hollow cylinders having this ratio also introduce errors unless the wall thickness is less than about $^1/_{10}$ of the radius, as discussed on page 404 of reference (15).

Detailed measurements of the two cylinders, having the greatest internal stresses, showed about 10 per cent less increase in outside diameter at the center of the cylinder than obtained 1 in. from either end. This means that the internal stresses given here are too high. After completion of these tests, S. Timoshenko suggested that the influence of the portions of the axle protruding at each end of the wheel fit should be determined. Measuring the diameter and length of the wheel seat before and after machining it from the axle would give data on this question, but the opportunity to make this study has not yet presented itself.

TABLE 3 CORRELATION OF PHYSICAL PROPERTIES, RESIDUAL STRESSES, AND FATIGUE STRENGTH OF AXLES

AXLE NO.	MATERIAL	ULTIMATE STRENGTH OF SURFACE SPECIMENS, PSI.	BRINELL HARDNESS NEAR SURFACE	RESIDUAL STRESS AT WHEEL SEAT O.DIA., PSI.		MAX. ALLOWABLE BENDING STRESS IN WHEEL SEAT TO PREVENT, PSI	
				LONGITUDINAL	TANGENTIAL	INITIATION OF FATIGUE CRACKS	BREAKING OFF OF AXLE
SOLID 4D2	M-101 0.39-0.43% C 0.54% Mn. As-Forged	79,800 to 84,500	156 to 167	-4,000	-3,300	9,000	16,000
SOLID 1B2	M-104 0.52-0.53% C 0.90% Mn. Norm. & Temp.	101,000 to 103,500	187 to 207	-600	Zero	9,000	9,500
	TUBULAR TYPE A 0.37% C 0.80% Mn. Quench & Temper	113,200 to 122,000	229 to 253	-34,300	-62,600	13,500 (b)	>19,000 (b)
3B2	TUBULAR TYPE B 0.50% C 0.73% Mn. FLAME Hardened	- - -	495	-105,500	-123,300	>22,000 (b)	>22,000 (b)
3T2	TUBULAR TYPE B 0.50% C 0.73% Mn. As-Rolled	103,500 to 106,000	236	-8,700	-8,500	12,000 (b)	12,000 (b)
3T5	TUBULAR TYPE B 0.50% C 0.73% Mn. Quench & Temper	119,000 to 120,000	298	+1,600	+2,000	<12,000 (b)	<12,000 (b)

(a) These residual stresses not measured for this axle but assumed to be the same as axle no. 4D2
(b) Allowable wheel seat stress given here on basis of tubular axle being solid - see text.

as the number of measurements so as to lower the cost and time element in this work considerably.

Correlating Residual Stresses and Fatigue Strength

The relationship between the surface residual stresses, Fig. 6, and the fatigue strength, obtained for the various axles, is shown in Table 3 and diagrammatically illustrated in Fig. 7. The general observations from this comparison are (*a*) that, in the order of their maximum fatigue strength, axles also exhibit the maximum surface residual compressive stresses, and (*b*) axles having surface residual tensile stresses are also accompanied by low fatigue values.

It is not intended to infer from Fig. 7 that the internal stresses are entirely responsible for the differences in fatigue strength of the various axles. All axles except type A were of similar design. Real differences exist in the microstructure of the several axles. Additional research is under way to determine any influence of microstructure upon the fatigue strength. The preliminary indication from such additional research with members subjected to high stress concentration, such as an axle with a pressed-on wheel, is as follows:

For plain medium-carbon steel, the large grain size and accompanying structure found in an as-forged axle give appreciably greater fatigue strength than a finer grain structure, such as is obtained by normalizing and tempering. In this comparison, the residual stresses are small and are believed to have less influence

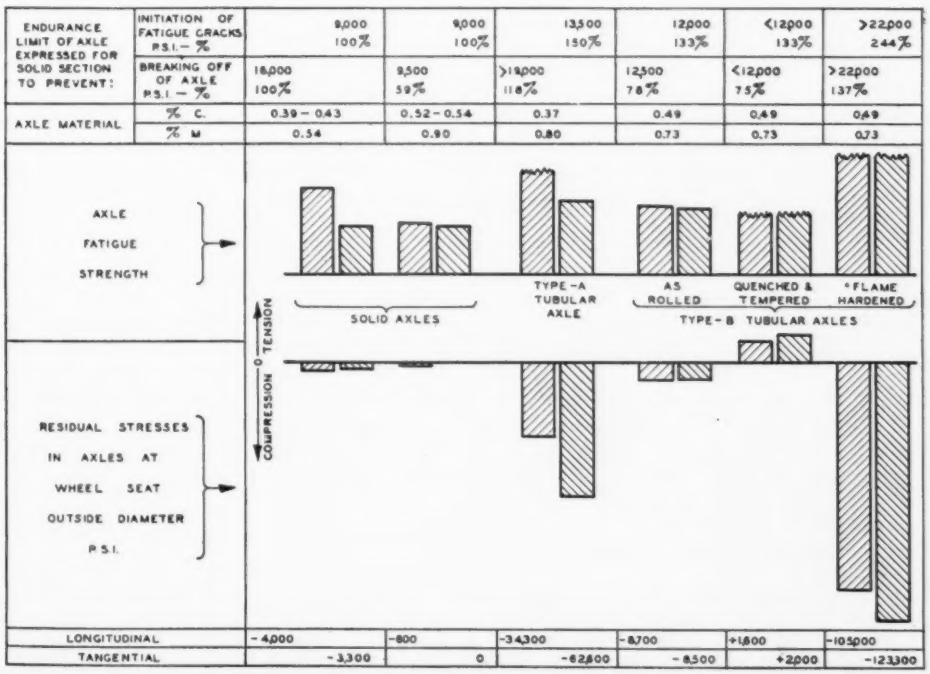


FIG. 7 DIAGRAMMATICAL CHART SHOWING RELATIONSHIP BETWEEN SURFACE RESIDUAL STRESSES AND FATIGUE STRENGTH

than the microstructure upon the fatigue strength. A possible explanation for this may be found from creep tests made at elevated temperature where a large grain structure exhibits superior creep properties than a finer grain structure. In these fatigue tests the local stresses are very high near the end of the wheel fit and some redistribution of stresses takes place. Another explanation may be that the type of structure accompanying large grain size is more resistant than the small grain size to the rubbing corrosion (fretting) occurring between the axle and wheel fit.

BIBLIOGRAPHY

1 "Internal Stresses—A Review," by C. S. Barrett, Contribution No. 48, Carnegie Institute of Technology, Metals Research Laboratory, Pittsburgh, Pa., 1934.

2 "The Fatigue of Metals," by H. J. Gough, Scott, Greenwood & Company, London, 1924.

3 "Molybdenum, Cerium, and Related Alloy Steels," by H. W. Gillett and E. L. Mack, Chemical Catalog Company, Inc., New York, N. Y., 1925.

4 "Fatigue and the Hardening of Steels," by H. J. French, Trans. American Society for Steel Treating, vol. 21, 1933, pp. 899–946.

5 "Some Observations on the Forging of Strong Aluminum Alloys," by G. Sachs, *Journal of the Institute of Metals*, vol. 64, no. 1, 1939, pp. 261–378.

6 "Internal Stresses in Piston Rods of a Large Diesel Engine Ocean Liner," by G. Sachs, Trans. American Society for Metals, vol. 27, 1939, pp. 821–836.

7 "Internal Stresses and Their Effect on the Fatigue Resistance of Spring Steels," by M. L. Becker and C. E. Phillips, *Journal of the Iron and Steel Institute*, vol. 133, no. 1, 1936, pp. 427–453.

8 "On the Effect of Residual Stresses on the Dynamic Strength," by H. Bühler and H. Buchholtz, *Mitteilung aus dem Forschungs-Institut der Vereinigte Stahlwerke, Dortmund*, vol. 3, 1933, pp. 235–248; also abstracted in *Stahl und Eisen*, vol. 53, 1933, pp. 1330–1332.

9 "The Determination of Internal Stresses in Rods and Tubes," by G. Sachs, *Zeitschrift für Metallkunde*, vol. 19, 1927, pp. 352–357.

10 "Mitteilungen aus dem Mechanisch-Technischen Laboratorium, Technische Hochschule," by J. Bauschinger, München, vol. 13, 1886, pp. 1–115; discussed in "Strength of Materials," by S. Timoshenko, D. Van Nostrand Company, Inc., New York, N. Y., vol. 2, 1934.

11 "Passenger Car Axle Tests $5^1/_2 \times 10$-In. Journals," Fifth Progress Report, Association of American Railroads, Chicago, Ill., June, 1941.

12 "Fatigue Comparison of 7-In. Diameter Solid and Tubular Axles," by O. J. Horger and T. V. Buckwalter, American Society for Testing Materials, preprint no. 32, 1941.

13 "The Measurement of Residual Stresses in Metal," by G. Sachs and G. Espey, *Iron Age*, vol. 148, 1941, Sept. 18, pp. 63–71, and Sept. 25, pp. 36–42.

14 "Practical Metallurgy," by G. Sachs and K. R. Van Horn, American Society for Metals, Cleveland, Ohio, 1940.

15 "Theory of Elasticity," by S. Timoshenko, McGraw-Hill Book Company, Inc., New York, N. Y., 1934.

16 "Theory of Plates and Shells," by S. Timoshenko, McGraw-Hill Book Company, Inc., New York, N. Y., 1940.

Plastic Flow as an Unstable Process

By L. H. DONNELL,[1] CHICAGO, ILL.

Instead of occurring simultaneously over regions which are apparently uniformly stressed, plastic flow frequently proceeds in a discontinuous manner, as in the formation of wedge-shaped plastic regions around the periphery of torsion specimens. It is contended in this paper that this phenomenon can be explained as an instability, brought about by stress concentrations which are caused, not by discontinuities in the shape of the specimen, but by the discontinuous behavior of the material around the yield point.

According to this explanation, yielding first occurs at some region of local weakness. The lagging of the stress in this yielded region causes a stress redistribution around the region, somewhat as if it were a hole, which retards stresses and therefore yielding in certain directions while accelerating them in other directions, thus leading to the spontaneous growth of characteristically shaped plastic regions.

Necking of Tensile Specimens

INSTABILITY is by definition a condition in which a small change in the state of a system brings into play forces or tendencies which increase the change, so that slight changes, which may occur accidentally, lead automatically to large changes.

A familiar example of unstable action in connection with plastic flow is the "necking," or localization of strain, which takes place during the latter part of a tensile test of a ductile material. This necking presumably starts with some slight accidental weakness of one section of the specimen relative to other sections, which is bound to be present because no specimen is absolutely uniform.

Due to its relative weakness, this section stretches slightly more under load than other sections. This slightly greater stretching is accompanied by slightly greater reduction of area, compared to other sections. This section is thereby still further weakened, which causes the stretching process to be yet further localized, and the section to be yet further reduced relative to other parts, etc., etc. The original accidental disturbance in the uniformity of the specimen thus starts a train of self-propagating actions, tending to localize the strains more and more.

There is also a "stabilizing" tendency present, in addition to the unstabilizing effects described. This stabilizing tendency is due to the phenomenon of strain hardening. This tends to make any section of the specimen which stretches more than other sections harder than the rest, and hence tends to inhibit further stretching at that section. These opposing tendencies are both present during most of a tensile test. It would be difficult to analyze them quantitatively, but it is evident that the stabilizing tendency is the dominant one up to the beginning of necking, at which time the unstabilizing tendency begins to dominate. The foregoing description is, of course, greatly oversimplified, although it probably includes the main factors affecting necking.

Plastic Flow in Bars Under Torsion

When a prismatical bar of ductile material such as mild steel is twisted until the yield point has been passed, studies of etched cross sections indicate that yielding has taken place in a highly discontinuous and yet remarkably regular manner.[2] In a circular bar, for example (the following discussion will be confined to circular bars for simplicity, although it applies equally well to other shapes), elastic theory indicates the stress to be a maximum and to be uniform in an annular region around the circumference, Fig. 1 (*a*). It would be natural to suppose therefore that, as the bar is twisted beyond the yield point, the regions of yielded material in the cross section would be more or less smooth annular regions which would be, successively, as indicated in Fig. 1 (*a*), (*b*), and (*c*).



Fig. 1



Fig. 2

Actually, the experiments show that yielding is confined, or at least is highly concentrated, in radial wedge-shaped regions in the cross section, which start at the periphery and gradually grow toward the center. As the yielding progresses, these regions grow in number as well as in size, but seem always to be distributed in a rather remarkably uniform manner about the circumference. They are quite slender but increase gradually in width as they grow in length, as indicated in Fig. 2 (*a*), (*b*), and (*c*), which shows typical successive stages of the process.

The author suggested an explanation for this phenomenon in a letter to Dr. Nádai in 1933, and it is this explanation which forms the bulk of this paper.[3] In brief the theory advanced is that the localization of the plastic flow is, like the necking in tensile tests, evidence of an unstable condition. In this case, the instability is caused by stress concentrations (it might be better to speak of strain concentrations in such a case as this, but the other term will be used because of its greater familiarity), which are caused, not by discontinuities in the shape of the

---

[1] Special Lecturer, Summer Engineering Structures Institute, University of Michigan, 1941. Professor of Mechanical Engineering, Armour College of Engineering, Illinois Institute of Technology. Mem. A.S.M.E.

Presented at the Annual Meeting, New York, N. Y., December 1–5, 1941, of The American Society of Mechanical Engineers.

Discussion of this paper should be addressed to the Secretary, A.S.M.E., 29 West 39th Street, New York, N. Y., and will be accepted until July 10, 1942, for publication at a later date. Discussion received after the closing date will be returned.

Note: Statements and opinions advanced in papers are to be understood as individual expressions of their authors and not those of the Society.

[2] "Plasticity," by A. Nádai, McGraw-Hill Book Company, Inc., New York, N. Y., 1931, chap. 20.

[3] An explanation along somewhat similar lines, making use of torsion analogies for elastic and plastic torsion, has been advanced by Reuss. See *Zeitschrift für angewandte Mathematik und Mechanik*, 1938, p. 347.

specimen, but by the discontinuous behavior of the material around the yield point. As this discontinuous behavior of the material (visualized by a break in the stress-strain curve) is a fundamental attribute of the yielding process, it is not surprising that localization of flow resulting from instability seems also to be quite a characteristic phenomenon in yielding.

Explanation of Radial Growth of Plastic Regions

Fig. 3 represents a cross section of a round bar in torsion with a semicircular notch cut in its edge. We know from the theory of elastic stress concentrations that the stress is greatly increased at the inner edge of the notch, at *b*, and is greatly decreased at the sides of the notch, at *mm*, in comparison to other parts of the cross section at the same radius, or in comparison to what would occur if there were no notch.

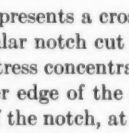


Fig. 3

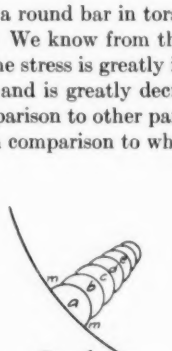


Fig. 4

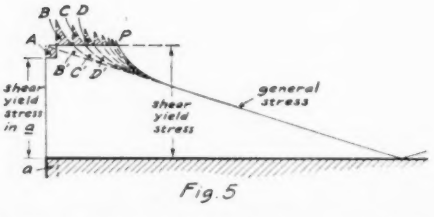


Fig. 5

These changes in the stresses at *b* and *mm* are obviously due to the elimination of the material of the notch. However, it is just as correct to say that it is due to the elimination of the *forces* which would otherwise be carried by the material of the notch, and which this material would transmit to the material outside the notch, because, obviously, the material of the notch has no effect on the material outside except through the forces it exerts on it.

Now, if the total elimination of these forces causes a large increase in stress at *b* and decrease at *mm*, then a partial elimination of the forces due to any cause will produce a proportionately smaller change in the stresses at *b* and *mm*. To put it in another way, instead of thinking of the elimination of these forces, we can think of counteracting forces being applied to the system. If such counteracting forces of a certain magnitude produce a certain result, i.e., a certain change in the stresses at *b* and *mm*, then, by the principle of superposition or linearity of action, counteracting forces of a fraction of that magnitude will produce the same fraction of the changes at *b* and *mm*.

Thus, since we know that complete elimination of the material of the notch increases the stress at *b* and decreases it at the corners *mm* by 100 per cent,[4] we can conclude that a 5 per cent decrease in the resistance of the material, and hence of the forces, taken by it and exerted by it across its boundaries, will cause about a 5 per cent increase of stress at *b* and decrease at *mm*. These changes will be much greater if the notch is elongated in the radial direction, instead of being of semicircular shape.

The formation of radially growing plastic regions in torsion can then be explained as follows: As the torsion increases, yielding first occurs at some region of local relative weakness such as must inevitably exist. Then the lagging of the stress in this yielded region relative to surrounding parts causes a stress redistribution around the region (of the same nature as if the region were a notch or hole, but of lesser magnitude) which retards stresses and therefore yielding in the tangential direction and accelerates them in the radial direction, thus leading to the elongation of the plastic region in the radial direction.

Considering this process in more detail, imagine that the material in a small region *a*, Fig. 4, is 5 per cent weaker—due perhaps to unfavorable orientation of the crystals—than the surrounding material. The material in this region will start to yield when the stress at the circumference reaches 95 per cent of the yield point. When the torsion is increased, the stress around this region will increase, but the stresses taken by and transmitted by the material within the region will remain substantially unaltered, assuming for simplicity that the material has a sharp yield point with a horizontal stress-strain curve after yielding.

When the stress has about reached the yield point on the circumference far from this region, there is therefore the equivalent of an elimination of about 5 per cent of the stress inside the region. This elimination would cause a rise in stress at *b* and a drop in stress at *mm* of 5 per cent, more or less, depending upon the shape of region *a*. But the stress at *b* was already nearly at the yield point, so that, with this increase, the stress in region *b* would have to be considerably greater than the yield point, and that at *c* just about at the yield point.

This is the condition which elastic theory indicates, i.e., a condition which satisfies equilibrium and continuity conditions everywhere. But the material cannot stand such a stress at *b* and will consequently yield, thus upsetting equilibrium again. This yielding is equivalent to an elimination of stresses in the region *b* of an amount equal to the excess they would otherwise have over the yield point. Thus, stresses have really been eliminated not merely over region *a* but over region *a* and *b* combined (which incidentally is a more pointed region than *a* alone, and hence causes a greater factor of stress concentration). This combined elimination of stress would require increased stresses at *c* for equilibrium, but again equilibrium is prevented because *c* was already at the yield point and its stress cannot increase. This amounts to a reduction of stress over *c* from the value required for equilibrium, which means that stress eliminations have occurred over *a*, *b*, and *c* combined, a still more pointed region. This leads to the yielding of regions *d*, *e*, etc., in succession.

Fig. 5 shows graphically the stress distribution along a radius passing through the region of original weakness, *a*. Area *A* indicates the stress reduction, below that otherwise required for equilibrium, which is due to the original weakness. Areas *B* and *B'* indicate the stress increase which this reduction would require, under elastic conditions, to maintain equilibrium. Area *B* represents a further stress reduction beneath what is required for equilibrium, due to yielding. Areas *C* and *C'* represent the stress increases due to this reduction, etc.

Actually, of course, the entire process would take place continuously instead of by steps. It might be described as a spreading of the plastic region (started by the original small weakness) toward the center in an effort to attain equilibrium, which is thwarted, for a time at least, by the continued yielding of the material under the influence of stress concentration. This self-perpetuating, or unstable, process will reach a definite end at some point such as *P*, Fig. 5, where, due to reduction in the general stress with the distance from the center, the sum of the general stress and stress increase is no longer above the yield

[4] "Strength of Materials," by S. Timoshenko, second edition, part 2, D. Van Nostrand Company, Inc., New York, N. Y., 1941, p. 325.

point. As the general stress is raised by increasing torsion, however, this point will move inward toward the center.

It should be emphasized that this explanation does not require that the material be weaker than normal anywhere except in the starting region, which can evidently be very small. Such minute points of weakness are bound to be distributed all over the cross section. The first yielding is naturally most likely to occur in one of the spots which is on or near the circumference, because the general stress is a maximum there. However, if yielding should first occur at an inside point, the yielded region would spread outwardly as well as inwardly, by the same process of reasoning as outlined. Such points of weakness act only as the initial disturbance or fuse which is necessary to *start* any unstable action, whereas after once being started the action is self-perpetuating. Similarly a strut, subjected to a load slightly above the critical, requires a slight disturbance or initial eccentricity to start the buckling, after which it continues unaided.

Even Distribution of Plastic Regions

The foregoing reasoning shows why slender radial plastic regions develop. Another remarkable fact, which has been mentioned, is that the regions are quite uniformly distributed around the circumference, instead of being closely bunched in some places and spread out in others, as might be expected if the distribution were entirely accidental. The explanation for this can obviously be found in the fact that, as has been pointed out before, the stresses are reduced at the sides of a plastic region, points *mm* Fig. 4, at the same time they are increased at the inner ends. The regions on either side of a plastic region are thus protected regions, safe harbors from stress and strain, where new regions are much less likely to start than elsewhere.

As the torque, and hence the general stress, is increased, more and more radial plastic regions are bound to be started, but, due to the protected flanks around those which have started, new regions will tend to start as far away as possible, i.e., about half way between those which have come before. Obviously, this would lead to the evenness of distribution which has been noted.

Increase in Width of Plastic Regions

The third and final feature of the phenomenon which requires explanation is the fact that, as the torsion progresses, the plastic

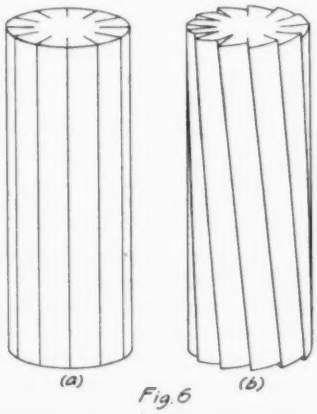


Fig. 6

regions gradually increase in width at the base or outside end. This fact seems to be directly opposed to the argument just cited, namely, that the stresses at the sides of the plastic regions are reduced, from which it might be expected that the plastic regions would remain narrow.

This widening of the plastic regions evidently represents a stabilizing tendency, which tends to change the unstable radial growth of Fig. 2, back toward the normal condition of Fig. 1, although it may never attain ascendancy over the unstable tendency as it does in the early stages of the tensile test. As in the tensile test, however, this stabilizing tendency is undoubtedly dependent upon the property of the material of strain-hardening after a certain amount of plastic flow has taken place. But in order to understand this fully, it will be necessary to consider more in detail the mechanism of the process.

Imagine a shaft in which a number of narrow radial slots have been cut, as shown in Fig. 6 (*a*). When this shaft is twisted it will present an appearance like Fig. 6 (*b*), the material between the slots undergoing very little distortion, while the sides of each slot slide relative to each other an amount which increases with the radius. The distortion of a shaft having plastic areas in the cross-sectional view, such as shown in Fig. 2 (*b*), must be similar to this. The plastic regions take the place of the slots, except that each plastic region will probably actually consist of numer-

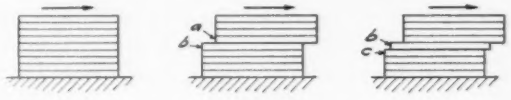


Fig. 7

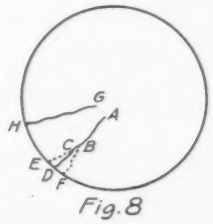


Fig. 8

ous surfaces each of which slides only a small part of the total. In any case, little distortion will take place in the unyielded material between the plastic regions, while large shear strains, increasing as the radius, will occur in the plastic regions.

After these shear strains reach a certain magnitude, the material which has been yielding stiffens up. If the relative sliding motion of the mass of the material on either side of the yielded region continues, then new planes of sliding must occur, say on either side of the stiffened material. Thus, the yielded region is widened. Fig. 7 illustrates such a process. A pile of plates is subjected to shear, sliding at first occurring between plates *a* and *b*. Due to heat of friction this surface seizes and plate *b* is dragged along with the top of the pile, creating a new sliding surface between *b* and *c*.

However, it is still not clear why the new sliding surface should occur next to the seized one, in preference to anywhere else. From the illustration, Fig. 7, it is apparently just as easy for it to occur next to the seized surface as anywhere else, but no easier. This does not conflict with what has previously been said regarding the reduction of stress at the sides of a yielded region. This reduction of stress is due to the *yielding* of the material in the region, but, as soon as this yielding ceases (as by stiffening of the material), the reduction of stress, and hence the immunity of material at the sides, ceases also.

If the stiffening of material due to strain-hardening occurred simultaneously all over the original surfaces of plastic flow, then there probably would be no reason for new surfaces to appear close to the old surfaces, and hence no explanation of the widening of the plastic region. But such simultaneous stiffening would be extremely unlikely. It is obvious that in practice stiffening will usually occur first at the outermost part of the sliding surface, where the relative motion is a maximum.

Assume for simplicity that there is only one original sliding surface in each plastic region, as in Fig. 6 (*b*) (the argument will be equally valid if there are many to start with, as would be probable). In Fig. 8 line *ABCD* shows the trace of such a surface in a cross-sectional view. Sliding proportional to the distance from the center occurs over this entire surface, and finally portion *CD* of the surface reaches the strain-hardening stage and in effect seizes. What happens then?

It seems obvious that a surface combining the still relatively weakened portion *ABC* with some new surface such as *CE*, will offer less resistance than an entirely new surface, such as *GH*. Or, to put the matter in a quite different way, after *CD* hardens, the surface *ABC* is still a plastic region, acting partially like an elongated hole, as discussed before, and causing stress concentration at both ends, *A* and *C*. Hence there is a strong tendency for the region to grow radially from *C*, and this growth will occur, not along the hardened path *CD*, but along some softer path such as *CE*. Similarly surface *BCE* will eventually harden, because all the outer sliding is now concentrated in it, leading to the formation of new surfaces, such as *BF*, etc. Thus plastic regions tend to widen at their outer ends, as well as to spread inwardly.

It is interesting to note that this is a process somewhat analogous to the case of a silt-carrying river, flowing over a gently sloping plain. When a portion of the original channel *CD* becomes choked with silt (strain-hardening), a backing up, or rise of water (stress concentration) occurs at *C*, leading to the formation of a new channel such as *CE*, etc., until we have a picture which is familiar in our geographies as that of many rivers at their mouths.

General Case—Formation of Lüders' Lines and Narrow Plastic Regions in Direction of Maximum Shear

In the case just considered it was found that the unstable localization of plastic flow was due to the tendency of an original sliding or shearing plane to spread laterally (that is, perpendicularly to the direction of sliding or of the shearing stress), under the influence of a concentration of shear stress of the type familiar to us in the case of twisted bars having discontinuities in their cross sections.

This sort of stress concentration is not confined to torsion specimens but will be produced whenever for some reason sliding or shearing starts locally. Fig. 9 shows such a case. Sliding has started in the vertical direction on surface *AA*, under the influence of vertical shearing forces and due, perhaps, to an initial crack or local weakness. A concentration of shear stress will be produced along the side of the surface, at points such as *p*, tending to make the surface spread horizontally in the direction of the dotted line, in exactly the same manner as in the torsion specimen Fig. 6 (*b*).

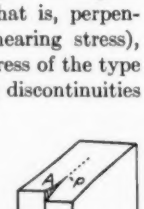


Fig. 9

This accounts for the spreading in the *lateral* direction of surfaces of sliding which start at minute points of weakness. However, it can easily be shown that a somewhat similar concentration of shear stress occurs at the *ends* of local sliding surfaces, which tends to make such surfaces spread in the direction of the sliding or of the shear stress, by exactly the same process as has been discussed.

Fig. 10 shows a portion of a body which is subjected to shear stress τ_0 and which contains an elliptical hole, with semiaxes *a* and *b*, in the directions of maximum shear stress. Intuition tells us that, if such a hole is elongated so that it approaches a crack, as shown in Fig. 10, there must be a high concentration of shear stress at points near the end of the crack, such as at *p*, while the shear stress will be nearly zero at the sides of the crack, as at point *q*. Intuition tells us this in spite of the fact that we know the shear stress must be zero exactly at the edge of the hole.

This case is included in Inglis' well-known study of the effect of elliptical holes,[5] although neither Inglis nor anyone else has apparently paid any attention to the concentration of *shear* stress at points such as *p*, perhaps because this stress is zero at the edge of the hole, and consequently it is not immediately apparent that a high stress concentration may exist just beyond the edge. From a previous paper[6] of the author's, containing a generalization of Inglis' work, it can be shown that the shearing stress τ, along the axis of symmetry a distance xa from the center of the hole, is

$$\tau = \frac{rx[r^2x^2(r^2+1) - (r^2+2)(r^2-1)] - 2r(r^2x^2 - r^2 + 1)^{3/2}}{(r^2x^2 - r^2 + 1)^{3/2}\,(r-1)^2}\,\tau_0 \qquad \ldots [1]$$

where $r = a/b$ is a measure of the slenderness of the hole.

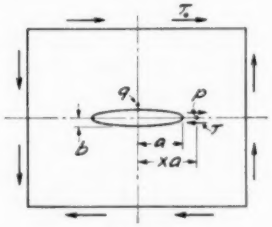


Fig. 10

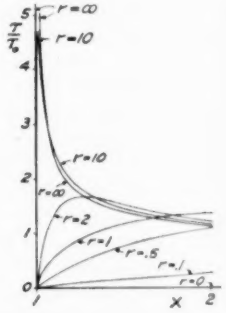


Fig. 12

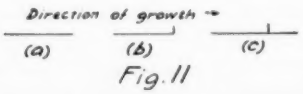


Fig. 11

Fig. 12 shows values of the shear stress concentration τ/τ_0, calculated from Equation [1], for various values of the slenderness r and the relative distance from the edge of the hole x. It can be seen that as the slenderness increases the stress concentration also increases, and its maximum value occurs closer to the edge of the hole, although the stress always comes down to zero at the edge itself (at $x = 1$). For $r = 10$, that is, for a hole 10 times as long as it is wide, a stress concentration of 4.7 occurs at a distance of about $0.01a$ from the edge. For $r = \infty$, that is, for a crack, there is an infinite stress concentration right at the edge of the hole; in this case the edge of the hole is a singular point where the stress concentration has values of both zero and infinity, depending upon whether the point is approached from the left or from the right. In the other direction, when r is small, the stress becomes very small near the hole; this evidently corresponds to the condition at points such as *q* in the middle of the broad side of the hole.

It now seems clear why surfaces of sliding, starting at minute points of weakness, tend to grow or spread, not only in the lateral direction, but in *all* directions along the surfaces of maximum shear stress. Sliding first starts, naturally along the direction of the surface of maximum shear stress, at some point where the resistance to sliding is less than in surrounding regions. As

[5] "Stresses in a Plate Due to the Presence of Cracks and Sharp Corners," by C. E. Inglis, Trans. Institution of Naval Architects, vol. 55, part 1, London, 1913, pp. 219–230.

[6] "Stress Concentrations Due to Elliptical Discontinuities in Plates Under Edge Forces," by L. H. Donnell, Theodore von Kármán Anniversary Volume, California Institute of Technology, Pasadena, Calif., 1941, p. 305.

the external loads increase, the shear resistance on this small yielded surface remains about constant, while the shear stresses increase elsewhere. By the time the stresses elsewhere have risen to the shearing yield point, there is the equivalent of the removal of a certain amount of internal resistance along the yielded surface.

Complete removal of this resistance would be equivalent to the existence of a crack, which would require for equilibrium large increases in the shear stress all around the periphery of the yielded surface, due to one or the other of the two types of stress concentration which have been discussed. Partial removal of the resistance requires proportionately smaller increases in the shear stress for equilibrium. The required increases cannot occur, because the material is already at the yield point and yields, so the yielded region has to spread yet further in search of equilibrium. At each stage of the process the surface which has already yielded forms a partial crack which tends to raise the stresses, and hence causes yielding, just beyond its borders.

As the yielded surface grows, it will tend to follow the original surfaces of maximum shear, because the combination of the original shear stress plus the increases due to stress concentration will obviously tend to be greater in that direction than in any other direction. There are, of course, at every point in a stressed body two mutually perpendicular surfaces of maximum shear. Since the shear stresses on these surfaces are equal it might be supposed that a yielded surface, in its growth, would find it just as easy to branch off at right angles at any point as to continue along the original surface in which it happened to start.

Actually, however, there is probably rather a strong tendency for it to continue along the original surface rather than to branch off, because the stress concentration at the end of a crack or partial crack of the shape shown in Fig. 11 (*a*) is probably higher than when the shape is as in Fig. 11 (*b*). Growth such as shown in Fig. 11 (*a*) tends to lengthen the original crack, and hence to increase the stress concentration. On the other hand, growth such as in Fig. 11 (*b*) probably has much the same general effect as widening the crack, and hence reducing the stress concentration. Thus, if such branches occur, growth along them will be slower than along the original direction. When the yielded region reaches the stage shown in Fig. 11 (*c*) growth along the branch path will tend to stop entirely because the whole branch will be in the protected zone at the side of the main crack.

How far such surfaces will grow will depend upon the variation in the general stress along the surface of maximum shear. When the general stress is uniform, as in a tensile specimen, so that the general stress is just about at the yield point everywhere before the growth starts, the sliding surfaces will grow completely across the entire specimen during a very slight change in the external load. Or, if the material is of the type which has an upper and a lower yield point, it is conceivable that they would spread explosively across the specimen without the external load changing at all.

When the general stress varies from point to point, as in torsion, bending, and around discontinuities, the sliding surfaces will, of course, tend to start at the most highly stressed points and spread until they reach a point where the decreased general stress plus the increase due to stress concentration is no longer above the yield stress. This will happen while the external loads are increasing only the slight amount necessary to balance statically the small localized increases in stress which this process entails. As the external loads increase, the yielded surfaces will, of course, also increase.

Similarly, the tendency to even spacing of yielded regions and the fact that they widen after considerable straining has occurred can be explained by the reduction of stress at the sides of yielded surfaces, strain-hardening, etc., for the general case in the same manner as for the twisted bar. It is believed that this discussion makes clear the mechanism of formation of Lüders' lines, which are the traces or intersections with the external surface of the yielded surfaces or narrow yielded regions, as well as all the other evidences which we have[7] that plastic flow tends to localize in narrow regions following the lines of maximum shear stress.

It can now be seen that the twisted bar first discussed is only a special case of the general phenomenon. There are some points in that case which we can now see in a somewhat different and clearer light. It was assumed previously that the region of starting weakness had the shape of a "notch cut in the edge" of a cross section. In order to produce the stress concentrations assumed, such a weakness would have to run the full length of the bar, or at least be considerably elongated in the direction of the length.

It is evident now that sliding will start on planes of maximum shear, such as an axial plane, at a point of weakness near the outer surface, and progress longitudinally by virtue of stress concentrations of the type of Fig. 10. The longitudinal surfaces of sliding thereby formed, will then spread in the radial direction in the manner originally discussed. We thus finally arrive at the spreading of the original sliding surface in all directions along maximum shear planes, as in the general case.

Moreover, the round shape which was assumed for the sake of the argument for the initial region of weakness can now be seen to have been unnecessarily pessimistic. Whatever shape the region of weakness may have, sliding will first start on surfaces of maximum shear. It is these sliding surfaces, having a shape to produce very high stress concentrations, which are the real starting point of the process.

Etching of sections of twisted bars seldom seems to reveal the presence of yielded surfaces in the circumferential direction.[8] There seems to be no ready explanation for their not forming as easily as longitudinal surfaces, unless it may lie in the "grain" or anisotropy of manufactured bars.

---

[7] Reference (2), chap. 16, 17, 20, 21, 25, etc.

[8] Reference (2), p. 145.

Discussion

Equiareal Pattern of Stress Trajectories in Plane Plastic Strain[1]

C. W. MacGregor.[2] A method is described in the paper by which the principal stress trajectories can be determined from their equiareal properties. These principal stress trajectories are very valuable in the analysis of any plastic-flow problem. We have approached the problem of their determination from the experimental point of view. The flow layers, which appear during early plastic flow, have been observed by a special equipment,[3] called a "plastiscope," in many problems such as: The cold-rolling of metals; the yielding of butt and lap welds; the plastic flow present in rollers compressed laterally; rivet holes punched in plates; and in many cases of stress concentration produced by notches, holes, etc. This equipment has been designed with considerable flexibility in mind. It can be applied equally well to the observation and recording of plastic flow in such cases as the rolling of metals, machining of metals, experiments in various testing machines, etc. In most cases motion pictures are made of the plastic flow as it is produced in each process; however, still photographs can also be made.

Having determined the pattern of flow layers experimentally in this manner, the principal stress trajectories can then be constructed easily from their property of cutting the family of flow layers at 45 deg.

It appears that the method described in the paper should be useful in supplementing and checking the method of construction outlined.

Modern Passenger-Car Ride Characteristics[1]

R. W. Brown.[2] The motorcar engineer has done an excellent job on the mechanical units of today's passenger cars. Possibilities for significant improvement appear to exist in working out the dynamic conditions which promote passenger comfort, decrease fatigue, and thereby increase safety.

The authors are to be congratulated for a concise, clear presentation of the complex performance of the various elastic and inertia elements of the car which are set into action when the wheel passes over even a single wave of simulated road inequality. Such articles provide a foundation for the statistical study of the thousands of vibrations to which the passenger is subjected in even a short ride.

The importance of "secondary" vibration has long been known to the ride engineers. Some recent research work[3] has been completed which emphasizes the importance of the seat cushion in isolating the passenger from uncomfortable effects of such vibrations. In a recent article,[4] dynamic performance of seat cushions was presented. Thus, a complete picture of the dynamic performance of the most important elastic systems of the motorcar under single-wave or repeated cyclic conditions has now been presented in the literature.

The Riding Comfort Research Committee of the Society of Automotive Engineers is active in encouraging and correlating efforts to the end that next year's motorcars will provide the passenger a constantly increasing freedom from the uncomfortable and fatiguing conditions incident to vibration, irrespective of its source. This work has substantiated the authors' contentions regarding mathematical analysis, importance of secondary vibrations, axle tramp, and interrelation of displacement and acceleration in bounce, pitch, and roll. The disclosure of axle motion is important, and their comment on rate of change of acceleration is interesting. It would appear that technical knowledge of suspension performance has received another worth-while addition.

Transient Torques in Induction-Motor Drives[1]

E. L. Davis.[2] Computations made by us from the data presented by the author indicate that couplings *A*, *B*, *C*, *D*, *E*, and *F* are separate and distinct designs of well-known manufacturers. We recognize coupling *E* as a Falk "steelflex" coupling.

After reviewing this paper, we agree that of all the couplings tested *A*, *B*, and *C* are properly applied on this particular drive. A coupling of the *E* type can be selected to give similar results. Obviously the coupling of the *E* type tested was not properly selected. The nonlinear torque-deflection characteristic of the type *E* coupling was not the cause of its undesirable effect on this drive. This coupling did not function properly because of its high average torsional-stiffness factor of 1,270,000 lb-in. per radian when compared to the low stiffness factors of couplings *A*, *B*, and *C*.

Table 1, herewith, shows the author's data in bold face and our calculations in regular face. The calculations shown in regular face were made from data shown in bold face, with the stiffness factor of the connecting shafts assumed to be 189,000,000 lb-in. per radian. Calculation gave 372,000 lb-in. per radian as the stiffness factor of coupling *D*. It was impossible to check the author's stiffness factors assigned to couplings *A* and *C* when working back from the frequencies he tabulated. Data, in Table 1, in regular face were also partly based upon the proportions of design that $I_r/(I_m + I_r) = 0.91$ and that $I_r = 10 \times I_m$ as stated by the author; where I_r = moment of inertia of roll, and I_m = moment of inertia of gear motor rotor, referred to the low-speed shaft.

---

[1] By M. A. Sadowsky, published in the June, 1941, issue of the Journal of Applied Mechanics, Trans. A.S.M.E., vol. 63, p. A-74.

[2] Associate Professor of Applied Mechanics, The Massachusetts Institute of Technology, Cambridge, Mass. Mem. A.S.M.E.

[3] "The Plastic Flow of Metals," by C. W. MacGregor, A.I.M.E., Technical Publication No. 1036, Metals Technology Division, April, 1939.

[1] By R. Schilling and H. O. Fuchs, published in the June, 1941, issue of the Journal of Applied Mechanics, Trans. A.S.M.E., vol. 63, p. A-59.

[2] In Charge, Automotive Research Division, The Firestone Tire & Rubber Company, Akron, Ohio.

[3] "Riding Comfort and Cushions," by W. E. Lay and L. C. Fisher, *S.A.E. Journal*, vol. 47, no. 5, Nov., 1940, pp. 482–496.

[4] "Engineering Properties of Rubber in Compression," by R. W. Brown, *S.A.E. Journal*, vol. 47, no. 4, Oct., 1940, pp. 432–444.

[1] By A. M. Wahl, published in the March, 1941, issue of the Journal of Applied Mechanics, Trans. A.S.M.E., vol. 63, p. A-17.

[2] Analyst, The Falk Corporation, Milwaukee, Wis.

TABLE 1 COUPLING DATA FROM PAPER[a] COMPARED WITH THOSE CALCULATED BY DISCUSSER[b]

Coupling	f_n	f	f_n/f	T_m/T_s calculated Case *b*	T_m/T_s calculated Case *a*	Highest test value	Volts	Stated locked power factor	Locked power factor, read from curves Figs. 4 and 5 Case *b*	Locked power factor, read from curves Figs. 4 and 5 Case *a*	T_s	T_s'	T_p	T_p'	T_m Case *b*	T_m Case *a*
A																
K = 112000	14	60	0.2335	2.5	2.2	2.6	440	0.52	0.6	0.75	600	3300	960	4800	8250	7260
K = 80000	14	40	0.3500	2.6	2.4	2.7	293		0.8	0.85	580[c]	2900[c]	840[c]	4200[c]	7540[c]	6960[c]
lb-in. per radian	14	20	0.7000				147	0.87			500	2500	720	3600		
B																
K = 170000	17	60	0.284	2.6	2.3	2.5	440	0.52	0.65	0.8	600	3300	960	4800	8570	7590
lb-in. per radian	17	40	0.425	2.9	2.7	2.7	293		0.84	0.8	580[c]	2900[c]	840[c]	4200[c]	8400[c]	7820[c]
	17	20	0.850				147	0.87			500	2500	720	3600		
C																
K = 193000	18	60	0.300	2.7	2.4	2.3	440	0.52	0.63	0.71	600	3300	960	4800	8910	7920
120000	18	40	0.450	3.1	2.7	2.7	293		0.75	0.84	580[c]	2900[c]	840[c]	4200[c]	8990[c]	7820[c]
lb-in. per radian	18	20	0.900				147	0.87			500	2500	720	3600		
D																
K = 372000	24	60	0.400	3.4	2.9	3.7	440	0.52	0.6	0.6	600	3300	960	4800	1210	9560
	24	40	0.600	4.3	3.6	4.3	293		0.8	0.76	580[c]	2900[c]	840[c]	4200[c]	12450[c]	10420[c]
avg lb-in. per radian	24	20	1.200				147	0.87			500	2500	720	3600		
E																
K = 1.27 × 10[6]	37.6	60	0.628	5.8	4.6	5.1	440	0.52	0.6[c]	0.6[c]	600	3300	960	4800	19150	15200
				4.6												15200
avg lb-in. per radian	37.6	40	0.94		5.9	5.7	293		0.8[c]	0.8[c]	580[c]	2900[c]	840[c]	4200[c]		17100[c]
	37.6	20	1.88			6.2	147	0.87			500	2500	720	3600		
F																
K = 2.335 × 10[6]	44.6	60	0.743		5.8	6.2	440	0.52			600	3300	960	4800	19100	
omitting lb-in. per	44.6	40	1.113		6.6	6.0	293				580[c]	2900[c]	840[c]	4200[c]	19100[c]	
radian backlash	44.6	20	2.225			7.8	147	0.87			500	2500	720	3600		

[a] Author's data are shown in bold-face type.
[b] Discusser's calculations are shown in regular-face type.
[c] Estimated.

NOMENCLATURE

K = stiffness factor, lb-in. per radian
f_n = natural frequency of systems, cycles per sec
f = electrical frequency, cycles per sec
T_m = peak torque, lb-in.
T_s = motor starting torque, lb-in.
T_s' = motor starting torque referred to low speed, lb-in.
T_p = motor plugging torque, lb-in.
T_p' = motor plugging torque referred to low speed, lb-in.

We agree with the author that for his test drive, which duplicates an existing roll-table drive at a steelmill, the ratio of $\frac{\text{natural frequency}}{\text{electrical frequency}}$ or f_n/f should be less than 0.6. For this reason couplings *A*, *B*, and *C* were successful for 60- and 40-cycle motors and not so successful for 20-cycle motors for this particular drive. By proper selection of coupling *E*, with the average stiffness factor the same as the constant stiffness factors of either couplings *A*, *B*, or *C*, coupling *E* will be suitable for this drive. In other words, it is possible to select a size and type *E* coupling having a ratio of f_n/f = 0.284 for 60 cycles.

This paper is helpful in showing conditions of stiffness factor for which a coupling should be selected or designed. Coupling *E* would have been ideal for certain mass-elastic systems of run-out tables other than those chosen for test comparison.

In design it is sometimes impossible to obtain proportions of f_n/f less than 0.6 due to space limitations or construction costs. When these items enter into the problem, one may be forced to select a design with proportions of f_n/f equal to 2 or greater. In this case coupling *E* as selected for the author's test would definitely be a better selection than couplings *A*, *B*, or *C* although none of the four would be adequate in capacity to transmit the peak torques. Fig. 1,[3] submitted with this discussion, shows that coupling *C* at 20 cycles with ratio of f_n/f = 0.9 (Table 1) will be in the range of resonance, whereas, coupling *E* will be beyond the range of resonance with a ratio f_n/f of 1.88.

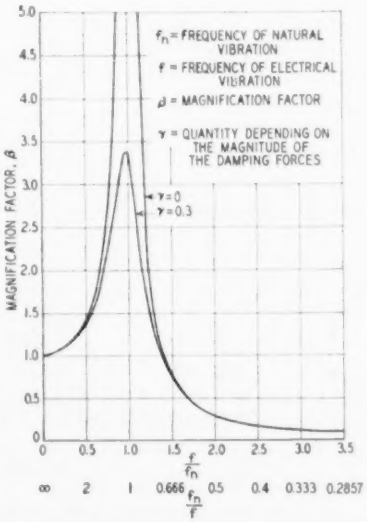


FIG. 1 CURVES SHOWING COUPLINGS WITHIN AND BEYOND RANGE OF RESONANCE

It is noteworthy that 55 couplings of type *E* have been successfully operating on run-out tables for 10 years on a 20-in. and 30-in. mill of a well-known steel company without mechanical failure. At another large steel mill, there are 486 type *E* couplings on run-out tables. A third steel mill reports excellent service from 25 type *E* couplings on run-out tables at the 84-in. hot-strip mill.

AUTHOR'S CLOSURE

Replying to Mr. Davis' discussion, the author would like to mention that the primary object of the paper has been to give designers a means of calculating the shaft torques set up in typical induction-motor drives during starting; the comparison of the results obtained by using various couplings was made primarily as a check on the method of calculation. The author agrees with the discusser that coupling *E* would not be satisfactory for an actual drive having the characteristics of the test drive. It was included as one of the test couplings in order to show how the shaft torque may be increased as a consequence of impact effects due to nonlinearity in the torque-angle characteristic of the coupling. It is clear that these impact effects could be greatly reduced by using a larger coupling of the *E* type such that the torque-angle curve would be practically linear for torques within the operating range.

Mr. Davis states: "The nonlinear torque-deflection characteristic of the type *E* coupling was not the cause of its undesirable effect on this drive. The coupling did not function properly because of its high average torsional-stiffness factor of 1,270,000 lb-in. per radian when compared to the low stiffness factors of

[3] "Vibration Problems in Engineering," by S. Timoshenko, second ed., D. Van Nostrand Company, Inc., New York, N. Y., 1937, p. 41.

couplings *A*, *B*, and *C*." Presumably the reasoning behind this statement is that this high stiffness factor tends to produce resonance. However, referring to Fig. 9 of the paper, the oscillogram obtained on coupling *E* shows a tendency toward resonance only at 20 cycles where the peak torque occurred on the second cycle; at 40 and at 60 cycles there is a sharp peak on the first cycle which is characteristic of an impact condition. For this reason the author believes that the high torque observed at 60 and at 40 cycles when using this type *E* coupling is due primarily to impact effects augmented by coupling nonlinearity and is only in part due to the relative stiffness of the coupling. At 20 cycles there is a combination of effects due to coupling nonlinearity and resonance which also results in relatively high torques. The author does agree, however, that conditions would be considerably improved as far as the test drive is concerned by using a type *E* coupling having the same average stiffness factor as for couplings *A*, *B*, or *C*. It should be noted that the average stiffness factor for a nonlinear coupling of this type increases with the applied torque, so that the peak torque must be specified if the average stiffness figure is to have meaning.

The values for natural frequencies f_n as given in Table 1 of the paper for couplings *A*, *B*, *C*, and *D* are approximate values obtained from actual oscillograph records. It was considered that this method would probably yield more accurate values than calculations based on the torque-angle curves as obtained from static tests on the couplings. The figures of 80,000 to 120,000 lb-in. per radian, given in the paper for the rubber-element couplings, were average values obtained by static torque-deflection tests. Under dynamic conditions it is quite possible that these stiffness values would be higher as indicated by the discusser.

Referring to Table 1 of the discussion, values of T_m/T_s were obtained by the author as follows: The nominal values of T_m/T_s for a load of infinite inertia were first found for the given values of f_n/f (or ω_n/ω) and locked power factor cos ϕ. Since the load inertia was not infinite these values were then corrected to take this into account by multiplying by $I_r/(I_m + I_r) = 0.91$ as mentioned in the paper. Thus for coupling *A* at 60 cycles, $f_n/f = 0.233$, cos $\phi = 0.52$, $T_m/T_s = 2.7$, assuming case (*b*) with infinite load inertia. Multiplying this by 0.91 gives a round figure of 2.5 for finite-load inertia. The discusser has evidently obtained the locked power factors given in his Table 1 by using the author's values of T_m/T_s and f_n/f in Figs. 4 and 5 of the paper without making this correction. In addition, the curves given in these figures are not plotted to a sufficiently accurate scale to enable this to be done accurately. This accounts for the differences shown in Table 1 between the discusser's values of locked power factor and those given by the author; the latter figures were based on actual electrical tests on the motor with the rotor locked.

It is suggested by the discusser that in cases where, due to space limitations or expense, a design with f_n/f less than 0.6 is not practical, a figure of f_n/f equal to 2 or greater be used. However, the author would like to point out that even where this is done, peak torques several times the nominal starting torque T_s may still occur depending upon the electrical characteristics of the motor. The reason for this is that, if f_n/f is high, i.e., if the shaft is very stiff, it may be expected that the peak shaft torque will be practically equal to the peak electrical torque acting on the rotor. This electrical torque in turn may be several times T_s, depending upon the locked power factor cos ϕ. It is shown elsewhere[4] that, for high-resistance motors of the type usually employed in this service, the peak electrical torque T_s (for nonsimultaneous voltage application on all phases) is given approximately by

$$T_s = T_s\left(1 + \frac{\sqrt{2}}{\cos\phi}\right) \quad \text{[1]}$$

For simultaneous voltage application the factor $\sqrt{2}$ is replaced by unity. Using Equation [1] and assuming a locked power factor of 0.5, the electrical torque becomes $T_s = 3.83\ T_s$, and as mentioned previously if f_n/f is very large this will also be the shaft torque.

Where f_n/f is not large (but yet considerably greater than unity so that damping may be neglected) a solution could be obtained for linear systems as follows: The expressions for transient electrical torque given by Equations [2] and [3] of the paper are taken in the differential equation for the system, Equation [7]. This equation is then solved using the proper boundary conditions. It will be found, however, that this method leads to considerable complication and for this reason the following approximate method may be used.

It may be shown that for high-resistance rotors of the type usually employed for this service, the term $\epsilon^{-\lambda_2 t}$ in Equation [3] of the paper dies out very rapidly during the first cycle of applied voltage, while for the usual motor with high magnetizing reactance the term $\epsilon^{-\lambda_1 t}$ may be taken as unity for several cycles of the applied voltage. Hence as an approximation (for nonsimultaneous voltage application) the electrical torque given by Equation [3] of the paper may be considered essentially as a constant torque T_s on which is superimposed an alternating torque at the electrical frequency f equal to $\frac{\sqrt{2}}{\cos\phi}\ T_s$. This alternating torque will be subject to a magnification as indicated by the discusser's Fig. 1. Neglecting damping this magnification is given by $1/[1 - (f/f_n)^2]$. Thus for $f_n/f = 2$ the magnification factor will be 1.33 and the alternating torque $\frac{1.33\sqrt{2}\ T_s}{\cos\phi}$. As an example for cos $\phi = 0.5$ the peak shaft torque then becomes $T_m = T_s\left(1 + \frac{1.33\sqrt{2}}{\cos\phi}\right) = 4.78\ T_s$. If a 20-cycle motor, having a locked power factor of 0.87 is used, the peak torque will be reduced to $T_m = T_s\left(1 + \frac{1.33\sqrt{2}}{0.87}\right) = 3.17\ T_s$ for the same ratio f_n/f. If there is some coupling nonlinearity an additional increase in torque may be expected. These examples show that torques of considerable magnitude may exist even if f_n/f is made 2 or larger.

The author wishes to take this opportunity to thank Mr. Davis for his contribution and interest in the problem.

[4] "Transient Starting Torques in Induction Motors," by A. M. Wahl and L. A. Kilgore, Trans. A.I.E.E., vol. 59, 1940, p. 605.

Analysis of Longitudinal Motions in Trains of Several Cars[1]

L. H. Fry.[2] This paper is an interesting contribution to the information available for analysis of the relative longitudinal motions of the individual cars in a railroad train. It is to be hoped that the author will be able to extend his method so that it may bring into account the friction action of the draft gears and the effect of slack between the couplers. The equations given in the paper are based upon cars connected by springs having uniform spring characteristics throughout closure and release.

[1] By W. M. Dudley, published in the December, 1941, issue of the Journal of Applied Mechanics, Trans. A.S.M.E., vol. 63, p. A-145.

[2] Railway Engineer, Edgewater Steel Company, Pittsburgh, Pa. Mem. A.S.M.E.

In reality the draft gears connecting the cars are designed to close and to release against relatively high friction. This is a vital element of draft-gear design. In every draft gear approved by the Association of American Railroads, the energy given up on release is less than 40 per cent of that put in during compression. This being the case, it is obvious that the wave of energy transmitted along the train will be damped rapidly and the wave reflected from the end will be very much less than is indicated in Figs. 6 and 7, in the paper.

The author suggests that the slack in the couplers between the cars will not come into play unless the amplitudes of vibration build up to several inches. In practice, any slack between the couplers must be alternately pulled out and taken up again during each cycle of vibration in which the draft gear goes from closure in buff to closure in pull.

It may also be pointed out that the numerical examples in the paper cover only five cars. In railroad work, the problems of practical interest involve trains of 100 cars or more. It appears that the direct application of the author's method to a 100-car train would lead to a group of Equations [14], involving 100 equations each containing 100 terms. The work involved in developing and then solving any such group of equations would be prohibitive.

O. R. Wikander.[3] To the writer's knowledge this is the first exact mathematical analysis which has been published, covering the action of an elastic chain, consisting of concentrated masses connected by frictionless springs. His use of the little-known "difference equations" for this purpose is also very interesting.

In his introductory remarks, the author compares his elastic-chain method with the known elastic-bar method and states that the results in his paper tend to show that the wave velocity in an elastic chain is only about two thirds of that in an equivalent elastic bar. We feel that this statement is misleading and that, on the contrary, the author's investigations tend to show that both methods give practically the same speeds of wave propagation.

The first example in the paper refers to a five-car train, represented by five concentrated, equal masses, connected by four identical frictionless springs.

The left-hand car approaches the rest of the train at a given speed and is coupled on, causing a speed-and-pressure wave to pass through the train.

In Figs. 2 and 3 of the paper, the car displacements and the velocities of the individual cars, as computed according to the author's method, are plotted against time.

Referring to the curves in these figures, the author points out that, according to the elastic-bar method, the wave would travel one car length in 1 time unit, while Fig. 3 shows a travel of one car length in 1.4 time units. This time is computed from the travel of the crest of the velocity wave, which is the resultant of a number of waves of different speeds, and thus continually changes its shape. If, instead, the author had measured the time interval between the moment when car No. 1 had moved the relative distance of one unit, until car No. 5 had moved the same distance, he would have found that exactly 4 time units had elapsed, showing a perfect agreement with the wave speed, as computed by the elastic-bar method.

In case of a seven-car train, the elastic chain would have 6 natural frequencies.

If the author's matrix method were used in solving the resulting difference equations, excessive time would be required to compute the displacements of all the cars.

For trains of more than ten cars, the amount of computation necessary when the author's method is used is so formidable as to appear prohibitive.

It is probable, however, that the method can be simplified and, at the same time, extended so as to apply to a wider field. This seems worth while, even if such simplifications should give only approximate, but truly comparative, results.

Fig. 10 in the paper is of particular interest. Curve A shows the velocity of wave travel at the lowest, curve B at the highest, natural frequency of trains consisting of from 2 to 45 cars.

Because of the great internal friction in the draft gears of any modern train, all higher harmonics will be effectively damped out, and it appears permissible to disregard all but the lowest natural frequency, represented by curve A. It will then be found that the velocity of wave travel increases from 90 per cent of that of an elastic bar in a two-car train to 95 per cent in a three-car train and to 100 per cent in any train of twelve cars or more.

In closing, the writer expresses the hope that the paper is only the beginning of the author's work in the comparatively virgin field of train dynamics.

Author's Closure

Messrs. Fry and Wikander both point out that the amount of calculation required to solve train problems by difference equations would be prohibitive if the train included more than about ten cars. This is implied in the title of the paper. It is true that for a train of 100 cars, the equation of motion of each car would contain 100 terms. It would probably not be necessary to compute the equations except for a few cars at important points of the train.

However, as Mr. Fry points out, such a solution would not be valid, owing to energy absorption in the draft gears. It seems unlikely that an exact solution will ever be calculated for problems involving slack or dry friction between cars. Both of these effects are mathematically discontinuous, that is, all the equations of the entire problem would have to be adjusted every time one pair of couplers reached the end of slack, or reversed its direction of relative slip. Furthermore, with dry friction, slip does not begin until the tension changes by a definite amount. It can be seen that it would take years to solve a problem involving a few cars, under these conditions.

If slack were eliminated and friction of the dashpot type (proportional to velocity) assumed, solutions could be obtained quite easily, as in long-distance telephoning problems, where the resistance of the line is included.

The writer does not agree entirely with Mr. Fry's comment that slack must inevitably come into play during vibrations. If the train is running, each pair of couplers carries the steady pull necessary to overcome running friction of the cars behind. Thus the vibrations are superposed on an average tension. Unless the compressive force of vibrations exceeds this tension, backlash or slack cannot occur.

Mr. Wikander's comments on the velocity of wave travel are interesting. It appears that the value found for this velocity will vary, depending upon whether one observes the times when cars first begin to move, when they have their maximum velocity, or when they have moved a definite distance.

In conclusion, it may be repeated that the paper is aimed at dynamic problems of short trains, such as passenger trains, involving not more than a dozen cars. For 100-car freights, it will probably always be necessary to distribute mass, stiffness, friction, and slack uniformly along the train, as is done in Mr. Wikander's well-known paper.[4] The author wishes to thank Messrs. Fry and Wikander for their encouragement and the discussions based on practical experience.

[3] Ring Spring Engineer, Edgewater Steel Company, Pittsburgh, Pa. Mem. A.S.M.E.

[4] "Draft-Gear Action in Long Trains," by O. R. Wikander, Trans. A.S.M.E., vol. 57, 1935, p. 317.

Note on Angular Motions of Ships[1]

H. O. Fuchs.[2] The author mentions the controversy involving the type of coupling between tank and ship. The question was whether the system had force coupling or inertia coupling.

Recently it has been shown[3] that the type of coupling (force or inertia) is not a characteristic of the physical system, but depends upon the arbitrary choice of co-ordinates. The same system (e.g., ship tank or double pendulum) will show force coupling with one set of co-ordinates and inertia coupling with another set. The controversy between Frahm and Schuler was without point; they were both right, but used different systems of co-ordinates. The various co-ordinates lead of course to the same result; their choice is a matter of convenience. Coupling by damping is inherently different by its phase. In undamped systems it is always possible to choose the natural modes as co-ordinates; the coupling then disappears from the equations; in damped systems, the coupling can be eliminated from the equations only under special conditions.

It follows that coupled systems cannot be classified by the type of coupling. Classification by invariant characteristics has been studied by Quade.[4]

Author's Closure

Mr. Fuchs has raised an interesting point which requires a far more extensive analysis than can be given here.

The situation which Mr. Fuchs mentions is created by the fact that the coupling terms appearing in the differential equations of a coupled system arise as the result of application of the Lagrangian equations to the systems. If, therefore, the latter equations are omitted and the differential equations with coupled terms are written by *a priori* considerations, as is usually done in the technical literature, one finds difficulty in attaching to these terms a definite physical interpretation, in so far as they do not stand in any direct relation with the fundamental invariants of the system; such as the law of energy, for example.

The matter gains in clarity, however, if instead of writing the differential equations with coupling terms introduced more or less *a priori*, one goes through a more laborious procedure of forming the Lagrangian equations. In so doing, one is obliged to form the expressions for the kinetic and potential energies of the system. The former is generally obtained without any particular difficulty. As to the latter, it requires an appropriate choice of the system of reference which is generally imposed by the problem itself.

In order to clarify this point, the following example will make apparent the underlying physical nature of the dynamical phenomena involved:

Consider a physical pendulum to which is attached a horizontal track in the plane of oscillation of the pendulum; on this track may roll a weight with negligible friction; the weight may be displaced by a cable driven by a motor.[5] It can be assumed that this cable passes through the axis of oscillation so that the inertial coupling, as usually defined, is negligible. Under these assumptions there is neither inertial nor frictional coupling provided in the system, comprising the pendulum and the weight. Assume that we control the motion of the weight as follows.

The weight arrives at the end of the track just at the instant when this end begins to rise in space owing to the motion of the pendulum and is kept there (e. g., by means of a catch) until this end reaches its maximum height. At this moment the catch is released, the weight slides "downhill," and the same phases are reproduced for the opposite swing.

Experiment shows that the motion of the pendulum is damped in such case (assuming that it was undamped with the weight fastened to its track).

The results are the same if the motion of the weight, instead of being discontinuous, is continuous of the form $x = k\,\theta$, where x is the departure of the weight from the middle of the track, $\dot{\theta}$ the angular velocity of the pendulum, and k a factor of proportionality.

It is easier, however, to discuss qualitatively the discontinuous arrangement.

The explanation of this phenomenon is very simple. The system in this case is conservative by our assumption. Since the weight is kept at the end of the track which is rising in space, the gravity performs a negative work, in so far as the weight always moves against the gravity. The work is thus absorbed and is converted into the potential energy of the raised weight. However, this absorption of energy can occur only at the expense of the diminution of the kinetic energy of the pendulum which, in fact, is observed since the amplitudes of oscillation decrease. The subsequent transfer of the weight downhill occurs at the expense of the potential energy so gained, but this has no effect on the pendulum in view of the fact that, in the arrangement described, the weight has neither potential nor frictional coupling with the pendulum.

One is tempted, therefore, to consider the coupling in this case as a kind of force coupling following Schuler's classification.

From the preceding explanation, it appears that the expression "potential coupling" is perhaps more appropriate. Furthermore, the following point of importance is to be noted: The increase of potential energy occurs with respect to the external field of force, i.e., the gravity ("Fernwirkung" using Klotter's term) and has nothing to do with the internal forces set up in the system itself.

These considerations can be easily generalized for the liquid-ballast transfer in a system of tanks. The only delicate point which arises in this case is the expression of the potential energy. This requires a particular choice of co-ordinates subordinated to Schuler's criterion, viz., there is no potential coupling between the ship and the ballast in a passive tanks system. In fact an inclination of the ship (θ_0) does not "incline" the free level in tanks in a steady-state condition. If, however, instead of the absolute level, one introduces the relative level φ_0 in tanks, the Schuler condition of passive tanks requires that $\theta_0 + \varphi_0 = 0$. Starting from this point, it is possible to express the potential energy of the system in terms of both parameters θ and φ and then form the Lagrangian equations. There appear no further ambiguities in this formulation in so far as the choice of co-ordinates is not arbitrary any more but becomes subordinated to the physical end of the problem.

The principal difficulty which Schuler encountered seems to be in the fact that, having established a correct criterion differentiating the passive performance of tanks from the active one, he came back to the differential equations with coupled terms instead of going through the formation of the Lagrangian equations, and thus found himself again in a vicious circle.

From this standpoint, Klotter's suggestion of building up the *actio in distans* theory is particularly interesting; it is then possible to use the Lagrangian equations, provided the expression of the potential energy is expressed in suitable co-ordinates, as has been explained.

The advantage of this procedure lies in the fact that it deals directly with the physical entities (the energies) of the system, so that the choice of suitable co-ordinates instead of being arbitrary becomes imposed by these physical considerations.

[1] By Nicholas Minorsky, published in the September, 1941, issue of the Journal of Applied Mechanics, Trans. A.S.M.E., vol. 63, p. A-111.

[2] Product Studies, General Motors Corporation, Detroit, Mich.

[3] "Kopplung mechanischer Schwingungen," by K. Klotter, *Ingenieur-Archiv.*, vol. 5, 1934, pp. 157–163.

[4] "Über die Schwingungsvorgänge in gekoppelten Systemen," by W. Quade, *Ingenieur-Archiv.*, vol. 6, 1935, pp. 15–34.

[5] "Control Problems," by Nicholas Minorsky, *Journal of The Franklin Institute*, vol. 232, 1941, p. 481.

Book Reviews

Torsional Vibration

PRACTICAL SOLUTION OF TORSIONAL VIBRATION PROBLEMS. By W. Ker Wilson. Second edition, John Wiley & Sons, Inc., New York, N. Y. Cloth, 6 × 9 in., Vol. 1, 1940, xx and 731 pp., 110 figs., $8; Vol. 2, 1941, xxi and 694 pp., 237 figs., $8.50.

REVIEWED BY GEORGE B. KARELITZ[1]

A single-volume edition of this book appeared in 1935. The second edition reflects the spectacular progress achieved during the intervening years in the field of general and torsional vibration. The author lists among others: A more general application of tuning mechanical oscillating systems, in order to place severe critical zones either above or below the operating speed ranges; the accumulation of data relating to fatigue phenomena; the introduction of the rotating pendulum vibration-absorber in aircraft engines; the investigation of the oscillating aero engine—air-screw system as a whole; the introduction of flexible mountings for engines and instruments; the study of "nonlinear" vibration systems.

All this new material, together with the author's desire to utilize a large amount of new practical design data, doubled the subject matter of the book and made the second edition a more valuable source of information for those who are working practically with torsional vibrations. The work can hardly be classified as a textbook in vibration and it does not intend to be. The reader should be familiar with the general elementary theory of vibration before undertaking the author's two volumes.

But these will be rather helpful as a means to translate the general principles into practical engineering forms. They are particularly timely at present, when so many engineers are concerned with torsional vibrations in plane, ship, or tank engines. The text is illustrated by frequent practical examples, with solutions worked out to final numerical values. Schemes to facilitate numerical computations are indicated in many instances. Useful and convenient tables of empirical design data are given, such as the comparative torsional stiffness of crankshafts of various designs. Valid physical approximations are suggested; for instance, the reasonable mass allowance is given for inertia of the water entrained by a vibrating marine propeller.

The book consists of twelve chapters, six in each volume, with appendixes to each volume. Chapter 1 recapitulates the relations governing the frequency of torsional vibration in systems with one degree of freedom. It shows also the approximate handling of systems with two, three, or more masses. Chapter 2 discusses the methods and arrangement of calculation for the natural frequency, for multimass systems in marine, automotive, and aviation machinery. Chapter 3 gives the torsional rigidities of practical crankshafts and the equivalent mass inertias of various details of engine installations, such as gears, propellers. A special chapter, the fourth, is devoted to the rigidity and design of flexible couplings. Chapter 5 treats the reduction of a geared system to an equivalent single shaft with several masses; the handling of gear transmissions used in aircraft is given particular attention. Chapter 6 deals with the determination of stresses at nonresonant speeds, i.e., torsional amplitudes in crankshafts. The effects of the number of cylinders and the firing order in engines of the in-line, vee, and radial types are discussed in detail.

Chapter 7 discusses stresses due to torsional vibration at resonant speeds and the effect of damping. Empirical numerical data are given on damping in commonly encountered designs of both engines and driven elements, as well as on the internal damping of structural materials. The permissible working stresses and the effect of stress concentration are indicated. Chapter 8 describes the design and operation of many commercial instruments for measuring torsional vibrations, while chapter 9 shows how to analyze and interpret records obtained by means of the torsiographs. Chapter 10 describes vibration-damping devices, for use with internal-combustion engines; numerous illustrations of vibration absorbers and friction dampers are given together with the theory of their action. Special importance is attached to the rotating-pendulum vibration absorber, in chapter 11. Designs of this device and their operation are discussed in detail. Chapter 12 gives the dynamic characteristics of electrical generating sets direct-coupled to internal-combustion engines, their torsional vibrations, governing, and flywheel effect.

The two volumes will be of assistance to mechanical engineers who are dealing with torsional vibration in their daily activity. The books will also be of interest to students of the science of vibrations, in bringing together many practical problems awaiting more rigorous solutions. Selected bibliographies at the end of each volume and detailed indexes add to the value of the book as a source of reference.

[1] Department of Mechanical Engineering, Columbia University, New York, N. Y. Mem. A.S.M.E.

Principles of Mechanics

PRINCIPLES OF MECHANICS. By J. L. Synge and B. A. Griffith. First edition. McGraw-Hill Book Company, Inc., New York, N. Y., 1942. Cloth, 6 × 9 in., xii and 514 pp., 162 figs., $4.50.

REVIEWED BY CHARLES W. MACGREGOR[2]

THE authors have stated their object in the preface as follows: "In a sense this is a book for the beginner in mechanics, but in another sense it is not. From the time we make our first movements, crude ideas on force, mass, and motion take shape in our minds. This body of ideas might be reduced to some order at high school (as crude ideas of geometry are reduced to order), but that is not the educational practice in North America. There is rather an accumulation of miscellaneous facts bearing on mechanics, some mathematical and some experimental, until a state is reached where the student is in danger of being repelled by the subject, as a chaotic jumble which is neither mathematics nor physics. This book is intended primarily for students at this stage. The authors' ambition is to reveal mechanics as an orderly self-contained subject."

This single volume treats the usual elementary subjects of statics, kinematics, and dynamics, but in addition covers the more advanced topics of vibration, kinematics, and dynamics in space together with a short chapter on the special theory of relativity. The scope of the book is therefore much broader than the usual text in this field which either treats only the more elementary phases of the subject or else, taking these for granted, embarks

[2] Associate Professor of Applied Mechanics, Massachusetts Institute of Technology, Cambridge, Mass. Mem. A.S.M.E.

on an extensive development of the more advanced subjects. The authors have also adopted a distinct departure in their division of the subject matter. They have elected to divide the treatment into plane mechanics and mechanics in space. In each of these parts, the subject of statics, kinematics, and dynamics are discussed separately. This means that the subject of statics in three dimensions is left until the subjects of kinematics and dynamics in the plane are disposed of. The customary procedure in the past has been to complete the treatment of both two- and three-dimensional statics before embarking on motion problems.

The mathematical background of the authors is well reflected in their attention to mathematical rigor, and even the most meticulous would feel quite satisfied on this score.

At the end of each chapter summaries are given of the more important formulas and conclusions developed, a procedure which has been adopted in too few cases in the past by authors on this subject. This enhances the value of the book greatly both as a text and as a reference work.

The first three chapters are devoted to a discussion of the equilibrium conditions in plane statics with applications to friction problems, thin beams, cables, and frames. In the development of the theory both the principle of virtual work and the parallelogram law are used in different places as basic premises. In the discussion of bending moments and shearing forces in beams it will be noted that the sign of the shearing force is taken opposite to the customary convention in this country. The treatment of cable problems is perhaps more rigorous than that appearing in many elementary texts since it is based on the differential equation rather than resorting to a "freezing technique" together with the three-force theorem.

Chapters 4 to 8 cover the subject of plane kinematics and dynamics with applications to the motion of projectiles with and without air resistance, vibration problems with and without damping, planetary orbits, plane motion, and impulsive motion.

Chapters 9 to 15 discuss mechanics in space, including statics, kinematics, and dynamics with applications to space frames, the spherical pendulum, the motion of a charged particle in an electromagnetic field, the spinning top, and gyroscopes. In chapter 15 Lagrange's equations are developed and applied to such problems as the determination of the normal frequencies of vibration of a system with two degrees of freedom, etc.

The special theory of relativity is discussed briefly in chapter 16. The Lorentz transformation connecting the co-ordinates of a pair of Galilean observers and the equations of motion in relative form are treated.

The very breadth and scope of the subject, encompassed as in this case in a single volume, has necessitated perhaps a somewhat briefer discussion of the various parts than is customary for engineering students in this country. The average engineering student who does not possess more than the commonly required undergraduate mathematical background also might experience some difficulty in certain portions of the book. This refers especially to the use of vector analysis in the discussion of mechanics in space. While many of the applications and examples given illustrate the theory very ably, the engineer might prefer less academic and more practical problems as illustrations. The authors have also preferred to omit any discussion of graphical methods used so generally in engineering practice. In spite of this, however, the book represents a very comprehensive exposition of the subject; and while it may be found to be most useful as a text in the education of mathematics and science students, or for a survey course for the more advanced engineering students, it is quite evident that many practicing engineers will find this volume a very welcome addition to their own reference libraries.

High-Pressure Plant and Fluids at High Pressure

THE DESIGN OF HIGH-PRESSURE PLANT AND THE PROPERTIES OF FLUIDS AT HIGH PRESSURES. By Dudley M. Newitt. The Oxford University Press, New York, N. Y., 1940. Cloth, 6¼ by 9½ in., viii and 491 pp., tables, diagrams, plates, $10.

REVIEWED BY JOSEPH H. KEENAN[3]

IN these busy days when the current professional literature waiting to be read piles higher and higher, and that Saturday afternoon when other things will not be pressing seems more and more remote, a book like this one should be warmly welcomed. It presents in 500 pages and in coherent form the literature of the experimental attack on the properties of fluids at elevated pressures.

In the preface the author states that, "In view of the rather specialized nature of the subject, it has been thought advisable to emphasize the experimental aspect and to devote several chapters to the design of high-pressure plant and to the methods of measuring high pressures." And so we find discussion of elastic and plastic properties of metals and the effects on these properties of the presence of gases under high pressure. Then comes a good chapter on devices for measuring pressures of magnitudes up to thousands of atmospheres.

The major part of the book is given over to a discussion of the properties of vapors and liquids at pressures that are high relative to the critical pressure. It requires no more than a limited acquaintance with this subject to appreciate the diligence and skill that has gone into the compilation and presentation of this material. It is generously illustrated with a fascinating collection of figures drawn largely from the literature. References are numerous and complete.

The disturbed state of the world will not readily permit the patient thorough work necessary to the preparation of a book of this sort. We shall, therefore, prize more highly those that have reached the stage of publication.

von Kármán Anniversary Volume

IN the review of this volume in the March issue of the JOURNAL it was stated in the first paragraph that Clark Millikan was the editor of this volume. This was an error since the volume was the work of friends of Theodore von Kármán, as stated in the heading of this particular review.

[3] Professor of Mechanical Engineering, Massachusetts Institute of Technology, Cambridge, Mass. Mem. A.S.M.E.

Torsional and Flexural Buckling of Bars of Thin-Walled Open Section Under Compressive and Bending Loads

By J. N. GOODIER,[1] ITHACA, N. Y.

The observed behavior of torsionally weak columns in buckling by twisting rather than, or as well as, bending is analyzed in this paper on the basis of a hypothesis due to Wagner. The theory is simplified, and extended to the general section, where results simpler than some already obtained by Kappus are given. It is further extended to bars, restrained by flexible sheets, and bars with constrained axes of rotation. Wagner's hypothesis is applied to the problem of lateral buckling, where it yields the accepted theory for symmetrical sections, but indicates results of novel form for unsymmetrical cases. Similar results are obtained in the problem of eccentric thrust, whatever the section.

Introduction

THE ordinary Euler buckling of a compressed bar does not always occur when the section is torsionally weak. Instead the bar may buckle by twisting, or by a combination of flexure and twist. It is easy to see how the purely flexural deformation, assumed in the Euler theory, can be maintained by bending moments of the thrust created by the deformation itself, but it is somewhat difficult to see how a torsional deformation can be maintained by thrust, in the general case.[2] In the special case of the angle section, such buckling may be explained by regarding each leg as a plate, as was done in 1910 by Timoshenko (1).[3] An analysis for the arbitrary open section was made by Wagner on different lines (2, 3), involving a tacitly assumed hypothesis, describing the torsional effect of the thrust. This hypothesis is adopted here, where it is used to obtain equations more general than Wagner's (which include further unessential assumptions and approximations), and more simple than those of Kappus (4), who replaced Wagner's hypothesis by an equivalent energy hypothesis, also employed here. Kappus' theory introduces two new constants of the section (R_x, R_y) which are found to be unnecessary. They do not appear when advantage is taken of certain properties of the shear center.

The theory of buckling by torsion and flexure under simple thrust is thereby given a simpler form than hitherto. It is extended to the case of a stiffener attached to a perfectly flexible sheet, which permits displacement of the line of attachment normal to it, but not parallel to it. Such a fundamental solution might be made the basis of a method of predicting the strength of stiffened panels, by including in the effective section the equivalent width of sheet indicated by a formula such as the well-known one of von Kármán.[4] Use of a stiffener section, augmented by von Kármán's effective width of sheet, in the Euler formula is current in aircraft design, but this of course takes no account of torsional effects.

The hypothesis of Wagner is further applied to the theory of lateral buckling, or buckling under bending loads, where it indicates that the present theory, due to Prandtl, Michell, and Timoshenko, will be inadequate except in special cases. In his original paper (2), Wagner considered the bar under eccentric thrust, attributing buckling entirely to the torsional effects of the thrust. The same problem, however, formed a part of the older theory of lateral buckling where it was attributed entirely to the bending moment of the eccentric thrust. The two effects are quite distinct, and evidently a complete theory must include both. This paper constitutes an attempt to do this, with various explicit results for critical loads in important special cases.

A fuller account of the subject is given in references (6) and (7).

Arbitrary Thin-Walled Section—Uniform Thrust

Buckling of the bar is taken to occur by twisting and bending deformations. The buckled form is specified by components of displacement, u, v of the shear center of the cross section, and a torsional rotation β about the shear center. The axe of x and y, Fig. 1, are taken with the origin at the shear center S, and directions, unless otherwise stated, parallel to the principal

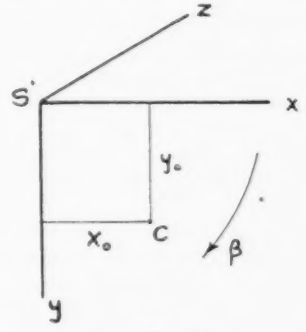


FIG. 1

axes of the section at the centroid. The z axis is the axis of shear centers.

It has been shown (6) that nonuniform torsion (the torsional moment varying along the bar) occurs by relative rotation of cross sections about the axis of shear centers (in the uniform tor-

[1] Professor of Mechanics, Cornell University. Mem. A.S.M.E.

[2] Torsional buckling has sometimes been entirely attributed to noncoincidence of centroid and shear center, but this is inadequate since such buckling can occur when these points are coincident.

[3] Numbers in parentheses refer to the Bibliography at the end of the paper.

Presented at the Annual Meeting, New York, N. Y., December 1–5, 1941, of THE AMERICAN SOCIETY OF MECHANICAL ENGINEERS.

Discussion of this paper should be addressed to the Secretary, A.S.M.E., 29 West 39th Street, New York, N. Y., and will be accepted until October 10, 1942, for publication at a later date. Discussion received after the closing date will be returned.

NOTE: Statements and opinions advanced in papers are to be understood as individual expressions of their authors, and not those of the Society.

[4] A method of this type, based on Wagner's formula for the torsional critical load of an unattached bar was proposed by E. E. Lundquist and C. M. Fligg: "A Theory for Primary Failure of Straight Centrally Loaded Columns," N.A.C.A. Technical Report No. 582, 1937.

sion of the Saint Venant theory the location of the axis of relative rotation is immaterial), and that the torsional moment M is given in terms of the rotation β of the section z by

$$M = GC\beta' - E\Gamma\beta''' \quad [1]$$

(primes denoting differentiation with respect to z) where GC is the Saint Venant torsional rigidity, G is the shear modulus, E is Young's modulus, and Γ a constant defined (6) in terms of the cross-sectional warping of the Saint Venant theory. This is a generalization of a similar relation obtained for the I-section by Timoshenko.[5] It was derived by Wagner (2).

Thus when the deformation u, v, β occurs, u produces bending stress forming a moment EI_1u'' in the x, z plane; v produces a moment EI_2v'' in the y, z plane, and β an axial moment as given by (1). I_1 and I_2 are the usual (centroidal) moments of inertia.

The stress on a cross section, besides forming the moments just discussed, must form a horizontal force P to balance the applied thrust P on the end. The former, being the resultant of

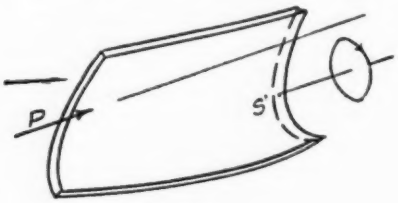


FIG. 2

uniform compressive stress only infinitesimally disturbed by the buckling, acts at the centroid of the displaced section. The components of displacement of the centroid are $(u - y_0\beta)$, $(v + x_0\beta)$, x_0 and y_0 being the co-ordinates of the centroid. The forces P, acting on the piece of the bar between the left end and the section z, thus form a couple $P(u - y_0\beta)$ in the x, z plane, $P(v + x_0\beta)$ in the y, z plane, the centroid of each end being undisplaced, and we have the equations (corresponding to the Euler theory)

$$EI_1u'' + Pu - Py_0\beta = 0 \quad [2]$$

$$EI_2v'' + Pv + Px_0\beta = 0 \quad [3]$$

The formation of a third equation requires Wagner's hypothesis. This presupposes that the stress on the cross section consists of the fiber stress—the fibers being of course inclined to the z axis—which is, except for small additions due to the deformation, simply uniform compression, σ, together with the (small) shearing stress of nonuniform torsion forming the moment [1]. There is also the shearing stress of bending, with resultant through the shear center.

Consider the moment, formed by the stress on the section, about an axis through the displaced shear center, but parallel to the z axis. The fiber stress σ forms a force σdA, on an element of area dA which, in virtue of the inclination of the fiber to the axis, has a moment of the type just defined of

$$\sigma dA\ [y(u' - y\beta') - x(v' + x\beta')] \quad [4]$$

in the sense of the curved arrow in Fig. 2. The total moment formed in this way is

$$Py_0u' - Px_0v' - P\rho^2\beta' \quad [5]$$

where P is written for σA, and ρ is the polar radius of gyration of the section about the shear center.

The moment formed by the shear stress of nonuniform torsion is given by [1], except perhaps for the cosine of a small angle as a factor, which is unimportant.

The shear stresses, associated with the bending, form no moment of the type in question since their resultant passes through the shear center. Thus moments [1] and [5] together must form zero moment so that

$$E\Gamma\beta''' + (P\rho^2 - GC)\beta' - Py_0u' + Px_0v' = 0 \quad [6]$$

Sections With Coincident Centroid and Shear Center

This case includes sections with two axes of symmetry, and sections with "point symmetry" such as the Z-section with equal flanges. Then $x_0 = y_0 = 0$ and Equations [2] and [3] become the usual Euler equations for buckling in the principal planes. Equation [5] becomes

$$E\Gamma\beta''' + (P\rho^2 - GC)\beta' = 0 \quad [7]$$

with the general solution

$$\beta = C_1 \cos kz + C_2 \sin kz + C_3$$

where

$$k^2 = (P\rho^2 - GC)/E\Gamma$$

A bar to which thrust is applied by ball joints, centered at the centroid of each end, would have the end condition $\beta = 0$ at $z = 0$, to eliminate rigid-body rotation. It is also necessary to have β'' at $z = 0$ and $z = l$, l being the length of the bar, since, as has been shown (6), nonuniform torsion involves an axial stress proportional to β''. It may be readily verified that these three conditions can only be satisfied if $kl = n\pi$ where n is an integer. This yields

$$P = \frac{1}{\rho^2}\left(GC + \frac{n^2\pi^2}{l^2}E\Gamma\right) \quad [8]$$

for the critical thrusts corresponding to modes

$$\beta = C_2 \sin n\pi z/l$$

C_2 remaining arbitrary. This is Wagner's critical thrust for torsional buckling. When it is less, with $n = 1$, than both the Euler critical thrusts, buckling will occur by twisting rather than bending.

This discussion does not exhaust all conceivable types of solution of Equation [7], but it has been shown (6) that the others have slight practical significance.

For fixed ends, the middle half of the bar will correspond to the solution given.

Sections With One Axis of Symmetry—Arbitrary Sections

The axis of symmetry being the x axis, $y_0 = 0$ and Equation [2] becomes the ordinary Euler equation. The critical thrust π^2EI_1/l^2 may be derived from it. However, Equations [3] and [6] are simultaneous equations in v and β, indicating that the other two modes of buckling are neither purely flexural nor purely torsional. A solution in the form $v = C_2 \sin n\pi z/l$, $\beta = C_3 \sin n\pi z/l$, corresponding to rotatable ends, leads to the critical condition

$$\begin{vmatrix} 1 - \dfrac{Q_n}{P} & x_0 \\ x_0 & \rho^2\left(1 - \dfrac{T_n}{P}\right) \end{vmatrix} = 0$$

where

$$Q_n = \frac{n^2\pi^2\,EI_2}{l^2}, \quad T_n = \frac{1}{\rho^2}\left(GC + \frac{n^2\pi^2}{l^2}E\Gamma\right)$$

[5] Bibliography (1), p. 256.

This quadratic yields

$$\frac{1}{P} = \frac{1}{2}\left\{\frac{1}{Q_n} + \frac{1}{T_n} \pm \sqrt{\left(\frac{1}{Q_n} - \frac{1}{T_n}\right)^2 + \frac{4}{Q_n T_n} \cdot \frac{x_0^2}{\rho^2}}\right\}$$

and it may be shown that one of the values of P is less than the smaller of Q_n, T_n, while the other exceeds the greater of Q_n, T_n.

For the arbitrary section, a solution of Equations [2], [3], and [6], as they stand, may be taken in the form

$$u = C_1 \sin\frac{n\pi z}{l}, \quad v = C_2 \sin\frac{n\pi z}{l}, \quad \beta = C_3 \sin\frac{n\pi z}{l}$$

corresponding to rotatable ends. The condition of consistency of the equations in C_1, C_2, C_3 obtained by substitution is the cubic in $1/P$

$$\left(1 - \frac{P_n}{P}\right)\left(1 - \frac{Q_n}{P}\right)\left(1 - \frac{T_n}{P}\right) - \left(1 - \frac{P_n}{P}\right)\frac{x_0^2}{\rho^2} - \left(1 - \frac{Q_n}{P}\right)\frac{y_0^2}{\rho^2} = 0$$

P_n being $n^2\pi^2 EI_1/l^2$. The lowest critical load will normally correspond to $n = 1$.

Bar Attached to Flexible Sheet

The attachment to the sheet, Fig. 3, imposes the condition $u - h\beta = 0$ all along the bar. If the bar is first imagined free, and buckled so that this condition is not fulfilled, as it would not be in general, forces must be applied in the plane of the sheet, to nullify the x displacement along the line of attachment.

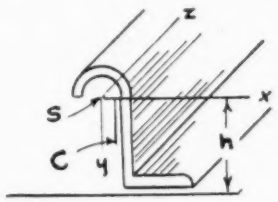


Fig. 3

These forces will exert both flexural and torsional actions. They are easily included in the differential equations, reference (6). The result of the calculation is that buckling of the form

$$u = hC_3 \sin\frac{n\pi z}{l}, \quad v = C_2 \sin\frac{n\pi z}{l}, \quad \beta = C_3 \sin\frac{n\pi z}{l}$$

can occur if the thrust P satisfies the quadratic

$$\left(1 - 2\frac{y_0}{h} + \frac{\rho^2 - x_0^2}{h^2}\right)P^2 - \left[P_n + \left(1 - 2\frac{y_0}{h} + \frac{\rho^2}{h^2}\right)Q_n + \frac{\rho^2}{h^2}T_n - 2\frac{x_0}{h}R_n\right]P + Q_n\left(P_n + \frac{\rho^2}{h^2}T_n\right) - R_n^2 = 0 \quad [9]$$

Here the axes x, y are no longer parallel to the principal axes through the centroid, but parallel and normal to the sheet, and $R_n = n^2\pi^2 EI_{12}/l^2$ where I_{12} is the product of inertia for axes through the centroid parallel to the x, y axes.

Ramberg, McPherson, and Levy (5) found stresses, at failure, in the Z-stringers of their test panels as given in Table 1.

TABLE 1 STRESSES AT FAILURE IN Z-STRINGERS OF TEST PANELS

	Sheet thickness 0.070 in.			Sheet thickness 0.025 in.			
Length, (fixed ends), in.	19	7.26	11.62	19	19	19	19	19
Stringer stress at failure, psi	36200	36400	37400	38400	31300	30200	30400	36200

From the dimensions given in their paper, the Euler critical stresses (for fixed ends, 19 in. length) work out to 27,400 and 176,000 psi, and the Wagner critical stress, Equation [7], for torsional buckling to 37,500 psi. The critical stresses obtained from the quadratic Equation [9] (with $l = 9.5$ in., $n = 1$), corresponding to attachment to a perfectly flexible sheet, are 31,600 and 157,000 psi. The lower value conforms to the observed values for the thinner sheet, and being close to the proportional limit of the material requires little if any correction on that score.

To take account of the stiffness of the sheet, an effective width of sheet, acting with the stiffener to form an augmented section, might be determined from von Kármán's formula, or an equivalent, and the critical stress redetermined from Equation [9].

If the section has an axis of symmetry normal to the perfectly flexible sheet, one possible mode of buckling is the ordinary Euler buckling by flexure in the plane of symmetry, unhindered by the sheet. The other mode, involving twisting, with bending parallel to the sheet, has the critical load

$$\left(P_n + \frac{\rho^2}{h^2}T_n\right) \Big/ \left(1 - 2\frac{y_0}{h} + \frac{\rho^2}{h^2}\right)$$

The value for a section with two axes of symmetry, normal and parallel to the sheet, is obtained by putting $y_0 = 0$.

Enforced Axis of Rotation

If the bar is constrained along a given axis, parallel to it, as by frictionless hinging, or its equivalent, the stability can be investigated by considering the forces exerted by the hinge when buckling occurs, or by the energy method (6). If the coordinates of the given axis are $x = a$, $y = b$, we have $u - b\beta = 0$, $v + a\beta = 0$, all along the bar. There is only one type of buckling, involving rotation of the cross sections about the hinge axis, and the critical load is found to be

$$\frac{GC + \frac{n^2\pi^2}{l^2}(\Gamma + I_1 b^2 + I_2 a^2 - 2I_{12}ab)}{a^2 + b^2 + \rho^2 - 2ax_0 - 2by_0}$$

Loading by Thrust, Bending, and Twisting

This more general problem is illustrated by Fig. 4. In addition to the thrust P, applied at the centroids of the end sections,

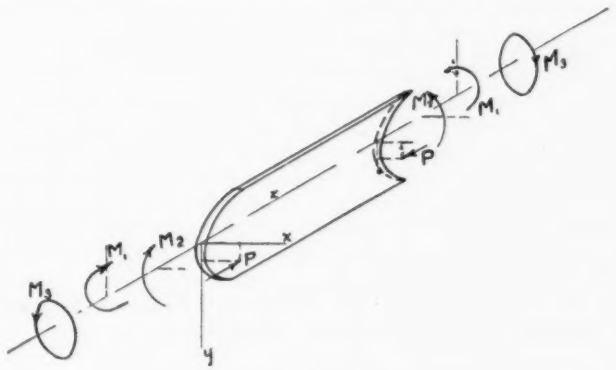


Fig. 4

and corresponding to uniform compression, the bar is bent by end couples M_1 in the x, z plane, M_2 in the y, z plane, and twisted by the torsional couple M_3. Thus the configuration of the bar, even if stable, involves flexure and torsion. In Fig. 5, which represents the piece of the bar between the left end and the section z, moments are represented by vectors. M_u and M_v

are the (bending) moments formed by the stress on the section. The torsional couple formed by the stress is omitted. The axes ξ, η are the displaced x, y axes of the section z. The equations of the type $\Sigma M_\xi = 0$, $\Sigma M_\eta = 0$ are

$$EI_1 u^{v} + Pu + M_3 v' + (M_2 - Py_0)\beta = -M_1 \ldots [10]$$

$$EI_2 v^{v} + Pv - M_3 u' - (M_1 - Px_0)\beta = -M_2 \ldots [11]$$

The x, y axes are here parallel to the principal centroidal axes.

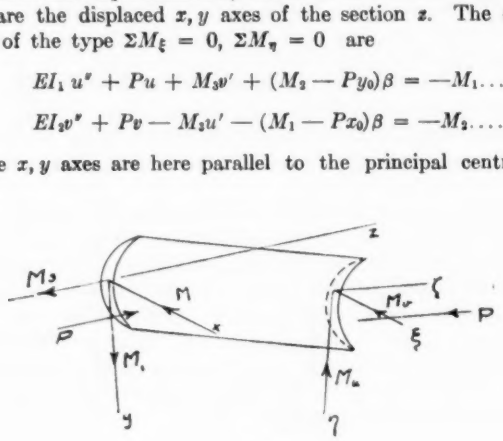


FIG. 5

The third equation is again obtained by taking moments about an axis through the shear center of the displaced section z, and parallel to the original axis of the bar. The compressive fiber stress is now, to a sufficient accuracy

$$\frac{P}{A} - \frac{M_1}{I_1}(x - x_0) - \frac{M_2}{I_2}(y - y_0)$$

When this is used in place of σ in [4], and the total moment computed by integration, we obtain instead of [5]

$$-P(x_0 v' - y_0 u' + \rho^2 \beta') + M_1\left(v' + \frac{\kappa_1}{I_1}\beta'\right) - M_2\left(u' - \frac{\kappa_2}{I_2}\beta'\right)$$

where

$$\kappa_1 = \int x(x^2 + y^2)\, dA - x_0 A\rho^2, \quad \kappa_2 = \int y(x^2 + y^2)\, dA - y_0 A\rho^2$$

The equation under consideration is thus found to be

$$E\Gamma\beta''' + \left(P\rho^2 - GC - M_1\frac{\kappa_1}{I_1} - M_2\frac{\kappa_2}{I_2}\right)\beta' + (M_2 - Py_0)u' - (M_1 - Px_0)v' = M_3 \ldots [12]$$

Equations [10, 11, 12] are three simultaneous equations for u, v, β which may be solved to determine the equilibrium configuration under the given loads, whether this is stable or not. To investigate the stability, let U, V, B be these equilibrium values, and let $(U + u_1)$, $(V + v_1)$, $(B + \beta_1)$ represent a neighboring configuration. Then u_1, v_1, β_1 satisfy Equations [10, 11, 12] with the right sides zero. These "stability" equations reduce to the simpler forms derived by Timoshenko[6] (with differences of sign accounted for by the different choice of axes) if we put $\Gamma = P = M_1 = M_3 = 0$ and take the section as doubly symmetrical, so that $x_0 = y_0 = \kappa_1 = \kappa_2 = 0$. The terms with $P\rho^2$, κ_1, κ_2 in Equation [12] appear to be new and result from Wagner's hypothesis.

Buckling Under Pure Bending

For this case we put $P = M_3 = 0$. A solution of the stability equations may be found in the form

$$u_1 = C_1 \sin\frac{n\pi z}{l}, \quad v_1 = C_2 \sin\frac{n\pi z}{l}, \quad \beta_1 = C_3 \sin\frac{n\pi z}{l} \ldots [13]$$

making the displacement and rotation vanish at $z = 0$ and $z = l$. On substitution, the condition that C_1, C_2, C_3 be different from zero is found to be

$$P_n M_1^2 + Q_n M_2^2 - P_n Q_n\left(\rho^2 T_n + M_1\frac{\kappa_1}{I_1} + M_2\frac{\kappa_2}{I_2}\right) = 0 \ldots [14]$$

As special cases we may consider the following:

Two Axes of Symmetry. Point Symmetry: On account of the symmetry

$$x_0 = y_0 = \kappa_1 = \kappa_2 = 0$$

and Equation [14] becomes

$$P_n M_1^2 + Q_n M_2^2 - P_n Q_n T_n \rho^2 = 0$$

For bending in one principal plane (y, z) only, $M_1 = 0$, and the critical bending moments are

$$M_2 = \pm\sqrt{P_n T_n \rho^2} \ldots [15]$$

which may be written

$$\pm\frac{n\pi}{l}\sqrt{EI_1\left(GC + \frac{n^2\pi^2}{l^2}E\Gamma\right)}.$$

For the I-beam this agrees with Timoshenko's result.[7]

One Axis of Symmetry. When this axis is normal to the plane

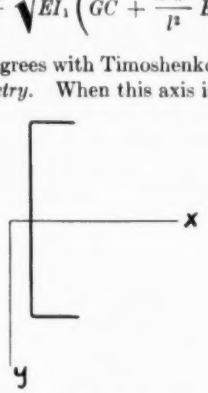


FIG. 6



FIG. 7

of bending, as in the channel section bent in the principal plane parallel to the web, Fig. 6, we have

$$y_0 = \kappa_2 = 0, \quad M_1 = 0$$

and again the critical moment is given by Equation [15].

However, if the axis of symmetry is in the plane of bending, as in the T-section, bent in the plane of the web, Fig. 7, we have $x_0 = \kappa_1 = 0$ and $M_1 = 0$, but

$$y_0 \neq 0, \kappa_2 \neq 0$$

Then Equation [14] becomes a quadratic for M_2 yielding

$$M_2 = \frac{1}{2}\left\{P_n\frac{\kappa_2}{I_2} \pm \sqrt{P_n^2\frac{\kappa_2^2}{I_2^2} + 4P_n T_n \rho^2}\right\} \ldots [16]$$

The positive sign yields a positive M_2 and the negative sign a negative M_2, whether κ_2 be positive or negative. Thus, the

[6] Bibliography (5), chap. 5.

[7] Bibliography (1), Equation [159], p. 261.

critical moment is different according as the beam is bent up or down. The quantity κ_2/I_2 as may be seen from the definition of κ_3 under Loading by Thrust, Bending, and Twisting, will be a length of the order of the over-all dimensions of the section. For a 90-deg-angle section with thin walls, κ_2/I_2 is $\sqrt{2}$ times the length of leg, the y axis being in the plane of symmetry. The quantity $P_n\kappa_2/I_2$ is of importance in Equation [16] if its square is comparable with $4\,P_n\,T_n\,\rho^2$ or if $(\kappa_2/I_2\rho)^2\,(P_n/4T_n)$ is comparable with unity. This is so if P_n and T_n are comparable, which is certainly the case for bars which are liable to buckle torsionally under thrust.

It may be shown that the fiber stress, corresponding to the moment [15] is of the order $\sqrt{P_1T_1/A^2}$ which will evidently be attainable when both P_1/A, T_1/A are within practical limits. This will be so for sufficiently thin-walled sections, or when the smallness of P_1/A compensates for largeness of T_1/A as in the thin rectangular section.

Other Loadings—Eccentric Thrust

The thrust is regarded as eccentric when its line of action, although parallel to the bar, does not pass through the centroids of the end sections. The components of eccentricity are e_1 and e_2 when the co-ordinates of the line of action are $(x_0 + e_1)$, $(y_0 + e_2)$. Then the eccentric thrust P is equivalent to a centroidal thrust P together with end moments M_1, M_2 equal to $-Pe_1$, $-Pe_2$, respectively. Using these values, and putting $M_3 = 0$ in Equations [10, 11, 12], a solution of the form [13] leads to the critical condition

$$\rho^2\left(1-\frac{P_n}{P}\right)\left(1-\frac{Q_n}{P}\right)\left(1-\frac{T_n}{P}\right)+\left(1-\frac{P_n}{P}\right)\left(1-\frac{Q_n}{P}\right)\left(\frac{e_1\kappa_1}{I_1}+\frac{e_2\kappa_2}{I_2}\right)-\left(1-\frac{P_n}{P}\right)(e_1+x_0)^2-\left(1-\frac{Q_n}{P}\right)(e_2+y_0)^2=0 \quad \ldots.[17]$$

the lowest of the three values of P being the critical load.

Two Axes of Symmetry. $x_0 = y_0 = \kappa_1 = \kappa_2 = 0$: The equation remains a cubic. However, if the line of thrust lies in a principal plane, say y, z, $e_1 = 0$ and the third term of Equation [17] disappears. One root is $P = Q_n$ corresponding to Euler buckling in the principal plane containing the thrust. There are two other types of buckling involving flexure and torsion at loads given by

$$\frac{1}{P}=\frac{1}{2}\left\{\frac{1}{P_n}+\frac{1}{T_n}\pm\sqrt{\left(\frac{1}{P_n}-\frac{1}{T_n}\right)^2+\frac{4\,e_2^2}{P_n\,T_n\,\rho^2}}\right\}$$

One of the values of P is less than the smaller of P_n, T_n the other exceeds the greater of P_n, T_n.

One Axis of Symmetry. Some simplification of Equation [17] occurs when the thrust is in the plane of symmetry. With the y axis as an axis of symmetry we have $e_1 = x_0 = \kappa_1 = 0$ and the reduced form of Equation [17] again yields $P = Q_n$ for one root. The others are the roots of the quadratic

$$\frac{1}{P^2}-\left(\frac{1}{P_n}+\frac{1}{T_n}+\frac{1}{T_n}\cdot\frac{e_2\,\kappa_2}{\rho^2 I_2}\right)\frac{1}{P}+\left[1+\frac{e_2\,\kappa_2}{\rho^2 I_2}-\frac{(e_2+y_0)^2}{\rho^2}\right]\frac{1}{P_n T_n}=0$$

The general problem can also be solved when the bar is attached to a flexible sheet, or has a constrained axis of rotation. The results are given in a current paper (7) by the author.

BIBLIOGRAPHY

1 "Theory of Elastic Stability," by S. Timoshenko, McGraw-Hill Book Company, Inc., New York, N. Y., 1936, chapt. 7.

2 "Torsion and Buckling of Open Sections," by H. Wagner, 25th Anniversary Publication, Technische Hochschule, Danzig, 1904–1929, pp. 329–343. Translated as Technical Memorandum No. 807, U. S. National Advisory Committee for Aeronautics, 1936.

3 "Torsion and Buckling of Open Sections," by H. Wagner and W. Pretschner, *Luftfahrtforschung*, vol. 11, 1934, pp. 174–180. Translated as Technical Memorandum No. 784, U. S. National Advisory Committee for Aeronautics, 1936.

4 "Twisting Failure of Centrally Loaded Open-Section Columns in the Elastic Range," by R. Kappus, *Luftfahrtforschung*, vol. 14, 1937, pp. 444–457. Translated as Technical Memorandum No. 851, U. S. National Advisory Committee for Aeronautics, 1938.

5 "Experimental Study of Deformation and Effective Width in Axially Loaded Sheet-Stringer Panels," by W. Ramberg, A. E. McPherson, and S. Levy, Technical Memorandum No. 684, U. S. National Advisory Committee for Aeronautics, 1939.

6 "The Buckling of Compressed Bars by Torsion and Flexure," by J. N. Goodier; forthcoming Bulletin of Cornell University Engineering Experiment Station.

7 "Flexural-Torsion Buckling of Bars of Open Section Under Bending, Eccentric Thrust, or Torsional Loads," by J. N. Goodier, forthcoming Bulletin of Cornell University Engineering Experiment Station.

8 "An Investigation of Sheet-Stiffener Panels Subjected to Compression Loads With Particular Reference to Torsionally Weak Stiffeners," by L. G. Dunn, Technical Memorandum No. 752. U. S. National Advisory Committee for Aeronautics, 1940.

Distribution of Stress in Built-In Beams of Narrow Rectangular Cross Section

By F. B. HILDEBRAND[1] and ERIC REISSNER,[1] CAMBRIDGE, MASS.

This paper deals with the problem of the distribution of stress in cantilever beams of narrow rectangular flanged cross section with one end of the beam rigidly built-in. Since an exact solution of this plane-stress problem appears difficult to obtain, an approximate solution is derived by applying the principle of least work. Instead of the linear normal stress distribution of the elementary beam theory, a third-degree polynomial is assumed, and the spanwise variation of this stress curve is determined by means of the calculus of variations. Numerical results are obtained with regard to the stresses at the built-in end of the beam, in their dependence upon (*a*) the span-height ratio of the beam, (*b*) the flange area–web area ratio of the beam, (*c*) Poisson's ratio of the material, and (*d*) the distribution of load along the span. It is found that the deviations from the results of the elementary theory may be appreciable when the distance of the center of gravity of the load curve from the built-in end of the beam is less than twice the height of the cross section of the beam.

Introduction

IT IS well known that the distribution of stress in bent beams as given by the elementary theory, as well as by known solutions of the exact theory, does not in general satisfy exactly prescribed conditions of support at the ends of the beam. It is also known that such deviations are of appreciable influence on the stress distribution when the cross-sectional dimensions of the beam are not small compared with the span length of the beam. The problem of the exact determination of the stresses for prescribed conditions of support, when formulated as a boundary-value problem of the general equations of the theory of elasticity, is one of considerable difficulty which thus far has found no exact solution in many interesting cases. In some instances approximate solutions have been obtained by the application of minimum-energy principles.

It is the purpose of this paper to add new approximate solutions of interest to those now existing, by investigating the distribution of stress in cantilever beams of flanged narrow rectangular cross section, one end of each beam built-in and the other end free. Results are obtained concerning the deviations of the stresses from those given by the elementary theory in their dependence upon the following:

1 The span-height ratio of the beam.
2 The flange area–web area ratio of the beam.
3 The distribution of load along the span.
4 Poisson's ratio of the material.

To obtain these results the principle of least work is employed in a form which has recently been found effective for the solution of problems somewhat related to those under consideration (1).[2] As will be seen this form of the method has the advantage of being more flexible than those forms of the least-work method previously applied (2, 3, 4, 5), and also, in a certain sense, it leads to more accurate results.

Formulation of the Problem

The determination of the stress distribution in a beam of narrow rectangular cross section may be considered as a problem in the theory of plane stress. If a system of coordinates (x, y) is introduced, the direction of x coinciding with the direction of the axis of the beam, and the direction of y perpendicular to the x axis, then according to the elementary beam theory, the normal stress σ_x is a linear function of y, the shear stress τ a quadratic function of y, and the transverse normal stress σ_y a negligible quantity. It is well known that these assumptions do not satisfy exactly the equations of the theory of plane stress, except for the case of a cantilever beam with concentrated end load, and that, moreover, this distribution of stress implies conditions of support of the beam not always met with in reality. In particular, it is known that these assumptions, concerning the distribution of stress, imply expressions for the components of the displacement of the elements of the beam which do not permit originally plane cross sections of the beam to remain plane after the load has been applied. For example, one of the possible conditions of support which cannot be satisfied by such a solution is that of a rigidly built-in end. It is known that the distribution of stress in the neighborhood of such an end section which is restrained from warping may deviate appreciably from the one given by the elementary beam theory (5, 6). The following developments are principally concerned with the problem of determining these deviations in their dependence upon the various factors mentioned in the introduction.

Starting with the expressions for the beam stresses in terms of Airy's stress function

$$\sigma_x = \frac{\partial^2 \phi}{\partial y^2} \qquad \sigma_y = \frac{\partial^2 \phi}{\partial x^2} \qquad \tau = -\frac{\partial^2 \phi}{\partial x \partial y} \quad \ldots\ldots [1]$$

it is known that the stress-strain relations

$$\frac{\partial u}{\partial x} = \frac{1}{E}(\sigma_x - \nu\sigma_y) \qquad \frac{\partial v}{\partial y} = \frac{1}{E}(\sigma_y - \nu\sigma_x) \qquad \frac{\partial u}{\partial y} + \frac{\partial v}{\partial x} = \frac{1}{G}\tau \quad \ldots\ldots [2]$$

require ϕ to be a solution of the biharmonic equation

$$\nabla^2\nabla^2\phi = 0 \quad \ldots\ldots [3]$$

For a flanged beam with one end rigidly built-in and the other end free or loaded in shear only, when for the purpose of simplification it is assumed that the manner of load application is such that σ_x is exactly an odd function of y, the boundary conditions of

---

[1] Instructor in Mathematics, Massachusetts Institute of Technology.

[2] Numbers in parentheses refer to the Bibliography at the end of the paper.

Presented at the Annual Meeting, New York, N. Y., December 1–5, 1941, of The American Society of Mechanical Engineers.

Discussion of this paper should be addressed to the Secretary, A.S.M.E., 29 West 39th Street, New York, N. Y., and will be accepted until October 10, 1942, for publication at a later date. Discussion received after the closing date will be returned.

Note: Statements and opinions advanced in papers are to be understood as individual expressions of their authors, and not those of the Society.

the problem are (Fig. 1)

$$x = 0 \quad u = 0 \quad v = 0 \ldots\ldots\ldots\ldots [4a, b]^3$$

$$x = l \quad \sigma_x = 0 \quad \tau = \tau_0(y) \ldots\ldots\ldots\ldots [5a, b]$$

$$y = \pm h \quad A_f \frac{\partial \sigma_f}{\partial x} = \pm t\tau(x, \pm h) \quad \epsilon_f = \epsilon_x(x, \pm h) \ldots [6a]$$

$$y = \pm h \quad \sigma_y = \mp {}^1/_2 p(x) \ldots\ldots\ldots\ldots [6b]$$

Equations [4] and [5] are self-explanatory. Equation [6a] expresses the fact that the variation of the flange normal stress is

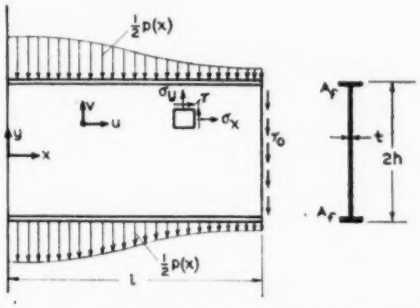


FIG. 1 FLANGED BEAM WITH ONE END RIGIDLY BUILT-IN, SHOWING LOAD APPLICATION

due to the shear acting between flange and web, and that flange and web normal strains coincide along the junction of the two structural members.[4] The particular type of load application, which is indicated by Equation [6b] and Fig. 1, has been chosen for the purpose of obtaining antisymmetry of the σ_x stresses about the axis of the beam, thus simplifying the analysis.

In order to obtain an approximate solution to this problem we write

$$\phi = F_e + F \ldots\ldots\ldots\ldots [7]$$

where F_e denotes the stress function corresponding to the elementary beam theory (which in general satisfies neither the differential Equation [3] nor all the boundary conditions). The function F determines the deviations from the elementary theory.

F_e can be written in the form

$$F_e = \frac{M(x)h^2}{I}\left[\frac{1}{6}\left(\frac{y}{h}\right)^3 - \left(m + \frac{1}{2}\right)\left(\frac{y}{h}\right)\right] = \frac{M(x)h^2}{I} g_e(y) = f_e(x)g_e(y) \ldots [8]$$

where $M(x)$ denotes the moment of the edge loads $tp(x)$ and $t\tau_0(y)$ at any section x = const, and

$$I = \frac{2}{3}h^3t(1 + 3m) \quad m = \frac{A_f}{th} \ldots\ldots\ldots\ldots [9]$$

are the moment of inertia and a form factor of the cross section. The function, Equation [8], satisfies the flange boundary conditions, Equations [5a] and [6], as well as Equation [5b] if the shear load at the free end is distributed in accordance with the assumptions of the elementary theory.

The correction term F is assumed in the form

$$F = \left[\frac{1 + 7m}{1 + 3m}\left(\frac{y}{h}\right) - 2\frac{1 + 5m}{1 + 3m}\left(\frac{y}{h}\right)^3 + \left(\frac{y}{h}\right)^5\right] h^2 f(x) = g(y)f(x) \ldots [10]$$

where $f(x)$ is a function yet to be determined. Term F has been chosen such that ϕ, as given in Equation [7], satisfies the flange-boundary conditions Equation [6]. Equations [5] for the free end are satisfied exactly by imposing appropriate boundary conditions on $f(x)$, while the remaining conditions, Equation [4] and the differential Equation [3], are satisfied approximately by minimizing the internal work of the beam, this procedure leading to a total differential equation and to additional boundary conditions for $f(x)$.

Expressions for the stresses follow from Equations [1, 7, 8, 10] in the form

$$\sigma_x = \left(\frac{y}{h}\right)\frac{M(x)h}{I} + \left[-12\frac{1 + 5m}{1 + 3m}\left(\frac{y}{h}\right) + 20\left(\frac{y}{h}\right)^3\right] f(x) \ldots [11]$$

$$\tau = -\left[\frac{1}{2}\left(\frac{y}{h}\right)^2 - \left(m + \frac{1}{2}\right)\right]\frac{M'(x)h^2}{I} - \left[\frac{1 + 7m}{1 + 3m} - 6\frac{1 + 5m}{1 + 3m}\left(\frac{y}{h}\right)^2 + 5\left(\frac{y}{h}\right)^4\right] hf'(x) \ldots [12]$$

$$\sigma_y = \left[\frac{1}{6}\left(\frac{y}{h}\right)^3 - \left(m + \frac{1}{2}\right)\left(\frac{y}{h}\right)\right]\frac{M''(x)h^3}{I} + \left[\frac{1 + 7m}{1 + 3m}\left(\frac{y}{h}\right) - 2\frac{1 + 5m}{1 + 3m}\left(\frac{y}{h}\right)^3 + \left(\frac{y}{h}\right)^5\right] h^2 f''(x) \ldots [13]$$

while for the curvature of the center line of the beam there is obtained

$$K = \left(\frac{\partial^2 v}{\partial x^2}\right)_{y=0} = \left[\frac{1}{G}\frac{\partial \tau}{\partial x} - \frac{1}{E}\left(\frac{\partial \sigma_x}{\partial y} - \nu\frac{\partial \sigma_y}{\partial y}\right)\right]_{y=0}$$

$$K = -\frac{1}{E}\left\{\frac{M(x)}{I} - 12\frac{1 + 5m}{1 + 3m}\frac{f(x)}{h^3} - (2 + \nu)\left[\frac{M''(x)h^2}{I}\left(m + \frac{1}{2}\right) - \frac{1 + 7m}{1 + 3m}\frac{f''(x)}{h}\right]\right\}$$

APPLICATION OF PRINCIPLE OF LEAST WORK

The function $f(x)$, occurring in Equations [11] to [13] for the stresses, will be determined by the method of least work, which in the present problem amounts to minimizing the internal energy W_i of the beam, given in terms of the stresses, by a suitable choice of $f(x)$.

Term W_i has the form

$$W_i = \frac{t}{2E}\int_0^l\int_{-h}^{h}\{\sigma_x^2 + \sigma_y^2 - 2\nu\sigma_x\sigma_y + 2(1 + \nu)\tau^2\}\, dydx + \frac{A_f}{E}\int_0^l \sigma_f^2 dx \ldots [14]$$

where the first integral represents the energy stored in the web,

---

[3] It should be noted that the conditions, Equations [4], of vanishing displacements at the built-in end are in practice never quite realizable due to flexibility of the support. The solution obtained without regard to this flexibility will therefore represent only an approximation in actual cases. An investigation of the limiting case seems, however, to be of interest in order to obtain an indication of trends.

[4] In order to avoid difficulties originating from the fact that, for a flanged beam, continuity of the strains at the transition from web to flange is not equivalent to continuity of the σ_x stresses when $\nu \neq 0$, it will be assumed that, in the formulas for the flanged beam, the applied load is either concentrated at the free end or uniformly distributed along the beam. Since in this case $\sigma_y(x, \pm h) = 0$ or c, it follows that $\frac{\partial \sigma_f}{\partial x} = \frac{\partial \sigma_x(x, h)}{\partial x}$. Also, in order to simplify the calculations, it is assumed that the flange area is concentrated along a line, which presupposes that the flange height is small compared with the height of the beam.

and the second integral the energy stored in the two flanges.[5]

The condition for a minimum value of W_i is, according to the rules of the calculus of variations, that the variation of W_i, δW_i vanish. Introducing Equations [1] into [14], δW_i takes the form

$$\delta W_i = \frac{t}{E}\int_0^l\int_{-h}^{h}\{\phi_{yy}\delta\phi_{yy} + \phi_{xx}\delta\phi_{xx} - \nu\phi_{xx}\delta\phi_{yy} - \nu\phi_{yy}\delta\phi_{xx} + 2(1+\nu)\phi_{xy}\delta\phi_{xy}\}\,dydx + \frac{2A_f}{E}\int_0^l [\sigma_f\delta\sigma_f]dx \quad [15]$$

By repeated integration by parts this is transformed into

$$\delta W_i = \frac{t}{E}\left\{\int_0^l\int_{-h}^{h}[\nabla^2\nabla^2\phi]\,\delta\phi dydx - \int_{-h}^{h}\left\{[\phi_{xxx} + (2+\nu)\phi_{xyy}]\delta\phi - [\phi_{xx} - \nu\phi_{yy}]\delta\phi_x\right\}_0^l dy - \int_0^l\left\{[\phi_{yyy} + (2+\nu)\phi_{yxx}]\delta\phi - [\phi_{yy} - \nu\phi_{xx}]\delta\phi_y\right\}_{-h}^{h} dx + 2(1+\nu)\left\{\left[\phi_{xy}\delta\phi\right]_0^l\right\}_{-h}^{h} + \frac{2A_f}{t}\int_0^l\sigma_f\delta\sigma_f dx\right\} = 0 \quad [16]$$

In view of the fact that the varied stresses must satisfy the same boundary conditions as the stresses themselves, it follows from [5*a*, *b*] and from [6*a*, *b*] that

$$x = l \qquad \delta\phi = 0 \qquad \delta\phi_x = 0 \quad [17a]$$

$$y = \pm h \qquad \delta\phi = 0 \qquad \pm\frac{A_f}{t}\delta\sigma_f + \delta\phi_y = 0 \quad [17b]$$

Thus all of the single integrals in Equation [16] are identically zero, with the exception of those which are taken along $x = 0$, where the displacements are prescribed,[6] and Equation [16] reduces to

$$\int_0^l\int_{-h}^{h}[\nabla^2\nabla^2\phi]\,\delta\phi dydx - \left\{\int_{-h}^{h}[(\phi_{xx} - \nu\phi_{yy})\delta\phi_x - (\phi_{xxx} + (2+\nu)\phi_{xyy})\delta\phi]dy\right\}_{x=0} = 0 \quad [17c]$$

Because of the arbitrariness of the variations occurring in Equation [17*c*], it is seen that the double integral and the two single integrals must vanish independently. Vanishing of the double integral leads to a differential equation for the function $f(x)$, and vanishing of the two single integrals results in conditions replacing the conditions of vanishing displacements at the built-in end of the beam. The results of this procedure, in addition to Equations [17*b*], constitute a fourth-order differential equation and four boundary conditions determining $f(x)$, as will now be shown.

Writing, in accordance with Equations [7, 8, 10]

$$\phi = g_s(y)f_s(x) + g(y)f(x) \quad [18]$$

then

$$\nabla^2\nabla^2\phi = g_s f_s^{IV} + 2g_s''f_s'' + gf^{IV} + 2g''f'' + g^{IV}f \quad [19]$$

$$\delta\phi = g\delta f \quad [20]$$

$$\phi_{xx} = g_s f_s'' + gf'' \qquad \phi_{yy} = g_s''f_s + g''f \quad [21]$$

$$\phi_{xxx} = g_s f_s''' + gf''' \qquad \phi_{xyy} = g_s''f_s' + g''f' \quad [22]$$

$$(\delta\phi_x)_{x=0} = g\delta f'(0) \qquad (\delta\phi)_{x=0} = g\delta f(0) \quad [23]$$

The least-work conditions, Equation [17*c*], then reduce to

$$\int_{-h}^{h}[g_s f_s^{IV} + 2g_s''f_s'' + gf^{IV} + 2g''f'' + g^{IV}f]\,gdy = 0 \quad [24]$$

$$\int_{-h}^{h}[g_s f_s''(0) + gf''(0) - \nu(g_s''f_s(0) + g''f(0))]\,gdy = 0 \quad [25]$$

$$\int_{-h}^{h}[g_s f_s'''(0) + gf'''(0) + (2+\nu)(g_s''f_s'(0) + g''f'(0))]\,gdy = 0 \quad [26]$$

The conditions, Equations [17*a*], are satisfied by prescribing

$$f(l) = 0 \qquad f'(l) = 0 \quad [27]$$

Equations [24, 25, 26] may be written in the form

$$a_4h^4\frac{d^4f}{dx^4} + 2a_2h^2\frac{d^2f}{dx^2} + a_0f = -b_4h^2\frac{d^4f_s}{dx^4} - 2b_2\frac{d^2f_s}{dx^2} \quad [28]$$

$$a_4h^2f''(0) - \nu a_2f(0) = -b_4f_s''(0) + \frac{\nu b_2}{h^2}f_s(0) \quad [29]$$

$$a_4h^3f'''(0) + (2+\nu)a_2hf'(0) = -b_4hf_s'''(0) - (2+\nu)\frac{b_2}{h}f_s'(0) \quad [30]$$

where the constants a_n and b_n are given by

$$a_4 = \frac{1}{h^5}\int_{-h}^{h}g^2dy = \frac{1}{(1+3m)^2}\left\{\frac{256}{3465} + \frac{4352}{3465}m + \frac{1280}{231}m^2\right\} \quad [31a]$$

$$a_2 = \frac{1}{h^3}\int_{-h}^{h}g''gdy = \frac{-1}{(1+3m)^2}\left\{\frac{256}{315} + \frac{256}{21}m + \frac{384}{7}m^2\right\} \quad [31b]$$

$$a_0 = \frac{1}{h}\int_{-h}^{h}g^{IV}gdy = \frac{1}{1+3m}\left\{\frac{128}{7} + \frac{1280}{7}m\right\} \quad [31c]$$

$$b_4 = \frac{1}{h^3}\int_{-h}^{h}g_sgdy = \frac{-1}{1+3m}\left\{\frac{64}{945} + \frac{256}{315}m + \frac{32}{21}m^2\right\} \quad [31d]$$

$$b_2 = \frac{1}{h}\int_{-h}^{h}g_s''gdy = \frac{1}{1+3m}\left\{\frac{16}{105} + \frac{32}{21}m\right\} \quad [31e]$$

Table 1 contains the numerical values of these constants for various values of the form factor m.

[5] To account for flexibility of the support it would be necessary to add a term for the work done in deforming the supporting structure.

[6] If, instead of prescribing the stresses at the free end ($x = l$) of the beam, conditions involving the displacements were prescribed, for instance v = constant instead of $\tau = \tau_0$, there would remain a single integral along $x = l$ leading to a further condition for $f(x)$ which would take the place of that following from $\tau(l, y) = \tau_0$. It is in this sense that the present least-work procedure is more flexible than a procedure utilizing an assumed function $f(x)$ with parameters to be determined from the minimum condition. In that case there would be no possibility of distinguishing between the two alternatives.

It may be added that Equation [16] is also suitable for a determination of the stresses in a beam, the middle section of which is at $x = 0$, with loading and support symmetrical about $x = 0$. In that case the condition, Equation [4b], of vanishing transverse displacement must be replaced by the symmetry condition of vanishing shear. This entails replacing part of the single integral in Equation [17*c*], by the condition $\delta\phi_x(0, y) = 0$ which is satisfied when $f'(0) = 0$. In that way it would be possible to obtain an approximate solution for a problem for which an exact Fourier integral solution has been given previously (7, 8).

TABLE 1 VALUES OF a_n AND b_n

m	a_4	a_2	a_0	b_4	b_2
0	0.07388	−0.81270	18.28571	−0.06772	0.15328
0.1	0.15082	−1.52681	28.13187	−0.12633	0.23443
1	0.42943	−4.24127	50.28571	−0.60106	0.41904
∞	0.61568	−6.09524	60.95238	$\approx -0.50794m$	0.50794

TABLE 2 VALUES OF $k = k_r + ik_i$

m	k_r	k_i
0	3.65591	1.53813
0.1	3.44840	1.32923
1	3.21699	0.68722
∞	3.15040	0.15784

In the foregoing developments the differential Equation [28] takes the place of the biharmonic equation for the stress function in an exact analysis. Equation [29] takes the place of the condition that, at the built-in end, the transverse displacement v vanishes and Equation [30] stands for the condition that the spanwise displacement u vanishes at that end. Equations [27] require that the approximate solution satisfy exactly the condition of vanishing σ_x and parabolic or vanishing τ at the free end.

Explicit Solution of Problem for Concentrated End Load and Uniformly Distributed Load

Restricting further discussion to the case of a concentrated end load $P = t\int_{-h}^{h}\tau_0 dy$ and a uniformly distributed load P_0, and setting

$$\frac{Plh}{I} = \sigma_0 \qquad \frac{P_0hl^2}{2I} = \sigma_1 \ldots\ldots\ldots\ldots [32]$$

it follows that

$$\left.\begin{aligned} M(x) &= \frac{I}{x}\left\{\sigma_0\left(1-\frac{x}{l}\right)+\sigma_1\left(1-\frac{x}{l}\right)^2\right\} \\ M''(x) &= \frac{2I}{hl^2}\sigma_1 \qquad M^{IV}(x) = 0 \end{aligned}\right\} \ldots\ldots [33]$$

and the differential Equation [28] as well as the boundary conditions Equations [27, 29, 30] for $f(x)$, in view of Equation [8], take the form

$$a_4h^4f^{IV}(x) + 2a_2h^2f''(x) + a_0f(x) = -4b_2\sigma_1\left(\frac{h}{l}\right)^2 \ldots [34]$$

$$a_4h^2f''(0) - \nu a_2 f(0) = -2b_4\left(\frac{h}{l}\right)^2\sigma_1 + \nu b_2(\sigma_0+\sigma_1) \ldots [35]$$

$$a_4h^3f'''(0) + (2+\nu)a_2hf'(0) = (2+\nu)b_2(\sigma_0+2\sigma_1)\left(\frac{h}{l}\right) \ldots [36]$$

$$f(l) = 0 \qquad f'(l) = 0 \ldots\ldots\ldots\ldots [37]$$

The solution of Equation [34] can be written

$$f = -4\frac{b_2}{a_0}\left(\frac{h}{l}\right)^2\sigma_1 + C_1e^{k\frac{x}{h}} + \bar{C}_1e^{\bar{k}\frac{x}{h}} + C_2e^{-k\frac{x}{h}} + \bar{C}_2e^{-\bar{k}\frac{x}{h}} \ldots [38]$$

where

$$2C_1 = A_1 + iB_1 \qquad 2C_2 = A_2 + iB_2 \ldots\ldots [39]$$

are complex constants of integration, bars indicating the conjugate complex, and

$$k = k_r + ik_i = \sqrt[4]{\frac{a_0}{a_4}}\left\{\cos\left[\frac{1}{2}\tan^{-1}\left(\frac{-1}{a_2}\sqrt{a_0a_4-a_2^2}\right)\right] + i\sin\left[\frac{1}{2}\tan^{-1}\left(\frac{-1}{a_2}\sqrt{a_0a_4-a_2^2}\right)\right]\right\} \ldots [40]$$

satisfies the characteristic equation

$$a_4k^4 + 2a_2k^2 + a_0 = 0 \ldots\ldots\ldots\ldots [41]$$

of the differential Equation [34].

While for the determination of the constants of integration it is convenient to take the solution in the complex form Equation [38], for the purpose of evaluation it is better to write it in terms of real variables

$$f = -4\frac{b_2}{a_0}\left(\frac{h}{l}\right)^2\sigma_1 + e^{k_r\frac{x}{h}}\left\{A_1\cos k_i\frac{x}{h} - B_1\sin k_i\frac{x}{h}\right\} + e^{-k_r\frac{x}{h}}\left\{A_2\cos k_i\frac{x}{h} + B_2\sin k_i\frac{x}{h}\right\} \ldots [38a]$$

To simplify the discussion, it shall now be assumed that the span length l is sufficiently large in comparison with the height $2h$, so that

$$e^{-k_r\frac{l}{h}} \ll 1, \text{ say } < 0.05 \ldots\ldots\ldots\ldots [42]$$

Under this condition, which is fulfilled when

$$\frac{h}{l} < \frac{k_r}{\ln 20} \approx 1 \ldots\ldots\ldots\ldots [43]$$

it is permissible to treat the effects at the built-in end ($x = 0$) and at the free end ($x = l$) separately.

As will be seen, there is no free-end correction necessary for the beam with free-end load only, whereas, correction terms do occur at the free end for the case of a uniformly distributed load p_0. This is in accordance with the known fact that the polynomial solutions for Airy's stress function which correspond to the case of the uniformly distributed load do not fulfill the conditions of vanishing stress at the free end (9). Since this effect however occurs at a section where the stresses are very small, a quantitative discussion of the required correction has not been undertaken here.

As can also be seen, in addition to the correction terms decreasing from the edges, there occurs a uniform correction term in f which is proportional to σ_1. (It is of some interest to notice that the magnitude of this correction depends only upon σ_1 and the ratio h/l and not on m and ν, the quantity b_2/a_0, from Equations [31c, e], having the constant value $\frac{1}{120}$.) In accordance with previous knowledge, this indicates that, for the uniformly distributed load, the linear bending-stress distribution is in any case only an approximation, whatever the conditions of support of the beam.

Taking

$$f = -\frac{1}{30}\left(\frac{h}{l}\right)^2\sigma_1 + Ce^{-k\frac{x}{h}} + \bar{C}e^{-\bar{k}\frac{x}{h}} \ldots\ldots [44]$$

and disregarding the conditions at the free end, there follow from Equations [35] and [36] two conditions determining C

$$(a_4k^2 - \nu a_2)C + (a_4\bar{k}^2 - \nu a_2)\bar{C} = \nu b_2(\sigma_0+\sigma_1) - \left(\frac{h}{l}\right)^2\left(2b_4 + 4\nu\frac{a_2b_2}{a_0}\right)\sigma_1 \ldots\ldots [45]$$

$$[a_4k^3 + (2+\nu)a_2k]C + [a_4\bar{k}^3 + (2+\nu)\bar{k}]\bar{C} = -(2+\nu)\left(\frac{h}{l}\right)b_2(\sigma_0+2\sigma_1) \ldots\ldots [46]$$

These equations give

$$C = \frac{1}{\Delta}\left\{\sigma_0\left[\nu b_2(a_4\bar{k}^2 + (2+\nu)a_2\bar{k}) + (2+\nu)\left(\frac{h}{l}\right)b_2(a_4\bar{k}^2 - \nu a_2)\right] + \sigma_1\left[\left\{\nu b_2 - \left(\frac{h}{l}\right)^2\left(2b_4 + 4\nu\frac{a_2b_2}{a_0}\right)\right\}\left\{a_4\bar{k}^2 + (2+\nu)a_2\bar{k}\right\} + 2(2+\nu)\left(\frac{h}{l}\right)b_2(a_4\bar{k}^2 - \nu a_2)\right]\right\} \quad [47]$$

where

$$\Delta = -2ik_i\{a_4(a_0 - 2a_2|k|^2) - \nu a_2[(2+\nu)a_2 + (k^2 + \bar{k}^2 + 2|k|^2)a_4]\} \quad [48]$$

It is convenient for the numerical evaluation of the preceding results to separate again the cases of concentrated end load and of uniformly distributed load.

Results for Beam With Concentrated End Load

Setting

$$\sigma_1 = 0$$

one has for the constant C occurring in $f(x)$, when in Equation [47] the real and imaginary parts are separated

$$C = \frac{1}{2}(A + iB) = \frac{b_2}{\Delta}\sigma_0\left\{(2+\nu)\left[a_4(k_r^2 - k_i^2) - \nu a_2\right]\frac{h}{l} - \nu k_r\left(\sqrt{a_0a_4} - \nu a_2\right)\right\} - i\frac{b_2k_i}{\Delta}\sigma_0\left\{2(2+\nu)a_4k_r\frac{h}{l} + \nu\left(\sqrt{a_0a_4} + \nu a_2\right)\right\} \quad [49]$$

The functions $f(x)$ and $f'(x)$ which, according to Equations [11] and [12], determine the distribution of σ_x and τ are given by

$$f(x) = e^{-k_r\frac{x}{h}}\left\{A\cos k_i\frac{x}{h} + B\sin k_i\frac{x}{h}\right\} \quad [50]$$

$$hf'(x) = e^{-k_r\frac{x}{h}}\left\{(-k_rA + k_iB)\cos k_i\frac{x}{h} + (-k_iA - k_rB)\sin k_i\frac{x}{h}\right\} \quad [51]$$

TABLE 3 VALUES OF CONSTANTS OF INTEGRATION IN $f(x)$

m	ν	A/σ_0	B/σ_0
0	0	$0.0508\left(\frac{h}{l}\right)$	$0.0497\left(\frac{h}{l}\right)$
0	1/3	$0.0506\left(\frac{h}{l}\right) + 0.0119$	$0.0660\left(\frac{h}{l}\right) - 0.0456$
0.1	0	$0.0463\left(\frac{h}{l}\right)$	$0.0511\left(\frac{h}{l}\right)$
0.1	1/3	$0.0460\left(\frac{h}{l}\right) + 0.0098$	$0.0677\left(\frac{h}{l}\right) - 0.0421$
1	0	$0.0379\left(\frac{h}{l}\right)$	$0.0848\left(\frac{h}{l}\right)$
1	1/3	$0.0374\left(\frac{h}{l}\right) + 0.0063$	$0.1115\left(\frac{h}{l}\right) - 0.0549$
∞	0	$0.0351\left(\frac{h}{l}\right)$	$0.3496\left(\frac{h}{l}\right)$
∞	1/3	$0.0346\left(\frac{h}{l}\right) + 0.0052$	$0.4589\left(\frac{h}{l}\right) - 0.2073$

Table 3 contains values of A and B for various values of the form factor m and for the two values of Poisson's ratio $\nu = 0$ and $\nu = 1/3$.

Introducing these values for A and B into Equations [50] and [51], which equations in turn are introduced into Equations [11] and [12], there result explicit expressions for τ and σ_x.

In particular, shear and normal stress at the built-in end of the beam have the form

$$\tau(0,y) = \sigma_0\frac{h}{l}\left\{\left[\frac{1}{2}\left(\frac{y}{h}\right)^2 - \left(m + \frac{1}{2}\right)\right] + \frac{l}{h}\left(k_r\frac{A}{\sigma_0} - k_i\frac{B}{\sigma_0}\right)\left[\frac{1+7m}{1+3m} - 6\frac{1+5m}{1+3m}\left(\frac{y}{h}\right)^2 + 5\left(\frac{y}{h}\right)^4\right]\right\} \quad [52]$$

$$\sigma_x(0,y) = \sigma_0\left\{\frac{y}{h} + \frac{A}{\sigma_0}\left[-12\frac{1+5m}{1+3m}\frac{y}{h} + 20\left(\frac{y}{h}\right)^3\right]\right\} \quad [53]$$

and the normal stress in the extreme fiber of the beam is given by

$$\sigma_x(x,h) = \sigma_0\left\{\left(1 - \frac{x}{l}\right) + \frac{8}{1+3m}\frac{f(x)}{\sigma_0}\right\} \quad [54]$$

To obtain a picture of the situation, these stresses have been calculated for a beam having equal height and length ($h/l = 0.5$).

Figs. 2(a, b, c, d) contain the normal stress distribution at the built-in end section ($x = 0$). It is seen that the maximum stress at the flange is higher than the one given by the elementary theory. Specifically, the magnitude of the stress correction increases with decreasing flange area–web area ratio m. It is noted that Poisson's ratio ν is of appreciable influence, the stress concentration being greater for $\nu = \frac{1}{3}$ than for $\nu = 0$. For the sake of comparison there is also given the result obtained by R. Sonntag (5) for the case $m = \nu = 0$, which is seen to give a correction for the maximum stress of about 89 per cent of the correction obtained here for the corresponding case.

Figs. 3(a, b, c) contain the shear-stress distribution over the built-in end of the beam. It is seen that this distribution deviates even more from the "elementary" distribution than the corresponding normal stresses and that the influence of Poisson's ratio ν is very pronounced. The point of maximum shear is no longer at the neutral axis but is moved toward the extreme

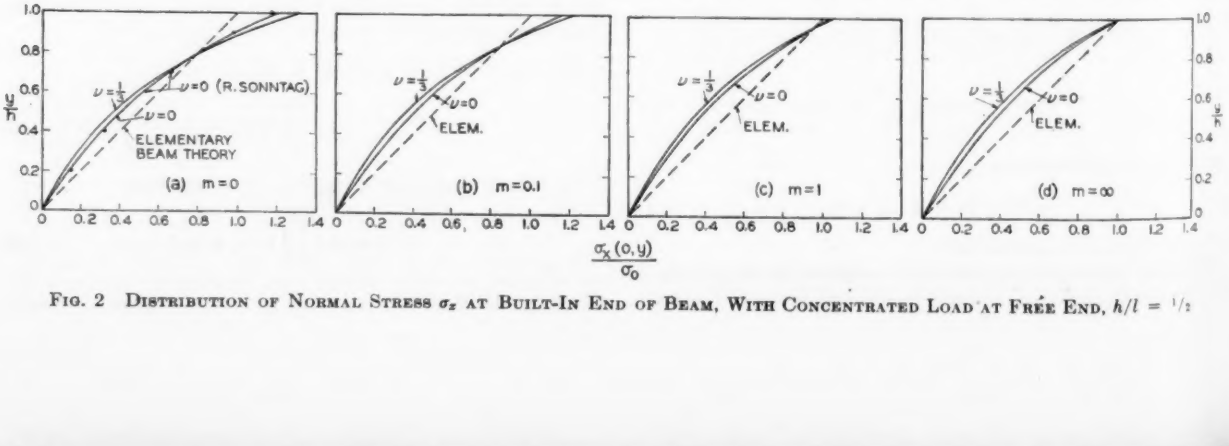


FIG. 2 DISTRIBUTION OF NORMAL STRESS σ_x AT BUILT-IN END OF BEAM, WITH CONCENTRATED LOAD AT FREE END, $h/l = 1/2$

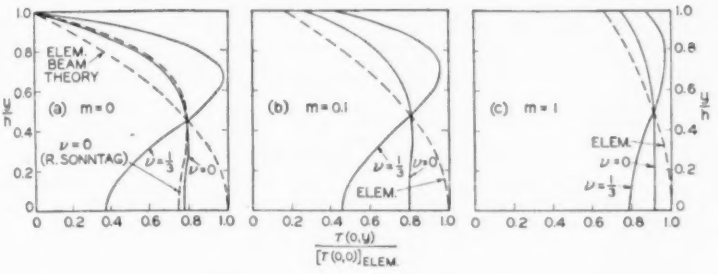


FIG. 3 DISTRIBUTION OF SHEAR STRESS τ AT BUILT-IN END OF BEAM, WITH CONCENTRATED LOAD AT FREE END, $h/l = 1/2$

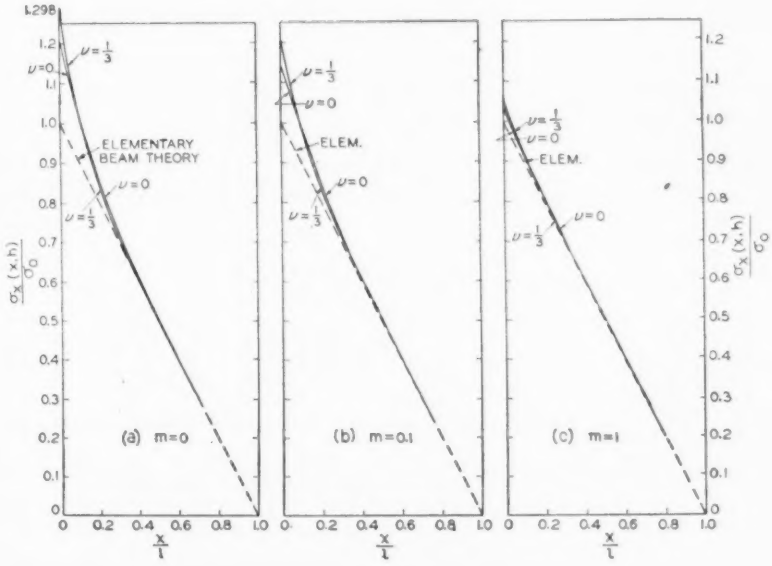


FIG. 4 SPANWISE DISTRIBUTION OF NORMAL STRESS σ_x IN THE EXTREME FIBER OF BEAM, WITH CONCENTRATED LOAD AT FREE END, $h/l = 1/2$

fibers, the further up the greater m. The value of the maximum shear is about the same for $\nu = 1/3$ as that given by the elementary theory, while for $\nu = 0$ it is considerably less.

Figs. 4(a, b, c) give the spanwise distribution of edge normal stress for various values of m and ν. They show that the deviation of the stresses from the stresses of the elementary theory does not extend effectively beyond a distance from the end section of about one half the height of the beam. They also show that the slight oscillation of the stresses about those of the elementary theory is too small to appear in the diagrams.

In Fig. 5, finally, values are plotted of what may be called a stress-concentration factor $\sigma_x(0, h)/\sigma_0$ for various values of m, ν, and h/l. Since the analytical expressions for this factor are fairly simple they are also reproduced in Table 4.

TABLE 4 VALUES OF RATIO OF MAXIMUM FIBER STRESS AND MAXIMUM ELEMENTARY FIBER STRESS, $\sigma_x(0, h)/\sigma_0$

m \ ν	0	1/3
0	$1 + 0.4065\,\frac{h}{l}$	$1.0954 + 0.4047\,\frac{h}{l}$
0.1	$1 + 0.2849\,\frac{h}{l}$	$1.0603 + 0.2830\,\frac{h}{l}$
1	$1 + 0.0759\,\frac{h}{l}$	$1.0125 + 0.0749\,\frac{h}{l}$
∞	1	1

Fig. 5 shows that the stress concentration increases with increasing height-length ratio h/l, and with increasing values of Poisson's ratio ν, and decreases with increasing form factor $m = A_f/th$. It is noteworthy that for $\nu \neq 0$ there is an increase of maximum stress even for $h/l = 0$. The explanation for this appears to be not the restraint against warping but the condition that the elements of the end section are also not permitted to move in a direction perpendicular to the beam axis.

It might finally be said that all these curves give the corrections to the elementary results which are compatible with the assumption of a third-degree polynomial for the σ_x stresses, with which it is not possible to satisfy exactly the condition of rigid clamping. Therefore it can only be said that the "average" warping has been reduced (presumably to a small fraction of the amount of warping which goes with the linear normal stress distribution). On the other hand, it is possible that the exact solution for rigid clamping may, for the beam with no flanges, lead to infinite stresses at the corners of the end section.[7] It appears not unreasonable to assume that in this case yielding, at

[7] It has, however, been established in reference (6) that no such singularity occurs if a material is assumed with no resistance to transverse (σ_y) stresses.

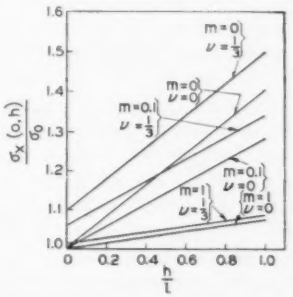


FIG. 5 VALUES OF RATIO OF MAXIMUM FIBER STRESS $\sigma_x(0, h)$, AND MAXIMUM FIBER STRESS OF ELEMENTARY THEORY σ_0, FOR VARIOUS VALUES OF FORM FACTOR $m = A_f/ht$, POISSON'S RATIO ν AND HEIGHT-SPAN RATIO $2h/l$ FOR BEAM WITH CONCENTRATED LOAD AT FREE END

TABLE 5 VALUES OF CONSTANTS OF INTEGRATION A AND B FOR CASE OF UNIFORMLY DISTRIBUTED LOAD

m	ν	A/σ_1	B/σ_1
0	0	$0.0486\left(\frac{h}{l}\right)^2 + 0.1016\left(\frac{h}{l}\right)$	$-0.1155\left(\frac{h}{l}\right)^2 + 0.0994\left(\frac{h}{l}\right)$
0	1/3	$0.0339\left(\frac{h}{l}\right)^2 + 0.1012\left(\frac{h}{l}\right) + 0.0119$	$-0.1296\left(\frac{h}{l}\right)^2 + 0.1320\left(\frac{h}{l}\right) - 0.0456$
0.1	0	$0.0494\left(\frac{h}{l}\right)^2 + 0.0926\left(\frac{h}{l}\right)$	$-0.1282\left(\frac{h}{l}\right)^2 + 0.1023\left(\frac{h}{l}\right)$
0.1	1/3	$0.0338\left(\frac{h}{l}\right)^2 + 0.0920\left(\frac{h}{l}\right) + 0.0098$	$-0.1452\left(\frac{h}{l}\right)^2 + 0.1354\left(\frac{h}{l}\right) - 0.0421$
1	0	$0.0916\left(\frac{h}{l}\right)^2 + 0.0759\left(\frac{h}{l}\right)$	$-0.4286\left(\frac{h}{l}\right)^2 + 0.1695\left(\frac{h}{l}\right)$
1	1/3	$0.0560\left(\frac{h}{l}\right)^2 + 0.0749\left(\frac{h}{l}\right) + 0.0063$	$-0.4912\left(\frac{h}{l}\right)^2 + 0.2230\left(\frac{h}{l}\right) - 0.0549$
$\to\infty$	—	$\to m\left(\frac{h}{l}\right)^2 \times$ const	$\to m\left(\frac{h}{l}\right)^2 \times$ const

the corners of the supporting medium as well as of the beam, will lead to a redistribution of stress which then can be represented by a third-degree polynomial. In this sense, it is necessary to use the results for the case of no flanges ($m = 0$) with a certain amount of caution.

Results for Beam With Uniformly Distributed Load

Setting

$$\sigma_0 = 0$$

in Equation [47], there follows for the constant of integration, after separating into real and imaginary parts

$$C = \frac{1}{2}(A + iB)$$

$$= \sigma_1 \frac{b_2}{\Delta}\left\{2k_r\left(\frac{b_4}{b_2} + 2\nu\frac{a_2}{a_0}\right)\left(\sqrt{a_0 a_4} - \nu a_2\right)\left(\frac{h}{l}\right)^2 + 2(2+\nu)\left[a_4(k_r^2 - k_i^2) - \nu a_2\right]\left(\frac{h}{l}\right) - \nu k_r\left[\sqrt{a_0 a_4} - \nu a_2\right]\right\}$$

$$+ i\sigma_1 \frac{b_2}{\Delta} k_i\left\{2\left(\frac{b_4}{b_2} + 2\nu\frac{a_2}{a_0}\right)\left(\sqrt{a_0 a_4} + \nu a_2\right)\left(\frac{h}{l}\right)^2 - 4a_4 k_r(2+\nu)\left(\frac{h}{l}\right) - \nu\left(\sqrt{a_0 a_4} + \nu a_2\right)\right\} \quad [55]$$

Table 5 contains the values of A and B for various values of m and ν, as functions of (h/l).

According to Equation [44] the function $f(x)$ is

$$f(x) = -\frac{1}{30}\left(\frac{h}{l}\right)^2 \sigma_1 + e^{-k_r\frac{x}{h}}\left(A\cos k_i\frac{x}{h} + B\sin k_i\frac{x}{h}\right) \quad [56]$$

As before, for the shear stress and normal stress at the built-in end, taking into consideration Equations [11, 12, 33], we obtain

$$\tau(0, y) = 2\sigma_1\frac{h}{l}\left[\frac{1}{2}\left(\frac{y}{h}\right)^2 - \left(m + \frac{1}{2}\right)\right] + \sigma_1\left(k_r\frac{A}{\sigma_1} - k_i\frac{B}{\sigma_1}\right)\left[\frac{1+7m}{1+3m} - 6\frac{1+5m}{1+3m}\left(\frac{y}{h}\right)^2 + 5\left(\frac{y}{h}\right)^4\right] \quad [57]$$

$$\sigma_x(0, y) = \sigma_1\frac{y}{h} + \sigma_1\left[-12\frac{1+5m}{1+3m}\frac{y}{h} + 20\left(\frac{y}{h}\right)^3\right]\left[\frac{A}{\sigma_1} - \frac{1}{30}\left(\frac{h}{l}\right)^2\right] \quad [58]$$

For the normal stress in the extreme fiber of the beam there follows

$$\sigma_x(x, h) = \sigma_1\left\{\left(1 - \frac{x}{l}\right)^2 + \frac{8}{1+3m}\frac{f(x)}{\sigma_1}\right\} \quad [59]$$

Again these stresses have been calculated for a beam having equal height and length ($h/l = 0.5$).

Figs. 6(a, b, c) contain the normal stress distribution over the end section, $x = 0$. For $m = 0$ and $m = 0.1$ there is qualitatively the same behavior as in the case of the concentrated load, i.e., the maximum stress is higher for $\nu = 1/3$ than for $\nu = 0$ and higher for $m = 0$ than for $m = 0.1$. Quantitatively, it is seen that the difference between the cases $\nu = 0$ and $\nu = 1/3$ is less noticeable than before and—most important—the difference between the maximum stress $\sigma_x(0, h)$ and the elementary extreme fiber stress σ_1 is more than twice as great as the corresponding difference for the same beam with concentrated end load. For $m = 1$ the maximum stress is again only slightly greater than the corresponding elementary stress, while in this case $\nu = 1/3$ gives a $\sigma_x(0, h)$ which is smaller than the corresponding value for $\nu = 0$.

Regarding the limiting case $m = \frac{A_f}{th} \to \infty$ it is seen that, while the end-section shear $\tau(0, y)$ behaves qualitatively as in the case

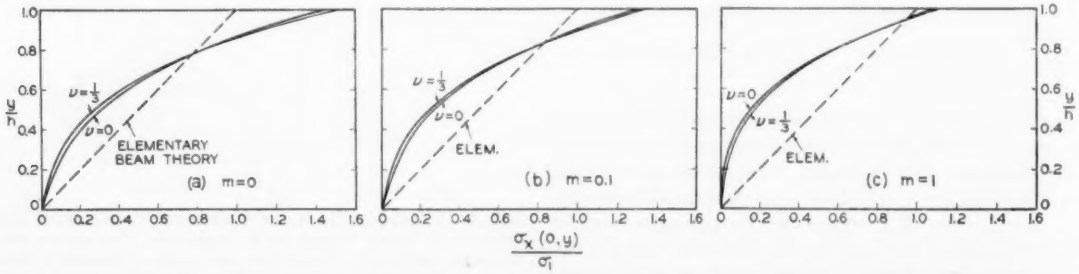


FIG. 6 DISTRIBUTION OF NORMAL STRESSES AT BUILT-IN END OF CANTILEVER BEAM, WITH UNIFORMLY DISTRIBUTED LOAD, $h/l = 1/2$

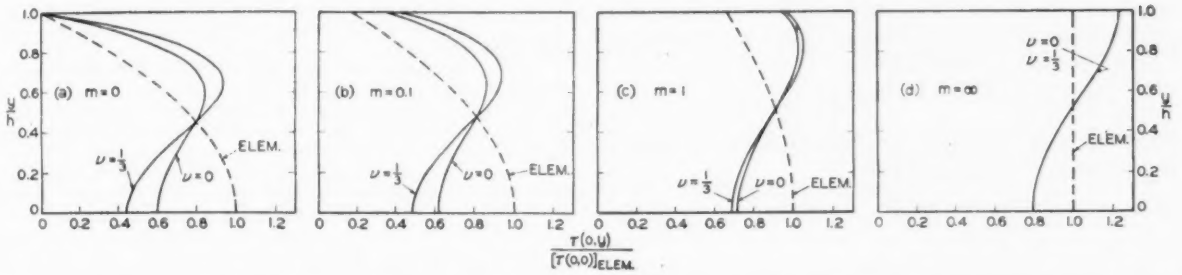


FIG. 7 DISTRIBUTION OF SHEAR STRESS τ AT BUILT-IN END OF CANTILEVER BEAM, WITH UNIFORMLY DISTRIBUTED LOAD, $h/l = 1/2$

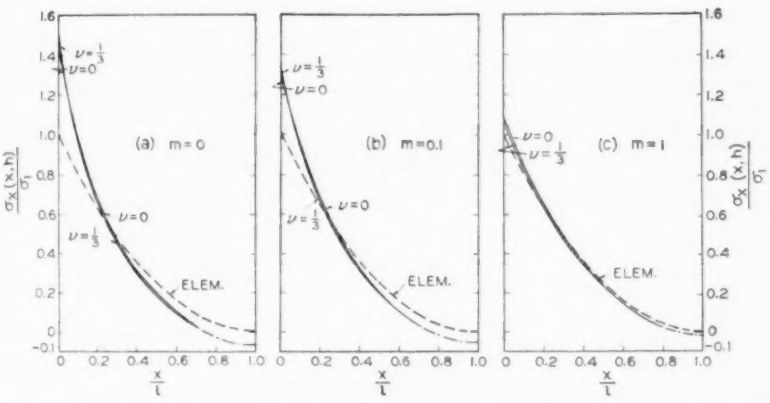


FIG. 8 SPANWISE DISTRIBUTION OF NORMAL STRESS σ_x IN EXTREME FIBERS OF CANTILEVER BEAM, WITH UNIFORMLY DISTRIBUTED LOAD, $h/l = 1/3$

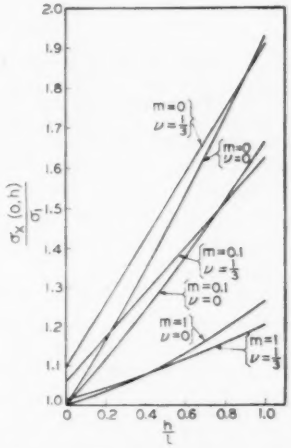


FIG. 9 VALUES OF RATIO OF MAXIMUM FIBER STRESS $\sigma_x(0, h)$ AND MAXIMUM FIBER STRESS OF ELEMENTARY THEORY σ_1 FOR VARIOUS VALUES OF FORM FACTOR $m = A_f/th$, POISSON'S RATIO ν, AND HEIGHT-SPAN RATIO $2h/l$ FOR A CANTILEVER BEAM WITH UNIFORMLY DISTRIBUTED LOAD

TABLE 6 VALUES OF $\sigma_x(0, h)/\sigma_1$ FOR A BEAM WITH UNIFORMLY DISTRIBUTED LOAD

$m \backslash \nu$	0	1/3
0	$1 + 0.8130\left(\frac{h}{l}\right) + 0.1220\left(\frac{h}{l}\right)^2$	$1.0954 + 0.8095\left(\frac{h}{l}\right) + 0.0047\left(\frac{h}{l}\right)^2$
0.1	$1 + 0.5699\left(\frac{h}{l}\right) + 0.0989\left(\frac{h}{l}\right)^2$	$1.0603 + 0.5661\left(\frac{h}{l}\right) + 0.0029\left(\frac{h}{l}\right)^2$
1	$1 + 0.1518\left(\frac{h}{l}\right) + 0.1164\left(\frac{h}{l}\right)^2$	$1.0125 + 0.1498\left(\frac{h}{l}\right) + 0.0453\left(\frac{h}{l}\right)^2$

of the concentrated end load, there is a fundamental difference in the behavior of $\sigma_x(0, y)$. Equation [58] and Table 5 indicate that for $m \to \infty$ also $\sigma_x(0, y) \to \infty$ except when $y = \pm h$ where the correction again becomes finite. Tracing back the reason for the behavior it is seen that the constants A and B behave like b_4 which according to Equation [31d] increases like m itself. Since b_4, according to Equation [35], occurs in the condition taking the place of $\epsilon_y(0, y) = 0$ in an exact analysis it is seen that the existence of the transverse normal stress σ_y is responsible for what happens. It is thought, however, that this result with regard to the limiting behavior of the present solution is not necessarily the same result which would be obtained from an exact solution so that the conclusive answer to the question as to what happens when $m \to \infty$ is yet to be given.

Figs. 7(a, b, c, d) contain the distributions of shear over the built-in section. Again the point of maximum shear is moved toward the extreme fibers of the beam and the value of the maximum shear stress is greater for $\nu = 1/3$ than for $\nu = 0$. While for $m = 0$ and $m = 0.1$, the maximum elementary shear stress is greater than $[\tau(0, y)]_{max}$, the opposite is true for $m = 1$ and $m \to \infty$.

In Figs. 8(a, b, c) are given the spanwise distribution of the extreme fiber stress $\sigma_x(x, h)$ for different values of m and ν. In the neighborhood of the free end ($x = l$), $\sigma_x(x, h)$ instead of going down to zero actually reverses its sign, with the magnitude of this stress about 5 per cent of the maximum elementary fiber stress. The reason for this behavior is to be found in the fact that two of the constants of integration in $f(x)$ have been set equal to zero instead of being determined from the conditions of vanishing stress at the free end. If the more elaborate calculation had been carried through, the result would have been $\sigma_x(l, y) = 0$ as it should be.

Fig. 9 incorporates the values of the stress-concentration factor $\sigma_x(0, h)/\sigma_1$, for different values of m, ν, and h/l, which are given by the functions of Table 6.

A comparison of Tables 4 and 6 gives the noteworthy result that the ratio $[\sigma_x(0, h) - \sigma_1]/\sigma_1$ for a beam with uniformly distributed load is about twice as great as the corresponding ratio for the same beam with concentrated end load.

A generalization of this statement can be obtained if one considers the stress in a beam of length l with distributed load as the resultant of stresses due to infinitesimal concentrated loads $p(\xi)d\xi$ applied at a distance ξ from the fixed end. Each such element of loading produces a distribution of stress at the fixed end nearly equal to that which would be produced if the beam were of length ξ and a load $p(\xi)d\xi$ were acting at the free end. This argument holds for any distribution of load and its quantitative result is that the concentration of stress characterized by the value of $[\sigma_x(0, h) - \sigma(0, h)_{elem.}]/\sigma(0, h)_{elem.}$ is about the same for a beam of length l, with arbitrary loading, as for a beam of length L, with concentrated end load, L being the distance between the fixed end and the center of gravity of the load curve.

Since, according to Table 4, the ratio $[\sigma_x(0, h) - \sigma_0]/\sigma_0$ is nearly proportional to $1/l$ and since for a uniformly distributed load $L = l/2$ it follows, in particular, that

$$[\sigma_x(0, h) - \sigma_1]/\sigma_1 \approx 2[\sigma_x(0, h) - \sigma_0]/\sigma_0$$

in accordance with the formulas of Tables 4 and 6. In general, for any spanwise distribution of load

$$\left[\sigma_x(0, h) - \frac{M(0)h}{I}\right] \Big/ \frac{M(0)h}{I} \approx \frac{l}{L}\,[\sigma_x(0, h) - \sigma_0]/\sigma_0$$

where the quotient of stresses on the right-hand side is given in Table 4.

BIBLIOGRAPHY

1 "Least Work Solutions of Shear Lag Problems," by E. Reissner, *Journal of the Aeronautical Sciences*, May, 1941, pp. 284–291.

2 "Beanspruchung eines Stabes von elliptischen Querschnitt, auf Drillen bei behinderter Querschnitt verwölbung," by A. Föppl, Berichte Bayerische Akademie der Wissenschaften, Munich, 1920, pp. 261–275.

3 "On the Approximate Solution of Two-Dimensional Problems in Elasticity," by S. Timoshenko, *Philosophical Magazine*, vol. 47 1924, pp. 1095–1104.

4 "... mpression of Rectangular Blocks and the Bending of Beams by Non-Linear Distributions of Bending Forces," by J. N. Goodier, Trans. A.S.M.E., vol. 54, 1932, paper APM-54-17, pp. 173.

5 "Über Biegung bei verhinderter Querschnittskrümmung," by R. Sonntag, *Ingenieur Archiv*, vol. 4, 1933, pp. 415–420.

6 "A Contribution to the Theory of Elasticity of Non-Isotropic Materials (With Applications to Problems of Bending and Torsion)," by E. Reissner, *Philosophical Magazine*, vol. 30, 1940, pp. 418–427.

7 "Über die Grundlagen der Balkentheorie," by Th. von Kármán, Abhandlungen Aerodynamisches Institut, Technische Hochschule, Aachen, vol. 7, 1927, pp. 3–10.

8 "Die Spannungen und Formänderungen von Balken mit rechteckigem Querschnitt," by F. Seewald, Abhandlungen Aerodynamisches Institut, Technische Hochschule, Aachen, vol. 7, 1927, pp. 11–33.

9 "Treatise on the Mathematical Theory of Elasticity," by A. E. H. Love, Fourth edition, Cambridge University Press, 1927.

10 "Über Biegung bei verhinderter Querschnittskrümmung," by R. Gran Olsson, *Ingenieur Archiv*, vol. 5, 1934, pp. 163–165.

11 "Erwiderung auf die Bemerkung von R. Gran Olsson zu meiner Arbeit, 'Über Biegung bei verhinderter Querschnittskrümmung,'" by R. Sonntag, *Ingenieur Archiv*, vol. 5, 1934, pp. 166–169.

Buckling of Semimonocoque Structures Under Compression

By TSUN KUEI WANG,[1] STANFORD UNIVERSITY, CALIF.

This paper presents an investigation of the strength of a stiffened cylindrical shell under the action of uniform axial compression. It is assumed that the cylindrical structure is a very thin tube of circular cross section; its reinforcements consist essentially of a great number of uniform longitudinal stiffeners and a great number of uniform transverse rings. It is often desirable to know the critical value of the compressive load for the buckling of such a structure.

IN aeronautical construction, the sheet covering of the semimonocoque structure is so thin that it contributes very little to the structural resistance in comparison with the stiffeners and rings. Thus, in attacking the problem of the over-all or general instability of this type of structure, a portion of the sheet covering is regarded as a part of the stiffeners, and the stability of a structural grid of effective longitudinal stiffeners and transverse rings is analyzed.

Several simplifying assumptions must be made in order to render the application of analytical methods possible. (1) It is assumed that the structure under consideration has a large number of identical equally spaced longitudinal stiffeners and a great number of identical equally spaced transverse rings. (2) A stiffener with its corresponding effective width of sheet is assumed to behave as a column which is not to fail torsionally and locally. The total deflection of this stiffener during buckling is determined by its two perpendicular components, i.e., by the radial displacement w_r and the tangential displacement w_t. (3) Each of the intermediate rings, originally plane, remains plane after bending. (4) The end rings of the structure are assumed to be absolutely rigid, while the longitudinal stiffeners are hinged to them.

Notations used in this paper are shown in Fig. 1. The origin is taken at the left end of the structure and the x axes are directed along the axes of the stiffeners. The radial deflection w_r is defined as positive toward the axis of the cylinder, and the tangential deflection w_t is defined in the counterclockwise direction. The angle ϕ is measured counterclockwise from the vertical radius of the cross section. Additional notations are used, as follows:

l = total length of cylinder
R = radius of rings
p = number of intermediate rings
q = total number of stiffeners
P = compressive force per stiffener

Calculating Critical Value of Compressive Force

In calculating the critical value of the compressive force P, the energy method will be used. The method consists essentially of assuming the radial deflection w_r of the cylindrical structure in the form of a double trigonometrical series of a type which satisfies the end conditions, obtaining the tangential deflection w_t by the assumption of the inextensional deformations of rings, and determining the critical value of the compressive force P from the general energy consideration (refer to Equation [4]). It is assumed initially that each of the stiffeners is perfectly straight and compressed by the centrally applied load P. If the compressive load is less than its critical value, the stiffener remains straight. By increasing gradually the compressive load P, a condition is reached in which the straight form of equilibrium becomes unstable and a slight lateral buckling occurs. The critical load is then defined as the smallest load that can keep the stiffener in a slightly bent form.

As assumed, the end rings of the cylinder do not change shape during buckling, therefore the deflections w_r and w_t along the end rings must be zero. At the same time the ends of the stiffeners can rotate freely with respect to the circumferential axes of the end rings, i.e., there are no bending moments along these end rings. Thus, the ends of the stiffeners will be considered as simply supported. The analytical expressions of the end conditions in this case are

$$w_r = 0 \text{ and } \frac{d^2w_r}{dx^2} = 0 \text{ for } x = 0, l$$

and

$$w_t = 0 \text{ and } \frac{d^2w_t}{dx^2} = 0 \text{ for } x = 0, l$$

In general, the radial displacements w_r can be represented in the form of trigonometric series and the tangential displacements

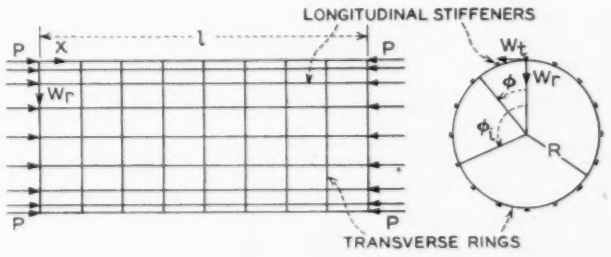


FIG. 1

w_t will be taken in such a form as to make the extension of the center line of the rings zero.[2] The final relation between w_r and w_t for this condition of inextensional deformation of the rings is

$$w_r = \frac{dw_t}{d\phi} \quad \ldots\ldots\ldots\ldots\ldots\ldots [1]$$

[1] Department of Mechanical Engineering, Stanford University.

Presented at the Annual Meeting, New York, N. Y., December 1–5, 1941, of THE AMERICAN SOCIETY OF MECHANICAL ENGINEERS.

Discussion of this paper should be addressed to the Secretary, A.S.M.E., 29 West 39th Street, New York, N. Y., and will be accepted until October 10, 1942, for publication at a later date. Discussion received after the closing date will be returned.

NOTE: Statements and opinions advanced in papers are to be understood as individual expressions of their authors, and not those of the Society.

[2] The discussion of inextensional deformations of rings and shells was originated by Lord Rayleigh. His investigation was based upon the fact, in the case of bending of thin rings, that the displacements due to extension of the center line of a ring are usually negligibly small in comparison with the displacements due to bending. Refer to "Theory of Sound," by John William Strutt, Baron Rayleigh, Macmillan & Company, Ltd., London, 1894–1896, chapter 2, Xa.

The deflection w_r of the structure during buckling can be represented by the following series

$$w_r = \sum_{m=1,2,3,\ldots}^{m=\infty} \sum_{n=2,3,4,\ldots}^{n=\infty} a_{mn} \cos n\phi \sin \frac{m\pi x}{l} \ldots [2]$$

where m and n indicate the numbers of half-waves and whole-waves in which the stiffeners and rings are deflected respectively during buckling.

Then the tangential displacement w_t may be obtained with the aid of Equation [1]

$$w_t = \sum_{m=1,2,3,\ldots}^{m=\infty} \sum_{n=2,3,4,\ldots}^{n=\infty} \frac{a_{mn}}{n} \sin n\phi \sin \frac{m\pi x}{l} \ldots [3]$$

Before buckling of the structure occurs, the total strain energy is stored only in the form of an axial compression. During buckling, the strain energy will increase, due partly to bending of the rings and partly to buckling of the stiffeners. At the critical value of the compressive load P, this increase in strain energy must be equal to the work done by the compressive load as the distances between the ends of the stiffeners shorten owing to buckling. Thus

$$\sum_{i=1}^{i=q} (V_{isr} + V_{ist}) + \sum_{i=1}^{i=p} V_{ir} = \sum_{i=1}^{i=q} (W_{ir} + W_{it}) \ldots [4]$$

where V_{ir} = strain energy stored in ith ring
V_{isr}, V_{ist} = strain energies stored in ith stiffener in radial and tangential directions, respectively
W_{ir}, W_{it} = works done by P during buckling of ith stiffener in radial and tangential directions, respectively.

Substituting x_i for x in Equation [2] and using the notation

$$A_{in} = a_{1n} \sin \frac{\pi x_i}{l} + a_{2n} \sin \frac{2\pi x_i}{l} + a_{3n} \sin \frac{3\pi x_i}{l} + \ldots \ldots [5]$$

the deflection curve of the ith ring is

$$w_{ir} = \sum_{n=2,3,4,\ldots}^{n=\infty} A_{in} \cos n\phi$$

The strain energy[3] of this ring can be expressed as

$$V_{ir} = \frac{EI_r}{R^3} \int_0^{\pi} \left[\left(\frac{d^2 w_{ir}}{d\phi^2} \right)^2 + 2w_{ir} \left(\frac{d^2 w_{ir}}{d\phi^2} \right) + w_{ir}^2 \right] d\phi$$

$$= \frac{EI_r \pi}{2R^3} \sum_{n=2,3,4,\ldots}^{n=\infty} (n^2 - 1)^2 A_{in}^2 \ldots [6]$$

where EI_r is the flexural rigidity of the rings.

In expressing the deflection curves for the ith stiffener, we may substitute ϕ_i for ϕ in Equations [2] and [3], respectively, and use the notations

$$\left.\begin{aligned} B_{mi} &= a_{m2} \cos 2\phi_i + a_{m3} \cos 3\phi_i + a_{m4} \cos 4\phi_i + \ldots\ldots \\ \text{and} \\ C_{mi} &= \frac{a_{m2}}{2} \sin 2\phi_i + \frac{a_{m3}}{3} \sin 3\phi_i + \frac{a_{m4}}{4} \sin 4\phi_i + \ldots \end{aligned}\right\} [7]$$

[3] "Strength of Materials," by S. Timoshenko, D. Van Nostrand Company, Inc., New York, N. Y., 1936, pp. 435 and 459.

Thus, the deflection curve for the ith stiffener in the radial direction is

$$w_{isr} = \sum_{m=1,2,3,\ldots}^{m=\infty} B_{mi} \sin \frac{m\pi x}{l}$$

and the bending energy[4] of the ith stiffener due to this deflection is

$$V_{isr} = \frac{EI_{sr}}{2} \int_0^l \left(\frac{d^2 w_{isr}}{dx^2} \right)^2 dx$$

where EI_{sr} is the flexural rigidity of the stiffeners in the radial direction.

Hence

$$V_{isr} = \frac{\pi^4 EI_{sr}}{4l^3} \sum_{m=1,2,3,\ldots}^{m=\infty} m^4 B_{mi}^2 \ldots\ldots\ldots\ldots [8]$$

The deflection curve for the ith stiffener in the tangential direction is

$$w_{ist} = \sum_{m=1,2,3,\ldots}^{m=\infty} C_{mi} \sin \frac{m\pi x}{l}$$

and the bending energy of the ith stiffener due to this deflection is

$$V_{ist} = \frac{EI_{st}}{2} \int_0^l \left(\frac{d^2 w_{ist}}{dx^2} \right)^2 dx$$

where EI_{st} is the flexural rigidity of the stiffeners in the tangential direction.

Hence

$$V_{ist} = \frac{\pi^4 EI_{st}}{4l^3} \sum_{m=1,2,3,\ldots}^{m=\infty} m^4 C_{mi}^2 \ldots\ldots\ldots\ldots [9]$$

During buckling of the cylinder, there is a longitudinal displacement or shortening between the end points of each stiffener due to the radial and tangential deflections. Owing to this displacement, the forces P produce work which can be expressed[5] for the ith stiffener as the sum of

$$W_{ir} = \frac{P}{2} \int_0^l \left(\frac{dw_{isr}}{dx} \right)^2 dx$$

$$= \frac{\pi^2 P}{4l} \sum_{m=1,2,3,\ldots}^{m=\infty} m^2 B_{mi}^2 \ldots\ldots\ldots\ldots [10]$$

and

$$W_{it} = \frac{P}{2} \int_0^l \left(\frac{dw_{ist}}{dx} \right)^2 dx$$

$$= \frac{\pi^2 P}{4l} \sum_{m=1,2,3,\ldots}^{m=\infty} m^2 C_{mi}^2 \ldots\ldots\ldots\ldots [11]$$

Substituting Equations [6] and [8] to [11] into Equation [4]

[4] "Strength of Materials," by S. Timoshenko.

[5] Ibid., p. 38; and "Theory of Elastic Stability," by S. Timoshenko, McGraw-Hill Book Company, Inc., New York, N. Y., 1936, p. 27.

and proceeding with a summation of the series as shown in the Appendix, we obtain

$$P = \frac{\pi^2 E I_{sr}}{l^2} \frac{n^2}{n^2+1}\left[\left(1+\frac{I_{st}}{n^2 I_{sr}}\right)m^2 + \frac{2I_r(p+1)l^3}{\pi^3 I_{sr} q R^3}\frac{(n^2-1)^2}{m^2}\right] \quad \ldots\ldots\ldots\ldots [12]$$

So far as n in this expression is concerned, the smallest value of the compressive load will be obtained by taking n equal to 2. The physical significance of this is that the cylindrical structure buckles in such a manner that there can be several half-waves in the longitudinal stiffeners but only 4 half-waves, or elliptical shape, in the transverse rings. Substitution of $n = 2$ in Equation [12], thus yields Equation [13], as follows:

$$P_{cr} = \frac{\pi^2 E I_{sr}}{l^2}\left\{\frac{4}{5}\left[\left(1+\frac{I_{st}}{4I_{sr}}\right)m^2 + \frac{18I_r(p+1)l^3}{\pi^3 I_{sr} q R^3}\times\frac{1}{m^2}\right]\right\} \quad \ldots\ldots\ldots\ldots [13]$$

where m can be taken equal to 1, 2, 3, ...

In Equation [13], the first factor represents the Euler load for the buckling of a bar with hinged ends and is designated by P_{eu} throughout the paper. The second factor indicates in what proportion the stability of the stiffeners reinforced by rings is greater than the stability of an isolated stiffener. The magnitude of the latter depends upon the numerical values of the ratios $\frac{I_r}{I_{sr}}, \frac{I_{st}}{I_{sr}}, \frac{l}{R}$, and $\frac{p+1}{q}$ as well as on the number m of the half-waves into which the stiffeners buckle. If, however, the geometrical dimensions of the cylinder are fixed, the number m can be uniquely determined.

Determining Number of Half Waves Into Which Stiffeners Buckle

The determination of this number m must be performed in such a way that its value should make the right-hand member of Equation [13] a minimum. This can be done graphically. Taking m equal to 1, 2, 3, ... in Equation [13] with any suitable value of I_{st}/I_{sr}, a system of straight lines for P_{cr}/P_{eu} against $2I_r(p+1)l^3/I_{sr}\pi^3 R^3 q$ is obtained. This is plotted in Fig. 2, with a value of I_{st}/I_{sr} equal to 0.5. With these lines, the critical value of the compressive load P for any given value of $2I_r(p+1)l^3$

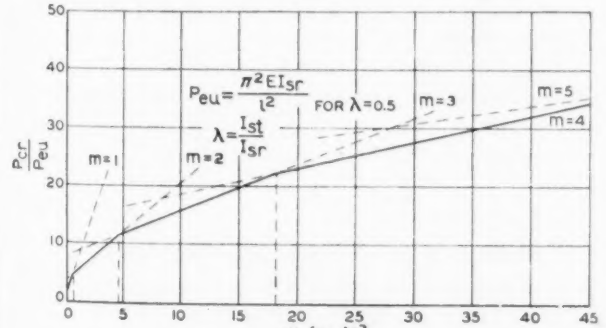


Fig. 2

$/I_{sr}\pi^3 R^3 q$ can be determined. It is only necessary to take the corresponding point on the axis of abscissas and to choose the line having the smallest ordinate for that point. We can see that for very short stiffeners, the line $m = 1$ gives the smallest ordinates. This corresponds to the buckling of the stiffeners into a single half-wave. Beginning with the point of intersection of lines $m = 1$ and $m = 2$, the second line has the smallest ordinates, i.e., the stiffeners buckle into two half waves, and this holds up to the point of intersection of lines $m = 2$, $m = 3$, etc. Since the slopes of the lines are all positive, the point of intersection of the lines $m = i$ and $m = (i + 1)$ evidently has the smallest ordinate for the segment of the line $m = (i + 1)$ between $m = i$ and $m = (i + 2)$. In Fig. 2 the portions of the lines defining the ratio of critical values of the compressive load P to the Euler load P_{eu} are shown by full lines.

Suppose the value of $2I_r(p+1)l^3/I_{sr}\pi^3 R^3 q$ has the magnitude at which the number of half-waves changes from i to $(i + 1)$. It is evident that this value corresponds to the transition point

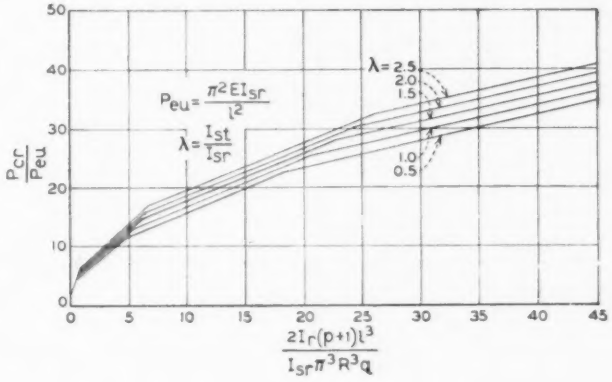


Fig. 3

from line $m = i$ to line $m = (i + 1)$ and, at this value, Equation [13] should give the same result for P_{cr} independently of whether $m = i$ or $m = (i + 1)$. By substituting the numbers i and $(i + 1)$ for m in Equation [13], respectively, and then equating these two expressions, we finally obtain

$$\left(\frac{9}{1+\frac{I_{st}}{4I_{sr}}}\right)\left(\frac{2I_r(p+1)l^3}{I_{sr}\pi^3 R^3 q}\right) = i^2(i+1)^2$$

This is the equation for calculating the transition points for curves with any suitable value of I_{st}/I_{sr}. In Fig. 2, these points are indicated by vertical dotted lines.

A family of broken lines of P_{cr}/P_{eu} against $2I_r(p+1)l^3/I_{sr}\pi^3 R^3 q$ for different values of I_{st}/I_{sr} is plotted in Fig. 3. From this figure or Equation [13], it is seen that the larger the value of I_{sr} or I_{st}, the greater will be the strength of the structure. However, the increase in strength is greater due to increase in I_{sr} than due to increase in I_{st}. This is very important for the practical application.

For larger values of m, the envelopes of the broken lines of Fig. 3 are very useful. Each of these envelopes is a curve which has the line elements of each broken line as tangents, and can be represented by the equation

$$\frac{P_{cr}}{P_{eu}} = \frac{24}{5}\left[\left(1+\frac{I_{st}}{4I_{sr}}\right)\frac{2I_r(p+1)l^3}{I_{sr}\pi^3 R^3 q}\right]^{1/2}$$

From this equation it can be seen that if all the members of these structures have the same geometrical dimensions, the critical values of the compressive load P per stiffener are proportional to the square roots of the numbers of their rings plus 1, and inversely proportional to the square roots of the numbers of their stiffeners, that is

$$P_{cr} \sim \left(\frac{p+1}{q}\right)^{1/2}$$

If the structures are considered as a whole, the total compressive load carried by each structure is qP, and the critical values of these loads are then proportional to the square roots of the products of the numbers of their rings plus 1 and stiffeners, that is

$$qP_{cr} \sim [(p+1)q]^{1/2}$$

The first statement means that, in the structure having fewer rings or more stiffeners, the buckling load per stiffener is smaller than that in the structure having more rings or fewer stiffeners; while the second statement means that the greater the number of rings or stiffeners or both, the higher is the total compressive load which the structure can carry.

Appendix

By making a substitution of Equations [6, 8, 9, 10, and 11] into Equation [4], the compressive force P at which a buckled form is possible will be

$$P = \frac{\dfrac{2EI_r}{R^3}\sum_{i=1}^{i=p}\sum_{n=2,3,4,\ldots}^{n=\infty}(n^2-1)^2A_{in}^2 + \dfrac{\pi^3EI_{sr}}{l^3}\sum_{i=1}^{i=q}\sum_{m=1,2,3,\ldots}^{m=\infty}m^4B_{mi}^2 + \dfrac{\pi^3EI_{sl}}{l^3}\sum_{i=1}^{i=q}\sum_{m=1,2,3,\ldots}^{m=\infty}m^4C_{mi}^2}{\dfrac{\pi}{l}\left(\sum_{i=1}^{i=q}\sum_{m=1,2,3,\ldots}^{m=\infty}m^2B_{mi}^2 + \sum_{i=1}^{i=q}\sum_{m=1,2,3,\ldots}^{m=\infty}m^2C_{mi}^2\right)} \quad \ldots [14]$$

To simplify the numerator and the denominator in Equation [14], the following steps will be taken:
By putting

$$\sin\frac{m\pi x_i}{l} = \sin\frac{m\pi i}{p+1} \qquad \sin n\phi_i = \sin\frac{2n\pi i}{q} \qquad \cos n\phi_i = \cos\frac{2n\pi i}{q}$$

and substituting them into Equations [5] and [7], the summation of the square of expression A_{in} from i to p and that of the squares of expressions B_{mi} and C_{mi} from i to q can be presented as follows

$$\left.\begin{aligned}
\sum_{i=1}^{i=p}A_{in}^2 &= \sum_{i=1}^{i=p}\left(a_{1n}\sin\frac{\pi i}{p+1} + a_{2n}\sin\frac{2\pi i}{p+1} + a_{3n}\sin\frac{3\pi i}{p+1} + \ldots\right)^2 \\
\sum_{i=1}^{i=q}B_{mi}^2 &= \sum_{i=1}^{i=q}\left(a_{m2}\cos\frac{4\pi i}{q} + a_{m3}\cos\frac{6\pi i}{q} + a_{m4}\cos\frac{8\pi i}{q} + \ldots\right)^2
\end{aligned}\right\} \quad [15]$$

and

$$\sum_{i=1}^{i=q}C_{mi}^2 = \sum_{i=1}^{i=q}\left(\frac{a_{m2}}{2}\sin\frac{4\pi i}{q} + \frac{a_{m3}}{3}\sin\frac{6\pi i}{q} + \frac{a_{m4}}{4}\sin\frac{8\pi i}{q} + \ldots\right)^2$$

It can be seen that Equations [15] contain the finite summations of the following type

$$\sum_{i=1}^{i=p}\sin\frac{m\pi i}{p+1}\sin\frac{n\pi i}{p+1}$$

For practical application only a few terms of the general expressions, Equations [2] and [3], need be taken with m and n as small integers, while the cylinder under consideration has a great number of longitudinal stiffeners and transverse rings so that integers p and q are relatively large. Thus, it can be assumed that either of m and n is not greater than both $\left(\frac{p+1}{2}\right)$ and $\frac{q}{2}$. Under this condition, it is concluded:[6]

1 Either $m+n$ or $m-n$ is not a multiple of $2(p+1)$, which causes

$$\sum_{i=1}^{i=p}\sin\frac{m\pi i}{p+1}\sin\frac{n\pi i}{p+1} = 0 \text{ when } m \neq n$$

2 Both $m+n$ and $m-n$ are not multiples of q, which cause

$$\sum_{i=1}^{i=q}\cos\frac{2m\pi i}{q}\cos\frac{2n\pi i}{q} = 0, \text{ when } m \neq n$$

3 Integer m is not a multiple of $p+1$, which causes

$$\sum_{i=1}^{i=p}\sin^2\frac{m\pi i}{p+1} = \frac{p+1}{2}$$

4 Integer $2n$ is not a multiple of q, which causes

$$\sum_{i=1}^{i=q}\cos^2\frac{2n\pi i}{q} = \frac{q}{2}$$

Hence, in Equations [15], those terms containing the products of the coefficients such as $a_{1n}a_{2n}$, $a_{1n}a_{3n}$, ..., $a_{m2}a_{m3}$, $a_{m2}a_{m4}$, . . . disappear and only those with squares of the coefficients remain. As a result of this fact, Equations [15] become

[6] "Elementary Treatise on Fourier Series and Spherical Harmonics," by W. E. Byerly, Ginn & Company, Boston, Mass., 1893, pp. 34–35.

$$\sum_{i=1}^{i=p} A_{in}^2 = \frac{p+1}{2}\left(a_{1n}^2 + a_{2n}^2 + a_{3n}^2 + \cdots\cdots\right) = \frac{p+1}{2}\sum_{m=1,2,3,\ldots}^{m=\infty} a_{mn}^2 \quad \ldots\ldots [16]$$

$$\sum_{i=1}^{i=q} B_{mi}^2 = \frac{q}{2}\sum_{n=2,3,4,\ldots}^{n=\infty} a_{mn}^2 \quad \ldots\ldots [17] \qquad \text{and} \qquad \sum_{i=1}^{i=q} C_{mi}^2 = \frac{q}{2}\sum_{n=2,3,4,\ldots}^{n=\infty} \frac{a_{mn}^2}{n^2} \quad \ldots\ldots [18]$$

By using the result of Equation [16], the following summation is obtained:

$$\sum_{i=1}^{i=p}\sum_{n=2,3,4,\ldots}^{n=\infty}(n^2-1)^2 A_{in}^2 = \sum_{n=2,3,4,\ldots}^{n=\infty}\left[(n^2-1)^2\sum_{i=1}^{i=p} A_{in}^2\right] = \sum_{n=2,3,4,\ldots}^{n=\infty}\left[(n^2-1)^2\frac{p+1}{2}\sum_{m=1,2,3,\ldots}^{m=\infty} a_{mn}^2\right]$$

$$= \frac{p+1}{2}\sum_{m=1,2,3,\ldots}^{m=\infty}\sum_{n=2,3,4,\ldots}^{n=\infty}(n^2-1)^2 a_{mn}^2 \ldots [19]$$

Similarly, using the results of Equations [17] and [18], we obtain

$$\sum_{i=1}^{i=q}\sum_{m=1,2,3,\ldots}^{m=\infty} m^4 B_{mi}^2 = \frac{q}{2}\sum_{m=1,2,3,\ldots}^{m=\infty}\sum_{n=2,3,4,\ldots}^{n=\infty} m^4 a_{mn}^2 \ldots [20]$$

$$\sum_{i=1}^{i=q}\sum_{m=1,2,3,\ldots}^{m=\infty} m^2 B_{mi}^2 = \frac{q}{2}\sum_{m=1,2,3,\ldots}^{m=\infty}\sum_{n=2,3,4,\ldots}^{n=\infty} m^2 a_{mn}^2 \ldots [21]$$

$$\sum_{i=1}^{i=q}\sum_{m=1,2,3,\ldots}^{m=\infty} m^4 C_{mi}^2 = \frac{q}{2}\sum_{m=1,2,3,\ldots}^{m=\infty}\sum_{n=2,3,4,\ldots}^{n=\infty} \frac{m^4}{n^2} a_{mn}^2 \ldots [22]$$

and

$$\sum_{i=1}^{i=q}\sum_{m=1,2,3,\ldots}^{m=\infty} m^2 C_{mi}^2 = \frac{q}{2}\sum_{m=1,2,3,\ldots}^{m=\infty}\sum_{n=2,3,4,\ldots}^{n=\infty} \frac{m^2}{n^2} a_{mn}^2 \ldots [23]$$

Substitution of the Equations [19, 20, 21, 22, 23] into Equation [14] yields

$$P = \frac{\dfrac{EI_r(p+1)}{R^3}\displaystyle\sum_{m=1,2,3,\ldots}^{m=\infty}\sum_{n=2,3,4,\ldots}^{n=\infty}(n^2-1)^2 a_{mn}^2 + \dfrac{\pi^2 EI_x q}{2l^3}\sum_{m=1,2,3,\ldots}^{m=\infty}\sum_{n=2,3,4,\ldots}^{n=\infty} m^4 a_{mn}^2 + \dfrac{\pi^2 EI_y q}{2l^3}\sum_{m=1,2,3,\ldots}^{m=\infty}\sum_{n=2,3,4,\ldots}^{n=\infty}\frac{m^4}{n^2} a_{mn}^2}{\dfrac{\pi q}{2l}\left[\displaystyle\sum_{m=1,2,3,\ldots}^{m=\infty}\sum_{n=2,3,4,\ldots}^{n=\infty}\left(m^2+\frac{m^2}{n^2}\right) a_{mn}^2\right]} \quad \ldots\ldots [24]$$

To find the critical value of the compressive load P, it is necessary to adjust the coefficients a_{mn} in such a manner as to make Equation [24] a minimum. This can be done on the basis of the following: Suppose we have a series of unequal fractions

$$\frac{a}{b}, \quad \frac{c}{d}, \quad \frac{e}{f} \quad \ldots\ldots [25]$$

where $a, b, c, \ldots\ldots$ are assumed positive. The fraction

$$\frac{a+c+e+\ldots\ldots}{b+d+f+\ldots\ldots} \quad \ldots\ldots [26]$$

in which the numerator is the sum of the numerators of series [25] and the denominator the sum of the denominators of series [25] is evidently of some intermediate value between the largest and the smallest of the fractions series [25]. Comparing series [25] and Equation [24], it can be concluded that the latter will be a minimum if we take only one term of the series in each numerator and denominator, that is, by making all coefficients a_{12}, a_{13}, a_{22}, $\ldots\ldots$, except one, equal to zero. If the coefficient is a_{mn}, different from zero, Equation [24] will be reduced to the form of Equation [12] as presented.

ACKNOWLEDGMENT

The author wishes to express his grateful appreciation to Prof. S. Timoshenko for his valuable suggestions and criticisms.

Graphical Analysis of Impact of Elastic Bars

By K. J. DeJUHASZ,[1] STATE COLLEGE, PA.

The object of this paper is to apply the methods of graphical analysis to the problem of longitudinal central impact of elastic bars, partly to compare the results of the graphical procedure with those arrived at mathematically, and partly to treat complicated cases not readily amenable to mathematical treatment.

THE group of problems on elastic impact to be discussed has a long history in the literature of engineering mechanics, which has been reviewed briefly by Timoshenko.[2] In the usual mathematical treatment, it has been assumed that the stress condition of the body is the same throughout the body at any given instant, i.e., the waves of stress and velocity are propagated with infinite velocity. This is tantamount to the assumption of a perfectly rigid body, i.e., a body incapable of storing potential energy. Yet on the other hand, it has been assumed that the transmission of energy from one body to the other takes place by means of elastic forces.

It has been found that experimental results agree with theoretical deductions in such cases in which the energy before and after the impact is purely in kinetic form. However, important deviations have been found in such cases where, after the impact, one or both of the impacting bodies contained potential energy in the form of traveling waves, according to Ramsauer.[3] Also, it has been recognized by several authors that this discrepancy is due to the contradiction in the basis of the theory mentioned. A more satisfactory theory was sought by assuming (correctly) a finite velocity of stress propagation. Important analytical work has been done on this basis by Saint Venant and Boussinesq,[4] who have treated the case of a body falling on the end of a long bar, supported by an infinite mass.

The mathematical difficulties are, however, of a high order and prevent the clear visualization and understanding of the phenomenon. Furthermore, some important questions, such as those relating to the energy state of the impacting bars after the impact, have remained unanswered.

A way out of the mathematical difficulties was sought, as in other engineering problems, by the use of graphical methods, by means of which important progress has been made by Donnell[5] and Bergeron.[4] The further development of the graphical method has been aided by the fact that several other types of similar engineering problems, such as surges in mechanical springs, in hydraulic systems, and in electric conduits have been solved by graphical means. As a result, the graphical method of analysis has been developed to a considerable degree of refinement, offering a clarity of visualization and adaptability of application unattainable by mathematical analysis.[6, 7, 8, 9] This method may

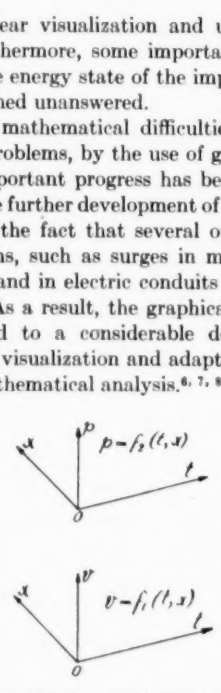


FIG. 1 CO-ORDINATE SYSTEM OF STEREOGRAMS OF STRESS AND VELOCITY AS FUNCTIONS OF TIME AND DISTANCE

be termed "graphic dynamics," because it bears a similar relationship to the mathematical dynamics as does the method of "graphic statics" to mathematical statics.

ESSENTIAL CONCEPTS OF THE GRAPHICAL METHOD

The derivation of the graphical method is fully given in the references.[4–9] However, in order to make this paper self-contained and obviate the necessity of referring to previous literature, a brief summary of the concepts and procedures of graphical analysis, as applied to elastic bars, will be given; the derivation of the formulas will be given in the Appendix.

The purpose of our inquiry is to describe the change of state

---

[1] Professor of Engineering Research, The Pennsylvania State College. Mem. A.S.M.E.

[2] "Theory of Elasticity," by S. Timoshenko, McGraw-Hill Book Company, Inc., New York, N. Y., 1934, chap. 12, pp. 381–403: "The Propagation of Waves in Elastic Solid Mediums" gives a summary of impact problems and their mathematical treatment. A history of treatment of these problems by numerous authors, namely, Young, Cauchy, Poisson, Saint Venant, and Boussinesq is briefly surveyed.

[3] "Experimentelle und theoretische Grundlagen des elastischen und mechanischen Stosses," by C. Ramsauer, *Annalen der Physik*, vol. 30, 1900, pp. 417–494. Discussion of the history of impact problems, listing the work of previous investigators. Experiments on the impact of bars of various lengths and cross-sectional areas.

[4] "Methode Graphique de Resolutions des Problems de Propagation d'Ondes Planes," by L. Bergeron, Fifth International Congress for Applied Mechanics, Cambridge, Mass., 1938, pp. 694–699. Treats graphically the impact of bars of different cross sections. Refers to the work of Saint Venant ("Théorie de l'élasticité des corps solides," by Clebsch, translated by Saint Venant, Dunod, Paris, 1883, p. 480), and of Boussinesq ("Application des potentiels à l'étude de l'équilibre et du mouvement des solides élastiques," Gauthier-Villars, Paris, 1885, p. 507) and finds agreement between their analytical results and his own graphical results.

Presented at the Annual Meeting, New York, N. Y., December 1–5, 1941, of THE AMERICAN SOCIETY OF MECHANICAL ENGINEERS.

Discussion of this paper should be addressed to the Secretary, A.S.M.E., 29 West 39th Street, New York, N. Y., and will be accepted until October 10, 1942, for publication at a later date. Discussion received after the closing date will be returned.

NOTE: Statements and opinions advanced in papers are to be understood as individual expressions of their authors and not those of the Society.

[5] "Longitudinal Wave Transmission and Impact," by L. H. Donnell, Trans. A.S.M.E., vol. 52, 1930, paper APM-52-14. Treats mathematically and also graphically a number of longitudinal-wave problems, such as impact of finite mass against infinite mass; maximum compression or unit stress in the bar during impact; longitudinal waves in railway trains; compression waves in helical springs; compression waves in liquid columns.

[6] "Graphical Analysis of Transient Phenomena in Linear Flow," by K. J. DeJuhasz, *Journal of The Franklin Institute*, vol. 223, no. 4, April, 1937, pp. 463–493; no. 5, May, 1937, pp. 643–654; no. 6, June, 1937, pp. 751–778. With extensive bibliography.

[7] "Graphical Analysis of Surges in Mechanical Springs," by K. J. DeJuhasz, *Journal of The Franklin Institute*, vol. 226, no. 4, October, 1938, pp. 505–526; no. 5, November, 1938, pp. 631–644. With extensive bibliography.

[8] "Graphical Analysis of Free Vibrations of Helical Springs," by K. J. DeJuhasz, *Journal of The Franklin Institute*, vol. 227, no. 5, May, 1939, pp. 647–672. With extensive bibliography.

[9] "Graphical Analysis of Transient Phenomena in Electric Circuits," by K. J. DeJuhasz, *Journal of The Franklin Institute*, vol 228, no. 3, September, 1939, pp. 339–373. With extensive bibliography.

in every cross section of an elastic bar, for every instant of time. In accomplishing this purpose, we deal with two co-ordinate systems:

(*a*) The $t - x$ diagram, in which a point identifies an instant of time t, as reckoned from a reference instant, and a cross section of the bar, situated at the distance x, as measured from a reference cross section.

(*b*) The $v - p$ diagram in which a point identifies an "elastic state," i.e., coexisting values of velocity and stress. We restrict our inquiry to cases in which the v, p values are the same at any point of a given cross section, which is tantamount to saying that the cross sections remain plane and parallel to each other at every instant of time.

Thus, the problem resolves into assigning a point in the $v - p$ diagram to every point in the $t - x$ diagram. If this is accomplished, then a pair of three-variable functions

$$v = f_1(t, x) \quad \text{and} \quad p = f_2(t, x)$$

can be derived which can be represented graphically by a pair of tridimensional diagrams, called "stereograms," showing the values of velocity and stress, respectively, erected over the time-distance, $t - x$ plane, as base, Fig. 1.

Such a pair of stereograms (if actually built of wood or plaster) describe completely the change of velocity and of stress in the elastic bar. Thus a section of the stereograms with an x = constant plane will give the velocity (or stress) values at that given cross section in the bar for every instant of time; such a section will be referred to as a "history diagram." A section of the stereograms with a t = constant plane will give the velocity (or stress) values at that particular instant for all cross sections in the bar; such a section will be referred to as a "gradient diagram."

The course of a phenomenon will depend upon a number of data, namely:

(*a*) The design data of the bar, i.e., its cross-sectional area F, and length L.

(*b*) The material constants of the bar, defining its elastic properties, i.e., its elastic modulus E (lb-in.$^{-2}$) and acoustic velocity a (in-sec^{-1}).

(*c*) The characteristics of the disturbance, involving the knowledge of the initial state v_1, p_1 before the disturbance, and the state v_2, p_2 after the disturbance.

There are two important relationships on which the graphical analysis is based, one referring to the $t - x$ diagram, the other to the $v - p$ diagram, as follows:

1 In an elastic bar a disturbance (i.e., change of an existing v_1, p_1 state to another v_2, p_2 state) is propagated along the bar with a constant velocity, which is the acoustic velocity

$$\frac{\Delta x}{\Delta t} = \text{const} = \pm a = \tan(\pm \varphi) \ldots\ldots\ldots [1]$$

This relationship is represented in the $t - x$ diagram by straight lines, called "disturbance lines," having a constant slope, tan ($\pm \varphi$) toward the t axis, Fig. 2. The slope is positive for disturbances in which with increasing time the x co-ordinate increases, and negative for disturbances in which, with increasing time the x co-ordinate decreases. The value of acoustic velocity for steel is a = 208,000 in-sec^{-1}.

2 In an elastic bar, a change of velocity involves a proportional change of stress, and vice versa

$$\frac{\Delta p}{\Delta v} = \text{const} = \pm \frac{E}{a} = \tan(\pm \alpha) \ldots\ldots\ldots [2]$$

which may be termed the "surge constant."

This relationship is represented in the $v - p$ diagram by straight lines, termed "directrixes," having a constant slope, tan ($\pm \alpha$) toward the v axis, Fig. 3. The slope is positive for a disturbance in which the velocity and stress both increase or both decrease; the slope is negative whenever the stress increases with decreasing velocity, or the stress decreases with increasing velocity. For steel E = 31,250,000 lb-in.$^{-2}$ and the surge constant is 151 lb-in.$^{-3}$ sec. This means that a velocity change by 1 in-sec^{-1} imposed on a steel bar is accompanied by 151 lb-in.$^{-2}$ change in the stress.

The validity of these relationships is restricted to such stress values which lie below the elastic limit of the material (for steel of the order of 30,000 lb-in.$^{-2}$), and to such values of velocity which are far below the acoustic velocity. Furthermore, it is assumed that all changes are perfectly elastic in nature, and no dissipation of energy due to hysteresis, damping, or friction takes place.

Energy in the Bar

Areas $v \cdot p$ in the $v - p$ diagram have the dimension of lb-in.$^{-1}$ sec^{-1}, i.e., that of work absorbed by or liberated by a bar of unit

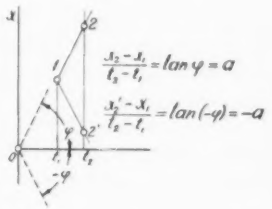


FIG. 2 PROPAGATION OF A DISTURBANCE ALONG AN ELASTIC BAR

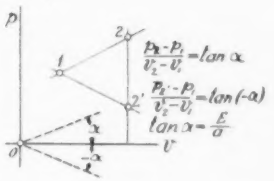


FIG. 3 VELOCITY-STRESS RELATIONSHIP IN AN ELASTIC BAR

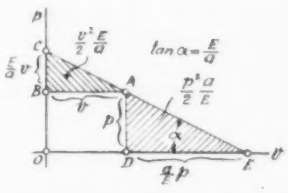


FIG. 4 KINETIC ENERGY AND POTENTIAL ENERGY IN AN ELASTIC BAR

cross-sectional area during 1 sec. As during 1 sec a length a is affected by a change, therefore, it is also correct to say that an area represents the work absorbed or liberated by a bar of unit cross-sectional area having a length a. Triangular areas, defined by a directrix drawn from a v_1, p_1 state (point A, Fig. 4) to the intersection of the v and p axes, represent the potential and kinetic energy, respectively, contained in the bar of unit cross-sectional area and length a, in virtue of its stress p and velocity v. Thus, in Fig. 4, the potential energy of the bar of unit cross-sectional area and of length a, having a stress p_A (point A) is represented by the hatched triangle ΔADE

$$H_p = \frac{p^2}{2}\frac{a}{E} = \Delta ADE$$

and the kinetic energy by the hatched triangle ΔABC

$$H_v = \frac{v^2}{2}\frac{E}{a} = \Delta ABC$$

For a length of bar L, of unit cross section, the corresponding energy values will be L/a times the hatched areas

$$U_p = \frac{L}{a}\,\Delta ADE; \quad U_v = \frac{L}{a}\,\Delta ABC$$

L/a being the interval of time necessary for a disturbance to travel from one end of the bar to the other end.

These properties of the $v - p$ diagram are useful for determining the energy content of the bar, by multiplying the areas of the proper triangles with the cross-sectional area of the bar, and the length portions characterized by the given v, p co-ordinates.

The derivation of the formulas included in this section is given in the Appendix.

Characteristics of Elastic Impact

The impact of elastic bars is characterized by the following facts:

1 While they are in contact with each other, the infinitesimal end slices of the two bars have a common velocity; hence their velocity relative to each other is zero.

2 From (1) it follows that there is no acceleration between the contacting surfaces; hence the forces acting on the contacting cross sections are equal and opposite in the two bars.

3 From (1 and 2), it follows that the state of both bars at the cross section of contact is defined by the same v and the same $P = F_1 p_1 = F_2 p_2$ values, where F_1 is the cross-sectional area of one bar, and F_2 is that of the other. For this reason, it is advantageous to represent the impact in $v - P$ instead of $v - p$ diagrams, because then, for the contacting cross sections, the v, P point will be the same. The directrixes then will be, for the bar with F_1, E_1, a_1 characteristics

$$\tan \alpha_1 = \frac{F_1 E_1}{a_1}$$

and for the bar with F_2, E_2, a_2 characteristics

$$\tan \alpha_2 = \frac{F_2 E_2}{a_2}$$

4 A free end of a bar is characterized by $P = 0$; an end of a bar in contact with an infinite mass is characterized by $v = 0$.

In possession of the relationships (1–4), we are able to proceed to the graphical solution of a number of representative impact problems.

Example 1 Impact of Bar Against Infinite Mass

Referring to Fig. 5, assume a bar AB of F cross-sectional area and L length, with elastic modulus E and acoustic velocity a. The bar is supported without friction in such a manner that it can move only longitudinally, and parallel with itself (e.g., by two bifilar suspensions from points C and D); it has initially zero stress, $P = 0$, and a v_1 velocity. Velocity to the right is chosen as positive, to the left, negative; compressional force is chosen as positive, tensional force, negative. At $t = t_1$ instant, the bar comes into contact with an infinite mass. This disturbance is characterized by the velocity becoming zero. In virtue of the relationship

$$\frac{\Delta P}{\Delta v} = \frac{EF}{a} = \tan (\pm \alpha)$$

this disturbance is represented in the $v - P$ diagram by a tan $(-\alpha)$ directrix drawn from the point 1 and intersecting the $v = 0$ line at point 2, defining the state of the bar at the B point at the $t = t_1$ instant. This disturbance travels toward the other end A of the bar with the acoustic velocity a, represented in the $t - x$ diagram by the slope tan φ, and attains the end A after the elapse of L/a interval. The A end is free and unrestricted, therefore, the value of P is zero; thus the state 2 is changed to

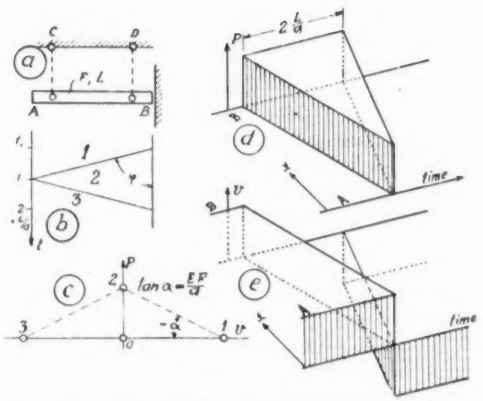


Fig. 5 Impact of Bar Against Infinite Mass
(*a* Schematic arrangement; *b* disturbance diagram; *c* velocity-force diagram; *d* stereogram of force; *e* stereogram of velocity.)

state 3, situated at the intersection of the tan α directrix drawn from point 2 with the $P = 0$ line. This disturbance travels toward the cross section B which it reaches after the elapse of another L/a interval of time. Erecting the v and P co-ordinates of the 1–2–3 points over the respective zones of the $t - x$ diagram, the stereograms of force and velocity are obtained, Fig. 5 (d, e). It is seen that the velocity after the impact is equal and opposite to that before the impact. It is of course evident that the postulata of conservation of momentum and of energy are satisfied.

Example 2 Impact of Moving Bar Against Similar Bar at Rest

Referring to Fig. 6, the values of E, a, and F being the same for both bars, the value of tan φ and of tan α is the same for both. In the $v - P$ diagram, the initial state of the bar AB is defined by point 1a and that of CD by point 1b, Fig. 6(c). When at the $t = t_1$ instant the two bars come into contact the velocity of the cross section B is reduced, and that of C is increased to the value corresponding to point 2 situated at the intersection of the tan $(-\alpha)$ directrix drawn from the point 1a with the directrix tan $(+\alpha)$ drawn from point 1b. The force is thereby increased from zero to that defined by point 2. This disturbance travels from B to A and from C to D with the acoustic velocity a and reaches the cross sections A and D, respectively, after the elapse of L/a interval of time. The state at both A and D is characterized by $P = 0$, therefore another disturbance takes place, defined for the cross section A by the point 3a situated at the intersection of the directrix tan $(+\alpha)$ drawn from point 2 with the $P = 0$ line, and for the cross section D by the point 3b situated at the intersection of the directrix tan $(-\alpha)$ drawn from point 2 with the $P = 0$ line. After the elapse of a further L/a interval these respective states will have traveled to the B and C cross sections, respectively, and the total bar AB will be at rest (point 3a), and the total bar CD will have the velocity 3b, which is of course equivalent to the initial velocity of bar AB. The stereograms of velocity and force are given in Fig. 6(d, e), from which for any cross section of the two bars the history of velocity and of force can be determined.

This problem has been also investigated experimentally by Fanning and Bassett,[10] and the oscillograms obtained confirm

[10] "Measurement of Impact Strains by Carbon-Strip Extensometer," by R. Fanning and W. V. Bassett, Journal of Applied Mechanics, Trans. A.S.M.E., vol. 62, 1940, p. A-24. The stress-time curve in an elastic bar, when the bar is struck by another bar, is determined by a resistance strain gage in conjunction with an oscillograph.

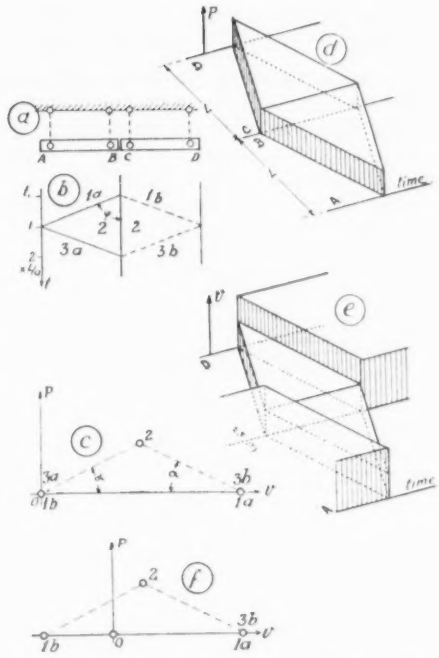


FIG. 6 IMPACT OF MOVING BAR AGAINST A SIMILAR BAR AT REST
(*a*, Schematic arrangement; *b*, disturbance diagram; *c*, velocity-force diagram; *d*, stereogram of force; *e*, stereogram of velocity; *f*, velocity-force diagram for both bars having an initial velocity.)

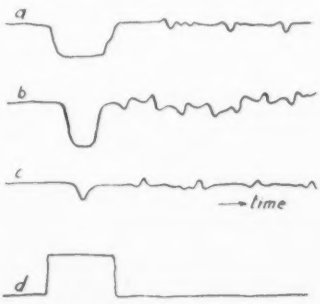


FIG. 7 OSCILLOGRAMS OF STRAINS IN IMPACTED BAR BY FANNING AND BASSETT
(*a*, Strains near impacted end; *b*, strains in middle of bar; *c*, strains at far end of bar; *d*, duration of electric contact at the contacting point of impact. The two bars were 6 ft long, and had the same cross-sectional area, having the impact end formed as a hemisphere.)

the results of the graphical analysis, Fig. 7. The deviation is due to the fact that, in the experimental arrangement, the two bars had a hemispherical shape at their impacting end. It is seen that the impacting and impacted bars exchange their velocities, and this is the case even when the bar *CD* has other than zero initial velocity, Fig. 6 (*f*).

EXAMPLE 3 IMPACT OF SHORT MOVING BAR AGAINST LONG BAR AT REST

In Fig. 8, it is assumed that the two bars have the same *E*, *a*, and *F* (hence tan α) values, but bar *CD* is twice as long as bar *AB*. The procedure and the $v - P$ diagram are similar to those in example 2. After the conclusion of the impact, the bar *AB* comes to rest (point 4) but bar *CD* does not attain a state of equilibrium. It goes through changes of velocity and force, the kinetic energy being converted into potential energy and vice versa, according to points 3–4–5–. . . . 11 in the $v - P$ diagram, which are valid in the similarly denoted zones of the $t - x$ diagram. In addition to the two stereograms, Fig. 8 (*d*, *e*), also the history of velocity for the end *C* is drawn Fig. 8 (*f*). It is seen that the velocity alternates between the value point 1 (original velocity of bar *AB*) and zero, each lasting for an L/a interval. The mean velocity is therefore one half of the original velocity of bar *AB*. The same value of mean velocity prevails for every cross section of the bar *CD*, as can be easily proved by intersecting the velocity stereogram with various x = constant planes.

It is of interest to compare this result with that obtained from mathematical theory for the elastic impact of point masses, according to which

v_1 = initial velocity of m_1 mass
v_2 = initial velocity of m_2 mass
v_1' = velocity after impact of m_1 mass
v_2' = velocity after impact of m_2 mass

$$v_1' = \frac{(m_1 - m_2)v_1 + 2m_2v_2}{m_1 + m_2}$$

$$v_2' = \frac{2m_1v_1 - (m_1 - m_2)v_2}{m_1 + m_2}$$

In example 3 $v_2 = 0$ and $m_2 = 2m_1$, hence

$$v_1' = -\frac{v_1}{3} \quad \text{and} \quad v_2' = \frac{2}{3}v_1$$

The surprising thing is that the graphical method yields a different result from the mathematical method. The former is

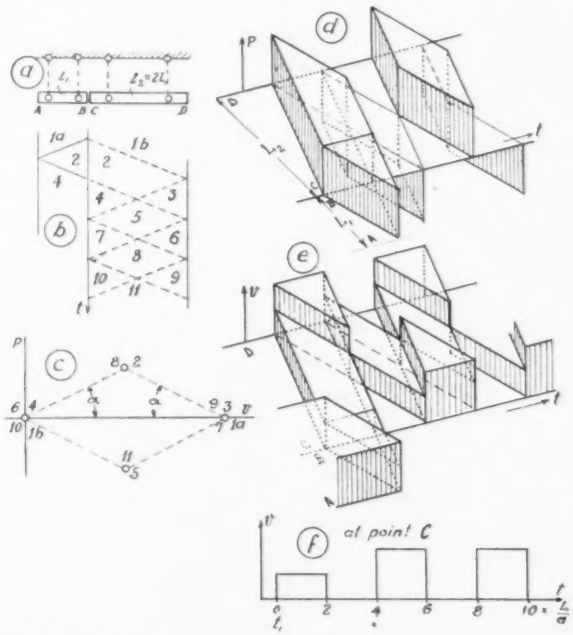


FIG. 8 IMPACT OF SHORT MOVING BAR AGAINST LONG BAR AT REST
(*a*, Schematic arrangement; *b*, disturbance diagram; *c*, velocity-force diagram; *d*, stereogram of force; *e*, stereogram of velocity; *f*, history of velocity at cross-section *D*.)

correct, and the latter is in error, owing to the assumption of infinite velocity of propagation of the disturbance, i.e., neglect of energy stored in the form of traveling waves. It will be shown in a later example that in particular cases the mathematical method and graphical method yield identical results.

EXAMPLE 4 IMPACT OF THREE BARS HAVING THE SAME CROSS SECTION

In Fig. 9, it is assumed that bar *AB* is moving with velocity v_1, bars *CD* and *EF* are at rest, and that they are in contact with each other. Bars *AB* and *EF* have the same length; the intermediate bar *CD* has a different length. From the $t - x$ and

$v - p$ diagrams, it can be seen that after the impact the impacting bar AB and the middle bar CD remain at rest, and the last bar EF receives the total velocity (and momentum, and energy) of AB. This result would be obtained regardless of the length of the interposed bar CD, or even if more than one bar is interposed,

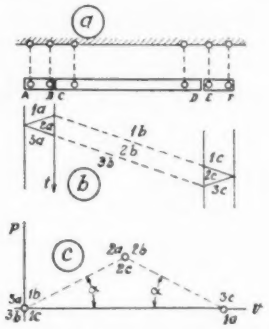


FIG. 9 IMPACT OF THREE BARS HAVING THE SAME CROSS SECTION
(a, Schematic arrangement; b, disturbance diagram; c, velocity-force diagram.)

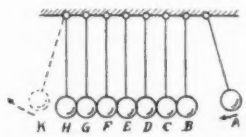


FIG. 10 EXPERIMENTAL ARRANGEMENT OF ROW OF BALLS WITH BIFILAR SUSPENSION
(When ball A is lifted and released and impacts against ball B, the last ball K will swing out, the others remaining at rest.)

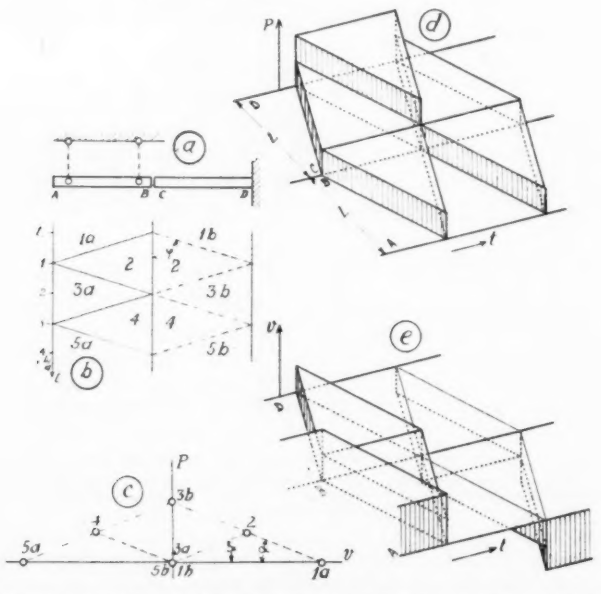


FIG. 11 IMPACT OF MOVING BAR AGAINST SIMILAR BAR AT REST, FIXED TO AN INFINITE MASS
(a, Schematic arrangement; b, disturbance diagram; c, velocity-force diagram; d, stereogram of force; e, stereogram of velocity.)

provided that the cross section of all bars is the same, and the first and last bars have the same length. This case is equivalent to the classic experiment of a row of contacting balls supported by bifilar suspension; lifting and releasing the first ball the last ball will swing out, the intermediate balls remaining at rest, Fig. 10.

EXAMPLE 5 IMPACT OF MOVING BAR AGAINST SIMILAR BAR AT REST, FIXED TO AN INFINITE MASS

In Fig. 11, the assumptions, reasoning, and procedure are similar to those of example 2, except for the fact that the cross section D of bar CD is fixed to an infinite mass, and therefore its velocity is zero at all times. The $t - x$ and $v - p$ diagrams are shown in Fig. 11 (b, c), and the resulting stereograms of velocity and force in Fig. 11 (d, e). It is seen that, after the conclusion of the impact, the bar AB has a velocity equal and opposite to

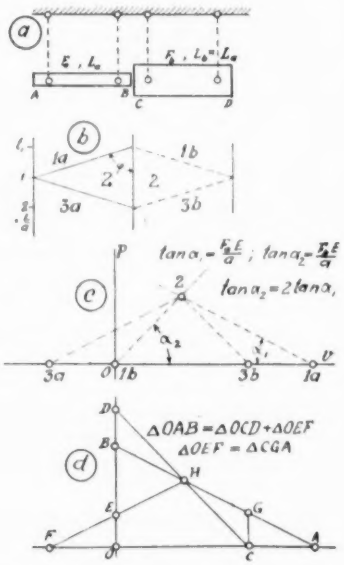


FIG. 12 IMPACT OF MOVING BAR AGAINST STATIONARY BAR HAVING THE SAME LENGTH AND DOUBLE CROSS SECTION
(a, Schematic arrangement; b, disturbance diagram; c, velocity-force diagram; d, energy diagram.)

the initial value (point 5a), which is, of course in full agreement with the mathematical analysis and experimental results.

EXAMPLE 6 IMPACT OF MOVING BAR AGAINST STATIONARY BAR HAVING SAME LENGTH AND DOUBLE CROSS SECTION

In the case shown in Fig. 12, the slope of the directrix of bar CD has double the value of that of bar AB

$$\text{For } AB, \tan \alpha_1 = \frac{EF_a}{a}; \quad \text{for } CD, \tan \alpha_2 = \frac{EF_b}{a} = 2 \tan \alpha_1$$

The $t - x$ and $v - P$ diagrams are shown in Fig. 12 (b, c). It is seen that after the impact the velocity of $AB = -\frac{1}{3} v_1$ and that of $CD = \frac{2}{3} v_1$. In this case, there remains no residual potential energy in the bar CD (as was the case in example 3), and the result of mathematical calculation is correct.

The initial energy of bar AB is represented in Fig. 12 (d) by $\frac{L}{a} \Delta OAB$, the energy of AB after the impact by $\frac{L}{a} \Delta OEF$, and that of bar CD by $\frac{L}{a} \Delta OCD$. It is seen that $\Delta OAB = \Delta OEF + \Delta OCD$.

EXAMPLE 7 IMPACT OF MOVING BAR AGAINST STATIONARY BAR FIXED TO INFINITE MASS, THE TWO BARS HAVING DIFFERENT LENGTHS AND CROSS-SECTIONAL AREAS

In Fig. 13, it is assumed that bar AB has a length L_a and cross

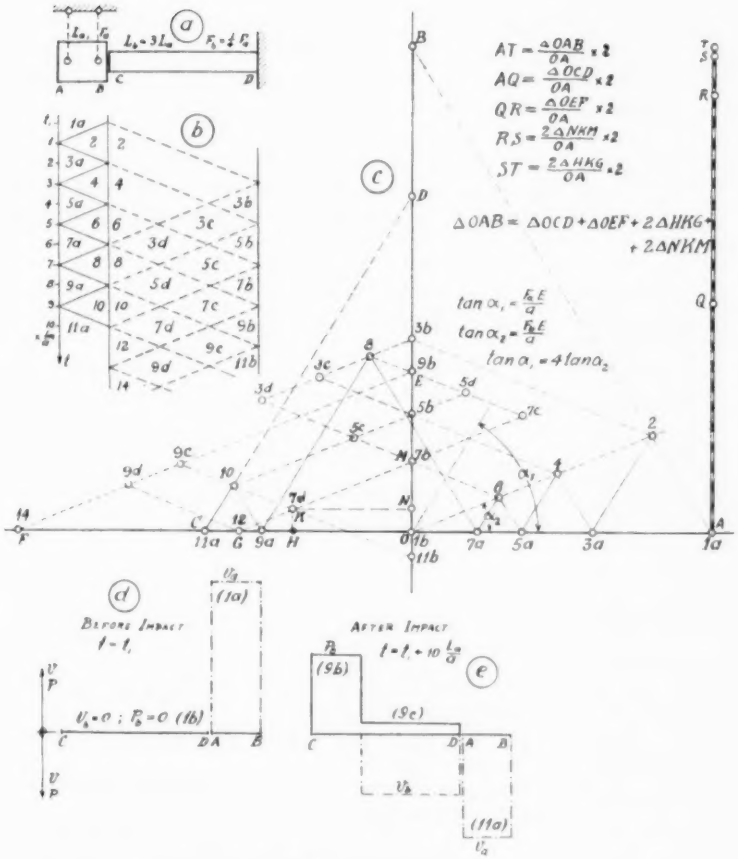


FIG. 13 IMPACT OF MOVING BAR AGAINST STATIONARY BAR FIXED TO INFINITE MASS, THE TWO BARS HAVING DIFFERENT LENGTHS AND CROSS-SECTIONAL AREAS

(*a*, Schematic arrangement; *b*, disturbance diagram; *c*, velocity-force diagram; *d*, state of bars before impact; *e*, state of bars after impact; *f*, stereogram of force; *g*, stereogram of velocity.)

section F_a; bar CD has a length $3L_a$ and cross-sectional area $^1/_4F_a$. Therefore, the slope of the directrix of bar AB is 4 times that of CD.

$$\tan\alpha_1 = \frac{EF_a}{a}; \quad \tan\alpha_2 = \frac{EF_b}{a} = {}^1/_4\tan\alpha$$

and the time interval of traverse in the bar CD is 3 times longer than in bar AB. The $t - x$ and $v - P$ diagrams are shown in Fig. 13 (*b*, *c*) from which the stereograms of velocity and of force can be constructed without difficulty, Fig. 13 (*f*, *g*). After the tenth L/a interval, the bar AB has the velocity denoted by point 11*a* and the impact is concluded. But the bar CD does not remain at rest; in it remain surges, $2L$ portion of it having the velocity and force according to point 7*d*, and $1L$ portion of it having a compression, according to point 9*b*. Fig. 13 (*d*) gives the state of both bars before the impact, and Fig. 13 (*e*) after the impact at the $t_1 = 10\,\frac{L_a}{a}$ instant. As these states are not in equilibrium, therefore, conversion of potential into kinetic energy and vice versa takes place in the successive intervals, as denoted in the $t - x$ diagram and in the $v - P$ diagram by identical figures. It can be proved, however, that the sum of the energies in bars AB and CD after the impact is equal to the initial kinetic energy of bar AB before the impact.

Referring to the derivations given earlier in this paper, the energies can be expressed as triangles in the $v - P$ diagram. Thus the initial kinetic energy of the bar AB is equivalent to $\frac{L}{a}\,\Delta OAB$; the final kinetic energy is equivalent to $\frac{L}{a}\,\Delta OCD$. For the CD bar, the potential energy corresponding to state 9*b* is

equivalent to $\frac{L}{a}\ \Delta OFE$. A $2L$ portion has the state $7d$, having both potential and kinetic energies: The potential energy is equivalent to $\frac{2L}{a}\ \Delta HKG$, and the kinetic energy is equivalent to $\frac{2L}{a}\ \Delta NKM$. By simple planimetering or counting of squares in the actual diagram, it can be proved that

$$\Delta OAB = \Delta OCD + \Delta OEF + 2\Delta HKG + 2\Delta NKM$$

or, clearer yet, these triangles can be converted by a simple graphical construction into equal-area triangles having the same base, e.g., the base OA. Then the areas will be proportional to the respective heights

$$AT = \frac{\Delta OAB}{OA/2};\ AQ = \frac{\Delta OCD}{OA/2};\ QR = \frac{\Delta OEF}{OA/2};\ RS = \frac{2\Delta NKM}{OA/2};$$

$$ST = \frac{2\Delta HKG}{OA/2}$$

from which it can be seen that

$$AT = AQ + QR + RS + ST$$

which is an added proof of the correctness of the graphical method.

A problem of such complexity is beyond the applicability of mathematical calculation, yet it can be treated without difficulty by the graphical method. Even more involved cases, composed of a number of impacting bars, each having different lengths, cross-sectional areas, and elastic properties, as well as different initial velocities, are well within the scope of applicability of the graphical treatment.

Appendix

Derivation of Basic Equations of Graphical Analysis

Assume an elastic bar, Fig. 14 (a), of modulus of elasticity E, specific volume V, of unit cross-sectional area, initially having v_1

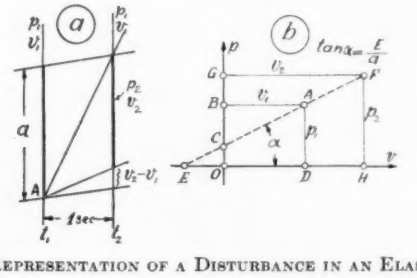


Fig. 14 Representation of a Disturbance in an Elastic Bar (a, History of change of state; b, velocity-stress diagram of disturbance.)

velocity and p_1 stress in its every cross section. At the instant t_1 the velocity is changed to v_2 at the point A. Thereby, the stress is changed to p_2 (the value of which is as yet unknown). The new state v_2, p_2 represents a disturbance which is propagated with constant velocity a (the value of which is yet unknown). After 1 sec has elapsed, a length a of the bar will have assumed the new state v_2, p_2. It is our purpose to determine p_2 and a.

After the elapse of 1 sec, the initial a length of the bar is changed to $a - (v_2 - v_1)$, and it can be written

$$\frac{a - (v_2 - v_1)}{a} = \frac{E - p_2}{E - p_1}$$

Assuming an elastic change, in which the values of p_2 and p_1 are very small in comparison with E, it can be written

$$1 - \frac{v_2 - v_1}{a} = 1 - \frac{p_2 - p_1}{E}$$

Denoting $p_2 - p_1 = \Delta p$ and $v_2 - v_1 = \Delta v$ it can be written

$$\frac{\Delta p}{\Delta v} = \frac{E}{a} \quad \ldots\ldots\ldots\ldots\ldots\ldots [3]$$

giving one fundamental equation of the graphical method.

From the postulatum of conservation of momentum, it can be written

$$(p_2 - p_1)\,\Delta t = m(v_2 - v_1)$$

Denoting $\Delta t = 1$ sec; $m = \frac{a}{V}$

which can be written $\Delta p = \frac{a}{V}\,\Delta v$

whence $\frac{\Delta p}{\Delta v} = \frac{a}{V}$

Combining with Equation [3] we obtain

$$\frac{a}{V} = \frac{E}{a}$$

whence $a = \sqrt{VE}$

giving the value of the velocity of propagation in terms of the properties of the material.

It is to be shown that these relationships satisfy the postulatum of conservation of energy.

For a length of bar a having co-ordinates of state v, p the energies can be expressed

$$\text{Kinetic energy} = Hv = \frac{mv^2}{2} = \frac{a}{V}\frac{v^2}{2} = \frac{E}{a}\frac{v^2}{2}$$

$$\text{Potential energy} = Hp = \frac{ap}{E}\frac{p}{2} = \frac{a}{E}\frac{p^2}{2}$$

that is, expansion of bar from p stress to zero stress, by a travel $a\frac{p}{E}$. If the initial state is $p = 0$, $v = 0$, then $p = \frac{E}{a}v$ and the kinetic energy is equal to the potential energy.

When the state of the bar is changed from state v_1, p_1 to state v_2, p_2 the work done per second (on length a because during 1 sec a length a of the bar is affected) is p_2v_2. Part of this work is expended in moving the bar against p_1 stress with v_1 velocity, i.e., p_1v_1. The balance appears as the change of kinetic plus potential energies in the bar. It can be written

$$p_2v_2 - p_1v_1 = \frac{1}{2}\frac{E}{a}(v_2^2 - v_1^2) + \frac{1}{2}\frac{a}{E}(p_2^2 - p_1^2)$$

$$= \frac{1}{2}\frac{E}{a}(v_2 - v_1)(v_2 + v_1) + \frac{1}{2}\frac{a}{E}(p_2 - p_1)(p_2 + p_1)$$

Substituting $p_2 - p_1 = \frac{E}{a}(v_2 - v_1)$

$$p_2v_2 - p_1v_1 = \frac{1}{2}(p_2 - p_1)(v_2 + v_1) + \frac{1}{2}(v_2 - v_1)(p_2 + p_1)$$

which expanded leads to an identity, q.e.d.

In the $v - p$ diagram for a length of bar a the kinetic energy is represented, for v_1, p_1 state (point A, Fig. 14) by the triangle ΔABC; and the potential energy by the triangle ΔADE. Similarly, for the v_2, p_2 state (point F) the respective triangles are ΔFGC and ΔFHE. It is readily seen that the difference $p_2v_2 - p_1v_1$ is $FGOH - ABOD = ABGFHD$.

Some Dynamic Properties of Rubber

By C. O. HARRIS,[1] CHICAGO, ILL.

The purpose of the investigation[2] described in this paper was to obtain information concerning the dynamic properties of rubber bonded to metal. Two properties of rubber were measured (*a*) the internal damping and (*b*) the dynamic modulus of elasticity. Two types of specimens were tested (*a*) rubber cylinders bonded to steel cylinders at the ends and stressed in compression and (*b*) specimens of rubber bonded to steel and stressed in shear. All specimens were of the same stock, 5140-V-4, manufactured by the U. S. Rubber Company. The hardness, as measured by the durometer, varied from 32 to 40. In the process of bonding to the steel, a $^1/_{32}$-in. layer of 60-durometer stock was added adjacent to each piece of steel. This represents standard practice of the U. S. Rubber Company in bonding soft stock to metal. All specimens were cured for 30 min at 279 F.

Previous Work

Kosten[3] tested massive rubber cylinders under forced vibrations. Three ratios of diameter to length were used, namely, 1, $^1/_2$, and $^1/_4$. All were tested in compression. He assumed a viscous damping and found that the product of frequency and damping coefficient was constant. He introduced the angle of loss as a variable. It is defined as $\tan^{-1}\frac{cp}{k}$, where c, p, and k represent damping coefficient, angular frequency, and spring constant, respectively. He concluded that:

1 The modulus of elasticity as calculated from dynamic tests is larger than the static modulus.

2 The dynamic modulus is independent of frequency.

3 The angle of loss has a tendency to increase with frequency and load.

Naunton and Waring[4] used a moving-coil driver unit which applied an alternating stress to two cylinders of rubber, each having a diameter of twice the length, placed on either side of a diaphragm attached to the moving coil. The system was tuned to resonance, and all calculations were made from measurements of amplitude and frequency at resonance. The following conclusions were reached:

1 The dynamic modulus of elasticity tends to increase with frequency.

2 The viscous resistance decreases with frequency and tends to become constant at higher frequencies.

Roelig[5] tested cylinders of rubber bonded to metal disks at the ends. The diameter and length were equal in all cases. A coil spring maintained a static load, and a dynamic load was superposed on this by means of an eccentric weight on the shaft of an electric motor. The load was measured by means of a dynamometer, and the displacement was taken as equal to that of the motor. A beam of light was reflected from two mirrors, one mounted on the casing of the motor and one in the dynamometer. This beam of light described a dynamic hysteresis loop on which calculations were based. Quantities measured include:

(1) Δw = energy lost per cycle (area of hysteresis loop).

(2) $\frac{\Delta w}{w}$ = ratio of energy lost to total energy (loop area divided by area between loop and axis of strain).

(3) Dynamic modulus of elasticity.

Roelig concluded that:

(1) Δw increases with increase of dynamic load while $\frac{\Delta w}{w}$ remains constant.

(2) Δw decreases with increase of static load while there is not much change in $\frac{\Delta w}{w}$.

(3) Both Δw and $\frac{\Delta w}{w}$ show a slight increase with increase of frequency.

(4) Δw increases with volume while $\frac{\Delta w}{w}$ decreases.

Of interest in regard to internal damping is a paper by Williams,[6] who states: "Energy expended on raw or vulcanized rubber is consumed largely by producing plastic flow and reversible elastic strain...Stress-strain curves obtained rapidly become straight lines through elimination of plastic flow." From this it would be expected that Δw would decrease with increase of frequency.

Hysteresis and Internal Damping

The energy lost by a unit volume of material in passing through a cycle of stress is equal to the area of the hysteresis loop. On the assumption that this loop maintains a constant shape, the area is proportional to ϵ_0^2 where ϵ_0 is the amplitude of strain. The area may be taken as $F\epsilon_0^2$, term F being a factor dependent upon material, type of stress, etc. For a bar of constant cross section, which has the same stress throughout its length, the total loss in energy is $F\epsilon_0^2$ times the volume, or $F\epsilon_0^2 Al$.

For a member of length l, with one end stationary and the other end subjected to a cyclic displacement of amplitude x_0, the damping force, taken as proportional to the velocity of the moving end, is $C\dot{x}$. The work done by the damping force in one cycle is $\pi C p x_0^2$ where p is the angular frequency of the motion. Equating this to the total hysteresis loss

$$\pi C p x_0^2 = F\epsilon_0^2 Al = F x_0^2 \frac{A}{l}$$

$$\frac{Cl}{A} = \frac{F}{\pi p} = C_2 \quad \ldots\ldots\ldots\ldots\ldots\ldots [1]$$

---

[1] Illinois Institute of Technology.

[2] A dissertation submitted in partial fulfillment of the requirements for the degree of Doctor of Science, at the University of Michigan, Ann Arbor, Mich.

[3] "Static and Dynamic Properties of Rubber in Compression," by C. W. Kosten, Proceedings Rubber Technology Conference, London, 1938, pp. 987–1002.

[4] "Fatigue in Rubber," by W. J. S. Naunton and J. R. S. Waring, Proceedings Rubber Technology Conference, London, 1938, pp. 805–820.

Presented at the Annual Meeting, New York, N. Y., December 1–5, 1941, of The American Society of Mechanical Engineers.

Discussion of this paper should be addressed to the Secretary, A.S.M.E., 29 West 39th Street, New York, N. Y., and will be accepted until October 10, 1942, for publication at a later date. Discussion received after the closing date will be returned.

Note: Statements and opinions advanced in papers are to be understood as individual expressions of their authors, and not those of the Society.

[5] "Dynamic Evaluation of Damping and Durability of Rubber Compounds," by H. Roelig, Proceedings Rubber Technology Conference, London, 1938, pp. 821–829.

[6] "Transformation of Energy by Rubber," by I. Williams, *Industrial and Engineering Chemistry*, vol. 21. 1929. p. 872.

Coefficient C_2 appears to be very convenient for use in specifying internal damping, since it permits comparison of specimens of different dimensions. Its physical significance may be seen by writing $C = C_2 \frac{A}{l}$ from which the damping force is $C_2 \frac{A}{l} \dot{x} = C_2 A \dot{\epsilon}$. Thus C_2 is a damping coefficient which is to multiply the velocity of strain and the area to give the damping force. Its units are $\frac{\text{lb-sec}}{\text{in.}^2}$. All damping data obtained in this investigation have been expressed by means of C_2. Equation [1] indicates that C_2 is inversely proportional to the frequency, if the hysteresis loop maintains the same shape at all frequencies. Any deviation of C_2 from such inverse proportionality would indicate that the frequency has an effect upon the shape of the hysteresis loop. If different values of C_2 are obtained for specimens of different shape, this would indicate a dependence of the condition of stress upon the shape.

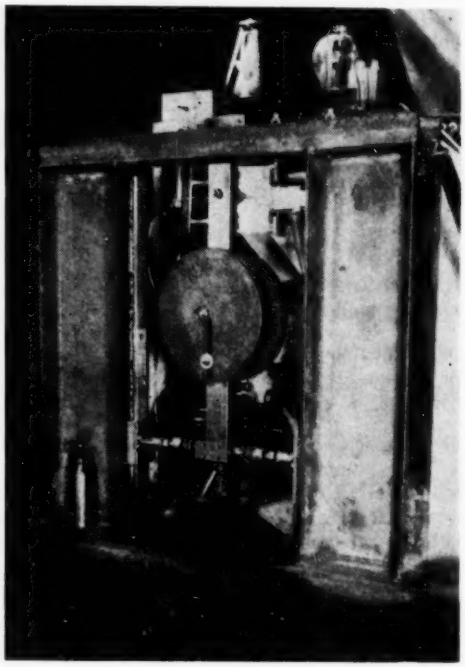


FIG. 1 GENERAL VIEW OF APPARATUS

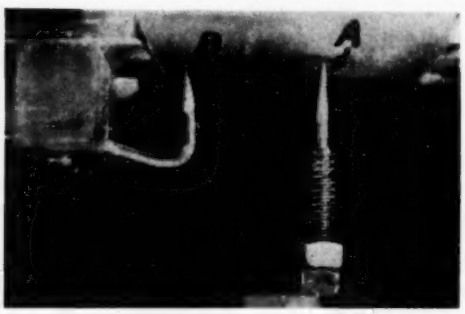


FIG. 2 HIGH-FREQUENCY-SPARK NEEDLES FOR RECORDING MOTION OF PENDULUM AND TIME

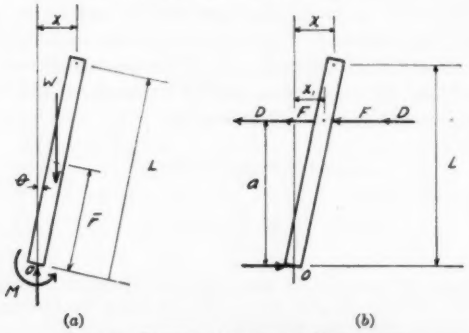


FIG. 3 FORCES ACTING ON PENDULUM
(*a*, Forces acting on pendulum alone; *b*, additional forces due to rubber specimens.)

APPARATUS AND MEASUREMENTS

A dynamic loading was superposed upon a static loading for a pair of specimens by means of a pendulum supported by an elastic hinge. A general view of the equipment is shown in Fig. 1. In this system, the rubber contributed to the damping and to the spring constant.

The rubber specimens were supported by means of conical points seating in conical holes of larger angle in the metal plates to which the rubber was bonded. The conical points on the rectangular frame could be adjusted by means of a screw so that the static deformation of the rubber specimens could be varied.

In order to start a free vibration, the pendulum was pulled to one side and held by means of a pin. Upon pulling out the pin, the pendulum would oscillate in a free vibration. The initial amplitude of the motion could be varied by adjusting the bar which held the pin.

The motion of the pendulum was recorded upon a strip of paper which moved across a metal plate. A needle A, on the end of the pendulum, discharged a high-frequency spark through the paper to the plate. The holes burned in the paper by the spark constituted the record of the motion. In addition, a second needle B discharged a series of sparks each second, giving a time measure. The two needles are shown in their positions adjacent to the paper strip in Fig. 2.

The frequency of the pendulum could be varied appreciably in three ways:

1 By changing the distance of the rubber specimens from the axis of rotation of the pendulum.

2 By adding auxiliary springs to the system.

3 By adding weights to the pendulum. One pair of weights appears in Fig. 1.

The natural frequency of the pendulum alone varied from 1.15 to 34.8 cycles per sec. The lowest frequency recorded for a vibration with rubber specimens was 3.93 cycles per sec; the highest was 46.2 cycles per sec.

The forces acting on the pendulum alone are shown in Fig. 3 (*a*). The moment about the axis of rotation exerted by the elastic hinge is proportional to the angular displacement and is $-k\theta$. If the damping is taken as proportional to the angular velocity of the pendulum, the moment due to damping is $-k_1\dot{\theta}$. The equation of motion for the pendulum is

$$I_0\ddot{\theta} = W\bar{r}\theta - k\theta - k_1\dot{\theta} \quad \ldots\ldots [2]$$

Since the linear displacement x is the quantity measured, it is best to change variables. For small displacements

$$\theta = \frac{x}{l}; \quad \dot{\theta} = \frac{\dot{x}}{l}; \quad \ddot{\theta} = \frac{\ddot{x}}{l}$$

Substituting

$$\ddot{x} + \frac{k_1}{I_0}\dot{x} + \frac{(k - W\bar{r})}{I_0}x = 0$$

This equation can be changed to standard form by letting $2q = \frac{k_1}{I_0}$ and $p^2 = \frac{k - W\bar{r}}{I_0}$. Then

$$\ddot{x} + 2qx + p^2\dot{x} = 0 \quad \ldots\ldots [3]$$

The solution of Equation [3] is

$$x = x_0 e^{-qt}\left(\cos\sqrt{p^2 - q^2}\,t + \frac{q}{\sqrt{p^2 - q^2}}\sin\sqrt{p^2 - q^2}\,t\right)$$

in which x_0 is the initial amplitude. For the small damping encountered in this investigation, this is approximately

$$x = x_0 e^{-qt}\cos pt \quad \ldots\ldots [4]$$

When two rubber specimens are added to the system, elastic forces F and damping forces D are exerted on the pendulum, Fig. 3 (*b*). The elastic force for each specimen is $F = \frac{Ex_1A}{l}$, or since $x_1 = \frac{ax}{L}$ then $F = \frac{EAa}{Ll}x$. The quantities E, A, and l are, respectively, modulus of elasticity, area, and length of the specimen. The inner end of the rubber specimen has the same velocity as the point on the pendulum at the distance a from the axis. The outer end is at rest. Assuming that the damping force D is proportional to the velocity of the moving end

$$D = C\dot{x}_1 \quad \text{or} \quad D = C\frac{a}{L}\dot{x}$$

The additional moment due to the rubber specimens is

$$-2\frac{EAa^2}{Ll}x - 2C\frac{a^2}{L}\dot{x}$$

When these terms are added to Equation [2], the following equation can be obtained

$$\ddot{x} + \left(2q + 2\frac{Ca^2}{I_0}\right)\dot{x} + \left(p^2 + 2\frac{EAa^2}{I_0 l}\right)x = 0$$

Putting

$$2q_1 = 2q + 2\frac{Ca^2}{I_0} \quad \ldots\ldots [5]$$

and

$$p_1^2 = p^2 + 2\frac{EAa^2}{I_0 l} \quad \ldots\ldots [6]$$

$$\ddot{x} + 2q_1\dot{x} + p_1^2 x = 0$$

This has for an approximate solution

$$x = x_0 e^{-q_1 t}\cos p_1 t \quad \ldots\ldots [7]$$

Equation [7] represents a cyclic motion with decaying amplitude. It has the period $\frac{2\pi}{p_1}$. The damping was measured in this investigation by means of the relation

$$N = \frac{\text{Amplitude after } n \text{ cycles}}{\text{Initial amplitude}} = e^{-2\pi n q_1/p_1} \quad \ldots\ldots [8]$$

The manner of using it was as follows:

Equation [8] was plotted on semilogarithmic paper (on which it is a straight line) for several values of n, Fig. 4. The quantity N was determined from the record of the vibration for the same values of n. Then each N was plotted on the proper line in Fig. 4. If points so plotted fall in a vertical line, the damping force is proportional to the velocity and the value of q_1/p_1 can be determined immediately. For each test performed in this investigation, the points plotted, as in Fig. 4, could be represented reasonably by a vertical line. The quantity n was increased in increments of 1, 2, or 10, depending upon the rate at which the oscillation died out. The frequency, in cycles per second, of the motion described by Equation [7] can be obtained easily from the vibration record. If this frequency is denoted by f, then $p_1 = 2\pi f$. Term q_1 is the product of q_1/p_1 and p_1. The quantities q and p for the pendulum alone can be determined in the same way as q_1 and p_1. Then from Equations [5] and [6]

$$C = \frac{I_0}{a^2}(q_1 - q)$$

and

$$E = \frac{I_0 l}{2Aa^2}(p_1^2 - p^2)$$

From Equation [1], the damping coefficient C_2 in terms of which the damping data herein obtained have been expressed is $C_2 = \frac{Cl}{A}$.

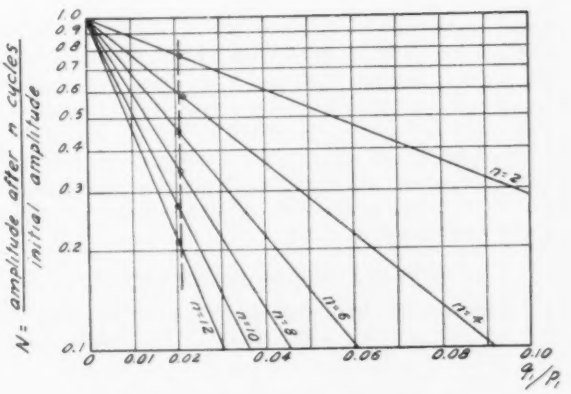


FIG. 4 CHART FOR EVALUATING q_1/p_1

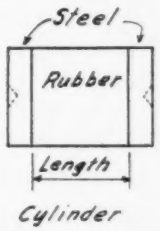


FIG. 5 TYPE OF TEST CYLINDER

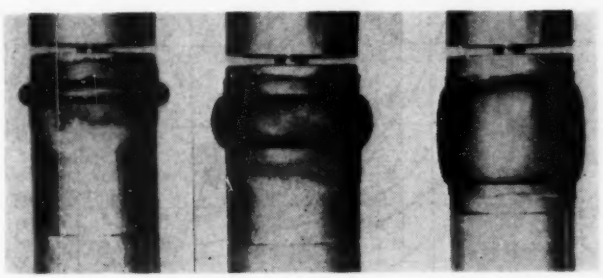


FIG. 6 THREE 1-IN. CYLINDERS

CYLINDERS IN COMPRESSION

Results are given in the following section for 17 pairs of cylinders tested in compression. These include cylinders of 1 in.

diam and lengths of 1 in. (3 pairs), 0.9 in., 0.8 in., 0.7 in., 0.6 in., 0.5 in., 0.4 in., 0.31 in., and 0.21 in.; 1.5 in. diam and lengths of 1.05 in., 0.45 in., and 0.35 in.; 2 in. diam and lengths of 1.05 in., 0.45 in., and 0.35 in. All were bonded to steel disks at the ends and were of the type shown in Fig. 5. Fig. 6 shows three cylinders of 1 in. diam under a strain of approximately 0.25. A pronounced end effect, which depends upon length, is evident. This made it desirable to test cylinders of several lengths for each diameter.

Damping of Cylinders in Compression

Fig. 7 shows the effect of frequency on the damping coefficient C_2 for a number of the cylinders tested. The results indicate

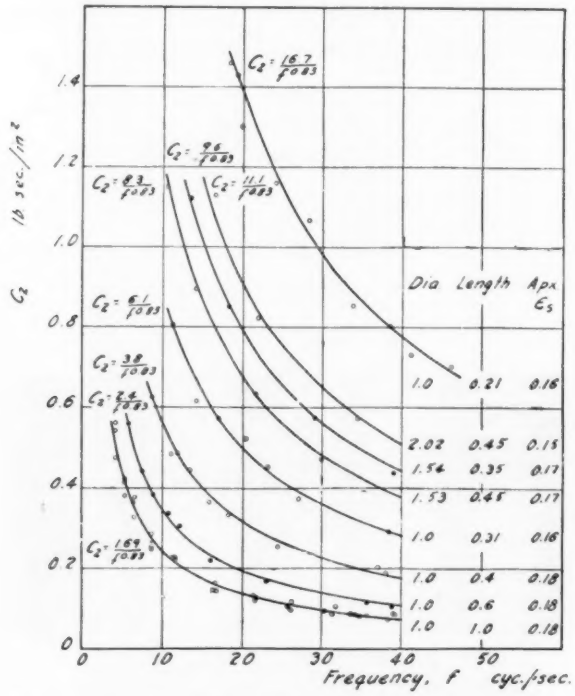


Fig. 7 Effect of Frequency on Damping Coefficient C_2
(Cylinders in compression; ϵ_s = static strain.)

that the damping is inversely proportional to $f^{0.83}$. Additional results are given in Table 1.

TABLE 1 RESULTS OF DAMPING TESTS

Diameter, in.	Length, in.	Approx. ϵ_s	$C_2 f^{0.83}$
1	0.9	0.18	1.64
1	0.5	0.18	2.47
1	0.7	0.18	1.76
1	0.8	0.14	1.76
2	1	0.15	2.12
2	0.35	0.15	16.5
1.5	1	0.17	1.65

The effect of static strain ϵ_s on the damping can be expressed by means of a function $A(\epsilon_s)$. Thus

$$C_2 = \frac{A(\epsilon_s)}{f^{0.83}} \quad \text{or} \quad C_2 f^{0.83} = A(\epsilon_s)$$

Fig. 8 shows the product $C_2 f^{0.83}$ plotted against the static strain for several pairs of cylinders. It appears that a linear relation is satisfactory for values of ϵ_s not exceeding 0.20, that is, $C_2 f^{0.83} = B_0 + B_1 \epsilon_s$, where B_0 is the intercept of the straight line on the vertical axis and B_1 is the slope.

The foregoing results indicate that the configuration of the

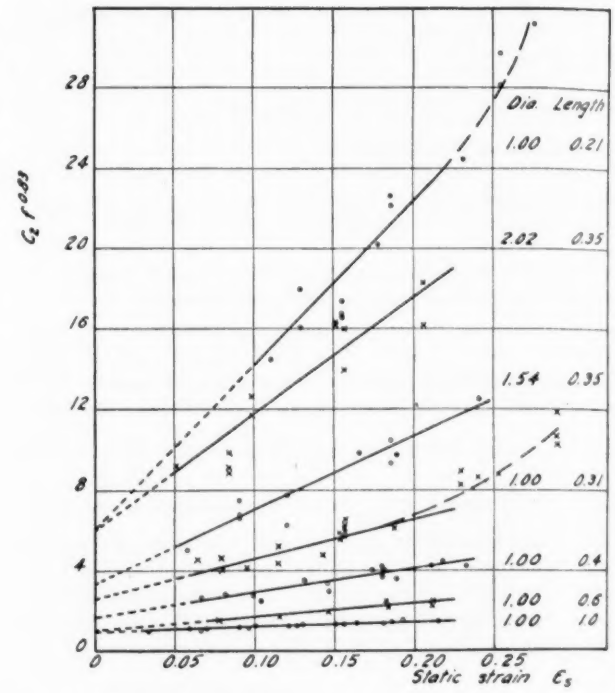


Fig. 8 Effect of Static Strain on Damping Coefficient C_2
(Cylinders in compression.)

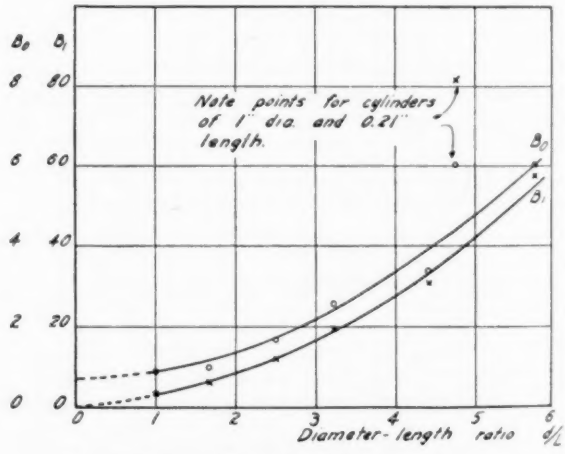


Fig. 9 Factors B_0 and B_1 Plotted Against d/L
(Cylinders in compression.)

cylinder has a considerable effect on the damping. A convenient way of describing the configuration is by means of the diameter-length ratio, d/L. Accordingly, the factors B_0 and B_1 from Fig. 8 have been plotted against d/L in Fig. 9. The factors for the cylinders of 1 in. diam and 0.21 in. length have values which are inconsistent with those for the other cylinders. This may be due to the $^1/_{32}$-in. layer of harder stock at each end. For this length, over 30 per cent of the specimen consists of the harder stock.

Dynamic Modulus of Elasticity

Fig. 10 shows the modulus of elasticity, as determined from the dynamic tests, plotted against frequency. In this range, the frequency appears to have no effect upon the dynamic modulus.

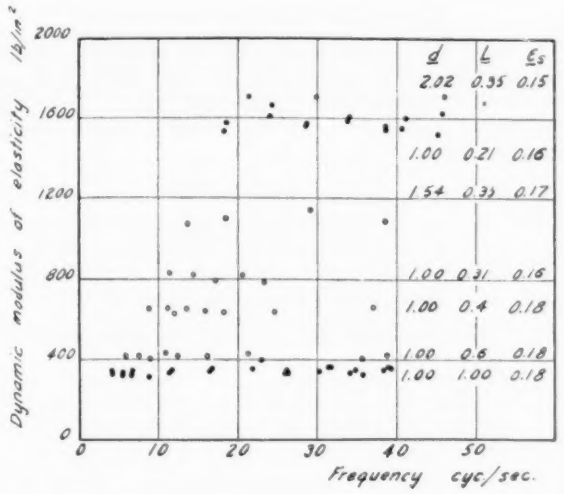


FIG. 10 EFFECT OF FREQUENCY ON DYNAMIC MODULUS OF ELASTICITY
(Cylinders in compression. d = diameter, L = length, ϵ_s = approximate static strain.)

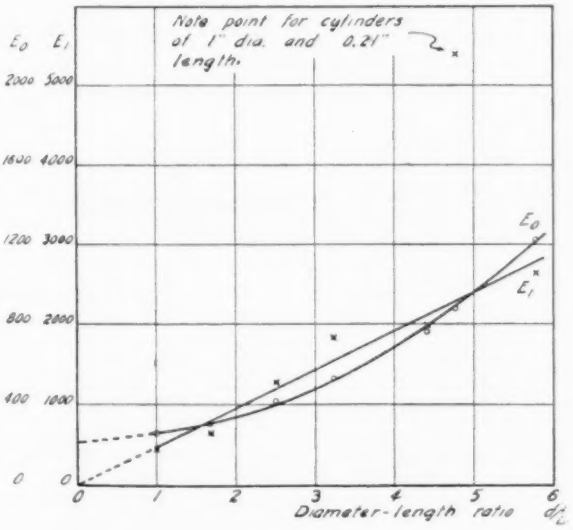


FIG. 12 EFFECT OF a/L UPON FACTORS E_0 AND E_1
(Cylinders in compression.)

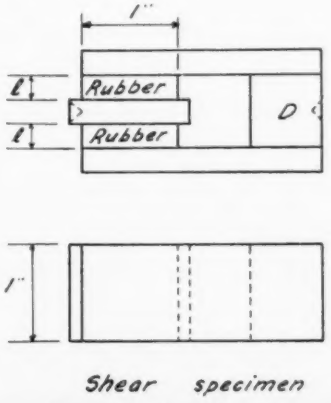


FIG. 14 SHEAR SPECIMEN

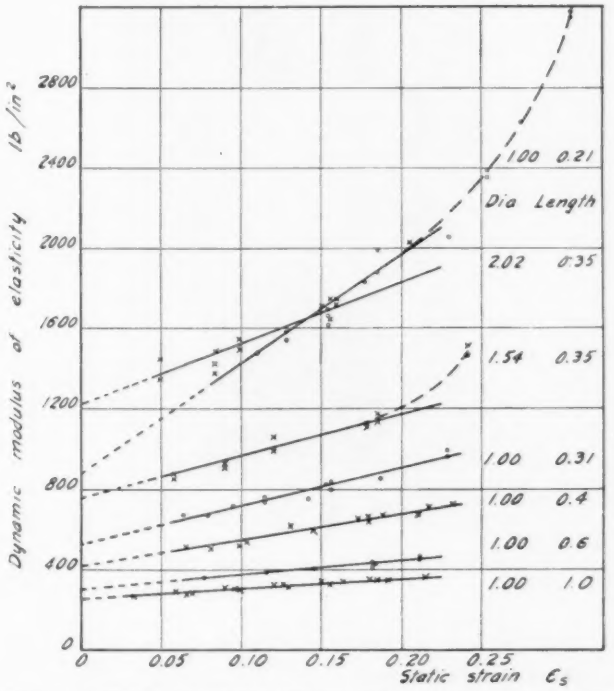


FIG. 11 EFFECT OF STATIC STRAIN ON DYNAMIC MODULUS OF ELASTICITY
(Cylinders in compression.)

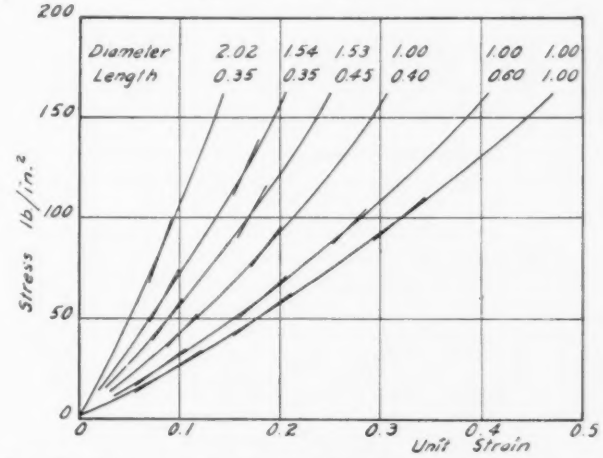


FIG. 13 COMPARISON OF DYNAMIC MODULUS OF ELASTICITY WITH STATIC MODULUS
(Cylinders in compression.)

The effect of static strain upon the dynamic modulus is shown in Fig. 11. The results may be represented as

$$E_{dyn} = E_0 + E_1\epsilon_s$$

for ϵ_s not exceeding 0.2.

Fig. 12 shows the effect of diameter-length ratio upon the factors E_0 and E_1.

Static stress-strain curves for some of the cylinders are shown in Fig. 13, in which the dynamic modulus of elasticity is shown in comparison with the static modulus. The short straight lines represent values of the dynamic modulus. In each case, the line has been drawn to intersect the static curve at the appropriate value of the static strain. It is evident that the dynamic modulus is slightly larger than the static modulus.

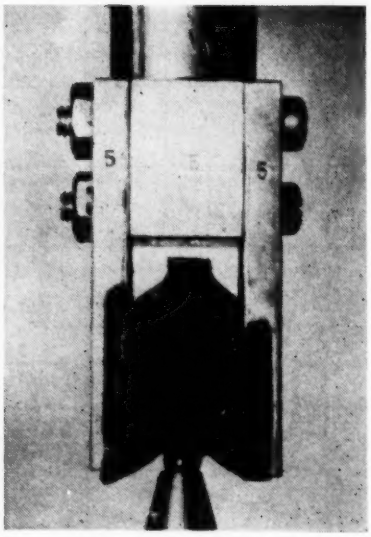


FIG. 15 SHEAR SPECIMEN UNDER STATIC STRAIN OF APPROXIMATELY 1

SHEAR SPECIMENS

Three pairs of specimens were tested in shear. All had the dimensions shown in Fig. 14. Fig. 15 shows a shear specimen under a static strain of approximately 1. There is no extreme end effect such as that seen in the cylinders in Fig. 6. The block D was added after molding and was held in place by means of dowel pins and machine screws. The dimension l was between 0.26 and 0.27 in. after molding. By means of the machine screws, this was brought down to 0.25 in. The latter value was used in calculations.

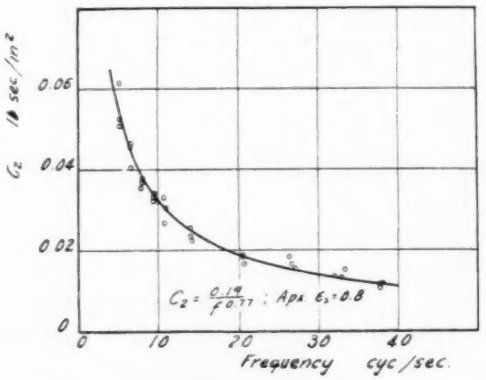


FIG. 16 EFFECT OF FREQUENCY ON DAMPING COEFFICIENT C_2 FOR SHEAR SPECIMENS

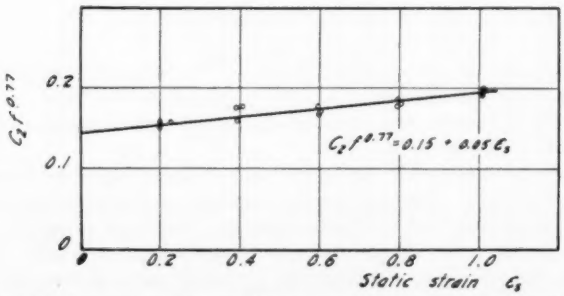


FIG. 17 EFFECT OF STATIC STRAIN ON DAMPING COEFFICIENT C_2 FOR SHEAR SPECIMENS

DAMPING OF CYLINDERS IN SHEAR

The effect of frequency on the damping coefficient C_2 for the shear specimens is shown in Fig. 16, from which it appears that the damping is inversely proportional to $f^{0.77}$.

In Fig. 17, the product $C_2 f^{0.77}$ has been plotted against the static strain ϵ_s

$$C_2 f^{0.77} = 0.15 + 0.05\epsilon_s$$

$$C_2 = \frac{0.15 + 0.05\epsilon_s}{f^{0.77}}$$

DYNAMIC MODULUS OF ELASTICITY

The dynamic modulus of elasticity for the shear specimens is

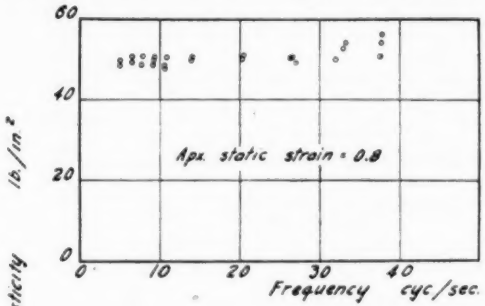


FIG. 18 EFFECT OF FREQUENCY ON DYNAMIC MODULUS OF ELASTICITY FOR SHEAR SPECIMENS

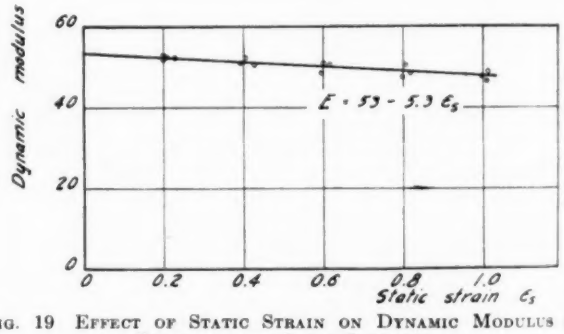


FIG. 19 EFFECT OF STATIC STRAIN ON DYNAMIC MODULUS OF ELASTICITY FOR SHEAR SPECIMENS

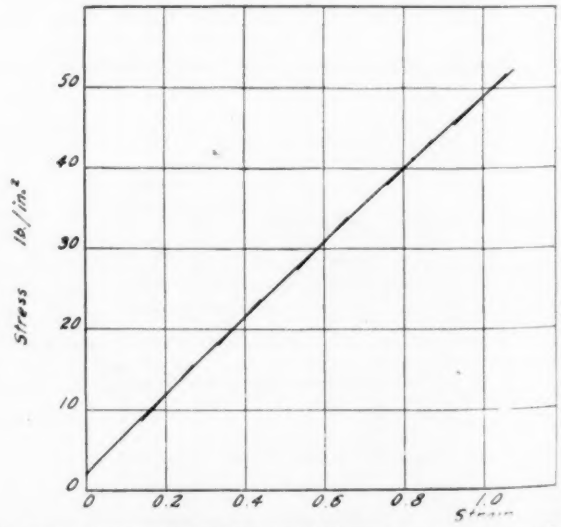


FIG. 20 COMPARISON OF DYNAMIC MODULUS OF ELASTICITY WITH STATIC MODULUS FOR SHEAR SPECIMENS

shown plotted against frequency in Fig. 18. The results indicate that frequency has no effect upon the dynamic modulus.

Fig. 19 shows the effect of static strain on the dynamic modulus. The results may be represented by

$$E_{dyn} = 53 - 5.3\epsilon_s$$

Fig. 20 shows an average static stress-strain curve for the six shear specimens, and a comparison between the dynamic modulus of elasticity and the static modulus. The short straight lines indicate values of the dynamic modulus, each line being drawn to intersect the static curve at the appropriate static strain. The dynamic modulus is slightly higher than the static modulus.

Comparison With Previous Work

In regard to damping, the results stated for cylinders in compression agree fairly well with the conclusions of Kosten[3] and Naunton and Waring.[4] To compare with Roelig,[5] it is necessary to express the results in terms of energy. Since all of Roelig's tests were made on cylinders having a diameter-length ratio of 1, this comparison is based upon results for cylinders of 1 in. diam and 1 in. length. In general

$$\Delta w = \pi C p x_0^2 = 2\pi^2 C f x_0^2$$

where the damping coefficient C is equal to $C_2 \frac{A}{l}$. Term C_2 can be obtained from Fig. 8 as $C_2 = \frac{0.94 + 3.6\epsilon_s}{f^{0.83}}$

$$\Delta w = 2\pi^2(0.94 + 3.6\epsilon_s) f^{0.17} \frac{A}{l} x_0^2 \quad \ldots\ldots\ldots [9]$$

The total energy is

$$W = \frac{1}{2} k x_0^2$$

For one cylinder

$$k = \frac{EA}{l}$$

From Fig. 11

$$E = 240 + 590\epsilon_s$$

so

$$w = \frac{1}{2}(240 + 590\epsilon_s) \frac{A}{l} x_0^2$$

Then

$$\frac{\Delta w}{w} = 4\pi^2 \left(\frac{0.94 + 3.6\,\epsilon_s}{240 + 590\,\epsilon_s}\right) f^{0.17} \ldots\ldots\ldots [10]$$

Equations [9] and [10] are in agreement with the first three conclusions of Roelig,[5] i.e., those in regard to the roles of dynamic load or amplitude, static load, and frequency in affecting the damping. In regard to the effect of volume, Equation [9] may be rewritten as

$$\Delta w = \frac{2\pi^3}{4}(0.94 + 3.6\,\epsilon_s) f^{0.17} x_0^2 l$$

since the diameter is equal to the length. Term Δw varies directly as the length and so increases with volume. Equation [10] shows that $\frac{\Delta w}{w}$ is unaffected by changing the volume.

Equation [9] does not agree with the conclusion of Williams.[6] The energy lost in 1 cycle of stress increases with the frequency.

Results for the dynamic modulus of elasticity agree with the conclusion of Kosten[3] that the dynamic modulus is not affected by change of frequency.

Conclusions

The following conclusions apply to rubber of the stock tested when bonded to steel:

1 For cylinders in compression and specimens in shear, the damping can be expressed in terms of a velocity coefficient. The damping decreases with increase of frequency; it increases with increase of static strain.

2 The dynamic modulus of elasticity is slightly larger than the static modulus and is not affected by change of frequency. It increases with increase of static strain for the cylinders and decreases for the shear specimens.

3 For cylinders in compression, both damping and modulus of elasticity are dependent upon the ratio of diameter to length.

Acknowledgments

The writer takes this opportunity to express his thanks to Prof. J. Ormondroyd, at whose suggestion and under whose direction the project was undertaken.

The specimens used were furnished by the U. S. Rubber Company. Messrs. C. M. Sloman and F. L. Yost were especially helpful in this connection.

Two Problems of Thermal Stress in the Infinite Solid

By N. O. MYKLESTAD,[1] CHICAGO, ILL.

The equations for thermal stress were first developed about 100 years ago by Duhamel (1),[2] who treated the cases of a sphere and a circular cylinder with radial variation of temperature only. As the problem of the cylinder can be considered one of plane strain, it appears that the problem of the sphere (2) is the only three-dimensional one for which a complete solution is available. Borchardt (3) has treated the thermal-stress problem of the sphere for a nonsymmetrical distribution of temperature. Recent developments of the theory (4) have made it possible to complete further solutions. In this paper results are obtained for an infinite solid in which a small internal region, in the form of an ellipsoid of revolution, or a long narrow region, in the form of a semi-infinite circular cylinder, is hotter than the surrounding material. In a finite solid the cylinder may alternately be considered as a blind hole filled with an oversize plug, or a similar shrink fit. The problem of the ellipsoid has some bearing upon the question of the effects of slag inclusion in metals. A discussion by B. P. Haigh (5) deals with the spherical inclusion, whereas, the results of this paper give some indication of the effect of shape variations. The shape of the ellipsoid varies from a flat pancake shape to a thin needle shape, and it is seen that both the pancake-shaped and the needle-shaped inclusions give rise to a higher stress than does the spherical one, for the same temperature variation.

IN THE two problems of this paper, the infinite solid is considered to have the uniform temperature zero outside the hot region, while inside this region the temperature has the constant value of T everywhere. The coefficient of thermal expansion α is considered to be constant, but a variation of α can easily be taken care of by carrying αT through as a single variable quantity. In the case of a small inclusion in the solid, α is the only variable, and T is then merely the uniform temperature change of the solid as a whole.

In Fig. 1 is shown the stress distribution around a hot ellipsoid of revolution in terms of the radii of curvature at the ends of the semiaxes a and c of the generating ellipse, the stresses being those along the extension of the axes. The maximum stress that occurs anywhere in this case is $\frac{E\alpha T}{1-\nu}$ and is normal to the surface of the ellipsoid at a point of minimum radius of curvature of the generating ellipse. This stress occurs only for the case of a pancake-shaped or needle-shaped ellipsoid. For a spherical inclusion, the maximum stress is $\frac{2}{3}\frac{E\alpha T}{1-\nu}$, and is also normal to the surface.

In general the stress in the cold exterior is a maximum at the surface of the ellipsoid of revolution and falls off rather rapidly for points farther out in the exterior. This is in accordance with Saint Venant's principle, and it is seen that, if the minimum dimension of the solid is about 3 times that of the maximum dimension of the inclusion, the solid can for all practical purposes be considered to be infinite.

The results of the second problem are interesting because of the sharp edge around the base of the semi-infinite circular cylinder. In Fig. 2 is shown the normal stresses along radial lines at various distances from the base of the cylinder. The letter n indicates the distance from the base of the cylinder in terms of the radius a.

Fig. 3 shows the normal stresses along lines parallel to the axis of the cylinder and at various distances from it. The letter p indicates the distance from the axis of the cylinder in terms of the radius a.

Fig. 4 shows the shear stress along the plane of the base of the cylinder and along a generator.

From Figs. 2 to 4, it is seen that, for external points, the stresses all drop off rapidly to negligible values in a radial direction and in the axial direction below the base. In the axial di-

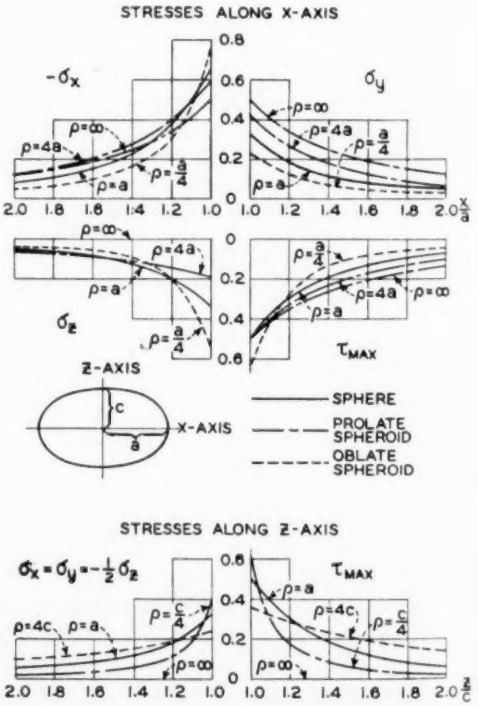


FIG. 1 STRESS DISTRIBUTION AROUND A HOT ELLIPSOID OF REVOLUTION FOR DIFFERENT VALUES OF THE RADIUS OF CURVATURE ρ

(ρ is expressed in terms of the lengths a and c of the semiaxes of the generating ellipse; all values for stress are to be multiplied by $E\alpha T/(1-\nu)$.)

[1] Assistant Professor of Machine Design, Armour College of Engineering of the Illinois Institute of Technology.

[2] Numbers in parentheses refer to the Bibliography at the end of the paper.

Presented at the National Meeting, of the Applied Mechanics Division, Philadelphia, Pa., June 20–21, 1941, of THE AMERICAN SOCIETY OF MECHANICAL ENGINEERS.

Discussion of this paper should be addressed to the Secretary, A.S.M.E., 29 West 39th Street, New York, N. Y., and will be accepted until October 10, 1942, for publication at a later date. Discussion received after the closing date will be returned.

NOTE: Statements and opinions advanced in papers are to be understood as individual expressions of their authors, and not those of the Society.

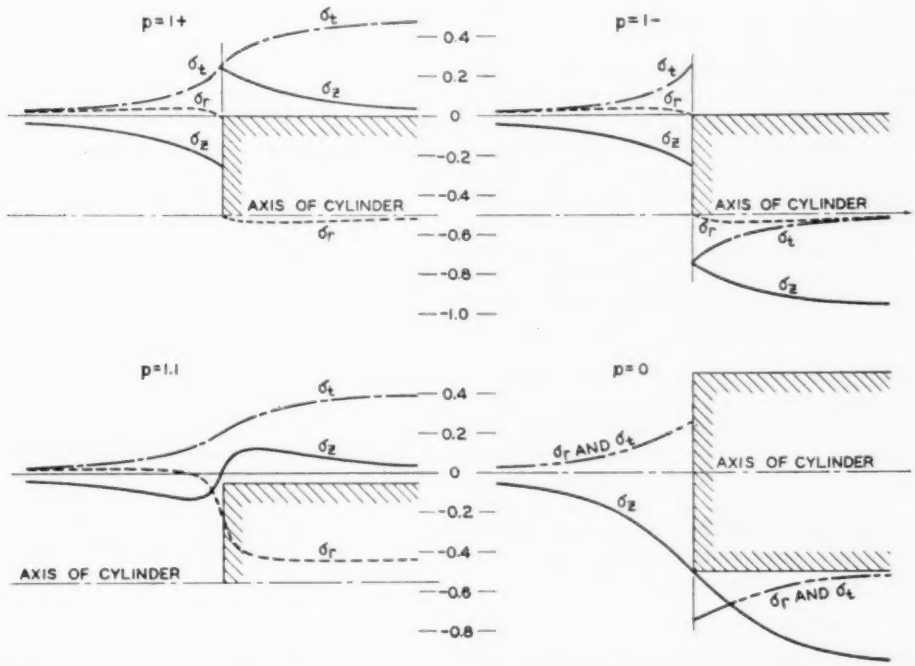


FIG. 3 NORMAL STRESSES, DUE TO A HOT SEMI-INFINITE CIRCULAR CYLINDER, ALONG LINES PARALLEL TO AXIS OF CYLINDER AND AT VARIOUS DISTANCES FROM IT

(p is the distance from the axis of the cylinder in terms of the radius a; all values for stress are to be multiplied by $E\alpha T/[1-\nu]$.)

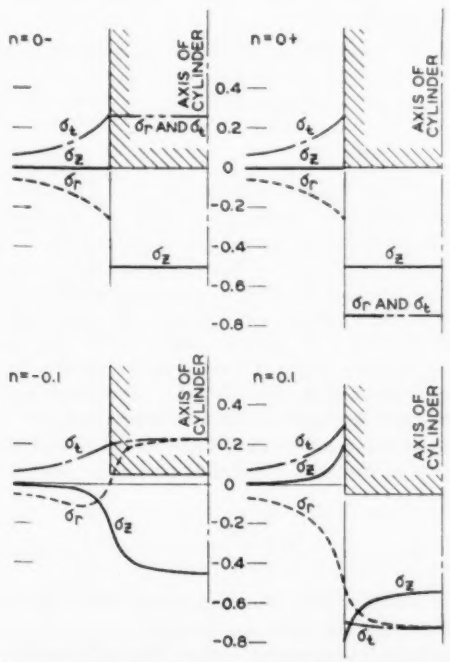


FIG. 2 NORMAL STRESSES, DUE TO A HOT SEMI-INFINITE CIRCULAR CYLINDER, ALONG RADIAL LINES AT VARIOUS DISTANCES FROM BASE OF CYLINDER

(n is the distance from the base of the cylinder in terms of the radius a; all values for stress are to be multiplied by $E\alpha T/[1-\nu]$.)

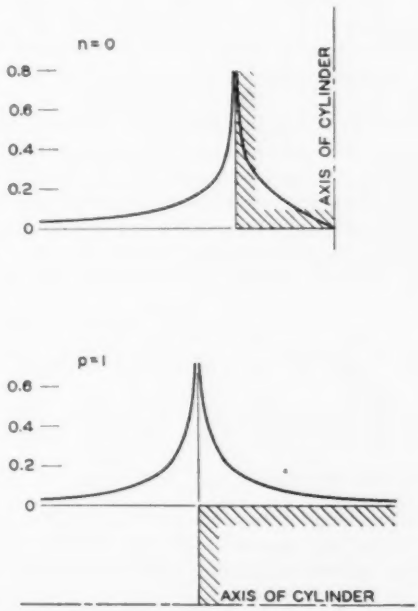


FIG. 4 SHEAR STRESS, DUE TO A HOT SEMI-INFINITE CIRCULAR CYLINDER, ALONG PLANE OF BASE OF CYLINDER AND ALONG A GENERATOR

(All values for stress are to be multiplied by $E\alpha T/[1-\nu]$.)

rection above the base of the cylinder, the radial and tangential stresses rapidly approach the values $-\frac{1}{2}\frac{E\alpha T}{1-\nu}$ and $\frac{1}{2}\frac{E\alpha T}{1-\nu}$, respectively, for points immediately outside the surface, while the axial stress falls off to a negligible value. Inside the cylinder, both the radial and tangential stresses approach the value $-\frac{1}{2}\frac{E\alpha T}{1-\nu}$ while the axial stress approaches the value $-\frac{E\alpha T}{1-\nu}$. To find the stresses in a semi-infinite solid when a blind hole is filled with hotter material, it is only necessary to cut the infinite solid with a plane perpendicular to the axis of the cylinder and at the

proper distance from its base. If a uniform pressure of $\frac{E\alpha T}{1-\nu}$ is applied to the plane of the cut where it is pierced by the cylinder, the same stress distribution is obtained as for the infinite solid. It is now only necessary to remove the local pressure on the surface of the semi-infinite solid to obtain the stress distribution for this case. As the effect of this local pressure is negligible at some distance below the surface, it will only affect slightly the stress distribution around the end of the cylinder. The results from the infinite solid may be used unchanged for the case of the semi-infinite solid when the length of the blind hole is more than twice the diameter. This will then take care of the case of a large solid with a blind hole into which a plug is shrunk or pressed.

From Figs. 2 to 4 it is also seen that at the sharp corner the normal stresses are discontinuous and the shear stress becomes infinite. This implies that the actual shear stress depends upon the degree of rounding of the corner, or that frictional slip will occur in the neighborhood. In the case of an oversize plug, the shear stress will evidently be limited by the degree to which friction can prevent slip between the plug and the hole surfaces. However, a small distance away from the corner the normal stresses will be nearly the same as the values found.

General Theory

When an elastic solid, which is unstressed at a uniform temperature, is given a nonuniform temperature $T(x, y, z)$ that is not linear in x, y, z, the natural expansion of a volume element will be restricted by the surrounding material and a state of stress will ensue. The difference between the actual strain and the natural expansion αT of a volume element is related to the stress through Hooke's law; α being the linear coefficient of thermal expansion. For simplicity, it is assumed that the original uniform temperature is zero. This makes no difference in the theory because a uniform change of temperature creates no stress in an isotropic solid. It is also assumed that the elastic constants of the material do not vary considerably over the temperature range in question, although a variation of α with temperature can be taken care of by carrying αT through as a single variable quantity.

Let u, v, w be the total displacements in the x, y, z directions, respectively, then the components of normal and shear strain are

$$\left.\begin{aligned} &\epsilon_x = \frac{\partial u}{\partial x}, \quad \epsilon_y = \frac{\partial v}{\partial y}, \quad \epsilon_z = \frac{\partial w}{\partial z}, \\ &\gamma_{xy} = \frac{\partial u}{\partial y} + \frac{\partial v}{\partial x}, \quad \gamma_{xz} = \frac{\partial u}{\partial z} + \frac{\partial w}{\partial x}, \quad \gamma_{yz} = \frac{\partial v}{\partial z} + \frac{\partial w}{\partial y} \end{aligned}\right\} \quad \ldots\ldots [a]$$

Also, the volume expansion $e = \epsilon_x + \epsilon_y + \epsilon_z$.

As a uniform change of temperature of a small volume element does not create any angular distortion of the element, the shear stresses will be unaffected by the term αT or, $\tau_{xy} = G\gamma_{xy}$, etc., where $G = \frac{E}{2(1+\nu)}$ is the modulus of elasticity in shear, E the modulus of elasticity in tension and compression (assumed equal), and ν Poisson's ratio. The normal stresses, however, are determined by the following equation

$$\sigma_x = \frac{E}{1+\nu}\left[\frac{\nu}{1-2\nu}\, e + \epsilon_x - \frac{1+\nu}{1-2\nu}\,\alpha T\right] \ldots\ldots [1]$$

and two more by interchanging x with y and z.

The three equations of equilibrium take the form

$$(\lambda + G)\frac{\partial e}{\partial x} + G\nabla^2 u - \frac{\alpha E}{1-2\nu}\frac{\partial T}{\partial x} = 0$$

and two more by interchanging x with y and z, and u with v and w. Also

$$\lambda = \frac{\nu E}{(1+\nu)(1-2\nu)} \quad \text{and} \quad \nabla^2 = \frac{\partial^2}{\partial x^2} + \frac{\partial^2}{\partial y^2} + \frac{\partial^2}{\partial z^2}$$

Substituting for λ and G these equations become

$$\frac{\partial e}{\partial x} + (1-2\nu)\nabla^2 u = 2\alpha(1+\nu)\frac{\partial T}{\partial x} \ldots\ldots [2]$$

etc. Equations [1] and [2] are the fundamental equations of the theory.

In order to obtain particular integrals of Equation [2], a function φ is introduced and defined in such a manner that

$$\frac{\partial \varphi}{\partial x} = u, \quad \frac{\partial \varphi}{\partial y} = v, \quad \frac{\partial \varphi}{\partial z} = w$$

By means of Equations [a], the strains can be expressed in terms of the function φ as follows

$$\epsilon_x = \frac{\partial^3 \varphi}{\partial x^3}, \quad \epsilon_y = \frac{\partial^3 \varphi}{\partial y^3}, \quad \epsilon_z = \frac{\partial^3 \varphi}{\partial z^3} \ldots\ldots [b]$$

$$e = \nabla^2 \varphi \ldots\ldots [c]$$

$$\gamma_{xy} = 2\frac{\partial^3 \varphi}{\partial x \partial y}, \quad \gamma_{xz} = 2\frac{\partial^3 \varphi}{\partial x \partial z}, \quad \gamma_{yz} = 2\frac{\partial^3 \varphi}{\partial y \partial z} \ldots\ldots [d]$$

Equation [2] can now be written

$$\frac{\partial}{\partial x}\left[(1-\nu)\nabla^2 \varphi - (1+\nu)\alpha T\right] = 0$$

etc. It is seen that Equation [2] is all satisfied when

$$\nabla^2 \varphi = \frac{1+\nu}{1-\nu}\,\alpha T \ldots\ldots [3]$$

Evidently any function φ, which satisfies Equation [3], provides a particular integral of Equation [2]. The state of stress and strain represented by this function φ will ordinarily require certain surface forces at the boundary of the solid. These surface forces can be determined from the conditions of equilibrium at the boundary and the stresses there, expressed in terms of φ. To complete the problem, it is necessary to apply equal and opposite forces to the surface of the solid and determine the stresses from these, as in an ordinary (isothermal) boundary-value problem. By superposition, the complete stress resulting from unequal heating of the solid can then be determined.

The function φ is called the "displacement potential."

By means of Equation [3], Equation [1] can now be written in the form

$$\sigma_x = 2G\left[\frac{\partial^2 \varphi}{\partial x^2} - \frac{1+\nu}{1-\nu}\,\alpha T\right] \ldots\ldots [1a]$$

etc. It is seen that only the second derivatives of φ are necessary to determine the stress components.

Equation [3] is of the same form as Poisson's equation $\nabla^2 V = -4\pi\rho$, and a particular integral is given by the Newtonian potential of a distribution of matter of density ρ per unit of volume

$$V = \int\int\int \frac{\rho}{r}\, d\xi d\eta d\zeta$$

In this equation V is the potential at the point (x, y, z), the co-ordinates ξ, η, ζ refer to a point in the solid where the density is ρ, and the integration is throughout the solid. The distance r, between the points (x, y, z) and (ξ, η, ζ), is given by the equa-

tion $r = \sqrt{(x-\xi)^2 + (y-\eta)^2 + (z-\zeta)^2}$. Putting $\frac{1+\nu}{1-\nu}\alpha T = -4\pi\rho$ the following equation for φ is obtained

$$\varphi(x, y, z) = -\frac{1+\nu}{1-\nu}\frac{\alpha}{4\pi}\int\int\int \frac{T(\xi, \eta, \zeta)}{r}\, d\xi d\eta d\zeta \quad [4]$$

When the inequalities of temperature are of a purely local nature in an infinite solid, $T = 0$ outside the hot part of the solid, φ will vanish at infinity because ξ, η, ζ are bounded, and consequently r goes to infinity when the point (x, y, z) goes to infinity. As $T(\xi, \eta, \zeta)$ is independent of (x, y, z), differentiation under the integral sign shows that the displacements will vanish as r^{-2} and the stresses as r^{-3}, when the point (x, y, z) goes to infinity. As this satisfies the boundary conditions for an infinite solid, the solution in this case is completely represented by Equation [4].

Discontinuous Temperature Distribution

The general Equation [2] implies the existence of the first derivatives of the temperature, and the validity of any solution at a surface S of temperature discontinuity therefore requires examination. By means of potential theory it is easily shown, however, that the solution of Equation [4] is also valid when T has surface discontinuities, and that any component of normal stress, acting on an element of area normal to, and at, the surface of discontinuity is discontinuous by an amount $\frac{E\alpha}{1-\nu}(T_i - T_e)$, while the component of normal stress acting on an element of the surface S is continuous. T_i is the temperature immediately inside the surface S and T_e is the temperature immediately outside S.

All these conclusions remain true even when the solid has finite boundaries. The boundary forces, corresponding to Equation [4], are to be canceled by superposing an isothermal stress distribution having equal and opposite boundary values. But any distribution of boundary forces, whether continuous or not, produces a stress that is continuous in the interior. The discontinuity of stress due to a temperature discontinuity remains unaffected, although the absolute values of the stresses on either side of S will in general be modified.

It is not necessary that S lie entirely within the boundary. It may cut it in one or more curves. When it does, the complementary surface forces on the boundary are discontinuous at these curves. When it does not, these forces are continuous all over the boundary.

Solution to Problem 1

Stresses set up in an "isotropic infinite solid" when part of it, bounded by an "ellipsoid of revolution," is at a higher uniform temperature than the rest of the solid.

Let the ellipsoid be formed by rotating an ellipse $\frac{x^2}{a^2} + \frac{z^2}{c^2} = 1$, with semiaxes a and c, about the z axis. The equation for the ellipsoid of revolution then becomes $\frac{x^2+y^2}{a^2} + \frac{z^2}{c^2} = 1$.

It is shown under "General Theory" that the stresses are found immediately from the potential of an ellipsoid of uniform mass density $\rho = -\frac{1+\nu}{1-\nu}\frac{\alpha T}{4\pi}$. The constant temperature of the ellipsoid is considered equal to T and in the cold exterior equal to zero.

The normal stresses are given by Equation [1a], and as $T = 0$ for the cold exterior, the stresses in this part of the infinite solid will be

$$\sigma_x = \frac{E}{1+\nu}\frac{\partial^2\varphi}{\partial x^2} \quad [5]$$

Both for external and internal points the shear stresses are

$$\tau_{xy} = \frac{E}{1+\nu}\frac{\partial^2\varphi}{\partial x \partial y} \quad [5a]$$

etc.

First consider the case of an "oblate spheroid" $a > c$, for which the potential (6) is

$$V = \frac{\pi\rho a^2 c}{a^2 - c^2}\left[\left(2\sqrt{a^2-c^2} - \frac{x^2+y^2-2z^2}{\sqrt{a^2-c^2}}\right)\sin^{-1}\sqrt{\frac{a^2-c^2}{a^2+\kappa}} + \frac{\sqrt{c^2+\kappa}}{a^2+\kappa}(x^2+y^2) - \frac{2z^2}{\sqrt{c^2+\kappa}}\right] \quad [6]$$

and κ is determined as being the positive root in the equation

$$\frac{x^2+y^2}{a^2+\kappa} + \frac{z^2}{c^2+\kappa} = 1 \quad [7]$$

By introducing the eccentricity $e = \frac{\sqrt{a^2-c^2}}{a}$, c can be eliminated. Also κ can be found by means of Equation [7]. Differentiation of Equation [6] then yields the following expressions for the stresses

$$\left.\begin{aligned}
\sigma_x &= \frac{E\alpha T}{1-\nu}\frac{a\sqrt{1-e^2}}{2e^2}\left[\frac{1}{ae}\sin^{-1}\frac{ae}{\sqrt{a^2+\kappa}} - \frac{\sqrt{c^2+\kappa}}{a^2+\kappa} - \frac{e^2a^2x}{(a^2+\kappa)^2\sqrt{c^2+\kappa}}\frac{\partial\kappa}{\partial x}\right] \\
\sigma_y &= \frac{E\alpha T}{1-\nu}\frac{a\sqrt{1-e^2}}{2e^2}\left[\frac{1}{ae}\sin^{-1}\frac{ae}{\sqrt{a^2+\kappa}} - \frac{\sqrt{c^2+\kappa}}{a^2+\kappa} - \frac{e^2a^2y}{(a^2+\kappa)^2\sqrt{c^2+\kappa}}\frac{\partial\kappa}{\partial y}\right] \\
\sigma_z &= \frac{E\alpha T}{1-\nu}\frac{a\sqrt{1-e^2}}{2e^2}\left[\frac{2}{\sqrt{c^2+\kappa}} - \frac{2}{ae}\sin^{-1}\frac{ae}{\sqrt{a^2+\kappa}} - \frac{e^2a^2z}{(a^2+\kappa)(c^2+\kappa)^{3/2}}\frac{\partial\kappa}{\partial z}\right]
\end{aligned}\right\} \quad [8]$$

and

$$\tau_{xy} = -\frac{E\alpha T}{1-\nu}\frac{a^3\sqrt{1-e^2}}{2(a^2+\kappa)^2\sqrt{c^2+\kappa}}\left[1 + \frac{r^2-e^2a^2}{\sqrt{(r^2-e^2a^2)^2+4e^2a^2z^2}}\right]xy$$

$$\tau_{xz} = -\frac{E\alpha T}{1-\nu}\frac{a^3\sqrt{1-e^2}}{2(a^2+\kappa)^2\sqrt{c^2+\kappa}}\left[1 + \frac{r^2+e^2a^2}{\sqrt{(r^2-e^2a^2)^2+4e^2a^2z^2}}\right]xz$$

$$\tau_{yz} = -\frac{E\alpha T}{1-\nu}\frac{a^3\sqrt{1-e^2}}{2(a^2+\kappa)^2\sqrt{c^2+\kappa}}\left[1 + \frac{r^2+e^2a^2}{\sqrt{(r^2-e^2a^2)^2+4e^2a^2z^2}}\right]yz$$

In the foregoing expressions $r^2 = x^2 + y^2 + z^2$ and

$$a^2 + \kappa = \frac{1}{2}\left[r^2 + e^2a^2 + \sqrt{(r^2-e^2a^2)^2 + 4e^2a^2z^2}\right]$$

$$c^2 + \kappa = \frac{1}{2}\left[r^2 - e^2a^2 + \sqrt{(r^2-e^2a^2)^2 + 4e^2a^2z^2}\right]$$

$$\frac{\partial \kappa}{\partial x} = \left[1 + \frac{r^2 - e^2a^2}{\sqrt{(r^2 - e^2a^2)^2 + 4e^2a^2z^2}}\right] x$$

$$\frac{\partial \kappa}{\partial y} = \left[1 + \frac{r^2 - e^2a^2}{\sqrt{(r^2 - e^2a^2)^2 + 4e^2a^2z^2}}\right] y$$

$$\frac{\partial \kappa}{\partial z} = \left[1 + \frac{r^2 + e^2a^2}{\sqrt{(r^2 - e^2a^2)^2 + 4e^2a^2z^2}}\right] z$$

Now consider the case of a "prolate spheroid" $c > a$, for which the potential is

$$V = \frac{\pi\rho a^2 c}{c^2 - a^2}\left[\left(2\sqrt{c^2 - a^2} + \frac{x^2 + y^2 - 2z^2}{\sqrt{c^2 - a^2}}\right)\sinh^{-1}\sqrt{\frac{c^2 - a^2}{a^2 + \kappa}} - \frac{\sqrt{c^2 + \kappa}}{a^2 + \kappa}(x^2 + y^2) + \frac{2z^2}{\sqrt{c^2 + \kappa}}\right]$$

This time a will be eliminated by means of the eccentricity $e = \frac{\sqrt{c^2 - a^2}}{c}$, and the formulas for stress will be

$$\left.\begin{aligned}
\sigma_x &= \frac{E\alpha T}{1 - \nu}\frac{c(1 - e^2)}{2e^2}\left[\frac{\sqrt{c^2 + \kappa}}{a^2 + \kappa} - \frac{1}{ec}\sinh^{-1}\frac{ec}{\sqrt{a^2 + \kappa}} - \frac{e^2c^2x}{(a^2 + \kappa)^2\sqrt{c^2 + \kappa}}\frac{\partial \kappa}{\partial x}\right] \\
\sigma_y &= \frac{E\alpha T}{1 - \nu}\frac{c(1 - e^2)}{2e^2}\left[\frac{\sqrt{c^2 + \kappa}}{a^2 + \kappa} - \frac{1}{ec}\sinh^{-1}\frac{ec}{\sqrt{a^2 + \kappa}} - \frac{e^2c^2y}{(a^2 + \kappa)^2\sqrt{c^2 + \kappa}}\frac{\partial \kappa}{\partial y}\right] \\
\sigma_z &= \frac{E\alpha T}{1 - \nu}\frac{c(1 - e^2)}{2e^2}\left[\frac{2}{ec}\sinh^{-1}\frac{ec}{\sqrt{a^2 + \kappa}} - \frac{2}{\sqrt{c^2 + \kappa}} - \frac{e^2c^2z}{(a^2 + \kappa)(c^2 + \kappa)^{3/2}}\frac{\partial \kappa}{\partial z}\right]
\end{aligned}\right\} \quad [9]$$

and

$$\tau_{xy} = -\frac{E\alpha T}{1 - \nu}\frac{c^3(1 - e^2)}{2(a^2 + \kappa)^2\sqrt{c^2 + \kappa}}\left[1 + \frac{r^2 + e^2c^2}{\sqrt{(r^2 + e^2c^2)^2 - 4e^2c^2z^2}}\right] xy$$

$$\tau_{xz} = -\frac{E\alpha T}{1 - \nu}\frac{c^3(1 - e^2)}{2(a^2 + \kappa)^2\sqrt{c^2 + \kappa}}\left[1 + \frac{r^2 - e^2c^2}{\sqrt{(r^2 + e^2c^2)^2 - 4e^2c^2z^2}}\right] xz$$

$$\tau_{yz} = -\frac{E\alpha T}{1 - \nu}\frac{c^3(1 - e^2)}{2(a^2 + \kappa)^2\sqrt{c^2 + \kappa}}\left[1 + \frac{r^2 - e^2c^2}{\sqrt{(r^2 + e^2c^2)^2 - 4e^2c^2z^2}}\right] yz$$

In the foregoing expressions put

$$a^2 + \kappa = \frac{1}{2}\left[r^2 - e^2c^2 + \sqrt{(r^2 + e^2c^2)^2 - 4e^2c^2z^2}\right]$$

$$c^2 + \kappa = \frac{1}{2}\left[r^2 + e^2c^2 + \sqrt{(r^2 + e^2c^2)^2 - 4e^2c^2z^2}\right]$$

$$\frac{\partial \kappa}{\partial x} = \left[1 + \frac{r^2 + e^2c^2}{\sqrt{(r^2 + e^2c^2)^2 - 4e^2c^2z^2}}\right] x$$

$$\frac{\partial \kappa}{\partial y} = \left[1 + \frac{r^2 + e^2c^2}{\sqrt{(r^2 + e^2c^2)^2 - 4e^2c^2z^2}}\right] y$$

$$\frac{\partial \kappa}{\partial z} = \left[1 + \frac{r^2 - e^2c^2}{\sqrt{(r^2 + e^2c^2)^2 - 4e^2c^2z^2}}\right] z$$

All stresses thus considered are for the cold exterior. The most interesting stresses in the cold exterior are those along the axis of the ellipsoid and along a line, through the centroid, perpendicular to the axis. These stresses, along the z and x axes, respectively, have been calculated for different radii of curvature ρ at the ends of the semiaxes of the ellipse $\frac{x^2}{a^2} + \frac{z^2}{c^2} = 1$. The results are plotted in Fig. 1.

Stresses in the Interior of the Hot Ellipsoid

From the form of the potential of an ellipsoid at interior points, it is easily seen that the shear stresses in the interior are all zero and that the normal stresses can be derived from Equations [8] and [9] by putting $\kappa = \frac{\partial \kappa}{\partial x} = \frac{\partial \kappa}{\partial y} = \frac{\partial \kappa}{\partial z} = 0$ and subtracting $\frac{E\alpha T}{1 - \nu}$ according to Equation [1a].

For an "oblate spheroid" these stresses become

$$\sigma_x = \sigma_y = -\frac{E\alpha T}{1 - \nu}\left[1 + \left(\sqrt{1 - e^2} - \frac{1}{e}\sin^{-1}e\right)\frac{\sqrt{1 - e^2}}{2e^2}\right]$$

$$\sigma_z = -\frac{E\alpha T}{1 - \nu}\left[1 + \left(\frac{1}{e}\sin^{-1}e - \frac{1}{\sqrt{1 - e^2}}\right)\frac{\sqrt{1 - e^2}}{e^2}\right]$$

and for a "prolate spheroid"

$$\sigma_x = \sigma_y = -\frac{E\alpha T}{1 - \nu}\left[1 + \left(\frac{1}{e}\sinh^{-1}\frac{e}{\sqrt{1 - e^2}} - \frac{1}{1 - e^2}\right)\frac{1 - e^2}{2e^2}\right]$$

$$\sigma_z = -\frac{E\alpha T}{1 - \nu}\left[1 + \left(1 - \frac{1}{e}\sinh^{-1}\frac{e}{\sqrt{1 - e^2}}\right)\frac{1 - e^2}{e^2}\right]$$

It is interesting to note that the normal stresses in the interior are all constant and dependent only upon the shape of the ellipsoid, as exemplified by the eccentricity e.

Inside a hot sphere it is easily seen that the normal stresses are all equal to $-\frac{2}{3}\frac{E\alpha T}{1 - \nu}$, while inside a pancake-shaped ellipsoid the stresses are found to be $\sigma_x = \sigma_y = -\frac{E\alpha T}{1 - \nu}$ and $\sigma_z = 0$. Inside a needle-shaped ellipsoid, the normal stresses are $\sigma_x = \sigma_y = -\frac{1}{2}\frac{E\alpha T}{1 - \nu}$ and $\sigma_z = -\frac{E\alpha T}{1 - \nu}$.

Solution to Problem 2

Stresses set up in an "isotropic infinite solid" when part of it, bounded by a "semi-infinite circular cylinder," is at a higher uniform temperature than the rest of the solid.

As far as the author has been able to ascertain, the potential of a semi-infinite circular cylinder is not known. However, it is the second derivatives of this potential which are required in order to find the stress, and the determination of these second derivatives constitutes the major part of this problem.

The first derivatives of the potential of a homogenous body can be found in terms of a surface potential by means of Gauss's

theorem. Then the attraction at a point P of a solid body of any form, when resolved parallel to any straight line (taken as the axis of x), is given as

$$\frac{\partial V}{\partial x} = \rho \int \frac{\cos\theta}{r}\, d\omega$$

where ρ is the constant density of the body, r the distance from P to any element $d\omega$ of the area of the surface, and θ is the angle the normal at $d\omega$, drawn inward, makes with the positive direction of x. This is true both for external and internal points.

The co-ordinate system is now located in such a manner that the origin is at the center of the base circle and the positive z axis forms the axis of the cylinder. The base of the semi-infinite circular cylinder, then, lies in the xy plane. The attraction in the z direction is readily seen to be the potential of the surface of the base of the cylinder with a mass density ρ per unit of area.

The potential (7) of a circular disk of radius a and mass density ρ per unit of area is

$$\frac{\partial V}{\partial z} = 2\rho a^2 \int_{\lambda_1}^{\infty} \sqrt{1 - \frac{r^2}{a^2+\psi} - \frac{z^2}{\psi}}\, \frac{d\psi}{(a^2+\psi)\sqrt{\psi}} \quad \ldots [10]$$

where the disk lies in the xy plane with the center at the origin. The quantity $r^2 = x^2 + y^2$, and λ_1 is the algebraically larger (positive) root of the equation

$$\frac{r^2}{a^2+\lambda} + \frac{z^2}{\lambda} = 1 \quad \ldots [11]$$

the smaller (negative) root of which is λ_2. Solving Eq. [11] gives

$$\left.\begin{aligned} \lambda_1 &= \frac{1}{2}\left[r^2 + z^2 - a^2 + \sqrt{(r^2+z^2-a^2)^2 + 4a^2z^2}\right] \\ \lambda_2 &= \frac{1}{2}\left[r^2 + z^2 - a^2 - \sqrt{(r^2+z^2-a^2)^2 + 4a^2z^2}\right] \end{aligned}\right\} \quad \ldots [12]$$

Differentiating Equation [10] and putting $\rho = -\dfrac{1+\nu}{1-\nu}\dfrac{\alpha T}{4\pi}$ yields

$$\left.\begin{aligned} \frac{\partial^2\varphi}{\partial x \partial z} &= \frac{1+\nu}{1-\nu}\frac{\alpha T}{2\pi} a^2 x \int_{\lambda_1}^{\infty} \frac{d\psi}{(\psi+a^2)\sqrt{(\psi+a^2)(\psi-\lambda_1)(\psi-\lambda_2)}} \\ \frac{\partial^2\varphi}{\partial y \partial z} &= \frac{1+\nu}{1-\nu}\frac{\alpha T}{2\pi} a^2 y \int_{\lambda_1}^{\infty} \frac{d\psi}{(\psi+a^2)\sqrt{(\psi+a^2)(\psi-\lambda_1)(\psi-\lambda_2)}} \\ \frac{\partial^2\varphi}{\partial z^2} &= \frac{1+\nu}{1-\nu}\frac{\alpha T}{2\pi} a^2 z \int_{\lambda_1}^{\infty} \frac{d\psi}{\psi\sqrt{(\psi+a^2)(\psi-\lambda_1)(\psi-\lambda_2)}} \end{aligned}\right\} \quad \ldots [13]$$

Evaluation of the elliptic integrals (8) in Equation [13] and substitution into the formulas for stress gives

$$\left.\begin{aligned} \tau_{xz} &= \frac{E\alpha T}{1-\nu}\frac{a^2 x}{\pi}\frac{K-E}{(a^2+\lambda_2)\sqrt{a^2+\lambda_1}} \\ \tau_{yz} &= \frac{E\alpha T}{1-\nu}\frac{a^2 y}{\pi}\frac{K-E}{(a^2+\lambda_2)\sqrt{a^2+\lambda_1}} \end{aligned}\right\} \quad \ldots [14]$$

everywhere in the infinite solid, and

$$\sigma_z = \frac{E\alpha T}{1-\nu}\frac{z}{\pi\sqrt{a^2+\lambda_1}}\left\{\frac{dn(v,k')}{k'^2 sn(v,k') cn(v,k')}\left[KE(v,k') + \left(\frac{\pi}{2} - KE'\right)\frac{v}{K'}\right] - K\right\} \quad \ldots [15]$$

for exterior points only. For interior points the normal stress in the direction of the axis of the cylinder is obtained from Equation [15] by subtracting $\dfrac{E\alpha T}{1-\nu}$, according to Equation [1a].

The functions entering into the foregoing formulas for stress are defined in the following manner

$$k = \sqrt{\frac{\lambda_2}{a^2+\lambda_1}} \quad \ldots [16]$$

which quantity is always smaller than 1, as λ_2 is smaller than λ_1. Also k is always taken as positive.

By means of Equation [12], k may be written

$$k = \frac{2ra}{r^2+z^2+a^2+\sqrt{(r^2+z^2-a^2)^2+4a^2z^2}} \quad \ldots [16a]$$

$$k = \frac{r^2+z^2+a^2-\sqrt{(r^2+z^2-a^2)^2+4a^2z^2}}{2ra} \quad \ldots [16b]$$

K and E are the complete elliptic integrals of the first and second kind, respectively, and K' and E' are the same complete elliptic integrals with modulus $k' = \sqrt{1-k^2}$.

Also

$$v = \int_0^{\varphi'} \frac{d\varphi}{\sqrt{1-k'^2\sin^2\varphi}}$$

$$E(v,k') = \int_0^{\varphi'} \sqrt{1-k'^2\sin^2\varphi}\, d\varphi$$

$$sn(v,k') = \sin\varphi'$$

$$cn(v,k') = \cos\varphi' = \sqrt{1-sn^2(v,k')}$$

$$dn(v,k') = \sqrt{1-k'^2\, sn^2(v,k')}$$

φ' is determined (9) by the equation $dn(v,k') = \dfrac{\sqrt{a^2+\lambda_2}}{a}$ and from this all the other elliptic functions, entering into Equation [15], can be found.

From Equation [16a], it is easily seen that k is the same for $z = +m$ as for $z = -m$, where m is any positive number, which then also holds for the elliptic functions and integrals. It follows immediately that the two shear stresses, Equations [14], are symmetrical with respect to the xy plane and that the normal stress σ_z, according to Equation [15] has equal, but opposite, stress for $z = +m$ and $z = -m$.

For the purpose of numerical calculation, the equations for stress can be greatly simplified by means of Equations [12] and [16a and b]; also by putting $r = pa$ and $z = na$, where a is the radius of the cylinder. By introducing cylindrical co-ordinates r, θ, z the two shear stresses, Equations [14], can immediately be reduced to one. Putting $x = r = pa$, $y = 0$, and $z = na$ gives

$$\left.\begin{aligned} \tau_{rz} &= \frac{E\alpha T}{1-\nu}\frac{1}{\pi}\sqrt{\frac{1}{pk}}\,(K-E) \\ \tau_{r\theta} &= 0 \end{aligned}\right\} \quad \ldots [17]$$

By expressing the elliptic functions entering into Equation [15] in terms of p and k and eliminating n by means (10) of Equation [16b] the normal stress σ_z can finally be written as

$$\sigma_s = \pm \frac{E\alpha T}{1-\nu}\left[\frac{K}{\pi}\left(E(v,k') - \frac{v}{K'}E' - \sqrt{\frac{(1-pk)(p-k)}{p}}\right) + \frac{1}{2}\frac{v}{K'}\right] \quad [18]$$

where the plus sign is to be used for positive z and the minus sign for negative z. Equation [18] is good for all external points except the z axis ($p = 0$). To obtain σ_s for internal points, it is only necessary to subtract $\frac{E\alpha T}{1-\nu}$ from the right-hand side of Equation [18].

Along the z axis it can be shown (11) that

$$\sigma_z = -\frac{1}{2}\frac{E\alpha T}{1-\nu}\left[1 + \frac{n}{\sqrt{1+n^2}}\right] \quad [19]$$

where n is positive when z is positive and negative when z is negative, and Equation [19] is good for both external and internal points.

Radial and Tangential Stresses

The radial and tangential stresses can also be found by means of Gauss's theorem. The attraction of the semi-infinite cylinder in the radial direction is the same as the attraction in the x direction for a point in the xz plane, and is equal to the potential of a cylindrical shell with a surface distribution of matter of $-\rho \cos\theta$, θ being the angle between the xz plane and a plane through the axis of the cylinder. As only the second derivatives are required in order to find the stress, it is not necessary to find the potential of the cylindrical shell, but only its attraction in the x direction upon a point in the xz plane. This is done by splitting the surface up into semi-infinite rods of width $a \cdot d\theta$ and mass per unit of length $\rho \cos\theta a d\theta$, and making use of the well-known formulas for the attractions of a semi-infinite rod of uniform mass density (12). This gives

$$\frac{\partial^2 V}{\partial r^2} = a\rho \int_0^{2\pi} \frac{r - a\cos\theta}{r^2 + a^2 - 2ar\cos\theta}\left(1 + \frac{z}{\sqrt{r^2+z^2+a^2-2ar\cos\theta}}\right)\cos\theta d\theta \quad [20]$$

where $r^2 = x^2 + y^2$.

To find the second derivative in the tangential direction of the potential of the solid cylinder, it is only necessary to turn the cylindrical shell 90 deg about its axis and find its attraction in the y direction upon a point in the xz plane. This gives

$$\frac{\partial^2 V}{\partial t^2} = a^2\rho \int_0^{2\pi} \frac{\sin^2\theta}{r^2 + a^2 - 2ar\cos\theta}\left(1 + \frac{z}{\sqrt{r^2+z^2+a^2-2ar\cos\theta}}\right)d\theta \quad [21]$$

Now put $z = na$ and, for r larger than a put $r = pa$, but for r smaller than a put $a = p'r$. Then Equations [20] and [21] will reduce to the form

$$\left.\begin{aligned}\frac{\partial^2 V}{\partial r^2} &= \rho \int_0^{2\pi} \frac{\rho\cos\theta - \cos^2\theta}{p^2 + 1 - 2p\cos\theta}\left(1 + \frac{n}{\sqrt{p^2+n^2+1-2p\cos\theta}}\right)d\theta \\ \frac{\partial^2 V}{\partial t^2} &= -\rho \int_0^{2\pi} \frac{1-\cos^2\theta}{p^2+1-2p\cos\theta}\left(1 + \frac{n}{\sqrt{p^2+n^2+1-2p\cos\theta}}\right)d\theta\end{aligned}\right\} \quad [22]$$

when r is larger than a, and to the form

$$\left.\begin{aligned}\frac{\partial^2 V}{\partial r^2} &= p'\rho \int_0^{2\pi} \frac{\cos\theta - p'\cos^2\theta}{p'^2 + 1 - 2p'\cos\theta}\left(1 + \frac{np'}{\sqrt{p'^2 + n^2p'^2 + 1 - 2p'\cos\theta}}\right)d\theta \\ \frac{\partial^2 V}{\partial t^2} &= -p'^2\rho \int_0^{2\pi} \frac{1-\cos^2\theta}{p'^2+1-2p'\cos\theta}\left(1 + \frac{np'}{\sqrt{p'^2+n^2p'^2+1-2p'\cos\theta}}\right)d\theta\end{aligned}\right\} \quad [23]$$

when r is smaller than a.

Integrating Equations [22] and [23] (13) the following results are obtained

$$\sigma_r = -\frac{E\alpha T}{1-\nu}\frac{1}{4\pi p^2}\left\{\pi + \frac{n}{\sqrt{(p+1)^2+n^2}}\left[\{(p+1)^2 + n^2\}(K-E) - (p^2+2p-1)K\right] \mp (p^2+1)\left[KE(v,k') - \frac{KE'v}{K'} + \frac{\pi v}{2K'}\right]\right\} \quad [24]$$

$$\sigma_t = \frac{E\alpha T}{1-\nu}\frac{1}{4\pi p^2}\left\{\pi + \frac{n}{\sqrt{(p+1)^2+n^2}}\left[\{(p+1)^2 + n^2\}(K-E) + (p-1)^2K\right] \mp (p^2-1)\left[KE(v,k') - \frac{KE'v}{K'} + \frac{\pi v}{2K'}\right]\right\} \quad [25]$$

for r larger than a and, by putting $p = \frac{1}{p'}$

$$\sigma_r = \frac{E\alpha T}{1-\nu}\frac{1}{4\pi}\left\{\pi - \frac{n}{p^2\sqrt{(p+1)^2+n^2}}\left[\{(p+1)^2 + n^2\}(K-E) - (p^2+2p-1)K\right] - \frac{p^2+1}{p^2}\left[KE(v,k') - \frac{KE'v}{K'} + \frac{\pi v}{2K'}\right]\right\} \quad [24a]$$

$$\sigma_t = \frac{E\alpha T}{1-\nu}\frac{1}{4\pi}\left\{\pi + \frac{n}{p^2\sqrt{(p+1)^2+n^2}}\left[\{(p+1)^2 + n^2\}(K-E) + (p-1)^2K\right] - \frac{p^2-1}{p^2}\left[KE(v,k') - \frac{KE'v}{K'} + \frac{\pi v}{2K'}\right]\right\} \quad [25a]$$

for r smaller than a. These are the stresses at exterior points. For interior points the stresses are

$$\sigma_r = -\frac{E\alpha T}{1-\nu}\frac{1}{4\pi}\left\{3\pi + \frac{n}{p^2\sqrt{(p+1)^2+n^2}}\left[\{(p+1)^2 + n^2\}(K-E) - (p^2+2p-1)K\right] - \frac{p^2+1}{p^2}\left[KE(v,k') - \frac{KE'v}{K'} + \frac{\pi v}{2K'}\right]\right\} \quad [24b]$$

$$\sigma = -\frac{E\alpha T}{1-\nu}\frac{1}{4\pi}\left\{3\pi - \frac{n}{p^2\sqrt{(p+1)^2+n^2}}\left[\{(p+1)^2+n^2\}(K-E)+(p-1)^2K\right] - \frac{p^2-1}{p^2}\left[KE(v,k') - \frac{KE'v}{K'} + \frac{\pi v}{2K'}\right]\right\} \quad [25b]$$

In Equations [24] to [25*b*], the elliptic integrals are determined by

$$k^2 = \frac{4p}{(p+1)^2+n^2}$$

$$k'^2 = 1-k^2 = \frac{(p-1)^2+n^2}{(p+1)^2+n^2}$$

$$sn^2(v,k') = \sin^2\varphi' = \frac{n^2}{(p-1)^2+n^2}$$

v and $E(v, k')$ are defined in the same manner as before in the expression for axial stress.

The stress formulas outlined do not hold when p equals zero, or for points along the z axis. In this case, however, it is quite simple to find the attractions of the cylindrical shell at points along its axis (14). This gives

$$\sigma_r = \sigma_t = \frac{1}{4}\frac{E\alpha T}{1-\nu}\left(1+\frac{n}{\sqrt{1+n^2}}\right) \quad [26]$$

for external points (n negative), and

$$\sigma_r = \sigma_t = -\frac{1}{4}\frac{E\alpha T}{1-\nu}\left(3-\frac{n}{\sqrt{1+n^2}}\right) \quad [26a]$$

for internal points (n positive).

From symmetry it is immediately seen that $\tau_{r\theta} = 0$.

The most interesting stresses are those near the end of the cylinder, and particularly at the sharp circular edge. The stresses have been calculated for different values of n and p, and the results are plotted in Figs. 2 to 4.

ACKNOWLEDGMENTS

The author wishes to express his gratitude to Dr. J. N. Goodier, professor of mechanics of engineering, Cornell University, for having suggested the problems of this paper and for invaluable aid in their solution. He also wishes to thank Dr. H. Poritsky, engineering general department, General Electric Company, for a valuable suggestion in the solution of the second problem.

BIBLIOGRAPHY

1 "Mémoire sur le Calcul des Actions Moléculaires developpées par les Changements de Température dans les Corps Solides," by J. M. C. Duhamel, Académie Royale des Sciences de L'Institute de France, vol. 5, 1838, p. 440.

2 "Theory of Elasticity," by S. Timoshenko, McGraw-Hill Book Company, Inc., New York, N. Y., 1934, p. 376.

3 "Untersuchungen über die Elasticität fester isotroper Körper unter Berücksichtigung der Wärme," by C. W. Borchardt, Monatsberichte der Königlich Preussichen Akademie der Wissenschaften zu Berlin, 1873, p. 9.

4 "On the Integration of the Thermoelastic Equations," by J. N. Goodier, *Philosophical Magazine*, vol. 23, 1937, p. 1017.

5 "Slag Inclusions in Relation to Fatigue," by B. P. Haigh, Trans. of the Faraday Society, vol. 20, 1924-1925, p. 153.

6 "Theory of the Potential," by W. D. MacMillan, McGraw-Hill Book Company, Inc., New York, N. Y., 1930, p. 62.

7 "The Stress Produced in a Semi-Infinite Solid by Pressure on Part of the Boundary," by A. E. H. Love, Philosophical Transactions of the Royal Society of London, series A, vol. 228, 1928-1929, p. 398.

8 "Two Problems of Thermal Stress in the Infinite Solid," by N. O. Myklestad, thesis for degree of Doctor of Philosophy, Graduate School, Cornell University, June, 1940.

9 Reference (8), p. 62.

10 Reference (8), p. 64.

11 Reference (8), p. 95.

12 "A Treatise on Analytical Statics," by E. J. Routh, Cambridge, England, vol. 2, 1892, p. 4.

13 Reference (8), p. 80.

14 Reference (8), p. 99.

Discussion

Solution of Problems of Elasticity by the Framework Method[1]

DOUGLAS MCHENRY.[2] The need for a simple versatile method of finding the numerical solutions of particular problems in elasticity has become rather pressing, and the author's description of the framework method may well serve to open an important new field in structural-design methods. To the writer, this need has recently become urgent. By coincidence, his attack upon the problem followed lines identical with those pursued by the author and resulted in what the writer has called a "lattice analogy." The term analogy is used for obvious reasons although, as shown by the author, the plate and the lattice may (as a limiting condition) become identical, in so far as concerns the solution of stress problems. The framework or lattice method was found to be best adapted to two-dimensional problems in plane stress, using the simple cross-braced square frame. For this type of problem, it offers about all that might be desired in the way of versatility and simplicity of computation. The restriction upon the value of Poisson's ratio is a matter of very slight practical importance. Problems involving any type of body forces may be handled readily, as may the formally intractable problem of stress due to temperature differentials. Only minor complications are introduced, if the section cuts through two or more materials of different densities, or different elastic properties (provided that μ is kept at $^1/_3$). Even reinforced concrete may be simulated by the lattice with an apparent degree of success and with little added difficulty in computation.

It is of particular interest to note that, in the braced framework, the state of stress or strain at each joint is completely specified in terms of three direct forces or three elongations, a specification which is in many respects more logical than the conventional one involving shearing stress and strain.[3] In solving a framework, the rather inconvenient concept of shear may be omitted completely.

The amount of labor required by a beginner in the method to reach a satisfactory solution of a practical problem is apt to be discouraging. However, the writer has solved several problems by this method (first, of course, those for which rigorous solutions were also available) and has found that familiarity with the method will suggest numerous devices to effect great savings in time and labor. The cost of a solution is in most cases probably comparable to that of a photoelastic analysis, and many problems can be handled satisfactorily by either method. However, for certain problems, one or the other of the two methods may possess a distinct superiority.

The method of solving the highly indeterminate framework may be selected to suit the preference of the computer, but some systematic method of successive approximation appears to be called for. The writer recommends that, in the plane-stress problem, the solution be carried out entirely in terms of displacements. The successive release of joints along a loaded boundary will yield a first approximation to the boundary displacements; then, with the boundary fixed in its new position, the interior displacements, resulting from the successive release of interior joints, may be computed without regard to the forces causing these displacements. The unbalanced forces may be computed as a final step to investigate the accuracy of the solution. Considering, for example, the four-frame assembly of the author's Fig. 7, if the horizontal and vertical components of displacement are designated h and v, with the joints lettered a, b, c, ... h, with a at the top center, then with given displacements assigned to the eight surrounding joints, we have for the corresponding displacement of the center joint, o

$$h_o = \frac{1}{12}\,(h_b + v_b + 4h_c + h_d - v_d + h_f + v_f + 4h_g + h_h - v_h)$$

$$v_o = \frac{1}{12}\,(4v_a + h_b + v_b - h_d + v_d + 4v_e + h_f + v_f - h_h + v_h)$$

The corresponding equations for other assemblies, either with or without boundary loads or body forces, may be easily derived.

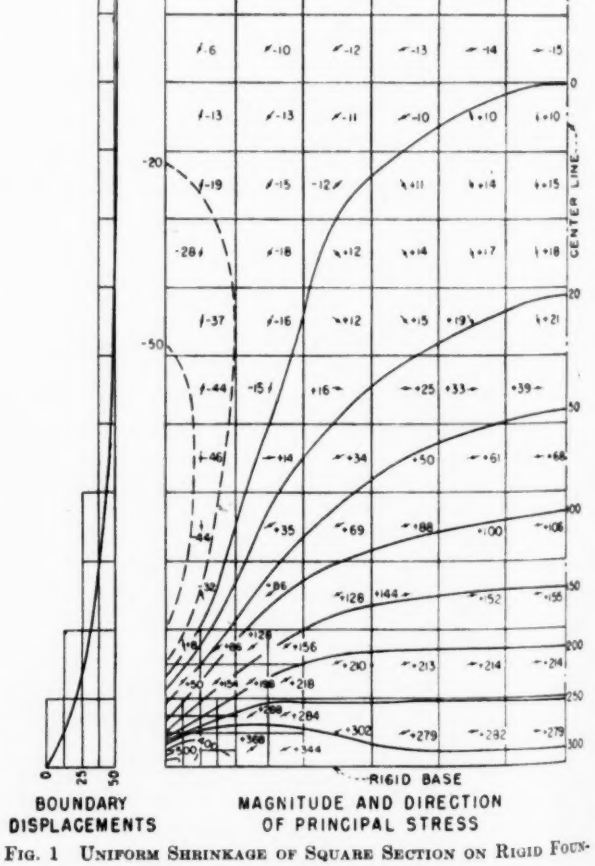


FIG. 1 UNIFORM SHRINKAGE OF SQUARE SECTION ON RIGID FOUNDATION

(Magnitude of numerically greatest stress shown by contours, direction by dashes. For uniform shrinkage of 100 millionths inch per inch, displacements are in millionths of base length and stresses are in pounds per square inch if $E = 3 \times 10^6$.)

[1] By A. Hrennikoff, published in the December, 1941, issue of the JOURNAL OF APPLIED MECHANICS, Trans. A.S.M.E., vol. 63, p. A-169.

[2] Engineer, U. S. Bureau of Reclamation, Denver, Colo.

[3] This point is discussed in "A New Specifying Method for Stress and Strain in an Elastic Solid," by Lord Kelvin, Proceedings of the Royal Society of Edinburgh, vol. 24, 1901–1902, pp. 97–101.

At each step, total displacements (rather than increments) are computed directly. Thus the shape of the deformed structure is continuously visualized, a condition which aids in introducing estimated displacements to speed the convergence of the process. Such estimates can and should be used freely; for the final result must be correct within some specified reasonable error regardless of the course by which it is reached.

The relaxation concept as described is a convenient one in that it assigns an easily visualized physical meaning to the adjustment process. However, it should be pointed out that mathematically the process is simply an iterative one, corresponding closely to the well-known method of solving Laplace's equation for given boundary conditions by averaging, at each point, assigned values at four equidistant surrounding points.

A typical solution of considerable practical interest is shown by Fig. 1 of this discussion, representing the stresses and the boundary displacements produced by uniform shrinkage of a square section on a rigid foundation. The framework method is particularly well adapted to this type of problem, for solutions from given displacements converge more rapidly than do those from given forces.

The possibility of constructing framework models for the solution of two-dimensional problems should receive consideration. The scheme appears to be entirely feasible provided the models are prestressed in tension to avoid buckling of the members under compressive stress.

Author's Closure

The similarity of the method of "lattice analogy," used by the discusser, with the author's framework method is very interesting, and the type of the lattice pattern, employed by the discusser, seems identical with the author's simple square framework. This type is suitable for solving all plane-stress problems in which the value of Poisson's ratio is $1/3$, as well as the problems involving other values of μ, in which the boundary conditions are represented by some known forces on the periphery of the framework. However, if some body forces, temperature distortions, or some known boundary displacements enter the question, the use of the simple square pattern is theoretically incorrect. This remark applies to the problem of shrinkage of a wall on a rigid foundation, illustrated in Fig. 1 of the discussion, since the value of Poisson's ratio of concrete is considerably below $1/3$. The use of the general type of square framework, suitable for any value of μ, would have obviated this error. This objection should not, however, detract from giving the discusser due credit for solving the problem of such complexity. The same criticism would apply also to photoelastic solutions of the problems just referred to, and in this fact there lies a distinct advantage of the framework method over the photoelastic method.

In analyzing framework stresses, the author has found the distribution procedure outlined in the paper to be the most convenient method of solution, especially in conjunction with the principles of symmetry and antisymmetry. It is true that the proficiency of such work depends a great deal upon the experience of the computer, and the results are likely to be discouraging for a beginner; but, once the technique of the distribution is mastered and the short cuts are well understood, some very formidable framework analyses may be accomplished expeditiously. Thus, in one of the problems solved by the author, an 8 by 12 simple square framework, acted upon by unsymmetrical forces, was analyzed and checked in approximately 200 hr, in which period of time the unbalanced joint forces were reduced from several thousand pounds to fractions of a pound. An equivalent solution by joint displacements, along the lines which are suggested by the discusser, would involve 231 simultaneous equations, and the labor required for it would be entirely out of the question.

The writer joins the discusser in recommending construction of a model of the square framework with $\mu = 1/3$. However, a model of the general type of square framework would seem to be impossible.

The Technical Cohesive Strength of Metals[1]

R. G. Sturm.[2] It is a real contribution to human progress when a new concept, such as technical cohesive strength of metals, or any other arbitrarily defined concept, is set forth for study and verification. Such a concept has been presented by W. Kuntze, who has shown considerable experimental evidence to establish trends in this "property" which he has introduced. It is a further contribution when such a new concept is critically examined and compared with the facts of human experience, in so far as such facts are obtainable. This the author has done very carefully. Inasmuch as Kuntze's work was written in German, it would have added considerable value to the author's paper if he had, at the beginning, outlined just what phenomena in the behavior of metals during the production of metal parts or in the service of these parts are indicated by the technical cohesive strength of metals.

The writer is not as familiar with Kuntze's work as he would like to be, but perhaps the author could give an answer to two specific questions for the benefit of practical physicists and engineers. Does the technical cohesive strength help to explain internal fractures sometimes encountered in overdrawn wire? Does the technical cohesive strength have anything to do with longitudinal splitting of brittle materials subjected to axial compression?

Apparently most investigators have found that in determining the technical cohesive strength, as in determining tensile strength, the speed of deformation is frequently a significant factor. For example, a recent test indicates that a bar held a sustained load of 50 per cent of the short-time tensile strength for $10^1/_2$ years and then failed. The elongation of the bar at the end of this long-time test was about 9 times the elongation obtained in the short-time test. It took approximately 8 years for the specimen to exhibit any indication of failure. This left $2^1/_2$ years for the failing process to continue. Actual stress based on the reduced area at fracture was 63 per cent of the nominal short-time tensile strength of the material. The question occurs: Did the material fracture when the actual stress reached the technical cohesive strength? If so, is this the technical cohesive strength of the original material in the bar or the material that has been elongated an amount equal to 9 times the elongation obtainable in a short-time test?

The writer would like further to supplement the author's examination of the technical cohesive strength obtained by notched specimens. It is true that, at the base of a notch of predetermined size and shape in a round specimen, the calculated stress concentration for an elastic material would be the same regardless of the over-all dimensions of the material, as long as the geometry of the notch and specimen is not changed. However, it is not possible to change grain size as we change specimen size. A sharp notch has a radius comparable to the grain size of metals. As soon as plastic action occurs at the base of a notch, the distribution of stresses in the vicinity of the notch is obviously changed, and the extent of this change in stress distribution would

[1] By D. J. McAdam, Jr., published in the December, 1941, issue of the Journal of Applied Mechanics, Trans. A.S.M.E., vol. 63, p. A-155.

[2] New Kensington, Pa. Mem. A.S.M.E.

be expected to vary with the amount of local deformation which takes place. Therefore at the center of the specimen there exists an entirely different phenomenon than exists immediately adjacent to the base of the notch. In view of the uncertainty in the determination of the technical cohesive strength, the author is quite justified in raising the question as to whether or not it is the technical cohesive strength or some other value which governs fracture of metals.

Author's Closure

Mr. Sturm has made a very welcome contribution to the discussion. His description of the results of a very lengthy test of a specimen under steady load is very interesting. The influence of the factors involved in this experiment will be discussed by the author in a paper now in preparation. Mr. Sturm's reference to the initial stress concentration and the deformation gradient in the cross section apparently indicates that he agrees with the views on this subject, expressed in the paper. The final sentence in his discussion, however, indicates a misunderstanding. The views expressed in the paper are in entire accord with the idea that fracture is determined by the technical cohesive strength, in the absence of an important stress gradient (premature fracture). The technical cohesion limit, however, has been shown to depend on the combination of principal stresses.

An Extension of the Sand-Heap Analogy in Plastic Torsion Applicable to Cross Sections Having One or More Holes[1]

R. E. Bruckner.[2] The method given in this paper for determining the torsional strength of irregularly shaped sections is so simple and readily understandable as to be of great value to the average designing engineer who is apt to be a bit rusty in his mathematics. The writer tried to check the author's Equation [1]

$$M = 2\frac{k}{m}V$$

as applied to a solid circular shaft against the conventional formula, such as that given by Timoshenko.[3]

Assume a shaft 5 in. diam of solid cross section with a value for the surface shear stress

$$S_s \text{ or } k = 5000 \text{ psi}$$

Calculated by the conventional method, the allowable torque load would be

$$(\pi/16)5^3 \times 5000 = 122{,}000 \text{ lb-in.}$$

Calculated by the author's Equation [1], and assuming various values for the slope m, the torque load becomes 164,000 lb-in., which is roughly 33 per cent larger than the allowable load calculated by the conventional formula, which considers the polar moment of inertia of the cross section. The present writer has been unable to resolve this discrepancy.

It is of interest to note that the ratio V/m is a constant for circular sections. Does this hold true for all sections? If so, this fact would be of importance.

A. Nádai.[4] Problems of finding the distributions of stress in perfectly plastic bodies, with cross sections connected in multiple, have some remarkable properties not encountered, for example, in the corresponding elastic states of stress. If a small disturbance is produced along one of the boundary curves of the area for which the plastic solution is sought, observation and also the theory show that it will propagate itself into the interior along definite curves. In the case of the plastic torsion of a bar, these curves are the normals of the boundary curve of the cross section of the twisted bar, i.e., the projections of the straight generatrices of the surface of constant slope which can be constructed above the boundary curves on the plane of the cross section.

If a small notch is made in the boundary line of the cross section, a small quantity of sand will run off from the surface of constant slope along the straight generatrix passing through the notch, but the shape of the sand heap otherwise will not be disturbed except along this narrow strip.

If the cross section has one or more holes in its interior, each point of the inner boundary curves must be considered as a center of a disturbance. The result of these disturbances is that new surfaces of constant slope will be generated around each hole and the external boundary line. The author is to be commended on having clarified the conditions to be met when the cross-sectional area has one or several holes, and of having determined the heights required of the planes in which the bases of these new surfaces of equal constant slope have to be assumed. An interesting fact becomes evident, namely, that the heights of the bases are independent of each other.

The rule which determines the heights is also extremely simple. The plane above a hole parallel to the base plane of the cross section must be raised to that height at which the generatrix, which marks the shortest distance between the external boundary curve and the boundary of the hole, intersects this latter curve. Therefore, the first thing to do is to draw the normals to the external boundary curve of the cross section and to find the ones having the shortest lengths measured between the external boundary curve and the nearest boundary of a hole. The heights at which these "shortest" generatrices reach the surfaces of the holes determine the inner edges of the surfaces of constant slope starting from the holes. The base planes above the holes have to be adjusted at such heights that the corresponding "inner" surfaces of constant slope do not cut away anything from the "shortest" generatrices.

This has been illustrated by three examples, shown by their contour lines in Fig. 1 (*a*), (*b*), and (*c*).[5] Following the schemes indicated by the author, brass models[6] were also made of the first two, as shown in Fig. 2 of this discussion. After correct adjustment of the tubes marking the inner edges, the sand heaps, Figs. 3 and 4, were produced. Since in these two models only circles and straight lines are used in the external boundary and in the curves determining the holes, the surfaces of constant slope which correspond to them are either straight circular vertical cones or planes, all having the same slope. The projections of the inner ridges along which the surfaces intersect each other

[1] By M. A. Sadowsky, published in the December, 1941, issue of the Journal of Applied Mechanics, Trans. A.S.M.E., vol. 63, p. A-166.

[2] Mem. A.S.M.E.

[3] "Strength of Materials," by S. Timoshenko, part 1, D. Van Nostrand Company, Inc., New York, N. Y., 1930, Equation [54], p. 70.

[4] Consulting Mechanical Engineer, Westinghouse Research Laboratories, East Pittsburgh, Pa. Mem. A.S.M.E.

[5] With particular reference to Fig. 1. (*a*), subsequent to the presentation of this discussion at the National Meeting of the Applied Mechanics Division, at Philadelphia, on June 20, 1941, Prof. N. M. Newmark of the University of Illinois advised the writer that a figure representing the stress surface of a round bar in torsion, having an eccentric circular hole, already had been published by H. M. Westergaard. ("Graphostatics of Stress Functions," by H. M. Westergaard, Trans. A.S.M.E., vol. 56, 1934, pp. 141–149, Fig. 3.) In that paper, the rule of using the shortest distance between the inner and outer boundaries was also mentioned.

[6] The models were constructed by S. W. Hagerling.

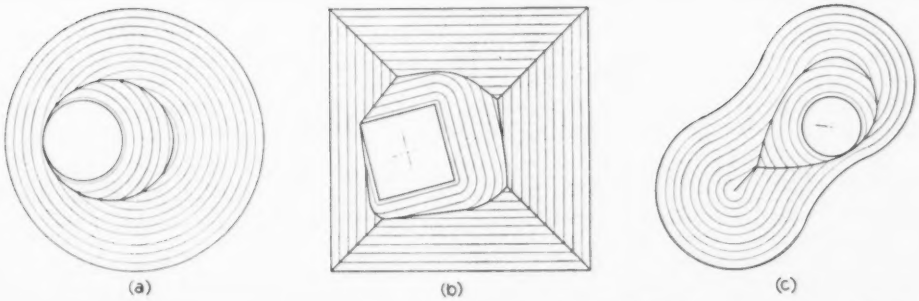


FIG. 1 PLASTIC TORSION; STRESS SURFACES FOR BARS HAVING CROSS SECTIONS WITH HOLES

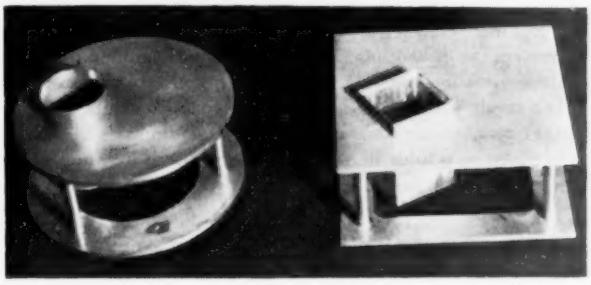


FIG. 2 FRAMES FOR PRODUCING SAND HILLS

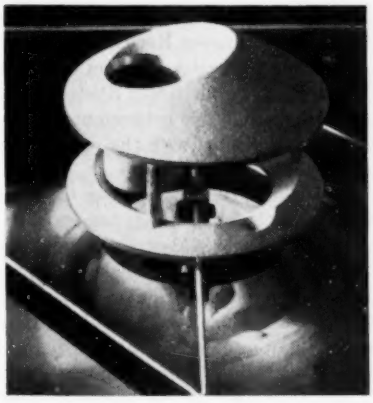


FIG. 3 STRESS SURFACE FOR CIRCULAR CROSS SECTION HAVING A CIRCULAR HOLE

are either portions of straight lines or else arcs of ordinary parabolas (intersection of a cone with a plane having the same slope as the generatrices of the cone).

The case of the plastic torsion of a bar with a circular cross section, having an eccentric circular hole, Figs. 1 (*a*) and 3, leads to a stress surface consisting of two equal circular cones. A "ridge"

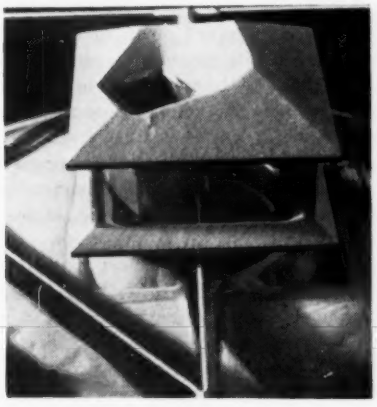


FIG. 4 STRESS SURFACE FOR SQUARE CROSS SECTION HAVING A SQUARE HOLE

appears in this case which has degenerated to a true ellipse both in space and in its projection on the base plane shown in Fig. 1 (*a*). It is perhaps of interest to note that, in the case of a square cross section with a square hole, the inner surface consists of four planes and of four inverted cones the apexes of which are situated in the corners of the holes. The sand heap around three of the re-entrant corners consists of such cones, as can indeed be verified by comparing the shape shown in Fig. 4.

AUTHOR'S CLOSURE

Mr. Bruckner rightly observes that the torsional moment, M, is smaller in elastic ("conventional") torsion than in plastic torsion. For a circular cross section the ratio of the corresponding torsional moments is 3:4 which confirms Mr. Bruckner's 33 per cent. The ratio V/m is constant for any shape of the cross section.

The author wishes to express his particular appreciation to Dr. Nádai and Mr. Hagerling for the experimental realization of the models and for the photographs.

Book Reviews

Track Stress Research

TRACK STRESS RESEARCH PROGRESS REPORT, November, 1935—November, 1938, Government of India Railway Department. By W. E. Gelson and E. A. Blackwood, Investigating Officers. East Indian Railway Press, Calcutta, India, 1939. Cardboard, 8½ × 13 in., Vol. 1, 113 pp., 74 figs.; Vol. 2 (Appendices), ix and 309 pp. of curves and figures. Each volume Rs. 10 or 16s.

REVIEWED BY B. F. LANGER[1]

THIS publication is a report of an investigation which was undertaken to find the answers to some specific problems regarding the adequacy of the track used in Indian railways. It is of interest to readers in this country because it is a good report on what was apparently a well-conducted study. The quantitative results must be considered with due regard for the differences between American and British track construction. The majority of tests were made on Bull head rails of less than 100 lb weight.

The subjects studied included the effect of speed, the adequacy of rail joints, the stability of track in the ballast (forces necessary to produce permanent distortion), the stresses in rails, and the forces produced by hunting movements of locomotives.

In the study of speed effect, the rail was considered in the conventional way as a beam on an elastic foundation, and the differential equations were solved for both static and moving loads. The theory was found to agree quite well with the measured stresses at low speed. At higher speeds the measured vertical deflections agreed fairly well with the theoretical values, but the bending stresses were found to be higher than those predicted except when the rails and fastenings were in excellent condition. Empirical formulas are given for the effect of speed, based on maximum test values for various types of vehicles.

On the subject of rail joints, it was found that most of those tested were inadequate. A joint always produces a discontinuity in track stiffness which can be at best only partly compensated by extra support at the joint. Therefore joints have an important effect on stresses produced by dynamic loads. It is the opinion of the investigators that a large part of the impact effect is due to inadequacy of the joints.

The problem of measuring the lateral force necessary to produce permanent distortion of the track has always been a difficult one because a moving load can displace the track in the ballast more easily than a static load. The investigators made static tests but also supplemented them with dynamic tests in which two locomotives were lashed together and run on parallel tracks. Lateral force was obtained by means of springs which pushed the locomotives apart. On the basis of 4 mm permanent distortion as the criterion of failure, the critical loads were found to vary from 12.2 to 14.9 English tons. The tests showed that the lateral strength of track depends chiefly on the tie spacing and the value of the grip the ties take in the ballast. The type of rail was found to have no appreciable effect within the limits of the experiments.

The investigators were well aware of the fact that failure of the rail itself is not generally produced by the primary bending stress but by secondary stresses associated with distortions of the rail cross section. Photoelastic tests were made in which the distortion measured in a full rail was reproduced in a two-dimensional xylonite model. These tests showed the importance of the fillet under the head as a possible point of failure under the action of eccentric vertical load.

Flange forces were measured on the locomotives during operation by means of tubular struts arranged so as to take the lateral forces between the flanges and the locomotive frame. The compression of the struts was measured with electromagnetic strain gages. Other instruments used included optical deflectometers for recording vertical rail deflection, Baldwin-Southwark inductor telemeters for measuring rail stress, and various simple but adequate devices for applying and measuring effects of static loads.

As a result of the tests the authors were able to draw many important conclusions, some of which are mentioned here, as well as to make up a table of safe speeds for various locomotives and cars on various types of track.

[1] Mechanics Department, Westinghouse Research Laboratories, East Pittsburgh, Pa.

Thermodynamics

THERMODYNAMICS. By Joseph H. Keenan. John Wiley and Sons, Inc., New York, N. Y., 1941. Cloth, 6 × 9 in., xi and 499 pp., 221 figs., $4.50.

REVIEWED BY MILTON C. STUART[2]

IT IS gratifying that Professor Keenan, who has long since attained pre-eminence in the development of tables of numerical values of thermodynamic properties of fluids, should now present an exposition of the relationships between properties and the heat and work quantities associated with the processes of science and engineering.

In a broad sense, this book accomplishes three things. It presents those basic principles of thermodynamics which are common to all processes, it illustrates the engineering applications in an unusually effective manner, and it breaks down the boundaries which have heretofore seemed to isolate into compartments the thermodynamics of mechanical engineering, physics, and chemistry. The present-day mechanical engineer needs to be able to apply in the expanding fields of engineering some parts of thermodynamics formerly held sacred as chemical thermodynamics. On the other hand, the chemical engineer may profit from a knowledge of the applications of the science which were exclusively within the province of the mechanical engineer.

A few of the headings of the twenty-six chapters reveal the scope of the book: The First Law of Thermodynamics, Properties of a Pure Substance, the Second Law of Thermodynamics, Reversibility, Availability, the Reciprocating Steam Engine, Steam Turbine, Heat Engine Cycles, Mixtures of Gases and Vapors, Refrigeration, Heat and Power From Combustion, the Flow of Fluids in Ducts, the Relation Between Pressure, Volume, and Temperature, Thermodynamic Temperature and the International Scale of Temperature, Equilibrium of a Pure Substance Supersaturated Vapor and Superheated Liquid, Chemical Equilibrium, and the Chemical Potential.

A brief survey of the author's definitions of the basic thermodynamic concepts will be of interest. Heat and work are both emphasized as being transient forms of energy. Heat is defined as energy "which transfers from one system to a second system at lower temperature, by virtue of the temperature difference . . ."

[2] Professor of Mechanical Engineering, Lehigh University, Bethlehem, Pa. Mem. A.S.M.E.

Work is interpreted in a generalized fashion as energy flowing "from a system (and to another) during a given operation if the sole effect external to the system could be the rise of a weight." Of the various possible avenues of approach to the internal-energy concept, the author chooses that which defines the internal-energy change of a system as the integral of the heat and work during a change of state of the system. The fact that this integral is zero for a cyclic process is the First Law, and leads to the important conclusion that the internal-energy change between any two states is independent of the type of process by which the system passes between two states. Internal energy thus joins the family of properties of a system.

The author rejects entirely the molecular view of internal energy because "it is generally true that the exposition of thermodynamics is simplified by ignoring the molecule." It must be pointed out, however, that the molecule is not ignored on page 366, where is explained the method of experimental determination of the internal energy of water vapor by examination of band spectra. There need be no quarrel here between different schools because all realize that thermodynamics is, as stated in the first sentence of Professor Keenan's book, only "the science of the relationship between heat, work, and the properties of systems." Numerical values of properties must be found by empirical methods borrowed from other sciences.

It has been said that there are at least fifty statements of the Second Law of thermodynamics. The author paraphrases Planck's statement, "It is impossible to construct an engine which will work in a complete cycle and produce no effect except to raise a weight and exchange heat with a single reservoir." As a consequence of this law, entropy is defined as the integral of dQ/T for any reversible path between two state points.

The temperature function is derived in a most satisfactory manner without fuss or feathers in chapter 21. The most violent purist could find no fault in the author's definition of other thermodynamic functions, such as enthalpy and the specific heats.

It is impossible to mention here the many features which are original or are treated in a unique manner. Among those which appeal to this reviewer are: The presentation of two categories of internal energy, one bearing the symbol U, which is a function of thermodynamic properties, the other bearing the symbol E, which includes U and all other forms of stored energy; the approach to the steady flow process through a more general treatment of an "open system;" the analysis of the steam turbine based on zero angles of approach and departure of the steam through the blading, and on the momentum equation; the emphasis which is placed on availability, in particular the availability studies of the ammonia-absorption cycle, the internal-combustion process, and the steam-power cycle; the use of the b function and the β function; the treatment of the metastable states of supersaturated vapor and superheated liquid; the explanation of the methods for determining numerical values for the properties of fluids; the criteria of equilibrium and the application of equilibrium principles to a pure substance; the use of the Fanno line and the Rayleigh line in flow analysis; and the study of chemical equilibrium and chemical potential, which will serve as an introduction to the mighty work of Gibbs.

An examination of the auxiliary features of the book reveals a list of symbols tabulated for ready reference at the end of the chapter. However, no reference is made to units. This omission may be a point of strength, because the formulas stand in any consistent system of units. At the end of each chapter is a list of ten to twenty problems and questions. Answers are not provided, but the data are well stated and instructions for proceeding are clear. A few examples are solved and explained, but the book has been written with a precision which requires a strong mathematical background for the student.

Professor Keenan has adopted a style which is characterized by comprehensiveness, clearness of exposition, and the avoidance of verbosity. He states in the opening sentence of the preface that "the object of this book is to give a simple and rigorous exposition of the First and Second Laws of thermodynamics." It is the opinion of this reviewer that this object has been attained.

Dynamics of Straight Railroad Track

BEITRAG ZUR DYNAMIK DES GERADEN EISENBAHNGELEISES (Contribution to the Dynamics of Straight Railroad Track). Dissertation completed at the University of Göttingen, Germany, by the reviewer in 1933. 28 pages, 15 × 22 cm., $2 per copy from author.

BY BERTRAM K. HOVEY[3]

BY substituting a substitution in the form of the sum of two exponential terms in a well-known, partial-differential equation of the fourth order for a bar on a continuous, massless, elastic foundation, the general form of the steady-state solution for the motion of the bar when acted upon by a sinusoidally varying force moving with uniform linear velocity along the bar was obtained. The solution consists of two components having damped sine-wave envelopes which disappear at infinity. One of these components proceeds and the other follows the moving load. All the arbitrary constants in the general solution were evaluated by boundary conditions which the two components were required to meet at the moving load. Since the differential equation is linear, the solution for any type of load consisting of a constant term plus harmonic terms can be obtained by superposition.

For the case of a single, sinusoidal load moving with uniform, linear velocity, an auxiliary relationship gives the critical limit for ideal railroad track in the form of a functional relationship between frequency and linear velocity. A calculation for a constant load plus a superimposed sinusoidal load with values selected to correspond to heavy loading of actual railroad track showed that the critical limit, which is lower for a combination of a constant plus a sinusoidal load than for a sinusoidal load alone, was exceeded for ideal railroad track. Evidently, when the loading of actual railroad track is such that this theoretical, critical limit is exceeded, factors not taken into account in the ideal solution limit the amplitude of motion of the track.

Elastic Energy Theory

ELASTIC ENERGY THEORY. By J. A. Van Den Broek, Ph.D., Professor of Engineering Mechanics, University of Michigan. Second edition. John Wiley & Sons, Inc., New York, N. Y., 1942. Cloth, 6 × 9 in., xvii and 298 pp., 95 figs., $4.50.

REVIEWED BY J. N. GOODIER[4]

IN Strength of Materials, and Theory of Structures, deformations are analyzed from (at least) two distinct points of view. One considers the deformations of the infinitesimal elements and builds them up by geometrical considerations into the over-all deflections required. The other avoids the geometry, or most of it, by considering the work-energy relations and deriving deflections from them. In Castigliano's theorem the strain energy is differentiated with respect to a force to give the deflection component in its direction at the point of action. A theorem equivalent to Castigliano's (any distinction between the two being merely in the order of the integration over the elements of the

[3] Instructor in Electrical Engineering, University of Pittsburgh, Pittsburgh, Pa.

[4] Professor in Charge, Department of Mechanics of Engineering, Sibley School of Mechanical Engineering, Cornell University, Ithaca, N. Y. Mem. A.S.M.E.

structure, and the differentiation with respect to the force) is obtained by considering a fictitious force applied where the deflection is to be found and writing down an equation of work which involves the required deflection. This is often called the method of virtual work.

The present book is based on an enthusiasm for this method, as superior to other available methods—notably that of the "elastic curve" in which the deflection curves of bars are separately determined and reconciled geometrically to the deflections of the rest of the structure (curvature is described as "very much of an abstraction"). It deals with a representative group of statically indeterminate problems: the deflections of simple frames; the deflections and stresses of redundant frames; beams, shafts, rings, arches, columns and beam columns (bars under direct thrust and lateral load); and has been the text of courses taught to seniors and advanced engineering students at the University of Michigan. There are 54 problems for the student. The style is close to that of a direct transcript of classroom exposition, salted here and there with statements of a downright quality. There is explicit insistence on logic, and on such points as clarity in rules of sign, in several interesting passages. Nevertheless this second edition of the book is not altogether free from unintended examples of confusion in word meanings, statements of assumptions, and definitions, stated and implied.

The book will continue to be valuable to those who share the author's preference for the method it advocates and expounds, and it will interest those who wish to estimate the place and scope of the method in structural theory. The second edition differs from the first (1931) mainly in a revision of notation to a more orthodox form, and in the addition of sections on piston rings, pipe problems, spiral springs, and the chapter on columns.

Mechanical Properties of Materials and Design

MECHANICAL PROPERTIES OF MATERIALS AND DESIGN. By Joseph Marin, Professor of Mechanics, The Pennsylvania State College, first edition, McGraw-Hill Book Co., Inc., New York, N. Y., 1942. Cloth, 6 × 9 in., viii and 273 pp., 142 figs., $3.50.

REVIEWED BY R. E. PETERSON[5]

A BOOK of this kind should be considered from two points of view—its use in engineering education and in engineering practice.

Concerning engineering education, the author states that he has used the material covered by the book both for a senior elective course and for a graduate course. The first few chapters are largely covered in the usual strength-of-materials course, but perhaps it is advisable to include these as a brief review in starting an advanced course. The latter part (about half) of the book is largely new material, speaking in terms of textbooks, and should be valuable to anyone preparing for design work.

With regard to engineering practice, this book should constitute a useful addition to the technical library of the more progressive engineers and designers. Professor Marin has concerned himself primarily with fundamental bases of design. In spite of the fact that in some cases the basic principles are not fully established, as the author points out, it is the reviewer's opinion that the most important feature of the book is the demonstration of rational approach in the development of design data. Too many engineers apply handbook formulas without knowing the assumptions on which the formulas are based. A study of Professor Marin's book should give the engineer a better appreciation of the difficulties involved in attempting to estimate the strength of a complicated machine part under a combination of operation conditions.

As to specific criticisms, the reviewer has only a few: Page 136, the "straight-line law" is no more than a convenient design *rule*, whereas the word *law* would imply an interpretation of actual failure conditions; page 123, the error due to transverse shearing stresses mentioned in connection with cantilever machines can be dismissed since these stresses are zero at the surface where failure starts; page 128, the difference between axial and bending fatigue strengths depends on the material and can amount to as much as 30 per cent for certain coarse-grained materials;[6] page 143, a value of unity for k_s is found in many cases if the shear energy theory is used.

The foregoing criticisms are obviously of a minor character; considering the entire book, the reviewer regards it to be of high order. It can apparently be used in special courses in engineering curricula and should also find use in industry in the design of critical machine parts.

Hydraulics of Steady Flow in Open Channels

HYDRAULICS OF STEADY FLOW IN OPEN CHANNELS. By S. M. Woodward and C. J. Posey, John Wiley and Sons, Inc., New York, N. Y., 1941. Cloth, 5¾ × 9 in., viii plus 151 pages, $2.75.

REVIEWED BY BRANDON G. RIGHTMIRE[7]

THIS book is intended not only for use as a text in senior and first-year graduate courses, but also as a guide to practicing engineers. The experience of the authors has enabled them in several instances to include valuable practical information or to detail quick methods of computation. These features make the book especially useful to the occasional worker in this field.

Both the stationary and moving hydraulic jump are treated; a convenient graphical solution being given. Backwater curves are discussed at length, starting with two-dimensional, frictionless flow, proceeding to Bresse's method of treating bottom friction in wide channels, and ending with graphical and step methods of wide applicability. An analysis is made of several typical flow problems, a method of attack on more complex problems being thus indicated. The concluding chapters deal with flow at bends and obstructions, and with nonsteady flow which changes so slowly that dynamic effects are negligible. A form of the continuity equation suitable for the latter flow is developed, and application is made to computing water levels in a pool with changing inflow and discharge rates dependent on the water level.

Throughout the book the fundamentals of hydraulics are assumed known. It has thus been possible to make the mathematical developments brief and to discuss at length the physical aspects of the phenomena. In only one instance is the treatment inadequate, in the opinion of the reviewer. Critical flow is introduced without a demonstration that small surface waves in shallow water move at the critical velocity, although this fact is used later in the book. The statement is merely made, without proof, that appreciable changes in level can exist without work being done on the water. This possibility is described as a condition of unstable, rather than neutral, equilibrium.

There are many figures, which beautifully supplement the text. Several worked examples are given, as well as problems. References to additional material are cited in frequent footnotes.

---

[5] Manager, Mechanics Department, Westinghouse Research Laboratories, East Pittsburgh, Pa. Mem. A.S.M.E.

[6] "Endurance Testing of Steel: Comparison of Results Obtained With Rotating-Beam Versus Axially Loaded Specimens," by R. D. France, Proceedings of the American Society for Testing Materials, vol. 31, part 2, 1931, p. 176.

[7] Assistant Professor of Mechanical Engineering, Massachusetts Institute of Technology, Cambridge, Mass. Mem. A.S.M.E.

Some Two-Dimensional Aspects of the Ejector Problem

By J. A. GOFF[1] and C. H. COOGAN,[2] PHILADELPHIA, PA.

Several investigators have attempted to analyze the performance of the ejector on a one-dimensional basis. Some doubt exists whether such analyses can lead to a rational ejector design because of the questionable validity of certain necessary assumptions. Recently, consideration has been given to the two-dimensional aspects of the problem, and while a rational design has not yet been evolved, the results attained seem to point in the right direction. The theory of turbulent mixing in jets, developed by Tollmien is used as the basis of the study reported in this paper. Tollmien's analysis of the mixing zone produced by a homogeneous air stream issuing into still air of the same pressure and density is reviewed. The authors then extend the theory to allow for the possibility that the driving and driven fluids may have widely different densities.

Introduction

SEVERAL attempts have been made to analyze the performance of the ejector on a one-dimensional basis. Notable among these are the analyses of Stodola (1),[3] Bošnjaković (2), and Flügel (3). All of these are based on the assumptions of uniform, unidirectional velocity over certain sections of interest and of adiabatic flow between sections. Under these assumptions, equations expressing conservation of mass, conservation of energy, and conservation of momentum are w itten down and solved simultaneously. The solution predicts the variation of flow ratio (ratio by weight of driven to driving fluids) with operating pressures and temperatures, and with various area ratios. It is doubtful whether such one-dimensional analyses can lead to a rational design of the ejector, particularly when efficiency is a principal consideration, because of the questionable validity of some of the necessary assumptions. Nevertheless, they have proved useful in the interpretation of experimental data on conventional ejectors and, in some cases, have led to minor improvements in design.

Recently, attempts have been made to consider the two-dimensional aspects of the problem. The starting point is the theory of turbulent mixing in jets first developed by Tollmien (4) as an application of the Prandtl (5) conception of apparent shear stress and mixing length. While none of these attempts has yet produced a rational design, nevertheless they seem to be pointed in the right direction. The present paper is intended as a contribution to further progress in this direction. Tollmien's analysis of the mixing zone produced by a homogeneous air stream issuing into still air of the same pressure and density is reviewed, paying closer attention to features of special importance in ejector design than did Tollmien himself. The theory is then extended to allow for the possibility that the driving and driven fluids may have widely different densities.

Tollmien's Solution

The first case, treated by Tollmien (4), is that of a plane parallel jet issuing into an atmosphere of the same fluid at the same pressure and density, Fig. 1. Tollmien assumes that the width of the mixing zone and, therefore, the magnitude of the mixing length l increase linearly with distance from the point where

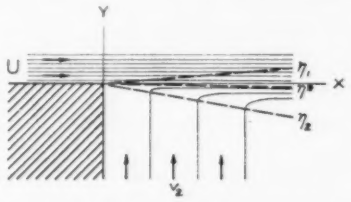


Fig. 1 Tollmien Streamlines

mixing begins. Accordingly, the expression for apparent shear stress becomes

$$\tau = \rho c^2 x^2 (\partial u/\partial y)^2 \quad \ldots\ldots [1]$$

where ρ is the density (assumed constant), c is an empirical constant to be adjusted by comparison with experiment, and u is the x component of the velocity. He then shows that the differential equations, expressing conservation of mass (continuity equation) and conservation of momentum in the x direction together with appropriate boundary conditions, can be satisfied by taking u to be a function of the ratio y/x. Thus, taking

$$u = F'(\eta) \quad (\eta = y/x) \quad \ldots\ldots [2]$$

the continuity equation requires that v, the y component of velocity, be also a function of y/x only, namely

$$v = -F(\eta) + \eta F'(\eta) \quad \ldots\ldots [3]$$

Taking account of Equations [1, 2, 3], the differential equation expressing conservation of momentum in the x direction reduces to

$$F(\eta) + 2c^2 F'''(\eta) = 0 \quad \ldots\ldots [4]$$

Equation [4] is an ordinary differential equation, the general solution of which may be written in the form

$$F/aU = be^{\zeta/2} [-e^{-3\zeta/2} + \cos\theta + f\sin\theta] \quad \ldots\ldots [5a]$$

$$F'/U = be^{\zeta/2} [+e^{-3\zeta/2} - \sin(\theta - \pi/6) + f\cos(\theta - \pi/6)] \quad \ldots [5b]$$

$$aF''/U = be^{\zeta/2} [-e^{-3\zeta/2} - \sin(\theta + \pi/6) + f\cos(\theta + \pi/6)] \quad \ldots [5c]$$

where $\zeta = \eta/a - \eta^*/a$ and $\theta = \sqrt{3}\zeta/2$, a being written for $(2c^2)^{1/3}$ and η^* denoting the solution of $F(\eta) = 0$. The three con-

---

[1] Dean, Towne Scientific School, University of Pennsylvania. Mem. A.S.M.E.

[2] Instructor in Mechanical Engineering, Towne Scientific School, University of Pennsylvania. Mem. A.S.M.E.

[3] Numbers in parentheses refer to the Bibliography at the end of the paper.

Presented at the Annual Meeting, New York, N. Y., December 1–5, 1941, of The American Society of Mechanical Engineers.

Discussion of this paper should be addressed to the Secretary, A.S.M.E., 29 West 39th Street, New York, N. Y., and will be accepted until January 11, 1943, for publication at a later date. Discussion received after the closing date will be returned.

Note: Statements and opinions advanced in papers are to be understood as individual expressions of their authors and not those of the Society.

stants b, f, η^*/a can be adjusted to satisfy appropriate boundary conditions.

The boundary conditions studied by Tollmien are: (a) Along $\eta = \eta_1$, $u = U$, $v = 0$, $\partial u/\partial y = 0$; ($b$) along $\eta = \eta_2$, $u = 0$, $\partial u/\partial y = 0$. These are equivalent to

$$(a)\ \eta = \eta_1;\ F'/U = 1;\ F/aU = \eta_1/a;\ aF''/U = 0$$
$$(b)\ \eta = \eta_2;\ F'/U = 0;\ aF''/U = 0$$

These five boundary conditions determine η_1/a, η_2/a, and the three constants of integration, η^*/a, b, f.

It happens that the two lower boundary conditions (b) themselves determine the values $\zeta_2 = -1.8498$, $f = 32.052$. With the value of f determined, the upper boundary conditions (a) determine the values of η_1/a, η^*/a, and b. The complete solution is as follows

$$\left.\begin{aligned} \eta_1/a &= 0.9814 \\ \eta^*/a &= -0.1855 \\ \eta_2/a &= -2.0353 \\ b &= 0.01985 \\ f &= 32.052 \end{aligned}\right\} \quad \ldots\ldots\ldots\ldots\ldots\ldots [6]$$

The corresponding velocity profiles at any distance x_0 from the origin are shown in Fig. 2. Tollmien (4) compared the theoretical profile u/U, Fig. 2, with that measured on a large wind-tunnel jet at the Aerodynamic Research Institute, Göttingen, and found that good agreement is obtained on taking $a = 0.0845$. Förthmann (6) investigated the open jet, partially open jet, and partially expanding jet. In the case of the open jet, Förthmann found minor systematic discrepancies from Tollmien's theoretical velocity profiles. Kuethe (7) extended Tollmien's theory to the case where the driven fluid has a velocity U_2 parallel to that of the driving fluid U_1.

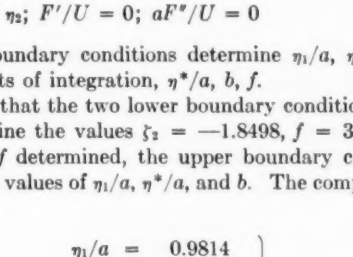


FIG. 2 TOLLMIEN VELOCITY PROFILES

Flow Ratio. This is a quantity which Tollmien neglected to mention, but which is of special interest in connection with the possible application of his analysis to ejector design. It is the ratio of the weight of fluid entering the mixing zone across η_2 between the origin and any section x_0, namely, G_2 (lb per sec), to that entering across η_1 between the origin and the same section x_0, namely, G_1 (lb per sec). Its value is easily computed as follows

$$\frac{G_2}{G_1} = \frac{-x_0F(\eta_2)}{x_0\eta_1U} = \frac{a}{\eta_1}\cdot\frac{F(\eta_2)}{aU} = 0.3868 \ldots\ldots\ldots [7]$$

It is important to note that, according to the Tollmien theory, the flow ratio has the nature of a universal constant, being independent of the velocity U of the driving fluid, independent of the density ρ, and independent of the empirical constant a. Its independence of the magnitude of the velocity U of the driving fluid suggests that the only reason for high values of U in the ejector is to provide the necessary kinetic energy to accomplish compression after mixing.

Kinetic Energy. In order to estimate the loss of kinetic energy due to mixing itself, it is convenient first to calculate separate items as follows:

(a) The kinetic energy crossing η_2 between the origin and any section x_0 per unit of kinetic energy crossing η_1 between the origin and the same section x_0, namely

$$-\frac{a}{\eta_1}\left[\frac{F(\eta_2)}{aU}\right]^3 a^2 = 10^{-2}a^2A \text{ (Fig. 4, } \rho_1/\rho_2 = 1)$$

(b) The kinetic energy crossing x_0 between η_2 and η_1 due to the x component of velocity per unit of kinetic energy crossing η_1 between the origin and x_0, namely

$$\frac{a}{\eta_1}\int_{\eta_2}^{\eta_1}\left(\frac{F'}{U}\right)^3 d(\eta/a) = 10^{-1}B \text{ (Fig. 4, } \rho_1/\rho_2 = 1)$$

(c) The kinetic energy crossing x_0 between η_2 and η_1 due to the y component of velocity per unit of kinetic energy crossing η_1 between the origin and x_0, namely

$$\left\{\frac{a}{\eta_1}\int_{\eta_2}^{\eta_1}\frac{F'}{U}\left[-\frac{F}{aU}+\frac{\eta}{a}\cdot\frac{F'}{U}\right]^2 d(\eta/a)\right\} a^2 = 10^{-3}a^2C$$
(Fig. 4, $\rho_1/\rho_2 = 1$)

(d) The loss of kinetic energy in the mixing zone per unit of kinetic energy crossing η_1 between the origin and x_0, namely

$$1 + 10^{-2}a^2A - 10^{-1}B - 10^{-3}a^2C = 10^{-2}D + 10^{-2}a^2E$$
(Fig. 4, $\rho_1/\rho_2 = 1$)

Numerically, this loss per pound of driving fluid is

$$(0.185 + 0.045a^2)\frac{U^2}{2g}$$

The definite integrals in items (b) and (c) were evaluated by mechanical quadrature aided by graphical integration. For $a = 0.0845$ as found by Tollmien, the second term within the parentheses is negligible in comparison with the first. Hence it appears that the kinetic-energy loss should not exceed approximately 18.5 per cent of the kinetic energy of the driving fluid regardless of the value of a.

Thermodynamics. The Tollmien theory assumes uniform pressure and uniform density throughout the mixing zone. Under these conditions the specific enthalpies of driving fluid, driven fluid, and mixed stream are the same; hence the total thermal energy convected out across any section x_0 between η_2 and η_1 is equal to that convected in across η_1 and η_2 between the origin and the given section x_0. Thus, it is necessary to reject heat of amount

$$-{}_0q_{x_0} = 0.185\,\frac{U^2}{2g} \ldots\ldots\ldots\ldots\ldots [8]$$

per unit weight of driving fluid.

In actual practice, it would be difficult, if not impossible, to provide means of rejecting any considerable quantity of heat from the mixing zone, and the mixing would be very nearly adiabatic. This would require an increase of specific enthalpy in the direction of flow and, therefore, if pressure is constant, a decrease in density. Consequently, the Tollmien theory cannot predict accurately the mixing process occurring in the actual ejector where the kinetic energy $U^2/2g$ must be fairly large in order to accomplish the necessary compression in the diffuser. At low velocities U, of course, this defect in the Tollmien theory is relatively unimportant.

TABLE 1 SUMMARY OF CALCULATIONS

θ_1	ρ_1/ρ_2	G_2/G_1	η_1/a	η^*/a	η_2/a	b_1	b_2	f_1	f_2
50	2.233	0.2309	0.8966	—0.1111	—1.961	0.09339	0.02423	6.942	32.05
52	1.822	0.2639	0.9203	—0.1277	—1.978	0.07579	0.02319	8.607	32.05
54	1.487	0.3009	0.9425	—0.1458	—1.996	0.05696	0.02211	11.38	32.05
56	1.214	0.3425	0.9631	—0.1655	—2.015	0.03799	0.02100	16.94	32.05
58	0.990	0.3893	0.9823	—0.1866	—2.036	0.01897	0.01985	33.61	32.05

Streamlines. The equation for a streamline is

$$xF(\eta) = \text{const} \quad [9]$$

The general character of the streamline is shown in Fig. 1. The streamline through the origin satisfies the equation $F(\eta) = 0$, and therefore coincides with the straight line $\eta = \eta^*$. Streamlines of the driving fluid are deflected downward at the line $\eta = \eta_1$ and approach the line $\eta = \eta^*$ asymptotically from above. The streamlines of the driven fluid are deflected to the right at $\eta = \eta_2$ and approach the line $\eta = \eta^*$ asymptotically from below. The theory, therefore, appears to deny the existence of mixing because it predicts distinct streamlines for driving and driven fluids, the driven fluid merely being accelerated by the action of a shearing force at the surface of separation $\eta = \eta^*$. However, it is necessary to remember that these are apparent or mean streamlines only, across which there occurs a continuous exchange of matter and momentum, giving rise to the apparent or mean shear stress.

Along a streamline of the driven fluid, the velocity may increase to a value well above acoustic. Still, the line is one of constant pressure and constant density, so that no compressibility effects and, hence, no critical phenomena should be expected. The only limitations of the theory with respect to the magnitude of the velocity U, besides that discussed under "Thermodynamics," appear to be that (*a*) at very low velocities true turbulent motion may not develop, but instead eddies are formed; (*b*) at velocities exceeding twice acoustic, according to Ackeret (8), the surface of separation between driving and driven fluids becomes stable and true turbulent mixing can only commence at some distance downstream from the nozzle end.

Density Effect

Consider an ejector supplied with air at 100 psi, 70 F exhausting a space filled with air at 0.3 psi, 70 F. The mixing-chamber pressure would be expected to approximate 0.3 psi, hence, in a correctly designed nozzle, the driving fluid would expand isentropically to 0.3 psi, —265 F. Thus the densities of driving and driven fluids would be in the ratio $\rho_1/\rho_2 = 530/195 = 2.72$. To this situation, the simple Tollmien theory cannot apply.

It is possible however on the basis of certain reasonable assumptions to extend the Tollmien theory to the case where driving and driven fluids have widely different densities. These assumptions may be enumerated as follows: (*a*) A line $\eta = \eta^*$ separates the mixing zone into two regions, the upper region having uniform density ρ_1 and the lower region, uniform density ρ_2; (*b*) the line of separation is a streamline in each region along which velocity and apparent shear stress are the same on either side; (*c*) the same boundary conditions apply at η_1 and η_2 as in the simple theory.

Now the magnitude of the shear stress at any point is given by

$$\tau = \rho c^2 x^2 \left(\frac{\partial u}{\partial y}\right)^2 = \rho c^2 [F''(\eta)]^2 \quad [10]$$

and it may be assumed that the constant c is independent of density. Hence, along the line of separation ($\eta = \eta^*$)

$$\eta_1^* = \eta_2^* \quad [11a]$$

$$F_1'(\eta^*) = F_2'(\eta^*) \quad [11b]$$

$$\rho_1^{1/2} F_1''(\eta^*) = \rho_2^{1/2} F_2''(\eta^*) \quad [11c]$$

At the upper boundary ($\eta = \eta_1$)

$$\frac{F_1(\eta_1)}{aU} = \frac{\eta_1}{a} \quad [12a]$$

$$\frac{F_1'(\eta_1)}{U} = 1 \quad [12b]$$

$$\frac{aF_1''(\eta_1)}{U} = 0 \quad [12c]$$

At the lower boundary ($\eta = \eta_2$)

$$\frac{F_2'(\eta_2)}{U} = 0 \quad [13a]$$

$$\frac{aF_2''(\eta_2)}{U} = 0 \quad [13b]$$

These boundary equations determine uniquely the constants η_1/a, η_2/a, η^*/a, f_1, f_2, b_1, b_2 for any given density ratio ρ_1/ρ_2. In the foregoing, the subscript 1 refers to the upper region of uniform density ρ_1, the subscript 2 to the lower region of uniform density ρ_2.

As in the simple theory, the quantities $\zeta_2 = (\eta_2/a - \eta^*/a)$ and f_2 are calculable from the two lower boundary conditions; and, since the density ratio does not appear in these, the values of ζ_2 and f_2 are the same as for the simple theory. The procedure followed in evaluating the remaining constants is to assume a value of $\theta_1 = \frac{\sqrt{3}}{2}\zeta_1$ and compute the corresponding value of f_1 using Equation [12*c*]; then to compute the values of b_1/b_2 and ρ_1/ρ_2 from Equation [11*b*] and [11*c*]; finally to compute η^*/a and b_1 from Equations [12*a*] and [12*b*]. After these constants have been determined, the corresponding value of G_2/G_1 can be computed from

$$\frac{G_2}{G_1} = \frac{\rho_2}{\rho_1} \cdot \frac{a}{1} \cdot \frac{F_2(\eta_2)}{aU} \quad [14]$$

Table 1 summarizes these calculations.

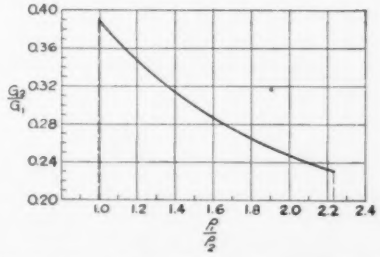


Fig. 3 Flow Ratio Versus Density Ratio

Flow Ratio. Fig. 3 shows the variation of flow ratio G_2/G_1 with density ratio ρ_1/ρ_2. As the density of the driving fluid increases relative to that of the driven fluid, the weight of driven fluid per unit weight of driving fluid decreases. Referring to the examples at the beginning of this section, if the driving fluid be preheated before being supplied to the ejector, its density will be decreased and a higher flow ratio will be obtained. Whether or not a net advantage results, considering the extra energy which must be

supplied, is a question which may be deferred until the applicability of the analysis to ejector design is fully demonstrated.

Kinetic Energy. Referring to the previous discussion of kinetic energy, the various ratios mentioned there can be calculated using the data in Table 1. It is necessary to divide the range of integration into subranges, η_2 to η^* and η^* to η_1; for the integral in the first subrange must be divided by the density ratio ρ_1/ρ_2. Also item (*a*) of the previous section on "Kinetic Energy," requires division by ρ_1/ρ_2. The results are given by the curves in Fig. 4, from which it appears that the loss of kinetic energy due to mixing decreases with increasing density ratio. This might

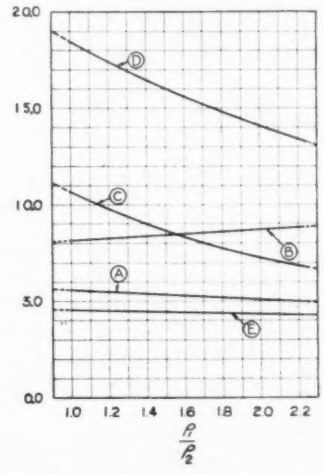


FIG. 4 KINETIC ENERGIES

([*a*] Kinetic energy crossing η_1 per unit kinetic energy crossing $\eta_1 = 10^{-2}a^2$ *A*; [*b*] kinetic energy crossing x_0 per unit kinetic energy crossing $\eta_1 = 10^{-1}$ *B* + $10^{-4}a^2$ *C*; [*c*] kinetic-energy loss per unit kinetic energy crossing $\eta_1 = 10^{-2}D + 10^{-2}a^2E$.)

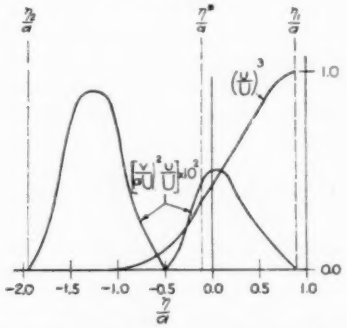


FIG. 5 VARIATION OF KINETIC ENERGY WITH η/a

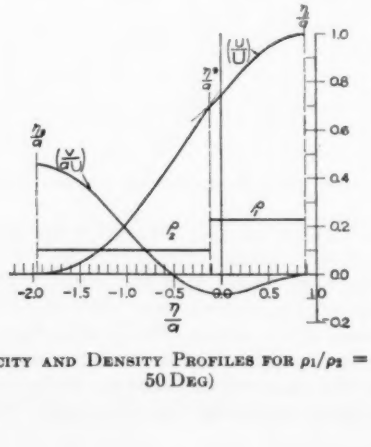


FIG. 6 VELOCITY AND DENSITY PROFILES FOR $\rho_1/\rho_2 = 2.233$ ($\theta_1 = 50$ DEG)

have been expected since the flow ratio also decreases with increasing density ratio. For a density ratio $\rho_1/\rho_2 = 2.233$, for example, the kinetic energy loss is

$$(0.133 + 0.042a^2)\frac{U^2}{2g}$$

per pound of driving fluid.

Fig. 5 is of some interest as showing the variation with η/a of the kinetic energy crossing x_0 on both the x and y components of velocity. Strictly speaking the ordinates to the left of η^*/a must be divided by the density ratio ρ_1/ρ_2 which, in Fig. 5, has the value 2.233.

SUMMARY

Fig. 6 shows velocity profiles similar to those of Fig. 2, but for a density ratio $\rho_1/\rho_2 = 2.233$. It is interesting to note the discontinuities in slope at η^*/a.

Fig. 6 also illustrates an important feature of the solutions obtained for density ratios different from unity by showing the assumed variation in density itself. In view of the analogy between heat transfer and momentum transfer in turbulent flow an abrupt change in density at η^* is not strictly compatible with a continuous velocity distribution. There are reasons to believe, however, that the solution is a good first approximation to the truth.

An apparatus has been designed to conform as closely as possible with the boundary conditions studied by Tollmien and has been tested with air as driven and driving fluid. The velocity of the driving fluid was arbitrarily taken as U = 300 fps, which dictated a pressure ratio of 0.95 for the nozzle. The driven air was supplied at atmospheric pressure by throttling some of the air from the pressure before the nozzle, hence, a density ratio of 1.015 in the mixing chamber. In calculating various dimensions, the value $a = 0.0845$ found by Tollmien was used. Beyond the mixing chamber proper, a convergent passage was added, the walls of which were made streamlines, according to the extended Tollmien theory, this passage being terminated at the point where the y component of velocity vanishes.

The experimental measurements showed a velocity distribution in substantial agreement with the theoretical; and a flow ratio of 0.34 was measured as against 0.382 predicted. It seems reasonable, therefore, to believe that the present theory can be used as a basis for design, though much additional experimentation is required.

BIBLIOGRAPHY

1 "Steam and Gas Turbines," by A. Stodola, McGraw-Hill Book Company, Inc., New York, N. Y., vol. 2, 1927, p. 927.

2 "Über Dampfstrahlgebläse," by F. Bošnjaković, *Zeitschrift für die gesamte Kalte-Industrie*, vol. 43, 1936, pp. 229–233.

3 "Berechnung von Strahlapparaten," by G. Flügel, V.D.I. *Forschungsheft* 395; Suppl. to *Forschung auf dem Gebiete des Ingenieurwesens*, Ausgabe B. vol. 10, March-April, 1939; Berlin, V.D.I. Verlag, 1939.

4 "Berechnung turbulenter Ausbreitungsvorgänge," by W. Tollmien, *Zeitschrift für angewandte Mathematik und Mechanik*, vol. 6, Heft 6, Dec., 1926, pp. 468–478.

5 "Bericht über Untersuchungen zur ausgebildeten Turbulenz," by L. Prandtl, *Zeitschrift für angewandte Mathematik und Mechanik*, vol. 5, 1925, pp. 136–139.

6 "Über turbulente Strahlausbreitung," by E. Förthmann, *Ingenieur-Archiv*, vol. 5, no. 1, 1934, pp. 42–54.

7 "Investigations of the Turbulent Mixing Regions Formed by Jets," by A. M. Kuethe, Trans. A.S.M.E., vol. 57, 1935, p. A-87.

8 "Über Luftkräfte bei sehr grossen Geschwindigkeiten insbesondere bei ebenen Strömungen," by J. Ackeret, *Helvetica Physica Acta*, vol. 1, 1928, pp. 301–322.

Experimental Determination of the Isostatic Lines

By AUGUSTO J. DURELLI,[1] CAMBRIDGE, MASS.

In this paper a direct method for obtaining the isostatics or stress trajectories is described. These lines indicate the directions of the principal stresses. The procedure used by the author can be applied almost without regard to the geometrical form of the object under stress. It also possesses the advantage in that the test is nondestructive and that in most cases it will yield values of the stress magnitudes within 10 or 15 per cent of the correct values. The technique consists in covering the surface of the body with a thin coat of lacquer which becomes brittle upon hardening. If the object being tested is painted under zero load and then stressed after the coating has hardened, the layer of lacquer will crack along lines perpendicular to the maximum tensile strain. The companion set of trajectories at right angles can usually be formed through relaxation. As an aid in photoelasticity this procedure has great possibilities as it eliminates the necessity for determining the isoclinic lines which are difficult to obtain.

Introduction

AT EVERY point in a two-dimensional system of stress there are two principal stresses, whose directions are at right angles. The stress trajectories or isostatics form orthogonal curves whose characteristic is that, at every point through which they pass, the principal-stress directions are normal and tangential to them. In order to construct the stress trajectories, one must know the directions of the principal stresses at all points in the field. However, because the directions of the principal stresses and principal strains coincide, the latter may be used for establishing the isostatics.

In the following paragraphs the author describes a direct method for utilizing the strains set up in a stressed body for constructing the stress trajectories.

General Application

If the surface of an unstrained body is painted with a thin coating of brittle lacquer, then when the load is applied the lacquer will follow the deformations of the body exactly and, if the strain is sufficient to rupture the lacquer, cracks will be formed in directions normal to the principal tensile strains, provided that the following conditions are fulfilled:

1 There must be perfect adhesion between the lacquer and the surface of the strained body.

2 The lacquer must be brittle and will rupture at a strain below the yield point of the material upon which it has been painted.

3 The lacquer must be able to resist small changes in temperature and humidity to avoid crazing.

With this procedure two sets of information can be obtained. Because the cracks follow the direction normal to the principal tensile strain, one family of the stress trajectories can be formed by loading a structure; and the family at right angles can be obtained by relaxation, that is, by releasing the load. In addition, an approximate value (usually within from 10 to 15 per cent of the correct value) of the strain intensity can be found because the lacquer will first crack at the region of highest strain and continue to crack at other regions as they reach the same strain, so that, by following the order of appearance of the cracks, it is possible to calculate the degree of the strain. The spacing or proximity of neighboring cracks will serve to give an indication of the strain at which the first cracks appear, by comparison with some object of known stress distribution. See Fig. 1. A convenient form of calibration specimen is a small cantilever beam, as shown in Fig. 2, in which the stress distribution varies linearly if a concentrated load is applied at the free end.

Strain-concentration factors can be determined very simply by this method without resort to the calibration specimen, provided that one knows the relation between the applied load and the strain at some point on the object under investigation. The point at which the strain is known can then be used as a reference. The loads corresponding to the appearance of the first cracks at the points of strain concentration and at the point of reference can be measured, and the ratio of these loads represents the value of the strain-concentration factor. A single test is usually insufficient for a representative value of the factor but a reasonably accurate value can be obtained as the mean of several observations.

In making use of this method of stress analysis the usual procedure is to spray a thin coating of lacquer on the surface of the object under investigation. This is usually allowed to harden for four or five hours. There are several substances which can be used for the coating (1 to 5)[2] but the writer has found those supplied by the Magnaflux Company (6) under the name of "Stresscoat" to be most convenient because they fulfill all the fundamental requirements and in addition they dry bubble-free without the necessity of heating the surface on which they have been sprayed.

The lacquer is usually applied to prototypes which in most cases are made of metal and in consequence are opaque. If the surfaces are brightly finished, photographs of the crack patterns can be made conveniently with reflected light: but if the surfaces are rough, an undercoating of aluminum paint is applied to produce the reflecting surface.

Although in many cases it is more desirable to work with prototypes, there are certain applications in which models can be used to great advantage. For large structures small scale models represent a great reduction in cost and at the same time permit one to apply materials which are easier to machine and which have a lower value of the elastic modulus in relation to the pro-

---

[1] Visiting Guggenheim Fellow, Department of Mechanical Engineering, Massachusetts Institute of Technology.

Presented at the National Meeting of the Applied Mechanics Division of THE AMERICAN SOCIETY OF MECHANICAL ENGINEERS, Cambridge, Mass., June 19–20, 1942.

Discussion of this paper should be addressed to the Secretary, A.S.M.E., 29 West 39th Street, New York, N. Y., and will be accepted until January 11, 1943, for publication at a later date. Discussion received after the closing date will be returned.

NOTE: Statements and opinions advanced in papers are to be understood as individual expressions of their authors and not those of the Society.

[2] Numbers in parentheses refer to the Bibliography.

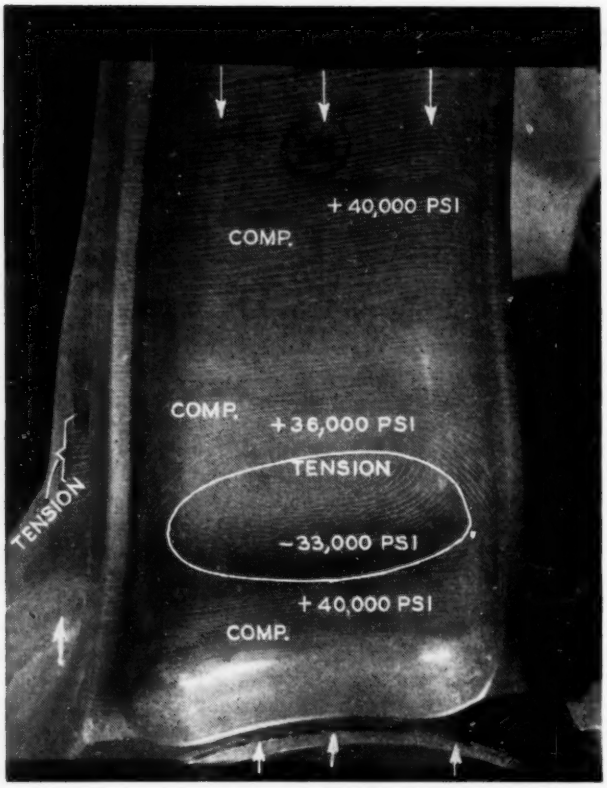


FIG. 1 "STRESSCOAT" PATTERN ON SURFACE OF A CONNECTING ROD
(The values are apparent stresses $E\epsilon$ for a compression load of 20,000 lb. Photographed with reflected light.)
Magnaflux Corporation

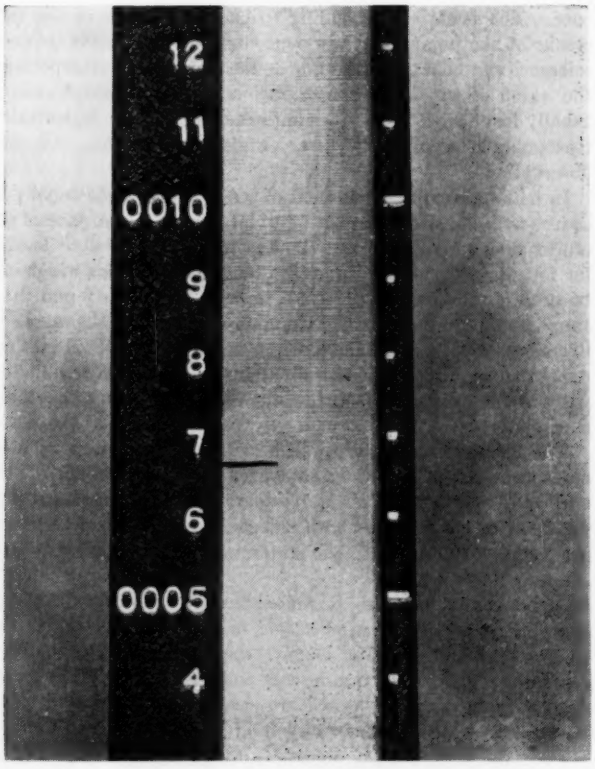


FIG. 2 CALIBRATION SPECIMEN
Magnaflux Corporation

portional limit. This latter consideration is of some importance since it permits a greater strain for a given stress and a corresponding increase in the number of isostatics and the area covered. As an example one might mention that the unit strain corresponding to the yield point in mild steel is about 0.001, whereas the corresponding strain in Bakelite is about 0.01, and for celluloid even greater.

When models are made from materials such as Lucite, Bakelite, and celluloid, which are transparent, photographs of the isostatics can often be made with transmitted light (9). If the models are made from flat plates of these materials then the use of transmitted light is simple and preferable.

APPLICATION TO PHOTOELASTICITY

The possibility of using the brittle lacquer on transparent flat plates at once suggests its application as an aid in photoelasticity. With present practice in photoelasticity, the use of the relatively sensitive synthetic resins is almost universal and the isochromatic lines giving the difference between the principal stresses can be determined conveniently and precisely. However, if one wishes to find the principal-stress directions, one must first locate the isoclinic lines and from these construct the stress trajectories. This is at best a somewhat uncertain procedure and represents the most inaccurate part of the photoelastic analysis. It is difficult to determine the exact position of the isoclinic lines, which must be located one by one, and the subsequent construction of the isostatics introduces still further possibility of error. In contrast to the photoelastic method of determining the stress directions, the application of brittle coatings to photoelastic models offers a relatively quick, easy, and direct means of obtaining the stress trajectories which can be recorded photographically over the whole field at once.

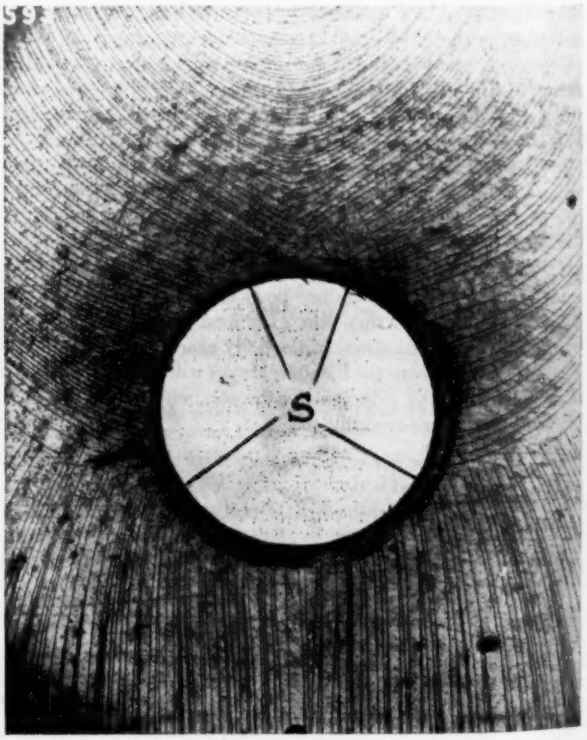


FIG. 3 ISOSTATICS NEAR THE POINT OF LOADING IN A SIMPLE BEAM OF LUCITE WITH A CIRCULAR HOLE
On the boundary there are four singular points. Photographed with transmitted light.)

In applying the lacquer to photoelastic models it is not necessary to use an intermediary coating. After testing, the surface is washed in succession with a solution of gasoline and oil, and gasoline alone. F. Stern also obtains very good results with turpentine alone or with dye in solution. The isostatics can then be photographed in a polariscope, after removal of the polarizing elements, or the model may be used in exactly the same manner as a photographic plate. If the latter procedure is adopted for making prints directly, the coated side of the model should be placed next to the printing paper. Since handling of the model is likely to chip off some of the coating it is advisable to make a photographic negative on film and to use this for printing.

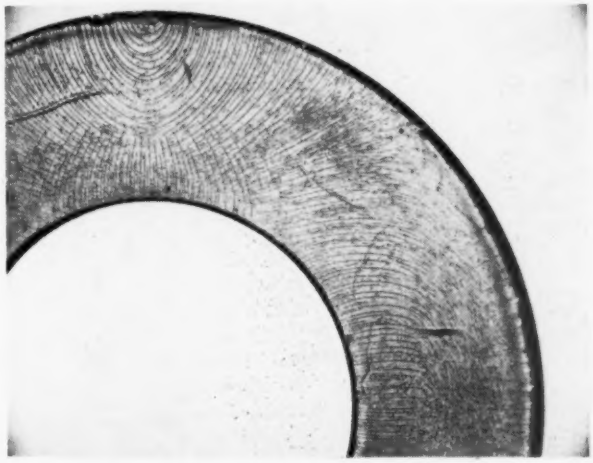


FIG. 4 ISOSTATICS IN A BAKELITE RING
(Width of ring is half its outer diameter.)

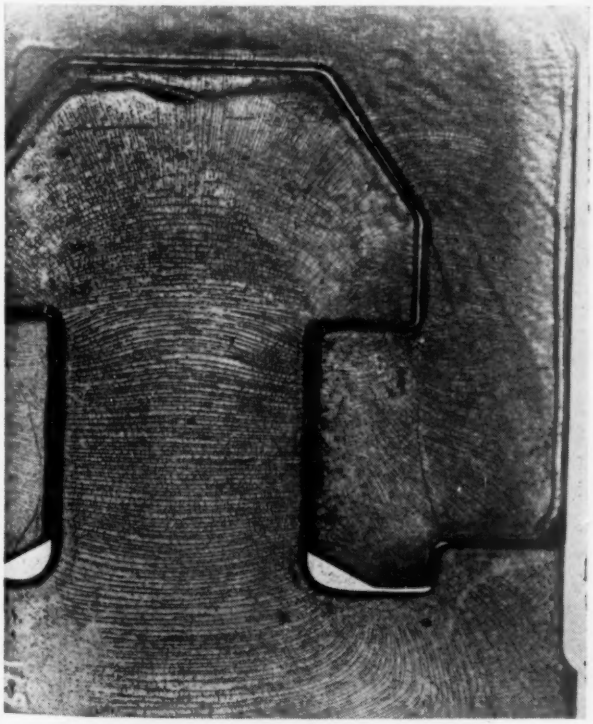


FIG. 5 ISOSTATICS IN A DOVETAIL JOINT
(Celluloid model.)

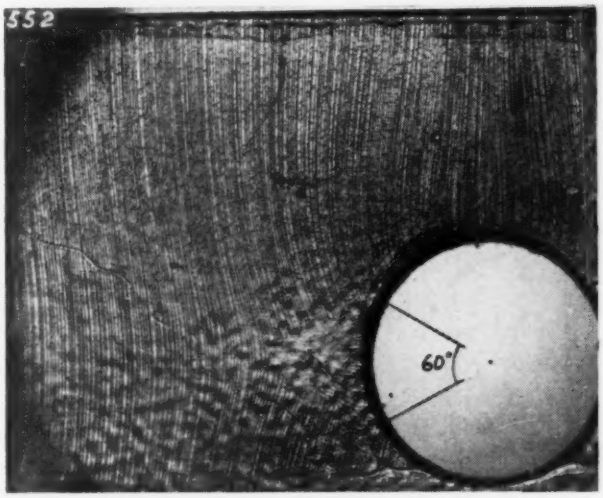


FIG. 6 ISOSTATICS AROUND A CIRCULAR HOLE IN A PLATE SUBJECTED TO PURE TENSION
(The boundary belongs to one set of isostatics and, after crossing the singular point, it changes to the other set.)

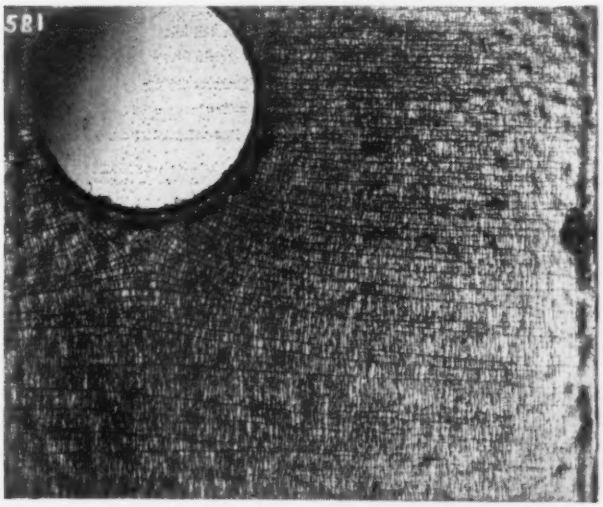


FIG. 7 ISOSTATICS AROUND A CIRCULAR HOLE IN A PLATE SUBJECTED TO PURE BENDING NORMAL TO THE PLANE OF THE PLATE
(The same set of isostatics prevails all along the boundary.)

Illustrations of the isostatics obtained on various models are shown in Figs. 3 to 6. These all represent cases of plane stress but the usefulness of brittle lacquer is by no means limited to such cases. There are other problems in which models of transparent material having a low elastic modulus can be used to great advantage, either as an aid to photoelasticity or an extension beyond the limits of the optical method of stress analysis. One problem of this nature is the determination of the stress condition around a discontinuity in a plate subjected to bending (7). Fig. 7 shows such an example with the directions of the principal stresses indicated at all points on the surface of the plate. A note of contrast should be observed between this picture and those in Figs. 3 and 6 where singular points are indicated. The absence of the singular points shows that there is no reversal of stress around the edge of the hole as in the case of pure tension.

As a point of academic interest, mention must be included of the fact that photographs can be made of photoelastic models in which the isostatics are superimposed on the isochromatics.

Fig. 8 illustrates two such sets of lines in a double-ended eyebar. The procedure for taking the picture was extremely simple; the model was first coated with the lacquer, which was allowed to dry, and then it was loaded in the testing machine of the polariscope.

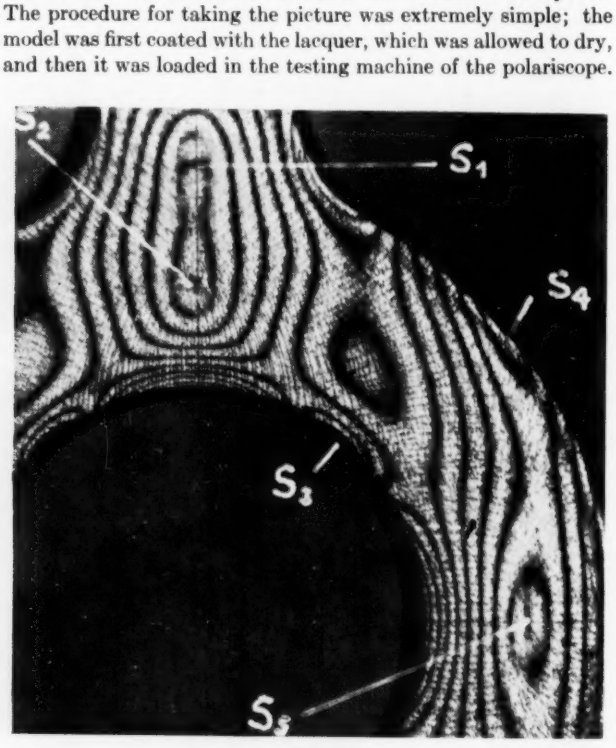


FIG. 8 ISOSTATICS AND ISOCHROMATICS IN AN EYEBAR
The singular points S_1, S_2, S_3, S_4, and S_5 of the isostatics are the points of zero order of interference in the isochromatic net.)



FIG. 10 ISOSTATICS IN AN EYEBAR
The brittle coating has not broken around the singular points.)

The usual photoelastic picture was taken with the crack pattern of the lacquer superimposed upon it. The interest in this procedure lies in the fact that it provides all the necessary information for determining the individual principal stresses and their directions at all points in the model.

So far in this discussion, the fact that the brittle coating cracks in a direction normal to the principal strain has been stated but no proof of the fact has been offered. If the illustrations are studied several proofs will appear. The fact that the cracks appear normal to free boundaries (where there is only one stress parallel with the boundary) and across the shank of the eyebar in Fig. 10, where a condition of pure tension exists, is proof for cases

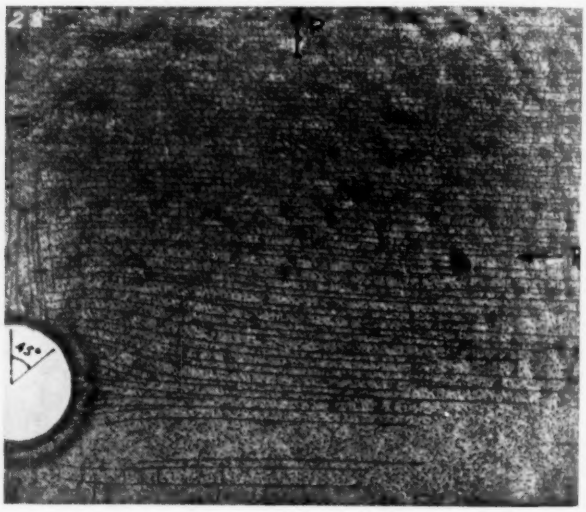


FIG. 9 PROOF THAT THE LACQUER BREAKS NORMAL TO THE PRINCIPAL TENSILE STRAIN IN COMPLEX STATE OF STRESS
(The specimen is under pure shear. The lines of fracture of the lacquer are normal to the tension.)

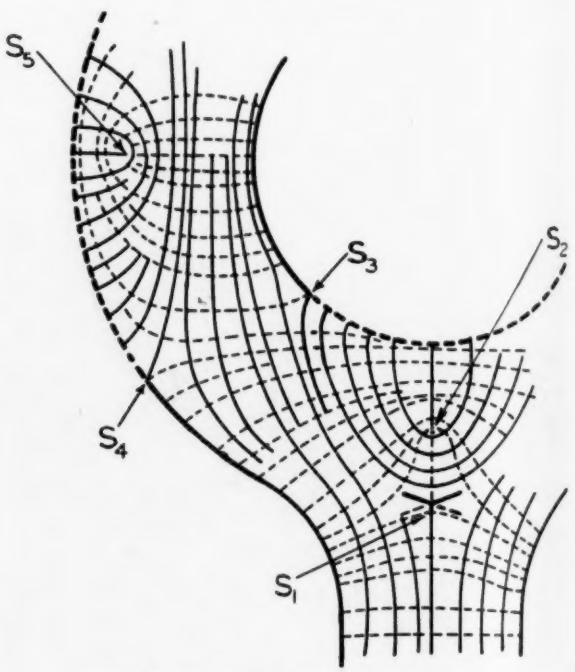


FIG. 11 ISOSTATICS IN AN EYEBAR
(S_2 and S_3 are singular points of first class. S_1 is a singular point of second class. On the boundary S_3 and S_4 are singular points of mixed character.)

of stress in one direction. For the condition of a complex state of stress similar proof is offered in Fig. 9 which shows the pattern in a model subjected to pure shear by the application of uniform and equal tension and compression in directions at right angles. Here the cracks are also normal to the tension (remote from the hole).

Limitations

A limitation in the use of the brittle-lacquer method of stress analysis arises from the fact that below a certain strain (about 0.0007 in. per in.) the lacquer will not rupture. For two-dimensional problems the principal strains are given by the equations

$$\epsilon_1 = (1/E)\ (\sigma_1 - \nu\sigma_2)$$

$$\epsilon_2 = (1/E)\ (\sigma_2 - \nu\sigma_1)$$

where ϵ_1 and ϵ_2 = the principal strains; σ_1 and σ_2 = the principal stresses; E = the modulus of elasticity; ν = Poisson's ratio. For Bakelite, $E \sim 700{,}000$ psi and $\nu = 0.36$, so that

$$\sigma_1 - 0.36\ \sigma_2 > \sim 500 \text{ psi}$$

to obtain the minimum strain of 0.0007 in. per in.

Even though there may be no stress at all in the direction normal to an isostatic, nevertheless the strain may produce a crack in the lacquer. The concentrated load on a semi-infinite plate is an example of such a case. See Fig. 12. If one considers the point of load application (for this case) as the point of reference in a system of polar co-ordinates then the principal stresses σ_1 and σ_2 will be the radial and tangential stresses, respectively.

The strain ϵ_1 produces the isostatics of set No. II and the strain ϵ_2 the isostatics of set No. I. The stress σ_2 is zero so that the strain ϵ_2 is due to stress σ_1. In other words, both sets of isostatics are produced by σ_1 which is the only stress acting. When the load is applied σ_1 is a compression but it acts like a tension at

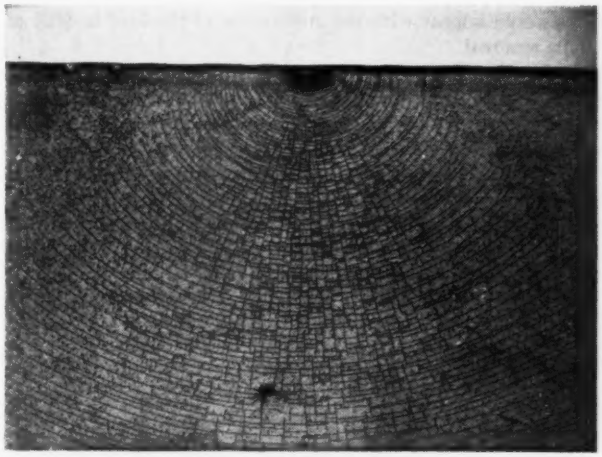


Fig. 12 Isostatics in a Plate of Bakelite, 3 × 1 × 0.25 In., Loaded on the Boundary by Means of a Cylinder 5/16 In. in Diameter

(Near the point of load application the stress is high and the lacquer has broken.)

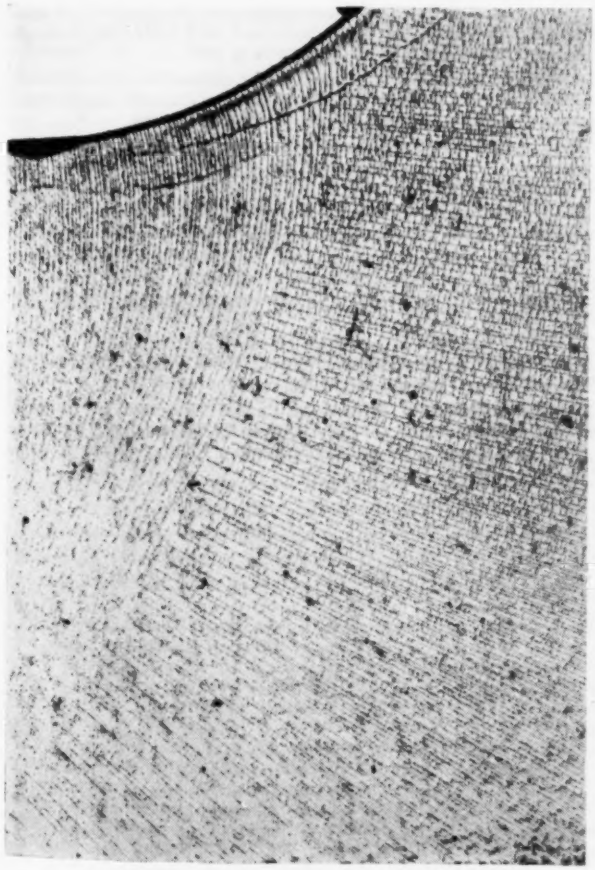


Fig. 13 Isostatics in an Eyebar

(The picture has been taken in the parallel field of the polariscope and enlarged about three and one-half times.)



Fig. 14 Isostatics in an Eyebar

(Printed directly from the transparent model of Bakelite. Enlarged about three times.)

right angles in producing ϵ_2. When the load is removed the relaxation of σ_1 produces the effect of a tension by creating the strain ϵ_1 directly.

A case might arise in which σ_2 would be a small compression such that $(\sigma_2/E) < (\nu\sigma_1/E)$. Under these circumstances although σ_2 would be a compression the strain ϵ_2 would be an extension and cracks would appear with the application of the load instead of with its removal.

The fact that the isostatics appear in the lacquer sooner at some regions than at others is a sign of greater strain but not always of greater stress. At the singular points, for instance, the stress required to produce cracks in the coating on a Bakelite model is about 800 psi; whereas if one of the principal stresses is zero the cracks will appear for stresses corresponding to about 500 psi. However, these considerations do not alter the fact that the directions of the principal stresses and principal strains coincide or that the singular points are the same for both.

To obtain the real value of the stress it would be necessary to make two tests, the first one giving ϵ_1 and the second one giving ϵ_2 by relaxation of the load.

Singular Points

At singular points, since $\sigma_1 = \sigma_2$, both principal stresses must be greater than about 800 psi to produce a crack. When these occur in regions of relatively low stress, it is often impossible to obtain the complete picture of the isostatics without overstressing some regions of the specimen.

Although there are several kinds of singular points (8), usually only those of the first and second order can be found. For example, in Fig. 11, S_2 and S_5 are singular points of the first order and S_1 is of the second order. On the boundaries the singular points can be mixed. In any case it is easy to recognize the type and to complete the picture of the isostatics.

This procedure is illustrated in Figs. 10 and 11 which show, respectively, the experimental determination of the isostatics and the completed diagram in which for clearness one family of curves has been put in with dotted lines.

Conclusions

Although the author does not claim that this method of stress analysis will by any means provide a solution to all problems, he feels that it is of wide use and application. The following are the general conclusions which can be drawn from his experience with it:

1 It has the advantage of being applicable to bodies of all kinds of irregular contour in three dimensions and will yield information where all other methods fail.

2 It is a method easy to apply and requires no very complicated apparatus.

3 It is nondestructive in character so that a part may be tested without impairing it for subsequent service.

4 As applied to photoelasticity it removes one of the major difficulties and inherent sources of error in that type of stress analysis.

5 One should be careful in interpreting the results to realize that the crack pattern formed is merely a function of strain and that stresses can be derived from these rather than observed directly.

Acknowledgment

The study described in the foregoing paragraphs was made at the Massachusetts Institute of Technology where the writer was a guest during 1940 and 1941. The author wishes to express his thanks and appreciation to authorities of the Massachusetts Institute of Technology for the privileges extended to him and in particular to Prof. W. M. Murray and to Prof. A. V. de Forest. To Mr. Ellis and Mr. Stern he is very grateful for assistance in the application of the brittle lacquer to problems in photoelasticity.

BIBLIOGRAPHY

1 "Das Dehnungslinienverfahren, ein Mittel zur Bestimmung der für die Bruchsicherheit bei Wechselbeanspruchung massgebenden Spannungsverteilung," by O. Dietrich and Ernst Lehr, *Zeitschrift des Vereines deutscher Ingenieure*, vol. 76, 1932, p. 973.

2 "Spannungsverteilung in Konstruktionselementen," by E. Lehr, V.D.I. Verlag, Berlin, 1934, p. 6.

3 "Procede d'etude de la distribution des efforts élastiques dans les pieces métalliques," by A. Portevin and M. Cymboliste, *Revue de Métallurgie, Memoires*, vol. 31, April 1934, p. 147.

4 "Anwendung des Dehnlinienverfahrens bei Zelluloidmodellen," by E. Siebel, W. Seufert, and W. Steurer, *Zeitschrift des Vereines deutscher Ingenieure*, vol. 84, November 16, 1940, p. 889.

5 "Brittle Lacquers as an Aid to Stress Analysis," by A. V. de Forest and Greer Ellis, *Journal of the Aeronautical Sciences*, vol. 7, March, 1940, p. 205.

6 "Stress-Strain Analysis From Crack Formations in Brittle Lacquer Coatings," *Product Engineering*, vol. 11, June, 1940, p. 266.

7 "Stress Concentration Around an Open Circular Hole in a Plate Subjected to Bending Normal to the Plane of the Plate," by C. Dumont, National Advisory Committee for Aeronautics, Technical Notes, 1939, No. 740.

8 "The Exploration of Stress in the Neighborhood of an Isotropic Point in an Elastic Plate," by L. N. G. Filon, *Philosophical Magazine*, series 7, vol. 22, July, 1936, p. 187.

9 "Distribution of Stresses in Partial Compression. A New Method of Determining the Isostatics in Photoelasticity," Proceedings of the Thirteenth Semi-Annual Eastern Photoelasticity Conference, June, 1941.

The Photoelastic Analysis of Transverse Bending of Plates in the Standard Transmission Polariscope

By D. C. DRUCKER,[1] ITHACA, N. Y.

In this paper the ideas of three-dimensional photoelasticity are applied to the analysis of plates under transverse bending, resulting in a simple photoelastic method, employing the standard two-dimensional transmission polariscope. The procedure used is to "freeze" a fairly high initial tension in bakelite or similar material, cut out the model at some angle to the direction of the tension, bend, and observe. Results of various tests are given; photographs of two cases, the circular hole and the semicircular notch, are included. Stress-concentration factors are also obtained and analyzed. The problem of the thick plate as contrasted with the thin plate, assumed in the usual theory, is discussed briefly.

Introduction

A NUMBER of methods have been proposed for the photoelastic analysis of plates under transverse bending, i.e., plates bent out of their plane, and other theoretically possible methods will occur to the reader as the problem is considered. However, until recently with the work of Goodier and Lee,[2] who used a reflecting foil in the middle plane of the plate, no successful method of analysis had been carried out accurately. Their procedure, in addition to requiring the cementing of a celluloid "sandwich," which is especially difficult in the important regions of stress concentration, does not have one very desirable feature—accurate usable photographic record of the results cannot be obtained.

From the standpoint of clarity of image, convenience, and accuracy of measurement, it is best to use transmitted light. Unfortunately, if a plate, originally free of stress, is bent and placed in a plane or circular polariscope so that light passes through in a direction perpendicular to the plate, as shown in Fig. 1(*b*), nothing can be observed. The tension side cancels the compression side and the net result is zero for both isochromatics and isoclinics. However, a standard transmission polariscope can be used if the following proposed procedure is employed.

First, a state of uniaxial tension is "frozen" in a large plate of bakelite or similar thermosetting material. This is done in the usual way. The bakelite is heated to about 110 C, loaded in pure tension, and then cooled under load. When down to room temperature, the load is removed. In so far as optical measurements are concerned, a state of simple tension remains in the bakelite which is not disturbed by slow and careful machining.[3] The stress which apparently exists in the material will be called $\sigma_t = n_t C/2h$, where n_t is the fringe order observed due to the frozen tension, C the room-temperature stress-optical coefficient in pounds per square inch for 1-in. thickness, and h the half thickness of the plate. The model is then cut from this larger plate at some angle to the direction of the tension, Fig. 1(*a*). When this smaller plate is placed in a circular polariscope and bent, it will be found that the fringe order appearing on the screen will

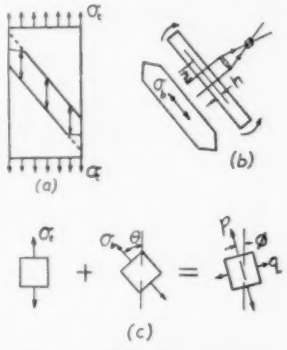


Fig. 1 Basic Procedure

increase as the bending moment increases but not in direct proportion. The tension side in bending no longer cancels the compression side.

Theory

The observed increase in retardation is a measure of the bending stresses produced. To find the relationship, it will first be assumed that the smaller plate is a thin rectangular plate under pure bending. As shown in Fig. 1(*c*), a state of pure bending has been added to a state of simple tension, the direction of the bending stress σ_b, at some angle θ to the direction of the tensile stress σ_t. The combination of these two states of stress at any point in the plate may be represented by the resulting principal stresses, p and q, and their orientation ϕ, say, with respect to the known direction of the tensile stress.

If light is passed through the plate perpendicularly, all that can be obtained photoelastically is something about the difference between the principal stresses p—q, and something about the orientation. Considering a co-ordinate z, measured from the middle plane of the thin plate, σ_b varies linearly with z and can be written as $\frac{\sigma_{bm}}{h}z$, where σ_{bm} is the value of the maximum bending stress. Terms p, q, and ϕ can then be expressed as functions of z, the frozen tension, and the maximum bending stress

[1] Instructor in Mechanics of Engineering, Sibley School of Mechanical Engineering, Cornell University.

[2] "An Extension of the Photoelastic Method of Stress Measurement to Plates in Transverse Bending," by J. N. Goodier and G. H. Lee, Journal of Applied Mechanics, Trans. A.S.M.E., vol. 63, 1941, p. A-27. Discussion, p. A-187.

Presented at the National Meeting of the Applied Mechanics Division, Cambridge, Mass., June 19–20, 1942, of The American Society of Mechanical Engineers.

Discussion of this paper should be addressed to the Secretary, A.S.M.E., 29 West 39th Street, New York, N. Y., and will be accepted until January 11, 1943, for publication at a later date. Discussion received after the closing date will be returned.

Note: Statements and opinions advanced in papers are to be understood as individual expressions of their authors and not those of the Society.

[3] "The Fundamentals of Three-Dimensional Photoelasticity," by M. Hetényi, Journal of Applied Mechanics, Trans. A.S.M.E., vol. 60, 1938, p. A-149.

$$p - q = \sigma_t \sqrt{1 + \left(2\frac{\sigma_{bm}}{\sigma_t}\cos 2\theta\right)\frac{z}{h} + \left(\frac{\sigma_{bm}}{\sigma_t}\right)^2\left(\frac{z}{h}\right)^2} \quad \ldots [1]$$

$$\tan 2\phi = \frac{\left(\frac{\sigma_{bm}}{\sigma_t}\sin 2\theta\right)\frac{z}{h}}{1 + \left(\frac{\sigma_{bm}}{\sigma_t}\cos 2\theta\right)\frac{z}{h}} \quad \ldots [2]$$

Were the orientations of the principal stress unchanged through the thickness, the retardation would add up algebraically as the light traveled through the model. The fringe order resulting would be

$$n = \int_{-h}^{+h} \frac{p - q}{C}\, dz \quad \ldots [3]$$

If the orientation changes continuously through the thickness as it does in this case, then the retardation will be somewhat higher than given by this expression, but the difference will be inappreciable in the working range that will be used[4] ($\sigma_{bm}/\sigma_t < 4$). Integrating Equation [3], and factoring out $n_t = \sigma_t 2h/C$, we obtain

$$n = n_t \left\{\frac{1}{4\frac{\sigma_{bm}}{\sigma_t}}\left[\left(\frac{\sigma_{bm}}{\sigma_t} + \cos 2\theta\right)\sqrt{1 + 2\frac{\sigma_{bm}}{\sigma_t}\cos 2\theta + \left(\frac{\sigma_{bm}}{\sigma_t}\right)^2}\right.\right.$$
$$\left. + \left(\frac{\sigma_{bm}}{\sigma_t} - \cos 2\theta\right)\sqrt{1 - 2\frac{\sigma_{bm}}{\sigma_t}\cos 2\theta + \left(\frac{\sigma_{bm}}{\sigma_t}\right)^2}\right]$$
$$\left. + \sin^2 2\theta \left\{\sinh^{-1}\left(\frac{\frac{\sigma_{bm}}{\sigma_t} + \cos 2\theta}{|\sin 2\theta|}\right) + \sinh^{-1}\left(\frac{\frac{\sigma_{bm}}{\sigma_t} - \cos 2\theta}{|\sin 2\theta|}\right)\right\}\right\}$$

$$n = n_t F(\sigma_{bm}/\sigma_t, \theta) \quad \ldots [4]$$

The retardation is thus equal to the retardation in the frozen plate before bending, multiplied by a function of the ratio of the maximum bending stress to the apparent frozen tensile stress and of the angle between their directions.

The preceding discussion is based upon bending in one direction only. In the general case there are two principal bending moments each of which, for thin plates, gives rise to linear distributions of bending stress. If σ_b is taken as representing the difference between the principal bending stresses and as acting in a principal direction, then the foregoing reasoning and results carry over without further change. The notation $(p-q)\sigma_b$ will be used in places where σ_b might be misinterpreted. Transverse shearing stresses which may appear will not affect the retardation.

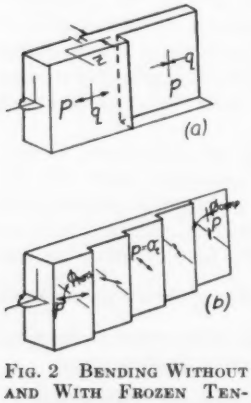


FIG. 2 BENDING WITHOUT AND WITH FROZEN TENSION σ_t
[(a) Without, and (b) with frozen tension.]

Let us now study the light as it passes through the bent plate. First suppose that the entering light is plane-polarized, the direction of vibration coinciding with the p direction of principal stress on entrance to the model. In the case of bending without initial frozen tension, Fig. 2(a), the direction of vibration coincides with the tension direction for the first half thickness of the plate, with the compression direction for the second half, and there is no change in orientation. In the case of initial tension, Fig. 2(b), the result is quite different. The orientation of the p direction changes continuously through the thickness and, providing the rate of change is not too rapid ($\sigma_{bm}/\sigma_t < 4$) for all practical purposes, the vibration will be in the p direction at every point in the model.[4] If the entering light has components in both the p and q directions, these components, with but negligible change in amplitude, will follow their respective directions about as they rotate.

From Equation [2]

$$\tan 2\phi_{tens} = \frac{\frac{\sigma_{bm}}{\sigma_t}\sin 2\theta}{1 + \frac{\sigma_{bm}}{\sigma_t}\cos 2\theta} \quad \ldots [5]$$

$$\tan 2\phi_{comp} = \frac{-\frac{\sigma_{bm}}{\sigma_t}\sin 2\theta}{1 - \frac{\sigma_{bm}}{\sigma_t}\cos 2\theta} \quad \ldots [6]$$

$$\sin 2\theta = \frac{\left(\frac{\sigma_{bm}}{\sigma_t}\right)^2 - 1}{2\frac{\sigma_{bm}}{\sigma_t}}\tan 2(\Delta\phi) \quad \ldots [7]$$

where $\Delta\phi = \phi_{comp} - \phi_{tens}$

EXPERIMENTAL PROCEDURE

Various experimental procedures can be worked out on the basis of the theory. For a complete analysis of a plate, the principal bending stresses and their orientations must be found at every point. In practice, only the maximum values, which occur at the surface of the plate, need be considered. Photoelastically, using the transmission-type polariscope, in a manner similar to that used in the case of plane stress, only the difference between the principal bending stresses at the surface, $(p-q)\sigma_{bm}$ and their orientation θ, can be found.

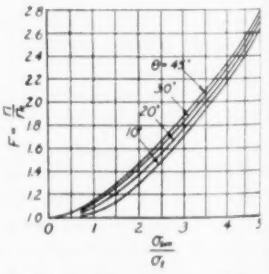


FIG. 3 RETARDATION AS FUNCTION OF RATIO OF MAXIMUM BENDING STRESS TO TENSILE STRESS, AND OF THE ANGLE BETWEEN THEIR DIRECTIONS

If θ is known, as it will be at most important points (free boundaries, axes of symmetry, and regions away from disturbance), one measurement is sufficient to determine $(p-q)\sigma_{bm}$. The simplest procedure is to measure the retardation n. Term n_t and the corresponding stress σ_t are known throughout the plate from measurements made before it is bent, so that the graph, Fig. 3, can be used directly. Values of θ from 0 to 45 deg are sufficient, for in so far as the function F is concerned, θ is the smallest angle between either of the principal bending stresses and the direction of the frozen tension. Values ± 20 deg, 90—20 deg = 70 deg, and —70 deg all lead to the same value of F.

As can be seen from Equations [5], [6], and [7], measurement of ϕ_{tens}, ϕ_{comp}, or $\Delta\phi = (\phi_{comp} - \phi_{tens})$ would also determine $(p-q)\sigma_{bm}$. Independent rotation of the polarizer and analyzer of a plane polariscope is required to find the first two. When the light passing through the model is extinguished at a point where the fringe order is fractional, the polarizer must be passing light

[4] "Stress Analysis by Three-Dimensional Photoelastic Methods," by D. C. Drucker and R. D. Mindlin, *Journal of Applied Physics*, vol. 11, 1940, pp. 724–732.

vibrating in a principal direction on entrance to the model, and the analyzer stopping the light vibrating in the rotated position of this principal direction on exit. The orientations must be determined by trial and, when found, the angle reading on the polarizer or analyzer gives a ϕ from which $(p—q)\sigma_{bm}$ can be computed. Such a procedure is obviously tedious and rather inaccurate. Term $\Delta\phi$ on the contrary can be measured easily if the retardation n is a whole number. At such a point, there will be a position of the analyzer which will extinguish the light for any position of the polarizer. The angular rotation of the analyzer from the original crossed position with the polarizer is the angle $\Delta\phi$. Unlike the corresponding plane-stress measurement, the polarizer does not have to be rotated.

For cases in which θ is known, angular measurements cannot compare in simplicity with measurement of retardation. An isochromatic, or fringe, photograph taken in a circular polariscope provides complete information and a permanent record.

At points where θ is not known, two independent measurements must be made. Two angles will suffice. The point-by-point investigation, using a plane polariscope and independent rotation of analyzer and polarizer just described, will give the information. However, measurement of retardation (i.e., a fringe photograph) and $\Delta\phi$ is much more convenient and accurate. As can be seen from Fig. 3, a 5-deg error in θ has a small effect on the retardation n, in the working range of $(p—q)\sigma_{bm}$ (roughly 1.3 to $4\sigma_t$). If θ is not known as closely as this, a value is assumed, the graph used to obtain a σ_{bm} which is substituted in Equation [7] with the measured value of $\Delta\phi$. This determines θ more accurately, which in turn enables more accurate determination of σ_{bm}. The final value is approached very rapidly. In many cases, one try will be sufficient; in most cases no more than two will be required.

The accuracy of work that can be expected, judging from Fig. 3, is not much less than that obtainable in photoelastic analysis of plane stress of the same precision of measurement. High accuracy, within 1 or 2 per cent, is possible if desired.

Check and New Experiments

Although the basic theoretical work had already been checked roughly for combined tension and torsion, it seemed desirable to obtain further experimental verification of the results.

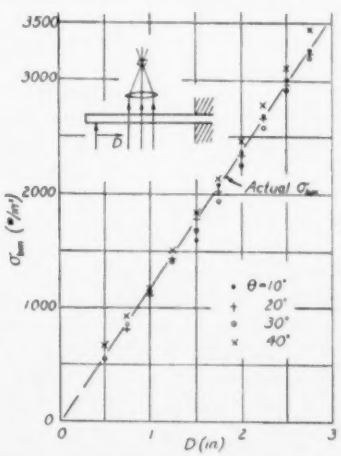


Fig. 4 Cantilever Bending as a Check for Theory

Plates in cantilever bending were used. The transverse shear stresses appearing have no effect on the retardation. Results of one series of tests on plates with four different values of θ are shown in Fig. 4. The points were obtained by computing the bending stress from the measured retardations using the graph of Fig. 3. The straight line gives the bending stress computed from the load and dimensions of the plate. In the range in which this work should be done, the error does not exceed 5 per cent.

The nearer the angle θ is to 45 deg, the smaller will be the bending stress that can be measured accurately.

Having established the accuracy and feasibility of the method on these test cases, the next step was to take a more complicated but well-known case. The bending of a thin plate with a circular hole has been solved analytically by Goodier[5] and checked at least partially by photoelastic and strain-gage measurements. A number of such plates were therefore made. The holes were bored carefully on a lathe, after it was found that drilling released

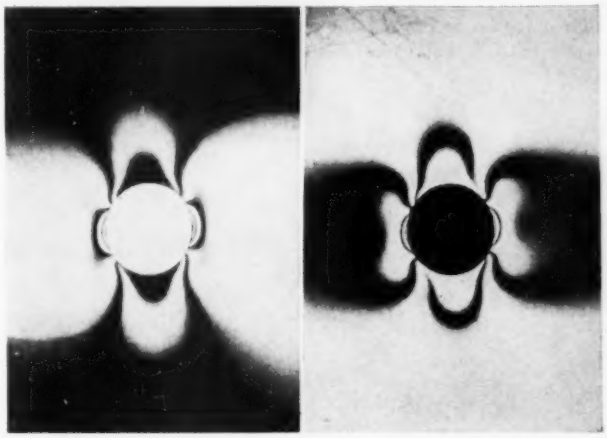


Fig. 5 Circular Hole in Plate Under Pure Bending

part of the frozen initial stress. Fig. 5 shows a typical case. The fringe patterns for both dark and light fields were obtained, for unless both are taken, it is not possible, without accurate scale measurements, to be sure that the true edge of the hole appears on the photograph. Errors of 20 per cent in regions of stress concentration are easily possible on this count alone if small models are used.

The results of a series of tests on different-sized holes in a $1^1/_8 \times {}^1/_4$-in. bakelite plate are shown in Fig. 6, indicating the precision that is possible in this work. The photographs were measured with a traveling micrometer, and care was taken to insure that the edge appearing on the photograph was actually the edge, and if not, where the edge really was. The agreement for the three different loads for the $^3/_8$-in-diam hole is very close. Precision of this order would, of course, not be required in a practical problem.

Analysis of Results

Fig. 7 shows the distribution of the difference between the maximum principal bending stresses all across the net section of the plate on the basis of the maximum bending stress in the gross section away from the hole being unity. Although two other series of tests checked these curves to within about 5 per cent, the results must be carefully scrutinized. The stress-concentration factors, which are based on the gross section, increase as the diameter of hole gets smaller, instead of decreasing as would normally be expected. The value of 2.3 for the $^3/_8$-in. hole is roughly what would be figured on the basis of Goodier's solution and checks with the experimental value obtained by Lee[2] using the reflection method. However, values of 2.5 for the $^1/_8$-in. hole

[5] "The Influence of Circular and Elliptic Holes on the Transverse Flexure of Elastic Plates," by J. N. Goodier, *Philosophical Magazine*, series 7, vol. 22, 1936, pp. 69–80.

and 2.4 for the 1/4-in. hole are far from the 1.8 predicted by the infinite-thin-plate theory.

The reason for the difference seems to lie in the "thinness" of the plate. The thin-plate theory postulates a plate whose thickness is very small compared to its lateral dimensions and the radius of curvature of any portion of the boundary. In the case of the hole in a plate, the diameter of the hole must be a number of times the thickness of the plate for the theory to apply closely. A 1/8-in-diam hole in a 1/4-in. plate certainly does not satisfy this condition, but a 3/8-in-diam hole might not involve large error. Consideration of the theory of moderately thick plates[6] shows that, although the thin-plate analysis satisfies the conditions of no moment and resultant force per unit of length on the free boundary of the hole, the stresses left on the boundary are as high as 1/2 the maximum stress in the plate for the small ratios of diameter to thickness used in the experiments.

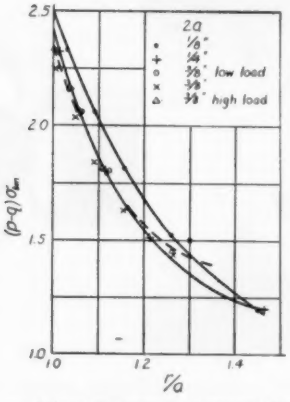


FIG. 6 RESULTS OF MEASUREMENTS ACROSS NET SECTION NEAR BOUNDARY OF HOLES
(Refer to Fig. 7.)

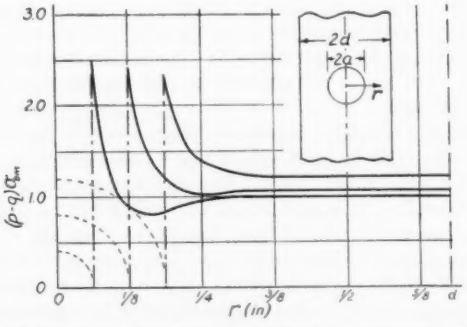


FIG. 7 DIFFERENCE BETWEEN PRINCIPAL BENDING STRESSES ACROSS NET SECTION FOR BENDING STRESS OF UNITY IN GROSS SECTION AWAY FROM HOLE
(Average of results from 1 1/8 × 1/4-in. bakelite plates.)

Partial confirmation of the high stress-concentration factors is found in an exact elastic solution which shows that the concentration factor is the same as for the plane-stress analog (uniaxial tension), i.e., 3, when the thickness of plate is very large compared to the hole diameter. Comparison of Fig. 7 with curves for the uniaxial-tension case and thin-plate bending indicates a much closer correspondence to the tension than the bending, both as to shape of curve and rapidity of falling off of the concentration with distance from the hole. On this basis, the factors of 2.4 and 2.5 for the 1/4- and 1/8-in. holes appear reasonable.

[6] "A Treatise on the Mathematical Theory of Elasticity," fourth edition, by A. E. H. Love, Cambridge University Press, 1927, p. 473.

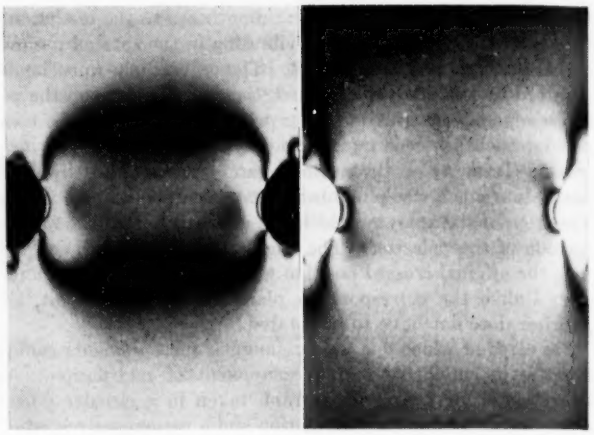


FIG. 8 SEMICIRCULAR NOTCHES IN PLATE UNDER PURE BENDING

Experimental work on semicircular notches, Fig. 8, gives concentration factors based on the gross section that are very nearly the same as for the circular hole. There is no theoretical solution available but reasoning from the corresponding plane-stress cases this result might well be expected.

CONCLUSION

After the initial tension is "frozen" in the plate, the work involved in the proposed method is almost the same as in the photoelastic analysis of a plane-stress problem. The same polariscope is used, and in each case a photograph of the isochromatic pattern is all that is required for most practical problems. If complete information is desired angle measurements must be made. In the analysis of plane stress, both polarizer and analyzer are rotated; in the analysis of plate bending, the polarizer remains fixed and the analyzer alone is rotated. The interpretation of the experimental data is, of course, more involved for bending. Use of Fig. 3 and Equation [7], however, makes the actual work simple.

The stress-concentration factor of 2.4 obtained for the circular hole and semicircular notch, in a plate under pure bending for a diameter equal to the thickness of the plate, is of practical interest. Further work is planned to obtain theoretical stress-concentration factors between the 1.8 for the thin plate and 3 for the small hole.

ACKNOWLEDGMENT

The author is indebted to Prof. R. D. Mindlin of Columbia University for recalling to mind[7] the possibility of the method which was originally used by the author in the equivalent problem of combined tension and torsion. He also wishes to express his thanks to the Sibley School of Mechanical Engineering of Cornell University for making available the facilities of the photoelasticity laboratory, and for a grant from the Westinghouse Research Fund.

[7] Discussion of paper[2] by R. D. Mindlin, JOURNAL OF APPLIED MECHANICS, Trans. A.S.M.E., vol. 63, 1941, p. A-187.

An Analytical Method for Determining the Flexibility of Piping Having Two or More Anchorages

By HARRY MILLER,[1] BROOKLYN, N. Y.

Reference is made to an analytical method for determining the flexibility of piping having two anchorages, as developed by H. C. E. Meyer and Prof. W. Hovgaard. This paper is an attempt to amplify the method in such a manner that the flexibility of piping having reverse bends may be conveniently and accurately computed. It is the author's objective also to remove the restriction on the number of anchorages. The mathematical development of the method was suggested in a previous paper by H. Poritsky and H. D. Snively.

Nomenclature

The following nomenclature is used in the paper:

O = origin of co-ordinates; fixed end of pipe

$\vec{i}$ = unit vector along reference X axis

$\vec{j}$ = unit vector along reference Y axis

$\vec{k}$ = unit vector along reference Z axis

$\vec{s}$ = unit vector tangential to pipe element ds

$\vec{r}$ = unit vector radial to pipe element ds

n = unit vector normal to pipe element ds

ρ = radius vector to point P_1, locating pipe element ds in space with respect to X, Y, Z axes

s = length of pipe from O to P_1 measured along pipe axis

F_0 = force reaction at O, due to loads on pipe length s

M_0 = moment reaction at O, due to loads on pipe length s

β = flexibility of pipe element ds

I = moment of inertia of pipe cross section about an axis in plane of cross section and passing through neutral axis of pipe

E = modulus of elasticity in tension

K = flexibility factor for moments normal to plane of an element of curved pipe of radius R

$$K = \frac{12h^2 + 10}{12h^2 + 1}, \quad \text{where } h = \frac{tR}{m^2}$$

t = wall thickness of pipe

m = mean radius of pipe

$[]\cdot[]$ = symbol for vector product

---

[1] Assistant Marine Engineer, Design Section, Navy Yard, New York, N. Y. Jun. A.S.M.E.

Presented at the National Meeting of the Applied Mechanics Division, Cambridge, Mass., June 19–20, 1942, of The American Society of Mechanical Engineers.

Discussion of this paper should be addressed to the Secretary, A.S.M.E., 29 West 39th Street, New York, N. Y., and will be accepted until January 11, 1943, for publication at a later date. Discussion received after the closing date will be returned.

Note: Statements and opinions advanced in papers are to be understood as individual expressions of their authors and not those of the Society.

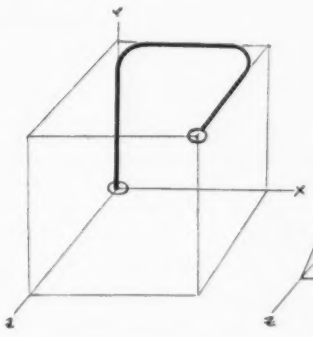


Fig. 1

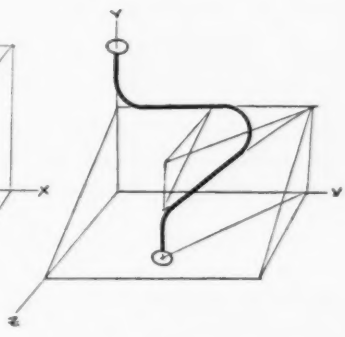


Fig. 2

Introduction

A method for determining analytically the flexibility of piping having two anchorages has been developed by H. C. E. Meyer, and Prof. W. Hovgaard of Gibbs and Cox, Inc., New York, N. Y. This method has been outlined in a paper by S. Noyes.[2] The method is restricted to piping arrangements of the type shown in Fig. 1, and requires that each of the tangent sections and the bends be parallel to at least one of the reference planes X, Y; Y, Z; or Z, X. Furthermore, the piping arrangement cannot have more than two anchorages. It is the purpose of this paper to generalize on this method, in such a manner that piping arrangements of the type shown in Fig. 2 may be conveniently and accurately handled, and also to remove the restriction on number of anchorages.

The mathematical development of this method was suggested in a paper[3] by H. Poritsky and H. D. Snively.

As originally submitted, the paper contained, in addition to the theoretical background of the subject, a series of 36 schedules and tables, which allowed the method to be used in practical problems. Two illustrative problems were offered, one showing the method as applied to a two-anchorage problem and the second as applied to a multianchorage problem. It was felt by the editors that the subject was of too limited interest to warrant publishing the entire paper. Accordingly, the paper was condensed and as herein presented contains only the mathematical development of the subject. For details of the method, as applicable to practical problems, reference may be made to the original paper, which is filed in the Engineering Societies Library, New York, N. Y.

Preliminary Considerations

1 A straight beam, Fig. 3, of length ds, which is subjected to a vector moment M normal to the length, causes the beam to con-

[2] "Thermal Expansion Stresses in Piping," by Mason S. Noyes, *Journal of the American Society of Naval Engineers*, vol. 53, 1941, pp. 275–374.

[3] "Stresses and Deflections of Three-Dimensional Pipe Bends," by H. Poritsky and H. D. Snively, Journal of Applied Mechanics, Trans. A.S.M.E., vol. 62, 1940, p. A-17.

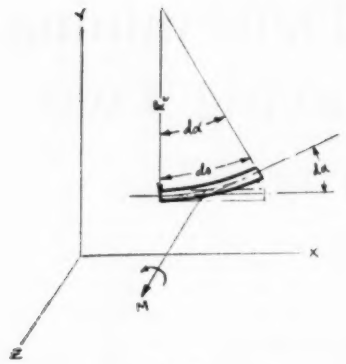


FIG. 3

form to a circle of radius R_e, the plane of R_e and ds also being normal to the vector moment M. The end of the beam rotates through an angle $d\alpha$. From the theory of beams

$$\frac{1}{R_e} = \frac{M}{EI} \quad \ldots\ldots [a]$$

where I is the moment of inertia of the beam cross section about an axis parallel with the vector moment and passing through the neutral axis of the beam, and E is the modulus of elasticity in tension.

$$d\alpha = \frac{ds}{R_e} = \frac{Mds}{EI} \quad \ldots\ldots [b]$$

Thus M/EI can be considered to be the rotation per unit length. It will be denoted by the symbol ψ.

2 If the beam element under consideration is a circular tube and is already bent to a radius R before the application of the vector moment, which is normal to the plane containing R and ds, von Kármán has shown that the rotation per unit length ψ is K times the rotation that would occur if the beam were straight. The "flexibility factor" K is a function of the radius of the bend R, the thickness of the tube, and the diameter of the tube.

3 If the vector moment is parallel to the length ds, the beam is subjected to torsion.

$$\psi = \frac{M}{E_t I_t} \quad \ldots\ldots [c]$$

where E_t is the modulus of elasticity in shear, and I_t is the moment of inertia of the beam cross section about an axis parallel to the length and passing through the neutral axis.

For circular steel pipe

$$E_t = \frac{E}{2.6}$$

$$I_t = 2I$$

$$\psi = \frac{M}{E_t I_t} = \frac{1.3M}{EI} \quad \ldots\ldots [d]$$

Determination of Flexibility of Piping Having Two Anchorages

Refer to Fig. 4

$$\rho = l_x\vec{i} + l_y\vec{j} + l_z\vec{k} \quad \ldots\ldots [1]$$

$$F_0 = P\vec{i} + Q\vec{j} + N\vec{k} \quad \ldots\ldots [2]$$

$$M_0 = M_{0x}\vec{i} + M_{0y}\vec{j} + M_{0z}\vec{k} \quad \ldots\ldots [3]$$

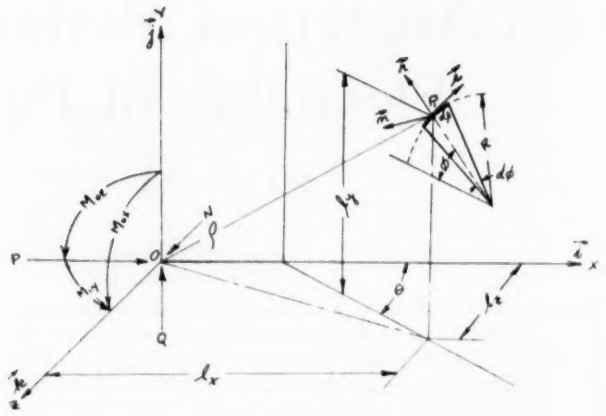


FIG. 4

For circular pipe

$$\beta = \frac{1}{EI}\vec{r} + \frac{1.3}{EI}\vec{s} + \frac{K}{EI}\vec{n} \quad \ldots\ldots [4]$$

$$= \frac{1}{EI}\left\{\vec{r} + \vec{s} + \vec{n}\right\} + \frac{1}{EI}\left\{0.3\vec{s} + (K-1)\vec{n}\right\} \quad \ldots [4a]$$

Let ψ = rotation of pipe per unit length
M = moment at P_1 due to reactions at O

$$\psi = \text{dyad product } [\beta \cdot M] \quad \ldots\ldots [5]$$

$$\left.\begin{aligned} M &= m_x\vec{i} + m_y\vec{j} + m_z\vec{k} \\ &= m_r\vec{r} + m_s\vec{s} + m_n\vec{n} \\ &= M_0 + [F_0 \cdot \rho] \end{aligned}\right\} \quad \ldots\ldots [6]$$

For pipes fixed at both ends and subjected to a thermal expansion $\Delta\epsilon$

$$\Delta\epsilon = \Delta x\vec{i} + \Delta y\vec{j} + \Delta z\vec{k} \quad \ldots\ldots [7]$$

$$\left.\begin{aligned} \int_{s_0}^{s_1} \psi ds &= 0 \\ \int_{s_0}^{s_1} [\psi \cdot \rho] ds &= -\Delta\epsilon \end{aligned}\right\} \quad \ldots\ldots [8]$$

where the integration is carried out from one fixed anchorage to the other.

$$\vec{s} = \cos\theta \sin\phi\,\vec{i} + \cos\phi\,\vec{j} + \sin\phi \sin\theta\,\vec{k} \quad \ldots\ldots [9]$$

$$\vec{n} = -\sin\theta\vec{i} + \cos\theta\vec{k} \quad \ldots\ldots [10]$$

Substitute Equations [9] and [10] in Equation [4a]

$$\beta = \frac{1}{EI} + \frac{1}{EI}\left\{0.3\cos\theta\sin\phi\,\vec{i} + 0.3\cos\phi\,\vec{j} + 0.3\sin\phi\sin\theta\,\vec{k} + (K-1)(-\sin\theta)\vec{i} + (K-1)\cos\theta\,\vec{k}\right\}$$

From Equations [6], [9], and [10], the dyad products

$$m_s \cdot \vec{s} = \cos\theta\sin\phi m_x\vec{i} + \cos\phi m_y\vec{j} + \sin\phi\sin\theta m_z\vec{k}$$

$$m_n \cdot \vec{n} = (-\sin\theta)m_x\vec{i} + \cos\theta m_z\vec{k}$$

$$\psi = \text{dyad product } [\beta \cdot M]$$

$$= \frac{M}{EI} + \frac{1}{EI}\Big\{0.3\cos^2\theta\sin^2\phi m_x\vec{i} + 0.3\cos^2\phi m_y\vec{j} + 0.3\sin^2\phi\sin^2\theta m_z\vec{k} + (K-1)\sin^2\theta m_x\vec{i} + (K-1)\cos^2\theta m_z\vec{k}\Big\}$$

$$= \frac{1}{EI}\Big\{[1 + 0.3\sin^2\phi\cos^2\theta + (K-1)\sin^2\theta]m_x\vec{i} + [1 + 0.3\cos^2\phi]m_y\vec{j} + [1 + 0.3\sin^2\phi\sin^2\theta + (K-1)\cos^2\theta]m_z\vec{k}\Big\} \quad \ldots [11]$$

Equation [6] can be written

$$M = M_0 + [P\vec{i} + Q\vec{j} + N\vec{k}]\cdot[l_x\vec{i} + l_y\vec{j} + l_z\vec{k}]$$
$$= M_0 + (Ql_z - Nl_y)\vec{i} + (Nl_x - Pl_z)\vec{j} + (Pl_y - Ql_x)\vec{k}$$
$$= (M_{0x} + Ql_z - Nl_y)\vec{i} + (M_{0y} + Nl_x - Pl_z)\vec{j} + (M_{0z} + Pl_y - Ql_x)\vec{k}$$

Therefore

$$\left.\begin{aligned} m_x &= M_{0x} + Ql_z - Nl_y \\ m_y &= M_{0y} + Nl_x - Pl_z \\ m_z &= M_{0z} + Pl_y - Ql_x \end{aligned}\right\} \quad \ldots\ldots\ldots [12]$$

Substitute Equations [11] and [12] in [8]

$$\int_{s_0}^{s_1}\psi ds = O = \frac{1}{EI}\int_{s_0}^{s_1}\{M_{0x} + Ql_z - Nl_y\}\{1 + 0.3\cos^2\theta\sin^2\phi + (K-1)\sin^2\theta\}\vec{i}\,ds + \frac{1}{EI}\int_{s_0}^{s_1}\{M_{0y} + Nl_x - Pl_z\}\{1 + 0.3\cos^2\phi\}\vec{j}\,ds + \frac{1}{EI}\int_{s_0}^{s_1}\{M_{0z} + Pl_y - Ql_x\}\{1 + 0.3\sin^2\theta\sin^2\phi + (K-1)\cos^2\theta\}\vec{k}\,ds$$

Therefore

$$\left.\begin{aligned} &\int_{s_0}^{s_1}\{M_{0x} + Ql_z - Nl_y\}\{1 + 0.3\cos^2\theta\sin^2\phi + (K-1)\sin^2\theta\}\,ds = 0 \\ &\int_{s_0}^{s_1}\{M_{0y} + Nl_x - Pl_z\}\{1 + 0.3\cos^2\phi\}\,ds = 0 \\ &\int_{s_0}^{s_1}\{M_{0z} + Pl_y - Ql_x\}\{1 + 0.3\sin^2\theta\sin^2\phi + (K-1)\cos^2\theta\}\,ds = 0 \end{aligned}\right\} \quad \ldots [13]$$

$$-EI\,\Delta\epsilon = \int_{s_0}^{s_1}[m_x\{1 + 0.3\sin^2\phi\cos^2\theta + (K-1)\sin^2\theta\}\vec{i} + m_y\{1 + 0.3\cos^2\phi\}\vec{j} + m_z\{1 + 0.3\sin^2\phi\sin^2\theta + (K-1)\cos^2\theta\}\vec{k}]\cdot[l_x\vec{i} + l_y\vec{j} + l_z\vec{k}]\,ds$$
$$= \int_{s_0}^{s_1}\{[1 + 0.3\cos^2\phi]l_xm_y - [1 + 0.3\sin^2\phi\sin^2\theta + (K-1)\cos^2\theta]l_ym_z\}\vec{i}\,ds + \int_{s_0}^{s_1}\{[1 + 0.3\sin^2\phi\sin^2\theta + (K-1)\cos^2\theta]l_zm_x - [1 + 0.3\sin^2\phi\cos^2\theta + (K-1)\sin^2\theta]l_xm_z\}\vec{j}\,ds + \int_{s_0}^{s_1}\{[1 + 0.3\sin^2\phi\cos^2\theta + (K-1)\sin^2\theta]l_ym_x - [1 + 0.3\cos^2\phi]l_xm_y\}\vec{k}\,ds$$

Therefore

$$\left.\begin{aligned} -EI\,\Delta x &= \int_{s_0}^{s_1}\{M_{0y} + Nl_x - Pl_z\}\{1 + 0.3\cos^2\phi\}\,l_z ds - \int_{s_0}^{s_1}\{M_{0z} + Pl_y - Ql_x\}\{1 + 0.3\sin^2\phi\sin^2\theta + (K-1)\cos^2\theta\}\,l_y ds \\ -EI\,\Delta y &= \int_{s_0}^{s_1}\{M_{0z} + Pl_y - Ql_x\}\{1 + 0.3\sin^2\phi\sin^2\theta + (K-1)\cos^2\theta\}\,l_x ds - \int_{s_0}^{s_1}\{M_{0x} + Ql_z - Nl_y\}\{1 + 0.3\sin^2\phi\cos^2\theta + (K-1)\sin^2\theta\}\,l_z ds \\ -EI\,\Delta z &= \int_{s_0}^{s_1}\{M_{0x} + Ql_z - Nl_y\}\{1 + 0.3\sin^2\phi\cos^2\theta + (K-1)\sin^2\theta\}\,l_y ds - \int_{s_0}^{s_1}\{M_{0y} + Nl_x - Pl_z\}\{1 + 0.3\cos^2\phi\}\,l_x ds \end{aligned}\right\} \quad \ldots [14]$$

Let

$$A_z = \int_{s_0}^{s_1}\{1 + 0.3\sin^2\theta\sin^2\phi + (K-1)\cos^2\theta\}ds$$
$$A_x = \int_{s_0}^{s_1}\{1 + 0.3\sin^2\theta\sin^2\phi + (K-1)\cos^2\theta\}l_x ds$$
$$A_y = \int_{s_0}^{s_1}\{1 + 0.3\sin^2\theta\sin^2\phi + (K-1)\cos^2\theta\}l_y ds$$
$$A_{x^2} = \int_{s_0}^{s_1}\{1 + 0.3\sin^2\theta\sin^2\phi + (K-1)\cos^2\theta\}l_x^2 ds$$
$$A_{y^2} = \int_{s_0}^{s_1}\{1 + 0.3\sin^2\theta\sin^2\phi + (K-1)\cos^2\theta\}l_y^2 ds$$
$$A_{xy} = \int_{s_0}^{s_1}\{1 + 0.3\sin^2\theta\sin^2\phi + (K-1)\cos^2\theta\}l_x l_y ds$$
$$B_z = \int_{s_0}^{s_1}\{1 + 0.3\cos^2\theta\sin^2\phi + (K-1)\sin^2\theta\}ds$$
$$B_y = \int_{s_0}^{s_1}\{1 + 0.3\cos^2\theta\sin^2\phi + (K-1)\sin^2\theta\}\,l_y ds$$
$$B_x = \int_{s_0}^{s_1}\{1 + 0.3\cos^2\theta\sin^2\phi + (K-1)\sin^2\theta\}l_x ds$$
$$B_{y^2} = \int_{s_0}^{s_1}\{1 + 0.3\cos^2\theta\sin^2\phi + (K-1)\sin^2\theta\}l_y^2 ds$$
$$B_{x^2} = \int_{s_0}^{s_1}\{1 + 0.3\cos^2\theta\sin^2\phi + (K-1)\sin^2\theta\}l_x^2 ds$$
$$B_{yx} = \int_{s_0}^{s_1}\{1 + 0.3\cos^2\theta\sin^2\phi + (K-1)\sin^2\theta\}l_y l_x ds$$
$$C_z = \int_{s_0}^{s_1}\{1 + 0.3\cos^2\phi\}ds$$
$$C_x = \int_{s_0}^{s_1}\{1 + 0.3\cos^2\phi\}l_x ds$$
$$C_x = \int_{s_0}^{s_1}\{1 + 0.3\cos^2\phi\}l_x ds$$
$$C_{x^2} = \int_{s_0}^{s_1}\{1 + 0.3\cos^2\phi\}l_x^2 ds$$
$$C_{x^2} = \int_{s_0}^{s_1}\{1 + 0.3\cos^2\phi\}l_x^2 ds$$
$$C_{xx} = \int_{s_0}^{s_1}\{1 + 0.3\cos^2\phi\}l_x l_x ds$$

It is to be noted that the integrations are along the pipe and extend from one anchorage to the other anchorage.

Equations [13] and [14] can now be written

$$\left.\begin{aligned} B_xM_{0z} + B_xQ - B_yN &= 0 \\ C_xM_{0y} + C_xN - C_xP &= 0 \\ A_xM_{0x} + A_yP - A_xQ &= 0 \end{aligned}\right\} \quad \ldots\ldots\ldots [13a]$$

$_1M_{ox}$	$_2M_{ox}$	$_3M_{ox}$	$_1M_{oy}$	$_2M_{oy}$	$_3M_{oy}$	$_1M_{oz}$	$_2M_{oz}$	$_3M_{oz}$
0	0	0	0	0	0	A_s +(11)	A_s −(22)	0
0	0	0	0	0	0	A_s +(11)+(12)	A_s +(12)	A_s −(33)
0	0	0	0	0	0	A_s +(11)+(12)+(44)	A_s +(12)+(44)	A_s +(44)
B_s +(11)	B_s −(22)	0	0	0	0	0	0	0
B_s +(11)+(12)	B_s +(12)	B_s −(33)	0	0	0	0	0	0
B_s +(11)+(12)+(44)	B_s +(12)+(44)	B_s +(44)	0	0	0	0	0	0
0	0	0	C_s +(11)	C_s −(22)	0	0	0	0
0	0	0	C_s +(11)+(12)	C_s +(12)	C_s −(33)	0	0	0
0	0	0	C_s +(11)+(12)+(44)	C_s +(12)+(44)	C_s +(44)	0	0	0
0	0	0	C_z −(11)	C_z +(22)	0	A_y +(11)	A_y −(22)	0
0	0	0	C_z −(11)−(12)	C_z −(12)	C_z +(33)	A_y +(11)+(12)	A_y +(12)	A_y −(33)
0	0	0	C_z −(11)−(12)−(44)	C_z −(12)−(44)	C_z −(44)	A_y +(11)+(12)+(44)	A_y +(12)+(44)	A_y +(44)
B_z +(11)	B_z −(22)	0	0	0	0	A_x −(11)	A_x +(22)	0
B_z +(11)+(12)	B_z +(12)	B_z −(33)	0	0	0	A_x −(11)−(12)	A_x −(12)	A_x +(33)
B_z +(11)+(12)+(44)	B_z +(12)+(44)	B_z +(44)	0	0	0	A_x −(11)−(12)−(44)	A_x −(12)−(44)	A_x −(44)
B_y −(11)	B_y +(22)	0	C_x +(11)	C_x −(22)	0	0	0	0
B_y −(11)−(12)	B_y −(12)	B_y +(33)	C_x +(11)+(12)	C_x +(12)	C_x −(33)	0	0	0
B_y −(11)−(12)−(44)	B_y −(12)−(44)	B_y −(44)	C_x +(11)+(12)+(44)	C_x +(12)+(44)	C_x +(44)	0	0	0

FIG. 6

$$
\left.
\begin{aligned}
-EI\,\Delta x &= C_s M_{0y} + C_{sx} N - C_{sz} P - A_y M_{0s} - A_{yz} P + A_{xy} Q \\
&= C_s \left\{ \frac{C_s P - C_x N}{C_s} \right\} + C_{sx} N - C_{sz} P - A_y \left\{ \frac{A_s Q - A_y P}{A_s} \right\} - A_{yz} P + A_{xy} Q \\
&= N \left\{ C_{sx} - \frac{C_x C_s}{C_s} \right\} - P \left\{ C_{sz} + A_{yz} - \frac{C_s^2}{C_s} - \frac{A_y^2}{A_s} \right\} + Q \left\{ A_{xy} - \frac{A_y A_x}{A_s} \right\} \\
-EI\,\Delta y &= A_s M_{0z} + A_{xy} P - A_{xz} Q - B_s M_{0x} - B_{sz} Q + B_{ys} N \\
&= A_s \left\{ \frac{A_s Q - A_y P}{A_s} \right\} + A_{xy} P - A_{xz} Q - B_s \left\{ \frac{B_y N - B_s Q}{B_s} \right\} - B_{sz} Q + B_{ys} N \\
&= N \left\{ B_{ys} - \frac{B_y B_s}{B_s} \right\} + P \left\{ A_{xy} - \frac{A_y A_x}{A_s} \right\} - Q \left\{ B_{sz} + A_{xz} - \frac{A_s^2}{A_s} - \frac{B_s^2}{B_s} \right\} \\
-EI\,\Delta z &= B_y M_{0x} + B_{ys} Q - B_{yz} N - C_x M_{0y} - C_{xz} N + C_{sx} P \\
&= B_y \left\{ \frac{B_y N - B_s Q}{B_s} \right\} + B_{ys} Q - B_{yz} N - C_x \left\{ \frac{C_s P - C_x N}{C_s} \right\} - C_{xz} N + C_{sx} P \\
&= -N \left\{ B_y^2 + C_s^2 - \frac{B_y^2}{B_s} - \frac{C_x^2}{C_s} \right\} + P \left\{ C_{sx} - \frac{C_x C_s}{C_s} \right\} + Q \left\{ B_{ys} - \frac{B_y B_s}{B_s} \right\}
\end{aligned}
\right\} \quad \text{.....[14a]}
$$

N_1	N_2	N_3	P_1	P_2	P_3	Q_1	Q_2	Q_3	=	
0	0	0	A_y +(11)	A_y −(22)	0	A_x −(11)	A_x +(22)	0	=	0
0	0	0	A_y +(11)+(12)	A_y +(12)	A_y −(33)	A_x −(11)−(12)	A_x −(12)	A_x +(33)	=	0
0	0	0	A_y +(11)+(12)+(44)	A_y +(12)+(44)	A_y +(44)	A_x −(11)−(12)−(44)	A_x −(12)−(44)	A_x −(44)	=	0
B_y −(11)	B_y +(22)	0	0	0	0	B_z +(11)	B_z −(22)	0	=	0
B_y −(11)−(12)	B_y −(12)	B_y +(33)	0	0	0	B_z +(11)+(12)	B_z +(12)	B_z −(33)	=	0
B_y −(11)−(12)−(44)	B_y −(12)−(44)	B_y −(44)	0	0	0	B_z +(11)+(12)+(44)	B_z +(12)+(44)	B_z +(44)	=	0
C_x +(11)	C_x −(22)	0	C_z −(11)	C_z +(22)	0	0	0	0	=	0
C_x +(11)+(12)	C_x +(12)	C_x −(33)	C_z −(11)−(12)	C_z −(12)	C_z +(33)	0	0	0	=	0
C_x +(11)+(12)+(44)	C_x +(12)+(44)	C_x +(44)	C_z −(11)−(12)−(44)	C_z −(12)−(44)	C_z −(44)	0	0	0	=	0
C_{zx} −(11)	C_{zx} +(22)	0	$A_y{}^2+C_z{}^2$ +(11)	$A_y{}^2+C_z{}^2$ −(22)	0	A_{xy} −(11)	A_{xy} +(22)	0	=	$EI\,\Delta x_{12}$
C_{zx} −(11)−(12)	C_{zx} −(12)	C_{zy} +(33)	$A_y{}^2+C_z{}^2$ +(11)+(12)	$A_y{}^2+C_z{}^2$ +(12)	$A_y{}^2+C_z{}^2$ −(33)	A_{xy} −(11)−(12)	A_{xy} −(12)	A_{xy} +(33)	=	$EI\,\Delta x_{13}$
C_{zx} −(11)−(12)−(44)	C_{zx} −(12)−(44)	C_{zx} −(44)	$A_y{}^2+C_z{}^2$ +(11)+(12)+(44)	$A_y{}^2+C_z{}^2$ +(12)+(44)	$A_y{}^2+C_z{}^2$ +(44)	A_{xy} −(11)−(12)−(44)	A_{xy} −(12)−(44)	A_{xy} −(44)	=	$EI\,\Delta x_{14}$
B_{yz} −(11)	B_{yz} +(22)	0	A_{xy} −(11)	A_{xy} +(22)	0	$A_x{}^2+B_z{}^2$ +(11)	$A_x{}^2+B_z{}^2$ −(22)	0	=	$EI\,\Delta y_{12}$
B_{yz} −(11)−(12)	B_{yz} −(12)	B_{yz} +(33)	A_{xy} −(11)−(12)	A_{xy} −(12)	A_{xy} +(33)	$A_x{}^2+B_z{}^2$ +(11)+(12)	$A_x{}^2+B_z{}^2$ +(12)	$A_x{}^2+B_z{}^2$ −(33)	=	$EI\,\Delta y_{13}$
B_{yz} −(11)−(12)−(44)	B_{yz} −(12)−(44)	B_{yz} −(44)	A_{xy} −(11)−(12)−(44)	A_{xy} −(12)−(44)	A_{xy} −(44)	$A_x{}^2+B_z{}^2$ +(11)+(12)+(44)	$A_x{}^2+B_z{}^2$ +(12)+(44)	$A_x{}^2+B_z{}^2$ +(44)	=	$EI\,\Delta y_{14}$
$B_y{}^2+C_x{}^2$ +(11)	$B_y{}^2+C_x{}^2$ −(22)	0	C_{zx} −(11)	C_{zx} +(22)	0	B_{yz} −(11)	B_{yz} +(22)	0	=	$EI\,\Delta z_{12}$
$B_y{}^2+C_x{}^2$ +(11)+(12)	$B_y{}^2+C_x{}^2$ +(12)	$B_y{}^2+C_x{}^2$ −(33)	C_{zx} −(11)−(12)	C_{zx} −(12)	C_{zx} +(33)	B_{yz} −(11)−(12)	B_{yz} −(12)	B_{yz} +(33)	=	$EI\,\Delta z_{13}$
$B_y{}^2+C_x{}^2$ +(11)+(12)+(44)	$B_y{}^2+C_x{}^2$ +(12)+(44)	$B_y{}^2+C_x{}^2$ +(44)	C_{zx} −(11)−(12)−(44)	C_{zx} −(12)−(44)	C_{zx} −(44)	B_{yz} −(11)−(12)−(44)	B_{yz} −(12)−(44)	B_{yz} −(44)	=	$EI\,\Delta z_{14}$

FIG. 6 (*continued*)

An inspection of the six simultaneous Equations, [13*a*] and [14*a*], which determine the end reactions, will show that they are relatively simple, once the A, B, and C coefficients have been determined. In order to simplify the determination of these coefficients, a series of 36 schedules have been drawn up which will handle the 36 most commonly recurring forms of pipe sections. For these cases, the general forms of the integrals have been determined as have their values for limits ranging between 0 and 90 deg at 15-deg intervals. As mentioned in the introduction to this paper, it is these schedules which have been omitted in this condensed paper.

Determination of Flexibility of Piping Having More Than Two Anchorages

Consider Fig. 5, which is shown in single plane. The method to be described is also applicable to piping systems in three dimensions. Some modification of the previous nomenclature is required as follows. The anchorages are labeled successively 1, 2, 3, . . . , etc., through n. The reactions at each anchorage are labeled ${}_1M_{0x}$, ${}_1M_{0y}$, ${}_1M_{0z}$, P_1, Q_1, N_1, ${}_2M_{0x}$, ${}_2M_{0y}$, . . . , etc. The coefficients ${}_1A_x$, ${}_1A_z$, ${}_1A_y$, ${}_1B_x$, . . . , etc., are integrations for the various branches, each considered separately. Let us

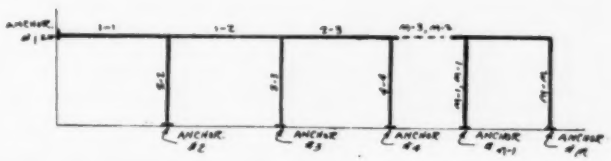


FIG. 5

return now to Equations [13*a*] and [14*a*]. They were derived from Equations [7] and [8]. It will be remembered that the integrations were carried out from one anchorage to the other. Where there are only two anchorages, the reactions at one anchorage are transmitted to the other anchorage through the medium of the connecting pipe and are constant. In the case where there are more than two anchorages, the reactions on the various branches are different. The integrations must thus be subdivided to correspond with the individual branches in which the reactions are constant but different from that of any other branch. Recognizing this, Equations [7] and [8] are modified as follows:

As regards rotations

$$
\left.
\begin{aligned}
&{}_{11}A_x({}_1M_{0x}) + {}_{11}A_y(P_1) - {}_{11}A_z(Q_1) = {}_{22}A_x({}_2M_{0x}) + {}_{22}A_y(P_2) - {}_{22}A_z(Q_2)\\
&{}_{11}A_x({}_1M_{0x}) + \ldots + {}_{12}A_x({}_1M_{0x} + {}_2M_{0x}) + \ldots + = {}_{33}A_x({}_3M_{0x}) + \ldots\\
&{}_{11}A_x({}_1M_{0x}) + \ldots + {}_{12}A_x({}_1M_{0x} + {}_2M_{0x}) + \ldots + {}_{23}A_x({}_1M_{0x} + {}_2M_{0x} + {}_3M_{0x}) = {}_{44}A_x({}_4M_{0x}) + \ldots\\
&\ldots\ldots\ldots

Buckling of Rectangular Plates With Built-In Edges

By SAMUEL LEVY,[1] WASHINGTON, D. C.

This paper presents an exact solution in terms of infinite series of the problem of buckling by compressive forces in one direction of a rectangular plate with built-in edges (zero slope, zero displacement in the direction normal to the plane of the plate). The buckling load is calculated for 14 ratios of length to width, ranging in steps of 0.25 from 0.75 to 4. On the basis of convergence, as the number of terms used in the infinite series is increased, it is estimated that the possible error in the numerical results presented is of the order of 0.1 per cent. A comparison is given with the work of other authors.

Introduction

IN THE design of thin plates buckled by compressive forces in their plane, the degree to which the edges are restrained has an appreciable effect on the buckling load. Approximate values of the buckling stress for a built-in rectangular plate, loaded by compressive stresses in one direction, have been computed by Faxén (1);[2] Sezawa and Watanabe (2); and Maulbetsch (3). The "built-in" edge condition is here defined as zero slope and zero displacement in the direction normal to the plane of the plate. The similar problem of a built-in square plate loaded by equal compressive stresses in two directions has been solved by Taylor (4) and Trefftz (5).

Faxén (1) solves the differential equation $\frac{\partial^4 w}{\partial x^4} + 2\frac{\partial^4 w}{\partial x^2 \partial y^2} + \frac{\partial^4 w}{\partial y^4} = \frac{-h\sigma_x}{D}\frac{\partial^2 w}{\partial x^2}$ (w = displacement normal to the plane of the plate), and gets an infinite set of simultaneous linear equations which must be satisfied in order to satisfy the boundary conditions. He obtains numerical solutions which satisfy up to six of these equations simultaneously. His results are given in the third column of Table 1.

Sezawa and Watanabe (2) solve the differential equation and expand the resulting hyperbolic and circular functions in trigonometric series, deriving an infinite set of simultaneous linear equations. They limit themselves to the first six of these equations in their numerical work. Their results are given in the fourth column of Table 1. They agree closely with Faxén's values.

Maulbetsch (3) extends Faxén's solution of the differential equation up to length-to-width ratios of $a/b = 4$. He obtains numerical solutions which satisfy up to six of the infinite set of simultaneous equations. The results are given in the fifth column of Table 1. Maulbetsch also solves the problem using the Ritz energy method and approximating the deflection surface by the normal modes of vibration of a bar clamped at both ends. He limits his numerical work with this method by requiring the lateral deflection along lines transverse to the direction of loading to be the same as the first normal mode of vibration of a bar clamped at both ends, and by allowing only up to three variations in the lateral deflection along lines parallel to the load. The results are given in the sixth column of Table 1.

TABLE 1 BUCKLING FACTORS $(\sigma_x)_{cr}b^2h/\pi^2D$ OBTAINED BY DIFFERENT AUTHORS

Length-width ratio, a/b	Number of buckles	$(\sigma_x)_{cr}b^2h/\pi^2D$ Faxén (1)	Sezawa and Watanabe (2)	Maulbetsch, diff. eq. (3)	Maulbetsch energy (3)	Table 2 of present paper
0.75	1	11.39	.....	....	12.77	11.66
1.00	1	10.07	10.04	....	10.48	10.07
1.25	2	9.20	.....	....	9.38	9.25
1.50	2	8.30	8.32	....	8.45	8.33
1.75	2	8.18	.....	....	8.17	8.11
2.00	3	7.87	7.88	7.84	8.06	7.88
2.25	3	.....	.....	....	7.96	7.63
2.50	3	.....	.....	....	7.99	7.57
2.75	4	.....	.....	7.13	7.76	7.44
3.00	4	.....	.....	6.93	7.59	7.37
3.25	4	.....	.....	....	7.86	7.35
3.50	5	.....	.....	6.81	7.37	7.27
3.75	5	.....	.....	....	7.40	7.24
4.00	5	.....	.....	....	7.45	7.23

The critical stresses obtained by the energy method are seen to be consistently higher than those obtained from an approximate solution of the differential equation. This is to be expected since the energy method generally gives an upper limit of buckling stresses, while the failure to fulfill all boundary conditions for built-in edges is equivalent to relaxing the end restraint and consequently should lead to a lower limit for buckling stresses. The differences between the upper and lower limits exceed 10 per cent in one case ($a/b = 0.75$), and they are of the order of 5 per cent in most cases. It appeared desirable therefore to investigate the possibility of obtaining more accurate values by an exact solution of the differential equation. The results of such an investigation are given in this paper.

Fundamental Equations

Nomenclature. Consider an initially flat rectangular plate of uniform thickness Fig. 1, and let

a = length in direction of load
b = width perpendicular to load
h = thickness
x, y, z = co-ordinate axes with origin at one corner of plate
w = displacement in direction of z axis normal to plane of plate
σ_x = stress in direction of load
$(\sigma_x)_{cr}$ = critical stress for buckling
D = flexural rigidity of plate $= Eh^3/12(1 - \mu^2)$
m_x = moment per unit length at edge $y = 0$
m_y = moment per unit length at edge $x = 0$
k_m = coefficient in expansion of m_x
l_n = coefficient in expansion of m_y
K = symbol in summation formulas

Deflection of Simply Supported Plate Under Combined Edge Moments and Axial Compression in One Direction. The plate with built-in edges may be regarded as a simply supported plate

[1] National Bureau of Standards, U. S. Department of Commerce.

[2] Numbers in parentheses refer to the Bibliography at the end of the paper.

Presented at the National Meeting of the Applied Mechanics Division, Cambridge, Mass., June 19–20, 1942, of The American Society of Mechanical Engineers.

Discussion of this paper should be addressed to the Secretary, A.S.M.E., 29 West 39th Street, New York, N. Y., and will be accepted until January 11, 1943, for publication at a later date. Discussion received after the closing date will be returned.

Note: Statements and opinions advanced in papers are to be understood as individual expressions of their authors and not those of the Society.

in which the slope along the edges is made equal to zero by suitably distributed edge bending moments. As a first step toward the solution of the problem we will therefore consider the lateral deflection of a simply supported plate under combined edge moments and axial compression in one direction.

This problem may be examined by substituting for the edge

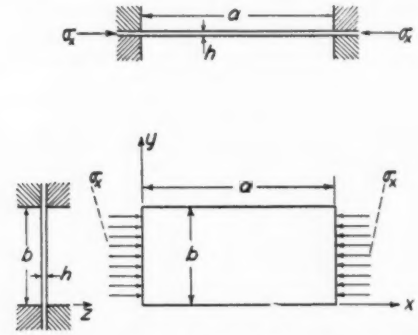


FIG. 1 FLAT RECTANGULAR PLATE WITH ALL EDGES BUILT-IN, LOADED BY UNIFORM COMPRESSION IN ONE DIRECTION

moments an equivalent pressure distribution. Timoshenko[3] has shown that if the lateral displacement is described by the trigonometric series

$$w = \sum_{m=1}^{\infty}\sum_{n=1}^{\infty} a_{m,n} \sin\frac{m\pi x}{a} \sin\frac{n\pi y}{b} \quad \ldots\ldots [1]$$

a concentrated force Q acting at a point (x, y) will be in equilibrium so long as

$$a_{m,n} = \frac{4Q \sin\frac{m\pi x}{a} \sin\frac{n\pi y}{b}}{abD\pi^4 \left\{\left[\left(\frac{m}{a}\right)^2 + \left(\frac{n}{b}\right)^2\right]^2 - \frac{m^2\sigma_x h}{\pi^2 a^2 D}\right\}} \quad \ldots\ldots [2]$$

The edge bending moment along an increment dx or dy of the edge may, on the basis of Saint Venant's principle, be considered equivalent to a couple consisting of a force dQ acting at a short distance c from the edge and a reaction $-dQ$ acting at the edge.

If we define as m_x and m_y the bending moments along those edges of the plate corresponding to the x and y axes, respectively, the value of dQ along these edges is, when $y = 0$

$$dQ = (1/c)m_x\, dx \quad \ldots\ldots [3a]$$

and when $x = 0$

$$dQ = (1/c)m_y\, dy \quad \ldots\ldots [3b]$$

The mode for the minimum buckling load always has a single half wave (n always odd) in the direction perpendicular to the load. The moment at the edge $y = b$ is, therefore, the same as that at $y = 0$ or, when $y = b$

$$dQ = (1/c)m_x\, dx \quad \ldots\ldots [3c]$$

The mode for the minimum buckling load may have either an odd (all values of m odd) or an even (all values of m even) number of half waves in the direction parallel with the load. If the number is odd the moments at the edges $x = 0$, $x = a$ will be equal or, when $x = a$ (m, odd)

$$dQ = (1/c)m_y\, dy \quad \ldots\ldots [3d]$$

[3] Reference (6), p. 317.

while, if the number is even the moments at the edges $x = 0$, $x = a$ will be of opposite sign or, when $x = a$ (m, even)

$$dQ = -(1/c)m_y\, dy \quad \ldots\ldots [3e]$$

The edge moments m_x and m_y may be expressed as trigonometric series with undetermined coefficients. Let

$$\left.\begin{aligned} m_x &= \frac{b^2}{4\pi} \sum_{m=1,2,3\ldots}^{\infty} k_m \sin\frac{m\pi x}{a} \\ m_y &= \frac{a^2}{4\pi} \sum_{n=1,3,\ldots}^{\infty} l_n \sin\frac{n\pi y}{b} \end{aligned}\right\} \quad \ldots\ldots [4]$$

Substituting Equations [4] and [3] in [2], integrating around the edge of the plate, and taking the limit as c approaches zero

$$a_{m,n} = \frac{nk_m + ml_n}{\pi^4 D\left[\left(\frac{m}{a}\right)^2 + \left(\frac{n}{b}\right)^2\right]^2 - \frac{\pi^2 m^2 \sigma_x h}{a^2}} \quad \ldots\ldots [5]$$

where n must always have odd values, and where the values of m must either be all odd or all even.

The lateral deflection is obtained by substituting Equation [5] into Equation [1]

$$w = \sum_{\substack{m=1,3,5\ldots \\ \text{or } 2,4,6\ldots}}^{\infty} \sum_{n=1,3,5\ldots}^{\infty} \frac{(nk_m + ml_n) \sin\frac{m\pi x}{a} \sin\frac{n\pi y}{b}}{\pi^4 D\left[\left(\frac{m}{a}\right)^2 + \left(\frac{n}{b}\right)^2\right]^2 - \frac{m^2\pi^2\sigma_x h}{a^2}} \quad \ldots [6]$$

where m has odd values from 1 to ∞ for buckling into an odd number of waves and even values from 2 to ∞ for buckling into an even number of waves.

Condition of Zero Slope at Built-In Edges. In Equation [6], we have a solution for the lateral deflection of a plate with simply supported edges under combined axial compression in one direction in its plane and moments on its edges. We will now adjust the undetermined coefficients k_m and l_n in the moment Equations [4] in such a way that the slope at the edges of the plate is zero. From Equation [6], setting the slope equal to zero

$$\left.\begin{aligned} 0 = \left(\frac{\partial w}{\partial x}\right)_{x=0,a} &= \sum_{m}^{\infty}\sum_{n}^{\infty} \frac{m\pi}{a} (-1)^m \\ &\frac{(nk_m + ml_n) \sin\frac{n\pi y}{b}}{\pi^4 D\left[\left(\frac{m}{a}\right)^2 + \left(\frac{n}{b}\right)^2\right]^2 - \frac{\pi^2 m^2 \sigma_x h}{a^2}} \\ 0 = \left(\frac{\partial w}{\partial y}\right)_{y=0,b} &= \sum_{m}^{\infty}\sum_{n}^{\infty} -\frac{n\pi}{b} \\ &\frac{(nk_m + ml_n) \sin\frac{m\pi x}{a}}{\pi^4 D\left[\left(\frac{m}{a}\right)^2 + \left(\frac{n}{b}\right)^2\right]^2 - \frac{\pi^2 m^2 \sigma_x h}{a^2}} \end{aligned}\right\} \quad \ldots [7]$$

In order to satisfy Equations [7] for all values of x and y, the coefficients of $\sin \frac{n\pi y}{b}$ and $\sin \frac{m\pi x}{a}$ must separately be zero. This leads to the doubly infinite sets of equations

$$\left.\begin{aligned} 0 &= \sum_{\substack{m=1,3,5\ldots \\ \text{or } 2,4,6\ldots}}^{\infty} \frac{mnk_m + m^2 t_n}{\left[m^2\frac{b^2}{a^2} + n^2\right]^2 - \frac{\sigma_x b^2 h}{\pi^2 D}\frac{m^2 b^2}{a^2}}, \quad (n = 1, 3, 5\ldots) \\ 0 &= \sum_{n=1,3,5\ldots}^{\infty} \frac{n^2 k_m + nmt_n}{\left[m^2\frac{b^2}{a^2} + n^2\right]^2 - \frac{\sigma_x b^2 h}{\pi^2 D}\frac{m^2 b^2}{a^2}}, \quad \begin{pmatrix} m = 1, 3, 5\ldots \\ \text{or } 2, 4, 6\ldots\ldots \end{pmatrix} \end{aligned}\right\} \ldots [8]$$

Solution

Condition for Buckling. In order to satisfy Equations [8], it is necessary either that k_m and t_n be zero (in which case there are no bending moments at the edges and no lateral displacement of the plate), or that σ_x have a value $(\sigma_x)_{cr}$ such that the determinant of the coefficients of k_m and t_n be zero. The smallest value of $(\sigma_x)_{cr}$ is then the desired critical buckling stress.

Summation Formulas. In making the computations it was found convenient to develop certain summation formulas. The method used is described by Guillemin[4] and is credited by him to A. Sommerfeld. These formulas are

$$\sum_{r=1,3\ldots}^{\infty} \frac{n^2}{\left[\frac{m^2b^2}{a^2} + n^2\right]^2 - K\frac{m^2b^2}{a^2}} = \frac{a/b}{4m\sqrt{K}}\left[\frac{\pi}{2}\sqrt{\frac{m^2b^2}{a^2} + \frac{mb}{a}\sqrt{K}}\tanh\frac{\pi}{2}\sqrt{\frac{m^2b^2}{a^2} + \frac{mb}{a}\sqrt{K}} - \frac{\pi}{2}\sqrt{\frac{m^2b^2}{a^2} - \frac{mb}{a}\sqrt{K}}\tanh\frac{\pi}{2}\sqrt{\frac{m^2b^2}{a^2} - \frac{mb}{a}\sqrt{K}}\right] \ldots [9]$$

$$\sum_{m=1,3\ldots}^{\infty} \frac{m^2}{\left[\frac{m^2b^2}{a^2} + n^2\right]^2 - K\frac{m^2b^2}{a^2}} = \frac{a^2/b^2}{2K\sqrt{1-\frac{4n^2}{K}}}\left[\frac{\pi an}{2b}\sqrt{1-\frac{K}{2n^2}\left(1-\sqrt{1-\frac{4n^2}{K}}\right)}\tanh\frac{\pi an}{2b}\sqrt{1-\frac{K}{2n^2}\left(1-\sqrt{1-\frac{4n^2}{K}}\right)} - \frac{\pi an}{2b}\sqrt{1-\frac{K}{2n^2}\left(1+\sqrt{1-\frac{4n^2}{K}}\right)}\tanh\frac{\pi an}{2b}\sqrt{1-\frac{K}{2n^2}\left(1+\sqrt{1-\frac{4n^2}{K}}\right)}\right] \ldots [10]$$

[4] Reference (7), p. 416.

$$\sum_{m=2,4,6\ldots}^{\infty} \frac{m^2}{\left[\frac{m^2b^2}{a^2} + n^2\right]^2 - K\frac{m^2b^2}{a^2}} = \frac{a^2/b^2}{2K\sqrt{1-\frac{4n^2}{K}}}\left[\frac{\pi an}{2b}\sqrt{1-\frac{K}{2n^2}\left(1-\sqrt{1-\frac{4n^2}{K}}\right)}\coth\frac{\pi an}{2b}\sqrt{1-\frac{K}{2n^2}\left(1-\sqrt{1-\frac{4n^2}{K}}\right)} - \frac{\pi an}{2b}\sqrt{1-\frac{K}{2n^2}\left(1+\sqrt{1-\frac{4n^2}{K}}\right)}\coth\frac{\pi an}{2b}\sqrt{1-\frac{K}{2n^2}\left(1+\sqrt{1-\frac{4n^2}{K}}\right)}\right] \ldots [11]$$

Convergence. The critical stress $(\sigma_x)_{cr}$ was computed by taking a sufficient number of terms in the determinant of the coefficients of k_m and t_n in Equations [8] so that the value of $(\sigma_x)_{cr}$ remained unchanged after taking additional terms.

Fortunately the convergence is rapid. For example, for the case of a square plate ($a = b$) the approximate value of $(\sigma_x)_{cr}$ which reduces the determinant involving t_1, k_1, k_3, k_5, and k_7 to zero is 10.047 (π^2D/b^2h); the approximate value of $(\sigma_x)_{cr}$ which reduces the determinant involving t_1, t_3, and k_1 to k_{13} to zero is 10.073 (π^2D/b^2h); the approximate value $(\sigma_x)_{cr}$ which reduces the determinant involving t_1 to t_5 and k_1 to k_{23} to zero is 10.074 (π^2D/b^2h); and the approximate value $(\sigma_x)_{cr}$ which reduces the determinant involving t_1 to t_7 and k_1 to k_{31} to zero is also 10.074 (π^2D/b^2h). Similar rapid convergence is indicated in Table 1 for ratios of length to width of 1.75, 2.5, 3.5, and 4. On the basis of these extensive computations, it seems reasonable to assume that, for length-to-width ratios up to 4, the approximate value of $(\sigma_x)_{cr}$ which reduces the determinant involving t_1, t_3, and k_1 to k_{13} to zero differs less than 0.1 per cent from the exact value of $(\sigma_x)_{cr}$ (which reduces the infinite determinant to zero).

Results. The results of the computation of the approximate values of $(\sigma_x)_{cr}$ which reduce finite determinants of the coefficients of k_m and t_n in Equations [8] to zero together with the estimated value (based on the convergence) of $(\sigma_x)_{cr}$ which would reduce the infinite determinant to zero are given in Table 2 for ratios of length to width from 0.75 to 4.

The results are plotted in Fig. 2. It is evident that as the ratio of length to width increases, the value of the critical stress approaches 6.97 (π^2D/b^2h), the value given by Dunn (8) for the critical stress for an infinitely long plate simply supported on the loaded edges and built-in on the other two edges. It is also evident that as the ratio of length to width approaches zero the

TABLE 2 BUCKLING STRESS OF RECTANGULAR PLATE WITH BUILT-IN EDGES, CRITICAL-STRESS RATIO $(\sigma_x)_{cr}b^2h/\pi^2D$

Length-width ratio, a/b	Number of buckles	Approximation: Including t_1 k_1 to k_7	Including t_1 to t_3 k_1 to k_{13}	Including t_1 to t_5 k_1 to k_{23}	Including t_1 to t_7 k_1 to k_{31}	Asymptotic value, estimated for infinite determinant
0.75	1	11.583	11.657	11.659	....	11.659
1.00	1	10.047	10.073	10.074	10.074	10.074
1.25	2	9.23	9.25	....	....	9.25
1.50	2	8.33	8.33	....	....	8.33
1.75	2	8.105	8.111	8.111	....	8.111
..	3	8.31	....	....	....	....
2.00	3	7.86	7.88	....	....	7.88
2.25	3	7.62	7.63	....	....	7.63
2.50	3	7.567	7.568	7.568	7.568	7.568
2.75	4	7.43	7.44	....	....	7.44
3.00	4	7.36	7.37	....	....	7.37
3.25	4	7.35	7.35	....	....	7.35
..	5	7.35	7.36	....	....	....
3.50	5	7.254	7.266	7.266	7.266	7.266
3.75	5	7.24	7.24	....	....	7.24
4.00	5	7.194	7.229	7.229	7.229	7.229

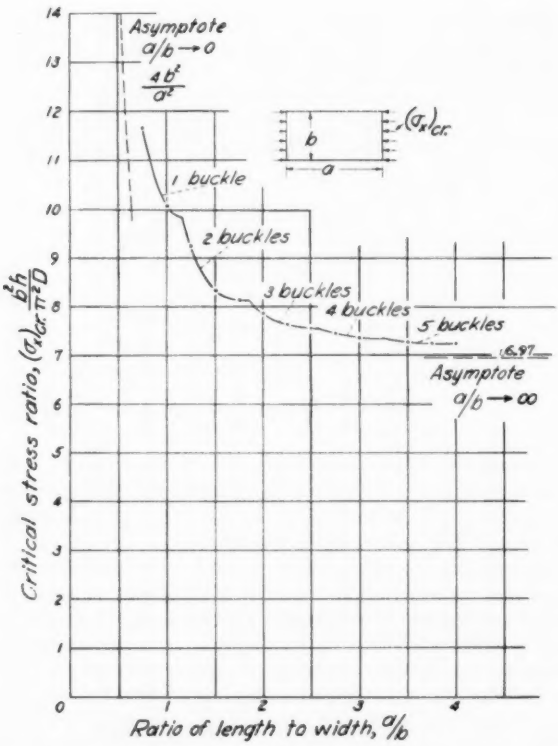


FIG. 2 BUCKLING STRESS OF RECTANGULAR PLATE WITH BUILT-IN EDGES, LOADED BY UNIFORM COMPRESSION IN ONE DIRECTION

value of the critical stress approaches $\frac{4b^2}{a^2}\frac{\pi^2 D}{b^2 h}$, the critical stress for a Euler column with built-in ends.

Comparison With Other Authors. The asymptotic values of critical-stress ratio derived in this paper are repeated in the last column of Table 1 for comparison with the values obtained by previous authors.

Faxén's results agree within about 2 per cent with the results in the present paper and are consistently equal to or lower except for $a/b = 1.75$. For $a/b = 1.75$, he derives a value of 8.18 which is even higher than the upper limit (energy solution) value of 8.17 given by Maulbetsch.

The results of Sezawa and Watanabe are equal to or lower than the results in the present paper by amounts up to about 0.3 per cent.

Maulbetsch has extended Faxén's solution of the differential equation up to values of $a/b = 4$. The results he obtained are consistently lower than the results in the present paper by amounts up to about 6 per cent. Maulbetsch's results using the Ritz energy method agree within about 10 per cent and are consistently higher than the results given in the present paper.

ACKNOWLEDGMENT

The author takes this opportunity to acknowledge the assistance of members of the Engineering Mechanics Section of the National Bureau of Standards, particularly that of W. Ramberg.

BIBLIOGRAPHY

1 "Die Knickfestigkeit rechteckiger Platten," by O. H. Faxén, *Zeitschrift für Angewandte Mathematik und Mechanik*, vol. 15, 1935, pp. 268–277.

2 "Buckling of a Rectangular Plate With Four Clamped Edges Re-Examined With an Improved Theory," by K. Sezawa and W. Watanabe, Tokyo Imperial University, Aeronautical Research Institute, Reports, vol. 11, no. 143, August, 1936, pp. 409–418.

3 "Buckling of Compressed Rectangular Plates With Built-In Edges," by J. L. Maulbetsch, JOURNAL OF APPLIED MECHANICS, Trans. A.S.M.E., vol. 59, 1937, p. A-59.

4 "The Buckling Load for a Rectangular Plate With Four Clamped Edges," by G. I. Taylor, *Zeitschrift für Angewandte Mathematik und Mechanik*, vol. 13, 1933, pp. 147–152.

5 "Die Bestimmung der Knicklast gedrückter, rechteckiger Platten," by E. Trefftz, *Zeitschrift für Angewandte Mathematik und Mechanik*, vol. 15, 1935, pp. 339–344.

6 "Theory of Elastic Stability," by S. Timoshenko, McGraw-Hill Book Company, Inc., New York, N. Y., 1936.

7 "Communication Networks," by E. A. Guillemin, John Wiley & Sons, Inc., New York, N. Y., 1931.

8 "An Investigation of Sheet-Stiffener Panels Subjected to Compression Loads With Particular Reference to Torsionally Weak Stiffeners," by Louis G. Dunn, U. S., N.A.C.A. Technical Note No. 752, 1940.

Investigation of Self-Excited Torsional Oscillations and Vibration Damper for Induction-Motor Drives

By A. M. WAHL[1] and E. G. FISCHER,[2] EAST PITTSBURGH, PA.

An unusual case of torsional oscillation was observed recently on several large induction-motor drives used for tunnel ventilation on the Pennsylvania Turnpike. These drives, which consist essentially of an induction motor driving a heavy centrifugal fan through a speed reducer, showed a severe torsional oscillation (with a double amplitude around 80 deg) at a point between two thirds and full speed during the accelerating period. These vibrations were found to be self-excited, as a consequence of the negative damping inherent in the shape of the speed-torque curve of the normal induction motor.

After consideration of various methods for eliminating the trouble, a torsional-vibration damper of relatively simple design was developed. Torsiograph records made on the actual drive showed that the oscillation was reduced to negligible values by the use of this damper.

Since induction-motor drives of this general type are used rather widely, it was felt that an account of this investigation, including the methods of calculating damper capacity, the laboratory tests on the damper, and the field tests on the actual drives would be of value to engineers, particularly those interested in vibration.

Introduction

An unusual case of self-excited torsional oscillation was encountered recently on a large induction-motor drive used for tunnel ventilation on the Pennsylvania Turnpike, as indicated schematically in Fig. 1. The torsional oscillation, which took place only when the drive was coming up to speed, was evidenced by chatter and noise at a point between two thirds and full speed, the noise being due largely to impact caused by torque reversal. The cause of the oscillation was the "negative damping" present as a result of the slope of the speed-torque curve of the motor. Since this type of oscillation is theoretically possible in all normal induction-motor drives (where the rotors are of relatively low resistance), it was felt that an account of the investigation of the vibration together with the results of tests made on the special damper used to control the oscillation, would be of value to engineers, particularly those interested in vibration.

Referring to Fig. 1 the drive consists essentially of a main motor and an auxiliary motor coupled to the high-speed shaft of a speed reducer by means of the couplings D and D'. The

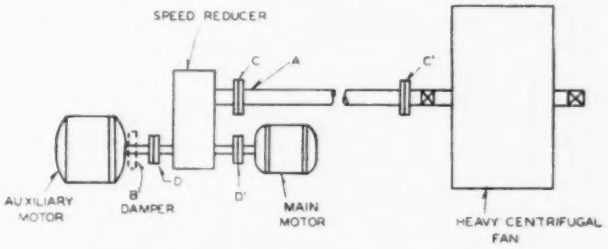


Fig. 1 Sketch of Fan Drive for Tunnel Ventilation (Blue Mt. and Kittatinny Mt. tunnels, Pennsylvania Turnpike.)



Fig. 2 Typical Torsiograph Record of Drive Without Damper

low-speed shaft of the speed reducer (which had a reduction ratio of about 7:1) is coupled to a heavy centrifugal fan through the couplings C and C'. In this case the equivalent inertia of the fan was about 90 times that of the motor while most of the flexibility of the system was in the long shaft between the couplings C and C'. In the drives under consideration, the auxiliary motor had a rating of either 40 or 50 hp; the main motor, $5\frac{1}{2}$ or $7\frac{1}{2}$ hp. The main motor is used most of the time, the auxiliary motor being used only occasionally when maximum speed is required.

To measure the torsional vibration, a Geiger torsiograph was belted to the low-speed shaft at A, Fig. 1. Because of the high inertia of the fan, the node in the system was practically at the fan hub. Thus the vibrograph measures essentially the twist in the shaft between point A and the fan hub. Because of the low acceleration during the starting period (which lasted around 25 to 45 sec for the drives tested), the seismic mass of the vibrograph did not come against the stops except when the vibration reached large amplitudes.

A sketch of a typical vibrograph record obtained during the starting period of these drives is shown in Fig. 2. At the start there is a transient oscillation of small amplitude at the torsional natural frequency of the system. This oscillation is due primarily to the electrical torque suddenly applied to the system and dies out after a few cycles. The torques set up through this transient condition may be calculated using the methods developed by one of the authors;[3] in the present instance such torques are low and of no concern. However, as seen from the torsiograph record, in the range from one half to full speed, a relatively severe oscillation continues to build up until full speed is almost reached after which it dies down.

This phenomenon may be explained as follows: The solid

[1] Research Engineer, Westinghouse Electric & Manufacturing Company. Mem. A.S.M.E.

[2] Westinghouse Electric & Manufacturing Company.

Presented at the Annual Meeting, New York, N. Y., December 1–5, 1941, of The American Society of Mechanical Engineers.

Discussion of this paper should be addressed to the Secretary, A.S.M.E., 29 West 39th Street, New York, N. Y., and will be accepted until January 11, 1943, for publication at a later date. Discussion received after the closing date will be returned.

Note: Statements and opinions advanced in papers are to be understood as individual expressions of their authors and not those of the Society.

[3] "Transient Torques in Induction-Motor Drives," by A. M. Wahl, Journal of Applied Mechanics, Trans. A.S.M.E., vol. 63, 1941, p. A-17.

line in Fig. 3 represents a typical speed-torque curve of a low-resistance induction motor of the type used for this service. From the curve it may be seen that in the range from *A* to *B* below full speed an increase in speed produces an increase in torque and vice versa. Thus for any small oscillation the alternating component of the torque is in phase with the alternating component of the angular velocity and energy will be put into the system. This condition is equivalent to "negative damping." If the positive damping present in the rest of the system is insufficient to compensate for this negative damping, the oscillation will build up, as shown in Fig. 2. When full speed is approached the slope of the curve is such as to give positive damping, Fig. 3, and this explains why the oscillation dies out near this point.

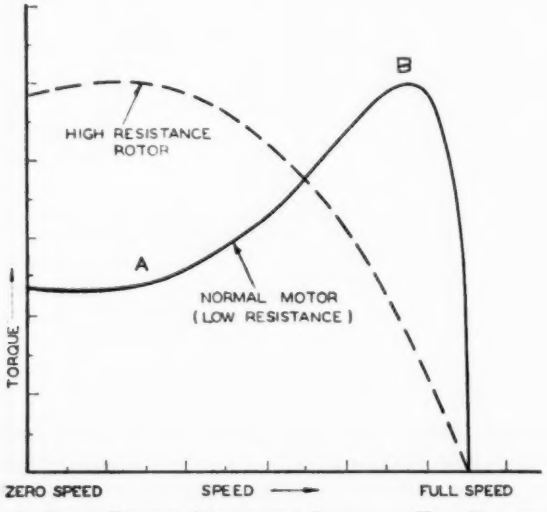


FIG. 3 SPEED-TORQUE CURVES FOR LOW- AND HIGH-RESISTANCE ROTORS

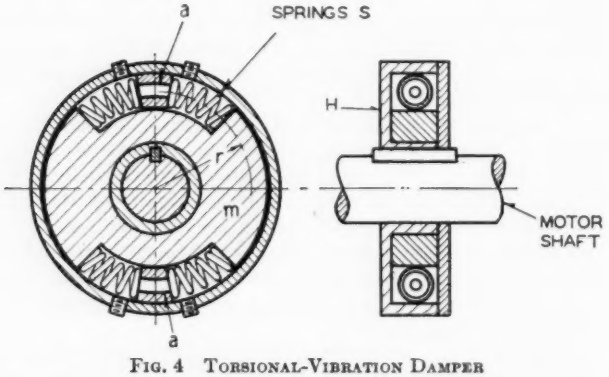


FIG. 4 TORSIONAL-VIBRATION DAMPER

It was considered advisable to eliminate these oscillations not only because of the noise and chatter produced but also because of the possible risk of eventual fatigue failure due to the stresses set up. Consideration was given to several methods for doing this, but all were found to involve certain disadvantages. One method is to use a squirrel-cage rotor of high resistance so that the slope of the speed-torque curve is changed as indicated by the dotted curve of Fig. 3. Here it is seen that during most of the accelerating period, the slope of the curve is such as to give a decrease in torque for an increase in speed, i.e., to give positive damping, in contrast to the normal curve for a low-resistance rotor (shown by the full lines) which yields an increase in torque with an increase in speed. However, a high-resistance rotor has lower efficiency at operating speeds and hence is not permissible. The use of a wound-rotor induction motor would enable a resistance to be inserted in the rotor circuit during the accelerating period and thus obtain a curve similar to the dotted curve of Fig. 3. While this method would give better results at operating speeds than the high-resistance squirrel-cage rotor alone, it involves added expense, and at the same time the efficiency at operating speeds is not as good as that obtained by means of a low-resistance squirrel-cage rotor.

An improvement could also be had by using a double-cage rotor but this does not completely eliminate the objectionable positive slope in the speed-torque curve and hence might not eliminate the trouble. In addition extra expense is involved.

After a consideration of these and other methods it was decided to use the relatively simple tuned vibration damper shown schematically in Fig. 4. This damper is keyed directly to the motor shaft at *B*, Fig. 1. It consists essentially of a mass *m*, mounted in a housing *H*, having an outside diameter of about 12 in. so that it may oscillate torsionally on the springs *S*. These springs are so chosen as to give the damper mass a frequency approximately equal to the lowest torsional natural frequency of the drive. By varying the size of the holes *a*, the amount of damping and shape of the resonance curve may be changed. If a light oil or fluid is used with an orifice of the proper size, the damping force will be proportional to the square of the velocity of flow in the orifice and will be practically independent of viscosity. Hence the damper operation may be made practically independent of temperature changes such as occur in service. As can be noted from Fig. 4, the complete assembly is self-contained and is permanently sealed so as to require practically no attention or maintenance. In addition, close clearances between the mass and housing are not required, thereby avoiding machining difficulties. Since the damper will only operate during the starting period no loss in efficiency during operation is involved by its use.

The object of the present investigation was primarily to obtain data on the energy absorption of the damper, to develop methods of calculation which may be used in the design of similar drives, and to check these methods by actual field tests on the drives. A further object was to obtain data on the actual positive damping present in drives of this type.

1—THEORETICAL ANALYSIS AND LABORATORY TESTS OF DAMPER

THEORY

For purposes of analysis the damper may be represented by the single-degree-of-freedom system shown in Fig. 5, the mass *m*

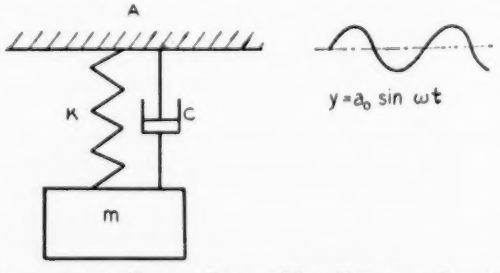


FIG. 5 SINGLE-DEGREE SYSTEM WITH VIBRATING SUPPORT

representing the damper inertia, and the spring constant *k* the torsional spring constant of the mass on the springs. Damping is represented by the dashpot *c*. It is assumed that the support *A* has a sinusoidal vertical motion $y = a_0 \sin \omega t$ which represents the torsional motion of the motor shaft on which the damper is mounted.

If it be assumed that the damping produced by the dashpot c is proportional to the relative velocity between the mass m and the support A, an exact solution of the problem of determining the energy absorption is available.[4] However, in the present instance where the clearances are such that little viscous damping occurs, provided a light oil is used, most of the damping is produced by flow of oil through a fixed orifice; here the damping force is proportional to the relative angular velocity squared. Some additional damping is produced by the rubbing of the mass m, Fig. 4, on its bearing; where a very light oil is used this may be considered as Coulomb damping. It therefore appears reasonable to obtain an approximate solution for this case by assuming a combination of velocity squared and Coulomb damping together with sinusoidal motion. On the basis of equal energy dissipation per cycle, an equivalent viscous-damping factor c is derived. In turn this factor c is used in the known expression for amplitude of motion for the case of viscous damping.[5]

The procedure is as follows:

The known solution for the single-degree system of Fig. 5 with viscous (or first power velocity) damping is

$$\frac{x_0}{a_0} = \frac{\omega^2/\omega_n^2}{\sqrt{\left(1 - \frac{\omega^2}{\omega_n^2}\right)^2 + \left(\frac{c\omega}{m\omega_n^2}\right)^2}} \quad \ldots\ldots [1]$$

where

a_0 = amplitude of motion of support
x_0 = peak amplitude of relative motion between mass and support
c = equivalent damping constant
ω = circular frequency of motion of support
k = spring constant
m = mass
$\omega_n = \sqrt{k/m}$ = undamped natural circular frequency

The equivalent damping constant c is calculated as follows:

Let $x = x_0 \sin \omega t$ be the relative motion between mass and support. Then for viscous damping the energy dissipated per cycle is

$$U = \pi c \omega x_0^2 \quad \ldots\ldots [2]$$

For velocity-squared damping where the damping force is taken as $c_1(\dot{x})^2$ the energy dissipated per cycle will be

$$U_1 = 4\int c_1(\dot{x})^2 dx = 4\int_0^{\pi/2\omega} c_1 x_0^3 \omega^3 \cos^3 \omega t \omega dt = \frac{8}{3} c_1 \omega^2 x_0^3 \quad \ldots\ldots [3]$$

The energy per cycle dissipated by Coulomb damping (which may be represented by a friction force F) is

$$U_2 = 4Fx_0 \quad \ldots\ldots [4]$$

The criterion of equivalent energy dissipation per cycle gives

$$U = U_1 + U_2 \quad \ldots\ldots [5]$$

$$\pi c \omega x_0^2 = \frac{8}{3} c_1 \omega^3 x_0^3 + 4Fx_0 \quad \ldots\ldots [6]$$

or

$$c = \frac{8}{3\pi} c_1 \omega x_0 \left(1 + \frac{3}{2}\frac{F}{c_1 \omega^2 x_0^2}\right) \quad \ldots\ldots [7]$$

Substituting this expression for c in Equation [1], and simplifying we find

$$\lambda = \frac{x_0}{a_0} = \frac{(1 - \tau^2)\sqrt{1 + \gamma_2}}{\sqrt{2}\,\tau^2 \gamma_1} \sqrt{\sqrt{1 + \lambda_1} - 1} \quad \ldots\ldots [8]$$

where λ = magnification of motion.

$$\lambda_1 = \frac{4\tau^2\gamma_1^2}{(1 - \tau^2)^4} \frac{(1 - \gamma_1^2\gamma_2^2/\tau^4)}{(1 + \gamma_2)^2} \quad \ldots\ldots [9]$$

$$\left.\begin{aligned} \tau &= \frac{\omega}{\omega_n} & \gamma_1 &= \frac{8}{3\pi}\frac{c_1 a_0}{m} \\ \gamma_2 &= \frac{3F}{2\omega_n^2 c_1 a_0^2} & \gamma_3 &= \frac{2\tau^2\gamma_1^2\gamma_2}{(1 - \tau^2)^2} \end{aligned}\right\} \quad \ldots\ldots [10]$$

When the forced frequency is equal to the natural frequency, i.e., when $\omega = \omega_n$, Equation [8] reduces to

$$\lambda_r = \sqrt{\frac{1}{\gamma_1} - \gamma_2} \quad \ldots\ldots [11]$$

where λ_r = magnification at $\omega = \omega_n$.

Using these equations in Equation [5], the energy dissipation per cycle becomes

$$U = \frac{8}{3} c_1 \omega^2 a_0^3 \lambda^2 + 4Fa_0\lambda \quad \ldots\ldots [12]$$

To apply these formulas to the damper shown on Fig. 4, the constant k is taken as the torsional spring constant, m as the torsional moment of inertia of the mass, and F as the friction torque. To calculate the constant c_1 which determines the damping torque in the equation

$$T_d = c_1(\dot{x})^2 \quad \ldots\ldots [12a]$$

where $\dot{x}$ in this case is the relative angular velocity between the mass and the housing, the procedure is as follows:

Let v = average velocity of fluid flow through orifice
v_p = velocity of motion at center line of springs at mean radius r (Fig. 4)

Then

$$v = \frac{A_p v_p}{A_h K_d} = \frac{A_p r \dot{x}}{A_h K_d} \quad \ldots\ldots [13]$$

where

A_p = piston area (or sectional area of openings for springs)
A_h = area of orifice
K_d = discharge coefficient

$$v_p = r\dot{x} \quad \ldots\ldots [14]$$

The pressure required to cause this flow is

$$p = \frac{\gamma v^2}{2g} \quad \ldots\ldots [15]$$

where γ is the weight of the oil per unit of volume and g the acceleration of gravity. Using Equation [13] in Equation [15]

$$p = \frac{\gamma}{2g}\left(\frac{A_p}{A_h K_d}\right)^2 r^2(\dot{x})^2 \quad \ldots\ldots [16]$$

Since for this case there are in effect two pistons, using Equation [16], the damping torque becomes

$$T_d = 2pA_p r = \frac{\gamma}{g}\frac{A_p^2}{A_h^2}\frac{r^3}{K_d^2}(\dot{x})^2 \quad \ldots\ldots [17]$$

[4] "Mechanical Vibrations," by J. P. Den Hartog, second edition, McGraw-Hill Book Company, Inc., New York, N. Y., 1940, p. 41.

[5] This method was suggested by L. S. Jacobsen, "Steady Forced Vibration as Influenced by Damping," Trans. A.S.M.E., vol. 52, 1930, paper APM-52-15, pp. 169–181; also, reference (4), p. 407.

from which

$$c_1 = \frac{\gamma}{gK_d^2} \frac{A_p^3 r^2}{A_h^2} \quad \ldots\ldots\ldots\ldots\ldots\ldots [18]$$

Tests on Dampers

As a check on the theory, a series of laboratory tests was made on dampers of two different sizes. The larger one had a mass of $10^3/_4$ in. OD with springs of $1^1/_2$ in. OD, the smaller a mass of $9^3/_4$ in. OD with $1^1/_4$-in. springs. The method of making the test was to mount the damper on a motor shaft (supported on ball bearings to reduce friction) and oscillate it back and forth through a small angle by means of the apparatus shown in Fig. 6.

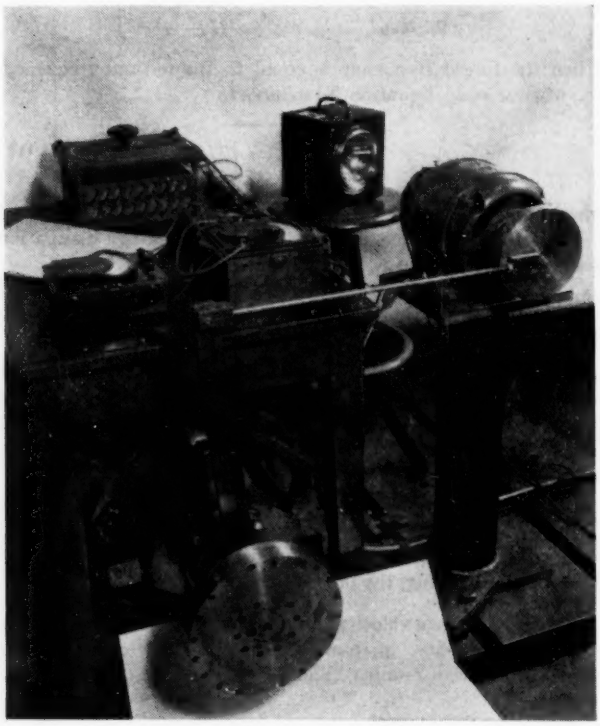


Fig. 6 Damper Test Arrangement

Essentially this consisted of a small 1-hp d-c motor having an eccentric mounted on its shaft. Holes in the eccentric enabled the stroke to be varied, while the frequency of oscillation could be changed by varying the speed of the motor. An accurate check of the frequency was possible by means of the stroboscope shown. In Fig. 7, a view of the test apparatus with the damper disassembled is shown.

The test procedure was as follows: The motor was operated at a constant speed, determined by the stroboscope and readings of armature current I, and voltage and watts were taken. Then the motor was stopped and the connecting rod disconnected from the eccentric. After the motor was started again, readings of the same quantities were taken at the same speed. From both the load and no-load wattage readings the I^2R losses were subtracted; the difference was then due to the energy absorption by the damper since the no-load run would give the losses due to hysteresis, bearing friction, windage, etc. As it was not found feasible to remove the damper from the shaft during the no-load run, a test was made with the damper mass blocked to determine the bearing losses of the damper shaft at various amplitudes and frequencies. These latter were found to be very small compared to the energy absorption of the damper except at points considerably removed from resonance. A further slight correction in the readings was therefore made taking these bearing losses into account.

Tests were made at various frequencies and amplitudes on both the large and the small damper using various sizes of orifices. Dimensions of the orifices used in the tests are shown in Fig. 8. In all cases, the damper was filled with Wemco C oil which is a very light oil having a viscosity of about 14 centipoises (or about 90 sec Saybolt) at room temperature.

The effect of varying the orifice diameter for the large damper is shown in Fig. 9, for frequencies near the resonant value and at a double amplitude of 8 deg (corresponding to a 3-in. stroke at the end of a $21^1/_2$-in. arm). On these curves the energy absorption, calculated from the wattage readings, is plotted against the frequency in cycles per minute. The orifices tested were of $^{13}/_{16}$, $^9/_{16}$, $^7/_{16}$, and $^5/_{16}$ in. diam. The reduction in energy absorption near the resonant frequency is quite pronounced for the smaller orifices. Similar curves for the small damper with orifice diameters of $^{19}/_{32}$, $^7/_{16}$, $^5/_{16}$, and $^3/_{16}$ in. are shown in Fig. 10.



Fig. 7 Damper Completely Disassembled

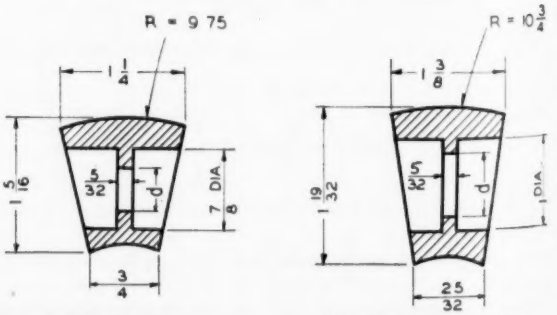


Fig. 8 Orifice Dimensions for Small and Large Dampers

The effect of varying the amplitude of oscillation on the energy absorption per cycle is shown in Figs. 11, 12, and 13, the full lines representing experimental results, the dotted lines the theoretical results (to be discussed later). In Fig. 11, the results on the small damper with the $^{19}/_{32}$-in-diam orifice are shown for double amplitudes of 8 and 5.3 deg. In Fig. 12, similar curves are shown for the large damper with the $^{13}/_{16}$-in. orifice and at the same amplitudes, while, in Fig. 13, the results obtained with this damper at amplitudes of 8 and 10.7 deg using the $^{9}/_{16}$-in. orifice are shown.

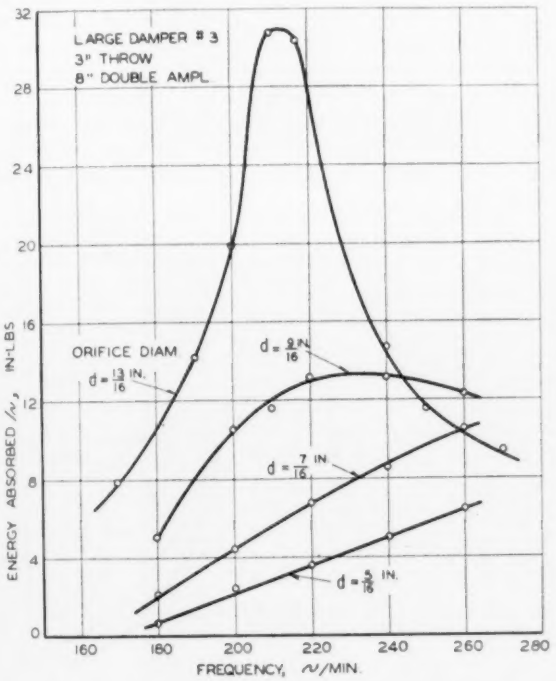


FIG. 9 ENERGY ABSORPTION VERSUS FREQUENCY FOR VARIOUS ORIFICE DIAMETERS, FOR LARGE DAMPER

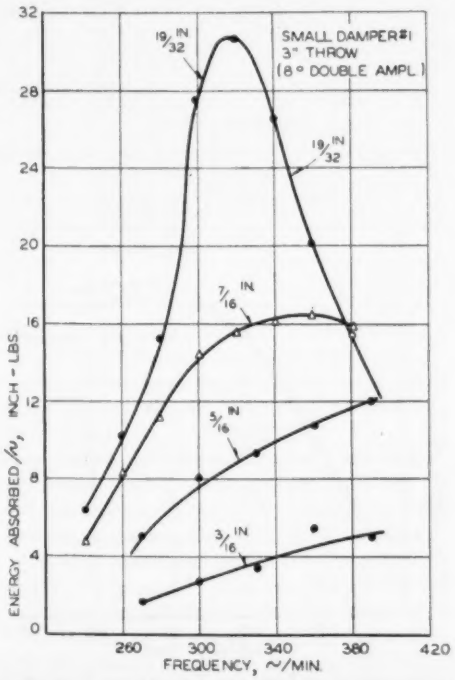


FIG. 10 ENERGY ABSORPTION VERSUS FREQUENCY FOR VARIOUS ORIFICE DIAMETERS, FOR SMALL DAMPER

It is interesting to note that, for the large damper, Fig. 12, using the 2-in. stroke (5.3 deg double amplitude), practically no damping occurred until the frequency reached 200 cycles per min. This may be explained as follows: There is always a slight amount of friction between the mass and its bearing on the housing. Until the amplitude and frequency of oscillation become great enough so that the torsional acceleration is sufficient to overcome this friction, no relative motion between mass and housing and hence no damping will take place. Calculations based on these tests indicate that a static coefficient of friction around 0.3 to 0.4 was present. In actual operation when mounted on a rotating motor shaft instead of a stationary one it may be expected that this coefficient of friction will be less. In the laboratory tests, a lower value may also be expected, except where the energy absorption is practically zero and no appreciable movement of the mass takes place.

This friction effect could be eliminated by mounting the mass on roller or ball bearings. In the present instance, however, this additional complication was not felt worth while, since as will be seen later, the use of the damper reduced the amplitude of oscillation to sufficiently low values

CALCULATION OF ENERGY ABSORPTION OF DAMPER AND COMPARISON WITH TEST

In calculating the energy absorption of the damper from Equation [12], it is necessary to know both the discharge coefficient K_d for the orifice and the friction coefficient μ between the mass m and the housing, Fig. 4. It is known that, for a plate orifice in a tube under steady-state flow conditions, the discharge coefficient will vary considerably depending upon the Reynolds number and on the ratio d/D between the orifice diameter and the tube diameter.[6] In addition the friction coefficient μ may vary considerably. An independent determination of these values for the conditions obtaining in the tests would be difficult. It was therefore felt that a satisfactory method of determining values of K_d and μ for use in calculation would be to assume some reasonable figures and compare the calculated curves obtained with the test curves. On this basis, a coefficient of friction μ = 0.2 and a discharge coefficient K_d = 0.8 were assumed for calculating the $^{9}/_{16}$-in. orifice in the larger damper and the $^{19}/_{32}$- and $^{7}/_{16}$-in. orifices in the smaller damper. Theoretical curves obtained by using these values in Equations [8] and [12] are shown by the dotted curves of Figs. 11, 13, and 14. It may be seen that, within the range covered by the tests, the agreement between test and calculated values may be considered as satisfactory for practical use in view of the approximate nature of the method of calculation.

In the case of the $^{13}/_{16}$-in. orifice in the larger damper, as indicated in Fig. 12, better results were obtained by assuming a discharge coefficient K_d = 0.9. This appears reasonable since, within the range of Reynolds numbers around 300 to 3000, as used in the tests, the value of K_d may be expected to be higher for the larger ratios of d/D; in the case of the $^{13}/_{16}$-in. orifice used on the larger damper, the ratio d/D was approximately 0.8, as compared with ratios of about 0.4 to 0.7 for the other orifices.

The numerical constants used in the calculations were as follows:

[6] For further discussion of this, refer to "Fluid Mechanics for Hydraulic Engineers," by H. Rouse, Engineering Societies Monographs, McGraw-Hill Book Company, Inc., New York, N. Y., 1938, p. 260; also "The Laws of Similarity for Orifice and Nozzle Flows," by J. L. Hodgson, Trans. A.S.M.E., vol. 51, 1929, paper FSP-51-42, pp. 303–332.

	Small damper	Large damper
m =	0.54 lb-in-sec^2	0.917 lb-in-sec^2
ω_n =	32.5 radians per sec	21.5 radians per sec
γ =	0.031 lb per cu in.	0.031 lb per cu in.
A_p =	1.71 sq in.	2.43 sq in.
r =	4.2 in.	4.6 in.
F =	7.7 in-lb	11.8 in-lb

The values of F given correspond to a friction coefficient $\mu = 0.2$ between mass and housing.

2—FIELD TESTS ON INDUCTION-MOTOR DRIVES

Torsiograph Tests With and Without Damper

As mentioned previously, tests were made by driving a Geiger torsiograph through a belt attached to the low-speed shaft at A, Fig. 1. (A photograph of one of the drives tested showing the damper A, the motors, and the speed reducer is shown in Fig. 15.) Besides the torsiograph records, speed and voltage readings were also taken so that the amplitude of oscillation as obtained from the torsiograph records could be correlated with motor speed.

Typical records obtained on three different units with the damper removed or blocked (so as to be inoperative) are shown on the records marked WB-1, WB-2, and EK-2 in Fig. 16. The records obtained for the same units with the damper on are also indicated; the improvement effected by using the damper is shown by comparison. In most cases the amplitude of oscillation without the damper was sufficient to cause the vibrograph pulley to strike the stops; this corresponds to an amplitude of about 12 deg at the low-speed shaft (or roughly 85 deg at the high-

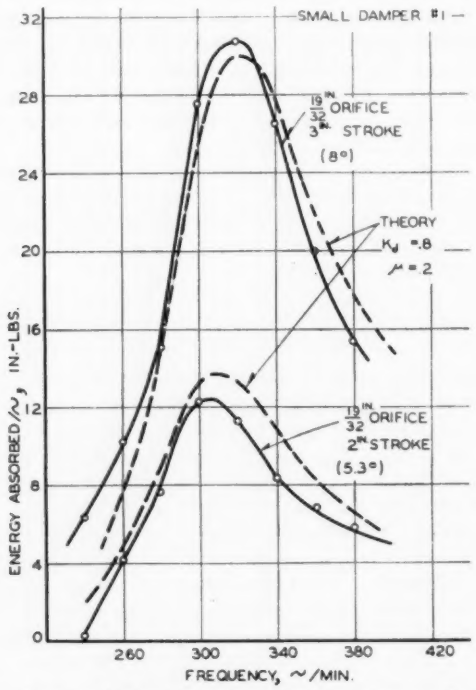


FIG. 11 ENERGY ABSORPTION VERSUS FREQUENCY AT DIFFERENT AMPLITUDES, FOR SMALL DAMPER

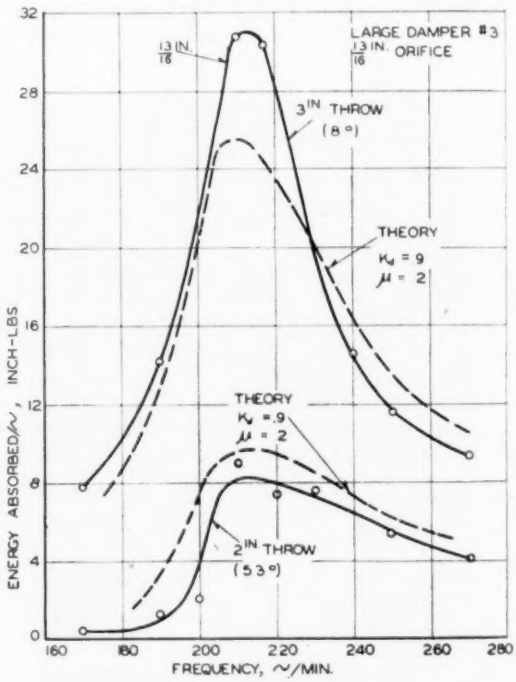


FIG. 12 ENERGY ABSORPTION VERSUS FREQUENCY AT DIFFERENT AMPLITUDES
(Large damper, 13/16-in. orifice.)

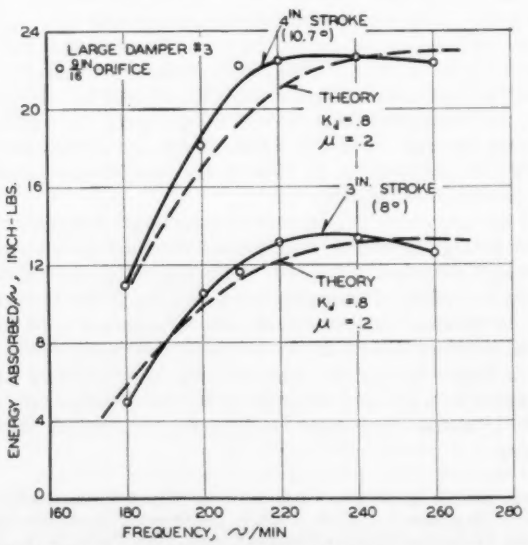


FIG. 13 ENERGY ABSORPTION VERSUS FREQUENCY AT DIFFERENT AMPLITUDES
(Large damper, 9/16-in. orifice.)

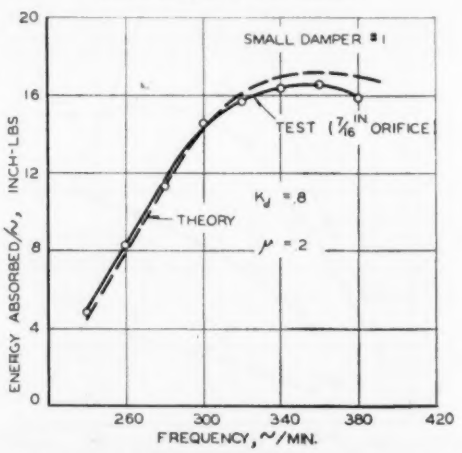


FIG. 14 COMPARISON OF TEST AND THEORY FOR ENERGY ABSORBED VERSUS FREQUENCY
(Small damper, 7/16-in. orifice.)

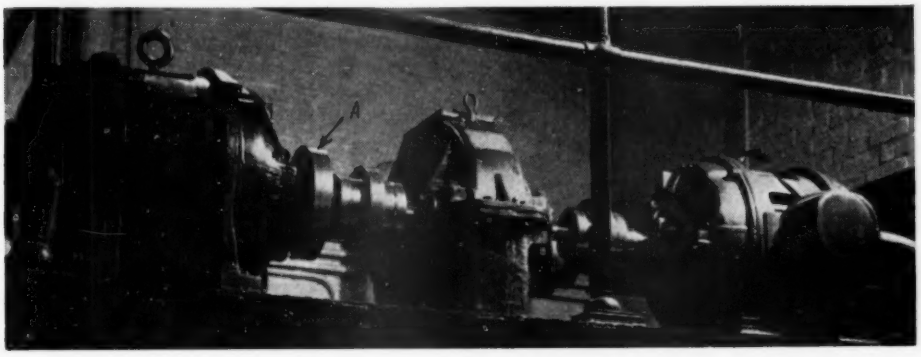


FIG. 15 VIEW OF ONE OF UNITS TESTED
(Damper shown at *A*.)

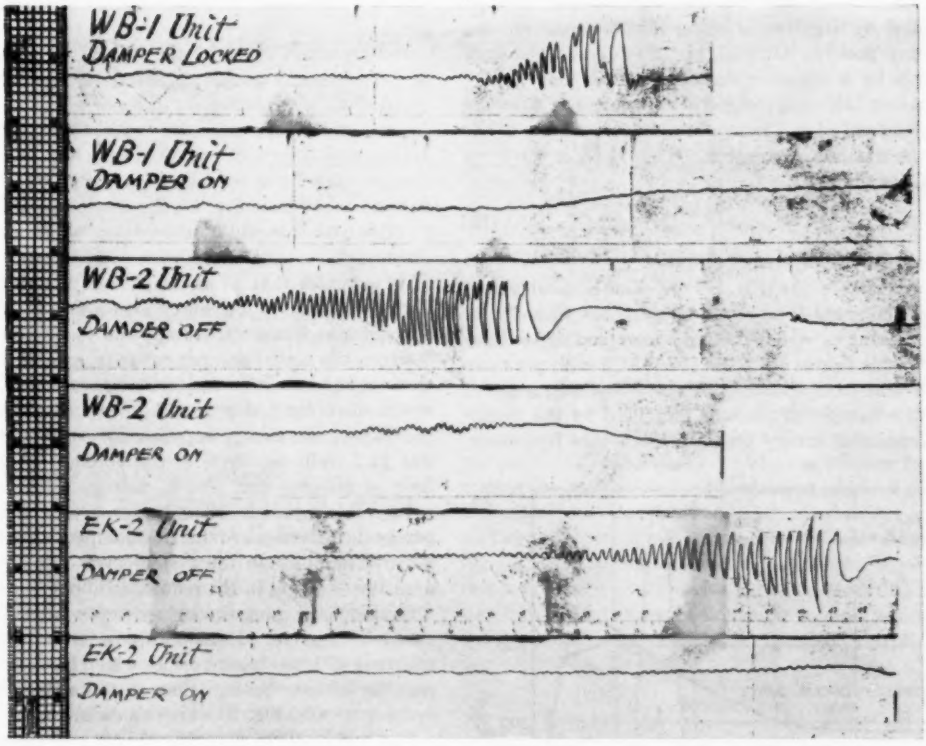


FIG. 16 TORSIOGRAPH RECORDS ON SEVERAL UNITS WITH AND WITHOUT DAMPER
(Scale, 0.085 in. = 1 deg at low-speed shaft.)

speed shaft). By using the damper, the double amplitude was reduced to less than 1 deg at the low-speed shaft, a value which is negligible from a stress standpoint. The natural frequency of oscillation for the units tested was about 5.8 cycles per sec for the smaller ones and 3.8 for the larger.

A typical curve of double amplitude of oscillation at the low-speed shaft versus speed, as determined from the torsiograph records and tachometer readings taken before the installation of the dampers, is shown together with the speed-torque curve in Fig. 17. It will be noted that during the first part of the accelerating period where the speed is low, no appreciable oscillation is present. The reason for this is that the slope of the speed-torque curve is less at the lower speeds, hence the negative damping at these speeds is not sufficiently great to overcome the positive damping in the system. As the speed increases, however, the slope increases and finally a point is reached where the negative damping sufficiently exceeds the positive damping in the system so that a rapid build-up of the oscillation may occur. After reaching a maximum amplitude the oscillations die out since, as mentioned before, the slope of the speed-torque curve is such as to give positive damping near full speed.

For comparison with the test results the dashed curve of Fig. 17 has been computed from the slope of the speed-torque curve by assuming that the positive damping in the system was equal to $^1/_2$ the negative damping supplied by the motor.[7] This was done by taking the amplitude equal to $Ae^{c_d t/2I}$ where c_d is the net damping constant, I the moment of inertia of the motor rotor, and A

[7] Further studies, based on the electrical characteristics of the motor, indicate that the negative damping may be determined with sufficient accuracy from the slope of the speed-torque curve, where the frequency of oscillation is low compared to the electrical-supply frequency as it was in the present case.

the initial amplitude.[8] It is seen that this assumption yields good agreement with the test curve; however, close agreement between test and theory in this case should not be expected since the positive damping in the system was not known with any great degree of accuracy.

From the records of Fig. 16 it may be seen that even with the damper in place there is still a small amplitude of oscillation. The explanation for this may be found in the slight friction existing between the damper mass and the housing. In order for the damper to function, the amplitude of oscillation must rise to a high enough value so that the acceleration is sufficient to overcome this friction and allow relative motion to take place. The variations in the amplitudes of motion with the damper in place may probably be ascribed primarily to variations in the positive damping present in the different units.

In order for the damper to be effective at any amplitude and frequency of motion the energy dissipated by the damper, as given by Equation [12] (or Figs. 9 to 14), must be greater than the energy supplied by negative damping at this amplitude and frequency, less any positive damping in the system. The work supplied per cycle by a negative damping torque may be obtained from Equation [2], using instead of c the negative damping constant c_0, and instead of x_0 the amplitude of motion a_0 of the shaft on which the damper is mounted. Thus if U_n is the work supplied by negative damping

$$U_n = \pi c_0 \omega a_0^2 \ldots\ldots\ldots\ldots\ldots\ldots [19]$$

where ω is the angular frequency of oscillation.

For the smaller (WB-1) units (Fig. 17) the value of c_0 calculated from the slope of the speed-torque curve was about 40 in-lb per radian per sec. Taking $a_0 = 0.07$ radian corresponding to 8-deg double amplitude, this figures out to be about 21.2 in-lb per cycle at 330 cycles per min (corresponding to the actual frequency of oscillation with the damper in place as measured by the torsiograph[9]). The measured energy absorption at this frequency,

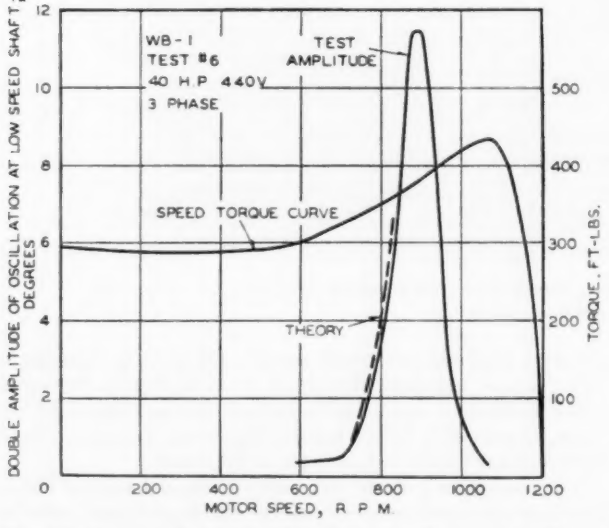


FIG. 17 TYPICAL CURVE OF AMPLITUDE OF OSCILLATION VERSUS SPEED DURING ACCELERATION, FOR SMALL DAMPER

[8] Reference (4), p. 325.

[9] The addition of a damper to the system considered should yield a 2-deg-of-freedom system with two natural frequencies, one slightly below and one slightly above the natural frequency without the damper. The figure of 330 cycles as measured on the WB-2 unit with the damper installed was about 5 per cent below the figure of 348 cycles measured on this unit without the damper. The higher natural frequency was not observed in any of the tests.

Fig. 10, was about 30 in-lb per cycle which indicates that the capacity of the damper was considerably greater than that required to take care of the negative damping at this amplitude; the positive damping present will increase this margin. At a double amplitude of 5.3 deg, the calculated value of energy supplied by negative damping was 9.5 in-lb per cycle which corresponds approximately to the test figure of 10 in-lb per cycle absorbed by the damper, Fig. 11. However, when the energy absorbed by the positive damping present is added to the energy absorbed by the damper, there may be an excess of damping capacity even at this low amplitude. This explains why the oscillation did not build up to this value in some cases.

TESTS TO DETERMINE POSITIVE DAMPING IN SYSTEM

In order to get an idea of the positive damping present in drives of this type, some further tests were made on two of the units. These tests were carried out by putting smaller orifices in the dampers so that the oscillation would build up; torsiograph records during the accelerating period were then taken.

Referring to Fig. 18 for the WB-2 unit with the $^{19}/_{32}$-in. orifice in the damper, a double amplitude of around 6 deg at the high-speed shaft was measured during acceleration. By putting in a $^{7}/_{16}$-in. orifice, the damping capacity of the damper was cut approximately in half at 330 cycles, Fig. 10, the energy absorption per cycle being reduced from about 30 to 16 in-lb. However, as will be seen from Fig. 18, the amplitude built up to only about $7^{1}/_{2}$ deg with this orifice in the damper. By using a $^{6}/_{16}$-in. orifice (energy absorption 9.3 in-lb per cycle) a large build-up occurred. This indicates that at an amplitude of around 8 deg, a $^{7}/_{16}$-in. orifice which gives an energy absorption of 16 in-lb per cycle is sufficient, and hence there appears to be a margin of about 2:1 between the actual damper capacity with the $^{19}/_{32}$-in. orifice and that required to limit the oscillation to about 7 deg at the high-speed shaft (or 1 deg at the low-speed shaft). As mentioned previously, the energy supplied by the motor at this amplitude was 21.2 in-lb per cycle at full voltage. Actually, there was a drop of about 5 per cent in voltage in the tests which would reduce this figure to 19 in-lb per cycle. Since about 16 in-lb per cycle are required in the damper, this indicates that the positive damping in the system (WB-2 unit) is roughly $^{1}/_{6}$ the negative damping in the motor (or about 3 in-lb per cycle).

Similar tests using the large damper on the EK-2 unit are also shown in Fig. 18. Here no appreciable build-up in amplitude occurred with the $^{9}/_{16}$-in. orifice which had about $^{1}/_{3}$ the damping capacity of the $^{13}/_{16}$-in. orifice at the observed frequency of 205 cycles per min, Fig. 9, which again indicates a margin between actual and required damping capacity of about 2:1. A build-up to about 18 deg occurred with the $^{7}/_{16}$-in. orifice in this damper. Referring to Fig. 9, this would indicate that an energy-absorption capacity of something under 11 in-lb per cycle is required to limit the amplitude to say 8 deg. Since the calculated energy supplied by the motor was about 17 in-lb per cycle (corrected for a voltage drop to 420 v as observed), this indicates that the positive damping in the system is about $^{1}/_{3}$ the negative damping supplied by the motor (or about 6 in-lb per cycle).

An estimate of the energy absorption due to hysteresis in the low-speed shaft of the drive was carried out assuming an average figure of 0.02 for specific damping capacity (carbon steel) at an alternating stress corresponding to 8 deg double amplitude at the high-speed shaft.[10] This yielded a figure of about 2 in-lb per cycle. However, in the actual drive, there is a steady stress superimposed on the alternating stress which would tend to raise this figure, while there are also other sources of damping in the

[10] "Damping Capacity of Materials," by G. S. Von Heydekampf. Proceedings, A.S.T.M., vol. 31, 1931, part 2, p. 164.

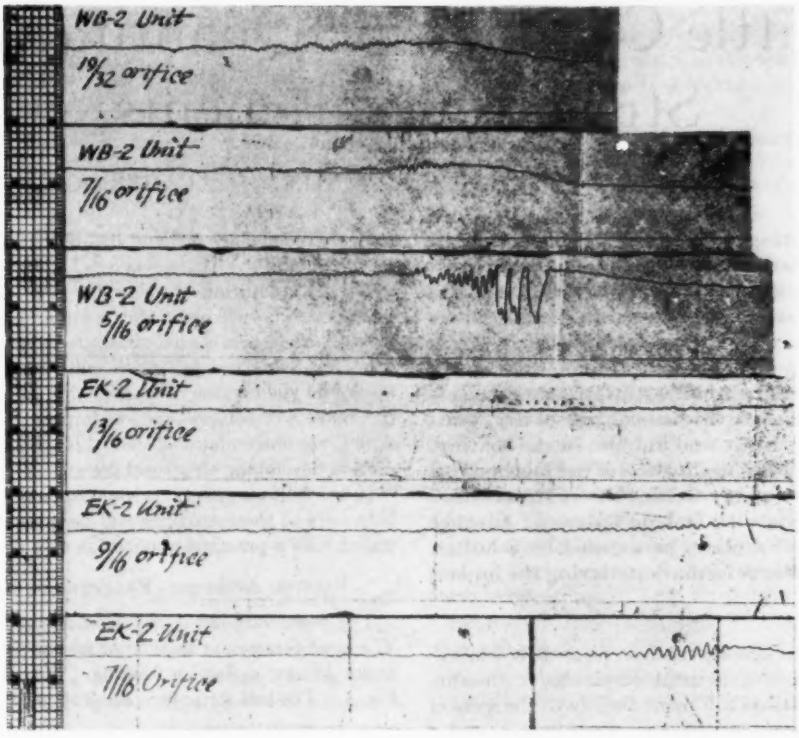


FIG. 18 TORSIOGRAPH RECORDS SHOWING INCREASE IN AMPLITUDE WITH DECREASE IN ORIFICE SIZE
(WB-2 and EK-2 units; scale, 0.085 in. = 1 deg at low-speed shaft.)

bearings, couplings, and gears. Consequently, the figures of 3 and 6 in-lb per cycle, as estimated from these tests, do not appear unreasonable, although they must be considered as very rough.

SUMMARY AND CONCLUSIONS

This study shows that, for a system consisting of an inertia load (such as a heavy fan or blower) which is driven by a low-resistance induction motor, there is danger of torsional oscillation due to negative damping during the accelerating period. If there is sufficient inherent positive damping in the system or drive, or if the accelerating time is relatively short, these torsional oscillations will build up only to a small extent, if at all. This is probably the situation in most induction-motor drives. On the other hand, if, as in the particular drives under consideration, the accelerating time is relatively long, while the positive damping present is low, the oscillations may build up to objectionable magnitudes, so that considerable noise and chatter occur.

Tests carried out on actual drives show that these objectionable oscillations may be eliminated by the use of a relatively simple tuned hydraulic damper mounted on the motor shaft.

For the design of similar drives, formulas are given for calculating the energy-absorption capacity of the damper at various amplitudes and for various orifice sizes. Laboratory tests indicate that a discharge coefficient of 0.8 to 0.9 may be assumed for the particular orifices tested. The use of these formulas in determining the margin between actual and required damping capacity is illustrated by application to an actual drive. Also tests made on two different units indicate that in these cases positive damping of about $^1/_6$ to $^1/_3$ the negative damping supplied by the motor is present. However, because of the considerable variation indicated, it appears advisable in design to neglect the positive damping in calculating the damper capacity unless definite test results are available.

ACKNOWLEDGMENT

The authors wish to express their appreciation to Dr. L. W. Chubb and Messrs. R. E. Peterson and L. A. Kilgore of the Westinghouse Company for their interest in the problem and the suggestions made, to Messrs. S. F. Henderson and F. Richards of the same company for information and advice during the course of the work, and to the Pennsylvania Turnpike Commission for permission to make field tests on the actual drives.

Brittle Coatings for Quantitative Strain Measurements

By A. V. de FOREST,[1] GREER ELLIS,[2] and F. B. STERN, JR.,[3] CAMBRIDGE, MASS.

The use of brittle coatings in stress analysis is discussed in this paper. Particular reference is made to the "Stresscoat" materials and method which can effect quantitative analyses within the elastic range by use of brittle coatings alone. In the plastic range, the flaking off of the coating is shown to be caused by a compression component of strain of about 1 per cent. Graphs and illustrations show the effect of such variables as coat thickness, time of dry, temperature and humidity, creep, and bubbles in the coating. Test procedure is outlined. Application of the method to a part from a high-speed sewing machine shows stress values and correlation of results with fatigue failures. Another application illustrated is a plate, penetrated by a bullet, showing elastic and plastic deformations during the impact loading.

BRITTLE coatings are among the most potentially convenient of strain gages. On the usual complicated engineering structure, such coatings will point directly to the areas of highest strain, show the direction of the principal tension, and if properly controlled can be made to yield quantitative values of sufficient accuracy for practical design purposes. Since fatigue failure in service usually correlates with maximum tension stress on the structure, direct correlation can be obtained between the brittle-coating patterns developed in a laboratory analysis and the likelihood of failure of that same structure in service. The analysis may be run on the structure itself or on models made of machined or cast plastics, cast iron, welded steel, or other material.

Compression strains can also be measured if desired, as long as the structure and its loading remain within the elastic range, by simply allowing the brittle coating to come to a neutral condition while the maximum load is on the structure. Then when the load is released, the relaxing compression strains will react as tension and fracture the coating.

In 1932, Dietrich and Lehr (1)[4] published the first recognized work on the use of brittle coatings for the indication of strains within the elastic range. Their use was purely qualitative in pointing to areas of highest strain and indicating the direction of the principal tension. Quantitative measurements were subsequently made with a special short-gage-length strain gage. Work on a brittle coating which could also be used to determine quantitative values was started in 1937 at the Massachusetts Institute of Technology (2) and has resulted in the present Stresscoat method.

Besides fracturing at relatively low values of tension strain, brittle coatings will also indicate larger values of strain by flaking off the surface of a coated structure in much the same way as the commonly observed flaking of mill scale. The flaking occurs in the initial yield region of most metals and correlates directly with the amount of compression strain present. Haigh (3) has made strong recommendations that this phenomenon be more fully used in developing structural designs.

In the following sections some basic data on the characteristic behaviors of these coatings will be presented and their use illustrated with a practical application to a design problem.

Factors Affecting Fracture of Brittle Coatings

The basic variable is of course the strain patterns produced. The most convenient method of test devised is a cantilever beam under known deflection loading. This apparatus is shown in Fig. 1. The test strips are pieces of spring steel 12 × 1 × 1/4 in.



Fig. 1 Method of Loading Test Strips

The loading rig embodies an adjustment screw at the rear to bring the strip into contact with the cam and a cam of definite deflection. This deflection is such that the upper surface of a coating 0.004 in. thick on the test strip will receive the graduated amount of strain along the strip, as indicated on the scale lying beside the loading rig. The testing procedure is simply to place a coated and dried strip in the loading rig, adjust the strip so that it will just touch bottom of the cam, and deflect the cam to its full extent. Reference marks can be made on the strip opposite the characteristic patterns being investigated, and the strip released from the rig and placed in the scale, from which the amount of strain is read. Tests reported here at other thicknesses of coating than 0.004 in. have been corrected back to this standard value.

Coating Thickness. Variation of the strain patterns with thickness of coating is one of the most important factors. Since it is practically impossible to produce a coating of uniform thickness on all surfaces of an irregular body, it is essential that the strain response of the coating be sensibly constant over a reasonable range of thickness of the coating. Fig. 2 shows a set of strips

---

[1] Professor of Mechanical Engineering, Massachusetts Institute of Technology. Mem. A.S.M.E.

[2] Manager, Stresscoat Division, Magnaflux Corporation.

[3] Research Engineer, Magnaflux Corporation. Jun. A.S.M.E.

[4] Numbers in parentheses refer to the Bibliography at the end of the paper.

Presented at the National Meeting of the Applied Mechanics Division, Cambridge, Mass., June 19–20, 1942, of The American Society of Mechanical Engineers.

Discussion of this paper should be addressed to the Secretary, A.S.M.E., 29 West 39th Street, New York, N. Y., and will be accepted until January 11, 1943, for publication at a later date. Discussion received after the closing date will be returned.

Note: Statements and opinions advanced in papers are to be understood as individual expressions of their authors and not those of the Society.

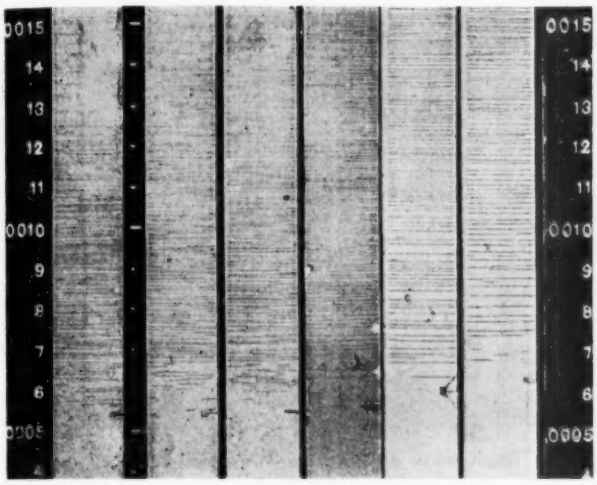


FIG. 2 APPEARANCE OF STRAIN PATTERNS WITH VARIATION IN AMOUNT OF STRAIN AND THICKNESS OF COATING
(Left to right, thickness 0.003, 0.004, 0.005, 0.006, 0.008, 0.01 in.)

with varying thickness of coating. Two characteristics immediately noted are that over the range from 0.003 to 0.006 in. thickness the patterns all start at about the same value of minimum strain, and that the spacing of the patterns becomes wider as the thickness increases. At the higher values of strain, where the spacing is stabilized, the average distance between crack patterns is 5 times the thickness of the coating. The fact that the pattern spacing is so regular and is directly proportional to the thickness of the coating indicates that pattern formation undoubtedly begins on the free surface of the coating. In the regions of lower strain, where the patterns are irregular, the average spacing is approximately 10 times the thickness of the coating. The most reliable quantitative indicators between all the strips are seen to be, first, the value of strain at which pattern formation starts, and next, the degree of regularity in the development of the evenly spaced full pattern.

Time of Dry. Although the coatings set hard enough to handle within a drying time of 5 minutes, the important drying processes which produce sufficient brittleness of coat for elastic-strain-indicating purposes require at least 3 hours before any indications below 0.0020 in. per in. strain can be obtained on a thickness of coating between 0.003 and 0.006 in. Fig. 3 shows how the region of constant strain sensitivity when plotted against thickness broadens as drying proceeds. Experience indicates 15 to 24 hours as the optimum drying time. A factor not indicated on the graph is that coatings dried more than 24 hours become noticeably more erratic in their pattern formation. It is possible to use 6 hours' drying time when necessary, as an experienced operator can maintain uniformity of coating thickness within limits of ±0.001 in. on simply shaped surfaces.

Temperature and Humidity. Atmospheric conditions during the drying and testing period affect the strain sensitivity of the coating. If the changes are gradual, providing that they were not so severe as to "craze" the coating at any time during the drying period, the coating will react as if the conditions which prevail at the time of test had been constant during the previous drying period. The strain sensitivity of a typical coating, when dried at different temperatures but at the same value of absolute humidity, is shown in Fig. 4. Absolute humidity is used as a parameter because it is the condition which usually prevails in a laboratory or in different rooms of the same building which are at different temperatures and are connected into the same ventilating system. Since the best working range for the coatings is in the sensitivity range of 0.0005 to 0.0009 in. per in. initial strain, it is seen that a coating picked for the optimum value of 0.0007 in. will have an allowable temperature fluctuation of ± 5 deg F. Because of the rapid variation of sensitivity with temperature, it is important that all bodies concerned in the same test be maintained at the same temperature.

Sensitivity also varies with change in relative humidity as shown in Fig. 5. However, this is not a critical point in the practical use of the coatings, as it is seldom that the humidity varies by much, except as caused by seasonal changes of weather.

In order to obtain the optimum coating for any condition of temperature or humidity, a graduated series of coatings of varying degrees of brittleness and a selection chart, such as that shown in Fig. 6, are used. The coating numbers apply to the valleys between the curves. The reactions of all coatings under their optimum conditions as indicated by the chart are the same.

Creep. Despite their brittleness the coatings are quite plastic materials. Fig. 7 shows how the amount of strain necessary initially to crack a coating varies with the time taken to reach that load. Correction for creep is an important factor in obtaining accurate quantitative measurements. Correction may be had either by loading all bodies involved in the test in the same length of time, or else by loading at a constant rate, observing the time at which patterns first appear, and correcting all values to a common time of loading by means of a chart similar to that in Fig. 7.

Bubbles in the Coating. The certainty of duplication of a definite strain pattern is enhanced by creating a formation of fine bubbles within the coating through proper spray-gun technique. Comparison of a series of test strips painted with clear coatings on the right and "bubbled" coatings on the left is shown in Fig. 8.

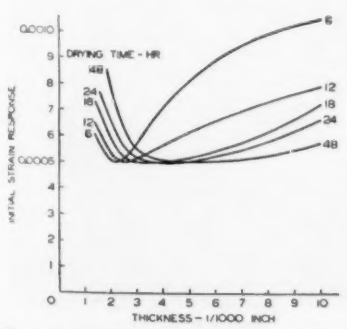


FIG. 3 VARIATION OF STRAIN SENSITIVITY WITH THICKNESS OF COATING AND TIME OF DRY

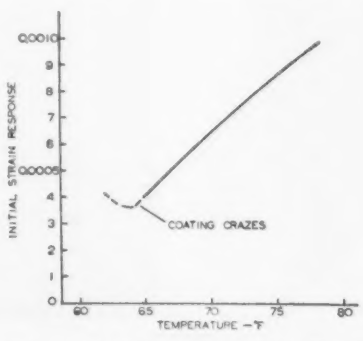


FIG. 4 VARIATION OF STRAIN SENSITIVITY WITH TEMPERATURE
(Absolute humidity maintained constant at 0.37 in. Hg; coating number 1204.)

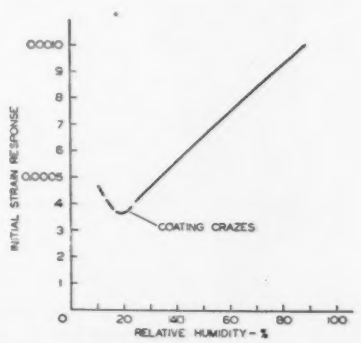


FIG. 5 VARIATION OF STRAIN SENSITIVITY WITH HUMIDITY
(Temperature maintained at 70 F; coating number 1204.)

The clear coatings have the characteristics of being more erratic in the initiation of pattern formation and, further, when a crack is started it tends to extend itself into areas of lower strain. A point of interest here is that there is approximately 6 per cent more tension strain in the center of these test strips than there is at the edges. The bubbled coatings exhibit more certainty of pattern formation in a given area and, further, exhibit less tendency to extend themselves into regions of lower values of strain. There is also some apparent increase in the sensitivity of the coating with bubbles present, but this is not as large a value as might be anticipated. An interesting fact is that the cracks in the brittle coating do not noticeably deviate in their direction because of the presence of bubbles in or beside their path.

All the data, except for the one illustration in Fig. 8, is for coatings with included bubbles.

Factors Affecting Flaking of Brittle Coatings

When the strain on the surface of the coated body has been carried to fairly high values which are at or slightly exceed the yield point of most structural materials, the proper grade of these brittle coatings will flake off. The initiation of flaking correlates directly with the amount of compression strain present, the optimum coating starting to flake at 1 per cent of the maximum compression-strain component,[5] regardless of the type of loading involved. This correlation is illustrated in Table 1.

TABLE 1 AMOUNT OF STRAIN TO INITIATE FLAKING OF COATING UNDER DIFFERENT LOADING CONDITIONS

	Strain	Compression-strain component
Tension loading	$\epsilon_t = 0.02$	$\epsilon_c = \nu_p \epsilon_t = 0.01$
Compression loading	$\epsilon_c = 0.01$	$\epsilon_c = 0.01$
Torsion loading	$\gamma = 0.02$	$\epsilon_c = {}^1/_2\gamma = 0.01$

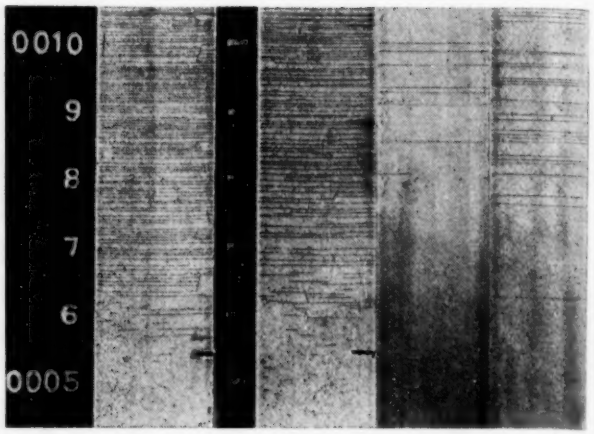


Fig. 8 Comparison of Coatings With and Without Included Bubbles
(Test strips on left have included bubbles.)

[5] It is of interest to note that the best brittle mill scale will flake at $^1/_2$ per cent compression-strain component, but that different mill scales vary widely in their brittle properties.

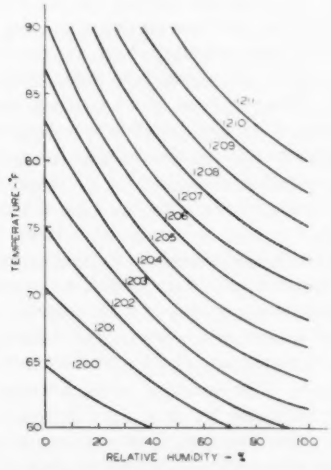


Fig. 6 Chart for Selecting Coating to Fit Prevailing Temperature and Humidity Conditions

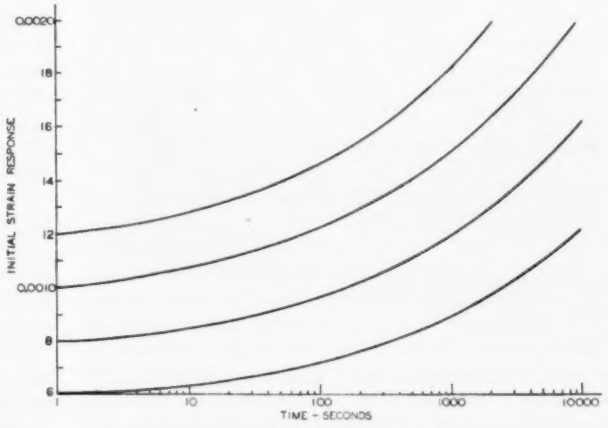


Fig. 7 Variation of Strain Sensitivity With Time of Loading
(Rate of loading maintained constant.)

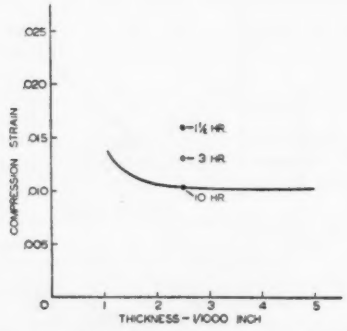


Fig. 9 Variation of Flaking Sensitivity With Thickness of Coating and Time of Dry

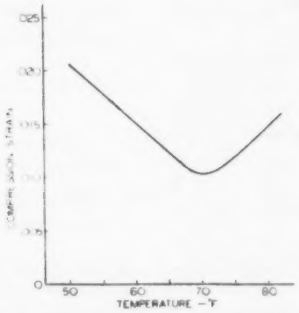


Fig. 10 Variation of Flaking Sensitivity With Temperature
(Absolute humidity maintained constant at 0.37 in. Hg; coating number 1208.)

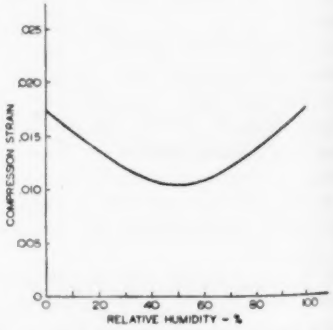


Fig. 11 Variation of Flaking Sensitivity With Humidity
(Temperature maintained at 70 F; coating number 1208.)

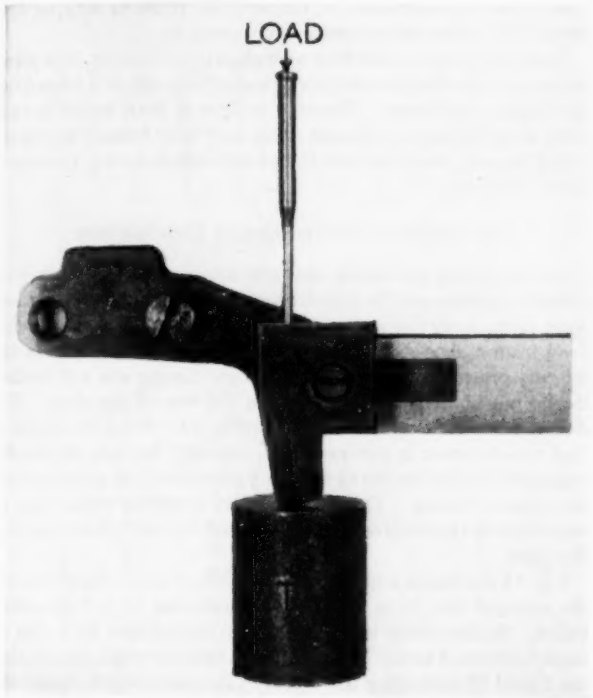


FIG. 12 STATIC SETUP SIMULATING SERVICE LOAD ON SEWING-MACHINE HEAD
(Courtesy of United Shoe Machinery Corporation.)

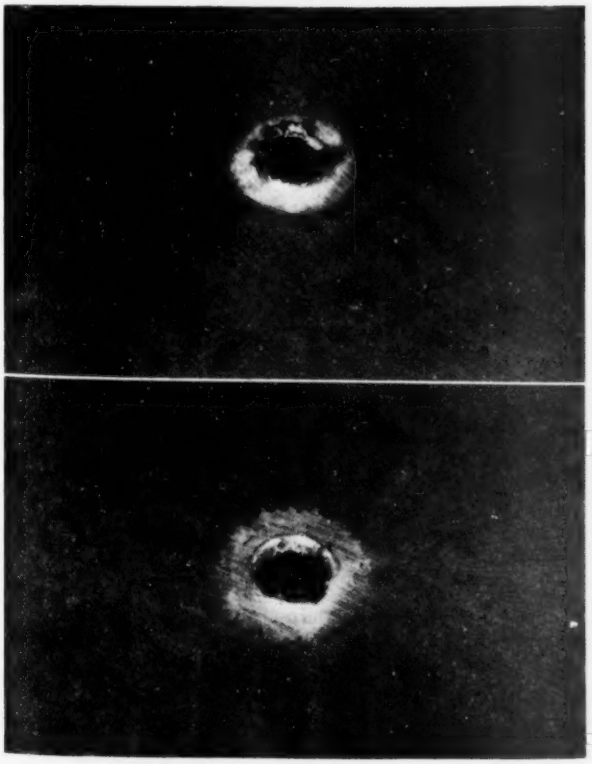


FIG. 14 ELASTIC- AND PLASTIC-DEFORMATION INDICATIONS ON A 3/8-IN. PLATE PENETRATED BY A 0.30-CALIBER BULLET
(Upper view is of entrance face; lower view is exit face; areas surrounding hole are: *a* Crown of heavily deformed metal; *b* plastically deformed metal from which brittle coating has flaked; *c* elastic-tension patterns.)

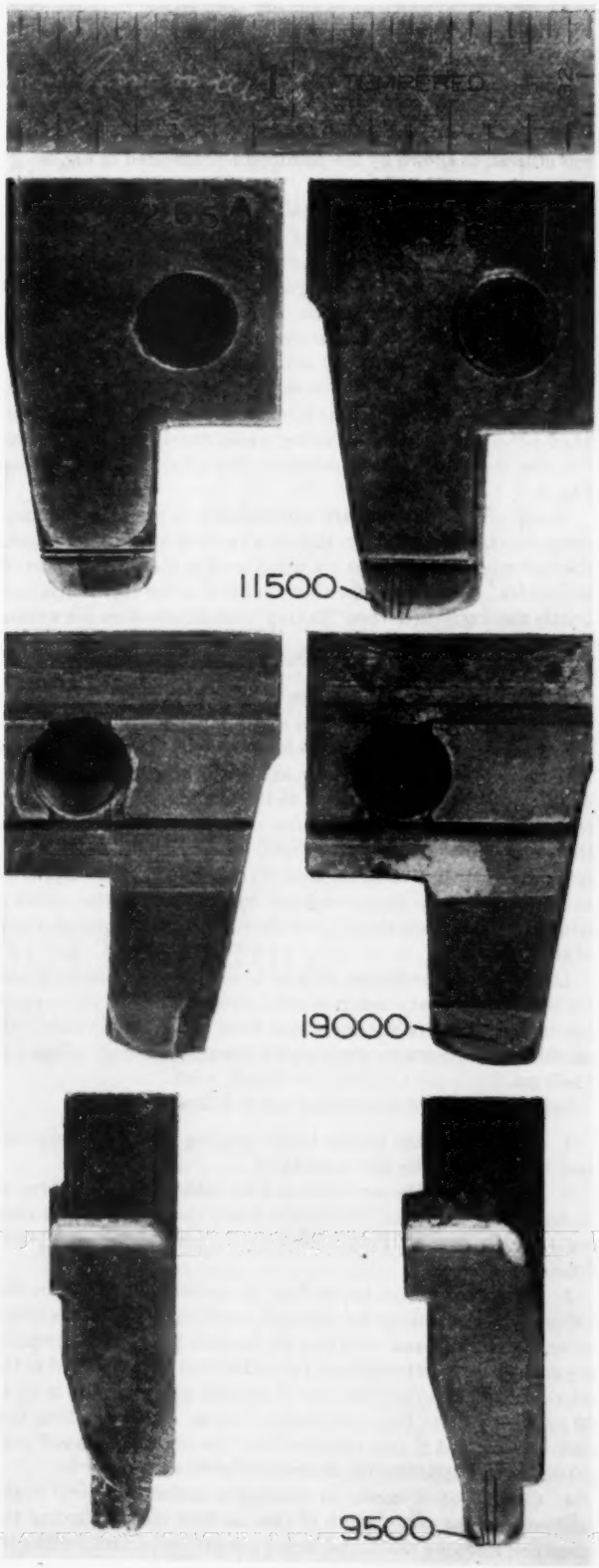


FIG. 13 RESULTS OF STRAIN ANALYSIS ON SEWING-MACHINE HEAD AND COMPARISON WITH SERVICE FAILURE
(Tension stresses in pounds per square inch at 250-lb load. Courtesy of United Shoe Machinery Corporation.)

Those factors, which have already been shown to influence the formation of elastic-strain patterns, differ somewhat in their influence on flaking of the coatings.

Thickness of Coating. Thickness of coating is less critical, as illustrated in Fig. 9.

Drying Time. The necessary drying time is shorter and also less critical, as shown by the point values indicated in Fig. 9.

Temperature and Humidity. The effects of temperature and humidity are moderately critical on the amount of quantitative compression strain indicated by flaking. Figs. 10 and 11 show that there are optimum values of temperature and of humidity at which a given coating requires a minimum amount of strain to start flaking. These optimum atmospheric conditions are the ones which promote a moderate crazing of the coating during drying and correspond to the minimums previously shown in the dotted portions of the curves in Figs. 4 and 5. The optimum coating, which operates at the minimums exhibited in Figs. 10 and 11, is obtained by using a coating whose number is 4 higher than the one indicated on the selection chart for the elastic range, Fig. 6.

Creep. Sufficient data are not available to present an accurate creep chart, but it is known that this variable is less severe than is the case when the coatings are being used as elastic-tension strain indicators. One reason for this condition is the fact that a more brittle coating is used when "flaking" indications alone are wanted.

Method of Making Strain Analyses

The most reliable quantitative indication in the elastic range is the amount of principal tension strain indicated when the strain patterns just start to form. As long as the structure and the distribution of loads remain within the elastic range, all local strains will vary directly in proportion to the amount of load, and therefore the measurement of one value of local strain, at any area at the value of load at which it occurs, will give sufficient data for a complete quantitative strain analysis of the structure. Apparent values of stress are then computed by multiplying the values of strain by the tension modulus of elasticity of that particular part of the structure.

Linear elastic conditions, such as have just been described, hold for the average static setup of solid structures, i.e., engine parts, but in general there are deviations from linear elastic conditions on thin-plate structures such as, for example, aircraft wings and fuselages.

Briefly the procedures for test are as follows:

1 Selection of the proper brittle coating for the temperature and humidity in the test laboratory.

2 Spraying on the structure and the calibration strips, first, an undercoating and then, 15 minutes later, the proper brittle coating, which is usually dried 15 to 24 hours, but may be used within 6 hours if necessary.

3 Running the test by loading the structure to a reasonable value of load, searching for patterns, marking any patterns which have just started, and returning to the base load. After remaining at the base load for at least twice the total time involved in the previous loading cycle, the load is applied again until it is 10 to 30 per cent greater than the previous value. After marking new patterns the load is again released and the cycles continued until patterns have appeared on all areas of interest.

4 Calibration is made by loading a calibration strip in the calibrator in the same length of time as that used in loading the structure, marking the initial strain pattern point and reading its value in the strain scale.

5 After the completion of the test, the patterns may be dye-etched if it is desired to increase their visibility.

Since the patterns will form at high rates of loading, it is possible to get a qualitative analysis of a structure which is loaded under impact conditions. The dye etchant is very useful in such tests, as it will reopen patterns which may have formed during the initial impact condition and then have closed during the subsequent vibration.

Illustrations of the Use of This Method

An interesting correlation between strain patterns obtained on a small machine part in a static test and fatigue failure of these same parts in service is shown in Fig. 13. The part is a sewing head from a shoe-stitching machine. The principal load is the internal pressure created by the plunger forcing the soft leather thread out of the head and through the sole of the shoe. The simple static-loading rig is shown in Fig. 12. Since the value of load which occurs in service is not definitely known, the results were simply computed to an arbitrary amount which gave reasonable values of stress. The exact amount of service stress is not as important as the relative values which will be useful in redesigning the part.

Fig. 14 illustrates a qualitative analysis of strain conditions on the surfaces of a $^3/_8$-in. steel plate penetrated by a 0.30-caliber bullet. In the center is the bullet hole, surrounded by a ring of highly deformed metal Next comes a band in which the coating has flaked off indicating the region of the plate which passed the yield point. The outer area with the coating intact shows the elastic strains present, radial tension predominating on the entrance side, and tangential-tension strain on the exit side.

BIBLIOGRAPHY

1 "Des Dehnungslinienverfahren," by O. Dietrich and E. Lehr, *Zeitschrift des Vereines deutscher Ingenieure*, vol. 76, 1932, pp. 973–982.

2 "Strain-Indicating Lacquers," by Greer Ellis, master's thesis, Aeronautical Engineering Department, Massachusetts Institute of Technology, 1937.

3 "Electric Welding as an Integral Part of Structural Design," by B. P. Haigh, Transactions of North East Coast Institution of Engineers and Shipbuilders, vol. 56, 1939–1940, pp. 43–82.

4 "Brittle Lacquers as an Aid to Stress Analysis," by A. V. de Forest and Greer Ellis, *Journal of the Aeronautical Sciences*, vol. 7, 1940, pp. 205–208.

5 "Procédé d'Étude de la Distribution des Efforts Élastiques dans les Pièces Metalliques," by A. Portevin and M. Cymboliste, *Revue de Métallurgie*, vol. 31, 1934, Memoires, pp. 147–158.

6 "Anwendung des Dehnlinienverfahrens bei Zelluloidmodellen," by E. Siebel, W. Seufert, and W. Steurer, *Zeitschrift des Vereins deutscher Ingenieure*, vol. 84, 1940, pp. 889–890.

7 "Stress-Strain Analysis From Crack Formations in Brittle Lacquer Coatings," anonymous, *Product Engineering*, vol. 11, 1940, pp 266–268

8 "A Short-Gage-Length Extensometer and Its Application to the Study of Crankshaft Stresses," by C. W. Gadd and T. C. Van Degrift, Journal of Applied Mechanics, Trans. A.S.M.E., vol. 64, March, 1942, p. A-15.

9 "Distribution of Stresses in Partial Compression and a New Method of Determining the Isostatics in Photoelasticity," by A. J. Durelli, Proceedings of the Thirteenth Semi-Annual Eastern Photoelasticity Conference, June, 1941, pp. 25–50.

10 "Stress Pattern Crazing," by Wolfgang B. Klemperer, Douglas Aircraft Company, Inc., Santa Monica, Calif., Applied Mechanics, von Kármán Anniversary Volume, 1941, pp. 328–337.

11 "Behavior of a Brittle Material at Failure," by M. M. Frocht, Journal of Applied Mechanics, Trans. A.S.M.E., vol. 58, 1936, p. A-99.

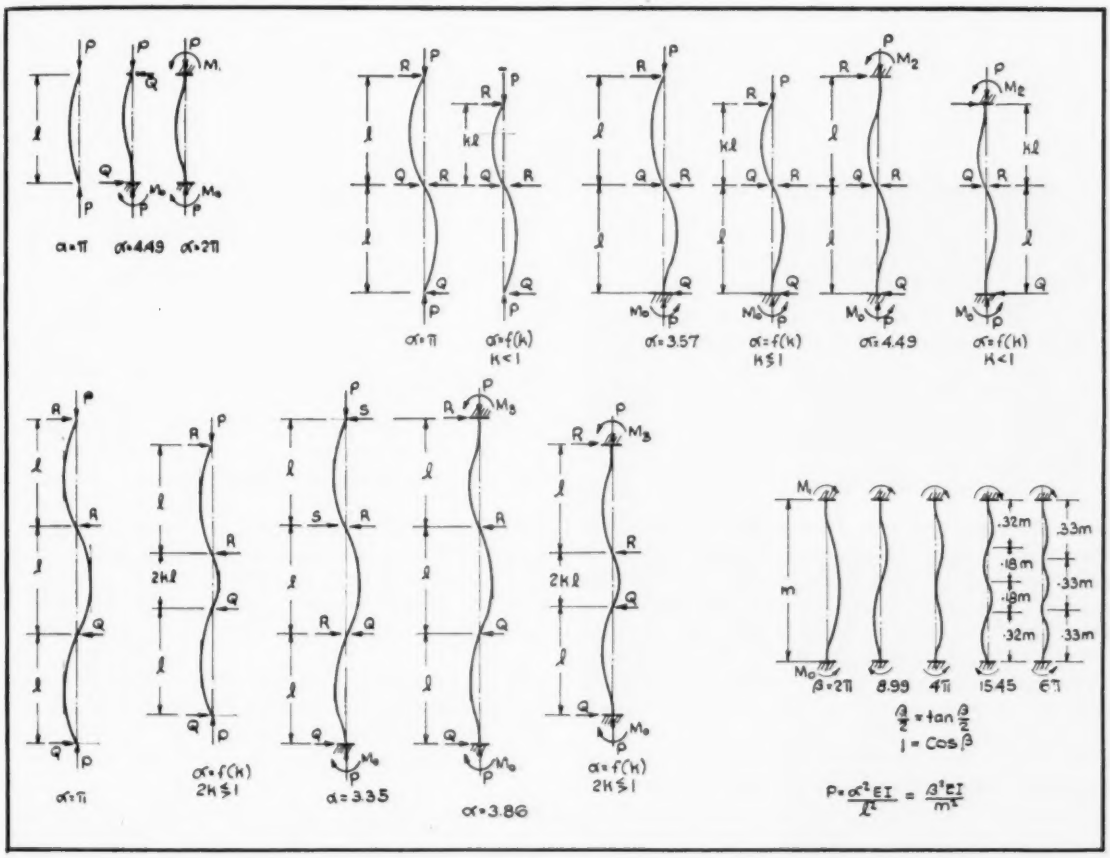


FIG. 1

Long Continuous Columns

BY F. G. SWITZER,[1] NEW YORK, N. Y.

IN connection with a design problem it became necessary to determine the strengths of long columns with intermediate guides. The guides were short, with clearance to the (moving) column and were assumed to offer no restraint to angularity. The solution offered here is the same as the Euler solution so well known for columns of a single loop.

An equation was written for each loop, constants of integration determined from the location of ends and guides on the load axis, and moments eliminated by slope equality through the guides. Buckling loads were finally found by satisfying given end conditions. Higher values of the single-loop solution were also investigated for two fixed ends. These are shown in the lower right-hand corner of Fig. 1.

Some explanation of the solutions, where $\alpha = 4\pi$, 6π, etc., is warranted. The axial tangents at the points of zero deflection are due to *two* guides, at distance zero apart. This interpretation is the same as saying that two points very close together on a

TABLE 1 BUCKLING LOADS AND GUIDE LOCATIONS FOR MAXIMUM LOAD

$P = \dfrac{\beta^2 E I}{m^2}$

m = total length of column
n = number of loops
$(n-1)$ = number of guides
β_{max} = two fixed ends; unequal lengths of loops
β_1 = two fixed ends; equal lengths of loops
β_2 = one fixed end, one round end; equal lengths of loops
β_3 = two round ends; equal lengths of loops

n	β_{max}	β_1	β_2	β_3
1	6.28	6.28	4.49	3.14
2	8.99	8.99	7.15	6.28
3	12.57	11.57	10.04	9.42
4	15.45	14.30	13.03	12.57
5	18.85	17.15	16.09	15.71
6	21.81	20.08	19.14	18.85

LOCATION OF GUIDES FOR β_{max} TWO FIXED ENDS

n	Distance from one end to guides
1	None
2	0.5 m
3	0.5 m, 0.5 m
4	0.32 m, 0.5 m, 0.68 m
5	0.33 m, 0.33 m, 0.67 m, 0.67 m
6	0.24 m, 0.34 m, 0.5 m, 0.66 m, 0.76 m

NOTE: With n odd, the guides are in pairs close together to give, in effect, a fixed end at each pair of guides.

[1] Division Engineer, New York City Board of Water Supply. Mem. A.S.M.E.

Discussion of this paper should be addressed to the Secretary, A.S.M.E., 29 West 39th Street, New York, N. Y., and will be accepted until January 11, 1942, for publication at a later date. Discussion received after the closing date will be returned.

NOTE: Statements and opinions advanced in papers are to be understood as individual expressions of their authors and not those of the Society.

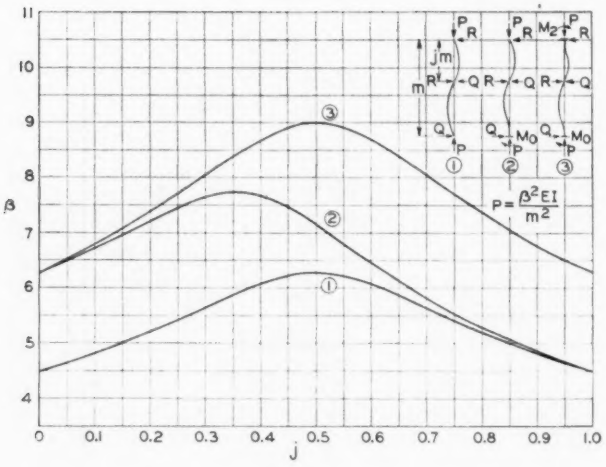


FIG. 2

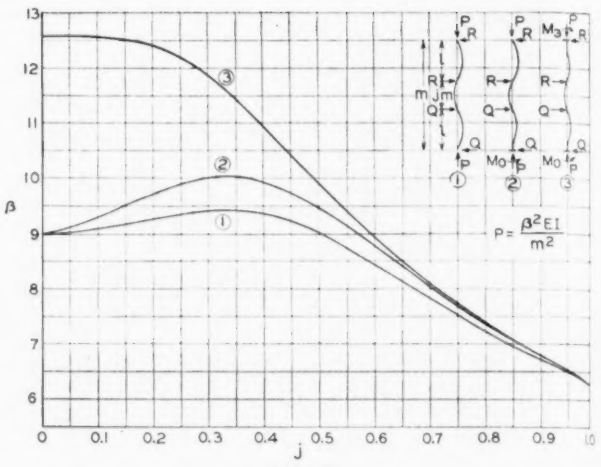


FIG. 3

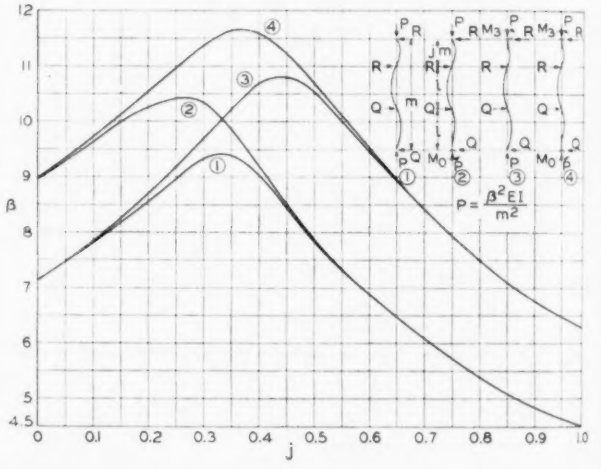


FIG. 4

line determine the slope of the line. Thus with two guides, three loops, and both ends fixed, the guides should be close together at the center and not at the third points as in the case with both ends round. The location of guides for maximum load are determined by the points of zero deflection. It should be noted that these are not equally spaced when the number of loops is even. Table 1 gives buckling loads and guide locations for maximum load, and also buckling loads for columns with equally spaced guides.

Figs. 2, 3, and 4 give buckling loads for long columns of two and three loops with guides at fixed locations. In the sketches of these three curve sheets, an end moment M_0, M_2, etc., indicates a fixed end with axial tangent. The absence of an end moment indicates a round end. The guide reactions Q, R, etc. are transverse forces only. The load is axial and centrally applied.

It has been assumed that these results may be applied to shorter columns than those within the Euler range by the use of a straight-line or parabolic formula derived on the basis of a given crushing stress, factor of safety, and tangency to the appropriate Euler equation, as is customary for single-loop columns.

This study was made in connection with sluice-gate extension-stem designs for the new Delaware Aqueduct. This work is under the direction of the New York City Board of Water Supply, composed of the following members: Commissioners, George J. Gillespie (president), Henry Hesterberg, Rufus E. McGahen; chief engineer, Charles M. Clark; deputy chief engineer, Roger W. Armstrong; and department engineer, Harry R. Bouton.

Discussion

A Short-Gage-Length Extensometer and Its Application to the Study of Crankshaft Stresses[1]

GREER ELLIS.[2] In connection with the use of Stresscoat brittle coatings which the authors mention in step 2 of their three steps in analyzing a structure, the writer would like to add the following information:

As the loading is increased on a structure under test, these coatings will fracture first in areas of maximum tension strain, with the direction of fracture always at right angles to the principal tension.

Compression strains may likewise be indicated as long as the load remains in the elastic range, by reversing the loading and coating processes. Maximum load is maintained while the coating sets to its normal neutral state. Then release of this load allows the relaxing compression strains in the structure to react as tension on the coating.

On practical structures which are usually complicated, qualitative analyses by brittle-coating patterns are great time savers in showing where and in what direction to place the mechanical gage. This is the use of brittle coatings referred to by the authors.

Sometimes, however, areas of interest are so located that the placing of a mechanical gage is difficult or impossible, while the placing of a lacquer film is feasible. Here the quantitative brittle-coating method of analysis, developed recently at the Massachusetts Institute of Technology, with careful handling, can provide values of the principal tension and compression strains to an accuracy of within ± 10 per cent of the true values.

[1] By C. W. Gadd and T. C. Van Degrift, published in the March, 1942, issue of the JOURNAL OF APPLIED MECHANICS, Trans. A.S.M.E, vol. 64, p. A-15.

[2] Managing Engineer, Stresscoat Division, Magnaflux Corporation, Cambridge, Mass.

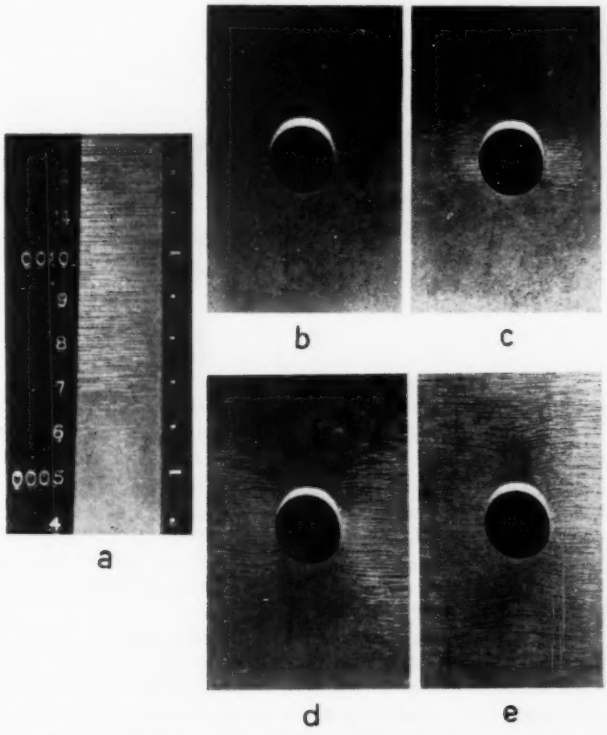


FIG. 2 METHOD OF USING STRESSCOAT QUANTITATIVELY

a Calibration strip
b Plate with hole, in tension, 5000-lb load
c Plate with hole, in tension, 9000-lb load
d Plate with hole, in tension, 14000-lb load
e Plate with hole, in tension, 17000-lb load

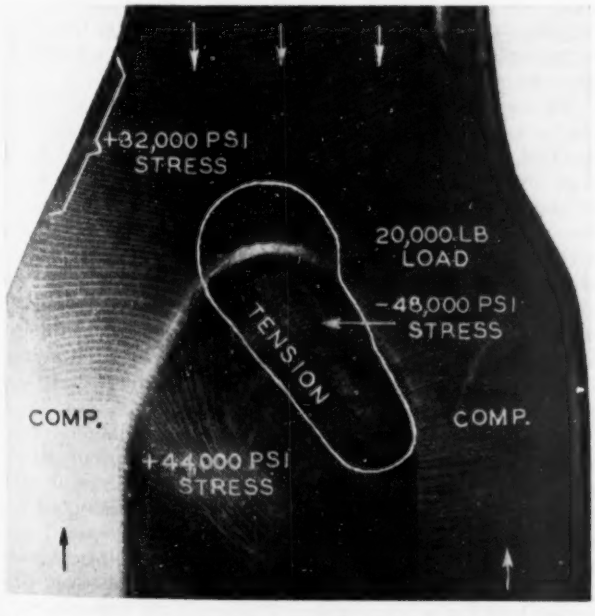


FIG. 1 STRESSCOAT PATTERNS ON FORKED CONNECTING ROD

Fig. 1 shows a forked connecting rod having indications within the crotch as well as on other more open sections. Since the patterns when once formed normally remain visible after release of load, the interiors of assembled structures may be coated, assembled, partially loaded and unloaded, and then disassembled for inspection. Repetition of the process at increasing loads enables one to follow the initiation and growth of all patterns. Even where there is a direct bearing fit, it has been found that the coating applied in a shallow channel $^1/_4$ in. wide and 0.01 in. deep, cut in the area under question, gives satisfactory results.

Fig. 2 illustrates the method of quantitative use. The location and the load at which initial patterns occur are the data taken on the structure. Matching the newly formed patterns on the structure with the lower-range patterns on the calibration strip in the strain scale, at the left, gives the amount of strain present. As long as the loads are kept within the elastic range of the structure, data of one value of strain at one value of load are sufficient for computation of strain at any other value of load by simply proportioning local strains to loads.

Fig. 3 shows the step of loading in the standardized loading

jig, the calibration strip which has previously been coated and dried along with the structure. Under cantilever-beam loading, the upper and lower surfaces of the calibration strip receive a linear gradation of strain from a maximum at the fixed end to zero under the cam. After release from the calibrator, the calibration strip is placed in the strain scale, which is marked off in terms of the strain imposed on the strip by the fixed-cam deflection.

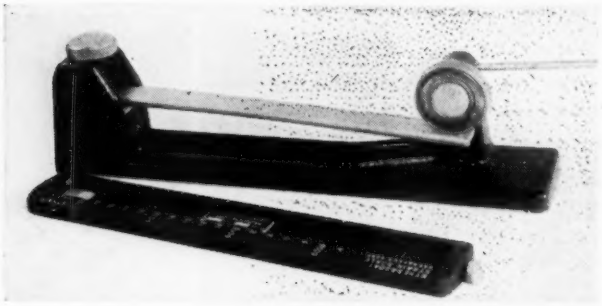


FIG. 3 CALIBRATION STRIP UNDER LOAD IN CALIBRATOR
(Strain scale in foreground.)

AUTHORS' CLOSURE

We agree with Mr. Ellis that brittle lacquer is a useful tool for the study of strains, used either qualitatively in conjunction with the extensometer or quantitatively on other problems, especially those not soluble by other methods.

The use of either brittle lacquer or an extensometer or strain gage permits measurements on the part in question itself. We have found this often to result in a considerable saving in time and expense in studying complicated structures, particularly if two or more parts must be assembled for the test with proper clearances and correct relation (as in a structure consisting of steel and aluminum) between the moduli of elasticity of the parts.

Buckling of the Circular Plate Beyond the Critical Thrust[1]

TH. VON KÁRMÁN.[2] The calculation of the deformation of a plate or shell beyond the buckling limit given by the classical theory of elastic stability requires the solution of a system of nonlinear partial differential equations. Because of the mathematical difficulties, until now only approximate solutions have been produced. The validity of these approximations is restricted either to the neighborhood of the buckling limit or to the very large value of the ratio between the actual and the buckling load. It is very fortunate that the authors found a special case in which the integration of the partial differential equation can be actually carried out so that the approximate methods can be checked. For this reason, the writer believes that this paper represents a definite step forward in the development of the theory of finite deformation.

It would seem that the simple method, which the writer applied years ago to the calculation of the ultimate stress of a flat square plate, supported freely along the longitudinal edges, might also be applied in this case, leading to a relation for the edge stress and buckling stress similar to that obtained by the authors, based on their asymptotic method of integration. The numerical constants involved in this relation might be different, since the writer's method represents a somewhat crude approximation. However, the form of the equation obtained by the two different methods is identical.

AUTHORS' CLOSURE

We have followed the suggestion of von Kármán and applied the Rayleigh-Ritz method to our problem; formulas of the correct type can thus be derived. In the treatment of von Kármán a simple assumption relating to the distribution of the membrane stresses was made. Instead, it is just as simple to determine the membrane stresses together with the bending stresses from the Rayleigh-Ritz method; then even a close numerical approximation can be obtained.

In the terminology of section 6, the potential energy is proportional to

$$V(Q) = \int_0^\infty \left\{ \left(\frac{dP}{d\beta}\right)^2 + \left(\frac{dQ}{d\beta}\right)^2 - PQ^2 \right\} d\beta$$

where

$$\frac{dP}{d\beta} = -\frac{1}{2}\int_\beta^\infty Q^2 d\beta \quad \text{.....cf [31]}$$

The function $Q(\beta)$ was assumed to be of the form $Q(\beta) = ag(\beta/b)$ and $V(Q)$ was minimized with respect to the parameters a and b. The membrane stresses were then obtained from $P = 1 + \int_0^\beta \frac{dP}{d\beta} d\beta$. Various assumptions were made for the function g; the closest approximation resulted from $g = (1 - \beta/b)^2$ for $0 \leq \beta \leq b$, $g = 0$ for $\beta \geq b$. We find, for example, 0.76 for the right member of Equation [37] instead of 0.728, while the tensile stress p_0 at the center is given almost exactly by $p_0 = -0.47\, p_r$.

That these results are so accurate is of course because of the fact that the correct asymptotic expression for the potential energy has been taken, i.e., that which leads to the asymptotic differential Equations [31, 32]. It would be highly desirable to refine the method which was introduced by von Kármán for the square plate along the same lines. Unfortunately, the proper asymptotic expression for the potential energy is not known for this case.

The authors have also made use of the Ritz method in attempting to decide the question raised in the paper as to whether the buckled state with radial symmetry might become unstable at high pressures, and a "second buckling" in waves relative to the original buckled state ensue. Lengthy computations have led always to negative results, i.e., the symmetrically buckled state seems, surprisingly enough, to be always stable. While the high concentration of compressive circumferential membrane stress in the boundary layer favors buckling into waves, this tendency would seem to be overbalanced by the small width of the boundary layer and by the positive contribution of the membrane stresses to the potential energy (the latter contribution is lacking in linear buckling problems).

Quite a different question is whether stable equilibrium states with nodes exist for which, under the same edge pressure p_r, the potential energy is lower than that of the radially symmetric state, even if the latter state is stable. Calculations by the Ritz method seem to indicate that this is also not the case and, hence, a sudden jump from one equilibrium state to another of lower energy seems not likely to occur. It is likely, however, that second buckling or jumping over will occur if the edge constraint is slightly weakened.

[1] By K. O. Friedrichs and J. J. Stoker, published in the March, 1942, issue of the JOURNAL OF APPLIED MECHANICS, Trans. A.S.M.E., vol. 64, p. A-7.

[2] Director, Guggenheim Aeronautical Laboratory, California Institute of Technology, Pasadena, Calif. Mem. A.S.M.E.

The Mechanism of Cavitation Erosion[1]

J. C. HUNSAKER.[2] The high-pressure tests on fused-quartz and glass specimens are interesting because they suggest that the liquids may have penetrated the surface of the glass or quartz. Three new experiments suggest themselves:

1 The repetition of the high-pressure tests on metal specimens.

2 The definite establishment of the presence of liquid molecules beneath the surface of a glass or other specimen previously immersed in the liquid under high pressure.

3 The testing of the protection against cavitation, afforded by previous immersion of a metal or other specimen in oil at high pressure.

The author states that cavitation and damage were produced at the surface of a vibrating specimen when the direction of motion of the surface was parallel with itself. A more complete description of the experiment is desirable to show how this motion can produce cavitation.

There is experimental and theoretical evidence available which shows that the maximum pressures occurring under damage-producing conditions in cavitation (1, 2, 3),[3] water impact (1, 2, 3), or compression-wave impingement (3, 4) are on the order of 5000 to 10,000 psi. This value is about 1 per cent of that which the author speculates may be reached.

Ackeret and de Haller (4) describe experiments on a compression-wave apparatus, in which they claim that no cavitation occurred, but during which damage was produced on metal and glass by very steep-fronted compression waves in water and gasoline. The amplitude of these waves was of the order of 3000 psi. On the other hand, no damage was caused by sinusoidal waves, even with amplitudes greater than 7500 psi. The frequency of each type of wave was about 16 cycles per sec. The pressure amplitude, measured by a piezoelectric crystal, was in fair agreement with that computed theoretically. The same authors also report measurements on instantaneous pressures in a cavitating venturi tube and in a water-impact machine (1).

At the Massachusetts Institute of Technology (5), photographs of the cavitation in a magnetostriction apparatus have been taken, from which have been made computations of the pressure-time relation at the test surface. The results show that the pressure is suddenly applied, once during each cycle, and that the maximum pressure is on the order of 6000 psi. The frequencies used were 5300 and 8750 cycles per sec.

These experiments indicate that a sudden application of pressure, on the order of 10,000 psi, causes damage, while a less rapid application of the same pressure may not do so. Further investigation of the effect on damage of changes in suddenness of application is necessary.

J. M. MOUSSON.[4] The author suggests that pitting due to cavitation is the result of fluid injection in molecular form under extremely high pressure. Actual failure supposedly takes place after the sudden release of the pressure due to the insufficiency of the cohesive forces of the material to retain the injected fluid particles. This is not the first time that such a theory has been proposed (6). However, despite the data made available in this paper, fluid injection under cavitation conditions does not appear to be substantiated. Moreover, a preponderance of evidence previously available would seem to be against it.

The results presented in the author's Fig. 1 indicate that fluid penetration requires extremely high pressures as well as a sustained pressure application; that is, the pressure must necessarily act over a sufficient length of time. Under cavitation conditions neither requirement may be fulfilled. While at first glance infinitely high stresses may be thought possible under impact due to collapsing cavities and vortices (7, 8), there are definite limitations in the magnitude as pointed out by Ackeret and de Haller (3). Even under extremely high relative velocities between fluid and boundary, that is, from 100 to 300 fps, the maximum stress may more likely be of the order of tens of thousands rather than hundreds of thousands of pounds per square inch (Fig. 1), or even 1,000,000 psi, as suggested to occur under cavity collapse. Stresses of the latter magnitudes are not only highly improbable but are believed to be unnecessary as a cause for severe pitting due to cavitation. The photomicrographic analyses of many low- and high-alloyed steels and nonferrous-metal specimens in various conditions have indicated that pitting as a result of cavitation is due to repeated pounding or pressure waves causing breakdown phenomena typical of this type of stress application (9, 10, 11). The phenomena observed were: Cold working, as evidenced through surface strain hardening, slip bands, and in certain instances twinning of crystals; yield in surface layers; fatigue cracks caused either by exhaustion of the capacity to yield or by reaching fatigue limits; cracks resulting from stress concentrations due to unfavorable grain shapes; break-throughs between impurities or nonmetallic inclusions or because stratification provided little bond between successive grain layers, etc. Keeping in mind that all these phenomena are the result of a very large number of stress applications, the stress magnitude may more likely be of the order of tens of thousands, rather than of hundreds of thousands, or even 1,000,000 psi.

In addition, two other factors should be given careful consideration. On the one hand, inter- or transcrystalline injection of fluid apparently requires a time interval during which these very high pressures are applied (refer to Fig. 1 of paper). Under cavitation conditions, the entire cycle from pressure rise to dissipation of energy is almost instantaneous. On the other hand, various practical experiences could be cited; although one of these may be sufficient. In some cases, cast carbon-steel propeller turbine blades have seriously pitted during relatively short periods of service, yet repairs of a permanent nature were possible by means of welded stainless-chromium-steel surfaces. Now, if the stresses under fairly severe cavitation conditions were of a magnitude as suggested in this paper, and if pitting were caused because of fluid injection, even the welded stainless steel could not possibly withstand the attack.

There has been an indication that cavitation as produced by means of magnetostriction oscillators may not necessarily be identical to that occuring in flowing water and simulated by test stands of the Venturi or nozzle type. The results obtained with the two types of apparatus check each other only along general lines but not in detail. This contention is illustrated very clearly by means of a comparison between the data obtained at the Massachusetts Institute of Technology (12), and at Holtwood (10), with oscillator- and Venturi-type apparatus, respectively. The author throws additional light on the subject in stating that stroboscopic observations at his laboratory showed vapor bubbles to form at the same point time and again. This phenomenon is not identical to that in flowing water where successive blows may fall at random anywhere in the target area producing a kneading type of stress application. Thus identical

---

[1] By T. C. Poulter, published in the March, 1942, issue of the JOURNAL OF APPLIED MECHANICS, Trans. A.S.M.E., vol. 64, p. A-31.

[2] Professor in Charge, Department of Mechanical Engineering, Massachusetts Institute of Technology, Cambridge, Mass. Past Vice-President A.S.M.E.

[3] Numbers in parentheses refer to the Bibliography at the end of the author's closure, covering references in all discussions of this paper.

[4] Project Engineer, Rustless Iron & Steel Corporation, Baltimore, Md. Mem. A.S.M.E.

results can hardly be expected with both types of laboratory methods.

The author states that there was no consistency between the pitting resistance of alloys and hardness. Without further qualification, this statement may be misleading. As hardness is not the only criterion to be considered, a consistent relation between hardness and pitting resistance may not be expected unless all other factors to be reckoned with remain unchanged, such as chemical composition, susceptibility to strain hardening, capacity to yield, fatigue limits, grain shapes, percentage of impurities, and nonmetallic inclusions, etc. With a change in material too many other factors change besides the hardness. For instance, taking those referred to by the author, lead and rubber can absorb substantial energy by means of plastic deformation, whereas, glass, cast iron, and carboalloys are very brittle. Rubber is particularly unusual because of its resilience. A series of tests with various types of protective rubber covers cemented to steel plates was made some years ago with the Holtwood cavitation test stand. The results indicated that the thinner the rubber sheet, the higher is the pitting resistance. Apparently appreciable heat is generated within the rubber sheet under the punishment by cavitation, and if this heat cannot be carried away quickly it may melt the rubber. While with thick rubber coverings heat is stored up, thin rubber sheets may apparently give off heat at a fairly rapid rate to the adjacent metal. This phenomenon may perhaps explain the results obtained by the author with molecular oil films.

F. G. Switzer.[5] The first part of this paper is interesting and informative. The data on the failure of glass and quartz upon the removal of pressure are not questioned. However, the writer is unable to follow through to the conclusion that this is the mechanism of cavitation erosion. It appears to be a well-established fact that cavitation erosion occurs in conjunction with the appearance and subsequent collapse of vapor bubbles in a flowing liquid. The collapse of the vapor bubbles results in the generation of high-pressure impacts lasting, as the author states, only a very small fraction of a second but repeated over and over again. The first part of the paper shows conclusively that the high pressure must be maintained for a substantial time of some seconds before failure is caused by the relief of the pressure. Under cavitation conditions, the high pressure does not last long enough to permit the entrance of liquid into the pores of the solid. Is it not much more likely that cracks in metal parts subjected to cavitation are fatigue cracks?

Author's Closure

In response to the various questions raised, concerning the material presented and the conclusions drawn, upon which was based what appears to the author to be the most logical explanation of the mechanism whereby tiny fragments are removed from the surface of a solid in the process commonly referred to as cavitation erosion, the author would like to make the following statements.

Although some experiments have been conducted along the line of those suggested by Professor Hunsaker before it became necessary temporarily to discontinue the work in favor of more urgent matters, additional work along these lines is definitely indicated. In connection with investigations involving high-pressure windows, it was observed that the window would be less likely to fracture in contact with water under pressure if previously it had been subjected to very high oil pressure, thus indicating but not proving an actual penetration.

In those specimens where the direction of motion was parallel with the surface of the specimen, the nickel tube was placed in a horizontal position, and a drop of water was placed on the top surface on the edge of the specimen. In this manner it is impossible for a compression wave to be set up by the movement of the flat surface of the specimen and travel through the liquid, around the corner of the specimen to produce the erosion on the specimen edge. However, the relative motion of the specimen with respect to the water produces the necessary rate of shear and turbulence in the water to produce cavitation and the resultant erosion. The experimental results of citations (1, 2, 3, 4) seem to be quite in agreement with the results obtained by the author, in that he has been unable to obtain any damage by means of a sinusoidal wave in the absence of cavitation.

It is the author's belief that, in spite of the fact that cavitation was not detected by Ackeret and de Haller (4), such was actually taking place whenever damage was produced, and that it would be impossible to measure directly the extremely high and localized pressure resulting from the collapse of the individual cavities. Perhaps one of the best indications that cavitation is actually taking place, and that it is the extremely high pressure localized at points on or near the surface, is that a compression wave, with sufficient amplitude to produce cavitation and therefore damage, ceases to produce damage when a hydrostatic pressure sufficient to prevent cavitation is superimposed on the liquid. If the superimposed hydrostatic pressure is equal to the pressure resulting from the sinusoidal compression wave, it is difficult to understand how doubling the maximum pressure could cause the erosion to cease. The author, therefore, contends that such a superimposed pressure merely prevents cavitation and the resultant extremely high and highly localized pressure sufficient to produce damage. It is also his contention that the mechanism described seems to be in agreement with the experimental data and theoretical consideration.

The fact that it is necessary to maintain pressure on a piece of glass for some seconds to obtain complete rupture of the piece of glass in a single cycle in no way indicates that, if such a pressure were applied several thousand times a second, it would not produce sufficient penetration during each cycle to give a rather rapid erosion. While the author makes no claims that pressures as high as 100,000 psi are necessary to produce erosion, it seems apparent that, since superimposing a hydrostatic pressure would tend to prevent and does minimize and in many cases prevent erosion, a pulsating pressure of only a few thousand pounds per square inch in most cases is insufficient to produce erosion of the type under discussion.

Since there seems to be no direct method of measuring the magnitude of the pressure caused by the collapse of a small cavity because of the extremely small space involved, and the fact that from theoretical considerations one would expect extremely high pressures to be produced, some indirect methods such as the one described can be a very helpful guide. As pointed out in the first of the paper, so many phenomena are involved in such a process that it is difficult, if not impossible, to isolate them completely. The mechanism described has served as a very useful tool in effecting a material reduction and in some cases complete elimination of erosion in certain commercial applications.

BIBLIOGRAPHY

1 "Untersuchungen über die durch Kavitation hervorgerufenen Korrosionen," by P. de Haller, *Schweizerische Bauzeitung*, vol. 101, 1933, pp. 243–246, and 260–264.

2 "La Corrosion par Cavitation et par Choc de Gouttes Liquides," by P. de Haller, *Schweizer Archiv*, vol. 6, 1940, pp. 61–68.

3 "Über die Zerstörung von Werkstoffen durch Tropfenschlag und Kavitation," by J. Ackeret and P. de Haller, *Schweizerische Bauzeitung*, vol. 108, 1936, pp. 105–106.

4 "Über Werkstoffzerstörung durch Stosswellen in Flüssig-

[5] Division Engineer, New York City Board of Water Supply, New York, N. Y. Mem. A.S.M.E.

keiten," by J. Ackeret and P. de Haller, *Schweizer Archiv*, vol. 4, 1938, pp. 293–294.

5 "Study of the Damage Producing Mechanism in Hydraulic Cavitation," unpublished thesis, by B. G. Rightmire, Massachusetts Institute of Technology, 1941.

6 "Cavitation and Erosion Investigated as a Problem in Fluid Mechanics," by W. W. Pagon, miscellaneous papers, A.S.M.E., 1935, no. 13.

7 "Mathematical Investigation of the Collapse of Water Cavities," by S. S. Cooks, *Engineering*, vol. 107, 1919, p. 519.

8 "Hydromechanische Probleme des Schiffsantriebs," Report of conference, edited by K. Kempf and E. Foerster, Hamburg, Germany, May, 1932, p. 243.

9 "Failure of Metals Due to Cavitation Under Experimental Conditions," by H. N. Boetcher, Trans. A.S.M.E., vol. 58, 1936, pp. 355–360.

10 "Pitting Resistance of Metals Under Cavitation Conditions," by J. M. Mousson, Trans. A.S.M.E., vol. 59, 1937, pp. 399–408.

11 "Practical Aspects of Cavitation and Pitting," by J. M. Mousson, Edison Electric Institute Bulletin, vol. 5, 1937, pp. 373–383, and 423–430.

12 "Determination of the Relative Resistance to Cavitation Erosion by the Vibratory Method," by S. L. Kerr, Trans. A.S.M.E., vol. 59, 1937, pp. 373–397.

Self-Excited Oscillations in Dynamical Systems Possessing Retarded Actions[1]

H. Poritsky.[2] The general conclusions reached by the author that self-excited oscillations might be due to retarded action, even if the latter occurs in a damping term, is of great interest. The term "hysterodifferential equations," used by the author for signifying the fact that there is a phenomenon of lag or hysteresis involved in the action, is more properly applied to cases where the "memory phenomena" extend not only to one preceding time instant but to all the past history of the system, for instance, in case of certain highly viscous solids. The title "retarded action" is more appropriate to the case at hand.

Mathematicians call differential equations which involve values of the function or its derivatives at t and $(t - \Delta t)$ "difference-differential" equations. The fact that a difference-differential equation is equivalent to a linear differential equation of infinite order, while of great interest, is hardly of any help in the actual solution of the problem. This solution may be obtained by assuming outright an exponential solution. Thus, assuming a solution of the author's Equation [4]

$$\theta = e^{\lambda t} \quad \ldots\ldots\ldots\ldots\ldots\ldots\ldots\ldots [1]$$

where λ is a proper constant, and substituting, there results upon factoring out the exponential $e^{\lambda t}$ the following equation for λ

$$J\lambda^2 + B\lambda + C + S\lambda e^{-\lambda \cdot \Delta t} = 0 \quad \ldots\ldots\ldots\ldots [2]$$

In general a linear difference-differential equation admits exponential solutions in a manner quite similar to that of an ordinary linear differential equation, except that, whereas in the latter case the determination of the exponents reduces to an algebraic equation, in the present instance it reduces to a transcendental one. There may now be an infinite number of exponentials. Instability obtains when a root exists with a positive real part.

The writer's colleague, Mr. C. Concordia, has called attention to a treatment of a similar problem of retarded action for synchronous-machine generators with regulators admitting a constant time of retardation, by Fritz Reinhardt.[3] The difference-differential equation treated in this case agrees precisely, except for notation, with the one discussed by the present author. The stability and other factors are discussed at great length.

Without wishing to detract from the value of the author's interesting investigation, the writer would like to point out that it is unlikely that even the system illustrated in the author's Fig. 1 possesses an exactly constant time of retardation. Very often in follow-up systems, the retardations are due to neglected inertias of moving parts. When these neglected inertias are taken into account, the order of the system is raised and instability sometimes appears. Again hunting may be due to lost motions such as might occur because of loose fitting between a pin and a sleeve bearing. That the latter may give rise to self-excited oscillations has been shown by C. Concordia[4] and others by means of differential-analyzer studies, and by the writer (in an unpublished paper) by direct investigation of linear systems.

Author's Closure

Mr. Poritsky raised a number of questions which can be discussed here only briefly.

As regards the classification of differential equations, the term "difference-differential equation" mentioned by Mr. Poritsky is probably more generally used than the term "hysterodifferential equation" used in this paper.

Equations in which the "memory phenomena" extend not only to one preceding time instant but to all the past history of the system are generally designated as "integrodifferential equations" following the nomenclature of V. Volterra.[5]

Equation [7′] of the paper by Fritz Rheinhardt,[3] cited by Mr. Poritsky, coincides exactly with the author's Equation [4], derived independently. Additional difference-differential equations encountered in the theory of controls are indicated in the paper.[6] More specifically, Equation [1] of the paper is the equation of a retarded automatic steering control with a purely directional control, and Equation [4] is encountered in the problem of water-ballast control in antirolling ship installations.

Consideration of the difference-differential equations as a limit of an ordinary differential equation of infinitely high order is helpful for two reasons:

1 From the latter point of view, the solution $e^{\lambda t}$ becomes obvious, although, from the former point of view, it is not so obvious.

2 Furthermore, if time lags are small, and the Taylor's expansion 3 converges rapidly, it is frequently convenient for numerical computations to neglect the terms of higher orders and consider only the first few terms of the expansion. In this manner, one has still an ordinary differential equation but of a higher order instead of a difference-differential Equation [8]. Such methods of approximation are described in a recent paper.[7] The increase in the order of the equation mentioned in the last paragraph of Mr. Poritsky's discussion appears then as the result of these approximations. If, however, one deals directly with the difference-differential Equation [8], there can be no question of raising its order, since this equation is nothing but an asymptotic

---

[1] By Nicholas Minorsky, published in the June, 1942, issue of the Journal of Applied Mechanics, Trans. A.S.M.E. vol. 64, p. A-65.

[2] Engineering General Department, General Electric Company, Schenectady, N. Y.

[3] "Der Parallelbetrieb von Synchrongeneratoren mit Kraftsmaschinenreglern Konstanter Verzögerungszeit," by Fritz Reinhardt, *Wissenchaftliche Veröffentlichungen* aus den Siemens-Werken, vol. 18, 1939, pp. 24–44.

[4] "Effect of Prime-Mover Speed Governor Characteristics on Power-System Frequency Variations and Tie-Line Power Swings," by C. Concordia, S. B. Crary, and E. E. Parker, Trans. A.I.E.E., vol. 60, 1941, pp. 559–567.

[5] "Leçons sur les Equations Integrales et les Equations Integrodifferentielles," by V. Volterra, Paris, 1913, chapt. 4.

[6] Ref. 1, p. A-71.

[7] "Control Problems," by Nicholas Minorsky, *The Journal of The Franklin Institute*, vol. 232, 1941, pp. 451–487 and 519–551.

form of an ordinary differential equation of an infinitely high order.

As regards the hypothesis concerning the constant time lag, like any other hypothesis, it is valid only if the experimental evidence justifies such an assumption. In experiments described in connection with Fig. 1, of the paper, the power of the motor was sufficiently great in comparison with the power needed to accelerate the weight and overcome its friction. The pendulum was rocked by a cam within a certain range of frequencies ω and moving pictures of the angle θ and the displacement x were taken. From the record of angle θ, a curve $\dot{\theta}$ of angular velocity was plotted and the phase angle $\varphi = \omega \Delta t$ between the $\dot{\theta}$ and x curves was thus obtained; from these computations it was found that the time lag Δt proper (as distinguished from the angular lag φ) was fairly constant, as was assumed in the theory.

Finally, in order to establish the existence of instability, it is sufficient to show that there is at least one positive root, as Mr. Poritsky points out and as is mentioned[8] in the paper.

[8] Ref. 1, p. A-67.

The criteria for stability are, however, more restrictive, since they require that the real parts of all roots must be negative. This condition is generally obtained by means of the so-called Hurwitzian criteria. The application of these criteria to Equation [14] of the paper presents no difficulty. It is not included here, because the purpose of the paper is to establish the conditions for instability rather than those for stability.

Finally, as regards the question of the stability of the amplitudes of self-excited oscillations (as distinguished from the question treated in this paper concerning the zones where these oscillations may occur), it can be stated that such stable self-excited oscillations can never occur in purely linear systems and are always associated with what Poincaré calls the "limit cycles" (cycles limites) of nonlinear systems. The relaxation oscillations studied by Van der Pol are typical in this connection, and it is to be expected that both mechanical and electromechanical systems must possess these features of nonlinearity if self-excited parasitic oscillations are to exist in a steady state. As far as is known, this question remains still relatively unexplored.

Book Reviews

Water and Carbon Dioxide

PROPERTIES OF ORDINARY WATER-SUBSTANCE. Compiled by N. Ernest Dorsey, Physicist, National Bureau of Standards, Washington, D. C. American Chemical Society Monograph Series. Reinhold Publishing Corporation, New York, N. Y., 1940. Cloth, 6 × 9 in., xxiv and 673 pp., $15.

CARBON DIOXIDE. By Elton L. Quinn and Charles L. Jones. American Chemical Society Monograph Series. Reinhold Publishing Corporation, 1936. Cloth, 6 × 9 in., 294 pp., $7.50.

REVIEWED BY JOSEPH H. KEENAN[1]

THE book by Dorsey is an amazingly comprehensive and complete collection of data on the properties of water in all its known phases. The plan of the compilation was made by a committee of the Bureau of Standards, but the reality is evidently the product of the diligence and skill of the author.

The backlog of the project is the International Critical Tables which provided information antedating January 1, 1923, though even this material has been supplemented. Information of later date was obtained by carefully combing the technical literature of all the civilized world.

Like the International Critical Tables this book presents source material rather than working tables such as the engineer employs. For example, one finds here all the data that have been used in the preparation of *steam tables* for engineering purposes, but not the *steam tables* themselves.

The material is of greater variety than would be required for ordinary engineering uses. Data are given on dissociation, heat of formation, characteristics of the molecule, rates of diffusion in various media, optical properties, emissivity, absorptivity, fluorescence, electrical characteristics, strength of the liquid in tension, photoelectric effects, and color.

The curiosity seeker will find here things to tickle his fancy. Samples of water taken from different depths of Lake Baikal had different densities, even after distillation. Negative pressures of 2300 lb per sq in. have been sustained by ordinary water. A reputable theory of the structure of ice maintains that "ice is a liquid jelly, with foam-walls of concentrated oily salt solution, which enclose foam cells containing viscous, doubly refracting, pure or nearly pure water."

The book is often difficult to read because the same type is used for text and tables. Where the text is interrupted by tables, which often extend over several pages and include explanatory paragraphs, the reader is sometimes at a loss to find the end of the interruption.

The vocabulary is occasionally troublesome, at least to the engineer. For instance on page 78 we learn that "by dilated water vapor is meant the vapor at a pressure that is less than its saturation pressure at the temperature concerned. The adjective 'dilated' is less ambiguous than the more frequently used 'unsaturated,' which is equally appropriate to the supersaturated condition." It appears that the author is unaware of the term *superheated vapor*, which has a more honorable history and far more general acceptance than the term *unsaturated* which he quotes. On page 271 we find that "the heat liberated by adiabatic compression" is the constant-temperature coefficient, $(\partial h/\partial p)_t$. This is a curious use of the term *adiabatic*. On page 269 it is stated that "the Joule-Thomson coefficient . . . . . is the increase in temperature on adiabatic compression."

These minor deficiencies should not, however, be overemphasized. The book is of first importance. To anyone working with H_2O it is the International Critical Tables brought up to date. It is something more than that, however. The Critical Tables are a mere skeleton of data. This book has flesh on its bones.

Dorsey devotes 670 pages to water; Quinn and Jones require less than half this number for carbon dioxide. And this despite the fact that half the discussion of carbon dioxide relates to manufacture and use—topics which do not appear in the volume on water.

The data on the properties of carbon dioxide are always meager and often questionable. It is a pity that the resources and the organization that until recently existed in America for research on water were not employed for research on carbon dioxide.

Nevertheless, many interesting items of information can be found among the data in this book. At high pressures solid CO_2 can exist at temperatures appreciably higher than the critical temperature. If water behaved similarly, ice could be red-hot. Fig. 14 in the book shows the Joule-Thomson coefficient as a function of pressure and temperature for liquid and vapor phases and above the critical point.

Although certain limited natural supplies of carbon dioxide rival soap in purity, the gas is commonly manufactured at low cost from products of combustion of fuel and from other sources. Descriptions are given of the manufacturing processes.

The manufacture of dry ice is considered in detail and the various processes employed are shown in diagrams. The preparation of the product for the market and its industrial uses are described.

The book is a happy combination of the scientific and the industrial points of view. The first half is a scholarly presentation of scientific data; the second half is an excellent presentation of engineering and manufacturing methods. If collaboration of a chemist and an engineer can be so fruitful it should be more common.

[1] Professor of Mechanical Engineering, Massachusetts Institute of Technology, Cambridge, Mass. Mem. A.S.M.E.

Materials Testing

MATERIALS TESTING. By Herbert J. Gilkey, Glenn Murphy, and Elmer O. Bergman, McGraw-Hill Book Company, Inc., New York, N. Y., 1941. Cloth, 8½ × 11 in., xii and 185 pp., $2.75.

REVIEWED BY W. M. MURRAY[2]

THIS book represents about twenty years' development of a manual for instruction in the fundamental principles of testing materials and their relation to various phases of engineering. Although the book is intended primarily for an introductory course, it has been prepared in such a manner as to indicate many of the more advanced aspects of testing. The authors have succeeded in the happy combination of a simple elementary text which is well written and easy to understand together with many suggestions showing how the procedures can be utilized in actual engineering practice.

The text is divided into twelve chapters starting with a detailed discussion of strain gages and testing machines. From the

[2] Assistant Professor of Mechanical Engineering, Massachusetts Institute of Technology, Cambridge, Mass. Mem. A.S.M.E.

point of view of a man already familiar with the subject this initial chapter might well be omitted, but for the beginner it will be of great interest and utility both because of the detailed illustrations and the variety of the equipment discussed. The second chapter is devoted to properties of materials and the third to the interpretation of test observations into terms of material properties. A section is devoted to the detail of each of the following types of tests: Tension, compression, shearing, and torsion, flexure, column, hardness, fatigue and impact, a long chapter on tests for concrete, and finally the text is concluded with a chapter on experimental aids in stress analysis.

Throughout the book there are numerous diagrams and detailed work sheets laid out to aid the student, as well as many questions and answers which have been designed to stimulate further study. As an aid to instructors a number of definite problems have been included to form the basis of a course which might be supplemental to lectures in applied mechanics or given as an independent subject.

One noticeable feature of the book lies in the fact that any student using it will be forced to consult the A.S.T.M. Standards very frequently. This will undoubtedly give excellent training in looking up references.

The writer regrets that the detail of the first few chapters is not maintained throughout the text. This is particularly noticeable in the chapters on hardness, impact, and fatigue which are not nearly so complete.

Although the book is elementary in character it includes an excellent list of references which carry on well beyond its own scope and for that reason it should prove most valuable to the beginner since it will indicate the direction in which to proceed after its own contents have been absorbed.

Thermodynamics

THE NATURE OF THERMODYNAMICS. By P. W. Bridgman. Harvard University Press, Cambridge, Mass., 1941. Cloth, 5¼ × 8 in., xii plus 229 pp., $3.50.

REVIEWED BY J. H. KEENAN[3]

PROFESSOR Bridgman states his object as follows: "to make an operational (as distinguished from a purely logical) analysis of the situation in thermodynamics and related fields, and at the same time cast the analysis in such a form as to bring out the role and consequences of the verbal requirements which have entered into forming the concepts. I shall attempt especially to make clear whether the operations involved are instrumental operations or 'paper and pencil' operations." The result is a distinct contribution to our literature of thermodynamics. It will help the advanced student, but many of the difficulties discussed are of too sophisticated a nature for the beginner who faces enough hurdles within his own scientific experience without having more dragged in from unfamiliar fields.

The discussion of temperature is good, but the treatment of heat and work is not clarifying. We find that the equation

$$dE = dW + dQ$$

"is also applicable . . . . . to regions in which the content of material substance is continually changing, as when it is applied in hydrodynamics." One's first impulse is to say that the example of a steam turbine adequately disproves this statement. But concealed in dW and dQ are Poynting vectors which make everything all right.

This vector concept leads to much argument which appears to end in anticlimax with the statements "it is not possible in general to analyze a flow of energy into two factors, one of which has all the properties of the velocity of a material thing," and "the probability is that even if such an analysis (of entropy flow into a velocity factor and a density factor) is possible, the necessity for it can be sidestepped."

Despite these criticisms, one finds many admirable features in the book. A good discussion of friction at the boundary surface of a system emphasizes the need for discretion in selecting the position of the boundary. The first law is stated in the form "dE is a perfect differential." The section on "the meaning of ΔE" is excellent. Concerning reversibility we read that "it is the recoverability of the original situation that is important, not the detailed reversal of the steps which led to the original departure from the initial situation." In the discussion of the definition of entropy we find this illuminating comment, "the entropy is in the first instance defined by means of reversible processes, just as energy was in the first instance defined for processes for which dW and dQ had a meaning."

The entropy of the universe is discussed intelligently and not in catch phrases, and there are helpful comments on the entropy of radiation. There is frequent reference to a new technique for analyzing irreversible processes which was discussed in the author's book on electrical phenomena in metals but which, unfortunately, is not restated here.

Kelvin once restricted his statement of the second law to inanimate agencies. On this point Bridgman has some interesting things to say, and his conclusion is that "as far as I am concerned there is not the slightest indication that such a conclusion (namely, that vital phenomena are outside the range of thermodynamics) will ever be necessary."

[3] Professor of Mechanical Engineering, Massachusetts Institute of Technology, Cambridge, Mass. Mem. A.S.M.E.

IN TWO SECTIONS—SECTION TWO

Transactions

of the

A.S.M.E.

SOCIETY RECORDS—PART 1

James W. Parker, President of The American Society of Mechanical Engineers, 1941-1942 ..... *Portrait and Biography*

Council and Committee Personnel ..... RI-1—RI-33

Officers and Council 1
Standing Committees 2
Special Committees 3
Special Council Committees 4
A.S.M.E. Representatives on Other Activities 5
Professional Divisions 6
Local Sections 10
Student Branches 18
Research Committees 20
Standardization Committees 22
Power Test Codes Committees 28
Safety Committees 30
Boiler Code Committees 32

Woman's Auxiliary to the A.S.M.E. RI-33
Awards RI-34
Honorary Members, Past-Presidents, Treasurers, and Secretaries RI-38
Index RI-40

SOCIETY RECORDS—PART 2

Constitution, By-Laws, and Rules RI-43
Index RI-54

FEBRUARY, 1942

VOL. 64, NO. 2

Transactions

of The American Society of Mechanical Engineers

Published on the tenth of every month, except March, June, September, and December

---

OFFICERS OF THE SOCIETY:

JAMES W. PARKER, *President*

W. D. ENNIS, *Treasurer* C. E. DAVIES, *Secretary*

COMMITTEE ON PUBLICATIONS:

F. L. BRADLEY, *Chairman*

C. R. SODERBERG E. J. KATES

A. R. STEVENSON, JR. L. N. ROWLEY, JR.

GEORGE A. STETSON, *Editor*

ADVISORY MEMBERS OF THE COMMITTEE ON PUBLICATIONS:

W. L. DUDLEY, SEATTLE, WASH. N. C. EBAUGH, GAINESVILLE, FLA. O. B. SCHIER, 2ND, NEW YORK, N. Y.

Junior Members

FRANKLIN H. FOWLER, JR., CALDWELL, N. J. J. A. CONNON, NEW YORK, N. Y.

Published monthly by The American Society of Mechanical Engineers. Publication office at 20th and Northampton Streets, Easton, Pa. The editorial department located at the headquarters of the Society, 29 West Thirty-Ninth Street, New York, N. Y. Cable address, "Dynamic," New York. Price $1.50 a copy, $12.00 a year; to members and affiliates, $1.00 a copy, $7.50 a year. Changes of address must be received at Society headquarters two weeks before they are to be effective on the mailing list. Please send old as well as new address. . . . By-Law: The Society shall not be responsible for statements or opinions advanced in papers or . . . printed in its publications (B13, Par. 4). . . . Entered as second-class matter March 2, 1928, at the Post Office at Easton, Pa., under the Act of August 24, 1912. . . .

Copyrighted, 1942, by The American Society of Mechanical Engineers. Reprints from this publication may be made on condition that full credit be given the Transactions of the A.S.M.E. and the author, and that date of publication be stated.

PRESIDENT



Craine

JAMES W. PARKER
1941-1942

James Wentworth Parker

James Wentworth Parker, President of The American Society of Mechanical Engineers for the year 1941-1942, is vice-president and chief engineer of The Detroit Edison Company, and has his residence in Ann Arbor, Michigan. He was born in Auburn, New York, in 1886, of people who had lived in that state for a generation or more but had originally come from New England. His family moved to Kentucky when he was four years old and his boyhood was spent in Louisville.

He prepared for college in the Louisville Male High School and was graduated from Cornell University in 1908, with the degree of mechanical engineer. In 1935 he was awarded the honorary degree of master of science in mechanical engineering by the Detroit Institute of Technology. He is a member of the honorary societies of Sigma Xi and Tau Beta Pi.

After graduation from Cornell, Mr. Parker served an apprenticeship, first with the DeKalb Power & Light Company in Illinois, and then with the Vincennes Street Railway Company, Vincennes, Ind. In 1910 he moved to Detroit to become boiler-room engineer with The Detroit Edison Company, and has been employed continuously by that Company to the present time, with the exception of a year's leave of absence for war service in 1918.

In the course of this employment he has organized and directed the various engineering projects which his company has accomplished in the last twenty years, notably the design and construction of its electric power plants, Trenton Channel, Marysville, Delray No. 3, and Conners Creek. In addition to supervising new construction, Mr. Parker has also general responsibility for the operation of The Detroit Edison electrical system and of its generating plants, and central-heating plants and system.

During the first World War he served in the Nitrate Division of the Ordnance Department, United States Army, as consulting mechanical engineer and head of that Division's inspection section.

He served ten years as a Trustee of Cornell University, elected by the alumni in 1929 and re-elected in 1934.

Mr. Parker has been a member of The American Society of Mechanical Engineers since 1913. From 1928 to 1933 he served as member of the Committee on Meetings and Program, and as Manager from 1935 to 1938, and Vice-President from 1938 to 1940. He served as a member of the Society's executive committee for four years.

He served a three-year term (1938-1941) as president of the Engineering Society of Detroit, of which he has been a director since the organization of the new society in 1936; and is a member of the Michigan Engineering Society and the Prismatic Club of Detroit.

The American Society of Mechanical Engineers

HEADQUARTERS: 29 West 39th St., New York, N. Y.
MID-WEST OFFICE: Room 1617, 205 West Wacker Drive, Chicago, Ill.

The members of the Council and of its standing and special committees given on the following pages are those in office on January 1, 1942, serving for the official year 1941-1942. The terms of office of members of other committees are not fixed by the official calendar.

OFFICERS AND COUNCIL

PRESIDENT

James W. Parker

PAST-PRESIDENTS

Terms expire December

James H. Herron (1942)
Harvey N. Davis (1943)
Alexander G. Christie (1944)
Warren H. McBryde (1945)
William A. Hanley (1946)

VICE-PRESIDENTS

Terms expire December, 1942

Samuel B. Earle
Frank H. Prouty
Edwin B. Ricketts

Terms expire December, 1943

Clarke Freeman
Clair B. Peck
William H. Winterrowd *
Willis R. Woolrich

MANAGERS

Terms expire December, 1942

Joseph W. Eshelman
Linn Helander
Guy T. Shoemaker

Terms expire December, 1943

Huber O. Croft
Paul B. Eaton
George E. Hulse

Terms expire December, 1944

William G. Christy
Herbert L. Eggleston
Thomas S. McEwan

TREASURER	SECRETARY
W. D. Ennis	C. E. Davies

CHAIRMEN OF STANDING COMMITTEES

Representatives on Council without vote

Finance, K. W. Jappe
Meetings and Program, A. L. Kimball
Publications, F. L. Bradley
Admissions, T. M. Knoop
Professional Divisions, G. B. Karelitz
Local Sections, J. N. Landis
Constitution and By-Laws, A. T. Dupont
Honors and Awards, Roy V. Wright
Relations with Colleges, A. C. Chick
Education and Training for the Industries, A. R. Stevenson, Jr.
Library, John Blizard
Research, W. Trinks
Standardization, J. E. Lovely
Power Test Codes, Francis Hodgkinson
Safety, A. W. Luce
Professional Conduct, W. H. Kenerson

EXECUTIVE COMMITTEE OF THE COUNCIL

James W. Parker, *Chairman*
Clarke Freeman, *Vice-Chairman*
George E. Hulse
Thomas S. McEwan
Clair B. Peck

Advisory Members: Chairmen of the Finance, Local Sections, and Professional Divisions Committees

SECRETARIAL STAFF

Ernest Hartford, *Executive Assistant Secretary* (Sections, Divisions, Student Branches, Membership, Meetings, etc.)
C. B. LePage, *Assistant Secretary* (Technical Committees)
R. L. Sackett, *Assistant to the Secretary*
George A. Stetson, *Editor*
Frederick Lask, *Advertising Manager*
D. C. A. Bosworth, *Comptroller*

* Deceased, December 7, 1941.

STANDING COMMITTEES

FINANCE

K. W. JAPPE, *Chairman** (1942)
G. L. KNIGHT, *Vice-Chairman* (1943)
E. J. GRIMMETT (1944)
J. J. SWAN (1945)
J. L. KOPF (1946)

Council Representatives

E. B. RICKETTS (1942)
W. G. CHRISTY (1943)

Junior Adviser

A. M. MILLER (1942)

MEETINGS AND PROGRAM

A. L. KIMBALL, *Chairman** (1942)
N. E. FUNK (1943)
L. K. SILLCOX (1944)
F. G. SWITZER (1945)
R. A. NORTH (1946)

Junior Adviser

R. A. ROBERTSON (1943)

PUBLICATIONS

F. L. BRADLEY, *Chairman** (1942)
C. R. SODERBERG (1943)
A. R. STEVENSON, JR. (1944)
E. J. KATES (1945)
L. N. ROWLEY, JR. (1946)

Advisory Members (1942)

W. L. DUDLEY
N. C. EBAUGH
O. B. SCHIER, II

Junior Advisers

F. H. FOWLER, JR. (1942)
J. A. CONNON (1943)

(Personnel of Special Committee, p. RI-3)

ADMISSIONS

T. M. KNOOP, *Chairman** (1942)
S. H. LIBBY (1943)
F. E. LYFORD (1944)
S. D. SPRONG (1945)
T. H. WICKENDEN (1946)

Advisory Member

H. E. MOLÉ (1942)

(Personnel of Advisory Committee, p. RI-4)

PROFESSIONAL DIVISIONS

G. B. KARELITZ, *Chairman** (1942)
W. A. CARTER (1943)
W. M. SHEEHAN (1944)
J. H. SENGSTAKEN (1945)
L. F. MOODY (1946)

Junior Adviser

K. J. BERRIAN (1943)

(Personnel of Professional Divisions' Executive Committees, p. RI-6)

* Representative on the Council.

LOCAL SECTIONS

J. N. LANDIS, *Chairman** (1942)
F. L. WILKINSON, JR. (1943)
F. W. MARQUIS (1944)
J. A. KEETH (1945)
OLIVER B. LYMAN (1946)

Junior Advisers

C. C. KIRBY (1942)
F. H. FOWLER, JR. (1943)

(Personnel of Local Sections' Executive Committees, p. RI-10)

CONSTITUTION AND BY-LAWS

A. T. DUPONT, *Chairman** (1942)
L. H. KENNEY (1943)
F. B. ORR (1944)
R. L. PARSELL (1945)
W. J. COPE (1946)

Junior Adviser

G. E. GOLDEN (1942)

HONORS AND AWARDS

ROY V. WRIGHT, *Chairman** (1942)
D. C. JACKSON (1943)
C. L. BAUSCH (1944)
L. W. WALLACE (1945)
GEO. A. ORROK (1946)

(Personnel of Special Committee, p. RI-3)

RELATIONS WITH COLLEGES

A. C. CHICK, *Chairman** (1942)
J. I. YELLOTT (1943)
H. E. DEGLER (1944)
G. L. SULLIVAN (1945)
R. P. REECE (1946)

Advisory Members (1942)

J. W. HANEY
B. T. MCMINN
R. H. PORTER

Junior Adviser

J. L. HALL (1942)

(Student Branches and Officers, p. RI-18)

EDUCATION AND TRAINING FOR THE INDUSTRIES

A. R. STEVENSON, JR., *Chairman** (1942)
M. R. BOWERMAN (1943)
A. C. HARPER (1944)
R. L. GOETZENBERGER (1945)
A. D. BAILEY (1946)

Advisory Members (1942)

R. BURDETTE DALE
L. J. FLETCHER
LINN HELANDER

PROFESSIONAL CONDUCT

W. H. KENERSON, *Chairman** (1942)
C. E. WADDELL (1943)
V. E. ALDEN (1944)
G. S. ARMSTRONG (1945)
P. W. THOMPSON (1946)

RESEARCH †

W. TRINKS, *Chairman** (1942)
M. D. HERSEY (1943)
HERMAN WEISBERG (1944)
W. R. ELSEY (1945)
J. F. D. SMITH (1946)

STANDARDIZATION †

J. E. LOVELY, *Chairman** (1942)
L. T. KNOCKE (1943)
T. E. FRENCH (1944)
W. H. HILL (1945)
J. H. TAYLOR (1946)

POWER TEST CODES †

FRANCIS HODGKINSON, *Chairman** (1944)
A. G. CHRISTIE, *Vice-Chairman* (1946)
H. H. MICHELSEN, *Junior Observer* (1942)
J. A. KEENE, *Junior Observer* (1943)

Term expires 1942

W. A. CARTER
HARTE COOKE
E. R. FISH
H. B. OATLEY
W. J. WOHLENBERG

Term expires 1943

LOUIS ELLIOTT
H. B. REYNOLDS
P. W. SWAIN
E. N. TRUMP

Term expires 1944

C. H. BERRY
FRANCIS HODGKINSON
D. S. JACOBUS
L. F. MOODY
E. B. RICKETTS

Term expires 1945

THEODORE BAUMEISTER
P. H. HARDIE
B. V. E. NORDBERG
R. J. S. PIGOTT
M. C. STUART

Term expires 1946

A. G. CHRISTIE
PAUL DISERENS
N. R. GIBSON
GEO. A. ORROK
E. B. POWELL

SAFETY †

A. W. LUCE, *Chairman** (1942)
A. E. WINDLE (1943)
H. C. HOUGHTON (1944)
E. R. GRANNISS (1945)
H. W. GABOR (1946)

LIBRARY

JOHN BLIZARD, *Chairman** (1945)
E. F. CHURCH, JR. (1943)
A. R. MUMFORD (1944)
The Secretary, C. E. DAVIES, *Ex-Officio*

† Personnel of all Technical Committees, pp. RI-20-31.

SPECIAL COMMITTEES

BIOGRAPHY

(Special Committee of Publications Committee)

ROY V. WRIGHT, *Chairman*
L. P. ALFORD *
R. E. FLANDERS
GEO. A. ORROK
J. W. ROE

BOILER CODE

D. S. JACOBUS, *Honorary Chairman*
E. R. FISH, *Chairman*
H. B. OATLEY, *Vice-Chairman*
J. W. SHIELDS, *Secretary*
M. JURIST, *Assistant Secretary*
C. A. ADAMS
H. E. ALDRICH
H. C. BOARDMAN
PERRY CASSIDY
R. E. CECIL
F. S. CLARK
A. J. ELY
V. M. FROST
C. E. GORTON
A. M. GREENE, JR.
W. G. HUMPTON
J. O. LEECH
I. E. MOULTROP
C. O. MYERS
C. W. OBERT
JAMES PARTINGTON
D. B. ROSSHEIM
WALTER SAMANS
S. K. VARNES
A. C. WEIGEL

Honorary Members

W. H. BOEHM
W. F. DURAND
T. E. DURBAN
C. L. HUSTON
W. F. KIESEL, JR.
M. F. MOORE
H. H. VAUGHAN
H. LEROY WHITNEY

(Personnel of Boiler Code Committees, pp. RI-32-33)

MEDALS

(Special Committee of Board of Honors and Awards)

Term expires 1942

ROY V. WRIGHT, *Chairman*
ALEX. KLEMIN
E. W. O'BRIEN
E. S. PEARCE

Term expires 1943

C. M. ALLEN
R. L. DAUGHERTY
D. C. JACKSON
R. C. MARSHALL, JR.

Term expires 1944

C. L. BAUSCH
FRANCIS HODGKINSON
L. C. MORROW
J. M. TODD

* Deceased, January 2, 1942.

MEDALS
(Continued)

Term expires 1945

A. D. BAILEY
J. W. BARKER
CLARKE FREEMAN
L. W. WALLACE

Term expires 1946

E. C. HUTCHINSON
W. H. KENERSON
ERIK OBERG
GEO. A. ORROK

REGULAR NOMINATING COMMITTEE FOR 1942

H. W. SMITH, *Chairman*
T. E. BELL, *Secretary*

I E. S. DENNISON, Groton, Conn
J. E. LOVELY, Springfield, Vt., *1st Alternate*
M. D. ENGLE, Boston, Mass., *2nd Alternate*

II WALDO McC. McKEE, New York, N. Y.

III F. C. STEWART, State College, Pa.
F. A. ALLNER, Baltimore, Md., *Alternate*

IV T. E. BELL, Atlanta, Ga., *Secretary*
JAMES ELLIS, Kingsport, Tenn., *1st Alternate*
A. M. ORMOND, Savannah, Ga., *2nd Alternate*

V H. W. SMITH, Ellwood City, Pa., *Chairman*
M. W. BENJAMIN, Dearborn, Mich., *1st Alternate*
M. R. Bowerman, Homeworth, Ohio, *2nd Alternate*

VI O. F. CAMPBELL, East Chicago, Ind.
L. H. Stark, Milwaukee, Wis., *1st Alternate*
C. A. JACOBSON, Beloit, Wis., *2nd Alternate*
M. P. CLEGHORN, Ames, Iowa, *3rd Alternate*

VII JULIUS BILLETER, Salt Lake City, Utah
W. J. COPE, Salt Lake City, Utah, *Alternate*

VIII E. C. BAKER, Stillwater, Okla.
A. L. HILL, Denver, Colo., *1st Alternate*
C. E. BROWN, Kansas City, Mo., *2nd Alternate*

LOCAL SECTIONS IN NOMINATING COMMITTEE GROUPS

GROUP I

BOSTON
BRIDGEPORT
GREEN MOUNTAIN
HARTFORD
NEW HAVEN
NORWICH
PROVIDENCE
WATERBURY
WESTERN MASSACHUSETTS
WORCESTER

NOMINATING COMMITTEE GROUPS
(Continued)

GROUP II

METROPOLITAN (N.Y.) AND MEMBERS OUTSIDE THE UNITED STATES (EXCEPT ONTARIO SECTION MEMBERS)

GROUP III

ANTHRACITE-LEHIGH VALLEY
BUFFALO
CENTRAL PENNSYLVANIA
PHILADELPHIA
PLAINFIELD
ROCHESTER
SYRACUSE
SUSQUEHANNA
WASHINGTON
ITHACA
BALTIMORE
SCHENECTADY

GROUP IV

ATLANTA
PIEDMONT-NORTH CAROLINA
EAST TENNESSEE
BIRMINGHAM
FLORIDA
GREENVILLE
MEMPHIS
RALEIGH
SAVANNAH
VIRGINIA

GROUP V

AKRON-CANTON
CINCINNATI
CLEVELAND
COLUMBUS
DAYTON
DETROIT
ERIE
ONTARIO
PITTSBURGH
PENINSULA
TOLEDO
WEST VIRGINIA
YOUNGSTOWN

GROUP VI

CENTRAL ILLINOIS
CENTRAL INDIANA
CHICAGO
FORT WAYNE
LOUISVILLE
MILWAUKEE
NEBRASKA
MINNESOTA
ROCK RIVER VALLEY
ST. JOSEPH VALLEY
ST. LOUIS
TRI-CITIES

GROUP VII

INLAND EMPIRE
OREGON
SAN FRANCISCO
SOUTHERN CALIFORNIA
UTAH
WESTERN WASHINGTON

GROUP VIII

COLORADO
KANSAS CITY
MID-CONTINENT
NEW ORLEANS
NORTH TEXAS
SOUTH TEXAS

SPECIAL COUNCIL COMMITTEES

(Dates in parentheses denote expiration of terms)

ADVISORY COMMITTEE TO COMMITTEE ON ADMISSIONS

H. A. Lardner, *Chairman*
R. E. Flanders
E. C. Hutchinson
Alfred Iddles
J. H. Lawrence
Roy V. Wright

BOARD OF REVIEW

W. A. Shoudy, *Chairman* (1942)
P. W. Swain (1943)
S. D. Sprong (1944)

BOARD ON TECHNOLOGY

C. B. Peck, *Chairman*
E. G. Bailey
R. F. Gagg
J. N. Landis (Local Sections)
A. L. Kimball (Meetings and Program)
G. B. Karelitz (Professional Divisions)
F. L. Bradley (Publications)
W. Trinks (Research)

CONSULTING PRACTICE

S. Logan Kerr, *Chairman*
P. L. Battey
M. X. Wilberding

DEPRECIATION

H. V. Coes
P. T. Norton, Jr.

DUES-EXEMPT MEMBERS' CONTRIBUTIONS

Harte Cooke, *Chairman*
F. D. Herbert
S. H. Libby
J. W. Roe
W. R. Webster
W. D. Ennis, *Treasurer*

ECONOMIC STATUS OF THE ENGINEER

C. J. Freund, *Chairman*
D. S. Kimball
H. B. Oatley
H. L. Whittemore
W. E. Wickenden
H. A. Winne

ECONOMIC STATUS OF THE ENGINEER

(Continued)

Junior Representatives

W. F. Carhart
W. B. Oakley, Jr.
Harry Ritterbusch

Chairmen of Committees on Local Sections and Relations With Colleges, *Ex-Officio*

ENGINEERS' CIVIC RESPONSIBILITIES

A. R. Cullimore, *Chairman*
Lillian M. Gilbreth
Walter Kidde
H. B. Oatley
J. W. Roe
Roy V. Wright
D. Robert Yarnall

Chairmen of Committees on Local Sections and Relations With Colleges, *Ex-Officio*

FREEMAN FUND

Clarke Freeman, *Chairman*
E. C. Hutchinson
Geo. A. Orrok

NATIONAL DEFENSE

J. L. Walsh, *Chairman*
C. E. Davies, *Secretary*

Advisory Members

W. L. Batt
Gano Dunn
E. A. Muller
W. I. Westervelt

Army and Navy Members

Brig. Gen. H. K. Rutherford (Army)
Capt. A. B. Anderson (Navy)

NATIONAL DEFENSE

(Continued)

General Committee

C. E. Brinley
H. V. Coes
K. H. Condit
J. D. Cunningham
H. N. Davis
W. C. Dickerman
W. F. Durand
R. E. Flanders
K. T. Keller
David Larkin
F. T. Letchfield
T. A. Morgan
R. C. Muir
T. E. Murray
A. C. Willard

REGISTRATION

V. M. Palmer, *Chairman*
S. H. Graf
J. A. McPherson
F. H. Prouty
W. K. Simpson

SOCIETY OFFICE OPERATION

Alfred Iddles, *Chairman*
Wallace Clark

GEORGE WESTINGHOUSE BUST

D. S. Kimball, *Chairman*
C. E. Davies, *Secretary*
K. T. Compton
S. W. Dudley
C. N. Lauer
W. G. Marshall
J. H. McGraw
L. A. Osborne
C. F. Scott
J. B. Wright
Roy V. Wright

A.S.M.E. REPRESENTATIVES ON OTHER ACTIVITIES

See also A.S.M.E. Representatives on Other Research Committees, etc., pages RI-21, 26, 29, 30, 33
(Dates in parentheses denote expiration of terms)

AMERICAN ASSOCIATION FOR THE ADVANCEMENT OF SCIENCE

SECTION M, ENGINEERING

R. F. Gagg
R. L. Sackett

AMERICAN STANDARDS ASSOCIATION

A. L. Baker (1942)
Alfred Iddles (1943)

Alternates

C. B. LePage (1942)
W. C. Mueller (1942)

AMERICAN YEAR BOOK CORPORATION

C. E. Davies

CENTER FOR SAFETY EDUCATION

E. R. Granniss

THE ENGINEERING FOUNDATION

K. H. Condit (1943)
A. A. Potter (1943)
E. R. Fish (1944)

RESEARCH PROCEDURE COMMITTEE

W. Trinks (1942)

ENGINEERING HISTORY

Geo. A. Orrok
J. W. Roe

ENGINEERING SOCIETIES LIBRARY BOARD

John Blizard
E. F. Church, Jr.
A. R. Mumford
Secretary, A.S.M.E., *Ex-Officio*

ENGINEERING SOCIETIES MONOGRAPHS COMMITTEE

E. J. Kates
G. B. Karelitz

ENGINEERING SOCIETIES PERSONNEL SERVICE, INC.

Ernest Hartford, *Vice-President*, National Board
R. D. Brizzolara, Chicago Board
C. J. Freund, Detroit Board
Ernest Hartford, *Chairman*, Metropolitan Board
H. J. Berg, San Francisco Board

* Deceased, January 2, 1942.

ENGINEERS' COUNCIL FOR PROFESSIONAL DEVELOPMENT

R. L. Sackett (1942)
A. R. Stevenson, Jr. (1943)
H. T. Woolson (1944)

ENGINEERS DEFENSE BOARD

K. H. Condit
H. V. Coes
R. M. Gates
J. W. Parker
W. R. Webster

ENGINEERS' NATIONAL RELIEF FUND

Ernest Hartford

JOHN FRITZ MEDAL BOARD OF AWARD

H. N. Davis (1942)
A. G. Christie (1943)
W. H. McBryde (1944)
W. A. Hanley (1945)

GANTT MEDAL BOARD OF AWARD

Lillian M. Gilbreth (1942)
L. P. Alford * (1943)
Wallace Clark (1944)

DANIEL GUGGENHEIM MEDAL FUND, INC.

Alex. Klemin (1942)
R. F. Gagg (1943)
E. E. Aldrin (1944)

JOSEPH A. HOLMES SAFETY ASSOCIATION

J. F. Barkley

HOOVER MEDAL BOARD OF AWARD

S. F. Voorhees (1943)
W. L. Batt (1945)
W. H. Kenerson (1947)

INTER-AMERICAN ENGINEERING COOPERATION

A. M. Greene, Jr.

INTERNATIONAL ELECTROTECHNICAL COMMISSION

U.S. NATIONAL COMMITTEE

H. N. Davis
Paul Diserens
Francis Hodgkinson

Alternate

C. Harold Berry

MARSTON AWARD

W. L. Abbott (1945)

NATIONAL BUREAU OF ENGINEERING REGISTRATION

V. M. Palmer

NATIONAL CONFERENCE ON ENGINEERING POSITIONS

W. F. Carhart
W. L. Cisler
H. B. Oatley
R. L. Sackett

NATIONAL FIRE WASTE COUNCIL

J. A. Neale

NATIONAL MANAGEMENT COUNCIL

L. P. Alford * (1943)—C. W. Lytle, *Alternate*
J. M. Talbot (1944)—Wallace Clark, *Alternate*
H. B. Bergen (1945)—J. R. Bangs, *Alternate*

NATIONAL RESEARCH COUNCIL

DIVISION OF ENGINEERING AND INDUSTRIAL RESEARCH

W. L. Batt (1942)

ALFRED NOBLE PRIZE

A. M. Greene, Jr.

POST-EMERGENCY PLANNING

R. E. Flanders

UNITED ENGINEERING TRUSTEES, INC.

H. A. Lardner (1942)
Walter Kidde (1943)
K. H. Condit (1944)

VERMILYE MEDAL ADVISORY COMMITTEE

W. D. Fuller (1947)

WASHINGTON AWARD COMMISSION

A. L. Rice (1942)
W. J. Sando (1943)

PROFESSIONAL DIVISIONS

ARTICLE B6A, PAR. 16: The Standing Committee on Professional Divisions shall, under the direction of the Council, have supervision of the Professional Divisions of the Society.

STANDING COMMITTEE

G. B. KARELITZ, *Chairman* (1942)
W. A. CARTER (1943)
W. M. SHEEHAN (1944)
J. H. SENGSTAKEN (1945)
L. F. MOODY (1946)

Junior Adviser

K. J. BERRIAN (1943)

Aeronautic

Organized, 1920

Reorganized, 1941

See Aviation

Applied Mechanics

Organized, 1927

H. L. DRYDEN, *Chairman*

EXECUTIVE COMMITTEE

H. L. DRYDEN, *Chairman*
J. H. KEENAN, *Secretary*
J. N. GOODIER
L. S. JACOBSEN
JESSE ORMONDROYD

Associates

J. P. DEN HARTOG
RUPEN EKSERGIAN
J. C. HUNSAKER
A. L. KIMBALL
G. B. PEGRAM
R. E. PETERSON
E. O. WATERS
H. M. WESTERGAARD
B. M. WOODS

Representative on Aviation Liaison Group

J. C. HUNSAKER

Representative, San Francisco Section

W. M. MOODY

Research Secretary

JESSE ORMONDROYD

JOURNAL OF APPLIED MECHANICS

J. M. LESSELLS, *Editor*

SPONSORS

Dynamics, F. M. LEWIS
Elasticity, STEPHEN TIMOSHENKO
Fluid Mechanics, H. W. EMMONS
Lubrication, G. B. KARELITZ
Plasticity, A. NÁDAI
Strength of Materials, C. R. SODERBERG
Thermodynamics, J. A. GOFF

Aviation

Organized, 1941

(Formerly Aeronautic)

J. E. YOUNGER, *Chairman*

EXECUTIVE COMMITTEE

J. E. YOUNGER, *Chairman*
J. M. CLARK, *Secretary*
E. E. ALDRIN
R. F. GAGG
CHAS. H. DOLAN, *Ex-officio*

Junior Advisers

F. H. FOWLER, JR.
HERBERT KUNEN

ADVISORY COMMITTEE

KARL ARNSTEIN
CARL BREER
E. C. CLARKE
H. M. CRANE
LOUIS DEFLOREZ
W. F. DURAND
A. J. GIFFORD
M. B. GORDON
WILLIAM HOVGAARD
J. C. HUNSAKER
P. G. JOHNSON
C. F. KETTERING
ALEX. KLEMIN
R. K. LEBLOND
W. B. MAYO
P. B. MORGAN
T. A. MORGAN
S. A. MOSS
E. A. SPERRY
A. R. STEVENSON, JR.
J. G. VINCENT
THEO. VON KARMAN
C. J. WARD
E. P. WARNER
B. M. WOODS
ORVILLE WRIGHT

Fuels

Organized, 1920

A. R. MUMFORD, *Chairman*

EXECUTIVE COMMITTEE

A. R. MUMFORD, *Chairman*
D. C. WEEKS, *Secretary*
O. F. CAMPBELL
H. F. HEBLEY
A. W. THORSON
J. E. TOBEY

Associates

J. F. BARKLEY
J. S. BENNETT, 3RD
T. C. CHEASLEY
W. G. CHRISTY
M. P. CLEGHORN
H. O. CROFT
B. J. CROSS
M. D. ENGLE

Associates (Cont.)

D. S. FRANK
E. R. KAISER
T. A. MARSH
M. A. MAYERS
W. E. REASER
R. L. ROWAN
R. A. SHERMAN
J. E. TOBEY
D. C. WEEKS

COAL TESTING CODE

Organized, 1939, Jointly with A.I.M.E.

R. L. ROWAN, *Chairman*
J. E. TOBEY, *Vice-Chairman*

A.S.M.E. Representatives

J. F. BARKLEY
H. C. CARROLL
R. A. FORESMAN
R. M. HARDGROVE
J. H. KERRICK
T. A. MARSH
M. A. MAYERS
A. R. MUMFORD
PERCY NICHOLS
R. A. SHERMAN
L. A. SHIPMAN
A. W. THORSON

COOPERATION WITH A.I.M.E.

J. E. TOBEY, *Chairman*

MODEL SMOKE LAW

J. F. BARKLEY, *Chairman*
O. F. CAMPBELL
A. G. CHRISTIE
T. A. MARSH
T. E. PURCELL
R. A. SHERMAN
R. R. TUCKER

PROGRAM

A. W. THORSON, *Chairman*
D. S. FRANK, *Assistant Chairman*
E. R. KAISER, *Junior Member*

REVIEW OF PAPERS

M. D. ENGLE
A. R. MUMFORD
A. W. THORSON
D. C. WEEKS

Graphic Arts

Organized, 1922

EXECUTIVE COMMITTEE

A. E. GIEGENGACK
F. W. HOCH
W. B. LAUGHTON
R. G. MACDONALD
W. M. PASSANO
B. L. SITES
B. D. STEVENS
B. L. WEHMHOFF

Heat Transfer

Organized, 1938

T. B. DREW, *Chairman*
W. S. PATTERSON, *Group Secretary*

EXECUTIVE COMMITTEE

T. B. DREW, *Chairman*
L. M. K. BOELTER
R. A. BOWMAN
E. D. GRIMISON
H. C. HOTTEL
R. H. NORRIS

Advisory Associates

C. E. LUCKE
A. K. SCOTT
J. H. SENGSTAKEN

Junior Representatives

J. L. MENSON
R. H. WOLIN

COORDINATION

W. S. PATTERSON, *Chairman*

Liaison Officer for Local Sections

A. K. SCOTT

Representative, San Francisco Section

W. M. MOODY

Representative on Aviation Liaison Group

L. M. K. BOELTER

Representatives of Other Divisions

Fuels, B. J. CROSS
Hydraulic, J. D. SCOVILLE
Iron and Steel, W. TRINKS
Oil and Gas Power, F. G. HECHLER
Petroleum, J. D. PETERSON
Power, O. F. CAMPBELL
Process Industries, ARNOLD WEISSELBERG
Railroad, L. H. FRY

Research Secretary

T. B. DREW

Members at Large

L. M. K. BOELTER
R. H. HEILMAN
G. L. TUVE

DIRECT-FIRED FLUID HEATERS AND BOILERS

E. D. GRIMISON, *Chairman*
JOHN BLIZARD
D. S. FRANK
L. B. SCHUELER
W. J. WOHLENBERG

INDUSTRIAL FURNACES AND KILNS

W. TRINKS, *Chairman*
H. C. HOTTEL
W. A. TICKNOR

PAPERS

R. A. BOWMAN
C. F. KAYAN
A. K. SCOTT
L. B. SCHUELER
R. A. SHERMAN

TESTING TECHNIQUE

H. C. HOTTEL, *Chairman*
B. J. CROSS
R. H. JACKSON
J. H. RUSHTON
A. K. SCOTT

THEORY AND FUNDAMENTAL RESEARCH

L. M. K. BOELTER, *Chairman*
A. P. COLBURN
T. B. DREW
MAX JAKOB
D. D. STREID

THERMO-PHYSICAL PROPERTIES OF MATERIALS

R. H. NORRIS, *Chairman*
O. KENNETH BATES
T. H. CHILTON
R. C. H. HECK
MAX JAKOB
R. J. S. PIGOTT
J. F. DOWNIE SMITH

SUBCOMMITTEE ON SPECIFIC HEAT OF GASES

MAX JAKOB, *Chairman*
W. L. DE BAUFRE
J. A. GOFF
A. C. GULLIKSON
R. C. H. HECK
R. J. S. PIGOTT
R. L. SWEIGERT

UNFIRED HEAT TRANSFER EQUIPMENT

B. E. SHORT, *Chairman*
R. A. BOWMAN
E. S. BUNN
G. A. HAWKINS
A. C. MUELLER
TOWNSEND TINKER
W. H. THOMPSON

Hydraulic

Organized, 1926

E. B. STROWGER, *Chairman*

EXECUTIVE COMMITTEE

E. B. STROWGER, *Chairman*
L. J. HOOPER, *Secretary*
J. D. SCOVILLE
F. G. SWITZER
R. V. TERRY

CAVITATION

E. B. STROWGER, *Sponsor*
L. F. MOODY, *Chairman*
R. T. KNAPP
J. M. MOUSSON
W. J. RHEINGANS
G. F. WISLICENUS

Representatives of Other Societies

American Society for Testing Materials, F. N. SPELLER
Engineering Institute of Canada, ERNEST BROWN
Institution of Mechanical Engineers, G. S. BAKER

Representative of France

A. TENOT

Representative, San Francisco Section

W. M. MOODY

HYDRAULIC PRIME MOVERS

R. V. TERRY, *Sponsor*
J. F. ROBERTS, *Chairman*
A. ABERLI
E. H. COLLINS
J. P. GROWDEN
L. F. HARZA
P. L. HESLOP
GEORGE JESSUP
F. H. ROGERS
F. SCHMIDT
S. O. SCHOMBERGER
S. H. VAN PATTER

PUMPING MACHINERY

F. G. SWITZER, *Sponsor*
R. L. DAUGHERTY, *Chairman*
B. F. TILLSON
HANS ULMANN

WATER HAMMER

Honorary Chairman, LORENZO ALLIEVI, Rome, Italy

J. D. SCOVILLE, *Sponsor*
S. LOGAN KERR, *Chairman*
N. R. GIBSON
EUGENE HALMOS
L. F. MOODY
R. S. QUICK
E. B. STROWGER

Affiliated Societies and Their Representatives

American Society of Civil Engineers, N. R. GIBSON and FORD KURTZ
American Water Works Association, F. M. DAWSON and L. H. KESSLER

Associate Members, Representing:

Australia, GEORGE HIGGINS
Brazil, A. W. K. BILLINGS and F. KNAPP
Engineering Institute of Canada, R. W. ANGUS and F. M. WOOD
France, LOUIS BERGERON and CHARLES CAMICHEL
Germany and Verein deutscher Ingenieure, D. THOMA
Great Britain and Institution of Mechanical Engineers, E. BRUCE BALL and A. H. GIBSON
Italy, GAUDENZIO FANTOLI and ALBINO PASINI
Switzerland, CHARLES JAEGER and O. SCHNYDER

Machine Shop Practice

Organized, 1921

Reorganized, 1941

See Production Engineering

Management

Organized, 1920

J. R. BANGS, *Chairman*

EXECUTIVE COMMITTEE

J. R. BANGS, *Chairman*
J. M. TALBOT, *Vice-Chairman*
G. M. VARGA, *Secretary*
L. A. APPLEY
J. M. JURAN
A. I. PETERSON

Representatives of Local Sections

Atlanta, S. C. HALE
Detroit, J. A. CARLIN
Kansas, A. H. SLUSS
Louisville, C. D. ELDRIDGE
Metropolitan, P. E. FRANK
Milwaukee, B. V. E. NORDBERG
New Orleans, P. F. HOOTS
Philadelphia, C. S. GOTWALS
Rochester, V. M. PALMER
San Francisco, B. A. GAYMAN
South Texas, V. M. FAIRES

Ammunition Group

CARLOS DEZAFRA

Education and Training Group

E. H. HEMPEL

Representative on Aviation Liaison Group

R. E. GILLMOR

Research Secretary

E. H. HEMPEL

General Committee

L. P. ALFORD *
R. M. BARNES
W. L. BATT
C. W. BEESE
H. B. BERGEN
F. B. BELL
WALLACE CLARK
H. V. COES
K. H. CONDIT
HOWARD COONLEY
CARLOS DEZAFRA
N. E. ELSAS
S. P. FISHER
W. D. FULLER
W. H. GESELL
LILLIAN M. GILBRETH
R. E. GILLMOR
C. H. HATCH
E. H. HEMPEL
P. E. HOLDEN
W. F. HOSFORD
D. S. KIMBALL
W. H. KUSHNICK
T. S. MCEWAN
L. C. MORROW
D. B. PORTER
F. E. RAYMOND
J. W. ROE
E. H. SCHELL
E. D. SMITH
L. W. WALLACE
J. A. WILLARD
A. WILLIAMS
J. E. YOUNGER

COMMITTEE CHAIRMEN

Administration Organization, L. A. APPLEY
Industrial Marketing, J. R. BANGS
Mathematical Statistics, A. I. PETERSON
Works Standardization, J. M. JURAN

DEPRECIATION STUDIES

H. V. COES
P. T. NORTON, JR.

* Deceased, January 2, 1942.

Materials Handling

Organized, 1920

G. E. HAGEMANN, *Chairman*

EXECUTIVE COMMITTEE

G. E. HAGEMANN, *Chairman*
R. B. RENNER, *Vice-Chairman*
C. H. BARKER, JR., *Secretary*
A. J. BURKE, *Assistant Secretary*
C. F. DIETZ
J. A. JACKSON
M. C. MAXWELL
F. J. SHEPARD, JR.

Associates

N. W. ELMER
H. C. KELLER
R. H. MCLAIN
F. E. MOORE
P. D. OESTERLE
E. D. SMITH
H. E. STOCKER
J. B. WEBB

Junior Associates

CORNELIUS CROWLEY
E. Z. GABRIEL
R. W. GRUNDMAN
D. D. JONES

Metals Engineering

Organized, 1927

Reorganized, 1940

(Formerly Iron and Steel)

J. H. HITCHCOCK, *Chairman*

EXECUTIVE COMMITTEE

J. H. HITCHCOCK, *Chairman*
R. A. NORTH, *Secretary*
M. J. DEMPSEY
G. L. FISK
W. TRINKS
W. R. WEBSTER

Associates

A. J. BOYNTON
J. A. CLAUSS
S. M. MARSHALL
B. C. MCFADDEN
J. H. ROMANN
W. M. SHEEHAN
M. D. STONE
R. J. WEAN
S. M. WECKSTEIN
T. H. WICKENDEN

Representative, San Francisco Section

WALTER KASSEBOHN

Oil and Gas Power

Organized, 1921

W. L. H. DOYLE, *Chairman*

EXECUTIVE COMMITTEE

W. L. H. DOYLE, *Chairman*
L. N. ROWLEY, JR., *Secretary*
H. E. DEGLER
E. S. DENNISON
C. W. GOOD
E. J. KATES

Associates

C. E. BECK
G. C. BOYER
M. M. DANA
G. J. DASHEFSKY
W. K. GREGORY
F. G. HECHLER
P. B. JACKSON
B. V. E. NORDBERG
M. J. REED
LEE SCHNEITTER

Junior Adviser

C. K. HOLLAND

Research Secretary

LEE SCHNEITTER

Representative, San Francisco Section

E. G. GOTHBERG

Liaison Representatives

American Society of Naval Architects and Marine Engineers, B. V. E. NORDBERG
Aviation Liaison Group, H. E. DEGLER
Heat Transfer Group, F. G. HECHLER
San Francisco Section, E. G. GOTHBERG

EDITING

E. J. KATES
ERNEST NIBBS
M. J. REED

METROPOLITAN SUBCOMMITTEE

E. J. KATES, *Chairman*
M. J. REED
LEE SCHNEITTER

OIL ENGINE POWER COST

H. C. MAJOR, *Chairman*
H. C. LENFEST, *Secretary*
B. B. BACHMAN
R. P. BOLSTER
L. T. BROWN
R. D. CAMPBELL
E. HALE CODDING
W. J. CUMMING
E. J. KATES
A. B. MORGAN
J. I. MOORE
G. D. NOILES
M. J. REED
R. TOM SAWYER
LEE SCHNEITTER
P. H. SCHWEITZER
H. C. THUERK
C. A. TRIMMER
STANLEY WRIGHT

OIL AND GAS POWER CONFERENCES

1942 General Arrangements Committee

F. L. MEYER, *Chairman*
R. E. MCCLAIN, *Secretary*
M. A. CLEMENTS
L. J. FLETCHER
R. T. MEES
C. G. A. ROSEN
C. O. SMITH
L. P. WEINER
L. G. BRIGGS, *Secretary, Peoria Association of Commerce*

Local Program Committee

R. E. MCCLAIN, *Chairman*
J. F. DEFFENBAUGH

1943 Location and Selection Committee

E. S. DENNISON, *Chairman*
H. E. DEGLER
C. W. GOOD

PUBLICITY

L. N. ROWLEY, JR.

TECHNICAL PROGRAM

G. C. BOYER, *Chairman*
R. D. CAMPBELL
E. S. DENNISON
LEE SCHNEITTER

Petroleum

Organized, 1925

Reorganized, 1937

W. F. HERBERT, *Chairman*

EXECUTIVE COMMITTEE

W. F. HERBERT, *Chairman*
W. H. CARSON, *Secretary*
E. H. BARLOW
H. L. EGGLESTON

Research Secretary

E. E. AMBROSIUS

Liaison Representative, San Francisco Section

HERMAN DISHINGTON

Power

Organized, 1920

O. F. CAMPBELL, *Chairman*

EXECUTIVE COMMITTEE

O. F. CAMPBELL, *Chairman*
J. N. LANDIS, *Secretary*
THEO. BAUMEISTER, *Research Secretary*
G. C. EATON
L. M. GOLDSMITH

Junior Adviser

(To be appointed)

Liaison Representative, San Francisco Section

E. C. GOTHBERG

Process Industries

Organized, 1934

J. W. HUNTER, *Chairman*

EXECUTIVE COMMITTEE

J. W. HUNTER, *Chairman*
T. R. OLIVE, *Secretary*
RICHARD O'MARA
WILLIAM RAISCH
A. F. SPITZGLASS
ARNOLD WEISSELBERG
W. R. WOOLRICH
J. I. YELLOTT
F. L. YERZLEY

Liaison Officer With Standing Committee on Professional Divisions

J. H. SENGSTAKEN

Junior Adviser

(To be appointed)

Research Secretary

ARNOLD WEISSELBERG

Other Liaison Representatives

Aviation Group
Industrial Instruments and Regulators Committee, E. A. SPERRY
Subdivision on Rubber and Plastics
W. F. BARTOE, Plastics
F. L. YERZLEY, Rubber
Heat Transfer Group, ARNOLD WEISSELBERG
Society of Automotive Engineers, F. L. YERZLEY

San Francisco Section, HERMAN DISHINGTON

COMMITTEE CHAIRMEN

Air Conditioning, C. F. KAYAN
Drying, ARNOLD WEISSELBERG
Food Processing, G. L. MONTGOMERY
Industrial Instruments and Regulators
E. S. SMITH, *Chairman*
A. F. SPITZGLASS, *Secretary*
J. C. PETERS, *Acting Secretary*
Mechanical Separation, RICHARD O'MARA
Papers, Awards, and Honors, C. E. LUCKE
Program, J. W. HUNTER
Sanitation, WILLIAM RAISCH
Sugar, F. M. GIBSON
Sulphur, B. E. SHORT
Vegetable Oils, R. W. MORTON

COMMITTEE ON INDUSTRIAL INSTRUMENTS AND REGULATORS

E. S. SMITH, *Chairman*
E. D. HAIGLER, *Vice-Chairman*
J. C. PETERS, *Secretary*

Executive Sub-Committee

P. G. EXLINE
R. L. GOETZENBERGER
P. W. KEPPLER
W. J. KING
E. S. LEE
H. L. MASON
G. W. SMITH
A. F. SPITZGLASS
I. M. STEIN
M. J. ZUCROW

Subdivision on Rubber and Plastics

EXECUTIVE COMMITTEE

J. F. D. SMITH, *Chairman*
G. M. KLINE, *Vice-Chairman*
E. F. RIESING, *Secretary*
G. F. JENKS, Research
L. E. JERMY, Publications
P. A. NORTH, Equipment
F. L. YERZLEY, Liaison
W. A. ZINZOW

Production Engineering

Organized, 1941

(Formerly Machine Shop Practice)

SOL EINSTEIN, *Chairman*

EXECUTIVE COMMITTEE

SOL EINSTEIN, *Chairman*
WARNER SEELY, *Secretary*
J. M. ALDEN
E. W. ERNEST
ERIK OBERG
C. L. TUTT, JR., *Staff Assistant*

Associates

HANS ERNST
A. M. JOHNSON
E. D. WATERS

Railroad

Organized, 1920

D. S. ELLIS, *Chairman*

EXECUTIVE COMMITTEE

D. S. ELLIS, *Chairman*
E. L. WOODWARD, *Secretary*
J. G. ADAIR
J. R. JACKSON
K. F. NYSTROM
W. M. SHEEHAN

Research Secretary

F. H. CLARK

Representative, San Francisco Section

M. P. TAYLOR

Textile

Organized, 1921

F. L. BRADLEY, *Chairman*

EXECUTIVE COMMITTEE

F. L. BRADLEY, *Chairman*
W. B. HEINZ, *Vice-Chairman*
W. W. STARKE, *Secretary*
H. H. ILER
J. D. ROBERTSON
E. R. STALL
E. WADSWORTH STONE

Associates

A. D. ASBURY
A. W. BENOIT
W. S. BROWN
WINN CHASE
M. A. GOLRICH, JR.
R. DEVERE HOPE

Southern Representative

S. B. EARLE

Research Secretary

JAMES W. COX

SUBCOMMITTEE CHAIRMEN

Activities, W. B. HEINZ
Air Conditioning, WENDELL BROWN
Drying, J. D. ROBERTSON
Lighting, EARLE MAULDIN
Lubrication, R. W. VOSE
Power and Heat Utilization, E. WADSWORTH STONE

Wood Industries

Organized, 1921

T. D. PERRY, *Chairman*

EXECUTIVE COMMITTEE

T. D. PERRY, *Chairman*
A. C. FEGEL, *Secretary*
SERN MADSEN, *Vice-Chairman*
D. R. GRAY
M. J. MACDONALD

Associates

C. L. BABCOCK
P. H. BILHUBER
H. B. CARPENTER
F. P. CARTWRIGHT
G. E. FRENCH
A. W. KEUFFEL
A. S. KURKJIAN
J. S. MATHEWSON
E. D. MAY
R. H. MCCARTHY
A. D. SMITH, JR.
H. M. SUTTON
CHARLES WHITE

COMMITTEE CHAIRMEN

Dimensional Limits and Allowances, SERN MADSEN
Use of Plywood as an Engineering Material, T. D. PERRY
Wood Finishing, M. J. MACDONALD

LOCAL SECTIONS

ARTICLE B6A, PAR. 17: The Standing Committee on Local Sections shall, under the direction of the Council, have supervision of the Local Sections of the Society.

STANDING COMMITTEE ON LOCAL SECTIONS

J. N. LANDIS, *Chairman* (1942)
F. L. WILKINSON, JR. (1943)
F. W. MARQUIS (1944)
J. A. KEETH (1945)
OLIVER B. LYMAN (1946)

Junior Advisers

C. C. KIRBY (1942)
F. H. FOWLER, JR. (1943)

REGIONAL GROUP DELEGATES TO ANNUAL CONFERENCES

Terms expire October, 1942

A. R. MUMFORD, *Speaker for 1941 Conference*, Group II
A. D. HUGHES, *Secretary*, Group VII
A. D. ANDRIOLA, Group I
J. S. MOREHOUSE, Group III
F. C. SMITH, Group IV
C. T. OERGEL, Group V
F. L. RUOFF, Group VI
C. W. CRAWFORD, Group VIII

Terms expire October, 1943

R. M. MATSON, *Speaker for 1942 Conference*, Group VIII
J. B. JONES, *Secretary*, Group IV
H. F. RAMM, Group I
W. H. LARKIN, 3RD, Group II
CARL SCHABTACH, Group III
A. M. SELVEY, Group V
B. G. ELLIOTT, Group VI
H. T. AVERY, Group VII

AKRON-CANTON

Organized: 1920
Territory: Counties of Richland, Ashland, Medina, Summit, Portage, Wayne, Stark, Holmes, Tuscarawas, Carroll, and Coshocton in Ohio
Place of Meeting: As selected monthly
Number of Members: 157

EXECUTIVE COMMITTEE

A. G. WALKER, *Chairman*
O. J. HORGER, *Vice-Chairman*
A. E. SHETLER, *Secretary-Treasurer*
M. R. BOWERMAN
D. H. CORNELL
H. G. DOSTER
JAMES FORREST
S. H. HAHN
L. B. HOLMES
E. HOMER KENDALL
J. H. VANCE

ANTHRACITE-LEHIGH VALLEY

Organized: 1920, as Lehigh Valley; reorganized, 1928, as Anthracite-Lehigh Valley
Territory: Counties of Bradford, Susquehanna, Wayne, Sullivan, Wyoming, Lackawanna, Columbia, Luzerne, Monroe, Pike, Schuylkill, Carbon, Berks, Lehigh, Northampton in Pennsylvania, and Warren in New Jersey
Place of Meeting: One meeting annually at Allentown, Bethlehem, Easton, Hazleton, Pottsville, Reading, Scranton, and Wilkes-Barre
Local Organization: The Engineers' Club of Lehigh Valley
Number of Members: 215

EXECUTIVE COMMITTEE

WALTER TALLGREN, *Chairman*
W. W. HAGERTY, C. M. MERRICK, R. H. PORTER } *Vice-Chairmen*
C. H. FOLMSBEE, *Secretary*
R. L. WILLIS, *Treasurer*
J. R. CONNELLY, J. A. GISH, JR., E. A. GORNEY, WALTER GREACEN, III, C. C. HERTEL, J. A. LLOYD, R. E. MOYER, JR., L. E. MYLTING } *Managers*
J. W. BLISS, C. R. DIECKMAN, C. H. FOLMSBEE, H. F. HATFIELD, W. G. MCLEAN, H. C. SCHWEIKART } *Assistant Managers*

ATLANTA

Organized: 1913
Territory: Radius of sixty miles from Atlanta, Ga.
Place of Meeting: Atlanta Athletic Club
Luncheon meeting every Monday at 12:30 p.m. at Atlanta Athletic Club
Number of Members: 93

EXECUTIVE COMMITTEE

A. H. KOCH, *Chairman*
J. M. RITTELMEYER, *Vice-Chairman*
R. N. BENJAMIN, *Secretary*
J. A. DODD
W. A. HINTON
A. C. KEISER, JR.
W. J. MCALPIN
J. W. PARKER, JR.

BALTIMORE

Organized: 1916
Territory: Radius of thirty miles from Baltimore, Md.
Place of Meeting: Engineers Club of Baltimore
Number of Members: 271

EXECUTIVE COMMITTEE

C. F. MERRIAM, *Chairman*
W. D. BOYNTON, *Secretary-Treasurer*
E. M. BENJES
SIDNEY HAUSMAN
HERMAN HOLLERITH, JR.
G. W. KEEN
J. M. MOUSSON, II
S. F. ROBERTSON
L. F. WELANETZ

JUNIOR GROUP

JOHN DOERING, *Chairman*
H. W. HYDE, *Secretary-Treasurer*
E. M. BENJES
L. R. HARTMAN
W. A. HAZLETT

BIRMINGHAM

Organized: 1915
Territory: Radius of sixty miles from Birmingham, Ala.
Place of Meeting: Tutwiler Hotel
Number of Members: 77

EXECUTIVE COMMITTEE

J. M. GALLALEE, *Chairman*
T. M. FRANCIS, *Vice-Chairman*
R. G. B. BOURNE, *Secretary*
J. B. BELL
H. S. KENT

BIRMINGHAM

(Continued)

JUNIOR GROUP

F. E. VANN, *Chairman*
A. V. JANNETTE
H. S. KENT

BOSTON

Organized: 1909
Territory: Radius of thirty miles from Boston, Mass.
Place of Meeting: Mass. Inst. of Technology
Local Organization: Engineering Societies of New England
Number of Members: 573

EXECUTIVE COMMITTEE

J. W. ZELLER, *Chairman*
H. J. BROWN, *Vice-Chairman*
R. A. SPENCE, *Secretary-Treasurer*
KERR ATKINSON
G. A. ORROK, JR.
S. S. PERRY

JUNIOR GROUP

W. J. O'MALLEY, *Chairman*
R. HERMANN, *Vice-Chairman*
R. A. SPENCE, *Secretary-Treasurer*
E. I. BOWER
SABIN CROCKER, JR.

BRIDGEPORT

Organized: 1917, as a Branch of Connecticut Section; reorganized as a Section, 1923
Territory: Fairfield County, Conn.
Place of Meeting: Stratfield Hotel
Local Organizations: The Bridgeport Tool Engineers Association; The Bridgeport Engineers Club
Number of Members: 125

EXECUTIVE COMMITTEE

RUDOLF BECK, *Chairman*
J. M. LUCARELLE, *Vice-Chairman*
W. H. SNIFFEN, *Secretary*
A. W. HAGAN, *Treasurer*
A. H. BEEDE
C. N. HOAGLAND
R. C. MOODY
O. J. RICHMOND
J. W. ROE
J. D. SKINNER
E. R. SPAULDING
C. P. WICKS

JUNIOR GROUP

E. L. UHL, JR., *Chairman*
E. A. SAMMIS, *Vice-Chairman*
A. H. BEEDE, *Secretary*
C. A. BUSS
A. E. LAROCQUE
W. E. VISCUSI

BUFFALO

Organized: 1915
Territory: Radius of thirty miles from Buffalo, N.Y.
Place of Meeting: Mareen Hotel, Main St. at Utica
Local Organization: Engineering Society of Buffalo
Number of Members: 206

EXECUTIVE COMMITTEE

N. C. BARNARD, *Chairman*
C. A. ROSS, *Vice-Chairman*
MELVILLE C. CASE, *Secretary*
CARLOS E. HARRINGTON, *Treasurer*
L. R. BURMESTER
H. W. S. LA VIER
W. A. MILLER
J. L. YATES, *Junior Adviser*
STEPHEN WAGNER, *Student Adviser*

CENTRAL ILLINOIS

Organized: 1937
Territory: All the territory in Central Illinois between the following counties on the northern boundary: Bureau, LaSalle, Knox, Stark, Putnam, Marshall, Livingston, Peoria; counties on the southern boundary: Pike, Scott, Morgan, Sangamon, Macon, Piatt, Douglas, and Edgar
Place of Meeting: Hotel Pere Marquette or Caterpillar Show Room
Number of Members: 81

EXECUTIVE COMMITTEE

C. G. A. ROSEN, *Chairman*
W. W. BABCOCK, *Vice-Chairman*
R. E. MCCLAIN, *Secretary-Treasurer*
J. L. DEFFENBAUGH, *Assistant Secretary*
L. E. JOHNSON
D. G. RYAN
F. L. MEYER, *Past-Chairman*

JUNIOR GROUP

L. WOLNAIK, *Chairman*

CENTRAL INDIANA

Organized: 1916
Territory: Radius of eighty miles from Indianapolis, within Indiana
Place of Meeting: Indianapolis Athletic Club
Local Organization: Indiana Engineering Society
Number of Members: 163

EXECUTIVE COMMITTEE

R. B. BASS, *Chairman*
C. L. KLINE, *Vice-Chairman*
R. W. GAUSMANN, *Secretary-Treasurer*
H. A. BOLZ
J. A. DROGUE
R. B. HOLMES
J. K. LOMAN

CENTRAL PENNSYLVANIA

Organized: 1921
Territory: Radius of approximately sixty miles from State College, Pa.
Place of Meeting: State College and Altoona, Pa.
Number of Members: 76

EXECUTIVE COMMITTEE

J. O. P. HUMMEL, *Chairman*
H. A. SORENSEN, *Secretary-Treasurer*
J. S. DOOLITTLE
G. L. GUILLET
F. T. MAVIS
R. Y. SIGWORTH
F. C. STEWART

CHICAGO

Organized: 1913
Territory: Radius of fifty miles from Chicago, Ill.
Headquarters: Mid-West A.S.M.E. Office, Room 1617, 205 West Wacker Drive, Chicago, Ill.
Place of Meeting: Civic Opera Bldg., 20 N. Wacker Dr.
Meetings: Tuesday, 7:30 p.m.
Local Organization: Western Society of Engineers
Number of Members: 826

EXECUTIVE COMMITTEE

C. C. AUSTIN, *Chairman*
H. M. BLACK, J. R. MICHEL, P. A. STEPHENSON } *Vice-Chairmen*
F. B. ORR, *Secretary-Treasurer*
R. H. BACON
E. L. BERRY
C. B. COLE
L. M. ELLISON
A. H. JENS
L. M. JOHNSON
N. R. KENDALL
J. S. KOZACKS
F. H. LANE
J. C. MARSHALL
W. T. MCCULLOUGH, JR.
T. S. MCEWAN
H. L. NACHMAN
C. W. PARSONS
H. S. PHILBRICK
J. G. REID
RALPH SARGENT
KARL TRANZEN
R. E. TURNER
C. L. WACHS
J. I. YELLOTT

JUNIOR GROUP

NORMAN KENDALL, A. W. MARBURG } *Co-Chairmen*
F. D. COTTERMAN, *Secretary*
W. G. CHAPPELL
R. C. CLOUGH
J. J. GAHAN
R. W. HELBIG
J. A. JOHNSTON
M. J. KILROY
D. I. PAYNE
A. W. VANDE VEN

CINCINNATI

Organized: 1912
Territory: Radius of thirty miles from Cincinnati, Ohio
Place of Meeting: Engineers' Club Rooms, Ninth & Race Sts.
Local Organization: Engineers' Club of Cincinnati
Number of Members: 192

EXECUTIVE COMMITTEE

E. H. MITSCH, *Chairman*
H. B. BRANDT, *Vice-Chairman*
R. L. SMITH, *Secretary-Treasurer*
J. J. BRAUN
HANS ERNST
R. S. HYATT
C. L. KOEHLER
R. E. LEBLOND
G. F. LOCKEMAN
F. W. SPALDING

CLEVELAND

Organized: 1918
Territory: Counties of Lorain, Cuyahoga Lake, Geauga, and Ashtabula in Ohio
Place of Meeting: Cleveland Engineering Society Club
Local Organization: Cleveland Engineering Society
Number of Members: 243

Executive Committee

J. P. Dearasaugh, *Chairman*
D. K. Wright, *Vice-Chairman*
E. R. McCarthy, *Secretary*
F. A. Barnes, *Treasurer*
M. E. Lange
McRea Parker
R. R. Slaymaker
W. G. Stephan
A. G. Trumbull

COLORADO

Organized: 1919
Territory: Entire State of Colorado
Place of Meeting: Albany Hotel, Denver, Colo.
Local Organization: Colorado Engineering Council (Colorado Society of Engineers)
Number of Members: 74

Executive Committee

R. F. Throne, *Chairman*
Durbin Van Law, *Vice-Chairman*
J. C. Reed, *Secretary-Treasurer*
L. D. Crain
A. L. Hill
F. A. Lockwood
N. A. Parker
F. H. Prouty
G. A. Richter
J. T. Strate
G. H. Woelbing

COLUMBUS

Organized: 1920
Territory: Counties of Union, Delaware, Licking, Madison, Franklin, Fayette, Pickaway, and Ross in Ohio
Place of Meeting: Battelle Memorial Institute and The Ohio State University
Number of Members: 78

Executive Committee

H. R. Limbacher, *Chairman*
H. M. Blank, *Vice-Chairman*
E. J. Lindahl, *Secretary-Treasurer*
A. I. Brown
C. Z. Gillivan
S. M. Marco
J. L. Purdy
E. M. Sampson

DAYTON

Organized: 1926
Territory: Counties of Drake, Miami, Champaign, Preble, Montgomery, Greene, and northern part of Butler and Warren in Ohio
Place of Meeting: Engineers' Club of Dayton
Local Organization: Engineers' Club of Dayton
Number of Members: 110

Executive Committee

L. R. Bridge, *Chairman*
C. W. Ball, *Vice-Chairman*
E. G. Johnson, *Secretary-Treasurer*
H. M. Gano
J. J. Healy
P. H. Kemmer
A. R. Weber
C. H. Wight

DETROIT

Organized: 1916
Territory: Radius of thirty miles from Detroit, Mich.
Place of Meeting: Place varies
Local Organization: Engineering Society of Detroit
Number of Members: 454

Executive Committee

A. M. Selvey, *Chairman*
J. W. Armour, *Secretary-Treasurer*
E. J. Abbott
C. L. Brattin
J. A. Carlin
L. W. Lentz
R. W. Parkinson
J. H. Spurgeon
H. L. Walton
R. K. Weldy
T. E. Winkler
Tom Jeffords, *Ex-Officio*

Junior Group

Paul Hoffman, *Chairman*
B. W. Lane, M. A. Simpson } *Committeemen*

EAST TENNESSEE

Organized: 1922
Territory: All counties in Tennessee east of the west boundary of Scott, Morgan, Cumberland, White, Warren, Coffee, Moore, Franklin; Belle County in Kentucky; and Rossville, Dade, Walker, Cattasa, Whitfield, Murray, Gordon, Chattooga in Georgia
Place of Meeting: Places varies
Local Organization: Chattanooga Engineers Club and Knoxville Technical Club
Luncheon Meeting every Monday noon at Chattanooga Engineers Club
Number of Members: 98

Executive Committee

Elmer Torok, *Chairman*
A. W. Harris, Horace Carpenter, C. H. Robinson } *Vice-Chairmen*
J. Mack Tucker, *Secretary-Treasurer*
T. C. Ervin
C. B. Kerns
W. S. Moorehouse
F. R. O'Brien
J. E. Rigby

Junior Group

Francis R. O'Brien, *Chairman*

ERIE

Organized: 1917
Territory: Radius of thirty miles from Erie, Pa.
Place of Meeting: Erie County Court House
Number of Members: 75

Executive Committee

H. J. Joyce, *Chairman*
G. H. Kaemmerling, *Vice-Chairman*
R. R. Blunt, *Secretary*
F. B. Schneider, *Treasurer*
G. W. Bach
F. G. Brinig
D. H. Corey
H. E. Goetz
E. C. Ims
C. I. Rainesale
MacDonald S. Reed
A. F. Wild

FLORIDA

Organized: 1925
Territory: State of Florida
Place of Meeting: Various Cities in State
Local Organization: Florida Engineering Society, Gainesville, Fla.
Number of Members: 82

Executive Committee

V. C. Couchman, *Chairman*
W. E. Drew, *First Vice-Chairman*
John Hunter, *Second Vice-Chairman*
C. F. Whitcomb, Jr., *Secretary-Treasurer*
T. H. Gardner
R. A. Thompson
E. P. Wood
R. R. Roberts, *Student-Chairman*

FORT WAYNE

Organized: 1939
Territory: Counties of LaGrange, Steuben, Noble, DeKalb, Whitley, Allen, Wabash, Huntington, Wells, Adams, Miami, Blackford and Jay in Indiana; Counties of Williams, Defiance, Paulding, Van Wert and Mercer in Ohio
Local Organization: Fort Wayne Engineers' Society
Number of Members: 30

Executive Committee

F. L. Ruoff, *Chairman*
F. T. McInerney, Jr., *Vice-Chairman*
K. K. Cooper, *Secretary*
W. H. Connor, *Treasurer*
N. T. Bourke
W. L. Knauss

GREEN MOUNTAIN

Organized: 1923
Territory: Entire State of Vermont and neighboring and closely related communities of Claremont and Hanover, N.H.
Place of Meeting: Springfield, Windsor, Vt., and Claremont, N.H.
Local Organization: Vermont Engineering Society
Number of Members: 37

Executive Committee

C. H. Adams, *Chairman*
F. T. Gear, *Vice-Chairman*
F. A. Johnson, *Secretary-Treasurer*
E. D. Clark
H. L. Daasch
D. T. Hamilton
J. B. Johnson

GREENVILLE

Organized: As a Branch, 1923; as a Section, 1927
Territory: Radius of sixty miles from Greenville, S.C.
Place of Meeting: Meetings held at Greenville, Clemson College, S.C., Canton, Asheville, and Enka, N.C.
Number of Members: 46

Executive Committee

J. W. Vaughan, Jr., *Chairman*
C. R. Hoey, Jr., *Vice-Chairman*
J. E. Waldrep, *Secretary-Treasurer*
J. A. McPherson
C. F. Mercer
W. P. Tindall
A. H. Vanderhoof
J. C. Whitehurst

HARTFORD

Organized: 1917, as Branch of Conn. Section; reorganized, 1923; New Britain Section merged with Hartford Section, July 1, 1940
Territory: Hartford County except that portion served by New Britain Section
Place of Meeting: Hartford Electric Light Company
Number of Members: 161

Executive Committee

H. F. Ramm, *Chairman*
Henry Michelsen, L. C. Smith } *Vice-Chairmen*
R. D. Keller, *Secretary-Treasurer*
P. W. Bauer
Herbert Burdick
E. P. Herrick
F. O. Hoagland
B. S. Lewis
E. R. Lewis
W. S. Paine
C. H. Richardson
C. C. Stevens
S. J. Teller
H. B. Van Zelm

INLAND EMPIRE

Organized: 1921
Territory: East of Columbia River in State of Washington, and Counties of Okanogan and Benton, and part of Northern Idaho
Place of Meeting: Davenport Hotel, Spokane
Luncheons Wednesdays at 12:00 noon, Davenport Hotel, Spokane
Local Organization: Associated Engineers of Spokane
Number of Members: 20

Executive Committee

J. G. McGivern, *Chairman*
F. W. Candee, *Vice-Chairman*
N. W. Humphrey, *Secretary-Treasurer*
Alexander Lindsay
E. B. Parker
L. J. Pospisil

ITHACA

Organized: 1936
Territory: Radius of thirty miles from Ithaca plus following cities: Binghamton, Corning, Endicott, Geneva, Painted Post
Place of Meeting: Alternately in different cities of Section territory, as announced.
Number of Members: 80

Executive Committee

C. L. Wilder, *Chairman*
S. S. Garrett, *Vice-Chairman*
F. S. Erdman, *Secretary-Treasurer*
D. S. Kimball, Jr.
W. M. Sawdon
M. P. Whitney
N. P. Wickersham

KANSAS CITY

Organized: 1921
Territory: Radius of sixty miles from Kansas City, Mo.
Place of Meeting: University Club
Local Organization: Engineers' Club of Kansas City
Number of Members: 118

Executive Committee

J. R. Stone, *Chairman*
R. V. Sutherland, *Vice-Chairman*
R. P. Hahn, *Secretary*
M. A. Durland, *Treasurer*
F. R. Applegate
C. E. Brown
E. M. Bruzelius
T. C. Cheasley
H. L. Crain
R. S. Tait

Junior Group

H. W. Cockrill, *Chairman*
Jack Weisbein, *Secretary*

LOS ANGELES *

Organized: 1915
Territory: South of southern boundaries of following counties: Monterey, Kings, Tulares, and Inyo, Calif.
Place of Meeting: Barker Bros. Store
Local Organization: Technical Societies of Los Angeles
Luncheon Meetings Thursdays at 12:00 noon at Engineers' Club
Number of Members: 560

Executive Committee

J. Calvin Brown, *Chairman*
E. M. Wagner, *Vice-Chairman*
C. E. McGinnis, *Secretary-Treasurer*
P. L. Armstrong
D. K. Coyle
R. B. Esselman
J. S. Gallagher
R. G. Roshong
C. H. Shattuck
H. S. Spaulding

Junior Group

John H. Hanna, *Junior Chairman*
LeRoy Barrett, *Secretary*
W. L. Parker, *Member at Large*

San Diego Sub-Section

John L. Bacon, *Chairman*
Louis Baldo, *Secretary-Treasurer*

LOUISVILLE

Organized: 1922
Territory: Radius of thirty miles from Louisville, Ky. (includes Lexington, Ky.)
Place of Meeting: University of Louisville, Louisville, Ky.
Local Organization: Engineers and Architects Club
Number of Members: 79

Executive Committee

W. F. Lucas, *Chairman*
H. C. Murphy, *Vice-Chairman*
C. D. Greffe, *Secretary*
J. K. Meyer, *Treasurer*
O. C. Krause
L. S. O'Bannon
J. H. Roman
Melvin Sack

MEMPHIS

Organized: 1923
Territory: Radius of sixty miles from Memphis, Tenn., and eastern half of Arkansas including all the territory east of a line drawn north and south through the western boundary of the city of Little Rock
Number of Members: 23

Executive Committee

R. H. Sogard, *Chairman*
W. H. Roberts, *Vice-Chairman*
J. A. Mollino, Jr., *Secretary-Treasurer*
T. H. Allen
E. J. Kueck

METROPOLITAN

Organized: 1910
Territory: Metropolitan District, New York and New Jersey
Place of Meeting: Engineering Societies Building, 29 West 39th Street, New York, N.Y.
Number of Members: 3,184

Executive Committee

F. D. Carvin, *Chairman*
G. J. Nicastro, *Secretary*
W. H. Larkin, 3rd, *Treasurer*
H. C. R. Carlson, *Chairman of Meetings and Program Committee*
E. J. Billings
P. E. Frank
W. S. Gleeson
P. T. Onderdonk
C. B. Peck
A. R. Mumford, *Ex-Officio*

Junior Group

J. L. Hall, *Chairman*
F. H. Fowler, Jr., *Vice-Chairman*
F. M. Gibson, Jr., *Secretary*
J. S. Hunter
C. C. Kirby
R. L. Robertson
H. D. Strong

MID-CONTINENT

Organized: 1919
Territory: Entire State of Oklahoma; territory in Arkansas not included in Memphis Section; part of Louisiana; and territory in Texas north of the southern boundaries of the counties of Gaines, Dawson, Bordon, Scurry, Fisher, Jones, and Shackelford

* Name changed to Southern California, November 30, 1941.

MID-CONTINENT

(Continued)

Place of Meeting: Usually Mayo Hotel, Tulsa, Okla.
Luncheon Meetings with Engineers Club of Tulsa, Mondays at 12:00 noon
Local Organization: Engineers Club of Tulsa
Number of Members: 130

Executive Committee

E. C. Baker, *Chairman*
A. N. Horne, *Vice-Chairman*
T. C. Webb, *Secretary*
E. H. Parker, *Treasurer*
E. E. Ambrosius
R. G. Ayers
D. O. Barrett
H. B. Bernard
A. G. Blanchard
W. L. Ducker, Jr.
R. L. Feagles
W. G. Heltzel
Gwynne Raymond
W. S. Sherman
H. A. Wienecke

MILWAUKEE

Organized: 1904
Territory: Radius of fifty miles from Milwaukee, Wis.
Place of Meeting: Wisconsin Club
Local Organization: Engineers' Society of Milwaukee
Luncheon Meetings once each month, 3rd Wednesday at Wisconsin Club
Number of Members: 214

Executive Committee

T. F. Eserkaln, *Chairman*
R. J. Smith, *Secretary-Treasurer*
James Brower
H. P. Dahlstrand
F. H. Dorner, Sr.
M. K. Drewry
Walter Ferris
O. A. Kisa
J. L. Martin
R. C. Newhouse

Junior Group

J. L. Martin, *Chairman*
J. H. Stanek, *Secretary*
Harry Gute
P. J. Imse
M. E. Ruess
W. T. Saveland, Jr.
R. C. Strassman

MINNESOTA

Organized: Minneapolis, 1913; St. Paul, 1913; the two Sections merged, 1934
Territory: Entire State of Minnesota
Place of Meeting: Minnesota Union, Univ. of Minnesota
Local Organization: Minneapolis Engineers Club, Minnesota Federation of Architectural and Engineering Societies
Number of Members: 98

Executive Committee

M. S. Wunderlich, *Chairman*
L. C. Sprague, *Vice-Chairman*
N. J. Sternal, *Secretary-Treasurer*
W. H. Erskine
Charles Foster
C. A. Herrick
L. G. Straub

NEBRASKA

Organized: 1922
Territory: State of Nebraska, and Council Bluffs, Iowa
Place of Meeting: Lincoln and Omaha
Local Organization: Engineers' Clubs of Lincoln and Omaha
Luncheon Meeting every Wednesday noon at the Omaha Engineers' Club—4th Monday Evening at Lincoln
Number of Members: 33

Executive Committee

J. W. Kurtz, *Chairman*
J. W. Haney, *Vice-Chairman*
G. A. Rogers, *Secretary-Treasurer*
E. V. Perkins, *Chairman of Meetings and Program Committee*
J. K. Ludwickson
A. A. Luebs
C. F. Moulton
W. F. Weiland

NEW HAVEN

Organized: 1912, reorganized, 1923
Territory: Portions of New Haven and Middlesex Counties, Conn.
Place of Meeting: Mason Laboratory, Yale University
Number of Members: 78

Executive Committee

L. H. Von Ohlsen, *Chairman*
I. T. Hook, *Vice-Chairman*
F. C. Richardson, *Secretary-Treasurer*
D. L. Bacon
A. F. Breitenstein
G. H. Eaton
L. C. Lichty

NEW ORLEANS

Organized: 1916
Territory: All of Louisiana except the northern part allotted to Mid-Continent Section
Place of Meeting: Room 422, St. Charles Hotel
Local Organization: Louisiana Engineering Society
Number of Members: 99

Executive Committee

G. R. Hammett, *Chairman*
L. J. Cucullu, *Vice-Chairman*
A. M. Hill, *Secretary-Treasurer*
E. L. Cowan
L. J. Lassalle
J. R. Rombach, Jr.
A. D. Stancliff
D. W. Stewart

Junior Group

J. R. Rombach, Jr., *Chairman*
H. W. Voelkel, *Vice-Chairman*
G. H. Schmitt, Jr., *Secretary*

NORTH TEXAS

Organized: 1922
Territory: All of Texas north of an approximately straight line through Del Rio, Fredericksburg, Georgetown, Cameron, Nacogdoches, and center, including the cities mentioned, and south of north boundaries of the counties of Parmer, Castro, Swisher, Briscoe, Hall, and Childress. Also the City of Texarkana, Ark.
Place of Meeting: Dallas Power & Light Co. Bldg. Auditorium
Local Organization: Technical Club of Dallas
Number of Members: 101

Executive Committee

F. C. Justice, *Chairman*
J. A. Noyes, *Vice-Chairman*
E. J. Wacker, *Secretary-Treasurer*
H. E. Chambers, Jr.
H. M. Robinson
C. H. Shumaker
Ray M. Matson, *Ex-Officio*

NORWICH

Organized: 1930
Territory: Counties of Tolland, Windham, and New London in Connecticut, and Westerly District in Rhode Island
Place of Meeting: New London Junior College, Pequot Ave., New London, Conn.
Number of Members: 50

Executive Committee

A. W. Luce, *Chairman*
Robert Wosak, *Secretary-Treasurer*
W. A. Morain, *Chairman of the Program Committee*
A. D. Andriola
W. E. Beaney
W. E. Edel
F. E. English
Dana Young

ONTARIO

Organized: 1917
Territory: Province of Ontario, Canada
Place of Meeting: Hart House, University of Toronto
Number of Members: 176

Executive Committee

H. H. Angus, *Chairman*
Ernest Jones, *Secretary-Treasurer*
T. H. Blair
A. C. Blue
S. G. Clarke
C. R. Davis
H. G. Hill
T. S. Jardine
W. G. McIntosh
W. E. Micklethwaite
A. A. Moline
W. D. Sheldon
Ered'k Truman

Junior Group

W. R. Trusler, *Chairman*
J. M. Van Winckle, *Secretary-Treasurer*
C. E. Beynon
J. H. Miller
F. Taylor

OREGON

Organized: 1919
Territory: State of Oregon and that territory in Washington within a radius of thirty miles from Portland, Ore.
Place of Meeting: Usually Public Service Bldg., Portland, Ore.
Local Organization: Oregon Society of Engineers
Number of Members: 45

OREGON

(Continued)

EXECUTIVE COMMITTEE

A. A. OSIPOVICH, *Chairman*
C. GORDON TUPLING, *Vice-Chairman*
E. P. WEISER, *Secretary-Treasurer*
A. J. CHAPUT
A. D. HUGHES
TOM PERRY
R. B. ROWAN

PENINSULA

Organized: 1923
Territory: West of the east boundaries of the following counties: Emmet, Charlevoix, Antrim, Kalkaska, Missaukee, Clare, Isabell, Gratiot, Clinton, Eaton, Calhoun, and Branch, Mich.
Place of Meeting: Grand Rapids, Mich.
Luncheon Meeting Fifth Thursday noon each month
Local Organization: Engineers' Club of Grand Rapids
Number of Members: 50

EXECUTIVE COMMITTEE

JOHN M. GORRIE, *Chairman*
DONALD MCSORLEY, *1st Vice-Chairman*
KENNETH CROWSER, *2nd Vice-Chairman*
CARL J. KUENZEL, *Secretary-Treasurer*
CHARLES BUCK
JANUS R. DE HAMER
GAROLD GEBBEN
CONRAD LOHMANN
GEORGE WARING
CHARLES A. HAMILTON, *Ex-officio*

PHILADELPHIA

Organized: 1912
Territory: Counties of Bucks, Montgomery, Chester, Philadelphia, Delaware, Pa., and the State of Delaware
Place of Meeting: Philadelphia Engineers' Club, 1317 Spruce Street, Philadelphia, Pa.
Local Organization: Philadelphia Engineers' Club
Luncheon Meeting every Thursday noon at 12:30 p.m. at Philadelphia Engineers' Club
Number of Members: 1,002

EXECUTIVE COMMITTEE

J. STANLEY MOREHOUSE, *Chairman*
C. S. GOTWALS, *Vice-Chairman*
L. N. GULICK, *Secretary-Treasurer*
L. P. HYNES
J. J. MCCARTHY
F. W. MILLER

JUNIOR GROUP

E. W. GRISCOM, *Chairman*
W. B. PEGRAM, *Vice-Chairman*
G. G. MARTINSON, *Secretary*
GEORGE FISHER, *Treasurer*
L. N. GULICK, *Senior Adviser*
J. P. CLARK
T. M. POMEROY, JR.
N. R. SEFING
R. D. STAFFER

PIEDMONT—NORTH CAROLINA

Organized: As a Branch, 1923; as a Section 1927; name changed from Charlotte Section to Piedmont—North Carolina, July 1, 1940
Territory: Radius of seventy-five miles from Charlotte, N.C.
Luncheon Meeting every other Monday at 1:00 p.m. at Efirds Department Store Dining Room
Local Organization: Charlotte Engineers Club
Number of Members: 46

EXECUTIVE COMMITTEE

R. W. OLIVE, *Chairman*
A. B. LECLERC, *Vice-Chairman*
W. B. FREEMAN, *Secretary-Treasurer*
B. L. COTTON
C. A. DEWEY
I. W. LEGGETT
R. P. REECE
T. O. SILLS

PITTSBURGH

Organized: 1920
Territory: Counties bounded by and including Beaver, Butler, Venango, Forest, Jefferson, Indiana, Somerset, Fayette, Greene, and Washington, Pa.
Place of Meeting: Engineers' Society of Western Pennsylvania, William Penn Hotel
Local Organization: Engineers' Society of Western Pennsylvania
Number of Members: 423

EXECUTIVE COMMITTEE

L. N. SHARANBERG, *Chairman*
T. J. BARRY, *Vice-Chairman*
C. A. HAHN, *Secretary*
K. F. TRESCHOW, *Treasurer*
S. B. ELY
J. N. EVANS
H. H. HALL
H. L. PARLETTE
R. E. PETERSON
KENNETH SEAVER
J. R. TANNER

PLAINFIELD

Organized: 1921
Territory: Plainfield and territory included between Elizabeth, Bound Brook, Metuchen, and Watchung, N.J.
Place of Meeting: Elizabeth Carteret Hotel, Elizabeth, and Plainfield Masonic Temple, Plainfield
Local Organization: Plainfield Engineers Club, Singer Engineering Society
Number of Members: 170

EXECUTIVE COMMITTEE

G. E. LEAVITT, JR., *Chairman*
F. C. SPENCER, JR., *Vice-Chairman*
E. E. FRANZ, *Secretary*
C. G. HOLMBERG, *Treasurer*
R. C. HECK, JR.
K. A. REEVE

PROVIDENCE

Organized: 1920
Territory: Radius of thirty miles from Providence, R.I.
Place of Meeting: Providence Engineering Society Building, 195 Angell St., Providence, R.I.
Local Organization: Providence Engineering Society
Number of Members: 159

EXECUTIVE COMMITTEE

J. D. ELDERT, *Chairman*
J. D. ROBERTSON, *Vice-Chairman*
R. M. SCOTT, *Secretary-Treasurer*
C. D. BILLMEYER
A. W. CALDER, JR.
J. S. CHAFEE
E. W. HARRINGTON
A. WILLIAM MEYER
P. V. MILLER
A. JOEL WARREN
G. E. WHEELER, JR.

RALEIGH

Organized: As a Branch, 1923; as a Section, 1927
Territory: Radius of sixty miles from Raleigh, N.C.
Places of Meeting: North Carolina State College, Raleigh, N.C.; Duke University, Durham, N.C.
Local Organizations: North Carolina Society of Engineers, Raleigh Engineers Club
Number of Members: 33

EXECUTIVE COMMITTEE

R. B. RICE, *Chairman*
F. B. TURNER, *Vice-Chairman*
R. G. CHAPMAN, *Secretary-Treasurer*
E. G. HOEFER
C. E. KERCHNER
R. M. ROTHGEB
R. S. WILBUR

ROCHESTER

Organized: 1919
Territory: Radius of thirty miles from Rochester, N.Y.
Place of Meeting: Rochester Engineering Society Rooms, Sagamore Hotel
Local Organization: Rochester Engineering Society, Sagamore Hotel
Luncheon Meeting every Tuesday at 12:15 p.m. at Sagamore Hotel
Number of Members: 109

EXECUTIVE COMMITTEE

I. S. BRADLEY, *Chairman*
W. D. WOOD, *Vice-Chairman*
I. G. MCCHESNEY, *Secretary-Treasurer*
K. H. HUBBARD
F. D. PUNNETT
A. E. SCHELL
A. W. SCHUSTER
J. H. SNYDER

ROCK RIVER VALLEY

Organized: 1926
Territory: Thirty miles east and west of Madison, Wis., and extending southward through Rockford, Ill.
Meeting Places: Madison, Wis., Beloit, Wis., and Rockford, Ill.
Local Organization: Rock River Valley Engineering Council
Number of Members: 73

EXECUTIVE COMMITTEE

C. A. JACOBSON, *Chairman*
B. G. ELLIOTT, *Vice-Chairman*
E. L. DAHLUND, *Secretary-Treasurer*
C. L. AVERY
M. W. DUNDORE
D. W. NELSON
F. J. ZIRCHER

ST. JOSEPH VALLEY

Organized: 1929
Territory: Counties of La Porte, Starke, Pulaski, St. Joseph, Marshall, Fulton, Elkhart, and Kosciusko in Indiana, and Cass and Berrien Counties in Michigan
Place of Meeting: South Bend, Ind.
Number of Members: 47

ST. JOSEPH VALLEY

(Continued)

EXECUTIVE COMMITTEE

E. J. WILLIAMS, *Chairman*
E. T. COBB, L. E. WADDINGTON, O. E. ZAHN } *Vice-Chairmen*
K. W. KNORR, *Secretary*
H. E. HOLLENSBE
J. A. MACLEAN
W. D. A. PEASLEE
L. E. WADDINGTON
C. C. WILCOX

ST. LOUIS

Organized: 1909
Territory: Radius of thirty miles from St. Louis, Mo.
Place of Meeting: Place varies
Local Organization: Engineers' Club of St. Louis
Number of Members: 205

EXECUTIVE COMMITTEE

R. W. MERKLE, *Chairman*
R. C. THUMSER, *Vice-Chairman*
HERBERT KUENZEL, *Secretary-Treasurer*
C. B. BRISCOE, *Chairman of the Program Committee*

SAN FRANCISCO

Organized: 1910
Territory: All territory north of the northern boundaries of the counties of San Luis Obispo, Kern, and San Bernardino
Place of Meeting: Engineers' Club, 206 Sansome St.
Luncheon Meetings, Tuesdays, California Hotel, Oakland; Thursdays, Engineers' Club, San Francisco
Local Organization: San Francisco Engineers' Club
Number of Members: 387

EXECUTIVE COMMITTEE

H. T. AVERY, *Chairman*
G. N. SOMERVILLE, *Vice-Chairman*
E. H. CAMERON, *Secretary-Treasurer*
V. F. ESTCOURT
R. S. QUICK
B. S. TRUETT
N. F. WARD

JUNIOR GROUP

V. F. ESTCOURT, *Chairman*
E. C. FLOYD
GEORGE L. SULLIVAN

SAVANNAH

Organized: 1923
Territory: Radius of 125 miles from Savannah in Georgia
Place of Meeting: Savannah Hotel
Local Organization: Engineers' Council of Savannah Chamber of Commerce
Number of Members: 19

EXECUTIVE COMMITTEE

W. L. MINGLEDORFF, *Chairman*
ALEX M. ORMOND, *Vice-Chairman*
B. J. SAMS, *Secretary-Treasurer*
W. H. ARTLEY
A. P. KEISKER
L. C. ROESEL

SCHENECTADY

Organized: As a Branch, 1919; as a Section, 1927
Territory: Radius of thirty miles from Schenectady, N.Y.
Place of Meeting: Rice Hall
Number of Members: 220

EXECUTIVE COMMITTEE

CARL SCHABTACH, *Chairman*
E. W. D. BUNKE, ALAN HOWARD, E. L. THEARLE } *Vice-Chairmen*
STANFORD NEAL, *Secretary*
L. A. GORE, *Treasurer*
H. E. BUNNELL, *Chairman of Program Committee*
R. G. MCANDREW
R. S. NEBLETT
A. R. STEVENSON, JR.

SOUTHERN CALIFORNIA

(See Los Angeles)

SOUTH TEXAS

Organized: 1919
Territory: South Texas and the northern part of the State not included in the North Texas Section territory
Place of Meeting: No fixed meeting place, but all meetings held in Houston
Number of Members: 173

EXECUTIVE COMMITTEE

C. L. ORR, *Chairman*
H. F. MOLLER, *Vice-Chairman*
J. J. KING, *Secretary-Treasurer*
C. W. CRAWFORD
H. E. DEGLER
V. L. DOUGHTIE
C. A. HALL
H. G. HIEBELER
S. G. KERSHNER
G. E. NEVILLE
W. B. PRESTON
J. G. H. THOMPSON
M. W. WILLIAMS

SUSQUEHANNA

Organized: 1927
Territory: Counties of Cumberland, Dauphine, Lebanon, Adams, York, and Lancaster
Place of Meeting: Engineering Society of York, and at Lancaster Twice a Year
Local Organization: Engineering Society of York and Engineers' Society of Pennsylvania, Harrisburg, Pa.
Number of Members: 76

EXECUTIVE COMMITTEE

O. E. WEBER, *Chairman*
S. P. SOLING, *Vice-Chairman*
E. T. P. NEUBAUER, *Secretary-Treasurer*
T. K. BREDA
JACOB FISCH
M. G. LEESON
M. E. SILBERGER

SYRACUSE

Organized: 1920
Territory: Radius of thirty miles from Syracuse, N.Y.
Place of meeting: Ball Room of the Onondaga Hotel
Local Organization: The Technology Club of Syracuse
Number of Members: 89

EXECUTIVE COMMITTEE

D. V. SHETLAND, *Chairman*
M. F. WILLIAMS, *Vice-Chairman*
E. A. FAILMEZGER, *Secretary-Treasurer*
L. E. POTTER, *Assistant Secretary*
H. T. AVERY
C. F. DIETZ
E. R. JEFFERSON
J. W. LINFORD
E. K. RHODES
G. I. VINCENT

TOLEDO

Organized: 1920
Territory: Radius of thirty miles from Toledo, Ohio
Place of Meeting: University Club, Toledo, Ohio
Local Organization: Affiliated Technical Societies of Toledo
Number of Members: 50

EXECUTIVE COMMITTEE

N. W. DORMAN, *Chairman*
H. R. SCHUTZ, *Vice-Chairman*
H. L. YARYAN, JR., *Secretary-Treasurer*
N. K. ANDERSON
F. S. BELL
C. W. FRAUTSCHI
T. L. HALLENBECK
H. H. KERR
W. C. LANG
GARLAND LUFKIN
R. H. MARKER
W. R. MORAN
R. J. MUGFOR
L. S. PLATOU
JOSEPH SEAMAN

TRI-CITIES

Organized: 1920
Territory: Radius of thirty miles from Moline, Ill.
Place of Meeting: Rock Island, Ill., Moline, Ill., and Davenport, Iowa
Luncheon Meeting every Wednesday, Davenport Hotel, 12:00 noon
Number of Members: 76

EXECUTIVE COMMITTEE

R. A. CROSS, *Chairman*
E. G. ERICKSON, *Vice-Chairman*
C. A. CARLSON, *Secretary-Treasurer*
P. E. ANDERSON
R. M. BARNES
K. R. HODGES

UTAH

Organized: 1923
Territory: State of Utah
Place of Meeting: University Club, Salt Lake City
Local Organization: Utah Society of Professional Engineers
Number of Members: 33

EXECUTIVE COMMITTEE

G. W. CARTER, *Chairman*
G. M. JONES, *Vice-Chairman*
R. D. BAKER, *Secretary-Treasurer*
C. B. BOWMAN
W. J. COPE
W. D. TURPIN

VIRGINIA

Organized: 1919
Territory: State of Virginia
Place of Meeting: Richmond, Norfolk, Blacksburg, Charlottesville, Roanoke, University, Petersburg
Local Organization: Central Virginia Engineers Club of Hampton Roads
Number of Members: 200

Executive Committee

G. C. Molleson, *Chairman*
J. B. Jones, *Vice-Chairman*
F. S. Roop, Jr., *Secretary*
W. J. Barber, *Treasurer*
G. L. Bascome
H. C. Hesse
H. R. Hopkins
M. L. Ireland, Jr.
Arthur Roberts, Jr.
H. C. Wintzer

WASHINGTON, D.C.

Organized: 1919
Territory: District of Columbia
Place of Meeting: Auditorium, Potomac Electric Power Co., 10th & E Sts., Washington, D.C.
Number of Members: 337

Executive Committee

W. B. Ensinger, *Chairman*
J. W. Huckert, *Vice-Chairman*
M. A. Mason, *Secretary-Treasurer*
C. E. Miller
T. R. Tate
J. E. Younger
G. F. Jenks, *Ex-Officio*

Junior Group

J. C. Phillips, *Chairman*
H. R. Booth
E. J. H. Lane
R. C. Meleney
F. M. Thuney
R. V. Vittucci

WATERBURY

Organized: 1917, as a Branch; reorganized as a Section, 1923
Territory: Litchfield County and a portion of New Haven County
Place of Meeting: Elton Hotel
Number of Members: 63

Executive Committee

A. L. Alves, *Chairman*
J. R. Hicks, *Vice-Chairman*
H. C. Ashley, *Secretary-Treasurer*
P. E. Peterson
W. C. Schneider
R. W. Shoemaker
R. S. Storrs

WESTERN MASSACHUSETTS

Organized: 1922
Territory: Includes counties of Berkshire, Franklin, Hampden, and Hampshire
Place of Meeting: Highland Hotel, Springfield, Mass.
Local Organization: Engineering Society of Western Massachusetts
Number of Members: 86

Executive Committee

C. Frank Dupee, *Chairman*
R. A. Packard, *Vice-Chairman*
D. A. Bartlett, *Secretary-Treasurer*
A. E. Benson
J. F. Malcolm
E. Lovell Smith

WESTERN WASHINGTON

Organized: 1919
Territory: State of Washington west of Columbia River with exception of territory included in 30-mile radius of Portland, Ore.
Place of Meeting: Engineers' Club, Seattle, Wash.
Local Organization: Seattle Engineers' Club
Luncheon Meetings daily at noon at Engineers' Club, Seattle
Number of Members: 168

Executive Committee

C. B. Shovar, *Chairman*
R. H. G. Edmonds, *Vice-Chairman*
S. Dan Hage, *Secretary-Treasurer*
R. E. Johnson
H. C. Krehbiel, Jr.
J. E. Mylroie

WEST VIRGINIA

Organized: 1925
Territory: State of West Virginia, South of Parallel 39
Place of Meeting: Charleston, W.Va.
Number of Members: 58

Executive Committee

A. H. Cannon, *Chairman*
J. Gilbert Miller, *Vice-Chairman*
J. L. Barker, Jr., *Secretary-Treasurer*
M. S. Bloomsburg
Minott Brooke
C. B. Cochran
H. C. Lewis

WORCESTER

Organized: 1915
Territory: Radius of thirty miles from Worcester, Mass.
Place of Meeting: Sanford Riley Hall, Worcester Poly. Inst.
Local Organization: Worcester Engineering Society
Number of Members: 130

Executive Committee

H. P. Crane, *Chairman*
G. H. MacCullough, *Vice-Chairman*
E. W. Armstrong, *Secretary-Treasurer*
L. R. Ball, *Chairman of Program Committee*
E. K. Allen, Jr.
J. A. Henrickson
F. R. Jones
C. M. McMahon
F. W. Naughton, Jr.
W. M. Wilcox

YOUNGSTOWN

Organized: 1928
Territory: Counties of Trumbull, Mahoning, and Columbiana in Ohio, and Mercer and Lawrence in Pennsylvania
Place of Meeting: Republic Rubber Co. Club Rooms, Albert St., Youngstown, Ohio
Number of Members: 55

Executive Committee

H. W. Smith, *Chairman*
L. A. Kline, *Vice-Chairman*
C. W. Foard, *Secretary-Treasurer*
F. J. Bowers
C. H. Legler
W. J. Longacher
H. E. Melin

STUDENT BRANCHES

ARTICLE B6A, PAR. 20: The Standing Committee on Relations With Colleges shall, under the direction of the Council, have supervision of the Student Branches of the Society and of such work of the Society as aims to further the education of engineers through the colleges and schools of accepted standing.

STANDING COMMITTEE, RELATIONS WITH COLLEGES

A. C. CHICK, *Chairman* (1942)
J. I. YELLOTT (1943)
H. E. DEGLER (1944)
G. L. SULLIVAN (1945)
R. P. REECE (1946)

J. W. HANEY, B. T. MCMINN, R. H. PORTER } *Advisory Members* (1942)

J. L. HALL, *Junior Adviser* (1942)

Communicate with Student Branch through Honorary Chairman

Name and Location	Year Authorized	No. of Members †	Chairman	Secretary	Honorary Chairman
Akron, Univ. of, Akron, Ohio	1924	31	FRED BROWN	ZACHARY HARRIS	F. S. GRIFFIN
Alabama Polytechnic Inst., Auburn, Ala.	1920	50	L. M. SAHAG	A. D. MULLIN	C. R. HIXON
Alabama, Univ. of, University, Ala.	1931	38	CLYDE PORTER	HOWARD FORSTER	D. H. MCCUAIG
Arizona, Univ. of, Tucson, Ariz.	1937	19	H. B. WEST	RAY WEAVER	M. L. THORNBURG
Arkansas, Univ. of, Fayetteville, Ark.	1910	16	B. B. DELAMAR	J. S. TOONE	R. G. PADDOCK
British Columbia, Univ. of, Vancouver, B.C., Can.	1938	21	S. C. ROONEY	H. M. CURRAN	H. M. MCILROY
Brown Univ., Providence, R.I.	1923	29	R. L. ROBERTS	S. M. TAYLOR	A. J. WARREN
Bucknell Univ., Lewisburg, Pa.	1916	24	R. W. DONEHOWER	M. A. CLARK	W. D. GARMAN
California Inst. of Tech., Pasadena, Calif.	1914	36	J. L. ALFORD	WILLIAM KENNEDY	R. L. DAUGHERTY
California, Univ. of, Berkeley, Calif.	1912	155	WALTER CONNOLLY	PETER BOWYER	R. G. FOLSOM
Carnegie Inst. of Tech., Pittsburgh, Pa.	1913	47	R. L. WAY	ROBERT DORIO	T. G. ESTEP
Case School of Applied Science, Cleveland, Ohio	1913	84	E. J. R. HUDEC	WILLIAM WEINKAMMER	R. R. SLAYMAKER
Catholic Univ. of America, Washington, D.C.	1922	39	E. B. GROSS	J. E. BEACH	M. E. WESCHLER
Cincinnati, Univ. of, Cincinnati, Ohio	1909	115	B. M. GEIGER	HAROLD HEMSTRAT	C. A. JOERGER
Clarkson College of Tech., Potsdam, N.Y.	1930	70	GEORGE COWIE	CHARLES BESIO	EDWARD MCHUGH
Clemson A.&M. College, Clemson College, S.C.	1921	..	E. B. BROWN	ATWELL SOMERVILLE	B. E. FERNOW
Colorado State College of A.&M. Arts, Fort Collins, Colo.	1914	29	MARVIN SCHACK	R. F. HUTCHISON	J. H. SCOFIELD
Colorado, Univ. of, Boulder, Colo.	1914	61	C. J. A. PERKO	R. F. BRACE	W. S. BEATTIE
Colorado School of Mines Division, Golden	——	1	L. B. LEIGH	F. G. KNIGHT	J. C. REED
Columbia Univ., New York, N.Y.	1909				
Management Division	——	2	.....	.....	.....
Mechanical Division	——	32	S. B. MENKES	R. G. VANMETRE	C. F. KAYAN
Connecticut, Univ. of, Storrs, Conn.	1941	(In process of organization)			
Cooper Union Inst. of Tech., New York, N.Y.	1920	49	MURRAY SACKSON	H. A. WELLS	W. A. VOPAT
Cooper Union Night School of Engineering, New York, N.Y.	1920	78	ANTHONY ORSINI	R. BLEECHER	E. A. SALMA
Cornell Univ., Ithaca, N.Y.	1908	104	H. M. ST. JOHN, JR.	H. E. OTTO	L. T. WRIGHT
Delaware, Univ. of, Newark, Del.	1929	25	A. H. GREEN	PIERCE HOLLINGSWORTH	LEO BLUMBERG
Detroit, Univ. of, Detroit, Mich.	1930	36	WALTER MAXIMOVICH	M. J. LEGARIE	J. J. UICKER
Drexel Inst. of Tech., Philadelphia, Pa.	1920	50	JACK SCHUSTER	WILLIAM BERNARD	A. H. REPSCHA
Duke Univ., Durham, N.C.	1935	51	JOHN GALT	KENT BOUTWELL	R. G. CHAPMAN
Florida, Univ. of, Gainesville, Fla.	1926	30	J. H. SINGER	R. E. MORLEY	R. A. THOMPSON
George Washington Univ., Washington, D.C.	1924	37	J. C. RITTER	R. L. FENTON	G. F. BUSH
Georgia School of Tech., Atlanta, Ga.	1915	88	T. R. VANDEN-HEUVEL	B. W. HASKELL	W. A. HINTON
Idaho, Univ. of, Moscow, Idaho	1925	46	N. L. FINCH	R. E. KENNEMER	H. F. GAUSS
Illinois Inst. of Tech., Chicago, Ill.	1940	179	RALPH JAHNKE	ALBERT WEGGER	J. S. KOZACKA
Illinois, Univ. of, Urbana, Ill.	1909	132	J. W. MCINTOSH	R. G. ESPY	D. G. RYAN
Iowa State College, Ames, Iowa	1919	69	T. B. ADAMS, JR.	PHIL GODDARD	D. L. ARM
Iowa, State Univ. of, Iowa City, Iowa	1913	22	DONALD ARGANBRIGHT	T. J. KINGSFORD	I. T. WETZEL
Johns Hopkins Univ., Baltimore, Md.	1917	42	W. H. THOMPSON	EDWARD VITEK	J. C. SMALLWOOD
Kansas State College, Manhattan, Kan.	1914	69	P. S. MYERS	J. M. BOWYER	WILSON TRIPP
Kansas, Univ. of, Lawrence, Kan.	1909	67	C. W. WALKER	E. J. LACROIX	R. S. TAIT
Kentucky, Univ. of, Lexington, Ky.	1911	23	T. C. JACKSON	M. C. RICE	C. C. JETT
Lafayette College, Easton, Pa.	1919	52	PETER PRUDDEN	JACK DONALDSON	W. G. MCLEAN
Lehigh Univ., Bethlehem, Pa.	1911	64	J. H. DUDLEY	T. M. BUCK	J. F. BAILEY
Louisiana State Univ., University, La.	1916	61	S. A. FUTRAL	R. H. TRULY	G. F. MATTHES
Louisville, Univ. of, Louisville, Ky.	1928	21	D. P. NEWHERN	E. K. HOLLOWAY	C. D. GREFFE
Maine, Univ. of, Orono, Maine	1910	65	R. F. GAY	D. B. HOPKINSON	I. H. PRAGEMAN
Marquette Univ., Milwaukee, Wis.	1923	19	R. K. LANGDON	W. F. SCHIER	J. G. WEBER
Maryland, Univ. of, College Park, Md.	1937	73	VAHL UNDERWOOD	FRED KOHLASS	W. P. GREEN
Massachusetts Inst. of Tech., Cambridge, Mass.	1909	78	S. J. FARRINGTON, JR.	H. R. O'HARA, JR.	ALVIN SLOANE
Michigan College of Min. & Tech., Houghton, Mich.	1930	62	R. G. G. PETAJA	G. A. HELLMAN	A. P. YOUNG
Michigan State College, E. Lansing, Mich.	1917	97	R. C. EDWARDS	W. C. DENT	J. M. CAMPBELL
Michigan, Univ. of, Ann Arbor, Mich.	1914	105	J. A. TEMPLER	GEORGE D. CAMERON	R. C. PORTER
Minnesota, Univ. of, Minneapolis, Minn.	1913	98	ROBERT WINTER	R. M. PETERSON	FULTON HOLTBY
Mississippi State College, State College, Miss.	1926	30	R. T. STATON, JR.	S. V. CRAFT	A. G. HOLMES

† As of December 15, 1941.

Name and Location	Year Authorized	No. of Members †	Chairman	Secretary	Honorary Chairman
Missouri School of Mines & Metallurgy, Rolla, Mo.	1930	46	C. T. Morris	R. F. Guilfoy	A. J. Miles
Missouri, Univ. of, Columbia, Mo.	1909	23	Harold Hilker	Richard Faucett	E. S. Gray
Montana State College, Bozeman, Mont.	1920	42	D. H. O'Brien	W. E. Cowles	R. T. Challender
Nebraska, Univ. of, Lincoln, Neb.	1909	70	C. E. Lee	F. J. Prochazka	J. K. Ludwickson
Nevada, Univ. of, Reno, Nev.	1928	9	J. W. Gross, Jr.	A. S. Weller	J. R. VanDyke
Newark College of Engineering, Newark, N.J.	1924	138	G. R. Fusner	Richard Hull	H. F. Ritterbusch
New Hampshire, Univ. of, Durham, N.H.	1926	41	Lester Rollins	William Clement	T. S. Kauppinen
New Mexico State College of A.&M. Arts, State College, New Mex.	1938	..	Edward Carmichael	C. F. Guillion, Jr.	A. M. Lukens
New Mexico, Univ. of, Albuquerque, New Mex.	1935	17	A. D. Ford, Jr.	Weston Mills	M. E. Farris
New York, College of the City of, New York, N.Y.	1922	77	Bernard Fishman	Martin Karp	S. J. Tracy
New York University, New York, N.Y.	1909				
Aeronautic Division	——	84	J. A. Arrighi	H. J. Studley	A. H. Church * F. K. Teichmann
Mechanical Division	——	49	Otto Reimer	Manten Kurutz	A. H. Church
New York Univ. Evening School, New York, N.Y.	1933	59	R. J. Seitz	Ralph Sloman	A. H. Church
North Carolina State College, Raleigh, N.C.	1920	67	J. B. Sibert	D. J. Hanse	F. C. Bragg
North Dakota Agricultural College, Fargo, N.D.	1929	23	J. R. Calhoun	Robert Perkins	R. M. Dolve
North Dakota, Univ. of, Grand Forks, N.D.	1923	16	G. G. Setterlund	J. H. Disher	A. J. Diakoff
Northeastern Univ., Boston, Mass.	1922	77	R. H. Murray	H. F. Morrow	A. E. Whittaker
Northwestern Univ., Evanston, Ill.	1935	15	L. V. Sloma	C. E. Spanjer	B. H. Jennings
Notre Dame, Univ. of, Notre Dame, Ind.	1929	34	John Gilbert	Edward Buenger	C. R. Egry
Ohio Northern Univ., Ada, Ohio	1922	17	H. M. Parks	H. A. Moon	J. A. Needy
Ohio State Univ., Columbus, Ohio	1911	59	R. W. Biser	Elizabeth Izant	Paul Bucher
Oklahoma A.&M. College, Stillwater, Okla.	1921	29	George Graff	Leigh McCaslin	C. M. Leonard
Oklahoma, Univ. of, Norman, Okla.	1917	102	J. R. Lesch	F. L. Spencer	L. H. Cherry
Oregon State Agricultural College, Corvallis, Ore.	1909	58	F. R. Young	F. L. Yoakum	A. D. Hughes
Pennsylvania State College, State College, Pa.	1909	67	W. G. Barger	R. S. Mucha	C. L. Allen
Pennsylvania, Univ. of, Philadelphia, Pa.	1925	57	R. T. Vogdes, Jr.	John Lundelius	August Ulmann, Jr.
Pittsburgh, Univ. of, Pittsburgh, Pa.	1917	45	C. C. Yates	Walter Logan, Jr.	T. G. Beckwith
Polytechnic Inst. of Brooklyn, Brooklyn, N.Y.	1909				
Day Division	——	53	J. G. Howard	C. F. Hefner	A. T. Kniffen
Polytechnic Inst. of Brooklyn Evening School, Brooklyn, N.Y.	1909	46	John Alico	Lucian Nogawski	A. T. Kniffen
Pratt Inst., Brooklyn, N.Y.	1923	109	F. E. Colgan	Alex Cherniachovsky	John Hunter
Princeton Univ., Princeton, N.J.	1926	29	S. W. Pach	H. Van Brewer	K. H. Condit
Puerto Rico, Univ. of, Mayaguez, P.R.	1923	26	E. Y. Acha	Fernando Sosa	Arturo Davila
Purdue Univ., W. Lafayette, Ind.	1909	234	D. A. Utley	K. W. Shaw	H. A. Bolz
Queen's College, Kingston, Ont., Can.	1941	..	.....	.....	W. A. Wolfe
Rensselaer Polytechnic Inst., Troy, N.Y.	1910	73	W. C. Osborne	D. H. Brown	H. A. Wilson
Rhode Island State College, Kingston, R.I.	1930	31	R. A. Houghton	Frank Nascenzi	E. L. Carpenter
Rice Inst., Houston, Tex.	1926	59	J. F. Dillard, Jr.	R. R. Bloss, Jr.	J. H. Pound
Rose Polytechnic Inst., Terre Haute, Ind.	1926	37	A. D. Owens	G. F. McConnell	I. P. Hooper
Rutgers Univ., New Brunswick, N.J.	1920	47	L. M. Zibko	T. A. Pierce	C. Carmichael
Santa Clara, Univ. of, Santa Clara, Calif.	1925	16	Bernard Bannan	George Sharp	H. C. Ames
South Dakota State College, Brookings, S.D.	1935	24	Thomas Grove	Paul Engelbretson	L. L. Amidon
Southern California, Univ. of, Los Angeles, Calif.	1929	50	James Nelson	Joseph McGowan	W. H. Shallenberger
Southern Methodist Univ., Dallas, Tex.	1933	25	Glyn Beesley	Robert Campbell	C. A. Shumaker
Stanford Univ., Stanford University, Calif.	1909	34	T. V. Jones	Harold Clyman	A. L. London
Stevens Inst. of Tech., Hoboken, N.J.	1908	74	R. S. Seybolt	J. S. Adkins	E. H. Fezandie
Swarthmore College, Swarthmore, Pa.	1921	29	C. W. Beck	D. S. Way	G. B. Thom
Syracuse Univ., Syracuse, N.Y.	1912	25	W. R. Bahn	H. S. Jones, Jr.	S. T. Hart
Tennessee, Univ. of, Knoxville, Tenn.	1923	30	D. E. Freeman	E. B. Russell	J. M. Tucker
Texas, A.&M. College of, College Station, Tex.	1921	182	E. R. Clark	T. J. Bolling, Jr.	V. M. Faires
Texas Technological College, Lubbock, Tex.	1930	44	Wesley Powell	Floyd Williams, Jr.	H. L. Kipp
Texas, Univ. of, Austin, Tex.	1921	86	Rudolph Guenzel	J. P. Wier	R. A. Bacon
Toronto, Univ. of, Toronto, Ont., Can.	1933	89	D. G. Huber	D. W. Knowles	G. R. Lord
Tufts College, Tufts College, Mass.	1917	50	Leonard Dozier	Richard Coar	D. A. Fisher
Tulane Univ. of Louisiana, New Orleans, La.	1933	38	A. A. Grant, Jr.	G. H. Menefee	N. L. Buck
U.S. Naval Academy, Postgraduate School, Annapolis, Md.	1925	..	.....	.....	P. I. Kiefer
Utah, Univ. of, Salt Lake City, Utah	1923	30	W. R. Mathews	L. G. Bywater	M. B. Hogan
Vanderbilt Univ., Nashville, Tenn.	1928	24	John Hutton	Syd Hailey, Jr.	Sidney E. Acker
Vermont, Univ. of, Burlington, Vt.	1922	20	W. L. Potter	John Williams	H. L. Daasch
Villanova College, Villanova, Pa.	1925	45	V. J. A. Gordon	T. J. DeSipin	K. J. Moser
Virginia Polytechnic Inst., Blacksburg, Va.	1915	66	J. G. Evans	B. W. Cunningham	A. E. Bock
Virginia, Univ. of, University, Va.	1923	31	J. P. March	David Guinter	A. F. Macconochie
Washington, State College of, Pullman, Wash.	1920	39	Norman Omodt	Arthur Tanasse	F. W. Candee
Washington Univ., St. Louis, Mo.	1911	39	Wilbert Jankowitz	N. H. Zimmerman	Herbert Kuenzel
Washington, Univ. of, Seattle, Wash.	1917	37	Gordon Sadick	H. W. Copenhagen	L. B. Cooper
West Virginia Univ., Morgantown, W. Va.	1922	22	J. M. Poindexter	Bill Downs	L. D. Hayes
Wisconsin, Univ. of, Madison, Wis.	1909	41	E. A. Meier, Jr.	F. E. Graper	B. G. Elliot
Worcester Polytechnic Inst., Worcester, Mass.	1914	99	P. P. Holz	R. G. Fritch	L. J. Hooper
Wyoming, Univ. of, Laramie, Wyo.	1925	37	G. T. Arkoosh	A. J. Castagne	C. E. Anderson
Yale Univ., New Haven, Conn	1910	45	L. G. Aust	R. I. Bonsal	S. W. Dudley

† As of December 15, 1941. * Faculty Adviser.

RESEARCH COMMITTEES

ARTICLE B6A, PAR. 24: The Standing Committee on Research shall, under the direction of the Council, have supervision of the research activities of the Society.

The first Standing Committee on Research was organized in 1909.

STANDING COMMITTEE

W. TRINKS, *Chairman* (1942)
M. D. HERSEY (1943)
HERMAN WEISBERG (1944)
W. R. ELSEY (1945)
J. F. D. SMITH (1946)

LUBRICATION

Appointed October, 1915, to investigate the fundamental problems of lubrication, to formulate results of investigations previously made, and to keep in touch with contemporary research in this field

(Reorganized May, 1936)

G. B. KARELITZ, *Chairman*
S. J. NEEDS, *Secretary*
A. L. BEALL
OSCAR BRIDGEMAN
W. E. CAMPBELL
H. A. EVERETT
A. E. FLOWERS
J. C. GENIESSE
RAYMOND HASKELL
M. D. HERSEY
B. F. HUNTER
C. M. LARSON
F. C. LINN
G. L. NEELY
B. L. NEWKIRK
E. S. PEARCE
ERNEST WOOLER

FLUID METERS

Appointed 1916 to develop the theory of fluid meters of all kinds and to report on the best methods for their installation and use

(Reorganized July, 1926)

R. J. S. PIGOTT, *Chairman*
J. R. CARLTON, *Secretary*
H. S. BEAN
S. R. BEITLER
R. K. BLANCHARD
B. O. BUCKLAND
LOUIS GESS
E. W. JACOBSON
A. J. KERR
T. H. KERR
M. P. O'BRIEN
W. S. PARDOE
L. K. SPINK
R. E. SPRENKLE
E. C. M. STAHL
T. R. WEYMOUTH
M. J. ZUCROW

THERMAL PROPERTIES OF STEAM

Appointed in December, 1921, to direct research on the thermal properties of water-vapor and steam from 0 C to the upper limits of temperature and pressure

(Reorganized April, 1929)

W. L. ABBOTT, *Vice-Chairman*
H. N. DAVIS
H. C. DICKINSON
A. M. GREENE, JR.
R. C. H. HECK
D. S. JACOBUS
MAX JAKOB
J. H. KEENAN
F. G. KEYES
L. S. MARKS
GEO. A. ORROK
R. J. S. PIGOTT
E. L. ROBINSON

STRENGTH OF GEAR TEETH

Appointed in December, 1921, to investigate factors affecting the strength and life of gear teeth

R. E. FLANDERS, *Chairman*
C. H. LOGUE, *Secretary*
EARLE BUCKINGHAM
A. M. GREENE, JR.
C. W. HAM
F. E. McMULLEN
E. W. MILLER
ERNEST WILDHABER

CUTTING OF METALS

Appointed in September, 1923, to study the problems of metal cutting, including tool materials, tool design, lubrication, cooling, and speeds and feeds

M. F. JUDKINS, *Chairman*
L. N. GULICK, *Secretary*
L. P. ALFORD *
O. W. BOSTON
R. C. DEALE
A. L. DELEEUW
C. M. THOMPSON, JR.

MECHANICAL SPRINGS

Appointed May, 1924, to determine the status of the mechanical-spring art, to promote and conduct necessary and adequate research, and to develop the art to the point of standardization

J. R. TOWNSEND, *Chairman*
C. T. EDGERTON, *Secretary*
R. W. COOK
W. T. DONKIN
RUPEN EKSERGIAN
G. E. HANSEN
BENJAMIN LIEBOWITZ
DAVID LOFTS
R. D. BRIZZOLARA (*Alternate*)
D. J. McADAM, JR.
L. C. PESKIN
R. E. PETERSON
J. W. ROCKEFELLER, JR.
B. W. ST. CLAIR
M. F. SAYRE
T. R. WEBER
KEITH WILLIAMS
J. K. WOOD
F. P. ZIMMERLI

ELEVATORS

Appointed June, 1924, to study the function and operation of elevator safeties and buffers and their associated mechanisms and to develop methods of test for the approval of elevator safety devices

(Reorganized August, 1940)

D. J. PURINTON, *Chairman*
D. L. LINDQUIST, *Vice-Chairman*
G. H. REPPERT (*Alternate*)
J. A. DICKINSON, *Secretary*
S. W. JONES, *Ex-officio*
E. M. BOUTON
E. B. DAWSON (*Alternate*)
K. A. COLAHAN
G. P. KEOGH
F. PAVLICEK (*Alternate*)
J. J. MATSON
M. B. McLAUTHLIN
C. R. CALLAWAY (*Alternate*)
W. S. PAINE
J. L. KEANE (*Alternate*)
C. A. PETERS, JR.

EFFECT OF TEMPERATURE ON THE PROPERTIES OF METALS

Appointed December, 1924, as a joint research committee of the A.S.T.M. and the A.S.M.E. to encourage the investigation and accumulation of data on the properties of metals used in the mechanic arts at extremely high and low temperatures

N. L. MOCHEL, *Chairman*
H. J. KERR, *Vice-Chairman*
J. W. BOLTON, *Secretary*
R. H. ABORN
W. H. ARMACOST
A. B. BAGSAR
A. D. BAILEY
F. E. BASH
C. L. CLARK
E. S. DIXON
F. B. FOLEY
J. R. FREEMAN, JR.
H. J. FRENCH
H. W. GILLETT
A. J. HERZIG
G. F. JENKS
J. J. KANTER
C. E. MACQUIGG
E. L. ROBINSON
A. E. WHITE
J. S. WORTH
Director, National Bureau of Standards, U.S. Department of Commerce
Representative of Bureau of Ships, U.S. Navy Department

BOILER FEEDWATER STUDIES

Appointed March, 1925, as a Joint Research Committee of the American Boiler Manufacturers Association, American Railway Engineering Association, American Water Works Association, Edison Electric Institute, the American Society for Testing Materials, and the A.S.M.E. to study methods of analysis and treatment of boiler feedwater for stationary and railroad practice

EXECUTIVE COMMITTEE (Total personnel 41)

C. H. FELLOWS, *Chairman*
R. C. BARDWELL, *Vice-Chairman*
J. B. ROMER, *Secretary*
A. G. CHRISTIE **
R. E. COUGHLIN
B. W. DE GEER
MAX HECHT
H. E. JORDAN
P. B. PLACE
S. T. POWELL
F. N. SPELLER
M. F. STACK

* Deceased, January 2, 1942.
** Official A.S.M.E. representative serving on this committee.

BOILER FEEDWATER STUDIES

(Continued)

G. E. TATE
E. H. TENNEY
A. E. WHITE *

CONDENSER TUBES

Appointed May, 1925, to investigate and report on the causes of failure of tubes used in steam condensers and similar heat interchange apparatus

A. E. WHITE, *Chairman*
D. C. WEEKS, *Vice-Chairman*
P. A. BANCELL
R. A. BOWMAN
D. K. CRAMPTON
C. A. CRAWFORD
H. M. CUSHING
R. E. DILLON
J. R. FREEMAN, JR.
V. M. FROST
C. F. HARWOOD
G. C. HOLDER
W. C. HOLMES
W. B. PRICE
J. S. RODGERS
M. F. STACK
W. R. WEBSTER
Director, Bureau of Ships, U.S. Navy Department

WORM GEARS

Appointed May, 1927, to investigate certain problems in connection with the action of worm gear drives and to recommend improvements in their design, manufacture, and use

EARLE BUCKINGHAM, *Chairman*
G. H. ACKER
L. R. BUCKENDALE
D. L. LINDQUIST
A. A. ROSS
B. F. WATERMAN
Representative of Bureau of Ships, U.S. Navy Department

STRENGTH OF VESSELS UNDER EXTERNAL PRESSURE

Appointed June, 1929, to develop reliable design data on the strength of cylindrical and spherical surfaces under external pressure, particularly with reference to jacketed vessels

F. V. HARTMAN, *Chairman*
W. D. HALSEY
M. B. HIGGINS
A. W. LIMONT, JR.
H. E. SAUNDERS
E. E. SHANOR
D. B. WESSTROM
F. S. G. WILLIAMS
D. F. WINDENBURG

WIRE ROPE

Appointed April, 1930, to investigate existing rope so that it may be better understood and more effectively used

W. H. FULWEILER, *Chairman*
H. LER. BRINK
D. L. LINDQUIST
G. W. MARTIN
A. H. MCDOUGALL
B. V. E. NORDBERG
W. S. PAINE
W. J. RYAN
GEORGE SIMPSON
L. E. YOUNG

* Official A.S.M.E. representative serving on this committee.

CRITICAL PRESSURE STEAM BOILERS

Appointed June, 1931, to study the characteristics of high-pressure forced-circulation steam-generating units

H. L. SOLBERG, *Chairman*
W. H. ARMACOST
A. D. BAILEY
E. G. BAILEY
F. S. CLARK
C. H. FELLOWS
H. J. KERR
G. A. OREOK
E. C. PETRIE
E. L. ROBINSON
P. W. THOMPSON

COTTONSEED PROCESSING

Appointed December, 1932, to study the mechanical problems involved in storing, conditioning, and cooking cottonseed meats

W. R. WOOLRICH, *Chairman*
HOMER BARNES
C. E. GARNER
J. F. LEAHY
R. W. MORTON
B. J. SAMS
R. B. TAYLOR

ROLLING OF STEEL (PLASTICITY)

Appointed October, 1938, to study plasticity in the particular field of rolling of steel

A. NADAI, *Chairman*
C. W. MACGREGOR, *Secretary*
E. C. BAIN
C. L. EKSERGIAN
J. H. HITCHCOCK
G. B. KARELITZ
MORRIS STONE
W. TRINKS

FURNACE PERFORMANCE FACTORS

Appointed in October, 1941, to collect and rationalize data on the performance of commercially important furnaces as an aid to design and operation

A. R. MUMFORD, *Chairman*
ALEX D. BAILEY
JOHN BLIZARD
S. P. BURKE
O. F. CAMPBELL
W. A. CARTER
B. J. CROSS
T. B. DREW
F. G. ELY
A. C. FIELDNER
J. H. HARLOW
H. C. HOTTEL
E. L. LINDSETH
W. H. MCADAMS
PERCY NICHOLLS
E. B. POWELL
A. A. RAYMOND
R. A. SHERMAN
PHILIP SPORN
HERMAN WEISBERG
W. J. WOHLENBERG

FORGING OF STEEL SHELLS

Appointed in October, 1941, to study methods of shell manufacture under modern conditions

M. D. STONE, *Chairman*
W. TRINKS, *Vice-Chairman*
JOHN DIERBECK
D. W. FLETCHER
W. M. FRAME
W. N. HOWLEY
A. F. MACCONOCHIE
F. C. MACDONALD
A. NADAI
GEORGE SACHS
A. E. VAN CLEVE
U. S. Army, Ordnance Department:
LT.-COL. H. U. WAGNER
MAJOR J. H. FRYE
MAJOR R. M. WOOD
U. S. Navy, Bureau of Ordnance:
LT.-COM. A. H. BATEMAN

A.S.M.E. Representatives on Other Research Committees

See also A.S.M.E. Representatives on Other Activities, page RI-5

AMERICAN COORDINATING COMMITTEE ON CORROSION

American Society for Testing Materials

S. L. KERR
C. H. FELLOWS (*Alternate*)

CORROSION COMMITTEE

American Society of Refrigerating Engineers

(To be appointed)

FATIGUE PHENOMENA OF METALS

American Society for Testing Materials

C. T. EDGERTON

HEAT-TREATMENT OF ROCK DRILL STEELS

Advisory Board of the National Bureau of Standards and Bureau of Mines

(To be appointed)

METALLURGICAL RESEARCH

Advisory Committee to the National Bureau of Standards

C. H. BIERBAUM

PROPERTIES OF REFRACTORY MATERIALS

Advisory Committee to the National Bureau of Standards

E. B. POWELL

WATER FOR INDUSTRIAL USES

American Society for Testing Materials

J. H. WALKER

STANDARDIZATION COMMITTEES

ARTICLE B6A, PAR. 23: The Standing Committee on Standardization shall advise the Council on the dimensional standardization work of the Society, including relations with the American Standards Association.

The first Standing Committee on Standardization was organized in April, 1911

STANDING COMMITTEE

J. E. LOVELY, *Chairman* (1942)
L. T. KNOCKE (1943)
T. E. FRENCH (1944)
W. H. HILL (1945)
J. H. TAYLOR (1946)

STANDARDIZATION AND UNIFICATION OF SCREW THREADS (B1)

* *Joint sponsorship with the Society of Automotive Engineers. Sectional Committee originally organized in June, 1921. Reorganized in February, 1929*

A.S.M.E. Members (Total personnel, 36)

R. E. FLANDERS, *Chairman* †
A. M. HOUSER, *Vice-Chairman* †
EARLE BUCKINGHAM, *Secretary*
E. J. BRYANT
G. S. CASE
T. G. CRAWFORD
H. C. E. MEYER
P. V. MILLER †
W. C. MUELLER
R. H. PERRY
G. T. TRUNDLE

SUBCOMMITTEE CHAIRMEN

Special Subcommittee on Revision of American Standard, P. V. MILLER
No. 1 on Scope, Arrangement, and Editing of American National Standard, R. E. FLANDERS
No. 4 on Acme and Other Similar Threads, Except Gages, EARLE BUCKINGHAM
No. 5 on Screw Thread Gages and Inspection, G. S. CASE
No. 6 on Threading of General Purpose Nuts, J. S. DAVEY
No. 7 on Screw Threads for High Temperature Bolting, W. H. GOURLIE

PIPE THREADS (B2)

* *Joint sponsorship with the American Gas Association. Sectional Committee originally organized in 1913. Reorganized May, 1927*

A.S.M.E. Members (Total personnel, 45)

A. S. MILLER, *Chairman*
C. B. LEPAGE, *Acting Secretary*
A. F. BREITENSTEIN †
E. J. BRYANT
C. S. COLE
E. S. CORNELL, JR.
J. J. CROTTY
A. P. DENTON
J. J. HARMAN
A. M. HOUSER †
P. V. MILLER †
F. H. MOREHEAD
W. C. MORRIS
S. F. NEWMAN
L. N. SHANNON
FRANK THORNTON, JR.
J. H. WILLIAMS

SUBCOMMITTEE CHAIRMEN

No. 1 on Editing and Gaging, A. M. HOUSER
No. 2 on Taper Pipe Threads, S. B. TERRY
No. 3 on Straight Pipe Threads, A. S. MILLER
No. 4 on Plumbers' Threads, A. F. BREITENSTEIN
No. 5 on Screw Threads for Rigid Steel Conduit, JAMES BARTON
No. 6 on Special Threads for Thin Tubes, C. C. WINTER
Special Subcommittee on Tolerances on Thread Elements, E. J. BRYANT
Special Editing Subcommittee on Taper Pipe Threads, S. B. TERRY
Special Editing Subcommittee on Straight Pipe Threads, P. V. MILLER
Special Subcommittee on Truncation, E. J. BRYANT

BALL AND ROLLER BEARINGS (B3)

* *Joint sponsorship with the Society of Automotive Engineers. Sectional Committee organized December, 1920*

A.S.M.E. Members (Total personnel, 20)

W. P. KENNEDY, *Vice-Chairman* †
D. E. BATESOLE †
L. A. CUMMINGS
O. H. DORER
F. G. HUGHES
G. E. HULSE †
W. L. ILIFF †
L. F. NENNINGER
S. M. WECKSTEIN †
ERNEST WOOLER

ALLOWANCES AND TOLERANCES FOR CYLINDRICAL PARTS AND LIMIT GAGES (B4)

* *Sole sponsorship. Sectional Committee originally organized in June, 1920. Reorganized in September, 1930*

A.S.M.E. Members (Total personnel, 40)

J. E. LOVELY, *Chairman* †
F. E. BANFIELD, JR.
F. S. BLACKALL, JR.
E. J. BRYANT
EARLE BUCKINGHAM †
F. H. COLVIN †
T. G. CRAWFORD
R. E. W. HARRISON
F. O. HOAGLAND
N. E. JACOBI
H. C. E. MEYER
P. V. MILLER
W. C. MUELLER
E. C. PECK †
R. H. PERRY
W. C. SCHOENFELDT
C. C. STEVENS
G. T. TRUNDLE

SUBCOMMITTEE CHAIRMAN

No. 1 on Tolerance Systems, R. E. W. HARRISON

SMALL TOOLS AND MACHINE TOOL ELEMENTS (B5)

* *Joint sponsorship with the National Machine Tool Builders' Association, and the Society of Automotive Engineers. Sectional Committee organized September, 1922*

A.S.M.E. Members (Total personnel, 33)

W. C. MUELLER, *Chairman* †
F. O. HOAGLAND, *Vice-Chairman*
J. B. ARMITAGE
O. W. BOSTON
E. J. BRYANT
EARLE BUCKINGHAM
F. H. COLVIN †
S. A. EINSTEIN
H. E. HARRIS †
JOHN HAYDOCK
J. P. LAUX †
J. E. LOVELY
A. F. MURRAY †
ERIK OBERG
FRANK THORNTON, JR.

TECHNICAL COMMITTEES

EXECUTIVE COMMITTEE

A.S.M.E. Members (Total personnel, 5)

W. C. MUELLER, *Chairman* †
F. O. HOAGLAND, *Vice-Chairman*
H. E. HARRIS †

No. 1 ON T-SLOTS

A.S.M.E. Members (Total personnel, 6)

ERIK OBERG, *Chairman*
J. B. ARMITAGE
HARRY CADWALLADER, JR.
S. A. EINSTEIN
F. O. HOAGLAND

No. 2 ON TOOL-POSTS AND TOOL SHANKS

A.S.M.E. Members (Total personnel, 8)

O. W. BOSTON, *Chairman*
F. S. BLACKALL, JR.
GRANGER DAVENPORT
M. E. LANGE

No. 3 ON MACHINE TAPERS

A.S.M.E. Members (Total personnel, 21)

E. J. BRYANT, *Chairman*
C. B. LEPAGE, *Acting Secretary*
J. B. ARMITAGE
F. S. BLACKALL, JR.
EARLE BUCKINGHAM
F. H. COLVIN †
J. B. DILLARD
(T. F. GITHENS, *Alternate*)
B. P. GRAVES
H. E. HARRIS †
F. O. HOAGLAND
J. H. HORIGAN
L. F. NENNINGER

SUBGROUP CHAIRMEN

Steep Tapers Series, S. MCMULLAN
Revision on Slow Taper Standard, E. J. BRYANT

* Note: All of these standards committees for which the Society is sponsor or joint sponsor, or on which it has representation, are organized under the procedure of the American Standards Association.

† Official A.S.M.E. representative serving on this committee.

SMALL TOOLS AND MACHINE TOOL ELEMENTS (B5)

(Continued)

No. 4 on Spindle Noses and Collets for Machine Tools

A.S.M.E. Members (Total personnel, 26)

J. E. Lovely, *Chairman*
L. F. Nenninger, *Secretary*
J. B. Armitage
B. P. Graves
F. O. Hoagland
A. M. Johnson
M. E. Lange
J. H. Mansfield
L. D. Spence

SUBGROUP CHAIRMEN

No. 1 on Milling Machines, Small and Medium, J. B. Armitage
No. 2 on Large Milling Machines, F. B. Kampmeier
No. 3 on Grinding Machine Spindles, H. J. Griffing
No. 5 on Drilling Machines and Horizontal Boring Machines, S. McMullan
No. 6 on Turning Machines, Including Automatic Screw Machines, Lathes, Automatic Lathes, Turret Lathes, and Automatic Chucking Machines, J. E. Lovely
No. 8 on Correlation of Counter Proposals for Spindle Noses, J. E. Lovely

No. 5 on Milling Cutters

A.S.M.E. Members (Total personnel, 20)

J. B. Armitage
A. N. Goddard
J. H. Horigan
G. L. Markland, Jr.
E. K. Morgan
Erik Oberg
E. D. Vancil

SUBGROUP CHAIRMEN

No. 1 on Profile Cutters, E. D. Vancil
No. 2 on Keyways, J. B. Armitage
No. 3 on Nomenclature, A. C. Danekind
No. 4 on Limits, J. H. Horigan
No. 5 on Formed Cutters, H. C. Hungerford
No. 6 on Hobs, G. L. Markland, Jr.
No. 7 on Inserted Tooth Cutters, J. B. Armitage

No. 6 on Designations and Working Ranges of Machine Tools

A.S.M.E. Members (Total personnel, 19)

John Haydock, *Chairman*
Earle Buckingham
T. H. Doan, Jr.
B. P. Graves
J. J. McBride
E. R. Smith

No. 7 on Twist Drill Sizes

A.S.M.E. Members (Total personnel, 6)

W. C. Mueller, *Chairman* †
J. H. Horigan

No. 8 on Jig Bushings

A.S.M.E. Member (Total personnel, 8)

J. H. Horigan

SUBGROUP CHAIRMEN

Subgroup on Liner Outer Diameters and Tolerances (to be appointed)

No. 9 on Punch Press Tools

A.S.M.E. Members (Total personnel, 15)

D. H. Chason
N. W. Dorman
E. W. Ernest
H. E. Harris †
D. M. Palmer

No. 10 on Forming Tools and Holders

A.S.M.E. Members (Total personnel, 10)

W. C. Mueller, *Chairman* †
L. D. Spence

No. 11 on Chucks and Chuck Jaws

A.S.M.E. Member (Total personnel, 10)

J. E. Lovely, *Chairman*

SUBGROUP CHAIRMEN

No. 1 on Master Chuck Jaws, J. E. Lovely
No. 2 on Adapters for Air Cylinders, J. E. Lovely

No. 12 on Cut and Ground Thread Taps

(Total personnel, 7)

No. 13 on Splines and Splined Shafts

A.S.M.E. Members (Total personnel, 15)

J. B. Armitage
R. E. W. Harrison
F. O. Hoagland
J. E. Lovely

No. 17 on Nomenclature for Small Tools and Machine Tool Elements

A.S.M.E. Members (Total personnel, 12)

O. W. Boston, *Chairman and Secretary*
F. S. Blackall, Jr.
F. H. Colvin †
H. E. Harris †
F. O. Hoagland

Ex-Officio Members

A. N. Goddard
W. C. Mueller †

No. 19 on Single-Point Cutting Tools

A.S.M.E. Members (Total personnel, 2)

F. H. Colvin, *Chairman* †
O. W. Boston, *Secretary*

No. 20 on Reamers

A.S.M.E. Members (Total personnel, 16)

F. H. Colvin
T. F. Githens
J. H. Horigan
H. E. Wells

SUBGROUP CHAIRMAN

No. 1 on Reamer Proposal, C. M. Pond

No. 21 on Tool-Life Tests for Single-Point Tools

A.S.M.E. Members (Total Personnel, 11)

O. W. Boston, *Chairman*
M. F. Judkins

GEARS (B6)

** Joint sponsorship with the American Gear Manufacturers Association. Sectional Committee organized June, 1921*

A.S.M.E. Members (Total personnel, 27)

Earle Buckingham, *Vice-Chairman* †
C. B. LePage, *Acting Secretary*
G. H. Acker
U. S. Eberhardt
L. H. Fry
C. B. Hamilton, Jr.
D. T. Hamilton
M. R. Hanna
O. A. Leutwiler †
G. L. Markland, Jr.
Carleton Reynell

SUBCOMMITTEE CHAIRMEN

Executive Committee (to be appointed)
No. 1 on Program (to be appointed)
No. 2 on Editing Reports (to be appointed)
No. 3 on Nomenclature, D. T. Hamilton
No. 4 on Tooth Form (Spur Gears), U. S. Eberhardt
No. 5 on Helical Gears, W. P. Schmitter
No. 6 on Worm Gears, T. R. Rideout
No. 7 on Bevel Gears, F. L. Knowles
No. 8 on Materials, C. B. Hamilton, Jr.
No. 9 on Inspection, J. P. Breuer
No. 10 on Horsepower Rating, Earle Buckingham

PIPE FLANGES AND FITTINGS (B16)

** Joint sponsorship with the Heating, Piping and Air Conditioning Contractors National Association, and the Manufacturers Standardization Society of the Valve and Fittings Industry. Sectional Committee organized October, 1921*

A.S.M.E. Members (Total personnel, 50)

C. P. Bliss, *Chairman* †
J. J. Harman, *Secretary*
A. L. Baker
L. W. Benoit †
A. L. Brown
Sabin Crocker
Ferdinand Fink
V. M. Frost
H. E. Haller
J. S. Hess
H. A. Hoffer †
E. L. Hopping
A. M. Houser
C. A. Kelting †
J. R. Kruse (John Blizard, *Alternate*)
M. B. MacNeille
F. H. Morehead
L. S. Morse
Ludwig Skog
J. R. Tanner †
J. H. Taylor
Rowland Tompkins
G. W. Watts
J. H. Williams

SUBCOMMITTEE CHAIRMEN

Executive Committee, C. P. Bliss
No. 1 on Cast Iron Flanges and Flanged Fittings, A. M. Houser
No. 2 on Screwed Fittings, F. H. Morehead
No. 3 on Steel Flanges and Flanged Fittings, C. P. Bliss
No. 4 on Materials and Stresses, A. M. Houser
No. 5 on Face to Face Dimensions of Ferrous Flanged Valves, J. R. Tanner

PIPE FLANGES AND FITTINGS (B16)

(Continued)

No. 6 on Malleable Iron or Steel Brass Seat Unions (to be appointed)
No. 7 on Rating of Pipe Fittings (to be appointed)
No. 8 on Marking of Pipe Fittings, F. H. MORELAND
No. 9 on Port Openings (to be appointed)

SHAFTING (B17)

** Sole sponsorship. Organized October, 1918*

A.S.M.E. Members (Total personnel, 13)

C. M. CHAPMAN, *Chairman* †
C. B. LEPAGE, *Secretary*
H. C. E MEYER
L. C. MORROW
J. M. SHIMER
G. N. VAN DERHOEF †
L. W. WILLIAMS †

BOLT, NUT, AND RIVET PROPORTIONS (B18)

** Joint sponsorship with the Society of Automotive Engineers. Sectional Committee organized March, 1922*

A.S.M.E. Members (Total personnel, 55)

W. C. STEWART, *Secretary*
H. E. ALDRICH
F. C. BILLINGS
B. G. BRAINE
G. S. CASE
T. G. CRAWFORD
H. P. FREAR
A. M. HOUSER †
HERMAN KOESTER
S. F. NEWMAN
R. J. WHELAN
E. M. WHITING
V. R. WILLOUGHBY
(J. J. MCBRIDE, *Alternate*)

SUBCOMMITTEE CHAIRMEN

No. 1 on Large and Small Rivets (to be appointed)
No. 2 on Wrench-Head Bolts and Nuts (to be appointed)
No. 3 on Slotted Head Proportions (to be appointed)
No. 4 on Track Bolts and Nuts (to be appointed)
No. 5 on Round Unslotted Head Bolts (Carriage Bolts) (to be appointed)
No. 6 on Plow Bolts (to be appointed)
No. 7 on Body Dimensions and Materials (to be appointed)
No. 8 on Nomenclature, G. S. CASE
No. 9 on Socket Head Cap and Set Screws, HERMAN KOESTER

PLAIN AND LOCK WASHERS (B27)

** Joint sponsorship with the Society of Automotive Engineers. Sectional Committee organized August, 1925*

A.S.M.E. Members (Total personnel, 39)

EUGENE CALDWELL
T. G. CRAWFORD
B. S. LEWIS †
C. H. LOUTREL
J. J. MCBRIDE
H. C. E. MEYER
W. C. MUELLER †
E. M. WHITING †

SUBCOMMITTEE CHAIRMEN

No. 1 on Plain Washers, W. L. BARTH
No. 2 on Spring Washers, E. COWLIN

TRANSMISSION CHAINS AND SPROCKETS (B29)

** Joint sponsorship with the Society of Automotive Engineers, and the American Gear Manufacturers Association. Sectional Committee organized September, 1917. Reorganized December, 1926*

A.S.M.E. Members (Total personnel 13)

W. J. BELCHER
C. B. JAHNKE †
JOSEPH JOY
L. V. LUDY †
D. B. PERRY
C. R. WEISS
G. A. YOUNG

SUBCOMMITTEE CHAIRMEN

No. 1 on Roller Chain Standardization (to be appointed)
No. 2 on Silent Chain Standardization, G. A. YOUNG

CODE FOR PRESSURE PIPING (B31)

** Sole sponsorship. Sectional Committee organized March, 1926. Reorganized December, 1937*

A.S.M.E. Members (Total personnel, 101)

E. B. RICKETTS, *Chairman*
R. E. BRYANT
C. S. COLE
H. C. COOPER
D. H. COREY
SABIN CROCKER
H. D. EDWARDS
E. R. FISH
CHARLES FITZGERALD
V. M. FROST
T. W. GREENE
H. E. HALLER
W. D. HALSEY
J. S. HAUG
H. A. HOFFER
G. G. HOLLINS
E. L. HOPPING
A. M. HOUSER †
ALFRED IDDLES †
D. S. JACOBUS
T. M. JASPER
C. A. KELTING
E. H. KRIEG
G. SINDING-LARSON
M. B. MACNEILLE
G. W. MARTIN
H. C. E. MEYER
J. W. MOORE
(J. D. CAPRON, *Alternate*)
F. H. MOREHEAD
(J. J. HARMAN, *Alternate*)
H. H. MORGAN
L. S. MORSE, SR.
R. M. NEE
E. W. NORRIS
C. W. OBERT
GEO. A. ORROK
A. L. PENNIMAN, JR.
C. S. ROBINSON †
J. H. ROMANN
D. B. ROSSHEIM
G. W. SAATHOFF
G. K. SAURWEIN
LUDWIG SKOG
H. S. SMITH
(H. H. MOSS, *Alternate*)
J. R. TANNER
J. H. TAYLOR
J. H. VANCE
H. L. WHITTEMORE
J. H. WILLIAMS
T. F. WOLFE

SUBCOMMITTEE CHAIRMEN

No. 1 on Plan, Scope, and Editing, SABIN CROCKER
No. 2 on Power Piping, ALFRED IDDLES
No. 4 on Gas and Air Piping, J. S. HAUG
No. 5 on Refrigeration Piping, A. B. STICKNEY
No. 6 on Oil Piping, A. D. SANDERSON
No. 7 on Piping Materials and Identification, F. H. MOREHEAD
No. 8 on Fabrication Details, LUDWIG SKOG
No. 9 on District Heating Piping, G. K. SAURWEIN

Special Committee to confer with Boiler Code Subcommittee on Material Specifications, the M.S.S., the A.S.T.M. and Sectional Committee B31 and Sectional Committee B16 to coordinate the several specifications relating to piping, valves and fittings

WIRE AND SHEET METAL GAGES (B32)

** Joint sponsorship with the Society of Automotive Engineers. Sectional Committee organized November, 1928. Reorganized November, 1939*

A.S.M.E. Members (Total personnel, 35)

A. P. COTTLE
E. W. ERNEST
J. F. HOWE †
F. G. WILSON †

SUBCOMMITTEE CHAIRMAN

Wire and Sheet Metal Gages, H. W. TENNEY

SCREW THREADS FOR HOSE COUPLINGS (B33)

** Sole sponsorship. Sectional Committee organized August, 1928*

A.S.M.E. Members (Total personnel, 28)

A. L. BROWN, *Secretary*
A. F. BREITENSTEIN †
J. J. CROTTY
W. L. CURTISS
W. E. DUNHAM †
J. J. HARMAN
(F. C. ERNST, *Alternate*)
A. M. HOUSER
H. C. E. MEYER
J. H. WILLIAMS

SUBCOMMITTEE CHAIRMEN

Special Subcommittee to Draft Recommended Specifications (to be appointed)
Subcommittee on Basic Thread Dimensions, D. R. MILLER

WROUGHT IRON AND WROUGHT STEEL PIPE AND TUBING (B36)

** Joint sponsorship with the American Society for Testing Materials. Sectional Committee organized April, 1928*

A.S.M.E. Members (Total personnel, 44)

H. H. MORGAN, *Chairman*
SABIN CROCKER, *Secretary*
J. S. ADELSON
H. E. ALDRICH
NEWELL HAMILTON
E. L. HOPPING
(A. B. MORGAN, *Alternate*)

WROUGHT IRON AND WROUGHT STEEL PIPE AND TUBING (B36)

(Continued)

A. M. Houser †
D. S. Jacobus †
(F. S. Clark, *Alternate*) †
J. J. Kanter
H. C. E. Meyer
F. H. Morehead
H. B. Oatley †
Ludwig Skoog †
J. R. Tanner
A. E. White

SUBCOMMITTEE CHAIRMEN

No. 1 on Plan, Scope, and Editing, H. H. Morgan
No. 2 on Pipe and Tubing for Low Temperature Service, J. J. Shuman
No. 3 on Pipe and Tubing for High Temperature Service, J. R. Tanner
No. 4 on Materials, F. H. Morehead

PRESSURE AND VACUUM GAGES (B40)

** Sole sponsorship. Sectional Committee organized July, 1930*

A.S.M.E. Members (Total personnel, 44)

M. D. Engle, *Chairman*
A. W. Lenderoth, *Secretary* †
E. J. Bryant
J. P. Cavanaugh †
Paul Diserens
C. H. Graesser
W. F. Jones
R. J. Kehl
J. C. McCune †
A. H. Morgan
H. B. Reynolds
W. C. Schoenfeldt

SUBCOMMITTEE CHAIRMEN

No. 1 on Plan and Scope, M. D. Engle
No. 2 on Definitions, C. F. Schwep
No. 3 on Gage Sizes and Mounting Dimensions, H. B. Reynolds
No. 4 on Accuracy and Test Methods, O. J. Hodge

STOCK SIZES, SHAPES AND LENGTHS FOR HOT AND COLD FINISHED IRON AND STEEL BARS (B41)

** Sole sponsorship Sectional Committee organized June, 1930*

A.S.M.E. Members (Total personnel, 25)

F. H. Dechant
E. W. Ernest
H. D. Tanner
L. W. Williams †
G. H. Woodroffe

SUBCOMMITTEE CHAIRMEN

No. 1 on Hot Rolled Steel, Henry Wysor
No. 2 on Cold Finished Steels, L. E. Creighton
No. 3 on Hot Rolled Iron (to be appointed)

SPECIFICATIONS FOR LEATHER BELTING (B42)

** Sole sponsorship. Sectional Committee organized February, 1931*

A.S.M.E. Members (Total personnel, 24)

H. T. Coates
R. W. Drake †
W. E. Emley
King Hathaway
P. G. Rhoads
G. A. Schieren

SUBCOMMITTEE CHAIRMEN

No. 1 on Standard Specifications (to be appointed)
No. 2 on Recommendations for Selection, Care and Installation, G. A. Schieren

MACHINE PINS (B43)

** Joint sponsorship with the Society of Automotive Engineers, Sectional Committee organized March, 1926*

A.S.M.E. Members (Total personnel, 13)

E. J. Bryant †
J. J. McBride
H. C. E. Meyer

SUBCOMMITTEES

No. 1 on Straight, Taper and Dowel Pins (to be appointed)
No. 2 on Split Pins (to be appointed)

CLASSIFICATION AND DESIGNATION OF SURFACE QUALITIES (B46)

** Joint sponsorship with the Society of Automotive Engineers. Sectional Committee organized May, 1932*

A.S.M.E. Members (Total personnel, 63)

E. J. Abbott
E. J. Bryant
T. G. Crawford
R. C. Deale †
U. S. Eberhardt
S. A. Einstein
R. F. Gagg
W. W. Gilbert
J. J. Harman
R. E. W. Harrison †
F. V. Hartman
F. O. Hoagland
H. J. Holtzclaw
R. T. Kent
H. F. Kurtz
F. C. Spencer
C. C. Stevens
W. C. Stewart
J. S. Tawresey
C. H. Whitaker
Ernest Wooler

SUBCOMMITTEE CHAIRMEN

Executive Committee (to be appointed)
No. 2 on Surfaces Produced by Molds, Dies, Rolls, or Any Other Means of Deforming Materials (to be appointed)
No. 3 on Coated Surfaces, G. B. Hogaboom
No. 4 on Symbols for Indicating Surface Quality on Drawings, T. G. Crawford
No. 5 on Ways, Means and Apparatus for Measuring Quality of Surface (to be appointed)
No. 7 on Standards for Appearance of Surfaces (to be appointed)

COMBUSTION SPACE FOR SOLID FUELS (B50)

** Sole sponsorship. Sectional Committee organized June, 1933*

A.S.M.E. Members (Total personnel, 21)

C. E. Bronson, *Chairman*
W. G. Christy
John Hunter
A. J. Johnson
V. G. Leach †
J. P. Magos
J. F. McIntire
F. L. Meyer
C. A. Reed
John Van Brunt †

SUBCOMMITTEE CHAIRMEN

No. 1 on Purpose and Scope, C. E. Bronson
No. 2 on Combustion and Design, B. M. Guthrie
No. 3 on Warm Air Furnaces, J. H. Manny
No. 4 on Steel Heating Boilers, W. B. Russell
No. 5. on Cast Iron Boilers, J. F. McIntire

SCHEME FOR IDENTIFICATION OF PIPING SYSTEMS (A13)

** Joint sponsorship with the National Safety Council. Sectional Committee organized June, 1922*

A.S.M.E. Members (Total personnel, 35)

E. E. Ashley
W. L. Bunker
Crosby Field
E. L. Hopping
H. L. Miner
H. S. Smith
Frank Thornton, Jr.
Frank Umbehocker †

SUBCOMMITTEE CHAIRMEN

Executive Committee, A. S. Hebble
Identification by Colors (to be appointed)
Classification, Crosby Field
Identification Markings Other Than Color (to be appointed)
Editing Subcommittee, A. S. Hebble

MINIMUM REQUIREMENTS FOR PLUMBING AND STANDARDIZATION OF PLUMBING EQUIPMENT (A40)

** Sole sponsorship. Sectional Committee organized August, 1928*

A.S.M.E. Members (Total personnel, 52)

C. B. LePage, *Acting Secretary*
J. F. Carney, *Alternate*
C. S. Cole
A. M. Houser
G. W. Martin
(A. H. Morgan, *Alternate*)
W. K. McAfee
Thorndike Saville †
W. R. Webster †

SUBCOMMITTEE CHAIRMEN

Research Committee on Plumbing (to be appointed)
No. 1 on Minimum Requirements for Plumbing, T. I. Coe
No. 2 on Staple Vitreous China Plumbing Fixtures, H. R. Van Sciver
No. 3 on Staple Porcelain (All Clay) Plumbing Equipment, H. R. Van Sciver
No. 4 on Enameled Sanitary Ware, A. H. Cline, Jr.
No. 5 on Traps, A. R. McGonegal
No. 6 on Brass Plumbing Products (to be appointed)
No. 7 on Brass Fittings for Flared Copper Tubes, F. L. Riggin
No. 8 on Cast Iron Soil Pipe and Fittings (to be appointed)

MINIMUM REQUIREMENTS FOR PLUMBING AND STANDARDIZATION OF PLUMBING EQUIPMENT (A40)

(Continued)

No. 9 on Gasoline, Oil and Grease Separators (to be appointed)
Joint Committee on Threaded Cast Iron Pipe, F. H. MOREHEAD
No. 11 on Soldered Fittings for Tubing, A. M. HOUSER
No. 12 on Minimum Air Gaps in Plumbing Systems, W. K. MCAFEE

ROLLED THREADS FOR SCREW SHELLS OF ELECTRIC SOCKETS AND LAMP BASES (C44)

** Joint sponsorship with the National Electrical Manufacturers Association. Sectional Committee organized March, 1929*

A.S.M.E. Members (Total personnel, 16)

E. J. BRYANT †
EARLE BUCKINGHAM †
A. B. MORGAN
E. S. SANDERSON †

LETTER SYMBOLS AND ABBREVIATIONS FOR SCIENCE AND ENGINEERING (Z10)

** Joint sponsorship with the American Association for the Advancement of Science, American Institute of Electrical Engineers, American Society of Civil Engineers, and the Society for the Promotion of Engineering Education. Sectional Committee organized January, 1926. Reorganized October, 1935*

A.S.M.E. Members (Total personnel, 43)

S. A. MOSS, *Vice-Chairman* †
K. H. CONDIT
R. J. S. PIGOTT †
(S. R. BEITLER, *Alternate*) †
FRANK THORNTON, JR.
E. P. WARNER

SUBCOMMITTEE CHAIRMEN

Executive Committee, H. M. TURNER
Steering Committee, H. M. TURNER
No. 1 on Letter Symbols and Signs for Mathematics, A. A. BENNETT
No. 2 on Symbols for Hydraulics, J. C. STEVENS
No. 3 on Symbols for Mechanics, R. E. PETERSON
No. 4 on Symbols for Structural Analysis, ALBERT HAERTLEIN
No. 5 on Symbols for Heat and Thermodynamics, S. A. Moss
No. 6 on Symbols for Photometry, E. C. CRITTENDEN
No. 7 on Aeronautical Symbols, G. W. LEWIS
No. 8 on Symbols for Electric and Magnetic Quantities (to be appointed)
No. 9 on Symbols for Radio, H. M. TURNER
No. 10 on Symbols for Physics, H. K. HUGHES
No. 11 on Abbreviations for Engineering and Scientific Terms, G. A. STETSON

DRAWINGS AND DRAFTING ROOM PRACTICE (Z14)

** Joint sponsorship with the Society for the Promotion of Engineering Education. Sectional Committee organized July, 1926*

A.S.M.E. Members (Total personnel, 51)

T. E. FRENCH, *Chairman*
H. P. FREAR
F. DER. FURMAN
A. C. HARPER
E. R. HILL
A. M. HOUSER
ALFRED IDDLES
SAMUEL KETCHUM †
C. W. KEUFFEL
F. R. LANEY
H. B. LANGILLE
RUDOLPH MICHEL, *Alternate*
F. W. MING
W. C. MUELLER
E. B. NEIL
J. W. OWENS
F. C. PANUSKA
E. S. SMITH †

SUBCOMMITTEE CHAIRMAN

Subcommittee on Revision, F. G. HIGBEE

GRAPHIC PRESENTATION (Z15)

** Sole sponsorship. Sectional Committee organized November, 1926*

A.S.M.E. Members (Total personnel, 31)

G. E. HAGEMANN, *Secretary* †
C. M. BIGELOW
WALLACE CLARK
T. E. FRENCH
D. B. PORTER †

SUBCOMMITTEE CHAIRMEN

No. 1 on Plan and Scope (to be appointed)
No. 2 on Terminology (to be appointed)
No. 3 on Preferred Practice for Time Series Charts, A. H. RICHARDSON
No. 4 on Engineering and Scientific Graphs, W. A. SHEWHART

SPEEDS OF MACHINERY (Z18)

** Sole sponsorship. Sectional Committee organized May, 1928*

A.S.M.E. Members (Total personnel, 30)

C. M. BIGELOW †
J. F. DAGGETT
R. C. DEALE †
PAUL DISERENS
F. S. ENGLISH
P. G. RHOADS
F. C. SPENCER

SUBCOMMITTEE CHAIRMEN

No. 1 on Plan and Scope, A. E. HALL
No. 2 on Questionnaire and Canvass to Industry, F. S. ENGLISH
No. 3—Special Reviewing Committee (to be appointed)

GRAPHICAL SYMBOLS AND ABBREVIATIONS FOR USE IN DRAWINGS (Z32)

** Joint sponsorship with American Institute of Electrical Engineers. Sectional Committee organized April, 1936*

A.S.M.E. Members (Total personnel, 51)

E. E. ASHLEY
J. M. BARNES
T. H. CHILTON
T. E. FRENCH †
G. F. HABACH
D. T. HAMILTON
A. M. HOUSER
(J. J. HARMAN, *Alternate*)
W. C. MUELLER
L. L. MUNIER
J. W. OWENS
F. C. PANUSKA †
W. C. STEWART
T. R. THOMAS

SUBCOMMITTEE CHAIRMEN

No. 1 on Symbols for Use in Mechanical Engineering, T. E. FRENCH
No. 2 on Symbols for Use in Electrical Engineering, H. W. SAMSON
No. 3 on Abbreviations for Use on Drawings, T. E. FRENCH

DEVELOPMENT OF STATISTICAL APPLICATIONS IN ENGINEERING AND MANUFACTURING

Joint Sponsorship with the American Mathematical Society, American Society for Testing Materials, American Statistical Association, Institute of Mathematical Statistics. Appointed in December, 1929

A.S.M.E. Members (Total personnel, 9)

A. G. ASHCROFT
L. K. SILLCOX †
J. S. TAWRESEY †

A. S. M. E. Representatives on Miscellaneous Standardization Committees

See also A.S.M.E. Representatives on Other Activities, page RI-5

ACOUSTICAL MEASUREMENTS AND TERMINOLOGY

** Sponsor body: Acoustical Society of America*

P. H. BILHUBER
(R. V. PARSONS, *Alternate*)
(J. S. PARKINSON, *Alternate*)

AERONAUTICS

** Sponsor body: Society of Automotive Engineers*

E. A. SPERRY, JR.

APPROVAL AND INSTALLATION REQUIREMENTS FOR GAS BURNING APPLIANCES

** Sponsor body: American Gas Association*

O. F. CAMPBELL

BUILDING CODE REQUIREMENTS FOR LIGHT AND VENTILATION

** Sponsor bodies: Federal Housing Administration, and U.S. Public Health Service*

F. R. SCHERER

COAL AND COKE

Committee of American Society for Testing Materials

R. M. HARDGROVE

DEFINITIONS OF ELECTRICAL TERMS

** Sponsor body: American Institute of Electrical Engineers*

C. H. BERRY

DRAINAGE OF COAL MINES

** Sponsor body: American Mining Congress*

O. M. PRUITT

ELECTRIC WELDING APPARATUS

** Sponsor bodies: American Institute of Electrical Engineers, and the National Electrical Manufacturers Association*

R. E. KINKEAD

FOREST FIRE PROTECTION

Committee of National Fire Protection Association

C. B. WHITE

GEAR LUBRICANTS

Committee of American Gear Manufacturers Association

G. B. KARELITZ

LOADING PLATFORMS AT FREIGHT TERMINALS AND WAREHOUSES

** Sponsor body: American Trucking Association, Inc.*

M. C. MAXWELL

MANHOLE FRAMES AND COVERS

** Sponsor bodies: ASA Telephone Group, and American Society of Civil Engineers*

ANTON HANSEN

MECHANICAL STANDARDS COMMITTEE

American Standards Association Committee

ALFRED IDDLES, *Chairman* †
(A. L. BAKER, *Alternate*) †
E. W. ERNEST
F. O. HOAGLAND
(M. E. LANGE, *Alternate*)
F. H. MOREHEAD
(A. M. HOUSER, *Alternate*)
H. H. MORGAN
FRANK THORNTON, JR.
H. L. WHITTEMORE, *Alternate*
Executive Committee, ALFRED IDDLES

METHODS OF TESTING WOOD

** Sponsor bodies: U.S. Forest Service, and the American Society for Testing Materials*

C. M. BIGELOW

MISCELLANEOUS OUTSIDE COAL-HANDLING EQUIPMENT

** Sponsor body: American Mining Congress*

(To be appointed)

PETROLEUM PRODUCTS AND LUBRICANTS

** Sponsor body: American Society for Testing Materials*

R. G. N. EVANS
G. B. KARELITZ
(H. J. MASSON, *Alternate*)
(S. J. NEEDS, *Alternate*)

PREFERRED NUMBERS

** Special Committee of ASA*

K. H. CONDIT

RATING OF RIVERS

** Sponsor body: U.S. Geological Survey*

D. W. MEAD

ROTATING ELECTRICAL MACHINERY

** Sponsor bodies: American Institute of Electrical Engineers, and National Electrical Manufacturers Association*

(To be appointed)

SPECIFICATIONS FOR CAST IRON PIPE AND SPECIAL CASTINGS

** Sponsor bodies: American Gas Association, American Society for Testing Materials, American Water Works Association, and the New England Water Works Association*

J. E. GIBSON
L. R. HOWSON

SPECIFICATIONS FOR CLEAN BITUMINOUS COAL

** Sponsor body: American Institute of Mining and Metallurgical Engineers*

R. A. SHERMAN
(E. L. LINDSETH, *Alternate*)

SPECIFICATIONS FOR FIRE TESTS OF BUILDING CONSTRUCTION AND MATERIALS

** Sponsor bodies: ASA Fire Protection Group, National Bureau of Standards, and the American Society for Testing Materials*

R. C. PARLETT

SPECIFICATIONS FOR SIEVES FOR TESTING PURPOSES

** Sponsor bodies: American Society for Testing Materials, and National Bureau of Standards*

R. M. HARDGROVE

THERMAL INSULATING MATERIALS

Committee of American Society for Testing Materials

R. H. HEILMAN

U.S. INTERDEPARTMENTAL COMMITTEE ON SCREW THREADS

EARLE BUCKINGHAM
A. M. HOUSER

VOLUME WATER HEATING

Committee of American Gas Association

MARC RESEK

WIRE ROPE FOR MINES

** Sponsor body: American Mining Congress*

(To be appointed)

POWER TEST CODES COMMITTEES

ARTICLE B6A, PAR. 27: The Standing Committee on Power Test Codes shall, under the direction of the Council, have supervision of all the activities of the Society in connection with the A.S.M.E. Power Test Codes, including the interpretation of such codes.

The first Standing Committee on Power Test Codes was organized in December, 1918, to revise and extend the Power Test Codes which had been formulated by various technical committees appointed to develop particular codes. This work began in 1884.

STANDING COMMITTEE

FRANCIS HODGKINSON, *Chairman* (1944)
A. G. CHRISTIE, *Vice-Chairman* (1946)
H. H. MICHELSEN, *Junior Observer* (1942)
J. A. KEENE, *Junior Observer* (1943)

Term expires 1942

W. A. CARTER
HARTE COOKE
E. R. FISH
H. B. OATLEY
W. J. WOHLENBERG

Term expires 1943

LOUIS ELLIOTT
H. B. REYNOLDS
P. W. SWAIN
E. N. TRUMP

Term expires 1944

C. H. BERRY
FRANCIS HODGKINSON
D. S. JACOBUS
L. F. MOODY
E. B. RICKETTS

Term expires 1945

THEODORE BAUMEISTER
P. H. HARDIE
B. V. E. NORDBERG
R. J. S. PIGOTT
M. C. STUART

Term expires 1946

A. G. CHRISTIE
PAUL DISERENS
N. R. GIBSON
GEO. A. ORROK
E. B. POWELL

---

(1) GENERAL INSTRUCTIONS

Appointed December, 1918
Reorganized, 1939

THEODORE BAUMEISTER, *Chairman*
PAUL DISERENS
HENRY KREISINGER
A. R. MUMFORD
R. H. SNYDER
C. R. SODERBERG
M. C. STUART
P. W. SWAIN

(2) DEFINITIONS AND VALUES

Appointed December, 1918
Reorganized, 1936

R. J. S. PIGOTT, *Chairman*
L. J. BRIGGS
W. F. DAVIDSON
L. S. MARKS
F. G. PHILO
J. C. SMALLWOOD
P. W. SWAIN
A. C. WOOD

(3) FUELS

Appointed December, 1918

W. J. WOHLENBERG, *Chairman*
E. G. BAILEY
B. L. BOYE
H. W. BROOKS
S. B. FLAGG
D. M. MYERS
F. G. PHILO
G. S. POPE
E. B. RICKETTS
F. M. ROGERS
E. X. SCHMIDT
NICHOLAS STAHL
E. N. TRUMP

(4) STATIONARY STEAM-GENERATING UNITS

Appointed December, 1918

E. R. FISH, *Chairman*
A. D. BAILEY
M. W. BENJAMIN
B. J. CROSS
MARTIN FRISCH
P. H. HARDIE
R. M. HARDGROVE
ALFRED IDDLES
E. L. LINDSETH
E. L. MCDONALD
E. B. POWELL
R. SHELLENBERGER
R. L. SPENCER

(5) RECIPROCATING STEAM ENGINES

Appointed December, 1918
Reorganized, 1931

A. G. CHRISTIE, *Chairman*
HARTE COOKE
K. S. M. DAVIDSON
HENRIK GREGER
J. A. HUNTER
H. G. MUELLER
B. V. E. NORDBERG
A. V. SAHAROFF
A. G. WITTING

(6) STEAM TURBINES

Appointed December, 1918

C. H. BERRY, *Chairman*
I. E. MOULTROP, *Secretary*
O. D. H. BENTLEY
W. E. CALDWELL
C. B. CAMPBELL
A. G. CHRISTIE
H. P. DAHLSTRAND
V. M. FROST
A. E. GRUNERT
FRANCIS HODGKINSON
S. A. MOSS
R. O. MULLER
T. E. PURCELL
G. B. WARREN

(7) RECIPROCATING STEAM-DRIVEN DISPLACEMENT PUMPS

Appointed December, 1918

R. D. HALL, *Chairman*
E. H. BROWN
J. N. CHESTER
J. E. GIBSON
G. L. KOLLBERG
M. B. MACNEILLE
D. W. MEAD
L. A. QUAYLE

(8) CENTRIFUGAL AND ROTARY PUMPS

Appointed December, 1918
Reorganized, 1936

R. L. DAUGHERTY, *Chairman*
H. E. BECKWITH
R. G. FOLSOM
R. C. GLAZEBROOK
W. B. GREGORY
R. T. KNAPP
J. B. LINCOLN
M. B. MACNEILLE
L. F. MOODY
ARVID PETERSON
F. H. ROGERS
W. C. RUDD
MAX SPILLMAN
F. G. SWITZER
W. M. WHITE
I. A. WINTER

(9) DISPLACEMENT COMPRESSORS AND BLOWERS

Appointed December, 1918
Reorganized 1935

PAUL DISERENS, *Chairman*
G. T. FELBECK
C. R. HOUGHTON
J. F. HUVANE
R. M. JOHNSON
J. F. D. SMITH

(10) CENTRIFUGAL AND TURBO-COMPRESSORS AND BLOWERS

Appointed December, 1918
Reorganized, 1929

M. C. STUART, *Chairman* (Fans)
E. L. ANDERSON
THEODORE BAUMEISTER
C. A. BOOTH
W. H. CARRIER
THOMAS CHESTER
E. D. CURLEY
L. E. DAY
Z. G. DEUTSCH
S. H. DOWNS
P. E. GOOD
J. J. GROB
H. F. HAGEN
PAUL HOFFMAN
F. H. JENKINS
H. D. KELSEY
A. L. KIMBALL
W. W. LAWRENCE
R. D. MADISON
L. S. MARKS
ARVID PETERSON

(12) CONDENSERS, WATER HEATING, AND COOLING EQUIPMENT

Appointed December, 1918

GEO. A. ORROK, *Chairman*
P. H. HARDIE, *Secretary*
C. H. BAKER, JR.
J. F. GRACE
D. W. R. MORGAN
H. B. REYNOLDS
P. E. REYNOLDS

(13) REFRIGERATING SYSTEMS

Appointed December, 1918
Reorganized May, 1939

B. H. JENNINGS, *Chairman* †
A. C. BUENSOD
(R. W. WATERFILL, *Alternate*)
J. C. CONSLEY
(H. B. POWNALL, *Alternate*)
R. J. EWER †
WALTER F. JONES †
M. A. NELSON †
A. W. OAKLEY
C. L. SVENSON
FRANK ZUMBRO †

(14) EVAPORATING APPARATUS

Appointed December, 1918

E. N. TRUMP, *Chairman*
B. N. BUMP
E. A. NEWHALL
H. L. PARR
L. C. ROGERS

(15) STEAM LOCOMOTIVES

Appointed December, 1918

E. C. SCHMIDT, *Chairman*
W. F. KIESEL, JR.
H. B. OATLEY
G. E. RHOADS
L. K. SILLCOX
W. E. WOODARD

(16) GAS PRODUCERS

Appointed December, 1918

C. D. SMITH

(17) INTERNAL-COMBUSTION ENGINES

Appointed December, 1918
Reorganized, 1939

LEE SCHNEITTER, *Chairman*
F. H. DUTCHER, *Secretary*
J. C. BARNABY
G. C. BOYER
HARTE COOKE
H. E. DEGLER
W. L. H. DOYLE
L. B. JACKSON
E. J. KATES
E. C. MAGDEBURGER
B. V. E. NORDBERG
RUSSELL PYLES
M. J. REED
O. D. TREIBER

† Official A.S.M.E. representatives serving on this committee.

(18) HYDRAULIC PRIME MOVERS

Appointed December, 1918
Reorganized, 1931

S. L. KERR, *Chairman*
C. M. ALLEN
L. M. DAVIS
H. L. DOOLITTLE
W. F. DURAND
N. R. GIBSON
J. P. GROWDON
T. H. HOGG
L. J. HOOPER
C. W. HUBBARD
E. C. HUTCHINSON
D. J. MCCORMACK
L. F. MOODY
W. J. RHEINGANS
J. F. ROBERTS
E. B. STROWGER
R. V. TERRY
W. M. WHITE

(19) INSTRUMENTS AND APPARATUS

Appointed December, 1918

W. A. CARTER, *Chairman*
C. M. ALLEN
W. C. ANDRAE
E. G. BAILEY
H. S. BEAN
L. J. BRIGGS
J. D. DAVIS
K. J. DE JUHASZ
R. E. DILLON
F. M. FARMER
J. B. GRUMBEIN
W. W. JOHNSON
W. H. KENERSON
E. S. LEE
E. L. LINDSETH
OSBORN MONNETT
S. A. MOSS
R. J. S. PIGOTT
E. B. RICKETTS
W. A. SLOAN
R. B. SMITH
I. M. STEIN

(20) SPEED, TEMPERATURE AND PRESSURE RESPONSIVE GOVERNORS

Appointed December, 1921
Reorganized February, 1940

C. R. SODERBERG, *Chairman*
C. L. AVERY
R. J. CAUGHEY
HARTE COOKE
W. L. H. DOYLE
HERBERT ESTRADA
S. N. FIALA
J. R. HAGEMANN
W. C. HOLMES
S. L. KERR
A. F. SCHWENDNER
R. B. SMITH
H. E. STICKLE

(21) DUST SEPARATING APPARATUS

Appointed October, 1934

M. D. ENGLE, *Chairman*
OLLISON CRAIG, *Secretary*
A. D. BAILEY
H. H. BUBAR
W. G. CHRISTY
H. O. CROFT
J. M. DALLAVALLE
H. O. DANZ
H. C. DOHRMANN
J. W. FEHNEL
H. F. HAGEN
P. H. HARDIE
C. W. HEDBERG
J. H. LEECH
H. E. MACOMBER
H. B. MELLER
H. C. MURPHY
B. F. TILLSON

A.S.M.E. Representatives on Other Technical Committees

See also A.S.M.E. Representatives on Other Activities, page RI-5

DEVELOPMENT OF DEFINITIONS FOR THE NET CALORIFIC VALUE AND GROSS CALORIFIC VALUE OF FUELS

Sponsor body: American Society for Testing Materials

W. J. WOHLENBERG

COMMITTEE ON REDEFINING SO-CALLED STANDARD TON OF REFRIGERATION

Sponsor body: American Society of Refrigerating Engineers

G. B. BRIGHT

COMMITTEE ON GASEOUS FUELS

Sponsor body: American Society for Testing Materials

E. X. SCHMIDT

COAL TESTING CODE COMMITTEE

Joint sponsorship with the American Institute of Mining and Metallurgical Engineers

A. R. MUMFORD

SPECIFICATIONS FOR PRIME MOVER SPEED GOVERNING

Joint sponsorship with the American Institute of Electrical Engineers

C. L. AVERY
R. J. CAUGHEY
HERBERT ESTRADA
C. R. SODERBERG
A. F. SCHWENDNER

SAFETY COMMITTEES

ARTICLE B6A, PAR. 25: The Standing Committee on Safety shall advise the Council on the activities of the Society having to do with engineering and industrial safety, except the activities of the Boiler Code Committee, for which special provision is made.

The first Standing Committee on Safety was appointed in October, 1921.

STANDING COMMITTEE

A. W. LUCE, *Chairman* (1942)
A. E. WINDLE (1943)
H. C. HOUGHTON (1944)
E. R. GRANNISS (1945)
H. W. GABOR (1946)

SAFETY CODE FOR ELEVATORS (A17)

* *Joint Sponsorship with The American Institute of Architects, and the National Bureau of Standards. Sectional Committee organized November, 1922*

Reorganized July, 1940

A.S.M.E. Members (Total personnel, 49)

O. P. CUMMINGS, *Vice-Chairman*
C. R. CALLAWAY
J. W. DEGEN
D. L. HOLBROOK †
D. L. LINDQUIST
N. O. LINDSTROM †
M. B. MCLAUTHLIN
W. S. PAINE
(W. H. SEAQUIST, *Alternate*) †
S. F. VOORHEES
H. L. WHITTEMORE

SUBCOMMITTEE CHAIRMEN

Emergency Elevator Rules, D. J. PURINTON
Executive Committee, D. J. PURINTON
Existing Elevators, D. J. PURINTON
Inspectors' Manual, K. A. COLAHAN
Mechanical Safety Equipment, D. L. LINDQUIST
Wire Rope, D. J. PURINTON
Working, G. H. REPPERT

SAFETY CODE FOR MECHANICAL POWER-TRANSMISSION APPARATUS (B15)

* *Joint sponsorship with the International Association of Industrial Accident Boards and Commissions, and the National Conservation Bureau. Sectional Committee organized February, 1921*

A.S.M.E. Members (Total personnel, 24)

G. M. NAYLOR, *Chairman* †
P. G. RHOADS, *Secretary*
D. C. WRIGHT †
(G. N. VAN DERHOEF, *Alternate*) †

SUBCOMMITTEE CHAIRMEN

No. 1 on Detail Classification of Belts (to be appointed)
No. 2 on Modification of Rule 223 for Cone Pulley Belts (to be appointed)
No. 3 on Mechanical Power Control (to be appointed)
No. 4 on Use of ASA Code Versus State Codes (to be appointed)
No. 5 on Statistics on Place of Occurrence of Accidents (to be appointed)
No. 6 on V-Belt Drives, D. C. WRIGHT

SAFETY CODE ON COMPRESSED AIR MACHINERY AND EQUIPMENT (B19)

* *Joint sponsorship with the American Society of Safety Engineers—Engineering Section, National Safety Council. Sectional Committee organized May, 1923*

A.S.M.E. Members (Total personnel, 24)

D. L. ROYER, *Chairman*
H. D. EDWARDS
W. J. GRAVES

SAFETY CODE FOR CONVEYORS AND CONVEYING MACHINERY (B20)

* *Joint Sponsorship with the National Conservation Bureau. Sectional Committee organized November, 1925, Reorganized, April, 1937*

A.S.M.E. Members (Total personnel, 53)

D. L. ROYER, *Chairman*
C. T. COLLEY
W. J. GRAVES
M. A. KENDALL †
(N. W. ELMER, *Alternate*) †
P. T. ONDERDONK
C. G. PFEIFFER
R. B. RENNER
F. J. SHEPARD, JR.
J. G. WHEATLEY

SUBCOMMITTEE CHAIRMEN

No. 1 on All Types of Chain Conveyors, Belt Conveyors, Belt Elevators Including Steel Belt, and Screw, Track or Scraper Conveyors, C. G. PFEIFFER
No. 2 on Gravity Conveyors and Chutes, Live Roll Conveyors, H. G. DALTON
No. 3 on Cable-Operated and Cable Flight Conveyors and Cableways, R. McA. KEOWN
No. 4 on Air, Steam, or Liquid Conveyors, J. J. MCNULTA
No. 5 on Tiering, Piling, and Stacking Conveyors, J. G. WHEATLEY

SAFETY CODE FOR CRANES, DERRICKS, AND HOISTS (B30)

* *Joint sponsorship with U.S. Navy Department, Bureau of Yards and Docks. Sectional Committee organized November, 1926*

A.S.M.E. Members (Total personnel, 54)

H. S. BROWN
LEWIS PRICE †
F. H. SCHWERIN
R. H. WHITE †
H. L. WHITTEMORE

SUBCOMMITTEE CHAIRMEN

Executive Committee, J. C. WHEAT
No. 1 on Overhead and Gantry Cranes, R. H. WHITE
No. 2 on Locomotive and Tractor Cranes, H. H. VERNON
No. 3 on Derricks and Hoists, LEWIS PRICE
No. 4 on Miscellaneous Equipment for Cranes and Hoists, L. W. HOPKINS
No. 5 on Jacks, E. W. CARUTHERS
Editing Committee, H. H. VERNON

* Note: All of the safety committees for which the Society is sponsor or joint sponsor, or on which it has representation, are organized under the procedure of the American Standards Association.

† Official A.S.M.E. representative serving on this committee.

A.S.M.E. Representatives on Other Safety Committees

See also A.S.M.E. Representatives on Other Activities, page RI-5

SAFETY CODE FOR ABRASIVE WHEELS

* *Sponsor bodies: Grinding Wheel Manufacturers Association of United States and Canada, and International Association of Industrial Accident Boards and Commissions*

J. B. CHALMERS

SAFETY CODE FOR CONSTRUCTION WORK

* *Sponsor bodies: The American Institute of Architects, and National Safety Council*

C. H. O'NEIL

COOPERATION WITH OTHER ENGINEERING SOCIETIES

Committee of American Society of Safety Engineers—Engineering Section of National Safety Council

H. L. MINER

ASA SAFETY CODE CORRELATING COMMITTEE

A. W. LUCE
(A. E. WINDLE, *Alternate*)

SAFETY CODE FOR EXHAUST SYSTEMS

* *Sponsor body: International Association of Industrial Accident Boards and Commissions*

T. F. HATCH

SAFETY CODE FOR FLOOR AND WALL OPENINGS, RAILINGS, AND TOE BOARDS

* *Sponsor body: National Safety Council*

A. E. WINDLE

SAFETY CODE FOR FORGING AND HOT METAL STAMPING

* *Sponsor bodies: American Drop Forging Institute and National Safety Council*

C. F. PARK

SAFETY CODE ON COLORS FOR IDENTIFICATION OF GAS MASK CANISTERS

* *Sponsor body: National Safety Council*

L. C. LICHTY

SAFETY CODE FOR LADDERS

** Sponsor body: American Society of Safety Engineers—Engineering Section of National Safety Council*

H. C. HOUGHTON

SAFETY CODE FOR LAUNDRY MACHINERY AND OPERATION

** Sponsor bodies: American Institute of Laundering, International Association of Governmental Labor Officials, and National Association of Mutual Casualty Companies*

E. J. CARROLL

SAFETY CODE FOR LIGHTING FACTORIES, MILLS, AND OTHER WORK PLACES

** Sponsor body: Illuminating Engineering Society*

A. W. LUCE

LOW VOLTAGE ELECTRICAL HAZARDS

Special Committee of the American Society of Safety Engineers—Engineering Section of National Safety Council

J. P. JACKSON

SAFETY CODE FOR MECHANICAL REFRIGERATION

** Sponsor body: American Society of Refrigerating Engineers*

O. A. ANDERSON
CROSBY FIELD
E. W. GALLENKAMP
W. F. JONES
(A. W. OAKLEY, *Alternate to all A.S.M.E. Representatives*)

SAFETY CODE FOR PAPER AND PULP MILLS

** Sponsor body: National Safety Council*

R. L. WELDON

SAFETY CODE FOR POWER PRESSES, AND FOOT AND HAND PRESSES

** Sponsor body: National Safety Council*

J. B. CHALMERS

SAFETY CODE FOR PREVENTION OF DUST EXPLOSIONS

** Sponsor bodies: National Fire Protection Association, and U.S. Department of Agriculture*

R. M. FERRY

SAFETY CODE FOR PROTECTION OF HEADS, EYES, AND RESPIRATORY ORGANS OF INDUSTRIAL WORKERS

** Sponsor body: National Bureau of Standards*

T. A. WALSH, JR.
(T. F. HATCH, *Alternate*)

SAFETY CODE FOR PROTECTION OF INDUSTRIAL WORKERS IN FOUNDRIES

** Sponsor bodies: American Foundrymen's Association, and National Founders Association*

H. M. LANE

SAFETY IN QUARRY OPERATIONS

** Sponsor body: National Safety Council*

REDFIELD PROCTOR

SAFETY CODE FOR RUBBER MACHINERY

** Sponsor bodies: National Safety Council, and International Association of Industrial Accident Boards and Commissions*

E. S. AULT

SPECIFICATIONS AND METHOD OF TEST FOR SAFETY GLASS

** Sponsor bodies: National Conservation Bureau, and National Bureau of Standards*

T. A. WALSH, JR.

SAFETY CODE FOR TEXTILES

** Sponsor body: National Safety Council*

M. A. GOLRICK, JR.

SAFETY CODE FOR VENTILATION

** Sponsor body: American Society of Heating and Ventilating Engineers*

T. F. HATCH

SAFETY CODE FOR WALKWAY SURFACES

** Sponsor bodies: The American Institute of Architects, and American Society of Safety Engineers—Engineering Section of National Safety Council*

G. K. PALSGROVE

SAFETY CODE FOR WORK IN COMPRESSED AIR

** Sponsor body: International Association of Industrial Accident Boards and Commissions*

L. J. EIBSEN

BOILER CODE COMMITTEES

ARTICLE B6A, PAR. 26: The Special Committee on Boiler Code shall, under the direction of the Council, have supervision of all the activities of the Society in connection with the A.S.M.E. Codes for Pressure Vessels, including the interpretations of these codes.

The first Special Committee on Boiler Code was organized in September, 1911.

SPECIAL COMMITTEE

D. S. JACOBUS, *Honorary Chairman*
E. R. FISH, *Chairman*
H. B. OATLEY, *Vice-Chairman*
J. W. SHIELDS, *Secretary*
M. JURIST, *Assistant Secretary*
C. A. ADAMS
H. E. ALDRICH
H. C. BOARDMAN
PERRY CASSIDY
R. E. CECIL
F. S. CLARK
A. J. ELY
V. M. FROST
C. E. GORTON
A. M. GREENE, JR.
W. G. HUMPTON
J. O. LEECH
I. E. MOULTROP
C. O. MYERS
C. W. OBERT
JAMES PARTINGTON
D. B. ROSSHEIM
WALTER SAMANS
S. K. VARNES
A. C. WEIGEL

Honorary Members

W. H. BOEHM
W. F. DURAND
T. E. DURBAN
C. L. HUSTON
W. F. KIESEL, JR.
M. F. MOORE
H. H. VAUGHAN
H. LEROY WHITNEY

CONFERENCE COMMITTEE

T. R. ARCHER, Delaware
L. M. BARRINGER, Seattle, Wash.
J. G. BOLLOCK, St. Joseph, Mo.
B. M. BOOK, Pennsylvania
E. J. BROCK, St. Louis, Mo.
H. S. BRUNSON, Minnesota
E. S. CARPENTER, Rhode Island
L. M. CAVE, Maryland
S. CHERRINGTON, Ohio
CITY BOILER INSPR., Parkersburg, W. Va.
D. J. CODY, Kansas City, Mo.
A. L. COLBY, Louisiana
A. J. CONWAY, Indiana
M. A. EDGAR, Wisconsin
C. W. FOSTER, Omaha, Neb.
M. R. FRANCIS, West Virginia
W. H. FURMAN, New York
F. D. GARVIN, Houston, Tex.
GERALD GEARON, Chicago, Ill.
C. H. GRAM, Oregon
J. A. GREGORY, Tampa, Fla.
C. W. HARNESS, Iowa
F. A. HECKINGER, Memphis, Tenn.
H. K. KUGEL, District of Columbia
JOE KUNSCHIK, Texas
P. N. LEHOCZKY, Ohio
M. L. LOBDELL, Washington
G. A. LUCK, Massachusetts
E. C. LUSTER, Miami, Fla.
C. E. MCGINNIS, Los Angeles, Calif.
H. H. MILLS, Detroit, Mich.
J. D. NEWCOMB, JR., Arkansas
W. L. NEWTON, Oklahoma
F. A. PAGE, California
L. C. PEAL, Nashville, Tenn.
E. K. SAWYER, Maine
J. F. SCOTT, New Jersey
J. N. SEIGER, Evanston, Ill.
C. I. SMITH, Utah
J. A. STRAIT, Tulsa, Okla.
WM. E. SMITH, Hawaiian Islands
JOHN H. THORPE, Michigan
C. E. WARD, North Carolina

EXECUTIVE COMMITTEE

D. S. JACOBUS, *Chairman*
H. E. ALDRICH, *Vice-Chairman*
E. R. FISH
V. M. FROST
C. E. GORTON
H. B. OATLEY
C. W. OBERT
JAMES PARTINGTON

SUBCOMMITTEES

BOILERS OF LOCOMOTIVES

JAMES PARTINGTON, *Chairman*
F. H. CLARK
J. M. HALL
H. B. OATLEY

CARE OF STEAM BOILERS AND OTHER PRESSURE VESSELS IN SERVICE

F. M. GIBSON, *Chairman*
D. C. CARMICHAEL
V. M. FROST
J. R. GILL
FRANK HENRY
J. A. HUNTER
H. J. KERR
P. B. PLACE
S. T. POWELL
C. W. RICE
J. B. ROMER
W. C. SCHROEDER
NICHOLAS STAHL
F. G. STRAUB

COORDINATION

V. M. FROST, *Chairman*
E. R. FISH
C. W. OBERT

FERROUS MATERIALS

D. B. ROSSHEIM, *Chairman*
A. B. BAGSAR
E. C. CHAPMAN
A. J. ELY
H. J. FRENCH
W. R. GRUNOW
M. B. HIGGINS
A. M. HOUSER
W. G. HUMPTON
A. HURTGEN
T. MCLEAN JASPER
J. J. KANTER
H. J. KERR
A. B. KINZEL
L. J. MASON
N. L. MOCHEL
E. L. ROBINSON
A. D. SANDERSON
A. P. SPOONER
S. K. VARNES
A. E. WHITE
R. L. WILSON

HEATING BOILERS

J. W. TURNER, *Chairman*
C. E. BRONSON
J. A. DARTS
WM. FERGUSON
C. E. GORTON
L. N. HUNTER
W. E. STARK

MATERIAL SPECIFICATIONS

PERRY CASSIDY, *Chairman*
A. M. GREENE, JR.
W. G. HUMPTON
J. O. LEECH
P. J. SMITH
A. C. WEIGEL

MINIATURE BOILERS

C. E. GORTON, *Chairman*
W. H. FURMAN
G. A. LUCK
C. W. OBERT

NONFERROUS MATERIALS

H. B. OATLEY, *Chairman*
J. J. AULL
W. F. BURCHFIELD
D. K. CRAMPTON
J. R. FREEMAN, JR.
A. M. HOUSER
E. F. MILLER
JOSEPH PRICE
R. L. TEMPLIN

POWER BOILERS

H. E. ALDRICH, *Chairman*
PERRY CASSIDY
E. R. FISH
V. M. FROST
D. L. ROYER
A. C. WEIGEL

RULES FOR INSPECTION

(This subcommittee is being reorganized)

SPECIAL DESIGN

D. B. WESSTROM, *Chairman*
H. C. BOARDMAN
R. E. CECIL
T. W. GREENE
D. B. ROSSHEIM
E. O. WATERS
F. S. G. WILLIAMS

UNFIRED PRESSURE VESSELS

E. R. FISH, *Chairman*
C. A. ADAMS
C. E. BRONSON
R. E. CECIL
PAUL DISERENS
H. S. SMITH
D. B. WESSTROM

WELDING

Members of A.S.M.E. Boiler Code Committee

JAMES PARTINGTON, *Chairman*
O. R. CARPENTER
E. C. CHAPMAN

J. H. Deppeler
W. D. Halsey
R. K. Hopkins
J. T. Phillips
L. A. Sheldon

Members of Conference Committee of American Welding Society

C. W. Obert, *Chairman*
C. A. Adams
H. C. Boardman
Walter Samans
A. C. Weigel

SPECIAL COMMITTEES

Approval of New Materials

C. A. Adams, *Chairman*

Clad Vessels

S. K. Varnes, *Chairman*

Extension of Fusion Welding Requirements

H. E. Aldrich, *Chairman*

Feedwater

C. W. Rice, *Chairman*

Issuance of Code Symbol Stamps

C. O. Myers, *Chairman*

Material Specifications for Piping Valves and Fittings

A. C. Weigel, *Chairman*

Radiographic Examination of Welded Joints

C. A. Adams, *Chairman*

Revision of Section VIII of the A.S.M.E. Boiler Code

E. R. Fish, *Chairman*

Rules for Bolted Flanged Connections

D. B. Wesstrom, *Chairman*

Rules for Dished Heads

H. C. Boardman, *Chairman*

Rules for Openings

T. D. Tifft, *Chairman*

Safety Valve Requirements

H. B. Oatley, *Chairman*

Work of Boiler Code Committee

H. E. Aldrich, *Chairman*

API-ASME COMMITTEE ON UNFIRED PRESSURE VESSELS

Walter Samans, *Chairman*

A.S.M.E. Representatives

R. E. Cecil
E. R. Fish
D. S. Jacobus
T. McLean Jasper
James Partington

A.P.I. Representatives

A. J. Ely
M. B. Higgins
K. V. King
Walter Samans
T. D. Tifft

THE WOMAN'S AUXILIARY TO THE A.S.M.E.

The Woman's Auxiliary to the A.S.M.E. was organized on May 10, 1923, and its Constitution and By-Laws was approved by the Council of the A.S.M.E. on October 27, 1924. The objects of the Auxiliary are to render service to all that pertains to the interest of the profession of mechanical engineering; to cooperate with any committees of the A.S.M.E.; and to assist the sons and daughters of the members of the Society or worthy students of mechanical engineering in obtaining scholarships; and to promote any other objects consistent with the aims or objects of the A.S.M.E.

OFFICERS

President, Mrs. F. M. Gibson
First Vice-President, Mrs. E. C. M. Stahl
Second Vice-President, Mrs. C. M. Sames
Third Vice-President, Mrs. R. F. Gagg
Fourth Vice-President, Mrs. E. F. Zeiner
Fifth Vice-President, Mrs. S. F. Duncan
Recording Secretary, Mrs. P. E. Frank
Corresponding Secretary, Mrs. A. R. Cullimore
Treasurer, Mrs. A. H. Morgan

STANDING COMMITTEE CHAIRMEN

Student Loan, Mrs. R. F. Gagg
Membership, Mrs. G. E. Hagemann
Calvin W. Rice Scholarship, Mrs. J. A. Brooks
Custodian, Miss Burtie Haar

COUNCIL REPRESENTATIVES

A. G. Christie
Warren H. McBryde

OFFICERS OF LOCAL SECTIONS

Cleveland

Chairman, Mrs. T. F. Githens

Los Angeles

Chairman, Mrs. S. F. Duncan

Metropolitan

Chairman, Mrs. J. Noble Landis
First Vice-Chairman, Mrs. Calvin W. Rice
Second Vice-Chairman, Mrs. C. H. Young
Third Vice-Chairman, Mrs. Earl Smith
Recording Secretary, Mrs. C. F. Kayan
Corresponding Secretary, Miss Burtie Haar
Treasurer, Mrs. C. E. Gus

Philadelphia

Chairman, Mrs. E. F. Zeiner

AWARDS

The following paragraphs deal with the medals, awards, scholarships, and loan funds which come within the jurisdiction of the A.S.M.E. Other awards available to Student Members are listed in *Mechanical Engineering*, February, 1938, page 183. The Society also participates with other engineering societies in a number of joint awards. Further details concerning all the awards will be found in a series of articles beginning in the October, 1938, issue of *Mechanical Engineering*.

Honorary Membership, to which persons of acknowledged professional eminence are elected by unanimous vote of Council under the provisions of the By-Laws and Rules. A list of honorary members is given on page RI-42.

Life Membership, which may be conferred by the Council for distinguished service to the Society; or secured by a member by payment for an annuity in accordance with the provisions of the By-Laws.

A.S.M.E. Medal, established by the Society in 1920 to be presented, together with an engraved certificate, for distinguished service in engineering and science. May be awarded for general service in science having possible application in engineering.

Holley Medal, instituted and endowed in 1924 by George I. Rockwood, Past Vice-President of the Society, to be bestowed, together with an engraved certificate, for some great and unique act of genius of engineering nature that has accomplished a great and timely public benefit.

Worcester Reed Warner Medal, provision for which was made in the will of Worcester Reed Warner, Honorary Member of the Society, is a gold medal to be bestowed, together with an engraved certificate, on the author of the most worthy paper received, dealing with progressive ideas in mechanical engineering or efficiency in management.

Melville Medal, established in 1914 by the bequest of Rear-Admiral George W. Melville, Honorary Member and Past-President of the Society, to be presented, together with an engraved certificate, for an original paper or thesis of exceptional merit, presented to the Society for discussion and publication, to encourage excellence in papers. The medal may be presented annually.

Spirit of St. Louis Medal, established by an endowment fund created in 1929 by citizens of St. Louis, Mo., to be awarded for meritorious service in the advancement of aeronautics. This medal will be awarded at the discretion of the Council of the Society at approximately three-year periods upon the recommendation of its Board of Honors and Awards.

Spirit of St. Louis Junior Award, established in 1938 by an endowment fund created by the General Committee for the 1935 Aeronautic Meeting in St. Louis; a cash award of $50, made every three years, for the best paper on an aeronautic subject presented at any A.S.M.E. meeting during the three-year period either personally by the author (a Junior Member of the Society under thirty years of age) or by a Junior Member designated by him, and submitted to the Committee on Medals within a reasonable period (to be determined by the Committee) after its initial presentation.

Pi Tau Sigma Medal Award, established in 1938, endowed by Pi Tau Sigma, the national honorary mechanical engineering fraternity, to be presented annually, together with an engraved certificate, to the young mechanical engineer for outstanding achievement in his profession within the ten years after graduation from a regular four-year mechanical engineering course of a recognized American college or university. Any mechanical engineering graduate, not more than thirty-five years of age, whose achievement has been all or in part in any field including industrial, educational, political, research, civic, etc., is eligible.

Junior Award, annual cash award of $50, established in 1914, from a fund created by Henry Hess, Past Vice-President of the Society, to be presented, together with an engraved certificate, for the best paper or thesis submitted by a Junior Member.

Charles T. Main Award, annual cash award of $150, established in 1919 from a fund created by Charles T. Main, Past-President of the Society, to be awarded, together with an engraved certificate, to a Student Member of the Society, for the best paper within the general subject of the influence of the profession upon public life. The exact subject is assigned by the Board of Honors and Awards, subject to the approval of the Council, and is announced each year through the Honorary Chairman of the Student Branches.

Student Awards, two annual cash awards of $25 each, established in 1914, from a fund created by Henry Hess, Past Vice-President of the Society, to be presented, together with engraved certificates, for the best papers or theses submitted by Student Members. The awards for 1932 and subsequent years have been given, one for undergraduate and the other for postgraduate work.

SCHOLARSHIPS AND LOAN FUNDS

Max Toltz: Loan Fund of $15,000 established by Major Max Toltz, former member of the Council of the Society, the income to be used for assistance to Student Members.

John R. Freeman: Fund of $25,000 established in 1926 by John R. Freeman, Past-President of the Society, the income to be used for travel scholarships and research.

Woman's Auxiliary: Scholarship or Fellowship offered by the Woman's Auxiliary to the Society to assist sons and daughters of members or worthy students of mechanical engineering.

RECIPIENTS OF AWARDS

The names of the recipients of the different awards to date are given in the following lists, together with the dates of presentation, and the services or papers for which the awards were made. There were no awards for the years not listed.

A.S.M.E. Medal

1921 Hjalmar Gotfried Carlson, in recognition of the services rendered the Government because of his invention and part in the production of 20,000,000 Mark III drawn steel booster casings used principally as a component of 75-mm high explosive shells, but also used extensively in gas shells and bombs

1922 Frederick Arthur Halsey, for his paper describing the premium system of wage payments presented before the Society at the Providence Meeting in 1891, as the adoption of the methods there proposed has had a profound effect toward harmonizing the relations of worker and employer

1923 John Ripley Freeman, for his eminent service in engineering and manufacturing by his meritorious work in fire prevention and the preservation of property

1926 R. A. Millikan, in recognition of his contributions to science and engineering

1927 Wilfred Lewis, for his contributions to the design and construction of gear teeth

1928 Julian Kennedy, for his services and contributions to the iron and steel industry

1929 William LeRoy Emmet, for his contributions in the development of the steam turbine, electric propulsion of ships and other power-generating apparatus

1931 Albert Kingsbury, for his research and development work in the field of lubrication

1933 Ambrose Swasey, for his contributions to the advancement of the engineering profession and for his part in the development of the turret lathe and the astronomical telescope

1934 Willis H. Carrier, in recognition of his research and development work in air-conditioning

1935 Charles T. Main, for distinguished achievements in the textile and other industries, in engineering education, and for eminent service to the engineering profession

1936 Edward Bausch, for meritorious mechanical development in the field of optics

1937 Edward P. Bullard, for outstanding leadership in the development of station-type machine tools

1938 Stephen J. Pigott, for outstanding leadership in marine propulsion and construction

1939 James E. Gleason, for service to the cause of safer and better transportation

1940 Charles F. Kettering, for outstanding inventions and research

1941 Theodor von Kármán, for his brilliance as a teacher, his researches in elasticity and many fields of physics and mechanics, and his distinguished leadership in the fields of aerodynamics and aircraft design.

Holley Medal

1924 Hjalmar Gotfried Carlson, for his inventions and processes which made possible the timely production of drawn steel booster casings for artillery ammunition, thereby aiding victory in the World War (diploma in recognition of achievements presented in 1921)
1927 Elmer Ambrose Sperry, for achievements and inventions that have advanced the naval arts, including the gyroscope that has freed navigation from the dangers of the fluctuating magnetic compass
1929 Baron Chuzaburo Shiba, for his contributions to knowledge through fundamental research, including the field of aerodynamics, by the development of ultra-rapid kinematographic methods
1934 Irving Langmuir, for his contributions to science and engineering, including the development of gas-filled incandescent lamps, thoriated filament for thermionic emission, atomic hydrogen welding, phase control operation of the thyratron tube, and fundamental research in oil films
1936 Henry Ford, for revolutionary influence through invention and practice on transportation and on mass production methods in manufacturing
1937 Frederick G. Cottrell, for preeminent public service—the invention of electric precipitation—advancement of the science of gas liquefaction—gifts for engineering research
1938 Francis Hodgkinson, for meritorious services in the development of the steam turbine
1939 Carl E. Johansson, in recognition of his pioneer work in the development of basic measuring gages
1940 Edwin Howard Armstrong, for his leadership in the field of radio communication
1941 John C. Garand, for the invention and development of the semi-automatic rifle, which has been adopted by the U.S. Army as the U.S. Rifle, Caliber .30, M1, an outstanding contribution to our national defense.

Worcester Reed Warner Medal

1933 Dexter S. Kimball, for his contributions to efficiency in management as exemplified by his recently revised "Principles of Industrial Organization" and by his many articles, engineering society papers, and public addresses
1934 Ralph E. Flanders, for his contributions to a better understanding of the relationship of the engineer to economic problems and social trends as exemplified by the many papers which he has presented
1935 Stephen Timoshenko, for his contributions to the theory of the design of elastic structures and the treatment of dynamics of moving machinery
1936 Charles M. Allen, for his early and continued hydraulic laboratory work and for the permanent value of the papers on his development of methods of testing large hydraulic turbine installations
1937 Clarence F. Hirshfeld, for his research and contributions to the theory and practice of heat-power engineering as exemplified by books and papers
1938 Lawford H. Fry, for contributions relating to improved locomotive boiler design and utilization of better materials in railway equipment
1939 Rupen Eksergian, for influential papers of permanent value in A.S.M.E. Transactions
1940 William Benjamin Gregory, for distinguished work in hydraulic engineering, which has been the basis for many engineering papers
1941 Richard Vynne Southwell, for his many distinguished services to engineering and science through papers and publications in many fields, including aeronautics, theory of structures, elasticity, and hydrodynamics.

Melville Medal

1927 Leon P. Alford, "Laws of Manufacturing Management"
1929 Joseph W. Roe, "Principles of Jig and Fixture Practice"
1930 Herman Diederichs and William D. Pomeroy, "The Occurrence and Elimination of Surge or Oscillating Pressure in Discharge Lines From Reciprocating Pumps"
1931 Arthur E. Grunert, "Comparative Performance of a Pulverized-Coal-Fired Boiler Using Bin System and Unit System of Firing"
1932 Alexey J. Stepanoff, "Leakage Loss and Axial Thrust in Centrifugal Pumps"
1933 William E. Caldwell, "Characteristics of Large Hell Gate Direct-Fired Boiler Units"
1935 Oscar R. Wikander, "Draft-Gear Action in Long Trains"
1936 H. A. Stevens Howarth, "The Loading and Friction of Thrust and Journal Bearings With Perfect Lubrication"
1937 Alfred J. Büchi, "Supercharging of Internal-Combustion Engines With Blowers Driven by Exhaust-Gas Turbines"
1938 Alphonse I. Lipetz, "Air Resistance of Railroad Equipment"
1939 Lester M. Goldsmith, for his paper, "High-Pressure High-Temperature Turbine-Electric Steamship *J. W. Van Dyke*"
1940 Carl A. W. Brandt, for his paper, "The Locomotive Boiler"
1941 Roger V. Terry, for his paper "Development of the Automatic Adjustable-Blade-Type Propeller Turbine."

Spirit of Saint Louis Medal

1929 Daniel Guggenheim, founder of the Guggenheim Fund for the Promotion of Aeronautics
1932 Paul Litchfield, for his work in encouraging and sponsoring airship design and construction in this country
1935 Will Rogers, for his splendid, constructive, and unselfish work in the achievement of aviation, and the building up of public confidence in aviation through his articles in the press, over the radio, and from the speaker's platform
1938 James H. Doolittle, for meritorious service in the advancement of aeronautics
1941 John E. Younger, for notable contributions to the science of airplane design, particularly in the conception, analysis, and supervision of the development of the fundamental design principles, requirements, and criteria which first assured the success of the pressure-cabin type of high-altitude airplane.

Spirit of Saint Louis Junior Award

1941 Wilbur W. Reaser, for his paper, "Calculation of the Heat Loss from an Airplane Cabin."

Pi Tau Sigma Medal

1938 Wilfrid E. Johnson, for his development work in the field of refrigeration
1939 John I. Yellott, Jr., in recognition of significant achievements in steam-flow research and engineering education; also contributions on "Supersaturated Steam" and "Condensation of Flowing Steam in Diverging Nozzles"
1940 George A. Hawkins, for significant achievements in high-pressure steam research and engineering education
1941 R. Hosmer Norris, for outstanding achievement in mechanical engineering, particularly in the heat-transfer field.

Junior Award

1915 Ernest O. Hickstein, "Flow of Air Through Thin Plate Orifices"
1916 L. M. McMillan, "The Heat Insulating Properties of Commercial Steam-Pipe Coverings"
1919 E. D. Whalen, "Properties of Airplane Fabrics"
1921 S. Logan Kerr, "Moody Ejector Turbine"
1922 R. H. Heilman, "Heat Losses From Bare and Covered Wrought-Iron Pipe at Temperatures up to 800 Degrees Fahrenheit"
F. L. Kallam, "Preliminary Report on the Investigation of the Thermal Conductivity of Liquids"
1923 S. S. Sanford and Sabin Crocker, "The Elasticity of Pipe Bends"
1924 R. H. Heilman, "Heat Losses Through Insulating Material"
1925 Gilbert S. Schaller, "An Investigation of Seattle as a Location for a Synthetic Foundry Industry"
1927 William M. Frame, "Stresses Occurring in the Walls of an Elliptical Tank Subjected to Low Internal Pressure"
1928 M. D. Aisenstein, "A New Method of Separating the Hydraulic Losses in a Centrifugal Pump"
1929 Arthur M. Wahl, "Stresses in Heavy, Closely Coiled Helical Springs"
1930 Ed Sinclair Smith, "Quantity-Rate Fluid Meters"
1931 M. K. Drewry, "Radiant-Superheater Developments"
1932 Edmond M. Wagner, "Frictional Resistance of a Cylinder Rotating in a Viscous Fluid Within a Coaxial Cylinder"
1933 Townsend Tinker, "Surface Condenser Design and Operating Characteristics"
1934 John I. Yellott, Jr., "Supersaturated Steam"
1935 Stanley J. Mikina, "Effect of Skewing and Pole Spacing on Magnetic Noise in Electrical Machinery"

1936 HARWOOD F. MULLIKAN, JR., "Evaluation of Effective Radiant Heating Surface and Application of the Stefan-Boltzman Law to Heat Absorption in Boiler Furnaces"
1937 LESLIE J. HOOPER, "American Hydraulic-Laboratory Practice"
1938 ARTHUR C. STERN, "Separation and Emission of Cinders and Fly Ash"
1940 ROBERT E. NEWTON, for his paper, "A Photoelastic Study of Stresses in Rotary Disks"
1941 JOHN T. RETTALIATA, for his paper, "The Combustion Gas Turbine."

CHARLES T. MAIN AWARD

1925 CLEMENT R. BROWN, Catholic University of America. Subject: "The Influence of the Locomotive on the Unity of the United States"
1926 W. C. SAYLOR, Johns Hopkins University. Subject: "The Effect of the Cotton Gin Upon the History of the United States During Its First Seventy Years"
1927 No Award. Subject: "Scientific Management and Its Effect Upon the Industries"
1928 ROBERT M. MEYER, Newark College of Engineering. Subject: "Scientific Management and Its Effect Upon Manufacturing"
1929 No Award. Subject: "The Influence of Engineering on Farm Production"
1930 JULES PODNOSSOFF, Polytechnic Institute of Brooklyn. Subject: "The Value of the Safety Movement in the Industries"
1931 ROBERT E. KLISE, University of Michigan. Subject: "Interchangeability—Its Development and Significance in Industry"
1932 MARSHALL ANDERSON, University of Michigan. Subject: "Apprenticeship and Vocational Training"
1933 GEORGE D. WILKINSON, JR., Newark College of Engineering Subject: "Progress in the Prevention of Smoke and Atmospheric Pollution"
1934 PHILIP P. SELF, Colorado State College. Subject: "Air Conditioning—Its Practicability and Relation to Public Welfare"
1935 G. LOWELL WILLIAMS, Lafayette College. Subject: "Coordinated Transportation—An Economic Comparison of Railroad, Bus, Truck, Water, and Air Transportation for Long and Short Haul"
1936 No Award. Subject: "Development in the Generation and Distribution of Power and Their Effect Upon the Consumer"
1937 ALLAN P. STERN, Case School of Applied Science. Subject: "The Influence of the Introduction of Labor Saving Machinery Upon Employment in the United States"
1938 EDWARD W. CONNOLLY, University of Detroit. Subject: "Economic Limitations in Engineering Design, With Concrete Examples"
1939 JAMES R. BRIGHT, Lehigh University. Subject: "The Economics of Investment in New Manufacturing Equipment—With Concrete Cases"
1940 FRANK DE POULD, Case School of Applied Science. Subject: "What Has Been the Effect of Technological Advance on Employment?"
1941 JOHN J. BALUN, University of Detroit. Subject: "The Need and Possibilities of Participation by Engineers in Public Affairs."

STUDENT AWARD

1916 BOYNTON M. GREEN, Stanford University, "Bearing Lubrication"
HOWARD E. STEVENS, Rensselaer Polytechnic Institute, "An Investigation of the Dynamic Pressure on Submerged Flat Plates"
M. ADAM, Louisiana State University, "The Adaptability of the Internal Combustion Engine to Sugar Factories and Estates"
1917 H. R. HAMMOND and C. W. HOLMBERG, The Pennsylvania State College, "Study of Surface Resistance With Glass as the Transmission Medium"
1919 C. F. LEH and F. G. HAMPTON, Stanford University, "An Experimental Investigation of Steel Belting"
W. E. HELMICK, Stanford University, "An Experimental Investigation of Steel Belting"
1920 HOWARD G. ALLEN, Cornell University, "Wire Stitching Through Paper"
1921 KARL H. WHITE, University of Kansas, "Forces in Rotary Motors"
RICHARD H. MORRIS and ALBERT J. R. HOUSTON, University of California, "A Report Upon an Investigation of the Herschel Type of Improved Weir"
1923 CHARLES F. OLMSTEAD, University of Minnesota, "Oil Burning for Domestic Heating"
H. E. DOOLITTLE, University of California, "The Integrating Gate: A. Device for Gaging in Open Channels"
1924 GEORGE STUART CLARK, Stanford University, "Two Methods Used for the Determination of the Gasoline Content of Absorption Oils in Absorption Plants"
L. J. FRANKLIN and CHARLES H. SMITH, Stanford University, "The Effect of Inaccuracy of Spacing on the Strength of Gear Teeth"
1925 HARRY PEASE COX, JR., Rensselaer Polytechnic Institute, "A Study of the Effect of End Shape on the Towing Resistance of a Barge Model"
W. S. MONTGOMERY, JR., and E. RAY ENDERS, JR., Pennsylvania State College, "Some Attempts to Measure the Drawing Properties of Metals"
1926 R. E. PETERSON, University of Illinois, "An Investigation of Stress Concentration by Means of Plaster of Paris Specimens"
CECIL G. HEARD, University of Toronto, "Pressure Distribution Over U.S.A. 27 Aerofoil With Square Wing Tips—Model Tests"
1927 ALFRED H. MARSHALL, Princeton University, "Evaporative Cooling"
ROGER IRWIN EBY, University of Washington, "Measurement of the Angular Displacement of Flywheels"
1928 CLARENCE C. FRANCK, Johns Hopkins University, "Condition Curves and Reheat Factors for Steam Turbines"
1929 FRANK VERNON BISTROM, University of Washington, "An Investigation of a Rotary Pump"
WILLIAM WALLACE WHITE, University of Washington, "An Investigation of a Rotary Pump"
1930 GERARD EDEN CLAUSSEN, Polytechnic Institute of Brooklyn, "High-Temperature Oxidation of Steel"
HAROLD L. ADAMS and RICHARD L. STITH, University of Washington, "A Wind Tunnel for Undergraduate Laboratory Experiments"
1931 JULES PODNOSSOFF, Polytechnic Institute of Brooklyn, "Pressure and Energy Distribution in Multi-Stage Steam Turbines Operating Under Varying Conditions"
1932 H. E. FOSTER, JR., University of Tennessee, "Factors Affecting Spray Pond Design" (Undergraduate Award)
WILLIAM A. MASON, Stanford University, "An Experimental Investigation of the Flame Propagation in Internal-Combustion Engines" (Postgraduate Award)
1933 HUGO V. CORDIANO, Polytechnic Institute of Brooklyn, "Thermal Analysis of Lithium-Magnesium System of Alloys" (Undergraduate Award)
JAMES A. OSTRAND, JR., Princeton University, "Sudden Enlargement in the Open Channel" (Postgraduate Award)
1934 H. REYNOLDS HUDSON, Georgia School of Technology, "Dynamic Balance and Functional Utility Applied to Automotive Design" (Undergraduate Award)
1935 CHARLES P. BACHA, Rutgers University, "The Behavior of Metals Subjected to Combined Stress" (Postgraduate Award)
ROBERT W. BEAL, Oregon State College, "Do Lubricating Oils Wear Out?" (Undergraduate Award)
1936 LEON B. STINSON, Oklahoma Agricultural and Mechanical College, "Polymerized Motor Fuels; Their Economic Significance" (Undergraduate Award)
DEWITT D. BARLOW, JR., Princeton University, "The Critical Speeds of Lateral Vibrations of Shafts with Gyroscopic Effects" (Postgraduate Award)
1937 GINO J. MARINELLI, Rensselaer Polytechnic Institute, "Investigation of the Towing Resistance of a Model Submarine Hull" (Undergraduate Award)
1938 MARSHALL C. LONG, Princeton University, "An Investigation Into the Angular Characteristics of an Adjustable Blade Current Meter" (Postgraduate Award)
DONALD C. MCSORLEY, Michigan State College, "Humidity Insulation" (Undergraduate Award)

1939 DAVID T. JAMES, Michigan State College, "Bells—Concerning Their Tones" (Undergraduate Award)

1940 GEORGE W. SHEPHERD, JR., Princeton University, "An Automatic Mechanical Control for Synchronizing Prime Movers" (Postgraduate Award)
EDWARD D. ROWAN, Oregon State College, "Powder Metallurgy (Undergraduate Award)

1941 G. WALKER GILMER, III, University of Florida, "Center of Pressure Characteristics of a Marconi Yacht Sail" (Undergraduate Award).

FREEMAN TRAVEL SCHOLARSHIP

1927 HERBERT N. EATON
1928 BLAKE R. VAN LEER
1929 ROBERT T. KNAPP
1931 REGINALD WHITAKER
1932 G. ROSS LORD
1933, 1934 H. J. CASEY
1935, 1936 VICTOR L. STREETER

HONORARY MEMBERS

HONORARY MEMBERS IN PERPETUITY

Alexander Lyman Holley, Founder of the Society. Died 1882.
John Edson Sweet, Founder of the Society. Died 1916.
Henry Rossiter Worthington, Founder of the Society. Died 1880.

DECEASED HONORARY MEMBERS

	ELECTED	DIED
Leon Pratt Alford	1941	1942
Horatio Allen	1880	1889
Lorenzo Allievi	1937	1941
Sir William Arrol	1905	1913
Sir John Audley Frederick Aspinall	1911	1937
William Wallace Atterbury	1925	1935
Sir Benjamin Baker	1886	1907
Johann Bauschinger	1884	1893
Sir Henry Bessemer	1891	1898
Sir Frederick Joseph Bramwell	1884	1903
John Alfred Brashear	1908	1920
Gustave Canet	1900	1908
Andrew Carnegie	1907	1919
Daniel Kinnear Clark	1882	1896
Rudolph Julius Emmanuel Clausius	1882	1888
Hutchinson I. Cone	1936	1941
Sir John Goode	1889	1892
Peter Cooper	1882	1883
Charles de Fréminville	1919	1936
Carl Gustaf Patrick de Laval	1912	1913
Rudolph Diesel	1912	1913
James Dredge	1886	1906
Victor Dwelshauvers-Dery	1886	1913
Thomas Alva Edison	1904	1931
Alexandre Gustave Eiffel	1889	1923
Marshal Ferdinand Foch	1921	1929
Sir Charles Douglas Fox	1900	1921
John Ripley Freeman	1932	1932
John Fritz	1900	1913
Major-General George Washington Goethals	1917	1928
Franz Grashof	1884	1893
Rear-Admiral Robert Stanislau Griffin	1920	1933
Otto Hallauer	1882	1883
Charles Haynes Haswell	1905	1907
Nathanael Greene Herreshoff	1921	1938
Friedrich Gustav Herrmann	1884	1907
Gustav Adolph Hirn	1882	1890
Joseph Hirsch	1889	1901
Ira N. Hollis	1928	1930
Robert Woolston Hunt	1920	1923
Benjamin Franklin Isherwood	1894	1915
Henri Léauté	1891	1916
Erasmus Darwin Leavitt	1915	1916
Henri Le Chatelier	1927	1936
Anatole Mallet	1912	1919
Charles H. Manning	1913	1919
Rear-Admiral George Wallace Melville	1910	1912
The Honorable Sir Charles Algernon Parsons	1920	1931
Charles Talbot Porter	1890	1910
Auguste C. E. Rateau	1919	1930
Sir Edward J. Reed	1882	1906
Franz Reuleaux	1882	1905
Calvin Winsor Rice	1931	1934
Palmer C. Ricketts	1931	1934
Henri Adolphe-Eugene Schneider	1882	1898
Charles M. Schwab	1918	1939
C. William Siemans	1882	1883
Viscount Ei-ichi Shibusawa	1929	1931
Ambrose Swasey	1916	1937
Elihu Thomson	1930	1937
Henry Robinson Towne	1921	1924
Henri Tresca	1882	1885
William Cawthorne Unwin	1898	1933
Samuel Matthews Vauclain	1920	1940
Oskar von Miller	1912	1934
Francis A. Walker	1886	1897
Worcester Reed Warner	1925	1929
George Westinghouse	1897	1914
Sir William Henry White	1906	1913
Sir Alfred Fernandez Yarrow	1914	1932

LIVING HONORARY MEMBERS

	ELECTED
William Lamont Abbott	1940
Robert W. Angus	1940
Edmund Bruce Ball	1939
Mortimer Elwyn Cooley	1928
Alex Dow	1936
William Frederick Durand	1934
Arthur M. Greene, Jr.	1940
Herbert Clark Hoover	1925
Clarence Decatur Howe	1941
David Schenck Jacobus	1934
Masawo Kamo	1929
Dexter Simpson Kimball	1939
Albert Kingsbury	1940
Charles Thomas Main	1939
George A. Orrok	1936
Grande Ufficiale Ing. Pio Perrone	1920
Edwin Jay Prindle	1939
Rear Admiral Samuel Murray Robinson	1941
James A. Seymour	1940
Aurel Stodola	1941
William H. Tschappat	1938
Henry Hague Vaughan	1939
Right Honorable Lord Weir	1920
Major General Charles Macon Wesson	1941
Orville Wright	1918

PAST-PRESIDENTS

A list of past vice-presidents, managers, treasurers, and secretaries will be found in the 1930 Record and Index, pages 10-12. Dates in parentheses denote year of death.

Alexander Lyman Holley, *Chairman of the Preliminary Meeting for Organization of The American Society of Mechanical Engineers* (1882)

1880–1882 Robert Henry Thurston (1903)
1883 Erasmus Darwin Leavitt (1916)
1884 John Edson Sweet (1916)
1885 Josephus Flavius Holloway (1896)
1886 Coleman Sellers (1907)
1887 George H. Babcock (1893)
1888 Horace See (1909)
1889 Henry Robinson Towne (1924)
1890 Oberlin Smith (1926)
1891 Robert Woolston Hunt (1923)
1892 Charles Harding Loring (1907)
1893–1894 Eckley Brinton Coxe (1895)
1895 Edward F. C. Davis (1895)
1895 Charles Ethan Billings (1920)
1896 John Fritz (1913)
1897 Worcester Reed Warner (1929)
1898 Charles Wallace Hunt (1911)
1899 George Wallace Melville (1912)
1900 Charles Hill Morgan (1911)
1901 Samuel T. Wellman (1919)
1902 Edwin Reynolds (1909)
1903 James Mapes Dodge (1915)
1904 Ambrose Swasey (1937)
1905 John Ripley Freeman (1932)
1906 Frederick Winslow Taylor (1915)
1907 Frederick Remsen Hutton (1918)
1908 Minard Lafever Holman (1925)
1909 Jesse Merrick Smith (1927)
1910 George Westinghouse (1914)
1911 Edward Daniel Meier (1914)
1912 Alexander Crombie Humphreys (1927)
1913 William Freeman Myrick Goss (1928)
1914 James Hartness (1934)
1915 John Alfred Brashear (1920)
1916 David Schenck Jacobus
1917 Ira Nelson Hollis (1930)
1918 Charles Thomas Main
1919 Mortimer Elwyn Cooley
1920 Fred J. Miller (1939)
1921 Edwin S. Carman
1922 Dexter Simpson Kimball
1923 John Lyle Harrington
1924 Frederick Rollins Low (1936)
1925 William Frederick Durand
1926 William Lamont Abbott
1927 Charles M. Schwab (1939)
1928 Alex Dow
1929 Elmer Ambrose Sperry (1930)
1930 Charles Piez (1933)
1931 Roy V. Wright
1932 Conrad N. Lauer
1933 A. A. Potter
1934 Paul Doty (1938)
1935 Ralph E. Flanders
1936 William L. Batt
1937 James H. Herron
1938 Harvey N. Davis
1939 Alexander G. Christie
1940 Warren H. McBryde
1941 William A. Hanley

TREASURERS

Apr. 1880—Dec. 1881	Lycurgus B. Moore *
Dec. 1881—Nov. 1884	Charles W. Copeland (1895)
1894—1925	William H. Wiley (1925)
1925—1935	Erik Oberg
1935—date	William D. Ennis

SECRETARIES

Organization Meeting, 1880	Samuel S. Webber, Jr. (1921)
Acting Secretary, Apr.-Nov. 1880	Lycurgus B. Moore *
Nov. 1880—Mar. 1883	Thos. Whiteside Rae *
1883—1906	Frederick R. Hutton (1918)
1906—1934	Calvin W. Rice (1934)
1934—date	Clarence E. Davies

* Deceased. Year not known.

Index to Society Records, Part 1

The page numbers in this section are preceded by the letters "RI," which are omitted in the following index.

Abbreviations and Symbols, Graphical, Comm.. 26
Abbreviations and Symbols, Letter, Comm.... 26
Abrasive Wheels, Rep. on Safety Comm..... 30
Acoustical Measurements, Reps. on Comm..... 26
Administration Organization, Comm..... 8
Admissions Comm.
  Special 4
  Standing 2
Advertising Manager, A.S.M.E..... 1
Aeronautic Div. *See* Aviation Div.
Aeronautics, Rep. on Standardization Comm.. 26
Air Conditioning, Comms., Process Industries and Textile Divs..... 9
Alfred Noble Prize, A.S.M.E. Rep..... 5
Allowances and Tolerances, Gages, Comm.... 22
American Association for the Advancement of Science, A.S.M.E. Reps..... 5
American Standards Association, A.S.M.E. Reps. 5
American Year Book Corporation, A.S.M.E. Rep. 5
Applied Mechanics Div., Comms..... 6
A.S.M.E. Medal
  Recipients 34
  Statement about 34
Assistant Secretaries, A.S.M.E..... 1
Aviation Div., Comms..... 6
Awards, A.S.M.E.
  Recipients 34
  Statements about 34
Awards Comm. *See* Honors and Awards Comm.
Ball and Roller Bearings, Comm..... 22
Biography Comm. 3
Board of Review..... 4
Board on Technology..... 4
Boiler Code
  Comm. Work 33
  Comm., Special 3, 32
  Conference Comm. 32
  Exec. Comm. 32
  Revision of Section VIII, Special Comm.. 33
  Subcomms. 32
Boiler Feedwater Studies, Comm..... 20
Boilers, Openings, Comm..... 33
Boilers, Power 32
Boilers, Rules for Inspection of, Comm..... 32
Boilers, Special Design of, Comm..... 32
Bolted Flanged Connections, Rules for, Comm.. 33
Bolt, Nut, and Rivet Proportions, Comm..... 24
Building Code for Light and Ventilation, Rep. on Comm. 26
Cast Iron Pipes, Reps. on Comm..... 27
Cavitation, Comm. 7
Center for Safety Education, A.S.M.E. Rep.... 5
Charles T. Main Award
  Recipients 36
  Statement about 34
Chucks and Chuck Jaws, Comm..... 23
Coal and Coke, Rep. on Comm..... 26
Coal, Clean Bituminous, Rep. on Comm..... 27
Coal-Handling Equipment, Rep. on Comm..... 27
Coal Mines, Drainage, Rep. on Comm..... 27
Coal Testing Code, Reps. on Comm..... 6, 29
Colleges, Relations With, Comm..... 2, 18
Compressed Air, Work in, Rep. on Safety Comm. 31
Compressed Air Machinery and Equipment, Safety Comm. 30
Compressors and Blowers
  Centrifugal and Turbo, Comm..... 28
  Displacement, Comm. 28
Comptroller, A.S.M.E. 1
Condensers, Water Heating, and Cooling Equipment, Comm. 29
Condenser Tubes, Comm..... 21
Constitution and By-Laws Comm..... 2
Construction Work, Rep. on Safety Comm.... 30
Consulting Practice, Comm..... 4
Conveyors and Conveying Machinery, Safety Comm. 30
Coordinating Comm. (Corrosion), Rep. on.... 21
Coordination Comm. (Boiler Code)..... 32
Coordination Comm. (Heat Transfer)..... 7
Correlating Comm. ASA Safety Code, Rep. on Comm. 30
Corrosion, Coordinating Comm., Rep. on..... 21
Corrosion, Rep. on Comm..... 21
Cottonseed Processing, Comm..... 21
Council, A.S.M.E.
  Exec. Comm. 1
  Members of 1
  Special Comms. 4
Cranes, Derricks, and Hoists, Safety Comm.... 30
Cut and Ground Thread Taps, Comm..... 23
Cutting of Metals, Research Comm..... 20
Cutting Tools, Single-Point, Comm..... 23
Daniel Guggenheim Medal Fund, Inc., A.S.M.E. Reps. 5
Definitions and Values, Power Test Codes, Comm. 28
Depreciation 4
Depreciation Studies, Comm..... 8
Dimensional Limits and Allowances, Comm... 9
Direct-Fired Fluid Heaters and Boilers, Comm. 7
Dished Heads, Comm..... 33
Displacement Pumps, Reciprocating Steam-Driven, Comm. 28
Drawings and Drafting Room Practice, Comm. 26
Drying, Comms., Process Industries and Textile Divs. 9
Dues-Exempt Members' Contributions, Comm.. 4
Dust Explosions, Rep. on Safety Comm..... 31
Dust Separating Apparatus, Comm..... 29
Economic Status of the Engineer Comm..... 4
Editor, A.S.M.E. 1
Education and Training for the Industries Comm. 2
Electrical Definitions, Rep. on Comm..... 26
Electric Sockets and Lamp Bases, Comm..... 26
Electric Welding Apparatus, Rep. on Comm... 27
Elevators, Comm. 20
Elevators, Safety Code, Comm..... 30
Engineering Foundation, A.S.M.E. Reps..... 5
Engineering History Comm., A.S.M.E. Reps.. 5
Engineering Registration, National Bur. of, A.S.M.E. Rep. 5
Engineering Societies, Cooperation in Safety Work, Rep. on Comm..... 30
Engineering Societies Library Board, A.S.M.E. Reps. 5
Engineering Societies Monographs Comm., A.S.M.E. Reps. 5
Engineering Societies Personnel Service, Inc., A.S.M.E. Reps. 5
Engineers' Civic Responsibilities, Comm..... 4
Engineers' Council for Professional Development, A.S.M.E. Reps..... 5
Engineers Defense Board, A.S.M.E. Reps..... 5
Engineers' National Relief Fund, A.S.M.E. Rep. 5
Evaporating Apparatus, Comm..... 29
Exhaust Systems, Rep. on Safety Comm..... 30
Feedwater, Boiler Code Comm..... 33
Feedwater Studies, Boiler, Comm..... 20
Ferrous Materials, Comm..... 32
Finance Comm. 2
Fire Tests, Building Construction and Materials, Rep. on Comm..... 27
Floor and Wall Openings, Railings, and Toe Boards, Rep. on Safety Comm..... 30
Fluid Meters, Comm..... 20
Food Processing, Comm..... 9
Forest Fire Protection, Rep. on Comm..... 27
Forging and Hot Metal Stamping, Rep. on Safety Comm. 30
Freeman Fund, Comm..... 4
Freeman Scholarships. *See* John R. Freeman Travel Scholarships
Fritz Medal Board of Award, A.S.M.E. Reps... 5
Fuels, Calorific Values, Rep. on Comm..... 29
Fuels, Power Test Code Comm..... 28
Fuels Div., Comms..... 6
Fuel Values, Calorific, A.S.M.E. Rep..... 29
Furnace Performance Factors, Comm..... 21
Fusion Welding Requirements..... 33
Gages, Pressure and Vacuum, Comm..... 25
Gantt Medal Board of Award, A.S.M.E. Reps.. 5
Gas Burning Appliances, Rep. on Comm..... 26
Gas Mask Canisters, Rep. on Safety Comm..... 30
Gas Producers, Comm..... 29
Gaseous Fuels, Rep. on Comm..... 29
Gear Lubricants, Rep. on Comm..... 27
Gears, Comm. 23
Gear Teeth, Strength of, Comm..... 20
George Westinghouse Bust Comm..... 4
Glass, Safety, Rep. on Comm..... 31
Graphic Arts Div., Comms..... 6
Graphic Presentation Comm..... 26
Guggenheim Medal Fund, A.S.M.E. Reps..... 5
Heating Boilers, Comm..... 32
Heat Transfer Div., Comms..... 7
Holley Medal
  Recipients 35
  Statement about 34
Holmes Safety Association, A.S.M.E. Rep..... 5
Honorary Members, List of..... 38
Honorary Membership, Statement about..... 34
Honors and Awards Comm..... 2
Honors and Awards, Special Comm. of Board of 3
Hoover Medal Board of Award, A.S.M.E. Reps.. 5
Hose Couplings, Screw Threads, Comm..... 24
Hydraulic Div., Comms..... 7
Hydraulic Prime Movers
  Hyd. Div. Comm..... 7
  Power Test Codes Comm..... 29
Industrial Furnaces and Kilns, Comm..... 7
Industrial Instruments and Regulators, Comm. 9
Industrial Marketing, Comm..... 8
Industrial Workers, Foundries, Protection of, Rep. on Safety Comm..... 31
Industrial Workers, Protection of, Rep. on Safety Comm. 31
Industries, Education and Training for, Comm. 2
Instruments and Apparatus, Power Test Codes, Comm. 29
Inter-American Engineering Cooperation, A.S.M.E. Rep. 5
Internal-Combustion Engines, Comm..... 29
International Electrochemical Commission, A.S.M.E. Reps. 5
Iron and Steel Bars, Comm..... 25
Iron and Steel Div. *See* Metals Engineering Div.
Jig Bushings, Comm..... 23
John Fritz Medal Board of Award, A.S.M.E. Reps. 5
John R. Freeman Travel Scholarships
  Recipients 37
  Statement about 34
Joseph A. Holmes Safety Association, A.S.M.E. Rep. 5
Journal of Applied Mechanics, Editor..... 6
Junior Award
  Recipients 35
  Statement about 34
Ladders, Rep. on Safety Comm..... 31
Laundry Machinery, Rep. on Safety Comm.... 31
Leather Belting, Comm..... 25
Library Comm. 2
Life Membership, Statement about..... 34
Lighting, Comm. 9
Lighting Factories, Mills, Rep. on Safety Comm. 31
Loading Platforms, Rep. on Comm..... 27
Local Sections
  Exec. Comms. 10
  Nominating Comm., Groups of..... 3
  Regional Group Delegates to Annual Conferences 10
  Standing Comm. 2, 10
Locomotives, Boilers of, Comm..... 32
Low Voltage Electrical Hazards, Rep. on Safety Comm. 31
Lubrication, Textile Div. Comm..... 9
Lubrication, Comm. 20
Machine Pins, Comm..... 25
Machinery, Speeds of, Comm..... 26
Machine Shop Practice Div. *See* Production Engineering Div.
Machine Tapers, Comm..... 22
Machine Tool Elements, Comm..... 22
Machine Tools, Designations and Working Ranges, Comm. 23
Main Award. *See* Charles T. Main Award
Management Div., Comms..... 8
Manhole Frames and Covers, Rep. on Comm.... 27
Marston Award, A.S.M.E. Rep..... 5
Materials Handling Div., Comms..... 8
Materials, New, Boiler Code Comm..... 33
Material Specifications, Comm..... 32
Mathematical Statistics, Comm..... 8
Max Toltz Loan Fund, Statement about..... 34
Mechanical Power-Transmission Apparatus, Safety Comm. 30
Mechanical Refrigeration, Reps. on Safety Comm. 31
Mechanical Separation, Comm..... 9
Mechanical Springs, Comm..... 20
Mechanical Standards, Reps. on Comm..... 27
Medals, Comm. 3
Meetings and Program Comm..... 2
Membership Comm. *See* Admissions Comm.
Melville Medal
  Recipients 35
  Statement about 34
Metallurgical Research, Rep. on Com..... 21
Metals, Cutting of, Comm..... 20
Metals, Effect of Temperature on, Comm..... 20
Metals Engineering Div., Comms..... 8
Metals, Fatigue Phenomena of, Rep. on Comm.. 21
Mid-West Office, Location of..... 1
Milling Cutters, Comm..... 23
Miniature Boilers, Comm..... 32
Model Smoke Law, Comm..... 6
Monographs Comm., A.S.M.E. Reps..... 5
National Bureau of Engineering Registration, A.S.M.E. Rep. 5
National Conference on Engineering Positions, A.S.M.E. Reps. 5
National Defense Comm..... 4
National Fire Waste Council, A.S.M.E. Rep... 5
National Management Council A.S.M.E. Reps.. 5
National Research Council, A.S.M.E. Rep..... 5
Noble Prize, A.S.M.E. Rep..... 5

Nomenclature, Machine Tools, Comm 23
Nominating Comm., 1942 3
Nonferrous Materials, Comm 32
Officers, A.S.M.E., for 1941-1942 1
Oil and Gas Power Div., Comms 8
Openings, Rules for, Boiler Code Comm 33
Paper and Pulp Mills, Rep. on Safety Comm .. 31
Past-Presidents, List of 38
Petroleum Div., Comms 9
Petroleum Products and Lubricants, Reps. on Comm. 27
Pipe and Tubing, Comm 24
Pipe Flanges and Fittings, Comm 23
Pipe Threads, Comm 22
Piping Systems, Identification, Comm 25
Piping Valves and Fittings, Material Specifications, Comm. 33
Pi Tau Sigma Award
Recipients 35
Statement about 34
Plumbing Equipment, Comm 25
Plywood, Use as Engineering Material, Comm .. 9
Post-Emergency Planning, A.S.M.E. Rep 5
Power Boilers, Comm 32
Power and Heat Utilization, Textile Div. Comm. 9
Power Div., Comms 9
Power Test Codes Comm., Standing 2, 28
Power Test Codes Comms., Technical 28
Power Test Codes, General Instructions, Comm. 28
Preferred Numbers, Rep. on Comm 27
Presses, Rep on Safety Comm 31
Pressure Piping, Code for, Comm 24
Pressure Vessels in Service, Care of, Comm ... 32
Pressure Vessels, Unfired
A.P.I.-A.S.M.E. Comm. 33
A.S.M.E. Comm. 32
Prime Movers
Hyd. Div. Comm 7
Power Test Codes Comm 29
Speed Governing Specifications, Rep. on Comm. 29
Process Industries Div., Comms 9
Production Engineering Div., Comms 9
Professional Conduct Comm 2
Professional Divs. Comm., Standing 2, 6
Professional Divs. Exec. Comms 6
Publications Comm.
Special 3
Standing 2
Pumping Machinery, Comm 7
Pumps, Centrifugal and Rotary, Comm 28
Pumps, Reciprocating Steam-Driven Displacement, Comm. 28
Punch Press Tools, Comm 23
Quarry Operations, Rep. on Safety Comm 31
Railroad Div., Comms 9
Rating of Rivers, Rep. on Comm 27
Reamers, Comm. 23
Refractory Materials, Properties of, Rep. on Comm. 21
Refrigerating Systems, Comm 29
Registration Comm. 4
Relations With Colleges Comm 2, 18
Representatives on Other Activities
A.S.M.E. 5
Boiler Code 33
Power Test Codes 29
Research 21
Safety 30
Standardization 26
Research Comm., Standing 2, 20
Research Comms., Technical 20
Research Procedure Comm. of Engineering Foundation, A.S.M.E. Rep 5
Research Secretaries
Applied Mechanics 6
Heat Transfer 7
Management 8
Oil and Gas Power 8
Petroleum 9
Process Industries 9
Railroad 9
Textile 9
Rock Drill Steels, Heat-Treatment of, Rep. on Comm. 21
Rolling of Steel (Plasticity), Comm 21
Rotating Electrical Machinery, Rep. on Comm .. 27
Rubber and Plastics, Subdivision 9
Rubber Machinery, Rep. on Safety Comm 31
Safety Comm., Standing 2, 30
Safety Comms., Technical 30
Safety Education, Center for, A.S.M.E. Rep ... 5
Safety Valve Requirements, Comm 33
St. Louis Junior Award. *See* Spirit of St. Louis Junior Award
St. Louis Medal. *See* Spirit of St. Louis Medal
Sanitation, Comm. 9
Scholarships and Loan Funds, Statement about 34
Screw Threads for Hose Couplings, Comm 24
Screw Threads, Standardization, Comm 22
Screw Threads, U. S. Comm., Reps. on 27
Secretarial Staff, A.S.M.E. 1
Secretaries, List of 39
Shafting, Comm. 24
Sieves for Testing Purposes, Rep. on Comm .. 27
Single-Point Cutting Tools, Comm 23
Single-Point Tool-Life Tests, Comm 23
Small Tools, Comm 22
Society Office Operation Comm 4
Solid Fuels, Combustion Space for, Comm 25
Specific Heat of Gases, Comm 7
Speed, Temperature and Pressure Responsive Governors, Comm. 29
Speeds of Machinery, Comm 26
Spindle Noses and Collets, Comm 23
Spirit of St. Louis Medal
Recipients 35
Statement about 34
Spirit of St. Louis Junior Award
Recipient 35
Statement about 34
Splines and Splined Shafts, Comm 23
Springs, Mechanical, Comm 20
Standardization Comm., Standing 2, 22
Standardization Comms., Technical 22
Standard Ton of Refrigeration, Rep. on Comm. 29
Standing Comms. 2
Statistics in Engineering and Manufacturing, Comm. 26
Steam Boilers, Critical Pressure, Comm 21
Steam Boilers in Service, Care of, Comm 32
Steam Engines, Reciprocating, Comm 28
Steam-Generating Units, Stationary, Comm 28
Steam Locomotives, Comm 29
Steam, Thermal Properties of, Comm 20
Steam Turbines, Comm 28
Steel, Rolling of (Plasticity), Comm 21
Steel Shells, Forging of, Comm 21
Strength of Gear Teeth 20
Strength of Vessels, Comm 21
Student Awards
Recipients 36
Statement about 34
Student Branches, List of 18
Sugar, Comm. 9
Sulphur, Comm. 9
Surface Qualities, Comm 25
Symbols and Abbreviations
Graphical, Comm. 26
Letter, Comm. 26
Symbol Stamps, Boiler Code, Comm 33
Technical Committees
Boiler Code 32
Power Test Codes 28
Research 20
Safety 30
Standardization 22
Technical Committees, Standing 2
Technology, Board on 4
Testing Technique Comm 7
Testing Wood, Rep. on Comm 27
Textile Div., Comms 9
Textiles, Rep. on Safety Comm 31
Theory and Fundamental Research, Comm 7
Thermal Insulating Materials, Rep. on Comm .. 27
Thermal Properties of Steam 20
Thermo-Physical Properties of Materials, Comm. 7
Toltz Fund. *See* Max Toltz Loan Fund
Tool Holders, Comm 23
Tool Posts and Shanks, Comm 22
Transmission Chains and Sprockets, Comm 24
Treasurers, List of 39
T-Slots, Comm. 22
Twist Drill Sizes, Comm 23
Unfired Heat Transfer Equipment, Comm 7
Unfired Pressure Vessels
A.P.I.-A.S.M.E. Comm. 33
A.S.M.E. Comm. 32
United Engineering Trustees, Inc., A.S.M.E. Reps. 5
Vegetable Oils, Comm 9
Ventilation, Rep. on Safety Comm 31
Vermilye Medal Advisory Comm., A.S.M.E. Rep. 5
Vessels, Clad, Comm 33
Vessels, Strength Under External Pressure, Comm. 21
Walkway Surfaces, Rep. on Safety Comm 31
Warner Medal. *See* Worcester Reed Warner Medal
Washers, Plain and Lock, Comm 24
Washington Award Commission, A.S.M.E. Reps. 5
Water for Industrial Uses, Rep. on Comm 21
Water Hammer, Comm 7
Water Heating, Volume, Rep. on Comm 27
Welded Joints, Radiographic Examination of, Comm. 33
Welding
Boiler Code Comm 32
Welding Apparatus, Electric, Rep. on Comm .. 27
Westinghouse Bust Comm 4
Wire and Sheet Metal Gages, Comm 24
Wire Rope, Comm 21
Wire Rope for Mines, Rep. on Comm 27
Woman's Auxiliary, Officers of 33
Woman's Auxiliary Scholarship 34
Wood Finishing, Comm 9
Wood Industries Div., Comms 9
Worcester Reed Warner Medal
Recipients of 35
Statement about 34
Works Standardization, Comm 8
Worm Gears, Comm 21

CONSTITUTION, BY-LAWS, AND RULES

Amended to June 16, 1941

Article C1, Name and Government

Sec. 1. The name of this Society is The American Society of Mechanical Engineers.

Sec. 2. The Society is a corporation, organized April 7, 1880, and chartered under the laws of the State of New York, December 24, 1881.* A supplemental charter** was issued on October 17, 1907, when the Society was consolidated with the Mechanical Engineers' Library Association.

The principal offices of the Society shall be in the City of New York.

Sec. 3. The Society shall be governed by this Constitution, the By-Laws, and the Rules.

Article B1, Government

Par. 1 Every question which shall come before a meeting of the Society or of the Council or of a committee, shall be decided by a majority of the votes cast, unless otherwise provided in the Constitution, the By-Laws and the Rules, or by the laws of the State of New York.

Par. 2 The Rules contained in "Robert's Rules of Order Revised" shall govern the Society in all cases to which they are applicable, when not inconsistent with the By-Laws or the Rules of this Society.

Article C2, Objects

Sec. 1. The objects of this Society are to promote the art and science of mechanical engineering and the allied arts and sciences; to encourage original research; to foster engineering education; to advance the standards of engineering; to promote the intercourse of engineers among themselves and with allied technologists; and severally and in cooperation with other engineering and technical societies to broaden the usefulness of the engineering profession.

Sec. 2. The Society may approve or adopt any report, standard, code, formula, or recommended practice, but shall forbid and oppose the use of its name, emblem, or initials in any commercial work or business, except to indicate conformity with its standards or recommended practices.

Article B2, Purposes

Par. 1 The objectives of the Society shall be accomplished by:

A Advancing the theory and practice of engineering and the allied arts and sciences by:

(*a*) Encouraging engineering research, tests, and other original work.

(*b*) Encouraging the preparation of original papers on engineering topics.

(*c*) Holding meetings for the presentation and discussion of original papers and participating in international engineering congresses.

(*d*) Publishing papers and reports and disseminating knowledge and experience of value to engineers.

(*e*) Developing and promulgating standards, codes, formulas, and recommended practices.

(*f*) Offering awards and other honors to encourage contributions to engineering; conferring awards and other honors in recognition of meritorious contributions to engineering.

(*g*) Furthering the purposes of the Engineering Societies Library, of which the Library of this Society forms a part.

(*h*) Encouraging intercourse among engineers for the mutual exchange of knowledge and experience.

B Enhancing the status of the engineer by:

(*a*) Maintaining high technical and cultural standards for entrance to the Society.

(*b*) Cooperating with educational institutions in the maintenance of high standards of engineering education.

(*c*) Requiring a high standard of ethical practice by members of the Society.

(*d*) Aiding in the adoption of a high standard of attainment for the granting of the legal right to practice professional engineering.

(*e*) Fostering among engineering students the study of philosophy and history, tradition and achievement, duties, and social functions of the engineering profession.

(*f*) Encouraging the personal and professional development of young engineers.

(*g*) Supporting activities looking to the increased employment of engineers and seeking new opportunities for engineering service.

C Increasing the usefulness of the organized engineering profession by:

(*a*) Cooperating with other engineering and technical societies.

(*b*) Encouraging a high standard of citizenship among engineers.

(*c*) Encouraging engineers to participate in public affairs.

(*d*) Cooperating with governmental agencies in engineering matters.

(*e*) Publicity for the engineering profession through the achievements of engineers.

Par. 2 The closest possible cooperation with universities and technical schools qualified and equipped to assist in the development and conduct of special research work is favored and is strongly urged.

Par. 3 Cooperative, not competitive, methods should be worked out with existing research laboratories and activities in other organizations. Such cooperation could take the form of publication of papers and groups of papers where a definite industry desires to bring to the attention of engineers for the development of the industry, any problem or special research, without commercial bias.

Par. 4 Each suggested research must be presented, on its individual merit, for approval by the Council, which will in turn refer the matter to the appropriate authority or committee.

Par. 5. Specific requests to the Council for solicitation of funds are to be accompanied with full details for proposed scope, method of solicitation, and budget.

Par. 6 No contributor is to be specially favored on account of any contribution for a research in which he is interested and a contribution can be received only on the basis of general benefit to the industry.

Article R2, Affiliated Organizations

Rule 1 The Council may approve the affiliation with the Society of any engineering society or legally organized group of engineers whose objects are in accord with the traditions, precedents, and objects of this Society.

Rule 2 The term "Affiliated with The American Society of Mechanical Engineers" shall be used by any society or by individual members of it only while the respective governing boards of both societies continue the affiliation.

*The original charter or certificate of incorporation was reproduced in facsimile form in the Transactions for 1937, pages RI-37–RI-42.

**The Supplemental Charter of October 17, 1907, also provided that the number of Directors shall be twenty-two (22).

RULE 3 Affiliation with this Society of any other organization shall in no wise be interpreted as interfering with the independence, autonomy, and self-control of that organization under its own constitution or by-laws.

RULE 4 The Society shall not be responsible for any act of any affiliated society.

RULE 5 Affiliation with this Society of any other organization may be terminated by the governing board of either giving sixty (60) days' written notice to the governing board of the other.

ARTICLE C3, MEMBERSHIP

Sec. 1. The corporate membership shall consist of Fellows, Members, and Junior Members. In addition there shall be Honorary Members, Associates, and Student-members.

Sec. 2. The rights and privileges of every member shall be personal to himself and shall not be transferable except that each corporate member shall be entitled to vote on any question before the Society either in person or by a proxy given to a corporate member.

Sec. 3. Every person admitted to membership shall be subject to the Constitution of the Society, and to any amendments that may be made from time to time.

ARTICLE B3, MEMBERSHIP

PAR. 1 The Council shall have power by resolution from time to time, to fix the number of Honorary Members.

PAR. 2 A proxy may be given to a member entitled to vote, but shall not be valid for more than six (6) months. Such proxy shall be signed, with an attesting witness, by the member giving it and shall be submitted to the Secretary for verification of the right of the member to vote at the meeting at which the proxy is to be used.

PAR. 3 Proffered resignations shall be presented to the Council for action, and shall be accepted if the requirements have been met. Each resignation presented to the Council after the fiscal year has commenced (October first) must be accompanied by a statement from the Secretary that the member has paid his dues up to and including the expired portion of the current fiscal year, unless such resignation is presented by January first, when no payment of current dues shall be required.

ARTICLE R3, MEMBERSHIP

RULE 1 Each member shall be entitled to a certificate of membership, signed by the President and the Secretary of the Society; it shall remain the property of the Society and be returned on demand. Each member requesting a certificate shall pay the cost of engrossing.

Rule 2 Abbreviations of the titles to be used by members are as follows:

Honorary Member	Hon. Mem. A.S.M.E.
Fellow	Fellow A.S.M.E.
Member	Mem. A.S.M.E.
Associate	Assoc. A.S.M.E.
Junior Member	Jun. A.S.M.E.
Student-member	Student A.S.M.E.

RULE 3 Each member shall be entitled to wear the emblem approved by the Council for his grade of membership.

RULE 4 Each member desiring to resign shall deposit with the Secretary any badge and certificate of membership in his possession, and upon acceptance of his resignation the Secretary shall make him the stipulated refund for his badge.

ARTICLE C4, QUALIFICATIONS FOR ADMISSION

Sec. 1. Members of all grades shall be elected by the Council.

Sec. 2. An Honorary Member shall be a person of acknowledged professional eminence.

Sec. 3. A Fellow shall be an engineer who shall have distinct engineering attainments, twenty-five (25) years of active practice in the profession of engineering or teaching of engineering in a school of accepted standing, and shall have been thirteen (13) years in the grade of Member. Graduation from an engineering school of accepted standing shall be considered equivalent to four (4) years of active practice.

Sec. 4. An engineer lacking the qualifications of Section 3 who has distinguished engineering or scientific attainments may be elected a Fellow by unanimous vote of Council members voting.

Sec. 5. A Member shall be an engineer or teacher of engineering who shall have reached the age of thirty (30) years and who shall have had nine (9) years active practice in the profession of engineering or teaching, three (3) years of which shall have been in a position of responsible charge of important work and who is qualified to design as well as direct such work. Graduation from a school of engineering of accepted standing shall be considered equivalent to four (4) years of active practice.

Sec. 6. An Associate need not be an engineer but must have a record of recognized leadership in some profession, or branch of industry, or science relating to engineering, and shall be qualified to cooperate with engineers in the practice of their profession and he must be at least thirty (30) years of age.

Sec. 7. A Junior Member shall be a graduate of a school of engineering of accepted standing or one who has equivalent attainments.

Sec. 8. A Student-member shall be a student regularly enrolled and pursuing an approved engineering curriculum in a school having a Student Branch of this Society.

ARTICLE B4, QUALIFICATIONS FOR ADMISSION

PAR. 1 A candidate for admission to the Society in any grade, except Honorary Membership, or a member desiring to change his grade, shall make application to the Council on an approved form.

PAR. 2 Fifteen (15) affirmative votes of the Council shall be required for the election of a candidate for any grade except Honorary Membership. Two (2) negative votes shall defeat an election.

PAR. 3 Each approved candidate shall be assigned by the Council to the grade of membership to which, in its judgment, his qualifications entitle him.

PAR. 4 Nomination for Honorary Membership may be made to the Council by at least twenty-five (25) members of the Society, who shall in all cases state in writing the grounds upon which the nomination is made.

PAR. 5 Election to Honorary Membership shall be by letter-ballot of the Council. Ballots shall be mailed by the Secretary to each member of the Council at least twenty-one (21) days in advance of the date set for the closure of such election. One (1) negative vote shall defeat an election to Honorary Membership.

PAR. 6 All matters relating to admissions to and promotions in membership shall be in charge of the Standing Committee on Admissions, under the direction of the Council.

PAR. 7 A Student-member may participate in all the activities of the Society but shall not be permitted to vote or hold an elective office except in the Student Branch located at the college of which he is a student.

PAR. 8 A Student-member shall not remain in this grade beyond the end of the Society's fiscal year in which he terminates his enrollment as a student.

ARTICLE R4, QUALIFICATIONS FOR ADMISSION

RULE 1 A candidate for admission to the Society as a Fellow, a Member, or an Associate, should refer to at least five (5) members who have personal knowledge of his qualifications and the grade of reference shall be as follows:

For Fellow, at least one (1) Fellow and the remainder Members
For Member, at least five (5) Fellows or Members

For Associate, at least three (3) Fellows or Members and the remainder Associates.

RULE 2 A candidate for admission to the Society as a Junior Member should refer to at least three (3) members who have personal knowledge of his qualifications, at least one of whom shall be a Fellow, Member, or Associate.

RULE 3 A candidate for admission to the Society as a Student-member must be endorsed by the Honorary Chairman in office at the Student Branch located at the college where he is a student.

RULE 4 An application for membership from a candidate who may not be able to give the necessary number of references may be recommended to the Council for ballot after sufficient evidence has been secured to show that the candidate is worthy of admission to membership. Such candidates may refer to officers or voting members of other societies of like standing.

RULE 5 An application may be referred by the Committee on Admissions to the executive committee of the Local Section to which the applicant would be logically attached, for information and comment by such local committee. If, after a period of twenty (20) days, no comment is received from the local committee, the Committee on Admissions will proceed with the consideration of the application.

RULE 6 The references for each candidate shall be requested to make such confidential communications to the Committee on Admissions as will enable it to arrive at a proper estimate of the eligibility of the candidate.

RULE 7 The Committee on Admissions shall report to each session of the Council the names of all candidates together with the recommendation on each. The Committee on Admissions shall meet monthly to receive and scrutinize applications, and shall seek further information as to the qualification of a candidate whose evidence of eligibility is not clear to them.

RULE 8 All confidential correspondence in relation to each candidate shall be destroyed by the administrative officer in charge of membership admissions within a reasonable period after acceptance of election by payment of the initiation or promotion fees and dues.

RULE 9 The Secretary shall mail to each member of the Council a ballot of the names and respective grades of the candidates for membership approved by the Committee on Admissions after having been duly posted in the publications of the Society. The voter shall prepare his ballot by crossing out the name of any candidate rejected by him, and shall enclose the ballot in an envelope and seal it. He shall enclose this envelope in a second envelope and sign it for identification. A ballot without the autographic endorsement of the voter on the outer envelope is defective and shall be rejected.

RULE 10 The Secretary shall count the ballots cast by the Council for election of new members, notify the applicants of their election, and regularly report the results of the ballot at the Council meeting next following each election. The names of applicants who are not elected shall neither be announced nor recorded.

ARTICLE C5, FEES AND DUES

Sec. 1. Initiation Fees:

Honorary Member	None
Fellow	$30
Member	25
Associate	25
Junior Member	10
Student-Member	None
Promotion Fees:	
From Member to Fellow	5
From Junior Member to Member or Associate (Except that an applicant under the age of 33 who has been a Junior Member in good standing for five consecutive years may be promoted without fee.)	10
From Student-member to Junior Member	None

Sec. 2. The annual dues for membership in each grade shall be:

Fellow	$25
Member	20
Associate	20
Junior Member until reaching the age of 30	10
Junior Member between the ages of 30 and 33	$15
Junior Member after reaching the age of 33	20
Student-member	as provided in the By-Laws

Sec. 3. The Council may permit any Fellow, Member, or Associate to become a life member in the same grade.

Sec. 4. The Council may remit the dues of any member for any special reason.

ARTICLE B5, FEES AND DUES

PAR. 1 The initiation fee and that part of the annual dues from the first month following the date of election to the first day of October, shall be due and payable on the first day of the month following the date of election. Only upon the payment of this amount shall the person elected be entitled to the rights and privileges of membership in the grade to which he is assigned. If such person does not comply with this requirement within three (3) months after notice of his election, the Council may declare his election void.

PAR. 2 The annual dues for each ensuing year shall be due and payable in advance on the first day of October.

PAR. 3 A bill for annual dues shall be mailed to each member by October first of each year. Notice of arrears shall be sent thereafter, as directed by the Council.

PAR. 4 At its first meeting in the calendar year the Secretary shall submit to the Council a list of members whose dues have remained unpaid for three (3) months. The Council may order the withholding of the publications for such delinquents.

PAR. 5 At its first meeting after the close of the fiscal year on September thirtieth, the Secretary shall submit to the Council a list of members whose dues have remained unpaid for twelve (12) months. Such delinquents shall, in the discretion of the Council, be stricken from the roll of membership and shall cease to have any further rights as members.

PAR. 6 If, in the case of non-payment of dues, the right to receive the publications of the Society or to vote be questioned, the books of the Society shall be conclusive evidence.

PAR. 7 The Council may temporarily excuse from payment of annual dues any member who from ill health, advanced age or good reason assigned is unable to pay such dues; and the Council may remit the whole or part of dues in arrears, or accept in lieu thereof desirable additions to the Library, or collections.

PAR. 8 The Council may restore to membership any person dropped from the rolls for non-payment of dues or otherwise, upon such conditions as it may deem best.

PAR. 9 The annual dues for a Student-member shall be $3.00 for the fiscal year beginning October first. Eight issues of *Mechanical Engineering*, October to May inclusive, shall be included in the dues for a Student-member.

PAR. 10 For distinguished service to the Society, the Council may confer life membership upon any Fellow or Member. Proposal for such action must be made at a regular meeting of the Council. Immediately following that meeting, the Secretary shall send to the members of the Council a letter ballot upon the proposal, this ballot to close in sixty (60) days. Fifteen (15) affirmative votes shall be required to approve and one (1) dissenting vote shall disapprove such proposal.

PAR. 11 A Fellow, Member, or Associate may become a Life Fellow, Life Member, or Life Associate by paying the Society at one time the present worth of an annuity equal to that member's dues for the period for which he is required to pay dues.

PAR. 12 The Council shall confer life membership upon any Fellow, Member, or Associate of the Society who has paid dues for thirty-five (35) years, or who shall have reached the age of seventy (70) years after having paid dues for thirty (30) years (Student-membership years not included).

Article R5, Fees and Dues

Rule 1 A Student-member recommended by the Honorary Chairman of his Student Branch may be elected by the Council to Junior membership, the election being subject to his graduation. The payment of dues as a Junior Member for one year at any time prior to September 30 of the calendar year following the calendar year in which he graduates, shall constitute acceptance of election and shall give him all the rights and privileges of the Junior Member grade from the date of such payment to September 30 of the calendar year following the calendar year in which he graduated.

Rule 2 The Student-member may pay an initial quarter year's dues, $2.50, to indicate acceptance of election. If he chooses this method, the remaining three quarter's of the dues, $7.50, shall be due not later than the first of the month following a three months' period thereafter. If he follows this procedure he will receive publications for the periods paid but no other services until election is accepted by payment of the full year's dues. If he does not accept or follow this procedure and complete his payments before September 30 of the calendar year following the calendar year in which he graduated, the automatic scheme of transfer without initiation fee expires and thereafter he must make a new application for Junior membership and if elected pay an initiation fee of $10.00.

Article C6, The Council (Directors)

Sec. 1. The affairs of the Society shall be managed by a Board of Directors, chosen from its membership and styled "The Council" which shall have full control of the activities of the Society, subject to the limitations of the Constitution and the results of letter ballots (Article B9, Par. 4 and Article B6, Par. 3).

Sec. 2. The Directors of the Society shall consist of a President, seven (7) Vice-Presidents, nine (9) Managers, and the last five (5) surviving Past-Presidents.

Sec. 3. The Directors may at any time, whenever sufficient cause shall appear to them, delegate to any corporate member of the Society the performance of any duties required by the Constitution to be performed by any Director.

Sec. 4. The Council shall meet immediately after the close of the Annual Meeting of the Society, at such other times as the Council may select, and at the call of the President. Eight members shall constitute a quorum of the Council.

Sec. 5. The Council shall present at the Annual Meeting of the Society a report verified by the President and the Treasurer or by twelve (12) members of the Council, showing the whole amount of real and personal property owned by the Society, where located, and where and how invested, and the amount and nature of the property acquired during the year immediately preceding the date of the report, and the manner of the acquisition; the amount applied, appropriated, or expended during the year immediately preceding such date, and the purpose, object, or persons to or for which such applications, appropriations, or expenditures have been made; also a report verified by the Secretary, giving the names and places of residence of the persons who have been admitted into membership in the Society during the year.

These reports shall be filed with the records of the Society, and an abstract shall be entered in the minutes of the proceedings of the Annual Meeting of the Society.

Article B6, The Council

Par. 1 The Council shall consider the failure of any incumbent, from inability or otherwise, to perform the duties of his office, and may, by a two-thirds vote, decree any elective office vacant. The Council shall thereupon appoint a member to fill the vacancy until the next election of officers, except for the office of the President, which shall be filled by the Vice-President serving his second year, who is senior by length of membership in the Society. Such appointment shall not render the appointee ineligible for election to any office.

Par. 2 An act of the Council which shall have received the expressed or implied sanction of the membership at the following meeting of the Society, shall be deemed to be an act of the Society and cannot afterward be impeached by any member.

Par. 3 The Council shall order the submission to the membership for decision by letter-ballot of any question of major importance involving a departure from usual custom. The Council shall appoint tellers to canvass such a ballot, the result of which shall be binding.

Article B6A, Standing and Special Committees

Par. 1 The Council shall at its first meeting of each year appoint from among its members an Executive Committee. Such committee shall consist of the President, two Vice-Presidents, and two Managers, with voting power; also the Chairman of the Finance Committee, the Chairman of the Committee on Professional Divisions and the Chairman of the Local Sections Committee, without voting power. During the intervals between sessions of the Council, the Executive Committee shall have and exercise all the general powers of the Council, except the power to fill vacancies in the Council, or to amend the By-Laws. The committee shall meet at the call of the President. The Secretary may take part in the deliberations of the Executive Committee, without vote. The Executive Committee shall keep minutes of its proceedings which shall be promptly reported to each member of the Council for approval.

Par. 2 Upon the recommendation of a business meeting of the Society or upon its own initiative, the Council shall have the power to appoint, as it may deem desirable, an Administrative Committee to assist in the conduct of the affairs of the Society. Any proposed expenditure of such a committee must be authorized by the Council before it is incurred.

Par. 3 Upon the recommendation of a business meeting of the Society or upon its own initiative, the Council shall have the power to appoint, as it may deem desirable, any Professional Committee to investigate and report upon a subject of engineering interest, except that the procedure of the American Standards Association shall be followed in organizing Sectional Committees. (See Paragraphs 10 and 11 of Article B6B.) Any proposed expenditure of such a committee must be authorized by the Council before it is incurred.

Par. 4 Administrative and Professional Committees shall be standing or special, as the By-Laws and Rules provide and the Council approves. The Chairmen of Standing Committees shall be entitled to a seat in the Council, but no vote. The term of office of one (1) member of each Standing Committee shall expire at the close of each Annual Meeting.

Par. 5 Each committee shall perform the duties required by the By-Laws and Rules, or assigned to it by the Council.

Par. 6 The Council may terminate membership on any committee on account of continued absence of the member, from inability or otherwise.

Par. 7 The President shall appoint a member to fill each vacancy in the Standing Committees.

Par. 8 Each committee shall at its first meeting elect a Chairman to serve for one (1) year.

Par. 9 A member of a Standing Committee whose term of office has expired, shall continue to serve until his successor has been elected or appointed.

Par. 10 On or before the fifteenth day of October of each year, each Standing Committee shall deliver to the Secretary a written report of its work for presentation to the Council. The Council may embody such report in its Annual Report.

Par. 11 On or before the fifteenth day of October of each year, each Special Committee shall deliver a written progress report to the Secretary for presentation to the Council. Upon receipt of this report, the Council may, in its discretion, continue the committee.

The committee shall be discharged upon the adoption of the final report.

PAR. 12 The Standing Committee on Finance shall, under the direction of the Council, have supervision of the financial affairs of the Society, including the books of account. The Committee shall consist of five (5) members of the Society, the term of one (1) member expiring at the close of each Annual Meeting, and two (2) members of the Council, the term of one (1) member expiring at the close of each Annual Meeting.

PAR. 13 The Standing Committee on Meetings and Program shall, under the direction of the Council, have supervision of the Meetings of the Society, except business meetings. The Committee shall consist of five (5) members, and the term of one (1) member shall expire at the close of each Annual Meeting.

PAR. 14 The Standing Committee on Publications shall, under the direction of the Council, have supervision of the publications of the Society. The Committee shall consist of five (5) members and the term of one (1) member shall expire at the close of each Annual Meeting.

PAR. 15 The Standing Committee on Admissions shall determine the eligibility of applicants for membership, and for transfer in membership grades, and shall make recommendation to the Council on each. The Committee shall consist of five (5) members and the term of one (1) member shall expire at the close of each Annual Meeting.

PAR. 16 The Standing Committee on Professional Divisions shall, under the direction of the Council, have supervision of the Professional Divisions of the Society. The Committee shall consist of five (5) members and the term of one (1) member shall expire at the close of each Annual Meeting.

PAR. 17 The Standing Committee on Local Sections shall, under the direction of the Council, have supervision of the Local Sections of the Society. The Committee shall consist of five (5) members and the term of one (1) member shall expire at the close of each Annual Meeting.

PAR. 18 The Standing Committee on Constitution and By-Laws shall, under the direction of the Council, have supervision of matters affecting the Constitution, By-Laws, and Rules, and shall report on all matters in this connection referred to it by the Council. The Committee shall consist of five (5) members and the term of one (1) member shall expire at the close of each Annual Meeting.

PAR. 19 The Standing Committee, designated as the Board of Honors and Awards shall, under the direction of the Council, have supervision of the awards of the Society as detailed in the Rules or prescribed by the Council. Recommendations for representatives of joint bodies of award shall be made to the Council by this Board. The Board shall consist of five (5) members and the term of one (1) member shall expire at the close of each Annual Meeting.

PAR. 20 The Standing Committee on Relations With Colleges shall, under the direction of the Council, have supervision of the Student Branches of the Society and of such work of the Society as aims to further the education of engineers through the colleges and schools of accepted standing. The Committee shall consist of five (5) members and the term of one (1) member shall expire at the close of each Annual Meeting.

PAR. 21 The Standing Committee on Education and Training for the Industries shall, under the direction of the Council, have supervision of such work of the Society as deals with education and training for the industries through agencies other than the colleges and engineering schools. The Committee shall consist of five (5) members and the term of one (1) member shall expire at the close of each Annual Meeting.

PAR. 22 There shall be a Standing Committee on Library, which shall represent the Society on the Library Board of the United Engineering Trustees, Inc. The number of members of this Committee and their terms of office shall be as required by the by-laws of the United Engineering Trustees, Inc.

PAR. 23 The Standing Committee on Standardization shall advise the Council on the dimensional standardization work of the Society, including relations with the American Standards Association. The Committee shall consist of five (5) members and the term of one (1) member shall expire at the close of each Annual Meeting.

PAR. 24 The Standing Committee on Research shall, under the direction of the Council, have supervision of the research activities of the Society. The Committee shall consist of five (5) members and the term of one (1) member shall expire at the close of each Annual Meeting.

PAR. 25 The Standing Committee on Safety shall advise the Council on the activities of the Society having to do with engineering and industrial safety, except the activities of the Boiler Code Committee, for which special provision is made. This Committee shall consist of five (5) members and the term of one (1) member shall expire at the close of each Annual Meeting.

PAR. 26 The Special Committee on Boiler Code shall, under the direction of the Council, have supervision of all activities of the Society in connection with the A.S.M.E. Codes for Pressure Vessels, including the interpretations of these codes. The Committee shall be appointed by the President and confirmed by the Council, and the President shall fill all vacancies in the Committee.

PAR. 27 The Standing Committee on Power Test Codes shall, under the direction of the Council, have supervision of all the activities of the Society in connection with the A.S.M.E. Power Test Codes, including the interpretation of such codes. The Committee shall consist of twenty-five (25) members and the terms of five (5) members shall expire at the close of each Annual Meeting.

PAR. 28 The Standing Committee on Professional Conduct shall, under the direction of the Council, have supervision of all matters relating to the Code of Ethics and its enforcement. The Committee shall consist of five (5) members and the term of one (1) member shall expire at the close of each Annual Meeting.

B6B, SOCIETY REPRESENTATION

PAR. 1 The Council may, in its discretion, appoint a member or members, or other person or persons, to represent it at meetings of societies of kindred aim or at public functions. Such delegates shall be designated as "Honorary Vice-Presidents," and their duties shall terminate with the occasion for which they are appointed.

PAR. 2 The President, subject to the approval of the Council, may nominate or appoint a member or members, or other person or persons, to represent the Society on professional or other committees organized by other societies or by Government departments or bureaus, or otherwise.

PAR. 3 The Council shall elect three (3) Trustees to serve on the Board of Trustees of the United Engineering Trustees, Inc., as required in the by-laws of that body.

PAR. 4 The Council shall appoint delegates to serve on the American Engineering Council as required in the by-laws of that body. If the number of delegates required to serve is at variance with the number elected or in office, the Council of the Society is empowered to make adjustments necessary. The President of the Society in office shall be the Chairman of the delegation of this Society to the meetings of the American Engineering Council, and the Chairman of the A.S.M.E. representatives on the Executive Board.

PAR. 5 The Council shall designate the Standing Committee on Library to serve as the Society's representatives on the Library Board of the United Engineering Trustees, Inc., as required in the by-laws of that body.

PAR. 6 The Council shall nominate to the United Engineering Trustees, Inc., two (2) members of the Society to serve on the Engineering Foundation as required in the by-laws of that body

PAR. 7 The Council shall appoint such number of members to represent the Society on the following agencies as may be required by the by-laws of those bodies, namely: John Fritz Medal Board of Award, Washington Award Commission of the Western Society of Engineers, Gantt Medal Board of Award, Daniel Guggenheim Medal Fund, Inc., Hoover Medal Board of Award, Alfred Noble Prize.

PAR. 8 The Council shall nominate three (3) members to represent the Society on the Division of Engineering of the

National Research Council as required in the by-laws of that body.

PAR. 9 The Council shall appoint three (3) members of the Society to represent the Society on the Engineers' Council for Professional Development.

PAR. 10 The Council shall designate such number of members to represent the Society on the American Standards Association as may be required by the constitution of that body.

PAR. 11 The representatives of the Society on Sectional Committees, organized under the rules of the American Standards Association, shall be appointed by the President, subject to the approval of the Council.

ARTICLE C7, ELECTION OF DIRECTORS

Sec. 1. The membership of the Society shall elect annually a Regular Nominating Committee, whose duty shall be to select candidates for the executive offices to be filled at each annual election.

Sec. 2. Other nominating committees having the same powers may be constituted by the membership of the Society.

Sec. 3. Directors shall be elected annually by sealed letter-ballot of the membership.

Sec. 4. The President shall be elected for one (1) year, the Vice-Presidents for two (2) years, the Managers for three (3) years. The Council shall have power to fill vacancies in its membership by appointment until the next election, except that the office of president shall be filled by the vice-president who is senior by length of membership in the Society.

ARTICLE B7, ELECTION OF DIRECTORS

PAR. 1 The Regular Nominating Committee of the Society shall consist of eight (8) members with eight (8) alternates elected at the Annual Meeting. The Chairman of the outgoing Nominating Committee shall serve as an advisory member, without vote, and the Secretary of the outgoing Committee may serve as alternate for him.

PAR. 2 The members and alternates of the Regular Nominating Committee shall be elected for one (1) year, and no member or alternate shall be eligible for more than two (2) consecutive terms. Serving as an alternate shall not affect the eligibility of a member to serve on the committee for two (2) terms.

PAR. 3 For the purpose of nominating members of the Regular Nominating Committee, the Council shall, on or before the first day of October of each year, associate the Local Sections into eight (8) groups, each group to be responsible for nominating one (1) member of the Committee. The Sections which will comprise these groups shall, as far as possible, be contiguous geographically to each other.

PAR. 4 The names of those elected to serve on the Regular Nominating Committee shall be published by the Secretary by the first week in February of each year, accompanied by a request for suggestions for nominees.

PAR. 5 A vacancy in a Regular Nominating Committee of the Society shall be filled by the alternate for that vacancy, or failing that, shall be filled by the Council.

PAR. 6 A Special Nominating Committee may be organized by any group of one (1) per cent of the membership of the Society in good standing certifying to the Secretary in writing their joint intention to organize such a Committee.

PAR. 7 Within two weeks following the Semi-Annual Meeting, the Regular Nominating Committee shall deliver to the Secretary in writing the names of its nominees for the elective offices to be filled at the next election, together with the written consents of the nominees.

PAR. 8 The names and qualifications of nominees for the various offices proposed by the Regular Nominating Committee shall be published by the Secretary immediately after the receipt of the report of the Nominating Committee.

PAR. 9 Candidates for the office of President and of Vice-President shall be of the grade of Fellow or of Member of the Society. Candidates for all other elective offices may be of any grade of corporate membership.

PAR. 10 Names of any nominees presented by any Special Nominating Committee must be in the hands of the Secretary by the first Tuesday in August of each year, and must be accompanied by the written consent of each nominee.

PAR. 11 On or before the third Thursday in August of each year, the Secretary shall mail to each member entitled to vote a ballot stating the names of the candidates for the elective offices to be filled at the next election.

PAR. 12 Voting for the election of Directors shall close at the City of New York at 10 o'clock in the forenoon on the fourth Tuesday in September in each year, and the ballots shall be canvassed.

PAR. 13 On or before the third Thursday in August of each year, the President shall appoint three (3) Tellers of Election of Directors, whose duty it shall be to canvass the votes cast. The term of office of the Tellers shall expire when their report of the canvass has been presented and accepted.

PAR. 14 By the first day of October, the Secretary shall notify the candidates having the greatest number of votes for their respective offices.

PAR. 15 The Directors shall be declared elected by the Presiding Officer at the Annual Meeting of the Society in December, and their terms of office shall begin on the adjournment of the Annual Meeting.

PAR. 16 If a tie occurs in the vote for any officer, the Presiding Officer at the Annual Meeting shall cast the deciding vote.

PAR. 17 In the election of the Vice-Presidents, three (3) shall be elected every other year and four (4) the alternate years to serve for two (2) years.

PAR. 18 In the election of the Managers, three (3) shall be elected each year to serve for three (3) years.

PAR. 19 A member in office shall not be eligible for immediate re-election to the same office at the expiration of the term for which he was elected, except the Secretary and the Treasurer.

PAR. 20 Members in office shall continue in their respective offices until their successors have been elected or appointed, and have accepted their offices.

ARTICLE R7, ELECTION OF DIRECTORS

RULE 1 The Chairman of the Committee on Local Sections, or in his absence, the senior member of the Committee, shall preside at the Conference of Group Representatives at the time action is taken on the Regular Nominating Committee.

RULE 2 At the business session of the Annual Meeting of the Society, the Chairman of the Committee on Local Sections shall present names recommended by the conference for the Regular Nominating Committee.

RULE 3 The names of the candidates proposed by the Regular Nominating Committee and by any other nominating committee, and the respective offices for which they are candidates, shall be printed in separate lists on the same ballot sheet, each list of candidates to be printed under the names of the members of the particular committee which proposed it.

RULE 4 Each list of names shall contain the name of only one (1) candidate for the office of President. For any other office than President, there may be more than one (1) candidate.

RULE 5 In the election of Directors, the voter shall prepare his ballot by crossing out the name of any candidate or candidates rejected by him and may write in the name of any eligible member of the Society, and shall enclose the ballot in an envelope and seal it. He shall then enclose this envelope in a second envelope marked "Ballot for Directors" and seal it, and he shall then write his name thereon for identification.

RULE 6 The Tellers shall not receive any ballot after the stated time for the closure of the voting.

RULE 7 The Secretary shall certify to the competency and signature of all voters.

RULE 8 The Tellers shall open and destroy the outer envelopes and then open the inner envelopes and canvass the results.

RULE 9 A ballot without the autographic endorsement of the voter on the outside envelope is defective and shall be rejected by the Tellers of Election.

RULE 10 A ballot containing more names than there are offices to be filled is defective and shall be rejected by the Tellers.

RULE 11 In counting the ballots for officers, the Tellers shall consider a ballot for any officer as valid providing the intent of the voter as to that particular office is clear, even though his ballot as to candidates for another office may for any reason be invalid.

ARTICLE C8, OFFICERS

Sec. 1. The Officers of the Society shall consist of the President, the Vice-President, the Secretary, and the Treasurer.

Sec. 2. At its first meeting after the Annual Meeting of the Society the Council shall appoint members of the Society to serve as Secretary and as Treasurer for one (1) year.

Sec. 3. Any vacancy in the office of Secretary or Treasurer shall be filled by appointment by the Council.

B8 OFFICERS

PAR. 1 The Officers shall perform the duties regularly or customarily attaching to their offices under the laws of the State of New York, and such other duties as may be required of them by the Council or the By-Laws.

PAR. 2 In the absence of the President his duties shall be performed by the Vice-President then present, who is serving his second year and is senior by length of membership in the Society, or in his absence or any other disability, by any other member of the Council designated by the Council.

PAR. 3 The Secretary and the Treasurer shall take part in the deliberations of the Council but shall have no vote therein.

PAR. 4 The Treasurer shall be the legal custodian of all funds of the Society. The investment of all trust funds and of other permanent or temporary investment of funds shall be made by the Treasurer with the approval of the Finance Committee and the Council.

PAR. 5 In the absence of the Treasurer his duties shall be performed by any other officer of the Society designated by the Council.

PAR. 6 The Secretary of the Society shall be the Secretary of the Council and of each of the committees.

PAR. 7 The Secretary shall receive a salary which shall be fixed by the Council.

PAR. 8 Any officer may be subject to removal for cause by a vote of fifteen (15) members of the Council at any time, after one (1) month's written notice has been given him to show cause why he should not be removed, and after he has been heard in his own defense, if he so desires.

R8, SECRETARY'S OFFICE

RULE 1 The office of the Secretary shall be open on business days from 9 a.m. to 5 p.m.; on Saturdays from 9 a.m. to 1 p.m.

RULE 2 The Secretary shall establish and enforce rules for the conduct of the business of his office.

RULE 3 The Secretary shall have charge of the rooms of the Society and furnishings, the historical relics and objects of art, and shall make suitable recommendations to the Council for their care and use.

ARTICLE C9, MEETINGS OF THE SOCIETY

Sec. 1. The Annual Meeting of the Society shall be held at such time and place as the Council shall appoint.

Sec. 2. The Semi-Annual Meeting of the Society shall be held at such time and place as the Council shall appoint.

Sec. 3. A special business meeting of the Society may be called at any time and place at the discretion of the Council, or shall be called by the Secretary upon the written request of at least one (1) per cent of the membership.

The call for the meeting shall be issued at least thirty (30) days prior to the date set for it, and shall state the business to be considered. No other business shall be transacted at the meeting.

Sec. 4. There shall be a business meeting of the Society during the Annual Meeting and during the Semi-Annual Meeting. At business meetings fifty (50) corporate members shall constitute a quorum.

Sec. 5. An action of a business meeting of the Society shall be deemed an action of the Society as a whole. Any expenditure required by such action is subject to approval and authorization by the Council.

Sec. 6. A General Meeting of the Society, primarily for the presentation and discussion of technical papers, may be held at such time and place as the Council shall appoint.

ARTICLE B9, MEETINGS OF THE SOCIETY

PAR. 1 A Semi-Annual Meeting shall be held upon the recommendation of the Committee on Local Sections, confirmed by the Committee on Meetings and Program, and authorized by the Council at its regular meeting at the previous Semi-Annual Meeting.

PAR. 2 A General Meeting shall be held upon the recommendation of the Committee on Local Sections, confirmed by the Committee on Meetings and Program, and authorized by the Council.

PAR. 3 Any business meeting of the Society at which a quorum is present may order the submission of any question to the membership for letter-ballot, and the result of the ballot shall be binding.

PAR. 4 Announcements of all Meetings of the Society shall be made in the publications. A notice of each meeting shall be given by the Secretary to each member not less than thirty (30) days before the date of that meeting.

PAR. 5 All Meetings of the Society, except business meetings, shall be in charge of the Committee on Meetings and Program, under the direction of the Council.

ARTICLE R9, MEETINGS OF THE SOCIETY

RULE 1 Subject to the approval of the Committee on Meetings and Program, any Local Sections participating in the conduct of a Semi-Annual or General Meeting shall appoint the necessary special local committees which shall function under the direction of the Committee on Meetings and Program.

ARTICLE C10, PROFESSIONAL DIVISIONS

Sec. 1. The Council may authorize the organization of Professional Divisions composed of members of any or all grades which shall operate under the provisions of the Constitution, By-Laws, and Rules.

ARTICLE B10, PROFESSIONAL DIVISIONS

PAR. 1 The object of each Professional Division shall be to provide, through an organization of members of any or all grades particularly interested in a branch of engineering included in the scope of the Society's activities, means for promoting the arts and sciences of that branch.

PAR. 2 A Professional Division of the Society may be organized upon acceptance by the Council of the written request of a satisfactory number of members. Such a Division shall be designated as the ..... Division of The American Society of Mechanical Engineers.

PAR. 3 The provisions of the Constitution, By-Laws, and Rules of the Society shall cover the procedure of all Professional Divisions, but no action or obligation of a Division shall be considered an action or obligation of the Society as a whole. This By-Law shall be imprinted on any publication issued by a Division.

PAR. 4 For the convenient conduct of its affairs, each Professional Division shall organize an executive committee. The executive committee shall elect its Chairman each year, and upon confirmation by the Council, he shall serve as Chairman of the Division.

PAR. 5 The function of the Standing Committee on Professional Divisions, under the direction of the Council, shall be to organize, foster, and coordinate Professional Divisions and their activities.

PROFESSIONAL GROUPS

PAR. 6 In case the number of members interested in a particular branch of the Society's work is not large enough to warrant the formation of a full Professional Division under the provisions of the By-Laws, the Council may authorize the formation of a Professional Group, and will itself appoint an executive committee to organize such a Group, and will designate the Chairman of the Committee. When a sufficient number of members become attached to this Group, it may petition for reorganization into a Professional Division.

ARTICLE R10, PROFESSIONAL DIVISIONS

RULE 1 When a number of members of the Society interested in a particular branch of the work of the Society favor the formation of a Professional Division for that branch, they may draw up a petition for the establishment of such a Division. Each such petition shall be sent to the Standing Committee on Professional Divisions for presentation to the Council with its recommendation. Upon approval of the petition by the Council, the Chairman of the Standing Committee on Professional Divisions shall appoint a temporary Chairman of the New Division.

RULE 2 The executive committee of each Professional Division shall consist of five (5) members and the term of one (1) member shall expire at the close of each Annual Meeting. The executive committee and such officers as the Division may require shall be selected from the membership of the Society. Other committees, advisors, and associates of the Division shall be appointed by the executive committee as required for a term not exceeding one (1) year.

RULE 3 Upon the organization of a Professional Division the initial selection of the executive committee shall be made by the President upon the nomination of the Standing Committee on Professional Divisions which will state the length of term of each appointee.

RULE 4 During the month of October of each year the executive committee of each Division will nominate to the President through the Standing Committee on Professional Divisions one or more individuals from whom the President shall appoint the member of the executive committee.

RULE 5 The executive committee of each Professional Division shall elect its own officers. No one shall be eligible for chairmanship until he has been a member of this committee for one year, except in the selection of the executive committee for a newly formed Division.

RULE 6 In case of resignation or decease, vacancies shall be filled by appointment of the executive committee subject to the approval of the President of the Society.

RULE 7 The executive committee may, subject to the approval of the Secretary of the Society, appoint or elect a secretary of the Division, who shall report the proceedings of that Division to the Secretary of the Society for notice in the publications. He shall perform the duties of secretary of the Division, and such other duties as may be prescribed by the executive committee.

RULE 8 Any expenditure for the purpose of a Division chargeable to the Society must be authorized by the Secretary of the Society before it is incurred, and must be provided for in the annual budget approved by the Council. Any liability otherwise incurred shall not be binding on the Society, and must be met by the Division itself.

RULE 9 Notice of all Professional Division meetings shall be given in writing to the Secretary of the Society and to the Chairman of the Standing Committee on Professional Divisions at least six (6) weeks in advance of the date set for such meetings.

PROFESSIONAL GROUPS

RULE 10 The functions and responsibilities of a Professional Group shall be the same as those of a Professional Division, except that the Chairman of the executive committee, although having a seat in the conferences of the Chairmen of the Professional Divisions shall have no vote.

RULE 11 The activities of a Professional Group shall be subject to the jurisdiction of the Standing Committee on Professional Divisions.

RULE 12 The Council reserves the right to disband any Professional Group on sixty (60) days' notice.

ARTICLE C11, LOCAL SECTIONS

Sec. 1. The Council may authorize the organization of Local Sections composed of members of any or all grades, which shall operate under the provisions of the Constitution, By-Laws, and Rules.

Sec. 2. The Local Sections shall be associated into geographical groups with annual meetings at which each Local Section shall be entitled to representation. Each geographical group shall be entitled to representation in a subsequent conference of group representatives at the Annual Meeting of the Society.

ARTICLE B11, LOCAL SECTIONS

PAR. 1 The object of a Local Section of the Society shall be to provide means for promoting the work of the Society by a local organization of members who are resident within a given territory.

PAR. 2 A Local Section shall consist of members of any or all grades.

PAR. 3 A Local Section of the Society may be organized upon acceptance by the Council of the written request of a satisfactory number of members. Such a Section shall be designated as the ..... Section of The American Society of Mechanical Engineers.

PAR. 4 The provisions of the Constitution, By-Laws, and Rules of the Society shall cover the procedure of all Local Sections, but no action or obligation of a Section shall be considered an action or obligation of the Society as a whole. This By-Law shall be imprinted on any publication issued by the Section.

PAR. 5 For the convenient conduct of its affairs, each Section shall organize an executive committee.

PAR. 6 The affairs of the Local Sections shall be in general charge of the Standing Committee on Local Sections, under the direction of the Council.

PAR. 7 The Council of the Society, on sixty (60) days' notice, may suspend or disband any Local Section.

PAR. 8. There shall be a group meeting of Local Section delegates of each group preferably between October fifteenth and November fifteenth of each year at some central point within the geographical limits of the group.

PAR. 9 Each Local Section shall be entitled to one voting delegate in the group meeting of Local Section delegates. In addition to such delegates the group representative serving his second year shall serve as chairman of the group meeting, but shall vote only in case of a tie.

PAR. 10 At such group meeting of Local Section delegates, one representative shall be elected to represent the group for two (2) years at the conference of group representatives.

PAR. 11 There shall be a conference of group representatives each year at the place and at the time of the Annual Meeting of the Society. There shall be sixteen (16) representatives to such annual conference, two (2) from each of the eight (8) groups, which groups shall conform geographically to those provided for in Article B7, Par. 3.

ARTICLE R11, LOCAL SECTIONS

RULE 1 When a number of members of the Society in any territory within the limits of North America, Hawaii, Puerto Rico and Cuba favor the formation of a Local Section in that territory, a preliminary meeting shall be called and notice sent to the entire membership of the Society residing in that territory. At this meeting a petition for the formaton of a Local Section, containing suggestions as to the territory to be included in the Section, may be presented, and, if adopted, shall be sent to the Standing Committee on Local Sections for recommendation to the Council.

RULE 2 Upon the approval by the Council of the petition, a meeting of the signers shall be held for the selection of a temporary executive committee of at least five (5) members. This committee shall have charge of, and be responsible for, the proceedings of the Local Section until the next election of officers.

RULE 3 The executive committee of a Local Section shall consist of a chairman, a secretary, and such other officers as may be found desirable. Such officers shall be elected by ballot of the members of the Society constituting the Section. The committee shall be elected before the first day of June each year and shall take office on the first day of July.

RULE 4 A member of the Society shall be entitled to vote or to hold office in not more than one (1) Local Section at a time.

RULE 5 The chairman of each Local Section shall have the privilege of attending all meetings of the Standing Committee on Local Sections.

RULE 6 The secretary of each Local Section shall report the proceedings of that Section to the Secretary of the Society for notice in the publications. He shall discharge the duties of secretary of the Section, and such other responsibilities as may be prescribed by the executive committee.

RULE 7 Any expenditure chargeable to the Society for the purpose of any Local Section must be provided for in the annual budget approved by the Council. No liability otherwise incurred shall be binding upon the Society.

RULE 8 Each Local Section shall use only such uniform stationery as is supplied by the Secretary of the Society.

RULE 9 For the convenient cooperation between the Local Sections and the Professional Divisions, each Local Section may appoint an individual or a committee to act as a correspondent with each Professional Division, with duties that will comprise generally the arranging with the Professional Division for the presentation of papers, holding of meetings, etc., within that particular Local Section, and as far as possible, to act as a means of furnishing information, secured within the Local Section, which might prove of interest to the Division.

RULE 10 A Local Section may affiliate with existing local engineering organizations, or form jointly with them new local engineering organizations, but the plan of such affiliation or organization, and the obligations assumed by the Local Section and the Society thereby, shall first be approved by the Council on recommendation of the Committee on Local Sections. Any expenditures incurred in such an affiliation shall be binding only on the Section and not on the Society as a whole.

RULE 11 A Local Section may arrange to hold joint meetings with other engineering organizations and may invite members of such organizations to attend its meetings, but all expenses incurred shall be binding only on the Section and not on the Society as a whole.

RULE 12 Each Local Section may adopt its own by-laws, for the conduct of its affairs, provided such are in harmony with the Constitution, By-Laws, and Rules of the Society, and provided also every publication of such by-laws be prefaced with a copy of this Rule.

RULE 13 Groups of members residing outside the limits of North America, Hawaii, Puerto Rico, and Cuba may engage in group activities with local members of the A.S.C.E., A.I.M.E., and A.I.E.E., in which case the Council may grant them nominal financial support, provided such group action is not in conflict with the policies and activities of any established national engineering societies in such foreign countries, and that such groups cooperate as permitted with such foreign societies.

ARTICLE C12, STUDENT BRANCHES

Sec. 1. The Council may authorize the organization of Student Branches which shall operate under the provisions of the Constitution, By-Laws, and Rules.

ARTICLE B12, STUDENT BRANCHES

PAR. 1 A Student Branch may be organized upon acceptance by the Council of the written request of at least fifteen (15) senior and junior students in any engineering school of accepted standing. Such a Branch shall be designated as the .... Student Branch of The American Society of Mechanical Engineers.

PAR. 2 The provisions of the Constitution, By-Laws, and Rules of the Society shall cover the procedure of all Student Branches, but no action or obligation of a Student Branch shall be considered an action or obligation of the Society as a whole. This By-Law shall be imprinted on any publication issued by the Student Branch.

PAR. 3 The function of the Standing Committee on Relations With Colleges under the direction of the Council shall be to organize, foster, and govern Student Branches and their activities.

PAR. 4 Annual regional conferences of delegates from Student Branches shall be held at the discretion of the Committee on Relations with Colleges.

ARTICLE R12, STUDENT BRANCHES

RULE 1 Upon the recommendation of a Student Branch, the President of the Society shall designate a corporate member of the Society as Honorary Chairman for one (1) year, to be a member ex officio of the governing body of the Student Branch.

RULE 2 Annually, each Student Branch shall select officers including a chairman and a governing body of at least three (3) Student-members.

ARTICLE C13, PUBLICATIONS AND PAPERS

Sec. 1. The papers and publications of the Society shall be issued in such manner as the Council may direct.

ARTICLE B13, PUBLICATIONS AND PAPERS

PAR. 1 All publications of the Society shall be in charge of the Standing Committee on Publications, under the direction of the Council.

PAR. 2 The publications of the Society shall consist of (*a*) the Transactions of the Society; (*b*) Mechanical Engineering; and (*c*) such other publications as the Council may direct.

PAR. 3 The policy of the Society shall be to give papers read before it the widest publicity.

PAR. 4 The Society shall not be responsible for statements or opinions advanced in papers or in discussion at meetings of the Society or of its Divisions or Sections, or printed in its publications.

PAR. 5 The Society reserves the right to copyright, at the discretion of the Council, any of its papers, discussions, reports, or publications.

ARTICLE C14, FUNDS

Sec. 1. The deposit, investment, and disbursement of all funds shall be subject to the direction of the Council.

ARTICLE B14, FUNDS

RECEIPTS

PAR. 1 All funds shall be paid in to the Secretary, who shall enter them in the books of the Society, and deposit them to the account of the Treasurer in a bank designated by the Council.

PAR. 2 All bills against members and others shall be made and collected by the Secretary.

PAR. 3 Income from initiation fees shall not be used for current expenses. At the close of each fiscal year, unless the Council then orders otherwise, this income shall be added to surplus.

PAR. 4 Funds may be solicited from sources outside of the Society for the conduct of research. All contributions to the Society for any specific purpose shall be disbursed under the direction of the Council.

PAR. 5 All gifts or bequests not designated for a specific purpose shall be invested and only the income shall be used.

PAR. 6 All gifts or bequests to the Society designated by the donors for a specific purpose, and all moneys permanently set aside by the Council for specific purposes, shall be invested and either the capital or income as so designated shall be used for that specific purpose for which it was designated.

PAR. 7 Except where otherwise definitely specified in a gift or bequest, the Secretary of the Society shall at the close of each fiscal year compute the interest and return received for the year on the Society's invested funds. The Secretary shall determine an average rate of income and shall recommend an apportionment of such return to each of the several funds for which investment is made. Upon approval and order of the Council these apportioned returns shall be duly entered in the books of account of the Society as the income for the year on the various funds.

PAR. 8 At the discretion of the Council income from any fund may be allowed to accumulate for expenditure in any subsequent year, or the income may be added to the original fund and invested with it. But in no case shall money be expended from such specially designated funds, either from capital or from income duly apportioned as detailed in paragraph 7, for the current expenses of the Society.

PAR. 9 Upon the maturity of any permanent investment the Treasurer shall reinvest such funds subject to approval by the Finance Committee and the Council.

PAR. 10 The securities of the Society, either principal or trust funds, may be sold, bought, or exchanged upon the written order of the Treasurer, the Secretary, and the Chairman of the

Finance Committee, and these three signatures must appear on any order to any broker, bank, or company. If any one or two of these officers be temporarily unavailable, then an equal number of members of the Executive Committee may be substituted.

Expenditures

Par. 11 All expenditures shall be made in accordance with the budget of appropriations as adopted by the Council.

Par. 12 Any obligations which may be incurred during the fiscal year and which will require the expenditure of the Society's funds outside of appropriations made by the Council shall first be referred to the Finance Committee for report by that Committee back to the Council.

Par. 13 The Secretary shall report to the Finance Committee each month the total expenditures incurred against each appropriation, together with the amount of each appropriation which is unexpended.

Par. 14 The annual appropriations approved by the Council, or so much thereof as may be required for the work of the Society, shall be expended by the Secretary, under direction of the committees.

Par. 15 All bills against the Society shall be in charge of the Secretary. Upon competent certification as to correctness and proper authorization, payment shall be made by the Secretary from the Cashier's Account.

Par. 16 The Treasurer shall reimburse the Cashier's Account for payments made therefrom only upon orders duly signed by the Secretary and the Chairman of the Finance Committee.

Article R14, Funds

Rule 1 The accounts of the Society shall be audited and approved annually by a chartered or other competent public accountant.

Rule 2 The Finance Committee shall hold monthly meetings for such business as shall come before it.

Rule 3 Each year the Finance Committee shall present with its report a detailed estimate of the probable income and expenditures of the Society for the following twelve (12) months.

Rule 4 Any contract or other obligations to pay money in the Society's work shall be valid only when signed by the Secretary.

Article C15, Professional Practice

Sec. 1. In all professional and business relations the members of the Society shall be governed by the Code of Ethics incorporated in the By-Laws.

Sec. 2. Any member who has violated the Constitution of the Society, or who is guilty of conduct rendering him unfit to remain a member, may be expelled by the vote of fifteen (15) members of the Council, after he has been given opportunity to be heard in his own defense.

Article B15, Professional Practice

Par. 1 All members of the Society shall subscribe to the following Code of Ethics, as required by the Constitution:

A Code of Ethics for Engineers

That the dignity of his chosen profession may be maintained, it is the duty of every engineer

1 To carry on his professional work in a spirit of fairness to employees and contractors, fidelity to clients and employers, and devotion to high ideals of personal honor.

2 To refrain from associating himself with, or allowing the use of his name by, any enterprise of questionable character.

3 To treat as confidential his knowledge of the business affairs or technical processes of clients or employers when their interests require secrecy.

4 To inform a client or employer of any business connections, interests, or affiliations which might influence his judgment or impair the disinterested quality of his services.

5 To accept financial or other compensation for a particular service from one source only, except with the full knowledge and consent of all interested parties.

6 To advertise only in a dignified manner, to refrain from using any improper or questionable methods of soliciting professional work, and to decline to pay or to accept commissions for work secured by such improper or questionable methods.

7 To refrain from using unfair means to win professional advancement and to avoid unfairly injuring another engineer's chances to secure and hold employment.

8 To cooperate in building up the engineering profession by the interchange of general information and experience with his fellow engineers and with students of engineering and also by contributions to the work of engineering societies, schools of applied science, and the technical press.

9 To interest himself in the public welfare and to be ready to apply his special knowledge, skill, and training in the public behalf for the use and benefit of mankind.

Article R15, Professional Practice

Rule 1 The Standing Committee on Professional Conduct, having in charge all matters connected with the Code of Ethics and its enforcement, shall cooperate with similar committees of other societies.

Rule 2 The Standing Committee on Professional Conduct shall follow the procedure below in considering cases presented to it:

(*a*) Cases for consideration may be:

(1) An interpretation of the code, or
(2) Rendering an opinion on the questionable conduct of a member of the Society.

(*b*) Cases and complaints are to be submitted to the Committee by the Secretary of the Society.

(*c*) Before a case is submitted to the Committee, the Secretary of the Society shall ascertain whether the person against whom a complaint has been made is a member of the Society, and if possible decide whether the case is of such importance as to be passed on by the Committee, or is of such a trivial nature that it can be handled by the Secretary.

(*d*) A case may be submitted by the Secretary of the Society either through the Chairman or jointly to each member of the Committee.

(*e*) On receipt of a case the Committee shall decide whether it can best make a finding by correspondence, or by a meeting of the Committee, and whether hearings shall be given to the interested parties.

(*f*) The Committee may appoint subcommittees to consider and report on cases too remote for the main Committee to act upon.

(*g*) All correspondence from members of the Committee should pass through the office of the Chairman of the Committee and not be sent direct to the Secretary of the Society. In order to facilitate filing and preparation of reports, a letter should cover only one case or subject.

(*h*) Reports and findings on cases shall be sent by the Chairman to the Secretary of the Society for consideration by the Executive Committee or Council of the Society, which may approve the findings or take such other action as may seem desirable or necessary.

(*i*) The Committee may, if it so desires, suggest action by the Executive Committee or Council.

(*j*) The Council shall have the power on recommendation of the Committee on Professional Conduct, either (1) to censure by letter the conduct of a member who has acted contrary to the Code, if the breach is of a minor character, or (2) to cause the member's name to be stricken from the rolls of the Society, as provided in C15, Sec. 2.

Article C16, Amendments to the Constitution

Sec. 1. At any Meeting of the Society any person entitled to vote may propose in writing an amendment to this Constitution, provided that it shall bear the written indorsement of at least twenty (20) corporate members in good standing.

Such proposed amendment shall not be voted on for adoption at that meeting, but shall be open to discussion and modification, and to a vote as to whether, in its original or modified form, it shall be mailed in printed form to the members of the Society for action.

If the members present at the meeting, not less than twenty (20) voting in favor thereof, shall so decide, then

the Secretary shall mail in printed form to each person entitled to vote, at least sixty (60) days previous to the next Meeting of the Society, a copy of the proposed amendment as so decided by said vote, accompanied by any comment the Council may elect to make.

A ballot shall be sent with the proposed amendment, and the voting shall be by sealed letter-ballot, closing at noon of the twentieth (20th) day preceding the meeting of the Society following the mailing.

The adoption of the amendment shall require a vote in its favor of two-thirds of the votes cast.

The Presiding Officer at the meeting of the Society following the close of the ballot shall announce the result, and if the amendment is adopted it shall thereupon take effect.

Sec. 2. Any changes in the order or numbering of paragraphs of the Constitution, By-Laws, and Rules required by an amendment shall be made under the direction of the Council.

Sec. 3. This Constitution shall supersede all previous rules of the Society, and shall go into effect upon the adjournment of the meeting of the Society at which the presiding officer announces its adoption.

Article B16, Amendments

Par. 1 At least fourteen (14) days before the closing of a ballot on an amendment to the Constitution, the President shall appoint three (3) Tellers whose duty it shall be to canvass the votes cast.

Par. 2 The Tellers shall canvass the ballots and shall certify the result to the Presiding Officer at the meeting of the Society at which the result is to be announced.

Par. 3 In the case of a tie vote on an amendment, the Presiding Officer at the Meeting of the Society shall cast the deciding vote.

Par. 4 The terms of office of the Tellers shall expire when their report of the canvass has been presented and accepted.

Par. 5 At any regular meeting, the Council may, by a two-thirds vote of its members present, adopt, or amend By-Laws in harmony with the Constitution, provided that such By-Laws or amendments shall have been submitted in writing at a previous meeting of the Council and the Secretary has mailed a copy to each member of the Council at least fifteen (15) days before the meeting at which action is to be taken. A By-Law or an amendment to a By-Law shall take effect immediately upon its adoption by the Council, and shall be published at once by the Secretary to all members of the Society.

Par. 6 At any regular meeting, by a majority vote of its members present, the Council may adopt or amend Rules in harmony with the Constitution and the By-Laws. A Rule or an amendment shall take effect immediately upon its adoption by the Council, and shall be published by the Secretary to all the members of the Society.

Article R16, Amendments

Rule 1 In voting on an amendment to the Constitution the voter shall prepare his ballot by crossing out that part of the amendment which he wishes to vote against. He shall then enclose the ballot in an envelope and seal it, and shall enclose this envelope in a second envelope marked "Ballot on Amendment" and seal it, and he shall then write his name thereon for identification.

Rule 2 The Tellers shall not receive any ballot after the stated time for the closure of the voting.

Rule 3 The Secretary shall certify to the competency and signature of all voters.

Rule 4 The Tellers shall open and destroy the outer envelopes and then open the inner envelopes and canvass the results.

Rule 5 A ballot without the autographic endorsement of the voter on the outside envelope is defective and shall be rejected by the Tellers.

Rule 6 The Tellers shall consider a ballot as valid provided the intent of the voter is clear, and provided also that he conforms with the regulations for voting.

Index to Constitution, By-Laws, and Rules

Abbreviations for grades of membership....R3(2)
Accounts, Public Accountant's auditing of....R14(1)
Administrative Committee....B6A(2)
Administration....C1(3); B1
Admission
  and promotions....B4(6)
  application for....B4(1)
  qualifications....C4
  without regular number of references....R4(4)
Admissions
  Standing Committee on....B6A(15)
Affiliated societies, non-responsibility for....R2(4)
Affiliation
  of Local Sections with engineering organizations....R11(10)
  with other societies....R2
Allied arts and sciences....C2(1); B2(1)A
Amendments to By-Laws and Rules....B16(5), (6)
  changes in numbering caused by....C16(2)
Amendments to the Constitution....C16; B16; R16
  changes in numbering caused by....C16(2)
  procedure on....C16(1); B16; R16
American Engineering Council, delegates to....B6B(4)
American Society of Mechanical Engineers—official name....C1(1)
American Standards Association....B6B(10)
  procedure....B6A(3)
Annual dues
  for various membership grades....C5(2); B5; R5
  regulations concerning....B5
Annual Meeting....C9(1)
Application for membership....B4(1)
Appropriations, monthly report by Secretary on...B14(11), (12), (13), (14)
Approval of commercial standards, codes, etc....C2(1)
Associate Member
  grade of....C3(1)
  qualifications of....C4(6)
Attainment standards, high....B2(1)B(d)
Auditing
  of bills and accounts....R14(1), (2)
  of bills by Finance Committee....B14(15)
Autographic endorsement of ballots....R16(5)
Awards and other honors, conferring of....B2(1)A(f)
Badges or emblems for members....R3(3)
Balloting
  for Directors....R7
  on amendments to the Constitution....C16; B16; R16
  on candidates....R4(9), (10)
Bequests and gifts, use of....B14(5), (6)
Bills
  Finance Committee's audit of....B14(15)
  Secretary makes out and collects....B14(2)
Board of Honors and Awards....B6A(19)
Boiler Code, Special Committee on....B6A(26)
Budget
  annual....R10(8)
  of appropriations....B14(11)
Business meetings....C9(4), (5); B9(3),(5)
  quorum at....C9(4)
  special....C9(3)
By-Laws, procedure regarding....B16(5)
Certificates of membership....R3(1)
Charters....C1(2)
Citizenship standards, high....B2(1)C(b)
Code of Ethics....C15(1)
  Members', Professional Conduct Committee and....R15
  Members required to subscribe to....B15; R15
  Members', violations of....R15
Colleges, Standing Committee on Relations with....B6A(20)
Commercial use of Society's name....C2(2)
Committee on Admissions and local committees....R4(5)
  confidential information for....R4(6)
  monthly consideration of applications by....R4(7)
  reports to Council by....R4(7)
Committee, Regular Nominating....C7(1); B7; R7
Committees
  appointed by the Council....B6A(2), (3)
  nominating....C7(1); B7(6)
  power of the Council over....B6A
  Sectional....B6B(11)
  special nominating....B7(6)
  standing and special....B6A
Conduct, Secretary's receipt of complaints on....R15
Confidential correspondence on candidates....R4(8)
Constitution
  amendments to the....C16; B16; R16
  and By-Laws, Standing Committee on....B6A(18)
  present....C16(3)
Contracts, Secretary's approval of....R14(4)
Contributions, specific, Council's disbursement of....B14(4)
Cooperation
  with educational institutions....B2(1)B(b); B2(2)
  with other societies....B2(1)C(a)
Cooperative methods in engineering problems....B2(3)
Copyright, Society reserves privilege of....C13(5)
Corporate membership....C3(1)
Council
  all members elected by the....C4(1)
  and solicitation of research funds....B2(5)
  appointment of committees by the....B6A(2), (3)
  appointment of Honorary Vice-Presidents by....B6B(1)
  appointment of Secretary by....C8(2), (3)
  appointment of Treasurer by....C8(2), (3)
  balloting by the....R4(9)
Council (*continued*)
  composition....C6(2)
  (Directors), The....C6; B6
  Executive Committee of the....B6A(1)
  expulsion of Members by the....C15(2)
  filling of elective offices by....B6(1)
  functions, important....B6B
  letter-ballots ordered by....B6(3)
  meetings of the....C6(4)
  procedure, members' approval of....B6(2)
  quorum for the....C6(4)
  report to Annual Meeting of A.S.M.E....C6(5)
  Secretary and the Executive Committee....B6A(1)
  Secretary, Society Secretary and....B8(6)
  selection of....C6(1)
  specific contributions disbursed by the....B14(4)
  submission of questions to members by....B6(3)
  voiding of elective offices by....B6(1)
Directors
  announcement of election of....B7(15)
  balloting for....R7
  beginning of terms of office....B7(15)
  (Council), The....C6; B6
  delegation of powers by....C6(3)
  election of....C7; B7; R7
  number of....C6(2)
  tellers, election of....B7(13)
  time of voting for....B7(12)
Division expenditures and the annual budget....R10(8)
Dues
  and fees....C5; B5; R5
  Council's remission of....C5(4), B5(7), (12)
  resignations and....B3(3)
Education and Training for the Industries, Standing Committee on...B16(21)
Educational institutions, cooperation with....B2(1)B(b)
Election of Directors....C7; B7; R7
  announcement of....B7(15)
Elective offices, Council in relation to....B6(1)
Eligibility, candidate for membership, confidential information on....R4(6)
Emblem of the Society....R3(3); C2(2)
Engineer, enhancing status of....B2(1)B
Engineering
  and allied arts and sciences, promotion of....B2(1)A
  Council, American, delegates to....B6B(4)
  Foundation, representatives for....B6B(6)
  organizations, local, and Local Sections....R11(10), (11)
  profession, increasing the usefulness of....B2(1)C
  Societies Library....B2(1)A(g)
  standards, promotion of....C2(1)
  students, fostering fine background for....B2(1)B(e), (f)
  Trustees, Inc., United....B6B(3), (6)
Engineers' Council for Professional Development....B6B(9)
Engineers, encouraging young....B2(1)B(f)
Entrance standards, high....B2(1)B(a)
Estimate of income and expenditures....R14(3)
Ethical standards, high....B2(1)B(c)
Ethics, Members' Code of....B15; C15(1); R15
Exchange of knowledge and experience....B2(1)A(b)
Executive Committee of the Council....B6A(1)
Expenditures
  and income, estimate of....R14(3)
  of the Society....B14(11)–(16)
  outside of Council's appropriations....B14(12)
  Report to Finance Committee....B14(13)
Expulsion of members....C15(2)
Fellow
  admission requirements of....R4(1)
  qualifications of....C4(3), (4)
Fellows....C3(1)
Fees and dues....C5; B5; R5
Finance Committee
  estimate of income and expenditures by....R14(3)
  monthly auditing of bills by....R14(2)
  special reports to the Council by....B14(12)
Finance, Standing Committee on....B6A(12)
Fritz Medal Board of Award, John....B6B(7)
Funds....C14; B14; R14
  Council's direction of....C14
  disbursed, Finance Committees' audit of....B14(16)
  disbursed, Secretary's approval of....B14(16)
  expenditures....B14(11)–(16)
  for research, outside sources of....B14(4)
  receipts....B14(1)–(10)
  return on invested....B14(7), (8)
  to Secretary, all....B14(1)
  Treasurer's disbursement of....B14(16)
Gantt Medal Board of Award....B6B(7)
General Meeting....C9(6); B9(2)
Gifts and bequests, use of....B14(5), (6)
Government of the Society....C1; B1
Governmental agencies, cooperation with....B2(1)C(d)
Grade requirements for holding office....B7(9)
Grades of membership, assignment of....B4(3)
Guggenheim Medal Fund, Daniel....B6B(7)
Headquarters....C1(2)
Honorary
  Member....C3(1); B3(1)
  Member, qualifications of....C4(2)
  membership, nomination and election to....B4(4), (5)
  Vice-Presidents....B6B(1)
Honors and Awards, Board of....B6A(19)
Hoover Medal Board of Award....B6B(8)

eachment of officers....B8(8)
come and expenditures, estimate of....R14(3)
dustries, Standing Committee on Education and Training for....B6A(21)
iation fees....C5; B5(1)
surplus receives income from....B14(3)
ternational congresses....B2(1)A(c)
vested funds, return on....B14(7), (8)
vestment, maturity of permanent....B14(9)
nior Member....C3(1)
admission requirements of....R4(2)
election to....R5(1)
qualifications of....C4(7)
brary
representatives for United Engineering Trustees, Inc....B6B(5)
Standing Committee on....B6A(22)
fe membership, eligibility for....C5(3); B5(11), (12)
cal Sections....C11; B11; R11
and Nominating Committee....B7(3)
annual budget of the Society and....R11(7)
at meetings....R9
Chairmen of....R11(5)
composition of....B11(2)
disbanding by the Council....B11(7)
executive committees of....B11(5); R11(2), (3)
foreign-country groups....R11(13)
geographical grouping of....C11(2)
government of....R11(12)
group meeting of delegates from....B11(8)–(11)
group representatives of....B11(9)–(11)
limitation of membership in....R11(4)
naming of....B11(3)
object of....B11(1)
office of correspondent in....R11(9)
official stationery of....R11(8)
organization of....C11(1)
petitioning the Council for....B11(3); R11(1), (2)
relations with local engineering organizations....R11(10),(11)
Secretary's duties in....R11(6)
separate responsibility of....B11(4)
Society rules and regulations regarding....B11(4)
Standing Committee on....B6A(17); B11(6)
nagers
number and election of....B7(18)
terms of office....B7(18); C7(4)
chanical Engineering, a Society publication....B13(2)
etings and Program, Standing Committee on....B6A(13); B9 (5)
etings of the Society....C9; B9; R9
announcement of....B9(4)
conduct of....B9(5)
Local Sections at....R9
etings, Society not responsible for opinions at....C13(4)
mber, qualifications of....C4(5)
mbers....C3(1)
approval of Council procedure by....B6(2)
Code of Ethics required of....B15; R15
Expulsion of....C15(2)
grades of....C3(1)
honorary....C3(1)
in group activities in foreign lands....R11(13)
Junior....C3(1)
Life....C5(2); B5(11), (12)
Student....C3(1)
titles, abbreviations of....R3(2)
mbership....C3; B3; R3; C4; B4; R4; C5; B5
abbreviations for grades....R3(2)
certificates of....R3(1)
corporate....C3(1)
grades, annual dues for....C5(2)
grades, dues and fees for....C5; B5
obligations....C3(3)
voting on....B4(2)
rights....C3(2); R3(3)
me and government of the Society....C1
me of Society, commercial use of....C2(2)
tional Research Council, Engineering Division of....B6B(8)
ble Prize, Alfred....B6B(7)
minating Committee, Regular....C7(1); B7; R7
minating committees....C7(1), (2)
special....B7(6), (10)
jects of the Society....C2
ficers
duties of the....B8
of the Society, grade requirements for....B7(9)
rule regarding reelection of....B7(19)
ices....C1(2)
inions at Meetings, Society not responsible for....C13(4)
iginal papers....B2(1)A(b), (c)
pers
presentation and discussion of....C9(6)
and publications....C13; B13
and publications, copyright privilege on....C13(5)
and publications, Council's direction of....C13; B13(1), (2), (5)
and publications—Society's responsibility on opinions and discussions....C13(4)
and reports, publication of....B2(1)A(d); B2(3)
reports, etc., Society's copyright privilege on....C13(5)
Society not responsible for opinions in....B13(4)
wide publicity to scientific....B13(3)
rmanent investment, maturity of....B14(9)
wer Test Codes, Standing Committee on....B6A(27)
sident
of A.S.M.E., substitute for the....B8(2)
of A.S.M.E., successor to....B6(1)
of A.S.M.E., term of office....C7(4)
ofessional Committee....B6A(3)
ofessional Conduct, Standing Committee on....B6A(28)
ofessional Development, Engineers' Council for....B6B(9)
Professional Divisions....C10; B10; R10
executive committees of....C10(4); R10(2)–(7)
in relation to Professional Groups....B10(6)
meetings, notice of....R10(9)
naming of....B10(2)
object of....B10(1)
petitioning for....R10(1)
Professional Groups subject to Standing Committee on....R10(11)
Standing Committee on....B6A(16); B10(5)
Professional Groups....B10(6); R10(10)–(12)
functions and responsibilities of....R10(10)
Professional Practice....C15; B15; R15
Promotion fees....C5
Promotion of engineering standards....C2(1)
Promotions in membership grades....B4(6)
Proxy....C3(2); B3(2)
Public Accountant, auditing of accounts by....R14(1)
Public affairs, encouraging participation in....B2(1)C(c)
Publications
and papers....C13; B13
and papers, copyright privilege on....C13(5)
of the Society....B13(2)
Standing Committee on....B6A(14)
Publicity through achievement....B2(1)C(e)
Purposes of Society....B2
Quorum at business and Council meetings....C9(4); C6(4)
Receipts of the Society....B14(1)–(10)
Reelection of officers, rules regarding....B7(19)
Refunds upon resignation....R3(4)
Regular Nominating Committee....C7(1); B7; R7
Reinvestment of permanent funds....B14(9)
Relations with Colleges, Standing Committee on....B6A(20)
Reports, annual....B6A(10), (11)
Representation, Society....B6B
Representatives of A.S.M.E., special....B6B
Research....B2(1)A(a); B2(2), (3), (4)
funds....B2(5), (6)
funds, contributors to....B2(6)
funds, outside sources for....B14(14)
laboratories, cooperation with....B2(3)
Standing Committee on....B6A(24)
Reserve account, initiation fees in....B14(3)
Resignations....B3(3); R3(4)
Rules
governing the Society, Robert's....C2(2)
procedure regarding....B16(6)
Safety Standing Committee on....B6A(25)
Secretary
all funds paid in to....B14(1)
and the Council....B8(3), (6)
annual Council appropriations expended by....B14(14)
approval of contracts by....R14(4)
bills charge of....B14(15)
bills made out and collected by....B14(2)
certification of voters by....R16(3)
conduct complaints received by....R15
Council's appointment of....C8(2)
disbursements approved by....B14(16)
duties of the....B8(6); R8
filling vacancy in office of....C8(3)
in balloting, duties of....R4(9), (10)
invested-funds return computed by the....B14(7)
monthly financial report by....B14(13)
of The Council, Executive Committee and the....B6A(1)
office of the....R8
reelection of....B7(19)
Society, Council, and committees'....B8(6)
term of office....C8(2)
Sectional Committees....B6A(3); B6B(11)
Securities of the Society....B14(10)
Semi-Annual Meeting....C9(2); B7(7); B9(1)
Society
Annual Meeting of the....C6(5)
group activities in foreign lands....R11(13)
Library and Engineering Societies' Library....B2, 1A(g)
publications....B3(2); B13(2)
representatives....B6B
Solicitation of research funds....B2(5)
Special
and standing committees....B6A
business meetings....C9(3)
Committee on Boiler Code....B6A(26)
Committees, discharge of....B6A(11)
nominating committees....B7(6)
representatives of the Society....B6B
Standardization, Standing Committee on....B6A(23)
Standards, codes, etc., development of....B2(1)A(e)
Standing and special committees....B6A
Standing Committee
on Admissions....B4(6); B6A(15)
on Constitution and By-Laws....B6A(18)
on Education and Training for the Industries....B6A(21)
on Finance....B6A(12)
on Honors and Awards....B6A(19)
on Library....B6A(22)
on Library and United Engineering Trustees, Inc....B6B(5)
on Local Sections....B6A(17)
on Meetings and Program....B6A(13)
on Power Test Codes....B6A(27)
on Professional Conduct....B6A(28)
on Professional Divisions....B6A(16); B10(5)
on Professional Divisions, Professional Groups subject to....R10(11)
on Publications....B6A(14)
on Relations with Colleges, Student Branches and....B12(3), (4)
on Research....B6A(24)
on Safety....B6A(25)
on Standardization....B6A(23)
report to Council by....B6A(10), (11)

Student Branches C12; B12; R12
and Standing Committee on Relations With Colleges ..... B12(3), (4)
annual regional delegate conferences ..... B12(4)
annual selection of officers for ..... R12(2)
Honorary Chairmen of ..... R12(1)
naming of ..... B12(1)
organization of ..... B12(1)
regulations regarding ..... B12(2), (3)
Student-members ..... C3(1)
admission requirements of ..... R4(3)
dues of R5
privileges of ..... B4(8)
qualifications of ..... C4(8)
Successors to officers, acceptance by ..... B7(20)
Tellers
in amendments to the Constitution. B16(1), (2), (4); R16(2); (4); (6)
election of Directors ..... B7(13)
Transactions of the Society ..... B13(2)
Treasurer
and the Council ..... B8(3)
appointment of ..... C8(2)
Cashier's Account reimbursement ..... B14(16)
duties of ..... B8(4), (5)
Treasurer (*continued*)
filling vacancy in office of ..... C8(3)
funds deposited by Secretary to account of ..... B14(1)
reelection of ..... B7(19)
term of office ..... C8(2)
United Engineering Trustees, Inc. ..... B6B(3), (6)
Library Board of ..... B6B(5)
Unusual problems submitted by Council to members ..... B6(3)
Vice-President
as substitute for the President ..... B8(2)
as successor to the President ..... B6(1)
Vice-Presidents
Honorary ..... B6B(1)
number and election of ..... B7(17)
term of office ..... C7(4)
Voters, Secretary's certification of ..... R16(3)
Voting
for Directors, time of ..... B7(12)
on membership applications ..... B4(2)
on questions ..... B1(1)
Washington Award Commission of Western Society of Engineers ..... B6B(7)
Young engineers, encouraging ..... B2(1)B(f)

Transactions *of the* A.S.M.E.

Memorial Biographies

SOCIETY RECORDS—Part 3

Parts 1 and 2 of Society Records for the year 1942, containing Council and Committee personnel and other general information, the directory of members, and the Constitution, By-Laws, and Rules, were issued as Section Two of the Transactions for February, 1942. Part 3 is published for inclusion with all bound copies of Volume 64 of the Transactions and distributed to members of the Society upon request.

OCTOBER, 1942

VOL. 64, NO. 7

Transactions

of The American Society of Mechanical Engineers

Published on the tenth of every month, except March, June, September, and December

---

OFFICERS OF THE SOCIETY:

JAMES W. PARKER, *President*

W. D. ENNIS, *Treasurer* C. E. DAVIES, *Secretary*

COMMITTEE ON PUBLICATIONS:

F. L. BRADLEY, *Chairman*

C. R. SODERBERG E. J. KATES

A. R. STEVENSON, JR. L. N. ROWLEY, JR.

GEORGE A. STETSON, *Editor*

ADVISORY MEMBERS OF THE COMMITTEE ON PUBLICATIONS:

N. C. EBAUGH, GAINESVILLE, FLA. O. B. SCHIER, 2ND, NEW YORK, N. Y.

Junior Members

F. H. FOWLER, JR., CALDWELL, N. J. J. A. CONNON, NEW YORK, N. Y.

Published monthly by The American Society of Mechanical Engineers. Publication office at 20th and Northampton Streets, Easton, Pa. The editorial department, located at the headquarters of the Society, 29 West Thirty-Ninth Street, New York, N. Y. Cable address, "Dynamic," New York. Price $1.50 a copy, $12.00 a year; to members and affiliates, $1.00 a copy, $7.50 a year. Changes of address must be received at Society headquarters two weeks before they are to be effective on the mailing list. Please send old as well as new address. . . .By-Law: The Society shall not be responsible for statements or opinions advanced in papers or . . . printed in its publications (B13, Par. 4). . . .Entered as second-class matter March 2, 1928, at the Post Office at Easton, Pa., under the Act of August 24, 1912. . . .

Copyrighted, 1942, by The American Society of Mechanical Engineers. Reprints from this publication may be made on condition that full credit be given the Transactions of the A.S.M.E. and the author, and that date of publication be stated.

Memorial Biographies

THE purpose of Memorial Biographies is to place on permanent record the biographical and professional data relating to deceased members of The American Society of Mechanical Engineers. Hence every effort is expended to insure accuracy and to make the memorials as inclusive as is reasonably possible.

The first source of information upon which these notices are based is the Society's file of membership applications and transfers. In the case of the more recent members, these application records are fairly complete. The applications of those who became members many years ago, however, contain less detailed data, and in many cases the sponsors are no longer alive, so that assistance from this source cannot always be obtained. If the member has been retired for several years prior to his death, his business associates are frequently hard to locate, and, in some cases, members of his family cannot be found. While all these factors add to the difficulty of obtaining accurate and fairly complete data, every possible source of information is explored, with the result that publication of the notice is delayed. Nearly all of the memorials in this issue have been prepared under these difficulties.

It is the practice of the Committee on Publications in the case of some deceased members to ask former friends and associates to prepare the obituary. The object is to secure a final record that will be more valuable for having been prepared by men who knew the deceased and are competent to evaluate his work. Memorials prepared in accordance with this policy are signed by those who wrote them or who collaborated in their preparation. To all persons who have thus co-operated, the Committee acknowledges its gratitude.

The Committee also appreciates and acknowledges the assistance that has been given by relatives, business associates, and friends in the preparation of all other memorials. It also acknowledges its debt to such sources as Who's Who in Engineering, Who's Who in America, and similar publications; the Encyclopedia of American Biography, and the National Cyclopedia of American Biography; the technical and daily press; colleges and universities and their alumni associations; and engineering and other societies which have supplied information from their records.

Relatives, business associates, and Local Section and Student Branch officers are urged to notify the Society promptly of the deaths of members. Newspaper clippings or obituaries in any other form should be sent whenever available and the names and addresses of those who can supply further information should be furnished. A special form for supplying complete details will be forwarded by the Office of the Society upon request.

THE COMMITTEE ON PUBLICATIONS

Memorial Biographies

EDWARD THOMAS ADAMS (1861–1939)

Edward Thomas Adams, a member of the A.S.M.E. since 1899, died in Los Angeles, Calif., on June 24, 1939, of coronary thrombosis. He had carried on a consulting practice in that city since 1919, specializing in the design of oil-well pumps and small Diesel engines, on which he had taken out a number of patents.

Mr. Adams was born on December 4, 1861, in Ohio, at Hampden, Geauga County, son of Edward Francis and Roah Elmira (Shattuck) Adams. His early education was obtained chiefly in schools in Chicago, Ill., then he spent about ten years, 1880–1890, on the Pacific Coast. During this period he was variously engaged as draftsman, millwright, and patternmaker with different firms, including the W. A. Woods Manufacturing Co., Santa Cruz Iron Works, and Gillispie Lumber Company (companies no longer existent); for two seasons he operated a mill in the redwood district.

In the years 1889 to 1891 he helped to establish and was in charge of a course of instruction in mechanical drawing in the city schools of Stockton, Calif. Subsequently he took two years' work in the Civil Engineering Department of Leland Stanford Junior University and in 1894 secured an M.E. degree from Cornell University. He worked as a draftsman for the Payne Engine Company, Elmira, N.Y., 1894–1895, then served as instructor in the Department of Mechanical Engineering at Cornell, 1895–1897, receiving his M.M.E. there in 1896.

After working as mechanical engineer for the Bullock Manufacturing Company for a year, Mr. Adams went into the Engineering Department of the Edward P. Allis Co., Milwaukee, Wis., in 1898, serving as private draftsman or assistant to Edwin Reynolds (Member A.S.M.E., president in 1902), general superintendent of the company. When the company was reorganized in 1901, Mr. Adams was made mechanical engineer of the Allis-Chalmers Company, and several years later he became manager and chief engineer of the Gas and Mill Engine Department. He designed and installed engines for various companies, including the Westinghouse company at Pittsburgh, Pa., and the Allis-Chalmers company at Milwaukee. Among these engines were those built for the U.S. Steel Corp., at Gary, Ind., said to be the largest gas engines, at that time, in the world.

Mr. Adams left the Allis-Chalmers Company in 1910 and subsequently served as president of the Wisconsin Engine Company, Corliss, Wis., and as chief engineer of M. Rumely Co., La Porte, Ind. In 1917–1918 he was consulting engineer for the Humphrey Gas Pump Company, Syracuse, N.Y. He then went to the West Coast and after some work for the Doble Laboratory, steam automobile engineers, in San Francisco, established his office as consulting engineer in Los Angeles.

Mr. Adams became a member of the A.S.M.E. in 1899. He served on a special committee of the Society on Power Tests from 1912 until 1918 when the committee organization for this work was revised. Mr. Adams was appointed a member of both the Main Committee and Individual Committee No. 17 on Gas and Oil Engines and he served on the Main Committee for five years and on No. 17 until April, 1928. He belonged to the University clubs in Milwaukee and Chicago and was a member of the Sigma Xi fraternity.

Mr. Adam's wife, Ester A. (Boschen) Adams, whom he married in 1891, died in 1931. He was survived by four daughters and two sons, as follows: Roah (Mrs. John Nahapiet) and Marion (Mrs. Raymond Sullivan), of San Francisco, Calif.; Adelaide (Mrs. Marshall Williams), of San Fernando, Calif.; Helen (Mrs. Thos. Monroe), of Tucson, Ariz.; and Thomas E. and E. Ernest Adams, of Los Angeles.

LEON PRATT ALFORD (1877–1942)

Leon Pratt Alford came of colonial ancestry on both sides. He was born at Simsbury, Conn., on January 3, 1877. His father was Emerson Alford, a manufacturer at Collinsville, Conn., and his mother Sarah Merriam (Pratt) Alford.

He prepared for college at the Plainville (Conn.) High School, learning the trade of house carpenter during his vacation periods. He was graduated at the Worcester Polytechnic Institute in 1896, with a high scholarship record, as a B.S. in E.E. when only nineteen years old. In 1905 he received a degree in M.E.

He married Grace Agnes Hutchins of Templeton, Mass., on January 1, 1900, and had one son Ralph I. Alford, a doctor in Montclair, N.J., and two grandchildren. He lived for the first ten years after graduation in various places about Boston, but throughout mid and later life his home was in Montclair.

Upon graduation in 1896 Alford entered the employment of the McKay Metallic Fastening Association at Winchester, Mass., where he secured his shop and drafting room experience. During the reorganization and consolidation of this and other companies engaged in the manufacture of boot and shoe machinery he rose from assistant machine-shop foreman to general foreman, assistant superintendent, and production superintendent of the various McKay companies which united to form part of the United Shoe Machinery Company. In April, 1902, he became division engineer and assisted in the designing and building of the United Shoe Machinery Plant at Beverly, Mass., at that time the largest reinforced-concrete machine shop in the world. Alford was responsible for much of the design and installation of the machinery and equipment, and for the general details of the buildings. In 1904 he became assistant mechanical engineer and in January, 1906, chief of the mechanical engineering department.

In 1907 his lifework took a different direction, for in that year he became an editor of the *American Machinist* and was made editor-in-chief in 1911. During his editorship the *Machinist* maintained and advanced its high position in its field. When he resigned this post in 1917 he wrote a friend that he was "through with journalism," but within a few months he became editor of *Industrial Management*. In July, 1921, he joined the Ronald Press Company and was editor of the journals in the management field which under several changes of name, *Management Engineering, Management and Administration*, etc., were published by that company until the merger of the magazine with *Factory and Industrial Management* in 1929. In 1925 Alford was elected director of the company and continued on its board until his death. He was vice-president from 1926 to 1937. In these capacities he headed up the editorial policies of the company.

His influence on the literature of management was far-reaching. He planned and edited "Management's Handbook," which became the standard reference book in that field, not only in this country but in England and Germany. With rare ability he drew together the experience and knowledge of other people and co-ordinated them into a complete whole. Through the books which he edited and those he wrote himself he rendered a distinguished service to the engineering field—the more so since the engineer engaged in management work has had far less reference literature to guide him than has the engineer engaged in other branches of engineering work.

In addition to editing "Artillery and Artillery Ammunition," 1917, "Management's Handbook," 1924, and "Cost and Production Handbook," in 1934, Alford was the author of "Bearings and Their Lubrication," 1911. His paper on "The Laws of Manufacturing Management" before the A.S.M.E. in 1927 won him the first award of the Melville Medal, and appeared in 1928 in book form and had a wide sale. He also wrote the "Life of Henry Laurence Gantt," 1934, and "Principles of Industrial Management for Engineers," 1940.

His contributions to the papers and reports of the A.S.M.E. are too many to be enumerated here in full. Outstanding among them is the series of progress reports on management. The first one in 1912, "The Present State of the Art of Industrial Management," was written for a committee of which he was secretary. A further review on "The Status of Industrial Relations" was prepared in 1919 at the request of the Committee on Meetings and Program. These were so successful that he wrote a continuation in 1922, "Ten Years' Progress in Management," and another with the same title in 1932. It was hoped that he might write a fourth one in 1942, but this was cut short by his death. His outstanding paper on the "Laws of Manufacturing Management" has been mentioned. The range of his papers included high-speed drilling, industrial relations, preferred numbers, factory construction and arrangement, production control, and a series of papers with J. E. Hannum on evaluating manufacturing operation, suggesting the "kilo man-hour" as the measuring unit. In addition to all these he wrote papers for the S.P.E.E., A.M.A., and the American Engineering Council, and others given in England, Japan, and Germany.

Valuable as were his contributions to the publications of the A.S.M.E., his work on its various committees was even more outstanding. Probably no one in all its membership had a longer and more varied service. There was no time from 1913 until his death that he was not serving on some committee, on the Council, or as A.S.M.E. representative on other bodies. The mere list of these assignments covers more than a closely typewritten page.

He served on most of the standing committees and on many special ones, of most of which he became chairman. The standing committees included those on Constitution and By-Laws, Professional Divisions, Meetings, and Honors and Awards. He had been a member of the executive and other committees of the Management Division, and

of many special committees dealing with research and technical problems, the Aims and Organization of the Society, Policies and Budget, and Administration, and he represented the Society on the American Engineering Council, Gantt Medal Board, National Management Council, etc.

No one can speak of Alford's work on the American Engineering Council with more authority than L. W. Wallace, executive secretary of the Council throughout most of its existence. He says, "Mr. Alford was for many years a member of the A.S.M.E. delegation and during much of the time was vice-chairman of the delegation. He attended the organization meetings of the Council, served on the committee which drafted its constitution and by-laws, and acted as temporary executive secretary for about three months, until I took over in April, 1921.

"Alford was a member of the Committee on Elimination of Waste in Industry, the first important study the Council made. He also contributed markedly to planning the study, conducting it, and especially the editing of the report, 'Waste in Industry.' He was one of the strong supporters of that report when it was adopted by the Administrative Board of the Council in June, 1921. He was also a member of the Committees on the Twelve-Hour Shift in Industry, on the Balance of Economic Forces, and on Safety and Production, and edited these reports. He was chairman of the original Committee on Publicity and Publications and served on it for many years. He also served for many years on the Public Affairs Committee and several times was its chairman. He was repeatedly a member of the Executive Committee and was on many of its subcommittees.

"Throughout the life of American Engineering Council no man served it in more capacities, or with greater courage, loyalty, and ability than did L. P. Alford. To it he gave unstintingly of his time, energy, and balanced judgment because of his belief in it as an instrument of public service."

His connection with the Council brought him into contact with various government problems as a consulting engineer. A study which he made in 1935 for the Textile Labor Relations Board led to a much more extended one on the manufacturing costs of telephone apparatus and equipment which he made for the Federal Communications Commission during 1935–1937, as a basis for recommendations on rates. The study reviewed the history of the Western Electric Company and its relation to the telephone industry; and made an examination of its cost and accounting procedures and those of its competitors, and an appraisal of its cost accounting practice. This report was made a part of the Commission's report to Congress.

With the completion of this work for the government, in 1937, Alford became professor of administrative engineering in New York University, and head of the Industrial (later Administrative) Engineering Department, which position he held until his death. He undertook this work with some hesitation, but on the advice of friends long experienced in this field who knew the man and assured him that as editor he had been teaching for thirty years. He fully justified this judgment and was happy in the work. He taught courses in management, industrial economics, etc., to seniors and graduates. His last book, "The Principles of Industrial Management for Engineers," published in 1940, was an outcome of this work. His long experience, wide contacts, and even wider viewpoint give it special value and it has taken its place among the standard textbooks in that field.

For some years he had been warned of heart trouble, but continued his work much as usual until his last brief illness. He died in the Flower Memorial Hospital in New York on January 2, 1942. It is characteristic of him that, quickly and unexpectedly as the end came, his immediate tasks were in order and the remaining lectures of his courses were written in anticipation of a rest he was planning to take.

Alford joined the A.S.M.E. as a junior member in 1900. He was elected a member in 1908 and a Fellow in 1936. He was vice-president from 1920 to 1922, and because of his long and distinguished service in the Society he was awarded honorary membership in 1941, only a month before his death. In 1932 the Worcester Polytechnic Institute conferred on him the honorary degree of Doctor of Engineering in recognition of his work in connection with machine tools.

He was a member of the American Management Association, the S.P.E.E., National Association of Cost Accountants, the Institut Scientifique d'Organisation et de Gestion, the Engineers' Club, New York, and Sigma Xi. He received the first award of the Melville Medal in 1927 and the Gantt Medal in 1931.

Alford's wide influence was not based so much on creative contributions, such as those of Taylor, Gantt, and Gilbreth, as on his singular clarity, breadth of view, and on his balance of judgment and capacity to see things as a whole and in true proportion. His writings were seldom the object of controversy because his presentations were so well grounded they found general acceptance. His handbooks were successful because they were well balanced, authoritative and helpful.

The A.S.M.E. has had few members who have given it more useful service. His presence on any committee strengthened it. It was especially valuable where the matter under consideration was controversial or confused. In discussion he was slow to speak, convincing, and apt to reserve comment until all points had been discussed. Then he would summarize the situation, and final action would often crystallize around his suggestions.

He stimulated and directed much valuable work by other men. The present writer acknowledges his debt to him. He was on the A.S.M.E. trip to Germany in 1913. At the close of the trip at Munich, Alford, impressed with the technical progress in Germany, proposed the writing of a series of articles on tool building and the development of machine tools, which started a life interest in that field.

His friends will long remember the quiet voice, the kindly eyes smiling behind his glasses, his friendliness and wise counsel. It is such men as he who have made the A.S.M.E. what it is. We are glad the Society's highest honor came to him in time for him to enjoy it. It must have meant much to one who had given so much.—[Memorial prepared by JOSEPH W. ROE, Southport, Conn. Fellow and Melville Medalist, A.S.M.E.]

DUDLEY BAIRD (1877–1939)

Dudley Baird, vice-president of the Pacific Foundry Company, Ltd., San Francisco, Calif., had been connected with that company more than thirty years when his death occurred on October 17, 1939. He entered its employ early in 1907 to design and erect chemical and metallurgical apparatus, and advanced through the position of secretary to the office of vice-president, in charge of engineering and operations.

Mr. Baird was born at Oakland, Calif., on February 14, 1877, his parents' names being Andrew and Julia Courtis Baird. After securing a B.S. degree at the University of California in 1898 he spent a year in postgraduate work in mining and metallurgy. During the following year he worked successively as stationary engineer in the steam-electric power plant of the Tesla (Calif.) Coal Mining Company, stamp mill assistant at Chips Mine, Sierra City, Calif., and chairman with a surveying party in Nome, Alaska.

After his return to California in August, 1900, he took a position with the Penn Mining Company, Campo Seco, Calif., as assayer and chemist. He was promoted to smelter superintendent and metallurgist in a few months and continued in that capacity for four years. Among other duties he was responsible for the design, erection, and operation of additional smelting, roasting, and ore-crushing units. In 1905–1907, prior to his connection with the Pacific Foundry Company, he was engaged with the erection and operation of a smelter for the Union Copper Mining Company, at Copperopolis, Calif.

Mr. Baird held many patents on multiple-hearth furnaces for roasting, calcining, and incinerating. He had been a member of the A.S.M.E. since 1921 and also belonged to the American Institute of Mining and Metallurgical Engineers and the Engineers Club of San Francisco. He married Viola Brainerd, of Middlebury, Vt., in 1910 and is survived by her and a son, Robert Baird.

JOHN JOSEPH BAKRADZE (1889–1937)

John Joseph Bakradze, whose death occurred in St. Luke's Hospital, New York, N.Y., on November 20, 1937, was born on January 1, 1889, at Vladikaukas, Russia. He secured his early education in that country and subsequently studied mechanical engineering in Germany. After returning to Russia in 1910, he was employed successively as a draftsman by Greefits & Co., Baku, as installation engineer by the Technical Bureau, Armavir, and the International Harvester Company of America, at Riga, and as engineering inspector in the car division of the Russian Army.

In 1920 he went to Constantinople, Turkey, where he was engaged by the Standard Oil Company as chief engineer on one of its barges. He came to the United States in the early part of 1923 and spent brief periods with the White Motor Car Company, on Long Island, and as draftsman for the Lutz Elevator Co., Inc., New York Edison Company, and the firm of Eadie, Freund & Campbell, all in New York.

Mr. Bakradze's work since 1924 had been with the firm of Sprague & Slocum and its successor, Slocum & Fuller, New York. First as draftsman and later as mechanical engineer, he was engaged in the field of heating and ventilating, and electric wiring, in connection with building construction. Since the reorganization of the firm in 1931 he had not been continuously employed.

Mr. Bakradze became an associate member of the A.S.M.E. in 1924 and was automatically transferred to the grade of member in 1935. He is survived by his widow, Pauline (Lobutzky) Bakradze.

OSCAR HOWARD BALDWIN (1863–1940)

Oscar Howard Baldwin, a member of the A.S.M.E. since 1889, died at his home, "Fairmount," Salcombe, South Devon, England, on February 14, 1940. He was born on November 4, 1863, in Newark, N.J., and was graduated from the Stevens Institute of Technology in 1885 with a degree in mechanical engineering. The following account of his work is taken from *The Engineer*, February 23, 1940.

"After serving a short time with the Pennsylvania Railway, he joined the firm of Westinghouse, Kerr and Co., which later became the Westinghouse Electric and Manufacturing Company. After being chief engineer in the lighting plant of Plainfield, N.J., for a year, he rejoined the Westinghouse Electric and Manufacturing Company and was chosen by the late George Westinghouse to look after its British interests. From 1889 to 1893 he was engineer of the Westinghouse Electric Company of London, and had charge of the engineering work of the firm, including the erection of the new plant at the Sardinia Street Station of the Metropolitan Electric Supply Company. In 1893 he returned to America for a year to take charge of the electrical exhibit of the Westinghouse Company at the World's Fair, and a year later was given charge of the foreign sales department of the company. About 1898 the offices of the Westinghouse Electric Company, Ltd., of London were established at 2, Norfolk Street, Strand, and Mr. Baldwin became the managing director of the firm. From 1900 to 1902 he was managing director of J. and G. White and Co., Ltd., of London. Eventually the Westinghouse Electric Company, Ltd., of London, became the British Westinghouse Electric and Manufacturing Company, Ltd., and works were built at Trafford Park, Manchester. Mr. Baldwin remained at the London office of the firm and became the district manager of the company. When the name of the company was changed to the Metropolitan Vickers Electrical Company, Ltd., he still remained at the London office, and for some years he was also joint European manager of the Westinghouse Electric International Company. He retired about 1920, and for a time went to live at Salcombe, South Devon. In 1927 he was entrusted by the Taylor Stoker Company, of America, with the management of its interests in England, and when the British company was formed he became director in London. Mr. Baldwin remained a director of the company till he finally retired in 1933."

HAROLD BUTLER BARNES (1880–1938)

Harold Butler Barnes was born at Springfield, Ill., on February 18, 1880, son of Phineas and Fanny (Ellsworth) Barnes. He took private tuition and attended the Thurston Preparatory School in Pittsburgh, and at the age of fourteen passed the entrance examinations for the engineering course at the Western University of Pennsylvania. Because of family considerations, however, he did not enter, but went to work for the Westinghouse Electric & Manufacturing Co., East Pittsburgh, where he spent about seven years in the operating and inspection departments.

During the years 1901–1903 Mr. Barnes was engaged in automobile work, first in charge of the electric garage of Banker Brothers Company, in Pittsburgh, then in the experimental and designing departments of the Pope Motor Car Company at its Waverly Plant, Indianapolis, Ind. He next designed, installed, and operated the electrical and mechanical equipment of the Launch & Gondola Concession Co. at the Louisiana Purchase Exposition at St. Louis, Mo., and also handled construction work for other concessions.

Following the exposition he was connected with the Peerless Motor Car Company for a time in its branch in New York, N.Y., after which he was located at Leadville, Colo., for several years, performing operating and maintenance work at the Yak Mill of the American Zinc Extraction Company, serving as superintendent of the electrostatic plant of the Lanyon Zinc Company, and engaging in the design, installation, and repair of mine and mill equipment.

In 1908 Mr. Barnes went to Denver, Colo., where he carried on business as a consulting electrical and mechanical engineer until his death on May 12, 1938. He specialized in labor-saving equipment and general power applications and pioneered in storage-battery applications to heavy haulage problems, such as haulage at the Big Five Mining Company, Idaho Springs, Colo. He designed many power installations for unusual conditions. He took a great interest in local construction works, whose progress he watched whenever he could. He contributed a number of articles on his work to the technical press.

Mr. Barnes became a member of the A.S.M.E. in 1920 and as a member of its Detroit Section served as chairman of the Hotels and Registration Committee for the 1934 Semi-Annual Meeting held in Denver. He also belonged to the American Institute of Electrical Engineers from 1919 to 1935 and had served as chairman of its Colorado Section and as alternate representative of the Institute on American Engineering Council. He was a member of the Technic Club, Denver, and of the Elks fraternal order.

Mr. Barnes married Marie Louise Warnecke, in Denver, in 1917, and was survived by her.

WILLIAM OLIVER BARNES (1864–1939)

William Oliver Barnes, consulting engineer, Worcester, Mass., died on September 8, 1939. He was born at Newburgh, N.Y., on May 16, 1864, son of David A. and Elsie E. (Ackerman) Barnes. His early education was secured in the public schools of Paterson, N.J., and he was graduated from Stevens Institute of Technology in 1884 with a mechanical engineering degree.

Following his graduation Mr. Barnes engaged in silk manufacture at Paterson under the firm name of Barnes and Reel for five years, then at Barmen, Germany, for two years, and again in Paterson until 1895, as superintendent of the Barnes Manufacturing Company. Then he followed the same line of work as superintendent of the Gregory Silk Manufacturing Company, Scranton, Pa., for a year.

Mr. Barnes turned to the design of tools and development of processes for the manufacture of typewriters, with the Blickensderfer Manufacturing Company, Stamford, Conn., in 1895, and continued there for five years. Subsequently he was engaged in design work on automobiles for the American Bicycle Company, Toledo, Ohio, then with the Mergenthaler Linotype Company, Brooklyn, N.Y., for a short time. From 1902 to 1908, he was connected with the Ross Rifle Company, of Hartford, Conn., the latter part of the time in charge of the company's factory at Quebec. In the following years he was, first, assistant superintendent of the Miller Lock Company, Philadelphia, Pa., then mechanical engineer at the Iver-Johnson Arms and Cycle Works, Fitchburg, Mass. During World War I he took an active part in machine tooling of one of the large ordnance plants in the eastern part of the United States. After the war he took up consulting practice in Leominster, Mass., later removing to Worcester and continuing until his death in development and inventive work in the machine tool and radio fields. He invented and manufactured the Barnes precision cutter grinder, which was widely used during the war both in the United States and abroad in arsenals and other manufacturing plants engaged in war work. Many other inventions had been patented by him.

Mr. Barnes married Grace D. Herdman in 1889. Her death, as well as that of their two children, William Oliver and Herdman Barnes, preceded his. A brother W. C. Barnes, of Chicago, survives him.

Mr. Barnes had been a member of the A.S.M.E. since 1908.

FREDERICK EMIL BAUSCH (1871–1938)

Frederick Emil Bausch, whose death occurred in St. Louis, Mo., on April 18, 1938, was born on January 8, 1871, at Mannheim on the Rhine, Germany. He came to the United States as a boy and prepared for college at the St. Louis High School. He was graduated from Washington University, St. Louis, with an E.E. degree in 1892 and an M.M.E. degree was conferred upon him by Cornell University four years later. He taught at the St. Louis Manual Training School during the years 1892–1895.

From 1896 to 1898 Mr. Bausch worked in the electrical laboratory of the Bell Telephone Company of Missouri, at St. Louis, and during the next two years was a draftsman in the Mechanical Department of the Missouri Edison Electric Company in that city. He was advanced to the position of assistant mechanical engineer in 1900, but soon afterward left to become chief engineer of the Pittsburgh Plate Glass Works at Crystal City, Mo. In 1901 he made another change, becoming western manager of The Hooven-Owens-Rentschler Company at St. Louis, the position which he occupied until 1930. In 1924 he also became owner of the Fred'k E. Bausch Fire Clay Mines. Since 1930 he had maintained his own office as sales engineer, in St. Louis.

Mr. Bausch was elected to membership in the A.S.M.E. in 1904. He was an active member of the St. Louis Section, which he served as secretary in 1913, chairman in 1914–1915, and member of the executive committee for the next two years. A brother, Adolph Bausch, of St. Louis, survives him.

PHILIP E. BLISS (1885–1939)

Philip E. Bliss, president of The Warner & Swasey Co., Cleveland, Ohio, died unexpectedly on April 11, 1939, after a brief hospitalization for treatment of a heart ailment. Surviving him are his widow, Loretta E. (Crane) Bliss, whom he married in 1904, and two children, Mary A. (Mrs. Edgar B. Gausby) and Charles William Bliss.

Mr. Bliss was born in Cleveland on December 14, 1885, son of

Julius E. and Arabel (Hauxhurst) Bliss. He attended the public schools in North Fairfield, Ohio, where his father was a well-to-do farmer, and had three years at Ohio Wesleyan University. Leaving there in 1904, he spent the next six years as a junior secretary in Y.M.C.A. work in Cleveland and New York. He returned to Cleveland in 1910 to enter the employ of The Warner & Swasey Co. as junior clerk in the accounting department. From that position he advanced to auditor, and later treasurer; in 1924 he was made a vice-president, and in 1928, president.

Quiet and self-effacing, Mr. Bliss was an outstanding leader among machine tool manufacturers. The depression years were particularly severe ones for this industry, but his courage never faltered, and his wise guidance not only brought his own company safely through, but also helped other organizations to weather the storm.

Mr. Bliss was tremendously interested in the welfare of his employees, and to help facilitate the solution of their problems he had the door to his private office removed so as to encourage them to seek discussion and friendly advice.

Mr. Bliss had numerous interests outside his immediate business activity. He was past-president (1927–1928) of the National Machine Tool Builders' Association, and had been serving as a member of the Executive Committee of the National Industrial Conference Board. He had a keen sense of civic duty, evidenced by serving several terms as a director of the Cleveland Chamber of Commerce; by being a Trustee of St. Luke's Hospital and Case School of Applied Science, a director of the Society for Savings, and vice-president of the Caxton Building Company, all of Cleveland.

Mr. Bliss belonged to numerous organizations and clubs. He became an associate of the A.S.M.E. in 1923, and served on its Committee on Education and Training for the Industries in 1935–1936. He was a member of the Board of Directors of the American Standards Association in 1937–1938. He also belonged to the Army Ordnance Association and the Cleveland Engineering Society, and was a member of Phi Delta Theta, the Union Club (Cleveland), and the Union League Club (New York).

ALBERT (HAMMOND) BUCKLER (1875–1939)

Albert (Hammond) Buckler, who died on December 1, 1939, was born on August 24, 1875, at Long Branch, N.J., son of Albert and Sarah A. (Hardover) Buckler. At the age of sixteen he became an apprentice machinist at the New York Navy Yard. During the period of his apprenticeship there he also took various engineering courses in evening classes at Pratt Institute. In later years he took courses at George Washington University and New York University. He was employed by the Navy Department until 1901, securing both machine shop and drafting room experience and spending some time at sea as an oiler in army transport service.

Early in 1901 Mr. Buckler took a position as engine draftsman with the William Cramp Ship & Engine Building Co. In the summer of 1903 he left that employment to become draftsman in the Turbine Department of the Westinghouse Machine Company, East Pittsburgh, Pa., where he spent about five years, part of the time as salesman for steam turbines and gas engines.

Mr. Buckler returned to government service in 1908 when he began a three-year period at the Naval Gun Factory, Washington, D.C., as draftsman and designer. Subsequently, from 1911 to 1919, he was in the U.S. Lighthouse Service, first as chief draftsman in the General Depot at New York, then from 1914 on as assistant superintendent of the Service. While in the Service he invented a boat for its use. He also taught marine engineering at Johns Hopkins University in 1917–1918.

During 1919–1920 Mr. Buckler was with the International Mercantile Marine Co., New York. While repair manager in the Construction Department, he was employed in connection with repairs on the S.S. *Leviathan*, and later, as assistant production engineer, he supervised the reconstruction of the twelve-story office building of the company at No. 1 Broadway, New York.

Mr. Buckler had been production engineer for Gibbs Brothers, Inc., and Gibbs & Cox, New York, since 1921. He installed production control and payment systems as applied to the construction and repair of ships, and engaged in estimating and design. He was intensely interested in everything pertaining to ships, the Navy, and related matters.

Mr. Buckler entered the A.S.M.E. as a junior member in 1905, became an associate-member in 1925, and was automatically transferred to the grade of member in 1935. He belonged to the Masonic fraternity. He is survived by his widow, Grace (Welch) Buckler, of Washington, D.C.

ELLWOOD BURDSALL (1856–1939)

Ellwood Burdsall, who died on March 10, 1939, after an illness of six months, had held membership in the A.S.M.E. since the year of its formation, having become a junior member in April, 1880. He was promoted to the grade of member in 1916. For many years he had been active in the technical committee work of the Society. He was a member of the Special Committee on Tolerances in Screw Thread Fits from the time of its formation in 1912 until it was discontinued in 1921. He continued his service in this field of standardization as a representative of the A.S.M.E. on the Sectional Committee on the Standardization and Unification of Screw Threads, organized in 1921, until the committee was reorganized in 1929. From its beginning in 1922, he was a member of the Sectional Committee on Bolt, Nut and Rivet Proportions and of its subcommittee on Wrench-Head Bolts and Nuts, and from 1924 until his death he was on its subcommittees on Round Unslotted Head Bolts and on Plow Bolts.

Mr. Burdsall was born on September 20, 1856, at Harrison, N.Y., a twin of Richard H. Burdsall, banker and industrialist. His parents were Ellwood and Hannah (Haviland) Burdsall. He attended the Friends Seminary in New York, N.Y., and Swarthmore College, and was graduated from Cornell University in 1878 with a B.M.E. degree.

Following his graduation he became draftsman for Russell, Burdsall & Ward, the bolt and nut company originally founded as the Union Screw Company in Port Chester, N.Y., in 1845 by his father, William E. Ward (a founder member of the A.S.M.E.), and Isaac D. Russell. Mr. Burdsall became secretary in 1880 and treasurer in 1915, and served in these offices until his death. The company was merged with the Port Chester Bolt & Nut Co. in 1901 to form the Russell, Burdsall & Ward Bolt and Nut Co.

He was also a member of the American Iron and Steel Institute. He was president of the First National Bank & Trust Co., of Port Chester, from 1915 until his death, and a former president of the Port Chester Savings Bank and local Board of Education. He was one of the founders of the Port Chester Rotary Club, a governor of the Old Port Chester Country Club, and a member of the Indian Harbor Yacht Club, and Red Spot Fishing Club, of Upton, Me. He was a devout Quaker and had been presiding officer of the New York Yearly Meeting.

Surviving him are two sons, Richard L. Burdsall and Robert L. Burdsall, both of Port Chester, N.Y. His wife, Luella T. (Morris) Burdsall, of Milton, Ind., whom he married in 1893, died in 1919. A third son, Dr. E. Morris Burdsall, died on April 21, 1939.

FRED JOSEPH CHATEL (1891–1939)

Fred Joseph Chatel, assistant engineer at the Delray Station of The Detroit Edison Company, died from a heart attack at his home in Detroit, Mich., on April 24, 1939.

Mr. Chatel was born at Kearsarge, Mich., on February 20, 1891, son of Joseph and Mary Louise (Doucette) Chatel. He prepared for college at the high school in Calumet, Mich., graduating in 1909, and received a B.M.E. degree from the University of Michigan in 1914. He had been connected with The Detroit Edison Company since then, except in 1917–1919, during World War I. Prior to the war he spent about six months in the Research Department, followed by something over two years as boiler room engineer at the Connors Creek plant. He returned to this position after the war for two years and a half, then was transferred to the Delray plant, where he held the title of technical engineer until 1929, when he was appointed assistant engineer. He contributed a paper on "Steam-Condenser Practice and Performance" to the 1927 Annual Meeting of the A.S.M.E., and was co-author with Paul W. Thompson of one on "Stoker Developments at the Detroit Edison Company's Delray Power House No. 3," presented at the 1932 Annual Meeting. These papers were published by the Society, the first in *Mechanical Engineering* for March, 1927, and the second in the Transactions, 1933. Mr. Chatel held a patent on a slag deflector for furnace walls.

During the war Mr. Chatel served in the navy, enlisting as a machinist's mate in April, 1917, and advancing to a lieutenant, junior grade, in the naval reserves. He was first chaplain of the Thomas A. Edison Post of the American Legion in 1931–1932 and senior vice-commander in 1937–1938.

Mr. Chatel was elected a member of the A.S.M.E. in 1938 and was a member of the Engineering Society of Detroit. He is survived by his widow, Genevieve M. (Doty) Chatel, whom he married in 1919, and by a daughter Elaine, and three sons, Paul F., John E., and Robert J. Chatel.

ERNEST LOWELL CLIFFORD (1883–1939)

Ernest Lowell Clifford, district sales manager of the Babcock & Wilcox Co. at Detroit, Mich., died on February 8, 1939.

Mr. Clifford became a member of the A.S.M.E. in 1914 and served on the Sectional Committee on the Safety Code for Conveyors and Conveying Machinery, representing the Associated General Contractors of America, from 1926 to 1936. He was also a member of this committee's Subcommittee No. 6 on Air, Steam, or Liquid Conveyors from 1927 to 1936. Other organizations to which Mr. Clifford belonged included the Western Society of Engineers, the Engineering Society of Detroit, Detroit Yacht Club, and masonic fraternity.

The son of Benjamin Franklin and Florence Lulu (Woollen) Clifford, Mr. Clifford was born in Indianapolis, Ind., on February 23, 1883. His early education was secured in public schools in Tacoma, Wash., and Chicago, Ill., and he was graduated from the Massachusetts Institute of Technology with a B.S. degree in 1904. Following his graduation he spent a year and a half as assistant to Prof. S. H. Woodbridge, of the M.I.T. faculty, in his private practice, chiefly heating and ventilation, in Boston, Mass., and Washington, D.C.

At the end of 1905 Mr. Clifford began work as draftsman for Pierce, Richardson & Neiler, mechanical and electrical consulting engineers, in Chicago. He was employed in that city and vicinity for about seventeen years. After leaving his first position in the spring of 1907, he spent about a year with the L. H. Prentice Co., heating and ventilating contractors, then for a short time was inspector for the village of Wilmette in connection with sewer construction. Next he was inspector of construction and assistant to the chief construction engineer, C. G. Y. King (Mem. A.S.M.E.), of the Cosmopolitan Electric Company, in the construction of the Grove Street Power Station. He was in charge of construction and engaged in power station engineering for Sargent & Lundy from early 1910 to the middle of 1913, then worked on designs and estimates for W. A. Pope, Chicago contractor, for a few months. Following this he was designer and construction superintendent for the Mead-Morrison Manufacturing Company, then became assistant chief engineer of the Cannon-Swenson Company, contractors for chemical and sugar plants. He later became a partner in this organization, and its vice-president.

From the fall of 1922 until April, 1927, Mr. Clifford was connected with McClellan & Junkersfeld, Inc., of New York, working on the design and construction of power stations and industrial plants. The Cahokia Power Station, at St. Louis, Mo., was one of the plants built under his direction. He began work for the Babcock & Wilcox Co. in 1932. He was in charge of the Detroit office from then until 1936, during which time it was part of the Chicago sales territory, operating under the Chicago district sales manager. In 1936 he was made district sales manager of the Detroit territory, reporting direct to the general offices in New York.

Mr. Clifford married Muriel Ruby King, a native of Liverpool, England, in 1907, who survives him, together with their three children, Margaret King, Jane Wingate King, and Franklin King Clifford.

DAVID BANKS CLOUDSLEY (1876–1934)

David Banks Cloudsley was born on December 16, 1876, at Toronto, Ont., Canada. He attended schools in that city and at Williamsport, Pa., where in 1892–1893 he served an apprenticeship with the Williamsport Engineering Supply Company, working on the manufacture of brass goods.

In 1894 Mr. Cloudsley went to Buffalo, N.Y., and after a short time in the drafting room of the Buffalo Forge Company he secured employment with the Buffalo General Electric Company as machinist and assistant engineer. He spent four years in this position, then in 1899 engaged in the design and construction of copper smelting furnaces with O. S. Garretson, of Buffalo.

During the years 1900–1901 he was employed by the Frontier Engine Works, Buffalo, as designer of gas and steam engines and special machinery. The following year he was working on traction engine design for the Buffalo Pitts Company.

In 1903 Mr. Cloudsley entered upon a long period of work for the City of Buffalo. At first he was in the Bureau of Engineering, designing a sewage pumping plant. Then he was transferred to the Bureau of Water, assigned to the design and installation of a boiler plant. Subsequently, as assistant to the chief engineer, he designed and superintended the installation of a new pumping station, of which he later became chief engineer. He served in this capacity until 1916. Two years later he became associated with the Zaremba Company, of Buffalo, as a design engineer, and he was employed by that organization until his death from a ruptured appendix on March 17, 1934.

Mr. Cloudsley became an associate of the A.S.M.E. in 1908. A brother, Arthur P. Cloudsley, of Buffalo, survived him.—[Biography compiled from best obtainable information, not all of which could be verified.]

WILLIAM LAWSON CONRAD (1873–1939)

William Lawson Conrad, a member of the A.S.M.E. since 1917 and active in the work of the Society's Textile Division, died at the Sibley Memorial Hospital, Washington, D.C., on November 29, 1939, from pneumonia. He is survived by his widow, Frances A. (Cushing) Conrad, whom he married in 1906.

Colonel Conrad was born at Topsfield, Mass., on September 17, 1873, son of Thomas Joshua and Margaret Agnes (O'Connor) Conrad. He attended school in Concord and Fitchburg, Mass., and after graduation from high school served an apprenticeship at the Fitchburg Machine Works. The record of his early experience, as taken from his application for membership in the A.S.M.E., lists the following: foreman, Putnam Machine Company, Fitchburg; assistant to assistant superintendent, United Shoe Machinery Company, Albany Street plant; and master mechanic, Sayles Bleacheries, Saylesville, R.I.

For many years Colonel Conrad was associated with Henry Laurence Gantt. According to the biography of Mr. Gantt, written by Leon P. Alford, the first contact was while Conrad was still a high school boy and was employed by Gantt during the organization of the Simonds Rolling Machine Company. Dr. Alford also lists Mr. Conrad as one of those trained in Gantt's methods at the Sayles Bleacheries. These early contacts grew into a close association which continued until Gantt's death in 1919. As a member of Gantt's organization, Colonel Conrad had part in many installations of modern methods of management in industrial organizations, and after the death of Mr. Gantt he continued in active practice as a consultant in production and management methods until his retirement in April, 1933. He had resided in Washington since then.

Another important part of his life was his military service. This was reported in detail in the January-February, 1940, issue of *The Quartermaster Review*, from which the following is taken:

"Colonel Conrad's first Army service came when, as a young man, he joined Company D, of the 6th regiment, National Guard, and was sent to Puerto Rico for service in the Spanish-American War. His next war service came on November 15, 1917, when he was mustered back into federal service as major, Q.M.C., N.G. (U.S., Mass.), and assigned to duty as camp quartermaster and sub depot quartermaster, Beauregard, La.

"In October, 1918, Colonel Conrad was assigned to duty as coast defense quartermaster and disbursing officer at Sandy Hook, N.J., where he served until September 26, 1919, when he was sent to Camp Alfred Vail as camp supply officer to stay until his discharge on October 31, 1919.

"On December 22, 1919, Colonel Conrad was appointed a lieutenant-colonel in the Quartermaster Reserve and on June 2, 1923, was promoted to colonel, Quartermaster Reserve. He was transferred to the Inactive Reserve on September 18, 1937, upon reaching retirement age.

"Colonel Conrad was a charter member of the Fitchburg Post, No. 10, American Legion, and of the Guanica Camp, U.S.W.V. He was also a member of the Massachusetts Commandery of the naval and military order of the Spanish-American War. He was the first Quartermaster Reserve officer to be elected national president of the Quartermaster Association and his best efforts went into fulfilling the responsibilities of that high office."

Colonel Conrad was on the Executive Committee of the A.S.M.E. Textile Division as its secretary from 1927 to 1930, as chairman in 1934, member in 1935, and associate from then until his death. He belonged to the Elks fraternal order and the Knights of Columbus and for a time was an advisor for the Nichols Junior College, Dudley, Mass.

L D CRAIN (1868–1942)

L D Crain, professor emeritus of mechanical engineering at Colorado State College, died unexpectedly at Long Beach, Calif., on March 15, 1942. Professor Crain had been in fairly good health and quietly passed into his last sleep while Mrs. Crain was reading to him. The A.S.M.E., and especially the Colorado Section, mourns the passing of one who has been very active in the Society affairs and who has played an important part in the success of the Colorado Section.

Professor Crain was born in Angola, Ind., on February 3, 1868, son of Abram and Hariet (Perry) Crain. He attended the local district school and the high school at Angola. After finishing high school he entered Purdue University, where he received the degree of Bachelor of Mechanical Engineering in 1892. Later he went to Cornell University and received the degree of M.M.E. in 1902.

He became assistant professor of mechanical engineering at Colorado State College in 1892. In 1903 he organized the Department of Electrical Engineering at that institution and became the first professor of electrical engineering at Colorado State College. From 1905 to 1912 he engaged in contracting and engineering work in Fort Collins, returning to the college in 1912 as associate professor of mechanical engineering. In 1917 he was appointed professor and head of the Mechanical Engineering Department, which position he held until his retirement in 1936.

Professor Crain became a junior member of the A.S.M.E. in 1895 and advanced to member in 1904. He relinquished his membership during the year 1906–1913, and was reinstated with the grade of member in 1914. He was a member of the Colorado Executive Committee from the time of its organization in 1919 until his death and was chairman of the Section from 1921 to 1923. At the time of his death Professor Crain was Section historian and was actively engaged in compiling a complete history of the A.S.M.E. in Colorado. He served on the Regular Nominating Committee of the Society in 1934.

He was a member of Sigma Xi, Phi Kappa Phi, Sigma Tau, and Rotary International. Because of his interest in civic affairs his fellow citizens elected him to various offices, including that of secretary of the Park Commission and president of the Chamber of Commerce of Fort Collins.

He was a 33rd degree Mason and Past Grand Master, A.F. & A.M., of Colorado. In 1928 he was appointed a trustee of the Colorado Masons Benevolent Fund Association and in 1934 he became the state chairman of the George Washington Masonic National Memorial Association.

In addition to his widow, Aureli (Bouton) Crain, whom he married in 1901, Professor Crain is survived by three sons, L D Crain, Jr., Richard W. Crain, and Clark Nixon Crain.

Professor Crain will long be remembered by his former students and associates as a man of splendid character and one who was always interested in the welfare of others.—[Biography prepared by J. T. STRATE, Ft. Collins, Colo. Mem. A.S.M.E.]

JOHN RORISON DOUGLAS (1883–1938)

John Rorison Douglas, chief construction engineer of Courtaulds, Ltd., Coventry, England, died on April 4, 1938, while on duty at the Preston Works branch of the company. He had been a member of the A.S.M.E. since 1931.

Mr. Douglas was born at Perth, Scotland, on August 1, 1883. He attended the Perth Academy and the Technical Section of Dundee University College. He served an apprenticeship with the Lily Bank Shipbuilding & Engineering Co., Dundee, from 1899 to 1903, and with Chas. Parker & Sons Ltd., Scotland, during the next three years. He was then employed by the J. M. Davidson Construction Co., Johannesburg, South Africa, and in 1908 became its chief engineer. In 1908–1909 he was engaged in the erection of a plant and equipment for the East Rand Gold Mines, and other construction work. He took a position as chief engineer for the Victory Hill Gold Mines, Barberton, Transvaal, in 1910, where he continued for about two years.

In 1912 Mr. Douglas designed and erected a complete textile plant at Odessa, Russia, and the following year, silk textile mills at Lyon, France. During the early part of 1914 he was chief engineer and manager of the New Port (Monmouthshire) Ship Repairing Co., repairing ocean-going ships. At the outbreak of World War I he joined the British navy as an aviator and during the most of the war served in that capacity. In 1917 he directed the raising of the S.S. *Kassandna* from the bed of the Mediterranean.

After the War he was engaged for a short time in the design and erection of an oil plant for extracting oil from peanuts and cereals for margarine manufacture. He joined the Courtaulds staff in 1921 and during the remainder of his life directed the design and erection of textile plants, many of them for the manufacture of rayon goods, in England, Germany, Canada, and other countries.

Surviving Mr. Douglas are Mrs. E. Douglas, of Coventry, and two sons. The elder, H. W. Douglas, is assistant plant manager of Courtaulds (Canada) Limited, Cornwall, Ont., Can., and the younger, A. J. Douglas, is a member of the engineering staff of the Bristol Aircraft Co. Ltd., Bristol, England.

OSWALD DUDA (1875–1938)

Oswald Duda, who had recently resigned as chief engineer for the American Well & Prospecting Co., Corsicana, Texas, died on June 2, 1938, of a heart attack. He had planned to go into business in partnership with his son.

A native of Austria, Mr. Duda came to the United States in August, 1907, and became a naturalized citizen at Houston, Texas, in 1912. He was born in Trzynietz, Silesia, on June 7, 1875. He secured his early technical education in the industrial school in Trzynietz and later took a course in mining and metallurgy in Leoben, Styria. From 1889 to 1893 he served an apprenticeship in the machine, metal spinning, and forging trades with the Erzherzog Albrecht Corporation, Silesia. He then worked on production estimating at the Union Blech Werke, Zolyom, Hungary, and, for six months, obtained foundry practice at the K.O.R.R. Works, Ruttka, Hungary. During the years 1898–1900 he took his course in the mining and metallurgical college at Leoben, then worked for a year for the Russian Shipbuilding Corporation, Nikolajeff, Russia, as a designer. From 1901 to 1907 he did similar work for the Rothschilds Werke, Witkowitz, Austria.

Mr. Duda's first position in this country was as a designer for the Union Iron Works, Houston, where he was engaged from 1907 to 1913. This employment was followed by similar work in 1914–1915 for the Calhoun Pattern & Foundry Co., and in 1915–1919 for the Houston Car Wheel & Machine Co., both of Houston. In 1919 he became chief mechanical engineer for the Reed Roller Bit Company, Houston. He remained with this company until 1930, when he was engaged as chief engineer of the American Well & Prospecting Co., in charge of designing and supervising the manufacture of oil well drilling machinery.

A number of patents had been taken out by him and copatentees and assigned in most cases to the last two companies for which he worked. These were on wrenches, deep-well-drilling apparatus, bits and reamers, and valve mechanisms.

Mr. Duda had been a member of the A.S.M.E. since 1927. He was a 32nd degree Mason and a Shriner, belonging to the Arabia Shrine Temple in Houston from 1927 until his death. He served as secretary of the Order of the Eastern Star in 1929–1930. He is survived by his widow, Emmanuela (Roszmetalsky) Duda, whom he married in 1904, his son, Erwin G. Duda, of San Antonio, Texas, and a daughter, Mrs. Inez (Duda) Schroeder.

CARL ERIC EKLIND (1878–1938)

Carl Eric Eklind, son of Carl Edward and Josephine (Conti) Eklind, was born in Orebro, Sweden, on October 8, 1878. He was educated in Sweden (with some postgraduate studies in Germany) and performed a year of required military service in the Swedish army, during which he received a rifle from the King as first prize in a marksmanship contest.

His first recorded work, after his graduation in 1900 from the University of Orebro as a mechanical engineer and chemist, was with the Pressed Steel Car Company, McKees Rocks, Pa., in 1903–1904. He then entered the employ of the Chicago, Topeka & Santa Fe Railway Co., Chicago, Ill, where he advanced from draftsman and checker on passenger and freight equipment to chief draftsman of the Car Construction Department. He became thoroughly familiar with every phase of car construction.

From 1924 until his death on December 1, 1938, he was associated with the Camel Company and Camel Sales Company of Chicago (dealers in railway specialties and supplies, taken over by the Youngstown Steel Door Company in 1935). He became assistant to the vice-president of the Camel Company in 1930 and at the time of his death was serving as vice-president of the Camel Sales Company.

Mr. Eklind had been a member of the A.S.M.E. since 1919. He belonged to the Illinois Athletic Club, Chicago, and the Acacia Golf Club. He married Ella Verdia Neun, of Pittsburgh, in 1908, and is survived by her and two children, Robert Warren Eklind, a lieutenant in the U.S. Army, and Marjorie V. Eklind, residing with her mother in Berwyn, Ill.

EDGAR CONWAY FELTON (1858–1937)

Edgar Conway Felton, a member of the A.S M.E. since 1885 and a manager of the Society for the term 1898–1901, was born at Thurlow (now Chester), Pa., on April 13, 1858, the son of Samuel Morse and Maria Low (Lippitt) Felton, and died at Haverford, Pa., on September 18, 1937.

He was prepared for college by Reginald Heber Chase, in Philadelphia, Pa., entered Harvard College, where he was graduated in 1879 with the degree of Bachelor of Arts.

He then spent one year in travel in Europe, returning in 1880 to begin work in the chemical laboratory of the Pennsylvania Steel Company at Steelton, Pa. The following year he was a laborer in the rolling-mill of the Sanderson Steel Company at Syracuse, N.Y., but he returned in 1883 to Steelton to take the position of mill superintendent. He rose rapidly through the grades of assistant superintendent and superintendent of works (1884–1893) and general

manager (1893–1896), and was elected president in 1896, serving until 1916, when the company was merged with the Bethlehem Steel Corporation, and he retired from active business. Under his management the departments of bridge building and shipbuilding were greatly enlarged.

While living at Steelton he was interested in the development of electric railways in that vicinity, and on the formation of the Harrisburg Traction Company was chosen its president.

During the World War he served as director of civilian service and labor, a department of the Pennsylvania Committee of Public Safety, and as examiner of the Shipbuilding Labor Adjustment Board for the Philadelphia District.

He was manager of the Gerard Trust Company and the Western Savings Fund Society, a director of the Pennsylvania Railroad, the General Asphalt Company, the DeLong Hook & Eye Co., and the Philadelphia & Western Railway Co., and a trustee of Drexel Institute, and he had served as president of the board of directors of the Steelton and the Haverford township schools. He had also served as secretary and treasurer of the Steelton Public Library.

Among the many other societies of which he had been a member were The Franklin Institute, the American Institute of Mining and Metallurgical Engineers, and the American Iron and Steel Institute (director).

He was also a member of the Harvard Club of Philadelphia (president), the University Club of Philadelphia (vice-president), the Philadelphia Club, and the Merion Cricket Club (governor).

To Harvard College he gave much of his time and interest, and he served as an overseer from 1914 to 1920 and from 1921 to 1927.

Fond of travel, he made several trips to Europe and visited Cuba and Jamaica. In 1911 he attended the conference of steel manufacturers of the world at Brussels, Belgium, and he made an automobile tour of France, England, and Wales.

In 1884 he married Alice Bent, daughter of Winslow Brigham and Jane Elizabeth (Tomlinson) Bent, of Ann Arbor, Mich., and Chicago, Ill., who survives him, together with six children, Mrs. Emmett Robinson Tatnall (Margaret Felton) of Haverford, Mrs. Sumner Rulon-Miller (Eleanor Felton) of Ardmore, Pa., Samuel Morse Felton, 3rd, of Boston, Mass., Cornelius Conway Felton of New York, N.Y., Edgar Conway Felton of Haverford, and Winslow Bent Felton, of Boston.—[Biography adapted from a memoir published in The New England Historical and Genealogical Register, January, 1938.]

FREDERICK CROMWELL FIELD (1875–1937)

Frederick Cromwell Field, who died at the Germantown Hospital, Philadelphia, Pa., on September 22, 1937, was born in Brooklyn, N.Y., on October 17, 1875, son of Richard Cromwell and Mary (Manning) Field. He attended the Friends School and Polytechnic Institute, in Brooklyn, then entered the Massachusetts Institute of Technology, where he studied for six years, taking both the electrical and mechanical engineering courses.

His first position, in 1898, was with the Edison Electric Illuminating Company of Brooklyn, in connection with switchboard operation. After a year there he was employed by the N.J. Foundry & Machine Co., New York, on estimating for engineering contracts; then in 1900–1901 was a member of the firm of Field and Everett, consulting engineers, New York. Subsequently he was engaged in estimating, designing, and construction work for Westinghouse, Church, Kerr & Co., New York; helped to establish and served as treasurer of the Engineer Company, which handled mechanical draft installations; was engineer of the building department of the N.Y. Telephone Co.; served as consulting engineer with Wendell and MacDuffie, New York; and did reporting and estimating for J.G. White & Co., Inc., New York, and E. I. du Pont de Nemours & Co., Wilmington, Del.

In 1911 Mr. Field became president and general manager of the Standard Arms Manufacturing Company, of Wilmington, and he continued with that organization until 1917. He was commissioned a captain in the Ordnance Reserve Corps in August, 1917, and assigned to active duty with the Remington Arms Company of Delaware, at Eddystone, Pa., as inspector in the Small Arms Division. He was promoted to the grade of major in the regular army in February, 1918, and in May of that year was transferred to the Inspection Division at Washington. He was again transferred, the following November, to the Philadelphia Ordnance District Office, in charge of the Tank, Tractor, and Trailer Division. He was honorably discharged from service on July 1, 1919.

Except for some consulting work in Philadelphia, Mr. Field had no professional business connections during the remainder of his life. In addition to his membership in the A.S.M.E., to the member grade of which he was elected in 1916, he belonged to the Engineers Club of Philadelphia, Crescent Club (Brooklyn), and Phi Beta Epsilon fraternity.

Surviving Mr. Field are his widow, Florence A. Field, two daughters, Mrs. C. F. Bond and Doris Field, and two sons, Harold A. and Frederick C. Field, Jr., all of Philadelphia at the time of his death.

CHARLES HARDY HARRIS (1878–1938)

Charles Hardy Harris, general engineer of the Virginia Electric & Power Co., Richmond, Va., an affiliate of the Stone & Webster Engineering Corp., of Boston, Mass., died at his home in Richmond on October 22, 1938. Although he had been in poor health for about a year, his illness was not regarded as serious until shortly before his death.

Mr. Harris was born in Natick, Mass., on September 3, 1878, the son of Charles O. and Alice D. (Osgood) Harris. He attended the Natick schools and was graduated from the Massachusetts Institute of Technology in 1901 with an S.B. degree in electrical engineering. He immediately entered the employ of the Stone & Webster Engineering Corp., at Boston, as an engineer-student. After a year he was transferred to Seattle, Wash., in the same capacity, completing his training with the Seattle Electric Company. During the remainder of his life he was assigned to service with different affiliated companies of the corporation. He was electrical and mechanical engineer of the Minneapolis (Minn.) General Electric Company, 1905–1912, superintendent of construction of the "Goat Rock" power development at Columbus, Ga., the following year, and subsequently was connected with the Mississippi River Power Company at Keokuk, Iowa, Western United Gas & Electric Co., Aurora, Ill., and Tampa (Fla.) Electric Company, before taking up his duties in Richmond in 1927.

Mr. Harris had been a member of the A.S.M.E. since 1921 and was a member of the executive committee of the Virginia Section in 1936–1937. He also belonged to the American Institute of Electrical Engineers, Central Virginia Engineering Society, Hermitage Country Club, and the masonic fraternity. His wife Elinor (Condon) Harris, whom he married in 1905, died on July 25, 1940. Two brothers, Dr. Leslie W. Harris, of Natick, Mass., and Dr. Lucien H. Harris, of Northampton, Mass., survive him.

DANIEL AUGUST HEIKEL (1859–1925)

Daniel August Heikel was born at Ny Karleby, Finland, on October 20, 1859, and died in his native country on April 29, 1925. A considerable part of his life, beginning in 1882, was spent in the United States, and he had been a member of the A.S.M.E. since 1899.

Mr. Heikel was educated in Finland, and received a degree in mechanical engineering in 1880 from the Polytechnical Institute of Finland. After about two years in drafting work in St. Petersburg, Russia, he emigrated to this country, where he secured work in August, 1882, with the Chicago, Milwaukee & St. Paul Ry., in Milwaukee, Wis. Subsequently he was employed by Crane Brothers Manufacturing Company, Chicago, Ill., Iowa Iron Works Company, Dubuque, Iowa, and Kansas City Bridge & Iron Co., Kansas City, Mo., all in drafting. For four years, 1887–1891, he was superintendent of the Engine Department of Hoffman & Billings Manufacturing Co., Milwaukee, then spent about five and one-half years with the Nordberg Manufacturing Company, of that city, as sales agent and engineer.

Mr. Heikel was next chief engineer and partner with C. H. Bradley, Jr. & Co., of Pittsburgh, Pa., consulting and contracting engineers. Later he carried on an independent consulting practice in Pittsburgh until his return in 1902 to Finland, where he continued his work as a consulting engineer and contractor. He came to the United States again for a period of about six years, 1905–1911, the most of which time he was employed by the Nordberg Manufacturing Company in Milwaukee and as its representative in Pittsburgh. Since 1911 he had resided in Åbo, Finland. His widow, Berta Heikel, survived him.

THOMAS HIBBARD (1854–1938)

Thomas Hibbard, of Milton, Mass., whose death occurred on October 4, 1938, was born on February 16, 1854, in East Boston, Mass., the son of William Charlton and Sarah Ann (Smith) Hibbard. He was graduated from the Massachusetts Institute of Technology in 1875 with an S.B. degree in mechanical engineering and for the next five years was draftsman at the Atlantic Works, East Boston, on the general designing of engines and boilers, principally for marine service. Then he was employed, first as designer and later as assistant superintendent, by the Boston Sugar Refining Company, rebuilding its plant. Upon the completion of this work he set up his

own office for general mechanical engineering practice in Boston, but gave it up after several years to become chief draftsman for the Deane Steam Pump Company, Holyoke, Mass. He remained with this company until about 1890, when he was made treasurer and mechanical engineer of the George Lawley & Son Corp., South Boston, builders of yachts of all kinds. Here he designed and equipped the plant for building steel hulls, and had charge of the design and installation of motive power in steam and motor vessels built by the company. He also was responsible for all the financial matters of the company, as treasurer. He retired in 1918 at his own request, but continued to hold an interest in the corporation, and in 1927 he returned to serve as president and director for three years.

Mr. Hibbard became a member of the A.S.M.E. in 1889. He was also a member of the American Society of Naval Engineers and of the Technology Club. He was twice married. His first wife, Jennie M. Blackinton, whom he married in 1880, died in 1889. He remarried in 1899, his second wife being Bertha Bartlett, who died in 1941. Two children by each marriage survive them.

ROBERT HATFIELD IRONS (1876–1939)

Robert Hatfield Irons, president of the Central Iron & Steel Co., Harrisburg, Pa., died of toxic poisoning in the International Hospital at Naples, Italy, on January 5, 1939. He was not well when he and Mrs. Irons left New York early in December for a two-month cruise to Italy, Egypt, and the Holy Land, and was obliged to go to the hospital the day after their arrival in Naples.

Mr. Irons had been president of the Central Iron & Steel Co. since 1916. He entered the employ of the company in 1892, at the age of sixteen, and after serving as mill superintendent from 1899 to 1912, was appointed general superintendent and chief engineer. Since his election to the presidency of the company four years later he had also served as a director and member of the executive committee.

The son of George D. and Rebecca (Hatfield) Irons, he was born at Halifax, north of Harrisburg, on August 7, 1876. Supplementary to his early public and private schooling, he attended the Wilkes-Barre Academy and studied engineering under a tutor.

Mr. Irons became a member of the A.S.M.E. in 1922. He was a member of the Executive Committee of the Susquehanna Section of the Society from 1927 to 1930, serving as chairman in 1929–1930. He represented the Society on the Sectional Committee on Standardization of Plain and Lock Washers, and on its Subcommittee No. 1 on Plain Washers, from 1927 to 1931.

Mr. Irons was past-president of the Association of American Steel Manufacturers. He was also a member of the American Iron and Steel Institute, (British) Iron and Steel Institute, American Institute of Mining and Metallurgical Engineers, American Society for Metals, American Society for Testing Materials, Engineers' Society of Western Pennsylvania, The Franklin Institute, India House (New York), the Harrisburg Club, and numerous civic organizations in Harrisburg. He was a member of the executive committee of the National Planning Committee for the Harrisburg area and long had been identified with the welfare federation which provides funds for local charities.

Mrs. Irons was the former Miss Nellie Brandt, of Harrisburg.

L(LYWELLYN) HOWARD (HARDING) JENKS (1862–1939)

L. Howard Jenks, Sr., a member of the A.S.M.E. since 1891 and active in the technical committee work of the Society for some years, died suddenly on November 15, 1939, in Wheeling, West Va., while returning home from a long western trip. Mr. Jenks represented the American Society of Refrigerating Engineers, of which he was president in 1926, on the Sectional Committee on Standardization of Pipe Flanges and Fittings from 1921 to 1938, and from 1924 to 1938 was a member of two of its subcommittees, No. 1 on Cast Iron Flanges and Flanged Fittings and No. 2 on Screwed Fittings. A charter member of the A.S.R.E., he gave valuable service to that organization in its formative years and continued active in its affairs until his death. Other groups to which he belonged included the National Association of Practical Refrigerating Engineers, the Pennsylvania Society of New York, and the masonic fraternity.

The son of Col. Barton H. Jenks and Elesa (Saurwen) Jenks, he was born on October 25, 1862, at Holly Hall, the Colonial homestead of the Jenks family on the Delaware River near Bridesburg, now a part of Philadelphia. After completing his early education in public and private schools he took a course in mechanical drawing at The Franklin Institute. Securing a competitive free scholarship, he entered the University of Pennsylvania in 1880 and acquired his B.S. degree four years later. A year of postgraduate work brought him a C.E. degree in 1885.

Mr. Jenks worked with his father on the development of a power multiple coal drill and other patents during the first year after his graduation, then was associated with J. J. de Kinder (Mem. A.S.M.E.), general superintendent of the Philadelphia Water Department, in water works construction, for two years. From 1888 to 1896 he was connected first with the Consolidated Ice Machine Company, of Chicago, Ill., in its New York branch, in sales and tests of refrigerating machinery, and later with the Hercules Ice Machine Company, of Aurora, Ill., as its general Eastern representative, with headquarters in New York. Subsequently, for two years he was general manager of the R.B.S. & C. Electric Light & Power Co., of Rutherford, N.J.

In 1898 Mr. Jenks became manager of the Philadelphia office of the Frick Company, of Waynesboro, Pa. Later he was appointed manager of the Eastern District of the company, with headquarters in New York, where he continued until his retirement in 1930. He had been granted several patents on refrigerating equipment, including one on a safety inverted compressor valve. He planned and executed the first fish-freezing system in the Orient, including transportation by rail and the equipment of a fleet of refrigerated vessels.

Mr. Jenks married Emma B. Loag, of Philadelphia, in 1890. Her death occurred in 1930. Surviving them are a daughter, Marjorie F. Jenks, and two sons, L. H. Jenks, Jr., and Barton L. Jenks, all of Rutherford, N.J., where the family had long resided.

FORREST ROBERT JONES (1861–1936)

Forrest Robert Jones, a member of the A.S.M.E. since 1890, died on March 27, 1936, in Bolivar, Texas, where he had lived with his daughter for a number of years.

The early part of his life was spent in Ohio. He was born at Sharon on December 12, 1861, son of Martin Ryan and Susan (Hageman) Jones. He attended public schools in Sharon and in 1888 was graduated from Cornell University with a degree in mechanical engineering. He had served an apprenticeship at the Niles Tool Works, Hamilton, Ohio, prior to entering college.

From Cornell, Mr. Jones went to Orange, N.J., where he worked in the laboratory and phonograph works of Thomas A. Edison. He was sent to Kearney, Neb., to take charge of electric railway and lighting plant construction and served in 1890–1891 as superintendent of the mechanical department of the Edison General Company.

In the fall of 1891, Mr. Jones became instructor in mechanic arts at the University of Tennessee, Knoxville. He transferred to the University of Wisconsin, Madison, in 1893 and taught machine design there until 1899. He then became professor of drawing and machine design at the Worcester Polytechnic Institute, Worcester, Mass. In 1902–1903 he visited the principal technical schools and many commercial manufacturing plants in England and on the Continent to study teaching methods and manufacturing developments, giving special attention to gas and oil engines and gas producers for power purposes. Upon his return he taught machine design at Sibley College, Cornell University, for two years, then spent an equal period as professor at the Manhattan Automobile School, New York. From 1908 to 1920 he was located in Knoxville, Tenn., except for the years 1915–1916 and for three weeks in January, 1918, when he was again on the faculty of the University of Wisconsin. From 1920 to 1925 he was located in New York, N.Y.

Mr. Jones was the author of a number of books, including his "Automobile Catechism" and "Electric Ignition for Combustion Motors," and also contributed papers to technical societies and periodicals. He had been a member of the Society for the Promotion of Engineering Education and belonged to the Sigma Xi fraternity. He is survived by his widow, formerly Miss Johnnie House Fletcher, of Knoxville, whom he married in 1892, and by his daughter, Mrs. David McAnulty, a resident of Union City, Tenn., after her father's death.—[Biography compiled from best obtainable information, not all of which could be verified.]

WILLIAM HARRISON KAVANAUGH (1873–1939)

William Harrison Kavanaugh, professor of experimental engineering at the Towne Scientific School of the University of Pennsylvania since 1916, died on May 6, 1939, at the Abington Memorial Hospital, Philadelphia, Pa., after a brief illness. Prior to his connection with the Towne school he was a member of the faculty of the University of Minnesota for fifteen years. In both cases he was in charge of the experimental laboratory.

During these years Professor Kavanaugh was also engaged by various organizations as a consultant or to conduct special investigations and tests of equipment. A number of these assignments were for city and state commissions. He was frequently called upon as an engineering expert in litigation over patents and he was a member of the International Jury of Awards of both the Panama-Pacific Ex-

position, at San Francisco, Calif., in 1915, and the Sesquicentennial Exposition at Philadelphia in 1926. He was director of the courses for training automobile mechanics at the Junior Plattsburg Camp, Plattsburg, N.Y., in 1918.

Professor Kavanaugh was born at Williamsport, Pa., on August 19, 1873, son of Daniel and Emma (Ramsey) Kavanaugh. Following his graduation from the local high school he entered Lehigh University, where he received an M.E. degree in 1894. He was principal of the Miners and Mechanics Institute at Freeland, Pa., the next year, but resigned to go into the mercantile business in Williamsport. In 1897 he re-entered the teaching field as instructor in mechanical engineering at the University of Illinois. After a year there he was employed by the Pennsylvania Railroad Company, becoming chief draftsman in the office of the superintendent of motive power. He continued in that position until he took up his duties at the University of Minnesota in 1901.

Much of Professor Kavanaugh's varied experience was recorded by him in technical papers and reports, only part of which has been published. He also found time for extensive service in the engineering societies to which he belonged—the A.S.M.E., of which he became a junior member in 1902 and a member in 1910, the Society for the Promotion of Engineering Education, and The Franklin Institute. While at the University of Minnesota he held various offices in the A.S.M.E. Minnesota Section and served as its chairman in 1915. When he went to Philadelphia he became affiliated with the Local Section there and served it in a number of capacities, including that of chairman in 1923–1924. He took part in the national work of the Society as a member of the Regular Nominating Committee in 1923, of the Standing Committee on Relations with Colleges from 1924 to 1927 (chairman in 1927), of the Standing Committee on Constitution and By-Laws, 1934–1938 (chairman in 1938), and of technical committees as follows: Power Test Codes Individual Committee No. 1 on General Instructions, chairman from the time of its formation in 1918 until his death; Standing Committee on Standardization, 1920–1923; and Special Research Subcommittee on Stresses Due to Vibration of Shafting, 1921–1925. His service to other societies included membership on the S.P.E.E. Council.

Surviving Professor Kavanaugh are his widow, the former Julia Sara Vogt of Allentown, Pa., whom he married in 1896; a son, Dr. William Ramsey Kavanaugh, of Kalamazoo, Mich., and a daughter, Emma Cosette (Mrs. William H. Regelman), of Hatboro, Pa.

FRED KEY (1869–1939)

Fred Key, whose death occurred on February 25, 1939, was born in Auburn, Ky., on January 19, 1869. At the age of seventeen he entered upon an apprenticeship with the Louisville & Nashville R.R. After the completion of four years' training in Nashville, Tenn., he was transferred to Louisville, Ky., where he worked for the railroad for four years as machinist and draftsman.

From 1894 to 1898 Mr. Key was chief engineer of the Kentucky Heating Company, Louisville, then spent two years with the Southern Division of the Illinois Central Railroad at Jackson, Tenn., as engineer on roadway maintenance and other work. After that he was for sixteen years connected with the Boiler and Flywheel Department of the Fidelity & Casualty Co., in Kansas City and St. Louis, Mo. In 1916 he became vice-president and general manager of the Key Boiler Equipment Company, St. Louis, and he continued with this company (which in 1935 became the Key Company, East St. Louis, Ill.), until his death. He was also for some years vice-president and general manager of the St. Louis Pressed Steel Company, which was taken over by the Key Boiler Equipment Company in 1925. He had invented and patented numerous devices for use in power plants and oil refineries, including a one-piece hand-hold cap for watertube boilers and return-bend fittings for oil refinery heating coils.

Mr. Key had been a member of the A.S.M.E. since 1918. He also belonged to the American Petroleum Institute, National Association of Power Engineers, and the masonic fraternity. The University of Tulsa conferred the degree of doctor of mechanical engineering upon him in 1937.

Surviving Mr. Key are three children, Mrs. David Mackey, Mrs. Philip Abel, and Elmer A. Key. His wife, Mattie J. Key, died on June 24, 1942.

LEONARD KIPP (1868–1939)

Leonard Kipp, who died at his home in New Haven, Conn., on September 9, 1939, was born in Wuerttemberg, Germany, on April 12, 1868. He attended the Stuttgart Politechnium and after coming to the United States studied for two years at Eastman's Technical School, New York, N.Y. Subsequently he took several courses through the International Correspondence Schools.

The first record of Mr. Kipp's work as an engineer is for the years 1898–1900, when he was employed as a draftsman for the Farrell Foundry & Machine Co., Waterbury, Conn. The next two years were also spent in drafting work, with the Scovill Manufacturing Company, in the same city.

In 1902 he became assistant to the chief engineer of the Chase Rolling Mill Company, Waterbury. In this capacity he was instrumental in working out the design of the first hydraulic tube extrusion press in this country. Later, as engineer in charge of design for this company, he was responsible for the design and building of hydraulic rod presses and hydraulic draw benches, as well as for much other developmental work. It was during this period that he also obtained a patent for an operating valve for extrusion presses.

After leaving the Chase Company in 1916 Mr. Kipp, working for the United States government, planned and designed the entire plant of the Mueller Brass Company, at Port Huron, Mich. This project included a rod and tube mill, a power plant, a casting shop with all the necessary equipment, a production set-up for 75-mm shells and fuses, railroad sidings, and all underground equipment.

From 1919 to 1923 Mr. Kipp engaged in business for himself. Among other contracts he handled the engineering work for a complete hydraulic plant for the Bristol Brass Company, Bristol, Conn., and also one for the Michigan Brass & Copper Co., Detroit, Mich.

In 1923 he took a position as mechanical engineer in charge of brass mill engineering for the Western Cartridge Company, East Alton, Ill. In this capacity he was continuously engaged in the supervision of the design of special machinery for nonferrous rolling mills. After an illness in 1926 he went abroad in an official capacity for the Western Cartridge Company, visiting brass plants in Germany, Austria, and Switzerland. On July 1, 1937, he was transferred to the Winchester Repeating Arms Company, in New Haven, Conn., a plant which the Western Cartridge Company had purchased some years before. Here his work was chiefly concerned with modernizing the rolling mill of this plant, and the installing of new equipment. He continued in this capacity until July 1, 1939, at which time he was forced to resign because of ill health.

Mr. Kipp became a member of the A.S.M.E. in 1934. He was a Mason and Knight Templar. He is survived by his widow, Margaret Ann (McKelvey) Kipp, whom he married in 1890, and by four daughters, Mrs. Irving J. Granger, Mrs. Victor H. Budge, Miss Margaret Kipp, and Miss Pauline Kipp, and by a son, George Kipp.

C. RUSSELL KIRSCH (1896–1939)

C. Russell Kirsch, whose death occurred on November 11, 1939, was a native of Waterbury, Conn., where he was born on October 23, 1896, son of Theodore F. Kirsch, Sr., and Amelia A. (Kreger) Kirsch. He attended the local Webster Grammar School and Crosby High School, then studied for two years at Pratt Institute, Brooklyn, N.Y., graduating in 1917.

Immediately following his graduation Mr. Kirsch went to work as a draftsman for the Western Electric Company, Inc., New York, N.Y., where he was assigned to radio layouts for the English, French, and American governments. After a few months of this work he took a position as instructor in mechanical drawing in Public School No. 12 (Gary Vocational) and in the High School, Passaic, N.J., where he developed his own courses of instruction for the seventh and eighth grades and vocational classes.

From August, 1918, to August, 1919, he served in the U.S. Army as sergeant, first class, attached to Base Hospital No. 113, A.E.F., in charge of the personnel office for evacuating wounded soldiers home from France.

After his return to the United States, Mr. Kirsch was employed by the U.S. Rubber Co., in New Haven, Conn., as machine designer until June, 1921. From then until November, 1938, he was mechanical engineer for the Waterbury Manufacturing Company Division of Chase Companies, Inc., and its successor, the Chase Brass & Copper Co., Inc. His duties included making factory plans and layouts, designing tools and machines, and checking costs involved in the manufacture of various novelties and brass goods. During the last year of his life he served as foreman of the Press Department of the Lux Clock Manufacturing Company, Waterbury.

Mr. Kirsch was elected to junior membership in the A.S.M.E. in 1922 and promoted to full membership in 1930. He had been active in the work of the Waterbury Section of the Society. He was also a past-president of the Chase Foreman's Association, and belonged to St. Paul's Methodist Church, in Waterbury, and to the masonic and Odd Fellows fraternal orders. He was a member of Corporal Coyle Post of the American Legion.

Mr. Kirsch married Esther M. Ford, of Waterbury, in 1920 and is survived by her and their daughter, Eleanor Ford Kirsch, as well as by his parents and a brother, T. Franklin Kirsch, Jr., all of Waterbury.

JAMES ROSS KNOX (1895–1939)

James Ross Knox, consulting engineer, of Newport, Fife, Scotland, died on October 18, 1939. He was a native of Scotland and returned there in 1934 after having spent about twelve years in the United States. He became associate-member of the A.S.M.E. in 1931 and was automatically transferred to the grade of member in 1935.

Mr. Knox was born at Kirkcaldy, Fife, on April 18, 1895, son of Alexander and Barbara Robertson (Ross) Knox. His technical education was secured at the Dundee Technical College, where he took evening courses for three years, and through supplementary courses at New York University (Evening Engineering School) and the International Correspondence Schools. He served an apprenticeship as a machinist with the Urquhart & Lindsay Co., Dundee, prior to World War I and worked on textile machinery for that company for several years after the war. He was an ordnance artificer in the Royal Navy, having care of gunnery machinery, from 1914 to 1919.

In this country, Mr. Knox was maintenance engineer for the Clark Thread Company, Newark, N.J., for about two years, and then was associated with the Lord & Burnham Co., greenhouse designers and manufacturers, Irvington, N.Y. He worked on designs and estimates for complete heating systems for a number of companies in the East.

Mr. Knox was also a member of the Institution of Heating and Ventilating Engineers and the American Society of Heating and Ventilating Engineers. He married Janet Scott Carmichael, of Dundee, in 1923, and was survived by her and two children, Alexander James and Jean Anderson Knox.

EDWARD LENZ (1894–1938)

Edward Lenz, manager of distribution operation for the New York Steam Corporation, New York, N.Y., died on March 18, 1938. Mr. Lenz was born in Brooklyn, N.Y., on April 13, 1894, the son of Zachary and Katherine (Krumn) Lenz. He attended the Eastern District High School of Brooklyn and later took evening courses at Pratt Institute, Brooklyn, and the Polytechnic Institute of Brooklyn.

A recognized authority on the distribution of central station steam service, Mr. Lenz was a prolific writer for the National District Heating Association and author of the chapter on steam distribution in the association's handbook. In 1937 he was elected third vice-president of the association and was chairman of its Distribution Committee, 1928–1931, and a member of the committee during the remainder of his life. Mr. Lenz became a member of the A.S.M.E. in 1929 and served on the Sectional Committee on a Code for Pressure Piping from 1929 to 1938.

After leaving high school, Mr. Lenz, in December, 1912, entered the employ of the New York Steam Company, predecessor of the present New York Steam Corporation, and remained in their employ until his death. Following three years in the Engineering Department, he was transferred to the office of the chief engineer as an assistant, having charge of testing laboratories, his work including the testing of meters and equipment. In 1919 he became district superintendent in charge of construction, operation, and maintenance of the Corporation's distribution system in the Downtown District. Subsequently, in 1924, Mr. Lenz was appointed to the post of general superintendent of distribution, having charge of the operation and maintenance of the entire distribution system; he became manager of distribution operation in 1936. During the more than twenty-five years of his employment with the company, Mr. Lenz participated in the extension of a service that increased ten times during his active years and to which he made substantial contribution.

Surviving Mr. Lenz are his widow, Louise (Koenig) Lenz, whom he married in 1922, and two daughters, Elizabeth Louise and Joan Marie Lenz.

RICHARD CHARLES LEWIS (1896–1938)

Richard Charles Lewis, sales engineer of the Farrel-Birmingham Company, Inc., Ansonia, Conn., was killed when a United Airlines plane crashed on May 24, 1938, just before reaching its destination, the Cleveland Airport.

At the time of his death Mr. Lewis was manager of the rolling mill sales division of the Farrel-Birmingham Company in charge of sales of rolling-mill equipment and roll-grinding machines. Previously he had been connected with the engineering department as division engineer in charge of engineering of rolling mills, metal-working machinery, roll grinders, sugar machinery, and other heavy equipment. He had had engineering and sales experience on practically all products of the company and had been granted a number of patents for mechanical devices he had invented. He was widely known throughout the steel and nonferrous rolling-mill industries as an experienced and capable engineer with a thorough knowledge of the design and operation of rolling-mill equipment.

Mr. Lewis was born at Derby, Conn., on December 20, 1896, son of Edward Herbert and Emma (Donnell) Lewis. He received his early education in the Ansonia public schools and was graduated with a B.S. degree in mechanical engineering from Worcester Polytechnic Institute in 1919, immediately after which he entered the employ of the Farrel Foundry & Machine Co. as a draftsman.

His college course was interrupted during World War I when he entered the Air Corps in April, 1918. He was commissioned a second lieutenant and served as a pilot and flying instructor in aviation training camps in Georgia and Louisiana until after the armistice. He was enthusiastic about flying and frequently used the airlines on business trips.

Mr. Lewis became a junior member of the A.S.M.E. in 1921 and a member in 1933. He was also a member of the American Society for Metals. Fraternally, he was affiliated with Theta Chi fraternity, George Washington Lodge, F.&A.M., and Naugatuck Lodge, I.O.O.F. He was a member of William H. Gordon Post, American Legion, and of Christ Episcopal Church of Ansonia.

He is survived by his widow, Adelaide Louise (Beach) Lewis, whom he married in 1923, and a son, Franklin Beach Lewis, both now residing in Orange, Conn., as well as by his father and a sister.

ROBERT RAMSBOTTOM LISTER (1853–1938)

Robert Ramsbottom Lister, who died on November 16, 1938, was born on November 23, 1853, at Keighley, Yorkshire, England, son of Charles Lister and nephew of John Ramsbottom. His early education in home schools was supplemented later at a technical school and at Owens College in Manchester, where he began an apprenticeship in 1869 at the Gorton Foundry of Beyer Peacock & Co. Ltd., locomotive builders. His ability and trustworthiness led in 1872 to his being put to assisting in the delivery of locomotives to various points in England and on the Continent. Early in 1874 he entered the drawing office, where he remained until 1880. He then served successively as assistant works manager and chief of the machine shops until 1887, when he was appointed works manager at the Broughton Copper Co. Ltd., Manchester. He returned to the Gorton Foundry in 1890 to take up the position of chief draftsman and, on the formation of a new company, was made works manager, which position he held until he retired in 1904.

In 1905 he built the Greenbank Laundry at Gatley, Cheshire, which he carried on until his death. He joined the old Northern Counties Laundry Association in 1906 and was a member of the Council of that body, also president for a period and a very prominent worker in the Manchester branch of the Association. After the N.C.L.A. became merged in the National Federation of Launderers Ltd., he occupied the positions of representative of the National Council, member of the National Executive, vice-president, and, in 1926–1927, was president of the Federation. He was also chairman of the North Western District Council and one of the members responsible for the formation of the British Launderers Research Association.

He had been a member of the A.S.M.E. since 1894 and also belonged to the Institution of Mechanical Engineers and Manchester Association of Engineers.

He was a well-known Freemason, being Almoner and Past Master of Fellowship Lodge No. 3650, Past Provincial Grand Deacon of East Lancashire, and Founder and Second Principal of Fellowship Royal Arch Chapter No. 3650.

He married Agnes, the daughter of Michael Hodgson of Witherslack, Westmoreland, and they celebrated their Golden Wedding in 1932. His wife died in 1933, leaving two sons and two daughters, who survived him.

WALLACE FORREST MacGREGOR (1874–1939)

Wallace Forrest MacGregor, associated with the J. I. Case Threshing Machine Co., Racine, Wis., since 1898, died on June 18, 1939. He was born at Janesville, Wis., on February 19, 1874, son of Alexander and Mary (Milne) MacGregor. He prepared for college in the Janesville schools and was graduated from the University of Wisconsin with a B.S. degree in mechanical engineering in 1897. He received an M.E. degree the following year.

Mr. MacGregor began to acquire his experience with threshing machinery when he was only thirteen years old, working in the field during school vacations. By the time he entered college he knew

enough about wood and metal working to enable him to work as a machinist and patternmaker in the university shops to help defray his expenses. He went into the drafting room of the Case Company in July, 1898, and five years later was made superintendent of the Experimental Department. He continued to work on research, design, and testing of farm machinery all his life, and held some fifty patents in this line. He was mechanical engineer and director of the company at the time of his death.

During World War I Mr. MacGregor served as first lieutenant in Company I, 7th Regiment, Wisconsin State Guard, and was branch chairman of the Military Training Camps Association. He was a member of the Racine Board of Education for eight years, four years of which he served as its president. He was a member and trustee of the First Presbyterian Church of Racine.

Mr. MacGregor married Jessie Louise Hand, of Racine, in 1905, and is survived by her and a married daughter, Jean Douglas (Mrs. Richard D.) Miller.

He became a junior member of the A.S.M.E. in 1901 and a member in 1914. He had been a member of the American Society of Agricultural Engineers since 1910 and in 1914 served as its seventh president. Several of his papers were published in The Transactions of that Society. He belonged to the Delta Phi and masonic fraternities and the Racine Country Club, Rotary Club, and Somerset Club.

CHARLES MARTI (1882–1939)

Charles Marti, for many years designer in the Standard and Experimental Department of the Burroughs Adding Machine Company, Detroit, Mich., died on February 8, 1939. His widow, formerly Frida Dasen, of Berne, Switzerland, whom he married in 1920, and their daughter Veronica, returned to Switzerland after his death.

Mr. Marti was also a native of Switzerland, having been born in the canton of Basel on June 4, 1882, son of Karl Marti and Lina Marti-Rieder. He attended primary school in Basel, high school in Berne, and technical college in Zurich, being graduated there in 1906. During the next two years he was engaged in automotive truck design for Automobile Fabrik, at Orion, Zurich, then spent an equal period as mechanic, fireman, and locomotive engineer for the Chemin-de-fer Federal Suisse.

Mr. Marti first came to this country in 1910. He worked as draftsman for different automobile factories in Detroit for a year, after which he went into the Experimental Department of the Burroughs Adding Machine Company. His work on design there was interrupted by World War I in 1914. He returned to Switzerland and served as an engineering officer in the Swiss Army, in connection with the construction of the St. Gotthard and other fortifications, until 1917. From May of that year until August, 1919, he was superintendent of the Compagnie du Chemin-de-fer du Congo-Belge, in Africa, a road some 185 miles in length, with three roundhouses, two locomotive repair shops, and sixty locomotives. In addition to having charge of the road's supplies and maintenance, involving adjustments of equipment to the tropical climate, Mr. Marti bore some of the responsibilities, such as regulation of water supply, for the white settlements established in connection with the road.

After returning to the United States in 1920 Mr. Marti worked on design in the Experimental Department of the Ford Motor Company, at Dearborn, Mich., for about six months and in 1921 was superintendent of sewer construction in Detroit. He re-entered the employ of the Burroughs Adding Machine Company in 1922 and continued there until his death.

Mr. Marti had been a member of the A.S.M.E. since 1925.

ALLAN PATTON McCLINTOCK (1887–1939)

Allan Patton McClintock was born at Mt. Vernon, N.Y., on December 31, 1887, son of David Patton and Anna Clara (Yates) McClintock. He attended the Mt. Vernon public schools and was graduated from Cornell University in 1910 with an M.E. degree.

Following his graduation Mr. McClintock was employed at the Homestead (Pa.) works of the Carnegie Steel Company, for something over a year, the latter part of the time as assistant to the steam engineer. In the fall of 1911 he went with the Babcock & Wilcox Co., at Bayonne, N.J. After some shop experience on boiler testing, he was transferred to the proposition department, where his duties included designing and estimating of boilers, stacks, superheaters, and other apparatus. He continued in that work until the spring of 1916, then spent about a year in the sales department of the Imperial Oil Co., Ltd., Toronto, Ont., Can., as engineer in connection with the mechanical use of oil and petroleum products. There followed a short period devoted to the reorganization of the plant of the Akron Company, Long Island City, N.Y., a machine shop for which in 1914 he had designed a steam power plant.

In July, 1917, Mr. McClintock was commissioned a first lieutenant in the Ordnance Department, U.S.A., and assigned to the arsenal at Frankford, Pa., where he was stationed until the end of 1918, directing artillery ammunition production and drilling the ordnance detachment at the arsenal.

During the early part of 1919 Mr. McClintock assisted the Philadelphia Claims Board in the settlement of claims growing out of the cancellation of war contracts after the armistice. Then he took a position as representative of the Locomotive Superheater Company, New York, with which he continued until 1922. For the next five years he was engaged in industrial construction work for Geo. E. Batcheller, Inc., New York, and subsequently he was sales manager for the eastern part of the United States for the Feather-Stone Company, with headquarters at New York, for two years. He then served successively as New York representative for the C. H. Cowdrey Machine Works, of Fitchburg, Mass., builders of special automatic machinery; the Caterpillar Tractor Company, as Virginia representative, located at Richmond; and the Beckwith Machinery Company, of Pittsburgh, Pa., handling sales of Diesel engines in Pennsylvania.

Mr. McClintock was inactive during the latter part of his life. After suffering a heart attack at his home in Mt. Vernon he resided with relatives at Meadville and Cochranton, Pa. His death occurred on October 6, 1939, at the Veterans Hospital in Aspinwall, Pa. He was unmarried. An aunt, Miss Jennie E. Yates, of Meadville, survives him.

Mr. McClintock became an associate-member of the A.S.M.E. in 1913 and was promoted to the grade of member in 1920.

FRANK RAYMOND McGEE (1873–1939)

Frank Raymond McGee, whose death occurred on December 5, 1939, was born on July 9, 1873, at McGees Mills, Clearfield County, Pa., son of Henry Lafayette and Agnes Ann Rose McGee. He attended the local country school and spent two years in the Preparatory Department of The Pennsylvania State College. He secured his B.S. degree in the mechanical engineering course at the college in 1897.

In December of that year Mr. McGee went to work in the drafting room at the Edgar Thomson Works, Bessemer, Pa., of the Carnegie Steel Company. Both this company and the National Steel Company, with which he was later employed, were acquired by the U.S. Steel Corp., and he was connected with them and with the Carnegie-Illinois Steel Corporation, a subsidiary of the U.S. Steel Corp., continuously until his death. For many years he had been at the works located at Mingo Junction, Ohio, serving as mechanical engineer there since 1905. During the course of his work he invented a thermal expansion goggle valve and open joint checkers, which he listed as the more important of his inventions, and also a flexible coupling, chimney valve, gas cleaner, and a single-pass hot blast stove.

Mr. McGee had been a member of the A.S.M.E. since 1912. Other societies to which he belonged were the American Iron and Steel Institute and the Engineers Society of Western Pennsylvania. He married Abbie Priscilla Ault, of Steubenville, Ohio, in 1904, and is survived by her and a daughter, Mary Agnes (Mrs. Lewis) Gray.

ARTHUR WILHELM MERKEL (1883–1939)

Arthur Wilhelm Merkel, vice-president in charge of production and design of the Continental Gin Company, Birmingham, Ala., died on May 6, 1939. He was a native of Alabama, having been born at Eureka, Talladega County, on August 1, 1883. His parents were William A. and Ada Brisbane (Arthur) Merkel.

Mr. Merkel obtained his technical education at the Alabama Polytechnic Institute, from which he was graduated with a B.S. degree in mechanical engineering in 1904. He entered the employ of the Continental Gin Company immediately following his graduation, being one of three men in his class recommended, in response to a request from the company, to work for it and learn the business. After experience in erecting the company's special cotton ginning machinery as well as other equipment, he was transferred to one of the factories. During ensuing years he learned all manufacturing details of the business and was given increasing responsibility, serving successively as assistant foundry superintendent, assistant to the factory superintendent, and head of the finishing department of the Avondale factory. In 1914 he was made assistant general superintendent of the company's factories, located in different parts of the South, with headquarters in Birmingham. For three years he had charge of designing new machinery for cotton gins, cottonseed oil mills, and power plants, and a full line of transmission machinery. He also engaged in capacity and efficiency tests of new machines, some developed for war work.

When the United States entered World War I in 1917 Mr. Merkel was commissioned a captain in the Coast Artillery, and served overseas in the antiaircraft section. After his discharge in 1919 he returned to the Continental Gin Company as superintendent of its plant at Atlanta, Ga. He was transferred to the Birmingham plant in the same capacity in 1924 and made general superintendent in 1930. He had been vice-president in charge of production and design since 1934. Several patents on gin machinery were taken out by him.

Mr. Merkel had been a member of the A.S.M.E. since 1921. Subsequent to his retirement from active war service he entered the Officers' Reserve Corps, in which he had advanced to the rank of colonel. He belonged to the masonic fraternity, Presbyterian Church, and Birmingham Country Club.

Mr. Merkel married Nora Izetta Duke, of Birmingham, in 1908 and is survived by her and two married daughters, Lona Brisbane (Merkel) Croft, and Lois Izetta (Merkel) Parker.

ARTHUR EUGENE MICHEL (1880–1939)

Arthur Eugene Michel, owner of the technical advertising firm of A. Eugene Michel and Staff, New York, N.Y., died of heart disease at his home in Douglaston, L.I., N.Y., on November 9, 1939. He had been engaged in advertising work since 1905. After securing a B.S. degree from Rose Polytechnic Institute in 1903 he was employed as designing draftsman with the Diamond Chain & Manufacturing Co., Indianapolis, Ind., and for a short time was with the Ewart Manufacturing Company, of the same city. While in college he had spent two summers in electric railway work with C. O. Mailloux, New York consulting engineer, and in 1905 he returned East and took a position as assistant manager of publicity for the International Steam Pump Company, of Harrison, N.J. Subsequently, before going into business for himself, he was office manager of Geo. N. Gibson Co., advertising agents, New York.

Mr. Michel was born at St. Louis, Mo., on March 4, 1880, son of Henry and Louise D. Michel. Three years after his graduation, Rose Polytechnic Institute conferred an M.S. degree upon him. In addition to his engineering and advertising work, he was greatly interested in philately, specializing in entires and government stationery. His collection of these items, considered one of the best in the United States, received a first award at the Philatelic Exposition in New York in 1935 and has been maintained in its entirety at the Smithsonian Institution in Washington. He was a member of the Collectors Club, New York. He wrote one book on philately, "Roving the Stamp World," and several others, including "The Use of Steel Sheet Piling," "Raising of the United States Battleship *Maine*," and "Steam Heating."

Surviving Mr. Michel are his widow, Lisette Albertine (de Saver) Michel, and a daughter, Celeste Michel.

Mr. Michel became a junior member of the A.S.M.E. in 1906 and an associate of the Society two years later.

JOHN FISHER GARR MILLER (1877–1939)

John Fisher Garr Miller, vice-president of the B. F. Sturtevant Co., Hyde Park, Boston, Mass., died on December 9, 1939, of a heart attack at his home in Brookline, Mass. He is survived by his widow, Helen B. (May) Miller, whom he married in 1934, and by two brothers.

Mr. Miller was born at Nineveh, Johnston County, Ind., on March 23, 1877, son of John Chapman and Elizabeth Ann (Garr) Miller. After a private preparatory education he entered Purdue University with the Class of 1903. During his college years he was captain of football, track, and basketball teams, and secured four letters in athletics. He was also elected to Tau Beta Phi, honorary engineering fraternity.

After his graduation with a B.S. degree in mechanical engineering, Mr. Miller served an apprenticeship in the shops and drafting room of the Chicago & Eastern Illinois R.R., at Danville, Ill., and with the Penberthy Injector Company at Detroit, Mich. Subsequently he was connected with several design and construction projects, including a heating system for a factory at Brazil, Ind., for the Wood Turret Machine Company; a lumber drying plant for the Cooper Carriage Wood Work Company, St. Louis, Mo.; a heating system for the Crystal City (Mo.) plant of the Pittsburgh Plate Glass Company; and a heating and power plant for the high school and negro manual training school at Muskogee, Okla.

He then became engineering salesman and manager of the St. Louis office of the American Blower Company, of Detroit, Mich., with which he was connected until 1933, becoming general sales manager, vice-president, and a director of the company. He had been vice-president, in charge of sales, advertising, and sales promotion, of the B. F. Sturtevant Company since 1933, and took particular pride in the effectiveness of the student sales engineering course which he inaugurated in 1934.

Mr. Miller was widely known and highly regarded in the fan and air conditioning industry. A member of the A.S.M.E. since 1910, he served from 1919 to 1931 on the Power Test Codes Individual Committee No. 9 on Displacement Compressors and Blowers. He was a past-president and director of the National Association of Fan Manufacturers, chairman of the board of directors and past-president of the Air Conditioning Manufacturers' Association, and past-president of the Industrial Unit Heater Association. He was a member of the American Society of Heating and Ventilating Engineers and of the University Club, Boston, and belonged to several country clubs in that vicinity.

GEORGE HERBERT NELSON (1901–1939)

George Herbert Nelson, a junior member of the A.S.M.E. since 1926, was drowned at Jones Beach, L.I., N.Y., on June 11, 1939.

Born in Worcester, Mass., on September 23, 1901, son of Peter A. and Paulina (Krafve) Nelson, he was graduated from the South High School, Worcester, and from Worcester Polytechnic Institute, receiving a B.S. degree in mechanical engineering in 1923. To familiarize himself with rolling mill machinery, he worked for a few months in the Assembly Department of the Morgan Construction Company, Worcester, then went into the Engineering Department of the company as a detail draftsman and designer of rolling mill machinery.

During the early part of 1925 Mr. Nelson took a position as special investigator at the National India Rubber Company, U.S. Rubber Co., Bristol, R.I. He carried on studies to improve production by the elimination of waste material and labor in the wire and shoe divisions of the company. After about two years on this work he went to the Sayles Finishing Plants, Inc., Plant A, at Saylesville, R.I., where he was employed first as a time study man and systematizer. He was later promoted through several departments to the position of superintendent of the dye works and related departments, a position which he held for about five years.

In September, 1933, Mr. Nelson entered the Harvard Graduate School of Business Administration as a candidate for a M.B.A. degree, which he received in June, 1935. Since then he had been employed as industrial engineer by the Eastman Kodak Company, Rochester, N.Y.

Mr. Nelson became a junior member of the A.S.M.E. in 1926.

CHARLES LADD NORTON (1870–1939)

Charles Ladd Norton, director of the Division of Industrial Co-operation at the Massachusetts Institute of Technology since 1921, a widely known inventor and engineer, died at his summer home in Annisquam, Mass., on September 8, 1939.

A pioneer in fire-prevention studies, Dr. Norton was the inventor of asbestos shingles and homogeneous asbestos-cement building sheets used in most modern structures. His inventions in this line paved the way for the asbestos industry.

Dr. Norton became prominent during World War I as the first person in the United States to manufacture magnesium metal for commercial purposes. The metal became an important constituent of flares used by the Army Air Service. Previously, magnesium metal had been manufactured only in Germany.

In association with the late Henry M. Whitney, of Boston, Dr. Norton collaborated with officials of the Johns-Manville Corporation in the manufacture of transite, a material widely used in the building industry to insure corrosion-proof water pipes. Among his many contributions to industry was a machine for making silica brick which superseded the old hand-molding method. His process is now used universally. He helped develop the application of X-rays to medicine and surgery in this country and was distinguished for early investigations in this field with Dr. Francis H. Williams, of Boston.

Altogether, Dr. Norton held more than one hundred American and foreign patents relating to the economies of heat and the diminution of fire loss. He was the director of many corporations and the founder of the Norton Laboratories, in Lockport, N.Y. His published papers, beginning with "The X-rays in Medicine and Surgery" in 1896, range over almost the entire field of industrial physics and number more than fifty.

Dr. Norton was born on December 11, 1870, at Springfield, Mass., son of Francis and Jennie Maria (Atwater) Norton. He attended the local schools and was graduated from the Massachusetts Institute of Technology in 1893, with an S.B. degree. In the same year he joined the M.I.T. physics department and remained a member of the faculty until his death. He became successively professor of industrial physics, director of the research laboratory of industrial

physics, and head of the physics department, before becoming director of the Division of Industrial Co-operation.

Dr. Norton became a member of the A.S.M.E. in 1910. He was a fellow of the American Academy of Arts and Sciences and a member of the Society for the Promotion of Engineering Education, American Physical Society, American Chemical Society, American Association for the Advancement of Science, American Ceramic Society, National Fire Prevention Association, American Society for Testing Materials, and many other organizations.

Surviving are three sons, Frederick H. Norton, of Winchester, Mass., John T. Norton, of Cambridge, Mass., and Charles L. Norton, Jr., of New York, and three daughters, Mrs. Joseph Bacheller, of Los Angeles, and Miss Margaret Norton and Miss Dorothy Norton of Boston. His wife, Mrs. Frances (Torrey) Norton, died in 1936. They were married in 1895.

FRED R. PATCH (1853–1938)

Fred R. Patch, who died on January 20, 1938, in Rutland, Vt., was born there on October 15, 1853, son of Joseph Lewis and Annette (Lull) Patch. He attended public schools in Rutland and Proctor, and his first work was with the Sutherland Falls Marble Company of Vermont, which had been organized by Redfield Proctor about 1870. In an address made by Mr. Patch at a conference in Proctor in June, 1926, he referred to one of his early assignments, as follows:

"Fifty years ago last fall Colonel Proctor sent me to the Hoosac Tunnel to take out and load on the cars about one hundred carloads of machines,—engines, boilers, air compressors, rock drills,—that had been used in building the tunnel. Some of the air compressors came here and were in operation for several years at the south end of the lower mill. There were no trains passing through the tunnel when I first got there and I walked from North Adams, through the tunnel, seven miles to the East End Shops, back and forth, a great many times. After a couple of months they began running one train through the tunnel from North Adams each morning and back in the evening. I still have the note from the state treasurer, Mr. Bond, to the train conductor, Mr. Miller, that passed me through the tunnel many times on this first train."

The Sutherland Falls Marble Company was combined with the Rutland Marble Company in 1880 to form the Vermont Marble Company, with which Mr. Patch was connected until 1890, rising to the position of general superintendent.

For a short time after leaving the Vermont Marble Company Mr. Patch was general superintendent of the Sheldon Marble Company in West Rutland. During the latter part of 1891 he entered into partnership with Newman K. and George T. Chaffee, of Rutland, under the name of F. R. Patch & Co. They purchased the foundry and machine shop of Mansfield and Stimson, who had manufactured stone working machinery. Less than a year afterward, the business was consolidated with the Charles P. Harris Manufacturing Co., and a corporation was formed under the name of the F. R. Patch Manufacturing Co., specialists in manufacturing machinery for working marble, granite, and stone. Mr. Patch served as president of the company until his retirement in 1933. He developed many new machines for stone working and lived to see them in use throughout the United States and in many other countries.

In 1917 the F. R. Patch Manufacturing Co. purchased the Glens Falls (N.Y.) Machine Works, which manufactured pulp and paper machinery, and Mr. Patch became its president, also. Later he was president for a number of years of the Madras Marble Corporation, of Sylacauga, Ala.

In the fall of 1927 the F. R. Patch Manufacturing Co. was consolidated with the Julius Wegner Machine Works, of Long Island City, N.Y., under the names of Patch-Wegner Company, Inc., Rutland, and Patch-Wegner Corporation, Long Island City. Mr. Patch was president of the former and vice-president of the latter.

Mr. Patch had written articles regarding progress in the stone and marble industry for publications in that field. He had been a member of the A.S.M.E. since 1929 and belonged to the Vermont Society of Engineers. He was the first president of the town of Proctor; commissioner of public safety in Rutland for several years beginning in 1909; commissioner of public works for Rutland County, 1915–1916; a former vice-president and director of the Rutland County National Bank; and past-president of the Evergreen Cemetery Association.

Mr. Patch is survived by his widow, Cigrid B. Patch. His first wife, Abbie (Loveland) Patch, whom he married in 1875, died in 1908.

JOE W. PIERSON (1893–1939)

Joe W. Pierson, who died on February 5, 1939, was born at Aberdeen, S.D., on May 27, 1893, son of Frank and Emma (Hamm) Pierson. He attended Aberdeen schools, including normal school, and was graduated from the University of Minnesota with a B.S. degree in 1919. He was in training for naval service during the summer of 1918, until the armistice was signed.

From the time of his graduation until his death Mr. Pierson was employed by the Commonwealth Edison Company in Chicago, Ill. Beginning as technical assistant on boiler and turbine testing, he was made assistant boiler room engineer at the Quarry Street Station in 1921 and at the Calumet Station two years later, boiler room engineer at the Crawford Avenue Station in 1924, and efficiency engineer of generating stations in 1934. He was serving in this capacity at the time of his death.

Mr. Pierson became a member of the A.S.M.E. in 1930. He is survived by his widow, Laura (Curtis) Pierson, whom he married in 1920, and by a daughter, Marjorie Ann Pierson.

JOSEPH HORACE POUND (1890–1942)

Joseph Horace Pound, professor of mechanical engineering at the Rice Institute, Houston, Texas, and consulting mechanical and petroleum engineer, died on May 23, 1942. He was born on June 24, 1890, at Hannibal, Mo., son of William L. and Zoretta (Burbank) Pound. He attended the Hannibal public schools and was graduated from the University of Missouri in 1913 with the degree of Bachelor of Science in Mechanical Engineering. Postgraduate work in summer sessions at the Universities of Missouri and Wisconsin led to an M.E. degree from the former in 1921.

After being employed with the Westinghouse Machine Company (now Westinghouse Electric & Manufacturing Co.), East Pittsburgh, Pa., in various departments and serving on the staff of the Casino Technical Night School (now Westinghouse Technical Night Schools), he joined the faculty of the Rice Institute in 1914. He had charge of the organization of the Department of Mechanical Engineering, including selecting, purchasing, and installing laboratory and shop machinery, building necessary structures, and forming the courses of instruction. He was head of the department until his death, except for the years 1917 to 1919, while serving in the U.S. Army. He was made assistant professor in 1919 and professor ten years later. He was a member of the faculty committees on Honours Courses and Advanced Degrees and on Examinations and Standings, and of the Faculty Club of the Institute.

An authority on petroleum production problems, Professor Pound contributed many papers and articles to trade and technical magazines serving that field. Nearly all of his summer vacations were spent in special work for various companies, including the Gulf Pipe Line Company, Reed Roller Bit Company, Texas Company, and Hughes Tool Company, all of Houston. He did much important work on design problems for these companies.

Professor Pound became a junior member of the A.S.M.E. in 1915 and a member in 1923. He was responsible for establishing the Society's Student Branch at Rice Institute in 1926 and served as its honorary chairman for many years. He was a member of the executive committee of the Houston (now South Texas) Section of the Society from 1925 to 1935, and its chairman in 1931-1932.

He was also an active member of the Society for the Promotion of Engineering Education and of the Houston Philosophical Society, of which he was treasurer in 1925 and president in 1933. He belonged to Tau Beta Pi and Sigma Xi, honorary scholastic fraternities, and was instrumental in founding student chapters of those organizations at the Rice Institute.

During World War I Mr. Pound entered the army as a private in the Ordnance Department. He attended Ordnance Schools and Engineer Officers' Training Camps and was commissioned a second lieutenant and sent overseas with the 546th Engineers in 1918. He served on highway work in the Argonne, St. Mihiel, and other sectors until after the armistice and then was an instructor at the A.E.F. University for several months. He left the service in July, 1919.

Professor Pound married Ruth Robinson in 1919 at Graham, Texas, and is survived by her and three children, John H., a student at Rice Institute, and David R. and Mary E. Pound, students in the Houston public schools.—[Memorial prepared by R. R. Crookston, Houston, Texas. Mem. A.S.M.E.]

EWALD PYZEL (1901–1939)

Ewald Pyzel was born at Tjepoe, Java, Dutch East Indies, on March 31, 1901, son of Daniel and Maria Catherina (von Glahn) Pyzel. After attending technical high school at The Hague, Netherlands, he came to the United States. He was graduated from Stanford University in 1925 with a B.S. degree in mechanical engineering.

Mr. Pyzel's first position after graduation was that of technical assistant at the Wood River (Ill.) Refinery of the Roxana Petroleum

Corporation (now Shell Oil Co., Inc.). He left there in 1929 to study the design of European synthetic ammonia and gasoline plants. In 1930 he was charged with the design and construction of a nitrogen fixation plant for the Shell Chemical Company at Pittsburg, Calif., and he superintended the operation of this plant from 1931 until his death. He held patents on a process and apparatus for the separation of liquids from gases, a process for the vapor phase hydrogenation of olefin polymers, and catalytic converters.

His widow, Mabel (Johnson) Pyzel, whom he married in 1925, and two children, Mary Catherine and Ewald Daniel, survive him, and also a brother, Frederic Pyzel, all of Piedmont, Calif. His death occurred on October 12, 1939, at the University of California Hospital, San Francisco, from a brain tumor.

Mr. Pyzel became a junior member of the A.S.M.E. in 1926 and also belonged to the Verein Deutscher Ingenieure. His interests outside his profession included painting, drawing, and the history of shipbuilding.

CHARLES DeLOS RICE (1859–1939)

Charles DeLos Rice, who had been issued some seventy-five patents on a variety of inventions, many relating to bicycles and typewriters, died on September 10, 1939, after a long illness. Retired from the Underwood Elliott Fisher Company (formerly Underwood Typewriter Company), with the title of vice-president in 1929, because of poor health, he was later able to take up further work on his inventions, which included improvements on pneumatic tires, gear-cutting machines, forging machines, milling and drilling machines, and a great variety of single-purpose mechanisms.

Mr. Rice was born at Auburn, N.Y., on April 15, 1859, son of Benjamin and Harriet M. Rice. His formal education, extending only through grammar school, was supplemented by home studies. As a general shop worker over a period of about ten years he became proficient in machine construction and toolmaking. He was associated during part of this time with the Caligraph Typewriter Company, at Corry, Pa. He moved to Hartford, Conn., with this company in 1885 and remained with it until 1888, when he joined the Yost Writing Machine Company at Bridgeport, Conn., while they were developing their machine. This led, in 1890, to the position of chief engineer of the Pope Manufacturing Company, of Hartford, builders of the Columbia bicycle. Located at the Columbia factory, he also guided the work of the company's allied plants.

Mr. Rice resigned this connection to become superintendent, on January 15, 1901, of the Underwood Typewriter Company, then located in Bayonne, N.J., but later moved to Hartford. He was made general manager in 1907 and as such subsequently directed the activities of more than five thousand employees.

Mr. Rice won honors at two expositions. At the one in Paris in 1900 he was awarded a medal for bevel gear-cutting machines, and in 1915, at the Panama-Pacific International Exposition in San Francisco he was given a gold medal for services rendered in the production of high-grade typewriters.

Mr. Rice had been a member of the A.S.M.E. since 1907. He had resigned from The Franklin Institute, to which he belonged for many years. He had served one term as councilman for the city of Hartford, and was a member of its school board for six years. Over a long term of years he had served on many directorates.

Surviving Mr. Rice are his widow, Anna C. (Hoagland) Rice, whom he married in 1882, and a daughter, Edna (Rice) Leavitt.

PAUL K. ROGERS (1889–1938)

Paul K. Rogers, president and treasurer of the Skinner Chuck Company, New Britain, Conn., accidentally fell from a fourth story window of the factory on January 11, 1938, and died before reaching the hospital.

Mr. Rogers was born in New Britain on February 4, 1889, the son of Daniel O. and Emma C. Rogers. After completing his studies at the New Britain High School he attended Princeton University for a year, then went to work for the Skinner Chuck Company as a clerk in the superintendent's office. Subsequently he spent some time in the Cost Department and also in the Purchasing Department. He was made treasurer of the company in 1915 and president in 1931.

Mr. Rogers organized a new bank in New Britain, known as the City National Bank, and was its president for six years until it was taken over by the New Britain National Bank in 1932. He was a deacon at the South Congregational Church of that city for a number of years, an office which both his father and grandfather had held. He was also much interested in civic affairs.

He became an associate of the A.S.M.E. in 1934 and had been a member of the Society of Automotive Engineers since 1932. He is survived by his widow, Greta (Clark) Rogers, whom he married in 1911, and by a son, Paul K. Rogers, Jr., of New Britain, and three daughters, Greta, of New Britain, Marjery, of New York, N.Y., and Jane (Rogers) Beebe, of Cornwall, Conn.

CHARLES WILLIAM RUSH (1886–1938)

Charles William Rush, who died on September 23, 1938, was born in London, England, on November 28, 1886, son of Charles William and Martha Ann (Bougen) Rush. After taking a course in mechanical engineering at the East London College of Engineering, he served an apprenticeship with the India Rubber Gutta Percha & Telegraph Co. in London, securing machine shop, drafting, and other experience. The following year he was an inspector for Robey & Co., Lincoln, England, in connection with high-speed engines, air compressors, and winding equipment for collieries. During the next three years he held the position of assistant chief inspector with the British Thomson Houston Company, at Rugby, also engaging in the design of tools, gages, and fixtures, and then he was in charge of machine shops for Crossley Bros., Manchester, directing work on various types of engines and turbines. At the outbreak of World War I he was appointed assistant superintendent and estimated and planned various war contracts and installed departments for producing naval ammunition.

Following the war, Mr. Rush became production manager for the Meccano Company, Ltd., Liverpool, in charge of the entire factory, employing some fifteen hundred people engaged in the manufacture of small electric motors, transformers, electric and mechanical trains, and other electric and mechanical toys. He contributed much to the success of the company through his design of special machines and layout work for mass production. In 1922 he was transferred to Paris as general superintendent of Meccano (France) Ltd., responsible for the establishment of another factory for such products. After supervising operations there for a time he came to the United States in 1924 to locate a factory at Elizabeth, N.J., and served as its general superintendent until 1930.

Mr. Rush left the Meccano Company to become assistant superintendent of the Meter Department of the Worthington Pump Company at Harrison, N.J., but after a few months there he went to Waterbury to take the position of superintendent of the Waterbury Manufacturing Company (now a subsidiary of the Chase Brass & Copper Co., Inc.), with which he was connected until his death, serving as plant engineer during the latter part of the time. He reconstructed and rearranged the various departments and installed new processes.

Mr. Rush had been a member of the Rugby Engineering Society and Manchester Association of Engineers, in England. He became a member of the A.S.M.E. in 1930 and served as secretary-treasurer of the Waterbury Section from 1936 to 1938. He also belonged to the Connecticut Society of Civil Engineers and masonic fraternity.

Surviving him are his widow, Eleanor S. (Alford) Rush, whom he married in London in 1911, and their daughter, Edna Nellie (Rush) Crane.

LEE GRISWOLD SHARPE (1893–1935)

Lee Griswold Sharpe, who became an associate of the A.S.M.E. in 1931, died suddenly on April 28, 1935, at Portland, Ore., from an acute heart attack, while on a business trip. He had been general sales manager of the Atlantic Paint Company, New York, N.Y., since 1918, covering territory west of the Mississippi, with headquarters at first in Oakland, later in Los Angeles, Calif.

Mr. Sharpe was born on October 19, 1893, at Denver, Colo., son of Alexander and Rachel Jane Sharpe. When he was two years old the family moved to San Francisco, where he was educated in the public schools. Prior to his connection with the Atlantic Paint Company he was manager of the Oakland Phonograph Company, Oakland, and of the Phonograph Department of the Benj. Curtez Music Company, San Francisco. He was an accomplished musician, playing the piano and trumpet and singing in various musical organizations. He had been tenor soloist in several churches, including the First Baptist Church of Oakland and the Episcopalian Church of the Advent, of San Francisco, of which he was a member. He was a member of the Glendale (Calif.) Lodge of Elks.

Mr. Sharpe married Mable Marshall, in Oakland, in 1917, and is survived by her. A sister, Gertrude (Sharpe) Martin, of Oakland, also survives him.

EDWIN COUPLAND SHAW (1863–1941)

Edwin Coupland Shaw, a resident of Akron, Ohio, since 1893, died at his home in that city on November 25, 1941, at the age of seventy-eight, noted both for his engineering and industrial work and his humanitarian and philanthropic projects.

Mr. Shaw's first position in Akron was that of superintendent of the Akron Light & Power Co., for which he was well fitted by a number of years' experience in the electrical industry. Born in Buffalo, N.Y., on February 1, 1863, the son of Edwin A. Shaw, a manufacturer of lumber and lumber products, and Clara (Coupland) Shaw, he attended public schools in Buffalo and entered the Sheffield Scientific School of Yale University. After securing his Ph.B. degree in 1886, he spent one season as assistant engineer on a cargo steamer on the Great Lakes. He then had a year with Otis Brothers & Co., elevator manufacturers, New York, N.Y., followed by a year in drafting work, part of the time with Charles M. Morse, consulting mechanical engineer, of Buffalo. In 1888-1889 he was engineer and draftsman, giving particular attention to gas engines, for the Binghamton (N.Y.) Hydraulic Power Company. He continued work of this character under his own name, with an office in Binghamton, until early in 1891, when he became general superintendent of the Thomson-Houston Electric Light & Power Co., Buffalo. During about two years there he reconstructed some of the stations.

With this background, Mr. Shaw took up his work in Akron. His ability was noted by the superintendent of the B. F. Goodrich Co., who persuaded him to join that organization on January 1, 1895, as mechanical and electrical engineer. His rise in the company was rapid. He became assistant superintendent in 1902, general manager four years later, and vice-president in charge of all factory operations in 1912. He retired from active management in 1919, but remained on the board of directors until 1926.

J. Henry Vance (Mem. A.S.M.E.), who entered the employ of the B. F. Goodrich Co. as a draftsman in 1894 and rose to the position of superintendent of power, has written the following account of Mr. Shaw's electrification of the Goodrich plant during his first years there.

"Here Mr. Shaw found a fertile field for the exercise of his ability as the industry was growing at a very fast pace, due largely to the pneumatic tire then coming into production for bicycles, and later for motorcycles and automobiles.

"Buildings had to be built, power facilities enlarged, and equipment developed to meet the ever-increasing demand for production.

"The principle type of buildings then in use had brick walls with wooden beams, columns, and floors. Mr. Shaw, seeking a more substantial and fireproof type of factory building, placed a contract for a reinforced-concrete building, the first of this type constructed in Akron. This building is still in use for manufacturing, and practically all later expansion was of the same type.

"The power plant at Goodrich, when Mr. Shaw took charge, consisted of about thirty steam engines and ten return-tubular boilers of 100-lb pressure. These engines were scattered all over the plant and ranged in size from 4 to 300 hp. They drove the rubber machinery by means of belting and line shafts.

"Mr. Shaw early became convinced that in order to take care of the rapidly increasing power demands and to have a system flexible enough to make possible an arrangement of equipment which would give a much higher efficiency, it would be necessary to consolidate the steam generating plants, which by this time consisted of three separate boilerhouses, and to generate sufficient electricity to drive all equipment, including mills and calenders, by motors and replace all gas by electric lighting.

"He made a careful and comprehensive study of this whole subject, and having no data of any kind to guide him as to the amount of power required to operate a gang of mills or an individual calender, he had carried out a long series of tests to establish facts on power requirements and, at the same time, looked into the use of alternating current as a means of lighting and power.

"The result was that in 1899, a layout of a consolidated powerhouse was completed and contracts placed for building boilers, coal-handling equipment, two 500-kw Westinghouse alternating-current, 60-cycle, 2-phase, 220-volt generators (each direct-driven by a cross-compound Harrisburg engine), and a synchronous rotary converter to furnish direct current for operation of calenders, as this type of direct-current drive allowed for a rather wide variation of speed of the calenders which had hitherto had but two speeds.

"All of this electrical equipment was so new as to type in this country, and the first of its kind installed west of Pittsburgh, that when the contract was written by Westinghouse a clause was inserted that stated that should the motor or generators not function to the full satisfaction of the B. F. Goodrich Co., the Westinghouse company would, at their own expense, remove all the alternating generators and motors and replace them with direct-current equipment; but when the plant was completed and started up in August, 1900, it was a complete success. The expansion of power demand was so rapid from then on that in 1902 a 400-kw turbine-driven generator, also the first of its kind shipped west by the Westinghouse company, was installed, and before the installation was finished, a 750-kw turbine-driven generator was ordered. Successive and larger turbines were installed at intervals of about two years until by 1907 five in all had been installed. At this time, it was decided to purchase all additional power required, as available condensing water facilities were exhausted."

Walter H. Allen, of Grosse Pointe, Mich., also associated with Mr. Shaw over a period of many years, refers to the electrification of the Goodrich plant as an "outstanding accomplishment which has stood the test of years and still remains best practice. Mr. Shaw conceived and directed the first application of central-station practice to rubber industry requirements. It was an enormous undertaking, requiring no small amount of foresight and confidence, and was carried through to a most successful conclusion in record time."

Charles F. Scott (Mem. A.S.M.E.), engineer at the Westinghouse works at the time of the electrification of the Goodrich plant, writing for the *Yale Scientific Magazine*, spring of 1942, also speaks of the task as a pioneer job, the plan for which was "ingenious, simple, and admirably adapted for the several services." Mr. Shaw, he says, was "a plain and quiet man; but he understood his problem and knew what he wanted."

Regarding other improvements inaugurated by Mr. Shaw, Mr. Vance writes:

"Mr. Shaw early recognized that the method of curing rubber goods in use when he entered the business was very wasteful of steam, and he did not hesitate to apply steam traps in place of hand-operated blow-off valves to remove the condensate from the vulcanizers, making the first installation of this kind in this country. He also introduced what is now called the quick-opening door, used throughout the country for opening and closing vulcanizers. He recognized the advantages of the principles of operation, and the economy of space requirements of centrifugal pumps, and purchased one of the first put out by the Worthington Pump & Machinery Corp. He introduced the use of electric clutches to disconnect quickly the rubber mills from their driving motor, should an employee become caught between the rolls."

Much has been recorded in the public press concerning Mr. Shaw's outstanding services as a humanitarian and philanthropist. But Mr. Shaw is said to have had a horror of being regarded as what he called "a long-haired uplifter." Dr. Scott has ably summarized the record of these services as follows:

"As an industrial manager he was a pioneer in the betterment of employee relations; interest in the health of employees extended to public health work and the establishment of a tuberculosis sanatorium, recently named for him. He was connected with scores of enterprises from Scouts to State Board of Pardons and Parole, and numerous state boards having to do with welfare. In civic leadership he was cited as one of Akron's finest citizens and a prominent contributor to everything he undertook."

With broad vision and foresightedness, Mr. Shaw recognized the importance of community and industrial health and he attacked these problems with the same energy and thought that he applied to those of engineering.

In fact, he used the same engineering principles in their solution that he had used in solving those of steam and electricity.

Careful planning, cautious testing, and thoughtful consideration of the methods to follow in establishing and maintaining a sure control led finally to the conversion of the ordinary county tuberculosis sanatorium which has been mentioned into one of national reputation; and of a county control of this disease that has reduced its mortality to a minimum. Because of his outstanding services in its behalf as a trustee, the name of the Sanatorium was changed by the county commissioners under date of August 10, 1934, to the Edwin Shaw Sanatorium.

It was through his efforts and by the same methods that the Akron Health Department was established on a full-time functioning basis.

Mr. Shaw's singleness of purpose, integrity of character, inherent honesty, and meticulous sense of honor and justice were attributes that marked him as a leader of men.

In recognition of these services the Akron Chamber of Commerce presented him a scroll in 1940, the inscription being:

"Your contribution to the business, industrial, and social well-being of this community, over the years since 1893 when you came to Akron, has been so fundamental and so outstanding that this chamber of commerce, here assembled this ninth day of February, 1940, is honored to have this opportunity to extend to you this token of its appreciation of your distinguished accomplishments, of its gratitude for your labors, and of its assurance that the benefits from them will continue long into the future."

Mr. Shaw's will directed that the bulk of his estate be used to support charitable, health, and educational institutions in Summit County, Ohio.

In 1933 Mr. Shaw received the honorary degree of LL.D. from the

University of Akron, the fourth to receive this honor. He held the fifty-year membership badge of the A.S.M.E., having joined the Society as a junior member in 1890; he was promoted to the grade of member two years later. Many other scientific and engineering organizations, as well as civic, fraternal, and social groups, were proud to count him as a member.

Probably no man in Akron had a keener appreciation of art. He was one of the original sponsors and a faithful supporter of the Akron Art Institute and had an excellent private collection of etchings and paintings. Gardening, and particularly the cultivation of rare specimens of peonies and iris, was another of his many interests, and he was also an ardent fisherman.

Mr. Shaw is survived by his sister, Caroline Coupland Shaw, who lived with him. His wife, Jennie (Bond) Shaw, whom he married in 1898, died in 1933.

ROBERT SHIRLEY (1869–1938)

Robert Shirley was born on February 5, 1869, in Glasgow, Scotland, son of Robert and Stewart (Sterling) Shirley. He received his early education at Hutcheson's Grammar School in Glasgow and subsequently attended the technical college there and served an engineering apprenticeship with Wm. Dixon & Co. Ltd. He was employed in drafting and shop work by this company and R. Napier & Sons, also of Glasgow, for several years before coming to the United States.

In this country, his first employment was with the Rensselaer Manufacturing Company, Cohoes, N.Y., designing valves and special tools for machining them. This led to the position of mechanical engineer with the Pratt & Cady Co., Hartford, Conn., with whom he remained until 1909. During the next nine years he was works manager of the Chapman Valve Manufacturing Company, Indian Orchard, Mass., then after a brief period in consulting work in Springfield, Mass., he went to Waterford, N.Y., to become works manager of the Eddy Valve Company. Poor health forced his retirement from active work in 1922.

After a period of traveling in this country and Europe, Mr. Shirley located in East Longmeadow, Mass., later moving to Springfield, where he spent the remainder of his life. He died of a cerebral hemorrhage in the Springfield Hospital on March 4, 1938.

During the latter part of his life Mr. Shirley did some consulting work and gave a great deal of time to the fraternal organizations to which he belonged. He was a Knight Templar, 32nd degree Mason, and Shriner, and had held a number of high offices in the masonic fraternity and related orders. He also served for a number of years as president of the Springfield Automobile Club and as director of the Automobile Association of America. He had been a member of the A.S.M.E. since 1906.

Mr. Shirley was a pioneer in steel valve design for superheated steam installations and while with the Pratt & Cady Co. designed and built some nine-foot cast-iron valves for the Ontario Power Company, Niagara Falls, Canada, at that time the largest valves of that kind in the world. He invented a double-gate valve, the patent for which was assigned to the Pratt & Cady Co. He lectured in Canada and Great Britain on American valve practices, particularly in large water works and power systems.

Surviving Mr. Shirley are two sons, John G. Shirley, of North Adams, Mass., a member of the A.S.M.E., and James G. Shirley, of Springfield, as well as a number of grandchildren, a brother, and a sister. His wife, Elizabeth A. (Gilchrist) Shirley, whom he married in 1891, died in 1936.

SVERRE SKAGEN (1882–1938)

Sverre Skagen, designing engineer for the Koppers Construction Company, Pittsburgh, Pa., since 1936, died in that city on July 6 1938. His widow, Yvonne Skagen, and one child, survive him.

Mr. Skagen was born at Bergen, Norway, on December 16, 1882, son of Peter Dankertsen and Anna Sophie (Hammerstad) Skagen. He attended the Anthonisen Grammar School, Cathedral High School, and technical college in Bergen, completing the mechanical engineering course in 1903. He studied marine engineering and shipbuilding in evening school in England the following year, while working as section chief at an iron foundry in that country. Later he returned to Oslo, where he engaged in marine consulting work for a number of years, was boiler and factory inspector for the Norwegian government from 1912 to 1914, and for several years was employed as chief draftsman by a Norwegian shipbuilding company.

Since the beginning of 1924 Mr. Skagen had been employed in this country as a designer, checker, and estimator, working for various companies, including the Carnegie Steel Company, the American Sheet & Tin Plate Co., the Jones & Laughlin Steel Corp., and the Gulf Refining Company, prior to his connection with the Koppers Construction Company. He was responsible for layouts and estimates for a number of new plants for these companies, involving expenditures of many millions of dollars.

Mr. Skagen had been a member of the Norwegian Engineering Society and Engineers' Society of Western Pennsylvania, and became a member of the A.S.M.E. in 1931. He was a naturalized citizen of the United States.

WLADIMIR BORISOVICH SOUNITZA (1885–1939)

Wladimir Borisovich Sounitza, mechanical engineer for the Emsco Derrick & Equipment Co., at Los Angeles, Calif., died at the Hospital of the Good Samaritan in that city on October 10, 1939, of an embolism following an operation.

Mr. Sounitza, who became a naturalized citizen of the United States in 1930, was born at Mglin, Russia, on July 11, 1885, son of Boris Pavlovich and Marie (Mishienko) Sounitza. He was educated in Moscow, completing his high school work in 1903. He carried on studies at the Imperial High Technological Institute for the next two years and from 1909 to 1915, in which year he received a master's degree in mechanical engineering. During the years 1905–1915 he was also engaged in teaching and engineering work. For about four years he taught mathematics and physics in a private school and spent considerable time in work in his own machine shop. Then he was engineer for the Construction Department of the Chetverikoff Woolen Mill, near Moscow.

Following the completion of his engineering course, Mr. Sounitza was successively employed by the Bocharov Engineering Company, Moscow, as draftsman and designer of boiler furnaces; in the Oil Engine Department of K. Wiegand, Revel, Russia, as designing engineer; and at the Lubertzy Plant, Moscow, of the International Harvester Company as engineer in charge of the Test Department of the Oil Engine Division.

In June, 1915, Mr. Sounitza took charge of the erection and operation of the Tolvol Plant of Nobel Brothers, in Baku, Russia, and later that year was made assistant oil field superintendent by the company. In January, 1916, the company sent him to the Bibi Eibat oil fields as chief engineer, and he continued in that position until August, 1918. From then until February, 1919, he served under General Bicherahov in the war against Turkey, part of the time in charge of an automobile repair shop and part as chief engineer on a gunboat in the Caspian Sea. For his services General Bicherahov bestowed upon him the order of St. Vladimir with the Swords.

Subsequently he returned to the employ of Nobel Brothers as assistant general manager of the Bibi Eibat oil fields. The following year he became associated in the capacity of chief engineer with the Engineering Department of Azneft—the nationalized oil industry in Baku—and he continued with that organization until 1928. In 1921–1923 he was also professor at the Technological Institute in Baku. He directed the Engineering Department of Azneft from 1921 to 1923, then came to the United States to serve as consulting engineer in charge of the selection and inspection of American machinery for oil fields and machine shops in Baku. He represented the Azneft organization but not the U.S.S.R. government itself and had no connection with the financial part of the transactions.

After leaving Azneft in 1928, Mr. Sounitza spent about a year in private practice as consulting engineer on the design of oil-field equipment before entering the employ of the Emsco company as engineer designer at Los Angeles. In April, 1935, he was transferred to Houston, Texas, as chief engineer of the Machinery Division of the company there. He was recalled to Los Angeles in January, 1938.

Mr. Sounitza wrote a textbook on kinetics of mechanisms, published in Russian about 1921. He held a number of patents on oil furnaces, oil-field equipment, and electric-arc cutting apparatus. He was talented in drawing and well-informed on classical music, literature, and history.

Mr. Sounitza became an associate of the A.S.M.E. in 1924 and was given the grade of member in 1928. Surviving him are his second wife, Elisabeth Ivanovna (Postnikova) Sounitza, whom he married in 1922, and an adopted son, Vadim Wladimir Sounitza. His first wife, Nadejda (Alexandrova) Sounitza, whom he married in 1906, died in 1919.

RALPH CHARLES STIEFEL (1862–1938)

Ralph Charles Stiefel, formerly vice-president of the Aetna-Standard Engineering Company, Ellwood City, Pa., and patentee in 1895 of a disk-piercing machine for making seamless steel tubes, died at his winter home in St. Petersburg, Fla., on March 15, 1938.

Born at Oerlikon, near Zürich, Switzerland, on February 17, 1862,

Mr. Stiefel received his technical training at the Maschinenfabrik Oerlikon and Technikum Zürich, graduating from the latter in 1881. After working in Swiss silk-spinning mills for a year he was employed for several years as chief draftsman in French establishments. He returned to Zürich in 1888 and worked as draftsman for Esher Wyss & Co. until October, 1889, when he went to Great Britain to work on seamless tube projects with the British Mannesmann Tube Company, Landore, Wales.

Mr. Stiefel came to the United States in 1894 and took the position of general superintendent of the Ellwood Weldless Tube Company, Ellwood City, which was acquired by the Shelby Tube Company in 1900. He was with this organization and the National Tube Company, both of which were taken over by the U.S. Steel Corp. in 1901, until 1912.

In the fall of 1902, Mr. Stiefel helped to organize the Standard Engineering Company, Ellwood City, manufacturers of seamless steel tube mill machinery, which was merged in 1926 with the Aetna Foundry & Machine Co., of Warren, Ohio, to form the present Aetna-Standard Engineering Company, with plants in the two cities. He retired as vice-president of the company in 1932.

Mr. Stiefel became a member of the A.S.M.E. in 1897 and served for two years on the Special Research Committee on Heavy Duty Anti-Friction Bearings, being appointed when the committee was formed in March, 1929, and resigning in 1931. He was a naturalized citizen of the United States.

Surviving Mr. Stiefel are his widow, Mary (Bowen) Stiefel, whom he married in 1895, a daughter, Mrs. Howell Jenkins, of New York, N.Y., and a son, R. Charles Stiefel, Jr., of Ellwood City.

CHARLES WATERMAN STONE (1874–1938)

Charles Waterman Stone, consulting engineer for the General Electric Company and connected with that organization for nearly forty years, died at his home in Schenectady, N.Y., on February 3, 1938, of a heart ailment which had confined him to bed for nine weeks.

Mr. Stone went to work for the General Electric Company as a draftsman in August, 1899. In 1901 he was assigned to switchgear engineering work and in 1904 was transferred to the Lighting Department as assistant engineer. He was named manager of the department (now known as the Central Station Department) in 1912, and continued in that position until 1928 when, at his own request, he was relieved of managerial responsibilities and became a consulting engineer for the company.

During his early connection with the company, Mr. Stone designed all the switchgear adopted by the U.S. government for warships for some years. Later he devoted his time to the design of large vertical frequency changer sets, vertical rotary converters, and various electrical apparatus. He designed many large railway and lighting central stations throughout the country, together with much of their equipment.

Experimenting at home on new physical and mechanical problems had been one of Mr. Stone's chief hobbies since childhood, so it was natural that he took more than ordinary interest in many of the company's important developments. Perhaps his chief interest was in radio and its associated developments, particularly the photophone, a device for recording the voice or music on film, the forerunner of the talking movie. He was also active in the affairs of the Radio Corporation of America from the time of its inception, and in 1927, while still manager of the Central Station Department of the General Electric Company, was named assistant to James G. Harbord, then president of R.C.A.

Seeing the possibilities of radio and other types of vacuum tubes in additional fields of the electrical industry, he became interested in the latter years of his life in the application of thyratron tubes as a cheaper and more efficient means in the distribution and conversion of electricity from alternating to direct current and vice versa.

Mr. Stone was born in Providence, R.I., on December 24, 1874, son of Waterman and Emily Clark (Steere) Stone. He attended public school in Providence and in Kansas City, Mo., and after his graduation from high school in the latter city, spent three and one-half years at Kansas State University. From then until he became associated with the General Electric Company he worked for the Franklin Electric Company, Kansas City, Mo., and the W. S. Hill Electric Co., New Bedford, Mass., where he served an apprenticeship as machinist and toolmaker and secured drafting experience, and the Hancock Equipment Company, Boston, Mass., as foreman of its Construction Department. His work for these companies included a complete survey of the elevated railway in Kansas City, and the building of several electric roads in New England.

Mr. Stone had been a member of the A.S.M.E. since 1907. He was a fellow of the American Institute of Electrical Engineers, which he had served in committee work and as a manager and vice-president. He also belonged to The Franklin Institute, Society for the Promotion of Engineering Education, American Association for the Advancement of Science, and a number of clubs in Schenectady and New York. He was a member of Beta Theta Pi fraternity and a life member of the Navy League, and had served on the Schenectady Chamber of Commerce. He contributed numerous papers before the organizations to which he belonged and had lectured before the Engineers School, Washington, D.C., Columbia University, and other institutions. He was president of the Pioneer Thresher Co., Inc., manufacturers of agricultural implements, Shortsville, N.Y.

Surviving Mr. Stone are his widow, Harriet Anna (Westinghouse) Stone, a native of Schenectady, whom he married in 1902, and two daughters, Clara Westinghouse (Stone) Howell, and Margaret Anna (Stone) Gibson.

FRANK GIFFORD TALLMAN (1860–1938)

Frank Gifford Tallman, vice-president and director of E. I. du Pont de Nemours & Co., Wilmington, Del., at the time of his death in 1938, had been associated with that company since 1905. He served as director of purchases until March, 1916, when he was elected a director, a member of the executive committee, and vice-president in charge of purchases. In 1919 he resigned from the executive committee and was made a member of the finance committee. Also in that year he was elected president of the Du Pont Building Corporation, Hotel Du Pont Company, and Du Pont Playhouse Company. In 1925, at his own request, he was placed on the retired list, subject to call. His death occurred on April 1, 1938, at the Delaware Hospital in Wilmington, after a long illness.

Mr. Tallman was born at Dubuque, Iowa, on January 26, 1860, son of Peleg and Maria (Hudson) Tallman. His early education was secured in private and public schools in Syracuse, N.Y., and from 1873 to 1876 he attended the Syracuse Classical School. During these years he spent his leisure time helping in the shops and rolling mill of his stepfather, William Avery Sweet, brother of Professor John Edson Sweet and founder of Sweet's Manufacturing Company, Syracuse.

Upon completion of his preparatory schooling he entered Cornell University, where he studied civil and mechanical engineering for a year, being one of Professor Sweet's "Boys." During 1877–1879 he worked again in the Sweet rolling mill and spring factory and served time as an apprentice patternmaker and draftsman. He also spent some time on the road erecting Sweet's producer gas furnaces and boilers.

For a short time in 1879, Mr. Tallman was superintendent of the Farist & Windsor Co., a small steel works at Windsor Locks, Conn. Then he went to Providence, R.I., to be assistant foreman in the machine shops and also special draftsman under George H. Corliss. There he became well versed in steam engines, their theory and construction.

In the fall of 1881, at the request of his stepfather, he returned to Syracuse and during the next four years he served first as assistant superintendent and later as superintendent of Sweet's Manufacturing Company. In connection with his application for membership in the A.S.M.E. at the beginning of this period Professor Sweet wrote of him: "I know no other man of Tallman's age who has so good a combination of mechanical and executive ability and who has them under so good control."

Mr. Tallman became general superintendent of the steel mills of Carnegie-Phipps & Co. in Beaver Falls, Pa., in 1885 and continued in that position until 1890. He next spent three years as mechanical consulting engineer in Pittsburgh, Pa., designing and building wire rod mills and rolling mills. He gave this up to become Pittsburgh sales manager of the Crane and Pulley Block Department of the Yale & Towne Manufacturing Co.

For ten years, beginning in 1895, he was connected with the Brown Hoisting Machinery Company, first as sales engineer at Pittsburgh and Chicago, and subsequently as manager of the company at Cleveland. He then took up his work with E. I. du Pont de Nemours & Co.

In his early life Mr. Tallman was granted patents on glass making machinery, glass containers, and wire drawing and rolling mill machinery. An honorary degree of Master of Arts was bestowed upon him by Bowdoin College in 1935. He had excellent taste in music and played the clarinet in orchestras for many years. He collected antiques, and Lincolniana, and had some rare pieces in his extensive collection of old silver. He was an ardent golfer and a veteran traveler.

Mr. Tallman's membership in the A.S.M.E. dated from 1881 and he served as a manager of the Society from 1905 to 1908. He was a member of the Historical Society of Delaware, New England Historic Genealogical Society, Massachusetts Society of Mayflower

Descendants, and Sons of the American Revolution, as well as of many professional, sport, and social clubs. He was a member of the National and Wilmington chambers of commerce, and until recent years was chairman of the Delaware Red Cross. He was also a member of the Board of Park Commissioners, director of the Wilmington Trust Company, director of the Boys' Club of Wilmington, chairman of the advisory board of the Salvation Army, and one of the proprietors of the Wilmington and Brandywine Cemetery.

Mr. Tallman was twice married. His first wife, Annie May Dickie, whom he married in Syracuse in 1881, died in 1922. In 1929 he married Mrs. Julia Hays Ashbrook, of Wilmington, who survives him. Five children by his first wife also survive him. They are William Sweet Tallman, of Sewickley, Pa., and Frank Gifford Tallman, Jr., of Wilmington, Mrs. Irving Warner and Mrs. Thomas W. Miller, also of Wilmington, and Mrs. Louis G. Bissell, of New York, N.Y.

JOHN IBBOTTSON THOMPSON (1883–1938)

John Ibbottson Thompson, president of the Koppers Rheolaveur Company, Pittsburgh, Pa., died at his home in the Ben Avon Heights section of that city on June 25, 1938.

Mr. Thompson was born in Braddock, Pa., on December 21, 1883, son of John Thomas and Mary Jane (Ibbottson) Thompson. At an early age he moved with his parents to Youngstown, Ohio, and later to Pueblo, Colo., where his father was for many years master mason in the plant of the Colorado Fuel & Iron Co.

When fifteen years of age he left school to work as a blueprint boy in the engineering department of the Colorado Fuel & Iron Co. He soon decided that he wanted to be an engineer and, therefore, resumed and completed his high school work at night. After years of work and study he was able to enter Leland Stanford University in 1905 and was graduated as a mechanical engineer in 1909.

His first employment after graduating was with W. F. Rust in the engineering department of the Youngstown Sheet & Tube Co., in Youngstown, Ohio. A year later he was employed by the Republic Iron & Steel Co., in Youngstown, where he remained until May, 1912, and then joined the Koppers organization in Chicago.

When, in the spring of 1915, the Koppers offices were moved from Chicago, to Pittsburgh, Mr. Thompson, as chief draftsman, with W. F. Rust as chief engineer, was faced with the task of building up the small nucleus of some fifteen engineers and draftsmen brought from Chicago, to one of the largest engineering organizations in the country. After two years the department had grown to over 300 employees and in August, 1927, it reached a peak of 730. Great administrative and engineering problems had to be met and successfully solved in organizing such a steadily growing force into a smoothly working assembly of well co-ordinated units. At the same time he had to establish the engineering principles governing the design of Koppers coke and gas plants to meet the standards already adopted for steel mill and power plant design.

Due to his recognized ability, Mr. Thompson was soon entrusted with greater responsibility. He served successively as assistant chief engineer, chief engineer, and vice-president in charge of engineering, construction, and purchasing, during one of the most active periods in the company's history.

At the time the Koppers Building was being planned, he, in addition to his other duties, served as chairman of the building committee and in this capacity was largely responsible for the successful completion of the entire building program.

When it was found desirable for Koppers to extend its activities to include coal washing plants, he was a member of the committee to investigate available processes. Largely due to his recommendations, the Rheolaveur Company was acquired and Mr. Thompson served, first, as vice-president and, since 1932, as president of the reorganized company, known as the Koppers Rheolaveur Company. As president, he devoted his entire time and effort to the management of the company and the establishment of its policies. During this period, through development work conducted under his direction, improvement in coal washing was accomplished and large coal preparation plants were constructed in the principal coal mining areas of the country.

Mr. Thompson took an active part in the community affairs in Ben Avon. He was responsible for much of the development work in connection with Ben Avon Heights and as first president of the Shannopin Golf Club, was an able leader in the organization of the club and the building of the club house and golf course. He was an active member of the Ben Avon Methodist Episcopal Church, which, at the time of his death, he was serving as president of its Board of Trustees.

Shortly after his graduation from Leland Stanford University, he married Adelaide Tillson, who survives him, with their two daughters, Mrs. Ruth Findlay and Jane Clare Thompson. He is also survived by three brothers, Frank, Peter B., and Carl Thompson.

Mr. Thompson had been a member of both the A.S.M.E. and the American Institute of Mining and Metallurgical Engineers since 1918. He also belonged to the Engineers' Society of Western Pennsylvania, Eastern States Blast Furnace and Coke Oven Association, and American Iron and Steel Institute, as well as to the Sigma Xi fraternity and the Duquesne Club of Pittsburgh and Medinah Country Club of Chicago.—[Adapted from a tribute in the *Koppers News*, August, 1938.]

ELIHU THOMSON (1853–1937)

In Swampscott, Mass., on March 13, 1937, death came to Professor Elihu Thomson, a few days before his 84th birthday. In his death there passes away the last member of that brilliant group of scientists and inventors who, in such amazingly rapid succession, discovered new fundamental scientific truths, contrived new theories and working hypotheses, and applied them to such a myriad of practical uses that they veritably started a new era. The names of Edison, Thomson, Steinmetz, and Westinghouse will ever be associated with the beginning and the early rapid growth of the adaptation of electricity to the industry, homes, and farms of America.

But Thomson, like the other three, by no means confined his genius to the electrical field. The fields of mechanical engineering, chemistry, and even astronomy were enriched by discoveries, applications, and improvements which constantly flowed from his laboratory as the result of his inspired thinking and brilliant experimentation. His early interests included the uniflow steam engine, the cream separator, and the automobile muffler. He made important contributions to the art of the heat treatment of steel, and was the first to propose the use of a mixture of helium and oxygen for workers in caissons and tunnel borings. For the field of astronomy he developed fused quartz for use in lenses and mirrors.

It is, however, for his achievements in the electrical field that he is best known. The three-coil dynamo, the Thomson electric meter, the resistance welder, and the alternating-current repulsion motor, are probably the best known of his inventions, but he was so prolific in this field that at his death he held the third largest number of patents ever issued to one inventor.

Professor Thomson was born in Manchester, England, on March 29, 1853, coming to the United States when he was 5 years old. Graduating from the Boys' Central High School, Philadelphia, at the age of 18, he became an instructor there, and so outstanding was his work that at the age of 23 he was made professor. Throughout these early years he was constantly conducting original experiments, mainly in electricity, making one invention after another, and delighting audiences by his astonishing demonstration lectures. It was during these early days that he antedated Hertz by over ten years and foreshadowed radio communication by sending wireless waves from one room to another through intervening walls and partitions.

In 1880, together with Professor Edwin J. Houston, also of the Philadelphia Central High School, and Edwin Wilbur Rice, Jr., one of their former pupils, he joined the newly formed American Electric Company in New Britain, Conn., forerunner of the Thomson-Houston Electric Company, which was established in Lynn, Mass., three years later. In 1892 this business was combined with the Edison General Electric Company to form the General Electric Company, Professor Thomson becoming the head of the now world-famous Thomson Research Laboratory. Here he continued his scientific investigations and development work up to about a year before his death, when his health began to fail. Throughout this long period, scientific discoveries and practical inventions continued to flow in an amazing stream from his active fertile brain. But he shunned publicity and his name rarely appeared in newspaper headlines, so the general public knew little of him. That the scientific and engineering world appreciated his greatness is attested by the numerous honorary degrees and medals conferred upon him by the outstanding scientific bodies of both Europe and America. From Great Britain he received the three most coveted scientific awards, the Hughes Medal of the Royal Society, the Lord Kelvin Medal, and the Faraday Medal. He was made chevalier and officer of the Legion of Honor of France, and was the second American to receive the Medal of Honor of the Verein Deutscher Ingenieure. In America, The Franklin Institute twice awarded him the John Scott Medal, and presented him with the Elliot Cresson Gold Medal and the Franklin Medal. He lectured before the Institute and the Thomson exhibit in its museum contains apparatus from the famous laboratory where he spent so much of his life. He also received the Rumford Medal of the American Academy of Arts and Sciences, and the John Fritz Medal of the four founder engineering societies.

As further evidence of appreciation, he was elected honorary mem-

ber of The A.S.M.E. in 1930, and had held the office of president of the American Institute of Electrical Engineers, the International Electrical Congress, and the International Electrotechnical Commission.

Professor Thomson was deeply interested in the Massachusetts Institute of Technology, serving as non-resident professor of electrical engineering, life member of the Corporation, and for over two years its acting president.

Honored by several great universities with the degree of Doctor, he preferred the simple title of Professor. "It is more friendly," he said. This is indicative of the man. His life was simple, his attitude friendly and unselfish, exemplifying the very spirit of co-operation and helpfulness. With a true scientist's and engineer's unselfish devotion to the common good, he took such an active part in civic and community affairs, that it won for him the confidence and enduring love of his fellow townsmen.—[Memorial prepared by Professor WILLIAM H. TIMBIE, Department of Electrical Engineering, Massachusetts Institute of Technology, Cambridge, Mass.]

EDWARD F. VOLKMER (1867–1934)

Edward F. Volkmer, who became a member of the A.S.M.E. in 1930, and whose death occurred on October 3, 1934, was a native of Germany. He was born at Seelow on November 27, 1867, and was educated in Germany, attending a technical high school in Berlin for a year and a half. For some fifteen years he was employed in that city, working for various firms, including Siemens & Halske and the C. P. Goerz Optical Co. Then he was at the Maxim gun works, Erith, Kent, England, for two and a half years.

The year in which Mr. Volkmer came to the United States is not known, but in 1906 he started a business here, it is thought in Newark, N.J., for the design and manufacture of automatic machinery and scientific instruments in the mechanical and electrical fields. This was later incorporated as the Volkmer Electrical Company, but reverses forced the company out of business. Between 1910 and 1918, when he reestablished himself in Newark as an independent designer and builder of automatic labor saving machinery, Mr. Volkmer served successively as superintendent of the Herschede Hall Clock Company, Cincinnati, Ohio, designing engineer for the Singer Sewing Machine Company, Elizabethport, N.J., and American Machine & Foundry Co., Brooklyn, N.Y., and superintendent of J. Mills Co., Brooklyn.

Mr. Volkmer's organization was known as E. F. Volkmer & Sons, Inc., until about 1930, when it became the Volkmer Radio Products Corporation, of which he was president and general manager. At that time he reported that a branch was being opened in Chicago, Ill. Whether this plan was carried out is not known, but in 1931 or 1932 the Volkmer Manufacturing Company, for the manufacture of special radio wire, was established in Long Island City, N.Y. After his death, this business was continued for a time by his son, Paul R. Volkmer.—[Biography compiled from best obtainable information, not all of which could be verified.]

EDGAR WHITE WAGENSEIL (1884–1938)

Edgar White Wagenseil, sales manager of the Hagan Corporation, Pittsburgh, Pa., and a resident of the Oakmont Section of that city, died suddenly on May 10, 1938, while engaged in his official duties.

Mr. Wagenseil was born at Port Huron, Mich., on November 16, 1884, son of George O. and Mary Adelia (White) Wagenseil. He attended the Port Huron schools and was graduated from the University of Illinois in 1905, with a B.S. degree in mechanical engineering. During the following summer he was employed by the B. F. Sturtevant Co., Chicago, as draftsman on indirect heating systems, then he became assistant to the master mechanic of the Illinois Steel Company at their South Works, Chicago, where he remained until June, 1907. The next six months were spent with the Warren Webster Company, Chicago, as salesman and draftsman on heating and ventilating installations.

In November, 1907, Mr. Wagenseil was made a deputy smoke inspector for the City of Chicago, and for two years he was engaged in various combustion engineering problems connected with that position. He then became sales manager and combustion engineer for the Burke Furnace Company, Chicago, in direct charge of furnace and stoker installations and boiler tests, and continued with that company until the United States entered World War I. As a lieutenant (junior grade) in the Naval Reserve Force, he served from July, 1918, to February, 1919, in the Naval Air Force in connection with the assembly and repair of Liberty motors, being stationed at a Reserve Flying Corps Repair Base in France part of the time.

After the war Mr. Wagenseil was employed for about two years by the Westinghouse Electric & Manufacturing Co. as district stoker engineer at Chicago. Subsequently he spent several years on sales of the Harrington stoker, first as sales manager for the Brady Foundry Company, later as district manager for the United Machine & Manufacturing Co., both in Chicago. When the latter was acquired by the Riley Stoker Corporation in 1924, he became secretary and treasurer of the Buckeye Dryer Company, Chicago. From 1927 to 1932 he was sales engineer for the Blaw-Knox Company, of Pittsburgh, Pa., handling air preheaters for the steel industry.

Mr. Wagenseil had been connected with the Hagan Corporation, combustion and chemical engineers, since 1932, serving first as sales engineer and later as general sales manager for the company and its subsidiaries, the Buromin Company and Hall Laboratories, Inc.

Mr. Wagenseil had been a member of the A.S.M.E. since 1916 and also belonged to the Engineers' Society of Western Pennsylvania, and to the Iron and Steel Electrical Engineers, and the Pittsburgh Field Club. He is survived by his widow, Ruth B. (Taylor) Wagenseil, whom he married in 1907, a son, John White Wagenseil, and a daughter, Martha.

LEE EARL WALKER (1881–1937)

Lee Earl Walker, district manager in charge of sales for the Good Roads Machinery Corporation's branch office at Philadelphia, Pa., died on December 18, 1937. The son of Curtis M. and Nancy Jane (Burleigh) Walker, he was born on August 10, 1881, in Johnstown, Pa., and attended public schools there and in Altoona, Pa. He served an apprenticeship as a machinist with the Pennsylvania Railroad, at Altoona, from 1899 to 1902, and then worked for nearly a year for the Westinghouse Machine Company, Pittsburgh, Pa., building gas and steam engines. From July, 1903, to January, 1905, he was employed by the Baldwin Locomotive Works, Philadelphia, Pa., as foreman of locomotive construction. During the next two years he was foreman of general locomotive repairs for the Atchison, Topeka & Santa Fe R.R. at Needles and San Bernardino, Calif. A survivor of the Johnstown flood as a boy, he also experienced the San Francisco earthquake during this period of employment in California.

In January, 1909, Mr. Walker returned to the Baldwin Locomotive Works, where he remained for about three years. At first he was night foreman of the erecting shop, then final engine inspector at the 26th Street shop. Later he went to the new Eddystone shops as assistant to the general foreman of the erecting department, and finally he was appointed traveling engineer, to set up locomotives and try them out on grade and tonnage tests on various railroads.

From early in 1912 until the latter part of 1914, Mr. Walker was connected with the American Road Machinery Company, Groton, N.Y., as assistant to the vice-president and general manager of the company, in direct charge of the entire plant. His duties included the design of jigs and fixtures, testing of machinery, and supervision of the drafting department, in addition to manufacturing. Early in 1915 Mr. Walker was transferred to the office of the Good Roads Machinery Company, in Philadelphia, the selling organization, as salesman and sales engineer. The following year he was made district salesman for this company, with headquarters in Washington, D.C.

During the World War period, 1917–1919, Mr. Walker served in the Ordnance Reserve Corps, advancing from the rank of first lieutenant to that of major. He was ordered to active duty in the Production Division of the Ordnance Department at Washington in October, 1917, and was officer in charge of the production of ordnance matériel at various plants during the following year. He was stationed at Amatol, N.J., in connection with the construction and operation of a shell-loading plant for several months following the Armistice, and from then until August, 1919, was on the staff of the commanding officer at the Amatol Arsenal, in charge of the Storage, Traffic, and Construction Department.

Mr. Walker returned to civilian life as district sales engineer and assistant manager of the Good Roads Machinery Company's branch office at Philadelphia. The Good Roads Machinery Corporation was incorporated in 1932, acquiring the Good Roads Machinery Company and also the American Road Machinery Company, and Mr. Walker continued with the organization as distributor until his death.

Mr. Walker became an associate of the A.S.M.E. in 1916; and associate-member in 1921; and was automatically promoted to the member grade in 1935. He was a member of the Engineers Club of Philadelphia, Philadelphia Art Club, and the Montgomery Lodge, in Philadelphia, of the masonic fraternity, in which order he held the 32nd degree. His main interest outside his work was his summer home, a farm in the Pocono Mountains.

Mr. Walker was twice married. He is survived by his second wife, Gertrude O. (Ferguson) Walker, and by two children, Sydney Lee Walker and Mrs. Juanita (Walker) Pelka.

IN TWO SECTIONS—SECTION TWO

Transactions

of the

A.S.M.E.

SOCIETY RECORDS—Part III

(Including Indexes to Publications)

[*Part I of Society Records for the year 1942 (containing Council and Committee Personnel and other general information) was issued as Section Two of the Transactions for February, 1942, and Part II (Memorial Biographies) October, 1942.*]

Depositories for A.S.M.E. Transactions in the United States RI-77

A.S.M.E. Transactions in Central and South America and Great Britain RI-80

Indexes to A.S.M.E. Papers and Publications RI-81

- Regular Society Publications, 1942 . . . . . RI-81
- Special Publications Issued in 1942 . . . . . RI-81
- How to Find Papers Presented at 1942 A.S.M.E. Meetings RI-81
- Publications Developed by the Technical Committees RI-81
- Biographies RI-83
- Books on Special Subjects RI-83
- Periodicals RI-83

Index to *Mechanical Engineering*, 1942 . . . . . RI-85

Index to Transactions, 1942 . . . . . RI-95

JANUARY, 1943

VOL. 65, NO. 1

Transactions

of The American Society of Mechanical Engineers

Published on the tenth of every month, except March, June, September, and December

---

OFFICERS OF THE SOCIETY:

HAROLD V. COES, *President*

W. D. ENNIS, *Treasurer* C. E. DAVIES, *Secretary*

COMMITTEE ON PUBLICATIONS:

C. R. SODERBERG, *Chairman*

F. L. BRADLEY, *Vice-Chairman* L. N. ROWLEY, JR.

E. J. KATES G. B. KARELITZ

GEORGE A. STETSON, *Editor*

ADVISORY MEMBERS OF THE COMMITTEE ON PUBLICATIONS:

N. C. EBAUGH, GAINESVILLE, FLA. R. F. GAGG, PATERSON, N. J. O. B. SCHIER, 2ND, NEW YORK, N. Y.

Junior Member

J. A. CONNON, NEW YORK, N. Y.

Published monthly by The American Society of Mechanical Engineers. Publication office at 20th and Northampton Streets, Easton, Pa. The editorial department is located at the headquarters of the Society, 29 West Thirty-Ninth Street, New York, N. Y. Cable address, "Dynamic," New York. Price $1.50 a copy, $12.00 a year; to members and affiliates, $1.00 a copy, $7.50 a year. Changes of address must be received at Society headquarters two weeks before they are to be effective on the mailing list. Please send old as well as new address. . . . By-Law: The Society shall not be responsible for statements or opinions advanced in papers or . . . printed in its publications (B13, Par. 4). . . . Entered as second-class matter March 2, 1928, at the Post Office at Easton, Pa., under the act of August 24, 1912. . . .

Copyrighted, 1943, by The American Society of Mechanical Engineers. Reprints from this publication may be made on condition that full credit be given the Transactions of the A.S.M.E. and the author, and that date of publication be stated.

Depositories for A.S.M.E. Transactions in the United States, Including Territories and Dependencies

BOUND copies of the complete Transactions of The American Society of Mechanical Engineers will be found in the libraries in the United States and other countries which are listed on the following pages.

Alabama

Auburn	Engineering Library, Alabama Poly. Inst.
Birmingham	Public Library
University	Library, University of Alabama

Arizona

Tucson	Library, University of Arizona

Arkansas

Fayetteville	Engineering Library, University of Arkansas

California

Berkeley	Library, University of California
Long Beach	Public Library
Los Angeles	Public Library
	University of Southern California
Oakland	Oakland City Library
	Teachers' Professional Library
Pasadena	Library, California Institute of Technology
Santa Clara	Library, University of Santa Clara
San Diego	Public Library
San Francisco	Engineers Club of San Francisco
	Mechanics Institute
	Public Library (Civic Center)
Stanford Univ.	Library, Stanford University

Colorado

Boulder	Library, University of Colorado
Denver	Public Library
Fort Collins	Colorado State College of Agriculture and Mechanic Arts

Connecticut

Bridgeport	Public Library
Hartford	Public Library
New Haven	Public Library and Yale University
Storrs	University of Connecticut
Waterbury	Silas Bronson Library

Delaware

Newark	University of Delaware
Wilmington	Wilmington Free Institute

District of Columbia

Washington	George Washington and Catholic Universities; Library of Congress; National Bureau of Standards Library; Scientific Library, U. S. Patent Office

Florida

Gainesville	University of Florida
Jacksonville	Free Public Library
Miami	Public Library
Tampa	Public Library

Georgia

Atlanta	Carnegie Public Library
	Georgia School of Technology
Savannah	Public Library

Hawaii

Honolulu	University of Hawaii Library

Idaho

Moscow	University of Idaho

Illinois

Chicago	John Crerar Library; Library, Illinois Institute of Technology; Museum of Science and Industry; Public Library of Chicago; Western Society of Engineers
Evanston	Northwestern University
Moline	Public Library
Peoria	Public Library
Urbana	University of Illinois

Indiana

Evansville	Public Library
Fort Wayne	Public Library
Indianapolis	Public Library and Indiana State Library
Notre Dame	Library, University of Notre Dame
Terre Haute	Rose Polytechnic Institute
West Lafayette	Library, Purdue University

Iowa

Ames	Iowa State College
Des Moines	Public Library
Iowa City	State University of Iowa

Kansas

Kansas City	Public Library, Huron Park
Lawrence	Library, University of Kansas
Manhattan	Kansas State College
Wichita	Wichita City Library

Kentucky

Lexington	University of Kentucky
Louisville	Speed Scientific School
	University of Louisville

Louisiana

Baton Rouge	Louisiana State University
New Orleans	The Howard-Tilton Memorial Library
	Louisiana Engineering Society
	Public Library
	Tulane University

Maine

Orono	University of Maine

Maryland

Annapolis	United States Naval Academy
Baltimore	Engineers Club of Baltimore
	Johns Hopkins University
	Public Library
College Park	Library, University of Maryland

Massachusetts

Boston	Boston Public Library
	Engineering Societies of New England
	Northeastern University
Cambridge	Harvard University (Engineering Library)
	Massachusetts Institute of Technology
Fall River	Public Library
Lynn	Free Public Library
New Bedford	Free Public Library
Springfield	Springfield City Library
Tufts College	Tufts College
Worcester	Free Public Library
	Worcester Polytechnic Institute

Michigan

Ann Arbor	University of Michigan
Detroit	Cass Technical High School
	Highland Park Public Library
	Public Library
	University of Detroit
East Lansing	Michigan State College
Flint	Public Library
Grand Rapids	Public Library
Houghton	Michigan College of Mining & Technology
Jackson	Public Library

Minnesota

Duluth	Public Library
Minneapolis	Minneapolis Public Library (Engineering and Circulating Libraries)
	University of Minnesota
St. Paul	James Jerome Hill Reference Library

Mississippi

State College	Mississippi State College

Missouri

Columbia.....University of Missouri
Kansas City.....Public Library
Rolla.....Missouri School of Mines and Metallurgy
St. Louis.....Engineers Club of St. Louis; Public Library; Washington University; Mercantile Library

Montana

Bozeman.....Montana State College

Nebraska

Lincoln.....University of Nebraska
Omaha.....Public Library

Nevada

Reno.....University of Nevada Library

New Hampshire

Durham.....University of New Hampshire

New Jersey

Bayonne.....Free Public Library
Camden.....Free Public Library
Elizabeth.....Free Public Library
Hoboken.....Stevens Institute of Technology
Jersey City.....Free Public Library
Newark.....Free Public Library
Newark College of Engineering
New Brunswick..Rutgers University
Paterson.....Free Public Library
Princeton.....Princeton University
Trenton.....Free Public Library

New Mexico

Albuquerque.....University of New Mexico
State College.....New Mexico State College

New York

Albany.....New York State Library
Brooklyn.....Polytechnic Institute
Pratt Institute
Brooklyn Public Library
Buffalo.....The Grosvenor Library
Engineering Society of Buffalo
Buffalo Public Library
Ithaca.....Cornell University
Jamaica, L. I.....Queens Borough Public Library
New York.....College of the City of New York
Columbia University
Cooper Union
Engineering Societies Library
New York Museum of Science and Industry
New York University Library
Public Library
Potsdam.....Clarkson College of Technology
Rochester.....Rochester Engineering Society
Schenectady.....Union College
Syracuse.....Public Library
Syracuse University
Troy.....Rensselaer Polytechnic Institute
Utica.....Public Library

North Carolina

Chapel Hill.....University of North Carolina
Durham.....Duke University
Raleigh.....North Carolina State College

North Dakota

Fargo.....North Dakota State Agricultural College.
Grand Forks.....University of North Dakota

Ohio

Ada.....Ohio Northern University
Akron.....Public Library
University of Akron
Canton.....Public Library
Cincinnati.....Engineers Club of Cincinnati
Public Library
University of Cincinnati
Cleveland.....Case School of Applied Science
Cleveland Engineering Society
Fenn College
Public Library
Columbus.....The Ohio State Library
Ohio State University
Public Library
Dayton.....Engineers Club of Dayton
Toledo.....Public Library
University of Toledo
Youngstown.....Public Library

Oklahoma

Norman.....Oklahoma University
Oklahoma City..Public Library
Stillwater.....Oklahoma A.&M. College
Tulsa.....Public Library

Oregon

Corvallis.....Oregon State College
Portland.....Portland Library Association

Pennsylvania

Allentown.....Free Library
Bethlehem.....Lehigh University
Easton.....Lafayette College
Public Library
Erie.....Public Library
Lewisburg.....Bucknell University
Philadelphia.....Drexel Institute
Engineers Club
Franklin Institute
The Free Library
University of Pennsylvania
Pittsburgh.....Carnegie Free Library of Allegheny
Carnegie Institute of Technology
Carnegie Library (Schenley Park)
Engineers' Society of Western Pennsylvania
University of Pittsburgh
Reading.....Public Library
Scranton.....Public Library
State College.....Pennsylvania State College
Swarthmore.....Swarthmore College
Villanova.....Villanova College
Wilkes-Barre.....Public Library

Puerto Rico

Mayaguez.....University of Puerto Rico

Rhode Island

Kingston.....Rhode Island State College
Providence.....Brown University
Providence Engineering Society
Public Library

South Carolina

Clemson College..Library, Clemson College

South Dakota

Brookings.....South Dakota State College

Tennessee

Kingsport.....Public Library
Knoxville.....University of Tennessee
Memphis.....Goodwin Institute
Nashville.....Vanderbilt University

Texas

Austin.....University of Texas
College Station...Texas Agricultural & Mechanical College
Dallas.....Public Library
Southern Methodist University
El Paso.....Public Library
Fort Worth.....Carnegie Public Library
Houston.....Public Library
Rice Institute
Lubbock.....Texas Technological College
San Antonio.....Carnegie Library

Utah

Salt Lake City...University of Utah
Public Library

Vermont

Burlington.....University of Vermont

Virginia

Blacksburg.....Virginia Polytechnic Institute
Charlottesville...University of Virginia

Lexington.....Virginia Military Institute
Norfolk.....Public Library
Richmond.....Virginia State Library

Washington

Pullman.....State College of Washington
Seattle.....Engineers Club
Public Library
University of Washington
Spokane.....Public Library
Tacoma.....Public Library

West Virginia

Morgantown.....West Virginia University

Wisconsin

Madison.....Library, University of Wisconsin
Milwaukee.....Marquette University
Public Library
Vocational School Library

Wyoming

Laramie.....Wyoming University

A.S.M.E. Transactions in Central and South America and Great Britain

Argentine

Buenos Aires	Biblioteca de la Sociedad Cientifica

Australia

Adelaide	Public Library of Adelaide
Melbourne	Public Library of Victoria
Perth	University of Western Australia Library
Sydney	Public Library of Sydney

Brazil

Rio de Janeiro	Bibliotheca da Escola Polytechnica
	Bibliotheca Nacional
São Paulo	Bibliotheca da Escola Polytechnica

Canada

Kingston	Queen's College
Montreal	Engineering Institute of Canada
	McGill University
Toronto	University of Toronto, Library
Vancouver	University of British Columbia

Chile

Santiago	Universidad de Chile, Facultad de Ciencias Fisicas y Matematicas (Engg. School)

Cuba

Havana	Cuban Society of Engineers

England

Birmingham	Birmingham Public Libraries
Bristol	University of Bristol
Cambridge	University of Cambridge
Leeds	University of Leeds
Liverpool	Liverpool Engineering Society
	Public Library of Liverpool
London	City and Guild Engineering College
	Institution of Automobile Engineers

England (continued)

	The British Coal Utilization Research Association
	The Institution of Mechanical Engineers
	Institution of Civil Engineers
	Institution of Electrical Engineers
	The Junior Institution of Engineers
	The Royal Aeronautical Society
Manchester	Manchester Public Libraries (Reference Library)
Oxford	Oxford University
Newcastle-upon-Tyne	The North-East Coast Institution of Engineers and Shipbuilders
Sheffield	Sheffield Public Libraries

India

Bangalore	Mysore Engineers Association
Calcutta	Bengal Engineering College
Poona	Poona College of Engineering
Rangoon	University of Rangoon

Ireland

Belfast	Queen's University of Belfast

Mexico

Mexico City	Asociacion de Ingenieros y Arquitectos de Mexico
	Library of the Escuela de Ingenieros Mecanicos y Electricistas

Scotland

Glasgow	Royal Technical College
	Mitchell Library

South Africa

Cape Town	University of Cape Town
Johannesburg	South African Institute of Engineers

Wales

Cardiff	Cardiff Public Library

Indexes to A.S.M.E. Papers and Publications

THIS and the following pages will serve as a guide to the current publications of the A.S.M.E. during the calendar year 1942 and also to publications developed by technical committees.

Regular Society Publications, 1942

Mechanical Engineering, monthly (see index on page RI-85)
A.S.M.E. Transactions, monthly (see index on page RI-95)
Mechanical Catalog and Directory, 1943 edition

Special Publications Issued in 1942

I.S.A. Tolerance System
1941 Oil Engine Power Cost Report
1942 Proceedings of the Oil and Gas Power Division
Surface Finish

American Standards

1942 Supplement to 1937 Safety Code for Elevators
C. I. Screwed Drainage Fittings
Pipe Threads
Code for Pressure Piping
Letter Symbols for Hydraulics
Letter Symbols for Mechanics of Solid Bodies

A.P.I.-A.S.M.E. Code for Unfired Pressure Vessels

1942 Addenda

Boiler Construction Code

1942 Addenda to:
- Locomotive Boiler Code
- Low Pressure Heating Boilers
- Miniature Boiler Code
- Power Boiler Code
- Unfired Pressure Vessel Code
- Specifications for Materials

Power Test Codes

Supplement to Hydraulic Prime Movers

Auxiliary Sections

Part 2, Pressure Measurement, Chapter 5, Liquid Column Gages
Part 12, Measurement of Time
Part 21, Leakage Measurements

How to Find Papers Presented at 1942 A.S.M.E. Meetings

THE technical programs of the meetings of the Society and of its Professional Divisions have been published in *Mechanical Engineering* and may be located by consulting the index on pages RI-85–94. A majority of these papers were published, or will be published, in *Mechanical Engineering* or the Transactions (including the *Journal of Applied Mechanics*) and may be located by reference to the indexes of these publications. Several additional papers and reports included in these 1942 programs were not published during the year in Transactions or *Mechanical Engineering* but were issued in mimeographed or photo-offset form.

Complete sets of these are on file for reference purposes at the office of the Society and the Engineering Societies Library, under the title of "Miscellaneous Papers Presented at A.S.M.E. Meetings, 1942." Photostat copies of any of the papers may be secured from the Library at twenty-five cents a page to members, or thirty cents a page to nonmembers.

Publications Developed by the Technical Committees

THE Society's technical committees, the first of which was organized many years ago and all of which have been continuously at work on codes, standards, research, and other special reports, have developed a series of publications of permanent value to the membership. The following list is presented here for record and for ready reference. This list covers the entire group of publications of these committees completed to date which are now available.

To assist the members in securing copies of these publications the sale price is also given. A discount of 10 per cent is allowed to A.S.M.E. members on standards and a 20 per cent discount on all other publications except where otherwise noted.

A.S.M.E. AMERICAN STANDARDS

Bolt, Nut, and Rivet Proportions

Large Rivets (B18.4—1937), $0.65
Plow Bolts (B18f—1928), $0.35
Round Unslotted-Head Bolts (B18.5—1939), $0.50
Slotted-Head Proportions: Machine Screws, Cap Screws, and Wood Screws (B18c—1930), $0.45
Small Rivets (B18a—1927), $0.30
Socket Set Screws and Socket-Head Cap Screws (B18.3—1936), $0.40
Tinners', Coopers', and Belt Rivets (B18g—1929), $0.35
Track Bolts and Nuts (B18d—1930), $0.40
Wrench-Head Bolts and Nuts and Wrench Openings (B18.2—1941), $0.65

Piping and Pipe Fittings

Brass Fittings for Flared Copper Tubes (A40.2—1936), $0.35
Cast-Iron Pipe Flanges and Flanged Fittings for 25 Lb Maximum Saturated Steam Pressure (B16b2—1931), $0.40
Cast-Iron Pipe Flanges and Flanged Fittings for 125 Lb Maximum Saturated Steam Pressure (B16a—1939), $0.60
Cast-Iron Pipe Flanges and Flanged Fittings for 250 Lb Maximum Saturated Steam Pressure (B16b—1928), $0.50
Cast-Iron Pipe Flanges and Flanged Fittings for 800 Lb Maximum Hydraulic Pressure (B16b1—1931), $0.35
Cast-Iron Soil Pipe and Fittings (A40.1—1935), $0.65
Cast-Iron Long Turn Sprinkler Fittings for 150 and 250 Lb Maximum Saturated Steam Pressure (B16g—1929) and Addendum (B16g1—1937), $0.50
Cast-Iron Screwed Fittings for 125 and 250 Lb Maximum Saturated Steam Pressure (B16d—1941), $0.40
Cast-Iron Screwed Drainage Fittings (B16.12—1942), $0.45
Code for Pressure Piping (B31.1—1942), $2.00
Face-to-Face Dimensions of Ferrous Flanged and Welding End Valves (B16.10—1939), $0.55
Malleable-Iron Screwed Fittings for 150 Lb Maximum Saturated Steam Pressure (B16c—1939), $0.50
Pipe Plugs (B16e2—1936), $0.35
Pipe Threads (B2.1—1942), $0.75
Scheme for the Identification of Piping Systems (A13—1928), $0.50
Steel Pipe Flanges and Flanged Fittings for 150 to 2500 Lb Maximum Steam Service Pressure (B16e—1939), $1.25

Soldered-Joint Fittings (A40.3—1941), $0.45
Steel Butt-Welding Fittings (B16.9—1940), $0.40
Wrought-Iron and Wrought-Steel Pipe (B36.10—1939), $0.50

Letter and Graphical Symbols and Charts

Abbreviations for Scientific and Engineering Terms (Z10.1—1941), $0.35
Drawings and Drafting-Room Practice (Z14.1—1935), $0.50
Engineering and Scientific Charts for Lantern Slides (Z15.1—1932), $0.50
Graphical Symbols for use on Drawings in Mechanical Engineering (Z32.2—1941), $0.50
Letter Symbols for Hydraulics (Z10.2—1942), $0.35
Letter Symbols for Mechanics of Solid Bodies (Z10.3—1942), $0.25
Letter Symbols for Heat and Thermodynamics (Z10c—1931), $0.30
Letter Symbols for Photometry and Illumination (Z10d—1930), $0.20
Time Series Charts (Z15.2—1938), $1.25

MISCELLANY

Fire-Hose Coupling Screw Thread (B26—1925), $0.25
Gear Materials and Blanks (B6.2—1933), $0.50
Hose Coupling Screw Threads (B33.1—1935), $0.25
Indicating Pressure and Vacuum Gages (B40—1939), $0.40
Preferred Thickness for Uncoated Thin Flat Metals (B32.1—1941), $0.25
Rolled Threads for Screw Shells of Electric Sockets and Lamp Bases (C44—1931), $0.35
Shaft Couplings (B49—1932), $0.35
Spur Gear Tooth Form (B6.1—1932), $0.45

Small Tools and Machine Tool Elements

Machine Tapers (B5.10—1937), $0.50
Milling Cutters (B5c—1930), $0.75
Taps—Cut and Ground Threads (B5.4—1939), $1.25
Terminology and Definitions for Single-Point Cutting Tools (B5.13—1939), $0.40
Adjustable Adapters (B5.11—1937), $0.50
Chucks and Chuck Jaws (B5.8—1936), $0.45
Circular and Dovetail Forming Tool Blanks (B5.7—1936), $0.40
Involute Splines, Side Bearings (B5.15—1939), $0.65
Jig Bushings (B5.6—1941), $0.35
Lathe Spindle Noses (B5.9—1936), $0.50
Reamers (B5.14—1941), $0.75
Rotating Air Cylinders and Adapters (B5.5—1932), $0.35
Tool Holder Shanks—Tool Post Openings (B5b—1929), $0.25
T-Slots, Their Bolts, Nuts, Tongues, and Cutters (B5a—1941), $0.35
Twist Drills (B5.12—1940), $0.55
Code for Design of Transmission Shafting (B17c—1927), $0.75
Shafting and Stock Keys (B17.1—1934), $0.45
Screw Threads for Bolts, Nuts, Machine Screws, and Threaded Parts (B1.1—1935), $0.60
Screw Thread Gages and Gaging (B1.2—1941), $0.60
Acme and Other Translating Threads (B1.3—1941), $0.45
Tolerances, Allowances, and Gages for Metal Fits (B4a—1925), $0.50
Woodruff Keys, Keyslots, and Cutters (B17f—1930), $0.35

BOILER CONSTRUCTION CODE

1942 Addenda to:
- Locomotive Boiler Code, $0.50
- Low-Pressure Heating Boilers, $0.50
- Miniature Boiler Code, $0.15
- Power Boiler Code, $0.45
- Unfired Pressure Vessel Code, $0.50
- Specifications for Materials, $0.85

Boiler Code Interpretation Service, $5.00 annually
API-ASME Code for Unfired Pressure Vessels
1942 Addenda, $0.40

POWER TEST CODES AND AUXILIARY SECTIONS

Test Codes for

Atmospheric Water-Cooling Equipment (1930), $0.45
Compressors and Exhausters (1935), $0.95
Displacement Compressors, Vacuum Pumps, and Blowers (1939), $0.75
Dust Separating Apparatus (1941), $0.90
Evaporating Apparatus (1941), $0.50
Feedwater Heaters (1927), $0.35
Gas Producers (1928), $0.55
Hydraulic Prime Movers (1938 with 1942 Addenda), $0.60
Internal-Combustion Engines (1930), $0.55
Liquid Fuels (1930), $0.35
Reciprocating Steam Engines (1935), $0.65
Reciprocating Steam-Driven Displacement Pumps (1927), $0.65
Refrigerating Systems (1927), $0.55
Solid Fuels (1931), $0.55
Speed-Responsive Governors (1927), $0.45
Stationary Steam-Generating Units (1936), $0.60
Steam Condensing Apparatus (1938), $0.65
Steam Locomotives (1941), $0.55
Steam Turbines (1941), $2.50

Auxiliary Sections

General Instructions (1929), $0.35
Definitions and Values (1931), $0.40
Part 1—General Considerations (1935), $0.35.
Part 2—Pressure Measurement
- Chapter 1, Barometers; Chapter 6, Tables, Multipliers, and Standards (1941), $0.60
- Chapter 2, Static and Total Pressure, Static Holes and Tubes, and Chapter 3, Pipes for Pressure Measurement (1936), $0.65
- Chapter 4, Bourdon, Bellows, Diaphragm, and Deadweight Gages (1938), $0.65
- Chapter 5, Liquid Column Gages (1942), $0.75

Part 3—Temperature Measurement
- Chapter 1, General; Chapter 5, Pyrometric Cones; Chapter 6, Liquid-in-Glass Thermometers; and Chapter 7, Bourdon Tube Thermometers (1931), $0.75
- Chapter 2, Radiation Pyrometers (1936), $0.55
- Chapter 3, Thermocouple Thermometers or Pyrometers (1940), $0.65
- Chapter 8, Optical Pyrometers (1940), $0.35

Part 4—Head Measuring Apparatus (1933), $0.35
Part 5, Chapter 4—Flow Measurement by Means of Standardized Nozzles and Orifice Plates (1940), $2.75
Part 6—Electrical Measurements (1934), $1.25
Part 8—Measurement of Indicated Horsepower (1941), $0.75
Part 9—Heat of Combustion (1932), $0.40
Part 10—Flue and Exhaust Gas Analyses (1936), $1.35
Part 11—Determination of Quality of Steam (1931), $0.45
Part 12—Measurement of Time (1942), $0.40
Part 13—Speed Measurements (1939), $0.45
Part 14—Linear Measurements (1936), $0.55
Part 15—Measurement of Surface Areas (1937), $0.75
Part 16—Density Determinations (1931), $0.30
Part 17—Determination of the Viscosity of Liquids (1931), $0.45
Part 18—Humidity Determinations (1932), $0.50
Part 20—Smoke-Density Determinations (1936), $0.65
Part 21—Leakage Measurements (1942), $0.60

RESEARCH

Fluid Meters:
- Part 1—Theory and Application (1937), $3.00
- Part 2—Description of Meters (1931), $1.75
- Part 3—Selection and Installation (1933), $1.50

Report of the A.G.A.-A.S.M.E. Committee on Orifice Coefficients (1935), $2.75
Tests on Electrical Equipment for Drilling Rotary Drilled Oil Wells (1933), $0.85
Tests on Steam Equipment for Drilling Rotary Drilled Oil Wells (1932), $0.85
Bibliography on Cutting of Metals (1866–1930), $1.25
Bibliography on Deterioration of Condensing Equipment (1845–1930), $1.25
Bibliography on Effect of Temperature Upon Properties of Metals (1928–1931), $1.25
Bibliography on Management Literature and Supplement (1903–1935), $2.75
Bibliography on Mechanical Springs (1678–1927), $1.25
Bibliography on Woods of the World (1928), $1.25
Bibliography on Marketing Research (1935), $1.00
Bibliography on Machining of Wood (1939), $1.25

SAFETY CODES

Safety Code for Elevators (A17.1—1937 with 1942 Supplement) (10 per cent discount), $1.00
Elevator Inspectors' Manual (A17.2—1937) (10 per cent discount), $0.75

Safety Code for Mechanical Power-Transmission Apparatus (10 per cent discount) (B15—1927), $0.35
Compressed-Air Machinery and Equipment (B19—1938), $0.30

BIOGRAPHIES

BIOGRAPHIES issued under the sponsorship of the A.S.M.E. Biography Committee are as follows:

Autobiography of John A. Brashear (1924), $5.00
Autobiography of an Engineer, by W. LeR. Emmet (1940), $3.50
Autobiography of John Fritz (1940), $3.25
Biography of James Hartness, by Joseph W. Roe (1937), $4.00
Biography of Fred J. Miller (1941), $1.00
Biography of John Stevens, by Archibald Douglas Turnbull (1928), $5.00
Biography of John Edson Sweet, by A. W. Smith (1925), $4.50
Biography of Robert Henry Thurston, by William F. Durand (1929), $5.00
Life of Henry Laurence Gantt, by L. P. Alford (1934), $5.00

BOOKS ON SPECIAL SUBJECTS

Aeronautical Dictionary (1929), $1.65
Corrosion-Resistant Metals (1936), $1.25
Engineering's Part in the Development of Civilization (1939), $1.50
Flow of Water in Pipes and Pipe Fittings (1941), $8.00
General Discussion on Lubrication (1938) (no discount), $6.50
Hydraulic Laboratory Practice (1929), $10.00
Hydraulic Structures (1937), $18.00
I.S.A. Tolerance System (1942), $2.50
Manual on Cutting of Metals (1939), $5.00
1943 A.S.M.E. Mechanical Catalog and Directory, $3.00 (set gratis to members upon request)
1941 Oil Engine Power Cost Report (1942), $1.25
Sixty Year Index to A.S.M.E. Technical Papers (1941), $3.75
Surface Finish (1942) (no discount), $3.25
Theoretical Steam Rate Tables (1937), $1.25

PERIODICALS

*Mechanical Engineering**—Annual Subscription rate in United States $6; to Canada $6.75; elsewhere, $7.50
A.S.M.E. Transactions,* including *Journal of Applied Mechanics*, Annual subscription rate in United States, $12, elsewhere, $12.75

* Subscription price included in A.S.M.E. membership dues.

Index photographed at the
beginning for the convenience
of the microfilm user.